IJACSA
WHERE WISDOM SHARES

International Journal of Advanced Computer Science and Applications

Volume 10 Issue 12

December 2019

ISSN 2156-5570(Online)
ISSN 2158-107X(Print)

SAI

www.ijacsa.thesai.org

Editorial Preface

From the Desk of Managing Editor…

It may be difficult to imagine that almost half a century ago we used computers far less sophisticated than current home desktop computers to put a man on the moon. In that 50 year span, the field of computer science has exploded.

Computer science has opened new avenues for thought and experimentation. What began as a way to simplify the calculation process has given birth to technology once only imagined by the human mind. The ability to communicate and share ideas even though collaborators are half a world away and exploration of not just the stars above but the internal workings of the human genome are some of the ways that this field has moved at an exponential pace.

At the International Journal of Advanced Computer Science and Applications it is our mission to provide an outlet for quality research. We want to promote universal access and opportunities for the international scientific community to share and disseminate scientific and technical information.

We believe in spreading knowledge of computer science and its applications to all classes of audiences. That is why we deliver up-to-date, authoritative coverage and offer open access of all our articles. Our archives have served as a place to provoke philosophical, theoretical, and empirical ideas from some of the finest minds in the field.

We utilize the talents and experience of editor and reviewers working at Universities and Institutions from around the world. We would like to express our gratitude to all authors, whose research results have been published in our journal, as well as our referees for their in-depth evaluations. Our high standards are maintained through a double blind review process.

We hope that this edition of IJACSA inspires and entices you to submit your own contributions in upcoming issues. Thank you for sharing wisdom.

Thank you for Sharing Wisdom!

Managing Editor
IJACSA
Volume 10 Issue 12 December 2019
ISSN 2156-5570 (Online)
ISSN 2158-107X (Print)

Editorial Board

CONTENTS

Local-Set Based-on Instance Selection Approach for Autonomous Object Modelling

Joel Luis Carbonera[1]
IBM Research, Rio de Janeiro, Brazil

Joanna Isabelle Olszewska[2]
University of West Scotland, UK

Abstract—**With the increasing presence of robotic agents in our daily life, computationally efficient modelling of real-world objects by autonomous systems is of prime importance for enabling these artificial agents to automatically and effectively perform tasks such as visual object recognition. For this purpose, we introduce a novel, machine-learning approach for instance selection called Approach for Selection of Border Instances (ASBI). This method adopts the notion of local sets to select the most representative instances at the boundaries of the classes, in order to reduce the set of training instances and, consequently, to reduce the computational resources that are necessary to perform the learning process of real-world objects by the artificial agents. Our new algorithm was validated on 27 standard datasets and applied on 2 challenging object-modelling datasets to test the automated object recognition task. ASBI performances were compared to those of 6 state-of-art algorithms, considering three standard metrics, namely, accuracy, reduction, and effectiveness. All the obtained results show that the proposed method is promising for the autonomous recognition task, while presenting the best trade-off between the classification accuracy and the data size reduction.**

Keywords—Machine learning; instance selection; autonomous systems; object modelling; visual object recognition; computer vision; machine vision

I. INTRODUCTION

Instance selection (IS) is a machine-learning, pre-processing task that consists in choosing a subset of instances among the total available data, in a way that the *subset* can support the machine learning task *with a low loss of performance* [1], [2]. Thus, every IS strategy faces a *trade-off* between the *reduction rate* of the dataset and the resulting *classification accuracy* [3], [4].

In Machine Learning, instance selection can be applied to reduce the data into a manageable subset, leading to a reduction of the computational resources (in terms of time and space) necessary to perform the learning process [5], [6], [7]. Besides that instance selection techniques can be used to improve the learned models through the deletion of useless, redundant, erroneous, or noisy instances [5], [8].

In this paper, we propose a new instance selection algorithm called ASBI (*Approach for Selection of Border Instances*) that applies the notion of *local set* [7] to guide the instance selection process. Hence, the proposed ASBI algorithm aims to preserve the most relevant instances at the *boundaries* of the data classes. Indeed, border instances provide relevant information to support discrimination between classes [7].

Moreover, we aim to use this method in Robotics for tasks such as autonomous object modelling, since object modelling for autonomous agents requires a reduced set of training instances to cope with the *in-situ* computational constraints [9], [10]. Furthermore, effective object modelling coupled with machine-vision-based recognition algorithms [11], [12] could lead to efficient autonomous object recognition, which is very challenging for robots and robot ecologies [13], [14].

The contribution of this paper is thus twofold and consists of (i) the new instance selection algorithm ASBI[1] and of (ii) the application of instance selection algorithms, in particular ASBI, to the automated object modelling for autonomous agents.

Thence, the ASBI algorithm was evaluated, on one hand, on a generic classification task and, on the other hand, on a specific visual recognition task. Its performance was then compared with the performance of 6 well-established algorithms such as the *Edited Nearest Neighbour* (ENN) algorithm [15], the *Decremental Reduction Optimization Procedure* (DROP1-DROP5) algorithm [16], the *Iterative Case Filtering* (ICF) algorithm [17], the *Local Set-based Smoother* (LSSm) algorithm [7], the *Local Set Border Selector* (LSBo) algorithm [7], and the *Local Density-based Instance Selection* (LDIS) algorithm [18]. For the classification task, it was evaluated on 27 standard datasets, considering the SVM classifier [19]. For the visual recognition task, it was evaluated on 2 challenging and well-known datasets, using the approach proposed in [12]. The results show that ASBI provides the best trade-off between accuracy and reduction, in comparison with the other state-of-the-art algorithms.

The remaining part of the paper is organized as follows: Section II presents the notation used throughout this paper, while our approach is explained in Section III. The experimental evaluation is presented in Section IV, and conclusions are drawn up in Section V.

II. NOTATIONS

In this section, we introduce the notations adopted from our previous papers, e.g. [18], [20], [21], [22], [23], [4], and used throughout this paper:

- $T = \{x_1, x_2, ..., x_n\}$ is the non-empty set of n instances (or data objects) representing the original dataset to be reduced in the instance selection process.

[1]The source code of our ASBI algorithm can be found at https://www.researchgate.net/publication/317788063_ASBI_Approach_for_selection_of_border_instances

- Each $x_i \in T$ is an $m - tuple$, such that $x_i = (x_{i1}, x_{i2}, ..., x_{im})$, where x_{ij} represents the value of the j-th feature of the instance x_i, for $1 \leq j \leq m$.
- $L = \{l_1, l_2, ..., l_p\}$ is the set of p class labels that are used to classify the instances in T, where each $l_i \in L$ represents a given class label.
- $l \colon T \to L$ is a function that maps a given instance $x_i \in T$ to its corresponding class label $l_j \in L$.
- $c \colon L \to 2^T$ is a function that maps a given class label $l_j \in L$ to a given set C, such that $C \subseteq T$, which represents the set of instances in T whose class is l_j. It is worth noting that $T = \bigcup_{l \in L} c(l)$. In this notation, 2^T represents the *powerset* of T, which is the set of all subsets of T, including the empty set and T itself.
- $d \colon T \times T \to \mathbb{R}$ is a *distance function* (or dissimilarity function) which maps two instances to a real number representing the distance (or dissimilarity) between them.
- $S = \{x_1, x_2, ..., x_q\}$ is a set of q instances such as $S \subseteq T$. It represents the reduced set of instances resulting from the instance selection process.

III. ASBI Algorithm

The proposed approach called ASBI (*Approach for Selection of Border Instances*) has been designed to reduce data in order to keep only a small number of data instances which are representative and which could be used in tasks such as autonomous object modelling and recognition. Indeed, ASBI preserves only the most representative instances at the boundaries of each class. It assumes that the instances at the boundaries can represent sufficient information to distinguish between classes and to support the classification of novel instances in their respective classes. This selection criterion is also adopted by other instance selection approaches, such as [7], but our approach improves the one proposed in [7] by adopting additional constraints for selecting the minimal set of border instances.

Hence, the ASBI algorithm adopts also the notion of *local set* (LS) [17], as follows:

Definition 1. The *local set* of a given instance i, with $i \in T$, is represented by $LS(i)$ and is the set of all instances contained in the bigger hypersphere centered at i, in a way that only instances whose class is $c(i)$ are included in the hypersphere. Let's consider $x \in T$ to be the nearest instance of i such as $c(i) \neq c(x)$, then $CL(i) = \{y | d(i, y) < d(i, x)\}$.

The notion of *local set* is represented in Fig. 1. This example considers two classes (i.e. the white circles and the black circles). In this scenario, the local set of the instance A is $LS(A) = \{A, B, C, D, E, F, G\}$. It is worth noting that the instances I, J, K, L, and M cannot be included due to the constraints imposed by the instance R to the size of the hypersphere (represented by a dashed circle). A bigger hypersphere would include the instance R, and $c(R) \neq c(A)$. The notion of local set allows thus the definition of the notion of *internality*.

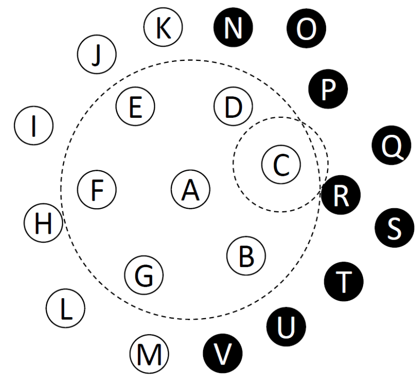

Fig. 1. Illustration of the notions of *internality* and *degree of potential noise*. The internality of A is $int(A) = |CL(A)| = |\{A, B, C, D, E, F, G\}| = 7$, while the *degree of potential noise* is $DPN(R) = |\{A, C\}| = 2$.

Definition 2. The *internality* of an individual i, with $i \in T$, is represented by $int(i)$ and is the cardinality of $LS(i)$, i.e. $int(i) = |LS(i)|$.

Closer to the border of its class is an individual, lower is its distance to instances of other classes and, therefore, lower is the cardinality of its local set. Thus, the internality of an instance can be used to estimate how close this instance is to the border of its class.

The notion of internality is illustrated in Fig. 1. In this case, the internality of A is given by $int(A) = |CL(A)| = |\{A, B, C, D, E, F, G\}| = 7$. On the other hand, the internality of C is given by $int(C) = |CL(C)| = |\{C\}| = 1$.

The ASBI algorithm adopts also the notion of *degree of potential noise* (DPN) of an instance.

Definition 3. The *degree of potential noise* of an instance i, with $i \in T$, is represented by $DPN(i)$ and is the number of instances in T which are classified in classes that are different from $c(i)$, where i is the closest instance in another class.

Fig. 1 illustrates also the notion of degree of potential noise. In this example, $DPN(R) = 2$, since there are two instances (namely, A and C) in T that have R as the closest instance of a different class. It is worth noting that higher is the $DPN(i)$, higher is the possibility of the instance i being harmful for the classification of novel instances of its class.

Besides that, our approach adopts the notions of *coherence* and *selectivity*.

Definition 4. The *coherence* of an instance i, with $i \in T$, is represented by $coherence(i) = |\{x | x \in T \wedge i \in LS(x)\}|$ and is basically the number of instances in T whose local set includes i. It measures the degree of coherence of an individual with the information abstracted by its class.

Definition 5. The *selectivity* of an instance $i \in T$ is defined as:

$$selectivity(i) = \frac{coherence(i)}{internality(i)}. \quad (1)$$

In this context, higher is the $selectivity(i)$, higher is the priority of the individual i being considered as a candidate in the process of instance selection.

Algorithm 1: ASBI (Approach for Selection of Border Instances)

Input: A set T of instances.
Output: A set S of instances, such that $S \subseteq T$.
begin
    $T^- \leftarrow$ Removing noisy instances from T (using the algorithm LSSm);
    $candidates \leftarrow \emptyset$;
    foreach $A \in T^-$ **do**
        if $int(A) > DPN(A)$ **then**
            $candidates \leftarrow candidates \cup \{A\}$;
    Sorting the $candidates$ set, in a descending order, according to the *selectivity* of each candidate;
    $S \leftarrow \emptyset$;
    foreach $A \in candidates$ **do**
        if $LS(A) \cap S = \emptyset$ **then**
            $S \leftarrow S \cup \{A\}$;
    return S;

According to the *selectivity* definition, higher is the *coherence* and lower is the *internality* of an instance i, higher is the selectivity of i. Thus, this heuristic assigns higher values for *border instances*, since they have a higher value of *internality*. Moreover, among these border instances, this heuristic prioritizes those that are *more coherent* with their classes.

Considering all these notions, Algorithm 1 formalizes the *Approach for Selection of Border Instances* (ASBI). Our algorithm takes as input a set T of instances. Firstly, the algorithm applies the LSSm algorithm [7] to remove noisy instances from T. The outcome of this step is the set T^-. Secondly, the algorithm includes in the set $candidates$ each instance $A \in T^-$ whose *internality* is higher than its *degree of potential noise*. If A does not meet this requirement, that means that A is considered potentially harmful for classifying new instances and, for this reason, A is ignored. This can be viewed as an additional step of candidate filtering, which selects only instances that are more typical of their classes and that have lower potential of harming the classification. In the next step, the algorithm sorts the $candidates$ set in a descending order, according to the *selectivity* of each instance. Next, the algorithm initializes the set S as an empty set. This set is used for storing the instances in T^- that will be selected. In the final step, for each instance $A \in candidates$, the algorithm verifies if there are some instances in $LS(A)$ already included in S, i.e. the algorithm checks if the intersection between S and $LS(A)$) is not empty. If the intersection is empty, the instance A is included in S to ensure that A and other instances similar to A will be correctly classified. At the end, the algorithm returns the set S as the set of selected instances.

It is worth noting that ASBI algorithm is different from LSBo in two main aspects. On one hand, ASBI performs an additional step of noise removal, where instances whose *DPN* are greater or equal to their *internality* are removed. On the other hand, ASBI uses the notion of *selectivity* to prioritize the instances that are evaluated first. According to this latter criterion, the ASBI algorithm evaluates first the instances with higher coherence and lower internality. Hence, our approach prioritizes the selection of instances that are near to the borders of their classes, i.e. instances with low internality, but that can represent more information about their neighbours, since they have a high coherence.

The most expensive steps of the ASBI algorithm are the phase of noise removal and the process of building the local sets of each instance. The time complexity of the LSSm algorithm is $O(|T|^2)$. The time complexity for building the local sets of every instance in T^- is $O(|T^-|^2)$. Consequently, the time complexity of the ASBI algorithm is also $O(|T|^2)$. Thus, the time complexity of ASBI is equivalent to the time complexity of other well-known instance selection algorithms such as [17], [7].

IV. Experiments

In order to evaluate our algorithm, we carried out two types of experiments. Hence, in Section IV-A, we tested our ASBI algorithm on a generic classification task, considering 27 well-known datasets, while in Section IV-B, we applied our ASBI algorithm to the autonomous object recognition task, using 2 challenging databases. For both experiments, the performance of our approach was compared with the ones of 6 state-of-art instance-selection (IS) algorithms, namely, LDIS, LSBo, DROP3, ICF, ENN, and LSSm.

In all experiments, we set $k = 3$ for DROP3, ENN, ICF, and LDIS, and we adopted the distance function $d\colon T \times T \to \mathbb{R}$, defined as follows:

$$d(x, y) = \sum_{j=1}^{m} \theta_j(x, y), \tag{2}$$

with

$$\theta_j(x, y) = \begin{cases} \alpha(x_j, y_j), & \text{if } j \text{ is a categorical feature,} \\ |x_j - y_j|, & \text{if } j \text{ is a numerical feature,} \end{cases} \tag{3}$$

where

$$\alpha(x_j, y_j) = \begin{cases} 1, & \text{if } x_j \neq y_j, \\ 0, & \text{if } x_j = y_j. \end{cases} \tag{4}$$

To evaluate the performance of the instance selection algorithms, we considered 3 standard metrics, namely, *accuracy*, *reduction* and *effectiveness* [7], [18].

The first 2 metrics are defined as follows:

$$accuracy = \frac{Success(Test)}{|Test|} \tag{5}$$

and

$$reduction = \frac{|T| - |S|}{|T|}, \tag{6}$$

where $Test$ is a given set of instances that are selected to be tested in a classification task, and $Success(Test)$ is the number of instances in $Test$ correctly classified in the classification task [7].

The third metric called *effectiveness* is then defined as follows:

$$effectiveness = accuracy \times reduction. \tag{7}$$

Indeed, the effectiveness is a measure of the degree to which an instance selection algorithm is successful in producing a small set of instances that allows a high classification accuracy of new instances [18].

TABLE I. DETAILS OF THE DATASETS USED IN THE CLASSIFICATION TASK.

Data set	**Instances**	**Attributes**	textbfClasses
Audiology	226	70	24
Breast cancer	286	10	2
Cardiotocography	2126	21	10
Cars	1728	6	4
Dermatology	358	35	6
Diabetes	768	9	2
E. Coli	336	8	8
Glass	214	10	7
Heart statelog	270	14	2
Ionosphere	351	35	2
Iris	150	5	3
Landsat	4435	37	6
Letter	20000	17	26
Lung cancer	32	57	3
Lymph	148	19	4
Mushroom	8124	23	2
Optdigits	5620	65	10
Page-blocks	5473	11	5
Parkinsons	195	23	2
Promoters	106	58	2
Segment	2310	20	7
Soybean	683	36	19
Spambase	4601	58	2
Splice	3190	61	3
Voting	435	17	2
Wine	178	14	3
Zoo	101	18	7

A. *Experiment 1*

In the first set of experiments, we run IS algorithms, such as ASBI, LDIS, LSBo, DROP3, ICF, ENN, and LSSm, to compare their performance in context of a classification task in 27 well-known, distinct datasets obtained from the UCI Machine Learning Repository[2], i.e. *audiology*, *breast cancer*, *cardiotocography*, *cars*, *dermatology*, *diabetes*, *e. coli*, *glass*, *heart statelog*, *ionosphere*, *iris*, *landsat*, *letter*, *lung cancer*, *lymph*, *mushroom*, *optdigits*, *page-blocks*, *parkinsons*, *genetic promoters*, *segment*, *soybean* (which combines the large soybean dataset and its test dataset), *spambase*, *splice junction gene sequences*, *voting*, *wine*, and *zoo*. Details of the data sets that were used are presented in Table I.

To evaluate the classification *accuracy* of new instances in each respective dataset, we adopted a SVM (*support vector machine*) classifier [24]. Following [25], we adopted the WEKA[3] 3.8 implementation of SVM that uses the sequential minimal optimization algorithm [26] for training the classifier, with the standard parametrization: $c = 1.0$, $toleranceParameter = 0.001$, $epsilon = 1.0E-12$, using a polynomial kernel and a multinomial logistic regression model with a ridge estimator as calibrator.

Besides that, the accuracy, reduction and effectiveness were evaluated in a *n-fold cross-validation* scheme [18], [23], where $n = 10$. Thus, the dataset is at first randomly partitioned in 10 equally sized subsamples. From these subsamples, a single subsample is selected as test data ($Test$), and the union of the remaining 9 subsamples is considered as the *initial training set* (ITS). Next, an instance selection algorithm is applied to reduce the ITS and thus to produce the *reduced training set* (RTS). At this point, the *reduction* of the dataset can be measured. Finally, the RTS is used as the training set for the classifier, to classify the instances in $Test$. At this point, the accuracy achieved by the SVM classifier can be measured using RTS as the training set. This process is repeated 10 times, with each subsample used once as $Test$. The 10 values of accuracy and reduction are averaged to produce the *average accuracy* (AA) and *average reduction* (AR), respectively [20]. The *average effectiveness* is calculated by considering AA and AR. Tables II-IV report the *average reduction*, the *average accuracy* and the *average effectiveness*, respectively, achieved in each combination of dataset and instance selection algorithm, using the SVM classifier. The best results for each dataset are marked in bold typeface.

[2]http://archive.ics.uci.edu/ml/
[3]http://www.cs.waikato.ac.nz/ml/index.html

TABLE II. COMPARISON OF THE *reduction* ACHIEVED BY EACH ALGORITHM FOR EACH DATASET IN THE CLASSIFICATION TASK.

Algorithm	**ASBI**	**LDIS**	**LSBo**	**DROP3**	**ICF**	**ENN**	**LSSm**	**Average**
Audiology	0.73	**0.75**	0.60	0.70	**0.75**	0.36	0.08	0.57
Breast cancer	0.84	**0.88**	0.73	0.77	0.85	0.30	0.13	0.64
Cardiotocography	0.80	**0.86**	0.70	0.70	0.71	0.31	0.13	0.60
Cars	0.85	0.84	0.74	**0.87**	0.81	0.18	0.12	0.63
Dermatology	0.81	**0.87**	0.73	0.64	0.70	0.15	0.13	0.58
Diabetes	0.84	**0.91**	0.75	0.77	0.86	0.30	0.13	0.65
E. Coli	0.89	**0.90**	0.82	0.72	0.86	0.16	0.09	0.64
Glass	0.82	**0.90**	0.72	0.75	0.69	0.32	0.14	0.62
Heart statelog	0.81	**0.92**	0.69	0.73	0.78	0.30	0.14	0.62
Ionosphere	0.89	0.90	0.86	0.80	**0.92**	0.11	0.04	0.65
Iris	**0.95**	0.89	0.93	0.71	0.59	0.04	0.06	0.60
landsat	0.91	**0.92**	0.88	0.72	0.90	0.10	0.05	0.64
Letter	**0.87**	0.83	0.83	0.68	0.81	0.05	0.04	0.59
Lung cancer	0.73	**0.84**	0.56	0.76	0.70	0.58	0.20	0.63
Lymph	0.82	**0.90**	0.74	0.71	0.81	0.20	0.11	0.61
Mushroom	**0.99**	0.87	**0.99**	0.86	0.94	0.00	0.00	0.67
Optdigits	**0.93**	0.91	0.90	0.71	0.92	0.02	0.02	0.63
Pageblocks	**0.97**	0.86	0.96	0.71	0.95	0.04	0.03	0.65
Parkinsons	**0.90**	0.80	0.86	0.71	0.75	0.15	0.11	0.61
Promoters	0.73	**0.83**	0.60	0.60	0.67	0.19	0.05	0.53
Segment	**0.93**	0.83	0.91	0.69	0.83	0.04	0.04	0.61
Soybean	**0.87**	0.78	0.83	0.69	0.57	0.09	0.05	0.55
Spambase	**0.86**	0.83	0.81	0.74	0.80	0.16	0.08	0.61
Splice	0.70	**0.81**	0.59	0.65	0.75	0.23	0.05	0.54
Voting	**0.91**	0.79	0.88	0.79	0.93	0.08	0.04	0.63
Wine	0.85	**0.87**	0.78	0.72	0.79	0.23	0.10	0.62
Zoo	**0.89**	0.62	0.88	0.65	0.30	0.06	0.06	0.50
Average	**0.83**	0.82	0.77	0.70	0.75	0.16	0.08	0.59

TABLE III. COMPARISON OF THE *accuracy* ACHIEVED BY EACH ALGORITHM FOR EACH DATASET IN THE CLASSIFICATION TASK, WITH THE SVM CLASSIFIER.

Algorithm	**ASBI**	**LDIS**	**LSBo**	**DROP3**	**ICF**	**ENN**	**LSSm**	**Average**
Audiology	0.71	0.55	0.77	0.65	0.69	0.68	**0.81**	0.70
Breast cancer	0.69	0.65	0.66	0.71	0.66	**0.72**	0.71	0.69
Cardiotocography	0.63	0.62	0.62	0.64	0.65	0.66	**0.67**	0.64
Cars	0.85	0.84	**0.91**	0.86	**0.91**	0.90	**0.91**	0.88
Dermatology	0.95	0.96	0.96	0.96	0.96	0.96	**0.97**	0.96
Diabetes	0.76	0.74	0.75	0.76	0.76	**0.77**	**0.77**	0.76
E. Coli	0.74	0.80	0.78	0.81	0.77	0.81	**0.82**	0.79
Glass	0.46	0.49	0.45	0.52	0.50	0.53	**0.55**	0.50
Heart statelog	0.81	0.79	0.82	0.81	0.81	**0.84**	**0.84**	0.82
Ionosphere	0.82	0.81	0.53	0.80	0.78	0.87	**0.89**	0.79
Iris	0.53	0.82	0.47	0.91	0.69	**0.96**	**0.96**	0.76
landsat	0.85	0.84	0.85	0.86	0.85	**0.87**	**0.87**	0.86
Letter	0.73	0.75	0.74	0.80	0.75	**0.84**	**0.84**	0.78
Lung cancer	**0.45**	0.32	0.40	0.33	0.38	0.38	0.40	0.38
Lymph	0.81	0.80	**0.84**	0.79	0.81	0.80	**0.84**	0.81
Mushroom	0.96	**1.00**	0.97	1.00	0.96	**1.00**	**1.00**	0.98
Optdigits	0.97	0.96	0.98	0.98	0.97	**0.99**	**0.99**	0.98
Pageblocks	0.93	0.93	0.92	0.93	0.93	**0.94**	**0.94**	0.93
Parkinsons	0.84	0.83	0.82	0.84	0.82	**0.87**	0.86	0.84
Promoters	0.85	0.76	0.86	0.85	0.79	**0.87**	0.86	0.83
Segment	0.85	0.89	0.81	0.91	0.90	**0.93**	0.92	0.89
Soybean	0.85	0.86	0.85	0.91	0.92	0.93	**0.94**	0.89
Spambase	0.89	0.88	0.89	**0.90**	**0.90**	0.89	**0.90**	0.89
Splice	0.93	0.91	0.92	**0.94**	0.93	**0.94**	**0.94**	0.93
Voting	**0.95**	0.93	**0.95**	**0.95**	**0.95**	**0.95**	**0.95**	0.95
Wine	0.94	0.94	**0.97**	0.96	0.94	0.96	**0.97**	0.95
Zoo	0.89	**0.95**	0.91	0.90	0.92	0.92	0.94	0.92
Average	0.78	0.78	0.76	0.80	0.78	**0.82**	**0.82**	0.79

TABLE IV. COMPARISON OF THE *effectiveness* ACHIEVED BY EACH ALGORITHM FOR EACH DATASET IN THE CLASSIFICATION TASK, WITH THE SVM CLASSIFIER.

Algorithm	ASBI	LDIS	LSBo	DROP3	ICF	ENN	LSSm	Average
Audiology	0.51	0.41	0.46	0.46	**0.52**	0.25	0.06	0.38
Breast cancer	**0.58**	0.57	0.48	0.55	0.56	0.21	0.10	0.44
Cardiotocography	0.50	**0.53**	0.43	0.45	0.46	0.21	0.08	0.38
Cars	0.72	0.71	0.68	**0.75**	0.74	0.16	0.11	0.55
Dermatology	0.77	**0.84**	0.70	0.62	0.67	0.15	0.12	0.55
Diabetes	0.64	**0.67**	0.57	0.59	0.65	0.23	0.10	0.49
E. Coli	0.66	**0.72**	0.64	0.58	0.66	0.13	0.08	0.50
Glass	0.38	**0.44**	0.32	0.39	0.34	0.17	0.08	0.30
Heart statelog	0.66	**0.73**	0.57	0.59	0.63	0.26	0.12	0.51
Ionosphere	**0.73**	**0.73**	0.45	0.65	0.72	0.10	0.04	0.49
Iris	0.51	**0.73**	0.44	0.64	0.40	0.04	0.06	0.40
landsat	**0.77**	**0.77**	0.75	0.62	**0.77**	0.08	0.04	0.54
Letter	**0.63**	0.62	0.61	0.54	0.60	0.04	0.03	0.44
Lung cancer	**0.33**	0.27	0.23	0.25	0.27	0.22	0.08	0.24
Lymph	0.67	**0.73**	0.62	0.56	0.65	0.16	0.09	0.50
Mushroom	0.95	0.87	**0.96**	0.86	0.91	0.00	0.00	0.65
Optdigits	**0.90**	0.88	0.88	0.70	0.89	0.02	0.02	0.61
Pageblocks	**0.91**	0.81	0.89	0.66	0.89	0.04	0.03	0.60
Parkinsons	**0.76**	0.66	0.71	0.59	0.62	0.13	0.10	0.51
Promoters	0.62	**0.63**	0.52	0.50	0.53	0.17	0.05	0.43
Segment	**0.80**	0.73	0.74	0.63	0.74	0.03	0.03	0.53
Soybean	**0.74**	0.67	0.71	0.62	0.53	0.08	0.05	0.49
Spambase	**0.77**	0.74	0.72	0.67	0.72	0.14	0.07	0.55
Splice	0.66	**0.74**	0.54	0.61	0.70	0.22	0.05	0.50
Voting	0.87	0.73	0.84	0.75	**0.88**	0.07	0.04	0.60
Wine	0.80	**0.82**	0.75	0.69	0.74	0.22	0.09	0.59
Zoo	0.79	0.59	**0.80**	0.58	0.28	0.05	0.05	0.45
Average	**0.67**	0.66	0.61	0.58	0.61	0.12	0.06	0.48

Table II shows that ASBI achieves the highest *reduction* in several datasets and has the highest average reduction rate. Table III shows that ENN and LSSm achieve the highest *accuracy* in most of the datasets, but they do not provide high reduction rates, since they were designed for removing noisy instances. On the other hand, Tables II-III show that in cases where the achieved accuracy by ASBI is lower than the accuracy provided by other algorithms, this is compensated by a high reduction. Table IV shows that, in several datasets, ASBI has the highest *effectiveness* as well as the highest average effectiveness. We can also observe that ASBI provides the highest reduction rates and the best trade-off between both accuracy and reduction (represented by the effectiveness).

It is also worth noting that ASBI does not have any free parameter that should be provided by the user. This could be an advantage, especially for autonomous systems.

B. Experiment 2

This set of experiments consists in applying instance selection algorithms to autonomous object modelling in context of the autonomous agent's visual object recognition task. For this purpose, we used 2 challenging, online-available databases[4] that are called *CMU10_3D* and *CMU_KO8*, respectively, and that contain instances of different visual objects [27].

In particular, *CMU10_3D* has a training dataset with 250 images with 2D ground truth of 10 classes of *grocery* objects and a testing dataset with 50 images per object class, while *CMU_KO8* dataset is split into 200 training images with 2D ground truth of 8 classes of *household* items and 800 images, with 100 instances per object class.

In order to evaluate the instance selection algorithms performance when applied to autonomous object modelling and recognition, each respective training visual data is first preprocessed using a modified version of visual object model, which was proposed by [12], in order to extract attributes such

[4]http://www.cs.cmu.edu/∼ehsiao/datasests.html

TABLE V. COMPARISON OF THE *reduction* ACHIEVED BY EACH ALGORITHM FOR EACH DATASET IN THE OBJECT RECOGNITION TASK.

Algorithm	ASBI	LDIS	LSBo	DROP3	ICF	ENN	LSSm	Average
CMU10 3D	0.85	**0.88**	0.73	0.75	0.53	0.30	0.14	0.60
CMU KO8	**0.89**	**0.89**	0.84	0.76	0.65	0.18	0.11	0.61
Average	0.87	**0.88**	0.78	0.76	0.59	0.24	0.12	0.61

TABLE VI. COMPARISON OF THE *accuracy* ACHIEVED BY EACH ALGORITHM FOR EACH DATASET IN THE OBJECT RECOGNITION TASK.

Algorithm	ASBI	LDIS	LSBo	DROP3	ICF	ENN	LSSm	Average
CMU10 3D	**0.72**	0.69	0.69	0.71	0.66	0.65	0.65	0.68
CMU KO8	**0.74**	0.72	0.70	0.69	0.67	0.66	0.66	0.69
Average	**0.73**	0.71	0.69	0.70	0.67	0.66	0.65	0.69

TABLE VII. COMPARISON OF THE *effectiveness* ACHIEVED BY EACH ALGORITHM FOR EACH DATASET IN THE OBJECT RECOGNITION TASK.

Algorithm	ASBI	LDIS	LSBo	DROP3	ICF	ENN	LSSm	Average
CMU10 3D	**0.62**	0.61	0.50	0.53	0.35	0.20	0.09	0.41
CMU KO8	**0.65**	0.64	0.58	0.52	0.44	0.12	0.07	0.43
Average	**0.64**	0.63	0.54	0.53	0.39	0.16	0.08	0.42

as object's name, height, width, centroid, perimeter, and area. Then, IS algorithms are run separately on this resulting training dataset in order to reduce the number of instances required to automatically build the corresponding, effective object model for each object class. At this stage, the autonomous object modelling is done. Next, the machine-vision algorithm called template matching algorithm, which was introduced in [12], can be applied on the entire testing dataset in order to perform the autonomous object recognition task, using separately each of the reduced object models based on the respective IS algorithms.

Results of this second type of experiments are reported in Tables V to VII, where the *average accuracy* (AA), *average reduction* (AR), and *average effectiveness* (AE) are computed respectively as the average of the obtained scores for each class, measure, dataset and IS algorithm; the best results for each dataset being marked in bold typeface.

From Tables V to VII, we can observe that the ASBI algorithm provides the best results in terms of visual object modelling, since ASBI achieves the highest scores for the average accuracy compared to the other IS algorithms. Furthermore, ASBI does not give the most reduced set of instances in every case, but achieves the best average effectiveness, i.e. the best trade-off between accuracy and reduction.

V. CONCLUSIONS

In this paper, we have proposed a new algorithm for instance selection, which enhances the notion of local set and which is well suited for the autonomous systems' object modelling. Indeed, our algorithm called ASBI (*Approach for Selection of Border Instances*) selects only the most representative instances at the borders of their classes. This approach was successfully tested on 29 well-known datasets. ASBI shows the best average *effectiveness*, i.e. the best trade-off between *accuracy* and *reduction*, when compared to 6 state-of-art algorithms. The experiments also suggest that the strategies adopted by ASBI are useful to build compact object models for the automated, visual object recognition task.

ACKNOWLEDGMENT

The authors would like to thank IBM Research Brazil for the support of this work.

References

[1] J. A. Olvera-Lopez, J. A. Carrasco-Ochoa, J. F. Martinez-Trinidad, and J. Kittler. A review of instance selection methods. *Artificial Intelligence Review*, 34:133–143, 2010.

[2] S. Garcia, J. Luengo, and F. Herrera. *Data Preprocessing in Data Mining*. Springer, 2015.

[3] C.-H. Chou, B-H. Kuo, and F. Chang. The generalized condensed nearest neighbor rule as a data reduction method. In *Proceedings of the IEEE International Conference on Pattern Recognition (ICPR)*, volume 2, pages 556–559, 2006.

[4] J. L. Carbonera and M. Abel. An efficient prototype selection algorithm based on dense spatial partitions. In *Proceedings of Artificial Intelligence and Soft Computing (ICAISC)*, pages 288–300, 2018.

[5] H. Liu and H. Motoda. On issues of instance selection. *Data Mining and Knowledge Discovery*, 6(2):115–130, 2002.

[6] W.-C. Lin, C.-F. Tsai, S.-W. Ke, C.-W. Hung, and W. Eberlem. Learning to detect representative data for large scale instance selection. *Journal of Systems and Software*, 106:1–8, 2015.

[7] E. Leyva, A. Gonzalez, and R. Perez. Three new instance selection methods based on local sets: A comparative study with several approaches from a bi-objective perspective. *Pattern Recognition*, 48(4):1523–1537, 2015.

[8] A. Zakeri and A. Hokmabadi. Efficient feature selection method using real-valued grasshopper optimization algorithm. *Expert Systems with Applications*, 119:61–72, 2019.

[9] H. Liu, Y. Liu, L. Huang, F. Sun, and D. Guo. Discovery of topical object in image collections. In *Proceedings of IEEE International Conference on Robotics and Automation (ICRA)*, pages 1886–1892, 2015.

[10] T. Faulhammer, R. E. Ambru, C. Burbridge, M. Zillich, J. Folkesson, N. Hawes, P. Jensfelt, and M. Vincze. Autonomous learning of object models on a mobile robot. *IEEE Robotics and Automation Letters*, 2(1):26–33, 2017.

[11] J. I. Olszewska. Active contour based optical character recognition for automated scene understanding. *Neurocomputing*, 161:65–71, 2015.

[12] J. I. Olszewska. "Where Is My Cup?" – Fully Automatic Detection and Recognition of Textureless Objects in Real-World Images. In *Proceedings of IAPR International Conference on Computer Analysis of Images and Patterns (CAIP). LNCS 9256, Part I*, pages 501–512, 2015.

[13] J. Calzado, A. Lindsay, C. Chen, G. Samuels, and J. I. Olszewska. SAMI: Interactive, multi-sense robot architecture. In *Proceedings of the IEEE International Conference on Intelligent Engineering Systems*, pages 317–322, 2018.

[14] J. I. Olszewska. Designing transparent and autonomous intelligent vision systems. In *Proceedings of International Conference on Agents and Artificial Intelligence*, pages 850–856, 2019.

[15] D. L. Wilson. Asymptotic properties of nearest neighbor rules using edited data. *IEEE Transactions on Systems, Man and Cybernetics*, SMC-2(3):408–421, 1972.

[16] D. R. Wilson and A. R. Martinez. Reduction techniques for instance-based learning algorithms. *Machine Learning*, 38(3):257–286, 2000.

[17] H. Brighton and C. Mellish. Advances in instance selection for instance-based learning algorithms. *Data Mining and Knowledge Discovery*, 6(2):153–172, 2002.

[18] J. L. Carbonera and M. Abel. A density-based approach for instance selection. In *Proceedings of IEEE International Conference on Tools with Artificial Intelligence (ICTAI)*, pages 768–774, 2015.

[19] M. Quinn and J. I. Olszewska. British sign language recognition in the wild based on multi-class svm. In *Proceedings of Federated Conference on Computer Science and Information*, pages 81–86, 2019.

[20] J. L. Carbonera and M. Abel. Efficient prototype selection supported by subspace partitions. In *Proceedings of the IEEE International Conference on Tools with Artificial Intelligence (ICTAI)*, pages 921–928, 2017.

[21] J. L. Carbonera. An efficient approach for instance selection. In *Proceedings of the International Conference on Big Data Analytics and Knowledge Discovery (DaWaK)*, pages 228–243, 2017.

[22] J. L. Carbonera and M. Abel. An efficient prototype selection algorithm based on spatial abstraction. In *Proceedings of the International Conference on Big Data Analytics and Knowledge Discovery (DaWaK)*, pages 177–192, 2018.

[23] J. L. Carbonera and M. Abel. Efficient instance selection based on spatial abstraction. In *Proceedings of the IEEE International Conference on Tools with Artificial Intelligence (ICTAI)*, pages 286–292, 2018.

[24] M. F. Akay. Support vector machines combined with feature selection for breast cancer diagnosis. *Expert Systems with Applications*, 36(2):3240–3247, 2009.

[25] I. M. Anwar, K. M. Salama, and A. M. Abdelbar. Instance selection with ant colony optimization. *Procedia Computer Science*, 53:248–256, 2015.

[26] J. C. Platt. 12 fast training of support vector machines using sequential minimal optimization. *Advances in Kernel Methods*, pages 185–208, 1999.

[27] E. Hsiao and M. Hebert. Gradient Networks: Explicit shape matching without extracting edges. In *Proceedings of AAAI International Conference on Artificial Intelligence*, pages 417–423, 2013.

Activation and Spreading Sequence for Spreading Activation Policy Selection Method in Transfer Reinforcement Learning

Hitoshi Kono[1], Ren Katayama[2], Yusaku Takakuwa[3], Wen Wen[4], Tsuyoshi Suzuki[5]
Department of Engineering, Tokyo Polytechnic University, Kanagawa, Japan[1]
Department of Electronics and Mechatronics, Tokyo Polytechnic University, Kanagawa, Japan[2]
Department of Information and Communication Engineering, Tokyo Denki University, Tokyo, Japan[3,5]
Department of Precision Engineering, The University of Tokyo, Tokyo, Japan[4]

Abstract—**This paper proposes an automatic policy selection method using spreading activation theory based on psychological theory for transfer learning in reinforcement learning. Intelligent robot systems have recently been studied for practical applications such as home robot, communication robot, and warehouse robot. Learning algorithms are key to building useful robot systems important. For example, a robot can explore for optimal policy with trial and error using reinforcement learning. Moreover, transfer learning enables reuse of prior policy and is effective for environment adaptability. However, humans determine applicable methods in transfer learning. Policy selection method has been proposed for transfer learning in reinforcement learning using spreading activation model proposed in cognitive psychology. In this paper, novel activation function and spreading sequence is discussed for spreading policy selection method. Further computer simulations are used to examine the effectiveness of the proposed method for automatic policy selection in simplified shortest-path problem.**

Keywords—Reinforcement learning; transfer learning; spreading activation theory; policy selection

I. Introduction

Intelligent robot systems are increasingly being developed to solve practical problems. For example, house cleaning, conveyance systems in warehouses, and agricultural systems [1]–[3]. Particularly, reinforcement learning framework is widely discussed in applications of machine learning such as deep Q-network [4], [5]. Reinforcement learning can be explored for optimal policy selection alternate to trial–and–error. This learning algorithm is used with other functions as framework in real world application. Traditional reinforcement learning techniques have long learning time; a disadvantage for implementation in robot systems. To address this problem, transfer learning is proposed for reinforcement learning [7], [8]. The concept of ç has appeared in psychology and education [9]. Transfer learning theory allows the application of a prior knowledge to another similar task. In reinforcement learning, a learning agent is used to draw and transfer policies from previous tasks (source task) to current tasks (target task) [7]. Advantages of transfer learning in reinforcement learning include [7], [8]:

- Fast adaptation to environments (Jump start).
- Learning faster than reinforcement learning (Time to threshold).
- Exploring more effective performances (Asymptotic performance).

The descriptions in parenthesis are the original representation of improvement in performance in transfer learning. In applications of transfer learning of reinforcement learning with pairs, source task and target task, the transfer schemes is called sequential transfer learning [10]. In sequential transfer learning, reusing policy is selected by humans as supervisors [11]–[13]. Parallel transfer learning [10] and multi-task and mutl-robot transfer [14] are proposed alternative approaches. They adopt multiple policy to improve performance of learning agents in target task. A typical disadvantage is if an agent includes an unprofitable policy. Fernández *et al.* and Takano *et al.* in [15]–[18] proposed some policy selection approach. Other related approaches are available in [19]–[21] Here, a learning agent selects a policy from stored multiple policies. Optimal policies are then selected for specific tasks. However, previous policy selection methods have high computational cost if an agent decides to reuse policy from sets of policies such as database.

For humans, many concepts are memorized using a schematic representation as network structure in brain. Spreading activation theory is regarded as realizing *cognitive economy* in cognitive process of humans [22]. Quillian in [23], [24] thoroughly discusses spreading activation theory. An example of semantic network structure for human memory is shown in Fig. 1. Each concept (*e.g.* red, orange, yellow, and green) is connected using paths with semantic distance. That is, connected concepts are related in semantic. In spreading activation theory, each concept has an activation value that can be activated or deactivated by external stimuli such as visual information. If activation value increases beyond the threshold value, the concept remain in human brain. This phenomena is called recall. Activated values spread to related concepts that are connected via paths of semantic distance. If a related concepts' activation value exceed threshold value, they get recalled.

Spreading activation model is an autonomous distributed

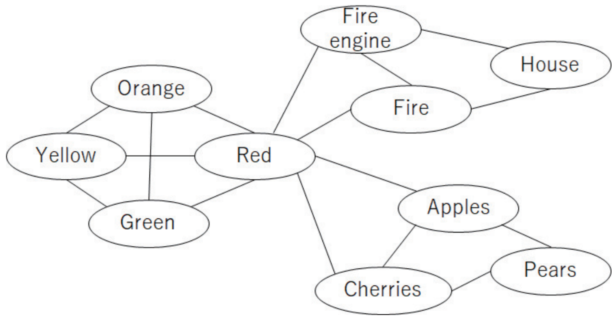

Fig. 1. A schematic representation of network structure including concepts. It is adapted from reference [22].

type. Many existing approaches have centralized decision system architecture. Thus, spreading activation model based on policy selection method is proposed in this study. Stored policies are connected to other policies in the network structure. The network paths denote the semantic distance of spreading activation model. All policies have values equal to the activation value. Concrete functions such as activate function, and spreading function are not formulated in psychological domain. Gaines *et al.* proposed SAN-RL learning algorithm that learns the structure of spreading activation network by reinforcement learning [25]. His study does not consider selecting and leveraging of policies. This study proposes some necessary functions for implementation in a policy selection method based on spreading activation model. From computer simulations, the proposed method for reinforcement learning enables selection of effective policies for task by a learning agent.

The rest of this paper is organized as follows. Section 2 gives an overview of learning algorithms such as reinforcement learning and transfer learning and spreading activation mode in cognitive psychology. Section 3 discusses spreading activation policy network and selection algorithm for transfer learning in reinforcement learning. Section 4 presents the computer simulation experiments and results. Section 5 presents concluding remarks.

II. Previous Works

A. Probabilistic Policy Reuse

Fernández *et al.* proposed a policy selection method using probabilities in [15], [16]. In this method called PRQ-learning, the reusing policy is decided based on Boltzmann distribution selection method (Eqn. (1)) from policy library $L = \{\Pi_1, \Pi_2, \cdots, \Pi_n\}$,

$$P(\Pi_i) = \frac{e^{\tau W_j}}{\sum_{p=0}^{n} e^{\tau W_p}},\ \forall \Pi_j, 0 \leq j \leq n. \tag{1}$$

where τ is a temperature parameter. The expected average reinforcement per episode, W, as defined by

$$W = \frac{1}{K}\sum_{k=0}^{K}\sum_{h=0}^{H}\gamma^h r_{k,h}, \tag{2}$$

where γ, ($0 \leq \gamma \leq 1$), denotes reducing value for future rewards, and $r_{k,h}$ represents immediate reward obtained in step h of the episode k in a total episodes K. Reusing policy decided using the above method enables an agent to reuse policy with the following π–reuse strategy.

$$a = \begin{cases} \Pi_{past}(s) & w/\text{prob.}\psi \\ \epsilon - \text{greedy}(\Pi_{new}(s)) & w/\text{prob.}(1-\psi) \end{cases}. \tag{3}$$

Here past policy is reused with probability ψ and new policy is exploited with probability $1 - \psi$.

PRQ-learning has remarkable success in computer simulation with navigation task based on grid world and keeps away soccer task . It adjusts policy selection based on expected rewards, and adjusts balance between policy reuse and exploring new policies. PRQ-learning does not consider environmental information where the agent act. In robotics applications, observable information are rich because aside reward information, they contain obstacle information from agent, environmental shape and color . Takano *et al.* noted that if a policy is selected; unnecessary actions are increased to select policy [18].

B. Transfer Learning with Forbidden Rule Set

Takano *et al.* proposed a policy selection method different from probabilistic policy reuse. It's selection is based on forbidden rules that pair with policy in policy library [17], [18]. Before policy selection, the agent records forbidden action and state information to the database as forbidden rules set F as a source task. If the agent executes a forbidden action, state and action pair (s, a) are added to F. After building database, the agent selects a policy using a step-by-step selection action in target task.

This approach is applicable in maze exploration simulation to prevent negative transfer until new learning in target task. It considers small maze environment between source task and target task. This method depends on forbidden rule generated in source task, and cannot modify the selection rule. In broad and dynamic environments, the selection frequency or the selection probability is desired to change flexibly.

III. Learning Algorithms and Psychological Theory

A. Reinforcement Learning

Reinforcement learning (RL) is a method of machine learning [4].RL agent explores for optimal solution via trial–and–error and creates its own policies. Thus, RL does not need training data sets unlike supervised learning. Many types of RL algorithms have been developed in decades. In this study, Q-learning is adopted as the learning algorithm [6]. Q-learning is defined by

$$Q(s,a) \leftarrow Q(s,a) + \alpha\{r + \gamma \max_{a' \in A} Q(s',a') - Q(s,a)\}, \tag{4}$$

where $s, s' \in S$ are state of environments in state space S, $a \in A$ is the action of agent in action space A, α is learning rate ($0 < \alpha \leq 1$), γ is discount rate ($0 < \gamma \leq 1$), and r denotes reward. $Q(s,a)$ called Q-table contains all state of environment and each action value pair.

In this study, Boltzmann distribution is adopted as action selection function. The action selection probability adapted from Boltzmann distribution is given by

$$P(a|s) = \frac{\exp\{Q(s,a)/T\}}{\sum_{b \in A} \exp\{Q(s,b)/T\}}, \tag{5}$$

where T is a parameter that determines the randomness of the action selection.

B. Transfer Learning

Transfer learning is a method that reuses prior knowledge in human brain. This concept has been applied in machine learning domain for decades. Transfer method is proposed for reinforcement learning [7]. Transfer policy is given by

$$Q_c(s,a) \leftarrow Q_t(s,a) + Q_s(s,a), \tag{6}$$

were, $Q_c(s,a)$ is current policy including reusing policy. $Q_t(s,a)$ is a policy in target task and $Q_s(s,a)$ is reusing policy from source task. However, $Q_c(s,a)$ has high probability of over fitting if Eq. (6) is used in the target task. To reduce the value of action in $Q_c(s,a)$, transfer rate is proposed to prevent over fitting [26]. Transfer rate similar parameter ζ is proposed by Takano [18]. ζ is analogously used to adjust value of reusing policy, and Kono *et al.* leveraging ζ (denoted by τ in his paper) to prevent over fitting. Transfer method including transfer rate τ $(0 < \tau \leq 1)$ is

$$Q_c(s,a) \leftarrow Q_t(s,a) + \tau Q_s(s,a). \tag{7}$$

In this study, Eq. (7) is adopted for implementation of transfer learning.

In using transfer learning for heterogeneous agents, Taylor *et al.* proposed mapping function, $\chi(\cdot)$, called inter-task mapping (ITM) between source task agent and target task agent. ITM presents the correspondence of state-space and action-space between source task and target task. In this study, homogeneous agents are assumed in source task and target task. Therefore, ITM $\chi(\cdot)$ is not needed for transfer learning.

In the transfer learning, if the agent obtains good effect through reusing policy, it is called positive transfer. In contrast, if the agent encounters the bad situation, this situation is called negative transfer in general.

C. Spreading Activation Model

Spreading activation model is proposed in cognitive psychology as a recall of concept in human brain [22]. In Fig. 1, if concepts "red" is recalled, the activation value of proximate concepts (*e.g.*"orange", "fire" and "Cherries") increase based on activation value of "red". This is spreading of activation value. If activation value is beyond the threshold value, the proximate concepts are recalled simultaneously. Activated concept's activation value can spread to neighboring concepts during the spreading activation process.

TABLE I. Variable declaration in proposed method

Character	Description
π_i	a policy
Π	Set of policies
$\mathbb{A}_i$	Activated value in π_i
A_a	Activation coefficient
Π^c	Set of candidate policies for selection
T_a	Threshold for activation of policy
T_r	Threshold for recall
$\Delta\mathbb{A}_i$	Decaying value for $\mathbb{A}_i$
w_{ij}	Weight in SAP–net between π_i and π_j
w_p	Adjustment value for w_{ij} with positive transfer
w_n	Adjustment value for w_{ij} with negative transfer

IV. Proposed Method

This section discuss the proposed method. Relevant parameters of the method is defined in Table I. The subsections in sequel explain necessary functions used in the proposed method. We commence with descriptions of preliminary functions. We assume that the agent has policies and policy network structure in initial state, and all policies have variable activated values.

1) The agent observes environmental information through sensors.
2) Extracted features form observed environmental information.
3) Corresponding policies are activated based on matches between extracted features and policies' label that are labeled using learned environmental information.
4) Activated value is spread to nearby policies from activated policy in this time.
5) Candidate policies are gathered using threshold value.
6) Selection of recall policies based on probabilistic function.
7) Transferring policy (This part is transfer learning).
8) Selecting action and learning (This part is reinforcement learning).
9) Evaluation of policy reuse effectiveness.
10) Adjusting of weights in policy network structure.
11) Back to process of 1).

From above, simplified system architecture of proposed method with reinforcement learning is shown in Fig. 2.

A. Spreading Activation Policy Network

To select the policy selection method in transfer learning through reinforcement learning method, spreading activation mode is adopted. Spreading Activation Policy Network (SAP–net) is a policy selection method of transfer learning in reinforcement learning. This was proposed by Takakuwa *et al.* in [27]. We propose effective functions based on Takakuwa *et al.*

In the initialization, obtained policy π_i is included in policy set Π as an undirected graph G is defined by $G = \{V, E\}$ where E denotes the set of edges between policies. SAP–net is defined as the adjacency matrix $\boldsymbol{A}$ given by G and the set of weights W, that is, $\boldsymbol{A} = (G, W)$.

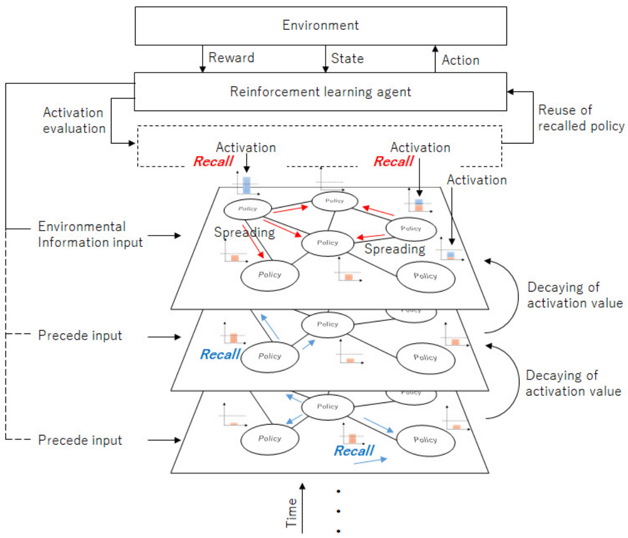

Fig. 2. Simplified system architecture of proposed method. This figure represents standard reinforcement learning concept overview with procedure of spreading activation for policy selection.

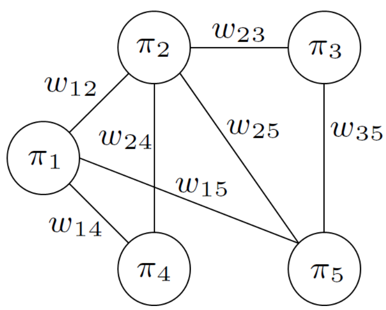

Fig. 3. Example of SAP–net. As default, all nodes are connected with full mesh. All path w_{ij} are assigned weight values and all π_k have activation value $\mathbb{A}_k$.

$$\boldsymbol{A} = \begin{array}{c c} & \begin{array}{ccccc} \pi_1 & \pi_2 & \pi_3 & \pi_4 & \pi_5 \end{array} \\ \begin{array}{c} \pi_1 \\ \pi_2 \\ \pi_3 \\ \pi_4 \\ \pi_5 \end{array} & \begin{pmatrix} 0 & w_{12} & 0 & w_{14} & w_{15} \\ w_{12} & 0 & w_{23} & w_{24} & w_{25} \\ 0 & w_{23} & 0 & 0 & w_{35} \\ w_{14} & w_{24} & 0 & 0 & 0 \\ w_{15} & w_{25} & w_{35} & 0 & 0 \end{pmatrix} \end{array} \tag{8}$$

is example adjacency matrix associated with Fig. (3) with $w_{ij} \in W$ and $w_{ij} \geq 1$. Note that large w_{ij} values indicate long paths. Initial state G is a full mesh network and behavior of graph depend on the weights w_{ij}. Extremely large w_{ij} indicate that path is disconnected asymptotically.

All policies have activated value $\mathbb{A}$. Therefore, node $v_i \in V$ of graph is configurated as $(\pi_i, \mathbb{A}_i)$. As the default $\mathbb{A}_i = 0$.

B. Activation Function

In match of a feature paired with corresponding policy, activated value $\mathbb{A}_i$ is updated by feature comparison function $C(\cdot,\cdot)$ between feature of observed environmental information

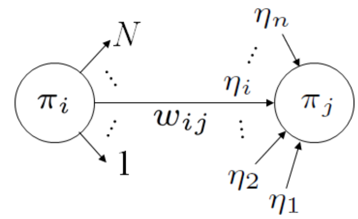

Fig. 4. Simplified illustration of spreading of activated value from π_i to π_j. In this situation, π_i is activated and outputs the activation value. π_j receives activated value η_i that is reduced by w_{ij}.

s and feature of policy that is environmental feature when the policy is obtained. Activation function is defined by

$$\mathbb{A}_i = \begin{cases} \mathbb{A}_i + A_a & (C(s, s_{\pi_i}) \geq T_a) \\ \mathbb{A}_i & (\text{Otherwise}) \end{cases}, \tag{9}$$

where A_a is activation coefficient value, $C(s, s_{\pi_i})$ is a function of extracted features similarity between s and s_{π_i}, and s_{π_i} is environmental feature when the policy π_i is obtained by the agent.

C. Spreading Function

Each policy included in SAP–net can spread the activated value to neighboring policies. A simplified spreading is depicted in Fig. 4. If policy π_i has activated value $\mathbb{A}_i$, it spreads to neighbor π_j as propagating activated value η_i.

$$\eta_i = \frac{1}{N}\mathbb{A}_i e^{-w_{ij}}. \tag{10}$$

Here, N is number of output path of policy π_i. Therefore, policy π_i outputs same activated value calculated from Eq. (10). Policy π_j receives more than one activated value from neighboring policies as shown in Fig. 4. The total activated value received by π_j is given by

$$\mathbb{A}_j \leftarrow \mathbb{A}_j + \sum_{k=1}^{n} \eta_k. \tag{11}$$

For example, if two spreading target are exit in the activation scene like Fig. 5, each spread activation value is calculated by Eq. (10). Policies π_j and π_k spread values to each other after spreading activation of π_i. Policy π_j received spread value η_l from π_k, and π_k received spread value η_m from π_j. Spreading direction and spreading activation value are decided by following equation.

$$\eta_l = \begin{cases} {}^{\triangle}\eta & ({}^{\triangle}\eta > 0) \\ 0 & (\text{Otherwise}) \end{cases}, \tag{12}$$

$${}^{\triangle}\eta = \frac{1}{N-1}\mathbb{A}_k e^{-w_{jk}} - \frac{1}{N-1}\mathbb{A}_j e^{-w_{jk}}. \tag{13}$$

Here, ${}^{\triangle}\eta$ is deference of propagating activation value from π_j and π_k. In calculating propagating activation value, N is changed to $N-1$ because a node as policy is prohibited to use receiving path (*e.g.* η_j and η_k) for output path.

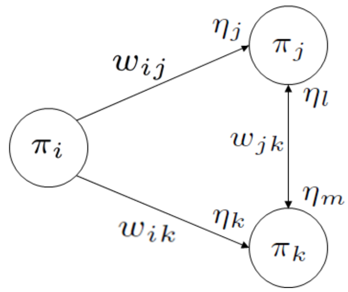

Fig. 5. Situation of multiple spreading of activation value. In this case π_j and π_k are affected to each other in same time. As a calculation result, activation value is propagated to either one like Eq. (13).

Note that, if SAP–net is contained with multiple nodes, and activation and spreading are emerged simultaneously, SAP–net will behave as the system, like a many-body problem. This SAP–net is set to sequential spreading of activation as a basic setting.

D. Threshold for Recall

Before selecting a reusing policy, candidate policy π_i is extracted with activation value $\mathbb{A}_i$. To create the set of candidate policies Π^c, π_i is filtered by following threshold function $\mathbb{T}(\cdot)$ using $\mathbb{A}_i$.

$$\mathbb{T}(\pi_i) = \begin{cases} \pi_i \in \Pi^c & (\mathbb{A}_i > T_r) \\ \pi_i \notin \Pi^c & (\mathbb{A}_i \leqslant T_r) \end{cases}, \tag{14}$$

where, Π^c is the set of candidate policies, and T_r is the threshold value. For the implementation, π_i is gives the optional value $\mathbb{A}_i^c$.

E. Policy Selection

We forbid the recall of multiple policy in same time. Therefore, a policy is selected by the following function. Reusing policies are selected from candidate policies Π^c. A reusing policy is decided by soft-max like function defined by

$$\mathbb{S}(\pi_i) = \frac{\exp \mathbb{A}_i}{\sum_{\pi_j \in \Pi^c} \exp \mathbb{A}_j}. \tag{15}$$

Reusing policy is decided in arbitrary timing. In further works, we will seek to reuse multiple policy in same time and their assimilation.

F. Decaying Process

Activated values decay in each time step. It synchronizes with time or actions. This mechanism is inspired by human oblivion phenomenon. Decay process is implemented for proposed method to re-flesh the state of SAP–net in long time learning.

In this study, decay value is calculated using

$$\Delta\mathbb{A}_i = \begin{cases} 0 & (\mathbb{A}_i = 0) \\ d & (\mathbb{A}_i > 0) \end{cases}, \tag{16}$$

where $\Delta\mathbb{A}_i$ is the decaying value for the activated value $\mathbb{A}_i$ in π_i, and d is the value of decay constant. This decaying value is used in the following equation to decrease present activated value $\mathbb{A}_i$

$$\mathbb{A}_i = \mathbb{A}_i - \Delta\mathbb{A}_i. \tag{17}$$

G. Activation Evaluation

Until an action by the agent, proposed method evaluates the effectiveness of selected policy reuse. If the agent observes positive transfer (PT) effect, weight in SAP–net is adjusted to small between previous used policy and current reuse policy. Thus, the network path's length becomes short in SAP–net. In case of negative transfer (NT), the weight is also adjusted to big value. Thus, the network path's length becomes long.

In this study, weights w_{ij} are adjusted in each action. Adjustment function is defined by.

$$w_{ij} = \begin{cases} w_{ij} - w_p & \text{if PT is emarged} \\ w_{ij} + w_n & \text{if NT is emarged} \end{cases}, \tag{18}$$

where w_{ij} is weight of connection between current reusing policy π_i and previous reused policyπ_j. Weight w_{ij} needs to be controlled using $w_{ij} < 1$ if positive transfer.

Activated policy's activated value is evaluated by action result. If negative transfer is emerged such as the agent collide obstacles based on action with selected policy, activated value gives penalty value. This function is defined by

$$\mathbb{A}_i = \begin{cases} \mathbb{A}_i - A_p & \text{(NT is emerged)} \\ \mathbb{A}_i & \text{(Otherwise)} \end{cases}. \tag{19}$$

V. Computer Simulation

A. Conditions

This experiment aims to confirm the emerging effect of transfer using the proposed method. To evaluate proposed method SAP–net, shortest path problem is adopted in this paper as the basic evaluation with single agent and learned multiple policies. Learning environment is set as Fig. 6 in computer simulation. In Fig. 6, if the agent achieved the goal, the agent can obtain reward from environment. Agent can observe self-localization and around environment such as wall or street with range defined by FOV (field of view) of agent. Reinforcement learning parameter is set as Table II. Positive reward is given to the agent if achieves goal position. Negative reward is given if the agent conflicts to the obstacle per every step, this situation means negative transfer in Eq. (18) and Eq. (19).

The agent has 100 policies that are learned as a source task, for random start and goal positions. When the agent is in a target task environment (Fig. 6), selecting policies include helpful and useless policies for transfer. Helpful policies refer to policies that can be contributed to solve shortest path in target task environment. In contrast, useless policies refer to those policies that are not related to solve the shortest path; these policies have the probability for emerging as negative transfers to use useless policies. Examples of helpful and

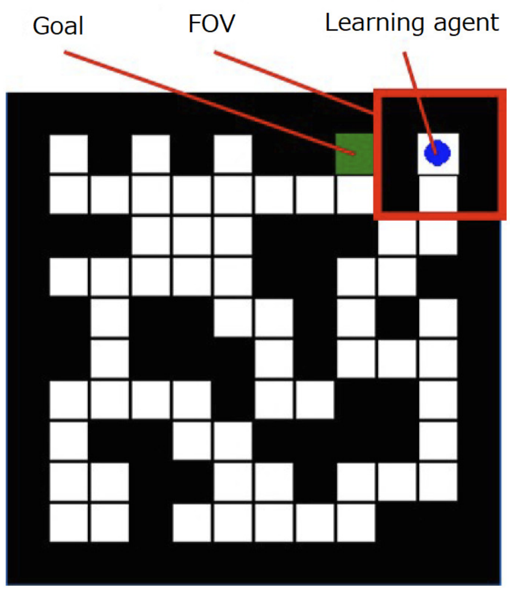

Fig. 6. Experimental environment in computer simulation. An environment includes an agent and a goal. The agent can observe self-localization and around environmental situation such as wall or street.

TABLE II. Set values of parameters for reinforcement learning and proposed method

Parameter	Source task	Target task
Learning rate α	0.9	0.9
Discount rate γ	0.1	0.1
Positive reward r^+	1.0	1.0
Negative reward r^-	0.0	-1.0
Boltzmann parameter T	0.01	0.01
Number of episodes	400	200
Number of trial	–	10

useless policies are shown in Fig. 7 and Fig. 8, respectively. The environmental shape of helpful policies are the same as the target task environment. In contrast, the environment of useless policies are different compared with target task environment. In this experiment, some shape of an environment is used in source tasks.

As default SAP–net configuration, all weights w_{ij} are five, all activation values $\mathbb{A}_i$ are zero. The network structure of the SAP–net is also set as a full mesh. The parameters of SAP–net are set as Table III. In this experiment, environmental information can be described with a discrete state, the feature comparison function $C(s, s_{\pi_i})$ helps determine whether the information is "matched" or not. Therefore, T_a needs not be adjusted in this experiment; the policy is activated only if there is a perfect matched between the current state s and the state s_{π_i}, which is observed when the policy π_i is learned.

B. Evaluation Factors

This experiment adopted the two types of basic evaluation factors. 1st is "learning" curve and area of learning curve, which is called "transfer ratio". The others are three main objectives in transfer such as "jumpstart improvement", "learning

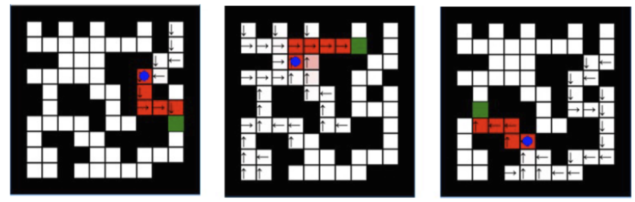

Fig. 7. Example of helpful policies for policy selection. Each learned path is included to the shortest path of the target task.

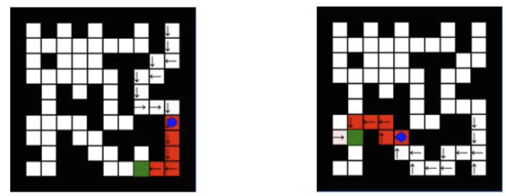

Fig. 8. Example of useless policies. The shape of the environment and path are slightly different.

TABLE III. Parameters setting for SAP–net for the experimental setup

Variable	value
Default activation value $\mathbb{A}_i$	0.0
Activation coefficient $\mathbb{A}_a$	1.0
Threshold for activation of policy T_a	Perfect match
Threshold for recall T_r	0.6
Decaying value $\Delta\mathbb{A}_i$	-0.001
Default weight between policies w_{ij}	5
Adjustment value of w_{ij} when PT	-0.5
Adjustment value of w_{ij} when NT	2.5

speed improvement", and "asymptotic improvement". Learning speed, asymptotic, and jumpstart improvement are proposed by Langlay in 2006 that are described in Lazaric's paper [8].

1) Learning curve: The learning curve is the most basic evaluation method among learning procedures. Reinforcement learning can also use the learning curve to evaluate the performance of the learning process (Fig. 9). The vertical axis of the learning curve denotes the performance of the learning agent, and the number of actions and problem solving time serve as its performance. The horizontal axis of the learning curve is time steps.

If the environment is defined as a Markov decision process (MDP), the learning curve is converged to optimum solution, which means that the fast problem-solving time, shortest path route, and so on. The converged learning curve aids understanding performance transition intuitively by humans. In a non-MDP environment such as a dynamic environment, learning curve is not converged; however, the shape of curve is emerged propensity for convergence with some fluctuations.

2) Jump start: Jump start is the difference between the value of the performance obtained with transfer and that without (Fig. 10). Normally, the learning curve of the initial state has some fluctuations; therefore, in this experiment, jump start value J_s is formulated as follow:

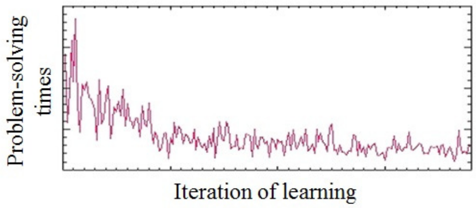

Fig. 9. Example of learning curve. This curve is not converged to optimal solution because this result is obtained by non-MDP environment experiment. However, an observer can read the increasing performance of the agent using this learning curve with every time step.

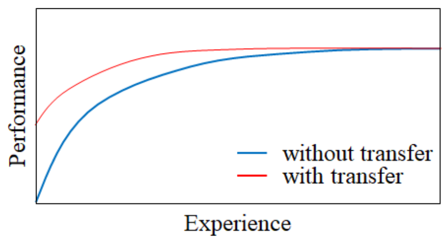

Fig. 10. Simplified example of the jump start that emerged in the learning curve. The blue curve explains the performance transition without transfer, which is the learning curve of reinforcement learning. The red curve denotes performance transition with transfer.

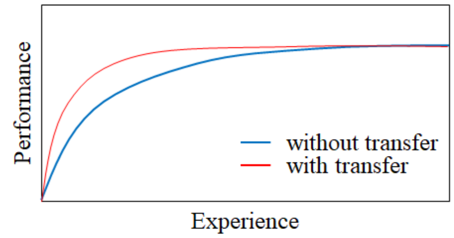

Fig. 11. Simplified example of learning speed improvement that emerged in the learning curve. The blue curve explains the performance transition without transfer, which is the learning curve of reinforcement learning. The red curve denotes performance transition with transfer.

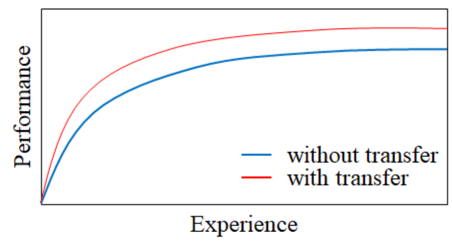

Fig. 12. Simplified example of asymptotic improvement which emerged in the learning curve. The blue curve explains the performance transition without transfer, which is the learning curve of reinforcement learning. The red curve denotes performance transition with transfer.

$$J_s = \frac{1}{n}\left(\sum_{i=1}^{n} L_t(i) - \sum_{i=1}^{n} L_{wt}(i)\right) \qquad (20)$$

Here, i is episode number of learning simulation. $L_t(t)$ is learning curve in transfer, and $L_{wt}(t)$ is learning curve without transfer, which means that pure reinforcement learning. Eq. (20) is formulated by Kono *et al.* [26]. If jump start is calculated with an upward curve such as Fig.10, the value of the jump start is positive; in other words, the performance is increasing. In contrast, if the jump start has a downward curve such as learning curve (Fig. 9), the value represents a negative that means that learning time is decreasing.

3) Learning speed improvement: Learning speed improvement means a reduction of area of the learning curve even if the start performance is the same value. Fig. 11 shows that learning curve converges faster than the learning curve without transfer. In other words, this phenomenon is represented as the speed of convergence.

If the initial performance and converged values of the learning curve are the same with or without transfer, learning speed improvement can help calculate transfer ratio r as defined below:

$$r = \frac{\sum L_t(t) - \sum L_{wt}(t)}{\sum L_{wt}(t)}. \qquad (21)$$

4) Asymptotic Improvement: Asymptotic improvement means that the final performance is improved by transfer. Fig. 12 shows the case of improvement; however, this emergence depends on the task and learned policy. This is because when depending on the task, there is an upper limit on performance, for example shortest path problem.

5) Transfer ratio: Taylor [7] proposed transfer ratio as a comparison method based on the area of the learning curves with or without transfer. If learning curve can be described as function $L(t)$, transfer ratio is defined by Eq. (21).

If the evaluation function is shaped as an upward curve (*e.g.* transition of rewards) as shown in Fig. 10, value r is positive. It represents the increasing performance or learning efficiency. In contrast, if the transfer ratio is evaluated as a downward curve, such as the learning curve, the value r becomes negative. It represents the decreasing of learning time or learning cost at the results .

C. Results and Discussions

First, criterial three learning curves are shown in Fig. 13. “Without transfer”, “Positive transfer” and “Negative transfer” are abbreviated as WT, PT and NT respectively. Proposed method as SAP–net is abbreviated as SAP. In the Fig. 13, represented learning curves are calculated averages from 10 trial, and standard deviation is represented with learning curve at 50 episode intervals. The red colored line is learning curve of WT equivalent to reinforcement learning. The blue colored line is learning curve of PT if the agent transferred policy from source task with helpful policy. This gives positive transfer. Green colored line is learning curve of NT. Here, the agent reused useless policy from the source task, and transferred policy inhibited learning in target task. This learning curve does not converge. It has huge fluctuation because the agent encountered dead lock with the wall in grid world, and it was difficult to re-learn the impeding behavior of dead lock until

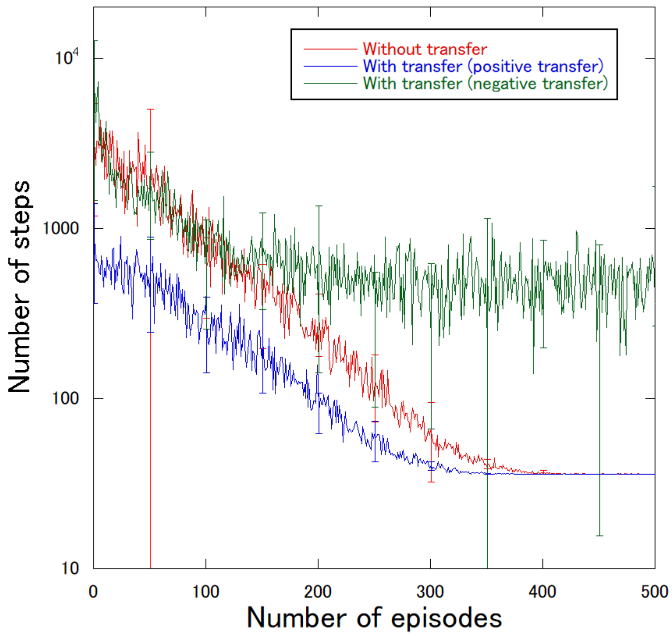

Fig. 13. Basic results of learning curve reinforcement learning, transfer learning with positive transfer and transfer learning with negative transfer.

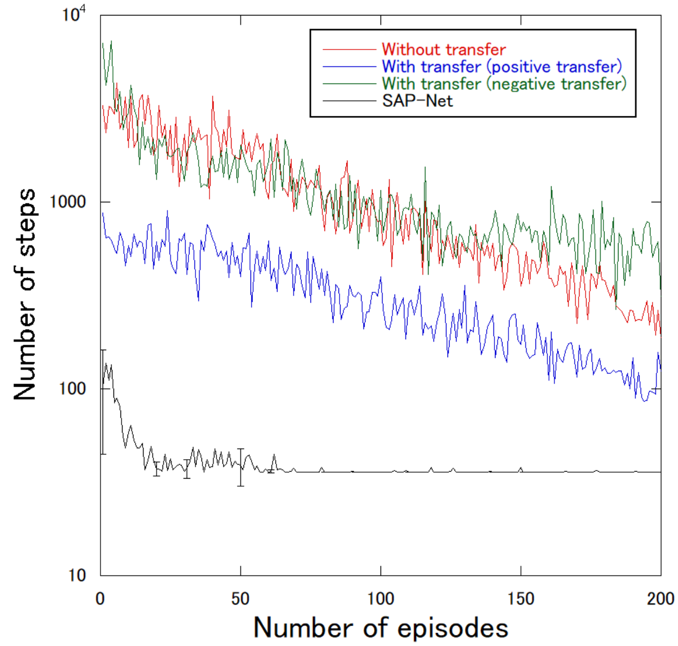

Fig. 14. Comparison among proposed method's learning curve and above basic results as Fig. 13. WT, PT and NT are the same as shown in Fig. 13.

1000 episodes. From the learning curve without transfer and learning curve on positive transfer, jump start and learning speed were improvement. However, asymptotic improvement did not occur because of optimal policy as shortest path in the grid world is the same between conditions without transfer and positive transfer.

The result of the learning curve with proposed method is shown in Fig. 14 represented with 200 episodes. Black colored line is learning curve of proposed method as SAP–net. It is a calculated 10 trials average. Standard deviation is represented at 50 episode intervals. SAP–net's learning curve extremely decreases compared to conditions WT, PT and NT, and convergence speed is faster than other conditions. Comparison of jump start value is indicated in Table IV. From WT, result of condition PT and SAP are exhibited jump start. This phenomenon means that the agent can solve the problem with fast time compared to WT. Moreover, SAP has a lower jumpstart value than PT, indicating that performance is high in the early stages of learning. Condition NT does not give jump start value, thus the performance worsens. A comparison of transfer ratio is shown in Table V. Condition PT and SAP decrease the value of transfer ratio thus the overall learning time is improved. In this result, WT and NT have near value of transfer ratio r. From Fig. 13, NT has a higher transfer ratio than WT. From these results, learning speed of condition PT is improved compared to WT. SAP can shorten the total learning time compared to condition PT. Therefore, not only PT but also SAP exhibited learning speed improvement. This result indicate that policy selection by proposed method has effectiveness for transfer learning in reinforcement learning. Additionally, in this experimental condition, shortest path has minimum limits, therefore asymptotic improvement is not achieved from this results.

Each activation value of policies is shown in Fig. 15 if the simulation is terminated. Activation value is averaged from 10 trials and standard deviation is calculated with 10 trials. Mainly seven policies are used and selected for solving shortest path problem. Initial activation value and weights of the path in SAP–net are same initialized value; therefore, activation value is adjusted by proposed method with learning in target task, and helpful policies' activation value become high value. Useless policies' activation value are not activated. Although some policies (*e.g.* policy number 36, 38 and 83) have low values, the activity value is updated a little. Transferred policies are generated in source task with random start position and goal position; therefore, a few policies selected were not effective. However, because the proposed method is learning algorithm, the process of selecting a policy through trial and error is important in transfer learning phase. Fig. 15 shows that final activation value of helpful policies are approximately 200; its higher value compared with initial activation value as 5. This is caused by insufficient tuning of decaying value

TABLE IV. COMPARISON IN JUMP START

Condition	Averaged steps (10 episodes)	Jump start
WT	3024.33	0.00
PT	623.07	−2401.26
NT	4253.29	1228.96
SAP	90.08	−2934.25

TABLE V. COMPARISON IN TRANSFER RATIO

Condition	Area under curve	Transfer ratio
WT	237463.40	0.00
PT	66689.40	−0.72
NT	248607.10	0.05
SAP	8033.40	−0.97

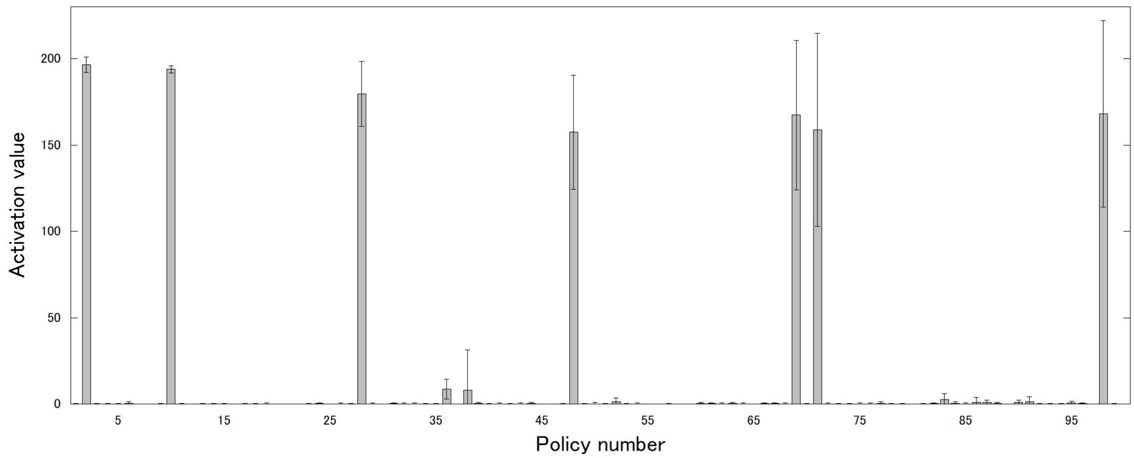

Fig. 15. Activation values when simulation terminated. Seven policies are founded useful from random generated source task's policy, and useless policies are not activated in SAP–net through this experiment.

$\Delta\mathbb{A}_j$. SAP–net is sensitive for parameter tuning, and many parameters are implemented. SAP–net effective from this experiment, however parameter setting needs to be discussed for generalization and applications.

VI. Conclusion

This paper proposed a novel policy selection method for transfer learning in reinforcement learning. Proposed method is inspired by the spreading activation theory discussed in cognitive science. SAP–net proposed contains functions such as networked stored policies, activation function, spreading function, decaying function, and recall function. Basic experiments were performed with shortest path problem using reinforcement learning agent that can select learned policies. From the experimental results, quantitative evaluation was performed, and results suggest that learning agent with SAP–net can solve the problem faster than WT and PT conditions. The agent with SAP–net selects policies adaptively from the environment.

As the future works, it is necessary to discuss the parameter settings. SAP–net is sensitive for activation and decaying and is related to trade-off. If a high activation value is set, the decaying value cannot cancel the activation value hence continues to rise. Further, decaying is strongly affected by the SAP–net and activation value may not rise. The proposed method is constructed with implementation as sequential, and calculation cost increases with number of policies. Order of proposed method is approximately $O(n^2)$, calculation is sequential processing. Parallelization method is also an important issue in implementation phase. Moreover, behavior SAP–net is connected to N-body problem, more theoretical consideration is required for system behavior.

Acknowledgment

This study was supported by JSPS KAKENHI Grant number JP18K18133 and JP19K12173, and this study was funded in part by the HAYAO NAKAYAMA Foundation for Science & Technology and Culture. We would like to thank Editage (www.editage.com) for English language editing.

References

[1] B. Ramalingam, A. K. Lakshmanan, M. Ilyas, A. V. Le, and M. R. Elara (2018). "Cascaded Machine-Learning Technique for Debris Classification in Floor-Cleaning Robot Application." *Applied Sciences* 8(12): 1–19.

[2] R. D. Andrea (2012). "Guest Editorial: A Revolution in the Warehouse: A Retrospective on Kiva Systems and the Grand Challenges Ahead." *IEEE Transactions on Automation Science and Engineering* 9(4): 638–639.

[3] T. Fukatsu, G. Endo, and K. Kobayashi (2016). "Field Experiments with a Mobile Robotic Field Server for Smart Agriculture." *Proceedings of the WCCA-AFITA2016*: pp.1–4.

[4] R. S. Sutton and A. G. Barto (1998). "Reinforcement learning: An introduction." MIT press.

[5] V. Mnih, K. Kavukcuoglu, D. Silver, A. A. Rusu, J. Veness, M. G. Bellemare, A. Graves, M. Riedmiller, A. K. Fidjeland, G. Ostrovski, S. Petersen, C. Beattie, A. Sadik, I. Antonoglou, H. King, D. Kumaran, D. Wierstra, S. Legg, and D. Hassabis (2015). "Human-level control through deep reinforcement learning." *Nature* 518: 529–533.

[6] C. J. C. H. Watkins and P. Dayan (1992). "Q-Learning." *Machine Learning* 8: 279-292.

[7] M. E. Taylor and P. Stone (2009). "Transfer learning for reinforcement learning domains: A survey." *Journal of Machine Learning Research* 10(Jul): 1633–1685.

[8] A. Lazaric (2012). "Transfer in Reinforcement Learning: A Framework and a Survey. Reinforcement Learning. Adaptation, Learning, and Optimization." Berlin, Heidelberg, Springer. 12: 143–173.

[9] J. M. Royer (1978). "Theories of Learning Transfer." *Technical report No. 79, University of Illinois at Urbana–Champaign*: 1–54.

[10] A. Taylor, I Dusparic, E. Dalván–López, C. Siobhán, and C. Vinny. (2014). "Accelerating learning in multi-objective systems through transfer learning." *2014 International Joint Conference on Neural Networks*: pp.2298–2305.

[11] M. E. Taylor (2009). "Transfer in Reinforcement Learning Domains." Studies in Computational Intelligence 216: Springer.

[12] B. Lakshmanan and R. Balaraman (2010). "Transfer learning across heterogeneous robots with action sequence mapping." *2010 IEEE/RSJ International Conference on Intelligent Robots and Systems*: pp.3251–3256.

[13] M. Koga, V. F. Silva, F. G. Cozman, and A. H. R. Costa (2013). "Speeding-up reinforcement learning through abstraction and transfer learning." *Proceedings of the 2013 international conference on Autonomous agents and multi-agent systems*: pp.119–126.

[14] C. Devin, A. Gupta, T¿ Darrell, P. Abbeel, and S. Levine (2017). "Learning modular neural network policies for multi-task and multi–

robot transfer." *2017 IEEE International Conference on Robotics and Automation*: pp. 2169–2176.

[15] F. Fernández, J. Garcia, and M. Veloso (2010). "Probabilistic policy reuse for inter-task transfer learning." *Robotics and Autonomous Systems* 58(7): pp. 866-871.

[16] F.Fernández, and M. Veloso (2013). "Learning domain structure through probabilistic policy reuse in reinforcement learning." *Progress in Artificial Intelligence* 2(1): 13-27.

[17] T. Takano, H. Takase, H. Kawanaka and S. Tsuruoka (2010). "Effective Reuse Method for Transfer Learning in Actor-critic." *Proceedings of the SCIS & ISIS 2010*: 137-141.

[18] T. Takano, H. Takase, H. Kawanaka, H. Kita, T. Hayashi, and S. Tsuruoka (2011). "Transfer Learning based on Forbidden Rule Set in Actor-Critic Method." *International Journal of Innovative Computing, Information and Control* 7(5(B)): pp. 2907–2917.

[19] M. Lanctot, V. Zambaldi, A. Gruslys, A. Lazaridou, K. Tuyls, J. Perolat, D. Silver, and T. Graepel (2017). "A unified game-theoretic approach to multiagent reinforcement learning." *Proceedings of the Neural Information Processing Systems* pp. 4190–4203.

[20] S. Doroudi, P. S. Thomas, and E. Brunskill (2017). "Importance Sampling for Fair Policy Selection." *Proceedings of the Thirty-Third Conference on Uncertainty in Artificial Intelligence*.

[21] A. Mittel and P. S. Munukutla (2019). "Visual Transfer Between Atari Games Using Competitive Reinforcement Learning." *Proceedings of the IEEE Conference on Computer Vision and Pattern Recognition (CVPR) Workshops*.

[22] A. M. Collins and E. F. Loftus (1975). "A spreading-activation theory of semantic processing." *Psychological Review* 82(6): 407-428.

[23] M. R. Quillian (1967). "Word concepts: a theory and simulation of some basic semantic capabilities." *Behavioral Science* 12: pp.410–430.

[24] M. R. Quillian (1969). "The teachable language comprehender: a simulation program and theory of language." *Computational linguistics* 12(8): pp.459–476.

[25] D. M. Gaines, J. White, M. Wilkes, K. Kusumalnukool, S. Thongchai and K. Kawamura (2001). "SAN-RL: combining spreading activation networks and reinforcement learning to learn configurable behaviors." *Proceedings of the Intelligent Systems and Advanced Manufacturing*.

[26] Hitoshi Kono, Akiya Kamimura, Kohji Tomita, Yuta Murata and Tsuyoshi Suzuki (2014) "Transfer Learning Method Using Ontology for Heterogeneous Multi-agent Reinforcement Learning." *International Journal of Advanced Computer Science and Application* 5(10): pp.156–164.

[27] Y. Takakuwa, H. Kono, W. Wen, and T. Suzuki (2019). "A Study on Policy Reuse Method Using Psychologically Inspired Model in Transfer Learning." *Proceedings of the 24th Robotics Symposia*: pp.86–89 (in Japanese)

Best-Choice Topology: An Optimized Array-based Maximum Finder

Marina Prvan[1], Julije Ožegović[2], Ivan Sočo[3], Duje Čoko[4]
Department of Electronics and Computing, Faculty of Electrical Engineering
Mechanical Engineering and Naval Architecture (FESB), Split, Croatia

***Abstract*—Extracting maximum from an unsorted set of binary elements is important in many signal processing applications. Since quite few maximum-finder implementations are found in the recent literature, in this paper we provide an update on the current topic. Generally, maximum-finders are considered array-based, with parallel bit-by-bit comparison of the elements, or more efficient tree-based structures, with the hierarchical maximum extraction. In this paper, we concentrate on array-based topologies only, since our goal is to propose a new maximum-finder design called Best-Choice Topology (BCT), which is an optimized version of the standard Array Topology (AT). The usual bit-by-bit parallel comparison is applied for extracting the maximum and its one-of-N address. Boolean expressions are derived for BCT logical design and the minimum-finder equivalent. Functionality of the proposed architecture and the reference designs is verified with Xilinx ISE Design Suite 14.5. Synthesis is done on Application Specific Integrated Circuit (ASIC) TSMC 65nm technology. The conclusion of the paper is two-fold. First, we confirm the timing efficiency of BCT compared to AT. Next, we show that BCT is more efficient than the recent maximum-finder design called Maximum Magnitude Generator (MaxMG) and it has a great potential to be used for real-time signal processing applications.**

Keywords*—*Array topology; best-choice topology; maximum finder; maximum magnitude generator

I. Introduction

The design of an efficient circuit for finding one or multiple maximum and/or minimum values in an unsorted set of binary numbers is very important. It is used by many applications [1-6] and depending on the purpose, circuits can be designed to produce value and/or the address of the winner element. For example, there are applications which require both maximum value and address [1, 7], while some others require only the fast computation of the maximum element [3, 8]. For example, finding minimum among distances to the cluster heads is crucial in clustering procedure or the neural network design [2, 5]. Extracting minimal distance to the stored database images or finding maximum among different image vectors is important in object recognition and classification [9]. The commonly used rank order filter requires fast computation of the central maximum, median or minimum [10].

Extracting one or multiple winner elements in a set can be solved by sorting the whole set and selecting the first or last few values [11, 12]. This approach is common in rank order filter algorithm, with complete or partial sorting used to extract the median. However, even though many efficient sorting algorithms are designed in hardware with optimized implementations [9, 13], sorting the whole set for extracting a single maximum/minimum value is not feasible when efficient throughput and latency are required. This raises the demand for the design of the dedicated hardware solutions.

Very few papers on the maximum-finder topologies have been published in recent years. This paper gives an update on the current topic and a solution of the maximum finding problem is proposed by a new logical design named Best-Choice Topology (BCT). It is an optimization of the standard Array Topology (AT), designed as a parallel combinational circuit that generates the value and one-of-N binary address of the maximum among N binary numbers. Minimum finder BCT can be easily derived with the minor change of the Boolean operations. The functionality of BCT and its reference designs is verified and simulated by using Verilog Hardware Definition Language (HDL). Synthesis is done on Application Specific Integrated Circuit (ASIC) TSMC 65 nm technology, by using Cadence Genus Synthesis Solution tool [14]. We show that BCT is faster than AT, especially for lower size of the binary input codewords. Also, it offers greater efficiency in timing, area and power than the recent Maximum Magnitude Generator (MaxMG) design.

The paper is organized as follows. Section II gives a summary of the existing topologies, with AT functionality explained in Section III. Next, in Section IV, a new maximum finder BCT design is proposed with optimization compared to AT. The general equivalent maximum and minimum finder BCT models are given. Section V and Section VI provide simulation and synthesis results. The BCT performance efficiency is evaluated and compared to referent designs. Limitations of the study are discussed in Section VII. Section VIII concludes the paper, followed by the references used.

II. Related Work

A literature survey is provided in [15], with circuits characterized as array-based or tree-based, depending on their logical design. The former ones are simpler, with bitwise comparisons of all candidates done in parallel, while the latter are more efficient in terms of latency. Authors propose the Array Based Topology (ABT) and some other designs using ABT as a basic building block. ABT is a compromise between performing a parallel comparison of all pairs of k-bit input data elements, and a tree-based hierarchical approach for the maximum extraction. They compare the proposed architecture with the simple Traditional Binary Tree (TBT) solution with comparator and multiplexer blocks, as well as its more efficient Parallel Binary Tree (PBT) variants like Ripple Carry (RCT) and Carry Select Topology (CST).

Recently, authors in [16] proposed an ABT-based architecture that is more efficient in timing but detrimental to area and power. On the other hand, an efficient maximum-finder topology called Maximum Magnitude Generator (MaxMG) is implemented in [17]. The design is combinational and array-based, so it works as a filter comparing all input data bits in parallel. It consists of three main levels of logic gates, as shown in Fig. 1. The first level extracts the MSB of the maximum element by using OR gates. The second level uses XOR gates for comparing MSB of all inputs with the previous level result MSB bit. Input data elements having the same MSB as the result could be potential maximums.

High signal generated from the second level is sent to the third level where XOR output is multiplied with each of the input MSBs. This level is a filter, providing a signal if the current element is still a potential maximum or it is excluded from the competition. Namely, AND output is transferred to the next level's AND for the next maximum element's bit calculation. If the output of the AND gate is low, the number is excluded from the maximum element competition. In case of the all input data elements having the MBS low, next XOR gate will have a high output, so that AND gate decide which number is chosen.

Authors in [18] propose an optimized maximum-finder circuit that is based on the Leading Zero Count Topology (LCT). The idea is to encode each k-bit binary input element so that a bitwise OR operation can be performed between the coded values. The count of the leading zeros in the result gives the position or index of the winner element. There are some other tree-like topologies in the literature, designed for the first two maximum or minimum values extraction, or calculating the kth best value in an unsorted list of elements, where the position k can be arbitrary [19-21].

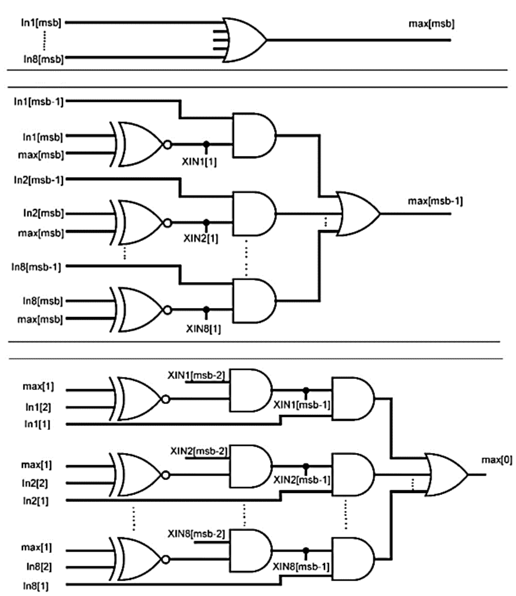

Fig. 1. Generalized MaxMG Topology [17].

III. Array Topology (AT)

BCT proposed in this paper is based on the optimized version of the Array Topology (AT) [15, 22], namely, AT is based on a filtering approach where all candidates are processed in parallel from the most to the least significant bit (MSB to LSB). Progressively, the number of candidates in the calculation of the maximum element is reduced by using the enable signal. This one disables the candidate that loses the chance to become a maximum when it has lost on a specific bit. As shown in Fig. 2, the basic building block of the topology is one AT-cell for each of the k candidate bits.

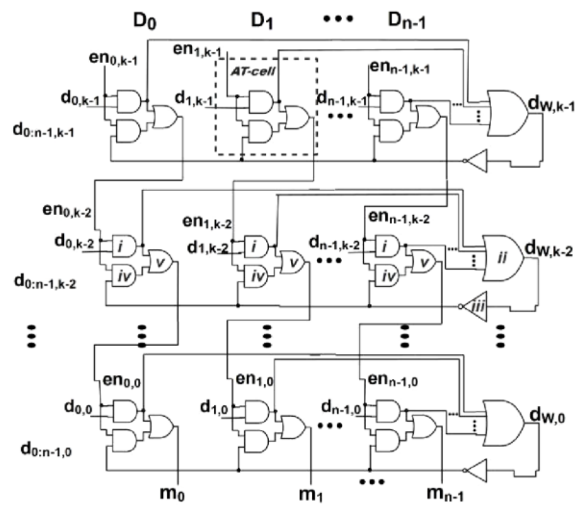

Fig. 2. Array Topology [15].

AT uses the 2-input AND gate (i) to select input data bits from n numbers that are enabled, and the signals are sent to the n-input OR gate (ii) providing the corresponding winner bit. Inverted winner data bit (iii) and 2-input AND gate (iv) ensure that even if all bits were zero, the result is still transferred to the next AT row, or the enable signals would all be low. Next, 2-input OR gate (v) generate the enable signal. Low/high output is generated depending on input signals, enabling/disabling the current input bit. The advantage is that we can get the winner element just after the first level if only one candidate has a high MSB bit, as AT will pass only the bits of that candidate. Besides the winner element, AT gives its corresponding address. It is generated by the enable signal propagated through the bits of each candidate. Value of the address bit is high if the candidate was enabled for all bits, and it is low otherwise.

IV. Proposed Best-Choice Topology (BCT)

A. Main BCT Concept

The solution for solving maximum-finder problem in the proposed BCT is defined again as a filtering approach. A bit-by-bit comparison of all candidates in parallel from MSB to LSB is applied, progressively reducing the number of candidates for the winner element. BCT functionality can be approximated with the self-organizing binary network that stabilizes when the maximum is found and settled on the result bus. This self-stabilizing concept is based on the combinational type of digital circuit, with binary signal comparison results obtained. The solution is accomplished by using only feedback coming from the lowest bit-level comparisons.

For example, if some of the N input elements receive negative feedback on a bit-level comparison, they exclude themselves from the winner competition, which is basically the calculation of the maximum element. On the other hand, if some element is high enough to become the winner (maximum), a positive feedback is generated, and system will advance in the maximum finding goal. Therefore, BCT logic can be summarized in two important aspects:

- The comparison is done bit-by-bit in parallel from MSB to LSB and extracting the winner element. This concept is like AT, but BCT uses an improved self-exclusion technique for the bit of the input element as well as fast propagation of the winner decision towards LSB.
- Feedback is implemented by a result (OR) bus where the winner bits are generated. It is important that this bus is unique, independent of the size of the input dataset. This means that there is no additional decision logic (such as in binary trees) but the OR bus realization. In ASIC technology this is the real OR-gates or wired-OR bus implemented with open-collector logic. Thus, additional delay remains only in the tree of OR gates of BCT structure.

Since the main winner competition is done on the lowest bit level, each of the input elements gives its high bit on the bus as if it was a winner and withdraws its high bit together with all the lower significant bits when it has lost the battle for the winner element. Thus, overall behavior of the BCT system is caused by the lowest bit-level components; every input element is entering the winner competition with its bits and it concludes if it is strong enough to be the winner. If it loses on the specific bit, it excludes itself from the further competition.

B. AT Optimization in BCT

BCT comparison starts from the basic Single Bit (SB) blocks working in parallel. SB comparator module consists of two AND gates, one OR gate and one inverter, as shown in Fig. 3. Inputs to the SB block are denoted as signals d (data bit) and r (result bit), because r is a bit on the result bus (the bit of the current maximum) and d is a current input data bit (the bit of the current candidate).

Comparison SB block output is marked wi and it becomes the enable signal t for the next bit. Signal t will be high and current input element is enabled while $d \geq r$. When $d < r$, it means that candidate has lost on a specific bit and t becomes low (Fig. 4). This disables the candidate from the further competition since output signal b will be zero for the current data bit and all further bits up to LSB.

BCT filtering concept is similar but more efficient than AT implementation, namely, in AT SB block, the next bit enable signal cannot be calculated before calculating previously the bit of the current maximum. This will cause one additional gate delay before calculating the winner bit, and shorter critical path delay as presented in Fig. 3. However, in BCT, enable signal for the next bit can be calculated immediately from the data bit, which means that we can have the maximum calculation started as soon as input data becomes available. This gives an enhancement of faster calculating the result element bits in BCT with respect to the traditional AT. BCT circuit area is foreseen to be the same as AT, since there is the same number of logic gates at the lowest level of SB comparators.

C. BCT Maximum Finder Example

BCT network stabilizes when winner is extracted on result bus. This means that there will be several result bus configurations that will change during the winner competition.

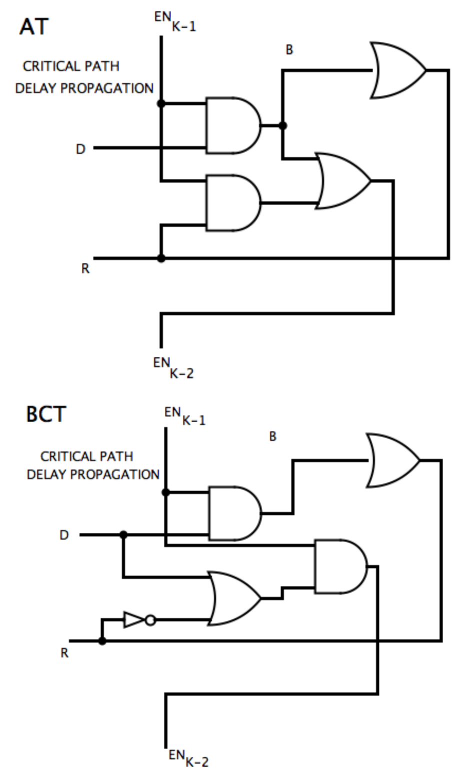

Fig. 3. The AT and BCT Single Bit (SB) Block.

t	d	r	b	wi
0	0	0	0	0
0	0	1	0	0
0	1	0	0	0
0	1	1	0	0
1	0	0	0	1
1	0	1	0	0
1	1	0	1	1
1	1	1	1	1

t \ dr	00	01	11	10
0				
1			1	1

b = t && d

r	d	¬r V d
0	0	1
0	1	1
1	0	0
1	1	1

t \ dr	00	01	11	10
0				
1	1		1	1

w = (t && ¬r) V (t && d)

w = t && (¬r V d)

Fig. 4. Boolean Expressions for the BCT SB Block.

result bus = {0 0 0 0 0 0 0 0}
x_0 = {0 0 0 1 0 1 0 1}$_{(2)}$ = 21$_{(16)}$ x_1 = {0 0 1 0 1 0 1 0}$_{(2)}$ = 42$_{(16)}$ x_2 = {0 0 1 1 0 1 0 1}$_{(2)}$ = 53$_{(16)}$ x_3 = {0 1 0 0 0 1 0 0}$_{(2)}$ = 44$_{(16)}$ x_4 = {1 0 0 0 1 0 0 0}$_{(2)}$ = 88$_{(16)}$ x_5 = {1 0 0 0 0 1 1 1}$_{(2)}$ = 87$_{(16)}$ x_6 = {1 1 0 1 0 1 1 0}$_{(2)}$ = D6$_{(16)}$ x_7 = {0 1 1 0 0 1 1 0}$_{(2)}$ = 66$_{(16)}$
result bus = {0 0 0 0 0 0 0 0}
bits$_{x0}$ = {0 0 0 1 0 1 0 1} bits$_{x1}$= {0 0 1 0 1 0 1 0} bits$_{x2}$ = {0 0 1 1 0 1 0 1} bits$_{x3}$ = {0 1 0 0 0 1 0 0} bits$_{x4}$ = {1 0 0 0 1 0 0 0} bits$_{x5}$ = {1 0 0 0 0 1 1 1} bits$_{x6}$ = {1 1 0 1 0 1 1 0} bits$_{x7}$ = {0 1 1 0 0 1 1 0}
result bus = {1 1 1 1 1 1 1 1}$_{(2)}$ = FF$_{(16)}$
bits$_{x0}$ = {0 0 0 0 0 0 0 0} bits$_{x1}$ = {0 0 0 0 0 0 0 0} bits$_{x2}$ = {0 0 0 0 0 0 0 0} bits$_{x3}$ = {0 0 0 0 0 0 0 0} bits$_{x4}$ = {1 0 0 0 0 0 0 0} bits$_{x5}$ = {1 0 0 0 0 0 0 0} bits$_{x6}$ = {1 1 0 0 0 0 0 0} bits$_{x7}$ = {0 0 0 0 0 0 0 0}
result bus = {1 1 0 0 0 0 0 0}$_{(2)}$ = C0$_{(16)}$
bits$_{x4}$ = {1 0 0 0 0 0 0 0} bits$_{x5}$ = {1 0 0 0 0 0 0 0} bits$_{x6}$ = {1 1 0 0 0 1 1 0}
result bus = {1 1 0 1 0 1 1 0}$_{(2)}$ = D6$_{(16)}$ address indicator = {0 1 0 0 0 0 0 0}

Fig. 5. BCT Maximum Extraction Example.

Example is given in Fig. 5. Initially, result bus is set to zero, so all input elements are winner candidates. This initial condition will reset the result bus and trigger the winner competition. It will put low bit of the result to high, enabling the enable signal generation. When the k-bit results of the SB comparisons are calculated for each of the input elements, array of k n-input OR gates is used for bitwise extraction of the temporary maximum bits on the result bus. This temporary result bus configuration forces each of the elements to compete by giving its high bits to the bus. Result is calculated when all candidates have lost the competition but the winner element that is larger or equal to the temporary result bus configuration. This configuration is generated by doing OR operation between each element's k-bit result bits. These are higher or equal to the winner, so that all maximum bits are extracted correctly after the OR operation. One-of-n binary address of the maximum is generated from the enable bits, where address bits are set low for all candidates but the winner position.

D. Generalized Maximum-Finder BCT Logic

Maximum or winner element is denoted as:

$$ymax = yk\text{-}1\ yk\text{-}2y1\ y0 \qquad (1)$$

It is computed in the following manner. As a first step, a parallel execution of n circuits with k slices produce n codewords which represent bitwise comparisons. Each codeword corresponds to the data k-bit number that is taken as input, as well as the enable signal wi which will enable or disable the current number from the further competition. We refer to these code words as bdata= bk-1 bk-2b1b0 where bi in each slice is calculated as:

$$bi = di \wedge ti, i=0, 1, 2, \ldots, k \qquad (2)$$

While data element is greater or equal to the winner element, its resulting bit bi will be high, and it will be put to low as soon as data element losses on a specific bit in the winner competition. Data bit is presented as di and the ith bit comparison element enable signal is marked as ti. Based on the annulment law in the Boolean algebra, as soon as enable signal becomes low, the result bit bi will be put to low as well, causing the data element to be disabled from the further winner competition. Enable or disable signal wi from the previous bit is transmitted to the next one in the ripple way:

$$tk\text{-}1 = t \wedge 1 = t$$

$$tk\text{-}2 = wk\text{-}1 \wedge t = wk\text{-}1 \wedge tk\text{-}1$$

$$tk\text{-}3 = wk\text{-}2 \wedge wk\text{-}1 \wedge t = wk\text{-}2 \wedge tk\text{-}2$$

$$t0 = w1 \wedge t1 \qquad (3)$$

Signal is propagating from MSB to LSB in the data element, enabling the calculation of the bdata codeword for each number competing for the winner position. One can see in the equations above that lower significance bit enable signals tk-2, tk-3,…,t0 depend on the win bits wk-1,wk-2,…,w1 where each win bit is enabling or disabling the next bit in the data element winner competition. This win signal tells if the current element is still in the competition or it has lost on the specific bit. Therefore, signal ti depends on wi+1 and once the data element loses the battle in the winning network, enable signals ti, ti-1,…,t1 will become zero, automatically annulling the corresponding bdata bits bi,bi-1,…,b1. Win bits wi are:

$$wi = ti \wedge (\neg ri \vee di) \qquad (4)$$

In the equation (4), data bit di of the current element is competing with the result bit ri of the winner element that is currently on the result bus. Result bus will obtain several configuration changes until the winner element is settled on the result bus and the winning network stabilizes in the search for the maximum element. For n elements competing in the network, result is put to zero at the very beginning. This reset of the result bus will start the competition and destabilize the network. Due to this initial zero configuration, each of the input data elements will be potential winner as they are all greater than the current result.

After the bitwise competition for n k-bit elements in parallel, winner is extracted on the result bus. It is done based on the bdata codewords of each data element as:

$$rk\text{-}1 = bdata0(k\text{-}1) \vee \ldots \vee b(data(n\text{-}1)(k\text{-}1))$$

$$rk\text{-}2 = bdata0(k\text{-}2) \vee \ldots \vee b(data(n\text{-}1)(k\text{-}2))$$

$$r1 = bdata01 \vee bdata11 \vee \ldots \vee bdata(n\text{-}1)1$$

$$r0 = bdata00 \vee bdata10 \vee \ldots \vee bdata(n\text{-}1)0 \qquad (5)$$

E. Minimum-Finder BCT

Minimum finder BCT (Fig. 6) is derived with a minor change of Boolean expressions in Fig. 4. Unlike previously calculating enable signal wi, we invert the data bit to obtain enable signal for minimum instead of the maximum:

$$wi = ti \wedge (ri \vee \neg di) \tag{6}$$

The minimum-finder BCT is based on the same concept as maximum-finder circuit. The exact difference is in the winner element extraction. Naturally, since the same logic gates are used, the bit d of the current element must be inverted, unlike the bit of the result r in the maximum-finder BCT variant.

t	d	r	w
0	0	0	0
0	0	1	0
0	1	0	0
0	1	1	0
1	0	0	1
1	0	1	1
1	1	0	0
1	1	1	1

r	d	r V ¬d	
0	0	1	d == r
0	1	0	d > r
1	0	1	d < r
1	1	1	d == r

t \ dr	00	01	10	11
0				
1	1	1		1

w = t ∧ (r V ¬d)

Fig. 6. Minimum Finder BCT Boolean Expressions.

V. Verilog Simulation Results

A. Experimental Setup

The referent designs used as competitors to BCT are array-topologies only, as our goal in the paper is not to compare array-based with tree-based topologies. Goal is to demonstrate the improvement over the state of the art with the proposed design, but only among array-based topologies. Therefore, to obtain a fair comparison, the competitors which are selected are AT and the recently introduced MaxMG. The topologies are implemented in Verilog HDL and simulated within the Xilinx ISE Design Suite 14.5 development environment. Timing and area results are given for the comparison of n k-bit input values in an unsorted set of elements where n={8,16,32,64} and k={8,16,32,64}. Synthesis is done with Cadence Genus synthesis tool on ASIC TSMC 65 nm technology, with constraints adjusted to virtual clock pulse of 20 ns. This working frequency represents the clock period of the integrated circuit used to implement the design and to constrain critical input/output path delay.

B. Xilinx ISE Simulation

The functionality of the topologies is verified by the simulation presented in Fig. 7. These are the results for the winner competition between n=8 input elements, each of them k=8 bits wide (example in Fig. 5). AT has the largest delay in the simulation, since more than 1 ns is needed for the winner extraction. On the other hand, MaxMG and BCT are faster, with 900ps delay. BCT configuration changes are presented on the result bus, where a SB-based competition between elements is done. It is shown in the simulation how BCT asynchronous network is destabilized with the changed input data and stabilized again when the winner is found on the result bus.

VI. ASIC Synthesis Results and Discussion

A. Area

The concise way of presenting the results is inspired by [15]. The area comparison of BCT with the reference circuits is given in Tables I and II. We present evaluation of the number of logic gates in ASIC, with area estimated in μm^2. In the theoretical calculation based on BCT and AT logical designs, BCT consists of the same number of logic gates as AT in the lowest level of SB comparators. Namely, when calculating number of gates from the digital logic scheme, an 8-bit maximum selector in a set of 8 input elements based on AT consists of:

- 128 2-input AND gates
- 64 2-input OR gates
- 8 8-input OR gates

That is in total 192 2-input gates and 8 8-input OR gates [23], where m-input logic gates can be implemented as a binary tree of m-1-unit gates [15]. This is in total 8*(8-1) = 56 gates for AT. BCT uses the same number of gates in SB blocks, i.e. 2 2-input AND gates and 1 2-input OR gate for each of the 64 SB blocks. Hence, BCT uses 192 gates for SB parallel comparisons, and with an array of n k-input OR gates for the result bus implementation, that is again 8*(8-1) =56 gates.

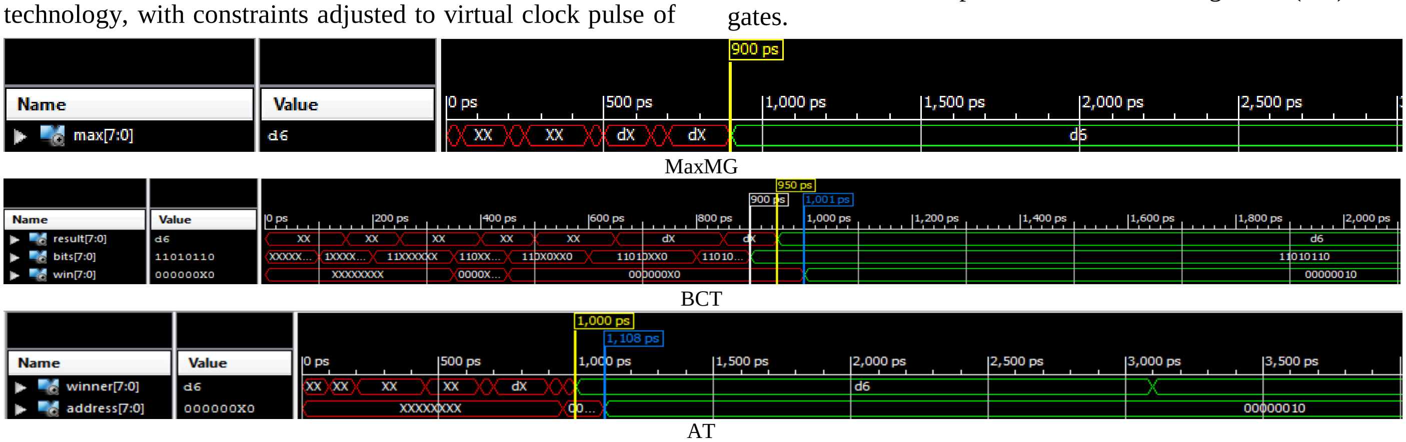

Fig. 7. Simulation Results.

TABLE. I. AREA (# LOGIC GATES)

k,n	MaxMG	AT	BC
8,8	143	147	**110**
8,16	292	251	**206**
8,32	601	524	**417**
8,64	1191	1078	**818**
16,8	315	281	**222**
16,16	655	465	**414**
16,32	1336	948	**841**
16,64	2670	1868	**1652**
32,8	646	429	**446**
32,16	1359	834	**830**
32,32	2758	1658	**1689**
32,64	5476	3254	**3314**
64,8	1315	862	**894**
64,16	2771	1667	**1662**
64,32	5598	3322	**3385**
64,64	11596	8394	**8394**

TABLE. II. AREA COMPARISON [UM^2]

k,n	MaxMG	AT	BC
8,8	293,40	335,88	**266,40**
8,16	637,56	592,92	**533,88**
8,32	1257,12	1223,28	**1058,40**
8,64	2913,48	2539,80	**2114,28**
16,8	623,52	630,00	**537,12**
16,16	1077,84	1129,32	**1077,84**
16,32	2138,40	2289,60	**2138,40**
16,64	4274,28	4572,00	**4274,28**
32,8	1281,24	1090,44	**1078,56**
32,16	2785,32	2139,84	**2160,72**
32,32	4296,60	4289,76	**4296,60**
32,64	8585,64	8545,68	**8585,64**
64,8	2599,20	2184,84	**2161,44**
64,16	5636,88	4284,36	**4328,28**
64,32	8609,76	8598,24	**8609,76**
64,64	19436,40	19459,80	**19436,40**

Similarly, the total number of logic gates for MaxMG implementation is dependent on the number of stages and input data elements, where the number of stages is equal to the number of input data bits. For example, in theoretical calculation from the MaxMG logic scheme, 8 bytes input maximum selector based on MaxMG consists of:

- 4 2-input OR gates in the first stage;
- 4 2-input OR gates, 8 XNOR gates and 8 AND gates in the second stage;
- 4 OR, 8 XNOR and 16 AND gates for each of the remaining 6 stages.

That is in total 4 gates in the first stage, 36 gates in second stage and 44*6=264 gates in total for the remaining MaxMG stages. This gives in total 304 gates for MaxMG, which is 22% larger than BCT in theoretical calculation. We consider in our calculation that XNOR is accomplished as XOR with an inverter, i.e. a single XOR gate area approximation. In the area comparison summarized in Fig. 8, we can see that the above theoretical calculations are verified. The synthesis result for BCT is almost the same as AT with small improvement factor. Also, BCT is more efficient than MaxMG, with the average improvement around 10%.

B. Propagation Delay

Timing efficiency is measured from the moment all input data is obtained, which is 3000 ps after the first data read-out. When the last signal is transferred to the final block in the design, the total propagation delay of the synthesized circuit is obtained. The results are presented in Table III.

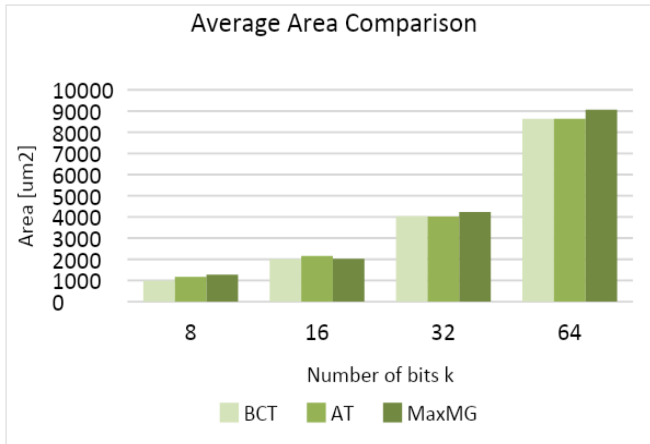

Fig. 8. Area Comparison.

TABLE. III. CRITICAL DATA PATH DELAY [NS]

k,n	MaxMG	AT	BC
8,8	9,926	5,687	**4,442**
8,16	10,317	6,026	**5,566**
8,32	11,592	6,975	**5,423**
8,64	11,672	7,381	**5,508**
16,8	18,331	7,536	**5,670**
16,16	18,695	7,033	**6,492**
16,32	19,504	7,697	**6,349**
16,64	19,734	7,542	**6,439**
32,8	34,903	8,336	**8,126**
32,16	35,368	8,758	**8,587**
32,32	35,951	8,886	**8,507**
32,64	36,019	8,914	**8,668**
64,8	68,107	13,144	**13,038**
64,16	68,314	13,610	**13,389**
64,32	69,546	13,769	**13,355**
64,64	71,521	15,576	**15,548**

It is shown that BCT outperforms referent designs in timing. Since BCT is the optimized version of AT, it provides more efficient calculation of the enable signal, and faster extraction of the winner on the result bus. There is no ripple effect in BCT which is present in AT, causing a poor timing result, namely, bits having the same significant values must wait on the output signal from other bits.

Even though each AT-cell in AT row can be executed in parallel, every AT-cell in the column is dependent of the previous one at the higher level. This means that lower-level AT-cell in the same column cannot begin its work before the enable signal for that AT-cell is calculated in former AT-cell. Also, enable cannot be calculated before the winner data bit is generated, and all the winner bits cannot be calculated until all enable bits settle down [15]. Since in AT circuit next bit enable signal cannot be calculated before calculating the bit of the current maximum, this will cause one additional gate delay before calculating the winner bit. However, in BCT, enable signal for the next bit can be calculated immediately from the data bit, which means that we can have the maximum element calculation started as soon as the input data becomes available. The comparison between BCT and AT is visualized in Fig. 9.

Fig. 10 shows the average propagation delay trendlines when BCT is compared with AT and MaxMG. We can see that BCT optimization is more present for smaller number of bits in the input data. In that case, BCT is faster in extracting the maximum from the dataset for around 20 % decrease in propagation delay. For larger number of bits, k>32, the average difference between BCT and AT is negligible (around 2%). This is caused by the enable signal propagation when larger number of input bits is compared in the input.

BCT is more efficient than MaxMG (Fig. 10(b)), since it is a parallel structure comparing all input bits at once in the winner competition. Maximum element can be settled on the result bus by using smaller number of logic gates causing on smaller delay on logic since BCT is a smaller circuit. BCT does not require k calculation stages processing in parallel for k-bit maximum value generation with a single bit carry propagation to the next stage. Therefore, BCT will calculate the maximum with at most (n/8k) +1 result bus configuration changes, where n is number of elements and k is number of data bits.

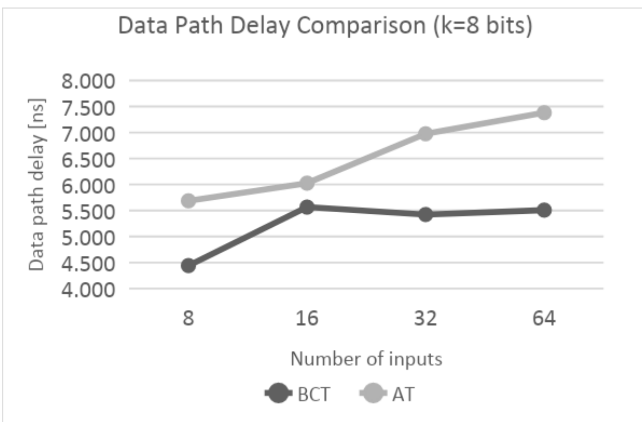

(a)

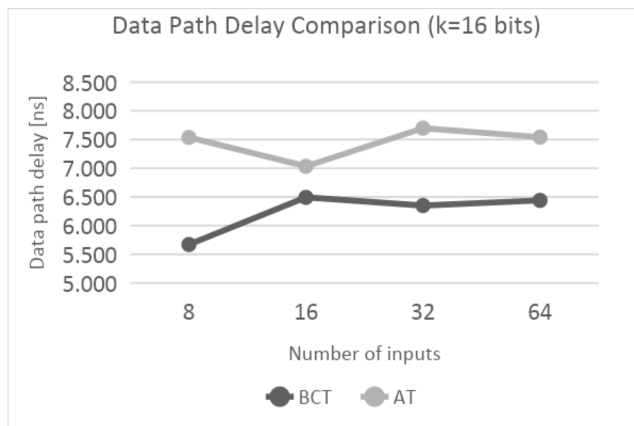

(b)

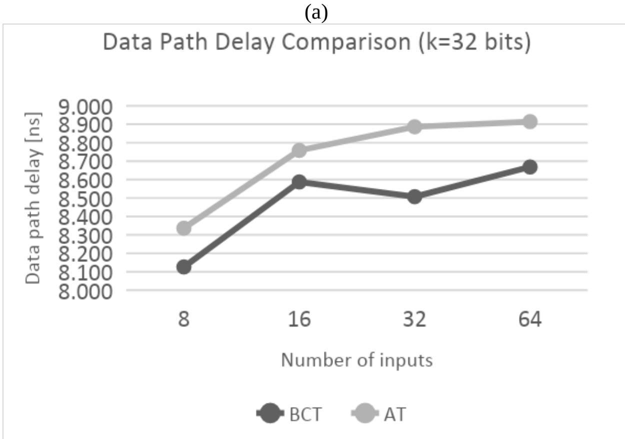

(c)

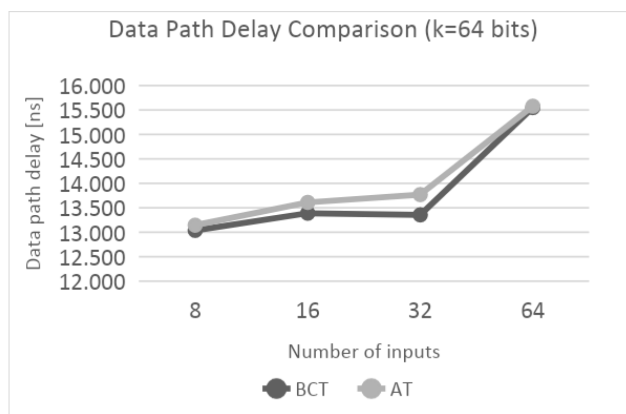

(d)

Fig. 9. Propagation Delay Comparison [ns].

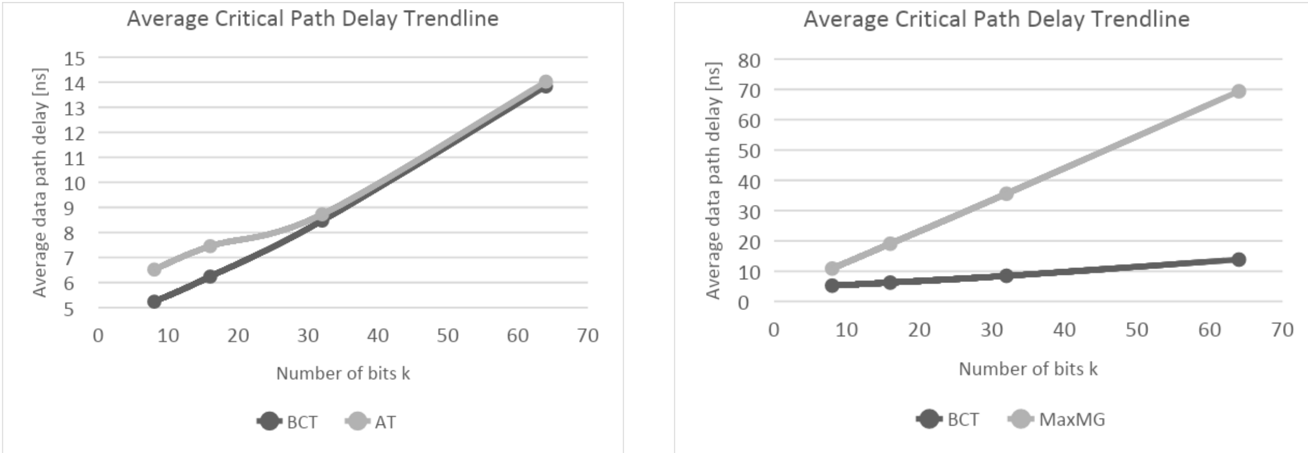

(a) (b)

Fig. 10. Average Propagation Delay Comparison. **(a)** BCT and AT, **(b)** BCT and MaxMG

C. Power Consumption

Dynamic power is energy that a digital circuit uses for its work. It represents the power consumed when the design runs, being calculated as the sum of the power supplied on logic and for input/output signals.

Table IV summarizes the results on the dynamic power consumption for ASIC circuit. The average power consumption is almost the same for BCT and AT as expected. MaxMG is considered one of the most energy efficient topologies in [17] outperforming tree-based and ABT-based circuits. However, in our experiment, MaxMG is almost three times slower than AT and BCT. Due to the larger number of logic gates and area, it has the highest switching activities causing the largest dynamic power consumption and power consumed on logic, especially with larger number of bits in the input code word. The average power trendlines for BCT and referent designs are given in Fig. 11 and visualizing the power comparison result.

D. Area and Power Delay Product (ADP and PDP)

Power-Delay-Product (PDP) and Area-Delay-Product (ADP) are commonly used to determine quality of a synthesized digital circuit [24-26]. PDP is a product of the average power consumption and gate delay. It estimates energy used per operation and estimates the average energy consumed per switching event [27]. ADP expresses trade-off between circuit area and average delay, as the main goal in the design of a digital circuit is to minimize area per logic gate.

It is shown in Tables V and VI that BCT is the best circuit in terms of standard measures for the quality of the logical design, namely, BCT outperforms the referent architectures, offering the minimized ADP and PDP metrics. It is straightforward since BCT has the smallest time and area complexity compared to MaxMG and lower delay and lower or equal area compared to AT when synthesized on ASIC TSMC 65 nm technology. Also, BCT is slightly more power efficient than AT in 50% of the measurement cases in our experiment. This provides an improvement when PDP is calculated, considering the lower propagation delay.

TABLE. IV. POWER CONSUMPTION [NW]

k,n	MaxMG	AT	BC
8,8	5232,62	6541,54	**5961,82**
8,16	15357,74	10120,18	**9993,22**
8,32	31692,88	19859,73	**18919,74**
8,64	77495,90	44881,81	**41692,10**
16,8	14003,28	7959,35	**7754,28**
16,16	36124,69	21215,25	**20935,51**
16,32	69477,02	30746,31	**31330,02**
16,64	152778,94	75189,38	**76165,04**
32,8	45535,67	13174,44	**13427,08**
32,16	91966,01	22596,36	**22724,47**
32,32	175197,80	47303,70	**48112,36**
32,64	316724,20	109041,50	**109650,40**
64,8	60469,86	21380,60	**21353,39**
64,16	140307,13	38008,61	**38225,02**
64,32	293379,06	81205,02	**82651,28**
64,64	738234,36	167856,56	**167039,52**

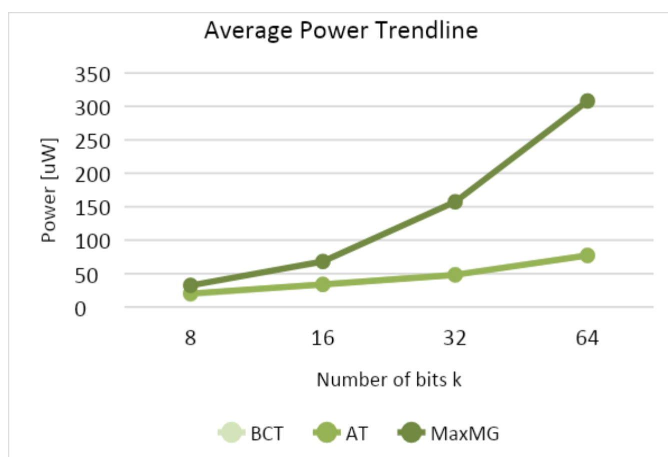

Fig. 11. Power Comparison.

TABLE. V. ADP RESULT [μM2*US]

k,n	MaxMG	AT	BC
8,8	2,91	1,91	**1,18**
8,16	6,58	3,57	**2,97**
8,32	14,57	8,53	**5,74**
8,64	34,01	18,75	**11,65**
16,8	11,43	4,75	**3,05**
16,16	20,15	7,94	**7,00**
16,32	41,71	17,62	**13,58**
16,64	84,35	34,48	**27,52**
32,8	44,72	9,09	**8,76**
32,16	98,51	18,74	**18,55**
32,32	154,47	38,12	**36,55**
32,64	309,25	76,18	**74,42**
64,8	177,02	28,72	**28,18**
64,16	385,08	58,31	**57,95**
64,32	598,77	118,39	**114,98**
64,64	1390,11	303,11	**302,20**

TABLE. VI. PDP RESULT [μJ]

k,n	MaxMG	AT	BC
8,8	51,94	37,20	**26,48**
8,16	158,45	60,98	**55,62**
8,32	367,38	138,52	**102,60**
8,64	904,53	331,27	**229,64**
16,8	256,69	59,98	**43,97**
16,16	675,35	149,21	**135,91**
16,32	1355,08	236,65	**198,91**
16,64	3014,94	567,08	**490,43**
32,8	1589,33	109,82	**109,11**
32,16	3252,65	197,90	**195,14**
32,32	6298,54	420,34	**409,29**
32,64	11408,09	972,00	**950,45**
64,8	4118,42	281,03	**278,41**
64,16	9584,94	517,30	**511,79**
64,32	20403,34	1118,11	**1103,81**
64,64	52799,26	2614,53	**2597,13**

VII. LIMITATIONS OF THE STUDY

The motivation for our application is in the Compact Muon Solenoid (CMS) detector design upgrade project [27]. BCT is tested as a selection algorithm applied in the front-end detector readout electronics chain. It offered a great potential to be implemented in front-end part of the concentrator ASIC design for selecting the data sent for further processing in the back-end architecture [28].

Current limitation of the study is that we only consider selection cases where a single maximum extraction is needed on a specific position. However, there exist many applications in which M largest numbers from N inputs must be selected. This is common in high-energy physics experiments and there are some dedicated solutions by using design parameterized and pipelined sorting units [29, 30]. Also, when several equal maximums are present in the input dataset, current BCT design provides a maximum value and an indicator array with all maximums' positions marked with the high bit. This means that, like in any array-based topology, if multiple equal winners exist in the input dataset, it requires some additional priority logic to filter out the most significant winner position.

VIII. CONCLUSION

In this paper, we propose a new optimized array-based topology BCT, used to extract maximum or minimum value from an unsorted set of N binary numbers, as well as its one-of-N binary address. BCT is based on the same concept as AT, but it is more efficient in timing, especially for smaller width of the input code word k<32. This makes BCT particularly important for applications that usually deal with these input sizes, such as high-speed network packet schedulers or the winner-take-all circuits. From the experimental results in the paper, the conclusion is two-fold. First, it is confirmed that BCT is indeed an optimized AT solution. Second, we show that it outperforms the recent referent design when synthesized on ASIC 65 nm technology. BCT extracts winner among N k-bit numbers with lower area and latency, consuming the smallest dynamic power. This makes BCT the best option among the existing array-based competitors when synthesized on ASIC technology.

IX. FUTURE WORK

To deal with the current limitations of the study, we will follow several additional future research directions. First, a research is foreseen on using BCT for data selection in the context where M of N elements must be extracted. It would be interesting to vary the (M, N) parameter pairs and to examine their influence on area, delay and power. Next, we will study the resource usage when priority logic is added to BCT, so that only a single maximum position is marked, where the one of the simplest implementations can be encoder-based. Finally, as this paper reveals a great potential of BCT to be used as an efficient maximum finder circuit in some real-time signal processing application, for our future work, we will consider using BCT in the rank order filter design. Due to simplicity of logic and fast extraction of the maximum, it is expected to obtain better results than existing research with MaxMG [31].

REFERENCES

[1] Monemi, A., Ooi, C. Y., Palesi, M., & Marsono, M. N. (2017). Ping-lock round robin arbiter. Microelectronics Journal, 63, 81-93.

[2] Azuma, Masaki and Hiroomi Hikawa. "Supervised learning of DPLL based winner-take-all neural network." 2014 IEEE International Conference on Evolvable Systems (2014): 117-124.

[3] Fan, R., Zhang, Y., Li, B. (2017). Motion Classification-Based Fast Motion Estimation for High-Efficiency Video Coding. IEEE Trans. on Multimedia, 19(5), 893–907. doi:10.1109/tmm.2016.2642786.

[4] Gaitan, V. G., Gaitan, N. C., & Ungurean, I. (2015). CPU Architecture Based on a Hardware Scheduler and Independent Pipeline Registers. IEEE Transactions on Very Large Scale Integration (VLSI) Systems, 23(9), 1661–1674. doi:10.1109/tvlsi.2014.2346542.

[5] Raghavan, R., & Perera, D. G. (2017). A fast and scalable FPGA-based parallel processing architecture for K-means clustering for big data analysis. 2017 IEEE Pacific Rim Conference on Communications, Computers and Signal Processing (PACRIM). doi:10.1109/pacrim.2017.8121905.

[6] Rongchun Li, Yong Dou, Dan Zou, Shi Wang, and Ying Zhang. (2015). Efficient graphics processing unit based layered decoders for quasicyclic low-density parity-check codes. Concurr. Comput. : Pract. Exper. 27, 1 (January 2015), 29-46. Doi: 10.1002/cpe.3193, http://dx.doi.org/10.1002/cpe.3193.

[7] Dimitrakopoulos, G., Kalligeros, E., Galanopoulos, K., “Merged switch allocation and traversal in network-on-chip switches”, IEEE Trans. Comput., 2013, 62, (10), pp. 2001–2012.

[8] Chakrabarti I., Batta K.N.S., Chatterjee S.K. (2015) Efficient Pixel Truncation Algorithm and Architecture. In: Motion Estimation for Video Coding. Studies in Computational Intelligence, vol 590. Springer, Cham, https://doi.org/10.1007/978-3-319-14376-7_6.

[9] Hu, C., Ye, M., Du, Y., Lu, X. “Vector projection for face recognition”, Comput. Electr. Eng., 2014, 40, (8), pp. 51–65.

[10] K. Vasanth, E. Sindhu, R. Varatharajan, VLSI architecture for Vasanth sorting to denoise image with minimum comparators, Microprocessors and Microsystems, Volume 71, 2019, 102880, ISSN 0141-9331, https://doi.org/10.1016/j.micpro.2019.102880.

[11] Farmahini-Farahani A., Duwe III, H.J., Schulte, M.J., Compton, K. “Modular design of high-throughput, low-latency sorting units”, Computers, IEEE Trans., vol. 62, no. 7, pp. 1389–1402, 2013.

[12] Kante, R.K., Thrimurthulu “Efficient Sorting Mechanism for Finding First W Maximum/Minimum Values”, Manager's Journal on Embedded Systems; Nagercoil Vol. 3 (3), (Aug-Oct 2014), pp. 39-44.

[13] Zuluaga, M., Milder, P., & Püschel, M. (2016). Streaming Sorting Networks. ACM Transactions on Design Automation of Electronic Systems, 21(4), 1–30. doi:10.1145/2854150.

[14] Genus Synthesis Solution, Genus Cadence Official, October 2019, https://www.cadence.com/content/cadence-www/global/en_US/home/tools/digital-design-and-signoff/synthesis/genus-synthesis-solution.html

[15] Yuce, B., Ugurdag, H. F., Goren, S., Dundar, G., “Fast and Efficient Circuit Topologies for Finding the Maximum of n k-Bit Numbers”, (2014), Computers, IEEE Transactions on. 63. 1868-1881. 10.1109/TC.2014.2315634.

[16] Smrithi SV., Agrawal, S. "A fast architecture for maximum/minimum data finder with address from a set of data," 2016 International Conference on Computer Communication and Informatics (ICCCI), Coimbatore, 2016, pp. 1-6. doi: 10.1109/ICCCI.2016.7479988.

[17] Kathirvel, S., Jangre R., and Ko, S. “Design of a novel energy efficient topology for maximum magnitude generator”, in IET Computers and Digital Techniques, vol. 10, no. 3, pp. 93-101, 5 2016.

[18] Huang, X. P., Fan, X. Y., Zhang, S. B., and Zhang, F. (2010, November). An optimized tag sorting circuit in WFQ scheduler based on leading zero counting. In 2010 10th IEEE International Conference on Solid-State and Integrated Circuit Technology (pp. 533-535).

[19] Amaru, L.G., Martina, M., Masera, G. “High speed architectures for finding the first two maximum/minimum values”, (2012). In: IEEE Transactions on Very Large-Scale Integration (VLSI) Systems, vol. 20 n. 12, pp. 2342-2346. ISSN 1063-8210.

[20] Biroli, A.D.G. and Wang, J. C. “A fast architecture for finding maximum (or minimum) values in a set”, 2014 IEEE International Conference on Acoustics, Speech and Signal Processing (ICASSP), Florence, 2014, pp. 7565-7569.

[21] Xiao, G., Martina, M., Masera, G., and Piccinini, G. “A Parallel Radix-Sort-Based VLSI Architecture for Finding the First W Maximum/Minimum Values”, in IEEE Transactions on Circuits and Systems II: Express Briefs, vol. 61, no. 11, pp. 890-894, Nov. 2014.

[22] Vai, Michael & Moy, Man. (1993). Real-Time Maximum Value Determination on an Easily Testable VLSI Architecture. Circuits and Systems I: Fundamental Theory and Applications, IEEE Transactions on. 40. 283 - 285. 10.1109/81.224304.

[23] Vinnakota, B., Rao, V.V. B. “A new circuit for maximum value determination”, IEEE Trans. Circuits Syst. I, vol. 41, pp. 929-930, Dec. 1994.

[24] Kiran, N.K. and Alok K. "Leakage Power Reduction and Power Delay Product (PDP) Improvement using Dual Stack Method." International Journal of Engineering and Technical Research (IJETR), ISSN: 2321-0869 (O) 2454-4698 (P), Volume-4, Issue-4, April 2016.

[25] Meher, P. K. and Park, S. Y. "Area-Delay-Power Efficient Fixed-Point LMS Adaptive Filter With Low Adaptation-Delay," in IEEE Transactions on Very Large-Scale Integration (VLSI) Systems, vol. 22, no. 2, pp. 362-371, Feb. 2014.doi: 10.1109/TVLSI.2013.2239321.

[26] Praveen, P., Zahid, A. "Variation of Power and Delay in Digital CMOS Circuit Design in DSM Technology", International Journal of Engineering Trends and Technology (IJETT), V45(9),449-453 March 2017. ISSN:2231-5381.

[27] Bilki B. and the CMS Collaboration (2015): ” CMS Forward Calorimeters Phase II Upgrade”. Journal of Physics: 16th International Conference on Calorimetry in High Energy Physics (CALOR 2014), Conf. Ser. 587 012014, doi:10.1088/1742-6596/587/1/012014.

[28] CMS Collaboration: “The Phase-2 Upgrade of the CMS endcap calorimeter Technical Design Report”, CERN-LHCC-2017-023, CMS-TDR-019, ISBN 978-92-9083-459-5, 2018.

[29] Farmahini-Farahani, A., Gregerson, A., Schulte, M., Compton, K. “Modular high-throughput and low-latency sorting units for FPGAs in the Large Hadron Collider.” 2011 IEEE 9th Symposium on Application Specific Processors (SASP) (2011): 38-45.

[30] T. N. Van, V. T. Thien, S. N. Kim, N. P. Ngoc and T. N. Huu, "A high throughput pipelined hardware architecture for tag sorting in packet fair queuing schedulers," 2015 International Conference on Communications, Management and Telecommunications (ComManTel), DaNang, 2015, pp. 41-45. doi: 10.1109/ComManTel.2015.7394257.

[31] Narasimha-Murthy, P., and Suryakala, S. V. "Rank order filter design using maximum magnitude generator." Wireless Communications, Signal Processing and Networking (WiSPNET), 2017 International Conference on. IEEE, 2017.

Words Segmentation-based Scheme for Implicit Aspect Identification for Sentiments Analysis in English Text

Dhani Bux Talpur[1]
School of Information and Communication Engineering
Guilin University of Electronic Technology
Guilin, China

Guimin Huang[2,*]
Guangxi Key Laboratory of Trusted Software
School of Computer Science and Information Security
Guilin University of Electronic Technology, Guilin, China

***Abstract*—Implicit and Explicit aspects extraction is the amassed research area of natural language processing (NLP) and opinion mining. This method has become the essential part of a large collection of applications which includes e-commerce, social media, and marketing. These application aid customers to buy online products and collect feedbacks based on product and aspects. As these feedbacks are qualitative feedback (comments) that help to enhance the product quality and delivery service. Whereas, the main problem is to analyze the qualitative feedback based on comments, while performing these analysis manually need a lot of effort and time. In this research paper, we developed and suggest an automatic solution for extracting implicit aspects and comments analyzing. The problem of implicit aspect extraction and sentiments analysis is solved by splitting the sentence through defined boundaries and extracting each sentence into a form of isolated list. Moreover, these isolated list elements are also known as complete sentence. As sentences are further separated into words, these words are filtered to remove anonymous words in which words are saved in words list for the aspects matching; this technique is used to measure polarity and sentiments analysis. We evaluate the solution by using the dataset of online comments.**

***Keywords*—Implicit aspect; explicit aspects; polarity; sentiments analysis**

I. Introduction

With the advancements in the field of technology more and more peoples are in touch with online shopping websites and these numbers are increasing day by day. This innovative move transfer street shopping into online shopping. The most popular trending websites includes Taobao, JD, Alibaba and Amazon etc. These e-commerce websites generally provide an easy and accessible platform for customers, where consumers can share the experience with feedback regarding products. With the help of these feedbacks it is easy to extract opinions and aspects of entities from various online comments of consumers as these reviews can help to provide opinion which can further use for prediction.

The feedback help consumers know about popular trends and aspects of these products to buy. Recently, different approaches are introduced on this field as few models were also proposed to process specific task. These specific tasks are the basic part of the NLP application is words segmentation, the procedure of separating and dividing the sentence into a single token of words is called Word Tokenization [1]. In Natural Language Processing (NLP) the term tokenization or word segmentation is thought as the most important task [2]. Mostly each application of NLP needs at a certain level the process of breaking its text into distinct tokens for processing. The tokenization and extraction method is done by identifying word borders in languages like English where punctuation marks or white spaces are used to isolate words [3].

Many sentiment analysis tools and applications have been developed to mine the opinions in user-generated content on the Web. However, the performances are very poor due to the complexity of natural language [4,5,6]. In essence, sentiment analysis is still a problem of natural language processing (NLP), which deals with the natural language documents, which are also called unstructured data [7]. Prior researches show that sentiment analysis is more difficult than the traditional topic-based text classification [8]. Although various methods have been projected to conduct sentiment analysis, it is still difficult to deal with some linguistic phenomena, such as negation and mix-opinion text. This indicates to low accuracy of sentiment classification [9,10]. Besides, it is insufficient to only determine the polarity of the opinions, since an opinion without a target is of limited use. The task of extracting the opinions and their targets simultaneously is also called aspect-level sentiment analysis in the research literature and is more difficult to achieve [11].

Furthermore, in order to achieve the finest information that is required for such analysis, the different aspects and features of a product or service must be identified in the comments section. There are different examples of such features include size, price, service and parts of product aspect which are mentioned in this text. Some of the examples are illustrated below.

“The mobile size is very large but picture quality is awesome and price is cheap”. In this sentence ‘size’,’price’ and ‘quality’ are all aspects on which sentiments is expressed.

In the proposed work, it is consider how to extract the implicit aspects and sentiments analysis on an aspect level.

The recent research has concluded that there was no parallel development available in which aspect extraction and sentiments analysis work together. The research work is

*Corresponding Author

divided into different portions. Section 2 describes an overview of related work with detailed methods of implicit sentiment analysis. However in Sect. 3 defines the research methodology and the results. Moreover in section 4 a detail overview of experiments and discussion analysis has been illustrated. Finally, the Section 5 gives brief outline of conclusion and future study.

II. Related Work

The sections of literature review discuss the literature of relevant fields which are concerned with implicit aspects extraction and sentiments analysis of customer reviews. Based on review analyzing the background and leverage some previous methodology of opinion mining and sentiment analysis to design solution by using distant methodologies. Furthermore sentiment analysis also deals with the computational treatment of sentiment, views and subjectivity in English text [12]. This approach is also known as opinion mining. Earlier developed schemes of natural language processing deals with sentiments analysis includes diverse aspects concerning how information about emotions, attitudes, perspectives and social identities is conveyed in the language.

There are two main approaches used for sentiments analysis which are further separated into lexicon-based and machine learning methodologies. The following approaches are combined to resolve issues related to sentiment analysis and aspects extraction Fig. 1 show different approaches:

The most useful approach in text classification as it is used for sentiment analysis with the help of machine learning. There are two different types of machine learning datasets required to perform classification one is known as training set and other is test set. Machine Learning uses text-classification approach for sentiment analysis. Two datasets are required to perform machine learning. The first one is called as training set and the other is test set. The training set is trained by an automatic classification to learn characteristics of documents while the test set is used to validate the performance of automatic classifier. It is also use to document level or sentence level sentiment analysis to predict whether the reviews are positive, neutral or negative. This segmentation can further be classified into supervised learning and unsupervised learning.

This can also be further classified into supervised learning and unsupervised learning.

a) Supervised Learning: Supervised learning is also known as label learning. It has various classifier algorithms to execute sentiment analysis of an opinion. It requires a labeled training data set to determine the invisible instances. Support Vector Machine (SVM), Naïve Bayes (NB), NBtree, J48 and LDA are some of the techniques used for this classification.

b) Unsupervised Learning: Unsupervised learning is also known as unlabeled learning. It uses set of inputs for clustering where labels are not known during the training of the data sets. Classification is performed based on opinion words and phrases.

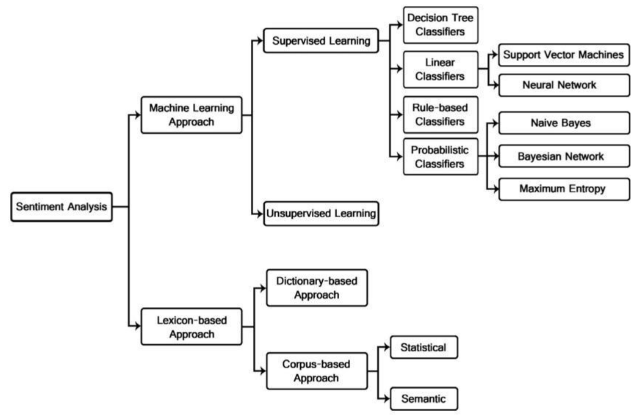

Fig. 1. Different Approaches for Sentiments Analysis.

The lexicon based approach depends on a collection of known and pre-determined domain sentiment terms. It is further classified into dictionary-based and corpus-based semantic methods used to find the polarity and score from large corpora. The dictionary-based approach searches the opinion word and finds its synonyms and antonyms in the seed list to measure the polarity from a dictionary. The corpus-based approach is an independent domain approach which is developed by the author according domain used. So, the sentiment words in the corpus are context specific.

The lexicon-based scheme is use for sentiments or subjectivity lexicons [13, 14, 15] to develop a corpus-based dictionary by remodeling the insights of the co-occurrence and conjunction method. These lexicons contain sentiment words that are also called opinion words listed with their polarity and strength. They tried the dictionary with the *Cornell Movie Review Data* and claim the accuracy of their measure up to 72.5%, which match the accuracy of machine learning classifiers [16]. In sentiment classification lexicon- based approach is applied by author, part of peech tagging, SentiWordNet and WordNet combined with a weighted model provided by Natural Language Processing (NLP)[17]. The dissimilarity in sentiments classification, opinion extraction goals are to produce wealthier information and need in-depth analysis of reviews [18].

The majority of approaches in the literature worked on extraction of the explicit features in sentences system are require to automatically find out and analyze the online opinionated texts (texts with opinions or sentiments), sentiment analysis grow out of its need. Some of the approaches are already mentioned in the reviews. However, implicit features have equally balance as explicit feature in the review. [19] It presents a fine-grained method for the labels of polar sentiment in text and for explicit sentiments on the other hand as well as implicit expressions of sentiment of polar facts.[20] The proposed scheme deals with a double-implicit problem in opinion mining and sentiment analysis. This methodology deals with recognizing features and polarities of opinionated reviews not consisting of opinion words and aspect terms. [21] It also Propose fuzzy-based information in engineering approach that has been developed for sentiment classification of a distinct group of such sentences that include the change or deviation from the desired range or value.

In the previous research works, most of the researches is done on implicit aspects extraction and sentiments analysis but a limited work has been done on the segmentation problem. The proposed classification approach uses words segmentation and a rule-based method to extract implicit features. However, aspect-based opinion mining gives attention on the task of extracting opinion about aspects. This research paper develops the implicit aspect extraction with a segmentation scheme and sentiment analysis approach for English text.

III. Research Methodology

A. Framework for Sentiment Analysis

In the real-world the sentiment analysis based on prior research identified by research gaps and requirements. In order to fulfill these research gaps is an effective approach for sentiment analysis; it is an innovative framework which is proposed in this research. By implementing proposed framework of sentiments analysis on customer reviews can predict the aspect level. It can not only analyze single-opinionated text but also mixed-opinion text. The framework provides an innovative way to detect sentimental words in the text through sentiment lexicon to gain more information from text. In addition to this the framework offers an effective approach to conduct aspect- level or feature-based sentiment analysis. Fig. 2 illustrates the component which includes segmentation, words matching, aspect-level analysis and sentiment classification.

B. Dataset

In this research paper can aid in observing a detail overview of data sets which are based on the proposed method and functionality. The data of dataset is the collection of reviews that are available online on websites includes implicit and explicit features. Whereas this dataset includes an electronics item which includes mobiles, laptops and cameras etc. these customers reviews are randomly collected from different online shopping websites and web portals. There are 4600 collected reviews from different domains like DVD player, mobile and camera in which analysis is made on 2024 reviews from these reviews based on this identification of the polarity of text through lexicon and sentiments analysis which are given in Table I.

C. Aspect-Level Analysis

The methodology proposed is a novel approach that concludes aspect level analysis which helps to explore potential aspects and feature which are clearly mentioned in the sentence. The parallel sentiment expression expressed regarding aspects need the extraction at the same time of the entity. Furthermore, many organization and companies are using aspect-based analysis.

There are some of advantages of aspect-level sentiment analysis which is opinion and its targets which can be captured and provide clear sentiment information of components of a product and services or its attributes. It is similar to evaluate sentiment classification in order to estimate the performance of aspect-level sentiment analysis were each aspect is needed to be examined on behalf of human verdict.

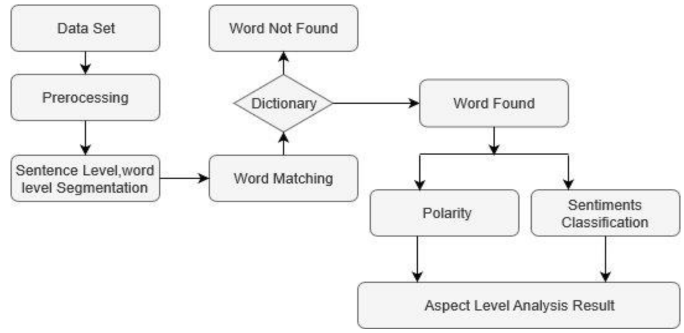

Fig. 2. Framework of System.

TABLE. I. Number of Reviews

Domain	Reviews	Words	Source
DVD Player	850	12980	Amazon
Mobile	600	9682	Amazon
Camera	654	11893	Amazon

D. Sentence Segmentation into Words

In this process sentence segmentation is converted into words in which English word are segmented and created from sentences and word boundaries are identified and marked. The boundaries are denoted by space character before and after of each word. The process begins with identifying word boundaries after that the isolated words are listed in the list which is clearly displayed in Fig. 3. The words are retrieved and analyzed to validate words to identify from lexicon. Token is created to identify the correct spelled word this can be accomplished by removing any unnecessary characters which are part of the original words. The process of filtration involves traversing with other words and to remove any or all special characters such as @, $, %, &, #. All these characters part of string and use previously. By using these hard space characters, new paragraph and newline symbols are cropped. The filtration process which is used to eliminate occurrence of English alphabet from documents and articles as it is most useful in some situation.

Fig. 3. Sentence Tokenization in Words.

E. Score Calculation and Word Matching

After the process of sentence segmentation and words matching the score calculation of English text the tokens are searched and matched with lexicons. In reality English text, contains multiple sentiment elements. Tokens are searched and matched with the help of lexicon after each token from English text has created. English text contains multiple sentiment elements. After the processes of segmentation and removal of stop words the remaining text is matched with lexicon and the values of each word is fetched at later stage. The value of sentiment English text can be calculated based on the corresponding calculation formulas. The text contains sentiments words and final sentiment value of English text which is calculated as follows:

Fig. 4 shows the score calculation algorithm in this algorithm the FinalValue represents the final sentiment value of the text. Sc represents the sentiment value of each aspect. The sentiment value will appear in following three states:

If FinalValue > 0, this output directs the sentiment of the text is positive.

If FinalValue = 0, it displays the sentiment of the English text as neutral.

If FinalValue < 0, it indicates the negativity of the text.

```
Input: English Text
Sentiment Polarity of Text
1.FinalValue=0;
2.A text divide into sentence n ,sentence divide into words w,
3. for(i=1;i++,i<=n)
4. { Sc=0;
5.for(j=1;j++;j<=w)
6. {Sc=sc+0;}
7.FinalValue=FinalValue+SC;
8. If (FinalValue>0)
9. Sentiment of text is positive;
 10. else If (FinalValue<0)
11. Sentiment of text is negative;
12. else
13. Sentiment of text is neutral
14. end if
15. end if
```

Fig. 4. Score Calculation Algoritm.

IV. Experimental Results and Analysis

In the section of experiments result and analysis the classification algorithm involves sentiment analysis in sentence tokenization which is performed by input of comments. The processing of tokenization split text into words as it is a critical stage in algorithm. However, the Sentences are tokenized into single words. The text classification method is used to extract implicit aspects with the help of word segmentation approach. The experiment in Table II illustrates the five different classification algorithms which are used to predict accuracy in the text.

TABLE. II. Evaluation Table without using Words Matching Algorithms Classification Methods

Classifier	Precision	Recall	F-Measure
Support Vector Machine	0.685	0.660	0.657
Naivebayes	0.744	0.429	0.735
NBTree	0.782	0.472	0.697
J48	0.801	0.576	0.781
LDA	0.843	0.595	0.801

Fig. 5 and Fig. 6 illustrate the results of proposed experiment model. In Fig. 5, the results are based on random algorithm by using machine learning classifiers like SVM, Naivebayes, Nbtree, J48 and LDA to prediction the performance of text classification. It clearly illustrate that the accuracy rate and F-measure is very high in LDA as compared to others. But the performances of Recall have decrease in all classifiers measure rate. The experiment analysis shows in Table III that not every classification is good in accuracy measure.

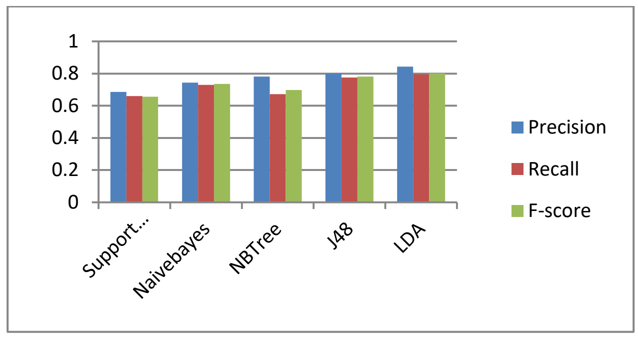

Fig. 5. Analysis of different Classifiers.

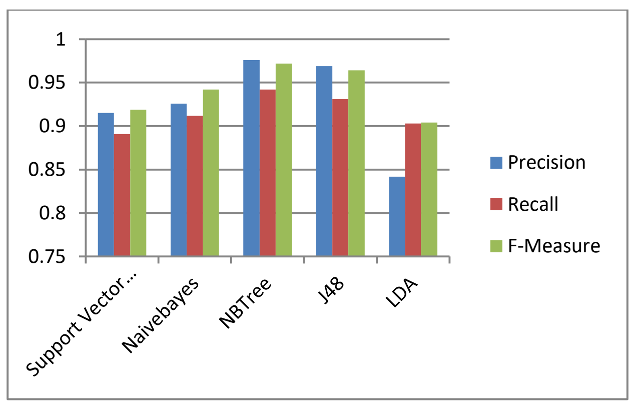

Fig. 6. Classifier with Framework.

TABLE. III. Evaluation Table using Words Matching Algorithms with Classifiers

Classifier	Precision	Recall	F-Measure
Support Vector Machine	0.915	0.891	0.919
Naivebayes	0.926	0.912	0.942
NBTree	0.976	0.942	0.972
J48	0.969	0.931	0.964
LDA	0.842	0.903	0.904

In Fig. 6, the classification framework is analyzed by using proposed word segmentation and matching algorithm. In the proposed algorithm data is purified and send for classification. Furthermore, it clearly displays that NBtree classification have the highest accuracy in all three measures precision, recall and F-Measure. The proposed method helps text classification to increase its prediction and performance.

V. Conclusion

To conclude, the analysis and experiments based on customer reviews help the different companies to improve the product quality and services. The research paper illustrates a new task of extracting implicit aspects from qualitative feedback comment from customers. The techniques like word segmentation and opinion mining are used to compare the effectiveness of different classifiers performance as well as text sentiment analysis. In the experiments section the observation has been made that NB tree classification provides better performance with F-Score. Furthermore, in future work the research will focus on recognizing the semantic polarity based on score of sentences and by applying distinct machine learning algorithm to identify positive and negative effects of the News Articles, Blogs and reviews etc.

Acknowledgement

This work was supported by the National Natural Science Foundation of China (no. 61662012).

References

[1] Mahar, J. A., Shaikh, H., Memon,G. Q., “A Model for Sindhi Text Segmentation into Word Tokens”, Sindh University Research Journal (Science Series), Vol.44 (1) pp.43-48 (2012).

[2] Haruechaiyasak, C.; Kongyoung, S.; Dailey,”A comparative study on Thai word segmentation approaches”,Electrical Engineering/Electronics, Computer, Telecommunications and Information Technology, 2008. ECTI-CON 2008. 5th International Conference on, vol.1, no., pp.125-128, 14-17 May 2008.

[3] Nadir D. And Sarmad H,”Urdu word segmentation. In Human Language Technologies”,The 2010 Annual Conference of the North American Chapter of the Association for Computational Linguistics (HLT '10). Association for Computational Linguistics, Stroudsburg, PA, USA, 528-536.

[4] Sobkowicz, P., Kaschesky, M. and Bouchard, “Opinion mining in social media: Modeling, simulating, and forecasting political opinions “, Government Information Quarterly, 29(4), pp.470-479.

[5] Mohammad, S. M., Kiritchenko, S. and Zhu, X “NRC-Canada: Building the state-of-the-art in sentiment analysis of tweets”, arXiv preprint arXiv:1308.6242.

[6] Maynard, D. G. and Bontcheva, “Challenges of Evaluating Sentiment Analysis Tools on Social Media”, Proceedings of LREC.

[7] Liu, B. (2012),”Sentiment analysis and opinion mining’, Synthesis lectures on human language technologies” 5(1), pp.1-167.

[8] Pang, B. and Lee, L. “Opinion mining and sentiment analysis”, Foundations and trends in information retrieval, 2(1-2), pp.1-135.

[9] Vinodhini, G. and Chandrasekaran, R. M,”Sentiment analysis and opinion mining: a survey”, International Journal, 2(6).

[10] Park, S., Lee, W. and Moon,”Efficient extraction of domain specific sentiment lexicon with active learning”,Pattern Recognition Letters, 56, pp.38-44.

[11] Lin, Y., Zhang, J., Wang, X., and Zhou, “An information theoretic approach to sentiment polarity classification”, In Proceedings of the 2nd Joint WICOW/AIRWeb Workshop on Web Quality, pp. 35-40. ACM.

[12] Pang, B. and Lee, “Opinion mining and sentiment analysis”, Foundations and trends in information retrieval, 2(1-2), pp.1-135.

[13] Turney, “Thumbs up or thumbs down? Semantic orientation applied to unsupervised classification of reviews”, In Proceedings of the Association for Computational Linguistics (ACL), pp. 417–424.

[14] Hu, M., and Liu, “Mining and summarizing customer reviews”, In R. Kohavi, J. Gehrke, W. DuMouchel, & J. Ghosh (Eds.), KDD-2004 - Proceedings of the Tenth ACM SIGKDD InternationalConference on Knowledge Discovery and Data Mining, pp. 168-177.

[15] Hu, M., and Liu, “Mining and summarizing customer reviews”, In Proceedings of the Tenth ACM SIGKDD International Conference on Knowledge Discovery and Data Mining, pp. 168-177.

[16] Ding, X., Liu, B., and Yu, P. S, “A holistic lexicon-based approach to opinion mining”, In Proceedings of the 2008 International Conference on Web Search and Data Mining, pp. 231-240. ACM.

[17] Marjan Van de Kauter .” The good, the bad and the implicit: a comprehensive approach to annotating explicit and implicit sentiment”, Lang Resources & Evaluation (2015) 49:685–720.

[18] Alexandra Balahur , Jesús M. Hermida, Andrés Montoyo,” Implicit Polarity and Implicit Aspect Recognition in Opinion Mining”, Proceedings of the 54th Annual Meeting of the Association for Computational Linguistics, pages 20–25,Berlin, Germany, August 7-12, 2016. c 2016 Association for Computational Linguistics.

[19] C acilia Zirn,Mathias ,Nieper,” Fine-Grained Sentiment Analysis with Structural Features”, Proceedings of the 5th International Joint Conference on Natural Language Processing, pages 336–344, Chiang Mai, Thailand, November 8 – 13, 2011.

[20] Alexandra Balahur, Jesús M. Hermida, Andrés Montoyo,”Detecting implicit expressions of emotion in text: A comparative analysis”.

[21] Amir Hossein Yazdavar a, Monireh Ebrahimi a, Naomie Salim ,” Fuzzy Based Implicit Sentiment Analysis on Quantitative Sentences”, Journal of Soft Computing and Decision Support Systems 3:4 (2016) 7-18.

Energy Balanced Two-level Clustering for Large-scale Wireless Sensor Networks based on the Gravitational Search Algorithm

Basilis Mamalis[1]
University of West Attica
Agiou Spyridonos, 12243, Egaleo
Athens, GREECE

Marios Perlitis[2]
Democritus University of Thrace
University Campus, 69100
Komotini, GREECE

***Abstract*—Organizing sensor nodes in clusters is an effective method for energy preservation in a Wireless Sensor Network (WSN). Throughout this research work we present a novel hybrid clustering scheme that combines a typical gradient clustering protocol with an evolutionary optimization method that is mainly based on the Gravitational Search Algorithm (GSA). The proposed scheme aims at improved performance over large in size networks, where classical schemes in most cases lead to non-efficient solutions. It first creates suitably balanced multihop clusters, in which the sensors energy gets larger as coming closer to the cluster head (CH). In the next phase of the proposed scheme a suitable protocol based on the GSA runs to associate sets of cluster heads to specific gateway nodes for the eventual relaying of data to the base station (BS). The fitness function was appropriately chosen considering both the distance from the cluster heads to the gateway nodes and the remaining energy of the gateway nodes, and it was further optimized in order to gain more accurate results for large instances. Extended experimental measurements demonstrate the efficiency and scalability of the presented approach over very large WSNs, as well as its superiority over other known clustering approaches presented in the literature.**

Keywords—Gravitational search algorithm; wireless sensors; network lifetime; nodes clustering; data collection

I. Introduction

Grouping sensors in clusters is an effective method for saving energy in large-scale WSNs [1]. Considering such a WSN, there are several sets of sensors called clusters and each one of them has a leader called 'cluster head'. The sensor nodes (after sensing the field) send the sensed data to the CH, and then the CH (after collecting the data) forwards them to the BS. A study in WSN clustering is given in [1]. Furthermore, a lot of scientists have adopted the use of a specific kind of nodes called 'gateway-nodes' which operate similarly to the normal sensor nodes, however they are usually equipped with more energy and communication capabilities and they cost more [2]. The gateway nodes finally behave as CH in the WSN, and forward the gathered data to the BS. Actually the scope of this idea is to create a stronger group of CH than in typical networks with cluster organization. On the other hand, their operation is still based on batteries, so they need to preserve their energy adequately while the network operates.

Let's suppose we have *m* gateway nodes and *n* sensors in the network, and there are *k* nodes in the range of the gateway nodes. The complexity for associating the *n* sensors to the *m* gateway nodes is naturally exponential. So, typical techniques can't normally lead to effective solutions that scale well. A lot of evolutionary methods could be applied to give a good approximate solution. The GSA [3] has been recently reported as a quite valuable such technique, driven by nature, which can manage effectively problems in hard computational form. Also, the particle swarm optimization technique and the ant colony method have been thoroughly studied [1].

A large number of research works can be found in the bibliography [1, 4-17, 22-32] following clustering schemes in WSNs (either centralized or distributed). The LEACH protocol [8] is the most known and one of the most effective. In this protocol the cluster-heads are chosen on the basis of a specified probability. The disadvantage of this protocol is that a sensor node of less energy could be chosen as a cluster head, thus limiting the network operation. PEGASIS [9] was proposed as an efficient alternative, but it can't lead to good scalability because of several constraints. A number of other schemes adopting clustering have further been met, trying to achieve sufficiently balanced depleting of energy and thus improving the network operation. Many of them [4,22-23,31-32] aim at solving the '*hot-spot'* problem and achieving ideal distribution in the depletion of energy for all the nodes, whereas others [28-30] try to gain efficiency and scalable secure behavior when dealing with large-scale networks and deployment areas.

Focusing on the schemes based on 'gateways', in [13] the authors propose a scheme of satisfactory balance, named LBC. In LBC the clusters are formed quite efficiently, but the algorithm doesn't take in account neither the distance between the sensor nodes and the gateway nodes nor the remaining energy of the gateway nodes. In [14] the authors propose an approach named GLBCA applying BFS, but when large-scale WSNs are considered non-satisfactory execution times are observed. In [15] the authors present an approach based on GA-clustering in order to elect a set of cluster heads among the regular sensors. In [16] the authors propose a scheme based on PSO by taking in account the energy and the distance within the clusters as main criteria, but on the other hand they don't consider the energy and the distance of the gateway nodes.

In [17], a clustering scheme of high efficiency is presented built over the GSA approach, in which the fitness function is properly selected considering not only the distance among the sensor nodes and the gateways/BS, but also the remaining energy of the gateway nodes. The eventually proposed scheme, named GSA-EEC, is evaluated based on several metrics, and it is proved to be very effective and performing better than most of the related approaches [13-16]. On the other hand, when large-scale networks are considered, these methods in most cases can't offer satisfactory results because of various problems met in the case of very high number of dimensions in the search space. More concretely, the GSA method in such cases is shown to have limited stability as well as low levels of accuracy due to the increased possibility to be trapped into local optimum solutions; additionally non-efficient execution times are observed. The above shortcomings restrict the worth of using the GSA technique in very large networks. The GSA approach has also been used in WSNs for nodes localization and relay/sink nodes placement, as shown in [18-21].

Trying to overcome the disadvantages referred in the previous paragraph with regard to the use of the GSA-oriented scheme [17] on large networks, we've designed a novel hierarchical clustering protocol that consists of two levels, and combines adequately the above GSA-oriented scheme with a classical gradient clustering scheme, similar to [22-23] and suitably modified in order to generate less number of clusters and fit better in the energy balancing needs of our proposed total scheme. The presented approach first constructs multihop clusters of evenly distributed energy reserves, in which the sensor nodes energy gets larger as coming closer to the cluster head. Thus, since the sensors near to the cluster head are more exhausted because of data forwarding, keeping the residual energy of those sensors high guarantees the prolonged and seamless operation of the WSN. Next, a suitable protocol based on the GSA runs to associate sets of cluster heads to specific gateway nodes for the eventual forwarding of data to the base station. Extended simulated experiments are presented to show the high efficiency and scalability of the proposed combined clustering scheme over very large WSNs, as well as its superiority over other clustering approaches of the literature [26-27,30-31]. Further experiments have been done to show the suitability of the proposed new fitness function against the one referred in [17], as well as the worth of using the proposed modified first-level clustering algorithm against the use of other alternatives (i.e. [22-23]).

The primary goal of our work is to build a clustering protocol able to achieve highly efficient behavior in *very large-scale* WSNs (i.e. not only for hundreds or one-two thousands of sensor nodes but also for 5000-10000 and even more sensor nodes; as it will be the case in future IoT/IoE applications). The existing clustering protocols unfortunately suffer from several shortcomings that lead to performance degradation in such *very large scale* WSNs, either relevant to the *hot spot* problem or to the fact that in order to face the *hot spot* problem they tend to generate quite large number of CHs and/or multihop routing overhead when we have large numbers of sensors (making their further use problematic, e.g. for data gathering etc.), and generally lead to not sufficiently scalable solutions. As a consequence a proper solution could be given by combining appropriately clustering protocols with specific features into corresponding two-level hierarchical schemes trying to gain efficiency and extent the scalability of the total scheme.

The main contribution of our work includes the following:

- The appropriate modification of the gradient-based clustering protocol presented in [22-23] in order to generate less number of clusters, achieve better execution times, and generally fit better in the balancing needs and the total behavior required as a first-level (only) clustering protocol.
- The appropriate modification of the GSA-based clustering protocol presented in [17], mainly with regard to its fitness function in order to have more accurate results (with regard to energy balancing), as well as with respect to the total behavior required as a second-level clustering protocol over a number of CH nodes.
- The integration of the above two basic clustering components (first-level and second-level) into a single combined (two-level) clustering approach that achieves both high energy efficiency and balancing, and also preserves its high scalability for very large WSN instances and relevant deployment areas due to its two-level nature.
- The extended evaluation (via carefully designed simulation experiments with Castalia simulator [25]) of both the two basic clustering components and the total proposed (two-level) clustering scheme, in order to demonstrate its high efficiency and scalability, in terms of energy consumption and network lifetime over very large WSNs, as well as its superiority over other relevant approaches.

The remaining text is organized as follows. In Section II some background is given with respect to the GSA. The proposed clustering scheme is described in Section III. In Section IV our simulated experiments are presented and discussed, and in Section V the main conclusions are stated.

II. Gravitational Search Algorithm

The description of the GSA technique in details is given in [3]. Let's assume we have a group of agents, N_A. Every agent is expected to give a part of the solution. The location of agent A_i, $1 \le i \le N_A$ in dimension d is x_i^d whereas its velocity is v_i^d, $1 \le d \le D$. Every agent has the same dimension. Every agent is evaluated to verify the suitability of the result based on a specific fitness function. Let the i^{th} agent's location be represented as $X_i = (x_i^1, x_i^2, \ldots, x_i^D)$. The following expression gives the force applied on the i^{th} agent by the j^{th} agent.

$$F_{ij}^d(t) = G(t)\frac{M_{pi}(t) \times M_{aj}(t)}{R_{ij}(t)}(x_j^d(t) - x_i^d(t))$$

M_{pi} represents the passive mass of the i^{th} agent, whereas M_{aj} stands as the corresponding active mass of the j^{th} agent, and α is a constant. $G(t)$ equals to $G_0(t_0/t_{max})^{\phi}$, in which G_0 represents also a constant. $R_{ij}(t)$ means the Euclidean distance from agent i

to agent j. The overall force applied by the group of agents over the i^{th} agent in dimension d is as follows.

$$F_i^d(t) = \sum_{j=1, j\neq i}^{N_A} rand_j \times F_{ij}^d(t)$$

The inertial mass as well as the gravitational mass is estimated by evaluating the fitness function. The heavier the mass of an agent the more efficient the agent is.

$$m_i(t) = \frac{fit_i(t) - worst(t)}{best(t) - worst(t)} + \varepsilon$$

In the above, ε is a limited constant, $fit_i(t)$ represents the fitness of agent i, whereas *worst (t) / best (t)* are as next.

$$best(t) = \min_{j\in\{1..N_A\}} fit_j(t) \quad worst(t) = \max_{j\in\{1..N_A\}} fit_j(t)$$

$$M_i(t) = \frac{m_i(t)}{\sum_{j=1}^{N_A} m_j(t)}$$

Further, let's assume M_{ai}, M_{pi}, M_{ii} and M_i are all equal to each other. Based on the 2nd law of Newton, we have the next.

$$a_i^d(t) = \frac{F_i^d(t)}{M_{ii}(t)}$$

In the above, the inertial mass of agent i is given by M_{ii}, whereas the acceleration of agent i is given by and $a_i^d(t)$.

III. Proposed Clustering Approach

As previously stated, the proposed approach has been developed on the basis of a hierarchical clustering protocol of two levels, named GC-GSA. First, the sensors and the gateway nodes are spread at random over a large deployment area. The deployed sensors / gateways are supposed to be static; no mobility is supported. Then, a two-phase network operation begins. In the first phase the necessary bootstrap and cluster formation procedures are completed. Initially, proper identities are assigned to all the sensors by the base station. Then, both the sensors and the gateway-nodes send their identities and other info to their neighbors using mac-level protocol. The gateway-nodes are finally informed with the identities of their neighbor sensors. Next, every gateway-node informs the base station with the collected info to complete the setup. The complete clustering routine is the run and all the sensors nodes get the necessary info with regard to their CH identity. In the second phase the network starts to operate steadily; the sensed data are gathered by the cluster heads and then by the gateway-nodes, and they finally directed to the base station.

A. First Level Energy-Balanced Clustering

With regard to the initial clustering, a suitable protocol based on multiple hops communication is adopted, aiming at building a robust hierarchy with controlled delay and sufficient coverage with respect to the secondary clustering (e.g. the size of the clusters and the positions of the selected cluster-heads). Further, the algorithm of [4] is primarily followed as the firstly applied clustering routine, whereas a proper adaptation has been incorporated aiming at inheriting the main advantages of approach described in [22, 23]. The remaining energy of the sensors is chosen as the basic factor while building the clusters, so a sufficiently balanced cluster hierarchy is built, the energy-hole problem (near to the cluster-heads) is effectively handled, and eventually the operation of the network is prolonged. A detailed description of the relevant procedure is given in [33].

From a qualitative point of view our modified clustering protocol is quite similar to the watershed-based clustering protocol presented in [22-23], with the main difference that it doesn't take in account separately (as separate clusters) the sets of sensors having almost equal to each other remaining energy. In our modified algorithm all the sensors are forced to follow a parent with larger residual energy (in the way described above) even if the residual energy is quite close (approximately the same) to the residual energy of the elected parent. As a result it leads to less number of CHs (which is a crucial factor in the context of the present gateways-based WSN environment), whereas also the execution of the cluster formation procedure is quite faster. On the other hand (validated also clearly by the corresponding simulations given in section 4.4), no actual 'loss' in the energy balancing performance is observed with respect to the present gateways-based WSN problem, if compared to the probable use of the watershed-based algorithm as the first-level clustering protocol in the same problem. Actually the slight loss that one would expect is counterbalanced by the energy savings due to the less number of cluster-heads and consequently the less heavy communication among the cluster-heads and the gateways, thus finally leading to slightly better overall performance (specifically when considering large and very large numbers of sensors).

On the basis of the above considerations, we have followed the use of the proposed modified algorithm as the first-level clustering protocol (as opposed to the use of the watershed-based algorithm of [22-23] or the use of the much simpler but weaker protocol of [4]), mainly because it has the potential to perform and scale better for large / huge numbers of sensor nodes and relevant deployment areas, in the context of this problem. Instead, in the context of other WSN environments and relevant applications (e.g. data gathering applications with mobile sinks where a number of sinks can be used to visit all the CHs, as in [22-23]) the performance of the watershed-based clustering protocol should be the preferable one.

B. Second Level GSA-based Clustering

Considering the next (second) level of building the cluster hierarchy, the GSA oriented protocol of [17] has been suitably modified and applied over the total set of cluster-heads elected in the first level (which is of relatively small size - i.e. avoiding the use over the complete WSN). The adopted GSA oriented scheme runs to associate sets of cluster-heads to specific gateway nodes for the eventual relaying of data to the base station. The initially chosen fitness function was further optimized and modified in order to keep the energy balanced over the gateway-nodes too, and gain more accurate results for large instances. The initialization of the basic group of agents (N_A) first takes place (note that each agent potentially stands as a part of the solution). More concretely, in the context of this stage of clustering the agents represent the associations of cluster-heads to corresponding gateway-nodes. If we assume that A_i stands as the agent i, every item $x_i^d(t)$ associates the relevant cluster-head to some gateway and $1 \leq i \leq N_A$, whereas also $1 \leq d \leq D$ (note that D equals to c). So, each agent may be denoted in the following form [17, 33], whereas our modified GSA protocol should then run as follows.

$$A_i = [x_i^1(t), x_i^2(t), x_i^3(t), \ldots, x_i^D(t)]$$

The Second-level GSA-based Clustering Algorithm

Input:

- Group of CHs: $H = \{h_1, h_2, h_3, \ldots, h_c\}$
- Set of gateway nodes: $G = \{g_1, g_2, g_3, \ldots, g_m\}$
- Initial group of agents with size equal to N_A
- Agent's dimensions = # of CHs = c

Output:

The optimal CHs associations to gateway-nodes

Description of the algorithm:

Agent A_i is initialized, $\forall i$, $1<=i<= N_A$

The mapping function is defined (for every h_d to a g_k)

do */* initially assume that t=0 */*

for *i=1 to* N_A

Fitness (A_i) is computed

The *best/worst* fitness values are updated of all agents

$M_i(t)$, $a_i^d(t)$ are computed of each agent of the system

The velocity and the position of A_i are updated

endfor

while the criteria for termination are not satisfied

C. Choosing the Fitness Function

The definition of fitness function (f) has to be appropriately specified considering not only (i) the residual energy of the gateway-nodes, but also (ii) the distance between the cluster-head and the gateway-node as well as between the latter and the base station. The gateway-nodes of high remaining energy reserves should be elected. Thus, the energy consumption is suitably balanced and the lifetime of the network is prolonged. Moreover they should be the ones having the less distance too. These requirements could be further described as follows (E_{gj} stands as the remaining energy of g_j, and l_{ij} equals to the number of gateway-nodes in the neighborhood of h_i).

Fitness Function #1:	
Object. 1: *Maximize f1 =*	$\sum_{i=1}^{c} E_{gj}$
Object. 2: *Minimize f2 =*	$\sum_{i=1}^{c} (d(h_i, g_j) + d(g_j, BS))$
Total Object.: *Fitness f =*	$a \times 1/f1 + \beta \times f2$
Get f minimized where $\alpha + \beta = 1$	

Several other functions denoting fitness (relevant fractions with a factor that minimizes the distance and a factor that maximizes the energy in the right place) could similarly be used and evaluated. Instead, the original fitness function given in [17] was initially adopted, aiming at having the same basis for comparing both approaches in our experimental evaluation. In our experiments α and β have been adequately defined to give us the best performance evaluation measurements in every instance. Beyond this fitness function (which was applied and tested as our basic selection due to comparison reasons), we've also chosen a suitable alternative function which is presented as follows (fitness function #2).

Fitness Function #2:	
Object. 1: *Maximize f1 =*	$\sum_{i=1}^{c} E_{gj}$
Object. 2: *Minimize f2 =*	$\sum_{i=1}^{c} (d(h_i, g_j) + d(g_j, BS))$
Total Object.: Minimize f =	$\frac{\beta \times f2 + t_1}{\alpha \times f1 + t_2}$

Note that α, β and t_1,t_2 are residual-energy/distance dependent and independent constants respectively, whereas the final value of the function is restricted adequately between 0 and 1 to normalize and optimize the result. The new proposed fitness function not only balances the weight of the two main factors (residual energy and distance) in the final computation, but also allows the designer to normalize (through α,β) conveniently the unpredictable (non-canonical) gaps caused by the potentially different measure units. It gives also the flexibility to take in account (through t_1,t_2) during the optimization process other significant parameters too (like data rates, transmission range, initial energy and energy consumption rates etc.). As it is shown in subsection IV.B the new fitness function leads both algorithms to better / more accurate execution behavior.

D. Discussion and Extensions

As it comes out of the literature, all the existing clustering protocols unfortunately suffer from several shortcomings that lead to performance degradation in very large scale WSNs, either relevant to the *hot spot* problem or to the fact that in order to face the hot spot problem they tend to generate quite large number of CHs and/or multi-hop routing overhead as the number of sensors increases, and generally lead to not sufficiently scalable solutions. As a consequence a proper solution could be given by combining appropriately clustering protocols with specific features into corresponding *two-level* hierarchical schemes trying to gain efficiency and extent the scalability of the total scheme.

In the above context, with the use of the GSA oriented scheme as the upper level cluster formation routine, we naturally get over the related disadvantages, due to the fact that it operates on a quite restricted number of nodes/cluster-heads. Thus, we may gain from its efficient behavior over such WSNs (of restricted size), and finally conclude to an outstanding performance gains if we use it in large / huge WSNs together with a lower level cluster formation scheme of similar efficiency (considering the balance of energy consumption), like the protocol referred as the basis of our approach.

Specifically, as it is also referred in section 4, the GSA oriented scheme behaves with great efficiency when applied over a set of e.g. 500 sensors. As a consequence, our combined approach may behave similarly over e.g. up to 500 cluster-heads, thus having the potential to lead to excessive total performance for large / huge networks of 5000-10000 and even more sensors.

On the contrary, one should also note that the proposed gradient-oriented algorithm applied for the initial clusters formation isn't suitable enough to cluster effectively the full large-scale WSN (despite of the fact that such cluster formation algorithms are considered quite efficient for this kind of WSNs too [22-23]). The basic disadvantage of such algorithms [4,22-23] relies on the fact that in many times they conclude to excessive numbers of cluster-heads when very large numbers of sensor nodes are deployed in the field. As a consequence the task of relaying of the data to the base station (or gathering with the use of a mobile sink) gets harder and completes in non-satisfactory total times. The ideal balancing of energy, preserving the number of cluster-heads in acceptable levels, is very hard to be achieved without applying a multi-level clustering procedure. Thus, by using additional gateway-nodes in the upper level, a hybrid scheme of great efficiency may naturally be built. Finally, it should be noted that the presented hybrid cluster formation procedure could be efficiently combined and integrated (in a straightforward manner - e.g. like in [21-24]) with one or more (mobile or not) sinks / collectors, thus forming a robust and flexible data gathering solution for very large-scale WSN application environments.

For example, following an approach similar to the one of [21] or [22-23] and considering a very large WSN where the number of gateways is also large enough, one should efficiently drive a set of one or more mobile sinks (or place a corresponding set of stationary sinks) to specific optimal (with respect to the locations of the gateways) route/locations to gather the data collected by the gateway-nodes.

IV. Simulation Results

Next, our relevant simulation experiments are presented, in which the proposed approach is shown to achieve high efficiency and scalability. Also our approach is compared to the original GSA oriented scheme given in [17] without any modifications. Specific sets of experiments have also been executed to show the suitability of the newly designed fitness function against the one referred in [17], as well as the worth of using the proposed modified first-level clustering algorithm against the use of the watershed-based one of [22-23]. The simulation experiments have been completed with the use of Castalia (a WSN simulator built on the basis of OMNeT++ [25]), and they focus on measuring the corresponding in each case protocol's efficiency (measuring the consumption of energy and lifetime of the WSN), over very large networks. In order to have a right comparison, the radio model used is the same as in [8, 17]. The consumption of energy for every node while sending a packet of *l bits* equals to the following:

$$E_{TX}(l,d) = \begin{cases} l \times E_{elec} + l \times \varepsilon_{fs} \times d^2, & if\ d < d_0 \\ l \times E_{elec} + l \times \varepsilon_{mp} \times d^4, & if\ d \geq d_0 \end{cases}$$

The energy consumption for transmitting or receiving one bit is E_{elec}, whereas the energy for amplification is based on the relevant model of the transmitting circuit, and d_0 stands as the limit for the maximum possible distance of transmission. Respectively, the energy consumption by the receiver for a packet of *l bits* equals to the following:

$$E_{RX}(l) = l \times E_{elec}$$

A. Comparing to the Native GSA-based Approach

Trying to compare the proposed hybrid scheme to the original GSA oriented scheme of [17], specific experiments have been run, considering different numbers of sensor nodes (*n* equal to 500, 1500, 2500), deployed at random (together with gateway-nodes) in a grid area with its side taking values between 200m and 500m (i.e. deployment areas of 200x200m^2, 360x360m^2 and 480x480m^2). The two first parameter values (500, 200x200m^2) stand as the main setup size chosen in the experimental evaluation of [17]. Based on the remaining two setup parameter values an approximate scale of 3x and 5x is simulated with respect to the experiments of [17]. With regard to the network setup factors considered in our simulations (transmission range, initial energy, etc. for both the sensors and the gateways) we have used the same values as given in the experiments of [17]; for comparison reasons too. The most important parameter values are summarized in Table I. Finally, it must be noted that for both algorithms the setup procedure is adjusted adequately to have equivalent behaviour with respect to the acceptable limit of coverage of the field where the sensors are deployed. The corresponding results are given in Fig. 1-4. By observing Fig. 1-3 one can easily conclude that considering the consumption of energy for each node, our proposed approach (GC-GSA) is definitely superior to the native GSA-EEC approach when n is equal to 1500 and 2500. On the other hand, it achieves almost the same performance (slightly worse) when n is equal to 500 nodes.

Specifically, for n equal to 1500, GC-GSA is shown to have a decrement of 15% with respect to the energy consumed on average, and this decrement becomes equal to 26% for n equal to 2500 sensor nodes. Instead, GSA-EEC has an almost ideal behaviour when n is equal to 500 sensor nodes, and its behaviour becomes gradually worse and worse as the WSN increases in size (which is a normal expectation because of the disadvantages of GSA technique, mainly when the number of dimensions is large). Moreover, Fig. 4 presents the lifetime of the network (which is measured as the life duration of the sensor node that dies first) with respect to the various test scenarios addressed above. One may easily observe that the GC-GSA approach leads to significant increments of the WSN lifetime when considering large networks (raising up to 30% - and even more - when n is equal to 2500 nodes). Also, the GSA-EEC scheme has a little better performance when n is equal to 500 nodes. It must also be noted that the disadvantages of GSA-EEC have a direct impact on the WSN lifetime, more important even than the energy consumed in average, because the energy consumption variance increases significantly too.

TABLE. I. PARAMETER VALUES FOR SIMULATION EXPERIMENTS

Parameter	Value
Sensor energy	1J
Gateway energy	5J
E_{elec} (bit energy dissipation)	50nJ/bit
ε_{mp} (multipath model amplification energy)	10pJ/bit/m^2
ε_{fs} (free space model amplification energy)	0.0013pJ/bit/m^4
d_{max} (sensor max. transmission range)	100m
d_0 (sensor threshold distance)	86m
R_{max} (gateway max. transmission range)	150m
R_0 (gateway threshold distance)	129m
Length of one data packet	4000bits
Size of one message	500bits

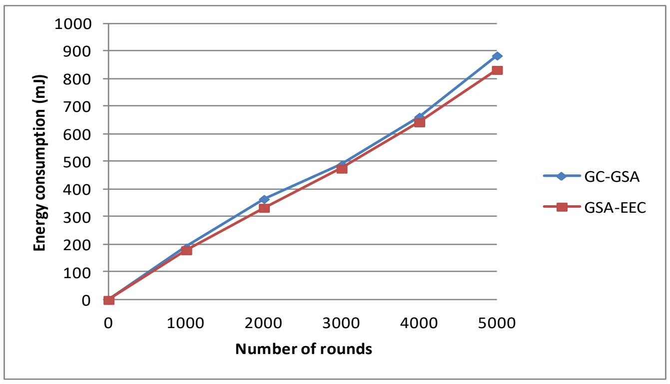

Fig. 1. Average Energy Consumption for n=500.

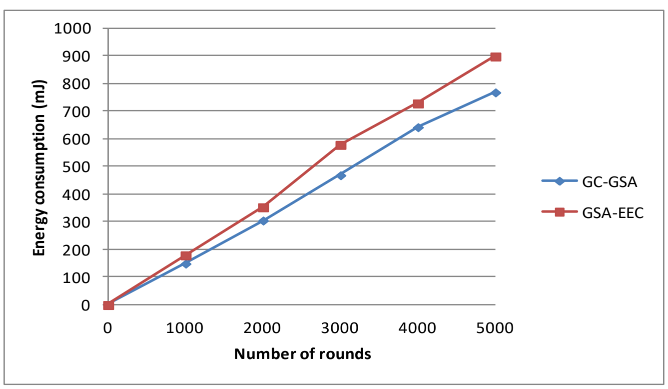

Fig. 2. Average Energy Consumption for n=1500.

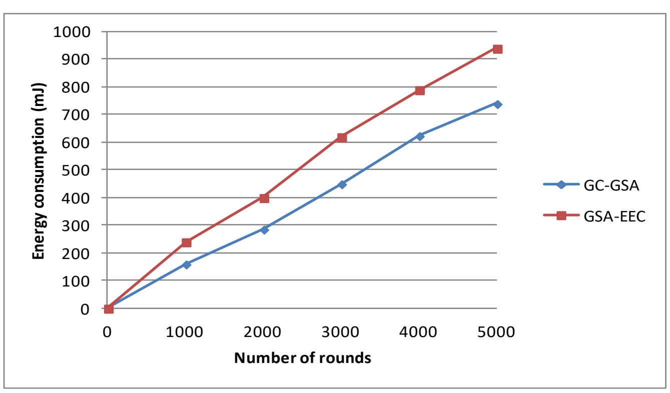

Fig. 3. Average Energy Consumption for n=2500.

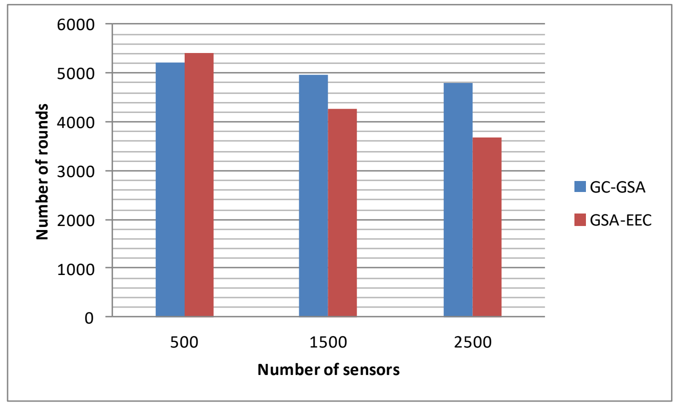

Fig. 4. Network Lifetime for Varying 'n'.

B. Evaluating the New Proposed Fitness Function

In the next set of experiments (summarized in Fig. 5 and 6) we present the improvements introduced due to the use of our new proposed fitness function (as described and discussed in subsection III.C). The corresponding measurements have been taken for n=2500 sensors over a 480x480m^2 terrain and present the energy consumed in average and the lifetime of the network for both the GC-GSA and GSA-EEC algorithms, for each one of the two fitness functions (the previously chosen in [17] - FF #1 - and the new proposed one here - FF #2).

As shown in Fig. 5, a significant improvement in the average energy consumption of the GC-GSA algorithm is achieved with the use of FF #2, which ranges form 5.5% to 9.5% depending on the number of rounds. Similarly, the average energy consumption of the GSA-EEC algorithm is also improved with the use of FF #2 (a decrease ranging from 3.5% to 5.5%); it remains however substantially worse than the one of the GC-GSA algorithm.

The improvements observed for the GSA-EEC algorithm are relatively smaller than the ones of the GC-GSA algorithm, mainly due to the fact that the performance of the GSA-EEC algorithm is influenced dramatically (in any case and more or less independently to the form of the fitness function) from the shortcomings met for large number of sensors (GSA dimensions etc. as it has been discussed earlier in Section 1). Furthermore, in Fig. 6 the corresponding improvements in network lifetime (due to the use of FF #2) are given for both algorithms.

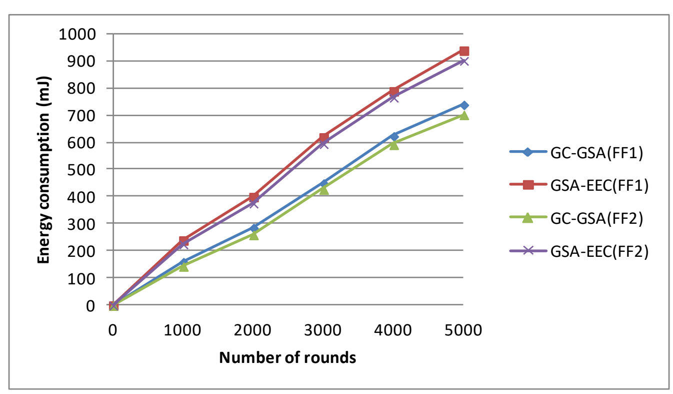

Fig. 5. Average Energy Consumption for Fitness Functions #1 and #2.

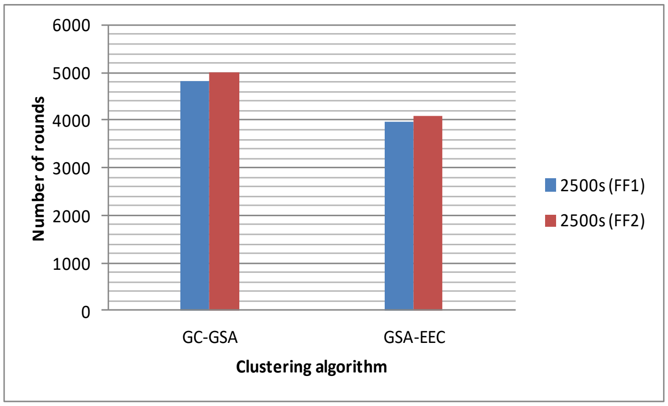

Fig. 6. Network Lifetime for Fitness Functions #1 and #2.

A relevant increase of approximately 4% is observed for the GC-GSA algorithm vs. an increase of approximately 2.5% for the GSA-EEC algorithm. As it was expected the network lifetime for both algorithms is not influenced in the same extent as the energy consumption (due to the fact that it has already reached quite high values for the specific number of sensors and the variance of the sensors' energy consumption has already been substantially restricted). As it is shown in all the measurements presented above, the proposed new fitness function leads to clearly better performance since it can represent more accurately the slight-extent modifications during the algorithm's execution and allows better balancing and accurate justification of the computed values.

C. *Evaluating the Scalability of our Combined Approach*

Moreover, in order to further examine the high efficiency and scalability of our combined protocol (GC-GSA algorithm) with use of the new proposed fitness function (FF #2), we've run additional experiments for very large WSN deployments - up to 10000 sensors. Specifically, we've examined the behavior of the GC-GSA protocol (considering the energy consumption and network lifetime as the basic performance metrics) for 4000, 6000, 8000 and 10000 sensor nodes, over a progressively growing deployment areas - from 800x800m^2 to 2000x2000m^2 (i.e. 800x800m^2, 1200x1200 m^2, 1600x1600m^2 and 2000x2000m^2 terrain respectively).

Moreover, we've used as the base for comparison the network lifetime achieved for 2500 sensor nodes with the use of FF #2, which is approximately equal (see also Fig. 6 and the relevant discussion) to 5000 rounds. We've chosen progressively growing deployment areas in order to test our approach in more realistic/practical cases; note here that if the size of the deployment area had been kept the same (i.e. 480x480m^2 as it was for 2500 sensors) our combined approach would lead to almost equal measurements (only a slight decrease would be observed in the network lifetime) since our first-level clustering protocol it is not influenced significantly (by its nature - see also [22-23] with respect to the quite similar watershed-based clustering protocol) by the increased density of sensors within the deployment area.

As it is shown in Fig. 8 there is a progressive decrease in the network lifetime when the number of the deployed sensors increase, which is more clear/significant for 10000 sensor nodes (over a 2000x2000 terrain). More concretely, the corresponding decrease for 4000, 6000, 8000 and 10000 sensors is approximately equal to 2%, 5,4%, 9.1% and 13.5% respectively. This decrease may not be considered insignificant, (at least for 8000 and 10000 sensors), however it is quite expected due to the large extent of the corresponding deployment areas. Due to the progressively growing deployment area the number of CHs and their sizes increase with a much less structured/controllable way (comparing to the case of keeping the deployment area the same), thus making much more difficult to keep the desired balance in energy consumption. Note here also that neither the GSA-EEC algorithm (GSA-based clustering algorithm only) or the WA-GSA algorithms would lead to better results (probably not even comparable) for such large numbers of sensors and deployment areas.

The observed decrease in the network lifetime is mainly caused by the relevant increase in the energy consumed by the sensor nodes (in average), as it is shown in more details in Fig. 7. In Fig. 7 one can easily observe (staring specifically at the relevant curves for 8000 and 10000 sensors) that the average energy consumption increases slightly till the execution of approximately 4000 rounds (due to the reasons referred above), and progressively more sharply afterwards, as the result of the energy exhaustion of some sensors and the end of network lifetime in every case. Overall, we can say that the proposed GC-GSA algorithm scales quite well even for very large number of sensors and deployment areas, thus making itself a promising choice for such extent realistic applications. Moreover, as it was also discussed in subsection III.D, it can be easily combined and integrated with one or more (mobile or not) sinks/collectors, thus forming a robust and flexible data gathering solution for very large-scale WSN based application environments.

D. *Comparing to other Large-Scale Clustering Approaches of the Literature*

Furthermore, in order to have a more clear sense of the performance of our two-level clustering protocol we've performed additional experiments comparing the proposed approach to other clustering approaches of the literature, such as (a) TL-LEACH [26] and EEHC [27], which are two of the most known two-level clustering protocols, and (b) the protocols presented in [30] and [31] which are two of the most valuable recent clustering approaches for large-scale WSN.

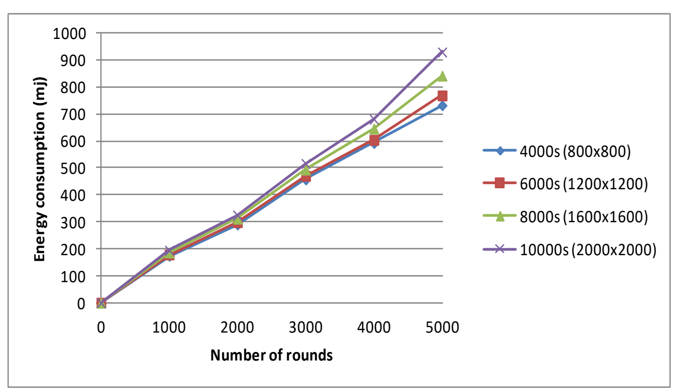

Fig. 7. Average Energy Consumption for Very Large Number of Sensors.

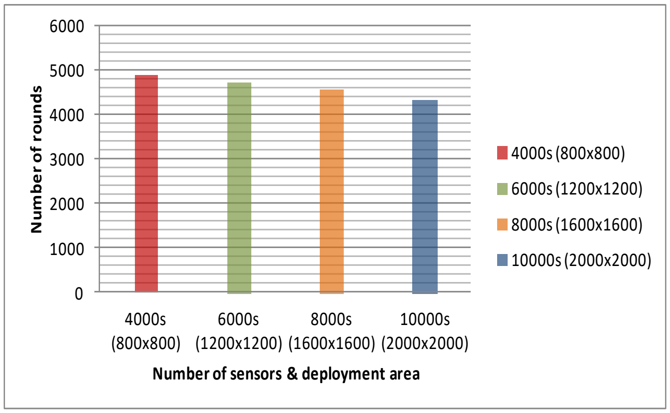

Fig. 8. Network Lifetime for Very Large Number of Sensors.

Specifically, we've run experiments for n=2500 sensors over a 480x480m2 terrain (which is a representative case of a very large WSN instance), and we've compared the performance of all the protocols over that instance. The corresponding results with regard to the energy consumption of all protocols in average are given in Fig. 9. In Fig. 10, the lifetime of the network for all the algorithms is shown (with additional measurements taken and presented for n=1500 sensors over a 360x360m2 for comparison reasons).

In [26] the authors propose a hierarchical protocol that consists of a two levels of clustering (TL-LEACH), aiming at managing the consumed energy in a more efficient way. The TL-LEACH protocol rotates both the first-level and second-level cluster-heads at random. In this way a two-level hierarchy is built, where it is possible, thus leading to a more efficient distribution of the energy reserves between the sensor nodes, which tends to be critical mainly when we have a quite dense WSN. Moreover, it is shown to perform much better than LEACH when the consumed energy and the lifetime of stand as the basic performance metrics. In [27], a random cluster-based hierarchy is proposed to organize the sensor nodes in a distributed manner. Their basic algorithm is then extended (EEHC) towards the construction of additional levels of cluster-heads, and finally a significant increase is observed with respect to the consumed energy. In [30] the authors first provide a thorough description and analysis with regard to the concept of cluster-based routing, and afterwards they introduce a corresponding combined cluster-based protocol (JCR), aiming at increased reliability and efficiency during the data gathering task in very large networks. In the JCR protocol the use of a back-off timer is followed, as well as a gradient-based protocol for routing, in order to conclude to a sufficiently connected network topology with efficient internal routing, given a specific maximum value with regard to the acceptable range of transmission. Further, in [31], the efficient solution of the 'hot spot' problem is the main objective of the authors. Their effort is based on the suitable rotation of the role of cluster-head between al the sensors, as well as adjusting appropriately the size of the formed clusters. The proposed protocol (UCF) first aims at selecting as probable cluster-heads the sensors that have more residual energy in the local area. Next, a fuzzy-logic technique is employed for the adjustment of the radius of the cluster radius. Simulation results show that the above protocol achieves significant improvements in the basic performance metrics.

As it is shown in Fig. 9 the energy consumption of the GC-GSA algorithm is less in average than all the competing protocols. The network lifetime (Fig. 10) is also steadily kept in high levels (around 5000 rounds), and its superiority over the other protocols is clear for both 1500 and 2500 sensors. The performance of TL-LEACH [26] is quite satisfactory, especially for 1500 sensors. However, although it also uses (among else) localized coordination to enable scalability, it employs a probability model for CH selection and so its energy efficiency can't be maximized. As a result it cannot preserve competitive efficiency comparing to GC-GSA for large and very large number of sensors. The EEHC protocol has similar behaviour with TL-LEACH since it's a randomized approach too; Moreover it performs slightly better due to its modular nature and the fact that it pays more attention in energy efficiency than TL-LEACH (stochastic geometry techniques are also used to improve the energy consumption). However for the same reasons it's also not highly competitive comparing to GC-GSA for large and very number of sensors.

The best performance among the other protocols is given by the UCF protocol [31], which leads to similar (slightly worse) network lifetime with GC-GSA and average network consumption, by combining unequal clustering and residual energy based CH selection with fuzzy logic to adjust the cluster radius. The fact that no other factors than the residual energy are taken in account for CH selection in each region, as well as the uncertainty nature of the fuzzy logic procedure makes UCF not scaling the same well for very large numbers of sensors (i.e. for 1500 and 2500 sensors in our case) as for smaller in size networks.

The JCR protocol [30] also performs very well for large networks since it selects a set of cluster-heads that helps (a) to organize a quite balanced cluster hierarchy (taking in account multiple factors for the procedure of CH selection), and (b) to construct a backbone of good connectivity for internal cluster-based routing. However it also doesn't scale the same well for very large numbers of sensors (and deployment areas), mainly because (as a result of the increase in the network size) the residual energy factor gets less critical (than it should be) on the computation of the back-off time of each node.

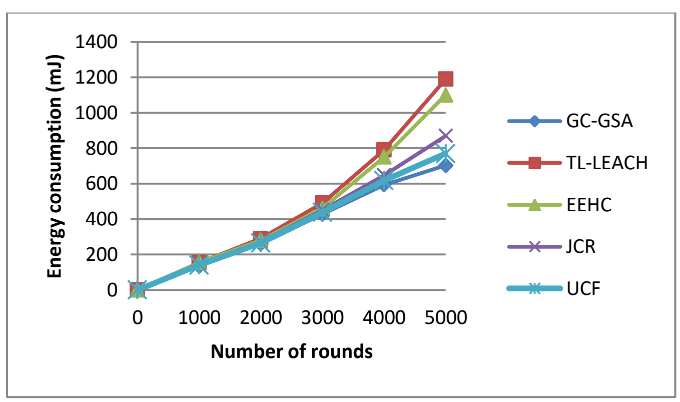

Fig. 9. Average Energy Consumption for GC-GSA, TL-LEACH, EEHC, JCR amd UCF (for 2500 Sensors).

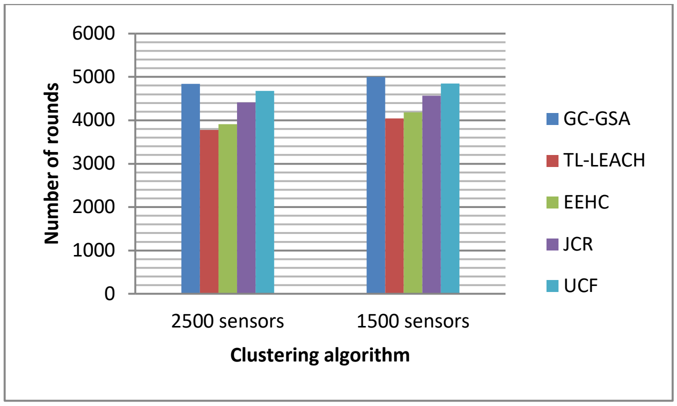

Fig. 10. Network Lifetime for GC-GSA, TL-LEACH, EEHC, JCR and UCF (for 1500 and 2500 Sensors).

E. Evaluating the First-Level Clustering Algorithm

Finally, in Table II and Fig. 11, 12 we've performed a basic set of experiments to show the worth of using the proposed modified first-level clustering algorithm instead of the more complex watershed-based algorithm given in [22-23]. More concretely, supposing that we use the algorithm of [22-23] as the first-level clustering algorithm in our combined approach, and keeping the GSA oriented algorithm as the cluster formation protocol of the second level, we conclude to a related alternative combined approach, i.e. WA-GSA. In the above context, we've run some of the experiments introduced in Section 4.1 (for n=1500 and n=2500 sensors over 360x360m2 and 480x480m2 terrains, respectively), aiming at a fair performance comparison of the two algorithms in large-scale WSN instances. For both algorithms (GC-GSA and WA-GSA) we've used the new proposed fitness function (FF #2) in order to have optimized performance behaviour.

As it is shown in Fig. 11 the average energy consumption of the WA-GSA algorithm is slightly larger than the one of the GC-GSA algorithm. Specifically, a slight increase is observed which ranges from 2.5% to 4% (depending on the number of rounds) for n=2500 sensors and from 2% to 3% for n=1500 sensors. Actually, in the beginning the behavior of both algorithms is approximately the same, whereas in the progress of the execution the WA-GSA algorithm tends to spend slightly more energy, which becomes more clear for larger number of sensors (n=2500). The latter is naturally expected, since with larger number of sensors we conclude to larger number of CHs in general (for both algorithms); and more concretely to larger differences in the number of cluster-heads between each other, which influences even more significantly the behaviour of the WA-GSA algorithm during its execution.

Furthermore, in Fig. 12 the corresponding difference in network lifetime is shown between the two algorithms. Here, one may notice also a slight decrease in the network lifetime for the WA-GSA algorithm, which is approximately equal to 2.5% and 1.5% for n=2500 and n=1500 respectively (the network lifetime is influenced in less extent for the same reasons as discussed for Fig. 6). As a general conclusion, the corresponding differences are not quite significant; however for large and very large number of sensors they make the choice of GC-GSA algorithm clearly preferable. As it was also discussed in Section 3.1 the slightly superior performance of our first-level clustering protocol against the watershed-based one of [22-23] is due to the less number of CHs it leads (which is a crucial parameter in the context of the present gateways-based WSN environment), whereas also the execution of the cluster formation procedure is quite faster. More concretely, the exact number of clusters (and CHs) produced for both algorithms in each set of experiments are given in Table II. Instead, in the context of other WSN environments (e.g. data gathering applications with a mobile collector, as in [22-23]) the performance of the watershed-based clustering protocol should be the preferable one.

TABLE. II. NUMBER AND SIZE OF CLUSTERS FOR GC-GSA AND WA-GSA

Sensors	# of Clusters (WA-GSA)	Nodes per Cluster (WA-GSA)	# of Clusters (GC-GSA)	Nodes per Cluster (GC-GSA)
500	105	4.8	94	5.3
1500	133	11.3	120	12.5
2500	187	13.4	171	14.6
4000	251	15.9	231	17.3
6000	321	18.7	295	20.3
8000	408	19.6	368	21.7
10000	495	20.2	447	22.4

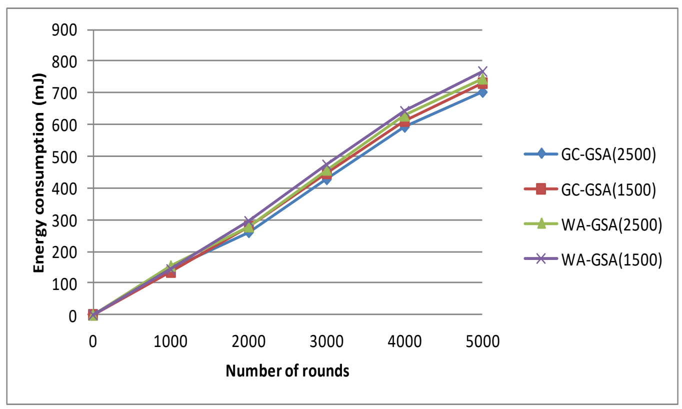

Fig. 11. Average Energy Consumption for GC-GSA and WA-GSA.

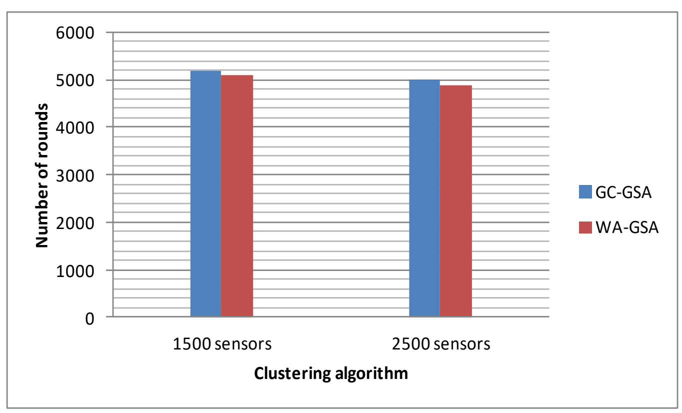

Fig. 12. Network Lifetime for GC-GSA and WA-GSA.

V. Conclusions

Throughout this paper the worth of using a novel hybrid clustering scheme that completes in two separate / hierarchical phases is demonstrated. It brings together a typical gradient protocol for clusters formation with an evolutionary optimization method that is mainly based on the recently introduced (the last decade) GSA algorithm, and trying to overcome its shortcomings on large networks. As a consequence it aims at better behaviour over large in size networks, where classical schemes in most cases lead to non-efficient solutions. The presented approach first constructs multihop clusters of evenly distributed energy reserves, in which the sensor nodes energy gets larger as coming closer to the cluster head. Thus, since the sensors near to the cluster head are more exhausted because of data forwarding, keeping the residual energy of those sensors high guarantees the prolonged and seamless operation of the WSN. Next, a suitable protocol based on the GSA runs to associate sets of cluster heads to specific gateway nodes for the eventual relaying of data to the base station. A fitness function was appropriately chosen considering both the distance from the cluster heads to the gateway nodes and the remaining energy of the gateway nodes. It was also further modified-optimized in order to gain more accurate results for large WSN instances (by providing the means for more discrete weighting of the overall formula). Extended simulated experiments have been completed to show the high efficiency and scalability of the proposed combined clustering scheme over very large WSNs, as well as its superiority over other clustering approaches of the literature. Additional sets of experiments demonstrate also separately the suitability of the proposed new fitness function against the previously existing one, as well as the worth of using the proposed modified first-level clustering algorithm against the use of other alternatives.

References

[1] B. Mamalis, D. Gavalas, C. Konstantopoulos, and G. Pantziou. 2009. Clustering in wireless sensor networks. In Y. Zhang, L. T. Yang, J. Chen (Eds.), RFID and sensor networks: Architectures, protocols, security & integrations, New York: CRC Press, Chap. 12, pp. 324–353.

[2] P.C.S. Rao, H. Banka, and P.K. Jana. 2016. PSO-based multiple-sink placement algorithm for protracting the lifetime of wireless sensor networks. In AISC, Springer, Heidelberg, vol. 379, pp. 605–616.

[3] R. Esmat, N. Hossein, and S. Saeid. 2009. GSA: A Gravitational Search Algorithm. Information Sciences, 179(13), 2232–2248.

[4] X. Bao, L. Liu, S. Zhang and F. Bao. 2010. An Energy Balanced Multihop Adaptive Clustering protocol for Wireless Sensor Networks. In Proceedings of the 2nd IEEE ICSPS (International Conference on Signal Processing Systems) Conf. vol. 3, pp. 47-51.

[5] M. Sabet, and H.R. Naji. 2015. A decentralized energy efficient hierarchical cluster-based routing algorithm for wireless sensor networks. AEU International Journal of Electronics and Communications, 69(5), 790–799.

[6] S.A. Sert, H. Bagci, and A. Yazici. 2015. MOFCA: multi-objective fuzzy clustering algorithm for wireless sensor networks. Applied Soft Computing 30, 151–165.

[7] D.S. Abbasi, and J. Abouei. 2015. Toward cluster-based weighted compressive data aggregation in wireless sensor networks. Ad Hoc Networks.

[8] W.B. Heinzelman, A.P. Chandrakasan, and H. Balakrishnan. 2000. Energy efficient communication protocol for wireless microsensor networks. In Proceedings of the 33rd Hawaii International Conference on System Sciences (*HICSS* 2000), p. 10.

[9] S. Lindsey, and C.S. Raghavendra. 2002. PEGASIS: power efficient gathering in sensor information systems. In Proceedings of the IEEE Aerospace Conference, pp. 1125–1130.

[10] P.C.S. Rao, P.K. Jana, and H. Banka. 2016. A particle swarm optimization based energy efficient cluster head selection algorithm for wireless sensor networks. Wireless Networks, Springer (online), 1-16.

[11] P.C.S. Rao, and H. Banka. 2017. Energy efficient clustering algorithms for wireless sensor networks: novel chemical reaction optimization approach. Wireless Networks, 23(2), 433–452.

[12] P.C.S. Rao, and H. Banka. 2017. Novel chemical reaction optimization based unequal clustering and routing algorithms for wireless sensor networks. Wireless Networks, 23(3), 759–778.

[13] G. Gupta, and M. Younis. 2003. Load-balanced clustering of wireless sensor networks. In Proceedings of IEEE International Conference on Communications, ICC 2003, vol. 3, pp. 1848–1852.

[14] C.P. Low, C. Fang, J.M. Ng, and Y.H. Ang. 2008. Efficient load-balanced clustering algorithms for wireless sensor networks. Computer Communications 31(4), 750–759.

[15] S. Hussain, A.W. Matin, O. Islam. 2007. Genetic algorithm for hierarchical wireless sensor networks. Journal of Networks 2(5), 87–97.

[16] N.M.A. Latiff, C.C. Tsemenidis, and B.S. Sheriff. 2007. Energy-aware clustering for wireless sensor networks using particle swarm optimization. In Proceedings of the 18th Annual IEEE International Symposium on Personal, Indoor and Mobile Radio Communications, pp. 1–5.

[17] P.C.S. Rao, H. Banka and P.K. Jana. 2015. Energy Efficient Clustering for Wireless Sensor Networks: A Gravitational Search Algorithm. In Proceedings of SEMCCO 2015 (International Conference on Swarm, Evolutionary and Memetic Computing), Springer, pp. 247-259.

[18] R. Krishnaprabha and A. Gopakumar. 2014. Performance of gravitational search algorithm in wireless sensor network localization, in Intl Conf. on Communication, Signal Processing and Networking (NCCSN), IEEE, pp. 1-6.

[19] Zhao Wei-Guo, Yang Shao-Pu, Li Kui and Wang Li-Ying. 2013. Gravitational Search Algorithm for Node Localization in Wireless Sensor Network. Information Technology Journal, 12, 5806-5811.

[20] J.M. Lanza-Gutierrez and J.A. Gomez-Pulido. 2017. A gravitational search algorithm for solving the relay node placement problem in wireless sensor networks, in Intl. Journal of Communication Systems, 30(2), 1-21.

[21] P.C.S. Rao, H. Banka and P.K. Jana. 2015. A Gravitational Search Algorithm for Energy Efficient Multi-sink Placement in Wireless Sensor Networks. In Proceedings of SEMCCO 2015 (International Conference on Swarm, Evolutionary and Memetic Computing), Springer, pp. 222-234.

[22] C. Konstantopoulos, B. Mamalis, G. Pantziou, and V. Thanasias 2012. Watershed-based Clustering for Energy Efficient Data Gathering in Wireless Sensor Networks with Mobile Collector. In Proceedings of Europar Conference, Springer, LNCS 7484, pp. 754-766.

[23] C. Konstantopoulos, B. Mamalis, G. Pantziou, and V. Thanasias. 2015. An image processing inspired mobile sink solution for energy efficient data gathering in wireless sensor networks. Wireless Networks 21(1), 227-249.

[24] B. Mamalis. 2013. A Residual Energy-based Data Gathering Solution for Wireless Sensor Networks with Delay Constraints", in Proceedings of ISCA ACC (Advanced Computing and Communications) 2013 Conference, pp. 59-66, September 25-27, Los Angeles, CA, USA.

[25] Castalia: WSNs and BANs simulator. 2007. National ICT Australia. URL: http:// castalia.npc.nicta.com.au/.

[26] Loscri, V & Morabito, G & Marano, Salvatore. 2005. A two-levels hierarchy for low-energy adaptive clustering hierarchy (TL-LEACH). In Proceedings of IEEE Vehicular Technology Conference, vol.3, pp. 1809-1813.

[27] Bandyopadhyay, Seema & Coyle, Edward. 2003. An Energy Efficient Hierarchical Clustering Algorithm for Wireless Sensor Networks. In Proceedings of IEEE INFOCOM Conference, vol.3, pp. 1713-1723.

[28] Tie Qiu, Aoyang Zhao, Feng Xia, Weisheng Si, Dapeng Oliver Wu, Tie Qiu, Aoyang Zhao, Feng Xia, Weisheng Si, and Dapeng Oliver Wu.

2017. ROSE: Robustness Strategy for Scale-Free Wireless Sensor Networks. IEEE/ACM Transactions on Networking, 25, 5, 2944-2959.

[29] M. Dong, K. Ota and A. Liu. 2016. RMER: Reliable and Energy-Efficient Data Collection for Large-Scale Wireless Sensor Networks. In IEEE Internet of Things Journal, vol. 3, no. 4, pp. 511-519.

[30] Z. Xu, L. Chen, C. Chen and X. Guan. 2016. Joint Clustering and Routing Design for Reliable and Efficient Data Collection in Large-Scale Wireless Sensor Networks. In IEEE Internet of Things Journal, vol. 3, no. 4, pp. 520-532.

[31] P Neamatollahi and M Naghibzadeh. 2018. Distributed unequal clustering algorithm in large-scale wireless sensor networks using fuzzy logic. In the Journal of Supercomputing, 74, 6, pp 2329-2352.

[32] A. Abro, D. Zhongliang, K. A. Memon, K. H. Mohammadani, N. ul Ain, S. Memon, I. Memon and M. A. Panhwar, 2019. Minimizing Energy Expenditures using Genetic Algorithm for Scalability and Longlivety of Multi hop Sensor Networks. In IEEE 9th Intl. Conf. on Electronics Information and Emergency Communication (ICEIEC), Beijing, China, 2019, pp. 183-187.

[33] B. Mamalis and M. Perlitis, Energy Balanced Clustering and Data Gathering for Large-Scale Wireless Sensor Networks, in Proceedings of the 21st Panhellenic Conference in Informatics (PCI 2017), ACM ICPS Series, 53:1-53:6, September 28-30, Larisa, Greece, 2017.

Application of Computer-Aided to Improve Industrial Productivity in Cement Factories by using a Novel Design of Quantitative Conveyor

Anh Son Tran[1]
Dept. of Manufacturing Engineering
HCMC University of Technology, VNU-HCM
Ho Chi Minh City, Vietnam

Ha Quang Thinh Ngo[*2]
Dept. of Mechatronics Engineering
HCMC University of Technology, VNU-HCM
Ho Chi Minh City, Vietnam

***Abstract*—To deal with the industrial evolution 4.0, many cement enterprises must be enhanced the productive ability. In this paper, the novel design of quantitative conveyor is introduced to improve the industrial productivity. Firstly, the test hardware platform is set-up based on customer's requirement. Then, the analysis and control of mechanical platform for quantitative conveyor is investigated. From the experimental results, the operation of conveyor is stable and precise to ensure the output products for cement factories.**

***Keywords*—Motion control; cement industry; conveyor; automation; robotics system**

I. Introduction

The more the economic develop, the more building is constructed. Many essential components of constructions such as cement; steel or concrete play an important role. For producers of cement, it is important to visualize the amount of this material. By knowing this information, it is needed for business trade, storage and distribution management. Since the need of cement becomes very large in market, its amount per day is huge and continuously. Hence, it is most often measured increment. In other words, it measures the volume of transported material. Traditionally, workers must measure the weight of cement in manual labor or in separated unit. This job is very limited because it costs much and low productivity. Furthermore, it is difficult to maintain the precise measurement due to restricted human resource. In reality, the weight is measured during the transport by means of conveyor. The problem is that the complicated measuring process and calibrating method often brings troubles to operators.

In the other fields, for example wood chips or mining, it is also required to maintain the industrial production and enhance the production line. In [1, 2], researchers introduced a mathematical relationship of computing volume measuring by a laser scanning method during transport on conveyor. The scanner SICK LMS400 hanging above conveyor and industrial PC monitoring overall process are combined together. The belt speed is constant and its information is transmitted via digital line. However, the cost of this method is expensive because of using laser scanner, it is hard for maintenance job. Especially, it cannot estimate the wood humidity. The study [3, 4] presented a distributed model of the transport conveyor which material moves along at the same speed to obtain the equations in closed form. Based on this model, the time delay between the arrival of the material at the inlet of the conveyor line and its outlet from the conveyor is calculated. Actually, the distribution of material on conveyor is not regular. And the material must be granulated form.

To control and monitor the conveyor system, a centralized system [5-8] including S7-300 PLC and peripheral devices is implemented. This system is to transport coal mine using PLC and touch screen to visualize. The hardware and software are matched together via Profibus DP. The components of this system are popular in market and un-expensive. Though, the effectiveness and feasibility of proposed system should be considered since this paper is just simulated. Once, these works in [9, 10] suggested a simulation tool for belt conveyor in bulk material transportation. They concentrate on role of conveyor in contribution to heavy industry. The results of research help the design process more rapid and simplified. The developers could shorten consuming time by analyzing the simulative data. The more convenient transportations are to apply the autonomous system in workshop [11-13]. In this method, a number of vehicles continuously operate to carry cargo around the workplace. Nonetheless, these drawbacks such as light weight carriage, sudden accidence or high maintenance cost could impact on the overall effectiveness of whole system.

In this paper, the overall scheme of quantitative conveyor for cement industry is proposed. From practical acquirements, the hardware platform is built up in the first period. Later, the system software and control algorithm are described in detail. Several experiences in calibrating method are discussed since proposed platform is operated. Finally, some conclusions are carried out for future development.

II. Basic Principle of Operation

There are several ways to measure how weight material is on conveyor. However, the effective and feasible method are not interested so much. As a result, the description of design system is detailed in Fig. 1. After material is poured, the belt conveyor brings matter based on rollers. The load-cell is located on one of rollers. This component is considered as weightbridge. The area in front of and after load-cell, named weight span, has length L. The controller collects signals from load-cell and speed sensor to calculate system parameters such as rate, load.

*Corresponding Author.

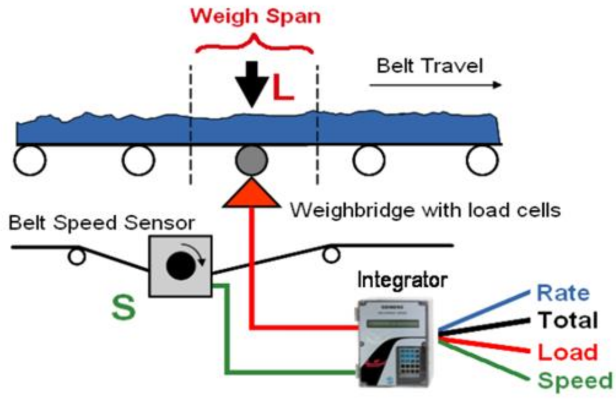

Fig. 1. Illustration of Proposed Approach.

In market, the products derived from cheal level are often large error, low firmness and suitable for small business. The others are expensive, high reliability and proper for mass production. For developing countries, there is a need to introduce a conveyor system which is high quality, low cost and durable. To solve the problems, the design process should be optimized and control method need to be effective and applicable.

III. Mechanical Model of Conveyor System

In this section, a belt conveyor with medium size is studied. The components platform as Fig. 2 are described in transportation system labeling as following. From feeding funnel, material drops on belt body and is delivered regularly by lever. There are many rollers distributed evenly along the length of conveyor. The rollers classifying into two sub categories, passive roller and active roller, are placed under belt. The active one is connected to driving motor directly while the others keep belt on a plane. To prevent the dimple, the adjusting bolt to tense belt is located in one side. The operator could handle to enhance the accuracy measurement. The material passing the area of weight span is estimated through load cell. The data is feedback to controller in real time to synthesize. The industrial productivity is able to visualize continuously.

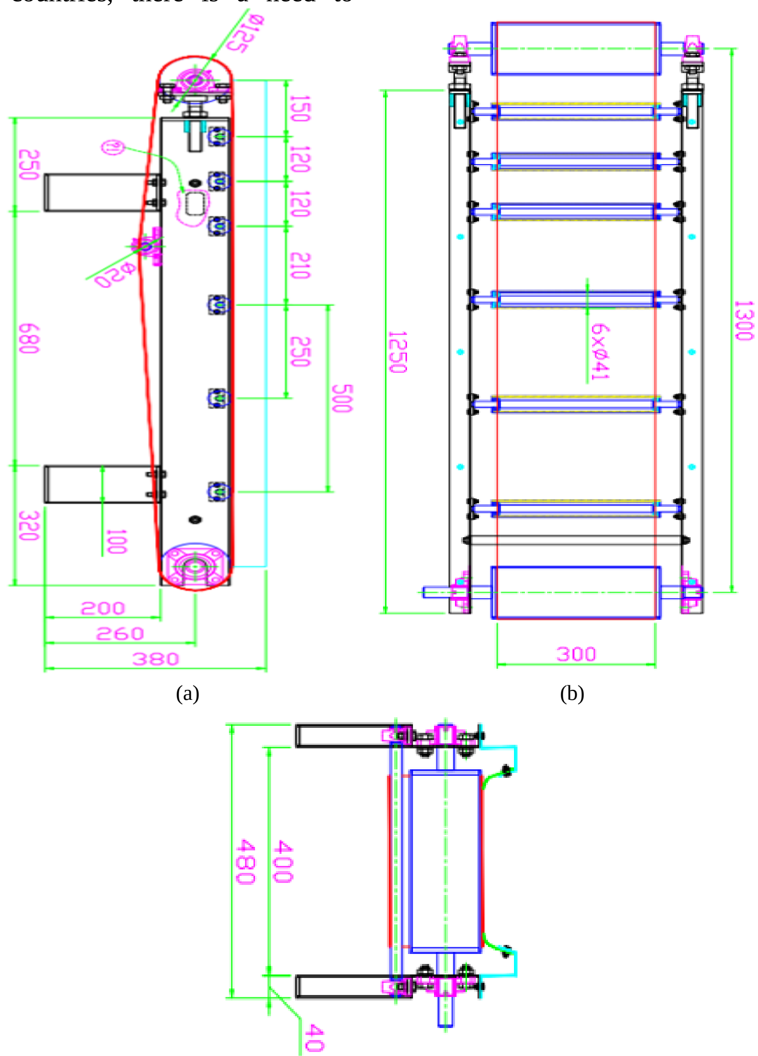

Fig. 2. Mechanical Scheme of Conveyor System, (a) Side View, (b) Upper View and (c) Front View.

IV. Monitoring Method and Control Approach

The monitoring and control of dynamic quantitative conveyor is based on integrated model, transpoting and weighing, when it operates. For easy supervision, HMI touch screen helps to show system parameters and control status. The controller obligates to certify system reliability, high repeated precision and standardization. The power circuit is embedded into inverter to drive AC motor. The data fusion between load cell and speedometer gives exact information to main CPU. In fact, there are two options instead of using load cell. Magnetoelastic sensor, being truly non-contact based, have inherent advantages over traditional solutions based on strain gauges regarding robustness and cost structures. A piezoelectric sensor is a device that uses the piezoelectric effect, to measure changes in pressure, acceleration, temperature, strain, or force by converting them to an electrical charge. Nevertheless, torque or load sensor will play an increasingly important role in many applications, enable critical benefits such as efficiency improvements, weight saving, operational safety, enhanced productivity and cost saving.

Since load sensor returns analog signal to controller while main CPU serves digital pulse as Fig. 3. A high precision analog-digital converter is necessary to add in control scheme. The more accuracy the converter is, the more exact the measuring data is. Additionally, the processing measurement results holds an important role. Each load sensor requires the particular processing algorithm. If the algorithm converges faster, the consuming time is shorter. The concerning system coefficients are length of weigh span, sampling time and velocity of conveyor.

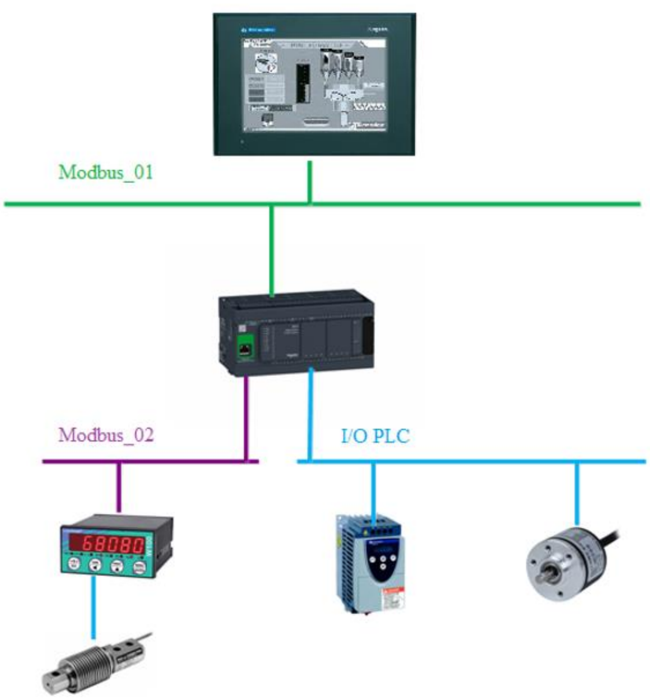

Fig. 3. Overview of Distributed Control Diagram.

V. Design of Industrial Controller

The embedded controller plays an important role in overall system. To interact with technical engineer, it is necessary to design a graphical tool under computer-aided. This program would handle entire missions in system: manage control signal and coefficients, control dynamic motor, output command values from controller and so on. In Fig. 4, the computer-aided software to design an interface on touch screen monitor is shown. Owing to its, the designer could carry out friendly program, fast debugging and easy to maintenance. After various tests and calibrations, a release version of graphical database has been packaged in Fig. 5.

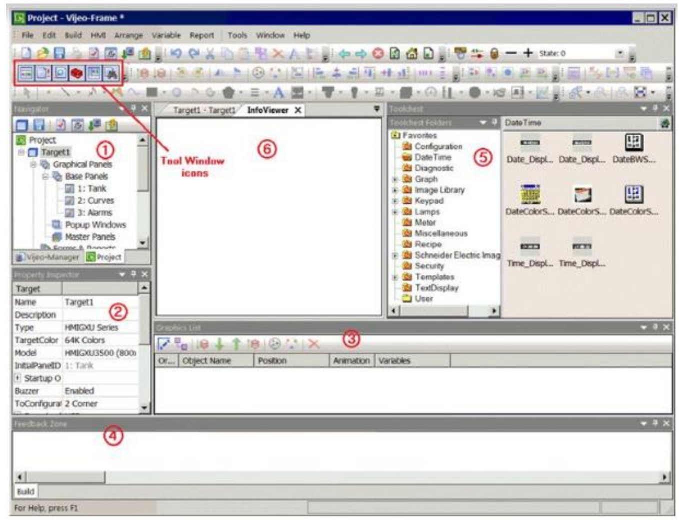

Fig. 4. Computer-Aided Graphical user Interface Program.

Fig. 5. Control Program of Embedded Controller on Central Panel.

VI. Results and Discussion

To verify the proposed design, the hardware platform is completed as Fig. 6. In this paper, a belt conveyor with medium size which is popular in developing country is studied. From this experimental model, a large-scale conveyor system could be considered to develop in future. After setting up the system instruments, the data connection is established. The control panel could be placed far from system, for instance in central control room, for convenient work. Fig. 7 shows practical layout of electrical control box. For the electrical safety, main CPU and AC inverter are separated if emergency case occurs. All electrical contact points are covered by isolation plastic elements. The outside layout of control panel box has monitoring screen, five buttons such as emergency stop, on, off and local/remote. LED signals perform status machine visibly.

Most of devices are from Schneider company except incremental encoder from Autonics Ltd. company and indicator from Laumas firm. The communication protocol is chosen as modbus network since the ability to reject noise of measurement system. All data wires are covered by shield outside.

The graphical user interface leaning on SCADA is demonstrated in Fig. 8. The AC inverter ATV11 drives feeding conveyor system depending on setting values from SCADA. PLC module is connected with inverter by analog signal, communicates with weight indicator W100 via Modbus protocol.

In Fig. 9, a monitoring page of control parameters is displayed to follow control process. The options Pid/Limit/Overflow indicate status of PID function. To tune PID coefficients, Man/Reset button is pressed to adjust up or down value. The chart on right side reveals information of SP/PV/Limit or flow. Based on experience of operator, it can be seen that the proposed system works well in industrial environment.

Fig. 6. Experimental Model of Proposed Material Transportation System.

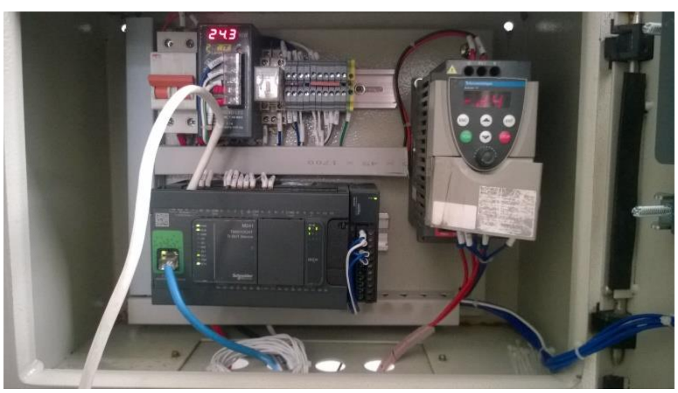

Fig. 7. Layout Inside Electrical Control Box.

Fig. 8. Experimental Software of Proposed Material Transportation System.

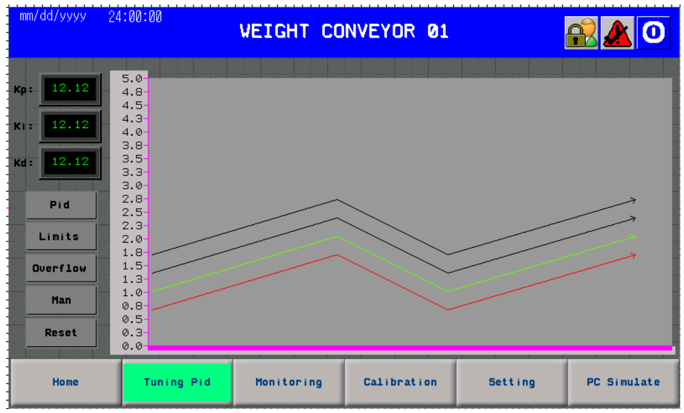

Fig. 9. Experimental Result of Tuning PID Control.

VII. Conclusions

In this paper, a medium sizing material transportation system is researched. From practical demand of industry, the conveyor system that guarantee high productivity and enhance precise measurement as well, is developed. The mechanical design and method to weight are considered to optimize the initial cost, easy to maintain and high production. From experimental results, it has been proved that the proposed system is effective and feasible in reality. It could be applied in various fields such as mining, cement.

Acknowledgment

The authors would like to thank the helping of Can Tho cement factory. This work is funded by Ngo Ha Gia Ltd. Co. under research grant no. NHG19-012-0008.

References

[1] D. Fojtik, "Measuring of the volume of material on the conveyor belt," Proc. of the 2014 International Carpathian Control Conference, pp. 121–124, 2014.

[2] H. Q. T. Ngo, T. P. Nguyen, T. S. Le, V. N. S. Huynh and H. A. M. Tran, "Experimental design of PC-based servo system," IEEE International Conference on System Science and Engineering, pp. 760–765, 2017.

[3] O. Pihnastyi, V. Khodusov, “Model of a composite magistral conveyor line,” IEEE First International Conference on System Analysis & Intelligent Computing, pp. 1–4, 2018.

[4] H. Q. T. Ngo, Q. C. Nguyen and T. P. Nguyen, “Design and implementation of high performance motion controller for 2-D delta robot,” IEEE International Conference on Information Science and Technology, pp. 129–134, 2017.

[5] Q. Lu, X. Wang and L. Zhuang, “Research and design of monitoring system for belt conveyor,” International Conference on Computer Science and Service System, pp. 1943–1945, 2012.

[6] H. Q. T. Ngo and A. S. Tran, “Using Fuzzy Logic Scheme for Automated Guided Vehicle to Track Following Path Under Various Load,” IEEE International Conference on Green Technology and Sustainable Development, pp. 312–316, 2018.

[7] Y. G, K. Hu, P. Wang and Y. Wang, “Dynamic simulation of belt conveyor based on virtual prototyping,” International Conference on Mechanic Automation and Control Engineering, pp. 5986–5988, 2010.

[8] H. A. M. Tran, H. Q. T. Ngo, T. P. Nguyen and H. Nguyen, “Implementation of vision-based autonomous moblie platform to control A* algorithm,” IEEE International Conference on Recent Advances in Signal Processing, Telecommunication and Computing, pp. 39–44, 2018.

[9] H. Q. T. Ngo, M. H. Phan, “Deisgn of an Open Platform for Multi-Disciplinary Approach in Project-Based Learning of an EPICS Class,” Electronics, 8(2), 200, 2019.

[10] L. Guangbu, L. Ruqiong, “Belt conveyor modeling and performance simulation based on AMESim,” International Conference on Information and Computing Science, vol. 4, pp. 304-307, 2009.

[11] H. Q. T. Ngo, T. P. Nguyen and H. Nguyen, “The fusing framework between lifting carrier and tractor-trailer for modern transportation,” Advances in Science, Technology and Engineering System Journal, vol. 4, no. 4, pp. 522–528, 2019.

[12] H. Q. T. Ngo, T. P. Nguyen, H. Nguyen, “A complete comparison to design complementary filter and kalman filter for aerial vehicle,” International Journal of Mechanical Engineering and Technology, vol. 9, pp. 502–513, 2018.

[13] Q. T. Truong, H. Q. T. Ngo, T. P. Nguyen, H. Nguyen and W. H. Kim, “A novel infrastructure design of industrial autonomous system,” International Journal of Fuzzy Logic and Intelligent Systems, vol. 19, no. 2, pp. 103-111, 2019.

Software Design using Genetic Quality Components Search

Evgeny Nikulchev[1], Dmitry Ilin[2], Aleksander Gusev[3]
MIREA – Russian Technological University
Russia

***Abstract*—The paper presents a software design methodology based on computational experiments for effective selection of software component set. The selection of components is performed with respect to the numerical quality criteria evaluated in the reproducible experiments with various sets of components in the virtual infrastructure simulating the operating conditions of a software system being developed. To reduce the number of experiments with unpromising sets of components the genetic algorithm is applied. For representing the sets of components in the form of natural genotypes, the encoding mapping is introduced, reverse mapping is used to decipher the genotype. In the first step of the technique, the genetic algorithm creates an initial population of random genotypes that are converted into the assessed sets of software components. The paper shows the application of the proposed methodology to find the effective choice of Node.js components. For this purpose, a MATLAB program of genetic search and experimental scenario for a virtual machine running Ubuntu 16.04 LTS operating system were developed. To guarantee the proper reproduction of the experimental conditions, the Vagrant and Ansible configuration tools were used to create the virtual environment of the experiment.**

Keywords—Software design; selection of software components set; numerical quality criteria evaluated; genetic algorithm

I. Introduction

Effective selection of software components based on assessments of the quality of service criteria [1] is becoming increasingly important problem [2] in connection with the spread of the framework approach to software development. This paper considers the problem in the context of highly loaded distributed client-server information systems (IS) implemented in the JavaScript.

The framework is a template of architectural solution. It allows the developer to unify the process of developing an IS based on a combination of the constant part of the IS (framework), which does not vary from configuration to configuration, and connected components that are compatible with the constant part. The JavaScript framework is a framework written in the JavaScript language that allows programmers to manipulate a set of compatible components (libraries) to solve a problem. The framework differs from the JavaScript library in the control flow: the library is always called by its parent code, while the framework defines the overall architecture of the IS and calls certain components to implement the functionality defined by the developer.

The research was performed as part of the state task of the Ministry of science and height education of Russian Federation, project 25.13253.2018 / 12.1 “Development of the technological concept of the Data Center for Interdisciplinary Research in Education”

The aim of this work is creating and experimentally testing a technique for effectively selecting the software components for the framework based on experimental evaluations of quality criteria.

The article consists of six sections. The first is Introduction. In the second section the review of the related works is presented. In the third section the problem is formulated. The fourth section describes the methods of genetic search and the configuration of the experimental stand. The fifth section provides the results of the genetic search. The sixth section discusses the results. The seventh section concludes the article.

II. Related Works

Solved with the help of JavaScript in recent years, the variety of tasks has led to the emergence of hundreds of frameworks. They can be divided into two groups. (1) Universal one (for example, Node.js), which allows the developers to use JavaScript for writing the server part of a web application as a general-purpose language with the ability to interact with I/O devices. (2) Frameworks for writing browser-based (front-end) applications running on the user's side, such as the followings: Angular.js, Angular (it is written in TypeScript, which is a backwards-compatible JavaScript modification), Vue.js, React.js and lots of others.

To support the optimal choice of the framework, various techniques were proposed earlier. Those techniques allowed the developers to assess the compliance of the framework with the general needs of the developer for a given set of components using the performance benchmark results [3] or expert evaluations [4]. However, an urgent task is creation of a methodology for selecting the efficient set of software components for the specified framework to provide the guaranteed quality of service [5] (QoS) and the efficiency of operation under given conditions. Those conditions include the specific development environment, computing infrastructure, computational loads during normal and peak operation, etc.

The basic element of such a technique should be the procedure for conducting reproducible computational experiments to assess the quality of the functioning of software components. Unlike the automated software testing [6], the experimental assessment of the quality of the functioning would provide more flexible approach to select the components for the IS even if there were no errors reported but the performance of the IS could be increased with effective selection of the components. By automating this procedure, it is generally necessary to solve the problem of reducing the number of iterations of software components in order to obtain the effective set. The solution can be found using genetic algorithms [7]. They have proven themselves to be useful in assessing the problem of multicriteria optimization in the field of software development: evolutionary software development cost estimation [8]; optimization of computing resources utilization [9, 10]; generating optimal test data sets [11]; evaluating [12] software reliability; optimization of software partitioning into modules [13]; prioritizing client requirements for software development [14]; software refactoring [15]; in solving problems of project management [16] and human resources allocation [17]; in other tasks, including those related to the development of cloud web – services with QoS-aware resource allocation and dynamic web-service composition [18–20].

III. Model and Research Methods

Let us consider n functional features $q_i,\ i=\overline{1,n}$, which should be implemented in the IS and t different configurations $\omega^k, k=\overline{1,t}$ of the virtual infrastructure, simulating the IS operating conditions; M is the set of all the software components available for the research, each of which implements at least one of the features q_i. The subset of alternative software components from M, suitable for implementing the feature q_i is denoted as $m_i, i=\overline{1,n}$. Let us consider the situation when there exist p technology stacks $s^j, j=\overline{1,p}$ i.e. such sets of software components, in which for every feature $q_i,\ i=\overline{1,n}$ there exists at least one software component from M. Let us denote the set of all possible stacks as S. We introduce then the set of f experimentally evaluated partial quality criteria $r_\xi^{k,j},\ \ \xi=\overline{1,f}$, values of which belong to the space R^{f}. Thus,

$$\forall\omega^k : s^j \rightarrow R^{k,j} \in \mathrm{R}^{\mathrm{f}},$$

$$R^{k,j}=(r_1^{k,j}, r_2^{k,j},\ldots, r_\xi^{k,j},\ldots, r_f^{k,j})^T, k=\overline{1,t}, j=\overline{1,p},$$

where $r_\xi^{k,j}, \xi=\overline{1,f}, k=\overline{1,t}, j=\overline{1,p}$ are the values of experimentally evaluated partial quality criteria for the configuration ω^k of the virtual infrastructure and the stack s^j being evaluated.

Let us introduce the integral quality criteria for the IS:

$$\Psi\left(\omega^k, s^j\right)=\sum_{\xi=1}^{f} w_\xi \tilde{r}_\xi^{k,j}, \tag{1}$$

where $\tilde{r}_\xi^{k,j}$ are the normalized values of partial quality criteria $r_\xi^{k,j}$; $\xi=\overline{1,f}$; $w_{\xi,}$ are the weights of the partial criteria. Herewith $\sum_{\xi=1}^{f} w_\xi=1$.

The problem of the effective choice of software components based on the experimental evaluation of the quality of operation (see Fig. 1) for the chosen configuration of the virtual infrastructure ω^k consists in the choice of the technology stack s^* satisfying the following condition:

$$s^*=\underset{s^j,\ j=\overline{1,p}}{\operatorname{argmin}}\ \Psi\left(\omega^k, s^j\right). \tag{2}$$

Using the above introduced approach let us consider the case of selecting Node.js components.

Table I shows the set of functional features and components that implement those features in a computational experiment. Thus, $n=10, p=216$.

The considered configuration $\omega^k, k=t=1$ of the virtual infrastructure is specified in Table II.

The evaluation of the quality of operation is performed with respect to the $f=14$ partial quality criteria defined in Table III.

The weighting factors for the criteria are $w_2=w_{11}=0.08$; $w_\xi=0.07(\xi=1,\ \xi=\overline{3,10},\ \xi=12)$, setting the target QoS.

When conducting the experiment, $r_\xi^{k,j}$ $(\xi=\overline{1,14}$, $k=\overline{1,t},\ j=\overline{1,p})$ are normalized with respect to their maximum values in the experiment and take their values in the segment [0; 1].

The task is selecting the stack s^* of Node.js components, solving the problem (2).

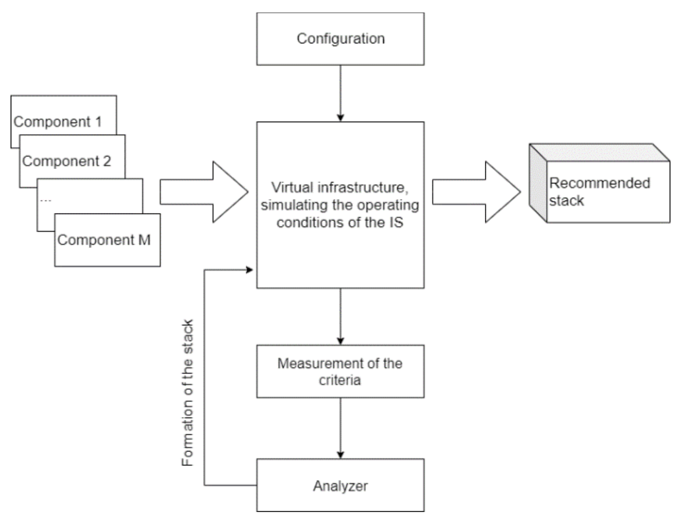

Fig. 1. The Effective Choice of Software Components based on the Experimental Evaluation of the Quality of Operation.

TABLE. I. LIST OF FUNCTIONAL FEATURES AND COMPONENTS

q_i	Name of the functional feature	Alternative components	Description
q_1	Filter	Lodash Underscore	Checks all the elements of an array against some condition and returns an array of elements for which the check gave "True"
q_2	First	Lodash Underscore	Returns the first element of an array
q_3	FsRead	Fs–extra Fs	Reads data from a file
q_4	FsReaddir	Fs–extra	Reads the contents of a directory
q_5	FsReaddirRecursive	Recursive–readdir	Recursively reads the contents of a directory
q_6	HashMD5	Hasha md5 Ts–md5	Calculates the MD5 hash for the specified data set
q_7	Map	Lodash Underscore JavaScript language tools	Applies the specified function to all the elements of the array, thereby returning a new array consisting of the transformed elements
q_8	PathResolve	Path	Generates the full path to the file or directory based on the specified array of path elements
q_9	StringReplace	JavaScript language tools	Finds and replaces a substring in the string passed
q_{10}	ZipCompress	Adm–zip Jszip Zipit	Performs archiving of the transferred file array and returns the generated Zip – archive

TABLE. II. VIRTUAL INFRASTRUCTURE CONFIGURATION $\omega^k (k = 1)$

Num.	Parameter	Value
1	CPU	Intel® Core ™ i7–7700
2	Number of cores	4
3	Number of logical processors	8
4	Clock frequency	3.60 GHz
5	RAM	12.0 GB
5	Host operating system	Ubuntu 16.04 LTS
6	Vagrant version	2.2.4
7	Node.js version	10.15.3
8	Virtual machine parameters	2 CPU cores 2.0 GB RAM Ubuntu 16.04 LTS
9	Provisioning software	Ansible
10	File exchange tools for the virtual machine	NFS–server + BindFS inside the virtual machine
11	Additional system software	– git – make – htop – iotop – rsync – node–gyp

TABLE. III. PARTIAL QUALITY CRITERIA ($k = 1, j = \overline{1, p}$)

Notation	Criterion	Unit
$r_1^{k,j}$	The microprocessor operating time spent on the initialization of the experiment	ms
$r_2^{k,j}$	The operating time of the microprocessor spent on the execution of system functions during the initialization of the experiment	ms
$r_3^{k,j}$	The increase in the Resident Set Size noted after the completion of the initialization of the experiment (including heap, code segment and stack)	byte
$r_4^{k,j}$	The increase in the heap size, marked upon completion of the initialization of the experiment	byte
$r_5^{k,j}$	The increase in the volume of the used heap, marked upon completion of the initialization of the experiment	byte
$r_6^{k,j}$	The increase in the amount of RAM used by C++ objects associated with JavaScript objects, marked after the experiment has been initialized	byte
$r_7^{k,j}$	The real time spent on the initialization of the experiment	ns
$r_8^{k,j}$	The microprocessor operating time spent on the experiment	ms
$r_9^{k,j}$	The microprocessor operating time spent on the execution of system functions during the experiment	ms
$r_{10}^{k,j}$	The increase in the Resident Set Size noted at the end of the experiment (including heap, code segment and stack)	byte
$r_{11}^{k,j}$	The increase in the heap size, marked at the end of the experiment	byte
$r_{12}^{k,j}$	The increase in the amount of the used heap noted at the end of the experiment	byte
$r_{13}^{k,j}$	The increase in the amount of RAM used by C ++ objects associated with JavaScript objects, marked upon completion of the experiment	byte
$r_{14}^{k,j}$	Real time spent on the experiment	ns

IV. EXPERIMENTAL METHODOLOGY

The automated methodology for selecting an effective set of software components involves the use of a genetic algorithm to generate and experimentally evaluate stacks of technologies (see Fig. 2).

The integration of the components of the stack is implemented using a functional approach, which is the most convenient way to combine various sets of software components. Each function which is being called during the experiment is a kind of software interface that is implemented using one of the stack components. Since components, as a rule, provide tools that go beyond a single function, they can be used to implement several functions. The use of a single component for performing a variety of tasks in the general case is preferable, since it reduces the amount of RAM needed by the IS.

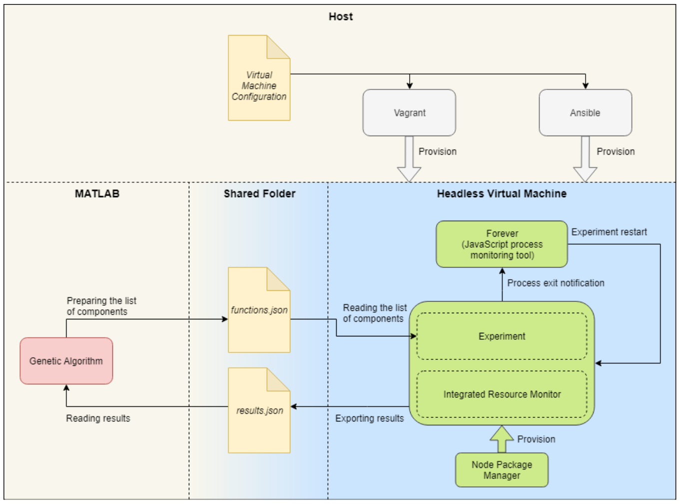

Fig. 2. Experimental Methodology.

At the initialization stage, the functions, which define the basic settings of the components, are called. Each of them forms a new anonymous function at the output, which has exclusive access to the component with the specified settings. Next, anonymous functions are placed in a single namespace with the names listed in Table III. To increase the reliability of the results obtained, the component cache (also known as Node.js module cache) is cleared before initialization.

After the initialization, the execution phase of the experimental algorithm begins. For research purposes, the following experimental algorithm is used:

1) Form the path to the directory with a set of subdirectories.

2) Read the list of subdirectories.

3) Exclude hidden subdirectories.

4) Form the path for each directory.

5) Do the followings for each path:

a) Read all the list of files recursively.

b) Read and load into the RAM all the files.

c) Create a Zip-archive in the RAM.

d) Calculate the MD5-hash for the created archive.

After the initialization procedure and the execution of the experimental algorithm are done, a json file results.json is generated. It contains the source data for the calculation of the integral criterion (1). This data is obtained through the interface of the "process" object of Node.js.

The genetic search configuration is specified in Table IV.

For the numerical representation of stacks, the encoding mapping is introduced as $C : S \to \Lambda \subseteq \mathrm{N}^n$. Thus, to each stack $s^j,\ j=\overline{1,p}$, which is called a phenotype, the natural set $\zeta^j = C(s^j),\ j=\overline{1,p}$, which is called a genotype, will correspond. The genetic algorithm treats genotypes as

$$\zeta_g^h = \left(\alpha_{1_g}^h \ldots \alpha_{n_g}^h\right), h=\overline{1,\left|\Theta_g\right|},$$

TABLE. IV. GENETIC SEARCH CONFIGURATION

Num.	**Parameter**	**Value**
1	MATLAB version	R2018a
2	Integer constraints	All the genes are integer-valued
3	Selection operator	Tournament selection [21]
4	Mutation operator	Extended power mutation [21]
5	Crossover operator	Laplace crossover [21]
6	Probability of mutation P_M	0.01
7	Probability of crossover P_K	0.8
8	Elite count	1
9	Population size	20
10	Max generations	100
11	Max stall generations	10
12	Function tolerance	0.01

where each $\alpha_{i_g}^h$ takes its values in the range from 1 to $\left|m_i\right|$, with respect to the sequence number of the selected alternative component from m_i ; Θ_g is a set of genotypes (population of individuals), which belong to the gth generation, $H = \left|\Theta_g\right|, H << p.$ The inverse mapping $C^{-1} : \Lambda \to S$ converts the genotype of a stack into its corresponding phenotype. Considering the above introduced notation, the initial problem (2) with the use of the genetic algorithm transforms into the following problem:

$$s_G^* = \underset{s_G^h, h=\overline{1,\left|\Theta_G\right|}}{\operatorname{argmin}} \Psi\left(\omega^k, s_G^h\right), \tag{3}$$

where G is the last population of individuals before the genetic algorithm stops.

Thereby, the algorithm of genetic search for the solution of problem (3) consists of the following steps:

1) Create the initial population: assign $g=1$; generate N random genotypes constituting the initial population $\Theta_1 = \{\zeta_1^1, \zeta_1^2, \ldots, \zeta_1^H\}$, get the corresponding choice of the software components $s_1^j = C^{-1}(\zeta_1^j)$ for each ζ_1^h , perform the computational experiment and calculate the value vector of the integral criterion (1) for each individual in the population $\mu = (\mu_1, \mu_2, \ldots, \mu_H)$, $\mu_i = \Psi(\omega^k, s_1^j,)$; set $\mu_{min} = \min_{j=\overline{1,H}} \mu_j$.

2) Start creating the next generation: assign $\kappa = 1$.

3) Select the first parent: assign $g = g+1$; using the specified selection method, choose $\zeta_g^{'\kappa}$ individual as the first parent.

4) Crossing-over: using the specified selection method, choose $\zeta_g^{''\kappa}$ individual as the second parent. With the probability P_K, cross over the parents $\zeta_g^{'\kappa}$ and $\zeta_g^{''\kappa}$ using the specified crossing-over operator. Mark the result (the child) as $\zeta_g^{'\kappa}$.

5) Mutation: with the probability P_M , act on the individual $\zeta_g^{'\kappa}$ with the specified mutation operator.

6) Create the next child: assign $\kappa = \kappa + 1$; if $\kappa = H$ then go to step 7, else go to step 3.

7) Select the elite individual: from the population Θ_g, the individual ζ_g^i with the lowest value of the quality criterion $\mu_i = \min_{j=\overline{1,H}} \mu_j$ is selected.

8) Complete creating next generation: create the population $\Theta_{g+1} = \{\zeta'^1_g, \zeta'^2_g, \ldots, \zeta'^H_g\}$ of individuals selected earlier; for each ζ'^κ_g get the corresponding choice of the software components $s'^j_g = C^{-1}(\zeta'^j_g)$, perform the computational experiment and compute the value vector of integral criterion (1) $\mu' = (\mu'_1, \mu'_2, \ldots, \mu'_H)$, $\mu'_i = \Psi(\omega^k, s'^j_g)$; set $\mu_{min} = \min_{j=\overline{1,H}} \mu_j$.

9) Stop condition check: if no termination condition is met then go to step 3, else issue the solution corresponding to the $\mu_{\min}$ as the answer and terminate the genetic search.

In the general case, plenty of methods including tournament selection, roulette wheel method, ranking method, uniform ranking, sigma – clipping, and modifications of these methods can be used as a selection operator. During the crossing-over process, a new individual is created by exchanging subsets of parameters between two parents. The mutation operator changes the genotype of an individual in a predetermined way.

However, when solving integer-constrained problems such as the one considered in this paper, the special set of genetic operators is used to produce the integer-valued genes. Those operators were described in detail in [20].

The algorithm can be stopped in the following cases: it reaches the limit number of generations, upon reaching the limit number of stall generations (the best fitness value among such consecutive generations does not change), when the change of the average fitness for a number of consecutive generations is less than the established threshold, at the request of the user, in other cases defined by the developer.

To implement the genetic algorithm in solving the problem (3) the ga library from the MATLAB Global Optimization Toolbox was used. The experiment was carried out on a virtual machine running Ubuntu 16.04 LTS, in which the Node.js 10.15.3 runtime was deployed. Creating a virtual machine is carried out using the Vagrant virtual development environment configuration tool. Ubuntu 16.04 LTS, in which the MATLAB R2018a system was installed, was also used as the Host operating system. It should be noted that the use of the virtual machine helps to ensure the reproducibility of the computational experiment, to avoid unrecorded changes in parameters, to reduce the influence of other random factors on the results of the experiment.

When the virtual machine starts, the reading of the functions.json is performed. That file is generated by the genetic search program. The functions.json file is a json representation of the framework configuration under study $s_i = C^{-1}(\zeta_i)$ which defines a set of alternative Node.js components for the experiment. The experiment consists of two main stages: the initialization of the components and the execution of the experimental algorithm with those components.

V. Results

As a result of the implementation of 11 generations of genetic search, the solution was found for the problem (3), corresponding to the value of the integral criterion of 0.242436. The average value of the integral criterion in the terminal generation was 0.284875. Genetic search took 71 seconds and ended when the specified threshold of convergence of the algorithm was reached (Function tolerance). Experimental measurements for the terminal generation of genetic search are presented in the Table V for the criteria $r_1^{k,j} ... r_6^{k,j} (k=1)$ and in the Table VI for the criteria $r_7 ... r_{10}^{k,j}, r_{12} ... r_{14}^{k,j}, \Psi(k=1)$. The r_{11} criterion is equal to zero for all the individuals in the terminal generation. The effective choice of components s_G^* is identified in the Table VII.

The graph of genetic search, reflecting the solution process for the problem of minimizing the integral quality criterion Ψ, is shown in the Fig. 3.

It should be noted that the slight "oscillation" in the genetic search graph was due to the unavoidable measurement noise caused by small variations of the real-time execution of the same process by the machine.

TABLE. V. Experimental Measurements for the Terminal Generation of the Genetic Search for the Criteria $r_1^{k,j} ... r_6^{k,j} (k=1)$

j	$r_1^{k,j}$	$r_2^{k,j}$	$r_3^{k,j}$	$r_4^{k,j}$	$r_5^{k,j}$	$r_6^{k,j}$
1	0.24	0	0.0754	0.6816	0.071	0.0873
2	0.24	0	0.0782	0.5243	0.0519	0.0672
3	0.28	0	0.1036	0.6291	0.0666	0.0807
4	0.2	0.4	0.1036	0.4719	0.055	0.0667
5	0.12	0.8	0.1032	0.5243	0.0565	0.0668
6	0.24	0	0.2392	0.6332	0.2689	0.1717
7	0.12	0.8	0.0766	0.5243	0.0584	0.0664
8	0.08	1.2	0.0782	0.5767	0.0564	0.0754
9	0.2	0.4	0.2388	0.6332	0.2689	0.1854
10	0.24	0	0.0766	0.6291	0.0586	0.0665
11	0.16	0.8	0.0774	0.5767	0.057	0.0674
12	0.2	0	0.1061	0.5767	0.0675	0.0892
13	0.16	0.4	0.1303	0.5243	0.0918	0.0754
14	0.16	0.8	0.1298	0.5243	0.0817	0.0667
15	0.16	1.2	0.2654	0.7381	0.3004	0.1714
16	0.2	0	0.0762	0.5243	0.0657	0.0748
17	0.24	0	0.1016	0.6291	0.0683	0.0829
18	0.2	0	0.1303	0.6291	0.0679	0.0748
19	0.2	0	0.1032	0.4719	0.0634	0.0745
20	0.2	0	0.1032	0.5243	0.0831	0.0668

Normalized, rounded to 4 decimal places, experimental measurements of the partial quality criteria in the terminal generation of genetic search. The measurements corresponding to the effective solution are **highlighted**

TABLE. VI. EXPERIMENTAL MEASUREMENTS FOR THE TERMINAL GENERATION OF THE GENETIC SEARCH FOR THE CRITERIA $r_7 ... r_{10}{}^{k,j}, r_{12} ... r_{14}{}^{k,j}, \Psi(k=1)$

j	$r_7^{k,j}$	$r_8^{k,j}$	$r_9^{k,j}$	$r_{10}^{k,j}$	$r_{12}^{k,j}$	$r_{13}^{k,j}$	$r_{14}^{k,j}$	Ψ
1	0.4283	0	0.4	0.2621	0.1709	0.96	0.4549	0.2682
2	0.5067	0.4	0	0.2376	0.1678	0.96	0.457	0.2583
3	0.4705	0.4	0	0	0.1726	0.96	0.4222	0.251
4	0.4299	0.8	0	0	0.1699	0.96	0.6203	0.3034
5	0.5538	0	0	0	0.1699	0.96	0.4606	0.2751
6	0.4578	0	0.4	0	0.162	0.96	0.4051	0.2757
7	0.4251	0.4	0	0.2376	0.1675	0.96	0.4323	0.3068
8	0.5054	0.4	0	0	0.1673	0.96	0.4534	0.3307
9	0.4913	0.4	0	0.2335	0.1599	0.96	0.4067	0.3244
10	0.3863	0.4	0	0.2417	0.4296	0.96	0.4274	0.2741
11	0.5028	0.4	0	0.2335	0.1696	0.96	0.4512	0.3199
12	0.4072	0.4	0	0.2294	0.1696	0.96	0.44	0.2552
13	0.4091	0.4	0	0	0.1703	0.96	0.4133	0.2654
14	0.5337	0.4	0	0	0.1711	0.96	0.469	0.3087
15	0.4411	0	0.4	0.2458	0.1596	0.96	0.4016	0.393
16	0.4049	0.4	0	0.2376	0.1728	0.96	0.4222	0.2477
17	0.4867	0.4	0	0.512	0.4318	0.96	0.4596	0.306
18	0.4159	0	0.4	0	0.1701	0.96	0.4152	0.2424
19	0.3574	0.4	0	0.2376	0.1742	0.96	0.482	0.2467
20	0.5173	0.4	0	0	0.1671	0.96	0.4737	0.2447

Normalized, rounded to 4 decimal places, experimental measurements of the partial quality criteria in the terminal generation of genetic search. The measurements corresponding to the effective solution are highlighted

However, as the genetic search proceeds, the genotype of the best choice begins to predominate from generation to generation (this can be seen as decreasing average value of Ψ) and the best choice is identified as the number of experiments attributable to the best genotype increases, which eliminates random factors in the assessment of this genotype.

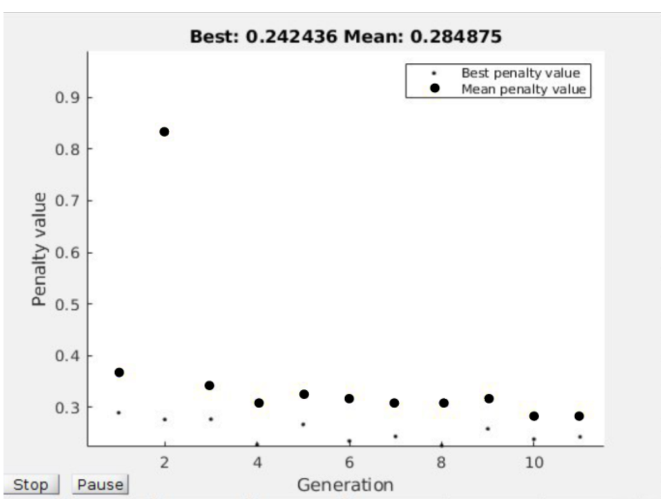

Fig. 3. Graph of Genetic Search. Penalty Value is Equal to the Ψ for the Specific Stack being Assessed in the Experiment. Best Penalty Value is the Minimal Ψ in the Generation. Mean Penalty Value is the Average Ψ in the Generation.

TABLE. VII. THE EFFECTIVE CHOICE OF COMPONENTS s_G^*

Genotype	Phenotype	
	Functional feature	**Component**
[2 3 2 1 1 1 2 2 1 1]	Filter	Underscore
	Map	Underscore
	First	Underscore
	PathResolve	JavaScript language tools
	StringReplace	JavaScript language tools
	ZipCompress	Adm–zip
	HashMD5	Md5
	FsRead	JavaScript language tools
	FsReaddir	Fs–extra
	FsReaddirRecursive	Recursive–readdir

VI. DISCUSSION

In the process of the development of the digital economy, the majority of data collection and exchange services are implemented using digital platforms and web portals. Those service range from public and municipal services and banking platforms to home control systems for household appliances. An important task of such systems development is to ensure effective interaction of components within the software system. Modern component-oriented development environments and interaction technologies provide a set of development tools, significant in number and approximately the same in functionality. Alternative technologies can bring different values of performance indicators depending on the functional features of the software system.

The paper deals with the framework architectural approach to the construction of software systems. A framework is a common form of template software structure that allows the developer to unify the software development process by combining the permanent piece of software (the framework) that does not change from configuration to configuration, and some plug-in components that are compatible with the permanent part. A component is a piece of software that has a specific interface and explicit context dependencies. Thus, the software system is created by selecting the appropriate components for the corresponding framework, while it is possible to use alternative sets of components that have a similar interface to implement similar functionality.

When there is a choice from a variety of components, the task of quality assessment is particularly important for the development and operation of software systems in the given conditions. The results of numerical evaluation of different variants of program interaction can be the basis for the formalization and finding the solution of the problem of choosing an effective set from a variety of alternatives.

In accordance with ISO/IEC 25041:2014, measurement procedure should be able to provide measurement to the quality characteristics of software. It should ensure that the measurements are made with the sufficient accuracy to determine the criteria and make the necessary comparisons. In the developed method, the physical execution time of the invariant algorithm of the experiment are measured with an accuracy of 10–9 seconds, the measurements of the amount of memory occupied are carried out with an accuracy of 1 Byte, the measurement of processor time spent on the execution of the experimental algorithm are carried out with an accuracy of 10^{-6} sec.

VII. CONCLUSIONS

A methodology of effective selection of software components based on experimental estimates of the criteria and the genetic algorithm was created. The methodology was experimentally approved in the task of effective selection of Node.js components to implement a specific set of functional features in accordance with the specified quality criteria. The configuration and parameters of the experimental stand as well as the parameters of the genetic algorithm were presented in the paper. The integral quality criterion was formulated, which allows to consider the contribution of a set of 14 experimentally evaluated partial quality criteria to the overall assessment of the effectiveness of the choice of software components. Experimental estimates of the quality criteria for the terminal generation of genetic search were also given in the paper. The effective selection of the software components was identified.

Future work will be aimed at evaluating the relative importance and the mutual influence of the partial quality criteria to reduce the dimension of the criteria space as well as considering some security criteria when choosing the set of software components.

REFERENCES

[1] Lun L., X. Chi and H. Xu, “Coverage criteria for component path-oriented in software architecture”, Engineering Letters, vol. 27, no. 1, pp. 40-52, 2019.

[2] S. Gerasimou, R. Calinescu and G. Tamburrelli, “Synthesis of probabilistic models for quality-of-service software engineering”, Automated Software Engineering, vol. 25, issue 4, pp. 785-831, 2018.

[3] A., Gizas S. Christodoulou and T. Papatheodorou, “Comparative evaluation of javascript frameworks,” In WWW’12 Companion Proceedings of the 21st International Conference on World Wide Web, 2012, pp. 513-514.

[4] J. Ferreira, “A javascript framework comparison based on benchmarking software metrics and environment configuration,” Masters dissertation, DIT, 2018. [Online]. Available: https://arrow.dit.ie/cgi/viewcontent.cgi?article=1142&context=scschcomdis.

[5] P. Kolyasnikov, E. Nikulchev, I. Silakov, D. Ilin and A. Gusev, “Experimental evaluation of the virtual environment efficiency for distributed software development,” International Journal of Advanced Computer Science and Applications, vol. 10, no. 5, pp. 309-316, 2019.

[6] B. M. Basok, V. N. Zakharov and S. L. Frenkel, “Iterative approach to increasing quality of programs testing,” Russian Technological Journal, vol. 5, no. 4, pp. 43-12, 2017.

[7] L. D. Chambers, “Practical handbook of genetic algorithms: Complex coding systems”. CRC press, 2001.

[8] S. Bilgaiyan, K. Aditya, S. Mishra and M. Das, “Chaos-based modified morphological genetic algorithm for software development cost estimation,” in Advances in Intelligent Systems and Computing, vol. 710, pp. 31-40, 2010.

[9] L. R. Still and L. S. Indrusiak, “Memory-Aware genetic algorithms for task mapping on hard real-time networks-on-chip,” in 2018 26th Euromicro International Conference on Parallel, Distributed and Network-based Processing (PDP), Cambridge, 2018, pp. 601-608.

[10] L. Liu, M. Zhang, R. Buyya and Q. Fan, “Deadline constrained coevolutionary genetic algorithm for scientific workflow scheduling in cloud computing,” Concurrency and Computation: Practice and Experience, vol. 29, no. 5, p. e3942, 2017.

[11] D. B. Mishra, R. Mishra, A. A. Acharya and K .N. Das, “Test data generation for mutation testing using genetic algorithm,” in Advances in Intelligent Systems and Computing, vol 817, pp. 857-867, 2019.

[12] R. Jain and A. Sharma, ‘Assessing software reliability using genetic algorithms,’ The Journal of Engineering Research, vol. 16, no. 1, pp. 11-17, 2019.

[13] A. C. Kumari, K. Srinivas and M. P. Gupta, “Software module clustering using a hyper–heuristic based multi–objective genetic algorithm,” in 2013 3rd IEEE International Advance Computing Conference (IACC), Ghaziabad, 2013, pp. 813-818.

[14] H. Ahuja, Sujata, U. Batra, “Performance Enhancement in Requirement Prioritization by Using Least-Squares-Based Random Genetic Algorithm,” in Studies in Computational Intelligence, vol. 713, pp. 251-263, 2017.

[15] A. Ouni, M. Kessentini, H. Sahraoui and M. S. Hamdi, “The use of development history in software refactoring using a multi–objective evolutionary algorithm,” in 15th annual conference on Genetic and evolutionary computation (GECCO '13), 2013, pp. 1461-1468.

[16] S. Kaiafa and A. P. Chassiakos, “A genetic algorithm for optimal resource-driven project scheduling,” Procedia Engineering, vol. 123, pp. 260-267, 2015.

[17] W. Almadhoun and M. Hamdan, “Optimizing the Self-Organizing Team Size Using a Genetic Algorithm in Agile Practices,” Journal of Intelligent Systems, 2018. Available: https://doi.org/10.1515/jisys-2018-0085.

[18] P. Devarasetty and S. Reddy, “Genetic algorithm for quality of service based resource allocation in cloud computing,” in Evolutionary Intelligence, pp. 1-7, 2019. Available: https://doi.org/10.1007/s12065-019-00233-6.

[19] C. Jatoth, G. R. Gangadharan, U. Fiore and R. Buyya, “QoS-aware Big service composition using MapReduce based evolutionary algorithm with guided mutation,” Future Generation Computer Systems, vol. 86, pp. 1008-1018, 2018.

[20] C. Jatoth, G. R. Gangadharan and R. Buyya, “Optimal Fitness Aware Cloud Service Composition using an Adaptive Genotypes Evolution based Genetic Algorithm,”, Future Generation Computer Systems, vol. 94, pp. 185-198, 2019.

[21] K. Deep, K. P. Singh, M. L. Kansal and C. Mohan, “A real coded genetic algorithm for solving integer and mixed integer optimization problems,” Applied Mathematics and Computation, vol. 212, no. 2, 505-518, 2009.

Resonance Mitigation and Performance Improvement in Distributed Generation based LCL Filtered Grid Connected Inverters

Danish Khan[1], Muhammad Mansoor Khan[2], Yaqoob Ali[3], Abdar Ali[4], Imad Hussain[5]
Department of Electrical Engineering
School of Electronic Information and Electrical Engineering
Shanghai Jaio Tong University
Shanghai, China

***Abstract*—Resonance turns into a growing issue of paramount importance for stable operation of LCL filtered grid-connected inverters. Active damping algorithms are widely adopted to restrain the resonance peak associated with LCL filters. The focus of this paper is to develop an improved active damping solution based on filter capacitor current for better control performance of three-phase LCL grid-connected inverters. In the proposed solution, an improved compensator is included across the LCL filter system and capacitor current feedback. A damping loop is implemented with the proposed combination, which is further feedback at a reference voltage point of the three-phase inverter to damp the aroused resonance peak. The substantial features of the proposed configuration are wide damping range of resonance frequency and high control bandwidth, which results in faster dynamic response in comparison with conventional capacitor current proportionally feedback. Moreover, the stability of current loop is examined in detail by implementing the proposed damping method under the filter parametric variations. Finally, the efficacy of the proposed method is validated by illustrating the outcomes based on steady state and transient responses through simulations and experimental results of the laboratory prototype.**

***Keywords*—LCL filter; high pass filter; grid connected inverters (GCI); stability analysis; robustness; SPWM technique; D-space**

I. Background

In recent years, growing concerns associated with climate change and increase in energy demand require new opportunities in the power sector[1]. Power quality issues along with stability issues of distribution Systems are becoming more significant with massive penetrations of Renewable Energy Resources. To build sustainable power systems for providing clean and renewable energy, low voltage power distribution system are frequently integrated with distributed generation units including wind power, photovoltaic power, and battery storage systems[2]. The mandatory and controlled active and reactive powers are injected through interfacing inverters known as pulse width modulated voltage source inverters [3].

Grid connected inverters have a considerable role in injecting power with high quality into power grids and utilized as an interface among the grid and renewable energy resource[4]. A filter is required to inject high quality power and to reduce high frequency harmonics produced due to pulse width modulation. The filter can be formed as either one inductor or two inductors with one capacitor LCL[5]. Among several available filters, LCL filter have drawn more attention due to enhance capability of current harmonics attenuation with lower value of inductance as compared to L and LC filters[6]. Furthermore, the grid side inductor in LCL filter limit the inrush current of capacitor and increase the robustness of inverter under grid impedance variation[5]. However, the presence of resonance phenomenon in LCL filter creates stability issues in control structure of the converter. The stability concern is raised due to high current gain produced by zero impedance at particular frequency that is called resonance frequency[7]. To prevent the instability issues in power grids produced by resonance effect, an appropriate damping approach is essential[8].

In general, for LCL filtered grid connected inverters, resonance suppression is achieved by employing active and passive damping approaches[9]. Passive damping approach is implemented by adding a passive component like inductor, resistor or both with the filter component. However, more power losses and reduced filter capability to suppress harmonics are the significant barriers of this approach[10]. Active damping approach has no damping losses by altering the control structure of an inverter [11]. However, the filter parameters variation and grid impedance may influenced the damping effectiveness of damping loop[12].

II. Introduction

Active damping can be implemented in different ways based on number of control loops to effectually handle the aforementioned problems. In active damping methods, depending on single control loop, damping of filter resonance is obtained without any further measurements[13]. Methods based on such approach are sensor less methods, grid current feedback and notched-filter based methods[13][14][15]. Generally, these methods have minimum robustness during parameter uncertainty and weak grid conditions[16].

In multi-loop active damping methods, additional measures are needed[9]. Filter capacitor voltage, capacitor current feedback and weighted average current control methods are associated with multi-loop active damping methods[17][18][19]. The robustness of these methods tends to be improved for filter parameter, and grid inductance variation is compared with single loop techniques.

Capacitor current feedback technique is mainly adopted in the literature due its simple operation, higher current quality, and damping effectiveness. The method is implemented with capacitor current is feedback through a coefficient for improved dynamics[20]. Furthermore, the stability features for this method are enhanced and the region of damping is extended by presenting a high pass filter and band pass filter in current control loop along with capacitor current[21][22]. These methods show reasonable effect of resonance damping; however, bandwidth is limited in case of grid impedance variation.

The focus of this paper is to introduce an alternative capacitor current method, which modify the damping loop with simple compensator adjustments in transfer function for capacitor current feedback damping method. The resonance peak is damped by further applying the capacitor feedback current across the LCL filter at a reference voltage. A modified controlled structure is demonstrated to improve the aforementioned issues. The proposed method presents better control performance of the system along with improvements in effective harmonic compensation region and control bandwidth of the system in comparison with the capacitor current active damping approaches method. Better robustness and faster dynamic response of the system even under week grid condition are substantial benefits of the proposed configuration.

The remainder of the paper is arranged as follows: Sections III explains the design of a typical three-phase system. Theoretical study of control and design of proposed compensator are presented in Section IV. Damping and comparative study analysis is examined in Section V. The simulation and prototype outcomes are illustrated in Section VI. Concluding comments are designated in Section VII.

III. System Description and Design Parameters

A three-phase grid connected inverter system is presented in Fig. 1 and design parameters of the system are described in Table I. The inverter system is comprised of four main parts including conversion unit, power grid, filter unit, and inverter control. The assumed Constant DC-link bus voltage is supplied at the input of three-phase voltage source inverter, which is connected with the grid through LCL filter. The filter contains inverter side inductor L_i, grid side inductor L_g and filter capacitor C_f. The filter capacitors are connected in delta. The resonance frequency of the LCL filter is given in equation (1).

$$f_{res} = \frac{1}{2\pi}\sqrt{\frac{L_i + L_g}{L_i L_g C_f}} \tag{1}$$

Control structure is employed to ensure the significant objectives, which includes high quality of injected current without resonance component and unity power factor. The control structure contains current control loop and inner damping loop that ensures good steady-state and transient performance of the system. The current control loop is implemented by measuring the grid current I_g, which is transferred into stationary reference frame by using the abc–αβ module and compared with the reference grid current I^*_g. The reference grid current I^*_g is obtained by measuring the angle of voltage at common coupling point v_{pcc} using phase lock loop (PLL). Proportional Resonant (PR) controller G_{pr} is used to regulate the error signal. The output of G_{pr} controller produces a reference value for the inner damping loop.

The inner damping loop is implemented by measuring the filter capacitor current I_c, which is transferred into stationary reference frame by using the abc–αβ module and compared with the reference current I^*_c. The reference capacitor current is achieved when the output of proportional P controller is feedback through a compensator in order to damp the resonance peak. This configuration is known as parallel feed-forward compensation. Furthermore, the output of inner damping loop is transferred into sinusoidal signal by using αβ–abc module in order to produce a modulating signal for the inverter.

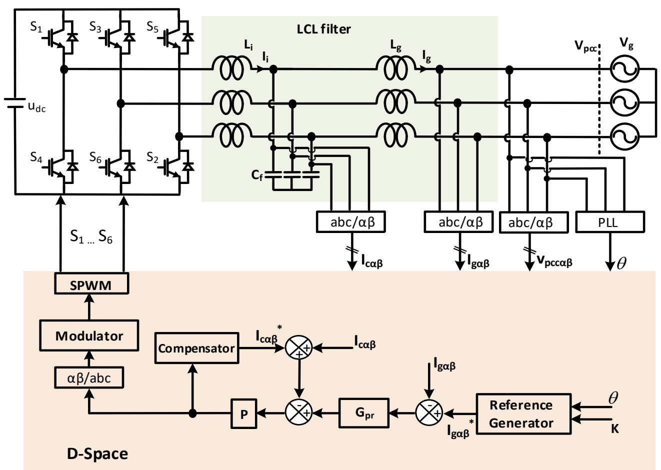

Fig. 1. Three-Phase LCL Filtered Grid Connected Voltage Source Inverter with Proposed Damping Loop.

TABLE. I. Grid Parameters

Parameter	*Symbol*	*Value*
Grid voltage	V_g	400V
DC-Bus voltage	V_{dc}	800V
Inverter-side inductor	L_i	3.6mH
Grid side inductor	L_g	1mH
Filter capacitor	C_f	4.7uF
Line frequency	f_l	50Hz
Sampling freq.	f_s	10kHz
Switching freq.	f_{sw}	10kHz
Resonance freq.	f_{res}	2.6kHz

IV. Control Loops Design

The linearized "Average Switching Model (ASM)" related to control structure of an inverter is given in Fig. 2 to design the current control loop and inner damping loop. In this model, the inverter switches are represented by its average value using a function over each carrier interval [23].

A. Proposed Damping Loop Design

The capacitor current feedback method used for active damping is initially proposed by Twining and Holmes[10]. In this method, the capacitor current is feedback through a coefficient H(s) with the output of current controller, which provides an additional damping in the closed loop.

In this paper, an alternative intuitive method is used to construct the damping loop known as Parallel Feed-forward Compensation (PFC). According to this technique, the damping compensator in feedback loop is visualized as a linear compensator across the plant to improve the stability characteristics, and the augmented plant output is feedback at the current controller output [24][25][26]. The considered plant in this case is LCL filter between inverter output voltage and capacitor current and transfer function K(s) is added as a compensator is illustrated in Fig. 2(b). From stability point of view the diagram shown in Fig. 2(b) is similar to Fig. 2(c) where the damping loop is applied separately by visualizing the controller of Fig. 2(b) in two sections as shown in Fig. 2(c). The basic idea is to increase the output impedance of the grid-connected inverter at higher frequencies, thus further enhancing the suppression capability.

The compensator K(S) can have different expressions. Here a first order high pass filter is used as compensator, because it provides adequate damping to oscillations and show robust response against grid inductance variation with good transient response[21]. The transfer function of high pass filter is given in equation (2).

$$K(s) = \frac{sk_{rc}(s)}{s+\omega_{rc}} \tag{2}$$

Where, k_{rc} and ω_{rc} represent gain and cut-off-frequencies respectively. Intuitively speaking, the high pass filter in feed-forward can be visualized as a resister and capacitor in parallel with the filter capacitor. With this alternative, the current through the filter capacitor i_c is multiplied by a gain k_{rc} to emulate the effect of a resistor in series with the filter capacitor. The cut off frequency ω_{rc} compensates the phase lag around the resonance frequency. At certain values of high pass filter parameters this configuration ensures a large stability margin, which is needed for accounting grid impedance variations. However, the high value of ω_{rc} may also shift the gain crossover frequency over a wide range, leading into instability. Therefore, it is very important to select proper values of k_{rc} and ω_{rc} to avoide instability. The compensator paramter are selected anaylitically from the stability plots as provided in Section IV.

For evaluating robustness and dynamic response subject to wider grid inductance variations, two transfer functions of the "plant" are necessary and derived accordingly. A linearized average switching model in 'S' domain of the proposed methodology is developed as shown in Fig. 3(a). Referring to Fig. 3(a), the transfer functions from the inverter output voltage $v_{inv}(s)$ to the grid current $I_g(s)$ and the capacitor current I_c (s) can be derived as follows:

$$G_{ig}(s) = \frac{I_g(s)}{V_{inv}(s)} = \frac{1}{L_i L_g C} \cdot \frac{1}{s^2+\omega_{res}^2} \tag{3}$$

$$G_{ic}(s) = \frac{I_c(s)}{V_{inv}(s)} = \frac{1}{L_i} \cdot \frac{s^2}{s^2+\omega_{res}^2} \tag{4}$$

From Fig. 3(a), the open damping loop with the proposed scheme can be calculated as

$$I_c(s) = \frac{PQ(s)}{1+P(K(s)+Q(s))} I_c^* \tag{5}$$

Where the Q(s)=F(s).R(s)

$$F(s) = \frac{G_{inv}}{L_i Cs^2+1}, R(s) = \frac{L_i Cs^2+1}{CL_i L_g s^3 + (L_i+L_g)s}$$

B. Current Control Loop Design

The control parameters are sinusoidal; therefore, PR controller is used.The PR controller removes the steady state error and results in low-settling and rise time around the line frequency. Moreover, it is easer to implement and requires less work for signal processing. Equation (6) shows transfer function of an ideal PR controller.

$$G_{PR} = K_p + \frac{2K_r s}{s^2+\omega_l^2} \quad (\omega_l = 2\pi f_l) \tag{6}$$

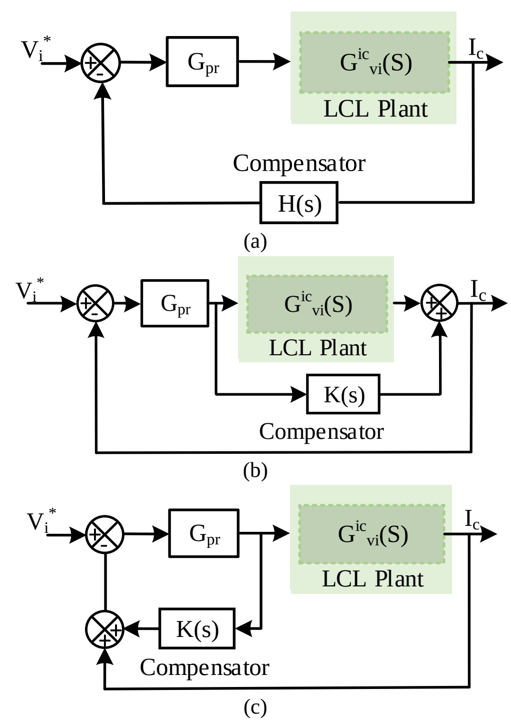

Fig. 2. Active Damping with (a) Proportional CCF Method (b) Parallel Feed-forward Configuration (c) Equivalent Control.

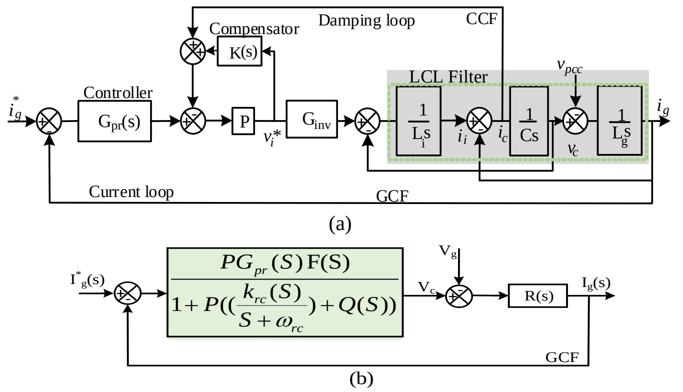

Fig. 3. (a) ASM Model of Proposed Method (b) Simplified Control Diagram.

Where ω_l, K_p and K_r are resonant frequency, proportional gain and resonant gain, respectively. Quasi-PR (Q-PR) controller is an developed form of PR controller, which is implemented because of better harmonics attenuation capability along with less severity to resonance frequency. Q-PR controller transfer function is shown in equation (7), where the variation in fundamental frequency is compensated with the bandwidth of resonant term ω_{PR}

$$G_{PR} = K_p + \frac{2K_r\omega_{PR}s}{s^2 + 2\omega_{PR}s + \omega_l^2} \tag{7}$$

Using Mason's rule, the average switching model model shown in Fig. 3(a) is simplified to Fig. 3(b) and injected grid current I_g is calculated. This current is equal to the sum of injected current by voltage V_g and reference grid current I^*_g given in equations (8).

$$\left.\begin{aligned} I_g(s) &= \frac{PG_{pr}(s).\mathrm{Q}(s)}{1+P[\mathrm{K}(s)+Q(s)(1+G_{pr})]}I_g^*(s) - \\ &\frac{\mathrm{R}(s).[1+P(\mathrm{K}(s)+Q(s))]}{1+P[\mathrm{K}(s)+Q(s)(1+G_{pr})]}v_g(s) \end{aligned}\right\} \tag{8}$$

Equations (5) and (8) show that the damping attributes of miserable or non -minimum phase system can be enhanced with suitable values of k_{rc} and ω_{rc}, which is discussed in this paper.

V. Design and Comparative Study

This section presents significant aspect of compensator parameter limits and comparative study of suggested method with conventional capacitor current feedback method. Furthermore, the stability performance of current control loop is analyzed with filter parameter variation. The design parameters are given in Table I.

A. Compensator Parameters Limits

The effects of gain and cut-off frequencies of high pass filter are illustrated in Fig. 4, where three scenarios are considered, in the 1st case, the value of ω_{rc} is considered smaller than ω_s (angular sampling frequency), while in the 2nd and 3rd case, the value is much higher than ω_s. To achieve similar magnitude in db and damping performance for all the cases, the damping k_{rc} need to be much higher for larger ω_{rc} and hence larger phase lag around the resonance frequency as shown in Fig. 4(b) and Fig. 4(c). For an acceptable system the gain and phase margin should be higher than 5db and 30 degree respectively. However, when the value of ω_{rc} increased, phase margin decreases dramatically below 30 degree as shown in Fig. 4(b) and Fig. 4(c). Therefore, to retain the system in acceptable margin a compromised range for the value of ω_{rc} might be $0.2\omega s<\omega rc<0.5\omega s$, where the upper limit shows the Nyquist frequency that should not be exceeded because of noise amplification of high pass filter in noisy environment.

B. Frequency Response

The frequency response of proposed method is compared with conventional capacitor current feedback method as shown in Fig. 5. From the figure, it can be observed that in each case the resonance peak is damped effectively because the gain margin is very close to each other. The gain margin curve also shows much higher bandwidth for proposed technique, which ensures faster dynamic response for the suggested method. Moreover, the higher phase margin of proposed technique results in better delay response of the system. The phase margin curve also indicates high compensation capability of delay for proposed method with high control bandwidth. The values for the proposed scheme are derived through methods used in[12][21][27][28][29]. Moreover, the values used for conventional capacitor current feedback are those which offer best performance for this technique.

In Fig. 5(b) the frequency response of proposed and conventional CCF methods are compared for resonance frequency less than $f_s/6$. The filter capacitance C value is increased from its nominal value of 4.7μF to 22.5μF to shift the resonance below $f_s/6$. From the figure it can be observed that the conventional capacitor current feedback method fail to damp the aroused resonance peak and the system is unstable. However, the proposed method damps the resonance peak with high phase margin. The proposed method maintains the stability of the system with wide range of resonance frequency.

C. Robustness Evaluation

The stability performance of current control loop is analyzed with filter parameter variation in Fig. 6(a), (b) and (c). When the inverter side inductor L_i varies 50% above and below its nominal value, the system remains stable as shown in Fig. 6(a). In this case, the open loop is stable and the phase margin is above 50 degree and the gain margin is above 5db. The system robustness and dynamic response reduces slightly for the lower value of L_i but remain in acceptable margin. On the other side, for high value of L_i, the dynamic response is still higher and gain margin remain in acceptable region. Similar changes in grid side inductor L_g are considered, which results in higher deviation in resonance frequency even the resonance frequency fall below 1/6th of the sampling frequency f_s as shown in Fig. 6(b). However, it shows greater phase margin and almost similar robustness as compared with variation in L_i. The current control loop is stable in both the cases. In Fig. 6(c), stability characteristics are observed under variation in filter capacitor; the overall result shows better phase margin with acceptable gain margin. The results shown in these graphs illustrate that proposed method is more robust to variation in resonance frequencies and can damp wide range of resonance frequencies with high phase margin.

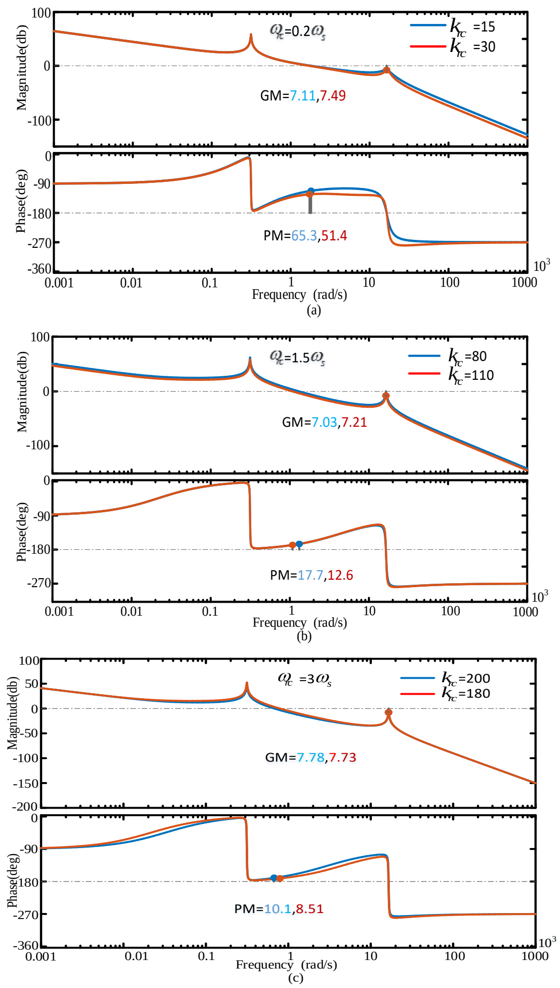

Fig. 4. Effect of (a) Low and (b and c) High Cutoff Frequencies Around LCL Resonance Frequency.

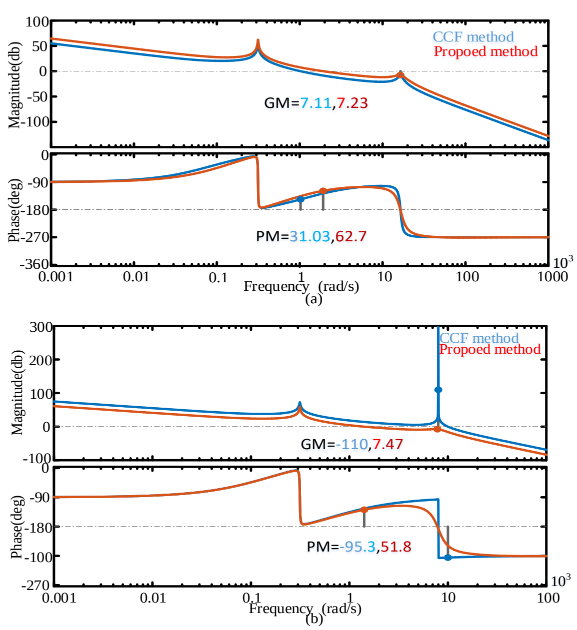

Fig. 5. Comparison of Proposed Method with Conventional CCF, and AD with PFC using Coefficient Gain.

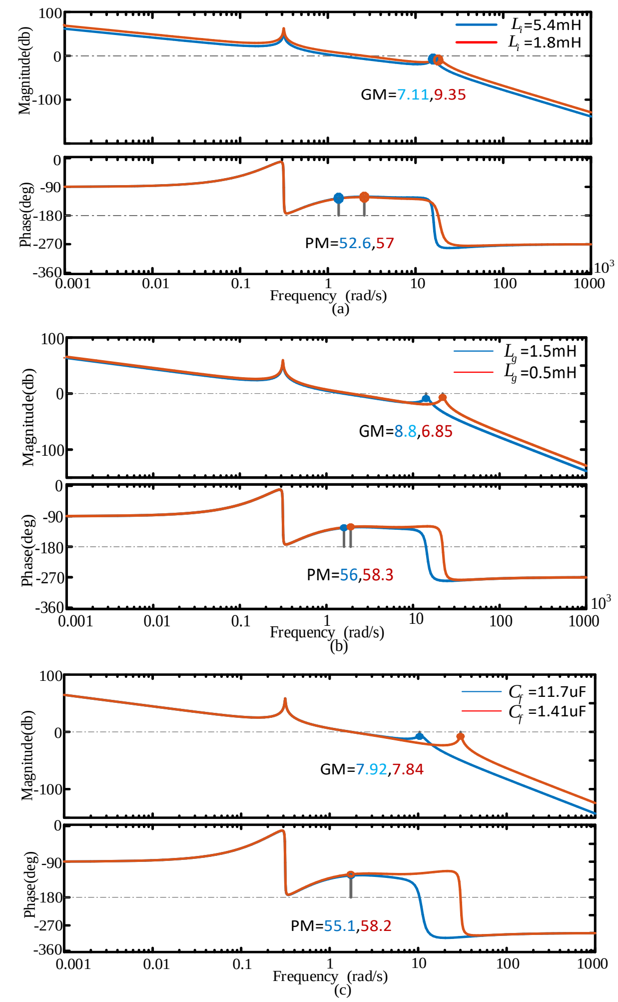

Fig. 6. Bode Plot under Filter Parameter Variation (a) Li+50%,-50% (b) Lg+50%, -50% (c) C+150%,-70%.

VI. Simulation and Experiment Results

To verify the effectiveness of proposed technique, a model of three-phase Grid-connected LCL filter is developed in MATLAB/Simulink environment. SPWM technique is used for gate signal generation. The design parameters of the system are described in Table I.

The steady-state injected current I_g and voltage V_{pcc} in phase A are shown in Fig. 7(a), Fig. 8(a) and Fig. 9(a) verifying the unity power factor operation. However, without the implementation of damping loop, the overall THD is 24.78% of the fundamental frequency where the contribution of resonance frequency region is highest as shown in Fig. 7(b).When conventional capacitor current feedback and proposed damping loop are applied, the overall THD is reduced to 6.39% and 3.28% respectively for the injected current, and the resonance peak is damped effectively as shown in Fig. 8(b) and Fig. 9(b). When damping is applied, half of the switching frequency region shows major contribution in the THD. However, with the proposed damping method the percentage is less than 5%, which is acceptable because the grid standards allow THD of less than 5% of fundamental frequency for stable operation.

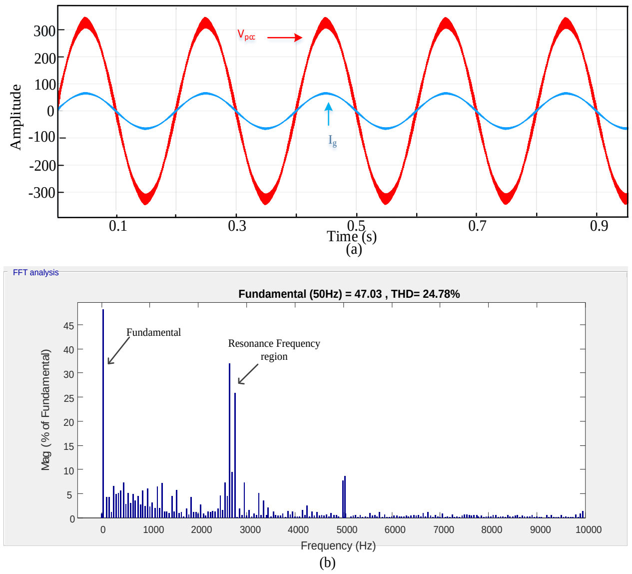

Fig. 7. Current Control Loop Response when no Damping Loop is Employed(a) I_g and v_{pcc}in Phase-A (b) Harmonic Spectrum of $I_g$in Phase-A.

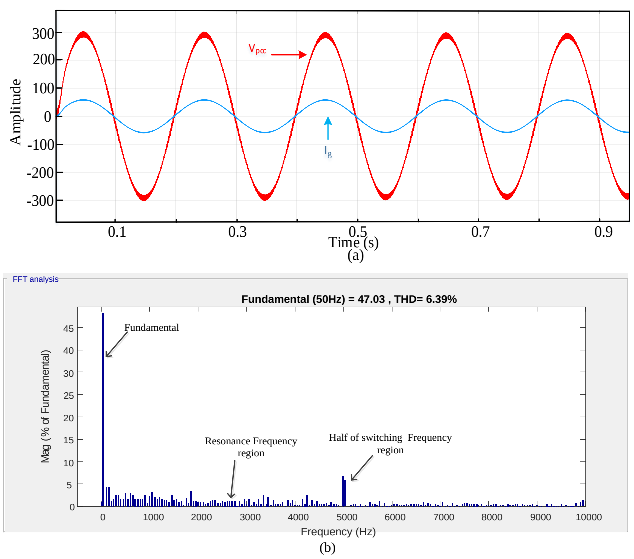

Fig. 8. Current Control Loop Response when CCF Damping Loop is Employed(a) I_g and v_{pcc}in Phase-A (b) Harmonic Spectrum of $I_g$in Phase-A.

To illustrate the effect of resonance frequency shift, the filter capacitance C value is increased from its nominal value of 4.7µF to 22.5µF. The stability and robustness of the system is examined for the resonance frequency of 1.2 kHz and ω_{rc}=0.2ω_s as shown in Fig 10. The system does not exhibit inherent damping because in this case the resonance frequency is lower than f_s/6. The figure illustrates that the conventional capacitor current feedback method fails to remove the resonance harmonics from the injected grid current and results in high THD and unstable system as shown in Fig. 10(a). However, with the proposed method the injected grid current tracks the reference current and also attenuate the resonance harmonics is shown in Fig. 10(b).

Fig. 11 verifies the better transient response of the system, when 50% reduction occurs in the reference load current, the measured current tracks the reference load current accurately. The resultant overshoot is between 7-8%, which is acceptable overshoot value, therefore, confirms the better transient response of the system.

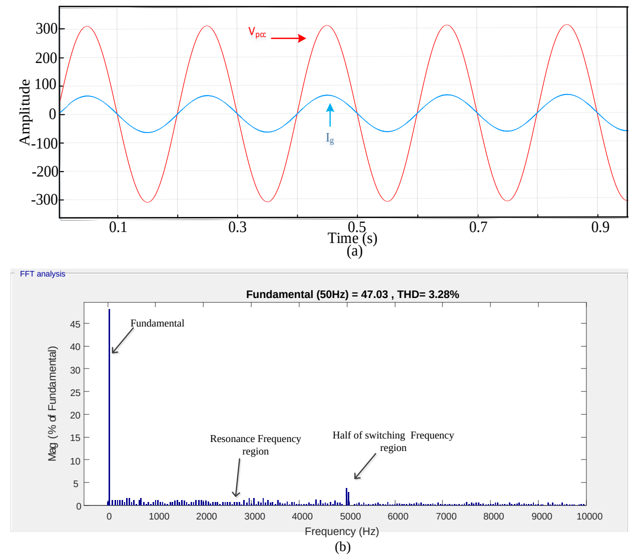

Fig. 9. Current Control Loop Response with Proposed Damping Loop (a) I_g and v_{pcc}in Phase-A (b) Harmonic Spectrum of $I_g$in Phase-A.

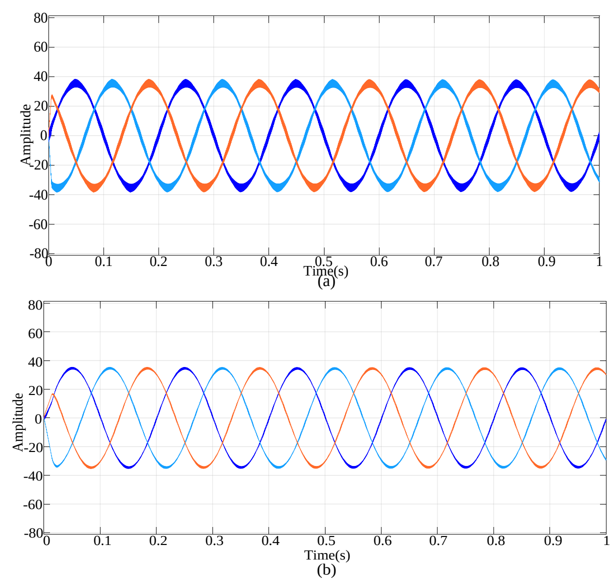

Fig. 10. Three Phase Injected Current behavior for Resonance Frequency Less than fs/6 (a) Conventional CCF (b) Proposed Method.

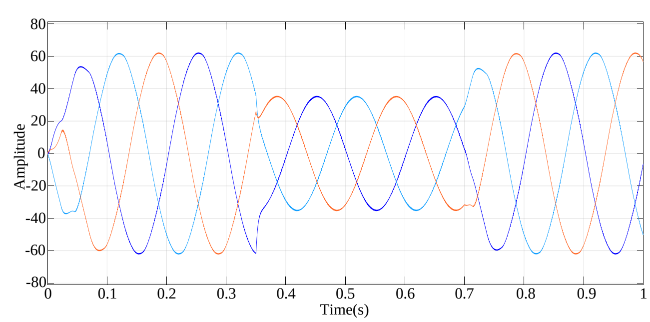

Fig. 11. Transient Response with Proposed Damping of Current Control Loop after Change in Reference Current.

A. Hardware Setup

A 1 kW experimental setup of inverter is used to evaluate the control dynamic response and harmonic attenuation capability of the proposed method. The experimental test bench consists of an inverter with constant DC power source and LCL filter connected with grid is shown in Fig. 12. The overall control strategy, presented in Fig. 1, including the proposed resonance damping is implemented on D-Space DS1006 control board based on parameter shown in Table I.

Different performances are observed for damping strategy in the presence of grid voltage harmonics. The control board link the inverter and MATLAB simulated model for real-time operation. The control board or PWM board generates sinusoidal plus-width modulation signal for the switching devices (IGBTs) of the inverter with the accomplishment of PR controller in synchronous reference frame. The sample or sensor board is used for the measurement of DC bus voltage, three-phase injected grid currents and voltages at common coupling point. The transferred power to grid is 1kW via three-phase inverter with 10 kHz switching frequency.

The steady-state response of the current loop is shown in Fig. 13(a), Fig. 14(a), Fig. 15(a). However, without the implementation of damping method, the overall THD is 16.31% of the fundamental frequency where the influence of resonance frequency region is the highest as shown in Fig. 13(b). When conventional capacitor current feedback and proposed damping loop are applied the overall THD is reduced to 5.512% and 2.91% respectively for the injected current, and the resonance peak is damped effectively as shown in Fig. 14(b) and Fig. 15(b). The three-phase grid injected currents with the proposed damping loop are shown in Fig. 16.

The conventional capacitor current feedback method fails to maintain the stability of the system at low resonance frequencies but with the proposed method the region can be enhanced. In this section, the system response is examined under resonance frequency less than 1/6th of the sampling frequency and $\omega_{rc}=0.2\omega_s$ as shown in Fig. 18. The filter capacitor c_f value is increased from 4.7uF to 22.5uF to demonstrate the effect of resonance frequency shift. The system does not exhibit damping in case of conventional capacitor current feedback as shown in Fig. 17(a). However, the system is stable with the proposed method and show evidence of damping as shown in Fig. 17(b).

To verify the better transient response of the proposed method, there is step change in reference current from 2 to 4A as shown in Fig. 18(a). Unlike proportional capacitor current feedback method discussed in [9] [10] and [28], there is no transient spikes and the injected current tracks the reference current smoothly with least amount of transient resonance and oscillation. The Phase-A line current THD for one cycle after the step change with the proposed damping loop is shown in Fig. 18(b).

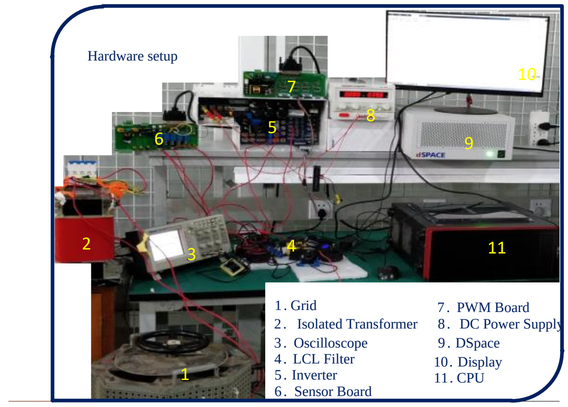

Fig. 12. Experimental Prototype of Three Phase Grid Connected Inverter using D-Space.

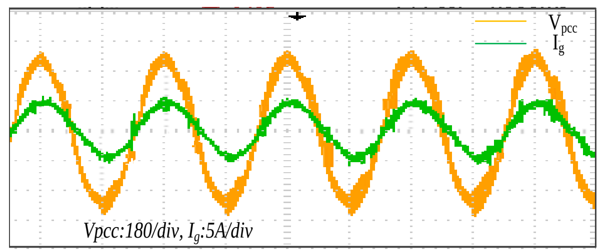

(a)

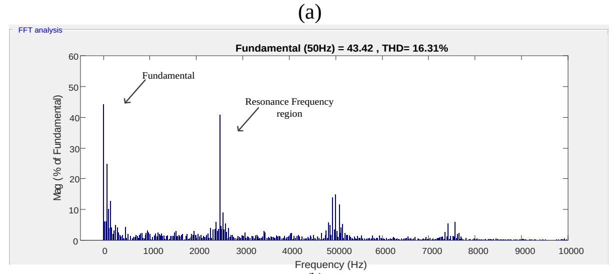

(b)

Fig. 13. Current Control Loop Response when no Damping Loop is Employed(a) I_g and v_{pcc}in Phase-A (b) Harmonic Spectrum of $I_g$in Phase-A.

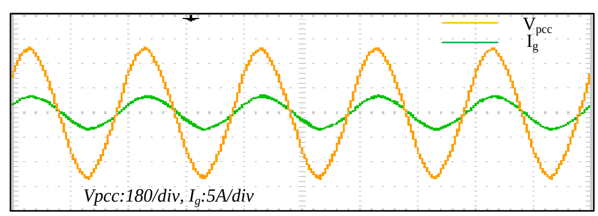

(a)

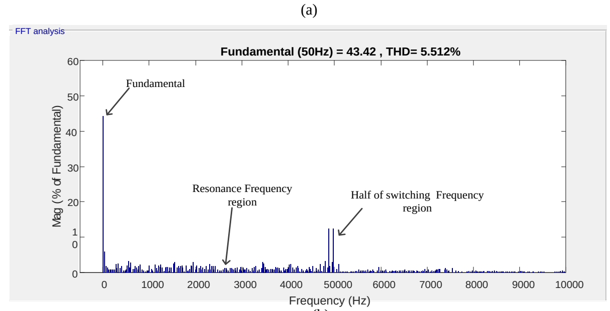

(b)

Fig. 14. Current Control Loop Response when CCF Damping Loop is Employed(a) I_g and v_{pcc}in Phase-A (b) Harmonic Spectrum of $I_g$in Phase-A.

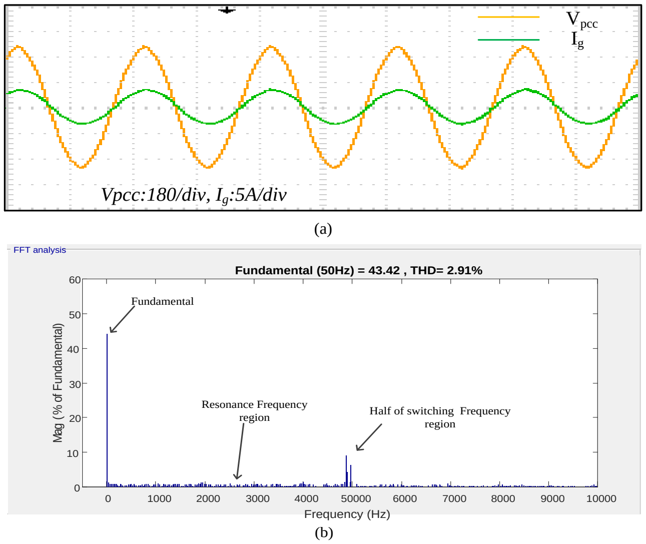

Fig. 15. Current Control Loop Response with Proposed Damping Loop (a) I_g and v_{pcc} in Phase-A (b) Harmonic Spectrum of I_g in Phase-A.

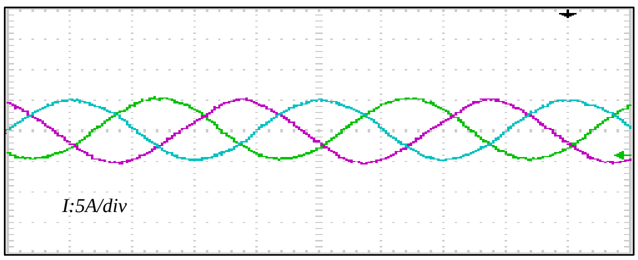

Fig. 16. Three-Phase Inject Current with Proposed Damping Loop

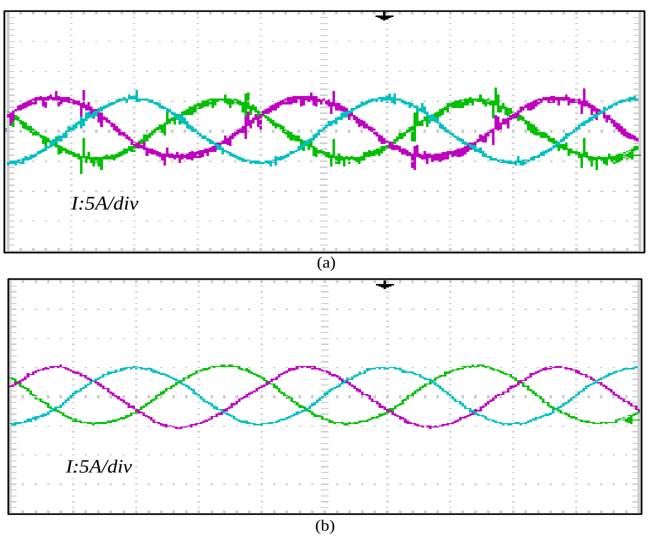

Fig. 17. Three Phase Injected Current behavior for Resonance Frequency Less than fs/6 (a) Conventional CCF (b) Proposed Method.

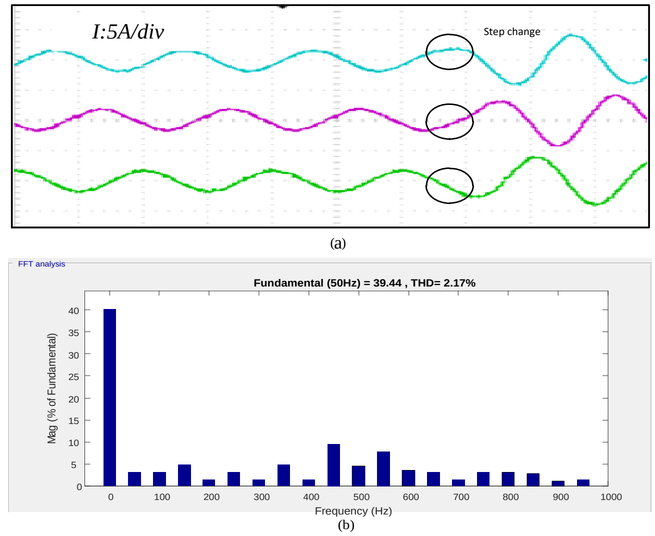

Fig. 18. (a) Transient Response and (b) Harmonic Spectrum, of Current Control Loop after Step Change in Reference Current.

VII. CONCLUSION

In this paper, active damping associated with three-phase grid connected LCL filter is explored with two different approaches. A new method is proposed, which is compared with the existing method to verify its efficacy. In the proposed strategy, a high pass filter is used as a compensator across the LCL filter to damp the arouse resonance peak. Based on proposed method, mathematical relation for grid injected current and capacitor damped current are derived. The proposed method gives faster dynamic response in comparison with conventional capacitor current feedback damping method. Moreover, the stability features with filter parameter variation illustrate that the proposed technique has potential to damp wide range of resonance frequencies as compared to the existing method. A case study of a 1 kW inverter is used to evaluate the control dynamic response and the harmonic attenuation capability. Different performances are observed for damping strategy in the presence of grid voltage harmonics. Finally, the simulation and experimental results validate the better dynamics response and damping effectiveness of the proposed methodology.

REFERENCES

[1] M. Huang, H. Li, W. Wu, and F. Blaabjerg, "Observer-Based Sliding Mode Control to Improve Stability of Three-Phase LCL-Filtered Grid-Connected VSIs," pp. 1–16, 2019.

[2] J. Park and K. Lee, "Performance Improvement for Reduction of Resonance in a Grid-Connected Inverter System Using an Improved DPWM Method," 2018.

[3] T. L. G. Converter, "Improved Capacitor Voltage Feedforward for," 2017.

[4] A. Saim, A. Houari, J. M. Guerrero, A. Djerioui, M. Machmoum, and M. A. Ahmed, "Stability Analysis and Robust Damping of Multi-Resonances in Distributed Generation based Islanded Microgrids," IEEE Trans. Ind. Electron., vol. PP, no. c, p. 1, 2019.

[5] Y. W. Li, "Control and Resonance Damping of Voltage-Source and Current-Source Converters With LC Filters," vol. 56, no. 5, pp. 1511–1521, 2009.

[6] A. Akhavan, H. Reza, and J. M. Guerrero, "A comprehensive control system for multi-parallel grid-connected inverters with LCL fi lter in

weak grid condition," Electr. Power Syst. Res., vol. 163, no. August 2017, pp. 288–300, 2018.

[7] Kang Zexin, Liu Chao, Sun Jiang, Ma Lin, You Haidong, and Jian Shuisheng, "Investigation on the Cladding Etched Single-Mode Fiber Acousto-Optic Tunable Filter and Its Axial Strain Characteristics," Acta Opt. Sin., vol. 33, no. 12, p. 1206003, 2013.

[8] X. Lu, K. Sun, and M. Liserre, "An Active Damping Method based on Biquad Digital Filter for Parallel Grid-interfacing Inverters with LCL Filters," pp. 392–397, 2014.

[9] C. C. Gomes, A. F. Cupertino, and H. A. Pereira, "Damping techniques for grid-connected voltage source converters based on LCL filter: An overview," Renew. Sustain. Energy Rev., vol. 81, no. April 2017, pp. 116–135, 2018.

[10] E. Twining, S. Member, and D. G. Holmes, "Grid Current Regulation of a Three-Phase Voltage Source Inverter With an LCL Input Filter," vol. 18, no. 3, pp. 888–895, 2003.

[11] X. Wang, X. Ruan, S. Member, S. Liu, and C. K. Tse, "Full Feedforward of Grid Voltage for Grid-Connected Inverter With LCL Filter to Suppress Current Distortion Due to Grid Voltage Harmonics," vol. 25, no. 12, pp. 3119–3127, 2010.

[12] X. Renzhong, X. Lie, Z. Junjun, and D. Jie, "Design and Research on the LCL Filter in Three-Phase PV Grid-Connected Inverters," vol. 5, no. 3, pp. 3–6, 2013.

[13] J. Xu, B. Zhang, Q. Qian, X. Meng, and S. Xie, "Robust control and design based on impedance-based stability criterion for improving stability and harmonics rejection of inverters in weak grid," Conf. Proc. - IEEE Appl. Power Electron. Conf. Expo. - APEC, pp. 3619–3624, 2017.

[14] H. Athari, M. Niroomand, and M. Ataei, "Review and Classi fi cation of Control Systems in Grid-tied Inverters," Renew. Sustain. Energy Rev., vol. 72, no. February 2016, pp. 1167–1176, 2017.

[15] M. Malinowski and S. Bernet, "A Simple Voltage Sensorless Active Damping Scheme for Three-Phase PWM Converters With an LCL Filter," Ieee Trans. Ind. Electron., vol. 55, no. 4, pp. 1876–1880, 2008.

[16] S. Gulur, V. M. Iyer, and S. Bhattacharya, "Stationary reference frame based current control structure with improved disturbance rejection for grid connected converters," Conf. Proc. - IEEE Appl. Power Electron. Conf. Expo. - APEC, vol. 2018-March, pp. 1031–1035, 2018.

[17] W. Yao, Y. Yang, X. Zhang, and F. Blaabjerg, "Digital Notch Filter based Active Damping for LCL Filters," 2015 IEEE Appl. Power Electron. Conf. Expo., pp. 2399–2406, 2015.

[18] T. Nhan, A. Luo, and M. Li, "A simple and robust method for designing a multi-loop controller for three-phase VSI with an LCL-filter under uncertain system parameters," Electr. Power Syst. Res., vol. 117, pp. 94–103, 2014.

[19] J. He, S. Member, Y. W. Li, S. Member, D. Bosnjak, and B. Harris, "Investigation and Active Damping of Multiple Resonances in a Parallel-Inverter-Based Microgrid," IEEE Trans. Power Electron., vol. 28, no. 1, pp. 234–246, 2013.

[20] T. Liu, Z. Liu, J. Liu, Y. Tu, and Z. Liu, "An Improved Capacitor-Current-Feedback Active Damping for LCL Resonance in Grid-Connected Inverters," 2017 IEEE 3rd Int. Futur. Energy Electron. Conf. ECCE Asia (IFEEC 2017 - ECCE Asia), pp. 2111–2116, 2017.

[21] X. Yan, J. Tang, W. Zhang, and Y. Zhang, "multi-objective optimization design for active damping lcl grid-connected filter."

[22] S. G. Parker, B. P. McGrath, and D. G. Holmes, "Regions of active damping control for LCL filters," IEEE Trans. Ind. Appl., vol. 50, no. 1, pp. 424–432, 2014.

[23] X. Wang, F. Blaabjerg, and P. C. Loh, "Virtual RC Damping of LCL - Filtered Voltage Source Harmonic Compensation," vol. 30, no. 9, pp. 4726–4737, 2015.

[24] M. T. Faiz, M. M. Khan, X. Jianming, S. Habib, and H. Tang, "Parallel feedforward compensation based active damping of LCL-type grid connected inverter," Proc. IEEE Int. Conf. Ind. Technol., vol. 2018-Febru, pp. 788–793, 2018.

[25] Z. Iwai and I. Mizumoto, "Realization of simple adaptive control by using parallel feedforward compensator," Int. J. Control, vol. 59, no. 6, pp. 1543–1565, 1994.

[26] I. Bar-Kana, "Parallel feedforward and simplified adaptive control," Int. J. Adapt. Control Signal Process., vol. 1, no. 2, pp. 95–109, 1987.

[27] J. He, S. Member, Y. W. Li, and S. Member, "Generalized Closed-Loop Control Schemes with Embedded Virtual Impedances for Voltage Source Converters with LC or LCL Filters," vol. 27, no. 4, pp. 1850–1861, 2012.

[28] M. T. Faiz, M. M. Khan, X. Jianming, M. Ali, and M. A. Mumtaz, "Active Damping of Capacitor Current based on Parallel Feedforward Compensation of LCL Grid Connected Inverter," 2018 Int. Conf. Electr. Eng., pp. 1–6.

[29] A.Ali, M. Mansoor Khan, J. Yuning, Y. Ali, M. T. Faiz and J. Chuanwen,"ZVS/ZCS Vienna rectifier topology for high power applications," in IET Power Electronics, vol. 12, no. 5, pp. 1285-1294, 1 5 2019. doi: 10.1049/iet-pel.2018.5875.

Automatically Extract Vertebra and Compute the Cobb Angle based on Spine's Features and Adaptive ASMs in Posteroanterior Radiographs

Pham The Bao
Computer Science Department, Information Science Faculty
Sai Gon University, Hochiminh city, Vietnam

***Abstract*—Nowadays, clinical diagnoses are more and more supported by medical equipment, but doctors still need a lot of time and effort to diagnosis. The construction of a system that can diagnose automatically will help doctors a lot when the doctor must handle many medical records. Many diseases need to be diagnosed by radiographs and they can be diagnosed automatically, especially bone diseases. The purpose of this paper is to introduce a new method to measure the curve of the spine in the X-ray images. We split this subject into two problems. The first problem is to extract the spine from the X-ray image. We use the threshold to remove redundant information from the images. Then an automatic mask is created to save the position of the spine and smooth the boundary of the spine. Based on the spine extracted from the previous steps, the Active Shape Model (ASM) which is designed from the characteristics of the vertebrae, is used to extract each vertebra from the spine. Finally, we measure the Cobb angle which is formed by vertebrae. The solution of two problems is implemented on X-ray images which have high quality, the results are more than 80% an area of the spine is extracted, and the Cobb angle is measured correctly, the accuracy of our method will decrease if the quality of the image is low.**

Keywords—Spine detection; spine extraction; vertebrae detection; cobb angle; adaptive active shape model

I. Introduction

A spine is a series of vertebrae extending from the skull to the small of the back, enclosing the spinal cord and providing support for the thorax and abdomen [Oxford Dictionaries]. Its responsibility is to support the body, move, and protect spinal marrow [1]. In the past and even in the present, spinal deformation is almost depended entirely on observing and diagnosing of orthopedic surgeons. Nowadays, there is a lot of model equipment like X-ray machine which can support doctors to diagnose diseases of the spine, especially scoliosis. To recognize scoliosis, doctors measure the Cobb angle, and this angle is defined as the angle formed between a line drawn parallel to the superior endplate of one vertebra above the fracture and a line drawn parallel to the inferior endplate of the vertebrae one level below the fracture. If the Cobb angle is more than 10 degrees, the spine is considered to be scoliosis. When society is more and more modern, many people want to take care of your health. It leads to a large number of medical records with many tasks such as reviewing, measuring, analyzing, and classifying; a doctor can not undertake all of them. The automatic system with artificial intelligence, which can detect vertebrae and calculate the Cobb angle from an X-ray image, will help doctors a lot. This system also helps other applications to model spine from 2D to 3D and detect diseases relating to the spine such as osteoporosis, gout in the spine, scoliosis, spondylolisthesis.

Many solutions have been applied to automatically detect lung, kidney, and bone from the radiograph. The aim of detecting the lung method [2, 3] is to identify the common features of the lung in an X-ray image and then use classifications. In another way, active models (Active Appearance Model - AAM [4] and Active Shape Model - ASM [5]) and their corresponding statistics [6] have been applied with the same basic idea, both of them try to fit the model of the sample (obtained by training data) to a new pattern by searching on the surrounding of points of new pattern. Smyth [7, 8] used the quantitative morphometry (QM) to build ASM of the lumbar vertebrae in the Dual-energy X-ray absorptiometry (DEXA) image to measure the shape. Robert [9] used AAM, which is characterized by a parameter model of the object. Finally, a method which gets good result is proposed by Luc Duong [10]. He reduces the noisy spine radiographs by using anisotropic filtering, and then the filtering process and pattern classification are devised to detect the spinal curve.

In this paper, we propose a new approach based on the characteristics of the X-ray image and the spine. This method is presented in five steps. First, we identify the region of interesting (ROI) in the X-ray images, which includes the spine [11], and the dynamic threshold which bases on the features of those areas, are applied for the ROI. Then we record the position of the spine in the image by an automatic mask. Third, based on the position of the spine, we proceed to adjust the spine correctly; this method is easier to apply than other methods, which is presented above. Fourth, we apply ASM to extract each vertebra from the spine. Finally, the Cobb angle is measured, and our system will give comments about whether the patients have scoliosis. Moreover, if scoliosis appears more than once in a spine, for example, Fig. 9, there are two signals of scoliosis (a left top curve and a right bottom curve), our method can solve that problem which other methods do not mention about.

II. Materials and Methods

A. General System

The input X-ray images must be taken posteroanterior and include the spine from the neck to the hipbone. The spine also has to be in a normal upright position, as shown in Fig. 1.

Our method is started by using thresholds to remove unnecessary pixels and follows as the flowchart 1.

B. Preprocessing

First of all, the X-ray image is grayed out because of its pixels that just change the bright between black and white.

A normal posteroanterior radiograph of the spine embraces two parts: upper half of the image has less bright than the lower, but the upper has more contras than the lower. It's because the lower half of the image is the region that contains many X-ray resistant things, organs [1]. Thus, we split this image into two parts vertically and create thresholds for each part base on its features.

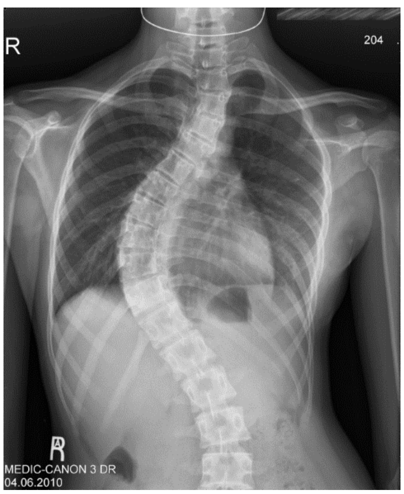

Fig. 1. Input Image.

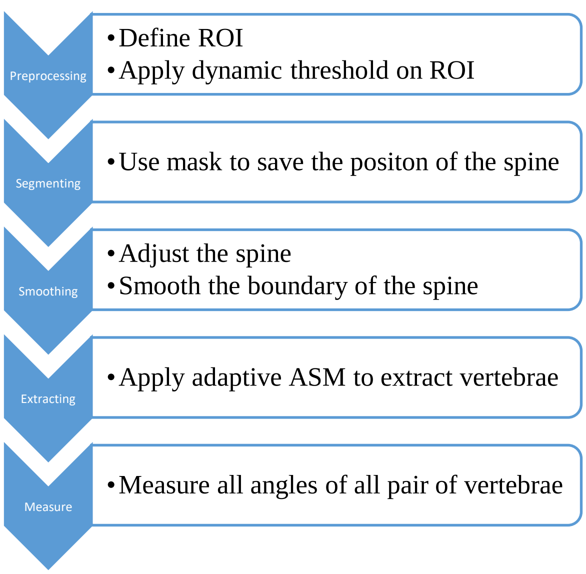

Flowchart. 1. Steps to Solve the Problem.

Each part of an X-ray image of the spine has a different threshold. We analyze the number of spinal pixels with its brightness's value statistically. Throughout empiric statistics for feedback characteristic X-ray of the spine, we have formula 1, where ave is the average brightness of the pixels having nonzero value of the image, max is the highest brightness's value of pixels of an image, α is coefficient of variation, and 0< α <1.

$$threshold = ave + (max - ave) \times \alpha \quad (1)$$

The threshold will only change if only α changes. Moreover, the threshold of the upper half of the image is lower than that of the lower half. With knowledge from doctors and experiments, we had found that α should be approximately 1/3 to get a good result for the upper half of the image. We remove all the pixels which are darker than the threshold in each part. We have a result in Fig. 2.

C. Segmenting

We start segmenting by binarizing an image. Almost people's bodies always are in an upright position, except sleeping time. Moreover, the middle spine is the region that changes status so much; for example, the middle spine must hunch when a person stops or turns the body. Hence, the middle part of spine is the most flexible part and the most pressure of the spine [11]. So, if the spine is scoliosis, the middle part is the most affected part. In addition, the size of vertebrae increases from the cervical region to the lumbar region [1]. We used morphology method to remove some small objects (noises). From these characteristics, we will detect the middle spine first.

Considering a horizon line in middle binary images, we refer the longest line segments with the white pixels passing through areas that are the backbone. The white pixels in the image are not continuous and fragment into sections, those lead to difficulties in finding the longest line segment. To handle this situation, we solve this problem by connecting all pixels in an error span (t) to a continuous segment line. We design the algorithm 1 – detecting the middle horizon line of spine.

Fig. 2. Result of the Preprocessing.

Algorithm 1

Input: A binary spine image, $A = \{a_{i,j} /\ i = \overline{1..r},\ j = \overline{1..c}\}$.

Output: middle line of spine, $L_{mid} = \{(x_{lmid}, y_{lmid}), (x_{rmid}, y_{rmid})\}$.

```
j = 1;
mid = [r/2];
end = begin = lj = j;
while (j<c) do
  if ((end - left)<(j-lj)) then {
        begin = lj;
        end = j;
        }
  if (A(mid,j) is black) then j++;
  else {
        lj = j;
        flag = 0;
        while (j<c and !flag) do
                if (A(mid,j+t) is white) then j=j +t;
                else    {
                                end = j;
                                begin = lj;
                                flag = 1;
                        }
        endwhile
        }
endwhile
xrmid = xlmid = mid;
yrmid = end;
ylmid = begin;
```

We use this segment line to determine the spine by moving it – L_{mid} – to the upper row and lower row from the middle of the spine. The determination process is executed as algorithm 2 – determining 02 parts of the spine; it was called upper-spine (UP) and lower-spine (LP). $UP = \{P_{left\_up} \oplus P_{right\_up}\}$, $LP = \{P_{left\_low} \oplus P_{right\_low}\}$ with $P_k = \{(x_i, y_i)\}$. We have resulted in Fig. 3.

D. Smoothing Boundary

After the segmentation step, the spine case is shown clearly, and we remove all the pixels that are outside the spine case by algorithm 3, and we have resulted in Fig. 4.

Although the obtained spinal that case contains most of the spine, the border is folded much. This problem leads to the deduction of some bones. We conduct a smoothing boundary algorithm to solve this problem, algorithm 4. The result is in Fig. 5.

Now, we have the new boundary of the spine. Most of the information on the spine is inside this boundary. With a normal spine or scoliosis without any disease else, its right or left boundary is a continuous curve that does not change the direction immediately.

Algorithm 2

Input: L_{mid} – result of algorithm 1. Defining value of neighbor of point (x,y) on x-axis, it was called

$$NE(x,y) = \{(x, y \pm \Delta y)/value\ of\ point\ is\ white\}.$$

Output: spinal region, $P_{left} = \{(x_l, y_l)\}$ and $P_{right} = \{(x_r, y_r)\}$

x = xlmid = xrmid;

$P_{left} = P_{right} = \emptyset$;

$P_{left} = P_{left} \cup \{(x_{lmid}, y_{lmid})\}$;

$P_{right} = P_{right} \cup \{(x_{rmid}, y_{rmid})\}$;

yl = y_{lmid};

yr = y_{rmid};

while(x still have value) do

x = x ⊗ 1; // opterator ⊗ is "+" in lower-spine process and "–"in upper-spine process.

if(NE(x,y1) or NE(x,yr) is not empty) then

{

yl = getCorrect(NE(x,y1));

yr = getCorrect(NE(x,yr));

$P_{left} = P_{left} \cup \{(x, y_l)\}$;

$P_{right} = P_{right} \cup \{(x, y_r)\}$;

}

endwhile

// function getCorrect(NE(x,y)) return the y-correct on spine in the set NE(x,y) based on value of pixel //and direction of y-axis of left and right boundary of spine.

Fig. 3. Result of the Region of the Middle Spine.

Algorithm 3
Input: UP and LP
Output: SP – the spine of image and CL – center line of spine. $SP = \{P_{left} \oplus P_{right}\}$, $CL = \{(x_i, y_i)\}$.
$SP.P_{left} = UP.P_{left} \cup LP.P_{left}$;
$SP.P_{right} = UP.P_{right} \cup LP.P_{right}$;
Sorting $SP.P_{left}$ by x increase.
Sorting $SP.P_{right}$ by x increase.
$CL = \varnothing$;
for each $x \in SP.P_{left}$ do
for y = 0 to c do
if $(y < SP(x).P_{left}.y_l \ or \ y > SP(x).P_{right}.y_r)$ then set A(x,y) is black
endfor
$CL = CL \cup \{(x, (SP(x).P_{left}.y_l + SP(x).P_{right}.y_r)/2)\}$;
endfor

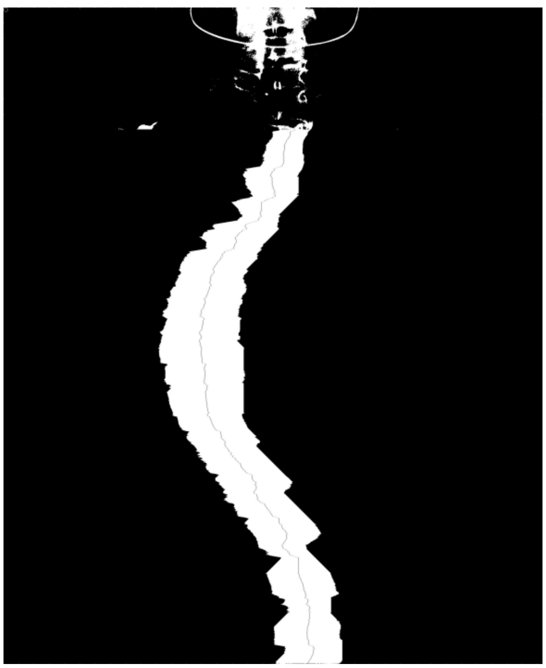

Fig. 4. Result of Segmentation.

We model and predict the curve by a regression model. This model uses the weighted linear least squares and the second-degree polynomial model. Then we use the robust version of this model by assigning lower weight to outliers in the regression. The boundary which is modified is shown in Fig. 6. After we have a new boundary of the spine, we update the CL.

E. Extracting Vertebrae

The region of the spine was extracted correctly; we perform to detect each vertebra in this region. The structure of any normal vertebrae is the same as each other when we view it from the same direction [13]. Hence, we propose to use Active Shape Models (ASMs) to detect vertebrae. We obtain a statistical model by marking 30 points on each vertebra and using ASM to train them. We use the statistical model of the vertebrae to locate better positions for points. For each landmark point, the Mahalanobis distance is used to relocate its position for a better result in our method.

However, if we look into the size, it is much difference between any pair of vertebrae. Moreover, with scoliosis, a vertebra can have many directions (a vertical position or a left tilt position or a right tilt position) [13, 14]. With the difference in the size and direction of the vertebrae, if we just use one sample model for all vertebrae, the result will not good. Thus, we design many sample models to detect vertebrae.

Algorithm 4
Input: SP – the spine image. SP was sorted by x-axis. Value d, the ratio of segment. α – The angle of x-axis and built line segment.
Output: SP – the updated spine image.
//smoothing for right boundary of spine.
for each $x \in SP.P_{right}$ form the smallest to biggest do
$t_x = (SP(x).P_{right}.y_r - SP(x).P_{left}.y_l)/d$;
$I_x = \emptyset$;
$\beta = \alpha$;
while (I_x is empty) do
Building the line segment l_x at point $A_x(x, SP(x).P_{right}.y_r)$ with angle β and the length is t_x. The form of line segment is $l_x(t) = \beta t + \gamma$.
$I_x = l_x \cap SP.P_{right}$;
Increase β;
endwhile
for $k = x \ to \ I_x.x$ do
$SP(k).P_{right}.y_r = l_x(k)$ // update value of right boundary of spine
endfor
endfor
//smoothing for left boundary of spine.
for each $x \in SP.P_{left}$ form the smallest to biggest do
$t_x = (SP(x).P_{right}.y_r - SP(x).P_{left}.y_l)/d$;
$I_x = \emptyset$;
$\beta = \alpha$;
while (I_x is empty) do
Building the line segment l_x at point $A_x(x, SP(x).P_{left}.y_l)$ with angle β and the length is t_x. The form of line segment is $l_x(t) = \beta t + \gamma$.
$I_x = l_x \cap SP.P_{left}$;
Decrease β;
endwhile
for $k = x \ to \ I_x.x$ do
$SP(k).P_{left}.y_l = l_x(k)$ // update value of left boundary of spine
endfor
endfor

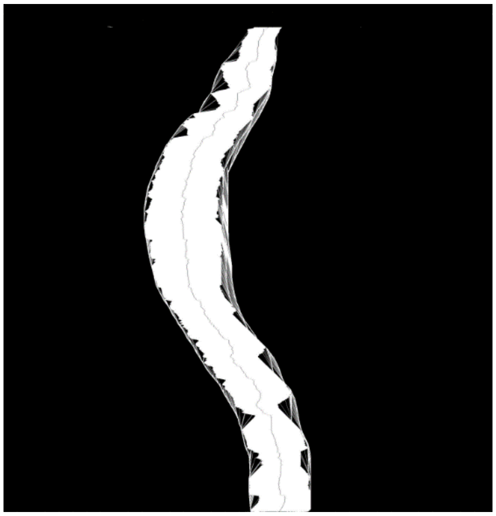

Fig. 5. A New Boundary of the Spine.

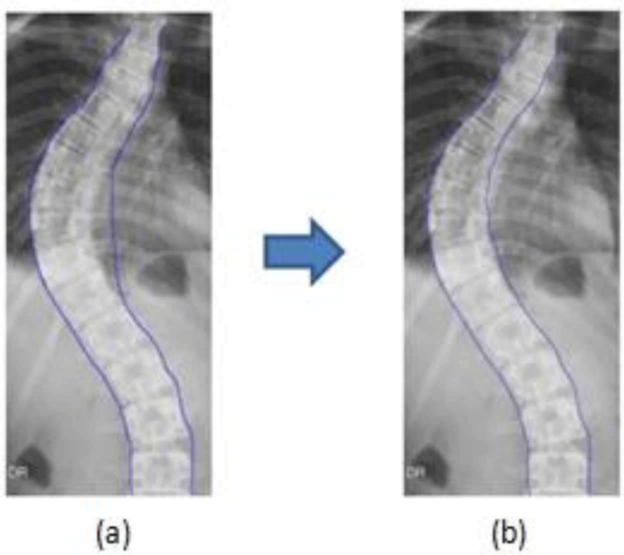

(a) Before using the Regression Model. (b) After using the Regression Model.

Fig. 6. The Boundary of the Spine.

At the bottom region of the spine, the vertebrae are much larger than the one in the top region [14], one model of ASM cannot change the size in a large range between the top vertebrae 's size and bottom vertebrae 's size. Thus, we have two models; one is a large model for the bottom region, and one is a small model for the top region. However, the height of vertebrae is increased steadily from top to bottom, Table I [13, 14].

The main purpose of this paper is to detect the spine, whether it is scoliosis or not, and the Cobb angle is the measurement to detect this. Simplify, The Cobb angle is defined as the angle formed by the intersection of two lines, one parallel to the superior endplate of a vertebra above the fracture and another line parallel to the inferior endplate of the vertebrae one level below the fracture. If the Cobb angle is more than 10 degrees, that is the symptom of scoliosis. The Cobb angle may be more than 60 degrees.

TABLE. I. VERTEBRAE INFORMATION

Kinds of vertebrae s	Averaged size (cm)	Number of vertebrae s
Cervical	12.5	7
Thoracic	28	12
Lumbar	18	5
Sacral	12.5	5
Coccyx		4

TABLE. II. LIST OF ASM MODELS

ASM model	Size	Direction
ASM_1	Large	Upright
ASM_2	Large	Left
ASM_3	Large	Right
ASM_4	Small	Upright
ASM_5	Small	Left
ASM_6	Small	Right

To cover all cases of vertebrae in scoliosis, we design three kinds of models of ASMs for each small model and large model above, each of three models which can rotate within at least 20 degrees angle. In other word, a model can rotate at least 10 degrees to the left and 10 degrees to the right. Specifically, first kind of model – normal model – is designed in the same direction of the vertical axis of spine, it can rotate 10 degrees to the left or the right; the second – left model – is designed to have the direction which slopes 20 degrees to the left of the spine's vertical axis; the third – right model – is the same of the second, but it slopes to the right. These ASM models, which are used, are developed by Tim Cootes and Chris Taylor [12]. In a word, with the different size and direction of each vertebra, we design six sample models as Table II. One model is trained by at least four samples which have the same corresponding characteristics.

To detect each vertebra more correct, we process three steps. Firstly, we detect all vertebrae s from bottom to top – algorithm 5 – we have $V_{up} = \{V_{up(i)}\}$ and the second is top to bottom – algorithm 6 – we have $V_{down} = \{V_{down(i)}\}$. The last, we check the correlation from results V_{up} and V_{down}; because the middle region of the spine is complicated to have the set of vertebrae $\{V_i\}$. The accuracy of bottom-up detection is higher than top-down detection because the last vertebra is stable and very clear to be detected. We use μ – the angle of the line (we regress all points on the centerline of the spine) with y-asix, the direction of vertebrae and the position of vertebrae to detect kind of ASM model, Table III and formula (1). We always detect the last and the first vertebrae of the spine, then the remaining sequential vertebrae. The intervertebral disc is between two vertebrae (V_{i-1} and V_i). We must calculate the size of the intervertebral disc ($inter_{disc}$), which is dependent on the height of two vertebrae [13, 14]. If V_{i-1} and V_i are the same feature then by ASM model of V_{i-1} and ASM model of V_i together in one of three sets: $\{AMS_1, AMS_4\}$, $\{AMS_2, AMS_5\}$ and $\{AMS_3, AMS_6\}$. Normally, the height of the intervertebral disc is approximately 20% of the height of the vertebrae [13, 14]. We use formula (3) to compute the height of the intervertebral disc. We have resulted in Fig. 7 and 8.

$$typeASM(x_1, x_2, \mu, , L_{mid}) = \left[\sqrt[4]{\frac{\mu}{10}}\right] \times [sign(x_1, x_2) + 2] + [sign(x_1, x_2, L_{mid}.x) + 1], \quad (2)$$

$$with\ 0 \le \mu \le 150, \quad x_1 > 0, \quad x_2 > 0\ and\ L_{mid}.x > 0$$

$$sign(x_1, x_2) = \begin{cases} 0 & if\ x_1 > x_2 \\ 1 & otherwise \end{cases} \quad and\ \ sign(x_1, x_2, L_{mid}.x) = \begin{cases} 0 & if\ L_{mid}.x > \dfrac{x_1 + x_2}{2} \\ 1 & otherwise \end{cases}$$

$$inter_{disc} = \left({}^{d}/_{100}\right) \times V_{i-1}.height \quad (3)$$

$$with\ d = \begin{cases} 20 & if\ \ V_i\ and\ V_{i-1} is\ the\ same\ in\ feature \\ sign(V_i.centerline, V_{i-1}.centerline) & otherwise \end{cases}$$

$$sign(V_i.centerline, V_{i-1}.centerline) = \begin{cases} 0 & if\ a > 20 \\ (20 - a) & otherwise \end{cases}$$

$a\ is\ degree\ angle\ between\ center\ line\ of$

$V_i\ and\ center\ line\ of\ V_{i-1}$

TABLE. III. APPLIED MODELS FOR VERTEBRAE

μ	Direction of vertebrae	Position of vertebrae	Kind of model
μ < 10 degrees		Lower half of spine	ASM_1
μ >= 10 degrees	$x_1 > x_2$	Lower half of spine	ASM_2
	$x_1 < x_2$	Lower half of spine	ASM_3
μ < 10 degrees		Upper half of spine	ASM_4
μ >= 10 degrees	$x_1 < x_2$	Upper half of spine	ASM_5
	$x_1 > x_2$	Upper half of spine	ASM_6

Fig. 7. Apply ASM for the Top Vertebrae: the Sample Model is in Blue; the Result is in Green Color.

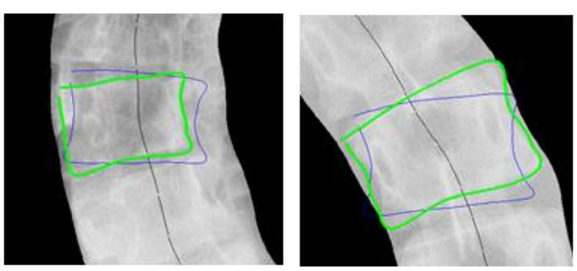

(a) Middle vertebrae (b) Bottom vertebrae.

Fig. 8. Apply ASM for the Sample Model is in Blue Color; The Result is in Red Color.

Algorithm 5. – **detecting all vertebrae s from bottom to up.**
Input: $SP,\ CL,\ L_{mid}$ and $ASM = \{ASM_i / i = 1..6\}$
Output: $V_{up} = \{V_{up(i)}\}$ – the set of vertebrae s, which are located from down to up of spine.
// detect the last vertebrae of spine
$h = \frac{\sum_{i=1}^{3} ASM_i.heigh}{3}$;
// check value of h with table 1.
$x_1 = max(CL.x)$;
// x_2, x_1 are on CL
$x_2 = x_1 - h$;
$temp = \dfrac{(x_1 + x_2)}{2}$;
$\mu = getAngle(x_1, x_2, CL)$;
$type = getTypeOfASM(x_1, x_2, \mu, temp, L_{mid})$;
//type = 1..6
$ASM_{type}.center = (temp, CL.y_{temp})$;
$ASM_{type}.window = \begin{pmatrix} x_1, x_2, SP.P_{left}(from\ x_1\ to\ x_2), \\ SP.P_{right}(from\ x_1\ to\ x_2) \end{pmatrix}$;
$ASM_{type}.active$;
$V_{up(1)} = result\ of\ ASM_{type}$;
$update\ CL, SP, x_2\ \ from\ \ ASM_{type}$;
// detect the remaining vertebraes
i = 2;
$type_{old} = type$;
while ($data\ remains\ on\ CL$) do
$h = V_{up(i-1)}.height$; // the height of previous located vertebrae was changed after ASM was run.
// the height of vertebrae is decreased by the result from ASM models.
$x_1 = x_2$;
$x_2 = x_1 - h$;
$temp = {(x_1 + x_2)}/_{2}$;
$\mu = getAngle(x_1, x_2, CL)$;
$type = getTypeOfASM(x_1, x_2, \mu, temp, L_{mid})$;
//type = 1..6
$inter_{disc} = getInterVertebralDisc\begin{pmatrix} V_{up(i-1)}, \\ type, type_{old}, x_1, x_2 \end{pmatrix}$;// the size of intervertebrae l
//disc
if($inter_{disc} > 0$) then
$x_1 = x_1 - inter_{disc}$;
$x_2 = x_1 - h$;
$temp = {(x_1 + x_2)}/_{2}$;
endif
$ASM_{type}.center = (temp, CL.y_{temp})$;
$ASM_{type}.window = \begin{pmatrix} x_1, x_2, SP.P_{left}(from\ x_1\ to\ x_2), \\ SP.P_{right}(from\ x_1\ to\ x_2) \end{pmatrix}$;
$ASM_{type}.active$;
$V_{up(i)} = result\ of\ ASM_{type}$;

$update\ (local\ range\ of\ CL\ and\ SP)\ and\ x_2\ \ from\ \ ASM_{type}$;
$type_{old} = type$;
i++;
endwhile

Algorithm 6. – **detecting all vertebrae s from top to down.**
Input: $SP,\ CL,\ L_{mid}$ and $ASM = \{ASM_i / i = 1..6\}$
Output: $V_{down} = \{V_{down(i)}\}$ – the set of vertebrae, which are located from down to up of spine.
// detect the first vertebrae of spine
$h = \frac{\sum_{i=4}^{6} ASM_i.heigh}{3}$;
// check value of h with table 1.
$x_1 = min(CL.x)$;
// x_2, x_1 are on CL
$x_2 = x_1 + h$;
$temp = \frac{(x_1 + x_2)}{2}$;
$\mu = getAngle(x_1, x_2, CL)$;
$type = getTypeOfASM(x_1, x_2, \mu, temp, L_{mid})$;
//type = 1..6
$ASM_{type}.center = (temp, CL.y_{temp})$;
$ASM_{type}.window = \begin{pmatrix} x_1, x_2, SP.P_{left}(from\ x_1\ to\ x_2), \\ SP.P_{right}(from\ x_1\ to\ x_2) \end{pmatrix}$;
$ASM_{type}.active$;
$V_{down(1)} = result\ of\ ASM_{type}$;
$update\ CL, SP, x_2\ \ from\ \ ASM_{type}$;
// detect the remaining vertebraes
i = 2;
$type_{old} = type$;
while ($data\ remains\ on\ CL$) do
$h = V_{down(i-1)}.height$;// the height of previous located vertebrae was changed after ASM was run.
// the height of vertebrae is increased by result from ASM models.
$x_1 = x_2$;
$x_2 = x_1 + h$;
$temp = {(x_1 + x_2)}/{2}$;
$\mu = getAngle(x_1, x_2, CL)$;
$type = getTypeOfASM(x_1, x_2, \mu, temp, L_{mid})$;
//type = 1..6
$inter_{disc} = getInterVertebralDisc\begin{pmatrix} V_{down(i-1)}, \\ type, type_{old}, x_1, x_2 \end{pmatrix}$;
//the size of

//intervertebrae l disc
if($inter_{disc} > 0$) then
$x_1 = x_1 + inter_{disc}$;
$x_2 = x_1 + h$;
$temp = {(x_1 + x_2)}/{2}$;
endif
$ASM_{type}.center = (temp, CL.y_{temp})$;
$ASM_{type}.window = \begin{pmatrix} x_1, x_2, SP.P_{left}(from\ x_1\ to\ x_2), \\ SP.P_{right}(from\ x_1\ to\ x_2) \end{pmatrix}$;
$ASM_{type}.active$;
$V_{down(i)} = result\ of\ ASM_{type}$;
$update\ (local\ range\ of\ CL\ and\ SP)\ and\ x_2\ \ from\ \ ASM_{type}$;
$type_{old} = type$;
i++;
endwhile

F. *Measuring Angle*

The Cobb angle is the angle that is formed by the intersection of two lines, one parallel to the superior endplate of a vertebra above the fracture and another line parallel to the inferior endplate of the vertebrae below the fracture.

We already had the exact position of each vertebra. An algorithm 7 – Measuring Cobb angle algorithm is designed to measure the Cobb angle for each pair of vertebrae. Before we compute the Cobb angle by getCobbAngle function, we must know the extreme point of the spine. From the extreme point, we chose a vertebrae (V_i) which is above extreme point and another vertebra (V_k), which is under extreme.

Function $getCobbAngle(V_i, V_k)$
Input: 02 vertebraes V_i and V_k.
Output: $angle_{Cobb}$ – the Cobb angle of vertebrae V_i and vertebrae V_k.
//each vertebra V_i, we have 05 line segments: upper, lower, left, right, center.
if ($V_i.center < V_k.center$) then
$V_1 = V_i$;
$V_2 = V_k$;
else
$V_1 = V_k$;
$V_2 = V_i$;
endif
Regressing all points on lower line segment of V_1 to the line L_{lower};
Regressing all points on upper line segment of V_2 to the line L_{upper};
$angle_{Cobb} = angle(L_{lower}, L_{upper})$;
return $angle_{cobb}$

Algorithm 7
Input: the set of all vertebrae $V = \{V_i\}\ i = \overline{1..M}$. It is ordered.
Ouput: the set of Cobb angle
$point_{center} = \emptyset$;
for (i=1 to M) do
$update\ V_i.centerline\ to\ CL$;
$point_{center} = point_{center} \cup \{V_i.center\}$;
endfor
Regressing all points of CL by least-square linear regress method to polynomial $euq_{CL}(x)$;
Solve equation $equ'_{CL}(x) = 0$ by numerical method fining a set of extreme points $point_{extreme}$;
Solve equation $equ''_{CL}(x) = 0$ by numerical method fining a set of inflection points $point_{inflection}$;
$Cobb = \emptyset$;
for (i=0 to $|point_{inflection}|$) do
with $point_{inflection}(i)$ get the $point_{extreme}(t)$ corresponding;
finding the $\sup(point_{extreme}(t))$ and $\inf(point_{extreme}(t))$ in $point_{center}$;
$V_1 = V(\sup(point_{extreme}(t)))$;
$V_2 = V(\inf(point_{extreme}(t)))$;
$Cobb = Cobb \cup \{getCobbAngle(V_1, V_2)\}$;
endfor

The equations of CL are approximated the CL become polynomial by least-square linear regress method, formula (4). We find the extreme points by solving the first-order derivative equation (5).

$$euq_{CL}(x) = a_n x^n + a_{n-1} x^{n-1} + \cdots + a_0 x^0 \tag{4}$$

$$equ'_{CL}(x) = 0 \tag{5}$$

Sometimes, we have some special cases which like Fig. 9; the spine of a patient has the left curve at the top and the right curve at the bottom. This patient needs to be treated two times, one for the left curve and one for the right curve. Then, we must detect and solve the problem, which likes Fig. 9. We must solve the second-order derivative equation to get the number of inflection points, also is the number of the left and right curls of the spine, equation (6). It shows us how many parts of the spine are split.

$$equ''_{CL}(x) = 0 \tag{6}$$

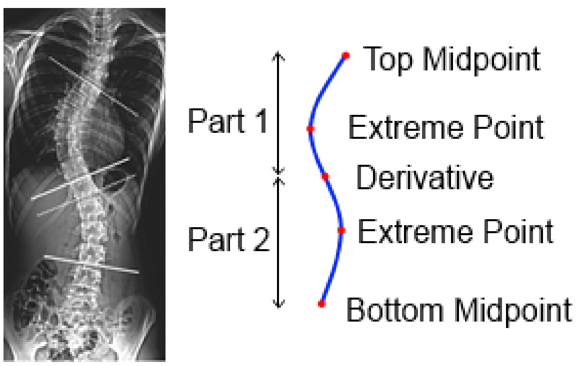

Fig. 9. Illustrate the Curve and Detect Some Important Points to Split the Spine into Parts.

Any pair of vertebra makes the Cobb angle more than 10 degrees is a symptom of scoliosis. We have four scales of evaluation: normal, low warning, high warning, and extreme warning. It bases on the largest Cobb angle of all pairs in this set. If the largest Cobb angle is more than 45 degrees, this is an extreme warning. If the largest Cobb angle of any pair is between 20 and 45 degrees, this is a high warning. If the largest Cobb angle of any pair is between 10 and 20 degrees, this is a low warning. The last, if all Cobb angles are less than 10 degrees, the spine is normal.

III. Results

We implemented our research on Laptop: chip Intel Core 2 Duo, CPU 2x2.0GHz, with 3GB RAM. The OS system is Windows 7 Professional 32-bit.

The testing database includes X-ray standard images used to illustrate the article, which is posteroanterior radiographs of a female, 16 years old, scoliosis patient.

The rest data in the testing database are from many sources, they are not original images, so their sizes are not uniformed, and many images have not good quality.

Fig. 10 shows two cases of testing. On the left case, the extracted area of the spine does not enough, and there is a noisy area on the left of the spine. The spine in the right case is extracted completely, and there is a little noise in the result.

Table IV shows the result of the first problem. The ratio of spine detection is measured manually because the dataset is not big, we count all pixels of the spine on the original image and all pixels of the extracting area of the spine on result image, then we calculate the ratio by doing the division and round operator. Most images are extracted at least 65% of the spine (excluding cervical vertebrae), and almost the unrecognized area of the spine in the region, which is near the cervical vertebrae. The average accuracy is high. In terms of program execution time, the small image will process quickly, but the bigger the image is, the more running time is increased. The noise magnitude is the area that is extracted but does not belong to the spine; this does not affect much to the vertebrae recognition problem. It's because we apply the ASM model to recognize exactly the bound of vertebrae, then these noises will be automatically ignored.

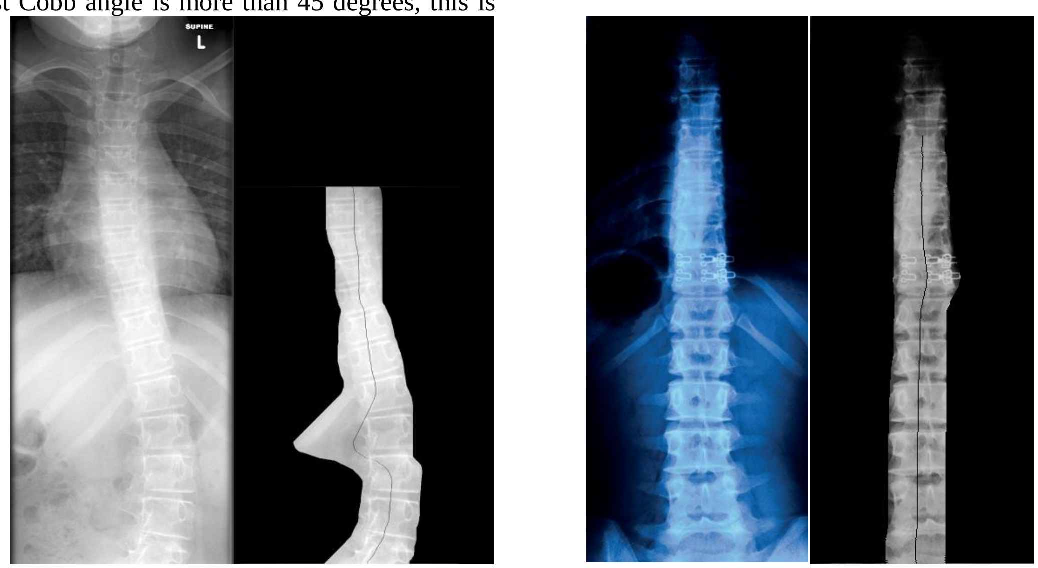

Fig. 10. Examples of Original Images (Left) and the Results of the First Problem (Right).

TABLE. IV. RESULT OF THE FIRST PROBLEM

Item	Size (pixel)	Recall	Time	Ratio of spine detection	Noise magnitude
1	2208x2688	10	40 mins	100%	very little
2	599x1741	10	20 mins	70%	big
3	1231x2420	10	30 mins	80%	medium
4	768x1024	10	5 mins	65%	big
5	1600x1600	10	10 mins	75%	very little
6	630x630	10	10 s	90%	little
7	250x683	10	7 s	100%	no
8	335x582	10	7 s	70%	medium
9	238x583	10	7 s	90%	medium

TABLE. V. RESULT OF THE SECOND PROBLEM

Item	Size (pixel)	Recall	Time	Auto Evaluation	Manual Evaluation
1	2208x2688	10	5 mins	Extreme	Extreme
2	599x1741	10	2 mins	Extreme	Extreme
3	1231x2420	10	3 mins	Extreme	High
4	768x1024	10	1 min	High	Low
5	1600x1600	10	2 mins	Normal	Normal

The sample models of ASM are trained on the standard image, and then we only test on the first 5 images which have high quality. However, because the size of images is different, when testing on each image, we must resize the models but keep the size's ratio between vertebrae 1 and the image manually. The result of the second problem for the standard X-ray image is good, Table V. Although the detection ratios of the spine are not high in some cases, in the detected region of the spine, vertebrae are extracted correctly, it leads to measure the exact Cobb angle on these vertebrae. The evaluation of the Cobb angle is mentioned in the last part. Our method evaluates on a scale, not on the exact degree of angle, then the lost vertebrae (in the unrecognized region) do not affect much to the evaluation. If these models are applied for low-quality images, the result is not good, and some vertebrae are skimpy or redundant when being extracted. Then, the Cobb angles are much erroneous.

IV. DISCUSSION

The method that we propose not only has good results but also it's simple and effective. In addition, by saving the midpoint, we can determine the direction of the curvature of the spine easily. The advantage of our method, when compared with other method is that our method can determine if a spine which has more than 1 curve, may be considered as scoliosis or not. Moreover, like other methods, our evaluations of the scoliosis are exactly.

A few areas are not handled well, especially the noisy vertebrae. Therefore, the program also needs to be studied more to improve accuracy; for example, he ASM can be combined with other edge detection methods or interpolation methods from the data which are recognized correctly.

The method applied for the second problem should be used for the same standard of an image, such as size, quality to get a good result. Small X-ray image should be applied by models which are trained by small standard image.

We will try to modify this method or find new approaches to improve the performance of this subject.

REFERENCES

[1] Henry Gray (2000). Anatomy of the human body. Bartleby.com (20th edition).

[2] McNitt-Gray MF, Huang HK, Sayre JW (1995). Feature selection in the pattern classification problem of digital chest radiograph segmentation. IEEE Transactions on Medical Imaging, 14, 537–547, https://doi.org/10.1109/42.414619.

[3] Luo H, Hao W, Foos DH, Cornelius CW (2006). Automatic image hanging protocol for chest radiographs in PACS. IEEE Trans. Inf. Technol. Biomed, 10, 302–311, https://doi.org/10.1109/TITB.2005.859872.

[4] Ginneken B (2002). Active Shape Model Segmentation with Optimal Features. IEEE Transactions on Medical Imaging, 21, 924–933, https://doi.org/10.1109/TMI.2002.803121.

[5] Cootes TF, Edwards GJ, Taylor CJ (2001). Active Appearance Models. IEEE Transactions on Pattern Analysis and Machine Intelligence, 23, 681–685, https://doi.org/10.1109/34.927467.

[6] Cootes TF, Taylor CJ (2004). Anatomical statistical models and their role in feature extraction. Br. J. Radiol, 77, 133–139, https://doi.org /10.1259/bjr/20343922.

[7] Smyth PP, Taylor CJ, Adams JE (1997). Automatic Measurement of Vertebrae l Shape using Active Shape Models. Image Vision Comput, 15, 575-581, https://doi.org/10.1016/S0262-8856(97)00006-1.

[8] Smyth PP, Taylor CJ, Adams JE (1999). Vertebrae l Shape: Automatic Measurement with Active Shape Models. Radiology, 211, 571-578, https://doi.org/10.1148/radiology.211.2.r99ma40571.

[9] Roberts M, Cootes T, Adams J (2003). Linking Sequences of Active Appearance Sub-Models via Constraints: an Application in Automated Vertebrae l Morphometry. The British Machine Vision Conference, 38, 1-10, https://doi.org/10.5244/C.17.38.

[10] Luc Duong, Cheriet F, Labelle H (2010). Automatic Detection of Scoliotic Curves in Posteroanterior Radiographs. IEEE Transactions on Biomedical Engineering, 57, 1143–1150, https://doi.org/10.1109/ TBME.2009.2037214.

[11] Long LR, Thomas GR (2001). Landmarking and feature localization in spine x –rays. J. Electron. Imaging, 10, 939–956, https://doi.org/ 10.1117/1.1406503.

[12] T.F. Cootes and C.J. Taylor and D.H. Cooper and J. Graham (1995). Active shape models - their training and application. Computer Vision and Image Understanding, 61, 38–59, https://doi.org/10.1006/cviu. 1995.1004.

[13] Charles Watson, George Paxinos, Gulgun Kayalioglu (2008). The Spinal Cord: A Christopher and Dana Reeve Foundation Text and Atlas. Academic Press (1st Edition).

[14] Henry Gray (2000). Anatomy of the human body. Bartleby.com (20th edition).

System for Monitoring People with Disabilities in the Event of an Accident using Mobile Terminals

Alexandra Fanca[1], Monica Cujerean[2], Adela Puscasiu[3], Dan-Ioan Gota[4], Honoriu Valean[5]
Department of Automation[1, 3, 4, 5]
Technical University of Cluj-Napoca, Cluj-Napoca, Romania[1, 2, 3, 4, 5]

***Abstract*—Being in the speed century, people around the world are busy scheduling every day and therefore, it is impossible to spend enough time with the elderly and people with disabilities or people who have a chronic illness. These persons need a lot more attention and care because they cannot cope with the daily activities like a healthy person would. Daily monitoring and assistance of elderly or disabled people is a very important task, both in the current activity, or, especially when emergencies can occur. Fortunately, we can easily use today's technologies, which are constantly developing to be able to monitor them remotely. This paper tries to find a solution to reduce cases of fatality due to accidents, by using advanced technologies of today, e.g. smartphones, fast communications. The use of these technologies can provide permanent monitoring of the elderly and persons with disabilities, without bounding their mobility and without affecting their quality of life. In this way, if emergency situations arise for the elderly or people with disabilities or chronic diseases, measures can be taken as soon as possible. The development of a mobile application capable to monitor the occurrence of accidents for the above-mentioned persons is obviously a help granted to the doctors involved in ensuring their health. Thus, the main objective of the application is to detect the accidental falls of the persons in the shortest possible time. Another objective is to provide an application that runs in the background of the mobile operating system, using as little as possible the power supply.**

Keywords—Smartphones; built-in smartphone sensors; monitoring people; android applications; accident detecting system

I. Introduction

One of the main problems of the community is those related to people's health. Over time, in finding ways to solve people's medical problems, both the academic community and research laboratories of large companies have been involved. Falls are considered major health hazards for both the elderly and the ill people, especially with chronic and neurodegenerative diseases [1].

People with disabilities or chronic illnesses must carry out their daily activities independently and that is a major challenge for them [2]. Almost half of these cases are not under medical supervision, and in the event of an accident followed by sudden falls or significant injuries, no one will be announced to provide medical care. In this situation, the injured person can be found in severe illness or even deceased.

According to the information provided by the National Statistical Institute, the number of deaths in Romania has remained constant over the last 20 years, ranging from 240,000 to 260,000 deaths annually. The average death rate recorded by Romania is above the mortality rate in the European Union (EU), respectively 13 deaths per thousand inhabitants, compared to the EU average of 10 deaths per thousand inhabitants [3]. This number would drop considerably if intelligent means of patient monitoring were used so that healthcare could intervene at critical times. Thus, in addition, 1 in 3 people could be saved on time. Accidents caused by slips and falls are ranked second place after road accidents and can lead to trauma and even death [4]. Chances of a person to be saved are increasing if assistance is received as soon as the accident has happened [5].

Smartphone has become a good tool used in mobile applications for the medical and safety fields, due to the increasing performance of the sensors and their ability to transmit and collect a large amount of data.

Following the introduction, the rest of the paper is organized as follows: Section II presents the existing main patients monitoring systems. In Section III the proposed system is developed and in Section IV some tests and results are presented. Section V focuses on some discussions, conclusions and future improvements.

II. State of the Art

Over the years the problem of monitoring and detecting human injuries/accidents has been intensively studied. In the literature, several systems based on different techniques for accident detection are reported.

Depending on the techniques used, we can find systems for monitoring people and/or detect falls that use acoustic sensors [6-9], video camera and image processing [10-13] or even sensors attached to the human body [14-16].

In [17] the authors proposed a system that is composed of a wearable accelerometer sensor, magnetic door sensor, Arduino Uno and a camera. For communication, a GSM module and a Wi-Fi module are used. This method is quite complex and also expensive and involves the use of a large number of components. It may not be reliable over time due to hardware degradation. In terms of usability, monitoring can be provided only indoor, where the camera and the magnetic sensor may have a use (there are doors). So, users can't use this technology if they go outside for a walk or shop.

Another fall detection system, proposed in [18], is based on image processing. The system proposed in this paper consists of a computer and a video camera, which can be installed inside a building, on the ceiling or the walls. The system can monitor a room for 24 hours without human intervention. It is based on artificial vision algorithms that monitor the presence of people in a room and detect if a person has fallen. When a fall is detected, an alarm message is sent to the attending physician along with a photograph. If the person recovers, another message is sent.

All these systems require the use of additional components compared to the systems that use sensors built into smartphones. Also, some systems are restricted only to be used inside the buildings.

III. Methods and Material

The purpose of this work is to implement a mobile application in order to remotely monitor people with disabilities or chronic diseases, using built-in sensors of smartphones. This application can be used by anyone with a phone with an Android operating system.

Once the application is installed on the phone, the user will be able to create an account by entering the personal data: first name, second name, email, password, personal phone number and two other telephone numbers as the emergency contact persons. Once registered, the user can log in with his credentials (email and password). After logging in, monitoring can begin at the user's request. Monitoring consists of constantly checking the coordinates of the accelerometer to detect a possible accident. The fall will be reported and filtered through the Linux machine's server, which sends an emergency message to the contacts instantly.

All user accident information will be displayed in the graphs. These graphs are implemented in Grafana and the access is granted only to the administrator. The displayed information will target the rate of accidents among the elderly, persons with disabilities or serious chronic diseases.

Another important objective is to use the phone's battery consumption as optimally as possible. For this purpose, a single sensor was chosen to be inspected by the application. This sensor, the accelerometer, is present in both older and state of the art phones.

The server part of the application is implemented as several services and allows performing complex operations.

A. Structural Specifications of the System

The system architecture is based on several independent services that communicate with each other. Thus, each service can be managed independently, without affecting the operation of other services.

This application is designed based on three-tier architecture. The data layer, the business logic layer, and the presentation layer are running on different servers so that it can be independent and can be accessed separately.

The system is composed of the following services:

- The service for users, representing the mobile application with a friendly interface, accessible to people of all ages. The available actions are: register, log in, edit profile, start the application or stop the application;
- The service managed by the admin that starts the Linux virtual machine and controls the filtering of the alerts received from the phone and also manages the graphs that monitor the accident rate on each user.

The connection between the user service and the service managed by the admin is made through a virtual machine API to which HTTP requests are sent.

The architecture of the system is presented in Fig. 1.

B. Functional Specifications of the System

The mobile application has several benefits that make it more flexible, qualitative, with a friendly interface. Regarding the functional specifications, a few examples can be listed:

- Reliability: the application architecture allows long-term operation, which can run on the phone's background for an indefinite period of time, without sending erroneous information to the server or without detecting an unfortunate accident;
- Accessibility: the user-friendly interface of the Android application can be used by anyone, regardless of age or technical knowledge. The users only need to start the application and have the phone permanently with them;
- Security: This targets the Android application as well as the admin's graphical interface (Grafana graphics). When creates an account, the user must fill in all the required fields, otherwise, registration cannot be done. When logs in, the credentials are checked in the database (email and password) and the user can only access the application if he/she enters the data correctly. The admin, in order to be able to access the statistics regarding the number of accidents produced in a period of time, must authenticate with the admin credentials (user and password);
- Database: There are two databases. The first is stored in Cloud Firebase and holds user information. The second database is a local database stored on Linux virtual machine that holds the information displayed by Grafana: user name, two indexes for the occurrence of the accident and the time at which the accident occurred;
- API usage: make possible the connection between the Linux machine and Android. The application sends HTTP requests to the Linux machine, which further filters the data about the user who had the accident and sends messages to the predefined contacts;
- Decomposition in services: the application is composed of several services, these being interconnected but also working independently. Each service is maintained on a different development platform;
- Limitations: The app can work on any phone that has Android operating system independent of the version. The used sensors, accelerometer and GPS are present on most smartphones.

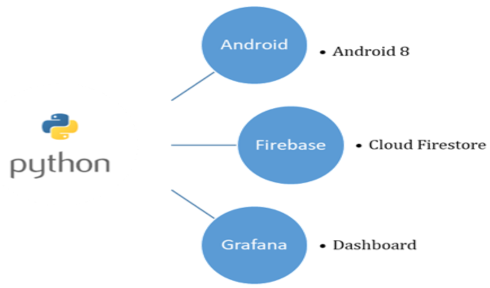

Fig. 1. The Architectural Presentation.

C. The Architecture of the Proposed System

The application architecture consists of several services that work independently. This facilitates the possibility to change the functionality of a service without degrading the rest of the services.

Qualitative requirements, such as functionality, reliability, accessibility, efficiency, security, independence from other platforms, require the design of a software system with a well-defined architecture. This is the reason for designing the service-based architecture. This architecture is relatively complex and is shown in Fig. 2.

As can be seen from the previous figure, the system consists of four important parts:

- Android application.
- Linux server.
- Database.
- Grafana.

The four components of the system are presented below.

1) Android Application: The smartphone allows the use of as many built-in sensors to perform different tasks or to monitor user's actions. For Android, for example, Google provides access to a set of libraries that allow developers to know when the user is in the car or riding a bicycle when entering or leaving a developer-defined perimeter. The proposed application uses the accelerometer to detect any possible impact, fall or other unusual situations that may occur. The Android application is divided into three major components at the logical level: authentication/registration, event monitoring and alerting.

2) Linux server: The role of this machine is to process and filter the information sent by the android application in order to send messages to the contacts in the event of an accident or strange behavior of the phone. It is installed on an AWS (Amazon Web Services) virtual machine under server mode.

The connection is made using an SSH (Secure Shell) key. The Admin connects using the Putty platform. He can set up a user name and password with which to connect in the future. The main libraries installed for optimum operation are Flask, Firebase-connector, Grafana, and MySQL.

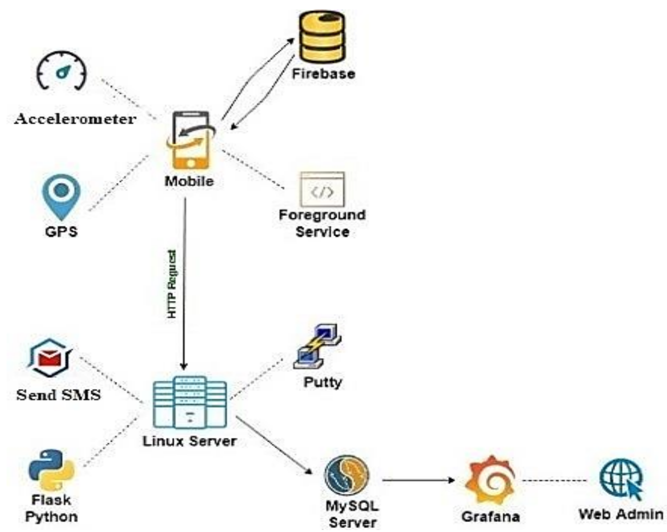

Fig. 2. The Architecture of the Proposed System.

3) Database: Regarding the data level, we can talk about two databases present:

- Firestore Cloud - dedicated database for mobile applications in general, but which can be used for other platforms, for example, node.js, Linux servers, and go java. In this context, the non-relational database is made up of a collection called users, which includes a set of documents, each having several fields, which the user must fill in through the registration process.
- Local Linux machine database - is used for the Grafana Dashboard, because the graphics cannot extract the required data directly from Firebase. Therefore, the database contains a table consisting of username, alert status (1 or 0, depending on the case) and the current date.

4) Grafana: Grafana Dashboard is a graphical interface installed on the Linux machine that can be accessed using the same API as the server. It can only be accessed by admin because authentication is required when accessing it. This includes the accident rate for each individual user, in the form of a graph, which is updated once a minute. Statistics can be maintained from the last 15 minutes to the last year of application usage by a user.

D. Use Case Diagram

One of the essential aspects of modeling a system is the presentation of its dynamic behavior. It is important to highlight the functionalities of the system, both at the client part and at the server part. Depending on its dynamic nature, the diagram highlights certain internal or external factors to make the interaction possible.

The use-case diagram is presented in Fig. 3 and includes the two possible actors of the system: the user of the mobile application and the admin of the server.

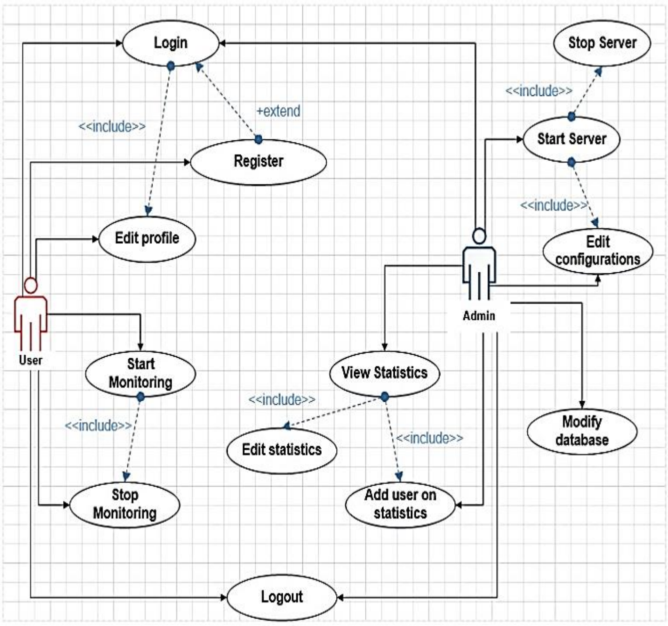

Fig. 3. Use Case Diagram.

As can be seen in the figure above, the roles of the actors are well defined.

Possible actions of the user:

- register to the application.
- log in to the application.
- start monitoring.
- stops monitoring.
- edit his profile with personal data.

The Admin has full rights over all services such as:

- start/stop the server.
- log in to the Grafana interface.
- edit the graphics, modify the logic behind them.
- add, delete users through the Grafana interface.
- add / delete graphs.
- configure the server; access the Firestore Cloud database.

E. Sequential Diagram

The sequence diagram is used to chronologically describe the events that take place within a system. The sequence diagram of the proposed system is shown below (Fig. 4).

As can be seen from the sequential diagram of the system, the sequence of actions is coherent and the steps in which the actions could be performed are finite and well defined.

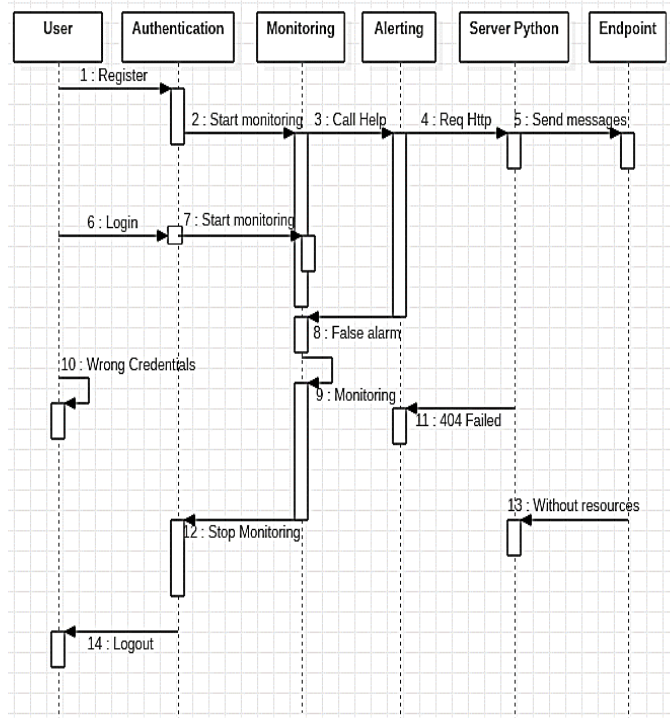

Fig. 4. Sequential Diagram.

In the first half of the diagram, the application implements all the actions that can take place without difficulties: registration, start monitoring, triggering the alert, sending request Http and sending messages. The chain of actions unfolds very quickly, there are no delays.

In the second half of the diagram, there are obstacles that may occur during the actions: logging in with incorrect credentials, false alarm, stopping the monitoring by the user, 404 could not make the call to the server or the server ran out of resources.

F. Implementation of the Android Application

The Android application is divided into three main components at the logical level: authentication/registration, event monitoring and alerting of events that have happened. Below are details on their implementation.

1) Authentication and registration: The login case is presented to the user after installing the application or after it has logged out. From the main activity, the authenticateUser() method is called when starting the application. This method receives the email stored in SharedPreferences as a parameter. The answer is delivered asynchronously via the LoginResponseListener interface back to MainActivity. If the answer is a successful one, the main screen of the application is presented. If the answer is negative, MainActivity presents LoginActivity for authentication. This flow is performed using the startActivityForResult() method, where it is verified that the authentication has been successfully performed. Below the class diagram for authentication is presented (Fig. 5).

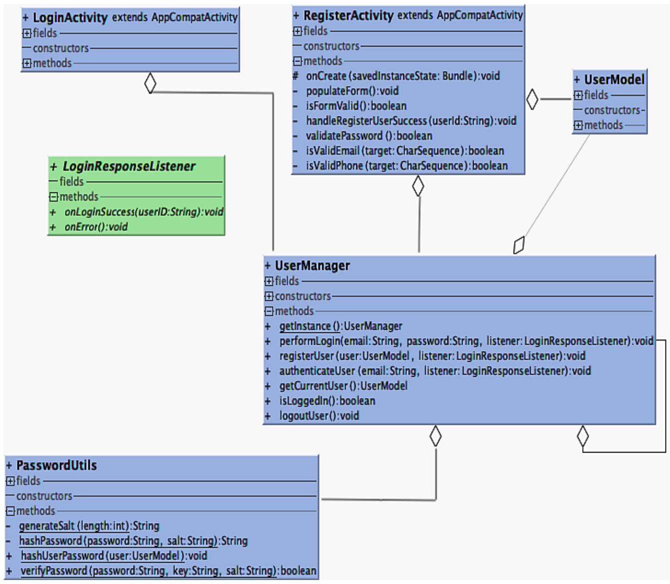

Fig. 5. Class Diagram for Authentication.

The data entered in the Register Activity is verified and validated by the isFormValid () method as follows: verified it respects the structure and checked and that no field is left blank:

- email - check the address format with a Regex.
- password - it is checked to be no more than 7 characters and coincides with the password confirmation field.
- name - it is only checked to be completed.
- phone numbers - check with a Regex for the formats: 0040000000000 and +40000000000. Verifying phone numbers with 100% accuracy is almost impossible due to the large number of variations of international phone number formats. This application is developed for demonstration and yet only national numbers are valid.

2) Event monitoring: Event monitoring is the main objective of the application. This is achieved by continuous monitoring of the events sent by the phone's accelerometer sensor. The application starts a service that runs all the time in the background. Monitoring Service has access to the accelerometer and registers to receive data from it at a range defined by the SensorManager constant "SENSOR_DELAY_NORMAL". At each event, the value of the acceleration is checked in m / s2 on the 3 axes. If the value exceeds the preset threshold by the constant "SENSOR_SENSITIVITY_THRESHOLD" with the value of 30, the user will be alerted by a notification, with an expiration time of 20 seconds. The value of 30 m/s2 was chosen following the studies present in the literature. The 20-second alert is accompanied by an alarm sound, and the user has the option to call for help or declare it a false alarm (for example, the phone was accidentally dropped from his hand). If the notification expires or the user confirms it, the phone will call a web service to which the current location and email of the user will be sent as parameters. The current location detection is done using the GPS of the phone in HIGH_ACCURACY mode and starts once the alarm has been activated. This results in lower energy consumption.

For obtaining data about the current acceleration of the device, the accelerometer of the phone has been used. The type of sensor "Sensor.TYPE_LINEAR_ACCELERATION" was chosen so that it returns a three-dimensional vector that indicates the value of the acceleration on the 3 axes in m/s2 and excludes gravitational acceleration. When the device is stationary, the returned values are close to 0.

The Android operating system offers multiple location detection strategies for devices that can be used, depending on the application. GPS_PROVIDER was used for the proposed system, as this method allows the location of the highest accuracy. Initially, we have tried to get the last known location of the operating system through "LocationManager. getLastKnownLocation". If this cannot be achieved or is less than 1 minute, a new location is required by the "Location Manager.requestLocationUpdates" method.

3) Event alert: NetworkManager is a singleton that has only one method, callHelp (String latitude, String longitude, String userId). This method uses the OkHttp library to make an Http request to the alert server. This is called by MonitoringService.

The purpose of the Linux server is to filter alerts, user information and to then send messages based on information received from the Android application. The figure below shows how the server works (Fig. 6).

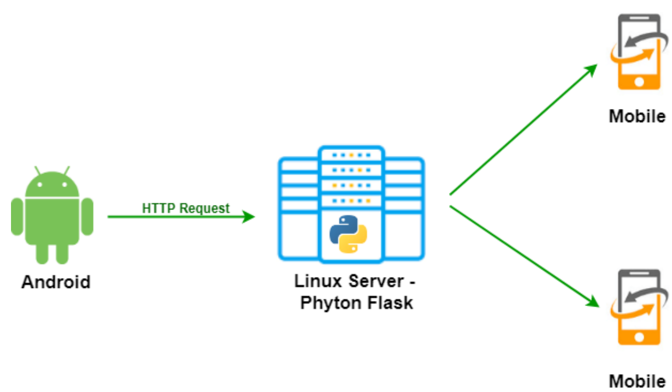

Fig. 6. How the Server Works.

Cento 6.9 was used to create the server (Linux virtual machine). This is an open-source operating system, used by a wide range of developers. Cento was installed on a virtual machine in AWS (Amazon Web Services) under server mode. This means that it has no graphical interface, all system configurations were done by accessing the server through SSH.

After the virtual instance was created in AWS, the connectivity part was set. The "brain" of the server application is implemented in the api.py file. The main function of the API is composed of several steps:

- It connects to Firebase (the online DB used by the Android application) and extracts all users with the related information, as those inserted into a dictionary variable. This is a feature of Python mode called Firebase;

- Parse the dictionary created above and verify that the email address sent by the Android application to this API is valid and belongs to a Firebase user;
- If the above condition is valid, some variables such as First Name, First Name, Telephone Number, etc. are extracted from the entries in Firebase of the user concerned;
- The SMS sending function is executed. This feature is a query of another API provided by AWS through which we can send SMS. This option was chosen because it is a secure solution that does not involve high costs and is available 100% without downtime.
- The last step of the function is to enter information into the local MySQL database about the user who queried this API. The person's name, date and value "1" are added. This helps us create a graph and see how many times a person has used this API using Grafana.

The messages are sent on two different phone numbers of the contact persons and contain information about: the name and surname of the person in danger, his telephone number and the location where he can be found. The message format is shown below (Fig. 7).

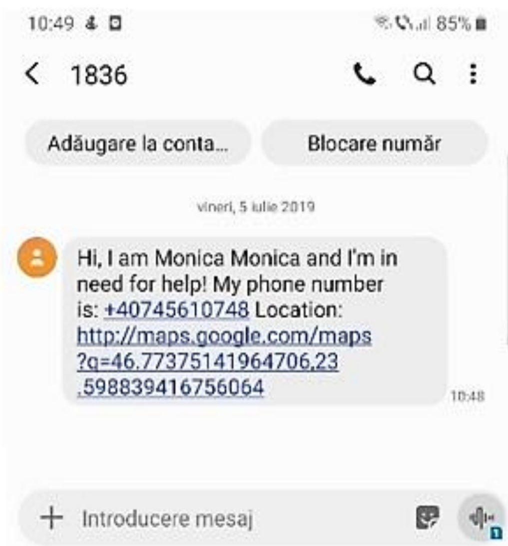

Fig. 7. Format Alert Message.

IV. Results

After the implementation of the system, it was required to test and validate it. Several tests were performed, such as:

- testing the functionality of the Android application;
- server security testing;
- optimization of battery consumption;
- production of statistics using Grafana.

As for testing the functionality of the mobile application, several aspects have been studied and tested, such as the login part, the register, the sending of Http requests in the most correct way.

Login is done by filling in the email and password fields (Fig. 8(a)). Failure to complete them or adding incorrect credentials, which are not found in the database, will trigger the following error: "wrong credentials". If the credentials match the values stored in the database, the user can open the main page of the application. There, it will be able to start monitoring, stop monitoring, but it also has a menu with two buttons: "My profile" and "Logout".

For the register part, the presence of certain rules established in the analysis and implementation part of the system was considered (Fig. 8(b)). The rules established for creating a user account include:

- filling in all the fields;
- the email must have an appropriate structure: zzzyy@gmail.com;
- the telephone numbers must have the prefix of Romania and 10 digits;
- the password must be of maximum 7 characters;
- "password" and "confirm password" must match.

"My profile" is the button that allows the user to edit their profile. It can change: name, surname, email, personal phone number, and phone numbers of the contact persons and also can reset his password. The editing part of the profile has the same rules as the registration ones.

Another important aspect of the Android part of the application is location permissions. Once the application is installed, if the location is not activated, the user receives a message which requests permission to the location of the smartphone. The application will not work without the enabled location.

For security purposes, the server can only be accessed by admin. Also, the Android application contains the exact path of the Http request to the server. Since the server is built on an AWS virtual machine, many hackers may try to access the server, but this is not possible due to server security. Any other application that tries to access the API will receive error 404. In conclusion, as far as server security is concerned, no other foreign application can access the Linux machine.

Another important objective of the paper was to achieve the lowest energy consumption. A battery consumption statistic was obtained through experiments (the application runs all the time in the background). The results are presented in Table I.

As can be seen from the performed tests, the proposed system requires a maximum consumption of 15.2% of the battery, without it being included in the list of applications for battery optimization.

Except for hardware malfunctions that may affect the sensors of the phone, the application has no issues in terms of life, because it works in optimal parameters.

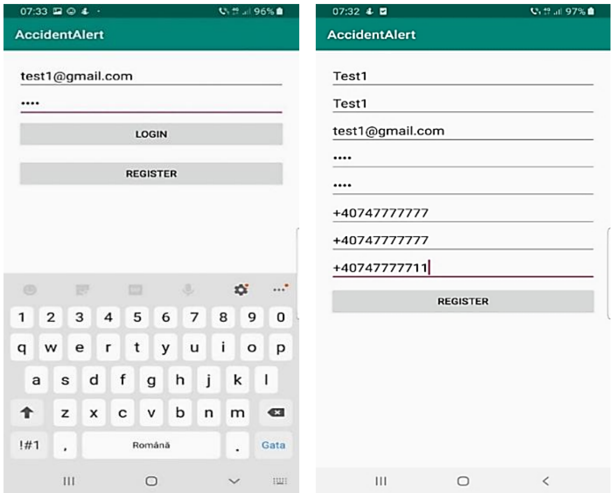

(a) (b)

Fig. 8. (a) Login Activity. (b) Register Activity.

TABLE. I. BATTERY CONSUMPTION

Time period	**Battery percentage**
One day	10,6 %
A day that sends at least 6 alerts, maximum 10 alerts	15,2 %

A. Making Statistics using Grafana Application

The proposed system offers, besides the mobile monitoring and a warning application in case of accident, the possibility of making statistics regarding the number of detected accidents for each user. This can be done by accessing the Grafana application which is also installed on the Linux virtual machine.

Logging into the Grafana application can only be done by the admin, using the username and password as credentials. Once logged in, the admin can view user accident statistics for a certain period of time. The server has a script set in the Linux scheduler to run every minute. This script is connected to Firebase and extracts the name of each user and inserts into the local MySQL database the user name, date and number '0'. In this way, we will have a table in the local database where there will be multiple lines with the names of the people and the digits 0 or 1. The value 1 is inserted only when the API is called by the Android application.

Fig. 9. Accident Statistics – June 2019.

The accident statistics for some users for June 2019 are presented (Fig. 9).

V. DISCUSSION AND CONCLUSIONS

One of the biggest challenges was to keep a service permanently running without affecting the rest of the applications. This is necessary to be able to monitor the users 24/24h. In the latest versions of Android, different process prioritization mechanisms have been implemented in order to save the battery and the processes are often stopped. Also, different phone manufacturers can change these mechanisms. For example, on Huawei, events sent by the accelerometer stop working after a few minutes. This issue can be solved by excluding the application from battery optimization in the phone settings. Also, a wake lock was used to increase service priority.

Another challenge is to detect the fall event and to remove false alerts. Determining the optimum acceleration threshold contributes to solve the problem only partially.

By combining all the technologies presented above, we have succeeded in implementing a modern solution, which adapts to the size of each mobile device and which is built on the principle of simplicity in use.

Looking at the context from the beginning of the paper, this application is very useful for helping people with disabilities, or the elderly, because it significantly reduces the risk of health hazard after an accident or even the risk of death. It can bring a huge contribution to the society, by allowing medical staff to do other works instead of monitoring people 24 hours a day at the hospital or at home.

A solution has been found to reduce the death of accidents due to the use of today's advanced technologies, for example, smartphones, sensors incorporated in smartphones, fast communication services. This will help the monitoring of helpless people even remotely. In this way, the elderly, people with disabilities or chronic diseases can be saved in time in the event of an unforeseen accident and also the monitoring of accidents is provided without affecting the mobility or quality of life.

In conclusion, the application complies with all the constraints set from the beginning, as can be seen from the results of testing and validation. The proposed application is not similar to other and works better by optimizing power consumption, displaying a user-friendly interface, using a database that updates very quickly and using a server that can send alert messages within three seconds of receiving alerts on smartphones.

As future improvement of the proposed solution, the use of machine learning technologies is desired. Firebase ML kit offers the possibility to train a sensor flow model for categorizing events and using artificial intelligence to decide whether it is a false alarm or not. It is possible to record the last sequence of values sent by the accelerometer and through the input of the user who decides whether it is a false alarm or not, to train the AI part of the application.

The statistics regarding the number of accidents are very important. These statistics can provide information on the number of falls produced in a given time, as well as information on which category of people are most prone to falls. So, another improvement may be the update of the dashboard with an automatically created graph when the application detects a new registered user. Now, it is up to the admin.

As a further development, the use of ML for falls detection and for minimizing false results can be a good solution. In this way, using the dataset obtained from the sensor, the application can learn the behavior of the user and can predict depending on the current movement if a fall is imminent or not.

References

[1] Mohammad Ashfak Habib, Mas S. Mohktar, Shahrul Bahyah Kamaruzzaman,Kheng Seang Lim, Tan Maw Pin, and Fatimah Ibrahim. "Smartphone-Based Solutions for Fall Detection and Prevention: Challenges and Open Issues", in Sensors (Basel) 2014 Apr.

[2] World Health Organization, Disability and health, 16 Junuary 2018, Article available online: .https://www.who.int/news-room/fact-sheets/detail/disability-and-health.

[3] National Institute of Statistics: General mortality rate, Available online: https://www.mediafax.ro/social/institutul-national-de-statistica-rata-mortalitatii-generale-dar-si-a-celei-infantile-mai-mare-in-romania-decat-media-ue-foto-14915507.

[4] World Health Organization, Falls, 16 Junuary 2018, Article available online: https://www.who.int/news-room/fact-sheets/detail/falls

[5] S. Rauscher, G. Messner, P. Baur, J. Augenstein, K. Digges, E. Perdeck, G. Bahouth, and O. Pieske. "Enhanced Automatic Collision Notification System- Improved Rescue Care Due To Injury Prediction- First Field Experiencee", 2009.

[6] Y. Li, K. C. Ho and M. Popescu, "A Microphone Array System for Automatic Fall Detection," in IEEE Transactions on Biomedical Engineering, vol. 59, no. 5, pp. 1291-1301, May 2012. doi: 10.1109/TBME.2012.2186449.

[7] A. Irtaza, S. M. Adnan, S. Aziz, A. Javed, M. O. Ullah and M. T. Mahmood, "A framework for fall detection of elderly people by analyzing environmental sounds through acoustic local ternary patterns," 2017 IEEE International Conference on Systems, Man, and Cybernetics (SMC), Banff, AB, 2017, pp. 1558-1563. doi: 10.1109/SMC.2017.8122836

[8] Y. Li, K. C. Ho and M. Popescu, "Efficient Source Separation Algorithms for Acoustic Fall Detection Using a Microsoft Kinect," in IEEE Transactions on Biomedical Engineering, vol. 61, no. 3, pp. 745-755, March 2014. doi: 10.1109/TBME.2013.2288783.

[9] Y. Zigel, D. Litvak and I. Gannot, "A Method for Automatic Fall Detection of Elderly People Using Floor Vibrations and Sound—Proof of Concept on Human Mimicking Doll Falls," in IEEE Transactions on Biomedical Engineering, vol. 56, no. 12, pp. 2858-2867, Dec. 2009. doi: 10.1109/TBME.2009.2030171.

[10] S. C. Agrawal, R. K. Tripathi and A. S. Jalal, "Human-fall detection from an indoor video surveillance," 2017 8th International Conference on Computing, Communication and Networking Technologies (ICCCNT), Delhi, 2017, pp. 1-5. doi: 10.1109/ICCCNT.2017.8203923.

[11] Z. Huang, Y. Liu, Y. Fang and B. K. P. Horn, "Video-based Fall Detection for Seniors with Human Pose Estimation," 2018 4th International Conference on Universal Village (UV), Boston, MA, USA, 2018, pp. 1-4. doi: 10.1109/UV.2018.8642130.

[12] A. Y. Alaoui, A. E. Hassouny, R. O. H. Thami and H. Tairi, "Video based human fall detection using von Mises distribution of motion vectors," 2017 Intelligent Systems and Computer Vision (ISCV), Fez, 2017, pp. 1-5. doi: 10.1109/ISACV.2017.8054942.

[13] G. M. Basavaraj and A. Kusagur, "Vision based surveillance system for detection of human fall," 2017 2nd IEEE International Conference on Recent Trends in Electronics, Information & Communication Technology (RTEICT), Bangalore, 2017, pp. 1516-1520. doi: 10.1109/RTEICT.2017.8256851.

[14] J. Limpanadusadee, P. Kesawattana, T. Wongsawat and D. Wongsawang, "EldTec: Improvement on Wearable Sensor for Elderly Fall Detection," 2018 Seventh ICT International Student Project Conference (ICT-ISPC), Nakhonpathom, 2018, pp. 1-6. doi: 10.1109/ICT-ISPC.2018.8523991.

[15] P. Pierleoni, A. Belli, L. Palma, M. Pellegrini, L. Pernini and S. Valenti, "A High Reliability Wearable Device for Elderly Fall Detection," in IEEE Sensors Journal, vol. 15, no. 8, pp. 4544-4553, Aug. 2015. doi: 10.1109/JSEN.2015.2423562.

[16] T. Tamura, T. Yoshimura, M. Sekine, M. Uchida and O. Tanaka, "A Wearable Airbag to Prevent Fall Injuries," in IEEE Transactions on Information Technology in Biomedicine, vol. 13, no. 6, pp. 910-914, Nov. 2009. doi: 10.1109/TITB.2009.2033673.

[17] K. Suganya, Dr. M. Saravanan, "A Survey on Monitoring and Fall Detection System for Old Aged Person", in International Journal for Research in Applied Science & Engineering Technology (IJRASET), vol. 6, Nov. 2018.

[18] Miguel K, Brunete A, Hernando M, Gambao E. "Home Camera-Based Fall Detection System for the Elderly". In Sensors (Basel). 2017;17(12):2864. Published 2017 Dec 9. doi: 10.3390/s17122864.

Embedding Adaptation Levels within Intelligent Tutoring Systems for Developing Programming Skills and Improving Learning Efficiency

Mohamed A. Elkot
Department of Computer Science
College of Science and Arts in Alrass, Qassim University, Qassim, Saudi Arabia

***Abstract*—Intelligent Tutoring Systems (ITSs) represent the virtual learning environment that provides learning needs, adapts to the characteristics of learners according to their cognitive and behavioral aspects, to reach desired learning outcomes. The purpose of this study is to investigate the impact of embedding some adaptation levels within intelligent tutoring systems on developing Object-Oriented Programming skills (OOP), as well as on learning efficiency for students of the computer science department, Faculty of Science and Arts at Qassem University. In this context, the author developed an Intelligent Tutoring System (ITS) that provides multiple levels of adaptation (Learner level, links level) to support automatic adaptation to each of the students' characteristics and investigate the effectiveness of the system on dependent variables. The random sample consisted of (n=44) students. Those students were divided into two similar groups, Experimental an (ITS), and Control (face-to-face, traditional). The findings revealed that there was a noticeable improvement in the students' performance for the experimental group than the control group how used face-to-face method for the programming skills and learning efficiency.**

Keywords*—*Intelligent Tutoring Systems (ITS); programming skills; adaptive e-learning; learning style; learning efficiency

I. Introduction

Intelligent tutoring systems (ITSs) based on artificial intelligence play a critical role as expert systems that provide an electronic learning environment that meets the needs of the learners and automatically adapts to their cognitive and behavioral characteristics, to achieve the highest educational return that can be reached [1]. (ITSs) will stimulate the learning process, stimulate the learner's motivation, direct his energies, and raise his motivation to continue the learning process [2]. This has been confirmed by many previous research and studies that have indicated the importance of these systems in learning programming languages that require higher cognitive levels in Thinking and problem-solving skills.

Many available current traditional e-learning management systems are intended for all learners, they do not take into account the individual characteristics and differences of learning abilities, experiences, skills, learning style, and the available educational materials through these systems do not allow for learning that takes into account the needs of individual learners as it is called "one-size-fits-all". In contrast, (ITSs) are adaptive learning systems developed to create a dedicated virtual environment to the learner and his individual needs at a suitable time and place, taking into account his abilities and skills. “One-on-one-teaching” [3, 5].

Adaptation is the solution to many of the limitations and weaknesses of traditional e-learning systems [6]. The main purpose of the adaptation process is to enhance learning by meeting the different needs of individual learners, [7] points out those adaptive systems are interactive systems that adapt their behavior according to the pattern and characteristics of each learner for the learning process and develop their skills. [8] think that in light of these characteristics; many previous studies have dealt with (ITSs) in many ways, especially with regard to the important question of how to achieve adaptation based on the learner characteristics? Thus, many studies have developed these systems based on specific characteristics such as learning style, motivation, cognitive traits, knowledge, learners' preferences… etc., and a few studies went to design adaptation process by combining multiple parameters together to build intelligent systems [9], these studies include:

A study [1] provided an introduction to integrating some learning styles into adaptive e-learning system based on hypermedia to measure the impact of that system at the learners' level. The results showed a clear improvement in learners' performance of the course using JavaScript.

In [4] study, which was concerned with the development of an adaptive e-learning system, based on the integration of some characteristics of adaptation levels, namely learning style and knowledge of the level of learners. To teach object-oriented programming and integrate with the level of presentation to display content by two factors, namely, the sequence and non-sequence in the presentation of content. The statistical results showed a significant improvement in students' learning levels of programming when they were exposed to the targeted adaptive learning system.

These systems have great credit in improving the cognitive and skillful level of learners. Especially in programming courses, as it was cited in previous research and studies [3,10] which led the author to think about developing an (ITS) based on the integration of some parameters (link generation, learning style), which are presented through different levels of adaptation (Learner level, Link level), which contribute to increase the amount of interaction with learners and identify the deficiencies in building their knowledge, skills, and rebuild them and determine the performance expectations, especially with object-oriented programming courses that represent difficulty in understanding and implementation, in addition, those courses represent the most challenge for students of the department of computer science [10,11, 12, 13] as learners need greater interaction with them in each step of problem-solving, writing a program, and training in problem-based thinking, so the aim of this study is to answer the following questions:

The main question "What is the impact of embedding adaptation levels within intelligent tutoring systems for developing programming skills and improving learning efficiency?"

1) What is the effect of integrating learning style and link generation with the proposed an (ITS) on the development of programming skills for students of computer science?

2) What is the effect of integrating learning style and link generation with the proposed an (ITS) on improving the learning efficiency for students of computer science?

II. Review of the Related Literature

A. Adaptation Levels within Intelligent Tutoring Systems

There are many levels of adaptation underpinning the building (ITSs), and the names of those levels differed from one study to another. In this study, the following names will be accredited for the following levels:

The first level of adaptation levels, which is Learner Level, which includes many characteristics and parameters like (learning style, motivation, cognitive traits, knowledge, learners' preferences, etc.), where this level represents the biggest challenge and the basis on which the system is built. This level is closely related to the next four other levels as indicated by [14]. The second level is the navigation or link level, which means the process of linking the learning objects (LOs) of the content and sequencing to facilitate the learner interaction with the system. This level includes many elements such as (Direct guidance, link hiding, and link generation)[15]. The third level is the content level, which involves the design of instructional content. It depends on the design and careful evaluation of (LOs) that can be reused and recalled with more than one learner at the same time depending on the type of characteristics of each individual learner. The fourth level is the presentation level. It is the way of displaying the content of each screen, as it is automatically generated to suit the nature of the learner individually, and it differs from a screen to another according to learners' classification. Finally, the level of learning path, which classifies learners into paths according to the characteristics of each learner to facilitate the recall and generation of learning elements appropriate for each learner individually and the following Fig. 1 shows adaptation levels in (ITSs).

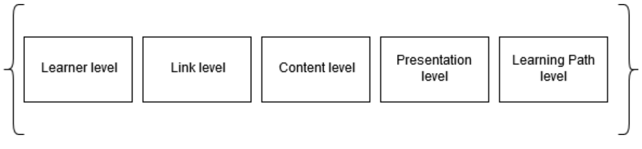

Fig. 1. Shows Levels of Adaptation in (ITSs).

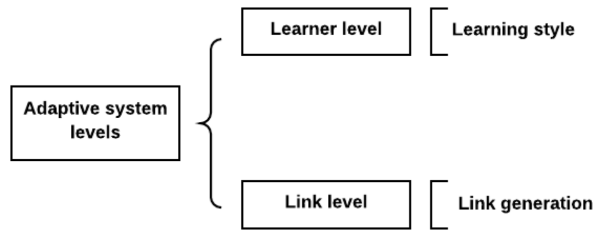

Fig. 2. Shows the Target Adaptation Levels in the Current Study.

The previous adaptation levels are very important in the design and construction of (ITSs) [4, 14]. These levels are linked together and overlapping, especially the link level, which the author believes the importance of this level in guiding the learner during the learning process within the system, specifically in terms of how content elements are sequenced, hidden and show links at the right time for each individual learner. Therefore the current study will be limited to merging two parameters from two different levels, the Learner Level (Learning style) with the Link level (link generation) as it is illustrated in Fig. 2.

B. Learning Objects (LOs) and Repositories

Learning objects are customizable and reusable interactive digital units in different contexts [15]. (ITSs) depend on Learning objects (LOs). To create learning content appropriate to the needs of learners, as well as, individual characteristics of students and their different capabilities [13], as the primary purpose is to reused with more than one learner to reduce the cost and speed of recall without loss of information. These objects are characterized by reusability, accessibility, scalability, manageability, durability, interoperability and manageability[16]. Whereas from a technological perspective, it is based on an idea of object-oriented programming, which we could use it many times in multi situations. This feature allows the idea of creating new and unique learning objects that can be used multiple times and there are several criteria that determine the structure of learning objects of the most important is SCORM standard "Shareable Content Object Reference Model" [17]. The design of these (LOs) is based on the idea of Metadata generation and reusability [15]. These objects require storage in a database called digital repositories, which act as a platform that store, retrieve, collect, and publish learning objects. Consequently, the current study depends on designing learning objects for intelligent tutoring systems by SCORM standards.

C. (ITSs) and Programming Skills

In fact, learning the programming languages, especially object-oriented programming (OOP) is one of the areas that are difficult to understand and implement. Besides, it represents the most difficult challenge for students [18, 19]. Because learners need more interaction with each step of problem-solving, writing programs, and the learner's need for help, ongoing mentoring, and problem-based thinking training. In contrast, (ITSs), which have been proven by many previous studies and research to be effective in teaching these courses, because they are adapted to the individual needs of the learner for each student individually according to their abilities, skills, and characteristics. In this regard, there are several relevant studies had adopted (ITSs) to learn computer courses including:

In [20] developed an adaptive e-learning system (AeLS) to learn computer graphics course for undergraduate students of a computer application program, they depend on the Felder Silverman learning style to build their system. Consequently, they divided learners into two groups (slow learners, face to face). Findings revealed that there is an obvious improvement with the slow learners group. In [19] developed an adaptive intelligent tutoring system to explore how adaptability is achieved in conventional intelligent tutoring systems and proposes an adaptive educational model that uses machine-learning techniques to define effective teaching methods appropriate for a particular student. The findings of the proposed model's test demonstrate the ability of the model to accurately identify the student subjects according to their learning style. [21] aimed to design an educational environment that supports smart classrooms, which included three aspects of content, collaboration, and hyperlinks. This proposal intended to obtain the data that helps in determining the appropriate learning materials for each learner according to his learning needs in programming languages subject, which includes the learning objects, knowledge, the skills of the students, as well as the educational activities. This proposal based on a system for managing learning objects (LOs) through a smart learning environment that meets learners' needs. Author in [22] provided an approach to factors influencing on designing and developing adaptive learning systems that include individual and group learning. This approach involves reinforcing and supporting learning to build intelligent environments based on artificial intelligence. Not only to provide appropriate methods that suggest learning materials that suit the needs of learners but to provide a good methodology for tracking student variables and status during the learning process, the finding indicated that the feasibility and effectiveness of the proposed approach. [23] aimed to provide an approach to design an adaptive learning system that not only depends on the learning style but also depends on the learning preferences. The experimental was applied for two groups. The firstly is the control group, that uses the traditional methods and the experimental group, which is used as a combination of variables within the adaptive learning environment, which provide learning according to learners' needs. The results showed the positive effect of the conducted of the system based on the integration of the third variables compared to the traditional system. Author in [24] investigated designing and developing adaptive courses used for learning programming basics which includes many kinds of personalized agents such as collect data from the user and tracking the response from students to present students appropriate materials of learning according to their learning styles. Author in [10] used intelligent tutoring system for learning java programming under multiple learning different methodologies such as problem-solving, knowledge space and overlays, they implemented the integration of cognitive and affective data to display emotions and empathy of the students, they used (ITS) open-source code in a programming language.

III. METHOD

For the current study, participants were (n=44) students. They were male students studying in the department of computer science at Qassim University, KSA. They split up randomly into two groups. The experimental group studied through the proposed system (ITS) and face-to-face group. There were (22) students in each group.

A. *Instrument*

The author developed the student's programming skills test in the Python Object-Oriented Programming course. The test consists of (15) questions in the inheritance unit. For the learning efficiency scale. The author relied on (SEL) scale for [25], which included (27) items to measuring self-efficacy for learning. While students' attitude towards an (ITS) was appeared by conducting personal interviews with students to know their views about the system, accessibility, and usability.

B. *Limitations of the Study*

The current study adopted the following limitations:

- Spatial Limitations: Faculty of Sciences and Arts, Qassim University, K.S.A.
- Python object-oriented programming language course (OOP).
- Human Limitations: Students in Level 8 and 9 in the Dep't. Of computer sciences.

C. *Design and Procedures*

There are many frameworks that can be used in designing adaptation systems such as, Generic Adaptation Framework (GEF) [14], Munich model [26], Adaptive Hypermedia Application model (AHAM) [27]. All these frameworks in general, should answer three questions: What can we adapt? to what do we adapt? In addition, how can we adapt? Accordingly, the current study adopted three components to answer the above questions, which used to design the proposed system (adaptation model, domain model, and learner model) as it is illustrated in Fig. 3. These components, in particular, constituted the common denominator for all previous frameworks [5].

1) Learner model: The learner model answers the question- What can we adapt? Accordingly, in this model, the adaptation system is based on learning style for each student, which refers to recognize the best way the learner perceives and interacts with the learning environment as well as, the individual's preferred method of learning [28]. In addition, knowing the needs of the learners and identifying their learning styles is essential in the design of content materials. [29]. Therefore, the present study relied on Felder- Silverman Learning style model (FSLSM). Which is one of the best models that presented many learning styles for learners, it includes four dimensions [Active: Reflective, Sensing: Intuitive, Visual: verbal, Sequential: Global], (FSLSM) considered more flexible than other most models. This model consists of 44 questions divided into four parts, each part involved a specific scope to reveal the learning style of each student, these questions are presenting after the login screen to the system. This domain also contains all the information and data for each individual student that is stored in the database by (Id).

2) Domain model: The domain model answers the question- To what do we adapt? It represents the educational content intended to be presented to the students through this system, this course is object-oriented programming using Python, where this content is presented as learning objects (LOs). These objects are stored classified in the system database (repository) according to the learning style for each individual learner.

3) Adaptation model: In view previous two models, this model answers the question- How can we adapt? Accordingly, an (ITS) relying on the two previous domains to build the process of adaptation, which is done in two ways. First is to determining the learning style of each learner to provide adaptation method based on the learning style, and then, call the learning object of each learner, as well as, all links related with advanced steps are hidden and presented in a timely manner, which depends on the interaction user with content. The second way is to monitor the screens to calculate the time taken. To provide feedback and instructions for each learner, in addition, providing feedback after the assessment and answer questions.

D. System Descriptions

A student is logged in by creating a new account via registration form to collect student's data, which is automatically stored in the database to take a unique ID number, then the student moves to the screen of the test to determine the learning style, which is consisted of 44 questions. Hence, saving the learning style code on the database and then the student moves to the educational content screen, which displays an educational module in a programming language with python shown to each student according to their learning style, and at the same time is tracking learner's behavior in terms of time spent and clicks on links. As well as, providing feedback, guidance, and counseling for each learner individually as shown in Fig. 4.

E. Experiment of the Study

The students were divided into two groups, each group twenty-two students (n=22). The pre-test was applied to the face-to-face control group as well as, the experimental group, which was implemented using an (ITS). The pre-test involved (15) questions about the inheritance unit within the python programming language. As well as, (SEL) scale to measuring self-efficacy, which includes (27) items. The experimental group was taught using an (ITS), whereas the control group learned face-to-face. After that, both of them exposed to the post-test. Fig. 4 shows the activity diagram for an (ITS).

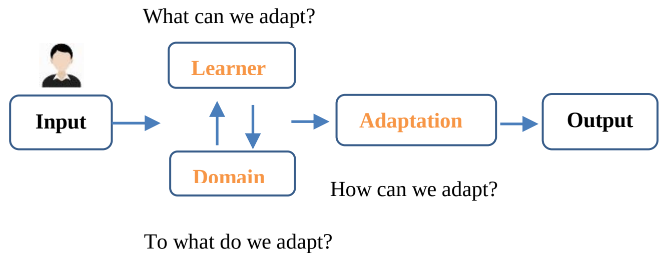

Fig. 3. Framework Architecture for Designing an (ITS).

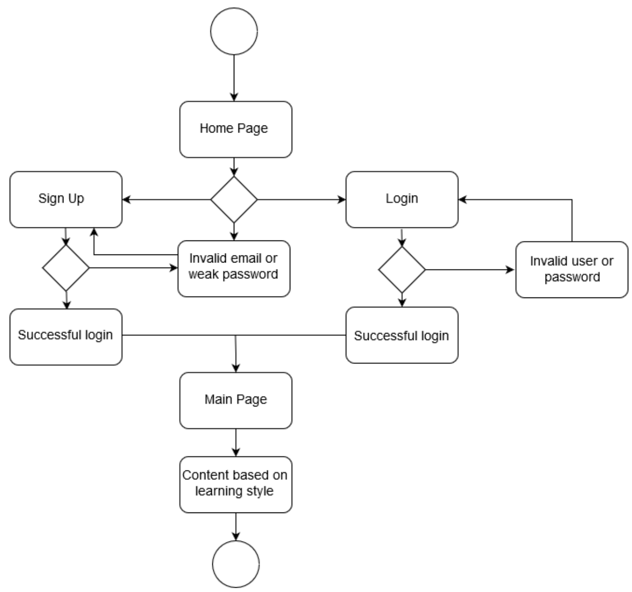

Fig. 4. Activity Diagram for an (ITS).

IV. Result and Discussion

To answer the study questions, the author used a descriptive statistical analysis program (SPSS). The first question asked if there was an effect of integrating learning style and link generation with the proposed an (ITS) on the development of programming skills for students. To check if there are initial differences between the pre-test and post-test for every single group. Paired-Sample T-test was used. In contrast, to comparing the two groups in the post-test, the Independent - Samples T-test was used.

Accordingly to Table I, there are significant differences between the mean scores of the pre-test (mean = 34.09) and the mean scores of the post-test (mean = 40.18) for experimental group, and T = 5.337 at a mean level (p = .000) less than the value of $\alpha = 0.05$ in favor of the post-test. This indicates that there is an improvement in students' programming skills after they exposed to the technological variable. Therefore, the obvious explanation for this result is that integrating learning style and link generation within an (ITS), have an effect on the performance of students. In addition, this result is consistent with many studies, which used an (ITS) for learning programming languages, such as [4, 10, 21, 23].

In contrast, the results in the previous table of the control group. Also indicates that there are significant differences between the mean scores of the pre-test (mean = 36.14) and the mean scores of the post-test (mean = 36.91), and T = 1.436 at a mean level (p = .166) less than the value of α = 0.05 in favor of the post-test. Despite there is a statistically significant difference, we note that the difference between the mean scores of the pre-test and post-test is very small, which indicates a weak improvement. The reason behind this is that the teaching of programming in the traditional system face-to-face, with the presence of large numbers of students, reduces the chance of student interaction with the professor, in addition to the traditional learning does not take into account the characteristics and individual needs of each learner regardless of the learning style for each student. This is consistent with previous research and studies, which point out that, such as [4, 6, 7, 30].

Accordingly to Table II, there are significant differences between the mean scores of the post-test (mean = 39.91) and the mean scores of the post-test (mean = 36.77), t-test = (1.964), degrees of freedom df = 42, at a mean level (p = .051) not greater than the value of α = 0.05 in favor of the experimental group. This result indicates that the learning outcomes for developing the programming skills of the experimental group are better than the learning outcomes of the control group. This confirms that an (ITS) used had a positive impact on the level of learning among students.

TABLE. I. DISPLAY THE DIFFERENCES BETWEEN PRE-TEST AND POST-TEST IN BOTH EXPERIMENTAL AND CONTROL GROUPS OF PROGRAMMING SKILLS FOR STUDENTS, USING THE PAIRED-SAMPLE T-TEST

	Control group					
	Mean	***SD***	***df***	***P-value***	***t***	***N***
Pre	36.14	5.276	21	.166	1.436	22
Post	36.91	5.255	21			22
	Experimental group					
	Mean	***SD***	***df***	***P-value***	***t***	***N***
Pre	34.09	6.796	21	.000	5.337	22
Post	40.18	5.086	21			22

TABLE. II. DISPLAY THE DIFFERENCES BETWEEN POST-TESTS FOR EXPERIMENTAL AND CONTROL GROUPS OF THE PROGRAMMING SKILLS, USING THE INDEPENDENT - SAMPLES T-TEST

	Experimental and control groups					
	Mean	***SD***	***df***	***P- value***	***t***	***N***
G1	39.91	5.362	42	.051	1.964	22
G2	36.77	5.228	41.9			22

TABLE. III. SHOWS THE DIFFERENCES BETWEEN PRE-TEST AND POST-TEST IN BOTH EXPERIMENTAL AND CONTROL GROUPS OF THE LEARNING EFFICIENCY FOR STUDENTS, USING THE PAIRED-SAMPLE T-TEST

	Control group					
	Mean	***SD***	***df***	***P- value***	***t***	***N***
Pre	30.50	9.324	21	.008	-2.944	22
Post	32.81	8.699	21			22
	Experimental group					
	Mean	***SD***	***df***	***P- value***	***t***	***N***
Pre	27.86	8.747	21	.000	-10.173	22
Post	40.14	7.692	21			22

To answer the second question: What is the effect of integrating learning style and link generation with the proposed an (ITS) on improving the learning efficiency for students of computer science? The author also used Paired-Sample T-test to check if there are initial differences between the pre-test and post-test for every single group as shown in Table III.

It is clear from Table III, there are significant differences between the mean scores of the pre-test (mean = 27.86) and the mean scores of the post-test (mean = 40.14) for experimental group, and T = 10.173 at a mean level (p = .000) less than the value of α = 0.05 in favor of the post-test. This result indicates that there is an improvement in students' learning efficiency after they exposed to the technological variable. Thus, the explanation for this result is that using an (ITS), has an effect on enhancing learning efficiency for students, this result is consistent with [31]. Besides, the results in the previous table of the control group. Also indicates that there are significant differences between the mean scores of the pre-test (mean = 30.50) and the mean scores of the post-test (mean = 32.81), and T = 2.944 at a mean level (p = .008) less than the value of α = 0.05 in favor of the post-test. Undoubtedly, there is an improvement in self-learning efficiency. However in a small percentage, and this is evident from the difference between the means. In addition, this is due to traditional learning, which does not take into account the characteristics and individual needs of each learner.

Undoubtedly, in Table IV, there are significant differences between the mean scores of the post-test (mean = 32.41) and the mean scores of the post-test (mean = 40.41), t-test = (3.234), degrees of freedom df = 42, at a mean level (p = .002) less than the value of α = 0.05 in favor of the experimental group. The current result indicates that the learning outcomes for enhancing the learning efficiency of the experimental group are better than the learning outcomes of the control group. This confirms that an (ITS) used had a positive impact on the level of learning among students.

Finally, all the students were invited to sharing in interviews. Regarding students' attitude towards an (ITS) was appeared by conducting personal interviews with students to know their views about the system, accessibility, and usability. The questions of the interviews were as the following:

1) What do you think about the merits of using an (ITS) on the development of programming skills*?*

2) What do you think about the merits of using an (ITS) on improving the learning efficiency for students*?*

3) What are the difficulties that you faced during learn from an (ITS)*?*

4) What are your suggestions for improving the system?

After the interviews, there seems to be some agreement among students about the following:

1) Ease of use of the system.
2) The lessons are clear.
3) Ease of code application.
4) Lessons need to increase the number of exercises.
5) Students cannot copy code from lesson pages.

TABLE. IV. DISPLAY THE DIFFERENCES BETWEEN POST-TESTS FOR EXPERIMENTAL AND CONTROL GROUPS OF THE LEARNING EFFICIENCY, USING THE INDEPENDENT - SAMPLES T-TEST

	Experimental and control groups					
	Mean	***SD***	***df***	***P- value***	***t***	***N***
G1	32.41	8.687	42	.002	3.234	22
G2	40.41	7.692	41.3			22

From the aforementioned, it may be deduced that an (ITS) used with the integration of some parameters had a clear impact on the development of programming skills among students, as well as on enhancing the learning self-efficacy among students of computer science.

V. CONCLUSIONS

The current study presented the effect of embedding adaptation levels (learner level and link level) via an intelligent tutoring system on developing programming skills and improving learning efficiency for students of computer science. Findings revealed that an (ITS) facilitated for students in improving their programming skills performance. As well as, there is also a positive effect on enhancing the learning self-efficacy, which is statistically evident from previous findings. As a future study, the current study recommends considering deeply at other parameters within other adaptation levels via intelligent tutoring systems. Specifically the presentation level and learning path level.

ACKNOWLEDGMENT

The author (Mohamed Ali Elkot) gratefully acknowledge Qassim University, represented by the Deanship of Scientific Research, on the material support for this research under the number (5144) during the academic year 1439 H / 2018AD.

REFERENCES

[1] Y. Eltigani, A. Mustafa, and S. M. Sharif, An approach to Adaptive E-learning Hypermedia System based on Learning Styles (AEHS-LS): Implementation and evaluation, vol. 3, no. 1. 2011.

[2] H. Peng, S. Ma, and J. M. Spector, "Personalized Adaptive Learning: An Emerging Pedagogical Approach Enabled by a Smart Learning Environment," Springer Singapore, 2019, pp. 171–176.

[3] S. Jiménez, R. Juárez-Ramírez, V. H. Castillo, J. José, and T. Armenta, Springer briefs in human computer interaction Affective Feedback in Intelligent Tutoring Systems A Practical Approach..

[4] M. T. Alshammari, "Adaptation based on Learning Style and knowledge Level in E-Learning Systems adaptation based on learnung style and knowledge level in e-learnin systems by School of Computer Science," 2016.

[5] P. Brusilovsky, "Adaptive hypermedia for education and training," Adapt. Technol. Train. Educ., pp. 46–66, 2012.

[6] S. Graf et al., "Adaptivity and Personalization in Learning Systems based on Students' Characteristics and Context," 1st Int. Symp. smart Learn. Environ., pp. 33–36, 2012.

[7] A. Jameson, "Adaptive Interfaces and Agents," pp. 105–130, 2009.

[8] S. Gross, B. Mokbel, B. Hammer, and N. Pinkwart, "Learning Feedback in Intelligent Tutoring Systems," KI - Künstliche Intelligenz, vol. 29, no. 4, pp. 413–418, 2015.

[9] H. M. Truong, "Integrating learning styles and adaptive e-learning system: Current developments, problems and opportunities," Comput. Human Behav., vol. 55, pp. 1185–1193, 2016.

[10] M. L. Barrón-Estrada, R. Zatarain-Cabada, F. G. Hernández, R. O. Bustillos, and C. A. Reyes-García, "An Affective and Cognitive Tutoring System for Learning Programming," 2015, pp. 171–182.

[11] M. A. Alket, "A Network-Based Peer Evaluation Strategy," Int. J. Mod. Educ. Comput. Sci., vol. 9, no. 4, pp. 32–42, 2017.

[12] D. Weragama and J. Reye, "The PHP intelligent tutoring system," Lect. Notes Comput. Sci. (including Subser. Lect. Notes Artif. Intell. Lect. Notes Bioinformatics), vol. 7926 LNAI, pp. 583–586, 2013.

[13] K. R. Premlatha and T. V. Geetha, "Learning content design and learner adaptation for adaptive e-learning environment: a survey," Artif. Intell. Rev., vol. 44, no. 4, pp. 443–465, 2015.

[14] E. Knutov, Generic Adaptation Framework for unifying adaptive web-based systems. 2012.

[15] L. P. A. Yela, A. D. O. Escobar, M. M. M. Anota, and J. M. Castillo, "Design of a mobile learning object repository (ROAM)," 2016 IEEE Int. Eng. Summit, IE-Summit 2016, 2016.

[16] V. Dagiene, D. Gudoniene, and R. Bartkute, "The integrated environment for learning objects design and storing in semantic web," Int. J. Comput. Commun. Control, vol. 13, no. 1, pp. 39–49, 2018.

[17] P. Kharat, G. Shekhar, and P. Gharpure, "Authoring tool based on learning object standards," Proc. - 2015 Int. Conf. Commun. Inf. Comput. Technol. ICCICT 2015, pp. 1–4, 2015.

[18] I. T. Machin Torres Ive, "Intelligent Tutor for Programming System Using Multiple Intelligences," IEEE Lat. Am. Trans., vol. 16, no. 2, pp. 634–638, 2018.

[19] M. Dlamini and W. S. Leung, Enhancing object-oriented programming pedagogy with an adaptive intelligent tutoring system, vol. 963. Springer International Publishing, 2019.

[20] L. Joseph and S. Abraham, "Adaptive e-Learning System for Slow Learners Based on Felder-Silverman Learning Style Model," vol. 1, pp. 123–135, 2019.

[21] D. Rivero-Albarrán, F. Rivas-Echeverria, L. Guerra, B. Arellano, and S. Arciniegas, "Design of a Recommender System for Intelligent Classrooms Based on Multiagent Systems," 2018, pp. 973–982.

[22] D. Shawky and A. Badawi, "A Reinforcement Learning-Based Adaptive Learning System," vol. 4, Springer International Publishing AG, 2018, pp. 221–231.

[23] A. Siddique, Q. S. Durrani, and H. A. Naqvi, "Designing Adaptive E-Learning Environment Using Individual Differences," Pak. J. Sci., vol. 69, no. 1, pp. 101–110, 2017.

[24] B. Vesin, M. Ivanović, A. Klašnja-Milićević, and Z. Budimac, "Personal Assistance Agent in Programming Tutoring System," in Smart Innovation, Systems and Technologies, vol. 38, 2015, pp. 441–451.

[25] J. E. Klobas, S. Renzi, and M. L. Nigrelli, "A scale for the measurement of self-efficacy for learning (SEL) at university," pp. 1–24, 2007.

[26] R. J. Sternberg and J. E. Davidson, Conceptions of giftedness. Cambridge University Press, 2005.

[27] N. Koch and M. Wirsing, "The Munich reference model for adaptive hypermedia applications," Lect. Notes Comput. Sci. (including Subser. Lect. Notes Artif. Intell. Lect. Notes Bioinformatics), vol. 2347 LNCS, no. May, pp. 213–222, 2002.

[28] T. Sheeba and R. Krishnan, "Automatic Detection of Students Learning Style in Learning Management System," in Smart Technologies and Innovation for a Sustainable Future, Advances in Science, Technology & Innovation, Springer International Publishing, 2019, pp. 45–53.

[29] M. Abdullah, W. H., R. M., M. Alzahrani, and M. Sadik, "The Impact of Learning Styles on Learner's Performance in E-Learning Environment," Int. J. Adv. Comput. Sci. Appl., vol. 6, no. 9, pp. 24–31, 2015.

[30] D. Hooshyar, R. B. Ahmad, M. Yousefi, M. Fathi, S. J. Horng, and H. Lim, "SITS: A solution-based intelligent tutoring system for students' acquisition of problem-solving skills in computer programming," Innov. Educ. Teach. Int., vol. 55, no. 3, pp. 325–335, 2018.

[31] T. Saba, "Implications of E-learning systems and self-efficiency on students outcomes: a model approach," Human-centric Comput. Inf. Sci., vol. 2, no. 1, pp. 1–11, 2012.

Neural Network-based Diabetic Type II High-Risk Prediction using Photoplethysmogram Waveform Analysis

Yousef K Qawqzeh
Department of Computer Science and Information
College of Science in Zulfi, Majmaah University
Al-Majmaah 11952, Saudi Arabia

***Abstract*—This work aims to predict and classify patients into diabetic and nondiabetic subjects based on age and four independent variables extracted from the analysis of photoplethysmogram (PPG) morphology in time domain. The study has two main stages, the first one was the analysis of PPG waveform to extract b/a, RI, DiP, and SPt indices. These parameters contribute by some means to the prediction of diabetes. They were statistically significant and correlated with the HbA1C test. The second stage was building a neural network based classifier to predict diabetes. The model showed an accuracy of 90.2% in training phase and an accuracy of 85.5% in testing phase. The findings of this research work may contribute towards the prediction of diabetes in early stages. Also, the proposed classifier showed a high accuracy in predicting the existence of diabetes in Saudi people population.**

***Keywords*—Diabetes; prediction; classification; photoplethysmogram; neural networks; diagnosis**

I. Introduction

The diabetes is considered as the most common chronic diseases in the world [1]. Normally, people having type 2 diabetes are exposed to different types of complications, which in turns leads to death [2]. In fact, the lack of insulin causes diabetes since it regulates sugar. Type 2 diabetes occurs when the insulin produced by pancreas is not effectively used by the body [3]. Changes in the lifestyle habits and foods worldwide increase the chance of having Type 2 diabetes among all societies [4-5]. Its expected by 2030 that diabetic patients will be increased by more than 100% [6]. This study utilized the photoplethysmogram (PPG) waveform analysis to extract features based on volumetric changes in PPG's contour that could by some means contribute to the prediction of type 2 diabetes. PPG signal represents the measurement of volumetric changes in blood tissues and vessels [7-8]. As there is no agreed definition about the origin of PPG waveform, it thought to represent the plethysmograph obtained optically [9]. Detecting of changes in blood volume in tissue microvascular bed can be achieved by PPG [10]. PPG's pulsatile components are related to blood volume changes inside arteries [11]. The well-known pulse oximeter is used to illuminate the skin (index finger, ear, or forehead) and then measure light absorption changes [12]. Different existed clinical applications utilized PPG technique in commercially available medical devices, such as pulse oximeters, blood pressure measurement systems, vascular diagnostics systems [13], and HR monitoring programs [14]. However, signal processing and features extraction will be elaborated in depth in research methods section.

Furthermore, the study implements an artificial neural network (ANN) classifier to predict and diagnose diabetic cases from non-diabetic ones. ANN represents a layered network structure that consists of an input layer, hidden layer(s), and an output layer. Each layer contains several nodes called neurons, were each neuron receives, processes its input and passes the output to the next layer [15]. ANN learning process consists of a training and testing phases in which the weights values are identified during the training phase [16]. Details on the input data (independent variables) and the target (the dependent variable) are demonstrated in research methods section.

II. Literature Reviews

Diabetes is considered as a global endemic that has a rapid increase in prevalence globally [17]. A good research work by [18] has proposed a PPG-based research work to assist the clinicians in diabetes screening and for the adopting of a suitable treatment plan towards the preventing of end-organ damage. In seeking the development of good and reliable classifiers for the prediction of diabetes, several classifiers were developed [19- 21]. A study by [22] claimed that they can use a deep learning algorithm for the detection of a prevalent diabetes by the analysis of PPG signal with a plausible difference.

The classification process is one of the most important topics in artificial intelligence area. Normally, the matter of classification happens when we want to assign an object to a predefined class depending on several attributes related to that object [23]. Classification plays a vital role in clinical diagnosis problems in which its outcomes will be used for further treatment [1].

The use of ANN in classification is considered very important in research and application areas [24]. One of the most common neural networks architecture that has been used for diseases prediction and diagnosis systems is the multi-layer neural networks architecture [25]. Additionally, a study by [26] used a deep convolutional neural networks (DCNN) to classify several types of cancer disease. To develop and evaluate a deep neural network learning classification and prediction models has been conducted for the diagnosis of patients with coronary heart disease [27]. A new convolutional neural network for breast cancer histopathology images classification has been designed by [28].

III. Research Methods

A. Subjects and Methods

This study aimed to study type II diabetic subjects, Saudi people at Zulfi General hospital, in a one-year time period (from Aug 2018 to Aug 2019). Normally, the patient will be diagnosed as type II diabetes if his HbA1C exceeds 6.5% [29]. The study hired a control group which has no diabetic history, and this health status is double checked by the analysis of a blood sample from each participant from the control group. A questionnaire-based data collection form is used to collect detailed information about participants, both diabetic and control subjects. Participants were advised to fast at least 6 hours before performing the HbA1C test and before the recording of PPG signal as well.

B. Data Collection

HbA1C tests are performed by analyzing a blood sample taken from participants by a specialized laboratory technician. The recorded HbA1C results are documented and labeled for each subject. The patient is then advised to move to an equipped research room to record his PPG signal using a customized PPG waveform recording system. A special instrument with a data acquisition board (NI cDAQ-9172) is used to digitize PPG signal locally and to transmit its digital data to a personal computer with a sampling rate of 5500 Hz. The recording of each PPG signal from each patient lasts for 1 minute approximately. The recording is repeated twice for each patient to allow for the selection of best PPG pulses. Subjects are requested to rest in a supine position in a quiet and controlled room temperature (25±1C^{o}) for 5 minutes to allow for cardiovascular stabilization. All participants received a brief orientation about the purpose of this study and about the expected outcomes of these recordings. Each subject showed his willingness to participate in this study by signing a written consent that declared his agreement. A customized algorithm is developed in MATLAB environment to analyze the PPG signals in time domain and then to extract features of interest from its morphology.

C. Measurements of Parameters

- HbA1C test: A blood sample for each subject has been taken and tested with Diazyme, enzymatic assay method by a specialized laboratory technician at Zulfi Hospital.
- The RI index: The RI index is calculated as the ratio of PPG's second wave peak to its first wave peak amplitudes. Fig. 1(a) also illustrates the calculation of RI index. The analysis of RI index variations could assist in the prediction of diseases and disorders associated with aging. A study by [7] reviewed the importance of PPG's RI index in the evaluation of atherosclerosis risk. Several studies focused on utilizing the RI index as an independent factor for the prediction of arterial stiffness and cardiovascular diseases. Its noteworthy to state that the RI index is declared to be highly related to age, as we age, the RI index will be increased.
- The b/a index: The b/a index is calculated as the ratio of "b" valley to the "a" peak, both a and b are extracted from PPG's second derivative morphology as shown in Fig. 1(b). The b/a index gained great attention from several researchers where they were looking for facilitating the interpretation of the original PPG's waveform using its derivatives. Early work by [30] has been conducted in which it concludes that the b/a index reflects arterial stiffness and atherosclerosis. Also, a study by [31] concluded that the b/a index is associated with peripheral arterial distensibility. Thereby, the b/a index is considered to be a very important factor in the examination of arterial wall elasticity. Other studies like [7; 32-33] stated that the b/a index is highly related to atherosclerosis and aging.
- The diastolic pulse peak (DiP): The Dpp represents the amplitude of PPG's second peak (the diastolic peak). The DiP tends to be clearly pronounced in healthy young subjects, while it tends to be less seen in old and diabetic subjects [34].
- The systolic peak time (SPt): The SPt is calculated as the time the PPG's systolic wave takes to arrive to its highest peak in milliseconds. As we age, the SPt index tends to increase in which it may reflect arterial stiffness.

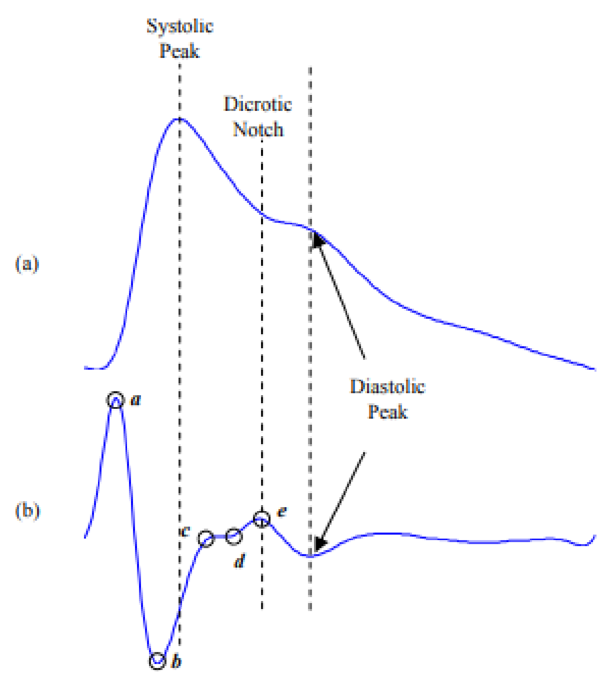

Fig. 1. The PPG Waveform were RI can be Calculated using the Systolic and Diastolic Peaks, (b) The Second Derivative of the PPG Waveform where the b/a Index can be Calculated. Source: [35].

D. Statistical Analysis

PPG parameters were expressed by their median ± SD values. Statistical analysis was implemented in the statistical package SPSS (version: IBM SPSS Statistics 25.0 for windows). Pearson correlation was used to examine the associations between the dependent (HbA1C) and the independent parameters. The value of P parameter <0.05 was considered statistically significant. Feedforward neural networks classifier using SPSS was used to predict the existence of HbA1C using the independent variables (IVs).

The neural network consists of one input layer, one hidden layer and one output layer. The input layer contains five independent variables namely b/a index, Age, RI, SPt, and DiP. Each one of them contributes by a certain amount towards the prediction of the dependent variable (HbA1C). The hidden layer utilized a Sigmund function that processes the inputs and classifies them into a diabetic or non-diabetic patient. The output layer falls into two binary outcomes, diabetic or non-diabetic.

IV. Results and Discussions

This section presents the multilayer perceptron. The case processing summary for the data is illustrated in Table I which shows the percent of the training sample (77%) and the percent of the testing sample (23%).

The network's information is explained in Table II which describes the input layer, hidden layer, and output layer elements. The input layer contains the following covariates as inputs parameters which are b/a index, Age, RI index, SPt index, and DiP index respectively. This network has one hidden layer that has three units with a Hyperbolic tangent as an activation function. Also, the output layer used the Softmax as an activation function to classify the dependent variable (the A1C index).

The network architecture is shown in Fig. 2. The architecture consists of three layers where the first column from the figure's left side represents the independent variables (inputs). The five indices in the input layer along with the Bias are used for classification. The output of each neuron (each input) is passed to all next neurons in the hidden layer which are multiplied by some weight and their product will be used to classify the samples into one binary class either diabetic or non-diabetic patient using a Softmax activation function.

In Table III, the model summary is elaborated which shows the performance of the model by looking to percent incorrect predictions error percentage in the training phase (9.8%) and in the testing phase (14.5%). The results claimed an accuracy of 90.2% in predicting the correct class in training time, and an accuracy of 85.5% in predicting the correct class during the testing time. As the error percent is approximately small in this model, we assume that this model performs well in predicting and classifying the patient into a diabetic or non-diabetic subject.

Parameter estimates in Table IV has two sections, the first left-upper part represents the result from the input layer to the hidden layer (predictors multiplied by weights), while the second right-down part represents the result from the hidden layer to the output layer. However, the classification results listed in Table V describe the overall percentage of model performance. In the training phase, the model classified 68 subjects correctly while 9 subjects were incorrectly classified as nondiabetic with an overall percentage of 90.2%. Besides, during the testing phase, the model performs well in diagnosing the subjects into 20 diabetic patients correctly while 3 subjects were classified incorrectly as nondiabetic patients with an overall percentage of 85.5%. Moreover, the model showed a better ability to predict the nondiabetic subjects by a percentage of 91.6% during the training phase where 9 subjects only have been classified incorrectly as diabetic patients.

TABLE. I. Case Processing Summary

		N	Percent
Sample	Training	184	77.0%
	Testing	55	23.0%
Valid		239	100.0%
Excluded		0	
Total		239	

TABLE. II. Network Information

Input Layer	Covariates	1	ba
		2	Age
		3	RI
		4	SPt
		5	DiP
	Number of Units[a]		5
	Rescaling Method for Covariates		Standardized
Hidden Layer(s)	Number of Hidden Layers		1
	Number of Units in Hidden Layer 1[a]		3
Output Layer	Dependent Variables	1	A1C
	Number of Units		2
	Activation Function		Softmax
	Error Function		Cross-entropy

a. Excluding the bias unit

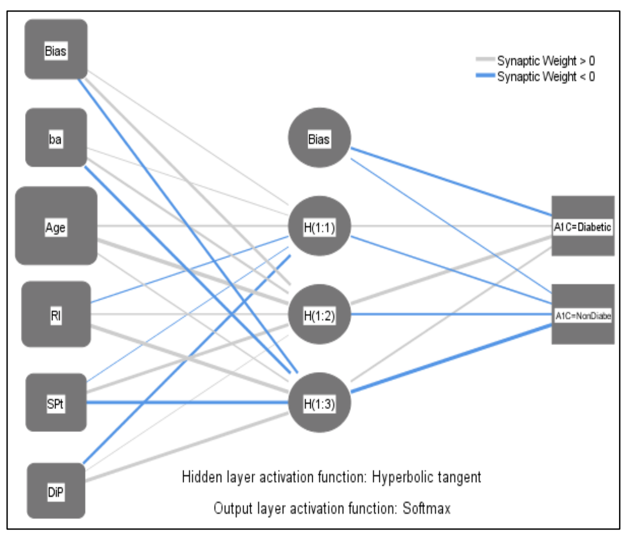

Fig. 2. The Architecture of the Developed NN Classifier.

TABLE. III. MODEL SUMMARY

Training	Cross Entropy Error	49.419
	Percent Incorrect Predictions	9.8%
	Stopping Rule Used	1 consecutive step(s) with no decrease in error[a]
	Training Time	0:00:00.05
Testing	Cross Entropy Error	18.105
	Percent Incorrect Predictions	14.5%
Dependent Variable: A1C		

a. Error computations are based on the testing sample

TABLE. IV. PARAMETER ESTIMATES

(Predicted)					
Predictor		H(1:1)	H(1:2)	H(1:3)	[Diabetic]	[Non diabetic]
Input Layer	(Bias)	.136	.819		
	ba	.063	.626		
	Age	.581	1.555		
	RI	-.259-	.431		
	SPt	-.042-	.957		
	DiP	-.738-	.013		
Hidden Layer 1	(Bias)			-.651-	-.244-
	H(1:1)			.480	-.455-
	H(1:2)			1.032	-.621-
	H(1:3)			.582	-1.077-

TABLE. V. CLASSIFICATION

Sample	Observed	Predicted		
		Diabetic	NonDiabetic	Percent Correct
Training	Diabetic	68	9	88.3%
	NonDiabetic	9	98	91.6%
	Overall Percent	41.8%	58.2%	90.2%
Testing	Diabetic	20	3	87.0%
	NonDiabetic	5	27	84.4%
	Overall Percent	45.5%	54.5%	85.5%

The classification of diabetic and nondiabetic patients is shown in Fig. 3. The boxplot demonstrates the Tukey's five numbers summary which are the minimum, first quartile (Q1), median, third quartile (Q3), and the maximum. For the diabetic group, the median value of those who are diagnosed correctly as a diabetic patient was 0.9. In the other hand, the median value of those who are diagnosed correctly as a nondiabetic patient was almost 0.95.

Moreover, a very interesting output from the developed model to look at is the independent variable importance which is illustrated in Table VI and in Fig. 4. Both Table VI and Fig. 4 showed that Age index (0.338) was the dominant index among the independent variables that contribute by some means to the prediction of diabetes as we age. The second important factor was RI index (0.225) in which it scored the second place of importance after Age. Finally, b/a index, SPt index and DiP index were contributed by a less amount towards the prediction of diabetes by 0.56, 0.152, and 0.129 percent, respectively. Note that the summation of all independent variables importance percent equals to 1.

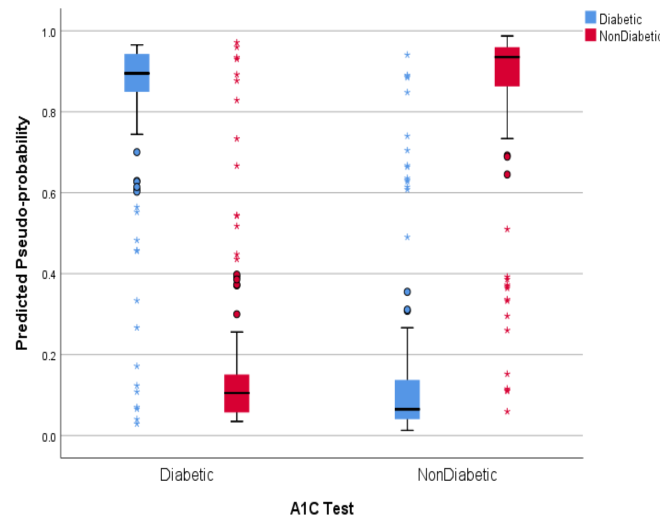

Fig. 3. Boxplot Diagram for the Classification of Diabetic and Nondiabetic Patients.

TABLE. VI. INDEPENDENT VARIABLE IMPORTANCE

	Importance	Normalized Importance
ba	.156	46.2%
Age	.338	100.0%
RI	.225	66.5%
SPt	.152	45.0%
DiP	.129	38.0%

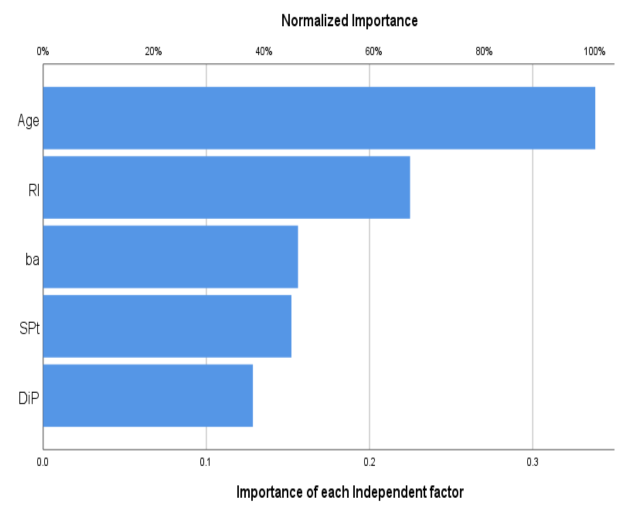

Fig. 4. The Normalized Importance of Each of the Dependent Variables in the Prediction of the Dependent Variable.

V. CONCLUSIONS

In this work, we recorded a PPG signals from two participant groups. The first one with established and clinical confirmed diabetic, while the second one with no history proof of diabetes. Their recorded PPG waveforms were analyzed in a customized algorithm to extract the parameters of interest which are RI, B/a, DiP, and SPt indices, respectively. After that an HbA1C test was conducted for all diabetic and nondiabetic groups and their measurement were recorded and documented. A Pearson correlation test was fired to examine the associations between the independent variables and the dependent variable. The study then performed a neural network classification model to investigate and examine the amounts of contribution that each independent variable did towards the prediction of diabetes. The developed classifier showed a high degree of accuracy in both training phase (90.2%) and in testing phase (85.5%) in which it makes the developed classifier a reliable model for diabetes evaluation and early diabetes stages prediction. The developed model may aid in the prevention of diabetes by predicting the high-risk diabetes in its early stages, which in turn might deliver a great benefit to both people and doctors in terms of prediction and classification.

ACKNOWLEDGMENT

The authors would like to thank the Deanship of Scientific Research at Majmaah University for supporting this work under project number No. R-1441-49.

REFERENCES

[1] K. Kannadasan, E. Damodar, and K. Venkatanareshbabu, "Type 2 diabetes data classification using stacked autoencoders in deep neural networks," Clinical Epidemiology and Global Health, 2018.

[2] O Abdulfatai, O. Olusegun, and O. Lateefat, "Type 2 Diabetes Mellitus: A Review of Current Trends," Oman Medical Journal, vol. 27, no. 4, 2012, pp269-273

[3] H. Chen, C. Tan, Z. Lin, and T. Wu, "The diagnostics of diabetes mellitus based on ensemble modeling and hair/urine element level analysis," Comput Biol Med, vol. 50, 2014, pp70–75

[4] EI. Mohamed, R. Linder, G. Perriello, ND. Di, S. Poppl, and AL. De, "Predicting type 2 diabetes using an electronic nose-based artificial neural network analysis," Diabetes, nutrition & metabolism, vol. 15, no. 4, 2002, pp215–221

[5] K. Polat and S. Gunes, "An expert system approach based on principal component analysis and adaptive neuro-fuzzy inference system to diagnosis of diabetes disease," Digit Signal Process, vol. 17, no. 4, 2007, pp702–710

[6] P. Manaswini and S. Ranjit, "Predict the onset of diabetes disease using Artificial Neural Network (ANN)," International Journal of Computer Science & Emerging Technologies, vol. 2, I 2, 2011, pp303-311

[7] Y. Qawqze, U. Rubins, and M. Alharbi, "Photoplethysmogram second derivative review: Analysis and applications," Scientific research and essays, vol. 10, no. 21, 2015, pp633-639

[8] A. Reisner, P. Shaltis, D. McCombie, and H. Asada, "Utility of the Photoplethysmogram in Circulatory Monitoring," Anesthesiology, vol. 108, no. 5, 2008, pp950-958

[9] J. Moraes et al, "Advances in photopletysmography signal analysis for biomedical applications," Sensors, vol. 18, no. 1894, 2018

[10] I. Challoner, "Non-Invasive Physiological Measurements," ed P Rolfe (London: Academic), 1979, pp125-151

[11] M. Elgendi, "The use of photoplethysmography for assessing hypertension," npj Digit. Med, vol. 2, no. 60, 2019, pp1-11

[12] K. Shelley and S. Shelley, "Pulse Oximeter Waveform: Photoelectric Plethysmography in Clinical Monitoring," Clinical Monitoring: Practical Applications for Anesthesia and Critical Care, pp420-428.

[13] J. Allen, "Photoplethysmography and its application in clinical physiological measurement," Physiol. Meas, vol. 28, ppR1-R39.

[14] Md. Shofiqul Islam, Md. Shifat-E-Rabbi, A. Dobaie, and Md. Hasan, "PREHEAT: Precision heart rate monitoring from intense motion artifact corrupted PPG signals using constrained RLS and wavelets," Biomedical Signal Processing and Control, vol. 38, 2017, pp212-223

[15] A. Al-Jarrah and H. Shatnawi, "Non-proliferative diabetic retinopathy symptoms detection and classification using neural network," Journal of medical engineering & technology, vol. 41, no. 6, 2015, pp498–505.

[16] K. Verma, L. Verma, and P. Tripathi, "Image classification using backpropagation algorithm," J Comput Sci Soft Appl, vol. 1, 2014, pp7–15.

[17] SI, Sherwani, HA. Khan, A. Ekhzaimy, A. Masood, and MK. Sakharkar, "Significance of HbA1c Test in Diagnosis and Prognosis of Diabetic Patients," Biomark Insights, vol. 11, 2016, pp95–104.

[18] N. Neelamshobha, R. Periyasamy, S. Bikesh, and K. Awanish, "Detection of type-2 diabetes using characteristics of toe photoplethysmogram by applying support vector machine," Biocybernetics and Biomedical Engineering, vol. 39, no. 1, 2019, pp38-51.

[19] E. Ubeyli, "Comparison of different classification algorithms in clinical decision-making," Expert Syst, vol. 24, 2007, pp17-31.

[20] J. Kandhasamy and S. Balamurali, "Performance analysis of classifier models to predict diabetes mellitus," Proc Comput Sci, vol. 47, 2015, pp45-51.

[21] N. Nai-Arun and R. Moungmai, "Comparison of classifiers for the risk of diabetes prediction," Proc Comput Sci, vol. 69, 2015, pp132-142.

[22] A. Robert, T. Geoffrey, K. Peter, M. Gregory, P. Mark, O. Jeffrey , and A. Kirstin, "Predicting diabetes from photoplethysmography using deep learning," J Am Coll Cardiol, vol. 73, no. I 9, s. 2, 2019.

[23] G. P. Zhang, "Neural networks for classification: a survey," IEEE Transactions on Systems, Man, and Cybernetics, Part C (Applications and Reviews), vol. 30, no. 4, 2000, pp451-462.

[24] K. Saravanan and S. Sasithra, "Review on classification based on artificial neural networks," International Journal of Ambient Systems and Applications (IJASA), vol. 2, no. 4, 2014, pp11-18.

[25] Er. Orhan, A. Tanrikulu, A. Abakay, F. Temurtas, "An approach based on probabilistic neural network for diagnosis of Mesothelioma's disease," Computers & Electrical Engineering – CEE, vol. 38, 2015, pp75-81.

[26] H. Nogay, "Classification of Different Cancer Types by Deep Convolutional Neural Networks," Balkan journal of electrical & computer engineering, 2018, pp54-59.

[27] M. Kathleen and M. Julia, "Coronary Heart Disease Diagnosis using Deep Neural Networks," International Journal of Advanced Computer Science and Applications (IJACSA), vol. 9, no. 10, 2018, pp1-8.

[28] Y. Jiang, L. Chen, H. Zhang, and X. Xiao, "Breast cancer histopathological image classification using convolutional neural networks with small SE-ResNet module," PLoS ONE, vol. 14, no. I 3, 2019, pp2-21.

[29] MayoClinic, "Type 2 diabetes," Retrieved form [https://www.mayoclinic .org/diseases-conditions/type-2-diabetes/diagnosis-treatment/drc-20351199] on Sep 25Th 2019.

[30] TN. Takazawa, M. Fujita, O. Matsuoka, T. Saiki, M. Aikawa, S. Tamura, and C. Ibukiyama, "Assessment of vasocative agents and vascular aging by the second derivative of photoplethysmogram waveform," Hypertension, vol. 32, 1998, pp365-70.

[31] I. Imanaga, H. Hara, S. Koyanagi, and K. Tanaka, "Correlation between wave components of the second derivative of plethysmogram and arterial distensibility," Jpn Heart J, vol. 39, 1998, pp775-84.

[32] B. Peskin and R. Rowen, "Breakthrough in Clinical Cardiology: InOffice Assessment with Pulse Wave Velocity (PWV) and Digital Pulse Analysis (DPA)," Clin. Cardiol, 2010, pp80-86.

[33] A. Alberto, "The finger volume pulse and the assessment of arterial properties," J. Hypertens, vol. 20, 2002, pp2341-2343.

[34] G. Papini, P. Fonseca, X. Aubert, S. Overeem, J. Bergmans, and R. Vullings, "Photoplethysmography beat detection and pulse morphology quality assessment for signal reliability estimation," 39th Annual International Conference of the IEEE Engineering in Medicine and Biology Society (EMBC), Seogwipo, 2017, pp117-120.

[35] M. Algendi, "On the Analysis of Fingertip Photoplethysmogram Signals. Current Cardiology Reviews, vol. 8, 2012, pp14-25.

Clustering Analysis for Malware Behavior Detection using Registry Data

Nur Adibah Rosli[1], Warusia Yassin[2], Faizal M.A[3], Siti Rahayu Selamat[4]
Faculty of Information and Communication Technology
Universiti Teknikal Malaysia Melaka
Malaysia

***Abstract*—The increase of malware attacks may increase risk in information technology industry such as Industrial Revolution 4.0 that consists of multiple sectors especially in cyber security. Because of that malware detection technique plays vital role in detecting malware attack that can give high impact towards the cyber world. In accordance with the technique, one of unsupervised machine learning able to detect malware attack by identifying the behavior of the malware; which called clustering technique. Owing to this matter, current research shows a paucity of analysis in detecting malware behavior and limited source that can be used in identifying malware attacks. Thus, this paper introduce clustering detection model by using K-Means clustering approach to detect malware behavior of data registry based on the features of the malware. Clustering techniques that use unsupervised algorithm in machine learning plays an important role in grouping similar malware characteristics by studying the behavior of the malware. Throughout the experiment, malware features were selected and extracted from computer registry data and eventually used in the proposed clustering detection model to be clustered as normal or suspicious behavior. The results of the experiment indicates that this proposed model is capable to cluster normal and suspicious data into two separate groups with high detection rate which is more than 90 percent accuracy. Ultimately, the main contribution based on the findings is the proposed framework can be used to cluster the data with the use of data registry to detect malware.**

Keywords—Malware; malware detection; behavior analysis; k-means clustering; data registry

I. Introduction

Developing a malware detection system model by using K-Means clustering approaches is demanding in IDS field. Even though clustering techniques causes a number of advantages in grouping similar malware characteristics, however unsupervised algorithm specifically against registry information is absent in machine learning techniques. First, clustering is one of the best method in recognizing similar binaries and put them in one group as used by [1]–[4]. Other researchers [4]–[9] shows that recognizing the malware in malware analysis by using K-Means clustering method is the best way. However, none of them use this method using registry information to analyze the malware. Thus, based on that matter, there is still low significant of malware analysis in this field. Second, Malware analysis by using registry information has been explored by previous researchers [10]–[15] with different methods of malware detection. Yet, K-Means algorithm is still not an alternative to cluster malware data to detect any malware causes low significant malware detection method. Even so, the use of K-Means clustering as malware detection in windows registry has been review by [16] in their survey and K-Means clustering method seems promising in malware detection field. Thus, this paper addresses the two issues, which are lack of data in detecting malware behavior and lack of further analysis in detecting malware behavior. K-Means clustering detection model with appoint of data mining, peculiarly clustering method is a notable field that can be explored to overcome this matter. It is a need to have continuous of IDS improvement in term of the accuracy of malware analysis, the detection time and the suitable detection approach; are the motivations for this research. Therefore, the objective of this research is to generate registry information in detecting malware behavior and secondly to propose clustering analysis against registry information for malware detection. This research focuses on the K-Means clustering as a method to analyze malware in windows registry, which accurately identify normal and suspicious behavior with minimum false positive and false negative as well as maximum true positive and true negative. In addition, the detection method is designed such that it could operate accurately in identifying intrusion in host-based intrusion detection system (HIDS).

II. Literature Review

A. Malware

Over the years, many security problems escalated because of excessive use of Internet usage and computer systems over network. Briefly, the interconnected systems such as Web servers, database servers and cloud computing servers are exposed to many threads that come from cyber attackers. Regarding this concern, CERT statistics [17] shows that the amount of intrusion every year, and distressingly, they keep growth excessively. Consequently, the attacks in the form of malicious intrusion exposing the network to vulnerabilities that causes serious impact to computer and information system besides violated the policies of computer security such as CIA or Confidentiality, Integrity and Availability. Malicious intrusion known as Malware is an intrusive software, which can be in term of file or code causing harm. It is a program that has malicious intentions, which is created and designed for clear objective to get access in information system without permission from the administrator [18]. This refers to [19] that described malware as developed malicious software which has an intention of lunching malignant tasks. Similar to [20], defined that malware is a type of program by accomplishing

Universiti Teknikal Malaysia Melaka (UTeM) and Cyber Security Malaysia (CSM) under CMERP Grant –GLUAR/CSM/2016/FTMK-CACT/100013.

something as such the attacker needs it to be. It also defined decades ago by [21] supported by [22] as a malicious software that fulfill harmful intention of an attacker such as “Viruses”, “Worms” and “Trojan horses”. In addition, there are many types of malware nowadays that has been created to take advantage as well as harming others such as “Botnet”, “Adware”, “Spyware” and “Ransomware”. Different category of malware act differently compare to each other:

1) Virus: A virus can be defined as a program that can 'infect' other programs by modifying them to comprise a possibly evolved version of itself [23]. Author in [24] also described virus as malicious program software that can replicate themselves and spread among computers. To be simplified, virus means a simple form of software that is loaded and launched without user’s permission while reproducing itself or infecting other software.

2) Worm: Similar to virus, worm can spread over the network but the different is it can replicate to other software. It is a self-replicating computer program and uses a network to send copies of itself to other nodes such as computers on the network without any user involvement [25]. Author in [26] also defined worms are generally self-propagating software, since they self-propagate but usually rely on the receiving user to activate them.

3) Trojan: Different to virus and worm, Trojan is a type of malware that appear as legitimate software. This malware class is used to define the malware types that aim to appear as genuine software. Because of this, the general spreading vector utilized in this class is social engineering, i.e. making people think that they are downloading the legitimate software [27].

4) Botnet: Botnet is an infected network of computers on the Internet with software robots, which is called as bots [28]. [29] Described botnets are large collections of computers called “zombies” that are under the control of a single attacker. Botnet also defined by [30] as collection of computer that has been infected by malicious software a; converts bots, drones, or zombies, which have been integrated into a bigger collection through a centralized command and control infrastructure. It means that in an infected computer, the information systems build a network of bots that receive instructions from a server known as command-and-control server.

5) Adware: Adware is an advertising supported programming that performs its activity by displaying or downloading the advertisement to a user computer after the installation of malicious application or programming [31]. Author in [32] also described that an ad-injecting browser extension such as of adware, analyzing all the malware activities of ad injecting extension also falls under the category of adware. The main purpose of adware is displaying advertisements on the computer and can lead to dramatic results. Adware are basically an applications which has a goal in getting maximal revenue to the developer while giving the user the minimal amount of value [33].

6) Spyware: A spyware is a malware; which follow the action of user silently without the client knowing. Standard actions of spyware are tracking search history to send personalized advertisements as well as tracking activities and afterwards selling them to the third parties. The gathered information can include the website, browser and system information which are visited by user. Spyware can likewise control over the framework [31].

7) Ransomware: Ransomare is a type of malware that aims to encrypt all the data on the machine and ask a victim to transfer some money as the ransom to get the decryption key. Usually, a machine infected by ransomware is “frozen” as the user cannot open any file, and the desktop picture is used to provide information on attacker’s demands. The Netskope Cloud Report of September 2016 revealed that 55.9% of malware-infected files found in cloud apps are shared publicly thus, the cloud is an attractive platform for attackers [34]. Currently, ransomware is a major threat faced by organizations and individuals alike. Ransomware is part of a recent malware trend that prevents or limits access to resources in the infected computer [35], Ranomware can be detected in registry as discussed by [36].

Data from the Malaysia Computer Emergency Response Team (MyCERT) shows the reported incidents of cyber-attacks [17]. Malware attacks rely under malicious codes and it is crucial incidents as it is in the top three of the statistics. Total cyber-attacks incidents in year 2017 are presented in Fig. 1.

Besides, statistic form Information Security Timelines and Statistics [37], in January 2018 malware hit a new maximum rate with 43.5%, which is the highest rate compared to the other attack vectors. Fig. 2 shows the attack vector statistic in January 2018.

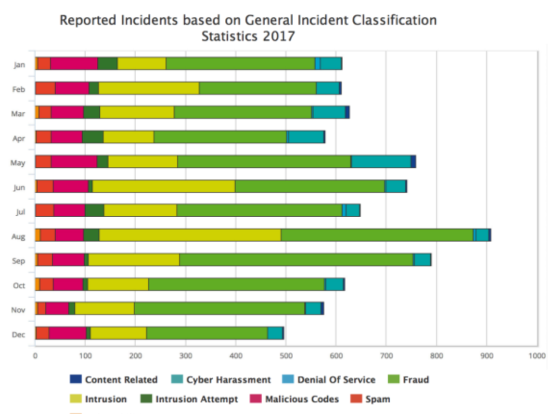

	JAN	FEB	MAR	APR	MAY	JUN	JUL	AUG	SEP	OCT	NOV	DEC	TOTAL
Content Related	2	5	9	2	9	2	1	4	2	2	5	3	46
Cyber Harassment	41	45	64	71	119	39	27	25	32	36	31	30	560
Denial of Service	11	0	3	3	1	3	8	6	2	2	1	0	40
Fraud	296	233	274	265	346	298	329	382	466	351	340	241	3821
Intrusion	98	201	148	101	138	284	146	363	181	121	119	111	2011
Intrusion Attempt	39	19	32	41	22	8	37	31	8	9	11	9	266
Malicious Code	94	68	65	62	92	71	62	56	64	60	46	74	814
Spam	26	38	24	30	31	32	36	30	29	26	17	25	344
Vulnerabilities Report	5	2	8	3	1	4	2	11	6	10	5	3	60
TOTAL	612	611	627	578	759	741	648	908	790	617	575	496	7962

Fig. 1. Statistic of Reported Incident, 2017.

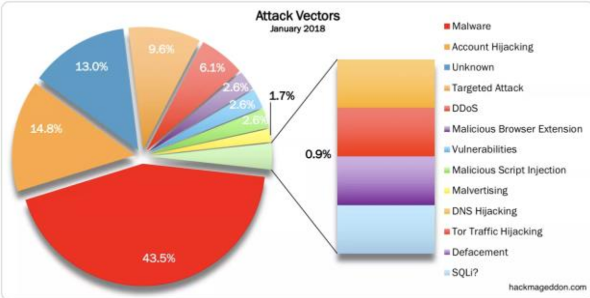

Fig. 2. Attacks Vector Statistic, January 2018.

Cyber-attacks become the biggest threat in computer and networks system around the world. Because of that it is important to merge IDS that can detect and analyze the data with high accuracy (i.e., true positives and negative) and low false detection (i.e., false positive and negative) in the minimal detection time. So, K-Means clustering detection model with appoint of data mining, peculiarly clustering method is a notable field that can be explored to overcome this matter. It is a need to have continuous of IDS improvement in term of the accuracy of malware analysis, the detection time and the suitable detection approach; are the motivations for this research.

B. *Malware Detection*

Malware interrupt the file registry when entering a computer and basically malware tend to create and modify computer files system and Windows registry entries besides the computer interprocess communication and basic network interaction [21]. Intrusion attack such as malwares are known to breach the policy of network security in organizations and continuously tries to interrupt the core fundamental of cybersecurity which are Confidential, Integrity and Availability or known as CIA. Therefore, previous cybersecurity researcher has proposed detection-based for malware intrusion, which is a framework that monitors the behavior of system activity. Then, the behavior will be analyzed by the framework and notify the users if there is a sign of intrusion. Furthermore, [24] define intrusion detection as an event monitoring process where it can be implemented in network or computer system and capable to send notification if there is any intrusion has been detected. Besides, scanning is vulnerability evaluation that has been used in intrusion detection to access the vulnerabilities over computers system or network. There are two types of attack that can be analyze by intrusion detection such an intrusion attack can be explained as an attack mainly from malware infect machine or network outside organization while on contrary, misuse attack can be define as an attack targeting within organization. In a nutshell, intrusion detection capable to monitor system activities including scanning vulnerabilities, system integrity and configuration, recognizing each attack patterns, analyzing irregular activities in operating system and tracing users if the users have break or violate policies.

At any cost, the detection of malware is important and crucial as it conquer more than half of malware attack that exploit on the computer registry; and it can be detected by using Intrusion Detection System as the early defense over the malware attack [36]. One of the solutions in detecting any intrusions is an Intrusion Detection System (IDS) to avoid the network and computer system from any cyber attack. There are many function and tasks in system security as discussed in most studies related to detection system. The uses of IDS protect computer system and ultimately improve the system security.

An IDS is a real time system that can monitor in spite of analyze network packet and system audit log for detecting and identifying malware behavior or any intrusion attempts in a computer system, before sending intrusion alerts to system administrators [38]. Another definition by [39] described that. IDS is a specific hardware and software that can monitor any occurring event automatically in computer system or network that collect and synchronize the event records as well as analyze them if there is any sign of security violation. Thus, an IDS is a type of security hardware and software that designed to give alert to the administrators automatically if there is any attacks, security policy violations or malicious activities that can compromise information system by monitoring system activity through examining vulnerabilities in the system and analyzing the vulnerabilities patterns bases on the mechanism of detection of previous attacks. In addition, IDS able to monitor the Internet search automatically to find any latest threats that could be future attacks based on the malware behavior.

In term of malware detection, this paper focusing on anomaly detection as it detects any intrusion through analyzing and make divergence from the pattern of the normal behavior [38]. Anomaly is an abnormality to a normal behavior and profiles pattern, which is a show as normal or usual behaviors. The anomaly detection is a derivation of information from monitoring regular computer activities, network connections, hosts or users over a specific time and sometimes it is called as Behavior-based Detection [40]. The profile of malware can be either static or dynamic, but still creating many attributes. After that, anomaly detection differentiates the normal profiles with the observed events to recognize significant attacks. As stated by [41] based on the abnormality anomaly-based intrusion detection characterize the baseline models that are normal and identifies any attacks from the models. This method is able to identify any unique attacks and capable to target a wide range of attacks. As an example, by is using low-level architectural and microarchitectural features that available from HPCs which is hardware performance counter, Tang also examine that the feasibility and limits of performing anomaly-based malware detection. Furthermore, based on the principle of detection, anomaly-based detection can be more promising techniques in discovering any computer intrusion or attacks [42] in term of monitoring and flags any network activities displaying significant deviation from legitimate traffic profiles as suspicious objects. Thus, this research used the concept of anomaly detection based on the benefit of anomaly detection to detect previous unknown intrusion or attack.

C. *Malware Detection in Windows Registry*

Windows Registry is known as hierarchical of database information, setting, option, and other value of hardware and software that stored in low-level settings of Microsoft Windows operating system. It can be accessed through registry key that analogous to file system directories [13]. Windows and every program are continually referencing the registry;

hence when there are any changes of them, changes are also made to suitable areas in the registry.

Detection of malware in windows registry by using K-Means clustering is a new topic in this field. Even though the previous researchers had discovered malware in the same location, which is in registry, however they have used different detection method as malware detection apart from K-Means clustering method.

In AccessMiner, which is using system-centric models achieve a large-scale collection for malware protection examine the diversity of system calls by [10]. The analysis of the data presents that simple malware detector by using alternative detection model that characterizes the general interactions between benign programs and the operating system (OS). The system-centric approach models analyze benign programs that access OS resources such as files and registry entries and it results in raising very few or even zero false positives malware detection.

Similar with Behavior-based Detection Model, HOLMES [11] also analyze files and registry by using another model. It presents an automatic technique to extract optimally discriminative specifications, which uniquely determine a class of the programs. The proposed technique is based on graph mining and concept analysis, scales to large classes of programs due to probabilistic sampling of the specification space. The proposed HOLMES can synthesize discriminative specifications that accurately distinguish between programs, sustaining an 86% detection rate on new, unknown malware, with 0 false positives rate.

Other than that, by using behavioral sequential patterns as malware detection method, [12] proposed dynamic malware detection system based on mining the API sequences and iterative patterns extracted from an executable trace of API calls. The framework is able to examine and detect malicious behavior as well as introduced the concept of iterative pattern mining in this field.

Moreover, to detect malware in virtual environment based on its behavior, a dynamic malware analyzer has been proposed [13]. This approach is able to bypass anti-VM detection technique in detecting malware and their behavior and also identify the technique that has been used by malware. The dynamic malware analyzer can monitor the resources of the system for example, network connection, file system, processes and also services. Then, it gives information regarding the malware attack to analyst and noted the changes of Windows registry. Finally, the accuracy test by using Pahadus public malware set is successful with high detection ratio which is 92%.

In experimental analysis of ransomware by [14], when a computer machine is attacked by ransomware, the analysis of ransomware, basically focus on the families evolution and characteristic of the. Ransomware interaction with the file system, registry activities, and network operations. The experimental results show that the detection of ransomware is achievable based on examining abnormal file system and registry activities in Windows environment. To check the effectiveness of the experiment, a computer machine is already had all inbuilt security procedures upgraded and running, which automatically detect and delete all those ransomware variants before it is infected by ransomware.

The last method in malware analysis and detection tools discussed by [15]. The author did an analysis of by comparing the well-known malware and benign programs. In the experiment, samples are taken which is 100 malware and 100 benign programs that come from many different sources and have been analyzed by using different type of Windows machines versions. The test results indicate that it is extremely difficult to detect the presence of malware by using only one tool. Thus, the new approach is by using both dynamic and static analysis tools; it can increase the detection rate as well as its accuracy.

The comparison of related works under detection malware on windows registry presented in Table I shows that different detection models are used in the same malware location, which is windows registry by different authors.

The comparison result shows that K-Means clustering is a new approach in detecting malware on windows registry. In addition, significant malware analysis by using K-Means clustering in high demand in analyzing malware accurately as well as better malware detection. All previous researchers had explored about K-Means clustering and applied the algorithm in different model to achieve the objectives. K-Means clustering is widely used in many different areas in detecting malware.

TABLE. I. PREVIOUS WORK (DETECTION OF MALWARE IN WINDOWS REGISTRY)

Author	Detection Model	Detection Location	Input Data	Result
[10]	System-Centric Models	Windows: system call, registry	Data collection (system call)	Increase false positive rate
[11]	Behavior-based Detection Model, HOLMES	Windows: registry, system call	Real malware samples (Honeypot)	Low false positive rate
[12]	Behavioral Sequential Patterns	Windows: file system, process, registry	Logging calls (API call)	Low false positive rate
[13]	Dynamic malware Analyzer	Windows: connections, processes, registry, file operations	Pahadus public malware set sample	High true positive rate
[14]	Analyzing samples of selected ransomware variants	Windows: file system, registry, network activity	Malware data sets collection (virus total, public malware repositories, security forums)	High true positive rate
[15]	Static and dynamic analysis tools	Windows: file system, registry, process activity	Program sample malware (Windows)	High true positive rate

D. Malware Detection by using K-Means Clustering

K-Means clustering is a method of cluster analysis in which the defined 'k' is separating the clusters with the existence of center value between all the grouped objects. However, in data mining perspective, the implemented K-Means clustering algorithm separates the time interval between the normal and abnormal data in the same training dataset. Differ from database manners, clustering can be referred as the capability of many servers or instances to connect to one database while in IDS, clustering technique is usually use within anomaly detection in exploring group of malware data information without knowing the former relationship knowledge of the data. So, clustering method clusters the objects according to their characteristic of data points, in such every single data point in a cluster is identical to those in the same cluster, but diverse from another clusters [43]. For this reason, clustering is one of the most admired concepts in the domain of unsupervised learning as the anomaly detection is generally unsupervised detection. The idea is the same data points tend to belong to same groups or clusters, as identified by the distance of the data from the local centroids. Fig. 3 shows the example of clustering in a graph.

The graph shows that there are only two centroids, which are marks as ‘X’. The ‘X’ mark depends on the number of cluster that is defined in the first step of the process. The resulting cluster centroids are then used for fast anomaly detection in monitoring of new incoming data [44]. The K-Means clustering algorithm is one of the simplest unsupervised learning algorithms as shown in Fig. 4 that resolves the clustering problem [8] by:

1) Collecting dataset of malware.

2) Identifying the number of clusters (*k*).

3) Initializing the k centroids (k-means) for the data.

4) Determining the distance of each malware from each centroid and then assign each malware to the cluster with centroid closest to it.

5) Recounting the centroids for each cluster.

6) Steps 4 and 5 are repeated until there is no change in cluster centroids.

7) If formed clusters do not look reasonable, repeat the steps 1-6 for different number of clusters.

In Fig. 4, clustering of data begins with identifying the number of cluster according to the characteristics of the data. Then the centroid of each cluster will be decided and accordingly, the distance of each data will be determined starting from the selected centroid. The data, which is in the minimum distance with the centroid, can be considered as the designed group otherwise it will be excluded from the group. The used of malware data in clustering method is suitable as malicious data characteristics almost similar to normal data, however somehow it cannot hide its different behavior compared to normal data behavior. Thus, the different behavior can be detected by using this clustering method. In data science, K-Means clustering is a type of algorithm that has been used to utilize the method of vector quantization specifically in signal processing field and most of the time examiners use it to solve clustering problems. According to [18], in K-Means clustering method, the whole dataset are transform to Voronoi cells by taking observations and finally create the ‘*k*’ groups in which every observation is a segment of a computed nearest mean cluster. It means that it creates 'k' similar clusters of data points and the data instances that fall outside of these groups could potentially be marked as anomalies. Thus, K-Means is a widely used clustering algorithm and this algorithm can be said as the most popular clustering algorithm among the geometric procedures [45] because of its computational simplicity, efficiency and ease of implementation [43], [46]. As it is straightforward algorithm, the computational time is faster then the other algorithm, thus the time of malware clustering process can be minimized [47].

Thus, K-Means Clustering detection method has been the focus of this research based on the motivation. In improving malware behavior detection, clustering analysis is a need by means of K-Means clustering as a new detection method especially in detecting malware.

The uses of DNS as carrier for its command and control determines and reverse engineered Feederbot, which is a botnet [5]. K-Means clustering is combined with Euclidean Distance based classifier correctly classified more than 14m DNS transactions of 42,143 malware samples concerning DNS-C&C usage then, uncovers another bot family with DNS C&C. In addition, this method correctly detected DNSC&C in mixed office workstation network traffic. For instance, DNS C&C provide a mechanism to detect DNS C&C in network traffic.

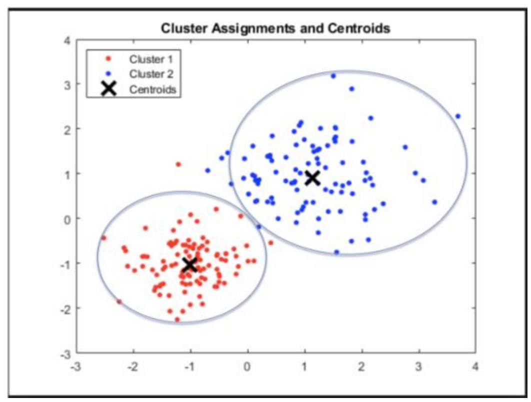

Fig. 3. Graph of Cluster Assignment and Centroid.

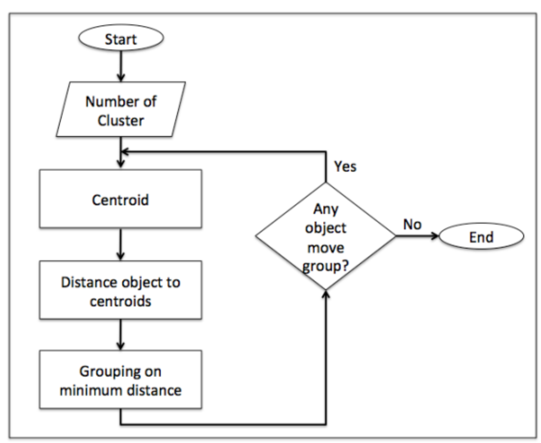

Fig. 4. Clustering Algorithm Flow Process.

In addition, a large-scale log analysis known as Beehive can detect suspicious activities in enterprise network has been proposed by [6]. This approach uses K-Means algorithm to solve data mining problem by extracting the information from data long produced by large enterprise. The improvised of signature-based technique can accurately detect many attack incidents and identify any suspicious behavior if data information. On top of that, Beehive evaluates the collected data log from the large enterprise and compares all the incidents to identify if there is any malicious events and violation of policies without being detected.

Apart from Beehive, the proposed semi-supervised approach only by using K-Means approach can self-merge the information of unknown malware which is unlabeled data into detection system as discussed by [7]. The semi-supervised approach extracts the information of the cluster before inserts the information into the SVM, which is support vector machine classification system by applying global K-Means clustering algorithm. As result, the experiment shows that the proposed approach reach high accuracy rate of detection compared to the existing supervised approach.

In genetic boosting classification to detect malware, the use a static analysis approach has been proposed by [4] can removes the samples that cannot be classified with adequate firmness and need. Thus, with the used of K-means clustering algorithm, the sample can be grouped into regions according to the features. Next, genetic algorithm guided the boosting process, to execute in every region besides evaluated using a test dataset discarding those regions, which do not reach a minimum accuracy threshold.

Malware detection using genetic algorithm (GA) optimized K-means and Hidden Markov Model (HMM) [8] considering the interrelated problem of malware classification. The HMMs is instructed for a variety of malware generators and variety of compilers. As per results, further classification was done using K-Means algorithm with GA in HMM. The GA tuned k-means clustering, and this approach is suggested for better malware detection.

Meanwhile, Distributed GHSOM which is Growing Hierarchical Self Organizing Maps is an unsupervised clustering algorithm for Big Data has been proposed by [9]. To fulfill the requirement on tolerance of variation between samples, the proposed method clusters the data samples dynamically. It pretends as an attractive unsupervised learning solution for data, which have finite information to decide the number of clusters in advance. It used parallel computation with scala actor models for GHSOM construction, distributing vertical and horizontal expansion tasks to actors and showing significant performance improvement.

In short, by using K-Means clustering approach in malware detection model may increase the accuracy of malware detection. However the used of this previous methods not truly focuses on specific malware location. Thus, this research will focus on K-Means clustering at Windows registry.

The comparison of related works under K-Means clustering algorithm as malware analysis can detect malware accurately is presented in Table II. The entire method listed in the table shows the result in term of detection rate which are true positive, true negative, false positive and false negative. As expected, the result is promising of the use of K-Means clustering in detecting malware accurately as proved by [47].

TABLE. II. PREVIOUS WORK (MALWARE DETECTION BY USING K-MEANS CLUSTERING)

Author	Detection Model	Method Used	Input Data	Result
[5]	DNS for Command and Control	K-Means clustering and Euclidean Distance based classifier	Malware binaries	High true positive rate.
[6]	Beehive: Large-Scale Log Analysis	K-Means clustering	Data collections (Log)	High true positive rate.
[4]	Genetic Boosting Classification	K-means clustering algorithm	Binary files	Low false positive rate.
[7]	Semi-supervise approach by using global K-Means clustering	K-Means clustering	Executable files (Win32-based systems)	High true positive rate.
[8]	GA optimized K-means and Hidden Markov Model (HMM)	Genetic Algorithm (GA) K-mean clustering	Pre-obtained dataset of malwares (API and opcode)	Low false positive rate.
[9]	Growing hierarchical self organizing maps (GHSOM)	K-means clustering algorithm	Malware executable (OWL database and Windows APIs)	Low false positive rates.

III. METHODOLOGY

The methodology of this paper consists of three steps started with data collection, followed by data preparation, and lastly data analysis. In data collection, the malware binary files are downloaded from the trusted website and sorted before they are used for the experiment. After the selection, the data was prepared running selected malwares in control environment and the registry features are extracted. Lastly, the extracted features are combined in a database for data analysis. All the process implemented based on the proposed Clustering Detection Model.

Fig. 5 shows the process flow of data clustering method that proposed in this study. There are four phases; which are binary execution phase, file extraction phase, registry data extraction phase and clustering phase. It is started with process 1 which is extracting normal file of registry from virtual machine. The process continued with process 2 by downloading binary file and injects it into the same virtual machine. Then, process 3 is extracting the infected file of registry from the virtual machine. In process 4, all the files are stored in a database and in process 5; which is registry data extraction phase, registry data is extracted and prepared. After that, process 6 begins by clustering all the data files by using K-Means clustering in clustering phase. Lastly, in process 7, the output data will be updated in the different table in the same database. All the processes are classified into four main phases and the phases of the detection model describes as follows:

Phases 1: Binary Execution Phase

In this phase, the binary file is run in virtual machine that is Drakvuf environment. Then, all the activities are captured as log format.

Phases 2: File Extraction Phase

Then, all the data, which is the malware activities are extracted in this phase. There are two types of data that are extracted; first, default file (normal activities) and second infected file (suspicious activities).

Phases 3: Registry Data Extraction Phase

After that, all the collected registry data is extracted and prepared in this phase, as the extracted data are imbalance data.

Phases 4: Clustering Phase

The last phase is clustering phase in which the balanced data is analyzed by using K-Means clustering algorithm to cluster the data either it is malware or not. Euclidean Distance formula is used to measure the distance of centroid and data points. The formula is shown in Fig. 6.

A. Binary Execution Phase

This phase is started by downloading binary files from the trusted website. The binary files of the malware are downloaded from trusted website which is mlawares.com (https://www. malwares.com/). Apart from containing malware binary files, malwares.com able to analyze various advance, newborn, mutated malicious code and URLs. So, this website is suitable for malware analysis as it provides latest malware for this project. The malwares are downloaded from this website for this experiment. Then the malwares are checked in the Lastline portal to ensure that the malware can be run in Windows 7 that suits for the experiment, which only focuses on Windows 7 operating system. The selected malwares and 2 normal files are uploaded into the database. One malwares contains around half million of data. After that, all the binaries are executed in Drakvuf environment.

B. File Extraction Phase

File extraction phase started by extracting default file, which is normal behavior, and extracting infected files, which is suspicious behavior from virtual machine that is Drakvuf environment. Drakvuf is a virtualization based agentless black-box binary analysis system that allows in-depth execution tracing of arbitrary binaries, which include operating system.

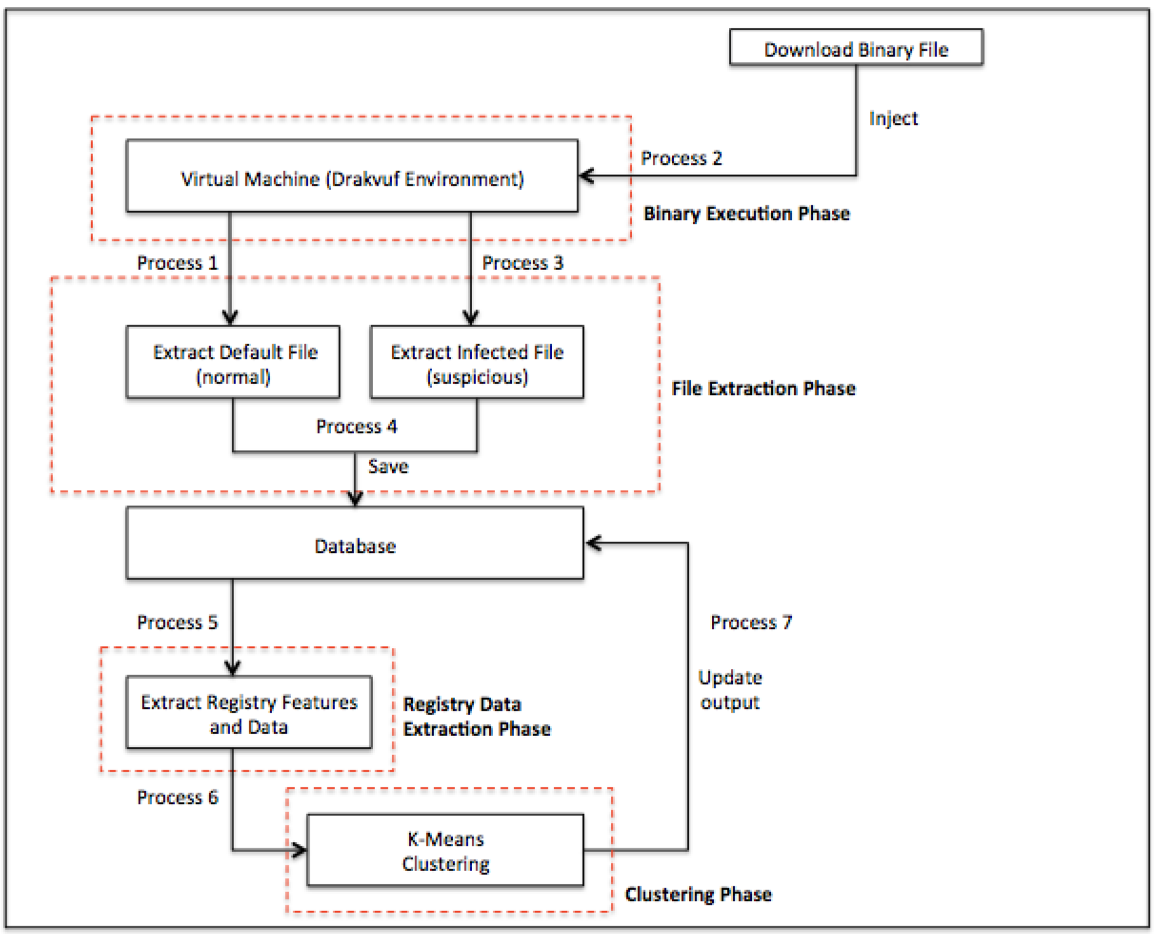

Fig. 5. Clustering Detection Model.

$$d(\mathbf{p},\mathbf{q}) = d(\mathbf{q},\mathbf{p}) = \sqrt{(q_1-p_1)^2 + (q_2-p_2)^2 + \cdots + (q_n-p_n)^2} = \sqrt{\sum_{i=1}^{n}(q_i-p_i)^2}.$$

Fig. 6. Euclidean Distance Formula.

C. Registry Data Extraction Phase

This phase started with uploading the data into database. By using SQL query, the data is selected based on targeted data for data analysis. The RegUtil system is used to upload the srp file of normal and infected file. It connected to database to store the data. The normal and infected files are uploaded through RegUtil system into a database. In the database, the data was extracted to get the only used data for the experiment by using SQLYog database. Then, the data is chunked into several paths before it can be used for analysis. To checked whether the path is correct or not, it was checked with regedit software.

D. Clustering Phase

Using Waikato Environment analyzes clustering phase started with uploading the prepared data for Knowledge Analysis (Weka) for clustering method implementation. The version of Weka used is 3.8.2. Weka is an information mining programming that uses an accumulation of machine learning calculations and the calculations can be associated direct to the information or called from the Java code. The apparatuses that can be utilized as a part of the information accumulation are relapse, grouping, affiliation, information pre-preparing, arrangement, and perception. In this undertaking, the instrument that had been utilized zone characterization. The balanced data is analyzed by using K-Means clustering algorithm to cluster the data either it is malware or not.

The performance of K-Means clustering detection in the field of Intrusion Detection is usually assessed using the following measurements:

- True Positive (TP) is the number of malware samples that has been detected accurately.
- True Negative (TN) is the number of normal samples that has been detected accurately.
- False Positive (FP) is the number or normal samples that is falsely detected as an attack.
- False Negative (FN) is the number of malware samples that is falsely detected as normal.

The detection rate is calculated by using the formula: Detection Rate = (TP) /(TP+FP). In addition, to detect intrusion attempt for unsupervised data, the features of the malware are needed, as there is no numeric number that can be used to calculate the distance between the points. Besides that, Elbow method is used to determine the value of K as well as the stop point after the result is plotted in the graph as discussed by [48]. To be exact, Elbow method is a method of interpreting and validating the consistency of the cluster analysis designed to help to find the best number of clusters in a dataset as shown in Fig. 7.

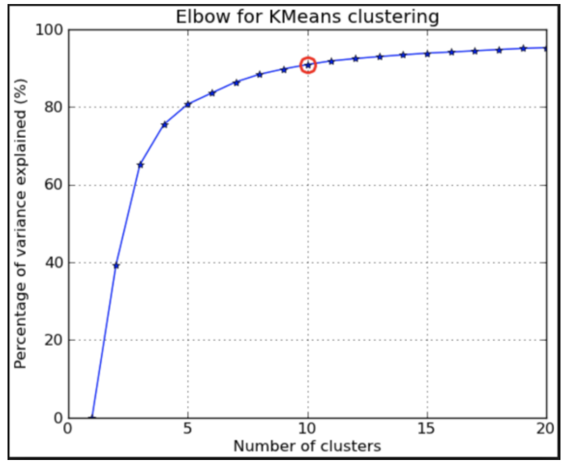

Fig. 7. Elbow Method Graph.

IV. Result, Analysis and Discussion

In this paper, the result of the experiment is based on the percentage of attack detection according to the number of cluster that has been identified during the experiment and it showed that cluster 20 has the highest percentage among the nine tested clusters, which is 96.41%. The percentage exceeds the acceptable detection rate, which is 90% for malware detection as stated by [18]. The percentage of attack is also presented in Fig. 8. It follows the principal of elbow method to find the value of K as stated in previous chapter. Thus, the number of K based on the result is 20, which is the best number that had the highest percentage of attack detection. In Table III, the high percentage of attack detection indicates that this method can highly detect the malware attack by clustering the normal and abnormal data. The normal data belongs to normal group while the abnormal data are excluded from the group. Thus the abnormal data are classified as malware as their behavior are different from the normal data and they are not in the same group with the normal group.

Based on the result, cluster 20 shows the best result among the other clusters. The detection rate is 96.41% however, the false alarm which is 3.55% causes the decreases number of malware detection. Because of that, some of the attacks can be missed to detect, as it is known as normal. Fig. 9 shows root cause of the miss-detected malware. Even though the label of the data is different for attack and normal, but all the features are same. Thus, it is hard to recognize the attack, as it is same with the normal features.

TABLE. III. Percentage of Attack Detection

Number of cluster	Percentage of Attack Detection (%)
5	76.48
10	80.78
15	92.9
20	96.41
25	92.23
30	92.43

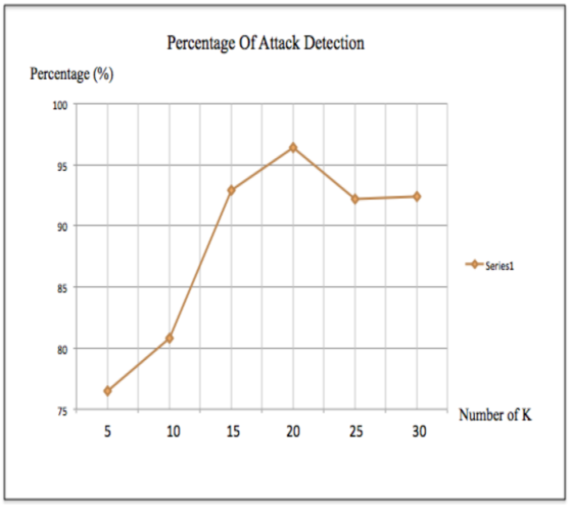

Fig. 8. Graph Percentage of Attack Detection.

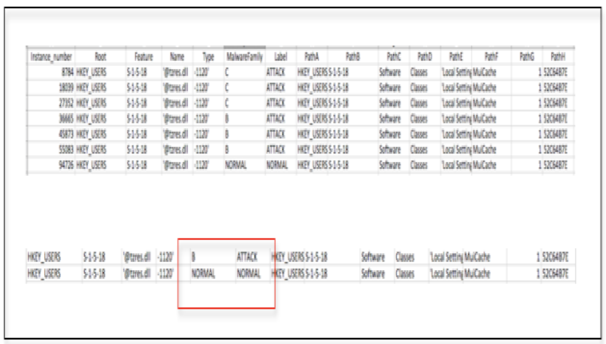

Fig. 9. Root Cause of the Miss-Detected Malware.

V. Conclusion and Future Works

Intrusion Detection System (IDS) is use as malware detector globally, causes many researchers in exploring this field. In this research project, clustering method is proposed for better malware detection. It is because of lack of analysis in detecting malware behavior causes low malware detection due to limited sources on this information especially in windows registry to identify malware activities. Clustering techniques that use unsupervised algorithm in machine learning plays an important role in grouping similar malware characteristics but this approach is absent in malware analysis environment specifically in registry information. Thus, the purpose of this research project is to study registry information and proposing clustering analysis against registry information to improve malware detection. Thus, the research project has been conducted successfully and proposing clustering analysis model against registry information to improve malware detection. Based on the result, the proposed method has a detection rate more than 90%. It is shows that the proposed method has high rate in detecting malware based on the features of the unknown file. According to the direction of this research project, it gives great benefit to community by providing guidance and steps on how to overcome the stated problem. Finally, it is a hope for community can fetch the importance of this research project and used it concerning to Information Technology and Computer Science area.

References

[1] J. Stiborek, T. Pevný, and M. Rehák, “Probabilistic analysis of dynamic malware traces,” Comput. Secur., vol. 74, pp. 221–239, 2018.

[2] T. Wüchner, M. Ochoa, and A. Pretschner, “Malware detection with quantitative data flow graphs,” pp. 271–282, 2014.

[3] A. D. James Baldwin, Omar Alhawi, “Leveraging Machine Learning Techniques for Windows Ransomware Network Traffic Detection,” 2017.

[4] A. Martín, H. D. Menéndez, and D. Camacho, “Genetic boosting classification for malware detection,” 2016 IEEE Congr. Evol. Comput. CEC 2016, pp. 1030–1037, 2016.

[5] C. J. Dietrich, C. Rossow, F. C. Freiling, H. Bos, M. Van Steen, and N. Pohlmann, “On botnets that use DNS for command and control,” Proc. - 2011 7th Eur. Conf. Comput. Netw. Defense, EC2ND 2011, pp. 9–16, 2012.

[6] T. Yen, A. Oprea, and K. Onarlioglu, “Beehive: large-scale log analysis for detecting suspicious activity in enterprise networks,” Proc. 29th Annu. Comput. Secur. Appl. Conf., pp. 199–208, 2013.

[7] S. Huda et al., “Defending unknown attacks on cyber-physical systems by semi-supervised approach and available unlabeled data,” Inf. Sci. (Ny)., vol. 379, pp. 211–228, 2017.

[8] A. Chanana and S. Singh, “Malware Detection Using GA optimized K-means and HMM,” pp. 355–362, 2017.

[9] C. H. Chiu, J. J. Chen, and F. Yu, “An Effective Distributed GHSOM Algorithm for Unsupervised Clustering on Big Data,” Proc. - 2017 IEEE 6th Int. Congr. Big Data, BigData Congr. 2017, pp. 297–304, 2017.

[10] A. Lanzi, D. Balzarotti, C. Kruegel, M. Christodorescu, and E. Kirda, “AccessMiner: Using System-Centric Models for Malware Protection,” ACM Conf. Comput. Commun. Secur. 2010, pp. 399–412, 2010.

[11] S. Jha, M. Fredrikson, M. Christodoresu, R. Sailer, and X. Yan, “Synthesizing near-optimal malware specifications from suspicious behaviors,” Proc. 2013 8th Int. Conf. Malicious Unwanted Softw. "The Am. MALWARE 2013, pp. 41–50, 2013.

[12] M. Ahmadi, A. Sami, H. Rahimi, and B. Yadegari, “Malware detection by behavioural sequential patterns,” Comput. Fraud Secur., vol. 2013, no. 8, pp. 11–19, 2013.

[13] A. Pektaş and A. Tankut, “A dynamic malware analyzer against virtual machine aware malicious software,” Secur. Commun. NETWORKS, vol. 7, no. 12, pp. 2245–2257, 2014.

[14] Monika, P. Zavarsky, and D. Lindskog, “Experimental Analysis of Ransomware on Windows and Android Platforms: Evolution and Characterization,” Procedia Comput. Sci., vol. 94, pp. 465–472, 2016.

[15] O. Aslan and R. Samet, “Investigation of Possibilities to Detect Malware Using Existing Tools,” 2017 IEEE/ACS 14th Int. Conf. Comput. Syst. Appl., pp. 1277–1284, 2017.

[16] D. Ucci, L. Aniello, and R. Baldoni, “Survey on the Usage of Machine Learning Techniques for Malware Analysis,” 2017.

[17] Anon, “Reported Incidents based on General Incident Classification Statistics 2016,” Reported Incidents bas ed on General Incident C las s ification Statis tics 2 014, 2017. [Online]. Available: https://www.mycert.org.my/assets/graph/pdf/2014-1.pdf.

[18] K. Kosmidis and C. Kalloniatis, “Machine Learning and Images for Malware Detection and Classification,” Proc. 21st Pan-Hellenic Conf. Informatics - PCI 2017, no. December, pp. 1–6, 2017.

[19] A. K. Ajay and J. C.D., “Automated multi-level malware detection system based on reconstructed semantic view of executables using machine learning techniques at VMM,” Futur. Gener. Comput. Syst., vol. 79, pp. 431–446, 2018.

[20] A. Souri and R. Hosseini, “A state-of-the-art survey of malware detection approaches using data mining techniques,” Human-centric Comput. Inf. Sci., vol. 8, no. 1, 2018.

[21] A. Moser, C. Kruegel, and E. Kirda, “Exploring multiple execution paths for malware analysis,” Proc. - IEEE Symp. Secur. Priv., pp. 231–245, 2007.

[22] M. Egele, T. Scholte, E. Kirda, and C. Kruegel, “A survey on automated dynamic malware-analysis techniques and tools,” ACM Comput. Surv., vol. 44, no. 2, pp. 1–42, 2012.

[23] J. Horton and J. Seberry, “Computer Viruses An Introduction,” vol. 19, no. 1, pp. 122–131, 1997.

[24] L. X. Yang and X. Yang, “A new epidemic model of computer viruses,” Commun. Nonlinear Sci. Numer. Simul., vol. 19, no. 6, pp. 1935–1944, 2014.

[25] B. Rajesh, Y. R. J. Reddy, and B. D. K. Reddy, “A Survey Paper on Malicious Computer Worms,” Int. J. Adv. Res. Comput. Sci. Technol., vol. 3, no. 2, pp. 161–167, 2015.

[26] C. Smith, A. Matrawy, S. Chow, and B. Abdelaziz, “Computer Worms: Architectures, Evasion Strategies, and Detection Mechanisms,” J. Inf. Assur. Secur., vol. 4, pp. 69–83, 2009.

[27] M. Moffie, W. Cheng, D. Kaeli, and Q. Zhao, “Hunting trojan horses,” Proc. 1st Work. …, no. January 2006, pp. 12–17, 2006.

[28] W. Kim, O.-R. Jeong, C. Kim, and J. So, “On botnets,” Proc. 12th Int. Conf. Inf. Integr. Web-based Appl. Serv. - iiWAS ’10, no. 2, p. 5, 2010.

[29] R. Wash, “Incentive design for home computer security,” CHI ’07 Ext. Abstr. Hum. factors Comput. Syst. - CHI ’07, p. 1681, 2007.

[30] R. Abdullah and M. Abdollah, “Revealing the Criterion on Botnet Detection Technique,” IJCSI Int. J. Comput. Sci. Issues, vol. 10, no. 2, pp. 208–215, 2013.

[31] P. Jyotiyana and S. Maheshwari, “Intelligent Systems Technologies and Applications 2016,” vol. 530, pp. 449–460, 2016.

[32] X. Xing et al., “Understanding Malvertising Through Ad-Injecting Browser Extensions,” Proc. 24th Int. Conf. World Wide Web - WWW ’15, pp. 1286–1295, 2015.

[33] I. Ideses and A. Neuberger, “Adware detection and privacy control in mobile devices,” 2014 IEEE 28th Conv. Electr. Electron. Eng. Isr. IEEEI 2014, 2014.

[34] A. Cohen and N. Nissim, “Trusted detection of ransomware in a private cloud using machine learning methods leveraging meta-features from volatile memory,” Expert Syst. Appl., vol. 102, pp. 158–178, 2018.

[35] P. B. Pathak, “A Dangerous Trend of Cybercrime: Ransomware Growing Challenge,” Int. J. Adv. Res. Comput. Eng. Technol., vol. 5, no. 2, pp. 371–373, 2016.

[36] R. Brewer, “Ransomware attacks: detection, prevention and cure,” Netw. Secur., vol. 2016, no. 9, pp. 5–9, 2016.

[37] P. Passeri, “January 2018 Cyber Attacks Statistics,” Information Security Timelines and Statistics, 2018. [Online]. Available: https://www.hackmageddon.com/2018/02/22/january-2018-cyber-attacks-statistics/.

[38] U. Ravale, N. Marathe, and P. Padiya, “Feature selection based hybrid anomaly intrusion detection system using K Means and RBF kernel function,” Procedia Comput. Sci., vol. 45, no. C, pp. 428–435, 2015.

[39] S. C. Satapathy, B. N. Biswal, S. K. Udgata, and J. K. Mandal, “Proceedings of the 3rd International Conference on Frontiers of Intelligent Computing: Theory and Applications (FICTA) 2014,” Adv. Intell. Syst. Comput., vol. 327, pp. 405–411, 2014.

[40] H. J. Liao, C. H. Richard Lin, Y. C. Lin, and K. Y. Tung, “Intrusion detection system: A comprehensive review,” J. Netw. Comput. Appl., vol. 36, no. 1, pp. 16–24, 2013.

[41] A. Tang, S. Sethumadhavan, and S. J. Stolfo, “Unsupervised anomaly-based malware detection using hardware features,” Lect. Notes Comput. Sci. (including Subser. Lect. Notes Artif. Intell. Lect. Notes Bioinformatics), vol. 8688 LNCS, pp. 109–129, 2014.

[42] Z. Zhiyuan Tan, A. Jamdagni, X. Xiangjian He, P. Nanda, and R. P. Ren Ping Liu, “A System for Denial-of-Service Attack Detection Based on Multivariate Correlation Analysis,” IEEE Trans. Parallel Distrib. Syst., vol. 25, no. 2, pp. 447–456, 2014.

[43] A. B. S. Serapião, G. S. Corrêa, F. B. Gonçalves, and V. O. Carvalho, “Combining K-Means and K-Harmonic with Fish School Search Algorithm for data clustering task on graphics processing units,” Appl. Soft Comput. J., vol. 41, pp. 290–304, 2016.

[44] S. Agrawal and J. Agrawal, “Survey on anomaly detection using data mining techniques,” Procedia Comput. Sci., vol. 60, no. 1, pp. 708–713, 2015.

[45] C. Bouveyron and C. Brunet-Saumard, “Model-based clustering of high-dimensional data: A review,” Comput. Stat. Data Anal., vol. 71, pp. 52–78, 2014.

[46] P. Louvieris, N. Clewley, and X. Liu, “Effects-based feature identification for network intrusion detection,” Neurocomputing, vol. 121, pp. 265–273, 2013.

[47] S. S. J and S. Pandya, “An Overview of Partitioning Algorithms in Clustering Techniques,” vol. 5, no. 6, pp. 1943–1946, 2016.

[48] P. Bholowalia and A. Kumar, “EBK-Means : A Clustering Technique based on Elbow Method and K-Means in WSN,” Int. J. Comput. Appl., vol. 105, no. 9, pp. 17–24, 2014.

Convolutional Neural Network Considering Physical Processes and its Application to Diatom Detection

Kohei Arai
Graduate School of Science and Engineering
Saga University, Saga City, Japan

***Abstracts*—Convolutional Neural Network (CNN) considering physical processes with time series of stages for diatom detection with remote sensing satellite derived physical data (Chlorophyll-a, Photosynthesis Available Radiance (PAR), Turbidity, Sea Surface Temperature (SST)) and meteorological data is proposed. Diatom is bloomed under the condition of suitable sea water temperature, nutrition rich water (Chlorophyll-a derived from river water flow), photosynthesis available radiance derived from solar irradiance, transparency of the sea water for photosynthesis (turbidity), and sea water convection between bottom sea water and sea surface water. Almost all the conditions can be monitored by remote sensing satellite-based radiometers. The proposed diatom prediction based on convolutional neural network with remote sensing satellite and meteorological data is validated. Through the experiments at Ariake bay area, Kyushu, Japan with gathered time series of remote sensing data of Moderate resolution of Imaging Spectroradiometer (MODIS) derived turbidity as well as chlorophyll-a data estimated for the winter seasons (from January to March) during from 2010 to 2018 together with measured and acquired meteorological data for the same winter seasons, the proposed method is validated.**

Keywords*—*Chlorophyl-a concentration; red tide; diatom; MODIS; satellite remote sensing; neural network; meteorological data

I. Introduction

One of the problems of DLM: Deep Learning Method (Convolutional Neural Network: NN, Recurrent Convolutional Neural Network: RCNN, etc.) is that DLM cannot consider time and spatial relations among data for input nodes. Also, another problem is that DLM is not supported physical processes nevertheless physical meaning is significantly important. The DLM method proposed here is to solve these problems. Namely, time series of physical processes are considered in the proposed DLM method.

In the previously proposed method [1], data gathering, and data analysis are featured for prediction of diatom appearance which occurs at Ariake Sea, Kyushu, Japan in winter season. The big data used in this research are Moderate resolution Imaging Spectroradiometer: MODIS derived turbidity and chlorophyll-a concentration data as well as meteorological data which are acquired for 9 years during from 2010 to 2018. As truth data of the diatom appearance are obtained from the shipment data of the number of cells of diatoms which are acquired with research vessel provided by the Saga Prefectural Institute of Ariake Fisheries Promotion: SPIAFP. DLM is used with the big data and the truth data.

The proposed method is required to predict when and where diatom will appear. Therefore, the prediction result must be displayed in a geographical representation. In this paper, it will be displayed onto MODIS [1] derived turbidity images because diatom appears in the not turbid sea areas usually (Photosynthesis becomes active). It is known that diatom appearance and blooming mechanism is as follows:

1) Diatom seeds are existing in sea water.

2) Nutrition rich water which is mainly containing in river water is increased in the low tide.

3) Sun illumination time which is required for photosynthesis is long enough in the low tide time period, and turbidity of sea water is small enough (transparent sea water).

4) Sea Surface Temperature: SST is appropriate for diatoms in the low tide time period, and chlorophyll-a concentration is high enough.

5) Relatively high wind which is required for convection of sea water blows during the low tide and the spring tide time periods.

6) Then diatoms appear in the spring tide time period (Blooming).

Although such these physical processes must be considered, CNN cannot consider the processes. Therefore, two stages of CNN are proposed here. Namely, turbidity, Photosynthetically Active Radiance: PAR[2], chlorophyll-a concentration as well as SST are monitored in a low tide time period as the first stage, then these parameters and wind direction and speed are also monitored in the following spring tide time period as the second stage.

All these data can be derived from MODIS of remote sensing satellite data except wind data. These imagery data which are acquired in a low tide time period can be input node data and diatom blooming distribution of imagery data can be output node data as truth data. These are training datasets for the first stage. These are same things for the second stage. These data which are acquired in the following spring tide time period are training data for the second stage. If these two stages of the result of rules are identical, then the rule can be used for diatom blooming detection. Thus, diatom blooming at the following spring tide time period can be predicted at the first stage of a low tide time period. The purpose of this study is to create a method for prediction of diatom detection by using

[1] https://modis.gsfc.nasa.gov/
[2] https://en.wikipedia.org/wiki/Photosynthetically_active_radiation

remote sensing data derived physical parameters based on physical process considered neural network.

Through experiments, it is found that the proposed prediction method for large diatom appearance is validated with the meteorological data and MODIS derived turbidity as well as chlorophyll-a data estimated for the winter (from January to March) in 2012 and 2015 [1]. This paper is to validate the proposed method with the acquired data in 2016-2018.

The research background and the related research works are described in the next section. Then proposed method is described in the following section followed by experiments. The experimental results are validated in the following section followed by conclusion with some discussions.

II. Research Background and Related Research

The Ariake Sea is the largest productive area of Nori (Porphyra yezoensis[3]) in Japan. In winters in 2012, 2013, 2014 and 2015, a massive diatom bloom appeared in the Ariake Bay, Japan [2]. In case of above red tides, bloom causative was Eucampia zodiacus[4]. This bloom has been occurred several coastal areas in Japan and is well reported by Nishikawa et al. for Harima-nada sea areas [3]-[11]. Diatom blooms have recurrently appeared from late autumn to early spring in the coastal waters of western Japan, such as the Ariake Bay [12] and the Seto Inland Sea [13], where large scale "Nori" aquaculture occurs. Diatom blooms have caused the exhaustion of nutrients in the water column during the "Nori" harvest season.

It is serious problem of red tide damage to Nori production. Approximately 30% of amount of Nori sales is getting down by discoloration of Nori due to red tide damage of diatom appearance. This damage can be avoided. Namely, the damage can be stopped by pulling the nori net above the sea at the time of red tide occurrence. Therefore, it is desirable to predict diatom appearance and inform some cautions to Nori fisherman.

The chlorophyll-a concentration algorithm developed for MODIS has been validated [14]. The algorithm is applied to MODIS data for a trend analysis of chlorophyll-a distribution in the Ariake Bay in winter during from 2010 to 2015 is made [14]. Also, locality of red tide appearance in Ariake Sea including Ariake Bay, Isahaya Bay and Kumamoto offshore is clarified by using MODIS data derived chlorophyll-a concentration [15].

Satellite and Ground based red tide detection method and system by means of peak shift of remote sensing reflectance is proposed [16]. Also, a method for red tide detection and discrimination of red tide type (spherical and non-spherical shapes of red tide) through polarization measurements of sea surface is proposed [17]. Red tide detection using remote sensing satellites, research vessels, and ground based red tide monitoring system and discrimination of red tide species is reported [18]. Comparative study on discrimination methods for identifying dangerous red tide species based on wavelet utilized classification methods is conducted [19]. Relation between chlorophyll-a concentration and red tide in the intensive study area of the Ariake Sea is investigated [20].

Trend analysis of relatively large diatoms which appear in the intensive study area of the Ariake Sea, Japan in winter (2011-2015) based on remote sensing satellite data is carried out [14]. Then, one of the possible causes for diatom appearance in Ariake bay area in Japan in the winter from 2010 to 2015 (Clarified with AQUA[5]/MODIS) is reported [21]. Relation between large sized diatom appearance and meteorological data in Ariake bay area in Japan in the winter in 2016 is reported [22]. Then, prediction method for large diatom appearance with meteorological data and MODIS derived turbidity and chlorophyll-a in Ariake bay area in Japan is proposed [1].

Rhizosolenia imbricata[6] as a large diatom in winter season has been suppressed by the shortage of sunshine and the like due to insufficient sunshine etc. after it is transferred from the open sea into the bay in the winter with high salinity and the conditions necessary for growth (high water temperature, high illuminance, high nutrient salt, etc. It is known that large occurrence occurs when the condition is met. In addition, small diatoms such as Skeletonema spp.[7] Proliferate, the density of Eucampia zodiacus (E. zodiacus) rapidly increases from late February after decline. In addition, E. zodiacus is widely distributed from the surface layer to the bottom layer, and the nutrient concentration decreases sharply with the growth of E. zodiacus. The cell density of E. zodiacus that was distributed in the bottom layer of the offshore region increased from the low tide to the high tide and the turbidity decreased mainly in the offshore region at the low tide period before the cell density of E. zodiacus increased. There is a tendency to do. In early March, when the cell density of E. zodiacus sharply increased, it is also known that there is a low salt water mass at the surface layer.

From Itoh et al. (2013) [2], it is considered important for the sedimented. zodiacus to improve the light environment at low tide in order to expand the population to the red tide level. In addition, from the comparison of observation results between 2007 and 2012, whether to rapidly expand the population at the high tide following E. zodiacus that was distributed in the deep layer at the time of tidal wave is related to river flow (supply of nutrient salt) It is said to be dependent. Author in [2] also described empirical mechanism of the diatom blooming. Therefore, the rules for prediction of diatom occurrence are compared to the empirically found mechanism. On the other hand, the occurrence of red tide caused by Asteroplanus karianus [8] (A. karianus) in the waters of Saga prefecture has been reported to be constantly increasing and densifying since FY 2007, and the cell density of A. karianus tends to increase after late December, A. Karianus is known to tend to be densified upstream of Shiotagawa river feeling tide area in the Ariake Sea Saga prefecture. Also, in the Ariake Sea,

[3] http://en.wikipedia.org/wiki/Porphyra
[4] http://www.eos.ubc.ca/research/phytoplankton/diatoms/centric/eucampia/e_zodiacus.html
[5] https://aqua.nasa.gov/
[6] http://www.marinespecies.org/aphia.php?p=taxdetails&id=149116
[7] http://www.marinebio.org/species.asp?id=4834
[8] http://www.godac.jamstec.go.jp/bismal/j/view/9031783

A. karianus has not reported the formation of red tide in areas other than the sea area of Saga prefecture.

Prediction method for large diatom appearance in winter with meteorological data and MODIS derived turbidity and chlorophyll-a in Ariake Bay Area in Japan is proposed. Mechanism for large diatom appearance in winter is discussed with the influencing factors, meteorological condition and in-situ data of turbidity, chlorophyll-a data with the measuring instruments equipped at the Saga University own Tower in the Ariake Bay area. Particularly, the method for estimation of turbidity is still under discussion. Therefore, the algorithm for estimation of turbidity with MODIS data is proposed.

III. Proposed Diatom Appearance Prediction

A. Big Data Anlysis

Because of remote sensing satellite imagery data and meteorological data are essentially big; a big data analysis must be done for diatom prediction (Estimation of time/location/size). Big data analysis can be done through the following procedure and typical tools.

1) Data gathering: Import.IO[9], etc.

2) Storage and management: Hadoop[10], Cloudera[11], MongoDB[12], Talend[13], etc.

3) Data cleaning: OpenRefine[14], Data cleaner[15], etc.

4) Data mining: IBM SPSS Modeler[16], Oracle Data Mining[17], Tera Data[18], Kaggle[19], etc.

5) Data analysis: Qubole[20], BigML[21], Statwing[22], Tableau[23], CartDB[24], Chartio[25], Plot.ly[26], Datawrapper[27], etc.

6) Data visualization: Tableau[28], CartDB[29], Chartio[30], Plot.ly, Datawrapper, etc.

7) Data integration: Blockspring[31], Pentaho[32], etc. and Data language of “R”, “Python”, “RegEx[33]”, “XPath[34]”, etc.

Import IO is used for gathering MODIS derived chlorophyll concentration and turbidity of the ocean areas in concern (Coastal areas of Ariake Bay which are situated in northern Kyushu, Japan). Hadoop is used for data management while OpenRefine is also used for data cleaning. On the other hand, DLM is used for learning diatom appearances. The learnt result for diatom appearance is compared to the empirical knowledge about diatom occurrences. As the results, the proposed method for diatom appearance prediction rules is reasonable in comparison to the empirical reasons.

B. Diatom Appearnce in Ariake Sea

Rhizosolenia imbricata (R. imbricate) is mainly assumed as a large diatom. In R. imbricata, the necessary conditions for growth (high water temperature, high illuminance, high nutrient salt, etc.) are established after small diatom growth is suppressed due to lack of sunshine, etc. due to lack of sunshine, etc. and a big outbreak. On the other hand, Eucampia zodiacus (E. zodiacus) has the following characteristics,

- Vertical axis length 13 to 100 μm.
- The cells are flat wedge-shaped, forming a spiral group consisting of several cells.
- Widely distributed in coastal areas around the world excluding the polar regions
- Can grow under a wide range of water temperature and salt conditions (optimal water temperature is 25° C).
- Growth requires relatively high light conditions.
- Maintains high nitrogen uptake ability even under low water temperature conditions
- The existence of dormant cells has not been confirmed.

These two major diatoms in the Ariake see in winter season. E. zodiacus is dominant recently. Therefore, it is important to predict E. zodiacus appearance.

C. Physical Proccesses for Diatom Appearance

From late February after the growth and decline of small diatoms such as Skeletonema spp., the cell density of E. zodiacus increased rapidly. E. zodiacus is widely distributed from the surface layer to the bottom layer.

As E. zodiacus grew, the nutrient concentration decreased rapidly. The cell density of E. zodiacus, which was distributed in the bottom of the offshore area, increased during the period from low tide to high tide.

The tendency of turbidity to decrease mainly in the offshore region during the tidal period before the cell density of E. zodiacus increases

In early March, when the cell density of E. zodiacus increased rapidly, there was a low-salt water mass on the surface layer.

D. Examples of Physical Proccesses for Diatom Appearance

For E. zodiacus, which is sinking, to expand its population to the red tide level, it is important to improve the light environment at low tide. From the comparison of observation

[9] https://www.import.io/
[10] https://ja.wikipedia.org/wiki/Apache_Hadoop
[11] https://www.cloudera.com/
[12] https://www.mongodb.com/
[13] https://qiita.com/kazu56/items/b089ded9af884426f008
[14] http://openrefine.org/
[15] https://datacleaner.org/
[16] https://www.ibm.com/products/spss-modeler
[17] https://www.oracle.com/technetwork/database/options/advanced-analytics/odm/overview/index.html
[18] https://www.teradata.jp/About-Us
[19] https://www.kaggle.com/
[20] https://www.qubole.com/
[21] https://bigml.com/
[22] https://www.statwing.com/
[23] https://www.tableau.com/ja-jp
[24] https://carto.com/
[25] https://chartio.com/
[26] https://plot.ly/
[27] https://www.datawrapper.de/
[28] https://tableau-i-ways.com/about
[29] https://en.wikipedia.org/wiki/CartoDB
[30] https://www.g2crowd.com/products/chartio/reviews
[31] https://www.blockspring.com/
[32] https://www.hitachivantara.com/go/pentaho.html
[33] https://docs.microsoft.com/jajp/dotnet/api/system.text.regularex pressions.regex?view=netframework-4.7.2
[34] https://ja.wikipedia.org/wiki/XML_Path_Language

results in 2007 and 2012, whether the population expands suddenly at the time of the storm followed by E. zodiacus distributed in the deep layer at the time of the low tide depends on the river flow (nutrient supply). Fig. 1 shows the diatom appearance mechanism and the examples of the mechanism for 2007 and 2012.

In 2012, precipitation on February 8, chlorophyll a and PAR increase after February 10, DIN (Dissolved Inorganic Nitrogen), PO_4-P (Phosphorus phosphate), SiO_2-Si (silicate silicon) increase on February 18, and temperature rises results in Skeletonema increases on February 24 Occurrence. Chlorophyll a and PAR increased after February 10, and DIN, PO_4-P, and SiO_2-Si increased until February 18, but the temperature dropped sharply from February 16 and the wind speed increased rapidly.

DIN, PO_4 -P, plummeted, then Skeletonema plummeted on February 24. There was precipitation on February 24, then PAR increased rapidly, the temperature rose on February 20-25, the surface SiO_2-Si continued, and then a large amount of Eucampia occurred. Since February 24, temperatures have fallen and chlorophyll a has decreased, but Eucampia, which does not require nutrients, has continued to occur.

Therefore, it would be better to consider the two stages in the learning process with DLM, namely, the first stage of "Low Tide" and the second stage of "Spring Tide" The input data of the first stage are Chlorophyll-a, turbidity, photosynthetically active radiance derived from MODIS data. Also, the desired output is true: diatom blooming or false: no diatom blooming. Meanwhile, the input data and the desired output of the second stage are same as the first stage. After the learning processes of the first and the second stages, the results must be associated as follows,

1) Diatom Blooming: True for the first and second stages.
2) No Diatom Blooming: the other cases.

The desired output can be obtained from the SPIAFP. SPIAFP provides the number of cells a ml in the Ariake sea areas by species by species and by the district by district (see Fig. 3(a)). Thus, physical mechanism and time sequence are considered in the proposed learning process.

River water can be monitored together with sunshine time a day. Also, wind direction and wind speed are monitored by meteorological agency. SST, chlorophyll-a concentration and Suspended Solid: SS can be monitored with satellite remote sensing data in a daily basis. Therefore, diatom appearance can be predicted. For SST, chlorophyll-a concentration and SS are represented as images. Therefore, machine learning can be done for prediction of SST, chlorophyll-a concentration and SS as well as diatom appearance.

Therefore, it is possible to predict diatom appearance with the time series of parameters. The proposed big data analysis-based method is based on the well-known machine learning with the time series of rainfall volume, river water volume, air temperature, tide level, wind direction / wind speed, solar radiation, turbidity sea surface temperature, and chlorophyll-a derived from time series of remote sensing satellite data. The machine learning process can learn the most appropriate prediction method. Using 9 years of these data (2010 to 2018), the machine learning is done and finds the most appropriate way and conditions are found.

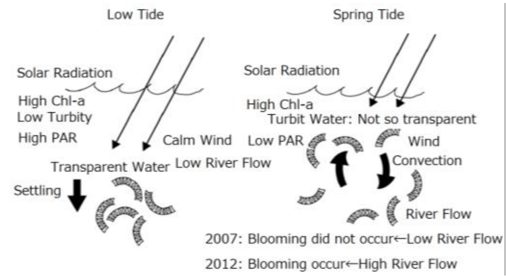

Fig. 1. Examples of Diatom Appearance Mechanism in 2007 and 2012.

For the input node, there are tidal data, sea surface temperature, river flow rate, wind direction and wind speed, turbidity and chlorophyll-a concentration derived from MODIS data. From the 9 years ground truth data of diatom appearance data are also inputted as desired outputs as training datasets. Thus, the proposed DLM can lean for diatom appearance detection.

IV. Experiments for Validation

A. Intensive Study Area

Intensive study areas of Ariake Sea, Isahaya Bay, and Kumamoto Offshore are shown in Fig. 2. Ariake Bay is a portion of Ariake Sea of which the width is around 20 km (in direction of east to west) and the length is approximately 100 km (in direction of north to south). It is almost closed sea area because the mouth of Ariake Sea is quite narrow. Sea water exchanges are, therefore, very small.

B. Truth Data and MODIS Derived Turbidity and Chlorophyll-a Concentration Data of Diatom Appearance

Truth data of diatom distribution which are measure with research vessels and MODIS data derived turbidity, chlorophyll-a concentration and PAR data in unit of Einstein unit of E/m^2/day as well as the time series of bi-monthly PAR data in the case of diatom appearance are shown in Fig. 3(a), (b), (c), (d) and (e), respectively. Also, Tables I and II show the measured diatom distribution together with the number of cells and diatom species, respectively.

Fig. 2. Intensive Study Areas.

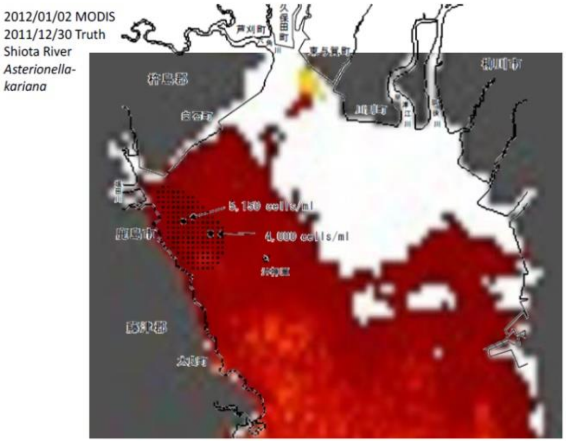

(a) Example of MODIS Derived Chlorophyll-a Concentration and Diatom Appearance.

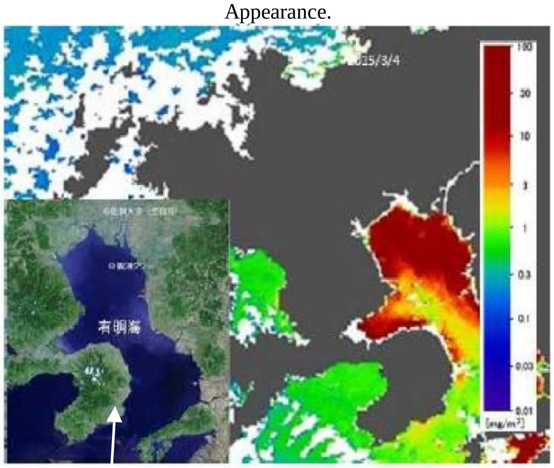

Ariake Sea (b) Chlorophyll-a Concentration.

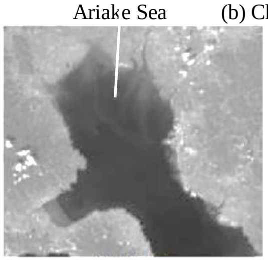

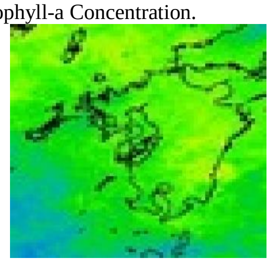

(c) Turbidity (d) Photosynthetically Active Radiance.

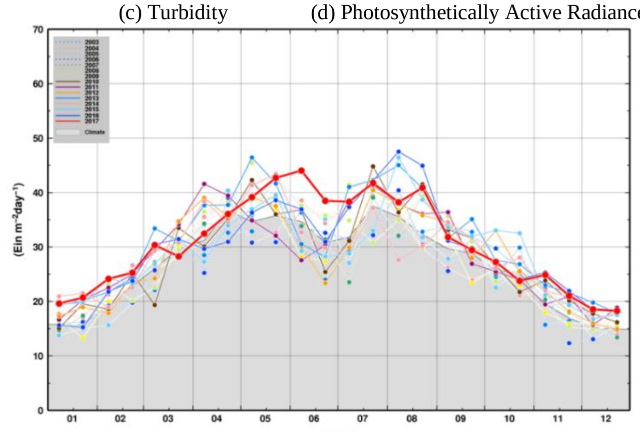

(e) Time Series Data of the Bimonthly PAR.

Fig. 3. Truth Data of Diatom Distribution which are Measured with Research Vessels and MODIS Data Derived Turbidity, Chlorophyll-a Concentration and PAR Data as well as the Time Series of bi-Monthly PAR Data in the Case of Diatom Appearance.

TABLE I. MAJOR SPECIES AND THE NUMBER OF RED TIDE INCLUDING DIATOMS APPEARED IN ARIAKE BAY AREA IN THE TIME PERIOD FROM JANUARY TO FEBRUARY IN 2010 TO 2018

January 21, 2010 Shiota river mouth and its surrounding areas Asteroplanus karianus; 3280 cells/ml Skeletonema costatum: 1330 cells/ml
January11 2011 Along with the Shiroishi town offshore to the Shiota river mouth and its surrounding areas, Asteroplanus karianus; 10150 cells/ml
February 25, 2011 Around the Kashima offshore Asteroplanus karianus; 4950 cells/ml
December 30, 2011 Around the Shiota River Mouth and its surrounding areas Asteroplanus karianus; 5150 cells/ml
January 23, 2012 around Shiota river mouth and its surrounding areas as well as Shiroishi offshore Skeletonema spp .: 5150 cells/ml
February 22, 2012 Along with the Kawazoe offshore to the Tara offshore Eucampia zodiacus: 1,090 cells/ml
December 31, 2012 Along with the Shiota river mouth and its surrounding areas to the Kashima offshore Skeletonema spp.: 6110 cells/ml
January 7, 2013 Along with the Shiota river mouth and its surrounding areas to the Shiroishi offshore Asteroplanus karianus 5630 cells/ml Skeletonema costatum: 3390 cells/ml
January 6, 2014 Shiroishi offshore Asteroplanus karianus; 4830 cells/ml
January 16, 2014 Shiroishi offshore Skeletonema spp.: 6110 cells/ml Thalassiosira spp.: 1510 cells/ml
February 6, 2014 Almost whole Ariake bay area except the Shiroishi offshore Eucampia zodiacus: 568 cells/ml
December 30, 2014 Along with the Shiroishi offshore to the Tara offshore Asteroplanus karianus; 3890 cells/ml Skeletonema costatum: 8750 cells/ml
March 6, 2015 Along with the Kashima offshore to the Tara offshore Eucampia zodiacus: 1310 cells/ml
March 24, 2016 Shiroishi offshore Skeletonem spp. of 12,880 cells/ml
December 29, 2016: Skeletonema, Asteroplanus karianus February 20, 2017 Skeletonema, Asteroplanus karianus , Kirosloth, Eucampier March 6, 2017: Skeletonema, Asteroplanus karianus March 13, 2017: Skeletonema, Asteroplanus karianus, Eucampia March 21, 2017: Skeletonema, Asteroplanus karianus
November 1, 2017: Skeetonema, Keatheros November 5, 2017: Skeetonema, Keatheros November 12, 2017: Skeetonema, Keatheros November 20, 2017: Skeletonema, Keatheros, Lisosolenia November 27, 2017: Skeletonema, Keatheros, Lisosolenia December 4, 2017: Skeetonema, Keatheros, Lisosolenia December 13, 2017: Skeletonema, Keatheros, Lisosolenia, Asteroplanus karianus, Eucampia December 28, 2017: Skeletonema, Keatheros, Lisosolenia, Asteroplanus karianus

TABLE. II. DAYS FOR MODIS DATA ARE ACQUIRED

(2010) January 1, 3, 9, 14, 16, 17, 18, 22, 24, 26, 27, 29, February 3, 4, 5, 6, 20, 21, 23, and 28 in 2010
(2011) January 1, 2, 7, 8, 14, 17, 22, 26, 27, February 1, 3, 4, 15, 21, 22, 24, and 26 in 2011
(2012) January 2, 6, 7, 12, 17, 20, 21, 23, 26, 29, 30, 31, February 4, 11, 12, 20, 24, and 29 in 2012
(2013) January 4, 6, 10, 11, 12, 15, 18, 25, 28, 30, 31, February 2, 3, 10, 13, 16, 20, 22, 23, 24, and 29 in 2013
(2014) January 10, 13, 15, 16, 19, 23, 24, 26, 27, 29, 30, February 4, 8, 11, 12, 20, 21, 23, and 24 in 2014
(2015) January 4, 6, 7, 8, 9, 10, 12, 17, 18, 20, 23, February 1, 3, 6, 9, 13, 14, 20, and 27 in 2015
(2016) January 7, 10, 16, 22, 30, February 3, 4, 9, 10, 18, 21, 24, 26 and March 1 in 2016
(2017) January 1, 3, 4, 6, 11, 14, 16, 17, 21, 25, 26, 28, 30, February 1, 2, 3, 6, 13, 15, 18, 19, 21, 28, March 2, 3, 5, 6, 9, 11, 14, 15, 16, 20, 21, 23, 27, 28
(2018) January 1, 2, 3, 6

One of the examples of MODIS derived chlorophyll-a concentration distribution and the truth data of diatom appearance which is occurred in 2012 is shown in Fig. 3(a). In the image, both images are superimposed. White portions of MODIS image are the cloud covered areas. The numbers in the truth data of image show the number of diatom cells per ml. Both images show a good coincide. Namely, the diatom appears at the areas of which chlorophyll-a is densely concentrated. This is a just one example. Other than this MODIS derived chlorophyll-a data, MODIS derived turbidity, SST, meteorological data of rainfall volume, river water volume, air temperature, tide level, wind direction/speed, solar radiation, are gathered.

C. Validation of the Proposed Method forWinter Diatom (2011-2012) Diatom Appearance Prediction Method

From the published paper, it is proposed the rule-based diatom appearance prediction method [1]. The previous paper indicates that the diatom appearance prediction can be done with rainfall volume, river water volume, air temperature, tide level, wind direction / wind speed, solar radiation, turbidity (which is corresponding to Suspended Solid: SS), sea surface temperature, and chlorophyll-a concentration derived from time series of remote sensing satellite data. One of the examples is shown in Fig. 4.

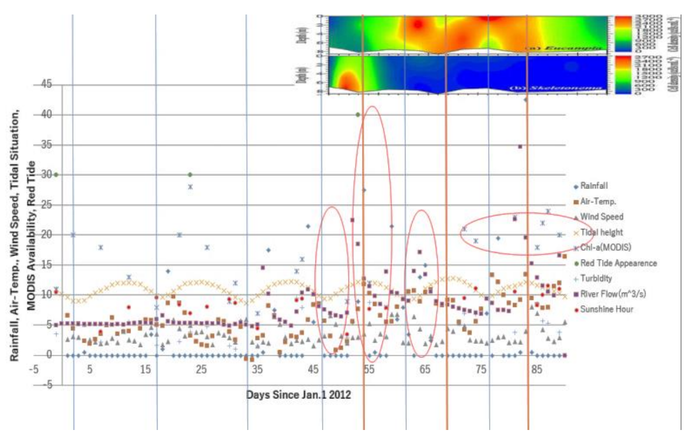

Fig. 4. Example of Diatom Appearance with the Conditions of Time Series of Data are Matched to the Threshold of the Appearance.

Relatively small size diatoms appear at western side of Ariake bay area in the middle of February and then large size diatoms appear in the whole area of Ariake bay area from 25 February to the middle of April 2012. The influencing factors, meteorological condition, turbidity, chlorophyll-a, river water flow, tidal height is collected from the Japanese Meteorological Agency: JMA, MODIS data and diatom appearance. These data of 2012 are plotted in Fig. 4. In the figure, Eucampia zodiacus (top) and Skeletonema spp. (bottom) appearances which are reported by the Ito et al. [1]. As a matter of fact, diatom needs nutrients, sunshine, appropriate sea temperature (22 to 26 degree Celsius) and salinity (15 to 28 ‰), as well as diatom seeds. Nutrients are provided by river water (source of nutrients) which is mainly caused by rainfall and run-off water. Therefore, river water flow is a key component for nutrients. Relatively large diatom (Eucampia zodiacus) seeds are situated in the bottom layer situated in Ariake bay while relatively small diatom seeds are situated from the sensory ranges of the specific rivers, Shiota- River for Skeletonema spp. and Asteroplanus karianus. Therefore, convection or vertical mixing in the sea water of Ariake bay is a key for the large diatom appearance at the sea surface.

The convection is usually occurred due to spring tide or strong winds from the north. Therefore, diatom bloom is used to be occurred in spring tide. Also, diatom seeds need sunshine, nutrients for blooming. Therefore, diatom bloom occurs after a relatively large river water flow followed by relatively small turbidity and sunshine as well as spring tide. These are mechanism for diatom appearance and blooming.

D. Validation of the Winter Diatom (2017 – 2018) Diatom Appearance Prediction Method

Furthermore, the diatom red tide occurrence situation from November 2017 to the present is as follows:

November/1: Skeetonema, Keatheros
November/5: Skeetonema, Keatheros
November/12: Skeetonema, Keatheros
November/20: Skeletonema, Keatheros, Lisosolenia
November/27: Skeletonema, Keatheros, Lisosolenia
December/4: Skeetonema, Keatheros, Lisosolenia
December/13: Skeletonema, Keatheros, Lisosolenia, Asteriopranos, Eucampia
December/28: Skeletonema, Keatheros, Lisosolenia, Asteriopranos

These diatom red tide spatial distributions are known. For instance, Skeletonema distribution, chlorophyll-a concentration and 10 days average of the sea surface temperature of January 4, 2018 is shown in Fig. 5(a), (b), and (c), respectively.

The diatom red tide space distribution is also known. In addition, sunshine hours, tide levels and river flow rates during this period are shown in Fig. 6, 7 and 8, respectively. In addition, Fig. 9 shows the wind speed northward from November 1, 2017 to January 31, 2018.

In these figures, blue colored down arrow denotes diatom occurrences. In particular, the last three arrow shows large diatom appearances. These figures show that the large diatom appearances are occurred in the spring tide time periods, relatively large river flow are observed in the November 2017, there are comparatively long sunshine hours in low tide time periods, and there are relatively strong winds from the north direction during the time periods from low tide and spring tide.

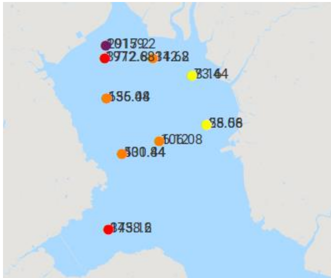

a) Skeletonema Distribution (the Numbers in the Figure shows the Number of Cells Per ml)

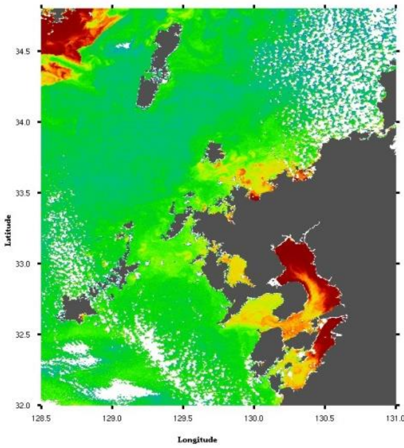

(b) Chlorophyll-a Concentration.

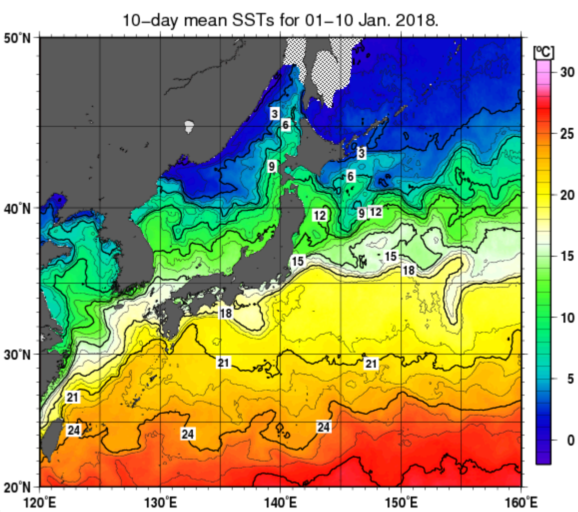

(c) Sea Surface Temperature of January 4, 2018.

Fig. 5. Skeletonema Distribution, Chlorophyll-a Concentration, and 10 Days Average of the Sea Surface Temperature of January 4, 2018.

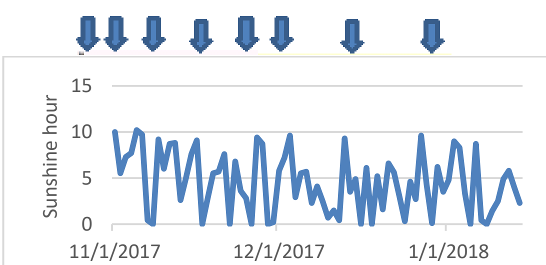

Fig. 6. Sunshine Hours from November 1, 2017 to January 31, 2018.

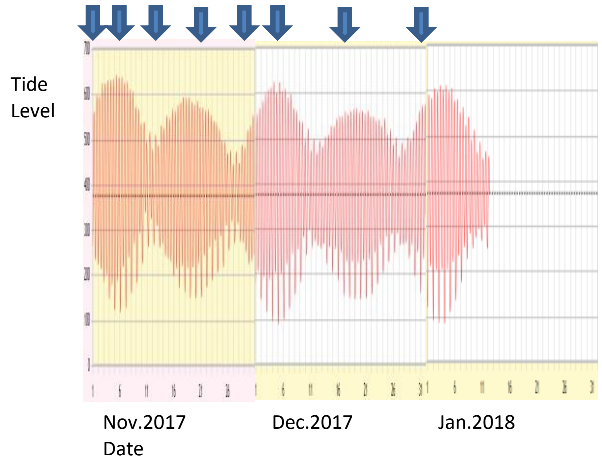

Fig. 7. Tide Level from 1 November 2017 to 31 March 2018.

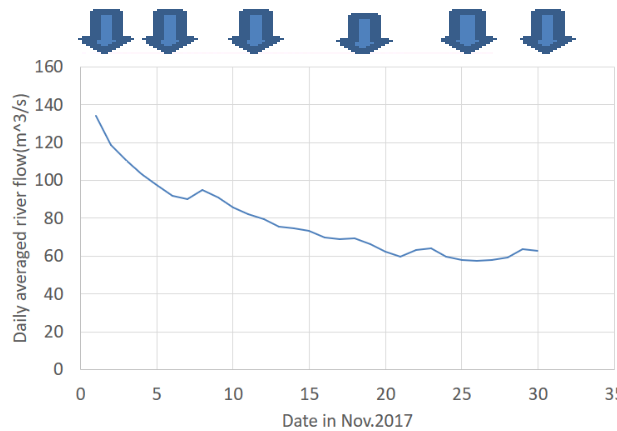

Fig. 8. River Flow Rate from November 1, 2017 to November 30, 2017.

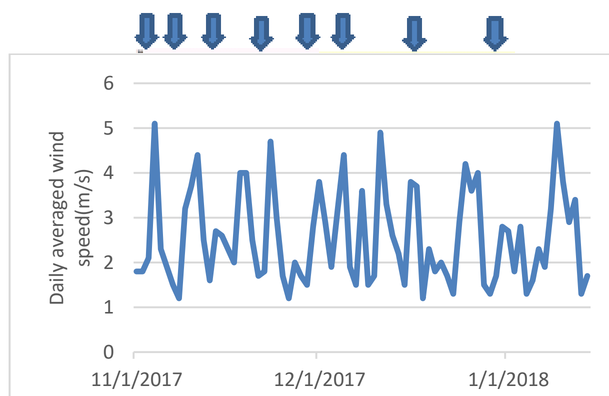

Fig. 9. Northernmost Wind Speed from November 1, 2017 to January 31, 2018.

Therefore, the proposed diatom detection method derived from the 9 years data of MODIS derived chlorophyll-a concentration data together with turbidity data as well as meteorological data is validated with the 2017 to 2018 data of these data.

The sea surface temperature declined after the middle of January 2017, but until then it has kept over 15 degrees and the condition of relatively high sea surface temperature continued.

Occurrence of Eucampia after February 20 is the high tide period, the wind to the north is stronger just before that, the turbidity is low in the low tide period before that, the solar radiation is large, and the river flow rate was large just before that.

From November 2017, although the amount is small, Skeetonema, Frequent Ketotheros, after 20 days Lysosrenia has occurred. Sea surface temperature declines from mid-December 2017, the sea surface temperature is lower than 2016. Increase of chlorophyll concentration after January 2018.

V. Conclusion

CNN considering physical processes with time series of stages for diatom detection with remote sensing satellite derived physical data and meteorological data is proposed. Previously proposed diatom prediction based on neural network with remote sensing satellite and meteorological data is validated. Through the experiments at Ariake bay area, Kyushu, Japan with gathered time series of remote sensing data of MODIS derived turbidity as well as chlorophyll-a data estimated for the winter seasons (from January to March) during from 2010 to 2018 together with measured and acquired meteorological data for the same winter seasons, the proposed method is validated.

Diatom appearance prediction method with big data of remote sensing satellite data and meteorological data is proposed together with validation of the proposed method. Through the experiments at Ariake bay area, Kyushu, Japan with gathered time series of remote sensing data of MODIS derived turbidity as well as chlorophyll-a data estimated for the winter (from January to March) during from 2010 to 2018 together with measured and acquired meteorological data for the same winter seasons, the proposed method is validated.

The sea surface temperature declined after the middle of January 2017, but it kept at least 15 °C until then, and the condition of relatively high sea surface temperature continued. Occurrence of Eucampia after February 20 is the high tide period, the wind to the north is stronger just before that, the turbidity is low in the low tide period before that, the solar radiation is large, and the river flow rate was large just before that. Also, since November 2017, although the amount is small, Skeletonema, Frequent Ketotheros occurred, Lisosolenia occurred after 20 days, the temperature of the sea surface declined since mid-December 2017, the sea surface temperature is lower than the year 2016. Chlorophyll concentration has been rising since January 2018. More importantly, it is found that the empirically found mechanism of diatom appearance shows coincide to the rules of diatom blooming predicted by the proposed method.

Further investigations are required for establishment of a method for predicting the seasonal surface environment Nowcasting to winter diatom red tide detection. Also, further study is required to check the possibility of using Japan Aeronautics Exploration Agency: JAXA satellite-borne SGLI[35] and Setinel-2, 3 / MSI[36] and try to use COMS / GOCI[37]. Applied to collaborative research with JAXA on research plan on winter diatom red tide prediction by SGLI, calibration of SGLI by Saga University observation tower data, etc. estimation of sea surface emission luminance, chlorophyll a, turbidity, etc. Estimation method will be studied.

[35] https://suzaku.eorc.jaxa.jp/GCOM_C/index_j.html
[36] https://sentinel.esa.int/web/sentinel/technical-guides/sentinel-2-msi
[37] https://oceancolor.gsfc.nasa.gov/data/goci/

Acknowledgment

The authors would like to thank Dr. Toshiya Katano of Tokyo University of Marine Science and Technology, Dr. Yuichi Hayami, Dr. Kei Kimura, Dr. Kenji Yoshino, Dr. Naoki Fujii of Saga University and Dr. Takaharu Hamada of the University of Tokyo for their great supports through the experiments.

References

[1] Kohei Arai, Prediction method for large diatom appearance with meteorological data and MODIS derived turbidity and chlorophyll-a in Ariake bay area in Japan, International Journal of Advanced Computer Science and Applications, 8, 3, 39-44, 2017.

[2] Yuji Ito, Toshiya Katano, Naoki Fujii, Masumi Koriyama**,** Kenji Yoshino, and Yuichi Hayami, Decreases in turbidity during neap tides initiate late winter large diatom blooms in a macrotidal embayment, Journal of Oceanography,69: 467-479. 2013.

[3] Nishikawa T (2002) Effects of temperature, salinity and irradiance on the growth of the diatom Eucampia zodiacus caused bleaching seaweed Porphyra isolated from Harima-Nada, Seto Inland Sea, Japan. Nippon Suisan Gakk 68: 356–361. (in Japanese with English abstract).

[4] Nishikawa T (2007) Occurrence of diatom blooms and damage tocultured Porphyra thalli by bleaching. Aquabiology 172: 405–410. (in Japanese with English abstract).

[5] Nishikawa T, Hori Y (2004) Effects of nitrogen, phosphorus and silicon on the growth of the diatom Eucampia zodiacus caused bleaching of seaweed Porphyra isolated from Harima-Nada, Seto Inland Sea, Japan. Nippon Suisan Gakk 70: 31–38. (in Japanese with English abstract).

[6] Nishikawa T, Hori Y, Nagai S, Miyahara K, Nakamura Y, Harada K, Tanda M, Manabe T, Tada K (2010) Nutrient and phytoplankton dynamics in Harima-Nada, eastern Seto Inland Sea, Japan during a 35-year period from 1973 to 2007. Estuaries Coasts 33: 417–427.

[7] Nishikawa T, Hori Y, Tanida K, Imai I (2007) Population dynamics of the harmful diatom Eucampia zodiacus Ehrenberg causing bleachings of Porphyra thalli in aquaculture in Harima- Nada, the Seto Inland Sea, Japan. Harmful algae 6: 763–773.

[8] Nishikawa T, Miyahara K, Nagai S (2000) Effects of temperature and salinity on the growth of the giant diatom Coscinodiscus wailesii isolated from Harima-Nada, Seto Inland Sea, Japan. Nippon Suisan Gakk 66: 993–998. (in Japanese with English abstract).

[9] Nishikawa T, Tarutani K, Yamamoto T (2009) Nitrate and phosphate uptake kinetics of the harmful diatom Eucampia zodiacus Ehrenberg, a causative organism in the bleaching of aquacultured Porphyra thalii. Harmful algae 8: 513–517.

[10] Nishikawa T, Yamaguchi M (2006) Effect of temperature on lightlimited growth of the harmful diatom Eucampia zodiacus Ehrenberg, a causative organism in the discoloration of Porphyra thalli. Harmful Algae 5: 141–147.

[11] Nishikawa T, Yamaguchi M (2008) Effect of temperature on lightlimited growth of the harmful diatom Coscinodiscus wailesii, a causative organism in the bleaching of aquacultured Porphyra thalli. Harmful Algae 7: 561–566.

[12] Syutou T, Matsubara T, Kuno K (2009) Nutrient state and nori aquaculture in Ariake Bay. Aquabiology 181: 168–170. (in Japanese with English abstract).

[13] Harada K, Hori Y, Nishikawa T, Fujiwara T (2009) Relationship between cultured Porphyra and nutrients in Harima-Nada, eastern part of the Seto Inland Sea. Aquabiology 181: 146–149. (in Japanese with English abstract).

[14] Kohei Arai, T. Katano, Trend analysis of relatively large diatoms which appear in the intensive study area of the ARIAKE Sea, Japan, in winter

(2011-2015) based on remote sensing satellite data, Internationa Journal of Advanced Research in Artificial Intelligence (IJARAI), 4, 7, 15-20, 2015.

[15] Kohei Arai, Locality of Chlorophyll-a Concentration in the Intensive Study Area of the Ariake Sea, Japan in Winter Seasons Based on Remote Sensing Satellite Data, Internationa Journal of Advanced Research in Artificial Intelligence (IJARAI), 4, 8, 18-25, 2015.

[16] Kohei Arai and Yasunori Terayama, Satellite and Ground based red tide detection method and system by means of peak shift of remote sensing reflectance, International Journal of Applied Science, 2, 3, 53-61, 2011.

[17] Kohei Arai and Yasunori Terayama, A method for red tide detection and discrimination of red tide type (spherical and non-spherical shapes of red tide) through polarization measurements of sea surface, International Journal of Applied Science, 2, 3, 62-70, 2011.

[18] Kohei Arai, Yasunori Terayama, Red tide detection using remote sensing satellites, research vessels, and ground based red tide monitoring system and discrimination of red tide species, Journal of Japan Society of Photogrammetry and Remote Sensing, 50, 6, 339-346, 2011.

[19] Kohei Arai, Comparative study on discrimination methods for identifying dangerous red tide species based on wavelet utilized classification methods, International Journal of Advanced Computer Science and Applications, 4, 1, 95-102, 2013.

[20] Kohei Arai, Relation Between Chlorophyll-a Concentration and Red Tide in the Intensive Study Area of the Ariake Sea, Japan in Winter Seasons by Using MODIS Data, International Journal of Advanced Research on Artificial Intelligence, 4, 10, 8-15, 2015.

[21] Kohei Arai, One of the Possible Causes for Diatom Appearance in Ariake Bay Area in Japan in the Winter from 2010 to 2015 (Clarified with AQUA/MODIS), International Journal of Advanced Research on Artificial Intelligence, 5, 4, 1-8, 2016.

[22] Kohei Arai, Relation between Large Sized Diatom Appearance and Meteorological Data in Ariake Bay Area in Japan, in Particular, in the Winter in 2016, International Journal of Engineering Science and Research Technology, 2, 2, 1-9, 2016.

AUTHOR'S PROFILE

Kohei Aarai He received BS, MS and PhD degrees in 1972, 1974 and 1982, respectively. He was with The Institute for Industrial Science and Technology of the University of Tokyo from April 1974 to December 1978 and also was with National Space Development Agency of Japan from January, 1979 to March, 1990. During from 1985 to 1987, he was with Canada Centre for Remote Sensing as a Post Doctoral Fellow of National Science and Engineering Research Council of Canada. He moved to Saga University as a Professor in Department of Information Science on April 1990. He was a councilor for the Aeronautics and Space related to the Technology Committee of the Ministry of Science and Technology during from 1998 to 2000. He was a councilor of Saga University for 2002 and 2003. He also was an executive councilor for the Remote Sensing Society of Japan for 2003 to 2005. He is an Adjunct Professor of University of Arizona, USA since 1998. He also is Vice Chairman of the Commission-A of ICSU/COSPAR since 2008. He wrote 30 books and published 580 journal papers.

Designing an Automated Intelligent e-Learning System to Enhance the Knowledge using Machine Learning Techniques

G. Deena[1]
Research Scholar, Computer Science & Engineering
Sathyabama Institute of Science & Technology
Chennai, Tamilnadu
India

Dr. K. Raja[2]
Department of Computer Science Engineering
Dhaanish Ahmed College of Engineering
Chennai, Tamilnadu
India

***Abstract*—The modern digital world requires its users to learn continuously in order to enhance their knowledge in the working environment and the academic sector. This kind of learning is significantly facilitated by the E-Learning platform, which is better than the traditional methods. As E-Learning offers benefits like time and space independence, many learners have made it their choice. However, since an abundant of E-Learning courses are available on websites, learners are confused as to which is the right one to choose. This paper proposes an Automated Intelligent Learning (AIL) methodology which covers the entire Teaching-Learning Process (TLP) to overcome this issue. It enables the selection of suitable topics and framing an appropriate course syllabus and assessment questions for the users. In it, the learner satisfies topic selection based on Bloom's taxonomy. This enables high-quality knowledge outcomes in the learner. The subject curriculum is framed by using Hierarchical clustering techniques. This helps the user to fix suitable topics and conveniently generate questions using machine learning techniques. The proposed methodology was evaluated by carrying out post and pre-assessment tests on undergraduate students from computer science courses. The performance analysis of the proposed methodology was compared with that of the existing methodology. It was observed that the proposed methodology is effective in applying the topic selection hierarchical method to make a perfect syllabus for the course, and assessment questions. Besides, it was found to enable the learner to learn without any confusion or distraction.**

Keywords*—e-Learning; teaching learning process; pre-assessment and post- assessment; blooms taxonomy; machine learning

I. INTRODUCTION

In the traditional educational system, the teaching-learning process takes place under the teacher-centric approach, where the teacher delivers as per their preferences. The impact of this method leads to frustration and a lack of interest in the student. Therefore, many students lose or discontinue the course. Later, the online system was developed to solve this issue. Learning has taken a gigantic transformation from classroom teaching to the online learning system. Information Technology has given a drastic change in the educational system by employing Information and communication technology (ICT). For a decade, research has been directed towards enhancing the teaching-learning process with the support of ICT. The modern teaching-learning process is commonly known as Intelligent Tutoring Systems, M-Learning, Pedagogical Agents, U-Learning, and Trainer Tutors [1].

In both the classical educational system and the E-Learning system, a human teacher understands the learning skill of the learners, and based on this, the skilled teacher trains them. However, the teacher has to spend a lot of time to understand the learners in the classical educational system [2]. The Intelligent Tutoring System (ITS) is designed in such a way that it helps to determine the cognitive level of a learner [3][4]. Thus, it teaches the learner with the highest preferences set by the learner.

Now- a- days, all the learning are being moved towards the electronic mode, where the learners feel highly comfortable to learn. The users are provided with the option of making additional choices of courses with the specific and appropriate syllabus. In the traditional system, users took up the classroom teaching i.e., the teacher-centric approach. This consumed a lot of time for enhancing knowledge due to the lack of resources and technology. Further, not all the users can avail of this kind of teaching system to enhance their knowledge, owing to the cost and time factors. Thus, there is a gap between the learner and the learning system in the traditional system. Today, the transition from the traditional to the E-Learning system has made it comfortable for the users to enrich their knowledge [5].

However, even after moving to E-Learning methodology some limitations are faced. If the users are learning the course through the web, they are exposed to unfavorable situations like the inability of course selection. This is due to confusion related to whether or not they are in the correct path of the course syllabus. To make E-Learners more comfortable, bloom-taxonomy has been introduced to check whether the syllabus of the particular subject is rightly framed from the basic level to the application level. It ensures that the syllabus is suitable for the learners to continue the course without any confusion.

e-Learning is a universally popular form of online education system widely accepted owing to it’s anytime anywhere learning benefits. Besides, it is also profitable to the management and the students. The learner can learn the content either individually or collaboratively as a team member. The collaborative method is the usual method selected by the learner, where they select the course as per their choice [6] to enhance their skill. Here come the domains like artificial intelligence, web ontology, and machine learning, which are emerging not only in the learning system but also to all sectors [7] and [8]. E-Learning is now moving towards the automated and integrated intelligence fields to make the user more comfortable in learning the course.

e-Learning is a learner-centric approach and a highly enabled computer-based system for enabling learning and knowledge enhancement. E-Learning has transformed the educational paradigm through its recent technologies. This learning system may be in any of the specified forms such as Virtual Education (VE), Web-Based Learning (WBL) or Computer Based Learning (CBL). The learning content is supplied via the tape-recorded format which may be in audio, video, text or image set-up, and can be supplied either in the CD form via the internet.

In this current era, the data storage in internet technology increase day by day. It is not easy for the learner to retrieve their specific data and information. In [9], Zhang proposed a personalized E-Learning system based on Google Web Toolkit to avoid confusion during the retrieval of information from the internet.

In the Automated Intelligent E-Learning system proposed by this paper, the preferences in the learner model are given to the learner's choice, the learning material is held by the domain model and the assessment of the model generates the assessment questions.

The rest of the paper is organized in the following manner: Section II discusses the related works, Section III presents the system architecture, Section IV presents the performance analysis, and Section V deals with the conclusion and future enhancement.

II. Related Work

In research filed, many researchers have been currently focusing on the personalized adaptability learning system, which was initially given by the author Brusilovsky & Peylo [10]. In this system, these authors suggested the determination of the cognitive factors and learner's learning style by a psychological test [11].

As per the adaptive educational system, the personalization of the subject for each student is provided as per the individual's knowledge level, skill, needs, and background. The adaptive system supports and guides the learner to enhance knowledge. Currently, many systems are designed using intelligent techniques and methods [12].

Artificial intelligence has several concepts related to Naive Bayes rule, Fuzzy Logic rule, etc. These can also be integrated with the frequent words search with relevance to form an appropriate course syllabus [13] and [14].

An instructional design process was used to assess the cognitive and learning style of a learner for web-based learning [15]. Personalization was enabled in an online educational system by designing the system to adapt the learner characteristics through ontology for the development of the content. This system collected the personal data of the learner and gave the recommendation to the teacher [16].

Apriori Algorithm was used in recommender E-Learning System to find the association between the features of the searching key element of the individual learning model. [17][18][19][20][21].

In [22], the author used an agent called mod-knowledge to completely track the learner's knowledge, and the internal and external structure of the learner using the machine learning algorithms. Authors in [23], called the cognitive skill as thinking skills. Higher the domain cognitive skill, the easier the problem-solving ability is. The sequence or the learning path would vary on the basis of the learner's performance.

The learning styles of an individual may also vary due to factors like the learner's mindset, the learning time, and the complexity of the course content. Learning Styles deliver a more prominent effect on the learning exhibitions, particularly in E-Learning situations.

In [23], authors Tee, T. K. et al., utilized the Learning style index designed by Felder and Silverman to examine the learning styles of students in a Malaysian vocational college's Business Management and Hospitality programs.

In [24], L.M. Al-Saud et al. proposed a methodology to decide the favored learning style of dental students at Saudi Arabia's King Saud University located at Riyadh. The experimental outcomes stated that there were multimodal learning inclinations in more than half of the students.

The domain model was constructed using fuzzy logic in [25]; the personalization model was adapted to fetch the learning content as per the learner's preference using the similarity index between the prerequisite model and the domain model. The subjective style was characterized as a person's predictable way of dealing with sorting out and handling data amidst considerations [26] [27].

An author in [28], applied the data mining techniques of the Bayesian network to discover the knowledge of the domain model. The computer system learner interacted with the learner to understand the knowledge level of the learner. The Bayesian network was utilized to design the student model and the domain model.

An existing methodology has shown the easy way to help continuous learning in an employee of an organization, but still, there is a lack of understanding of the concept [29]. The present and future situation of the organization seeks to improve their business further by making the learners continue their learning without any distractions [30].

Most of the existing e-Learning courses are available with multiple course contents, but the focus has not been directed on how effectively these help the user in enhancing knowledge.

In the proposed system, the complete teaching-learning process has been designed to determine the student's knowledge level to train them effectively using Bloom's taxonomy followed in the domain model. Assessments were carried out before and after the course to determine their level of understanding of the concept.

III. System Architecture

To make the learner a more efficiently knowledgeable person, we have developed an Automated Intelligent E-Learning a system, which covers the complete set of the teaching-learning process. It identifies the cognitive knowledge level, frames the syllabus, and conducts the assessment to the user. The learner model accesses the students for their flexibility of accessing the learning content. Learning contents are developed by experts as per the hierarchical clustering techniques. Each file is represented as the learning element. The target of the assessment model is to generate the procedural and declarative question using Natural Language Processing techniques. The proposed system's architecture is given in Fig. 1.

A. Learner Model

Woolf has identified the Student model as a significant model in Intelligent Tutoring System (ITS). The learner model is an important part of adaptive E-Learning systems. This is commonly referred to as a user or student model. Generally, the learner has to spend too much time in identifying the appropriate learning content. In general, two types of information are collected from each learner, namely the domain-independent and domain-dependent information. Domain-specific the information pertains to the learner's subject knowledge. The pre-requisite knowledge of the subjects has to be identified and stored for further process. The domain-independent knowledge implies their cognitive behavior, their style of learning, their current understanding capability level, and their preferences of learning. In [31], author Paramythis & Loidl-Reisinger specified that this model sustains the learner's account. In the online educational system, the learning style improves the learner model.

1) Cognitive style: Cognitive learning styles are data handling tendencies of a person. Individuals are different in their capacities. Cognizance depicts a man's normal capacity of seeing, reasoning, the critical thinking and recalling. The subjective style is usually depicted as an identity measurement that affects the qualities, social collaboration and states of mind, and can characterize as a person's predictable way to deal with data [32].

The cognitive skill is an essential part of the process of learning information. The author in [33], states that cognitive style implies the mechanism of processing the received information into knowledge and that it is totally different for each individual. When the cognitive level is high, the learner concentrates more on learning the subject at high speed. Otherwise, there are chances of quitting the course.

In the proposed system, the cognitive skill of the learner has to be identified and based on that skill; the content will be supplied for further training or coaching of the material. Before taking up the course, learner pre-requisite subject knowledge has to be identified by conducting a simple assessment. The assessment questions are generated automatically as per Bloom's order. Bloom's taxonomy is the best classifier that classifies information into two viz., the lower level and the higher level. Lower level covers factors including Knowledge, Understanding, and Application; and higher-level covers Analysis, Synthesis and Evaluation of the concept. The Learner model is given in Fig. 2.

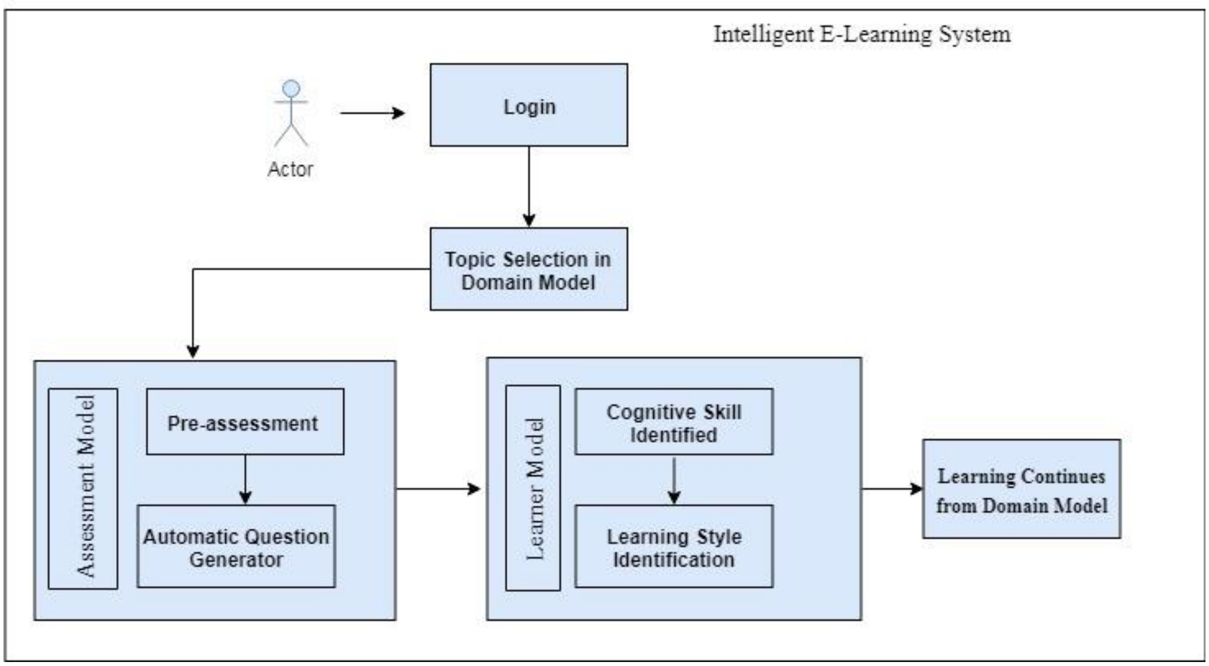

Fig. 1. Intelligent E-Learning System.

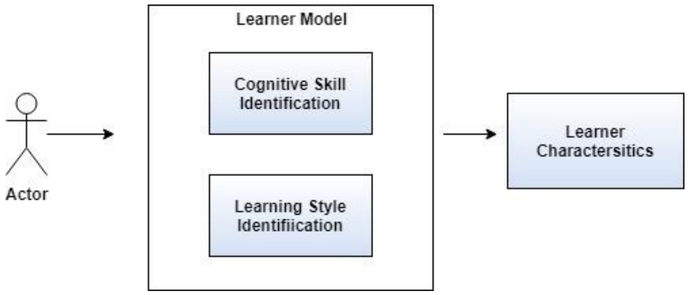

Fig. 2. Learner Model.

In [34], the author used the demographic information of the learner, specifically the name, age, experience, and qualification. However, the proposed system, the learner characteristics like learning style and subject knowledge are considered. A pre-assessment was conducted using a familiar diagnostic method like multiple-choice questions to check the knowledge level, but not to classify learners. When a learner crosses the threshold level of the mark, they will proceed to the next level of the material. If not, the current topic will be continued to refresh information and give the learner more clarity of the content.

Each learner has an individual learning style that has the most important role in the learning process to help learn the material more effectively [35]. Felder-Silverman [36] is the most appropriate method used in the E-Learning system to determine the learning style. This method classifies learners into any one of the styles including the active, the sensing, the visual, the verbal and the sequential type learner.

2) Felder-Silverman learning style: Styles are the psychological facet of the learner which enables learning. This is important in the online educational system for enhancing the technology supporting system. The learners grasp and process the information in different ways. Felder-Silverman model uses any of the techniques to motivate learning, to generate solid information, explicit illustration, provide balanced material for practical problem solving, computer-assisted instruction and scientific method [37]. Once the learning style has been determined, suitable content can be mapped to the learner. Felder suggested four types of learning styles, of which the proposed system includes two viz., the visual and the verbal for our system.

- Active Learner: Learner recognizes the information only by doing the concept learned from the learning material. This type of learner joins a group to work in it as a team member.
- Sensing Learner: Learner prefers to consider the solid learning material and facts. They like to solve the problem in fixed methods, are patient with available details, and are fine at learning by performing hands-on work and rote facts.
- Visual Learner: Learners learn the best by way of what they have seen. They focus more on study materials like demonstrations, pictures, flow charts and visual aids.
- Verbal Learners: Learners learn best from vocal and written explanations delivered by experts. They like to follow storytelling techniques during learning.
- Sequential Learners: Learners learn in a sequential ladder and progress in a linear fashion. Even at times when they have not completely comprehended the concept, they still are capable of doing something with the concepts learned.

Our Proposed System has been developed for the visual and verbal type of learners, who are higher in number in the online educational system. The readily available printed materials are given as the source. The Learner characteristics are identified from the cognitive skill identification and Learning style using the pre-assessment. Once the learner characteristics are identified, the learner becomes ready to learn the suitable content without any disappointment and boredom. The learner's knowledge of the subject will be thus enhanced, and that can be compared with the existing methodologies.

B. Domain Model

The central part of the learning process is the domain model. The learning materials are organized in a specific manner, where the learner's choice may be the text, image or video format as per the learning style predicted by using LSI. The materials are developed by a domain expert and converted into the digital format. The materials are classified as per blooms taxonomy from the low-level content to high-level content.

Hierarchical clustering is the unsupervised algorithm it contains a set of a similar item in a group. The syllabus is organized using the hierarchical clustering technique as follows. The similar topics come under the subject, and the sub-topics are related to the main topics, which form a cluster. As per hierarchy, the learning material is divided into units, the units are divided into topics, and the topics are divided into sub-topics, and so on as given in Fig. 3. This type of organized material is stored in the database, where each content is represented as an object. The object is utilized whenever there is a need for the material.

Learning content accessed by the learner is as per the learner characteristics [38] such as the knowledge level, the cognitive style, and the learning style. This way, the basic concept of the subject is well understood by the learner, and the learner keeps continuing to the next level without any frustration owing to learning. Before and during the learning process, a diagnostic assessment will be conducted for which the important sentences have to be identified automatically using the Latent Semantic Analysis (LSA) [39].

In our proposed system, the content of topics is stored in a hierarchical order. This content undergoes some pre-processing to get rid of the stop words and the least occurring words from the input file to generate some meaningful questions. The domain model has to follow the information retrieval techniques such as Sentence Scoring, Input Matrix and Singular Value Decomposition (SVD).

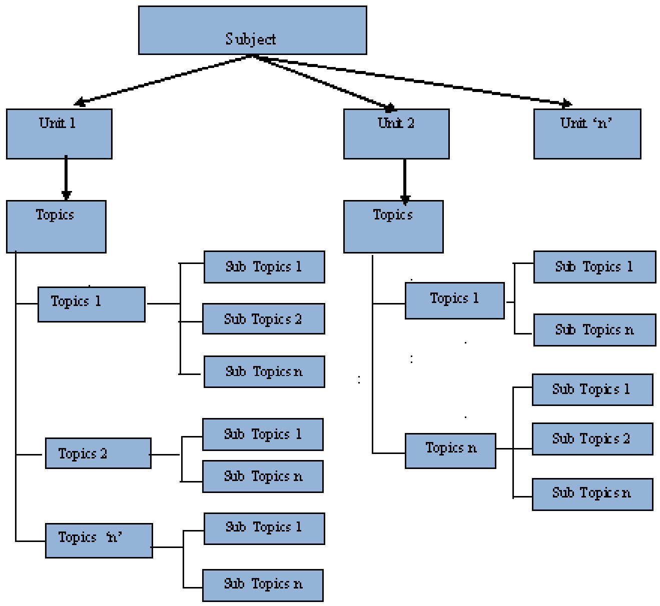

Fig. 3. Syllabus in Hierarchical Format.

1) Latent semantic analysis: Latent Semantic Analysis involves the application of natural language processing and the techniques of information retrieval. This unsupervised algorithm helps in coming up with the most significant sentences from the course material without any human interference.

With the supplied keywords from the phrases, it helps in determining the relevant learning content with a high degree of correlation to the target sentence. Arithmetic processes are used to calculate the similarity of the sentences from the material with the support of Singular Value Decomposition. Analyzing the relationships between a set of words and a set of concepts is done by Latent Semantic Indexing (LSI). It also helps in judging the quality of the content in the sentences.

2) Singular value decomposition: Singular value decomposition (SVD) matrix finds the correlation between each word in the sentences by analyzing the phrases and their relation to the learning material. The original matrix is created from the orthogonal factors and large words in the input file by linear combination. The original matrix is decomposed into three matrices:

$$A=USV^T$$

A is the m*n Matrix, row and column value

U and V is an orthogonal matrix

S is the diagonal Matrix

3) Sentence scoring: Sentence tokenizer has been used to frame individual sentences from the input topic file. Sentence scoring has been applied to evaluate the similarity between the two non-zero vectors of the words by using cosine similarity method. The value of each sentence is allocated using the number of occurrences of the words in the sentences. For every sentence, the vector coordinate is evaluated with the help of the following formula.

$$\text{Similarity}(qn, dn) = \frac{q.\,d}{|q||d|}$$

The similarity of the sentences is supplied to the input matrix to generate the matrix.

4) Input matrix: The original input matrix is represented as 'd'. It is decayed into three individual sub-matrices viz., U, V and $\sum$. Now, the query matrix is raised with the available terms, the keywords and the noun. The most important word used for summarizing the material is the noun. Query matrix 'Q', consists of the significant noun related terms, is given by nk_i. Q= [nk1, nk2… nkn]. Term Frequency (TF) of the word is set in the binary format, where '1' fixes for the word's presence in the sentence, and '0' for the nonexistence of the word in it. Based on this, the important sentences are identified and supplied to the assessment model.

The diagnostic assessment questions are generated automatically using the machine learning techniques in the form of multiple-choice questions or fill in the blanks and the procedural type. Sentence selection is the critical point in framing the questions.

C. Assessment Model

In the educational system, assessment plays the highest role in determining the learning skill level of the learner. Assessment can be of different types, typically the procedural and the declarative. Declarative types of questions are highly used to test the learner's basic skill level. The learner will answer the question in one word. The questions will have multiple choice answers or fill up the blank space form of questions [40]. This type of question is easily implemented to test the skill level of the learner to check whether he/she belongs to the low level, middle level or high level.

Each time before taking the course, the learners are advised to take up the pre-requisite test to know their basic knowledge in the subject. Using Bloom's taxonomy, pre-assessment questions are generated from low order to high order thinking [41]. In traditional E-Learning, assessment questions were framed by a teacher who takes much time for it. Since the learner has to wait until the teacher evaluates his knowledge level and creates a question paper, it leads to time complexity.

To avoid time complexity like that in the existing methodologies, the proposed system generates questions automatically using machine learning techniques without any question bank concept. Each and every time the learner fetches the new set of questions without any human intervention. Since the answers to the questions are also evaluated immediately, immediate identification of subject knowledge is facilitated. When the learner's score crosses the threshold level, they step into the next topic. Otherwise, the current topics are reinforced. The process continues to the end without making the learner lose interest or get disturbance.

In the proposed system, an input file is fetched from the domain model and sent for the document preprocessing, where the entire file is split into the individual sentences, and the stops words such as 'is, was, be, of, on, because and so on are removed. With the available list of words, the keywords, which may be the most frequently occurring words in the sentence, are identified. And finally, noun identification, which is the most important part of the pre-processing, is done. This noun is used to frame questions to test the skill level of the learner.

The problem to be solved is known as stem, which is nothing but the assessment question. The machine learning techniques are used to generate the Fill up the blank questions and the multiple choice questions (MCQ) [42]. A new set of questions are generated every time using the randomization algorithm.

1) Declarative type question: There are two types of declarative questions in general, viz., Fill up the blanks type and Multiple Choice Question (MCQ) type. In the proposed system, the noun is replaced by the blank space in the fill-up the blank. A sample question is given in Fig. 4.

In Fig. 4, the input sentence is supplied to the question generator, where the preprocessing takes place, and finally, the important noun keyword is replaced by the blank space to generate the assessment. Each time the learner gets a new set of questions to test the skill level.

2) Multiple Choice Questions (MCQ): Another declarative type question is MCQ. Stem is selected by sentence tokenizer and sentence scoring; and the distractors are generated by Named Entity Recognizer (NER), which is a Natural Language Processing (NLP) Technique. NER splits the information into small pieces as an entity name and entity type. tagged_tree.leaves() and tagged_tree.label() are operated to identify the chunked data. Noun filter is used to extract the noun, and Rapid Automatic keyword extraction (RAKE) is used to extract the keywords for generating the distractor and the correct answer. The keyword or the noun is the correct answer, and the other distractors are selected by entity type and their entity names. The answers are instantly evaluated, and the marks are shown to the learner. The marks are not to classify the learner, but help to them upgrade their knowledge of the learning content. The sample MCQ is given in Fig. 5, which is implemented in python language.

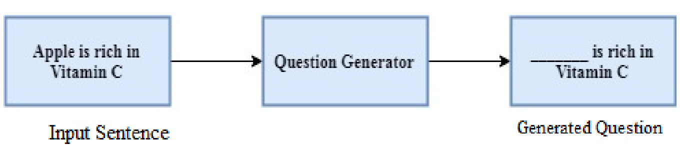

Fig. 4. Fill up the Blank Question.

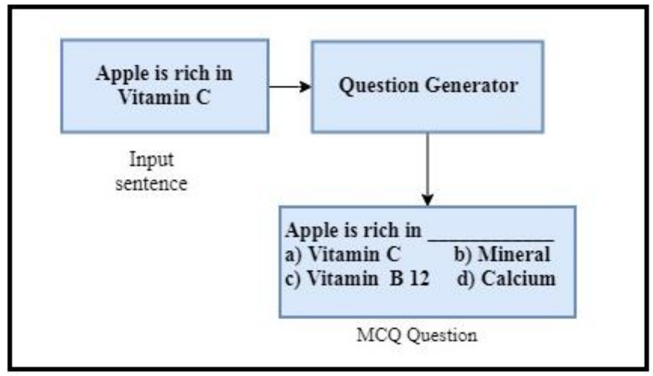

Fig. 5. MCQ Generator.

IV. Performance Analysis

In the proposed Intelligent E-Learning system, the learner's attributes are identified via the individual's cognitive skill and learning style in the learner model. The domain model keeps the syllabus in the hierarchical clustering method, which helps the learner to fetch the content easily. The relevant topics are grouped together as subtopics. The material is processed using Latent Semantic Analysis of NLP techniques to identify the important sentences, and to generate the questions. Finally, the assessment is automatically carried out without any support from the teacher or trainer, by employing NLP techniques. As a result, the suitable course content is supplied to the learner as per the blooms' hierarchy. The learner continues the course with full interest, and the subject knowledge in the particular domain is highly increased as compared to the existing traditional E-Learning systems. The satisfaction level is highly increased by the proposed system. The system was tested with the different categories of school students, and the performance is shown in Fig. 6. It shows the accuracy of the proposed system is increased.

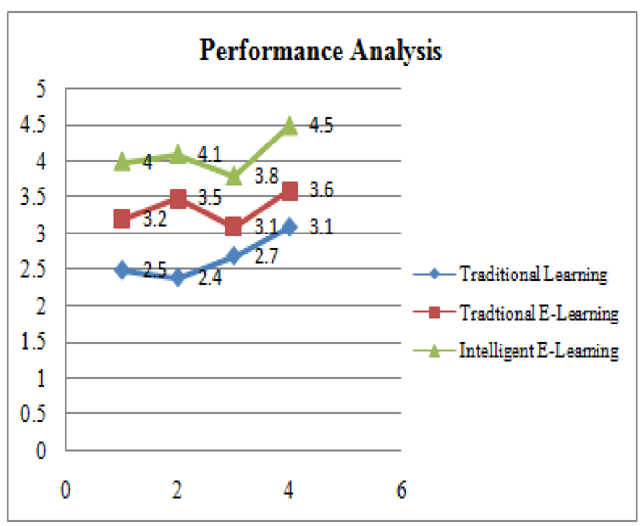

Fig. 6. Performance Analysis.

Each learner is assessed with three different learning systems such as the traditional teaching method highly teacher–centric, traditional E-Learning as student-centric approach and finally with proposed system. The different learners are given in the x-axis; their marks are given in y-axis for the grade scale of 5 point. Each learner is trained and assessed with all type of teaching method and their result is given in the performance analysis. Finally, achieved the learners are highly satisfied with the proposed system.

V. Conclusion

The proposed AIL methodologies have overcome the problem of learners in selecting the course material by determining the learner's cognitive skill and learning style using machine learning techniques. The syllabus was framed in hierarchical ordering, and the assessment questions were generated automatically using machine learning techniques. The subject knowledge and satisfaction level of the learners are highly increased through the proposed system. From the analysis, we have concluded that by using the proposed methods, the course outcome can be enhanced in terms of better understanding and suitable topics selection as per the blooms taxonomy. In future, the E-Learning system can be designed using any other advanced method like big data, deep learning automatically, etc.

References

[1] Luis Alfaro1, Claudia Rivera2, Jorge Luna-Urquizo, "Using Project-based Learning in a Hybrid e-Learning System Model", International Journal of Advanced Computer Science and Applications, Vol. 10, No.10, pp. 426-436, 2019.

[2] Markowska-Kaczmar U., Kwasnicka H., Paradowski M., "Intelligent Techniques in Personalization of Learning in e-Learning Systems", Studies in Computational Intelligence, Springer, Berlin, Heidelberg, Vol. 273, pp. 1–23, 2010.

[3] Etienne, Wenger. "Artificial intelligence and tutoring systems." Computational and Cognitive Approaches to the Communication of Knowledge. Morgan Kauffmann, Los Altos, San Francisco, CA USA, 1987.

[4] Ohlsson, Stellan. "Some principles of intelligent tutoring", Instructional Science, Vol.3, No.4, pp. 293-326, 1986.

[5] Mark Nichols, "A theory for eLearning," Journal of Educational Technology & Society, Vol. 6, No. 2, pp. 1-10, 2003.

[6] M. Alavi. "Computer mediated collaborative learning: An empirical, evaluation", MIS Quart., Vol.18, No.2, pp.159-174, 1994.

[7] Nicola Henze, Peter Dolog and Wolfgang Nejdl, "Reasoning and Ontologies for Personalized E-Learning in the Semantic Web," Journal of Educational Technology & Society, Vol. 7, No. 4, pp. 82-97, 2004.

[8] Jeroen J. G., van Merriënboer and Paul A. Kirschner, "Ten Steps to Complex Learning A Systematic Approach to Four-Component Instructional Design," Taylor & Francis Group, 2017.

[9] Zhanga, Ye Jun, and Bo Songb. "A Personalized e-Learning System Based on GWT." In: International Conference on Education, Management, Commerce and Society, pp. 183-187, 2015.

[10] Brusilovsky, P., Peylo, C., "Adaptive and intelligent web-based educational systems", International Journal of Artificial Intelligence in Education Vol. 13, pp. 156–169, 2003.

[11] Brusilovsky, P. "Adaptive Hypermedia", User Modeling and User-Adapted Interaction", Vol. 11, No.2, pp.87-110, 2001.

[12] K. Chrysafiadi, M. Virvou, "Student modelling approaches: A literature review for the last decade", Expert Systems with Applications, Vol. 40, Issue 11, pp. 4715–4729, 2013.

[13] Wai Lam and Fahiem Bacchus, "Learning Bayesian Belief Networks: An Approach Based on the MDL Principle," Computational Intelligence, Vol. 10, No.3, pp. 269-293, 1994.

[14] Russell, Stuart J. Norvig and Peter., "Artificial Intelligence : A Modern Approach," Pearson Education Limited, 2016.

[15] Santally, M.I., Alain, S," Personalisation in web-based learning environments", International Journal of Distance Education Technologies, Vol. 4, No.4, pp. 15–35, 2006.

[16] Lazcorreta, E., Botella, F., Fernaández-Caballero, A.: Towards personalized recommendation by two-step modified Apriori data mining algorithm. Expert Systems with Applications, Vol.35, No.3, pp. 1422–1429, 2008.

[17] Romero, C., Porras, A., Ventura, S., Hervás, C., Zafra, "A using sequential pattern mining for links recommendation in adaptive hypermedia educational systems", In: International Conference Current Developments in Technology-Assisted Education, pp. 1015–1020, 2006.

[18] Rigou, M., Sirmakessis, S., Tsakalidis, "A.: Integrating Personalization in E-Learning Communities", Journal of Distance Education Technologies, vol. 2, No. 3, pp. 47–58, 2004.

[19] Tsai, C.J., Tseng, S.S., Lin, C.Y.,"A Two-Phase Fuzzy Mining and Learning Algorithm for Adaptive Learning Environment", ICCS-Computational Science, Vol. 2074, pp. 429–438. Springer, .2001.

[20] Markellou, P., Mousourouli, I., Spiros, S., Tsakalidis, "A.: Using semantic web mining technologies for personalized e-Learning experiences". In: Proceedings of the web based education, pp. 461–826, 2005.

[21] Trifa, A., Hedhili, A. & Chaari, W.L, "Knowledge tracing with an intelligent agent, in an e-Learning platform.", Education and Information Technologies, Vol.24, 2019.

[22] Wei-Lun Lin and Yi-Ling Shih, "The developmental trends of different creative potentials in relation to children's reasoning abilities: From a cognitive theoretical perspective," Journal of Thinking Skills and Creativity, Elsevier Publications, Vol. 22, pp. 36 – 47, 2016.

[23] T.K.Tee, J.Md Yunos, B.Kuppusamy, M.H.Yee, MimiMohaffyza Mohamad, W.Othman, R.CheRus and Z.Hanapi, " The Pattern of Learning Styles among Second Year Students in Business Management and Hospitality Programs at One of The Vocational College in Northern Zone," Procedia - Social and Behavioral Sciences, Elsevier Publications, Vol. 204, pp. 62 – 72, 2015.

[24] Al-Saud LM, "Learning style preferences of first-year dental students at King Saud University in Riyadh, Saudi Arabia: influence of gender and GPA," US National Library of Medicine National Institutes of Health, Vol. 77, Issue. 10, 2013.

[25] Ali Aajli, Karim Afdel, "Generation of an adaptive e-Learning domain model based on a fuzzy logic approach", In 13th International Conference of Computer Systems and Applications, Dec. 2016, Agadir, Morocco.

[26] Karl O. Jones, Janice Harland, Juliet M.V. Reid and Rebecca Bartlett, "Relationship between examination questions and bloom's taxonomy," in proc. of 39th IEEE Frontiers in Education Conference, FIE '09, 2009.

[27] Ana Lidia Franzoni ; Saïd Assar ; Bruno Defude ; Javier Rojas, "Student Learning Styles Adaptation Method Based on Teaching Strategies and Electronic Media," in proc. of 8th IEEE International Conference on Advanced Learning Technologies, ICALT '08, 2008,

[28] Aarij Mahmood Hussaan, Karim Sehaba, "Learn and Evolve the Domain Model in Intelligent Tutoring Systems Approach Based on interaction Traces", Jan 2014.

[29] Mushtaq Hussain et.al, "Student Engagement Predictions in an e-Learning System and Their Impact on Student Course Assessment Scores", Computational Intelligence and Neuroscience, 2018.

[30] Arthur James Swart, "Evaluation of Final Examination Papers in Engineering: A Case Study Using Bloom's Taxonomy," IEEE Transaction on education, Vol. 53, Issue. 2, pp. 257 – 264, 2010.

[31] Alexandros Paramythis and Susanne Loidl-Reisinger, "Adaptive Learning Environments and e-Learning Standards", Electronic Journal on e-Learning, Vol.2 Issue 1, pp. 181-194, 2004.

[32] Karl O. Jones, Janice Harland, Juliet M.V. Reid and Rebecca Bartlett, "Relationship between examination questions and bloom's taxonomy," In proc. of 39th IEEE Frontiers in Education Conference, FIE '09, 2009.

[33] Richard J. Riding, “On the Nature of Cognitive Style”, An International Journal of Experimental Educational Psychology, Vol.17, pp.22-49, 2010.

[34] Ninni Singh, Amit Kumar, Neelu Jyothi Ahuja, “Implementation and Evaluation of Personalized Intelligent Tutoring System”, International Journal of Innovative Technology and Exploring Engineering, Vol.8 , Issue-6C, April 2019.

[35] Loreta Leka, Alda Kika, Silvana Greca,, ”Adaptivity In E-Learning Systems”, RTA-CSIT, 2016.

[36] G.Deena, Dr.K.Raja , “A study on knowledge based e-Learning in teaching learning process”, In Int.Conf on Algorithms, Methodology, Models and Applications in Emerging Technologies (ICAMMAET), 2017.

[37] G. Deena and K. Raja, "The Impact of Learning Style to Enrich the Performance of Learner in E-Learning System", Journal of Web Engineering, Vol.17, No.6, pp.3407-3421, 2018.

[38] Amit Kumar, Neelu Jyoti Ahuja, “ In Adaptive Framework of Learner Model Using Learner Characteristics for Intelligent Tutoring Systems”, Intelligent Communication, Control and Devices, pp. 425-433, 2020.

[39] G.Deena, and K.Raja, “Sentence Selection Using Latent Semantic Analysis for Automatic Question Generation in E-Learning System”, International Journal of Innovative Technology and Exploring Engineering, ISSN: 2278-3075, Volume-8 Issue-9, July 2019.

[40] G Deena, and K.Raja, NizarBanu, P. K., & Kannan, K.,, Implementing Bloom’s Taxonomy to determine the cognitive level of E-Learner through Automatically Generated Questions. Proceedings of Second International Conference of Computing and Informatics ICC, Egypt, 2019.

[41] G Deena, K Raja and K Kannan, “An Automatic Question Generation System using Rule-Based Approach in Bloom’s Taxonomy”, Recent Advances in Computer Science and Communications, Vol.13, Iss.1, 2020.

[42] Rakangor, S., & Ghodasara, Y. R., “Automatic Fill in the blanks with Distractor Generation from given Corpus”, International Journal of Computer Applications, Vol. 9, PP:. 1-8.

A Comparative Study of Supervised Machine Learning Techniques for Diagnosing Mode of Delivery in Medical Sciences

Syeda Sajida Hussain[1], Rabia Riaz[3]
The University of Azad Jammu and Kashmir
Muzaffarabad, 13100
Pakistan

Tooba Fatima[2]
SQA Engineer, DataCheck Limited
Mezzanine Floor Bahria Complex III
M T Khan Road Near American Embassy
Karachi, Pakistan

Sanam Shahla Rizvi[4]
Raptor Interactive (Pty) Ltd, Eco Boulevard
Witch Hazel Ave, Centurion 0157, South Africa

Farina Riaz[5]
Independent Researcher, Australia

Se Jin Kwon[*6]
Dept. of Computer Engineering
Kangwon National University, 346 Joongang-ro
Samcheok-si, Gangwon-do 25913, Korea

***Abstract*—The uses of machine learning techniques in medical diagnosis are very helpful tools now-a-days. By using machine learning algorithms and techniques, many complex medical problems can be solved easily and quickly. Without these techniques, it was a difficult task to find the causes of a problem or to suggest most appropriate solution for the problem with high accuracy. The machine learning techniques are used in almost every field of medical sciences such as heart diseases, diabetes, cancer prediction, blood transfusion, gender prediction and many more. Both supervised and unsupervised machine learning techniques are applied in the field of medical and health sciences to find the best solution for any medical illness. In this paper, the implementation of supervised machine learning techniques is performed for classifying the data of the pregnant women on the basis of mode of delivery either it will be a C-Section or a normal delivery. This analysis allows classifying the subjects into caesarean and normal delivery cases, hence providing the insight to physician to take precautionary measures to ensure the health of an expecting mother and an expected child.**

Keywords*—Machine learning; supervised learning; bioinformatics; medical sciences

I. Introduction

Bioinformatics is now-a-days the most important field that is associated with the concepts of machine learning. Almost every main medical problem can now be solved by implementing the machine learning techniques such as classification, regression analysis, clustering, etc. [1] [2] [3]. Both supervised and unsupervised machine learning techniques can be implemented on medical datasets, based on the nature of the data and the type of results to be inferred from the data.

There is a huge corpus of data available for applying machine learning techniques related to the medical problems. In almost every field of Bioinformatics, the techniques of machine learning are implemented and providing very helpful results for the diagnosis of the disease. The use of these techniques is very helpful for the medical technicians and doctors as well as practitioners to correctly perform the treatment of a disease. These techniques are also supportive for the future researchers to devise more ways of solving the problems related to any medical issue effectively. In short, machine learning has provided a new life span to the field of Bioinformatics for solving medical related issues.

Many datasets are also available online about the domain of maternity related cases. Many different types of judgements can be performed related to those datasets, such as gender prediction of a child, weight of new born baby, mode of delivery of the baby and many more. The correct prediction about the birth mode of a child is important, not only for the survival of the new born but also for the health of a becoming mother. So, decision about the mode of delivery of a woman should be carried out very carefully. In this research, a medical dataset consisting of the real-world values from the medical records of the pregnant women has been obtained for evaluating machine learning techniques to select the most appropriate technique for solving such type of problems.

Machine learning is a scientific discipline which focuses on how machines learn from the given data. Machine learning is a field of artificial intelligence, that provide a system of automated learning and producing the desired outcome from the given dataset based on the previous examples from the same domain.

Samuel, the father of machine learning term divided it in Supervised and Unsupervised categories [4]. In supervised learning, we have a training data, with a defined set of rules. Based on those rules, the testing data will be evaluated. The

*Corresponding Author

main goal of supervised machine learning is to predict a known output or target from a huge volume of the input data. Because of these predictions, the evaluation of the learning methods will be performed by classifying some metrics. Supervised machine learning techniques are very important for performing Classification, Inference or Regression analysis on a set of data [5] [6] [7]. A study [8] discussed that a supervised machine learning model is built by dividing a dataset into two parts: One set is used for building a classification model by assigning every attribute to one of the defined class labels. The other is for testing the classification model.

In unsupervised learning, there are no group boundaries defined and patterns are matched and recognized from the data that has no labels for identification of the data. Unsupervised learning is a type of machine learning algorithm used to draw implications from datasets consisting of input data without labelled responses. The most common unsupervised learning method is cluster analysis, which is used for exploratory data analysis to find hidden patterns or grouping in data.

The main motivation for this research is to provide aid to the pregnant women for getting their new born baby healthier and in a safe way. No doubt, the maternity related issues are very delicate to handle and solve as, it is the matter of two lives and a concern of a whole family. So, in this research, the focus is to perform some affective work for the betterment of expecting women and to help the medical officers for performing the maternity related delicate decision about the mode of delivery very carefully and correctly.

The problem to be solved in this research work is about the classification of the data of pregnant women in to Caesarean Section or Normal, identifying their mode of delivery based on the number of attributes describing different aspects of a pregnant woman. The Supervised machine learning techniques of Classification are applied on the sampled dataset for assigning a class label of either 0 or 1 to an expecting woman. This classification will be done by using the techniques of Neural Networks, Support Vector Machines (Linear) and Tree based classification (Random Forest, CTree, RPART).

The rest of the paper is organized as follows. Related previous work is reviewed in Section II. Section III describes the data used in the research and the techniques and tools adopted to perform the classification techniques. The results of the experiments in the form of accuracy metrics, ROC curves and graphs are discussed in Section IV. Section V provides conclusion and recommendations for the future work.

II. LITERATURE REVIEW

There is a huge volume of research work performed to determine relationship between C-Sections and inter related risk factors. Defined maternal age of above 44 has more chances of medical complications [9] e.g. hypertension and diabetes and results in higher rate of C-Section delivery. They used machine learning techniques [10] to find if high blood pressure and pulse rate, lack of education and low income, previous surgery and multivitamins are causes of C-Section delivery. Hueston defined site to site variations have chances of C-Section delivery [11]. They said that patients of age greater than or equal to 35 cannot effect in C-Section delivery but if weight is greater than 3600gm and age is also greater than 35 than there are more chances of C-Section delivery [12].

A research about C-Section delivery in 2015 reported that wealth and education effect C-Section delivery [13]. 23 to 35 per cent C-Section deliveries occur in high income people and 12 per cent C-Section deliveries of low income group. Same as higher education have higher C-Section deliveries, the women with no education have C-Section birth rate 7.5 and the metric, secondary and higher education have 21, 31 and 41 per cent, respectively. If there was a previous C-Section birth, then there are more chances of C-Section birth.

Another research described that many factors are involved in C-Section [14]. Major factors for C-Section delivery showed the relationship between section birth, wealth, education, age, ultrasonography, pregnancy completions. Private hospitals have more C-Section delivery as compare to the public. A study said that maternal age affects the C-Section delivery [15]. The authors divided the age in 3 groups. One group is less than 35, another is between 35 and 39 and one group is above 40. Authors defined that the age of 35 -39 have increasing risk of miscarriage and felt chromosomes abnormalities and age of 40 and above have risk factors of gestational diabetes, placenta Persia, placenta abrupt and C-Section delivery.

A reasonable amount of work has been performed on the coeliac disease effect on the new born [16]. They studied that if father suffered from any coeliac disease, new born have lower birth weight and shorter pregnancy duration. If mother suffer from coeliac then birth weight of new born will also be low. The factors of cigarette smoking and hypertension during pregnancy increase the risk in placental abruption [17]. Women that use less calcium level in diet, have more chances of increase blood pressure in their pregnancy [18]. Deficiency of calcium level creates more chances of preeclampsia in the women in pregnancy. They need calcium supplementation to decrease hypertension disorders. Effect of rotation of the head direction of the foetus inside the uterus has a great impact on the mode of delivery of a baby [19]. The researchers studied the effects of rotation of the foetal head on the probable outcome of the delivery mode.

The effects of medical complications that cause C-Section are very important to handle with great care. In a study [20], they discussed the scope of elective caesarean section without any medical complications. They discussed that the rate of C-Section deliveries is increasing day by day mostly due to the elective mode of delivery. A survey was conducted by interviewing the expected mothers about their own choice of the mode of birth and most of the women selected C-Section, because majority of women think that it is a safe way for the baby as compared to the vaginal birth.

The maternal age of the expecting mother also influences the mode of delivery either it will be a C-Section or a normal birth. They performed an analysis about the impact of the maternal age on the mode of delivery of an expecting woman [21]. They discussed that the women with age more than 35 years have a caesarean section of about 46.1% and that of the age between 30 to 34 years was 40.9%. They showed that only age is not the influencing factor on the mode of delivery. Besides age there are many other factors such as stress, fatigue, posture of working, economic status is also affecting the birth mode of a becoming mother.

The effect of maternal age and the foetal sex are also considered a cause of C-section in most of the expecting women. They discussed that the foetal sex and maternal age combine affect the mode of delivery of a woman [22]. They showed that the risk of operative deliveries increased with a woman of age >40 and carrying a male foetus. The risk of maternal diabetes and increased hospitalization of the women having age<40, but carrying a male foetus also become a cause of operative or caesarean section delivery.

A smart decision support system is available for performing statistical analysis for finding different results. An analysis applied machine learning techniques on smart decision support systems for prediction of the correct treatment methods for a pregnant woman [23]. A comparison between two Bayesian classifiers is performed to classify hypertensive disorder severity among the pregnant women and the results showed that the Bayesian classifier produces the best results with a precision of 0.400 as compared to AODE which has a precision of 0.275.

III. Methodology

The attributes of the dataset are listed with their types and full description in the Table I. Besides all these attributes, a class attribute is used for performing the classification of the data based on the values given to the attributes about a specific entity. Based on the values of the attributes, it is decided that a specific entity is assigned to a class with label 0 or 1. The accuracies of the applied techniques are calculated and the Kappa values for these accuracies are also observed. Based on these calculations, the best methods for solving such type of problems are suggested.

The techniques of Artificial Neural Networks (ANNs), Support Vector Machines (SVM), Random Forests (RF), Recursive Partitioning (RPART) and Conditional inference Tree (CTree) are applied on the dataset. After applying these techniques, the results are recorded and presented in the form of tables, curves and graphs.

TABLE. I. Attribute Description for the Dataset

S#	Name	Description	Type
1	Age	Age of the patient	Integer (17-40)
2	Fp	First pregnancy or not	Binary
3	Pcp	No. of pregnancies before the current pregnancy	Integer
4	Lb	No. of live births	Integer
5	Boys	No. of boys	Integer
6	Girls	No. of girls	Integer
7	Abortin	No. of abortions	Integer
8	Miscag	No. of miscarriages	Integer
9	Last_mode	Mode of last delivery	Binary
10	Inherited	Husband having any inherited disease or not	Binary
11	Menstrual	Having menstrual regular or not	Binary
12	Days_mentcal	No. of days of menstruation cycle	Integer
13	Last_time	Last time of menstruation	Integer
14	Bleeding	Having bleeding or not	Binary
15	Fatigue	Feeling fatigue during pregnancy or not	Binary
16	Diabetic	Having any diabetes disease or not	Binary
17	Breathing	Having breathing issue or not	Binary
18	Headache	Having headache or not	Binary
19	Fast_bet	Having fast heart beat or not	Binary
20	Surgery	Having any surgery before or not	Binary
21	Hemoglobin	Hemoglobin level	Integer
22	BMAX	Blood pressure maximum	Integer
23	BMIN	Blood pressure minimum	Integer
24	BPORNOT	Having BP issue or not	Binary
25	Medcin	Taking any medication or not	Binary
26	Headic	Any sort of tension or not	Binary
27	Hyperten	Having any hypertension disorder or not	Binary
28	FA	Taking Folic Acid tablets or not	Binary
29	Iron	Taking iron supplements or not	Binary

IV. Performance Evaluation

In this section, we discuss the experimental setup and tools used for evaluation. Further, the results are presented and discussed in detail.

A. Experimental Setup

The evaluation of algorithms is carried out by using RStudio tool, which is the most user-friendly tool available for performing machine learning tasks on any given dataset. Before processing the data using RStudio, the dataset was converted into CSV format. The evaluation results of ANN, SVM, RF, RPART and CTREE algorithms are gained and a comparison between the results is performed to judge the most appropriate technique for performing such type of classification jobs.

Further, the evaluation of the algorithms is carried out by using the cross-validation method, which is the most frequently used method for performing the validation on a collected set of data for statistical analysis. The 10-fold cross validation is the most important type of validation that is mostly used in evaluation of different machine learning techniques. In this method, the whole dataset is divided into 10 equal parts/folds. The evaluation is performed by selecting one of the folds as a test set and the remaining 9 folds as the training data. The same procedure is repeated each time for every fold of the data set. In this way, 10 iterations will be performed on the supplied data for validation of the results of the accuracies required by the given machine learning techniques.

The dataset is divided into two halves of 75% and 25% size. One is used as training dataset and the other is used for testing the results based on the training dataset values. After doing this process, the most accurate results about the analysis of the data are obtained.

B. Implementation Tools

RStudio is a free open source Integrated Development Environment tool available online for performing machine learning tasks with the help of statistical analysis. It provides an interactive environment that provides the facility of coding, debugging, plotting different types of graphs and viewing the history of the previous code run. It contains a set of built in libraries and functions for performing different tasks. It provides an interactive environment to the users for making the implementation of different machine learning techniques easy and efficient. We can perform classification and clustering of data using RStudio. The ROC curves can be created using RStudio for viewing the result of the applied techniques graphically for comparison or analysis. RStudio provides an environment to the user for performing the data manipulation easily and efficiently. All the coding is done in the R language by using different packages and libraries. There are many built-in libraries and packages available with the RStudio application software. R programming Language is the base of the RStudio application. Any computer running RStudio must have installed R language prior to RStudio.

C. Results

The accuracies and Kappa statistic values for the data are calculated and the results are shown in the tabular form for interpretation. Next the Receiver Operating Curves are created for each technique to check the overall accuracies of the mentioned techniques. After that graphs are plotted for interpretation of accuracies and Kappa values of all the folds in 10-fold cross validation. Table II shows the accuracy values of RF, SVM, RPART, CTREE and NNET. Results show that the accuracy of RF Algorithm is highest among all the five mentioned techniques followed by NNET, RPART, CTREE and SVM in the descending order. RF has highest accuracy value of 0.9972. The accuracy of NNET is 0.9863, RPART is 0.9838, CTREE is 0.9835, and SVM is 0.9784.

Table III shows the Kappa statistics values for all the five classifiers and provides an insight about the performance of the classification algorithms. Results show the Kappa statistics values for RF, SVM, RPART, CTTREE and NNET. These values depict that Random Forest algorithm shows the highest Kappa value of 0.9941 for the given data. The Neural Net has second highest value 0.9710, after that the value of Recursive Partitioning is 0.9666, then CTREE has 0.9657 and at last SVM has the value 0.9551. These statistics show that RF shows highest associativity among the values of different attributes of the given dataset.

TABLE. II. Accuracy Values of Classifiers

Classifier	**Min.**	**1st Quadrant**	**Median**	**Mean**	**3rd Quadrant**	**Max.**	**NA's**
RF	0.9722	1.0000	1.0000	0.9972	1	1	0
SVM	0.8947	0.9722	0.9861	0.9784	1	1	0
RPART	0.9211	0.9722	1.0000	0.9838	1	1	0
CTREE	0.9444	0.9722	0.9868	0.9835	1	1	0
NNET	0.9722	0.9724	0.9865	0.9863	1	1	0

TABLE. III. Kappa Statistics Values of Classifiers

Classifier	**Min.**	**1st Quadrant**	**Median**	**Mean**	**3rd Quadrant**	**Max**	**NA's**
RF	0.9408	1.0000	1.0000	0.9941	1	1	0
SVM	0.7847	0.9412	0.9712	0.9551	1	1	0
RPART	0.8403	0.9423	1.0000	0.9666	1	1	0
CTREE	0.8861	0.9423	0.9721	0.9657	1	1	0
NNET	0.9417	0.9423	0.9712	0.9710	1	1	0

The results of training and validation accuracies are combined for performing a comparative analysis of training and validation results of the data. Fig. 1 shows the comparison of training and validation accuracies of the classification techniques. CTREE has highest set of values for both training and validation results of the data and RPART has highest accuracy values. NNET with third highest accuracy, RF has values 96.15616 and 100 for training and validation respectively. SVM shows lowest values among all. This plot shows that all the applied techniques have better accuracy values for the validation data set as compared to the training part of the data. RPART and CTREE have highest points in this plot.

Next the ROC curves for all the five classifiers are obtained by using the RStudio. Fig. 2 shows the overall accuracies of NNET, SVM, RF, RPART and CTREE as a whole. Results show the classification of the given dataset into normal and C-Section values according to given class labels assigned. The area under the curve shows the sensitivity over specificity for NNET is 1.000, SVM is 0.993, RF is 1.000, RPART is 1.000 and CTREE is 1.000. Results depict that NNET, RPART, CTREE and RF have maximum sensitivity to specificity ratio.

Fig. 3 depicts the training and testing accuracies of all the techniques. Results show that in the testing phase, Tree-based techniques are providing better accuracy values as compared to other techniques on the given dataset.

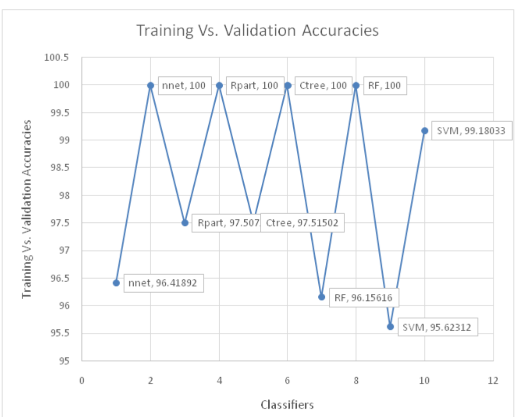

Fig. 1. Training vs Validation Accuracies of Classifiers.

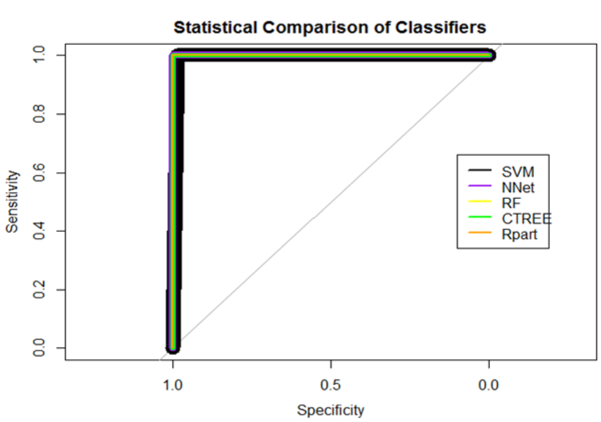

Fig. 2. Area under the Curve of All the Classifiers.

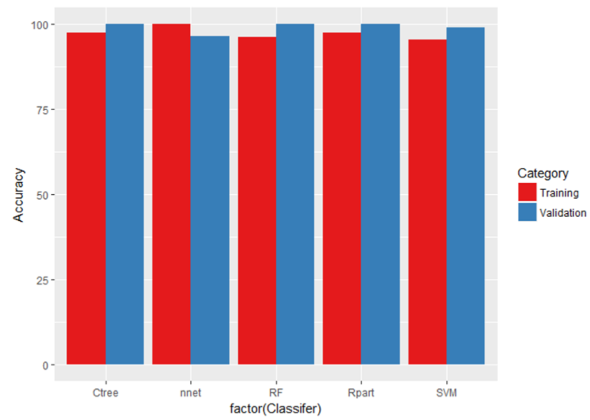

Fig. 3. Comparison of Training and Testing Accuracies of Classifiers.

Table IV shows the accuracies of the classifiers for all the 10 folds individually. Every fold performs a complete run on the data for every technique separately and the result is returned at the end of complete run of the data. Every fold has specific values for the classification of the data. The value 1 shows the maximum accuracy of the classifiers.

Table V shows the Kappa values of the classifiers for all the 10 folds in a 10-fold cross validation process. Results show that in each iteration, as the values of training and testing data are changed, so the results for the evaluation of algorithms are also changed accordingly.

TABLE. IV. ACCURACIES OF CLASSIFIERS FOR 10-FOLD CROSS VALIDATION

Folds	RF	SVM	RPART	CTREE	NNET
Fold01	1	1	1	1	1
Fold02	1	0.9722	0.9722	1	0.9722
Fold03	0.9722	0.8947	0.9210	0.9444	1
Fold04	1	1	1	0.9722	0.9729
Fold05	1	0.9722	0.9722	0.9722	1
Fold06	1	1	1	0.9722	1
Fold07	1	1	1	1	0.9722
Fold08	1	0.9722	1	1	1
Fold09	1	0.9722	0.9722	1	0.9729
Fold10	1	1	1	0.9736	0.9722

TABLE. V. KAPPA STATISTICS OF CLASSIFIERS FOR 10-FOLD CROSS VALIDATION

Folds	RF	SVM	RPART	CTREE	NNET
Fold01	1	1	1	1	1
Fold02	1	0.9423	0.9423	1	0.9423
Fold03	0.9407	0.7847	0.8403	0.8860	1
Fold04	1	1	1	0.9423	0.9417
Fold05	1	0.9423	0.9423	0.9423	1
Fold06	1	1	1	0.9423	1
Fold07	1	1	1	1	0.9423
Fold08	1	0.9407	1	1	1
Fold09	1	0.9407	0.9407	1	0.9417
Fold10	1	1	1	0.9442	0.9423

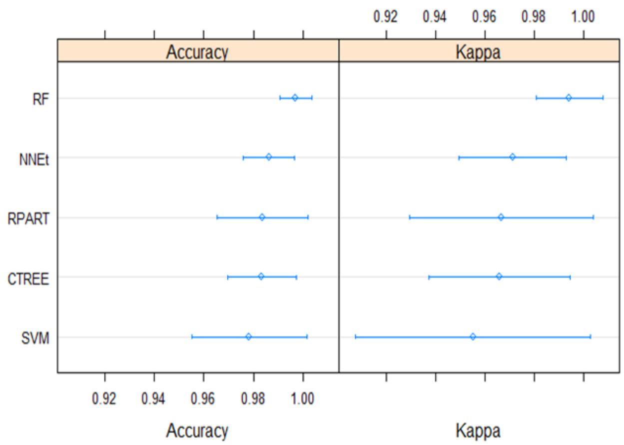

Fig. 4. Comparison of Accuracies and Kappa Values of Classifiers at Confidence Level 0.95.

Fig. 4 shows the comparison of Accuracies and Kappa Statistics values for all the five mentioned techniques. Results show the performance evaluation of Random Forest, SVM, NNet, RPART and CTREE for the classification accuracy of data of the pregnant women. This comparison shows that RF has the highest accuracy value as well as kappa value among all. The accuracy of RF is 0.9972. the Kappa value of RF is also highest as 0.9941. RPART and CTREE have highest training accuracies. Except SVM, all the techniques have maximum validation accuracies and AUC values.

V. Conclusion

In this paper, we show the accuracies of classification algorithms on the dataset of pregnant women for classifying the data into two groups based on the mode of delivery of a woman. The techniques of Support Vector Machines, Neural Networks, Random Forest, Recursive Partitioning and Conditional Inference Tree are applied on the given dataset and the results in the form of accuracy tables, ROC curves and different plots are recorded for further interpretation of the data.

The results show that the tree-based techniques are best suited for the classification of data into normal and C-Section classes as compared to the kernel based approach. Among the tree based techniques, Random Forest shows the maximum accuracy value for the classification of the given data. The Accuracy of Random Forest is highest as calculated 0.9972. The Kappa Statistics for Random Forest is also higher than all the other implemented techniques and is calculated to be 0.9941.

It can be concluded from all the above discussion and the presented results that the technique of Random Forest is best suited for this type of data as it provides the maximum value for accuracy on the given dataset.

References

[1] Snyder, R. M. (2015). An Introduction to Topic Modeling as an Unsupervised Machine Learning Way to Organize Text Information. Association Supporting Computer Users in Education.

[2] Jordan, M. I., & Mitchell, T. M. (2015). Machine learning: Trends, perspectives, and prospects. Science, 349(6245), 255-260.

[3] Holzinger, A. (2016). Interactive machine learning for health informatics: when do we need the human-in-the-loop? Brain Informatics, 3(2), 119-131.

[4] Samuel, A. L. (1959). Some studies in machine learning using the game of checkers. IBM Journal of research and development, 3(3), 210-229.

[5] Kotsiantis, S. B., Zaharakis, I., & Pintelas, P. (2007). Supervised machine learning: A review of classification techniques. Emerging artificial intelligence applications in computer engineering, 160, 3-24.

[6] Caruana, R., & Niculescu-Mizil, A. (2006). An empirical comparison of supervised learning algorithms. Paper presented at the Proceedings of the 23rd international conference on Machine learning.

[7] Phyu, T. N. (2009). Survey of classification techniques in data mining. Paper presented at the Proceedings of the International MultiConference of Engineers and Computer Scientists

[8] Krishnaiah, V., Narsimha, G., & Chandra, N. S. (2014). Survey of classification techniques in data mining. International Journal of Computer Sciences and Engineering, 2(9), 65-74.

[9] Dulitzki, M., Soriano, D., Schiff, E., Chetrit, A., Mashiach, S., & Seidman, D. S. (1998). Effect of very advanced maternal age on pregnancy outcome and rate of cesarean delivery. Obstetrics & Gynecology, 92(6), 935-939.

[10] Sana, A., Razzaq, S., & Ferzund, J. (2012). Automated Diagnosis and Cause Analysis of Cesarean Section Using Machine Learning Techniques. International Journal of Machine Learning and Computing, 2(5), 677.

[11] Hueston, W. J. (1995). Site-to-site variation in the factors affecting cesarean section rates. Archives of Family Medicine, 4(4), 346.

[12] Adashek, J. A., Peaceman, A. M., Lopez-Zeno, J. A., Minogue, J. P., & Socol, M. L. (1993). Factors contributing to the increased cesarean birth rate in older parturient women. American journal of obstetrics and gynecology, 169(4), 936-940.

[13] Nazir, S. (2015). Determinants of cesarean deliveries in Pakistan. Pakistan Institute of Development Economics.

[14] Leone, T. (2014). Demand and supply factors affecting the rising overmedicalization of birth in India. International Journal of Gynecology & Obstetrics, 127(2), 157-162.

[15] Malone, F. D., Canick, J. A., Ball, R. H., Nyberg, D. A., Comstock, C. H., Bukowski, R., . . . Craigo, S. D. (2006). First-Trimester or Second-Trimester Screening, or Both, for Down's Syndrome. Obstetrical & gynecological survey, 61(4), 226-228.

[16] Ludvigsson, J. F., & Ludvigsson, J. (2001). Coeliac disease in the father affects the newborn. Gut, 49(2), 169-175.

[17] Ananth, C. V., Smulian, J. C., & Vintzileos, A. M. (1999). Incidence of placental abruption in relation to cigarette smoking and hypertensive disorders during pregnancy: a meta-analysis of observational studies 1. Obstetrics & Gynecology, 93(4), 622-628.

[18] Sultana, R., Singh, K. R., & Joshi, V. Original Research Article Role of Serum Calcium Level in Pregnancy Induced Hypertension.

[19] Romano, A. M. (2007). Research summaries for normal birth. The Journal of perinatal education, 16(3), 53.

[20] Miesnik, S. R., & Reale, B. J. (2007). A review of issues surrounding medically elective cesarean delivery. Journal of Obstetric, Gynecologic, & Neonatal Nursing, 36(6), 605-615.

[21] Benli, A. R., Benli, N. C., Usta, A. T., Atakul, T., & Koroglu, M. (2015). Effect of maternal age on pregnancy outcome and cesarean delivery rate. Journal of clinical medicine research, 7(2), 97.

[22] Weissmann-Brenner, A., Simchen, M. J., Zilberberg, E., Kalter, A., & Dulitzky, M. (2015). Combined effect of fetal sex and advanced maternal age on pregnancy outcomes. Medical science monitor: international medical journal of experimental and clinical research, 21, 1124.

[23] Moreira, M. W., Rodrigues, J. J., Oliveira, A. M., Saleem, K., & Neto, A. V. (2016). An inference mechanism using bayes-based classifiers in pregnancy care. Paper presented at the e-Health Networking, Applications and Services (Healthcom), 2016 IEEE 18th International Conference on.

Affective Educational Application of Fish Tank Hydroponics System

Rodolfo Romero Herrera[1]
Departamento de Ciencias e Ingeniería de la Computación
Instituto Politécnico Nacional-ESIME-ESCOM
Ciudad de México, México

Francisco Gallegos Funes[2]
Sección de Estudios de Posgrado e Investigación
Instituto Politécnico Nacional- ESIME
Mexico

***Abstract*—This project develops algorithms for the design and implementation of an embedded system in hydroponic gardens for homes located on roofs, terraces, and even in kitchens in the house; since a fishbowl is used. Vegetables, flowers, etc. are contemplated. One plant was obtained per seed. The development and care of Nature is also a special theme of this project with the objective of educating in the care of the environment, for which it is essential not to overlook the affection that one has for life. It is here that it is important to ensure that plants can transmit the physical conditions in which they find themselves through an emotional interface that translates the lack of water into an emotional state of sadness; or enough moisture with a state of joy. Thus a technique is presented, which allows through affective or emotional interfaces to educate owners about the care of the plant and take advantage of the emotional states of the people for the development of educational software.**

***Keywords*—Hydroponics; affective interface; embedded system; gardens; educational software**

I. Introduction

The inhabitants of the cities live in houses with small gardens, patios and/or balconies. Thus, keeping plants alive is complicated. Vegetation requires care; and in most cases, there are no educational tools to guide the owner [1], and much less equipment is available for plants to communicate with us.

The educational material developed is a consequence of the reflection of the impact of plants on our planet [2]. Currently, there are government programs for the care of the environment [3]; such as those based on indigenous knowledge or those promoted by the Government Commissions [4].

There are several educational proposals [5], such as those that develop interactive software tools with touch screens [2]; and in urban environments, there are school gardens, which require the development of materials for students [6]; and virtual models allow simulating the cultivation of fruit trees [7]; In addition, there are websites that contain information about plant care [8]; however, there is still a shortage of applications that bring the person to consider their plants as part of the family. Many people in the home take great care of their pets; So why not consider your plants with equal attention. After all, they provide us with several benefits.

Because most housewives or end-users lack knowledge and interest in plant care, it is proposed to develop a system that considers both hardware and software development that facilitates the approach to raise awareness about the protection of nature. For this, it is proposed to use the affection that a user feels for what is his property, in this case, the plants.

II. Objectives

A. General

Develop a system that translates the physical conditions of a plant into a simulation of affective states using advanced technologies in a hydroponics fish tank and educational software.

Thus, happiness is interpreted as sufficient humidity; and sadness like dry land or low humidity. Also, the ambient temperature is related to reflect anger and the level of ph with fear.

B. Specific

- Development of affective interface module through images that reflect moods depending on humidity, temperature and pH sensor readings.
- Development of a learning tool for plant care with recommendations and indications ranging from germination to harvest or flowering.
- Development of a system for sensing plant conditions.

III. Methodology and Development

Plants need 16 elements, 9 macronutrients that must be provided in greater quantities (Hydrogen, Carbon, Oxygen, Nitrogen, Calcium, Phosphorus, Magnesium, Potassium and Sulfur) and 7 micronutrients (Chlorine, Zinc, Boron, Iron, Copper, Manganese, Molybdenum) that are required in smaller proportions [9]. Oxygen and CO2 are obtained from the environment; Hydrogen and oxygen are obtained from water. In the case of hydroponics, macronutrients and micronutrients dissolve in water (nutrient solution).

Fish hydroponics was chosen, as it is economical and easily accessible for the home. The main advantages of the system are control, efficient water consumption and full use of the substrate.

A. Hydroponics

Hydroponics is used to grow plants where soil use is not necessary [10]. The proposed hydroponic system does not consider traditional NFT [11]. But use a circulating nutrient solution (see Fig. 1).

(a) NFT System. (b) Proposed System.

Fig. 1. Hydroponic Systems.

The realized system has automatic irrigation. Hydroponics requires maintaining a water level; so a liquid level sensor is used. Materials such as cotton or some fiber absorb liquid and nutrients (see Fig. 2). For hot days a water spray system was implemented; When a certain level of aridity is reached, an electronic key is opened for water to flow and the spray pump is activated; the water pumping system closes when there is a certain level of temperature and humidity [12]. For cold days there is a fish tank heater.

To avoid the nutrient solution plate on the water surface, a pump was used to recycle the fish tank liquid (see Fig. 3).

B. Algorithms - Agent for Automation

The system is controlled by an Arduino Uno card, which obtains sensible information, that activates the corresponding actuators [13]; the result is transmitted wirelessly via WiFi to a cell phone, tablet or PC. Thresholds are used to determine simulated emotions. The data are taken from the sensors and can be adjusted (see Fig. 4).

Fig. 2. Spray System.

Fig. 3. Pumping System.

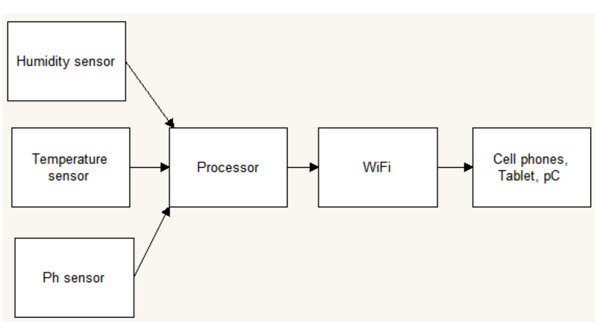

Fig. 4. Sensing Process.

C. Sensing Humidity and Water Level

To detect the water level, a soil moisture sensor (hygrometer FC28) was used. If there is greater humidity the conductivity increases and if the soil is very dry the conductivity decreases. A card (comparator LM393) was added for sensing analogously or digitally [14]. The zero value corresponds to soil with high conductivity and the 1023 value to practically dry soil. The digital output delivers the value "HIGH" when the humidity threshold is exceeded and LOW when it is below, this level can be modified through the potentiometer (see Fig. 5).

If analog signal A0 is used, the value is read; and the serial port is used to transmit information to a computer (see Fig. 6).

D. Temperature Sensing Agent

An RTD (resistance temperature detector) is a resistive temperature sensor; it is based on the variation of the resistance of a conductor that is proportional to the increase or decrease in temperature [15]. The LM35 was used (see Fig. 7). You can calculate the temperature based on the voltage with equation (1) and use the diagram in Fig. 8 for the program.

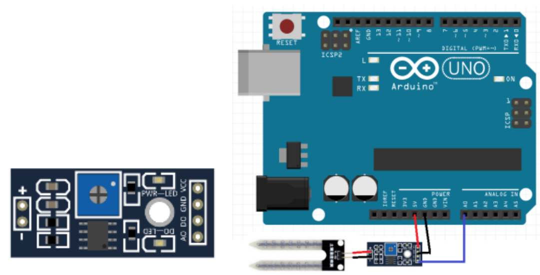

Fig. 5. Mounting the Humidity and Liquid Level Sensing System.

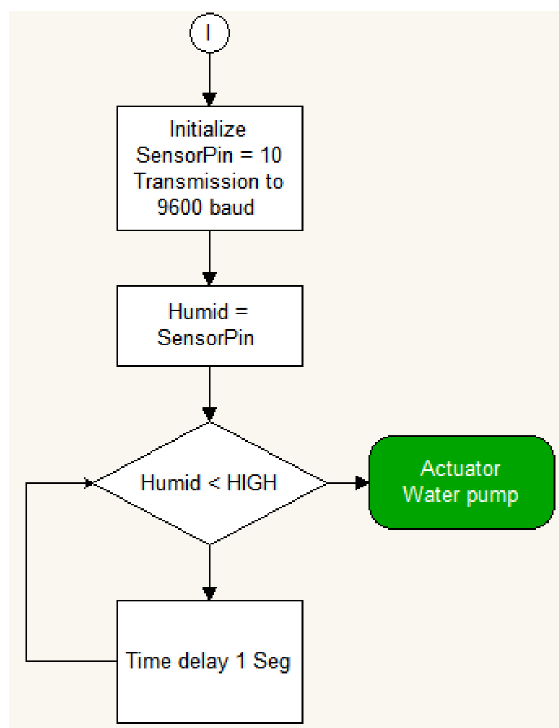

Fig. 6. Flow Diagram of the Humidity Sensing by a Digital Input.

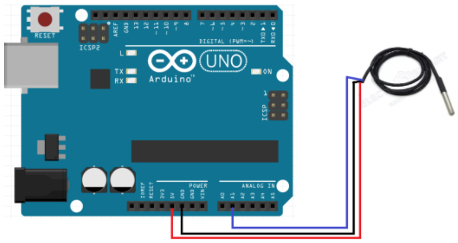

Fig. 7. Temperature Sensor.

To set the analog reference, an Arduino one function is used, which sets the reference for the entry with a value of 1023. If the INTERNAL option is used, 1.1v can be used for higher resolution.

$$\text{Temperature} = \text{Value} * 1.1 * 100/1024 \quad (1)$$

The code that we must load corresponds to the flowchart of Fig. 8.

E. Ambient Light Sensor Agent

Artificial lighting was used in the case of closed environments. The LED strips are automatically turned on by time and by lumens in the room (see Fig. 9).

The TEMT6000 sensor is sensitive to the visible spectrum. The output of this sensor is analog, so it connects to the Arduino ADC. In this case, the ambient light is the measured variable; When the module does not detect enough light, a signal is emitted to the Arduino to turn on the LED strip; otherwise, if the light is sufficiently intense, the Arduino is instructed to turn off the LED strip (see Fig. 10).

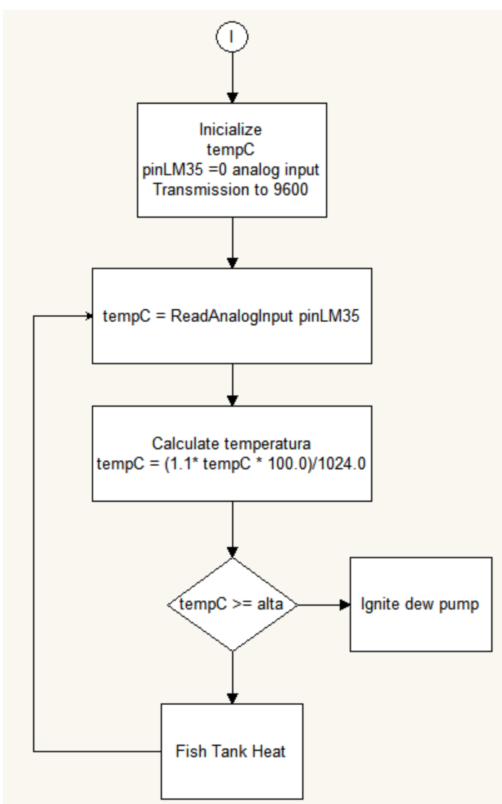

Fig. 8. Flow Chart of Temperature Sensing with the INTERNAL Option.

Fig. 9. Lighting System.

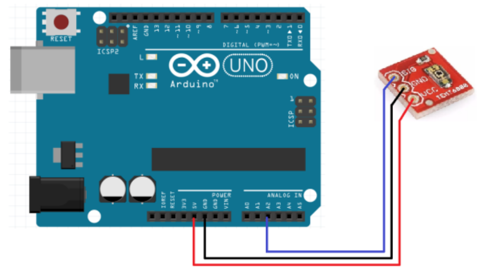

Fig. 10. Mounting the Ambient Light Sensing System.

In the diagram of Fig. 11, first are assigned the input and output ports on the microcontroller and the ranges that were used for the variable "sunlight" (this is adjustable). It is set to 0 for the sensor to send the signal to turn off the microcontroller once it detects light. When the sensor does not register enough light in the room, it will send the signal to the microcontroller to turn on the LED strip.

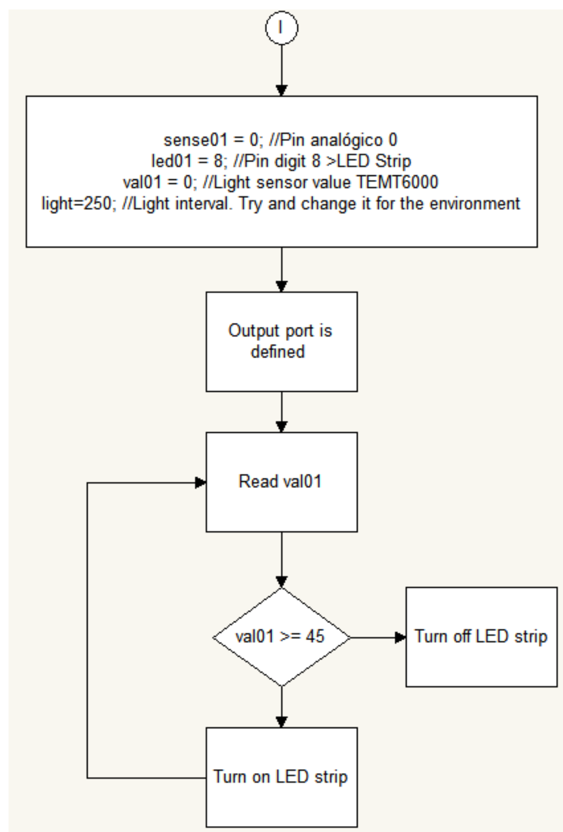

Fig. 11. Flow Chart - LED Strip Ignition.

F. ESP8266 Wifi Transmission

Wireless communication through Wi-Fi to a cell phone or PC was chosen (see Fig. 12). The ESP8266 was used with the microcontroller as an Arduino connected to its serial port and managed with Hayes commands [4]. The connection diagram is shown in Fig. 12. The ESP8266 is a Wi-Fi chip with a TCP / IP stack and an MCU (Micro Controller Unit).

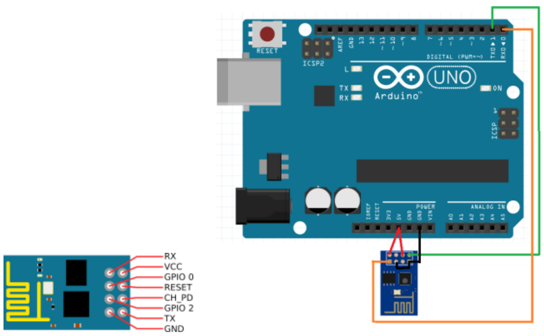

Fig. 12. Connection Diagram.

IV. Educational Interface for Plants Care

To design the software, we proceeded under the methodology proposed by Becerra and Torres in [2]. An initial inquiry was made with general aspects to identify the main problems in plant cultivation. In the second stage, the Educational didactic model was selected with a teaching-learning approach; in order to make people aware of their responsibility in the care of nature. In the third stage, The contents of the module were structured with information on each of the main problems during planting. germination, growth care, harvesting, and pruning. See Fig. 13.

For the design of the didactic model, a proposal was taken as in reference [8] in 10 points:

1) The genesis of the idea.
2) Pre-design or functional design.
3) Feasibility study and project framework.
4) Design report and project framework.
5) Programming and development of the alpha-test prototype.
6) Writing the program documentation.
7) Internal evaluation.
8) Adjustments and development of the beta-test prototype.
9) External evaluation.
10) Adjustment and development of version 1.0.

Although the software development process seems linear, it is rather iterative; since the operation should be checked, and the results evaluated.

The initial idea is to create a tool based on the measurement of temperature, humidity and ph sensors. This idea creates the seed of WHAT (matter and level) for the realization of the work. The HOW (didactic strategy) was developed during the first design of the program.

For the pre-design, a script of the program was formed. Emphasis was placed on the pedagogical aspects of the project: content, objectives, teaching strategy, etc. For the development of the software, bibliographic sources were consulted as well as housewives and books dedicated to the care of plants and fruit trees, for example in [16].

Indications for plant care are provided through easy to understand diagrams; for example, for the preparation of the substrate is used in the Fig. 14.

The plant can communicate its "emotional" state by activating emoticons in animated gifs. See Table I. Showing an animated icon solves the problem of dealing with numbers or data that are strange to the end-user. Fig. 15 shows one of the generated screens; the interpreted state of the plant is observed by means of animation.

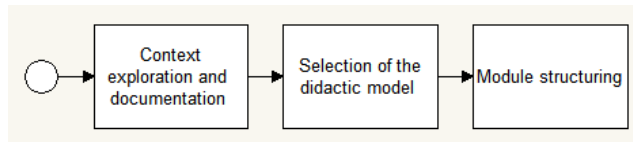

Fig. 13. Stages for Design.

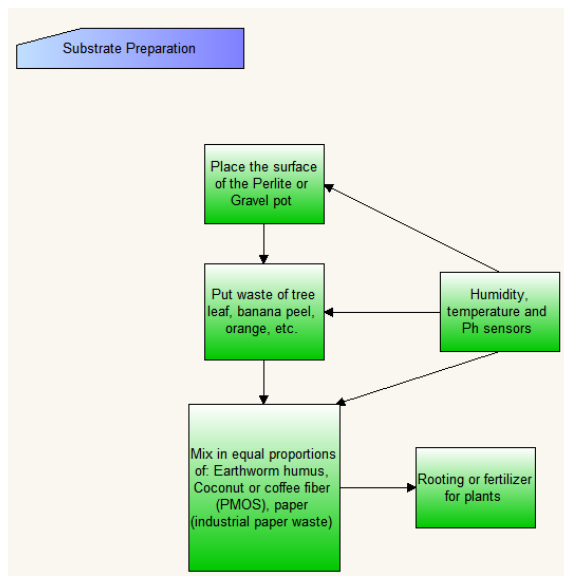

Fig. 14. Substrate Preparation.

TABLE I. Emoticons vs State

Emotion	State	Sensor
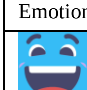	Happiness	Humidity
	Anger	Temperature
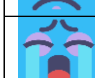	Sadness	Humidity
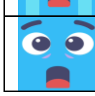	Fear	PH

Fig. 15. Main Interface.

V. Results

Plants were taken care of from planting to harvest. The system was tested for several days. He underwent continuous work for 2 months without interruption; Without presenting problems. The energy system is low consumption and does not work continuously since it depends on the atmospheric conditions, The energy system is low consumption and does not work continuously, since it depends on the atmospheric conditions, and is sufficient for the needs of the circuit. Wireless communication works properly within a 10 m radius. If you need more communication radius, you can use the internet.

The software tests performed are unitary. It was divided into modules to apply logical tests; that is, detection of learning styles, cognitive level and the proportion of educational resources.

The white box test cases are created from the selected units. For which input values were defined for the detection of learning styles and cognitive level. The proportion of educational resources is based on learning and cognition style.

As proof of usability, user interaction with the software was verified, to ensure that the interface provides navigation. The usability was made based on gender, location, age, and income level through questionnaires to a total of 65 people.

The graph in Fig. 16 shows that most people have a good opinion about the implementation of technology to assist their learning and awareness; Similarly, most respondents have used a mobile device such as laptops, tablets or smart-phone to search for information.

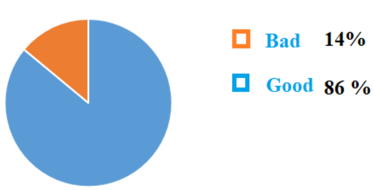

Fig. 16. The Opinion of the People Interviewed Regarding the use of Technology.

The graph in Fig. 17 shows that the majority (67.7%) of respondents use an application to support their daily activities. Similarly, 56.9% agree that a mobile application can help them improve their performance.

Some of the reasons why users used the application are:

- Difficulty in understanding the care of plants.
- They consider that it helps to understand more easily.
- Facilitates the development of the solution to the problem.

Finally, 87.7% of the interviewees consider that if they were provided with a resource for the care of plants, they would benefit from the care of nature and obtain an economic income.

As for the plants with which the experiment was performed, the results shown in Table II were obtained. From the vegetables, lucrative crops of 10 lettuces have been obtained on average per house room, one per seed. Estevia harvest of 20 plants on average, and generation 3 plants of bell pepper. In watermelon, there are problems for the survival of the plant, as it requires special conditions. The strawberry requires more care, does not exceed a transplant. Notorious success stories were cilantro, onion, pumpkin, and tomato.

Pests have been successfully fought for tomato. Thus, slugs, aphids, and ants have been fought successfully. Fig. 18 shows the system for the case of stevia, where it was decided to leave the plants inside the fish tank to protect them and create an ecosystem.

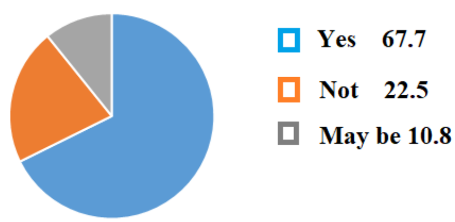

Fig. 17. People who use Applications to Rely on their Activities.

TABLE. II. Emoticons vs State

Plant	Crecimiento	Cosecha
Watermelon	30 cm	Not harvested
Stevia	1.5 m	It yields 1 liter per plant. 20 Harvest
Coriander	10 cm	Harvested
Strawberry	Germ	Not harvested
Pumpkins	20 m	10 Pumpkins diameter 60 cm
Tomato	147 cm	100 fruits per week
Onion	20 cm	From 10 seeds / 10 were harvested
Lettuce	10 Cm	One per seed
Pepper	80 cm	50 Peppers of 3 plants

Fig. 18. Fish Tank for Hydroponics. Stevia Plant.

VI. Conclusions

The tests carried out showed the autonomy of the system; since it can work 24 hours a day without setback. There is no problem in wireless communication, nor with the detection of the different measurements. It is feasible to implement the system with another microprocessor, although the Arduino system provides a method of easy implementation and economical. Flowcharts are useful if you need to use another embedded system.

The costs for both the hydroponic system are really low compared to the benefits. An even feasible product was obtained from being commercialized and a cultivation system for cities that can satisfy food needs in a short time, due to the success in production.

People, in general, have a good opinion regarding the use of computer technology as a support for learning and caring for plants.

If we consider the existing population in the cities, we can think that the software can reach a large number of people and therefore of possible users; which according to respondents can benefit and improve plant production. All expressed feeling great affection for nature after the use of the application and the harvest obtained.

In the area of affective computation, it allows expanding knowledge in the area of Life Sciences, generating an effective interaction with the plant.

VII. Future work

Develop an embedded system and affective or emotional software for the care of dwarf trees.

Acknowledgment

The authors thank the National Polytechnic Institute for the support received.

References

[1] Resh, Howard M.Cultivos hidropónicos: nuevas técnicas de producción: una guía completa de los métodos actuales de cultivo sin suelo para técnicos y agricultores profesionales, así como para los aficionados especializados. No. 631.585. Mundi-Prensa,, 1997.

[2] J. D. Becerra-Barón and N. Y. Torres-Merchán, "El diseño de material didáctico como aporte al abordaje de los problemas ambientales en entornos educativos y comunitarios," Revista Educación, vol. 38, (2), pp. 1, 2014.

[3] M. Cebrián-de-la-Serna and J. Noguera-Valdemar, "Conocimiento indígena sobre el medio ambiente y diseño de materiales educativos," Comunicar, vol. 17, (34), pp. 115-124, 2010;2009.

[4] A. Molina, "Ensenara pirinola a cuidar los árboles," El Norte, 2005.

[5] J. P. Chacón et al, "Los contenidos curriculares digitalizados: Voces y silencios en el ámbito editorial/ The digitized curriculum: voices and silences in the publishing field," Educatio Siglo XXI, vol. 33, (3), pp. 39, 2015.

[6] Hezkuntza, L.. Huertos Escolares. Editorial CEIDA, Centro de educación e investigación didáctica ambiental, España., 1998.

[7] F. Lescourret et al, "QualiTree, a virtual fruit tree to study the management of fruit quality. I. Model development," Trees, vol. 25, (3), pp. 519-530, 2011.

[8] Dávila Sanabria, D. T., Galvis Álvarez, A. C., & Vivas Granados, R. Sitio web como estrategia de enseñanza en la educación para la sostenibilidad. Praxis & Saber, 6(11), 115-138, 2015.

[9] Huterwal, G. O. "Hidroponía: cultivo de plantas sin tierra." (1956).

[10] Barbado, José Luis. Hidroponía; su empresa de cultivos en agua. No. 631.585 B228. Albatros, 2005.

[11] Baixauli Soria, C., and J. M. Aguilar Olivert."Cultivo sin suelo de hortalizas: aspectos prácticos y experiencias." No. C057. 013. Generalitat Valenciana, 2002.

[12] Rodríguez Delfín, Alfredo, et al.Manual práctico de hidroponía. No. 631.585 M294m. Lima, PE: Universidad Agraria La Molina, 2004.

[13] Pan, Tianhong, and Yi Zhu. "Getting Started with Arduino."Designing Embedded Systems with Arduino. Springer, Singapore, 2018. 3-16

[14] Valdéz, Jorge, Daniel Pandolfi, and Andrea Villagra. "Redes de sensores inteligentes para monitoreo de datos remotos."XIX Workshop de Investigadores en Ciencias de la Computación (WICC 2017, ITBA, Buenos Aires). 2017.

[15] Castro, Jorge R.Building a Home Security System with Arduino. Packt Publishing Ltd, 2015.

[16] Geoffrey R. Dixon Dixon et al, Horticulture: Plants for People and Places, Volume 1: Production Horticulture. (2014th ed.) 2014. DOI: 10.1007/978-94-017-8578-5.

Memory-based Collaborative Filtering: Impacting of Common Items on the Quality of Recommendation

Hael Al-bashiri[1], Hasan Kahtan[2]
Awanis Romli[4]
Faculty of Computing, Univirsity Malaysia Pahang
Gambang, Kuantan, Malaysia

Mansoor Abdullateef Abdulgabber[3]
Faculty of Computer and Cyber Sciences
University of Prince Mugrin, Madinah
Saudi Arabia

Mohammad Adam Ibrahim Fakhreldin[5]
Faculty of Computer Science and Information Systems, Jazan University,
Jazan, Saudi Arabia

Abstract*—In this study, the impact of the common items between a pair of users on the accuracy of memory-based collaborative filtering (CF) is investigated. Although CF systems are a widely used recommender system, data sparsity remains an issue. As a result, the similarity weight between a pair of users with few ratings is almost a fake relationship. In this work, the similarity weight of the traditional similarity methods is determined using exponential functions with various thresholds. These thresholds are used to specify the size of the common items amongst the users. Exponential functions can devalue the similarity weight between a pair of users who has few common items and increase the similarity weight for users who have sufficient co-rated items. Therefore, the pair of users with sufficient co-rated items obtains a stronger relationship than those with few common items. Thus, the significance of this paper is to succinctly test the impacting of common items on the quality of recommendation that creates an understanding for the researchers by discussing the findings presented in this study. The MovieLens datasets are used as benchmark datasets to measure the effect of the ratio of common items on the accuracy. The result verifies the considerable impact exerted by the factor of common items.

Keywords—Collaborative filtering; memory-based; similarity method; data sparsity

I. Introduction

Currently, Internet users have faced information overload issues. Therefore, these users resort to traditional recommendation methods to make their decisions, such as asking friends, scanning newspapers and following advertisements. These basic solutions might help alleviate information overload [1]. However, the amount of information on the Internet increases tremendously every day, thus complicating the decision-making process of Internet users. To assist the users in dealing with information overload, researchers have developed a recommender system (RS) that can provide a list of preferable items among the huge amount of items available by predicting users' preferred items [2-7]. State-of-the-art RSs can be grouped into content-based, collaborative filtering (CF) or combined (i.e. hybrid) approaches [4, 8-11].

CF, which is one of the most successful recommendation methods, uses the feedback provided by the users to generate recommendations [2, 12-15]. CF can be classfied as model- or memory-based [1, 16]. In the former, a part of the dataset is used to build a model that can predict the preferred items. By contrast, the latter does not require a model. Instead, user feedback (e.g. ratings) is used to compute the similarity amongst the users directly. The computation of the similarity can be conducted in the space of users (user-based) or items (item-based) [1, 8, 17]. The idea behind CF is that the users will have similar favourites in the future if they have shared similar preferences in the past [18, 19]. The key step in CF is finding the right neighbours. Therefore, selecting the appropriate similarity is fundamental to the system's performance. Several methods have been introduced in CF systems, including Pearson's correlation coefficient (PCC), cosine similarity and other derivative methods [20, 21]. However, the key challenge faced in a CF system is providing high-quality recommendations to users who do not have enough information preferences. Most users do not evaluate a sufficient number of items in the database, thereby making the user–item rating matrix sparse [22-27]. As a result, calculating the similarity amongst these users may lead to locating unsuccessful neighbours and consequently low performance.

Therefore, the primary goal of this study is to investigate the impact of co-rated item size based on sigmoid function on enhancing the accuracy of the recommendation. This evaluation will rely on the various sizes of common items, which will be represented by threshold values, to measure the impact on solving the issue of data sparsity. PCC and cosine similarity will be used and modified by adopting a sigmoid function under several thresholds. The correlation weight between the pair of users should be devalued if the number of the co-rated items is smaller than the threshold. The experiments will be conducted using MovieLens benchmark datasets.

The remainder of this paper is organized as follows. Section 2 presents the literature review. Then, the developed similarity method and its phases are discussed in Section 3. In Section 4, the evaluation process and the experimental results are presented. The conclusions are provided in Section 5.

II. Related Work

Given the great impact of the quality of similarity measure on the accuracy of recommendation, several similarity measures have been developed based on the ratio of common items. In this section, certain methods that consider the proportion of co-rated items in improving the accuracy of recommendation will be presented, as well as how these factors influence the quality of recommendation.

Resnick, et al. [2] applied PCC similarity measures to compute the linear correlation between two objects. The outcome was between 1 and −1, where 1 denoted the total positive correlation, 0 meant no correlation and −1 denoted complete negative correlation. However, the PCC similarity method exerted a remarkable influence on the sparsity of data. Therefore, the correlation calculation amongst users who had few co-rated items was difficult and might lead to high/low similarity and weak recommendations. To scale the similarity properly when the number of common items was not enough, [28] introduced a significant factor ($\min[I_{x,y},\gamma]/\gamma$) to devalue the similarity weights. They applied these weights for the users who had fewer common co-rated items than the threshold. In addition, they used threshold γ to determine the minimum number of co-rated items. In their experiments, when $\gamma \geq 25$, the accuracy of the predicted ratings improved; the optimal result was when $\gamma = 50$. However, the proportion of the common ratings was not considered. Thus, the sparsity issue still influenced the determination of neighbours who had common items that were bigger than the threshold.

In [24], the authors introduced a heuristic measure called Proximity–Impact–Popularity (PIP), which consisted three essential factors that played important roles in identifying the relationship amongst users. PIP utilised the ratings given by a set of users to enhance the accuracy of RS under cold-star conditions. However, PIP ignored the proportion of the common ratings and performed excessive similarity computations [29]. Author in [30] proposed a weighted item-based similarity measure based on the sigmoid function. This function devalued the similarity weight if few co-ratings were available. If the size of the set of common items was sufficiently large, the weight value was 1. Otherwise, the weight value was 0.6. Another improved similarity measure was introduced by adding the similarity impact factor ε to the traditional similarity measure to alleviate the effect of data sparsity [31]. This factor represented the proportion of the common items rated by a pair of users. If the pair of users did not have co-rated items, then the in-between similarity was 0, which was considered a weakness in this method. Author in [32] formulated a weight distance model to compute the association between two users based on the ratio of the common ratings and the relationship between the target and the co-rated items. The proportion of the common ratings was computed using the Jaccard index, whereas the relationship between the target and the co-rated items were computed using PCC. A singularity-based similarity measure was introduced in [33]. This method hypothesised that a stronger relationship existed between two users if they rated the items that had been rated by few users than if they rated the items that had been rated by numerous users. The singularity values of each user replaced the similarity value to improve the PCC method. The Jaccard measure was then modified based on singularity to consider the proportion of the common items.

A new weight similarity model called NWSM was proposed by Zang, et al. [34]. This model took into account the proportion of the common rating, user rating preference and the different contributions of other users to the target. To improve the accuracy of the recommendation, the final similarity formula was obtained by integrating three factors: (1) the PCC method with influence weight (i.e. neighbourhood's rating information), (2) the Jaccard measure to compute the proportion of co-ratings and (3) the mean variance of the rating to calculate the differences in the preference of each user. Zhang, et al. [35] presented a new effective CF method to decrease the impact of data sparsity based on user preference clustering. The users were first grouped into clusters according to preferences before the neighbour for the active user was selected from these clusters. Zhang and Yuan [26] presented an improved similarity method to overcome the problem of data sparsity by analysing the shortcomings of a traditional memory-based CF similarity method. In the enhanced similarity method, the relationship between the users' common rating items and all items rated by the target user was considered. Author in [29] proposed a new linear combination similarity method called weight-based modified heuristic similarity measure to solve the problem of data sparsity.

The above-mentioned studies highlighted the significance of the ratio of common item in the process of developing a similarity measure that can improve the recommendation accuracy. However, studies on the determination of the optimal size of co-rated items amongst users are lacking. Therefore, the sigmoid function will be used in this study to test the impact of the item size on the accuracy of recommendation using co-rated items with various sizes.

III. Methodology

This section details the step in obtaining the ratio of the common items. Firstly, the Bray–Curtis (BC) distance measurement is used to compute the distance between two different sites based on the counts at each site [36]. Normalisation is performed using absolute difference divided by the summation. The output value of the BC ranges from 0 and 1, where a value of 0 indicates a complete matching of the two data records in the n-dimensional space, and 1 means that the records are different. The BC distance performed better than the 10 and 9 distance measures used in [37, 38], respectively. The general formula for the BC distance can be expressed as

$$\mathrm{Bc}\,(\mathrm{u},\mathrm{v}) = 1/(1+\frac{\sum_{\mathrm{g}=1}^{\mathrm{k}}|\mathrm{w}_{\mathrm{u},\mathrm{g}}-\mathrm{w}_{\mathrm{v},\mathrm{g}}|}{\sum_{\mathrm{g}=1}^{\mathrm{k}}\mathrm{w}_{\mathrm{i},\mathrm{g}}+\sum_{\mathrm{g}=1}^{\mathrm{k}}\mathrm{w}_{\mathrm{v},\mathrm{g}}}) \quad , \tag{1}$$

where k represents the number of item categories in the database, and the $w_{u,g}$ and $w_{v,g}$ represent the ratio rating of type g for users u and v, respectively. The computation of ratio rating values are provided in the previous work [21].

Then, the BC similarity is multiplied by the sigmoid function (Sf) to devalue the similarity in cases of few co-ratings. The θ in the equation below is used to determine the minimum size of co-rated items. If the size of the set of common items is sufficiently large, then the sigmoid value will be higher than 0.9. Otherwise, the value will be less than 0.9. For example, if θ = 1 and the number of the common ratings of the pair of users is equal to 0, the sigmoid value will be 0.5. If the size of co-rated items is greater than 3, the sigmoid value will be greater than 0.95. The sigmoid function can be computed as

$$Sf(u,v) = Sf(v,u) = \frac{1}{1+Exp^{(-\frac{|I_{u,v}|}{\theta})}} \quad , \tag{2}$$

where $|I_{u,v}|$ represents the number of items rated by users u and v. The Blazing Signature Filter (BSF) method can then be defined as

$$BSF\ (u,v) = \frac{1}{1+\frac{\sum_{g=1}^{k}|w_{v,g} - w_{v,g}|}{\sum_{g=1}^{k} w_{v,g} + \sum_{g=1}^{k} w_{v,g}}} * sf(u,v). \tag{3}$$

Several denominator values of the sigmoid function are tested to determine the acceptable number of common items.

After the similarity is computed, the most similar users in the database will be located as neighbours. Then, the adjusted weighted method is used to compute the predictions score for the user u on each neighbours' item as can be defined in Eq. 4.

$$P_{u,i} = \bar{r_u} + \frac{\sum_{v \in k} \text{sim}^{\text{BSF}}(u,v)}{\sum_{v \in N} |sim(u,v)|} \tag{4}$$

Where $P_{u,i}$ is the prediction value for u about a specific item i, and N is the nearest neighbour of user u.

In the next phase, M-top items will be provided to the target user as a set of recommendation.

Finally, the performance accuracy of the BSF similarity method is evaluated using MovieLens 100K dataset with holdout splitting methods using selected metrics (MAE, Recall, Precision, and F-measure). All these steps are presented in Fig. 1.

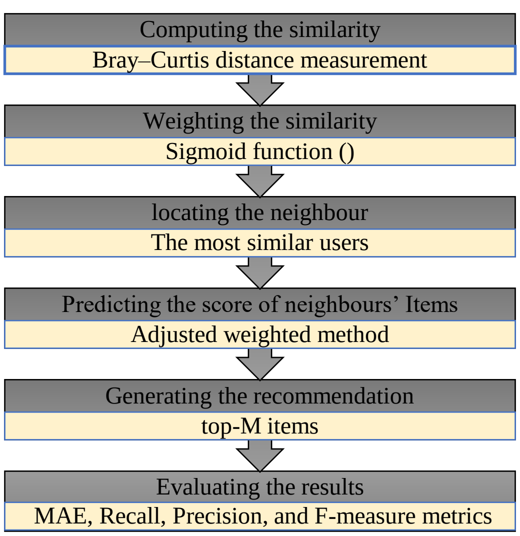

Fig. 1. Methodology.

IV. Experiment and Result

To include the proportion of the common ratings in the calculation of the similarity between a pair of users, the necessary size of the co-rated items to increase or decrease the weight of similarity between the pair of users should be determined. The use of the sigmoid function depends on the denominator value. Therefore, several experiments have been conducted to determine the appropriate denominator value that can improve the similarity measure and produce acceptable results. Table I presents the description of various initial testing denominator values and their corresponding effect on the sigmoid value.

Fig. 2 illustrates the mean absolute error (MAE) rate for the CF-BSF using MovieLens 100K. The numbers of neighbourhoods were 30, 50, 70, 100 and 150. A slight improvement can be observed in the MAE value when the number of neighbours increases. Similarly, the MAE value increases when the denominator increases. In summary, the MAE values are acceptable when the size of the neighbours is 150 in all denominator values. Moreover, the lowest MAE rate is observed when the denominator is equal to 13. When the denominator is nine, the MAE rate is approximately near the optimal value.

TABLE. I. Description of Various Denominator Values

θ	Description
5	The sigmoid value will be greater than 0.9 if the number of co-rated items is more than 10. Otherwise, the value will be less than 0.9. However, if the number of the common ratings of the pair of users is equal to 0, the sigmoid value is equal to 0.5.
7	The sigmoid value will be greater than 0.9 if the number of co-rated items is more than 15. Otherwise, the value will be less than 0.9.
9	The sigmoid value will be greater than 0.9 if the number of co-rated items is more than 20. Otherwise, the value will be less than 0.9.
11	The sigmoid value will be greater than 0.9 if the number of co-rated items is more than 25. Otherwise, the value will be less than 0.9.
13	The sigmoid value will be greater than 0.9 if the number of co-rated items is more than 30. Otherwise, the value will be less than 0.9.

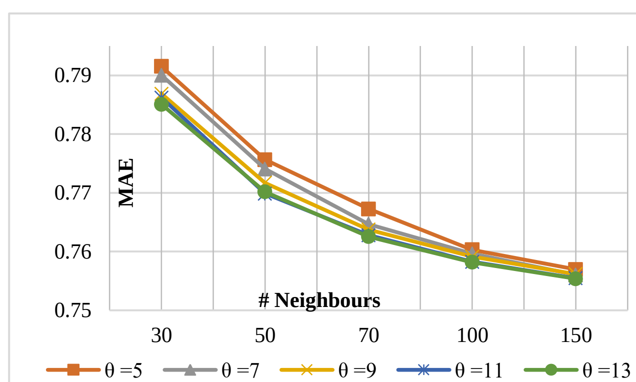

Fig. 2. MAE of CF-BSF vs. $\boldsymbol{\theta}$.

Fig. 3 presents the comparison of the recall rates for CF-BSF using the initial denominator values. The subfigures A, B, C, D and E represent the respective recall rates for neighbour sizes 10, 20, 30, 40 and 50. The horizontal axis represents the sizes of the recommendations. Based on the illustrations, the recall rates in most cases are the highest when the denominator value is 9. Similarly, the recall percentages in some cases demonstrate a good rate when the denominator is less than 9. The lowest recall values are observed when the denominator exceeds 9.

Fig. 4 shows the precision rate of CF-BSF under five different denominator values: 5, 7, 9, 11 and 13. The subfigures represent the respective precision rates of neighbour sizes 10, 20, 30, 40 and 50. When the denominator value is 9, the rate of precision is the highest in most cases. The opposite is true for the denominator values equal to 11 and 13. Moreover, the precision rate does not exceed the precision rate of the denominator values less than 9. The highest precision rate is observed when the number of recommended items is small. The precision rate slightly decreases when the number of recommended items increases. In summary, the precision rate has exhibited variations, wherein the precision is higher than any other values when the denominator is equal to 9.

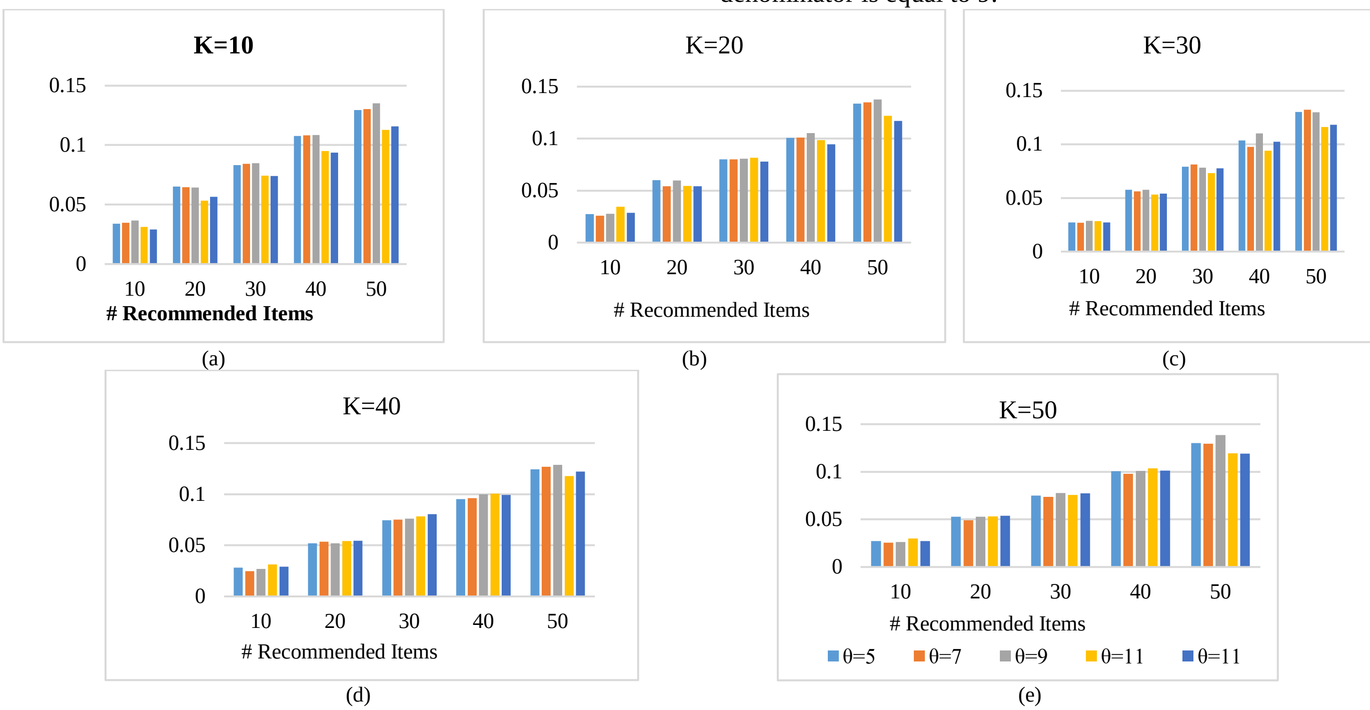

Fig. 3. Recall of CF-BSF vs. $\boldsymbol{\theta}$.

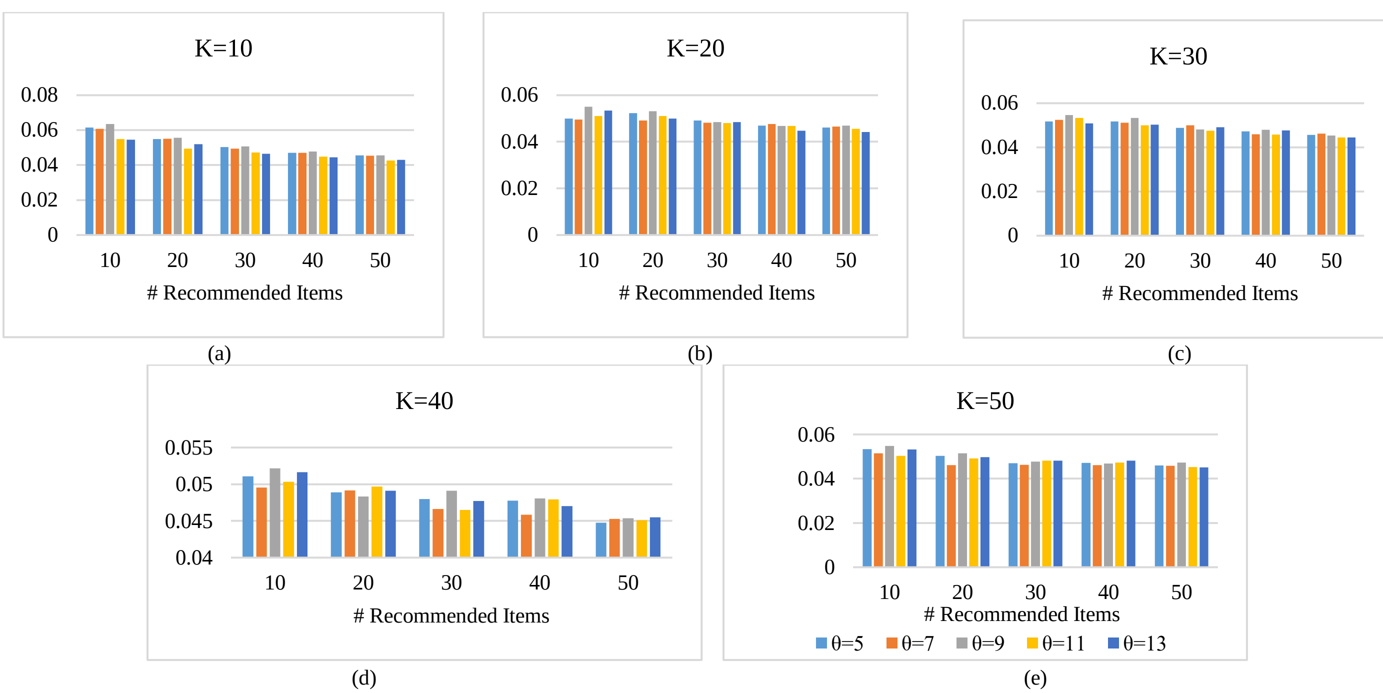

Fig. 4. Precision of CF-BSF vs. $\boldsymbol{\theta}$.

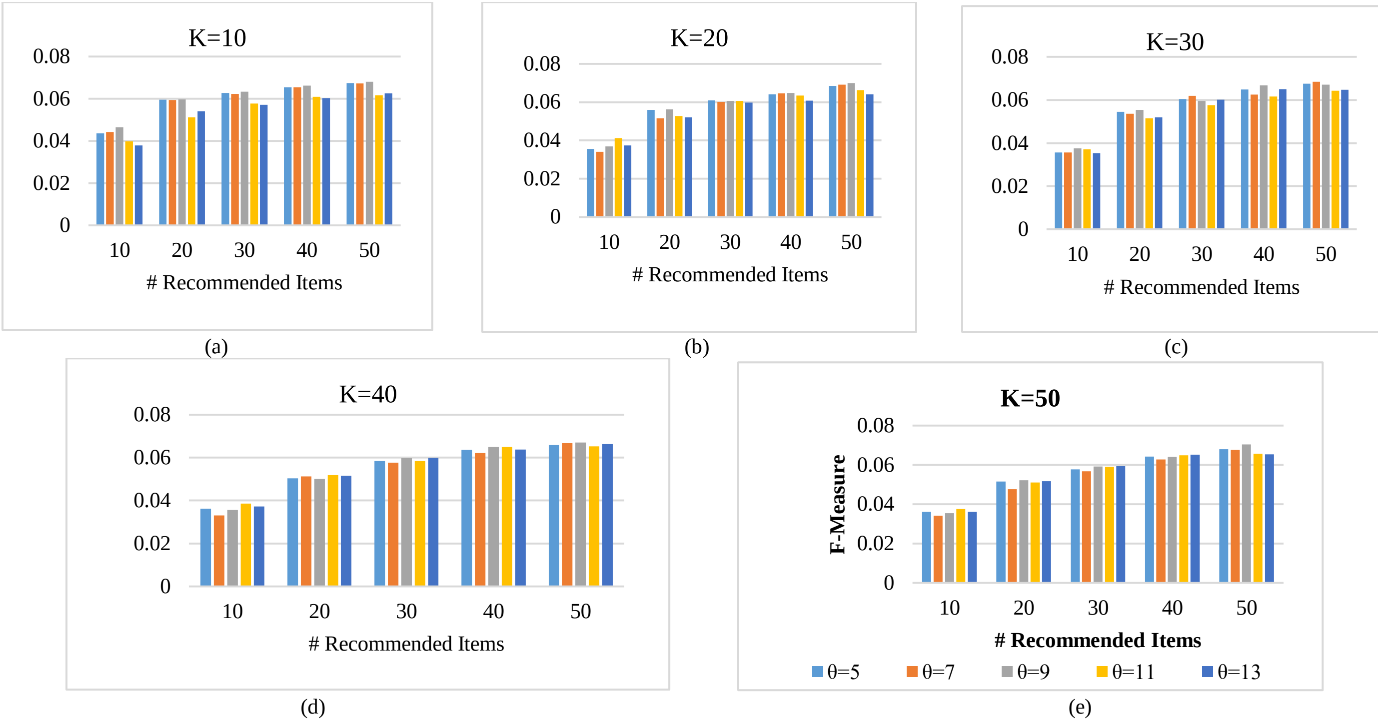

Fig. 5. F-Measure of CF-BSF vs. $\boldsymbol{\theta}$.

Fig. 5 depicts the F-measure rate of CF-BSF under the five initial denominator values. The result shows that the highest rate is observed when the denominator value is equal to 9, and the lowest rate appears when the denominator is equal to 11 and 13. For denominator values less than 9, the F-measure rate has approximately the same rate as when the denominator value is 9. The highest percentage of F-measure is observed when the number of recommended items is 50. The F-measure rate was slightly enhanced when the number of recommended items increases. Similar to the results of the precision rates, the F-measure rates exhibit variation under the five denominator values. Nevertheless, the F-measure rate almost reaches the highest value when the denominator is equal to 9.

V. Discussion and Finding

Fig. 1 to 4 indicates that the denominator value has affected prediction and performance accuracies. In addition, the size of neighbours and the number of recommended items, as significant variables, have an impact on both metrics. As previously mentioned, the aim of these experiments is to determine the appropriate value of the denominator. This value will be used as a primary input for the sigmoid function to identify the right number of the common rating items amongst the users. If the number of co-rated items between a pair of users is insufficient, the similarity weight will be devalued using the sigmoid function.

Although the MAE rate is superior to the other rates for denominators higher than 9, the recall, precision and F-measure rates do not produce acceptable values. By contrast, the MAE rate is the lowest when the value of the denominator is less than 9; the recall, precision and F-measure percentages are not higher than the percentages when the denominator is equal to 9. In conclusion, the most appropriate value for the denominator is 9. However, the result is dependent on the type and size of the dataset. Thus, using datasets with different sizes and types might produce different results.

VI. Conclusion

In this work, the effect of the size of co-rated items among users on recommendation accuracy was tested using exponential function. Sparsity problems had a negative impact on the accuracy of memory-based CF. The similarity weight between a pair of users with a small number of ratings, regardless if the similarity was high or low, produced an unrealistic relationship amongst users compared with a real relationship with either a high or low similarity. Therefore, the exponential function using varying threshold values was used to determine the optimal number of the common items amongst the users to revalue the similarity weight of the traditional similarity methods. The exponential function could devalue the similarity weight between a pair of users who had few co-rated items. Consequently, the similarity weight between users who had sufficient co-rated items would be increased. Moreover, the MovieLens 100K was used as the benchmark dataset to quantify the impact of the ratio of co-rated items on memory-based CF accuracy. The results showed that the factor of common items exhibited a significant impact on the accuracy. Several evaluation metrics were utilised for the investigation, namely, MAE, recall, precision and F-measure. A similarity method can be developed in the future to improve the accuracy of memory-based CF by considering the co-rated item size and the different rating degrees of users and different datasets.

Acknowledgment

This research is supported by the Department of Research and Innovation of University Malaysia Pahang under RDU190365 grant.

References

[1] X. Su and T. M. Khoshgoftaar, "A survey of collaborative filtering techniques," Advances in artificial intelligence, vol. 2009, 2009.

[2] P. Resnick, N. Iacovou, M. Suchak, P. Bergstrom, and J. Riedl, "GroupLens: an open architecture for collaborative filtering of netnews," in Proceedings of the 1994 ACM conference on Computer supported cooperative work, Chapel Hill, North Carolina, USA, 1994, pp. 175-186.

[3] U. Shardanand and P. Maes, "Social information filtering: algorithms for automating "word of mouth"," in Proceedings of the SIGCHI conference on Human factors in computing systems, Denver, Colorado, USA 1995, pp. 210-217.

[4] P. Resnick and H. R. Varian, "Recommender systems," Communications of the ACM, vol. 40, pp. 56-58, 1997.

[5] O. S. Revankar and Y. Haribhakta, "Survey On Collaborative Filtering Technique In Recommendation System," IJAIEM, vol. 4, pp. 85-91, 2015.

[6] N. Salehudin, H. Kahtan, M. A. Abdulgabber, and H. Al-Bashiri, "A Proposed Course Recommender Model based on Collaborative Filtering for Course Registration," International Journal of Advanced Computer Science and Applications(IJACSA), vol. 10, pp. 162-168, 2019.

[7] H. Al-bashiri, M. A. Abdulgabber, A. Romli, and H. Kahtan, "An improved memory-based collaborative filtering method based on the TOPSIS technique," PloS one, vol. 13, p. e0204434, 2018.

[8] F. Ricci, L. Rokach, and B. Shapira, Introduction to recommender systems handbook: Springer, 2011.

[9] L. Sharma and A. Gera, "A survey of recommendation system: Research challenges," International Journal of Engineering Trends and Technology (IJETT), vol. 4, pp. 1989-1992, 2013.

[10] J. A. Konstan, J. Riedl, A. Borchers, and J. L. Herlocker, "Recommender systems: A grouplens perspective," in Recommender Systems: Papers from the 1998 Workshop (AAAI Technical Report WS-98-08), 1998, pp. 60-64.

[11] L. Lü, M. Medo, C. H. Yeung, Y.-C. Zhang, Z.-K. Zhang, and T. Zhou, "Recommender systems," Physics Reports, vol. 519, pp. 1-49, 2012.

[12] J. B. Schafer, D. Frankowski, J. Herlocker, and S. Sen, "Collaborative filtering recommender systems," in The adaptive web, ed: Springer, 2007, pp. 291-324.

[13] M. D. Ekstrand, J. T. Riedl, and J. A. Konstan, "Collaborative filtering recommender systems," Foundations and Trends in Human-Computer Interaction, vol. 4, pp. 81-173, 2011.

[14] B. Sarwar, G. Karypis, J. Konstan, and J. Riedl, "Item-based collaborative filtering recommendation algorithms," in Proceedings of the 10th international conference on World Wide Web, Hong Kong, Hong Kong, 2001, pp. 285-295.

[15] J. L. Herlocker, J. A. Konstan, K. Terveen, and J. T. Riedl, "Evaluating collaborative filtering recommender systems," Acm Transactions on Information Systems, vol. 22, pp. 5-53, Jan 2004.

[16] R. Zhang, Q.-d. Liu, and J.-X. Wei, "Collaborative Filtering for Recommender Systems," in Advanced Cloud and Big Data (CBD), 2014 Second International Conference on, 2014, pp. 301-308.

[17] G. Adomavicius and A. Tuzhilin, "Toward the next generation of recommender systems: A survey of the state-of-the-art and possible extensions," Knowledge and Data Engineering, IEEE Transactions on, vol. 17, pp. 734-749, 2005.

[18] D. Jannach, M. Zanker, A. Felfernig, and G. Friedrich, Recommender systems: an introduction: Cambridge University Press, 2010.

[19] H. Al-bashiri, M. A. Abdulgabber, A. Romli, and F. Hujainah, "Collaborative Filtering Similarity Measures: Revisiting," in Proceedings of the International Conference on Advances in Image Processing, 2017, pp. 195-200.

[20] Q. Cheng, X. Wang, D. Yin, Y. Niu, X. Xiang, J. Yang, et al., "The new similarity measure based on user preference models for collaborative filtering," in Information and Automation, 2015 IEEE International Conference on, 2015, pp. 577-582.

[21] H. Al-Bashiri, M. A. Abdulgabber, A. Romli, and N. Salehudin, "A Developed Collaborative Filtering Similarity Method to Improve the Accuracy of Recommendations under Data Sparsity," International Journal of Advanced Computer Science and Applications(IJACSA), vol. 9, pp. 135-142, 2018.

[22] H. Koohi and K. Kiani, "A new method to find neighbor users that improves the performance of Collaborative Filtering," Expert Systems with Applications, vol. 83, pp. 30-39, 2017.

[23] B. K. Patra, R. Launonen, V. Ollikainen, and S. Nandi, "A new similarity measure using Bhattacharyya coefficient for collaborative filtering in sparse data," Knowledge-Based Systems, vol. 82, pp. 163-177, Jul 2015.

[24] H. J. Ahn, "A new similarity measure for collaborative filtering to alleviate the new user cold-starting problem," Information Sciences, vol. 178, pp. 37-51, Jan 2 2008.

[25] O. S. Revankar and Y. Haribhakta, "Survey On Collaborative Filtering Technique In Recommendation System," IJAIEM, ISSN 2319-4847, vol. 4, 2015.

[26] B. Zhang and B. Yuan, "Improved collaborative filtering recommendation algorithm of similarity measure," in AIP Conference Proceedings, 2017, pp. 020167-1–020167-6.

[27] H. Al-Bashiri, M. A. Abdulgabber, A. Romli, and F. Hujainah, "Collaborative Filtering Recommender System: Overview and Challenges," Advanced Science Letters, vol. 23, pp. 9045-9049, 2017.

[28] J. L. Herlocker, J. A. Konstan, A. Borchers, and J. Riedl, "An algorithmic framework for performing collaborative filtering," in Proceedings of the 22nd annual international ACM SIGIR conference on Research and development in information retrieval, 1999, pp. 230-237.

[29] S. Kg and G. S. Sadasivam, "Modified Heuristic Similarity Measure for Personalization using Collaborative Filtering Technique," Appl. Math, vol. 11, pp. 317-325, 2017.

[30] M. Jamali and M. Ester, "Trustwalker: a random walk model for combining trust-based and item-based recommendation," in Proceedings of the 15th ACM SIGKDD international conference on Knowledge discovery and data mining, 2009, pp. 397-406.

[31] J. Mao, Z. Cui, P. Zhao, and X. Li, "An improved similarity measure method in Collaborative Filtering Recommendation Algorithm," in Cloud Computing and Big Data (CloudCom-Asia), 2013 International Conference on, 2013, pp. 297-303.

[32] B.-H. Huang and B.-R. Dai, "A Weighted Distance Similarity Model to Improve the Accuracy of Collaborative Recommender System," in Mobile Data Management (MDM), 2015 16th IEEE International Conference on, 2015, pp. 104-109.

[33] L. Shunpan, M. Lin, and Fuyongyuan, "A singularity-based user similarity measure for recommender systems," IJICIC, vol. 11, pp. 1629-1638, 5 October 2015.

[34] X. Zang, T. Liu, S. Qiao, W. Gao, J. Wang, X. Sun, et al., "A New Weighted Similarity Method Based on Neighborhood User Contributions for Collaborative Filtering," in Data Science in Cyberspace (DSC), IEEE International Conference on, 2016, pp. 376-381.

[35] J. Zhang, Y. J. Lin, M. L. Lin, and J. H. Liu, "An effective collaborative filtering algorithm based on user preference clustering," Applied Intelligence, vol. 45, pp. 230-240, Sep 2016.

[36] J. R. Bray and J. T. Curtis, "An ordination of the upland forest communities of southern Wisconsin," Ecological monographs, vol. 27, pp. 325-349, 1957.

[37] M. Kokare, B. Chatterji, and P. Biswas, "Comparison of similarity metrics for texture image retrieval," in TENCON 2003. Conference on Convergent Technologies for the Asia-Pacific Region, 2003, pp. 571-575.

[38] S. Viriyavisuthisakul, P. Sanguansat, P. Charnkeitkong, and C. Haruechaiyasak, "A comparison of similarity measures for online social media Thai text classification," in Electrical Engineering/Electronics, Computer, Telecommunications and Information Technology (ECTI-CON), 2015 12th International Conference on, 2015, pp. 1-6.

Winning the Polio War in Pakistan

Prediction and Visualization of Polio Cases

Toorab Khan[1], Waheed Noor[2], Junaid Babar[3], Maheen Bakhtyar[4]
Department of CS and IT, University of Baluchistan
Quetta, Pakistan

***Abstract*—Polio is one of the most important issues which have caught the global attention. It has been eradicated globally except Pakistan and Afghanistan. Its quiet alarming, where whole world is polio free, still polio cases are emerging from Pakistan. The major motivation behind this research is to study and analyze the past cases (trend analysis) and to predict the number of future cases and obstacles hindering Pakistan to eliminate polio. The areas with peak level of influx could be prioritized for effective tracking, planning and monitoring of vaccination activities and better utilization of human resources for targeted and controlled interventions. It shall provide better management and resource allocation decisions for speedy eradication of this epidemic syndrome. Polio cases are displayed on Google Maps for localization and clustering, and trend analysis is performed for future prediction using linear regression.**

***Keywords*—Prediction; visualization; regression; clustering**

I. Introduction

Poliomyelitis causes lifelong paralysis and once suffered it cannot be cured. However, it can be prevented by getting proper and in time vaccination. Since 1988, 99% of polio cases have been reduced as a whole. In 2011, poliomyelitis existed only in four republics of the world i.e. Afghanistan, Nigeria, India and Pakistan. Then in 2014 only three countries reported confirmed polio cases i.e. Afghanistan, Nigeria and Pakistan [1]. At the current stage, polio is confined to only two countries i.e. Pakistan and Afghanistan. Pakistan caught the global attention of the world in the year 2014 when 306/359 confirmed polio cases were reported. While whole world got polio free, Pakistan reporting such a large figure was such an alarming situation.

II. Background

Developing countries are facing very serious health issues along with severe shortage of resources. One of such serious health threats is named as 'Poliomyelitis' [2]. A British physician Michael Underwood described this disease for the first time in 1789 [3]. Word 'Poliomyelitis' is derived from Greek words i.e. 'polio' (meaning grey), 'myelon' (meaning marrow) that of spinal cord and Latin suffix 'itis' (meaning inflammation) [4].

It is one the most deadly and stable virus. It can stay alive in contaminated food and water for several weeks. Patients of poliomyelitis are mostly in the age between two and five years old in the developing countries where the hygienic conditions are pathetic [5].

The global health officials and state health officials in Pakistan had anticipated an endgame for polio in Pakistan. The upward trend in the number of polio cases after 2005 suggested these predictions and indications as premature. Polio eradication activities had been initiated in Pakistan in 1994 by conducting its first Supplementary Immunization Activities (SIAs) for polio. Acute flaccid paralysis (AFP) surveillance started in 1995.

Pakistan achieved significant progress in polio eradication during 1994-2013. During this time period, the average annual polio cases were reduced by nearly 95% as compared to the pre-vaccine time period.

III. Literature Review

This literature review section has been compiled through surveys, books, profound articles, and the other sources relevant to the current specific issue. This review is intended to produce an outline of sources explored whereas researching the spread and cure practices of this disease. It's unquestionable that this analysis fits inside a bigger field of study.

In year 2012 [6] authors used Google Earth for mapping and dissecting the neighborhood food generation regions in the city of Chicago, Illinois. Its motivation was to highlight the urban regions of Chicago where the food production existed. It was carried out with the help of high satellite pictures taken from Google Earth. To show the agribusiness urban zones, Google Earth was utilized to outline urban horticulture locales which were recently reported. Next, they superficially broke down the pictures/map for those reported nourishment creation destinations and found the holes, for example removed some new destinations of urban agribusiness which were already unreported. At that point they completed ground truthing by visiting those destinations. Based on visual investigation of the recorded, final dataset was made and results were assessed including all unlisted and unreported instances.

In year 2013 [7] a contextual investigation is exhibited in which creators shows a web-based mapping application to show a huge number of nurseries in USA on guide. In this application, a business database is utilized for information stockpiling and the application gives modern functionalities to the clients. Instruments used to build up this application were Google Geocoder along with Google Maps API, the database structure of MS SQL, and dynamic webpages were created with the help of MS aspx.NET.

In year 2014 [8] presented trend analysis of obesity in Canada using linear regression. Number of adults (18 years and above) per year was taken as dependent variable and BMI (Body Mass Index) was taken as independent variable.

In 2015 [9] proposed an energy signature heat balance equation and showed thermal performance line of the building. They correlated energy consumption with weather variables. The basics of simple and multiple linear regression analysis were applied.

In year 2016 presented an assessment of relative contribution of heritable versus non-heritable factors, they performed a systems-level analysis on healthy twins between. They measured 204 different parameters and found that 58% almost completely determined by non-heritable influences.

Prediction of dengue outbreak was studied in 2016 by [10]. This analysis composes of a comparative set of prediction models including meteorological and lag disease surveillance variables. Generalized linear regression models were used to fit relationships between the predictor variables and the dengue surveillance data as outcome variable. Model fit were evaluated based on prediction performance in terms of detecting epidemics, and for number of predicted cases. An optimal combination of meteorology and autoregressive lag terms of dengue counts in the past were identified best in predicting dengue incidence and the occurrence of dengue epidemics. Past data on disease surveillance, as predictor alone, visually gave reasonably accurate results for outbreak periods, but not for non-outbreaks periods. A combination of surveillance and meteorological data including lag patterns up to a few years in the past showed most predictive of dengue incidence and occurrence in Yogyakarta, Indonesia.

In 2016 [11] have adapted a simple regressive method in Microsoft Excel that is easily implementable and creates predictive indices. This method trends consumption of antibiotic drugs over time and can identify periods of over- and underuse at the hospital level.

In 2017 [12] , developed a dynamic forecasting model for Zika virus (ZIKV), based on Google Trends (GTs). It was designed to provide Zika virus disease (ZVD) surveillance and detection for Health Departments, and predictive numbers of infection cases, which would allow them sufficient time to implement interventions. In this study, they found a strong correlation between Zika-related GTs and the cumulative numbers of reported cases (confirmed, suspected and total cases; p<0.001). Then, they used the correlation data from Zika-related search in GTs and ZIKV epidemics to construct an autoregressive integrated moving average (ARIMA) model for the dynamic estimation of ZIKV outbreaks. The forecasting results indicated that the predicted data by ARIMA model, which used the Google trends search data as the external regressor to enhance the forecasting model and assist the historical epidemic data in improving the quality of the predictions, are quite similar to the actual data during ZIKV epidemic.

IV. METHODS

The different aspects of this research including data collection, re-arranging and data pre-processing steps were the compulsory requirement for further utilization of the data. The essentials tasks are explained below:

A. Data Gathering

The required dataset for polio cases in Pakistan was got from National Emergency Operation Center Government of Pakistan, Islamabad with proper permission letter. The dataset obtained, contained the record of confirmed polio cases in Pakistan along with the dataset of missed children, untrained team members and refusal cases for last four years i.e. 2013, 2014, 2015 and 2016. It was available in MS Excel spread sheets. Fig. 1 shows the sample snapshot of acquired data.

B. Data Re-structuring

The accumulated information was not organized in the manner, to be used by Google Maps. There were numerous futile fields of data which were not required, so real task was to remove the useless fields and to organize data in legitimate and admissible format. Some portion of the area names were incorrectly spelled in the accumulated information which were amended accordingly.

C. Data Mapping and Clustering

In this stage, the reformatted information was mapped on Google MyMaps, moreover clustering technique was applied on the information. Fig. 2 shows the snapshot of plotted and clustered data of "Polio cases for the year 2014 on Google MyMaps".

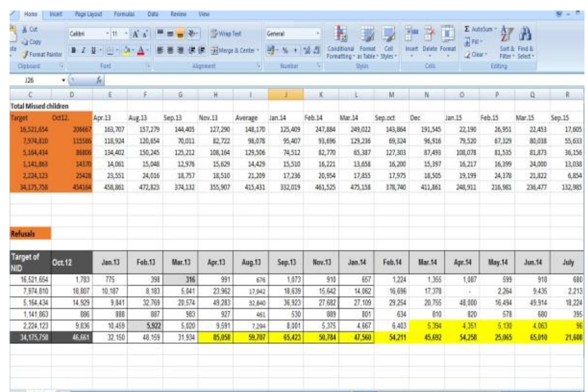

Total Missed children

Target	Oct12.	Apr.13	Aug.13	Sep.13	Nov.13	Average	Jan.14	Feb.14	Mar.14	Sep.oct	Dec	Jan.15	Feb.15	Mar.15	Sep.15
16,521,654	208667	163,707	157,279	144,405	127,290	148,170	125,409	247,884	249,022	143,864	191,545	22,190	26,951	22,453	17,605
7,974,810	115586	118,924	120,654	70,011	82,722	98,076	95,407	93,696	129,236	69,324	96,916	79,520	67,329	80,038	55,633
5,164,434	86806	134,402	150,245	125,212	108,164	129,506	74,512	82,770	65,387	127,303	87,493	108,078	81,535	81,873	36,156
1,141,863	14370	14,061	15,048	12,976	15,629	14,429	15,510	16,221	13,658	16,200	15,397	16,217	16,399	24,000	13,038
2,224,123	25428	23,551	24,016	18,757	18,510	21,209	17,236	20,954	17,855	17,975	18,505	19,199	24,378	21,822	6,854
34,175,758	454164	458,861	472,823	374,132	355,907	415,431	332,019	461,525	475,158	378,740	411,861	248,911	216,981	236,477	132,985

Refusals

Target of NID	Oct.12	Jan.13	Feb.13	Mar.13	Apr.13	Aug.13	Sep.13	Nov.13	Jan.14	Feb.14	Mar.14	Apr.14	May.14	Jun.14	July
16,521,654	1,783	775	398	316	991	676	1,073	910	657	1,224	1,365	1,087	599	918	680
7,974,810	18,807	10,187	8,183	5,041	23,962	17,942	18,639	15,642	14,062	16,696	17,378	-	2,264	9,436	2,213
5,164,434	14,929	9,841	32,769	20,574	49,283	32,840	36,923	27,682	27,109	29,254	20,756	48,000	16,494	49,914	18,224
1,141,863	686	888	887	983	927	461	530	889	801	634	810	820	578	680	395
2,224,123	9,836	10,459	5,922	5,020	9,591	7,294	8,001	5,375	4,667	6,403	5,394	4,351	5,130	4,063	96
34,175,758	46,661	32,150	48,159	31,934	85,058	59,707	65,423	50,784	47,560	54,211	45,692	54,258	25,065	65,010	21,608

Fig. 1. Dataset by National Emergency Operation Center.

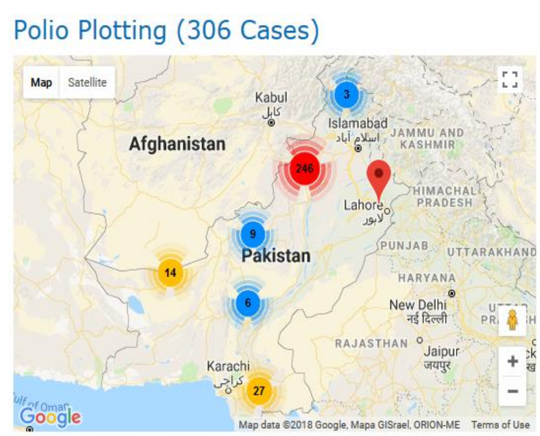

Fig. 2. Polio Plotting for the Year 2014 on Google MyMaps.

Clustering of markers (polio cases) is done by using the Google Maps API and a utility library. This API was available in Java and JavaScript for Android and Web respectively. Our system was web based so we used web API written in JavaScript, namely, "MarkerCluster for Map v3" (Fig. 3).

Mapping and clustering were done so as to give comprehension of the epidemic for further breaking down the patterns and making determinations. Fig. 4 shows the snapshots of geo coordinates data, required for plotting on Google Map.

D. Graphical Representation of Data

In this stage, the information was shown with the assistance of charts and tables to make correlations among the information. Correlations were made among polio cases in various areas for 2013, 2014, 2015 and 2016 and afterward looking at polio cases for the referenced four years inside and out. Fig. 5 shows the bar chart epidemic curve bar chart of confirmed Polio cases in Pakistan for the years 2013-2016.

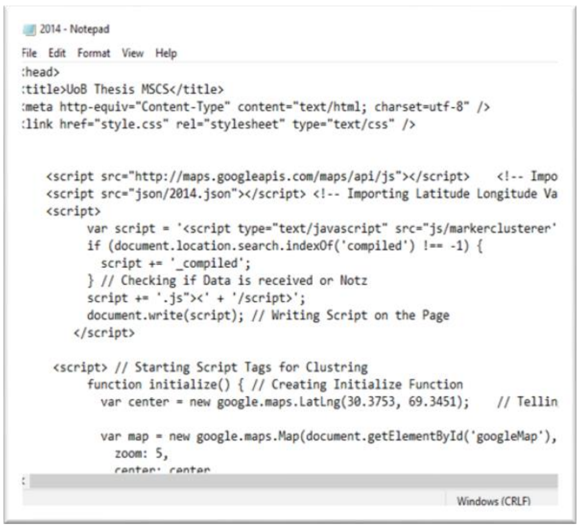
```
2014 - Notepad
File  Edit  Format  View  Help
:head>
:title>UoB Thesis MSCS</title>
:meta http-equiv="Content-Type" content="text/html; charset=utf-8" />
:link href="style.css" rel="stylesheet" type="text/css" />

   <script src="http://maps.googleapis.com/maps/api/js"></script>   <!-- Impo
   <script src="json/2014.json"></script> <!-- Importing Latitude Longitude Va
   <script>
         var script = '<script type="text/javascript" src="js/markerclusterer'
         if (document.location.search.indexOf('compiled') !== -1) {
           script += '_compiled';
         } // Checking if Data is received or Notz
         script += '.js"><' + '/script>';
         document.write(script); // Writing Script on the Page
       </script>

    <script> // Starting Script Tags for Clustring
         function initialize() { // Creating Initialize Function
           var center = new google.maps.LatLng(30.3753, 69.3451);    // Tellin

           var map = new google.maps.Map(document.getElementById('googleMap'),
             zoom: 5,
             center: center
Windows (CRLF)
```

Fig. 3. JavaScript MarkerCluster API Code Snapshot.


```
2015.json - Notepad
ile  Edit  Format  View  Help
ar data = {
"locations": [
 {
   "id": "1",
   "lat": "24.834803",
   "long": "67.356297",
   "title": "Bin Qasim, Sindh."
 },
 {
   "id": "2",
   "lat": "32.989724",
   "long": "70.603833",
   "title": "Bannu, Khyber Pakhtunkhwa."
 },
 {
   "id": "3",
   "lat": "32.674906",
   "long": "71.278512",
   "title": "Isakhel,Mianwali,Punjab."
 }
```

Fig. 4. Geo-Coordinated of Lat/Long Provided to Google MyMaps.

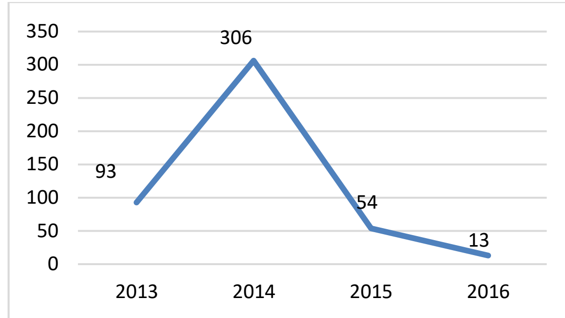

Fig. 5. Epidemic Curve of Polio Cases, 2013-2016.

V. Findings

After evaluating the data visually and graphically, next stage was to discover out the aspects fluctuating polio in Pakistan. After thorough study and discussions with the polio experts in Pakistan, we concluded three basic factors being the reasons behind polio in Pakistan [11].

- Missed Children: Children who are left unvaccinated (unavailability of child due to any reason).
- Refusals: Parents refuse to vaccinate their child. The main reasons behind refusal are misconceptions regarding vaccine that it contains forbidden ingredient or it causes infertility etc.
- Untrained team: It includes the team members who fail to deliver polio vaccines. Reasons include security issues, lack of supervision on team members, untimely payments to the team members, team members who do not know how to enter a record etc.

On the basis of these three dependent factors, we calculated the influence of these variables on effective Polio campaign. Regression Analysis was carried out with comparison to number of Polio cases for each year. After concluding out the factors, trend analysis was carried out of the dependency of the polio cases on the above mentioned three factors using linear regression method.

VI. Results

The relationship between the number of cases for the four years and the missed children for the respective years was analyzed and estimates for the next three years were made using linear regression method. Although the methods could be used to predict future Polio cases for any number of years. MS Excel was the tool used for this purpose. The linear regression equation is.

$$y = a + bx$$

Where Y is independent variable, x is dependent variable, a is y-intercept and b denotes the slope of projected line.

In our prediction model, the number of polio cases depends upon the effective vaccination coverage therefore missed children, refusal cases and untrained team members data are represented by x (on x-axis) as being independent variable and polio cases are represented by y (on y-axis) as being dependent variable. The below listed data was provided by National Emergency Operation Center Government of

Pakistan, Islamabad. The given data for x variables and y variables were fed to MS Excel analysis tool pack function of Regression and further Linear Regression was selected among various regression techniques. The data was fed category wise separately for missed children, refusal cases and untrained team members respectively. The Regression function returned the following regression equations against each category of input data. The regression function also returned the predicted y variables values for future years. The predicted values are plotted on bar chart in this paper "Table I".

The predicted values are plotted on bar chart, with comparison of confirmed Government sources and WHO unconfirmed sources later in this paper.

E. Prediction Results

The results of all three predictive variables are compiled together for better understanding. The trend analysis shows that government is making low progress in Polio data compilation. The progress slow because of many challenges such as the adoptability in remote areas where polio cases still exists. People in remote area of Pakistan are not cooperating with the polio workers and the Government. The second issue is the infrastructure. People are living on the small units spread over the peaks of the mountains where polio workers can't reach easily nor contact them.

TABLE. I. INPUT DATA TO PREDICTION SYSTEM

Description	Year	X Variable	Y Variable	Regression Equation
Missed Children Data	2013 2014 2015 2016	431022 409838 577236 323410	93 306 52 20	y = 158 – 0.00009248x
Refusal Data	2013 2014 2015 2016	53118 45815 56613 48847	93 306 52 20	y= 37-6.467077982x
Untrained Team Data	2013 2014 2015 2016	13319 12554 9116 7734	93 306 52 20	y= 1016.8 – 0.017593x

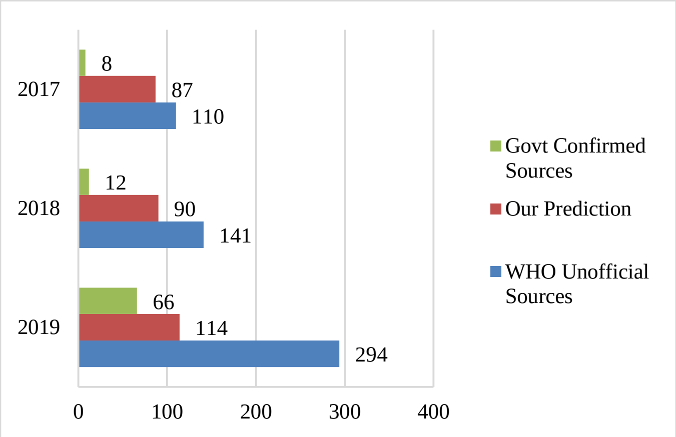

Fig. 6. Future Prediction of Polio Cases.

Our prediction model found the following conclusions:

- We identified an increase in the number of polio cases in future despite the eradication claims made the Government and other Health Organizations.
- The record keeping of confirmed Polio cases by Government agencies does not depict true picture.
- The government still needs to spend more resources on proper vaccination coverage and training of health workers.
- Our prediction model trend analysis is upheld by the unconfirmed sources cited above which are taken from WHO HQ unofficial sources [12].

VII. Conclusion and Discussion

In this research, online portal is created to visualize and predict the Polio cases. Although the same prediction model had been used in many similar trend analyses as presented in literature review, the following short comings handicapped the accuracy and precision of our model: (1) The system relied upon the available data maintained by the Government sources. Which may not reflect true population. (2) The high peak of y variable for the year 2014 i.e. 306 cases may pull the trend line irrationally.

Future work include to make visulization of other related diseases, and inlcude all countries rather only Pakistan.

References

[1] S. Kanwal, A. Hussain, S. Mannan and S. Parveen, "Regression in polio eradication in Pakistan: A national tragedy," J Pak Med Assoc, vol. 66, 2006.

[2] T. Ahmad, S. Arif, N. Chaudry and S. Anjum, "Epidemiological Characteristics of Poliomyelitis during the 21st century (2000-2013)," in Proceedings of the International Conference on Software Testing Analysis & Review, 2000.

[3] N. H. D. Jesus, "Epidemics to eradication: the modern history of poliomyelitis," Virology Journal, PubMed NCBI, 2007.

[4] A. Artenstein, "Vaccines," New York: Springer, 2010.

[5] B. Seytre and M. Shaffer, The death of a disease, New Brunswick: Rutgers University Press, 2005.

[6] J. R. Taylor and S. T. Lovell, "Mapping public and private spaces of urban agriculture in Chicago through the analysis of high-resolution aerial images in Google Earth," Landscape and Urban Planning, vol. 108, 2012.

[7] S. Hu and T. Dai, "Online Map Application Development Using Google Maps API, SQL Database, and ASP.NET," International Journal of Information and Communication Technology Research, vol. 3, 2013.

[8] L. K. Twells, D. M. Gregory, J. Reddigan and K. W. Midodzi, "Current and predicted prevalence of obesity in Canada: a trend analysis," CMAJ Open, vol. 2, 2014.

[9] N. Fume and R. Biswas, "Regression analysis for prediction of residential energy consumption," Renewable and Sustainable Energy Reviews, 2015.

[10] L. Aditya, L. Lutfan, L. H. Yien, H. Asa, K. Hari and R. Joacim, "Prediction of Dengue Outbreaks Based on Disease Surveillance and Meteorological Data," PLOS One, 2016.

[11] J. Ahmad, S. Anjum and S. Razzaq, Interviewees, Factors fluctuating polio in Pakistan. [Interview]. 2015.

[12] WHO, "Wild virus type 1 reported from other sources," Data in WHO HQ, 19 Nov 2019. [Online]. Available: http://polioeradication.org/wp-content/uploads/2016/08/Weekly-GPEI-Polio-Analyses-wpv-20191119.pdf.

Investigation of Different Modulation Formats for Extended Reach NG-PON2 using RSOA

S. Rajalakshmi[1]
ECE, SENSE, VIT, Vellore,
Tamil Nadu, India

T. Shankar[2]
ECE, SENSE, VIT, Vellore,
Tamil Nadu, India

***Abstract*—Global market forecasts predicted that by 2020, more than 26 billion internet devices and connections universally interconnected will require nearly 3 times the data traffic generated when compared to the year 2015. The increase in data traffic, demands for enormous bandwidth capacity. The potential to deliver 10 Gbps of huge data to individual businesses and households will be of paramount importance and a challenging issue for the present day service providers. An intensive study is carried out for the Fiber-To-The-Home Passive Optical Network (FTTH PON) for their use in the optical communication, due to their high data rates and more bandwidth. The current evolution of Next Generation-Passive Optical Networks Stage 2 (NG-PON2) network is the primary key technology for the growing demands of higher bandwidth and transmission of the data to the subscribers present in the access network from the service providers. Time Wavelength Division Multiplexing PON (TWDM-PON) architecture is the viable essential solution for NG-PON2 which provides more bandwidth for bidirectional transmission. This article proposes a design for extended reach TWDM-PON based on reflective semiconductor optical amplifier (RSOA). The exclusive feature of the RSOA is the wavelength conversion, which replaces the transmitters in the subscriber end. The Quality of Service (QoS) performance is critically analyzed for different optical modulation formats in proposed extended reach TWDM-PON using RSOA. The TWDM-PON using RSOA is simulated and investigated for different photodetectors. The analysis is also carried for various distance and data rates. The results exhibited that APD receivers have better performance of minimum bit error rate obtained is 10^{-11} and minimum Q factor is 6.2 when compared with PiN receivers. The comparative analysis of different modulation formats shows that the Carrier Suppressed Return to Zero- Differential Phase Shift Keying (CSRZ-DPSK) gives the best performance for longer distance and large data rates and Return to Zero(RZ) gives the least performance.**

Keywords*—Fiber To The Home (FTTH); Passive Optical Network (PON); Next Generation-Passive Optical Networks Stage 2 (NG-PON2); Quality of Service (QoS); Reflective Semiconductor Optical Amplifier (RSOA); Time and Wavelength Division Multiplexing (TWDM)

I. Introduction

In today's world we are bombarded with high performance networking system like laptops, smartphone, and their applications requiring more bandwidth like Internet of Things (IoT), remote medical services, cloud computing, file sharing, cloud storage, video and web conference, online audio and video streaming. The rapid increase in bandwidth demand for commercial applications drives the intensive tremendous need of high data rates at the subscriber end. Subscribers with high bandwidth are facilitated with faster data transfer speed, reduced crashes, bounces or busy signals, faster application performance, allows for more simultaneous users, increased data transfer capability and enabling more interactivity etc. NG-PON2 technology is outstripping the user demand. Flexible services towards the consumer are also provided by NG-PON2. Low latency and Quality of Experience (QoE) will be guaranteed to the customers by NG-PON2. The modern technique to get high data rates at end users is by implementing NG-PON2 network.

The TWDM-PON has been a key technique for NG-PON2. It is the first point to multi point wavelength access that provides data rate of 40 Gbps, for a distance of 40 Km without amplifier which is cost effective solution and has very high efficiency. Service operators require NG-PON2 systems for having higher capacity, huge bandwidth, more users and for longer reach. The article describes about the TWDM-PON for upstream using burst mode and downstream using continuous mode for 50Gb/s transmission using Non-return-to-Zero(NRZ) modulation formats and optical amplifiers [1].

In this article, a bidirectional TWDM-PON is proposed using NRZ modulation format for high capacity of 80 Gbps for a distance of 50 Km with minimum BER by using power optimization process of 5 to 10 dBm [2]. This paper explains the analysis of the performance of TWDM-PON for different reach and wavelength variation in ONU by using NRZ and Pulse-amplitude modulation (PAM4) in intensity modulation and direct detection [3]. In this paper they analyzed Manchester, Differential Phase Shift Keying (DPSK) and Differential Quadrature Phase Shift Keying (DQPSK) for different distances and different data rates. They described in terms of Bit Error Rate (BER) and Quality factor (Q- factor) for optical systems [4].

In this paper they have investigated the necessary pre-request required for NRZ Feed forward Equalization(FFE) and Decision Feedback Equalizer(DFE) and Duo-binary based adaptive equalization techniques for the design of 25 Gigabit-Ethernet Passive Optical Network(G-EPON). They demonstrated and compared for different number of taps and modulation formats, where duo binary shows better results than NRZ [5]. The NG-PON2 based on Nyquist NRZ technique for downstream transmission based on Direct Modulated Laser (DML) and APD. It shows superiority as -28.4 dBm in receiver sensitivity for TWDM-PON network [6]. The article analyzed and compared the advance modulation formats such NRZ, RZ, Duobinary and PAM-4 for 8 channel WDM-PON for different data rates without amplifiers and dispersion compensation [7].

The article investigates the performance of residual dispersion, dispersion tolerance and spectral efficiency, for correlative coding using NRZ and RZ for intensity modulation using direct detection an coherent receiver for 40 Gbps data transmission for 30 km Standard Mode Fibre (SMF) [8]. Using SMF and Dispersion Compensation Fiber (DCF) design composition of pre, post and symmetrical fiber composition, they achieved high data rate and long transmission over existing fibre optic systems [9]. Demonstration of 100G-PON based on NRZ transmission using Germanium and Silicon Avalanche Photo detector (APD) proved sufficient power budget for high data rate transmission [10].

In this paper they simulated asymmetrical Next Generation-passive Optical Network (XG-PON) for a upstream and downstream transmission using RZ and CSRZ. They analyzed these modulation schemes for different fiber length. The performance is affected by Polarization Mode Dispersion (PMD) and CSRZ provides best performance when compared to RZ format [11]. A new NG-PON2 is designed for 2048 users using TWDM-PON architecture for long reach of 100 Km using optical amplifiers. The amplifier emission noise power and saturation power of optical amplifier and splitter losses are simulated and evaluated. The design is analyzed for QoS parameter [12].

The article gives the summary of different modulation schemes such as RZ, RZ-DPSK, NRZ, NRZ-DPSK, CSRZ-DPSK and DB in the design of WDM-PON data transmission[13]. The author investigated DPSK signal for downstream in the proposed WDM-PON with RSOA in ONU for a distance of 25 Km. The upstream signal remodulated noise is reduced by using Orthogonal Frequency Division Multiplexing(OFDM). The results exhibited better BER of10^{-10}[14]. The paper investigates currently used modulation formats such as NRZ, RZ, CSRZ and DB in terms of BER, Q factor, optical reach and distance, they analyzed under polarization effects, dispersion and spectral efficiency [15].

This paper reviews the different types of advanced modulation formats supported proposed architectures used to carry high capacity of 400 Gigabit Ethernet links. Their optical link power budget, digital complexity, and power dissipation are compared via simulations. The challenges of implementing the physical layer are discussed [16]. Advanced modulations formats and detection techniques based on low power and integrated optical modulators are used in this design to reduce the cost and energy. The impairments induced by all kinds of defects and bandwidth limitation of opto-electronic components and the corresponding compensation techniques based on DSP algorithms have also been discussed in the experiments [17].

Design of downlink/uplink unicast 8 channel of each 2.5 Gb/s and one 10 Gb/s broadcast channel with the use of the cyclic property of arrayed waveguide grating with reflective capabilities of the fiber Bragg grating which produces colourless operation in TWDM-PON. The maximum allowable power budget loss for the network is about 36.5 dB with the receiver sensitivity for all ONUs obtained is 29.83 dBm [18]. RSOA is used to design a TWDM-PON for do transmission and DML for upstream transmission with filters for analyzing the power budget for different modulation formats [19].

This article proposes a WDM–OFDM–RoF system based on optical coupling tandem single-sideband (O-TSSB) transmitter. The impact of harmonic distortion and intermodulation distortion in this system is theoretically investigated and demonstrated to reduces the nonlinear distortion effectively by the use of (O-TSSB) transmitter with modulation index of 0.6 for distance of 50Km with a BER of 10^{-3}[20]. The author presents a comparative analysis of power sensitivity of the receiver under different modulation formats in SMF. Four modulation techniques were used namely “Return to Zero” (RZ), “Non Return to Zero” (NRZ), Duobinary (DB) and Differential Quadrature Phase Shift Keying (DQPSK). The result indicated DQPSK to be the smartest among all followed by DB. NZR showed moderate performance in general. RZ showed the worst performance in WDM system [21].

We propose four strategies for TDHMF Tx operation. BER minimization permits PM-QPSK/PM-16QAM performance similar to PM-8QAM's. In TDHMF nonlinear propagation, predistortion and/or polarization interleaving enables the maximum reach predicted by GN-model [22]. The 40 Gbps is PON is designed using different modulation formats such as NRZ-OOK, RZ-OOK, RZ-DPSK, and RZ-DQPSK for 20 km distance using TDMA and OCDMA with zero dispersion at BER less than 10^{-3} [23]. The paper discusses the WDM-PON for long reach and short reach applications. They calculated the loss budget for different modulation [24]. The manuscript analysis about the performance of the design of WDM-PON by using advanced modulation formats which requires intensity modulation and phase modulation for the service factor of power, noise, crosstalk, dispersion and polarization [25].

The article is organized as follows: the introduction section consists of the background literature survey. The second section describes the proposed design methodology with the suitable codes and standards adopted in NG-PON2. Then next section explains the summary and discussion of the results obtained for different modulation formats used in NG-PON2 network.

II. Proposed Design of NG-PON2

The proposed design of NG-PON2 is based on Hybrid TWDM-PON architecture for extended reach, which consists of 3 sections, a Central office (CO), Optical Distribution Network (ODN) and Optical Network Unit (ONU). The hybrid TDM-WDM PON is shortly called as TWDM-PON. The principle of operation of NG-PON2 is based on TWDM-PON architecture. NG-PON2 is designed to operate in bidirectional direction. When the data is carried from OLT to ONU it is called Down Stream (DS) transmission and when the data is carried from ONU to OLT it is called Up Stream (UP) transmission. During DS it follows Wavelength Division Multiplexing (WDM) principle and during US it follows Time Division Multiplexing (TDM) principle.

The NG-PON2 consist of 8 number of OLT which includes eight DS transmitter unit and eight US receiver unit. The ODN consists of multiplexer/demultiplexer, circulator, bidirectional fiber and 1:8 power splitter and eight ONU DS receiver and eight ONU US transmitters are present in this design. Here NG-PON2 is arranged according to the wavelength stacking technology for an extended reach of 100 Km using RSOA. The proposed design of TWDM-PON network is considered for direct detection system and for non-polarization multiplexing signals. Direct detection is typically used for 40Gb/s or lower-speed systems. In a direct detection receiver, its photo-detector only responds to changes in the receiving signal optical power, and cannot extract any phase or frequency information from the optical carrier. The proposed TWDM-PON architecture for extended reach NG-PON2 is shown in Fig. 1.

Basic formats like Non- Return to Zero (NRZ), Return to Zero(RZ) and DB and advanced formats such as Non- Return to Zero-Differential Phase Shift Keying (NRZ-DPSK), Return to Zero- Differential Phase Shift Keying (RZ-DPSK), and Carrier Supressed Return to Zero- Differential Phase Shift Keying (CSRZ-DPSK) are considered in this article. The basic modulation formats supports 200 GHz to 100 GHz channel spacing with spectral efficiency of 0.5 bits/sec/Hz and supports shorter distance of 200 miles. The advanced modulation formats supports 100 GHz to 50 GHz with spectral efficiency of 1 bits/sec/Hz.

The downstream operation consist of eight OLT transmitters with eight wavelength channels specified from 187.1–187.8 THz with fixed channel spacing of 100 GHz grid.

The eight wavelengths are modulated with different modulation formats starting with basic NRZ modulation as shown in Fig. 1. The modulated downstream signals are then multiplexed using an optical multiplexer and transmitted through a single mode optical fibre running for 90 Km is fed to the eight ONU by using passive power splitter with 1:8 ratio.

The downstream data transmission acts as a broadcast transmission, which splits the equal optical power to different wavelength ONU DS receivers. Semiconductor photodiodes are the most commonly used detectors in optical fiber systems since they provide good performance, being small in size, and are of low cost. The DS optical signal from power splitter is detected by PIN photodetector. The power splitter and the DS ONU are connected by a distribution fiber running for 10 Km. therefore the total distance achieved is 100 Km. The same DS signal is given to RSOA via Fabry perot free spectral range (FPF) to separate the DS signal from US signal.

The DS signal wavelength is reused by RSOA for US wavelength transmission. It considerably reduces the ONU transmitters and the cost also. Therefore no synchronization problem exists. The upstream signal is once again remodulated by RSOA. The same process will be continued for other remaining seven wavelength and feed to the optical fiber cable (OFC) via 1:8 splitter following TDM. The US signal then travels the OFC and reaches the US receiver. The US and DS signals are separated by using the circulator present at both OLT and ONU ends. The US signals are detected by PiN photodetector and perform O-E conversion. Subsequently, the converted electrical signals are sent to Bessel LPF for filtration process and followed by 3R generator for reshaping, restoring and retiming of the original electrical signal. The original electrical signal is fed to BER analyser to measure the BER value. BER is measured at both ONU receiver for DS and OLT for US receiver.

In the basic Fig. 1 the downstream OLT transmitter is designed separately according to the different modulation types considered in this article. Fig. 2 shows the DS OLT NRZ transmitter, Fig 3 shows the DS OLT RZ transmitter, Fig. 4 shows the DS OLT NRZ-DPSK transmitter, Fig. 5 shows the DS OLT RZ-DPSK transmitter, Fig. 6 shows the DS OLT CSRZ-DPSK transmitter, Fig. 7 shows the DS OLT DB transmitter. These different modulation transmitters are incorporated in the basic design of wavelength stacking NG-PON2 (Fig. 1) and simulated separately.

The OLT unit consists of Phase Pattern Generator (PPG) period of 27^{-1} to examine the high speed connections. A randomly generated sequence is then coded with NRZ pulses for reference encoder. CW laser source generates a continuous optical beam of having a power of 3 dBm. CW laser and NRZ pulses is further fed for the process of modulation into the MZM. The optical wave amplitude is controlled by MZM having ratio of extinction at 30 dB. The signal is then modulated optically. The simulation operation process is repeated for different modulation formats given in figure from Fig. 2 to Fig. 7. The simulation input specifications are given in the Table I.

TABLE. I. SIMULATION KEY PARAMETERS USED

Parameters	**Values**
Data Rate	10Gbps
Transmitter Power	0 dBm
Fibre Back Haul length	90 Km
Fiber distribution section	10 Km
Fiber dispersion coefficient	16.75ps/nm/km
Extinction ratio	30 dB
Attenuation coefficient	0.30 dB/km
Channel spacing	100 GHz
Power splitter insertion loss	1.5 dB
PIN Receiver responsivity	0.6 A/W
APD Responsivity	0.9 A/W
Receiver Sensitivity	-20 dBm
Receiver Electrical Bandwidth	7.5 GHz
RSOA Bias Current	50 mA
RSOA Output Power	1.85 dBm
RSOA average Gain	15.78 dB

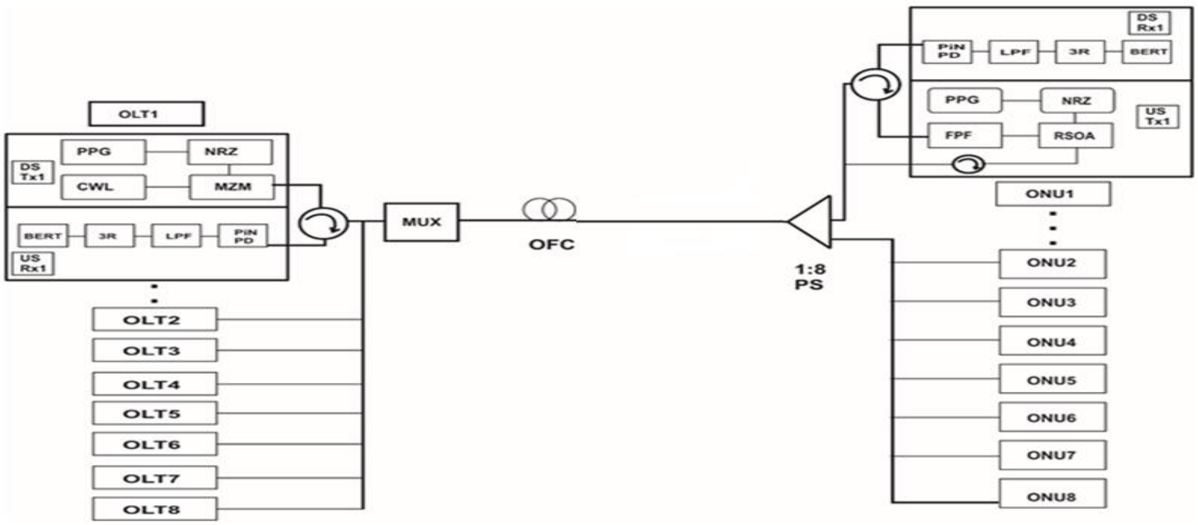

Fig. 1. The Schematic Stacked Wavelength Model for NG-PON2.

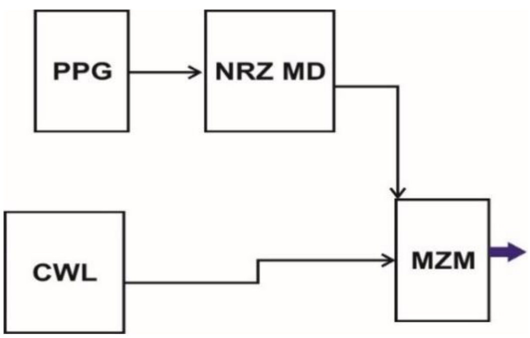

Fig. 2. DS OLT NRZ Transmitter.

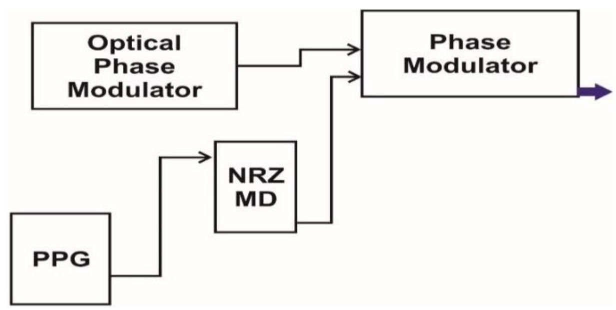

Fig. 5. DS OLT RZ-DPSK Transmitter.

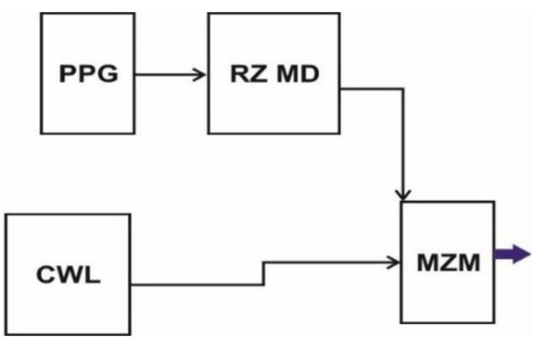

Fig. 3. DS OLT RZ Transmitter.

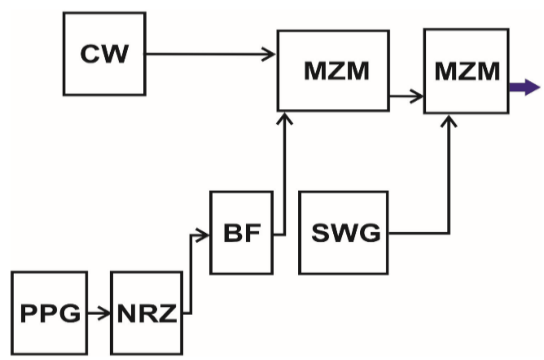

Fig. 6. DS OLT CSRZ-DPSK Transmitter.

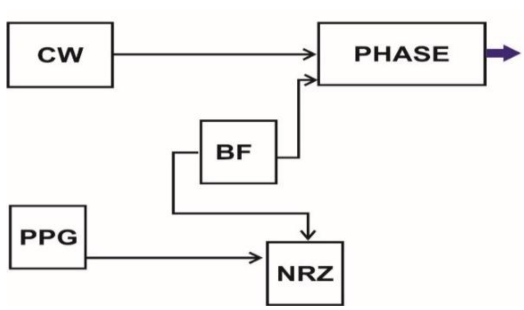

Fig. 4. DS OLT RZ-DPSK Transmitter.

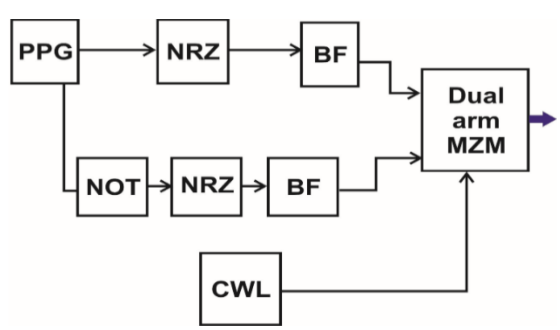

Fig. 7. DS OLT Duobinary Transmitter.

III. Results and Discussion

The proposed wavelength stacking NG-PON2 network is designed and implemented in Optisystem 13.0 simulation tool using Optiwave photonic software. The simulation is carried out and investigated for different distance from 10 Km to 100 Km for different modulation formats. The simulation is also carried out and investigated for different data rate from 10 Gb/s to 80 Gbps for different modulation formats The analysis is also investigated for different types of receiver configuration like PIN photodetector and APD photo detector for the above conditions of distance and data rate for different modulation. In this article QoS analysis have been carried out mainly for 2 important factors like Bit Error Rate (BER) and Q-Factor for different modulation formats such as NRZ, RZ, NRZ-DPSK, RZ-DPSK, CSRZ-DPSK and Duobinary. The analysis is also done for downstream transmission and upstream transmission.

A. PIN Receivers Performance

1) BER analysis for various distance: The effect of distance factor is analyzed using PIN receiver. It is shown in the Fig. 8. The effect of distance is analyzed in terms of BER and it is compared with all the six types of modulation formats. CSRZ-DPSK modulation format gives the best performance of BER value of $5*10^{-9}$, the next good performance is given by NZR-DPSK of BER value of $2.5*10^{-9}$, followed by RZ-DPSK and the least performance of $5*10^{-7}$ for RZ format at 10 Km. At 100 Km distance the BER value increases from $4*10^{-8}$ to 10^{-7}. For the long distance data communication, choosing the optimum BER in CSRZ-DPSK, NRZ-DPSK, RZ-DPSK can be used for optimum distance. Similar performance characteristics is obtained for upstream transmission also.

2) Q factor analysis for various distance: The effect of distance factor is analyzed using PIN receiver. It is shown in the Fig. 9. The effect of distance is analyzed in terms of Q factor and it is compared with all the six types of modulation formats. CSRZ-DPSK modulation format gives the best performance of Q factor value of 6.19, the next good performance is given by NZR-DPSK of q factor value of 5.96 followed by RZ-DPSK and the least performance is given by RZ format of value 5.25 and is observed at 10 Km.

For maximum distance of 100 Km, the Q factor decreases from 5.97 to 5.12. For the long distance data communication, choosing the optimum Q factor in CSRZ-DPSK, NRZ-DPSK, RZ-DPSK can be used for optimum distance. As the distance increases, the Q factor decreases. Similar performance characteristics are obtained for upstream transmission.

B. APD Receivers Performance

1) BER analysis for various distance: The effect of distance factor is analyzed using PIN receiver. It is shown in the Fig. 10. The effect of distance is analyzed in terms of BER and it is compared with all the six types of modulation formats. CSRZ-DPSK modulation format gives the best performance of BER value of $5.7*10^{-11}$, the next good performance is given by NZR-DPSK of BER value of $4*10^{-11}$ followed by RZ-DPSK and the least performance is RZ format is $5*10^{-8}$ at the distance of 10 Km. . At 100 Km the BER value increases from $5*10^{-9}$ to $3*10^{-8}$. For the long distance data communication choosing the optimum BER in CSRZ-DPSK, NRZ-DPSK, RZ-DPSK can be used for optimum distance Similar performance characteristics is obtained for upstream transmission.

The effect of distance factor is analyzed using PIN receiver. It is shown in the Fig. 11. The effect of distance is analyzed in terms of Q factor and it is compared with all the six types of modulation formats. CSRZ-DPSK modulation format gives the best performance of Q factor value of 6.1, the next good performance is given by NZR-DPSK of q factor value of 6.0 followed by RZ-DPSK and the least performance is given by RZ format of value 5.42 observed at 10 Km. For maximum distance of 100 Km, the Q factor decreases from 5.96 to 5.25. For the long distance data communication choosing the optimum Q factor in CSRZ-DPSK, NRZ-DPSK, RZ-DPSK can be used for optimum distance. As the distance increases, the Q factor decreases. Similar performance characteristics are obtained for upstream transmission.

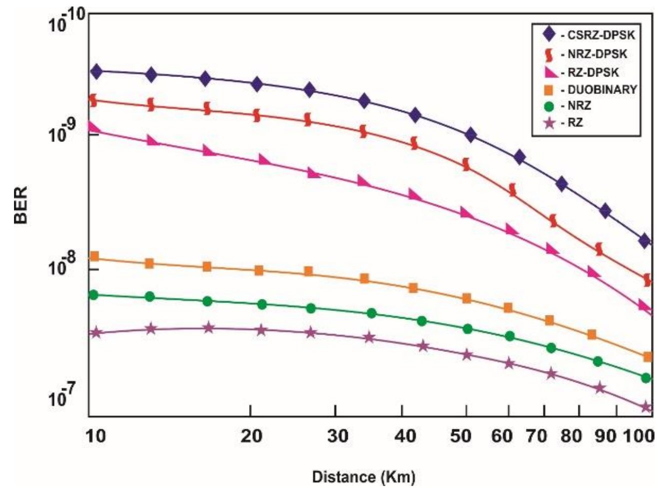

Fig. 8. Performance of BER for Distance Factor using PIN Receivers.

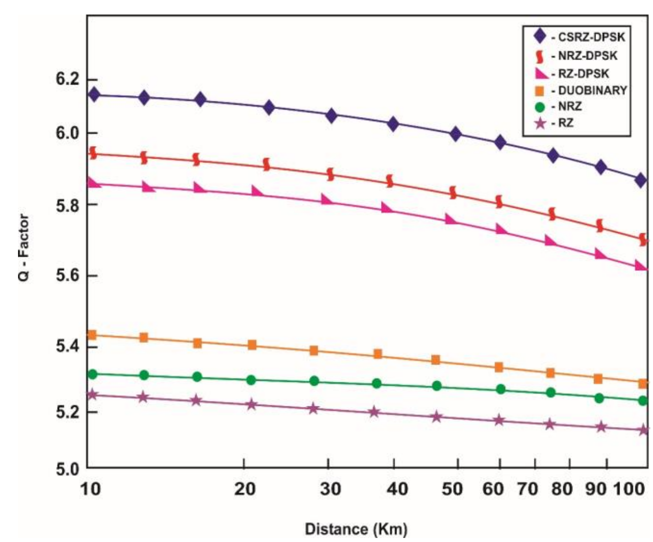

Fig. 9. Performance of Q Factor for Distance Factor using PIN Receivers.

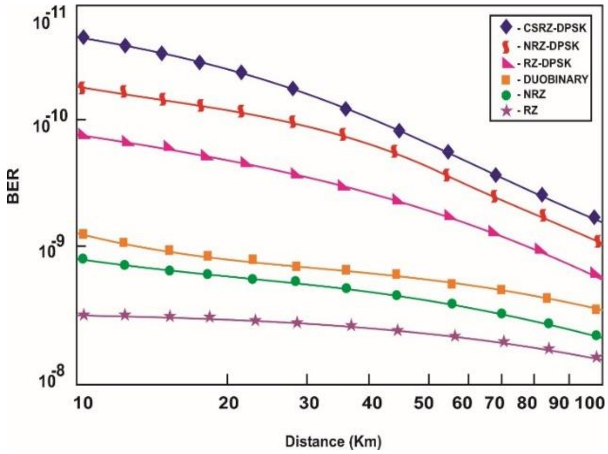

Fig. 10. Performance of BER Factor for Distance Factor using APD Receivers.

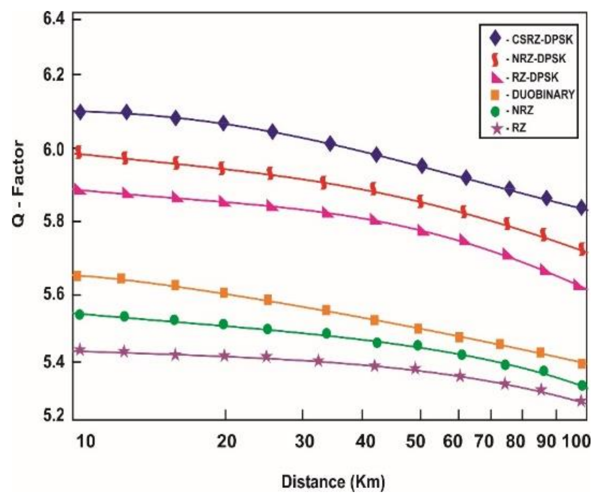

Fig. 11. Performance of Q Factor for Distance Factor using APD Receivers.

C. PIN Receivers Performance

1) BER analysis for various Data rate: The effect of data rate is analyzed using PIN receiver. It is shown in the Fig. 12. The effect of data rate is analyzed in terms of BER and it is compared with all the six types of modulation formats. CSRZ-DPSK modulation format gives the best performance of BER value of $7*10^{-10}$, the next good performance is given by NZR-DPSK of BER value of $5*10^{-10}$, followed by RZ-DPSK and the least performance of $5*10^{-7}$ for RZ format at 10 Gb/s data rate. At 80 Gb/s distance the BER value increases from $8*10^{-9}$ to $2*10^{-7}$. For increased data rate choosing the optimum BER in CSRZ-DPSK, NRZ-DPSK, RZ-DPSK can be used. Similar performance characteristics is obtained for upstream transmission

2) Q factor analysis for various Data rate: The effect of distance factor is analyzed using PIN receiver. It is shown in the Fig. 13. The effect of data rate is analyzed in terms of Q factor and it is compared with all the six types of modulation formats. CSRZ-DPSK modulation format gives the best performance of Q factor value of 6.1, the next good performance is given by NZR-DPSK of q factor value of 5.9 followed by RZ-DPSK and the least performance is given by RZ format of value 5.22 observed at 10 Gbps. For maximum data rate of 100 Gbps, the Q factor decreases from 5.97 to 5.2. For the long distance data communication choosing the optimum Q factor in CSRZ-DPSK, NRZ-DPSK, RZ-DPSK can be used for optimum distance. As the distance increases, the Q factor decreases. Similar performance characteristics is obtained for upstream transmission.

D. APD Receivers Performance

1) BER analysis for various Data rate: The effect of data rate is analyzed using PIN receiver. It is shown in the Fig.14.The effect of data rate is analyzed in terms of BER and it is compared with all the six types of modulation formats. CSRZ-DPSK modulation format gives the best performance of BER value of $8*10^{-11}$, the next good performance is given by NZR-DPSK of BER value of $5*10^{-11}$, followed by RZ-DPSK and the least performance of $5*10^{-8}$ for RZ format at 10 Gb/s data rate. At 80 Gb/s distance the BER value increases from $7*10^{-10}$ to $2*10^{-8}$. For increased data rate choosing the optimum BER in CSRZ-DPSK, NRZ-DPSK, RZ-DPSK can be used. Similar performance characteristics is obtained for upstream transmission.

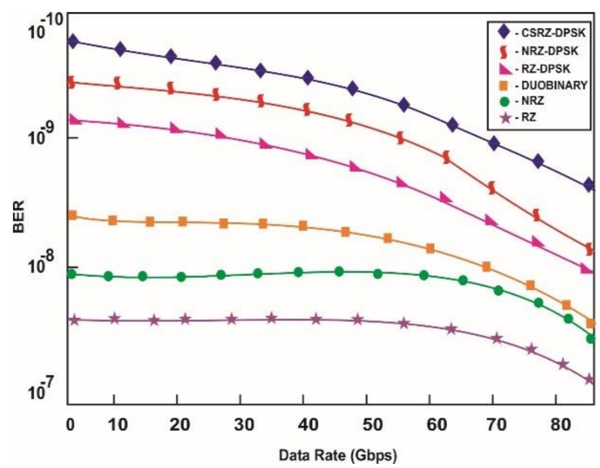

Fig. 12. Performance of BER for Various Data Rate using PIN Receivers.

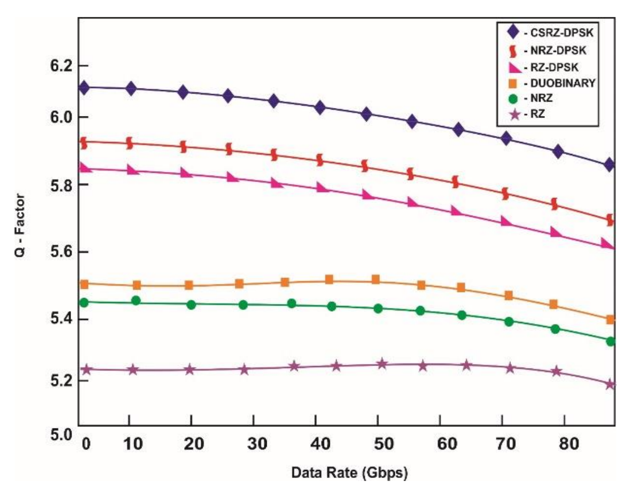

Fig. 13. Performance of Q Factor for Various Data Rate using PIN Receivers.

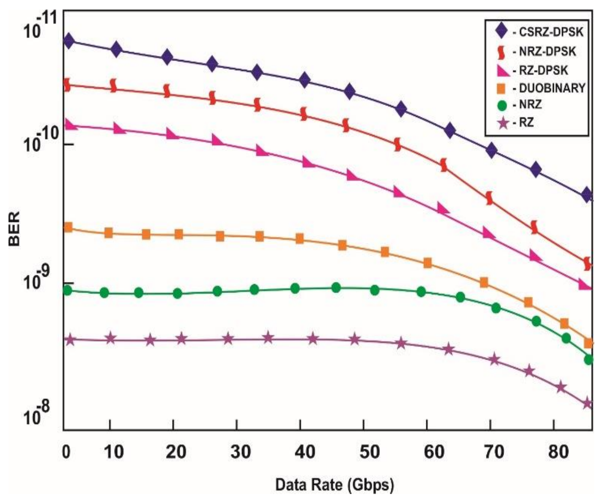

Fig. 14. Performance of BER for Data Rate Factor using APD Receivers.

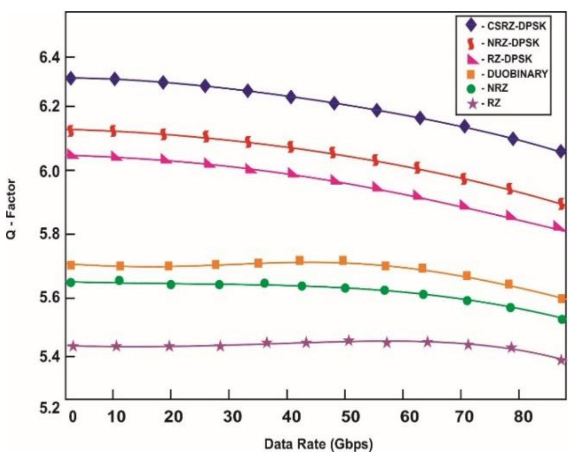

Fig. 15. Performance of Q Factor for Data Rate Factor using APD Receivers.

The effect of distance factor is analyzed using PIN receiver. It is shown in the Fig. 15. The effect of data rate is analyzed in terms of Q factor and it is compared with all the six types of modulation formats. CSRZ-DPSK modulation format gives the best performance of Q factor value of 6.1, the next good performance is given by NZR-DPSK of q factor value of 5.9 followed by RZ-DPSK and the least performance is given by RZ format of value 5.22 observed at 10 Gbps. For maximum data rate of 100 Gbps, the Q factor decreases from 5.97 to 5.2. For the long distance data communication choosing the optimum Q factor in CSRZ-DPSK, NRZ-DPSK, RZ-DPSK can be used for optimum distance. As the distance increases, the Q factor decreases. Similar performance characteristics are obtained for upstream transmission.

IV. Conclusion

In this article wavelength stacking architecture of NG-PON2 for extended reach is designed, implemented and simulated for various modulation formats using RSOA. The design is analyzed for various factor of increasing distance and increasing data rate. The factors are also investigated for different receiver operation and also for both downstream and upstream transmission. Similar characteristics are observed for upstream and downstream. CSRZ-DPSK gives minimum BER performance of 5 * 10^{-9} and minimum Q factor of 5.22 at the maximum distance of 100 Km than all other codes in downstream transmission. The APD receivers' receiver performs better when compared to PIN receivers for both distance and data rate factor. RZ gives the least performance.

Acknowledgment

This research was done in VIT, Vellore, but not funded by VIT Vellore. The author would like to acknowledge the management VIT for supporting this work to be carried out in the successful manner.

References

[1] Borkowski, R., Schmuck, H., Cerulo, G., Debrégeas, H., & Bonk, R., "Single-Wavelength Symmetric 50 Gbit/s Equalization-Free NRZ IM/DD PON with up to 33 dB Loss Budget and Fiber Transmission over> 40 km", Optical Fiber Communication Conference, pp. W2A-26, 2019.

[2] Aly, M. H., & Saleh, M. B, "Evaluation and optimization of TWDM-PON system capacity over single bidirectional optical fiber: Migration promising solution for the next generation PONs", International Conference on Computer and Information Sciences, pp. 1-6, 2019.

[3] Houtsma, V., Chou, E., & van Veen, D., "50 Gbps TDM-PON using Neural Network Enabled Receiver Equalization Specialized for PON",, Optical Fiber Communications Conference and Exhibition, pp. 1-3, 2019.

[4] Gill, H. K., Walia, G. K., & Grewal, N. S, "Performance analysis of mode division multiplexing IS-OWC system using Manchester, DPSK and DQPSK modulation techniques", Optik, vol 177, pp. 93-101, 2019.

[5] Xia, J., Li, Z., Li, Y., Xu, T., Chen, J., Song, Y., & Wang, M, "Comparison of NRZ and duo-binary format in adaptive equalization assisted 10G-optics based 25G-EPON", Optics Communications, vol. 410, pp. 328-332, 2018.

[6] Zhang, H. B., Wang, W. Q., Zheng, Z., & Jiang, N, "Experimental demonstration of 25-Gb/s downstream transmission using 10-Gbps optics for next-generation PONs", Optics Communications, vol. 427, pp. 209-214, 2018.

[7] Spolitis, S., Kurbatska, I., & Bobrovs, V, "Considering of PAM-4, DB, NRZ and RZ for Implementation in Next-Generation PONs", International Conference on Software, Telecommunications and Computer Networks, pp. 1-6, 2018.

[8] Dong-Nhat, N., Elsherif, M. A., Le Minh, H., & Malek mohammadi, A., "NRZ versus RZ over absolute added correlative coding in optical metro-access networks", Optics Communications, vol. 387, pp. 30-36 2017.

[9] Paloi, F., Mirza, T., & Haxha, S, "Optimisation of dispersion compensating in and long-haul fibre for RF transmission of up to 100 Gbit/s by using RZ and NRZ formats", Optik, vol. 131, pp. 640-654, 2017.

[10] Guo, Y., Yin, Y., Song, Y., Huang, M., Li, Y., Kuang, G., Li, M, "Demonstration of 25Gbit/s per channel NRZ transmission with 35 dB power budget using 25G Ge/Si APD for next generation 100G-PON", Optical Fiber Communications Conference and Exhibition, pp. 1-3, 2017.

[11] Kaur, A., Sheetal, A., & Miglani, R., "Impact of optical modulation formats on 10 G/2.5 G asymmetric XG-PON system", Optik, vol.149, pp. 351-358, 2017.

[12] S. Rajalakshmi., T. Shankar., "Optimization of Optical Amplifier Saturation power in NG-PON2 using 2048 way Splitter", Pakistan Journal of Biotechnology, Vol. 14 (Special Issue II) pp. 28-32, 2017.

[13] Kurbatska, I., Alsevska, A., Gegere, L., & Bobrovs, V., "Comparison of modulation formats for use in the next generation passive optical networks", Progress in Electromagnetic Research Symposium, pp. 3783-3787, 2016.

[14] Choudhury, P. K., & Khan, T. Z, "Symmetric 10 Gb/s wavelength reused bidirectional RSOA based WDM-PON with DPSK modulated

downstream and OFDM modulated upstream signals", Optics Communications, vol 372, pp.180-184, 2016.

[15] Agalliu, R., & Lucki, M., "System improvements in dense wavelength division multiplexing networks by using advanced optical modulation formats", International Conference on Transparent Optical Networks, pp. 1-4, 2015.

[16] Wei, J., Cheng, Q., Penty, R. V., White, I. H., & Cunningham, D. G, " 400 Gigabit Ethernet using advanced modulation formats: performance, complexity, and power dissipation", IEEE Communications Magazine, vol 53(2), pp. 182-189, 2015.

[17] Xu, X., Zhou, E., Liu, G. N., Zuo, T., Zhong, Q., Zhang, L., & Li, Z, "Advanced modulation formats for 400-Gbps short-reach optical inter-connection". Optics express, vol 23(1), pp. 492-500, 2015.

[18] S. Rajalakshmi, T. Shankar "Carrier Reuse using RSOA in TWDM-PON for Broadcast and multicast Transmission", International Journal of Pharmacy and Technology, Vol 8, no 4, pp. 21470-21481, 2016.

[19] Yi, L., Li, Z., Bi, M., Wei, W., & Hu, W., "Symmetric 40-Gb/s TWDM-PON with 39-dB power budget", IEEE Photonics Technology Letters, vol. 25, no.7, 644-647, 2013.

[20] Ji, W, "40 Gbit/s per wavelength channel in WDM-RoF-PON with polarization multiplexing and CSRZ-QDPSK modulation", Optik, vol 125(1), pp. 366-369, 2014.

[21] Badhan, N, Sharma, N, "Comparative analysis of CSRZ, DB and DPSK modulation formats for single channel 40Gb/s system", International Conference on Medical Imaging, m-Health and Emerging Communication Systems, pp. 95-100, 2014.

[22] Curri, V., Carena, A., Poggiolini, P., Cigliutti, R., Forghieri, F., Fludger, C., & Kupfer, T. (2014, March). Time-division hybrid modulation formats: Tx operation strategies and countermeasures to nonlinear propagation. In OFC 2014 (pp. 1-3). IEEE.

[23] Maneekut, R., Sakchaichanchon, T., Ket-Urai, V., & Kaewplung, P., "Recent progress of the next generation 40-Gbps signal transmission over passive optical network using the advance modulation formats", International Conference on Optical Communications and Networks, pp. 1-4, 2012.

[24] Iwatsuki, K., "Application and technical issues of WDM-PON", Broadband Access Communication Technologies IV, Vol. 7620, p. 76200C. 2010.

[25] Winzer, P. J., & Essiambre, R. J., "Advanced modulation formats for high-capacity optical transport networks", Journal of Lightwave Technology, vol. 24, no.12, pp 4711-4728, 2010.

Distributed Shadow Controllers based Moving Target Defense Framework for Control Plane Security

Muhammad Faraz Hyder[1]
Department of Software Engineering
NED University of Engineering & Technology
Karachi, Pakistan

Muhammad Ali Ismail[2]
Department of Computer and Information Systems
Engineering, NED University of Engineering & Technology
Karachi, Pakistan

***Abstract*—Moving Target Defense (MTD) has drawn substantial attention of research community in recent past for designing secure networks. MTD significantly reduced the asymmetric advantage of attackers by constantly changing the attack surface. In this paper Software Defined Networking (SDN) based MTD framework SMTSC (SDN based MTD framework using Shadow Controllers) has been proposed. Although the previous work in SDN based MTD targets the Data plane security, we exploit MTD for the protection of Control plane of SDN. The proposed solution uses the concept of Shadow Controllers for producing dynamism in order to provide security at the Control plane of SDN environment. We proposed the concepts of Shadow Controllers for throttling the reconnaissance attacks targeting Controllers. The advantage of our approach is multifold. First it exploits the mechanism of MTD for providing security in the Control plane. The other advantage is that the multi-controller approach provides higher availability in the SDN network. Another critical gain is the lower computational overhead of SMTSC. Mininet and ONOS Controller are used to implement the proposed framework. The effectiveness and overheads of the framework is evaluated in terms of attacker's effort, defender cost and complexity introduced in the network. Results demonstrated promising trends for the protection of Control plan of SDN environment.**

Keywords*—Control plane security; moving target defense; shadow controllers; software defined networks

I. Introduction

Cyber Security is a critical challenge of today's connected world. The emergence of technologies like Internet of Things (IoT), Web of Things (WoT), 5G have significantly increased the opportunities of Cyber-attacks. Cyber Security is a never-ending game between attacker and defender in which attackers always have the advantage. In current Cyber Security scenario, attackers have ample amount of time to analyze and launch attacks on the systems. The reason is that targeted systems and networks are static. Therefore, analyzing these systems from the perspective of vulnerabilities is much easier.

Moving Target defense (MTD) is an emerging area in cyber security. The motivation behind MTD is to make Cyber Systems dynamic and thus making them harder to discover, predict and attack. MTD removes the asymmetric advantages of attackers and make the cyber security field an equal playing ground. The term Moving Target Defense (MTD) was introduced for the first time in 2009 [1]. It is one of the game changing themes of cyber security defense. The main objective of MTD is to make the cyber security an equal playing field for both attackers and defenders. MTD eliminate the asymmetric advantage of adversaries by continuously changing the attack surface. Attack surface [2] of a system is basically a set of resources available in the systems that can be exploited by the attacker.

MTD ensures that attackers are not provided with slowly-changing /constant and predictable attack surface. MTD can be broadly classified as Network Based, Host based, Application based and Hybrid Approaches, etc. [3]. There are different parameters at each of these levels which can be changed in order to increase the difficulty level for attackers. Such attributes may include IP Address, Ports, OS versions, MAC Address, Routing paths etc.

SDN is a popularly growing networking paradigm. It fundamentally decouples the network control plane from forwarding data plane [4]. In recent past, there is a trend to design MTD solutions using Software Defined Networking (SDN) [5-8]. SDN substantially enhance the utilization of resources in the network, provides simplified network management, reeducation in operating cost and provides opportunities for network innovation and evaluation. SDN has a 3-layer architecture comprising of Application, Control and Data planes as shown in Fig. 1. Application Plane contains different application for numerous functionalities like network management, security and policy management etc. In the Control Plane SDN has SDN controller which is the brain of SDN network. In the Data Forwarding plane SDN has switches which forwards the packet based upon the directions from the Controller. The fundamental model behind SDN is OpenFlow [4]. It operates between the Control and Data planes. Its main role is defining the communication mechanism between the controller and switches in the data planes. The Controller has a clear unified view of the network. This global visibility of the Control plane enhances the network security. Control plane has the capability of network wide monitoring, vulnerabilities diagnostics and security policy deployment etc.

There has been a lot or research work in the domain of SDN security and MTD based SDN. Moreover, Distributed Controllers and Control planes security are also very active area of research. However, to the best of our knowledge there is no previous work which used the concept of MTD for the security of Control plane of SDN.

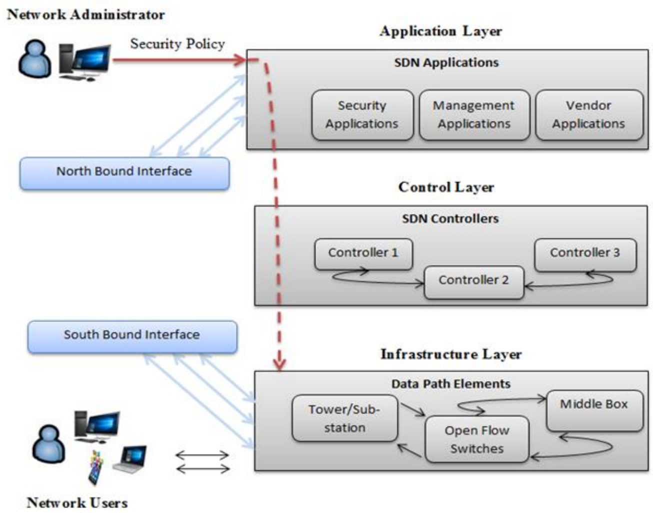

Fig. 1. Software Defined Networking Architecture.

The previous works for the protection mechanisms of control plane of SDN mainly focus on load balancing and mitigation of DDoS attacks [9-11]. Most of these solutions are reactive in nature, lacking a proactive approach like MTD. Moreover, these works do not take into consideration the first stage of Cyber kill chain which is reconnaissance. These solutions do not prevent the critical information collected by malicious attackers in the first stage of cyberattacks. The accurate information collected by the attackers is one of the main reasons of attackers' success. There is a need to design a solution which can prevent such attacks against the control plane of SDN at the first stage of cyber kill chain. This is one of the main motivations of this work. The proposed approach substantially protects against the reconnaissance attacks targeted towards the controller. The proposed approach will substantially enhance the DDoS protection of SDN control plane. The proposed MTD approach will make it difficult for the attackers to detect the actual controllers.

In this paper we proposed the idea of MTD for securing the Brain of SDN network i.e. Controller. The Brain of SDN has been the target of number of attacks. Its security is pivotal for the successful operations of SDN as it is the central controlling part of SDN. We used the concept of shadow Controllers for protecting against reconnaissance attacks which is the first stage of cyber-attack chain. The notion is to detect the reconnaissance traffic targeted against Controllers and provide manipulated response. Our proposed scheme has many advantages like increase difficulty level for the attacker to predict the correct Controller, higher availability and reliability due to the use of distributed Controllers and very low overhead for MTD implementation. Mininet emulator [12] and ONOS Controller [13] are used to implement the prototype of SMTSC.

Rest of the paper is outlined as follows: section 2 highlights the related work in the domain of SDN based MTD. Problem definition and threat model is presented in Section 3. The proposed SMTSC is explained in Section 4. Performance evaluation of SMTSC is presented in Section 5 whereas Section 6 covers the conclusion.

II. Related Work

One of the very first works in the domain of SDN based MTD was done in [5]. It provides the randomization of IP addresses in order to thwart the scanning attacks. It exploits OpenFlow to provide virtual IP address to different nodes in the network using a predefined frequency. Aydeger et al [6] proposed a MTD framework using SDN and Network Function Virtualization (NFV). The main motivation of their work is to exploit the benefits of both SDN and NFV for MTD design along with forensic capabilities. The framework utilizes three different MTD techniques to protect against the reconnaissance phase of cyber kill-chain [8].The framework was implemented in Mininet and considered indirect DDoS attacks as the threat model. An SDN based MTD was proposed in [7] securing the data plane. Their solution comprises of hopping of IP addresses. The solution protects against unauthorized access and reconnaissance attacks. The work substantially reduced the controller overhead by reducing its involvement in the MTD strategies. However, this may lead to some security problems and risks. An MTD using SDN with collaborative network mutation was proposed in [8]. It combines the idea of network and endpoint mutation for enhancing the security benefits. The collaborative model also utilized the hypothesis tests in order to adapt against the reconnaissance tactics of attackers. It also used the satisfiability modulo theories for generating optimal strategies. CHAOS which is an MTD system was proposed in [14]. It utilized the concept of CTS (Chaos Tower Structure). It divides the hosts based upon the security levels and then obfuscates the resources correspondingly. It used IDS to detect abnormal traffic patterns. The key strategy is to keep the legitimate traffic pass through the network normally while mystifying the abnormal traffic. An MTD utilizing SDN for protection against Fingerprinting attacks was proposed in [15]. The author proposed a method based upon hopping of Fingerprinting information (FPH). The main idea is to protect against fingerprinting attacks which are primarily used to gather the Operating System information. To devise an optimal strategy for proposed MTD, the FPH model fingerprinting attack and its defense as game. Authors in [16] developed SDN based MTD based on the concept of multiplexing of virtual IP addresses. The model was named as FRVM which is for multiplexing of virtual IPs in random fashion. There is a de-multiplexing module which provides the mapping of real IP address to virtual IPs. The proposed random mapping may suffer from performance degradation. A model to collect SDN Controller information was presented in [17]. The attack model proposed in this paper assumed that attacker is connected in Data plane of SDN. The model utilized simple TCP based measurement techniques to detect the Controller's platform. The authors in [18] proposed a mechanism to collect critical information of SDN based network without being detected. The attack KYE (Know your enemy) can collect critical information like network virtualization, threshold values against different probing attacks, QoS parameters and different security mechanisms implemented in a given SDN network. The authors also proposed a mechanism to protect against such attacks. SDN based virtual topologies for countering the Reconnaissance attacks was proposed in [19]. The work also proposed mechanism for the identification of malicious nodes generating scanning through statistical information. An MTD analysis framework was proposed in [20]. The work primarily focused on the developing a framework for the evaluation of SDN based MTD. A proactive security using MTD was proposed in [21] to secure the web servers running behind proxy servers in cloud environment. The work fundamentally focused on the botnets attacking the web servers. Proxy servers change at specific rate making a Moving target effect. A framework for the evaluation and optimization of container based cloud was proposed in [22]. The DSEOM framework provides mechanism for the analysis of MTD in dynamic cloud environment. It also provides optimization of different MTD techniques in the Cloud environment. Authors in [23] proposed the idea of MTD based protection for SDN enabled smart grids. These cyber physical have a high security requirements as security breach can cause substantial damage. Therefore, authors provide the idea of securing such systems with MTD based dynamic security techniques. The SFV which is security function virtualization was proposed in this paper. MTD based mechanism for privacy enhancement was proposed in [24]. The work targeted privacy leakage protection using MTD. For the experimental verification of the work, Domain Name system (DNS) was used. A Smart collaborative distribution provides protection against privacy leakage due to DNS queries using Moving Target Defense. A Cyber deception method based on MTD was proposed in [25] to counter the insider threats. Previous MTD work focused on the external attacks, while this is one of its kind works that exploited MTD for countering the insider threats. A Moving target defense approach was presented in [26] to counter adversarial machine learning approach of attackers. Stackelberg game based approach was used model the problem between attacker and defender.

III. Methodology

A. Threat Model

Our threat model assumes that attacker can run scanning to gather the information of Controller. Attackers in our work can be a host which is connected to target SDN network either directly or indirectly. Attackers target is to detect the SDN based System and then run different scanning attacks to gather information regarding Controller which is the brain of SDN network. In different previous work of SDN based MTD the attack model focused predominantly on the Data plane of SDN Network. However, our threat model assumes that attacker fundamentally targets the Controller of SDN. Modern attackers [18] can detect the presence of security mechanisms of SDN by observing the Controller and switch communication.

B. Proposed SMTSC Model

Fig. 2 presents the overall concept of SMTSC. In this framework there are "n" Controllers for building a distributed SDN network. All large SDN system uses the Distributed Controllers in order to run a reliable, highly available network. SMTSC also utilizes shadow Controllers. There are "k" shadow controllers. The reason for incorporating extra "k" controllers is to provide protection against the reconnaissance traffic generated by the attacker against Controllers. These "k" virtual controllers will generate responses against the reconnaissance traffic in order to constantly changing the attack surface and thus providing an MTD effect. There are other advantages of this approach as well. First one is fault tolerance. In case of failure in the "n" clusters, these shadow controllers may also provide backup support.

Fig. 3 represents the SMTSC internal components and the Data plane of SDN. According to our threat model discussed in the previous section, after successfully detecting the presence of an SDN based Network, the attacker will run the reconnaissance traffic against the Controller to capture critical information like Controller's platform etc. The notion is to exploit vulnerabilities of Controller. The proposed SMTSC framework will come into play now. It will detect the reconnaissance traffic using its Reconnaissance Detection Module (RDM). RDM is implemented primarily using SNORT [27] which is an open source Intrusion Detection System. We have modified its configuration to detect the reconnaissance traffic directed against the Controllers. After the successful detection of Probing traffic, next task is performed by Movement Decision Module (MDM). Its fundamental role is the selection of strategy for movement. It will select one of the "k" shadow controllers to generate a response for the probing traffic. This selection is based upon the Round Robin fashion. There is another critical module which MTD Monitoring engine. Its responsibility is the overall monitoring of the proposed MTD framework. MDM also has capability to store the mapping of probing traffic and responses generated by respective k controller. It will be beneficial for the forensic analysis by tracking the footprints of attackers.

Algorithm 1 represents method of detection of interesting traffic. The required SDN network comprises of N distributed and K shadow Controllers is initialized. PacketArrival received the packets with their respective source and destination TCP/IP information. It checks for the interesting traffic directed towards controller. Once it detects the interesting scanning traffic, it will call the MTD Selection Algorithm. Algorithm 2 represents MTD Strategy and Shadow Controller Selection. This algorithm selects the shadow controllers from the list on Round Robin basis.

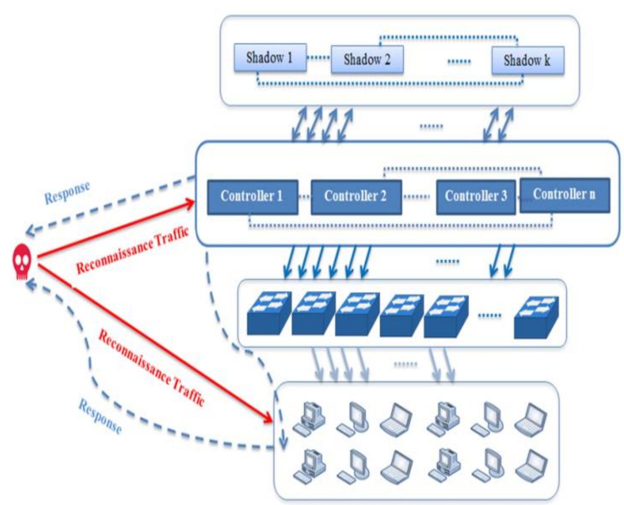

Fig. 2. SMTSC Block Diagram Indicating Distributed and Shadow Controllers.

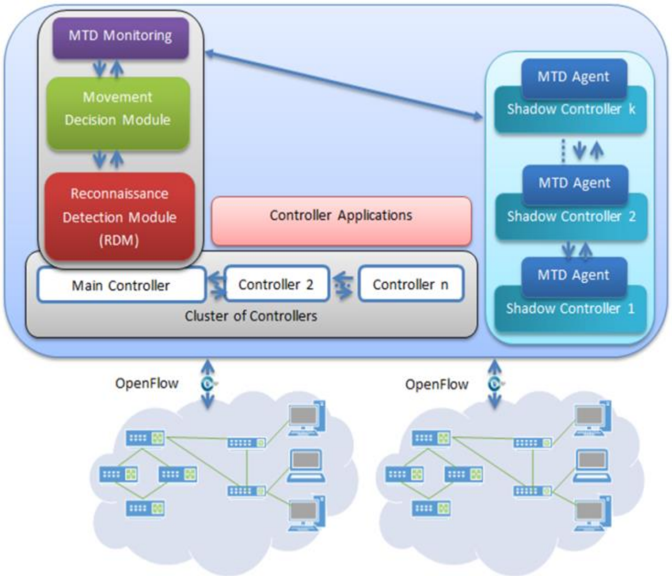

Fig. 3. SMTSC Internal Components.

Algorithm 1 Shadow Controller interesting traffic received

1: [Initialization of SDN based Network with Distributed and Shadow Controllers]
2: **function** PacketArrival (srcIP, srcPort, dstIP, Protocol)
3: **if** (dstIP = = ControllerIP) AND (srcIP ! = switch_IP) AND (Protocol ! = LLDP) **then**
4: SC ⟵ ShadowControllerSelection ()
5: Prepare_Response_probabing_traffic
6: Set IP_SC =IP_Probed_Controller
7: Set Ports_SC=Port_Probed_Controller
8: Attacker ⟵ SendResponse_to_probing_traffic
9: **endif**
10: **else**
11: Normal_SDN_Forwarding ()
12: **end function**

Algorithm 2 Shadow Controller Selection

1: **function** ShadowControllerSelection
2: SelectedShadowcontroller = = RoundRobinSelection (list of K controllers)
3: Return SelectedShadowcontroller
4: **end function**

Fig. 4 represents the workflow of SMTSC. The MTD Application is constantly monitoring the reconnaissance traffic. As discussed in the previous sections, the network is running using Distributed SDN controllers. There are k shadow controllers as well in the system. The Data plane comprises of different switches and hosts connected to these switches. Both benign and malicious are present in the system. Traffic generated by legitimate users will pass through different switches and controllers as per the requirements. The Controller will install the required flows. However, the malicious users will generate the probing traffic directed towards the SDN controllers. The MTD application will detect this reconnaissance traffic. It will select one of the shadow controllers to respond to this traffic. The shadow controller will be selected based upon round robin fashion.

C. *Experimental Setup*

The experimental setup for the proposed framework comprises of Dell Server (Intel Xeon CPU E5-2620 2.1GHz) with 32 GB RAM. The platform for the distributed SDN Controller is ONOS [13]. The proposed network topology was implemented in Mininet simulator. The topology comprises of Distributed Controllers. All practical implementation of SDN requires Disturbed Control Plane for redundancy, higher availability and scalability. For the detection of reconnaissance traffic Snort was configured in an IDS (intrusion detection system) mode. We used Nmap [28] for running scanning traffic against the Controllers. Fig. 5 represents the implemented topology.

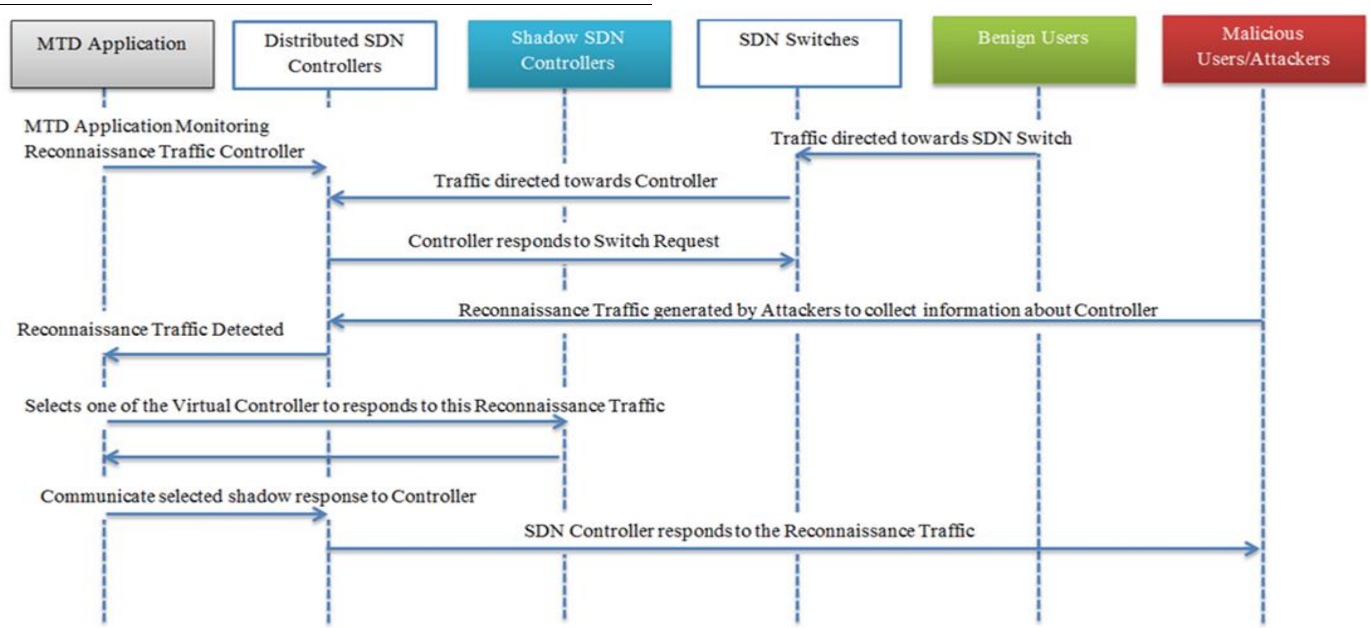

Fig. 4. Workflow of SMTSC.

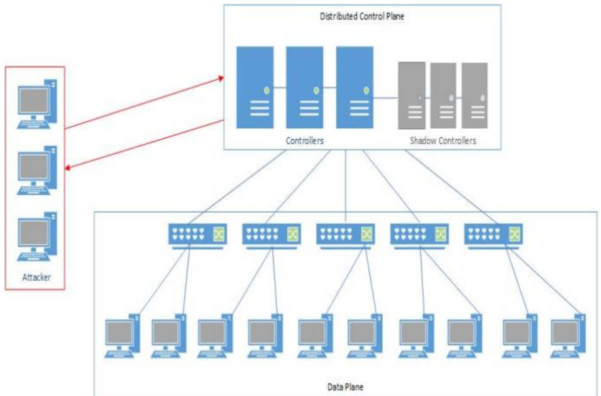

Fig. 5. Simulation Setup of SMTSC.

IV. Results and Discussion

Table I represents the time elapsed while the attacker is running Nmap scan against the Controllers for all possible ports. After several scans the following time ranges has been obtained with respect to number of controllers. As it is evident from the table that as the number of Controllers increased, the time required to scan will increase and hence the attacker's effort. Therefore, it is useful to have a Distributed Control plane for SDN in order to increase its security against reconnaissance attacks. Fig. 6 represents the box plot of Scanning time for different controllers.

A. Attacker Cost

The main objective of MTD is the increase in attacker's effort to attack a system. In this section, attacker's cost is analyzed. After incorporating the SMTSC, the snort configuredin IDS mode intercepts the reconnaissance traffic and redirect it one of the shadow Controllers as per Algorithms 1 and 2. The attacker will get response from one of those shadow controllers. Table II represents the attacker accurate detection with respect to total number of scans for different number of Shadow Controllers (SC). The accurate detection here means that attacker is able to correctly identify the Real Controller rather than getting response from one of the shadow Controllers. As evident from table, the attacker's success rate ranges from 15% to 20.55% after the adaptation of SMTSC.

For the purpose of experimental analysis, a maximum of 2000 scans were performed. Fig. 7 presents the graph of Attacker's success.

Attacker's cost is dependent on various factors like the accuracy of scanning traffic detection by IDS, the number of shadow controllers, and the number of scans by the attacker. Accurate detection by IDS is critical as it is the first step of our framework. The number of shadow Controllers plays important role. The higher number of Shadow Controller will increase the probability of successful response from these controllers and making it difficult for the attacker to identify the manipulated response. The number of scans performed by the attacker increases the probability of attacker's success. The reason is that the attacker scan may be able to get through the scanning detection mechanism without being detected. Hence, the increase in the number of shadow controllers decreases the attacker's success rate. However, increasing the number of shadow controllers beyond 6-7 doesn't substantially increase the attacker effort as evident from Fig. 7.

$$C_{attacker} = N_{scan} + N_{shadowcontroller} + A_{detection} \qquad (1)$$

TABLE. I. NMAP Scan Time with Single and Multiple Controllers

Scan time with 1 Controller (seconds)	Scan time with 2 Controllers (seconds)	Scan time with 3 Controllers (seconds)
1753-1882	2963-3062	3663-3721

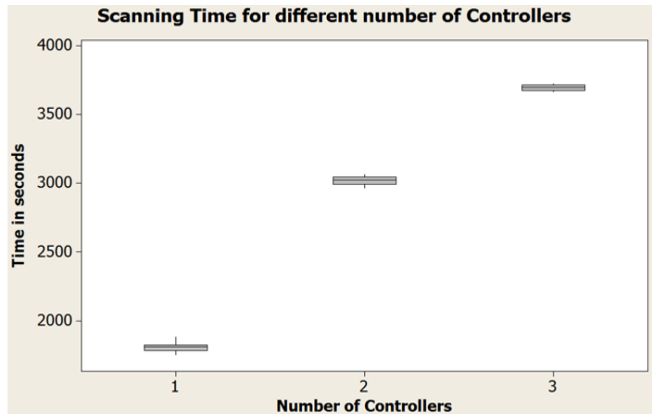

Fig. 6. Scanning Time for different Number of Controllers.

TABLE. II. Accurate Detection by Attacker after SMTSC for different Number of Shadow Controllers

Controllers	Number of Scans		Number of Shadow Controllers (SC)					
			SC=2	SC=3	SC=4	SC=5	SC=6	SC=7
3	100	Attacker Success (%)	18	17	16	16	15	15
3	200		18.5	17	16.5	16.5	15.50	15
3	400		19.25	17.75	17.25	16.75	16.50	16.25
3	800		19.62	18.50	17.75	17.62	17.37	17.12
3	1600		20.06	19.68	18.62	18.50	18.18	17.93
3	2000		20.55	19.65	19.15	18.85	18.2	18.05

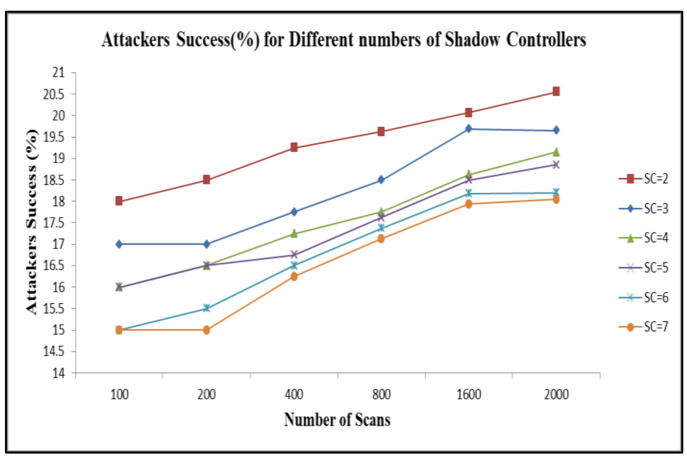

Fig. 7. Accurate Detection by Attacker.

Where $C_{attacker}$ is the attacker cost, N_{scan} is the number of scans attacker perform, $N_{shadowcontroller}$ is the number of shadow controllers and $A_{detection}$ is the accuracy of scanning traffic detection.

B. Defender Cost

One of the main challenges of MTD is the overhead it introduced in the existing system. The proposed SMTSC model takes into consideration this problem. It utilizes the concept of Shadow Controllers which are running as different Virtual Machines. Moreover, it doesn't reset any IP address or Port address of running connections, therefore no such network overhead added in the original system. The SMTSC, stores the footprint of interesting traffic for the purpose of forensic analysis. For this purpose it requires minimal storage which won't incur substantial cost. For analysis purpose, a storage entry will require 17 bytes. It includes 2 bytes for ID field, 4 bytes for source IP address, entry date and time field comprises of 7 bytes and 4 bytes for Controller IP.

$$C_{storage} = Number\ of\ Scans \times Storage\ Required\ for\ one\ scan \quad (2)$$

The overall Defender's cost comprises of Number of Shadow Controllers present in the model and the computation power required by each controller. It also includes the storage cost required for storing the logs for analysis and reconnaissance detection mechanism cost.

$$\boldsymbol{C_{defender}} = \boldsymbol{k} \times \boldsymbol{C_{processing}} + \boldsymbol{C_{storage}} + \boldsymbol{C_{\text{reconnaissancedetection}}} \quad (3)$$

Where, $\boldsymbol{k}$ is the count of shadow controllers, $\boldsymbol{C_{processing}}$ is the processing required by each shadow controller. $\boldsymbol{C_{storage}}$ is the storage cost and $\boldsymbol{C_{reconnaissancedetection}}$ is the cost of reconnaissance detection module.

For each shadow controller, we implemented a Virtual Machine (VM) with 2 CPUs, 2GB RAM, and 20GB hard disk. Therefore, $\boldsymbol{C_{processing}}$ is the computational cost of each VM. For SMTSC, the storage cost is $C_{storage} = 2000 \times 17 = 34Kbytes$. $\boldsymbol{C_{reconnaissancedetection}}$ is cost associated with reconnaissance detection module. Since all modern network protection scheme requires probing detection as the part of their IDS system. Therefore, this cost may be ignored for SMTSC as it will already be covered. Hence the main cost of SMTSC is cost of Shadow Controllers. Fig. 8 depicts the Defenders' success (%) for different number of scans.

The proposed framework was analyzed for maximum of 2000 scans. An attacker cannot perform very large number of scans as it will get permanently detected by the defender system. As evident from Fig. 8 and Table III, our framework can sustain realistic number of scans with a maximum accuracy of 85%.

C. Control Plane Security Analysis after SMTSC

In this section we analyzed the control plane security before and after the SMTSC. Attacker's success increases as the number of scans increased. Table IV presents Reconnaissance of SDN Network with and without SMTSC. Fig. 9 represents the attacker success on SDN Network with and without SMTSC.

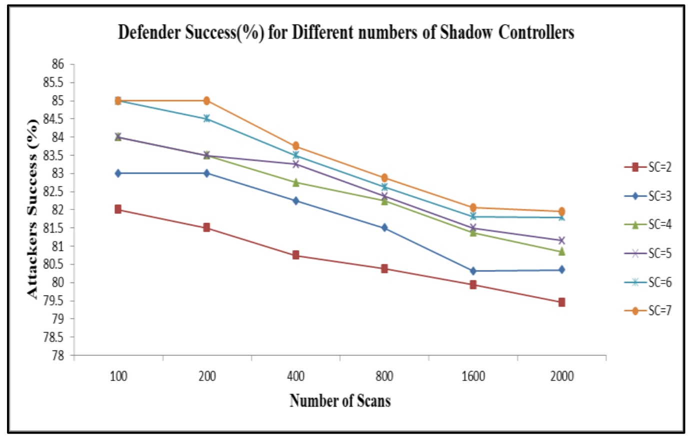

Fig. 8. Successful Response from Shadow Controllers.

TABLE. III. DEFENDER SUCCESS AGAINST NUMBER OF SCANS AND DIFFERENT NUMBER OF SHADOW CONTROLLERS

Controllers	Number of Scans		Number of Shadow Controllers(SC)					
			SC=2	SC=3	SC=4	SC=5	SC=6	SC=7
3	100	Defender Success (%)	82	83	84	84	85	85
3	200		81.5	83	83.50	83.5	84.5	85
3	400		80.75	82.25	82.75	83.25	83.5	83.75
3	800		80.37	81.50	82.25	82.37	82.62	82.87
3	1600		79.93	80.31	81.37	81.50	81.81	82.06
3	2000		79.45	80.35	80.85	81.15	81.8	81.95

TABLE. IV. RECONNAISSANCE OF SDN NETWORK WITH AND WITHOUT SMTSC

Controllers	Number of Scans	Attacker Success against Native SDN	Number of Shadow Controllers(SC)					
			SC=2	SC=3	SC=4	SC=5	SC=6	SC=7
3	100	97	18	17	16	16	15	15
3	200	195	37	34	33	33	31	30
3	400	391	77	71	69	67	66	65
3	800	788	157	148	142	141	139	137
3	1600	1569	321	315	298	296	291	287
3	2000	1962	411	393	383	377	364	361

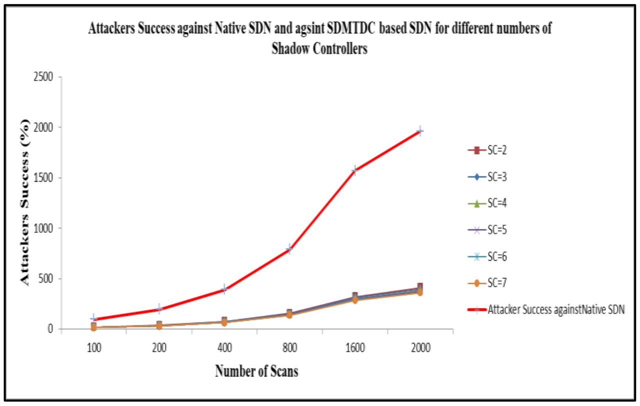

Fig. 9. Reconnaissance of SDN Network with and without SMTSC.

V. Conclusion

In this paper SDN based MTD SMTSC has been proposed. The SMTSC is distributed SDN Controller based system. It uses shadow Controllers to respond to the reconnaissance traffic directed towards the SDN Controllers. The notion is the protection of the brain of SDN. Another benefit of SMTSC is the distributed control plane for providing high availability and resilience for SDN network. The proposed model was analyzed against Reconnaissance attacks as well the overhead it introduces in the network. The results showed significant increase in the attackers' cost at minimum overhead in the system.

In future, we want to investigate in detail the impact of Multi-controller approach on users' privacy and protection against such privacy leakages. Moreover, another area that we will target is the crossfire attacks DDoS protection using this framework.

References

[1] F. Chong, R. Lee, A. Acquisti, W. Horne, C. Palmer, A. Ghosh, et al., "National Cyber Leap Year Summit 2009: Co-chairs' Report," NITRD Program, 2009.

[2] P. K. Manadhata, "Game theoretic approaches to attack surface shifting," in Moving Target Defense II, ed: Springer, 2013, pp. 1-13.

[3] J. Zheng and A. S. Namin, "A Survey on the Moving Target Defense Strategies: An Architectural Perspective," Journal of Computer Science and Technology, vol. 34, pp. 207-233, 2019.

[4] B. G. Assefa and Ö. Özkasap, "A survey of energy efficiency in SDN: Software-based methods and optimization models," Journal of Network and Computer Applications, 2019.

[5] J. H. Jafarian, E. Al-Shaer, and Q. Duan, "Openflow random host mutation: transparent moving target defense using software defined networking," in Proceedings of the first workshop on Hot topics in software defined networks, 2012, pp. 127-132.

[6] Aydeger, N. Saputro, and K. Akkaya, "A moving target defense and network forensics framework for ISP networks using SDN and NFV," Future Generation Computer Systems, vol. 94, pp. 496-509, 2019.

[7] S.-Y. Chang, Y. Park, and B. B. A. Babu, "Fast IP Hopping Randomization to Secure Hop-by-Hop Access in SDN," IEEE Transactions on Network and Service Management, vol. 16, pp. 308-320, 2019.

[8] H.-q. Zhang, C. Lei, D.-x. Chang, and Y.-j. Yang, "Network moving target defense technique based on collaborative mutation," computers & security, vol. 70, pp. 51-71, 2017.

[9] A. Abdou, P. C. Van Oorschot, and T. Wan, "Comparative analysis of control plane security of sdn and conventional networks," IEEE Communications Surveys & Tutorials, vol. 20, pp. 3542-3559, 2018.

[10] F. Bannour, S. Souihi, and A. Mellouk, "Distributed SDN control: Survey, taxonomy, and challenges," IEEE Communications Surveys & Tutorials, vol. 20, pp. 333-354, 2018.

[11] N. Z. Bawany and J. A. Shamsi, "SEAL: SDN based secure and agile framework for protecting smart city applications from DDoS attacks," Journal of Network and Computer Applications, vol. 145, p. 102381, 2019.

[12] B. Lantz, B. Heller, and N. McKeown, "A network in a laptop: rapid prototyping for software-defined networks," in Proceedings of the 9th ACM SIGCOMM Workshop on Hot Topics in Networks, 2010, p. 19.

[13] P. Berde, M. Gerola, J. Hart, Y. Higuchi, M. Kobayashi, T. Koide, et al., "ONOS: towards an open, distributed SDN OS," in Proceedings of the third workshop on Hot topics in software defined networking, 2014, pp. 1-6.

[14] Y. Shi, H. Zhang, J. Wang, F. Xiao, J. Huang, D. Zha, et al., "CHAOS: An SDN-Based Moving Target Defense System," Security and Communication Networks, vol. 2017, 2017.

[15] Z. Zhao, F. Liu, and D. Gong, "An SDN-based fingerprint hopping method to prevent fingerprinting attacks," Security and Communication Networks, vol. 2017, 2017.

[16] D. P. Sharma, D. S. Kim, S. Yoon, H. Lim, J.-H. Cho, and T. J. Moore, "Frvm: Flexible random virtual ip multiplexing in software-defined networks," in 2018 17th IEEE International Conference On Trust, Security And Privacy In Computing And Communications/12th IEEE International Conference On Big Data Science And Engineering (TrustCom/BigDataSE), 2018, pp. 579-587.

[17] A. Azzouni, O. Braham, T. M. T. Nguyen, G. Pujolle, and R. Boutaba, "Fingerprinting OpenFlow controllers: The first step to attack an SDN control plane," in 2016 IEEE Global Communications Conference (GLOBECOM), 2016, pp. 1-6.

[18] M. Conti, F. De Gaspari, and L. V. Mancini, "A novel stealthy attack to gather SDN configuration-information," IEEE Transactions on Emerging Topics in Computing, 2018.

[19] S. Achleitner, T. F. La Porta, P. McDaniel, S. Sugrim, S. V. Krishnamurthy, and R. Chadha, "Deceiving Network Reconnaissance Using SDN-Based Virtual Topologies," IEEE Transactions on Network and Service Management, vol. 14, pp. 1098-1112, 2017.

[20] A. Chowdhary, A. Alshamrani, D. Huang, and H. Liang, "MTD analysis and evaluation framework in software defined network (MASON)," in Proceedings of the 2018 ACM International Workshop on Security in Software Defined Networks & Network Function Virtualization, 2018, pp. 43-48.

[21] D. Fleck, A. Stavrou, G. Kesidis, N. Nasiriani, Y. Shan, and T. Konstantopoulos, "Moving-target Defense against Botnet Reconnaissance and an Adversarial Coupon-Collection Model," in 2018 IEEE Conference on Dependable and Secure Computing (DSC), 2018, pp. 1-8.

[22] H. Jin, Z. Li, D. Zou, and B. Yuan, "DSEOM: A Framework for Dynamic Security Evaluation and Optimization of MTD in Container-based Cloud," IEEE Transactions on Dependable and Secure Computing, 2019.

[23] G. Lin, M. Dong, K. Ota, J. Li, W. Yang, and J. Wu, "Security Function Virtualization Based Moving Target Defense of SDN-Enabled Smart Grid," in ICC 2019-2019 IEEE International Conference on Communications (ICC), 2019, pp. 1-6.

[24] F. Song, Y.-T. Zhou, Y. Wang, T.-M. Zhao, I. You, and H.-K. Zhang, "Smart collaborative distribution for privacy enhancement in moving target defense," Information Sciences, vol. 479, pp. 593-606, 2019.

[25] K. Park, S. Woo, D. Moon, and H. Choi, "Secure cyber deception architecture and decoy injection to mitigate the insider threat," Symmetry, vol. 10, p. 14, 2018.

[26] A. Roy, A. Chhabra, C. A. Kamhoua, and P. Mohapatra, "A moving target defense against adversarial machine learning," in Proceedings of the 4th ACM/IEEE Symposium on Edge Computing, 2019, pp. 383-388.

[27] M. Roesch, "Snort: Lightweight intrusion detection for networks," in Lisa, 1999, pp. 229-238.

[28] G. F. Lyon, Nmap network scanning: The official Nmap project guide to network discovery and security scanning: Insecure, 2009.

Scientific Text Sentiment Analysis using Machine Learning Techniques

Hassan Raza[1], M. Faizan[2], Ahsan Hamza[3], Ahmed Mushtaq[4], Naeem Akhtar[5]
School of Computer Sciences
National College of Business Administration and Economics
Lahore, Pakistan

***Abstract*—Over time, textual information on the World Wide Web (WWW) has increased exponentially, leading to potential research in the field of machine learning (ML) and natural language processing (NLP). Sentiment analysis of scientific domain articles is a very trendy and interesting topic nowadays. The main purpose of this research is to facilitate researchers to identify quality research papers based on their sentiment analysis. In this research, sentiment analysis of scientific articles using citation sentences is carried out using an existing constructed annotated corpus. This corpus is consisted of 8736 citation sentences. The noise was removed from data using different data normalization rules in order to clean the data corpus. To perform classification on this data set we developed a system in which six different machine learning algorithms including Naïve-Bayes (NB), Support Vector Machine (SVM), Logistic Regression (LR), Decision Tree (DT), K-Nearest Neighbor (KNN) and Random Forest (RF) are implemented. Then the accuracy of the system is evaluated using different evaluation metrics e.g. F-score and Accuracy score. To improve the system' accuracy additional features selection techniques, such as lemmatization, n-graming, tokenization, and stop word removal are applied and found that our system provided significant performance in every case compared to the base system. Our method achieved a maximum of about 9% improved results as compared to the base system.**

Keywords—Sentimental analysis; scientific citations; machine learning; scientific literature; classification

I. Introduction

Sentiment analysis of scientific citation is very well discussed and interesting topic in this era where WWW is excessively loaded with an enormous amount of text data [62]. This data contains tons of important information inside itself that can be very beneficial after being analyzed based on requirements. Sentimental analysis is also known as opinion mining that means to find out or identify the positive, negative, neutral opinions, views, attitudes, impressions, emotions and feelings indicated in the text [8]. Opinion mining from the citations is of prime importance because citations from the papers reinforce arguments and connect it to intellectual [25][47][84]. From the last decade, the importance opinion mining or sentimental analysis is mentioned by [86][91][93][94] as a research on a citation function.

We choose more specifically scientific domain as a problem statement in order to analyze the sentiments of citation sentences extracted from different scientific research papers just because of linguistic differences in this domain. A lot of work has been done previously in other genres like English and Chinese as compared to the scientific domain. Following are the problems related to scientific text has been mentioned in literature: usually, sentiments in scientific citations are hidden and not well expressed, scientific citations are often neutral, prevalent style of writing [9], objective style and personal biased of authors have to be hedged [35][64]. Conventionally scientific citations are written in dual-mode and that is also a problem in scientific literature. Some authors apply the strategy of dual-mode like prefacing some criticism after a light appraisement[55]. Identifying such opinions is a challenging task. Such kind of expressions are also found in other types of literature as well [96].

In this work citation sentence refers to the reference of other's papers in the text of a given scholarly work, the former will be known as cited and the latter is called citing paper as well. Along with the citation sentences usually, the citation references are mentioned using different styles and standards. One such famous standard of writing citations' references is "Harvard Style" that uses the author's last name followed by the year of publication [9].

In this research work, we have done sentimental analysis of scientific citations by using an annotated corpus consists of citation sentences developed by [9]. The corpus is made up of 8736 citation sentences constructed from the scientific domain related research papers extracted from ACL (Association for Computational Linguistics) Anthology. The corpus is annotated using some rules to assign the polarity to citation sentences. We have developed a system based on six different machine learning algorithms including Naïve-Bayes, Support Vector Machine, Logistic Regression, Decision Tree, K-Nearest Neighbor and Random Forest. Accuracy of the classification algorithms has been evaluated using different evaluations measures e.g., F-Score and Accuracy score to evaluate the classification system' correctness. To improve our system' performance, we have used different features selection techniques like lemmatization, n-gaming, tokenization, stop words and punctuation removal. After successful experimentation we have found that our system outperforms in each case as compare to the method adopted by the[9]. The maximum outperformance we achieved is 87% F-score as compare to 78% F-score reported by [9] which results in 9% improvement than [9].

II. Literature Review

To carry out this study, literature review is held out to analyze the current state of the domain. In the last couple of years, the interest towards the research in sentimental analysis has been increased for different domains but less work has been done on the scientific literature due to some problems mentioned above.

Sentimental classifiers can be developed using two machine learning approaches named Supervised and Unsupervised learning [50]. The most famous approach to build a classifier is supervised learning. In supervised approach, the classifier requires labeled training data. Yet the training data is to be annotated using manual or automatic approaches on the basis of some predefined rules. Using predefined rules the citation sentences are annotated as positive, negative and neutral. For the purpose of annotations, human annotators are required. While in the case of an unsupervised approach, there is no need for labeled training data. Instead, there is a need for sentiment lexicon to assign polarities to citation sentences. This approach is very difficult because it requires different varieties of a lexicon for different genres. From the literature review, we found that many researchers used supervised while others relyied on unsupervised approach.

Author in [23] worked on automatic citataion classification. Another work has been done in order to analyze the behaviors of authors, readers of research papers in the scientific field by [39]. The analysis was regarding the authors of research papers, how they frame their citations, how readers become interested in the citations of authors and how these processes contribute towards the maturity of Natural Language Processing (NLP). For the sake of analyzing the contributions and purpose of citations based on behavioral analysis, authors classify their data using two different schemes [20]. They prepared the data set of citation sentences extracted from 52 papers from ACR (Anthology Reference Corpus) and annotated the data set using some guidelines based on ACR [16]. They used core aspects of prior citation based on annotation schemes mentioned by [30][31][94][95]. BRAT Tool was used to perform the annotations [85]. They used the Random Forest classifier implemented using Sickit-learn [101]. The major reason of choosing this classifier is its ability to perform effecient for larger feature sets [21][98]. Structural features and grammatical features were used for the classification [28][30][31]. They compared their evaluation results with [89]. Their method with different features shows salient behavior of writers, readers and domain. We have also used a supervised learning approach and developed a system in which multiple machine learning classifiers are implemented. As input, our system takes corpus consisted of labeled citation sentences, to performs classification and also evaluate the classification accuracy of the system. To Increase the efficiency and system accuracy, we have applied different features selection techniques in the data pre-processing phase. Our data set consists of a huge set of citation sentences. Our system performed better than [9].

While processing the citations, finding the implicit citation is also a problem and this problem was addressed by [63]. In their work, the major goal was to identify the implicit citations with the help of improving citation context detection methods [63]. As the research work by [10] was restricted up to the detection of the author's sentiments towards citation reference. In order to create a summary of reference citations, text data may also helpful [72]. Mostly the negative opinions are appeared in explicit citations [10]. [81] claimed that researchers only read 20% of the papers to get the desired information. Different authors have different intentions towards the citations. The intentions of the author were classified using manually constructed and compared cue-phrases against citation context [90]. Citations' context detection is also helpful for creating summaries of different research topics that can support researchers to get a detailed and convenient view of papers [72]. The importance of citation context can also be felt from the fact that all the information retrieval systems that incorporate the concept of citation context have better retrieval effectiveness [73]. The authors developed a system in which data set prepared by [12] and [10] were tested using the method from the work of [72]. The data set consisted of 852 papers from ACL Anthology. To boost up the efficiency and accuracy results of the system authors applied some new classification features like sentence features and sentence similarity measures. The accuracy of the system was evaluated and find out that the system performed better. Our approach is totally different in which we have used new and different classification algorithms and different features have been used by us to improve the system accuracy scores. And our system outperformed the state of the art.

Another work is done in the domain of sentimental analysis which is not in English, Chinese or scientific domain but specifically in the Urdu domain [59], as very less work was done in the Urdu language [56]. They used the data set based on Urdu reviews related to movies, politics, mobile, dramas and miscellaneous domains extracted using scrapers as well as manual. The data set was then classified using different types of supervised learning classifiers and compare their results with each other.

Author in [67] used labeled data for the purpose of classification, they preferred the supervised learning approach. For the purpose of classification, the Naïve Bayes classifier is used. In this work, they have used a dataset of movie reviews. The reviews were classified as positive or negative based on their ratings. After the experimental evaluations, the system achieved an accuracy score of 83%. We have followed a totally different approach in this work as our method is based on the scientific domain. Our approach is comprised of not only one classifier as well as our system accuracy score is better than [67].

Another work following the supervised approach is done by [96]. They have developed a system that distinguishes between sentence-level as well as contextual polarity. In this work, their data set was comprised of 8984 sentences extracted from 425 documents. Their method gave 76 % accuracy.

In sentimental analysis, researchers used semi-supervised and unsupervised learning approaches. The importance of the ML approaches is based on the need and specific scenario. In the sentiment analysis of English text, the impact of an adjective in sentence is of potential effect. First, there should be the identification of adjective orientation in a sentence. The orientation of adjectives will decide the state of a sentence whether should be positive or negative. One such work that contributed towards the identification of adjective orientation is done by [28] and they followed the unsupervised approach. They presented a method for identifying adjectives' semantic orientation in a sentence. They suggested that orientation' information depends upon the conjunction between adjectives, where AND refers to similar conjunction e.g. "Fair and Honest" while BUT refers to different orientation e.g. "Simple but popular". They used a well-known lexicon named Wall Street Journal Corpus for extracting the conjunctions of adjectives. For the sake of determining orientation, they used a log-linear model and achieved 78% accuracy of the system. Similar work was done by [92] following the unsupervised mechanism, also worked on the orientation of words. They found out the estimated Point Mutual Information of each phrase to calculate semantic orientation and the system achieved an accuracy score of 74%. [92] extracted the sentences that contain adjectives using the POS tag pattern lexicon. They found that the large size of lexicon can be better to achieve outperform classification results.

One such work is presented by [87] in which expansion towards the lexicon is considered by using the concept of text position. They used the position of text in order to expand lexicon to get better-classified results. They used the concept of assigning weights to the parts of the text. They tend to assign more weight to more subject-oriented part while less weight to the less subject-oriented part. This method achieved an accuracy score of 65%, later they found that this technique is not as efficient as they expected. The authors expanded the lexicon by measuring the co-occurrence of words inside the sentence. For the classification of data semantic orientation of each sentence is calculated, and by applying the density estimation positive and negative polarities are assigned to sentences. This system achieved an accuracy score of about 90%.

III. Methodology

The purpose of the methodology is defined in this section. Our methodology is depicted in Fig. 1. First of all, we used the annotated dataset prepared by [12] mentioned in section V. We used python based machine learning library named Scikit-Learn [68] for implementing the system**.** Scikit-Learn is a well-known machine learning library tightly integrated with Python language and provides easy-to-interact interface [68]**.** First of all our system reads the data stored in the file having(Tab Separated Values) format. After reading, preprocessing phase is applied to clean and prepare the data for the use of machine learning algorithms. Directly text data cannot be given to machine learning algorithms, it should be converted into a suitable type. Using Scikit-Learn module named "count vectorizer", the text data firstly convert into numeric format and prepare the matrix of tokens count, now the data is ready for machine learning algorithms. Then 60% of data is splitted randomly to train the classifier and 40% for testing the classifier' accuracy. We perform our experiments in two phases, firstly we just apply N-grams (Length 1-3) features on data and compute accuracies using equation (1) and equation (2). Secondly, in order to improve the accuracy scores, we apply other features like(stop words & punctuation removal, lemmatizationnm, etc.) along with n-grams and then again compute the accuracies. The latter approach helps to reduce the noise and complexity of the data. Thirty iterations of each experiment were conducted to compute average results and a total of six experiments were performed. After computing the accuracies of each phase, we then select the best feature which is giving the best result and which classifier is better in a specific scenario.

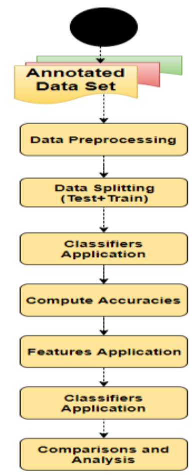

Fig. 1. Step by Step Flow of System Working.

IV. Evaluation Metrics

The evaluation of any research product decides the status and quality of that specific research work. This section briefly describes the metrics used to evaluate the sentimental analysis system we developed. The performance of sentimental analysis system is evaluated by computing the accuracy of the classification results given by the system. Accuracy of the system is to be mentioned in the form of some units that include F-score and Accuracy score. In our evaluation phase, we have calculated both Macro-F Score as well as Micro-F Score. Where FP is considered an error of type-1 and FN is considered an error of type-2. F-score is commonly used, a harmonic mean between precision and recall.

$$\text{Fscore} = (1+\beta^2)\frac{\text{Precision}*\text{Recall}}{\beta^2*\text{Precision}+\text{Recall}} \quad (1)$$

$$\text{Accuracy} = \frac{TP+TN}{TP+FN+FP+TN} \quad (2)$$

V. Corpus Construction

As mentioned earlier, we have used the data set prepared by [9]. However, we are going to highlight the process of corpus construction. As the authors restricted themselves to the field of computational logistics**,** they preferred to use the ACL (Association for Computational Linguistics) anthology mentioned by [16][29]. This digital archive contains journal and conference papers in PDF format since 1965 [15]. At the time of work done by the [9] the archive contains about 21,800 papers. The ACL anthology neither provides fully machine-readable text nor citation information that was a problem so this problem was solved by the resource of ACL anthology that provides the paper text converted from PDF using automated tools. The detailed corpus data is consists of 8736 citation sentences.

A. Citation Sentiment Annotations

Data annotation was done according to some defined rules. Citation sentences are classified into 3-classes positive, negative and neutral. The guidelines used for the annotation are as follows:

B. Annotation Guidelines Negative

- If direct mention of the problem or shortcoming of cited paper.
- If citing paper improves upon the cited paper.
- If citing paper gives outperform evaluation than cited paper.

Positive:

- If direct mention of the positive attribute of the cited paper.
- If citing paper not improves upon the cited paper.
- If citing paper gives not outperform evaluation than cited paper.

Neutral:

- If neither positive nor negative sentiment regarding the citation sentence is mentioned it will be tagged as neutral.

C. Total Annotated Corpus Statistics

The final sentiment corpus consists of 8736 sentences which were annotated using the above-mentioned rules. Here is the statistics of the sentiment annotated sentiment corpus in Table I.

TABLE. I. CORPUS ANNOTATION STATISTICS

Class	**Count**	**Percentage**
Positive	829	9.5 %
Negative	280	3.2 %
Neutral	7,627	87.3 %
Total	8,736	100 %

VI. CLASSIFICATION PROCESSING

This section gives brief details about the classification process used in this paper. The classification process is comprised of multiple processes like Data Pre-processing, Features Selections and classification classifiers used are discussed in details.

A. Data Pre-Processing

As mentioned in section V that corpus used for sentimental analysis classification is prepared or constructed by the [9]. This data set is comprised of a total of 8,736 citation sentences annotated as positive, negative, and neutral after applying rules. From total citation sentences, 60% of sentences were chosen randomly for training the classifier and the rest of 40% data was used for classifier' testing. The data set was cleaned to get the highest accuracy of the system. The following mentioned rules are used for normalization as shown in Table II.

TABLE. II. DATA NORMALIZATION RULES

No	**Original Sign**	**Convert into**
1	,	No change
2	:	No change
3	^	No Change
4	(jing , 2008)	<CIT>
5	(	-LRB-
6	)	-RRB-
7	[	-LRB-
8	]	-RRB-
9	{	-LCB-
10	}	-RCB-
11	.	Eliminate
12	\	Eliminate
13	|	Eliminate
14	**%**	**\%**
15	**Successive Citation**	**<OTH>**
16	**‘**	**\’**
17	*****	*****

B. Features Selection

For the sake of developing a system for sentiment analysis, different features are provided by ML framework [67][96][54]. We have used various features e.g. lemmatization, n-grams, stop words and term-document frequency to evaluate the classifier' accuracy. Later the evaluation results will be displayed.

C. Lemmatization

Lemmatization is a process of normalizing the inflected forms of words [70]. Homographic words cause ambiguity that disturbs searching accuracy and this ambiguity may also occur due to inflectional word forms [44]. For instance, words like “Talking”, “Talks” and “Talked” are the inflected forms of the word “Talk”. The process of lemmatization and stemming is similar with minor changes [70], while the benefits of both approaches are the same. We have applied only lemmatization and avoid stemming due to the problems of stemming process. The stemming process is worthwhile for short retrieval lists [11][27][34], while our system has to deal with large data set and processing lists so we did not apply stemming. Stemming performs normalization of inflected words by keeping different variations of words along with their derivation process [4][46][69]. The stemming process produces more potential results for the languages other than English – for example, Slovenian [71], French, modern Greek [41], Arabic [1] and Swedish [74], because other languages include less inflected form of words than English. In our case, we are dealing with the data set containing the Citation Sentences written in the English language.

D. N-Grams

N-grams refer to the combination of sequenced words in a text, where n means the number of words in that combination. If the N = 1, then it means a single word in a text if N = 2 then it leads to the combination of two sequenced words. We used 3 different kinds of N-grams in our classification that generate different results. The example of these N-grams with different values of N based on the sentence “I like to do research” is given in Table III.

Author in [67] claimed that uni-grams and bi-grams performed well for movie reviews data. In our work, we have applied tri-grams because tri-grams play a substantial part in scientific text [40].

E. Stop Words and Punctuation

English text contains a lot of meaningless and non-informative words [52] called stop words. These are not required in classification because their presence just increase the size of data. So we applied stop words removal technique in order to cleanse the data for better and efficient classification [80]. Some research works support the stop words removal from the data set to reduce the dimensions of data [13][7][66][24][45][83], while some researchers are against the removal of stop words because these words contain sentiment information [75][57][32][33]. The earliest work that contributes to the removal of stop words by [53], in which they advised that words can be categorized into two types (i) keywords and (ii) non-keywords and the latter were called as stop words. There are also pre-compiled stop word lists such as Van, Brown [22], called classic stop or standard stop lists. Later these stop word lists are criticized for being out dated [82][52]. We have used the latest and up to date, NLTK stop words list that provides 180 plus stopwords.

F. Term Document Frequency

Term document frequency refers to the count of specific words in the document [99]. We also used the concept of finding the term document using vectorizer.

G. Classification Classifiers

After preprocessing and features selection the very next step is to apply classification algorithms. Many text classifiers have been purposed in literature [19][36]. We have used 6 algorithms of machine learning including Naïve-Bayes (NB), Support Vector Machine (SVM), Logistic Regression (LR), Decision Tree (DT), K-Nearest Neighbor (KNN), and Random Forest (RF).

a) Naïve Bayes: Naïve- Bayes is the most popular classification algorithm due to its simplicity and effectiveness [42][76]. This classifier works according to the concept of Bayes theorem [26]. It’s a kind of module classifier [102] that follows the idea of probabilities for the purpose of classification. Bernoulli and multinomial are the models of naïve Bayes classifier [49][2][58], Binarized Naïve Bayes model is described by [26].

b) Support Vector Machine: In the world of machine learning one such supervised learning algorithm that achieves enough improvements on a variety of tasks is a Support vector machine classifier [37]. Particularly in the case of analyzing the sentiments, SVM has demonstrated good results [67][96][54][43]. In-text classification the SVM contributes towards excellent precision scores while poor recall scores while adjusting the thresholds recall scores can be adjusted [36]. Adjustment of thresholds is of vital importance, a study by [78] described the mechanism of automatically adjusting the thresholds of SVM.

TABLE. III. N-GRAM EXAMPLE

N values	Called	Example
N=1	Unigram	I, like, to, do, research
N=2	Bi-gram	I like, like to, to do, do research
N=3	Trigram	I like to, like to do, to do research

c) Decision Tree: In various fields of text classification the use of decision tree classifier can be seen and analyzed [61]. Its popularity is based on the nature of classification rules that make it interesting for NLP researchers [14]. The decision is constructed by selecting the data from the data set randomly [3]. The information gain is calculated for all values and the feature with the highest information gain value becomes the tree's root [59] and the whole tree is constructed by finding the features for the next level again and again. The fast decision tree algorithm is developed by [38]. So the solution for such kind of a scenario is presented by [60].

d) Random Forest: [18] mentioned the importance of a random forest classifier and compared its performance with the other classifiers. [5][18] claimed that the random forest algorithm provides efficient and discriminative classification, as a result, it is considered an interesting classifier. [48][65] were the first who discussed the importance of random forest classifier in the field of computer vision. [97][79] Introduced class recognition based on random forest. [100][101] used random forest for bi-layer video segmentation, [17] used it for image classification, and [6] used it for personal identification.

e) K-th Nearest Neighbour: KNN is a simple and efficient classifier [88]. Called lazy learner because its training phase contains nothing but storing all the training examples as classifiers [77]. KNN requires a lot of memory while storing the training values [59]. The performance issue of KNN can also be solved by efficient estimations of parameters [51].

VII. RESULTS

For the sake of performing the experimental task, we have used the data set mentioned in Section V. The data is labeled using positive, negative, and neutral classes using annotated rules mentioned in Section V. Different machine learning algorithms used for the classification discussed in Section VI. The evaluation metrics mentioned in Section IV (Equation 1, 2) were used to validate the system. The detailed description of the experimental results using evaluation metrics is defined in Table IV, and Table V. In these tables terms, A1, B1, C1 denotes simply unigram, bigram, trigram features while A2, B2, and C2 denote the application of unigram, bigram, trigram along with other features. Table IV shows that Overall DT using n-grams gives the best F-score in macro while RF is best in case of micro average. LR is also overall best in the micro average without applying extra features. Uni-gram plays support in better performance of LR and DT, uni-gram along with other features plays significant performance in NB, KNN, and RF. DT gives better performance in the case of uni-grams, bi-grams, and tri-grams. LR performance is significant in case of uni-grams only, k-th nearest neighbor outperforms in case of n-grams along with other features and give worst performs without other features while RF performs best as same as KNN. The overall discussion describes that uni-gram, bi-gram, and tri-gram without other features perform best where uni-gram is at first position.

Table V shows that Overall SVM, LR, and RF performed very best with the highest accuracy scores. N-grams play significant performance in NB, SVM gives the best accuracy using uni-gram, LR performance is significant in case of bi-grams and tri-grams, KNN outperforms in case of n-grams without other features and gives worst performs with other features. The overall discussion describes that uni-gram, bi-grams, and tri-grams without other features performs best and give significant accuracy scores.

TABLE. IV. F-SCORES AFTER THIRTY ITTERATIONS

Features	**NB**		**SVM**		**LR**		**DT**		**KNN**		**RF**	
	Macro Scores %	**Micro Scores %**	**Macro Scores %**	**Micro Scores %**	**Macro Scores %**	**Micro Scores %**	**Macro Scores %**	**Micro Scores %**	**Macro Scores %**	**Micro Scores %**	**Macro Scores %**	**Micro Scores %**
A1	36	87	37	88	49	88	49	85	33	87	44	88
A2	49	83	48	87	46	87	48	85	34	87	46	88
B1	34	87	31	87	46	88	49	86	32	87	44	88
B2	46	79	47	87	46	87	48	85	34	87	46	88
C1	36	87	31	87	44	88	49	86	32	87	42	88
C2	45	77	46	87	46	87	48	85	34	87	46	88

TABLE. V. ACCURACY SCORES AFTER THIRTY ITTERATIONS

Features	**NB %**	**SVM %**	**LR %**	**DT %**	**KNN %**	**RF %**
A1	87	87	87	87	87	88
A2	83	88	84	87	86	88
B1	87	88	88	87	87	88
B2	79	88	85	87	86	88
C1	87	88	88	87	87	88
C2	77	88	86	87	86	88

VIII. CONCLUSION

In this research work, we presented a sentiment analysis system for scientific text. We have used different machine learning classifiers namely NB, SVM, DT, LR, KNN and RF along with different features to process the data and optimize the classification results. Experiments are performed on the data set prepared by the [9]. Data set is partitioned into training and testing sets according to the ratio of 60:40 and. Accuracies of the classifiers are computed by using various evaluation metrics like F-score, and Accuracy score. The results show that SVM performs better than other classifiers. After SVM Naïve Bayes performs well. In the case of the macro average, the performance of SVM classifier is best while computing F-score, and accuracy measures while the random forest is best in case of micro average. Uni-grams, bi-grams, and tri-gram features performed very well and support the classifiers to achieve highest accuracy scores.

We compared our findings with [9] in the experimental phase based on different features. We used the n-grams approach together with the lemmatization process to reduce the data dimensions as the latter approach was not applied by the [9]. Table VI describes the comparative analysis of our work and the work of [9].

The author of [9] used NB and SVM classifier and compute the accuracies of the system using an F-score. In this paper, we have implemented six classifiers LR, DT, KNN, and RF including NB, SVM used by [9]. We computed the accuracies by increasing the number of evaluation metrics F-score and accuracy including F-score used by [9] to evaluate the accuracies with the base system. Our results showed significant improvement like in the case of Naïve Bayes using uni-gram feature we achieved micro-F 87% while the base system described the result of micro-F = 78% and our results are approximately 9 % better.

Macro-F scores using uni-gram mentioned in the research work of [9] is 48% and we achieved the macro-F = 49% by reducing the data dimensions by using the lemmatization process and stop words removal mechanism. Based on bi-gram and tri-gram features our system achieved the same result of micro-F = 87%. The micro-F of [9] based on bi-gran and tri-gram features decreased from 78% to 76%. In our case, the micro-F based on bi-gram and tri-gram features increased by 11 %. While in the case of bi-gram and trigram research work of [9] showed the macro-F score of 47%, where our method achieved a macro-F score of 46% using bi-gram and 45% using tri-gram. Overall using Naïve Bayes classifier [9] work achieved maximum of (micro-F score = 78%, macro-F score = 48) while we improved our results to extant and achieved maximum of (micro-F = 87%, macro-F = 49%) that shows the significant improvement of our work.

TABLE. VI. COMPARATIVE ANALYSIS OF OUR WORK WITH [9]

Characteristics	[9]	Our Method
Classification algorithms used	2	6
Evaluation metrics used	1	2
Naïve Bayes F-scores	78 %	87 %
SVM F-scores	86 %	88 %

The second classifier used by the [9] is SVM. We also implemented SVM based on the same features and our results outperform [9]. In the case of using uni-gram, bi-gram and tri-gram features in SVM classifier the author [9] reported the micro-F = 86% and our result with micro-F = 88% for uni-gram and shows the significant improvement.

We also implemented other classifiers like DT, LR, KNN, and RF and achieved significant results. LR and DT performed well. In the case LR, we achieved the micro-F score = 88% and for DT micro-F score = 87% and for both macro-F score = 49%. If we compare this result with [9] results than the F-scores show the improvement of approximately 2% for macro-F scores for both LR and DT and approximately 10% for micro-F-score of LR. KNN and RF classifiers give improved results than [9] in the case of an F-score micro average with the improvement of approximately 10 %.

ACKNOWLEDGMENT

First of all, authors would like to thank Almighty Allah for His grace and blessings. Authors would also like to pay thanks their parents, friends and colleagues for their support and encouragement.

REFERENCES

[1] Abu-Salem, H., Al-Omari, M., & Evens, M. W. (1999). Stemming methodologies over individual query words for an Arabic information retrieval system. Journal of the American Society for Information Science, 50(6), 524-529.

[2] Aghila, G. (2010). A Survey of Na\" ive Bayes Machine Learning approach in Text Document Classification. arXiv preprint arXiv:1003.1795.

[3] Ali, J., Khan, R., Ahmad, N., & Maqsood, I. (2012). Random forests and decision trees. International Journal of Computer Science Issues (IJCSI), 9(5), 272.

[4] Alkula, R. (2001). From plain character strings to meaningful words: Producing better full text databases for inflectional and compounding languages with morphological analysis software. Information Retrieval, 4(3-4), 195-208.

[5] Amit, Y., & Geman, D. (1997). Shape quantization and recognition with randomized trees. Neural computation, 9(7), 1545-1588.

[6] Apostolof, N., & Zisserman, A. (2007, September). Who Are You?-Real-time Person Identification. In BMVC (pp. 1-10).

[7] Asiaee T, A., Tepper, M., Banerjee, A., & Sapiro, G. (2012, October). If you are happy and you know it... tweet. In Proceedings of the 21st ACM international conference on Information and knowledge management (pp. 1602-1606). ACM.

[8] Athar, A. (2011, June). Sentiment analysis of citations using sentence structure-based features. In Proceedings of the ACL 2011 student session (pp. 81-87). Association for Computational Linguistics.

[9] Athar, A. (2014). Sentiment analysis of scientific citations (No. UCAM-CL-TR-856). University of Cambridge, Computer Laboratory.

[10] Athar, A., & Teufel, S. (2012, July). Detection of implicit citations for sentiment detection. In Proceedings of the Workshop on Detecting Structure in Scholarly Discourse (pp. 18-26). Association for Computational Linguistics.

[11] Avoy, J. (1999). A stemming procedure and stopword list for general French corpora. Journal of the American Society for Information Science, 50(10), 944-952.

[12] Awais Athar. Citation Context Corpus. http://www.cl.cam.ac.uk/~aa496/citation-context-corpus/. Accessed: 2015-05-13.2,5).

[13] Bakliwal, A., Arora, P., Madhappan, S., Kapre, N., Singh, M., & Varma, V. (2012). Mining sentiments from tweets. In Proceedings of the 3rd Workshop in Computational Approaches to Subjectivity and Sentiment Analysis (pp. 11-18).

[14] Ben-Haim, Y., & Tom-Tov, E. (2010). A streaming parallel decision tree algorithm. Journal of Machine Learning Research, 11(Feb), 849-872.

[15] Bienz, T., Cohn, R., & Adobe Systems (Mountain View, Calif.). (1993). Portable document format reference manual (p. 214). Boston^ eMA MA: Addison-Wesley.

[16] Bird, S., Dale, R., Dorr, B. J., Gibson, B., Joseph, M. T., Kan, M. Y., & Tan, Y. F. (2008). The acl anthology reference corpus: A reference dataset for bibliographic research in computational linguistics.

[17] Bosch, A., Zisserman, A., & Munoz, X. (2007, October). Image classification using random forests and ferns. In 2007 IEEE 11th international conference on computer vision (pp. 1-8). Ieee.

[18] Breiman, L. (2001). Random forests. Machine learning, 45(1), 5-32.

[19] Breiman, L. (2017). Classification and regression trees. Routledge.

[20] Chubin, D. E., & Moitra, S. D. (1975). Content analysis of references: Adjunct or alternative to citation counting?. Social studies of science, 5(4), 423-441.conference on Empirical methods in natural language processing (pp. 129-136). Association for Computational Linguistics.

[21] Fernández-Delgado, M., Cernadas, E., Barro, S., & Amorim, D. (2014). Do we need hundreds of classifiers to solve real world classification problems?. The Journal of Machine Learning Research, 15(1), 3133-3181.

[22] Fox, C. J. (1992). Lexical Analysis and Stoplists.

[23] Garzone, M., & Mercer, R. E. (2000, May). Towards an automated citation classifier. In Conference of the canadian society for computational studies of intelligence (pp. 337-346). Springer, Berlin, Heidelberg.

[24] Gokulakrishnan, B., Priyanthan, P., Ragavan, T., Prasath, N., and Perera, A. (2012). Opinion mining and sentiment analysis on a twitter data stream. In Advances in ICT for Emerging Regions (ICTer), 2012 International Conference on, pages 182–188. IEEE.

[25] Goodwin, J. (1980). Eugene Garfield, Citation Indexing-Its Theory and Application in Science, Technology, and Humanities (Book Review). Technology and Culture, 21(4), 714.

[26] Gupte, A., Joshi, S., Gadgul, P., Kadam, A., & Gupte, A. (2014). Comparative study of classification algorithms used in sentiment analysis. International Journal of Computer Science and Information Technologies, 5(5), 6261-6264.

[27] Harman, D. (1991). How effective is suffixing?. Journal of the american society for information science, 42(1), 7-15.

[28] Hatzivassiloglou, V., & McKeown, K. R. (1997, July). Predicting the semantic orientation of adjectives.

[29] In Proceedings of the 35th annual meeting of the association for computational linguistics and eighth conference of the european chapter of the association for computational linguistics (pp. 174-181). Association for Computational Linguistics.

[30] Hernández-Alvarez, M., & Gomez, J. M. (2016). Survey about citation context analysis: Tasks, techniques, and resources. Natural Language Engineering, 22(3), 327-349.

[31] Hernández-Alvarez, M., & Gómez, J. M. (2015, October). Citation impact categorization: for scientific literature. In 2015 IEEE 18th International Conference on Computational Science and Engineering (pp. 307-313). IEEE.

[32] Hu, X., Tang, J., Gao, H., & Liu, H. (2013, May). Unsupervised sentiment analysis with emotional signals. In Proceedings of the 22nd international conference on World Wide Web (pp. 607-618). ACM.

[33] Hu, X., Tang, L., Tang, J., & Liu, H. (2013, February). Exploiting social relations for sentiment analysis in microblogging. In Proceedings of the

sixth ACM international conference on Web search and data mining (pp. 537-546). ACM.

[34] Hull, D. A. (1996). Stemming algorithms: A case study for detailed evaluation. Journal of the American Society for Information Science, 47(1), 70-84.

[35] Hyland, K. (1995). The Author in the Text: Hedging Scientific Writing. Hong Kong papers in linguistics and language teaching, 18, 33-42.

[36] Ikonomakis, M., Kotsiantis, S., & Tampakas, V. (2005). Text classification using machine learning techniques. WSEAS transactions on computers, 4(8), 966-974.

[37] Joachims, T. (1998, April). Text categorization with support vector machines: Learning with many relevant features. In European conference on machine learning (pp. 137-142). Springer, Berlin, Heidelberg.

[38] Johnson, D. E., Oles, F. J., Zhang, T., & Goetz, T. (2002). A decision-tree-based symbolic rule induction system for text categorization. IBM Systems Journal, 41(3), 428-437.

[39] Jurgens, D., Kumar, S., Hoover, R., McFarland, D., & Jurafsky, D. (2016). Citation classification for behavioral analysis of a scientific field. arXiv preprint arXiv:1609.00435.

[40] Justeson, J. S., & Katz, S. M. (1995). Technical terminology: some linguistic properties and an algorithm for identification in text. Natural language engineering, 1(1), 9-27.

[41] Kalamboukis, T. Z. (1995). Suffix stripping with modern Greek. Program, 29(3), 313-321.

[42] Kim, S. B., Rim, H. C., Yook, D., & Lim, H. S. (2002, August). Effective methods for improving naive bayes text classifiers. In Pacific Rim International Conference on Artificial Intelligence (pp. 414-423). Springer, Berlin, Heidelberg.

[43] Korde, V., & Mahender, C. N. (2012). Text classification and classifiers: A survey. International Journal of Artificial Intelligence & Applications, 3(2), 85.

[44] Korenius, T., Laurikkala, J., Järvelin, K., & Juhola, M. (2004, November). Stemming and lemmatization in the clustering of finnish text documents. In Proceedings of the thirteenth ACM international conference on Information and knowledge management (pp. 625-633). ACM.

[45] Kouloumpis, E., Wilson, T., & Moore, J. (2011, July). Twitter sentiment analysis: The good the bad and the omg! In Fifth International AAAI conference on weblogs and social media.

[46] Krovetz, R. (1993, July). Viewing morphology as an inference process. In Proceedings of the 16th annual international ACM SIGIR conference on Research and development in information retrieval (pp. 191-202). ACM.

[47] Latour, B. (1987). Science in action: How to follow scientists and engineers through society. Harvard university press.

[48] Lepetit, V., & Fua, P. (2006). Keypoint recognition using randomized trees. IEEE transactions on pattern analysis and machine intelligence, 28(9), 1465-1479.

[49] Lewis, D. D. (1998, April). Naive (Bayes) at forty: The independence assumption in information retrieval.

[50] In European conference on machine learning (pp. 4-15). Springer, Berlin, Heidelberg.

[51] Lim, H. S. (2004, November). Improving kNN based text classification with well estimated parameters. In International Conference on Neural Information Processing (pp. 516-523). Springer, Berlin, Heidelberg.

[52] Lo, R. T. W., He, B., & Ounis, I. (2005, January). Automatically building a stopword list for an information retrieval system. In Journal on Digital Information Management: Special Issue on the 5th Dutch-Belgian Information Retrieval Workshop (DIR)(Vol. 5, pp. 17-24).

[53] Luhn, H. P. (1957). A statistical approach to mechanized encoding and searching of literary information. IBM Journal of research and development, 1(4), 309-317.

[54] Maas, A. L., Daly, R. E., Pham, P. T., Huang, D., Ng, A. Y., & Potts, C. (2011, June). Learning word vectors for sentiment analysis. In Proceedings of the 49th annual meeting of the association for computational linguistics: Human language technologies-volume 1 (pp. 142-150). Association for Computational Linguistics.

[55] MacRoberts, M. H., & MacRoberts, B. R. (1984). The negational reference: Or the art of dissembling. Social Studies of Science, 14(1), 91-94.

[56] Malik, M. K. (2017). Urdu named entity recognition and classification system using artificial neural network. ACM Transactions on Asian and Low-Resource Language Information Processing (TALLIP), 17(1), 2.

[57] Martínez-Cámara, E., Montejo-Ráez, A., Martín-Valdivia, M. T., & Ureña-López, L. A. (2013). Sinai: Machine learning and emotion of the crowd for sentiment analysis in microblogs. In Second Joint Conference on Lexical and Computational Semantics (* SEM), Volume 2: Proceedings of the Seventh International Workshop on Semantic Evaluation (SemEval 2013) (Vol. 2, pp. 402-407).

[58] McCallum, A., & Nigam, K. (1998, July). A comparison of event models for naive bayes text classification. In AAAI-98 workshop on learning for text categorization (Vol. 752, No. 1, pp. 41-48).

[59] Mehmood, K., Essam, D., & Shafi, K. (2018, July). Sentiment Analysis System for Roman Urdu. In Science and Information Conference (pp. 29-42). Springer, Cham.

[60] Mehta, M., Agrawal, R., & Rissanen, J. (1996, March). SLIQ: A fast scalable classifier for data mining. In International conference on extending database technology (pp. 18-32). Springer, Berlin, Heidelberg.

[61] Mitchell, T. M. (1997). Does machine learning really work?. AI magazine, 18(3), 11.

[62] Moravcsik, M. J., & Murugesan, P. (1988). Some Results on the Function and Quality of Citations: Social Studies of Science. 研究 技術 計画, 3(4), 538.

[63] Murray, J. (2015). Finding Implicit Citations in Scientific Publications: Improvements to Citation Context Detection Methods.

[64] Oppenheim, C., & Renn, S. P. (1978). Highly cited old papers and the reasons why they continue to be cited. Journal of the American Society for Information Science, 29(5), 225-231.

[65] Ozuysal, M., Fua, P., & Lepetit, V. (2007, June). Fast keypoint recognition in ten lines of code. In 2007 IEEE Conference on Computer Vision and Pattern Recognition (pp. 1-8). Ieee.

[66] Pak, A., & Paroubek, P. (2010, May). Twitter as a corpus for sentiment analysis and opinion mining. In LREc (Vol. 10, No. 2010, pp. 1320-1326).

[67] Pang, B., Lee, L., & Vaithyanathan, S. (2002, July). Thumbs up? sentiment classification using machine learning techniques. In Proceedings of the ACL-02 conference on Empirical methods in natural language processing-Volume 10(pp. 79-86). Association for Computational Linguistics.

[68] Pedregosa, F., Varoquaux, G., Gramfort, A., Michel, V., Thirion, B., Grisel, O., ... & Vanderplas, J. (2011). Scikit-learn: Machine learning in Python. Journal of machine learning research, 12(Oct), 2825-2830.

[69] Pirkola, A. (2001). Morphological typology of languages for IR. Journal of Documentation, 57(3), 330-348.

[70] Plisson, J., Lavrac, N., & Mladenic, D. (2004). A rule based approach to word lemmatization. Proceedings of IS-2004, 83-86.

[71] Popovič, M., & Willett, P. (1992). The effectiveness of stemming for natural-language access to Slovene textual data. Journal of the American Society for Information Science, 43(5), 384-390.

[72] Qazvinian, V., & Radev, D. R. (2010, July). Identifying non-explicit citing sentences for citation-based summarization. In Proceedings of the 48th annual meeting of the association for computational linguistics (pp. 555-564). Association for Computational Linguistics.

[73] Ritchie, A. (2009). Citation context analysis for information retrieval (No. UCAM-CL-TR-744). University of Cambridge, Computer Laboratory.

[74] Rosell, M. (2003). Improving clustering of Swedish newspaper articles using stemming and compound splitting. In NoDaLiDa 2003, Reykjavik, Iceland 2003 (pp. 1-7).

[75] Saif, H., He, Y., & Alani, H. (2012, November). Semantic sentiment analysis of twitter. In International semantic web conference (pp. 508-524). Springer, Berlin, Heidelberg.

[76] Schneider, K. M. (2005, February). Techniques for improving the performance of naive bayes for text classification. In International

Conference on Intelligent Text Processing and Computational Linguistics (pp. 682-693). Springer, Berlin, Heidelberg.

[77] Sebastiani, F. (2002). Machine learning in automated text categorization. ACM computing surveys (CSUR), 34(1), 1-47.

[78] Shanahan, J. G., & Roma, N. (2003, September). Improving SVM text classification performance through threshold adjustment. In European Conference on Machine Learning (pp. 361-372). Springer, Berlin, Heidelberg.

[79] Shotton, J., Johnson, M., & Cipolla, R. (2008, June). Semantic texton forests for image categorization and segmentation. In 2008 IEEE Conference on Computer Vision and Pattern Recognition (pp. 1-8). IEEE.

[80] Silva, C., & Ribeiro, B. (2003, July). The importance of stop word removal on recall values in text categorization. In Proceedings of the International Joint Conference on Neural Networks, 2003. (Vol. 3, pp. 1661-1666). IEEE.

[81] Simkin, M. V., & Roychowdhury, V. P. (2002). Read before you cite! arXiv preprint cond-mat/0212043.

[82] Sinka, M. P., & Corne, D. W. (2003, October). Towards modernised and web-specific stoplists for web document analysis. In Proceedings IEEE/WIC International Conference on Web Intelligence (WI 2003) (pp. 396-402). IEEE.

[83] Speriosu, M., Sudan, N., Upadhyay, S., & Baldridge, J. (2011, July). Twitter polarity classification with label propagation over lexical links and the follower graph. In Proceedings of the First workshop on Unsupervised Learning in NLP (pp. 53-63). Association for Computational Linguistics.

[84] Spiegel-Rosing, I. (1977). Science studies: Bibliometric and content analysis. Social Studies of Science, 7(1), 97-113.

[85] Stenetorp, P., Pyysalo, S., Topić, G., Ohta, T., Ananiadou, S., & Tsujii, J. I. (2012, April). BRAT: a web-based tool for NLP-assisted text annotation. In Proceedings of the Demonstrations at the 13th Conference of the European Chapter of the Association for Computational Linguistics (pp. 102-107). Association for Computational Linguistics.

[86] Swales, J. (1986). Citation analysis and discourse analysis. Applied linguistics, 7(1), 39-56.

[87] Taboada, M., & Grieve, J. (2004, March). Analyzing appraisal automatically. In Proceedings of AAAI Spring Symposium on Exploring Attitude and Affect in Text (AAAI Technical Re# port SS# 04# 07), Stanford University, CA, pp. 158q161. AAAI Press.

[88] Tan, S. (2006). An effective refinement strategy for KNN text classifier. Expert Systems with Applications, 30(2), 290-298.

[89] Teufel, S. (1999). Argumentative zoning: Information extraction from scientific text (Doctoral dissertation, University of Edinburgh).

[90] Teufel, S., Siddharthan, A., & Tidhar, D. (2006). An annotation scheme for citation function.

[91] Teufel, S., Siddharthan, A., & Tidhar, D. (2006, July). Automatic classification of citation function. In Proceedings of the 2006 conference on empirical methods in natural language processing (pp. 103-110). Association for Computational Linguistics.

[92] Turney, P. D. (2002, July). Thumbs up or thumbs down?: semantic orientation applied to unsupervised classification of reviews. In Proceedings of the 40th annual meeting on association for computational linguistics (pp. 417-424).Association for Computational Linguistics.

[93] Valenzuela, M., Ha, V., & Etzioni, O. (2015, April). Identifying meaningful citations. In Workshops at the Twenty-Ninth AAAI Conference on Artificial Intelligence.

[94] White, H. D. (2004). Citation analysis and discourse analysis revisited. Applied linguistics, 25(1), 89-116.

[95] White, H. D., Wellman, B., & Nazer, N. (2004). Does citation reflect social structure?: Longitudinal evidence from the "Globenet" interdisciplinary research group. Journal of the American Society for information Science and Technology, 55(2), 111-126.

[96] Wilson, T., Wiebe, J., & Hoffmann, P. (2009). Recognizing contextual polarity: An exploration of features for phrase-level sentiment analysis. Computational linguistics, 35(3), 399-433.

[97] Winn, J., & Criminisi, A. (2006). Object class recognition at a glance. In Video Proc. CVPR.

[98] Xia, R., Zong, C., & Li, S. (2011). Ensemble of feature sets and classification algorithms for sentiment classification. Information Sciences, 181(6), 1138-1152.

[99] Y. Yang and J. O. Pedersen. A comparative study on feature selection in text categorization. In International Conference on Machine Learning, pages 412–420, 1997.

[100] Yanjun Qi., "Random Forest for Bioinformatics". www.cs. cmu.edu/~qyj/papersA08/11-rfbook.pdf.

[101] Yin, P., Criminisi, A., Winn, J., & Essa, I. (2007, June). Tree-based classifiers for bilayer video segmentation. In 2007 IEEE Conference on Computer Vision and Pattern Recognition (pp. 1-8). IEEE.

[102] Yong-feng, S., & Yan-ping, Z. (2004). Comparison of text categorization algorithms. Wuhan university Journal of natural sciences, 9(5), 798-804.

Enrichment Ontology with Updated user Data for Accurate Semantic Annotation

Haytham Al-Feel[1], Hanaa Ghareib Hendi[2], Heba Elbeh[3]
Faculty of Computers & Information
Fayoum University, Fayoum, Egypt

***Abstract*—Annotation is considered one of the main applications that semantic web applies. The idea beyond annotation focused on adding metadata to existing information which facilitates machines dealing with data that have meanings and can be readable. Semantic annotation is one of the techniques used for the enrichment of web content semantically, which facilitates writing comments and evaluate previously annotated resources that can lead to better search results. Our framework aims to enrich ontology via embedding data directly to ontology in order to have completed and accurate data.**

Keywords—Ontology; Semantic Web; Semantic Annotation; RSS News

I. Introduction

The current web has many problems and limitations where most of the web pages can't be understood by machines, which makes the web flat, boring and also misunderstandings [1]. Semantic Web has many definitions but most of them refer to it as an extension for the current web that links information to each other. It also could link data to anything that could have a Unified Resource Identifier and in this way, the web will be enabled for accurate retrieval [2]. Absolutely, the work is not easy like this but it will include many sophisticated technologies and languages such as the Resource Description Framework (RDF), Web Ontology Language (OWL) and SPARQL as a query language.

Semantic annotation can be defined as adding metadata to available documents that add value and explanation to the web, facilitates the searching process and finding any piece of information especially when these data resources linked to each other [3] [4] [5]. Annotation is a set of explanatory notes that accompanies a text [6].

Ontology considered one of the main players of the semantic web and the backbone for the annotation process that explained as the formal specification for a specific domain explaining its concepts semantically [7]. Ontology triples have main three parts they are: subject which describes a specific resource and identified by a URI, predicate which identifies a property and an object which can be another resource or value as shown in "Fig. 1". Because of syntax and structure which has a lot of details, specifications, and recommendations, regular users do not have the full awareness of ontology to deal with or insert, update and delete data. The task of annotation could enrich content and ontologies in different domains.

Our paper presents a Semantic annotation tool that facilitates the user adding data to available resources according to specific rules and privileges determined by the admin of each website. Admin reviews the user's insertion, whether true or false. If the user insertion is acceptable, in this case, data inserted will be stored in the ontology triple store to enrich ontology. Users do not need to have any background about semantic and ontology to use our tool and framework, just he/she will insert data that will be transformed in the form of subject, predicate, and object.

The remainder of this paper is organized as follows: Section 2, highlights semantic annotation techniques. While Section 3, presents our framework and evaluation. Finally, Section 4 presents our conclusions and further research.

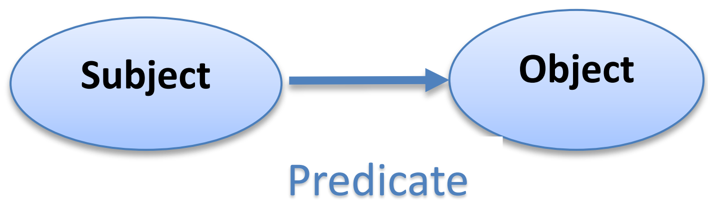

Fig. 1. Ontology Triple Structure.

II. Semantic Annotation

Remarks, comments, notes and any explanations added to a part of web documents are considered annotations to these web documents and if these annotations based on ontologies and semantic web techniques; in this situation, we call them semantically annotated [8]. Semantic annotation is defined as the process of adding data related to ontological concepts to have full metadata description about concepts. The purpose of a semantic annotation is to specify the meaning and properties of an annotated information resource in a generally understandable way [9]. It recognizes the parts of the text and converts into pieces in a data processing mechanism that can be linked to a broader context of data that already exist [10]. In [11] we developed a Semantic Annotation Framework for News Feeds (SANF) which annotates RSS news titles and provides additional information for concepts on the news domain via an ontology contains different categories and concepts in this domain as shown in "Fig. 2". In this paper, we added new features for enhancing the system via adding full authority to the user to add a comment on what retrieved from an ontology which could be later accepted or refused from the administrator. In addition to this, even if a particular user needs a brief annotation of an unannotated object the system does not stand idly; it acts intelligently by looking for an object online in order to perform an annotation process as fully as possible.

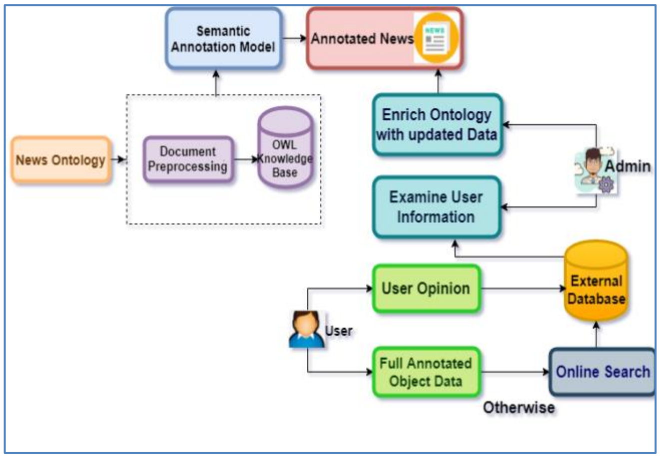

Fig. 2. System Architecture.

III. System Framework

We enhance our proposed system to support the user to have the full ability to insert his/her own metadata into the system repository. After that, the system admin examines and reviews the inserted one in order to enrich ontology with updated data to enrich the data repository.

Each class in the developed ontology has many individuals with its properties and relations which in turn clearly illustrates the components of this class as shown in "Fig. 3".

The system validates URLs entered by users and apply the required process of news titles to finally provide a semantic annotation model to map concepts with its related ontology class. The final stage of the system is an annotated web page of news feeds as shown in "Fig. 4".

If the user selects any of the annotated words, the full annotation would be retrieved then the user can insert his/her reviews about the information retrieved from the ontology as shown in "Fig. 5" where it is stored successfully in an external repository.

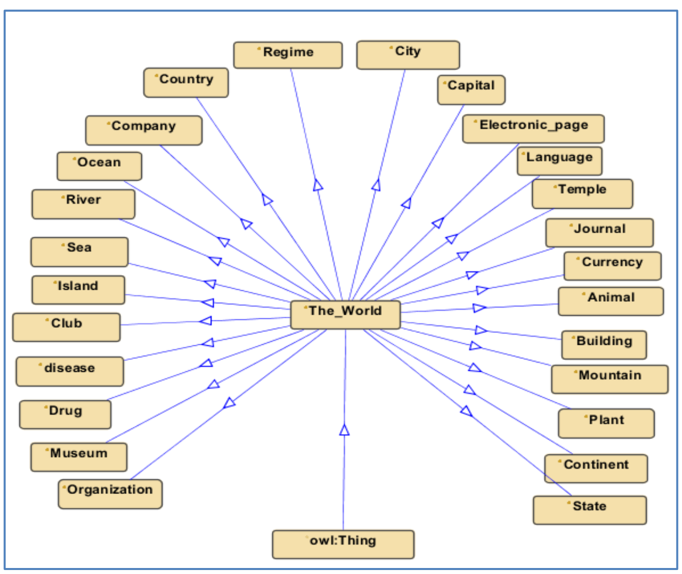

Fig. 3. Top Level Ontology Class.

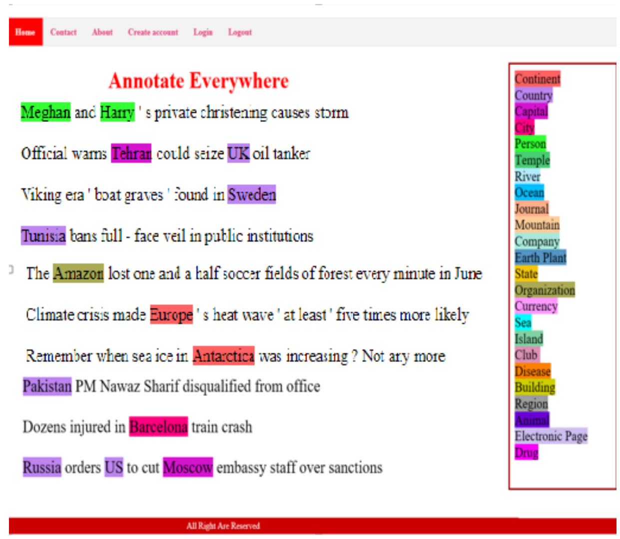

Fig. 4. RSS Final Annotation.

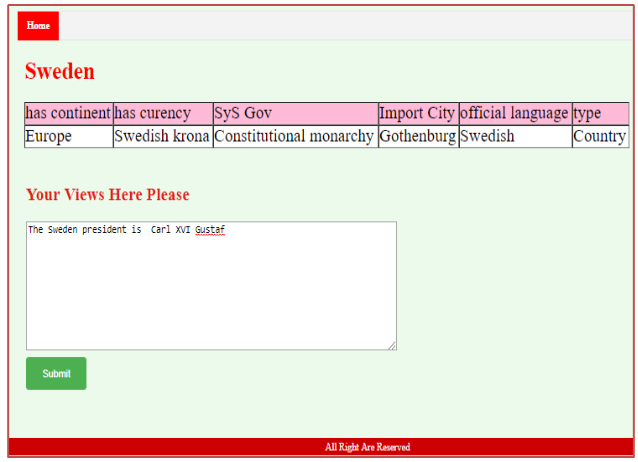

Fig. 5. The Full Annotated Object with Insertion form.

After that, the entered information would be examined and validated in order to enrich the ontology with updated information. If the user needs to know more information about the un-annotated text, the system will search online about the selected topic and treated as an object in the triple store if it is annotated. For example, the user selects an un-annotated word which is "Las Vegas" as shown in "Fig. 6".

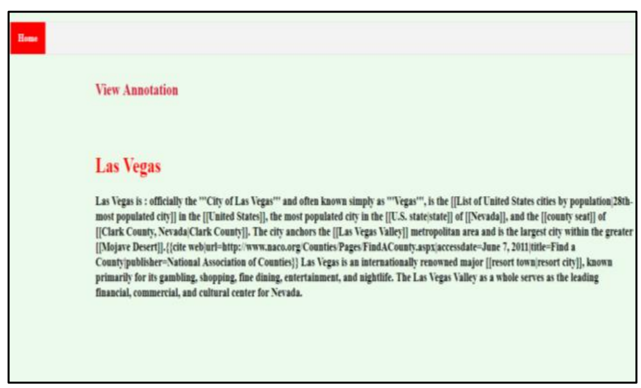

Fig. 6. Online Information about un-annotated Objects.

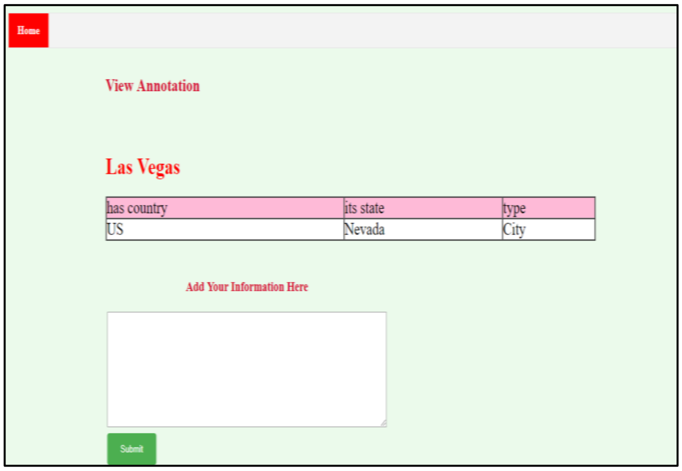

Fig. 7. Enrichment of Ontology with Online Search.

After that, the viewed text on the un-annotated selected object stored in an external database so that it achieve one of two things; one of them, when another user selects the same object; the annotation will be retrieved from the database instead of searching for it once again. The second, If the object belongs to one of the predefined ontology classes; then the system will recommend admin to add this piece of information to the ontology with full description to enrich it. If the user selects it again it will be retrieved directly from the ontology as shown in “Fig. 7”.

IV. System Evaluation

The performance of our SNFA tool is our target in this section and how to enhance our annotation tool will be evaluated later on here. To evaluate the performance of updated SNAF semantic tool [11] as we mentioned before, Precision, Recall, and F-measure are calculated based on “equation (1)”, “equation (2)” and “equation (3)” [12] [13] [14].

$$\text{recall} = \frac{accurate}{all} \quad (1)$$

$$\text{precision} = \frac{accurate}{accurate+inaccurate} \quad (2)$$

$$\text{F-measure} = 2 * \left(\frac{recall \times precision}{recall+precision}\right) \quad (3)$$

The idea beyond the calculation of F-measure concluded in its ability to reflect accurately the performance of our tool. We applied our experiment on 8 different RSS URLs in the news domain, measured evaluated and compared with results gained from our previous work.

As shown in Table I, values before and after enhancement are presented. The precision almost the same because the same entities retrieved the OWL repository. The average F-measure is improved from 86.9% to 95.5%. This is what we want to reach to achieve the highest efficiency of our system in order to obtain better results every time. On the other hand, “Fig. 8” shows the recall, precision and F-measures variance comparison of our tool before and after enhancement.

TABLE. I. Recall, Precision and F-Measure of SNFA tool before and after Enhancement

RSS NO.	Old System			New Updated System		
	Precision (%)	*Recall (%)*	*F-measure (%)*	*Precision (%)*	*Recall (%)*	*F-measure (%)*
1	100	90	94.7	100	98	98.9
2	90	70	78.75	100	93	93.6
3	100	82.4	90.4	100	95	97.4
4	95	75	83.8	100	90	94.7
5	100	68.8	81.5	100	80	88.9
6	100	63.6	77.8	100	90	94.7
7	95.7	88	91.7	100	95	97.4
8	90	81.8	85.7	95	90	92.4
Avg			**86.9**			**95.5**

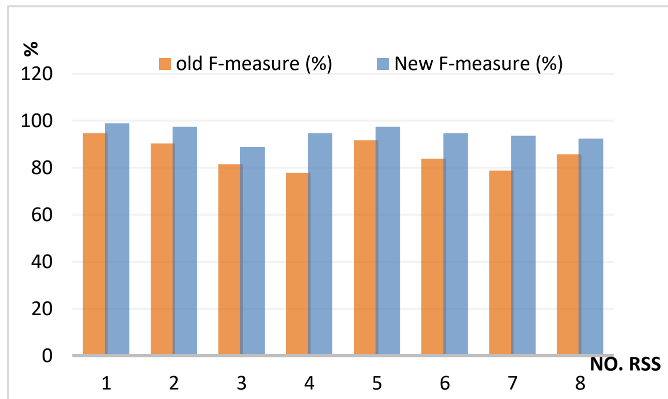

Fig. 8. F-Measure Comparision of SNFA Tool before and after Enhancement.

V. Conclusion and Future Work

Our paper presents an effective framework that allows people to add their annotations. Even if no annotation found, the system will have to search them online and store them in the ontology to be used next time. Our experimental shows that our tool and approach lead to accurate annotations that facilitate information retrieval with high precision and high recall.

We will focus on improving the accuracy of the annotation document by automating the process of extending and enriching the ontology by using machine learning methods in our future work.

References

[1] T.Berners-Lee, M. Fischetti, and M.L. Dertouzos Weaving the Web: The Original Design and Ultimate Destiny of the World Wide Web by Its Inventor, HarperInformation, 2000, p. 244.

[2] O.Rodríguez Rocha,I.Vagliano and C.Figueroa, "Semantic Annotation and Classification in Practice," IT Professional , vol. 17, no. 2, pp. 33-39, 2015.

[3] "Annotation," [Online]. Available: https://en.wikipedia.org/wiki/. [Accessed 15 May 2019].

[4] F. van Harmelen, "The semantic Web: what, why, how, and when," in IEEE Distributed Systems Online, 2004.

[5] Bontcheva, Kalina, and Hamish Cunningham, "Semantic annotations and retrieval: Manual, semiautomatic, and automatic generation," in Handbook of semantic web technologies, 2011.

[6] Yongxin Liao, Mario Lezoche, Hervé Panetto, and Nacer, "Why, where and how to use semantic annotation for systems interoperability," in 1st UNITE Doctoral Symposium, 2011.

[7] Thomas R.Gruber, "Toward principles for the design of ontologies used for knowledge sharing?," International Journal of Human-Computer Studies, vol. 43, no. 5-6, pp. 907-928, 1995.

[8] "Annotating documents," [Online]. Available: https://www.w3.org/Amaya/User/doc/Annotations.html. [Accessed 24 OCT 2019].

[9] M. P. Kogalovskii, "Semantic Annotating of Text Documents: Basic Concepts and Taxonomic Approach," Automatic Documentation and Mathematical Linguistics, vol. 52, no. 0005-1055, p. 19–26, 2018.

[10] "What is Semantic Annotation?," [Online]. Available: https://www.ontotext.com/knowledgehub/fundamentals/semantic-annotation/. [Accessed 20 10 2019].

[11] Hanaa G.Hendi, Haytham Al-Feel, Ehab E.Hassanein, "Semantic Annotation for News Feeds," in IEEE 8th IEEE Annual InformationTechnology, Electronics and Mobile Communication Conference (IEMCON), Canada, 2017.

[12] K.Holvoet, "What is RSS and how can libraries use it to improve patron service?," Library Hi Tech News, vol. 23, no. 8, pp. 32-33, 2006.

[13] J. Makhou, F.Kubala, R.Schwartz, and Ralph, "Performance Measures For Information Extraction," Proceedings of DARPA broadcast news workshop, 1999.

[14] Powers, D. Martin, "Evaluation: from precision, recall and F-measure to ROC, informedness, markedness, and correlation," Journal of Machine Learning Technologies, vol. 2, no. 1, pp. 37-63, 2011.

Detecting Fake Images on Social Media using Machine Learning

Njood Mohammed AlShariah[1], Abdul Khader Jilani Saudagar[2]
Information Systems Department, College of Computer and Information Systems
Imam Mohammad Ibn Saud Islamic University (IMSIU)
Riyadh, Saudi Arabia

***Abstract*—In this technological era, social media has a major role in people's daily life. Most people share text, images, and videos on social media frequently (e.g. Twitter, Snapchat, Facebook, and Instagram). Images are one of the most common types of media share among users on social media. So, there is a need for monitoring of images contained in social media. It has become easy for individuals and small groups to fabricate these images and disseminate them widely in a very short time, which threatens the credibility of the news and public confidence in the means of social communication. This research attempted to propose an approach to extracting image content, classify it and verify the authenticity of digital images and uncover manipulation. Instagram is one of the most important websites and mobile image sharing applications on social media. This allows users to take photos, add digital photographic filters and upload pictures. There are many unwanted contents in Instagram's posts such as threats and forged images, which may cause problems to society and national security. This research aims to build a model that can be used to classify Instagram content (images) to detect any threats and forged images. The model was built using deep algorithms learning which is Convolutional Neural Network (CNN), Alexnet network and transfer learning using Alexnet. The results showed that the proposed Alexnet network offers more accurate detection of fake images compared to the other techniques with 97%. The results of this research will be helpful in monitoring and tracking in the shared images in social media for unusual content and forged images detection and to protect social media from electronic attacks and threats.**

Keywords*—*Convolution Neural Network (CNN); Image forgery; Classification; Alexnet; Rectified Linear Unit (ReLU); SoftMax function; Features extraction

I. Introduction

It is a fact that social media have changed the way people interact and carry on with their everyday lives. Social networking sites are a prominent media phenomenon nowadays, and have attracted a large number of people. Worldwide, the number of users [1] now exceeds three billion. In the Gulf region, growth in the number of active users has exceeded 66% [2]. Saudi Arabia ranks seventh in the world in terms of social media use; more than 75% of its estimated 25 million people [3] are active users of social media. Social media are based on specific foundations that bring people together and empower them to express themselves, share their interests and ideas, and forge new friendships with others who share their interests. Facebook, Twitter, and Instagram are among the most popular social networking sites of the day. It is a widespread practice to share images online through social networking services such as Instagram. At least 80 million images [4] are currently shared via Instagram every day. Instagram enables users to take photographs, apply digital photographic filters, and upload the pictures to website for social networking together with short captions. People upload and share billions of pictures [5] every day on social media.

A huge number of people have become victims of photo forgery in this technological age. Some criminals use software to exploit and use pictures as evidence to confuse the courts of justice [17]. To put an end to this, all photographs exchanged via social media should be labeled as true or fake. Social media is a great platform for knowledge sharing and dissemination. Yet If there is no caution, people may be fooled and even induced by unintended false propaganda. Though most image editing using Photoshop is clearly evident, some of these images may indeed appear really due to pixelization and shoddy jobs by novices [16]. In particular, in the Policy arena, edited images can break the credibility of a politician. In this research using machine learning algorithms [6, 7], the researcher will attempt to propose a classifier model via a convolutional neural network (CNN) that is capable of take advantage of knowledge to take an image from social media and then classify and detect it.

This research proposes an approach that takes an image as input and classifies it, using an effective system (the CNN model) [20]. The result of this proposed research will be helpful in monitoring and tracking social media content and in discovering fraud on social networking sites, especially in the field of images.

II. Literature Review

Very little work has been finalized around detecting forge audio, images, and videos. Yet, several studies and tasks are underway to identify what can be done around the incredible proliferation about counterfeit pictures online. Adobe recognizes the way in which Photoshop is misused and has tried to offer a sort of antidote [8]. The following provide a summary of a few of these studies:

According to a study [9] conducted by Zheng et al. (2018), the identification of fake news and images is very difficult, as fact-finding of news on a pure basis remains an open problem and few existing models Can be used to resolve the problem. It has been proposed to study the problem of "detecting false news." Through a thorough investigation of counterfeit news, many useful properties are determined from text words and pictures used in counterfeit news. There are some hidden characteristics in words and images used in fake news, which can be identified through a collection of hidden properties derived from this model through various layers. A pattern called TI-CNN has been proposed. By displaying clear and embedded features in a unified space, TI-CNN is trained with both text and image information at the same time.

Raturi's 2018 architecture [10] was proposed to identify counterfeit accounts in social networks, especially on Facebook. In this research, a machine learning feature was used to better predict fake accounts, based on their posts and the placement on their social networking walls. Support Vector Machine (SVM) and Complement Naïve Bayes (CNB) were used in this process, to validate content based on text classification and data analysis. The analysis of the data focused on the collection of offensive words, and the number of times they were repeated. For Facebook, SVM shows a 97% resolution where CNB shows 95% accuracy in recognizing Bag of Words (BOW) -based counterfeit accounts. The results of the study confirmed that the main problem related to the safety of social networks is that data is not properly validated before publishing.

In 2017 study by Bunk et al [11], two systems were proposed to detect and localize fake images using a mix of resampling properties and deep learning. In the initial system, the Radon conversion of resampling properties is determined on overlapping pictures corrections. Deep learning classifiers and a Gaussian conditional domain pattern are then used to construct a heat map. A Random Walker segmentation method uses total areas. In the next system, for identification and localization, software resampling properties are passed on overlapping object patches over a long-term memory (LSTM)-based network. In addition, the detection/ localization performance of both systems was compared. The results confirmed that both systems are active in detecting and settling digital image fraud.

Aphiwongsophon and Chongstitvatana [12], aimed to use automated learning techniques to detect counterfeit news. Three common techniques were used in the experiments: Naïve Bayes, Neural Network and Support Vector Machine (SVM). The normalization method is a major step to disinfect data before using the automatic learning method to sort information. The results show Naïve Bayes to have a 96.08% accuracy in detecting counterfeit news. There are two other advanced methods, the Neural Network Machine and the Support Network (SVM), which achieve 99.90% accuracy.

In [13] by Kuruvilla et al., a neural network was successfully trained by analyzing the 4000 fake and 4000 real images error level. The trained neural network has succeeded in identifying the image as fake or real, with a high success rate of 83%. The results showed that using this application on mobile platforms significantly reduces the spread of fake images across social networks. In addition, this can be used as a false image verification method in digital authentication, court evidence assessment, etc. It develops and tests reliable fake image detection program by combining the results of metadata analysis (40%) and neural network output (60%).

According to [15] Kim's and Lee's, digital forensics techniques are needed to detect manipulation and fake images used for illegal purposes. Thus, the researchers in this study have been working on an algorithm to detect fake images through deep learning technology, which has achieved remarkable results in modern research. First, a converted neural network is applied to image processing. In addition, a high pass filter is used to get at hidden features in the image instead of semantic information in the image. For experiments, modified images are created using intermediate filter, Gaussian blurring, and added white Gaussian noise.

This research develops an approach that takes an image as input and classifies it, using the CNN model. For a completely new task/problem, CNNs are very good feature extractors. It extracts useful attributes from an already trained CNN with its trained weights by feeding your data at each level and tuning the CNN a bit for the specific task. This means that a CNN can be retrained for new recognition tasks, enabling to build on pre-existing networks. This is called pre-training, where one can avoid training a CNN from the beginning and save time. CNN can carry out automatic feature extraction for the given task. It eliminates the need for manual feature extraction, since the features are learned directly by the CNN. In terms of performance, CNNs outperform many methods for image recognition tasks and many other tasks where it gives a high accuracy and accurate result. Another key feature of CNNs is weight sharing, which basically means that the same weight is used for two layers in the model. Due to the above features and advantages, CNN is used in this research in comparison to other deep learning algorithms.

III. Research Methodology

This research explores a supervised machine learning classification problem [14,18], where the label or category of the input sample is known as the training phase. There are two labels or classes: the original image class and the fake image class. The researcher uses the deep learning technique via a conventional neural network (CNN).

A. *Input Features for Neural Networks*

Features in a neural network are the variables or attributes in the data set where extraction of features is a fundamental step in automated methods based on approaches to machine learning. The goal is to obtain useful data characteristics. In order to classify images, convolution neural networks use features. Such features are taught by the network during the training process itself. Features aim to reduce the number of features in a dataset by creating new features from the existing ones (and then discarding the original features). Then this new simplified set of features should be able to summarize most of the details in the original set of features. Therefore, from a combination of the original set, a condensed version of the original features can be produced.

B. *Devloping Fake Image Detection Algorithm Architecture*

Convolution neural network (CNN) architecture is illustrated in Fig. 1.

- Target images will be extracted from the Instagram application, where these images represent the dataset that is relevant to find answers to the research questions, test the hypothesis and assess the results.

- Construct CNN convolution layer, the convolutional layer is responsible for extracting image features, using conventional mathematical operations. These convolutional operations act as applying digital filters with two dimensions. Assuming the image tile is 4X4 pixels and the conventional filter is 2X2 matrix filter, the Fig. 2, Fig. 3 and Fig. 4 illustrates the conventional operation, where each image tile block matrix with dimensions equal to the filter dimension will be multiplied by the filter matrix.

- Construct the Activation function. Fig. 5 illustrates the activation function layer, contained in the yellow oval. The activation function layer is a layer between the conventional layer and the feature map, which, as in any traditional neural network activation function, removes un-wanted pixels, e.g. negative values.

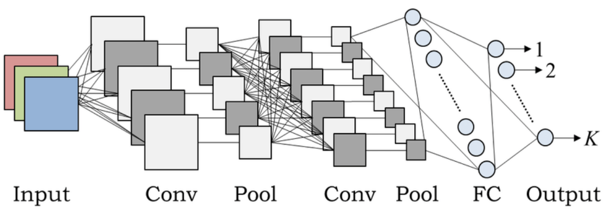

Fig. 1. Convolution Neural Network Architecture.

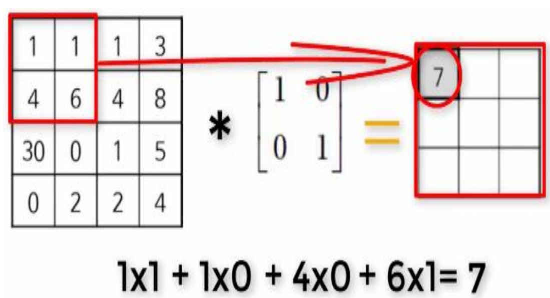

Fig. 2. Conventional Operation 1.

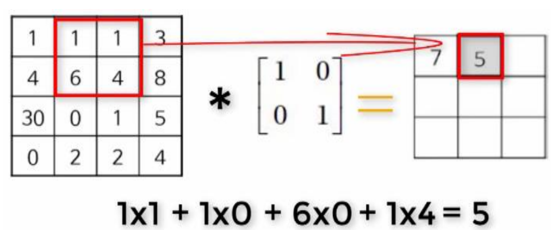

Fig. 3. Conventional Operation 2.

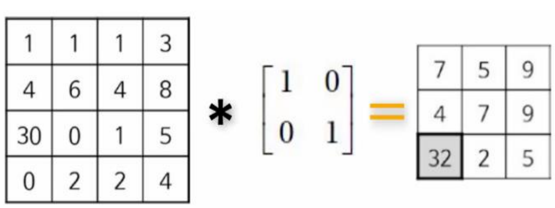

Fig. 4. Overall Conventional Operation.

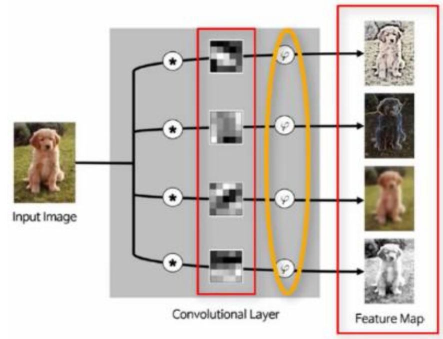

Fig. 5. Activation Function Layer.

- Due to the nonlinear nature of image data, the researcher will use a non-linear activation function called The Rectified Linear Unit (ReLU). The rectifier job is defined as the positive section of its argument, as shown in the Fig. 6.

- To reduce the size of the array in the precise step, we downsample it using an algorithm called max pooling to modify the output of the layer. Further pooling helps to make the representation almost invariant with respect to small translations of the input.

Fig. 7 illustrates the max pooling operation on an image tile example with max pooling at a 2X2 dimension size:

- Make a prediction, this neural network decides whether the image is, or is not, a match. To differentiate it from the convolution process, it is referred to as a “fully connected” network. Before constructing a fully connected network, the pooled feature map data must convert to the single column to be suitable as a neural network input. This process is known as “flattening,” as shown in the Fig. 8.

- Fig. 9 illustrates the fully connected network architecture.

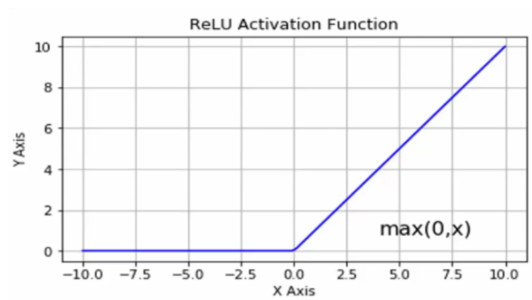

Fig. 6. Rectified Linear unit Activation Function.

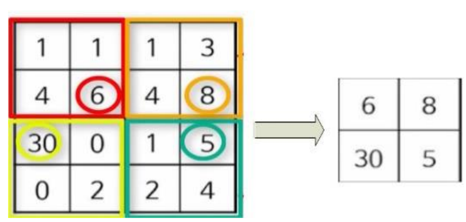

Fig. 7. Max-Pooling Features Mapping.

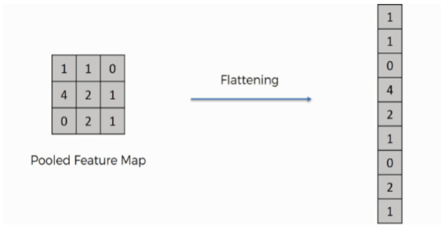

Fig. 8. Flattening Process.

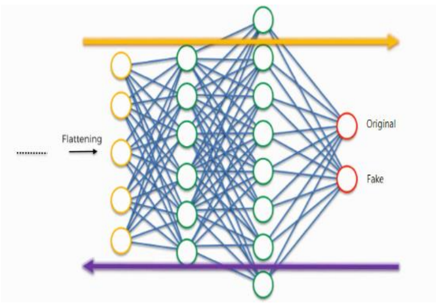

Fig. 9. Fully Connected Network Architecture.

- Construct the SoftMax Function and the classifier module (image classification). The result of the SoftMax function can be used to represent a categorical distribution; that is, a probability distribution of various possible outcomes. The SoftMax function helps the output to appear in the form of probabilities.
- Testing and Results, when the neural network is finished with its training, the dataset is tested and we extract the confusion matrix, which contains several variables through which the neural network accuracy is calculated.

IV. Implementation

Applying MATLAB software with the Deep Learning Toolbox helps you to train your own CNN from scratch or use a pretrained model to conduct transfer learning. The method you choose depends on the resource you have, the type of application you are creating and the purpose of the application. In order to train the network from scratch, the number of layers and filters must be determined and the other requirements adjusted. Training a specific model from the start also requires enormous amounts of data, based on millions of samples, which can take a long time. An appropriate alternative to CNN training from scratch is the use of a pre-training model to automatically extract properties from a new dataset. Known as transfer learning, this is an easy way to apply deep learning without a great data set and a long period spent on calculation and training.

A. *Create Simple Deep Learining Networks for Classification*

There are three networks: Alexnet, Classic CNN, and Alexnet using transfer learning. For each network, there are a training dataset and a test dataset. There are also cases in which the test data is from training data and vice versa. There are two datasets in our experiment. The first dataset contains 1400 images for training and 400 images for testing. The second dataset contains 400 images for training and 40 images for testing. In the second dataset, the fake images in the training data are extracted from the original images and, for each original image, three fake images were made. The researcher modified the original images via addition, deletion, changing colors. The dataset training steps are described as follow by using CNN network.

1) Load and analyze image data: Load the data of the sample as a data store for the image. Image Datastore automatically labels images based on the name of the folder and stores the data as an object of the image datastore. An image datastore helps you to store large image information when training a convolution neural network and interpret image batches efficiently.

2) Define the network architcture: Determine the convolutional neural network architecture and create network layers.

3) Define training options: Defines the training options after defining the architecture of the network. Learning rate, number of epochs, momentum and batch size.

4) Train the network: Train the network using layer-defined architecture, training data & the training options.

5) Predict the labels of new data and measure the classification accuracy

Predict the labels of the data using the trained network, and measure the final accuracy.

Note that Alexnet network and Transfer Learning network follow the same training steps but with some additions where the load pretrained network is additional step in Alexnet network and the replace final layers is additional step in transfer learning.

B. *Test Datasets*

In this step the researcher used codes to choose an image from amongst the images; then it determines whether the image is original or fake as shown in Fig. 10 and Fig. 11.

Fig. 10. Image Classification.

Fig. 11. Image Classification.

V. Results and Discussion

The performance measures of the proposed methodology are discussed in detail. The major goal of this work is to detect both normal and fake images in an accurate manner. For this purpose, a convolution neural network is utilized in this work. This CNN comprises four layers: the convolution layer, pooling layer, activation layer, and SoftMax layer. Each layer performs a specific task individually. First, the input image is obtained from the image acquisition. Then the image is converted into non-overlapping patches, from these patches. Further, the values of the features are normalized and down sampled to obtain a reduced feature set. Finally, the probability of the output is determined to classify the given image as normal or fake. Here, the approach developed in this research is evaluated, based on performance metrics and relative with the current techniques.

A. Performance Measures

The performance of the anticipated methodology is evaluated using different performance metrics, such as sensitivity, specificity, accuracy, precision, and recall.

1) Sensitivity: Sensitivity refers to the calculation of the ratio of True Positives that are recognized accurately. It can be defined as,

$$Sensitivity = \frac{TP}{TP+FN} \quad (1)$$

2) Specificity: Specificity is defined as the ratio of correctly detected True Negatives. This can be defined as,

$$Specificity = \frac{TN}{TN+FP} \quad (2)$$

3) Accuracy: Accuracy is known as the ratio of correct intrusions of classification to the total number of data. It is clarified as follows,

$$Accuracy = \frac{TP+TN}{TP+TN+FP+FN} \quad (3)$$

4) Precision: Precision is the ratio of the number of intrusions that are correctly identified to the total number of intrusions in the process. This is denoted by,

$$Precision = \frac{TP}{TP+FP} \quad (4)$$

5) Recall: Recall is the ratio of the number of properly detected intrusions to the number of intrusions that are relevant. This can be represented as,

$$Recall = \frac{TP}{TP+FN} \quad (5)$$

B. Performance Analysis

The quality of the technique proposed is tabulated and shown in the tables below. The accuracy of the results is shown to vary among networks. Alexnet is the most accurate, followed by Alexnet using TL and then Classic CNN. Table I illustrates comparison among three network types (Alexnet Network, Alexnet Using Transfer Learning, and Classic CNN) regarding the performance accuracy of results when the testing data is from outside the training data. The findings reveal differences among the three networks, in favor of Alexnet (93.4), followed by Alexnet using transfer learning (93.2) and, finally, classic CNN (70.1). The findings also reveal differences among the three networks when testing data from the training data. These are again in favor of Alexnet (99.3), followed by Alexnet using transfer learning (94.0) and, finally, classic CNN (83.9). The results in the table below are specific to the first dataset.

Fig. 12 illustrates Mean scores of performance accuracy results, when testing data from outside the training data and from the training data

Table II compares among the three network types (Alexnet Network, Alexnet Using Transfer Learning, and Classic CNN) regarding the performance accuracy of results when testing data from outside the training data. The findings reveal no statistically significant differences in the performance accuracy of results among the three network types. The value of significance level amounted to 0.172; this means it is greater than 0.05, which is not statistically significant. There were, however, differences amongst the three networks when testing data from the training data, in favor of Alexnet (91.1), followed by Alexnet Using Transfer Learning (78.4) and, finally, Classic CNN (64.5). The results in the table below are specific to the second dataset.

TABLE. I. Kruskall-Wallis Test of the Differences between the Mean Scores of Performance Accuracy Results when the Testing Data is from Outside the Training Data and from the Training Data (Alexnet, TL, Classic CNN)

Performance results when testing data is		**Mean**	**SD**	**Chi-Square**	**p. value**
Outside the trainin g data	Alexnet Network	93.4	2.0	9.482	0.009
	Alexnet Using Transfer Learning	93.2	3.08		
	Classic CNN	70.1	0.22		
From the trainin g data	Alexnet Network	99.3	0.45	12.635	0.002
	Alexnet Using Transfer Learning	94.0	0.93		
	Classic CNN	83.9	3.17		

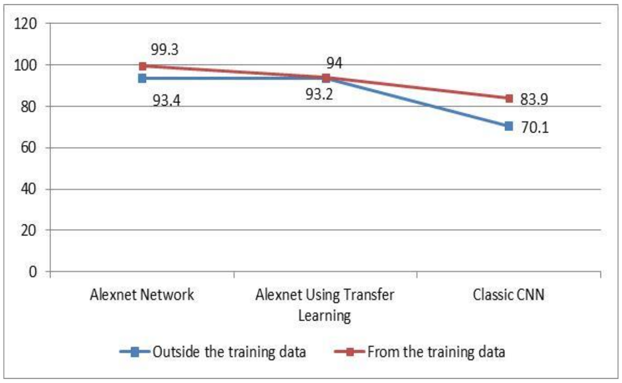

Fig. 12. Mean Scores of Performance Accuracy Results, when Testing Data from Outside the Training Data and from the Training Data.

TABLE. II. KRUSKALL-WALLIS TEST OF THE DIFFERENCES BETWEEN THE MEAN SCORES OF PERFORMANCE ACCURACY RESULTS WHEN TESTING DATA FROM OUTSIDE THE TRAINING DATA AND FROM THE TRAINING DATA (ALEXNET, TL, CLASSIC CNN)

Performance results when testing data from		**Mean**	**SD**	**Chi-Square**	**p. value**
Outside the training data	Alexnet Network	80.9	9.5	3.519	0.172
	Alexnet Using Transfer Learning	66.2	21.7		
	Classic CNN	64.8	16.8		
From the training data	Alexnet Network	91.1	3.4	7.559	0.023
	Alexnet Using Transfer Learning	78.4	17.6		
	Classic CNN	64.5	25.8		

Fig. 13 illustrates Mean scores of performances accuracy results when testing data from outside the training data and from the training data

After running the code, the values of precision, recall, accuracy, specificity, and sensitivity are extracted from the confusion matrix by calculating the value of True positive, True Negative, False positive and False Negative for example in Alexnet network the confusion matrix shown in Table III.

From the above table the values are calculated where accuracy is 93.3, precision is 95.5, recall is 91.4, specificity is 95.3 and sensitivity is 91.4.

The performance of Alexnet, CNN, and TL is evaluated using several measures, such as accuracy, sensitivity, specificity, precision, recall, true positive rate, and true negative rate [19]. The performance of the methodologies is also evaluated and compared with current techniques. From the outcomes, it is concluded that the proposed Alexnet approach offers more accurate detection of fake images compared to conventional techniques. This proves the superiority of the developed methodology.

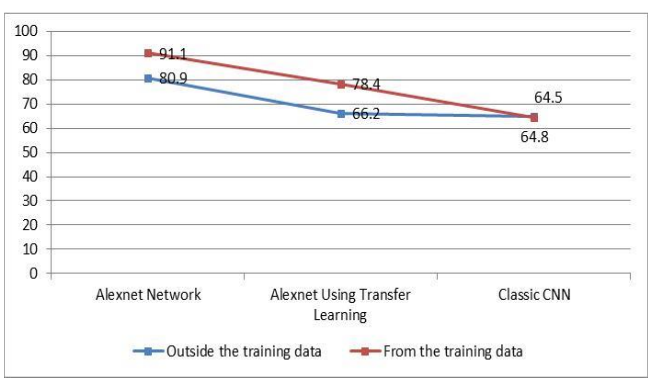

Fig. 13. Mean Scores of Performance Accuracy Results when Testing Data from Outside the Training Data and from the Training Data.

TABLE. III. CONFUSION MATRIX OF ALEXNET NETWORK

n = 400	**Actual Fake**	**Actual Normal**
Predicted Fake	TN 182	FP 9
Predicted Normal	FN 18	TP 191

VI. CONCLUSION

Recently, electronic attacks have spread in Saudi Arabia. There is currently no clear vision nor a unified framework to protect us against the dangers of piracy and threats, especially about the penetration of social media and the spread of false accounts. This has led Saudi Arabia to invest in information security, which is concerned with protecting the technical infrastructure from hacking and focuses on developing techniques and tools to protect social media from electronic attacks and threats. This research has contributed to the rapid detection of fraud in social media, especially in the field of images, thus solving the problem of spreading rumors and promoting false news on social networking sites and helps communities seeking to protect their technical infrastructure from piracy and cyber threats and to strengthen their information security, where the crime of image forgery poses a danger to societies. There are some problem and limitations in neural networks including it computationally expensive, requiring the use of powerful and distinct processing units. Without a good CPU, neural networks are quite slow to train for complex tasks.

Another problem with neural networks is that they depend on the amount of data provided to them. If the quantity of data is small, then one can expect poor network performance and vice versa. Neural networks contain millions of parameters that require a huge amount of data. The use of neural networks thus requires a large amount of training data and takes time to train these neural networks.

It is clear—from the results of the model used—that a large, deep convolutional neural network is capable of achieving record-breaking results on a highly challenging dataset using supervised learning where the results of this research achieved high accuracy of up to 97%. The results of this research will be helpful in monitoring and tracking social media content and in discovering fraud on social networking sites, especially in the field of images. To effectively identify objects, the convolution neural network architecture implicitly combines the benefits obtained from standard neural network learning with the convolution process. Like a neural network, CNN and its variants can also be optimized to large datasets, which is often the case when classifying objects.

The recommendations for future work are for example using a more complex and deeper model for unpredictable problems. Integration of deep neural networks with the theory of enhanced learning, where the model is more effective. Neural network solutions rarely take into account non-linear feature interactions and non-monotonous short-term sequential patterns, which are necessary to model user behavior in sparse sequence data. A model may be integrated with neural networks to solve this problem. The dataset could be increased and another type of images could be used for training, for example gray-scale images.

REFERENCES

[1] G.Mohamed Sikandar, "100 Social Media Statistics You must know," [online] Available at: https://blog.statusbrew.com/social-media-statistics-2018-for-business/ [Accessed 02 Mar 2019].

[2] Damian Radcliffe, Amanda Lam, "Social Media in the Middle East,"[online]Available:https://www.researchgate.net/publication/323185146_Social_Media_in_the_Middle_East_The_Story_of_2017 [Accessed 06 Feb 2019].

[3] GMI_BLOGGER,"Saudi Arabia Social Media Statistics," GMI_ blogger. [online] Available at:https://www.globalmediainsight.com/blog/saudi-arabia-social-media-statistics/ [Accessed 04 May 2019].

[4] Kit Smith,"49 Incredible Instagram Statistics,". Brandwatch. [online] Available at: https://www.brandwatch.com/blog/instagram-stats/ [Accessed 10 May 2019].

[5] Selling Stock. (2014). Selling Stock. [online] Available at: https://www.selling-stock.com/Article/18-billion-images-uploaded-to-the-web-every-d [Accessed 12 Feb 2019].

[6] Li, W., Prasad, S., Fowler, J. E., & Bruce, L. M. (2012). Locality-preserving dimensionality reduction and classification for hyperspectral image analysis. IEEE Transactions on Geoscience and Remote Sensing, 50(4), 1185–1198.

[7] A. Krizhevsky, I. Sutskever, & G. E. Hinton, (2012). Imagenet classification with deep convolutional neural networks. In Advances in Neural Information Processing Systems, 1097–1105.

[8] K. Ravi, (2018). Detecting fake images with Machine Learning. Harkuch Journal

[9] L. Zheng, Y. Yang, J. Zhang, Q. Cui, X. Zhang, Z. Li, et al. (2018). TI-CNN: Convolutional Neural Networks for Fake News Detection. United States

[10] R. Raturi, (2018). Machine Learning Implementation for Identifying Fake Accounts in Social Network. International Journal of Pure and Applied Mathematics, 118(20), 4785-4797.

[11] J. Bunk, J. Bappy, H. Mohammed, T. M. Nataraj, L., Flenner, A., Manjunath, B., et al. (2017). Detection and Localization of Image Forgeries using Resampling Features and Deep Learning. University of California, Department of Electrical and Computer Engineering, USA.

[12] S. Aphiwongsophon, & P. Chongstitvatana, (2017). Detecting Fake News with Machine Learning Method. Chulalongkorn University, Department of Computer Engineering, Bangkok, Thailand.

[13] M. Villan, A. Kuruvilla, K. J. Paul, & E. P. Elias, (2017). Fake Image Detection Using Machine Learning. IRACST—International Journal of Computer Science and Information Technology & Security (IJCSITS) .

[14] S. Shalev-Shwartz, & S. Ben-David, (2014). Understanding Machine Learning: From Theory to Algorithms. New York: Cambridge University Press.

[15] D.-H. Kim, & H.-Y. Lee, (2017). Image Manipulation Detection using Convolutional Neural Network. International Journal of Applied Engineering Research, 12(21), 11640-11646.

[16] M. D. Ansari, S. P. Ghrera, & V. Tyagi, (2014). Pixel-based image forgery detection: A Review. IETE Journal of Education, 55(1), 40–46.

[17] D. Strigl, K. Kofler, & S. Podlipnig, (2010). Performance and scalability of GPU-based convolutional neural networks. In 18th Euromicro Conference on Parallel, Distributed, and Network-Based Processing.

[18] Y. Li, & S. Cha, (2019). Face Recognition System. arXiv preprint arXiv:1901.02452.

[19] R. Kohavi, (1995, August). A Study of cross-validation and bootstrap for accuracy estimation and model selection. In Ijcai, 14(2), 1137–1145.

[20] R. Saracco, (2018). Detecting fake images using artificial intelligence. IEEE Future Directions.

Optimal Global Threshold based on Two Dimension Otsu for Block Size Decision in Intra Prediction of H.264/AVC Coding

Sawsan Morkos Gharghory
Computers and Systems Department
Electronics Research Institute
Giza, Egypt

***Abstract*—The Advanced Video Coding (H.264/AVC) has proved its ability in finding the tradeoff between the compressed bit rate value and the visual quality of video comparing to the others of traditional coding. One of the most encoder stages consuming time is the intra prediction in which different sizes of a block are exhaustively examined for selecting the suitable block size to the best block mode decision. In this paper, an efficient approach is suggested to select the best block size for the intra prediction adaptively to achieve high compression efficiency. The proposed approach exploits the idea of quad tree decomposition for blocks partitioning based on a predefined threshold value. An optimal global threshold value based on two dimension Otsu technique is suggested for the decision of block division in this work. The proposed technique is carried out on different set of videos resolutions with different quantization parameters using Matlab software. The comparison of the proposed approach with the reference JM18.6 video coding is done in terms of bit rate (BR), time saving and peak signal to noise ratio (PSNR). A tangible acceleration on the running time can be accomplished besides improvement in both of visual quality and bit rate with some of QCIF and CIF videos resolution by the proposed technique. The simulation results demonstrate saving in time by average 42% to 68% with CIF and QCIF videos. Concerning the visual quality in terms of Bjontegaard Delta parameters, the PSNR improved in which its value increased from 0.2 to 1.6, while the value of BR reduced from 0.79 to 15.3 respectively with some videos of resolutions QCIF, CIF and 720p. In addition, the performance of the suggested approach with the high resolution videos achieves minor improvement with some of them while has a slightly degradation with others of them.**

***Keywords*—H.264/AVC coding; intra prediction; block size decision; Otsu two dimensions method**

I. Introduction

H.264/AVC coding [1] has becoming among the pioneers in video coding, it has proved its ability in achieving a preferable performance comparing to the others. The most important parameters for advancing H.264 coding performance are: the intra prediction to a block in spatial domain, the motion estimation for variable block size, reference frames, and finally the rate distortion optimization (RDO) [2-3]. Intra prediction in the spatial domain is one of the most encoder stages consuming time and is considered in this paper. The intra prediction process goal is to reduce the data size needed to the sufficient representation of the concerning block samples of video frame. Intra prediction is used for editing of video sequence, coding of static image and finally for the significantly changes in the content of scene. The fast intra prediction algorithm was categorized into two types; the block size decision and block mode decision. As follow in the standard H.264/AVC, the determination of block size for the intra prediction was by examining all block sizes exhaustively to the nine modes or the four modes for optimal mode decision which is time consuming. Many fast algorithms have been presented concerning the block size decision for the reduction of computation time. Huang et al. [4] suggested fast block type selection for intra block coding based on the texture complexity of a macro-block (MB). Lin et al. [5] used the ratio of AC and DC coefficient energy to predict the intra prediction block size. Zhang et al. [6] proposed a fast block size decision algorithm based on the relationship between the smoothness of macro-blocks and the block type of intra prediction. The smoothness of a block was assessed by DC and AC coefficients in DCT domain. Wei et al. [7] used the variance of DC coefficients which is obtained from DCT for block size decisions. Many of the above mentioned researches suffered from determining the optimal threshold value required for preferring between different block sizes. So, the setting of optimum threshold value was a very important issue. If the threshold value is set too high, it may be resulted in error of block prediction which consequently leads to a dissipation in coding.

In this paper, the idea of quad tree decomposition based on optimal global threshold for block size decision is suggested for the intra prediction manner. Quad tree decomposition method in partitioning is based on the calculation of intensity variation (homogeneity) value within the macro blocks and its comparison to the global threshold value in order to decide whether performing a new partitioning or not. In this paper, the calculation of optimal global threshold value is based on the two dimension (2-D) Otsu, considering the between classes variance feature for block size decision. The 2-D Otsu method utilizes both of the gray level information of each pixel and its spatial correlation information within the neighborhood. The proposed technique is implemented on sequences of different videos with different quantization parameters (QP) and different resolutions such as QCIF, CIF and high resolution such as 720p and 1080p using Matlab Software. Both Peak signal to noise ratio (PSNR), time saving and bit rate are considered as criterions for evaluating the efficiency of the proposed technique relative to the standard technique. The simulation results prove the superiority of the suggested approach compared to those of the reference JM18.6 in terms of the aforementioned metrics. The results of simulation achieve time saving by average 48% to 68% with CIF and QCIF videos accompanied with improvement in both of visual quality and bit rate with some of them. Beside, the performance of the suggested approach with the high resolution videos achieves a little improvement with some of them while has a slightly degradation with others of them either of visual quality or bit rate.

The rest of paper is organized as follows. The intra prediction is detailed in Section 2. Code tree decomposition and the suggested global threshold value based two dimension Otsu for block size decision is depicted in details in Section 3. Section 4 presents the proposed algorithm and its flow chart. Finally, the simulation results of the proposed algorithm to different videos sequences with different resolutions and different quantization parameters are reviewed in Section 5. Section 6 concludes the work and results discussion.

II. Intra Prediction

H.264/AVC performs the intra prediction to the block for reducing the redundancy in the spatial domain in various manners to the previous video coding which used the reconstructed pixels from the adjacent blocks. In intra prediction stage, H.264 code supports the luminance pixels in a macro block (MB) three intra modes representative to different blocks sizes which are: intra 4×4 (I4MB), intra 8×8 (I8MB), and intra 16×16 (I16MB). The luminance (luma) components in block with size 4x4 or 8x8 have nine prediction modes, while the luminance components in block size 16x16 have only four prediction modes [1]. On the other hand, chrominance (chroma) components have only 8 × 8 block size with four prediction modes. Practically, the blocks of small sizes are used for encoding the texture regions, while the large sizes blocks are often used for encoding the smooth (homogenous) regions. The luma sample label and the direction of intra prediction modes of I4MB are illustrated in Fig. 1 and 2, respectively [4].

M	A	B	C	D	E	F	G	H
I	**a**	**b**	**c**	**d**				
J	**e**	**f**	**g**	**h**				
K	**i**	**j**	**k**	**l**				
L	**m**	**n**	**o**	**p**				

Fig. 1. Samples Labeling in Luma 4x4 Intra Prediction.

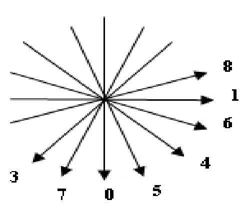

Fig. 2. The Directions of Prediction Modes in I4MB.

The sixteen lowercase letters from (a to p) in the mentioned figure are the pixels to be encoded, while the capital letters from A to M around the block are used for predicting this block. In Fig. 2, the second prediction mode that is dc mode is not shown because it has not direction and is estimated by calculating the average value to the number of luminance pixels from A to L surrounding the block to be coded shown in Fig. 1. Concerning the intra prediction coding of Luma 8×8, the number of its prediction modes besides their directions is similar to that in the Luma 4×4 and is only different in size. On the other hand, the encoding of both of Luma 16×16 and Chroma 8×8 blocks have three prediction modes in addition to the dc mode which can be calculated by the average intensity value to the surrounding coding block pixels [8-13]. Intra prediction modes for Chroma 8x8 and Luma 16x16 blocks are shown in Fig. 3.

In intra prediction stage of H.264/AVC, the encoder calculates and compares the rate of distortion (RD) of all prediction modes to different sizes of the block to be coded. Finding the optimal block size corresponding to the best prediction mode is implemented by minimizing the cost function for rate distortion (RD). Consequently, the intra prediction objective is to achieve an optimal visual quality for each block in the frame under certain bit rate cost and with a given quantization parameter (QP). The number of calculations for the RD before utilizing the suggested method in finding the optimal prediction mode with the suitable block size decision can be obtained by the following equation:

$$N = Mode_{(\mathrm{Chroma}_8)} \times (Mode_{(\mathrm{Luma}_4)} \times 16 + Mode_{(\mathrm{Luma}_8)} \times 4 + Mode_{(\mathrm{Luma}_{16})}) \quad (1)$$

Where: $\mathrm{Modes}_{(\mathrm{Chroma}_8)}$, $\mathrm{Modes}_{(\mathrm{Luma}_4)}$, $\mathrm{Modes}_{(\mathrm{Luma}_8)}$ and $\mathrm{Modes}_{(\mathrm{Luma}_{16})}$ are the prediction modes number for the coding blocks Chroma 8 × 8 which equals 4, Luma 4 × 4 with number of modes equaling 9, Luma 8 × 8 in which it has 9 modes and finally Luma 16 × 16 with 4 modes, respectively [14]. As depicted in equation (1), each number of luma prediction modes is multiplied by the number of coding blocks, in which there are sixteen coding blocks of size 4 × 4 and four coding blocks with size 8 × 8 in an MB. Consequently, the number of RDO calculations needs 763 computations in the latest JM version of H.264/AVC encoder for each macro block (MB) which is considered as a heavy computation [14]. With the previous version of JM reference software which is JM 9, the number of RDO computations equals 576 when the selected block size for coding is 4x4. The optimal mode for intra prediction is determined based on minimizing the cost function of RDO process as depicted in equation (2):

$$J = SSD(Mode|QP) + \lambda_{mode} \times R\ (Mode|QP) \quad (2)$$

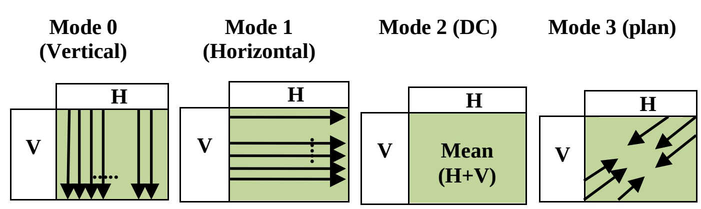

Fig. 3. Directions of Luma 16x16 and Chroma 8x8 Intra Predictions.

Where: SSD is summing the square difference between the original MB and its reconstructed pixels, QP is the parameter of quantization, R is the bit rate of encoding block in which λ_{mode} has a significant control on the rate of distortion and is determined by $0.85 \times 2^{QP-\frac{12}{3}}$, and finally J is the cost of the current intra-prediction mode [14]. To reduce the cost function aforementioned, the components of I-frame are partitioned into square sizes blocks and then the best block size corresponding to the optimal prediction mode for each MB in these components will be estimated through iterative computations of RDO.

Concerning the issue of reducing the number of RDO computations to find the suitable block size with its optimal mode, the block size decision based on the concept of code tree decomposition with global threshold based on two dimension Otsu is proposed. Both of the suggested tree decomposition code and two dimension Otsu method for determining the global threshold value is detailed in the following sections.

III. Quad Tree Decomposition

Quad- tree approach is used to split an image into partitions based on the measurement of blocks homogeneity such as coefficient variation or variance. The decomposition code of quad-tree is initialized firstly by partitioning an image into four equal size parts named nodes, each of them represents either a macro block (MB), or it is considered as a leaf. To evaluate if the macro block represented by the node homogeneous or not is through a performed test comparing its intensity variation with the variation of intensity of its parent. If the test is negative the node becomes a MB and it is divided, otherwise the node not divided and became a leaf. The partitioning process is iteratively for all nodes represented by MB till reach to the desired block size in image. Each parent node representing a macro block in the tree has four children called micro blocks (mB) in which each one has a quarter of its parent area. The structure of the tree and the implementation on image are depicted in Fig. (4a), (4b) and (4c). As shown in Fig. (4c), the content of the image or video frame is divided into four macro blocks (MB_k), and each MB_k will be divided into four micro-blocks (mB_{ki}) or not based on its homogeneity and then each mB_{ki} will be iteratively post subdivided or not based on the achievement of this criterion. In this paper, the optimal threshold based variance using two dimensions Otsu method is suggested to determine whether the block is homogenous or not so that the division decision can be taken [15].

The proposed global threshold based on two dimensions Otsu is presented in the following section in details.

A. *Two Dimension Otsu Technique*

Normally, the Otsu's method calculates the between-classes and within-class variance using the one Dimension (1-D) image histogram. To determine the optimal threshold value, the cost function for minimizing the within-class variance or maximizing the between-classes variance is used. This concept is extended to multilevel threshold as well. It is noted that 1-D Otsu's method is considered as the fastest and the simplest of all methods because the threshold value is mostly determined by the 1-D histogram of the image. However, 1-D histogram does not depict the spatial correlation between the pixels in image or video frame. For this reason, images having complex boundaries may yield a poor threshold performance. Therefore, Otsu's 1-D method is extended to the 2-D version, where the 2-D histogram of an image is used [16-18]. Also, the 2-D Otsu's criteria has been extended to be implemented to multilevel threshold. The between class variance concept of 2-D Otsu is presented below in details.

Let I represent a gray scale image of size M × N with L gray levels g = [1, 2,.., L] and total number of pixels equals M × N. Also, suppose f (x, y) is the gray value of the pixel located at coordinate (x, y) where x ∈ {1, 2, . . ., M}, y ∈ {1, 2, . . ., N}. Let h(x, y) represents the local average gray value for a window of size w × w with center at the location (x, y), and is given by equation 3:

$$h(x,y) = \frac{1}{wxw}\sum_{m=-(\frac{w-1}{2})}^{m=(\frac{w-1}{2})}\sum_{n=-(\frac{w-1}{2})}^{n=(\frac{w-1}{2})} f(x+m, y+n) \qquad (3)$$

The window size w is odd and may be equal to 3x3 or 5x5 and so on. Let q_{ij} is the occurrence time of the pair (i, j), where f (x, y) = i and h(x, y) = j. Then, the frequency of occurrence of pair (i, j) is calculated as follows:

$$P_{ij} = \frac{q_{ij}}{MxN}, \; 1 \leq i \leq L, \; 1 \leq j \leq L, \text{ and } L=256 \qquad (4)$$

If the image is segmented into to two classes C_o and C_1 (background and objects) by a threshold at level value k, in which the background C_o contains pixels taking the level values from: 1 to k, and C_1 contains pixels with levels [k + 1, ,L]. If the current threshold value is (t, s) where t named the gray threshold and s is the local average threshold, the probability distribution of the background and object classes ω_0 and ω_1 are calculated respectively, through equations 5 and 6. Also, the mean class vectors μ_0 and μ_1 for each of them with gray and local average features are calculated by the equations from 7 to 8.

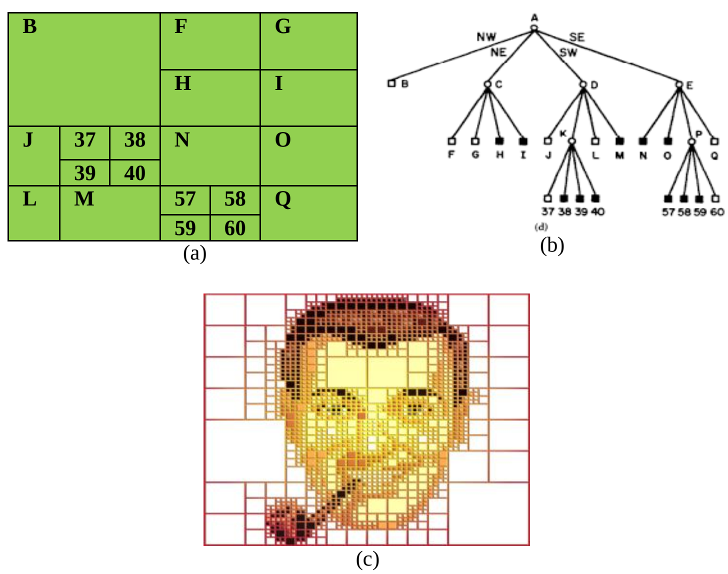

Fig. 4. (a-c) Quad- Tree Decomposition Approach.

$$\omega_0 = \mathrm{P}(C_0) = \sum_{i=1}^{S}\sum_{j=1}^{t} \mathrm{P}_{i,j} \quad (5)$$

$$\omega_1 = \mathrm{P}(C_1) = \sum_{i=S+1}^{L}\sum_{j=t+1}^{L} \mathrm{P}_{i,j} = 1 - \omega(k) \quad (6)$$

$$\mu_0 = (\mu_{00}, \mu_{01})^{\mathrm{T}} = \left[\frac{\sum_{i=1}^{S}\sum_{j=1}^{t} \mathrm{i}*\mathrm{P}_{i,j}}{\omega_0}, \frac{\sum_{i=1}^{S}\sum_{j=1}^{t} \mathrm{j}*\mathrm{P}_{i,j}}{\omega_0}\right]^{T} = \frac{\mu(k)}{\omega(k)} \quad (7)$$

$$\mu_1 = (\mu_{10}, \mu_{11})^{\mathrm{T}} = \left[\frac{\sum_{i=S+1}^{L}\sum_{j=t+1}^{L} \mathrm{i}*\mathrm{P}_{i,j}}{\omega_1}, \frac{\sum_{i=S+1}^{L}\sum_{j=t+1}^{L} \mathrm{j}*\mathrm{P}_{i,j}}{\omega_1}\right]^{T} = \frac{\mu_T - \mu(k)}{1-\omega(k)} \quad (8)$$

Where: $\omega(k) = \sum_{i=1}^{k} P_i \quad \mu(k) = \sum_{i=1}^{k} i * P_i$

Both of $\omega(k)$ and $\mu(k)$ are the zero-order and the first-order cumulative moments of the histogram up to the k^{th} level. The total mean vector μ_T is given by equation 9:

$$\mu_T = (\mu_{T0}, \mu_{T1})^{\mathrm{T}} = \left[\sum_{i=1}^{L}\sum_{j=1}^{L} \mathrm{i} * \mathrm{P}_{i,j}, \sum_{i=1}^{L}\sum_{j=1}^{L} \mathrm{j} * \mathrm{P}_{i,j}\right]^{T} \quad (9)$$

Where: $\omega_0 + \omega_1 \approx 1$ and $\omega_0\, \mu_0 + \omega_1\, \mu_1 \approx \mu_T$ and $\omega_1 \approx 1 - \omega(k)$

The two classes variance are calculated as described in equations 10 to 11 as follows:

$$\sigma_0^2(k) = \sum_{i=1}^{k} (i - \mu_0)^2\, \mathrm{P}_{i,j}/\omega_0 \quad (10)$$

$$\sigma_1^2(k) = \sum_{i=k+1}^{L} (i - \mu_1)^2\, \mathrm{P}_{i,j}/\omega_1 \quad (11)$$

The within class variance is given by equation 12:

$$\sigma_W^2 = \omega_0\mu_0^2 + \omega_1\mu_1^2 \quad (12)$$

The between class variance σ_b^2 is computed by:

$$\sigma_b^2 = \omega_0((\mu_0 - \mu_T)^2) + \omega_1((\mu_1 - \mu_T)^2)$$

$$\sigma_b^2 = \omega_0((\mu_{00} - \mu_{T0})^2 + (\mu_{01} - \mu_{T1})^2) + \omega_1((\mu_{10} - \mu_{T0})^2 + (\mu_{11} - \mu_{T1})^2) \quad (13)$$

For simplification, by substituting in equation 13 using equation 5 and 6, the between classes variance σ_b^2 is given by equation the equation 14:

$$\sigma_{\mathrm{b}}^2\,(\mathrm{k}) = \frac{(\mu(\mathrm{k}) - \mu_{\mathrm{T}}\omega(\mathrm{k}))^2}{\omega(\mathrm{k})(1-\omega(\mathrm{k}))} \quad (14)$$

The between class variance σ_b^2 is calculated by the mean of class subtracted from the total mean level of the original frame multiplied by probability of occurrence of this class divided by the multiplication of probability of this class occurrence and the probability of the other class occurrence.

The maximization of the between class variance value gives the optimal threshold for image partition as depicted in equation 15:

$$t_{opt}, S_{opt} = \arg\ max_{t,S} = \{\sigma_b^2(t,S)\} \text{ in which } 1 \le t, S \le L \quad (15)$$

The optimal threshold value k^* is calculated by the maximizing $\sigma_b^2\,(k)$, which is termed by $max_{1\le k\le \mathrm{L}}\, \sigma_b^2\,(k)$. Fig. 5 (d to f) shows the implementation of the two dimension Otsu method to the I-frame from sequences of different test videos with different resolutions such as CIF and 1080p as shown in Fig. 5 (a to c).

(a) I- frame of News video with resolution CIF (352x288)

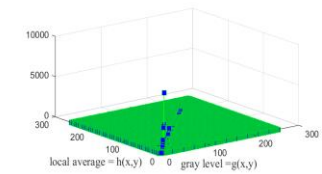
(d)Two dimension Otsu for I- frame of News video


(b) I-frame of football video with resolution CIF (352x240)

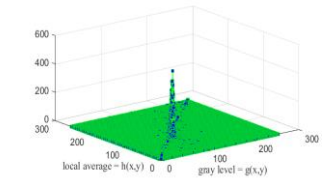
(e) Two dimension Otsu for I- frame of football video


(c) I- frame of Highway video with resolution CIF (352x192)

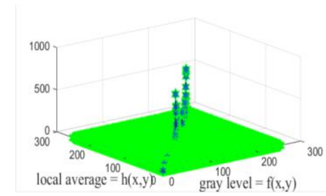

(f)Two dimension Otsu for I- frame of Highway video

Fig. 5. (a-c) Sequences of Videos with different Resolutions and (d-f) the Two Dimension Otsu for the Test Videos

Variance-based optimal threshold using 2-D Otsu method is suggested in this paper to partition the I-frame into blocks with different sizes which is presented in details in the following section.

IV. The Proposed Technique

This paper suggests the determination of optimal threshold value based on automatic algorithm for partitioning the frame under consideration into different blocks sizes. The proposed algorithm is employed for block size decision in intra prediction stage in which it utilizes the idea of quad-tree decomposition technique based on a global threshold value determined by two dimension Otsu method. An input frame will be divided into blocks either of 4×4 or 16×16 pixels according to the smoothness or the complication of the macro block through utilizing the statistical measurements of homogeneity feature of block. Each large square block in the frame will be divided if the homogeneity feature measured by the difference between maximum and minimum intensity values within the block exceeds a threshold value T, otherwise, the block is not divided. Thus, the value of threshold plays a very crucial role in which the independent selection to the threshold value without considering input frame statistical features may lead to bad compression characteristics. This problem is addressed in this paper by utilizing the aforementioned 2-D Otsu method to calculate the optimal threshold value which consequently leads to accurate decision about the blocks division into sub blocks. Once the frame is optimally decomposed into suitable blocks, the intra prediction to the block with final size either 4x4 or 16x16 are implemented using the corresponding prediction modes. After that, the predicted block is passing by the following processes: the DCT transformation, the quantization to the difference between the original block and the predicted block, the entropy coding on this quantized difference and finally the inverse process to both the quantization and DCT transformation. The flowchart of the proposed technique is shown in Fig. 6. Also The Pseudo code concerning the block size decision in H.264/ AVC intra prediction coding is described as follows.

The Pseudo code of the proposed approach

1) Determine the optimal global threshold to the I frame from the input video sequence using the variance-based two dimension Otsu method.

2) Then, I frame is divided into equally blocks of sizes 16x16, decompose each one of these blocks into sub-blocks of size 4x4 using the idea of Quad tree decomposition based on the optimal threshold value T calculated from the previous step.

3) Check if the difference between maximum and minimum intensity values of the square block exceeds the optimal threshold value T, it means the block is non-homogeneous and it should be divided, otherwise the block is not divided.

4) Finally the whole frame is becoming blocks with 4x4 or 16x16 sizes.

5) The resulted block is encoded using 4x4 intra prediction if its size 4x4, which it is well suited for coding the region of significant details, otherwise it is encoded by 16x16 intra prediction which is suitable for the smoothness region [1].

6) After that, the difference between the original and the predicted block called the residual coefficients block are calculated, transformed by DCT, quantized, coded by the entropy encoding that yields the bits of the quantized residual coefficients of block and finished by the bit streams for all I-frame blocks.

7) On the other path of the quantization process, the inverse quantization and the inverse transformation is applied to the residual coefficients block. Finally the re-constructed block is built from adding the predicted block to that block of the residual coefficients.

8) The result of encoding process is frame bits streams and re-constructed frame after encoding.

The metrics used to evaluate the efficiency of the proposed method comparing to the standard H.264 video coding are PSNR, run time saving and bite rate of the compression process and they are calculated in the equations 16-18.

$$\Delta\, PSNR = \frac{PSNR(\text{Proposed}) - PSNR(\text{JM})}{PSNR(\text{JM})} \times 100\% \tag{16}$$

$$\Delta\, Time = \frac{Time(\text{Proposed}) - Time(\text{JM})}{Time(\text{JM})} \times 100\ \% \tag{17}$$

$$\Delta Bitrate = \frac{Bitrate(\text{proposed}) - Bitrate(\text{jm})}{Bitrate(\text{jm})} \times 100\ \% \tag{18}$$

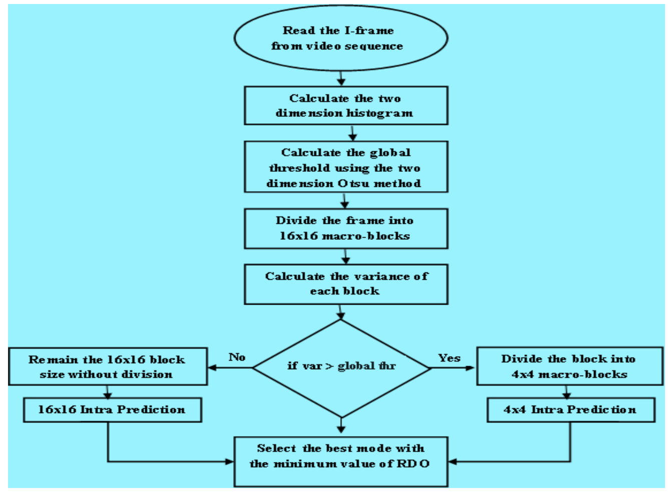

Fig. 6. The Flowchart of the Proposed Technique with the Mode Selection using Minimum ORD.

Also, the Sum of Absolute Differences (SAD) is used as other metric for measuring the error between the original frame and the predicted frame in intra prediction stage. Each of PSNR and SAD is depicted in the following equations.

$$\text{PSNR} = 10 \log \frac{255^2}{\text{MSE}} \tag{19}$$

$$MSE = \frac{SSD}{H \times W} \tag{20}$$

$$SSD = \sum_{x=0}^{H-1} \sum_{y=0}^{W-1} ((p(x,y) - p_r(x,y))^2 \tag{21}$$

$$SAD = \sum_{x=0}^{H-1} \sum_{y=0}^{W-1} |(p(x,y) - p_r(x,y)| \tag{22}$$

Where: H and W are the height and the width of the frame, each of $p(x, y)$ and $\mathrm{p_r}(x,y)$ represents the original and reconstructed frame pixels at location x and y , as well as both of MSE and SSD are Mean Square Error and Sum of Square Differences between the predicted and the original blocks respectively.

V. Simulation Results

The proposed block size decision in intra prediction based on global threshold using 2-D Otsu method is employed for different sets of test videos sequences with different resolutions. The performance of the proposed algorithm is evaluated and compared numerically with the standard version of H.264/AVC (JM18.6) in terms of Bjontegaard Delta bit rate, Bjontegaard Delta PSNR and run time [19]. Different set of videos with different resolutions at frame rate of 30Hz are used for testing and are depicted in Table I as follows:

TABLE. I. Set of Videos Sequences with different Resolutions

Videos Resolution	**Tested Video Sequences**
1080p	Station2 and Pedestrian (1920x1080)
720p	Johnny and kristenandsara (1280x720)
576p	Harbour and Soccer (704x576p)
CIF	Stefan, Container, Hall and Mother-daughter (352x288)
QCIF	Claire, Akiyo, Hall and News (176x144)

The setting parameters for the proposed technique are:

1) A group of IIII........I frames from the test videos for luminance components of the frames, while the intra prediction based block size 8 is applied on the chrominance components of I frames.

2) Entropy coding of Context Adaptive Variable Length Coding (CAVLC),

3) Quantization parameters (QP) are setting at 20, 24, 28 and 32.

The performance of the proposed algorithm is evaluated through its comparison to the standard reference video coding JM 18.6 and the results of simulation in terms of different metrics are presented to demonstrate the suggested approach efficiency. The simulation results and BD curves of the proposed method using the Bjontegaard Delta (BD) parameters to the set of test videos with resolutions QCIF, CIF, 576p, 720p and 1080p comparing to that of the reference coding JM18.6 are visually shown in Fig. 7 (a to d), Fig. 8 (a to d) and Fig. 9 (a to f), respectively. Additionally, the numerical results to the performance of the proposed algorithm in terms of BD measurements of both bit rate (BDBR) and peak signal to noise ratio (BDPSNR) are depicted in Tables II and III for the video sequence with different resolutions including the high definition (HD) video resolution 1080p. While the setting parameters for JM18.6 are: enabling for both of RD-Optimization, RD-quantization and slice mode equals zero. Also, QP equals 20, 24, 28 and 32 and CAVLC are used with the reference code JM18.6.

Where: BD_PSNR and BD_ Bit Rate are the average PSNR difference and average percentage of time saving between the reference JM18.6 video coding and the proposed technique, respectively.

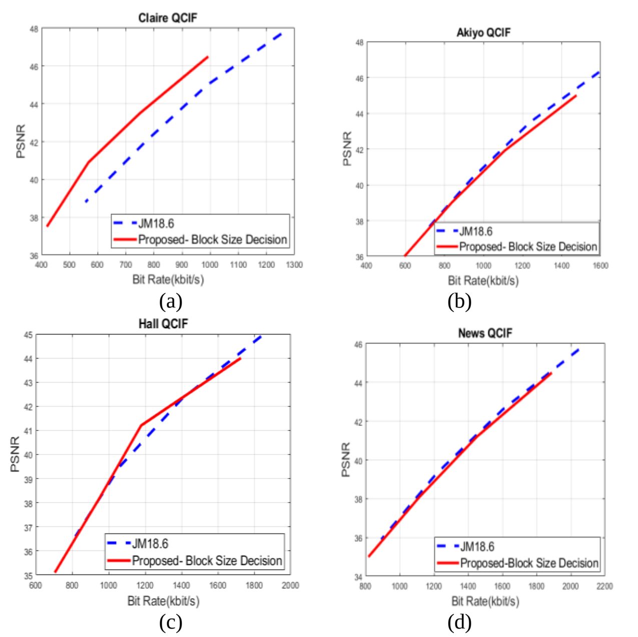

Fig. 7. (a-d) BD Curves for QCIF Test Video Sequences with the Proposed Approach and JM18.6.

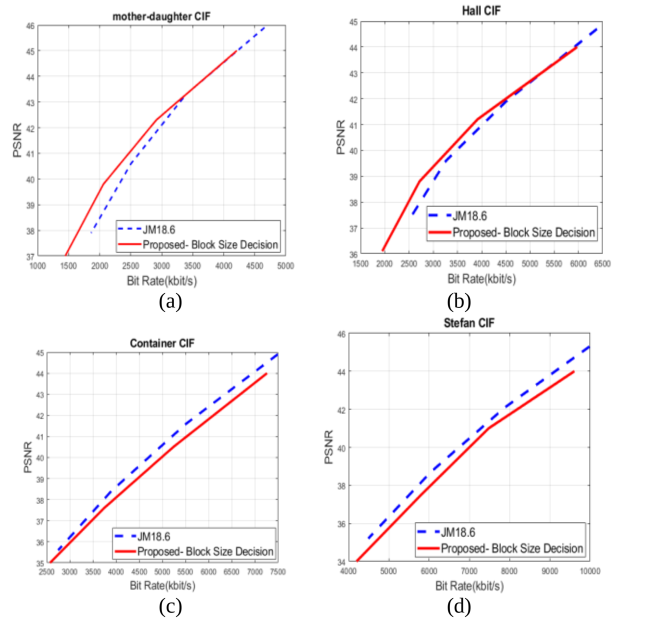

Fig. 8. (a-d) BD Curves for CIF Videos Sequences to the Proposed Approach and JM18.6.

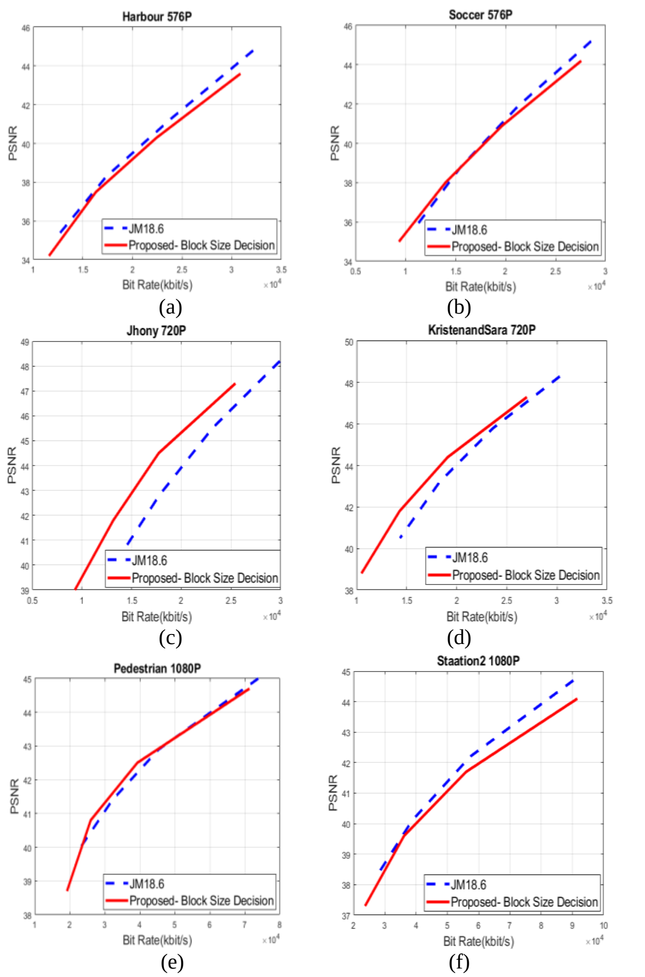

Fig. 9. (a-f) BD Curves for Test Video Sequences of 576p, 720p and 1080p Resolutions to the Proposed Approach and JM18.6.

The sign (-) means value decreasing while the sign (+) means increasing in value. As demonstrated in Table III, the proposed method achieve best simulation results for the video sequences with QCIF resolution in which the values of BDPSNR increased from 0.2 to 1.6 for both of videos sequence Claire and hall, and the values of BDBR to aforementioned videos decreased by percentage values range from 0.79 to 14.9. In contrast, with the videos sequences Akiyo and News QCIF resolution; the BD-PSNR values slightly decreased by percentage values ranging from 0.17 to 0.24 and the BDBR increased from 1.5 to 2.3, respectively.

Concerning the simulation results for the videos sequences with CIF resolution, the values of BDPSNR increased for both of Mother-daughter and Hall videos from 0.49 to 0.58 respectively, while slightly decreased for both of the videos sequence Stefan and Container from 0.47 to 0.6, respectively. On the other hand, the values of BDBR decreased from 5.5 to 6.2, respectively for both of the videos sequences Mother-daughter and Hall, while BDBR value increased from 5.1 to 5.3 for the videos sequences Stefan and Container. The percentage values in the time saving of the proposed algorithm for the videos sequences with QCIF and CIF resolutions was from 0.42 to 0.68.

Regarding the high resolutions videos, the simulation results of BDPSNR of the proposed technique as depicted in Table II slightly decreased by percentage values from 0.005 to 0.3 for the videos sequence with resolutions 576p and 1080p. While BDPSNR increased from 0.96 to 1.5 for the videos sequences with 720p resolution. The results of BDBR increased by percentage values from 0.4 to 3.5 for both of the videos sequences with resolutions 576p and Station2 video with 1080p resolution. While, BDBR decreased from 1.8 to 15.3 for 720p video sequences and Pedestrian video with 1080p.

TABLE. II. THE COMPARISON OF THE PROPOSED APPORACH IN TERMS OF BDPSNR AND BDBR TO HIGH RESOLUTIONS VIDEOS: 576P,720P AND 1080P

Reso-lution	Video Test	QP	PSNR (dB)			Bit rate (Kbits)		
			JM 18.6	Proposed	BD PSNR	JM 18.6	Proposed	BD BR%
576P	Harbour	20	**44.8**	43.6	-0.35	**32165**	30880	3.59
		24	**41.3**	40.3		**23937**	22436	
		28	**38.3**	37.5		**17368**	16321	
		32	**35.2**	34.2		**12405**	11588	
576P	Soccer	20	**45.2**	44.2	-0.005	**28554**	27562	0.45
		24	**41.9**	40.9		**21255**	19660	
		28	**38.8**	38		**15520**	13980	
		32	**35.7**	35		**10927**	9337	
720P	Johnny	20	**48.2**	47.3	1.51	**29901**	25428	-15.3
		24	**45.5**	44.5		**23115**	17715	
		28	**42.8**	41.8		**17769**	13145	
		32	**40.4**	39		**13870**	9284	
720P	Kristen And Sara	20	**48.3**	47.3	0.96	**30278**	26991	-8.27
		24	**45.8**	44.4		**23606**	19083	
		28	**43.2**	41.8		**18272**	14285	
		32	**40.5**	38.8		**14326**	10484	
1080P	Station2	20	**44.7**	44.1	-0.3	90346	91590	0.4
		24	**42.2**	41.7		57316	56010	
		28	**40.1**	39.6		38707	36151	
		32	**38.3**	37.3		27509	23681	
1080P	Pedestrian	20	**45**	**44.7**	-0.07	73870	71339	-1.8
		24	**42.9**	**42.5**		45419	39282	
		28	**41.4**	**40.8**		32186	25991	
		32	**40**	**38.7**		23104	19217	

TABLE. III. THE COMPARISON OF THE PROPOSED APPROACH WITH JM18.6 IN TERMS OF BDPSNR AND BDBR TO QCIF, CIF RESOLUTIONS VIDEOS AND THE RUNNING TIME

Resolution	Sequence	QP	PSNR (dB)			Bit rate (Kbits)			Running Time (Sec)		
			JM 18.6	Proposed	BDPSNR	JM 18.6	Proposed	BDBR %	JM 18.6	Proposed	Average Time Saving %
QCIF	Claire	20	47.7	46.4	1.6124	**1253**	993	-14.953	**47**	11.5	%-56
		24	45	43.5		**990**	750		**34**	11	
		28	42	40.9		**770**	567		**26**	10.8	
		32	38.8	37.5		**556**	419		**20**	10.5	
QCIF	Hall	20	44.9	44	0.2041	**1837**	1726	-0.7940	**71**	13.3	%-68
		24	42.3	41.2		**1401**	1178		**55**	12.5	
		28	39.5	38.2		**1061**	950		**41.5**	12	
		32	36.6	35.1		**817**	704		**31.3**	11.5	
QCIF	Akiyo	20	46.3	45	-0.2409	**1592**	1476	2.3738	**56**	12.8	%-57
		24	43.5	41.9		**1238**	1107		**42**	12.3	
		28	40.3	39		**935**	836		**31**	11.8	
		32	37.3	36		**692**	594		**23**	11.6	
QCIF	News	20	45.7	44.5	-0.17	**2047**	1889	1.5	**82**	16	-68%
		24	42.6	41.2		**1602**	1451		**64**	13	
		28	39.3	38.1		**1215**	1116		**48**	12.8	
		32	35.9	35		**892**	817		**35**	12.7	
CIF	Mother-daughter	20	45.9	45	0.5811	**4656**	4209	-6.2416	**156**	44	%-42
		24	43.3	42.3		**3392**	2912		**113**	42	
		28	40.6	39.8		**2503**	2059		**85**	41	
		32	37.9	37		**1862**	1444		**69**	40	
CIF	Hall	20	44.7	44	0.4973	**6382**	5972	-5.5747	**228**	44	-61%
		24	41.9	41.2		**4506**	3914		**165**	42	
		28	39.6	38.8		**3263**	2716		**124**	40	
		32	37.3	36.1		**2497**	1946		**96**	37	
CIF	Stefan	20	45.3	44	-0.6	**9982**	9605	5.1	**369**	61	%-68
		24	42.1	41		**7882**	7478		**293**	58	
		28	38.7	37.5		**6040**	5800		**216**	54	
		32	35.2	34		**4487**	4196		**159**	52	
CIF	Container	20	44.9	44	-0.47	**7494**	7260	5.3	**304**	47	-66%
		24	41.6	40.5		**5509**	5235		**227**	44	
		28	38.4	37.6		**3891**	3738		**161**	41	
		32	35.6	35		**2744**	2568		**114**	40	

VI. Conclusion

In this paper, an efficient technique for block size decision to the intra prediction stage of H2.64 video coding is suggested. An optimal global threshold based on the 2-D Otsu method is suggested for block partitioning. The proposed method considers the between classes variance as feature for the block size decision. The suggested technique achieved acceptable results comparing to the reference JM18.6 video coding. By the proposed approach, a tangible acceleration on the code running time was accomplished with improvement in both of PSNR and bit rate with some of CIF and QCIF videos. While with some others CIF and QCIF videos, the running time acceleration was accompanied with slightly degradation in the visual quality and increasing in bit rate. Also with high video resolutions, the increasing of PSNR may be accompanied occasionally with decreasing in bit rate while it may be accompanied with increasing in bit rate with others. The results of simulation demonstrate saving in time by average 42% to 68% with QCIF and CIF videos. Besides, the visual quality in terms of BDPSNR improved in which its value increased from 0.2 to 1.6, while the value of BDBR reduced from 0.79 to 15.3 respectively with some videos of resolutions QCIF, CIF and 720p. While with high videos resolutions there is some improvement in visual quality but on expense of running time and increasing in bit rate.

References

[1] Draft ITU-T Recommendation and Final Draft International Standard of Joint Video Specification, document JVT-G050.doc, ITU-T Rec. H.264 and ISO/IEC 14496-10 AVC, 2003.

[2] T. Wiegand, G. J. Sullivan, G. Bjontegaard, and A. Luthra, “Overview of H.264 video coding standard,” IEEE Trans. Circuits Syst. Video Technol., vol. 13, no. 7, pp. 560–576, Jul. 2003.

[3] G. J. Sullivan and T. Wiegand, “Rate-distortion optimization for video compression,” IEEE Signal Process. Mag., vol. 15, no. 6, pp. 74–90, Nov. 1998.

[4] Yi-Hsin Huang; Tao-Sheng Ou; Chen, H.H.; , "Fast decision of block size, prediction mode, and intra block for H.264 intra prediction," Circuits and Systems for Video Technology, IEEE Transactions on , vol.20, no.8, pp.1122-1132, Aug. 2010.

[5] Y. K. Lin and T. S. Chang, “Fast block type decision algorithm for intra prediction inH.264 frext,” in Proc. IEEE Int. Conf. Image Process., Sep. 2005,vol. 1, pp. 585–588.

[6] Tianruo Zhang, Guifen Tian, Satoshi Goto, "A frequency-based fast block type decision algorithm for intra prediction in H.264/AVC high profile," Circuits and Systems, 2008. APCCAS 2008. IEEE Asia Pacific Conference on , vol., no., pp.1292-1295, Nov. 30 2008-Dec. 3 2008.

[7] Yung-Chiang Wei, Chao-Hsuing Tseng, "Transformed domain block size and intra mode decision for advanced video coding," Computer Communication Control and Automation (3CA), 2010 International Symposium on , vol.1, no., pp.221-224, 5-7 May 2010.

[8] J. Ostermann et al., “Video coding with H.264/AVC: Tools, performance, and complexity,” IEEE Circuits Syst. Mag., vol. 4, no. 1, pp. 7–28, Jan./Mar. 2004.

[9] S.-K. Kwon, A. Tamhankar, and K. R. Rao, “Overview of H.264/MPEG-4 part 10,” J. Vis. Commun. Image Represent., vol. 17, no. 2, pp. 186–216, Apr. 2006.

[10] T. Wiegand, G. J. Sullivan, G. Bjøntegaard, and A. Luthra, “Overview of the H.264/AVC video coding standard,” IEEE Trans. Circuits Syst. Video Technol., vol. 13, no. 7, pp. 560–576, Jul. 2003.

[11] Sara Hamdy, AbdelhalimZekry and Wael A. Mohamed , "Development of the best prediction matrix mode algorithm for-intra prediction in h.264 encoder", International Journal of Engineering & Technology, 7 (4) (2018) 3847-3853.

[12] Manjanaik.Na, Parameshachari B Db Hanumanthappa S Nc, Reshma Banud, "Intra Frame Coding In Advanced Video Coding Standard (H.264) to Obtain Consistent PSNR and Reduce Bit Rate for Diagonal Down Left Mode Using Gaussian Pulse" IOP Conf. Series: Materials Science and Engineering 225 (2017) 012209, doi:10.1088/1757-899X/225/1/012209.

[13] Kyungmin Lim, Seongwan Kim, Jaeho Lee, Daehyun Pak and Sangyoun Lee, "Fast Block Size and Mode Decision Algorithm for Intra Prediction in H.264/AVC", IEEE Transactions on Consumer Electronics, Vol. 58, No. 2, May 2012.

[14] Lih-Jen Kau, Member and Jia-Wei Leng, " A Gradient Intensity-Adapted Algorithm With Adaptive Selection Strategy for the Fast Decision of H.264/AVC Intra-Prediction Modes", IEEE TRANSACTIONS ON CIRCUITS AND SYSTEMS FOR VIDEO TECHNOLOGY, VOL. 25, NO. 6, pp: 944-957, JUNE 2015.

[15] Carlos Mera and Maria Trujillo, "Using Dispersion Measures for Deterring Block-Size In-Motion Estimation", DYNA, Vol. 79, Num. 171 , pp. 97-104 , (2012).

[16] N. Otsu, "A threshold selection method from gray level histograms", IEEE TRANSACTIONS ON SYSTEMS, MAN, AND CYBERNETICS, VOL. 9, No. 1, pp. 62-66, JANI'ARY 1979.

[17] Wuli Wang, Liming Duan and Yong Wang, "Fast Image Segmentation Using Two-Dimensional Otsu Based on Estimation of Distribution Algorithm", journal of Electrical and Computer Engineering, Article ID 1735176, PP.1-12 , September 2017,Hindawi, https://doi.org/10.1155/2017/1735176.

[18] Fangyan Nie , Yonglin Wang , Meisen Pan , Guanghan Peng and Pingfeng Zhang, "Two-dimensional extension of variance-based thresholding for image segmentation", (2013) 24:485–501, © Springer Science+Business Media, DOI 10.1007/s11045-012-0174-7

[19] G. Bjontegaard, “Calculation of average PSNR differences between RD curves,” presented at the 13th VCEG-M33 Meeting, Austin, TX, Apr. 2001.

A Framework for Cloud Security Risk Management based on the Business Objectives of Organizations

Ahmed E. Youssef
College of Computer and Information Sciences
King Saud University, Riyadh, Saudi Arabia
Faculty of Engineering, Helwan University, Cairo, Egypt

***Abstract*—Security is considered one of the top ranked risks of Cloud Computing (CC) due to the outsourcing of sensitive data onto a third party. In addition, the complexity of the cloud model results in a large number of heterogeneous security controls that must be consistently managed. Hence, no matter how strongly the cloud model is secured, organizations continue suffering from lack of trust on CC and remain uncertain about its security risk consequences. Traditional risk management frameworks do not consider the impact of CC security risks on the business objectives of the organizations. In this paper, we propose a novel Cloud Security Risk Management Framework (CSRMF) that helps organizations adopting CC identifies, analyze, evaluate, and mitigate security risks in their Cloud platforms. Unlike traditional risk management frameworks, CSRMF is driven by the business objectives of the organizations. It allows any organization adopting CC to be aware of cloud security risks and align their low-level management decisions according to high-level business objectives. In essence, it is designed to address impacts of cloud-specific security risks into business objectives in a given organization. Consequently, organizations are able to conduct a cost-value analysis regarding the adoption of CC technology and gain an adequate level of confidence in Cloud technology. On the other hand, Cloud Service Providers (CSP) is able to improve productivity and profitability by managing cloud-related risks. The proposed framework has been validated and evaluated through a use-case scenario.**

Keywords—Information security; data privacy; cloud security risks; risk management; business objectives; cloud computing

I. Introduction

The importance of Cloud Computing (CC) is increasing and it is receiving a growing interest by many scientific and business organizations [11]. According to the National Institute of Standards and Technology (NIST) [32], cloud computing is a model for enabling convenient, ubiquitous, on-demand access to a shared pool of configurable resources (e.g., networks, servers, storage, and applications) which can be easily delivered with different types of service provider interaction that follow a simple Pay-As-You-Go (PAYG) model. In PAYG model, the Cloud Service Consumers (CSC) can request the computing services as needed to their business; the services are provided on-demand by the Cloud Service Providers (CSP), and the CSC only pay for the services they have used. The many advantages that CC brings to organizations, such as high scalability and flexibility, excellent reliability and availability, economy of scale, consolidation and energy saving, are well-documented [35]. Furthermore, CC is poised to be a significant growth area, according to Forbes, CC market is projected to reach $411B by 2020 [30]. LogicMonitor has conducted a survey to explore the landscape for cloud services in 2020, one of the interesting findings in this survey is that 83% of enterprise workloads will be in the Cloud by 2020 [36].

Although the benefits of CC are significant for many organizations, it has brought many risks that influence its confidence and feasibility. Fig. 1 shows the most important risks for organizations adopting CC [36]. Security is considered one of the top ranked risks of CC [12,13], From the CSC perspective, the main reasons for distrust on CC are its multi-tenancy nature and the outsourcing of sensitive data, critical applications and infrastructure onto the cloud. On the other hand, from CSP perspective, security issue in CC is also a challenge because of the complexity of the cloud model that results in a large number of heterogeneous security controls that must be consistently managed.

Organizations have many security concerns about migration to the cloud such as loss of control over their data, lack of security guarantees, and sharing their data with malicious users. These risks often create fears in the side of organizations causing them to rethink their decisions in adopting CC technology. No matter how strongly the cloud model is secured, organizations continue suffering from lack of trust on cloud and remain uncertain about its economic feasibility. Although the provision of zero-risk service is not practically possible, an effective security risk management framework may lead to a higher confidence of organizations in CC and help them take well-informed decisions regarding the adoption of this emerging technology. Traditional risk management frameworks do not fit CC well due the assumption by those frameworks that the assets are owned and fully managed by the organization itself. Moreover, none of them considers organization's security requirements and the effect of CC security risks on its business objectives.

This paper proposes a novel Cloud Security Risk Management Framework (CSRMF) that helps organizations and CSP identify, analyze, evaluate security risks in CC platforms, and establish the best course of action to avoid or mitigate them. Unlike traditional risk management framework, CSRMF considers organization's security requirements and is driven by the impact of CC security risks on the achievement of its business objectives. It allows any organization adopting CC to be aware of cloud security risks and align their low-level management decisions according to high-level business objectives. In essence, it is designed to address impacts of cloud-specific security risks into business objectives in a given organization. Consequently, organizations are able to conduct a cost-value analysis and take a well-informed decision regarding the adoption of CC technology. On the other hand, CSP are able to improve productivity and profitability by managing cloud-related risks. This framework provides an adequate level of confidence in CC for organizations and a cost-effective productivity for CSP.

Fig. 1. The Biggest Challenges for Organization Engaged with CC.

The rest of this paper is organized as follows: section 2 briefly introduces the main concepts in risk management. In section 3, related work is reviewed. Section 4 describes the proposed framework (CSRMF) in detail. In Section 5, we evaluate the framework through a use case scenario. Finally, in section 6, we give our conclusions and future work.

II. Risk Management

Risk is defined as the possibility of a hazardous event occurring that will have an adverse consequence on the achievement of the objectives of an organization [2]. Risks are unavoidable and persistently exist in our daily life in almost every situation [10]. The main concepts related to risks are: Asset: something to which an organization assigns value and hence it needs protection. Threat: a potential undesired event that harms or reduces the value of an asset. Vulnerability: a flaw or deficiency that may be exploited by a threat to harm assets. Risk likelihood: the probability that a risk occurs. Risk impact: the degree by which a risk influences (i.e., causes loss of satisfaction of) an organization's objective(s). Risk level: the severity of a risk derived from its likelihood and impact. Risk tolerance: the amount of satisfaction or pleasure regarding the risk level. For example, a server is considered as an asset, a threat could be a backdoor virus attack, and a vulnerability is a virus scan not up to date. The likelihood that a computer is infected by this virus is medium, but its impact on data integrity is high [1, 2].

Risk management is the art and science of identifying, analyzing, evaluating and responding to risks throughout the service lifecycle. It enables an organization to recognize uncertain events that may result in unfortunate or damaging consequences and to set the best course of action to avoid or mitigate them [4,15]. However, in order to apply risk management effectively, it is vital to first identify the overall vision, mission and objectives of an organization. Risk management is about making decisions that contribute to the achievement of an organization's objectives such as costs with benefits and expectations in investing limited public resources. It protects and adds value to the organization and its stakeholders by:

- Enhancing safety and security in an organization.
- Protecting organization's assets and reputation.
- Optimizing operational efficiency.
- Supporting the achievement of organization's objectives by satisfying stakeholders' expectations and improve their confidence and trust.
- Improving decision making by comprehensive understanding of business activities in organizations.

A Risk Management Framework (RMF) is a set of components that provide the foundations for risk management throughout the organization. Fig. 2 shows the evolution of RMF [37].

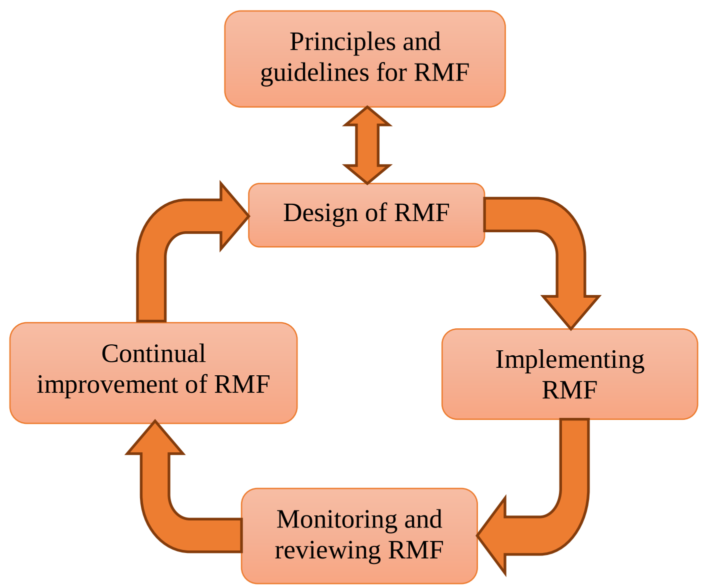

Fig. 2. Standard Risk Management Framework Evolution.

III. Related Work

In literature, there are many frameworks that help in security risk management [3,5-9,14,20-29,39], however, these traditional risk management frameworks do not fit CC well due to the complexity of CC environment and the assumption by those frameworks that the assets are owned and fully managed by the organization itself. In addition, none of them considers organization's security requirements and the effect of CC security risks on the business objectives and goals of the organizations. The work presented in this paper aims to develop an RMF that is driven by the impact of CC security risks on the business objectives of organizations adopting CC technology. The existing information security risk management frameworks are described below.

QUIRC: a quantitative impact and risk assessment methodology for CC projects developed to assess the security risks associated with CC platforms [8]. This framework uses the definition of risk as a combination of the probability of a security threat event and its severity, measured as its impact. Six key security criteria (Confidentiality, Integrity, Availability, Multiparty trust, Auditability, and Usability) are identified for cloud platforms, they are referred to as the CIAMAU framework, and it is shown that most of the typical attack vectors and events map under one of these six categories. QUIRC employs a quantitative approach that gives vendors, customers and regulation agencies the ability to comparatively assess the relative robustness of different cloud vendor offerings and approaches in a defensible manner. Limitations of this approach include that it requires the meticulous collection of input data for probabilities of events, which requires collective industry inputs.

OPTIMS: an effective and efficient risk assessment framework for cloud service provision [1, 2]. Four risk categories, namely legal, technical, policy, and general were identified. This framework is beneficial for end-users and Service Providers (SP) approaching the cloud to deploy and run services, as well as Infrastructure Providers (IP) to deploy and operate those services. These benefits include supporting various parties for making informed decisions regarding contractual agreements. The risk assessment framework is fully integrated in the OPTIMIS toolkit, which simplifies cloud self-management, optimizes the cloud service lifecycle, and supports various cloud architectures. However, the SP dynamic risk assessment is limited due to the lack of support for service consumer's side monitoring tools and the limited availability of shared monitored data from IPs.

CARAM: is a qualitative and relative risk assessment model that helps CSC select CSP that fit their risk profile the best [9]. It consists of tools that complements the various recommendations of ENISA [33] and CSA [40]. These tools include a questionnaire for CSC, an algorithm to classify the answers to Cloud Assessment Initiative Questionnaire (CAIQ) to discrete values, a model that maps the answers to both questionnaires to risk values, and a multi criteria decision approach allowing to quickly and reliably compares multiple CSP. However, there are limitations that may affect the accuracy of the results mainly stemming from the analyzed input data such as: Vague formulation of the CAIQ answers provided by the analyzed CSP, Possibility for deliberate misinformation in the CAIQ, and Ineffective implementation of the security controls by the analyzed CSPs.

CRAMM: a risk analysis and management method that includes a comprehensive range of risk assessment tools that are fully compliant with ISO27001 and address tasks such as: asset dependency modeling, identifying and assessing threats and vulnerabilities, assessing risk levels, and identifying required controls [14,22]. It provides a staged and disciplined approach embracing both technical (e.g. hardware and software) and non-technical (e.g. physical and human) aspects of security. The major flaws in CRAMM are: 1) quantitative risk assessment cannot be provided. Hence, there is need to extend this methodology in this direction and 2) it does not clearly talk about the security attributes e.g. Confidentiality, Integrity, and Availability [23].

COBRA: a risk assessment model that consists of a range of risk analysis, consultative and security review tools which were developed largely in recognition of changing nature of IT and security, and the demands placed by business upon these areas [39]. The default risk assessment process usually consists of three stages: questionnaire building, risk surveying, and report generation. The major weaknesses of COBRA are 1) risk assessment technique is not clearly mentioned; hence, there is need to extend this methodology in this direction and 2) threats and vulnerabilities play a very important role in the process of risk assessment; but how these are taken into consideration, is not clearly given in COBRA [23].

IV. The Proposed Framework

We propose a Cloud Security Risk Management Framework (CSRMF) that implies methods for identifying, analyzing, evaluating, treating, and monitoring security risks throughout the cloud service lifecycle. In this context, assets include data hosted on the cloud, physical nodes, virtual machines, and other cloud resources as well as the Service Level Agreement (SLA), risks are potential security threats attacking the assets in CC platforms causing loss of satisfaction of organization's objectives. The proposed CSRMF aims at:

- Identifying the risks that present threats to the cloud within the context of organization's concerns.
- Analyzing and evaluating identified risks with respect to organization's goals and objectives.
- Applying the best course of treatment actions to reduce the likelihood and/or the impacts of these risks.
- Monitoring the currency of identified risks regularly to ensure that treatment actions are valid.
- Establishing a dynamic relationship between the organization and CSP during risk management process to ensure the compliance to SLA.

Fig. 3 shows the main components of the proposed framework. In the following subsections, we discuss each one of these components.

A. *Identifying Organization's Business Objectives*

Organizational objectives are short-term and medium-term goals that an organization seeks to accomplish. Achievement of these objectives helps an organization reach its overall strategic goals. Therefore, the proposed framework, CSRMF, is driven by the organization's high-level objectives. Organizational objectives are established through understanding the overall internal culture (e.g. vision, mission, etc.) of the organization and a number of environmental analyses that include identifying the constraints and opportunities of the operating environment.

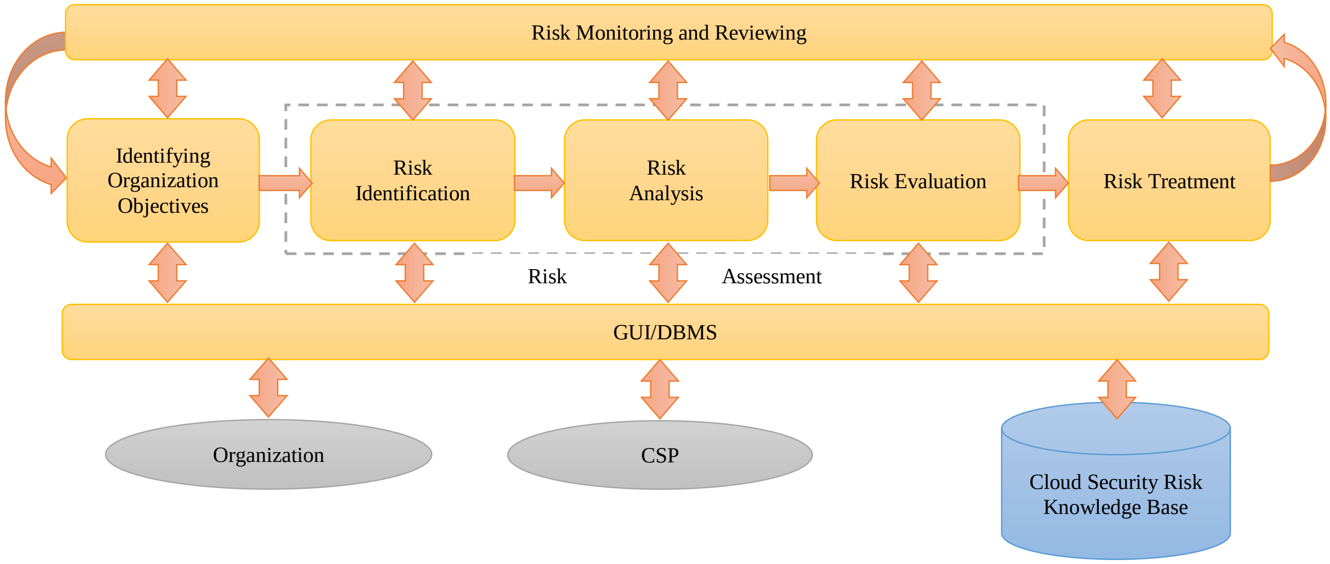

Fig. 3. The Proposed Framework (CSRMF).

To set the organization's objectives, CSRMF proposes to conduct SWOT analysis [41] where organizations identify their internal Strengths and Weaknesses as well as external Opportunities and Threats. This information allows CEO to develop objectives and strategies that are relevant and realistic to their organizations. In CSRMF, organizational objectives should follow the SMART model (i.e., should be Specific, Measurable, Attainable, Relevant, and Time bound). To apply the SMART model, CEO have to ask themselves the following questions when setting their organizations' objectives:

- Specific – What type of company do you want to be the best at? On what scale do you want to compete? Do you want to be the best company in your area or in the world?
- Measurable–How will you know when you have achieved your objective? What benchmarks are you going to use to measure your success?
- Attainable–Is this objective achievable given your resources? What are the obstacles that you are going to encounter and can you get past the hurdles?
- Relevant–How relevant is this objective to the company and its employees? Will it benefit your organization?
- Time bound–When do you want to achieve this objective by?

Examples for good organization objectives are: achieving financial success, increasing sales figures, improving human resources, retaining talented employees, focusing on customer service, and establishing brand awareness.

B. *Risk Identification*

The second phase in CSRMF is to identify risks that are likely to affect the achievement of the objectives of the organization. The identification of security risks affecting cloud services in organizations that adopt CC is the most critical step in risk management. The better identifying and understanding these risks, the more meaningful and effective will be the risk management process. The appropriate risk identification method will depend on the application area (i.e., nature of activities and the hazard groups), the nature of projects in organization, resources available, regularity requirements and client requirements as to objectives, desired outcome and the required level of detail. However, there is no single scientific method that guarantees identification of all risks [10].

Risks are caused by security threats that may exploit vulnerabilities in CC platform to harm organization's assets and consequently affect the achievement of its objectives. Therefore, in order to identify risks precisely, we need to identify assets, vulnerabilities, and threats in CC platform. Since there is no single scientific approach that guarantees identification of all risks, CSRMF employs a hybrid approach that combines two techniques for risk identification. This combination will be more effective for full and adequate coverage of risks. Risk identification techniques that are employed by CSRMF are: documented knowledge acquisition and brainstorming.

C. *B.1. Documented Knowledge Acquisition*

This technique implies collecting and reading documents about CC risk domain such as books, surveys, articles, and regulations. Many documents in literature have attempted identifying CC risks and threats [31-33, 38,40]. One of the most useful documents regarding CC risk is the one provided by the European Network and Information Security Agency (ENISA) [33] that affords generic lists of risks for CC. Examples of such risks are Lock-in, Resource Exhaustion, Isolation Failure and Malicious Insider, a sample of these risks is shown in Fig. 4. However, these lists do not reflect the organization objectives nor they reveal a specific class of business applications.

R.1 LOCK-IN

Probability	HIGH	Comparative: Higher
Impact	MEDIUM	Comparative: Equal
Vulnerabilities	V13. Lack of standard technologies and solutions V46. Poor provider selection V47. Lack of supplier redundancy V31. Lack of completeness and transparency in terms of use	
Affected assets	A1. Company reputation A5. Personal sensitive data A6. Personal data A7. Personal data - critical A9. Service delivery – real time services A10. Service delivery	
Risk	**HIGH**	

Fig. 4. A Sample of ENISA CC Risk Identification (LOCK-IN Risk).

The documented knowledge acquisition technique is an important prerequisite to other techniques. However, the huge amount of available documentation may lead to irrelevant details and outdated information. An effective solution that we employed to solve this issue is to use meta-knowledge (know what you need to know and what you do not need to know) to prune the document space. The knowledge acquired in this step is stored in a cloud security risk knowledge base for use in the next step (i.e., brainstorming).

D. B.2. Brainstorming

Brainstorming a semi-structured creative group-based activity, used most often in ad-hoc business meetings to come up with new ideas for solving problems, innovation or improvement [34]. It usually involves a group, under the direction of a facilitator and implies two stages:

1) Idea generation: generate as many ideas as possible to address the problem from each participant without criticism.

2) Idea evaluation: by all participants together according to agreed criteria (e.g. value, cost, feasibility) to prioritize ideas.

In CSRMF, members of a team that comprises information security experts and a diverse group of stakeholders in the organization meet to identify organization's assets, vulnerabilities, and potential threats. Risks identification takes place in a series of group workshops; group sessions provide a wider exploration of issues and more creative ways for identifying risks. The group uses the knowledge acquired in the previous step to identify different risks. The outcome of this step is a list of identified risks which is reviewed by an independent stakeholders group. If satisfaction is achieved the risk management process proceeds to the next phase, otherwise, it goes through another round of risk identification.

E. Risk Analysis

Risk analysis involves the estimation of risks likelihoods and impacts. CSRMF deploys a quantitative approach for risk analysis and assumes the following:

- Objective weight (w_j): the importance of an objective $o_{j,}$ $(0 \leq w_j \leq 1, \sum_j w_j=1,\ j = 1,2,\dots,m)$
- Risk Likelihood L(r_i): the probability of occurrence of risk r_i. $(0 \leq L(r_i) \leq 1,\ i = 1,2,\dots,n)$.
- Risk Impact I(r_i^j): the effect of r_i on o_j, $(0 \leq I(r_i^j) \leq 1)$, where 0 means no loss of satisfaction in o_j, 1 means total loss of satisfaction in o_j, m and n are numbers of objectives and risks respectively.

The goal of risk analysis phase is to estimate values for $L(r_i)$ and $I(r_i^j)$. A widely accepted consensus-based estimation technique is the Delphi method [8, 16-19]. Three essential characteristics of Delphi method are: 1) structured and iterative information flow, 2) anonymity of the participants in order to alleviate peer pressure and other performance anxieties, and 3) iterative feedback of the participants until consensus is reached. We adapted the Delphi technique for the estimation of security risk likelihood and impacts; this is shown in Fig. 5.

In CSRMF Delphi technique, a moderator is used to control and facilitate information gathering from a selected group of Subject Matter Experts (SME). SME are knowledgeable about the likelihoods and impacts of risks on the organization's particular type of business. During the Delphi process, each participant is asked to provide his best numerical estimates of w_j, $L(r_i)$ and $I(r_i^j)$. Following this step, the moderator collects the estimates from all participants in anonymous presentation, shares and analyses the combined results with all participants. The participant are encouraged to iteratively reconsider and modify their estimates based on the feedback from previous discussion. When estimates reach a consensus (e.g. 85% or more), the moderator reports the final estimates to be used in the next phase.

F. Risk Evaluation

Risk evaluation implies estimate of the risk level (i.e., risk severity) to be able to decide whether the risk is tolerable (i.e., acceptable) by the organization or not. Tolerable risk criteria must be defined, approved, and documented by relevant committee from experts and stakeholders. Should the estimated risk level greater than the tolerable level then the specific risk needs treatment or improved countermeasures. In CSRMF, risks are evaluated using a quantitative approach, the level of risk r_i ($Level(r_i)$) is estimated using equation 1.

$$Level(r_i) = L(r_i) \sum_{j=1}^{m} w_j\, I(r_i^j) \tag{1}$$

$$0 \leq Level(r_i) \leq 1$$

Risk level ($Level(r_i)$) ranges between 0 and 1, where 0 means r_i has no effect (min. severity) on the organization's objectives and 1 means r_i has significant effect (max. severity) on organization's objectives. A risk , r_i, may be considered acceptable (tolerable) if $Level(r_i)$ is less than threshold α, otherwise r_i requires treatment. This threshold $(0 \leq \alpha \leq 1)$ is predetermined by the organization. By applying this condition an organization can achieve an acceptable Global Risk Level (GRL) which is given by equation 2.

$$GRL = \sum_{i=1}^{n} Level\,(r_i) \tag{2}$$

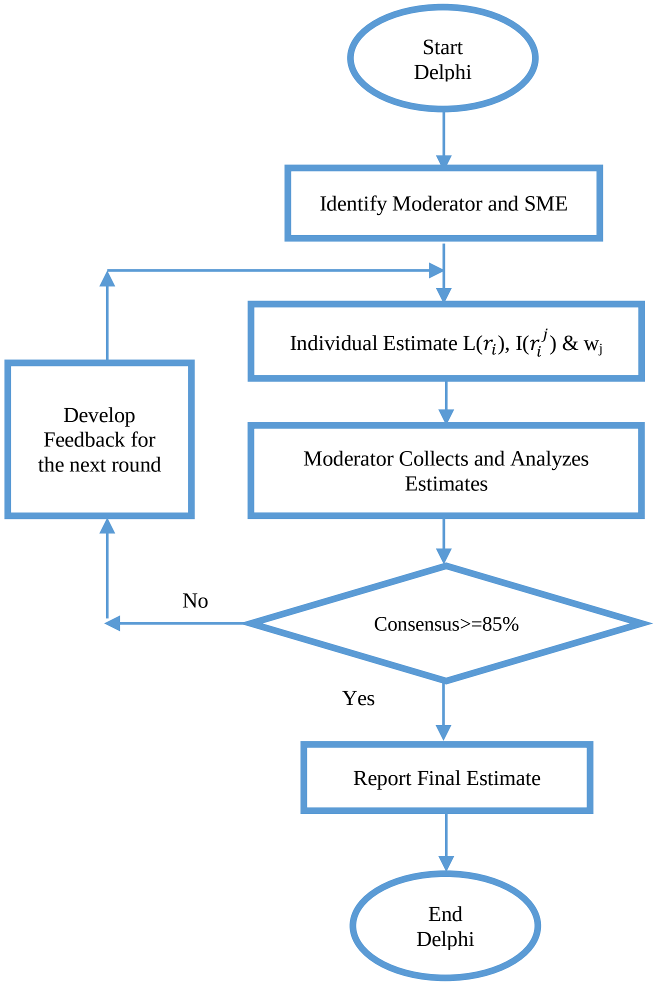

Fig. 5. The Delphi Process for Risk Analysis as used in CSRMF.

G. Risk Treatment

Any unacceptable risk should be treated, which means to reduce its risk level to become less than the threshold α. The objective of risk treatment is to develop cost effective options for treating unacceptable risks. Different treatment options may be employed, which are not necessarily mutually exclusive or appropriate in all circumstances such as risk avoidance, risk transfer or share with a third party and risk mitigation (reduction) which means controlling the likelihood of risk occurrence, or controlling the impact of the consequences if the risk occurs.

CSRMF employs risk mitigation approach for risk treatment. The ultimate goal is to reduce GRL by reducing $Level(r_i)$ for each unacceptable risk. Risk likelihood, $L(r_i)$, can be reduced through preventative maintenance, or quality assurance and management, change in business systems and processes. On the other hand, risk impact, $I(r_i^j)$, can be reduced through contingency planning, minimizing exposure to sources of risk or separation/relocation of an activity and resources. Risk mitigation actions can be determined using a combination of documented knowledge acquisition and brainstorming techniques. Examples for CC risk mitigation actions (countermeasures) adopted in CSRMF are shown in Table I.

TABLE. I. EXAMPLES OF RISK COUNTERMEASURES USED IN CSRMF

CC risk	**Countermeasures**
Account or service hijacking	-Identify and access management guidance -Dynamic credentials
Data leakage	-Fragmentation Redundancy Scattering (FRS) -Digital signature -Encryption
Customer data manipulation	-Web application scanners
Malicious VM	-Protecting aegis from live migrations of VMs
Sniffing/spoofing virtual Net	-Virtual Network security guarantees

H. Risk Monitoring

The last phase in CSRMF is to monitor and evaluate the effectiveness of the preferred risk treatments and current control activities. To do this, we need to estimate the risk level reduction after applying a countermeasure technique. Suppose that c_k (k=1,2,3, …) is a countermeasure that can be applied to mitigate a risk (i.e., reduce its level). The Delphi approach described in section 4.C can be used to estimate risk level reduction of r_i after applying c_k which is denoted as $LevelRed(r_i|c_k)$. $LevelRed(r_i|c_k)$ is a measure to the amount by which a countermeasure c_k mitigates (reduces the level of) risk r_i . Its value ranges between 0 and 1 $(0 \le LevelRed(r_i|c_k) \le 1)$ where 0 means no reduction, 1 means risk elimination.

The *Combined Risk Reduction* (CRR) of a risk r_i which measures the resultant (i.e., joint) mitigation in r_i after applying a course of countermeasures is given by equation 3. Its value ranges between 0 and 1 $(0 \le CRR(r_i) \le 1)$ where 0 means no reduction, 1 means risk elimination. This metric is used to decide whether a treatment course for a risk is successful or not.

$$CRR(r_i) = 1 - \prod_{k=1}^{p}(1 - LevelRed(r_i|c_k)) \tag{3}$$

$0 \le CRR(r_i)$
≤ 1 (p is the number of countermeasures applied to r_i)

The Global Risk Reduction (GRR) for the organization is given by equations (4).

$$GRR = \sum_{i=1}^{n} CRR(r_i) \tag{4}$$

V. FRAMEWORK VALIDATION AND EVALUATION

In order to validate the proposed framework for usability and applicability, we provide a step-by-step use-case scenario that shows how an organization can benefit from the proposed framework to manage Cloud security risks. Advanced Telecom (AT) is a leading telecommunications company that has a broad range of customers, whom it offers integrated communications services. AT's services bundle includes fixed landlines, Internet and mobile communications. AT employs 80 thousand employees, who spare no effort or time to reach customers and provide best services. The CEO of AT thought that it would be a great idea to develop several Intranet site applications that would allow employees in AT to share their knowledge. He also thought it would make sense to make some information available to the company's clients. For example, the company could provide advertisements about products, articles, links to other sites, and an Ask the Expert feature to help build relationships with current and future clients. He has heard about the cutting-edge CC technology and thought that it would probably be a good idea to adopt the Cloud technology in his company to support the Intranet project; however, he was worried about the security risks associated with that technology. Since AT emphasizes the importance of high-payoff projects, he wanted to explore the management of security risks in CC environment before adopting this technology in his company. Our goal is to help AT company take a decision on the adoption of CC using our proposed CSRMF.

A. Phase 1: Identifying Organization's Objectives

AT uses SWOT analysis and SMART model to help identify its business objectives. AT's representatives would provide the underlying information on AT's business objectives and the security requirements to protect these objectives against security risks as well as information concerning risk tolerance criteria. This Information is stored in the risk knowledge base and is used as a profile for the organization. The outcomes of this phase are shown in Tables II and III.

B. Phase 2: Risk Identification

A team consists of seven members of information security experts (i.e., SME) and a diverse group of stakeholders in AT uses documented knowledge such as those described in section 4.B to gather information on security risks related to CC that are likely to affect the organization's objectives. Information regarding identified risks are stored in the risk knowledge base. The team then meets, conducts brainstorming session, and uses the knowledge stored in the risk knowledge base to prepare a final list of possible risks. This list is shown in Table IV.

C. Phase 3: Risk Analysis

The team utilizes the Delphi technique explained in section 4.C to estimate the weight w_j of each objective o_j , the likelihood $L(r_i)$ of each risk r_i , and the impact $I(r_i^j)$ of r_i on o_j. These information are shown in Table V. For example, the weight of o_2 *is* $w_2 = 0.2$, the likelihood of r_3 is $L(r_3) = 0.5$, while the impact of r_3 on o_2 is $I(r_3^2) = 0.3$ (all shaded in gray).

D. Phase 4: Risk Evaluation

The levels of identified risks are evaluated using equations 1, the results are shown in Table VI. This evaluation allows the organization to decide whether the risk is tolerable (i.e., acceptable) or not. Tolerable risk criteria have been defined, approved, and documented by the relevant committee of experts and stakeholders in phase 1. The committee has agreed that the risk level for a tolerable risk should not exceed 0.25 (i.e., $\alpha = 0.25$), this means that r_1 and r_4 need treatment to lower their risk levels below 0.25. The GRL (the sum of all risk levels) has been estimated using equation 2.

E. Phase 5: Risk Treatment

Unacceptable risks (r_1, r_4) require treatment; the objective of this phase is to identify countermeasures to mitigate unacceptable risks. The ultimate goal is to reduce GRL for the organization. Risk countermeasures are identified by the team using a combination of knowledge acquisition and brainstorming techniques. Countermeasures used by AT for r_1 and r_4 are listed in Table VII.

TABLE. II. BUSEINESS OBJECTIVES FOR AT ORGANIZATION

Symbol	Objective (o_j)
o_1	Enhance customer trust and build relationships with current and future customers
o_2	Boost employees' relationships and allow knowledge share among them
o_3	Provide perfect customer services and improve customer satisfaction
o_4	Increase profitability and decrease operational costs

TABLE. III. SECURITY REQUIREMENTS FOR AT ORGANIZATION

Security requirements	Confidentiality – medium Integrity – high Availability – high
Risk tolerance	0.25

TABLE. IV. IDENTIFIED RISKS FOR AT ORGANIZATION

Symbol	Risks
r_1	Account hijacking
r_2	Data leakage
r_3	Denial of services
r_4	Insecure VM migration
r_5	Sniffing/spoofing virtual networks

TABLE. V. RISK IMPACT MATRIX FOR AT ORGANIZATION

$\downarrow w_j \quad L(r_i) \rightarrow$	r_1 /0.6	r_2 /0.2	r_3 /0.5	r_4 /0.7	r_5/0.3
o_1 / 0.2	0.65	0.15	0.4	0.85	0.1
o_2 / 0.2	0.85	0.35	0.3	0.8	0.3
o_3 /0.3	0.75	0.8	0.25	0.7	0.7
o_4 /0.3	0.8	0.65	0.1	0.6	0.2

TABLE. VI. RISK LEVELS FOR AT ORGANIZATION

r_i	$Level(r_i)$
r_1	0.46
r_2	0.11
r_3	0.12
r_4	0.50
r_5	0.11
GRL	1.30

TABLE. VII. RISK COUNTERMEASURES EMPLOYED BY AT ORGANIZATION

Symbol	**Countermeasure used to mitigate risks**	**Risk Mitigated**
c_1	Identify and access management guidance	r_1
c_2	Dynamic credentials	r_1
c_3	Protecting aegis from live migrations of VMs	r_4

F. Phase 6: Risk Monitoring

Using the Delphi technique, the team would estimate $LevelRed(r_i|c_k)$ for r_1 and r_4 as per Table VII. This is given in the risk reduction matrix shown below in Table VIII. For each unacceptable risk, the risk reduction matrix shows risk reduction by each alternative countermeasure and estimates its CRR as per equation 3.

From Table VIII, we can see that CRR(r_1) = 0.98 which means that the new risk level of r_1 after treatment is 0.46*(1-0.98) = 0.01 < 0.25 and CRR(r_4) = 0.9 which means that the new risk level of r_4 after treatment is 0.50*(1-0.9) = 0.05 < 0.25. The new value of GRL after treatment =0.40, compared to 1.30 before treatment with %69 risk reduction, this is shown in Table IX. The global risk reduction in AT organization GRR= 0.98+0.9= 1.88. Finally, the organization should continuously monitor the occurrence of the identified risks to ensure that the treatment actions are still valid and to identify new risks that may occur.

TABLE. VIII. RISK REDUCTION MATRIX FOR AT ORGANIZATION

c_k	$LevelRed(r_1\|c_k)$	$LevelRed(r_4\|c_k)$
c_1	0.8	0
c_2	0.9	0
c_3	0	0.9
$CRR(r_i)$	**0.98**	**0.9**

TABLE. IX. RISK LEVELS FOR AT ORGANIZATION

r_i	Risk Level	
	Before mitigation	After mitigation
r_1	0.46	0.01
r_2	0.11	0.11
r_3	0.12	0.12
r_4	0.50	0.05
r_5	0.11	0.11
GRL	1.30	0.40

VI. CONCLUSION AND FUTURE WORK

CC offers numerous advantages to organizations in terms of economical saving, elasticity, flexibility, and minimal management effort. However, security and privacy concerns of CC have always been the focus of the impediments to its widespread adoption by businesses. Over time, organizations tend to relax security risks associated with CC, however, this relaxation requires a regular effective security risk management. In this paper, we proposed a novel framework for cloud security risk management that helps organizations and CSP identify, analyze, evaluate, and mitigate security risks in their CC platforms. It allows any organization adopting CC to be aware of cloud security risks and align their low-level management decisions according to high-level business objectives. In essence, it is designed to address impacts of cloud-specific security risks into business objectives in a given organization. Consequently, organizations are able to conduct a cost-value analysis and take a well-informed decision regarding the adoption of CC technology. On the other hand, CSP are able to improve productivity and profitability by managing cloud-related risks. This framework provides an adequate level of confidence in CC for organizations and a reliable and cost-effective productivity for CSP. In the future, we plan to explore quantitative techniques based on statistical analysis for risk management in CC so that we can reach a higher level of confidence in this emerging technology for organizations.

REFERENCES

[1] Karim Djemame, Django Armstrong, Mariam Kiran, and Ming Jiang, “A Risk Assessment Framework and Software Toolkit for Cloud Service Ecosystems”, 2ndInternational Conference on Cloud Computing, GRIDs, and Virtualization, 2011.

[2] Karim Djemame, Django Armstrong ,Jordi Guitart, and Mario Macias, “A Risk Assessment Framework for Cloud Computing”, IEEE Transactions on Cloud Computing, Vol. 4 , Issue. 3 , 2016.

[3] MohemedAlmorsy, John Grundy and Amani S. Ibrahim, “Collaboration-Based Cloud Computing Security Management Framework”, IEEE 4th International Conference on Cloud Computing, Washington, DC, USA, 2011.

[4] Drissi S.,Houmani H. and Medromi H, “Survey: Risk Assessment for Cloud Computing”, International Journal of Advanced Computer Science and Applications (IJACSA), Vol. 4, No. 12, 2013.

[5] Xuan Zhang , NattapongWuwong , Hao Li and Xuejie Zhang, “Information Security Risk Management Framework for the Cloud Computing Environments”, 10th IEEE International Conference on Computer and Information Technology, Bradford, UK, 29 June-1 July 2010.

[6] Rana Alosaimi and Mohamed Alnum,“A Proposed Risk Management Framework for Cloud Computing Environment”, Inernational Journal of Computer Science and Information Security, Vol. 14, No.8, 2016.

[7] Rana Alosaimi and Mohamed Alnum, “Risk Management Framework for Cloud Computing: A Critical Review”, International Journal of Computer Science and Information Technology, Vol.8, No. 4, 2016.

[8] Prasad Saripalli and Ben Walters, “QUIRC: A Quantitative Impact and Risk Assessment Framework for Cloud Security”, IEEE 3rd International Conference on Cloud Computing, Miami, FL, USA, 5-10 July 2010.

[9] Erdal Cayirci, Alexandr Garaga, Anderson Santana and Yves Roudier, “A Risk Assessment Model for Selecting Cloud Service Providers”, Journal of Cloud Computing: Advances, Systems and Applications, 5:14, 2016.

[10] Heinz-Peter Berg, “Risk Management: Procedures, Methods and Experiences”, RT&A, Vol. 1, No. 2(17), 2010.

[11] BlessonVarghese and RajkumarBuyya, “Next generation cloud computing: New trends and research directions”, Future Generation Computer Systems, Vol. 79, Part 3,pp. 849-861, February 2018.

[12] Keiko Hashizume, David G Rosado, Eduardo Fernández-Medina, and Eduardo B Fernandez, “An analysis of security issues for cloud computing”, Journal of Internet Services and Applications, 4:5, 2013.

[13] SaurabhSingh,Young-SikJeong, and Jong HyukPark, “A Survey on Cloud Computing Security: Issues, Threats, and Solutions”, Journal of Network and Computer Applications, Vol. 75, pp. 200-222, 2016.

[14] CRAMM: Information Security Risk Assessment Toolkit, [online] Available: http://www.cramm.com.

[15] https://www.theirm.org/media/4709/arms_2002_irm.pdf.

[16] H.A. Linstone, The Delphi Method: Techniques and Applications, Addison-Wesley, 1975.

[17] L.M. Stuter, "The Delphi Technique: What is it?", Lynn's Educational and Research Network, March 1996.

[18] RAND Corporation 2007, “A collection of RAND publications on the Delphi method”, Jan 2010.

[19] E. Teijlingen, E. Pitchfork, C. Bishop, E. Russell, "Delphi method and nominal group techniques in family planning and reproductive health research", Journal of Family Planning and Reproductive Health Care, Vol. 31, No. 2, pp. 132-135, 2005.

[20] Umesh Kumar Singh and Chanchala Joshi, "Comparative Study of Information Security Risk Assessment Frameworks", International Journal of Computer Application, Vol. 2, Issue 8, 2018.

[21] Filipe Macedo and Miguel Mira da Silva, "Comparative Study of Information Security Risk Assessment Models", available online: https://fenix.tecnico.ulisboa.pt/downloadFile/395139415147/resumo.pdf

[22] Ahmad Amini and Norziana Jamil, "A Comprehensive Review of Existing Risk Assessment Models in Cloud Computing", Journal of Physics: Conference Series, Volume 1018, 2018.

[23] S. K. Pandey and K. Mustafa, "A Comparative Study of Risk Assessment Methodologies for Information Systems", Bulletin of Electrical Engineering and Informatics, Vol.1, No.2, pp. 111-122, June 2012.

[24] Mohammed Alnuem, HalaAlrumaih and Halah Al-Alshaikh, "A Comparison Study of Information Security Risk Management Frameworks in Cloud Computing", The Sixth International Conference on Cloud Computing, GRIDs, and Virtualization, CLOUD COMPUTING 2015.

[25] Neeta Shukla and Sachin Kumar, "A Comparative Study on Information Security Risk Analysis Practices" International Journal of Computer Applications, Special Issue on Issues and Challenges in Networking, Intelligence and Computing Technologies, 2012.

[26] MounaJouinia, Latifa Ben ArfaRabaia, "Comparative Study of Information Security Risk Assessment Models for Cloud Computing systems", The 6th International Symposium on Frontiers in Ambient and Mobile Systems, Procedia Computer Science 83, pp. 1084 – 1089, 2016.

[27] Vivek Agrawal, "A Comparative Study on Information Security Risk Analysis Methods", Journal of Computers, Vol. 12, No. 1, January 2017.

[28] Nada Mannane , Youssef Bencharhi, BrahimBoulafdour and BoubkerRegragui, "Survey: Risk assessment models for cloud computing: Evaluation criteria", 3rd International Conference of Cloud Computing Technologies and Applications , Rabat, Morocco, 24-26 Oct. 2017.

[29] K.V.D.Kiran, SaikrishnaMukkamala, AnudeepKatragadda and L.S.S.Reddy, "Performance And Analysis Of Risk Assessment Methodologies In Information Security", International Journal of Computer Trends and Technology (IJCTT),Vol. 4, Issue 10, October 2013.

[30] https://www.forbes.com/sites/louiscolumbus/2017/10/18/cloud-computing-market-projected-to-reach-411b-by-2020/#1317df7078f2.

[31] https://www.idc.com/.

[32] https://www.nist.gov/.

[33] https://www.enisa.europa.eu/publications/cloud-computing-risk-assessment.

[34] https://www.mindtools.com/brainstm.html.

[35] Ahmed E. Youssef, "Exploring Cloud Computing Services and Applications", Journal of Emerging Trends in Computing and Information Sciences, VOL. 3, NO. 6, July 2012.

[36] https://www.forbes.com/sites/louiscolumbus/2018/01/07/83-of-enterprise-workloads-will-be-in-the-cloud-by-2020/#6ae3cce76261.

[37] https://www.iso.org/standard/43170.html.

[38] "The Top Cyber Security Risks", SAN Institute Report, Sept. 2009.

[39] COBRA: Introduction to Security Risk Analysis. Available on: http://www.security-risk-analysis.com/.

[40] https://cloudsecurityalliance.org/.

[41] https://www.mindtools.com/pages/article/newTMC_05.htm.

Handwritten Arabic Text Recognition using Principal Component Analysis and Support Vector Machines

Faisal Al-Saqqar[1], Mofleh Al-Diabat[3], Mesbah Aloun[4]
Department of Computer Science
Al al-Bayt University, Mafraq, Jordan

Atallah. M AL-Shatnawi[2]
Department of Information Systems
Al al-Bayt University, Mafraq, Jordan

***Abstract*—In this paper, an offline holistic handwritten Arabic text recognition system based on Principal Component Analysis (PCA) and Support Vector Machine (SVM) classifiers is proposed. The proposed system consists of three primary stages: preliminary processing, feature extraction using PCA, and classification using the polynomial, linear, and Gaussian SVM classifiers. In this proposed system, text skeleton is first extracted and the images of the text are normalized into uniform size for extraction of the global features of the Arabic words using PCA. Recognition performance of this proposed system was evaluated on version 2 of the IFN/ENIT database of handwritten Arabic text using the polynomial, linear, and Gaussian SVM classifiers. The classification results of the proposed system were compared with the results produced by a benchmark. TRS that is depending on the Discrete Cosine Transform (DCT) method using numerous normalization sizes of Arabic text images. The experimental testing results support the effectiveness of the proposed system in holistic recognition of the handwritten Arabic text.**

Keywords*—Handwritten Arabic text; holistic recognition; principal component analysis; support vector machines

I. Introduction

The ultimate objective of any Arabic Text Recognition System (ATRS) is to imitate the human understanding abilities so that the computer can read, understand, and accomplish activities on texts that are similar to the ones which the human mind executes [2, 3, 4, 7, 26]. The Arabic language is universal language and the official language of 25 countries and greater than 300 million individuals in the world. Additionally, many Arabic characters are utilized in numerous languages such the Iranian, Jawi, and Urdu languages [1, 7, 3]. Review of the literature uncovers that, so far, there are two major systems for offline Arabic text recognition; segmentation-free systems (holistic recognition approaches) and segmentation-based systems [25, 12]. In the former systems, recognition is applied on the entire representation of the text or word, which is treated as one unit with no segmentation. In the segmentation-based systems, however, cursive text is often segmented into characters or small segments called primitives. This approach, thus, suffers from varying problems, including overlapping and ligatures, short distances between connected characters, and the Arabic writing properties [6]. Details on characteristics of the handwritten Arabic text can be found in Al-Shatnawi et al. [6] and Al-Shatnawi [4]. For the holistic approaches in text recognition, a universal feature vector is computed for the indivisible input texts or words for them to be classified by using any of a number of machine learning approaches [13].

The ultimate objective of feature extraction is to produce efficient representation of the image of the text using a group of distinctive characteristics. These characteristics may be categorized into three classes: (i) high-level characteristics, which are drawn from the entire image of the text or word, (ii) medium-level characteristics that are derived from the characters, and (iii) low-level characteristics, which are usually extracted from the related sub-characters [18]. In other respects, the handwritten Arabic text may be recognized using various classifiers like the Support Vector Machines (SVM), Hidden Markov Model (HMM), the k-nearest neighbors (kNN), and the Artificial Neural Network (ANN) classifiers [11, 12, 26].

This study proposes a multi-stage Offline Holistic Handwritten Arabic Text Recognition System (OHATRS) based on Principal Component Analysis (PCA) and SVM classifiers. This suggested system progresses in three steps: preliminary preprocessing, feature extraction using PCA, and classification using the polynomial, linear, and Gaussian SVM classifiers. The primary contributions of this paper can be abbreviated as follows: (i) extracting the statistical handwritten Arabic text features using the PCA technique, (ii) testing and evaluating the extracted features on version 2 of the IFN/ENIT database of handwritten Arabic text using the polynomial, linear, and Gaussian SVM classifiers, and (iii) comparing the recognition results of the proposed OHATRS with benchmark ATRS that is depending on the Discrete Cosine Transform (DCT) method.

The remainder of this paper is organized as follows: Section 2 overviews previous holistic handwritten ATRSs while Section 3 presents the proposed OHATRS. Thereafter, Section 4 presents the experimental recognition results of the herein proposed system and discusses them. Then, Section 5 outlines the conclusions of this study and highlights directions for future research.

II. Related Work

Several previous research efforts have examined the offline holistic approaches to recognizing the handwritten Arabic cursive scripts. For instance, El-Bashir [21] suggested recognition of Arabic sub-words using PCA as the means of feature extraction. Recognition was carried in his study by using different norms that are, ENorm and EEuclidean norm. The suggested system was verified on dataset of two groups, one comprising two-character sub-words and the other including three-character sub-words. The evaluation results exposed that the classification accuracies related with the first norm, ENorm, second norm, and EEuclidean were 74.3%, 76.8%, 76.8%, and 77.17%, respectively, in the instance of the two-character sub-words and 75.85%, 77.45%, 78.2%, and 78.49%, respectively, in the instance of the three-character sub-words.

Sagheer et al. [27] suggested holistic recognition model for the handwritten Urdu words depending on sets of integrated features and the SVM classifier. Their suggested system incorporated the gradient, or directional, features and the structural features that were extracted from the handwritten Urdu words. When tested on the CENPARMI Urdu Words Database, this proposed system achieved a recognition accuracy of 97.00%.

Nemmour and Chibani [15] presented an offline holistic model for recognition of the handwritten Arabic text based on combination of the SVMs and Ridgelet transform. The Ridgelets were employed to generate relevant features of handwritten words whereas classification was based on the 'One-Against-All' multi-class operation of the SVMs. This system was then tested on vocabulary of 24 words taken from the IFN/ENIT database. Ridgelet performance was evaluated in this study relative to the results produced by the Radon and uniform grid (zoning) feature method. The performance evaluation outcomes spotlight reliability of the combination of the SVM and Ridgelet tools for recognition of the handwritten Arabic words.

EI Qacimy et al. [11] suggested offline, word-based system for recognition of the handwritten Arabic text depending on the DCT features and a SVM classifier that is improved by reject option. This system comprised four key processes, namely, preprocessing, segmentation into sub-words, extraction based on DCT features, and classification by the SVM RBF classifier. The system was then evaluated on 2,000 word images that were chosen randomly from the IFN/ENIT database of handwritten Arabic words that were separated into a training sub-set of 1,500 images and a testing sub-set of 500 images. Afterwards, performance of this suggested system was verified with the ranks of performance of state-of-the-art schemes that used DCT features for classification of the Arabic handwritten text. The results disclosed effectiveness of this proposed system in holistic classification of the Arabic words.

Kadhm and Abdul [24] developed an offline holistic system for recognition of the handwritten Arabic words that is based on SVM classifiers. The HOG and DCT were both employed for feature extraction. Then, this system was verified on the AHDB Database, which contains 2,913 images of handwritten Arabic words by the SVM linear, polynomial, and RBF kernel classifiers. These three classifiers produced recognition accuracies of 96.32%, 92.63%, and 91.50%, respectively.

Hassan and Alawi [9] developed a holistic, offline, system for recognition of the handwritten Arabic words depending on the SVM with the Gaussian kernel and the Discrete Wavelet Transform (DWT) transforms. This system was established based on four levels of the DWT by segmenting the wavelet space into 16x16 blocks. Then, the standard deviation was calculated for every block. Performance of this system was then evaluated on database of 1,160 word images of names of Iraqi cities that had been handwritten by 30 writers of differing educational backgrounds and ages using the SVM Gaussian, polynomial, and linear kernel classifiers, which produced recognition accuracies of 89.17%, 90.00%, and 90.65%, respectively.

III. The Proposed Text Recognition System

This paper presents a multi-stage system for holistic recognition of the handwritten Arabic text that is based on PCA and SVM classifiers. The proposed (OHATRS) has three basic processes: preliminary preprocessing, feature extraction using PCA, and classification using the Gaussian, linear, and polynomial SVM classifiers. Architecture of this proposed system is presented in Fig. 1. In the preliminary stage, text skeleton is first extracted and images of the text are then normalized into uniform size for the purpose of extraction of the universal features of the Arabic text using PCA. The extracted features are then used to classify the handwritten Arabic text using the aforementioned SVM classifiers. Stages of the OHATRS are illustrated in the following sub-sections.

A. *Preliminary Stage*

The preliminary processing stage prepares the text data under consideration for the successive stages. It enhances uniformity of the texts, which is an essential requirement of the recognition system. Preliminary processing is concerned with representation of the Arabic text images and normalization processes. At this stage, the skeleton of the word is first extracted by means of the skeletonization-based morphological process so as to eliminate the unnecessary pixels via extraction of the text skeleton at the single-pixel width level. Afterwards, the image of the text of concern is normalized into suitable size for extraction of the global features of the Arabic text using the PCA technique. A briefing of the two operations making up this stage follows.

B. *The Skeleton Extraction Process*

In the skeleton extraction process, skeleton of the input text image is extracted via the skeletonization-based morphological operation method. As such, this process refines text shape and minimizes the size of the data that needs handling for the purpose of feature extraction and recognition [5]. This particular approach was selected to thin the handwritten Arabic text because it proved (e.g., [2]) to be having high performance in thinning the handwritten Arabic text. An example on skeletons of handwritten Arabic texts that have been extracted using the skeletonization-based morphological method is presented in Fig. 2.

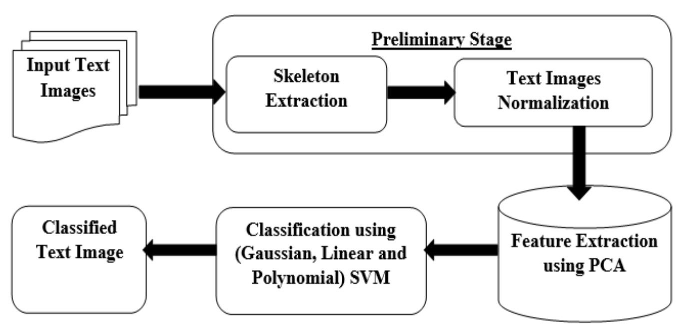

Fig. 1. Architecture of the Proposed OHATRS.

(a) Original Image. (b) Produced Skeleton.

Fig. 2. Example of (a) Handwritten Arabic Text before thinning and (b) Extracted Skeleton of this Text.

C. Normalization

Normalization of the text images is a very important step in the text recognition process. Because the styles of writing differ from one person to another, the size normalization process is often employed to convert the sizes of the characters or words into a uniform standard size [16]. In view of importance of this process and its effect on the recognition results of the system proposed in this paper (OHATRS), recognition performance of this system was tested on text images of varying sizes, taking into consideration the smallest and largest image sizes in the relating databases so as to select the best results and compare performance of this proposed system with levels of performance of another recognition system. Those sizes and their effects on performance of the proposed system are discussed in the experimental results and discussion section.

D. Feature Extraction using Principal Component Analysis

Feature extraction is the most important process in the recognition systems of the handwritten texts. Best recognition usually depends on successful use of efficient feature extraction methods [9]. The eventual goal of feature extraction is to produce efficient representation of the entire text image through set of features [18].

Principal Component Analysis (PCA) is a statistical linear transform technique. It was developed originally by Pearson [20]. It is broadly employed for differing pattern recognition applications like character recognition (e.g., Abandah et al. [14]), data compression (e.g., da Rocha Gesualdi and Seixas [8]), and face recognition (e.g., Bansal et al. [17]).

This study applied PCA to extract and select the relevant features of handwritten Arabic text as a global statistical text feature extraction technique for the extracted features to be classified by the SVM classifiers. The PCA is commonly employed as feature extraction method so as to reduce dimensions of images to manageable sizes. PCA begins by calculating the mean of the data matrix. Then, it computes the covariance of the data. Thereafter, the Eigenvalues and Eigenvectors are estimated [28]. The PCA aims at finding the space that represents direction of the maximal variance of the data under consideration. It defines low-dimensional space, or a PCA space (W), that can be employed to transform the data (X = {x1, x2, . . . , xn}, where n is number of observations or samples and xi is the ith observation, sample, or pattern) from high-dimensional space into low-dimensional space [10].

Principal Component Analysis has been already applied successfully in feature extraction and in dimension reduction in numerous recognition systems of isolated Arabic characters. For example, Ali and Shaout [28] employed PCA for feature extraction in recognition of isolated, handwritten, Arabic characters using the Adaptive Neural Network Fuzzy Inference System (ANFIS). As well, Khan et al. [19] employed PCA in recognition of isolated Urdu characters. In addition, Abandah et al. [14] employed PCA for reduction of the dimensionality of the features extracted from isolated Arabic letters (characters) for text recognition purposes by using five classifiers: Linear Discriminant Analysis (LDA), Quadratic Discriminant Analysis (QDA), Diagonal Quadratic Discriminant Analysis (DQDA), k-NN, and Diagonal Linear Discriminant Analysis (DLDA).

In this process, the PCA is applied to extract and select global Arabic text features according to the following six steps [10]:

Step 1: The two-dimensional (2D) text image is transformed into mono-dimensional vector by concatenating every column (or row) in the 2D matrix in order to create long vector. If we have an M vector of the size N that represents sample image, then

$$X_i = [p_1 \dots p_N]^T, i = 1, \dots, N \tag{1}$$

where X_i is a vector, px is pixel value Xi, and T is tanspose of the vector set.

Step 2: Find mean, μ, of the image, which can be calculated as follows:

$$\mu = \frac{1}{m}\sum_{i=1}^{m} x_i \tag{2}$$

Step 3: Find the mean center of the image, wi:

$$w_i = X_i - \mu \tag{3}$$

Step 4: Calculate the covariance matrix, S. This matrix measures the relations between two dimensions or more. It can be computed from the equation:

$$S = \frac{1}{m}\sum_{i=1}^{m}(x_i - \mu)(x_i - \mu)^{T_i} \tag{4}$$

Step 5: Calculate the Eigenvalue, λ, and Eigenvector, V, of S according to the equation

$$SV_i = \lambda_i V_i\,, for\ i = 1,2 \dots n. \tag{5}$$

Afterwards, sort the eigenvectors based on their concomitant eigenvalues.

Step 6: Choose the eigenvectors which have the highest eigenvalues, W = {v1. . . vk}. The chosen W values correspond to the projection space of the PCA. Thereafter, project those W values on the low-dimensional space of the PCA.

E. Classification using SVM Classifiers

The SVM is a relatively modern classifier that employs kernels to find the optimum decision boundary and, then, separate between the potential classes in the high-dimensional feature spaces. Algorithm of the SVM was introduced originally by Vapnik [30]. It was proposed initially for the binary separation problems. However, it may be generalized easily to the multi-class classification problems. The fundamental form of the linear SVM classifier attempts to discovery the optimum hyperplane that separate the best set of samples that belong to differing classes [11].

In classification in the present study, the multi-class polynomial, Gaussian, and linear SVM classifiers were used for classification of images of handwritten Arabic text by using the sequent SVM kernel functions [22]:

The linear function: K(x, y) = (K(xi, xj) = (xixj))

The polynomial function: K(x, y) =(K(xi, xj)=(γxixj + coef)

The Gaussian function: K(x, y) = exp−γ||xi−xj ||2)

The proposed (OHATRS), which is based on the PCA and the Gaussian, linear, and polynomial SVM classifiers is presented in the following algorithm:

Algorithm (1): The proposed system for holistic recognition of the handwritten Arabic text based on PCA and the Gaussian, linear, and polynomial SVM classifiers.

Input: Images of Handwritten Arabic Text

Output: Classified Word

{Read the image of the handwritten Arabic text,
prepare the data of the text image using the following two preliminary steps:
- Extract the text skeleton using the skeletonization-based morphological operation method,
- Normalize the text image size to a suitable size,

Extract the global text features using PCA,
and then classify the text images using the Gaussian, linear, and polynomial SVM classifiers,
end}

IV. Experimental Results and Discussion

In this study, both the proposed and benchmark Arabic text recognition systems were implemented in the MATLAB 2017a environment in personal computer with an i3 processor, a speed of 1.90 GHz, and a memory of 6 GB. The various systems under study were tested on version 2.0 of the IFN/ENIT Arabic handwritten text database. This database is made up of 32,492 images of handwritten Arabic names of Tunisian villages and towns. The names are categorized into five sub-sets; a, b, c, d, and e sub-sets [23, 29]. The (a), (b), (c), and (d) sub-sets were employed for training purposes whereas the (d) and (e) sub-sets were utilized for testing purposes. All sub-sets are provided with ground truth information that has been employed in labeling the recognition observations.

For the purpose of verifying performance of the herein proposed OHATRS, the recognition results of the proposed system were compared with those of a benchmark recognition system that is based on DCT. The DCT method was employed by EI Qacimy et al. [11] for holistic classification of Arabic texts with the reject option on the basis of sub-word segmentation.

The OHATRS proposed here and the benchmark ATRS were tested on the (d) and (e) sub-sets of the IFN/ENIT database using (i) the polynomial, Gaussian, and linear SVM classifiers, and (ii) five normalized word image sizes: 75x75, 100x100, 125x125, 150x150, and 175x175. The cassification accuracies of both systems when tested on sub-set (d) of the IFN/ENIT database are summarized by Table I.

As Table I shows, the proposed OHATRS produced better classification accuracies than the benchmark ATRS system when applying the aforementioned five normalized image sizes on sub-set (d) of the IFN/ENIT database and using the Gaussian (RBF), linear, and polynomial SVM classifiers. The recognition accuracies of the proposed and the benchmark systems are shown in Fig. 3. The best classification accuracy (89.96%) achieved by the proposed OHATRS was concomitant with 125x125 image normalization size and the Gaussian SVM classifier. On the other hand, the best classification accuracy (79.14%) achieved by the benchmark ATRS was achieved with the 75x75 image normalization size and the Gaussian SVM classifier, too. This finding supports effectiveness of the proposed OHATRS in holistic recognition of the handwritten Arabic text. Table II shows the classification accuracies of both the proposed OHATRS and the benchmark ATRS when tested on sub-set (e) of the IFN/ENIT database.

Table II uncovers that better classification accuracies are associated with the proposed OHATRS than with the benchmark ATRS system when using (i) the same five normalized image sizes on sub-set (e) of the IFN/ENIT database and (ii) the Gaussian (RBF), linear, and polynomial SVM classifiers. The recognition accuracies of both systems are presented in Fig. 4. The best classification accuracy (77.80%) produced by the proposed OHATRS was associated with the 125x125 image normalization size and the Gaussian SVM classifier. Meanwhile, the best classification accuracy (68.46%) generated by the benchmark ATRS was concomitant to the 100x100 image normalization size and the polynomial SVM classifier. This result suggests effectiveness of the proposed OHATRS in holistic recognition of the handwritten Arabic text.

TABLE. I. THE CLASSIFICATION ACCURACIES OF THE PROPOSED OHATRS AND THE BENCHMARK ATRS WHEN TESTED ON SET (D) OF THE IFN/ENIT DATABASE USING THE SVM CLASSIFIERS

	Normalization size	Classification accuracy		
		Gaussian	Linear	Polynomial
Proposed system based on PCA	75x75	86.64%	83.99%	85.54%
	100x100	89.18%	87.42%	89.07%
	125x125	89.96%	87.53%	88.62%
	150 x150	89.51%	87.41%	88.51%
	175x175	89.07%	87.75%	88.52%
Benchmark system using the DCT method	75x75	79.14%	74.94%	77.37%
	100x100	78.48%	77.37%	77.26%
	125x125	75.49%	75.48%	73.07%
	150x150	73.18%	74.83%	69.76%
	175x175	70.97%	74.50%	65.56%

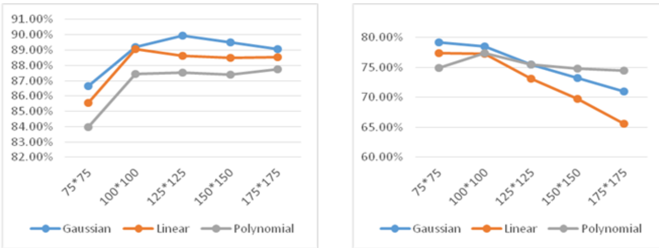

(a) The proposed OHATRS. (b) The benchmark ATRS.

Fig. 3. Classification Accuracies of (a) The Proposed OHATRS and (b) The Benchmark ATRS when Tested on Sub-Set (d) of the IFN/ENIT Database using Five Normalized Image Sizes and the SVM Classifiers.

TABLE. II. THE CLASSIFICATION ACCURACIES OF THE PROPOSED OFFLINE HATRS AND THE BENCHMARK ATRS WHEN TESTED ON SET (E) OF THE IFN/ENIT DATABASE USING THE SVM CLASSIFIERS

	Normalization size	Classification accuracy		
		Gaussian	Linear	Polynomial
Proposed system based on PCA	75x75	75.22 %	73.21%	74.50%
	100x100	77.72%	76.19%	77.47%
	125x125	77.80%	76.51%	77.47%
	150 x150	77.79%	76.43%	76.99%
	175x175	77.55%	76.11%	76.99%
Benchmark system using the DCT method	75x75	67.34%	66.37%	68.30%
	100x100	66.93%	67.81%	68.46%
	125x125	66.93%	67.82%	68.30%
	150x150	63.15%	65.81%	63.15%
	175x175	61.62%	66.05%	60.66%

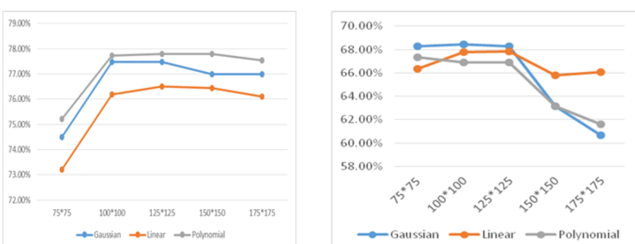

(a) The proposed OHATRS. (b) The benchmark ATRS.

Fig. 4. Classification Accuracies of (a) The Proposed OHATRS and (b) The Benchmark ATRS when Tested on Sub-Set (e) of the IFN/ENIT Database using Five Normalized Image Sizes and the SVM Classifiers.

V. CONCLUSIONS AND FUTURE DIRECTIONS

This study proposed a holistic, multi-stage, system for recognition of the handwritten Arabic text that is based on PCA and SVM classifiers (OHATRS). Text recognition in this proposed system is performed at three stages: preliminary processing, feature extraction using PCA, and classification using the Gaussian, linear, and polynomial SVM classifiers. At the preliminary stage, text skeleton is extracted and text image is normalized into a uniform size for extraction of the universal Arabic word features using PCA. These extracted features are then used to classify the handwritten Arabic words using SVM classifiers.

The herein proposed OHATRS and the benchmark ARTS were evaluated on the (e) and (d) sub-sets of the IFN/ENIT database using (i) five word image normalization sizes (75x75, 100x100, 125x125, 150x150, and 175x175) and (ii) the Gaussian, linear, and polynomial SVM classifiers. The best classification accuracies (89.96% and 77.80%) produced by the proposed OHATRS were achieved using the 125x125 image normalization size and the Gaussian SVM classifier when this system was evaluated on the (d) and (e) sub-sets of the IFN/ENIT database, respectively. On the other hand, the best classification accuracies (79.14% and 68.46%) produced by the benchmark ARTS were achieved using the 75x75 and 100x100 image normalization sizes, respectively.

This study finds that the Arabic text recognition results of the proposed OHATRS are promising; the system produced better classification accuracies than the benchmark ATRS. As was highlighted in the foregoing section, the testing outcomes support effectiveness of the proposed system in recognition of the handwritten Arabic words. The experimental results underscore that the 125x125 word image size is the best size for optimum system performance and recognition results. For similar future studies, the researcher suggests training the proposed OHATRS using a combination of structural and statistical features.

REFERENCES

[1] A. Al-Shatnawi and K. Omar, "Methods of Arabic language baseline detection -the state of art". IJCSNS, 8 (10), 2008.

[2] A. Al-Shatnawi, "A Non-Iterative Thinning Method Based on Exploited Vertices of Voronoi Diagrams", PhD Thesis, University Kebangsaan Malaysia, Malaysia, 2010.

[3] A. Al-Shatnawi, "A Novel Baseline Estimation Method for Arabic Handwritten Text Based on Exploited Components of Voronoi Diagrams", International Arab Journal of Information Technology (IAJIT), 13(3), 2016.

[4] A. Al-Shatnawi, "A Preprocessing Model for Hand-Written Arabic Texts Based on Voronoi Diagrams", International Journal of Computer Science and Information Technology (IJCSIT), 7(6), (p.p 1-18) December 2015.

[5] A. Al-Shatnawi, "A skew detection and correction technique for Arabic script text-line based on subwords bounding", In Computational Intelligence and Computing Research (ICCIC), IEEE International Conference on, (pp. 1-5), IEEE, 2014.

[6] A. Al-Shatnawi, A. S. Safwan, F. AL-Zawaideh, and K. Omar, "Offline Arabic Text Recognition–An Overview". World of Computer Science and Information Technology Journal (WCSIT), 1(5), (pp.184-192), 2011.

[7] A. Al-Shatnawi, and K. Omar, "The Thinning Problem in Arabic Text Recognition-A Comprehensive Review", International Journal of Computer Applications, 103(3), (pp. 0975-8887), 2014.

[8] A. Da Rocha Gesualdi, and J. M. de Seixas, "Character recognition in car license plates based on principal components and neural processing", In VII Brazilian Symposium on Neural Networks Proceedings, (pp. 206-211), IEEE, (November, 2002).

[9] A. K. Hassan, and Alawi. M, "Proposed Handwriting Arabic Words classification Based on Discrete Wavelet Transform and Support Vector Machine", Iraqi Journal of Science, 58(2C), (pp.1159-1168), 2017.

[10] A. Tharwat, "Principal component analysis-a tutorial", International Journal of Applied Pattern Recognition, no. 3 (pp.197-240), 2016.

[11] B. El Qacimy, A. Hammouch, and M. A Kerroum, "A review of feature extraction techniques for handwritten Arabic text recognition", In 2015 International Conference on Electrical and Information Technologies (ICEIT), (pp. 241-245), IEEE. 2015.

[12] B. El Qacimy, M. A Kerroum, and A. Hammouch, “Word-based Arabic handwritten recognition using SVM classifier with a reject option”, in 2015 15th international conference on intelligent systems design and applications (ISDA), (pp. 64-68), IEEE, December 2015.

[13] F. Nashwan, M. A. Rashwan, H. M Al-Barhamtoshy, S. M. Abdou, and A. M. Moussa, ”A holistic technique for an Arabic OCR system”, Journal of Imaging, 4(1), 6, 2018.

[14] G. A. Abandah, K. S. Younis, and M. Z. Khedher, “Handwritten Arabic character recognition using multiple classifiers based on letter form”, In Proceedings of the 5th International Conference on Signal Processing, Pattern Recognition, and Applications (SPPRA) (pp. 128-133), February 2008.

[15] H. Nemmour, and Y. Chibani, ”Handwritten Arabic word recognition based on Ridgelet transform and support vector machines”, In 2011 International Conference on High Performance Computing & Simulation, (pp. 357-361), 2011.

[16] J. H. AlKhateeb, “Word based off-line handwritten Arabic classification and recognition: design of automatic recognition system for large vocabulary offline handwritten Arabic words using machine learning approaches”, Ph.D. dissertation, University of Bradford, 2010.

[17] K. Bansal, and S. Arora, “Face Recognition using PCA & LDA Algorithms,” Second International Conference on ACCT, (pp. 251-254), 2012.

[18] K. Jayech, M. A. Mahjoub, and N. E. Amara, “Synchronous multi-stream hidden markov model for offline Arabic handwriting recognition without explicit segmentation”, Neurocomputing, (pp. 958-971), 2016.

[19] K. Khan, R. Ullah, N. A Khan, and K. Naveed, “Urdu character recognition using principal component analysis”, International Journal of Computer Applications, 60(11), 2012.

[20] K. Pearson, "On Lines and Planes of Closest Fit to Systems of Points in Space", Philosophical Magazine, 2 (11), (pp.559–572), 1901.

[21] M, El-Bashir, “Principal components analysis for Arabic sub-word recognition”, 2010 International Conference on Intelligent Network and Computing (ICINC 2010) (pp. 432–434), 2010.

[22] M. Amara, K. Ghedira, K. Zidi, and S. Zidi, “A comparative study of multi-class support vector machine methods for Arabic characters recognition”, In 2015 IEEE/ACS 12th International Conference of Computer Systems and Applications (AICCSA), (pp. 1-6), IEEE, (November 2015).

[23] M. Pechwitz, S. S. Maddouri, V. Märgner, N. Ellouze, and H. Amiri, “IFN/ENIT-database of handwritten Arabic words”, In Proc. of CIFED, Vol. (2), (pp. 127-136), October 2002.

[24] M. S. Kadhm, and A. P. Abdul, “Handwriting word recognition based on SVM classifier”, International Journal of Advanced Computer Science & Applications, 1, (pp.64-68), 2015.

[25] M. S. Khorsheed, “Off-line Arabic character recognition–a review”, Pattern analysis & applications, 5(1), (pp. 31-45), 2002.

[26] M. T. Parvez, and S. A Mahmoud, “Offline Arabic handwritten text recognition: a survey”, ACM Computing Surveys (CSUR), 45(2), 23, 2013.

[27] M. W. Sagheer, C. L. He, N. Nobile, and C. Y. Suen, “Holistic Urdu handwritten word recognition using support vector machine”. In 2010 20th International Conference on Pattern Recognition, (pp. 1900-1903), IEEE, August 2010.

[28] O. B. Ali, and A. Shaout, “Hybrid Arabic Handwritten Character Recognition Using PCA and ANFIS”, In International Arab Conference on Information Technology (ACIT’2016), 2016.

[29] V. Märgner, and H. El Abed, “ICDAR 2009 Arabic handwriting recognition competition”, In 2009 10th International Conference on Document Analysis and Recognition, (pp. 1383-1387). IEEE, (July 2009).

[30] V. Vapnik, ”Statistical learning theory”, Vol. 1, 1998, New York: Wiley.

5G Enabled Technologies for Smart Education

Delali Kwasi Dake[1], Ben Adjei Ofosu[2]
Department of ICT Education
University of Education, Winneba
Winneba, Ghana

***Abstract*—5G technology use cases depicts the prospects of 5G network model to revolutionize Industry and Education is not an exception. The 5G model in general is made up of three main blocks: Enhanced Mobile Broadband, Massive Machine Type Communication and Ultra Reliable and Low Latency Communication. Within these blocks are the services 5G offers to users. In this paper, we focus on Educational users as beneficiaries of 5G technologies. The modern day Educational Institutions can benefit from the deployment of 5G-enabled services adapted to this sector. We proposed frameworks relating 5G and its disruptive technologies in advancing tools that will propel the idea of a Smart Educational System. This paper hence provides a comprehensive discussion on 5G technologies that will facilitate new teaching and learning trends in Educational environment.**

Keywords*—5G Networks; smart education; smart campus; machine learning; artificial intelligence; big data; internet of things

I. Introduction

5G technology stands for 5th Generation of the Mobile Technology (MT). This MT has evolved from the past four decades starting from 1G (1st Generation), 2G (2nd Generation), 3G (3rd Generation), 4G (4th Generation) and now the expected 5G [1]. 1G is being used for voice calls, 2G for SMS which was later improved to 2.5 to help support browsing activities on the internet. 3G is for mobile television with Global Positioning System (GPS) and video conferencing which are all in use today. 4G is an improvement on 3G with extra services for higher data exchange. Long Term Evolution (LTE) is the standard for high speed wireless communication and boosted the abilities of 4G with a higher downloading and uploading speed rates.

The 5G MT will bring about a "Network Society" where many network technologies including Millimeter Wave (mmWave), Massive Multiple Input Multiple Output (mMiMo), Full Duplex, Cognitive Radio (CR) Technology, ZigBee, Bluetooth Low Energy (BLE) and Dynamic Spectrum Access (DSA) would be integrated to provide improvement in terms of reliability, availability, flexibility, energy efficiency and low latency. These technologies are important requirements for advancements in Internet of Things (IoT) [2]. The integration of these technologies for 5G also offers support for Augmented and Virtual Reality which are effective technologies applicable to Education. Therefore the imminence arrival and commercialisation of 5G and its technologies must lead to a discussion about its potential benefit to Education.

The rapid integration of Information communication and technology tools (ICTs) in education in aiding synchronous and asynchronous lesson delivery and new ways to access information and knowledge are important in the teaching process. Instructors and Learners mostly adopt the YouTube in accessing educational video contents with most institutions integrating web based educational platforms: the Moodle, Edmodo and Edsby [3] to facilitate school assessments and management. Other smart devices have also emerged in adaptation to intelligent tutoring systems, personalized learning and Recommender Systems [4]. Academic Institutions are yet to fully benefit from the Integration of Internet of Things (IoT) in Education that will completely lead to the idea of Smart Education.

The data generated by these IoT devices and mobile phones on campuses will lead to an era of Big Data that can be analysed to shape and create a dynamic educational system with intelligent gathering concepts. The intelligence gathered can suggest new learning patterns, curriculum re-design and better management decisions on running academic institutions based on facts.

5G is going to disrupt the ICT ecosystem thereby having a greater impact on the concept of Smart Education (SmE), Smart University (SmU) and a Smart Campus (SmC). This has exerted pressure on Education to adapt all the necessary technology advancement to attain the level of the new age of industry (Industry 4.0). From various perspectives, 5G will be a facilitator and a quickening agent of Industry 4.0 and SMART Education (SmE, SmU, SmC).

II. Review of Literature

Author in [5] concentrated on the architecture of the ecosystem of 5G network. The research addressed the three main categories of the 5G Ecosystem which are the Enhanced Mobile Broadband (eMBB), Ultra-reliable and Low-latency Communications (uRLLC), and Massive Machine Type Communications (mMTC). It continued to elaborate on the various services within the three blocks of the 5G Ecosystem. It uncovered other services that seeks to meet the demands of individuals and industries. Due to the lack of recognition for Education in the 5G Ecosystem Model, the researcher proposed a modification of the model to fully concentrate on services that could directly be applied in Education.

Author in [6] focused on the attributes of 5G such as higher data rates, low latency and efficient use of spectrum with coexistence of heterogeneous networks for a successful compatibility of 5G and Internet of Things. This paper proposed the incorporation of Artificial intelligence as a necessity to make competent decisions based on the immense data produced by the activities of users of IoT devices. It addressed the use of Artificial intelligence to help analyze data in other to extract patterns and make sense of it and then prescribe action to the end devices. It also recommended the need for Artificial Intelligence in IoT devices for device self-analysis.

Author in [7] fixated the research on 5G as a compatibility for wireless technology and how 5G network seeks to be a foundation for the development of the World Wide Wireless Web (WWWW) and the Dynamic Adboc Wireless network (DAWN). This research work discussed the reason why the world needs 5G with its use cases for supporting interactive multimedia, internet and other broadband services and have bi-directional accurate traffic statistics.

Author in [8] explained the significance of IoT and why IoT is an integral part of the daily learning and teaching methodologies. The article concluded that the effective use of IoT systems will improve personalised and interactive learning. This article again focused on the importance of IoT in the mobility tracking of students using intelligent cameras. In [8], author also explained the importance of effective educational applications in leveraging on IoT to transform teaching and learning.

Author in [9] fixated on the educational field where critical learning spaces are prepared to utilize Internet of things. A system was proposed that enables and understudies interfaces with physical objects virtually connected with a subject of learning. The result of their experiment proved that their model improves outcomes in teaching and learning.

Author in [10] research paper recommended cloud computing as a solution to cater for the rapid growth of data. The paper discussed the three models of the cloud computing services which defines the paradigm of what users would use technology for. The three main models of the cloud service in this paper explains what each of the provisions from the cloud computing structure provides. The Software as a Service (SaaS) provides the complete application to a cloud end user. This provides an already made and executable software running over the internet. The Platform as a Service (PaaS) is a virtual environment for provisioning and developing cloud applications and the third model which is the Infrastructure as a Service (IaaS) provides an access of a layer to the IT resources services such as data storage resources, computing resources and communications channel pooled under this service. This service makes it possible for users to use all the intelligence of the cloud service which becomes an appropriate infrastructure for Data Analytics.

III. 5G INTEGRATED TECHNOLOGIES IN EDUCATION

Considering the services expected of 5G, this research adopted a model from the 5G ecosystem proposed by Huawei Technology Company Limited, with an integrated concept ‘Smart Education’ that grouped the services provided by 5G and adapted to Education as shown in Fig. 1.

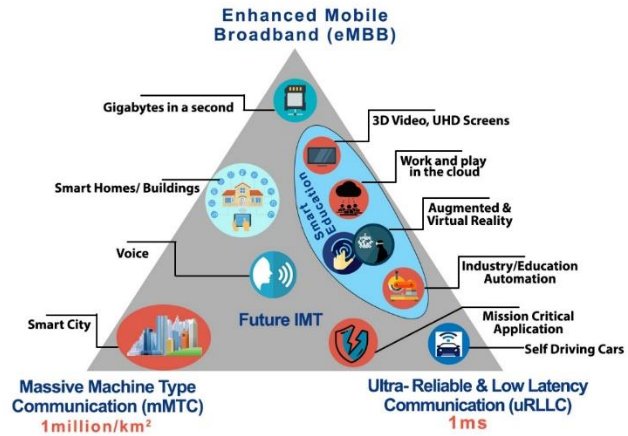

Fig. 1. Smart Education Concept Integrated in Huawei 5G Model.

A. 3D Video, UHD Screens

3D visualization technologies make computer generated images appear more lifelike. This technology has helped in delivering content which are very abstract and difficult to re-create. With 3D virtualization technology, learners sense a greater depth in understanding than just reading. 3D technology led to computer generated images which are equivalent to real world content. This technology has helped integrate simulations and animations in education to better deliver most complicated educational content. Due to the immense benefit of videos in Education, 3D videos adoption to assist in teaching and learning process has become one of the most trending technology to revolutionize Education. Downloading and uploading speed has been a challenge for accessing 3D videos with Fully/Ultra High Definition quality on academic institutions. 5G provides heterogeneous air interfaces to improve spectral efficiency exponentially. 5G provides eMBB data rates for uplink (UL) and downlink (DL) up to 10 Gb/s and 20 Gb/s, respectively. Having such data rate makes it possible for not only downloading and uploading but also, to have a full high definition live video communication with a lower latency. The application of this service in education can assist in synchronous lecture delivering with real time Question and Answer sessions and a live communication between an instructor and a student.

B. Work and Play in the Cloud

Cloud Computing is a type of Internet-based computing where different services such as server, storage and applications are delivered to an organization's computers and devices through the Internet [11]. 5G services provide the opportunity to work and play in the cloud thus taking advantage of cloud computing technologies with the help of eMBB, uRLLC and mMTC. With this technology, the various departments of an academic institution can take advantage of this provision in reducing the cost of computation, application hosting, content storage and delivery. To be able to fully utilize the services offered by the 5G Ecosystem, the various models of cloud computing are important. The Ultra Reliable speed with lower latency of 5G will be the catalyst for the application of this service. Considering the centralised architecture of cloud service providers, there is a prominent delay in accessing contents even with a relatively fast internet connectivity. However with 5G, users should be able to use the cloud base models without delays with the aid of Lower latency, higher network availability and ultra-fast data rate exchange. This will keep the responses and executions in real time.

1) Software as a Service (SaaS): As shown in Fig. 2, this model offers a complete application to consumers, as a service on demand. A single instance of the service runs on the cloud and multiple end users are serviced. With the customers (institutions such as UEW), there is no need for upfront investment in software licenses. The SaaS model provides subscription based option online. Currently, SaaS is offered by companies such as Google, Salesforce, Microsoft and Zoho. A service of its kind could be used by Students and Lecturers and can be extended to Departments and Administration.

2) Platform as a Service (PaaS): As shown in Fig. 3, this model offers a layer of software, or development environment that is encapsulated and offered as a service, upon which other higher levels of service can be built. The customer or institution can build applications that will run on the provider's infrastructure. To meet manageability and scalability requirements of the applications, PaaS providers offer a predefined combination of Operating Systems (OS) and application servers that are highly robust and efficient. Students, lecturers and departments related to application and software development can have access to such service without the need to physically install any software on their computers. The PaaS will aid in collaborative projects irrespective of distance.

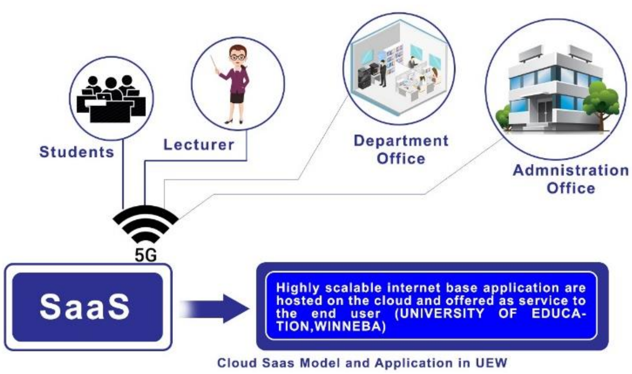

Fig. 2. Cloud SaaS Model and Application in UEW.

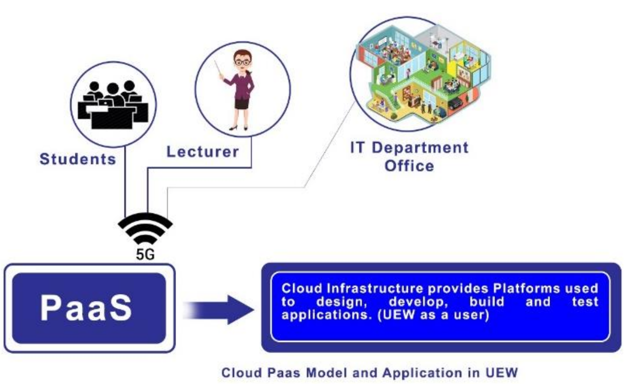

Fig. 3. Cloud PaaS Model and Application in UEW.

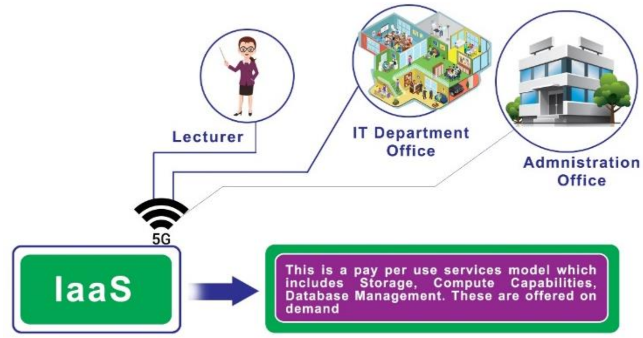

Fig. 4. Cloud IaaS Model and Application in UEW.

3) Infrastructure as a Service (IaaS): As shown in Fig. 4, IaaS provides basic storage and computing capabilities as standardized services over the network. Computer server, storage systems, networking equipments and data centers are pooled and made available to handle workloads. The customer (or institutions such as UEW) would typically deploy their software on the infrastructure.

C. Augumented and Virtual Reality

As shown in Fig. 5, the virtual reality is an interactive and haptic computer-generated environment in which users are physically connected through a simulation device to collaboratively execute tasks by perceiving the objects through many senses such as audio-visual, touch and smell senses [12]. Augmented reality is the combination of computer generated and a real content in a constructive view point of the user. Augmented and virtual reality technologies can be combined to achieve a desired objective. The main challenge of these technologies is the available bandwidth, network speed and latency to run it. The solution is offered by 5G services. These two technologies supported by 5G can essentially provide enormous benefit to Education in creating smart student, smart instructors and smart administrative team.

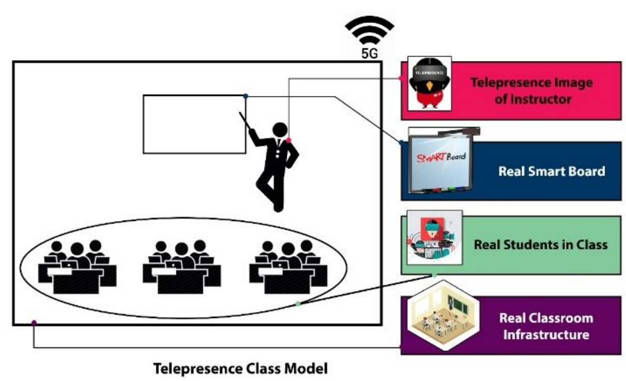

Fig. 5. Augmented and Virtual Reality Applicable to Education.

1) Telepresence Mode (TM): The concept of telepresence could be seen as 'telexistence' where users are enabled by both augmented and virtual visualization to be present at a remote location in a form [13]. The evolution of this concept has led to a technology which is capable of advancing education. Though telepresence with a high end-to-end audio and video conference call was integrated in education, somehow much of the precise face-to-face communication such as body language, eye contact, physical presence is still lacking. This face to face communication is one of the reasons that makes traditional classroom interesting. It is therefore important to integrate this immersive communication system in the telepresence concept. Holoportation is an end-to-end system for augmented and virtual reality where users are enabled by both augmented and virtual visualization to be present at a remote location exactly as they are not in any other form [14]. This system is skilled to capture people, objects and motions in full 360 degrees within a constructive room using group of custom depth cameras and then transmitted to a remote participants over a network in real time. The transmission of this communication generate a very large amount of data which makes it challenging to keep communication happening in real time. One factor that needs to be present before holographic communications can wind up completely is an impressive increment in network capacity. The presence of 5G with eMBB and uRLLC will solve this problem. 5G will enable full utilization of this technology. As shown Fig. 5, students in physical classroom are to wear AR or VR Head Mounted Display (HMD) such as Hololens or HTC Vive to see their holoported instructor. The instructor being an agent of knowledge is enabled to continue the transfer of knowledge regardless of the proximity. Students enrolled in Distance Learning modules can use this technology at the comfort of their homes.

2) *Full and Hybrid Virtual Model:*

a) Full Virtual Class Model: Full Virtual Class Model (FVCM) is a class where the delivering of learning content, teaching materials and evaluations are fully implemented using virtual and augmented content [15]. Section A in Fig. 6 depicts students accessing augmented and virtual content at the comfort of their desired location. Here, students access contents through the use of electronic devices and Head Mounted Display (HMD). Students accessing such virtual contents would have an in-depth instruction of the topic being delivered. Using the case of Haptic Augmented Technology and Tactile internet, this application can be modified for students to experience the texture of object on Mars. Teaching about Mars by Geography Department at UEW can make good use of such application to help student have a full understanding of this planet which is a futurist travel. Full Virtual Class Model could be adopted by UEW to help strengthen the provision of the Distance Education Program. FVCM doesn't restrict students to their location thereby making it easy for students to have access to class regardless of their location. FVCM can be implemented to help distance education students experience a replication of the traditional classroom.

b) Hybrid Virtual Class Model: Hybrid Virtual Class Model (HVCM) is a class where the delivering of contents and evaluations are accomplished using both traditional classroom and augmented and virtual content. Fig. 6, section B represents a regular class (Traditional Classroom) where there is an instructor and students using HMD. Content of abstract being delivered using the VR content to explain the reality of a concept. The instructor will serve as a guide in directing students on the visuals and help leaners with questions and answers. Example is using the Boulevard application for museum excursions.

D. *Industry / Educational Automation*

5G networks will have a Software-Defined Networking (SDN) architecture that comprises of the control and data planes. Most of the control plane intelligence will instruct data plane to drive the infrastructure [16] [17]. Fig. 7 depicts a scenario of an automated 5G Education setting to enable an intelligent university campus. The emergence of 5G will provide communication and automation within the classroom and administration offices where Educational Internet of Things (EIoT) and Industrial Internet of Things (IoT) are being used. Educational application "A" represent administration offices with cloud sensor devices and computerized system to perform computation. Educational application "B" is a classroom with Educational IoT wireless devices such as Smartboard 7000 Series IQ with image detective sensor, sensored door with actuator, sensored chair, smart table with embedded touch screen computer, room temperature sensor, motion and facial expression cameras.

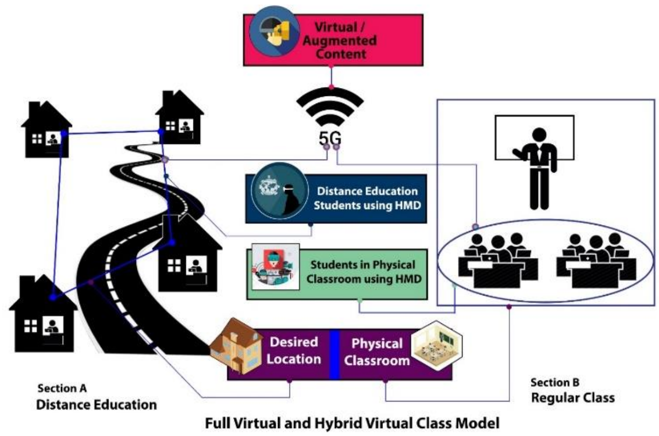

Fig. 6. Full Virtual and Hybrid Class Model.

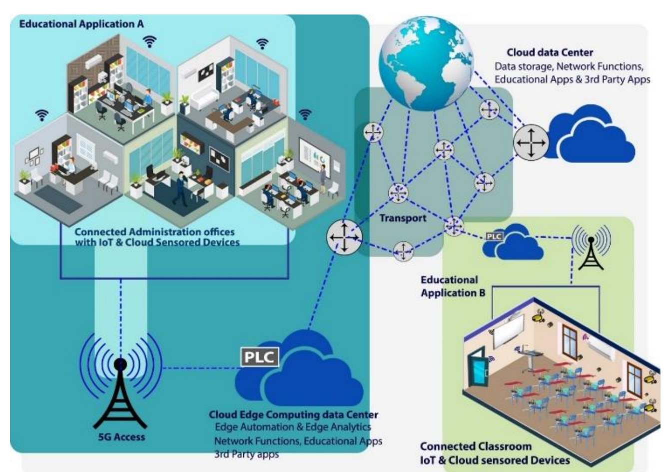

Fig. 7. Prospect Application Scenario of 5G – Enabled Automation in Education.

Existing automation in Education is highly focused on systems that promote personalised learning through the use of E-Learning system such as the Massive Open Online Courses (MOOCs) [18] and Adaptive Intelligent Tutoring Systems (AITSs) [19]. MOOCs enables flexibility in learning new skills with progress tracking. AITS incorporate built-in expert systems to monitor students' performance and to personalise instructions based on adjustment to students' learning style, current knowledge level and suitable teaching procedures. In addition, Adaptive Hypermedia system is another educational use case which adapts what the student is offered depending on a model of the learner's objectives, proclivity and knowledge. Automation in education over the years has improved learner understanding. These systems are educational interventions to automate education in a different way and improve teaching and learning. However, as far as the prospect of automation in education by 5G is concerned, machines, devices and humans are to communicate and interact to achieve educational goals. Machines are expected to be intelligent enough to make decisions without the intervention of humans.

Research shows that the revolution in industry (industry 4.0) is pressuring education with demands to keep pace with industry evolution. Therefore it would be very appropriate to adopt the core driving force of industry revolution (automation) and apply it in education. The prospect of automation from 5G in education takes a different trend from the existing automation in Education. The automation in 5G seeks to consume the three models of the 5G Ecosystem: eMBB, uRLLC and mMTC thereby utilizing the characteristics of automation, smart interconnection, real-time monitoring and collaborative control. These characteristics enable fast machine learning (ML), machine to machine/man technology (M2M) and Device to Device (D2D) technology.

1) The Role of ML, M2M, D2D in Automation: Machine-learning (ML) framework involves capturing and maintaining up a rich organised data in order to convert it into a structured information base for various use cases. This enables computers or instructing machines to learn from every past data set and settle on intelligent choices in making best decisions. Machine learning in education helps to personalised learning and instructions. Deployment of this technology interpret patterns and human interaction to support deeper learning and provide users with fast and accurate data in education. M2M is direct connection and communication that can exist between machine to machine, man to machine, machine to man, and machine to mobile network [20]. D2D represent a method of direct communication between two peer nodes [21]. With ML, M2M and D2D, communication between machines, machines and man, and device to device can have an accurate transfer of information to ensure perfect prescription, description and making the best decisions. These technologies work base on established procedures from the obtained data to make decisions and then issues control commands to actuators. Regardless of M2M or D2D, the core problem is the data rate transmission which 5G will provide.

2) ML, M2M and D2D FOR Automation in Education: With reference to Fig. 7, an example of the application of ML, M2M and D2D automation can be cited. In Application “B” there is a door with QR code reader to read student’s ID card or programmable wearable device. Communication is established between the sensor reader and the actuator to get the door opened. Upon the credentials read from the door’s QR code reader, a feed is sent to the Smartboard 7000 Series IQ to power on. The Instructor stores lesson materials on the cloud. With the help of date and time the smartboard automatically makes the e-learning materials available to the instructor. Students on the other hand would have their smart tables turned on using the feed from the sensor in the chairs. Students’ smart tables automatically access lesson materials from the cloud. There is room temperature sensor monitoring the temperature of the class. Air-conditioner get powered on and regulated by the feeds from the room temperature sensors. This communication between these machines provide data that is then stored in the cloud for analytics. With data analytics instructors and students can be monitored and report sent to the appropriate office machines at the administration office in Educational application “A”. With the eMBB offered by 5G network model, large amount of data is transmitted in every second whiles the mMTC keeps all the IoT sensors connected. The uRLLC keeps all devices connected with consistent data exchange.

E. *Tactile Internet, Over 5g*

The Tactile Internet increases the capacity to human-to-machine communication by empowering tactile and haptic sensations, and improves the interactions of machines. Tactile internet is a holistic network or grid of networks for remotely getting to, seeing, manipulating, and controlling genuine or virtual objects [22]. This is a sure way for students to have an interactive and haptic feel of Augmented and Virtual reality contents respectively. A typical example is a learner having an aquatic augmented reality excursion. Students can feel the exact temperature of the water body, have a haptic feeling of aquatic plant and animals using Haptic Augmented Reality Technology. For a student to experience the sensational feelings of touching a Wale, it would be an expensive and a highly risky attempt to get a Wale in a real world that would be reachable for a touch, however with the emergence of Tactile Internet, students can have the sense of touching a wale in a virtual classroom. To achieve these interactive haptic feedback in real time, the speed involved in data exchange as well as the latency should meet the exact natural reactions time. Hence a network with Lower Latency is needed. The 5G Ecosystem can provide the possibility in deploying the Tactile Internet Technology.

IV. CONCLUSION

The realization of 5G networks will revolutionize not only industry but will propel a change in Academic Institutions. In this paper, we proposed frameworks and discussed the possibility of using the 5G Ecosystem and adapting its relevant technologies to Education. This paper discussed the transformation 5G Networks will bring especially in strengthening the teaching and learning process. From this research, the possible deployment 5G technologies in

Education and the emergence of IoT devices on campuses will serve as a turning point in students learning process, instructors' research and content delivery mechanisms.

References

[1] Meraj, M., & Kumar, S. (2015). Evolution of mobile wireless technology from 0G to 5G. International Journal of Computer Science and Information Technologies, 6(3), 2545-2551.

[2] N. Javaid, A. Sher, H. Nasir and N. Guizani, "Intelligence in IoT-Based 5G Networks: Opportunities and Challenges," in IEEE Communications Magazine, vol. 56, no. 10, pp. 94-100, OCTOBER 2018. doi: 10.1109/MCOM.2018.1800036.

[3] Gros, B. (2016). The design of smart educational environments. Smart Learning Environments, 3(1), 15.

[4] Klašnja-Milićević, A., Vesin, B., Ivanović, M., Budimac, Z., & Jain, L. C. (2016). E-learning systems: intelligent techniques for personalization (Vol. 112). Springer.

[5] Demestichas, P., Georgakopoulos, A., Karvounas, D., Tsagkaris, K., Stavroulaki, V., Lu, J., ... & Yao, J. (2013). 5G on the horizon: Key challenges for the radio-access network. IEEE vehicular technology magazine, 8(3), 47-53.

[6] Javaid, N., Sher, A., Nasir, H., & Guizani, N. (2018). Intelligence in IoT-Based 5G Networks: Opportunities and Challenges. IEEE Communications Magazine, 56(10), 94-100.

[7] Patil, G. R., & Wankhade, P. S. (2012). 5G Wireless Technology. world, 1(1).

[8] Lee, I. (2017). Big data: Dimensions, evolution, impacts, and challenges. Business Horizons, 60(3), 293-303.

[9] Gómez, J., Huete, J. F., Hoyos, O., Perez, L., & Grigori, D. (2013). Interaction system based on internet of things as support for education. Procedia Computer Science, 21, 132-139.

[10] Sharma, M. M., Husain, S., & Ali, M. S. (2017). Cloud computing risks and recommendations for security. International Journal of Latest Research in Science and Technology, 6(1), 52-56.

[11] Li, X., Jiang, W., Jiang, Y., & Zou, Q. (2012, June). Hadoop applications in bioinformatics. In 2012 7th Open Cirrus Summit (pp. 48-52). IEEE.

[12] Bower, M., Howe, C., McCredie, N., Robinson, A., & Grover, D. (2014). Augmented Reality in education–cases, places and potentials. Educational Media International, 51(1), 1-15.

[13] Kaber, D. B., Riley, J. M., Zhou, R., & Draper, J. (2000, July). Effects of visual interface design, and control mode and latency on performance, telepresence and workload in a teleoperation task. In Proceedings of the human factors and ergonomics society annual meeting (Vol. 44, No. 5, pp. 503-506). Sage CA: Los Angeles, CA: SAGE Publications.

[14] Orts-Escolano, S., Rhemann, C., Fanello, S., Chang, W., Kowdle, A., Degtyarev, Y., & Tankovich, V. (2016, October). Holoportation: Virtual 3d teleportation in real-time. In Proceedings of the 29th Annual Symposium on User Interface Software and Technology (pp. 741-754). ACM.

[15] Chiu, H. P., Kaelbling, L. P., & Lozano-Pérez, T. (2007). Virtual training for multi-view object class recognition. In 2007 IEEE Conference on Computer Vision and Pattern Recognition (pp. 1-8). IEEE.

[16] Kim, H., & Feamster, N. (2013). Improving network management with software defined networking. IEEE Communications Magazine, 51(2), 114-119.

[17] Shin, M. K., Nam, K. H., & Kim, H. J. (2012, October). Software-defined networking (SDN): A reference architecture and open APIs. In 2012 International Conference on ICT Convergence (ICTC) (pp. 360-361). IEEE.

[18] Kizilcec, R. F., Piech, C., & Schneider, E. (2013, April). Deconstructing disengagement: analyzing learner subpopulations in massive open online courses. In Proceedings of the third international conference on learning analytics and knowledge (pp. 170-179). ACM.

[19] Phobun, P., & Vicheanpanya, J. (2010). Adaptive intelligent tutoring systems for e-learning systems. Procedia-Social and Behavioral Sciences, 2(2), 4064-4069.

[20] Wu, G., Talwar, S., Johnsson, K., Himayat, N., & Johnson, K. D. (2011). M2M: From mobile to embedded internet. IEEE Communications Magazine, 49(4), 36-43.

[21] Hakola, S., Chen, T., Lehtomaki, J., & Koskela, T. (2010, April). Device-to-device (D2D) communication in cellular network-performance analysis of optimum and practical communication mode selection. In 2010 IEEE wireless communication and networking conference (pp. 1-6). IEEE.

[22] Cheng, J., Chen, W., Tao, F., & Lin, C. L. (2018). Industrial IoT in 5G environment towards smart manufacturing. Journal of Industrial Information Integration, 10, 10-19.

A Multi-Layered Security Model for Learning Management System

Momeen Khan[1]
Department of Computer Science
IIC University of Technology
Phnom Penh
Cambodia

Tallat Naz[2]
Department of Information Systems and Computer Science
King Khalid University, Tohama Branch, Mahayil Asir, Saudi Arabia

Mohammad Awad Hamad Medani[3]
Department of Information Systems
King Khalid University, Tohama Branch, Mahayil Asir, Saudi Arabia

***Abstract*—A learning management system is a web-based software application that is used for the documentation, administration, tracking, reporting and delivery of training programs and educational courses. It is an efficient and effective way to give valuable information to the students in a short time. With the evolution of e-learning, the learning management system is widely adopted in the education sector as well as in corporate market. Thus, it became a valued target for attackers to focus their attacks on LMS platforms. Most of the popular learning management systems available now a day don't pay enough attention to the security mechanism and that gives opportunity to intruders to gain unauthorized access by manipulating the security gaps and breach into the system. The result is information leakage, unwanted data deletion or modification and compromised integrity of the data. The aim of this research paper is to focus on the need of security concerns and to provide a solution that can make the learning management system secure from any possible potential threats and attacks. In this paper, a complete multi-layered security model is proposed. The implementation of proposed model will provide a very secure environment for any learning management system.**

Keywords*—Multi-layered security model; designing a security model for learning management system; learning management system

I. Introduction

The application of Information Communication Technology tools in education expanded the learning methods and introduced new ways of learning. The development of Information Communication Technology includes various ways of communication [1], such as smart phones and mobiles that gives the learners the opportunity to learn anywhere and anytime. Learning management system is a platform that facilitates the learners to carry out e-learning related tasks. It is a mechanism that powers e-learning [2]. Learning management system or E-Learning is a kind of learning method that shares and distributes information and it can be used as an alternate of traditional classroom for the learners, who may not be able to attend the traditional classroom environment.

There is a noticeable increase in the number of learners that are using online learning [3] or a learning management system as compared to traditional face to face learning environment [4]. As a result, many learning institutes and organizations have adopted learning management system to increase their revenue and pedagogy. According to the statistics of the US National Center for education, almost one million students enrolled in distance learning [5], which was 35% of solely online students. From this, it is quite clear that learning management system is becoming popular in education sector and is considered as a main building block of learning and training activities. Considering its importance, there is a need to make it secured and protected against any possible attack.

Learning management systems uses the internet to share and distribute data and information. However, the internet as a backbone of any learning management system is insecure. Security is one of the significant issues in a learning management system where multiple databases are connected through the common gateway [6]. Therefore, the learning management system is subject to software and hardware attacks. These attacks may have an effect on intellectual property such as copyright and privacy. To our knowledge, little work tried to find a solution that can ensure a safer learning environment. Moreover, learning management system includes vital information and knowledge about the learners and institutes or organizations that is always considered as a critical asset.

Learning management systems have several security issues that include protection against manipulation, authentication, availability, confidentiality and data integrity. Over time, many features are usually added to the learning management system. Therefore, efforts should be made to make this sensitive information as much secured as possible. Such information should be restricted to only the authorized groups. The security threats of the learning management system have common features to E-Systems threats, therefore, managing security is also common. Managing the security of learning management systems should include content and services to ensure usable and available system [7]. For the safe and smooth operation of learning management system with a high quality, it is a challenge for institutions and organizations is to provide an immense security plan after assessing the risks and their potential impact in detail [8]. Hence, by the development of security mechanism and use of tools for security will guarantee the availability of high-quality services with a low cost.

In section 2, studies the literature review. In section 3, we discussed about the security issues in the learning management system. In section 4, we proposed a multi-layered security model for the learning management system. In section 5, we did discussion and in the last section 6, we wrote the conclusion.

II. Literature Review

In the literature review, it was found that many researchers elevated several issues concerning the security in learning management system. Some of these issues are data protection, anonymous use, privacy, and authentication. Due to the vulnerability of the networks to the hackers, an entire system can be damaged by a single virus and thus may result in the infection of other systems that are connected to the network [7]. The institutes are worried about the protection of their data. In the meanwhile, the researchers are trying to find ways to protect and secure data and learning environment.

Learning management systems are complex systems. They are open, heterogeneous and they are wide spread. There is a greater chance for them to expose to risks and threats. Therefore, security is a difficult and important challenge. It is of great concern to focus on the security of learning management system platforms and to learn about the authentication, availability, confidentiality and integrity. A high-quality learning process would be the result of a more stable and secure learning platform.

A researcher talked about user authentication as an essential issue to think in the security of learning management system [9]. His work explained that policies and strategies should be laid while changing the requirements for the software and hardware to guarantee suitable authentication of the learner. The highlighted security issues include identity theft, inadequate authentication and impersonation [10]. Various sources of security threats for a learning management system are authenticity, access control, confidentiality, integrity, availability, and non-repudiation [11] [12]. Furthermore, some of security risks or threats in learning management system includes confidentiality violation, integrity violation, denial of service, etc. and providing remedies to minimise all these risks.

From the above literature, the security issues in Learning management system can be categorised as following:

A. Authorization

Authentication checks whether the authenticated person has the right or privilege to access the contents of the system [13].

B. Identification and Authentication

Identification tries to identify legitimate users to whom access has been granted. While Authentication tries to verify that the user is the same as whom, he claims to be.

C. Availability

In Learning management system, availability is the assurance that the Learning management system's environment is accessible by authorised users, whenever it is needed. Availability can be divided into two: Denial of Service attack (DoS)–an attack that stops access to authorized users of a website, so that the site is forced to offer a reduced level of services or in some cases, ceases operation completely that results in the loss of data processing capabilities. The Learning management system users are dependent on the information on the Internet; therefore, the availability of materials and information to be accessed at any point in time and at any location is crucial [7]. Failing to fulfil this will have a huge impact on Learning management system users and providers.

D. Confidentiality

This is the protection of information in the system so that unauthorised persons cannot gain access.

E. Integrity of information

This is the protection of data from unauthorised changes (i.e. only authorised users or processes can alter contents and no changes can be made illegally). Integrity depends on access controls; therefore, it is important to positively and uniquely identify all persons who attempt access. Integrity can be compromised by hackers, masquerades, unauthorised user activity, unprotected downloaded files, LANs, and unauthorised programs (e.g., Trojan horses and viruses). Each of these threats can lead to unauthorised changes to data or programs.

III. Security Issues in Learning Management System

The security design of the learning management system is always part of discussions theoretically. However, it is important to understand the attacks in a way to correctly identify the factors that are affecting the security mechanism. It will help in the designing of the security services.

A. Authentication Attacks

The attack is to gain access to system information by using stolen passwords, keys or credentials. An attacking device pretend as a legitimate device trying to gain access to the system. These types of attacks may lead to unauthorized modification of contents and breach of confidentiality. Examples include brute force attack, dictionary attack, login spoofing attacks, key management attacks, replay attacks, Man-in-middle attacks. To counter these attacks, strong authentication method such as multi-factor authentication security system should be implemented.

B. Authorization Attack

An attack that occurs as a result of unauthorised access to specific content. Unauthorized use or elevation of access can be countered by using the principle of least privilege; strong access control lists (ACL's) or strong role-based security mechanism should be used.

C. Availability Attack

This is an attack that occurs when services of a system and contents are unavailable to legitimate users for some time. Examples of such attacks include Denial of Service, Node attacks, Line attacks, Network infrastructure attacks. A Good backup system is a way of countering these attacks, use of a scrubbing cloud DDoS mitigation technique and load sharing among several servers carrying the learning management system.

D. Confidentiality Attack

This attack tries to expose the confidential data to unauthorized users. This may be transfer of e-contents to the unauthorized persons or obtaining secret passwords. Example includes: Group session eavesdropping, Group session traffic analysis, and Group identity disclosure [14]. Strong encryption methods should to be used to counter confidentiality attack. Ex. RSA-265, Hash or above.

E. Integrity Attack

This aims to destroy or modify the contents of the system. Due to the integrity attack, the legitimate users will not get the correct contents. Examples are malicious code attacks, message injection, traffic modification**,** traffic deletion. To counter integrity attacks, digital signature, data hashing and shining can be used effectively. Authorization should be strong enough to keep unauthorized users at bay to stop them from many chances to alter the information. Protocols should be tempered resistant across communication links.

The main asset of an organization is the information that is obtained from the useful data. If the access is made easy for everybody then it will be not hard for anyone to gain access despite of the fact that that have good or bad intentions. As a result, the information is exposed to a variety of threats and vulnerabilities.

IV. Problem Statement

Implementing learning management system is not an easy task. Regardless of gaining many benefits from learning management system there are also many challenges and issues while trying to make the learning management system successful. Despite the deployment of advanced security methodologies, there are still several loopholes that must be filled. It is important to properly assess the security properties that are associated with learning management system.

V. Research Objective

Based on this assessment, a security model should be proposed that offers technological security mechanism to secure learning management system. It is of great importance to treat the security mechanism in learning management system more seriously by designing more complex security models. Therefore, a new security model based on multi-layers security mechanism is proposed.

VI. Proposed Security Model for Learning Management System

In order to ensure authentication, availability and integrity for learning management system we have developed a model with four main layers and five sub layers as shown in Fig. 1. Distribution of tasks on different layers ensures better management of security on each layer.

A. Physical Layer

In order to ensure maximum security for learning management system we will use the design as shown in Fig. 2. It will help to ensure authentication, availability and integrity. On physical layer only authorized people are given access to sensitive hardware which includes routers, proxy server, web server, database server, file server and backup server.

Users connect with router to access learning management systems. Router sends data to the firewall and a honey pot. Data travels from firewall to web server after passing through intrusion detection prevention system (IDPS) and proxy server. Database is placed on a separate server and files are placed on a separate server. While everything on the web server, database server and file server is backed up on a separate server. All these things will be discussed in more detail under other layers.

The presence of proxy server in front of the web server increases privacy and caches data. Cached data helps in faster delivery of data.

B. Network Layer

Network layer primarily deals with data coming in from internet and going out on internet. It also deals with connection of different devices for successful operation of Learning Management System.

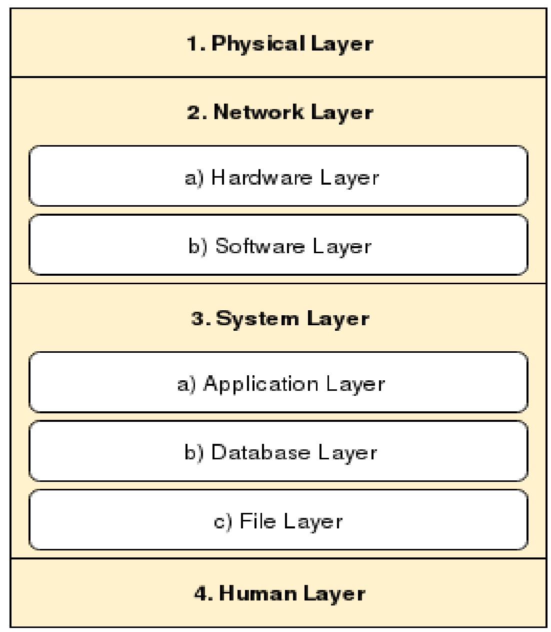

Fig. 1. Layers in LMS Security Model.

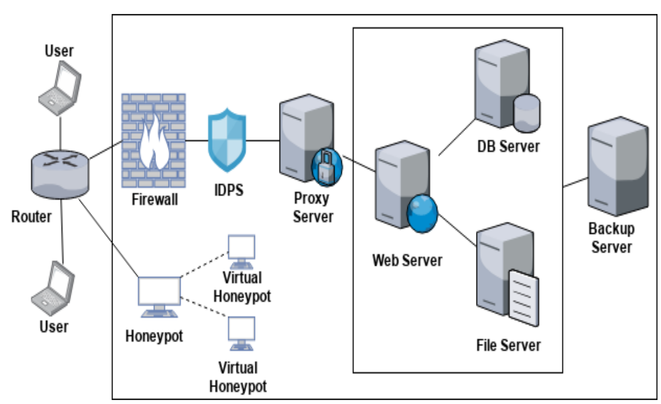

Fig. 2. Infrastructure at Physical Layer.

a) Hardware layer: On hardware layer of network layer, we have router. Routers can be helpful in the following:

- Restricting unauthorized devices from connecting to the network to ensure safety of the network.
- Cisco routers have a hardware firewall which can be used to filter traffic.
- Router can also help in restricting websites which we don't want to be opened on the network. Certain websites can contain viruses, malwares, trojans, spywares etc. These can harm devices present on our network. So, it is much better to block such websites completely.

b) Software layer: On software layer of network layer, we have the following:

- A software firewall is used to filter traffic and protect LMS from malicious traffic sent by attackers. It also logs the traffic so if needed later behavioral analysis can be performed on the logs to detect unwanted behavior.
- Intrusion prevention systems (IPS) also known as Intrusion detection prevention systems (IDPS) are used to deeply monitor the packets on the network. When any malicious activity is detected, IPS / IDPS will log and block it. It will also report this activity to alert the system administrators.

C. System Layer

On system layer we use various mechanisms to ensure security of the system, which will be discussed below:

a) Application layer: LMS is placed on the web server and following measures are taken for its security:

- Access control list (ACL) is used for authentication and it ensures that only authorized people are allowed to access the system. Whenever a user requests a resource on the LMS, it is first checked in ACL to make sure that this user is authorized to access that resource. If that user is authorized, then he / she is given access to that particular resource otherwise if that user is not authorized then access is not granted.
- Hyper Text Transfer Protocol (HTTP) is the protocol through which data is transferred between our browser and website or server to which we are connected through an insecure connection. Any attacker can get the data which is being transferred over HTTP and steal login details of legitimate users because the connection is insecure. Using Hyper Text Transfer Protocol Secure (HTTPS) encrypts the connection making it difficult for attacker to steal any information from the data being transferred over HTTPS. So, we will install SSL to ensure use of HTTPS
- All the forms in the application will use POST method instead of GET to secure login details and the data transferred.
- Prepared statements are always used while making a query to the database, it helps to protect the application against SQL injection attacks. Prepared statements help to ensure integrity because data present in the database can't be affected or changed by attacker.

Honey pot is connected with the router. Honeypots appear as vulnerable parts of the system to attackers and they mislead the attacker on concentrating all their energy on the honeypot instead of the actual system. Whenever anyone tries to connect with honeypot it gives us a clear signal that an attacker might be scanning the system and will eventually try to penetrate it. When someone scans the Honeypot, more virtual honeypots are created, and the attacker will start to scan them also. It alerts the staff to take appropriate action before any serious damage is done to the system.

Distributed Denial of Server (DDoS) Attack are well known for making the website / system unavailable for legitimate users. Honeypot can also protect against Distributed Denial of Server (DDoS) Attack and make sure that LMS is available for legitimate users.

b) Database layer: Database is deployed on the database server and following measures are taken for its security:

- Table level access control is applied. Only authorized people are allowed to read, write, update or delete anything from table.
- Sensitive information stored on database server is encrypted using hardware security module (HSM). HSM are specially designed hardware components for cryptography.
- In case of data loss, data can be retrieved from backup server to ensure data is available for legitimate users.

c) File layer: All files are stored on the file server and following measures are taken for its security:

- To ensure integrity of files a file check sum will be calculated and stored for all the files. Whenever file integrity needs to be checked, we will simply recalculate the check sum of file and then compare it with the check sum which we have already calculated and stored in the past. If checksum is same it means file is not tampered but if checksum is different, it means file is tampered and it should be deleted. After deleting such files, original files can be retrieved from the backup server.
- All directories in which files are uploaded don't have execute permissions. Only read and write permissions are given.
- Only files of the following format are allowed to be uploaded: doc, docx, ppt, pptx, xls, xlsx, pdf, png, jpeg other ones will be rejected by system. It will ensure no malicious file is uploaded on the file server.

d) Human layer

- Training for staff is vital and is of paramount importance. They need to be trained to check the URLs in address bar of browser before entering any sensitive details in the system. They should make sure that the protocol being used in HTTPS and not HTTP.

- Staff should also be made aware of the social engineering tactics used by attackers.

VII. Discussion

The success of a learning management system needs to resolve all the challenges in the implementation, specially the security challenges. The proposed security model is designed to be a purely defense in depth model for security of LMS.

- It ensures every step is taken to stop attackers on each layer.
- It ensures authentication by application of ACL at application layer (a sub layer of system layer), encryption at database layer (a sub layer of system layer) and filtering unauthorized devices at hardware layer (a sub layer of network layer).
- It ensures availability by using proxy server, high bandwidth and backup server.
- It ensures integrity by using SSL, POST method in forms, Reputation check with checksums, prepared statements to protect against SQL injection.
- Honeypots connected to router help to detect attackers before any damage is done to the actual system.
- Honeypots can protect LMS against DoS attacks and ensure availability of LMS for respected users.

Traffic logs are maintained at a sub layer of network layer called software layer, these help in behavioral analysis of the traffic to find out any malicious traffic being sent to our network.

VIII. Conclusion

The major challenge in learning management systems today is the issue of security. In this research paper, the researchers highlighted several issues in the security of learning management system. The researchers also proposed a multi-layered model that can ensure the security mechanism of a learning management system. As per the proposed solution might seem costly in its implementation but it's return of investment (ROI) is worthwhile. The implementation of this security model shall be of great use for enterprises holding a learning management system and will make sure that both users and professors will gain trust towards a system that is well secured against tampering and manipulation of their data.

References

[1] Ally M (2007). Mobile Learning. Int. Rev. Res. Open Distance Learn. Volume 8, Number 2. ISSN: 1492-3831.

[2] Tallat Naz and Momeen Khan, "Functionality Gaps in the Design of Learning Management Systems" International Journal of Advanced Computer Science and Applications(ijacsa), 9(11), 2018. http://dx.doi.org/10.14569/IJACSA.2018.091152.

[3] Allen E, Seaman J (2014). Tracking Online Education in the United States. Babson Survey Research Group and Quahog Research Group, LLC.

[4] Pastore R, Chellman A (2009). Motivations for residential students to participate in online courses. Q. Rev. Distance Educ. 10(3):263-277.

[5] Akanegbu, Anuli (2012). 50 Striking Statistics about Distance Education in Higher Education https://edtechmagazine.com/higher/article/2012/07/50-striking-statistics-about-distance-learning-higher-education.

[6] Momeen Khan, Tallat Naz, Khalid Mahmood, (2019) "Using Blockchain to resolve Database Distribution and Security Issues in The Learning Management Systems (LMS)" International Journal of Computer Science and Network security (IJCSNS), Vol. 19 No. 11 pp. 139-150. http://paper.ijcsns.org/07_book/201911/20191120.pdf

[7] Alwi N, Fan IS (2010). E-Learning and Information Security Management. Int. J. Digit. Soc. 1(2).

[8] May M, George S (2011). Privacy concerns in e-Learning: Is using a tracking system a threat? Int. J. Inf. Educ. Technol. 1(1):1-8 [Online]. Available: http://liris.cnrs.fr/Documents/Liris5266.pdf[Accessed 25 09 2014].

[9] Levy D (2011). Lessons learned from participating in a connectivist massive online open course (MOOC). In Y. Eshet-Alkalai, A. Caspi, S. Eden, N. Geri & Y. Yair (eds.), Proceedings of the Chais conference on instructional technologies research: Learning in the technological era, (pp. 31-36). Available online at http://www.openu.ac.il/research_center/chais2011/download/f-levyd-94_eng.pdf.

[10] Chen Y, He W (2013). Security risks and protection in online learning: A survey. Int. Rev. Res. Open Distrib. Learn. 14(5).

[11] Saleh MM, Wahid FA (2015). A Review of Security Threats by the unauthorized in the E-learning. Int. J. Comput. Technol. 14(11):6240-6243.

[12] Barik N, Karforma S (2012). Risks and remedies in e-learning system. Int. J. Netw. Secur. Appl. 4(1):51-59.

[13] Assefa S, Solms V (2009). An Information Security Reference Framework for e-Learning Management Systems (ISRFe-LMS)," Proceedings of 9th WCCE, 2009.

[14] Cardenas R, Sanchez E (2005). Security challenges of Distributed E-learning systems. ISSADS, 2005.LNCS 3563 pp. 538-544.Springer Verlag Berlin Heidelberg.

Comparative Study between Lean Six Sigma and Lean-Agile for Quality Software Requirement

Narishah Mohamed Salleh[1], Puteri NE Nohuddin[2]
Institute of Visual Informatics
National University of Malaysia
Bangi 43600 Malaysia

***Abstract*—Requirement Elicitation is one of the challenging phases in the entire software development life cycle. It is the process of extracting and analyzing the requirements from customers to understand thoroughly of what system needs to be built. Despite all the advances in methodologies and practice approaches, extracting and establishing the right requirements are still part of the research debate. The objective of this paper is to compare the characteristics of two hybrid development approaches; Lean Six Sigma vs. Lean Agile. Most of the comparative studies done by most of the research compared within its relative knowledge such as; Lean vs. Six Sigma, Define-Measure-Analyze-Improve-Control vs. Design-For-Six-Sigma or Lean vs. Six Sigma vs Lean Six Sigma. Whereas in software industries, the comparative studies were focused on Lean vs. Agile, Agile vs. Waterfall, Lean vs. Kanban vs. Agile, which compared the project size, process cycle time, sequential or iterative process. The following parts of the study is to explore the differences and similarities in principles and practices. The study contributes significantly to the business analysts to systematically address the solutions and actions to ensure continuous improvement in producing quality software requirement.**

Keywords—Lean Six Sigma; Lean Agile; DMAIC; SCRUM; Requirement Elicitation

I. INTRODUCTION

Requirement Engineering is a process of eliciting, analyzing, specifying, validating and managing the requirements to meet end users' objective [1], [2]. The core of requirements engineering is Requirement Elicitation (RE), the process of identifying what the customer needs and understanding the problems to resolve from the software engineering perspective[3], [4]. Without an accurate understanding of what the stakeholders' specification, tendency of projects to be failed is at high degree. It is observed about 12% to 71% of the project failure are attributed to poor requirements[5]. Standish report in 2014 revealed that most of significant factors contribute to the software project challenges are Lack of User Input and Incomplete Requirements. Getting the absolute requirements has always been the challenge in the current global and complex business process supply chain. [6], [7] confirmed that a combination of elicitation techniques was required to resolve different types of requirement challenges. Many software methodologies were created to assist team in understanding and providing the optimum solutions; such as Waterfall, Incremental Prototyping, Agile, Lean Software Development (LSD) and hybrid Lean-Agile. All with the same objective to improve quality, to meet customers' needs, reduce software delivery cycle time and reduce the cost of reworks.

The purpose of the research is to investigate similarities and differences of principles and practices between LSS and LA approach. This will assist analysts and researchers to find the benefits, limitations and strengths in software requirement gathering process. The rest of the paper is organized as follows: Section 2 contains characterization and definition of Requirement Elicitation, Lean-Agile and Lean-Six Sigma methods and related work of comparison analysis in the hybrid approach. Section 3 details on discussion and analysis. Section 4 provides the conclusion and summary of the topic.

II. LITERATURE REVIEW

A. Requirement Elicitation

RE is the process of determining, understanding "what is customer's wants" which is then to be translated into a reality. The process consists of five principles activities [8]. The first principle is the understanding of knowledge domain. The second principle is to identify the main stakeholders in the entire life cycle. The third principle is to analyze the characteristic and behavior of the stakeholders. It is also to evaluate the impact of stakeholders in the project scope. The fourth principle is RE selection techniques. The fifth principle is to extract the requirement from stakeholders or end users. The common RE techniques are Interviews, Discussion, Focus group, Surveys, Observations, Requirements Workshops, Prototyping and others. Researchers confirmed which is impossible to perform stand-alone activity for RE techniques. It is required a combination of RE techniques to achieve the project goals.

Authors in [7], [9], [10] categorized the elicitation techniques into Traditional, Collaborative, Cognitive and Observational which are summarized in Table I. Each group has different technique to be applied during the requirement elicitation process.

Table I outlines a summary of what RE techniques should be applied at different types of situation. For example, if the end users are well knowledgeable, the interviews and discussions are more than enough to extract the requirement and user specification in full capacity. Despite the category of RE techniques, there are few practices in the RE process recommended by [11], [12] that were based on value chain analysis:

- RE preparation – Define objective, scopes and stakeholders, business function scenario and business requirement.
- Non-Functional Requirement and Constrain – Availability, reliability and sustainability.
- RE Audition and Negotiations – Control and feedback, evaluate consistency of requirements and describe demand rationality.
- RE Completion – RE process will stop once the requirements met the user's expectation else, the process will be in iterative mode.

Those are the main elements to further elaborate between LSS and LA development model.

B. Lean Six Sigma (LSS)

Lean Six Sigma (LSS) is a methodology which derived from Six Sigma and Lean Management approach [13]. It is the integrated methodology with a systematic approach to improve organizational performance by removing process wastes and reducing variation through diagnosis and analysis capabilities of Six Sigma. In recent years, more companies have decided to combine Lean and Six Sigma methodologies [14] to improve business process efficiency and to deliver the highest quality to customers. Table II summarized the LSS principles based on previous literatures [15], [16] :

The methodology can be divided into five phases known as DMAIC (Define, Measure, Analyze, Improve and Control) which occurs in sequential order where tollgate review will be done at end of each phases.

Define is the first step to define objective, to identify the stakeholders, to understand and explore customer's requirement. Authors in [20], [21] applied Project Charter template in the research as the outcome at Define Phase which constitute of comprehensive strategy and planning to identify problems, project objective and business goal, scope and boundaries, time of completion and list of stakeholders involved for extrusion process and project costing. Author in [14] recommended few important tools at this phase; problem identification, Voice of Customers (VOC), Drill Down Tree Diagram, High level process map (SIPOC), Critical to Process Qualities and Project Charter.

Measure phase is the second phase which most of the tools are adopted to collect data, to understand current organization which basically to understand "What-Is" scenario data [22]. However, [23], [24] utilized this phase to explore and to investigate the base line of manufacturing process.

The third phase is Analyze which to perform the analysis and to identify the root cause of the problems. It is similar with requirement analysis in traditional Requirement Engineering process. The fourth phase is Improve which is to implement optimized solutions to solve the problem. In requirement engineering, it is known as Design and development phase. The last phase is Control which is to sustain the improved results which is similar concept as Verification and Validation phase in SDLC or Requirement Engineering cycle.

C. Lean Agile

Agile was established in 2001 when Agile Manifesto was formulated with the main objective to resolve fluctuating demand or requirement changes in software development. Lean is a management philosophy focused on providing maximum customers' value through end-to-end focus on delivering to customer's needs, efficient work streams, empowered teams and continuous improvement initiatives [25].

TABLE. I. SUMMARY OF ELICITATION TECHNIQUES

Situational Challenges	*Category*	*Technique*
• Stakeholders have deep domain knowledge. • End users were cooperative and can be accessed easily • System is stereotype	Conversational	Interviews Discussion
• End users have shallow knowledge and unable to express what they want. • Business Analyst is new at the domain. • End users were not cooperative • Documents were insufficient and incomplete	Observational Synthetic	Protocol Analysis Observation Scenarios Prototype JAD/ RAD
• Procedures were properly documented	Analytical	Content Analysis Requirement Reuse
• Systems involved with many end users	Analytical Observational	Content Analysis, Requirement Reuse

TABLE. II. PRINCIPLES OF LSS

Principles	*Description*
Focus on Customers	It is a principle of creating values to the customer. Any processes that do not benefit customers will be considered as a waste [17]
Value Stream	Identifying and understanding how the works get done through value stream mapping is crucial to visualize the current process before new solution is proposed
Focus on value-add process	Value Stream analysis, all non-value added tasks should be eliminated from the process to ensure the smoothness of the flow [18]
Manage, improve and smooth the process flow	Lean principle itself is about managing a smooth flow not only in operations, but also the information and the material flow where complexity should be managed and improved.
Manage by fact and reduce variation	LSS emphasizes that problems are based on solid evidence and baseline data where process improvement is derived from a structured statistical analysis [19]
Undertake improvement activity in a systematic way	LSS followed systematic and proven statistical tools which is applied to ensure business efficiency and customer's satisfaction.
Involve and equip the people in the process	Resources is the most important element in LSS principle where increasing values through respect, empowerment and growth of learning are vital to improve collaboration and teamwork.

This philosophy was adopted by [26] who considers lean thinking as a "platform upon which to build agile software development practices". Author in [27] argued that although agile and lean have fundamental differences, yet they complement each other by addressing different "components" of systems development. Consequently, software development is interpreting the combination of agile and lean in a different way than in manufacturing. Author in [28] summarized in a research that most of Lean principles have similar objective with agile principle. The focus of related theory in this paper is to explore Lean-Agile principles, methodologies and elicitation process.

Scale Agile Inc developed a framework applied Lean and Agile principles in building large enterprise class software. Scale Agile Framework described nine LA principles which tabulated in Table III. Application of the principles had improved employee involvement, speed up time-to-market, product quality and productivity in Scale Agile Inc.

TABLE. III. PRINCIPLE OF LEAN AGILE

Principles	***Description***
Take an economic view	It is about the principle of business values which to understand the economic impact of the decision been made [26]
Apply system thinking	It is a holistic approach which consists of design, development, deployment and maintenance. It also the process of optimizing the full value stream with an integrated end-to-end solution.
Assume variability and preserve options	According to Scale Agile framework (Scaled Agile Inc.2016), this principle emphasizes of the need to design multiple options of solutions to ensure speed of delivery and to avoid hiccup in development.
Incremental Development Approach with Integrated Continuous Improvement	Iterative development is critically important to allow fast feedback from customers and to reduce risk by designed and developed solutions in a series of short iteration [26]. This is similar to Scrum sprint review [29].
Manage by fact and reduce variation	LSS emphasizes that problems are based on solid evidence and baseline data where process improvement is derived from a structured statistical analysis.
Systematic Milestones Objective evaluation	Gates milestones is essential to evaluate the status of each phase dateline, cost, resources and objectives to ensure return of investments.
Applying Kanban Principle to improve visualization, managing que lengths and work-in-progress (WIP)	KANBAN recommends small batches, visualize and control Work-In-Progress (WIP) and minimize queue of length to ensure continuous flow, reduces waste and increase predictability of outcomes [30], [31] .
Unlock the intrinsic motivation of knowledge workers	It is a principle of creating an environment of mutual influence, self-direct and respect each other. This is aligned with Lean Thinking principle and Agile manifesto where team empowerment is a significant philosophy to drive for project success
Decentralize decision making	Decentralize decision making is the process of making a quick decision based on the expertise, policies and rules to improve cycle time, product delivery, continuous flow and facilitates faster feedback.

Both LSS and LA emphasize "The Principles" as the core values to optimize sustainability in global competitive advantage. Cost reductions, faster time-to-market and high-quality products and services are the main pillars in many software developments companies. That is the main reason why the first principle for both LA and LSS is focusing on the customers' values. Author in [32] summarized that any extra steps, processes or features that do not give values to customers are considered wastes which not only impact productivity but also efficiency. Both LA and LSS principles agree that the importance of human involvement in the development cycle where respect, trust and motivation should be restored. LA methodology in software is not specifically a set of method that is designed for Lean-Agile itself. However, it is more on the application of Lean principles into agile processes in different practices for different purpose. Author in [33] had performed a study using hybrid approach which combined Scrum and Kanban method to improve software performance metrics.

One of the significant elements in Lean-agile methodology is communication. Statistic shows that face-to-face communication is the most effective way to convey information which has many advantages. For example, when customers and developers work collectively; if any question or issue or problem arises then it can be solved immediately.

D. *Comparative Study*

There were many studies done to compare Lean and Agile approaches in terms of principles, methodologies, practices and tools to assist the researcher to evaluate and characterize similarities and differences at different perspective. Authors in [32], [23] performed a comparative study between Agile Methodologies towards Heavyweight software development by analyzing the differences between Waterfall and Agile in principles, project size, perspectives and strategies. Author in [34] presented the comparison study of seven agile methodologies to understand the characteristics, advantages and disadvantages. Methodologies of focused were Lean Software Development (LSD), Scrum, Extreme Programming and FDD. The study explored the definition, characteristics and to understand the advantages and disadvantages of agile methods.

The impact of Lean and Agile methods in real application has been performed to evaluate the performance between Lean and Agile methodology. Author in [30] had performed a statistical study to compare SCRUM and Kanban which observed that the Kanban method had performed better than the Scrum method in terms of managing project schedule.

E. *Summary of Literature*

Most of the comparative studies done were to compare within the subject itself, for example; Lean vs. Agile, Lean-Agile vs. heavyweight methods, Lean vs. Six Sigma, and Lean-Sigma vs. Six Sigma or Lean-Sigma vs. Total Quality Management methods. Most of agile methodologies research is done from software related domain while Lean-Sigma is focused on manufacturing product and process cycles. There was no analysis done to compare between hybrid methodologies such as Lean-Sigma vs. Lean-Agile at requirement gathering process for software requirement. Characterization analysis of principles and methodologies will be much help for analysts and researchers to explore the differences or similarities. In this research, a comparison study of two hybrid methodologies, LA and LSS, was performed to characterize principles and methodologies in relation to RE process. Understanding main differences and commonalities between the hybrid technologies will speed up development process, project cycle time and cost.

III. Discussion and Analysis

In this section, the similarities and differences of the principles, methodologies and practices between LSS and LA are discussed and analyzed. The principles will be analyzed and characterized based on the relationship of RE which are; Understanding Knowledge Domain, Identify Stakeholders, Analyze stakeholders' characteristics and behavior, RE Selection techniques, Documentation and Refinement.

A. Comparative Analysis of Principles

[10],[25] in the book title as "Lean Integration", confirmed that lean concept is embedded in agile which many of the principles are aligned to each other. Comparative analysis for this research is to evaluate any similarities and differences between LSS and LA in relations to RE principles. Table IV listed the comparison of principles between LA, LSS and Requirement Elicitation;

TABLE. IV. Comparison by Principles

Lean Agile	***LSS***	***RE***
• Take an economic view	• Focus on Customer	• Understand what customer wants • Identify stakeholder
• Apply system thinking	• Identify and understand how the works were done	• Stakeholder analysis • Elicitation techniques selection
• Incremental Development Approach with Integrated Continuous Improvement	• Sequential and Continuous Improvement • Integrated Management approach	• Iterative elicitation process
• Visualize and limit WIP, reduce batch size and manage queue lengths	• Streamlining and Lean process flow	
• Assume variability, preserve options	• Remove non-value add tasks • Managed by fact and reduced variations	
• Base milestones on objective evaluation working system • Apply cadence, synchronize with cross-domain planning	• Undertake improvement activities in systematic ways	
• Unravel the underlying motivation of knowledge workers	• Involve and equip the people in the process	

Table IV summarizes the relationship of LSS vs LA from RE principles perspective. First RE principle is to understand the business functions or domain knowledge of the specific area. LSS and LA main elaborate this principle by concentrates on the customer and economic values respectively. Customer values is translated into economic gain that is direct correlation towards understanding the domain of knowledge. For example, Insurance process flow, Financial Supply Chain Management, Manufacturing Planning and Scheduling, Financial Payment and Billing process, Human Resources, Engineering and others. Understanding business process is related to process owners. The second and third principles for RE are to identify stakeholders and stakeholder analysis.

The second and third principles for RE are to identify stakeholders and stakeholder analysis. Stakeholders are the primary sources of the information which known as the Subject Matter Expert for specific domain. LSS and LA principles cover this principle related to Customer Focus and Economic View. That is why identify who are the stakeholders are vital to both LSS and LA principles to ensure knowledge extracting process would be done efficiently. For stakeholder analysis, LSS is exploring and investigating how the entire process is currently done through high level process map. While LA is applying systems thinking that consists of comprehensive approach with several aspects in software development. Selecting elicitation techniques based on situational background has been discussed in Table I which is correlated with the result of stakeholder analysis.

The fourth RE principle is quite difficult to adopt because it requires a high technical and experienced team to discover information from the affected users. It is highly dependent on the knowledge of its relative domain. In LSS, principle of stakeholder analysis is elaborated detail with principle of "Focus to Customer". Any process that do not added values at customer process, such feature should have not been developed. Non- valued added activities can be identified from the value stream map which can be extracted from Voice of Process and Voice of Business. The Fifth RE principle is documentation and refinement knowledge discoveries which correlated with Incremental Development and Continuous Improvement Approach principle in LA. Incremental development is the process where respective requirements are captured and stored in product backlog. Reviewing each requirement at every sprint with continuous enhancement is considered critical to optimize the process. This principle also known as adaptive approach where LA focuses towards solution with a series of short iterations to gain fast feedback from customers that translated to minimize the risks [35].

Iterative principle is in the opposite with LSS which emphasizes problem solving management approach known as data and facts driven. Problems is defined based on actual data through comprehensive statistical analysis and lean applications before proposed solutions are provided. Refinement discoveries is aligned with iterative which the process will go through cycle of activities where it will end once the requirements are confirmed by users. But LSS is practically ensure a smooth and uninterrupted process flow and focuses only on customers' values. Six Sigma particularly stresses "critical to quality" processes or operations and reduces costs by reducing variability. Another key principle is to empower the organization for LSS and employee's motivation for LA. Both LSS and LA enforce the important values of human capital development to maximize profitability and sustainability. These are the important elements that were expanded from RE principles. Most of LA principles elaborate the important roles from development.

Overall, the principles defined for LSS and LA are completing each other with the goal to achieve similar customer's objective. Technically, in software development, applying LSS or LA with respective of its underlying foundation of knowledge did not interrupt the objectives of the projects. In fact, both principle of knowledge for both LSS and LA are driven towards customer's goal and objectives.

B. *Comparative Analysis of LSS and LA towards Requirement Process*

This section of comparative analysis is to evaluate the practices and tools applied either in LA or LSS based on DMAIC and SCRUM. The focus phase is related to "Definition" for LA and "Define and Measure" for LSS. Main elements to study are regarding the requirement known as; Requirement Preparation, Requirement Representation, Requirement Refinement and Requirement Confirmation. This section analyzed the practices between LSS and LA with regards to requirement elicitation process.

Requirement Preparation is the initial phase for analysts and team to start the planning and preparation activities. LSS applied Project Charter as the main guidance which represents all the key information to start on the project such as objectives, identify stakeholders, knowledge domain, project scope and limitations, estimate cost and others. Table V summarized the findings:

TABLE. V. SUMMARY BY PROCESS

Requirement Elements	Definition Phase (LA)	Define and Measure Phase (LSS)
• Requirement Preparation	• Planning meeting with stakeholders • Kick Off Meeting to define structure	• Prepare Project Charter Template • Elaborate Project Charter for Objective, Stakeholders and key metrics
• Requirement Specification	• Define User Stories • Product Backlogs	• SIPOC • Voice of Customers (VOC) • Voice of Process (VOP) • CTQ metrics
• Requirement Refinement	• Face to Face Communication • Frequent Meetings • On Site Meeting • Product backlogs update	• Enforce "What-Is" through process mapping (Swimlane Diagram) • Transfer Functions • Lean Waste Analysis
• Requirement Confirmation	• Prototyping • Adaptive process	• Process Performance Analysis • Process Mapping Optimization • Drill Down Tree Diagram

Table V showed that LA main tasks are planning meeting with stakeholders to understand the objective, to prepare all the relevant questions to the respective team. Kick Off meeting is the recommended tool [36] to define the structure with the customers. It is highly depending on the competent skills of analysts to ask the right questions to the customers. At this phase, the assumption is customers know what is needed.

Requirement Specification phase is the process to identify the systems that needs to be built. LA best practices focuses on the involvement of users such as user stories and product backlogs. User stories are the notation of expressing the requirements which commonly used in Agile development. It is practical with the assumption that users able to articulate the situations that currently done. Product backlogs are the inputs from all the stakeholders which can be categorized as Functional and Non-Functional Requirements.

While LSS recommended VOC or QFD to understand and to discover the requirement specifications. VOC is the comprehensive tools to discover the implicit and explicit requirements from end users. Not only that, SIPOC is used to understand the overview of the process in the entire supply chain [17], [37].

Daily meeting and product backlog updates at each sprint are common practice done in LA for requirement refinement purpose. Product backlog is also known as checklists thus both parties are on the mutual agreement of the subject domain. In fact, it is also act as a communication medium among developers and Scrum Masters for effective tracking purpose [38]. However, LSS is applying detail process mapping such as swim lane diagram to understand tasks and detail task. Swim lane diagram helps analysts to visualize the interaction of the processes and the roles for each stakeholder within that domain of supply chain [39], [40].

Requirement confirmation or documentation is the phase where proper documentation is signed off to confirm on the policy, rules and agreement. At this phase, LA approach utilized early prototyping at each iterations process to gather fast feedback. Once the preferred options are selected, the detailed requirement is explored using storyboards, situational scenarios and prototyping techniques. Again, an iterative approach is used at this stage in order to develop a final operational prototype. From "What-Is" process mapping, team able to propose "To-Be" solutions, either using automation through script development to optimize value essentials process or to explore knowledge base rules to refine the specification. The next phases in LSS which known as Analyze, Improve and Control will elaborate further of the validation process.

The main difference in the two methods are the practices applied at different phases of the cycle where LSS applies many different tools to acquire and to represent the requirements, while LA focuses more on the effective communications among the stakeholders at every sprint review. Prototyping is a technique that is quite often mentioned in the LA approach compared to LSS especially at the end of the sprint review. This is due to the principle of LA itself where the development projects deliver its functionality incrementally at every phase. It is due to the change of requirement whenever there is new knowledge observed. Incremental delivery is a process where developer provides a solution with added functionality based on the feedback of every sprint review. But LSS is more on the structure and systematic management problem approach where systematic tools and practices are in place to understand and visualize current process before solutions were proposed. The DMAIC framework could be utilized not only at software solution and development projects but also at the feasibility study phase where fuzzy problems occurred.

IV. Conclusion

In Agile perspective, every aspects of development, requirements need to be revisited to ensure conformance. This principle empowers team to continuously re-plan the product release to be more comparative and flexible with current economic uncertainty. Lean Six Sigma (LSS) is becoming popular in almost all organizations from many different industries globally. It is a management philosophy which provides a world class business strategy that requires an organizational change, leadership, promotes successful teamwork, in systematic and structured approach. The entire methodology is the explorative process from unknown to a clear defines solutions because it is data and facts driven. Thus, LSS is very beneficial to new analysts or experienced researchers to discover the real problems in the organization.

Lean and Agile are two different origins but some of the practices can be combined to face volatile demand in customer responsiveness. Producing a software system that fulfills 100% of customers' needs is no way possible. However, there is a standard methodology and practices that would resolve the challenges at a very comparative cost. Lean-Agile focuses on customer satisfaction, flexibility and rapidly embrace changes at most effective economical approach to improve business or product value. However, Lean-Agile is highly depending on the stakeholders as the main input which contributes to high risk of uncertainty. Though LA is very adaptive and flexible in managing frequent requirement changes, the chances of cost over-run is at high stake.

If analyzing based on methods and practices, LSS is very promising due to its systematic and structured guidelines. Each phase, there are proven recommended tools to be utilized by analysts or researchers to move forward. LSS typical framework, the process is well defined from Define stage to Implementation and Control stage where researchers could forecast the project planning efficiently. The recommended tools applied at each phase have its own steps and procedure to guide researcher to refine the requirement process. DMAIC methodology is used to incorporate Six Sigma and Lean tools to improve processes by systematically reducing the variations, while creating even flow with the objective to delight customers by focusing on quality and speed.

Future research might extend the work to perform a case study between LA and LSS at specific phases; for example: requirement development phase. This is to confirm how LSS and LA difference in practicality.

References

[1] L. R. Wong, D. S. Mauricio, and G. D. Rodriguez, “A systematic literature review about software requirements elicitation. Journal of Engineering Science and Technology,” J. Eng. Sci. Technol., vol. 12, no. 2, pp. 296–317, 2017.

[2] E. Schön, D. Winter, and M. J. Escalona, “Agile Processes in Software Engineering and Extreme Programming,” vol. 283, pp. 37–51, 2017.

[3] T. Iqbal, “Requirement Elicitation Technique : - A Review Paper,” Int. J. Comput. Math. Sci., vol. 3, no. 9, pp. 1–6, 2014.

[4] V. Singh, S. Sankhwar, and D. Pandey, “A framework for requirement elicitation,” no. February, 2014.

[5] B. Davey and K. R. Parker, “Requirements elicitation problems: a literature analysis,” Issues Informing Sci. Inf. Technol., vol. 12, pp. 71–82, 2015.

[6] F. A. and R. Razali, “A Practical Guide to Requirements Elicitation Techniques Selection - An Empirical Study,” Middle-East J. Sci. Res., vol. 11, no. 8, p. 9, 2012.

[7] S. Tiwari and S. S. Rathore, “A Methodology for the Selection of Requirement Elicitation Techniques,” 2017.

[8] L. Bormane, J. Gržibovska, S. Bērziša, and J. Grabis, “Impact of Requirements Elicitation Processes on Success of Information System Development Projects,” Inf. Technol. Manag. Sci., vol. 19, no. 1, 2016.

[9] S. Tiwari, S. S. Rathore, and A. Gupta, “Selecting requirement elicitation techniques for software projects,” in 2012 CSI Sixth International Conference on Software Engineering (CONSEG), 2012, pp. 1–10.

[10] R. Egas, “Requirements elicitation , which method in which situation ?,” Open Univ. Netherlands, p. 70, 2015.

[11] N. Jacob and H. Dekkers, “Requirements Elicitation Technique : Improving the Interview Technique,” Univ. Amsterdam, no. 10629505, pp. 1–26, 2015.

[12] H. Liao, “Requirement Elicitation Based on Value Chain Analysis,” J. Theor. Appl. Inf. …, vol. 50, no. 2, 2013.

[13] M. P. J. Pepper and T. A. Spedding, “The evolution of lean Six Sigma,” Int. J. Qual. Reliab. Manag., vol. 27, no. 2, pp. 138–155, 2010.

[14] A. Tenera and L. C. Pinto, “A Lean Six Sigma (LSS) Project Management Improvement Model,” Procedia - Soc. Behav. Sci., vol. 119, pp. 912–920, 2014.

[15] A. Mirela and C. Munteanu, “Comparative Analysis between Lean, Six Sigma and Lean Six Sigma Concepts,” J. Manag. Econ., vol. 2, no. 1, pp. 78–89, 2017.

[16] R. Yousef and T. Almarabeh, “An enhanced requirements elicitation framework based on business process models,” vol. 10, no. 1, pp. 279–286, 2015.

[17] J. Antony, D. Setijono, and J. J. Dahlgaard, “Total Quality Management & Business Excellence Lean Six Sigma and Innovation – an exploratory study among UK organisations,” vol. 27, no. December, pp. 37–41, 2014.

[18] R. Panat*, V. Dimitrova, T. Selvy Selvamuniandy, K. Ishiko, and D. Sun, “The application of Lean Six Sigma to the configuration control in Intel’s manufacturing R&D environment,” Int. J. Lean Six Sigma, vol. 5, no. 4, pp. 444–459, 2014.

[19] T. Reijns, “The advantages and limitations of Lean Six Sigma in process (re) design,” no. June, p. 32, 2010.

[20] S. Kelly, “Towards an evolutionary framework for agile requirements elicitation,” in Proceedings of the 2nd ACM SIGCHI symposium on Engineering interactive computing systems - EICS ’10, 2010, p. 349.

[21] W. Behutiye, P. Karhapää, D. Costal, M. Oivo, and X. Franch, “Non-functional requirements documentation in agile software development: Challenges and solution proposal,” Lect. Notes Comput. Sci. (including Subser. Lect. Notes Artif. Intell. Lect. Notes Bioinformatics), vol. 10611 LNCS, pp. 515–522, 2017.

[22] X. Q. Xu, C. Huang, and H. Lu, “Application of Lean Six Sigma Methodology in Software Continuous Integration,” Key Eng. Mater., vol. 693, pp. 1893–1898, 2016.

[23] J. A. Garza-Reyes, M. Al-Balushi, J. Antony, and V. Kumar, “A Lean Six Sigma framework for the reduction of ship loading commercial time in the iron ore pelletising industry,” Prod. Plan. Control, vol. 27, no. 13, pp. 1092–1111, 2016.

[24] A. C. Tonini, M. De Mesquita Spínola, and F. J. B. Laurindo, “Six sigma and software development process: DMAIC improvements,” Portl. Int. Conf. Manag. Eng. Technol., vol. 6, no. c, pp. 2815–2823, 2006.

[25] R. Suomela, “Using Lean Principles to Improve Software Development Practices in a Large-Scale Software Intensive Company,” 2015.

[26] M. Poppendieck and T. Poppendieck, Lean Software Development: An Agile Toolkit. 2003.

[27] E. Bjarnason, K. Wnuk, and B. Regnell, “A case study on benefits and side-effects of agile practices in large-scale requirements engineering,” Proc. 1st Work. Agil. Requir. Eng. - AREW ’11, pp. 1–5, 2011.

[28] N. Schmidt and C. Meures, “‘Mind the Gap’: An Analysis of Communication in Agile Global Outsourced Software Development Projects,” 2016 49th Hawaii Int. Conf. Syst. Sci., pp. 501–510, 2016.

[29] K. Petersen and C. Wohlin, “Measuring the flow in lean software development,” Software-Practice Exp., vol. 41, no. 9, SI, pp. 975–996, 2011.

[30] H. Lei, F. Ganjeizadeh, P. K. Jayachandran, and P. Ozcan, “A statistical analysis of the effects of Scrum and Kanban on software development projects,” Robot. Comput. Integr. Manuf., pp. 1–9, 2015.

[31] E. Corona, F. Eros, and P. Diee, “A Review of Lean-Kanban Approaches in the Software Development,” vol. 10, no. 1, pp. 1–13, 2013.

[32] A. K. R. Pillai, A. K. Pundir, and L. Ganapathy, “Implementing Integrated lean six sigma for software development: A flexibility framework for managing the continuity: Change dichotomy,” Glob. J. Flex. Syst. Manag., vol. 13, no. 2, pp. 107–116, 2012.
S. Khan1, A. B. Dulloo2, and M. Verma3, “Systematic Review of Requirement Elicitation Techniques,” Int. J. Inf. Comput. Technol., vol. 4, no. 2, pp. 133–138, 2014.

[33] S. Merzouk, S. Elhadi, H. Ennaji, A. Marzak, and N. Sael, “A Comparative Study of Agile Methods : Towards a New Model-based Method,” vol. 9, no. 4, pp. 121–128.

[34] B. Kola, “Thinking Lean in Agile Software Development Projects,” 2014.

[35] R. Vallon, L. Wenzel, M. E. Brüggemann, and T. Grechenig, “An Agile and Lean Process Model for Mobile App Development: Case Study into Austrian Industry,” J. Softw., vol. 10, no. 11, pp. 1245–1264, 2015.

[36] S. M. Saad and M. Khamkham, “Development of Lean Six-Sigma Conceptual Implementation Model for Manufacturing Organisations,” Adv. Manuf. Technol. Xxx, vol. 3, pp. 497–502, 2016.

[37] N. Ramadan and S. Megahed, “Requirements Engineering in Scrum Framework,” Int. J. Comput. Appl., vol. 149, no. 8, pp. 24–29, 2016.

[38] M. L. George et al., The Lean Six Sigma Pocket Toolbook: A Quick Reference Guide to Nearly 100 Tools for Improving Process Quality, Speed, and Complexity The Lean Six Sigma Pocket Toolbook: A Quick Reference Guide to Nearly 100 Tools for Improving Process Quality, Speed, and. McGraw-Hill, 2005.

[39] T. Bortolotti, P. Romano, and B. Nicoletti, “Lean first, then automate: An integrated model for process improvement in pure service-providing companies,” IFIP Adv. Inf. Commun. Technol., vol. 338 AICT, pp. 579–586, 2010.

Indonesian Words Error Detection System using Nazief Adriani Stemmer Algorithm

Anton Yudhana[1], Abdul Fadlil[2]
Electrical Engineering Department
Universitas Ahmad Dahlan Yogyakarta, Indonesia

Muhamad Rosidin[3]
Informatics Engineering Department
Universitas Ahmad Dahlan, Yogyakarta, Indonesia

***Abstract*—Stemming in each language has a different process and is determined according to the structure of the language. Stemming is mostly used as a complete step in the processing of words and phrases. There are many stemming algorithms available, and some used as a process for word processing. One function of stemming is to detect word errors in Indonesian. In this study, researchers created the Indonesian words error detection system using Nazief and Adriani algorithm. In the trials conducted, the system will accept text input obtained from the user. Then the system will preprocess the text. In this study, there are three stages of preprocessing, namely tokenization, case folding, and filtering. After the stages in preprocessing are finished, the system will call each word for the process of stemming. The results of the stemming will be compared with the base words available in the database. If it does not match, then the word is highlighted and is considered an error word. The first finding is the Nazief Adriani's algorithm can be able to detect words error until 100%. The second finding is the Nazief Adriani's algorithm also detect non-words error, the accuracy of detecting is 97.464%.**

***Keywords*—Indonesian; word error; stemming; Nazief and Adriani stemmer algorithm; detection system**

I. Introduction

Affixes can be easily found in Indonesian because it uses a lot of affixes. Affixes can be used in all Indonesian words and it can be combining each other [1]. There are three types of affixes in Indonesian, namely prefixes, insertions, and suffixes. It is not simple to separate words that contain affixes into base words. There are base words whose letters initially change when given an affix. This rule makes it difficult to use the right words. The word that containing affixes can be changed into base words using the stemming algorithm. The implementation of stemming is very large because stemming is the most important part of text mining. An example of stemming development can be found in research about plagiarizing. Indeed, the phenomenon of plagiarizing in the scope of Indonesian education has long occurred so that educational institutions are tainted by plagiarism act [2]. Based on the description above, the researchers will develop the Indonesian words error detection system using Nazief Adriani's algorithm.

Typing has two ways, namely typing by looking at the keyboard and typing without looking at the keyboard [3]. Nowadays, to detect error words in a document is very difficult because it has been checked manually.

In the previous study, stemming algorithm implementation has been carried out in detecting word errors, for example, in the research of Marsel Widjaja and Seng Hansun (2015) [4]. The stemming can be done with Nazief and Adriani, Porter, Confix Stripping, Enhanced Confix Stripping, Porter Stemmer, and Modified Porter Stemmer algorithm.

II. Research Method

A. Proposed Method

The ability of the algorithm used in this method will be tested. Then the test results showed error words and processing time. The steps used in this study can be seen in Fig. 1.

In Fig. 1, it can be seen that the initial stage in carrying out this research is the design of the Indonesian words error detection system. Then implement a design that has been created using the PHP programming language. Then enter the Nazief Adriani algorithm into the Indonesian words error detection system. At the last stage is the testing of system functions.

B. *Nazief Adriani's Stemmer Algorithm*

The stemming algorithm in this study is based on Nazief and Adriani's algorithm [5]. The flow chart of the Nazief Adriani algorithm can be seen in Fig. 2.

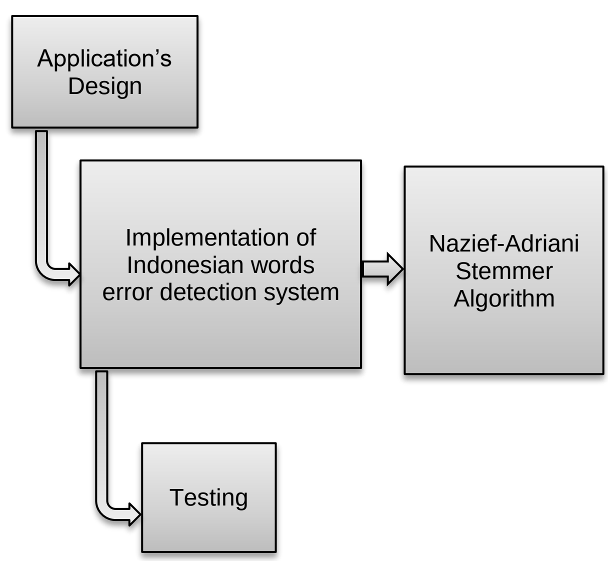

Fig. 1. Proposed Method.

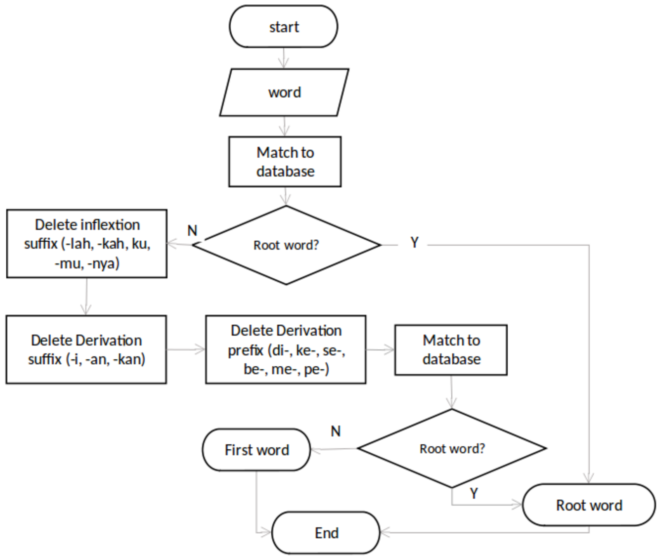

Fig. 2. Flow Chart of the Nazief Adriani Stemmer Algorithm.

Nazief Adriani's algorithm has been used in research [6], [7], [8], dan [9]. The algorithm created by Bobby Nazief and Mirna Adriani has the following stages:

1) Check the original word: The algorithm checks the original word towards a base word dictionary. If it works, thus algorithm stops, and the word is declared as the base word. If it fails, the algorithm goes to the next step.

2) Remove the inflection suffix: The algorithm removes the inflection suffix ("- lah", "–kah", "-ku", "-mu", "-nya"). If it works and the inflection suffix is a particle ("-lah" atau "-kah"), the algorithm eliminates possessive pronoun inflection ("-ku", "-mu", "-nya").

3) Remove the derivation suffix: The algorithm removes the derivation suffix ("-i", "-an", "-kan"). If it works, thus the algorithm continues to step 4. If step 4 fails, the algorithm continues to step a, as follow:

a) Delete the character "-k": If the derivation suffix is "-an" and the last character of the word is "-k", the algorithm removes the "-k". Then, proceed to step 4. If it fails, go to step b.

b) Restore the original word: The algorithm returns the deleted suffix ("-i", "-an", "-kan") to the original word.

4) Remove the derivation prefix: The algorithm removes the derivation prefix, consists of several steps:

a) Unauthorized prefixes and suffixes: If the removal of inflection suffixes in step 3 is performed, the algorithm checks for unauthorized prefixes and suffixes. If the algorithm finds it, the algorithm will returns.

b) Similar prefixes: Check if the current prefix is similar to the previous prefix, then the algorithm is returned.

c) Limitation of derivation prefix deletion: If removal of derivation prefix has been performed three times, the algorithm is returned.

d) Check and delete the derivation prefix: The algorithm checks the type of derivation prefix and removes the prefix.

e) Find the root word: If the root word is found, the algorithm is returned. Instead, step 4 repeats again to removes the second prefix.

f) Recoding: The algorithm does the recoding process, depending on the type of prefix.

5) Recording: The algorithm is recording the process.

If the algorithm is failed in doing all steps above, then the first word is assumed to be the base word. So the process is complete [10].

III. Proposed System

A. Flowchart System

The design's process of the study uses the main flowchart that can be observed in Fig. 3.

Fig. 3 shows the main flowchart in this study. Initially, the system will accept text input obtained from the user. Then the system will be preprocessing the text. There are three stages of preprocessing. The first stage is case folding, where the contents of the text will be changed to the default form, usually lowercase. The second stage is tokenizing, where the system will parse the input text into units of words. The third stage is filtering, where the system will eliminate characters that are not needed in the next process. After the preprocessing stages are completed, the system will call each word using an array to perform the stemming process using the Nazief Adriani algorithm. The results of the stemming will be matched with the base words available in the database to confirm their validity. If it does not match, then the word is highlighted and is considered an error word.

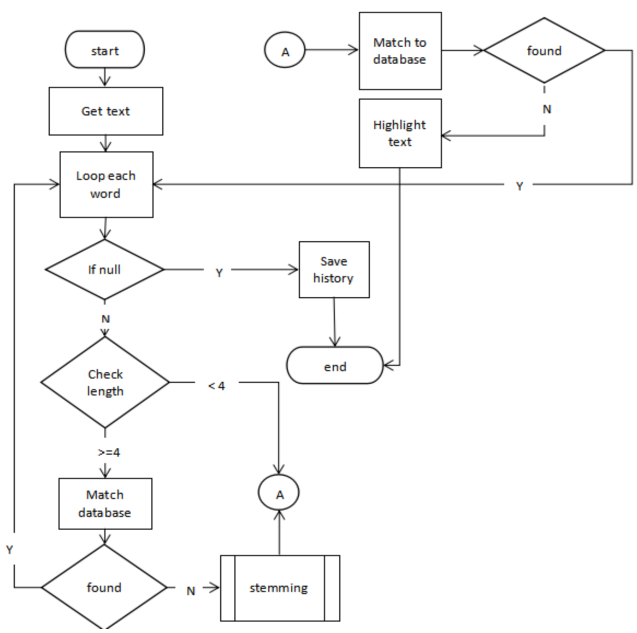

Fig. 3. Main Flowchart System.

B. Information Retrieval

Information Retrieval is the stage in identifying or retrieving documents from directories (files) as feedback in requests for information [11]. Information retrieval of researchers explains that queries are the basis for providing better search engine performance [12]. Specific techniques are needed to retrieve documents relevant to user requests, one of the techniques that can be used is Information Retrieval (IR) [13].

C. Text Processing

Text preprocessing is part of building the text corpus. Building a text corpus has two main steps, namely collecting and preprocessing [14]. Text preprocessing is an early stage of semantic analysis (meaning accuracy) and syntactic analysis (arrangement accuracy) [15]. The steps in Indonesian text processing consist of; case folding, tokenizing, stopword removal, and stemming. Before the process of stemming begins, the document must be preprocessed. In this study, text processing consists of tokenization, case folding, filtering and stemming [16].

D. Preprocessing

Preprocessing is to eliminate characters and words that are not relevant to the document [17]. Omitting the information will facilitate and improve word processing [18]. Preprocessing in text mining is expected to reduce the processing time by eliminating unnecessary words or text from texts or documents. [19]. At this stage, a combination of four preprocessing methods that are commonly used includes: tokenization, case folding, stop word removal, and stemming.

1) Case folding: The process of changing a capital letter into lowercase letters in a document (a-z). In this study, the case folding process is done by calling a function directly in the PHP programming language.

2) Tokenizing: Tokenizing is the stage used to separate or eliminate input strings based on each word from its constituents or separate each word arranged in the document. The omitted part can be numbers, characters or symbols, and punctuation in addition to the letters of the alphabet [20].

3) Filtering: Remove words that have been listed in the stopword or stoplist. Stopwords are words that often appear in large amounts of text and are considered to have no significance [21]. In this study, there is no words are deleted because each word will be verified in the database.

4) Stemming: The stemming process in Indonesian is more complicated than English because there are variations of affixes that must be removed to get the base word [22]. The structure of Indonesian morphology has a higher level of complexity than English [23]. Besides Indonesian and English, stemming can be used in Arabic, as in research [24]. Stemming is more efficient for Arabic retrieval than for English [25]. Stemming is the process of determining the base words of words that contain affixes. Nazief Adriani is one of the most commonly used stemming algorithms. [26]. There is also a pretty good porter algorithm in the process of stemming [27]. Stemming is implemented in the appropriate affix. In Indonesian, the same intonation can give different meanings depending on the topic domain of the word or term. For example, the Indonesian greeting "kemeja" with the same intonation can be written as "ke meja" (go to the table) or "kemeja" (a dress) [28].

IV. Result and Analysis

A. System Interface

Display system interface created using the PHP programming language. Processed documents will be stored in the system. Display on the head of the page for the title of the application. In the middle, there is a document input form and an upload button. If the upload button is clicked, it will display the contents of the document. At the bottom, there are algorithms and process buttons. If the process button is clicked, it will display the word that has been highlighted and interpreted as a word error. In addition, there is also a table view of the results of stemming. The system interface display can be seen in Fig. 4 and highlights the words in Fig. 5.

In addition to the page containing the word error highlight in Fig. 5, there is also a table displaying the results of the stemming process using Nazief and Adriani's algorithm. The words displayed are only words that have an affix and the results of the stemming. But with the wrong word, the results of stemming cannot be seen. The stemming result table can be seen in Fig. 6.

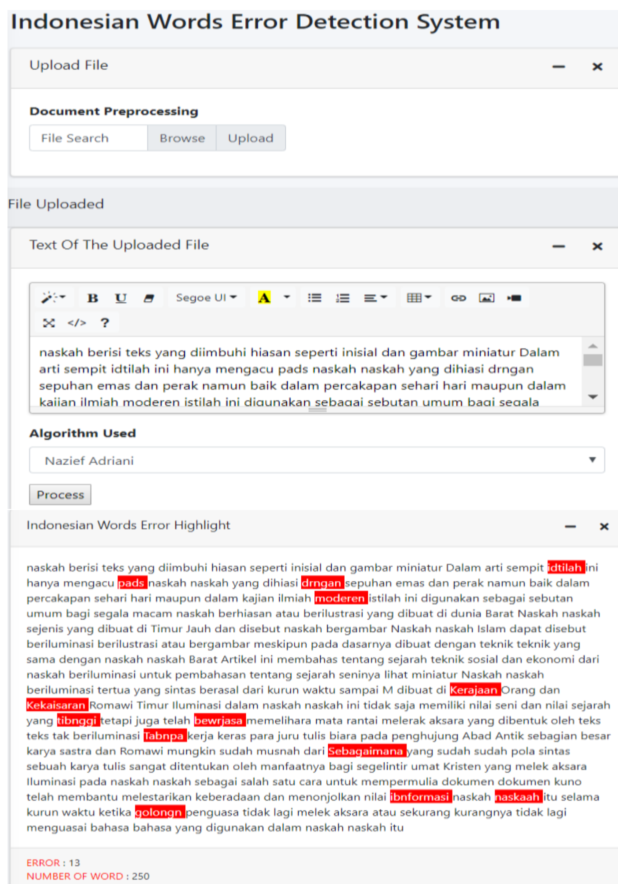

Fig. 4. Interface of Indonesian Words Error Detection System.

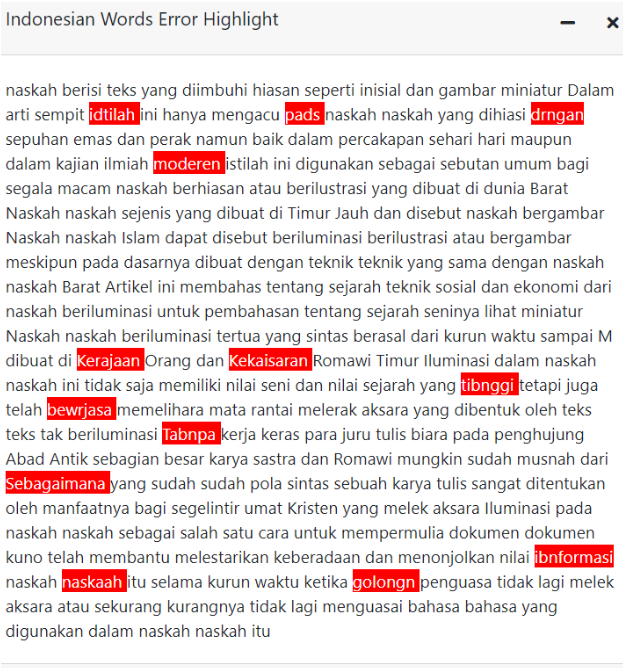

Indonesian Words Error Highlight

naskah berisi teks yang diimbuhi hiasan seperti inisial dan gambar miniatur Dalam arti sempit idtilah ini hanya mengacu pads naskah naskah yang dihiasi drngan sepuhan emas dan perak namun baik dalam percakapan sehari hari maupun dalam kajian ilmiah moderen istilah ini digunakan sebagai sebutan umum bagi segala macam naskah berhiasan atau berilustrasi yang dibuat di dunia Barat Naskah naskah sejenis yang dibuat di Timur Jauh dan disebut naskah bergambar Naskah naskah Islam dapat disebut beriluminasi berilustrasi atau bergambar meskipun pada dasarnya dibuat dengan teknik teknik yang sama dengan naskah naskah Barat Artikel ini membahas tentang sejarah teknik sosial dan ekonomi dari naskah beriluminasi untuk pembahasan tentang sejarah seninya lihat miniatur Naskah naskah beriluminasi tertua yang sintas berasal dari kurun waktu sampai M dibuat di Kerajaan Orang dan Kekaisaran Romawi Timur Iluminasi dalam naskah naskah ini tidak saja memiliki nilai seni dan nilai sejarah yang tibnggi tetapi juga telah bewrjasa memelihara mata rantai melerak aksara yang dibentuk oleh teks teks tak beriluminasi Tabnpa kerja keras para juru tulis biara pada penghujung Abad Antik sebagian besar karya sastra dan Romawi mungkin sudah musnah dari Sebagaimana yang sudah sudah pola sintas sebuah karya tulis sangat ditentukan oleh manfaatnya bagi segelintir umat Kristen yang melek aksara Iluminasi pada naskah naskah sebagai salah satu cara untuk mempermulia dokumen dokumen kuno telah membantu melestarikan keberadaan dan menonjolkan nilai ibnformasi naskah naskaah itu selama kurun waktu ketika golongn penguasa tidak lagi melek aksara atau sekurang kurangnya tidak lagi menguasai bahasa bahasa yang digunakan dalam naskah naskah itu

Fig. 5. Indonesian Words Error Highlight.

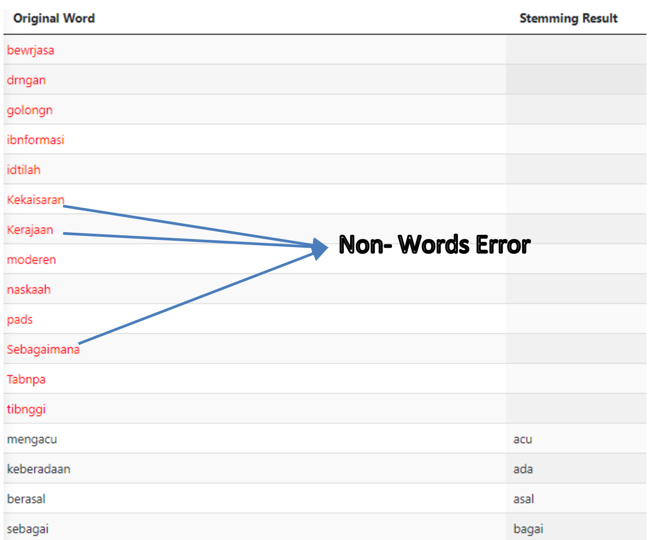

Original Word	Stemming Result
bewrjasa	
drngan	
golongn	
ibnformasi	
idtilah	
Kekaisaran	
Kerajaan	
moderen	
naskaah	
pads	
Sebagaimana	
Tabnpa	
tibnggi	
mengacu	acu
keberadaan	ada
berasal	asal
sebagai	bagi

Fig. 6. The Interface of Stemming Result Table.

B. Document Testing

The documents to be tested in the word error detection system contain sentences in Indonesian. The amount of documents tested is six documents that can be seen in the following Table I.

C. Test Result

The results of the word error detection system in Indonesian using the Nazief Adriani algorithm are quite good. In the six documents tested, 100% succeeded in detecting word errors in the document, but some words that were considered correct were also detected as errors. As seen in document text1, the detection ability is 98.75%, complete data on the test results are presented in Table II, and the graph can be seen in Fig. 7.

Based on all the experimental results in Table II, it can be concluded that the Nazief Adriani algorithm can analyze all the wrong words up to (100%). However, there are still deficiencies in analyzing the correct words. Based on the results shown in Table II, it can be concluded that the average accuracy of Nazief Adriani's algorithm in analyzing the correct words is 97.464. The results of the analysis of Table II are presented below in the graphical form.

TABLE. I. TEST DOCUMENT INFORMATION

Document Name	Number of Words	Description
text1.pdf	250 words	Randomly copy articles on the internet.
text2.pdf	500 words	Randomly copy articles on the internet. Including text1.pdf
text3.pdf	1000 words	Randomly copy articles on the internet. Including text1 and text2.pdf
cerpen1.pdf	1384 words	Copied from compass stories titled “Seragam” written by clippers
cerpen2.pdf	1592 words	Copied from compass stories, titled “Dua Wajah Ibu” written by clippers
cerpen3.pdf	1630 words	Copied from compass stories, titled “Tangan-Tangan Buntung" written by clippers

TABLE. II. WORD ERROR DETECTION SYSTEM

Document			**Number of Words**		**Number of Word Highlight**	
No	***Type***	***Words***	***True***	***False***	***True***	***False***
1	text1.pdf	250	240	10	3 (98,75%)	10 (100%)
2	text2.pdf	500	480	20	12 (97,5%)	20 (100%)
3	text3.pdf	1000	960	40	23 (97,6%)	40 (100%)
4	cerpen1.pdf	1400	1384	16	33 (97,6%)	16 (100%)
5	cerpen2.pdf	1620	1592	28	84 (94, 72%)	28 (100%)
6	cerpen3.pdf	1650	1630	20	68 (95,87%)	20 (100%)
Average					97,464 %	100 %

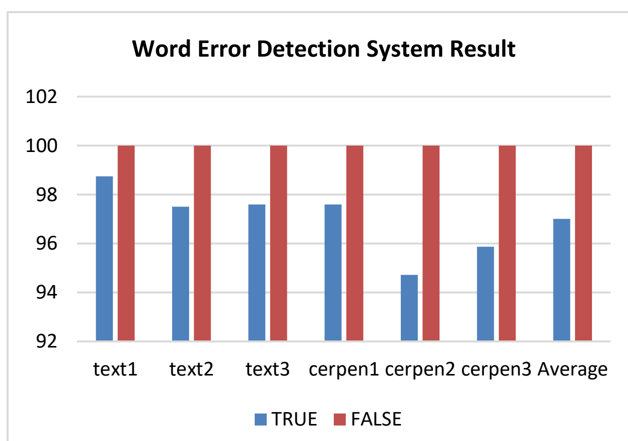

Fig. 7. Chart of Word Error Detection System Result.

Nazief Adriani's algorithm has more complex steps and is designed to minimize errors and lack of other stemming algorithms in the process of analyzing correct words. Based on the results of the study, it was found there were differences between the studies conducted by Marsel Widjaja and Seng Hansun (2015). That study implemented the porter stemmer modified algorithm in the Indonesian word error detection plugin application and was able to analyze all the wrong words up to (100%). However, there are still deficiencies in analyzing correct words with an average of 96.31%. Whereas in this study, the Indonesian word error detection system using Nazief Adriani algorithm can analyze all the wrong words up to (100%). However, there are still deficiencies in analyzing correct words with an average of 97,464%. Thus, it can be concluded that the Nazief Adriri algorithm has an average accuracy that is better than the modified porter stemmer algorithm.

The results of the processing speed on the word error detection system in Indonesian documents with the stemming process using the Nazief Adriani stemmer algorithm is quite good. In the six documents that were tested with three attempts, the average time required to process one word is smaller or equal to 0.030 seconds/word, the data on the complete test results are presented in Tables III, IV, and V.

Table III explains the details of the processing speed in the first experiment. In the text1.pdf document containing 250 words, it has a processing time of 6.8554 seconds with a processing speed of 0.0274 seconds/word. In a text2.pdf document containing 500 words, it has a processing time of 13.9129 seconds with a processing speed of 0.0278 seconds/word. In the text3.pdf document containing 1000 words has a processing time of 27.6677 seconds with a processing speed of 0.0277 seconds/word. In the cerpen1.pdf document containing 1400 words has a processing time of 40.4160 seconds with a processing speed of 0.0289 seconds/word. In the cerpen2.pdf document containing 1620 words has a processing time of 41.2138 seconds with a processing speed of 0.0254 seconds/word. In the cerpen3.pdf document containing 1650 words has a processing time of 47.3358 seconds with a processing speed of 0.0287 seconds/word.

Table IV explains the details of the processing speed in the second experiment. In the text1.pdf document containing 250 words, it has a processing time of 6.8958 seconds with a processing speed of 0.0276 seconds/word. In a text2.pdf document containing 500 words, it has a processing time of 13.7238 seconds with a processing speed of 0.0274 seconds/word. In the text3.pdf document containing 1000 words has a processing time of 27.9247 seconds with a processing speed of 0.0279 seconds/word. In the cerpen1.pdf document containing 1400 words has a processing time of 41.3115 seconds with a processing speed of 0.0295 seconds/word. In the cerpen2.pdf document containing 1620 words has a processing time of 41.4399 seconds with a processing speed of 0.0256 seconds/word. In the cerpen3.pdf document containing 1650 words has a processing time of 46.9563 seconds with a processing speed of 0.0285 seconds/word.

Table V explains the details of the processing speed in the third experiment. In the text1.pdf document containing 250 words, it has a processing time of 6.8409 seconds with a processing speed of 0.0274 seconds/word. In a text2.pdf document containing 500 words, it has a processing time of 13.8641 seconds with a processing speed of 0.0277 seconds/word. In the text3.pdf document containing 1000 words has a processing time of 27.7267 seconds with a processing speed of 0.0277 seconds/word. In the cerpen1.pdf document containing 1400 words has a processing time of 42.2806 seconds with a processing speed of 0.0302 seconds/word. In the cerpen2.pdf document containing 1620 words has a processing time of 41.2279 seconds with a processing speed of 0.0254 seconds/word. In the cerpen3.pdf document containing 1650 words has a processing time of 47.1392 seconds with a processing speed of 0.0286 seconds/word.

The average processing speed of all experiments can be seen in Table VI and graphs in Fig. 8.

TABLE. III. PROCESSING SPEED OF TRIAL 1

No	Document		Trial 1	
	Type	***Words***	***Time(s)***	***s/word***
1	text1.pdf	250	6.8554	0.0274
2	text2.pdf	500	13.9129	0.0278
3	text3.pdf	1000	27.6677	0.0277
4	cerpen1.pdf	1400	40.4160	0.0289
5	cerpen2.pdf	1620	41.2138	0.0254
6	cerpen3.pdf	1650	47.3581	0.0287

TABLE. IV. PROCESSING SPEED OF TRIAL 2

No	Document		Trial 2	
	Type	***Words***	***Time(s)***	***s/word***
1	text1.pdf	250	6.8958	0.0276
2	text2.pdf	500	13.7238	0.0274
3	text3.pdf	1000	27.9247	0.0279
4	cerpen1.pdf	1400	41.3115	0.0295
5	cerpen2.pdf	1620	41.4399	0.0256
6	cerpen3.pdf	1650	46.9563	0.0285

TABLE. V. PROCESSING SPEED OF TRIAL 3

No	Document		Trial 3	
	Type	***Words***	***Time(s)***	***s/word***
1	text1.pdf	250	6.8409	0.0274
2	text2.pdf	500	13.8641	0.0277
3	text3.pdf	1000	27.7267	0.0277
4	cerpen1.pdf	1400	42.2806	0.0302
5	cerpen2.pdf	1620	41.2279	0.0254
6	cerpen3.pdf	1650	47.1392	0.0286

TABLE. VI. THE AVERAGE OF THREE TRIALS

No	Doc		Avg	
	Type	*Words*	*Time(s)*	*s/word*
1	text1.pdf	250	6.8640	0.0275
2	text2.pdf	500	13.8336	0.0277
3	text3.pdf	1,000	27.7730	0.0278
4	cerpen1.pdf	1,400	41.3360	0.0295
5	cerpen2.pdf	1,620	41.2939	0.0255
6	cerpen3.pdf	1,650	47.1512	0.0286

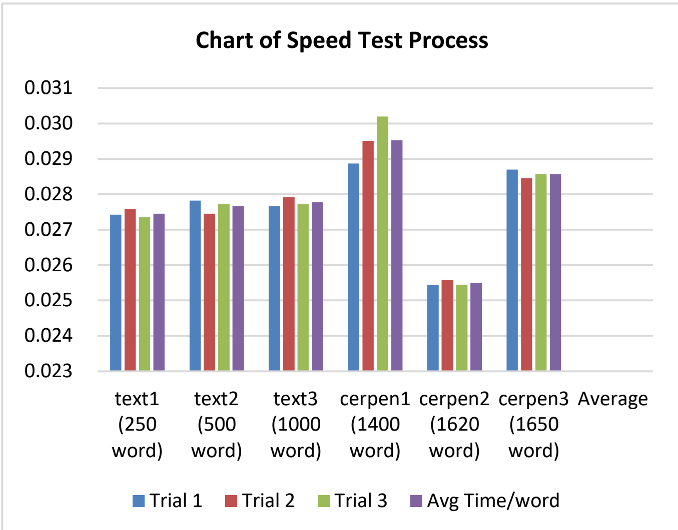

Fig. 8. Chart of Speed Test Process.

V. CONCLUSION

Indonesian words error detection system is good enough to detect word errors. From the trials conducted, the Nazief Adriani algorithm is 100% successful in detecting incorrect words in the six documents prepared. But some words that should be correct or non-word errors are detected as word errors, so they are highlighted by the system. Thus, Nazief Adriani's algorithm has been successfully implemented in the system and gives good results. In improving the accuracy of Nazief Adriani's algorithm, algorithm modifications can be made. Besides being modified, other algorithms can also be added, such as porter stemmer, confix stripping (CS), or enhanced confix stripping (ECS). The development of an Indonesian word error detection system can be improved by adding other features, such as automatic correction and correct word suggestions.

REFERENCES

[1] S. Vinsensius B. Vega S., Bressan, "Indexing the Indonesian Web: Language Identification and Miscellaneous Issues." Poster Proceedings of the tenth International World Wide Web Conference, pp. 46–47, 2001.

[2] S. Sunardi, A. Yudhana, and I. A. Mukaromah, "Plagiarism Detection Implementation Using N-Gram and Jaccard Similarity Methods On Winnowing Algorithm (English)," Transmisi, vol. 20, no. 3, p. 105, 2018.

[3] M. I. K. Islam, M. T. Habib, M. S. Rahman, M. R. Rahman, and F. Ahmed, "A context-sensitive approach to find optimum language model for automatic Bangla spelling correction," Int. J. Adv. Comput. Sci. Appl., vol. 9, no. 11, pp. 184–191, 2018.

[4] M. Widjaja and S. Hansun, "Implementation of porter's modified stemming algorithm in an Indonesian word error detection plugin application," Int. J. Technol., vol. 6, no. 2, pp. 139–150, 2015.

[5] J. Asian, H. E. Williams, and S. M. M. Tahaghoghi, "Stemming Indonesian," Conf. Res. Pract. Inf. Technol. Ser., vol. 38, no. January, pp. 307–314, 2005.

[6] A. S. Rizki, A. Tjahyanto, and R. Trialih, "Comparison of stemming algorithms on Indonesian text processing," Telkomnika (Telecommunication Comput. Electron. Control., vol. 17, no. 1, pp. 95–102, 2019.

[7] T. Mardiana, T. B. Adji, and I. Hidayah, "Stemming influence on similarity detection of abstract written in Indonesia," Telkomnika (Telecommunication Comput. Electron. Control., vol. 14, no. 1, pp. 219–227, 2016.

[8] A. F. Hidayatullah, C. I. Ratnasari, and S. Wisnugroho, "Analysis of Stemming Influence on Indonesian Tweet Classification," Telkomnika (Telecommunication Comput. Electron. Control., vol. 14, no. 2, pp. 665–673, 2016.

[9] T. Winarti, D. Kerami, E. T. P. Lussiana, and S. A. Sudiro, "Improving stemming algorithm using morphological rules," Int. J. Adv. Sci. Eng. Inf. Technol., vol. 7, no. 5, pp. 1758–1764, 2017.

[10] A. Rahmatulloh, N. I. Kurniati, A. Z. Asyikin, I. Darmawan, and J. D. Witarsyah, "Comparison between the stemmer porter effect and nazief-adriani on the performance of winnowing algorithms for measuring plagiarism," Int. J. Adv. Sci. Eng. Inf. Technol., vol. 9, no. 4, pp. 1124–1128, 2019.

[11] H. L. Agnew, "Our Natural Language," Orig. Czech Natl. Renasc., no. 1982, pp. 51–92, 2017.

[12] N. Yusuf, M. A. B. M. Yunus, and N. B. Wahid, "A comparative analysis of web search query: Informational vs. navigational queries," Int. J. Adv. Sci. Eng. Inf. Technol., vol. 9, no. 1, pp. 136–141, 2019.

[13] G. Mediamer, - Adiwijaya, and S. Al Faraby, "Development of Rule-Based Feature Extraction in Multi-label Text Classification," Int. J. Adv. Sci. Eng. Inf. Technol., vol. 9, no. 4, pp. 1460–1465, 2019.

[14] S. M. Isa, R. Suwandi, and Y. P. Andrean, "Optimizing the hyperparameter of feature extraction and machine learning classification algorithms," Int. J. Adv. Comput. Sci. Appl., vol. 10, no. 3, pp. 69–76, 2019.

[15] W. C. F. Mariel, S. Mariyah, and S. Pramana, "Sentiment analysis: A comparison of deep learning neural network algorithm with SVM and naïve Bayes for Indonesian text," J. Phys. Conf. Ser., vol. 971, no. 1, pp. 0–8, 2018.

[16] P. M. Prihatini, I. K. G. D. Putra, I. A. D. Giriantari, and M. Sudarma, "Stemming Algorithm for Indonesian Digital News Text Processing," Int. J. Eng. Emerg. Technol., vol. 2, no. 2, pp. 1–7, 2017.

[17] A. Yudhana, Sunardi, and I. A. Mukaromah, "Implementation of winnowing algorithm with dictionary English-Indonesia technique to detect plagiarism," Int. J. Adv. Comput. Sci. Appl., vol. 9, no. 5, pp. 183–189, 2018.

[18] H. Alani and S. Saad, "Schema matching for large-scale data based on ontology clustering method," Int. J. Adv. Sci. Eng. Inf. Technol., vol. 7, no. 5, pp. 1790–1797, 2017.

[19] M. Javed and S. Kamal, "Normalization of unstructured and informal text in sentiment analysis," Int. J. Adv. Comput. Sci. Appl., vol. 9, no. 10, pp. 78–85, 2018.

[20] A. Fadlil, "Application of Student Questionnaire Retrieval System Using Application of Information Retrieval for Student Opinion (English)," J. Teknol. Inf. dan Ilmu Komput., vol. 6, no. 1, pp. 33–40, 2018.

[21] A. Yudhana, Sunardi, and A. Djalil, "Implementation of Pattern Matching Algorithm for Portable Document Format," Int. J. Adv. Comput. Sci. Appl., vol. 8, no. 11, pp. 509–512, 2017.

[22] F. Z. Tala, "A Study of Stemming Effects on Information Retrieval in Bahasa Indonesia," M.Sc. Thesis, Append. D, vol. pp, pp. 39–46, 2003.

[23] E. Da Costa, H. Tjandrasa, and S. Djanali, "Text mining for pest and disease identification on rice farming with interactive text messaging," Int. J. Electr. Comput. Eng., vol. 8, no. 3, pp. 1671–1683, 2018.

[24] H. Omar, M. Dahab, and M. Kamal, "Stemmer Impact on Quranic Mobile Information Retrieval Performance," Int. J. Adv. Comput. Sci. Appl., vol. 7, no. 12, pp. 135–139, 2016.

[25] A. Nwesri, "Effective Retrieval Techniques for Arabic Text," 2008.

[26] A. Yudhana, A. D. Djayali, and Sunardi, "Plagiarism Detection System for Scientific Papers Using Pattern Matching Algorithms (English)," Jurti, pp. 178–187, 2017.

[27] S. Alnofaie, M. Dahab, and M. Kamal, "A Novel Information Retrieval Approach using Query Expansion and Spectral-based," Int. J. Adv. Comput. Sci. Appl., vol. 7, no. 9, pp. 364–373, 2016.

[28] S. N. Hidayatullah and Suyanto, "Developing an adaptive language model for Bahasa Indonesia," Int. J. Adv. Comput. Sci. Appl., vol. 10, no. 1, pp. 488–492, 2019.

Problems Solving of Cell Subscribers based on Expert Systems Neural Networks

Ahmad AbdulQadir AlRababah
Faculty of Computing and Information Technology, King Abdulaziz University,
Rabigh 21911, Kingdom of Saudi Arabia

***Abstract*—With the growing demand for telecommunications services, the number of calls to telecommunications companies related to issues of using services, setting up and maintaining equipment, as well as resolving possible problems arising in the process of using services is also growing. From the point of view of system analysis, the problem is the mismatch between the existing and the required (target) state of the system for a given state of the environment at the moment in time. Based on this definition, we consider the problem of the subscriber of the cellular network a mismatch between the existing and the required state of the cellular network in this state of the environment at the moment in time. The state of the cellular network is characterized by the functioning of all devices, the proposed range of services. A short time for analyzing problem situations and making decisions, a large amount of information characterizing the current situation, the difficulty of solving poorly formalized and poorly structured tasks in the absence of complete and reliable information about the state of the cellular communication network and the functioning of its elements lead to a mismatch of human capabilities to effectively solve these problems. In this regard, the development and implementation of a precedent based neural network expert system for solving the problems of subscribers of a cellular communication network is an urgent scientific and technical task.**

Keywords*—*Neural network expert system; telecommunications companies; system analysis; cellular network; structured tasks; reliable information; human capabilities; telecommunications services

I. Introduction

Development of precedent based neural network expert system on an integrated approach to the problem of effective relationship management with subscribers of a cellular communication network [4,17,31], including the use of expert systems technologies, neural networks, case-based reasoning, as well as the creation of models [10,24,37], algorithms and support programs for decision-makers interacting with subscribers of a cellular communication network.

Research Objectives of this manuscript are considered analysis of the most popular systems for managing cellular networks [5,19,32,40] and customer relationships; research of existing methods and techniques for decision support for tasks of managing relationships with subscribers of cellular communication networks; analysis of various technologies of intelligent systems, methods of their interaction and combination [15,29]; building mathematical models of precedent based neural network expert system components: a production fuzzy knowledge base about subscriber problems[16,30,42], a fuzzy controller based on a neural network, a knowledge base of precedents for problems; development of a complex of algorithms: processing subscriber applications, finding solutions to subscribers' problems based on precedents and using a fuzzy neural network[3,18,34]; creation of a neural network expert system based on precedents for solving problems of subscribers of a cellular communication network; study of the effectiveness of the developed precedent based neural network expert system using the following groups of indicators: functional suitability, efficiency, reliability, cost-effectiveness of the system[2,8,39]; development and implementation in trial operation of the precedent based neural network expert system software[6,13] to solve the problems of cellular network subscribers.

Scientific novelties of this research are mentioned in the existing approaches to solving the problems of managing the relationships of operator companies with subscribers of cellular networks[11,25]; theoretically substantiated a new approach to building an intelligent system to solve the problems of subscribers of a cellular communication network, based on the integrated use of technology expert systems, neural networks, fuzzy logic and reasoning based on precedents; software was developed for building a precedent based neural network expert system, including: a production fuzzy knowledge base about problems of subscribers, a fuzzy controller based on a neural network[7,20], a knowledge base of precedents for problems; algorithms have been created for finding solutions to subscribers' problems based on precedents and using a fuzzy neural network; a neural network expert system based on precedents was developed to solve the problems of subscribers of a cellular communication network[21,33,38]; experimental studies were conducted to verify the effectiveness of the developed system.

The practical value of this research was explored as a first version of the software neural network expert system based on precedents for solving the problems of subscribers of a cellular network after testing and evaluating specialists in 2009, where it was used to apply as an integrated approach to the development of precedent based neural network expert system, methods for building knowledge bases of fuzzy products and use cases[1,14,41], algorithms for finding solutions based on use cases and a neural networks.

II. Research Framework

The first stage of the research will focus on analyzes methods and software tools for solving problems associated with servicing subscribers of cellular communication networks[9,22]. The study showed that making decisions in the field of telecommunication network management, and in particular, in solving problems of servicing subscribers of such networks is a complex and multi-criteria task [23,28]. One of the bottlenecks in its solution is the procedure for finding the cause of problems with the provision of cellular services to the subscriber. This task requires a minimum of time to solve it and a maximum of reliability of the found solution to the identified problem [12,35]. The complexity of the problem also lies in the fact[26,38,43] that the state and dynamics of the processes of functioning of a cellular communication network cannot be unambiguously described using clear mathematical models.

Based on the analysis of operators serving cellular network subscribers, it is concluded that it is necessary to use intelligent systems (IS) [7,39] that combine previously accumulated experience in the field of operation of a cellular communication network. As a result of research on various IS technologies and methods of their interaction, the feasibility of hybridization of various intellectual components is substantiated [5,27,36]. This stage of the work concludes with the goals and objectives of the study.

III. Proposed Methodology

The next stage of this research discusses the theoretical foundations and resolves issues of developing mathematical support for a precedent based neural network expert system to solve the problems of subscribers of a cellular communication network. The mathematical description of a neural network expert system based on precedents has the form:

$$NES^{p} =< KB, KB_p, A(p), R'', I^{np}, I^{n2}, I^{p} >$$

In a precedent based neural network expert system, the knowledge base contains knowledge in the form of products KB and in the form of precedents KB_p , R'' - systemic relations of IS. The search for solutions is divided into a neural network I^{n2} and case law I^{p} with $A(p)$ - an algorithm for determining similar use cases. Neural network training I^{np} is based on data from precedents.

A model of a system for solving subscriber servicing problems is presented as a nonlinear object (Fig. 1) with many inputs $\{x_i\}$ and output variables $\{y_k\}$:

$$\begin{cases} \{x_i\}, i=\overline{1,n}; \\ \{y_k\} = f_y(x_1, x_2, ..., x_n), k=\overline{1,q} \end{cases} \tag{1}$$

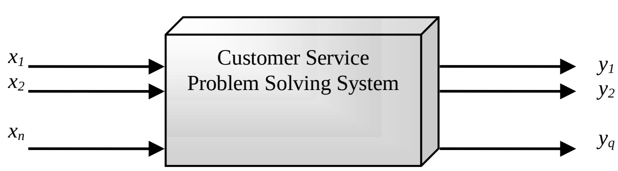

Fig. 1. Model of a System for Solving Problems of Customer Service.

Input variables are characteristics of the problem that the subscriber has. The output variables are the causes of the problem. Input $\{x_i\}, i=\overline{1,n}$ and outputs $\{y_k\}, k=\overline{1,q}$ variables can take only qualitative values, and the set of all possible values of these variables is known

$$U = \{u_j, u_{j+1}, ..., u_m\} \tag{2}$$

Where u_j - score corresponding to the lowest value of the input x_i or outputs y_k variable; u_m - score corresponding to the largest input value x_i (or output value y_k) variable *m* is the power of the set *U*.

We accept that the vector $X^* = \{x_1^*, x_2^*, \ldots, x_n^*\}$ - fixed values of input variables of the considered system model, where $x_i^* \in U, i=\overline{1,n}$.

The task of finding a solution is based on the vector X^* define output vector $Y^* = \{y_1^*, y_2^*, \ldots, y_q^*\}$. Input and output variables will be considered as linguistic variables defined on universal sets *U*.

To evaluate linguistic variables, qualitative terms from the following term set are used:

$$A = \{a_j, a_{j+1}, \ldots, a_m\}, \tag{3}$$

Where *A* is the term set of variables x_i and y_k, a_j - j-th linguistic term of a variable x_i or y_k, $i=\overline{1,n}$, $j=\overline{1,m}$, $k=\overline{1,q}$.

Linguistic terms $a_j, a_{j+1}, \ldots, a_m$ are calculated as follows: $a_j = \sum_{p=1}^{l} \mu^{a_j}(u_j^p)/u_j^p$, where $\mu^{a_j}(u_j^p)$ - degree of membership of an element $u_j \in U$ of term $a_j \in A$, $p=\overline{1,l}$, $j=\overline{1,m}$. The task of constructing membership functions of elements $u_j \in U$ term set $A = \{a_j, a_{j+1}, \ldots, a_m\}$ comes down to determining degrees of belonging $\mu^{a_j}(u_j^p)$ for all $p=\overline{1,l}$, $j=\overline{1,m}$.

In accordance with (1), the MIMO structure (Multiple Input - Multiple Output) of a fuzzy knowledge base of the form:

If ($x_1=a_1^{\,l}$) and ($x_2=a_2^{\,l}$) and … and ($x_n=a_m^{\,l}$), then ($y_1=b_1^{\,l}$) and ($y_2=b_2^{\,l}$) and … and ($y_n=b_m^{\,l}$) (4)

Where *l* is the rule number, $l=\overline{1,L}$, L is the number of rules, a_j^l and b_j^l - fuzzy terms to evaluate the input variable

x_i and output variable y_k, ($i=\overline{1,n}$, $j=\overline{1,m}$, $k=\overline{1,q}$) in the *l*-th rule, respectively.

We transform the system of logical statements (4) using operations $\cup$(or), $\cap$(and):

$$\bigcup_{p=1}^{t_k}\left[\bigcap_{i=1}^{n}\left(x_i=a_j^{kp}\right)\right]\rightarrow\bigcup_{p=1}^{t_k}\left[\bigcap_{k=1}^{q}\left(y_k=b_j^{kp}\right)\right] \quad (5)$$

Where

$j=\overline{1,q}$, $k=\overline{1,q}$, $p=\overline{1,t_k}$

IV. Implementations and Experemental Results Discussions

To implement the process of extracting knowledge from a fuzzy knowledge base, a neuro-fuzzy logical inference mechanism is used in the form of a fuzzy controller based on a neural network - NNFLC (Neurons Network Fuzzy Logic Controller) (Fig. 2).

Structurally, NNFLC is a multilayer network for direct signal propagation, and different layers perform different functions.

Layer 1: represents membership functions implemented as radial basis neurons: $y_i^{(1)}(x)=\exp\left[-(x_i-c_i)^2/2\cdot\sigma_i^2\right]$.

Layer 2: models the and- conditions of the rules: $y_i^{(2)}=\min\left[y_1^{(1)},\ldots,y_n^{(1)}\right]$.

Layer 3: is an OR combination of rules with identical terms in consequents: $y_i^{(3)}=\max\left[y_1^{(2)},\ldots,y_n^{(2)}\right]$. In the training mode, the layer adjusts the parameters of the membership functions of the output variables. In operating mode, forms an output.

Layer 4: in operating mode, neurons perform defuzzification: $z_i^{(4)}=\sum_j \omega_{ji}\cdot y_i^{(3)}$. In training mode, this is an additional input that performs normalization, which allows you to configure the membership function of the output variable: $y_i^{(4)}\left(z_i^{(4)}\right)=\sum_j y_i^{(3)}\cdot\left[\omega_{ji}\big/\sum_j \omega_{ji}\right]$.

The structure of a fuzzy neural network NNFLC is initialized on the basis of the formation of a complete matrix of rules.

The mathematical definition of the knowledge base of precedents has the form: $BP=\left\{\langle\pi_1,\pi_2,\ldots,\pi_n\rangle,K,I\right\}$, where $\langle\pi_1,\pi_2,\ldots,\pi_n\rangle$ - a lot of precedents, *I* - a set of index terms that determine whether the precedent belongs to class *K*.

Next stage of this research discusses the architectural features of precedent based neural network expert system (Fig. 3) to solve the problems of subscribers of a cellular communication network. Fig. 3 shows the structural diagram of the system. The input data for the precedent based neural network expert system is information from the application submitted by the network subscriber. The application contains general data, technical parameters, a list of actions carried out on the application.

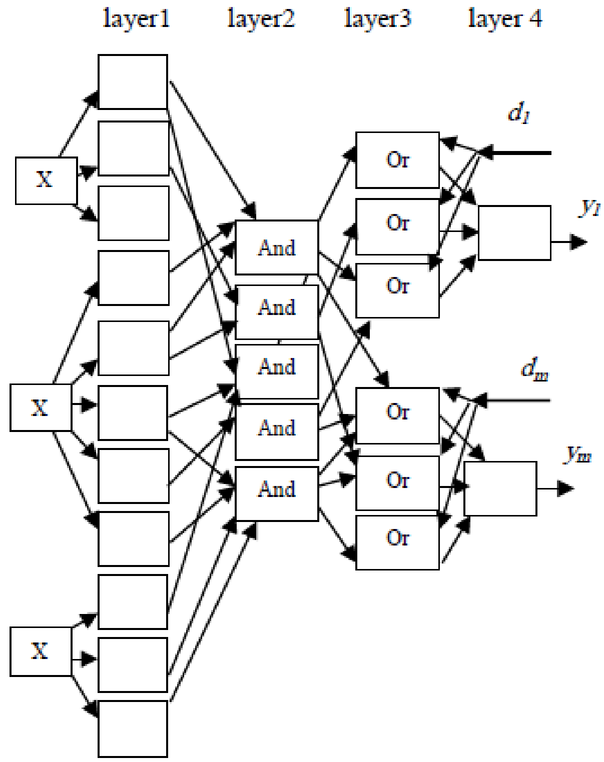

Fig. 2. The Structure of the Neuro-Fuzzy Controller NNFLC.

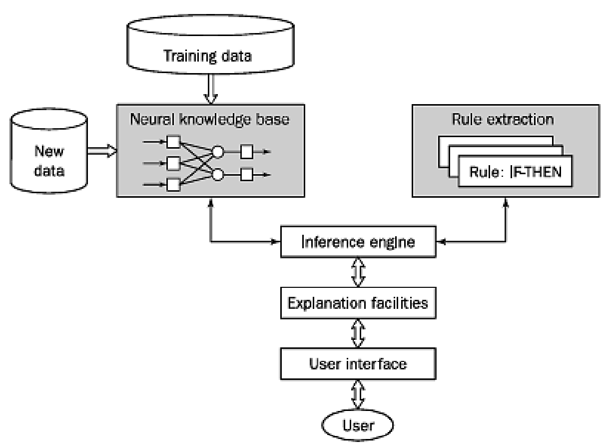

Fig. 3. Structure of Neural Network Expert System.

An algorithm for extracting precedents from the knowledge base using the Euclidean metric is developed. The input to the algorithm is:

1) a description of the subscriber's problem $P=\{p_1, p_2,..., p_n\}$, including *n* values of parameters characterizing the situation;

2) *BP* is a non-empty set of precedents;

3) $W=\{W_1, W_2,..., W_n\}$ - weight (importance factors) parameters;

4) *M* - the number of precedents under consideration from the knowledge base,

5) *K* - threshold value of the degree of similarity.

Output: a lot of precedents *SP*, which have a degree of similarity greater than (or equal to) the threshold value *K*.

Step 1. *SP*=∅, *j*=1 and go to the next step.

Step 2. If $j \leq M$ we choose the use case A_j from the set *BP* ($A_j \in BP$) and go to step 3, otherwise the use cases are considered and go to step 7.

Step 3. We calculate the distance according to the Euclidean metric between the selected use case *Aj* and the current situation *P*, taking into account the importance factors of the parameters: $D(P, A_j)=\sqrt{\sum_{i=1}^{n}(a_i - p_i)^2} \cdot w_i$

Step 4. We calculate the distance according to the Euclidean metric for the boundary values of the parameters: $D_{\max}(P)=\sqrt{\sum_{i=1}^{n}(p_{\max} - p_{\min})^2} \cdot w_i$

Step 5. In this step, we calculate the degree of similarity $S(A,P)=(1-D/D_{\max})$ or as a percentage $S(A,P)=(1-D/D_{\max})\cdot 100\%$, if the threshold value of K is set in percent, and go to step 6.

Step 6. If $S(A,P)\geq K$, then this precedent *Aj* is added to the result set *SP* ($A_j \in SP$), means we extract this precedent from the knowledge base. After checking, *j = j + 1* and go to step 2.

Step 7. If *SP*=∅, then no precedents for the current problem situation were found and go to step 9 with a message for the operator about the need to reduce the threshold value *K*, otherwise the precedents for the current situation were successfully extracted and go to the next step.

Step 8. The found precedents are sorted in decreasing order of similarity with the current situation and presented to the operator.

Step 9.The end (completion of the algorithm).

Neural network training is as follows:

In step 1. A training sample is set, consisting of many examples of the following form: $\left(x_1^{(k)}, x_2^{(k)}, x_3^{(k)},..., x_n^{(k)}, y_1^{(k)}, y_2^{(k)}, y_3^{(k)},..., y_q^{(k)}\right)$, $k=\overline{1,K}$, where $x_i^{(k)}$ - values of input variables x_i ($i=\overline{1,n}$) and $y_j^{(k)}$ - values of output variables y_j ($j=\overline{1,q}$)in k-th example; *K* is the total number of examples in the training set. The values of the input and output variables are determined by the membership functions of the corresponding terms: $\left(\mu_{a_1}\left(x_1^{(k)}\right),..., \mu_{a_n}\left(x_n^{(k)}\right), \mu_{b_1}\left(y_1^{(k)}\right),..., \mu_{b_q}\left(y_q^{(k)}\right)\right)$, $k=\overline{1,K}$.

We introduce the notation $x_i^{(k)}$ and $y_j^{(k)}$ as values of membership functions of the terms of input and output variables, respectively.

In step 2. Configuring the parameters of membership functions includes determining the centers c_i and widths σ_i for membership functions represented by shape functions: $y_i^{(1)}(x)=\exp\left[\frac{-(x_i - c_i)^2}{2\cdot\sigma_i^2}\right]$

The training data self-organization algorithm is used, which automatically divides the space into clusters. The center c_i of the cluster is identified with the center of the radial basis function. The preliminary selection of centers is carried out randomly on the basis of uniform distribution.

The matrix of bond weights ω_{ji} is specified following the conditions: $\begin{cases} \omega_{ii}=1, \\ -\frac{1}{T-1}<\omega_{ji}<0, i\neq j, \end{cases}$ where T is the number of neurons in the input layer.

After presentation of the k-th vector $x^{(k)}$ the center is selected from the training set c_i closest to $x^{(k)}$ according to the Euclidean metric: $\left\|x^{(k)} - c_i\right\|=\sqrt{\sum_{t=1}^{T}(x_t - c_i)^2}$.

This center is subject to refinement in accordance with the winner algorithm (WTA algorithm):

$c_i(k+1)=c_i(k)+\eta(t)\cdot\left[x^{(k)} - c_i(k)\right]$, where $\eta(t)$ - monotonously decreasing level of training. Other centers do not change. All training vectors $x^{(k)}$ presented several times in random order until the stabilization of the values of the centers.

Width Adjustment σ_i carried out heuristically, on the principle of "first closest neighbor": $\sigma_i=(\sigma_i - \sigma_\omega)/\lambda$, where λ is the overlap parameter. The outputs of each layer are calculated by the formulas:

$$y_i^{(2)}=\min\left[y_1^{(1)},..., y_n^{(1)}\right],$$

$$y_i^{(3)}=\max\left[y_1^{(2)},..., y_n^{(2)}\right],$$

$$y_i^{(4)}=\sum_j y_i^{(3)}\cdot\left[\omega_{ji}\Big/\sum_j \omega_{ji}\right]$$

Winner Algorithm Looks For Weight Matrix ω_{ji}, which evaluates the quality of relations between the left and right parts of the rules: $\omega_{ji}(n+1) = \omega_{ji}(n) - \eta \cdot \Delta\omega$, where $\Delta\omega = y_j^{(3)} \cdot \left(y_i^{(2)} - \omega_{ji}\right)$.

In step 3. The combination of rules is carried out with the participation of an expert.

In step 4. Final configuration of membership functions is performed using the error back propagation algorithm for the error function $e_i = \left(y_i^{(4)} - d_k\right)^2$ regarding vectors $x^{(k)}$.

For K learning pairs, the objective error function is defined as:

$$E = \frac{1}{2}\sum_{k=1}^{K}\left(y_k^{(4)} - d_k\right)^2 = \frac{1}{2}\sum_{k=1}^{K}\left[\sum_{t=0}^{T}\omega_i \cdot y_t^{(4)}(x_k) - d_k\right]$$

The magnitude of the error determines the gradient vector of the objective function relative to specific centers c_{ij} and width σ_{ij}:

$$c_{ij}(n+1) = c_{ij}(n) - \eta \cdot \frac{\partial E}{\partial c_{ij}(n)},$$

$$\sigma_{ij}(n+1) = \sigma_{ij}(n) - \eta \cdot \frac{\partial E}{\partial \sigma_{ij}(n)}.$$

Repeated training cycles lead to complete and fast network learning.

The search for a solution to the subscriber's problem using the neural network mechanism is carried out according to the created algorithm (Fig. 4).

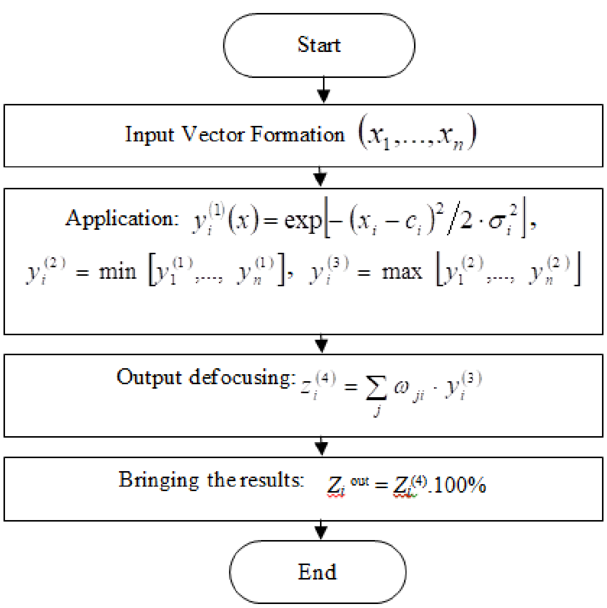

Fig. 4. Algorithm for Neural Network Search for a Solution to a Problem.

The next main stage of this research discusses the features of the software implementation of a precedent based neural network expert system. The choice of the object-oriented programming language Java as a part of the Microsoft Visual Studio with a program development environment as the main precedent based neural network expert system programming tool is substantiated. The modern database development tools are analyzed and the choice is made in favor of the Microsoft SQL Server DBMS.

A production fuzzy knowledge base has been developed for a system for solving problems of cellular network subscribers, training data sets have been generated for a neural network search mechanism. A software implementation of a fuzzy neural network was made, an algorithm for training and finding a solution using a neural network was implemented. A database of customer applications has been developed. A precedent presentation form is defined, a precedent knowledge base is built (Fig. 5), and a software implementation of the use case search is implemented.

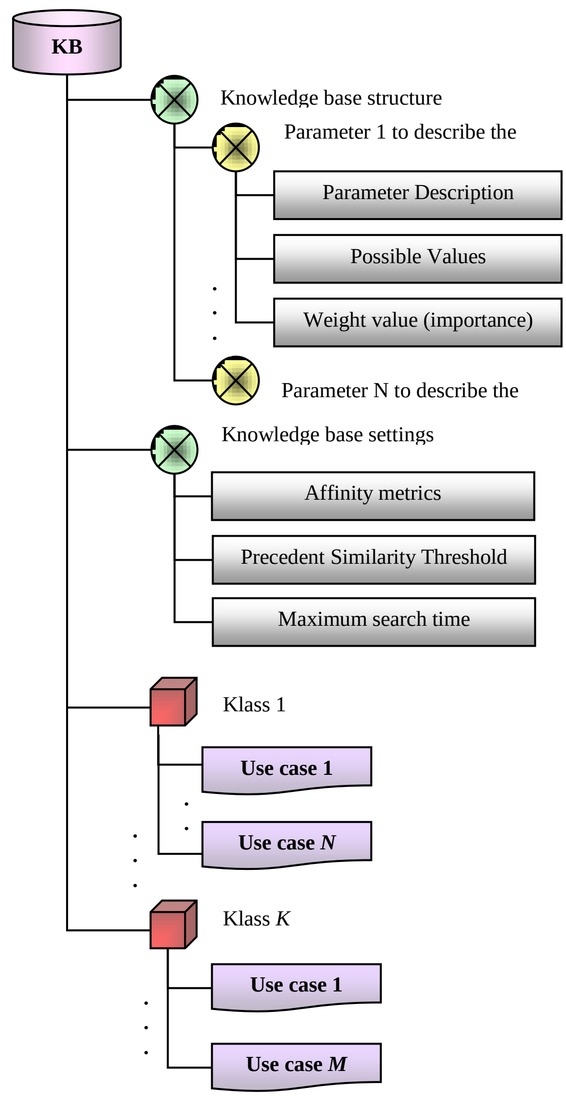

Fig. 5. Knowledge base Structure of Precedent based Neural Network Expert System.

To increase the speed and efficiency of the search for a precedent in the knowledge base, the full space of precedents is classified by the number of incidents in the precedent.

V. Results Analysis and Practical Strenghs

Next main important stage in this research is devoted to an experimental study of the operability and effectiveness of precedent based neural network expert system to solve the problems of subscribers of a cellular communication network. Four groups of indicators were selected as performance indicators: functional, operational, economic indicators and reliability indicators (Table I).

TABLE. I. A List of Indicators for Assessing the Effectiveness of Precedent based Neural Network Expert Systems

№	Indicator	Assessment Object
1) Functionality		
1.	The total number of applications of subscribers	System as a whole
2.	Problem Identification Factor	Use Case Search Subsystem Neural Network Search Subsystem System as a whole
3.	The ratio of unprocessed applications	Use Case Search Subsystem Neural Network Search Subsystem System as a whole
4.	Problem Identification Criteria Accuracy	Use Case Search Subsystem Neural Network Search Subsystem System as a whole
5.	Problem Level	System as a whole
2) Efficiency		
6.	Application Processing Duration	System as a whole
7.	Duration of finding a solution to a problem	Intellectual part of the system The non-intellectual part of the system
8.	Average processing time	Use Case Search Subsystem Neural Network Search Subsystem The non-intellectual part of the system
9.	The number of operators	
3) Reliability		
10.	System uptime	System as a whole
4) Profitability		
11.	Development cost	System as a whole
12.	Operation cost	System as a whole
13.	The average cost of processing one subscriber application	System as a whole
14.	Annual cost savings	System as a whole
15.	Annual economic effect	System as a whole
16.	Coefficient of economic efficiency	System as a whole
17.	Payback period (years)	System as a whole

A technique has been developed for conducting an experiment to check the operability and effectiveness of the developed information system. When testing a precedent based neural network expert system in real conditions, the system was installed on the computers of two operators of the call center of cellular network subscribers. One operator used only the database of customer requests, and another used an additional intelligent subsystem for servicing applications. The experiment was carried out during the week around the clock to take into account the influence of the day of the week and time of day on the frequency of receipt and processing time of subscribers' applications (Table II).

An economic assessment of the effectiveness of the implementation of a neural network expert system based on precedents for solving the problems of subscribers of a cellular network was carried out according to the following particular criteria: development cost, operating cost, annual cost savings, annual economic effect, cost recovery period.

The calculations showed that the costs of creating and maintaining the system pay off for 3.5 years of operation, and the use of intellectual support of the precedent based neural network expert system in the work of the mobile operator gives well enough annual savings.

TABLE. II. Results of Testing Precedent based Neural Network Expert System in Real Conditions

<table>
<tr><th rowspan="2">Indicator</th><th colspan="2">Intelligent Subsystem</th><th rowspan="2">The non-intellectual part of the system</th><th rowspan="2">System as a whole</th></tr>
<tr><th>Use Case Search Subsystem</th><th>Neural Network Search Subsystem</th></tr>
<tr><td rowspan="2">Total number of customer requests</td><td>347</td><td>471</td><td rowspan="2">572</td><td rowspan="2">1390</td></tr>
<tr><td colspan="2">818</td></tr>
<tr><td rowspan="2">Problem Identification Factor</td><td>93,37%</td><td>100,00%</td><td rowspan="2">91,96%</td><td rowspan="2">95,11%</td></tr>
<tr><td colspan="2">96,69%</td></tr>
<tr><td rowspan="2">The ratio of unprocessed applications</td><td>6,63%</td><td>0,00%</td><td rowspan="2">8,04%</td><td rowspan="2">4,96%</td></tr>
<tr><td colspan="2">6,63%</td></tr>
<tr><td rowspan="2">Problem Identification Criteria Accuracy</td><td>96,50%</td><td>99,72%</td><td rowspan="2">81,33%</td><td rowspan="2">92,52%</td></tr>
<tr><td colspan="2">98,11%</td></tr>
<tr><td rowspan="2">Application processing time (hours)</td><td>35,16</td><td>24,54</td><td rowspan="2">143,00</td><td rowspan="2">168</td></tr>
<tr><td colspan="2">59,59</td></tr>
<tr><td rowspan="2">Duration of finding a solution to a problem</td><td>1,39</td><td>0,59</td><td rowspan="2">12,45</td><td rowspan="2">4,51</td></tr>
<tr><td colspan="2">1,09</td></tr>
<tr><td rowspan="2">Average processing time</td><td>5,54</td><td>3,13</td><td rowspan="2">15</td><td rowspan="2">7,59</td></tr>
<tr><td colspan="2">4,33</td></tr>
<tr><td>The number of operators</td><td colspan="2">1</td><td>1</td><td>2</td></tr>
</table>

VI. Conclusion

The main scientific results of this research is a theoretical justification, a study of construction methods and the development of a neural network expert system based on precedents for solving the problems of subscribers of a cellular communication network.

It was also investigated modern systems for managing cellular networks and customer relationships. The methods for solving problems that arise during the operation of a cellular communication network are analyzed, and it is concluded that it is advisable to hybridize various intelligent technologies in order to create a single advisory system for solving subscribers' problems. Also a mathematical model of a neural network expert system based on precedents for solving the problems of subscribers of a cellular communication network is developed; the system components and the processes of interaction of its intellectual components are mathematically described. In additional, a mathematical model of a fuzzy knowledge base with a MIMO structure has been built, including knowledge about the problems that subscribers have during the operation of a cellular network. The composition is determined and the characteristic of input and output linguistic variables and their terms is given. Beside the previous mentioned outputs and concludes a mathematical model of a fuzzy neural network output system using a fuzzy controller based on the NNFLC neural network has been developed. The use of a neural network approach to the implementation of fuzzy inference is justified. A module for explaining the solution obtained by the neural network search engine has been implemented.

A neural network expert system based on precedents for solving the problems of subscribers of a cellular network is implemented programmatically. A database of subscriber applications has been developed, which is used both for registering applications and for creating precedents and knowledge base rules on their basis. Also performance indicators of the developed precedent based neural network expert system are determined. An experiment to verify the health and effectiveness of the system. The calculated indicators suggest that the developed precedent based neural network expert system has reliable software, good ability to identify the causes of subscribers' problems, and can identify these causes with a high degree of reliability and high speed.

Acknowledgement

This project was funded by the Deanship of Scientific Research (DSR), King Abdulaziz University, Jeddah, under grant No. (DF-749-830-1441). The authors, therefore, gratefully acknowledge DSR technical and financial support.

References

[1] Guimarães, Augusto Junio, et al. "Using fuzzy neural networks to the prediction of improvement in expert systems for treatment of immunotherapy." Ibero-American Conference on Artificial Intelligence. Springer, Cham, 2018.

[2] AlRababah, Ahmad Abdul Qadir. "Watermarking implementation on digital images and electronic signatures." International Journal of Advanced and Applied Sciences 4.10 (2017): 160-164.

[3] Bui, Nhan X., et al. "Reliable data reading with data set screening by error injection." U.S. Patent Application No. 10/262,681.

[4] AlRababah, Ahmad AbdulQadir. "Data Flows Management and Control in Computer Networks." International Journal of Advanced Computer Science and Applications 9.11 (2018): 207-217.

[5] Li, Xiaodong, et al. "Rapid, robust, and reliable blind deconvolution via nonconvex optimization." Applied and computational harmonic analysis 47.3 (2019): 893-934.

[6] Rondinelli, Dennis A. Applied methods of regional analysis: the spatial dimensions of development policy. Routledge, 2019.

[7] Tang, Jinjun, et al. "Lane-changes prediction based on adaptive fuzzy neural network." Expert Systems with Applications 91 (2018): 452-463.

[8] Zhang, Chiya, et al. "Spectrum Sharing of Drone Networks." Handbook of Cognitive Radio (2019): 1279-1304.

[9] AlRABABAH, A.A., Implementation of Software Systems Packages in Visual Internal Structures. Journal of Theoretical & Applied Information Technology, 2017. 95(19).

[10] Shen, Kai-wen, Xiao-kang Wang, and Jian-qiang Wang. "Multi-criteria decision-making method based on Smallest Enclosing Circle in incompletely reliable information environment." Computers & Industrial Engineering 130 (2019): 1-13.

[11] Bui, Dac-Khuong, et al. "A modified firefly algorithm-artificial neural network expert system for predicting compressive and tensile strength of high-performance concrete." Construction and Building Materials 180 (2018): 320-333.

[12] AlRababah, Ahmad AbdulQadir. "Lempel-Ziv Implementation for a Compression System Model with Sliding Window Buffer."

[13] Huberman, Gur, Jacob Leshno, and Ciamac C. Moallemi. "An economic analysis of the Bitcoin payment system." Columbia Business School Research Paper 17-92 (2019).

[14] Anand, S. Krishna, TG Sundara Raman, and S. Subramanian. "Implementing a neuro fuzzy expert system for optimising the performance of chemical recovery boiler." International Journal of Artificial Intelligence and Soft Computing 4.2-3 (2014): 249-263.

[15] Mukherjee, Sayandev. "Distribution of downlink SINR in heterogeneous cellular networks." IEEE Journal on Selected Areas in Communications 30.3 (2012): 575-585.

[16] Deliyannis, Theodore, Yichuang Sun, and John Kelvin Fidler. Continuous-time active filter design. CRC press, 2019.

[17] Pelusi, Danilo, et al. "Neural network and fuzzy system for the tuning of Gravitational Search Algorithm parameters." Expert Systems with Applications 102(2018):234-244.

[18] Pearlson, Keri E., and Carol S. Saunders. Managing and using information systems: A strategic approach. John Wiley & Sons, 2019.

[19] Silva Araújo, Vinícius Jonathan, et al. "Using resistin, glucose, age and bmi and pruning fuzzy neural network for the construction of expert systems in the prediction of breast cancer." Machine Learning and Knowledge Extraction 1.1 (2019): 466-482.

[20] AlRababah, A.A., A. AlShahrani, and B. Al-Kasasbeh, Efficiency Model of Information Systems as an Implementation of Key Performance Indicators. International Journal of Computer Science and Network Security (IJCSNS), 2016. 16(12): p. 139.

[21] Reichling, Markus, and Tim Otto. "The environmental impact of the new economy: Deutsche Telekom, telecommunications services and the sustainable future." The ecology of the new economy. Routledge, 2017. 119-129.

[22] Naderializadeh, Navid, Mohammad Ali Maddah-Ali, and A. Salman Avestimehr. "Cache-aided interference management in wireless cellular networks." IEEE Transactions on Communications 67.5 (2019): 3376-3387.

[23] Bar-Yam, Yaneer. Dynamics of complex systems. CRC Press, 2019.

[24] Kristjanpoller, Werner, and Marcel C. Minutolo. "A hybrid volatility forecasting framework integrating GARCH, artificial neural network, technical analysis and principal components analysis." Expert Systems with Applications 109 (2018): 1-11.

[25] AlRababah, A.A., A new model of information systems efficiency based on key performance indicator (KPI). management, 2017. 4: p. 8.

[26] AL-Qutami, Tareq Aziz, et al. "Virtual multiphase flow metering using diverse neural network ensemble and adaptive simulated annealing." Expert Systems with Applications 93 (2018): 72-85.

[27] Reichling, Markus, and Tim Otto. "The environmental impact of the new economy: Deutsche Telekom, telecommunications services and the sustainable future." The ecology of the new economy. Routledge, 2017. 119-129.

[28] Al-Rababah, Ahmad A., Taghreed AlTamimi, and Najat Shalash. "A New Model for Software Engineering Systems Quality Improvement." Research Journal of Applied Sciences, Engineering and Technology 7.13 (2014): 2724-2728.

[29] Moustafa, Akram, et al. "A New Dynamic Model for Software Testing Quality." Research Journal of Applied Sciences, Engineering and Technology 7.1 (2014): 191-197.

[30] Rendón, Claudio Marco Cartagena, et al. "Proposed Model for Measuring Customer Satisfaction with Telecommunications Services." Mediterranean Journal of Social Sciences 8.2 (2017): 15-25.

[31] Hadi, Mohammed S., et al. "Patient-Centric Cellular Networks Optimization using Big Data Analytics." IEEE Access 7 (2019): 49279-49296.

[32] AlRababah, Ahmad. "Digital Image Encryption Implementations Based on AES Algorithm." VAWKUM Transactions on Computer Sciences 13.1 (2017): 1-9.

[33] Smith, Trevor D., et al. "Methods and systems for distributing fiber optic telecommunications services to local area." U.S. Patent No. 8,805,152. 12 Aug. 2014.

[34] Al Ofeishat, H.A. and A.A. Al-Rababah, Real-time programming platforms in the mainstream environments. IJCSNS, 2009. 9(1): p. 197.

[35] Wang, Yueying, Xixiang Yang, and Huaicheng Yan. "Reliable fuzzy tracking control of near-space hypersonic vehicle using aperiodic measurement information." IEEE Transactions on Industrial Electronics (2019).

[36] Chougdali, Sallami, et al. "New air traffic management approach based on expert system and using real-time scheduling algorithms." International Journal of Intelligent Engineering Informatics 4.3-4 (2016): 305-321.

[37] Zahariadis, Nikolaos. "The multiple streams framework: Structure, limitations, prospects." Theories of the Policy Process, Second Edition. Routledge, 2019. 65-92.

[38] AlRababah, Ahmad Abdul Qadir. "On the associative memory utilization in English-Arabic natural language processing." International Journal of Advanced and Applied Sciences 4.8 (2017): 14-18.

[39] Bolz, Ray E. CRC handbook of tables for applied engineering science. CRC press, 2019.

[40] Zurkirch, Manfred, and Inge Reichart. "Environmental Impacts Of Telecommunications Services: Two life-cycle analysis studies." The Ecology of the New Economy. Routledge, 2017. 130-149.

[41] Chen, Min, et al. "Mobility-aware caching and computation offloading in 5G ultra-dense cellular networks." Sensors 16.7 (2016): 974.

[42] Goddard, John B., and Andrew E. Gillespie. "Advanced telecommunications and regional economic development." Managing the city. Routledge, 2017. 84-109.

[43] Al Rababah, Ahmad Abdul Qadir. "Embedded Architecture for Object Tracking using Kalman Filter." JCS 12.5 (2016): 241-245.

Understanding Students' Motivation and Learning Strategies to Redesign Massive Open Online Courses based on Persuasive System Development

Mohamad Hidir Mhd Salim[1], Nazlena Mohamad Ali[2], Mohamad Taha Ijab[3]
Institute of Visual Informatics, The National University of Malaysia
Bangi, Selangor, Malaysia

***Abstract*—Electronic learning or E-learning is currently flourishing immensely in areas such as secondary and tertiary education, lifelong learning programs and adult education. Within recent years, massive open online courses (MOOCs) have received profound attention within the field of E-learning. Persuasive principles can be implemented to enhance the system design and motivate students to engage with the system. The aim of this study is to identify students' motivation and learning strategies that affect their academic performance in using MOOCs among tertiary education students. 40 students enrolled in the Ethnic Relations course participated in the online survey. Motivated Strategies for Learning Questionnaire (MSLQ) is the instrument used in this study while Automatic Linear Modelling (ALM) and Multiple Linear Regression (MLR) were used in the analysis. The result shows that there is a correlation between students' motivation, learning strategies and their academic performance. It is found that resource management, cognitive and metacognitive and value component are the main scales that influenced their motivation and learning strategies towards excellent academic performance. The results can be used to fulfil the first phase of designing a persuasive system based on the Persuasive System Design (PSD) model which is to understand the issues behind a system.**

***Keywords*—Persuasive; MOOCs; motivation; learning strategies**

I. Introduction

Electronic learning or E-learning is currently flourishing immensely in areas such as secondary and tertiary education, lifelong learning programs and adult education [1]. Due to the advantages that E-learning brings to tertiary education institutions particularly the absence of reliance on the time requirements, the capacity to pose inquiries without timidity and access of materials from anyplace [2], the implementation of E-learning has become widely implemented [3]. E-learning is defined as the development of knowledge and skills using information and communication technologies (ICTs) to support interactions (i) with content, (ii) learning activities and tools, and (iii) other people. Internet learning, Web-based learning, and online learning are examples of E-Learning [4].

Massive open online courses (MOOCs) are online courses that developed for open, unlimited enrolment via the internet [5]. MOOCs are often released by third-party online platforms and developed independently by academics [6]. There are a few tertiary education institutions in Malaysia that have embarked on MOOCs initiative and they are currently at the implementation phase. These Malaysian universities are Universiti Putra Malaysia, Universiti Kebangsaan Malaysia, Universiti Malaysia Sarawak and Universiti Teknologi MARA. Malaysia's approach can be portrayed as exploratory. Hence, the implementation is focusing less on reaching the huge number of users or competing with established providers like edX, Udacity and Coursera, but more on educating the user to use web-based technology to complement current educational delivery systems at the higher education level as a way of familiarizing MOOCs to the general Malaysian audience [7]. There are four compulsory courses for Malaysia's undergraduate students namely Islamic and Asian Civilization, Ethnic Relations in Malaysia, Introduction to Entrepreneurship, and Information Communication Technology (ICT) Competency that use MOOCs as its learning platform [8].

There are issues regarding the use of MOOCs among tertiary students. These issues have to do with MOOCs themselves and their platforms, including learning engagement difficulty in MOOCs due to the limited of social presence, as well as lack of support and interaction in the platform [9]. Furthermore, learners lacking in learning strategies will not get much from open-ended learning [10] and it still uncertain on how MOOCs might affect students' motivations and participation, and how these later will impact their academic performance. By implementing persuasive technology, it might help solve these issues [11]. "Captology" (Computer as Persuasive Technology) or "persuasive technology" refers to a technology designed to influence users' behaviour without coercion [12]. This technology can be implemented in an e-learning system as assistance to improve students' behaviour [11] and elicit positive emotions in students using the persuasive principles according to the suitability to improve students' trust towards the system [13]. According to the persuasive system design (PSD) model, the development of persuasive systems involve three different phases: 1) understanding key issues behind the persuasive system, 2) analyzing the persuasion context, 3) designing the system qualities [14]. This paper will explain about the history of MOOCs, Persuasive System Development Model, Fogg Behaviour Model, and the instrument used in this study which is Motivated Strategies and Learning Questionnaire (MSLQ). This study aims to fulfil the first phase of persuasive system development by identifying students' motivation and learning strategies that can improve their academic performance. Understanding this relationship has important pedagogical and practical implications for future MOOC improvement [15].

II. Background Study

We are currently at the beginning of the fourth industrial revolution (4IR). The industrial revolution commonly is a concept that changed the economy and society. Huge changes occurred within a short time. [16]. Tertiary education will also change significantly due to the impact of 4IR. [17]. This section reviews the history of MOOCs and the Malaysian universities efforts in implementing MOOCs, the persuasive system development process, the behaviour change model for persuasive design to give insight on how persuasive technology can affect behaviour and the instrument used to identify learning strategies and motivation factors.

A. Massive Open Online Courses (MOOCs)

The report State of the Field Review on E-learning argues that E-learning does not encompass a specific technology and can be used in hybrid approaches [4]. Research in the area of E-learning has demonstrated that the advantages offered by this environment are convenience and flexibility offered by the ‘anytime and anywhere’ accessibility [4]. Students can work at their own style of learning and this feature is crucial for a certain group of learners. However, some claim the web-based or online learning is not as effective as the traditional classroom because of it is lacking face to face interaction which caused learners felt disconnected from others due to lack of facial expression and other common features found in a traditional way of learning [18].

The development and implementation of e-learning have become a necessity for academic institutions. This is because of the benefits E-learning brings to universities [3]. To make this happen, technologies and innovations such as Massive Open Online Courses (MOOCs) are implemented. A few years back, MOOCs have become popular in the field of e-Learning [19]. Although traditional online courses and MOOCs share commonalities because they are both offered online, both are different in terms of course structure and aims [20]. Unlike traditional online courses, MOOCs attract massive numbers of users and typically require little (or no) prior knowledge [21]. This kind of technologies will create greater dynamism and personalization of students’ learning experience.

cMOOCs is the first phase of MOOCs development period in the comparatively short history of MOOCs. cMOOCs (the connectivist MOOCs) are based on "connectivist distributed peer learning model. Courses are typically developed and led by academics through open source web platforms" (Wulf, Blohm, & Brenner, 2014, p. 6) [22]. xMOOCs is the second phase of MOOCs development. The xMOOCs period included online courses that are structured in a more conventional way and delivered through not simple web platforms but via some learning management platforms such as Coursera, EdX, Udacity, Udemy, Iversity, MiriadaX and Futurelearn. Some xMOOCs (content-based MOOCs) are also delivered through proprietary learning management platforms of institutions or individual academics [6].

There are five pillars in The National e-Learning Policy created by the Malaysian government which include curriculum and content, the structure of the organization, professional development and enculturation to enable Malaysia higher learning institutions to implement their initiatives towards e-learning. One of the benefits that MOOCs offer to Malaysian higher education system is by increasing students’ enrolment and improve the quality of instruction at the same time to do all the necessary in a cost-efficient manner. The first of its kind in the world, these undergraduate courses bring together all first-year students from 20 Malaysian universities on a single platform. This launch is significant as it marks the first foray of Malaysian public universities into MOOCs [23].

MOOCs offer competence development and even certification. As a stand-alone solution, MOOCs offer chances for reflecting on and constructing new knowledge, but often they involve a minimum amount of live interaction. Many MOOCs continue to be online replications of classrooms primarily consisting of video lectures, multiple-choice quizzes, Q&As and more informal after-class discussions in online discussion forums [24]. Students may have developed comprehension monitoring skills that imply when the material is insufficiently understood but may not use those skills if they are not having enough effort to really understand the contents. Understanding student learning, therefore, needs taking into consideration the dynamic exchange between cognition and motivation [25], [26].

B. Persuasive System Development

There are three phases in persuasive system development. Understanding the key issues behind the persuasive system is the first phase need to be taken. After getting a thorough understanding of the issues, the system can be analysed and designed by recognizing the intent, event and strategies for the use of persuasive systems. When those elements have been identified, the actual system qualities for a new system can be designed [27]. The first phase of the process is identified by getting significant learning strategies and motivation factors that affect students’ academic performance.

Analyzing the persuasion context is the next phase in persuasive system development. It consists of three aspects which are the intent, the event and the strategy [27]. According to [28] there are three sources of intentions which are endogenous, exogenous, and autogenous. Endogenous belongs to people that produce interactive technology. While exogenous belongs to people that distribute or give the interactive technology access to others and autogenous belongs to people that adopting interactive technology. It is very important to determine these three sources of intention due to the reason that computers do not have intentions of their own [27]. The event involves understanding the situations around the behaviour to influence. There are three contexts that need to identify in the event including use context, user context and technological context. The use of context can be identified by understanding the features arising from the problem domain. While user context can be identified by focusing the end-user’s individual differences which determine their level of technology literacy. Because of information technologies are expanding rapidly nowadays, identifying technological context is very crucial where the strength and weaknesses, along with the risk and opportunities of technological platforms need to be wholly recognised [27]. The strategy is the last aspect that needs to be identified in this phase. It is about the message that reaches the end-users. Having a proper message will increase the level of persuasion. Therefore, a deeper understanding of the message and how it works to persuade the end-users are important [29].

Design of system qualities is the last phase in persuasive system development. There are four categories in persuasive design principles which has been outlined by [30] in Persuasive System Design (PSD) model which are Primary Task Support, Dialogue Support, System Credibility Support and Social Support. Each category has its own design principles that need to be suitably selected to design an effective persuasive system. Primary task support consists of a set of principles that help simplify user's main task. While dialogue support is very useful to keep the end-users towards their target behaviour by implementing computer-human dialogue support. System credibility support explains about the way to design a credible persuasive system. Where the more credible a system is, the more persuasive it can be [27]. Lastly, the interaction between people through a computer has significant implication for persuasion [12]. To ensure that the end-users will remain motivated, social support will do the task by providing social interaction features between users. According to [31], there is proof that changing social norms would affect behaviour change.

C. Behaviour Model

There are some theories related to behaviours such as The Stage of Change Model and SNAP model. SNAP stands for "staying the old behaviour, new behaviour engagement, attempting to change and planning to change". Both theories describe the process of behaviour to occur. However, these theories are not explaining behaviour change [11]. This is because of a persuasive system is developed to influence users' behaviour. It is crucial to understand behaviour change model to ensure the system can deliver its purpose. Fogg Behaviour Model (FBM) explains a new way to understand factors that could give an impact on users' behaviour. The persuasive design could fail because of misunderstanding on these three021 factors which are motivation, ability and triggers. Users must have these three factors at the same time to ensure they perform the target behaviour [32]. Fig. 1 shows the visualization of The Fogg Behaviour Model. The figure shows that when users have high motivation, high ability with an appropriate type of triggers, it would be easy for users to perform the target behaviour.

Every factor in this model has its elements. Elements in motivation consist of pleasure/ pain, hope/ fear and social acceptance/ rejection. Pleasure/pain is a primitive response that functions adaptively in activities related to self-preservation and the response is immediate. While the difference between hope and fear is the anticipation of good or bad situations that will happen if certain behaviours occur. Social acceptance/ rejection are elements that depend on users' surrounding because some users prefer to be socially accepted rather than socially rejected. Although users have high ability to perform a target behaviour, without having a certain level of motivation, the tendency for them not to reach the target behaviour is high [32].

The persuasive system must provide features that are simple to increase users' abilities to perform target behaviour. This factor has six elements, where every element is related. Those elements are time, money, physical effort, brain cycles, social deviance and non-routine. By considering users' time, the designer of a persuasive system will simplify the tasks given. For users that have limited financial resources, money would affect their ability to perform a target behaviour. The physical effort might not be simple for users who have problems with their health. Hence, this element should be considered before designing tasks for a persuasive system. While brain cycle is an element that requires users to think before they manage to complete a task. If the tasks are complicated, it will not persuade users to change behaviour. Social deviance means that if any tasks in the systems require users to against the norm, it is not simple for certain users. The last element in this factor is non-routine. Usually, users prefer to do tasks that can be performed in their routine unless they have enough motivation to do it. Users' abilities are different. Some users have money but do not have time. While some other users have time but cannot perform brain cycles activity and vice versa [32].

The last factor in the FBM model is triggers. Three types of triggers that contribute to behaviour change which are "spark", "facilitator" and "signal". The tendency for users to perform a target behaviour without enough motivation is low, even though they could do it. In this case, "spark" plays an important role to ensure users perform a target behaviour. "Spark" could be a video or a highlighted text that is designed to inspire users. "Facilitator" is a type of trigger for users who do not have the ability to perform target behaviour. The purpose of this type of trigger is to facilitate users to perform target behaviour while triggering them. It could be in a form of video, highlighted text, pictures and others. The last type of trigger is "signal". "Signal" is for users who have both motivation and ability. It works as a reminder for users and this type of trigger will not contribute to users' motivation or simplify tasks. All of these triggers are very useful to ensure users perform a target behaviour at the specific moment when users have both motivation and ability [32].

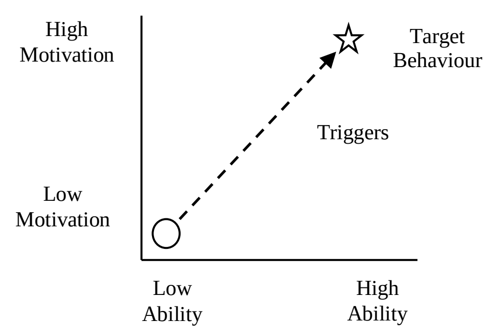

Fig. 1. The Fogg behaviour Model [32].

D. Motivation Strategies and Learning Questionnaire (MSLQ)

Two of the scales resulting from this previous work are the Learning and Study Strategies Index (LASSI) and the Motivated Strategies for Learning Questionnaire (MSLQ). One of the advantages of the MSLQ over LASSI is that there is no implied internal model that must be used to interpret results. The scales are also designed to be modular so as to allow a researcher to develop a model structure to fit the needs of a particular study [33]. This ability to customize the MSLQ makes it an appropriate choice for use in the present study as our research is of an exploratory in nature and therefore requires greater freedom in interpreting the data collected [11].

Table I shows the MSLQ components. The MSLQ consists of 81 items broadly categorized as part of either the motivation or learning strategies scales [33]. Those scales are divided into two levels of subscales and it comes together with the specific study behaviours. It is crucial to understand students' study behaviours before designing a persuasive system. Learning includes many different skills and abilities and so there are a lot of study behaviours that either has a positive or negative impact on learning performance. Previous research has thus sought to identify and categorize the types of study behaviours and strategies students typically have [34]. The MSLQ was developed using a social-cognitive view of motivation and learning strategies with the student represented as an active processor of information whose beliefs and cognitions mediated important instructional input and task characteristics [35].

TABLE. I. MOTIVATION STRATEGIES AND LEARNING QUESTIONNAIRE (MSLQ) COMPONENTS [33]

Motivation Scales	
Scale	**Subscale**
Value	Intrinsic Goal Orientation
	Extrinsic Goal Orientation
	Task Value
Expectancy	Control of Learning Beliefs
	Self-efficacy
Affective	Test Anxiety
Learning Strategies Scales	
Scale	**Subscale**
Cognitive and Metacognitive	Rehearsal
	Elaboration
	Organization
	Critical Thinking
	Metacognitive Self-regulation
Resource Management	Time and Study Environment
	Effort Regulation
	Peer Learning
	Help-Seeking

III. METHODOLOGY

To identify students' motivation and learning strategies that affect their study behaviours, an online survey targeting students that were taking Ethnic Relations course using MOOCs was conducted. The online questionnaire is referred to as the MSLQ instrument with some modification. This part will explain every modification that has been made to the MSLQ instrument and the statistical approach used to analyze the results to determine the most factors that affect students' study behaviours.

The online questionnaire consists of four sections. The first and second sections are focusing on motivation and learning strategies for the students. These two sections have been going through some changes. Changes were made to the original form of the MSLQ questionnaire because the original MSLQ questionnaire was designed to be focused on the traditional ways of learning. This study focused on online learning. Hence, the generalization should be made to make it understandable and precise about the learning requirements. In order to address the issue, words related to traditional learning styles in MSLQ questionnaire like 'teacher' has been changed to "instructor", 'classroom' has been changed to "environment" and others have been changed according to the suitability of online learning.

The third section is about students' academic performance. This section is added because the original MSQL questionnaire did not ask about academic performance in which it is necessary for the researcher to do the assessment using their current performance in the course. These following questions were added to the questionnaire regarding students' academic performance:

1) What do you think about your academic performance as a student on this subject?

2) How frequently did you receive high grades (of over 80%) for assignments, quizzes for this subject?

The last section consists of three open-ended questions, which are to identify students' opinion about the factors that affect their academic performance, their suggestions to improve current MOOCs system and the preferable features that they think can persuade students to use MOOCs system. Students had to answer all the questions using a 7-point Likert scale, which 1 indicates "not all true of me" and 7 indicates "very true of me" except for students' academic performance section which 1 indicates "poor" and 7 indicates "excellent" for the first question and for the second question, 1 indicates "never" and 7 indicates "often".

Forty (40) students who enrolled in Ethnic Relations course using the MOOCs system were the participants in this study. Ethnic Relations was chosen because the course is compulsory for every tertiary student in Malaysia. All forty participants are from Universiti Kebangsaan Malaysia and this experiment was not restricted to any years of study. To distribute the questionnaire, the web-based survey approached had been used which is Google Form. The process took about six weeks. The survey link was distributed through social media such as Facebook. To reach the exact group of students, the link had been shared in a specific Facebook group which is related to the course. Facebook was selected because it is a popular choice among the students and lecturers to communicate and sharing things regarding academic matters. Other than that, the link also had been shared using WhatsApp messaging application to increase the potential for reaching the students to answer the questionnaire. This platform was aiming at students who do not have Facebook accounts.

SPSS software was used to analyze the data. Automatic Linear Modelling (ALM) and Multiple Linear Regression (MLR) were the statistical analysis that had been applied to narrowing the students' motivation and learning strategies according to the MSLQ questionnaire. ALM was used to rank the list of variables and their impact factors. We chose academic performance as the dependent variable and all the MSLQ items as independent variables. Top ten variables with the largest impact factors had been considered as significant. To form an equation, the top ten variables selected from ALM had gone through the MLR process. The variables that did not fall below 0.5 significance were excluded. This process stops until significant variables appeared within the Durbin-Watson value range between 1 and 3 [36].

IV. Results and Discussion

In this part, the findings in terms of students' demographic (Section 1), motivation (Section 2), learning strategies (Section 3) and their opinions about the current MOOC system (Section 4) are reported. All of them have experienced using the MOOCs system specifically in the Ethnic Relations course.

As Table II summarizes, this study involved 45% of male and 55% of female students. 20% of them are from Art & Humanities discipline and 80% of them are from the Science & Technology discipline. Most of them were second-year students which consisted of 47.5% of students, 32.5% of them were third-year students and 20% of them were fourth-year students. 72.5% of students involved in this study were taking more than five subjects and 22.5% of them were taking two to five subjects during the current term. Most of them took about one to ten hours a week to study which consisted of 80% of students and only 20% of students took about 10 to 30 hours a week to study for the course.

Table III displays the students' academic performance. Most of them described that their academic performance was at a good level. 75% of students chose 5 to 6 which indicate that they performed well in their academic. 20% of them chose 4 which is neutral and only 5% of them chose 3 and 2 which imply that they have nearly poor academic performance. Almost half of the students which is 67.5% of students that involved in this study stated that they often received high grades for assignment, quizzes for the subject and 27.5% of students chose neutral in response to the statement and only 5% of students chose 3 to 1. From all the data above, most of the students involved in this study are well-performed students which received a grade of above 80% and can be categorized as students that have a real understanding on the subject [37]. This is indicating that good students incline to answer a survey compared to students that have poor academic performance. Since most of the students participated in this study are well-performing students, the data collected are inclined towards only one group of students. But the result is still valid to test whether there is a correlation between students' motivation, learning strategies and their good academic performance.

Table IV shows the reliability results for the model. 88.2% ALM accuracy and the Durbin-Watson values were in an acceptable range of 1 to 3, shows that the model satisfies the reliability criteria. An explanation of the model is presented below.

$$f(x) = (0.554)x1 + (0.364)x2 + (-0.325)x3 + (0.212)x4 + (-0.229)x5 + (0.196)\,x6 + 1.18$$

TABLE. II. Demographic Information

Items	Statements	Response	(n=40) %
1.	Gender	Male	18 (45%)
		Female	22 (55%)
2.	What discipline you are in your study?	Art & Humanities	8 (20%)
		Science & Technology	32 (80%)
3.	What year you are now in tertiary education?	2nd Year	19 (47.5%)
		3rd Year	13 (32.5%)
		4th Year	8 (20%)
4.	How many subjects are you taking this term?	2 subjects	3 (7.5%)
		3 subjects	0
		4 subjects	1 (2.5%)
		5 subjects	5 (12.5%)
		More than 5 subjects	29 (72.5%)
5.	How many hours a week do you study for this course?	1 to 10 hours	32 (80%)
		10 to 20 hours	1 (2.5%)
		20 to 30 hours	7 (17.5%)
		30 hours and above	0

TABLE. III. Students' Academic Performance

Items	Statements	Response	(n=40) %
1.	What do you think about your academic performance as a student for this subject?	1 (Poor)	0
		2	1 (2.5%)
		3	1 (2.5%)
		4	8 (20%)
		5	18 (45%)
		6	8 (20%)
		7 (Excellent)	4 (10%)
2.	How frequently did you receive high grades (of over 80%) for assignments, quizzes for this subject?	1 (Never)	0
		2	1 (2.5%)
		3	1 (2.5%)
		4	11 (27.5%)
		5	15 (37.5%)
		6	8 (20%)
		7 (Often)	4 (10%)

TABLE. IV. Reliability Results

	ALM Accuracy	Durbin-Watson	r2
Overall model	88.2%	1.815	0.882

Where f(x) = How would you describe your academic performance as a student? x1 = I make sure that I keep up with the weekly readings and assignments for this course, x2 = I log in to the system regularly, x3 = I try to think through a topic and decide what I am supposed to learn from it rather than just reading it over when studying for this course, x4 = I rarely find time to review my notes or readings before an exam (reversed), x5 = Whenever I read or hear an assertion or conclusion in this course, I think about possible alternatives, x6 = If I can, I want to get better grades in this course than most of the other students.

Based on Table V, it shows that there are six study behaviours represent students' motivation and learning strategies that affect academic performance. Based on the MSLQ questionnaire, every statement has its scale and subscale that related to students' study behaviours. These study behaviours will be considered as target behaviours as the first step to redesign MOOCs based on persuasive system development.

Study behaviour 1 *(x1)* specifies that students with good academic performances will ensure that they keep up with the weekly readings and assignments for the course they are taken. Good students will prepare themselves before the learning process started. This could be one of the factors that lead to excellent performance in academic. According to the study results, most of them are well-performed students. Hence, we could say that they do not face motivational and ability issues. To encourage this category of students to keep up with the weekly readings, factors such as triggers should be considered. "signal" is the type of trigger that could help students to perform study behaviour 1 (*x1*) by reminding them if a new material uploaded by instructors.

Study behaviour 2 *(x2)* shows that students who login to the system (MOOCs) frequently will have the potential to perform better than other students who seldom log in to the system. Therefore, the appropriate reason to log in the system should be highlighted as a motivation factor. Reasons like getting news about assignments, quizzes or any new materials uploaded by the instructors could encourage students to frequently login to the system as well as improving their academic performance. "Spark" and "signal" also can trigger students to perform the behaviour.

Metacognitive self-regulation is the subscale that we use to represent students that try to think through a topic and decide what they are supposed to learn rather than just reading it over when study for the course just like study behaviour 3 *(x3)*. This kind of study behaviour may also lead to good academic performance. To let them perform this behaviour, the system should suggest related sources and trigger them by giving a signal with an appropriate message. It will save their time and decrease the brain cycle of the students. However, decreasing students' brain cycle would discourage students to think critically. Hence, instructors should plan the tasks by considering the critical thinking aspect of the students.

Students who may not have time to review the notes given by the instructors before an exam will have a difficult time to score in their exams. It shows in study behaviour 4 *(x4)*. To overcome this issue, the system should emphasize the importance of reviewing notes before an exam by considering "hope/fear" element by reminding them to review the notes provided by the instructors. Other than that, the system should provide simplified features to ensure the system is easy to use while saving students' time to access and review notes. In other words, the efficiency of the system should be increased to ensure the students can perform the behaviour.

Critical thinking is another subscale that characterizes students who try to think possible alternatives, whenever they found an assertion or conclusion. Critical thinking is a crucial process, especially for tertiary students. It teaches them to complete problem-solving assessments. Study behaviour 5 *(x5)* belongs to the critical thinking subscale that would encourage students to have a good score in their academic. Because of the critical thinking process requires students to deeply think, it would decrease the students' motivation to perform the behaviour. Hence, to overcome this issue, the system should optimize the elements of simplicity and implementing suitable types of triggers such as "spark" and "facilitator" to let them focus on the task without facing any unnecessary problems.

The last study behaviour that will increase students' academic performance is when they try to compete with their friends to get better grades *(x6).* Social deviance is one of the elements in the Fogg Behaviour Model (FBM) that falls under the "ability" factor. If getting a good grade is a norm for students, it will boost their spirit to give extra effort and perform well in their academic. Therefore, the system should motivate students by giving them hope to perform the behaviour and consistently trigger them with positive messages.

TABLE. V. RELATED MSLQ SCALES AND SUBSCALES

Equation	Study Behavior	Scale	Subscale
x1	I make sure that I keep up with the weekly readings and assignments for this course	Resource Management Strategies (Learning Strategies)	Time and Study Environment
x2	I log in to the system regularly	Resource Management Strategies (Learning Strategies)	Time and Study Environment
x3	I try to think through a topic and decide what I am supposed to learn from it rather than just reading it over when studying for this course	Cognitive and Metacognitive Strategies (Learning Strategies)	Metacognitive Self-Regulation
x4	I rarely find time to review my notes or readings before an exam (reversed)	Resource Management Strategies (Learning Strategies)	Time and Study Environment
x5	Whenever I read or hear an assertion or conclusion in this course, I think about possible alternatives	Cognitive and Metacognitive Strategies (Learning Strategies)	Critical Thinking
x6	If I can, I want to get better grades in this course than most of the other students	Value Component (Motivation)	Extrinsic Goal Orientation

The last section in the questionnaire asks the students about their opinions on the existing MOOC. Time management and motivation are two popular answers given by the students in this study to become the factors that affect their academic performance. These two answers indicate that time and study environment plays an important role in their learning process. When they can manage their time effectively, they tend to be successful in their academic. Furthermore, when they surround themselves with positive people, it will encourage them not to waste their time. There are some suggestions to improve the existing MOOC. As one of the students wrote that "give notification through email if the deadline of a task is near the corner" shows that positive trigger gives an impact to their study behaviour. A statement like "easily access using a smartphone" indicates that there are students who prefer to learn using a mobile application instead of the web system. Other than that, students also want to have extra features like animated user interface and live chat. These features will let them communicate with their instructor and friends easily. They also suggest putting some gamification elements to make the application seems interesting to the students. It will also attract the students to log in to the system frequently. All the above statements are the popular statements given by the students in this section. It signifies that students are interested to learn through MOOC but there are some improvements that still can be made to the existing system to expand students' potential.

V. Conclusion and Implications

The result concludes that there are six study behaviours that significant to be the factors that affect students' academic performance using MOOCs in Ethnic Relations course. All these study behaviours can be used as target behaviours to redesign MOOCs according to the Persuasive System Design (PSD) model. The study also fulfils the first phase of designing a successful persuasive system which is understanding the key issues behind a persuasive system. Five study behaviours represent learning strategies and only one study behaviour represents motivation. Time and study environment is the subscale which affecting students' academic performance the most. It signifies that students must be able to manage and regulate their time and study environments. Scheduling, planning, and managing are time management routines that should be applied by students. Metacognition self-regulation consists of three general processes which are planning, monitoring, and regulating. It assists students to apply their prior knowledge to understand the subject material before the learning process even begins. Students' critical thinking can be tested by letting them apply their previous knowledge to solve a problem. Reasons such as grades, rewards, performance, evaluation by others would be the factors to encourage students to score in their subjects. This subscale refers to the general orientation of the course.

This study has implications for instructors and system developers of MOOCs. Study behaviours that found in this study can give an insight for instructors on how students can improve their academic performance in MOOCs. By understanding the relationships between study behaviours and how it affects students' academic performance, instructors will be able to develop their contents for future MOOCs and influence students to perform better. However, the roles of instructors are limited to only prepare contents and utilize the existing system's features. Instead of instructors, the study results also contribute insight to system developers. By understanding the study behaviours that represent students' motivation and learning strategies which could affect academic performance, system developers can use the resulted study behaviours to redesign the system's features that able to empower students to improve their academic performance and increase the effectiveness of the system.

VI. Limitations and Future Directions

Despite the constructed model that has been produced in this study, there are few limitations of the research identified. The sample size was considered small. Even though it was enough to compute the statistical analysis, the model produced was restricted according to only a group of students. A variety group of students in different subjects should be involved in the future study to get a more holistic model because students' academic performance also relied on the subjects they took in their previous semester. To get an in-depth understanding of the students' motivation and learning strategies, students that received poor academic result also need to be involved. A comparison can be made between these two types of students to identify the factors that are still lacking in the current MOOCs system. This comparison study is indispensable to ensure that every level of students can get benefit from the system. MOOCs is a technology concept that is very useful for tertiary education students. But still, it needs some improvements to increase the persuasiveness of the system. In addition, to improve the system, students also need to change their study behaviour to excel in their academic. Technology is just a tool to ease the learning processes. Instructors and students should try to create teaching and learning outcomes. On the other hand, instructors including lecturers and teachers are the one who must have an in-depth understanding of their content and pedagogical aspects.

References

[1] H. Kimiloglu, M. Ozturan, and B. Kutlu, "Perceptions About and Attitude Toward the Usage of E-Learning in Corporate Training," Comput. Human Behav., vol. 72, pp. 339–349, 2017.

[2] J. A. Rudy, "EDUCAUSE Core Data Service. 2009," Summ. Rep., 2007.

[3] W. M. Al-rahmi, M. S. Othman, and L. Mi Yusuf, "The Effectiveness of Using E-Learning in Malaysian Higher Education: A Case Study Universiti Teknologi Malaysia," Mediterr. J. Soc. Sci., vol. 6, no. 5, pp. 625–637, 2015.

[4] S. Folinsbee, "Online Learning for Adults: Factors That Contribute to Success," 2008.

[5] A. M. Kaplan and M. Haenlein, "Higher education and the digital revolution: About MOOCs, SPOCs, social media, and the Cookie Monster," Bus. Horiz., vol. 59, no. 4, pp. 441–450, 2016.

[6] M. H. Baturay, "An Overview of the World of MOOCs," Procedia - Soc. Behav. Sci., vol. 174, pp. 427–433, 2015.

[7] M. Fadzil, L. Abdol, L. Tengku, and A. Munira, "MOOCs in Malaysia: A Preliminary Case Study," E-ASEM Forum Renewing Lifelong Learn. Agenda Futur., pp. 1–17, 2016.

[8] Prime Minister's Department, "Transforming Education System," 2016.

[9] X. Wang, A. H. Hall, and Q. Wang, "Investigating the implementation of accredited massive online open courses (MOOCs) in higher education: The boon and the bane," Australas. J. Educ. Technol., vol. 35, no. September 2013, pp. 1–14, 2018.

[10] R. Azevedo, "Using Hypermedia as a Metacognitive Tool for Enhancing Student Learning? The Role of Self- Regulated Learning," Educ. Psychol., no. October 2014, pp. 199–209, 2005.

[11] J. Filippou, C. Cheong, and F. Cheong, "Modelling the Impact of Study Behaviours on Academic Performance to Inform the Design of a Persuasive System," Inf. Manag., vol. 53, no. 7, pp. 892–903, 2016.

[12] B. J. Fogg, Persuasive Technology: Using Computers to Change What We Think and Do. 2003.

[13] W. N. W. Ahmad and N. M. Ali, "A Study on Persuasive Technologies: The Relationship between User Emotions, Trust and Persuasion," Int. J. Interact. Multimed. Artif. Intell., vol. inPress, no. inPress, p. 1, 2018.

[14] H. Oinas-kukkonen and M. Harjumaa, "Persuasive Systems Design : Key Issues , Process Model , and System Features," Commun. Assoc. Inf. Syst., vol. 24, no. 28, pp. 485–500, 2009.

[15] P. De Barba, J. Lodge, G. Kennedy, L. Corrin, and A. Brooker, "A tale of two MOOCs: How student motivation and participation predict learning outcomes in different MOOCs," Australas. J. Educ. Technol., vol. 34, no. 1, pp. 73–87, 2017.

[16] J. Bloem, M. Van Doorn, S. Duivestein, D. Excoffier, R. Maas, and E. Van Ommeren, "The Fourth Industrial Revolution Things to Tighten the Link Between it and ot," 2014.

[17] N. W. Gleason, Higher Education in the Era of the Fourth Industrial Revolution. 2018.

[18] M. Sohn and J. Lee, "UP health: Ubiquitously Persuasive Health Promotion with an Instant Messaging System," 25th SIGCHI Conf. Hum. Factors Comput. Syst. 2007, CHI 2007, pp. 2663–2668, 2007.

[19] S. S. Noesgaard, R. Ørngreen, S. Schack, and K. Foundation, "The Effectiveness of E-Learning: An Explorative and Integrative Review of the Definitions, Methodologies and Factors that Promote e-Learning Effectiveness," Electron. J. e-Learning, vol. 13, no. 4, pp. 278–290, 2015.

[20] L. W. Perna et al., "Moving Through MOOCs: Understanding the Progression of Users in Massive Open Online Courses," Educ. Res., vol. 43, no. 9, pp. 421–432, 2014.

[21] B. K. Pursel, L. Zhang, K. W. Jablokow, G. W. Choi, and D. Velegol, "Understanding MOOC students: Motivations and behaviours indicative of MOOC completion," J. Comput. Assist. Learn., vol. 32, no. 3, pp. 202–217, 2016.

[22] J. Wulf, I. Blohm, and W. Brenner, "Massive open online courses: Higher Education's Digital Moment?," Bus. Inf. Syst. Eng., vol. 6, no. 2, pp. 111–114, 2014.

[23] Ministry of Education Malaysia (MoE), "Malaysia Education Blueprint 2015-2025 (Higher Education)," Minist. Educ. Malaysia, vol. 2025, p. 40, 2015.

[24] S. Schack and K. Foundation, "The Effectiveness of E-Learning : An Explorative and Integrative Review of the Definitions , Methodologies and Factors that Promote e-Learning Effectiveness," Electron. J. e-Learning, vol. 13, no. 4, pp. 278–290, 2015.

[25] P. R. Pintrich and B. Schrauben, "Students' motivational beliefs and their cognitive engagement in classroom academic tasks," in Student perceptions in the classroom, 1992, pp. 149–183.

[26] P. R. Pintrich, "The dynamic interplay of student motivation and cognition in the college classroom.," in Advances in motivation and achievement: Vol. 6. Motivation enhancing environments, 1989, pp. 117–160.

[27] H. Oinas-kukkonen and M. Harjumaa, "Communications of the Association for Information Systems Persuasive Systems Design : Key Issues , Process Model , and System Features Persuasive Systems Design : Key Issues , Process Model , and System Features," Commun. Assoc. Inf. Syst., vol. 24, no. 28, pp. 485–500, 2009.

[28] B. J. Fogg, "Persuasive computers: perspectives and research directions," in Analysis, 1998.

[29] J. Filippou, C. Cheong, and F. Cheong, "Combining the Fogg Behavioural Model and Hook Model To Design Features in a Persuasive App To Improve Study Habits," Australas. Conf. Inf. Syst., 2015.

[30] H. Oinas-Kukkonen and M. Harjumaa, "A Systematic Framework for Designing and Evaluating Persuasive Systems," Persuas. Technol. Third Int. Conf. Persuas. 2008, Oulu, Finland, June 4-6, 2008. Proc., pp. 164–176, 2008.

[31] B. Dohnke, E. Weiss-Gerlach, and C. D. Spies, "Social influences on the motivation to quit smoking: Main and moderating effects of social norms," Addict. Behav., 2011.

[32] B. Fogg, "A Behavior Model for Persuasive Design," 2009.

[33] P. R. Pintrich, D. A. F. Smith, T. Garcia, and W. J. McKeachie, "A Manual for the Use of the Motivated Strategies for Learning Questionnare," no. August, pp. 4–75, 1991.

[34] E. D. Fitkov-Norris and A. Yeghiazarian, "Measuring study habits in higher education: The way forward?," J. Phys. Conf. Ser., vol. 459, no. 1, 2013.

[35] T. G. Duncan and W. J. Mckeachie, "The Making of the Motivated Strategies for Learning Questionnaire," Educ. Psychol., vol. 40, no. 2, pp. 117–128, 2005.

[36] A. Field, J. Miles, and Z. Field, Discovering Statistics Using SPSS, vol. 81, no. 1. 2013.

[37] J. H. Block and R. B. Burns, "1: Mastery Learning," Rev. Res. Educ., vol. 4, no. 1, pp. 3–49, 1976.

Integrated Methodological Framework for Digital Transformation Strategy Building (IMFDS)

Zineb Korachi[1], Bouchaib Bounabat[2]
ALQUALSADI Team, ADMIR Laboratory
ENSIAS/Mohamed V University in Rabat, Rabat, Morocco

***Abstract*—There is still a conflict among the definitions, frameworks, and formulation of the digital transformation strategy in the literature. Despite extensive research on Digital Transformation Strategies and Digital Transformation Assessment, there is not a clear and global meta-model describing the general concepts and guidelines of the digital transformation to frame and drive a successful digital transformation. Several digital transformation approaches have been presented in the literature, these approaches are focusing on specific cases and specific concepts. The present paper describes the digital transformation and its relationship with IT governance. It presents how IT governance can lead the digital transformation. A literature review has been conducted on the most well-known IT Frameworks (COBIT, ITIL, CMMI) and their structure in order to provide a standard and known framework by practitioners. This paper proposes an Integrated Methodological Framework for Digital Transformation Strategy Building. The proposed framework is called IMFDS, it is based on IT governance elements (Business Strategic Planning, IT Strategic Planning, IT Organizational Structure, IT Reporting, IT Budgeting, IT Investment Decisions, Steering committee, IT Prioritization Process and IT Reaction Capacity). It provides specific guidelines to help organizations formulating, implementing and monitoring their transformation strategies. IMFDS is articulated across 9 blocks (steps) and 34 processes.**

Keywords—Digital transformation strategy; digital transformation assessment; IT governance; IT framework

I. Introduction

Digital transformation has become a high priority on leadership agendas, with nearly 90% of business leaders in the U.S and U.K expecting digital technologies to make an increasing strategic contribution to their business in the coming decade [1]. As a result, organizations need to quickly adapt to the digital era in order to gain competitive advantages and offer added-value to their customers, based on a digital transformation strategy [2]. Recent research has contributed to increase our understanding of specific aspects of the digital transformation phenomenon [3]. Researchers highlight the importance of formulating and evaluating a digital transformation strategy, although this field has not been fully investigated [2]. Digital transformation strategy is still an ongoing area of research, which leads to immature literature and inadequate understanding.

However, despite the multiplicity of new technologies and recipes for their implementation, whether in business, public governance and private life, real digital transformation is taking much longer and facing more difficulties than it has been expected [4]. Organizations want to make a digital transformation of their businesses to take advantage of the digital revolution, but most of them do not know from where to start, what standards to adopt, what are the costs, what are the benefits, what are the challenges, what are the opportunities, what are the strategies to follow, what are the right metrics to use, what are the technologies suitable for their business or activity, what is the percentage of success of this digital transformation, there are hundreds of questions that go through the head of organizations' leaders. To answer all these questions and meet the digital transformation challenges organizations need specific guidelines for building their digital transformation strategy. The most cited articles focus on the understanding of specific aspects of the digital transformation phenomenon. Therefore, they do not provide specific guidelines for organizations to formulate, implement, and evaluate digital transformation strategies. While the building blocks of a digital strategy are known, clearly specified guidelines for managers on how to approach digital transformation and implement a well-defined digital transformation strategy are lacking [1].

Digital transformation needs mature and superb IT governance which helps conduct business processes [5]. Companies with matured IT governance are more likely to engage in digital initiatives and have a better starting point for digital transformation [5]. Some works have presented how IT Governance Objectives can drive digital transformation [6]. Several digital transformation strategies have been presented in the literature, each of these strategies is focused on specific cases and specific concepts. The contribution of this paper is to describe: What are the relationship between IT governance and digital transformation? And How IT governance can drive digital transformation? This work presents an Integrated Methodological Framework for building Digital Transformation Strategies. The proposed framework is constructed based on IT governance components. It is a cyber-strategy framework that consists of two integrated systems. The first system is articulated across nine building blocks and it provides organizations specific guidelines for building their digital transformation strategy. The second one provides an evaluation system (KPIs, dashboard, and maturity model) to evaluate the results and progress of the digital transformation and to continually improve the digital transformation strategy.

The paper is structured as follows: the next section explores related works, followed by a section describing the proposed solution (IMFDS framework), followed by discussion, conclusion, and suggestions for future research.

II. Literature Review

A. Digital Transformation Strategy

A digital transformation is the use of technology to radically improve performance or reach of organizations [7,8]. The digital transformation is an important cornerstone for helping organizations improve their business processes in order to create business values and competitiveness. This transformation will be effective if it is established within the framework of a digital strategy [9].

Several works have studied the digital transformation concepts and concerns, they have studied: digital strategy definitions, characteristics of failed and successful digital strategies [10], standard for IT governance [11], standard for IT service management [12], maturity models [13], The stages of the digital transformation [14], the challenges of digital transformation [14], areas of focus for the digital transformation[14], Steering committee [14,9], IT Opportunities [14], digital transformation priorities [14], digital strategy in a specific domain [15], digital strategy assessment [16], and digital strategies for building smart cities [16, 17]. Despite the prior research, specific guidelines for organizations on how to build and evaluate digital transformation strategies are still not clear, and both academics and practitioners need to further investigate this field [2].

Researchers tried to find out a process that supports business goals and business strategy, through the development of Information Systems [18]. An in-depth study of literature about digital transformation strategy has been conducted, the most cited articles focus on understanding the digital transformation definitions, concepts, dimensions, phases, and components. Therefore, they do not propose an integrative framework that provides clear guidelines for building and monitoring digital transformation strategies.

B. Digital Transformation Assessment

The transformation strategy should be revisited and evaluated on a regular basis and make sure that the action plan for implementing the strategy is on the right track [17]. To stay competitive as an organization, there is a need for having a continual process of improvement that scrutinizes the company's positioning in terms of its IT capabilities and the quality of its properties and services [19]. For digital transformation assessment and monitoring, there are several evaluation systems and maturity models in the literature, and each of them deals with a specific problem. For example; The World Health Organization and International Telecommunication Union suggested the use of KPIs (Key Performance Indicators) and Dashboards for evaluating the progress of the eHealth strategy [15].

Appropriate Key Performance Indicators are required in order to assess the contribution that the digital transformation is making toward the organization, but for efficient use and analysis of these metrics, organizations need to exploit them within an evaluation system that provides the ability to analyze and generate information from these metrics. For example; MMDSA (Maturity Model for Digital Strategy Assessment) is a maturity model using KPIs to monitor the progress of the digital strategy [9]. In the literature, there are also some evaluation systems for evaluating the digital transformation of a city [20,16]. For example, there is a smart city evaluation system that is articulated across 4 components: Key Performance Indicators, Ranking System, Control system, and Dashboard [16]. The same components can be used to develop a system for assessing the digital transformation strategy.

C. IT Governance, IT frameworks, and Digital Transformation

IT governance is an integral part of corporate governance exercised by the board and addresses the definition and implementation of processes, structures and relational mechanisms in the organization that enable both business and IT people to execute their responsibilities in support of business/IT alignment and the creation of business value from IT-enabled business investments [6]. Many sources identify five areas or domains of attention in the context of IT governance that need to be addressed [6, 21]: Strategic alignment, Value delivery, Risk management, Resource management, and Performance measurement. These five areas are the concerns of the digital transformation. For this reason, the adoption of IT governance can drive digital transformation and resolve their concerns.

Strategy and strategic plan should be conceptual, visionary and directional, and should be different from the operational plan [22]. A literature review has been conducted on IT governance, IT management, and IT frameworks in order to take advantage of their structure, components, and limitations to propose a clear and simple integrated methodological framework for digital transformation strategy building.

On the market, there are several tools and frameworks for IT management and governance in fashion such as COBIT (Control Objectives for Business & Related Technology), ITIL (Information Technology Infrastructure Library), CMMI (Capability Maturity Model Integration), EFQM (European Foundation for Quality Management), BSC (Balanced Scorecard), Ect. Using these frameworks independently prevents organizations from achieving the full benefits of IT Governance because every practice has its limitations on its application to specific IT areas and all these practices overlap [23, 24]. For example, the important thing about ITSM and therefore ITIL or COBIT is to improve the quality of IT services [11]. To see if it is achieved, the quality should be measured. But neither COBIT nor ITIL measures the quality, so it is necessary to use other methodologies [11]. EFQM is proposed for this purpose because it is the best methodology to measure the quality [25]. ITIL provides the how for service management aspects, COBIT helps to define what should be done and EFQM defines and measures the how of quality improvement [11]. Together, they can make a great combination for improving the quality of IT services [11].

TABLE. I. THE NINE ELEMENTS OF IT GOVERNANCE [21]

IT Governance Practice	Supporting Literature
Business Strategic Planning: capturing and synthesizing how the organization can reach its vision.	[30]
IT Strategic Planning: conceptualizing and assimilating how the organization can meet its vision by leveraging IT.	[31, 32, 33, 34]
IT Organizational Structure: the way the IT function is structured (e.g., centralized, decentralized, federated) and where the IT decision-making authority is located within the organization.	[35, 36]
IT Reporting: who manages the senior IT executive and IT function; and how.	[37, 38]
IT Budgeting: financial control (processes for allocating financial resources; is IT managed as a cost center, investment center, profit center, etc.)	[39, 40]
IT Investment Decisions: how IT asset spending is allocated and reviewed (e.g., cost-based, creating business value, etc.), and by whom.	[41, 42]
IT Steering Committee(s): strategic, tactical, and operational teams commissioned to allocate and oversee IT initiatives, priorities, spending, and resource allocation.	[43, 44, 45]
IT project prioritization process: how IT projects are selected, and by whom.	[46, 47]
IT Reaction Capability: IT's ability to quickly respond to the organization's changing business needs/demands	[48, 49]

Based on previous studies, none of these frameworks can provide an integrated work, and they cited that to cover and treat all IT organizations' concerns, it is necessary to choose a good combination of these frameworks. To adopt IT Governance, organizations are being forced to adopt and integrate multiple IT standards and frameworks to comply with the increasing demands of the industry coupled with compliance requirements [26] but struggle with the complexity and difficulty of understanding and adopting several practices at the same time [27]. The integration of IT standards and best practices has many benefits. The primary one is the enabling of features that would be unavailable through the use of practices individually, leading to a more comprehensive and efficient approach [28, 29]. Hence the need for an integrated solution to consolidate the best combination of IT standards and their best practices. In order to create a digital strategy approach that is based on IT governance and take advantage of its components, IMFDS framework will be articulated across IT Governance components (Table I) [21]: Business Strategic Planning, IT Strategic Planning, IT Organizational Structure, IT Reporting, IT Budgeting, IT Investment Decisions, Steering committee, IT Prioritization Process and IT Reaction Capacity.

D. IT Frameworks Structure

A literature review has been conducted on the most well-known IT Frameworks in the literature (COBIT, ITIL, BSC, CMMI, and EFQM) and their structure in order to provide a standard and known framework by practitioners. Meta-Models of these frameworks have been studied in order to define the structure and the most common elements between them. Meta-models allow the analysis and presentation of existing concepts of a model and how these concepts relate to each other, giving an idea of how the model works [50]. Meta-models allow reducing the perceived complexity of IT frameworks by representing their concepts and relationships with graphical concepts. Meta-models facilitate the learning of IT standards (reduce the perceived complexity), as well as understand their main components and their relationships. Several works have studied and developed meta-models of the well-known IT frameworks and have proposed some integration between these models: ITIL Meta-Model [23], COBIT Meta-Model [51, 52], ITIL and COBIT Meta-Models integration [23], CMMI Meta-model [50], ISO 27001 Metamodels [53].

Based on this review, it has been deduced that the common structural elements between these frameworks are that they give a toolbox to solve a specific problem or several problems in the information system of the organization. This toolbox contains processes, best practices, criteria, goals, activities, and metrics. To maintain the same structure that is standard and known by practitioners, the IMFDS framework is also designed as a toolbox that contains processes, goals, good practices, and metrics to guarantee a successful digital transformation.

III. PROPOSED SOLUTION: IMFDS FRAMEWORK DESCRIPTION

This section describes the components and structure of the suggested methodological framework IMFDS.

IMFDS framework provides an approach to guide the implementation of an efficient digital transformation in different organizations. It is composed of two systems as illustrated in Fig. 1. The first system is dedicated to define the strategic plan for the digital transformation while the second one is dedicated on the one hand to assessing and monitoring the progress of the implementation of the digital strategy, and on the other hand to continually improve the digital strategy and its components. The following figure (Fig. 1) provides an overview of the systems and the key components involved by the proposed framework in the process of establishing a digital strategic planning.

A. IMFDS Components

The following figure (Fig. 2) shows the complete set of processes within the IMFDS framework (34 processes).

1) Digital strategy building system: The Digital Strategy Building System of the IMFDS framework is articulated across the following blocks: Business Strategic Planning, IT Strategic Planning, IT Organizational Structure, IT Reporting, IT Budgeting, IT Investment Decisions, Steering committee, IT Prioritization Process and IT Reaction Capacity. To build a digital transformation strategy, organizations should follow these guidelines:

Step 1 - Build the Business Strategic Planning

The business strategic planning is composed of a strategic vision and an action plan to reach this vision.

- Strategic Vision: The first challenge of a digital transformation is to develop the strategic vision in which you determine why the organization needs a digital transformation, what are strategic goals, changes, and desired outcomes of this transformation, and what are resources required to perform the digital transformation.
- Action Plan: An action plan is a set of planned projects, programs, activities, and resources to reach the strategic vision.

Step 2 - Define the IT Organizational Structure

To define the IT organizational structure organizations should determine how people work together in the IT department to create value and benefits. The IT organizational structure should facilitate company growth, increases profits, and optimizes internal operations. To build such a good IT Organizational structure, organizations determine the following elements:

- Required skills in the IT department for digital transformation [54].
- Critical problems that should be solved by the IT department.
- The conception of an optimal combination of Internal IT Department Vs Outsourced IT staff who will contribute to the digital transformation.
- Flexible IT Department Structure that can be Adapted easily.

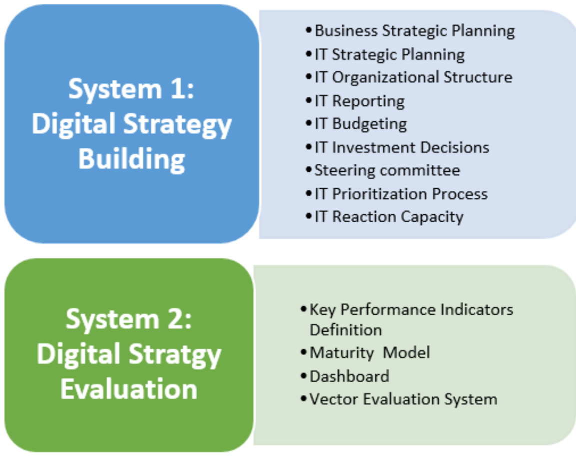

Fig. 1. IMFDS Components.

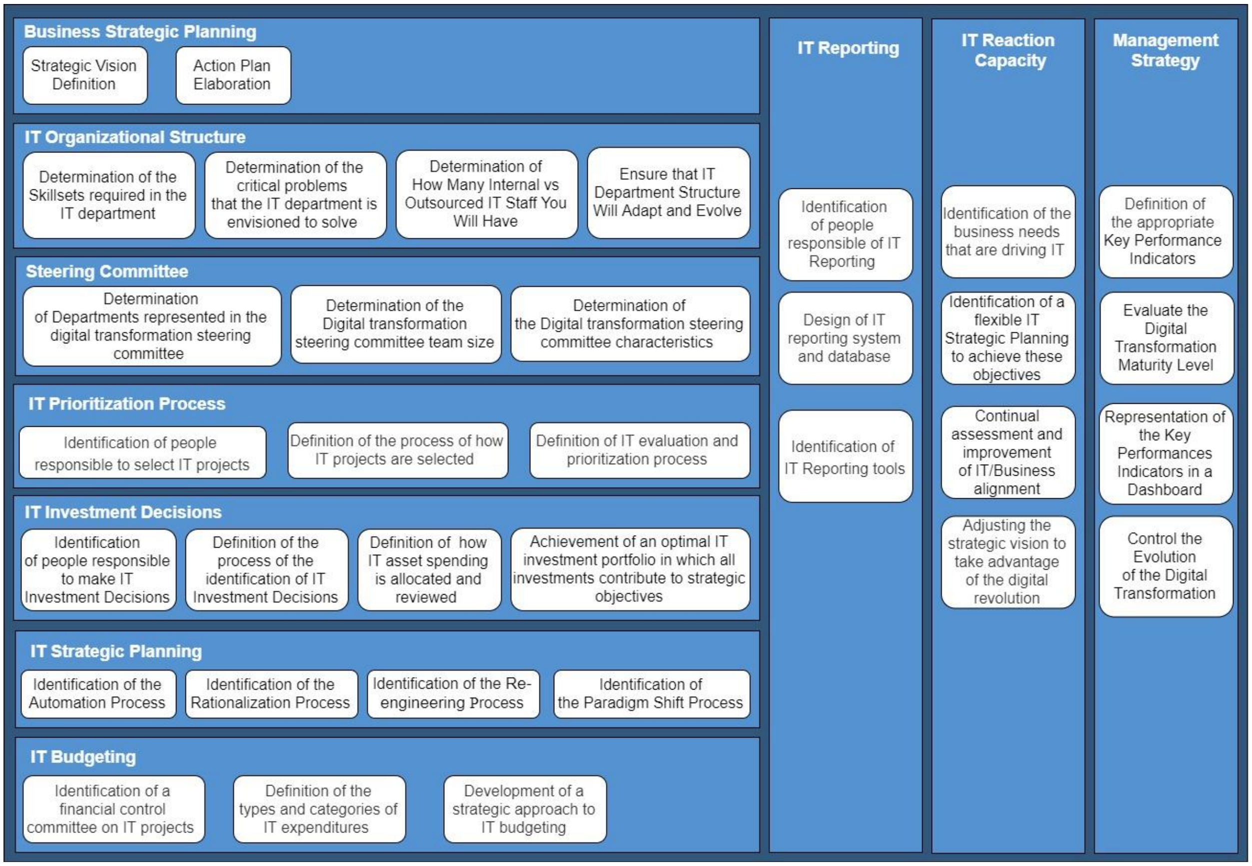

Fig. 2. IMFDS Processes (34 Processes).

Step 3 - Build the Steering committee

A steering committee is composed of strategic, tactical, and operational teams commissioned to allocate and oversee IT initiatives, priorities, spending, and resource allocation [21]. Steering committees include cross-functional and interdepartmental members and are essential to driving meaningful change across the enterprise [14]. In order to build the steering committee company executives should determine:

- Departments represented in the digital transformation steering committee (ex: IT, customer service, marketing, innovation, e-commerce, human resources, employee engagement, R&D, product groups).
- Digital transformation steering committee team size.
- Digital transformation steering committee characteristics (Formal or Informal Committee)

Step 4 - Define the IT Prioritization Process

It is a process of management of the portfolio of IT projects. This process defines how IT projects are selected and identify people responsible to select IT projects. The process defines also the priorities of IT projects [9]. For evaluating and prioritizing projects, organizations should:

- Identify people responsible to select IT projects.
- Identify the process of how IT projects are selected (Identify project drivers).
- Identify the process of how IT projects are evaluated and prioritized. Once you have gathered the list of IT projects, AHP (Analytic Hierarchy Process) [55] Model can be adopted in order to priorities IT projects based on the creation of an evaluation and prioritization matrix.

Step 5 - Define How IT Investment Decisions are made and How made them.

Define How IT asset spending is allocated and reviewed (e.g., cost-based, creating business value, etc.), and identify people responsible to do this study [21]. A decision is made in a process that follows two stages, the first of which is the formulation of the decision, in which the decision is prepared and ends with the specific commitment to action; in the second stage, the decision is implemented [56]. Compared with other types of decisions, IT investment decisions have some specific Characteristics [56]:

- IT investments require funds or budgets.
- IT investment decisions cannot be taken in isolation.
- Achievement of an optimal IT investment portfolio in which all investments contribute to strategic objectives.
- IT investment decisions should follow the two stages of decision-making: the formulation and the implementation stage.

Step 6 - Build IT Strategic Planning

IT strategic planning and business strategic planning complement each other to achieve the strategic vision. The IT Strategic Planning should define how new technologies can achieve the organization's vision, improve its business process, impel the competitiveness and improve its smartness [9]. It should highlight the four types of organizational change enabled by IT namely, automation, rationalization, reengineering and paradigm shift [9]:

- Automation: refers to the application of IT to assist employees in performing their jobs more efficiently and to speed up the performance of existing tasks.
- Rationalization of procedures: streamlining of standard operating procedures, eliminating bottlenecks so that automation makes the procedures more efficient.
- Reengineering: refers to the radical redesign of business processes with the goal of reducing significantly the costs of business and take advantage of IT.
- Paradigm shift: a more radical form of reengineering, involves the radical reconceptualization of the nature of the business and the nature of the organization.

Step 7 - Define How IT Budgeting is Managed

Organizations struggle with IT budgeting. To manage IT projects funding it is necessary to:

- Identify a financial control committee on IT projects [9].
- Define the types and categories of IT expenditure.
- Develop a strategic approach to IT budgeting [57].

Step 8 - Define the IT Reporting System

The reporting function is more than preparing an annual report, quoting statistics, and informing your staff of current developments [58]. The reporting function compares how you are doing with what you set out to do. IT Reporting allows Identifying who manages the senior IT executive and IT function; and how [21]. IT reporting should focus on the things that quantify the value that IT delivers to the organization. It should illustrate the percentage of successful change implementations that have been triggered using IT. To perform a good IT Reporting, organizations should:

- Identify people responsible for managing and monitoring IT function, IT objectives and IT results.
- Identify the conception of characteristics, data, and measures that should be included in IT Reports.
- Identify IT reporting tools that will be used by the organization.

Step 9 - Define the IT Reaction Capacity Process

Organizations should study, measure and evaluate the ability of IT to be aligned easily to any change in the business process of the organization and to respond quickly to new demands [9]. IT managers deal with external environmental changes, changing internal customer needs, and rapid technology changes [49]. Studies suggest that to manage change and prepare for uncertainty, IT leaders should create an organization that is more flexible [49]. The alignment between Business and IT requires the definition of a process. This process should be based on anticipation, agility, and adaptability [49]. The main steps that must be included in this process are:

- Identification of the strategic objectives that are driving the digital transformation (Strategic Vision).
- Identification of a flexible IT Strategic Planning to achieve these objectives.
- Continual assessment and improvement of IT/Business alignment.
- Adjusting the strategic vision to take advantage of the digital revolution.

2) Digital strategy evaluation system: The Digital Strategy Evaluation System of the proposed framework is a system designed to help the organization establishing a Management Strategy to manage the digital transformation strategy. A strategy is a continual process that needs management and monitoring. To monitor the digital transformation strategy, organizations need a management strategy. KPIs are useful tools for efficiently monitoring the digital transformation strategy. In this regard, an appropriate set of relevant indicators must be established and properly evaluated [16]. A management strategy should define a list of indicators that include the perspective of stakeholders and allow to monitor the digital strategy progress, assess the digital strategy results, make appropriate decisions [16]. The Digital Strategy Evaluation System of the proposed framework helps the organization to:

- Define Key Performance Indicators: by implementing the Goal Question Metric Method. Goal Question Metric (GQM) is a suitable approach to define relevant KPIs [16]. It is a well-known paradigm proposed by Basili for defining the software measurements [59]. The GQM approach identifies three steps, it provides a method for defining Goals, refining them into Questions and then defining the Metrics to collect data. This approach has been applied successfully in several contexts [16] and it will be successful also in the context of this work. GQM defines a top-down approach based on three levels: a conceptual level (Goal); an operational level (Question); and a quantitative level (Metric). This method will help to exploit KPIs for assessing strategic goals.
- Evaluate the Digital Transformation Maturity Level: IMFDS framework integrates MMDSA (The Maturity Model for Digital Strategy Assessment) Model. MMDSA is a maturity model for monitoring the digital strategy progress, evaluating the alignment between the business strategy and the digital strategy, and assessing the benefits of IT projects [9].
- Represent the Key Performances Indicators in a Dashboard: dashboards allow quick access to key performance indicators via data visualizations and simple metrics.
- Control the Evolution of the Digital Transformation: to evaluate the progress of the digital strategy and control the achievement of the strategic goals, Key Performance Indicators will be used. These KPIs will allow assessing and monitoring the achievement of the associated strategic goal using Control Theory in order to control the variation and development of KPIs measurements at any moment of time [16]. The control theory studies the possibility of acting on a dynamical system dependent on the temporal variable in order to lead the state of this system to a given state at a given instant. The dynamical system in this work is RSgObj vector, it is the ranking vector of KPIs, it provides a clear idea of the reality of achievement of the strategic goals at a given moment in time.

$$\begin{pmatrix} R_{SgObj1}(t_0) \\ R_{SgObj2}(t_0) \\ \vdots \\ R_{SgObjn}(t_0) \end{pmatrix} \Rightarrow \begin{pmatrix} R_{SgObj1}(t) \\ R_{SgObj2}(t) \\ \vdots \\ R_{SgObjn}(t) \end{pmatrix} \Rightarrow \begin{pmatrix} R_{SgObj1}(t_1) \\ R_{SgObj2}(t_1) \\ \vdots \\ R_{SgObjn}(t_1) \end{pmatrix} \qquad (1)$$

AsIs **ToBe**

$\mathbf{R_{SgObji} = \sum_{j=1}^{m}(Vj * Wj)}$: *Rank of KPIs associated to the strategic goal i.*

n*: Number of strategic goals.*

m*: Number of KPIs associated to the strategic goal i.*

t0*: The initial moment.*

t1*: Moment of reaching objective values of KPIs.*

B. IMFDS Structure

IMFDS framework is designed as a toolbox that contains processes, goals, good practices, and metrics (Fig. 3). The following figure (Fig. 3) illustrates the meta-model of IMFDS framework (this meta-model is designed using ArchiMate [60]). The core elements of this framework are processes. A process can be seen as the glue that connects people, tools and equipment, and procedures and methods in a consistent way through a set of interrelated activities that, together, interact to achieve objectives. An objective is controlled by metrics.

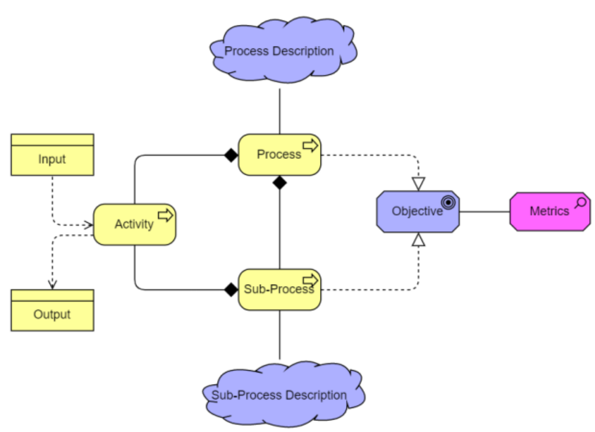

Fig. 3. IMFDS META-Model.

TABLE. II. IMFDS AND ARCHIMATE ONTOLOGICAL MAPPING

IMFDS Concept	IMFDS Concept Description	Archi-Mate Notation	ArchiMate Concept Description [61]	Archi-Mate Representation
Process	Set of interrelated activities and sub-processes which generate an objective	Business Process	Behavior element that groups behavior based on an ordering of activities	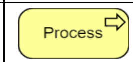
Sub-Process	Set of interrelated activities and sub-processes which achieve a goal	Business Process	Behavior element that groups behavior based on an ordering of activities	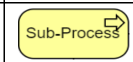
Objective	An objective is the output of a process or a sub-process	Goal	An end state that a stakeholder intends to achieve.	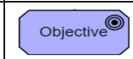
Metrics	Metrics are used to control the achievement of objectives	Assessment	The outcome of some analysis of some drivers.	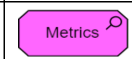
Composition	Composition	Composition	Composition	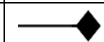
Realization	Realization	Realization	Realization	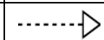
Description	Process description	Meaning	The knowledge or expertise present in a business object or its representation, given a context.	
Activity	A set of actions designed to consumes inputs and generates outputs within a period time	Business Process	Behavior element that groups behavior based on an ordering of activities	
Input	An activity consumes inputs	Business Object	A passive element that has relevance from a business perspective.	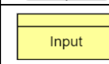
Output	An activity consumes outputs	Business Object	A passive element that has relevance from a business perspective.	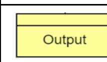
Consume /Generate	Representation of consummation and generation relations	Influence	Influence	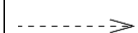

Table II illustrates the description of IMFDS META-MODEL components and their mapping with ArchiMate ontological.

IV. DISCUSSION

Several works have studied the concepts, concerns, and strategies of the digital transformation. However, specific guidelines for organizations on how to build and monitor digital transformation strategies are still not clear. The purpose of the paper is to propose a framework of digital transformation strategy building using IT governance components as constructed blocks of the proposed framework. The suggested framework provides specific guidelines on how to build and monitor a digital transformation strategy. To build an integrative and user-friendly framework, a literature review has been conducted about IT governance and about the structures, components, and limitations of the well-known IT frameworks (COBIT5, ITIL4, CMMI-DEV, BSC, and EFQM). Based on this review, the structure and the core components of IMFDS framework have been defined as follows: Processes, Activities, Input/Output, Goals, and Key Performance indicators. IMFDS framework is based on IT governance elements, and its processes will take advantage of the processes, and limitations of the following frameworks: COBIT5, ITIL4, CMMI-DEV, BSC, and EFQM.

V. CONCLUSION

This research was developed with the purpose of taking advantage of IT governance components for developing a digital transformation framework to help originations building and monitoring the digital transformation strategy. The proposed framework is composed of two systems. The first one is a Digital Strategy Building System; it provides nine steps for building the digital transformation strategy. The second one is a Digital Strategy Evaluation System, it allows defining key performance indicators, evaluating the digital transformation maturity level, representing the key performance indicators in a dashboard, and controlling the evolution of the digital transformation. This paper presents the different blocks and processes of IMFDS framework. The following promising future directions of the current work can be considered in future research:

- IMFDS framework is based on IT governance only and this can be a limitation. Future research should also consider additional digital strategy concepts and dimensions as the basis of digital transformation strategies.
- Analysis of the individual IT Governance elements impact on the digital strategy.
- Design and definition of the processes, objectives, metrics, and activities of IMFDS framework (analysis and comparison of the proposed approach with some well-known frameworks like COBIT, ITIL, CMMI-DEV, BSC, and EFQM to take advantage of their best practices).

REFERENCES

[1] Hess, T., Matt, C., Benlian, A., Wiesböck, F. (2016). Options for Formulating a Digital Transformation Strategy. June 2016 (15:2)| MIS Quarterly Executive.

[2] Mitroulis D., Kitsios F. (2019). Digital Transformation Strategy: A Literature Review. Department of Applied Informatics University of Macedonia Thessaloniki, Greece *tm1133@uom.edu.gr. 6Φοιτητικό Συνέδριο ΕΕΕΕ / 28.2-3.3, 2019 / Ξάνθη. ISBN: 978-618-80361-9-2.

[3] Vial, G., (2019). Understanding digital transformation: A review and a research agenda. Journal of Strategic Information Systems, https://doi.org/10.1016/j.jsis.2019.01.003.

[4] Zinder, E., Yunatova, I. (2016). Synergy for digital transformation: person's multiple roles and subject domains integration. In: Digital Transformation and Global Society, pp. 155–168 (2016).

[5] Mario Spremic. (2017). Governing digital technology – how mature IT governance can help in digital transformation? International Journal of Economics and Management Systems. http://www.iaras.org/iaras/journals/ijems. Volume 2, 2017. ISSN: 2367-8925.

[6] De Haes, S., Caluwe, L., Huygh, T., & Joshi, A. (2020). Governing Digital Transformation. Management for Professionals. doi:10.1007/978-3-030-30267-2.

[7] Westerman, G., Bonnet, D., McAfee, A., (2014). The nine elements of digital transformation. 7,from https://sloanreview.mit.edu/article/the-nine-elements-of-digitaltransformation/.

[8] Westerman,G., Calméjane, C., Bonnet, D., Ferraris, P., McAfee, A. (2011). Digital transformation: a roadmap for billion-dollar organizations. In: MIT Center for Digital Business and Capgemini Consulting, pp. 1–68.

[9] Korachi, Z. and Bounabat, B. (2019a). Towards a Maturity Model for Digital Strategy Assessment. Second Edition of the International Conference On Advanced Intelligent Systems for Sustainable Development Applied To Agriculture, Energy, Health, Environment Industry and Economy. VOLUME 4 (ISBN 978-3-030-3667-35): Advanced Intelligent Systems for applied Computing Sciences. AI2SD, 08-11 July 2019, Marrakech, Morocco.

[10] Christine, M., and Megan, H. (2018). Digital Strategy Environmental Scan for the Concordia University Digital Strategy Committee. Athenaeum21 Consulting for Concordia University, © June 2018. https://www.concordia.ca/content/dam/concordia/docs/strategic-directions/Concordia-University-Digital-Strategy-Environmental-Scan.pdf.

[11] Peña, S., José, J., Vicente, F., E., Ocaña, M., A. (2013). ITIL, COBIT and EFQM: Can They Work Together? International Journal of Combinatorial Optimization Problems and Informatics. IJCOPI Vol. 4, No. 1, Jan-April 2013, pp. 54-64. EDITADA. ISSN: 2007-1558.

[12] Long, J. O. (2012). ITIL® 2011 At a Glance. SpringerBriefs in Computer Science. doi:10.1007/978-1-4614-3897-7.

[13] Ayyagari, M. and Atoum I. (2019). CMMI-DEV Implementation Simplified. International Journal of Advanced Computer Science and Applications. 2019;10(4). doi:10.14569/ijacsa.2019.0100455.

[14] Solis, B. (2019). The state of digital transformation. 2018-2019 edition. by brian solis, principal analyst. Altimeter Report.

[15] World Health Organization and International Telecommunication Union. (2012). National eHealth Strategy Toolkit.

[16] Korachi, Z. and Bounabat, B. (2019b). Integrated Methodological Framework for Smart City Development. ISBN: 978-989-8533-90-6 © 2019. International Conferences ICT, Society, and Human Beings 2019; Connected Smart Cities 2019; and Web Based Communities and Social Media 2019, Porto, Portugal.

[17] Korachi, Z. and Bounabat, B. (2019c). Towards a Platform for Defining and Evaluating Digital Strategies for Building Smart Cities. IEEE ISBN: 978-1-7281-3848-0. The 3rd. International Conference on Smart Grid and Smart Cities (ICSGSC 2019), University of California, Berkley, USA, June 25-28, 2019.

[18] Kamariotou M., Kitsios F. (2017). Department of Applied Informatics University of Macedonia Thessaloniki, Strategic Information Systems Planning: Implementing a Digital Strategy. DOI: 10.4018/978-1-5225-2255-3.ch078. In book: Encyclopedia of Information Science and TechnologyEdition: Fourth EditionChapter: 78Publisher: IGI Global PublishingEditors: Mehdi Khosrow-Pour.

[19] Boström, E., Can Celik, O. (September 2017). Towards a Maturity Model for Digital Strategizing A qualitative study of how an organization can analyze and assess their digital business strategy.

[20] Korachi, Z. and Bounabat, B. (2018). Data Driven Maturity Model for Assessing Smart Cities. ICSDE'18, October 18– 20, 2018, Rabat, Morocco; © 2018 Association for Computing Machinery; ACM ISBN 978-1-4503-6507-9/18/10; ENSIAS Rabat; Morocco.

[21] Luftman, J., Ben-Zvi, T., Dwivedi, R., & Rigoni, E. H. (2010). IT Governance. International Journal of IT/Business Alignment and Governance, 1(2), 13–25. doi:10.4018/jitbag.2010040102.

[22] Maqbool, M. H. (2015). A consolidated model for putting Balanced Scorecard into action in Pakistan's textile industry. Journal of Strategy and Performance Management, 3(1), 40-46.

[23] Percheiro, I., Almeida, R., Pinto, P. L., & da Silva, M. M. (2017). Towards Conceptual Meta-Modeling of ITIL and COBIT 5. Lecture Notes in Business Information Processing, 478–491. doi:10.1007/978-3-319-65930-5_38.

[24] Gehrmann, M. (2012). Combining ITIL COBIT and ISO/IEC 27002 for structuring comprehensive information technology for management in organizations. Navus-Rev. Gest˜ao Tecnol.2(2), 66–77 (2012).

[25] Michalska, J. (2008) Using the EFQM excellence model to the process assessment, Vol . 27, No. 2. Journal of Achievements in Materials and Manufacturing Engineering, 2008.

[26] Looso, S., Goeken, M. (2010). Application of best-practice reference models of IT governance. In: ECIS (Paper 129).

[27] Pardo, C., Pino, F.J., Garc´ıa, F., Piattini, M., Baldassarre, M.T. (2012). An ontology for the hamonization of multiple standards and models. Comput. Stand. Interfaces34, 48–59.

[28] Cater-Steel, A., Tan, W.G., Toleman, M. (2006). Challenges of adopting multiple process improvement frameworks. In: 14th European Conference on Information Systems (ECIS).

[29] Ula, M., Ismail, Z., Sidek, Z.M. (2011). A framework for the governance of information security in banking system. J. Inf. Assur. Cyber Secur.2011, 1–12.

[30] Mintzberg, H., Ahlstrand, B., & Lampel, J. (2000). Safari de estratégia. Porto Alegre, Brazil: Bookman.

[31] Peterson, R. (2004). Crafting information technology governance. Information Systems Management, 21(4), 7–22. doi:10.1201/1078/44705.21.4.200409 01/84183.2.

[32] Lee, G., & Bai, R. (2003). Organizational mechanisms for successful is/it strategic planning in the digital era. Management Decision, 41(1), 32–42. doi:10.1108/00251740310445536.

[33] Jiang, J., & Klein, G. (1999). Project selection criteria by strategic orientation. Information & Management, 36(2), 63–75. doi:10.1016/S0378-7206(99)00009-9.

[34] Teo, T., & King, W. (1997). Integration between business planning and information systems planning: an evolutionary-contingency perspective. Journal of Management Information Systems, 14(1), 185–214.

[35] Sambamurthy, V., & Zmud, R. (1999). Arrangements for Information Technology Governance: A Theory of Multiple Contingencies. Management Information Systems Quarterly, 23(2), 261–290. doi:10.2307/249754.

[36] Brown, C., & Magill, S. (1994). Alignment of the IS Functions with the Enterprise: Toward a Model of Antecedents. Management Information Systems Quarterly, 18(4), 371–403. doi:10.2307/249521.

[37] Raghunathan, T. (1992). Impact of the CEO's participation on information systems steering committees. Journal of Management Information Systems, 8(4), 83–96.

[38] Smaczny, T. (2001). Is an alignment between business and information technology the appropriate paradigm to manage IT in today's organisations. Management Decision, 39(10), 797–802. doi:10.1108/EUM0000000006521.

[39] Venkatraman, N. (1997). Beyond Outsourcing: Managing IT Resources as a Value Center. Sloan Management Review, 38(3), 51–64.

[40] Jensen, M., & Meckling, W. (1998). Divisional performance measurement . In Foundations of Organizational Strategy. Cambridge, MA: Harvard University Press.

[41] Gunasekaran, A., Love, P., Rahimi, F., & Miele, R. (2001). A model for investment justification in information technology projects. International Journal of Information Management, 21, 349–364. doi:10.1016/S0268-4012(01)00024-X.

[42] Boonstra, A. (2003). Structure and analysis of IS decision-making processes. European Journal of Information Systems, 12(3), 195–209. doi:10.1057/ palgrave.ejis.3000461.

[43] Weill, P., & Ross, J. (2004). IT Governance - How Top Performers Manage IT Decision Rights for Superior Results. Boston, MA: Harvard Business School Press.

[44] Mintzberg, H. (2003). Criando organizações eficazes: estruturas em cinco configurações. Porto Alegre, Brazil: Atlas.

[45] Karimi, J. (2000). The Effects of MIS Steering Committees on Information Technology Management Sophistication. Journal of Management Information Systems, 17(2), 207–230.

[46] Wu, L., & Ong, C. (2008). Management of information technology investment: A framework based on a Real Options and Mean–Variance theory perspective. Technovation, 28(3), 122–134. doi:10.1016/j.technovation.2007.05.011.

[47] Wen, H., & Shih, S. (2006). Strategic Information Technology Prioritization. Journal of Computer Information Systems, 46(4), 54–63.

[48] Schildt, K., Beaumaster, S., & Bailey, S. (2006). Organization Antecedents of Successful IT Management. In Proceedings of the 39th Annual Hawaii International Conference on System Sciences.

[49] Patten, K., Whitworth, B., Fjermestad, J., & Mahinda, E. (2005). Leading IT Flexibility: Anticipation, Agility and Adaptability. In Proceedings of 11th Americas Conference on Information Systems Engineering.

[50] Valverde, L., Mira da Silva, M., & Gonçalves, M. R. (2018). CMMI-DEV v1.3 Reference Model in ArchiMate. On the Move to Meaningful Internet Systems. OTM 2018 Conferences, 191–208. doi:10.1007/978-3-030-02671-4_11.

[51] Almeida, R., Pinto, P.L., da Silva, M.M. (2016). Using ArchiMate to integrate COBIT and COSO metamodels. In: European, Mediterranean and Middle Eastern Conference on Information Systems, Krakow, Poland, p. 5.

[52] Souza Neto J and Ferreira Neto A. (2013). Metamodel of the IT Governance Framework COBIT. Journal of Information Systems and Technology Management. 2013;10(3):521-540. doi:10.4301/s1807-17752013000300004.

[53] Lourinho, R., Almeida, R., Mira da Silva, M., Pinto, P., & Barafort, B. (2017). Mapping of Enterprise Governance of IT Practices Metamodels. Lecture Notes in Business Information Processing, 492–505. doi:10.1007/978-3-319-65930-5_39.

[54] Sousa, M. J., & Rocha, Á. (2018). Digital learning: Developing skills for digital transformation of organizations. Future Generation Computer Systems. doi:10.1016/j.future.2018.08.048.

[55] Teknomo, K. (2006). Analytic hierarchy process (AHP) tutorial. Revoledu. com. Available at: https://people.revoledu.com/kardi/tutorial/AHP/. Accessed September 23, 2019.

[56] Van den Berg, M., Slot, R., van Steenbergen, M., Faasse P, van Vliet H. (2019). How enterprise architecture improves the quality of IT investment decisions. Journal of Systems and Software. 2019;152:134-150. doi:10.1016/j.jss.2019.02.053.

[57] Hu, Q., & Quan, J. (2006). The Institutionalization of IT Budgeting. Information Resources Management Journal, 19(1), 84–97. doi:10.4018/irmj.2006010105.

[58] Waldron, M., W., Vsanthakumar, J., and Arulraj, S. (1998). Chapter 13 - Improving the organization and management of extension. Improving agricultural extension. A reference manual. ISBN 92-5-104007-9.

[59] Basili, V. R. (1993). Applying the Goal/Question/Metric paradigm in the experience factory (pp. 21–44). Software Quality Assurance and Measurement: A Worldwide Perspective.

[60] Desfray, P., and Raymond, G. (2014). ArchiMate. Modeling Enterprise Architecture with TOGAF, 249–258.doi:10.1016/b978-0-12-419984-2.00014-8.

[61] The Open Group. (2013). ArchiMate® 2.1 Specification. Pubs.opengroup.org. https://pubs.opengroup.org/architecture/archimate2-doc/. Published 2012- 2013. Accessed September 23, 2019.

Real-Time Carpooling Application based on k-NN Algorithm: A Case Study in Hashemite University

Subhieh El Salhi[1], Fairouz Farouq[2], Randa Obeidallah[3], Yousef Kilani[4], Esra'a Al Shdaifat[5]

Department of CIS
Hashemite University Jordan

***Abstract*—The current revolution of mobile technology in different aspects of community directs the researchers and scientists to employ this technology to identify practical solutions for daily life problems using mobiles. One of the major challenges in our developing countries is the public transportation system. Public transportation system is an essential requirement for the welfare of modern society and has a critical impact on the people productivities and thus on the entire economic development process. Therefore, different solutions had been investigated to find applicable solutions. "Carpooling" is one of the initiative solutions that based on the usage of a single shared car by a group of people heading to the same location on a daily basis. In addition, carpooling can be considered as an efficient alternative to overcome the limitations of the conventional transportation system with an easier, quicker and more environmentally friendly car journeys. This paper presents an intelligent carpooling mobile app to commute students of the Hashemite University. The proposed solution is founded on using data mining technique, and more specifically the k-Nearest-Neighbour (k-NN) technique.**

Keywords*—*Mobile Application; Carpooling; Data mining; Classification; k-NN algorithms

I. Introduction

Jordan as many countries is effected by the increasing number of vehicles on streets. The enormous number of vehicles causes environmental pollution, social problems, traffic congestion and not enough parking spaces. The extensive number of vehicles on roads is a natural result for the inefficient public transportation system that leads to vehicle dependency and ownership.

Transportation Demand Management is a collection of strategies and administrative regulations to encourage efficient traffic patterns to reduce travel demand and to reorganize mobility in space and time. Transportation Demand Management provides several solutions for traffic congestion. One solution to reduce the increasing number of vehicles on streets is car sharing. Car sharing is also known as carpooling. Carpooling is involved with a group of people who have similar time slots and going to the same office or school such that they share a vehicle owned by the driver [1].

Information and Communication Technology (ICT) play a major role for bringing potential carpoolers together and encourage carpooling. ICT contribute to establish communication with potential passengers, and make it available to a large number of potential users with enough variation in demographic and trip characteristics (e.g. timing, geography, etc.).

Many algorithms were used in Carpooling systems to calculate the best route, shortest path and find potential passengers. Carpooling systems use algorithms and data mining techniques to allow both passengers and drivers to find a convenient trip route and to support a billing system. Examples of these mining algorithms are Dijkstra's algorithm, Bellman Ford's algorithm, Floyd–Warshall's Algorithm and k-Nearest Neighbor algorithm [2]. However, one of the most popular machine learning algorithms is the k-Nearest Neighbor algorithm (k-NN). Generally speaking, k-NN is an efficient, simple and easy-to-implement supervised machine learning algorithm that can be used to solve different classification and regression problems [3].

The University is located in city of Zarqa in Jordan. Students and employees of the Hashemite University (HU) have critical difficulties during their daily journey to the campus because of the poor public transportation. The lack and delay in public transportation system while travelling from different locations such as Amman, Zarqa and Irbid to campus motivate us to develop a carpooling application that directed mainly to students. Obviously, the proposed carpooling app is directed to a particular class of users --the students of the Hashemite University where the idea is to provide them with a reliable, safe and rapid ride to the campus with minimum fees. The proposed carpooling app based on the well-known k-NN algorithm and the novelty of our application comes from its simplicity where the app use the same recognized road to the university with predetermining stopping points to pick the student from or drop them in. Therefore, the k-NN is employed to identify the closest drivers at certain time. Taking into consideration that eligible drivers only are sent to passengers to select the most suitable one. The Deanship of Student Affairs at the Hashemite University determines the eligibility with accordance to its policy to assure the safety of the students.

Our main goals of developing carpooling app are: (i) to minimize the overall travel cost and distance from students' houses to HU campus that is located in ZARQA city, (ii) to reduce pollution and traffic jam and (iii) to help students to be comfortable and satisfied with their ride to the university and this would absolutely has a positive impact on the students productivity. Furthermore, an ethical value added since this app highlights the initiatives and high responsibilities towards community problems. Being initiatives and part of the suggested solution would raise the value of the team work as well to face different types of life problems.

The main contribution of the presented work is to use the k-NN algorithm in generating an intelligent carpooling application for the students of the Hashemite University.

The paper is organized as follows: Section II presents a solid background and a general overview of related work. The proposed mobile application is discussed in Section III in terms of the Architecture specifications and the employed k-Nearest-Neighbour (k-NN) Algorithm and the functionality of the application. Section IV demonstrates the implementation and interface of the mobile app. Finally, Section V presents a summary and some directions for future work.

II. Related Work

Carpooling usually consists of two to four persons shuttling with a driver [4]. Carpooling is involved with a group of people who have similar time slots and going to the same office or school such that they share a vehicle owned by the driver [1].

Many studies were conducted to conclude the benefits and advantages of using carpooling service. There are benefits for individuals and the entire community. For individuals; the most important reason to use carpooling is to reduce transportation expenses and reduce travel time [4]. Researchers found that the most important reason to use carpooling is to decrease expenses of car fuel and transportation fees [5] [1] [6]. Carpooling is considered to be a good alternative to public transportation and taxi services.

Furthermore, riding with a group of people with similar interest is a good way to spend the travel time. It is a good way to reduce the total travelling time and driving stress [7]. The work presented in [6] noted that being able to ride and socially interact with others rather than to drive is a cause for carpooling. The study of using carpooling in Massachusetts Institute of Technology campus showed that travel distance was reduced 9% to 27% [11].

For communities; carpooling is a mean to reduce traffic congestion and pollution. Some studies identified environmental responsibility as a motivation for carpooling [6]. However, others pointed the benefits of carpooling from a social point perspective; less fuel consumption, less CO2 production, less traffic congestion and more social interaction [7]. Gargiulo et al. showed how applying carpooling in Dublin would decrease the amount of CO2 in the air [8]. The case study proposed by [4] showed the efficiency of carpooling in moderating congestion in Delhi.

On the other hand; carpooling is affected by transportation policies. Legal restrictions in some countries do not allow carpooling, such that a vehicle will get a traffic violation ticket, if it is used as a carpooling. Additionally, in case of traffic accidents, insurance coverage policies will not cover the damages and hits that might occur to passengers [9] [1].

Moreover, travel schedule in carpooling is strict and does not allow personal freedom mobility during work day neither allows to change route or to stop during the trip [12]. In addition, it is hard to connect with an appropriate carpooling schedule with unknown passengers.

Today, Information and Communications Technology (ICT) is used to enhance carpooling services. Technology plays an important role in carpool creation [10]. Online map services are available and used in carpooling systems, such as: Google Maps Directions API that calculates directions between locations using HTTP requests and Bing Map which calculates and display directions and routes on the map with direction API module or with Bing Map Rest services.

The use of smart phone devices with internet connectivity and GPS navigation technology ease the way to connect potential carpoolers together and arrange travel route. Most of the developed carpooling systems use algorithms and data mining techniques to allow both passengers and drivers to find a convenient trip route, in addition to support a billing system to manage fees and payment [2]. Nourineja et al. presented a centralized (binary integer programming) and decentralized (dynamic auction-based multi-agent) optimization algorithms to match passengers and drivers [13]. Montes et al. developed an online community for car sharing called Teranga Go!. Teranga GO! is a multi-criteria decision making system using Hesitant Fuzzy Linguistic terms to present judgment of both drivers and passengers [14].

To the best of our knowledge, extensive works and researches have been conducted to produce a carpooling app for general purpose where the machine learning and data mining techniques were employed to find the “best” and the most optimal route to the desired destination. However, identifying the optimal and shortest route present a neat solution but with high complexity. For instance, Bicocchi et al. developed an application for ride sharing based on the extraction of suitable information from mobility traces and use a clustering algorithm that is applied to labeled trajectories [15]. An android carpool application was developed to allow passengers to collaborate, plan for their journey and share expenses [16]. In [7], author presented two applications; the SplitCar application and the Buddy application for shared-use mobility in the metropolitan area of Bacău, Romania. The authors integrated different computing languages, standards and technologies. Mallus et al. developed CLACSOON application; a dynamic carpooling services in urban areas for real time carpooling service using multi-objective route matching algorithm [17]. The carpooling app employs the k-NN in order to queries are launched based on location/region. Menaka et al. proposed carpooling system with three modules; user module, LBS module and route saver module [18]. The authors used k-NN to find intermediate route for the destination point and display the reservation chart of the vehicle allotted to the user.

Our proposed mobile carpooling application aims to generate a simple intelligent carpooling app that help students and employees of the Hashemite University (HU) to find the most nearby drivers that match the passenger’s preferences (i.e. gender) and thus to serve the ultimate goal of minimizing the overall travel distance, effort and the waiting time from students’ homes to HU campus located in ZARQA city.

III. Proposed Mobile App

In this section, the proposed carpooling apps are presented in terms of architecture and design in Section A. The k-Nearest-Neighbour (k-NN) Algorithm and its functionality are demonstrated in Section B and Section C, respectively.

A. Architecture Overview and Design

The architecture of the proposed system comprises of the following components (as shown in Fig. 1):

1) Users: Three types of users are involved in the proposed system: driver, passenger and system administrator. Passenger – a student requesting carpooling Services while Driver– the student providing carpooling Services using his own car. Typically, drivers and passengers are students who are registered in the current academic semester. However, the system administrator is a staff member of the Computer Centre (CC) of the Hashemite University.

2) Carpooling System: A web based system developed by the computer centre of the Hashemite University to manage, support and control all administration tasks. It is the most substantial component and considered as the heart of our proposed mobile application. The system encompasses of:

a) System administrator – a staff member who is responsible for controlling and managing the system. The main administration tasks include (but not limited to): (i) accept new drivers' requests, (ii) accept new passengers' requests, (iii) give the students (drivers and passengers) their account details to start using the system and (iv) generate reports about the registered drivers and all related information about their cars (i.e., car brand, colour, and seat availability).

b) Database – contains the actual database for all employees and students of the Hashemite University.

c) Computer Centre Web Server (CC server) – this type of server contains the actual desired database of the registered and activated users necessary to operate the mobile application. Registered users are eligible drivers and/or passenger, but the activated users are those drivers who are currently ready to start a trip and commute passengers.

1) Stop points – well-known predetermined meeting points (stations) located along the way to the Hashemite University to pick-up and drop-off the passengers from. Normally, the passenger chooses the nearest stop points to wait the driver.

2) Wi-Fi network – maintains and supports the connection of drivers, passengers and the carpooling system.

It is worth to mention that the eligibility requirement for the drivers are summarised in two main points; the driver should: (i) be a legal registered student in the current academic semester and (ii) provide the university with a qualified driving behaviour report obtained from the Central Traffic Department of the Public Security Directorate. This report shows the traffic offences and used as a safety indicator.

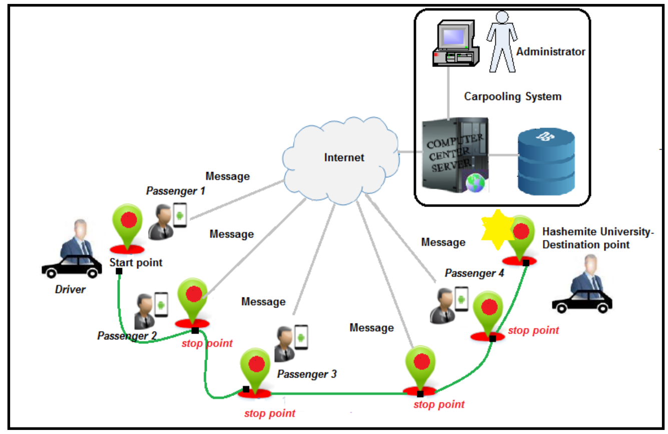

Fig. 1. The Architecture of the Proposed Carpooling Mobile Apps.

The steps of the proposed system are illustrated below based on the system architecture:

1) Initially, the legal drivers and passengers apply for the carpooling system by sending a request to join the carpooling mobile application.

2) Once the administrator assures the eligibility, especially for the drivers, the accounts are created and the details are provided to students to start using the carpooling mobile application.

3) With respect to driver, the driver log in to the mobile app and determine the start-up time (time to be in the nearest stop point), end-time (time to leave the university) and the seat availability.

4) With respect to passenger, the passenger sends a request that determines the pick-up time, stop point (meeting station) and the preferred gender of the driver (optional).

5) Once the passenger request arrives to the carpooling system, the k-NN algorithm is applied on the available drivers to provide the passenger with the "best"- matched drivers (i.e. top five drivers). The k value of the k-NN algorithm reflects the available active drivers. In our case, the value of the best available driver is set to three drivers (k=3)[1]. Typically, the value is set by the system administrator. The passenger is informed with the set of the best-matched drivers obtained by the k-NN. The set of the best-matched drivers are shown as coloured cars on the map (pink car stands for female drivers and blue cars stands for male drivers). Then he/she selects the driver/s so that the request is forwarded to them.

6) Finally, the system sends a confirmation note contains the driver details, pick-up time and stop point.

7) The system provides the drivers with the suitable passenger requests fit the driver start-up and end-time. Also, the seat availability is considered. The driver can check the details of the passenger easily and accept the desired requests.

8) For each accepted passenger, the number of the available seats is decreased automatically. Consequently, if the available seats become zero then the driver cannot be

[1] Our experiments show that k=3 is empirically the best value to operate the *k*-NN algorithm.

nominated to other passengers and no new request will be forwarded.

9) Finally, the carpooling system will generate a small notification (report) with the stop points along with the number of passengers should be collected from each.

The default case of the proposed system assumes all the students are passengers until the eligibility of the driver requirements are met and satisfied.

B. An overview of the k- Nearest-Neighbour (k-NN) Algorithm applied in the carpooling

The k-NN is one of the most popular machine learning algorithms and it is considered an attractive classification algorithm because it is very simple, flexible and highly efficient algorithm. The k-NN is a non-parametric learning algorithm. The term "non-parametric" term means that the complexity of the model cultivates with an increasing amount of data. Moreover, the boundary of the k-NN decision occurs on any form and it makes no assumption about the data distribution, which makes the flexibility of k-NN's decision boundary an enormous advantage. Since there is no previous information available in k-NN, the decision of k-NN is highly reliant on the distance metrics. Therefore, the k-NN algorithm was adopted with respect to carpooling problem to support making a decision as shown in Algorithm 1.

In the context of carpooling problem, the k-NN produces encouraging results as it does not lose any details since it scans all registered drivers, calculates the distance between each driver d_i and the passenger P and compares the obtained results to make a decision to select the nearest drivers (to determine the "best"- matched drivers).

Algorithm 1: k-NN for carpooling system (P, DR)

```
{
Input:
P:passenger request details that contains the coordinate,
pick-up time (t) and gender (g)
DR: the set of active registered drivers where each driver
d_i contains t_i: pick-up time and g_i: gender (if determined)
Output:
S: The set of three nearest matched-drivers
1. S= θ; L= θ;
2. For each d_i ∈ DR
3. If d_i (t_i, g_i) == P(t, g) then
4. Calculate dist_i(x_i, y_i): the distance between d_i and P;
5. L = ADD (d_i, dist_i)
6. Endif
10. End for
S=arrange L in descending order with respect to dist_i.
Return S
}
```

With respect to the presented work, the adopted form of the distance metric dist(x, y) is the Euclidean distance, which is calculated as:

$$\mathbf{dist}(\mathbf{x},\mathbf{y}) = \sqrt{\sum_{\mathbf{i}}(\mathbf{x_i} - \mathbf{y_i})^2} \quad (1)$$

When computing Euclidean distance, it is important to mention that the weighs of the passengers and drivers are the same to the total distance. Each data point (passengers/drivers) is represented by its latitude and longitude values. However, the Euclidean distance does not make sense when it is calculated from latitudes and longitudes, which are not coordinates in a Cartesian coordinate system. In order to calculate the distance between two points on the earth, given by latitudes and longitudes points it proceeds in two phases: i) calculate the Euclidean distance between two points by computing the Cartesian coordinates of the points from their latitudes and longitudes then ii) convert this distance to one measured along the surface of the earth.

Thus, suppose we are given two points P1 and P2 determined by their latitudes and longitudes values: P1(α1, β1) and P2 (α2, β2). The Euclidean distance dist in Cartesian coordinates is computed as:

$$\mathbf{dist^2} = (\mathbf{x_1} - \mathbf{x_2})^2 + (\mathbf{y_1} - \mathbf{y_2})^2 + (\mathbf{z_1} - \mathbf{z_2})^2 \quad (2)$$

Where

$x = R\cos\alpha\cos\beta$

$y = R\cos\alpha\sin\beta$

$z = R\sin\beta$

and

$R \approx 6371$ km

Taking into consideration that R is the average radius of the earth, which is equal to approximately 6.371 x 10^6 m according to NASA's Goddard Space Flight Centre. Next, convert the distance d in Cartesian coordinates to the distance D measured along the surface of the earth, which is defined by the following formula:

$$\mathbf{D} = \mathbf{R}\,\mathbf{sin^{-1}}\left(\frac{\mathbf{d}}{\mathbf{2R^2}}\sqrt{\mathbf{4R^2} - \mathbf{d^2}}\right) \quad (3)$$

C. System Functionality

As previously mentioned, the carpooling app provides a set of services to the registered students; passengers and drivers. In order to describe each service, the details of each functional requirement (FR) are listed below using Cockburn template [20][19].

Typically, the student is set as "passenger" once the account is created. However, the student is transformed to "driver" when he provides the necessary documents such as driving licence and driving offences report to the Deanship of student affairs in the Hashemite University. Fig. 2 shows the use case diagram of the main functionalities for each type of users: Passenger, Driver and Admin.

FR1: Create Student Account (i.e., registration) including the following:

- Use case Title: Log in
- Primary Actor: Passenger, Driver, Admin
- Stakeholder: Students, Driver, Admin

- Precondition: The students (passengers and drivers) need to download the carpooling app and enter valid data.
- Minimal Guarantee: Failed to create the user account.
- Success Guarantee: The new account is created and users can start using the carpooling app successfully.
- Trigger: the user asks the admin to register in the carpooling app

Main success scenario:

1) Student send a sign up request to the admin to register in the app

2) Admin accept the request

Extensions:

1) If the sign up not successfully completed

a) Users should roll back to sign up again

FR2: Check Safety Report including the following:

- Use case Title: Check safety Report
- Primary Actor: Admin
- Stakeholder: Driver, Admin
- Precondition: Users need to register in to the carpooling App and log in to their account successfully
- Minimal Guarantee: Safety report are not handed in or not considered by the admin
- Success Guarantee: The safety report is checked and recorded.
- Trigger: The driver need to hand in the report to admin.

Main success scenario:

1) Driver obtain the safety report from the Central Traffic Department

2) Driver hand in the report to the admin at the Deanship of Student Affairs at the Hashemite University

3) Admin receives and checks the report

4) Admin register the student as legal “Driver”

Extensions:

1) If the safety report is not received and considered by the Deanship of Student Affairs

a) The students accounts registered as “Passenger” Only

FR3: Request Driver including the following:

- Use case Title: Request Driver
- Primary Actor: Passenger
- Stakeholder: Passenger, Admin
- Precondition: Passenger send a request for a driver after logging in to their account successfully
- Minimal Guarantee: The request is not sent
- Success Guarantee: The request is received and the suggested list of drivers are provided
- Trigger: The passenger need to log in successfully and send a driver request

Main success scenario:

1) Passenger filled the details of his journey correctly

2) The request is received and the k-NN is applied on the available drivers

3) A suggested list of drivers is provided to passenger

4) Passenger select a driver from the list and the request is automatically forwarded to the Driver”

Extensions:

1) If the passenger is not able to fill the preferences and journey details easily and correctly

a) Quit the carpooling app

b) Tack action to gain access to the app

2) A list of suggested drivers is not provided (empty list)

Passenger needs to roll back and starts the request again

FR4: Receive Passenger Request including the following:

- Use case Title: Receive Passenger Request
- Primary Actor: Driver
- Stakeholder: Passenger, Driver
- Precondition: Passenger received a suggested list of drivers and select some of them successfully
- Minimal Guarantee: N/A
- Success Guarantee: One of the driver accept the passenger request
- Trigger: The driver need to receive a passenger request

Main success scenario:

1) Passenger received a suggested list of available drivers

2) Passenger selects one or more drivers

3) The passenger request is forwarded to selected drivers

4) Driver accepts the request

5) Other services such as Chat and Rate become available and can be used

Extensions:

1) The passenger request is not forwarded to the selected drivers

a) Passenger needs to roll back and sends the request again

1) Driver does not accept the request

a) Passenger is informed after a predefined time stamp. Passenger needs to select another driver

IV. Application Implementation and Interface

With respect to implementation specifications for the proposed application, the app encompasses of the following main components:

1) Server-Side: uses Java language including .NET and JavaScript is mainly used to develop the server-side part, especially the k-NN algorithm. Furthermore, when passenger submits queries and asks for available driver, the server will operate the k-NN algorithm on the activated registered students stored on the database and forward the best matched result back to the passenger. Moreover, PHP was used to generate an interface with the database. The PHP scripts are invoked to handle the applications requests for a data manipulation. Finally, the specifications of the CC server are: 6th generation Intel Octa Core i7 3.4 GHz processor, sixteen GB SDRAM and one TB SSD hard disk.

2) Database: In order to handle the database manipulations smoothly and efficiently Firebase real time database technology was adopted. Firebase depends on the concepts of using JavaScript Object Notation (JSON) where Data is stored as a node with reference key. In addition, NoSQL is adopted for the proposed carpooling application as it provides a flexible supported way for scalable database than the traditional relational SQL (the attributes of an object may be created on fly if there is a need, so space is not taken if an attribute is empty). Moreover, NoSQL enhance the performance as it formats data in the same way of using JSON so there is no need to reformat data.

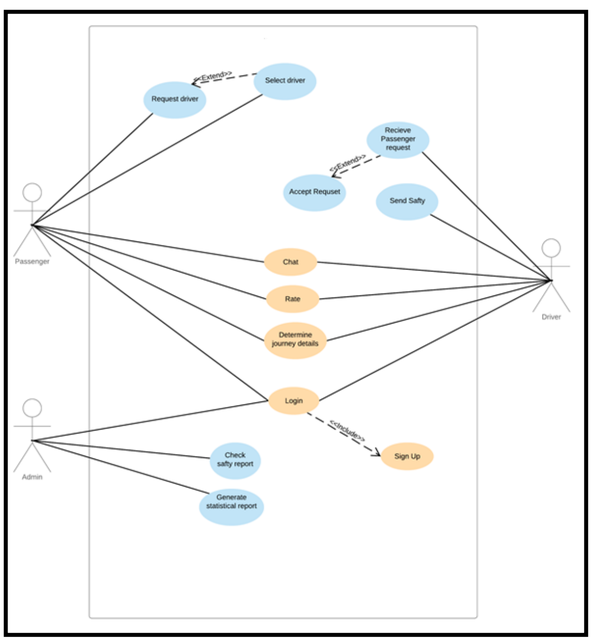

Fig. 2. The use-Case Diagram of the Carpooling Apps.

3) Client-Side: includes the developing of the Android SDK application which will be installed later on the students' mobiles. Firebase Cloud Messaging (FCM) which is an improved version of the Google Cloud Messaging was adopted to handle the messages between server applications and mobile client apps in a more easy and efficient way as the FCM is built on Google Play Services. A wide range of mobile devices were used such as: Sony Xperia, Samsung Galaxy S4, Samsung Galaxy S6, and LG G2. The application worked smoothly and properly on the different devices.

4) Others: Google Maps API and Google Maps directions API are used to download and display maps in order to show passenger and driver locations, available drivers to select one of them. Moreover, APIs allow user interaction with the map (zoom, rotate, scale the map and open the map in full screen mode) easily and effectively.

The screenshots in Fig. 3 shows the app log in page and Fig. 4 illustrates the main services provided by the carpooling app.

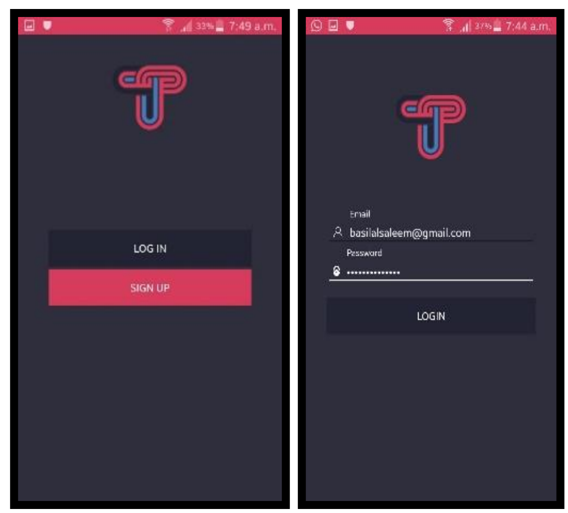

Fig. 3. Application Login Page to Create user Account, user can either Choose to Log in or Register (Sign up) from this Page.

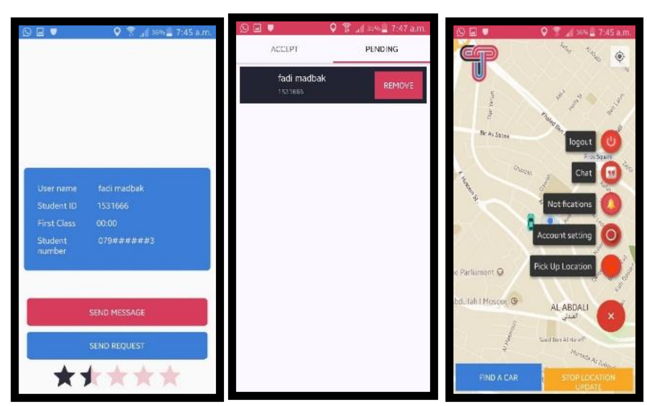

(a) (b) (c)

Fig. 4. Screenshots of the main App Services. (a) The user asks for a Driver by Sending a Request. Send Message Option is Activated when the Driver is Selected and Assigned Successfully to Passenger. Also, the Rate for the Selected Driver is Clearly shown (using Stars). (b) The Passenger Details are shown to Selected Driver. (c) The main Services of the App: (i) Find a Car used to Find the Best Match Driver, (ii) Logout Option, (iii) Chat Services, (iv) Notification: used for Confirmation, (v) Account Setting used to Set Any Preferences and Finally (vi) Pick up Location to Determine the Stop Point to Meet the Driver.

V. Summary and Future Work

Transportation difficulties becoming more serious challenge, day after day. The pollution, fuel consumption, congestion, travelling cost and stress have a great impact on our daily lives. Therefore, an intelligent carpooling app is proposed in this paper as a solution for the aforementioned mentioned problems. The ultimate goal is to provide the students of the Hashemite University with an applicable, portable and easy to use mobile application for the transportation problem. An intelligent and reliable carpooling solution aids not only the students but also enrich the societal benefits in terms of strengthen the social relationship. The intelligent carpooling system app is based on the data mining techniques and more specifically the k-NN technique. Preliminary model have been designed and developed where the drivers are evaluated using the k-NN and a list of best match drivers are provided to passenger taking into consideration their preferences. Also a set of services are provided and included in the app such as: (i) a simple rating technique was used to give a feedback about the drivers and (ii) chat service between the drivers and passengers was activated once the driver accept the request of the ride. In addition, the traffic offences reports for drivers are checked on regular base to offer safe and sound rides.

The Hashemite University is satisfied with the initial values obtained from applying the carpooling app as the transportation problems eliminated and reduced for the student without any additional resources or cost. A set of suggestion are listed below to give a significant addition to the current version of the carpooling app is considered to be the next step for our future work:

- Employ other machine learning algorithms such as Convolution Neural Network (CNN).
- Operate the proposed app by the Ministry of Higher Education in Jordan to cover other universities in this application. Taking into consideration that there are two more universities located on the same road of the Hashemite University; Al Bayet University and Private Zarqa University.
- Integrate the app with Public Security Directorate– Traffic Department (Drivers and vehicles Licensing Department). This type of cooperation would easily control and manage different drivers services support the safety concerns such as traffic offenses and license queries.

Acknowledgment

The authors would like to thank the Hashemite University for the continuous help and endless support to implement and evaluate the mobile app of this research.

References

[1] M. Do, and H. Jung, “The Socio-Economic Benefits of Sharing Economy: Colleague-Based Carpooling Service in Korea”.(2018), J. Open Innov. Technol. Mark. Complex. 2018, 4, 40.

[2] Ferreira J, Trigo P, Filipe P. “Collaborative car pooling system. World academy of Science, Engineering and technology”. 2009 Jun 20;54:721-5.

[3] J. Han, M. Kamber, and J.Pei, “Data mining concepts and techniques”, third edition. The Morgan Kaufmann Series in Data Management Systems, pp.83-124.,2011.

[4] K. Dewan, K. and I. Ahmad. . “Carpooling: A Step to Reduce Congestion (A Case Study of Delhi).” Engineering Letters 14 (1): 61–66,2007.

[5] F. Alpizar, and F.Carlsson, “Policy implications and analysis of the determinants of travel mode choice: an application of choice experiments to metropolitan Costa Rica”. Environment and Development Economics, 8, 603-619, 2003.

[6] Benkler Y. “Sharing nicely: On shareable goods and the emergence of sharing as a modality of economic production”. Yale LJ. 2004;114:273.

[7] E. Nechita, GC. Crişan, SM. Obreja,and CS. Damian, “Intelligent Carpooling System”. In: Nakamatsu K., Kountchev R. (eds) New Approaches in Intelligent Control. Intelligent Systems Reference Library, vol 107. Springer, Cham, 2016.

[8] E. Gargiulo, R. Giannantonio, E. Guercio C. Borean, and G. Zenezini, G. ,”Dynamic ride sharing service: Are users ready to adopt it?” Procedia Manuf. 2015, 3, 777–784.

[9] B. Taylor, “Putting a Price on Mobility- Cars and Contradictions in Planning”. Journal of the American Planning Association, 72(3), 279-284, 2006.

[10] R. Calvo, F.de Luigi, P. Haastrup, and V. Maniezzo, “A distributed geographic information system for the daily carpooling problem”. Computers & Operations Research, 31, 2263-2278, 2004.

[11] A. Amey, “A proposed methodology for estimating rideshare viability within an organization, applied to the MIT community”. In Proceedings of the Transportation Res Boar 90th Annual Meeting (TRB 2011), Washington, DC, USA, 23–27 January 2011; pp. 1–16.

[12] J. Andrey, K. Burns, and S. Doherty. “Toward sustainable transportation: Exploring transportation decision making in teleworking households in a mid-sized Canadian city”. Canadian Journal of Urban Research, 13(2), 257, 2004.

[13] M. Nourinejad, M. Roorda. “Agent based model for dynamic ridesharing”. Transp. Res. C Emerg. Technol. 2016; 64:117–132.

[14] R. Montes A.M. Sanchez, P. Villar , and F. Herrera , “Teranga Go!: Carpooling Collaborative Consumption Community with multi-criteria hesitant fuzzy linguistic term set opinions to build confidence and trust. Appl”. Soft Comput. 2017.

[15] N. Bicocchi, and M. Mamei,. “Investigating ride sharing opportunities through mobility data analysis”. Pervas. Mob. Comput. 2014;14:83–94.

[16] A. Antao, V.Corria, and S.Gonsalves, "Carpooling application in android", International Journal of Current Engineering and Technology, 2015, Vol.5, No.2 pp. 955-958 ISSN 2277-4106.

[17] M. Mallus, G. Colistra, L. Atzori, M. Murroni, M., and V.Pilloni. “Dynamic Carpooling in Urban Areas: Design and Experimentation with a Multi-Objective Route Matching Algorithm”. Sustainability 2017, 9, 254.

[18] R. Menaka, B. Ashadevi, L. Viji, T. Premamala, and T.K. Kartheeswari, “Leveraging Route Saver Based On Location Service in Carpooling System Using K-NN Algorithm” International Journal of Advances in Computer and Electronics, Vol. 3, No. 8, pp. 9-14, August 2018.

[19] A. Cockburn, “Structuring Use Cases with Goals. Journal of Object-Oriented Programming (JOOP Magazine)”, Sept-Oct and Nov-Dec, 1997.

[20] A. Cockburn, (2000), “Writing Effective Use Cases”. Addison-Wesley.

Cardiovascular Disease Diagnosis: A Machine Learning Interpretation Approach

Hossam Meshref
Associate Professor, Computer Science Department
College of Computers and Information Technology
Taif University, Taif, Saudi Arabia

***Abstract*—Research on heart diseases has always been the center of attention of the world health organization. More than 17.9 million people died from it in 2016, which represent 31% of the overall deaths globally. Machine learning techniques have been used extensively in that area to assist physicians to develop a firm opinion about the conditions of their heart disease patients. Some of the existing machine learning models still suffers from limited predication ability, and the chosen analysis approaches are not suitable. As well, it was noticed that the existing approaches pay more attention to building high accuracy models, while overlooking the ability to interpret and understand the recommendations of these models. In this research, different renowned machine learning techniques: Artificial Neural Networks, Support Vector Machines, Naïve Bayes, Decision Trees and Random Forests have been investigated to help in building, understanding and interpreting different heart disease diagnosing models. The Artificial Neural Networks model showed the best accuracy of 84.25% compared to the other models. In addition, it was found that despite some designed models have higher accuracies than others, it may be safer to choose a lower accuracy model as a final design of this study. This sacrifice was essential to make sure that a more transparent and trusted model is being used in the heart disease diagnosis process. This transparency validation was conducted using a newly suggested metric: the Feature Ranking Cost index. The use of that index showed promising results by making it clear as which machine learning model has a balance between accuracy and transparency. It is expected that following the detailed analyses and the use of this research findings will be useful to the machine learning community as it could be the basis for post-hoc prediction model interpretation of different clinical data sets.**

Keywords*—Heart diseases; machine learning; artificial neural networks; support vector machines; Naïve Bayes; decision trees; random forests; model interpretation; feature ranking cost index

I. Introduction

The field of machine learning has been progressing tremendously as its techniques became more popular and easily accessible. Applications ranged from face detection, system security, disease diagnosis, drug discovery, and many other revolutionary areas that impacted the lifestyle of many individuals. The basic idea behind building machine learning applications is different from most conventional programming methods. Basically, Machine learning models learn from patterns in the provided training examples without using explicit instructions, and then use inference to come up with useful predictions.

Some machine learning techniques, such as Artificial Neural Networks (ANN) and Support Vector Machines (SVM), are very well known as successful prediction models, but sometimes they have problems. The main problem lies in the fact that they remain as black boxes after the model is built. In most of the cases, prediction models are built using historical data to make predictions about future situation that may take place. Understanding the reasoning behind the model prediction response could save organizations' stakeholders a lot of trouble as they may be carefully investigating different situations, while choosing the right medical treatment or assessing the risk of an investment plans for example. Some designed machine learning models play a very critical role in the health care system, and the designed system could recommend performing surgery on a patient. That decision should be extremely accurate to avoid life threatening situations. Making such a tough decision requires a thorough understanding of the reasons behind the model final recommendation before actually going on with the surgery.

In order to build machine learning models that could perform heart patient diagnosis, patients' data set examples need to be used. There are a few trusted websites that most researchers use when they collect data for analysis, such as UCI and Kaggle. The data set that has been used in this research is from the UCI Machine Learning Repository, and it is called the Cleveland Heart Disease data set, which consists originally of 76 features and has 303 instances. The data was originally collected from Cleveland Clinic Foundation, Cleveland, Ohio, and provided by Robert Detrano, M.D., Ph.D. of the V.A. Medical Center, Long Beach, CA [1].

At the UCI website, there were 4 heart diseases data sets to choose from: The Cleveland, Hungarian, Switzerland, and Long Beach, VA data sets. However, the Hungarian and the Cleveland data sets were the most promising in terms of the number of data instances and quality of data. Particularly, the Cleveland data set was almost complete with 303 instances, while the Hungarian data set had 294 instances, but some features were incomplete such as slope, ca and thal. On the other hand, the other two data sets, Switzerland and Long Beach, had 123 and 200 instances respectively, and they even have more incomplete features such as chol, exang and thalach.

Having introduced the available heart disease data sets, it is necessary to have a second look at the two major data sets that have more records than the rest: the Cleveland and the

Hungarian data sets. It was noticed that the distribution of heart disease categories in the Hungarian data set were proportional, whereas the in the Cleveland land data set, some disease categories such as Dis-Cat1 was more represented, see Fig. 1 and Fig. 2. In almost all the research work done on heart data sets, all the disease categories were grouped into one group. Therefore, that note was not important, and the vote for which data set to use was won by the Cleveland data. That led to having almost a balanced category of disease instances versus no-disease: 160 instances of people without heart disease versus 137 instances of people with chance for heart decease.

Most research papers that investigated the Cleveland data set have used only 13 features out of the original 76 features. The last column in the data set is num, which is a categorical variable having values: 0 for no disease, and 1, 2, 3 and 4 for variation of presence of heart disease, see Table I. However, as mentioned earlier, the heart disease variation levels, 1 to 4, have not been specified in the UCI available data sets description. Therefore, in this research, since it was logical to group all the disease levels 1, 2, 3 and 4 in one category, the num variable had only two categories: Dis, or NoDis.

The structure of this paper is organized as follows: Section two shed some light on the related research that has been done in heart disease diagnosis using machine learning. Section three focuses on the theory behind different methodologies used in this paper. Section four covers results and discussion, followed by a related section: models' interpretations, which complements the models' design processes as we try to achieve the best diagnosing model. Finally, section six concludes the presented work and provides a glimpse into possible future research avenues.

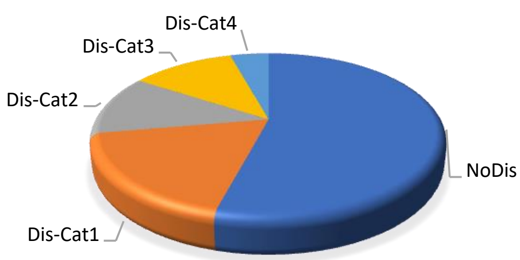

Fig. 1. Cleveland Data Categories.

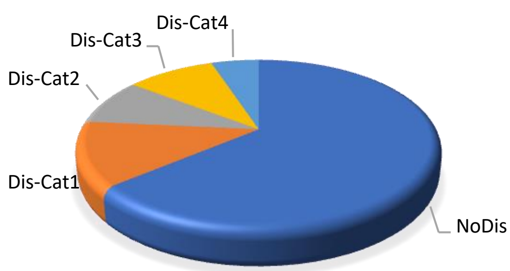

Fig. 2. Hungarian Data Categories.

TABLE. I. LIST OF FEATURES AND THEIR DESCRIPTIONS IN THE HEART DISEASE DATASET

Name Feature	Description
age	age in years
sex	patient sex
cp	chest pain type
trestbps	resting blood pressure
chol	serum cholesterol
fbs	fasting blood sugar
restecg	resting electrocardiographic result
thalach	maximum heart rate achieved
exang	exercise induced angina
oldpeak	ST depression induced by exercise relative to rest
slope	the slope of the peak exercise ST segment
ca	number of major vessels (0-3) colored by fluoroscopy
thal	Exercise thallium scintigraphy
num	Response: diagnosis of heart disease

II. RELATED WORK

Different learning techniques have been used successfully in many medical applications to leverage human health conditions. For example, some applications addressed Liver Fibrosis prediction in Hepatitis patients as well as a decision support system for Diabetes diagnosis using soft computing fuzzy techniques [2,3]. Other applications focused on diagnostic systems for Heart Disease prediction for Coronary diseases using machine learning approaches. The machine learning methods used in these applications ranged between using a single machine learning technique such as hidden Naïve Bayes (NB), SVM, optimized ANN and Decision Tree (DT) classifiers [4,5,6,7], to using a collective or hybrid machine learning techniques [8,9,10]. Since the focus in this proposed research is on heart disease diagnosis, more attention will be devoted to its related literature.

The literature on using machine learning techniques to diagnose Heart Diseases were abundant. That was expected as the topic is very critical and is the center of attention of the World Health Organization as mentioned earlier. However, to build reliable machine learning models, rich data sets are needed. Unfortunately, most of the trusted data sources on heart diseases such as UCI or Kaggle have a relatively small number of instances when compared to Diabetes data sets for example [11]. Some machine learning techniques could be affected by that small number of instances such as ANN, which will eventually lead to building low accuracy models.

A few researchers have addressed the heart data instances sparsity issue and developed some techniques to handle it [12,13,14,15]. Some have combined two major heart data sets, the Cleveland and the Hungarian, to form a bigger set aiming to design better machine learning models and eventually achieve better results. Other researchers have used surrogate data sets that include synthetic observations in order to increase the number of instances in a heart disease data set. These models have done good efforts to improve the overall accuracy of the designed machine learning model despite data sparsity.

In general, most of the literature on using machine learning for heart disease diagnosis utilized two major techniques: the ANN [16,17,18,19] and the SVM [20,21,22,23]. They both have high classification accuracy, but they suffer from low learning speed when the number of instances or the number of features is huge. These facts make them great candidates for analyzing the Cleveland heart disease data at hand, since the number of instances and the features are relatively low. Most of the research focus in these two techniques tried improving the classification Accuracy and other validation metric scores such as the F-score.

In some applications that were based on ANN models research was focused on a serious pathophysiological heart condition, the Congestive Heart Failure (CHF), which is difficult to diagnose in some cases. Despite facing that difficulty, the combined design of convolutional neural network (CNN) and a distance distribution matrix (DDM) classification models was efficient enough to discriminate CHF patients from normal ones. The applications on deep learning continued to be used effectively in other research efforts focused on the same CHF heart condition. An important feature predictor, the Heart Rate Variability (HRV), which is an effective predictor, was used to analyze the designed model. Despite the challenges associated with the use of this predictor, the researchers have deployed an effective ensemble method for CHF detection using short-term HRV measured data and deep neural networks. They have added an extra analysis step, which is considered very important in model validation. They have conducted feature importance analysis to see if it agrees with their deep learning designed model chosen features. We Believe that the validation step is very important in model design, and we are going to use this step as well in our proposed research.

On the other hand, in some other applications that were based on SVM models, research was focused also on the CHF pathophysiological heart condition. One application deployed the same approach by using the HRV measures as input features to the support vector machine classifier. Their designed model was able to detect the CHF cases effectively, and therefore could be valuable if applied in other biomedical signal processing applications. One application using the support vector machine learning technique was focused on detecting patients with Heart Failure (HF). In it, researchers have utilized a hybrid grid search algorithm that can optimize multiple support vector machine models simultaneously. That algorithm showed an improvement over using the conventional stand-alone support vector machine models.

As a general comment on the literature, most of the applications found were focusing on getting the best performance model to perform predictions based on the available data. However, these efforts stopped at that point in most of the applications, and there were no further attempts of model interpretation. The focus in our research is not only to have the best performance model, but also to have a transparent model that could give interpretable trusted results. With interpretation, more useful information could be extracted from the data set in addition to prediction. This is a recent research trend in machine learning and the efforts in this area are growing in a promising direction.

This paper uses the UCI Machine Learning Repository Cleveland heart disease data set with the intention of performing the following main objectives: (1) to understand the heart disease data set at hand, to perform suitable data pre-processing, and to explore the best features to use during analysis (2) to build different machine learning classifiers and to use them to achieve the best prediction model. (3) to interpret the results achieved using these classification models and to provide suitable analysis about the transparency of these classifiers and the reasons to trust their resulted predictions. As much as the first two objective are considered as valuable contributions of this paper, the latter objective is considered to have more contribution by proposing the new metric: the Feature Ranking Cost index. In this research, that index was informative enough during the analysis phase to asses trust of different designed machine learning models based on their feature-sets used for prediction. We believe that it is a must-need step for every researcher who claim to have designed a robust machine learning model. We hope that it becomes a practice to adopt post-hoc validation techniques such as the one that we are proposing to guarantee the design of efficient and authentic machine learning models.

III. Theoritical Background

In this research, a few supervised machine learning techniques have been chosen to build a diagnosing model for the Cleveland heart disease data set: MLP, NB, and a SVM, and Random Forests (RF) classifiers [24,25,26]. For experimentation, a 10-fold cross validation method was used to evaluate each model performance. During the validation process, the data set is divided into 10 folds. Each fold is held in turn for testing, while the other 9 folds are used for training. This validation process is repeated 10 times to guarantee that each data instance is used once for testing and 9 times for training. To further enhance the performance of the designed models in this research, stratified cross validation has been deployed where each fold used in the validation is balanced by having the right proportion of the class labels. In the following sections, a brief theoretical background about the deployed machine learning techniques will be introduced.

A. The ANN Model

ANN is designed based on the biological neural networks, which form the building blocks of the human nervous system. Multi-layer ANN consists of more than one processing layer of neurons, which represent the mathematical realization for the biological neural networks. During supervised learning, an ANN learns and gains experience from a set of predefined training examples. The error minimization process is supervised by a teacher. In this research use of the ANN model, a supervised training method is used to perform non-linear mapping in pattern classification based on back-propagation. During the training phase, the input examples are applied to the network, and the resulting, actual, response is compared with the desired response. If the actual response differs from the target response, an error signal is back propagated to adjust the network weights, see Fig. 3.

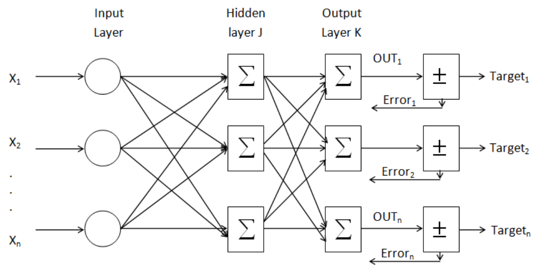

Fig. 3. The Back-Propagation ANN Structure.

The directions of two basic signal flows in a backpropagation network are: forward propagation of function signals and back-propagation error signals. For the forward propagation Pass:

1) Calculate output_j : actual-net-output
2) Calculate error (target_j – output_j) at the output units

The basic back-propagation algorithm is based on minimizing the error of the network using the derivatives of the error function. The most common measure of error is the mean-square error:

$$E = 1/2\,(\text{target} - \text{actual})^2 \tag{1}$$

A small step, learning rate α, in the opposite direction will result in the maximum decrease of the local error function. Therefore, the new weight will be given by:

$$W_{new} = W_{old} - \propto \frac{\partial E}{\partial W_{old}} \tag{2}$$

For the backward propagation Pass:

1) Compute Δw for all weights of the output layer:

$\delta_j = f'(net_j)(\text{target}_j - \text{output}_j)$, therefore:

$$W_{new} = W_{old} + \alpha\, \text{output}_i f'(net_j)(\text{target}_j - \text{output}_j) \tag{3}$$

2) Compute Δw for all weights from hidden layer(s) back to input layer:

$\delta_j = f'(net_j)(\sum \delta_k W_{kj})$, therefore:

$$W_{new} = W_{old} + \alpha\, \text{output}_i f'(net_j)(\sum \delta_k W_{kj}) \tag{4}$$

B. The SVM Model

The key difference that discriminate SVM from other classifiers is that it focuses on the data points which are hard to classify, whereas in most other classifying techniques, the focus is on all the data points. For example, the basic Perceptron, in ANN, is searching for linear separability for each data point in the training set and stops when that condition is satisfied. However, these lines are not guaranteed to be the best separators. On the other hand, the SVM linear classification algorithm goal is to maximize the distance between the two hyper planes defined by: $wX - b = -1$ for the first class, and $wX - b = 1$ for the second class, see Fig. 4. The problem of finding that max-margin hyperplane, defined by $wX - b = 0$, could be solved by finding the distance:

$$\max_{w} \frac{2}{\|w\|} \tag{5}$$

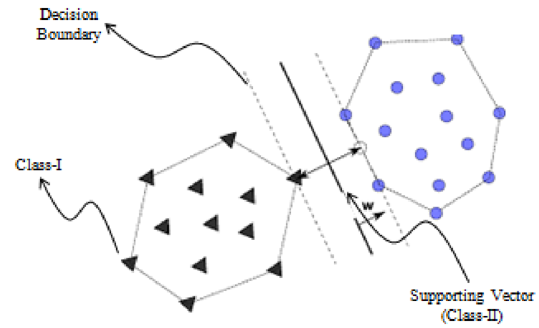

Fig. 4. The Concept behind the SVM Technique.

C. The NB Model

The Bayesian classifier is considered to be one of the most commonly used classification techniques in machine learning. The NB classifier, in particular, base its prediction on Bayes theorem, while assuming independence between the data set attributes, which makes its model easy to build. However, the assumption of independence is not accurate all the time and based on that NB classifiers may be considered less accurate than other more sophisticated machine learning algorithms. On the other hand, there are some advantages of its use such classification speed, tolerance to missing values and fewer model parameter handling. Therefore, when speed is needed during the analysis of big data sets, the NB classifier could be an appropriate choice. The Naive Bayes classification problem could be solved by estimating a classification ratio C, see equation (6). If C is greater than 1, then the first class is predicted, if not, then predict the second class.

$C = \frac{P(i|X)}{P(j|X)}$, therefore:

$$C = \frac{P(i) \prod P(X|i)}{P(j) \prod P(X|j)} \tag{6}$$

Where,

- $P(i|X)$ is the posterior probability of the target class, given a predictor (i.e. attribute X).
- $P(X|j)$, is the likelihood (i.e. the probability of predictor given class).
- $P(i)$ and $P(j)$ are the priori probability of first class i and second class j respectively.

D. The DT and RF Models

One major advantage of DT, unlike most other machine learning models, that it is transparent as you can follow its hierarchical structure to understand how the classification decision took place. In DT, Entropy measures disorder in the data, and can give an indication of how untidy the data is. For that reason, it is used as an algorithm to tidy the data by separating it and grouping the samples in the classes they belong to. A data set could be considered ordered, or tidy, when all the data items in it share the same label and is considered untidy if it has a blend of items with different labels. The DT algorithm uses the Entropy equation while looping around the training data set make sure that each sub data group is tidy and carries the same label, see equation (7).

In this research, J48 DT algorithm is used, which is an open source java implementation of the C4.5 algorithm. The information gain, Gain, is calculated based on testing the attributes, and the best attribute with the highest gain is used as a base for further branching, see equation (8). Given a node (attribute) split argument $\vec{S}$ by a certain value i, to calculate its Entropy we use the following equations:

$$\mathrm{Entropy}(\vec{S}) = -\sum_{j=1}^{n} \frac{|S_i|}{|\vec{S}|} \log\left(\frac{|S_i|}{|\vec{S}|}\right) \tag{7}$$

And the overall Gain is calculated for an attribute j as:

$$\mathrm{Gain}(\vec{S}, j) = \mathrm{Entropy}(\vec{S}) - \mathrm{Entropy}(j/\vec{S}) \tag{8}$$

The DT classifier that we have discussed so far is the basic building block of the RF classifier. In the RF classifier a subset of the original features is used when constructing a given tree. Then, the algorithm searches over sets of random features, e.g. N1 to N4, to choose the best one. Since there are different features for different DT, it is anticipated that it will form with different sizes, and eventually, the formed de-correlated DT are expected to produce different predictions. Based on that assumption, the RF classifier forms its final classification decision by majority voting, which is averaging all the predications of the formed sub trees #1-4, see Fig. 5.

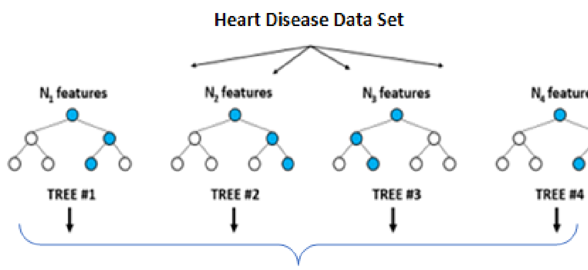

Fig. 5. The Concept behine the RF Technique.

E. Model Evaluation Metrics

During model evaluation, the confusion matrix played an important role in understanding the results obtained in this research, see Table II. True Positive value (TP) were those values that represent the number of patients who originally has heart disease and were actually predicted correctly. True Negative (TN), on the other hand, represented the number of patients who originally did not have heart disease and were actually predicted correctly. Conversely, False Positive (FP) were those patients, who originally did not have heart disease, but were predicted as positive. False negative (FN) on the other hand, were those patients predicted as negative, but originally did have a heart disease.

TABLE. II. THE CONFUSION MATRIX STRUCTURE

Actual			Predicted
		Negative	Positive
	Negative	TN	FP
	Positive	FN	TP

Recall Precision

Based on the previous definitions of TP, TN, FP and FN, the accuracy of the designed models in this research has been calculated using the following evaluation metric:

$$\mathrm{Accuracy} = \frac{TP+TN}{TP+FN+FP+TN} \tag{9}$$

It refers to the ratio between the sum of the total true-positives and true-negatives results to the number of examined instances of the training data. However, in most research papers, scholars agreed that accuracy should not be the end-all measure of model evaluation. Other metrics such as Precision, Recall, and F_1 score should also be considered:

$$\mathrm{Precision} = \frac{TP}{TP+FP} \tag{10}$$

$$\mathrm{Recall} = \frac{TP}{TP+FN} \tag{11}$$

$$F_1\mathrm{Score} = 2\left(\frac{\mathrm{Precision}\times\mathrm{Recall}}{\mathrm{Precision}+\mathrm{Recall}}\right) \tag{12}$$

Precision, or confidence, refers to the ratio between the positively predicated values and the total predicted positive values, whereas Recall, or sensitivity, is the ratio between the positively predicated values and the total actual positive values. The F_1 score on the other hand utilizes both Precision and Recall producing a new harmonic average that shows the balance between them.

IV. RESULTS AND DISCUSSION

A. Heart Data Set Pre-Processing

In this data set, there were 13 features and one target class value as a label. Missing values were not noticed in most of the attributes; however, only 6 missing values were found, 2 in thal, and 4 in ca. The instances that included these missing values were fully deleted, leaving 297 instances for further analysis. Since eventually we need to interpret the designed machine learning model, the idea of implementing feature reduction was not recommended. Instead, feature selection was implemented to identify those features that effectively contribute to the classification process.

It was necessary to remove outliers and extreme values to guarantee robustness of the designed machine learning models. The interquartile range (IQR) technique was used as a measure of the statistical dispersion for the data set features. There was one patient data instance with outliers in the chol feature with a value of 564, which deviates remarkably from the rest of the values in the data set. That instance was removed to avoid skewing in the result as it could have a significant effect on the mean and standard deviation.

As for the extreme values, it was found that there are 43 instances with extreme values, which constitutes 14.5% of the data records. However, for fear of falling into bias problems during models' design, the effect of the removal of these extreme records had to be checked. It was found that the 43 instances are divided almost equally between the two disease categories: 23 patients have a heart disease and 20 patients do not have a heart disease. That balance between the two class instances gave an indication that it is less likely to have class bias, and therefore, those 43 records were removed. Having done this step, it was necessary to follow with a check for feature ranges to make sure that they are homogeneous.

It was noticed that the range of the features in the heart data set vary in a way that could affect the design of the machine learning models. For example, the maximum value for age and oldpeak are 77 and 6, while chol and thalach are 564 and 200 respectively, see Fig. 6. One effective method that was used in this research is to standardize all numeric attributes in the data set to have zero mean and unit variance. Overall, by conducting the previous pre-processing steps, the heart disease data set was ready for the models' design stage. All the models' performance evaluation results during the pre-processing stage are summarized in Table III.

As illustrated in Table III, the initial raw instances of the heart disease data set were used to build four different classifier models: MLP, NB, SVM, and RF. The SVM, NB, and the RF models showed the best performances compared to the MLP model, and significantly better than the base case classifier model: the ZeroR. Because there were a small number of instances with missing value and outliers, models' performances were not noticeably affected after their removal. However, removal of instances with extreme values as well as feature standardization led to an improvement in the MLP model accuracy reaching 81.88%, see also model building speeds in Fig. 7. The experiments were run on an Intel(R) Core (TM) i-2400S CPU @ 2.50GHZ processor, with 6.00 GB RAM, on a 64-bit operating system, x64-based processor system. Having dealt with the previous data processing steps, it was imperative to perform feature selection hoping to improve the performance of the models under investigation.

B. *Feature Selection and Model Design*

In this research, simple fast attribute selection methods have been studied such as single attribute evaluator with ranking and attribute subset selection methods. However, the single attribute method can allow redundancy, which is not recommended and may lead to inaccurate results. For example, problems such as redundancy have strong impact on the performance of the NB classifier, while overfitting could badly impact the MLP classifier. The attribute subset selection method, on the other hand, removes redundancy as well as irrelevant features, hence it was chosen in this research as a base method for feature selection.

Careful measures have been considered while applying that attribute selection method to the heart disease data set, with cross-validation, to have fair classification results. A problem could have happened if the entire data set is used to decide on the attribute subset. Therefore, in this research, attributes have been selected based on the training data only. Then, each designed classifier model has been trained on the training data as well with cross-validation in effect, followed by model evaluation using the test data.

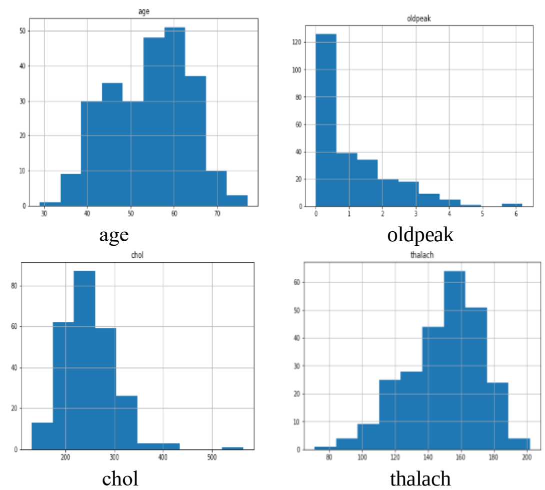

Fig. 6. Selected Features' Histograms.

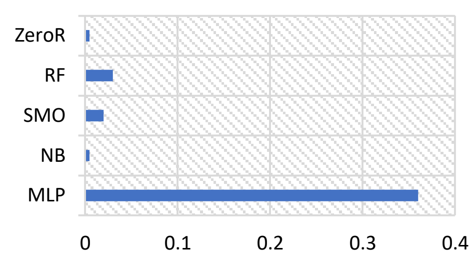

Fig. 7. Models' Building Speeds in Seconds.

TABLE. III. EFFECT OF PRE-PROCESSING STAGES

	Performance%	**MLP**	**NB**	**SVM**	**RF**	**ZeroR**
Original Data	Accuracy	78.88	83.5	83.82	81.85	54.12
	Precision	78.9	83.6	83.9	82.3	29.3
	Recall	78.9	83.5	83.8	81.8	54.1
	F_1	78.8	83.4	83.8	81.7	38.0
Missing & Outliers	Accuracy	78.37	83.11	83.44	82.43	53.72
	Precision	78.4	83.2	83.5	82.5	28.9
	Recall	78.4	83.1	83.4	82.4	53.7
	F_1	78.3	83.0	83.4	82.3	37.5
Extrems, Missing & Outlier	Accuracy	81.88	81.88	82.68	75.9	53.94
	Precision	81.9	81.9	82.7	76.2	29.1
	Recall	81.9	81.9	82.7	76.0	53.9
	F_1	81.9	81.9	82.6	76.0	37.8
-Standardization	Accuracy	81.88	82.28	82.67	79.13	53.93
	Precision	81.9	82.3	82.7	79.7	29.1
	Recall	81.9	82.3	82.7	79.1	53.9
	F_1	81.9	82.2	82.6	79.2	37.8

One good recommended practice, when performing attribute selection, is to use the same classification method as a wrapper substitute evaluator method. However, all possibilities have been tested in this research to find the best attribute selection method, and eventually come up with that specific set of features that lead to the best results. This feature-set is expected to be authentic in a sense that it actually affects the results at hand. In the following table, the row entries represent the used technique within the wrapper substitute evaluator method, while the column entries represent the classification technique used in building the models. Different model performance evaluation metrics such as accuracy, precision, recall, and F_1-score are presented in a separate column, see Table IV. It worth mentioning that the time taken for attribute selection and classifier training using MLP in the wrapping process was considerably long compared to other techniques, see a sample run in Fig. 8.

The best accuracy result obtained, 84.25%, after feature extraction, was for the MLP classifier with SVM as a feature selection wrapper substitute evaluator method. The NB and the SVM classifiers had a lower, but comparable, results at 83.07% and 82.28% respectively. The RF classifier came last with 78.35% accuracy despite the fact that the redundant features have been removed. Recalling an earlier comment in this paper about the practice of using the same classification method as a wrapper substitute evaluator method, it was noticed that SVM has the best accuracy performance at 82.28%, see the lightly shaded diagonal cells at Table IV.

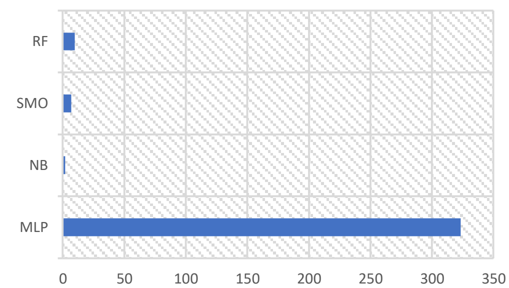

Fig. 8. Feature Extraction and Classification Model Building Speeds in Seconds.

During the feature selection analysis, different features have been selected by different wrapper substitute evaluator method. For example, MLP came up with 8 features in its recommended feature-set, followed by 5 features feature-sets for NB, SVM, and RF, see Table V. Up to this point of analysis, it could be fair to assume from Tables IV and Table V that the longer the run-time, while deciding on the best selected feature-set, the more the numbers of features selected. However, how authentic are these feature-sets required further analysis. The following section focuses on using one of the well-known model interpretation techniques, the DT, to find reasonable explanations for the resulted models' performances.

TABLE. IV. EFFECT OF FEATURE SELECTION METHODS

	Performance%	MLP	NB	SVM	RF
MLP	Accuracy Precision Recall F_1	79.13 79.1 79.1 79.1	79.92 80.2 79.9 80.0	79.53 79.5 79.5 79.5	80.32 80.4 80.3 80.3
NB	Accuracy Precision Recall F_1	81.1 81.1 81.1 81.1	81.1 81.1 81.0 81.0	82.7 82.8 82.7 82.6	78.35 78.3 78.3 78.3
SVM	Accuracy Precision Recall F_1	84.25 84.4. 84.3 84.2	83.07 83.2 83.1 83.0	82.28 82.3 82.3 82.2	78.35 78.4 78.3 78.4
RF	Accuracy Precision Recall F_1	78.3 78.3 78.3 78.3	80.71 80.9 80.7 80.7	77.56 77.7 77.6 77.6	79.92 79.9 79.9 79.9

TABLE. V. FREQUENCY OF SELECTED FEATURES

	age	sex	cp	trestbps	chol	fbs	resteg	thalach	exang	oldpeak	slope	ca	thal
MLP	√	√		√	√					√	√	√	√
NB			√					√		√		√	√
SVM		√	√						√			√	√
RF		√									√	√	√

V. Prediction Level Interpretation

All the machine learning models used in this research deploy supervised learning methods. These methods used the instances of heart disease data set to learn and to produce general hypotheses as predictions. DT is one of the supervised machine learning models that is frequently used to solve classification problems. One major advantage of DT models is that they could map non-linear relationships, while providing clear interpretation, and for that reason DT will have more focus in this section.

Further analysis was done using the J48 DT classifier, while performing attribute selection and using the same classification method, J48, as a wrapper substitute evaluator method, see Table VI. The DT designed model took 1.1 seconds to be build using the same earlier machine specs used for the other machine learning models: MLP, NB, SVM, and RF. The resultant model accuracy was 76.38%, which is considered low compared to those previous models except for the RF model. Most of those earlier models, despite having better accuracy, were not transparent, and therefore were hard to interpret.

Comparing Table V and Table VI, it was noticed that they are almost identical, except for one attribute difference between the RF and the DT models as wrapper substitute evaluator methods. Both models agreed on selecting attributes sex, ca and thal, but disagreed on slope and oldpeak. Focusing on table VI, one could conclude that the most frequently selected attributes for the J48 DT model were thal, ca, oldpeak, sex, and maybe cp as well. The following classification trees' samples were generated, while the designed DT models were evaluated, see Fig. 9 to Fig. 12. The root node in each illustrated classification tree is considered the attribute with the highest purity as it is more capable of discriminating between patients with and without heart disease and so forth down the tree.

From the model interpretation point of view, the purity of these features could be a reference point for measuring their contribution to the accuracies of their corresponding analyzed models. For example, if we look at classification Tree-1, in Fig. 9, it could be fair to deduce that in order to decide if a patient has heart disease or not, thal status need to be checked first. As well, the next feature to be checked in that tree is ca, whether the answer at the previous thal-node was Yes or No. One can comprehend such reasoning even at the third level of the tree while checking for sex and age. However, as we go deeper in that tree, we may get confused during analysis. That confusion could be more noticeable at classification Tree-4, which was build during the design of the MLP model.

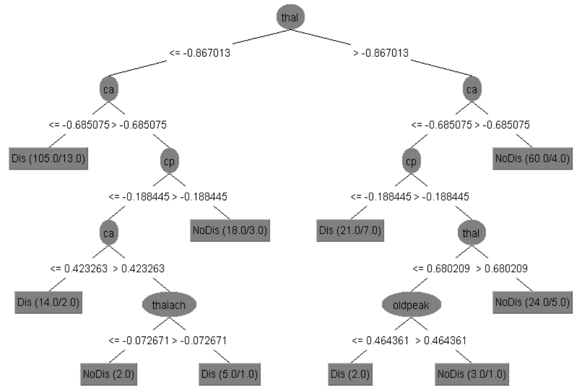

Fig. 9. Classification Tree-1.

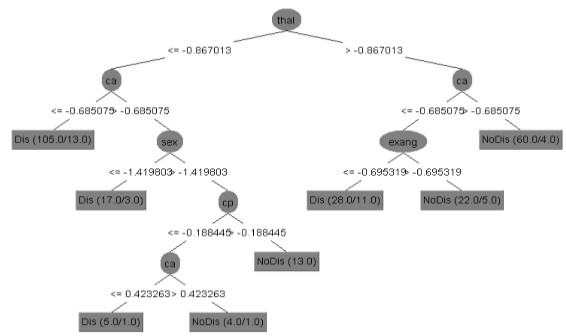

Fig. 10. Classification Tree-2.

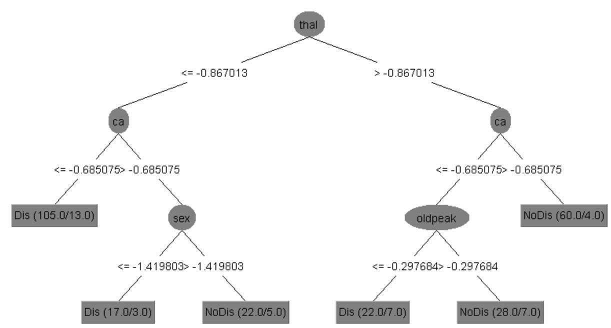

Fig. 11. Classification Tree-3.

TABLE. VI. Frequency of Selected Features-DT Only

	age	sex	cp	trestbps	chol	fbs	restecg	thalach	exang	oldpeak	slope	ca	thal	Accuracy (%)
Tree1 NB			√					√		√		√	√	77.17
Tree2 SVM		√	√						√			√	√	79.53
Tree3 DT		√								√		√	√	76.38
Tree4 MLP	√	√		√	√					√	√	√	√	78.35

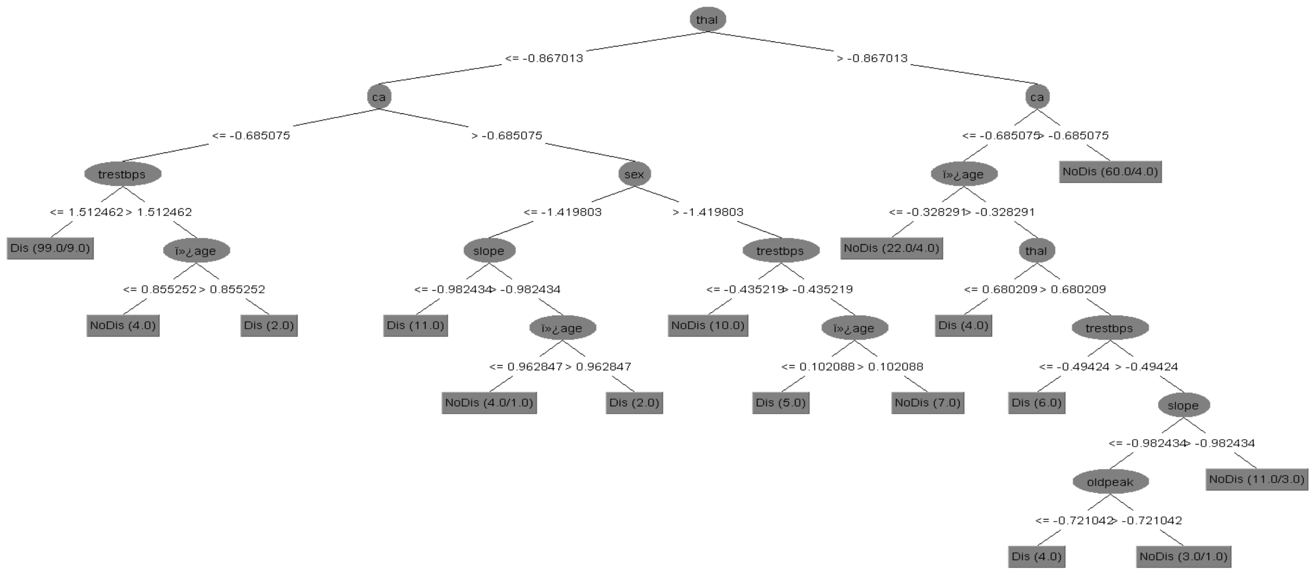

Fig. 12. Classification Tree-4.

A well-known method to handle the previous confusion problem is to use feature importance analysis using ensemble method of DT. The values representing feature importance are relative values, or scores, comparing the performance of the desired model with and without that specific feature. In this research, all features in the heart disease data set have been considered for feature analysis, see the chart shown in Fig. 13. Values of importance ranged between Zero for the fbs feature to 1.75 for the thal feature, which is considered for this model to be the most predictive value. Based on that concept, removing a feature such as thal is expected to considerably affect the designed model, while removing a feature such as fbs should not have an effect, and so forth for rest of the feature importance values.

Further analysis has been conducted using a new proposed technique, Feature Ranking Cost, to better understand and interpret the performances of the designed models: MLP, NB, SVM, and RF. The concept behind the creation of this new metric is to come up with a simple post-hoc technique that can help in evaluating the worthiness of a model performance based on the importance of its feature-set. After evaluating the designed models from that point of view, a simple corrective action could be taken by choosing the best final model that is capable of producing the best authentic result as much as possible.

Table VII illustrates how this index could be calculated with the support of the chart in Fig. 13 as well. The Feature Ranking Cost (FRC) index for a specific model M as well as the best model FRC could be calculated using Equation (13) and Equation (14) respectively.

$$M_{FRC_i} = \sum_{i=1}^{n} FIR_i \qquad (13)$$

$$M_{Authentic_j} = \min_j M_{FRC_j},\ j{:}1 \rightarrow m \qquad (14)$$

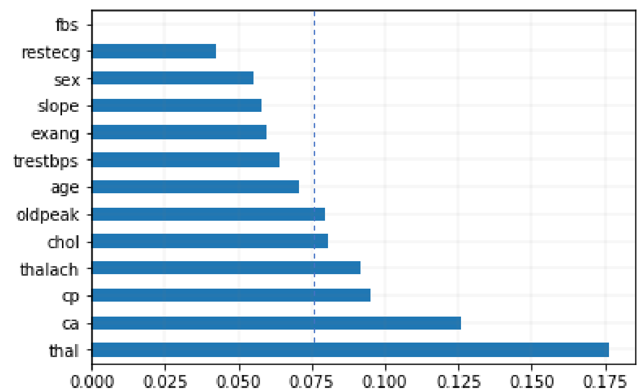

Fig. 13. Most Important Features based on DT– Entropy Function.

TABLE. VII. CREATION OF FEATURE RANKING COST INDEX

Feature Importance	Feature	MLP	NB	SVM	RF
0.07041383	age	7			
0.05492301	sex	11		11	11
0.09525694	cp		3	3	
0.06413777	trestbps	8			
0.08089077	chol	5			
0.0	fbs				
0.04242536	restecg				
0.09190829	thalach		4		
0.05973358	exang			9	
0.07978184	oldpeak	6	6		
0.05797686	slope	10			10
0.12622297	ca	2	2	2	2
0.17632879	thal	1	1	1	1
	Σ Cost @ 0.075	14	16	6	3

Where M_{FRC} is the sum of ranks for all the feature-set items of a model M given its Feature Importance Ranks (FIR's), and $M_{Authentic}$is the minimum authentic value amongst all the m models (m=4 in this research). The FIRs could be found from Fig. 13 in an ascending order: 1 for thal, 2 for cp, and so forth until 13 for fbs. The reason behind choosing the minimum authentic value is that the most authentic model is expected to have the most important set of features and to show the best performance at the same time. It worth mentioning that the sum of all the feature importance values adds up to one. Therefore it is recommended when conducting research with a larger feature data set to use a Weighted Feature Ranking Cost to avoid computational problems. It could be calculated by multiplying each FIR by its corresponding Feature Importance Score (FIS), and then follow the previous calculation procedures:

$$M_{WFRC} = \sum_{i=1}^{n} FIR_i \times FIS_i \quad (15)$$

Deciding how many features should be in each feature-set is a challenging task. In other words, at what rank should we stop to perform the calculation of the M_{FRC} indices? In this research, the approach was to calculate the whole FIS range, and then use that as a reference as where to set the threshold value. Specifically, for Table VII, 50% of the whole FIS range was used, and every feature that has a lower value was not included in the features' analysis pool. Based on that range of choice, approximately 46% of the attributes in the feature importance chart were covered: thal, ca, cp, thalach, chol, and oldpeak.

The FIR values for each classification model were added to calculate its M_{FRC}. The lowest FRC index was for the RF model, using the RF wrapping attribute select method. It was chosen based on that criterion as it has the most relevant attribute-set than the other models: MLP, NB, SVM. As a final concluding point, recalling Table IV, the MLP model, at an accuracy of 84.25%, seemed to be the right choice for the heart disease final classification model design. However, after conducting the pos-hoc FRC analysis, it could be more accurate to resort to a safer lower accuracy model in our final design by choosing the RF model at an accuracy of 79.92%. By doing that the final designed model in this research will have a balance between accuracy and transparency.

It has been noticed that the RF model has around 40% of the most effective feature, while the MLP has around 65%. However their feature ranking cost (FRC) are 3 and 14, see Fig. 14. It is believed that the values of the feature ranking cost FRC should be proportional to the values of the feature count ratio, shown in Fig. 15, for each designed model. A few modification have been applied to equation (13) by introducing a new term, the feature count ratio C_i, see equations (16) and (17). To further enhance the proportional relation between FRC for each model and its C_i, it was necessary to factor it by the corresponding Feature Importance Ranks (FIR), see equation (18). Table VIII shows the new re-calculated FRC's for the four designed models, and it shows that the RF model still has the lowest cost, which means that the previous post processing analysis still holds. Fig. 16 combines the new values for feature ranking costs for each model compared to its feature count ratio based on the new equations. It has been noticed that the values of the feature ranking cost FRC have better proportion to the values of the feature count ratio. That result assures, as well, that despite the previous modifications, the choice of the RF model is still an authentic choice and more safer to rely on.

$$C_i = \frac{m_i}{n_\theta} \quad (16)$$

$$M_{FRC_i} = \frac{1}{C_i} \sum_{i=1}^{n} FIR_i \quad (17)$$

$$M_{WFRC_i} = \frac{1}{C_i} \sum_{i=1}^{n} FIR_i \times FIS_i \quad (18)$$

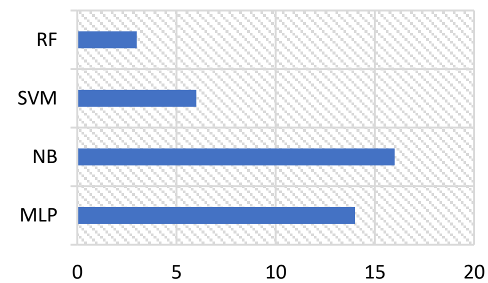

Fig. 14. Feature Ranking Costs based on Equation 13.

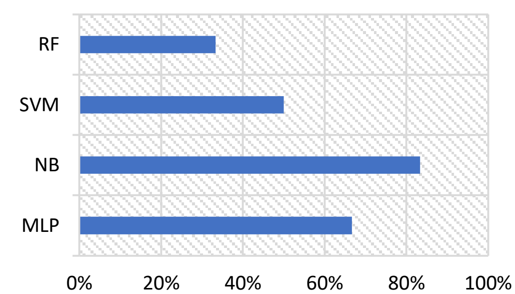

Fig. 15. Feature Count Ratio.

TABLE. VIII. CREATION OF WEIGHTD FEATURE RANKING COST INDEX

Feature Importance	Feature	MLP	NB	SVM	RF
0.07041383	age	0.4929			
0.05492301	sex	0.6042		0.6042	0.6042
0.09525694	cp		0.2858	0.2858	
0.06413777	trestbps	0.5131			
0.08089077	chol	0.4045			
0.0	fbs				
0.04242536	restecg				
0.09190829	thalach		0.3676		
0.05973358	exang			0.5376	
0.07978184	oldpeak	0.4787	0.4787		
0.05797686	slope	0.5798			0.5798
0.12622297	ca	0.2524	0.2524	0.2524	0.2524
0.17632879	thal	0.1763	0.1763	0.1763	0.1763
	Σ Cost @ 0.075	1.9679	1.8730	1.4291	1.2863

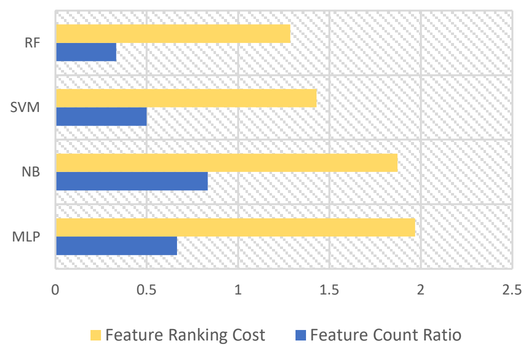

Fig. 16. Feature Ranking Costs Vs Feature Count Ratio.

VI. Conclusion

In this paper it was shown that we have conducted thorough analyses and understanding of the Cleveland heart data set. As well, different machine learning classifiers were designed and used to achieve the best diagnosing model. However, the previous discussion in the interpretation section highlight a few issues that need to be considered as we try to understand the machine learning designed models. If the design for the four models: MLP, NB, SVM, and RF was concluded based merely on calculating the initial used metrics: accuracy, precision, recall, and F1, there could have been a chance of ending up with an inaccurate model. For example, the MLP model, based on an SVM wrapping attribute select method, resulted in an 84.25% accuracy, but used an 8-features set to achieve that result. Based on the 50% threshold used in this research, its feature ranking score, M_{FRC}, was 15, which is a triple of the RF model score. This result indicated that it would not have been accurate to choose the MLP as a base for heart disease diagnosis model.

The investigation analysis done in this research have laid a reasonable foundation in exploring the nature of the heart disease data set. These efforts have been complemented by the interpretation analysis, which added more clarification of the designed models by the introducing the new FRC index. That index was an informative metric and led to a clear discrimination between the models based on their feature-set importance. The final chosen RF model, based on the post-hoc interpretation analysis, had a 79.92% accuracy, which was not a far compromise from the MLP model accuracy. In fact, it was a necessary step to choose the RF model instead of the MLP model to ensure that the final chosen model is authentic and has a balanced compromise between its transparency and its accuracy. It is anticipated that the use of the previous findings will be useful to the machine learning community as it could be the basis for post-hoc prediction model interpretation analysis on different clinical data sets.

For future work, a few main points could be considered. First, combing the Cleveland & Hungarian data sets and performing the required analysis may improve accuracy and give more insight into the transparency of each designed model. New challenges could arise such as missing data, but the 100% data instances increase may compensate for that problem. Second, performing association rule analysis could help in model interpretation and help in understanding the designed DT models, but rule post-processing may be needed to remove redundancy. Lastly, further in-depth post-hos prediction model interpretation analysis could be done to better understand and validate the designed models.

References

[1] Detrano, R., Janosi, A., Steinbrunn, W., Pfisterer, M., Schmid, J., Sandhu, S., Guppy, K., Lee, S., and Froelicher, V., "International application of a new probability algorithm for the diagnosis of coronary artery disease," Am. J. Cardiol. vol.64, pp.304–310, 1989.

[2] S. El-Sappagh, F. Ali, A. Ali, A. Hendawi, F. A. Badria and D. Y. Suh, "Clinical Decision Support System for Liver Fibrosis Prediction in Hepatitis Patients: A Case Comparison of Two Soft Computing Techniques," in IEEE Access, vol. 6, pp. 52911-52929, 2018.

[3] S. El-Sappagh, J. M. Alonso, F. Ali, A. Ali, J. Jang and K. Kwak, "An Ontology-Based Interpretable Fuzzy Decision Support System for Diabetes Diagnosis," in IEEE Access, vol. 6, pp. 37371-37394, 2018.

[4] M. A. Jabbar and S. Samreen, "Heart disease prediction system based on hidden naïve bayes classifier," 2016 International Conference on Circuits, Controls, Communications and Computing (I4C), Bangalore, pp. 1-5, 2016.

[5] M. Ahmad, V. Tundjungsari, D. Widianti, P. Amalia and U. A. Rachmawati, "Diagnostic decision support system of chronic kidney disease using support vector machine," 2017 Second International Conference on Informatics and Computing (ICIC), pp. 1-4, Jayapura, 2017.

[6] M. Kumar, A. Sharma and S. Agarwal, "Clinical decision support system for diabetes disease diagnosis using optimized neural network," 2014 Students Conference on Engineering and Systems, Allahabad, pp. 1-6, 2014.

[7] Purushottam, K. Saxena and R. Sharma, "Efficient heart disease prediction system using decision tree," International Conference on Computing, Communication & Automation, Noida, pp. 72-77, 2015.

[8] M. Gudadhe, K. Wankhade and S. Dongre, "Decision support system for heart disease based on support vector machine and Artificial Neural Network," 2010 International Conference on Computer and Communication Technology (ICCCT), Allahabad, Uttar Pradesh, pp. 741-745, 2010.

[9] Dewan and M. Sharma, "Prediction of heart disease using a hybrid technique in data mining classification," 2015 2nd International Conference on Computing for Sustainable Global Development (INDIACom), New Delhi, pp. 704-706, 2015.

[10] Sowmiya and P. Sumitra, "Analytical study of heart disease diagnosis using classification techniques," 2017 IEEE International Conference on Intelligent Techniques in Control, Optimization and Signal Processing (INCOS), pp. 1-5, Srivilliputhur, 2017.

[11] J. Collins, J. Brown, C. Schammel, K. Hutson, and W. Edenfield, ”Meaningful Analysis of Small Data Sets: A Clinicians Guide,” Greenville Health System Proc., vol.2, no.1, pp. 16-19, June, 2017.

[12] Gárate-Escamilla, A.; El Hassani, A. and Andres, E., “Dimensionality Reduction in Supervised Models-based for Heart Failure Prediction,” In Proceedings of the 8th International Conference on Pattern Recognition Applications and Methods – Volume 1: ICPRAM 2019, pp. 388-395, 2019.

[13] A. Sabay, L. Harris, V. Bejugama, and K. Jaceldo-Siegl, "Overcoming Small Data Limitations in Heart Disease Prediction by Using Surrogate Data," SMU Data Science Review, vol.1, no.3, 2018.

[14] S. Torgyn, and N. Khovanova, ”Handling limited datasets with neural networks in medical applications: A small-data approach,” Artificial intelligence in medicine, vol.75, pp. 51-63, 2017.

[15] L. Masitah, M. Azah, Y. Zeratul, M. Noor, and A. Mohd. "Handling a Small Dataset Problem in Prediction Model by employ Artificial Data Generation Approach: A Review," Journal of Physics: Conference Series, 2017.

[16] Y. Li et al., "Combining Convolutional Neural Network and Distance Distribution Matrix for Identification of Congestive Heart Failure," in IEEE Access, vol. 6, pp. 39734-39744, 2018.

[17] L. Wang, W. Zhou, Q. Chang, J. Chen and X. Zhou, "Deep Ensemble Detection of Congestive Heart Failure Using Short-Term RR Intervals," in IEEE Access, vol. 7, pp. 69559-69574, 2019.

[18] S. Rajamhoana, C. A. Devi, K. Umamaheswari, R. Kiruba, K. Karunya and R. Deepika, "Analysis of Neural Networks Based Heart Disease Prediction System," 2018 11th International Conference on Human System Interaction (HSI), Gdansk, pp. 233-239, 2018.

[19] S. Harjai and S. K. Khatri, "An Intelligent Clinical Decision Support System Based on Artificial Neural Network for Early Diagnosis of Cardiovascular Diseases in Rural Areas," 2019 Amity International Conference on Artificial Intelligence (AICAI), Dubai, Unitsed Arab Emirates, pp. 729-736, 2019.

[20] B. Hu, S. Wei, D. Wei, L. Zhao, G. Zhu and C. Liu, "Multiple Time Scales Analysis for Identifying Congestive Heart Failure Based on Heart Rate Variability," in IEEE Access, vol. 7, pp. 17862-17871, 2019.

[21] L. Ali et al., "An Optimized Stacked Support Vector Machines Based Expert System for the Effective Prediction of Heart Failure," in IEEE Access, vol. 7, pp. 54007-54014, 2019.

[22] C. Yang, B. An and S. Yin, "Heart-Disease Diagnosis via Support Vector Machine-Based Approaches," 2018 IEEE International Conference on Systems, Man, and Cybernetics (SMC), pp. 3153-3158, Miyazaki, Japan, 2018.

[23] L. Ali et al., "An Optimized Stacked Support Vector Machines Based Expert System for the Effective Prediction of Heart Failure," in IEEE Access, vol. 7, pp. 54007-54014, 2019.

[24] Witten, I.H., Frank, E. and Hall, M.A., Data Mining: Practical Machine Learning Tools and Techniques. Morgan Kaufmann Publications, 2011.

[25] Michael Bowles, Machine Learning in Python: Essential Techniques for Predictive Analysis. John Wiley & Sons Publications, 2019.

[26] Simon Haykin, Neural Networks and Learning Machines. Pearson Prentice Hall Publications, 2009.

Towards the Development of Collaborative Learning in Virtual Environments

Benjamin Maraza-Quispe[1], Nicolás Caytuiro-Silva[2], Eveling Castro-Gutierrez[3], Melina Alejandro-Oviedo[4]
Walter Choquehuanca-Quispe[5], Walter Fernandez-Gambarini[6], Luis Cuadros-Paz[7], Betsy Cisneros-Chavez[8]
Facultad de Ciencias de la Educación, Universidad Nacional de San Agustín, Arequipa-Perú[1, 4, 5, 6, 7, 8]
Facultad de Ciencias e Ingenierías Físicas y Formales Universidad Católica de Santa María, Arequipa-Perú[2, 3]

***Abstract*—The objective of the research is to evaluate strategies such as Wikis, Forums and Chat in the development of collaborative learning in higher education students. A collaborative experience was developed with 25 students in an asynchronous e-learning environment. The activities consisted of forum discussions, chat and project development in a wiki environment. The research method includes a quantitative analysis whose forum rating was developed by applying a rubric. The use of didactic strategies such as Wikis, Forums and Chat in the learning sessions promotes collaborative learning where the main factors for this to happen are the degree of appropriation of these technologies by students and the mastery of their use by teachers. It is not possible to affirm the superiority of one tool over another because each has its own characteristics and could be used for different purposes, besides having complementary functions, they must organize and complement each other to develop collaborative learning.**

***Keywords*—Wikis; forums; chat; learning; collaborative**

I. Introduction

"Technological progress, and especially information and communication technologies have influenced many fields, one of which is the education sector" [1], bringing consequently changes from routine learning environments to others characterized by constant transformation and innovation.

The importance and purpose of this research lies in knowing the social and ethical impact of collaborative learning tools and at the same time promote the use of these tools in students because in most cases the teaching-learning processes are carried out routinely, through non-participatory methodologies that directly involve students to develop collaborative processes. The justification for this research lies in the exchange of information, knowledge and dialogues, through active collaboration among team members; allowing self-evaluation and measurement of individual and collective performance, which will facilitate access to a large amount of shared information, as well as the management of such information.

According to [2] "Collaborative Learning consists in learning with others and from others" that is to say, students have the opportunity to be at the center of their own learning, this leads them to determine or plan their objectives, methodology and strategy that promote collaborative learning through a descriptive-experimental study which is analyzed in a sample of 25 students.

A collaborative experience was studied with 25 students in an asynchronous e-learning environment. The activities lasted 24 days and consisted of difficulties in forums, chat and development of a project in a wiki environment. The research method includes a quantitative analysis whose forum rating will be applied in an application based on the following evaluation criteria: (1) Number of entries, (2) Importance of the topic, (3) Contribution of new ideas, (4) quality of interventions and (5) Interaction with peers. The following evaluation criteria will be used to rate the Wikis: (1) Number of entries, (2) Content and quality of contributions, (3) Respect and collaboration, (4) Links and sources and (5) Language management. And to rate the chat, the following evaluation criteria will be used: (1) Language management, (2) Subject mastery, (3) Conventions and (4) Consistency.

II. State of the Art

A. Web 2.0, e-Learning and Moodle

Web 2.0 [3], is a set of Internet utilities and services that are supported by a database, which can be modified by users of the service. Users can add, change, delete and exchange information, either in the form of presenting them in the content or in both simultaneously. In this context, Web 2.0 combines a variety of learning events with tutorial support to facilitate the transmission of tacit knowledge, [4].

Consequently, Web 2.0 is characterized by the easy management of information, and by promoting a collaborative teaching-learning scheme in which the student is the protagonist of his or her own learning process.

According to [5] currently, the most innovative modality in Web-based distance education are e-Learning systems or environments, which make use of the services and facilities of the Internet, to make the process of collaborative teaching-learning possible; as well as the Web has enabled educational possibilities at certain levels and with very specific applications.

In this context, e-Learning platforms constitute teaching-learning systems mediated by technology, where one of the fundamental requirements is the existence of an Internet connection.

According to [6], Moodle based its design on collaborative learning and ideas of constructivism in pedagogy that assert that knowledge is constructed in the student's mind rather than being transmitted unchanged from books or teachings.

In this context, Moodle bases its approach on a collaborative learning teaching system, where the student is the center of the process.

B. Moodle Tools

According to [6], the tools that distinguish the Moodle virtual learning platform are the Forums, Wikis and Chats; [7], classifies the resources available in Moodle into three categories, to which the communication tools can also be added: (a) Transmissive resources, (b) interactive resources, (c) collaborative resources: Moodle includes the following collaborative tools: Forums, Workshops and Wikis [8], cited by [7], (d) In this context collaborative resources are tools oriented to interaction and exchange of ideas, these tools are forums, wikis, workshops, among others, (e) communication tools [8] available in Moodle are: E-mail, Chats, Messages, Consultations and Surveys.

In this context, chats as well as forums and wikis allow interaction and exchange of ideas among participants, creating collaborative learning environments and teamwork, as it allows interaction between teacher-student and student-student at the same time.

C. Collaborative Learning

According to [8], collaborative learning enables students to build their own knowledge through a complex interactive process involving three key elements: the students, the content, and the teacher, who acts as facilitator and mediator between the two.

In other words, the student is the active author of the acquisition of his or her own knowledge, through an interactive process in which the content and the teacher are also involved.

According to [9], collaborative learning mediated through ICT tools gives rise to what is known as Computer-Based Collaborative Learning.

According to [10] a constructivist learning environment is based on collaborative learning, a place where students must work together to help each other, using a variety of tools and computing resources that allow the pursuit of learning objectives and activities to solve the problem.

For [11] collaborative learning is based on cognitive theories. In the constructivist theory of [2], learning requires the action of a mediating agent to access the area of proximate development, he will be responsible for setting up a scaffolding that provides security and allows him to appropriate the knowledge and transfer it to his own environment. In the same way, regarding the educational implications of the above [10], it defines teaching as "a continuous process of negotiation of meanings, of establishment of shared mental contexts, fruit and platform, at the same time, of the negotiation process", which allows to verify the connections between learning, interaction and cooperation.

In this context, collaborative learning is another of the constructivist postulates that conceives education as a process of socio-construction in order to know the different perspectives of approaching a given problem, develop tolerance around diversity and the ability to re-elaborate a joint alternative.

According to [11], in order to define a learning environment, it is important to first determine the environment, understanding as environment all that surrounds the teaching-learning process, that is, the space that surrounds the student while participating in said process, constitutes it from material elements such as the infrastructure and facilities of the campus, as well as different factors that directly influence the student such as physical, affective, cultural, political, economic, social, family and even environmental factors; which combine and have a favorable effect or not so much in the student's learning.

In this context, communication between those who are within the teaching-learning process, that is, teacher-students, vice versa, and student-student, measured by the environment that surrounds it and by technologies such as a virtual classroom (CMS Moodle), are environments and factors that often promote the process of collaborative teaching-learning.

D. Collaborative Learning and Constructivism

According to [12] collaborative learning is based on cognitive theories.

One of these is the constructivist theory of [2], where the apprentice requires the action of a mediating agent to access the zone of proximate development, this will be responsible for having a scaffolding that provides security and allows that the apprentice appropriates the knowledge and transfers it to his own environment. As for the educational implications.

E. CMS Tools that Contribute to the Development of Collaborative Learning

According to [12], the Wiki is an instrument that allows everyone to participate in it; they can be visited, edited or changed. The use of this tool begins to gain strength in the academic field in virtual spaces.

On the other hand [13] they affirm that the student is promoted to develop an autonomous learning, in which, under his responsibility he appropriates his formation, exchanging knowledge and ideas with other students, incorporating himself in this way in a collaborative learning. As opposed to what happens in a classroom, the wiki can extend the notes with the collaboration of all; wikis can also be used in parallel with forums or chat.

In this context [5], he affirms that the use of a virtual classroom contributes to improving students' inter-learning; new resources are integrated that help to improve teaching practice, communication, motivation, and orientation; improving the interaction between teacher-student and student-student.

Likewise [14] virtual learning environments offer an asynchronous learning space that provides students with course materials, as well as collaboration and interaction during the implementation of a virtual forum.

Some of the benefits of the application [15] of virtual discussion forums: (1) It reinforces learning and improves its significance; (2) It allows students to know their attitudes towards certain topics; (3) It favors the development of social skills through interaction and helps to improve written communication skills.

For [16] They consider that asynchronous school activities, either through educational platforms CMS promote collaborative work between peers, through the use of forums teachers and students participate on educational topics, interacting with peers, exchanging knowledge, experiences, and expressing their ideas with more freedom and ease, in addition to being able to participate from different geographical locations.

For [17] the objective of a forum is none other than to create reflection, through contributions, to achieve a clear and precise concept, building it little by little, from the contributions of the participants.

Simultaneously [18] emphasizes the potentials of peer collaboration and social negotiation in an asynchronous online environment, individuals are able to build knowledge and relate what they learn to their prior knowledge.

Regarding the rules of courtesy [19], they mention that [...] the forums are regulated by rules of courtesy and that their participants maintain a collaborative and co-evaluative attitude, in order to contrast their points of view, and thus generate a process of knowledge construction.

In this context, the application of virtual spaces, as in the case of virtual forums, which contribute to promoting collaborative learning [20], allow for the strengthening of learning processes in order to reach knowledge.

III. Materials and Methods

The TISG area (Information Technology in a Global Society) considers people as the central axis around which the TISG study revolves [21], the case studies proposed in the experimentation consider the use of IT (Information technology) and its effects on users.

Participation in the forums, wikis and chats will be evaluated using the headings found in Fig. 1 and in detail described in the following Technical Report[1].

IV. Research Design

A. Sample Population

The population is made up of 25 randomly selected students who take the TISG course.

As can be seen in Table I.

Two case studies are analyzed: Case A and Case B, where each case corresponds to the issues: IT in the home and leisure,

Modelling and simulations respectively.

Table II shows the heading used to rate student participation in the Forums.

Table III shows the heading used to rate the participation of students in the Chat.

Table IV shows the heading used to rate the participation of students in the Wiki.

V. Analysis of Results

A. Instruments

The wikis, forums and chat will be implemented under the following criteria and conditions as can be seen in Table V.

As for the data collection instruments, use the Wikis, Forums and Chat, as can be modified in Table V.

TABLE. I. STUDENTS PARTICIPATING IN THE RESEARCH PHASE

Case Study	**Students**	**Teachers**	**Duration**
A	25	1	12 days
B	25	1	12 days
Total participants in A-B cases	25	1	-

TABLE. II. ASSESSMENT RUBRIC-FORUM

Objectives Criteria	**Excellent (4 points)**			
Participation	Participate in the forum with at least 3 interventions.	Very well (3 points).	Needs improvement (1 point each item)	Does not (0 points each item)
Importance of the topic	The interventions show, in a broad way, that he did the reading and analyzed it based on the guide.	Participate in the forum with at least 2 interventions.	Participate in the forum with at least 1 intervention.	Does not participate in the forum.
Contribution of new ideas	Provides new ideas and justifies them (minimum 4 aspects for Internet planning).	The interventions show that he did the reading and considered some of the guiding questions.	Interventions show little analysis of reading and use of the guide.	It performs the intervention but does not show any analysis of the reading and the guide.
Quality of interventions	The interventions are very clear, concise and respectful.	Provides new ideas and justifies them (minimum 2 aspects for Internet planning).	It provides at least one idea for Internet planning).	He doesn't bring new ideas.
Interaction with peers and tutor	Establishes a dialogue with peers and tutor, debating and defending ideas, and building new contributions together.	Interventions are clear, concise and respectful.	The interventions are unclear, concise and respectful.	Interventions are not clear, concise and respectful.

TABLE. III. ASSESSMENT RUBRIC- CHAT

Aspects to evaluate/Performance scales	Outstanding	Satisfactory	Needs improvement	Insufficient
Language skills	In his participations, he expresses his ideas clearly and structurally.	In the participations, he expresses his ideas with sufficient clarity.	Some of his ideas are clear and some are confusing.	It is not clearly expressed in its participations.
Mastery of the theme	Shows understanding of the subject and uses appropriate notation and terminology to express opinions.	Makes some mistakes in the terminology used and shows some gaps in the understanding of the topic.	He makes many mistakes in terminology and shows deep conceptual gaps.	He shows no knowledge of the subject matter.
Conventions	Makes good use of the conventions of the medium: he waits his turn to intervene; he uses lowercase letters when he writes (he does not "shout" in capital letters); he is respectful of the opinions of his peers; he expresses ideas briefly; he uses polite language; he uses contrasting color for his interventions; he uses emoticons.	It uses most of the conventions of the medium.	Use some of the conventions of the medium.	Use few or none of the conventions of the medium.
Coherence	Listen (read) carefully to what others contribute and follow the thread of the conversation with congruent comments.	In general, your comments are accurate and respect the main topic of the chat.	Some comments deviate from the theme.	He makes trivial and off-topic comments.

TABLE. IV. ASSESSMENT RUBRIC - WIKI

Aspects to evaluate / Performance scale	Outstanding	Satisfactory	Needs improvement	Insufficient
Participation	Edit an existing article or create a new one, with formatting and images.	Edit an existing article or create a new one.	You have a lot of difficulty editing an existing article or creating a new one.	You cannot edit or create an article.
Content and quality of contributions	In their contributions, they express extensive knowledge on the subject and integrate useful information and knowledge that enrich the text. He presents arguments and his ideas are clear and profound.	In their contributions, they demonstrate knowledge about the subject and integrate certain information and knowledge that help to enrich the text. Most of his ideas are clear and he argues for them.	Their contributions demonstrate vague knowledge on the subject and integrate information or knowledge with difficulty. Few of their ideas are clear.	Your contributions demonstrate that you have no knowledge of the subject and do not integrate additional data or information. Ideas are confusing and superficial. Expresses only opinions and does not argue.
Respect and collaboration	He collaborates in a respectful way in his participations and in case of disagreement, he resorts to dialogue.	Collaborate respectfully but, in case of disagreement, avoid conflict or respond with little self-criticism.	Sometimes he is not respectful with the rest of the collaborators and can respond aggressively.	He is not respectful in his contributions or responses to other collaborators. Does not accept criticism and is not capable of constructing a group text.
Links and sources	The article created or the contribution made has at least two links that work or at least two sources of its arguments completely.	The article created or the contribution made has a link that works or cites a source of its arguments in a complete way.	The article created or the contribution made has a link that does not work or in the contribution cites the sources of its arguments incompletely.	The article created or the contribution made has no links or quotations, and no reference to sources.
Language skills	In his participations he expresses his ideas with total clarity and structuring; he applies correctly the orthographic, grammatical and syntax rules.	In his participations, he expresses ideas with sufficient clarity; in most cases, he applies the rules of spelling, grammar and syntax correctly.	In his participations, he does not express ideas clearly and applies the rules of spelling, grammar and syntax, with errors.	He does not express himself clearly in his participations; apply them to orthographic, grammatical and syntax rules, with many errors.

TABLE. V. DATA COLLECTION INSTRUMENTS

forums	News forum Forum questions and discussion of the case study Forum to discuss any topic	A Case Study	The number of units and contributions made measures it. Forums are evaluated according to the evaluation rubric.
wikis	Wiki News Wiki doubts and debate the case study Wiki to discuss any topic	Case Study B	The number of units and contributions made measures it. Wikis are evaluated according to the evaluation rubric.
Chat	General:	It applies to both cases	It is measured by the number of units and inputs, and was evaluated according to the column.

VI. Obtaining and Analyzing Results

A previous study was carried out to obtain data on the tools in both Case Studies (CS), and then to make the comparison, see Fig. 1

A. *Comparison of Number of Shares Forum Case Study A and B*

In the graph in CS-A, two students have a total of 06 participations, representing 6%, while four students only participated once, representing 3% of the total number of students. Similarly, in CS-B, two students have a total of 06 and 05 participations, while 08 students have an average between 03 and 04 participations.

On the basis of the results obtained we can analyze that in the forum of the CS-B, a smaller number of participations is presented, however, the quality of interventions has improved considerably with respect to the CS-A, this because the students were already familiar with the use and functionality of the forums.

B. *Comparison of the Average of Ratings According to the Evaluation Rubric of Forum CS - A and B, see Fig. 2*

In the CS - A, with respect to the average grades by criterion according to the rubric, it can be observed that the highest average belongs to the participation criterion; while the lowest average corresponds to the criterion of interaction with peers and tutor. In the sense it can be inferred that students participate actively, however, it is at a basic level of collaboration and the quality of interventions with peers and tutor is poor.

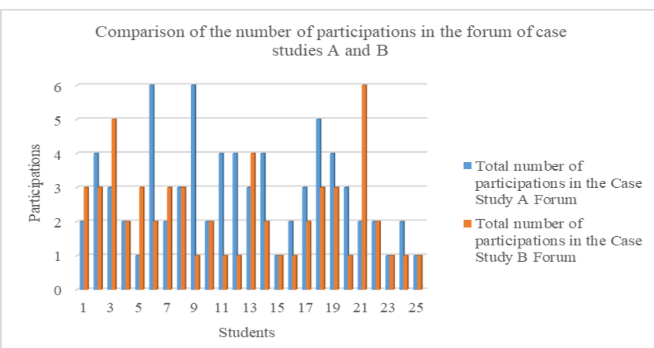

Fig. 1. Comparison of Number of Shares Case Study forum A and B.

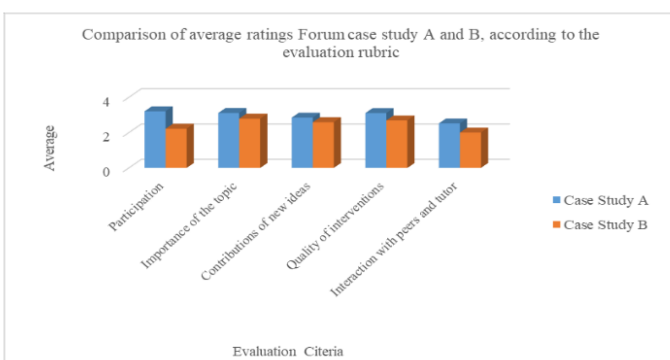

Fig. 2. Comparison of the Grade Point Average According to the Evaluation Rubric.

While in CS-B, the quality of the interventions and the importance of the topic present a higher average than the weighted average, so it can be interpreted that the forums are used to build quality knowledge from the contributions of other peers, regardless of the number of interventions.

C. *Comparison of the Number of Wiki, CS - A and B Participations, see Fig. 3*

In CS-A, the results show that students are familiar with participation through the wiki tool, since most participations range from 3 to 4 participations, which shows that there is participation and collaboration on the part of the students. Similarly, in CS-B the results show that students are familiar with participation through the wiki tool, since most participations range from 5 to 4 participations, which shows that there is student participation and collaboration.

D. *Comparison of Average Ratings According to the Wiki Evaluation Rubric Case study A and B, see Fig. 4*

In the CS - A the content and quality of participations, the respect and collaboration on the part of the students represent a superior average to the weighted average, reason why we can interpret that the wikis help the students to make good contributions fomenting the respect and collaboration with theirs. In the same way in the CS - B the content and quality of participations, links and sources, represent a higher average than the weighted average, so it can be said that wikis help students to develop better skills such as research and analysis and interpretation of the sources consulted to support their ideas.

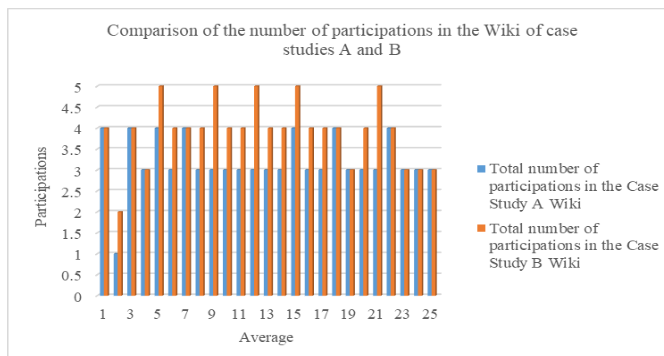

Fig. 3. Comparison of the Number of CS - A and B Wiki Participations.

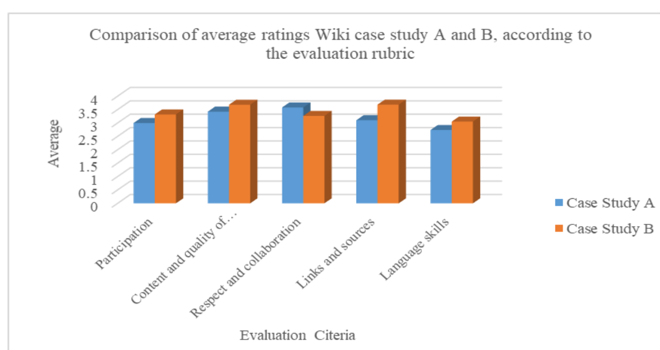

Fig. 4. Comparison of the Average of Ratings According to the Evaluation Rubric of Forum CS - A and B.

E. Comparison of the Number of Shares Chat Case study A and B, see Fig. 5

In both Case Studies, students are familiar with participation through the chat tool, since most participations range from 4, 5 to 6 participations, demonstrating that student collaboration and participation has developed significantly.

F. Comparison of the Average of Ratings According to the Chat Evaluation Rubric Case Study A and B, see Fig. 6

From the case of Study B we can analyze that the domain of the subject on the part of the students and the conventions used by these, represent a superior average to the weighted average, reason why we can interpret that the chat, encourages the students to that these read more on the subject, have a greater domain on the subject and be respectful with their other companions. While in Case Study A, the conventions of the medium are used correctly: it waits its turn to intervene; it uses lowercase letters when it writes, and so on. This represents a higher average than the weighted average, so we can interpret that chat helps students to be respectful and develop assertive communication.

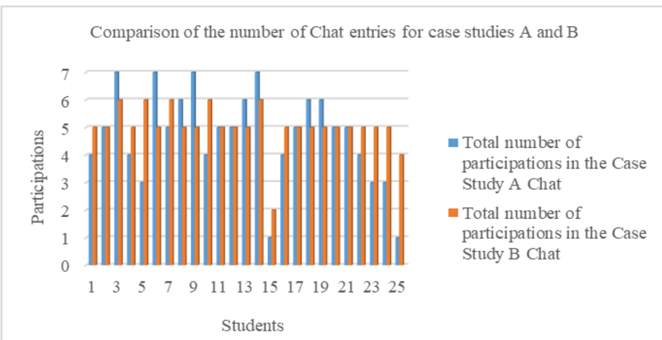

Fig. 5. Comparison of the Number of Shares Chat Case Study A and B.

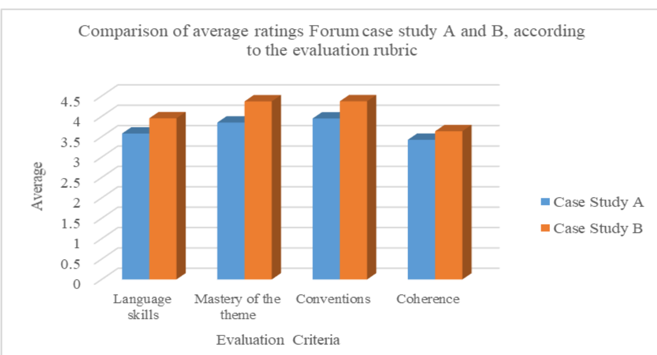

Fig. 6. Comparison of the Grade Point Average According to the Chat Evaluation Rubric Case Study A and B.

VII. Discussion

It is not possible to affirm the superiority of one tool over another because each one has its own characteristics and could be used for different purposes. The forums, wikis and chat could have complementary functions and should be organized to complement each other to develop collaborative learning. The digital divide for the use of these technologies can cause students who do not have access to them to be disadvantaged

VIII. Conclusions

From the evidence shown in the investigation, one can conclude:

- The use of didactic strategies such as Wikis, Forums and Chat in the sessions promote collaborative learning. The main factors for this to happen are the degree of appropriation of these technologies by students and the mastery of their use by teachers.
- The digital divide for the use of these technologies can cause students who do not have access to IT to be disadvantaged.
- Wikis, Forums and Chat encourage and enhance students' reflection on their own practice, in an interactive way, encouraging critical analysis and autonomous and collaborative work.
- The experimentation carried out is useful not only for students, but for all teachers who want to promote collaborative learning.
- Some doubts or topics are difficult to address from chat sessions, for this we use the forums that are the most appropriate to develop collaborative learning.

IX. Future works

It is necessary to use learning analytics in order to use the information collected and the analysis and reporting of data on students and their contexts, in order to understand and optimize learning and the environments in which it occurs.1 A closely related field is educational data mining.

References

[1] L. Emiro, C. Bravo, and F. D. P. Santander, “Incorporación de las TIC en procesos Industriales,” vol. 7, pp. 11–23, 2016.

[2] L. Vigotsky, “Internalizacion de las funciones psicologicas superiores.,” El Desarro. los procesos psicológicos Super., pp. 87–116, 1978.

[3] F. X. Ribes Guardia, “La Web 2.0. El valor de los metadatos y de la inteligencia colectiva,” Telos Cuad. Comun. Tecnol. y Soc., no. 73, pp. 0036–0043, 2017.

[4] C. F. M. Tamayo, “Universidad Complutense de Madrid Plataformas Virtuales Como Recurso para la Enseñanza en la Universidad: Análisis, Evaluación y Propuesta de Evaristo Alejandro Nafría López,” 2016.

[5] Gómez García Melchor, Estudio teórico, desarrollo, implementación y evaluación de un entorno de enseñanza colaborativa con soporte informático (CCCL) Para matemáticas. 2016.

[6] J. Cabrera, “Creación de un aula virtual en la Plataforma Moodle como complemento en el interaprendizaje de la informática de los jóvenes de la Unidad Educativa Salesiana Domingo Savio de Cayambe”. 2017.

[7] E. Jay, M.; Pérez, “Plataforma virtual Moodle y su incidencia en la calidad del proceso de enseñanza aprendizaje de estudiantes universitario,” VI Congr. Virtual Iberoam. Calid. en Educ. Virtual y a Distancia, 2015.

[8] María García, “Análisis del desarrollo de extensiones para Moodle: Desarrollo de un módulo para la gestión de laboratorios docentes,” 2015.

[9] Gómez García Melchor, Estudio teórico, desarrollo, implementación y evaluación de un entorno de enseñanza colaborativa con soporte informático (cscl) Para matemáticas. 2016.

[10] V. Álvares, “Aprendizaje colaborativo mediado por TIC en la enseñanza universitaria: un acercamiento a las percepciones y experiencias de profesores y estudiantes de la Universidad Autónoma de Chihuahua,” Univ. Salamanca, 2016.

[11] M. E. Calzadilla, “Aprendizaje Colaborativo y TIC,” Rev. Iberiamericana Educ., vol. 1, no. ISSN: 1681-5653, pp. 1–10, 2014.

[12] Marianella Castro; María Morales, “Los ambientes de aula que promueven el aprendizaje, desde la perspectiva de los niños y niñas escolares,” 2015.

[13] D. A. Padilla Beltrán, José E; Vega Rojas, Paula L; Rincón Caballero, “Revista Academia y Virtualidad Revista Academia y Virtualidad,” Acad. y Virtualidad, vol. 6, no. 1, pp. 34–55, 2015.

[14] L. G. Aretio and E. Bened, “Wiki en contextos educativos,” Uned, 2016.

[15] N. K. Subramaniam and M. Kandasamy, “The virtual classroom: A catalyst for institutional transformation,” Australas. J. Educ. Technol., vol. 27, no. 8, pp. 1388–1412, 2017.

[16] D. Ornelas, “El uso del Foro de Discusión Virtual en la enseñanza,” Rev. Iberoam. Educ., vol. 44, 2007.

[17] M. Lima, J. Villarruel, and R. Rivera, “La utilidad del foro virtual para el aprendizaje colaborativo, desde la opinión de los estudiantes,” Campus Virtuales, vol. 5, no. 2, pp. 122–133, 2016.

[18] V. Cuenca, “El foro virtual como estrategia de enseñanza en la educación superior,” vol. 2, no. 1, pp. 23–31, 2015.

[19] J. Abawajy, “Analysis of Asynchronous Online Discussion Forums for Collaborative Learning,” Int. J. Educ. Learn., vol. 1, no. 2, pp. 11–22, 2017.

[20] A. Arbey Sánchez-Upegui, “Investigación Pedagógica New Modes of Educational Interaction: Linguistic Analysis of a Virtual Forum Novos modos de interação educativa: análise lingüística de um foro virtual,” vol. 12, no. 2, pp. 29–46, 2015.

[21] B. Garibay, M.; Concari, S; Ordóñez, “Desarrollo del aprendizaje colaborativo empleando tareas mediadas por foros virtuales,” vol. ii, 2016.

Modification of Manual Raindrops Type Observatory Ombrometer with Ultrasonic Sensor HC-SR04

Anton Yudhana [1], Jessy Rahmayanti[2], Son Ali Akbar[3]
Electrical Engineering Department
Universitas Ahmad Dahlan
Yogyakarta, Indonesia

Subhas Mukhopadhyay [4]
Mechanical / Electronic Engineering
Macquaire University
NSW, Australia

Ismail Rakip Karas[5]
Computer Engineering Department
Karabük University
Karabük, Turkey

***Abstract*—Water, in any way it comes, is important for the life of all living things. Indonesia is an area of tropical equatorial with a variation of rain, which is quite high. The regularity of the distribution of rainfall is one of the aspects most important to the activity of the community. As the development of technology, the intensity of rainfall can be measured manually using Ombrometer Observatory tool. The manual tool for measuring the rain precipitation, Ombrometer Observatorium, is used to take data manually. Samples should be taken at 7.00 a.m. everyday using a measuring cup to know the height of the water contained. However, the type is prone to error at the high rainfall intensity, since the drainage of the samples is conducted every 24 hours. Therefore, much water is wasted. To solve the problem, a modification of a rainfall gauge was made, that is Ombrometer Observatory with ultrasonic sensor HC-SR04. The height of the water in the container is sent through a server of which the data is stored in the database every ten minutes to reduce the risk of evaporation. It also minimizes the error in measuring the rainfall intensity. The results have been compared to the ones by BMKG (Meteorology, Climatology, and Geophysics Agency). The correlation value of the measurement ratio reached 0.9739 or 97.39%.**

***Keywords*—Observatory Ombrometer; rainfall; database; ultrasonic sensor; IoT; rain gauge**

I. Introduction

Water plays significant role for the life of all living things on earth. Water is the essence of life and essential nutrients for humans, animals, plants, and the environment [1]. Water that comes from rain can meet the daily needs of any living things. For example, water is a part of community livelihoods as well as irrigation for farmers [2][3][4]. Farmers also need water to determine the quality of the soil as a planting medium [5]. Water and soil quality on agricultural land is very important to determine the types of plants suitable for planting [6]. Water that has good quality is the one that is not too polluted by chemicals [6],[7].

Related to water is the climate. The two main elements of climate formation are temperature and rainfall. Temperatures that have relatively high or low values of water vapor will produce certain humidity [8]. The impact of extreme climate change will cause an irregular change of seasons and ecological disasters, such as floods and long droughts, that may lead to losses [9],[10]. Indonesia lies in a tropical equator with high rainfall variation [11]. The regularity of rainfall patterns and distribution in an area is an important aspect of the ongoing activities of certain sectors of society [12]. Rainfall shows spatial structure in the form of closed contours in statistics [13]. Rainfall data is very useful for areas relying on agriculture and urban management [14]. High rainfall that exceeds the capacity of nature can cause disasters, such as floods [15].

Various ways have been conducted to overcome disasters due to high rainfall intensity, such as environmental management by increasing water infiltration and irrigation. Water absorption systems to reduce the vulnerability of disasters can neither accommodate in the event of extreme rainfall [16]. The need for a hydrological information system regarding water resource management has been regulated in Law No. 7 of 2004. The appendix to the Presidential Regulation of the Republic of Indonesia Number 28 of 2012 concerning Management Policies on Hydrology, Hydrometeorology, and Hydrogeology at the national level, mentions that hydrological data that is accurate, correct, sustainable, and timely is one of the factors that determine the implementation of resource management optimal water.

As technology develops, rainfall intensity can be measured automatically using an instrument called Automatic Rain Gauge (ARG). Several types of rain gauges have been developed, such as weighing gauges, capacitance gauges, tipping-bucket (TB) gauges, optical gauges, disdrometers, underwater acoustic sensors, and others [17]. Estimating the rainfall is necessary to estimate the rainfall data of an area[18]. In the Meteorology Climatology and Geophysics Agency in several areas, to get rainfall data, two types of equipment are used, namely Ombrometer Observatory (OBS) and Hellman and Tipping Bucket. Manual rain gauges are the type of rain gauge of which the data are not recorded, while the automatic rain gauge Hellman and Tipping Bucket do the opposite. In the rain gauge, the Tipping Bucket type is connected to a logger that will count each end of the rainwater that enters the rainfall gauge. Rainfall data will be sent automatically to the server during a rain event and every 24 hours with the help of sensors [19][20][21].

At weather stations in Indonesia, a manual type Observatory Ombrometer is often installed in a tool park to estimate the season in an area [22]. Observatory Ombrometer rain gauge is widely used in Indonesia because it is considered easier to operate and has a very economical price compared to other types of rain gauge.

The weakness of Observatory Ombrometer rain gauge is that the reading of rainfall data is still done manually using a measuring cup that is vulnerable to an error in reading the samples at high rainfall intensity. In the event of rain with high intensity, this type of manual tool cannot collect rainwater, because of the overflowing water in the cup. This condition will hamper the process of measuring rainfall if there is more than one rain event in a day, keeping in mind that the data collection and drainage of the container in the Observatory Ombrometer type rainfall gauge is only conducted every 24 hours at 07.00 am.

The solution to this problem is the manufacture of a manual rainfall gauge Ombrometer Observatory using the HC-SR04 ultrasonic sensor that will change the data collection automatically without using a measuring cup. In addition, the drainage of water in the tube will also be modified automatically by adding valves and relays.

The HC-SR04 ultrasonic sensor is a sensor that uses sonar to determine the distance to an object. This sensor has pretty good accuracy and a fairly stable reading. Operations are not influenced by sunlight or dark-colored material but are influenced by acoustic material. This sensor has a specification ranging from 2 cm to 400 cm with a resolution of 0.3 cm, and an angle range of less than 15 degrees which will minimize data retrieval errors during high rainfall, in which the tube can no longer hold water [23].

II. Research Method

A. Hardware Research Tools

In the modified schematic circuit of Fig. 1, it is explained that the input voltage of the rain gauge modifier is 12V. At the 12V input, voltage will be supplied to the DC-DC step-down module so that the output voltage from the step-down raise from 7V to 9V. The output voltage from the step-down will be supplied to the Arduino input voltage. It is used to adjust the reference voltage of the Arduino specification. The voltage sensor is used to determine the remaining capacity of the input voltage source [24].

The HC-SR04 ultrasonic sensor is connected to Arduino to find out the range of water level held in the rain gauge. The results of the water level range will be displayed on the LCD.

If the range of water level detected by the HC-SR04 ultrasonic sensor reaches 10 cm and the RTC DS3231 on the circuit schematic that functions as a real-time indicator has shown at 07.00 Western Indonesian Time, the ultrasonic sensor gives instructions to Arduino to send signals to the relay to start the pump to drain for 2 minutes 30 seconds. Realtime time generated by RTC DS3231 will be displayed on the LCD.

Data transmission to the ceerduad.com website platform is carried out with the help of the ESP8266 wifi module, which is communicated with Arduino. The data transmission is carried out in two conditions. The first is once every 10 minutes until 07.00 WIB to reduce evaporation in the event of extreme hot weather. Second is when the water stored in the rain gauge has been detected by an ultrasonic sensor HC-SR04 as high as 10 cm. Drain on the container is carried out at a height of 10 cm or 100 mm because it is adjusted to the maximum range in the value of low rainfall intensity, between 0 mm - 100 mm.

B. Software Research Tools

Overall, the software used in this study is Arduino IDE Fig. 2. Rainfall data will be sent to the website www.mhs.ceerduad.com in Fig. 3 through the Wifi Module.

- Platform Ceerduad: The ceerduad platform is an IoT platform service that is communicated using TCP / IP Fig. 3 using the data posting method and uses the PHP programming language to receive, store, and process the data to display graphics.
- System Work Principle:In general, the system consists of a controller in the form of an Arduino IDE, an HC-SR04 ultrasonic sensor, a wifi module that is used as a data sender, and a power supply in the form of a 12V battery. Block diagram of the system is shown in Fig. 4:

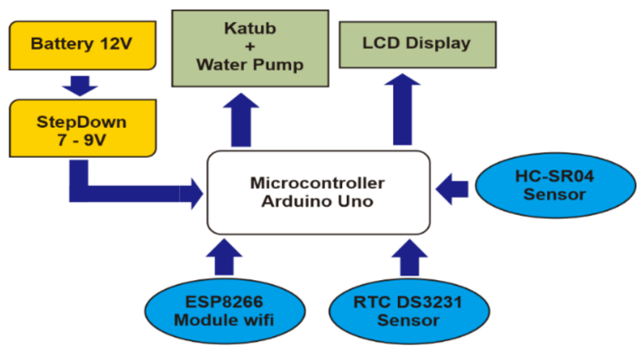

Fig. 1. Block Diagram of Hardware.

Fig. 2. Arduino IDE.

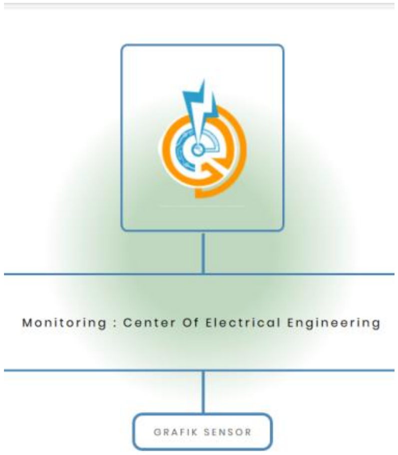

Fig. 3. Server Display Ceerduad.

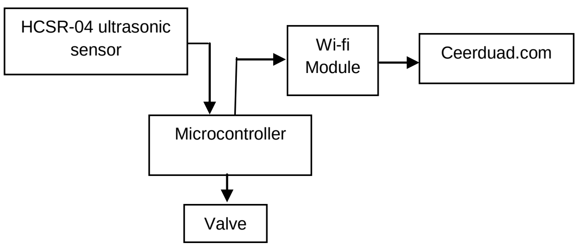

Fig. 4. Block Diagram of the System.

The basic principle of this Observatory Ombrometer type manual rain gauge modification tool is the HC-SR04 ultrasonic sensor which has been set to detect the height of the water in the reservoir when filled with rainwater, then the signal from the HC-SR04 Ultrasonic sensor will send data to the microcontroller. In the microcontroller, the data will be processed and sent by the computer through the wifi module and at the same time, the drain valve will open due to the signal from the microcontroller. As mentioned previously the system works in two condition: every day at 7.00 a.m. and when the water reaches the sensor.

III. Results and Discussion

Rainfall intensity has several specifications shown in Table I.

To measure the height of water in a tube the formula is used:

$$H = \frac{\text{Volume}}{\text{Cross-sectional area}} \qquad (1)$$

With

H = Water level

TABLE I. Rainfall Specifications

Rain Category	Rainfall / Day (mm)
Low	0-100
Intermediate	100-300
High	300-500
Very high	≥ 500

With a program as stated in Pseudocode 1:

```
void HCSR04() {
// put your main code here, to run repeatedly:
digitalWrite(trigPin, LOW);
delayMicroseconds(2);
digitalWrite(trigPin, HIGH);
delayMicroseconds(10);
digitalWrite(trigPin, LOW);

duration = pulseIn(echoPin, HIGH);
//jarak =duration*0.0343/2;
jarak = duration/58.2;
jarak2 = jarak*10;
jarak3 = jarak2-147.4;
jarak4 = jarak3*(-1);
if (jarak4 < 0){
jarak4=0;
}
```

Pseudocode. I. Data Retrieval Function HC-SR04

- Tool Development: In the design of the modified form of an ombrometer observatory type manual rain gauge is on a container that has a height of 26.5 cm with a diameter of a 15 cm funnel. In the modification tool, the reservoir tube is coated with styrofoam and the outer layer is coated using aluminum foil. This is to reduce the evaporation of the floating water during extreme heat or drought.

Inside the reservoir tube, there is an HC-SR04 ultrasonic sensor placed on the radius of the tube to minimize sensor reading errors. Just below the reservoir tube is a beam that is used as a place to store various circuits such as mini-systems, pumps, adapters, and batteries.

The results of the water level read by the ensors that will be sent to the online database server, which then displayed on the LCD offline. On the LCD, several buttons are used to switch on / off, and reset, to check the water level and the Internet connection [25]. The LED located next to the LCD is used as an indicator when the instrument is being operated and as an indicator when the instrument is draining the tubes. The modification system design can be seen in Fig. 5.

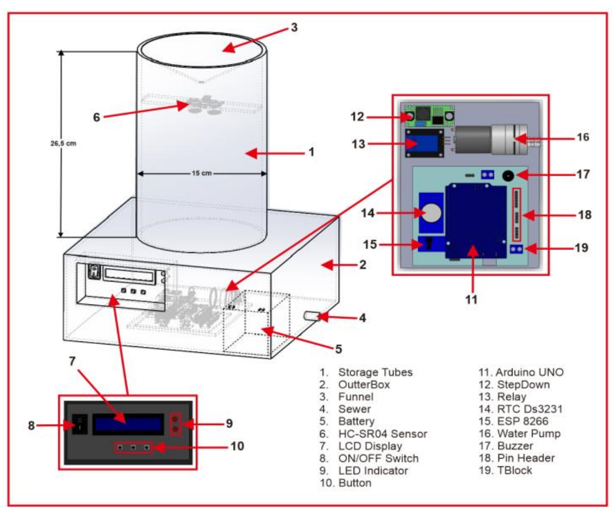

Fig. 5. Tool Development.

TABLE. II. COMPARISON RAINFALL SPECIFICATIONS

Days to -	Date month Year	Manual Measurement (mm)	Modification Measurement (mm)	Rainfall Intensity
1	26 April 2019	0	0	Low
2	27 April 2019	0	0	Low
3	28 April 2019	17.1	-	Low
4	29 April 2019	76.5	73.2	Low
5	30 April 2019	3.2	-	Low
6	1 May 2019	0	0	Low
7	2 May 2019	6.4	3	Low
8	3 May 2019	0	1	Low
9	4 May 2019	0	1	Low

- Measurement Analysis Data: The measurement results obtained using the BMKG manual with modifications using the HC-SR04 ultrasonic sensor are as follows which are listed in the Table II.

Fig. 6 shows relatively small value of the rainfall. From the results of the comparison of measurements of manual tools with modified tools, the correlation value reached 97.39%.

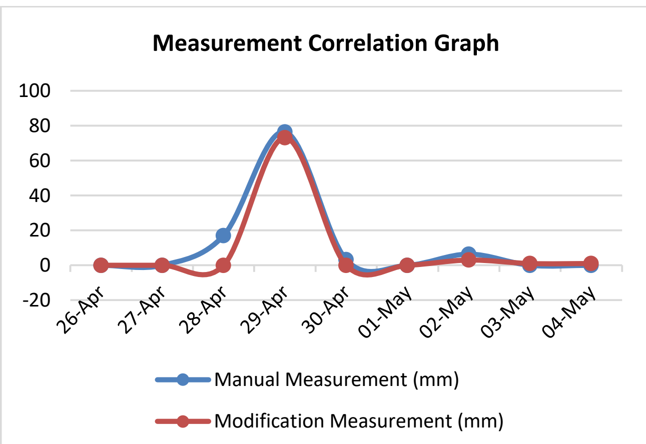

Fig. 6. Measurement Correlation Graph.

IV. CONCLUSION AND SUGGESTION

To conclude, sending the rainfall data in the field can be conducted automatically using the Wi-Fi ESP8266 module. The concept works successfully. Based on the data and the comparison with those by BMKG, the correlation of rainfall measurement reached the 07.39%.

To get optimal and stable values, it is necessary to replace sensors with a higher level of accuracy. This will reduce the error factor in reading the data. Also, the addition of an SD card is needed to handle data storage if the data is not sent successfully on the server due to the lack of internet network.

ACKNOWLEDGMENT

Acknowledgments are given to LPPM UAD for providing PKLN 2019 research funds with contract numbers PKLN-PI-001/SP3/LPPM-UAD/IV/2019.

REFERENCES

[1] M. A. Yunus And S. C. Mukhopadhyay, "Development Of Planar Electromagnetic Sensors For Measurement And Monitoring." IOP Publishing, Pp.01-09, 2017.

[2] A. Yudhana And A. C.Kusuma, I. O. P. C. Series And M. Science, "Water Quality Monitoring At Paddies Farming Based On Android," IOP Conference Series: Materials Scient and Engineering, Vol. 1, Pp.09-13, 2018.

[3] Sunardi, S. A. Akbar, F. Noviyanto, E. Wibowo, And R. Naufal, "Irigation Distribution Automatization Based On Scheduling System," Iop Conf. Ser. Mater. Sci. Eng., Vol. 403, No. 1, 2018.

[4] S. A. Akbar, Sunardi, Harianto, And F. Noviyanto, "Irrigation Distribution System For Agriculture Using Fuzzy Control And Android-Based Water Monitoring," In Proceedings Of The 2019 Ahmad Dahlan International Conference Series On Engineering And Science (Adics-Es 2019), 2019, Vol. 189, Pp. 45–49.

[5] A. Yudhana And S. A. Akbar, "Kelompok Tani Desa Argorejo," Pp. 298–302.

[6] U. Syafiqoh And A. Yudhana, "Pengembangan Wireless Sensor Network Berbasis Internet Of Things Untuk Sistem Pemantauan Kualitas Air Dan Tanah Pertanian," Jurnal Pengembangan IT (JPIT), Vol.03, No. 02, Pp. 285–289, 2018.

[7] Menteri Kesehatan Republik Indonesia, "Peraturan Menteri Kesehatan Nomor : 416 / Men . Kes / Per / Ix /1990 Tentang Syarat-Syarat Dan Pengawasan Kualitas Air," Pp. 1–10, 1990.

[8] J. Ascorbe, J. Corres, F. J. Arregui, I. R. Matias, And S. C. Mukhopadhyay, "High Sensitivity Optical Structures For Relative Humidity Sensing," Pp. 55–79.

[9] B. H. N. Ryke Nandini, "Kajian Perubahan Curah Hujan, Suhu Dan Tipe Iklim Pada Zone Ekosistem Di Pulau Lombok (Study Of Rainfall, Temperature And Type Of Climate Change In Lombok Island Ecosystem Zone)," Jurnal Kebijakan Kehutanan, No. August 2017, Pp. 228–244, 2011.

[10] L. Warlina, "Pencemaran Air: Sumber, Dampak Dan Penanggulangannya," Pp. 1–26, 2004.

[11] E. Hermawan, "Pengelompokkan Pola Curah Hujan Yang Terjadi Di Beberapa Kawasan Pulau Sumatera Berbasis Hasil Analisis Teknik Spektral," J. Meteorol. Dan Geofis., Vol. 11, No. 2, Pp. 75–85, 2010.

[12] W. Estiningtyas "Penentuan Wilayah Kunci Keragaman Iklim Indonesia Menggunakan Indikator Global untuk Mendukung Adaptasi Perubahan Iklim" J. Agromet Indonesia, Vol. 21, No. September, Pp. 1669–1672, 2006.

[13] C. Enjamio, E. Vilar, F. P. Fontan, A Redaño, And D. Ndzi, "Dimensions And Dynamic Evolution Of Microscale Rain Cells," No. 1, 1999.

[14] C. Jing, M. Du And Et Al, "Research On Accuracy Assessment Of Urban Rainfall Spatial Interpolation From Gauges Data School Of Geomatics And Urban Spatial Information Of Beijing University Of Civil Engineering And Architecture , Beijing , China Key Laboratory For Urban Geomatics Of National Administration Of Surveying , Mapping And Geoinformation , Beijing , China," IEEE Geoscience And Remote Sensing Symposium, Pp. 3121–3124, 2014.

[15] A. Muliantara, N. Agus, And S. Er, "Perancangan Alat Ukur Ketinggian Curah Hujan Otomatis Berbasis Mikrokontroler," J. Ilm. Ilmu Komput., Vol. 8, No. 2, Pp. 31–37, 2015.

[16] P. Willems And J. Olsson, "Climate Change Impact Assessment On Urban Rainfall Extremes And Urban Drainage : Methodologies And," Change, Vol. 6, No. 1, Pp. 149–154, 2009.

[17] E. Habib, W. F. Krajewski, And Et Al, "Sampling Errors Of Tipping - Bucket Rain Gauge Measurements" No. April, Pp. 159–166, 2001.

[18] U. Lewlomphaisarl And P. Saengsatcha, "High Accuracy Tipping Bucket Rain Gauge," Proceedings of SICE Annual Conference (SICE), Pp. 372–375, 2012.

[19] W. Bunganaen, "Analisis Hubungan Tebal Hujan Dan Durasi Hujan Pada Stasiun Klimatologi Lasiana Kota Kupang," Jurnal Teknik Sipil, Vol. Ii, No. 2, Pp. 181– 190, 2013.

[20] T. Karuturi And V. Raghava, “Internet Enabled Tipping Bucket Rain Gauge,” International Conference on Computer Communication and Informatic, Pp. 1–5, 2014.

[21] M. D. Amico, S. L. Jong, And C. Riva, “Tipping Bucket Data Processing For Propagation Application,” Electrobic Letters, Vol. 49, No. 8, Pp. 49–51, 2013.

[22] Sunarno, “Rancang Bangun Sistem Pengukur Curah Hujan Jarak-Jauh Real Time Sebagai Peringatan Banjir Lahar Dingin,” Forum Tek., vol. 33, pp. 175–180, 2010.

[23] U. M. Arief, “Pengujian Sensor Ultrasonik PING untuk Pengukuran Level Ketinggian dan Volume Air,” J. Ilm. “Elektrikal Enjiniring” UNHAS Vol. 9 No. 2 Mei-Agustus 2011, vol. 9, no. 2, pp. 72–77, 2011.

[24] A. Yudhana And J. Rahmawan, “Eontex Conductive Strechtable Sensor Response On Smart Glove For Sign Language,” Ahmad Dahlan Conference Series on Engineering and Science (ADICS-ES 2019), Vol. 189, Pp. 22–25, 2019.

[25] A. Yudhana and H. S. Purnama, Proyek Instrumentasi Medis Berbasis Internet of Things.

Clustering based Privacy Preserving of Big Data using Fuzzification and Anonymization Operation

Saira Khan[1], Khalid Iqbal[2], Safi Faizullah[3], Muhammad Fahad[4], Jawad Ali[5], Waqas Ahmed[6]
Department Computer Science, COMSATS University Islamabad, Attock Campus, Pakistan[1,2,4]
Faculty of Computer and Information System, Islamic University of Madinah, Saudi Arabia[3]
Malaysian Institute of information Technology (MIIT), University Kuala Lumpur, Kuala Lumpur, Malaysia[5]
UniKL Business School (UBIS), University Kuala Lumpur, Kuala Lumpur, Malaysia[6]

***Abstract*—Big Data is used by data miner for analysis purpose which may contain sensitive information. During the procedures it raises certain privacy challenges for researchers. The existing privacy preserving methods use different algorithms that results into limitation of data reconstruction while securing the sensitive data. This paper presents a clustering based privacy preservation probabilistic model of big data to secure sensitive information..model to attain minimum perturbation and maximum privacy. In our model, sensitive information is secured after identifying the sensitive data from data clusters to modify or generalize it.The resulting dataset is analysed to calculate the accuracy level of our model in terms of hidden data, lossed data as result of reconstruction. Extensive experiements are carried out in order to demonstrate the results of our proposed model. Clustering based Privacy preservation of individual data in big data with minimum perturbation and successful reconstruction highlights the significance of our model in addition to the use of standard performance evaluation measures.**

Keywords*—Big data; clustering; privacy preservation; reconstruction; perturbation

I. Introduction

The big data refer to the massive amount of structured and unstructured data with an increase of 2.5 ExaBytes per day. This rapid increase in data volume is due to web-services [1], mobile data [2, 3], health care data [4], GPS signals, Youtube, digital cameras and file hosting websites, and social media like facebook and twitter [5]. Generally, Big data can be classified into Volume, Velocity and Variety [5, 7]. First, Volume is the amount of data larger than tera bytes and peta bytes. Second, Velocity represents the speed of in and out, share and seized of data. Lastly, Variety means the explosion of new data types from social sites, mobile computing and machine devices. Big Data is used to bring improvements in businesses and society known as Big Data Analytics [6]. However, the combination of personal and external data increases the vulnerability of sensitive attributes. Prevention of sensitive information from disclosure is known as Big data privacy. The causes of privacy violation are the massive volume of data, management, storage, manipulation and data analytics [8]. Big data privacy can either be preserved by design or by rules and regulation as shown in Fig. 1.

Sanitization is common technique to remove the sensitive attribute in order to secure the quasi and sensitive information while preserving privacy of big data. The removal of sensitive and quasi attributes may lead to the incorrect mining results in different fields i.e., Healthcare and Bank Datasets [8]. The sensitive attributes in the datasets can either be numeric or categorical such as patient name, zip code, DOB, gender or sex, salary, balance, disease, race and Phone Numbers. These attributes threaten the individual privacy. To secure the individual privacy of structured data, annonymization algorithm is presented by Mohammad et al. [9] that probabilistically generalizes the data by adding noise to guarantee differential privacy. The advantage of generalization is to build a decision tree effectively. However, generalization is ineffective in re-construction of attribute. Sanitization lowers the re-construction ability of sensitive data over large scale [8]. A framework is proposed to conceptualize and measure service quality for internet of things. This study establishes the IoT-SERVQUAL model with four dimensions (i.e., Privacy, Functionality, Efficiency and Tangibility) of multiple service quality models and security issues[29].

On the other hand, Abitha et. Al [11] used min-max normalization, fuzzy logic, rail fence and map range to preserve the privacy of individual by masking the sensitive attributes. The use of fuzzy logic reduced the number of iterations and processing time that enhanced the clustering efficiency. However, S-shape membership function presented better results than the traditional data masking algorithms. In addition, Min-max normalization, rail-fence method and map range can only use for specific ranges in a given data, categorical data and numeric data respectively.

In this paper, a probabilistic method based privacy preservation model is proposed to modify the sensitive/quasi attribute sensitive values in a given dataset. The goal is to generalize the sensitive data rather than sanitization of sensitive/quasi attribute. Hierarchical clustering is used to split the data into clusters with objective of managing data chunks. For each sensitive attribute in a given cluster, attribute frequency distribution is formed to find the probability of values ranging from the lower-class limit to the upper-class limit. Median is chosen as a threshold to declare sensitive data in a given cluster. The sensitive numeric data is modified using S-shape membership function and sensitive categorical data is generalized by anonymization operation. At the end, sensitive and non-sensitive data is combined for mining operations. Data mining techniques can classify, cluster or make a decision tree without disclosing the individual information. For empirical analysis Bank Marketing and Adults datasets are used.

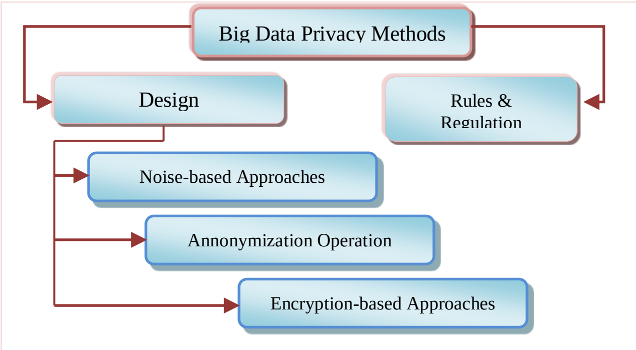

Fig. 1. Big Data Privacy Approaches.

Remaining part of paper is organized as follows; Section II contains related work done by previous researchers, in Section III we proposed our methodology, Section IV contains experimental section and Section V presents conclusion.

II. Literature Review

This section review the earlier studies by highlighting the opportunities of data analysis for miners as well as the challenges faced by the researchers. The major challenges are storage, processing and privacy & security of Big data. First, the rapid origination of large volume of electronic data causes the incremental requirement of storage. Second, Big data is collection of different types of data such as structured, semi-structured and unstructured that make complicated the mining process. Lastly, security and privacy refer to keep it safe from attackers and preventing Big data in processing phase while using data mining techniques for knowledge discovery. In current era, privacy of an individual and organizational data in Banks and Hospital is a major challenge for their sensitive and quasi information [13, 14, 15]. The mining process is a threat to disclose the identity of an individual using their sensitive attributes like salary, Balance and disease. Using quasi attributes such as zipcode, sex and DOB, 85% to 87% individuals of U.S. residents can be identified by Joining quasi attributes with external/publicly available voter list dataset can be misused after the disclosure of privacy of an individual [10].

Another easier target, that reveal sensitive information, is health care data. In 2009, 120 million health care records were manipulated. Theft resource center reported 1190 breach cases of health care data between 2005 to 2014. About 307000 patient's records were inadvertently placed accessible on internet containing sensitive information such as patient name, DOB and phone number. In the first three months of 2015, 91 million health care records were hacked. These mentioned cases increased the demand of Big data analytics [9]. To preserve privacy, perturbation algorithm is proposed by Adebayo et al. [8] that removes sensitive attributes like gender, race, religious views and political views from the data. The removal of attributes refers to the sanitization. The use sanitization process almost eliminates the reconstruction ability of sensitive data over a large scale. [11, 12] considered min-max normalization, fuzzy logic, rail-fence and map range to mask the sensitive attributes to preserves the privacy of an individual. The use of fuzzy logic is not only enhanced the efficiency of clustering, but also reduced the number of passes and processing time. Min-max normalization transformed numeric data into specific range while rail fence is more suitable to mask categorical data and map range is appropriate on numeric data only.

Besides this, an augmented anonymization method with better privacy performance is proposed by Rajalakshmi et al. [16]. Data is transformed into sub-clusters using isometric transformation. Quasi identifiers are modified to hide the association between individual and its actual record. To the best of our knowledge, data anonymization is considered as a simple procedure with better privacy preservation of data. However, numerical attributes can only be preserved by [16] and supports similarity attack upto some extent. Another data-leak detection (DLD) is presented by Xiaokui et al. [17] to solve the privacy problem of sensitive information. For this purpose, fuzzy finger print technique is used data-leak detection model to figure out, design and implement with an aim to enhance the privacy during data-leak detection operations. On the other hand, fuzzy logic is used to protect privacy of data by transforming numerical attributes into linguistic information. Sensitive data is made public with fuzzy draft rate. Fuzzy based experimental results were better than k-anonymity method in context of loss and performance. The performance and information loss are minimized 48% to 59% and 40% to 50% respectively [18].

III. Probabilistic Model for Privacy Preservation in Big Data

In this section, the generalized view of our probabilistic Model for privacy preservation in Big data is presented as shown in Fig. 2. Big data analysis computationally discover trends, patterns and associations related to human relations and actions according to their behavior. Therefore, trends, patterns and association visualization are hard to show with in a table or graphically. In this perspective, clustering is the best solution to split Big data into manageable groups. These clusters contain the sensitive/Quasi and non-sensitive attributes. Assuming sensitive/quasi attributes in each cluster as given , a frequency/probability distribution is obtained on quasi numeric attribute (e.g. age) data by finding the probabilities for the lower-class limit to upper class limit. In case of categorical attributes, frequent data values are considered as sensitive for sensitive/quasi attributes with an ANDing operation on the entire set of sensitive attributes. The median of these probabilities is used as threshold to find sensitive and quasi attributes values with an aim to apply S-shaped fuzzy membership function and anonymization operation to preserve the privacy of the data.

A. *Big Dataset*

A dataset ranging from tera bytes to peta bytes or exa bytes is considered as Big data. The origination of Big data on daily basis is increasing due to posts on social media like twitter and facebook, and digital pictures and videos on YouTube, mobile computing, file hosting and transactional records. There are four types of attributes in Big datasets [19].

- Identifier: An identifier is used to identify an individual uniquely such as CNIC_No, Social_Security_number and Employee_No.

- Quasi Attribute: Attributes that identify an individual by linking data with external data are known as quasi attributes. Quasi attributes can be categorized into two types and shown in Fig. 3.
  - Quasi numeric Attributes: Attributes based on numeric values such as age, zipcode and Date_of_Birth.
  - Quasi Categorical Attributes: Attributes consisted of textual information or combination of characters, for example sex.

- Sensitive Attributes: Sensitive attributes provide an insight of an individual's private and confidential data. These attributes can also have classified into two types.
  - Sensitive Numeric Attributes: Attributes with numeric values such as account_balance, salary and income.
  - Sensitive Categorical Attributes: Textual values-based attributes or combination of characters are known as sensitive categorical attributes. Examples are race, occupation and disease.

- Non-Sensitive Attributes: Attributes that does not help in revealing the privacy of an individual.

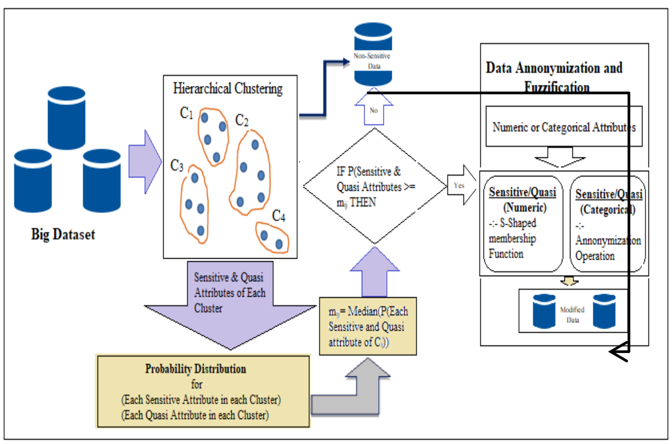

Fig. 2. Probabilistic Model for Privacy Preservation of Big Data.

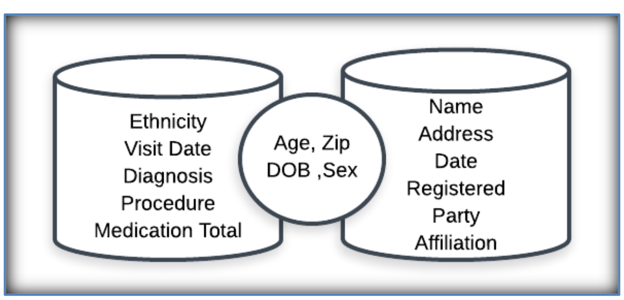

Medical Data Quasi Identifiers Voter List

Fig. 3. Quasi Identifier.

B. Clustering

Clustering is an unsupervised learning to group similar data of sensitive attributes. The goal of clustering is to find the fundamental groups in a set of unlabelled Big datasets, for example healthcare and bank marketting dataset. Data clustering can be used in various research domains such as data mining, pattern recognition, spatial databases, DNA analysis, Market analysis, medical domain and web statistics [20,21, 22]. Hierarchical clustering algorithm constructs a hierarchy among sensitive attributes values in order to split them into two or more clusters either on the basis of closeness or using a reversible process to merge clusters attributes values [23]. The outcome of the hierarchical can be represented by dendrogram [24, 25, 26]. For N sensitive attributes to be clustered, the basic process of *N*x*N* distance similarity matrix of hierarchical clustering is as below:

Assign each sensitive attribute data values to cluster based on similarities. Find the closet pair of cluster to merge clusters. Compute similarities b/w new & old clusters. Repeat step-2 & 3 untill all sensitive attributes are clustered.

C. Probability Distribution of Sensitive Attributes

After clustering sensitive attributes, a probability distribution is obtained using the frequency of all sensitive and quasi attributes in each cluster. The probability of all sensitive and quasi attributes is computed according to the *age* attribute. This attribute is used to define the class ranges and the occurrences of *age* values in in each of these classes resulted in frequency of different people. The probability of each class can be obtained by equation 1.

$$P(A_{ij}(v)) = \frac{\left|A_{ij}^{c_i}(v)\right|_{lcl}^{ucl}}{\left|c_i\right|} - \qquad (1)$$

Where $A_{ij}(v)$ represent the sensitive/quasi attribute of i^{th} cluster of j^{th} attribute's v^{th} value, c_i is the cluster number and *lcl* & *ucl* represent the lower-class limit and upper-class limit.

Median of $P(A_{ij}(v))$ is computed by equation 2 as a threshold to determine the sensitive/quasi attribute information that should be private before application of data mining technique. The probability above or equal to *M* is private data.

$$M = median(P(A_{ij}(v))) - \qquad (2)$$

For the remaining sensitive attributes, ANDing operation is applied after thresholding (as given by equation 2) to consider sensitive/quasi attribute as private either by modifying it through S-shaped membership function or by anonymization operation.

D. Fuzzification and Anonymization Operation on Sensitive Attributes Values

Fuzzy logic is considered as a remarkable method for data distortion with minimum information loss. Data distortion is the process of hiding sensitive attributes values without information loss. In this perspective, fuzzy transformation method is used to distort the sensitive/quasi attributes values by using the fuzzy membership function. The process of generating membership values for a fuzzy variable using membership function is termed as fuzzification [27, 28]. A membership function defines the mapping of membership value of input space between 0 and 1. The mapping of membership values of each sensitive/quasi attributes values (input space) can computed by equation 3.

$$S(\alpha,\beta,\gamma)=\begin{cases} 0, & \alpha \le \beta \\ 2\left(\dfrac{\alpha-\beta}{\gamma-\beta}\right)^2, & \beta \le \alpha \le \dfrac{\beta+\gamma}{2} \\ 1-2\left(\dfrac{\alpha-\gamma}{\gamma-\beta}\right)^2, & \dfrac{\beta+\gamma}{2} \le \alpha \le \gamma \\ 1, & \alpha \ge \gamma \end{cases} - \tag{3}$$

Where α is the original data, β represents minimum value in data set and γ represents maximum value in data set. S shaped fuzzy membership function transforms the numeric sensitive information in each cluster into fuzzified form. Transformed data range between 0.0 and 1.0 [30].

For sensitive/quasi categorical attributes, anonymization operation replaces, modify and generalize the informative attributes values. The objective of anonymization operation is not to disclose or re-identify the sensitive/quasi categorical attributes data [31]. Anonymization operation can generalize, suppress, anatomization, permutation operation and perturbation operation [32]. First, generalization operation replaces sensitive and quasi attributes with some less specific values. For example, *age* can be generalized into ranges. Second, suppression operation uses special value (e.g. an asterisk '*') to replace sensitive/quasi attributes values. Third, anatomization dissociate the correlation observed between quasi and sensitive attributes data. Fourth, permutation operation shuffle values of sensitive/quasi attributes by partitioning records into groups. Lastly, Perturbation operation modifies the original data by transforming values with synthetic values.

E. Algorithm for Modified and Generalized view of Data

The above-mentioned steps can be turned into algorithmic steps with an aim to modify and generalize the informative data of sensitive/quasi attributes. The important steps of the proposed algorithm are presented.

With the use of above algorithm, input dataset is modified only for sensitive and quasi attributes record with an aim to the minimal effect to the original data. Sensitive/quasi attributes modified using fuzzification through S-shape membership function can be re-constructed. However, re-construction is out of scope of the algorithm. In addition, Sensitive/quasi attributes modified through anonymization operation cannot be re-constructed. The reason is that the sensitive/quasi attributes records are generalized. In this way, our proposed probabilistic model preserves the privacy of sensitive information of an individual before outsourcing the actual dataset.

1. Input D// Dataset
2. Set $C_i = HierarchicalClust(D)$
3. $Assume\ Sensitive(S), Quasi\ Attributes(Q)\ \&\ Non-Sensitive\ Attributes(N)$
   $S=\{A_1,A_2,A_3,...,A_j\}, Q=\{B_1,B_2,B_3,...,B_k\}\ \&\ N=\{I_1,I_2,I_3,...,I_k\}\ in\ each\ C_i$
4. $FOR\ each\ C_i$
5. $\quad IF\ A_j \in S\ THEN$
6. $\quad\quad Compute\ P(A_j)\ in\ each\ C_i$
7. $\quad IF\ B_k \in Q\ THEN$
8. $\quad\quad Compute\ P(B_k)\ in\ each\ C_i$
9. $\quad m_{ij} = median(P(A_j(v)))$
10. $\quad m_{ik} = median(P(B_k(v)))$
11. $IF\ type(A_j)\ \&\&\ type(B_k) = False\ THEN\ //\ Numeric$
12. $\quad IF\ P(A_j(v)) \ge m_{ij}\ AND\ P(B_k(v)) \ge m_{ik}\ THEN\ //\ Numeric\ (Sensitive/Quasi)$
13. $\quad\quad DA_{jk} = [A_j,1],[B_k,1]\ \&\ Apply\ S-Shape\ Membership\ Function\ //\ Equ.3$
14. $\quad ELSE$
15. $\quad\quad RA_{jk} = [A_j,0],[B_k,0]$
16. $ELSE\quad //\ Categorical$
17. $\quad IF\ P(A_j(v)) \ge m_{ij}\ AND\ P(B_k(v)) \ge m_{ik}\ THEN\ //\ Categorical\ (Sensitive/Quasi)$
18. $\quad\quad MA_{jk} = [A_j,1],[B_k,1]\ \&\ Apply\ Anonymization\ operation$
19. $\quad ELSE$
20. $\quad\quad UA_{jk} = [A_j,0],[B_k,0]$
21. $SC_i = FD_s = [DA_{jk}; RA_{jk}], AD_s = [MA_{jk}; UA_{jk}]\ //\ Fuzzified, Anonymized\ and\ Non-Sensitive\ Records$
22. $DC_a = concat(SC_i, N)$
23. END

IV. EXPERIMENTAL RESULTS

In this section, experimental results are discussed to demonstrate the cluster wise privacy of numeric and categorical attributes. Numeric and categorical attributes in each cluster can be divided into direct identifier, sensitive attributes and quasi attributes. Cluster wise probability-based threshold (e.g. median) is calculated for sensitive and quasi attributes. Numeric sensitive and quasi attributes having a median greater than probability is assumed as sensitive need to modify. Sensitive numeric information in the data set is modified by using S-shaped fuzzy membership and sensitive categorical information is transformed by using anonymization operation. After modifying all the sensitive numeric and categorical information of each cluster, probabilistic based model creates modified view of data without any loss of data and leak of privacy any one can use modified data for analysis purpose freely without any privacy issue. To test our proposed probabilistic based model, we considered UCI machine learning adult's dataset and bank marketing data set [31] for validating the results in comparison with sanitization. Both dataset information is presented in Table I.

To protect health related information in United States, HIPAA (Health Insurance Portability and Accountability Act) defines 18 elements that can be removed or generalized for ensuring privacy of data. Besides this, several sensitive and quasi attributes are commonly existing in most of the dataset that can reveal the privacy of individual. Therefore, sensitive and quasi attributes information should be private. Direct identifiers of HIPAA, Sensitive and Quasi attributes are presented in Table II.

TABLE. I. ATTRIBUTES TYPES IN ADULTS AND BANK MARKETING DATASET

Data Set	Instances	Attributes	Attrb. Types	No. Attr. Types	Sensitive Attributes	Quasi Attributes
Adults	32561	15	Identifiers	0	Race, Income, Occupation	Age, Sex
			Sensitive	3		
			Quasi	2		
			Non-Sensitive	10		
Bank Marketing	4521	17	Identifiers	1	Balance, Loan, Job	Age
			Sensitive	3		
			Quasi	1		
			Non-Sensitive	12		

TABLE. II. DIRECT IDENTIFIERS OF HIPAA, SENSITIVE AND QUASI ATTRIBUTES

Direct Identifiers of HIPAA	Sensitive Attributes	Quasi Attributes
Invidual Name Individual Address(including street address, city county, and zip code) Dates related to an individual (including birthdate, admission date, discharge date, date of death, and exact age if over 89) Phone# Fax# Email_ID Social Security # (SSN) Medical record # Account # Certificate/licence # Vehicle/device serial# Web URL Internet Protocol (IP) Address Finger/voice print Photographic image	Salary, Disease Balance, loan status Race, Occupation Religion, income	Age Sex DOB Zip code

A. Clusters based Privacy of Adults and Bank Marketing Data

To split Big dataset into small and manageable fragments, hierarchical clustering is used to get clusters as shown in Fig. 4. Five clusters and three clusters were obtained from Adults and Bank Marketing dataset respectively after performing extensive experiments.

For each cluster, S-shape membership function and anonymization operation is used to secure the sensitive information according to the attributes type. These operations only modify the sensitive values which satisfy the probabilistic median based threshold criteria.

B. Privacy through S-Shape Membership Function

S-shape fuzzy membership function, as given by eq. 3, distorts the sensitive/quasi numeric attributes by changing their values with re-construction ability. The reason is that S-shape fuzzy membership function mapps values in a range from 0 to 1 for each cluster. For example, age and balance attributes values are sensitive if threshold criterion is satisfied. Therefore, sensitive/quasi numeric values are modified by S-shape fuzzy membership function as shown in Table III.

The fuzzified view of Table III for sensitive attributes can be used for further analysis without breaching the individual privacy. However, the re-construction of both attributes (i.e. *Agea* and *Balance)* is out of scope.

C. Privacy through Anonymization Operation

Anonymization operation replaces, modify and generalize individual data with an aim not either to disclose or re identified. For restricting disclosure or re-identification of data, data is anonymized before releasing it to the users.

Our proposed probabilistic model for privacy of data can handle categorical and numerical attributes for data mining by generalizing the attributes values. Data anonymization is the simplest procedure with better privacy. The application of anonymization operations can either be on categorical or quasi categorical attributes such as race, sex and occupation. The use of S-shaped fuzzy membership and anonymization operation ensures the best modification of direct, sensitive and quasi attributes by generalizing and fuzzified view of data for users. Table IV and Table V present the before and after modified view of data.

Similarly, S-shaped membership function and anonymization can also be used to ensure Big data privacy by modifying sensitive and quasi attributes values. Table VI and Table VII presents the results obtained on Bank Marketing dataset before and after modification for a better comparison.

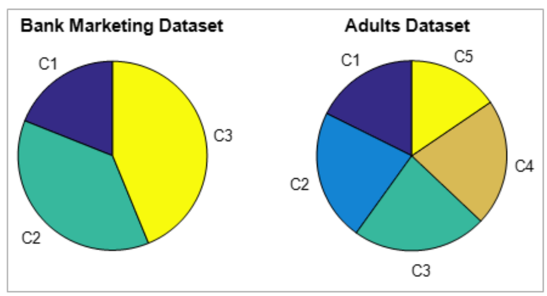

Fig. 4. Clusters of Big Datasets.

TABLE. III. BEFORE AND AFTER MODIFICATION OF ATTRIBUTES VALUES BY S-SHAPE FUZZY MEMBERSHIP FUNCTION

Before modification		After modification	
Age	Balance	Age	Balance
50	3143	0.817	0.00687
40	2096	0.397	0.01581
26	12519	0.061	0.03941
28	11262	0.091	0.88158
43	343	0.507	0.84953

TABLE. IV. SAMPLE OF ADULTS DATA SET BEFORE MODIFICATION

Cluster ID	Age	Marital Status	Ocupation	Race	Sex	Income
1	50	Divorced	Other-service	Asian-Pac-Islander	M	<=50K
1	19	Never-married	Sales	White	M	<=50K
2	61	Married-civ-spouse	Prof-specialty	White	M	<=50K
2	40	Married-civ-spouse	Craft-repair	White	M	<=50K
3	18	Never-married	Other-service	Black	M	<=50K
3	26	Married-civ-spouse	Prof-specialty	White	M	<=50K
4	28	Married-civ-spouse	Sales	White	M	<=50K
4	71	Married-civ-spouse	Farming-fishing	Amer-Indian-Eskimo	M	<=50K
5	73	Married-civ-spouse	Sales	White	M	>50K

TABLE. V. SAMPLE OF ADULTS DATA SET AFTER MODIFICATION

Cluster ID	Age	Marital Status	Ocupation	Race	Sex	Income
1	0.817	Divorced	Unkonwn	Unkonwn	Person	Unkonwn
1	19	Never-married	Sales	White	Male	<=50K
2	61	Married-civ-spouse	Prof-specialty	White	Male	<=50K
2	0.397	Married-civ-spouse	Unkonwn	Unkonwn	Person	Unkonwn
3	18	Never-married	Other-service	Black	Male	<=50K
3	0.061	Married-civ-spouse	Unkonwn	Unkonwn	Person	Unkonwn
4	0.091	Married-civ-spouse	Unkonwn	Unkonwn	Person	Unkonwn
4	71	Married-civ-spouse	Farming-fishing	Amer-Indian-Eskimo	Male	<=50K
5	73	Married-civ-spouse	Sales	White	Male	>50K

TABLE. VI. SAMPLE OF BANK MARKETING DATA SET BEFORE MODIFICATION

Cluster ID	Age	Job	balance	Day	month	Loan
1	33	management	3143	29	Jun	No
1	45	management	2096	21	Nov	No
1	47	admin.	1934	14	May	Yes
2	50	blue-collar	12519	17	Apr	No
2	60	Technician	11262	26	Aug	No
2	68	Retired	4189	14	Jul	No
3	26	management	63	28	Jul	No
3	32	Services	182	6	May	No

TABLE. VII. SAMPLE OF BANK MARKETING DATA SET AFTER MODIFICATION

Cluster ID	Age	Job	balance	Day	month	Loan
1	0.155	Unknown	0.0069	29	Jun	Unknown
1	0.228	Unkown	0.0158	21	Nov	Unknown
1	45	management	2096	21	Nov	Yes
2	0.831	blue-collar	0.0394	17	Apr	Unknown
2	0.369	Unknown	0.8816	26	Aug	Unknown
2	68	Retired	4189	14	Jul	No
3	26	management	63	28	Jul	No
3	0.165	Unknown	0.7405	6	May	Unknown

V. Comparison of Results with Existing Approaches

After modification of cluster wise attributes values, the entire data of all clusters for sensitive, quasi and non-sensitive attributes were combined for open access. In this combined open access data, anonymized attributes cannot be re-constructed due to generalization. However, fuzzified view of sensitive and quasi attributes can be re-constructed. Fig. 5 presents the percentage of sensitive attributes including the total number of records and total number of attributes in each dataset.

Similarly, Fig. 6 presents the cluster wise records, modified records percentage and a probabilistic threshold used for sensitive attributes. Fig. 6(a) and Fig. 6(b) present the modification through S-shaped membership function on Adults and Bank marketing datasets, respectively.

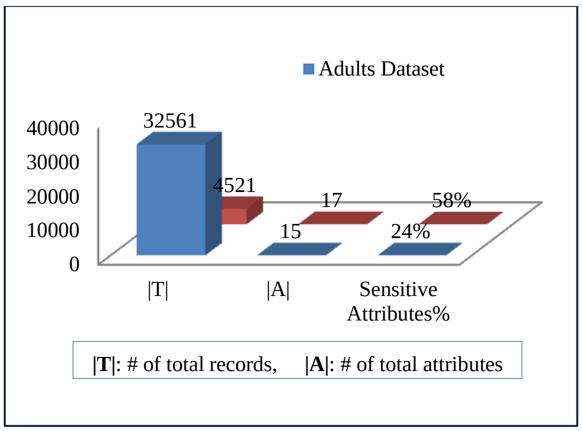

Fig. 5. Sensitive Information in Datasets.

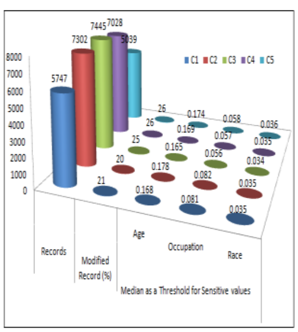

(a) Adults Dataset (Cluster Wise) Records, Modified view and Probabilistic Threshold.

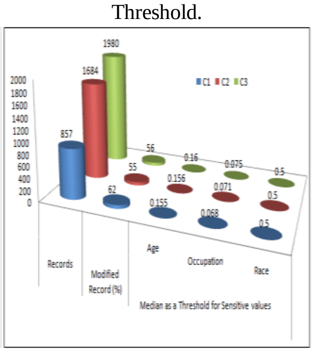

(b) Bank Marketting Dataset, Cluster Wise Records, Modified view and Probabilistic Threshold.

Fig. 6. Cluster Wise Modified View of Records.

Furthermore, our probabilistic threshold-based model for privacy preservation of big data is compared with the sanitization-based approaches [8] to validate the presented work. The objective of sanitization is to remove the sensitive attributes like gender, race, religious views, political view etc. from dataset. The problem with sanitization is left with only generalization and limits the application of data mining techniques for knowledge extraction. Sanitization restricts the re-construction of attributes upto 20% after removal of sensitive attributes. On the other hand, our probabilistic based threshold model can re-construct the fuzzification based modified data without removing any attribute. However, sanitization and our proposed model cannot re-construct the generalized attribute values. Thus, our model is more useful for users with the use of anonymization and fuzzification. In this perspective, our model modified only sensitive values of each cluster attributes upto 24% and 58% for adults and Bank Marketting dataset.

VI. Discussion

Social networking applications allow user to create content freely data which can cause a dramatic increase in data volume known as Big Data. Big Data have to be managed and analyzed efficiently to retrieve useful information to enhance business and improve society. Privacy preserving data mining emerged as a field to discuss privacy problem arise in data mining techniques to large scale individual data. Predictive Privacy harm itself is greater harm to individual privacy cause by sensitive attributes.

Sensitive attribute are part of mining process. Removal of sensitive attribute and quasi attribute causes data loses due to which big data is not useful for future data mining context. Browsing through a big data set would be difficult and time consuming to extract useful information from unstructured, invaluable, imperfect and complex data. Big data is divided into clusters using hierarchical clustering. Hierarchical clustering is more flexible and efficient approaches for clustering divide the data into different clusters using ward's method. Cluster wise probability and median of all sensitive and quasi attribute is calculated. Sensitive and quasi attributes whose probability is greater than median are declare as sensitive.

Probabilistic threshold based Big data privacy model creates fuzzified and anonymized view of sensitive values cluster wise using S shaped fuzzy membership function and anonymization operations. S shaped fuzzy membership function is applied upon numeric sensitive values enhance privacy of individual data by creating fuzzified view of sensitive information. Anonymization operation is performed upon sensitive values of categorical attributes and quasi identifier to preserve the privacy of individuals by creating anonymized view of big data. The Proposed model creates modified view of data by combining fuzzified, anonymized, non-sensitive attributes and values cluster wise. Modified Data can be used for analysis purpose. Modified data can be freely use for data mining purpose. The Proposed model reduce data lose and leak of privacy by creating modified view of data and modifying minimum no of attributes cluster wise.

VII. Conclusion and Future Work

Privacy preservation turns out to be an important aspect in Big data to restrict the disclosure of sensitive information before applying data mining techniques. In our proposed model, we tend to preserve the the individual privacy in baig data.with zero or minimum side effects.Main goal is to uncover and conceal those sensitive items by Anonymization and fuzzification participate in exposing individual privacy to external world. The objective of the model is to preserve the individual privacy by anonymization and fuzzification for each cluster. Anonymization generalize the individual's data while fuzzification modifies the individual data with the re-construction capability unlike previous approaches. Different pervasive tests over case studies and different datasets are held to validate the effectiveness and accuracy of proposed work. After resulting data is obtained,it is assembled back as single cluster for data minig purposes. The experimental results have proven the better privacy over sanitization-based methods. However, re-construction of modified data is yet to consider as our future work. In future, k-mean clustering can be helpful in locating the most sensitive data based cluster with additional feature of finding more accurate sensitive item which can further be reconstructed to maintain the originality of big data.

References

[1] Sedayao, Jeff, Rahul Bhardwaj, and Nakul Gorade. "Making big data, privacy, and anonymization work together in the enterprise: experiences and issues." In Big Data (BigData Congress), 2014 IEEE International Congress on, pp. 601-607. IEEE, 2014.

[2] Garber, Lee. "Security, Privacy, Policy, and Dependability Roundup." IEEE Security and Privacy 11, no. 1 (2013): 6-7.

[3] Musolesi, Mirco. "Big mobile data mining: Good or evil?." IEEE Internet Computing 18, no. 1 (2014): 78-81.

[4] Patil, Harsh Kupwade, and Ravi Seshadri. "Big data security and privacy issues in healthcare." In Big Data (BigData Congress), 2014 IEEE International Congress on, pp. 762-765. IEEE, 2014.

[5] Yu, S., Liu, M., Dou, W., Liu, X., & Zhou, S. (2017). Networking for big data: A survey. IEEE Communications Surveys & Tutorials, 19 (1), 531-549.

[6] Thuraisingham, B. (2015, March). Big Data Security and Privacy. InProceedings of the 5th ACM Conference on Data and Application Security and Privacy (pp. 279-280). ACM.

[7] Sagiroglu, S., &Sinanc, D. (2013, May). Big data: A review. In Collaboration Technologies and Systems (CTS), 2013 International Conference on (pp. 42-47). IEEE.

[8] Adebayo, J, &Kagal, L. (2015, May). A privacy protection procedure for large scale individual level data. In Intelligence and Security Informatics (ISI), 2015 IEEE International Conference on (pp. 120-125). IEEE.

[9] Mohammed, N., Chen, R., Fung, B., & Yu, P. S. (2011, August). Differentially private data release for data mining. In Proceedings of the 17th ACM SIGKDD international conference on Knowledge discovery and data mining (pp. 493-501). ACM.

[10] van der Aalst, W. M. (2016). Green Data Science. ICEIS 2016, 9.

[11] Sarada, G., N. Abitha, G. Manikandan, and N. Sairam. "A few new approaches for data masking." In Circuit, Power and Computing Technologies (ICCPCT), 2015 International Conference on, pp. 1-4. IEEE, 2015.

[12] T. Ali Syed, A. Alzahrani, S. Jan, M. S. Siddiqui, A. Nadeem and T. Alghamdi, "A Comparative Analysis of Blockchain Architecture and its Applications: Problems and Recommendations," in IEEE Access, vol. 7, pp. 176838-176869, 2019. doi: 10.1109/ACCESS.2019.2957660.

[13] Hirsch, Dennis D. "The Glass House Effect: Big Data, the New Oil, and the Power of Analogy." Maine Law Review 66 (2014): 2.

[14] Katal, Avita, Mohammad Wazid, and R. H. Goudar. "Big data: Issues, challenges, tools and Good practices." In Contemporary Computing (IC3), 2013 Sixth International Conference on, pp. 404-409. IEEE, 2013

[15] J. Ali, A. S. Khalid, E. Yafi, S. Musa, and W. Ahmed, "Towards a Secure Behavior Modeling for IoT Networks Using Blockchain," CEUR Workshop Proceedings (Vol. 2486, pp. 244–258) 2019.

[16] Rajalakshmi, V., & Mala, G. A. (2013, December). Data Anonymization Using 1100]Augmented Rotation of Sub-Clusters for privacy preservation in data mining. In Advanced Computing (ICoAC), 2013 Fifth International Conference on (pp. 22-26). IEEE.

[17] Shu, Xiaokui, Danfeng Yao, and Elisa Bertino. "Privacy-preserving detection of sensitive data exposure." IEEE transactions on information forensics and security 10, no. 5 (2015): 1092-1103.

[18] Xie, M. B., & Qian, Q. (2016, May). Fuzzy set based data publishing for privacy preservation. In Software Engineering, Artificial Intelligence, Networking and Parallel/Distributed Computing (SNPD), 2016 17th IEEE/ACIS International Conference on (pp. 569-574). IEEE.

[19] Dashora, R., Bajaj, H., & Dube, A. (2013). Parallel Algorithm for the Chameleon Clustering Algorithm using Dynamic Modeling. International Journal of Computer Applications, 79(8).

[20] J. Ali, T. Ali, Y. Alsaawy, A. S. Khalid, and S. Musa, "Blockchain-based Smart-IoT Trust Zone Measurement Architecture," in Proceedings of the International Conference on Omni-Layer Intelligent Systems - COINS '19, 2019, pp. 152–157.

[21] Joshi, S., Khan, F. U., & Thakur, N. (2014). Contrasting and Evaluating Different Clustering Algorithms: A Literature Review.

[22] Xu, L., Jiang, C., Wang, J., Yuan, J., & Ren, Y. (2014). Information security in big data: privacy and data mining. Access, IEEE, 2, 1149-1176.

[23] B. C. M. Fung, K. Wang, R. Chen, and P. S. Yu, ``Privacy-preservingdata publishing: A survey of recent developments," ACM Comput. Surv.vol. 42, no. 4, Jun. 2010, Art. ID 14.

[24] Ayed, A. B., Halima, M. B., & Alimi, A. M. (2014, August). Survey on clustering methods: Towards fuzzy clustering for big data. In Soft Computing and Pattern Recognition (SoCPaR), 2014 6th International Conference of (pp. 331-336). IEEE.

[25] Fahad, A., Alshatri, N., Tari, Z., Alamri, A., Khalil, I., Zomaya, A. Y., & Bouras, A. (2014). A survey of clustering algorithms for big data: Taxonomy and empirical analysis. Emerging Topics in Computing, IEEE Transactions on, 2(3), 267-279.

[26] T. A. Syed, S. Musa, A. Rahman and S. Jan, "Towards Secure Instance Migration in the Cloud," 2015 International Conference on Cloud Computing (ICCC), Riyadh, 2015, pp. 1-6. doi: 10.1109/ CLOUDCOMP.2015.7149664

[27] Murtagh, F., & Legendre, P. (2014). Ward's hierarchical agglomerative clustering method: which algorithms implement Ward's criterion?. Journal of Classification, 31(3), 274-295.

[28] Xie, M. B., & Qian, Q. (2016, May). Fuzzy set based data publishing for privacy preservation. In Software Engineering, Artificial Intelligence, Networking and Parallel/Distributed Computing (SNPD), 2016 17th IEEE/ACIS International Conference on (pp. 569-574). IEEE.

[29] S. M. Hizam and W. Ahmed, "A conceptual paper on SERVQUAL-framework for assessing quality of Internet of Things (IoT) services". International Journal of Financial Research, vol. 10, no. 5, pp. 387–397, 2019. doi: 10.5430/ijfr.v10n5p387

[30] Ahmed, S. M. T., Haque, S., & Tauhid, S. F. (2014). A fuzzy based approach for privacy preserving clustering. Int. J. Sci. Eng. Res, 5(2), 1067-1071.

[31] Sarada, G., Abitha, N., Manikandan, G., &Sairam, N. (2015, March). A few new approaches for data masking. In Circuit, Power and Computing Technologies (ICCPCT), 2015 International Conference on (pp. 1-4). IEEE.

[32] Xu, L., Jiang, C., Wang, J., Yuan, J., & Ren, Y. (2014). Information security in big data: privacy and data mining. Access, IEEE, 2, 1149-1176.

Flooding and Oil Spill Disaster Relief using Sentinel of Remote Sensing Satellite Data

Kohei Arai
Faculty of Science and Engineering
Saga University, Saga City
Japan

***Abstract*—Flooding and oil spill disaster relief using Sentinel of remote sensing satellite data is conducted. Kyushu, Japan had severe heavy rain from 26 August to 30 August 2019. Optical sensor and Synthetic Aperture Radar: SAR onboard remote sensing satellite is used for disaster relief. NDVI and SWIR data derived from the Sentinel data are used for disaster relief. Merits and demerits of the optical sensor and SAR instrument are compared from the disaster relief of point of view.**

Keywords—Sentinel; disaster relief; satellite remote sensing; flooding; oil spill; synthetic aperture radar; optical sensor; vegetation index

I. Introduction

On the morning of August 26, the front line near the southern part of Kyushu moved northward to the vicinity of the Tsushima Strait on the 27th day. For this reason, it was a record heavy rain in Saga Prefecture. About record short-term heavy rain (analytical rainfall) from 04:00 to 04:50 on the 28th, Taku City, Takeo City, Ogi City, Kohoku Town, Saga City, Omachi Town, Shiraishi Town, Kanzaki City, Yoshinogari Town It was analyzed from about 110 mm to over 120 mm per hour in the vicinity. Due to the heavy rain, landslide and oil spill disaster is occurred. Such disaster can be relieved from space, spaceborne mission instrument data.

There are many kinds of mission instruments onboard remote sensing satellites. Typical instruments of passive type are optical sensors, visible to near infrared radiometer, shortwave infrared radiometers, thermal infrared radiometers and microwave radiometers while those of active instruments, Synthetic Aperture Radar: SAR. Both types of mission instruments have merits and demerits for disaster relief. It would be desirable to use both mission instrument data considering their merits and demerits.

Typically, SAR data can be used under all-weather condition, day and night as well as cloudy and rainy conditions. On the other hand, optical sensors do not work under the conditions, night time, and cloudy and rainy conditions. Physical quantities derived from these mission instruments are also different from each other. Essentially, SAR data reflect surface slope, roughness, soil moisture, and so on. Meanwhile, SWIR data, moisture index, vegetation index, land cover types etc. can be derived from the optical sensors. Therefore, depending on the purposes, both instrument data can be used separately or collaboratively.

In order to conduct disaster relief of flooding area detection and oil spill area detection, Sentinel-1 of SAR data and Sentinel-2 of optical sensor data are used collaboratively in this research. Results show effectiveness and efficient usage of SAR and optical sensor data for landslide and oil spill disaster relief.

The next section describes related research works followed by the research background of this study. Then, experimental results are described followed by conclusions together with some discussions.

II. Related Resrach Works

There are some related studies on disaster relief and mitigation research works, method for estimation of damage grade and damaged paddy field areas due to salt containing sea breeze with typhoon using remote sensing imagery data is proposed and validated [1]. Back-up communication routing through Internet satellite WINDS for transmitting of disaster relief data are also proposed [2]. On the other hand, cellular automata for traffic modeling and simulation in a situation of evacuation from disaster areas are proposed [3]. Meanwhile, micro traffic simulation with unpredictable disturbance based on Monte Carlo simulation: effectiveness of the proposed agent cars of Sidoarjo hot mudflow disaster is discussed [4] while probabilistic cellular automata based approach for prediction of hot mudflow disaster area and volume is proposed and validated [5]. In the meantime, two dimensional CA approach for disaster spreading is proposed [6]. Micro traffic simulation with unpredictable disturbance based on Monte Carlo simulation and effectiveness of the proposed agent cars of Sidoarjo hot mudflow disaster is discussed already [7].

Probabilistic cellular automata based approach for prediction of hot mudflow disaster area and volume is reviewed and re-evaluated [8] together with new approach of prediction of Sidoarjo hot mudflow disaster area based on probabilistic Cellular Automata: CA [9]. Cellular automata for traffic modeling and simulation in a situation of evacuation from disaster areas -Cellular Automata Simplicity behind Complexity- is discussed [10].

Sensor network for landslide monitoring with laser ranging system avoiding rainfall influence on laser ranging by means of time diversity and satellite imagery data based landslide disaster relief is proposed and validated [11]. Task allocation model for rescue disable persons in disaster area with help of volunteers is also proposed [12]. Deceleration in the evacuation from disaster area is discussed [13]. Cell based GIS as cellular automata for disaster spreading predictions and required data systems are proposed and validated already [14]. On the other hand, visualization of 5D assimilation data for meteorological forecasting and its related disaster mitigation utilizing VIS5D of software tool is proposed and well reported [15].

Meanwhile, vital sign and location/attitude monitoring with sensor networks for the proposed rescue system for disabled and elderly persons who need a help in evacuation from disaster areas is proposed and validated [16] together with method and system for human action detection with acceleration sensors for the proposed rescue system for disabled and elderly persons who need a help in evacuation from disaster areas [17]. Vital sign and location/attitude monitoring with sensor networks for the proposed rescue system for disabled and elderly persons who need a help in evacuation from disaster areas is discussed and re-evaluated [18].

Method and system for human action detection with acceleration sensors for the proposed rescue system for disabled and elderly persons who need a help in evacuation from disaster areas is proposed and well validated [19], [20].

III. Research Background

On the morning of August 26, the front line near the southern part of Kyushu moved northward to the vicinity of the Tsushima Strait on the 27th day. For this reason, it was a record heavy rain in Saga Prefecture. Saga prefecture is situated in the north portion of Kyushu, Japan as illustrated in Fig. 1.

Fig. 1. Location of Saga Prefecture.

Fig. 2 shows MTSAT (Japanese Meteorological Satellite in the geostationary orbit) imagery data acquired (a) at 3 a.m. on August 26 2019 and (b) at 21:00 on August 30 2019, respectively. During from 26 to 30 August 2019, heavy rain was continued recursively. The heaviest rainfall was observed in the morning on 28 August 2019 as shown in Fig. 3. Much greater than 100 mm / hour was recorded in the morning. Also, rainfall rate and accumulated rainfall measured during from 28 to 30 August 2019 is shown in Fig. 4. Accumulated rainfall reached to 500 mm while the peak rainfall rate reached to 100 mm, respectively. As the results, landslide (collapsed) and oil spill were occurred in the Omachi-Town in Saga prefecture.

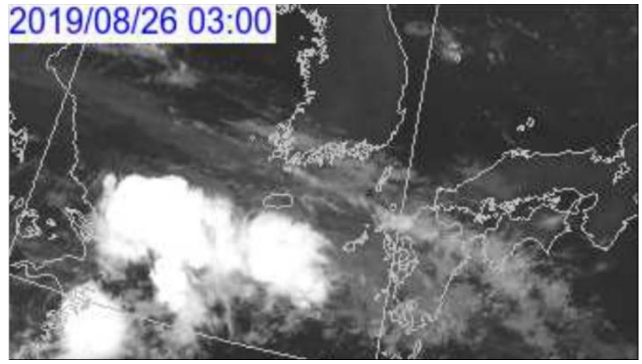

(a) 3:00 on August 2019.

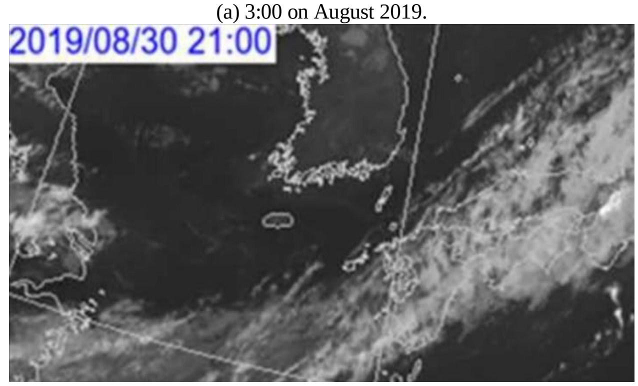

(b) 21:00 on August 2019.

Fig. 2. MTSAT (Japanese Meteorological Satellite in the Geostationary Orbit) Imagery Data Acquired (a) at 3 a.m. on August 26 2019 and (b) at 21:00 on August 30 2019.

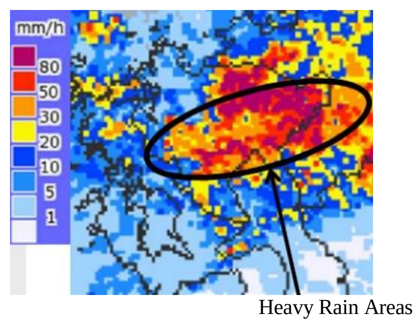

Fig. 3. Rain Radar Derived Rainfall Distribution which was Observed in the Morning on 28 August 2019.

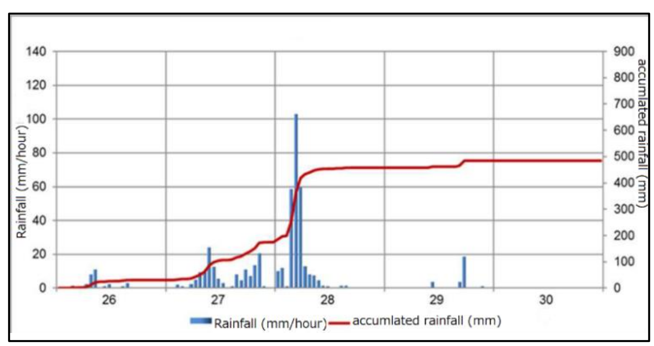

Fig. 4. Rainfall Rate and Accumulated Rainfall Measured During from 28 to 30 August 2019.

IV. Disaster Relief with Satellite Data

A. Intensive Study Area

In the morning of 28th, “Botayama Wanpaku Park” in Omachi-Town, Saga Prefecture, was affected by heavy rain, and the slope collapsed about 50 meters wide and about 20 meters high, blocking the town road leading to the park. Fig. 5(a) shows photo of collapsed area while Fig. 5(b) shows photo of oil spill area in Omachi-Town. These disaster areas are situated in the Omachi-Town shown in Fig. 6.

The oil spill was occurred at the bottom left corner in Fig. 6(b) and (c) while the collapsing was happened at the top right corner in Fig. 6(b) and (c), respectively.

B. Remote Sensing Satellite Data Analysis

Sentinel-1 of SAR data is used for detection of oil spill and collapsed area detection. There are two Sentinel-1 satellite, 1A and 1B. Both of repetition cycle is 12 days. Therefore, it is possible to observe the earth surface every 6 days. Also, there are two polarization of available SAR data, VV and VH (V and H stands for vertical and horizontal polarization so that VV means emit V polarization of Electromagnetic Wave: EM (C band) and receive V polarization of EM return echo from the earth surface. Spatial resolution of SAR on the ground is 5 m. Table I shows major specification of Sentinel-1 of SAR.

(a) Collapsed Area.

(b) Oil Spill Area.

Fig. 5. Photos of the Collapsed Area and Oil Spill Area Due to Heavy Rain.

(a) Location.

(b)Oil Spill and Collapsed Areas on Google Map.

(c) Oil Spill and Collapsed Areas on Google Map.

Fig. 6. Intensive Study Areas of Omachi-Town, Saga Prefecture.

TABLE. I. Major Specification of Sentinel-1 of SAR

Stripmap	80 km	5 m × 5 m	HH-HV, VV-VH

Fig. 7(a) shows topographic map of Omachi town while Fig. 7(b) shows ortho rectified VV sigma note (back scattered cross section of the earth surface) in unit of decibel of the areas of oil spill and collapsed acquired at 09:21 UTC on August 14 2019 (just before oil spill and collapse are occurred). Meanwhile, Fig. 7(c) shows same area of ortho rectified VH sigma note (back scattered cross section of the earth surface) in unit of decibel of the areas of oil spill and collapsed acquired at the same time.

Meanwhile, Sentinel-2 carries 10 m resolution of visible to short wave infrared radiometer. Table II shows major specification of optical sensor onboard Sentinel-2 Band 12 is Short Wave Infrared SWIR band while band 8 is Near Infrared: NIR band. Also, band 4 is red color band so that Normalized Deviation of Vegetation Index: NDVI and be retrieved with the following equation.

$$NDVI = (B8 – B4) / (B8 + B4) \quad (1)$$

(a) Topographic Map.

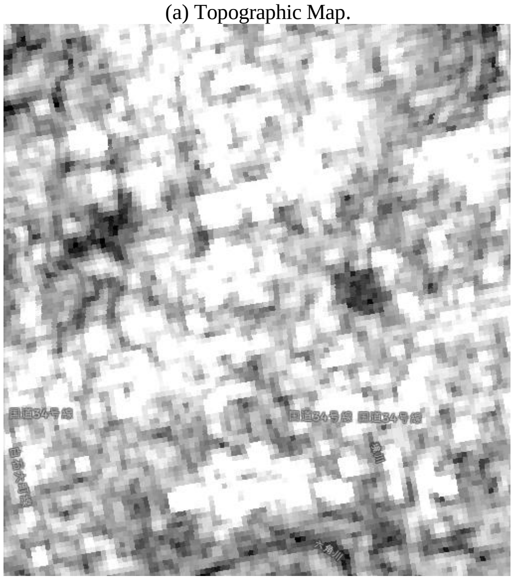

(b) Ortho Rectified VV Sigma Note (Back Scattered Cross Section of the Earth Surface) in unit of Decibel of the Areas of Oil Spill and Collapsed Acquired at 21;17 UTC on August 15 2019.

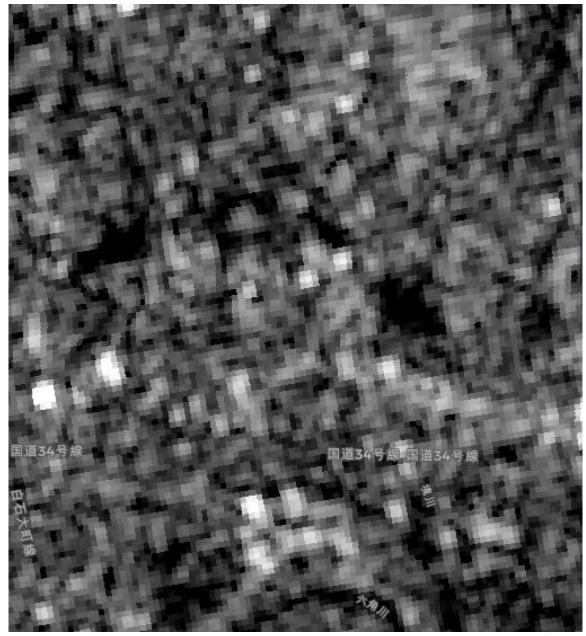

(c) Ortho Rectified VH Sigma Note (Back Scattered Cross Section of the Earth Surface) in unit of Decibel of the Areas of Oil Spill and Collapsed Acquired at the Same Time.

Fig. 7. Disaster Relief Result.

At the top right corner, Botayama Wanpaku park of collapsed area is situated while oil spill area is situated bottom left corner, respectively. On the other hand, Fig. 8(a) shows ortho rectified VV sigma note (back scattered cross section of the earth surface) in unit of decibel of the areas of oil spill and collapsed acquired at 09:22 UTC on September 1 2019 (just after oil spill and collapse are occurred). Meanwhile, Fig. 7(b) shows same area of ortho rectified VH sigma note (back scattered cross section of the earth surface) in unit of decibel of the areas of oil spill and collapsed acquired at the same time.

It is quite obvious that VV sigma note at the collapsed area acquired after the collapse is occurred is much higher than that of before the collapsing. Also, it is found that VV sigma note at the oil spill area acquired after the collapse is occurred is much lower than that of before the oil spill. These are almost same for the VH sigma note.

TABLE. II. MAJOR SPECIFICATION OF OPTICAL SENSOR ONBOARD SENTINEL-2

B1	443 nm	60 m
B2	490 nm	10 m
B3	560 nm	10 m
B4	665 nm	10 m
B5	705 nm	20 m
B6	740 nm	20 m
B7	775 nm	20 m
B8	842 nm	10 m
B8a	865 nm	20 m
B9	940 nm	60 m
B10	1375 nm	60 m
B11	1610 nm	20 m
B12	2190 nm	20 m

Also, SWIR color composite image can be derived from Band 12, Band 8A and Band 4 while false color composite image can be derived from Band 8, 4, and 3 where Band 3 is green color band.

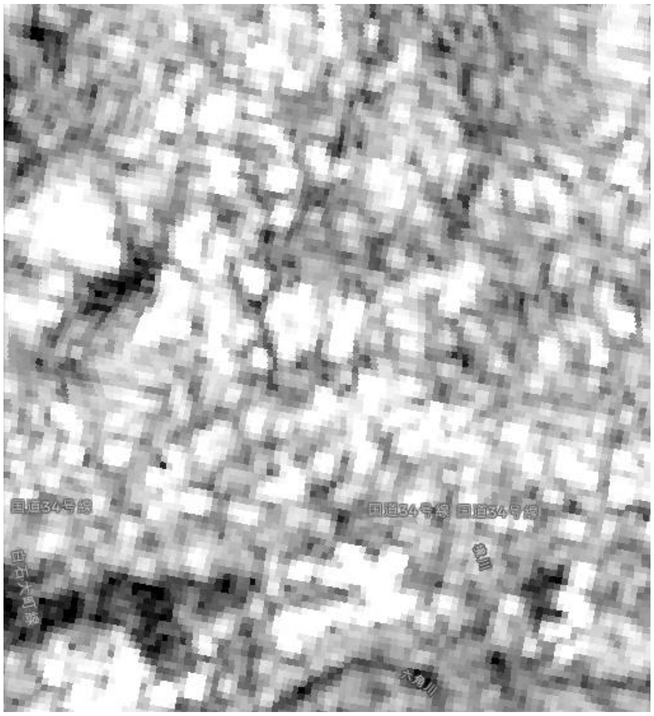

(a) Ortho Rectified VV Sigma Note (Back Scattered Cross Section of the Earth Surface) in unit of Decibel of the Areas of Oil Spill and Collapsed Acquired at 09:22 UTC on September 1 2019.

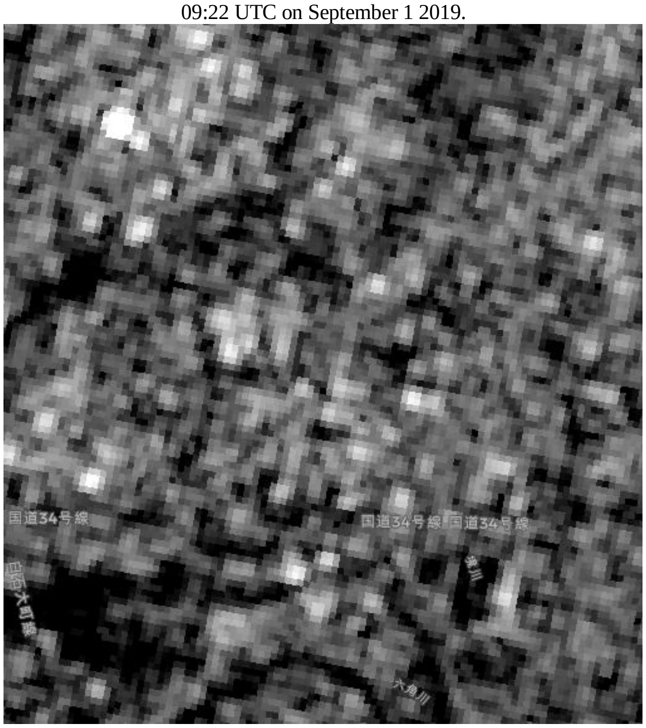

(b) Ortho Rectified VH Sigma Note (Back Scattered Cross Section of the Earth Surface) in unit of Decibel of the Areas of Oil Spill and Collapsed Acquired at the Same Time.

Fig. 8. Disaster Relief Result.

Sentinel-2 data derived false color image which is acquired at 02:08 on August 13 2019 is shown in Fig. 9(a) while NDVI is shown in Fig. 9(b). Also, Fig. 9(c) shows SWIR color composite image. These imagery data are acquired just before the heavy rain.

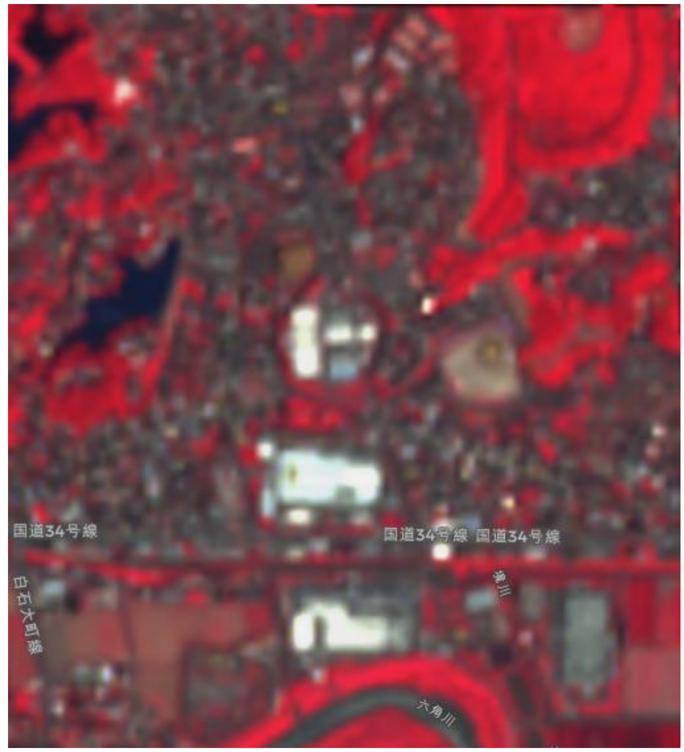

(a) False Color.

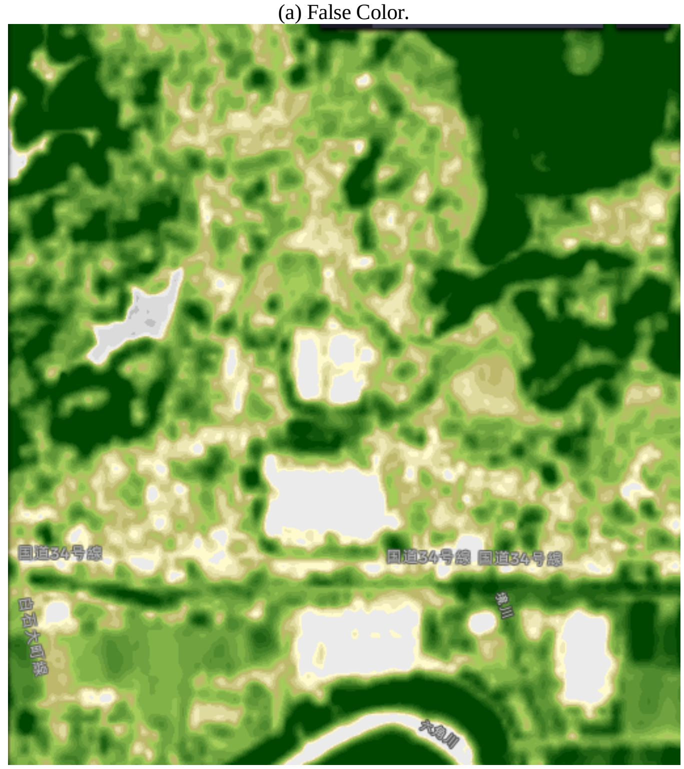

(b) NDVI.

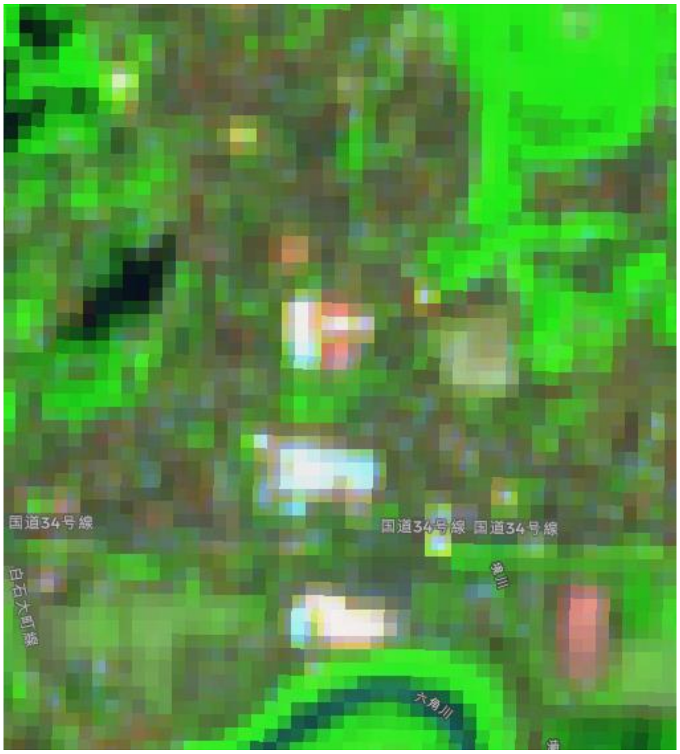

(c)SWIR color

Fig. 9. Sentinel-2 Data Derived False Color Image which is Acquired at 02:08 on August 13 2019 and NDVI as well as SWIR Color Composite Image.

In the figure of NDVI, color scale is as shown in Fig. 10.

On the other hand, Sentinel-2 data derived false color image which is acquired at 02:08 on September 9 2019 is shown in Fig. 9(a) while NDVI is shown in Fig. 9(b). Also, Fig. 9(c) shows SWIR color composite image. Due to heavy rain condition, it was not acquired a good Sentinel-2 data on the following dates, August 15, 18, 20, 23, 25, 28, 30, September 2, 4, and 7 2019.

Because of poor spatial resolution of optical sensor, it is not clear the collapsed area (it has to be situated at the top right corner). Meanwhile, it can be detect the oil spill disaster at the bottom left corner of the false color, NDVI, and SWIR color composite imagery data through a comparison between Fig. 9 and Fig. 11 (just before and after the disaster). Due to the oil spill, surface vegetation is covered with oil so that the surface reflectance and NDVI are decreased.

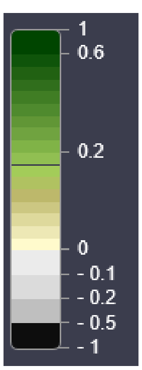

Fig. 10. NDVI Color Scale.

In these figure, the oil spill areas are situated at the bottom left corner while the collapsed area is situated at the top right corner, respectively. Spatial resolution of visible wavelength channels (10m) is different from shortwave infrared wavelength channels (20m). In particular for collapsed area is just 20 m by 50 m so that it is not easy to recognize the location of collapsed area in the SWIR image while it can be found the collapsed area in the visible wavelength channels of false colored images. On the other hand, oil spill areas are identified at the bottom left corner in both visible and SWIR images.

(a) False Color.

(b) NDVI.

(c) SWIR.

Fig. 11. Sentinel-2 Data Derived False Color Image which is Acquired at 02:08 on September 9 2019 and NDVI as well as SWIR Color Composite Image.

V. Conclusion

Flooding and oil spill disaster relief using Sentinel of remote sensing satellite data is conducted. Kyushu, Japan had severe heavy rain during from 26 August to 30 August 2019. Optical sensor and Synthetic Aperture Radar: SAR onboard remote sensing satellite is used for disaster relief. NDVI and SWIR data derived from the Sentinel data are used for disaster relief. Merits and demerits of the optical sensor and SAR instrument are compared from the disaster relief of point of view.

Through experiments, it can be detect the oil spill disaster at the bottom left corner of the false color, NDVI, and SWIR color composite imagery data through a comparison between Fig. 9 and Fig. 11 (just before and after the disaster). Due to the oil spill, surface vegetation is covered with oil so that the surface reflectance and NDVI are decreased. Also, it is found that both of oil spill and collapsed disaster areas are detected through a comparison between SAR data which are acquired just before and after the disaster even if the weather condition.is not good and in the night time and day time.

VI. Future Research Works

Further experimental studies are required for the validation of the proposed method. Also, applicability of the proposed method has to be confirmed through further experiments.

Acknowledgment

The author would like to thank Professor Dr. Hiroshi Okumura for his valuable discussions.

References

[1] Kohei Arai, Method for estimation of damage grade and damaged paddy field areas sue to salt containing sea breeze with typhoon using remote sensing imagery data, International Journal of Applied Science, 2, 3, 84-92, 2011.

[2] Kohei Arai, Back-up communication routing through Internet satellite WINDS for transmitting of disaster relief data, International Journal of Advanced Computer Science and Applications, 2, 9, 21-26, 2011.

[3] 28. Kohei Arai, Tri Harsono, Achmad Basuki, Cellular automata for traffic modeling and simulation in a situation of evacuation from disaster areas, Cellular Automata-Simplicity Behind Complexity, Edit. Aiejandro Salcido, ISDN:978-953-307-230-2, InTech Publishing Co.Ltd., 193-218, 2011.

[4] 83. Kohei Arai, Disaster Monitoring from Space (Remote Sensing Satellites), Research Note for Natural Disaster, No.23, pp.29-34, Mar. 1999.

[5] Kohei Arai, Tri Harsono, Achmad Basuki, Micro traffic simulation with unpredictable disturbance based on Monte Carlo simulation : effectiveness of the proposed agent cars of Sidoarjo hot mudflow disaster, Journal of Emitter, 1, 1, 1-10, 2010

[6] Achmad Basuki, Tri Harsono and Kohei Arai, Probabilistic cellular automata based approach for prediction of hot mudflow disaster area and volume, 1, 1, 11-20, 2010.

[7] Achmad Basuki and Kohei Arai, Two dimensional CA approach for disaster spreading, Innovation Online (INOVASI), 18,12,19-26, 2010.

[8] Kohei Arai, Tri Harsono, Achmad Basuki, Micro traffic simulation with unpredictable disturbance based on Monte Carlo simulation and effectiveness of the proposed agent cars of Sidoarjo hot mudflow disaster, Journal of EMITTER, 1, 1, 10-19, 2010.

[9] Achmad Basuki, Tri Harsono, Kohei Arai, Probabilistic cellular automata based approach for prediction of hot mudflow disaster area and volume, Journal of EMITTER, 1, 1, 1-9, 2010.

[10] Kohei Arai, Achmad Basuki, New Approach of Prediction of Sidoarjo Hot Mudflow Disaster Area Based on Probabilistic Cellular Automata, Geoinformatica - An International Journal (GIIJ), 1, 1, 1-11, 2011.

[11] Kohei Arai, Tri Harsono, Achmad Basuki, Cellular automata for traffic modeling and simulation in a situation of evacuation from disaster areas -Cellular Automata Simplicity behind Complexity-, Edit. Aiejandro Salcido, ISBN:978-953-307-230-2, InTech Pub. 193-218, 2011.

[12] Kohei Arai, Sensor network for landslide monitoring with laser ranging system avoiding rainfall influence on laser ranging by means of time diversity and satellite imagery data based landslide disaster relief, International Journal of Applied Sciences, 3, 1, 1-12, 2012.

[13] Kohei Arai, T.X.Sang, N.T.Uyen, Task allocation model for rescue disable persons in disaster area with help of volunteers, International Journal of Advanced Computer Science and Applications, 3, 7, 96-101, 2012.

[14] T.Harsono, Kohei Arai, Deceleration in the evacuation from disaster area, Journal of Electronics, Mechanics & Robotics, Informatics & Computer, Telecommunications (EMITTER), 2, 2, 203-210, 2012.

[15] Kohei Arai, Cell based GIS as cellular automata for disaster spreading predictions and required data systems, Advanced Publication, Data Science Journal, Vol.12, WDS 154-158, 2013.

[16] Kohei Arai, Visualization of 5D assimilation data for meteorological forecasting and its related disaster mitigation utilizing VIS5D of software tool, International Journal of Advanced Research in Artificial Intelligence, 2, 9, 24-29, 2013.

[17] Kohei Arai, Vital sign and location/attitude monitoring with sensor networks for the proposed rescue system for disabled and elderly persons who need a help in evacuation from disaster areas, International Journal of Advanced Research in Artificial Intelligence, 3, 1, 24-33, 2014.

[18] Kohei Arai, Method and system for human action detection with acceleration sensors for the proposed rescue system for disabled and elderly persons who need a help in evacuation from disaster areas, International Journal of Advanced Research in Artificial Intelligence, 3, 1, 34-40, 2014.

[19] Kohei Arai, Vital sign and location/attitude monitoring with sensor networks for the proposed rescue system for disabled and elderly persons who need a help in evacuation from disaster areas, International Journal of Advanced Research in Artificial Intelligence, 3, 1, 24-33, 2014.

[20] Kohei Arai, Method and system for human action detection with acceleration sensors for the proposed rescue system for disabled and elderly persons who need a help in evacuation from disaster areas, International Journal of Advanced Research in Artificial Intelligence, 3, 1, 34-40, 2014.

AUTHOR'S PROFILE

Kohei Arai, He received BS, MS and PhD degrees in 1972, 1974 and 1982, respectively. He was with The Institute for Industrial Science and Technology of the University of Tokyo from April 1974 to December 1978 also was with National Space Development Agency of Japan from January, 1979 to March, 1990. During from 1985 to 1987, he was with Canada Centre for Remote Sensing as a Post Doctoral Fellow of National Science and Engineering Research Council of Canada. He moved to Saga University as a Professor in Department of Information Science on April 1990. He was a councilor for the Aeronautics and Space related to the Technology Committee of the Ministry of Science and Technology during from 1998 to 2000. He was a councilor of Saga University for 2002 and 2003. He also was an executive councilor for the Remote Sensing Society of Japan for 2003 to 2005. He is an Adjunct Professor of University of Arizona, USA since 1998. He also is Vice Chairman of the Science Commission "A" of ICSU/COSPAR since 2008 then he is now award committee member of ICSU/COSPAR. He wrote 37 books and published 570 journal papers. He received 30 of awards including ICSU/COSPAR Vikram Sarabhai Medal in 2016, and Science award of Ministry of Mister of Education of Japan in 2015. He is now Editor-in-Chief of IJACSA and IJISA. http://teagis.ip.is.saga-u.ac.jp/index.html.

Analysis of Multi-hop Wireless Sensor Networks using Probability Propagation Models

Komgrit Jaksukam*[,1], Teerawat Tongloy[2]
Santad Chuwongin[3]
Center of Industrial Robot and Automation (CiRA)
College of Advanced Manufacturing Innovation (AMI)
King Mongkut's Institute of Technology Ladkrabang
Bangkok, Thailand

Siridech Boonsang[4]
Department of Electrical Engineering
Faculty of Engineering
King Mongkut's Institute of Technology Ladkrabang
Bangkok, Thailand

***Abstract*—This paper presents a formula for estimating the probability of collecting a given amount of data from a propagation model and multi-hop wireless sensor networks (WSNs) based on Monte Carlo simulation with cluster-tree topology. The probabilistic model is based on an analytical model of the IEEE 802.15.4 MAC protocol. The probability of successful node transmission is extended to the probabilities of successful collection at the cluster P(X=k) and sink node P(X ⩾ k). A numerical example has been provided for comparing the probabilities. We propose a model to calculate the probability from the ratio of the collection rate to the total number of nodes and therefore provide the likeliness of complete data collection. Finally, the results from our analysis provide an estimation of the probability of achieving successful transmission in WSNs.**

Keywords—Probabilistic modelling; wireless sensor network; multi-hop networks; data collection scheme; Monte Carlo simulation; probability propagation models; probabilistic analysis

I. Introduction

Wireless network communication technology has been widely used owing to its infrastructure network that can link and exchange data based on an ad hoc network [1]. The ad hoc network uses distributed node computing without any control centres [2-5, 16]. In addition, it is a self-organization wireless network [6] having a significant number of sensor nodes that respond to several physical aspects, for example, agricultural parameter controlling, transportation planning, logistics planning, and structural testing [7, 24]. This can be achieved by physical data measurement and collection from sensor nodes; the data is then transferred to the coordinator nodes and finally to the sink nodes, based on data exchange of trade-off networks [3-4, 21].

General wireless sensor networks (WSNs) can support single-hop data transfer where the sink node is located at a far distance, which causes energy loss during data transfer. For multi-hop data transfer, the sensor nodes are linked together from the node source to the node sink. In the case of a large network, the data transfer becomes complicated and accumulates more data as the number of hops increase. This contributes to the weakness of multi-hop wireless communication, causing packet loss from the network traffic load, which in turn creates data overflow and network congestion [10, 11]. This then results in channel access failure. For this reason, it was found that general WSNs could not guarantee packet transfer from the sensor to the sink nodes in multi-hop data transfer. Some probability models, based on the IEEE 802.15.4 standard of CSMA/CA protocol [6], have been proposed to solve the aforementioned problem. An example is the model proposed by Marco et al. [9]. This model focuses on the impact of the reliability and delay at the MAC layer on the routing algorithm's performance [2, 20]. This is done by balancing traffic distribution through the adjustment of three parameters: macMinBE, macMaxCSMABackoffs, and macMaxFrame-Retries. However, this model does not directly guarantee packet transfer to the sink nodes.

This paper presents a new model for calculating the probability of a successful collection. The proposed model was developed from the analytical model of the IEEE 802.15.4 MAC layer networks proposed by Buratti et al. [8]. The Buratti model for single-hop is expanded and applied to the probability framework of WSNs with multi-hop. Extending into a cluster-tree topology, the model for multi-hop networks is formulated by using a propagation model or by following a Monte Carlo simulation of the probability of successful reception for each cluster [12]. A simple numerical result is given to demonstrate the application of our proposed model to estimate the probability of a successful collection rate.

This paper is divided into six sections. In Section II, the statement of contribution is to analyse multi-hop wireless communication in the related works, the underlying analysis model for IEEE 802.15.4 networks is explained. This is followed by the development of multi-hop WSNs based on cluster-tree topology, in Section IV. Section V presents the numerical results that express the probability of successful reception in the propagation model and a probabilistic modelling based on Monte-Carlo simulation at the sink node of WSNs. Finally, the conclusions are provided in Section VI.

II. Related Works

For applications based on IEEE 802.15.4 WSN, there are two types of simulation models to evaluate the performance of the data transfer as follows: (1) simulation model using a computer simulation program, (2) simulations models using the probability model for WSNs based on Markov chain's principle. In the first type of simulation model, a computer program, consisting of the OMNeT++[16, 17], TinyOS [18] and the NS3 [20], is used to arrange the network in various

*Corresponding Author.

kind of topologies by ways of random data to achieve different results. The weakness of this method is some limitations in adjusting some MAC-layer parameters.

For the second type of simulation model [8-9, 12, 19, 22], which is the simulation using the probability model for WSNs based on Markov chain's principle, this simulation described that WSN work mechanism includes two steps, that is, the transition state diagram and the process of every event with the transition probability. In this simulation type, the probability of successful data transfer can be easily calculated and adjusted by changing MAC-layer parameters. Due to these strong points, the topology designed [23] in this research was based on this type of this simulation model. The specific model used in this paper was the IEEE 802.15.4, which was non beacon-enabled model presented by Buratti et al. [8]. The model determines the trade-off between the probability success and energy consumption [22, 25] by adjusting three MAC parameters consists of number of nodes, number of time slots and size of packet. Subsequently, the MAC losses are reduced.

In view of the above, one of the probability models that have been proposed to analyse the performance of IEEE 802.15.4 is the one developed by single hop model [8]. On one hand, this model allows the calculation of the probability of success for a transmission packet. On the other hand, it is based on single-hop communication and can be operated only in a short range due to low-power radio. Some other probability models have been proposed based on multi-hop communication. However, in the case of an extensive network, data collection becomes complicated, and more data is accumulated as the number of hops increases. This contributes to the weakness of multi-hop wireless communication [5], causing packet loss from the network traffic load, which creates data overflow and network congestion [10]. Finally, this leads to channel access failure [11]. Therefore, there is no guarantee that the data packet will be transferred from the sensor to the sink nodes for multi-hop data collection.

The proposed probabilistic model used to express the probability of successful collection at the sink node of WSNs is based on two topology parameters, namely cluster size and hop distance. The simulation was repeated using the Monte Carlo method. From the simulation results, a histogram was created to obtain the probability distribution of data collection. This study provides a reliable multi-hop WSN topology, which can guarantee packet transfer at an acceptable confidence percentage. The analytical multi-hop network has a uniform cluster-tree topology structure composed of small clusters. All clusters are connected to each other via collect and forward methods. In each cluster, the probability of data transfer is calculated based on the Buratti's model for single-hop data transfer. The overall probability of success is then calculated by probability propagation and classified using the number of nodes and hops. They also focus on the reception rate and the probability of success in data collection in WSNs.

III. Single Hop Communication Model

The analytical model, the symmetrical topology design of multi-hop WSNs using probability propagation models in this study was based on this type of analytical model [23, 25], which was presented by single hop model [8]. These are the hypotheses and assumptions for a multi-hop WSN in this study: (1) no hidden nodes, (2) no data retransmission, (3) no acknowledgement for node sensors, and (4) no propagation delay (no data collision). The WSN had a star topology structure and a query-based application. Spaces between each node were equal or symmetric, where each cluster had N nodes (N = 1,2,..,N). The data comprised the size of packet (D) which is an integer, the backoff time ($d_b = 20T_s$, where T_s = 16 μs), the time slot (j), and the maximum data transmission time (T_{max} = 120). The size of the data transmitted by each node was 10*D bytes. The time for sending a packet is D*d_b.

The IEEE 802.15.4 non-beacon-enabled model explains the behaviour of the nodes' operation in one cluster with single-hop communication, as shown in Fig. 1(a). Each single hop consists of 4 statuses: backoff, sensing, transmission, and idle. The procedure starts when the transmission node needs to transmit data. It will check the status of the channel, whether the node is busy or free, by using probability sensing of slot j or $P\{S_i^j\}$. If the status is busy, then the node will keep increasing the number of backoff slots each time until it finds a free channel. Once the data transmission is completed, the probability that a node transmits its packet in slot j for the final node, $P\{T^j\}$ can be calculated. Then the subsequent transmission node, which is in idle status, will start the data transmission procedure once again, where the number of nodes, N, increases from N-1 to N until the data transmission is completed. As N increases, the number of slots j decreases. This mechanism is shown in Fig. 1(b).

From the data transmission mechanism of a single-hop cluster [8], once the probability $P\{T^j\}$is determined, the probability that a node transmits its packet with success in slot j, j ∊ [0, T_{max}+D-1], where $P\{Z^j\}$ can be calculated and expressed as follows.

$$P\{Z^j\} = \left(1 - p_b^{j-D}\right)P\{C^{j-D}\}\prod_{i=0}^{NB_{max}}\left(1 - P\{S^{j-D}\}\right)^{N_c^{j-D}-1} \quad (1)$$

where the probability, $P\{Z^j\}$ depends on other probabilities: the probability of a busy channel p_b^j, the probability of a node to sense a channel $P\{C^j\}$, and $P\{S^j\}$. Therefore, the probability success, p_s, of data transmission in every node in the cluster can also be determined by

$$p_s = \sum_{j=0}^{t_{max}+D-1} P\{Z^j\} \quad (2)$$

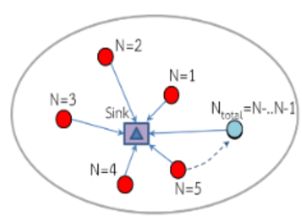

(a) Star Topology.

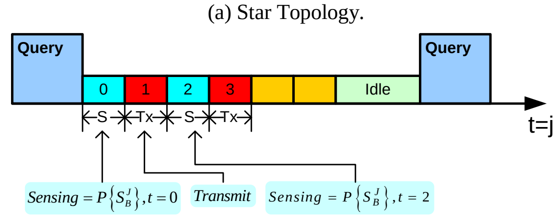

(b) Pattern of Data Transmission Node.

Fig. 1. Single-Hop Cluster using a Probability Model.

In addition, the function of accumulative probability $P\{Z^j\}$ is affected by the number of nodes, N, and the size of the packet, D, from the following equation:

$$F\{Z^j\} = \sum_{v=0}^{j} P\{Z^v\} \quad (3)$$

where $F\{Z^j\}$ is a cumulative function for the probability that a node successfully transmits its packet in time slot j. Furthermore, the probability model is an algorithm with $N \geqslant 1$, $D \geqslant 1$, and $T_{max} \geqslant 120$ for single-hop, developed using a MATLAB script as follows: (1)

1) Initialize MAC parameters for j = 0.
2) Loop for $j \leq (T_{max} + D - 1)$
   a) Set $N_c^j = N$.
   b) Compute probability p_b^j.
   c) Compute probabilities $P\{S_0^j\}$, $P\{S_1^j\}$, $P\{S_2^j\}$, $P\{S_3^j\}$, and $P\{S_4^j\}$.
   d) Compute probabilities $P\{C^j\}$, $P\{Z^j\}$, p_s.
   e) Compute probabilities $P\{T^j\}$, $P\{R^j\}$.
   f) Compute cumulative probability $F\{Z^j\}$

The performance limitations of multi-hop networks were studied by evaluating the probability of success based on an assumption of star topology. We studied the effects of changing the size of packet (D) on p_s, accumulated probability $F\{Z^j\}$. There were two cases studied of the probability for a data transfer in a single hop cluster: The first case studied for the effects of size of packet (D) in the network to by fixing D are set 1, 3, 6, 9, 12 and the maximum data transmission time T_{max} at 120. For the effect of D on p_s, N is varying due to 50 nodes while p_s for each is calculated and the result is show in Fig. 2(a).

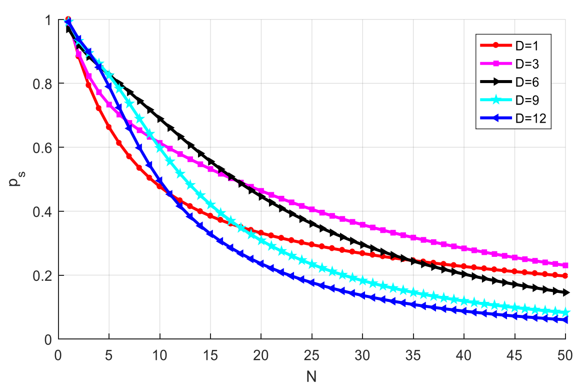

(a) The Effect of N and D on the Probability ps.

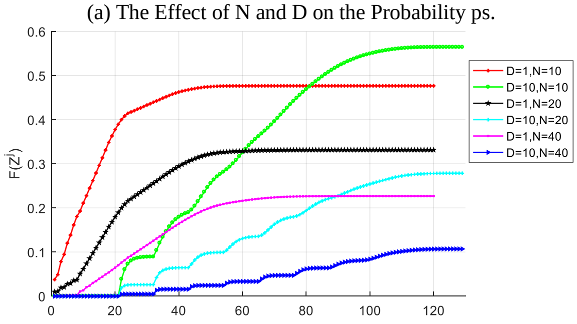

(b) The Effect of D and N on Accumulative Probability F{Zj}.

Fig. 2. Effect of Data Transfer in a Single hop Cluster.

The result show that the very low probability success as having a chance of occurrence of less than 0.25%, this caused N and D were increasingly. Second case studied for the effect D in the network on accumulated probability $F\{Z^j\}$ by D was set 1, 10 and N was set to 10, 20, 40 nodes in each case shows that the node was transferring data in the network when time slot (j) was increased due to steady-state, as show in Fig. 2(b). We are specifically interested in the channel distribution access in time slot j within the maximum data transmission time (T_{max}).

IV. Multi-Hop Wireless Sensor Networks

A. Analysis Probability of Single-Hop Model

We studied the effects on the probability p_s of N and the number of hops (H) in the network to learn which terms of data transfer were increasing with N per cluster and H per cluster. The varying parameters in the network were as follows: (1) N was set to 12 nodes per cluster and, for no data transfer, H was set to 0. The total for each node is equal to $p_s(N=12,H=0)$ of $N_{totol}=12$, as shown in Fig. 3(a). (2) N was set to 4 nodes per cluster with H set to 1, which makes the total per node equal to $p_s(N=4,H=1)$ of $N_{totol}=12$, as shown in Fig. 3(b). In Fig. 3(c), the comparison of probability p_s between N and H in the network shows that N has more impact than H on probability p_s. In case studies, we showed that the very low probability p_s could be improved by increasing the H of data transmission.

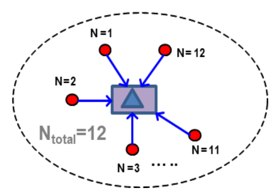

(a) Single-hop Transmission (H=0) with N=12, D=1.

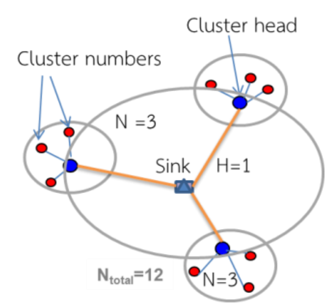

(b) Two-hop Transmission (H=1) with N=3, D=4.

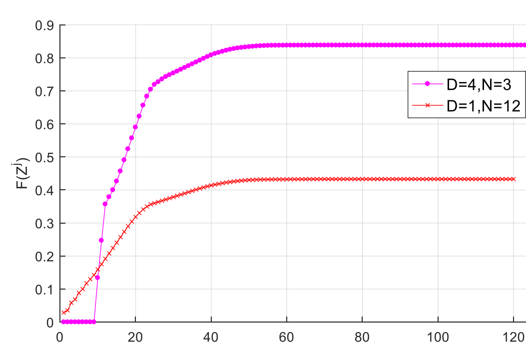

(c) A Comparison of the Probability ps between N, H in the Network.

Fig. 3. Effect of Data Transfer of N, H Parameters in Network.

B. Model of Multi-hop WSNs

As the previous model is for single-hop data transfer, it can be extended to support the multi-hop model. From the data transmission mechanism of a single-hop cluster, it was found that the effects of data collected in a single hop have a very low probability. The ideal goal would be to design a multi-hop uniform cluster-tree topology composed of small clusters, as shown in Fig. 4. According to the reasons mentioned above, we propose data transfer in-network, where small clusters are collected, and data is forwarded in each small cluster until it reaches the sink node. Each cluster is built by extending the single hop into the multi-hop network.

The model given in Section III is valid for WSNs with star topology. Considering its application to a multiple infrastructure network, there is a limitation due to the radius of low-power radio. Therefore, an extended model is proposed to multi-hop WSNs topology using a probability framework that can link and exchange data based on an ad hoc network. The cluster-tree formulation is one of the widely used topologies to expand the coverage area of WSNs to be larger than the distance of IEEE 802.15.4 radio. The multi-hop data transmission with cluster-tree formulation [12] with a simplifying model consists of clusters of single-hop models. The topology consists of clusters and a sink node in which each cluster is formed as a star network, which then forwards data to a next-hop router.

In addition, the model of multi-hop WSNs is based on the assumptions given in Section III. Symmetrical topology is assumed in the cluster-tree structure, as depicted in Fig. 3. In this study, we make four assumptions: (1) All nodes are identical. (2) All clusters have the same size. (3) Tree structure is uniform with respect to hop distance. (4) WSN communications use a collect-and-forward protocol, statistically independent in each layer. There were two types of distribution of the nodes in the network: the depth branch is increasing the H that data is transmitted over, and the breadth branch is increasing the number of child nodes in each cluster (N).

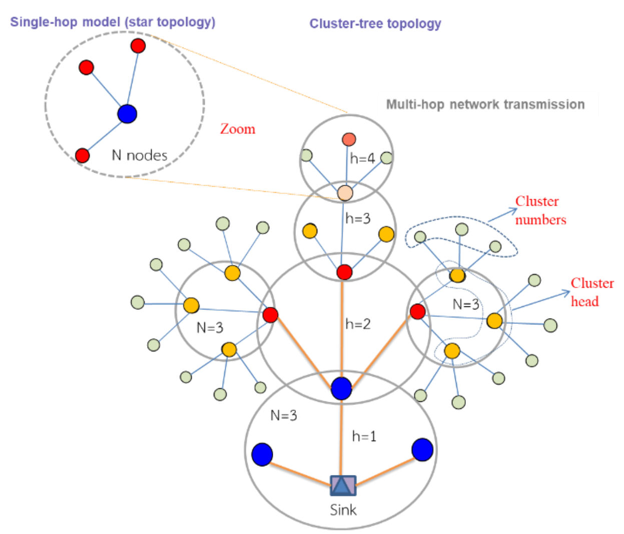

Fig. 4. Cluster-Tree Topology as Multi-Layer Star Topologies.

C. Probabilistic Modelling based on Monte-Carlo Simulation

We can quickly solve this simplified model with a Monte Carlo simulation. A method for analysing the collected data in multi-hop WSNs with cluster-tree topology is to examine the probability of collected data in each hop independently. In this study, a probability propagation model was created using a pseudo-random Monte Carlo simulation [14, 15]. Such Monte Carlo simulation has been used to compute the concrete probability of successful collection rates to deploy node sensors in a network.

The probability distribution of internal communication networks with probability models was calculated using a pseudo-random method [15] with a uniform distribution [0, 1] of Monte Carlo simulation. Then the value p_s in each cluster was calculated. The value converges to the random number of the successful data transmitted (X=0, 1, 2,.., N) by parameters N and H in the network. The expected value convergence is given by.

$$E\left[P(X=k)\right] = \frac{1}{L}\sum_{i=1}^{L} X_i \tag{4}$$

where E[P(X=k)] is the expected amount of collected data in each cluster, and L is the number of simulation loops. The estimated mean to be expected for collected data in a network can be realistically predicted by running enough simulations. The Monte Carlo model is computed further in loop simulations for the amount of data to be obtained using N and H parameters in WSNs that are closer to the behaviour of the data transmission within the networks.

The packet size per node (D) in each cluster by H hops equals to (N+1) * D bytes is given by

$$D^h = ((N+1)*D^{h-1})+1 \quad \text{h=1, 2, 3,..,H} \tag{5}$$

Then, the total number of nodes in the network (N_{totol}) is increasing by

$$N_{total} = \sum_{h=0}^{H+1} N^h \tag{6}$$

In this paper, multi-hop network transmission is considered to be a collect-and-forward protocol; thus, the probability of reception rate P (X= k) is statistically independent in each layer. In order to use the packet size to depend on the probability of data collected in each such cluster, nodes have to compute the probability of successful transmission (p_s).

Therefore, the tree structure is created according to the parameters of WSNs, namely N and H. Then hop count = h, p_s in each cluster is calculated recursively from the cluster at hop distance = H, and the loop ends at the sink node.

The algorithm to estimate the collected data of WSNs is calculated by following steps: (2)

1) Initialization for N, H parameters.
2) Loop for L ⩾ 10000
   a) Generate cluster-tree topologies (N,H)

b) Compute probability $p_s(N,D)$ in each cluster in WSN as H is decreasing.

c) Compute probability $p_s \leqslant$ pseudo-random $[0,1] \rightarrow X=0,1$ in each cluster.

d) Compute path, counting the number of 1-valued nodes in the cluster; otherwise, it is equal to 0.

e) Compute cumulative probability of reception rate $P(X=k)$.

This $P(X=k)$] is the amount of data collection that will be used in the cluster that is closer to the sink node. The calculated value converges to the expected value when the number of simulation loops approaches infinity. The diagram of estimating collected data is outlined in Fig. 5.

In addition, to the algorithm to estimate the number of nodes of the data transmission, we calculate the p_s value for different N and D values by forming a tree topology. Each cycle of tree generation starts with N and H, which define the size of the network.

D. Probability propagation

This study analyses the performance limitations of data transmission from each node in the network. Then, we contribute to guidelines for a topology design [23, 25] with the optimal parameters $\{N, H, N_{total}\}$, based on their relationship to the probability p_s. The efficiency of data transfer can be calculated from the probability of success of collect-then-forward data passing to a cluster that is closer to the sink node.

Considering p_s as the probability for a successful collection from a child node, we can derive the probability of successful reception from k identical child nodes using the theory of binomial probability [26] for the data distribution by evaluating the success of data transfer in each H for all paths separately. The definitions of the variables are as follows: the number of independent nodes in each cluster is N+1, and the number of sample space (N(S)) has the sequence of the total probability as $\{X_0, X_1, X_2, X_3, ..., X_N\}$ where the number N(S) of nodes equals N, and k is the number of successful data transfers (k=0, 1, 2, …, N), which means that N-k is the number of failed data transfer in each cluster. In addition, the determination of D and H in each cluster will be evaluated for the worst-case scenario, which equals to k+1.

The probability p_s of data transfer in each cluster can be calculated to wait for data until T_{max} by using Equation (7):

$$P^{[l]}(X=k) = \binom{N}{k} p_s^{k} (1-p_s)^{N-k} \tag{7}$$

where $0 \leq k \leq N$, l is the layer number of a hop, $P^{[l]}(X=k)$ is the probability of success for data transfers for each number of hops. Additionally, we studied the probability distribution that affects the probability p_s of data collection, and we can substitute $p_s(T_{max}, D, N)$ with following the layers of data collection in the network. Thus, the probability as well as the sink node can be determined by the maximum amount of data that can be collected at the sink. The total probability of success equals to

$$p_s^{topology} = \prod_{i=1}^{\ell} \left(p_s \rightarrow p_s' \,|\, p_s'' \rightarrow p_s'' \,|\, p_s''' \rightarrow ..... \rightarrow p_s(sink) \,|\, p_s'^{....'} \right) \tag{8}$$

A method for analysing and classifying the propagation model in multi-hop WSNs with cluster-tree topology, where the relationship between N, D, j and H at T_{max} is assumed to be fixed. We studied the effect of generating the tree by probability of successful collection in which each cluster communicates independently from the others. For example, the application of the probability propagation [13] for successful data transmission into two nodes. The probability of success (X) of each cluster which has the probability distribution equals to N(S), and the factor of probability consists of{{V}, {V,A}, {V,B}, {V,C}}, as expressed in equation (9):

$$p_s = p_s^{V} p_s^{A|V} p_s^{B|V} p_s^{C|V} \tag{9}$$

The expanding of the relationship of the joint probability distribution for {V, A, B, C} was shown in Fig. 6(a) by setting {A,B,C} as X and by letting A equal to 0, B equal to 1, and C equal to 2, as shown in Fig. 6(b).

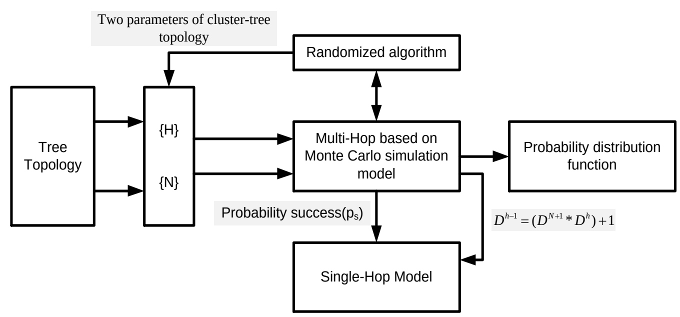

Fig. 5. Block Diagram of the Monte-Carlo Simulation Model.

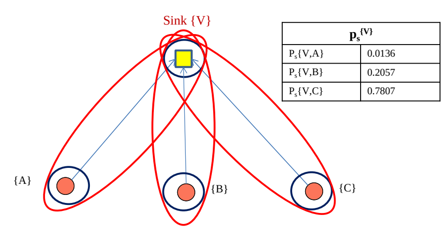

(a) Joint Probability Distribution.

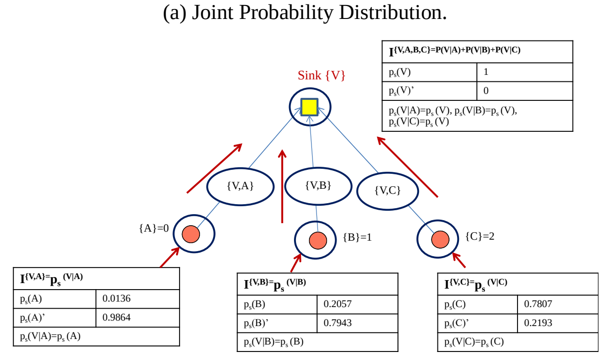

(b) Joint Probability Distribution of ps for 2 Nodes.

Fig. 6. Probability Propagation.

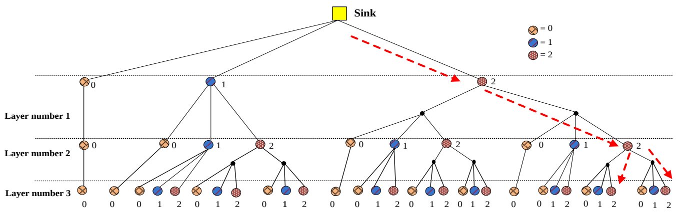

Fig. 7. Probability Propagation for WSNs with N = 2 and H = 3.

Fig. 7 illustrates the backpropagation approach to calculate the probability of successful transmission from m nodes at the sink node. The amount of collected data can be computed by traversing down the tree where each cluster communicates independently from the others. For example, a set of arrows in Fig. 7 shows branches representing the scenario of which all 14 data can be collected in the networks. We can derive the probability of successful collection from m nodes at the sink node using the concept of probability propagation [13].

$$P(X=m)=\prod_{h=H}^{l} P_{h-1}\left(x=k_{h-1} \mid \prod_{l=1}^{k_{h-1}} P_h^{(l)}\left(x=k_h^{(l)}\right)\right) \tag{10}$$

where $0 \le m \le (N_{total}\text{-}1)$. Term $P_h(x=k_h \mid \prod P_h+1(l)(x=k_h+1(l)))$ denotes the probability of successful collection from k_h nodes at hop h considering the probability of successful collection for each cluster at the next hop. Equation (10) leads to an approach for estimating the amount of collected data at hop h by back-propagating P(x=k) from the last hop.

For WSNs with star topology, the packet length D is an independent parameter and may be treated as a fixed value. However, the packet length of a node in WSNs with cluster-tree topology depends on both cluster size (N) and hop distance (h). Due to imperfections in transmission, a function D(N, h) is a random process with its upper bound given by.

$$D(N,h) \le \sum_{p=0}^{H-h+1} N^p \tag{11}$$

To avoid random variables in the model expressed by (7) and (10), local maxima of D(N,h) may be used as an approximation for the computation of p_s at each hop.

V. Numerical Results

For developing a model used to predict the behaviour of the internal data collection, the structure tree is assumed to have a uniform cluster-tree topology, and N and H are set to 2 and 3, respectively. This corresponds to the total number (N_{total}) = 14. The main results are as follows: There are two methods, namely propagation modelling and probabilistic modelling based on the Monte-Carlo simulation, which is used to calculate the probability of successful collection (see Section IV).

E. Analysis of Multi-hop WSNs based on Monte Carlo Simulation

For numerical comparison, we used a model for estimating the probability of collecting a given amount of data from multi-hop WSNs based on Monte Carlo simulation with cluster-tree topology. Based on the analytical model of IEEE 802.15.4 MAC, the probability of successful node transmission p_s is extended to the probabilities of successful collection at the cluster P(X=k) and sink node P(X ⩾ k).

Fig. 8 shows the simulation results, demonstrating the effectiveness of our proposed model for the probability of data collection at the sink node, for N=2 and H=3. The cluster-tree structure has a uniform topology with N = 2 and H = 3, and N_{total}=14.

F. Analysis of Multi-hop WSNs based on Propagation Probability

The probability propagation model has been used to calculate the probability distribution of internal communication in WSNs. We considered a multi-hop WSN with N = 2 and H = 3. We name each node by concatenating the characters ‘A’ and ‘B’ to denote the hop distance from the sink node marked by ‘V’. That is, a cluster “VA” consists of “VAA” and “VAB” nodes. Similarly, the “VAA” node also forms a cluster by collecting data from “VAAA” and “VAAB” nodes. There are eight nodes belonging to four clusters at the last hop (h = 2), namely “VAAA”, “VAAB”, “VABA”, “VABB”, “VBAA”, “VBAB”, “VBBA”, and “VBBB”. For these clusters, the probability of successful collection from k nodes is deterministic and can be calculated from (3) using N = 2 and D = 1. For a cluster with h=1, e.g. “VA”, the probability of successful collection can be approximated conservatively from (4) by using D = 3.

Fig. 9 illustrates the backpropagation approach to calculate the probability of successful collection, if the number of successful transmissions at each cluster is provided. The completed collection in Fig. 10, it shows that the calculation of all nodes of the network can be successfully transferred 14 data sets by considering the reduced hop distance and a growing size of data will be increased according to reduced hop distances located on near the sink node. Also, the probability of successful transmission of a data will be decreased according to a growing size of data by collecting data at the sink node (X= 14), and the probability of successful transmission of a data at 14 (P(X=14) was 0.3600.

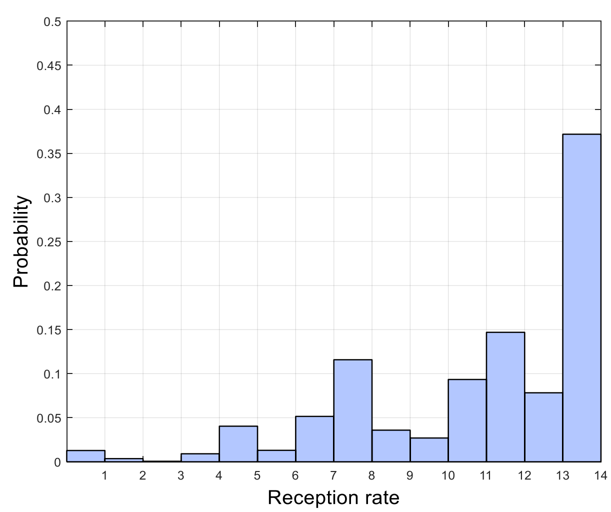

Fig. 8. Histogram of the Reception Rate with N = 2, H = 3.

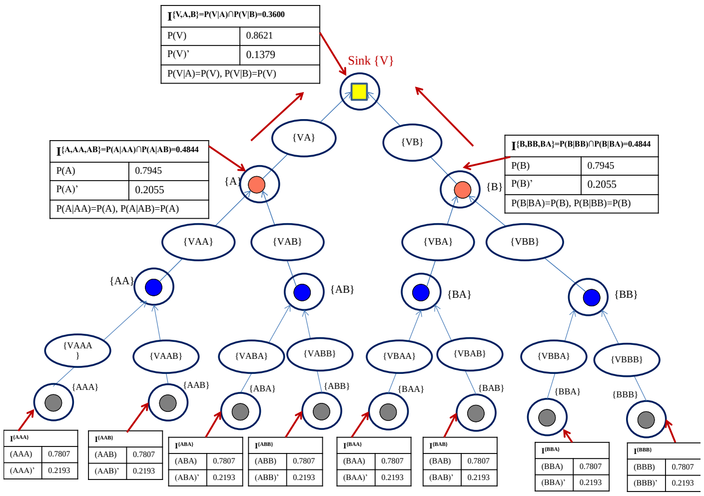

Fig. 9. Probability Propagation for WSNs with N=2, H=3.

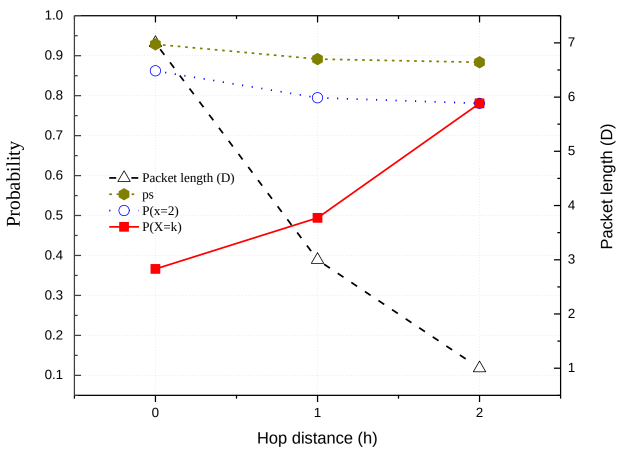

Fig. 10. Probability of Successful Collection with P(X=14).

The calculation of the probability of data collection viewed as an imperfect transmission in WSNs was at X=11of N=14. The consideration of the probability of data collection to gather data of N=2, H=3 can be successfully transmitted in some sink nodes considered as imperfect transmissions in WSNs (X=11) consisting of the probability of propagation of imperfect transmission {7, 4}, {6, 5} , {5, 6} and {4, 7}.

This leads to the current researcher selects this model in order to explain the imperfect transmitting data to sink node. To test the probability propagation in imperfect transmission, the calculation of the probability for data collection was to gather transferring data at X=11 according to the formulation presented m_i=(7,4), (6,5), (5,6) and (4,7) as mentioned term $P(X = 11) = \sum_{m_i} \prod_{h=H}^{l} P_{h-1} \left(X = k_{h-1} \mid \prod_{l=1}^{k_{h-1}} P_{h-1}^{(l)} (X = k_h^l\right)$ as presented in Table 1.

Fig. 11 shows the probability of successful collection, which represents the reception rate, for X = 2, 7, 11, and 14. Both propagation and probabilistic modelling based on the Monte-Carlo simulation results are reported: the P(X=k) value according to (4) and the probabilistic modelling process in Section IV.

TABLE. I. THE CALCULATION OF THE PROBABILITY FOR DATA COLLECTION AT X=11 IN WSNS

Probability of successful collection P(X=11) in WSNs		
Pattern Probability propagation	P(X=k)	$\sum_{m_1}^{m_4} \{P(X=11)\}_{m_i}$
m_1=7,4	0.01418256	0.0722
m_2=6,5	0.0076	
m_3=5,6	0.0076	
m_4=4,7	0.01418256	

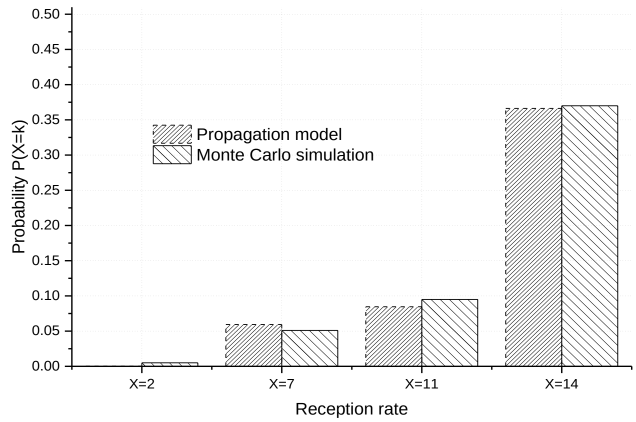

Fig. 11. Comparison of Probability Propagation vs Monte Carlo Simulation with N = 2 and H = 3.

As we can see, the two proposed models provide approximately the same results, and neither presents relevant differences with respect to simulations; therefore, the model is validated. The comparison of results obtained from the propagation and simulation models confirms that the proposed model used for probabilistic analysis of multi-hop WSNs leads to changing the N and H parameters in the topological structure of large-scale WSNs. From the case study of the multi-hop model, we considered the pattern of the probability distribution. The uniform topology structure for perfect transmission of the total packet has H set to 3, T_{max} set to 120, and D set to 1. In addition, we categorized the calculated probabilities of success for a perfect transmission packet (X=14 nodes) into three hops, as presented in Table 2.

G. *Design Topology of Multi-hop WSNs*

The designed multi-hop topology has a uniform cluster-tree topology which is composed of small clusters. All clusters are connected to each other via a collect-and-forward method. From the design of the uniform cluster-tree topology, which the number of nodes was set to 14 nodes, the probability of success was evaluated using the probability propagation. Additionally, the result of perfect transmission of total packet at 14 nodes and imperfect transmission of total packet at 10 nodes, it was found that the p_s was equal to 20.22% and 0.89%, respectively. Furthermore, in Fig. 12, there were other parameters in the network such as N, D, j and H, and all of these parameters contributed to the reliability of data collection and forwarding for the multi-hop WSNs.

TABLE. II. THE PROBABILITY SUCCESS VALUE FOR ATTRIBUTION

Number of received packet (X)	Number of hop: 3		Number of hop: 2		Number of hop: 1		$p_s^{topology}$ (%)
	Parameters /cluster	$p_s^{[3]}$ (%)	Parameters/cluster	$p_s^{[2]}$ (%)	Parameters /cluster	$p_s^{[1]}$ (%)	
X=10 (5-5)	N=2,D=1, X=1	20.57	N=2,D=2, X=2	77.93	N=2,D=5, X=2	82.7	0.89
	N=2,D=1, X=1	20.57	N=2,D=2, X=2	77.93	N=2,D=5, X=2	82.7	
X=10 (5-5)	N=2,D=1, X=0	1.354	N=2,D=3, X=2	79.45	N=2,D=5, X=2	82.68	0.005
	N=2,D=1, X=2	78.07	N=2,D=3, X=2	79.45	N=2,D=5, X=2	82.68	
:	:	:	:	:	:	:	:
X=14	N=2,D=1, X=2	78.07	N=2,D=3, X=2	79.46	N=2,D=7, X=2	86.21	20.22
	N=2,D=1, X=2	78.07	N=2,D=3, X=2	79.46	N=2,D=7, X=2	86.21	

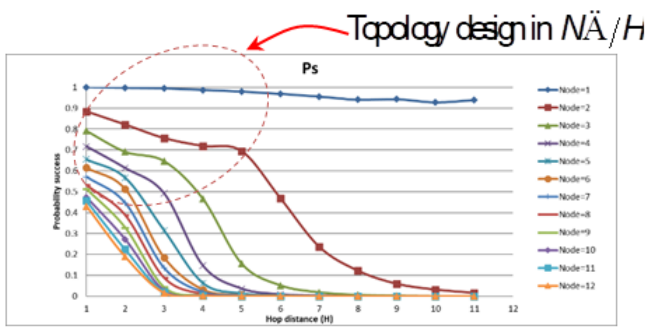

Fig. 12. WSNs Topology for Optimal Data Collection from N and H with P(X=k).

As future work, we plan to design an algorithm for multi-hop WSN by optimising a technique that increases the data reception ratio (PRR) and is suitable for the usage of maximum topology with deep learning approaches.

VI. CONCLUSION

This study presents an analysis model for multi-hop WSNs based on the Monte Carlo simulation model for the probability of data collection in cluster-tree WSNs using the IEEE 802.15.4, MAC protocol with the probability of success in data transmission (p_s) of each node in the cluster by data transmission network expansion with a probability of obtaining data on each cluster P (X = k) and at the sink node P(X $\geqslant$ k), respectively.

The model for multi-hop WSNs with simulation data collection within WSNs for data received at the sink node is applied to calculate the probability of success for a maximum topology of a network model. The objective of this study was to create a model with an explanation of the conditions for collecting/forwarding data over a network with adjustable parameters, N and H, which have an effect on data collection, hop distance, and the number of nodes in each cluster. Results from the analysis of the collected data were applied in a probabilistic analysis of multi-hop WSNs, comparing probability propagation to probabilistic modelling based on Monte-Carlo simulation as an important indicator of WSNs data collection abilities.

REFERENCES

[1] I.F. Akyildiz and M.C. Vuran, Wireless Sensor Networks. Wiley, 2010.

[2] Kiruthika.A 1, Sugandhi.N, “The Efficient Energy Aware Routing and Data Aggregation in Multi-Hop Wireless Sensor Network”, International Journal of Innovative Research in Science, Engineering and Technology, Vol. 4, Issue 1, January 2015.

[3] N. Patwari, J.N. Ash, S. Kyperountas, A.O. Hero, R.L. Moses, and N.S. Correal, “Locating the Nodes: Cooperative Localization in Wireless Sensor Networks” IEEE Signal Processing Magazine, vol. 22, pp. 54 - 69, July 2005.

[4] PRABHA. N and ASHWIN.M, M.E,” Mobile Data Collection in Wireless Sensor Networks Using Bounded Relay Hop”, International Journal of Innovative Research in Science, Engineering and Technology, Volume 3, Special Issue 1, February 2014.

[5] Senthil.T1, Bifrin Samuel.Y, “Energy Efficient MAC Protocol for Wireless Sensor Networks Using Multi hop Optimization”, International Journal of Innovative Research in Science, Engineering and Technology, Volume 3, Special Issue 3, March 2014.

[6] (2006). "IEEE Standard for Information technology--Local and metropolitan area networks-- Specific requirements-- Part 15.4: Wireless Medium Access Control (MAC) and Physical Layer (PHY) Specifications for Low Rate Wireless Personal Area Networks (WPANs)." IEEE Std 802.15.4-2006 (Revision of IEEE Std 802.15.4-2003): 1-320.

[7] E. Callaway, P. Gorday, L. Hester, J.A. Gutierrez, M. Naeve, B. Heile, and V. Bahl, “Home Networking with IEEE 802.15.4: a Developing Standard for Low-rate Wireless Personal Area Networks”, IEEE Communications Magazine, vol. 40, pp. 70-77, August 2002.

[8] Buratti and R. Verdone, “Performance Analysis of IEEE 802.15.4 Non Beacon-Enabled Mode”, IEEE Trans. on Vehicular Technology, vol.58, pp. 3480-3493, September 2009.

[9] P. Di Marco, P. Park, C. Fischione, K. H. Johansson, “Analytical Modeling of Multi-hop IEEE 802.15.4 Networks”, IEEE Transactions on Vehicular Technology, Vol. 61, No. 7, pp. 3191--3208, September 2012.

[10] B. Hull, K. Jamieson and H. Balakrishnan , “Mitigating congestion in wireless sensor networks “,Proceedings of the 2nd international conference on Embedded networked sensor systems, 2004, Baltimore, MD, USA.

[11] Z. Fu "The Impact of Multihop Wireless Channel on TCP Throughput and Loss", IEEE INFOCOM 2003, 2003.

[12] K.Jaksukam and S.Vorapojpisut, “A Study on Data Collection Behaviors for a Class of Multi-Hop Wireless Sensor Networks Based on Probability Model”, International Review on Computers and Software 10(6):635, June 2015.

[13] G. Shafer and P.P. Shenoy, “Probability Propagation”, Annals of Mathematics and Artificial Intelligence, vol. 2, pp. 327-351, 1990.

[14] R. Ricardo, H. G. Xiong, Q. Gao, A. Magallanes and F. Candilio,"Monte Carlo Analysis of nodes deployment for large-scale Wireless Sensor Network using range-free location methods", 2010 IEEE 2nd Symposium on Pages: 484-489, 16-17 Aug. 2010.

[15] Rubinstein RY. Simulation and the Monte Carlo method. John Wiley & Sons,lnc.; 1981.

[16] Fatima Laassiri, Mohamed Moughit and Noureddine Idboufker, "Improvement of the Vertical Handover Decision and Quality of Service in Heterogeneous Wireless Networks using Software Defined Network" International Journal of Advanced Computer Science and Applications (IJACSA), 9(12),2018. http://dx.doi.org/10.14569/IJACSA.2018.091210

[17] F. Chen and Falko Dressler, : A Simulation Model of IEEE 802.15.4 in OMNeT++, in Proceedings of 6. GI/ITG KuVS Fachgespräch Drahtlose Sensornetze, Poster Session, Aachen, Germany, July (2007), pp. 35-38.

[18] O. Gnawali, R. Fonseca, K. Jamieson, D. Moss and P. Levis, Collection tree protocol, Proceedings of the 7th ACM Conference on Embedded Networked Sensor Systems, (2009).

[19] Jurcik, P., A. Koubaa, et al.: A Simulation Model for the IEEE 802.15.4 protocol: Delay/Throughput Evaluation of the GTS Mechanism. Modeling, Analysis, and Simulation of Computer and Telecommunication Systems, MASCOTS (2007).

[20] Nouredine Seddiki and Bassou Abedsalem, "Study of the Performance of Multi-hop Routing Protocols in Wireless Sensor Networks" International Journal of Advanced Computer Science and Applications(ijacsa), 8(2), 2017. http://dx.doi.org/10.14569/IJACSA.2017.080248.

[21] Omar Fouad Mohammed, Burairah Hussin and Abd Samad Hasan Basari, "On the Probability of Detection Ability in Observing Dynamic Environmental Phenomena using Wireless Sensor Networks" International Journal of Advanced Computer Science and Applications (ijacsa), 8(5), 2017.

[22] Hui, J. and H. Aida,: An analytical approach to optimization of throughput for IEEE 802.15.4 slotted CSMA/CA networks., CCNC 2011, (2011).

[23] Buratti, C. and R. Verdone : Tree-based Topology Design for Multi-Sink Wireless Sensor Networks. Personal, Proceedings of the IEEE 18th International Symposium on Personal, Indoor and Mobile Radio Communications, PIMRC 2007, 3-7 September 2007.

[24] Chen, F., N. Wang, et al.: Simulation study of IEEE 802.15.4 LR-WPAN for industrial applications. Wireless Communications and Mobile Computing vol 10(5), (2010),p.609-621.

[25] Martalo, M., C. Buratti, et al. : Optimum Topology in Clustered IEEE 802.15.4 Sensor Networks with Decentralized Detection, Vehicular Technology Conference (VTC Spring), (2011).

[26] Jianguo Ding: Probabilistic Inferences in Bayesian Networks, Bayesian Network. Ahmed Rebai (Ed.), Teck, (2010), p. 39-52.

Cloud- Edge Network Data Processing based on User Requirements using Modify MapReduce Algorithm and Machine Learning Techniques

Methaq Kadhum[1], Saher Manaseer[2], Abdel Latif Abu Dalhoum[3]
King Abdullah II School for Information Technology
The University of Jordan, Amman, Jordan

***Abstract*—Edge computing extends cloud computing to enhancing network performance in terms of latency and network traffic of many applications such as: The Internet of Things (IoT), Cyber-Physical Systems (CPS), Machine to Machine (M2M) technologies, Industrial Internet, and Smart Cities. This extension aims at reducing data communication and transmission through the network. However, data processing is the main challenge facing edge computing. In this paper, we proposed a data processing framework based on both edge computing and cloud computing, that is performed by partitioning (classification and restructuring) of data schema on the edge computing level based on feature selection. These features are detected using MapReduce algorithm and a proposed machine learning subsystem built on user requirements. Our approach mainly relies on the assumption that the data sent by edge devices can be used in two forms, as control data (i.e. real-time analytics) and as knowledge extraction data (i.e. historical analytics).We evaluated the proposed framework based on the amount of transmitted, stored data and data retrieval time, the results show that both the amount of sending data was optimized and data retrieval time was highly decreased. Our evaluation was applied experimentally and theoretically on a hypothetical system in a kidney disease center.**

***Keywords*—Edge computing; cloud computing; data processing; data partitioning; MapReduce; machine learning; feature selection; user requirement**

I. Introduction

Recently many applications seek to improve society by sharing distributed devices and processing their data, such as the Internet of Things (IoT) [1], Cyber-Physical Systems (CPS) [2], Machine to Machine (M2M) technologies [3], Industrial Internet [4], and Smart Cities [5].

However, there are great challenges to efficiently process, store, and manage the data collected by these applications. Since cloud computing (CC) has virtually an unlimited capacity in terms of storage and processing power; hence, cloud computing provides an opportunity to properly approach these tasks by integrating these networks and cloud computing [6].

To cope with these problems, Edge computing architecture has been proposed to support the CC applications and their requirements [7]. Edge computing can be considered as a layer or gateway between the applications' device's layer (edge devices) and the cloud layer (server in the cloud). This layer allows for speedy and direct processing of data produced by edge devices, rather than sending them to the central cloud infrastructure, enabling the CC applications to impose smaller latencies and to alleviate the traffic overhead on the network to the cloud [8]. Moreover, this layer has the power to process data and make intelligent decisions according to the data produced by the edge devices even before the data is processed by the cloud [7]. Consequently, the main functionality of an Edge Computing layer, when integrated with Cloud networks, is improving performance in terms of latency, and network traffic load through processing the data; hence, data processing is the main issue in edge computing [8]. Data processing in the edge layer is a relatively new topic, few studies have focused on this topic, although, there are still many open issues [9]. However, many researchers have addressed the issue of improving network performance in different ways to improve the quality of service and network performance in edge cloud networks [10]. Consequently, we observe that some of these researchers employed edge as a service [11] while others employed it to reduce the overload data with deep learning [12], and others use the edge as a fundamental tool [13]. Du B, et al. (2018) [11] designed Things-edge-cloud computing architecture to enable edge servers to cooperatively work with the cloud and achieve traffic-data as a service. Xu, X. et al. (2017)[14] presented edge Analytics as a service; rule-based analytics model equipped to edge node to prop the management of real-time analytic on edge. Alturki, B et al. (2017) [15] leveraged edge computing to provide low latency and network traffic by using confusion technique to preprocessing data in edge layer and Fu, J. et al, (2018) [13]proposed data processing schemes that combine fog computing and cloud computing to improve the quality of service in terms of latency, security, and flexibility and build object-oriented index to enhance data retrieval.

The main issues in CC that are faced by edge computing are storage, bandwidth, and real-time data analytics; this work presents a new method for improving edge cloud network's performance through data processing in the edge layer before sending it to the cloud. This is performed by processing the data schema on the edge computing level. Basically, the proposed technique of data processing is Data Partitioning, this procedure involves classifying the data and restructuring the data schema based on feature selection techniques. The objective of Data Partitioning is to partition the table into smaller tables in a manner, to allow the queries which access only a fraction of the data to run faster because there are fewer data to scan, as well as to allow knowledge extraction data to be transmitted to the cloud, with low transmission time and low cost of bandwidth, because there are fewer data to load. Without loss of generality, we assume that smaller tablets are more likely to be located as close as possible to the CPU in the memory hierarchy, i.e, in the cache or the main memory.

Feature selection is a data preprocessing strategy based on dimension reduction, it directly selects a subset of relevant features, by removing irrelevant, redundant and noisy features from data; hence, preventing sending unnecessary data to the cloud to reduce the utilization of resources in the cloud (i.e. storage, bandwidth) as well as providing lower latency with data retrieval by only choosing relevant features [16], Feature selection techniques reduce storage and computational costs while avoiding significant loss of information [17]. Feature selection algorithms can be divided into wrapper, filter, and embedded methods. [18]. Wrapper Methods generate models with subsets of features and gauge their model performances. In this work, we presented a solution based on the forward search wrapper method.

In our proposed, features are detected using a modify MapReduce algorithm (M-MapReduce) and proposed a novel machine learning subsystem that are applied on user requirements (also called functional specifications in software engineering) [19]. These requirements reflect expectations for a new or modified product, requirements should be quantifiable, relevant and detailed.

The importance of this work is reflected from the main contribution of this paper, which is to develop a data processing framework based on both edge computing and cloud computing, by integrating the functions of data preprocessing that involves classifying, restructuring, storage, and retrieval. Therefore, this work focuses on the structure of the stored data as well as the transmitted data.

The infrastructure of the proposed framework consists of five main components as shown in Fig. 1: cloud-computing layer, edge computing layer, edge device layer, cloud computing queries, and edge device queries.

- Edge device collects data and then sends the data to the edge layer. In this work we assume that the data sent by edge devices can be used in both control data (i.e. real-time analytics) as well as knowledge extraction data (i.e. historical analytics). Control data is the streaming data that is processed in real time or time-limited data, on those data parts, real-time decisions are made e.g. monitoring, detecting fraud. While, Knowledge Extraction Data is the data stored for mining purposes and analyzing for support decision e.g. run reports, queries, and inferences from historical data [13].

- Edge layer where data is partitioned into control data (time-limited data) and knowledge extraction data; control data are extracted and processed in this layer. On the other hand, knowledge extraction data is uploaded to the cloud server layer. Thus edge layer is assumed to be stronger in both power and computing capability for model construction as well as the preprocessing and real-time analytics of the raw data sent by the edge device.

- Cloud computing layer for the data mining purpose and machine learning.

- Edge device queries are the search process in the device layer that is responsible for real-time decision making, constitute the queries in this layer (i.e. user requirements in devices layer such as control data). These queries are sent to a feature selection algorithm based on machine learning concepts, in order to extract key features that will assist in defining the real-time data.

- Cloud computing queries are the queries in the cloud layer that are executed for the mining process to extract knowledge from the data in the cloud layer (e.g. user requirements, data warehouse and data cube) that serves in other applications such as decision support systems. Moreover, these queries are also sent to the machine learning features extraction tool, in order to update feature extraction rules in order to accurately select features data to be sent to the cloud.

The proposed method in this paper fundamentally relies on the following assumptions:

First, the way we access data can help to restructure the data in a way that improves its locality characteristics such that the transaction time is reduced. In this work, we take note of the fact that data which exhibits good locality structure can be accessed in a much better way than data with the poor locality. By locality, we refer to a particular access pattern that can improve the efficiency of local memory (main memory or cache) in any system [20].

Second, the space-time product of a task or a set of tasks is inversely proportional to the throughput of the system [21].

Consequently, the main issues in the process of designing our framework are the detecting of accurate features for partitioning (classification and restructuring) the data without losing information, and implementing an efficient restructuring data algorithm. To illustrate our approach, we apply it on an imaginary system in a kidney disease center. We assumed that the edge cloud system is deployed in a chronic kidney disease center to monitor the patient's status and we use data from the UCI repository for chronic kidney disease (CKD) [22].

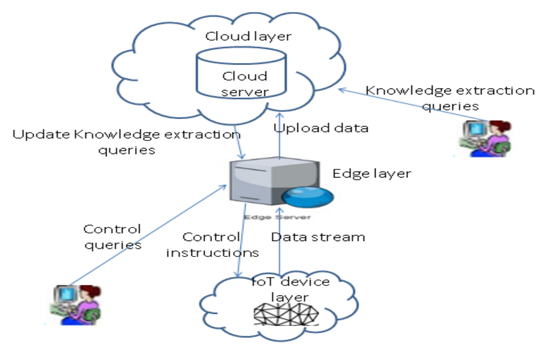

Fig. 1. The System of Preprocessing Data Classification, Restructuring, Storage and Retrieval.

The paper is organized as follows: Section 2 summarizes the edge computing, Section 3 presents the related work followed by a description of the proposed framework architecture in Section 4. Section 5 lists the details of the experiment environment and discusses the obtained results. Finally, Section 6 concludes the paper.

II. Edge Computing

With virtually unlimited computing power and storage resources, clouds are conceived to be the perfect platform for large-scale data analytics, while storage efficiencies also provide easy management of different applications. However, with cloud-based applications, most data must be sent to the data centers in the Cloud [23]. During the expansion of these applications, the volume of data increases and a large amount of data from these applications (e.g., IoT devices) are moved to the Cloud causing network bottlenecks due to bandwidth constraints. As time-sensitive and location-aware applications are developed (e.g., patient monitoring, real-time applications, transportation systems), the remote cloud will fail to fulfill the low-latency requirements of these applications; the round trip delay is too great [24].

Edge computing (e.g., Cloudlet, Mobile Edge Computing, and fog computing)[25][26] is proposed to overcome the problems faced by cloud-based applications [27] by offloading computing tasks to the edge of the cloud network. Using installed computing resources and intelligence at the network edge layer, a prompt response can be delivered to applications and the transmission of redundant data to remote clouds is avoided [28]. One more feature of edge computing is its distributed mode and support for device mobility inside heterogeneous network [29].

The Edge computing layer lies between cloud and end edge network devices; however, there is no commonly agreed-upon framework to capture the functionality of this computing paradigm. Recently, IBM and some researchers have proposed a three-layer paradigm as the high-level architectures, this is illustrated in Fig. 2 [30] [31].

Edge computing [32] is introduced for extending the Cloud Computing paradigm to the edge of the network to support many of cloud application (IoT, M2M, and CPS). Many characteristics have been found in edge computing, including low-latency, location awareness, mobility, and wide-spread geographical distribution, etc. These features make Edge computing suitable for different cloud applications.

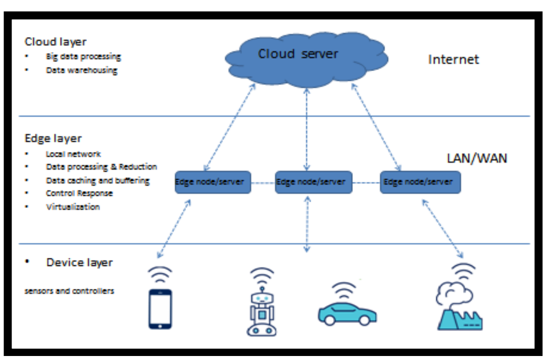

Fig. 2. An Example of an Edge Computing Architecture.

III. Related Work

Recently, many applications developed are internet-enabled such as surveillance, virtual reality, and real-time systems (e.g. monitoring)requiring fast processing and quick response time [33][34] . The core service and processing of these applications are performed on cloud servers; cloud computing provides an opportunity to these applications via an unlimited capacity in terms of storage and processing [6]. These applications produce a significant amount of data. This creates a number of challenges, such as high communication latency, and network traffic overhead, which is raised by transmitting all data to the cloud for processing and analysis. To overcome these challenges edge computing has been [35][36][37] proposed to extend the cloud computing paradigm to the edge of the network, consequently, the data processing is the main challenge posed by integrating cloud computing with edge computing, it demands researchers to discuss and develop high-performance data processing architectures.

Many researchers provide a hybrid approach between edge computing and cloud computing such as, Du B, et al. (2018)[38] designed Things-edge-cloud computing architecture to enable edge servers to cooperatively work with the cloud and achieve traffic-data as a service. Xu, X. et al. (2017) [14]presented edge Analytics as a service; rule-based analytics model equipped to edge node to prop the management of real-time analytic on edge. Alturki, B et al. (2017)[15] leveraged edge computing to provide low latency and network traffic by using confusion technique to preprocessing data in edge layer and (Fu, J. et al, 2018) [13] proposed data processing schemes which combine the fog computing and cloud computing to improve the quality of service in terms of latency, security, and flexibility and build object-oriented index to enhance data retrieval. They also discuss the impact of distributed services between Fog and cloud Architecture for IoT; four types of architectures have been evaluated with three types of datasets. This evaluation displays the importance of distributed services between fog nodes and cloud computing. In Bittencourt, L. et al, (2018) [39] they discussed the integration of IoT-Fog-Cloud system and provided a review for different aspects such a system are organized managed, and how applications can benefit from it.

Others researchers presented the functionality that edge computing should provide it. Consequently, In (Ai Y et al, 2018) [40], the authors comprehensively present a tutorial on three typical edge computing technologies, namely Mobile Edge Computing, Cloudlets, and Fog computing. In particular, the standardization efforts, principles, architectures, and applications of these three technologies are summarized and compared. From the viewpoint of radio access network, the differences between mobile edge computing and the fog computing are highlighted, and the characteristics of the fog computing-based radio access network are discussed. Finally, open issues and future research directions are identified as well.

Machine learning has an essential role in edge computing thus, Yuuichi Teranishi et al (2017)[41] propose a novel dynamic data flow platform for Internet of Things (IoT) applications in edge computing environments. To avoid the overloads on network and computational resources that are caused by IoT applications, the proposed platform replicates processes and changes the structure of the data flow dynamically on the distributed computational resources located at network edges and data centers. M. Mahdavinejad et al. (2018) [42] assesses the various machine learning methods that deal with the challenges presented by IoT data by considering smart cities as the main use case. The key contribution of this study is the presentation of the taxonomy of machine learning framework explaining how different techniques are applied to data in order to extract higher level information. The potential and challenges of machine learning for IoT data analytics are also addressed. Sneha Sureddy et al. (2018) [43] present a proposal of Flexible Edge Computing (FEC) architecture as a flexible system to perform edge computing using deep learning in IoT. Combination of these two models that are deep learning and flexible edge computing significantly improve the performance of the system and optimize the task assignment between edge layer and cloud layer.

IV. Data Partitioning Framework

The main functionality of an Edge Computing layer, when integrated with Cloud network, is to improve performance in terms of latency, and network traffic load through processing data. Hence, data processing is the main issue in edge computing in cloud computing real-time application networks such as IoT, CPS, and M2M [44].

In an attempt to overcome the data processing issue, we construct data processing framework over the Edge-cloud network by integrating the function of data partitioning, restructuring, storing and retrieving, to enhance the performance of Edge-cloud network in terms of lower latency level and network traffic. The architecture of the proposed framework consists of three main layers as presented in the flowchart shown in Fig. 3, These layers are edge device layer, edge computing layer, cloud layer.

- Edge device layer: in this layer, several devices are connected and employed for different purposes and these devices are responsible for the aggregation and integration of the data in order to be delivered to the edge node via wireless or wired communication by using a suitable routing algorithm. We also propose that the data sent by edge devices can be used in both control data (i.e. real-time analytics) as well as knowledge extraction data (i.e. historical analytics).

- Edge computing layer: is a communication layer between cloud and end device levels, it is connected to the cloud server through the Internet. This layer receives raw data from the edge device and inputs this data into a uniform preprocessing procedure that issues both cleaning and integration of data. This preprocessed data would form a schema i.e. is stored in a database that facilities data access and search. After that, this schema is partitioned (classified and restructured) based on the features that are selected from user requirements to permit fast access and search on the database as well as to reduce the amount of data transmitted to cloud computing and for saving the bandwidth resources and storage in the cloud layer.

- Cloud layer is employed to perform several processes, such as:

a) Store the transformed data in the cloud data center.

b) Mining tools execute the search operations on data to extract knowledge and new patterns. Data analytic tool are used on historical data for support decision.

c) Analytic tools execute the search operations on data to support decisions.

d) In the training phase, the training classifier and feature selection algorithm are executed at the cloud layer.

e) Queries are updated and added to the queries accumulator accordingly.

f) Control attributes are imposed on the network to provide higher quality of results.

In the following we describe the design issues and constraints on the implementation of the framework and present the data workflow also the network throughput calculation.

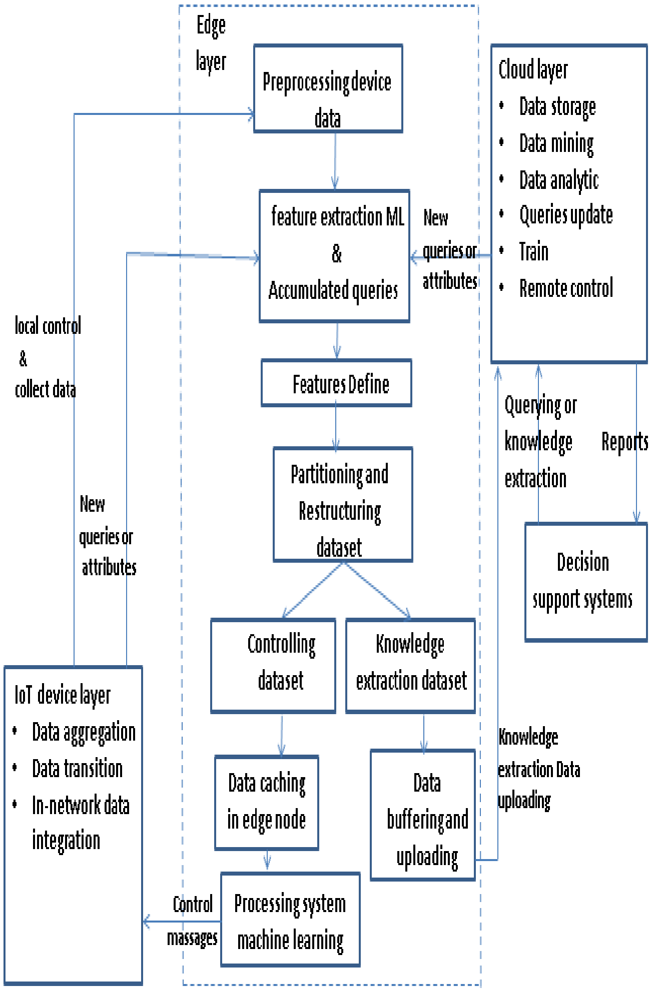

Fig. 3. The Proposed Framework Architecture.

A. Design Issues

Before implementing our framework, there are three important design issues that should be addressed, the requirements analysis to selected features, data classification as control data and knowledge extraction, and the extraction of the subset of features to restructure data schema. These issues are discussed for our proposed framework as follows:

1) Requirements analysis: the requirements analysis issue, as mentioned above, features are selected from user requirements, these requirements can be obtained from a given stream of queries generated over a time period for existing systems or from queries generated by network requirements for a new system. It is the responsibility of the system analysts to extract and detect the features and relationships among them for many large problems.

It is important to mention that user requirements can be past referenced behavior for existing systems; the past referenced behavior is obtained from a given stream of queries generated over a time period. While the requirement for building a new system, are obtained from the users' requirements and network analysis, thus a large sequence of queries can be generated by these requirements, which represents the system referencing behavior.

However, when the requirements queries' size grows too big, the process of analyzing the requirements queries for detecting the features and their frequency is excessively prohibitive. Hence, MapReduce [45] technique was used to overcome this issue.

a) Modify MapReduce algorithm: The traditional MapReduce a programming model [46] was inspired from the Functional Programming model introduced by Google, which uses the Divide and Conquer technique to process large amounts of data. It works in three functions [47]: the map function, the Shuffle Function and the reduce function. The Mapper stage splits the queries into features by whitespaces, and the output of the Mapper is the pair of features with their frequencies known as (key, value) pair, where key is the feature and value is a count of features. Then, in the intermediate phase, Shuffle sorts the (key, value) pair according to the key and sends it to the Reducer. Pairs that have the same key go to the same Reducer.

The Reducer stage collects all (key, value) pairs with the same key and sums the values for each key.

In this paper, we modify the MapReduce algorithm to support our work to find features from user requirements by resetting all values for each key to one as shown in algorithm 1, we reset list (count) number for each feature (attribute) to one, to avoid the duplication of features in one query. The output of this stage is a list that combines the feature Ai with its total frequency where i is the location of the attribute.

2) Data classification: The second issue is the classification of accumulated data into control data and knowledge extraction data based on feature extraction from user requirements. Thus, we used extreme learning classifier with feature selection to classify our data.

Algorithm 1: M-MapReduce algorithm.

1.***map***(file, queries) {

for each features in queries. *Split*(){

output (word, 1);

}

}

2. ***Reduce*** (word, list (count)) {

Reset all # in list (count) to 1

Output (word, sum (count));

}

3) Features subset extraction: The third issue is extracting the subset of features that have an inherent locality structure, in other words, grouping the features that form temporal locality in the same subset. The features that are requested in the same query, construct temporal locality. The locality structure is discussed in detail in the next subsection. In this dissertation, we proposed using the k-mean algorithm [48][49][50] which is modified according to our approach, combined with the features selection Wrapper methods which is performed in a new way to cope with our approach as shown in Fig. 4 [51] [52]. This combination provides a machine learning subset system that is used to find a subset of features.

a) Machine Learning Subset System: In this dissertation a machine learning subset system was used in establishing a subset of features; it groups features into subsets according to their frequency.

The traditional k-means algorithm consists of two stages. The first stage adjusts k based on the number of groups [49][50]. The second stage detects initial centroid randomly from the dataset for each group. In this dissertation, we used k-means with modifying its stages (M_k-means), where the initial centroid is determined based on a features frequency (i.e., taking the higher and lower frequency) and the number of groups K determines based on used a wrapper feature selection method. However, we illustrated the steps of this system as follows:

The M K-means algorithm as shown in Algorithm 2 in uses iterative refinement to produce a final result. The algorithm inputs are the number of groups K and the data set. The data set is a collection of features (data attributes) and frequency for each feature. The algorithm starts with two groups; the first group takes the high value of a feature frequency as a centroid while the second group takes the lower value of a feature frequency as a centroid. The initial value of group centroid(fai) was defined to avoid the oscillation with iterative refinement to produce a final result.

Modify k-mean algorithm: The K means algorithm is used to establish a subset of features, it groups features into subsets according to their frequency [49][50]. Traditional K means algorithm consists of two stages. The first stage adjusts k based on the number of groups. The second stage detects initial centroid randomly from the dataset for each group. In this paper, we used k-means with modifying the second stage (M_k-means), where the initial centroid is determined based on feature's frequency (i.e. taking the higher and lower frequency) as shown in algorithm 2.

Algorithm 3.2: M_ K-means Algorithm

Input:

F = {f1a1, fa2,......,fnai} // fai is a feature frequency ,i is a feature # and n is the number of feature.

k // Number of desired subset

Output:

A set of k subset.

Steps:

Phase 1: Determine the initial centroids of the subset (group) by taking high and low frequency (fnai).

Phase 2: Calculate new mean for each cluster;

Until convergence criteria is met.

The algorithm iterates between three steps and iterates among these steps until a stopping criterion is met. These steps illustrated in detail as follows:

Data Assignment Step 1

In this step, each data point is assigned to its nearest centroid, based on its frequency fi. More formally, if ci is the centroid in cluster C, then each data point x is assigned to a cluster based on the following:

$$dif\ (fi, ci) \quad (1)$$

Where $dif\ (\cdot)$ is the difference between the feature's frequency and cluster's centroid. Let the number of features assignments for each ith cluster centroid is S_i.

Centroids Update Step 2:

In this step, the centroids are recomputed. This is done by taking the mean of all frequency of features to that centroid's cluster.

$$Ci = \frac{1}{|si|} \sum_{fi \in si} fi \quad (2)$$

Choosing K Step 3:

In the previous two steps, the clusters and data set labels were found for a particular pre-chosen k. In this step, we discuss how wrapper feature selection is used in a new method to choose the number of clusters K.

Some of the techniques that are commonly used to find k are: cross-validation, information criteria, the information-theoretic jump method, the silhouette method, and the G-means algorithm. In this dissertation we proposed a new method of wrapper feature selection to find the value of k.

The wrapper is a feature selection method, that evaluates feature subsets by the quality of the performance on a modeling algorithm, which is taken as a black box evaluation [51] [52]. In our approach, the wrapper will evaluate subsets based on the performance of executing queries on the new tables that are built on the feature subset.

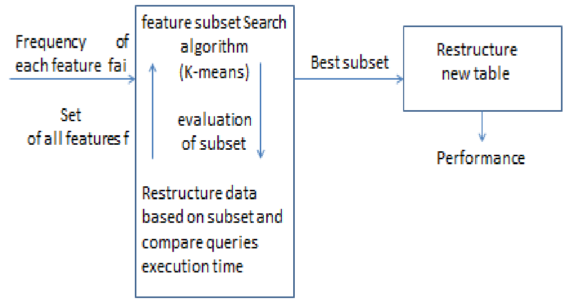

Fig. 4. Our Approach Wrapper Feature Selection.

The evaluation is repeated for each subset and the subset generation is dependent on the k-means algorithm as shown in Fig. 4.

B. Data Scheme Partitioning Workflow

The Preprocessing data scheme was partitioned by some processes as shown in the flowchart in Fig. 3 which is assigned by a dotted line. These processes and their design issues can be described in the following two parts. First, requirement analysis (feature selection) and Second, partitioning data schema.

1) Requirement analysis (feature selection): This part is responsible for detecting the locality structure of control data and knowledge extraction data; it relies heavily on user requirements or query stream analysis.

The objective of this part is to group attributes, which are likely to be referenced together , in a partition or table. The more frequently the attributes are referenced together, the more likely for them to belong to one locality structure. for example, in a monitaring system in a factory, the monitoring devices share the same identifier, also in medical systems the diseases may be chronic or not chronic.

Query stream analysis is used to find the frequency of a given query execution and the frequency of attributes requested within the same query. Furthermore, query analysis is used to detect the adjacency of attributes, where adjacency is defined as the attributes referenced within the same query. Attribute Ai is said to be adjacent to Aj: AJ (Ai,Aj) if Ai and Aj are requested within the same query Q_k. By default, adjacent attributes form a temporal locality, since they are referenced within the same query and their access to the data storage falls within the same time period. Note that adjacent attributes Ai and Aj may or may not be stored within the same virtual page or in close space proximity.

For example, assume that query Qk is used to select attribute Ai and attribute Aj from table T1. Thus, the attributes Ai and Aj are adjacent within the query Q. Ai and Aj certainly form a temporal locality, in the sense that both are referenced within the same period. The system will access both A_i and A_j and return their values as requested. However, A_i and A_j may be very well located in different memory regions, or more precisely could be located in two different pages in the virtual space. If Q_k is referenced n times, then it is only reasonable to have A_i and A_j stored in close proximity, e.g., in the same page or the same page block, such that when the page or page block is transferred from virtual storage to main memory or cache, then the requested items A_i and A_j will have been located in main memory already.

For illustration purposes, assume that the data table has 10^9 which is ≈ (2^{30}) records, and attributes A_i and A_j are both of type real with 8 bytes each. This means that each column representing attributes A_i and A_j is 2^{33} bytes. Assume further that a page size (using virtual memory paging representation), is 1024 Kbytes (2^{20} bytes). Thus the number of pages representing each attribute is given by $2^{33}/2^{20} = 2^{13}$ pages (≈ 8 GBytes). If attributes A_i and A_j are requested as adjacent attributes frequently, i.e., they appear in the same query or in different queries N times, where N is relatively large, then it is worthwhile to convert the temporal locality of A_i and A_j to spatial locality, in the sense that A_i and A_j should be adjacent in space allocation scheme. Fig. 5 shows a temporal and spatial locality example.

Consequently, data are restructured based on adjacency of attributes where the unrelated attributes are removed. Furthermore, these steps' outline is illustrated in Algorithm 3.

Moreover, the attributes that have the highest frequency value (Ati) will be collected in the same new table.

2) Partitioning data scheme: This part is responsible for partitioning the dataset based on features that are selected in the previous part. Partitioning aims to classify the data in order to remove unrelated data to reduce the size of data. As well as grouping a set of attributes in a subset, where the subset will be used to create a new table of data with the attributes given in the subset. In essence, the process of partitioning leads to the auto reconstructing of the original schema, which was originally used to represent the data. This part includes the following steps.

a) Classifying the data as controlling data and knowledge extraction data using feature selection in part 1. Machine learning classification algorithm (classifier) with feature selection is used to classify the data instance, this classifier learning in the cloud layer is based on features that were selected from user requirements. Then it is used to classify data in the edge layer.

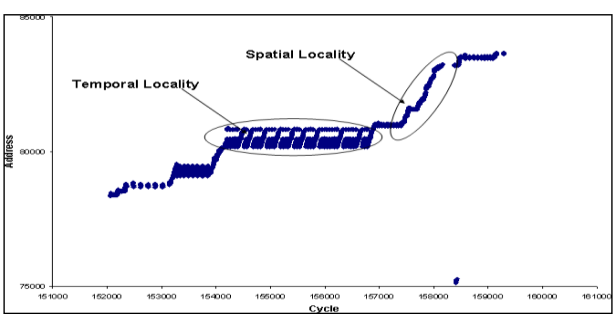

Fig. 5. Temporal and Spatial Locality Example.

ALGORITHM 3: GENERATE ATTRIBUTE ADJACENCY

1. Generate and collect a set of queries {Q1}{q1}&{q2}. // Requirements analysis (Requirements engineering).
2. Analyze queries and extract the following parameters:
   a. For each query (q), find the frequency of its execution f(q).
   b. Build adjacency matrix for all attributes contained within the set of queries {Q}.
      i. Two attributes Ai and Aj are said to be adjacent if both attributes are referenced within the same query.
      ii. The number of attributes Ai that is shared between the query Qi and Qi, is given by the similarity S (q).
      iii. The number of appearance Ai within different queries is given by fai.
      iv. The total frequency of an attribute Ati = fqi * fai
3. Build adjacency list for features selected from q1 contained within the set of queries {Q1}.
4. Build adjacency list for features select from q2 contained within the set of queries {Q2}.

b) For the control data, create a new table for each subset in the set Si, these new tables are stored in the edge layer for real-time analysis. For this step, we develop algorithm 3.

c) Creating a new table for the knowledge extraction data is suitable for the data mining technique using feature selection from q2 and uploading to the cloud layer for storing and analysis.

These steps are performed on our framework by applying algorithms 4.

C. Network Throughput

Without loss of generality and accuracy, we will ignore the complexity of algorithms 3.3 and 3.4, since they will be performed one time whenever the structuring of the DB schema is required. Henceforth, we are not concerned with the complexity of the algorithms; rather our concern is with the complexity of the data access time as well as data transmission time before and after partitioning.

Algorithm 4 Partitioning Data Schema

1) Create list A of attribute Ai and frequency n (Ai ,n).
2) Sort Ai in list A according to largest frequencyn.
3) Using the wrapper feature selection method with the execution time of query as an evaluation strategy.
   a) Running k-means algorithm to Grouping attribute in a subset Si = {s1, s2…sn}.
   b) Evaluate Si using the evaluation function
   c) While (stopping function not met)
   d) Fined new Si
   e) Evaluate function
   f) End while
   g) Output: the best Si
4) If Have new query go to step 1
5) Terminate Algorithm.

Assume that the DB tables are stored in a column wise schema, where the data belonging to one attribute are stored sequentially. Then to retrieve one record in a table, it is required to scan all attributes in the record. Given that the number of attributes in a table is N; this leads us to consider the space occupied by the table as a major cost of the system. When multiplied by the overall time required executing a query, or the time required transmitting this table the complexity naturally lends itself to the space time product as the main tuning parameter.

It has been shown that the space-time product of a task or a set of tasks is inversely proportional to the throughput of the system (Denning & Buzen, 1978). In other words, if we want to maximize the throughput (X), which is defined as the number of tasks performed within a time period(T), then we have to minimize the space-time cost (Y), i.e., the total space (S) consumed by the tasks within the same time period (T). This implies the following relationship.

$$X \approx 1/Y, \text{ where } Y = S*T \quad (3)$$

1) Data retrieval complexity: In term of data access time and reduce latency, for a given query (Q_i), the space consumed during the query execution equals the space of the tables referenced by Q_i. For example, assume that Q_i has the following structure:

$Q_i \rightarrow (\{A_i\})$ from Tables $\{T_k\}$

Where a set of attributes A_i , i =1, .. n are referenced in tables T_k, k = 1, … m

The space occupied by Q_i is thus given by Equation 2

$$S(Q_i) = \Sigma S(T_k) \text{ , } k = 1,\dots m \quad (4)$$

And the time required to execute the queries is given by:

$$T = t*An \quad (5)$$

Where A_n is the number of attributes referenced in Q_i and t is the time required to process each attribute.

Thus the space time cost of a query Q_i is given by:

$$Y = T_i*S \quad (6)$$

If the frequency of Q_i is f then the total space time cost for Q_i is given by:

$$Y = f* T_i*Si \quad (7)$$

2) Data transmission complexity: While, in term of data transmission time, for transmitted a table Tk, the transmission time is related to the space of the table. For example assume that the table T has Ai attributes where Ai , i =1, n are referenced in tables and Rj records, j= 1…..m

The space occupied by T is given by equation 6

$$S(T)= \Sigma \text{ Rj Ai} \quad (8)$$

And time required to transmit the table Tk is Tt

$$Tt= t* An \quad (9)$$

where A_n is the number of attributes referenced in Tk and t is the time required to transmit each attribute.

Thus, the space time cost of a table Tk is given by:

$$Y = T_t*S(T) \quad (10)$$

The objective of the proposed method is to maximize the throughput of the system by minimizing the space-time product for the data access (i.e., reduce latency), and data transmission (i.e., saving bandwidth). Therefore, the throughput is increased with decreasing space (S).

V. Analysis and Results

To verify the performance of the proposed framework of data partitioning, we assumed there is an edge cloud network deployed in a chronic kidney disease center to monitor the patient's status. We experimented our proposed framework on this network and compared it to the same network, without our framework. We compared between these networks in term of data transmission amount, storage space and queries execution time (data retrieval efficiency). The proposed framework is experimented with different queries and different sizes of data. The utilized dataset, experiment environment, queries generation, and the results with their discussion are given as follows.

This verification takes on two aspects:

- Experimental Verification which begins by defining the experiment processes, dataset used, environment, and query generation, followed by a discussion of the results in Section A.
- Theoretical Verification which covers the theoretical verification for the proposed framework on this network and is discussed in Section B.

A. Experimental Verification

This section describes, in detail, the experiment performed to verify our framework.

1) Processes

a) Requirements analysis with M-MapReduce.

b) Data classification using ELM classifier.

c) Data restructuring using our subsystem machine learning.

d) Generation of queries executed against the new data schema.

2) Dataset: In this research, we use data from the UCI repository. The data collected from the Apollo Hospital, India by b. Jerlin Rubini. The number of instances in the dataset are 400 instances with 25 attributes (including attribute classes), where 250 instances include those who have chronic kidney disease (ckd) and the remaining 150 who did not have chronic kidney disease (notckd) as in Table I.

3) Environment: In this experiment, our edge server consisted of a laptop computer with a 2.6 GHz Intel Core processor, Window 7 operating system and 4 GB of RAM. As discussed previously, the edge server handles running the network and analyses the pre-processed data. Our cloud server was a desktop computer with a 3.6 GHz Intel Core processor, Windows 7 operating system and 8 GB of RAM.

The edge server connects to the cloud server through the Internet and pre-processes the raw data. We used MATLAB® R2018b extreme learning machine (ELM) libraries for the classification methods and a k-means function for the clustering method.

The MapReduce algorithm is used to identify suitable features. We first taught the classifier in the cloud server, and then applied steps one and two in the previous section on our data to define the features that are used in restructuring the data. We also created the database structures necessary for the new tables that are created.

4) Edge layer query generation and cloud layer feature selection: Based on the users' requirements, we generated random queries to apply our approach. Specifically, from the users' requirements in the edge layer, 120 queries are generated randomly. In Table II, the 10 edge layer generation queries that had the highest frequency are listed. From the expert and user requirements in the cloud layer, we can extract and select relevant feature subsets. These subsets, shown in Table III, are used to restructure the data passed to the cloud layer.

Based on the requirements noted above, as well as from network requirements, we selected the features that classified the data into two groups: CKD, and not CKD. The ELM, using a wrapper method for feature selection, was used to classify this data [53][54].

We applied Algorithm 3 on the generated queries, to select the features to use in restructuring the data. Table IV (an adjacency matrix for all the attributes within the set of queries and a list for each attribute with its frequency), Table V and Table VI illustrate the features for the controlling data and knowledge extraction data, respectively. After the feature selection, we performed the following two steps.

TABLE. I. ATTRIBUTES OF CKD DATASET

No.	Code	Parameter	Value
1	Age	Age	In the year
2	Blood pressure	Blood pressure	In mm/Hg
3	Specific gravity	Specific gravity	(1.005,1.010,1.015,1.020,1.025)
4	Albumin	Albumin	(0,1,2,3,4,5)
5	Sugar	Sugar	(0,1,2,3,4,5)
6	Red blood cells	Red blood cells	Normal / Abnormal
7	Pus cell	Pus cell	Normal / Abnormal
8	Pus cell clumps	Pus cell clumps	Present / NotPresent
9	ba	Bacteria	Present / NotPresent
10	bgr	Blood glucose random	In mgs/dl
11	bu	Blood urea	In mgs/dl
12	sc	Serum creatinine	In mgs/dl
13	sod	Sodium	In mEq/L
14	pot	Potassium	In mE1/L
15	hemo	Hemoglobin	In gms
16	pcv	Packed cell volume	In %
17	wc	White blood cell count	In cells/cumm
18	rc	Red blood cell count	In millions/cmm
19	htn	Hypertension	Yes / No
20	dm	Diabetes mellitus	Yes / No
21	cad	Coronary artery disease	Yes / No
22	appet	Appetite	Good / Poor
23	pe	Pedal edema	Yes / No
24	ane	Anemia	Yes / No
25	Class	Class	Ckd, notckd

TABLE. II. EDGE LAYER GENERATION QUERIES

Q1→ bp, sg, bu, sod, pot, hemo, ckd	Q7→ bp, bu, sod, hemo, ckd
Q2→ bp, sg, bu, sc, sod, hemo, ckd	Q8→ bp, sg, pot, hemo, ckd
Q3→ bp, sg, bu, sc, sod, ckd	Q9→ bp, sg, bu, sc, pot, ckd
Q4→ bp, sg, bu, sod, hemo, ckd	Q10→ sg, bu,sod
Q5→ bp, bu, sc, sod, pot, hemo, ckd	Q11→ pb, sg, bu, sc, sod, pot, hemo, ckd
Q6→ bp, sc, sod, pot, ckd	----

TABLE. III. CLOUD LAYER GENERATION QUERIES

Q1→Hypertension, CKD
Q2→Diabetes mellitus, Hypertension, CKD
Q3→Diabetes mellitus, CKD

TABLE. IV. FEATURES OF CONTROLLING DATA (ADJACENCY MATRIX)

Attr / Q	Age	Bp	sg	al	su	rbc	Pc	pcc	ba	bgr	Bu	sc	sod	pot	Hemo	pcv	Wc	Rc	htn	Dm	cad	appet	pe	ane	Fq
Q1	0	1	1	0	0	0	0	0	0	0	1	0	1	1	1	0	0	0	0	0	0	0	0	0	4
Q2	0	1	1	0	0	0	0	0	0	0	1	1	1	0	1	0	0	0	0	0	0	0	0	0	4
Q3	0	1	1	0	0	0	0	0	0	0	1	1	1	0	0	0	0	0	0	0	0	0	0	0	3
Q4	0	1	1	0	0	0	0	0	0	0	1	0	1	0	1	0	0	0	0	0	0	0	0	0	4
Q5	0	1	0	0	0	0	0	0	0	0	1	1	1	1	1	0	0	0	0	0	0	0	0	0	3
Q6	0	1	0	0	0	0	0	0	0	0	0	1	1	1	0	0	0	0	0	0	0	0	0	0	3
Q7	0	1	0	0	0	0	0	0	0	0	1	0	1	0	1	0	0	0	0	0	0	0	0	0	4
Q8	0	1	1	0	0	0	0	0	0	0	0	0	0	1	1	0	0	0	0	0	0	0	0	0	3
Q9	0	1	1	0	0	0	0	0	0	0	1	1	0	1	0	0	0	0	0	0	0	0	0	0	4
Q10	0	0	1	0	0	0	0	0	0	0	1	0	1	0	0	0	0	0	0	0	0	0	0	0	3
Q11	0	1	1	0	0	0	0	0	0	0	1	1	1	1	1	0	0	0	0	0	0	0	0	0	48
Fai for 120 q	**5**	**93**	**97**	**5**	**16**	**17**	**5**	**5**	**16**	**5**	**103**	**94**	**96**	**98**	**96**	**18**	**20**	**8**	**17**	**15**	**16**	**15**	**19**	**19**	

TABLE. V. FEATURE OF KNOWLEDGE EXTRACTION DATA

Hypertension
Diabetes mellitus
Class

TABLE. VI. KNOWLEDGE EXTRACTION DATA SCHEMA

Hypertension	Diabetes mellitus

TABLE. VII. CONTROLLING DATA SCHEMA

Blood	Specific-Gravity	Blood-Urea	Serum Creatinine	Sodium	Potassium	Hemoglobin

Firstly, we restructured the knowledge extraction data in one table by using the features in Table V and buffered it for transmission to the cloud. This table schema is shown in Table VI.

Secondly, we used Algorithm 4 on Table IV to restructure new tables for the controlling data. The k-means algorithm was applied twice, once with k = 2 and again with k = 3. A superior subset was achieved with k = 3. The algorithm provided three subsets, and two of these subsets contained features with low frequency. Consequently, we built only one table using the subset that contained features with high frequency, and that represented the controlling data which is then stored in the edge layer. The schema of this new table is shown in Table VII.

5) Results: As previously mentioned, our framework is tested for data transmission time, storage space and queries execution time (i.e., data retrieval efficiency).

a) Data Transmission Time and Storage Space: As mentioned above, from user requirements and network requirements, the pre-processing data were separated into two classes: CKD, and not CKD. Only the CKD class is relevant. Thus, the amount of the processing data was reduced. This conclusion is supported by Fig. 6 which shows both the original data and relevant classification data plots. The classification data clearly required a lower amount of storage and analysis.

Fig. 7(a) compares the amount of data transmitted over the network from the edge layer to the cloud layer for storage. The two bars represent the two datasets: the red bar for original dataset before any partitioning, and the blue bar for the dataset after partitioning (classification and restructuring, as shown in Table VI). Clearly the volume of data transmitted over the network for the original dataset is extremely high relative to the volume transmitted over the network for the dataset after partitioning. Fig. 7(b) portrays the corresponding transmission times of the two datasets. This result confirms that a network with our framework can reduce network resource requirements (i.e., bandwidth and storage space) and, as a direct consequence, reduce network traffic because of the increased rate of data transmission.

In Fig. 7(a) the plotted bar of stored value indicates the amount of stored data is 92 KB for the network for the original dataset and only 6.95 KB for our partitioned dataset. This represents a 92.4% reduction in storage space required. Similarly, in Fig. 7(b), the plotted bar of stored value indicates the amount of transmission time is 0.007376 S for the original dataset and only 0.000556 S our partitioned dataset. This represents a 92.5% reduction in time required for transmission.

b) Query Execution Time (Data Retrieval Efficiency): In this section, we compare the execution time of the 11 queries in Table II with different size datasets, and examine the outcome for two additional queries in Table VIII on both the original dataset and our new schema dataset(partitioning dataset) (see Table VII).

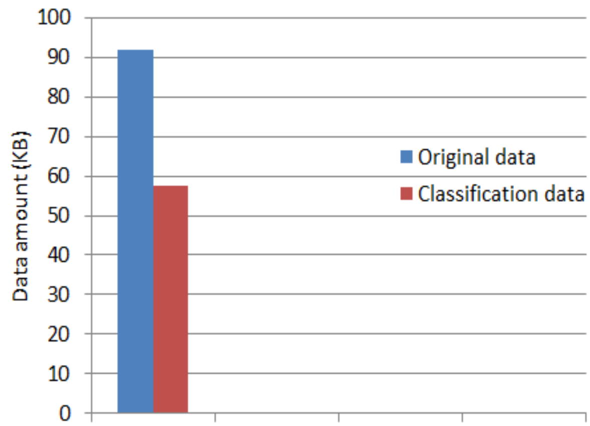

Fig. 6. Data Classification Amount.

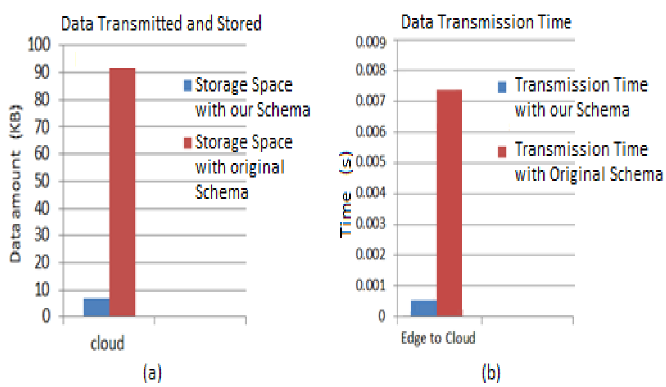

Fig. 7. (a) Data Storage Space and (b) Transmission Time.

Table VIII shows the execution time of the 11 queries in both our schema dataset and the original dataset. The results show significant differences in the execution times between the two datasets. Obviously, our schema dataset requires a shorter execution time than the original dataset because it has a smaller size as well as greater spatial locality of reference. In other words, the network with our framework has low latency and high performance. These differences can be shown by analyzing the bar chart in Fig. 8. Furthermore the average execution time for these 11 queries was decreased by 79.841%.

An interesting observation is the execution time of the Q5 which is low in both datasets because the temporal locality of the query schema is virtually identical to the spatial locality of both types of data schema.

Table IX shows the execution times produced using a relatively large dataset. By comparing Table IX with Table VIII, we observe that the proposed framework consistently has the shorter execution time despite the change in data size. Fig. 9 illustrates graphically that the difference between execution times persists in spite of the change in the dataset size.

We conclude that changes in dataset size do not adversely affect the results, meaning our proposed framework can achieve its objectives in different networks with different dataset sizes.

Fig. 10 compares the execution times of the two additional queries in Table X against each of the two sizes of dataset. Again, the proposed framework has a consistently shorter execution time compared to the original system.

TABLE. VIII. QUERY EXECUTION TIME FOR NORMAL SIZE DATASET

Query	Execution Time with Our Schema	Execution Time with Original Data
Q1	0.0025	0.0027
Q2	0.0020	0.0025
Q3	0.0015	0.0025
Q4	0.0023	0.0025
Q5	0.0005	0.0010
Q6	0.0022	0.0025
Q7	0.0020	0.0025
Q8	0.0015	0.0025
Q9	0.0020	0.0025
Q10	0.0012	0.0025
Q11	0.0025	0.0026

Fig. 8. Query Execution Times.

TABLE. IX. QUERY EXECUTION TIMES FOR LARGE SIZE DATASET

Query	Execution Time with Our Schema	Execution Time with Original Data
Q1	0.0040003	0.0080003
Q2	0.0050003	0.0070003
Q3	0.0040003	0.0060005
Q4	0.0030003	0.0040003
Q5	0.0022000	0.0030003
Q6	0.0025000	0.0030000
Q7	0.0030000	0.0040000
Q8	0.0030003	0.0035000
Q9	0.0040001	0.0045005
Q10	0.0025005	0.0030000
Q11	0.0040000	0.0060005

Fig. 9. Query Execution Times (Large Dataset).

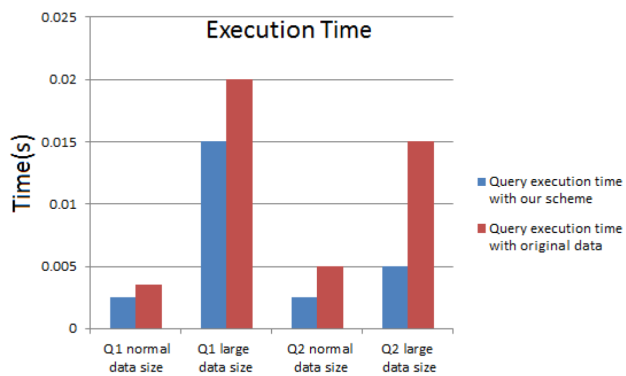

Fig. 10. Queries Execution Time.

TABLE. X. TWO SUGGESTED QUERIES

Q1→	Blood, Specific_Gravity, Blood_Urea, Sodium, Potassium, Hemoglobin where Specific_Gravity like "1"
Q2→	Blood group by Hemoglobin

B. Theoretical Analysis and Verification

This section describes the use of the throughput calculation functions in Section IV to theoretically evaluate our framework in the proposed system. This calculation involves two elements, provided by Equations 5 and 7: the first element is the measurement of data access time, performed by calculating the space-time for demand query. The second element is to calculate the data transmission volume, performed by computing the space-time product for data moving through the network.

1) Dataset access time: As mention before, the original dataset of our system has 400 instances and 25 attributes. Considering our approach, this dataset after classification and restructuring to identify a controlling dataset, a new dataset was built. This new dataset has 250 instances and 7 attributes as shown in Table VII.

Table XI displays the results of performing equation 5 (i.e., Y = f * Ti * Si) on the queries in Table II, to calculate the space-time product of the proposed network with and without our framework.

As shown in Table XI, where the first column identifies the query, the second column shows the space-time product for the original dataset, and the third column displays the space-time product for the new dataset. Our proposed framework consistently showed a more favorable result. This conclusion is further reinforced when examining the bar chart shown in Fig. 8 showing execution times for both the original dataset and new dataset. Indeed, a lower latency is invariably achieved by our approach. The average execution time was reduced by 98%.

The storage of data is critical to the process of retrieving data in real-time. By extension, it necessarily has a material impact on network latency. The result in Table IX shows that best throughput is achieved with our approach when the data storage is considered and takes into account the fact that data which exhibits good locality structure can be accessed more easily than data with poor locality.

2) Data transmission time: The original dataset of our system has 400 instances and 25 attributes. Using our approach, this dataset, after classification and restructuring to establish a knowledge extraction dataset, a new dataset was built containing 250 instances and only two attributes.

Thus, the data transmission space-time before partitioning data may be expressed by the following equation:

$$Y = T * S(T)$$

$$Y = 400 * 25 * t = 10000\ t$$

The data transmission space-time after partitioning data is expressed as follows:

$$Y = 250 * 2 * t = 500\ t$$

According to the results of the space-time product of transmission data, our framework proves a better approach for analyzing the dataset. This is confirmed by observing the chart in Fig. 6 which shows the amount of data transmitted to the cloud layer and stored there as well the time required to transmit the data. The space-time product of transmission data rate was reduced by 95%

TABLE. XI. CALCULATION OF SPACE-TIME PRODUCT

Query Number	Space-Time Product of Original Dataset	Space-Time Product of New Dataset
Q1	4 * 6 * 400 * 25 =240 000	4 * 6 * 250 * 7 = 42 000
Q2	4 * 6 * 400 * 25 =240 000	4 * 6 * 250 * 7 = 42 000
Q3	3 * 5 * 400 * 25 =150 000	3 * 5 * 250 * 7 = 26 250
Q4	4 * 5 * 400 * 25 =200 000	4 * 5 * 250 * 7 = 35 000
Q5	3 * 6 * 400 * 25 =180 000	3 * 6 * 250 * 7 = 31 500
Q6	3 * 4 * 400 * 25 =120 000	3 * 4 * 250 * 7 = 21 000
Q7	7 * 4 * 400 * 25 =280 000	7 * 4 * 250 * 7 = 49 000
Q8	3 * 4 * 400 * 25 =120 000	3 * 4 * 250 * 7 = 21 000
Q9	4 * 5 * 400 * 25 =200 000	4 * 5 * 250 * 7 = 35 000
Q10	3 * 3 * 400 * 25 =90 000	3 * 3 * 250 * 7 = 15 750
Q11	48 * 7 * 400 * 25 =3 360 000	48 * 7 * 250 * 7 = 588 000

Network throughput quantifies the amount of data, during a defined time interval that a network can send or receive. Throughput must take into account the entire network overhead as well as contention on the transmission links. Multiple data flows on a link will each use some percentage of the overall bandwidth, thereby reducing the total throughput of each. It follows that increasing data flow causes an increase in both network traffic and contention on the links.

Bandwidth is the number of bits per second that a link can send or receive, including all flows. Data rate (or data transfer rate) is the volume of data transferred through a connection within one second. The data rate cannot exceed the bandwidth of the connection; data rate is closer to bandwidth. Thus, the reducing the required data rate reduced traffic overhead on the network; in other words, a reduced data rate leads to a reduce bandwidth requirement.

VI. Conclusion

In this paper, efficient data storage and retrieval frameworks are proposed based on both the edge computing and cloud computing techniques. The main challenges in terms of data partitioning and requirements analysis are summarized, and appropriate solutions are also provided. Specifically, the data partitioning (classification and restructuring) framework is provided to support low latency and save network bandwidth based on MapReduce algorithms, wrapper feature selection method and a machine learning proposed subsystem, in addition, a new algorithm for restructuring the data was proposed.

The components of the proposed framework flowchart are discussed; data partitioning (knowledge extraction and control data) and requirements generation are presented from a wider view. The functionalities of each point of the proposed framework are displayed in detail.

The framework is verified on a case study and approved its efficiency that is evaluated using Data time, storage space, and data retrieval time.

For future work, other data restructuring algorithms can be used and other types of requirements analysis models can be explored.

References

[1] K.-D. Kang, D. S. Menasche, G. Küçük, T. Zhu, and P. Yi, “Edge computing in the Internet of Things,” Int. J. Distrib. Sens. Networks, vol. 13, no. 9, p. 155014771773244, 2017.

[2] B. Omoniwa, R. Hussain, M. A. Javed, S. H. Bouk, and S. A. Malik, “Fog/Edge Computing-based IoT (FECIoT): Architecture, Applications, and Research Issues,” IEEE Internet Things J., no. October, 2018.

[3] D. Boswarthick, O. Elloumi, and O. Hersent, M2M communications: a systems approach. John Wiley & Sons, 2012.

[4] P. C. Evans and M. Annunziata, “Industrial internet: pushing the boundaries of minds and machines, 2012,” Available(accessed 4.10. 2016) https//www. ge. com/docs/chapters/Industrial_Internet. pdf, 2015.

[5] A. Zanella, N. Bui, A. Castellani, L. Vangelista, and M. Zorzi, “Internet of things for smart cities,” IEEE Internet Things J., vol. 1, no. 1, pp. 22–32, 2014.

[6] L. Qian, Z. Luo, Y. Du, and L. Guo, “Cloud computing: An overview,” in IEEE International Conference on Cloud Computing, 2009, pp. 626–631.

[7] N. Takahashi, H. Tanaka, and R. Kawamura, “Analysis of process assignment in multi-tier mobile cloud computing and application to edge accelerated web browsing,” in 2015 3rd IEEE International Conference on Mobile Cloud Computing, Services, and Engineering, 2015, pp. 233–234.

[8] J. Lin, W. Yu, N. Zhang, X. Yang, H. Zhang, and W. Zhao, “A Survey on Internet of Things: Architecture, Enabling Technologies, Security and Privacy, and Applications,” IEEE Internet Things J., vol. 4, no. 5, pp. 1125–1142, 2017.

[9] “□,” 2016.

[10] Y. Zhang, H. Wang, J. Zhao, and B. An, “SeCEE: Edge Environment Data Sharing and Processing Framework with Service Composition,” in International Conference of Pioneering Computer Scientists, Engineers and Educators, 2018, pp. 33–47.

[11] B. Du, R. Huang, Z. Xie, J. Ma, and W. Lv, “KID Model-Driven Things-Edge-Cloud Computing Paradigm for Traffic Data as a Service,” IEEE Netw., vol. 32, no. 1, pp. 34–41, 2018.

[12] H. Li, K. Ota, and M. Dong, “Learning IoT in Edge: Deep Learning for the Internet of Things with Edge Computing,” IEEE Netw., vol. 32, no. 1, pp. 96–101, 2018.

[13] J. S. Fu, Y. Liu, H. C. Chao, B. K. Bhargava, and Z. J. Zhang, “Secure Data Storage and Searching for Industrial IoT by Integrating Fog Computing and Cloud Computing,” IEEE Trans. Ind. Informatics, vol. 14, no. 10, pp. 4519–4528, Oct. 2018.

[14] X. Xu, S. Huang, L. Feagan, Y. Chen, Y. Qiu, and Y. Wang, “EAaaS: Edge Analytics as a Service,” Proc. - 2017 IEEE 24th Int. Conf. Web Serv. ICWS 2017, no. 1, pp. 349–356, 2017.

[15] B. Alturki, S. Reiff-Marganiec, and C. Perera, “A hybrid approach for data analytics for internet of things,” in Proceedings of the Seventh International Conference on the Internet of Things, 2017, p. 7.

[16] J. Li and H. Liu, “Challenges of feature selection for big data analytics,” IEEE Intell. Syst., vol. 32, no. 2, pp. 9–15, 2017.

[17] I. Guyon, S. Gunn, M. Nikravesh, and L. A. Zadeh, Feature extraction: foundations and applications, vol. 207. Springer, 2008.

[18] Z. Hu, Y. Bao, T. Xiong, and R. Chiong, “Hybrid filter–wrapper feature selection for short-term load forecasting,” Eng. Appl. Artif. Intell., vol. 40, pp. 17–27, 2015.

[19] K. Pohl, Requirements engineering: fundamentals, principles, and techniques. Springer Publishing Company, Incorporated, 2010.

[20] R. Bunt and C. Williamson, Temporal and spatial locality: A time and a place for everything. na, 2003.

[21] P. J. Denning and J. P. Buzen, “The operational analysis of queueing network models,” ACM Comput. Surv, vol.10, no.3, pp. 225–261, 1978.

[22] A. S. Levey and J. Coresh, “Chronic kidney disease,” Lancet, vol. 379, no. 9811, pp. 165–180, 2012.

[23] B. Ravandi and I. Papapanagiotou, “A self-learning scheduling in cloud software defined block storage,” in 2017 IEEE 10th International Conference on Cloud Computing (CLOUD), 2017, pp. 415–422.

[24] B. Zhang et al., “The cloud is not enough: Saving iot from the cloud,” in 7th {USENIX} Workshop on Hot Topics in Cloud Computing (HotCloud 15), 2015.

[25] Y. Jararweh, A. Doulat, O. AlQudah, E. Ahmed, M. Al-Ayyoub, and E. Benkhelifa, “The future of mobile cloud computing: Integrating cloudlets and mobile edge computing,” in 2016 23rd International conference on telecommunications (ICT), 2016, pp. 1–5.

[26] M. Satyanarayanan, “The emergence of edge computing,” Computer (Long. Beach. Calif)., vol. 50, no. 1, pp. 30–39, 2017.

[27] M. Satyanarayanan, P. Bahl, R. Caceres, and N. Davies, “The case for vm-based cloudlets in mobile computing,” IEEE pervasive Comput., no. 4, pp. 14–23, 2009.

[28] C. M. S. Magurawalage, K. Yang, L. Hu, and J. Zhang, “Energy-efficient and network-aware offloading algorithm for mobile cloud computing,” Comput. Networks, vol. 74, pp. 22–33, 2014.

[29] K. Dolui and S. K. Datta, “Comparison of edge computing implementations: Fog computing, cloudlet and mobile edge computing,” in 2017 Global Internet of Things Summit (GIoTS), 2017, pp. 1–6.

[30] T. H. Luan, L. Gao, Z. Li, Y. Xiang, G. Wei, and L. Sun, “Fog computing: Focusing on mobile users at the edge,” arXiv Prepr. arXiv1502.01815, 2015.

[31] M. Taneja and A. Davy, "Resource aware placement of data analytics platform in fog computing," Procedia Comput. Sci., vol. 97, pp. 153–156, 2016.

[32] F. Bonomi, R. Milito, J. Zhu, and S. Addepalli, "Fog computing and its role in the internet of things," in Proceedings of the first edition of the MCC workshop on Mobile cloud computing, 2012, pp. 13–16.

[33] N. Hassan, S. Gillani, E. Ahmed, I. Yaqoob, and M. Imran, "The Role of Edge Computing in Internet of Things," IEEE Commun. Mag., vol. 56, no. 11, pp. 110–115, 2018.

[34] M. Liu, F. R. Yu, Y. Teng, V. C. M. Leung, and M. Song, "Distributed resource allocation in blockchain-based video streaming systems with mobile edge computing," IEEE Trans. Wirel. Commun., vol. 18, no. 1, pp. 695–708, 2018.

[35] P. Wang, C. Yao, Z. Zheng, G. Sun, and L. Song, "Joint Task Assignment, Transmission, and Computing Resource Allocation in Multilayer Mobile Edge Computing Systems," IEEE Internet Things J., vol. 6, no. 2, pp. 2872–2884, 2018.

[36] Y. Sahni, J. Cao, and L. Yang, "Data-aware task allocation for achieving low latency in collaborative edge computing," IEEE Internet Things J., vol. 6, no. 2, pp. 3512–3524, 2018.

[37] J. Ren, Y. He, G. Huang, G. Yu, Y. Cai, and Z. Zhang, "An edge-computing based architecture for mobile augmented reality," IEEE Netw., 2019.

[38] B. Du, R. Huang, Z. Xie, J. Ma, and W. Lv, "KID model-driven things-edge-cloud computing paradigm for traffic data as a service," IEEE Netw., vol. 32, no. 1, pp. 34–41, 2018.

[39] L. F. Bittencourt et al., "The Internet of Things, Fog and Cloud Continuum: Integration and Challenges," 2018.

[40] Y. Ai, M. Peng, and K. Zhang, "Edge computing technologies for Internet of Things: a primer," Digit. Commun. Networks, vol. 4, no. 2, pp. 77–86, 2018.

[41] Y. Teranishi, T. Kimata, H. Yamanaka, E. Kawai, and H. Harai, "Dynamic Data Flow Processing in Edge Computing Environments," Proc. - Int. Comput. Softw. Appl. Conf., vol. 1, pp. 935–944, 2017.

[42] M. S. Mahdavinejad, M. Rezvan, M. Barekatain, P. Adibi, P. Barnaghi, and A. P. Sheth, "Machine learning for internet of things data analysis: a survey," Digit. Commun. Networks, vol. 4, no. 3, pp. 161–175, 2018.

[43] S. Sureddy, K. Rashmi, R. Gayathri, and A. S. Nadhan, "Flexible Deep Learning in Edge Computing for IoT," Int. J. Pure Appl. Math., vol. 119, no. 10, pp. 531–543, 2018.

[44] V. C.P and D. A. A. Chikkamannur, "IOT future in Edge Computing," Int. J. Adv. Eng. Res. Sci., vol. 3, no. 12, pp. 148–154, 2016.

[45] R. Grossman and Y. Gu, "Data mining using high performance data clouds: experimental studies using sector and sphere," in Proceedings of the 14th ACM SIGKDD international conference on Knowledge discovery and data mining, 2008, pp. 920–927.

[46] J. Dean and S. Ghemawat, "MapReduce: simplified data processing on large clusters," Commun. ACM, vol. 51, no. 1, pp. 107–113, 2008.

[47] A. F. Gates et al., "Building a high-level dataflow system on top of Map-Reduce: the Pig experience," Proc. VLDB Endow., vol. 2, no. 2, pp. 1414–1425, 2009.

[48] Y. Kim, W. N. Street, and F. Menczer, "Evolutionary model selection in unsupervised learning," Intell. data Anal., vol. 6, no. 6, pp. 531–556, 2002.

[49] K. A. A. Nazeer and M. P. Sebastian, "Improving the Accuracy and Efficiency of the k-means Clustering Algorithm," in Proceedings of the world congress on engineering, 2009, vol. 1, pp. 1–3.

[50] C. Slamet, A. Rahman, M. A. Ramdhani, and W. Darmalaksana, "Clustering the Verses of the Holy Qur'an using K-Means Algorithm," Asian J. Inf. Technol., vol. 15, no. 24, pp. 5159–5162, 2016.

[51] N. Hoque, D. K. Bhattacharyya, and J. K. Kalita, "MIFS-ND: A mutual information-based feature selection method," Expert Syst. Appl., vol. 41, no. 14, pp. 6371–6385, 2014.

[52] L. Yu and H. Liu, "Efficient feature selection via analysis of relevance and redundancy," J. Mach. Learn. Res., vol. 5, no. Oct, pp. 1205–1224, 2004.

[53] G.-B. Huang, Q.-Y. Zhu, and C.-K. Siew, "Extreme learning machine: theory and applications," Neurocomputing, vol. 70, no. 1–3, pp. 489–501, 2006.

[54] H. A. Wibawa, I. Malik, and N. Bahtiar, "Evaluation of Kernel-Based Extreme Learning Machine Performance for Prediction of Chronic Kidney Disease," in 2018 2nd International Conference on Informatics and Computational Sciences (ICICoS), 2018, pp. 1–4.

Proof of Credibility: A Blockchain Approach for Detecting and Blocking Fake News in Social Networks

Mohamed Torky[1]
Information Technology Department
Faculty of Computer and Information System
Islamic University of Madinah
Madinah, Saudi Arabia
Higher Institute of Computer Science and Information Systems
Culture and Science City Academy
6 October-Giza-Egypt
Scientific Research Group in Egypt (SRGE)
ORCID No: 0000-0002-3229-9794

Emad Nabil[2]
Computer Science Department
Faculty of Computer and Information System, Islamic University of Madinah, Madinah, Saudi Arabia
Faculty of Computers and Artificial Intelligence
Cairo University, Giza, Egypt

Wael Said[3]
Computer Science Department, Faculty of Computers and Informatics, Zagazig University, Zagazig, Egypt

***Abstract*—Rumors and misleading information detection and prevention still represent a big challenge against social network developers and researchers. Since newsworthy information propagation is a traditional behavior of most of the users in social media, then verifying information credibility and reliability is indeed a vital security requirement for social network platforms. Due to its immutability, security, tamper-proof and P2P design, Blockchain as a powerful technology can provide a magical solution to overcome this challenge. This Paper introduces a novel blockchain approach called *Proof of Credibility (PoC)* for detecting fake news and blocking its propagation in social networks. The functionality of the PoC protocol has been simulated on two datasets of newsworthy tweets collected from different news sources on Twitter. The results clarified a satisfying performance and efficiency of the proposed approach in detecting rumors and blocking its propagation.**

Keywords—Blockchain technology; social networks; fake news detection

I. Introduction

Sharing newsworthy information on social media platforms like Facebook, Twitter, and Instagram without evaluating its credibility has popped out a big challenge. Disseminating Misleading information and fake news across social networks represent a big dilemma against researchers and Social Network Service Providers (SNPs) [1]. The political elections are the best witness to sharing a lot of rumors patterns across social media. For instance, more than 1,000 reports on politics and election were declared as fake in the Jakarta Gubernatorial Election in 2017 [2]. Also, Fake news and misleading information can misuse the reputation of countries as well as jeopardize international relations. In 2017, the Twitter account of Qatar's state news agency had been penetrated and published false news to criticize aspects of the Arab Gulf and US foreign policy towards Iran. The neighbor countries like UAE, Bahrain, Saudi Arabia, and Egypt broke diplomatic ties with Qatar [3]. With advances in AI technologies like Machine learning [4], deep learning [5] and digital animations [6], developing malicious social bots for propagating fake news represents a big challenge. According to Gartner's predictions for 2018, most of the people will read and believe more false news than real news by 2020 [7]. Although AI has the best opportunity of recognizing misleading information, it is seriously able to create fake content on social media. Unfortunately, recently, the power of AI algorithms for identifying fake news is lower than its ability to create it [8]. Therefore, it has become an essential need to search for an alternative robust and efficient technology for handling this problem. Developing blockchain-based solutions have the potential to change the way of information creation and propagation [9]. Blockchain can provide trustable, immutable, verifiable, reliable, and transparent transactions for designing a trusted social system [10]. In this paper, we investigate the possibility of using blockchain theory for developing a novel protocol called Proof of Credibility (PoC) able to verify shared information and detect misleading information across social networks. The proposed protocol is simulated on 1003 newsworthy tweets around the trending topic #ISIS, and 802 newsworthy tweets around the trending topic #Halamadrid which are collected from different news sources on Twitter. The results clarified the possibility of developing a standard blockchain consensus for verifying information credibility as well as blocking rumor propagation across social networks. PoC will represent the first blockchain protocol that can be utilized for solving the problem of fake news and misleading information in social networks. The rest of this paper can be organized as follows: Section 2 presents the literature review. Section 3 discusses the proposed blockchain protocol. Section 4 presents the simulation results. Finally, Section 5 presents the conclusion and future work.

II. Literature Review

There is a relatively small body of literature that is concerned with using blockchain as a solution tool for solving social network security problems. Moreover, unfortunately, there are relatively few historical blockchain approaches utilized for solving fake news and misleading information problem specifically. However, the literature introduced some blockchain techniques for handling specified problems in social networks. For example, A blockchain is configured as a data bank accessible by social network nodes based on rules and preferences of the nodes upon authorization by the blockchain configured data bank for facilitating social integrity networking [11]. Another work in investigating some of the recent blockchain platforms to determine if they fulfill Metcalfe's Law for modeling social media networks based on digital currency protocols [12]. The authors in [13] investigate the potential of utilizing the U-share-blockchain mechanism to enable users to manage and track all posted contents they share over the social network. Yahiatene et al. in [14] introduced a novel framework that depends on two main components: Software-Defined Vehicular Networks (SDVN) and Blockchain for authenticating the transactions and providing anonymity of data in a distributed manner across the social network. Moreover, blockchain-based social networks can be utilized for combining fog computing to develop security architecture for managing IoT systems by creating tamper-proof digital identities in a trustless domain [15]. An additional blockchain contribution to social networks is Tweet-chain [16]. Tweet-chain is a novel social network model-based on blockchain for managing public posts based on Proof of Concept protocol [17] to ensure social transaction security instead of proof of work. It can work without the required trustworthiness assumption for the social network provider. Fakechain [18] is another blockchain consensus –based on data mining algorithms for authenticating shared information [19] across the social network and detecting fake news [20]. Detecting fake news can be achieved by utilizing the functionality of Ethereum blockchain combined with the Breadth-First Search (BFS) algorithm [21].

III. Proof of Credibility (PoC) Approach

Automatic rumors recognition and blocking it propagation are indeed very hard challenges to design trusted social networks. There are a number of techniques that have been developed to fight against misleading information in social networks [22][23]. The recent researches utilize the benefits of Artificial Intelligence (AI)-based techniques for detecting misleading information [24] [25]. Other methods have been based on sentiment analysis combined with IP network analysis [26] for detecting social network rumors. Moreover, some studies tried to solve this problem based on Natural Language Processing techniques [27]. However, these studies have a lot of limitations and inaccurate results in detecting fake news. For example, while AI-based techniques can help in limiting the rise of misleading information, it is not invincible. Such that, It may occasionally make a lot of False Positive and False Negative errors. So, Social network systems can be re-designed with blockchain to give control of the shared posts back to the users themselves in P2P communication. The major advantages of utilizing blockchain-based techniques for detecting misleading information are:

1) Better privacy and protection.
2) Decentralized social network architecture.
3) User control based on a distributed content.
4) Online automatic verification for shared information.
5) Grants a robust authentication and ensures anonymity.

In this paper, we propose a novel Blockchain algorithm called Proof of Credibility (PoC) for detecting and blocking fake news in social networks. The idea behind PoC is that re-engineering the social networks as decentralized networks, where users are represented as peers. Each peer shares a distributed ledger, which represented as an immutable, cryptographically secured record of detected rumors. The distributed ledger is designed as a sequence of blocks, where each block in the blockchain represents a new detected number of rumors. For example, a new block is added to the chain if the blockchain system detected 10 rumors. Moreover, The detection functionality is executed by PoC chain code which is shared also with all peers in the social network platform. They can execute POC chain code via a blockchain browser. "Fig. 1" shows the conceptual view of the blockchain-based social network system, and Fig. 2 explains the design model of the PoC protocol.

With PoC –based social network systems there is no need for the third party to verify the shared information and identifying rumors, such that peers will do this task based on the PoC blockchain system. Each block in the blockchain involves a fixed number of fake news. This number is agreed by the peers of social networks and is defined in the PoC consensus. For example, a new block is added to the chain after identifying 100 rumors in the social networking system.

The idea behind PoC is evaluating the credibility of the source who shared the information. As we interested in newsworthy information, the source may be an online newspaper, magazine, TV-News channel, Radio, Wire services, or a blog by users. The functionality of PoC is based on the Best Match technique (BM25F) metric [28]. It can be used for evaluating the credibility of online sources of newsworthy information [29].

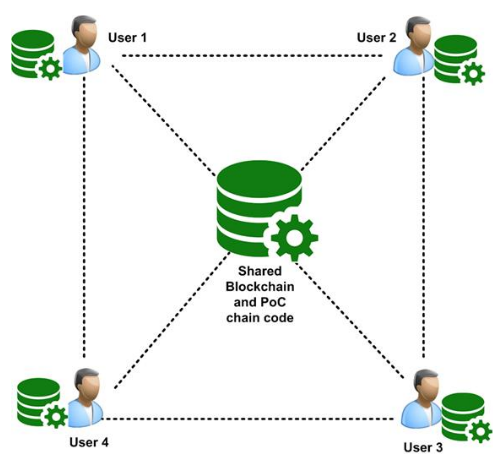

Fig. 1. Conceptual view of the Blockchain-based Social Network System.

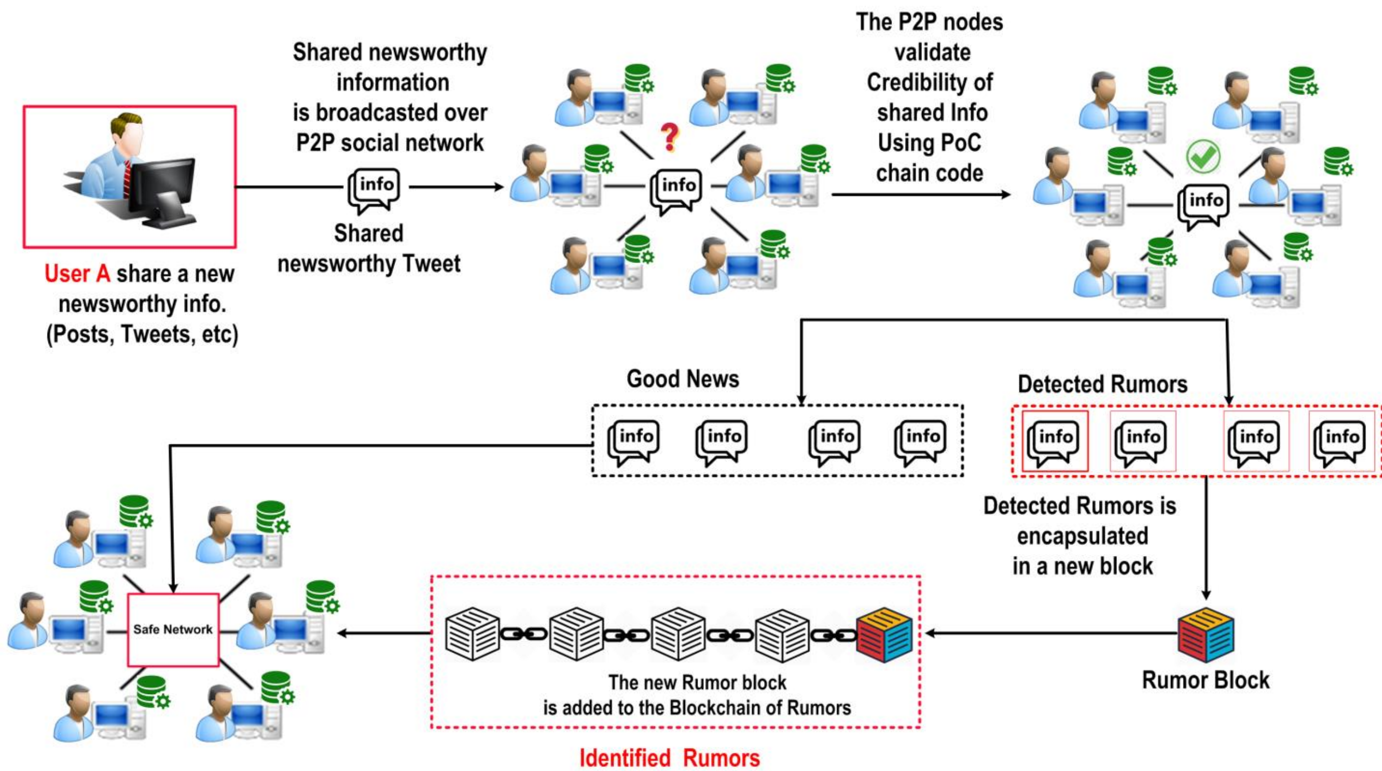

Fig. 2. Proof of Credibility (PoC) Design Model.

Source credibility can be calculated based on two dependent factors. The first factor is $W\ (Si)$, which is used for producing the credibility weight (W) value to Information Sources as formulated in equation (1).

$$W(S_i) = \frac{Occure \times Boost}{[(1-b)+b\times\frac{\#Posts}{\#Followers}]} \tag{1}$$

Where *occur* is the number of *posts/ tweets* that are associated with the source S_i in all shared Posts/Tweets of a specific trending topic in a specific time *t*. *Boost* is called boost factor, which applied according to the type of the source of information as presented in Table I, the boost values are taken from News Trust [30] which is a review tool rate the news based on journalistic quality, not just popularity. So, the handled information must be classified according to the source type to assign the appropriate *boost* value from Table I. *b* is a constant, such that $0.5 < b < 0.8$. *#Posts* is the number of all posts that are shared by the source S_i. *#followers* is number of followers who follow the source S_i. The second factor is Logarithmic Ratio (LR) of the number of posts/tweets in the collection (i.e. the number of shared information within a specific period defined in PoC protocol) that share the same source of news as in equation (2).

$$LR(S_i) = Log\,\frac{N+n(S_i)+0.5}{n(S_i)+0.5} \tag{2}$$

Where *N* is the number of *posts* in the collection and $n(S_i)$ is the number of posts, which are associated with (S_i). Finally, the Source Credibility (SC) value can be calculated as in equation (3).

$$SC(S_i) = \frac{W(S_i)}{K_1 + W(S_i)} \times LR(S_i) \tag{3}$$

Where, K_1 is a constant value used as a free Parameter, such that $1.2 < K_1 < 2$.

TABLE I. BOOST VALUES OF THE MOST COMMON SOURCES OF NEWSWORTHY INFORMATION [30]

News Source	**Boost values**
Newspapers	3.29
Magazines	3.68
TV-News Channels	3.54
Online Sites	3.69
Radio	3.60
Wire Service	3.48
Blogs	3.55

The PoC-chain code which implements the detection methodology and evaluates information credibility can be implemented as in Algorithm 1.

Algorithm 1: PoC Detection Methodology

1: Input: Time $T = \{t_1, t_2, t_3, \ldots . t_n\}$
2: Input: News = $\{N_1, N_2, N_3, \ldots . N_P\}$
3: Output: Blockchain of Rumors BR= $\{B_1, B_2, B_3, \ldots . B_n\}$
4: Procedure Rumors Detection
5: While (is share news())
6: for each $N \in News\ \mathbf{in}\ t_i\ Do$
7: if $(N_i.url\ IsTrue())\ Then$
8: $Source\_News \leftarrow N_i$
9: else
10: $Blog\_News \leftarrow N_i$
11: End if
12: End for
13: for each $N_i \in Source\_News$
14: $Score(N_i) = SC\ (N_i.source)$
15: $Cred_{Threshold\ 1} = \sum_{i=1}^{i=n1} \frac{Score(N_i)}{n1}$
16: if $(Score(N_i) < Cred_{Threshold})$
13: $B_j \leftarrow N_i$
14: else
15: $Good\ info \leftarrow Ignore\ (N_i)$
16: End if
17: End for each
18: for each $N_i \in Blog\_News$
19: $Score(N_i) = \frac{\#Reshare}{\#Fllowers} \times 100$
20: $Cred_{Threshold\ 1} = \sum_{i=1}^{i=n2} \frac{Score(N_i)}{n2}$
21: if $(Score(N_i) < Cred_{Threshold})$
22: $B_j \leftarrow N_i$ // Add N_j to the Block B_j
23: else
24: $Good\ Info \leftarrow Ignore\ (N_i)$
25: return B_j
26: $BR \leftarrow B_j$ // Add B_j to the blockchain
27: Open (New Block B_{j+1})
28: End While
29: End Procedure

IV. Simulation Results

For investigating the realism and effectiveness of the proposed PoC approach, a simulation experiment has been applied in two datasets collected from Twitter. The two datasets are described as two trending topics (#ISIS, and #Halamadrid) that involve several newsworthy tweets that have been tweeted by multiples sources of information. The Twitter R library tool [31] has been used as a software tool for collecting tweets of each trending topic across four-time intervals. The general description of the two datasets can be summarized in Table II. The simulation results of applying the PoC algorithm on the two mentioned datasets show that the PoC algorithm could detect the fake news in the two mentioned datasets as follows, 215 tweets in block 1, 284 tweets in block two, 224 in block three, and 208 in block four as depicted in Table III. Fig. 3 depicts also the total numbers of fake news for the seven sources types of information. The results show that online newspapers are the most source type of fake news in the #ISIS dataset, while Wire Service is the most source type of fake news in the #Halamadrid dataset. The pi plot in Fig. 4 depicts the percentages of detected fake news in the two studied datasets.

For verifying this obtained results, the set of detected fake news (i.e.931 tweets) and good news (i.e. 874 tweets) are outsourced to the Xpertin platform [32]. It has a set of the best experts in social media services. The verification results and feedback of Xpertin reported that only 91% of detected fake news is indeed fake (i.e. only 847 tweets are fake news) and 86% of good news is indeed good (i.e. only 752 tweets are good news). According to Xpertin's feedback, this result means that the PoC technique failed to recognize 84 tweets as fake tweets and 57 tweets as good tweets. So, according to True Positive (TP), False Positive (FP), True Negative (TN) and False Negative (FN) values, Precision, Recall, and Accuracy can be calculated as in equations 4, 5, 6. Fig. 5 presents the Precision, Recall, and Accuracy results of the PoC technique.

$$Precision = \frac{TP}{TP+FP} \tag{4}$$

Such that *TP* is the number of True Positive tweets and *FP* is the number of False Positive tweets.

$$Recall = \frac{TP}{TP+FN} \tag{5}$$

Such that *TP* is the number of True Positive tweets and *FN* is the number of False Negative tweets

$$Accuracy = \frac{TP+TN}{P+N} \tag{6}$$

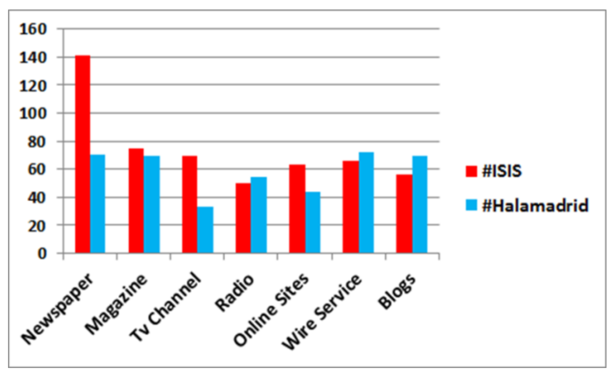

Fig. 3. The Total Numbers of Fake News for the Seven Sources Types of Information in the Two Studied Datasets after Constituting Four Blocks in the Blockchain.

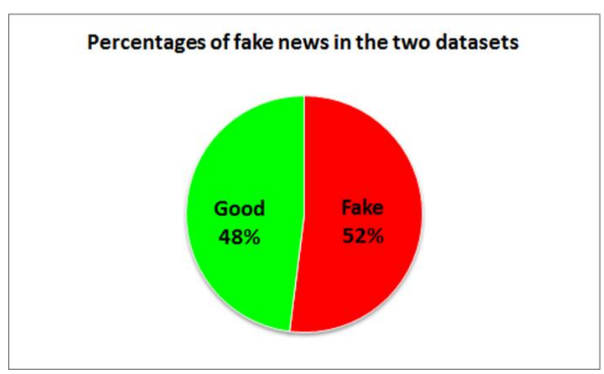

Fig. 4. The Total Percentages of Detected Fake News in the Two Data Sets.

TABLE. II. TWO DATASETS DESCRIPTION, #ISIS, AND # HALAMADRID

	#ISIS					#Halamadrid				
Source	**# Tweets**	**t1**	**t2**	**t3**	**t4**	**# Tweets**	**t1**	**t2**	**t3**	**t4**
Newspapers	281	66	73	59	83	183	39	46	57	41
Magazines	149	46	34	38	31	156	47	28	37	44
TV Channels	132	36	29	43	24	108	25	22	43	18
Radios	99	25	16	22	36	101	29	33	17	22
Online Sites	114	22	35	30	27	97	16	26	19	36
Wire Service	109	26	38	26	19	50	14	15	10	11
Blogs	119	25	23	39	32	107	30	22	26	29
Sum	**1003**	**246**	**248**	**257**	**252**	**802**	**200**	**192**	**209**	**201**

TABLE. III. NUMBER OF DETECTED FAKE NEWS IN #ISIS AND #HALAMADRID DATASETS WITH RESPECT TO FOUR TIME PERIODS (I.E. 4 BLOCKS IN THE BLOCKCHAIN) AND SEVEN SOURCES

Source	**t1**		**t2**		**t3**		**t4**	
	#ISIS	**#Halamadrid**	**#ISIS**	**#Halamadrid**	**#ISIS**	**#Halamadrid**	**#ISIS**	**#Halamadrid**
Newspaper	41	16	44	23	22	14	34	17
Magazine	20	11	23	17	19	29	13	12
TV Channels	24	9	20	4	10	17	15	3
Radio	8	9	11	17	15	10	16	18
Online Sites	15	12	24	13	7	9	17	10
Wire Service	12	20	18	28	23	16	13	8
Blogs	6	12	25	17	14	19	11	21
Sum/Block	**B1= 215**		**B2= 284**		**B3= 224**		**B4= 208**	

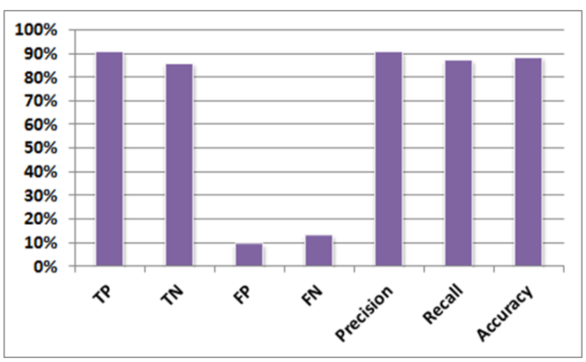

Fig. 5. TP, TN, FP, FN, Precision, Recall, Accuracy Results.

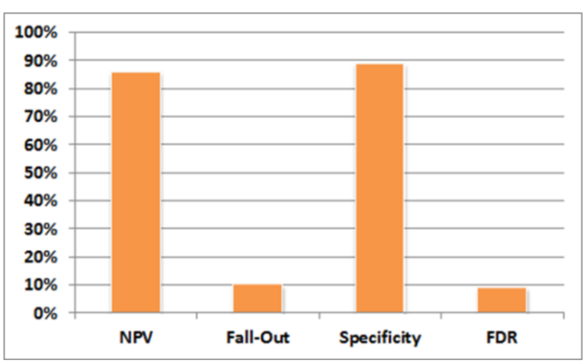

Fig. 6. NPV, Fall-Out, Specificity, and FDR Results.

Such that P = (TP + FN), and N = (FP + TN) and TN is the True Negative tweets.

Moreover, the Negative Predictive Value (NPV), Fall-Out, Specificity, and False Discovery Rate (FDR) are evaluated for PoC mechanism as in equations 7, 8, 9, 10 and the results depicted in Fig. 6.

$$NPV = \frac{TN}{TN+FN} \quad (7)$$

$$Fall - Out = \frac{FP}{FP+TN} \quad (8)$$

$$Specificity = \frac{TN}{TN+FP} \quad (9)$$

$$FDR = \frac{FP}{FP+TP} \quad (10)$$

V. DISCUSSION

Prior studies that have noted the importance of utilizing blockchain for detecting and preventing fake news in social networks didn’t introduce a novel and real blockchain technique for solving this problem [19-23]. These studies were limited to only present some state of the art about the problem without proposing a novel blockchain-based algorithm able to detect fake news in social networks. This study set out with the aim of proposing the first blockchain consensus called Proof of Credibility (PoC) for detecting and preventing fake news and rumors in social networks. The most interesting finding of this study is the satisfied value of accuracy (89%) in detecting fake news although the proposed algorithm is an initial blockchain algorithm that may require more functions and metrics for future improvements. Other interesting findings are the low values of Fall-Out and False Discovery Rate (FDR) which are 10% and 9% respectively in recognizing rumors and Fake news. It is somewhat surprising that about 52% of the total number of tweets in the two-handled datasets is recognized as fake news. This finding was unexpected and suggests that it should be there are more considerations to additional features (such as consistency and coherency of news, and general commons and acceptability [33]) of handled online newsworthy information for assessing its credibility in more accuracy. However, these findings support and encourage utilizing blockchain algorithms in managing and controlling the information propagation in social networks. As this result has not previously been described, and all previous studies handled the problem as jus as a theoretical investigation and review of the literature [19-23], so there are no comparison factors we can investigate. However, this study introduces the first real blockchain algorithm that can be compared with other blockchain-based algorithms in detecting fake news in social networks, which can be developed in the future. These findings must be interpreted with caution because the proposed algorithm is simulated on a limited amount of newsworthy tweets collected from two trending topics on twitter. For more accurate analysis and evaluation, the proposed algorithm should be improved and applied on benchmark and standardized datasets and should be applied within more periods of time for investigating the growth of blockchain of rumors in more tracing. However, this finding, while preliminary, suggests utilizing the first blockchain-based algorithm for managing and controlling information dissemination in social networks in order to detect fake news and misleading information. Improving the proposed algorithm with more measures of information credibility and simulating its functionality in benchmark and standardized datasets are more important issues for future research.

VI. Conclusion

The aim of the present research was to examine utilizing a novel blockchain-based algorithm for detecting and preventing fake news and misleading information across social networks. The study proposed a novel blockchain consensus called Proof of Credibility (PoC) for detecting fake news in social media platforms. The study has shown satisfying preliminary results obtained from simulating the proposed algorithm on two trending topics from Twitter. The experimental results have clarified the effectiveness of PoC in detecting Fake news with an accuracy of about 89 %, Fall-Out, and False Discovery Rate about 10% and 9% respectively. An implication of these results is the possibility of proposing additional blockchain algorithms for managing and controlling online information dissemination across social networks and can be compared with the proposed one. Before this study, the idea of utilizing blockchain for detecting fake news was purely anecdotal. This study was limited by the absence of a benchmark and standardized datasets for investigating PoC efficiency in more accuracy. However, this study introduces valuable insight into leveraging Blockchain and developing novel consensuses for more managing and controlling rumors propagation in social networks. More research using benchmark datasets and controlled trials is needed for improving PoC functionality and efficiency in recognizing rumors and fake news in the next studies.

References

[1] Vosoughi S, Roy D, Aral S. The spread of true and false news online. Science. 2018 Mar 9;359(6380):1146-51.

[2] BBC News, How fake news and hoaxes have tried to derail Jakarta's election, [online], available, https://www.bbc.com/news/world-asia-39176350 (accessed 5 Oct. 2019).

[3] Robert W and William M. A, Who Planted the Fake News at Center of Qatar Crisis?, [online], available, https://www.nbcnews.com/news/world/who-planted-fake-news-center-qatar-crisis-n784056 (accessed 5 Oct. 2019).

[4] Kumar A, Sangwan SR. Rumor Detection Using Machine Learning Techniques on Social Media. International Conference on Innovative Computing and Communications 2019 (pp. 213-221). Springer, Singapore.

[5] Gong Q, Chen Y, He X, Zhuang Z, Wang T, Huang H, Wang X, Fu X. DeepScan: Exploiting deep learning for malicious account detection in location-based social networks. IEEE Communications Magazine. 2018 Nov 19;56(11):21-7.

[6] Hou R, Pérez-Rosas V, Loeb S, Mihalcea R. Towards Automatic Detection of Misinformation in Online Medical Videos. arXiv preprint arXiv:1909.01543. 2019 Sep 4.

[7] Gartner, “Gartner Top Strategic Predictions for 2018 and Beyond”, 2017.Available: https://www.gartner.com/smarterwithgartner/gartner-topstrategic-predictions-for-2018-and-beyond/ [Accessed 6 Oct. 2019].

[8] Paschen J. Investigating the emotional appeal of fake news using artificial intelligence and human contributions. Journal of Product & Brand Management. 2019 May 6.

[9] Tee WJ, Murugesan RK. Trust Network, Blockchain and Evolution in Social Media to Build Trust and Prevent Fake News. In2018 Fourth International Conference on Advances in Computing, Communication & Automation (ICACCA) 2018 Oct 26 (pp. 1-6). IEEE.

[10] Chen Y, Li Q, Wang H. Towards trusted social networks with blockchain technology. arXiv preprint arXiv:1801.02796. 2018 Jan 9.

[11] Shah SN, inventor; Netspective Communications LLC, assignee. Device-driven non-intermediated blockchain system over a social integrity network. The United States patent application US 15/372,699. 2017 Mar 30.

[12] Alabi K. Digital blockchain networks appear to be following Metcalfe’s Law. Electronic Commerce Research and Applications. 2017 Jul 1;24:23-9.

[13] Chakravorty A, Rong C. U-share: user-controlled social media based on blockchain. InProceedings of the 11th international conference on ubiquitous information management and communication 2017 Jan 5 (p. 99). ACM.

[14] Yahiatene Y, Rachedi A. Towards a blockchain and software-defined vehicular network approaches to secure vehicular social network. In2018 IEEE Conference on Standards for Communications and Networking (CSCN) 2018 Oct 29 (pp. 1-7). IEEE.

[15] Zhu X, Badr Y. Fog Computing Security Architecture for the Internet of Things using Blockchain-based Social Networks. In2018 IEEE International Conference on the Internet of Things (iThings) and IEEE Green Computing and Communications (GreenCom) and IEEE Cyber, Physical and Social Computing (CPSCom) and IEEE Smart Data (SmartData) 2018 Jul 30 (pp. 1361-1366). IEEE.

[16] Buccafurri F, Lax G, Nicolazzo S, Nocera A. Tweetchain: An alternative to blockchain for crowd-based applications. In International Conference on Web Engineering 2017 Jun 5 (pp. 386-393). Springer, Cham.

[17] Song G, Kim S, Hwang H, Lee K. Blockchain-based Notarization for Social Media. In2019 IEEE International Conference on Consumer Electronics (ICCE) 2019 Jan 11 (pp. 1-2). IEEE.

[18] Gomes AJ, Fernandes AM, Leithardt VR. FakeChain: A Blockchain Architecture to Ensure Trust in Social Media Networks. In Quality of Information and Communications Technology: 12th International

Conference, AQUATIC 2019, Ciudad Real, Spain, September 11–13, 2019, Proceedings (p. 105). Springer Nature.

[19] Huckle S, White M. Fake news: a technological approach to proving the origins of content, using blockchains. Big data. 2017 Dec 1;5(4):356-71.

[20] Tee WJ, Murugesan RK. Trust Network, Blockchain and Evolution in Social Media to Build Trust and Prevent Fake News. In2018 Fourth International Conference on Advances in Computing, Communication & Automation (ICACCA) 2018 Oct 26 (pp. 1-6). IEEE.

[21] Paul S, Joy JI, Ahmed S, Sarker S, Das AK. Fake News Detection in Social Media using Blockchain., 2019 7th International Conference on Smart Computing & Communications (ICSCC).

[22] A. Campan, A. Cuzzocrea, and T.M. Truta, “Fighting fake news spread in online social networks: Actual trends and future research directions”, 2017 IEEE International Conference on Big Data (Big Data), 2017.

[23] E. Mustafaraj and P. T. Metaxas, "The Fake News Spreading Plague: Was it Preventable?", Proceedings of the 2017 ACM on Web Science Conference, Troy, New York, USA, 2017.

[24] Singhania S, Fernandez N, Rao S. 3han: A deep neural network for fake news detection. In International Conference on Neural Information Processing 2017 Nov 14 (pp. 572-581). Springer, Cham.

[25] Ahmed H, Traore I, Saad S. Detection of online fake news using N-gram analysis and machine learning techniques. In International Conference on Intelligent, Secure, and Dependable Systems in Distributed and Cloud Environments 2017 Oct 25 (pp. 127-138). Springer, Cham.

[26] Hannah Rashkin, Eunsol Choi, Jin Yea Jang, Svitlana Volkova, Yejin Choi, “Truth of Varying Shades: Analyzing Language in Fake News and Political Fact-Checking” Conference on Empirical Methods in Natural Language Processing, September 7–11, 2017, Copenhagen, Denmark, 2017.

[27] Oshikawa R, Qian J, Wang WY. A survey on natural language processing for fake news detection. arXiv preprint arXiv:1811.00770. 2018 Nov 2.

[28] Gupta A, Kuru P. Credibiliumaragty ranking of tweets during high impact events. InProceedings of the 1st workshop on privacy and security in online social media 2012 Apr 17 (p. 2). Acm.

[29] Melgy A, Ibrahim H, Torky M, “ Recognizing and Stopping Rumors Patterns in Social Networks”, Indian Journal of Science and Technology, 10 (28), 2017.

[30] "Your Guide to Good Journalism-New Trust" (2015),(Online), http://newstrust.net/.(Access, Oct 2019).

[31] J. Gentry "Package Twitter R", [Online] available: http://cran. rproject.org/web/packages/twitterR/twitterR.pdf , 2011, (Access 14 May. 2015).

[32] Xpertin, https://www.xpertin.com/en/pages/how_it_works (Access, 1 Nov. 2019).

[33] Kumar KK, Geethakumari G. Detecting misinformation in online social networks using cognitive psychology. Human-centric Computing and Information Sciences. 2014 Dec;4(1):14.

Predictive Control for Distributed Smart Street Light Network

Pei Zhen Lee[1], Sei Ping Lau[2], Chong Eng Tan[3]
Faculty of Computer Science and Information Technology
University Malaysia Sarawak (UNIMAS)
94300, Kota Samarahan, Sarawak
Malaysia

***Abstract*—With the advent of smart city that embedded with smart technology, namely, smart streetlight, in urban development, the quality of living for citizens has been vastly improved. TALiSMaN is one of the promising smart streetlight schemes to date, however, it possesses certain limitation that led to network congestion and packet dropped during peak road traffic periods. Traffic prediction is vital in network management, especially for real-time decision-making and latency-sensitive application. With that in mind, this paper analyses three real-time short-term traffic prediction models, specifically simple moving average, exponential moving average and weighted moving average to be embedded onto TALiSMaN, that aim to ease network congestion. Additionally, the paper proposes traffic categorisation and packet propagation control mechanism that uses historical road traffic data to manage the network from overload. In this paper, we evaluate the performance of these models with TALiSMaN in simulated environment and compare them with TALiSMaN without traffic prediction model. Overall, weighted moving average showed promising results in reducing the packet dropped while capable of maintaining the usefulness of the streetlight when compared to TALiSMaN scheme, especially during rush hour.**

Keywords—Traffic prediction; adaptive street lighting; smart cities; energy efficient; network congestion

I. Introduction

Street lighting is an essential public service that ensures the road safety for the public during the night [1]. The number of streetlights increased when an area is getting urbanise. Thus, the electricity and energy consumption of street lighting also increased linearly with streetlight. According to [2], this has various impacts such that it has significantly affected the cities' energy use and burden the municipal budgets.

With the notion of Networked Street Lighting, also known as intelligent streetlight system, street lighting can be operated autonomously by observe the changes in surroundings. [3] indicated that intelligent streetlight system can reduce high electricity and energy consumption of traditional streetlights, while ensuring public safety and economic growth.

One way to manage Networked Street Lighting is implementing the Wireless Sensor Networks (WSNs) onto the lamp pole. Application of WSN consists of issues where constant monitoring and manual resolving is impossible. WSN need to be able to adapt the real time network traffic to ensure quality of service and avoid malfunction.

There have been a few attempts on street lighting management, among many of them, distributed Traffic-Aware Street Lighting Scheme Management Network (TALiSMaN) [4] is one of the promising schemes for the adaptive streetlight system. As it is distributed, TALiSMaN performs dynamically and remotely without depending on human intervention. Based on [4], TALiSMaN was equipped with WSNs to improve the efficiency in power consumption and to facilitate network communication among the lamp pole effectively.

TALiSMaN could work well in urban area, but that is not the case for rural areas. Due to poor access to power grid, TALiSMaN-Green [5], which was an improved version of TALiSMaN scheme that made use of green energy to power the streetlights. TALiSMaN-Green aimed to further improve energy consumption efficiency, cost saving and less carbon footprint. TALiSMaN-Green adopted solar panels and battery [5], to ensure the power supplying is ample for the usage until the next daylight, and implements Artificial Intelligence (AI) to predict energy demand and allocate energy accordingly.

On the contrary, the urbanisation process and urban population expansion bring great pressure to the urban traffic management that result in traffic congestion [6]. This is a burden for both TALiSMaN and TALiSMaN-Green as the scheme requires real-time data to transfer among streetlights. Besides, road traffic congestion will lead to network overload, due to constant sensing and broadcasting in both schemes, which prone to network congestion, delay in data transmission, packet lost as well as wastage of energy.

In smart streetlight scheme, even a slight delay is unbearable as operation of networked streetlight is totally dependent on the information exchange between streetlights. Streetlight expects instant lights on before the commuters are approaching. A slight delay of the scheme could lead to streetlight unable to illuminate on time, thus reducing commuters' visibility and perception of safety when in a dark environment. This is crucial as it might affect the utility of TALiSMaN schemes and may cause more harm.

Moreover, when packet dropped increases, streetlight is unable to receive the packet to turn off the light, thus causing drainage of energy and result in performance degradation. The issue of energy wastage is affecting TALiSMaN-Green the most as it only possesses limited energy budget for each sensor node.

Traffic forecasting is crucial for efficient development of road networks [7]. In this study, we enhance TALiSMaN with three moving average computation technique to ease the severity of packet drop and network congestion. The aim of this study is to use road traffic volume predictor to establish a stable connection and efficient throughput to ensure the attainability of streetlight throughout the entire night, thereby achieving streetlight usefulness from evening until the next morning. We evaluate the performance of proposed solution by comparing with the original TALiSMaN scheme using a linear streetlight topology. From the simulation results, the proposed solution reduces packet dropped and maintains the usefulness of TALiSMaN scheme throughout the whole night.

The rest of this paper proceeds with the background study of the previous work on intelligent streetlight and the issues occur. Followed by, the related works on prediction models. Next, a brief description on the main idea and structure of the proposed system. Then, evaluation of proposed system compared with TALiSMaN scheme. Finally, conclude the paper and highlights recommendation for future work.

II. Background

A. TALiSMaN and TALiSMaN-Green

TALiSMaN is a traffic-aware lighting scheme management network that makes use of sensors for autonomous control of the brightness of each streetlight via a distributed network [4]. Instead of depending on a centralised operational control, TALiSMaN is designed to be adaptive to the different behaviours of road users and enable each streetlight to operate independently using a short-range mesh network.

According to [5], 150 meters is the range where optimum lighting condition in the surrounding of a pedestrian should have. For the purpose of efficient energy usage, the light intensity of the streetlight decreases gradually in the range of 150m from every direction (distance between S1 to S5 and S5 to S9) when the sensors detect the presence of pedestrian progress further; while ensures ample of visibility in that environment, as shown in Fig. 1. As for motorists, streetlights within a 100m radius from the detected vehicle are completely turned on, as presented in Fig. 2. Author in [5] claimed that TALiSMaN can reduce energy usage by 45-98% based traffic condition of the road.

In TALiSMaN, consistent delivery of data and network congestion control are necessary to achieve the full potential of TALiSMaN. Since the sensor in TALiSMaN scheme has no knowledge of the travel direction of detected users, all the streetlight will keep on broadcast data to each other under the predefined perimeter via a refined flooding protocol. In other words, if the road user is located at S5 in Fig. 1, the streetlight will start broadcasting data to S4 and S6. If S1 to S9 is within 150m perimeter, then the broadcast will proceed from S4 to S3 and S5, S6 to S5 and S7, and continue the broadcasting until S9 to S8 and S1 to S2. The broadcast of data packet will repeat every 0.5 seconds and stop broadcasting after 15 seconds. When the road user approaching to S6, S5 will still broadcast the same data to other streetlight, and at the same time S6 also starts to broadcast the same data as S5, by means of informing other streetlight the distance of road user and to predefined light intensity based user's distance.

One of the setbacks of TALiSMaN is that it is vulnerable to data transmission delay. In the predefined area, it requires an instant end-to-end transmission to all the streetlights. Fig. 2 can further describe the important of the high precision on data transmission in TALiSMaN. Assume that the distance between streetlight in Fig. 2 is 30m apart from each other, a car is travelling with a constant speed of 40km/h through a 120m of street, TALiSMaN needs to ensure generated data packets takes about 2 seconds to broadcast across the street distance (120m) [8]. The reason is to ensure the streetlights within 100m surrounding the car is turned on when the car is approaching the next streetlight. When streetlight did not turn on before the car arrive, it will reduce the usefulness [5] of the streetlight.

There is another setback during heavy road traffic. During heavy traffic, the WSN prompts to be congested which causes packet loss at the rate of between 23% and 29%. As discussed previously the data broadcast between streetlights is delay sensitive and it might cause TALiSMaN-Green fails to operate until the next day. This is because when sensor node is not receiving packet, the streetlight may remain switch on, which causes overburden of sensor node and resulting in rapid drainage of energy. If the scheme is unable to ensure instant transmission of data to the neighbouring streetlight, it will be dampening the potential and performance of this scheme, and hence resulting in streetlights slow to respond to the road users' movements and less efficiency of energy consumption.

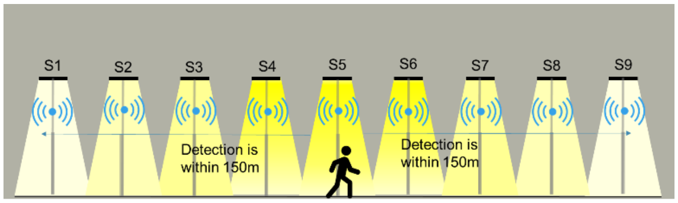

Fig. 1. TALiSMaN Street Lighting Distribution for Pedestrian Adopted from [5].

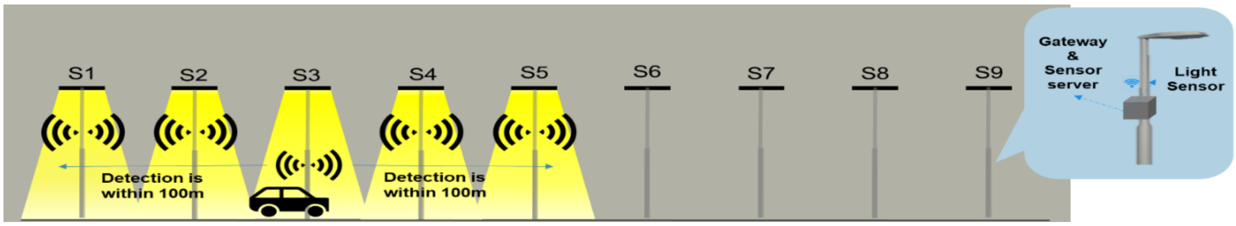

Fig. 2. Street Lighting Distributions for Motorist Adopted in TALiSMaN [4].

B. Related Work on Prediction Model

There have been some attempts on tackling the issue of network congestion, one of the methods is applying the prediction model to forecast the situation of transmission of data in real time of a network, then determine the action to best prevent the happening of network congestion. There comes another challenge in this part which is to perform model selection that best suited for the TALiSMaN scheme since there are so many kinds of the prediction model to opt for. Statistical model and Artificial Intelligence model for traffic forecasting are compared in [9]. This section discusses the various techniques or algorithms of predictions and their respecting use case.

Statistical model such as Auto Regressive Integrated Moving Average (ARIMA) has been quite popular around as a predictive model for various domains, especially transportation research in [10], [11] and [12]. Author in [13] realised the importance of high accuracy in traffic prediction for resource management in cloud computing. ARIMA was apt to predict short term traffic conditions, but in order to gain accurate results it required huge amount of historical data which is not ideal for a limited available memory on a WSN node.

Artificial Intelligent models such as Machine Learning and Deep Learning are some buzzwords these days. Machine Learning is a subset of artificial intelligence that can create and perform algorithm itself without human intervention [14]. Deep learning is a subset of Machine Learning that consist of numerous layers of algorithms, also known as artificial neural networks [15]. Author in [16] proposed a machine-learning technique, namely support vector machine (SVM) [17] to predict vehicle travel times. Author in [18] suggested a neural network incorporate with a fuzzy method to manage non-linear data in traffic data. In 2017, [19] adopted Long Short-Term Memory Neural Network (LSTM) for travel prediction by utilising temporal–spatial correlation techniques through a two-dimensional network. The cost for training these models is computationally expensive, even though frequent updating is being prohibitive [20]. While these approaches can perform well, there is one drawback that is these models are technically difficult to implement on large scale networks.

ARIMA is more advanced version of Statistical Model, it combines the technique of Auto Regression and Moving Average. However, it is not a suitable solution in our study as the computing resource is limited for TALiSMaN-Green that operating with a WSN node. Thus, we argue that the weightage on deciding the prediction model should give to efficiencies over performance. Whereas Artificial Intelligence, other than heavy taxing on computing resource, it is far too complex to implement on TALiSMaN-Green. Thus, this study is more favourable on simpler approach for the prediction model.

III. Proposed Solution

The proposed solution is illustrated in Fig. 3. The purpose of this scheme is to enhance the performance of TALiSMaN by reducing packet drop to ensure the accessibility of streetlight during heavy rush hour, so that streetlight can turn on when it is required. Furthermore, the proposed solution aims to maintain the usefulness of TALiSMaN even after adopting the proposed scheme, as to ensure it can perform in TALiSMaN-Green. Reason is that, with the reduction in duplicate packet broadcast, there are low probability of network congestion and exhaustion of sensor node, thus allow TALiSMaN-Green to reserve ample energy to operate during the next day while maintain the usefulness of TALiSMaN. As mentioned before, due to the challenges of network congestion in TALiSMaN and limited power budget in TALiSMaN-Green, a proper measure must be taken. The following subsections detail the proposed approach to meet these requirements.

Fig. 3 presents the overall idea of the proposed solution. LED is the core component of the TALiSMaN scheme as it is more energy efficient compare to compact fluorescent lamps (CFL) and Incandescent Light Bulbs [21]. It also provides better brightness and have a longer lifespan [22]. Under this scheme, each of the streetlight is powered by electrical grid to ensure sufficient and stable power supply [23], [24]. The backbone of this networked streetlight is powered by WSN, that enable transmission of data for different purposes, such as monitoring, adjusts brightness of LED or merely for notification purpose [4], [5]. TALiSMaN is embedded with AI capability that allows autonomously performance by responding to the type of road users and dynamically adjusts the lighting scheme based on users' proximity.

The prediction model technique (shown in blue colour box in Fig. 3) acts as a place holder that will swap in and out and to find out which prediction model will yield the best result possible. The prediction model consists of three phase, namely forecast phase, detection phase, control phase. This study proposes to use some simple short-term prediction models that are known for consuming less power to perform the computation of the prediction model. The prediction model is used to predict traffic for the next t period and categorise the traffic into light or heavy traffic based on the historical traffic pattern, then control the packet propagation to maintain the usefulness of the existing scheme. When prediction shows the occurrence of heavy traffic during the next t period, the proposed solution will signal the streetlight to remain turn on until the prediction shows light traffic. When prediction shows light traffic for the following t period, the streetlight operation will proceed as predefined in TALiSMaN scheme. Fig. 4 illustrates the workflow of the proposed system.

A. Traffic Prediction Model

The moving average is a smoothing method that estimates future values that heavily depends on the historical data. This study will explore three moving average algorithms to plug and play with the TALiSMaN scheme to determine which is the most power efficient method and yet most effective in reducing the network congestion. These algorithms are Simple Moving Average, Exponential Moving Average and Weighted Moving Average.

Before delving into how these prediction methods implement into TALiSMaN, we need to determine three moving average parameters that include the traffic data at time period t, the lengths of the moving average periods n and the type moving average method from those stated above. We apply root mean square error (RMSE) [25] to evaluate the accuracy of the method to predict road traffic data x_t.

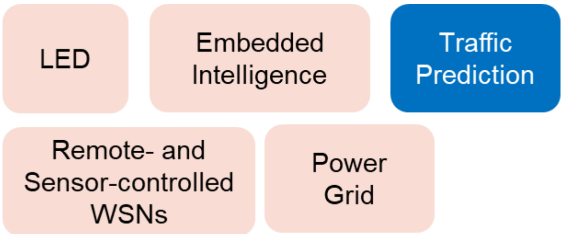

Fig. 3. Components of Refined TALiSMaN.

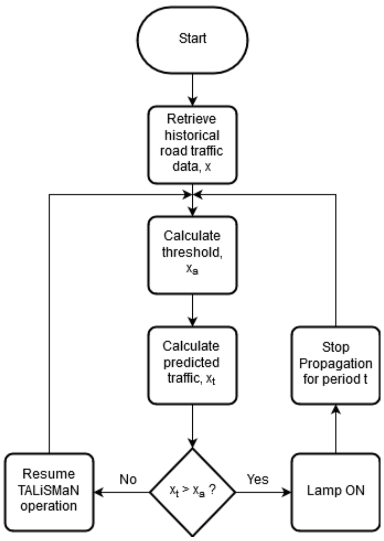

Fig. 4. Workflow of Proposed Syetem.

$$\text{RMSE} = \sqrt{\left(n^{-1}\sum_{i=1}^{n}(x_{f_i} - x_{t_i})^2\right)}, n > i \qquad (1)$$

Where:

x_{f_i} = forecasts traffic value at period t

x_{t_i} = actual traffic value generated by TALSMaN scheme at period t

n = number of periods

The following is an explanation of the steps to obtain those three parameters.

Step 1: (Generation of initial data): Historical traffic data is collected over a time interval from the simulation of TALiSMaN. The simulation is set to run from Monday until Sunday, where streetlights operate from 16:00 to 08:00 the next day, with 3508 [26] road users per day, over a period of 100 weeks. Three datasets are generated, where 10,000 sets of data are for training; 950 datasets each for testing and validation purpose. Note that there is no real data used as the simulated traffic pattern is based on the traffic distribution profile adopted from [27]. The generated road traffic data is adequate and equivalent to real life road traffic scenario, as the car is randomly injected at any point of the road, either moving to the left or right. The car is also randomly added at any time based on the traffic ratio predefined in the road distribution profile for that specific time period.

Step 2: (Aggregation of data); Simulation results are accumulated into weekly format. Since the road traffic profiles indicate perceptible trends throughout the days of week as shown in Fig. 5, thus it is realistic to assume historical traffic data from previous week of the same day and time can provide a more accurate prediction than previous day data. For instance, when predicting for time period 17:00 on Monday, assuming prediction length is two days of week, the prediction calculation should be the generated traffic data for time period 17:00 of Monday from two previous weeks.

Step 3: (Determination of t value): To produce an accurate traffic volume prediction, time period t = {24, 288, 1440} is considered. The time period t = {24, 288, 1440} represent one-hour, five-minutes and one-minute time frame respectively. The equation to calculate the time period is shown below.

$$t = \frac{tal\ hours\ in\ a\ day*3600\ sec}{selected\ time\ period*60\ sec} \qquad (2)$$

Based on Fig. 6, t = 1440 shows the most accurate prediction with the lowest error value, when evaluated with three of the prediction methods.

Step 4: (Determination of n value): Since data aggregation is in weekly format, the moving average prediction length n will represent the number of previous n days. The n value varies from 1 to 50 days, with t = 1440 are evaluated with RMSE for the three prediction methods. From Fig. 7(a), (b) and (c), the RMSE values that has the lowest minimum values of each predictor is chosen as their respective n values. Hence, n = 4 is chosen for three of the predictors as they have the least minimum error.

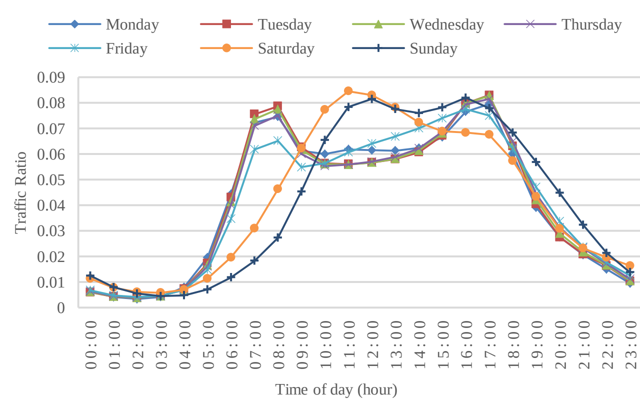

Fig. 5. Road Traffic Distribution Ratio throughout the Week based on [27].

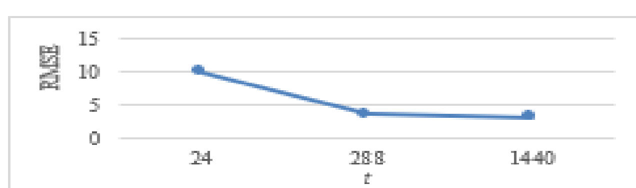

Fig. 6. Average Prediction Error of Predictors with n = 4 Days Against t Values.

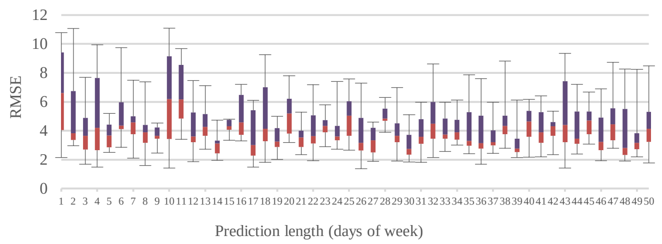

(a) SMA

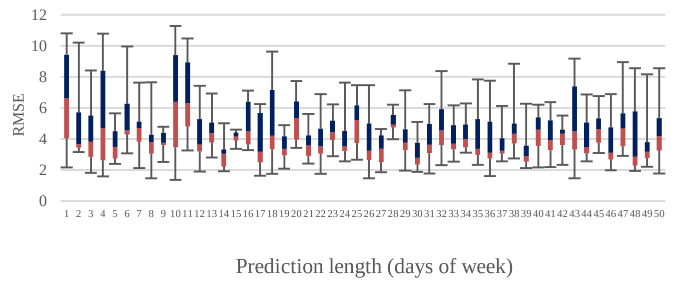

(b) EMA

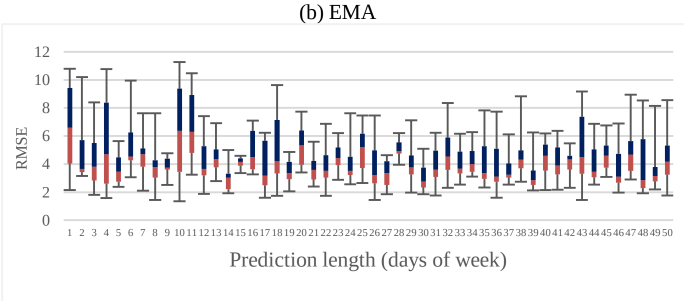

(c) WMA

Fig. 7. The Interquartile Ranges of RMSE Result for different Predictors at different Prediction Length, n Values. The Error bars Indicate the Minimum and Maximum of MAE values.

Step 5: (Determination of prediction model): In this step, three of the prediction methods are simulated and tested with $t = 1440$ and $n = 4$ at traffic volume of 3508. To illustrate, the scheme initially divides the total time in a day into t equal size timeslot that is in every one-minute traffic predictor predict traffic volume for the future timeslot (next one-minute) while collecting actual traffic one second after the previous timeslot. Thus, the calculation for each predictor is derived in the subsection below. Before delving into which prediction methods is more suitable to implement into TALiSMaN, some brief description is made on each of the algorithms.

1) Simple moving average: There are many variants of the moving average method, Simple Moving Average (SMA) as the name of method is the simplest method to construct among them. As shown in the formula (3), the calculation of SMA is by taking the average of traffic volume data x_t at period t for previous n days of week. Since mentioned above $t = 1440$ and $n = 4$, in order to calculate SMA at timeslot 196, the x_{196} from previous four days are used for obtaining the average value.

$$SMA_t = \frac{x_t + x_{t-1} + \ldots + x_{t-(n-1)}}{n}$$
$$= n^{-1} \sum_{i=0}^{n-1} (x_{t-i}), \; n > i \quad (3)$$

Where:

x_t = road traffic volume at time period t

n = number of days of week

2) Exponential moving average: The main difference between Exponential Moving Average (EMA) and SMA is the sensitivity towards variation in the most current data during calculation [28]. Based on the equation, the weighting factor decreases for older historical traffic data while provide more weightage towards recent traffic data to accurately predict the traffic trend. The accuracy of EMA relies on the smoothing factor of the recent data and the prediction length [29]. As when prediction length is longer, the lesser the weightage value causing it to be insignificance towards change.

$$EMA_t = a * x_t + (1 - a) * EMA_{t-1} \quad (4)$$

Where:

$a = \frac{2}{1+n}$ [29]

x_t = road traffic volume at time period t

n = number of days of week

EMA_{t-1} = Forecast of past time period road traffic volume

3) Weighted moving average: Like EMA, Weighted Moving Average (WMA) applies less weight on the past data while more on the current data. This is due to the calculation of multiplying each current value by a weighting factor as follows:

$$WMA_t = \frac{\sum_{i=0}^{n-1} (n-i)\, x_{t-i}}{a}, \; n > i \quad (5)$$

Where:

$$a = n * \frac{1+n}{2}$$

x_t = road traffic volume at time period t

n = number of days of week

B. Congestion Detection based on Traffic Pattern

Every sensor node will store up to a month of historical road traffic data and will undergo categorisation before proceeding with prediction process. The categorisation of predicted traffic data will utilise the road traffic threshold value as a metric to determine the congestion situation. The calculation for road traffic threshold value (assume is x_a) is compute using the average value of the road traffic data on a specific day from previous week.

For instance, the first step is determining the operating hours of streetlight in a day then perform data collection. Typically, the operation hour of a streetlight in a day starts from 12am until 8am, then 4pm until 11pm, as shown in Fig. 8 The traffic threshold value is obtained by taking the average value of the road traffic data in Fig. 8, where x_a is 107 vehicles. After the prediction is performed, the prediction result at time period t (assume is x_f) will be compared with the average value obtained previously (which is 107 as mentioned above). Predicted traffic data greater than the threshold value (i.e. $x_f > 107$) is categorise as congested, while predicted data lesser than threshold value ($x_f < 107$) is categorise as non-congested period.

$$x_a = \frac{\sum_{i=1}^{n} x_{t_i}}{n}, n > i \quad (6)$$

Where:

x_a = road traffic threshold value for a day

x_t = road traffic volume at time period t

n = number of time periods

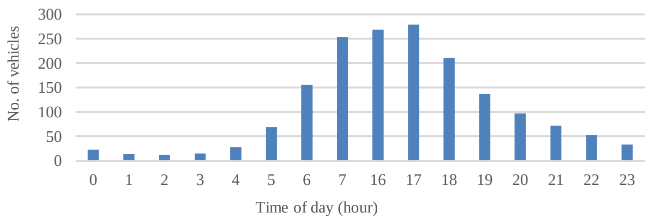

Fig. 8. The Simulation Results of Monday Vehicle Distribution Generated by StreetlightSim with 3508 Road users Per Day.

C. Congestion Control Strategy

The prediction models will be applied to TALiSMaN after obtaining prediction value to determine the action for the next period t (i.e. one-minute). If the result of prediction x_t indicates there is going to have a congestion for a certain amount of time t, then TALiSMaN will stop the broadcasting of data among streetlight, while the streetlight remains turned on at time t. To illustrate, if prediction results indicate there will be heavy traffic from 4.00pm to 4.05pm, then TALiSMaN will stop the packet propagation of every sensor node and keep the streetlight on for one-minute. On the other hand, if there is no congestion, then packet propagation will proceed as intended in TALiSMaN.

IV. Result Analysis and Discussion

This study proposed prediction model to determine the heavy traffic congestion period that affects the packet dropped rate, and provide control measures to reduce packet dropped, while ensure attainability of streetlight. By predicting the future traffic volume at time period *t*, it is possible to reduce packet dropped through traffic condition detector and packet propagation controller. The proposed scheme implemented with each of the prediction model is analysed and discussed based on the comparison with TALiSMaN. This section will also describe the simulation tools, configuration, assumptions and evaluation parameters.

A. Simulation Setup

The proposed scheme is implemented in StreetlightSim. StreetlightSim is an open-source simulation environment that is used to implement TALiSMaN as well as TALiSMaN-Green [26]. The simulation environment utilised both OMNeT++ and SUMO tools, to represent all the performance and operation of streetlights, such as traffic detection, traffic pattern generation, and evaluation of the practicality of the TALiSMaN and TALiSMaN-Green schemes through the perspective of road user. The following parameters were used:

- Streetlights apply a linear streetlight topology in a residential area.
- The topology consists of 12 streetlights assign across the road of 360m wide, shown in Fig. 9.
- Streetlights operate from 16:00 until the next day 08:00, to represent the streetlight operational hours in real life.
- The total road traffic is set to 3508 vehicles per day [26].
- The road traffic users will be added randomly into the simulation at any point of the road and anytme based on the traffic pattern predefined in the traffic distribution profile obtained from Southampton City Council [27].
- The simulation is run for 100 days.
- The t (time period) is set to 1440, representing 1440s (i.e. 1 minutes).
- The n (prediction length) is 4 days of week for every predictors.

B. Evauation Parameters

In this paper, the performance of proposed solution is evaluated in terms of Packet Dropped Ratio (PDR), Total Utility (TU) and Total Energy Consumption (TEC) as to demonstrate the effectiveness of real-time short-term traffic prediction in adaptive streetlighting.

PDR is chosen as the parameter as it shows the number of packets that are dropped during data transmission among streetlights. Furthermore, PDR can be used to identify problems that might lead to poor throughput or poor load distribution.

TU represents the measurement of the usefulness of streetlighting to road users obtained using utility model [29]. The usefulness model can be used as a parameter to determine the correctness, competence and impact of the proposed scheme towards existing scheme.

TEC refers to the total energy consumed by a streetlight in a day. As mentioned above, energy constraint is one of the factors affecting the performance of TALiSMaN that occurs when implement with the off-grid power supply. Since the battery used in off-grid scheme is very bulky and heavy to carry around, it is not feasible to constantly replace the batteries once it fails. It is crucial to extend the network lifetime as to ensure TALiSMaN scheme can perform effectively.

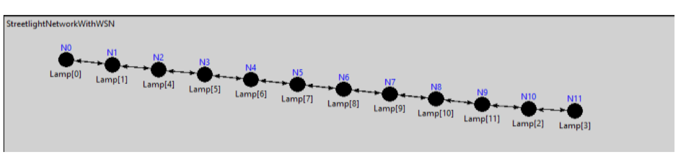

Fig. 9. A Linear Topology Set up with Twelve Streetlights.

C. Analysis and Discussion of Simulation Result

Fig. 10 shows the interquartile ranges of packet dropped ratio for TALiSMaN with and without prediction generated throughout the night. The simulation results shown below incorporate with all the above-mentioned prediction parameters, which include the traffic volume of 3508, t value of 1440 and n equals to 4. Through observation, the SMA, EMA and WMA successfully reduce the packet drop of TALiSMaN scheme, with the range of 71.2% to 74.6%, 75.4% to 75.7% and 71.2% to 74.6% respectively. Without the traffic prediction, TALiSMaN has experienced a consistent packet dropping ratio, ranging between 636 to 680. Based on the simulation results, SMA and WMA have similar result, while EMA shows a slightly higher reduction in packet drop compare to SMA and WMA. This indicates that EMA is a better predictor in reducing packet dropped for TALiSMaN scheme.

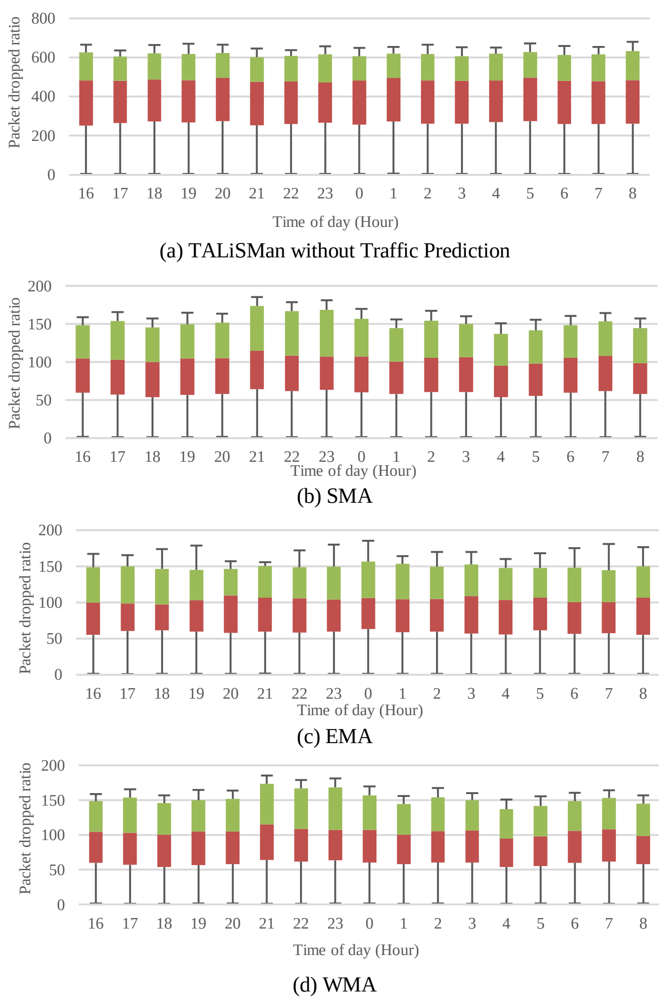

Fig. 10. Average Packet Dropped Throughout the Operation Hour of the Streetlight between 16:00 to 08:00 the following Day. The Error bars Indicate the Minimum and Maximum Values of the Packet Dropped Ratio.

Fig. 11 shows the usefulness the application of the SMA, EMA and WMA in TALiSMaN scheme throughout the simulation days. It clearly shows that WMA provide consistent usefulness throughout the operation which is the highest among all scheme. Whereas SMA achieves the least usefulness, by dropping onto 0.6 on the 16th day and produce consistent usefulness throughout the operation days. TALiSMaN and EMA produce similar result throughout the simulation.

Fig. 12 illustrated the average energy usage in a day. Based on observation, all three predictors consume more energy than TALiSMaN because more energy is consumed to turn on the streetlight in full brightness when prediction indicates congested traffic condition. Overall, SMA consumed the most energy, whereas the energy consumption of EMA and WMA is nearly equal.

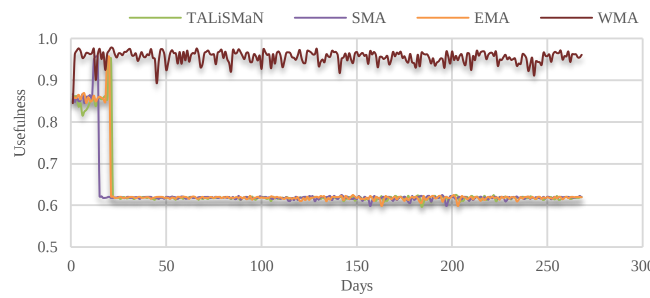

Fig. 11. Total usefulness Produced when Implemented with different Scheme at different Simulation Days.

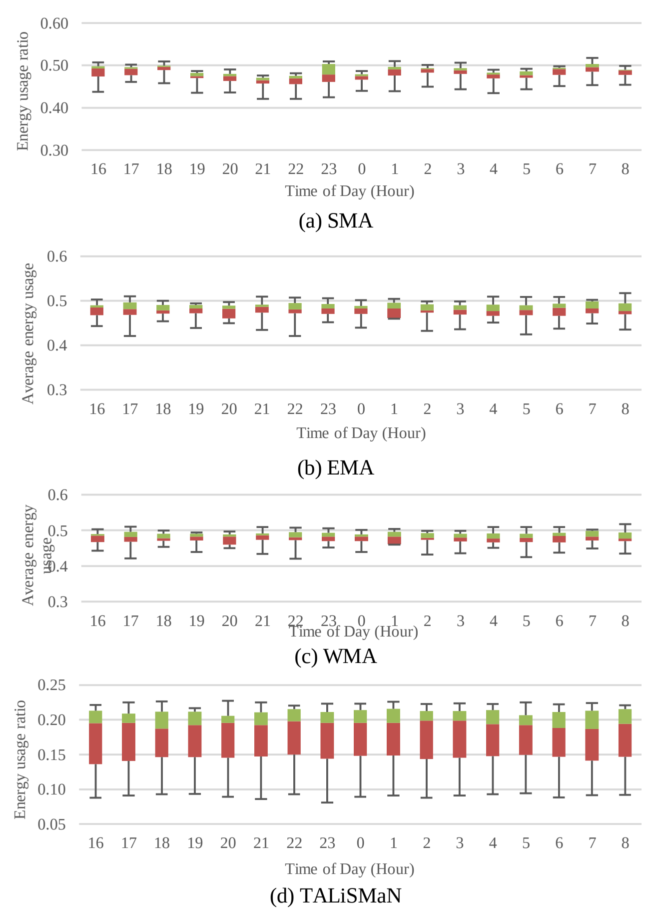

Fig. 12. Average Energy usage Throughout the Operation Hour of Streetlight from 16:00 to 08:00 the following Day. The Error Bars Indicate the Minimum and Maximum Values of the Energy Consumed.

V. Conclusion

The issue of network congestion in networked streetlighting system causes an increase in packet drop and network latency. Consequently, the streetlight is unable to utilise the full potential of TALiSMaN scheme if it fails or late to receive the signal to switch on or off. A streetlight is practically useless when it is unable to switch on in the dark. Contrary, streetlight continuously turn on throughout the night can cause excessive drainage of energy and prompt to operational failure. In order to tackle this issue in the networked streetlight system, a non-heavy computation prediction model to mitigate network congestion and packet dropped is adopted.

This study proposed and implemented three real-time short-term predictions for TALiSMaN, an adaptive networked streetlighting system. These techniques utilise the historical traffic data, first to obtain the threshold value to detect the congestion condition, second, is to forecast periodic traffic volume. The forecast results are then used for signalling the streetlight to adjust the lighting, sensing and broadcasting operation to manage the congestion. The performance and analysis of TALiSMaN implemented with SMA, EMA, and WMA is measured and compared using packet dropped and energy efficiency.

VI. Future Work

In the future work, it can be continuing with other more advanced short-term prediction method, potentially ARIMA, one thing to note that power consumption should keep in mind when selecting the method for future work. The performance of the scheme can be further enhanced by undergoing more tests on different structure of road and different time frame.

References

[1] N. R. Velaga and A. Kumar, "Techno-economic evaluation of the feasibility of a smart street light system: a case study of rural India," Procedia-Social and Behavioral Sciences, vol. 62, pp. 1220-1224, 2012.

[2] S. A. E. Mohamed, "Smart street lighting control and monitoring system for electrical power saving by using VANET," International Journal of Communications, Network and System Sciences,vol.6,no.8,p.351, 2013.

[3] F. Marino, F. Leccese and S. Pizzuti, "Adaptive street lighting predictive control," Energy Procedia, vol. 111, pp. 790-799, 2017.

[4] S. P. Lau, G. V. Merrett and N. M. White, "Energy-efficient street lighting through embedded adaptive intelligence," in 2013 International Conference on Advanced Logistics and Transport, 2013.

[5] S. P. Lau, A. S. Weddell, G. V. Merrett and N. M. White, "Energy-neutral solar-powered street lighting with predictive and adaptive behaviour," in Proceedings of the 2nd International Workshop on Energy Neutral Sensing Systems, 2014.

[6] Z. Diao , D. Zhang, X. Wang, M. IEEE, K. Xie, S. He, X. Lu and Y. Li, "A Hybrid Model For Short-Term Traffic Volume Prediction In Massive Transportation Systems," IEEE Transactions on Intelligent Transportation Systems, vol. 20, no. 3, pp. 935 - 946, 2018.

[7] A. Singh, S. Ahamd, R. Singh, Ranjeet and R. Dubey, "Traffic Forecasting," International Journal of Scientific Research and Review , vol. 7, no. 3, pp. 1565-1568, 2019.

[8] S. P. Lau, A. S. Weddell, N. M. White and G. V. Merrett, "Poster: Solar-Powered Adaptive Street Lighting Evaluated with Real Traffic and Sunlight Data," in Proceedings of the 13th ACM Conference on Embedded Networked Sensor Systems, 2015.

[9] M. G. Karlaftis and E. I. Vlahogianni, "Statistical methods versus neural networks in transportation research: Differences, similarities and some insights," Transportation Research Part C: Emerging Technologies, vol. 19, no. 3, pp. 387-399, 2011.

[10] K. Kumar, M. Parida and V. K. Katiyar, "Short term traffic flow prediction for a non urban highway using artificial neural network," Procedia-Social and Behavioral Sciences, vol. 104, pp. 755-764, 2013.

[11] A. Das, S. Barua and K. C. Roy, " Estimation of traffic arrival pattern at signalized intersection using ARIMA model," International Journal of Computer Applications, vol. 128, no. 1, pp. 1-6, 2015.

[12] B. Moghimi, A. Safikhani, C. Kamga and W. Hao, "Cycle-length prediction in actuated traffic-signal control using ARIMA model," Journal of Computing in Civil Engineering, vol. 32, no. 2, p. 04017083, 2017.

[13] H. Mehdi, Z. Pooranian and P. G. Vinueza Naranjo, "Cloud traffic prediction based on fuzzy ARIMA model with low dependence on historical data," Transactions on Emerging Telecommunications Technologies, p. e3731, 2019.

[14] F. Jiang, Y. Jiang, H. Zhi, Y. Dong, H. Li, S. Ma, Y. Wang, Q. Dong, H. Shen and Y. Wang, "Artificial intelligence in healthcare: past, present and future," Stroke and vascular neurology, vol. 2, no. 4, pp. 230-243, 2017.

[15] A. B. Levine, C. Schlosser, J. Grewal, R. Coope, S. J. Jones and S. Yip, "Rise of the machines: Advances in deep learning for cancer diagnosis," Trends in cancer, vol. 5, no. 3, pp. 157-169, 2019.

[16] C. H. Wu, J. M. Ho and D. T. & Lee, "Travel-time prediction with support vector regression," IEEE transactions on intelligent transportation systems, vol. 5, no. 4, pp. 276-281, 2004.

[17] N. G. Polson and S. L. Scott, "Data augmentation for support vector machines," Bayesian Analysis, vol. 6, no. 1, pp. 1-23, 2011.

[18] C. Quek, M. Pasquier and B. B. S. Lim, "POP-TRAFFIC: A novel fuzzy neural approach to road traffic analysis and prediction," IEEE transactions on intelligent transportation systems, vol. 7, no. 2, pp. 133-146, 2006.

[19] Z. Zhao, W. Chen, X. Wu, P. C. Y. Chen and J. Liu, "LSTM network: a deep learning approach for short-term traffic forecast," IET Intelligent Transport Systems, vol. 11, no. 2, pp. 68-75, 2017.

[20] Y. Kamarianakis, W. Shen and L. Wynter, "Real-time road traffic forecasting using regime-switching space-time models and adaptive LASSO," Applied stochastic models in business and industry, vol. 28, no. 4, pp. 297-315, 2012.

[21] F. G. Montoya, A. Peña-García, A. Juaidi and F. Manzano-Agugliaro, "Indoor lighting techniques: An overview of evolution and new trends for energy saving," Energy and buildings, vol. 140, pp. 50-60, 2017.

[22] M. S. Islam, N. A. Chowdhury, A. K. Sakil, A. Khandakar, A. Iqbal and H. Abu-Rub, "Power quality effect of using incandescent, fluorescent, CFL and LED lamps on utility grid," in 2015 First Workshop on Smart Grid and Renewable Energy (SGRE), Doha, 2015.

[23] P. Nikolaidis and A. Poullikkas, "Cost metrics of electrical energy storage technologies in potential power system operations," Sustainable Energy Technologies and Assessments, vol. 25, pp. 43-59, 2018.

[24] P. T. Krein and M. A. Fasugba, "Vehicle-to-grid power system services with electric and plug-in vehicles based on flexibility in unidirectional charging," CES Transactions on Electrical Machines and Systems, vol. 1, no. 1, pp. 26-36, 2017.

[25] T. Chai and R. R. Draxler, "Root mean square error (RMSE) or mean absolute error (MAE)?–Arguments against avoiding RMSE in the literature," Geoscientific model development, vol. 7, no. 3, pp. 1247-1250, 2014.

[26] S. P. Lau, G. V. Merrett, A. S. Weddell and N. M. White, "StreetlightSim: A simulation environment to evaluate networked and adaptive street lighting.," in 2014 IEEE Asia Pacific Conference on Wireless and Mobile, 2014.

[27] European Platform on Mobility Management, "TEMS - The EPOMM Modal Split Tool," [Online]. Available: http://www.epomm.eu/tems. [Accessed 4 July 2013].

[28] J. Raiyn and T. Toledo, "Real-time short-term forecasting based on information management," Journal of Transportation Technologies, vol. 4, no. 1, p. 11, 2014.

[29] "Moving Averages - Simple and Exponential," [Online]. Available: https://school.stockcharts.com/doku.php?id=technical_indicators:moving_averages. [Accessed 23 12 2019].

Developing a Framework for Potential Candidate Selection

Farzana Yasmin[1], Mohammad Imtiaz Nur[2], Mohammad Shamsul Arefin[3]
Computer Science and Engineering, Chittagong University of Engineering and Technology
Chattogram, Bangladesh

***Abstract*—Recruitment is the process of hiring the right person for the right job. In the current competitive world, recruiting the right person from thousands of applicants is a tedious work. In addition, analyzing these huge numbers of applications manually might result into biased and erroneous output which may eventually cause problems for the companies. If these pools of resumes can be analyzed automatically and presented to the employers in a systematic way for choosing the appropriate person for their company, it may help the applicants and the employers as well. So in order to solve this need, we have developed a framework that takes the resume of the candidates, pull out information from them by recognizing the named entities using machine learning and score the applicants according to some predefined rules and employer requirements. Furthermore, employers can select the best suited candidates for their jobs from these scores by using skyline filtering.**

Keywords—Information extraction; named entity recognition; machine learning; skyline queries

I. Introduction

Information extraction (IE) infers the process of automatically gisting of information in a strucutred way from unstructured and/or semi-structured machine-readable documents. The task involves the utilization of natural language processing (NLP). The present purpose of IE refers to the growing amount of information available in unstructured form [1].

Nowadays huge volume of documents are found online and offline. Extracting information from these vast volumes of data manually is time consuming. Moreover generating some pattern from the extracted information has recently been a new challenge and prime concern of the modern technological era.

Recruitment is the process of searching and selecting best candidates for filling the vacant positions of an organization. Recruitment process requires planning, requirements setup strategy, searching candidates, screening the candidates according to the requirements and evaluation of the candidates. These steps are usually conducted by the Human Resource (HR) department of any company. Whenever there is a job opening for the vacant positions, large amount of applications are dropped. On the other hand, the recruiters may search applicants from a job portal placing their requirements. In both cases, searching and screening the best candidates from these applicants after assessing the ablites and qualifications manually, takes huge amount of time, cost and effort of the HR department as the volume of data are big. If we can develop an efficient system for extracting information from the resumes and process these information in an automated way so that only the relevant applications are presented to the recruiters, it will ease the work of the HR management. An automated system for choosing the potential candidates that best suits the position’s requirements can increase the efficiency of the HR agencies greatly.

Therefore, in order to make the recruitment process easy, effective and automated, we have developed a framework of potential candidate selection system. To perform this task we have chosen a domain of document information extraction which can be helpful in choosing the best potential candidates for any job openings i.e. CV/resume document. This development task involves the information extraction based on natural language processing i.e. tokenization, parsing, named entity recognizer (NER) and utilizes skyline query processing which works well in filtering the non-dominating objects from database and also makes a new addition to this domain.

So the objectives of the system development can be summerized as follows: 1) To design an efficient information extraction system from documents like curriculum vitae, 2) To generate scores on different features based on extracted information, 3) To perform appropriate filtering of information using skyline queries and 4) To generate proper ranking system for candidate selection.

The rest of the paper is presented as follows: In Section II related works of the candidate ranking system development has been portrayed. The system architecture and design is elaborated in Section III. Section IV represents the implementation of our work with some experimental results. And finally, a conclusion over the work has been drawn in Section V.

II. Related Work

D. Celik [2] proposed an information extraction system for candidate selection where the information extraction was based on ontology. The proposed methodology used Ontology-based Resume Parser(ORP) to convert English and Turkish documents into ontological format. The proposed method constructed seven reference ontologies to extract the information and categorize them into one of these ontologies. Though the methodology worked good on information extraction but it did not describe any score generation mechanism to rank the candidates.

Another form of candidate selection was proposed by S. Kumari et. al. [3] where candidate selection was done by using

Naïve Bayes algorithm for classifying the candidate profiles. They also considered employers importance criteria. No description given of how the information extraction are done. Also it requires GPRS connection every time as it is online based.

R. Farkas et al. [4] worked on a method of extracting information for career portal where the information of applicants' are stored in a uniform data structure named HR-XML format. They used a CV parser to automatically extract data from the CV. It is basically template specific method and doesn't work for all formats of documents.

In [5], the authors used a hybrid cascade model for information extraction from CVs. In the first pass, the proposed method segments resume using Hidden Markov Model. The second pass uses HMM and SVM to extract further detailed information. The cascaded pipeline suffers from error propagation i.e. errors from first step are passed in the second pass and the precision and recall value decreases subsequently.

Information is extracted from resumes using basic techniques of NLP like word parsing, chunking, reg ex parser in [6]. Information like name, email, phone, address, education qualification and experience are extracted using pattern matching in this work. Some other online resume parsers are found in [7] & [8].

An algorithm for CV information extraction is developed in [9] which works in two step. In the first step, raw texts are retrieved as resume blocks. Then in the next step they developed a mechanism to identify the fact information from the resume like named entities.

There also have been developed some works using skyline queries. [10], [11] & [12] describes some algorithms for processing skyline queries with their implementation.

S. Patil et al. [13] developed a method for learning to rank resumes with the help of SVM rank algorithm. In [14], X. Yi et. al. applied a Structured Relevance Model to select resumes for a given post or to choose the best jobs for a given candidate based on their CV. İn [15] job narration are transformed into queries and lookup in database is performed. The top-ranked candidates get selected automatically from these queries. Some authors exploit additional information like social media information along with information gained directly from resumes [16]. Moreover, [17] takes consideration of data collected from the LinkedIn profile and personality traits from the personal blogs of the candidates. In [18], digital resumes of candidates are generated by extracting data from social networking sites like Facebook, Twitter and LinkedIn. Candidates are evaluated based on their digital resume and ranked accordingly. In [19], CVs are filled in a predefined format and the scoring and ranking process is based on Analytic Hierarchy Process (AHP).

Though many works have been developed for candidate recruitment, the use of skyline query in this sceneraio is relatively new approach and we have implemented this novel approach in our framework.

III. System Architecture and Design

The proposed framework works in 4 modules according to Fig. 1: Document processing module, Query Execution Module, Analysis & Output module and Storage module.

A. Processing Module

1) CV upload: First, the candidates may upload their resumes in the interface. After resumes are uploaded to the system it is considered as input for the processing module.Then information extraction process begins and we used a NLP module named spaCy [20] for the rest of the processing steps. Suppose, sample resumes as Fig. 2(a), (b) and (c) are uploaded in the system.

2) Conversion to text: The standard format of resumes for our system is considered english resumes in PDF format. At first, we need to convert the pdf into plain text using UTF-8 encoding. From [21], UTF stands for Unicode Transformation Format and '8' means it uses 8-bit blocks to represent a character. The number of blocks needed to represent a character varies from 1 to 4. UTF-8 is a compromise character encoding that can be as compact as ASCII but can also contain any Unicode characters.

3) Tokenization: After conversion to text, now we have our necessary text file. We start reading the text file and tokenize the whole document. Tokenization is the process of splitting a document into its smallest meaningful pieces named tokens. Tokenization is done using the language rule i.e. removing the white space, checking the exception rules like punctuation checking, abbreviation rules, etc.

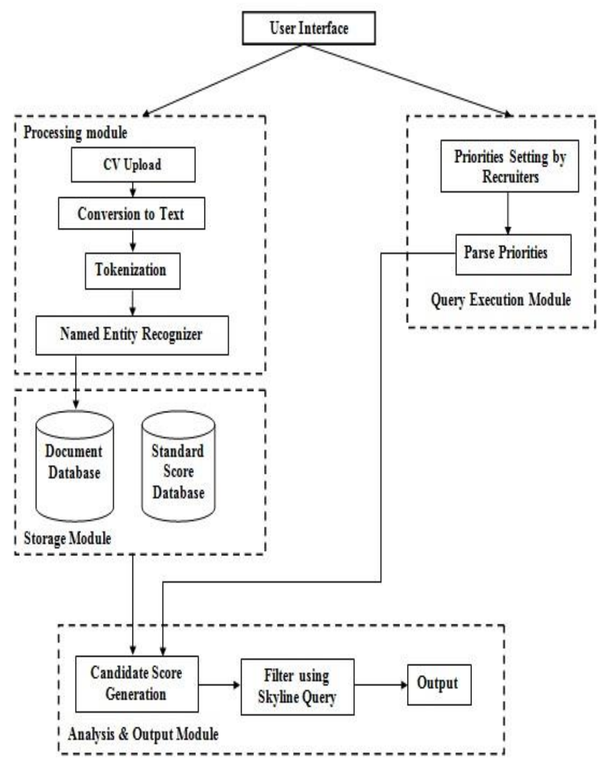

Fig. 1. System Architecture of Potential Candidate Selection System.

Adam Wang (Male)

XXXX Company of Bejing,
Beijing City, 100007
1364-110-XXX
wangXXX@hotmail.com

Education Background
From Sept. 2000 to Apr. 2003, I got master degree from University of XXX in computer software engineering.
From Sept. 1996 to July. 2000, I got bachelor degree from School of XXX and major in computer science and technology.

Experience
From March 2003 to now, working on Human Face Recognition System in XXXX Company of Beijing
From June 2001 to March 2003, working on Content-Based Intelligent Image Retrieval System in Research Center of XXX Company
From Sept. 2000 to May 2001, working on Intelligent Highway Distress Detection System in National Lab. Of XXX University

Interests
Reading, music, and jogging

(a)

ABC

Cell: +880 1680671851
E-mail: abc@gmail.com,

RESEARCH INTEREST
Data Mining, Artificial Intelligence, Machine Learning, Algorithm Design, Data Structure.
EDUCATIONAL QUALIFICATIONS
- **B.Sc. in CSE**- October 2015
CUET, Bangladesh.
Result: CGPA 3.81 (out of 4.00)
Class Position: 2nd out of 113 students
WORK EXPERIENCES
- **Chittagong University of Engineering & Technology, Chittagong-4349, Bangladesh**
  - Joined as ***"Lecturer"*** as on 2016
  - Duration : 2016- Present

(b)

Ishraq Rayeed Ahmed
+880 1717 342569, ishraqrayeed@gmail.com,
www.irahmed.wordpress.com
Research Interests
Pavement Materials and Design, Urban and Public Transportation System, Traffic Emissions and Air Quality, Transportation Safety, Intelligent Transportation System
Education
Bachelor of Science, Civil Engineering, March 2016
BUET at Dhaka, Bangladesh
CGPA: 3.24/4.00
Technical Skills
Scientific Computing & Simulation Tools: MATLAB, R Project, ArcGIS, VisSim, EPAnet
Structural Design Software: AutoCAD, SAP, ETABS, GRASP
Programming Languages: C++, Python
Graphics Design Software: Adobe Photoshop, Adobe Illustrator, 3D Studio Max
Publications
- Ahmed, I.R; Mondal, A.R; Noor, A.U, *"Assessment Of Pedestrian Perception Towards Pedestrian Crossing Facilities In Dhaka Metropolitan City: A Study Based On Observation and Survey"*, (IICSD-2015), DUET, Dhaka.

(c)

Fig. 2. (a), (b) and (c) Sample Resumes.

4) Named entity recognition: Named entity recognition (NER) is the most important task to do next. The success of the extraction process mainly depends on the accurately recognized entities from a resume. The subtask of information extraction that seeks to locate and classify named entity mentions in unstructured text into pre-defined categories such as the person names, organizations, email, phone, address, time, quantities, numeric values, etc. can be defined as Named entity recognition [22]. A statistical model is used to classify our desired entities in a standard resume like name, date of birth, email, phone number, university, education, major, publications, experience, skills, etc. The NER training model is designed using incremental parsing and residual CNNs. In case of training our model (Fig. 3) with the desired annotation we used resumes in JSON format.

The adapted algorithm of spaCy's NER training module is provided below:

Algorithm 1: Named Entity Recognition Training
Input: Tokens of the resumes
Goal: To identify the named entities required for information extraction

1. **Begin**
2. Annotate the training data manually
3. Initialize the annotated model, no. of iterations, output directory path
4. **If** model not loaded **do**
5.   Load the initialized model
6. **End if**
7. **If** ner pipeline is not set **do**
8.   Create *ner pipe*
9.   Add the *ner pipe*
10. **Else** get *ner pipe*
11. **For** *annotations* in training data **do**
12.   **For** *entities* in *annotations* **do**
13.   Add *labels* of *entities*
14.   **End for**
15. **End for**
16. Disabling other pipeline, begin the training
17. **For** iterations in range **do**
18.   Shuffle the examples in batches
19.   For each example update the model
20. **End for**
21. Save the model in the output directory
22. Test the model with the test data

At first, we have to manually annotate our training data in JSON format (2). Then we load or build the NER model (step 4-6). For training the NER model with our custom entities, now we add the labels for each annotations (step 11-15). For starting the training of our NER model, we must disable other pipeline components like tokenizer, tagger of spaCy (step 16). Then we shuffle and loop over our training examples (step 18). At each word the model makes a prediction. It then consults the annotations to see whether it was right. If it was wrong, it makes adjustment of the weight so that the correct action will score higher next time (step 19). Then we save the model (step 21) and test it to make sure the entities in the test data are recognized correctly (step 22).

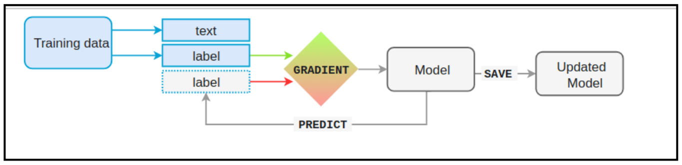

Fig. 3. SpaCy's NER Model Training Process (Source: [23]).

After the validation of the training of the NER model, now we use this model to extract the values of the entities from the resumes as blocks. The recognized entity values are stored block-wise in a row of a table for each candidate in the storage module. If we send the resumes in the NER model, the table of the extracted information takes the form like Table I, Table II, Table III, Table IV and Table V.

B. Storage Module

Storage module stores information processed by the processing module. The extracted information table after the entites are recognized are stored in the document database. We set the scores for different criterias based on some predefined hypothetical rules. The total storage is required for the candidate score generation in the analysis and output generation phase. The rules and scores that are set as lookup tables (Tables VI and VII) in the score database are given.

Rule for Experience:

If (*Designation==Required experience designation*)
If (*Experience == Required position experience*)
Score[Experience] = 5
Else
If (*Total Experience* ≥ *Required experience*)
Score[Experience] = 2
Else *Score*[Experience] = 0}

Rule for Skills:

If (Candidate_skill== Required skill)
Score[skill]= *Score*[skill]+ 1
Else *Score*[skill] = 0

Rule for Certification:

If (Candidate_certification== Required certification)
Score[Certification]= Score[Certification]+ 1
Else *Score*[Certification] = 0

TABLE. I. EXTRACTED INFORMATION OF PERSONAL INFORMATION BLOCK

Name	Phone	Email	Date of Birth
Farzana Yasmin	01680671851	farzanaefu@gmail.com	30 Sep 1993
Mohammad Imtiaz Nur	01818772617	imti.nur@gmail.com	07-09-1992
Ohidul Islam	01617224955	ohid@gmail.com	14-12-1989
Faisal Karim	01826564578	faisal90@outlook.com	13.05.1994
Md. Intishar ur	01747678878	intishar788@gmail.com	6/1/1983
Ananna Das	01918793180	anannadas@yahoo.com	5-23-1987
Hasibul Haq	01922935210	h.haq602@yahoo.com	3 April 1990

TABLE. II. EXTRACTED INFORMATION OF EDUCATIONAL INFORMATION BLOCK

Name	Degree	Major	Institution	CGPA
Farzana Yasmin	B.Sc	CSE	Chittagong University of Engineering & Technology	3.81
Mohammad Imtiaz Nur	Bachelor in Science	CSE	CUET	3.01
Ohidul Islam	B.Sc., M.Sc.	Electrical Engineering	BUET, Jahangirnagar University	3.72,3.96
Faisal Karim	B.Sc., PhD	CSE	Chittagong University, University of Houston	3.50
Md. Intishar Nur	Bachelor in Science	Computer Science	IUT	3.46
Ananna Das	LLB	Law	Premier University	3.22
Hasibul Haq	Bachelor in Business Administration	Finance	IIUC	2.90

TABLE. III. EXTRACTED INFORMATION OF PUBLICATION BLOCK

Name	Publication
Farzana Yasmin	International Journal, International Conference
Mohammad Imtiaz Nur	--
Ohidul Islam	International Conference
Faisal Karim	International Journal, International Journal, International Journal, International Conference
Md. Intishar Nur	--
Ananna Das	--
Hasibul Haq	--

TABLE. IV. EXTRACTED INFORMATION OF EXPERIENCE BLOCK

Name	Company Worked at	Experience	Designation
Farzana Yasmin	CUET	3 yrs	Lecturer
Mohammad Imtiaz Nur	SAPL	2 yrs	Executive Programmer
Ohidul Islam	PDB	7 yrs	Executive Engineer
Faisal Karim	MatWorks	2.5 yrs	Senior Programmer
Md. Intishar Nur	BSRM	6 months	Assistant Programmer
Ananna Das	--	0	--
Hasibul Haq	Dhaka Bank Ltd.	5 yrs	Senior Officer

TABLE. V. EXTRACTED INFORMATION OF OTHERS BLOCK

Name	Skills	Certification
Farzana Yasmin	C, C++, PHP, Python, HTML, Java Script	CCNA
Mohammad Imtiaz Nur	Angualar, JavaScript, PHP, Java	Mobile Apps Training
Ohidul Islam	Python, Java, Javascript, Rubi on rails	--
Faisal Karim	C#, C++, PHP, Html, CSS, Javascript	--
Md. Intishar Nur	Matlab, C++	--
Ananna Das	MS Word, MS Office	--
Hasibul Haq	MS Word, MS Office, Linux	--

TABLE. VI. SCORE LOOKUP TABLE (PUBLICATION)

International Journal						Conference			
Indexing	Score	Publisher	Score	Impact Factor	Total	International Conference	Score	Others	Score
SCI	1	Nature	1	Value	Sum of Indexing, Publisher and Impact Factor score	Match the keyword ‘International Conference’	.2	If doesn’t satisfy other criteria of publication	.1
SCIE	.75	Springer, IEEE, Wiley, Elsevier	.5						
SCOPUS	.5	Others	.1						
Others	.4								
Predatory	0								

TABLE. VII. SCORE LOOKUP TABLE (EDUCATION)

Inst. Ranking	***PhD Score***	***M.Sc. Score***	***B.Sc. Score***	***CGPA***		***Major***	
1-200	10	5	2	***Rule***	***Score***	***Rule***	***Score***
201-500	9.5	4.8	1.9	$\geq$ 3.75	4	Keyword Matching with Requirement	2
501-1000	9	4.6	1.8	3.5-3.74	3		
1001-1500	8.5	4.4	1.7	3.0 -3.49	2		
1501-2000	8	4.2	1.6	2.5-2.99	1		
2001-2500	7.5	4	1.5	Others	0		
2501-3000	7	3.8	1.4				
3001-3500	6.5	3.6	1.3				
3501-4000	6	3.4	1.2				
Others	5.5	3.2	1.1				

TABLE. VIII. REQUIREMENT SETTING TABLE

Job_criteria	Keywords
Skills	C++, Java, PHP
Experience	0-3 yrs as Executive/ Senior Programmer
Major	CSE, EEE

C. Query Execution Module

1) Priorities setting by the recruiter: In the UI, employers set the requirements for the vacant positions of their company. For example, for Senior Programmer position, the employer sets the following requirements as Table VIII for each criteria.

2) Parse priorities: The system will then parse these requirements of the employer in the query execution module.

D. Anaysis and Output Module

1) Candidate Score Generation: After parsing the requirement of the employer, the system will start the score table generation of each candidate according to the employer priority and previously set standard score for different categories from the score database. The algorithm of candidate score generation is given below:

Algorithm 2: Candidate Score Generation
Input: Extracted information stored in Excel file
Goal: To generate score of each candidate in each criterion

```
1.  Begin
2.  Initialize Scores object with unique job_criteria
3.  Initialize an empty Score_table list
4.  For each row in excel do
5.        Set Scores object value to zero
6.        For each job_info details do
7.           Find(Excel(column))
8.           If job_criteria == Excel(column) do
9.                 If keyword matches with column value do
10.                Calculate the Scores value as:
                   Scores [job_criteria] += score set for the
                   criteria in the score database
11.                Else skip
12.          Else skip
13.       End For
14. Push Scores values in Score_table
15. End for
16. Set the mandatory required job_criteria
17. If Scores [mandatory_job_criteria] = 0 do
18.       Delete the score row from the Score_table
```

The extracted information stored in the lookup table in document database is retrieved (step 7-8) and matched with the keywords stored in the job_info_details table (step 9). If match found, the corresponding values are calculated as the rules set in the standard score table (step 10).

If multiple keywords are matched for a specific criteria, then they are stored as aggregated sum. For example, if multiple skills match, then all the skill values are added and stored in the skill column for that candidate.

For education score generation, the degrees and the ranking of the institutions they are acquired from are checked and scores for the institution and degree is put on the score table.

For the publication column, internation conference, international journal keywords are searched and matched. İf found, the number of occurences are counted. The lists of SCI, SCIE, SCOPUS and predatory journals are sotred in the database. The journal names are matched with these list. If match found, scores are calculated accordingly.

For the experience column, at first it is checked that the candidate is fulfilling the requirements for the given job. If yes, the experience score is calculated. If relevant experience is not fulfilled according to the requirements, the total experience is checked and given a score.

For skills an certifications score calculation, the requirement of the employers are checked. If matched, the information is given a value for each matched keywords.

If any column information contains missing value, then they are considered as zero in the score calculation. The calculated score is stored in that specific criteria column of the score table. After being scored in each criteria, now a table is generated which is score of each candidate (step 14).

The sample score table of the resumes of Table I are depicted below in Table IX.

TABLE. IX. SAMPLE SCORE TABLE

CV no.	Degree	Publication	CGPA	Skills	Experience	Major	Total
1	1.1	.2	4	1	2	2	10.3
2	1.1	0	2	2	5	2	12.1
3	5	.1	8	1	0	2	16.1
4	10.1	54.2	3	2	5	2	76.3
5	1.1	0	2	0	2	2	7.1
6	0	0	2	0	2	0	4
7	0	0	1	0	0	0	1

The first candidate had a B.Sc degree from Chittagong University of Engineering & Tech. And its ranking goes to institution category others. So the value for degree from the lookup Table VI is 1.1. She also has an international conference publication so the score is .2. The first candidate had the matching skill C++, experience of 3 years but as lecturer and major CSE. So the first candidate get scores according to the rules.

The scores of the other candidates will be calculated as the 1st candidate. The degree of 6th and 7th candidate doesn’t match the required degree database as we have only condidered technical degrees and so the missing value is scored as zero. Accordingly, the 5th, 6th and 7th candidates doesn’t match the skills requirement and so they get a zero in skills field. Now if we select any field as mandatory, the row containing zero in that field will be deleted.

2) Filter using skyline query: A skyline is defined as those points in a dataset those cannot be worse than any other point. A point dominates other points if it is as greater or equal in all criteria and greater in at least one criterion. A study in [24] states that during the past two decades, skyline queries are applied in several multi-criteria decision support problems. Skyline query utilizes the idea of skyline operator. There are several algorithms for the implementation of skyline operator like using directly in SQL queries, block nested loop, divide and conquer (D&C), branch and bound, map reduce etc. We have used the block nested loop (BNL) and D&C method. Applying skyline queries on the score table according to employers' priorities, now the dominant applicants will be filtered. We can explain the working procedure of skyline query using Table IX. According to BNL, we compare all the data points with all other points. We keep the points that can dominate other points in all criteria and at least in one dimension. The points dominated are discarded from the list. Those points are considered to be skyline that dominates others or maybe a part of the skyline if they neither dominates nor dominated by others. For performing skyline filtering, the categories are to be selected by the recruiters. As the employer placed the requirements for only skills, major and experience category, so comparing the data points of these categories of Table IX we find that Candidate 2 and 4 dominates the other candidates in the required criteria as they contain either equal or higher value in every criteria than the other five. After applying skyline we get that candidate 2 & 4 best suits for the job and others are discarded from the list as depicted in Table X.

According to D&C, first we will divide the list into m partitions recursively. Then a local skyline is calculated for each partition. Then we merge these local skylines for calculating the global skyline. And finally these global skylines are the best candidates for the job.

3) Output generation: The system output will show the result of the potential candidates after the filtering process. The output will be sorted according to the score obtained and personal details like name, email, phone number of each candidate will be displayed. The sample output generation is shown in Table XI.

The algorithm is depicted below:

Algorithm 3: Filtering Using Skyline Query (BNL method)
Input: Generated *Score_list,* candidate (1), candidate (2),…. candidate(n)
Goal: To filter the total candidate, create the best candidates list and remove the non dominant candidates

1. **Begin**
2. Initialize an empty *best_candidates* list
3. Set flag 'passed'= true for all Candidates
4. **For** i to n of *score_list*
5.   **If** (passed==false || candidate(i)== candidate(n))
6.   Continue
7.   Set *compare_list* = *score_table* filtered by (passed=true && candidate(i)
8. **For** each *job_criteria* do
9.   **If** (candidate (i).[criteria] ≥candidate (i+1).[criteria])
10.   Candidate (i+1).passed= false
11.   **Else if** (candidate (i).[criteria] < candidate (i+1).[criteria])
12.   { Candidate (i).passed= false
13.   Break}
14.   **End If**
15. **End for**
16. Set *best_candidates* list = candidates with (passed= true)
17. **End for**

Algorithm 3: Filtering Using Skyline Query (D&C method)
Input: Generated *Score_list,* candidate (1), candidate (2),…. candidate(n)
Goal: To filter the total candidate, create the best candidates list and remove the non dominant candidates

1. **Begin**
2. Initialize an empty *best_candidates* list
3. Keep the *Score_list* in N
4. Divide N using the median value of each criteria
5. Call BNL for calculating partial skyline of each partition
6. Merge the partial results
7. Call the BNL for calculating global skyline
8. Add the global skylines to *best_candidates* list
9. **End**

TABLE. X. SCORE TABLE AFTER FILTERING USING SKYLINE QUERY

CV no.	Skills	Experience	Major
2	2	5	2
4	2	5	2

TABLE. XI. OUTPUT GENERATION

CV No.	Name	Phone	Email	Skills	Experience	Major
2	Mohammad Imtiaz Nur	01818772617	imti.nur@gmail.com	2	5	2
4	Faisal Karim	01826564578	faisal90@outlook.com	2	5	2

IV. IMPLEMENTATIONS AND EXPERIMENTS

In this section, we have described the implementation and experimental setup of our system with necessary illustrations.

A. Experimental Setup

Potential candidate selection system has been developed on a machine having Windows 10, 2.50GHz Core i5-3210 processor with 12GB RAM. The system has been developed in Python 3.7.3, Asp.Net Core and Angular5 in the front end and MS SQL Server is used in the back end for storing related data to complete this project.

B. Implementation

At the beginning of our system workflow, resume documents are fed into the system. All the resumes are stored in a file according to the specific job id. These resumes are then converted into text format using UTF-8 encoding and stored in a file named lookup.py.

Once we have found the extracted information table, it is stored in the document database.

On the other hand, employers set the necessary information for setting the requirements of each criteria. Job_info_details table holds the columns like Job_info ID, Keyword, Job Criteria Name i.e. the information set by the recruiters on the requirements setting step. For the specific job position, extracted information table can be uploaded next for score generation.

After scoring according to the rules set, the system generates the score table. This table can be downloaded by the recruiter. Next the recruiter is given the option to choose the mandatory requirement criteria. If any of the criteria is chosen and candidates holding zero value in that specific criterion is removed before applying skyline query. Applying skyline query on the score table now returns the dominant applicants for the specified job by comparing each data points with each other. Then the unique dominant candidates holding maximum values in any of the criteria are returned.

The best candidates with score and personal details are shown in the output generation page (Fig. 4) in a descending score order.

C. Performance Evaluation

Potential candidate selection system performance is evaluated in two different phases- Information extraction performance, and filtering using skyline queries. We tested the performance of our system using 150 resumes of engineering background.

For the training of our NER model, we used a dataset of 300 manually annotated resumes and validated the model using resumes from the dataset. We found some incorrect values for extracted information and also some missing values. The precision, recall and F-measure of each block of information of the NER model is given below in Tablse XII, XIII and XIV. The extraction time is depicted in Table XV for different number of resumes.

We have tested the candidate filtering using skyline query with three different job criteria- Software Engineer with 2-4 years experience, Research Assistant with CGPA above 3.5 and 2 publications and Assistant Programmer with skills Java, JavaScript, HTML and CSS. We have scored the 150 resumes for these three different job positions. The returned output showed that the top scored candidates were different for the 3 job positions as the requirements were placed different. Comparing with the manual processing, we found that the filtering were accurate with a faster response. So based on the observations we can come to the conclusion that the accuracy of the skyline query depends on the accuracy of the scores generated. If the score generation is accurate, the skyline query returns those candidates that are best for the vacant position quite accurately and within few seconds.

We have also compared the response time of the skyline filtering using BNL and D&C method. The execution time for different number of resume data and with different number of dimensions is given in Table XVI. The table shows that the D&C method performs faster than BNL method because D&C method doesn't compare all the points naively as BNL does. The graphical comparison of each method for different criteria is shown in Fig. 5, 6 and 7.

TABLE. XII. PERSONAL INFORMATION EXTRACTION PERFORMANCE

Entity	Accuracy	Precision	Recall	F- measure
Name	99.77	0.99	0.99	0.99
Email	100.0	1.0	1.0	1.0
Phone	100.0	1.0	1.0	1.0
Date of Birth	99.87	1.0	0.99	0.99

TABLE. XIII. EDUCATIONAL INFORMATION EXTRACTION PERFORMANCE

Entity	Accuracy	Precision	Recall	F- measure
University	99.87	1.0	0.99	0.99
Degree	99.25	0.99	0.99	0.98
Major	98.36	0.99	0.98	0.98
CGPA	100.0	1.0	1.0	1.0

TABLE. XIV. PUBLICATION, SKILLS AND CERTIFICATION INFORMATION EXTRACTION PERFORMANCE

Entity	**Accuracy**	**Precision**	**Recall**	**F- measure**
Publication	98.71	0.98	0.98	0.98
Skills	94.84	0.99	0.94	0.96
Certification	93.21	0.92	0.93	0.93

TABLE. XV. INFORMATION EXTRACTION TIME OF THE SYSTEM

No of CV	Extraction Time (msec)
10	11.08
20	20.53
50	28.5
100	60.64
150	83.81

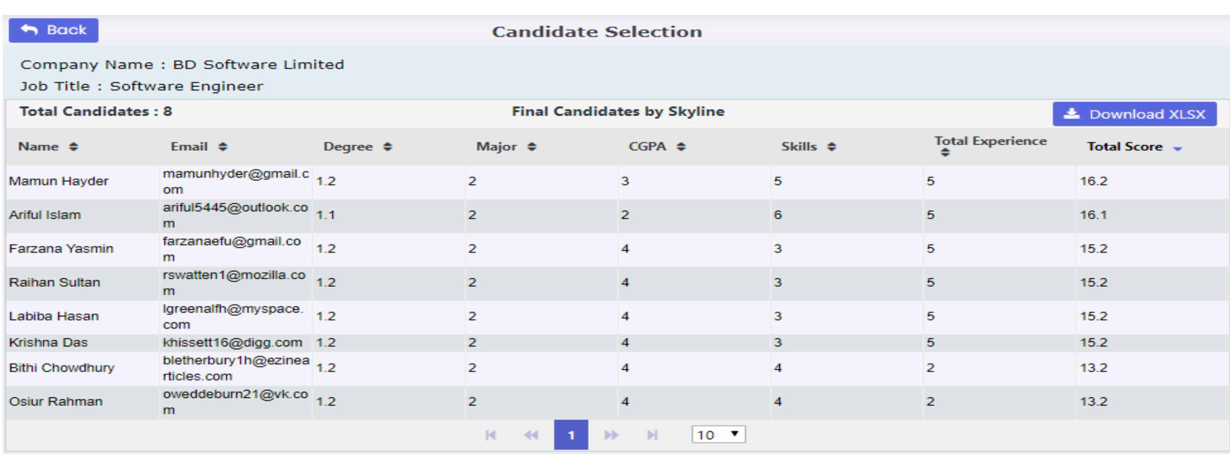

Fig. 4. Output Generation.

TABLE. XVI. RESPONSE TIME OF SKYLINE FILTERING

No of Resume	Response time (msec)					
	5 criteria		7 criteria		9 criteria	
	BNL	D&C	BNL	D&C	BNL	D&C
10	3.09	3.08	6.24	3.98	15.41	6.55
50	13.01	3.73	24.00	5.61	32.69	10.17
100	13.49	4.10	24.08	7.66	40.85	19.26
200	17.33	4.98	24.466	7.77	48.445	22.90

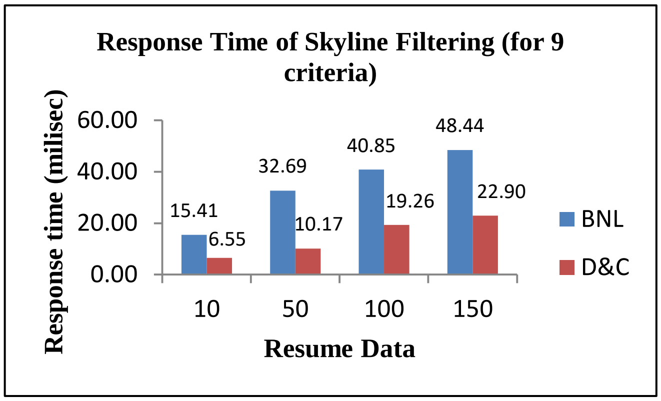

Fig. 5. Response Time of BNL & D and C for 9 Criteria.

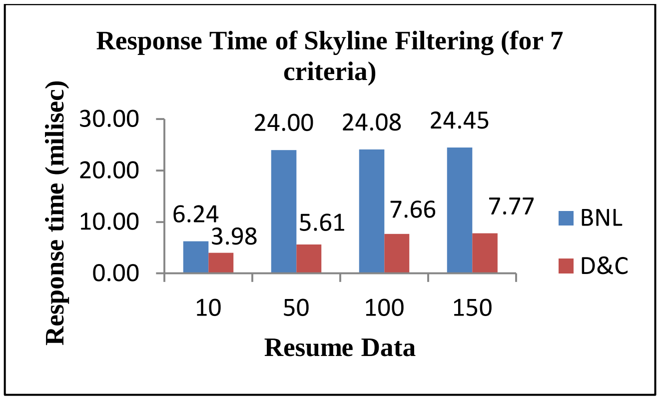

Fig. 6. Response Time of BNL and D and C for 7 Criteria.

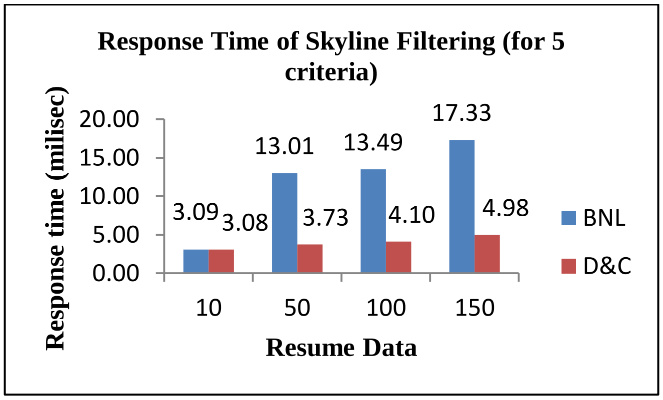

Fig. 7. Response Time of BNL and D and C for 5 Criteria.

V. CONCLUSION

In this paper, we narrated the idea of a candidate selection system which finds the best potential candidates by extracting information and filtering using skyline query. Automating the total task may help the HR agencies by reducing time, cost and effort of searching and screening the pioneer applicants from vast applications. There are many automated candidate ranking system available online. But we have developed a novel idea of using skyline query in filtering and returning the dominant candidates for the job specified. Skyline queries are mostly applied in multidimensional decision application. In candidate filtering, the implementation of skyline is new and we have applied this novel approach in an efficient manner. In the system performance evaluation, we have used 150 resumes of technical background in testing of the system and found that, the system works in an efficient way of returning best candidates by matching the given requirements with qualifications of the candidates. Altogether the system performs better in filtering the documents as well as the candidates based on the information extracted from the resume documents. We have also compared the performance of two skyline filtering method and found out that D&C method returns faster response than BNL method. Our system works for only English documents currently. In future, we hope to extend it for Bangla resumes as it is fifth most spoken native language in the world by incorporating Bangla Language Processing and test the system performance accordingly.

REFERENCES

[1] Information Extraction, https://en.wikipedia.org/wiki/Information_extraction.

[2] Celik, D., “Towards a semantic-based information extraction system for matching resumes to job openings,” Turkish Journal of Electrical Engineering & Computer Sciences. vol. 24, pp. 141-159 (2016).

[3] Kumari, S., Giri, P., Choudhury, S., Patil, S.R., “Automated resume extraction and candidate selection system,” In: International Journal of Research in Engineering and Technology, e-ISSN. 2319-1163, p-ISSN. 2321-7308, vol. 03, issue. 01 (2014).

[4] Farkas, R., Dobó, A., Kurai, Z., Miklós, I., Nagy, Á., Vincze, V., Zsibrita, J., “Information extraction from hungarian, english and german cvs for a career portal,” In: Prasath R., O’Reilly P., Kathirvalavakumar T. (eds) Mining Intelligence and Knowledge Exploration. Lecture Notes in Computer Science, vol. 8891, Springer, Cham (2014).

[5] K. Yu, G. Guan, M. Zhou, “Resume information extraction with cascaded hybrid model,” In Proceedings of the 43rd Annual Meeting of the Association for Computational Linguistics, pp. 499–506, Ann Arbor, June 2005.

[6] Information Extraction from CV, https://medium.com/@divalicious.priya/information-extraction-from-cv-acec216c3f48.

[7] Writing Your Own Resume Parser, https://www.omkarpathak.in/2018/12/18/writing-your-own-resume-parser/.

[8] Resume Parser, https://github.com/bjherger/ResumeParser.

[9] Chen, J., Zhang, C., Niu, Z., “A two-step resume information extraction algorithm,” Mathematical Problems in Engineering, vol. 2018, Article ID 5761287 (2018).

[10] Shah, S., Thakkar, A., Rami, S., “A survey paper on skyline query using recommendation system,” In: International Journal of Data Mining And Emerging Technologies, vol. 6, issue. 1, pp. 1-6, ISSN. 2249-3212 (2016).

[11] Kalyvas, C., Tzouramanis, T., “A survey of skyline query processing,” 2017.

[12] Papadias, D., Tao, Y., Fu, G., Seeger, B., "An optimal and progressive algorithm for skyline queries," In: ACM SIGMOD International Conference on Management of Data, pp. 467-478 (2003).

[13] Patil, S., Palshikar, G.K., Srivastava, R., Das, I., "Learning to rank resumes," In: FIRE, ISI Kolkata, India (2012).

[14] Yi, X., Allan, J., Croft, W.B., "Matching resumes and jobs based on relevance models" In: SIGIR, Amsterdam, The Netherlands, pp. 809–810 (2007).

[15] Rode, H., Colen, R., Zavrel, J., "Semantic CV search using vacancies as queries," In: 12th Dutch-Belgian Information Retrieval Workshop, Ghent, Belgium, pp. 87–88 (2012).

[16] Bollinger, J., Hardtke, D., Martin, B., "Using social data for resume job matching," In: DUBMMSM, Maui, Hawaii, pp. 27–30 (2012).

[17] Faliagka, E., Ramantas, K., Tsakalidis, A., Tzimas, G., "Application of machine learning algorithms to an online recruitment system," In: Seventh International Conference on Internet and Web Applications and Services, Stuttgart, Germany, pp. 215–220 (2012).

[18] Dandwani, V., Wadhwani, V., Chawla, R., Sachdev, N., Arthi, C.I., "Candidate ranking and evaluation system based on digital footprints," In: IOSR Journal of Computer Engineering (IOSR-JCE), e-ISSN. 2278-0661, p-ISSN. 2278-8727, vol. 19, issue. 1, ver. 4, pp. 35-38 (2017).

[19] Faliagka, E., Ramantas, K., Tsakalidis, A., Viennas, M., "An ıntegrated e-recruıtment system for cv rankıng based on ahp," In: 7th International Conference on Web Information Systems and Technologies, Noordwijkerhout, The Netherlands, (2011).

[20] SpaCy, https://spacy.io/.

[21] UTF-8 encoding, https://www.fileformat.info/info/unicode/utf8.htm.

[22] Named Entity Recognition, https://en.wikipedia.org/wiki/Named-entity_recognition.

[23] spaCy NER training model, https://course.spacy.io/chapter4.

[24] Tiakas, E., Papadopoulos, A. N., Manolopoulos, Y., "Skyline queries: An introduction," In: 6th International Conference on Information, Intelligence, Systems and Applications (IISA), DOI: 10.1109/IISA.2015.7388053, E-ISBN: 978-1-4673-9311-9**,** July (2015).

Identification of People with Parkinson's Suspicions through Voice Signal Processing

Brian Meneses-Claudio[1], Witman Alvarado-Diaz[2], Avid Roman-Gonzalez[3]
Image Processing Research Laboratory (INTI-Lab)
Universidad de Cienciasy, Humanidades
Lima, Perú

***Abstract*—Parkinson is considered a disease with a very random prognosis, in addition to its origin due to a multisystemic neurodegenerative process that affects the central nervous system, which is responsible for motor control of the body and also produces chronic joint pain if the patient is not treated also suffers states of depression. This disease currently has no cure so it recommends the patient's family to provide quality of life, the age of incidence is from 40 years, according to the INCN (Instituto Nacional de Ciencias Neurológicas) indicates that there are 3,000 cases of Parkinson in Peru annually. In this research paper, it proposes the creation of an algorithm in MATLAB capable of extracting the characteristics of the voice spectrum through the voice signal processing to provide an early detection so that they can receive treatment, appease and slow down Parkinson's disease. This processing will consist of submitting the audio by the Fast Fourier Transform (FFT), identifying the signal bodies, separating by frequency periods, to finally find the average and maximum values. It was identified that in the lower frequencies are where there are major differences, in addition the test was done with patients who has Parkinson's suspicions and the same differences were obtained resulting in the frequency periods [9Hz – 13Hz], [20Hz –30Hz] and [40Hz – 54Hz]. Also note that the period of 20 Hz to 30 Hz is where if the values in this frequency are less than 3.5 in amplitude they are principles of suspicion of Parkinson's disease.**

Keywords—Voice signal processing; Parkinson Disease (PD); Fast Fourier Transform; speech signal segmentation; audio treatment

I. Introduction

Parkinson's disease (PD) is caused by a multisystemic neurodegenerative process that primarily affects the central nervous system, also characterized as bradykinesia (slow movement), stiffness, tremor and progressive loss of postural control [1]. The progressive damage is random for each person, and the causes of this disease are not known with certainty. This disease is not fatal means that the affected person is not going to die from PD, in other words the life expectancy of a patient with PD is equal to that of a normal person. Unfortunately, there is currently no definitive cure for PD, which is why it is called chronic and incurable disease [2].

According to the INCN (Instituto Nacional de Ciencias Neurológicas), of the Ministerio de Salud (MINSA), it indicated that Parkinson's disease affects approximately 30 thousand people and also the current incidence in Peru is 3,000 cases of patients with PD annually [3]. Some more common symptoms that manifest at the beginning and continue in the disease process are, for example: joint pain, extreme tiredness means that feels the body tired very frequently in some cases without physical effort, dragging the foot, writing difficulties due to the tremor generated by his body, broken voice and long-term depressive symptoms [4].

According to the INCN, Parkinson's disease affects men and women, because it does not exclude sex, in addition, it indicates that 90% of cases of this disease happens since the age of 40 years old, however, the average age of incidence of the disease is between 50 and 60 years old [5]. The INCN also indicates that there are many medical investigations for the treatment and discovery of the cause of this chronic disease that affects the central nervous system and control of body movement [6]. The neurologist, Carlos Cosentino Esquerre, indicates that these patients with PD mostly have states of depression and that is why they should be provided with quality of life as well as motivation for the practice of the exercises and walking for periods of time [7].

Parkinson is classified by degrees from I to V, usually beginning with mild symptoms only in the middle of the body, then in the second grade, it presents throughout the body, after postural instability, these symptoms can already be observed but the patient remains independent; continuing with the next grade, the patient will present a severe disability, in addition to the well-marked symptoms; finally, when the patient is in the last grade, it is already when the patient becomes dependent and needs help for everything, just be sitting or in bed [8]. In all grades, constant tremor occurs in their bodies. There are currently medical and non-medical treatment to reduce symptoms, slow the evolution of the disease and effectively improve the quality of life of patients [9].

The identification of people with PD can help the early medication and in many cases prevent visible symptoms, in addition to slowing down the PD process. It is known that a patient who is not treated in time about this disease, its chronic pain will be very strong and the progress of the disease is fast. In addition to stressing the physical effort that must be made or practiced to keep the body active as well, avoiding depression and disease progression [10].

The interruption of motor speech control is very frequent, as well as notable in patients with PD, there is an estimate that more than 90% of these patients present and develop a speech disorder known as Hypokinetic Dysarthria (HD) [11]. Among other speech symptoms associated with HD, vocalization abnormalities are the most frequent and widely observed in patients with PD. It can be characterized by the general reduction in tone and volume during the prolongation of speech, in addition to the self-control of abnormal speech [12].

In [13], they explain the creation of an electronic device that will provide speech exercises proposed for the patient with Parkinson's Disease for their voice spectrum analysis, their analyzes were carried out in closed environments to avoid ambient noise thus obtaining data without distortions also indicated that the frequency range of 10 Hz to 30 Hz is where different anomalies were presented to the audios of a normal person. This research paper explains the defragmentation of the voice signal of the patient with PD for each exercise, obtaining notable characteristics, such as distortion at low frequencies and low amplitudes, these same results were obtained in this paper with low frequencies being one of the most differentiated.

In [14], this research paper explains the voices at rest of Parkinson's Disease patients, which have a peculiarity because after obtaining the voice signal, they defragment it to obtain samples of the signal, then analyze the variations that the peaks and falls of the signal occur, resulting in the letters where there are more difficult to pronounce for patients with PD. In addition, they presented that the frequencies where the greatest variation is identified compared to people who do not suffer from this disease was between 15 and 45 Hz. Also, in this research paper, they used medical equipment such as dopamine to know how the patient improved, obtaining as a result, and an improvement in the pronunciation of the words up to certain phrases. Voice spectrum analysis is important for the identification of patients with PD due to its characteristic frequency and amplitude.

In [15], this research paper shows a predictive analysis of people with possible suspicions of PD through the analysis of the voice spectrum, samples were taken from people who had tremor in the voice and then represent it in the time and amplitude domain, In addition, they analyzed people with PD to identify in what time periods a difference and time difference is obtained. This analysis was done to prevent and accelerate the symptoms of Parkinson's disease, in addition, by applying artificial intelligence methods, they trained a system to be able to identify people who have possible signs of having Parkinson's disease.

The main objective of the research paper is the identification of people with Parkinson Disease through voice processing because these patients have a tremor at the time of reading or speaking, this is why audios of these patients with PD and people that do not suffer from this disease were recorded, to then process both voices signals and compare them, thus obtaining the most notable differences and also identify the frequencies, the average and the maximum value where there is a significant variation.

Digital voice processing is the study of voice signals and the techniques used for processing these signals; it is used for voice knowledge, voice coding, voice analysis and etc. Also in the biomedical environment, voice treatment can be used for the treatment of the voice spectrum and then use filtering techniques because it knows that we can obtain noise in the recording, which must be eliminated. Currently, it uses voice processing for voice distortion and pattern recognition as specific words [16].

Digital signal processing is the mathematical manipulation of an information signal to modify or improve it with respect to a parameter, they are usually represented in the time and frequency domain, but in the case it wants to compare signals or identify differences, These signals have to be filtered so that they are all in the frequency domain and their amplitude to identify the average and maximum values. This procedure will serve to verify differences between other voice compositions, this process is widely used in voice tuners to modulate it at different frequencies and powers. In this research paper, it will be used to know the amplitude and average of the frequency periods and to know the differences of patients with Parkinson's disease and who do not suffer from it.

The following research paper is structured as follows: In Section II, the digital voice processing methodology for conversion to the frequency and amplitude domain will be presented, in addition to filtering the ambient noise to obtain the real voice signal. In Section III, bar diagrams will be shown indicating the maximum values and the average of the frequency periods identifying the differences in voice between patients with early PD and patients who do not suffer from this disease. Finally in Section IV, we will present the discussions and conclusions of the research work.

II. Methodology

In this section, it will present the steps that were followed for the Identification of People with Parkinson's Suspicions through voice processing, in addition in Fig. 1, the process of the algorithm is shown, as the reader can see, several processes were used to obtain clean audio without any external noise.

A. Audio Acquisition

For audio acquisition, a Smartphone was used for recording because the audio recording was required to be as close to the person as shown in Fig. 2.

In addition, a Bachelor of Literature Milton Gonzales was required to generate paragraphs that require a lot of good modulation for the pronunciation of words. These paragraphs consisted of fragments of Peruvian literary books being the following:

Audio 1: "Un poema es una obra. La poesía se polariza, se congrega y aísla en un producto humano: cuadro, canción, tragedia. Lo poético es poesía en un estado amorfo; el poema es creación, poesía erguida. Sólo en el poema la poesía se aísla y revela plenamente" [17].

Audio 2: "Apenas desviamos los ojos de lo poético para fijarlos en el poema, nos asombra la multitud de formas que asume ese ser que pensábamos único. ¿Cómo asir la poesía si cada poema se ostenta como algo diferente e irreducible? La ciencia de la literatura pretende reducir a géneros la vertiginosa pluralidad del poema" [17].

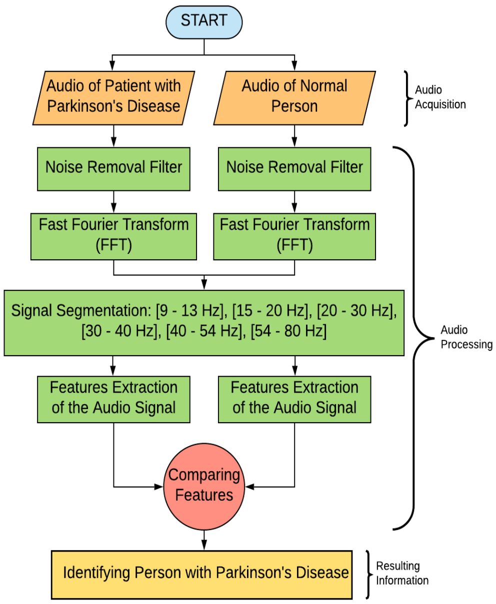

Fig. 1. Process Flow Diagram for the the Identification of People with Parkinson's Suspicions.

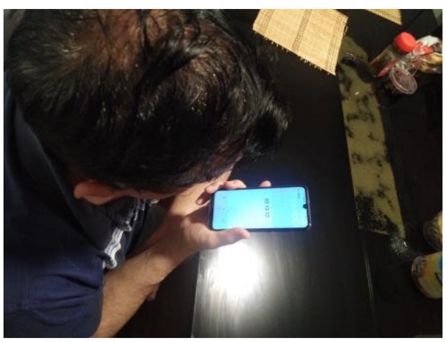

Fig. 2. Acquisition of Voice Data of a Patient with Parkinson's Disease through a Smartphone Device.

After obtaining the audios, these were changed from format to .wav because it is preferred to use this format when using MATLAB software for the following voice processing. In addition, it should be taken in mind that it does not matter how much time each person takes because it will be analyzed in the frequency and its amplitude domain.

To declare the audio files, it must indicate that these audios have two variables being the Data and the Sampling Frequency (Fs), the following programming:

```
[data,fs]=audioread('audio_patient.wav');
```

These variables will be used for programming and use in the following steps of voice processing, this signal is like the one shown in Fig. 3(a).

B. Audio Processing

At this stage, the voice signal was already declared in the software, so filters must be applied to improve the voice signals, because of that, the first filter that is applied is the noise elimination. This filter helped us to sector the frequencies where the relevant data was for the analysis and eliminate the others.

After eliminating the external noise, the Fast Fourier Transform was applied to the voice signals; this process helps to change the domains of the signal so that they can then be analyzed. The software makes a sum by means of complex numbers where the frequency, time and amplitude of the signal are taken into account, as shown in Fig. 3(b) for that it extracts data using the following programming in the software:

```
n = length(data);
y = fft(data);
f = (0:n-1)*(fs/n)/10;
power = abs(y).^2/n;
```

As shown in the previous programming, the length of the data and the sampling frequency are important to graph the signal submitted to the Fast Fourier Transform, in addition to the "Power" section, it is observed that it uses absolute value to the signal after the FFT because there are negative values.

The next step for voice processing is to identify the signal bodies, this process is done to know the frequency periods to which the signal must be segmented and thus extract the characteristics of each of the periods [18]. The frequencies sectored by observing the bodies as shown in Fig. 3(c), the following frequency periods were observed: [9 Hz – 13 Hz], [15 Hz – 20 Hz], [20 Hz – 30 Hz], [30 Hz – 40 Hz], [40 Hz – 54 Hz], [54 Hz – 80 Hz].

These partitions by frequency period can be visualized in Fig. 3(d), where each one adapts to its amplitude and parameterized frequency. For this reason, the following programming was used:

```
control = 1;
for i=1:length(f)
  if f(i) > frecuencia1
    if f(i) < frecuencia2
      C(control) = f(i);
      control=control+1;
    end
  end
end
```

As shown in the programming, a "For" loop was used because the algorithm was required to review data by data to sectored a certain frequency range and also create a frequency matrix to position the data. After that, it indicates in the software that each frequency position has an assigned data, for that the following programming was used:

```
variable1 = C(1);
variable2 = C(control-1);
data1 = find(f==variable1);
data2 = find(f==variable2);
```

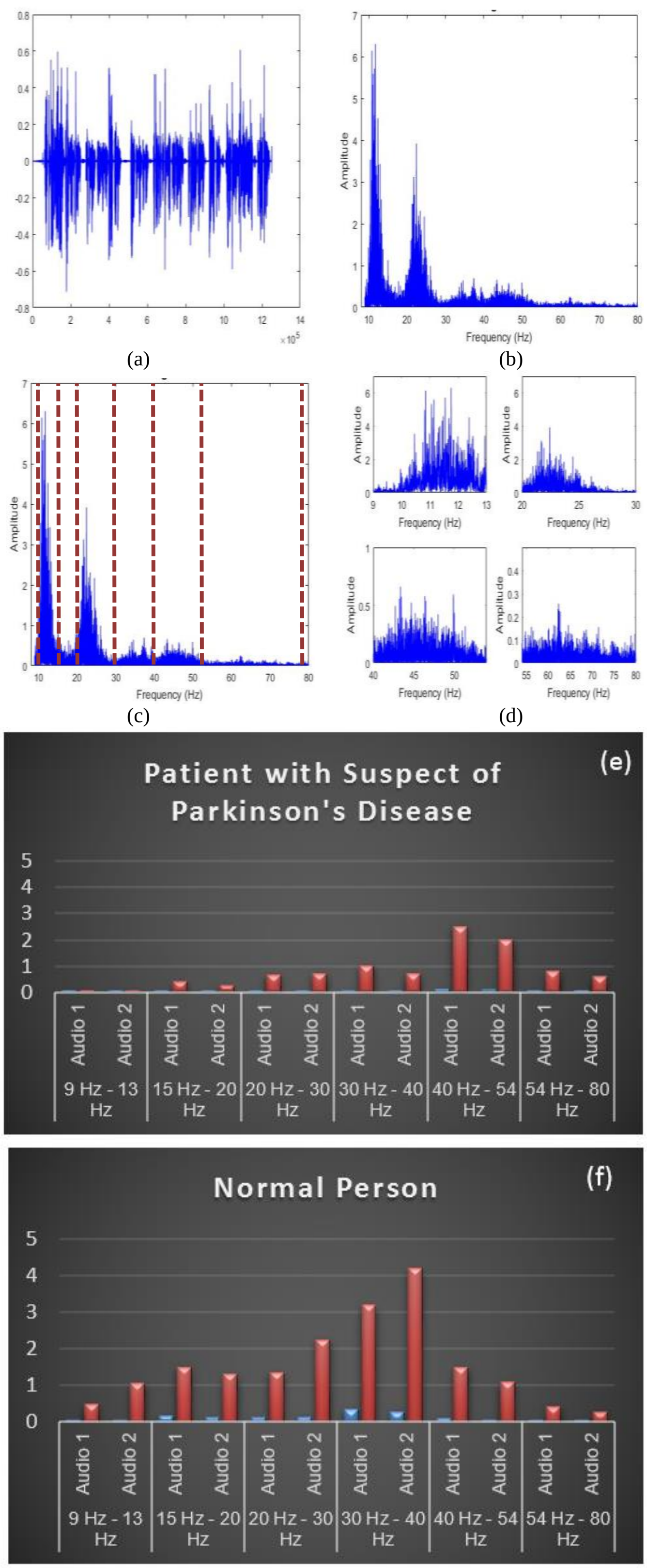

Fig. 3. Identification of People with Parkinson's Suspicions through Voice Signal Processing. (a) Original Signal. (b) Filtered Voice Signal. (c) Identification of Bodies in the Signal. (d) Voice Signal Divided by Frequency Ranges. (e) and (f) Average and Maximum of People with and without Parkinson.

It uses the "find" function because each frequency is assigned a data and because of that, the algorithm knows that its amplitude data is in the same position of the frequency so that it can be plotted. To graph the voice signal in the declared frequency range, as well as find its average and maximum value, the following programming is used:

```
plot(f(data1:data2),power(data1:data2));

mean = mean(power(data1:data2));

max = max(power(data1:data2));
```

Finally, when obtaining the data, it will graph the averages and the maximum values to identify the differences, as can be seen in Fig. 3(e) and (f), in these bar graph, it can be denoted that at low frequencies, it is where the difference between the voice spectrum of a person with PD and a person who does not suffer from this disease is mostly presented.

III. Results

Voice audios were acquired from the same paragraphs because the differences of all audios are required. This analysis was performed on 10 people of which 2 of them are patients with Parkinson's disease are confirmed clinical states, 3 were people had early symptoms of Parkinson's disease and 5 people who do not suffer from this disease. Each one of them was taken 2 audios, which means that 20 data were obtained that were analyzed in the algorithm to recognize suspicions of people with Parkinson's disease.

As mentioned earlier, the first symptoms of Parkinson's disease are dysfunction of the motor control of the body, in addition to the voice with tremors and with a lower volume than normal, these tremors cause a variation in frequencies and when compared with audios of people who do not have this disease, the differences are remarkable.

In Table I, the characteristics extracted from the voice signals of the Parkinson's patient are shown, in which they were sectored by periods, audios, average and maximum value, as can be verified, the data is much lower in addition to having maximum values very low.

TABLE. I. Characteristics of Patient's Audios with Parkinson's Disease

Periods	Audios	Average	Max Value
9 Hz - 13 Hz	Audio 1	0.00015185	0.0024172
	Audio 2	0.000050975	0.00079106
15 Hz - 20 Hz	Audio 1	0.030011	0.40081
	Audio 2	0.022719	0.26129
20 Hz - 30 Hz	Audio 1	0.038021	0.67023
	Audio 2	0.040266	0.72365
30 Hz - 40 Hz	Audio 1	0.047363	1.0247
	Audio 2	0.032152	0.71534
40 Hz - 54 Hz	Audio 1	0.13886	2.5033
	Audio 2	0.11137	2.0071
54 Hz - 80 Hz	Audio 1	0.057259	0.79477
	Audio 2	0.039726	0.58931

Table II shows the characteristics extracted from the voice signals of a person who does not suffer from this disease, in the same way that the previous table was divided by the different variables that were taken into account. In addition, it can be identified that the data are higher at the first frequencies and also the maximum values that become higher compared to the patient with Parkinson's disease.

TABLE. II. CHARACTERISTICS OF THE AUDIOS OF A PERSON WITHOUT PARKINSON'S DISEASE

Periods	Audios	Average	Max Value
9 Hz - 13 Hz	Audio 1	0.72048	6.3013
	Audio 2	0.74735	6.5805
15 Hz - 20 Hz	Audio 1	0.10601	1.1277
	Audio 2	0.13828	1.5766
20 Hz - 30 Hz	Audio 1	0.24961	3.9177
	Audio 2	0.25488	3.8277
30 Hz - 40 Hz	Audio 1	0.074909	0.69614
	Audio 2	0.069628	0.77149
40 Hz - 54 Hz	Audio 1	0.071098	0.66055
	Audio 2	0.062307	0.68884
54 Hz - 80 Hz	Audio 1	0.021494	0.25681
	Audio 2	0.017134	0.21275

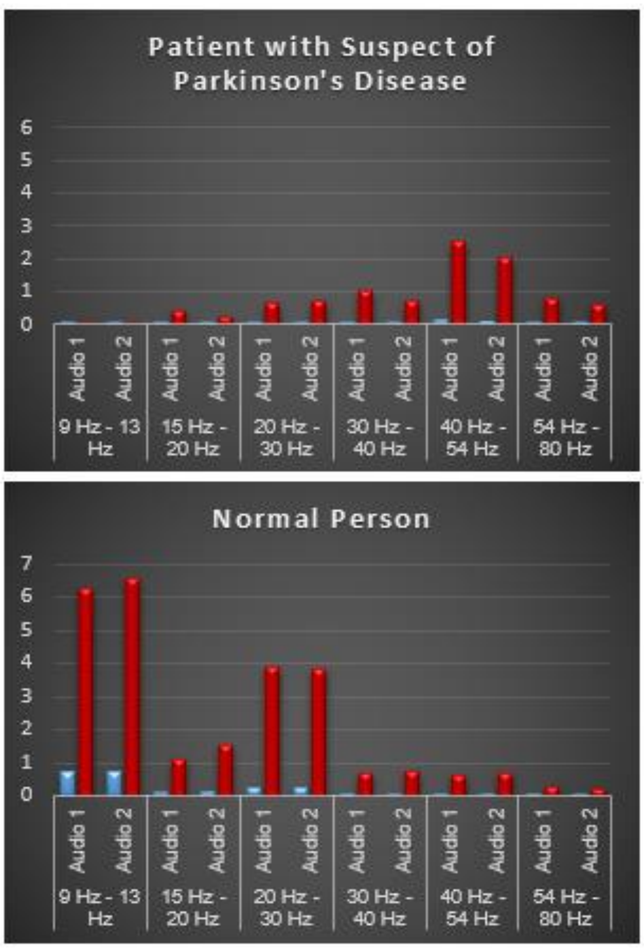

Fig. 4. Bar Chart of the Data in Table I and II.

As can be seen in Fig. 4, the blue bars represent the average and the red bar, the maximum value of the frequency range, the most notable differences are in the first frequency ranges from 9 Hz to 30 Hz, as well as they were mentioned in the background previously studied.

The same test was applied to a patient with possible suspicions of Parkinson's disease, because it presented some symptoms such as motor dysfunction but in early stages, in addition to the trembling voice and the volume of the same. So in Table III, the characteristics extracted from the voice signals of the patient with Parkinson's disease suspicions are shown, where similarities can be identified with the data obtained in the patient with Parkinson's disease.

These data were compared with the voice data of another person who does not suffer or have suspicions of Parkinson's disease, as can be seen in Table IV, has higher maximum values in the lower frequency ranges. This same result being in the previous tests and also being similar to the results obtained by previous papers on the analysis of the voice processing of patients with Parkinson's disease.

TABLE. III. CHARACTERISTICS OF A PATIENT'S AUDIOS WITH PARKINSON'S DISEASE SUSPECTS

Periods	Audios	Average	Max Value
9 Hz - 13 Hz	Audio 1	0.042599	0.48363
	Audio 2	0.033672	1.0534
15 Hz - 20 Hz	Audio 1	0.18416	1.504
	Audio 2	0.12795	1.3005
20 Hz - 30 Hz	Audio 1	0.12629	1.3458
	Audio 2	0.14664	2.2469
30 Hz - 40 Hz	Audio 1	0.36163	3.1787
	Audio 2	0.28522	4.175
40 Hz - 54 Hz	Audio 1	0.11892	1.4972
	Audio 2	0.068878	1.0798
54 Hz - 80 Hz	Audio 1	0.049341	0.42559
	Audio 2	0.029901	0.2781

TABLE. IV. CHARACTERISTICS OF THE AUDIOS OF A PERSON WITHOUT PARKINSON'S DISEASE

Periods	Audios	Average	Max Value
9 Hz - 13 Hz	Audio 1	0.11899	1.8299
	Audio 2	0.10968	1.4951
15 Hz - 20 Hz	Audio 1	0.09504	0.78943
	Audio 2	0.075898	0.84714
20 Hz - 30 Hz	Audio 1	0.29918	4.5561
	Audio 2	0.30901	4.8064
30 Hz - 40 Hz	Audio 1	0.10745	0.92966
	Audio 2	0.0743	0.65491
40 Hz - 54 Hz	Audio 1	0.18932	2.2626
	Audio 2	0.1251	1.2111
54 Hz - 80 Hz	Audio 1	0.043824	1.1407
	Audio 2	0.037408	1.0797

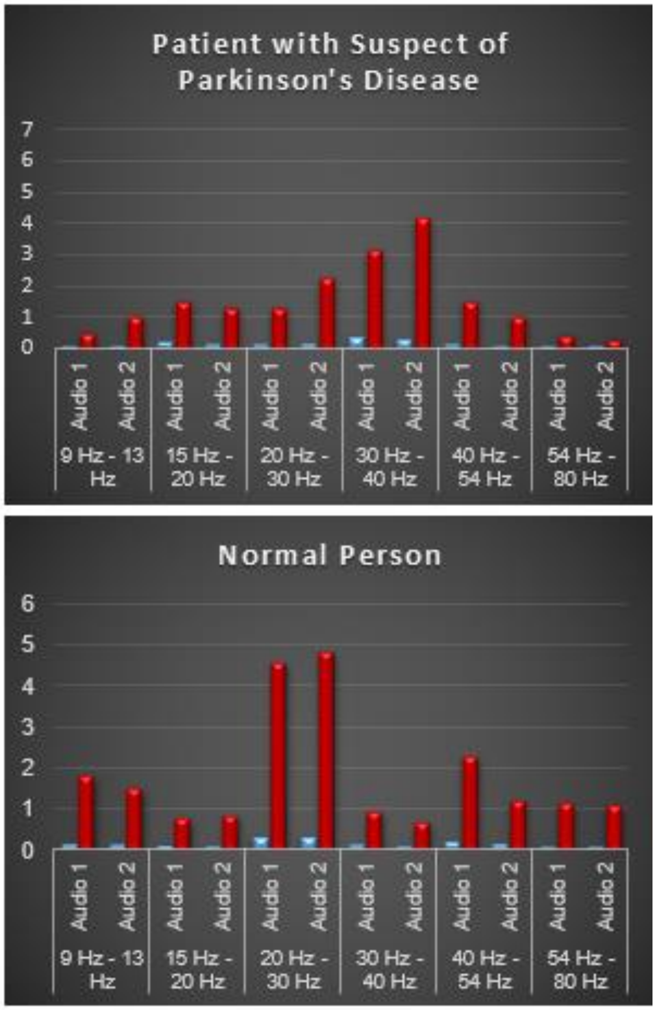

Fig. 5. Bar Diagram of the Data in Table III and IV.

As can be seen in Fig. 5, in the same way the blue bars represent the average and the red bars represent the maximum value of the frequency period represented in the lower part, the differences are also found in the lower frequencies and also with the added of the signals of patients with suspected Parkinson's disease have more noticeable maximum values at higher frequencies.

Concluding both analyzes, it can be indicated that the frequency periods where notable differences are shown are:

[9 Hz – 13 Hz], [20 Hz – 30 Hz] y [40 Hz – 54 Hz]

This means that mostly in lower frequencies different notables can be found and in addition to maximum values,they are also variants, but in both studies in the frequency range of 20 Hz - 30 Hz a higher maximum value was presented as well as the averages of the data.

IV. Discussion and Conclusions

The research paper confirms the use of voice processing techniques for the detection of suspicions of people with Parkinson’s disease due to analysis of the voice spectrum and knowing the frequency periods where a greater difference is appearing. In addition, knowing the importance of the early detection of this disease to slow down and soothe the chronic damage suffered by patients with this disease.

This research paper was focused on frequency and amplitude because it knows that when it records audios in different environments, not everyone can say a sentence at the same speed as another, because of this, the axes of the signal were changed to identify the spectrum of voice in periods of time and maximum observable values in the amplitude.

It is concluded, people with suspicions of Parkinson's disease have a lower voice volume and also choppy being nonlinear. These differences are verified more in the range of frequency and the amplitude of the signal that is why in this research paper the average and the maximum value of the data were found.

It is concluded that the signal was separated by frequency periods because notable bodies were present in such periods, in addition a range was parameterized to subject all the analyzed signals; this was done to parameterize all the analyzes of the voice spectra and thus obtain results when comparing them.

As a work in the future, we want to implement the algorithm in a device where more tests can be done, thus improving its accuracy and also detecting this disease in time to prevent its prolongation and also knowing if they have Parkinson's suspicions.

Acknowledgment

We would like to thank the graduate in literature Milton Gonzales Macavilca for his search for excerpts from a literature book that contains words where a good pronunciation is required in addition to containing long sentences in order to detect the tremor in the voice of patients with suspected Parkinson's disease.

References

[1] W. Poewe et al., “Parkinson disease,” Nat. Rev. Dis. Prim., vol. 3, pp. 1–21, Mar. 2017.

[2] O. B. Tysnes and A. Storstein, “Epidemiology of Parkinson’s disease,” Journal of Neural Transmission, vol. 124, no. 8. Springer-Verlag Wien, pp. 901–905, 01-Aug-2017.

[3] Peru 21, “Alrededor de 30 mil personas tienen enfermedad del Parkinson en el Perú, informó Minsa Lima | Peru21.” [Online]. Available: https://peru21.pe/lima/ministerio-salud-minsa-30-mil-personas-peru-enfermedad-parkinson-nndc-471293-noticia/.

[4] L. Pinto, C. Alva Diaz, and L. Torres, “Associated factors with depressive symptoms in patients with Parkinson’s disease,” Med. Clin. (Barc)., vol. 150, no. 3, pp. 119–120, Feb. 2018.

[5] O. Rodríguez Vega, L. Torres Ramírez, K. Meza Capcha, R. López Cabanillas, H. Ruiz García, and C. Cosentino Esquerre, "Estreñimiento como factor asociado a mayor severidad en pacientes con enfermedad de Parkinson del Instituto Nacional de Ciencias Neurológicas del Perú," Diagnóstico, vol. 57, no. 4, pp. 180–183, Apr. 2019.

[6] S. Bhat, U. R. Acharya, Y. Hagiwara, N. Dadmehr, and H. Adeli, "Parkinson's disease: Cause factors, measurable indicators, and early diagnosis," Computers in Biology and Medicine, vol. 102. Elsevier Ltd, pp. 234–241, 01-Nov-2018.

[7] V. Dueñas Vicuña, L. Torres Ramírez, C. Cosentino Esquerre, and H. Ruiz García, "Frecuencia de disfagia en una cohorte de pacientes con enfermedad de Parkinson," Diagnóstico, vol. 57, no. 4, pp. 175–179, Apr. 2019.

[8] S. Yu et al., "Clinical features and dysfunctions of iron metabolism in Parkinson disease patients with hyper echogenicity in substantia nigra: a cross-sectional study," BMC Neurol., vol. 18, no. 1, p. 9, Dec. 2018.

[9] N. Yoshiki, S. Sayuri, M. Yasuaki, U. Akihiro, I. Shinji, and M. Tatsuro, "Fatigue evaluated using the 16-item Parkinson Fatigue Scale (PFS-16) predicts Parkinson's disease prognosis," Fujita Med. J., vol. 5, no. 2, pp. 45–48, 2019.

[10] A. J. Noyce, R. N. Rees, A. P. Acharya, and A. Schrag, "An early diagnosis is not the same as a timely diagnosis of Parkinson's disease [version 1; referees: 2 approved]," F1000Research, vol. 7. F1000 Research Ltd, 2018.

[11] M. C. T. dos Santos et al., "Evaluation of cerebrospinal fluid proteins as potential biomarkers for early stage Parkinson's disease diagnosis," PLoS One, vol. 13, no. 11, p. e0206536, Nov. 2018.

[12] S. L. Oh et al., "A deep learning approach for Parkinson's disease diagnosis from EEG signals," Neural Comput. Appl., 2018.

[13] H. Dubey, J. C. Goldberg, M. Abtahi, L. Mahler, and K. Mankodiya, "EchoWear: Smartwatch technology for voice and speech treatments of patients with Parkinson's disease," in Wireless Health 2015, WH 2015, 2015.

[14] S. Sharma, R. K. Gupta, and K. Anil, "Processing and analysis of human voice for assessment of Parkinson disease," J. Med. Imaging Heal. Informatics, vol. 6, no. 1, pp. 63–70, Feb. 2016.

[15] A. B. New et al., "The intrinsic resting state voice network in Parkinson's disease," Hum. Brain Mapp., vol. 36, no. 5, pp. 1951–1962, May 2015.

[16] J. Rusz, "Detecting Speech Disorders in Early Parkinson's Disease by Acoustic Analysis," 2018.

[17] P. Octavio, La casa de la presencia, no. 532. 1994.

[18] C. Misra and M. K. Hota, "Hybrid Technique for Voice Recognition, Encryption and Analysis using MATLAB," in Proceedings of the 2018 IEEE International Conference on Communication and Signal Processing, ICCSP 2018, 2018, pp. 200–203.

Towards the Identification of Student Learning Communities using Centrality

Intissar Salhi[1], Hanaa El Fazazi[2], Mohammed Qbadou[3], Khalifa Mansouri[4]
Laboratory Signals, Distributed Systems and Artificial Intelligence ENSETM
University Hassan II, Casablanca
Morocco

***Abstract*—Emergence of universities towards "digital university" has already been present for some years. The use of digital is largely developed to ensure a good quality of education. Universities therefore use large-scale learning management systems to manage the interaction between learners and teachers. Teachers can provide online training and educational materials for students following their classes and courses, monitor their participation and evaluate their performance. Students can use interactive features such as discussion threads, videoconferences, and discussion forums. These online tools make it possible to create new social networks or connect online social interactions. This will allow us to understand the structure of this complex network and extract useful information. In this article, we report our research on the detection of student learning communities based on learner activity. We found that it is possible to group students in communities through their messages and response structures using standard community detection algorithms. Also, that their behaviours can be strongly correlated with their closest peers who belong to the same community.**

Keywords—Student's learning communities; complex network; learner activity; community detection

I. Introduction

Learning using educational technologies has become an integral part of modern schools[1]. Scientific and technological advances are constantly improving to ensure good quality education and facilitate the engagement of students and teachers[2]. The processes for improving educational programs and teaching principles require constant adaptation to the new conditions and capacities of modern software tools[3]. Students now complete the traditional course structure with online materials. Instructors can share class materials online, have an online discussion forum, or complete questionnaires and homework submissions online. This in turn provides a wealth of new behavioural data that we can use to group students into communities using standard community detection algorithms to create qualitative and accessible software systems that will allow teachers to constantly improve their educational approaches.

The concept of community, commonly clusters or modules, is specific to online and offline social networks [4]. A community is defined in a current graph as a group of nodes that are particularly interconnected and weakly connected to the rest of the network [5]. For example, they may be individuals who interact a lot with each other and little with others. It is particularly interesting to identify these groups in order to bring out the underlying structure of the graph. It can thus be divided into natural groups of individuals (no overlap, i.e. a node belongs to a single group) that can be of any size. This identification will take into account only the structure of the graph, as well as weights of edges that provide additional information, as the level of activity of a relationship.

Communities are interesting for a variety of reasons. For example, users in a community tend to interact frequently, share interests, and trust each other to some degree. Therefore, communities are useful, for example, to guide, identify typical profiles [6], carry out targeted actions, better adjust recommendations [7], reorganize and identify central or influential actors [8], etc.

In previous work in the educational field, in paper [9], the authors have shown that students can be grouped into stable communities according to their online question and answer model. They also showed that the students' final scores were significantly correlated with those of their peers closest to the community group. In paper [10] they have also shown that learners belonging to these communities, although homogeneous in terms of performance, are not united by their incoming motivations to register for the course nor by their level of prior experience.

Until today, these results have only been found in MOOCs and the user forum, where almost all of the relevant interactions in the course occur online and where the relationship between students is the direct connection between each other's. In this paper, we have shown that interaction on forums is not the only way to establish a relationship between students in order to create communities, but that their activity can also establish it. Thus, we found that it is possible to group students in communities through their messages and their response structures using standard community detection algorithms. Furthermore, that their behaviours can be strongly correlated with their closest peers who belong to the same community.

In this article, we start with a review of the literature on community detection through social network analysis, then we explain the notions of centrality as well as the most used community detection techniques. After that, we continue with a discussion about the algorithms we used to create a student community. The resulting student community will be tested on a database and discussed. And we conclude with some recommendations for future studies.

II. Community Detection

Community detection has received a lot of attention in the research community over the last decade and several approaches have been proposed [11]. However, the majority of existing approaches mainly deal with social and biological networks, viral marketing, [12][13][14][15] etc.

In the pedagogical field, and in a set of students, the detection of subsets of vertices more densely connected than others, called student learning communities, is a problem that we find strongly as it can be beneficial to us. To control all students enrolled in an institution and even within a class and given an idea of the behaviour of each based on the descriptive characteristics of the community to which they belongs. Within a class, these communities play an important role in his organization and structure.

As a result, it is necessary to determine classes in a graph. This problem is therefore strongly related to the problem of partitioning, with the following specificity: according to the application that we want to do with these communities, classes can (or must) be disjointed or not. So we can analyse network interaction between learners to, among other things, predict, quite reliably, a list of recommendations. Just as in clustering, there are many individuals who belong to more than one community, and in this case it is reasonable to build not a partition, but a collection, that is, a system of overlapping classes. It is the same in social networks, [16] where individuals can belong to several groups.

A. *Social Network Analysis*

The social graph refers to the mapping of relationships within a social network [17]. Nodes are usually the interacting social actors and the links are the relationships between them. The social graph in its simplest form is modelled to form an analysable structure where all the significant links between the nodes are studied. The same goes for structural holes vertices [18], or "network closures" where there is an absence of direct links between two.

B. *Presentation of a Social Network*

A social network can be represented by a graph G (V, E) where V represents the set of vertices (nodes), E the set of edges and can be represented using the so-called adjacency matrix A_{ij} which indicates the connections between the nodes.

III. Notion of Centrality

In social network analysis, centrality [19] is an important concept which can be applied to all kinds of networks. The identification of the actors with the greatest centrality (leaders or influential person) makes it possible to define the structure of the network [20][21],more precisely, these actors should normally play a key role in the simulated and real behaviours.

In this part we will talk about the notion of centrality within a network.

A. *Identification of Central Nodes*

The importance of a vertex in a graph can be quantified simply by its neighbourhood, and it is said that a node is central if it has many neighbours [19], here we talk about the degree of centrality; it may be in terms of distance. A central node may be distant from others, so we talk about centrality closeness [22]; or more subtly, it constitutes a node of passage by the shortest way to transit from one summit to another, this is explained by centrality betweenness [23][24]. In the following parts, we will highlight these three algorithms:

1) Degree centrality: The Degree Centrality measure can help us find popular nodes in a graph. Indeed, it is the ratio between the number of outcoming links and the maximum degree possible in a network of a possible size. Thus, for a node called i and a total number of nodes n in the network:

$$\mathrm{D_c(i)} = \frac{\mathrm{d_s(i)}}{\mathrm{(n-1)}} \quad (1)$$

The degree centrality reflects only a local view of the relationships between nodes in a network and does not provide information about the overall structure of the network.

2) Closeness centrality: This is the most widely used measure of centrality. The centrality of proximity of the actor i is defined as the inverse of the average degree d (i, j):

$$C_c(i) = \frac{(n-1)}{\sum_{i\neq j} d(i,j)} \quad (2)$$

If the node i has a strongest value c_c it implies that i is a central node.

The multiplication by {n-1}, where n is the number of nodes in the graph. This adjustment allows comparisons between nodes of graphs of different sizes.

3) Betweenness centrality: Intermediary is the measure of centrality of a vertex in a graph. Intermediate centrality counts the number of times a node acts as a waypoint along the shortest path between two other nodes (geodesic distance).

It is based on the counting of the geodesic distance δ_{ij} between the actors i and j, and by looking at the number δ_{ij}(m) passing through the actor m.

$$C_b(m) = \frac{2}{(n-1)(n-2)} \sum_{i\neq m} \sum_{i<j\neq m} \left(\frac{\delta_{ij}(m)}{\delta_{ij}}\right) \quad (3)$$

The larger C_b is, the higher the vertex is central since it is located at the crossroads.

The betweenness may be normalized by dividing through the number of pairs of vertices not including v, which for directed graphs is (n-1)(n-2) and for undirected graphs is (n-1)(n-2)/2.

B. *Individual Relay*

Problems often arise when people no longer talk to each other or interact with one another. In this case some individuals can act as relays between the two nodes[25]. These individuals belong to the shortest path between the two people.

To form groups and partition the network into disjoint sets, we must consider connections between the nodes globally. This phase is based on: the measurement of the similarity between the nodes [26], latent space model [27], approximation of the block model [28]… etc.

In this study we are interested in calculating the similarity between individuals, which is defined by the similarity of their interaction models. And we say that two nodes are structurally equivalent if they are connected to the same set of actors. The similarity in the graphs is defined in terms of neighbourhood, that means that two vertices are close (similar) if there is a strong overlap between their neighbourhoods. And it can be calculated by several approaches, namely, Jaccard coefficient [29] and cosine similarity [30].

1) Jaccard coefficient: The Jaccard coefficient is used in statistics to compare the similarity and the diversity between individuals who belong to given samples. Discovery of communities. It is the relationship between the cardinal of the intersection of the edges N connecting a node to the other nodes and the cardinal of the same edges. Let two nodes i and j, the Jaccard coefficient is as indicated below:

$$Jaccard(i,j) = \frac{|N_i \cap N_j|}{|N_i \cup N_j|} \tag{4}$$

2) Cosine similarity: The cosine similarity or cosine measure makes it possible to calculate the similarity between two nodes by determining the cosine of the angle between them. The cosine similarity between two nodes i and j is the number of common neighbours divided by the geometric mean of their degrees. This value oscillates between 0 and 1. The value 1 indicates that the two vertices have exactly the same neighbourhood, while the value 0 means that they have no neighbours in common. The cosine similarity is technically indefinite if one or both vertices have a degree of 0, but according to the convention it is said that the cosine similarity is 0, in these cases.

The cosine similarity is calculated according to formula (5) below:

$$Cosine(i,j) = \frac{|N_i \cap N_j|}{\sqrt{|N_i|.|N_j|}} \tag{5}$$

IV. Community Discovery

The discovery of communities within a network is done using several approaches, as follow:

Agglomerative Approche (hierarchical cluster analysis)

The hierarchical cluster analysis (HCA) is an iterative classification method [31].

In the case of graphs we define firstly similarity between vertices based on the adjacency matrix, and we can chain with a HCA. is the pseudocode of the HCA algorithm.

A. *Divisive Approche (Girvan–Newman Algorithm)*

The importance of the connection between two vertices can be materialized by the "edge betweenness"[32]. It indicates the frequency with which it is borrowed when considering the shortest path between each pair of nodes.

$$E_b(m) = \sum_i \sum_{i>j} \frac{\delta_{ij}(m)}{\delta_{ij}} \tag{6}$$

Algorithm 1: The hierarchical ascending classification

```
given a dataset (d1, d2, d3, ....dN) of size N
# compute the distance matrix
for i=1 to N:
  # as the distance matrix is symmetric about
  # the primary diagonal so we compute only lower
  # part of the primary diagonal
  for j=1 to i:
    dis_mat[i][j] = distance[di, dj]
each data point is a singleton cluster
repeat
  merge the two cluster having minimum distance
  update the distance matrix
until only a single cluster remains
```

The higher the value, the more important the connection is, because it establishes a "bridge" between groups of vertices.

The divisive approach consist to iteratively remove connections with the highest values of edge betweenness. Here is the pseudocode of the algorithm:

Algorithm 2: Girvan–Newman algorithm

1. For a given graph G = (V, E), carry out the following steps for each pair of vertices in the same component:
2. For a given pair of vertices u, v assign one unit of flow in total.
3. Find the number, k(u, v), of shortest paths from u to v.
4. Assign 1/k(u, v) units of the flow to each shortest path from u to v.
5. For each shortest (u, v)-path, record the edges in the path. After all this is finished:
6. For each edge e ∈ E count up how much flow goes through the edge e adding over all shortest paths between all pairs of vertices u, v ∈ V which use the edge e.

V. New Application: In the Educational Field

The detection of communities in an educational network aims to identify groups of learners maintaining a special relationship, so they have the same level of skills. In addition, the identification of the most influential person (Leader) may be beneficial to the teacher (learning agent) because it will facilitate his interaction with his students. In addition, the identification of the most influential person (the leader) can be beneficial for teachers (learning agents) because it will facilitate their interaction with their students. This data analytics approach will allow them to pinpoint their students, including, the behaviour, the performance and the student satisfaction in courses, it will allow them too, the prediction of the level of learners and their skills focusing only the leader, in order to enhance the learning experience by providing informed advice and optimizing learning materials and then give a list of possible recommendations.

This theme is experiencing a resurgence of interest in recent years with the development of social media (like LinkedIn, Twitter, Facebook, E-learning platform forums, etc.), multiplying the opportunities for interaction between individuals. A community is a group of nodes with a high density of connections. This article is about to show that social network analysis techniques and community detection can be used in other areas, namely, the educational field, to control a given set of students.

We consider a particular situation where the graph is undirected, the connections between people, if they exist, are symmetrical and unweighted that is to say that the connections have the same intensity.

A. Study Case

The anonymised Students' Academic Performance Dataset [33][34] is an educational dataset which is collected from a learning management system (LMS) called Kalboard 360. Kalboard 360 is a multi-agent LMS, designed to facilitate learning through the use of leading-edge technology. Such system provides users with a synchronous access to educational resources from any device with Internet connection.

The data is collected using the experience API (xAPI), which is a learner activity tracker tool. This component is a part of the training and learning architecture (TLA) that enables to monitor learning progress and learner's actions such as reading an article and watching a training video and all activities and objects describing the learning experience.

The dataset consists of 480 student records and 16 features, between these features we choose 4 that we judged essentials to describe the behaviour of such a student. That are:

- Raised hand: define how many times the student raises his/her hand on classroom.
- Visited resources: define how many times the student visits a course.
- Viewing announcements: define how many times the student checks the new announcements.
- Discussion groups: define how many times the student participate on discussion groups.

And in order to test our program and see how it can identify communities. At first, we chose to select 20 random instances.

B. Construction of the Network

The network must be described by a symmetric Boolean adjacency matrix (values 1/0) indicating the privileged relationships (or not) maintained by the learners. To this end, we must use the database we have available to construct this adjacency matrix that will be used to build the graph and then define the leaders and determine the communities.

The adjacency matrix is calculated firstly by the cosines similarity and as a result we had a cosines similarity matrix between each instance and the others. And secondly by transforming this matrix on a Boolean one by replacing values by 0 or 1 compared on a threshold. Here the threshold is set at 0.89. Finally, we construct the graph represented in Fig. 1. Where each node in our social network represents an individual participant in the class. And the relationships between the participants are presented as arcs. We define a relationship between them by a higher degree of similarity.

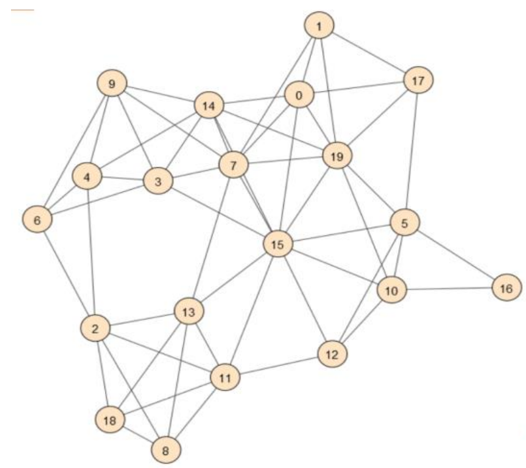

Fig. 1. The Graphical Representation of 20 Instances Chosen Randomly.

C. Identification of Central Nodes

After the calculation centrality, the program have as results the three Tables I, II and III, representing respectively the degree centrality, closeness centrality and betweenness centrality.

Reading is easier if we display the most important values in descending order by associating them with the names of the nodes.

In Table I, the vertices 15, 19, 7, 14 and 13 are highlighted. That means that these are candidate points to be central points.

Same for Table II, vertices 15, 19, 7, 14 and 13 are highlighted. Except that summit 7 is second this time.

In Table III, we observe a certain coherence with the previous results.

Obviously, individuals 15 and 7 are at the centre of relationships between group members. Then, the program choose these nodes whose highlights in the graph using appropriate colours. As shown in the following Fig. 2.

TABLE. I. TOP 5 FIRST VALUES OF THE DEGREE CENTRALITY IN DESCENDING ORDER

Node name	***degree***
15	10
19	8
7	8
14	7
13	6

TABLE. II. TOP 5 FIRST VALUES OF THE CLOSENESS CENTRALITY IN DESCENDING ORDER

Node name	***closeness***
15	0.678571
7	0.612903
19	0.558824
14	0.558824
13	0.558824

TABLE. III. Top 5 First Values of the Betweenness Centrality in Descending Order

Node name	***Betweenness***
15	49.775000
7	22.591667
13	19.250000
11	15.700000
19	15.075000

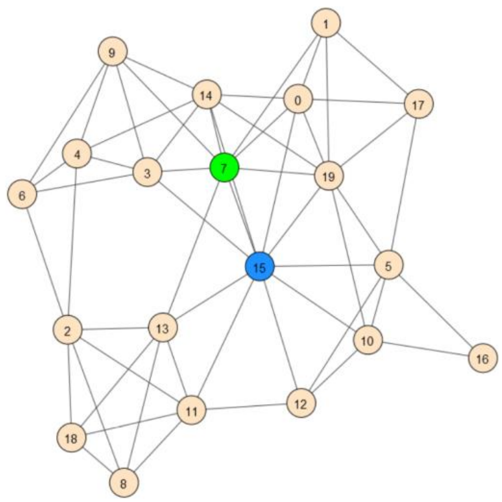

Fig. 2. The Graphical Representation with Highlighted Central Nodes.

D. Discovering Communities

We are interested in a divisive approach based on the notion of "edge betweenness". We obtain a net partition (crisp), i.e. an individual belongs to one and only one group.

In a possible partition into two groups, we note that the troublemakers' individuals 7 and 15 will actually be separated as shown in the resulting dendrogram of the hierarchical ascending classification (Fig. 3) and so this appears explicitly in the graph (Fig. 4) where both communities appear clearly.

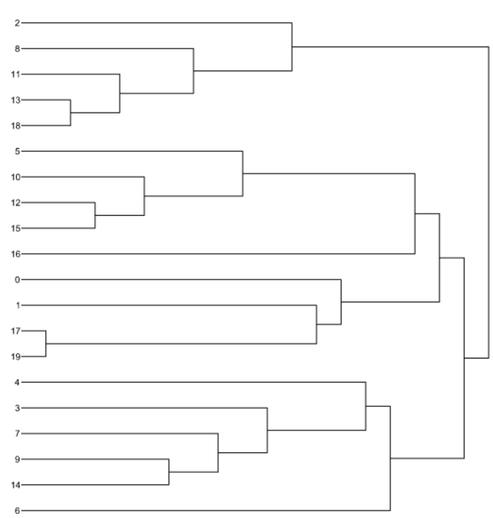

Fig. 3. The Resulting Dendrogram of the Hierarchical Ascending Classification.

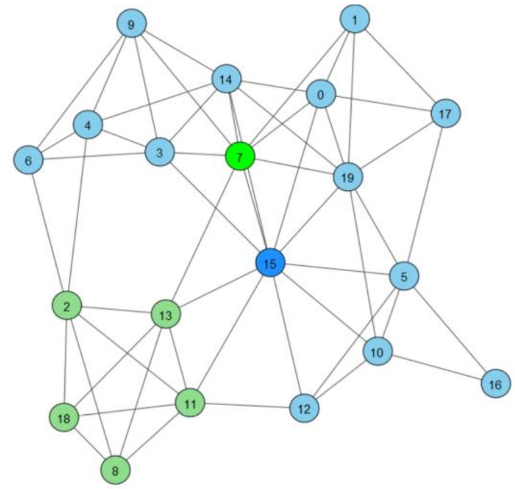

Fig. 4. The Graphical Representation with Highlighted Two Communities.

We performed the Girvan Newman clustering and the resulting clusters can be seen in Fig. 4. In this graph, nodes with dark colours represent leaders of their communities. And moreover, they are the students who can be traced to get a global idea on the other students belonging to the same community.

Community users tend to interact frequently, share interests, and trust each other to some extent. Therefore, our method will help teachers to reduce the efforts made to manage a very large number of students, to a minimum effort. In other words, to manage their students, teachers only have to observe the central players who constitute all the influential students to carry out targeted actions, organize the structure of the class, guide the learners, and adjust the recommendations, for all students belonging to the same communities.

VI. Conclusion

With recent technological advances, huge amounts of data are accumulating at a frantic pace in various areas of human activity, namely, the learning activity. Understanding both the universal and specific characteristics of the networks associated with this data has become a real and important task. Knowing the structure of the community makes it possible to predict certain essential characteristics of the systems under study. For example, with our approach, it is possible to discover student learning communities in the pedagogical system. We then provide a tool based on the notion of centrality and standard community detection algorithms for interpreting the local organization of a student network within a learning management system, which can be used to identify standard profiles, perform targeted actions, and better adjust recommendations. For our future work, we want to spread our study on our university students in order to integrate it in the module of recommendation of pedagogical resources of a learning management system.

References

[1] R. Raja and P. C. Nagasubramani, "Impact of modern technology in education," J. Appl. Adv. Res., vol. 3, no. S1, p. 33, May 2018.

[2] P. Serdyukov, "Innovation in education: what works, what doesn't, and what to do about it?," J. Res. Innov. Teach. Learn., vol. 10, no. 1, pp. 4–33, Apr. 2017.

[3] W. D. Haddad and A. Draxler, "The dynamics of technologies for education," Acad. Educ. Dev., pp. 2–17, 2002.

[4] P. Bedi and C. Sharma, "Community detection in social networks," Wiley Interdiscip. Rev. Data Min. Knowl. Discov., vol. 6, no. 3, pp. 115–135, May 2016.

[5] F. Radicchi, C. Castellano, F. Cecconi, V. Loreto, and D. Paris, "Defining and identifying communities in networks," Proc. Natl. Acad. Sci. U. S. A., vol. 101, no. 9, pp. 2658–2663, 2004.

[6] H. Cai, V. W. Zheng, F. Zhu, K. C. C. Chang, and Z. Huang, "From community detection to community profiling," Proc. VLDB Endow., vol. 10, no. 7, pp. 817–828, 2017.

[7] F. Gasparetti, A. Micarelli, and G. Sansonetti, "Community Detection and Recommender Systems," in Encyclopedia of Social Network Analysis and Mining, New York, NY: Springer New York, 2017, pp. 1–14.

[8] R. Missaoui and I. Sarr, Eds., Social Network Analysis - Community Detection and Evolution. Cham: Springer International Publishing, 2014.

[9] R. Brown et al., "Good Communities and Bad Communities: Does membership affect performance?"

[10] R. Brown et al., "Communities of performance & communities of preference." CEUR-WS, 2015.

[11] B. S. Khan and M. A. Niazi, "Network Community Detection: A Review and Visual Survey," 2017.

[12] M. Planti and M. Crampes, "Survey on Social Community Detection To cite this version : Survey on Social Community Detection," pp. 65–85, 2013.

[13] A. Dhumal and P. Kamde, "Survey on Community Detection in Online Social Networks," Int. J. Comput. Appl., vol. 121, no. 9, pp. 35–41, 2015.

[14] G. Jia et al., "Community Detection in Social and Biological Networks Using Differential Evolution," Springer, Berlin, Heidelberg, 2012, pp. 71–85.

[15] S. Combéfis, "Viral marketing and Community detection algorithms," p. 89, 2007.

[16] Q. Wang, "Overlapping community detection in dynamic networks," 2012.

[17] C. P. Diehl, G. Namata, and L. Getoor, "Relationship Identification for Social Network Discovery," AAAI Work. - Tech. Rep., vol. WS-08-04, pp. 9–14, 2008.

[18] M. Gargiulo and M. Benassi, "Trapped in Your Own Net? Network Cohesion, Structural Holes, and the Adaptation of Social Capital," Organ. Sci., vol. 11, no. 2, pp. 183–196, 2000.

[19] L. C. Freeman, "Centrality in Social Networks Conceptual Clarification," Soc. Networks, vol. 1, no. 1968, pp. 215–239, 1978.

[20] S. P. Borgatti, "Centrality and network flow," Soc. Networks, vol. 27, no. 1, pp. 55–71, Jan. 2005.

[21] S. P. Borgatti and M. G. Everett, "A Graph-theoretic perspective on centrality," Soc. Networks, vol. 28, no. 4, pp. 466–484, Oct. 2006.

[22] G. Sabidussi, "The centrality index of a graph," Psychometrika, vol. 31, no. 4, pp. 581–603, Dec. 1966.

[23] L. C. Freeman, "A Set of Measures of Centrality Based on Betweenness," Sociometry, vol. 40, no. 1, p. 35, Mar. 1977.

[24] U. Brandes, "A faster algorithm for betweenness centrality*," J. Math. Sociol., vol. 25, no. 2, pp. 163–177, Jun. 2001.

[25] Z. Lu, X. Sun, Y. Wen, G. Cao, and T. La Porta, "Algorithms and Applications for Community Detection in Weighted Networks," IEEE Trans. Parallel Distrib. Syst., vol. 26, no. 11, pp. 2916–2926, 2015.

[26] A. Rawashdeh and A. L. Ralescu, "Similarity measure for social networks-a brief survey," CEUR Workshop Proc., vol. 1353, pp. 153–159, 2015.

[27] D. K. Sewell and Y. Chen, "Latent Space Approaches to Community Detection in Dynamic Networks," Bayesian Anal., vol. 12, no. 2, pp. 351–377, Jun. 2017.

[28] E. Abbe, "Community detection and stochastic block models: Recent developments," J. Mach. Learn. Res., vol. 18, pp. 1–86, 2018.

[29] B. Bank, Jacob and Cole, "Calculating the jaccard similarity coefficient with map reduce for entity pairs in wikipedia," Wikipedia Similarity Team, 2008.

[30] S. Tariq, M. Saleem, and M. Shahbaz, "User Similarity Determination in Social Networks," Technologies, vol. 7, no. 2, p. 36, 2019.

[31] E. Cuvelier et al., "Graph Mining and Communities Detection," 2012.

[32] M. Arasteh and S. Alizadeh, "A fast divisive community detection algorithm based on edge degree betweenness centrality," Appl. Intell., vol. 49, no. 2, pp. 689–702, Feb. 2019.

[33] E. A. Amrieh, T. Hamtini, and I. Aljarah, "Mining Educational Data to Predict Student's academic Performance using Ensemble Methods," Int. J. Database Theory Appl., vol. 9, no. 8, pp. 119–136, Aug. 2016.

[34] E. A. Amrieh, T. Hamtini, and I. Aljarah, "Preprocessing and analyzing educational data set using X-API for improving student's performance," in 2015 IEEE Jordan Conference on Applied Electrical Engineering and Computing Technologies, AEECT 2015, 2015.

Visualising Image Data through Image Retrieval Concept using a Hybrid Technique: Songket Motif's

Nadiah Yusof[1], Amirah Ismail[2], Nazatul Aini Abd Majid[3]
Faculty of Information Science and Technology
Universiti Kebangsaan Malaysia (UKM) Bangi Selangor Darul Ehsan Malaysia

***Abstract*—It has been proven that the massive dataset is strictly complex in Content Based image Retrieval (CBIR) because the present strategies in CBIR might have faced difficulties in feature extraction of the images. Moreover, technological constraints encountered in the analysis and extraction of the image arrays are how the system customizes the primitive geometric structures known as polygonal approximations structure. Hence, this study has discovered that image feature extraction is utilized by applying the Principal Component Analysis (PCA) technique, which is primarily based on the matrix of image representation that will enlarge the similarity of detection. The PCA approach needs to be enhanced resulting from the lack of the extraction of features in songket motives images. Therefore, this study proposes a new hybrid model that will integrate PCA with geometric techniques for image feature extraction to increase the recall and precision result. This paper employs the use of a qualitative experimental design model that involves three phases of activities. First, the analysis and design phase, secondly is a development phase, and lastly is the testing and evaluation phase. This paper focuses on those two phases in terms of design and development phases. The outcome process of the empirical phase is followed by designing the algorithm and model based on the result of literature review. This study has found that the hybrid between the principal component analysis model and the geometry technique will help to reduce the problems faced by the basic engineering technique model, which is the constraint in analysing and extracting the image features to customize the geometric primitive structure.**

Keywords*—Multimedia; image; content-based image retrieval (CBIR); image retrieval; near-duplicate; principal component analysis (PCA); geometric

I. Introduction

Malays are rich in fine art heritage, inherited since immemorial time. Weaving, embroidery, engraving and fine arts are so synonymous with Malay custom. Creativity and fine arts are reflected in each of these traditional handicrafts. The fine arts of Malay cultural heritage include weaving, batik art, fireplace, stick, dastard, beads, engraving, brass, and songket. [1],[2]. Songket is a fine art heritage with many privileges. The important part of the songket fabric is the structure of songket motif's image that shows the different philosophy and meaning [3]. Table I shows that preservation aspects of songket motif's from many websites are not solely the main purpose but focuses towards the commercialization aspects and concerns [4]. Researchers play an important role in preserving the continuity of the Malay cultural heritage from extinction in this modern era [2]. Songket preservation and conservation efforts can be undertaken by digitizing the principal component of songket fabric; the songket motif's arrangement.

The arrangement of songket motif's is an important element of songket fabric which provides and avenue for the songket motives image digitization research and studies. The digitization of songket motif's will help to preserve the songket motif's from extinction and allow the continuation of heritage for future generations. While defining features and structure of images will help to facilitate a database of songket motif's proceeds with the clustering process according to a specific category. This process eases the users to store and retrieve the image of songket motif's without having to categorize the songket motif's image manually. Thus, automatic clustering of songket motif's can be performed by the implementation of near-duplicate image retrieval technique. Various image retrieval techniques have exploited and included those traditional image retrieval techniques which have been implemented through the content-based image retrieval (CBIR).

Content-based image retrieval [6] field has been rather popular among researchers through a rapid study along with other popular research areas such as Database Management, Natural Language Processing, Signal Processing, Computer Vision, Network Systems and Human-Computer Interaction [7]. Since studies on the field of image retrieval have proliferated, the main issue is how to expect the user's preferences [8] to the result of the image obtained through the image retrieval system [9],[10],[11]. Various models of image feature extraction were introduced through the implementation of the development on a variety of retrieval systems. The developed system uses multiple models of processing query image features to represent the information space contained in the image, whether in the query or the database space.

The implementation of a model description of the image feature in the field of image retrieval has been extended through the customization of the model in the field of pattern recognition to help analyse the query image features and images contained in the database to fit the image retrieval field. Implementation of the study mentioned above is part of the detect and matching process to retrieve near-duplicate images. The precision of the image can almost be seen from the point of similarity found in image features (such as; shapes, textures, text, sketches, and colours). The features mentioned are part of the basic content-based image retrieval technique. All these techniques can assist the process of near-duplicate image entirely, as evidenced by various studies that have been carried out [10],[12],[13],[14]. However, the techniques involved in

CBIR face obstacles in processing image datasets in high-dimensional clusters [15],[16],[17]. Technological constraints encountered in the analysis and extraction of image arrays indicate how to customize primitive geometric structures and are better known as polygonal approximations.

TABLE. I. SURVEY ON QUERY TECHNIQUE ON RELATED SONGKET WEBSITE : [5])

Survey on Query Techniques	
Website	***Explanation/Content***
Institut Kraf Negara (www.ikn.gov.my)	Craft institution website
Visit Terengganu (www.visit-terengganu.net)	Tourist and advertisement website
Songket Moden (songketmoden.com)	Product commercialize
Warisan Budaya Melayu (malaysiana.pnm.my)	Malaysian culture heritage website
Azizah Songket Terengganu (azizahsongket.wordpress.com)	Product commercialize
Songket Restaurant (www.songketrestaurant.com)	Product commercialize
Bibah Songket (www.bibahsongket.com)	Product commercialize
Atikah Songket TTDI (www.atikahsongket.com)	Product commercialize
Aura Batik (aura-batique.blogspot.com)	Product commercialize
Kain Songket.com (kainsongket.com)	Product commercialize

Therefore, this study has found that the hybrid between the Principal Component Analysis [18] model and the geometry implemented help to reduce the problems faced by the basic Engineering technique model, which is the constraint in analysing and extracting the image outline for the purpose of customizing the geometric primitive structure where the problem can solved by emphasizing aspects image representations of the primitive data structure angles within the image [19],[20] which include image size, image depth, angle and compression of images. These are the components found in the Principal Component Analysis model. Also, the principal component analysis model will help to decrease each dimension of the image features and structure [16], while geometric techniques are identified to help detect the global space within the image and continued with scale, rotation, small and big size of images.

The paper is organized as follows. In Section 2, a brief review of relevant works is presented, and labelled as Research Background; Section 3 presents the research flow described as Method. Meanwhile, Section 4 discusses the structure of the system and development; The experimental results of the studies on algorithm evaluation are presented in Section 5 and the paper is concluded in Section 6.

II. RESEARCH BACKGROUND

Multimedia data (text, images, audio, and video) have always inundated websites [21], including YouTube, Google videos, Facebook, Instagram, Twitter, and Flickr [22]. In addition to providing information and connecting to the world without boundaries, it can also harm database information management in managing the flow of multimedia data, especially images. Uploading images again will increase a similar image and is known as a near-duplicate image. Currently, almost all images on various websites show over 80 percent similarity [23],[24]. This issue necessitates the study of near-duplicate image retrieval in order to match and cluster the near-duplicate image in unique characteristic.

A. Challenges in Near-Duplicate Image Retrieval

There are two challenges in detecting the near-duplicate image. The first challenge is that the selection of features extraction technique aims to compute the percentage of similarity of image features in large-scale databases [25]. The second challenge is the process of image clustering with an existing template in a database. Assignments in the clustering process involve time, angles, illumination and resolution of the image that need to be detailed and compared for similarity properties, which makes the process involved in clustering process complicated than the implementation of near-duplicate image retrieval tasks [17], [26]. However, the two tasks are mutually required to enable image processing in the search system.

B. Image Features Extraction

The essential element in near-duplicate image retrieval is through the technique of matching and comparison between query images and stored images in the database [26]. Furthermore, several characteristics are related to near-duplicate image retrieval whereby detection for near-duplicate image involves two-part of images; the first part is a query images and the second part is images inside the database. Category of images divided into two main sections, the general image, and the specific image category. Commonly, general images are images of various activities provided by users through the social media sites, image management centres, personal blogs, online drivers such as Google Drive, Dropbox and others [17] whereas the specific image is a group of images that come from different areas such as medical image scan, cultural heritage, criminal image, chemical structure, and building structure. Usually, specific images database is provided only for a specific user and private databases. Besides, to extract the image features, the image needs to be extracted based on the structural primitive contained within the image.

Image features are analyzed through the calculation of structural primitives and the technique of placement within the image because that technique is very effective against complex image structures. While the other technique method of calculating similar structure of images is based on statistics that include Fourier Power Spectrum Statistics [27], Co-Occurrence Matrices [28], [29], Fixed-Invariant Principal Component Analysis (SPCA) [19],[30], Tamura Feature [31], Wold Decomposition [32], Random Markov Fields [33], Fractal Models [34], and Multi-Resolution Filtering Techniques such as Gabor and Wavelet Transform [11]. The features found in texture techniques are statistically performed through the distribution of image intensity [11],[29],[31], [26],[35],[36]. This technique is very effective in measuring the shape of the images matrix to obtain the different surfaces of the objects [37],[38]. However, the constraints encountered are that the boundaries between objects that have a similar tone of objects that are difficult to be identified, thus, the process to to decipher the structure of each object in the image being executed is hindered.

Furthermore, research on near-duplicate image retrieval also includes Sketch-Based Image Retrieval (SBIR), and it has begun as early as the 1990s [39],[4]. This study was sparked by the domain of cartoon images. The primary purpose of this technique is to help those who are not able to read especially children. This technique allows the user to retrieve the cartoon image by sketching the imaged bone into the sketch canvas, and the system initiates the sketch structure in order to match a similar image by sketch bone. This technique has been proven to be more effective in assisting users than textual techniques and is more user-friendly, especially for children [5],[4],[40]. In general, almost all researchers in the field of image retrieval support and agree that content-based image retrieval techniques will allow the users retrieve similar image much more efficiently and effectively [7],[4]. However, the technique in CBIR encounters barriers with image issues as more complex and challenging images are required to determine the similarity of queries that users aim to reach, and this is a complex task for the CBIR system to perform [4],[41]. Therefore, various technological innovations have been proposed by subsequent researchers who aim to assist in the process of features extraction of the near-duplicate image retrieval structure.

Furthermore, the process of extraction of image features needs a calculation on the precision value of the similarities between the query image and the stored image in the database. Additionally, the value of similarity in image retrieval is measured based on the estimated empirical values contained in the near-duplicate image characteristics that have been identified by the system and is shown in Fig. 1. The similarities between query images and stored images may impede the measurement of the retrieval value and image accuracy in determining the effectiveness of the developed image retrieval system [43].

Moreover, various studies and techniques involving near-duplicate image retrieval have been conducted recently in order to solve some issues and problems pertaining the related technique, which is the bag of visual word and Min-Hash [44],[16], This technique focuses on clustering the near-duplicate images through the matching of space and position within the image. Meanwhile, the Singular Value Decomposition-Scale Invariant Feature Transform (SVD-SIFT) technique [45] implements a catalyst method to speed up the image detection process. Subsequent Salient Riemannian Visual technique [22] aims to identify the prominent space within the processed image. Furthermore, the data duplication technique [46],[47],[48],[49] optimizes database usage by reducing subsequent data match and comparing to bits of help reduce electricity consumption which can increase heat production. Another technique is Similarity Join Operator Technique [42],[50] that evaluate image similarity based on absolute ratios, whereas, Fourier Mellin Transform technique [51] helps image detection via image rotation, image scaling and invariant changes found in the image, followed by the Haar-wavelet technique [52],[53] that assist to extract features vector that is included in the image in order to find the Manhattan distance of the object in the image. Furthermore, kernel hashing technique [54] helps to detect the near-duplicate image by examining the various features contained within the image to detect the differences of each image and convert it to binary of images to place within the kernel space. Although most of the techniques mentioned above focus more on image features extraction for low dimensionality, but when applied to high dimensional images, the system has to deal with the time-consuming problems in image feature extraction and can cause the delay of the process [17]. In consequence, this problem has suggested several solutions.

Therefore, among other techniques that have been introduced in order to solve image features extraction problems for a massive dataset, the locality-constrained linear coding (LLC) & max-idf [17] technique has been proposed to improve features extraction structure of the image through the fragmentation of the matrix contained in the image and continue with clustering the near-duplicate image by dividing the image into several baskets following by the essential features. Furthermore, the next step is to apply to a matching technique within the space for the image clustering task based on the image feature extraction. The hashing technique [16],[48] also will help to extract the features on the image in large-scale images dataset, the process following by detecting Jaccard similarity structure where the images have high precision included in the same cluster. Another technique used is the Min-Hash & tf-idf weighting technique [55],[56] whereas those techniques are more focused on detecting near-duplicate images in local space of images. As shown in Table II, almost all of the researchers focused only on local space while only one researcher focused on the two spaces (local & global) in the image [26].

A study conducted by Hassanian [23] agreed whereby focusing on the two spaces within the image helps to improve the image accuracy results. This combination, therefore, enhances the effectiveness and overall efficiency of image features extraction almost immediately [57]. Also, this statement was supported by [58], which stated that a combination of global and local features helped to increase accuracy by up to 65.5 percent. The global space is the basic structure in the image, while the local space is the space that meets the basic structure.

Fig. 1. Framework of Near-Duplicate Image Proposed by [42].

TABLE. II. SUMMARY OF PREVIOUS TECHNIQUES HAVE BEEN USED TO DETECT NEAR-DUPLICATE IMAGE RETRIEVAL PROBLEM

Previous Techniques in Near-Duplicate Image Retrieval		
References	***Technique***	***Local /Global***
[22]	Rotation, Scale, Translation (RST) Invariance features + Salient Covariance Matrix (SCOV) + ICA Independent component analysis	Global
[59]	Scale In variance Features Transform (SIFT)	Local
[60]	Scale In variance Features Transform (SIFT)	Local
[61]	Scale In variance Features Transform (SIFT) + Histograms of oriented Gradient (HoG) + BoF + KMean Clustering	Local
[62]	Locality Sensitive Hashing + K-Nearest Neighbor SIFT + K means + BoVW	Local
[63]	Colour Texture Moment (CTM)	Local
[64]	Strong Geometry Consistency (SGC) + Scale Weighting	Local
[65]	Bag of Visual Word (BoV)	Local
[26]	Color Moment + Wavelet Transform + SIFT	Local & Global
[66]	Bag of Visual Word (BoVW)	Local
[67]	K-Nearest Neighbor	Local
[16]	Min-Hashing + Jaccard Similarity	Local
[68]	Bag of Word	Local
[69]	K-Mean Clustering + Bag of Word	Local
[42]	K-Mean Clustering	Local
[17]	Locality Linear Coding + MaxIDF-cut + K-Means clustering	Local
[55]	Canny Edge Detection+ Great Deluge Algorithm	Local
[23]	Min-Hash + Locality Sensitive Hashing	Local

III. METHOD

This section focuses on three main phase's iteration; first, is the analysis and design phase, secondly is a development phase, and lastly is the testing and evaluation phase. Fig. 2 shows the interconnection between the three phases implemented in the research, but only two phases which are coloured has been applied in this paper.

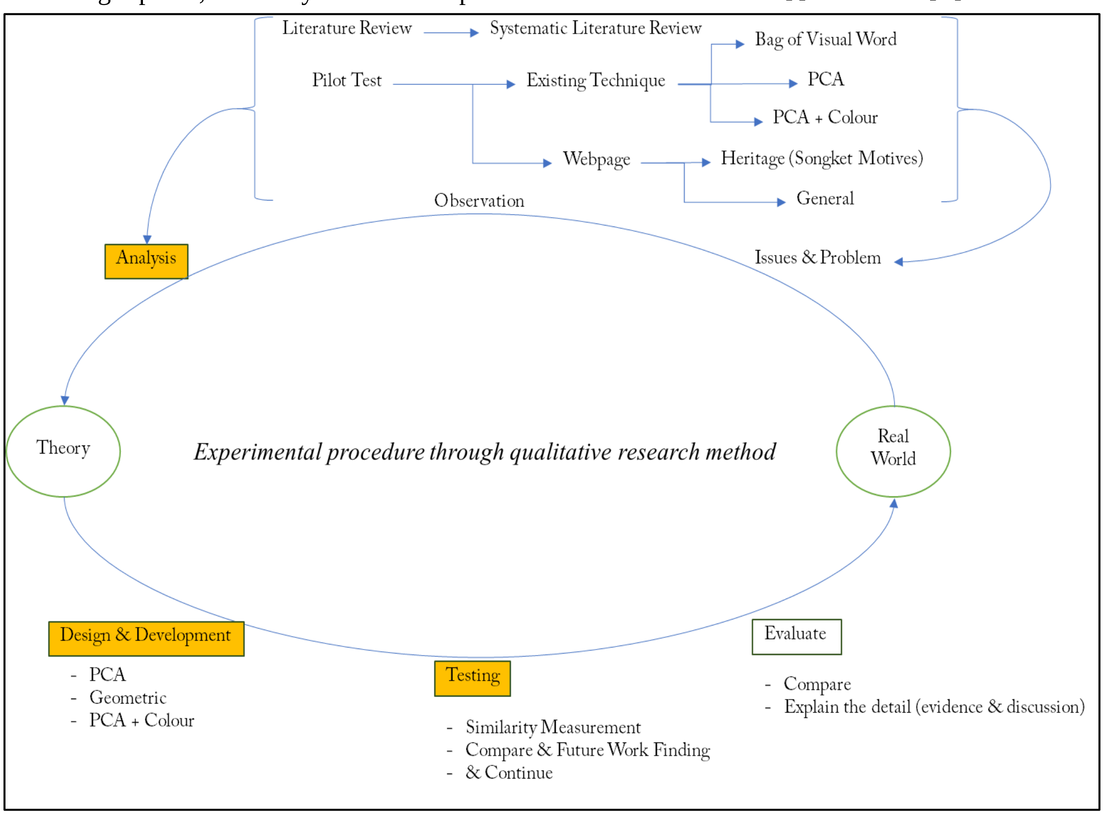

Fig. 2. The Interconnection between the Three Phases has Implemented in the Paper[70].

The analysis phase divided is into two main categories of the process. The process is followed by analysing more than 400 articles, that include books, in order to structure and prepare a systematic literature review on a variety of techniques that have been applied and proposed in near-duplicate image retrieval and clustering. The advantages of a systematic literature review will help the readers to find a new significant contribution that can contribute to the body of knowledge in image retrieval research field. Also, it is important to look at the advantages and disadvantages of each proposed technique and, which techniques are appropriate to be applied to the cultural heritage domain and various other domains in general. As can be seen, the songket motif's image structure is more geometric, so the hybrid of the two techniques is assumed to coincide with the image structure described earlier after obtaining technique suitable for near-duplicate image retrieval. Subsequent design and algorithm development were performed using MATLAB 2019a software. Finally, after image detection algorithms were almost fully utilized, the PCA technique was developed. Technical testing is performed by applying Local Binary Pattern and similarity measurement technique to see image results and is a guide to improvements to the development of hybrid image detection of hybrid algorithms.

IV. System Implementation

System implementation starts with applying principal component analysis technique with eigenvalues on images (query/databases) in order to proceed on comparison of image size following by converting the images into double-precision value using sin & cos algorithm (%(sj*sin hj – si*sin hi)^2) calculation, then proceeding with the features extraction process.

Features extraction process is followed by computing, selecting, and normalizing the eigenvalue of images. The number of eigenvalues is always lower or equal than the number of the original image (i.e., K<M), and the process in normalization is to remove all the standard features in the images in order to get the lower dimension of images. A method on normalizing shape value using principal component analysis following by calculation of average shape value then calculating the mean (average) shape value to urge the normalizing of the shape value. Consequently, to calculate eigenvalue in images, the system must be used and calculate the covariance matrix first and the algorithm is shown in (1) and Fig. 3 below is an example direction and calculation of features extraction using principal component analysis on the images.

$$\% \; cov(X, Y) = \frac{1}{n} \sum^{n} (X_1 \vec{X})(Y_1 - \vec{Y}) \qquad (1)$$

Principal component analysis eigenvalues will be considering each pixel in an image as a separate dimension. For example, N*N images has N2 pixels; therefore, the value in N2 has a dimension (e.g., 236*236 = 55696), that values are showing a vast amount number, and the calculation process will make the system slower, and run out of memory, and computation calculation on that amount requires a vast process. The system will process to a reduced dimension of images by calculating the eigenvalue from covariance matrix using principal component analysis into lower dimension (100*100 = 10000) of size images in order to recognize the vital image structure and known as a principal component. Fig. 4. shows the process of a reduced dimension of geometric images by computing, selecting, and normalizing the dimension inside the image's matrix.

Rotation changes the spatial relationships between the grid cells and the object boundaries, which leads to a completely different matrix number representation for a similar object. Therefore, objects should be through the normalizing process for a geometric shape rotation. The most important axis of the shape will be accomplished by connecting the two points on the shape boundary furthest faraway from one another.

The shape is then rotated to create a significant parallel to the coordinate axis. An example of rotation normalization in Fig. 4 shows an object before rotation normalization and scale normalization of an object [72] and the whole process in the system is also shown in Fig. 5. The principal component analysis is improved by enhancing the process of rotation, scale, and normalization using a geometric algorithm calculation. By describing the direction of rotation, an example is shown in Fig. 6 from 0 to 315 degree [71].

```
Features Extraction
% compute, select & normalize eigenvector
          [V, D] = eigs(cov([M1(:) M2(:)]));
% matrix D containing the eigenvalue on the main
diagonal
% matrix V whose columns are the corresponding
eigenvalue

...............Direction of image scan
|          | Rows (:,n);
|    C     |
|    O     |
|    L     |
|    U     |
|    M     |
|    N     |
|    S     |
| (m,:);   |

if (D(1,1) > D(2,2))
  a = V(:,1)./sum(V(:,1));
else
  a = V(:,2)./sum(V(:,2));
end;
```

Fig. 3. Image Features Extraction Process using Covarians Matrix.

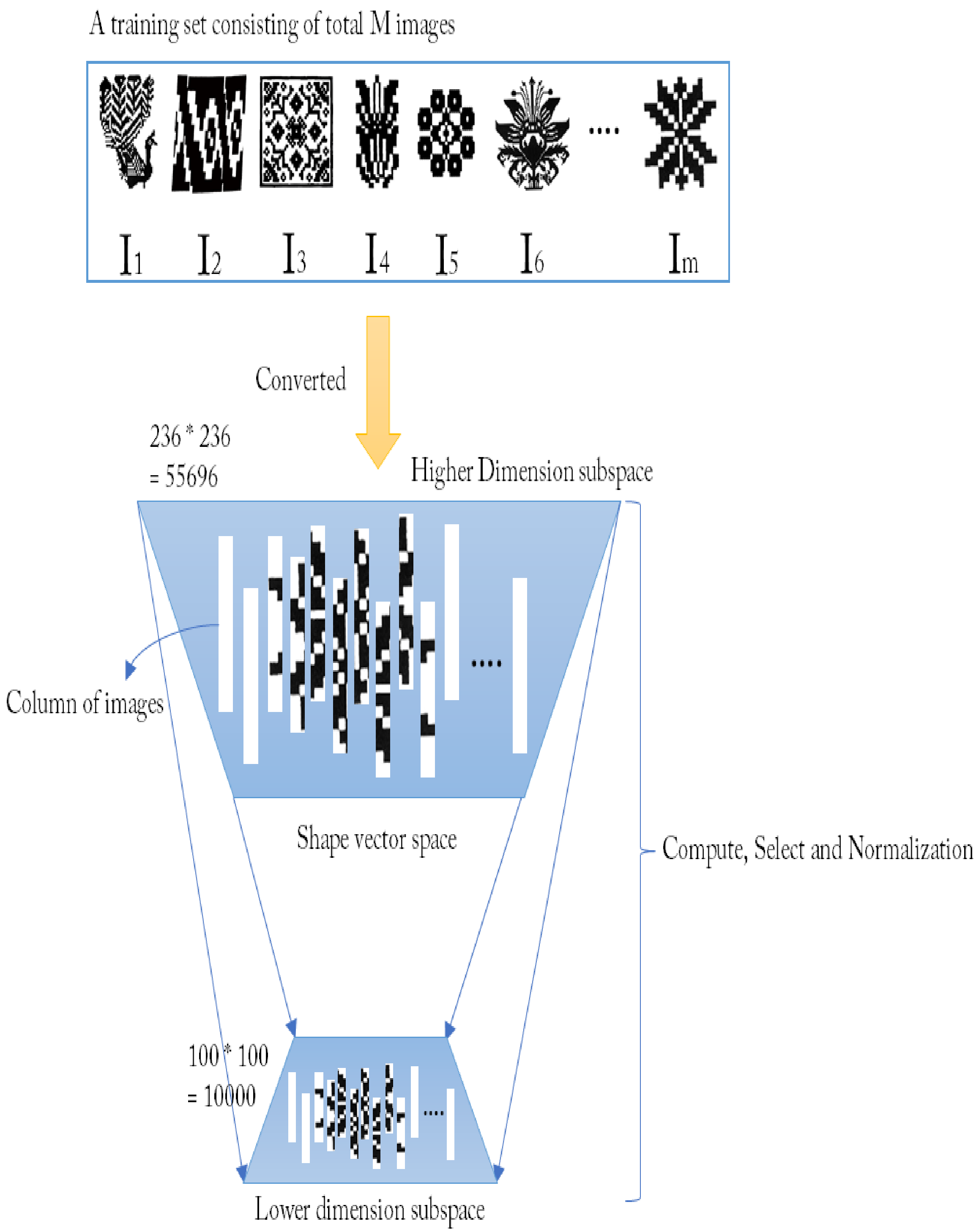

Fig. 4. A Step of Compute, Select and Normalize the Image Vector Space.

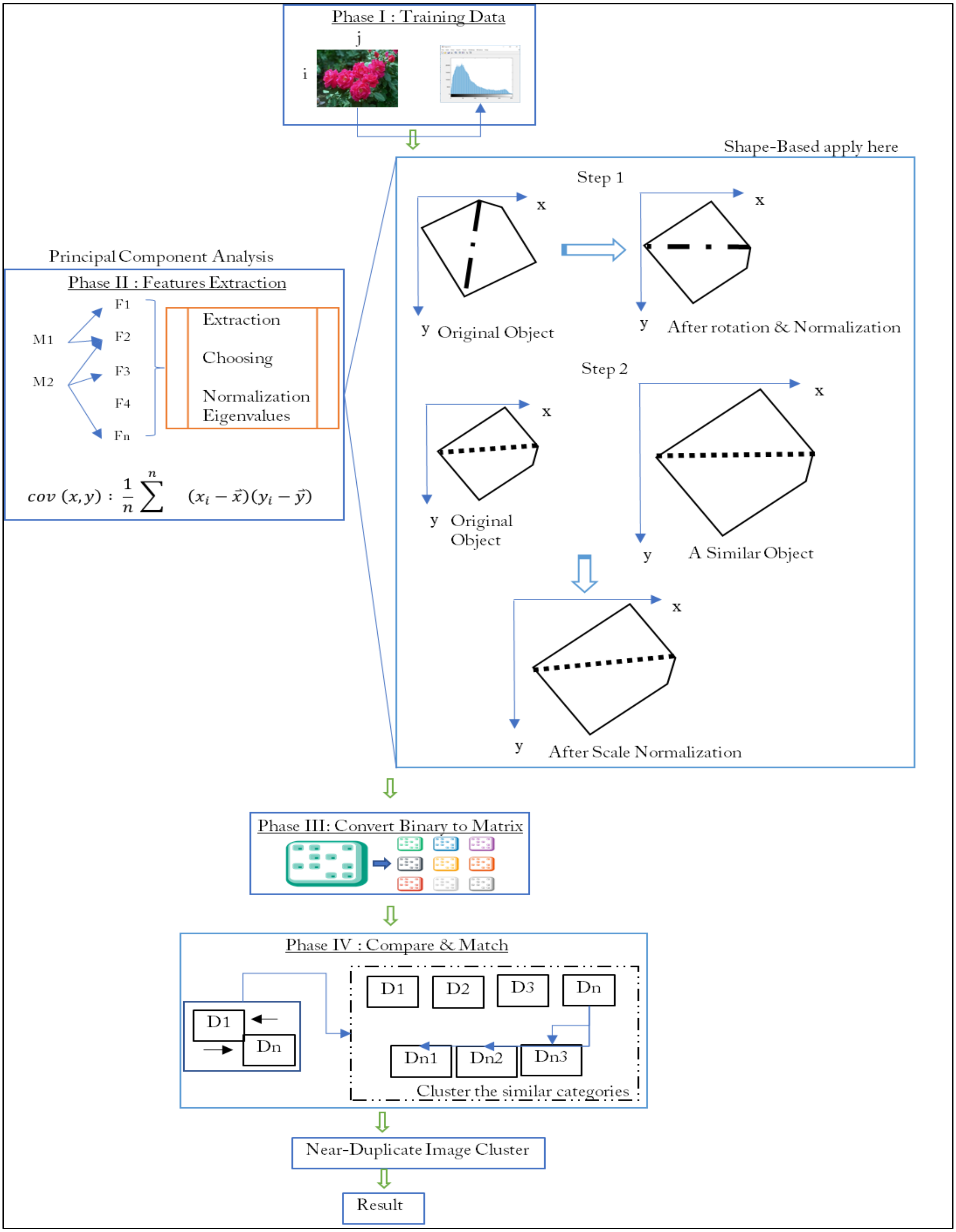

Fig. 5. The System Flows for Near-Duplicate Image Retrieval.

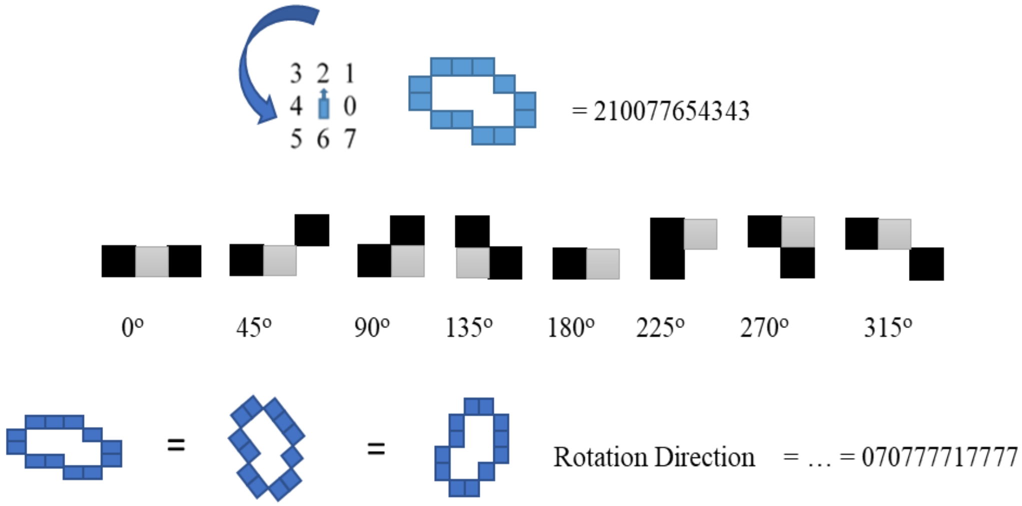

Fig. 6. The Degree of Direction Applying in the System in Order to Help Improve the Detection of Near-Duplicate Images Redrawn from [71].

V. Result and Discussion

The testing recall results using songket motives images data that has been deployed in two different techniques in order to prove the theory conception of this paper. Table III could be a half part of the recall result using principal component analysis technique. Table V shows a half part of a recall result using a bag of visual word technique, while Table IV (PCA) and Table VI (BoVW) show a full result of recall and precision for the two technique that has been tested in this paper.

Based on the preliminary tests conducted on the principal component analysis technique and the bag of visual words technique, the percentage of image precision value is calculated by local binary pattern and similarity measurement technique showed that the principal component analysis technique result is higher than the bag of visual word technique as in Fig. 7. The bag of visual words technique analysed the image through the chuck of the image, and it is difficult to finalize the real shape structure of image template, and thus, the results obtained are less accurate than the principal component analysis techniques. Whereas the principal component analysis technique is seen to produce higher precision results in image retrieval but lacking with less recall of images. It is seen as limiting the choice of the user; based on the suggestion by Prof. Dr. Nursuriati Jamil during the interview (May 2019) session, result of retrieve images can be further enhanced by improving image rotation, image scaling, improvising the image size by enlarging and reducing the size of images. According to her suggestions, the suitable technique is the implementation of a hybrid technique together with the principal component analysis and quadratic distance algorithm to be applied in the near future in order to improve a recall result and precision result of image songket motives.

TABLE. III. A Partially of Principal Component Analysis Technique on Songket Motives Images Retrieval Result

A part of Principal Component Analysis						
Query	***Result***					
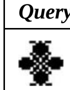						
						

TABLE. IV. A Full Average of Principal Component Analysis Technique on Songket Motives Images Retrieval Result

Query images										
	1	***2***	***3***	***4***	***5***	***6***	***7***	***8***	***9***	***10***
Principal component analysis Precision Value of Songket Motives	1.0	1.0	1.0	1.0	1.0	1.0	1.0	1.0	1.0	1.0
	0.41	0.37	0.38	0.86	0.79	0.71	0.70	0.71	0.66	0.77
	0.41	0.38	0.46	0.81	0.77	0.72	0.91	0.73	0.69	0.78
	-	0.48	0.48	0.92	-	0.63	0.81	-	0.71	0.74
	-	0.59	-	0.71	-	-	-	-	-	-
	-	0.59	-	0.62	-	-	-	-	-	-
Average result	0.61	0.57	0.58	0.82	0.85	0.76	0.85	0.81	0.76	0.82

TABLE. V. A PARTIALLY OF BAG OF VISUAL WORD TECHNIQUE ON SONGKET MOTIVES IMAGES RETRIEVAL RESULT

A part of Bag of Visual Word	
Query	***Result***

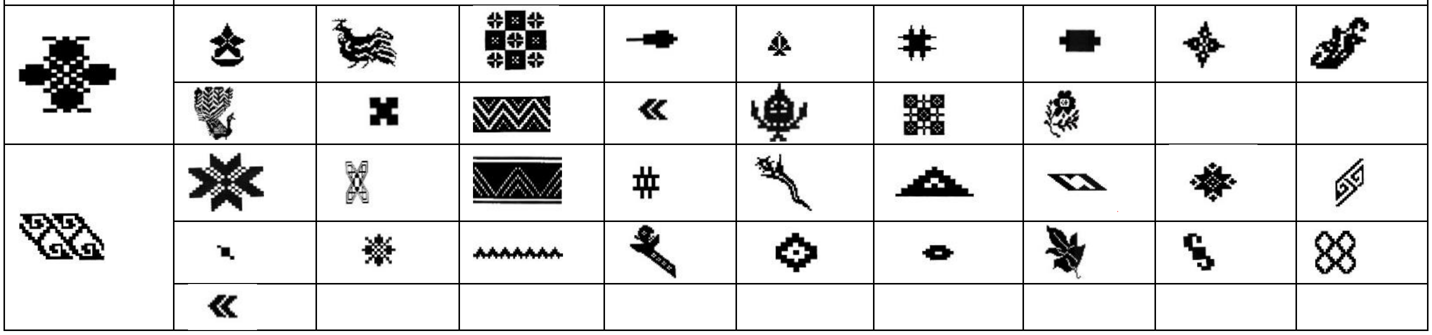

TABLE. VI. A FULL AVERAGE OF BAG OF VISUAL WORD TECHNIQUE ON SONGKET MOTIVES IMAGES RETRIEVAL RESULT

	Query Image									
	1	***2***	***3***	***4***	***5***	***6***	***7***	***8***	***9***	***10***
Bag of Visual Word Precision Value of Songket Motives	0.99	1.0	1.0	1.0	1.0	1.0	1.0	1.0	1.0	1.0
	0.99	0.37	0.49	0.37	0.55	0.77	0.83	0.69	0.76	0.62
	0.41	0.55	0.75	0.82	0.45	0.43	0.85	0.72	0.57	0.78
	0.33	0.47	0.45	0.82	0.55	0.72	0.91	0.75	0.55	0.85
	0.41	0.60	0.58	0.81	0.58	0.73	0.95	0.67	0.72	0.80
	0.40	0.53	0.78	0.83	0.57	0.76	0.78	0.72	0.67	0.86
	0.47	0.59	0.56	0.83	0.47	0.77	0.77	0.77	0.42	0.50
	0.45	0.61	0.75	0.84	0.48	0.73	0.92	0.66	0.32	0.92
	-	0.61	0.77	0.74	-	0.39	0.35	0.49	0.76	0.67
	0.43	0.59	0.77	0.83	0.55	0.76	0.82	0.68	0.59	0.72
	0.42	0.63	0.76	0.81	0.33	0.74	0.82	0.68	0.64	0.87
	0.33	0.63	0.75	0.79	0.53	0.81	0.41	0.76	0.64	0.48
	0.41	0.59	0.76	0.49	0.46	0.64	0.57	0.73	0.58	0.79
	0.37	0.54	0.55	0.82	0.35	0.50	0.89	0.76	0.69	0.79
	0.44	0.61	0.77	0.54	-	-	0.31	0.78	0.61	0.65
	0.46	0.62	-	0.78	0.48	0.31	-	0.76	0.57	0.66
	0.43	0.47	0.75	0.30	0.57	0.75	0.66	0.76	0.77	0.41
	0.43	0.59	0.64	0.75	0.57	0.85	0.69	0.61	0.74	0.94
	0.42	0.45	0.44	0.80	0.33	0.86	0.78	0.71	0.30	0.82
	-	0.62	0.73	0.48	0.37	0.89	0.86	0.36	0.74	0.42
Average result	0.43	0.58	0.65	0.72	0.46	0.67	0.71	0.70	0.63	0.73

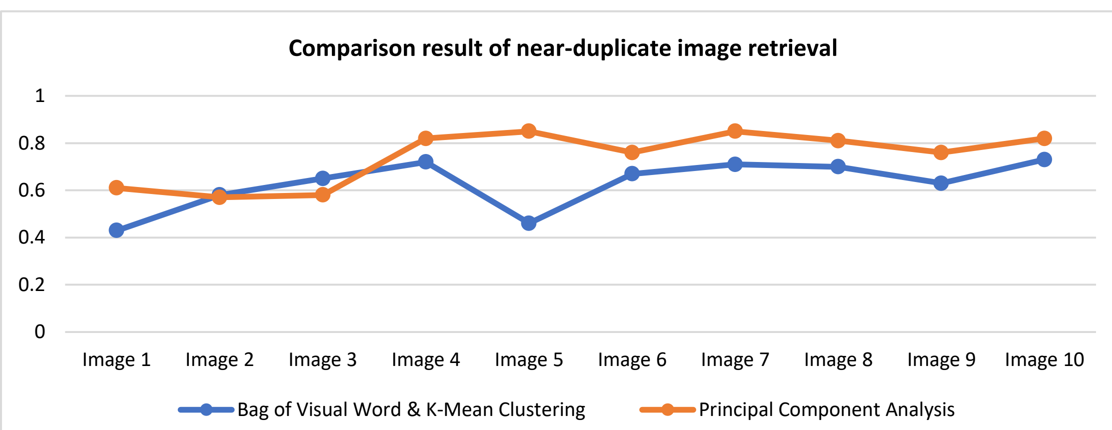

Fig. 7. Calculation by Local Binary Pattern and Similarity Measurement Technique.

VI. Conclusion

Similarity calculation in near-duplicate images retrieval faces several issues primarily based on unique images dataset and cluster. Furthermore, the image is in line with their category, which has comparable features that may want to assist the system and as a result, it will enlarge the percentage of recall and precision incomparable image retrieval and detection. The motive is that the way to increase the percentage of similar image detection is to center the attention on more detail of two areas - local and global image representation. This can be executed by utilizing hybrid PCA and geometric techniques. This solution is predicted to cater to the near-duplicate image retrieval issues that contain mostly local and global feature extraction.

Acknowledgment

This research was supported by GGP-2017-077, MyPHD MyBrain and Universiti Kebangsaan Malaysia. Special appreciation to our associates who provided the skill and knowledge that enormously assisted in the exploration of this research.

References

[1] N. Nawawi, A. Aziz, N. Legino, RafeahAhmad, and N. Ismail, “the Nature of Malay Songket Textile,” Bus. Manag. Q. Rev., vol. 6, no. (2/3), pp. 41–56, 2015.

[2] N. bt Yusof, T. S. M. T. Wook, and S. F. M. Noor, “Comparison Result of Songket Motives Retrieval through Sketching Technique with Keyword Technique,” Int. J. Comput. Sci. Netw., vol. 3, no. 2, pp. 70–76, 2014.

[3] Tenas Effendy.., “Falsafah Dalam Motif’s Songket Melayu,” Seminar Antarabangsa Tenun Nusantara. pp. 1–17, 2009.

[4] N. Yusof, T. S. M. T. Wook, and S. F. M. Noor, “Songket Motives Retrieval through Sketching Technique,” Procedia Technol., vol. 11, no. Iceei, pp. 263–271, 2013.

[5] N. Yusof, “Pencarian Imej Motif’s Songket Mengguna Teknik Lakaran,” Universiti Kebangsaan Malaysia, 2014.

[6] M. A. Hannan, M. Arebey, R. A. Begum, H. Basri, and M. A. Al Mamun, “Content-based image retrieval system for solid waste bin level detection and performance evaluation,” Waste Manag., vol. 50, pp. 10–19, 2016.

[7] S. Noah and S. Sabtu, “Binding Semantic to a Sketch Based Query Specification Tool,” Int. Arab Inf. Technol., vol. 6, no. 2, pp. 116–123, 2006.

[8] A. Othman, T. S. M. T. Wook, and S. M. Arif, “Quantization selection of colour histogram bins to categorize the colour appearance of landscape paintings for image retrieval,” Int. J. Adv. Sci. Eng. Inf. Technol., vol. 6, no. 6, pp. 930–936, 2016.

[9] Q. Dao Thi Thuy, Q. Nguyen Huu, C. Phuong Van, and T. Ngo Quoc, “An efficient semantic – Related image retrieval method,” Expert Syst. Appl., vol. 72, pp. 30–41, 2017.

[10] N. Jamil, Z. A. Bakar, and T. M. T. Sembok, “Image retrieval of songket motif’ss using simple shape descriptors,” in GMAI ’06 Proceedings of the conference on Geometric Modeling and Imaging: New Trends, 2006, vol. 2006, pp. 171–176.

[11] A. Verma, “Content Based Image Retrieval Using Color , Texture and Shape Features,” vol. 4, no. 5, pp. 383–389, 2014.

[12] T. Bui, L. Ribeiro, M. Ponti, and J. Collomosse, “Compact descriptors for sketch-based image retrieval using a triplet loss convolutional neural network,” Comput. Vis. Image Underst., 2017.

[13] J. Kalpana and R. Krishnamoorthy, “Color image retrieval technique with local features based on orthogonal polynomials model and SIFT,” Multimed. Tools Appl., vol. 75, no. 1, pp. 49–69, 2016.

[14] G. Lu and A. Sajjanhar, “Region-based shape representation and similarity measure suitable for content-based image retrieval,” Multimed. Syst., vol. 7, no. 2, pp. 165–174, 1999.

[15] E. Coppa, “On Data Skewness , Stragglers , and MapReduce Progress Indicators,” pp. 139–152, 2015.

[16] S. Kim, X. J. Wang, L. Zhang, and S. Choi, “Near duplicate image discovery on one billion images,” in 2015 IEEE Winter Conference on Applications of Computer Vision, 2015, pp. 943–950.

[17] W. Zhao, H. Luo, J. Peng, and J. Fan, “MapReduce-based clustering for near-duplicate image identification,” Multimed. Tools Appl., vol. 76, no. 22, pp. 23291–23307, 2016.

[18] L. S. Xue, N. A. A. Majid, and E. A. Sundararajan, “Dynamic virtual machine allocation policy for load balancing using principal component analysis and clustering technique in cloud computing,” J. Telecommun. Electron. Comput. Eng., vol. 10, no. 3–2, pp. 47–52, 2018.

[19] P. Sanguansat, Principal Component Analysis - Multidisciplinary Applications. Croatia: InTech, 2012.

[20] X. Zhu, X. Li, S. Zhang, Z. Xu, L. Yu, and C. Wang, “Graph PCA Hashing for Similarity Search,” IEEE Trans. Multimed., vol. 19, no. 9, pp. 2033–2044, 2017.

[21] S. A. M. N. Yanti Idaya Aspura Mohd Khalid, “The electronic library,” Collect. Manag., vol. 35, no. 6, pp. 1191–1214, 2017.

[22] L. Zheng, Y. Lei, G. Qiu, and J. Huang, “Near-duplicate image detection in a visually salient riemannian space,” IEEE Trans. Inf. Forensics Secur., vol. 7, no. 5, pp. 1578–1593, 2012.

[23] R. Hassanian-esfahani and M. javad Kargar, “Sectional MinHash for near-duplicate detection,” Expert Syst. Appl., vol. 99, no. 1 June 2018, pp. 203–212, 2018.

[24] W. Youzhong, D. Zeng, Z. Xiaolong, and W. Feiyue, “Propagation of online news: Dynamic patterns,” in 2009 IEEE International Conference on Intelligence and Security Informatics, ISI 2009, 2009, pp. 257–259.

[25] J. Huang, R. Zhang, R. Buyya, J. Chen, and Y. Wu, “Heads-Join: Efficient Earth Mover’s Distance Similarity Joins on Hadoop,” IEEE Trans. Parallel Distrib. Syst., vol. 27, no. 6, pp. 1660–1673, 2016.

[26] J. Li, X. Qian, Q. Li, Y. Zhao, L. Wang, and Y. Y. Tang, “Mining near duplicate image groups,” Multimed. Tools Appl., vol. 74, no. 2, pp. 655–669, 2014.

[27] E. Sokic and S. Konjicija, “Phase preserving Fourier descriptor for shape-based image retrieval,” Signal Process. Image Commun., vol. 40, pp. 82–96, 2016.

[28] J. M. Patel and N. C. Gamit, “A review on feature extraction techniques in Content Based Image Retrieval,” 2016 Int. Conf. Wirel. Commun. Signal Process. Netw., pp. 2259–2263, 2016.

[29] V. I. Patil and S. Kotyal, “Survey on Content Based Image Retrieval Using Color and Texture Features,” Int. J. Adv. Electron. Comput. Sci. ISSN 2393-2835, vol. 2, no. 10, pp. 1424–1429, 2015.

[30] I. T. Jolliffe, Principal Component Analysis, Second Edition, vol. 98, no. 3. 2002.

[31] H. Zhu, Z. Shen, L. Shang, and X. Zhang, “Parallel Image Texture Feature Extraction under Hadoop Cloud Platform,” Springer Int. Publ., pp. 459–465, 2014.

[32] J. M. Francos, A. Narasimhan, and J. W. Woods, “Maximum Likelihood Parameter Estimation of Textures Using a Wold-Decomposition Based Model,” IEEE Trans. Image Process., vol.4, no. 12, pp. 1655–1666, 1995.

[33] C. Wang, N. Komodakis, and N. Paragios, “Markov Random Field Modeling, Inference & Learning in Computer Vision & Image Understanding : A Survey,” Comput. Vis. IMAGE Underst., vol. 117, no. 11, pp. 1610–1627, 2013.

[34] H. Jiang, T. Feng, D. Zhao, B. Yang, L. Zhang, and Y. Chen, “Statistical Fractal Models Based on GND-PCA and Its Application on Classification of Liver Diseases,” Biomed Res. Int., vol. 2013, pp. 1–8, 2013.

[35] S. Deb, Multimedia systems and content-based image retrieval. 2004.

[36] J. Yue, Z. Li, L. Liu, and Z. Fu, “Content-based image retrieval using color and texture fused features,” Math. Comput. Model., vol. 54, no. 3–4, pp. 1121–1127, 2011.

[37] M. K. Alsmadi, “Query-sensitive similarity measure for content-based image retrieval using meta-heuristic algorithm,” J. King Saud Univ. - Comput. Inf. Sci., 2017.

[38] T. S. Kumar, V. V. Kumar, and B. E. Reddy, “Image retrieval based on hybrid features,” ARPN J. Eng. Appl. Sci.,vol.12,no.2,pp.591–598, 2017.

[39] R. Datta, D. Joshi, J. I. A. Li, and J. Z. Wang, "Image Retrieval : Ideas , Influences , and Trends of the New Age," J. ACM Comput. Surv., vol. 40, no. 2, pp. 1–60, 2008.

[40] C. Wang, J. Zhang, B. Yang, and L. Zhang, "Sketch2Cartoon : Composing Cartoon Images by Sketching," in Proceeding MM '11 Proceedings of the 19th ACM international conference on Multimedia, 2011, pp. 789–790.

[41] H. Wang and C. Wang, "MindFinder : Interactive Sketch-based Image Search," in Proceeding MM '10 Proceedings of the 18th ACM international conference on Multimedia, 2010, pp. 1605–1608.

[42] L. O. Carvalho, L. F. D. Santos, W. D. Oliveira, A. J. M. Traina, and C. Traina, "Self Similarity Wide-Joins for Near-Duplicate Image Detection," in Proceedings - 2015 IEEE International Symposium on Multimedia, ISM 2015, 2015, pp. 237–240.

[43] D. Feng, W. C. Siu, and H. Zhang, Multimedia Information Retrieval and Management, 1st (2003). New York: Springer, 2003.

[44] J. Feng, Y. Liu, and L. Wu, "Bag of Visual Words Model with Deep Spatial Features for Geographical Scene Classification," Comput. Intell. Neurosci., vol. 2017 (2017, p. 14, 2017.

[45] H. Liu, H. Lu, and X. Xue, "SVD-SIFT for web near-duplicate image detection," in Proceedings - International Conference on Image Processing, ICIP, 2010, pp. 1445–1448.

[46] Q. He, Z. Li, and X. Zhang, "Data Deduplication Techniques," in 2010 International Conference on Future Information Technology and Management Engineering, 2010, pp. 430–433.

[47] N. Mandagere, P. Zhou, and M. A. Smith, "Demystifying Data Deduplication," pp. 12–17, 2008.

[48] J. Zhang et al., "IM-Dedup: An image management system based on deduplication applied in DWSNs," Int. J. Distrib. Sens. Networks, vol. 2013, 2013.

[49] J. Zhang, T. Li, and Y. Pan, "Parallel rough set based knowledge acquisition using MapReduce from big data," in BigMine '12 Proceedings of the 1st International Workshop on Big Data, Streams and Heterogeneous Source Mining: Algorithms, Systems, Programming Models and Applications, 2012, pp. 20–27.

[50] L. Chen and F. Stentiford, "Comparison of near-duplicate image matching," Cvmp06, 2006.

[51] S. H. Srinivasan and N. Sawant, "Finding Near-duplicate Images on the Web using Fingerprints," in Proceeding of the 16th ACM international conference on Multimedia MM 08, 2008, pp. 881–884.

[52] M. Chen, Y. Wang, X. Zou, S. Wang, and G. Wu, "A duplicate image deduplication approach via Haar wavelet technology," Proc. - 2012 IEEE 2nd Int. Conf. Cloud Comput. Intell. Syst. IEEE CCIS 2012, vol. 2, pp. 624–628, 2013.

[53] S. G. Lakshmi and N. R. Gayathiri, "a Framework for Hosting Image Compression in Cloud," Int. J. Comput. Sci. Mob. Comput., vol. 3, no. 3, pp. 845–848, 2014.

[54] F. Zou, Y. Chen, J. Song, K. Zhou, Y. Yang, and N. Sebe, "Multiple Kernel Hashing," IEEE Trans. Multimed., vol. 17, no. 7, pp. 1006–1018, 2015.

[55] M. K. Alsmadi, "An efficient similarity measure for content based image retrieval using memetic algorithm," Egypt. J. Basic Appl. Sci., vol. 4, no. 2, pp. 112–122, 2017.

[56] O. Chum, J. Philbin, and A. Zisserman, "Near Duplicate Image Detection : min-Hash and tf-idf Weighting," in Proceedings of the British Machine Vision Conference, 2008, vol. 810, pp. 812–815.

[57] D. P. Tian, "A review on image feature extraction and representation techniques," Int. J. Multimed. Ubiquitous Eng., vol. 8, no. 4, pp. 385–395, 2013.

[58] D. A. Lisin, M. A. Mattar, M. B. Blaschko, E. G. Learned-Miller, and M. C. Benfield, "Combining Local and Global Image Features for Object Class Recognition," 2005 IEEE Comput. Soc. Conf. Comput. Vis. Pattern Recognit. - Work., vol. 3, pp. 47–47, 2005.

[59] L. Bueno, E. Valle, and R. da S. Torres, "Bayesian approach for near-duplicate image detection," in Proceeding ICMR '12 Proceedings of the 2nd ACM International Conference on Multimedia Retrieval, 2012, pp. 1–8.

[60] W. Dong et al., "High-Confidence Near-Duplicate Image Detection," in Proceeding ICMR '12 Proceedings of the 2nd ACM International Conference on Multimedia Retrieval, 2012, pp. 3304--3311.

[61] H. Wang, Y. Shen, L. Wang, K. Zhufeng, W. Wang, and C. Cheng, "Large-Scale Multimedia Data Mining Using MapReduce Framework," in 2012 IEEE 4th International Conference on Cloud Computing Technology and Science, 2012, pp. 287–292.

[62] Z. Li and X. Feng, "Near duplicate image detecting algorithm based on bag of visual word model," J. Multimed., vol. 8, no. 5, pp. 557–564, 2013.

[63] G. Kalaiarasi and K. K. Thyagharajan, "Visual Content Based Clustering of Near-Duplicate Web Search Images," in 2013 International Conference on Green Computing, Communication and Conservation of Energy (ICGCE), 2013, vol. 6, pp. 767–771.

[64] J. Wang, "Strong Geometry Consistency for Large Scale Partial-Duplicate Image Search," in MM '13 Proceedings of the 21st ACM international conference on Multimedia, 2013, pp. 633–636.

[65] L. Li, S. Jiang, Z. J. Zha, Z. Wu, and Q. Huang, "Partial-Duplicate Image Retrieval via Saliency- Guided Visual Matching," IEEE Multimed., vol. 20, no. 3, pp. 13–23, 2013.

[66] S. Battiato et al., "Aligning codebooks for near duplicate image detection," Multimed. Tools Appl., vol. 72, no. 2, pp. 1483–1506, 2014.

[67] L. Liu, Y. Lu, and C. Y. Suen, "Variable-length signature for near-duplicate image matching," IEEE Trans. Image Process., vol. 24, no. 4, pp. 1282–1296, 2015.

[68] F. Nian, T. Li, X. Wu, Q. Gao, and F. Li, "Efficient near-duplicate image detection with a local-based binary representation," Multimed. Tools Appl., vol. 75, no. 5, pp. 2435–2452, 2015.

[69] H. Wang, F. Zhu, B. Xiao, L. Wang, and Y. Jiang, "GPU-based MapReduce for large-scale near-duplicate video retrieval," Multimed. Tools Appl. J., vol. 74, no. 23, pp. 10515–10534, 2015.

[70] N. Yusof, A. Ismail, N. Aini, and A. Majid, "A Hybrid Model for Near-Duplicate Image Detection in MapReduce Environment," TEM J., vol. 8, no. 4, pp. 1252–1258, 2019.

[71] R. Raieli, Multimedia Information Retrieval (Theory and Techniques), vol. 1, no. 1. 2013.

[72] M. H. Safar and C. Shahabi, Shape Analysis and Retrieval of Multimedia Objects, First Edit. USA: Kluwer Academic Publishers, 2003.

Accurate Speech Emotion Recognition by using Brain-Inspired Decision-Making Spiking Neural Network

Dr. Madhu Jain[1]
Electronics and Communication Engineering Department,
Jaypee Institute of Information Technology, A-10,
Sector 62, Noida

Ms. Shilpi Shukla[2*]
Mahatma Gandhi Mission's College of Engineering and Technology, A-9
Sector 62, Noida

***Abstract*—A portion of speech recognition is taken away by emotion recognition which is a smart update and it is necessary for its gain massively. Feature selection is an indispensable stage among the furtherance of various schemes in order to implement the classification of sentiments in speaking. The communication among features prompted from the alike audio origin has been rarely deliberated at present, which might yield terminated features and cause an upswing in the computational costs. To resolve these defects the deep learning-based feature extraction technique is used. An incredible modernization in speech recognition in recent years incorporates machine learning techniques with a deep structure for feature extraction. In this paper, the speech signal obtained from the SAVEE database is used as an input for a deep belief network. In order to perform pre-training in the network, the layer-wise rapacious feature extraction tactic is implemented and by using systematic samples, the smearing back-propagation method is accomplished for attaining fine-tuning. Brain-inspired decision-making spiking neural network (SNNs) is used to recognize different emotions but training by deep SNNs remains a challenge, but it improves the determination of the result. In order to enhance the parameters of SNNs, a social ski-driver (SSD) evolutionary optimization algorithm is used. The results of the SNN-SSD algorithm are related to artificial neural networks and long short term memory with different emotions to refine the classification for authorization.**

Keywords*—Brain-inspired decision-making spiking neural network (BDM-SNN); deep belief network; social ski-driver (SSD) optimization; emotion recognition

I. Introduction

Speech recognition is gaining a lot of attention, which deals with the recognition of speech and conversion into text by the computer. This origination of speech recognition can expand human-computer communication [1]. The speech recognition principle has been improved to speech emotion recognition (SER) which is proved to be a developing investigation area [2]. This, in turn, attempts to decide the emotion from the speech signals. The advancement in emotion recognition will convert everything to ease and hence making our lifestyle more comfortable through various researches [3]. Emotion recognition is actually very tricky in certain criteria's since reactions may be in accordance with the surroundings, principles, singular face response leads to vague discoveries; the emotion cannot be concluded just by using speech quantity and if there is a deficiency of speech databank in voluminous languages [4].

The focal investigation disputes in speech emotion recognition are an optimal feature set selection from the provided speech signals [5, 6]. The speech emotion recognition deals with a greater part of the past through various investigations of speech rhythm features and ethereal data [7, 8]. The speech emotion recognition uses some novel feature parameters which may include the Fourier parameters. Numerous validated acoustic parameters are found in order to hold emotional data, execution of various triumphs such that a lot of features that are executed dependably over various conditions [9]. In the same way, most of the analysts want to utilize a unification feature set that is made out of numerous sorts of features comprising of contemporary emotional data [10]. Utilizing the blending feature set may cause increment too high measurement and reduction of speech features, thus the learning procedure is being elaborated for most machine learning calculations and develops the probability of overfitting. Utilizing an assortment of modalities SER frameworks are being created by the analysts, a few examples of varying media signals are sound, pictures, video, and electroencephalogram (EEG). There are various reasons why the identification of emotions from human speech is fascinating. Sound nearness of emotions is one such reason in the acoustic channel of speech which is similar to semantic channel and this as the simple way to show off the emotion. In real-time, speech can be effectively acquired and prepared yet different modalities, for example, video or EEG are hard to get, which is a crucial factor remembering potential applications [11]. Emotions depend on language and culture, appropriate acoustic features and their correlation.

Traditional machine learning strategy and the deep learning strategy are the two classes of the SER techniques. In traditional machine learning techniques for automatic emotion recognition (AER), the strategy shadowed is feature determination, which is forthrightly branded with the precision of recognition [12]. The pitch frequency feature, the vitality related feature, the formant feature, the ghastly feature, etc. are integrated into the most eminent feature extraction strategy [13]. Artificial neural network (ANN), Bayesian network model, hidden Markov model (HMM), support vector machine (SVM) [14], Gaussian mixture model (GMM) [14],

*Corresponding Author

and multi-classifier fusion [15] are primed by utilizing the machine learning strategy and all these are done after separation of the features.

The above-used techniques are cooperative for recognizing explicit emotion; there is no authoritative strategy to reveal intertwined adoring states. Due to two prime reasons, the existing speech emotion recognition innovation is veracity. The only cause is that the recurrence of speech emotion data prompts the fall of the conclusive recognition rate and the long training time of sample data, and handling the information of numerous speech data obstructs the ongoing feedback of the planned framework. An additional cause is that the overall efficacy of the calculations hooked on the speaker-free highlights which can be connected to SER is comparatively compact and it additionally sways the practicability of speech feeling recognition innovation.

The essential bit of leeway of this strategy is to train a model in the lack of exceptionally huge information. While the inconvenience is that it is hard to pass judgment on the nature of the feature and some key features may be absent, which will diminish the precision of acknowledgment. Meanwhile, it is hard to guarantee the great outcomes that can be accomplished in an assortment of databases. Contrasted and the customary artificial intelligent (AI) technique, the deep learning can separate the abnormal state features, and it has been appeared to surpass human execution in visual assignments. Right now, deep learning has been connected to the SER by numerous researchers. Many optimization techniques have been used for increasing the performance of the system by optimizing the weights, hidden layers and other parameters of neural network. The results are very promising [16]-[23]

This paper recaps the allied work in Section 2, however, information concerning the speech recognition and deep neural network (DNN) is accessible in Section 3. The methodology used to conduct this review is précised in Section 4. In Section 5 the results are demonstrated, where Section 6 accomplishes this paper.

II. Related Work

Certain overviews lead the territory of speech emotion recognition. Badshah et al. [24] in 2017 presented a technique to identify emotions in the speech by means of convolutional neural network (CNN) along with rectangular kernels. Outcomes publicized that rectangular kernels and max pooling operations in rectangular neighborhoods are appropriate for SER via spectrograms. This technique effectively learns discriminative features from speech spectrograms. The propounded technique can be additionally improved if further labeled data can be collected and a much deeper CNN having rectangular kernels could be successfully trained. Zhao, J., et al. [25] in 2019 describes 1D and 2D CNN long short term memory (LSTM) networks for Speech emotion recognition. The results obtained determine that the designed networks accomplish the best performance on the task of distinguishing speech emotion. The investigational outcomes prove that the designed networks attain tremendous performance while recognizing speech emotion; particularly the 2D CNN LSTM network is better compared to the traditional methods, deep belief network (DBN) and CNN on the chosen databases. The proposed method provides less accuracy which can be enhanced in future works.

Gupta, S., et al. [26] in 2019 proposed a novel CNN architecture with a spatial pyramid pooling (SPP) layer that function on varying length feature representation of speech signals to accomplish emotion classification task. A constraint of the propounded kernel is that it necessitates a CNN model to attain varying size feature maps. These restrictions found in the proposed techniques are reduced in upcoming works. Xu, H., et al. [27] in 2019 proposed an attention mechanism with the ASR system to learn the alignment between the original speech and the recognized text, which is then used to fuse features from two modalities. The outcomes prove that the projected method is better than other methodologies concerning emotion identification ability. But the computational time is high and so it has taken under consideration in forthcoming works.

Hook, J., et al. [28] in 2019 describes a minor set of features presented a competitive performance in SER. The feature set used in this work performs well for both male and female speakers. The primary results appear to be hopeful and permit an additional investigation. In future works, supplementary testing on other ESDs to evaluate the quality of the recommended features must be accomplished moreover enhanced discrimination amid anger and happiness owing to the worldwide nature of the difficulty in the SER field for both machines and humans. Mohanty, M.N. et al. [29] in 2019 presented few models for the recognition which are depending upon the NN frameworks. The elementary organization as a multilayer perceptron (MLP), radial basis function network (RBFN), and probabilistic neural network (PNN) are utilized with various spectral features. The DNN model is confirmed with all these features. Consequently, the description of speech emotions in dissimilar levels and various domains is to be performed in the future work which has the ability to decide the combination type that can be enhanced than the current work.

III. Proposed Methodology

SER is an interdisciplinary research region which aims to naturally recognize the emotional condition of a person. It is critical to improving human-PC connection in numerous perspectives, for instance, a non-human communicator should be aware of the proper emotional condition of the voice to recognize dual implications of a similar term. Emotions are not that much easier to detect by machines that need a lot of intelligence and training. If controllable intelligence is developed, human-machine interaction can be made much easier than before. It is found that some emotions are recognized accurately, other emotions lead to an ambiguous condition in inferring and classifying the emotion. The efficient characterization of dissimilar emotions by the extraction of appropriate features comes under the design of an SER system which is a significant dispute. An accurate selection of features significantly distresses the performance of classification since the pattern recognition techniques are hardly independent of the problem domain.

The defect can be erased but we need an efficient deep learning technique that is necessary which is a need of deep learned automated speech recognizer with a combined accuracy rate for the effective results with improved recognition rate. In this work, a system using SNN is proposed that performs emotion recognition from standard raw speech database and report results with the help of the SAVEE database as shown in Fig. 1. The noteworthy stepping tool in accomplishing a decent presentation of the SER system is feature extraction. It is the process of extraction of certain types of emotion from the speech.

This paper utilizes a learning approach deep belief network (DBN) that normally assumes huge operations on data to extract out meaningful information based on the training condition of raw data. The classification or recognition stage is the decision making part of the recognition system. A DBN-SNN is used in this work for classifying and recognizing the speech emotion using the advantage of automatic differentiation. This technique can automatically and analytically afford the derivatives to the training algorithm, which will be optimized using an SSD optimization algorithm.

A. Formulation of a Dataset for Speech Recognition

Initially, the voice database D_s is utilized to extract relevant information from the database containing different emotions. *Ds* comprises both structured and unstructured data which comprises sonic-visual data which are recorded with English articulations in six distinct emotions namely anger, disgust, fear, happiness, sadness, surprise plus neutral. $d_1, d_2, d_3 \ldots d_n$ are the categorical labels of each utterance and can be displayed as follows.

$$D_s = d_1 + d_2 + d_3 + \ldots . d_n \tag{1}$$

The above equation (1) is selected because of the consideration of speech data. Experiments make use of speech alone as the input. The information from all speakers which is part of the training set is 70%, the validation set is 15% and a test set 15%. The audio data are having noises, and this data is fed into the preprocessing steps for the accurate extraction that is explained in the sections.

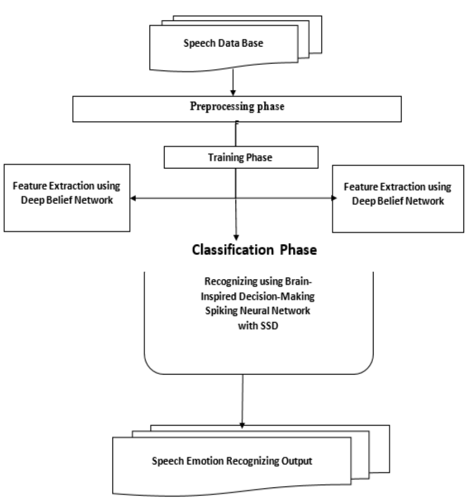

Fig. 1. Overall Schematic Diagram for Speech Emotion Recognition.

B. Data Augmentation

Over-fitting and aid generalization is diminished by means of a significant advance [21] termed as data augmentation. Since numerous data are necessary for DNNs, the preparation data was increased to orchestrate additional data. This analysis, this progression has fundamentally enhanced the generalization of the connected technique. Data in the preparation set was amplified by performing resampling the first sound at four diverse sampling frequencies, the first sampling recurrence. Few data augmentation procedures were investigated, for example, including Gaussian noise, yet were observed to be less effective than the detailed technique.

C. Preprocessing for Noise Removal

During the progress of the ASR system, pre-processing is the first phase in order to differentiate the voiced or unvoiced signal and to construct feature vectors in speech recognition. The speech signal, x (n), is being modified by preprocessing only then a noise-free input can be given for feature extraction analysis. Here x (n) must be tested to eradicate the background noise d (n).

$$x(n) = s(n) + d(n) \tag{2}$$

Where s (n) is the clean speech signal.

Different methods to diminish the noise are approved to work on a noisy speech signal. Spectral subtraction and adaptive noise cancellation are the two key methods under a noise reduction algorithm to develop a perfect speech recognition system.

D. Feature Extraction using Deep belief Network

In this paper, DBN is utilized, utilizing speech acquired from the crude speech databases. Reenactment of the progressive way that the cerebrum forms the information is cultivated by a deep encoder or deep learning; it is the current propelled machine learning technique that connects with the deep structure to display the information circulation and inward structure. At first extraction of features from low level to abnormal state is executed by presenting deep learning technique which starts progressive structure. The next level is a grouping of the info. Incredible achievement is being envisioned quite a while back in PC vision and programmed speech acknowledgment through deep learning techniques. Indeed, even now the conventional machine learning technique is picked to be deep learning and just consideration on the precision with various low dimensional physically unmistakable features. The main sort of deep learning technique is shared by DBN, is acquainted with extracting meaningful emotional features from the data which is displayed in Fig. 6.

a) A brief introduction to DBN

By stacking various restricted Boltzmann machines (RBMs), DBN which is a generative model is being constructed, as illustrated in Fig. 2. Three components are needed to compose a common recognition model: collecting detecting signals, removing features and building connections; all these components need many manual efforts. DBN gives a foundation to make sense of the model straight from what we see to what we need to know. A sort of hierarchical feature representation is resolved as the layer-by-layer structure. The brainwork-consuming feature-extracting segment is replaceable in light of the fact that the network training procedure is self-versatile. The layer by layer training procedure is directed via massive unlabeled samples.

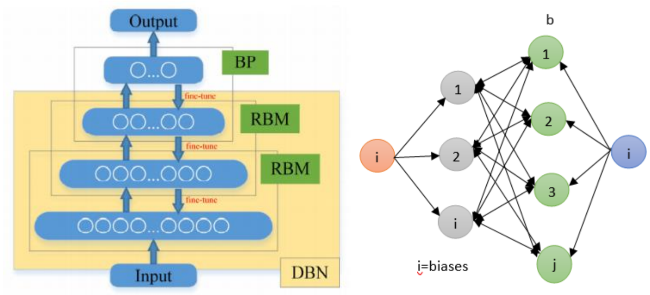

(a) (b)

Fig. 2. Architecture of (a) RBM and (b) DBN.

Learning a likelihood conveyance over the preparation set is set up by RBM which is a generative stochastic counterfeit neural system dependent on statistical mechanics. Two layers of two-fold stochastic units are perceived as an obvious layer and a concealed layer. As to as an undirected graphical model, every single noticeable unit is related to every shrouded unit and nonattendance associations inside each layer. The visible unit biases G, hidden units biases I and connection weight J are the parameters included. The hypothetical inference of RBM starts from the meaning of framework vitality for a particular framework state, which describes a likelihood circulation over the joint state of the noticeable units and the shrouded units, formulated as:

$$J(b,m)=x(n)-\sum_{j=1}^{sB} g_j b_j-\sum_{i=1}^{sM}\sum_{j=1}^{sB} m_i C_{ij} b_j-\sum_{i=1}^{sM} h_i m_i \tag{3}$$

The visible unit i and the hidden unit j has the binary states as b_i and m_i. The number of visible units and hidden units is represented as sB and sM respectively. The joint distribution of these units is formulated as:

$$J(b,m)=\frac{1}{A}e^{-J(b,m)} \tag{4}$$

Where $A=\sum_{b,m} e^{-J(b,m)}$ is called the partition function. Among the associated two margin distributions are

$$U(b)=\frac{\sum_m e^{-J(b,m)}}{A}=U(m)=\frac{\sum_b e^{-J(b,m)}}{A}$$
$$U(b\mid m)=\frac{U(b,m)}{U(m)}=\frac{e^{-J(b,m)}}{\sum_{\tilde{m}} e^{-J(b,\tilde{m})}} \tag{5}$$

$$=\frac{\exp\left(\sum_{j=1}^{sB} g_j b_j+\sum_{i=1}^{sM}\sum_{j=1}^{sB} m_i C_{ij} b_j+\sum_{i=1}^{sM} h_i m_i\right)}{\sum_{\tilde{m}}\exp\sum_{j=1}^{sB} g_j b_j+\sum_{i=1}^{sM}\sum_{j=1}^{sB} \tilde{m}_i C_{ij} b_j+\sum_{i=1}^{sM} h_i \tilde{m}_i} \tag{6}$$

Similar derivation can be done to U(b|m)

$$U(b\mid m)=\prod_{j=1}^{sM}\frac{\exp\left(g_i b_j+\sum_{j=1}^{sB} m_i C_{ij} b_j\right)}{\sum_{\tilde{b}} b_j+\exp\left(g_i\tilde{b}_j+\sum_{j=1}^{sB} m_i C_{ij}\tilde{b}_j\right)} \tag{7}$$

$$U(b\mid m)=\prod_{j=1}^{sM}\frac{\exp\left(g_i b_j+\sum_{j=1}^{sB} m_i C_{ij} b_j\right)}{\sum_{\tilde{b}} b_j+\exp\left(g_i\tilde{b}_j+\sum_{j=1}^{sB} m_i C_{ij}\tilde{b}_j\right)}$$

Because of the nonattendance certain connections, the units in a single layer are restrictively free while other layers are provided, so we can obtain.

$$U(m_i=1\mid b)=\frac{1}{1+\exp(-\sum_{j=1}^{sM} C_{ij}\tilde{b}_j+\sum_{i=1}^{sB} m_i C_{ij}-h_i} \tag{8}$$

$$U(b_i=1\mid m)=\frac{1}{1+\exp(-g_i\sum_{i=1}^{sB} m_i C_{ij}} \tag{9}$$

A maximum likelihood estimation is the best technique to train the RBM. The log-likelihood of the model for a single training sample is given below.

$$Q(\theta)=\log U(b\mid m)=\log\sum_m e^{-J(b,m)}-\log\sum_{b,m} e^{-J(b,m)} \tag{10}$$

Where Θ = {C, g, h} is the parameters to be evaluated. The gradient can be given as:

$$\frac{\partial(Q)}{\partial(\theta)}=\frac{\partial}{\partial(\theta)}\left(\sum_m e^{-J(b,m)}-\log\sum_{b,m} e^{-J(b,m)}\right) \tag{11}$$
$$=\frac{\sum_m e^{-J(b,m)}}{\sum_{b,m} e^{-J(b,m)}}\left(-\frac{\partial J(b,m)}{\partial(\theta)}\right)-\sum_{b,m}\frac{e^{-J(b,m)}}{\sum_{b,m} e^{-J(b,m)}}\left(-\frac{\partial J(b,m)}{\partial\theta}\right)$$
$$=\sum_m U(b\mid m)\left(-\frac{\partial J(b,m)}{\partial(\theta)}\right)-\sum_m U(b\mid m)\left(-\frac{\partial J(b,m)}{\partial\theta}\right)$$

Dual symbols are introduced to simplify the equation which is equated below:

$$\langle\theta\rangle_{data}=\sum_m U(b\mid m)\left(-\frac{\partial J(b,m)}{\partial(\theta)}\right)\quad \langle\theta\rangle_{model}=\sum_m U(b\mid m)\left(-\frac{\partial J(b,m)}{\partial\theta}\right) \tag{12}$$

The partial derivative of energy function to model parameters is briefed as follow:

$$-\frac{\partial J(b,m)}{\partial(\theta)}=b_i m_j \quad -\frac{\partial J(b,m)}{\partial\theta}=b_j \quad \frac{\partial J(b,m)}{\partial}=m_i \tag{13}$$

$\langle\theta\rangle_{data}$ can be calculated easily while the $\langle\theta\rangle_{model}$ needs to traverse all the probable value mixtures of the hidden units and visible units, this is called an NP-hard problem. The Gibbs inspecting begins with a training test, and on the other hand tests the shrouded units and unmistakable units utilizing condition (8) and (9) by k ventures, as delineated underneath:

$$b^{(0)} = t, \quad m^{(0)} \sim U(m \mid b^{(0)})$$

$$b^{(1)} \sim U(b \mid m^{(0)}), = t, \quad m^{(0)} \sim U(m \mid b^{(1)})$$

$$b^{(k)} \sim U(b \mid m^{(k-1)}), = t, \quad m^{(k)} \sim U(m \mid b^{(k)}) \tag{14}$$

When k->∞ the accurate model distribution can be gained and $\langle\theta\rangle_{\text{model}}$ can be calculated. In practice, Pro. Hinton brought up that the CD learning with k =1 can give satisfactory outcomes to appropriately gauge the model gradient. Therefore the subsequent term can be assessed utilizing $\langle\theta\rangle_{\text{model}}$ Gibbs sampling as

$$\langle\theta\rangle_{\text{model}} = \sum_{b,m} U(b,m)\left(-\frac{\partial E(b,m)}{\partial\theta}\right)$$

$$\langle\theta\rangle_{\text{model}} = \sum_{b} U(b) \sum_{m} U(b \mid m)\left(-\frac{\partial E(b,m)}{\partial\theta}\right) \tag{15}$$

$$\langle\theta\rangle_{\text{model}} = \frac{1}{l}\sum_{b}\sum_{m} U(b \mid m)\left(-\frac{\partial E(b^{(1)},m^{(1)})}{\partial\theta}\right)$$

In handy application, the training data is partitioned into mini-batches to upgrade the registering effectiveness. What's more, a typical system is set l equivalent to the size of the mini-group. Partition of "mini-batch" from the total gradient by the information size mini-clump to abstain from varying the learning rate when the size of mini-group changes. Along these lines, with the stochastic gradient descent algorithm, the refreshing standards of the parameters can be formulated as:

$$\theta = \theta + \varepsilon\Delta\theta = \theta + \varepsilon(<\theta>)_{data} - <\theta>_{\text{model}} \tag{16}$$

Where ε is considered as the learning rate. The gradient for a size 1 mini-batch is equated as:

$$\Delta C_{ij} = \frac{\sum_{x=1}^{l} (m_{(x)}^{(0)} b_{(x)}^{(0)} - m_{(x),i}^{k} b_{(x),j}^{(k)}}{l} \tag{17}$$

$$\Delta g_j = \frac{\sum_{x=1}^{l} (b_{(x),j}^{(0)} - b_{(x),j}^{(k)})}{l}$$

$$\Delta h_i = \frac{\sum_{x=1}^{l} m_{(x),j}^{(0)} - m_{(x),j}^{(k)})}{l}$$

Where the $(.)_{(x),i}^{k}$ notation signifies the parameter of the x^{th} training sample's i^{th} element, Furthermore, k infers the example got after k-step Gibbs sampling. The entire construction is arranged avariciously layers one after the other using unlabeled preparing data on a course of action RBM units, and RBMs are all around arranged, their parameters are then spread out to the DBN network, and BP algorithm is accomplished to align the entire system using a much little game plan of named data. We accept that the degrees of deliberation associated with mapping a matrix of pixel esteems to an emotion class make it especially appropriate for examining profound structures. When these highlights have been learned in solo preparing, we expect that the model will effectively get familiar with the specific characterization task. Also, we anticipate that more profound designs will outflank shallow systems since our assignment was picked so advance progressive portrayals. We have less refined expectations concerning the impact of the size of concealed layers, yet for the most part, anticipate that driving data pressure by lessening the number of units in the shrouded layer will bring about better abstractions.

E. Brain-Inspired Decision-Making Spiking Neural Network

Deep learning uses engineering with numerous layers of trainable parameters and has exhibited remarkable execution in AI and AI applications. DNNs are prepared to start to finish by utilizing advancement calculations typically dependent on BP. The multi-layer neural design in the primate's cerebrum has enlivened specialists to focus on the profundity of non-straight neural layers as opposed to utilizing shallow networks with numerous neurons. Additionally, hypothetical and test results show preferable execution of deep rather over wide structures. DNN extricate complicated highlights by means of consecutive neuron layers prepared by nonlinear, differentiable activation functions to give a suitable stage to the BP calculation.

For most portrayal issues, a softmax module is utilized as the yield layer of a significant framework. One-hot encoding is utilized during the preparation vector. In a one-hot encoding, every vector segment is matched to the potential classes. This vector is parallel with precisely one section set to 1 that identifies with the ideal objective class. The softmax module for the yield layer provides assurances that the estimations of all of the yield units fall inside the range (0, 1) and total to 1. This gives a great deal of on a very basic level inconsequential and far-reaching probability regards. The softmax recipe now and again called the normalized exponential,

$$D_i = \frac{\exp(x_i)}{\sum_j \exp(x_j)} \tag{18}$$

Where, x_i, is the net input to a particular output unit, j indexes the set of output units, and D_i is the value of output unit i, which falls in the range (0, 1).

The input undergoes pre-processing through the input layer. The data is then sent to a progression of hidden layers, the quantity of which can fluctuate. As the data proliferates through hidden layers, includes that are increasingly mind-boggling are separated and learned.

a) Social Ski-Driver (SSD) Optimization Algorithm

The conduct of SSD which is a novel optimization algorithm was motivated by various evolutionary optimization algorithms. Its name compliments to the way that its stochastic exploration in some way or another looks like the ways that ski-drivers take downhill. SSD has numerous parameters; a short depiction of these parameters is given beneath.

1) The places of the agents (Xi € Řn) are utilized to figure the target work in the same area, where n is the search space element.

2) The best position previously P_i: The fitness function helps in determining the fitness value for all operators.

Contrasting the fitness value for every specialist is performed and it puts away both the present position and the best position. This is like the PSO algorithm.

3) Mean global solution M_i: In our algorithm, as in the GWO, the agents are directed toward the global point which signifies the mean of the finest three solutions given by eq (19).

$$R_i^t = \frac{x_\alpha + x_\beta + x_\gamma}{3} \tag{19}$$

Where X_α, X_β, and X_γ are the three solutions that are considered to be the finest.

The velocity of the agents (V_i): The agents' positions are updated by adding the velocity Vi as follows

$$X_i^{t+1} = X_i^t + B_i^t \tag{20}$$

Where

$$B_i^{t+1} = \begin{cases} h\sin(w_1)(u_i^t - x_i^t) + \sin(w_1)(R_i^t - x_i^t) & \text{if } w_2 \le 0.5 \\ h\cos(w_1)(u_i^t - x_i^t) + \cos(w_1)(R_i^t - x_i^t) & \text{if } w_2 > 0.5 \end{cases} \tag{21}$$

Where B_i is the velocity of X_i, w_1 and w_2 are consistently created random numbers in the range of [0, 1], u_i is the superlative clarification of the ith agent, R_i is the mean global solution for the entire population, and h is a parameter makes the exploration constancy to the exploitation which is calculated as $h^{t+1} = \alpha h^t$, where the current iteration is denoted as t and $0<\alpha<1$ is used to decrease h value. Hence, $h \sin(w_1) < 0$and $h \cos(w_1) > 0$, where $t \to t_{max}$ and t_{max} is the highest times the iteration occurs. Equation (21) indicates, the moving directions for the agents are reversed as in GWO or PSO, and the reason behind this is the sine and cosine functions. Fig. 4 pictures an example with double agents moving in the SSD algorithm. Thus an offered calculation provides a superior guided investigation capacity and creates the hunt bearings to be differentiated,

Searching for near-optimal solutions in space is the main objective of the SSD. The dimension of that space is being determined by the number of parameters that must be optimized which is displayed in Fig. 3. In SSD, the agent's positions (Xi) are arbitrarily set, where the number of agents is fixed by the user. By the accumulation of the velocity to the previous position, the new position is being updated as in equation (20). The agents' velocities are also haphazardly initialized, and it is adapted based on equation (21).In this equation, the agent's adjusted velocity relies upon the partition amid the present positions, Xti, other than the past best position Pi, (2) the detachment between the present position, Xti, moreover the mean worldwide arrangement Mi. Hence, the agents in SSD advance in the direction of the mean of the finest three arrangements which makes the SSD calculation additional social compared to PSO. Furthermore, the SSD administrators are moved not a reasonable way, which in turn provides the SSD computation enhanced investigation precision. Fig. 4 clearly describes the flow of our proposed framework.

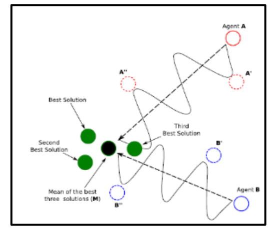

Fig. 3. Diagrammatic Representation of an Instance of how Two Agents (A and B) using the SSD Algorithm.

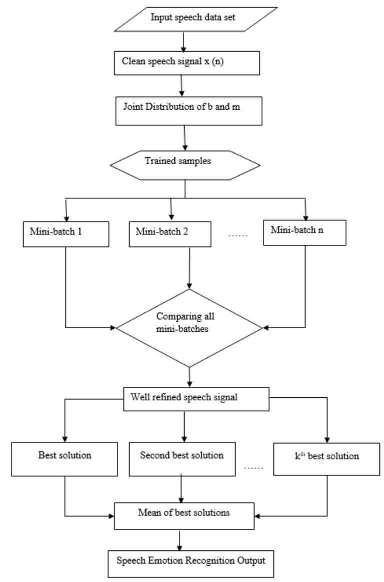

Fig. 4. Flow of our Proposed Framework.

IV. Simulation Results

System configuration: Operating System: Windows 8, Processor: Intel Core i3, RAM: 4 GB and Platform used is MATLAB.

A. Dataset Description

SAVEE [20] is an audio-visual database that includes 480 English articulations from four male entertainers in seven unique feelings, which are anger, disgust, fear, happiness, sadness, surprise plus neutral. Utterances were categorically labeled. The information collected from almost all the speakers as audio was randomly part in training (70%), validation (15%) and test (15%) sets. The mentioned sets are fundamentally unrelated.

B. Performance Evaluation

The performance of the proposed method was employed with some criteria such as accuracy, precision, recall F-measure. The formulation for precision, recall, accuracy, F-measure, is given below.

a) Precision

The precision is equated as follows

$$\Pr ecision(p) = \frac{Sum of\ relevant\ data\ \det ected}{Total\ sum of\ data\ \det ected} \tag{22}$$

b) Recall

The recall is equated as follows.

$$Recall(r) = \frac{Sumof\ accurate\ data\ detected}{Total\ sumof\ relevant\ data\ inthedatabase} \quad (23)$$

c) Accuracy

The data accuracy is equated by an equation which is given below.

$$Accuracy = \frac{p+r}{2} * 100 \quad (24)$$

C. Simulation Results

Exploration of various deep learning architectures and their influences on the classification is by making use of SAVEE database. Solidly, the influences of the quantity of hidden layers neurons for a permanent quantity of layers and the number of layers for a permanent quantity of neurons per hidden layer will be taken under consideration for the study. In this way, a thorough report on measurements for the picked design for the SAVEE databases is seen. Fig. 5 portrays the input SAVEE voice dataset which is converted to be a speech signal that is the mixture of different emotions like anger, fear, happiness, sad and neutral, etc. Fig. 6 shows the feature extracted using DBN.

D. Comparative Analysis

a) Proposed different parameter value with a different emotion

Table I describes the performance of the SAVEE database on the proposed system with different emotions to attain the required values and its bar graph is displayed in Fig. 7. The overall precision value is 96.94%, recall value attained is 97.42% and accuracy values is 98.21%. The different emotion values of proposed parameters are depicted in Fig. 8 which describes precision, recall, f-score and accuracy for different emotions.

b) Performance evaluation with the proposed and existing technique

In Table II, the CNNs and LSTM network-based SER results are compared with our proposed methodology that is depicted in Fig. 9 which describes the different emotion with different attributes. The training and testing accuracy graph is displayed in Fig. 10.

Fig. 9 describes the parameter values of different emotions compared with different algorithms, like CNN [30], LSTM [30] and proposed technique. When compared to all other methodology, the recommended technique gives the better result. The overall average of CNN precision value is 87.49% and LSTM value is 80.78%, average recall value of CNN is 85.94% and LSTM is 83.83% and average F-score values for CNN and LSTM is 85.77% and 79.85, respectively. The proposed methodology has average precision value of 95.64%, average recall value is 96.06% and average F-score value 97.59% which is far better compared to CNN and LSTM techniques. Training accuracy values of proposed technique 96.32% and testing accuracy value is 94.25% compared to various existing works like support vector machine and DNN along with extreme learning machine (ELM) technique plotted in Fig. 10.

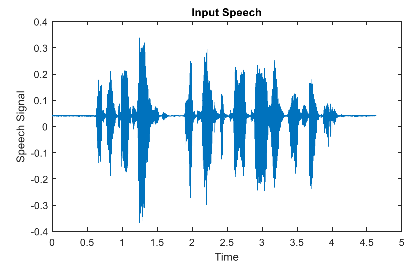

Fig. 5. Input Voice Database.

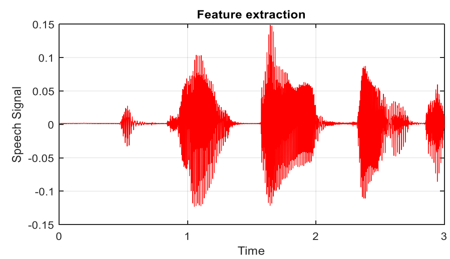

Fig. 6. Feature Extraction using Deep belief Network.

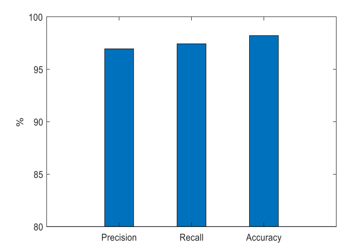

Fig. 7. Overall Proposed Performance Values.

TABLE. I. PERFORMANCE METRICS ON THE SAVEE DATABASE WITH A DIFFERENT EMOTION

EMOTION	PRECISION	RECALL	F-SCORE	ACCURACY
Anger	95.36	96.32	97.36	97.25
Disgust	97.25	95.32	96.87	96.32
Fear	95.36	97.25	97.98	96.21
Happiness	94.25	95.32	97.25	96.21
Neutral	96.32	95.32	98.78	96.32
Sadness	95.31	95.32	97.32	97.32
Surprice	95.32	96.32	97.25	98.32
All	98.32	94.56	97.22	98.57

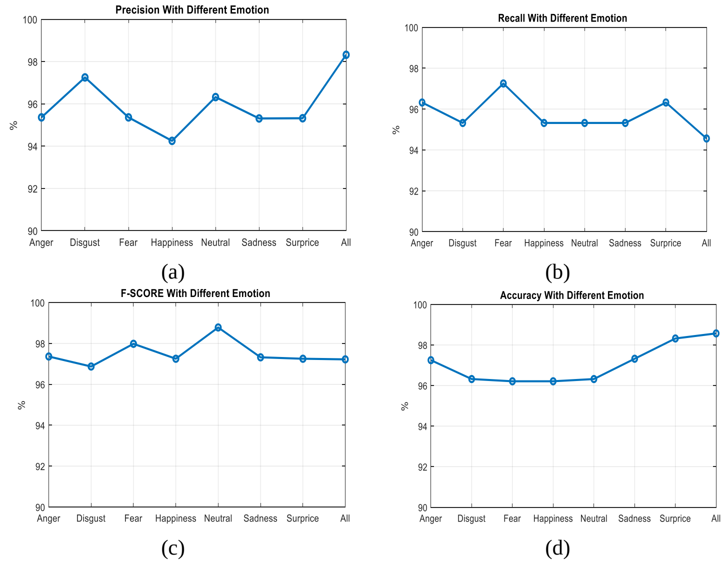

Fig. 8. Proposed Values with different Parameter (a) Precision (b) Recall (c) F-Score and (d) Accuracy.

TABLE. II. PERFORMANCE ANALYSIS OF THE PROPOSED AND EXISTING TECHNIQUE

	CNN [30]			**LSTM[30]**			**PROPOSED**		
EMOTION	P	R	F	P	R	F	P	R	F
Anger	87.16	92.58	89.48	84.82	89.04	86.46	95.36	96.32	97.36
Disgust	87.76	90.30	88.48	80.18	82.60	80.56	97.25	95.32	96.87
Fear	87.56	80.22	82.70	84.90	94.08	79.76	95.36	97.25	97.98
Happiness	80.88	68.86	73.26	73.90	66.84	68.78	94.25	95.32	97.25
Neutral	91.58	85.32	87.16	75.28	76.36	74.58	96.32	95.86	98.78
Sadness	90.04	98.40	93.56	85.62	94.08	88.96	95.31	96.32	97.32

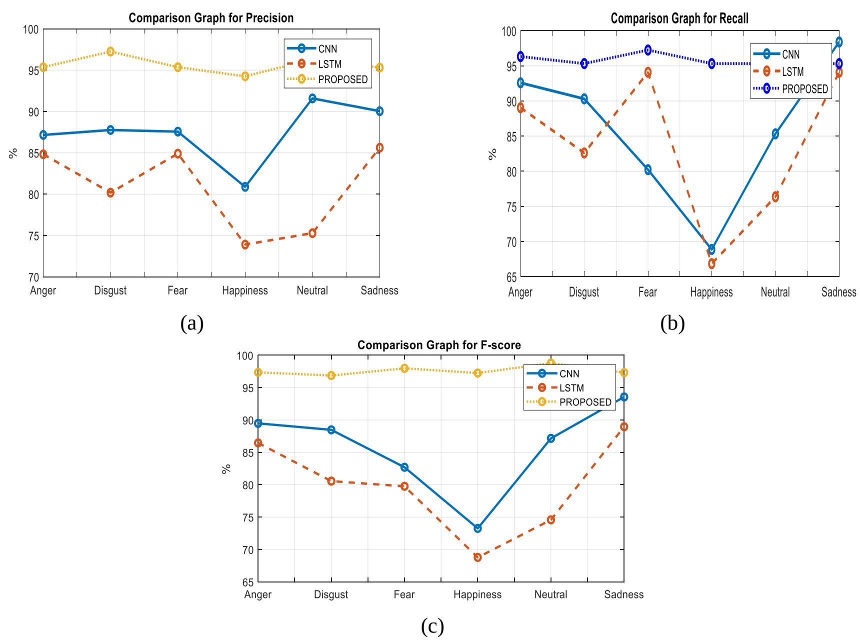

Fig. 9. Comparison Values of Existing and Proposed Methodology (a) Precision (b) Recall and (c) F-Score.

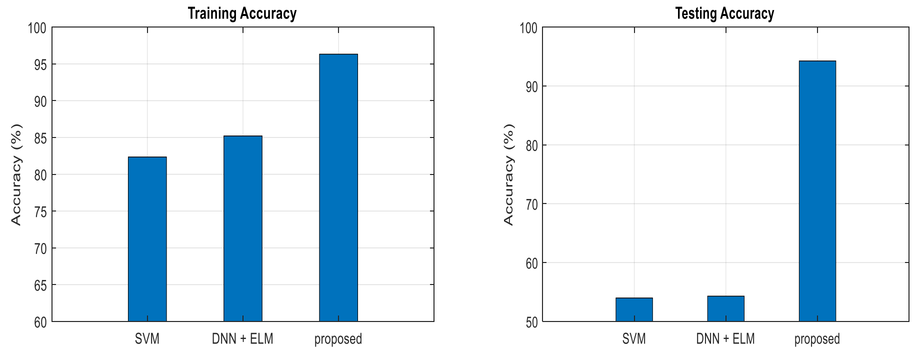

Fig. 10. Training and Testing Accuracy Graph.

V. Conclusion

The field of profound learning is adequately new to at present be quickly growing, frequently from development in new formalizations of profound learning issues driven by reasonable applications. Be that as it may, perceiving emotions from discourse is as yet a difficult issue. In this paper, we proposed the profound learning system brain-inspired decision-making spiking neural network with a social ski-driver (SSD) optimization-based network without utilizing any conventional hand-made highlights to characterize emotional discourse. For SER, we examined the recognition result by contrasting and the essential CNNs and LSTM based emotion recognition results. In all the existing methods adequate upswing in the computational costs was noticed which is being eradicated by introducing the deep learning-based feature extraction technique. Thus the results obtained by implementing the SNN-SSD algorithm related to artificial neural networks and long short term memory provides a refined classification of different emotions. At this point when contrasted with existing work our proposed work achieved better outcomes with a precision of about 96.94%, recall value of 97.42% and accuracy of about 98.21%. In the future the sound/video-based multimodal emotion recognition task can be implemented.

References

[1] Morganti, F., & Riva, G. Ambient Intelligence for Rehabilitation. In G. Riva, F. Vatalaro, F. Davide, & M. Alcañiz (Eds.), Ambient Intelligence: The evolution of technology, communication and cognition towards the future of human-computer interaction (p. 281–292), 2005.

[2] Petrushin, “Emotion in speech: Recognition and application to call centers,” In Proceedings of ANN in engineering, vol. 710, pp. 22, 1999.

[3] Picard, Rosalind & Vyzas, Elias & Healey, Jennifer. Toward Machine Emotional Intelligence: Analysis of Affective Physiological State. IEEE Transactions on Pattern Analysis and Machine Intelligence, 2001.

[4] Parkinson, M. H. Reviews : The Dual Voice. Free Indirect Speech and Its Functioning in the Nineteenth-Century European Novel. By Roy Pascal. Manchester: Manchester University Press, and Totowa, New Jersey: Rowman and Littlefield, 1977. Journal of European Studies, 9(35), 210–211,1979.

[5] M. El Ayadi, & F. Karray, “Survey on speech emotion recognition: Features, classification schemes, and databases,” in Journal Pattern Recognition vol. 44, no. 3, pp. 572-587, 2011.

[6] J. Edwards, & P.E. Pattison, “Emotion recognition via facial expression and affective prosody in schizophrenia: a methodological review,” CPR, vol. 22, no. 6, pp. 789-832, 2002.

[7] Y.L. Lin, “Speech emotion recognition based on HMM and SVM,” ICMLC, vol. 8, pp. 4898-4901, 2005.

[8] A.V. Haridas, & V.G. Sivakumar, “A critical review and analysis on techniques of speech recognition: The road ahead,” KBIES, vol. 22, no. 1, pp. 39-57, 2018.

[9] K. Wang, & L. Li, “Speech emotion recognition using Fourier parameters,” vol. 6, no. 1, pp. 69-75, 2015.

[10] B. Schuller, & D. Seppi, “Recognising realistic emotions and affect in speech: State of the art and lessons learnt from the first challenge,” Speech Communication , pp. 1062-1087, 2011.

[11] S. Pouyanfar, S.C. Chen, & S.S. Iyengar, “A survey on deep learning: Algorithms, techniques, and applications,” CSUR, vol. 51, no. 5, pp. 92, 2019.

[12] A. Hassan, “On automatic emotion classification using acoustic features”, Doctoral dissertation, University of Southampton, 2012.

[13] L. Li, & H. Sahli, “Hybrid Deep Neural Network--Hidden Markov Model (DNN-HMM) Based Speech Emotion Recognition,” HACACII, pp. 312-317, 2013.

[14] M. Sheikhan, & D. Gharavian, “Modular neural-SVM scheme for speech emotion recognition using ANOVA feature selection method,” NCA, vol. 23, no. 1, pp. 215-227, 2013.

[15] X. Cheng, & Q. Duan, “Speech emotion recognition using gaussian mixture model,” In Proceedings of the 2012 International Conference on CASM, 2012.

[16] S. Shukla, M. Jain & Dubey R,K, “Increasing the Performance of Speech Recognition System by Using Different Optimization Techniques to Redesign Artificial Neural Network,” Journal of Theoretical and Applied Information Technology, vol. 97, no. 8, pp. 2404-2415, 2019.

[17] Shukla, S. & Jain, M. International Journal of Speech Technology, 22: 959. https://doi.org/10.1007/s10772-019-09639-0 ,2019.

[18] M. Gupta, & B. Kumar, “Novel class of stable wideband recursive digital integrators and differentiators,” IET Signal Processing, vol.4, iss.5, pp.560–566, 2010.

[19] M. Jain, M. Gupta, and N. Jain, “Linear Phase Second-Order Recursive Digital Integrators and Differentiators,” in Radioengineering, vol. 21, no. 2, 2012.

[20] M. Gupta, & B. Kumar, “Wideband digital integrator and differentiator,” IETE Journal of Research, pp. 166-170, 2012.

[21] M. Jain, & N.K. Jain, “The Design of the IIR Differentiator integrator and its Application in Edge Detection,” Journal of Information Processing Systems, vol. 10, iss. 2, pp. 223 - 239, 2014.

[22] M. Jain, M. Gupta, and N.K. Jain, “Design of half sample delay recursive digital integrators using trapezoidal integration rule,” International Journal of Signal & Imaging Systems Engineering, vol. 9, iss. 2, pp. 126 - 134, 2016.

[23] M. Jain, & N.K. Gupta, “Analysis and design of digital IIR integrators and differentiators using minimax and pole, zero, and constant optimization methods,” ISRN Electronics, vol. 2013, pp. 1 - 14, 2013.

[24] A.M. Badshah, & S.W. Baik, “Deep features-based speech emotion recognition for smart affective services,” MTA, vol. 78, no. 5, pp. 5571-5589, 2017.

[25] J. Zhao, X. Mao, & L. Chen, "Speech emotion recognition using deep 1D & 2D CNN LSTM networks," BSPC, vol. 47, pp. 312-323, 2019.

[26] S. Gupta, K. De, D.A. Dinesh, & V. Thenkanidiyoor, "Emotion Recognition from Varying Length Patterns of Speech using CNN-based Segment-Level Pyramid Match Kernel based SVMs", NCC, pp. 1-6, 2019.

[27] Xu, H., Zhang, H., Han, K., Wang, Y., Peng, Y., Li, X. "Learning Alignment for Multimodal Emotion Recognition" from Speech. Proc. Interspeech pp 3569-3573, DOI: 10.21437/Interspeech.2019-3247,2019.

[28] J. Hook, F. Noroozi, O. Toygar, & G. Anbarjafari, "Automatic speech-based emotion recognition using paralinguistics features," Bulletin of the polish academy of sciences technical sciences, vol. 67, no. 3, 2019.

[29] M.N. Mohanty, & H.K. Palo, "Segment based emotion recognition using combined reduced features," IJST, vol. 22, no. 4, pp. 865-884, 2019.

[30] W. Lim, D. Jang, & T. Lee, "Speech emotion recognition using convolutional and recurrent neural networks," APSIPA, pp. 1-4, 2016.

Power Quality Evaluation for Electrical Installation of Hospital Building

Agus Jamal[1], Sekarlita Gusfat Putri[2], Anna Nur Nazilah Chamim[3], Ramadoni Syahputra[4]
Department of Electrical Engineering, Faculty of Engineering
Universitas Muhammadiyah Yogyakarta
Yogyakarta, Indonesia

***Abstract*—This paper presents improvements to the quality of power in hospital building installations using power capacitors. Power quality in the distribution network is an important issue that must be considered in the electric power system. One important variable that must be found in the quality of the power distribution system is the power factor. The power factor plays an essential role in determining the efficiency of a distribution network. A good power factor will make the distribution system very efficient in using electricity. Hospital building installation is one component in the distribution network that is very important to analyze. Nowadays, hospitals have a lot of computer-based medical equipment. This medical equipment contains many electronic components that significantly affect the power factor of the system. In this study, power quality analysis has been carried out on the building installation of one of the largest hospitals in Yogyakarta, Indonesia. In the initial condition, the power losses at the facility were quite high. Installation of power capacitors in these installations can improve the power factor, and ultimately improve the performance of the electrical installation system in the hospital building.**

Keywords*—*Power quality; power capacitor; hospital building; electrical installation

I. Introduction

The estimated electricity demand is calculated based on the intensity of the need for electricity usage. With the addition of an ever-increasing amount of load, it must be followed by reliable supply and excellent quality electricity services by maintaining the quality of the system voltage [1]-[3]. In the distribution of electricity from electric power sources to consumers who are located far apart, there will be losses in the form of power losses and voltage losses. The amount of power losses and voltage losses on the distribution channel depends on the type and length of the conduit, the kind of distribution network, the capacity of the transformer, the kind of load, the power factor, and the amount of installed power and the number of inductive loads that cause an increase in demand reactive power [4]-[6].

Reduced electrical power, followed by a large number of systems that use energy, will result in not optimal performance of each component and will cause several problems faced, including high line current, low power factor, and power losses [7]-[9]. The load contained in the distribution network can be either capacitive or inductive, but in general, it is an inductive load. If the inductive and capacitive reactive loads get higher, it will increase the current, increase the power losses, and reduce the power factor [10].

Considering how vital electrical energy services are to consumers, good quality electricity is needed [11]. There are several methods to correct the voltage drop in a system, namely by increasing the cross-section wire, changing the feeder section from one phase to a three-phase system, sending the load through a new feeder. The three methods above show ineffectiveness both in terms of infrastructure and in terms of cost. Another technique that allows for more productive work is by using a Bank Capacitor [12].

The addition of capacitor banks can improve the power factor, supply reactive power so that it can maximize the use of complex power, reduce voltage drops, avoid overloaded transformers, provide additional power available, save efficiency, can cause current to flow in the conductor to be small, so as to reduce the magnitude of power losses so as to improve the power factor, and bank capacitors can also reduce other losses on electrical installations [13]-[14].

Besides, along with the advancement in electrical appliances, more and more electrical equipment is included in the non-linear loads. Besides being practical, non-linear loads are also easy to operate, so that non-linear loads are widely used. Non-linear loads are generally made of semiconductor materials and electronic elements that can produce harmonics in an electric power system.

Related to previous studies concerning harmonics concluded that the harmonic component could cause an increase in power losses because harmonics is an event produced by the use of non-linear loads on the electric power system. This incident can cause problems in terms of power quality, which will eventually result in various kinds of losses and damage to some electrical equipment [15].

Therefore calculating the need for capacitors and harmonic distortion in the conductor can help reduce power losses. Voltage decreases typically occur at the end of the line, and voltage regulation worsens and can also minimize damage to electrical equipment due to the presence of harmonic distortion that can cause harm to both producers, in this case, PLN as the electricity provider and consumer. Based on the background of the problems above, the authors are compelled to research on improving the quality of electric power in hospital buildings using active filters.

II. Power Quality in Hospital Building Installation

Along with the times, the need for electricity consumption will continue to increase. Therefore, improvement in the quality and quantity of electrical energy is one of the reasons why utility companies need to pay attention to the issue of electric power quality. Attention to the issue of the quality of electric power in industrial consumers who need supplies because the machines in the industry are sensitive to surge or voltage instability. Therefore it is necessary to try an electrical distribution system that can provide services that meet the criteria desired by consumers [16].

Since the late 1980s, the quality of electric power has become an important issue in the industry. The quality of electric power is a picture of the pros and cons of an electricity system in dealing with disturbances that might occur in the system [17]-[19].

Four main reasons for the need for more attention to power quality issues [20]:

1) Electrical devices used today are very sensitive to the quality of electrical power, where microprocessor-based devices and other power electronics require stable voltage service, and voltage levels must also be maintained.

2) The emphasis is on the overall power efficiency of the electrical system, which results in continued growth in high-efficiency equipment applications, such as regulating the speed of the electric motor and the use of bank capacitors for power factor correction to reduce losses. This increases the level of harmonics in the power system and can reduce the quality of power.

3) Increased consumer awareness of power quality problems, where consumers become more aware of problems such as interruptions, sags, and transient switching and expect electrical utilities to improve the quality of power delivered.

4) The electric power system currently has a lot of interconnection between networks, which gives a consequence that the failure of each component will fail other components.

Poor power quality can cause problems in the power system in the form of problems with surges or large voltage changes, high currents, and frequencies that will cause failure or damage to the equipment where this failure can damage electrical equipment both on the sending and receiving sides. Therefore to anticipate losses that can occur both from the PLN and consumers, the PLN must strive for a good electrical system.

A. Electric Power

Electric power is the energy expended to do business. In an electric power system, power is the amount used to do work or business. Power has units of Watt, which is the product of voltage (volts) and currents (amperes). Electric power is stated in P, the electric voltage is expressed in V, and the electric current is expressed in I, so the amount of electric power is expressed in [18]:

$$P = V\ I\ \text{Cos}\ \varphi \tag{1}$$

Active power is the power that is used to carry out actual energy. The active power unit is watts. The active power equation is as follows [6]:

$$\text{For three phases (P)} = V\ I\ \text{Cos}\ \varphi \tag{2}$$

$$\text{For thirteen phases (P)} = \sqrt{3}\ V\ I\ \text{Cos}\ \varphi \tag{3}$$

This power is commonly used by consumers and is converted in the form of work.

Reactive power is the amount of power required for the formation of a magnetic field. From the structure of the magnetic field, magnetic field flux will form. Examples of power that cause reactive power are transformers, motors, and others. The unit of reactive power is Var. The reactive power equation is as follows [6]:

$$\text{For one phase } Q = V\ I\ \text{Sin}\ \varphi \tag{4}$$

$$\text{For three phases } Q = \sqrt{3}\ V\ I\ \text{Sin}\ \varphi \tag{5}$$

Apparent power is the power produced by the multiplication of voltage and current in a network. The apparent power unit is VA. The equation in active power is as follows [6]:

$$\text{For one phase } S = V\ I \tag{6}$$

$$\text{For three phases } S = \sqrt{3}\ V\ I \tag{7}$$

The power triangle is a triangle that describes the mathematical relationship between apparent power, active power, and reactive power based on the principle of trigonometry.

B. Power Factor

The power factor (Cos φ) is the ratio between active power (Watt) and real power (VA) used in an AC circuit or phase angle difference between V and I which is usually expressed in cos φ [6].

Power Factor = Active Power (P) / Apparent Power (S)

= kW / kVA

= V I Cos φ / V I

$$= \text{Cos}\ \varphi \tag{8}$$

Lagging power factor is a state in which the current power factor has the following conditions; load or electrical equipment requires reactive power from the system, or the load is inductive, and the voltage (V) precedes I with an angle φ resulting in a backward current (I) from the source.

Leading power factor is a state when the power factor has the following conditions; loads or electrical equipment provide reactive power from the system or capacitive loads, and the voltage (V) is backward from the current with an angle φ which results in the current passing the voltage.

The power factor has a range between 0-1 and is expressed as a percent (%). A good power factor is when the value of the power factor is close to one.

$$\text{Tan } \varphi = \text{Reactive Power (Q) / Active Power (P)}$$
$$= \text{kVAR / kW} \quad (9)$$

Active power generally has a fixed value, while the values of apparent power (kVA) and reactive power (kVAR) have values that vary according to the value of the power factor [6].

$$\text{Reactive Power (Q)} = \text{Active Power (P) x Tan } \varphi \quad (10)$$

To improve the power factor, the formula for calculating the required capacitor rating is as follows [6],

$$\text{Reactive power at initial pf} = \text{Active Power (P) x Tan } \varphi_1 \quad (11)$$

$$\text{Reactive power improved pf} = \text{Active Power x Tan } \varphi_2 \quad (12)$$

The capacitor ratings needed to improve the power factor are [6]:

$$\text{Reactive Power} = \text{Active Power x (Tan } \varphi_1 \text{ - Tan } \varphi_2) \quad (13)$$

Increasing the power factor will have several advantages, including:

a) The electricity bill becomes smaller (PLN will give a fine if the pf value is below 0.85).

b) The distribution capacity of the electric power system will increase.

c) Reducing power losses in the system.

d) Increasing the voltage will minimize the voltage drop that occurs in the electric power system.

If the pf value is less than 0.85, the active power capacity (kW) used will decrease because the smaller the pf value, the reactive power value is higher.

C. Harmonics in Electrical Installation System

In the electric power system, there is a phenomenon called harmonics, in which the current waveform or voltage from the supply will be distorted so that it can cause damage to electrical equipment. Another definition of harmonics is the phenomenon of the formation of waves with different frequencies, which are multiplications of integers with their fundamental frequencies. The electric power system is designed to operate at frequencies of 50 Hz or 60 Hz, but in reality, several loads cause the appearance of currents and voltages with frequencies above 50/60 Hz. Loads whose frequency capacity exceeds a predetermined capacity are called non-linear loads. Whereas 50 Hz or 60 Hz frequencies are called fundamental frequencies, and multiples are called harmonics or harmonics.

An electric power system has a fundamental frequency of 50 Hz, so for both frequencies, it is a wave with a frequency of 100 Hz, the third harmonic is a wave with a frequency of 150 Hz, and so on. In an electrical system, harmonics are currents and voltages that are distorted and deviate from the sinusoidal waveform. Periodic distortion of sine waves of current, voltage, or power with a waveform is multiple outsides of one of the fundamental frequencies. The system is designed to operate at 50 Hz or 60 Hz. These waves then hitch a ride on pure or original waves so that a defective wave is formed, which is the sum between the instantaneous pure wave and the harmonic wave, as shown in Fig. 1.

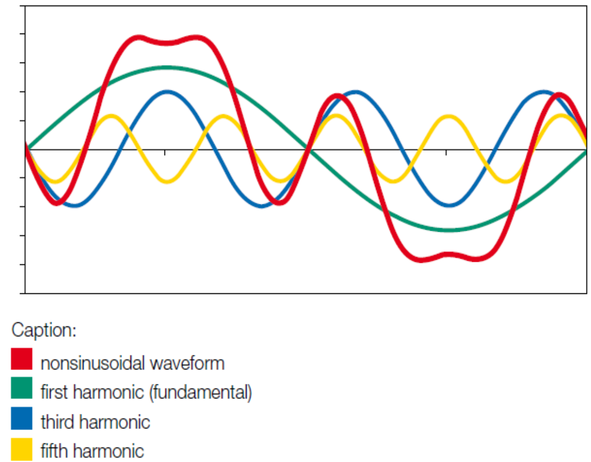

Fig. 1. Harmonic Waveform.

In 1916 Steinmetz first examined the harmonic phenomenon in the electric power system. Steinmetz observed the 3rd harmonic that appeared in the 3 phase system. The 3rd harmonic is caused by the saturation of the iron core in the transformer and electric machines. In 1930-1940, the 3rd order harmonic problem was resolved well. But in this day and age, electronic device's power is the cause of the appearance of harmonics [20].

Power electronic circuits are widely used in switching power supplies, UPS, computers, printers, fluorescent lamps, and other equipment. The reason many parties use power electronics is that it is efficient and easy to control, but this device can draw non-sinusoidal AC currents from an AC source. When this current acts with system impedance, it will generate harmonic voltage and current. Voltage and current harmonic waves move as if they were against the direction of the voltage and current coming from the source. If this harmonic wave joins with its fundamental wave, then the fundamental wave will experience distortion and change its shape to an imperfect sinusoidal wave.

Harmonic is an event that takes place periodically, and in the form of a steady-state, the existence of continuous harmonics can cause distortion in the sine wave voltage and current and will adversely affect the system or electrical equipment. The distortion signal itself is the sum of several harmonics together.

All equipment that is connected to a system that contains harmonics will have different effects. The equipment experiencing a decrease in performance or can also be damaged and will also influence the power quality of the electric power system. This harmonic distortion can disrupt or increase the workload of tools connected to the same network. Some things that can be caused by harmonics are as follows:

- It causes increased heating and losses at switchgear, thereby reducing the ability to flow current and shorten the life of some insulator components.
- The emergence of mechanical vibrations in electrical panels which are mechanical resonance vibrations due to harmonics of high-frequency currents.

- Harmonics can cause additional torque on kWh-meters of an electromechanical type that uses a rotating induction disk. As consequently, the disk rotation will be faster, or there is a measurement error on the kWh-meter because the induction disk is designed only to operate at a fundamental frequency.
- Reduces the life of the transformer, decreases efficiency in generator power, transmission, and usage
- The working temperature of the equipment is also getting higher and will eventually reduce the life of the equipment. Also, increasing losses will reduce equipment efficiency.
- Damage to the power factor correction tool (capacitor bank).

Harmonics are the formation of waves, which are multiples of fundamental frequencies [21]. Voltage and current waves, which were originally pure sinusoidal, will be distorted to no longer pure sinusoidal. The index is called THD (Total Harmonic Distortion), where THD is a comparison of the value of fundamental components that are usually in the form of a percent (%). In general, THD is used to determine the type of current and voltage waveform deviations that contain harmonics against the original sine wave every one period.

The difference between THD_V and THD_I is if THD_V is to determine the quality of the voltage from the source, while at THD_I to assess the quality of the current from the load. In general, the cause is designed to flow the voltage close to the original sine so that the THD value of the allowable voltage is much smaller than THD_I. The danger that THD_I can cause is overheating. However, the presence of abundant current harmonics will create a high THD_V.

The level of harmonic interference in the electric network reflects the distortion factor that exists in the electrical power system. One measurement that is generally used is THD that will be used in this study, for voltage or current.

The basic concept of the filter current is:

$$\text{Filter Current} = \text{Fundamental Flow} - \text{Load Current} \tag{14}$$

From the formulation above, it is found that the filter current is the fundamental current multiplied by THD [22]:

$$I_{filter} = I_1 \text{ x } THD_I\ (\%) \tag{15}$$

With a Safety Factor of 20% we get the following equation [22]:

$$I_{filter} = I_{RMS} \text{ x } \frac{\sqrt{THD\ (I)^2\ (\%)}}{THD\ (I)^2(\%)+100^2} \text{ x FS} \tag{16}$$

$$\text{Voltage, } THD_V = \frac{\sqrt{\sum_{h>1}^{\infty} V^2 h}}{V_1} \tag{17}$$

$$\text{Current, } THD_I = \frac{\sqrt{\sum_{h>1}^{\infty} I^2 h}}{I_1} \tag{18}$$

Equations (18) and (19) are equations used to express the THD values of current and voltage.

D. Maintaining the Integrity of the Specifications

The template is used to format your paper and style the text. All margins, column widths, line spaces, and text fonts are prescribed; please do not alter them. You may note peculiarities. For example, the head margin in this template measures proportionately more than is customary. This measurement and others are deliberate, using specifications that anticipate your paper as one part of the entire proceedings, and not as an independent document. Please do not revise any of the current designations.

III. Methodology

This study discusses energy audits and their mitigation efforts. The object of this study is a hospital building, which is a multi-story building that has a very complicated electrical installation, where the electrical loads are complete medical devices. The hospital building is located in an area in the city of Yogyakarta, the province of Yogyakarta Special Region, Indonesia.

The rare steps of this research are shown in Fig. 2.

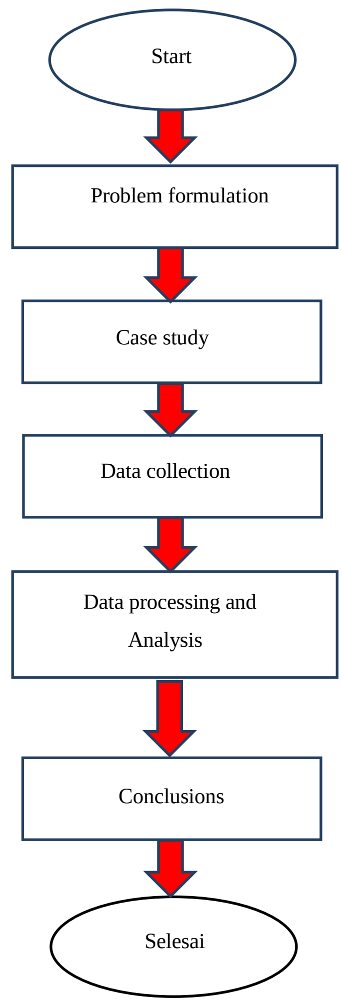

Fig. 2. The Steps of this Research.

Based on the data obtained by various sources, the data is processed by calculation according to standard procedures. The estimate of the value of the bank capacitors and the harmonic distortion obtained is then analyzed so that it can be seen how much the capacity of the capacitor of the bank and what percentage of the harmonic distortion. The next step is data processing, which is done by ETAP (Electric Transient and Analysis Program) software. The modeling method in ETAP is software that supports the electric power system. This device is capable of working offline for electric power simulations, online for real-time data management or used to control the order in real-time.

IV. Results and Discussion

A. Electric Energy Audit on Hospital Electrical Installations

Before analyzing data calculations, the thing to do is first to know what data is needed in the forecast that will be done. The LVMDP (Low Voltage Medium Distribution Panel) schedule is the central panel after the transformer is in the leading powerhouse, containing the main MCCB (Molded Case Circuit Breaker) of the building. Data on LVMDP measurement results at hospital electrical installations are shown in Table I.

B. Modeling in ETAP Software

After knowing the entire load data installed in the hospital building then the design of the load is carried out, as shown in Fig. 3. This design is carried out in ETAP 12.6.0 software by entering the load data in Table I. This software can simulate in an offline state and can analyze data such as voltage drops, current flowing at load, active, reactive, and apparent power. In Fig. 3, you can see modeling on the PLN power source using the toolbar power grid. The power grid in ETAP is an ideal voltage source in the sense of being able to supply power with a fixed voltage even though the energy absorbed is changing. For loads that do not contain non-linear loads using static loads, static loads in ETAP are loads that do not provide many electric motors. Then for loads that contain lots of electric motors, use a lumped load. Fig. 4 shows modeling LVMDP load on ETAP before installing power capacitors for calculation of electric current and apparent power.

Fig. 3 and Fig. 4 are modeling as well as simulating the calculation of active power (kW), recative power (kVAR), apparent power (kVA), current and also the voltage that exists at the hospital electrical installation load before installing a capacitor bank using ETAP 12.6.0 software. At the time before using capacitors, the apparent power at the voltage source and transformer is large enough and the current flowing is quite large. The greater the current flowing, the more heat the cable can cause to decrease the life of the cable and can also damage other protection components. Measurement data before installation of power capacitors was shown in Table II.

TABLE. I. DATA ON LVMDP MEASUREMENT RESULTS AT HOSPITAL ELECTRICAL INSTALLATIONS

NO	PANELS	LOCATION	LOAD CAPACITY					PF (%)	NORMAL LOAD				
			S (KVA)	P (KW)	I_R (kA)	I_S (kA)	I_T (kA)		S (KVA)	P (KW)	I_R (kA)	I_S (kA)	I_T (kA)
1	SDP EMERGENCY	Rooftop	145.8	105.0	220.9	220.9	220.9	0.5	66.0	44.3	100.1	100.1	100.1
2	SDP.AC	Basement 1	1110.0	761.3	1687.2	1678.5	1679.9	0.8	861.5	588.7	1309.3	1302.7	1303.7
3	LP.B.3	Basement 3	8.1	6.9	12.6	11.8	12.6	0.7	5.7	4.8	8.8	8.2	8.8
4	LP.B.2	Basement 2	6.4	5.4	10.0	9.5	9.6	0.7	4.5	3.8	7.0	6.6	6.7
5	LP.B.1	Basement 1	7.2	6.1	10.9	11.3	10.7	0.7	5.1	4.3	7.6	7.9	7.5
6	PP.ELECTRONICS	Lower Ground	8.9	7.6	15.0	13.4	12.3	0.7	6.3	5.3	10.5	9.4	8.6
7	LP.LG	Lower Ground	11.7	10.0	17.6	17.4	18.4	0.7	8.2	7.0	12.3	12.2	12.9
8	PP.LG	Lower Ground	45.6	38.8	67.9	70.9	68.4	0.7	31.9	27.1	47.5	49.6	47.9
9	PP.LAB	Lower Ground	52.8	42.2	80.0	80.0	80.0	0.7	37.0	29.6	56.0	56.0	56.0
10	PP.RADIOLOGY	Lower Ground	320.0	256.0	484.8	484.8	484.8	0.5	160.0	128.0	242.4	242.4	242.4
11	PK.ESCALATOR 1	Ground floor	16.9	11.0	25.6	25.6	25.6	1.0	16.9	11.0	25.6	25.6	25.6
12	PK.ESCALATOR 2	Ground floor	16.9	11.0	25.6	25.6	25.6	0.75	12.7	8.3	19.2	19.2	19.2
13	LP.D	Ground floor	7.1	6.0	9.2	11.1	11.9	0.7	4.9	4.2	6.4	7.8	8.3
14	PP.D	Ground floor	29.9	25.4	47.1	44.4	44.4	0.7	20.9	17.8	32.9	31.1	31.1
15	LP.1	Floor 1	6.3	5.4	9.2	9.7	9.8	0.7	4.4	3.8	6.4	6.8	6.8
16	PP.1	Floor 1	24.8	21.1	37.7	36.1	39.0	0.7	17.4	14.8	26.4	25.3	27.3
17	LP.2	Floor 2	6.7	5.7	9.9	11.1	9.3	0.7	4.7	4.0	6.9	7.8	6.5
18	PP.2	Floor 2	26.9	22.9	41.2	41.4	39.6	0.7	18.8	16.0	28.8	29.0	27.7
19	PP.KEMOTERAPI	Floor 2	7.7	6.6	12.8	11.2	11.0	0.7	5.4	4.6	9.0	7.9	7.7
20	LP.3	Floor 3	6.0	5.1	9.0	9.5	8.8	0.7	4.2	3.6	6.3	6.6	6.2
21	PP.3	Floor 3	34.8	29.6	52.7	52.9	52.4	0.7	24.3	20.7	36.9	37.1	36.7
22	LP.4	Floor 4	26.3	29.6	40.1	39.6	39.6	0.7	18.4	20.7	28.1	27.7	27.8
23	SDP.ATAP	Rooftop	17.9	13.5	27.5	27.5	26.4	0.7	12.6	9.6	19.4	19.4	18.5
24	PP.PH	Power House	1.6	1.4	3.5	2.7	1.3	0.7	1.1	0.98	2.5	1.9	1.0
Total			**1946,3**	**1433,3**	**1946.3**	**1433.3**	**2957.9**	**2946.9**	**2942.4**		**1352.8**	**982.7**	**2056.4**

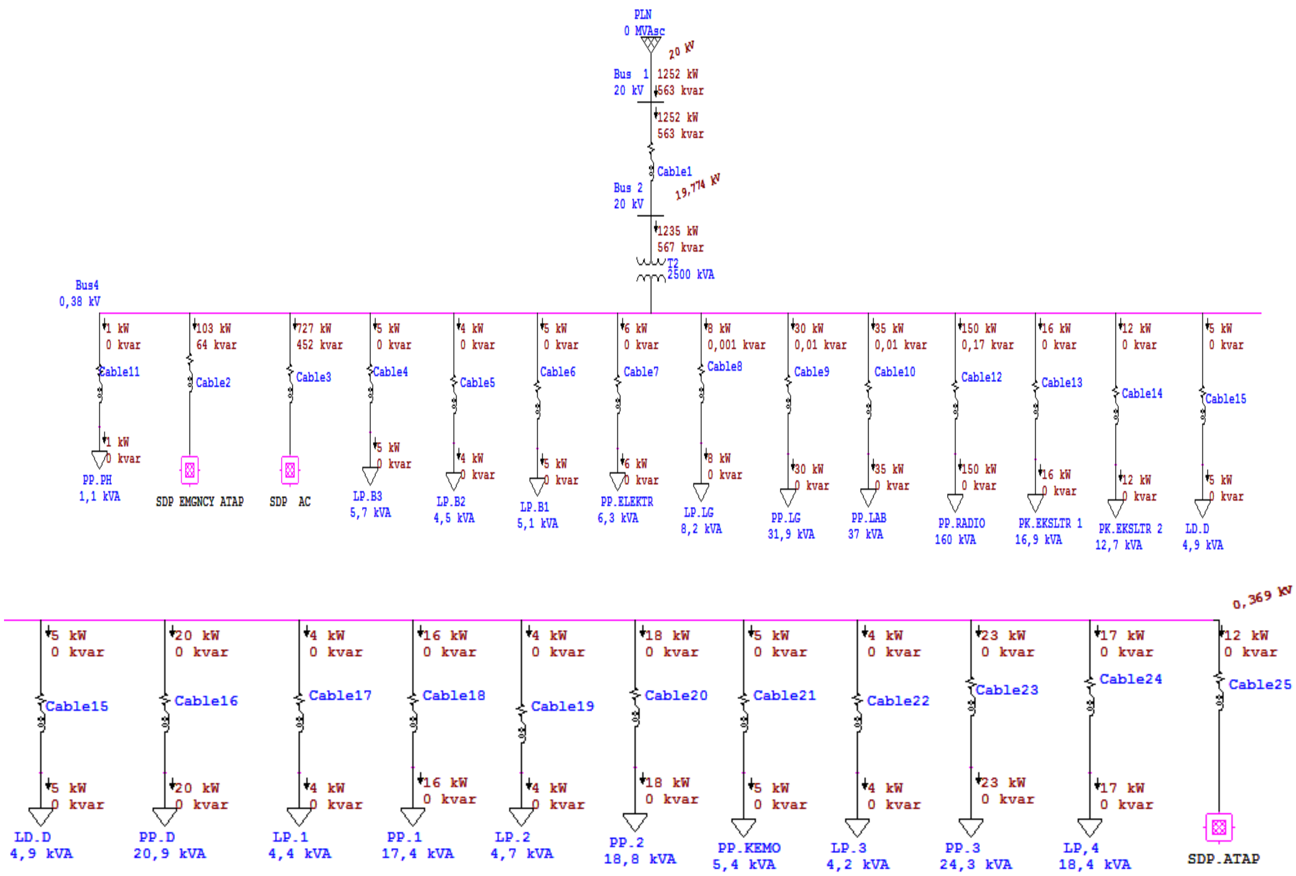

Fig. 3. Modeling LVMDP Load on ETAP before Installing Power Capacitors for Calculation of Active and Reactive Power.

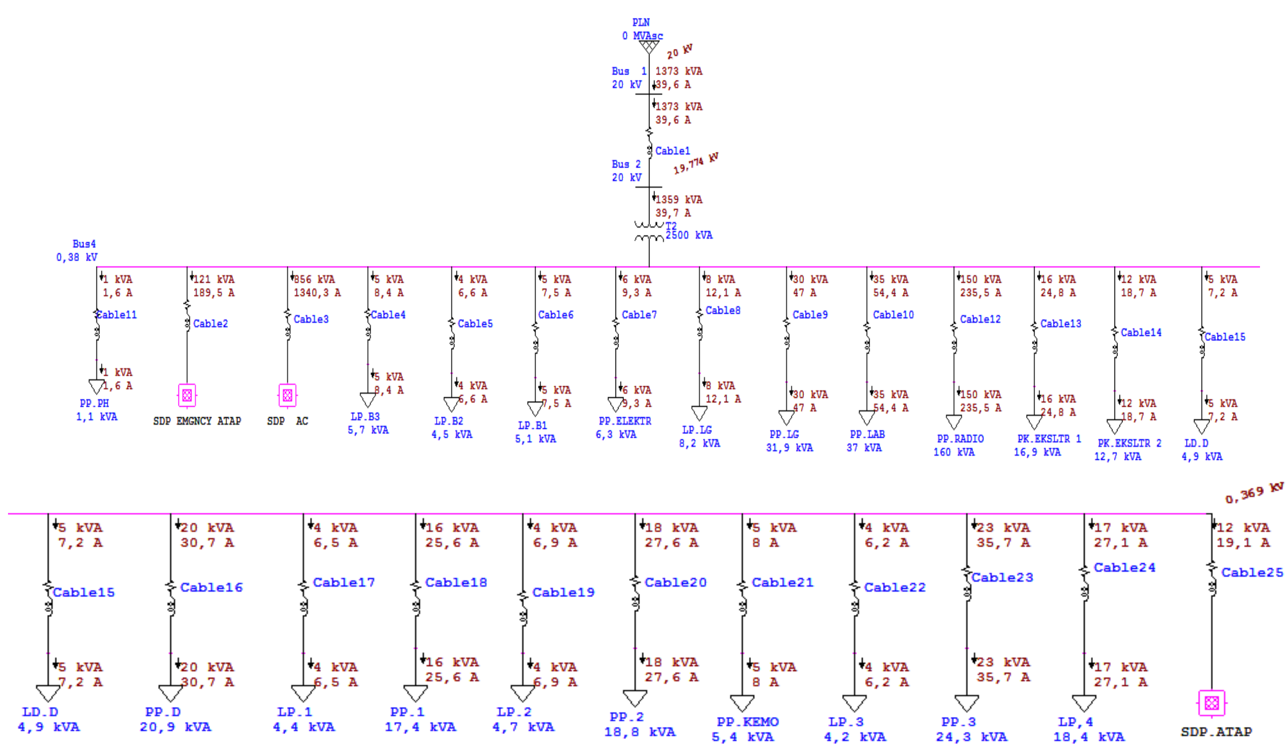

Fig. 4. Modeling LVMDP Load on ETAP before Installing Power Capacitors for Calculation of Electric Current and Power.

TABLE. II. MEASUREMENT DATA BEFORE INSTALLATION OF POWER CAPACITORS

No.	Components	Voltage (kV)	Power			Electric Curents (A)
			P (kW)	Q (kVAR)	S (kVA)	
1.	Busbar 20 kV	20	1252	563	1373	39,6
2.	Busbar 0,38 kV	0,369	1235	567	1359	39,7
3.	Busbar SDP Emergcny	0,368	103	64	121	189,5
4.	Busbar SDP AC	0,365	727	452	856	1340,3
5.	Busbar SDP Atap	0,368	12	0	12	19,1

After knowing the needs of the bank capacitors with the desired cos phi fix from 0.7 to 0.9 through calculations, then a simulation of the use of the bank capacitors on the distribution channel. Installation of bank capacitors using the Global Compensation method, namely, the installation of bank capacitors on the main panel, has been recommended. This method serves to be able to receive more active power needed. Fig. 5 and Fig. 6 show the modeling of the placement of capacitor banks in the electrical insulating system of a hospital building.

Reactive power on the side of the voltage source and transformer decreases, and active power increases from the state before the capacitor is installed. Because the function of installing capacitors with the global compensation method is to reduce the supply of the transformer, thus the electricity load will be able to receive more active power needed and reduce the power tariff for excess kVAR consumption.

Fig. 5 and Fig. 6 show the LVMDP load scheme with a simulation of apparent power calculation (kVA) and the current flowing. Both images show installation when using capacitors. The apparent power available at the voltage source and transformer is reduced from the state before using the capacitor bank. Based on the report data from the ETAP 12.6.0 simulation, where the 20kv PLN voltage source goes to the loads that exist in the hospital installation, it can be seen that the ratio of losses and power factors as shown in Table III.

Based on Table III, it can be concluded that the effect of the use of bank capacitors on hospital installations can reduce power losses as evidenced by a decrease in active power losses of 3.0 kW. The results of the comparison of the amount of active power, reactive power and apparent power before and after the installation of capacitors are as in Table IV.

In Table IV, it can be seen that all observed variables have improved with the installation of power capacitors in hospital building installations in Yogyakarta, Indonesia. These variables are the system voltage, which has developed a profile, and the electric current has decreased. This condition makes the power losses smaller. Variable active power, reactive power, and apparent power measurement results after the installation of power capacitors also improved.

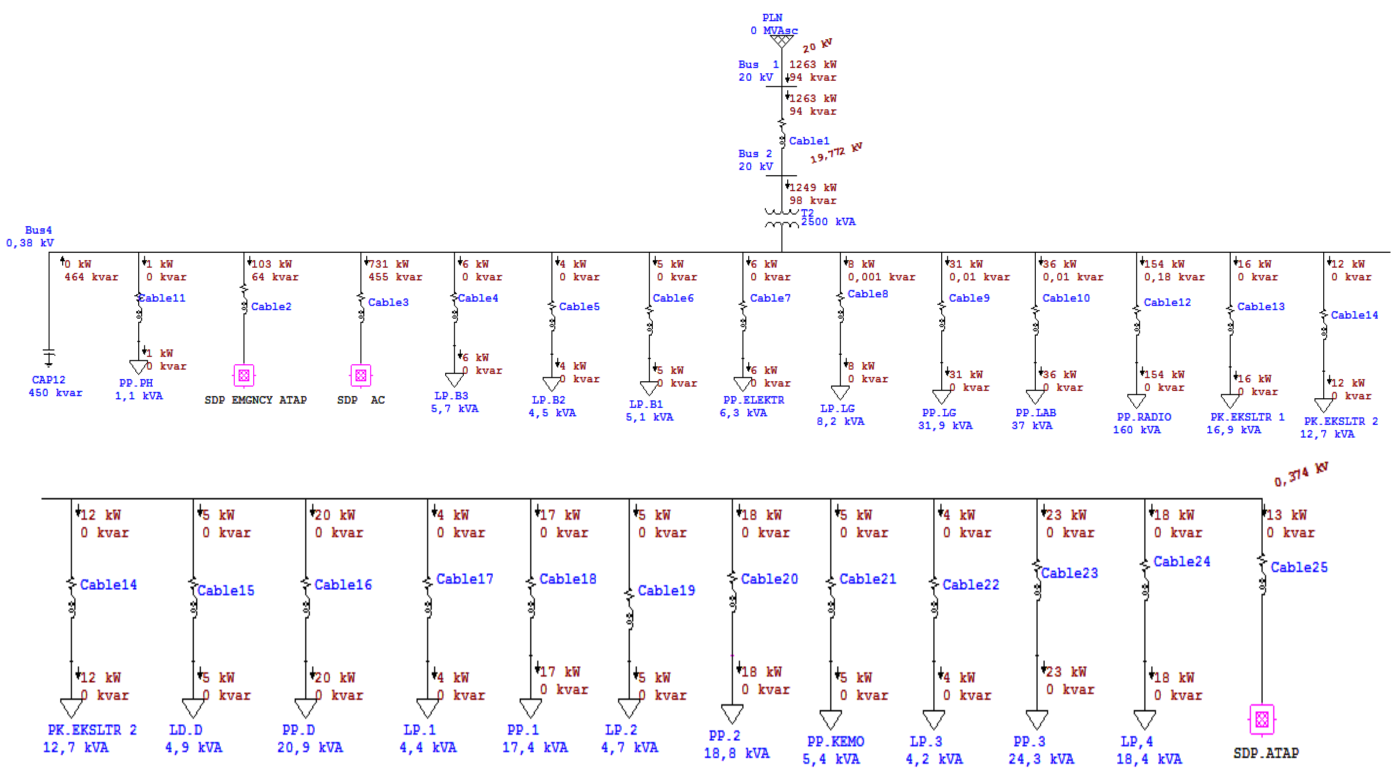

Fig. 5. Modeling LVMDP Load on ETAP after Installing Power Capacitors for Calculation of Active and Reactive Power.

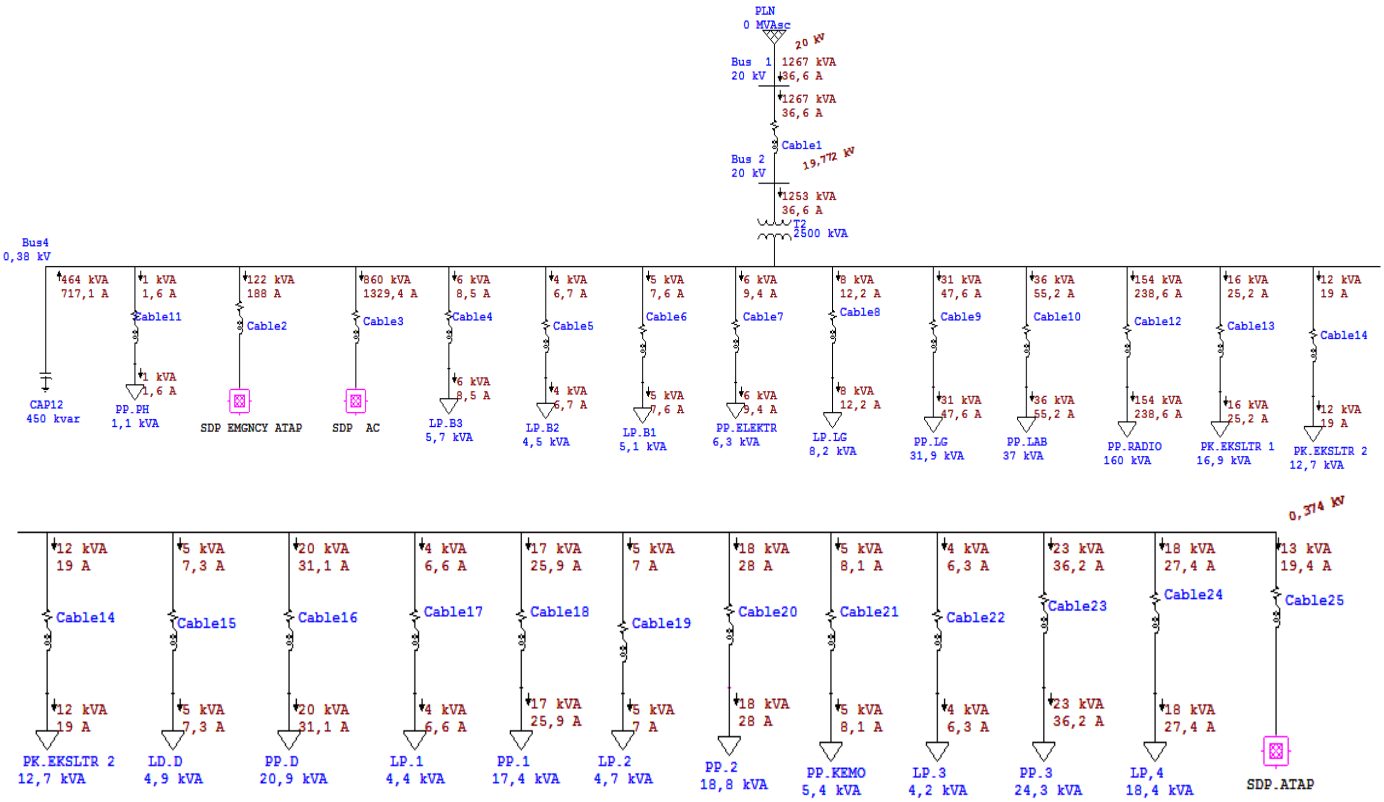

Fig. 6. Modeling LVMDP Load on ETAP after Installing Power Capacitors for Calculation of Electric Current and Apparent Power.

TABLE. III. POWER LOSSES BEFORE AND AFTER INSTALLATION OF BANK CAPACITOR

No.	Hospital Installation	Power Losses	
		P (kW)	Q (kVAR)
1.	Before installation of bank capacitor	17.0	50.8
2.	After installation of bank capacitor	`14.0	43.2

TABLE. IV. HOSPITAL BUILDING INSTALLATION BEFORE AND AFTER INSTALLATION OF BANK CAPACITOR

No.	Components	Voltage (kV)		Electric Currents (A)		Power					
						Reactive Power (kVAR)		Active Power (kW)		Apparent Power (kVA)	
		Before	After	Before	After	Before	After	Before	After	Before	After
1	Busbar 20 kV	20	20	39.7	36.6	563	94	1252	1263	1373	1267
2	Busbar 0.38 kV	0.369	0.374	2088.5	2083.8	567	98	1235	1249	1359	1253
3	Busbar SDP Emergency	0.368	0.373	189.5	188.0	64	64	103	103	121	122
4	Busbar SDP AC	0.365	0.37	1340.3	1329.4	452	455	727	731	856	860
5	Busbar SDP Rooftop	0.368	0.373	19.4	19.1	0	0	12	13	12	13

V. CONCLUSIONS

After making improvements to the power factor by raising cos phi, which was initially from 0.73 to 0.9, it can reduce the amount of reactive power (kVAR), apparent power (kVA), increase the active power (kW), and cause a decrease in the load current. Thus it can supply power to more loads and can reduce the voltage drop. This condition also reduced the number of losses from the initial state of active power by 17 kW to 14 kW and reactive power before the installation of capacitors by 50.8 kVAR to 43.2 kVAR. This fact shows that the higher the value of the power factor, the smaller the current flowing in the distribution network. This phenomenon dramatically affects electrical equipment, both cable size, electrical safety, and other electrical equipment. By increasing the power factor above 0.85, PLN will not provide compensation due to high kVAR. Improving the power factor from 0.73 to 0.9 requires a bank capacitor to compensate for reactive power of 455 kVAR. However, the capacity of existing bank capacitors in the market is 50 kVAR, so the capacitor banks that will be installed to be 480 kVAR are connected as many as 12 steps with each capacitor value of 50 kVAR.

ACKNOWLEDGMENT

The authors gratefully acknowledge the contributions of the Directorate General of Development and Research Enhancement, Ministry of Research, Technology and Higher Education of the Republic of Indonesia, for funding this research.

REFERENCES

[1] L. Tang, W. Xu, C. Mu, “Analysis for step-size optimisation on MPPT algorithm for photovoltaic systems”, IET Power Electronics, Vol. 10, No. 13, pp. 1647 – 1654, 2017.

[2] A. Jamal, R. Syahputra," UPFC Based on Adaptive Neuro-Fuzzy for Power Flow Control of Multimachine Power Systems", International Journal of Engineering Science Invention (IJESI), Vol. 2, No. 10, pp. 5-14, 2013.

[3] Syahputra, R., Soesanti, I., Ashari, M. (2016). Performance Enhancement of Distribution Network with DG Integration Using Modified PSO Algorithm. Journal of Electrical Systems (JES), 12(1), pp. 1-19.

[4] Syahputra, R., Robandi, I., Ashari, M. (2015). Performance Improvement of Radial Distribution Network with Distributed Generation Integration Using Extended Particle Swarm Optimization Algorithm. International Review of Electrical Engineering (IREE), 10(2). pp. 293-304.

[5] Syahputra, R., Robandi, I., Ashari, M. (2014). Optimization of Distribution Network Configuration with Integration of Distributed Energy Resources Using Extended Fuzzy Multi-objective Method. International Review of Electrical Engineering (IREE), 9(3), pp. 629-639.

[6] H. Saadat, (1999). Power System Analysis, Singapore, McGraw-Hill, 1999.

[7] Syahputra, R. (2017). Distribution Network Optimization Based on Genetic Algorithm. Jurnal Teknologi, Journal of Electrical Technology UMY (JET-UMY), 1(1), pp. 1-9.

[8] Mujaahid, F., Fauzi, A.M., Syahputra, R., Putra, K.T., Purwanto, K. Potentials of Organic Waste Conversion in a Green Campus Concept. Journal of Electrical Technology UMY (JET-UMY), 1(4), pp. 183-188.

[9] Ahmed, J., Salam, Z. (2018). An Enhanced Adaptive P&O MPPT for Fast and Efficient Tracking Under Varying Environmental Conditions, IEEE Transactions on Sustainable Energy, 9(3), pp. 1487 – 1496.

[10] Soesanti, I., Syahputra, R. (2016). Batik Production Process Optimization Using Particle Swarm Optimization Method. Journal of Theoretical and Applied Information Technology (JATIT), 86(2), pp. 272-278.

[11] Syahputra, R., Robandi, I., Ashari, M. (2015). PSO Based Multi-objective Optimization for Reconfiguration of Radial Distribution Network. International Journal of Applied Engineering Research (IJAER), 10(6), pp. 14573-14586.

[12] Hui, J.C.y., Bakhshai, A., Jain, P.K. (2016). An Energy Management Scheme With Power Limit Capability and an Adaptive Maximum Power Point Tracking for Small Standalone PMSG Wind Energy Systems, IEEE Transactions on Power Electronics, 31(7), pp. 4861 - 4875.

[13] Soedibyo, Ashari, M., Syahputra, R. (2014). “Power loss reduction strategy of distribution network with distributed generator integration”, Proceeding of 2014 1st International Conference on Information Technology, Computer, and Electrical Engineering (ICITACEE) 2014, UNDIP Semarang, pp. 404 - 408.

[14] Jamal, A., Suripto, S., Syahputra, R. (2015). Multi-Band Power System Stabilizer Model for Power Flow Optimization in Order to Improve Power System Stability. Journal of Theoretical and Applied Information Technology (JATIT), 80(1), pp. 116-123.

[15] Syahputra, R., Soesanti, I. (2016). Application of Green Energy for Batik Production Process. Journal of Theoretical and Applied Information Technology (JATIT), 91(2), pp. 249-256.

[16] R.G. Andrei, M. Ahmed; H.K. Tumageanian, J. C. Smith. “World's first commercial bridge capacitor bank installation on the American Electric Power System”, IEEE Transactions on Power Delivery, Vol. 16, No. 2, pp. 342-345, 2001.

[17] Jamal, A., Syahputra, R. (2016). Heat Exchanger Control Based on Artificial Intelligence Approach. International Journal of Applied Engineering Research (IJAER), 11(16), pp. 9063-9069.

[18] Syahputra, R., Soesanti, I. (2016). An Optimal Tuning of PSS Using AIS Algorithm for Damping Oscillation of Multi-machine Power System. Journal of Theoretical and Applied Information Technology (JATIT), 94(2), pp. 312-326.

[19] Syahputra, R., Soesanti, I. (2017). Modeling of Wind Power Plant with Doubly-Fed Induction Generator. Jurnal Teknologi, Journal of Electrical Technology UMY (JET-UMY), 1(3), pp. 126-134.

[20] R.G. Andrei, A.J.F. Keri, R.J. Albanese, P.B. Johnson, “Bridge capacitor bank installation concept reactive power generation in EHV systems”, IEEE Transactions on Power System, Vol. 8, No. 4, pp. 1463 – 1470, 1993.

[21] K.D. McBee and M.G. Simões, “Evaluating the Long-Term Impact of a Continuously Increasing Harmonic Demand on Feeder-Level Voltage Distortion,” IEEE Transactions on Industry Applications, Vol. 50, No. 3, May-June 2014, pp. 2142 – 2149.

[22] D. Shmilovitz, “On the definition of total harmonic distortion and its effect on measurement interpretation,” IEEE Transactions on Power Delivery, Vol. 20, No. 1, Jan. 2005, pp. 526 – 528.

Dynamic Performance of Synchronous Generator in Steam Power Plant

Ramadoni Syahputra[1], Andi Wahyu Nugroho[2], Kunnu Purwanto[3], Faaris Mujaahid[4]
Department of Electrical Engineering, Faculty of Engineering
Universitas Muhammadiyah Yogyakarta, Yogyakarta, Indonesia

***Abstract*—This paper presents dynamic performance of synchronous generator in steam power plant. Steam power plants are the most popular power plants to date. Until the end of 2018, 48.43% of the total installed capacity of power plants in Indonesia is this type of power plant. The largest steam power plant in Indonesia is in Paiton, Probolinggo, East Java, which is the object of this research. In its operation, the generator in this generator experiences dynamics as electricity load changes. This study discusses the analysis of the performance of synchronous generators to changes in electrical load. The analysis includes the voltage, active power, reactive power, power factor, and generator efficiency variables. The results showed that the generator performance remained good despite serving a very dynamic electricity load.**

Keywords—Synchronous generator; steam power plant; dynamic performance; efficiency

I. Introduction

Electrical energy is vital in all activities of human life to meet daily needs. Along with the development of technology that is very rapid, of course, the level of electricity demand every day is increasing in every human and industrial activity [1]-[4]. Power generation to produce electrical energy is also increasing and where the nature of electrical energy is easily channeled and converted into other forms of energy, such as mechanical energy, light energy, heat energy, and others [5]-[7].

Steam turbines play a significant role in the generation and distribution of electricity in an electric power system. Steam turbines are one of the essential components in steam power plants [8]-[10]. The steam turbine is a prime mover that converts steam potential energy into kinetic energy and then is converted into mechanical energy in the form of turbine shaft rotation [11]. Therefore, the steam turbine must be protected from all possible causes of disturbances and abnormal conditions that occur, both interference originating from the steam turbine itself or interference or abnormal conditions originating from other parts of the electric power system [12]-[14].

A generator is a system that functions to change power mechanics into electric power. Mechanical power is the result of generator input power, while electric power is the result of generator output power [15]-[19]. Generator efficiency is the ratio between the output power of the generator and the generator input power [20]. The generator input power is the same as the force generated by the turbine because the turbine and generator work together and can be separated [21]-[24].

The efficiency of the turbine generator will affect the performance of the Steam Power System. The higher the efficiency of the turbine generator, the better the reliability and performance of the generator. Turbines and generators are a unified system that cannot be separated, so turbines and generators have the same problem [30]. The problem is a decline in turbine generator efficiency due to several factors, such as the overload requested from the grid. So that the turbine will be overloaded, which causes the turbine to accelerate at the maximum rate and the generator does not work to the maximum, the factors of maintenance duration and errors in operation and maintenance [25]-[28].

PT Paiton Energy is the first private generating company in Indonesia. PT Paiton Operation and Maintenance Indonesia (POMI) are one of the electrical energy plants which have three units, namely unit 3, unit 7, and unit 8, which supply to Java and Bali and have a total capacity of 2045 MW. The Paiton Steam Power Plant has experienced very vital problems because the imbalance between the loads from the generator exceeds the limit. So that with the excess limit the turbine speed is breakneck and will undoubtedly damage the turbine itself and other effects all units in the Paiton trip due to the problem of imbalance between the turbine and generators. While the Paiton Steam Power Plant units 3, 7, and 8 supply the entire Java and Bali region so the performance of the turbine generator is very influential for channeling electrical energy because it discussed the analysis of the performance of the turbine generator at the Steam Power Plant of PT Paiton Operation and Maintenance, Indonesia. By calculating the turbine generator efficiency, it can be seen that the turbine and generator are working optimally or less optimally and know the problems that often occur with turbines and generators.

The purpose of this study is to identify the problems that cause the performance of generators in the PT POMI Paiton unit 7, know the turbine and generator power output in the PT POMI Paiton unit 7, and determine the generator performance in the PT POMI Paiton unit 7.

II. Fundamental

A. Steam Power Plant of PT POMI Paiton unit 7

Steam power plants are plants that use coal combustion sources to heat water to convert water to steam to produce electricity. In Fig. 1, a schematic of steam power plant Paiton unit 7 is shown.

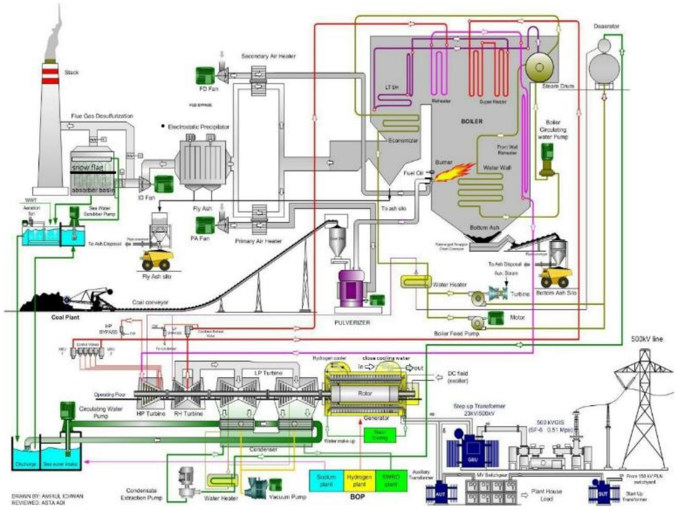

Fig. 1. A Schematic of Steam Power Plant Paiton unit 7.

Coal is moved from coal carriers on the jetty to the conveyor belt using a stacker by a coal removal device called a ship unloader. After the coal is moved from the coal carrier to the conveyor belt, then the coal is transported to the coal reservoir (stockpile) with the conveyor belt [29]. The placement of coal in the stockpile is also arranged according to its quality. There are four central stockpiles and one reserve stockpile. Coal in the stockpile does not need to be covered with a roof because the water content in coal will not exceed 40%.

From this stockpile, coal is transported to a bunker (coal silo) using a conveyor belt. From coal silos, coal is fed into the pulverizer/mill via a coal feeder. A pulverizer is a place for crushing coal so that it becomes fine grain so that it resembles powder. The coal feeder is a regulator of coal capacity that must go into the pulverizer. At the same time, coal is sampled and examined in a laboratory to determine its water content and quality. After the pulverizer, the powdered coal will rise to the furnace because of the hot air push from the PA (Primary Air) Fan. Aside from being a booster, this hot air also functions as a coal dryer, which has been in the form of powder so that it is faster in the combustion process in furnaces. The air from the PA (Primary Air) is also the main component so that combustion can occur inside the furnace [30].

The process of combustion in the furnace begins with fuel, namely diesel fuel, as a fuel used for starting a spray on a spark-plug such as a motor vehicle. There are 8 Spark-plugs found in each corner (corner) of the furnace. After the combustion process starts, slowly, coal is replaced by diesel fuel as fuel until finally only coal is used as fuel. If the quality of the coal used is inferior, the coal will be difficult to burn. As a result, more coal will be needed to produce the same amount of heat. Water to be converted into steam in a boiler comes from the WTP (Water Treatment Plant). The water used is seawater that is purified so that it becomes demineral water and is used to supply boilers.

The water used in the steam turbine cycle is called Demineral Water (Demineralized), which is water that has a conductivity level of 0.015 μs (micro-cements). In comparison, the mineral water we drink daily has a conductivity of around 100 - 200 μs. To get this demineral water, each PLTU unit is usually equipped with a Desalination Plant and Demineralization Plant that functions to produce this demineral water.

The water in the boiler comes from the sea, which goes through various processes in the Water Treatment Plant (WTP) to become demineral water. The initial process of producing demineral water starts from seawater that has been filtered out with its impurities and then pumped by the Sea Water Feed Pump to the Coagulant Storage Tank (seawater is given a coagulant to condense particles such as sand, mud, etc. in order to precipitate). Then the water is pumped to the Primary Sea Water Filter to filter the particles that have been compressed if it is still not filtered; it will be filtered back on the Polishing Filter. Filtered water is then collected in a Filtered Water Storage Tank and then pumped to the Cartridge Filter after being given antiseptic, acid, and sodium bisulfite.

In the cartridge filter, the water is filtered again to get purer water, which is then turned into freshwater through a reverse-osmosis desalination process. However, this water still contains much carbon. Then the carbon is separated in the Decarbonate Tank. Water is transferred to the Permeate Storage Tank using a Decarbonate Pump and Decarbonate Blower. Water from Permeate Storage Tank can be used to supply daily needs, but cannot be used to supply boilers.

Water from the Permeate Storage Tank using the Permeate Supply Pump is then processed again with the second reverse osmosis and then collected in Mixed Beds. This water is called demineral water and is collected in a Demin Water Tank.

The water collected at the WTP is first supplied to the condenser. By using a Condenser Extraction Pump, the water is transferred to the deaerator. In deaerators, oxygen levels are reduced so that there is not too much oxidation. Because if oxidation occurs, the pipe will easily corrode and can cause leakage. The oxygen-depleted water is collected in the Feed Water Storage Tank.

Furthermore, the water in the Feedwater Storage Tank is transferred to the economizer of the Boiler Feedwater Pump. In the economizer, the water gets warmed up from the furnace for the first time even though it has been warmed up several times by the heater. Out of the economizer, water that has been mixed with steam is stored in a Water Separator to be separated between water and steam. Then it will be heated at the superheater. At this superheater, the central heating because these Superheater boiler pipes come into direct contact with the fire. Here the steam will be increased in temperature to around 542 ˚C.

The steam that has been heated in the superheater will go directly to High-Pressure Turbine (HP Turbine). The steam that comes out after turning the HP Turbine is heated again in the boiler through the reheater. Steam heated in a reheater is not as hot as the steam produced by a superheater.

Then the steam from the reheater will go to the Intermediate Pressure Turbine (IP Turbine). After coming from IP Turbine, the steam goes directly to the Low-Pressure turbine (LP Turbine) without being heated up again. Then after the steam rotates LP Turbine, steam will flow into the condenser and condensed. The condensation water is collected and pumped again, and so on. When the steam rotates the turbine, the turbine shaft will also rotate. The turbine shaft itself is integrated between the HP Turbine, IP Turbine, and LP Turbine. The rotation of the shaft is used to rotate the generator and exciter.

The existence of water is essential in the Paiton Unit 7 power plant because it is used for various purposes, namely as the main ingredient in producing steam. Water is put into the boiler to be heated later with very high temperatures and transformed into water vapor. Besides that, water is also used for the cooling process or condenser cooling, which is used to absorb heat from the machines that are being used and as an absorber in the process of flue gas desulfurization (FGD).

There are two types of ash produced from coal combustion in the boiler, namely, fly ash and bottom ash. Fly ash is ash, which is quite small in size so that it is mixed with combustion gases (flue gas). Some of the ash produced from the combustion process will stick to the walls of the boiler pipe, accumulate, compact, and one day it will fall to the bottom of the boiler. This falling ash is known as bottom ash.

Flue gas combustion results in the boiler will be partially exhaled by the primary air fan and used to help the process of drying and heating coal when in the pulverizer. Most of the flue gas produced by combustion flows through the Electrostatic Precipitator (ESP). Electrostatic Precipitator functions to catch dust from coal combustion (fly ash). Smoke will pass through the electrodes, which causes the smoke to become electrically charged. Then by itself, the fly ash will stick to the second electrode wall. Then periodically, the second electrode wall will be shaken to drop the fly ash and be accommodated in the fly ash silo. Combustion smoke that has passed through the Electrostatic Precipitator will pass through the flue gas desulfurization (FGD). In the flue gas desulfurization, there are water curtains that will absorb the sulfur content in the combustion smoke, so that the exhaust gas that comes out through the stack (chimney) will be environmentally friendly.

B. Steam Turbine

A steam turbine is a mechanical device that extracts thermal energy from high-pressure steam into a rotary motion to drive a generator. Steam turbines are the main components in a Steam Power Plant [31] Fig. 2.

The basic working principle of a steam turbine is the combustion of coal to heat water and convert water into hot steam, commonly called thermal energy. Then heat energy is converted into kinetic energy; the process of converting heat energy into kinetic energy occurs in the turbine nozzle. At the nozzle, water vapor increases the speed/acceleration and causes a pressure differential between the sides before the nozzle and after the nozzle. Furthermore, kinetic energy is transformed into mechanical energy in the form of rotary energy from the turbine rotor, where then the rotation on the shaft will also turn the generator to produce electrical energy. Following is a general description of the working principle of a steam turbine.

In general, steam turbines have types of steam turbines that help the turbine work, including:

a) High-Pressure Turbine (HP Turbine): The High-Pressure Turbine (HP) turbine is the first turbine to accept the main steam from a superheater. After that, the steam output will be heated at the reheater. The High-Pressure Turbine (HP turbine) tip is connected to the Governing Valve (GV), and the other end is connected to the Intermediate Pressure (IP) turbine. HP turbine has several parts, namely casing, nozzle chamber, blade ring, dummy ring, LP dummy ring, blading, rotor, bearing, and gland. In this turbine, there is also a valve that is useful for regulating the amount of steam entering the turbine.

b) Intermediate Pressure Turbine (IP Turbine): The steam that has been heated in the reheater enters and plays an IP Turbine. Whereas for the IP turbine, the end is related to the LP turbine. IP Turbine has several parts, namely IP blading and IP rotors.

c) Low-Pressure Turbine (LP Turbine): Dry steam that comes out of the Intermediate Pressure Turbine (IP) is continued to be expanded to LP Turbine without further heating. The steam that comes out of LP Turbine is immediately accommodated and cooled by a condenser to be condensed with cooling media in the form of seawater. After using water, it will be used again as boiler fill water. LP Turbine is of double-flow type because, in this turbine, two output channels go to the condenser.

C. Synchronous Generator

The generator is a tool to generate electricity. The central part of the generator itself is the stator, rotor, and air gap. The working principle of a generator based on electromagnetic induction is that the prime mover rotates the rotor. Thus the poles that are on the rotor will rotate. If a direct voltage supplies the polar coil, then a magnetic field will emerge that rotates at the same speed as the polar rotation [32].

Fig. 2. Steam Turbine.

Fig. 3. Generator in a Steam Power Plant.

Based on Faraday's Law, if the conductor windings are rotated across the lines of magnetic force, then the conductor emits EMF (Electro Motive Force) or GGL (Electric Motion Force) or induced voltage. GGL generated by anchor conductor is an alternating voltage (AC). Fig. 3 shows the generator in a steam power plant.

Types of generators based on the location of the poles are grouped into the following.

a) Inner Pole Generator: Polar generators are generators whose magnetic fields are located in the rotor.

b) Outer Pole Generator: The outer pole generator is a generator whose magnetic field is located on the stator.

The type of generator based on the type of current generated

a) Synchronous Generator: Synchronous generators are electric generating machines that convert mechanical energy into electrical energy as output. The output voltage of a synchronous generator is alternating, therefore a synchronous generator is also called an AC generator. According to Anderson (1982), synchronous generators can produce energy sources, namely alternating voltage (AC). It says synchronous generator if the phase sequence must be the same, the voltage must be the same, the frequency must be the same, and the phase angle must be the same.

b) Asynchronous Generator: Basically, there is no asynchronous generator but that on an asynchronous motor.

Generator type based on the type of current generated

a) Direct Current Generator (DC): The direct current (DC) generator described can be converted into a DC generator, replacing the contact ring with a mechanical switch. A simple switch can be made with a metal ring divided into two separate parts (segments), mounted on an axis. This type of commutator is a denominational collector.

Each loop terminal is connected to the collector segment. When the loop is rotating, an AC voltage is induced in the coil, just like in an AC generator. However, before reaching the load, the induced voltage is converted to DC voltage by the collector, which functions as a mechanical rectifier. The contact segment of the collector moves to a different brush every half loop, keeping the direct current flowing through the electrical load of the circuit.

The rotation speed must be well determined so that the final result is expected. As stated earlier, the rotational speed affects the amplitude and frequency of the induced voltage.

b) Alternating Current Generator (AC): A loop of wire rotates in a magnetic field generated by a magnet, which induces an AC voltage between the loop terminals. The periodic change of voltage polarity is due to changes in the position of the coil relative to the magnetic pole. The voltage amplitude depends on the strength of the magnetic field and is also directly proportional to the rotational speed (1, 2, 3, and 4). If the magnetic field is uniform and the rotational speed is constant, the voltage induced between the loop terminals is sinusoidal with an average value of zero. The frequency is the same as the number of revolutions per second executed by the loop. Each loop terminal is connected to a metal ring. Contact with the ring is made with a fixed brush. If the brush is connected to an electrical load, an alternating current will be formed in the circuit.

III. Methodology

This research uses materials in the form of data related to power in turbines and generators as well as problems that cause turbines and generators that often disrupt the steam power plant of PT POMI Paiton. The location of this research is on Jalan Surabaya - Situbondo km 141, Binor, Paiton, Probolinggo, East Java, Indonesia.

In this study requires tools and materials in the form of hardware and software, namely:

1) Hardware: The hardware used in this study is a unit of Asus core i7 laptop.

2) Software: The software used in this research is Microsoft Word 2016 and Microsoft Excel 2016.

The rare steps of this research are shown in Fig. 4. Based on Fig. 4, it can be explained about the steps in this study. Research preparation is the first stage carried out in writing the final project. In this step, a field study was carried out by observing, interviewing directly the situation of the power plant of PT Paiton POMI and data acquisition licensing related to power in turbines and generators as well as problems that often occur in turbines and generators.

The next step is to identify and formulate the problem. The issue raised as a topic in the discussion of this paper is the analysis of the performance of turbines and generators at the PT POMI Paiton steam power plant. Therefore it is necessary to do a case study and collect data needed to support research in this thesis. The data about the performance of the turbine and generator will make it easier to solve the problems that occur.

The next step is a literature study. This stage has the aim of finding information about theories, methods, concepts, and references in the form of textbooks, journals, internet, manual books relating to the issues raised and can be used as a reference in solving the problems of this research and strengthening the theoretical basis for solve research problems.

This data collection phase is based on primary data. Primary data is data obtained directly from the research subject or source; in this case, the researcher obtains data or information directly using predetermined instruments. In collecting data based on primary data, there are interview and observation methods. The interview is one of the data collection techniques, where its implementation can be done directly dealing with research subjects through oral media by asking questions. Observation is a data collection technique by direct observation of the object under study for observations that researchers do to obtain data by direct observation of the company. After the data is collected, the next step is data processing. This data processor determines the results of the performance analysis of turbines and generators by calculating turbine power, generator, and turbine-generator efficiency, and the data is processed into tables and graphs.

After processing the data, we will get results that can be analyzed based on these data. To find out the performance of the turbine and generator at the PT POMI Paiton steam power plant, it is necessary to analyze the power output of the turbine and generator. Furthermore, these data can determine efficiency, from the efficiency that can determine the performance of turbines and generators and analyze problems that occur in turbines and generators.

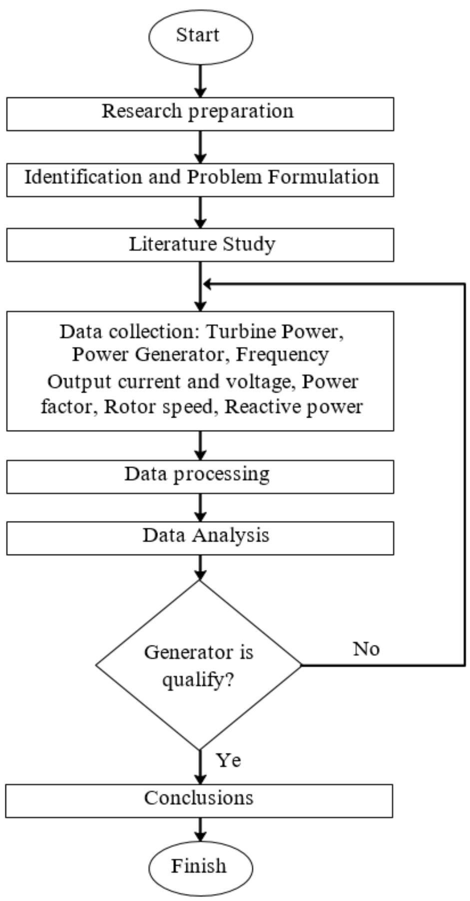

Fig. 4. The Steps of this Research.

IV. Results and Discussion

A. Synchronous Generator of Steam Power Plant

The type of generator used at PT POMI's unit 7 steam power plant is a synchronous generator. This type of generator is very suitable for use in power plants that have high-speed turbines such as steam power plants. In principle, a generator is said to be a synchronous generator if the rotation of the stator field is the same as the rotation of the rotor. If the generator wants to be on grid right, the generator is said to be synchronous if the phase sequence, instantaneous voltage, frequency, and phase angle must all be the same as the grid network. The working principle of synchronous generators is based on electromagnetic induction. When the prime mover is connected to the rotor, the rotor will rotate at a speed corresponding to the number of revolutions produced by the turbine. If the DC voltage as the source of the amplifier field supplies the coil to the field pole, then the magnetic field line appears on the surface of the rotating pole at the same speed as the pole. The lines of the rotating magnetic force will cross the coil anchors contained in the stator so that the EMF (electromotive) coil appears. Next, the EMF generated at the conductor anchors is the AC voltage, which is the generator output voltage.

B. Characteristics of Generators and Turbines in PT POMI Unit 7 Steam Power Plants

At the PT POMI unit 7, the steam power plant has a total capacity of 615 MW, including turbines and generators. In turbines, there are three types of turbines, namely High-Pressure turbines. Intermediate Turbine Pressure and Low-Pressure Turbine. And the power in this turbine is to determine the efficiency of the generator's performance. The generator used is a synchronous generator, which is said to be asynchronous if the phase sequence must be the same, the voltage must be the same, the frequency must be the same, and the phase angle must be the same. Table I shows the characteristics of the turbine while Table II shows the characteristics of the generator. Fig. 2 shows the nameplate of the turbine and generator.

To determine the performance of the 280T330 generator in the Paiton unit 7 steam power plant, there are several parameters such as generator output, power factor, frequency, efficiency, the relationship between active power, reactive power, and power factor and excitation system and power supply voltage. The performance of the generator determines the performance of the generator from 1 December 2018 - 30 December 2018.

TABLE. I. Characteristics of the Turbine

Manufacture	General Electric
Type	280T330
Rated Output	670 KW
Pressure	2400 PSIG
Temperature	1000 °F
Reheat Temperature	1000 °F
Exhaust Pressure	2.18 HGA

TABLE. II. CHARACTERISTICS OF THE GENERATOR

Rated Output	846,231 KVA
Armature Voltage	23 Kv
Armature Current	21,242 A
Power Factor	0.85
Phase	3
Frequency	50 Hz
Rotation speed	3000 RPM
Excitation voltage	683 Volt
Gas Pressure	75 PSIG
Connection	2-Y
Field Ampere	4,670 A

To analyze the performance of 280T330 generator Paiton steam power plant unit 7 with the generator output power output using the unit 7 daily operating power output data. Daily operating data to be analyzed for 30 days, starting from 1 December 2018 to 30 December 2018. The following are power output generator unit 7 for 30 days.

Active power is real power or power that is fed to the load. The size of the active power is influenced by voltage, and current, the higher the current and voltage, the active power will be even more significant and vice versa if the smaller the current and voltage, the active power will also be smaller. The active power of the generator output at the PT POMI Paiton steam power plant is shown in Fig. 5.

In Fig. 5, the generator performance can be observed based on changes in active power with time. The output power of the generator concerning time from December 1, 2018, to December 30, 2018, has fluctuated. The highest active power occurred on December 13, 2018, amounting to 604.85 MW due to the large current and voltage generated, and the load demand by the PLN grid is also significant. The lowest active power occurred on December 16, 2018, amounting to 465.74 MW because the current and voltage generated are small, and the load demand by the PLN grid is also small.

The generator in PT POMI unit 7 steam power plant has an output voltage specification of 23 kV with 3 phases. The generator output voltage is affected by consumer load, frequency, and excitation. Generator output voltage decreases when consumer load increases, conversely generator output voltage rises when the consumer load decreases. In Fig. 6, the graph shows the change in the output voltage of the generator with time for one month.

In Fig. 6, it can be observed the performance of the generator based on changes in the output voltage concerning that of the generator output voltage concerning time from December 1, 2018, to December 30, 2018, experiencing fluctuations. The highest output voltage occurs on December 1, 2018, in the amount of 21.6299 kV because the load generated is large, and the lowest output voltage occurs on December 22, 2018, in the amount of 21.3461 kV because the load generated is small.

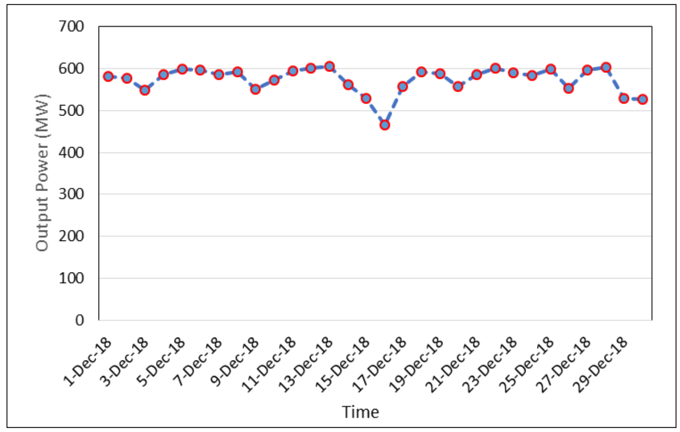

Fig. 5. The Active Power of the Generator Output at the PT POMI Paiton.

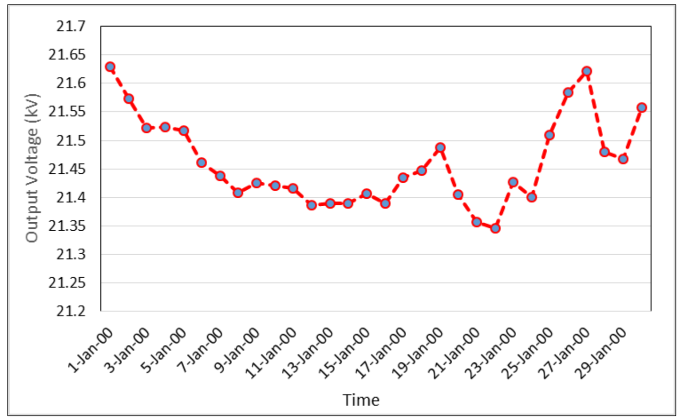

Fig. 6. The Output Voltage of the Generator at the PT POMI Paiton.

In addition to active power, the reactive power of synchronous generators is also analyzed. This reactive power cannot be used directly by the load but instead is converted into another form of energy in the form of magnetic power to generate magnetic electricity in industrial electrical equipment. There are two types of reactive power, namely inductive reactive power used to generate magnetic flux in industrial equipment and capacitive reactive power used to reduce the use of reactive power. Fig. 7 shows the change in reactive power in MVAR concerning time during one month of observation.

In Fig. 7, it can be observed the performance of the generator based on the change in reactive power concerning time from December 1, 2018, to December 30, 2018. The reactive power of the generator during that period fluctuates. The highest reactive power occurred on December 7, 2018, in the amount of 231.7503 MVAR because the excitation current injected to the generator produced was large, and the lowest reactive power occurred on December 25, 2018, in the amount of 11.2169 MVAR because the current injected into the generator produced was small.

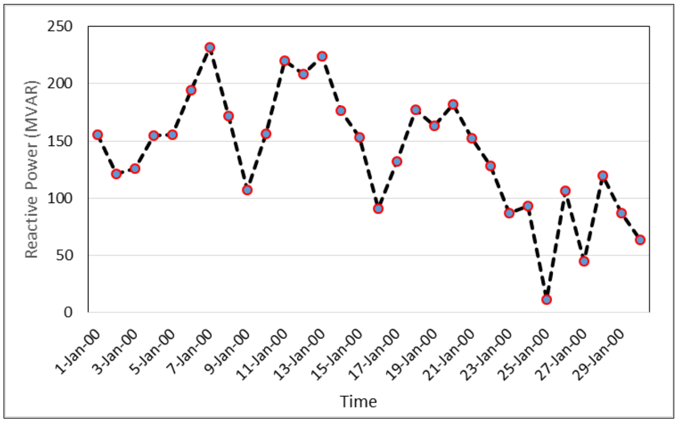

Fig. 7. The Reactive Power of the Generator at the PT POMI Paiton.

The next generator performance analysis is the generator power factor variable. The power factor is influenced by active power and apparent power. The higher the active power and the smaller the apparent power, the higher the power factor so that it approaches the value of 1 and vice versa if the smaller the active power and the higher the apparent power, the smaller the power factor. Fig. 8 shows the graph of changes in power factor from December 1, 2018, to December 30, 2018.

From Fig. 8, it can be observed that the generator performance based on the power factor starting December 1, 2018, until December 30, 2018, has fluctuated. The highest power factor occurred on December 25, 2018, at 0.998 because the reactive power generated was small, and the lowest power factor occurred on December 7, 2018, in the amount of 0.9298 because the reactive power generated was immense. The higher the power factor or a value of 1, the resulting factor can be said to be good.

In Fig. 9, it can be observed the efficiency of synchronous generators at the PT POMI Paiton unit 7 steam power plant. Observations were made from December 1, 2018, to December 30, 2018. The results of observations show that the efficiency of the generator still meets the design with a tolerance of ± 5. The efficiency of generators is affected by losses. The higher the losses, the smaller is the efficiency and vice versa, the smaller the losses, the higher the efficiency.

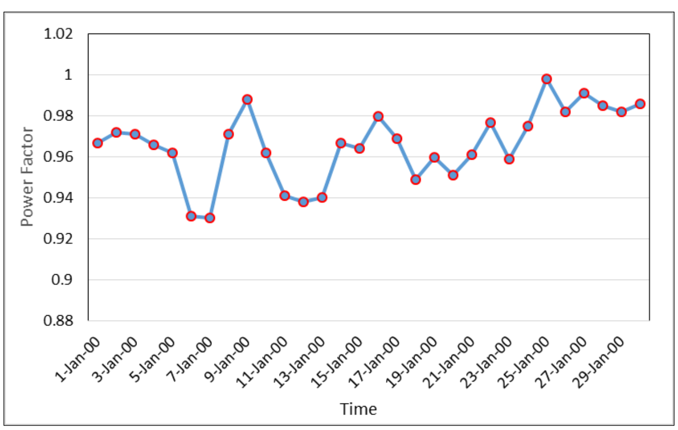

Fig. 8. The Power Factor of the Generator at the PT POMI Paiton.

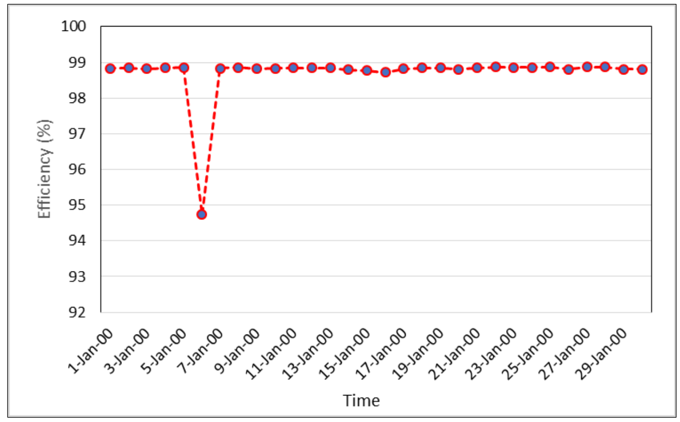

Fig. 9. The Efficiency of the Generator at the PT POMI Paiton.

Based on Fig. 9, it can be observed that the performance of generators based on generator efficiency from December 1, 2018, to December 30, 2018, has fluctuated. On December 6, 2018, it experienced a very drastic decrease because at 06:00 PM, because no output power was detected in the turbine because it was under maintenance and the highest efficiency occurred on December 25, 2018, amounting to 98.87% due to the large load generated.

V. Conclusions

In this research, an analysis of the performance of synchronous generators at the PT POMI Paiton Unit 7 steam power plant includes analysis of changes in active power, changes in output voltage, changes in reactive power, changes in power factors, and changes in generator efficiency. Based on observations during December 2018, it shows that the generator characteristics are in good condition, although experiencing dynamics due to changes in electricity load. In general, the losses on generators are relatively small, so they are not a problem.

Acknowledgment

The authors gratefully acknowledge the contributions of the Universitas Muhammadiyah Yogyakarta, for funding this research.

References

[1] Brusco, G., A. Burgio, D. Menniti, A. Pinnarelli, N. Sorrentino. (2014). Optimal Sizing of DGs for a CHP-Based Agro-Industrial Microgrid with a Priority Criteria Operational Strategy, International Review of Electrical Engineering (IREE), 9(2), pp. 351-362.

[2] Syahputra, R., Soesanti, I. (2017). Modeling of Wind Power Plant with Doubly-Fed Induction Generator. Jurnal Teknologi, Journal of Electrical Technology UMY (JET-UMY), 1(3), pp. 126-134.

[3] Syahputra, R., Soesanti, I. (2016). DFIG Control Scheme of Wind Power Using ANFIS Method in Electrical Power Grid System. International Journal of Applied Engineering Research (IJAER), 11(7), pp. 5256-5262.

[4] Syahputra, R., Wiyagi, R.O., Sudarisman. (2017). Performance Analysis of a Wind Turbine with Permanent Magnet Synchronous Generator. Journal of Theoretical and Applied Information Technology (JATIT), 95(9), pp. 1950-1957.

[5] Syahputra, R., Soesanti, I., Ashari, M. (2016). Performance Enhancement of Distribution Network with DG Integration Using Modified PSO Algorithm. Journal of Electrical Systems (JES), 12(1), pp. 1-19.

[6] Syahputra, R., Robandi, I., Ashari, M. (2015). Performance Improvement of Radial Distribution Network with Distributed Generation Integration Using Extended Particle Swarm Optimization Algorithm. International Review of Electrical Engineering (IREE), 10(2). pp. 293-304.

[7] Syahputra, R. (2017). Distribution Network Optimization Based on Genetic Algorithm. Jurnal Teknologi, Journal of Electrical Technology UMY (JET-UMY), 1(1), pp. 1-9.

[8] Mujaahid, F., Fauzi, A.M., Syahputra, R., Putra, K.T., Purwanto, K. (2017). Potentials of Organic Waste Conversion in a Green Campus Concept. Journal of Electrical Technology UMY (JET-UMY), 1(4), pp. 183-188.

[9] Ahmed, J., Salam, Z. (2018). An Enhanced Adaptive P&O MPPT for Fast and Efficient Tracking Under Varying Environmental Conditions, IEEE Transactions on Sustainable Energy, 9(3), pp. 1487 – 1496.

[10] Hui, J.C.y., Bakhshai, A., Jain, P.K. (2016). An Energy Management Scheme With Power Limit Capability and an Adaptive Maximum Power Point Tracking for Small Standalone PMSG Wind Energy Systems, IEEE Transactions on Power Electronics, 31(7), pp. 4861 - 4875.

[11] Hui, J.C.y., Bakhshai, A., Jain, P.K. (2015). A Sensorless Adaptive Maximum Power Point Extraction Method With Voltage Feedback Control for Small Wind Turbines in Off-Grid Applications, IEEE Journal of Emerging and Selected Topics in Power Electronics, 3(3), pp. 817 - 828.

[12] Syahputra, R., Robandi, I., Ashari, M., (2012), “Reconfiguration of Distribution Network with DG Using Fuzzy Multi-objective Method”, International Conference on Innovation, Management and Technology Research (ICIMTR), May 21-22, 2012, Melacca, Malaysia.

[13] Syahputra, R., Robandi, I., Ashari, M. (2014). Optimization of Distribution Network Configuration with Integration of Distributed Energy Resources Using Extended Fuzzy Multi-objective Method. International Review of Electrical Engineering (IREE), 9(3), pp. 629-639.

[14] Jiang, R., Han, Y., Zhang, S. (2017). Wide-range, high-precision and low-complexity MPPT circuit based on perturb and observe algorithm, Electronics Letters, 53(16), pp. 1141 - 1142.

[15] Peng, B.R., Che, K., Liu, Y.H. (2018). A Novel and Fast MPPT Method Suitable for Both Fast Changing and Partially Shaded Conditions, IEEE Transactions on Industrial Electronics, 65(4), pp. 3240 - 3251.

[16] Hossain, M.K., Ali, M.H. (2013). Overview on Maximum Power Point Tracking (MPPT) Techniques for Photovoltaic Power Systems. International Review of Electrical Engineering (IREE), 8(4). pp. 1363-1378.

[17] Tang, L., Xu, W., Mu, C. (2017). Analysis for step-size optimisation on MPPT algorithm for photovoltaic systems, IET Power Electronics, 10(13), pp. 1647 - 1654.

[18] Ghasemi, M.A., Ramyar, A., Eini, H.I. (2018). MPPT Method for PV Systems Under Partially Shaded Conditions by Approximating I–V Curve, IEEE Transactions on Industrial Electronics, 65(5), pp. 3966 - 3975.

[19] Farhat, S., Alaoui, R., Kahaji, A., Bouhouch, L., Ihlal, A. (2015). P&O and Incremental Conductance MPPT Implementation. International Review of Electrical Engineering (IREE), 10(1). pp. 116-122.

[20] Soesanti, I., Syahputra, R. (2016). Batik Production Process Optimization Using Particle Swarm Optimization Method. Journal of Theoretical and Applied Information Technology (JATIT), 86(2), pp. 272-278.

[21] Syahputra, R., Robandi, I., Ashari, M. (2015). PSO Based Multi-objective Optimization for Reconfiguration of Radial Distribution Network. International Journal of Applied Engineering Research (IJAER), 10(6), pp. 14573-14586.

[22] Metry, M., Shadmand, M.B., Balog, R.S., Abu-Rub, H. (2017). MPPT of Photovoltaic Systems Using Sensorless Current-Based Model Predictive Control, IEEE Transactions on Industry Applications, 53(2), pp. 1157 - 1167.

[23] Jamal, A., Syahputra, R. (2016). Heat Exchanger Control Based on Artificial Intelligence Approach. International Journal of Applied Engineering Research (IJAER), 11(16), pp. 9063-9069.

[24] Syahputra, R., Soesanti, I. (2016). Design of automatic electric batik stove for batik industry. Journal of Theoretical and Applied Information Technology (JATIT), 87(1), pp. 167-175.

[25] Soedibyo, Ashari, M., Syahputra, R. (2014). “Power loss reduction strategy of distribution network with distributed generator integration”, Proceeding of 2014 1st International Conference on Information Technology, Computer, and Electrical Engineering (ICITACEE) 2014, UNDIP Semarang, pp. 404 - 408.

[26] Jamal, A., Suripto, S., Syahputra, R. (2015). Multi-Band Power System Stabilizer Model for Power Flow Optimization in Order to Improve Power System Stability. Journal of Theoretical and Applied Information Technology (JATIT), 80(1), pp. 116-123.

[27] Syahputra, R., Soesanti, I. (2015). Power System Stabilizer model based on Fuzzy-PSO for improving power system stability. 2015 International Conference on Advanced Mechatronics, Intelligent Manufacture, and Industrial Automation (ICAMIMIA), Surabaya, 15-17 Oct. 2015 pp. 121 - 126.

[28] J. Ahmed, Z. Salam. (2018), “An Enhanced Adaptive P&O MPPT for Fast and Efficient Tracking Under Varying Environmental Conditions", IEEE Transactions on Sustainable Energy, Vol. 9, No. 3, pp. 1487 – 1496.

[29] Syahputra, R., Soesanti, I. (2016). Application of Green Energy for Batik Production Process. Journal of Theoretical and Applied Information Technology (JATIT), 91(2), pp. 249-256.

[30] L. Tang, W. Xu, C. Mu, “Analysis for step-size optimisation on MPPT algorithm for photovoltaic systems”, IET Power Electronics, Vol. 10, No. 13, pp. 1647 – 1654, 2017.

[31] Sher, H.A., Addoweesh, K.E., Al-Haddad, K. (2018). An Efficient and Cost-Effective Hybrid MPPT Method for a Photovoltaic Flyback Microinverter, IEEE Transactions on Sustainable Energy, 9(3), pp. 1137 - 1144.

[32] Syahputra, R., Soesanti, I. (2016). An Optimal Tuning of PSS Using AIS Algorithm for Damping Oscillation of Multi-machine Power System. Journal of Theoretical and Applied Information Technology (JATIT), 94(2), pp. 312-326.

The Impact of using Social Network on Academic Performance by using Contextual and Localized Data Analysis of Facebook Groups

Muhammad Aqeel[1], Mukarram Pasha[2], Muhammad Saeed[3], Muhammad Kamran Nishat[4]
Maryam Feroz[5], Farhan Ahmed Siddiqui[6], Nasir Touheed[7]
Department of Computer Science/UBIT, University of Karachi, Karachi, Pakistan[1, 2, 3, 5, 6]
Department of Computer Science, Karachi Institute of Economics and Technology, Karachi, Pakistan[4]
Department of Computer Science, Institute of Business Administration, Karachi, Pakistan[7]

***Abstract*—Social Networks due to their intrinsic nature of being addictive have become an integral part of our civilization and plays an important role in our daily interactions. Facebook being the largest global online network, is used as a primary platform for carrying out our study and hypothesis testing. We built a web crawler for data extraction and used that data for our analysis. Primary goal of this study is to identify patterns among members of a Facebook group using a contextual and localised approach. We also intend to validate some hypotheses using a data driven approach like comparison of student's social participation and activeness with actual class participation and its impact on his/her grades. We have also used user interactions in Facebook groups for identifying close relationships. The polarity of content in a group's comments and posts defines a lot about that group and is also conferred in this paper.**

Keywords—Social networks; data analysis; data mining; NLP; sentiment analysis

I. Introduction

Social network like Social networking sites like Facebook and Twitter have become ubiquitous in our everyday life. With more than 2 Billion active users Facebook is undoubtedly the most used social networking site. Young students are in majority among these users. Students use it as a platform to share their ideas and collaborate on projects in addition to socializing with other students and people. There have been many studies to understand the impact of social media on the grades of undergrad students [5, 8, 9, 19, 20]. Results of these studies are mixed there is evidence of both positive and negative impact of social media usage on the academic performance of students. For our analysis, we built a web crawler for extracting data from Facebook and used its data throughout our analysis. The data extraction process and building the appropriate schema itself was a challenging task and is also presented in this paper. We extracted profiles of students in an undergraduate class studying computer science in Pakistan. First, we anonymize their data to protect their privacy. Then we study the correlation between their activeness on Facebook and their grades. We applied different data analysis techniques and some well-established correlation test to quantify the impact of social media.

The structure of the paper is as follows. Section 2 explores the related work in this area in detail. Section 3 describes our methodology and our dataset used in this study. Section 4 discusses the results of our study and Section 5 concludes the paper.

II. Related Work

With the advent of online social networking websites, there has been an explosion of user data and information and thus a lot of work has been done in the field of social network analysis. Previous studies involving Facebook data can be subcategorized into following three categories.

A. Social Network Analysis

Social network analysis is the study of analysing social structures using networks and graphs. Networks are built using existing user data available on online social networking sites like Facebook, Twitter etc. Graph data structures are extensively used to model such scenarios. Users are represented in the form of nodes of a graph and their relationships are represented by edges. As Berry Wellman [1] discussed in his paper in 2001, "Computer networks are inherently social networks, linking people, organizations, and knowledge".

Social network analysis is categorized in two types:

1) Sociocentric (whole) network analysis: This involves sociological quantification of interaction among a group of people. It focuses on the identification of global structural patterns. Most SNA research in organizations in recent times concentrates on this sociometric approach.

2) Egocentric (personal) network analysis: This emerged from anthropology and psychology and involves quantification of interactions between an individual (called ego) and all other persons (called alters) related (directly or indirectly) to ego. It is not so difficult to collect data for such studies especially after the advent of online social networking websites. Some generalizations are made if there is some missing data of an ego.

Similar work is in Social Network Analysis.

Many studies have been carried out to understand and better model sociocentric and egocentric networks. J. Ugander et al. [2] in 2011 analysed the global structure of the Facebook user network graph and characterized the assortative patterns present in the graph by studying the basic demographic and network properties of users. Similar study was carried out by Traud et al. [3] in which they examined the roles of user attributes in a Facebook network of one hundred American colleges and universities.

Many of the work have been done to find relation between social media usage and its effect on academic performance of students Daniel Z. Grunspan et. al. [11] analysed two study networks from a single classroom and study interactions among students at exam time. Nikolaos K Tselios et al. [n1] examines the use of social media site Facebook and its correlation with academic accomplishments. Justyna P. Zwolak et al.[10] used Social Network Analysis to identify patterns of interaction that contribute to taking the advanced course of MI after taking a first course, in this paper they try to prove that social integration of students during course study increase their persistence towards that course. G. Han et al. [12] performed analysis on social network's data to measure student's collaboration in a capstone project, their study suggests the instructor should include structures activities that emphasizes student collaboration to help develop strong information networks in other courses. Eric Brewe et. al. [13] applied sequential multiple regression modelling to evaluate factors which contribute to participation in the learning community PLC (Physics Learning Center - that support the development of academic and social integration), their model indicates that gender and ethnicity were not good predictors of participation in social learning group.

B. Natural Language Processing

Natural language processing can be referred to as a range of computational techniques that attempts to understand, analyse and perform linguistic analysis on naturally occurring text to achieve human like language processing, which is helpful in many tasks. Sentiment Analysis (also known as opinion mining or emotion AI) is an NLP technique used to analyse opinions, sentiments, evaluations, attitudes and emotions from the text. With the growth of social media, individuals and organizations are now extensively using public opinions for making decisions based on sentiment analysis.

Natural language processing can be applied on text, audio, video and voice with some pre-processing. Basically, all formats are usually first converted to text and then the relevant NLP techniques are applied. NLP based on text can lead to discussion analysis, opinion mining, contextual study, dictionary building or corpus building, linguistic study, semantics, ontological study etc.

Machine translation is one of the most studied topics in NLP and significant advances have been made in this field. Machines are now capable of translating almost any human language efficiently and in real time.

Similar work is in NLP.

Substantial work has been done on Facebook's dataset involving NLP techniques. P. Dewan et al. [3] proposed and extensive feature set based on entity profile, textual content, metadata, and URL features to identify malicious content on Facebook in real time. In other work, F Krebs et al. [4] proposed methods for predicting reactions/emotions on user posts on pages of supermarket chains. Their final model predicted the distribution of reactions with an MSE of 0.135. Bharat Gaind [17] et al. also did similar work to detect emotions from the Facebook and Twitter, they applied two-fold approaches comprised of NLP and Machine Learning which yields significantly good results on test data.

SNA and NLP applications are being built using social networks' data in almost every field Adil Rajput. 2019. [14] gives a good overview of sentiment analysis from social network's data of patients and application of NLP to mental health. Hiroki Takikawa [15] conducted both large-scale social network analysis and natural language processing on Japan's political Twitter data, they applied community detection method to identify the five most common communities they also use topic modelling technique their results also showed if topic is solely propagated by left or right wing. Glen Coppersmith et al. [16] used natural language processing and machine learning techniques to detect quantifiable signals around suicide attempts.

C. Data Analysis

There are endless possibilities for data analysis using Facebook's data and people have used it to extract many insights and trends.

Data analysis can be classified into various types

1) Descriptive analysis: Descriptive analysis answers the "what happened" by summarizing past data usually in the form of dashboards. The biggest use of descriptive analysis in business is to track Key Performance Indicators (KPI's). KPI's describe how a business is performing based on chosen benchmarks.

2) Diagnostic analysis: After asking the main question of "what happened" you may then want to dive deeper and ask why did it happen? This is where diagnostic analysis comes in. A critical aspect of diagnostic analysis is creating detailed information. When new problems arise, it is possible you have already collected certain data pertaining to the issue.

3) Predictive analysis: Predictive analysis attempts to answer the question "what is likely to happen". This type of analytics utilizes previous data to make predictions about future outcomes. Business applications of predictive analysis include risk assessment, sales forecasting, etc.

4) Prescriptive analysis: Prescriptive analysis utilizes state of the art technology and data practices. It is a huge organizational commitment and companies must be sure that they are ready and willing to put forth the effort and resources.

Similar work in Data Analysis

Mariam Adedoyin-Olowe et al. [18] provided a survey of data mining and data analysis techniques for Social Media Analysis much of the work is done in this dimension R. Farahbakhsh et al. [6] crawled 479K random user profiles on Facebook and studied the sensitivity of various attributes and listed few which are rarely disclosed by users and are considered private. In another study, S. Mohammadi et al. [7]

explored the popularity evolution for professional users in Facebook. They monitored 8K most popular professional users on Facebook over a period of 14 months and concluded that being active and famous correlate positively with the popularity trend.

III. Methodology

This section includes detailed step by step explanation of our analysis.

A. Data Extraction

We choose to extract data from profile of users whom we can later verify our results with. Data extraction was done in three steps from specialization to generalization and following a localized approach.

1) Same class: Initially, we extracted data from a group of students belonging to the same batch. There were 85 members in that group and had 1207 posts, 4436 comments and 3177 replies.

2) Same major: Our next group had 532 members and all members had the same major. The group had 348 posts, 906 comments and 805 replies.

3) Same university: Lastly, a public group of university including members from all majors was scraped. There were 1593 members in that group and had 323 posts, 1355 comments and 881 replies.

For extracting data from these groups, we made use of python-client of web crawling library - Selenium. As Facebook renders only a small number of posts when a group is opened, we had to automate the scrolling of a page by executing some JavaScript code. We also had to expand all comments and replies in each post as those are collapsed by default. Once the page was completely rendered, we extracted the page source and parsed the HTML using Beautiful Soup library.

B. Schema

We created separate tables for posts, comments and replies and used their URLs as primary keys. We decided to follow this fragmented structure because it would help us in carrying out our analysis independently. Tables can also be merged later when needed.

We designed a separate schema for reactions, because all posts, comments and replies contain reaction_url. In addition, another table for each group was maintained which included information of each user’s mentions to other users of that group.

C. Data Cleaning

Data extracted from Facebook was in raw form and had to be cleaned before carrying out any analysis. Cleaning of the data included:

- Text in most of the posts, comments and replies was in roman-Urdu and was converted to English.
- User profile links were URL encoded and had to be formatted correctly.
- An anonymous alias was assigned to each user profile to ensure user privacy.
- Removal of any trailing spaces, punctuations and links in the text so that it would later be used to find out subjectivity and polarity.

D. Polarity and Subjectivity

Polarity can be referred as the negativity or positivity of the text. Its value ranges from -1 to +1. Negative content has polarity less than 0 and positive content has polarity greater than 0, while polarity of 0 denotes the neutrality of the text.

Subjectivity expresses some personal feelings or belief. Content addressing general issue tends to be more objective than texts which contain information about a specific topic. Value of subjectivity lies between 0 and 1. Texts with values below 0.5 tends to be more objective and texts with values greater than 0.5 are interpreted as subjective.

After cleaning and preprocessing of the data, sentiment analysis was carried out on texts of posts, comments and replies to find subjectivity and polarity. For sentiment analysis python TextBlob library was used.

We can clearly see (Table I) that first example is positive and objective as it is addressing public while the second example is more positive than the first one and is also more subjective, because in the second example “Ali” is being addressed by his friend particularly and more positive sentiments are used. In the third example, subjectivity is quite high as it is talking about last class and Friday but is not polar as there are no sentiments involved.

E. User Participation in different Communities

We selected users who were members of all three of the groups we crawled and used their interactions in each group to identify participation patterns in communities of different sizes. We found a total of 14 members who were members of all three groups and counted number of posts, comments and replies of each user in each group.

It is visible (Fig. 1, Fig. 2, Fig. 3) that many of the students are the silent members of other groups except their class’s group as they have lesser or no participation there. We can observe the trend as most of the members are very active in their closed class group, less active in their department’s group and least active in public group but there is also an exception as one of our subject “Talha” has no post in class’s group, but he is active in public group.

TABLE. I. EXAMPLES OF POLARITY AND SUBJECTIVITY

Example	Sentence	Polarity	Subjectivity
1	Congratulations everyone, what a team work.	0.4	0.16
2	Congratulations Muhammad Ali on winning Trophy you did it once again brother <3	0.75	0.87
3	I forgot my calculator in last class on friday, did anyone find?	0.00	0.06

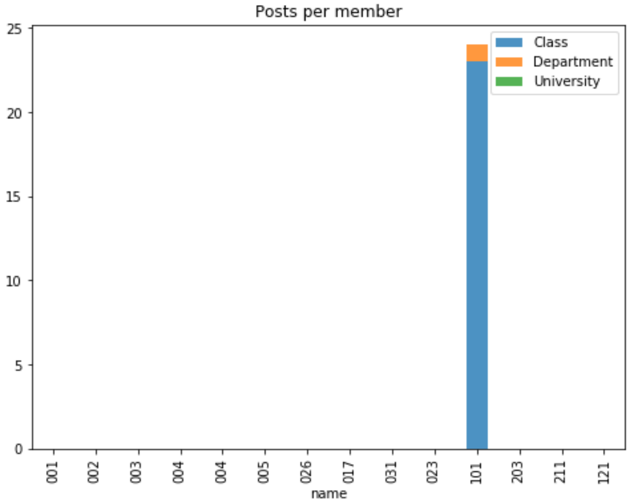

Fig. 1. Number of Posts in Each Group by Common Member.

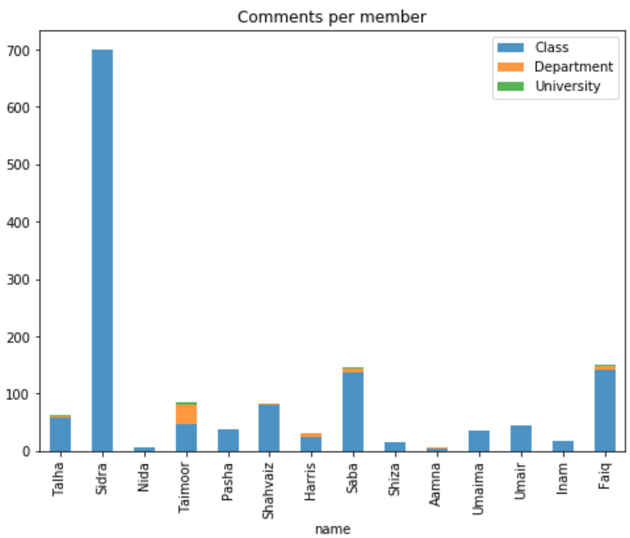

Fig. 2. Number of Comments in Each Group by Common Member.

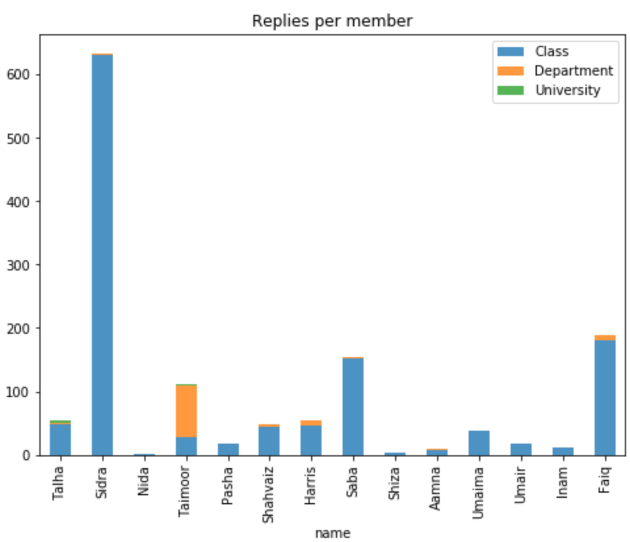

Fig. 3. Number of Replies in Each Group by Common Member.

F. *User Interaction Frequencies*

Using our existing data tables, we created a frequency matrix determining each user's interaction (mentions) with every other user (Fig. 4). The higher the frequency of user pairs, the stronger is the relationship. Building on these bi-pair user frequencies we can create groups of N members by setting a threshold frequency.

We can clearly see from mention frequency graph that very few users mention every user in the group otherwise most of the users are mentioned by the group of their groups or close friends.

G. *Correlation between Grades and Activeness on Social Study Group*

As we already have access to user's activity on Facebook class study group; their posts, comments and replies are all available in our dataset, we can make use of this and analyse whether there is any sort of correlation between social network usage and students' grades.

1) Hypothesis: Our hypothesis was that generally students who are active on social study groups should have good grades compared to those who do not participate in discussions happening over the study group.

2) Analysis: We aggregated the student's interaction on the study group by summing their posts, comments and replies. A data frame was built containing all study group members along with their CGPA and total interaction.

We calculated the correlation of CGPA and student's activity on social group and found it to be *0.0065*. Which meant there wasn't any impact of social study group activeness and student's grades. We then decided to dig into this problem a little deeper and segment the data based on some metrics to identify the correlation within the sub groups.

3) Segmenting Students Based on Their CGPA: We decided to create sub groups from the existing pool of study group members based on their CGPA. We partitioned into three separate bins.

a) Good Students - Students with CGPA greater than or equals to 3.

b) Average Students - Students with CGPA greater than 2 and less than 3.

c) Bad Students - Students with CGPA less than or equals to 2.

4) Correlation within Sub Groups: We then decided to analyse the correlation of each sub group separately. Average student's sub group showed no correlation but interesting patterns were identified within subgroups of Good and Bad students.

Correlation Heatmap of good and bad student's sub groups can be seen.

It can be seen clearly from the heatmap (Fig. 5) that there is a strong negative correlation of CGPA with every other social interaction feature. This indicates that those students who have good grades do not participate actively in study group discussions. For good students, increased participation in an online study group can have a negative impact on their CGPA.

Correlation heatmap of bad students (Fig. 6) indicates an opposite scenario. Bad students who participate actively in online study groups, can have higher CGPA than those bad students who do not. CGPA for bad students is positively correlated, those who participate actively tends to get higher CGPA.

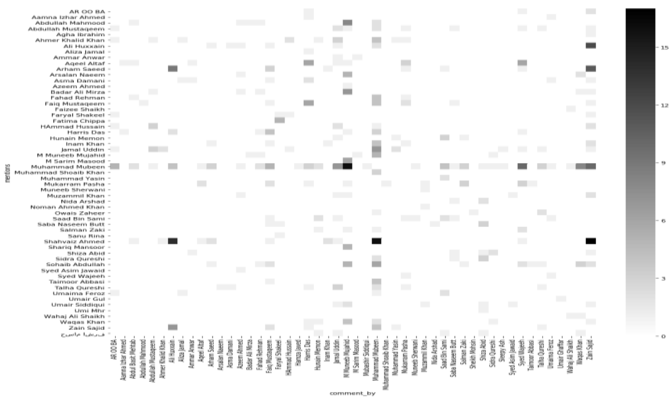

Fig. 4. Heatmap of user Interaction Frequencies.

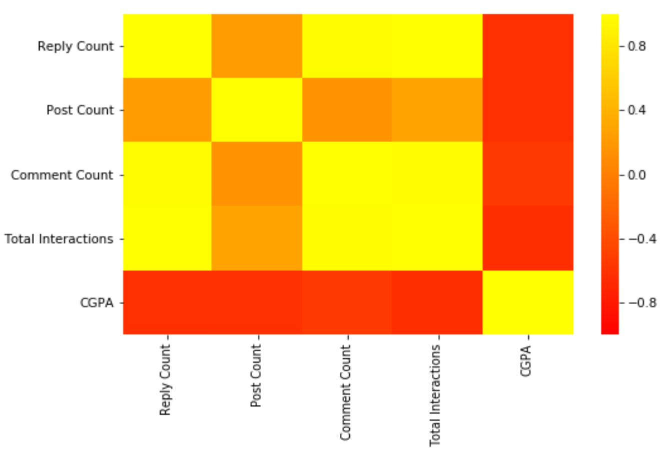

Fig. 5. Correlation Heatmap of Good Student's Sub Group.

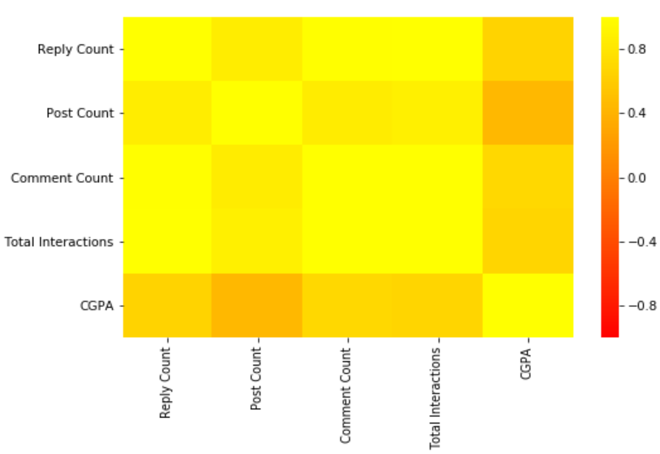

Fig. 6. Correlation Heatmap of Bad Student's Sub Group.

IV. Results

From user participation plots, it's evident that many users are comfortable interacting within their localized communities. This localized approach was helpful in carrying out analysis of student's social participation and was later compared with their actual class participation by their teacher's feedback.

This analysis came up with some good outcomes that students participating on all the forums actively are also vocal in their classes and the students who does not actively participate at all over social media but are active in class have very good grades.

Study of correlation between CGPA and student's interaction in study group generated interesting results as well. Students who are generally good does not need to participate actively in discussions instead the opposite is true for them. One the other hand, students who aren't good have better chances of getting higher CGPA if they participate actively in study groups.

V. Conclusions

Facebook is by far the most popular social networks among students in Pakistan. In this paper we study the relationship between social media usage and GPA score in a Pakistan.

In this study using real profiles and comments we come to a conclusion that mostly extensive use of Facebook on all the forums affects studies negatively in their academic life. On the other hand, actively participating in class group is positively correlated with good grades.

VI. Future Work

From existing data, we can dig out many other interesting insights and prove various hypotheses, few possible options are:

- Analysis on how e-learning using Facebook group is affecting the grades.
- Personality traits using NLP techniques.
- Detection of friend circles and closeness of users.
- We can use a weighted aggregation scheme for scoring student's interaction in study groups.

References

[1] Barry Wellman, "Computer Networks as social networks", 2001.

[2] J. Ugander, B. Karrer, L. Backstrom, C. Marlow, "The Anatomy of the Facebook Social Graph," Arxiv Nov. 2011.

[3] A. L. Traud, P. J. Mucha, and M. A. Porter, "Social Structure of Facebook Networks," Feb. 2011.

[4] P. Dewan and P. Kumaraguru, "Detecting Malicious Content on Facebook," arXiv:1501.00802 [cs], Jan. 2015.

[5] F. Krebs, B. Lubascher, T. Moers, P. Schaap, and G. Spanakis, "Social Emotion Mining Techniques for Facebook Posts Reaction Prediction," Dec. 2017.

[6] R. Farahbakhsh, X. Han, A. Cuevas, and N. Crespi, "Analysis of publicly disclosed information in Facebook profiles," May 2017.

[7] S. Mohammadi, R. Farahbakhsh, and N. Crespi, "Popularity Evolution of Professional Users on Facebook," arXiv:1705.02156 [cs], May 2017.

[8] Mathews Nkhoma, Hiep Pham Cong, Bill Au, Tri Lam, Joan Richardson, Ross Smith, and Jamal El-Den ,"FaceBook as a tool for learning purpose ".

[9] Georgia Sapsani, Nikolaos Tselios , "Facebook use, personality characteristics and academic performance: A correlational study".

[10] Justyna P. Zwolak, Eric Brewer ,"The impact of social integration on student persistence in introductory Modeling Instruction courses".

[11] Daniel Z. Grunspan, Benjamin L. Wiggins, Steven M. Goodreau, "Understanding Classrooms through Social Network Analysis: A Primer for Social Network Analysis in Education Research" CBE life sciences education· January 2014.

[12] G. Han, OP McCubbins and T.H. Paulsen,"Using Social Network Analysis to Measure Student Collaboration in an Undergraduate Capstone Course". NACTA Journal, June 2016.

[13] Eric Brewe, Laird H. Kramer, Vashti Sawtelle, "Investigating Student Communities with Network Analysis of Interactions in a Physics Learning Center". Physical Review Special Topics - Physics Education Research, 2012.

[14] Adil Rajput, "Natural Language Processing, Sentiment Analysis and Clinical Analytics".

[15] Hiroki Takikawa, Kikuko Nagayoshi, "Political Polarization in Social Media: Analysis of the "Twitter Political Field" in Japan".

[16] Glen Coppersmith, Ryan Leary, Patrick Crutchley Patrick Crutchley, "Natural Language Processing of Social Media as Screening for Suicide Risk".

[17] Bharat Gaind, Varun Syal, Sneha Padgalwar, "Emotion Detection and Analysis on Social Media".

[18] Mariam Adedoyin-Olowe, Mohamed Medhat Gaber, Frederic Stahl, "A Survey of Data Mining Techniques for Social Media Analysis".

[19] Tariq, W., Mehboob, M., Khan, M. A., & Ullah, F. (2012). The impact of social media and social networks on education and students of Pakistan. International Journal of Computer Science Issues, 9, 407–411.

[20] Al-Khalifa, H. S., & Garcia, R. A. (2013). The state of social media in Saudi Arabia's higher education. International Journal of Technology and Educational Marketing (IJTEM), 3, 65–76.

GPLDA: A Generalized Poisson Latent Dirichlet Topic Model

Ibrahim Bakari Bala[1], Mohd Zainuri Saringat[2]
Faculty of Computer Science and Information Technology
Universiti Tun Hussein Onn Malaysia
Johor, Malaysia

***Abstract*—The earliest modification of Latent Dirichlet Allocation (LDA) in terms of words or document attributes is by relaxing its exchangeability assumption via the Bag-of-word (BoW) matrix. Several authors have proposed many modifications of the original LDA by focusing on model that assumes the current topic depends on the words from previous topic. Most of the earlier work ignored the document length distribution since it is assumed that it will fizzle out at the modelling stage. Thus, in this paper, the Poisson document length distribution of LDA model is replaced with Generalized Poisson (GP) distribution which has the strength of capturing complex structures. The main strengths of GP are in capturing overdispersed (variance larger than mean) and under dispersed (variance smaller than mean) count data. The Poisson distribution used by LDA strongly relies on the assumption that the mean and variance of document lengths are equal. This assumption is often unrealistic with most real-life text data where the variance of document length may be greater than or less than their mean. Approximate estimate of the GPLDA model parameters was achieved using Newton-Raphson approximation technique of log-likelihood. Performance and comparative analysis of GPLDA with LDA using accuracy and F_1 showed improved results.**

Keywords*—Bag-of-word; generalized Poisson distribution; topic model; latent Dirichlet allocation

I. INTRODUCTION

In recent years, a stochastic generative model that has been used widely in the field of computer science with the focus on text mining and information retrieval is referred to as a topic model. Since the early proposition of the model, it has been used by many researchers in several fields such as text mining [2], computer vision [1], population genetics, and social networks [3].

Topic modelling can be traced to latent semantic indexing (LSI) by [4]. It is the basis of the developing topic models. However, LSI is not a probabilistic model. Hence uncertainty is not quantifiable. After the era of LSI, towards the search for a realistic probabilistic model, probabilistic latent semantic analysis (PLSA) by [5] was developed and served as the basis of modern topic models. As a further earlier extension of PLSA, [6] proposed latent Dirichlet allocation (LDA). The model was referred to as a complete generative stochastic model. Nowadays, there is a growing number of probabilistic models that are based on LDA via combination with particular tasks.

Since the introduction of topic models, researchers have introduced this approach into the fields of text mining. Because of its superiority in the analysis of large-scale document collections, better results have been obtained in such fields as text mining [7] and clinical informatics [8-9]. On the other hand, most of these studies follow the classic text-mining method of a topic model.

In LDA, we let d denotes the document indicator, z for the topic, w for word and consequently N is the number of words in a specific document d. Also, we define $P(z|d)$ as the conditional distribution of topic z in the document d and $P(w|z)$ as the conditional distribution of words w in topic z. The two conditional probability distributions, $\boldsymbol{P}(\boldsymbol{z}|\boldsymbol{d})$ and $\boldsymbol{P}(w|z)$, are presumed to follow multinomial distributions such that the topics in the entire documents have common Dirichlet prior distribution $P(\boldsymbol{\alpha})$ and the word conditional distributions on topics have common Dirichlet prior $P(\boldsymbol{\beta})$ [10].

Algorithm 1: Pseudocode of LDA Algorithm

Sample N from Poisson $\mathbf{P}(\mathbf{N}=\mathbf{n}|\boldsymbol{\lambda})$
for each topic $\mathbf{k} \in \{\mathbf{1},\mathbf{2},\mathbf{3},\ldots,\mathbf{K}\}$:
    for each document $\mathbf{d} \in \{\mathbf{1},\mathbf{2},\mathbf{3},\ldots,\mathbf{N}\}$:
        Simulate $\boldsymbol{\theta}_{\mathbf{d}} \sim \mathbf{Dir}(\boldsymbol{\theta}_{\mathbf{d}}|\boldsymbol{\alpha})$
            for each word w $\in \mathbf{d} \in \{\mathbf{1},\mathbf{2},\mathbf{3},\ldots,\mathbf{N}\}$:
                Simulate $\mathbf{z}_{\mathbf{dn}} \sim \mathbf{Mult}(\mathbf{z}_{\mathbf{dn}}|\boldsymbol{\theta}_{\mathbf{d}})$
                Simulate $\mathbf{w}_{\mathbf{dn}} \sim \mathbf{Mult}(\mathbf{w}_{\mathbf{dn}}|\mathbf{z}_{\mathbf{dn}},\boldsymbol{\beta})$
            end for w
    end for d
end for k

After the selection of appropriate prior hyperparameters $\boldsymbol{\alpha}$ and $\boldsymbol{\beta}$ for a document d, a conditional distribution of K topics with parameter θ is formed and it is assumed to be multinomially distributed from the Dirichlet distribution $Dir(\theta|\alpha)$. Also, for a specific topic k, a conditional distribution of V words are formed, and it is assumed to be multinomially distributed from the Dirichlet distribution $Mult(w|z,\beta)$. The Dirichlet prior distribution is choosing because of the conjugacy property between the multinomial and Dirichlet distribution which thus makes the statistical inference of LDA easy.

II. Related Work

The earliest modification of LDA in terms of words attributes is relaxing the exchangeability assumption of LDA via the BoW matrix by [11]. Wallach proposed a model that assumes that the current topic depends on the words from the previous topic. The method involves using a hierarchical procedure by combining the *n*-grams statistics procedure and latent topic models. Specifically, Wallach [11] extended the unigram topic model to include the properties of a hierarchical Dirichlet bigrams model. The author reported that the hybrid model is better than either of the unigram topic model or the Dirichlet bigram model. The results were inferred from two datasets consisting of 150 documents each. The model was supported by [12] with the claim that it is unrealistic to impose the exchangeability of words as orders of words matters when dealing with words contexts. Hu et al. [8] countered the class of models that either supported the exchangeability assumptions or relaxes it. The authors claimed the models are not interactive but rather employ several *apriori* fixes that are unrealistic. In addition, Inouye et al. [13] also exemplify that these class of models do not incorporate word dependencies within a topic but rather incorporates inter-topic word correlation which is the major strength of models such as Bigrams language model by [11].

Reisinger et al. [14] modified the word absences drawback features of LDA. The algorithm specifically improved the accuracy of LDA in terms of increasing the possibility of modelling rare words. The procedure addresses the use of multinomial draws by proposing the Von-Mises Fishers distribution for topics.

Most of the existing modifications targeted one or the other loopholes in LDA, but none has considered the overdispersed or under dispersed drawback that is inherent in text data. Thus, in this paper, the Poisson document length distribution of the Latent Dirichlet Allocation (LDA) model is replaced with Generalized Poisson (GP) distribution which has the strength of capturing complex structures. The new model referred to as GPLDA was tested on the 20-newsgroup dataset to facilitate comparison with the LDA.

III. Generalized Poisson Distribution

Suppose we have N documents that assumed Poisson distribution with rate λ, the probability mass function of having n realizations of N is given by [15]:

$$P(N=n|\,\lambda\,)=\frac{\exp(-\lambda)\,\lambda^{n}}{n!},n=0,1,2 \qquad (1)$$

The Generalized Poisson (GP) [15-18] which is the extension of (1) can be defined in terms of additional dispersion parameter η as:

$$P(N=n|\,\lambda\,,\eta)=\lambda(\lambda+\eta n)^{n-1}\frac{\exp(-\lambda-\eta n)}{n!},n=0,1,2 \qquad (2)$$

It is obvious from (2) that GP can be reduced to Poisson when $\eta=0$. The behaviour of the dispersion parameter η tell about the direction of disparity. If $\eta<0$, underdispersion is suspected and $\eta>0$ overdispersion is suspected.

A. *Generalized Poisson Latent Dirichlet Allocation Model (GPLDA)*

The GPLDA assumes the same structure as LDA except for the change in document length distribution. Mathematically, the joint distribution of document N, topics z, word w and topic mixture θ is defined as:

$$P(\theta,z,w|\alpha,\beta,\lambda\,,\eta)$$

$$=P(\theta|\alpha)\prod_{n=1}^{N}P(z_n|\theta)\,P(w_n|z_n,\beta)\times P(N=n|\,\lambda\,,\eta)$$

where;

$$P(\theta|\alpha)=\frac{\Gamma\left(\sum_{i=1}^{k}\alpha_i\right)}{\prod_{i=1}^{k}\Gamma(\alpha_i)}\theta_1^{\alpha_1-1}\dots\theta_k^{\alpha_k-1}$$

$$P(z_n|\theta)=\prod_{n=1}^{N}\frac{\Gamma\left(\sum_{i=1}^{k}z_{ni}+1\right)}{\prod_{i=1}^{k}\Gamma(z_{ni}+1)}\prod_{i=1}^{k}\theta_i^{z_{ni}}$$

$$P(w_n|z_n,\beta)=\prod_{n}\prod_{v=1}^{V}\frac{\Gamma\left(\sum_{i=1}^{k}w_{ni}+1\right)}{\prod_{i=1}^{k}\Gamma(w_{ni}+1)}\prod_{i=1}^{k}\beta_{iv}^{w_{ni}}$$

Therefore,

$$P(\theta,z,w|\alpha,\beta,\lambda\,,\eta)$$

$$\begin{aligned}=&\frac{\Gamma(\sum_{i=1}^{k}\alpha_i)}{\prod_{i=1}^{k}\Gamma(\alpha_i)}\theta_1^{\alpha_1-1}\dots\theta_k^{\alpha_k-1}\\&\times\prod_{n=1}^{N}\left\{\left[\prod_{n=1}^{N}\frac{\Gamma\left(\sum_{i=1}^{k}z_{ni}+1\right)}{\prod_{i=1}^{k}\Gamma(z_{ni}+1)}\prod_{i=1}^{k}\theta_i^{z_{ni}}\right]\right.\\&\times\left[\prod_{n}\prod_{v=1}^{V}\frac{\Gamma\left(\sum_{i=1}^{k}w_{ni}+1\right)}{\prod_{i=1}^{k}\Gamma(w_{ni}+1)}\prod_{i=1}^{k}\beta_{iv}^{w_{ni}}\right]\\&\left.\times\left[\lambda(\lambda+\eta n)^{n-1}\frac{\exp(-\lambda-\eta n)}{n!}\right]\right\}\end{aligned}$$

The marginal distribution of document D can be obtained by marginalizing the joint distribution $P(\theta,z,w|\alpha,\beta,\lambda\,,\eta)$ as follows:

Algorithm 2: Pseudocode of GPLDA Algorithm

1. Sample N from Generalized Poisson $\mathbf{P(N=n|\boldsymbol{\lambda}\,,\boldsymbol{\eta})}$
2. **for** each topic $\mathbf{k}\in\{\mathbf{1},\mathbf{2},\mathbf{3},\dots,\mathbf{K}\}$:
3.   **for** each document $\mathbf{d}\in\{\mathbf{1},\mathbf{2},\mathbf{3},\dots,\mathbf{N}\}$:
4.   Simulate $\boldsymbol{\theta}_{\mathbf{d}}\sim\mathbf{Dir}(\boldsymbol{\theta}_{\mathbf{d}}|\boldsymbol{\alpha})$
5.   **for** each word w $\in\mathbf{d}\in\{\mathbf{1},\mathbf{2},\mathbf{3},\dots,\mathbf{N}\}$:
6.   Simulate $\mathbf{z}_{\mathbf{dn}}\sim\mathbf{Mult}(\mathbf{z}_{\mathbf{dn}}|\boldsymbol{\theta}_{\mathbf{d}})$
7.   Simulate $\mathbf{w}_{\mathbf{dn}}\sim\mathbf{Mult}(\mathbf{w}_{\mathbf{dn}}|\mathbf{z}_{\mathbf{dn}},\boldsymbol{\beta})$
8.   **end for w**
9.   **end for d**
10. **end for k**

$$P(D|\theta_d, z, w, \alpha, \beta, \lambda, \eta) = \prod_{d=1}^{M} \int \left(\frac{\Gamma\left(\sum_{i=1}^{k} \alpha_i\right)}{\prod_{i=1}^{k} \Gamma(\alpha_i)} \theta_{d1}^{\alpha_1 - 1} \dots \theta_{dk}^{\alpha_k - 1} \times \prod_{n=1}^{N} \left\{ \left[\prod_{n=1}^{N} \frac{\Gamma\left(\sum_{i=1}^{k} z_{ni} + 1\right)}{\prod_{i=1}^{k} \Gamma(z_{ni} + 1)} \prod_{i=1}^{k} \theta_{di}^{z_{ni}} \right] \times \left[\prod_{n}^{N} \prod_{v=1}^{V} \frac{\Gamma\left(\sum_{i=1}^{k} w_{ni} + 1\right)}{\prod_{i=1}^{k} \Gamma(w_{ni} + 1)} \prod_{i=1}^{k} \beta_{iv}^{w_{ni}} \right] \times \left[\lambda(\lambda + \eta n)^{n-1} \frac{\exp(-\lambda - \eta n)}{n!} \right] \right\} \right) d\theta_d$$

B. Parameter Estimation of GPLDA

In this section, we present an approximate procedure for estimating the parameters of the GPLDA model. The Newton-Raphson approximation technique is employed by obtaining the log-likelihood of the distribution. The log-likelihood of the distribution of corpus of words in document D is:

$$\log[P(D|\theta_d, z, w, \alpha, \beta, b, a)] = \sum_{d=1}^{M} \int \left(\frac{\Gamma\left(\sum_{i=1}^{k} \alpha_i\right)}{\prod_{i=1}^{k} \Gamma(\alpha_i)} \theta_{d1}^{\alpha_1 - 1} \dots \theta_{dk}^{\alpha_k - 1} \times \prod_{n=1}^{N} \left\{ \left[\prod_{n=1}^{N} \frac{\Gamma\left(\sum_{i=1}^{k} z_{ni} + 1\right)}{\prod_{i=1}^{k} \Gamma(z_{ni} + 1)} \prod_{i=1}^{k} \theta_{di}^{z_{ni}} \right] \times \left[\prod_{n}^{N} \prod_{v=1}^{V} \frac{\Gamma\left(\sum_{i=1}^{k} w_{ni} + 1\right)}{\prod_{i=1}^{k} \Gamma(w_{ni} + 1)} \prod_{i=1}^{k} \beta_{iv}^{w_{ni}} \right] \times \left[\lambda(\lambda + \eta n)^{n-1} \frac{\exp(-\lambda - \eta n)}{n!} \right] \right\} \right) d\theta_d$$

The procedure involves obtaining the first and second partial derivatives which are intractable from the $\log[P(D|\theta, z, w, \alpha, \beta, b, a)]$. Thus, the Newton-Raphson approximation technique is used. The procedure involves finding the approximate derivatives of the $\log[P(D|\theta, z, w, \alpha, \beta, b, a)]$. The Newton-Raphson procedure for obtaining the parameters of GPLDA can be summarized below as:

1) Obtain the log-likelihood of the marginal distribution that is $\log[P(D|\theta_d, z, w, \alpha, \beta, b, a)]$.

2) Find the first derivative w.r.t to each parameter in the parameter space $\omega = \{\theta, \alpha, \beta, b, a\}$ and obtain the iterative estimate of parameter Ω using;

$$\omega_{t+1} = \omega_t - \frac{\log[P(D|z, w, \omega)]}{\partial \log[P(D|z, w, \Omega)]/\partial\omega}$$

The process continues until $|\omega_{t+1} - \omega_t| \le \varepsilon$ where $\varepsilon \to 0$.

IV. Simulation Experiment

The behaviour of the GPLDA is observed by simulating several Generalized Poisson distributed variates with varying parameter $\eta =$ -0.5, -0.4, -0.3, -0.2, -0.1, 0, 0.1, 0.2, 0.3, 0.4, 0.5 and fixing rate parameter $\lambda = 5$. Fig. 1 shows the behavioural patterns for both under dispersed and overdispersed scenarios. All analyses were carried using the R package.

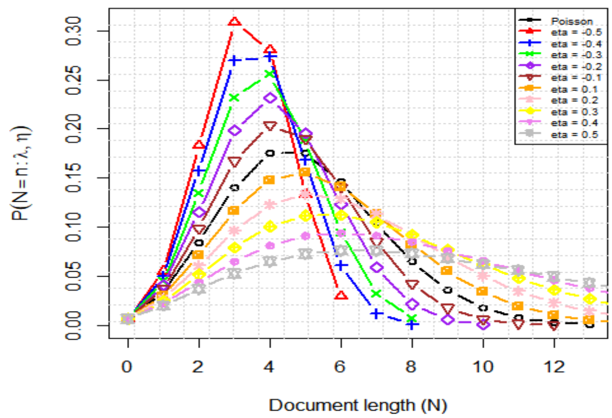

Fig. 1. Document Length Distribution at Various Dispersion Parameter $\eta =$ -0.5, -0.4, -0.3, -0.2, -0.1, 0, 0.1, 0.2, 0.3, 0.4, 0.5.

V. Performance Evaluation using 20-Newgroup Dataset

Performance evaluation of the GPLDA algorithm was achieved using the 20-Newsgroup dataset [19-22]. There are 18846 documents in the dataset, and it cut across 20 different topics categories. The topics in the classes include sports, politics, religion etc., which is diverse enough. The **Precision (P)** was used as class-specific index while **Recall (R)** (also known as sensitivity) is the proportion of the total amount of relevant cases that were actually retrieved [23-29]. The F_1 is a measure of the accuracy of the test dataset and it is defined as:

$$F_1 = \frac{2 \times Recall \times Precision}{Recall + Precision}$$

VI. Results and Discussion

The plot in Fig. 1 confirms that when $\eta = 0$ the Generalized Poisson distribution reduces to Poisson distribution and consequently the GPLDA will reduce to LDA. The underdispersed situation yields observations with high probability of having values close to zero than Poisson while the overdispersed situation yields observation with low probability of having values close to zero than Poisson. The graph also confirms that the Poisson distribution only assumes the midpoint position by averaging the scenarios, this may be true but not in all cases.

TABLE. I. Performance Comparison for LDA and the Proposed GPLDA using 20-New Group Dataset

Performance	**LDA**	**GPLDA**	**Relative Increase (%)**
Accuracy	0.42	0.77	83.3
Micro F_1	0.60	0.87	45.0
Macro F_1	0.48	0.84	75.0

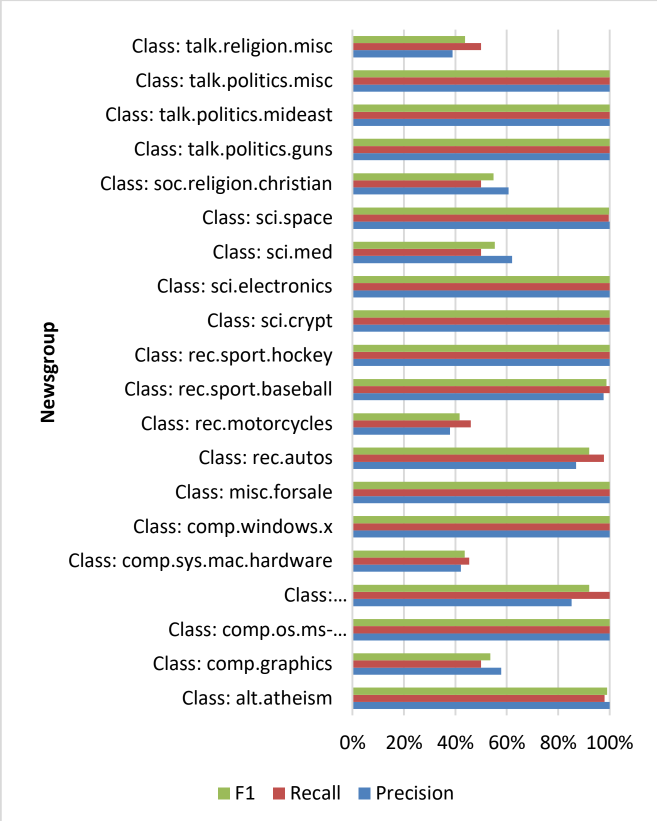

Fig. 2. Precision, Recall and F_1 Score in Percentage for Each News Group Class using GPLDA.

The predictive classification results performance analysis in Fig. 2 showed that the GPLDA algorithm results are high in terms of precision, recall and F_1 scores in 14 of the 20 classes but average on the other 6 topics/class. Performance comparison with LDA in Table I shows that the algorithm showed significant improvement over LDA. For Accuracy, GPLDA has about 83.3% percentage increased from the LDA result likewise for Micro F_1 45% increase and 75% increase for Macro F_1.

VII. Conclusion

This paper considered a new class of LDA using the Generalized Poisson distribution to model the length of a document. The Poisson distribution assumed by LDA has many stringent assumptions which are often violated in most real-life data. Thus, we propose the Generalized Poisson LDA (GPLDA) in order to provide a better fit. Estimation procedure was achieved using Newton-Raphson procedure and data calibration was done with the 20-Newsgroup dataset. The results from the simulation show that the Poisson distribution only assumes the midpoint position by averaging the scenarios which are not always correct. The results from the classification of 20-Newsgroup dataset showed that the GPLDA has an improved prediction over LDA. The results also established that the diversity in the Generalized Poisson over Poisson resulted in significant improvement. The GPLDA can be combined with the distributed learning system such as *word2vec* [10] to form a hybrid system like *lda2vec* by [30].

References

[1] W. Luo, B. Stenger, X. Zhao, and T.K., Kim. "Automatic topic discovery for multi-object tracking", In Twenty-Ninth AAAI Conference on Artificial Intelligence. March 2015.

[2] L. C. Chen. "An effective LDA-based time topic model to improve blog search performance", Information Processing & Management. Vol. 53, no. 6, pp. 1299-1319, November 2017.

[3] S. Jiang, X. Qian, J. Shen, Y. Fu, and T. Mei. "Author topic model-based collaborative filtering for personalized POI recommendations", IEEE Trans Multimedia, vol. 17, no. 6, pp. 907–918, March 2015.

[4] Deerwester S, Dumais ST, Furnas GW, Landauer TK, Harshman R (1990) Indexing by latent semantic analysis. J Am Soc Inf Sci 41(6):391

[5] Hofmann T (2001) Unsupervised learning by probabilistic latent semantic analysis. Mach Learn 42(1–2):177–196.

[6] Blei, D. M., Ng, A. Y., & Jordan, M. I. (2003). Latent dirichlet allocation. Journal of machine Learning research, 3(Jan), 993-1022.

[7] Wang X, Zhu P, Liu T, Xu K (2016) BioTopic: a topic-driven biological literature mining system. Int J Data Mining Bioinform 14(4):373–386.

[8] Hu QV, He L, Li M, Huang JX, Haacke EM (2014) A semi-informative aware approach using topic model for medical search. 2014 IEEE international conference on bioinformatics and biomedicine (BIBM) 2014, pp 320–324.

[9] Huang Z, Dong W, Ji L, Gan C, Lu X et al (2014) Discovery of clinical pathway patterns from event logs using probabilistic topic models. J Biomed Inform 47:39–57.

[10] Xue, M. (2019). A Text Retrieval Algorithm Based on the Hybrid LDA and Word2Vec Model. In 2019 International Conference on Intelligent Transportation, Big Data & Smart City (ICITBS) (pp. 373-376). IEEE.

[11] Wallach HM (2006) Topic modeling: beyond bag-of-words. In: Proceedings of the 23rd international conference on Machine learning, pp 977–984.

[12] Gruber, M., Gruber, S. B., Taube, W., Schubert, M., Beck, S. C., & Gollhofer, A. (2007). Differential effects of ballistic versus sensorimotor training on rate of force development and neural activation in humans. Journal of strength and conditioning research, 21(1), 274-282.

[13] Inouye, D., Ravikumar, P., & Dhillon, I. (2014a). Admixture of Poisson MRFs: A topic model with word dependencies. In International Conference on Machine Learning (pp. 683-691).

[14] Reisinger, J., & Mooney, R. J. (2010). Multi-prototype vector-space models of word meaning. In Human Language Technologies: The 2010 Annual Conference of the North American Chapter of the Association for Computational Linguistics (pp. 109-117).

[15] Chandra, N. K., Roy, D., & Ghosh, T. (2013). A generalized Poisson distribution. Communications in Statistics-Theory and Methods, 42(15), 2786-2797.

[16] Consul, P. C. (1989). Generalized Poisson Distributions. New York: Dekker.

[17] Consul, P. C., & Famoye, F. (2006). Lagrangian probability distributions (pp. 21-49). Birkhäuser Boston.

[18] Joe, H., & Zhu, R. (2005). Generalized Poisson distribution: the property of mixture of Poisson and comparison with negative binomial distribution. Biometrical Journal: Journal of Mathematical Methods in Biosciences, 47(2), 219-229.

[19] Albishre, K., Albathan, M., & Li, Y. (2015). Effective 20 newsgroups dataset cleaning. In 2015 IEEE/WIC/ACM International Conference on Web Intelligence and Intelligent Agent Technology (WI-IAT) (Vol. 3, pp. 98-101). IEEE.

[20] Inouye, D. I., Ravikumar, P. K., & Dhillon, I. S. (2014b). Capturing semantically meaningful word dependencies with an admixture of Poisson MRFs. In Advances in Neural Information Processing Systems (pp. 3158-3166).

[21] Jiang, B., Li, Z., Chen, H., & Cohn, A. G. (2018). Latent topic text representation learning on statistical manifolds. IEEE transactions on neural networks and learning systems, 29(11), 5643-5654.

[22] Liu, L., Tang, L., Dong, W., Yao, S., & Zhou, W. (2016). An overview of topic modeling and its current applications in bioinformatics. SpringerPlus, 5(1), 1608.

[23] Jamil, S. A. M., Abdullah, M. A. A., Kek, S. L., Olaniran, O. R., & Amran, S. E. (2017). Simulation of parametric model towards the fixed covariate of right censored lung cancer data. In Journal of Physics: Conference Series (Vol. 890, No. 1, p. 012172). IOP Publishing.

[24] Olaniran, O. R., Olaniran, S. F., Yahya, W. B., Banjoko, A. W., Garba, M. K., Amusa, L. B., & Gatta, N. F. (2016). Improved Bayesian feature selection and classification methods using bootstrap prior techniques. Annals. Computer Science Series, 14(2), 46-52.

[25] Olaniran, O. R., & Yahya, W. B. (2017). Bayesian hypothesis testing of two normal samples using bootstrap prior technique. Journal of Modern Applied Statistical Methods, 16(2), 34.

[26] Olaniran, O. R., & Abdullah, M. A. A. (2017). Gene Selection for Colon Cancer Classification using Bayesian Model Averaging of Linear and Quadratic Discriminants. Journal of Science and Technology, 9(3).

[27] Olaniran, O. R., & Abdullah, M. A. A. (2019a). Bayesian Variable Selection for Multiclass Classification using Bootstrap Prior Technique. Austrian Journal of Statistics, 48(2), 63-72.

[28] Olaniran, O. R., & Abdullah, M. A. A. B. (2019b). BayesRandomForest: An R implementation of Bayesian Random Forest for Regression Analysis of High-dimensional Data. In Proceedings of the Third International Conference on Computing, Mathematics and Statistics (iCMS2017) (pp. 269-275). Springer, Singapore.

[29] Olaniran, O. R., & Abdullah, M. A. A. B. (2019c). Bayesian Random Forest for the Classification of High-Dimensional mRNA Cancer Samples. In Proceedings of the Third International Conference on Computing, Mathematics and Statistics (iCMS2017) (pp. 253-259). Springer, Singapore.

[30] Moody, C.E., 2016. Mixing dirichlet topic models and word embeddings to make lda2vec. arXiv preprint arXiv:1605.02019.

A Mobile Agent Team Works based on Load-Balancing Middleware for Distributed Computing Systems

Fatéma Zahra Benchara[1], Mohamed Youssfi[2]
Department of Computer Science, Laboratory SSDIA
ENSET Mohammedia, Hassan II University of Casablanca, Mohammedia, Morocco

***Abstract*—The aim of this paper is to present a load balancing middleware for parallel and distributed systems. The great challenge is to balance the tasks between heterogeneous distributed nodes for parallel and distributed computing models based distributed systems, by the way to ensure HPC (High performance computing) of these models. Accordingly, the proposed middleware is based on mobile agent team work which implements an efficient method with two strategies: (i) Load balancing Strategy that determines the node tasks assignment based on node performance, and (ii) Rebalancing Strategy that detects the unbalanced nodes and enables tasks migration. The paper focuses on the proposed middleware and its cooperative mobile agent team work model strategies to dynamically balance the nodes, and scale up distributed computing systems. Indeed, some experimental results that highlight the performance and efficiency of the proposed middleware are presented.**

***Keywords*—Load balancing; middleware; parallel and distributed systems; parallel and distributed computing models; high performance computing; mobile agents; distributed computing**

I. Introduction

Distributed systems play a great role by providing a promising distributed computing environment for big data applications, in order to meet their requirements, and ensure the HPC. Therefore, distributed systems have been introduced as a promising solution for HPC thanks to two main features: interconnection network speed such as: Ethernet, 4G, 5G and, their effective Middleware such as: CORBA, RMI, AMQP. These make distributed systems as a cooperative parallel and distributed environment able to implement parallel and distributed computing models, and ensure the collaboration of heterogeneous machines in order to achieve the processing power required by big data [1] applications, and reduce the computing time.

Consider the two principal distributed system challenges that these applications have to deal with. Their scalability and efficiency depends on their ability to manage the message passing paradigm, and the heterogeneity of node performance. For example, performing an application of big data classification based parallel and distributed computing models. It involves a wide number of heterogeneous distributed computing system nodes to achieve the required processing power. The heterogeneity of distributed system nodes influences negatively the performance of these models if unbalanced task assignment is performed between nodes. Therefore, an effective task assignment strategy is required to deal with the load balancing challenge.

In this paper, a new load balancing middleware is proposed, which is based on mobile agents, and implements effective method for task assignment and migration. Besides, the proposed middleware integrates a cooperative mobile agent team work model, which elaborates well defined load balancing strategies to balance the distributed computing system. Consider the great challenge of nodes performance heterogeneity in parallel and distributed systems. We will present a load balancing model that achieves these requirements. This paper is organized as follows:

- The middleware and its innovative components for load balancing process are presented in Section 3.
- The Section 4 is focused on presenting the method used by the mobile agent team work in order to elaborate load balancing strategies.
- The efficiency of proposed load balancing middleware is demonstrated, by performing an SPMD application in parallel and distributed computing system (Section 5).

II. Background

To set the scene of this paper, we begin with a brief overview of distributed computing systems [2], and their ability to perform HPC application based on parallel and distributed computing models. Consider this application is composed by a set of NT tasks $T_k\{k=1,\ldots, NT\}$, which is executed in parallel and distributed computing system of n nodes $N_i\{i=1,\ldots, n\}$. In case of homogenous system, the same number of tasks (load LB) is assigned for each node Ni with $LB_i=\frac{NT}{n}$. Otherwise, the load LB depends on the node's performance index NPI_i, by means that for each node Ni the assigned load LBi is given by:

$$LB_i=\frac{NT}{n}\times NPI_i \qquad (1)$$

Therefore, a load balancing method for HPC applications based distributed system is required. This method has to take into account the node performance index NPI_i, and grants the same computation time for all nodes. Thus, the computation time Ω^{MIN} of node N_i^{MIN} (slowest node) is equal to Ω^{MAX} of node N_j^{MAX} (faster node) with $i\neq j$.

The Mobile agents [3],[4] have impressive skills, such as asynchronous communication ability, autonomy, adaptability, and mobility. They can move from overloaded nodes to under loaded ones, and perform a balanced system. The agent's mobility can be an effective mechanism for dynamic load balancing of the system. Additionally, the mobile agents cooperate asynchronously by exchanging messages, which significantly reduces the load balancing strategy time. Further, their adaptability skill makes the proposed middleware flexible with different distributed computing systems. Thus, the mobile agents ensure effective features for scalable load balancing middleware.

III. Proposed Load Balancing Middleware

A. Middleware Overview

The proposed middleware (Fig. 1) implements a load balancing method, which behaves when an application is deployed, and performed in the system. Once, it is deployed this method defines the initial performance index by getting the node's performance capabilities. If the metadata of task is known, the defined index is used to estimate the load assignment LB_i for each node N_i. Else, the initial performance index will be used for running the application. For an iterative application, before the next iteration, this method decides the required load migration. Thus, the middleware can balance the node's load effectively.

B. Aspect based Load-balancing Middleware

The proposed middleware integrates the LoadBalancer aspect to the system. This aspect is based on AOP (Aspect Oriented Programming) approach [5],[6], which is useful for separating the functional aspects from the technical ones in an application, and allows to dynamically modify the program behavior. To do so, the middleware adds two aspects (behaviors) to the system, by the way that it can get metadata and provide the results needed to balance the system. These behaviors are described as follows:

- Load Assignment Aspect This aspect is performed when an application is deployed in order to get the load assignment of nodes.
- Rebalancing Aspect This aspect is executed when an application is running in order to get the required load migration, and rebalance the system before performing the next iteration.

IV. Effective Load Balancing Method

The proposed middleware implements an effective load balancing method (Fig. 2) for distributed computing system. This is done according to three method's main step; Initial nodes performance Determination, Load Assignment Prediction, Load Rebalancing. This method is implemented on cooperative mobile agent team works composed by two principal agents: Team Load Balancer Agent (TLBA agent), and Team Node Performance Monitor Agents (TNPMA agents) one per node. Main steps of this method are detailed as follows:

Step 1. Initial nodes performance Determination

- Metadata MDT_0 Determination
- Computing the initial performance index NPI^{T0}
- Computing the initial load LB^{T0}

Step 2. Load Assignment Prediction

- Metadata MDT_k Determination
- Computing the Node Performance index NPI^{Tk}
- Computing the initial load LB^{Tk}

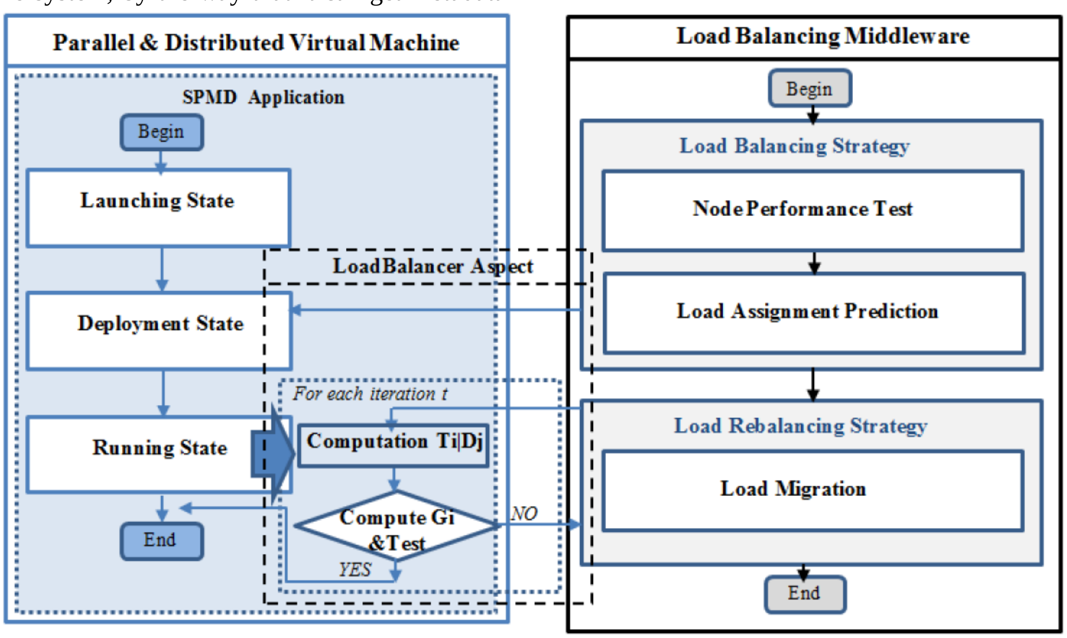

Fig. 1. Load Balancing Middleware Architecture.

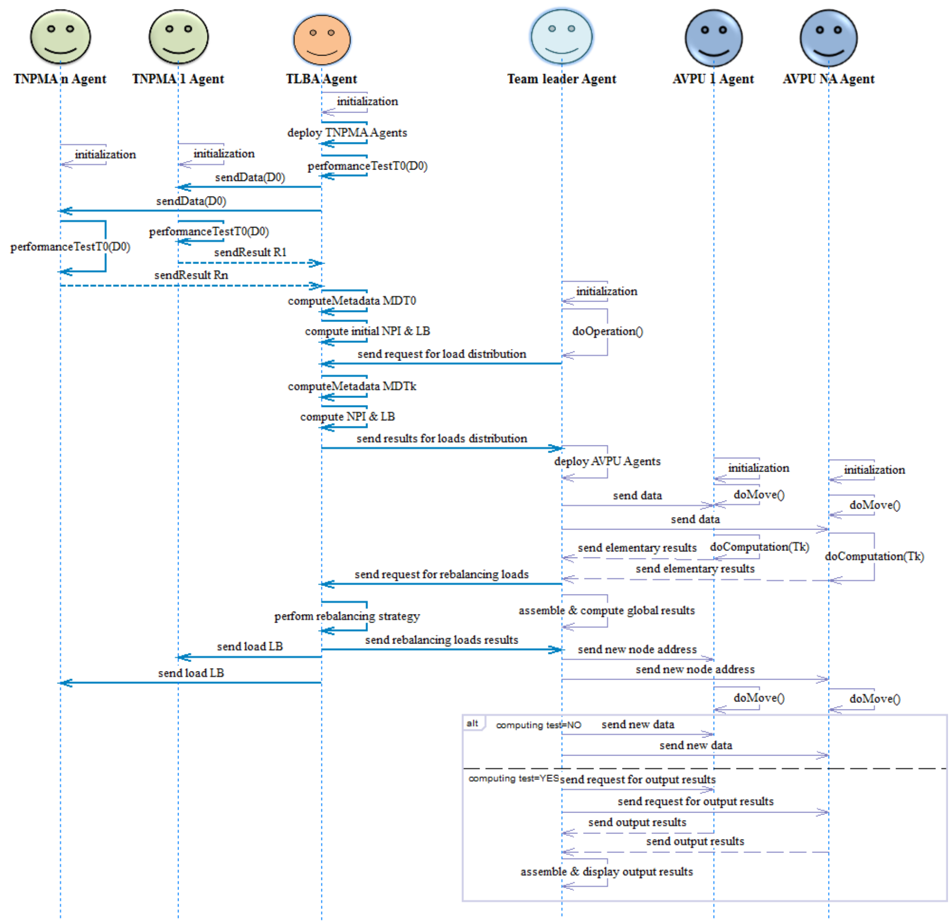

Fig. 2. Sequence Diagram of Mobile Agent Team Works Load-Balancing Method.

Step 3. Load Rebalancing

The load balancing method's steps are detailed as follows:

Step 1. Initial nodes performance Determination

- Metadata MDT_0 Determination

a) The TLBA agent deploys TNPMA(i) agent for each node N_i, after its initialization by the task T_0(initial performance task with complexity C_0) and the data D_0(initial data of size x_0).

b) The TLBA agent executes the performance test of its node N_0.

c) The TLBA agent sends the data D_0 for each TNPMA(i) agent.

d) Each TNPMA(i) agent gets the data D_0 and executes the task T_0 on data D_0.

e) Each TNPMA(i) agent returns the results R_i (the size of result y_0, and the execution time $\theta t_i^{T_0}$) to the TLBA agent.

f) The TLBA agent receives the result R_i from each TNPMA(i) agent at $t_1(i)$, and computes the communication latency $\theta l_i^{T_0}$ between the node N_i and N_0 by:

$$\theta l_i^{T_0} = \omega_i^{T_0} - \theta t_i^{T_0} \qquad (2)$$

Where: $\boldsymbol{\omega_i^{T_0}}$ computation time of the task T_0 in the node N_i, which is given by:

$$\omega_i^{T_0} = t_1(i) - t_0 \qquad (3)$$

- Computing the initial performance index NPI^{T0}

The TLBA agent computes the initial performance $NPI_i^{T_0}$of each node N_i by:

$$NPI_i^{T_0} = \frac{MIN(\omega_i^{T_0})}{\omega_i^{T_0}} \qquad (4)$$

- Computing the initial load LB^{T0}

The TLBA agent determines the initial load LB^{T0} of each node N_i by:

$$LB_i^{T_0} = LB_{ref} \times \frac{NPI_i^{T_0}}{\langle NPI_i^{T_0} \rangle} \qquad (5)$$

Where:

LB_{ref} The referenced load of each node N_i in homogeneous distributed system, which is computed by (6), where NT is the total number of tasks, and n the total number of nodes.

$$LB_{ref} = \frac{NT}{n} \qquad (6)$$

$\langle \boldsymbol{NPI_i^{T_0}} \rangle$ The average of node performance index NPI_i that is computed by.

$$\langle NPI_i^{T_0} \rangle = \frac{\sum_{i=0}^{n-1} NPI_i^{T_0}}{n} \quad (7)$$

Step 2. Load Assignment Prediction

- Metadata MDT_k Determination

The TLBA agent predicts the execution time $\theta t_i^{T_k}$, and the communication latency $\theta l_i^{T_k}$, and the computation time $\omega_i^{T_k}$, respectively by:

$$\theta t_i^{T_k} = \frac{\theta t_i^{T_0} \times C_k}{C_0} \quad (8)$$

$$\theta l_i^{T_k} = \frac{\theta l_i^{T_0} \times Z_k}{Z_0} \quad (9)$$

$$\omega_i^{T_k} = \theta t_i^{T_k} + \theta l_i^{T_k} \quad (10)$$

- Computing the Node Performance index NPI^{T_k}

The TLBA agent gets the computed value of $\omega_i^{T_k}{}_i$, and computes the node performance index $NPI_i^{T_k}$ by:

$$NPI_i^{T_k} = \frac{MIN(\omega_i^{T_k})}{\omega_i^{T_k}} \quad (11)$$

- Computing the initial load LB^{T_k}

The TLBA agent gets the node performance index $NPI_i^{T_k}$, and computes the load assignment LB_i by :

$$LB_i^{T_k} = LB_{ref} \times \frac{NPI_i^{T_k}}{\langle NPI_i^{T_k} \rangle} \quad (12)$$

Where :

$\langle NPI_i^{T_k} \rangle$ The average of node performance index NPI_i that is computed by:

$$\langle NPI_i^{T_k} \rangle = \frac{\sum_{i=0}^{n-1} NPI_i^{T_k}}{n} \quad (13)$$

Step 3. Load Rebalancing

1) The TLBA agent computes the experimental computation time ω_i^{EXP} by:

$$\omega_i^{EXP}(t) = \frac{\Omega_i^{EXP}(t)}{LB_i(t-1)} \quad (14)$$

2) The TLBA agent computes the new performance index NPI_i^{EXP} by:

$$NPI_i^{EXP} = \frac{MIN(\omega_i^{EXP}(t))}{\omega_i^{EXP}(t)} \quad (15)$$

3) The TLBA agent computes the new load $LB_i^{EXP}(t)$ by:

$$LB_i^{EXP}(t) = LB_{ref} \times \frac{NPI_i^{EXP}(t)}{\langle NPI_i^{EXP}(t) \rangle} \quad (16)$$

4) The TLBA agent tests the overload ΔLB_i by:

$$\Delta LB_i = LB_i^{EXP}(t) - LB_i^{EXP}(t-1) \quad (17)$$

$$\begin{cases} ON_i = N_i & if \quad \Delta LB_i < 0 \\ UN_i = N_i & if \quad \Delta LB_i > 0 \\ NN_i = N_i & if \quad \Delta LB_i = 0 \end{cases} \quad (18)$$

5) The TLBA agent determines the required load migration by running the given algorithm (Agent migration determination).

Algorithm Agent Migration Determination

```
1 : int overLNode;
2 : int underLNode;
3: for(int i=0;i<NO.size();i++){
4: overLNode=NO.get(i);
5:   for(int j=0;j<NU.size();j++){
6:   underLNode=NU.get(j);
7:    if(deltaLB[underLNode]>0){
8:      originMigration.add(overLNode);
9:      destinationMigration.add(underLNode);
10:     if(deltaLB[underLNode]>deltaLB[overLNode]){
11:       nbAgentsMigration.add(deltaLB[overLNode]);
12:             deltaLB[underLNode]=deltaLB[underLNode]-
deltaLB[overLNode];
13:             deltaLB[overLNode]=0;
14:             break;
15:     }
16:     else if(deltaLB[underLNode]<deltaLB[overLNode]){
17:        nbAgentsMigration.add(deltaLB[underLNode]);
18:             deltaLB[overLNode]=deltaLB[overLNode]-
deltaLB[underLNode];
19:        deltaLB[underLNode]=0;
20:     }
21:      else{
22:        nbAgentsMigration.add(deltaLB[overLNode]);
23:             deltaLB[overLNode]=0;
24:             deltaLB[underLNode]=0;
25:             break;
26:         }
27:      }
28:  }
29: }
```

The load deltaLB(overLNode) (line 3) which corresponds to the overloaded node is compared with deltaLB(underLNode) of the under loaded node. This is done, to decide the required load migration with the node destination. When deltaLB(underLNode) is greater than deltaLB(overLNode) (line 10), the load will move to the under loaded node (line 11). At the end, this algorithm provides the three output results:

1) originMigration list of nodes from where the load will move.

2) destinationMigration list of nodes that will receive the load.

3) nbAgentsMigration list of agents load that will move from their origin node to the appropriate destination node.

V. Results and Discussion

The proposed middleware is integrated in the parallel and distributed virtual machine [7], which is constituted by distributed computing system of 10 heterogeneous nodes. To do so, an SPMD application is chosen in order to perform the image processing of ne × me = (20×50) elementary images of size (1024×768) pixels. Thus, NA=1000 of AVPU(Agent Virtual Processing Units) agents have to execute the same task

T_k at the same time in the system. To illustrate the effectiveness feature of this middleware two case studies are considered:

Case 1 Task assignment by initial performance test

In this case the task assignment is performed by using the LB^{T0} in Table I. The initial performance test is executed by using task T_0 of complexity $C_0(x)=O(x^3)$ and data D_0 (matrix (80×80) where $x_0=6400$ and $y_0=6401$). For example in Table III, the value of ΔLB_8 at the node N_8 is equal to -5. This means that the node is overloaded by 5 agents, which have to move to under loaded nodes given in Table V.

Case 2 Task assignment by prediction using the metadata $MDT_{K.}$

The node task assignment is performed by using the LB^{Tk} in Table II. The predicted LB^{Tk} is based on the metadata of task T_k (complexity $C_k(x)=O(x^2)$, and data size ($x_k=786432$, $y_k=786433$), and the metadata MDT_0. In this case the load $\Delta LB_8=LB_8^{EXP(t)} - LB_8^{EXP(t-1)}$ of node N_8 is equal to -1 in Table IV. This means that the node is overloaded by only one agent, which has to move to under loaded nodes given in Table VI.

By comparing the two cases (Fig. 3), the system is balanced from the first iteration in case 2. Therefore, in case 1 it becomes balanced after the second iteration. This means that case 2 grants effective load balancing strategy of the system at the first iteration. The Fig. 4 presents that the system becomes balanced after performing the load rebalancing.

TABLE. I. RESULTS OF LOAD ASSIGNMENT BY INITIAL PERFORMANCE TEST

	Ni	Metadata MDT0	$\mathbf{NPI_i^{T_0}}$	$\mathbf{LB_i^{T_0}}$	$\Omega_i^{TH}(\omega_i^{T_0} * \mathbf{LB_i^{T_0}})$ (ms)		
		$\omega_i^{T_0}(ms)$	$\theta t_i^{T_0}(ms)$	$\theta l_i^{T_0}(ms)$			
	0	7826,00	7818	8	0,811014567	94,66	740843,0833
	1	7658,00	7640	18	0,828806477	96,74	740843,0833
	2	8072,00	8050	22	0,786298315	91,78	740843,0833
	3	7673,00	7640	33	0,827186237	96,55	740843,0833
	4	7249,00	7230	19	0,875569044	102,20	740843,0833
	5	6998,00	6980	18	0,906973421	105,86	740843,0833
	6	7155,00	7133	22	0,887071978	103,54	740843,0833
	7	8011,00	7980	31	0,792285607	92,48	740843,0833
	8	6347,00	6322	25	1	116,72	740843,0833
	9	7449,00	7430	19	0,852060679	99,46	740843,0833
$MIN(\omega_i^{T_0})$		6347,00	-	-	-	-	-
$MAX(\omega_i^{T_0})$		8072,00	-	-	-	-	-
SUM(LBT0)		-	-	-	-	1000,00	-
AVG(NPIT0)		-	-	-	0,85672663	-	-

TABLE. II. RESULTS OF LOAD ASSIGNMENT BY PREDICTION

	Ni	Metadata MDTk			$\mathbf{NPI_i^{T_k}}$	$\mathbf{LB_i^{T_k}}$	$\mathbf{\Omega_i^{TH}}$
		$\omega_i^{T_k}(ms)$	$\theta l_i^{T_k}(ms)$	$\theta t_i^{T_k}(ms)$			
	0	19428,016	983,040	18444,976	0,925852089	103,22	2005359,82
	1	20236,861	2211,840	18025,021	0,888846789	99,09	2005270,60
	2	21695,693	2703,360	18992,333	0,829080199	92,43	2005332,89
	3	22080,061	4055,040	18025,021	0,814647611	90,82	2005311,18
	4	19392,430	2334,720	17057,710	0,927551072	103,41	2005371,19
	5	18679,726	2211,840	16467,886	0,962940743	107,35	2005268,59
	6	19532,218	2703,360	16828,858	0,92091277	102,67	2005372,86
	7	22636,462	3809,280	18827,182	0,794623703	88,59	2005364,18
	8	17987,469	3072,000	14915,469	1	111,48	2005243,08
	9	19864,289	2334,720	17529,569	0,90551789	100,95	2005300,00
$MIN(\omega_i^{T_k})$		17987,469	-	-	-	-	-
$MAX(\omega_i^{T_k})$		22636,462	-	-	-	-	-
SUM(LBTk)		-	-	-	-	1000,00	-
AVG(NPITk)		-	-	-	0,89699729	-	-

TABLE. III. RESULTS OF LOAD REBALANCING (CASE 1)

N_i	$LB_i^{EXP}(t-1)$	$\Omega_i^{EXP}(t)$ (ms)	$\omega_i^{EXP}(t)$ (ms)	$NPI_i^{EXP}(t)$	$LB_i^{EXP}(t)$	$\Delta LB_i(t)$	State
0	95	1845662	19428,01613	0,92585209	103	8,00	Under
1	97	1962976	20236,86144	0,88884679	99	2,00	Under
2	92	1996004	21695,6928	0,8290802	92	0,00	Normal
3	97	2141766	22080,06144	0,81464761	91	-6,00	Over
4	101	1958635	19392,43008	0,92755107	103	2,00	Under
5	106	1980051	18679,72608	0,96294074	107	1,00	Under
6	104	2031351	19532,21837	0,92091277	103	-1,00	Over
7	94	2127827	22636,46208	0,7946237	90	-4,00	Over
8	116	2086546	17987,46931	1	111	-5,00	Over
9	98	1946700	19864,28928	0,90551789	101	3,00	Under

TABLE. IV. RESULTS OF LOAD REBALANCING (CASE 2)

N_i	$LB_i^{EXP}(t-1)$	$\Omega_i^{EXP}(t)$ (ms)	$\omega_i^{EXP}(t)$ (ms)	$NPI_i^{EXP}(t)$	$LB_i^{EXP}(t)$	$\Delta LB_i(t)$	State
0	103	2020514	19428,01613	0,92585209	104	1,00	Under
1	99	2043923	20236,86144	0,88884679	101	2,00	Under
2	92	1996004	21695,6928	0,8290802	92	0,00	Normal
3	91	2009286	22080,06144	0,81464761	91	0,00	Normal
4	103	1997420	19392,43008	0,92755107	103	0,00	Normal
5	107	1961371	18679,72608	0,96294074	105	-2,00	Over
6	103	2011818	19532,21837	0,92091277	103	0,00	Normal
7	90	2037282	22636,46208	0,7946237	90	0,00	Normal
8	111	1978622	17987,46931	1	110	-1,00	Over
9	101	2006293	19864,28928	0,90551789	101	0,00	Normal

TABLE. V. RESULTS OF AGENT'S MIGRATION (CASE 1)

	Origin Migration N_i	Destination Migration N_i	Nb Agents Migration	Load Migration Percentage
	3	0	6	37,50%
SUM	-	-	6	37,50%
	6	0	1	6,25%
SUM	-	-	1	6,25%
	7	0	1	6,25%
	7	1	2	12,50%
	7	4	1	6,25%
SUM	-	-	4	25,00%
	8	4	1	6,25%
	8	5	1	6,25%
	8	9	3	18,75%
SUM	-	-	5	31,25%

TABLE. VI. RESULTS OF AGENT'S MIGRATION (CASE 2)

	Origin Migration N_i	Destination Migration N_i	Nb Agents Migration	Load Migration Percentage
	5	0	1	33,33%
	5	1	1	33,33%
SUM	-	-	2	66,67%
	8	1	1	33,33%
SUM	-	-	1	33,33%

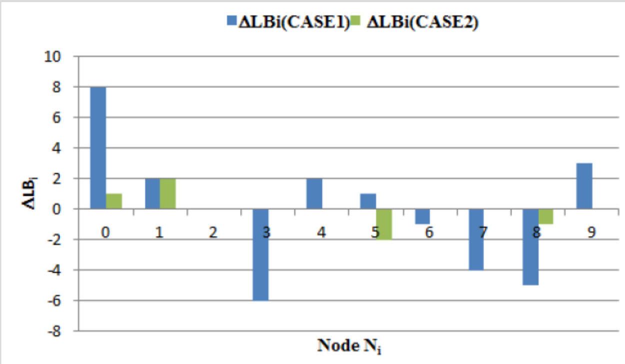

Fig. 3. Comparison of Overload in Case 1 and Case 2 of Each node N_i.

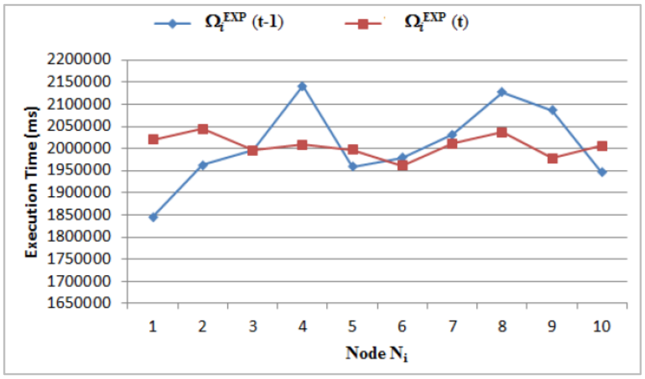

Fig. 4. Execution Time of the Task T_k before and after Load Rebalancing.

By analyzing the execution time (Fig. 5) of both cases compared with the case 3 (unbalanced system where each node receives LB_i^{NB} =100 agents), the following conclusions are achieved:

- In case 1 (Table VII) the obtained unbalance DES is DES1=$\Omega_{MAX}^{EXP}(LB_i^{T_0}) - \Omega_{MIN}^{EXP}(LB_i^{T_0})$ = 296,104s, and for case 2 is DES2=$\Omega_{MAX}^{EXP}(LB_i^{T_k}) - \Omega_{MIN}^{EXP}(LB_i^{T_k})$ = 41,2778496 s. These present the efficiency of task assignment based on prediction compared to the one based on initial performance test.
- The gain of performance φ compared to case 3, provides to the following results:
  - In case 2 the gain of performance is $\varphi 2 = \frac{\Omega_{MAX}^{EXP}(LB_i^{NB}) - \Omega_{MIN}^{EXP}(LB_i^{NB})}{\Omega_{MAX}^{EXP}(LB_i^{T_k}) - \Omega_{MIN}^{EXP}(LB_i^{T_k})}$ = 5,631 at the first iteration.
  - In case 1 the gain of performance is $\varphi 1 = \frac{\Omega_{MAX}^{EXP}(LB_i^{NB}) - \Omega_{MIN}^{EXP}(LB_i^{NB})}{\Omega_{MAX}^{EXP}(LB_i^{T_0}) - \Omega_{MIN}^{EXP}(LB_i^{T_0})}$ = 1,570 at the first iteration, which is enhanced to $\varphi'1$= 5,631 after de second iteration.
  - The obtained gain of performance of case 2 $\varphi 2$ is equal to $\varphi'1$, which illustrates the effectiveness of the load rebalancing step based on load migration.

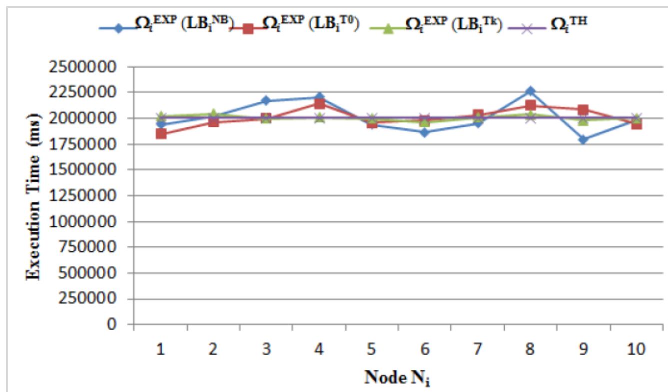

Fig. 5. Execution Time Comparison between Theoretical Execution Time Ω_i^{TH}, and Experimental One of Case 1 $\Omega_i^{EXP}(LB_i^{T_0})$ and Case 2 $\Omega_i^{EXP}(LB_i^{T_k})$ and Case 3 $\Omega_i^{EXP}(LB_i^{T_{NB}})$.

TABLE. VII. COMPARISON BASED EXECUTION TIME IN THREE CASES OF LOAD ASSIGNMENT

N_i	Ω_i^{TH}(ms)	CASE 1		CASE 2		CASE 3
		$\Omega_i^{EXP}(LB_i^{T_0})$ (ms)	$\varepsilon_i(LB_i^{T_0})$	$\Omega_i^{EXP}(LB_i^{T_k})$ (ms)	$\varepsilon_i(LB_i^{T_k})$	$\Omega_i^{EXP}(LB_i^{NB})$ (ms)
0	2005359,82	1845661,53	0,079635728	2020513,677	0,007556677	1942801,61
1	2005270,60	1962975,56	0,021091936	2043923,005	0,019275406	2023686,14
2	2005332,89	1996003,74	0,00465217	1996003,738	0,004652171	2169569,28
3	2005311,18	2141765,96	0,068046686	2009285,591	0,001981942	2208006,14
4	2005371,19	1958635,44	0,023305286	1997420,298	0,003964798	1939243,01
5	2005268,59	1980050,96	0,012575687	1961371,238	0,021891009	1867972,61
6	2005372,86	2031350,71	0,012954125	2011818,492	0,003214181	1953221,84
7	2005364,18	2127827,44	0,061067841	2037281,587	0,015916015	2263646,21
8	2005243,08	2086546,44	0,040545389	1978621,624	0,013275925	1798746,93
9	2005300,00	1946700,35	0,029222386	2006293,217	0,000495296	1986428,93

VI. Related Work

There are several inspiring load balancing approaches which have presented interesting results. Some of them are proposed for distributed systems [8], grid [9],[10], P2P systems [11],[12], and also for cloud computing systems [13],[14], and heterogeneous computing systems [15],[16],[17]. The main idea behind the considered challenge is the effective method for task assignment. To do so, the approaches in [18],[19] are based on the states of the nodes, which are grouped on domains. In [20], it is based on an index of load that is defined by the summation of the active services duration in the node; without taking into account the communication latency. The load prediction method is also investigated in load balancing models; such as [21] for dynamic load balancing of HLA based distributed simulations. However, system can further be unbalanced when running an application. This leads authors to propose dynamic load balancing algorithm based-load migration [22] in order to move the load from the overloaded nodes to the under loaded ones. It is performed by moving just one unit per iteration [23],[24],[25],[26], or a fixed number [27],[28]. Further, in [29] it's achieved by exchanging the load between neighbor nodes.

Multi-agent based load-balancing approach has been investigated as a promising paradigm for this challenge. The agent is used in [30] to represents the node for load balancing process, and in [31] it is implemented to monitor and detect the congestion in the nodes, and [32] to perform the load assignment. Further, in [33] the agent is deployed to encapsulate the tasks that will be executed.

Thereby, the mobile agents allow the load migration between nodes even in [34] homogeneous distributed system, or heterogeneous one based on node prediction algorithm. Accordingly, the proposed middleware combines two methods; task assignment according to node performance, and task migration, by the way to assign a set of tasks T_k $\{k=1,\ldots, NT\}$ to a set of $N_i\{i=1,\ldots, n\}$ nodes. Through, thanks to these several interesting works, the proposed work develops their foundation in the following ways. In this paper, a new load balancing middleware for distributed computing systems is proposed and implemented with three main focuses:

- Effective task assignment method using node performance prediction based on communication latency of each node, with integrated task migration algorithm.
- Optimized load balancing time by using the asynchronous communication mechanism between agents.
- Scalable Load balancing middleware for SPMD applications based parallel and distributed computing systems.

VII. Conclusion

The proposed load balancing middleware based cooperative mobile agents team work is a new paradigm, which is implemented using the aspect oriented approach for separating the load balancing aspect from distributed system. Through, this middleware can be integrated with different distributed computing systems for node task assignment problem. The proposed middleware deploys the mobile agent for each node in order to get the node performance. When the program is deployed the mobile agents perform an initial performance test based on referenced task in order to compute the appropriate task assignment of each node. In the case when the application tasks metadata; the complexity and the data size are known, the proposed method can predict with precision the task assignment for each node. When the application is running, if the system becomes unbalanced, the middleware executes the rebalancing algorithm to identify and decide the required load migration and rebalance the system. The obtained results, related to the execution time of each node and the gain of performance, demonstrates that the proposed middleware can ensure effective balanced distributed computing system and enhance its performance. Further, it is interesting to have a load balancing solution which handles the middleware failures. To do so, an extended work is driven in order to propose and implement a fault tolerance module for the proposed load balancing middleware.

References

[1] M. D. Assunção, R. N. Calheiros, S. Bianchi, M. A. S. Netto, and R. Buyya, "Big Data computing and clouds: Trends and future directions," J. Parallel Distrib. Comput., vol. 79, pp. 3–15, 2015.

[2] A. Puder, K. Romer, and F. Pilhofer, "Distributed Systems Architecture," Morgan Kaufmann Publ., vol. 53, no. 9, pp. 1689–1699, 2006.

[3] W. R. Braun, P., & Rossak, Mobile agents: Basic concepts, mobility models, and the tracy toolkit. 2005.

[4] F. Bellifemine, G. Caire, and D. Greenwood, Developing Multi-Agent Systems with JADE. 2007.

[5] E. Hilsdale and J. Hugunin, "Advice Weaving in AspectJ," in Proceedings of the 3rd International Conference on Aspect-oriented Software Development, 2004, pp. 26–35.

[6] M. Lippert and C. V. Lopes, "A Study on Exception Detection and Handling Using Aspect-oriented Programming," in Proceedings of the 22Nd International Conference on Software Engineering, 2000, pp. 418–427.

[7] F. Z. Benchara, M. Youssfi, O. Bouattane, H. Ouajji, and M. O. Bensalah, "A New Distributed Computing Environment Based on Mobile Agents for SPMD Applications BT-Proceedings of the Mediterranean Conference on Information & Communication Technologies 2015," 2016, pp. 353–362.

[8] Y. Jiang, "A Survey of Task Allocation and Load Balancing in Distributed Systems," IEEE Trans. Parallel Distrib. Syst., vol. 27, no. 2, pp. 585–599, 2016.

[9] D. S. Acker and S. Kulkarni, "A dynamic load dispersion algorithm for load-balancing in a heterogeneous grid system," in 2007 IEEE Sarnoff Symposium, 2007, pp. 1–5.

[10] M. Li, P. He, and L. Zhao, "Dynamic Load Balancing Applying Water-Filling Approach in Smart Grid Systems," IEEE Internet of Things Journal, vol. 4, no. 1. pp. 247–257, 2017.

[11] D. R. Karger and M. Ruhl, "Simple Efficient Load Balancing Algorithms for Peer-to-peer Systems," in Proceedings of the Sixteenth Annual ACM Symposium on Parallelism in Algorithms and Architectures, 2004, pp. 36–43.

[12] R. Bhardwaj, V. S. Dixit, and A. K. Upadhyay, "A propound method for agent based dynamic load balancing algorithm for heterogeneous P2P systems," 2009 International Conference on Intelligent Agent & Multi-Agent Systems. pp. 1–4, 2009.

[13] H. C. Hsiao, H. Y. Chung, H. Shen, and Y. C. Chao, "Load Rebalancing for Distributed File Systems in Clouds," IEEE Trans. Parallel Distrib. Syst., vol. 24, no. 5, pp. 951–962, 2013.

[14] J. Zhao, K. Yang, X. Wei, Y. Ding, L. Hu, and G. Xu, "A Heuristic Clustering-Based Task Deployment Approach for Load Balancing Using

Bayes Theorem in Cloud Environment," IEEE Transactions on Parallel and Distributed Systems, vol. 27, no. 2. pp. 305–316, 2016.

[15] J. Shen, A. L. Varbanescu, Y. Lu, P. Zou, and H. Sips, "Workload Partitioning for Accelerating Applications on Heterogeneous Platforms," IEEE Transactions on Parallel and Distributed Systems, vol. 27, no. 9. pp. 2766–2780, 2016.

[16] E. Hwang, S. Kim, T. k. Yoo, J. S. Kim, S. Hwang, and Y. r. Choi, "Resource Allocation Policies for Loosely Coupled Applications in Heterogeneous Computing Systems," IEEE Transactions on Parallel and Distributed Systems, vol. 27, no. 8. pp. 2349–2362, 2016.

[17] J. Y. Jang, H. Wang, E. Kwon, J. W. Lee, and N. S. Kim, "Workload-Aware Optimal Power Allocation on Single-Chip Heterogeneous Processors," IEEE Transactions on Parallel and Distributed Systems, vol. 27, no. 6. pp. 1838–1851, 2016.

[18] F. auf der Meyer Heide, B. Oesterdiekhoff, and R. Wanka, "Strongly adaptive token distribution," Algorithmica, vol. 15, no. 5, pp. 413–427, 1996.

[19] P. Berenbrink, T. Friedetzky, and R. Martin, "Dynamic Diffusion Load Balancing BT - Automata, Languages and Programming: 32nd International Colloquium, ICALP 2005, Lisbon, Portugal, July 11-15, 2005. Proceedings," L. Caires, G. F. Italiano, L. Monteiro, C. Palamidessi, and M. Yung, Eds. Berlin, Heidelberg: Springer Berlin Heidelberg, 2005, pp. 1386–1398.

[20] Y. Qiao and G. v. Bochmann, "A Diffusive Load Balancing Scheme for Clustered Peer-to-Peer Systems," 2009 15th International Conference on Parallel and Distributed Systems. pp. 842–847, 2009.

[21] R. E. De Grande, A. Boukerche, and R. Alkharboush, "Time Series-Oriented Load Prediction Model and Migration Policies for Distributed Simulation Systems," IEEE Transactions on Parallel and Distributed Systems, vol. 28, no. 1. pp. 215–229, 2017.

[22] G. Cybenko, "Dynamic load balancing for distributed memory multiprocessors," J. Parallel Distrib. Comput., vol. 7, no. 2, pp. 279–301, 1989.

[23] A. Cortés, A. Ripoll, F. Cedó, M. A. Senar, and E. Luque, "An asynchronous and iterative load balancing algorithm for discrete load model," J. Parallel Distrib. Comput., vol. 62, no. 12, pp. 1729–1746, 2002.

[24] Y. F. Hu and R. J. Blake, "An improved diffusion algorithm for dynamic load balancing," Parallel Comput., vol. 25, no. 4, pp. 417–444, 1999.

[25] E. Luque, A. Ripoll, A. Cortes, and T. Margalef, "A distributed diffusion method for dynamic load balancing on parallel computers," Proceedings Euromicro Workshop on Parallel and Distributed Processing. pp. 43–50, 1995.

[26] T. A. Murphy and J. G. Vaughan, "On the relative performance of diffusion and dimension exchange load balancing in hypercubes," in PDP, 1997.

[27] P. Berenbrink, T. Friedetzky, and Z. Hu, "A new analytical method for parallel, diffusion-type load balancing," J. Parallel Distrib. Comput., vol. 69, no. 1, pp. 54–61, 2009.

[28] F. Cedo, A. Cortes, A. Ripoll, M. A. Senar, and E. Luque, "The Convergence of Realistic Distributed Load-Balancing Algorithms," Theory Comput. Syst., vol. 41, no. 4, pp. 609–618, 2007.

[29] I. Konstantinou, D. Tsoumakos, and N. Koziris, "Fast and Cost-Effective Online Load-Balancing in Distributed Range-Queriable Systems," IEEE Transactions on Parallel and Distributed Systems, vol. 22, no. 8. pp. 1350–1364, 2011.

[30] S. Banerjee and J. P. Hecker, "A Multi-agent System Approach to Load-Balancing and Resource Allocation for Distributed Computing BT - First Complex Systems Digital Campus World E-Conference 2015," P. Bourgine, P. Collet, and P. Parrend, Eds. Cham: Springer International Publishing, 2017, pp. 41–54.

[31] X.-J. Shen et al., "Achieving dynamic load balancing through mobile agents in small world P2P networks," Comput. Networks, vol. 75, pp. 134–148, 2014.

[32] O. Rihawi, Y. Secq, and P. Mathieu, "Load-Balancing for Large Scale Situated Agent-based Simulations," Procedia Comput. Sci., vol. 51, pp. 90–99, 2015.

[33] S. Hunt, Q. Meng, C. Hinde, and T. Huang, "A Consensus-Based Grouping Algorithm for Multi-agent Cooperative Task Allocation with Complex Requirements," Cognit. Comput., vol. 6, no. 3, pp. 338–350, Sep. 2014.

[34] J. Liu, X. Jin, and Y. Wang, "Agent-based load balancing on homogeneous minigrids: macroscopic modeling and characterization," IEEE Trans. Parallel Distrib. Syst., vol. 16, no. 7, pp. 586–598, 2005.

An Efficient Method for Speeding up Large-Scale Data Transfer Process to Database: A Case Study

Ginanjar Wiro Sasmito[1], M. Nishom[2]
Informatics Engineering
Polytechnic of Harapan Bersama
Tegal, Indonesia

***Abstract*—Among the of characteristics of Large Data complexity comprising of volume, velocity, variety, and veracity (4Vs), this paper focuses on the volume to ensure a better performance of data extract, transform, and load processes in the context of data migration from one server to the other due to the necessity of update to the population data of Tegal City. An approach often used by most programmers in the Department of Population and Civil Registration of Tegal City is conducting the transfer process by transferring all available data (in specific file format) to the database server regardless of the file size. It is prone to errors that may disrupt the data transfer process like timeout, oversized data package, or even lengthy execution time due to large data size. The research compares several approaches to extract, transform, and load/transfer large data to a new server database using a command line and native-PHP programming language (object-oriented and procedural style) with different file format targets, namely SQL, XML, and CSV. The performance analysis that we conducted showed that the big scale data transfer method using LOAD DATA INFILE statement with comma-separated value (CSV) data source extension is the fastest and effective, therefore recommendable.**

***Keywords*—Big data; speeds up; data processing; data transfer**

I. Introduction

The existence of an information system in an organization can help improve different aspects, namely improving the organization's efficiency and effectiveness of the business process, decision making, productivity, and competitive advantages[1]. In an organization, data are processed on a daily basis and stored in the server, therefore the volume is always increasing every year [2]. Indonesia, as the fourth biggest country in terms of population [3], has utilized information system to manage its population data. The volume size of population data is increasing every year, and it requires new server upgrade as well as database migration to server. In practice, there are several methods that can be used in the database migration, namely data import to database server using default (built-in) import feature, third party application suite like phpmyadmin [4] and navicat [5], and using standalone application developed by the programmer itself using Extract, Transform, Load (ETL) Procedures. The Procedures are performed by collecting the data from different sources as needed, modifying it according to the needs, and uploading it to specific database server to be processed or displayed as needed [6]. The most frequently used tools for ETL process are spreadsheet, relational database, non-SQL database, and many more [7].

During the ETL process, selecting correct file format to import or transfer large data is a challenge for the programmer and database administrator, because as the size getting bigger, it affects the execution or transfer time. In the MySQL database server, the data loading process can be performed using different file formats, namely SQL, XML, CSV format, or Excel spreadsheet [5]. Some authors chose different file format to import the data, like [8] chose CSV file format because it is accessible through excel spreadsheet application and data is presented in tabular form, therefore it is easier to access and modify according to the specific needs, and chose SQL format or text file by using mysqldump and mysql to export and import the data [9][10][11], while delisle (in his book) used phpmyadmin to import the data [12]. Other than file format, selecting the appropriate method in the transfer process also need to be considered, such as whether the data is transferred using single-row INSERT statement method, or using INSERT statement with multiple VALUES lists (or generally referred to as extended INSERT) to include all data simultaneously, or using LOAD DATA statement. LOAD DATA Statement is the most appropriate method to transfer large data [13].

One of the issues frequently faced by a database administrator even the programmer is the allowed limit of package size per connection (packet too large). In server MySQL terminology, a package is a request sent to the server and processed by the server in a chunk or batch, simultaneously the server allocates the temporary memory to sore each package and ensures that the memory of servers is still sufficient to prevent a server from running out the memory [14]. The default value for a package allowed in MySQL 8.0 server is 64 MB, but we can set a bigger value for this system variable as the size of package will depend on the availability of memory in the server [15]. The rule of thumb for this is that buffer_pool must be set to 75% or 80% of the server's memory. However, the ratio does not have sufficient basis, therefore only works intermittently, but no guarantee whether it will be working better in a specific case [16]. Hence, in a big size data transfer, an appropriate approach or selection of statement used and file format are required to ensure smooth data transfer.

For that reason, this research aims to achieve the above objectives by comparing the ETL process using different file formats with different statements to find the most appropriate and efficient method to transfer large data into the database server.

II. Methods

In general, the data transfer process into the server is performed regardless of the file size or amount of data to be transferred, while the database server usually has certain limitations to process the data transfer, such as the maximum file size for transfer, the limit of allowed package size on each statement and transaction, and the net buffer size limit. Despite in practice it is possible to change the value of these limits; such changes may affect the execution time, which may relatively need a longer time and the possibility of transfer failure due to timeout as the result of processing significant amount of data. The approach proposed in the research is Extract-Transform-Load (ETL) approach using appropriate file format and statement. The concept of this approach is performing data source extraction process, transforming data to SQL, XML, and CSV file format, increase buffering and decrease durability in the server configuration, and transferring the data and test the speed of its execution time.

III. Results and Discussion

A. Extraction and Transformation of Data Source to the Expected Format File

The file or data source used in the research is the population data of Tegal City obtained from the Depatment of Population and Civil Registration of Tegal City. The file is an Excel spreadsheet sized 106MB containing 284917 data rows consisting of 55 fields/columns. The Excel spreadsheet was chosen because data source can be presented in tabular format and enables the stakeholders to customize the data according to their needs. First, data source is extracted using PHP language program to determine the value of data to be transferred to the new database server. Second, the result of the extraction then converted into different file formats, namely SQL, XML, and CSV. Table I shows the conversion of data source to the file format to be used in the data transfer tests, and each file has a different size.

Table I explains the conversion scenario to obtain SQL format file using two approaches, i.e. using single-insert statement (one-row insert per statement) and extended-insert (multiple-row insert per statement) in a transaction.

TABLE. I. Result of Data Source Conversion to File Formats to be Transferred

Data Source	Output Format	Statement	Transaction	Output File Size
Excel Spreadsheet (106MB)	SQL	Single-insert (one-row per statement)	1	136 MB
	SQL	Extended-insert (multiple-row per statement)	1	126 MB
	XML	LOAD XML INFILE	1	704.2 MB
	CSV	LOAD DATA INFILE	1	120.2 MB

B. Methods used for Data Transfer

This research used MySQL as the database. The configuration is applied to speed up processing, shown in Table III. There are two ways to transfer the data into the database server online. First, data sources (*.sql, *.csv, and *.xml extension files) are uploaded to the directory of the root server using FTP or cPanel. Second, data is imported or transferred using specified approaches. The import/transfer of data to database server can be performed using several methods. First, database is imported using mysql command using command line (Windows, Linux, or Unix); the file format used was SQL (single-row insert and multiple-row insert per statement). However, this method of data import sometimes takes time especially if the size of the file being imported is large or extensive. Secondly, using LOAD DATA INFILE statement, the file format used is CSV. The third, using LOAD XML INFILE statement to transfer the data using XML file format. Since the server used is an online server, the command line is executed using SSH network protocol using the third-party application. From all three methods, the result of the test showed that the data transfer process using LOAD DATA INFILE statement is the fastest compared to other statements, as shown in Table II. The average of total data transferred per second is shown in Fig. 1.

TABLE. II. Comparison of Data Transfer Time using Several Approaches

File Format	Statement	Transaction	Rows	Transfer Time
Command Line Way				
SQL	Single-insert	1	284917	21.6 sec
	Extended insert	1	284917	18.6 sec
XML	LOAD XML INFILE	1	30000	7 min 34 sec
CSV	LOAD DATA INFILE	1	284917	6.05 sec
Native-PHP: Prosedural Way				
SQL	Single-insert	1	284917	18.73 sec
	Extended insert	1	284917	13.74 sec
XML	LOAD XML INFILE	1	30000	8 min 2.3 sec
CSV	LOAD DATA INFILE	1	284917	6.56 sec
Native-PHP: Object Oriented Way (MySQLi)				
SQL	Single-insert	1	284917	18.65 sec
	Extended insert	1	284917	13.35 sec
XML	LOAD XML INFILE	1	30000	8 min 2.2 sec
CSV	LOAD DATA INFILE	1	284917	6.68 sec
Native-PHP: Object Oriented Way (PDO)				
SQL	Single-insert	1	284917	18.55 sec
	Extended insert	1	284917	13.7 sec
XML	LOAD XML INFILE	1	30000	8 min 2.6 sec
CSV	LOAD DATA INFILE	1	284917	6.7 sec

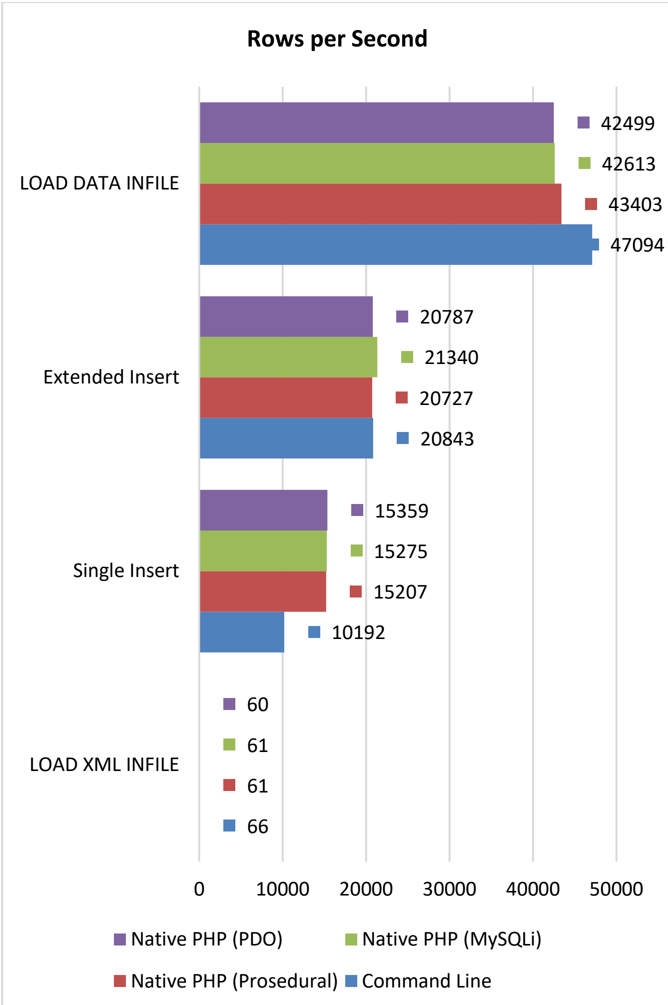

Fig. 1. The Average of Total Data Transferred Per Second using Several Approaches.

TABLE. III. INCREASE PACKET AND BUFFERING, AND DECREASE DURABILITY FOR SPEEDS UP PROCESSING

Name	**Value**	**Description**
max_allowed_packet	2048M	Adjust size for handling big queries
key_buffer	64M	Speeds up of index reads
innodb_buffer_pool_size	4096M	25% of physical memory (tested using 16G)
innodb_log_file_size	1024M	25% of buffer pool size
innodb_log_buffer_size	256M	25% of log file size

C. *Recommendation and Challenge of Data Transfer Methods*

Fig. 1 present the result of the tests using several methods related to the number of transferable data rows to server per second. This transfer method using single-row insert statement is deemed to be less effective in data transfer process (of big size), as it takes a longer time, therefore not recommended. Different from single-row insert statement, the extended-insert statement has slightly better performance. Unfortunately, there is no comprehensive approach to determine the number of ideal data rows in each per package data transfer process. Since the data transfer using extended-insert statements relies heavily on the maximum configuration of maximum allowed packet), therefore the probability of timeout even error is high. For that reason, a database administrator or programmer must be able to determine the number of maximum packets allowed according to the specifications of the server's hardware products. The specification of hardware used (ideally must be more significant than the size of the data source to be transferred). The better the server specification to be used and the bigger the configuration size or value will prevent the issues from occurring during the transfer data process using this statement. Nevertheless, using this statement is recommended as it is faster than the single-row insert statement. To speed up the processing, it is better to increase the Buffer Pool size by 20-50% from the physical memory size, and increase the Log File size to 25% from the Buffer Pool size.

Different from the previous two statements, the data transfer method using LOAD XML statement has poor time performance. The bigger the file size, the longer the execution process or data transfer. The LOAD DATA statement is inversely proportional to extended-insert statement and does not rely on the server configuration (the maximum size of allowed packet size per statement); therefore, this method is the most suitable for large data transfer process. Moreover, the statement has excellent data transfer speed as described in Fig. 1, that data transfer using LOAD DATA statement is the best way as it is the fastest in processing data transfer.

IV. CONCLUSION

The objective of the research is to determine the most efficient method to transfer the data in large size to database server. The testing of the methods was performed by using extract-transform-load approach using single-insert statement, multiple-insert (extended-insert) statement, LOAD XML statement, and LOAD DATA statement. The result of the tests showed that the data transfer data method with single-insert statement is not recommended due to low-speed transfer. Multiple-insert statement to transfer large data is also not recommended because the possibility of timeout or errors if the packet delivered per statement exceeds the allowed packet value in the server configuration. The data transfer method using LOAD XML statement is the worst choice and suggested not to be used for large scale data transfer. Instead, data transfer method using LOAD DATA is the most recommended method to transfer large data. However, a database administrator or programmer must consider the appropriate server configuration to avoid problems during large scale data process.

ACKNOWLEDGEMENT

The author would like to thank the Depatment of Population and Civil Registration and Statistics Agency of Tegal City for sharing the data source and Ministry of Technology Research and Higher Education of the Republic of Indonesia for funding this research.

REFERENCES

[1] R. M. Stair and G. W. Reynolds, Fundamentals of Information Systems, 8 ed., Boston: Cengage Learning, 2014.

[2] K. A. I. Hammad, M. A. I. Fakharaldien, J. M. Zain and M. A. Majid, "Big Data Analysis and Storage," in International Conference on Operations Excellence and Service Engineering, Florida, 2015.

[3] CIA, The World Factbook, Langley: Central Intelligence Agency, 2019.

[4] P. McFedries, Web Coding & Development All-in-One For Dummies, Hoboken: Wiley, 2018.

[5] G. Ozar, "MySQL Management and Administration with Navicat," Birmingham, 2012.

[6] L. Baldacci, M. Golfarelli, S. Graziani and S. Rizzi, "QETL: An approach to on-demand ETL from non-owned data sources," Data & Knowledge Engineering, vol. 112, pp. 17-37, 2017.

[7] S. Challawala, J. Lakhatariya, C. Mehta and K. Patel, MySQL 8 for Big Data: Effective data processing with MySQL 8, Hadoop, NoSQL APIs, and other Big Data tools, Birmingham: Packt publishing, 2017.

[8] R. J. Dyer, Learning MySQL and MariaDB: Heading in the Right Direction with MySQL and MariaDB, Sebastopol: O'Reilly Media, 2015.

[9] S. K. Cabral and K. Murphy, MySQL Administrator's Bible, Hoboken: Wiley, 2009.

[10] P. DuBois, MySQL Cookbook, 3 ed., Sebastopol: O'Reilly Media, 2014.

[11] P. Zhang, Practical Guide to Large Database Migration, Boca Raton: CRC Press, 2019.

[12] M. Delisle, Mastering Phpmyadmin 3.4 for Effective MySQL Management, Birmingham: Packt Publishing, 2012.

[13] P. Scobey and P. Lingras, Web Programming and Internet Technologies: An E-commerce Approach, Burlington: Jones & Bartlett, 2012.

[14] S. Pachev, Understanding MySQL Internals: Discovering and Improving a Great Database, Sebastopol: O'Reilly Media, 2007.

[15] C. Mehta, A. K. Bhavsar, H. Oza and S. Shah, MySQL 8 Administrator's Guide: Effective guide to administering high-performance MySQL 8 solutions, Birmingham: Packt Publishing, 2018.

[16] B. Schwartz, P. Zaitsev and V. Tkachenko, High Performance MySQL: Optimization, Backups, and Replication, Sebastopol: O'Reilly Media, 2012.

A Systematic TRMA Protocol for Yielding Secure Environment for Authentication and Privacy Aspects

Anusha R[1]
Department of Electronics and Communication Engineering,
N. M. A. M. Institute of technology, (Visvesvaraya Technological University, Belagavi) Nitte 574110
Udupi District, Karnataka, India

Veena Devi Shastrimath V[2]
Professor, Dept. of ECE
NMAM Institute of Technology
NITTE, Udupi
India

***Abstract*—RFID is a system that uses the radio waves to scrutinize and capture data pertained to a tag for an object attached to it. In spite of RFID's wide application in industries, it poses a severe security issue. There is high susceptibility that RFID might be attacked with future attacks to invade the privacy and data in the system. To protect the RFID system against such attacks, the Pad-generation (Pad-Gen) function is used. This paper presents a mutual authentication scheme Tag Reader Mutual Authentication (TRMA) that is implemented using two approaches, the XOR operation and the MOD operation by modifying the Pad-Gen function. The proposed framework is executed on low-cost Artix7 FPGA XC7A100T-3CSG324, and its hardware verification is done on chip scope pro tool.**

Keywords—Mutual Authentication; Modified Pad-Gen; Radiofrequency Identification (RFID); Privacy; Security; Tag-Reader Mutual Authentication (TRMA)

I. Introduction

RFID is an emerging wireless technology that operates over the radio signals to recognize and track the various objects that consist of a distinctive serial identification [1]. The RFID system comprises majorly of three different sections, which are the transponder/tag, a database, or an interrogator/reader. It uses the general frequency bands, which are the Ultra High-Frequency Band (860 MHz- 930MHz), High Frequency (13.56MHz), and Low Frequency (125 kHz – 134 kHz) [2]. An RFID tag individually owns a unique identification code called the Electronic Product Code (EPC) [3]. The two kinds of tags are the active tags and the passive tags separable by the implications, specifications, and storage capacity. The passive tags don't need a battery as it charges itself from the charge availed from the electromagnetic signals of the reader's request side, whereas the active tag demands battery back-up. Passive tags are built to enable lower storing capacities lesser than the values of 1KB, used in shorter applications range from those of 4 inches to 15 feet. It has the capability wherein it can read once and write many. Hence these are the read-only tags. Opposite to this, active tags have a storage ability of 512KB, implied in the utilization of massive applications until 300 feet [4]. The role of the RFID reader is to write and read the information available on the tag. The details are preserved in a database consisting of integrated circuitry that concerning the password of tags individually, EPC, and reader [5]. Usually, there is a requirement for a dynamic protocol to establish a secured communication taking place among the RFID reader and the tag. For various security applications, a vital role is played by the Linear Feedback Shift Register (LFSR) [6]. This operates generating random numbers together at the side of the tag and reader. The two kinds of LFSR architectures are the Galois and the Fibonacci LFSRs. Out of the two, the Fibonacci LFSR is the one which is most commonly applied to the hardware implementation use [7].

A new version of EPC Class-1 has been ratified. This is EPC Class-1 version in Generation 2 that is compatible along with the old version, to provide a set of a new type of featured series intends on improvising the security parameter giving an opportunity to the manufacturers to perform the customization using cryptographic authentication ways for verification of identities and avoid the unauthorized access [8]. As per the previous standard, the new EPC standard also supports Cyclic Redundancy Check (CRC), Pseudo-Random Number Generator (PRNG), and the XOR function. A security protocol is considered as EPC compliant only if it solely makes use of one or more functions [9]. Moreover, the functions mentioned are not cryptographic functions themselves. Various other measures should be ensured to provide an acceptable security level of computations as there only 500-5000 elements of gates present on a tag [10]. Therefore, this paper proposes a framework to provide a secure environment for RFID to transfer data. Section II focuses on the background of RFID along with the description of a problem statement. Section III foregrounds the existing techniques in securing the privacy concern of RFID.

Further, the hardware architecture of the proposed mechanism is given in Section IV. The results are discussed in Section V. The performance analysis of both the approaches is carried out in Section VI. The conclusion is followed in Section VII.

II. Background and Challenging Issue

The RFID mutual authentication protocol establishes the communication between the reader and the tag that is encoded using a password. The communication in RFID is initiated by transferring a signal request from the reader. Radio signals are emitted from the reader section, and as the tag is made to enter the range, it responds towards the reader's request [11]. These protocols mentioned below, have a unique procedure for encrypting and decrypting along with few benefits as well as drawbacks.

A. Standard of EPC Global Class-1 Generation-2

The standard utilizes a bitwise EX-OR operation that performs the function of the cover code string. The scheme does not guarantee a secure environment as it provides support only for the reader's authentication. This helps in creating fake cloning tags that utilize the unencrypted password in the form of a cover code that is generated using primary bitwise operation. The non-volatile features that should be pertained to an RFID tag are briefed as follows:

- Password- Two passwords individually consisting of 32 bits that operate at the transmitter and receiver section to access/kill the tag forever hold space in the reserved memory.
- Object Identification and user Memory- To identify the object to which tag is attached, the memory space of the tag has an EPC section comprising of Protocol Control bits (PC-16). CRC bits (16) in the PC accomplish the task of object identification. The data that is processed as per the user's instructions are stored in the user memory [12].

B. Mutual Authentication Protocol- PadGen

A computational procedure that encrypts and decrypts the password accordingly is called the PadGen operation for a mutual authentication scheme. In a mutual authentication scheme, two passwords are made. This involves the process of four numbers randomly consisting of two rounds each; the PadGen computes the cover code password further. The initial around would of PadGen comprises of the Access password, and another round has the Kill password [13]. Also, the hardware realization of the protocol is not accomplished. Following which the same PadGen function is used but pertained to a different computational procedure [14].

C. Standard of EPC Global Class-1 Generation-2

The standard utilizes a bitwise EX-OR operation that performs the function of the cover code string. The scheme does not guarantee a secure environment as it provides support only for the reader's authentication. This helps in creating fake cloning tags that utilize the unencrypted password in the form of a cover code that is generated using primary bitwise operation. The non-volatile features that should be pertained to an RFID tag are briefed as follows:

- Password- Two passwords individually consisting of 32 bits that operate at the transmitter and receiver section to access/kill the tag forever hold space in the reserved memory.
- Object Identification and user Memory- To identify the object to which tag is attached, the memory space of the tag has an EPC section comprising of Protocol Control bits (PC-16). CRC bits (16) in the PC accomplish the task of object identification. The data that is processed as per the user's instructions are stored in the user memory [12].

D. Mutual Authentication Protocol- PadGen

A computational procedure that encrypts and decrypts the password accordingly is called the PadGen operation for a mutual authentication scheme. In a mutual authentication scheme, two passwords are made use of. This involves the operation of four numbers randomly consisting of two rounds each; the PadGen computes the cover code password further. The initial around would of PadGen comprises of the Access password, and another round has the Kill password [13]. Also, the hardware realization of the protocol is not accomplished. Following which the same PadGen function is used but pertained to a different computational procedure [14].

III. Existing Techniques in Securing the Privacy Concerns of RFID Systems

There are numerous schemes presented by various researchers concerning the aspect of RFID security. This section stresses the techniques incorporated for enabling securer RFID access in a wireless environment. Sarma et al. [16] showed that the Auto-ID Center is an emerging way to develop a cost-effective RFID system as an extension to the bar code use. Due to the constrained RFID resources and also with the interconnections, low-cost RFID is not ideal for the functioning of wireless devices. Yuan et al. [17], designed encoder architecture for UHF –Ultra High Frequency, RFID purposes. Two schemes, namely the Miller Modulated Subcarrier (MMS), and Bi-phase space applicable in Class-1, Gen 2 UHF RFID implications scenarios have been designed. Avoine and Oechslin [18] stressed that there is a chance of high susceptibility to attacks over RFID technology, threatening the privacy of the network. The study introduced a scheme for eliminating the scalability constraint in the overall mechanism. This indeed ensured that the system exhibits the function of forwarding privacy and privacy. Kim et al. [19] propose an interference model that is derived from the interference statistics from a reader-to-reader over a nominal level of the desired reader in the model.

Peris-Lopez et al. [20] presented a lightweight protocol for mutual authentication among the tag and the reader. This suggested adequate privacy and security levels, capable enough of being applicable in most systems for real-time operations as it has a fundamental requirement to accomplish the operation of only 300 gates. Garfinkel et al. [21], foregrounded the potential privacy threats faced by activists with the increasing employment of RFID in multiple areas. The work of Li and Wang [22], analyze security vulnerabilities respective to two ultra-light weighted mutual authentication protocols. By identifying two attacks, the functioning of the protocol is tested. Bogdanov et al. [23], focused on the drawback of utilizing the cheap tags for RFID operation that tend to compromise with the security and privacy measure in the network. Hash function working is described, whereas it also highlights the major issues designing lightweight functions. The study of Want [24], showed that the necessity to incorporate RFID sensors would be mostly in the use of environmental sensors. Thiesse et al. [25] presented the primary ideas and implications of the EPC network, the integration of it along with the enterprise systems involving its functionality for data communication among supply chain organizations. Eom et al. [26] concentrated on the issue of collisions among readers in RFID. The study proposed an effective algorithm for anti-collision between readers. The work of Lopez et al. [27], surveyed the crucial technical limitations of RFID systems.

Sun et al. [28] proposed a framework of the novel Gen2 authentication protocol for cost-effective RFID tags. The protocol ensures that readers can access the reading of new tags. Peris-Lopez et al. [29] proposed a new scheme of the mutual authentication protocol for the light-weight RFID tag-readers based on the EPCglobal mechanism. Konidala et al. [29], introduced a fundamental, reliable, low cost enabled, the lightweight mutual authentication scheme for the RFID tag-reader. The scheme addresses the approach of two standards, namely, a protocol of EPCglobal Class 1 Gen2 Ultra High-Frequency RFID and EPCglobal framework architecture. The schemes make use of Access and Kill Password that is indeed successful in achieving three aims of detecting the cloned fake tags, allowing the manufacturer to keep track of the genuine products and removing the malicious snooping readers.

The study of Han et al. [30] described a model for the effective localization in indoor robots used in mobiles incorporating the technology of RFID systems. Juels [31], surveyed over the difficulties in security and privacy concerns of RFID systems. The surveys investigate an approach to protect the privacy and integrity of the system.

Lee et al. [32] presented an RFID tag chip that, in the compact in size, completely integrated into the HF-band, enabling the security and authentication function. Eisenbarth et al. [33], surveyed the implementations reading the Lightweight cryptography. The high-cost requirements and implementation limitations of the products pertaining to high-volume involving the smart cards and RFID secure tags, mandatorily need cryptographic implementations. The work carried out by Piramuthu [34], carry out the study and estimation of protocols from an individual stream of security, recognizing the vulnerabilities and hence design an optimal solution. The security analysis respective to the proposed settlement is being conducted. Anusha R and Veena Devi Shastrimat [35] have presented qualitative evaluation over efficiency of the security methods to safeguarding NFC tools and its services. Anusha R and Veena Devi Shastrimat [36] have an efficient method for Mutual verification of the RFID wireless schemes. Anusha R and Veena Devi Shastrimat [37] have a proficient Lightweight cryptographic Block cipher design. The hardware architecture of Tiny Encryption Algorithm (TEA) has been designed and which is very simple, elastic, less computations needed and simple key development.

IV. Hardware Architecture

The proposed TRMA protocol hardware architecture uses 32-bit passwords. To establish mutual authentication in RFID, the tag and reader individually generates a 16-bit password, which together makes it the 32-bit password. The hardware protocol that functions on the Exclusive OR operation requires interchanging information among the tag and reader to accomplish a secure communication path. The access password and kill password are identical two 32-bit values that are stored in the memory space of tag. Before the data interchange process between the tag and reader, the reader needs to indicate a confirmation regarding the password validity. This step is mandatory to set up a password for RFID communication. Fig. 1 depicts the hardware architecture of the modified pad generated TRMA using the XOR method for RFID. To ensure a secure environment for RFID data exchange, Access Password (AP) and Kill Password (KP) reserve memory space and are represented in equations (1-6). Both the passwords use 32-bits in the memory, individually pertaining to 16 bits of data. The LSB and MSB for the two 16 bit passwords are as follows:

Access Password,

AP = ap0ap1……..ap31 (1)

For MSB, APM =ap16ap17....ap31 (2)

For LSB, APL=ap0ap1…….ap15 (3)

Kill Password,

KP = kp0kp1………..kp31 (4)

For MSB, KPL=kp0kp1…….kp15 (5)

For LSB, KPM=kp16kp17…..kp31 (6)

The MSB (8 bits) and LSB (8 bits) are concatenated to obtain the resulting 16bits of AP and KP, respectively.

An algorithm of TRMA using XOR operation as follows:

1. *Process Initialization* $\leftarrow$ *The request (R) is transferred from the reader to tag*
2. *LFSR generates a 16-bit random number concerned to tag (R_{Tx}).*
3. *A communication path is established through EPC.*
4. *LFSR generates a 16-bit random number concerned to a manufacturer (R_{mx}).*
5. $R_T \oplus_M \leftarrow R_T \oplus R_M$
6. $Rv \leftarrow$ *Pad-gen(R_{TX},R_{MX})---[Apsd]*
7. $Rw \leftarrow$ *Pad-gen(R_T,$R_T \oplus_M$)---[Apsd]*
8. $R_V \oplus_W \leftarrow R_V \oplus R_W$
9. *PAD1* $\leftarrow$ *Pad-gen(Rv, Rw) ---[Kpsd]*
10. *PAD2* $\leftarrow$ *Pad-gen (Rv, $Rv \oplus_W$) ---[Kpsd]*
11. $CCPSD_M \leftarrow Apsd_M \oplus PAD1$*---(Code covered password MSB)*
12. $CCPSD_L \leftarrow Apsd_L \oplus PAD2$*---(Code covered password LSB)*
13. *Tag Verification and Authentication* $\leftarrow$ *The tag verifies the password validity and reader authenticates the tag.*

The hardware architecture modified Pad-Gen TRMA using the MOD method is illustrated in Fig. 2. The steps in involved in the operation of TRMA using MOD [15] operation are explained as follows:

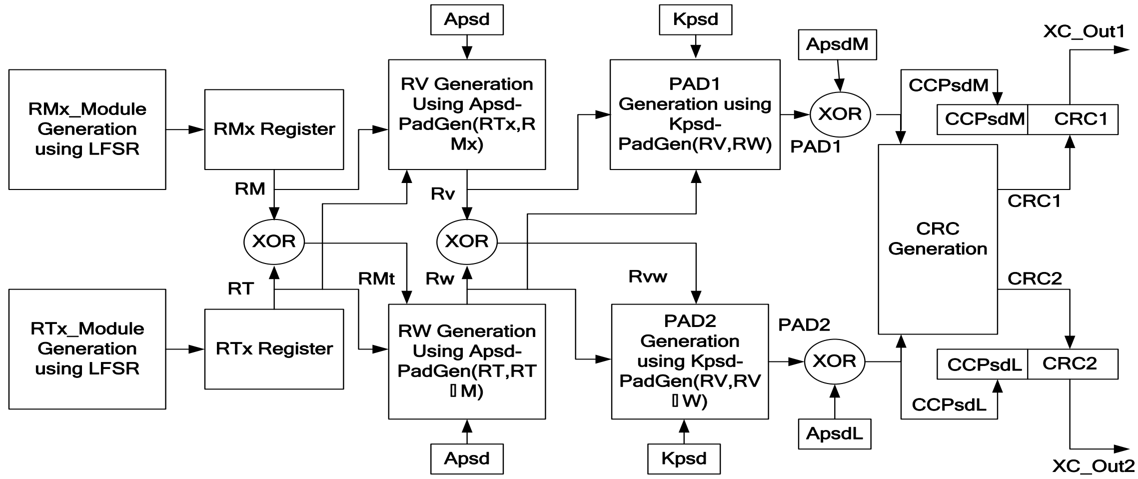

Fig. 1. Hardware Architecture of Modified Pad-Gen Design using XOR Method for RFID –TRMA Protocol.

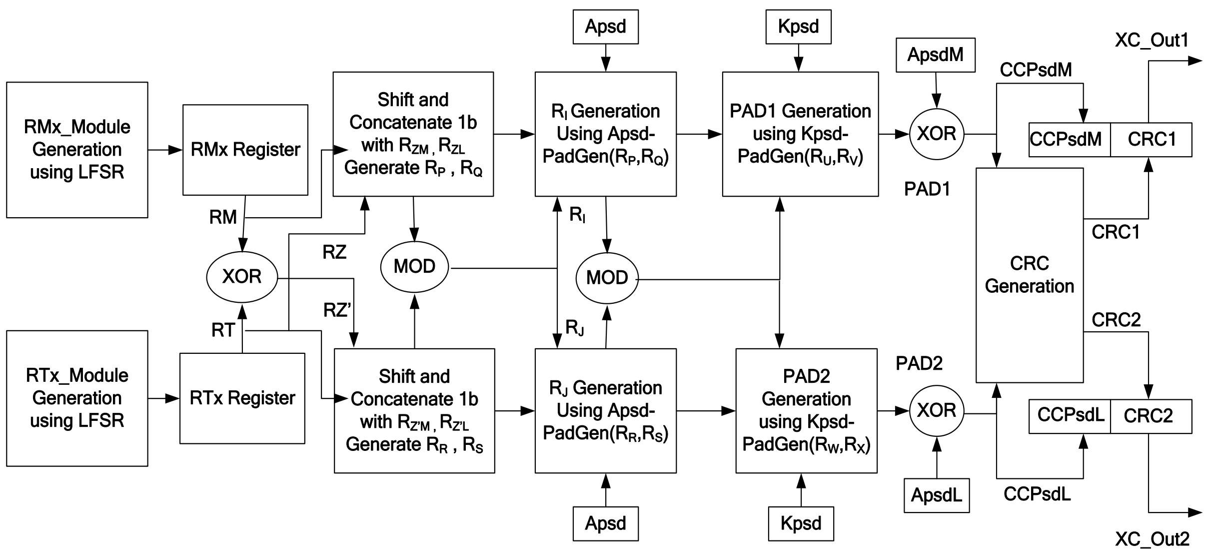

Fig. 2. Hardware Architecture of Modified Pad-Gen Design using MOD Method for RFID –TRMA Protocol.

The algorithm of TRMA using MOD operation as follows:

1. *Process Initialization $\leftarrow$ The request (R) is transferred from the reader to tag*
2. *LFSR generates a 16-bit random number concerned to tag (R_{Tx}).*
3. *A communication path is established through EPC.*
4. *LFSR generates a 16-bit random number concerned to the manufacturer (R_{mx}).*
5. *$R_T \oplus_M \leftarrow R_T \oplus R_M = R_Z$, [$RZ = R_{ZM} \,||\, R_{ZL}$]*
6. *Shifting by one bit left and concatenate$\leftarrow R_{1+ZM} = \{1, R_{ZM}\}$, $R_{1+ZL} = \{1, R_{ZL}\}$*
7. *Mod-Operation for MSB (R_P) $\leftarrow Mod_1(R_T) \,||\, Mod_1(R_M)$*
8. *Mod-Operation for LSB (R_Q) $\leftarrow Mod_1(R_T) \,||\, Mod_1(R_M)$*
9. *$R_I \leftarrow$ Pad-gen (R_P, R_Q) --- [Apsd]*
10. *$R_Z' \leftarrow$ bit reversal (R_Z)*
11. *Shifting by one bit left and concatenate$\leftarrow R_{1+ZM} = \{1, R_{ZM}\}$, $R_{1+ZL} = \{1, R_{ZL}\}$*
12. *Mod-Operation for MSB (R_R) $\leftarrow Mod_1(R_T) \,||\, Mod_1(R_M)$*
13. *Mod-Operation for LSB (R_S) $\leftarrow Mod_1(R_T) \,||\, Mod_1(R_M)$*
14. *$R_J \leftarrow$ Pad-gen (R_R, R_S) --- [Apsd]*
15. *ReplaceR_P, R_Q, R_R, R_S with R_U, R_V, R_W, R_X and repeat the process from step5*
16. *PAD1 $\leftarrow$ Pad-gen (R_U, R_V) --- [Kpsd]*
17. *PAD2 $\leftarrow$ Pad-gen (R_W, R_X) --- [Kpsd]*
18. *Tag Verification and Authentication $\leftarrow$ The tag verifies the password validity and reader authenticates the tag.*
19. *$CCPSD_M \leftarrow Apsd_M \oplus PAD1$---(Code covered password MSB)*
20. *$CCPSD_L \leftarrow Apsd_L \oplus PAD2$---(Code covered password LSB)*
21. *Authentication and Verification*
22. *Cyclic Redundancy Check (CRC)$\leftarrow$ after the generation of code covered passwords, the CRC can be incorporated to provide the next level of security in the mutual authentication process.*

V. Result Discussion

The simulation outcomes relevant to the modified PadGen of TRMA are described in Fig. 3. Additionally, the physical verification of the outcomes is depicted in Fig. 4. The design is implemented using Verilog coding on Xilinx 14.7 ISE. The device used is Artix7 FPGA with Modelsim 6.5f. As the clock is triggered high along reset pulled to logic 0, the output for the PAD1 and PAD2 are observed. AP and KP are predefined values before the process of sending a request to the tag. The crc_en signal uses the LFSRs to generate the crc_out. The output XC_Out1 and XC_Out2 are attained by performing concatenation operation on CCPSDM, CCPSDL with crc_out1, and crc_out2.

And further on-chip scope pro- tool for hardware verification. The design of the TRMA protocol for XOR implementation is integrated with ILA and ICON IP core. This aids in prototyping the architecture on the FPGA platform.

The inputs are pre-defined both in case of simulation and physical verification. The input pins like reset, enable, and crc_en are provided input via FPGA pins. The values of XC_Out1 and XC_Out2 are verified on the simulation result and the chip scope pro tool. This proves that both while performing simulation and hardware verification, the same values were attained.

The simulation outcomes and physically verified results of TRMA protocol using the MOD method are shown in Fig. 5 and Fig. 6, respectively. At first, the bit file is dumped on FPGA and further over chip scope pro tool for hardware verification. As observed from the simulation result in Fig. 5, when reset is pulled low, XC_Out1 and XC_Out2 use the first four bits from $CCPSD_M$ and $CCPSD_L$. Rest to fill the place of the remaining four bits; zero is appended. In the further cycle, the zeroes are replaced by the output generated from crc_out1 and crc_out2. Hence the process keeps continuing by considering the first four bits to be taken from $CCPSD_M$, $CCPSD_{L,}$ and the next four bits to be taken from the

It can be seen that the values obtained in the simulation result and the figure depicting the hardware verification are the same. In both cases, XC_Out1 and XC_Out2 hold up the value 5A3C and 1E5A, respectively. Here, only MSB bits are taken into consideration for verifying the output of Modified Pad-Gen TRMA using the MOD method on-chip scope pro-tool.

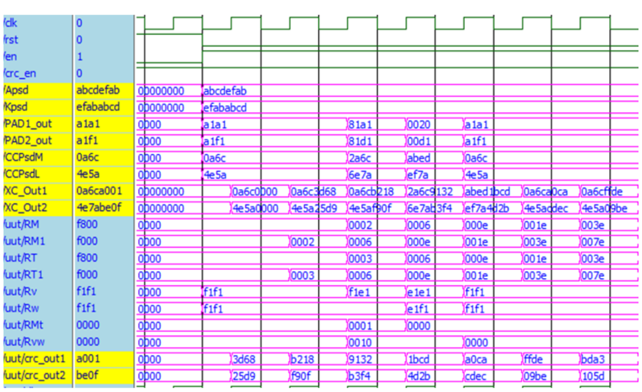

Fig. 3. Simulation Results of TRMA Protocol using XOR Method.

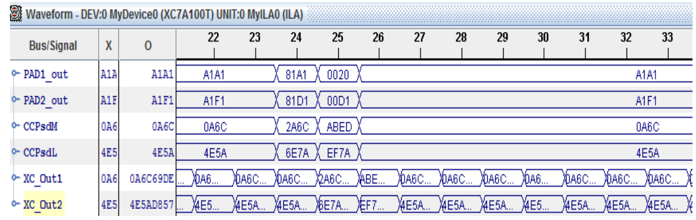

Fig. 4. Chip Scope Verified Results of Modified Pad-Gen Design using the XOR Method.

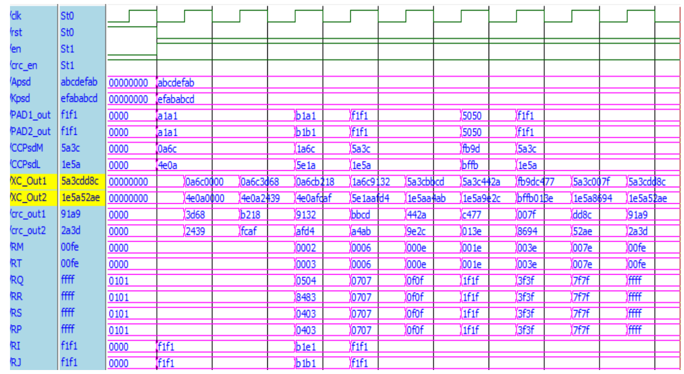

Fig. 5. Simulation Results of TRMA Protocol using MOD Method.

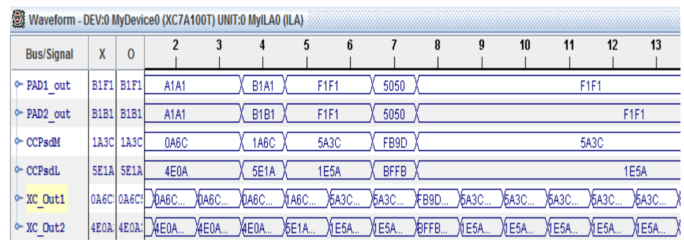

Fig. 6. Chip Scope Verified Results of Modified Pad-Gen Design using MOD Method.

VI. Performance Analysis

On comparing the performance of the performance parameter for both XOR and MOD schemes, it was observed that the XOR method yielded better outcomes. Metrics such as the Number of slice registers, LUT-FF pairs were found to be approximately the same in both ways.

In the case of the Number of Slice LUTs, a huge variation is seen. In the XOR method, it is found to be 172 operating at a maximum frequency of 262.158MHz. For the MOD method, the number increased to 227, operating at a reduced frequency value of 222.408 MHz. On the whole, with the observation made using all the performance metrics, it can be concluded that the XOR method exhibits better performance illustrated in Fig. 7.

Fig. 8 and 9 show the comparative analysis of power and Area parameters between the XOR and MOD methods, respectively. Fig. 8 highlighting the graph of total power versus operating frequency for XOR, and the method indicates that the XOR method consumes less power when compared to the MOD method. Hence this enables the XOR method to be a more suitable approach for the mutual authentication process of the tag and reader.

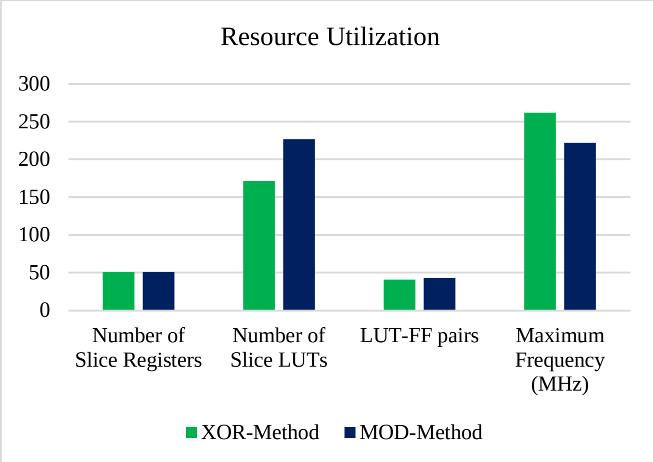

Fig. 7. Comparative Performance Analysis between XOR and MOD Method.

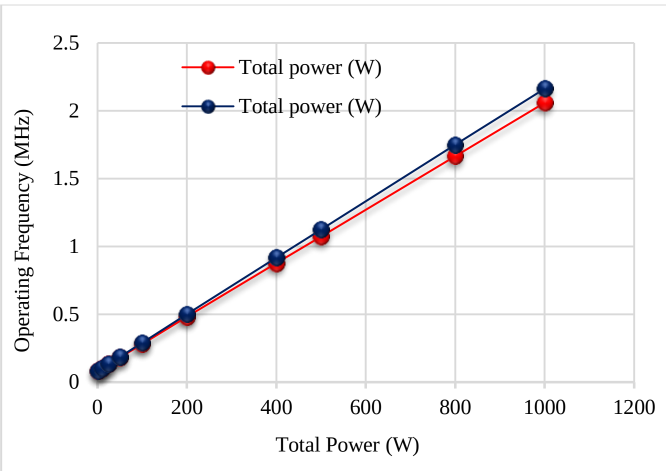

Fig. 8. Comparative Power Analysis between XOR and MOD Method.

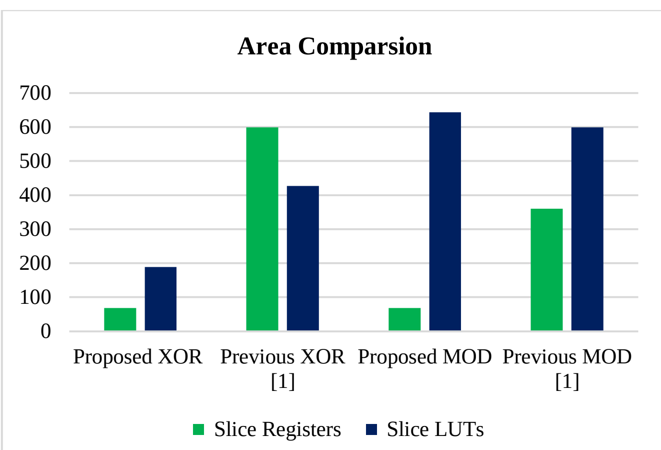

Fig. 9. Comparative Area Analysis between Proposed and Previous XOR and MOD Schemes.

The comparative analysis of the proposed and previous approach of XOR and MOD schemes are illustrated in Fig. 9. The graph foregrounds the count of slice registers and LUTs respective to both the methods. The number of slice registers and slice LUTs was found to be 68 and 189 for the proposed XOR operation of the mutual authentication protocol, respectively. That for the previous XOR approach was seen to be 599 and 427. For the proposed MOD operation, the number of slice registers and slice LUTs was 64 and 643, whereas in the case of the previous approach was found to be 360 and 599, respectively. Out of all the approaches investigated, it was seen that the proposed XOR method consumes the least power with an optimized area, utilizing fewer performance metrics and hence is an efficient way to establish mutual authentication among the tag and reader of the RFID system.

VII. Conclusion

To ensure the protection of the user's data privacy, a mutual authentication mechanism based on the modified Pad-Gen function is proposed in this paper. On comparing both the implementation methods, i.e., the XOR operation and MOD operation, it was seen that when mutual authentication is performed using XOR operation, enhanced performance metrics are yielded. The proposed design is capable of eliminating the security and privacy attacks concerns in the EPC-C1G2 authentication standard. Simulation outcomes were obtained on the cost-effective Artix-7 FPGAdevice XC7A100T-3CSG324. Physical verification of the resultant was confirmed on the Chipscope pro tool. CRC inclusion in the framework provides a security shield for the next level of operation in RFID tags. In future, incorporate the proposed work for real time NFC applications.

References

[1] Huang, Yu-Jung, Wei-Cheng Lin, and Hung-Lin Li. "Efficient implementation of RFID mutual authentication protocol." IEEE transactions on industrial electronics 59.12 (2012): 4784-4791.

[2] Korkmaz, Evsen, and Alp Ustundag. "Standards, security & privacy issues about radio frequency identification (RFID)." RFID Eurasia, 2007 1st Annual. IEEE, 2007.

[3] Chen, Chin-Ling, and Yong-Yuan Deng. "Conformation of EPC Class 1 Generation 2 standards RFID system with mutual authentication and privacy protection." Engineering Applications of Artificial Intelligence 22.8 (2009): 1284-1291.

[4] Peris-Lopez, Pedro, et al. "EMAP: An efficient mutual-authentication protocol for low-cost RFID tags."OTM Confederated International Conferences" On the Move to Meaningful Internet Systems". Springer, Berlin, Heidelberg, 2006.

[5] Yeh, Tzu-Chang, et al. "Securing rfid systems conforming to epc class 1 generation 2 standard." Expert Systems with Applications 37.12 (2010): 7678-7683.

[6] Kardas, Suleyman, et al. "Cryptanalysis of lightweight mutual authentication and ownership transfer for RFID systems." Lightweight Security & Privacy: Devices, Protocols and Applications (LightSec), 2011 Workshop on. IEEE, 2011.

[7] Lee, Young Sil, et al. "RFID mutual authentication protocol with unclonable RFID-tags." Mobile IT Convergence (ICMIC), 2011 International Conference on. IEEE, 2011.

[8] Yeh, Tzu-Chang, et al. "Securing rfid systems conforming to epc class 1 generation 2 standard." Expert Systems with Applications 37.12 (2010): 7678-7683.

[9] Chen, Yalin, Jue-Sam Chou, and Hung-Min Sun. "A novel mutual authentication scheme based on quadratic residues for RFID systems." Computer Networks 52.12 (2008): 2373-2380.

[10] Kulseng, Lars, et al. "Lightweight mutual authentication and ownership transfer for RFID systems." INFOCOM, 2010 Proceedings IEEE. IEEE, 2010.

[11] Rofougaran, Ahmadreza Reza. "Radio frequency identification (RFID) carrier and system." U.S. Patent Application No. 11/527,085.

[12] Mu, Haibing, and Zhenlong Zheng. "A dynamic key authentication protocol for RFID system." International Journal of Mobile Network Design and Innovation 7.3-4 (2017): 210-215.

[13] Sadaiyappan, T., K. K. Manoj, and S. A. Subhasakthe. "FPGA Implementation of Mutual Authentication Protocol Using Modular Arithmetic." (2014).

[14] Mohanavelu, S., and T. Ramya. "Secured Authentication Protocol for RFID System Using XOR Scheme."

[15] Beuchat, J-L. "Some modular adders and multipliers for field programmable gate arrays." Parallel and Distributed Processing Symposium, 2003. Proceedings. International. IEEE, 2003.

[16] Sarma, Sanjay E., Stephen A. Weis, and Daniel W. Engels. "RFID systems and security and privacy implications." International Workshop on Cryptographic Hardware and Embedded Systems. Springer, Berlin, Heidelberg, 2002.

[17] Yuan, Ching-Chien, et al. "The design of encoding architecture for UHF RFID applications." Microwave Conference, 2008. APMC 2008. Asia-Pacific. IEEE, 2008.

[18] Avoine, Gildas, and Philippe Oechslin. "A scalable and provably secure hash-based RFID protocol." Pervasive Computing and Communications Workshops, 2005. PerCom 2005 Workshops. Third IEEE International Conference on. IEEE, 2005.

[19] Kim, Do-Yun, et al. "Effects of reader-to-reader interference on the UHF RFID interrogation range." IEEE Transactions on Industrial Electronics 56.7 (2009): 2337-2346.

[20] Peris-Lopez, Pedro, et al. "LMAP: A real lightweight mutual authentication protocol for low-cost RFID tags." Proc. of 2nd Workshop on RFID Security. 2006.

[21] Garfinkel, Simson L., Ari Juels, and Ravikanth Pappu. "RFID privacy: An overview of problems and proposed solutions." IEEE Security & Privacy 3.3 (2005): 34-43.

[22] Bogdanov, Andrey, et al. "Hash functions and RFID tags: Mind the gap." International Workshop on Cryptographic Hardware and Embedded Systems. Springer, Berlin, Heidelberg, 2008.

[23] Want, Roy. "Enabling ubiquitous sensing with RFID." Computer 37.4 (2004): 84-86.

[24] Thiesse, Frédéric, et al. "Technology, standards, and real-world deployments of the EPC network." IEEE Internet Computing 13.2 (2009): 36-43.

[25] Eom, Jun-Bong, Soon-Bin Yim, and Tae-Jin Lee. "An efficient reader anticollision algorithm in dense RFID networks with mobile RFID readers." IEEE Transactions on industrial electronics 56.7 (2009): 2326-2336.

[26] Peris-Lopez, Pedro, et al. "RFID systems: A survey on security threats and proposed solutions." IFIP international conference on personal wireless communications. Springer, Berlin, Heidelberg, 2006.

[27] Sun, Hung-Min, and Wei-Chih Ting. "A Gen2-based RFID authentication protocol for security and privacy." IEEE Transactions on Mobile Computing 8.8 (2009): 1052-1062.

[28] Peris-Lopez, Pedro, Tong-Lee Lim, and Tieyan Li. "Providing stronger authentication at a low cost to RFID tags operating under the EPCglobal framework." Embedded and Ubiquitous Computing, 2008. EUC'08. IEEE/IFIP International Conference on. Vol. 2. IEEE, 2008.

[29] Konidala, Divyan M., and Kwangjo Kim. "RFID tag-reader mutual authentication scheme utilizing tag's access password." Auto-ID Labs White Paper WP-HARDWARE-033(2007).

[30] Han, Soonshin, HyungSoo Lim, and JangMyung Lee. "An efficient localization scheme for a differential-driving mobile robot based on RFID system." IEEE Transactions on Industrial Electronics 54.6 (2007): 3362-3369.

[31] Juels, Ari. "RFID security and privacy: A research survey." IEEE journal on selected areas in communications 24.2 (2006): 381-394.

[32] Lee, Jong-Wook, et al. "A Fully Integrated HF-Band Passive RFID Tag IC Using 0.18-$\mu\hbox {m} $ CMOS Technology for Low-Cost Security Applications." IEEE Transactions on Industrial Electronics 58.6 (2011): 2531-2540.

[33] Eisenbarth, Thomas, and Sandeep Kumar. "A survey of lightweight-cryptography implementations." IEEE Design & Test of Computers 24.6 (2007).

[34] Piramuthu, Selwyn. "Protocols for RFID tag/reader authentication." Decision Support Systems 43.3 (2007): 897-914.

[35] Anusha, R. "Qualitative Assessment on Effectiveness of Security Approaches towards safeguarding NFC Devices & Services." International Journal of Electrical and Computer Engineering 8, no. 2 (2018): 1214.

[36] Anusha, R., and V. Veena Devi Shastrimath. "TRMA: An Efficient Approach for Mutual Authentication of RFID Wireless Systems." In Computer Science On-line Conference, pp. 290-299. Springer, Cham, 2018.

[37] Anusha, R., and V. Veena Devi Shastrimath. "LCBC-XTEA: High Throughput Lightweight Cryptographic Block Cipher Model for Low-Cost RFID Systems." In Computer Science On-line Conference, pp. 185-196. Springer, Cham, 2019.

Face Recognition on Low-Resolution Image using Multi Resolution Convolution Neural Network and Antialiasing Method

Mario Imandito[1], Suharjito[2]
Computer Science Department, BINUS Graduate Program-Master of Computer Science
Bina Nusantara University, Jakarta, Indonesia 11480

***Abstract*—Video surveillance applications usually take pictures of faces that have a low resolution (12x12) due to distance, lighting and shooting angles Most of face recognition algorithm have the poor performance accuracy and poor identify face on low resolution. Based on the problem, identifying the face of the query in low resolution, based on high resolution (64x64) proves to be a huge challenge. The aim of this research is to develop a new model for face recognition of low-resolution image in order to increase the accuracy of recognition. A Multi-Resolution Convolutional Neural Network (MRCNN) is proposed to address the problem. First, Antialiasing is used in preprocessing phase, then use MRCNN to extract the feature of the image. LWF (Labeled Face in Wild) will be used to evaluate the model. The result of this study is increasing the accuracy of face recognition on low-resolution image compared to the previous MRCNN model.**

Keywords—Face recognition; low resolution; convolutional neural network; antialiasing

I. Introduction

Security in one of the most concern problem in almost every application. Face recognition is one of many samples of security method. The existing face recognition system such as Principal Component Analysis (PCA) [1], Linear Discriminant Analysis (LDA) [2], and the most popular Super Resolution (SR) [3] have achieved satisfactory performance, in case that the face images that collected are in high resolution and are well aligned. But in case of video surveillance system, as the face target are far away from the cameras, the captured facial images are usually in low resolution (32x32). This affects the accuracy of facial recognition system. This issue of face recognition is known as low-resolution face recognition (LRFR). Besides, video surveillance system usually used to identify someone in a secure area such as workspace, data center etc. To identify person in low resolution based on high resolution image proves to be a huge challenge.

Because of that, some research in face recognition for low resolution image has been done. In 2014 [4] proposed a fusion method where they take several video frames as an input and fuse it into one image in order to derive rich feature. At the same year, [5] proposed Multi-resolution Feature Fusion (MFF). At their research, they employ a Gabor – feature hallucination method to estimate the higher resolution Gabor features from low resolution (LR) from the LR Gabor Features followed by feature extraction. The result of their research is outperforming the previous research on the ORL and FERET databases. Still at 2014, [6]proposed Coupled Basis & Distance (CBD) method. They are matching biometric data from disparate domains. Min-Chun Yang in 2015 [7] joint face recognition and hallucination algorithm based on sparse representation. Instead performing recognition as standard approaches, their model can learn a person-specific face hallucination with recognition guarantees. Where the result of the experiment outperformed the previous method. In 2016 [8] proposed a method using Low-Resolution Convolutional Neural Network (CNN) by proposing an appropriate network architecture. The input is from low-resolution video face recognition with a manifold-based track comparison strategy. In the next year in 2017 [9] proposed a multi-resolution convolutional neural network (MRCNN). This model is proposed in order to study the consistent feature representation from high-resolution and low-resolution face images.

The main problem of this research is a low-resolution image as the input process. The state-of-the-art method [9] works on feature extraction phase, and Bicubic as their preprocessing phase. Their experiment result showed great value in recognition rate. But as mentioned before, the state-of-the-art use Bicubic where Bicubic is an old method and the output is not good enough. There is better method in preprocessing phase. This study replaces Bicubic as their preprocessing phase with hallucination as proposed by [10] hopefully can increase the face recognition performance. This method is proved in their research have better result than Bicubic. And with the better input, the accuracy of face recognition will increase.

In this paper, MRCNN [9] method is proposed to achieve better accuracy of face recognition of low-resolution image. Anti-alias [11] is used to generate a high resolution (HR) image from low resolution (LR) probe and MRCNN is carefully designed to learn the consistent feature representations of both the gallery images and the generated ones. This paper uses Anti-alias, Anti-alias produce better image rather than Bicubic that is used in state of the art [9].

The remainder of this paper is organized as follows. In Section II, related work in face recognition on low-resolution image. Section III, Research method will be explained that was used in this study. Section IV will explain the result of the study. Section V is Conclusion and future works.

II. Related Works

As we know that security is so much important in application development. Because if there is no security, the data can be harmed. Because this motivation, may research try to build a strong security method. And one of security system is face recognition. In last decade of research, face recognition has been solved. But as far as technology goes, there are comes a new challenge in face recognition. One of them is face recognition on low resolution image. This kind of problem make researcher challenged to solve the problem.

In 2014 [4] make a research in surveillance system. They see that the captured faces are often very small resolution. In their research for pre-processing phase, they use Histogram Equalization for reducing illumination variation. After that, the images will be fused using curvelet feature. In order to enhance face feature, they proposed a super-resolution based on face recognition algorithm. They use 2 methods here. First, they use of sparsity signal representation to train low-resolution image. The second method is Eigen-subspace feature of human face. Both of high-resolution face image are then combined into one image with pixel by pixel decision making. After combining all blocks together, the final enhanced face image will be used for recognition.

In the same year [5] the do the research on face recognition on low resolution as well. As same as the previous research above, they focus on feature fusion method. They proposed Multi-resolution Feature Fusion (MFF). The research starts with Gabor Wavelet for extracting local features following by Canonical Correlation Analysis (CCA) for measuring the linear relationship between two multidimensional variables, Generalized Canonical Analysis (GCCA) and Generalized Canonical Projective Vector (GCPV). After that MFF method for face recognition presented. Different with above [6] they focus on the problem of comparing a low-resolution image with the high-resolution one. The previous coupled mapping methods do not fully exploit the high-resolution information, or they do not simultaneously use samples from both domains during training. Because of that, they proposed Coupled Basis & Distance (CBD) that learns coupled distance metrics. The method learns coupled distance metrics in two steps. In addition, they propose to jointly learn wo semi-coupled bases that yield optimal representation. In particular, the high-resolution images are used to learn a basis and distance that result in increased class-separation. The low-resolution images are used to learn a basis and distance metric that map to low-resolution data to their class-discriminated high-resolution pairs. And at the end, the two-distance metrics are refined to simultaneously enhance the class separation of both high-resolution class-discriminant and low-resolution projected images.

In 2016 [8] as same as [4], they do their research on surveillance system. They proposed Convolutional Neural Network (CNN) for the low-resolution video face recognition. They transfer the success of CNN on high-resolution image into low-resolution image by proposing an appropriate network architecture. Their focus is on efficiency of track matching strategy. Because related literature employs an effective but inefficient many-to-many comparison. Instead, they reduce the necessary comparisons by defining a fixed number of local patches in the face descriptor set and show that low numbers of patches are sufficient for superior comparison result.

Next research in 2017 [12] proposed a cluster-based regularized simultaneous discriminant analysis (C-RSDA) based on SDA. Next year in 2018 [13] proposed a method called low-rank representation and locality-constrained regression (LLRLCR) to learn occlusion-robust representation features. Last research found in 2019 proposed by [3] they called SSR2 (Sparse Signal Recovery) for single-image super-resolution on faces with extreme low resolution.

Based on the literature review result on Table I, the goal of the research is to increase the recognition rate. Our research focus is on CNN method and the model in [9] is the state-of-the-art of our research. We found that the state-of-the-art use Bicubic for the preprocessing phase. Where there is better method that has better result than Bicubic. And from literature review, we will use Eigen transformation Hallucination that proposed by [10] to replace Bicubic. Another research from [7] that uses Hallucination also shows better result than Bicubic.

TABLE. I. Related Work Comparison

Author	Method	Dataset	Result
[10]	Eigen transformation based on Hallucination method.	XM2VTS	Increasing recognition rate
[4]	Fusion method from video surveillance system.	FRGC, AR, ScFace and Curtin Face.	Increasing recognition rate
[5]	Multi-resolution Feature Fusion (MFF)	ORL and FERET	Increasing recognition rate
[6]	Coupled Basis & Distance (CBD)	ScFace and Multi-PIE (Pose, Illumination, and Expression)	Increasing recognition rate
[7]	Joint method Hallucination and Face recognition	CMU MULTI-PIE and FRGC	Increasing recognition rate
[8]	Low-Resolution Convolutional Neural Network (CNN)	YTF	Increasing recognition accuracy
[9]	multi-resolution convolutional neural network (MRCNN)	CMU-PIE and Extended Yale B	Increasing recognition rate
[12]	Cluster-based regularized simultaneous discriminant analysis (C-RSDA)	Feret, LFW, SCFace	Increasing recognition rate
[13]	Low-rank representation and locality-constrained regression (LLRLCR)	AR face and Extended Yale B	Increasing recognition rate
[3]	SSR2 (Sparse Signal Recovery)	MPIE	Increasing recognition rate

Multi-resolution Convolutional Neural Network (MRCNN) was proposed by [9] to study the consistent feature representation from high resolution and low-resolution face images. First, the corresponding labelled multi-resolution face images are utilized to train the MRCNN model. After that process, the trained model is used as the feature extractor in order to obtain features for the targets in the gallery and query images respectively. Finally, the nearest neighbor is applied as the classifier for the purpose of final identification. The preprocessing phase of this method using Bicubic interpolation to ensure that the network inputs are of similar size. For the feature extraction, they use CNN. The input or MRCNN architecture is the mixed gray facial images from the gallery images and the generated gallery images. After the features are obtained, the cosine distance is used to measure the similarity between the probe feature and the gallery feature.

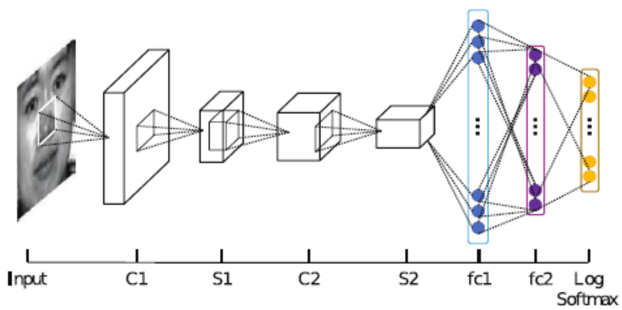

Fig. 1. The Architecture of MRCNN [9].

Fig. 1 shows the architecture of MRCNN. The mixed gray facial image from gallery image and the generated high-resolution image are the input for the network of MRCNN above. For extract local information they use two convolutional layers following by max-pooling layers. For the activation function, they use ReLu function. And after the convolutional operation, they obtained 64 vectorized feature maps. A fc1 or Fully Connected layer is used to fuse the global information and the output of it are used to the features. Finally, from the fig x, the combination between fc2 and the Log SoftMax layer is used as classifier in order to compute the probability that the input belongs to a certain class.

III. Research Methods

A. Research Steps

The research steps to build a new model of face recognition method by Multi Resolution CNN and Anti-alias are: model development, model implementation such as training and testing model, and analysis the result. The flow this study is shown in Fig. 2. The research begins with define research background and the scope of the result. Literature study is to know more about face recognition on low resolution image and the state of the art for this research. Besides that, literature review can be used for guiding of the methods to be used.

The second step is data collection. In this study the data of face was collected from internet. LWF (Labeled Face in Wild) was used to develop the model of low-resolution face recognition. Based on literature review, the research can define what model will be made. Third step is model implementation including training and testing model. The fourth step is analysis the result, what the benefits and limitation compared with the previous research. And the final step is conclusion.

This research was based on [9] where we replace Bicubic as their preprocessing phase with Eigen transformation-based hallucination. In Fig. 3 shows the proposed model that was used in this study. After preprocessing phase using the mentioned method above, the feature extraction phase using Multi Resolution Convolutional Neural Network and the output will be used as classifier to compute probability that the input belongs to a certain class.

B. Proposed Model

The First step of this model is data preparation, HR images with 250x250 are resize into 32x32 and down sampled into LR images 12x12. After the LR images are created, then upscaled using Anti-alias and called generated HR or HR'. The LR image and HR' images furthermore will be blended into one image. And the blended images will be used as train and validate the CNN model.

In this model, the method of feature extraction used CNN. The inputs are mixed gray scaled face image between HR' image and HR image. The input size is 1x32x32. Two convolutional layers, followed by Max-pooling layers, are used to extract local information. The kernel size is 5×5. ReLU function is used as the activation function. After the convolutional operation, 64 feature maps of size 5×5 are obtained. Those maps are vectorized and a fully connected layer (fc1) is used to fuse the global information to form a global feature and the outputs of the fc1 layer are taken as the features. Finally, the combination of fc2 layer and the Log SoftMax layer is used as the classifier to compute the probability that the input belongs to a certain class.

C. Evaluation Methods

LWF (Labeled Face in Wild) [14] contains 5.749 persons and 13.223 images. Each person has variety number of images. This study will run 2 training model. The first one is training model for classification into 2 classes (top 2 person with the most images which are George W Bush with 530 images and Collin Powel with 236 images) and the second one is training model for classification into 143 classes (person with images more than 10 images). This study will use 70%, 20%, and 10% images for training data, validation data, and testing data respectively for each person. For evaluating the proposed model, this study used accuracy and execution time. The result of evaluation will be compared with the state of the art of this model [9].

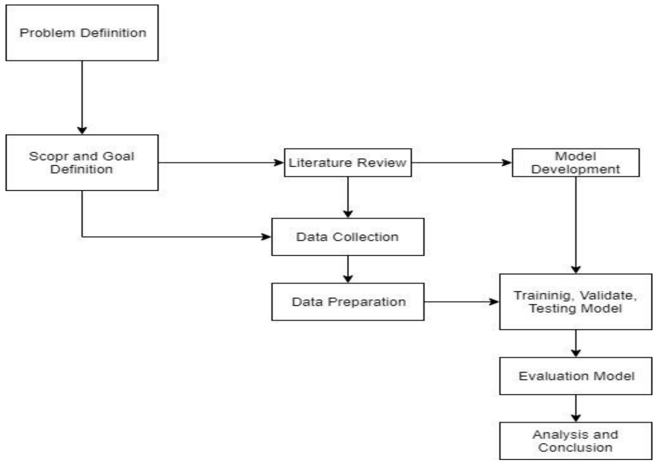

Fig. 2. Research Steps.

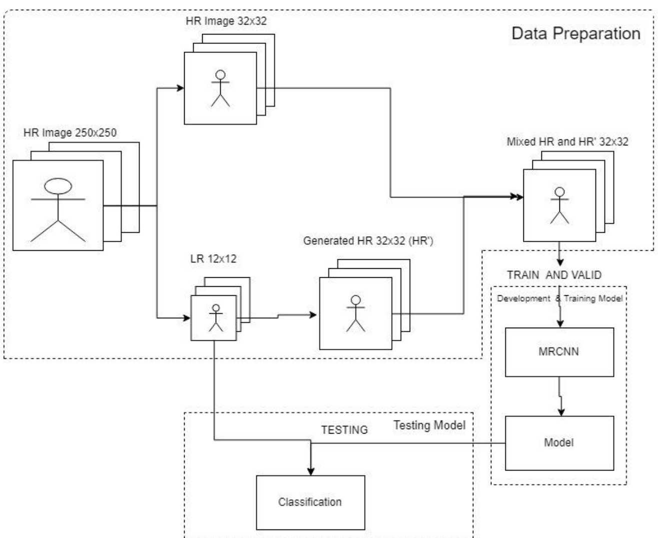

Fig. 3. Proposed Model

IV. Results and Discussion

Fig. 4 shows data pre-processing using Antialiasing method.

Based on Fig. 4, it can be seen that the input model are the HR image using 250x250 size. These images were resize into 32x32 as HR Image. The input images were down sampling into LR image with size 12x12. After that the LR image will be built using the antialiasing method to be generated HR with a size of 32x32. Then the resized HR image from input and generated HR is combined as an MRCNN modeling input in the training and testing process.

Fig. 4 shows example of data pre-processing using Bicubic that has been proposed in [9]. This study used 648 face images for 2 classes. The evaluation result for 2 classes faces recognition were shown in Table II.

Based on Table II, the accuracy of MRCNN model using Antialiasing method for pre-processing was greater than MRCNN model that using Bicubic interpolation method. Bicubic interpolation method acquired 61% in accuracy on low resolution face recognition. While Antialiasing acquired 70% in accuracy of on low resolution face recognition. The differences of this accuracy result were 15%, it indicates that the performance of the proposed method is outperform than the state-of-the-art model [9].

Table III shows the execution time comparison between the proposed model and the state of the art. The execution time was count in generating image from LR into generated HR.

As shown in Table III, Bicubic took less time to generated HR image from LR image. Bicubic interpolation method needed 2,199 second in generating HR image from LR. Antialiasing method used 3,434 for generating HR image from LR image. It means that Bicubic interpolation method is faster than Antialiasing method that used an Eigen transformation based on hallucination method.

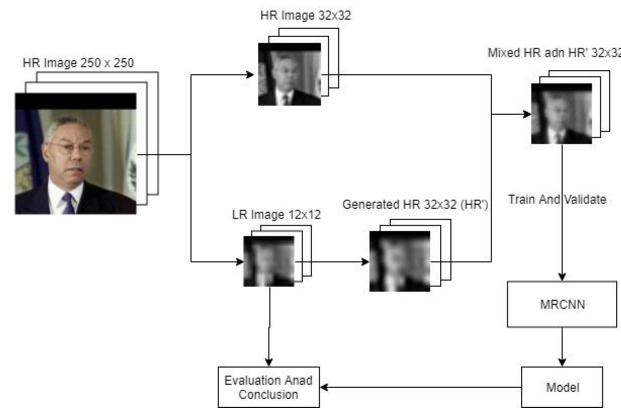

Fig. 4. Modelling step using Anti-alias for 2 Classes image

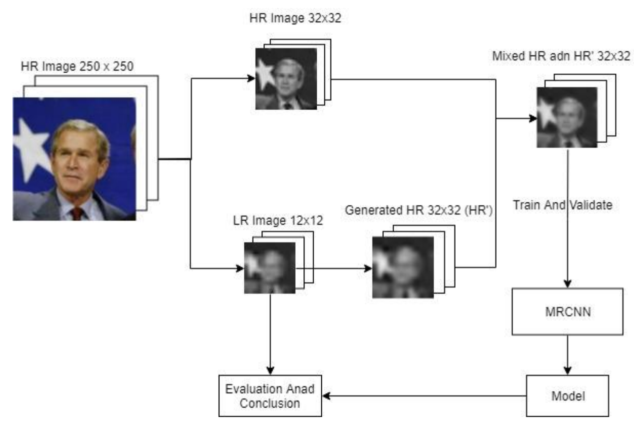

Fig. 5. Modelling step using Bicubic for 2 Classes image

TABLE. II. Comparation of Accuracy Rate

Method	Accuracy Rate (%)
Bicubic	61
Antialiasing	**70**

TABLE. III. Comparation of Execution Time

Method	Time (sec)
Bicubic	2.199
Antialiasing	3.434

V. Conclusion and Future Works

This paper proposes a new Multi Resolution Convolutional Neural Network model with Antialiasing techniques as a pre-processing method. The results of the comparison of this pre-processing method with the Bicubic method shows that the antialiasing pre-processing method produces better accuracy than the Bicubic pre-processing method. The proposed model can increase the accuracy by 15% in face recognition using the multi-resolution convolutional Neural Network method. However, the antialiasing pre-processing method uses a longer processing time compared to the Bicubic pre-processing method. Therefore, for further research will be directed to obtain a hybrid pre-processing method that can adapt to facial image characteristics that will be recognized based on differences in resolution and lighting.

Acknowledgment

This research was supported by Research Grant No. 225/SP2H/LT/DRPM/2019 from Ministry of Research Technology and Higher Education of Republic of Indonesia.

References

[1] S. K. Dandpat and S. Meher, "Performance improvement for face recognition using PCA and two-dimensional PCA," in International Conference on Computer Communication and Informatics, 2013.

[2] M. Kan, S. Shan, H. Zhang, S. Lao and X. Chen, "Multi-view discriminant analysis," IEEE transactions on pattern analysis and machine intelligence, vol. 38, pp. 188--194, 2015.

[3] R. Abiantun, F. Juefei-Xu, U. Prabhu and M. Savvides, "SSR2: Sparse Signal Recovery for Single-Image Super-Resolution on Faces with Extreme Low Resolutions.," Pattern Recognition., vol. 90, pp. 308-324., 2019.

[4] X. Xu, W. Q. Liu and L. Li, "Low resolution face recognition in surveillance systems.," Journal of Computer and Communications, vol. 2, pp. 70-77, 2014.

[5] H. K. Pong and K. M. Lam, "Multi-resolution feature fusion for face recognition.," Pattern Recognition, vol. 47(2), pp. 556-567, 2014.

[6] P. Moutafis and I. A. Kakadiaris, "Semi-coupled basis and distance metric learning for cross-domain matching: Application to low-resolution face recognition.," In Biometrics (IJCB), 2014 IEEE International Joint Conference on, pp. (pp. 1-8), 2014.

[7] M. C. Yang, C. P. Wei, Y. R. Yeh and Y. C. F. Wang, "Recognition at a long distance: Very low resolution face recognition and hallucination.," In Biometrics (ICB), 2015 International Conference on, pp. (pp. 237-242), 2015, May.

[8] C. Herrmann, D. Willersinn and J. Beyerer, "Low-resolution convolutional neural networks for video face recognition..," In Advanced Video and Signal Based Surveillance (AVSS), 2016 13th IEEE International Conference on, pp. (pp. 221-227), 2016.

[9] C. Ding, T. Bao, S. Karmoshi and M. Zhu, "Low-resolution face recognition via convolutional neural network.," In Communication Software and Networks (ICCSN), 2017 IEEE 9th International Conference on, pp. (pp. 1157-1161), 2017, May.

[10] X. Wang and X. Tang, "Face hallucination and recognition.," In International Conference on Audio-and Video-Based Biometric Person Authentication, pp. pp. 486-494, 2003, June.

[11] B. Dai, R. Zhuo, S. Yin, M. Lv, R. Hong, Q. Wang, and X. Wang, "Ultrafast imaging with anti-aliasing based on optical time-division multiplexing," Optics letters, vol. 41, pp. 882--885, 2016.

[12] Y. Chu, T. Ahmad, G. Bebis and L. Zhao, "Low-resolution face recognition with single sample per person.," Signal Processing, vol. 141, pp. 144-157, 2017.

[13] G. Gao, Z. Hu, P. Huang, M. Yang, Q. Zhou, S. Wu and D. Yue, "Robust low-resolution face recognition via low-rank representation and locality-constrained regression.," Computers & Electrical Engineering, vol. 70, pp. 968-977., 2018.

[14] G. B. Huang, V. Jain and E. Learned-Miller, "Unsupervised Joint Alignment of Complex Images," in In 2007 IEEE 11th International Conference on Computer Vision , 2007.

Research Trends in Surveillance through Sousveillance

Siraj Munir[1]
Department of Computer Science
Mohammad Ali Jinnah University
Karachi, Pakistan

Syed Imran Jami[2]
Faulty of Computer Science
Mohammad Ali Jinnah University
Karachi, Pakistan

***Abstract*—Collective Intelligence is an immense research area that has wide application to cross-disciplines, like social, legal, and computation. Research trends in Surveillance find its place in the work of this area generating curated data set helpful in answering complex queries. Sousveillance is a recent term coined by researchers and had been discussed in different literatures. However our findings suggest that integration of Surviellance through Sousviellance data set has not been given much importance in collective fashion. In this literature we introduced an effective model of collective intelligence by integrating surveillance through sousviellance in a campus environment. For testbed networking devices are used to generate sousvillance data to provide validation, and cleaning to enable reliability and trust in the target object.**

Keywords—Semantics; querying; profiling; IoT; surveillance; sousveillance

I. Introduction

Recent advancement in technology has given rise to several practical implications of surveillance and sousveillance. Sousveillance is a French origin word sous means below and veiller means watch combinational it means watching from below. Sousviellance Term was coined by Steve Mann et al. in [1, 2], that can be described as inverse of surveillance, surveillance on-demand and activity of particular entity for example person, officer, politician etc. using wearable computing. Analytics for Surveillance is still an active area in research community as researchers recently proposed some outstanding techniques for surveillance as shown in [3, 4]. Several use cases are identified for integration of surveillance with sousveillance, for better results in terms of accuracy in answering complex queries. Consider a scenario of police officer's behavior with citizens. It has been noticed in several incidents that on personal biasness, officer's behavior was non ethical and main concern is that these type of events were also surveilled. In some events no action was taken or either surveillance clip was not present that is somehow deleted. This raises a huge question mark on surveillance systems, and therefore requires the support of sousveillance. Surveillance has already proven its usage by providing potential solutions in different areas including computer science, and social sciences. Integrated approach of Surveillance with Sousveillance would help in resolving different queries that are complex to solve. A detailed taxonomy of veillance is presented in Fig. 1 which clearly differentiates types of veillance and their sub-categories. There are eleven different categories of veillance as reported in [1]. Each category of veillance has its role like Dataveillance is used for doing veillance over online activities, while Counterveillance is using veillance for recording own actions. Beinveillance deals with the usage of veillance for benefits like presence of sence and turning on lights using sensors. Malveillance is veillance for malicious intent and Coveillance is peer-to-peer veillance like veillance of neighbors, family members etc. Other areas include Kineveillance and Stativeillance that are veillance of mobile and stationary objects like electromagnetic waves etc. Autoveillance is veillance of quantified self/ body hacking. Uberveillance is surveillance which can be embedded in human body using state-of-the-art IoT based wearable computing. Some major problems with surveillance are:

1) Surveillance is a type of veillance about/ around a fix point.

2) What if surveillance system was on update while certain event happened.

3) What if any high profile person uses his/ her resources and delete surveillance data from system.

4) What if server was down when X terrorism event happened.

These are some of the major queries that require resolution using intelligent query engine. A potential solution to these queries is the integration of surveillance systems with sousveillance. The ongoing digital age where technology and computing are ubiquitous, the tracking of generated data through viellance will eventually help in solving many hurdles of our daily life. The major contribution of this work is the identification of problem with the discussion on research trends in ongoing work and proposed an integrated approach of Sousviellance with surveillance in the campus setting. Next section will discuss research trends in surveillance through sousveillance.

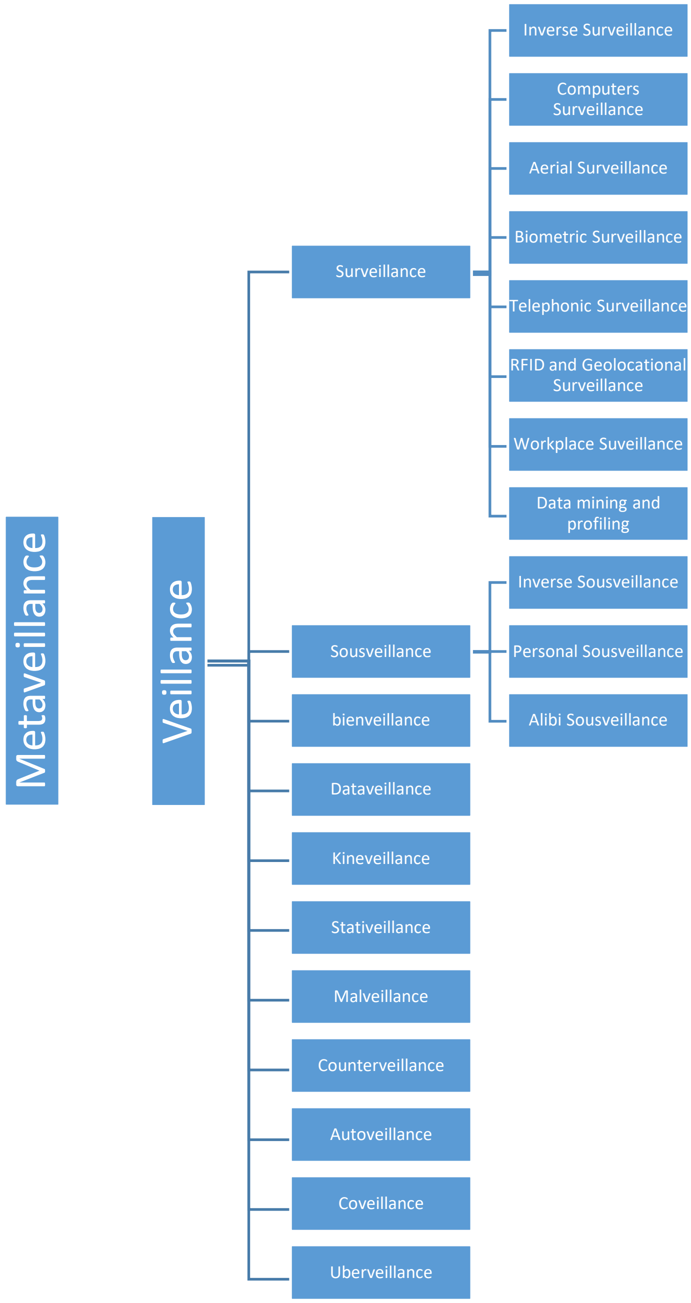

Fig. 1. Taxonomy of Veillance [2].

II. Research Trends in Surveillance and Sousveillance

Surveillance is a French originated word sur means over and veiller means watch collectively it means watching from above or about any fixed point. Furthermore, it can also be described as monitoring of individual/ individuals through different available sources that is social media, physical cameras etc. Moreover, there are two types of surveillance: Preconstructive surveillance and Reconstructive surveillance. Preconstructive surveillance is about to veillance any individual or group of individuals in a closed room under CCTV (Closed Circuit Television) while Reconstructive Surveillance is about veillancing using different law and technological tools including fingerprinting, phone tapping, internet tracking etc. Several ways are available for surveillance including telephones, physical cameras, social network analysis, biometric surveillance, aerial surveillance etc. Recent research trends show wide range of problems to be solved in surveillance through computer vision [3, 4, 5, 7, 8, and 10]. Research in surveillance through computer vision deals with the analysis on huge bulk of collection of images and videos and provision of solutions in the identification and tracking of target object. In [3] authors have provided insights of video surveillance, with four million CCTV cameras by BSIA (British Security Industry Association) who deployed across the Britain states alone. A novel technique for hierarchical architecture was proposed as FVSA (Fused Video

Surveillance Architecture) which can provide multi-layer hardware abstraction which can effectively use with Internet of Things (IOT) based systems. The work in [4] discusses detection of gender using surveillance images. This is applicable for cold climate where detection and surveillance of gender based approach can help to law enforcement departments to catch guys with malicious intent. Proposed technique includes RCNN (Region-based Convolutional Network) and transfer learning. In [5], the authors discussed behavior of employee under organizational surveillance through computer-mediated technique. They surveyed full time adult employees and tried to observe organizational trust, privacy, commitment to organization etc. This study also shows surveillance application in social life style and workplace life. A study has been carried out in [11] that tried to determine how can 'Surveillance of Things' can be connected to IOT. Authors used Sigfox, a wireless network for IoT based devices, with assumption that the gathered surveillance data is incorrect and thus can have impact on people. Moreover, authors also established a linkage for surveillance of people to surveillance of things. The literature in [12] puts lights on usage of Big Data for surveillance specifically for digital citizenship and contemporary democracy. Authors proposed critical analysis of existing research works alongwith the suggestion on the working of ambivalent digital citizen mechanism that should be constructed to target every citizen. In [13], the authors proposed usage of RFID for object detection which can be used for surveillance purpose. In [14], authors proposed a new open source database for video surveillance, tracking, recognition and re-identification. Database contains collection of high resolution images which can be used for several task like evaluation of algorithms. The work in [15] reviews classic and recent approaches for object detection in dynamic environment. Authors also discussed different areas where object detection can help to resolve critical issues. Authors in [16] briefs usage of social media data surveillance for different aspects including behavioral analysis, medical insights/ news etc. In [6] authors briefed usage of video surveillance of moving objects and it's challenges and in response to these challenges they proposed different techniques to resolve the highlighted problem. Author in [17] highlighted usage of surveillance in computer vision to assist drivers on safety critical event. Furthermore, they evaluated proposed system on challenging dataset. Author in [7] proposes a bridge between classical object detection techniques. As literature describes in real world we have huge collection of surveillance videos. Detection of dynamic objects from these long-term video is a complex task. In this literature authors proposed a framework using Bag-of-word and classification approach which can resolve the aforementioned problem effectively with the highest accuracy of 92% on LOST (Longterm Observation of Scenes (with Tracks)) dataset. Author in [8] explored cost effective and optimized technique for dynamic object detection. Author in [9] puts light on current and future status of surveillance. Authors discussed different techniques for object detection, image enhancement, object tracking, object recognition etc. Further, authors stressed on usage of latest techniques including fog, cloud, edge computing and DL. Literature summed up on expected future of surveillance using AR (Augmented Reality). [10] highlighted multi-cue object detection in dynamic environment and proposed a novel technique under different modularity's with state-of-art results. Further, they claimed that many literatures discussed multi-cue pros but only some literatures brief its modularity: singular or plural. [18] proposed an effective approach for crowd segmentation and classification. Literature introduced intelligent video surveillance for crowd using four metrics: crowd density, crowd saliency, crowd segmentation and statistical analysis. Steve Mann in [2, 17] carried various forms of veillance including surveillance (viewing from top from a fix point), sousveillance (viewing from below through mobile locations pervasively or non-pervasively), autoveillance (extreme level of surveillance is autoveillance), kineveillance (sensing through moving frame-of-reference), dataveillance (continuous tracking user digital data and personal data through social media, online transactions etc.), coveillance (simply peer-to-peer surveillance), countersurveillance (measure or practices taken to counter surveillance), malveillance (dangerous type of surveillance), stativeillance (surveillance of static frame-of-reference), bienveillance (machine sensing our presence and respond accordingly), uberveillance (surveillance using embedded devices). The discussions on these veillances have been made in the domains of social sciences and its related perspective but their algorithmic implementation using pervasive approaches have not explored yet. In this work we evaluated research literatures in the area of Sousviellance and we have found no progress since last three years surveillance. Steve Mann worked on Sousveillance [1] starting with a neck worn camera in 1997, however, in 2003 Microsoft introduced a slightly modified version of neck worn camera, while in 2006 Mann again released another modified version and finally in 2013 Memoto released version of neck worn camera device. This leads to the development of glass based devices including Meta, Google Glass, EyeTap, etc. Next section will discuss proposed methodology along with the results.

III. Proposed Methodology and Results

In this section we have proposed an effective model for Citizen Profiling using surveillance and sousveillance. Citizen profiling can also be done through surveillance but as discussed in previous sections there can be various limitations to surveillance based system, which can be solved through the integration of surveillance with sousveillance. The work in [19] briefly discussed the issue of 'sousviellance less' surveillance systems and considered such systems as a half-truth: "if buildings can wear cameras why humans cannot" [19].

In this work we have proposed a model which can be adopted to use collective benefits of both surveillance and sousveillance which is still an open research question to solve issues related to Collective Intelligence. In Fig. 2, we proposed a model for citizen profiling. Proposed model consist of five steps: (i) data acquisition (using surveillance and sousveillance), (ii) storage, (iii) data representation, (iv) semantic engine, and (v) querying.

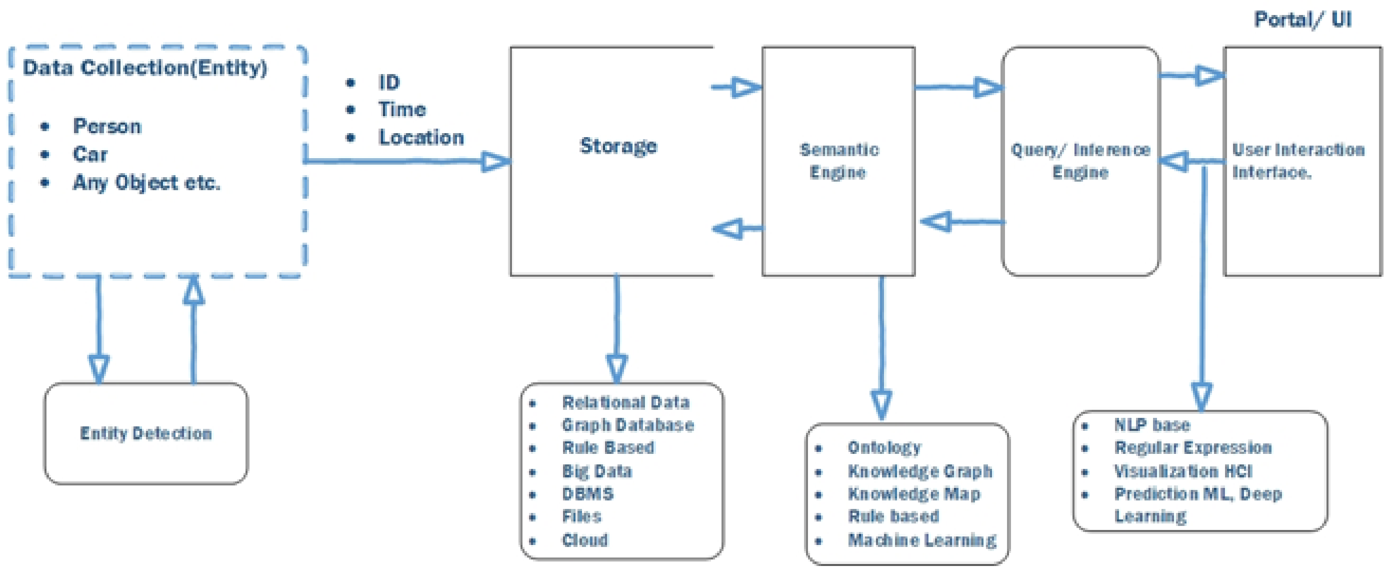

Fig. 2. Model for Citizen Profiling.

In Data acquisition the curated data is collected from environment using sensors and cameras that are dumped into storage as raw data. Storage can be of any variant of available services i.e. Relational database, graphs, NoSQL, etc. whose usage is dependent on the scenario related to the magnitude of organization from small scale to large scale to social media. In campus setting we employed NoSQL for fast processing where it does not require structure. To maintain semantics among entities, Semantic engine is implemented using ontology and Knowledge Graph to employ temporal data from sousviellance devices. Other potential soultions include Rule based or Machine Learning approaches to learn rules and infer them on the creation of new entities. Fourth and fifth phases deal with the querying engine and user interface, that may use NLP, Regular Expression, Machine Learning / Deep learning to search out object data in storage and display profile data to end-user. For proof of concept we made a dataset of network traces having three columns namely (Timestamp having time and date, MAC address represents each individual device and switch id represents location). We randomly generated data for aforementioned columns. Furthermore, we collected data from NMS (Network Management System) through smartwatch where smartwatch is supposed to be used as a sousveillance device. Here Fig. 3 shows how our data looks like in general format.

Some sample semantic queries are as follows:

1) Where was XYZ person at time X.

2) At what timestamp X person visited library.

3) Through which switch did Person X having MAC XX was connected.

4) Who was connected to switch X at XYZ time?

The result of sample query 4 is shown in Fig. 4.

	TimeStamp	MAC_add	Switch_id
0	2018-05-10 5:19:26	10:AA:BE:CC:CE:26	3
1	2018-05-30 16:2:51	12:BA:CD:RW:01:89	7
2	2018-04-19 8:12:33	SW:NI:TE:MO:ET:98	7
3	2018-05-22 0:16:36	OL:JQ:OK:QR:UL:16	6
4	2018-05-16 22:59:8	NA:HF:LU:TF:RX:98	8

Fig. 3. Surveillance and Sousveillance Data.

```
         TimeStamp             MAC_add  Switch_id
2018-05-30 16:2:51  12:BA:CD:RW:01:89          7
```

Fig. 4. Query Result.

Surveillance devices are used in detection of objects while Sousveillance data is gathered from network monitoring devices. The network monitoring devices help in verifying, validating and cleaning the object detection data from the surveillance fields. Result in Fig. 4 is showing that the object having network device with given MAC address is currently located at the given location (where switch number 7 is placed) at the given time and date.

IV. Conclusion

In this paper we proposed a model for citizen profiling which uses surveillance and sousveillance for data aquisition. We also reviewed some recent research work for surveillance and sousveillance. Previous sections highlighted key problems and solutions of surveillance and sousveillance with the discussion on detailed taxonomy for veillance. Our results show that integration of sousveillance with surveillance system will give extended data that will increase reliability and trust.

Several extensions are planned in next phase. The increasing amount of data in terms of velocity and variability will require big data based solutions in analytics. Furthermore, automated learning algorithms based on Machine Learning can be devised on the basis of network stream. This work did not provide any solution for interface in translating queried result to natural language using NLP which is another area of research.

REFERENCES

[1] S. Mann, J. Nolan, and B. Wellman, "Sousveillance : Inventing and Using Wearable Computing Devices for Data Collection in Surveillance Environments," 2002.

[2] S. Mann, "Surveillance (Oversight), Sousveillance (Undersight), and Metaveillance (Seeing Sight Itself)," in 2016 IEEE Conference on Computer Vision and Pattern Recognition Workshops (CVPRW), 2016, pp. 1408-1417.

[3] S. O. Ajiboye, P. Birch, C. Chatwin, and R. Young, "Hierarchical video surveillance architecture: a chassis for video big data analytics and exploration," in SPIE/IS&T Electronic Imaging, 2015, p. 10.

[4] D. Chahyati, M. I. Fanany, and A. M. Arymurthy, "Man woman detection in surveillance images," in 2017 5th International Conference on Information and Communication Technology (ICoIC7), 2017, pp. 1-4.

[5] R. M. Chory, L. E. Vela, and T. A. Avtgis, "Organizational Surveillance of Computer-Mediated Workplace Communication: Employee Privacy Concerns and Responses," Employee Responsibilities and Rights Journal, vol. 28, pp. 23-43, March 01 2016.

[6] P. K. Mishra and G. P. Saroha, "A study on video surveillance system for object detection and tracking," in 2016 3rd International Conference on Computing for Sustainable Global Development (INDIACom), 2016, pp. 221-226.

[7] M. M. Saemi, J. See, and S. Tan, "Lost and found: Identifying objects in long-term surveillance videos," in 2015 IEEE International Conference on Signal and Image Processing Applications (ICSIPA), 2015, pp. 99-104.

[8] S. Sajjanar, S. K. Mankani, P. R. Dongrekar, N. S. Kumar, Mohana, and H. V. R. Aradhya, "Implementation of real time moving object detection and tracking on FPGA for video surveillance applications," in 2016 IEEE Distributed Computing, VLSI, Electrical Circuits and Robotics (DISCOVER), 2016, pp. 289-295.

[9] V. Tsakanikas and T. Dagiuklas, "Video surveillance systems-current status and future trends," Computers & Electrical Engineering, vol. 70, pp. 736-753, 2018/08/01/ 2018.

[10] G. S. Walia and R. Kapoor, "Robust object tracking based upon adaptive multi-cue integration for video surveillance," Multimedia Tools and Applications, vol. 75, pp. 15821-15847, 2016/12/01 2016.

[11] P. Doucek, A. Pavlicek, and L. Luc, "Internet of Things or Surveillance of Things?," in Research and Practical Issues of Enterprise Information Systems, Cham, 2018, pp. 45-55.

[12] J. Duncan, "Uncertainty and Desire: Big Data Surveillance and Digital Citizenship," The iJournal: Graduate Student Journal of the Faculty of Information, vol. 3, 2018.

[13] N. Fescioglu-Unver, S. H. Choi, D. Sheen, and S. Kumara, "RFID in production and service systems: Technology, applications and issues," Information Systems Frontiers, vol. 17, pp. 1369-1380, December 01 2015.

[14] M. Fularz, M. Kraft, A. Schmidt, and J. Niechciał, "The PUT Surveillance Database," Cham, 2016, pp. 73-79.

[15] J. S. Kulchandani and K. J. Dangarwala, "Moving object detection: Review of recent research trends," in 2015 International Conference on Pervasive Computing (ICPC), 2015, pp. 1-5.

[16] S. Liu and S. D. Young, "A survey of social media data analysis for physical activity surveillance," Journal of Forensic and Legal Medicine, vol. 57, pp. 33-36, 2018/07/01/ 2018.

[17] E. Ohn-Bar, A. Tawari, S. Martin, and M. M. Trivedi, "On surveillance for safety critical events: In-vehicle video networks for predictive driver assistance systems," Computer Vision and Image Understanding, vol. 134, pp. 130-140, 2015/05/01/ 2015.

[18] S. Yang, H. Yang, J. Li, and J. Zhu, "An Effective Crowd Property Analysis System for Video Surveillance Application," in Digital TV and Wireless Multimedia Communication, Singapore, 2017, pp. 115-127.

[19] S. Mann, R. Janzen, M. A. Ali, and K. Nickerson, "Declaration of veillance (Surveillance is Half-Truth)," in 2015 IEEE Games Entertainment Media Conference (GEM), 2015, pp. 1-2.

Outlier Detection using Graphical and Nongraphical Functional Methods in Hydrology

Insia Hussain[1]
Department of Statistics
University of Karachi, Karachi
Pakistan

***Abstract*—Graphical methods are intended to be introduced in hydrology for visualizing functional data and detecting outliers as smooth curves. These proposed methods comprise of a rainbow plot for visualization of data in large amount and bivariate and functional bagplot and boxplot for detection of outliers graphically. The bagplot and boxplot are composed by using first two score series of robust principal component following Tukey's depth and regions of highest density. These proposed methods have the tendency to produce not only the graphical display of hydrological data but also the detected outliers. These outliers are intended to be compared with outliers obtained from several other existing nongraphical methods of outlier detection in functional context so that the superiority of the proposed graphical methods for identifying outliers can be legitimated. Hence present paper aims to demonstrate that the graphical methods for detection of outliers are authentic and reliable approaches compare to those methods of outlier detection that are nongraphical.**

Keywords—Rainbow plot; bivariate bagplot; functional bagplot; bivariate boxplot; functional boxplot

I. Introduction

Methods of visualization help in exploring those characteristics which might have been neglected when using summary statistics and mathematical models. This area of study did not receive much attention when analysing data in a functional context.

Reference [1] bought this matter under consideration and introduced graphical tools for visualizing functional data and detecting functional outliers. These proposed graphical tools include three new methods the rainbow plot, the bagplot and the boxplot for displaying functional data graphically since it was aimed to make a contribution to the analytic toolbox of functional data. The bagplot and boxplot have the benefit of identifying outliers graphically which might not be visible through the original data plot. Curves of outliers may either located outside the data range and represent "magnitude outliers" or they may locate within the data range but having different shape compare to other existing curves and appear as "shape outliers" or they might exhibit due to these combined features. Outliers of all types should be dealt while attempting to identify curves of outliers. The proposed graphical methods were also legitimated as the better approaches for detecting outliers by comparing them with various other existing nongraphical methods of outlier detection.

The proposed graphical methods for data visualization and outlier detection were practised by [2-4] on hydrological data. Hence the work of [1, 2] is intended to be implemented on a daily flow series of Taunsa Barrage on Indus river in Pakistan.

II. Literature Review

Functional data are gaining immense importance in numerous fields, therefore latest statistical tools are required to be developed so that functional data can be analysed. Hence, the analysis of data comprises of the smooth curve are of interest in the present paper. Authors in [5-7] present surveys in detail regarding many nonparametric techniques to analyse functional data.

Most of the studies emphasis on functional data clustering, modelling and forecasting with visualization having a minor role to play. The phase-plane plot and the rug plot presented by [8] and [9], respectively, are of notable exceptions for highlighting characteristics of important distributions using first and second functional data derivatives. A plot of singular value decomposition introduced by [10] is another exception, which shows the latent component changes due to an increase in the dimensionality or sample size.

The work of [1] has been extended for identification of outlier curves with respect to shape or magnitude or combination of magnitude-shape features. Outliergram was introduced by [11] for detecting shape outliers, [12] presented functional outliers taxonomy by proposing methods of visualization for detecting outliers whereas [13] introduced plots for displaying outlier curves having combined magnitude-shape features. Several other methods have also been recently developed by [14-17] for data visualization and outlier detection in functional framework. The study conducted by [2] in hydrology has been employed for classification of hydrograph by [18] and for the purpose of streamflow forecasting by [19].

This paper is organized as follows: Section 2 contains the discussion about graphical and nongraphical functional methods. The description of employed hydrological data is presented in Section 3. Section 4 contains the application, discussion and results of the discussed methods on the employed hydrological data and the corresponding conclusion are presented in Section 5.

III. Methodology

This section represents a functional graphical method for visualizing data and also functional graphical and nongraphical methods for detecting and computing outliers, respectively. The rainbow plot provides data visualization graphically whereas bagplot and boxplot are graphical methods for outlier detection. Outliers are computed nongraphically using functional mathematical methods which include methods of likelihood ratio test, integrated error square, functional depth and robust Mahalanobis distances.

A. Functional Graphical Methods for Data Visualization and Outlier Detection

Outliers are observations which are unusual and required to be detected and treated [20]. A crucial phase before modelling in data analysis is to detect and treat outliers since outliers also affect the analysis, modelling and forecasting of data in hydrology, therefore detailed study in this regard was conducted by [2] in hydrology. Hence, the present section contains functional graphical methods for outlier detection to explore and analyse unusual observations.

Various methods were presented in some works of literature of functional context for outlier detection by [21-23]. However, [1] introduced new tools for detection of outliers which do not only identify outliers accurately and have fast computing speed but also provide a graphical presentation of outliers to observe the behaviour of unusual observations. These proposed graphical approaches contain rainbow plot for visualization of data pattern whereas bagplot and boxplot are the tools for identifying outliers graphically. The observations or curves which locate within or outside the range of data due to unusual structure or shape are identified as outliers. Practically, results may vary between the two methods proposed for outlier detection depending on the nature of employed data.

1) Rainbow plot: The rainbow plot introduced by [1] and implemented by [2,4] in hydrology for the purpose of visualizing a complete set of employed data through a single plot having a distinct feature of displaying data curves using rainbow colour palette following data order. Two indices are used for data ordering that are functional depth and data density. The bivariate score depth and kernel density estimates are used for computation of the data ordering indices. The bivariate score depth is written as

$$OT_j = d\left(z_j, Z\right),\ \ Z = \{z_j \in \mathbb{R}^2; k = 1, \ldots\ldots, n\} \qquad (1)$$

where $d(.,.)$ is the function of half-space depth introduced by [24]. Depth function by Tukey for bivariate score series z_j of first two principal components is defined as the amount of smallest observations present in closed half-space with z_j points on the boundary. The observations arrange decreasingly following depth values OT_j order. The first curve according to the depth order is the median curve having highest OT_j whereas curve having lowest OT_j is the outermost curve. The median curve based on Tukey's depth function is obtained using a bivariate score series z_j as observations of the curve which is adopted as an alternate approach to original data for simplification. The series z_j as observations of functional data are also ordered using kernel density estimate [25] as follows:

$$OD_j = \hat{f}\left(z_j\right) = \frac{1}{n}\sum_{k=1}^{n}\frac{1}{h_k}K\left(\frac{z_j - z_k}{h_k}\right),\ j \neq k, j = 1, \ldots, n \qquad (2)$$

where $K(.)$ is a kernel function and smoothing parameter h_k is a bandwidth of *k*th point $\{z_k\}$. The observations are arranged decreasingly following OD_j order. Hence, the mode curve is the first curve containing the highest *OD* whereas the curve containing the lowest *OD* is an outlying curve. The curves ordered according to *OT* and *OD* are displayed according to order of rainbow colour in such a way that the curves closest to median or mode appear in red whereas outlying curves appear in violet colour.

2) Functional bagplot: The bivariate bagplot based on half-space depth function was introduced by [26]. This plot was employed in multivariate and functional context by [27] and [2,4] respectively in hydrology using streamflow data. The functional bagplot is obtained following the pattern of bivariate bagplot which is composed using the first two score series $z_j = (z_{j,1}, z_{j,2})$ of principal components in such a way that each bivariate bagplot point correspond to each functional bagplot curve. Three elements that are the central median curve surrounded by inner region enclosed in an outer region cause the formation of bivariate bagplot which also contribute to the composition of functional bagplot. The inner region captures total observation of 50 per cent and surrounded by 95 or 99 per cent of total observation bounded by the outer region which is formed by inflating inner region according to ρ factor. Author in [1] suggested ρ value 1.96 for 95 per cent inflation and 2.58 for 99 per cent inflation since the standard normal distribution is followed by score series z_j. Finally, the points appear outside the inflated outer region are outliers.

3) Functional boxplot: The bivariate boxplot based on highest density region is composed by the first two z_j score vector of the principal component was introduced by [28]. The pattern employed for the formation of bivariate boxplot is followed for the composition of a functional boxplot. The detailed study regarding functional boxplot was organized by [1] and practised by [2,4] in hydrology. Recently, applications of boxplot in functional context have been conducted by [29,30].

As discussed in subsequent section, three elements correspond to bivariate boxplot, combine to compose a functional boxplot such that mode curve is formed in the centre of inner region containing 50 per cent data observations enclosed in an outer region having 95 or 99 per cent of total observation while the observations not bounded by outer region and located outside the region are outliers.

The difference in outliers obtained by bagplot and boxplot are due to the approaches used for establishing inner and outer regions since median and depth function belong to bagplot whereas mode and density estimate belong to boxplot. Hence, outliers displayed by bagplot are unusual observations compared to median whereas boxplot display outliers which are unusual with respect to mode.

B. Detection of Outliers using Nongraphical Functional Methods

Reference [1] proposed the comparison of graphical methods (i.e. bagplot & boxplot) with various nongraphical methods for detecting functional outliers, performed on discretized functions. The graphical method has been legitimated better able to detect outliers than other nongraphical methods. The nongraphical methods for detecting functional outliers are as follows:

1) Method of likelihood ratio test: Reference [22] proposed a method for detecting outlier which calculates a statistic of likelihood ratio test for each $y_j(x)$ curve. An outlier is a value when most of the test statistics exceed a given c critical value. This outlier value is then removed and the new outlier is obtained from the remaining data. This process stops when no more values of outliers are detected. Following equation based on depth function is used for this test

$$o_j = \int D\left(y_j(x)\right) dx \tag{3}$$

A univariate measure of depth for a particular x value is $D\left(y_j(x)\right)$. According to this definition, the curves are ordered increasingly by an order of $\{o_j\}$, such that a curve with the lowest depth function is the first curve whereas a curve with the highest depth function is the last curve.

2) Method of integrated error square: Author in [31] proposed a method for detecting outliers which contains the principal component analysis of robust function. Let the integration of error square for jth observation be

$$\upsilon_j(x) = \int_x e_j^2(x) g dx = \int_x \left(y_j(x) - \sum_{l=1}^{L} z_{j,l}\phi_l(x)\right)^2 dx \tag{4}$$

where L is a number of pre-specified components; usually 2, $\{\phi_l(x)\}$ are the functions of principal components and $z_{j,l}$ are their related scores. This provides an accurate measure of the approximated principal component for *j*th observation. High integrated error square indicates points with high likelihood as outliers. If $e_j(x)$ is distributed normally, then $\upsilon_j(x)$ follows a chi-square (χ^2) distribution with $\mathrm{E}(\upsilon_j(x)) = 0.5Var(\upsilon_j(x))$ then the probability that $\upsilon_j < c$, where $c = m + \lambda\sqrt{m}$ and $m =$ median $(\{\upsilon_1, \dots, \upsilon_n\})$, is approximately $\Phi(\lambda/\sqrt{2})$, where $\Phi(.)$ is the standard normal distribution function. For example, $\Phi(3.29/\sqrt{2}) = 99\%$ when $\lambda = 3.29$.

3) Method of functional depth: Author in [32] proposed a method for detecting outliers by employing functional depth including all curves as well as trimmed curves. The centre of a group of curves is measured using the functional depth. Hence, a group of curves ordered in the outward centre is obtained through depth. In fact, the curve having maximum depth can be considered as an estimate for the functional distribution centre. Therefore, depth is an inverse notion of outlyingness and curves of functional outliers which are supposed to be located far from the central region of the data, are the curves with low depth. Hence, functional outlier curves are detected having comparatively lower depth.

4) Method of robust mahalanobis distances: The Robust Mahalanobis distance is a multivariate method for detection of outliers which is applicable on discretized curves $\{y_j(x_k); k = 1, \dots, p\}$. Suppose the functional data are obtained on an equal distance $\{x_1, \dots, x_p\}$dense grid, the Mahalanobis distance square is defined as

$$r_j = (y_j(x_k) - \hat{\mu}(x_k))'\hat{\Sigma}^{-1}(y_j(x_k) - \hat{\mu}(x_k)),\ k = 1, \dots, p \tag{5}$$

where the mean of a sample is $\hat{\mu}(x_k)$, $\hat{\Sigma}$ is a covariance matrix robust estimate of $\{y_j(x_k)\}$ which is assumed to be a positive definite, such that $\hat{\Sigma}^{-1}$ is nonsingular. The comparison of resultant distance with a critical value follows χ^2 distribution having degrees of freedom *p*. For α=99%, a predefined level, observations are considered to be outliers that contain Mahalanobis distance square greater than $\chi^2_{0.99,p}$critical value . The Robust Mahalanobis distance variations are further discussed by [21,33].

IV. Data Description

The major data source in hydrology is daily streamflow. Flows of water are also recorded instantly, hourly or on other time scales. The data series of the daily flow of Taunsa barrage are available from Sindh Irrigation department, Sindh Secretariat, Karachi, Pakistan.

Taunsa barrage is built in Taunsa Tehsil of Dera Ghazi Khan District located in Punjab province on the Indus River in Pakistan. It has a discharge capacity of up to 1,000,000 cusecs (i.e. approximately 28300 m^3s^{-1}). Fig. 1 indicates the geographical location of the Taunsa Barrage.

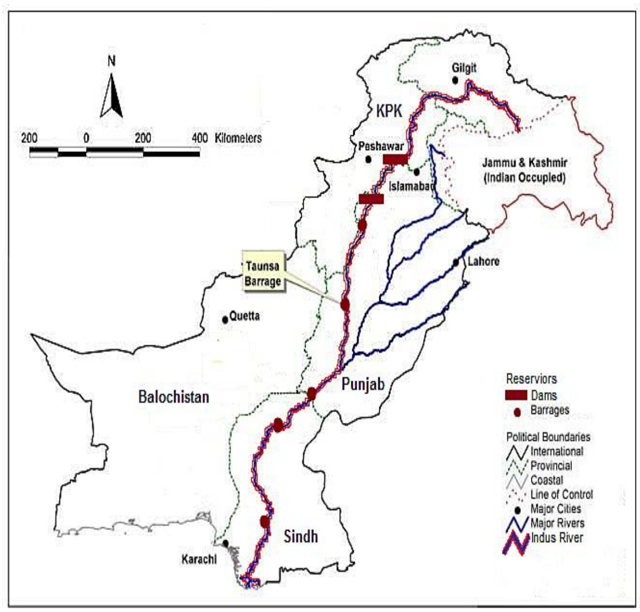

Fig. 1. Geographical Location of Taunsa Barrage

Some studies use data of entire year while some use data of only high flow season depending on what region is considered as an area for flood analysis. Data used in the present study are the observations of 6 months ($T = 183$ days) for the duration of years 1977 to 2017 (*n*=41 years) since high flow season is observed during April to September in Pakistan. The series of observations are $Y_j = \left(y_j(t_1), \dots, y_j(t_T)\right)$, $j = 1, \dots, n$, $k = 1, \dots, T$, where *n*=41 years, $T = 183$ days and $y_j(t_k)$ is the recorded discrete flow value on t_k day in the jth year. Before any calculation is performed the values of streamflow which are recorded originally in cusec (a volume flow rate) are required to be converted into cubic meter per second ($m^3 s^{-1}$).

V. Analysis

Specific formats of data ordering are followed by all the proposed graphical methods. Rainbow plot displays the curves of all the data in a single plot having a distinct feature of colour palette following the order of rainbow colours. By default, time order is followed by the curves of rainbow plot in such a way that the curve of the recent past appear in violet whereas curve belongs to remote past is appear in red colour.

The rainbow plot is the simplest way of displaying all the data in the functional format ordered with respect to time. Due to the overlapping of the number of curves, “median curve” or “mode curve” is not easily identified or it is difficult to locate where the majority of data curves present. Also, outliers are difficult to be identified if other curves obscure them. Therefore, there are also other options for ordering functional data using (1) and (2), respectively. This ordering is done using rainbow plot such that curves colour then follows the pattern of rainbow according to depth or density ordering. The curve near the core of data appears in red, whereas the curve in violet is an outlying curve. Since plotted curves follow either depth or density ordering, the red data curves are usually obscure, whereas data curves in violet are seen distinctly even if they are overlapped by other data curves.

The simple rainbow plot follows time ordering as shown by Fig. 2(a), but some data sets required to be ordered according to the data value themselves. Therefore, two optional ordering methods stated earlier i.e. depth or density uses the first two scores of principal components for measuring either “depth” or “density” of data according to the order of data values.

Tukey’s depth is described as the number of smallest data values present in an enclosed half-plane. The data values are then increasingly ordered as the $OT_i = d(z_i, Z)$ distance, using (1). The curve we first obtain by this order is considered as a curve of the median, while the last order curve is the outlying curve among all curves where a distance from the median to each curve is defined as depth. Depth ordering rainbow plot is depicted in Fig. 2(b). The black curve in the centre represents the median, the curve in purple is an outlying curve and the curve in red, near the median, is not clearly seen due to the other data curves are overlapping.

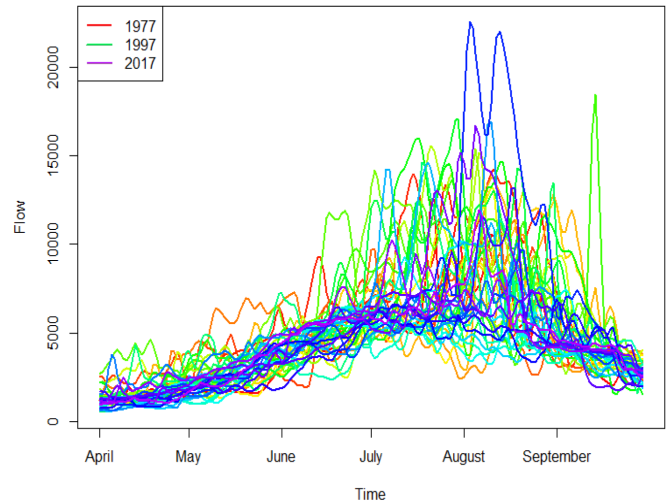

(a)

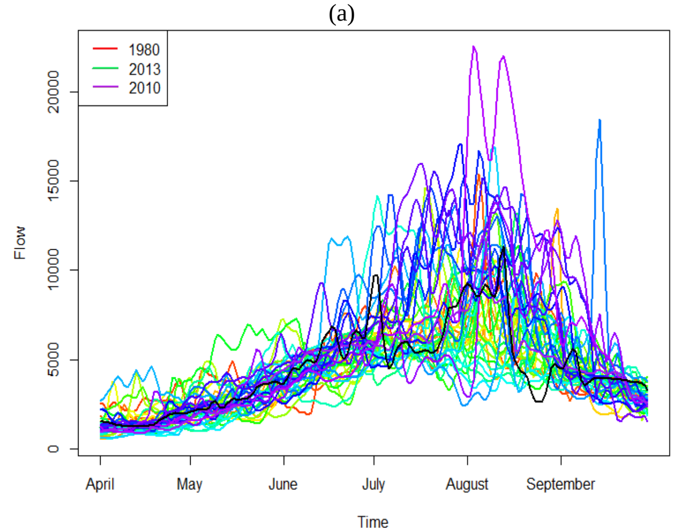

(b)

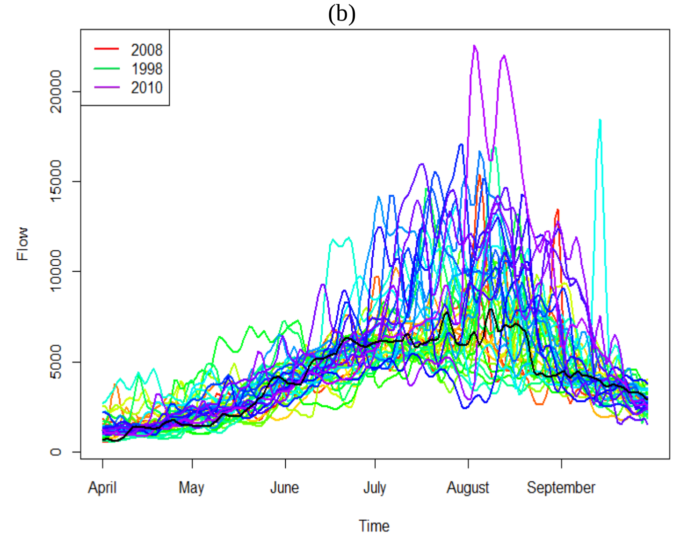

(c)

Fig. 2. Rainbow Plots with (a) Time (b) Depth and (c) Density Ordering for Years 1977-2017.

The third way for ordering data points is by the estimate of kernel density at each data value, using (2). The values of $\{OD_i\}$ decreasingly order the functional data, such that the first order curve is the curve of highest density and considered as "mode curve" whereas the last order curve is the curve of lowest density and considered as an unusual outlying curve. It can be noted that the values of the last curve obtained through this ordering is possibly remain the same compared to the other curves and its (z_1, z_2) bivariate scores might be in the centre of (z_1, z_2) scatter plot such that no other points are around it and hence having the value of lower density. Results reveal that both ordering methods may follow a similar order, especially for high ordering years. Density ordering rainbow plot is depicted in Fig. 2(c). The black curve in the centre represents a mode, the curve in purple is an outlying curve and the curve in red, near mode, is not clearly seen due to the other data curves are overlapping.

The data observations ordered by depth and density, lead to the formation of bivariate and functional bagplot and boxplot, as described in the subsections of 2.1. The association of bivariate and functional bagplot and boxplot to the first two scores of principal components for the probability coverage of 95% and 99% are illustrated in Fig. 3 and Fig. 4. The bivariate bagplot and boxplot exhibit median and mode, respectively, the inner region which covers 50% and an outer region which accumulate 95% or 99% of data values depending on the selected values of factor ρ i.e. either 1.96 or 2.58. The functional bagplot and boxplot contain curve of median and mode, respectively, area of the inner region and outer region. The functional bagplot and boxplot inner and outer region contain 50% and 95% or 99% of all the data curves, respectively.

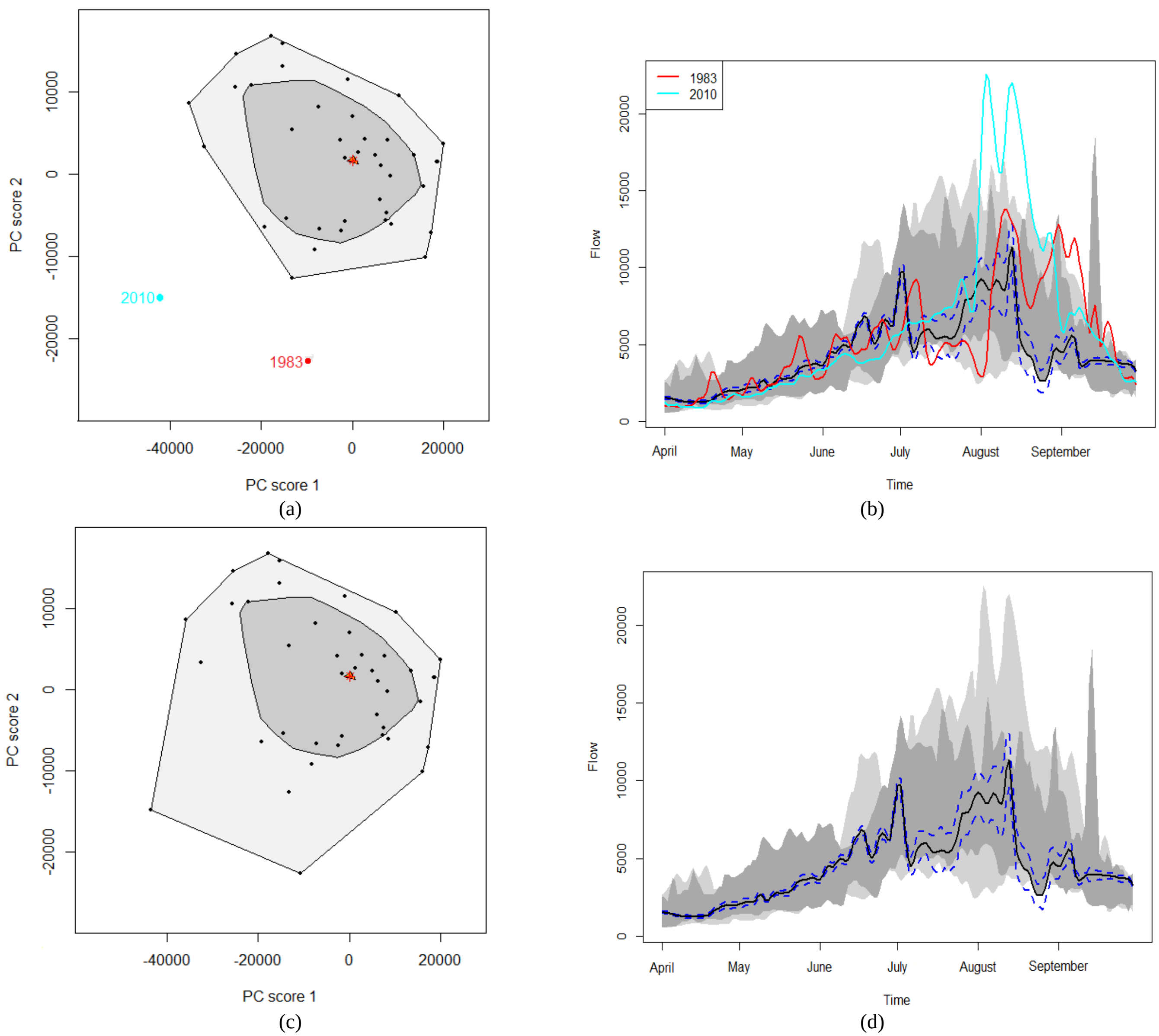

Fig. 3. (a) The bivariate and (b) Functional Bag Plot with 95%, whereas (c) The Bivariate and (d) Functional Bag Plot with 99% of Probability Coverage.

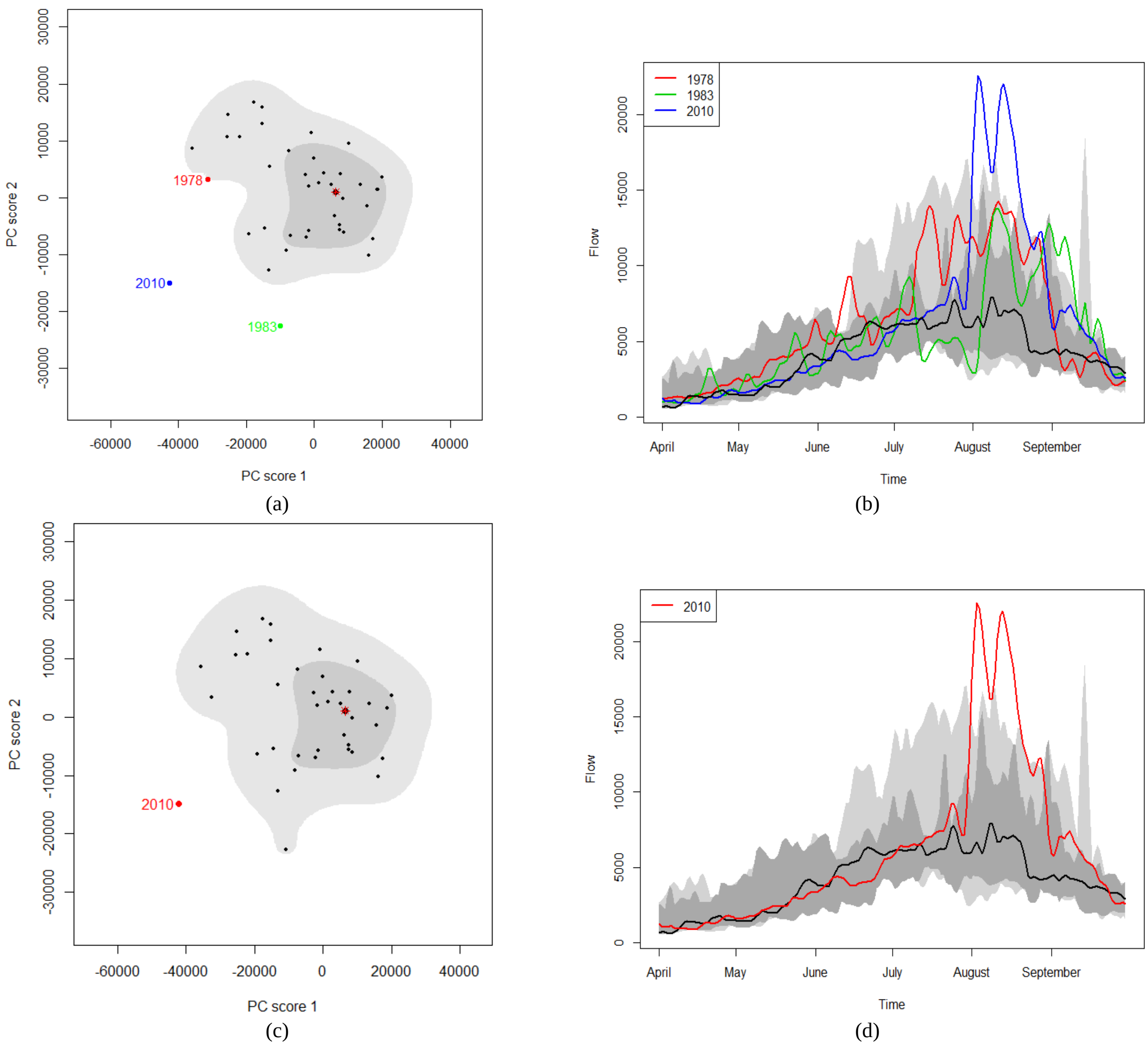

Fig. 4. (a) The Bivariate and (b) Functional Boxplot with 95%, While (c) The Bivariate and (d) Functional Boxplot with 99% of Probability Coverage.

The dark grey shaded area of bivariate bagplot and boxplot displays inner 50% region whereas area in light grey shade exhibits outer 95% and 99% region. These shaded areas correspond to the region of functional bagplot and boxplot with same shades. Points that appear beyond the outer region are detected as outliers. The bivariate bagplot and boxplot outliers appear in several colours match to the colour of functional bagplot and boxplot outlier curves. The median and mode display as the mark of a red asterisk (Fig. 3(a) and 3(c)) and (Fig. 4(a) and 4(c)), respectively, which corresponds to the black curve of median and mode appears in functional bagplot and boxplot (Fig. 3(b) and 3(d)) and (Fig. 4(b) and 4(d)), respectively.

It is clearly observed from Fig. 3 that the years 1983 and 2010 are identified as outliers when 95% region of both bivariate and functional bagplots are considered as displayed by Fig. 3(a) and 3(b). Besides this, no outlier is located outside the 99% region of bivariate and functional bagplots, as exhibited by Fig. 3(c) and 3(d). Note that, usually when outliers are found near the median, it is difficult to be detected by bagplot [1]. Therefore, it is authentic to use more appropriate approach and that is boxplot. The years 1978 and 1983 appear beyond 95% outer region as shown by Fig. 4(a) and 4(b). The only outlier detected with the probability coverage of 99% is the year 2010 which is displayed outside the bivariate and functional boxplot outer region as displayed by Fig. 4(c) and 4(d). It can be deduced that the outlying year 1978 is close to the median, therefore, it was not detected by bagplot whereas the outlying years 1986 and 2010 are not close to the median. It can be concluded that the flow corresponds to the year 2010 is an outlier having different shape and magnitude compared to the curve of other years. The year 2010 is an authentic outlier identified through both bagplot and boxplot. Hence, boxplot is considered a more reliable approach for the detection of outliers than bagplot.

As discussed earlier in Section 2.1 that the bagplot and boxplot are the graphical methods for detecting and identifying functional outliers. These detected outliers are compared to the outliers detected by various nongraphical methods for detecting functional outliers, as discussed in Section 2.2. The purpose of conducting this comparison is to legitimate that the graphical methods are better able to detect outliers than nongraphical methods in a functional context. The nongraphical methods for detecting outliers were applied to the smoothed flow data for years 1977-2017. Outputs of nongraphical methods; likelihood, integrated error, depth and Robust method, and graphical methods; bagplot and boxplot for functional data are tabulated in Table I with the computation time of each method.

VI. Results

The results displayed by Table I demonstrates that likelihood method is unable to detect any outliers, the integrated method detected several outliers, a similar result is also produced by depth method while robust method provides a comparatively better result. Hence, the likelihood method produced the worst performance with respect to accuracy and computation time. The integrated method detected many years, among them only a few exist as outliers. The depth method is unable to encounter shape outliers according to [34] analysis, therefore results show false detection and slow computation time. In contrast, the highest accuracy and fastest time computation for detecting outliers are achieved by functional bagplot and boxplot, compare to other earlier implemented methods i.e. likelihood, integrated error, depth and Robust method.

The graphical methods to visualize functional data and identify functional outlier have advantages that they not only accurately detect outliers but also simultaneously give the graphical presentation to visualize those outliers. Hence, resultant values in Table I demonstrate that the performance of proposed graphical methods is explicitly better than existing nongraphical methods for detecting outliers. In spite of the fact that sometimes the method of bagplot could not detect those outliers which are around the curve of median and such outliers can be identified correctly by boxplot, the bagplot and boxplot are authentic methods for detecting correct functional outliers.

TABLE I. A Comparison of the Outlier Detection Performances

Methods	**Detected outliers**	**Time (mins)**
Likelihood ratio test	None	1.54
Integrated squared error	1978, 1979, 1981, 1983, 1984, 1987, 1988, 1989, 1990, 1991, 1992, 1994, 1995, 1996, 1997, 1998, 2005, 2006, 2010, 2015	2.33
Functional depth	2010, 20111, 2012, 2013, 2014, 2015, 2016, 2017	2.19
Robust Mahalanobis Distance	2010	0.45
Functional bagplot	None	0.01
Functional HDR boxplot	2010	0.37

VII. Conclusion

In this paper, three graphical methods for visualization of functional data and identification of functional outliers have been employed. Ranking scores of principal components using depth or density of data is performed in a two-dimensional space so that inliers and outliers are separated. The graphical presentation is obtained by scores matching, displayed by both bivariate bagplot and boxplot followed by functional curves. The approaches employed in this paper have the benefits of accurately detecting outliers with a fast-paced computation while simultaneously representing it graphically.

The results obtained from the implementation of the proposed method on the data of Taunsa Barrage illustrate that the graphical methods are better in performance compare to existing nongraphical methods for detecting outliers, which either detect miss obvious or spurious outliers.

Besides this, the method of depth-based which contribute in the formation of bagplot is not able to detect outliers that are close to the curve of median whereas the method of density-based which contribute in the formation of boxplot can detect such outliers authentically. Hence boxplot is more reliable compared to bagplot nevertheless both the graphical approaches are authentic for displaying and detecting concrete outliers.

VIII. Future Scope

Functional data modelling, analysing and forecasting are seriously affected due to the outlier presence. Statistical analysis can lead to invalid conclusions if the identification and treatment of outliers are ignored. Hence, a crucial phase before modelling is to detect and treat outliers so that outliers do not affect the analysis and forecasting of data in hydrology.

Acknowledgment

The author wants to express gratitude to Sindh Irrigation Department, Sindh Secretariat, Karachi, Pakistan for graciously catering with data of Taunsa Barrage for executing this study. The author also thanks the authors of Rainbow R packages [35].

References

[1] R. J. Hyndman and H. L. Shang, “Rainbow plots, bagplots, and boxplots for functional data,” Journal of Computational and Graphical Statistics, vol. 19, no. 1, pp. 29–45, 2010. doi:10.2307/25651298.

[2] F. Chebana, S. Dabo-Niang and T. B. Ouarda, “Exploratory functional flood frequency analysis and outlier detection,” Water Resources Research, vol. 48, no. 4, W04514, 2012. doi:10.1029/2011WR011040.

[3] L. Millán-Roures, I. Epifanio and V. Martínez, “Detection of anomalies in water networks by functional data analysis,” Mathematical Problems in Engineering, vol. 2018, no.1, 2018. doi:10.1155/2018/5129735.

[4] I. Hussain and M. Uddin, “Functional and multivariate hydrological data visualization and outlier detection of Sukkur Barrage,” International Journal of Computer Applications, vol. 178, no. 28, pp. 20-29, 2019. doi:10.5120/ijca2019919097.

[5] J. O. Ramsay and B. W. Silverman, Functional Data Analysis, Springer, New York, NY, USA, 2nd edition, 2005.

[6] F. Ferraty and P. Vieu, Nonparametric Functional Data Analysis: Theory and Practice, Springer, 2006 doi:10.1007/0-387-36620-2.

[7] J.-L. Wang, J.-M. Chiou, and H.-G. Müller, "Functional data analysis," Annual Review of Statistics and Its Application, vol. 3, no. 1, pp. 257-295, 2016. doi:10.1146/annurev-statistics-041715-033624.

[8] J. O. Ramsay, and J. B. Ramsay, "Functional data analysis of the dynamics of the monthly index of nondurable goods production," Journal of Econometrics, vol. 107, no. 1-2, pp. 327-344, 2002. doi:10.1016/S0304-4076(01)00127-0.

[9] V. Hyde, J. Wolfgang, and G. Shmueli, "Investigating concurrency in online auctions through visualization," The American Statistician, vol. 60 no. 3, pp. 241-250, 2006. doi: 10.1198/000313006X124163.

[10] L. Zhang, J. S. Marron, H. Shen, and Z. Zhu, "Singular value decomposition and its visualization," Journal of Computational and Graphical Statistics, vol. 16, no. 4, pp. 833-854, 2007. doi:10.1198/106186007X256080.

[11] A. Arribas-Gil and J. Romo, "Shape outlier detection and visualization for functional data: the outliergram," Biostatistics, vol. 15, no. 4, pp. 603–619, 2014. doi:10.1093/biostatistics/kxu006.

[12] M. Hubert, P. J. Rousseeuw, and P. Segaert, "Multivariate functional outlier detection," Statistical Methods and Applications, vol. 24, no. 2, pp. 177–202, 2015. doi:10.1007/s10260-015-0297-8.

[13] W. Dai and M. Genton, "Multivariate functional data visualization and outlier detection," Journal of Computational and Graphical Statistics, vol. 27, no. 4, pp. 923–934, 2018. doi:10.1080/10618600.2018.1473781.

[14] W. Xie, S. Kurtek, K. Bharath, and Y. Sun, "A geometric approach to visualization of variability in functional data," Journal of the American Statistical Association, vol. 112, no. 519, pp. 979-993, 2017. doi:10.1080/01621459.2016.1256813.

[15] F. Yu, L. Liu, L. Jin, N. Yu, and H. Shang, "A method for detecting outliers in functional data," IECON 2017 - 43rd Annual Conference of the IEEE Industrial Electronics Society, Beijing, pp. 7405-7410, 2017. doi: 10.1109/IECON.2017.8217297.

[16] P. J. Rousseeuw, J. Raymaekers, and M. Hubert, "A measure of directional outlyingness with applications to image data and video," Journal of Computational and Graphical Statistics, vol.27, no. 2, pp. 345-359, 2018. doi:10.1080/10618600.2017.1366912.

[17] W. Dai and M. Genton, "Directional outlyingness for multivariate functional data," Computational Statistics & Data Analysis, vol. 131, pp. 50–65, 2019. doi:10.1016/j.csda.2018.03.017.

[18] C. Ternynck, M. A. B. Alaya, F. Chebana, S. Dabo-Niang, and T. B. M. J. Ouarda, "Streamflow hydrograph classification using functional data analysis," Journal of Hydrometeorology, vol. 17, no. 1, pp. 327–344, 2016. doi: 10.1175/JHM-D-14-0200.1.

[19] P. Masselot, S. Dabo-Niang, F. Chebana, and T. B. Ouarda, "Streamflow forecasting using functional regression," Journal of Hydrology, vol. 538, pp. 754-766, 2016. doi: 10.1016/j.jhydrol.2016.04.048.

[20] V. Barnett and T. Lewis, Outlier in Statistical Data, John Wiley, Chichester, U.K, 3rd edition, 1998.

[21] J. Hardin and D. M. Rocke, "The distribution of robust distances," Journal of Computational and Graphical Statistics, vol. 14, no. 4, pp. 928-946, 2005. doi:10.1198/106186005X77685.

[22] M. Febrero-Bande, P. Galeano, and W. González-Manteiga, "A functional analysis of NOx levels: location and scale estimation and outlier detection," Computational Statistics, vol. 22, no. 3, pp. 411–427, 2007. doi:10.1007/s00180-007-0048-x.

[23] P. Filzmoser, R. Maronna, and M. Werner, "Outlier identification in high dimension," Computational Statistics & Data Analysis, vol. 52, no. 3, pp. 1694-1711, 2008. doi:10.1016/j.csda.2007.05.018.

[24] J. W. Tukey, "Mathematics and the picturing of data," Proceedings of the 1975 International Congress of Mathematics, vol. 2, pp. 523-531, 1975.

[25] D. W. Scott, Multivariate Density Estimation: Theory, Practice, and Visualization, John Wiley, New York, NY, USA, 1992.

[26] P. Rousseeuw, I. Ruts, and J. W. Tukey, "The bagplot: A bivariate boxplot," The American Statistician, vol. 53, no. 4, pp. 382-387, 1999. doi:10.1080/00031305.1999.10474494.

[27] F. Chebana and T. B. Ouarda, "Depth-based multivariate descriptive statistics with hydrological applications," Journal of Geophysical Research, vol. 116, D10120, 2011b. doi:10.1029/2010JD015338.

[28] R. J. Hyndman, "Computing and graphing highest density regions," The American Statistician, vol. 50, no. 2, pp. 120-126, 1996. doi:10.2307/2684423.

[29] W. Dai, T. Mrkvicka, Y. Sun, and M. G. Genton, "Functional outlier detection and taxonomy by sequential transformations," arXiv e-prints, 2018.

[30] C. Zhao and J. Yang, "A robust skewed boxplot for detecting outliers in rainfall observations in real-time flood forecasting," Advances in Meteorology, vol. 2019, pp. 1-7, 2019. doi:10.1155/2019/1795673.

[31] R. J. Hyndman and M. S. Ullah, "Robust forecasting of mortality and fertility rates: A functional data approach," Computational Statistics & Data Analysis, vol. 51, no. 10, pp. 4942–4956, 2007. doi:10.1016/j.csda.2006.07.028.

[32] M. Febrero-Bande, P. Galeano, and W. González-Manteiga, "Outlier detection in functional data by depth measures, with application to identify abnormal NOx levels," Environmetrics, vol. 19, no. 4, pp. 331 – 345, 2008. doi:10.1002/env.878.

[33] C. Becker and U. Gather, "The largest nonidentifiable outlier: a comparison of multivariate simultaneous outlier identification rules," Computational Statistics & Data Analysis, vol. 36, no. 1, pp. 119-127, 2001. doi:10.1016/S0167-9473(00)00032-3.

[34] S. López-Pintado and J. Romo, "On the concept of depth for functional data," Journal of the American Statistical Association, vol. 104, no. 486, pp. 718–734, 2009. doi:10.1198/jasa.2009.0108.

[35] H. L. Shang and R. J. Hyndman, Rainbow: Rainbow Plots, Bagplots and Boxplots for Functional Data, R package version 3.4, 2016.

Heart Disease Prediction based on External Factors: A Machine Learning Approach

Maruf Ahmed Tamal[1], Md Saiful Islam[2]
Md Jisan Ahmmed[3], Md. Abdul Aziz[4], Pabel Miah[5]
Department of Computer Science and Engineering
Daffodil International University, Dhaka, Bangladesh

Karim Mohammed Rezaul[6]
Faculty of Arts, Science and Technology
Wrexham Glyndŵr University
Wrexham, UK

***Abstract*—Technology has immensely changed the world over the last decade. As a consequence, the life of the people is undergoing multiple changes that directly have positive and negative effects on health. Less physical activity and a lot of virtual involvements are pushing people into various health-related issues and heart disease is one of them. Currently, it has gained a great deal of attention among various life-threatening diseases. Heart disease can be detected or diagnosed by different medical tests by considering various internal factors. However, this type of approach is not only time-consuming but also expensive. Concurrently, there are very few studies conducted on heart disease prediction based on external factors. To bridge this gap, we proposed a heart disease prediction model based on the machine learning approach which enables predicting heart disease with 95% accuracy. To acquire the best result, 6 distinct machine learning classifiers (Decision Tree, Random Forest, Naive Bayes, Support Vector Machine, Quadratic Discriminant, and Logistic Regression) were used. At the same time, sklearn.ensemble.ExtraTreesClassifier has been used to extract relevant features to improve predictive accuracy and control over-fitting. Findings reveal that Support Vector Machine (SVM) outperforms the others with greater accuracy (95%).**

Keywords*—*Heart disease; Risk prediction; Decision Tree (DT); Support Vector Machine (SVM); Naive Bayes (NB); Random Forest (RF); Logistic Regression (LR); Quadratic Discriminant Analysis (QDA); Machine learning

I. Introduction

Recently, heart disease has become the leading cause of human death comparing other life-threatening diseases. As human life itself depends on the heart's function effectively, if it does not function properly, it will affect various parts of the human body. Heart disease (also known as a coronary disease) continues the world's major cause of death for centuries. 1/3 deaths of the world are caused by coronary disease and the death rate is higher than cancer mortality rates [1]. A large number of people around the world are struggling to control the risk factors of cardiovascular disease. Several factors are responsible for heart diseases like a family history of coronary illness, smoking, poor eating methodology, high pulse, cholesterol, high blood cholesterol, obesity, physical inertia, overweight, high blood pressure, stress or hypertension, chest pain, taking a drug, etc. [2, 3]. The diagnosis of cardiac disease is usually based on the patient's signs, external symptoms, and physical tests (Electrocardiogram (ECG), Holter monitoring, Echocardiogram, Stress test, Cardiac catheterization, Cardiac computerized tomography (CT) scan, etc.), but the main challenge facing by medical providers is to provide quality services at manageable cost [5]. At the same time, overall diagnosis processing is time-consuming [6] which has a negative impact on patients, especially those in need of emergency treatment. To remove this barrier, researchers are trying to utilize different Machine Learning (ML) algorithms like Decision Tree (DT) [4], Multi-layer perceptron (MLP), Artificial Neural Network (ANN) [6] [5], Naïve Bayes (NB) , K-closest neighbor (K-NN) and Support vector machine (SVM) [6] [7] [8] for distinguishing and extricating valuable data from the clinical dataset with insignificant client inputs and efforts [9]. Nevertheless, there are still very few effective measures to solve these problems. Detecting heart disease is still now a big challenge because of the overall diagnosis process and cost [10]. Researchers are relentlessly trying to develop an early heart disease detection system to minimize the death rate. Nevertheless, the lack of diversity in previous studies is a matter of great concern. As a result, improvement in this field is being hampered. Table I shows that almost all the past studies [5, 6, 7, 10, 12, 14, 15, 16, 8, 19] were conducted on the secondary data [11] which was published by UCI (Machine Learning Repository) where the features were almost same. At the same time, this dataset is a little bit outdated too (donated in 1988). So, the lack of innovation is a major concern here. Concurrently, most of the existing studies have been performed on both internal and external factors (see Table I) where heart disease diagnosis using internal factors (MRI, ECG, Echocardiogram, Blood Test, etc.) is not only costly but also time-consuming. Another downside of previous studies is less predictive accuracy (see Table I). A limited data set [5, 6, 7, 14, 18] as well as a lack of features extraction [5, 6, 13, 14], are the main reasons behind this poor accuracy. On the other hand, a model has been [5] proposed where a multilayer perceptron neural network with backpropagation was used which gained 100% accuracy. However, they did not clarify the methodologies well. The following specific objectives were followed to resolve all these gaps in order to achieve the main objective of this paper:

1) Detecting heart disease at an initial stage using machine learning based on external factors.

2) Providing less time-consuming services for a more reliable diagnosis of heart disease.

TABLE. I. SUMMARY OF THE PREVIOUS STUDY

Ref	Data Size	Type of data	Type of Approach	No. of features	Features extraction	Algorithm used	Based on	Accuracy
[7]	270	Secondary	Machine Learning	13	Yes	SVM	External + internal factors	Max. 88.34%
[6]	270	Secondary	Machine Learning	13	No	ANN, kNN, SVM, LR, CT	External + internal factors	Max. 83%
[5]	182	Secondary	Data Mining	15	No	MPNN with backpropagation	Internal factors	100%
[12]	1190	Secondary	Statistics	14	Yes	Fuzzy system	Internal + External factors	Av. 92.3%
[10]	N/A	Secondary	Data Mining	14	No	DT, K-mean Clustering	Internal + External factors	N/A
[13]	1000	Secondary	Data Mining	13	No	Decision Support and NB	Internal + External factors	Max. 88.33%
[14]	300	Secondary	Data Mining	14	Yes	DT, SVM, NB	Internal + External factor	Max. 84.85%
[15]	N/A	Secondary	fuzzy decision support system	14	Yes	NN, Clinical Decision support system, RF, J48	External + internal factors	Almost 80%
[16]	4146	Secondary	Machine learning	16	Yes	LR,NN	External + internal factors	81.163%
[17]	370	Primary +Secondary	Data Mining	13	No	KStar, J48, SMO, Bayes Net, MLP	External + internal factors	89%
[18]	303	Secondary	Machine Learning	**14**	Yes	ANN, BNN	External + internal factors	**95%**
[19]	N/A	Secondary	Data Mining	11	Yes	NN, Bayesian Networks, DT, SVM	External + internal factors	93%

N.B. MPNN = Multilayer Perceptron Neural Network, ANN = Artificial Neural Network, DT = Decision Tree, NN = Neural Network, SVM = Support vector Machine, NB = Naïve Bayes, SMO = Sequential Minimal Optimization, BNN = Backpropagation Neural Network.

II. RESEARCH METHODOLOGY

The primary purpose of this study is to explore the best predictive model based on external symptoms for diagnosing heart disease. Fig. 1 represents the methodological framework of the current study. The methodological part was separated into several sections to clearly reflect the overall study.

A. Data Collection

A substantial literature review was performed at the beginning of the study to identify the gap in the existing studies. Simultaneously, significant study issues were found through literature review which assisted to collect relevant data and factors. This study was conducted between July 2018 and September 2019 at Dhaka, Bangladesh. Primary data was collected through both field surveys and online surveys. A web-based questionnaire (Google form) was sent to the targeted audience of various ages.

B. Participants

A total of 3500 questionnaires were distributed and 1247 valid records were gathered (field survey: 952 internet survey: 295), including spontaneous female (43% and male (57%) participants. The ethical factors of the respondent have been closely assured to keep their privacy strictly and confidentially secret.

C. Data Preprocessing

In order to obtain the precise value, the dataset was fully prepossessed until irrelevant, incomplete, inconsistent information was removed. Several python libraries were used to preprocess the raw data. At the same time, we also carried out data transformation from string to numerical value in order to fit the data with the classifiers.

D. Feature Extraction

Feature extraction is a process of minimizing dimensionality by reducing less effective features from raw data which to helps extract relevant features to improve predictive accuracy and control over-fitting. Fig. 2 indicates more significant features from bottom to top. From 14 features, we took the first 11 features that helped us get more accuracy. To extract the important features “sklearn.ensemble.ExtraTrees Classifier” class has been used.

E. Model Selection

The final data set was split into a training set (80%) and a testing set (20%). The top six common algorithms have been selected to explore the best-performance machine learning classifier for predicting heart disease.

a) Decision Tree (DT): A non-parametric supervised classification and regression learning method. The goal is to create a model that predicts the value of a target variable by learning simple rules of a decision based on data characteristics.

b) Support Vector Machine (SVM): A Vector Support Machine (SVM) is formally defined as a biased classifier by a particular hyper plane. The determination function of SVMs relies on some of the training data sub-sets called support vectors.

c) Naïve Bayes (NB): It is one of the learning algorithms that are commonly used. The NB classifier is a Bayes rule-based probabilistic model. We used GaussianNB in this current study to create a predictive model.

d) Random Forest (RF): Random forest (RF) is a meta estimator that suits a variety of decision tree classifiers on different data set sub-samples and uses the average to boost predictive precision and over-fitting power.

e) Logistic Regression (LR): It is a probabilistic classifier, generally applied to problems of binary classification.

f) Quadratic Discriminant Analysis (QDA): A quadratic classifier is used to distinguish observations from two or more groups of artifacts or occurrences by a quadric layer in ML and numerical classification.

In this study, all of the above algorithms were implemented using Scikit-learn which is a Python-based open-source machine learning library.

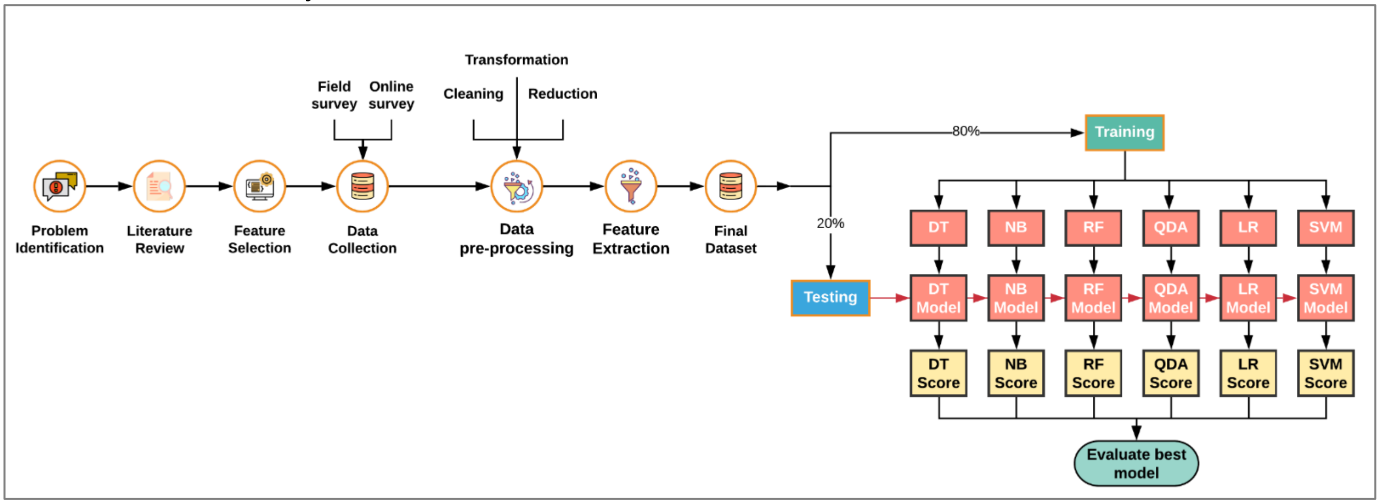

N.B. DT= Decision Tree, SVM=Support Vector Machine, NB=Naive Bayes, RF=Random Forest, LR=Logistic Regression, QDA= Quadratic Discriminant Analysis

Fig. 1. Methodological Framework.

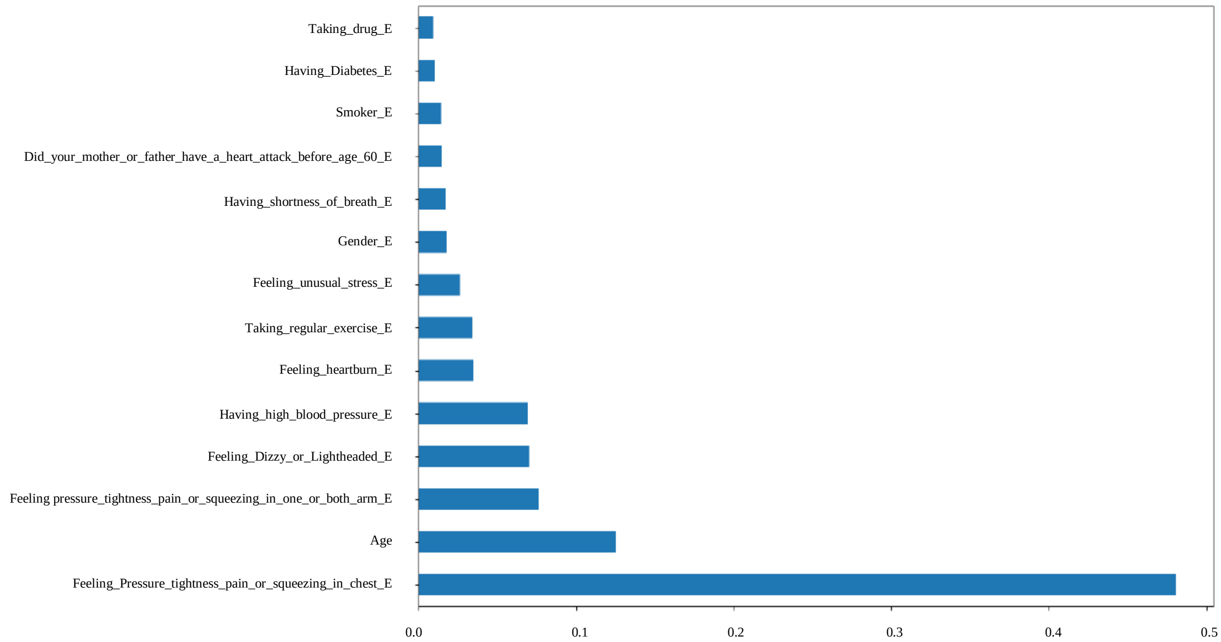

Fig. 2. Feature Importance.

III. Data Analysis and Result

A. Respondents based on Gender

3,500 survey questionnaires had been distributed to collect the primary data, over the heart patients and normal people. Total 1247 responses were collected and preprocessed. After removing the irrelevant, incomplete, inconsistent records, 1201 records were selected for analysis. The proportion of participants among male and female were 57% and 43% respectively. Where the participants ' age ranged from 10 to 95. Table II represents the frequency distribution of the overall dataset according to gender.

B. Materials and Feature Selections

As our key objective is to early predict heart disease without performing any medical test, we focused on the external symptoms of heart disease to design survey questionnaires. 14 individual factors were identified and selected for survey questionnaires to achieve the research goal. To improve prediction accuracy and control over-fitting, feature selection algorithm was performed and 12 out of 14 most important features were selected for final analysis (see Table III and Fig. 2).

C. Performance Measurement of Classification Algorithms

a) Confusion matrix: A confusion matrix is represented by a table (see Table IV) that measures the performance of a classification model. By using certain terminologies (TP, TN, FP, FN), it summarizes a classifier's correct and incorrect predictions. In a confusion matrix, True Positive (TP) represents the correctly predicted positive values, True Negative (TN) represents correctly predicted negative values, False Positive (FP) represents that the classifier predicted the value as positive but it was false, False Negative (FN) represents that the classifier predicted the value as negative but it was false. Fig. 3 represents the summary of the confusion matrix of the selected classifiers.

b) Precision: Precision represents the ratio of correctly predicted positive observations of the total predicted positive observations. High precision indicates that the classification model has a low false-positive rate. Table V shows the performance evaluation of the selected classifiers where the Support Vector Machine (SVM) gives high precision.

Precision (P) = TP/ (TP+FP)

c) Recall: Recall which is commonly known as sensitivity represents the ratio of correctly predicted positive observations to all observations in the actual class. Recall measures what proportion of people that actually had heart disease was diagnosed by the classifier as having heart disease. Support Vector Machine (SVM) gives a high recall rate among all other classifiers (see Table V).

Recall (Sensitivity) = TP/TP+FN

d) F1-score: F1-Score represents the weighted average of Precision and Recall that measures a test's accuracy. In our study, Support Vector Machine (SVM) gives a high F1-score rate among all other classifiers (see Table V).

F1-Score = 2*(Recall * Precision) / (Recall + Precision)

TABLE. II. Frequency Distribution According to Sex

Gender	Frequency	Frequency distribution	People type	
			Heart patient	***Normal***
Male	711	57%	51.6%	48.4%
Female	536	43%	52.1%	47.9%

TABLE. III. Feature Details

Features	Feature rank according to the importance	Final feature selection status
Feeeling_pressure_tightness _pain_or_squeezing_in_chest	1	Yes
Age	2	Yes
Feeling_pressure_tightness_pain_or_squeezing_in_one_or_both_arm	3	Yes
Feeling_Dizzy_or_Lightheaded	4	Yes
Having_high_blood_pressure	5	Yes
Feeling_heartburn	6	Yes
Taking_regular_extercise	7	Yes
Feeling_unusual_stress	8	Yes
Gender	9	Yes
Having_shortness_of_breath	10	Yes
Having_parents_heart_attack_before_age_60	11	Yes
Smoker	12	Yes
Having_Diabetes	13	No
Taking_drug	14	No

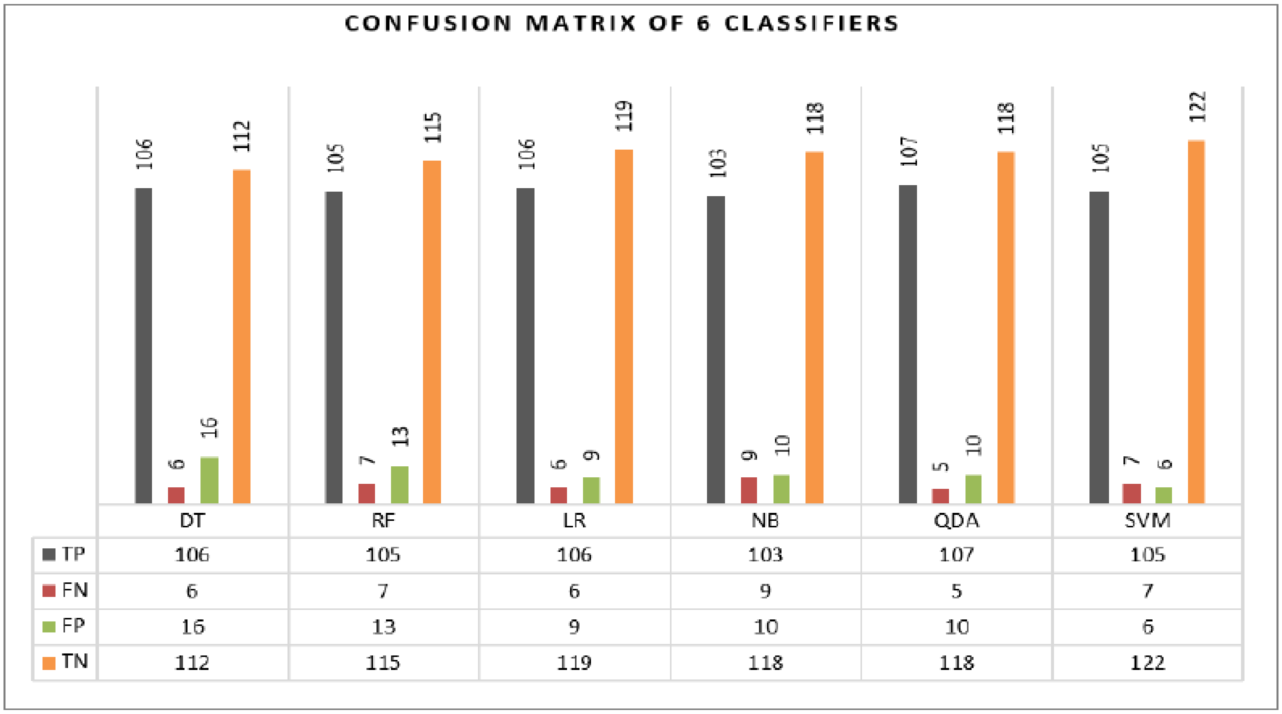

N.B. TP = True Positive, TN = True Negative, FN = False Negative, FP = False Positive, DT = decision tree; SVM = Support Vector Machine, NB = Naive Bayes, RF = Random Forest, LR = Logistic Regression, QDA = Quadratic Discriminant Analysis

Fig. 3. Summary of the Confusion Matrix of the Selected Classifiers.

TABLE. IV. CONFUSION MATRIX

	Predicted **0**	Predicted **1**
Actual **0**	**TN**	**FP**
Actual **1**	**FN**	**TP**

TABLE. V. PERFORMANCE EVALUATION OF THE SELECTED CLASSIFIERS

Classifier	Accuracy	Class	Precision	Recall	F1-score	Support
Naïve Bayes	92%	Heart Patient	0.91	0.92	0.92	112
		Normal	0.93	0.92	0.93	128
Quadratic Discriminant Analysis	94%	Heart Patient	0.91	0.96	0.93	112
		Normal	0.96	0.92	0.94	128
Logistic Regression	94%	Heart Patient	0.92	0.95	0.93	112
		Normal	0.95	0.93	0.94	128
Support Vector Machine	**95%**	**Heart Patient**	**0.95**	**0.94**	**0.94**	**112**
		Normal	**0.95**	**0.95**	**0.95**	**128**
Decision Tree	91%	Heart Patient	0.87	0.95	0.91	112
		Normal	0.95	0.88	0.91	128
Random Forest	92%	Heart Patient	0.89	0.94	0.91	112
		Normal	0.94	0.90	0.92	128

IV. Discussion

The diagnosis of cardiac disease is usually based on the patient's signs, external symptoms, and physical tests. Since the diagnosis of heart disease is time-consuming and expensive, this type of treatment cannot be adopted by everyone. So providing quality services at manageable cost has become a major issue. The purpose of the present study is to find an effective and less expensive way to predict heart disease based on the external risk factors.

The overall study was conducted on 1247 samples where 51% of the sample had heart disease and 49% of the sample was normal (see Table II). A total of 14 external risk factors were identified (see Table III) and 12 factors were eventually selected for further analysis based on the importance of the feature. Six distinct machine learning classifiers (Decision Tree, Random Forest, Naive Bayes, Support Vector Machine, Quadratic Discriminant, and Logistic Regression) were used to obtain the best result. The confusion matrix of prediction results is presented in Fig. 3. The result shows that the Support Vector Machine performed best to identify True negative values. Concurrently, Quadratic Discriminant Analysis did its best to define True Positive values. Overall results (see Table V), however, show that SVM outperformed all other machine learning classifiers with a peak classification accuracy of 95%, whereas LR and QDA (94%) achieved second-highest classification accuracy. Through contrast, the overall recall of 94.5 percent, 94 percent and 94 percent was shown by all three classifiers. At the same time, NB, DT, RF displays 92%, 91%, and 92% accuracy, respectively.

V. Conclusion and Future Work

Globally, heart disease (also known as cardiovascular disease) has become a major concern due to its destructive behaviour. It can be detected or diagnosed by different medical tests by considering various internal factors. Predicting heart disease (based on internal factors) using Machine Learning is a common approach. However, there are very few studies conducted on heart disease prediction based on external factors. In this study, we proposed a heart disease prediction model (based on external factors) using a machine learning approach that enables predicting heart disease with 95% accuracy. To acquire the best result, six distinct machine learning classifiers (Decision Tree, Random Forest, Naive Bayes, Support Vector Machine, Quadratic Discriminant, and Logistic Regression) were used. Findings reveal that Support Vector Machine (SVM) outperforms the others with greater accuracy (95%). This study's future work involves designing an Android-based application that is based on the results of the current study and helping the general public predict their cardiovascular disease at no cost.

References

[1] Y. Gultepe and S. Rashed, “The Use of Data Mining Techniques in Heart Disease Prediction,” International Journal of Computer Science and Mobile Computing, vol. 8, no. 4, pp. 136–141, Apr. 2019.

[2] J. Thomas and R. T. Princy, "Human heart disease prediction system using data mining techniques," 2016 International Conference on Circuit, Power and Computing Technologies (ICCPCT), Nagercoil, 2016, pp. 1-5.doi: 10.1109/ICCPCT.2016.7530265.

[3] AK. Peters A. Dewan and M. Sharma, "Prediction of heart disease using a hybrid technique in data mining classification," 2nd International Conference on Computing for Sustainable Global Development (INDIACom), New Delhi, 2015, pp. 704-706.

[4] S. Pouriyeh, S. Vahid, G. Sannino, G. De Pietro, H. Arabnia and J. Gutierrez, "A comprehensive investigation and comparison of Machine Learning Techniques in the domain of heart disease," 2017 IEEE Symposium on Computers and Communications (ISCC), Heraklion, 2017, pp. 204-207.doi: 10.1109/ISCC.2017.8024530.

[5] P. Singh, S. Singh, and G. S. Pandi-Jain, “Effective heart disease prediction system using data mining techniques,” International Journal of Nanomedicine, vol. 13, pp. 121–124, 2018.

[6] A. K. Dwivedi, “Performance evaluation of different machine learning techniques for prediction of heart disease,” Neural Computing and Applications, vol. 29, no. 10, pp. 685–693, 2016.

[7] C. B. Gokulnath and S. P. Shantharajah, “An optimized feature selection based on genetic approach and support vector machine for heart disease,” Cluster Computing, vol. 22, no. S6, pp. 14777–14787, 2018.

[8] 22nd IEEE Symposium on Computers and Communication (ISCC 2017): Workshops - ICTS4eHealth 2017.

[9] Srinivas, K., Rani, B.K., Govrdhan, A., 2010. “Applications of data mining techniques in healthcare and prediction of heart attacks”. Int. J. Comput. Sci. Eng. (IJCSE), 2010, Vol. 2, No. 2, pp. 250–255.

[10] S. Babu et al., "Heart disease diagnosis using data mining technique," 2017 International conference of Electronics, Communication and Aerospace Technology (ICECA), Coimbatore, 2017, pp. 750-753. doi: 10.1109/ICECA.2017.8203643.

[11] Archive.ics.uci.edu. (1988). UCI Machine Learning Repository: Heart Disease Data Set. [online] Available at: https://archive.ics.uci.edu/ml/datasets/heart+Disease [Accessed 26 Dec. 2019].

[12] A. K. Paul, P. C. Shill, M. R. I. Rabin, and K. Murase, “Adaptive weighted fuzzy rule-based system for the risk level assessment of heart disease,” Applied Intelligence, vol. 48, no. 7, pp. 1739–1756, Jun. 2017.

[13] Mamatha Alex P and Shaicy P Shaji, “Prediction and Diagnosis of Heart Disease Patients using Data Mining Technique " International Conference on Communication and Signal Processing, April 4-6, 2019, India.

[14] S. Bashir, Z. S. Khan, F. Hassan Khan, A. Anjum and K. Bashir, "Improving Heart Disease Prediction Using Feature Selection Approaches," 16th International Bhurban Conference on Applied Sciences and Technology (IBCAST), Islamabad, Pakistan, 2019, pp. 619-623. doi: 10.1109/IBCAST.2019.8667106.

[15] A. K. Paul, P. C. Shill, M. R. I. Rabin and M. A. H. Akhand, "Genetic algorithm based fuzzy decision support system for the diagnosis of heart disease," 5th International Conference on Informatics, Electronics and Vision (ICIEV), Dhaka, 2016, pp. 145-150. doi: 10.1109/ICIEV.2016.7759984.

[16] J. K. Kim and S. Kang, “Neural Network-Based Coronary Heart Disease Risk Prediction Using Feature Correlation Analysis,” Journal of Healthcare Engineering, vol. 2017, pp. 1–13, 2017.

[17] M. Sultana, A. Haider and M. S. Uddin, "Analysis of data mining techniques for heart disease prediction," 2016 3rd International Conference on Electrical Engineering and Information Communication Technology (ICEEICT), Dhaka, 2016, pp. 1-5. doi: 10.1109/CEEICT.2016.7873142.

[18] T. Karayılan and Ö. Kılıç, "Prediction of heart disease using neural network," 2017 International Conference on Computer Science and Engineering (UBMK), Antalya, 2017, pp. 719-723. doi: 10.1109/UBMK.2017.8093512.

[19] K. Mathan, P. M. Kumar, P. Panchatcharam, G. Manogaran, and R. Varadharajan, “A novel Gini index decision tree data mining method with neural network classifiers for prediction of heart disease,” Design Automation for Embedded Systems, vol. 22, no. 3, pp. 225–242, Nov. 2018.

Embracing Localization Inaccuracy with a Single Beacon

Anisur Rahman[1]
Dept. of Computer Science and Engineering
East West University, Dhaka, Bangladesh

Vallipuram Muthukkumarasamy[2]
School of Information and Communication Technology
Griffith University, Gold Coast, Australia

***Abstract*—This paper illustrates a new mechanism to determine the coordinates of the sensors using a beacon node and determines the definitive error associated with it. In UWSNs (underwater wireless sensor networks), actual and precise location of the deployed sensors which accumulate data is vital, because the accumulated data without the location information has less significance. Moreover it has limited value in the domain of location based services. In UWSN, trilateration or multilateration is exploited to assess the location of the deployed hosts; having three or more reference nodes to localize a deployed sensor is not pragmatic at all. On the other hand, non-linear equations are usually solved in conventional method where degree-of-freedom is uncertain to lead to an exclusive solution. In this paper, associated localization inaccuracies has been shown for a unique configuration where a single beacon is used to determine the coordinates of three deployed sensors simultaneously. Cayley-Menger determinant is used for the configuration and system of nonlinear distance equations have been linearized for better accuracy and convergence. Simulations with Euclidean distances validate the propounded model and reflect the acquired accuracies in sensors' coordinates and bearings. Moreover, an experiment has been conducted with ultrasonic sensors in terrestrial environments to validate the proposed model; the associated inaccuracies were found to be generated from the distance measurement errors; on the other hand, considering Euclidean distances proves the model to be precise and accurate.**

Keywords*—Underwater localization; linearization; mobile beacon; Cayley-Menger determinant; bearing; underwater wireless sensor network

I. Introduction

Localization has become very prominent to provide location oriented services in terrestrial environment as well as in underwater. There are many underwater domains where localization of the submerged sensors and devices sometimes become crucial. Among them data collection for the sustenance of marine biome, finding lost objects, estuary monitoring and autonomous underwater vehicles control for military or research purposes are very common. These sorts of marine exploration are not only for the profusion of wealth the ocean has, it is also very vital for geological research to detect the movement of tectonic plates [1]. Some of these objectives require accurate localization for meaningful interpretation sensed data [2]. Erroneous localization is quite common; the degree of error in coordinates of the devices plays a vital role in comprehension of the problem and to provide solutions.

Location oriented services are become popular nowadays; to meet the demand, a plethora of methods have been proposed. These methods can be categorized as range-based and range-free schemes. Range based mainly depends on the distances between nodes, whereas range-free deals with profiling of the environment. Between these methods, accuracy of range based scheme is higher than that of range-free. In addition to that, former can be applied to a dynamic ever changing environment; whereas later performs well if environment is static. Generally multiple reference nodes are used for underwater localization; however, having one or many reference node is quite impractical. In this research paper, we have propounded a model that consists of single mobile beacon (boat/buoy) and at least three deployed sensors – a very realistic situation and typical configuration as depicted in Fig. 1. Moreover, acoustic signal is used for measuring inter node distances. In underwater wireless sensor networks, acoustic signals propagation and channels are naturally employed for distance measurements in contrast to radio signals [1,3].

Having no preinstalled infrastructure in a dynamic configuration that can occur anytime is obvious. Hence, the proposed model kept in mind the natural occurrence and pragmatic nature of solutions. The model uses Cayley-Menger determinant and linearization of non-linear system of equations. Among few assumptions, surfing boat's plane and the deployed sensors' plane are in parallel state, which is sometimes the case in a water tank. Besides, voluntary and/or uncontrolled mobility of the nodes and in-situ measurement of speed of acoustic signals are kept for future exploration. This paper covers a simulation as well as hardware experiment in terrestrial environment. The results suggest negligible errors if true Euclidean distances are considered between beacon and deployed nodes. Positional errors found to be in 10^{-12} to 10^{-14}m range for a 150m water column. If Gaussian error is added, the positional errors still remain within acceptable range for a sensor with a size of 0.25-0.5m in length. It is conspicuous that distances between devices are the controlling factor for pin pointing the nodes. These negligible errors in simulations and experiments validate the proposed model.

The organization of the remaining paper is as follows. Section II focuses on acoustic signals propagation and distance measurement algorithm. Section III explains the proposed mathematical model; simulation, experimental results and analysis are elaborated in Sections IV, V and VI, respectively. Section VII states related works with associated constraints and finally conclusions in Section VIII.

II. Flight Time of Acoustic Signals

To determine the distances between beacon and deployed sensors, average speed of underwater acoustic signal is generally accepted to be 1500m/s. Propagation of radio signals has limitations; acoustic signals travel much slower than radio signal; on the contrary, acoustic's propagation distance is much higher than that of radio in underwater. Nowadays, researchers shown a fervent interest in using radio underwater; in line of such a drive, we tend to use each of its merit. In hardware experiment in terrestrial, electrical signals has been used instead of radio; in the distance measurement method, we propose radio to be used for synchronization and acoustic for signal transfer.

A. Assumptions:

- Radio and acoustic signals can be generated simultaneously by the beacon node.
- Sensor nodes are stationary; beacon and sensor nodes are in parallel plane state.

Steps:

Radio and acoustic signals are generated simultaneous by beacon $S_j, j = 4,5....$ at t_0 (S_j : possible positions of the beacon)

Submerged sensors position $S_i, i = 1,2,3$ as in Fig. 1

1) Sensors receive the radio signals immediately at $t_{Ra(rec)} = t_0 + \varepsilon$ (ε : flight time of radio signal between beacon and sensors).

2) Sensor receives the acoustic signals after a while at $t_{Ac(rec)}$; here $(t_{Ac(rec)} - t_0) >> (t_{Ra(rec)} - t_0)$ due to high speed of radio signals.

Time of acoustic signals travelled from beacon to sensors:

$$T_{ij(Travel)} = t_{Ac(rec)} - t_{Ac(tra)} = t_{Ac(rec)} - t_{Ra(tra)} \quad \because t_{Ac(tra)} = t_{Ra(tra)}$$

$$\therefore T_{ij(Travel)} \approx t_{Ac(rec)} - t_{Ra(rec)} \quad \because t_{Ra(rec)} = t_0 + \varepsilon \approx t_{Ra(tra)}$$

$T_{ij(Travel)}$: time beacon gets once sensors send with individual ID using radio signals

Eventually the distances between the beacon and sensors are computed by: $d_{ij} = \overline{\mathrm{v}} \times T_{ij(travel)}$ (here, $\overline{\mathrm{v}}$ is average speed of acoustic signals for the water column).

III. Coordinates Determination

B. Coordinates of the Sensors(Origing at the Sensor)

The prime intention of localization process is to determine positions and bearing accurately with the use of gathered distances between beacon and deployed sensors. Distances are the only values available; traditionally it is assessed as a problem of optimization where objective functions that require minimization have residuals of distance equations. Typically in principle, number of equations should be at least equal to the number of unknown variables in the system. This concept known as degree-of-freedom may not guarantee a unique solution for a non-linear system of equations. Conventionally, multilateration is applied in solving this sort of non-linear system i.e. to determine locations or coordinates, in partial or full. In [4], Guevara et al. showed that initial condition is vital for the convergence of optimization algorithms; where they linearized the nonlinear equations and bypassed associated convergence problem.

Fig. 1 depicts the domain comprises of the beacon node $S_j, j = 4,5...9$ and deployed three sensors $S_i, i = 1,2,3$. One of the underwater sensors $S_i, i = 1,2,3$ is considered to be the origin $(0,0,0)$ of the Cartesian system and found trilateration equations are grouped in two. The distances between the beacon node and sensors are measured values $d_{14}, d_{24}, d_{34}....$ and internode distances d_{12}, d_{13}, d_{23} as well as volume of tetrahedron V_t which is formed by surfaced beacon and underwater sensors are unknown. Depending on the local positioning system configuration depicted in Fig. 1, we determine the equations that include all known and unknown distances. So, Cayley-Menger determinant is used to determine the volume of tetrahedron V_t as follows:

$$288\, V_t^2 = \begin{vmatrix} 0 & 1 & 1 & 1 & 1 \\ 1 & 0 & d_{12}^2 & d_{13}^2 & d_{14}^2 \\ 1 & d_{12}^2 & 0 & d_{23}^2 & d_{24}^2 \\ 1 & d_{13}^2 & d_{23}^2 & 0 & d_{34}^2 \\ 1 & d_{14}^2 & d_{24}^2 & d_{34}^2 & 0 \end{vmatrix} \qquad (1)$$

By expanding (1), we obtain:

$$d_{34}^2 d_{23}^2 - d_{34}^2 d_{12}^2 + d_{34}^2 d_{13}^2 - \frac{d_{14}^2 d_{23}^4}{d_{12}^2} + d_{23}^2 d_{14}^2 + \frac{d_{13}^2 d_{14}^2 d_{23}^2}{d_{12}^2} - \frac{d_{24}^2 d_{13}^4}{d_{12}^2} + \frac{d_{13}^2 d_{23}^2 d_{24}^2}{d_{12}^2} + d_{13}^2 d_{24}^2 - d_{13}^2 d_{23}^2 - 144 \frac{V_t^2}{d_{12}^2} + \frac{d_{14}^2 d_{23}^2 d_{24}^2}{d_{12}^2} + \frac{d_{14}^2 d_{23}^2 d_{34}^2}{d_{12}^2} - \frac{d_{23}^2 d_{24}^2 d_{34}^2}{d_{12}^2} - \frac{d_{14}^4 d_{23}^2}{d_{12}^2} + \frac{d_{13}^2 d_{24}^2 d_{34}^2}{d_{12}^2} - \frac{d_{13}^2 d_{14}^2 d_{34}^2}{d_{12}^2} + \frac{d_{13}^2 d_{14}^2 d_{24}^2}{d_{12}^2} - \frac{d_{13}^2 d_{24}^4}{d_{12}^2} - d_{34}^4 + d_{24}^2 d_{34}^2 + d_{14}^2 d_{34}^2 - d_{14}^2 d_{24}^2 = 0$$

By separating known variables from unknown, we get:

$$d_{34}^2\left(d_{12}^2 - d_{23}^2 - d_{13}^2\right) + d_{14}^2\left(\frac{d_{23}^4}{d_{12}^2} - d_{23}^2 - \frac{d_{13}^2 d_{23}^2}{d_{12}^2}\right) + d_{24}^2\left(\frac{d_{13}^4}{d_{12}^2} - \frac{d_{13}^2 d_{23}^2}{d_{12}^2} - d_{13}^2\right) - \left(d_{14}^2 d_{24}^2 + d_{14}^2 d_{34}^2 - d_{24}^2 d_{34}^2 - d_{14}^4\right)\frac{d_{23}^2}{d_{12}^2} - \left(d_{34}^2 d_{24}^2 - d_{14}^2 d_{34}^2 + d_{14}^2 d_{24}^2 - d_{24}^4\right)\frac{d_{13}^2}{d_{12}^2} + \left(144 \frac{V_t^2}{d_{12}^2} + d_{13}^2 d_{23}^2\right) = \left(d_{24}^2 d_{34}^2 - d_{34}^4 + d_{14}^2 d_{34}^2 - d_{14}^2 d_{24}^2\right)$$

Here, $\left(\frac{d_{23}^4}{d_{12}^2} - d_{23}^2 - \frac{d_{13}^2 d_{23}^2}{d_{12}^2}\right)$, $\left(\frac{d_{13}^4}{d_{12}^2} - \frac{d_{13}^2 d_{23}^2}{d_{12}^2} - d_{13}^2\right)$, $\left(d_{12}^2 - d_{23}^2 - d_{13}^2\right)$, $\frac{d_{23}^2}{d_{12}^2}$, $\frac{d_{13}^2}{d_{12}^2}$, and $\left(144 \frac{V_t^2}{d_{12}^2} + d_{13}^2 d_{23}^2\right)$ are considered as unknown variables.

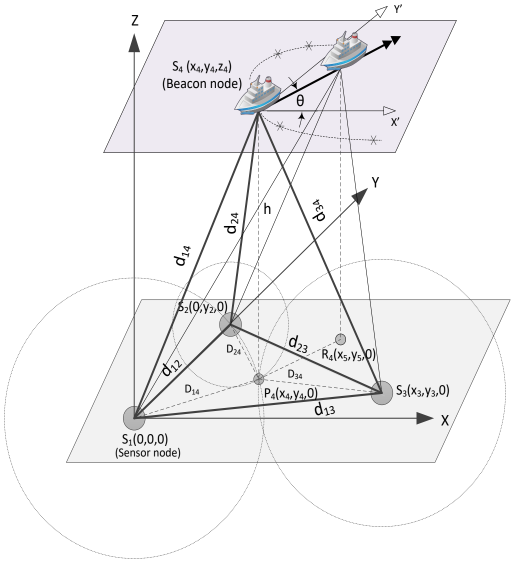

Fig. 1. Coordinates Determination.

So, we get:

$$d_{14}^2 X_1 + d_{24}^2 X_2 + d_{34}^2 X_3 - \left(d_{14}^2 - d_{34}^2\right)\left(d_{24}^2 - d_{14}^2\right) X_4 - \left(d_{24}^2 - d_{14}^2\right)\left(d_{34}^2 - d_{24}^2\right) X_5 + X_6 = \left(d_{24}^2 - d_{34}^2\right)\left(d_{34}^2 - d_{14}^2\right) \quad (2)$$

Equation (2) has six unknowns, which matches with the linear form of $a_1 x_1 + a_2 x_2 + \cdots + a_n x_n = b_1$. As there are six unknowns, to solve we have taken six measurements. The measurements can be taken following aforesaid procedure by steering the beacon node $S_j, j = 4,5....9$ to different area of the water surface. These six measurements can be taken at the vicinity of S_4, it is worth mentioning that the deployed underwater sensors are considered to be static at the time of measuring distances. By omitting references to the variables we get an array of all coefficients recognized as augmented matrix, where first row of the array represents the first linear equation and so on as $AX = b$ form. So, system of linear equations can be expressed as following:

$$A = \begin{bmatrix} d_{14}^2 & d_{24}^2 & d_{34}^2 & -\left(d_{14}^2 - d_{34}^2\right)\left(d_{24}^2 - d_{14}^2\right) & -\left(d_{24}^2 - d_{14}^2\right)\left(d_{34}^2 - d_{24}^2\right) & 1 \\ d_{15}^2 & d_{25}^2 & d_{35}^2 & -\left(d_{15}^2 - d_{35}^2\right)\left(d_{25}^2 - d_{15}^2\right) & -\left(d_{25}^2 - d_{15}^2\right)\left(d_{35}^2 - d_{25}^2\right) & 1 \\ \vdots & \vdots & \vdots & \vdots & \vdots & \vdots \\ d_{19}^2 & d_{29}^2 & d_{39}^2 & -\left(d_{19}^2 - d_{39}^2\right)\left(d_{29}^2 - d_{19}^2\right) & -\left(d_{29}^2 - d_{19}^2\right)\left(d_{39}^2 - d_{29}^2\right) & 1 \end{bmatrix}$$

$$X = \begin{bmatrix} \left(\frac{d_{23}^4}{d_{12}^2} - d_{23}^2 - \frac{d_{13}^2 d_{23}^2}{d_{12}^2}\right) \\ \left(\frac{d_{13}^4}{d_{12}^2} - \frac{d_{13}^2 d_{23}^2}{d_{12}^2} - d_{13}^2\right) \\ \left(d_{12}^2 - d_{23}^2 - d_{13}^2\right) \\ \frac{d_{23}^2}{d_{12}^2} \\ \frac{d_{13}^2}{d_{12}^2} \\ \left(144\frac{V_t^2}{d_{12}^2} + d_{13}^2 d_{23}^2\right) \end{bmatrix} \qquad b = \begin{bmatrix} \left(d_{24}^2 - d_{34}^2\right)\left(d_{34}^2 - d_{14}^2\right) \\ \left(d_{25}^2 - d_{35}^2\right)\left(d_{35}^2 - d_{15}^2\right) \\ \vdots \\ \left(d_{29}^2 - d_{39}^2\right)\left(d_{29}^2 - d_{19}^2\right) \end{bmatrix}$$

From the above representation, after finding X_1, X_2, X_3, X_4, X_5 and X_6 we calculate d_{12}, d_{13} and d_{23} as follows:

$$d_{12}^2 = \frac{X_3}{\left(1 - X_4 - X_5\right)},\ d_{13}^2 = \frac{X_3 X_5}{\left(1 - X_4 - X_5\right)},\ d_{23}^2 = \frac{X_3 X_4}{\left(1 - X_4 - X_5\right)}$$

Here, coordinates of deployed underwater sensors S_1, S_2 and S_3 are considered to be $(0,0,0)$, $(0, y_2, 0)$ and $(x_3, y_3, 0)$ respectively; so, the inter sensor distances can be stated with respect to coordinates of the sensors are as follows:

$$d_{12}^2 = y_2^2,\ d_{13}^2 = x_3^2 + y_3^2,\ d_{23}^2 = x_3^2 + \left(y_3 - y_2\right)^2$$

So, the unknown variables can be derived as:

$$y_2 = d_{12},\quad y_3 = \frac{d_{12}^2 + d_{13}^2 - d_{23}^2}{2d_{12}},\ x_3 = \sqrt{\left(d_{13}^2 - \left(\frac{d_{12}^2 + d_{13}^2 - d_{23}^2}{2d_{12}}\right)^2\right)}$$

Here d_{12}, d_{13} and d_{23} are computed distances. Coordinates of the sensors for the proposed problem domain are illustrated in Table I as follows.

C. Coordinates of the Sensors (origing at the beacon)

So far we calculated the coordinates of the sensors with respect to S_1 which was considered to be the origin of the system. To find with respect to beacon, following steps need to be followed.

By incorporating depth sensor with the deployed nodes, the depth h in Fig. 1 can be measured as depicted in [5]. After measuring the vertical distance h in between the beacon node $S_4(x_4, y_4, z_4)$ and the XY plane, we can assume the projected coordinate of the beacon node $S_4(x_4, y_4, z_4)$ on the plane XY is $P_4(x_4, y_4, 0)$. To find x_4 and y_4, we can apply trilateration in the following manner assuming the distances between S_1, S_2, S_3 and P_4 are D_{14}, D_{24} and D_{34} respectively and device following relations.

$$D_{14}^2 = x_4^2 + y_4^2 \quad (3)$$

$$D_{24}^2 = x_4^2 + \left(y_4 - y_2\right)^2 \quad (4)$$

$$D_{34}^2 = \left(x_4 - x_3\right)^2 + \left(y_4 - y_3\right)^2 \quad (5)$$

TABLE. I. COORDINATES OF THE SENSORS

Sensors	Coordinates
S_1	$(0,0,0)$
S_2	$(0, d_{12}, 0)$
S_3	$\left(\sqrt{\left(d_{13}^2 - \left(\frac{d_{12}^2 + d_{13}^2 - d_{23}^2}{2d_{12}}\right)^2\right)}, \frac{d_{12}^2 + d_{13}^2 - d_{23}^2}{2d_{12}}, 0\right)$

From (3), (4) and (5) we obtain the projected beacon's coordinates $P_4(x_4, y_4, 0)$, where

$$x_4 = \frac{1}{2d_{12}}\sqrt{\left(4d_{12}^2 D_{14}^2 - (D_{14}^2 - D_{24}^2 + d_{12}^2\right)^2},$$

$$y_4 = \frac{1}{2d_{12}}\left(D_{14}^2 - D_{24}^2 + d_{12}^2\right)$$

As d_{14}, d_{24} and d_{34} are the hypotenuse of the $\Delta S_1P_4S_4$, $\Delta S_2P_4S_4$ and $\Delta S_3P_4S_4$ respectively, so it is possible to obtain D_{14}, D_{24} and D_{34} using Pythagorean Theorem. So the coordinate of the beacon node $S_4(x_4, y_4, z_4)$ would be (x_4, y_4, h) where all the elements are known.

$$\therefore S_4(x_4, y_4, h) =$$

$$S_4\left(\frac{1}{2d_{12}}\sqrt{\left(4d_{12}^2 D_{14}^2 - (D_{14}^2 - D_{24}^2 + d_{12}^2\right)^2}, \frac{1}{2d_{12}}\left(D_{14}^2 - D_{24}^2 + d_{12}^2\right), h\right)$$

By linear transformation, the origin (one of the sensor's coordinates) of the Cartesian system has been transferred to coordinates of the beacon; found sensors' coordinates with respect to beacon S_4 are depicted as in Table II.

TABLE. II. COORDINATES WITH RESPECT TO THE BEACON

	Coordinates
S_4	(0,0,0)
S_1	$\left(\frac{\sqrt{4d_{12}^2D_{14}^2 - \left(D_{14}^2 - D_{24}^2 + d_{12}^2\right)^2}}{2d_{12}}, \quad -\frac{1}{2d_{12}}\left(D_{14}^2 - D_{24}^2 + d_{12}^2\right), \quad -h\right)$
S_2	$\left(\frac{\sqrt{4d_{12}^2D_{14}^2 - \left(D_{14}^2 - D_{24}^2 + d_{12}^2\right)^2}}{2d_{12}}, \quad \frac{1}{2d_{12}}\left(d_{12}^2 - D_{14}^2 + D_{24}^2\right), \quad -h\right)$
S_3	$\left(\left(\sqrt{\left(d_{13}^2 - \left(\frac{d_{12}^2 + d_{13}^2 - d_{23}^2}{2d_{12}}\right)^2\right)} - \frac{\sqrt{4d_{12}^2D_{14}^2 - \left(D_{14}^2 - D_{24}^2 + d_{12}^2\right)^2}}{2d_{12}}\right), \quad \frac{1}{2d_{12}}\left(d_{13}^2 - d_{23}^2 - D_{14}^2 + D_{24}^2\right), \quad -h\right)$

IV. SIMULATION RESULTS

A simulation environment is created in Matlab for the aforesaid problem domain taking a sensor as the beacon (boat/buoy) and three sensors. The depth of the problem domain is considered for a 150m water column. The complexity of the simulated environment is discussed as well as positional errors for sensors have been elaborated in Table III. In [6], coordinates of the sensors with respect to beacon has been shown. With the simulated environment, it is possible to determine 3D coordinates of the sensors with bearing information; as the beacon is at the surface of the water, the coordinates could be known by GPS.

To validate the proposed model, three sensors are placed in random fashion on the XY plane and beacon, which is mobile is kept above XY plane. As the positions are random, one of the sensors is considered as the origin of the Cartesian system; the other sensors are on the y-axis and on any point of XY plane respectively. The model suggests that the beacon should be steered in six different locations to measure distances between the sensor above and the sensors on the XY plane. However, the sensors on the XY plane are considered to be static while the sensor (beacon) steers in six different locations. To verify the proposed mathematical model, at first true Euclidean distances were considered; afterward Gaussian errors in the distances added.

The orientations of the mobile beacon and its effects have been explored in [7]; straight line, circular line and angular Archimedean spirals of different radius (5-50m) are among them. Archimedean arc lengths of spirals of different radius are calculated according to (6) and (7).

$$r = a + b\theta \tag{6}$$

$$L = \int_a^b \sqrt{r^2 + \left(\frac{dr}{d\theta}\right)^2}\, d\theta \tag{7}$$

Here, r and θ are distance from origin and span from a to b respectfully.

We have found that true Euclidean distances between beacon and deployed sensors produce negligible errors. For a 150 m water column, positional errors remain within 10^{-12} to 10^{-14} m range, so we can conclude that for a sensor that has radius in meters, this negligible error validates the proposed mathematical model. The accuracy of the coordinates are denoted in Table III. It is worth noting that these errors in nanometre range produced from the linearization process of non-linear equations. It also illustrates that the beacon's orientation can be in any form other than straight movement; straight line mobility generates singular matrix. Moreover, span of the sensor mobile trajectory has no effect on coordinates. However, if the distance measurements are taken in close proximity, then generated errors can be kept minimal.

TABLE. III. POSITIONAL ERRORS FOR S_1, S_2 AND S_3 (WITH RESPECT TO BEACON :EUCLIDEAN DISTANCES)

Orientation (circular) (radius)	Positional Error		
	S_1(m)	S_2(m)	S_3(m)
5m	1.11×10^{-12}	1.99×10^{-12}	3.51×10^{-12}
10m	4.39×10^{-13}	8.93×10^{-13}	1.59×10^{-12}
15m	1.44×10^{-13}	2.15×10^{-13}	1.15×10^{-12}
20m	7.12×10^{-15}	5.70×10^{-14}	7.31×10^{-13}
50m	7.09×10^{-15}	4.24×10^{-14}	1.05×10^{-13}
Orientation (spiral) (single turn increase)	Positional Error		
	S_1(m)	S_2(m)	S_3(m)
5m	6.05×10^{-13}	1.20×10^{-12}	3.24×10^{-12}
10m	4.56×10^{-13}	9.26×10^{-13}	2.61×10^{-12}
15m	8.54×10^{-13}	1.67×10^{-12}	3.15×10^{-12}
20m	5.75×10^{-13}	1.15×10^{-12}	7.75×10^{-13}
50m	1.03×10^{-13}	2.56×10^{-13}	8.58×10^{-14}

V. Experimental Setup and Results

A. Description of the Setup

The problem domain suggests that at least three sensors need to be deployed underwater and a single beacon would remain on the surface of the water. Usually sensors are deployed in various numbers underwater to accumulate data; the number can range from a few to many. Among various methods, in our experiment flight time of the signals is considered to measure distances between beacon and deployed sensors as in [8]. We also assume that the experimental water column is considered to be homogeneous; though temperature, salinity and pressure (depth) affects the speed of acoustic signals. Most of the papers consider 1500m/s to be the speed of acoustic signals underwater; however, speed measurement of acoustic signal is not covered in this paper. Besides, signals propagation in this adverse environment and various other factors left unaddressed.

The experiment requires us to take multiple measurements according to the proposed model; we have also considered the plane i.e. the plane where beacon surfs and the plane of sensors to be in parallel state. However, non-parallel state scenario has not been considered in this paper. Besides, for simplicity, we considered the deployed sensors would be in static state while taking six measurements. The mobility of the sensors we tend to address in future. Fig. 1 illustrates a solvable configuration of the experiment in line of proposed model.

B. Devices and Setup

The experiment has been performed with an Arduino board connected to four HC-SR04 ultrasonic sonic sensors as in Fig. 2 and 3. Ultrasonic sensors are mainly used to determine distances with bouncing technique; which is, generated signal bounces back from the nearest obstacles that are positioned in front of the sensor. If the object's position is placed in angular fashion, i.e., is positioned not right in front of the sensor, HC-SR04 sensor will not be able to receive the bounced back signals. In this experiment we have customized the sensors as such that it does not measure the distance with bouncing signal,

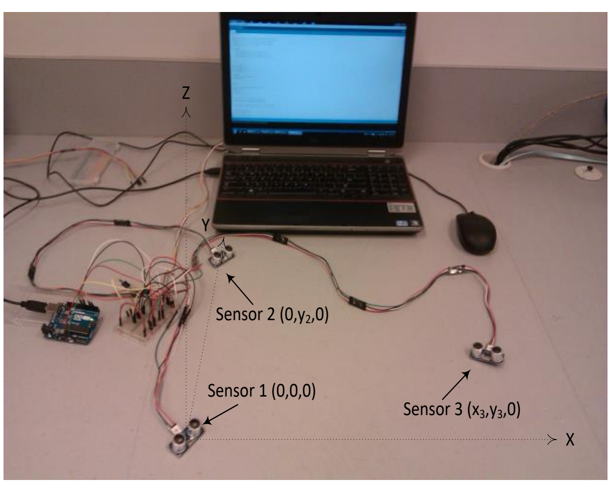

Fig. 2. Experimental Setup with Sensors in Terrestrial Environment with Sensors on the Floor and Beacon at the Ceiling.

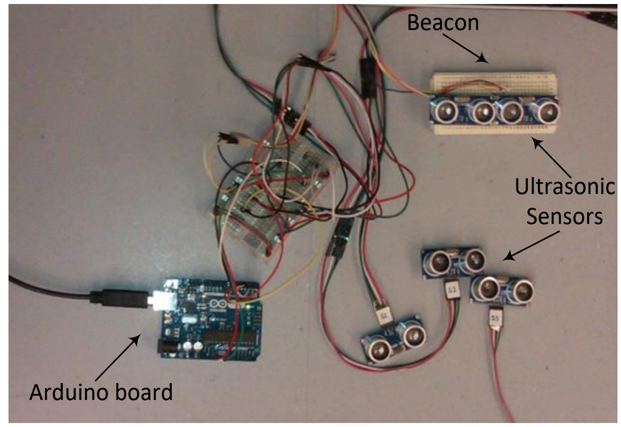

Fig. 3. Different ultrasonic Sensors and Board used in Experiment.

whereas the table top sensors detect the presence of signal that has been generated by the beacon sensor at the ceiling.

C. Experimental Results

The experiment has been conducted in two different orientations; four tests have been performed in each scenario as in Fig. 4 and 5. For each scenario positional errors are shown in Tables IV and V.

For the scenario 1, we can see that keeping the origin at the S_1, positional error for S_2 and S_3 are within 0.2 to 4cm range. Accuracy in distance measurements with the ultrasonic sensor generates accurate positional error: 0.17cm, whereas in extreme case it is 3.85cm.

For the scenario 2, we can see that keeping the origin at the S_1, positional error for S_2 and S_3 are within 0.5 to 6cm range. Accuracy in distance measurements with the ultrasonic sensor generates accurate positional error: 0.47cm, whereas in extreme case it is 5.90cm.

TABLE. IV. Positional Error for Scenario 1

	S_1(cm)	S_2(cm)	S_3(cm)
Test 1	0	0.17	0.42
Test 2	0	0.55	0.98
Test 3	0	0.73	1.02
Test 4	0	2.28	3.85

TABLE. V. Positional Error for Scenario 2

	S_1(cm)	S_2(cm)	S_3(cm)
Test 1	0	1.28	3.41
Test 2	0	1.12	2.97
Test 3	0	0.47	2.71
Test 4	0	2.11	5.90

Scenario 1:

Original coordinates of sensors:

S_1: (0,0,0); S_2: (0,20,0); S_3: (30,15,0)

Test 1

	S_1	S_2	S_3
R1	54.14	52.31	50.36
R2	57.96	52.65	51.10
R3	51.32	50.56	52.87
R4	61.11	52.49	55.71
R5	59.90	58.57	48.99
R6	60.14	55.04	50.17

Calculated Coordinates:

S_1: (0,0,0)
S_2: (0,19.83,0)
S_3: (29.58,14.94,0)

Test 2

	S_1	S_2	S_3
R1	62.57	57.27	52.20
R2	60.31	54.78	53.17
R3	53.39	52.60	55.01
R4	63.58	54.62	57.96
R5	62.32	60.94	50.98
R6	56.34	54.42	52.40

Calculated Coordinates:

S_1: (0,0,0)
S_2: (0,20.55,0)
S_3: (30.88,15.45,0)

Test 3

	S_1	S_2	S_3
R1	60.76	55.20	53.57
R2	56.76	54.83	52.79
R3	53.80	53.00	55.43
R4	64.06	55.03	58.40
R5	62.79	61.41	51.36
R6	63.04	57.71	52.60

Calculated Coordinates:

S_1: (0,0,0)
S_2: (0,20.73,0)
S_3: (30.93,15.42,0)

Test 4

	S_1	S_2	S_3
R1	65.58	59.57	57.81
R2	61.26	59.18	56.97
R3	58.06	57.20	59.82
R4	69.13	59.39	63.03
R5	67.77	66.27	55.43
R6	68.04	62.28	56.76

Calculated Coordinates:

S_1: (0,0,0)
S_2: (0,22.28,0)
S_3: (33.48,16.65,0)

Fig. 4. Calculated Coordinates of the Sensors According to Scenario 1.

Scenario 2:

Original coordinates of sensors:

S_1: (0,0,0); S_2: (0,25,0); S_3: (35,10,0)

Test 1

	S_1	S_2	S_3
R1	59.85	57.26	48.71
R2	50.32	53.25	51.74
R3	53.70	53.04	49.86
R4	51.20	49.57	53.90
R5	57.65	55.37	48.92
R6	55.25	50.62	52.43

Calculated Coordinates:

S_1: (0,0,0)
S_2: (0,23.72,0)
S_3: (33.26,12.94,0)

Test 2

	S_1	S_2	S_3
R1	65.34	62.51	53.19
R2	54.94	58.15	56.49
R3	55.90	54.13	58.85
R4	58.63	57.91	54.44
R5	62.95	60.46	53.42
R6	60.32	55.26	57.25

S_1: (0,0,0)
S_2: (0,26.12,0)
S_3: (36.55,12.54,0)

Test 3

	S_1	S_2	S_3
R1	56.77	52.01	53.88
R2	51.71	54.73	53.17
R3	55.18	54.51	51.24
R4	52.61	50.94	55.39
R5	59.25	56.90	50.28
R6	61.50	58.84	50.06

S_1: (0,0,0)
S_2: (0,24.53,0)
S_3: (34.33,12.63,0)

Test 4

	S_1	S_2	S_3
R1	65.85	63.24	55.88
R2	57.47	60.83	59.09
R3	61.33	60.58	56.95
R4	68.35	65.40	55.64
R5	58.47	56.62	61.57
R6	63.10	57.81	59.89

S_1: (0,0,0)
S_2: (0,27.11,0)
S_3: (37.85,15.17,0)

Fig. 5. Calculated Coordinates of the Sensors According to Scenario 2.

VI. Analysis and Discussions

Pragmatic approach of this method is having a single beacon at the water surface and sensors underwater. Having a boat or buoy in the time of crisis is natural than having multiples. Besides, this method won't require any preinstalled reference points; but still it can determine the coordinates of the sensors dynamically with negligible error. The proposed model is validated by considering true Euclidean distances; later on Gaussian error has been added to acquired distances. By taking true Euclidean distances, it has been shown that accuracy of distance determination would generate accuracy in coordinates.

The acquired result has been reinforced by experimenting three ultrasonic sensors on the table top and a beacon above those emulating the configuration as depicted earlier. Flight time i.e. the propagation time of acoustic signals is used to calculate the distances between beacon and underneath sensors. This way of measuring distance helps us to avoid multipath fading affect present in RSSI. It also shows that it is possible to calculate the distances between sensors as the pulses travel the shortest Euclidean distance. Fig. 6 shows the intended distance to be measured and acquired distances are considered to calculate coordinates of the sensors in Matlab.

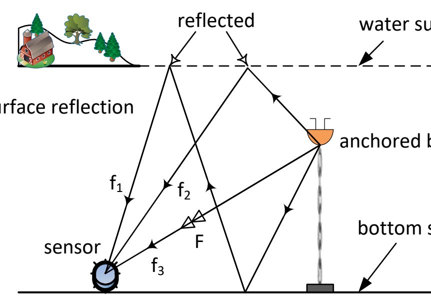

Fig. 6. Multipath Fading can be Avoided to Measure Shortest Euclidean Distance.

A. Internode Distances from Acoustic Signals' Flight Time

Ultrasonic sensor at the top generates TTL impulses in 40 KHz frequency and 3 sensors at the bottom receive the pulses and record the time. Speed of acoustic signal in normal environment in terrestrial is considered 340m/s i.e. it takes 29µs to travel 1cm of distance; by measuring the flight time of the acoustic signal it then calculates the distance between the beacon and the sensors. It is worth noting that clocks of all the sensors including the beacon at the top are synchronized as it is connected to the same Arduino board; besides the pulse generation time and a sample of generated impulse by the beacon is made available to the sensors to determine the signals' arrival time as soon as it travel the shortest Euclidean distance.

B. Problems and Challenges Encountered in Experiments

Mathematical model has been validated in simulated environment concluding the accuracy of the distance measurements are the limiting factor of the precise coordinates determination. Different scenario has been chosen for the experiment and each scenario is tested multiple times. In each test we needed to read the distances six times from different positions of the beacon. While reading the values time to time some readings were such that it does not comply with the real distance, and eventually did not converge in Matlab. In those cases we had to go for another test that ultimately converges. In each reading the measured distances for S_1, S_2 and S_3 have to be consistent.

The off the shelf sensors has 12^0 sentry angle which limits the beacon's movement span. Within this sentry angle, acquired positional errors are in the range of 0.5-6cm. Having an acoustic sensor with 4.5x1.5x1.5cm in size, this range of error is within acceptable range. In simulation, Cartesian coordinates has been used and one of the sensor is placed at the origin. The 150m water column has not been emulated in Matlab as distances between beacon and sensors are determined by considering flight time and its average speed. Besides, multipaths fading due to obstruction are left unaddressed in this paper. The simulation results also suggest that beacon's movement has limited effect on coordinates of the sensor. We have shown that angular and circular movement do not affect localization method except moving the beacon in straight line which leads to unsolvable singular matrix. In practice, moving in a very straight line is rare where current is present. In the method, expanded Cayley-Menger determinant is used calculate the volume of tetrahedron and derived equations are non-linear. Besides, due to six unknown variables, six individual measurements were necessary to solve linearized system of equations.

VII. Related Works

There are many localization algorithms where known values of few sensors are usually used to determine their positions, among them distances between sensor in time interval and bearing of any moment are common. Localization in terrestrial is popular field of research due to the demand of location oriented services. However, techniques that are used in terrestrial sometime may not be used in UWSNs due to different characteristics and heterogeneous nature of underwater world. Guevara et al. proposed a closed-form method where positions of nodes are not required to localize multiple static reference nodes in [4]; distances between mobile nodes and static reference nodes are sufficient for the proposed method. Recently, the preciseness of the model with Euclidean distances between beacon and sensors has been elaborated in [6]. The paper showed that the produced negligible errors were due to linearization process of the method. Moreover, the effect of Gaussian noise in distance measurements and its implication on coordinates and bearing have been shown in [7].

Signals propagation model for this type of heterogeneous environment is quite different than that of terrestrial environment; Chandrasekhar et al. explored and showed signal propagation difficulties and limitations in UWSNs in [9]. Among the plethora of proposed localization algorithms, few have shown the merit to be explored. In [10], three dimensional Euclidean distance estimation has been proposed; where a specific number of submerged nodes are required to measure internode distances. Besides, generated error in distance measurement propagates through the system due to its recursive behaviour. On the other hand, proposed method in [11] requires mobile sensors to communicate with moored nodes (buoys) for detecting its location. Besides, 3D positioning system in [12] requires four separate positions to determine the coordinates of the beacon. The major limitation of these methods are static inherently, dynamicity of localization is absent. Node requires to be moored to the waterbed in advance, which is cumbersome as well as possess inconveniences.

Duff and Muller delineates incorporates nonlinear least square method in their model to solve the system of multilateration equations in [13]. In the proposed model, authors have focused on the necessity of multiple equations that is gathered from different locations of the nodes – a criterion of degree-of-freedom analysis of system of linear equations. The proposed model has been validated in [14] by incorporating of Kalman filter with many folds. However, the complexity and inherent nature of degree-of-freedom have been shown in [15], which showed that it does not guarantee a unique solution for nonlinear system, such as trilateration. Trilateration or multilateration may not be solved when only parameter available is distances between nodes. Moreover, the prerequisites to have initial configuration of nodes have been justified with rigidity theory as well.

This paper focuses on the method of determining coordinates and bearing of submerged sensors and associated inaccuracies; a pragmatic method has been proposed where a single mobile node will be used to localize deployed submerged sensors. Having a single beacon without any preinstalled reference points is dynamic by nature. Recently, localization of submerged nodes with a single beacon has been illustrated in [16] for non-parallel state situation, i.e. the plane where the beacon surfs and the plane where three of the submerged sensors are deployed are not parallel. The paper also showed that it is the distance between beacon and nodes which affects the model, not the state of the planes.

VIII. Conclusions

Steadfast positioning is indispensable in various applications and services due to safety and research. Location oriented services are the demand of time regardless of terrestrial or underwater environment for conveniences. Among the plethora of localization models, this paper illustrates associated inaccuracies in the proposed mathematical model to determine coordinates and bearings of sensors with a single beacon (node) in real time considering the environment. The practical orientation of the proposed domain and the aforesaid model has been validated with simulation results having negligible errors. This paper showed the practicality of having a single boat/buoy (beacon) at the water surface while localizing deployed nodes instead of three or more beacons.

Simulation results showed negligible errors in coordinates of the nodes while Euclidean distances were considered. It also delineates the produces errors are due to erroneous distance determination between beacon and nodes. The accuracy of the distance measurements lead to pin pointing the nodes. Moreover, beacon's mobility and span has limited or almost no effect on coordinates. Experimental results performed in terrestrial environment also suggest that the inter node distances can be measured by calculating the flight time of acoustic signals with the help of electrical signal for clock synchronization. As acoustic signal is affected by environmental constraints; inaccuracies in distance determinations were due to signals propagations and signal processing limitation of the ultrasonic sensors. Eventually coordinates of the sensors can be determined with a single beacon following proposed model with inevitable error due to inaccuracies in distance determinations.

In future, we intend to address voluntary mobility of the autonomous underwater vehicles and involuntary mobility of the freely deployed sensors due to currents in the proposed model.

REFERENCES

[1] J. H. Cui, J. Kong, M. Gerla, and S. Zhou, "The challenges of building mobile underwater wireless networks for aquatic applications," Network, IEEE, vol. 20, pp. 12-18, 2006.

[2] L. Hu, B. Liu, K. Zhao, X. Meng, and F. Wang, "Research and Implementation of the Localization Algorithm Based on RSSI Technology," Journal of Networks, vol. 9, pp. 3135-3142, 2014.

[3] P. Xie, J. H. Cui, and L. Lao, "VBF: vector-based forwarding protocol for underwater sensor networks," Networking Technologies, Services, and Protocols; Performance of Computer and Communication Networks; Mobile and Wireless Communications Systems, pp. 1216-1221, 2006.

[4] J. Guevara, A. Jiménez, J. Prieto, and F. Seco, "Auto-localization algorithm for local positioning systems," Ad Hoc Networks, vol. 10, pp. 1090-1100, 2012.

[5] I. Vasilescu, K. Kotay, D. Rus, M. Dunbabin, and P. Corke, "Data collection, storage, and retrieval with an underwater sensor network," in Proceedings of the 3rd international conference on Embedded networked sensor systems, pp. 154-165, 2005.

[6] A. Rahman, V. Muthukkumarasamy, and E. Sithirasenan, "Coordinates Determination of Submerged Sensors Using Cayley-Menger Determinant," in Distributed Computing in Sensor Systems (DCOSS), IEEE, pp. 466-471, 2013.

[7] A. Rahman, V. Muthukkumarasamy, and X. Wu, “Coordinates and Bearing of Submerged Sensors Using a Single Mobile Beacon (CSMB)”, Journal of Networks, Vol. 10 No. 8, 2015.

[8] A. Rahman, V. Muthukkumarasamy, and E. Sithirasenan, "Localization of Submerged Sensors Using Radio and Acoustic Signals with Single Beacon," in Ad-hoc, Mobile, and Wireless Network. LNCS. vol. 7960, J. Cichoń, M. Gębala, and M. Klonowski, Eds., ed: Springer Berlin Heidelberg, pp. 293-304, 2013.

[9] V. Chandrasekhar, W. K. G. Seah, Y. S. Choo, and H. V. Ee, "Localization in underwater sensor networks: survey and challenges," in International Conference on Mobile Computing and Networking: Proceedings of the 1st ACM international workshop on Underwater networks,pp. 33-40, 2006.

[10] Z. Zhou, J. H. Cui, and S. Zhou, "Efficient localization for large-scale underwater sensor networks," Ad Hoc Networks, vol. 8, pp. 267-279, 2010.

[11] T. C. Austin, R. P. Stokey, and K. M. Sharp, "PARADIGM: a buoy-based system for AUV navigation and tracking," in OCEANS 2000 MTS/IEEE Conference and Exhibition, pp. 935-938 vol.2, 2000.

[12] J. C. Prieto, A. R. Jiménez, J. Guevara, J. L. Ealo, F. Seco, J. O. Roa, and F. Ramos, "Performance evaluation of 3D-LOCUS advanced acoustic LPS," IEEE Transactions on Instrumentation and Measurement, vol. 58, pp. 2385-2395, 2009.

[13] P. Duff and H. Muller, "Autocalibration algorithm for ultrasonic location systems," in Seventh IEEE International Symposium on Wearable Computers, 2003. Proceedings, pp. 62-68, 2003.

[14] E. Olson, J. Leonard, and S. Teller, "Robust range-only beacon localization," in Autonomous Underwater Vehicles, IEEE/OES, pp. 66-75, 2004.

[15] J. Guevara, A. R. Jimenez, A. S. Morse, J. Fang, J. C. Prieto, and F. Seco, "Auto-localization in Local Positioning Systems: A closed-form range-only solution," in IEEE International Symposium on Industrial Electronics (ISIE), pp. 2834-2840, 2010.

[16] A. Rahman and V. Muthukkumarasamy, , "Localization of Submerged Sensors with a Single Beacon for Non-Parallel Planes State", in 10th International conference on Ubiquitous and Future Networks (ICUFN), pp. 525-530, 2018.

Joint Demographic Features Extraction for Gender, Age and Race Classification based on CNN

Zaheer Abbas[1], Sajid Ali[2], Muhammad Ashad Baloch[3], Hamida Ilyas[4], Moneeb Ahmad[5]
Mubasher H. Malik[6], Noreen Javaid[7], Tanvir Fatima Naik Bukht [8]
Department of Computer Science, Institute of Southern Punjab Multan, Pakistan[1, 4, 5, 6, 7, 8]
Department of Computer Science, University of Education Lahore, Pakistan[2]
Department of Computer Science, NCBA&E Multan, Pakistan[3]

***Abstract*—Automatic verification and identification of face from facial image to obtain good accuracy with huge dataset of training and testing to using face attributes from images is still challengeable. Hence proposing efficient and accurate facial image identification and classification based of facial attributes is important task. The prediction from human face image is much complex. The proposed research work for automatic gender, age and race classification is based on facial features and Convolutional Neural Network (CNN). The proposed study uses the physical appearance of human face to predict age, gender and race. The proposed methodology consists of three sub systems, Gender, Ageing and Race. Therefore different feature are extracted for every sub system. These features are extracted by using Primary, Secondary features, Face Angle, Wrinkle Analysis, LBP and WLD. The accuracy of classification is based on these features. CNN used to classify by using these features. The proposed study has been evaluated and tested on large database MORPH II and UTKF. The performance of proposed system is compared with state of art techniques.**

Keywords*—*Appearance features; age; gender; wrinkle analysis; face angle; classification; race; LBP

I. INTRODUCTION

The face of human holds significant amount of qualities and data about the human identification, for example, appearance, race, gender classification, and age. Humans can identify and examine these data effectively, for example, most of human can perceive human attributes like gender classification [1], and they can judge if the human is male or female by just observing face. They can estimate the age of the individual and state whether this individual is a kid or a grown-up. Without a doubt, most of programmed facial characteristic arrangement frameworks depend on machine vision and machine acknowledgment. Computer vision incorporates strategies and procedures for comprehension, breaking down, and removing data from pictures. In [2] the plan of a machine acknowledgment framework includes three principle parts, which are pre-handling, highlights extraction, and order. Age predicting gender classification and race forecast frameworks has been developing quickly as of late due its significant modules and valuable uses for some machine vision applications in seeing a particular portion of individuals. Estimation of gender and age forecast frameworks are presently being utilized by lodgings, air terminals, transport stations, club, government stations, colleges, clinics, films, and so forth to build the degree of security and tackling any potential threats or lacks. In the security apps, age and gender forecast methods are utilized likewise in social insurance frameworks, data recovery, scholarly examinations and investigates, and (ECRM) frameworks, customers are conveyed to various gender classification and age gatherings like youngsters, adolescents, old citizens and senior old citizens not withstanding decide if they male or female. Moreover, assembling some client's day by day life data like exercises, propensities, customs, needs and so forth may assist the enterprises with classifying items and administrations relying upon their gender classification or age gatherings that lead to expand their earnings and procure more cash [3]. In [4] For instance, clothing stores may offer suitable styles for guys or females as per their age gatherings; cafés required to know the mass prominent suppers for each age or gender classification gathering, multiple organizations need to make explicit publicizing to explicit spectators relying upon their gender, age and race estimation structures [4].

There are totally different algorithmic program and techniques are already for age, gender, and race classification severally or combination of two techniques. There's no multitasked design for age, gender and race classification conjointly. The problem statement is taken from [22]. The planned work is organized for race, age and gender estimation conjointly, during this study multilayer design developed for age, gender and race classification supported by Convolutional Neural Network (CNN). All structured are learned and radio-controlled by auxiliary demographic data, since alternative demographic data (i.e., gender and race) is helping for age estimation. Every cascaded structure is embodied in an exceedingly main network and several other sub networks. The applied frameworks gender trained by gender data, then two sub networks are trained by the male and female samples, severally. We have a tendency to use the options extracted from the physically structure with mathematician method regression that may enhance the performance for age estimation, gender prediction and race classification. The Experimental results on the MORPH II and UTKF datasets have gained superior performances compared to the progressive ways with state of art techniques. This paper organized as follow, Section 2 described related work. The Methodology is delineated in the Section 3. Experimental result discussed in Section 4. The conclusion and future work is presented in Section 5.

II. Related Work

Facial image recognizable research has consisted 30 decades as stated by previous work. However face traits, for example, age, gender orientation and ethnicity recognizable proof from facial pictures has effectively developing in late 1996s as per the previous. Research on facial quality acknowledgment, for example, age, gender, ethnicity and facial feelings have been begun almost 10 years back. In this way there are just a couple of research arrangements presented for facial property grouping from human face image. It is fundamental to present new techniques with higher correctness for face characteristic grouping from facial images. As indicated by the writing, the majority of the exploration arrangements depend on characterizing the pictures into one of the traits yet not for a mix of properties. The absolute first association did with age grouping from facial pictures in 1999 by Y. H. Kwon et, al [5]. Wen-Bing Horng et al. [6] built up a calculation to distinguish age from gray level pictures by utilizing an Artificial Neural Network (ANN) classifier. Proposed strategy can characterize pictures into one of the four classifications from children, young, old, moderately aged, and older aged. K B Raja et al [7] proposed an estimation period of life and gender orientation classifier utilizing ANN framework and back class likelihood. The calculation comprises of three primary stages, preprocessing, include extraction and characterization. Feng GAO and Haizhou Ai [8] built up their own calculation to confront the test of age order utilizing buyer pictures in different state. Gabor highlight is separated for face image portrayal and a fluffy rendition of Linear Discriminate Analysis is utilized for arrangement. They [9] exhibited a novel strategy for face gender characterization by utilizing totally skewed information, for example, made an interpretation of or turned information into the preparation set and got a momentous exactness. Proposed approach utilized two classifiers for the examination. One depends on feeble highlights; for example, LBP histograms depend on SIFT key focuses. At long last the proposed framework has accomplished a high precision of 92.5%. The neighborhood qualities are usually known to all the more likely arrange an individual into age bunches as they insert specific attributes that separate distinctive age gatherings. Instead of the neighborhood highlights, they contended that the worldwide partners are better for evaluating increasingly exact age data and contain the age characteristics, however further individual-related qualities as personality, feeling and ethnic foundation. Half breed highlights which are created through joining nearby and worldwide highlights are found to offer unrivaled execution for different face related applications. This is a direct result of the wastefulness found in each sort of highlight can be remunerated prompting the end that cross breed highlights are alluring for precise age estimation. One of the prior chips away at sexual orientation acknowledgment utilizing CNNs was exhibited in paper [10]. The arrangement comprised of a face location and sexual orientation acknowledgment module – both utilizing neural systems. The engineering included three layers (two covered up and yield). Info pictures had 32×32 pixels goals. The announced precision on the FERET dataset was 97.2%. A large portion of the business related to the DCNNs showed up in 2015 and later. In the article two methodologies were thought about: "great" and DCNN based. In the first case the accompanying highlights were considered: HOG, LBP and SURF. As relapse the CCA (Canonical Correlation Analysis) was connected. In the second, a wide range of variations of system designs were inspected (the Caffe library was utilized). The arrangement comprised of a face discovery and sexual orientation acknowledgment module – both utilizing neural systems. The engineering included three layers (two covered up and yield). Information pictures had a 32×32 pixels goals. The revealed exactness on the FERET dataset was 97.2%. The vast majority of the business related to the DCNNs showed up in 2015 and later. In the article [10] two methodologies were looked at: "great" and DCNN based. In the first case the accompanying highlights were considered: HOG, LBP and SURF. As relapse the CCA (Canonical Correlation Analysis) was connected. In the second, various variations of system designs were inspected (the Caffe library was utilized). The best outcome was gotten for two Convolutional and one completely associated layer. Info pictures had 50 × 50 pixels size. The creators noticed significantly lopsidedness between the time required for learning and real activity in the two cases. At last, for the MORPH database, the "work of art" arrangement got 4.25 and DCNN 3.88 mean outright blunder (MAE) esteem. In the work [11] a DCNN for age and sexual orientation estimation was proposed. The system had three Convolutional and two completely associated layers. Information pictures of size 256×256 were edited to 227 × 227. The creators did not utilize a pre-prepared system model opposed to numerous different methodologies. There are totally different algorithmic program and techniques are already for age, gender, and race classification severally or combination of 2 techniques. There's no multitasked design for age, gender and race classification conjointly. The planned work is organized for age, gender and race estimation conjointly, during this study multilayer design developed for age, gender and race classification supported Convolutional Neural Network (CNN). All structured are learned and radio-controlled by auxiliary demographic data, since alternative demographic data (i.e., gender and race) is helping for age estimation. Every cascaded structure is embodied in an exceedingly main network and several other sub networks. as an example, one in every of the applied frameworks may be a gender trained by gender data, then 2 sub networks are trained by the male and female samples, severally. We have a tendency to use the options extracted from the physically structure with mathematician method regression that may enhance the performance for age estimation, gender prediction and race classification. The Experimental results on the MORPH II and UTKF datasets have gained superior performances compared to existing techniques.

III. Proposed Methodology

The main purpose of proposed system is estimated jointly gender, age and race on the basis of specific human facial features. The human extraction of facial features is important phase in the proposed algorithm. Fig. 1 demonstrates the proposed system architecture flow that clearly shows that the most important steps in proposed system (preprocessing, Feature extraction and classification).

Primary landmarks getting is the more significant stage in the examination. Primary landmarks in the face image are nose, eyes, eyebrow and mouth. They present a particular district where every face component falls in a picture and in this manner. The quest landmark for a facial element could be limited. As per this perception, face region can be separating into a few pieces and begin to find each element point utilizing a prepared classifier for each component. Each element is found utilizing prepared classifiers for every element. Face districts are first sent to the comparing identifier to identify the separate component regions. At that point subsequent stage is to discover the closest enormous enough district including the found component territory.

A. Gender Classification

A particular number of parameters are needed to proceed with gender prediction. Fig. 2 demonstrates the used features of gender classification.

The description of the parameters is given below:

$$\hat{E} = \frac{X_1+X_2}{2} \tag{1}$$

Here $\hat{E}$ is height of eye.

$$\rho = \frac{Y_1+Y_2}{2} \tag{2}$$

Here ρ Distance between Eye and Eye brow.

$$\Gamma = \frac{b(d+f)}{2} \tag{3}$$

Here Γ height of Nose.

$$\omega = h - b \tag{4}$$

Here ω space between Nose and Lip.

Eyebrow width = Q

$$\tau = e - c \tag{5}$$

Here τ distance between Eyes.

$$\lambda = \frac{h-(f+d)}{2} \tag{6}$$

Here λ Eye to upper Lip distance.

$$R_1 = \frac{\varsigma}{\Gamma} \tag{7}$$

Here ς distance between Eyes and Γ height of Nose.

$$R_2 = \frac{\varsigma}{\lambda} \tag{8}$$

Here ς distance between Eyes and λ Eye to upper Lip distance.

B. Age Estimation

The features of appearance face have consisted of two features, shape and facial skin texture features. During the changes in the age from childhood to adult the shape features also changed considerably. The shape features are very helpful for estimating the age of adult instead of babies. In other hand facial skin texture feature is more efficient to differentiate between adult and senior adult. Thus texture and shape features are provided useful information for estimating age. Therefore facial texture and shape features are used to develop age estimation phase. In the proposed age estimation phase face angle and geometric ratios are used as shape landmarks and (LGBPH) [12] of skin features is used as texture features.

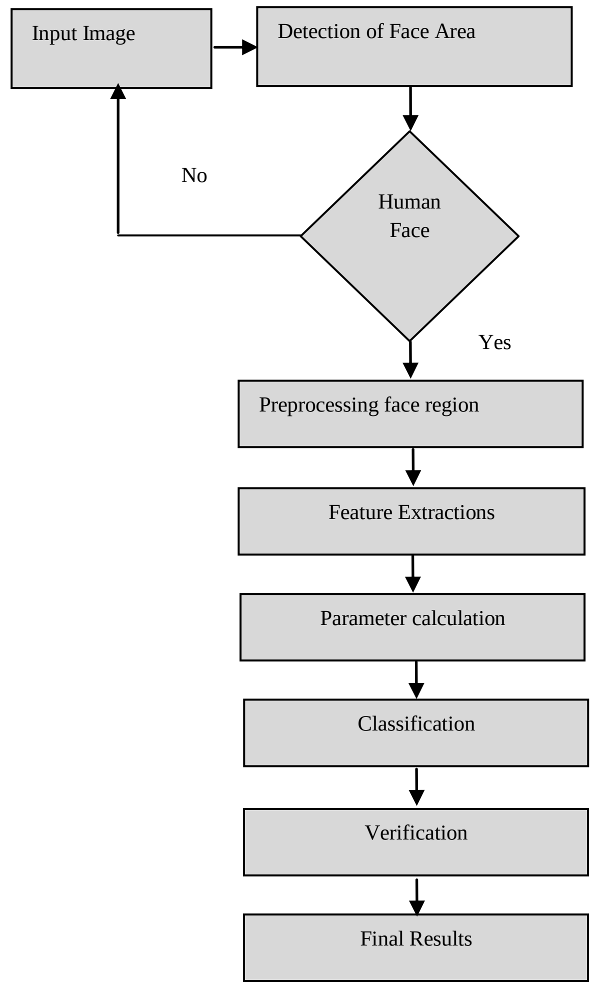

Fig. 1. Demonstrate Flow of Proposed System.

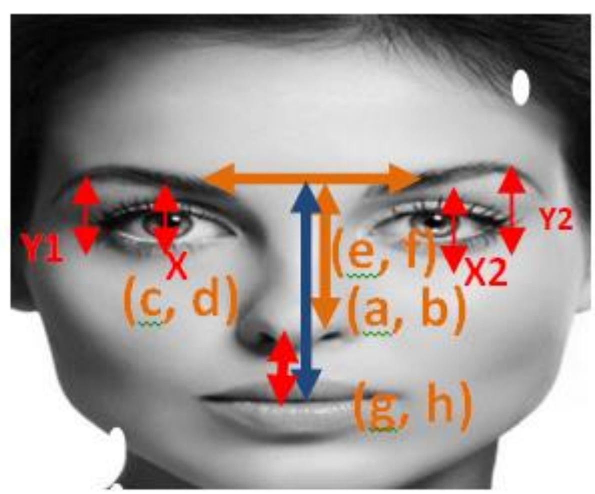

Fig. 2. Gender Classification Parameter.

The general equation of calculating ratios is follow:

$$R_i = \frac{D_{hi}}{D_{vi}} \tag{9}$$

R_i is demonstrate the ratio which are calculate by using vertical and horizontal distance between different face angles D_{hi} horizontal distances and D_{vi} vertical distance.

$$R_1 = \frac{D_{heni}}{D_{veei}} \tag{10}$$

D_{heni} Span middle of eyes and nose tip D_{veei} span middle of eyes.

$$R_2 = \frac{D_{hemi}}{D_{veei}} \tag{11}$$

D_{hemi} Span middle of eyes and centre of mouth D_{veei} span middle of eyes.

$$R_3 = \frac{D_{heci}}{D_{veei}} \tag{12}$$

D_{heci} Span middle of eyes and chin tip D_{veei} span middle of eyes.

$$R_4 = \frac{D_{heni}}{D_{vemi}} \tag{13}$$

D_{heni} Span middle of eyes and nose tip D_{vemi} span middle of eyes and centre of mouth.

$$R_5 = \frac{D_{heni}}{D_{veci}} \tag{14}$$

D_{heni} Span middle of eyes and nose tip D_{veci} span middle of eyes and chin tip.

$$R_6 = \frac{D_{heni}}{D_{veci}} \tag{15}$$

D_{heni} Span middle of eyes and centre of mouth D_{veci} span middle of eyes and Chin tip.

1) Face angle: The angle of face image is extracted as demonstrate in Fig. 3 is measured by applying the law of cosines, which used to extract as another shape landmark in the presented age estimation architecture.

2) Facial skin textural features: The characteristics of facial skin extracted from LGBPH described by Zhang et al. (2005) have been used successfully for face recognition and their effectiveness has been proven in comparison to conventional LBP features or Gabor features.

3) Wrinkle analysis: The wrinkle analysis comprises of wrinkle highlight extraction utilizing LGBPH and wrinkle thickness includes extraction. Wrinkle includes extraction utilizing LGBPH is completed with slight adjustments in the method talked about for face skin textural highlight extraction utilizing LGBPH. The reaction of Gabor channel is a most extreme toward wrinkles.

$$W_d = \frac{W_p}{T_p} \tag{16}$$

The wrinkle density is represented by W_d, the count of wrinkle pixels and the count of total pixels in the region of interest is represented by W_p and T_p, respectively.

C. Race Classification

The proposed race identification methods are used to extract standardized information from face pictures: LPB and WLD [13]. The CNN classifier is utilized for distinguishing the race. We have experimented with numerous distance measures.

1) Local binary pattern: LBP has been the for the most part used descriptor and best performing surface descriptors in present years. This administrator names the pixels of a picture by thresholding the 3 × 3 neighborhood of each pixel with the inside worth and thinking about the outcome as a double number.

The central value from Fig. 4 is calculated by the binary values which obtained by writing clock wise binary number from 3*3 matrix.

CW = 11000110 = 198

The LBP is computed using the following equation:

$$LBP_{P.R} = \sum_{i-1}^{P-1} 2^i \times S(P_i - P_c \quad) \tag{17}$$

Where P_c is the center pixel and the thresholding operation is

$$S\,(Pi - Pc) = \begin{cases} 1, & p_i - p_c \geq 0 \\ 0, & P_i - p_c < 0 \end{cases} \tag{18}$$

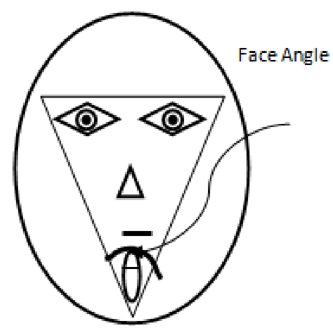

Fig. 3. Face Angle.

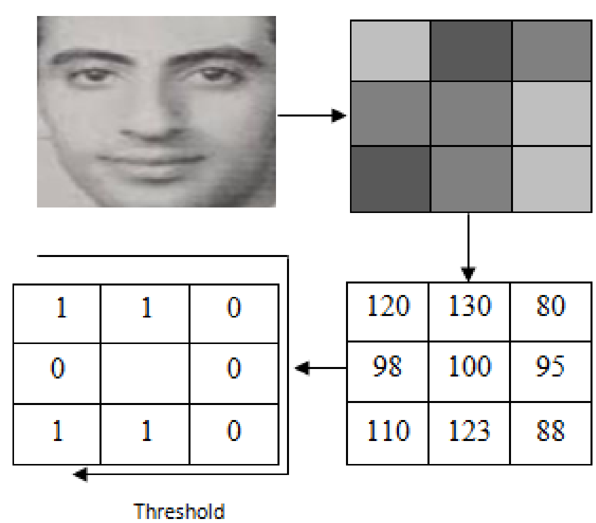

Fig. 4. Shows the LBP Operator.

2) Weber Law Descriptor: WLD can be a solid and ground-breaking nearby handle as of late created. It is blend of two sub parts: differential excitation and direction. The WLD was dazzled by a mental law known as the Weber Law [13]. The proposed law shows that the difference in information, (for example, sound, lighting) that might be felt might be a consistent proportion of the first info. Since the progressions are not as much as this association with a fixed worth, the animal would remember it as a foundation signal rather than a genuine sign and concentrate the sides of the picture accurately even within the sight of noteworthy commotion and is solid against light change.

D. Convolutional Neural Network

Classification takes place in three main steps. Gender classification first identifies the gender of source image. Fig. 5 demonstrates the structure of CNN.

Then source image forward to the age classifier to identify the relative age order and forward to the race classifier to classify the race. Gender classification is basically using the facial features on features of face, age range based on wrinkle analysis, face angle and the classification of the race, which is done LBP and WLD. Identification process completed by utilizing calculated parameters of Convolutional Neural Networks. Convolutional Neural networks are trained using data taken from nearly 2,400 images of two genders, different age groups and four races, which are front and near front images. Fig. 5 shows the structure of the neural network used for age classification. The parameters are sent to the CNN to classify the images per gender, age and race. CNN used for gender prediction having 5 input and 2 output nodes 0 and 1 resembling the 2 gender teams, male (0 – 0.5) and feminine (0.5 – 1.0). Output worth from the Convolutional Neural Network is employed to classify the image into one amongst the gender teams. The neural network wont to classify the given input image in to a corresponding age bracket has eight input nodes and also the output layer contains four nodes particularly zero, 1, 2, 3, 4, 5, 6 and 7 to represent the age teams 0-5, 6-11, 12-17, 18-30, 31-60, 61-74 and 75-95 respectively. The somatic cell with the best response is taken into account because the output of the age orders CNN projection technique. Thus manual classification takes place for the incorrectly detected pictures.

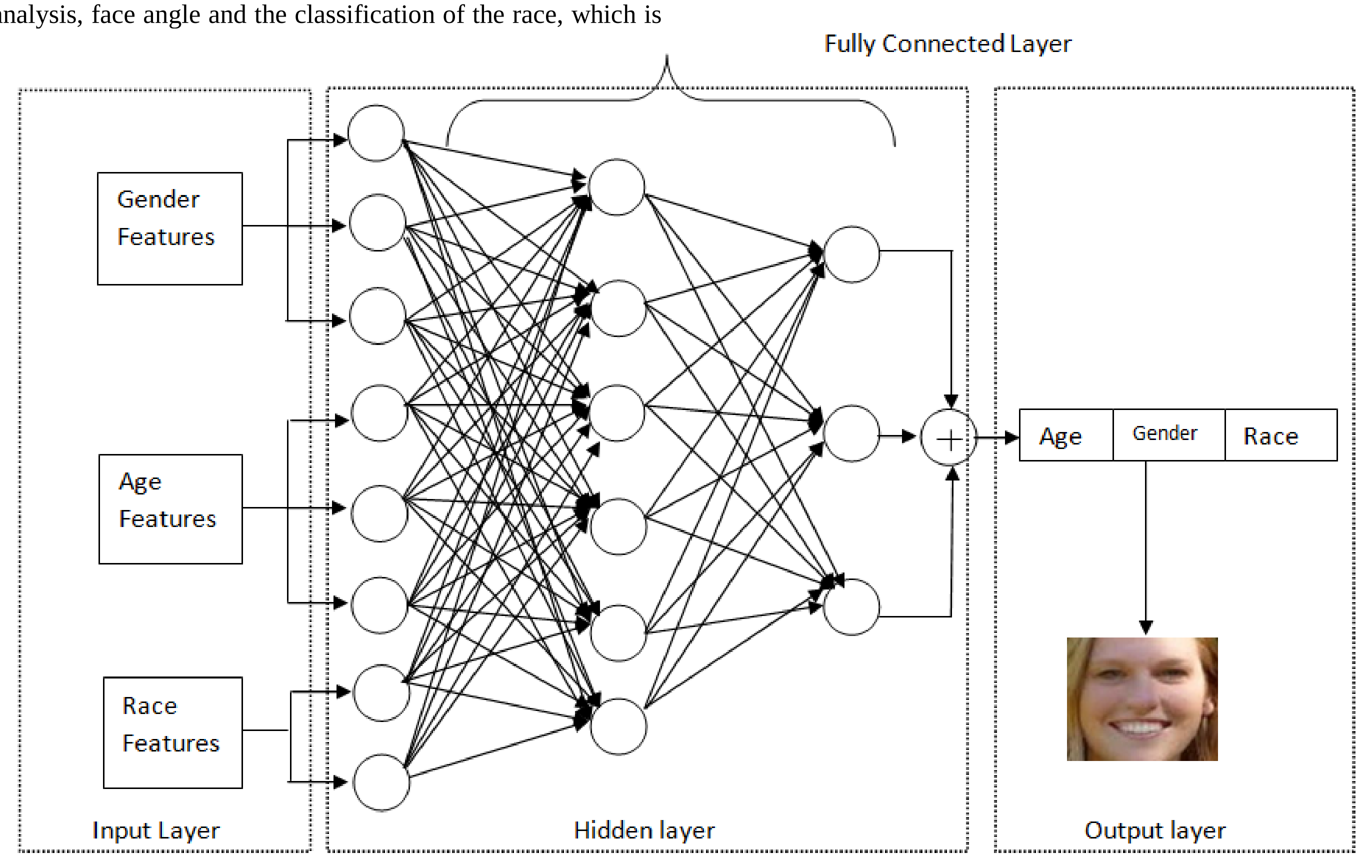

Fig. 5. Neural Network Framework for Age, Gender and Race Classification.

IV. Results and Experiments

The proposed work is organized for gender, age and race estimation conjointly, during this study multilayer design developed for age, gender and race classification supported Convolutional Neural Network (CNN). All structured are learned and radio-controlled by auxiliary demographic data, since alternative demographic data (i.e., gender and race) is helping for age estimation. Every cascaded structure is embodied in an exceedingly main network and several other sub networks. as an example, one in every of the applied frameworks may be a gender trained by gender data, then two sub networks are trained by the female and male samples, severally. We have a tendency to use the feature extraction from the physically structure with mathematician method regression that may enhance the performance for age estimation, gender prediction and race classification. The Experimental results on the UTKF and MORPH II datasets have gained superior performances comparison in progressive ways with state of art techniques. The experiments compiled on Lenovo i3, 6 GB RAM, windows 10 operating system, Matlab 2019. The proposed system Gender, Age and Race classification trained and testing on MORPH II and UTKF faces database. More than 2400+ images are trained and number of test applies on trained dataset. The propose framework are consisted on three phases which are briefly described in chapter 3. The first phase is performing pre-processing on input image and pass to second phase. It is most important phase of proposed framework, it calculated feature of input image for age, gender and race. After successfully extracting features (the feature extracting techniques are briefly described in Section 3), the results will pass to third phase, in this the phase classification were done by using CNN. We trained more than 2400 images and more than 1200 images are tested for experiments. The result are extracted from testing images are follow. Gender prediction performance accuracy is extremely dependent on specific landmarks that extract from input face. Landmarks just like height of eye (D1), span of eye brow corner and eye corner (D2), nose height (D3), span of nose and lip (D4) and breadth of eye brow (D5). Set of results taken for the five parameters from the take a look at image is shown within the Table I. These parameters in brief delineate in Section 3.

Tables II, III and V show the confusion matrix of gender, age and race, respectively.

The performance of projected framework is described by exploitation Table III referred to as confusion matrix. The first column of Table III shows actual seven age classes of the input face photos. Initial row of Table III shows foretold age classes of the input take a glance at face photos by the projected age organization. The count inside the diagonal cell of Table III is incremented, if the anticipated class is same as actual class for the input take a glance at face image. Therefore, the diagonal entries of Table III shows the count of accurately classified input take a glance at face photos for corresponding age classes. Non-diagonal entries of Table III show the count of misclassified input take a glance at face photos. Total of count of accurately classified and misclassified entries across the rows of Table III offers total type of face photos inside the express people. The illustration confusion matrix in graphs clearly shows the accuracy old-time detection. Some inaccurate results jointly show in confusion matrix and graphs that indicate the wrong detection by projected style. In this paper, we use the MAE for accuracy calculation. For the MAE calculation, it computes he MAE between the true age and the predicted age in the testing set. Formally, MAE is calculated as:

$$MAE = \frac{1}{N}\sum_{m=1}^{N}|l_m - l'_m| \quad (19)$$

Where l_m and l'_m denotes the ground truth age and predicted age of the m_{th} image, respectively, and N is the number of testing images. If the value of MAE is lower, the performance is better. Table IV demonstrates the age results and Fig. 6 shows graphical representation on MORPH II database.

TABLE. I. Parameters Values for Gender Classification

Image	**D1**	**D2**	**D3**	**D4**	**D5**
A01	0.20	0.30	0.55	0.23	0.08
A02	0.16	0.14	0.55	0.36	0.06
N01	0.16	0.20	0.64	0.32	0.11
N02	0.14	0.13	0.63	0.37	0.13
A03	0.16	0.17	0.53	0.27	0.06
A04	0.16	0.21	0.64	0.24	0.6
N03	0.17	0.14	0.51	0.35	0.10
N04	0.16	0.28	0.67	0.31	0.8
A05	0.16	0.25	0.65	0.25	0.08

TABLE. II. Shows Confusion Matrix of Gender Classification

	Male	Female
AG1	98	2
AG2	1	99
AG3	99	1
AG4	2	98

TABLE. III. Shows Confusion Matrix of Age classification

	S1	S2	S3	S4	S5	S6	S7
AGS1	116	3	1	0	0	0	0
AGS2	2	114	2	2	0	0	0
AGS3	1	3	110	3	3	0	0
AGS4	0	0	1	87	2	0	0
AGS5	0	0	1	1	87	1	0
AGS6	0	0	0	1	2	85	2
AGS7	0	0	0	0	2	2	86

TABLE. IV. Experimental Results on Morph II Database

Method	MAE
AGES [14]	8.83
CA-SVR [15]	5.88
OHRank [16]	5.69
DLA [17]	4.77
VGG+SVR [18]	3.45
DEX [19]	3.33
OURS	3.29

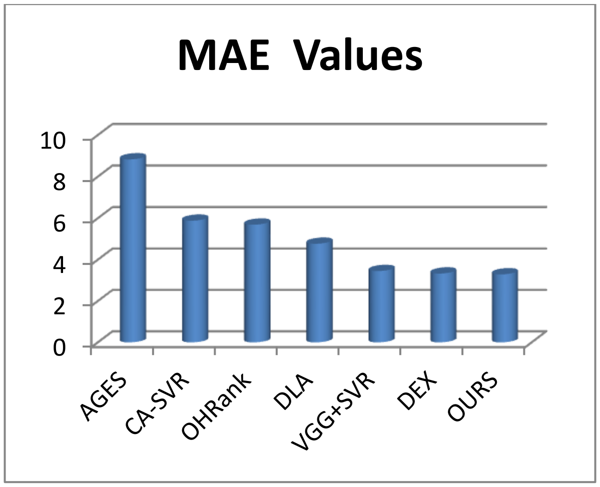

Fig. 6. Comparison with State of the Art Existing Technique.

Fig. 7 demonstrates the race accuracy on different races (Mongolian, Indian, Black, and White).

In Table VI shows the result comparisons with state of art techniques.

Fig. 8, 9 and 10 show the overall accuracy of proposed accuracy with other state of art techniques gender age and race respectively. In the proposed study we have been create a framework to classify age, gender and race jointly. The proposed work based on facial human feature. The feature extracted by using different appearance features. The experiments clearly show in this chapter the proposed work better than existing techniques. The proposed performance compared with state of art techniques overall and also by sub modules. Every module and overall performance clearly demonstrated that the proposed system work comparatively better.

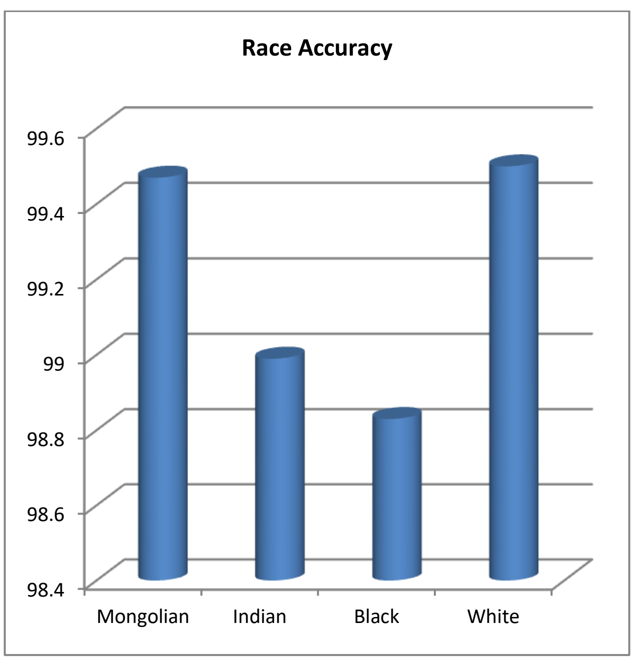

Fig. 7. Shows Accuracy of Race Classification.

TABLE. V. CONFUSION MATRIX OF RACE ACCURACY

	Mongolian	Indian	White	Black
AG1	99.47%	-	-	0.53%
AG2	-	98.99%	-	1.01%
AG3	-	-	98.83%	1.17%
AG4	0.25%	0.25%	-	99.50%

TABLE. VI. DEMONSTRATE THE COMPARISON OF PROPOSED METHOD WITH STATE OF ART TECHNIQUES

M	TS	GA	RA	AM	AM
CCA [20]	S_1	95.2%	97.8%	5.39	5.37
	S_2	95.2%	97.8%	5.35	
KCCA [20]	S_1	98.5%	98.9%	4.00	3.98
	S_2	98.4%	99.0%	3.35	
PLS [21]	S_1	97.3%	98.7%	4.58	4.56
	S_2	97.4%	98.6%	4.54	
KPLS [21]	S_1	98.4%	99.0%	4.07	4.04
	S_2	98.3%	99.0%	4.01	
OURS	S_1	98.69%	99.1%	3.29	3.31
	S_2	98.60%	99.2%	3.33	

*TS- Training Set *GA- Gender Accuracy
* RA- Race Accuracy * AM- Age MAE

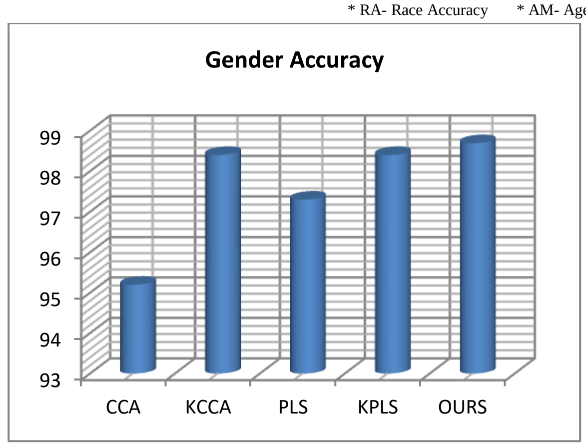

Fig. 8. Overall Gender Accuracy.

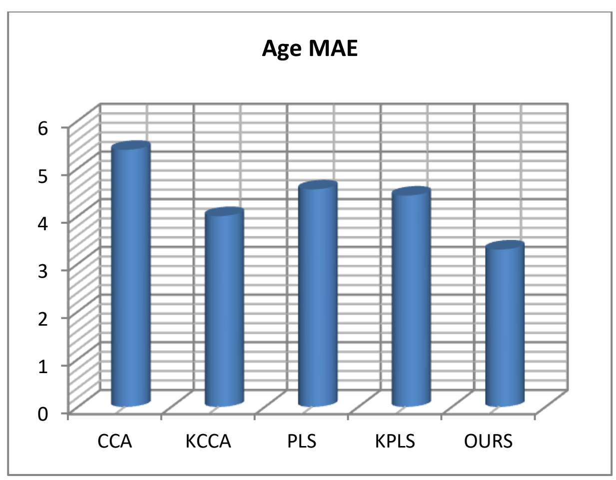

Fig. 9. Demonstrate the Overall MAE of Age.

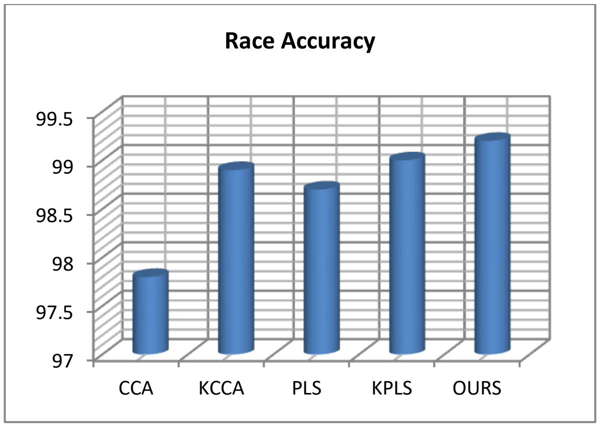

Fig. 10. Demonstrate the Overall Race Accuracy.

V. Conclusion

The proposed architecture based on Convolutional Neural Network, which is learned by Primary, Secondary, Wrinkle analysis, LBP and WLD. The proposed system classify the gender, age and race very efficiently. The overall accuracy of proposed work is 98%. The sub module accuracy is 98.63% for gender classification, 99.2% for Race prediction and 3.31 MAE for age estimation. For the verification the efficiency of the proposed methods, we tested them on several databases. Consequently, we got nearly the same performance on two different databases (MORPH II and UTKF). The overall performance of proposed system is very efficient. The proposed system results compare with state of art methods. The comparison results show that the proposed system detect gender, age and race is more accurately than existing techniques. Generally, from the performance of proposed methods, we noticed that CNN classifiers more accurate than SVM, KNN and ANN. Our future work will focus to design such a framework that can detect age, race and gender on the basis of single appearance feature.

References

[1] Nguyen, P., Tran, D., Huang, X., & Ma, W. (2013, November). Age and gender classification using EEG paralinguistic features. In 2013 6th International IEEE/EMBS Conference on Neural Engineering (NER) (pp. 1295-1298). IEEE.

[2] Eidinger, E., Enbar, R., & Hassner, T. (2014). Age and gender estimation of unfiltered faces. IEEE Transactions on Information Forensics and Security, 9(12), 2170-2179.

[3] Khan, S. A., Ahmad, M., Nazir, M., & Riaz, N. (2014). A comparative analysis of gender classification techniques. Middle-East Journal of Scientific Research, 20(1), 1-13.

[4] Lin, F., Wu, Y., Zhuang, Y., Long, X., & Xu, W. (2012). Human Gender Classification: A Review. International Journal of Biometrics.

[5] Kwon, Y. H., & da Vitoria Lobo, N. (1999). Age classification from facial images. Computer vision and image understanding, 74(1), 1-21.

[6] Horng, W. B., Lee, C. P., & Chen, C. W. (2001). Classification of age groups based on facial features. 淡江理工學刊, 4(3), 183-192.

[7] Ramesha, K. B. R. K., Raja, K. B., Venugopal, K. R., & Patnaik, L. M. (2010). Feature extraction based face recognition, gender and age classification.

[8] Gao, F., & Ai, H. (2009, June). Face age classification on consumer images with gabor feature and fuzzy lda method. In International Conference on Biometrics (pp. 132-141). Springer, Berlin, Heidelberg.

[9] Mayo, M., & Zhang, E. (2008, November). Improving face gender classification by adding deliberately misaligned faces to the training data. In 2008 23rd International Conference Image and Vision Computing New Zealand (pp. 1-5). IEEE.

[10] Tivive, F. H. C., & Bouzerdoum, A. (2006, July). A gender recognition system using shunting inhibitory convolutional neural networks. In The 2006 IEEE International Joint Conference on Neural Network Proceedings (pp. 5336-5341). IEEE.

[11] Levi, G., & Hassner, T. (2015). Age and gender classification using convolutional neural networks. In Proceedings of the iEEE conference on computer vision and pattern recognition workshops (pp. 34-42).

[12] Hermosilla, G., Ruiz-del-Solar, J., Verschae, R., & Correa, M. (2012). A comparative study of thermal face recognition methods in unconstrained environments. Pattern Recognition, 45(7), 2445-2459.

[13] Chen, J., Shan, S., He, C., Zhao, G., Pietikainen, M., Chen, X., & Gao, W. (2009). WLD: A robust local image descriptor. IEEE transactions on pattern analysis and machine intelligence, 32(9), 1705-1720.

[14] Geng, X., Zhou, Z. H., & Smith-Miles, K. (2007). Automatic age estimation based on facial aging patterns. IEEE Transactions on pattern analysis and machine intelligence, 29(12), 2234-2240.

[15] Chen, K., Gong, S., Xiang, T., & Change Loy, C. (2013). Cumulative attribute space for age and crowd density estimation. In Proceedings of the IEEE conference on computer vision and pattern recognition (pp. 2467-2474).

[16] Chang, K. Y., Chen, C. S., & Hung, Y. P. (2011, June). Ordinal hyperplanes ranker with cost sensitivities for age estimation. In CVPR 2011 (pp. 585-592). IEEE.

[17] Wang, X., Guo, R., & Kambhamettu, C. (2015, January). Deeply-learned feature for age estimation. In 2015 IEEE Winter Conference on Applications of Computer Vision (pp. 534-541). IEEE.

[18] Rothe, R., Timofte, R., & Van Gool, L. (2016). Some like it hot-visual guidance for preference prediction. In Proceedings of the IEEE conference on computer vision and pattern recognition (pp. 5553-5561).

[19] Rothe, R., Timofte, R., & Van Gool, L. (2018). Deep expectation of real and apparent age from a single image without facial landmarks. International Journal of Computer Vision, 126(2-4), 144-157.

[20] Guo, G., & Mu, G. (2013, April). Joint estimation of age, gender and ethnicity: CCA vs. PLS. In 2013 10th IEEE International Conference and Workshops on Automatic Face and Gesture Recognition (FG) (pp. 1-6). IEEE.

[21] Guo, G., & Mu, G. (2011, June). Simultaneous dimensionality reduction and human age estimation via kernel partial least squares regression. In CVPR 2011 (pp. 657-664). IEEE.

[22] Wan, J., Tan, Z., Lei, Z., Guo, G., & Li, S. Z. (2018). Auxiliary demographic information assisted age estimation with cascaded structure. IEEE transactions on cybernetics, 48(9), 2531-2541.

A Novel Method for Patients Identification in Emergency Cases using RFID based RADIO Technology

Eman Galaleldin Ahmed Khalil[1]
College of Computing & Information Technology
Shaqra University, Afif
Saudi Arabia

Asim Seedahmed Ali Osman[2]
College of Computing & Information Technology
Shaqra University, Shaqra
Saudi Arabia

***Abstract*—Medical records provide an important role in the process of providing health care in hospitals and in various types of medical institutions. Medical records play a vital role in maintaining the information of the entire patients which includes the basic information, medical information, history of operation and medication etc. These medical records have been produced for the purpose of identifying a patient. In this paper, a novel method for identification of patients using the Radio Frequency Identification (RFID) technology is proposed. This paper explains the concept of electronic medical record and explains how to use RFID based technology in order to create an electronic medical-card for patients. The proposed methodology also aims to identify patients quickly in the case of emergencies using the magnetic card reader device, which provides detailed medical information for the patient file. It also helps the doctors who are present in the ambulance of patient. The proposed methodology is importance in some emergency cases where patients cannot provide their information to the hospital because they didn't know their identity and medical history.**

Keywords—Medical records; radio frequency identification; magnetic card reader; patient; emergency; electronic health record; laboratory

I. Introduction

Information technology is the basis for providing the quality of service in hospitals. It is effective in solving the problems of data loss and loss of time. It is also observed that the main aim of this information technology is to increase the efficiency and also the performance of staff who are working there, accuracy and utilization of the data available to the hospital in order to obtain the desired results. It also aims to improve the accuracy of how to train the people who have access to the system. The Electronic Health Record (EHR) [2] is a systematic collection of health information of patients which are electronically in nature and stored in digital format. These records can be shared across different healthcare institutions. These Records are shared through network or enterprise-wide information systems or other information networks for exchanging the data. E-health records may include a set of data, including demographics, medical history, medications, allergies, immunization status, laboratory test results, radiographs, vital signs and personal statistics such as age, weight, and billing information etc. [3, 5].

Hospitals are facing various problems nowadays, despite the use of electronic records [8]. These include the difficulty in identifying patients in the case of emergency, in the case of a traffic accident or fainting etc. In these cases, it is difficult for the doctors to identify the person or his medical record whether he has any chronic diseases, his medical history since they don't have the enough information about the previous treatments done. This leads to the loss of time in treating the patient. Identifying the medical history without contacting the patient provides high flexibility in many emergency cases so that it will be easier to provide the electronic medical record of the patients. This can be achieved by an RFID-RADIO based technology in which the patient can be identified by radio waves through the smart chip which is implanted in the patient's body by the Ministry of Health.

RFID chips are smart chips which send and receive the digital signals in the form of radio waves. The scanner present in the hospital captures the digital data which were encoded in the smart chip and labels attached to the patient's body. It locates the point of issue, read the data present in it and stores it in the reader. As soon as the patient enters the hospital (emergency department), the nurse uses an RFID reader for capturing the signals from the smart chip present in the patient's body via radio waves. All the information collected from the chip is transmitted through the communication interface to the computer system connected to the reader. Thus, the patient's identity, personal data and medical records were identified quickly and the information about whether he or she suffers from any chronic diseases or permanent treatment can also be found.

The physical components of a RFID system is shown in Fig. 1. The smart chip present in the RFID controller contains an encrypted integrated circuit. It does not have any battery. All the data are entered into the smart chip via a computer, which is directly connected to a machine. Doctors can store data and then it is inserted in the patient's body. The RFID reader captures digital signals from these smart chips by radio waves and then stores the information on the computer which is connected to it. The computer is programmed with an electronic system which is compatible with the RFID based technology.

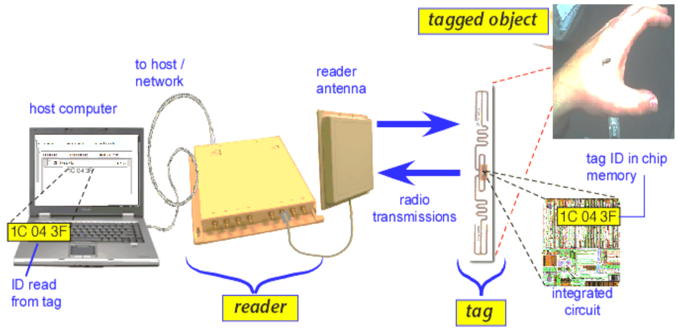

Fig. 1. Physical Components of the RFID System.

RFID smart label tag RFID RADIO COMPUTER

Fig. 2. RFID, Its Tag and the Computer Connected to it.

This paper discusses the proposal of development and working of a system with the application of the RFID based technology in hospital. When a patient was bought to the hospital in case of an emergency, the employee present in reception use the RFID Radio Reader to read the data in the chips which it present in the body of patient. The reader collects the data and it searches the database in order to identify the information about the patient and it retrieves his record. This information helps the doctors and nurses to treat the patient at once. RFID, its tag and the computer connected to it is shown in Fig. 2. This proposed approach can save the time of treatment because the time taken to search the patients information in some emergency cases is more and also, in the case of an emergency, the patient need quick action to save his life. This paper is organized as follows: Section 2 depicts the literature review focusing on various methods proposed by earlier researchers. Section 3 depicts the Components of an RFID system, discusses the proposed methodology, its phased and the modules, etc. Section 4 depicts the result and discussion section, conclusion and future works are shown in Section 5.

II. Literature Review

The RFID is a technology which uses radio waves to transfer data from an electronic tag, called RFID tag which is attached to a person. The data is accessed through a reader for the purpose of identifying and tracking the information about the person. The RFID based technology has been already used by various researchers [1-3] to track and trace the victims in a situation of disaster. Data which were collected in real time in the case of an emergency is saved time in the RFID chip. Various applications such as crisis management teams, hospitals and emergency personnel, have access to data through a computer database present inside the RFID chip [3].

The RFID was the first explored in the 1940s as a method to identify allied airplanes [4]. Nowadays, the RFID system have been applied successfully to various applications in the manufacturing, supply chain management, agricultural applications, transportation, healthcare, etc. [5]. Various errors in medical field can be prevented by building a safer healthcare based system. Recently, the RFID has been applied in hospital management [16]. The RFID is valuable for quickly retrieving patient information and monitoring patient locations in the hospital [6, 7]. There have been few previous by reports researchers based on on-site experiments shows that the RFID is suited best for the application in hospital [8]. Resources from various organizations and technical structures such as hardware and software are the most essential requirements in the re-design of electronic projects [9].

Chao et al, proposed a novel methodology for improving the safety of patient with the combination of RFID and mobile based technology. In general, medical errors can be classified into five categories such as the poor decision making, poor communication, inadequate monitoring of the patient, misidentification of the patient, inability to respond rapidly and poor patient tracking, etc. Adopting information technologies based methodologies in enhancing these deficiencies are the main goals of current trend in enhancing patient safety [10]. The result showed that the RFID adoption though assigned with low level of awareness; adoption capital recompense and infrastructural challenges in the health sector also has high and great tendencies to thrive. As a result of the second research, question revealed that the health care service delivery can harness the benefits of the information technology solution system to function in its servicing in forms like authentication and identification of personnel, patients' data and blood verification; drug dispensary among others [11].

Barriers and critical success factors towards Radio-frequency identification technology adoption [12] in South-East Asian healthcare industry showed that most respondents think the reason of that barrier from the budget and less information, and there is difficulty to use the technology and systems.

The respondents also think the success factor are the integration of collected data, collaboration between units, supporting from top management, and finally they can create a small Radio-frequency identification project [13].

Yao et al proposed that the RFID technology offers healthcare practitioners various advantages to improve safety of patient, time saving, and costs reduction but. It also causes critical issues for successful implementation of the RFID based technology. In order to increase the acceptance and wide use of RFID in healthcare, more customized the RFID systems, more institutional support, and integration with existing HIS, and various regulations to protect privacy are needed [14].

III. Components of an RFID System

The proposed Radio-frequency identification system in this paper consists of different Component which are integrated in a system and shown in Section 4. The integration of the Radio-frequency identification components enables the implementation of an Radio-frequency identification solution [15]. Components of the Radio-frequency identification system is as follows:

- Transponder (tag that it can attached to human).
- RFID Antenna (To detect the transponder).
- RFID Reader (use to receive the data from transponder).
- Connections (enable Transponder, Antenna, and Reader to work together by using information technology infrastructure).
- Web-Based System (Database / User interfaces).

IV. Proposed Methodology

Various methods have been proposed in literature for the RFID based patient authentication. In this paper, a system based on the incremental model is proposed which has the development stage, requirements and then design stage until it reaches the final stage. It is shown in Fig. 3. Design stage is the phase of testing and implementation [17]. Main objective of this paper is to identify the patient's in emergency cases when he was bought to the hospital using the radio-frequency identification technology. This also provides an interface to manage the follow-up of patients. In the proposed system, the programmer designs, implements and tests all the components of the system. To apply this proposed methodology, we have to develop a system which is work with the RFID technology.

A. Use Case Diagram

Fig. 4 shows the use case diagram of the proposed system. In Fig. 4, first actor represents the system administrator. He has the authority to access the entire system and manage the medical record by adding new patient and update and delete the patients. He also has the authority to add doctor, he can identify the patients using RFID Reader to identify the patient, and he can also show the EHR of patients. The second actor represents a doctor. He can write a report, insert the medicine, and also, he can send data to the lab.

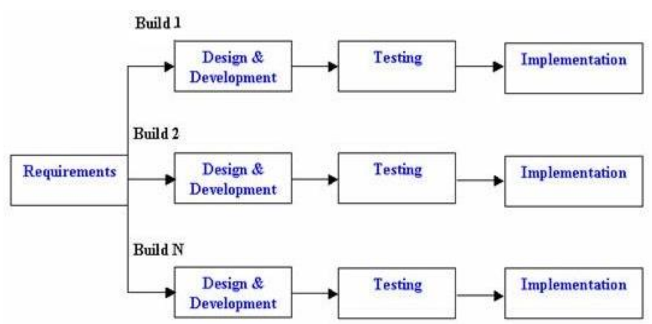

Fig. 3. Schematic Representation of an Incremental Model.

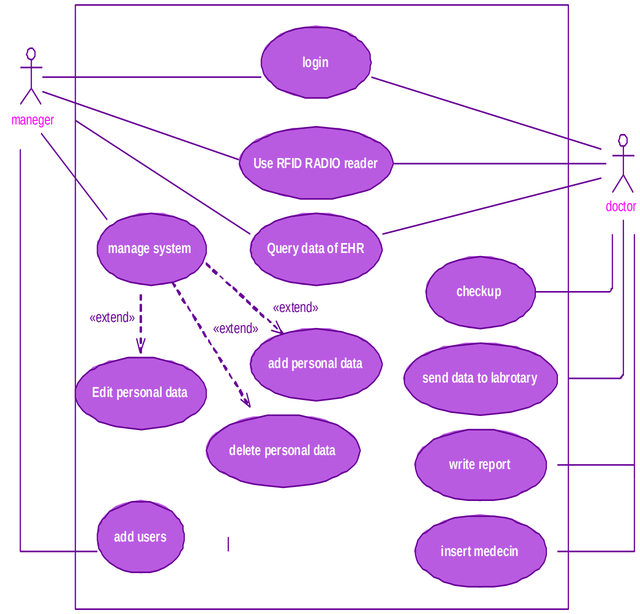

Fig. 4. Use Case Diagram for the Proposed System.

B. Findings and Discussion

Fig. 5 shows the Main interface for the Administrator which will allows him to enter the personal data of the patient for the process of saving it in the chips. By this screen, he can read the data from the chips using reader to query about patients in the cases of emergency. He can view the reports and show the electronic health record which belongs to the patients.

Main interface for the doctor is shown in the Fig. 6. It also shows how to quickly the query of a patient's data can be retrieved through tag smart reader is also shown. Inquiry about the full medical record of the patient, i.e. tests and previous medicines are also shown. Two buttons are there for the purpose of sending the data towards the laboratory tests and radiology.

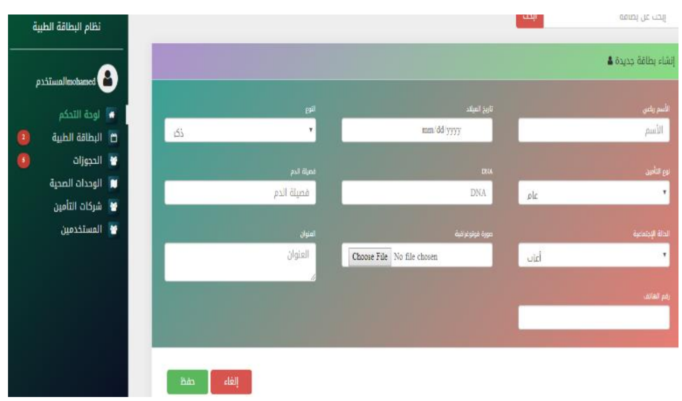

Fig. 5. Main Interface for the Administrator.

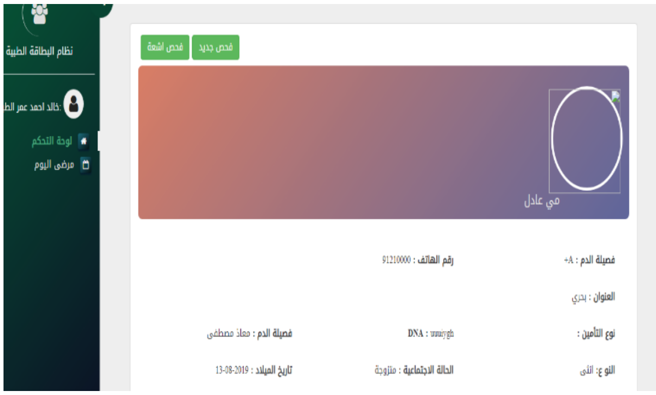

Fig. 6. Main Interface for the Doctor.

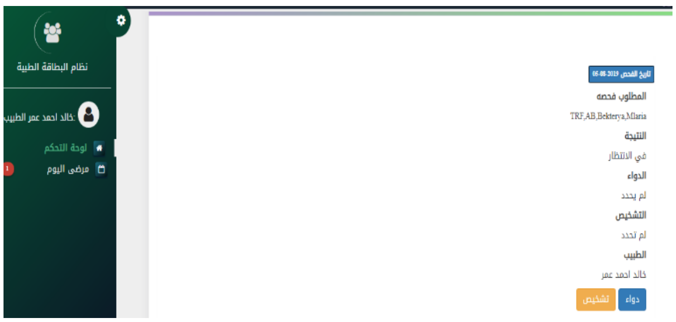

Fig. 7. Interface for Diagnosis.

Fig. 7 shows the interface for previous diagnosis of the patient and the type of examination required by the doctor and dispatched laboratory medical laboratories. The interface screen also contains a form in which the doctor can fill the report and enter the type of medicine for the purpose of sending it to the pharmacy.

V. Conclusion and Future Enhancements

Radio-frequency identification systems have been successfully applied in various areas of manufacturing, Production, agriculture, Logistic services and healthcare services. In the healthcare industry, there are other advantages for example; increase accuracy tasks, reduce human errors, improve safety, and patient satisfaction. In the coming years there is no doubt for using the RFID in the healthcare industry and it will become a primary requirement. Although, the complete usage of RFID will not be able meet expectation of health care organizations. In this paper, a novel methodology for identifying the person's information using the RFID chip in case of an emergency is proposed. The RFID reader present in the hospital is used to read the data or previous information about the patient in case of any emergency is done. If the proposed methodology is used alone, health care organizations and many patients will be faced with numerous advantages. Integrating the proposed methodology with Hospital Information Systems (HIS), electronic health records (EHRs) and also with the Clinical Decision Support Systems (CDSS) could be the feature enhancements.

References

[1] Nambiar AN. II. San Francisco, USA: 2009. RFID technology: A review of its applications. Proceeding of the World Congress on Engineering and Computer Science October 20-22

[2] Booth, P., P.H. Frisch & S. Miodownik, 'Application of rfid in an integrated healthcare environment', Proceedings of the 28th IEEE EMBS Annual International Conference, 2006.

[3] Ajami S, Akbari B, editors. Isfahan, RFID in Earthquake Information Management System: Work in progress. In Health system, risk management And Disaster, Iran: Health Management and Economics Research Center, Isfahan University of Medical Sciences; 2012.

[4] Landt J. Potentials, The history of RFID New York: IEEE Institute of Electrical and Electronics Engineers; 2005.; pp. 8–11. Vol. 24.

[5] Nambiar AN. II. San Francisco, USA: 2009. RFID technology: A review of its applications. Proceeding of the World Congress on Engineering and Computer Science October 20-22.

[6] Lai CL, Chien SW, Chang LH, Chen SC, Fang K. New York: IEEE Institute of Electrical and Electronics Engineers; 2007. Enhancing medication safety and healthcare for inpatients using RFID.

[7] Bates DW, Gawande AA. Improving safety with information technology. N Engl J Med. 2003;348:2526–34.

[8] Britton J. An investigation into the feasibility of locating portable medical devices using radio frequency identification devices and technology. J Med Eng Technol. 2007;31:450–8.

[9] Ajami S, Ketabi S, Isfahani SS, Heidari A. Readiness assessment of electronic health records implementation. Acta Inform Med. 2011;19:224–7.

[10] Chao CC, Jen WY, Chi YP, Lin B. Improving patient safety with RFID and mobile technology. Int J Electron Healthc. 2007;3:175–92.

[11] Abiona O. Thesis. Lahti University of Applied Sciences in Lahti of Finland; 2012. Adoption possibilities and use of RFID in Nigeria health sector.

[12] Fuhrer P, Guinard D. Switzerland: Proceedings of the 1st European Conference on eHealth (ECEH06), Fribourg; 2006. Oct 12-13, Building a Smart Hospital using RFID technologies.

[13] Vanany I, Shaharoun AB. Barriers and critical success factors towards RFID technology adoption in South-East Asian Healthcare Industry. 2008

[14] Yao W, Chu CH, Li Z. New York: IEEE Institute of Electrical and Electronics Engineers; 2010. The use of RFID in healthcare: Benefits and barriers.

[15] Ahsan K, Shah H, Kingston P. RFID applications: An introductory and exploratory study. IJCSI Int J Comput Sci Issues. 2010, 7:1–7.

[16] Kafi Mohammad Ullah's Lab, K. M. Ahsan - Uz - Zaman, Kafi Mohammad Ullah, Omar Faruk Tasin, Md. Shaidul Kabir Milon, RFID Based Hospital Laboratory Automation System, 2nd International Conference on Electrical & Electronic Engineering (ICEEE), July 2017.

[17] Asim Seedahmed Ali Osman and Ahmed Seedahmed Ali Osman, Evaluating Employee Performance using Automated Task Management System in Higher Educational Institutions, Indian Journal of Science and Technology, Vol 12(9), March 2019.

Multi-Label Classification using an Ontology

Yaya TRAORE[1], Didier BASSOLE[3]
Mathematics and Informatics Laboratory (LAMI)
University Joseph KI-ZERBO (UJKZ)
Ouagadougou, BURKINA FASO

Sadouanouan MALO[2], Abdoulaye SERE[4]
Mathematics and Informatics Laboratory (LAMI)
University Nazi Boni (UNB)
Bobo-Dioulasso, BURKINA FASO

***Abstract*—During these last few years, the problem of multi-label classification (ML) has been studied in several domains, such as text categorization. Multi-label classification is a main challenging task because each instance can be assigned to multiple classes simultaneously. This paper studies the problem of Multi-label classification in the context of web pages categorization. The categories are defined in an ontology. Among the weakness of the multi-label classification methods, exist the number of positive and negative examples used to build the training dataset of a specific label. So the challenge comes from the huge number of labels combinations that grows exponentially. In this paper, we present an ontology-based Multi-label classification which exploit dependence between the labels. In addition, our approach uses the ontology to take into account relationships between labels and to give the selection of positive and negative examples in the learning phase. In the prediction phase, if a label is not predicted, the ontology is used to prune the set of descendant labels. The results of experimental evaluation show the effectiveness of our approaches.**

Keywords—Multi-label classification (ML); Binary Relevance (BR); ontology; categorization; prediction

I. Introduction

In recent years, Multi-label classification (ML) has been studied in several domains, such as text categorization with its many applications on the World Wide Web. Multi-label classification is a main challenging task because each instance can be assigned to multiple classes simultaneously. This paper studies the problem of Multi-label classification in the context of web pages categorization. The categories are defined in an ontology. So the challenge comes from the huge number of labels combinations that grow exponentially. In text categorization, Multi-label (ML) classification problem [1], [12] consist in predicting the categories of a new instance according to its features. In our context, categories are looked upon as text labels. Binary Relevance (BR) [14] is the most intuitive method for multi-label classification. It decomposes the multi-label classification task into a set of binary classification tasks. This approach is easy to understand and learn. However, this approach has a deficiency. The semantic relations between the labels are ignored.

In order to use dependence between the labels to build the training dataset, we associate an ontology with ML method. An ontology [2] is used to present the domain knowledge. In this paper, we propose a novel approach that uses a method of ML based on ontology to predict the categories of a new web page. Experiments are implemented to evaluate the performance of the proposed approach on the datasets of the uniprot[1] web site. The results of experimental evaluation indicate that the approach has a better performance.

The remainder of the paper is organized as follows: Section 2 presents Multi-label classification task for web page. Section 3 presents an external Ontology used to annotate the page of semantic web platform. Section 4 presents related work. In Section 5, we describe and give details on the proposed approach. Section 6 specifies primary experiment results. Finally, Section 7 ends with a conclusion and perspectives.

II. Multi-Label Classification (ML)

According to [9], traditional classification tasks deal with assigning instances to a single label. Multi-label classification is an extension of traditional classification, where the task is to find the set of labels that an instance can belong. In this case, each instance may belong to many classes simultaneously. For the rest of paper, we apply a ML for web page categorization to illustrate our proposed method. A multi-label classification for web page in Semantic web platform deals with a situation where web page [19] can belong to more than one category. Semantic web platform is basically defined by a set of categories and pages. Each page is assigned to one or more categories and includes a set of tags. Formally, semantic web platform web is defined by:

- P is the finite set of web pages, let n the number of pages,
- Let T the finite set of tags and $R_T \subseteq P \times T$ a binary relation between P and T, let m the number of tags. We denote : $\forall\, i \in [0, n]$, $\forall\, j \in [0, m]$, $\forall\, P_i \in P$,$\forall\, T_j \in T$, $R_T(P_i, T_j) = t_{ij}$ with $t_{ij} = 1$ if the page $P_i \epsilon P$ is tagged by $T_j \epsilon T$ and 0 otherwise,
- C the finite set of categories and $R_C \subseteq P \times C$ a binary relation between P and C , let k the number of categories. We denote : $\forall\, i \in [0, n]$, $\forall\, j \in [0, k]$, $\forall\, P_i \in P$,$\forall\, C_j \in C$, $R_C(P_i, C_j) = c_{ij}$ with $c_{ij} = 1$ if the page $P_i \epsilon P$ is categorized by $C_j \epsilon C$ and 0 otherwise. We define the function g which allows to obtain all the pages associated with a category as follows:
- $g: C \rightarrow P$ such that, $\forall c \in C$, $g\,(c) = \{p \,/\, p \in P \; and \; R_C\,(p, c) = 1\}$.

[1] https://www.uniprot.org/

TABLE. I. TRAINING DATA OF MULTI-LABEL CLASSIFICATION FOR WEB PAGE CLASSIFICATION

	T_1	....	T_m	C_1	...	C_k
P_1	t_{11}	....	t_{1m}	c_{11}	...	c_{1k}
....	....	....	....	....	... .	....
P_n	t_{n1}	....	t_{nm}	c_{n1}	... .	c_{nk}
P_{n+1}	$t_{(n+1)1}$	....	$t_{(n+1)m}$	?	?	?

Table I shows the training data for multi-label classification for web page classification.

There are multiple approaches to deal the Multi-Label classification problem. We distinguish two methods families proposed in [13]: transformation methods and adaptation methods. We focus on the transformation methods. The popular approach is Binary Relevance (BR) method. In this approach we can use k binary classifiers. Let h the classifier of ML. BR [14] decomposes the learning of h into a set of binary classification tasks where each single model h_l (using only the information of that particular label) is learned independently, and ignoring the information of all other labels. Hence, $h_l(x)$ =1, if the label l is predicted for the instance x. $h(x)$ gives the set of relevant labels predicted by h for the instance x. Thus, for the categorization of a new example x, BR [14] outputs the union of the labels predicted by the k classifiers.

Table II shows BR method of ML problem with training dataset for n=3, m=3 and k=2.

TABLE. II. TRANSFORMED DATASETS PRODUCED BY BINARY RELEVANCE (BR) METHOD

	T_1	T_2	T_3	C_1
P_1	t_{11}	t_{12}	t_{13}	c_{11}
P_2	t_{21}	t_{22}	t_{23}	c_{21}
P_3	t_{31}	t_{32}	t_{33}	c_{31}

	T_1	T_2	T_3	C_2
P_1	t_{11}	t_{12}	t_{13}	c_{12}
P_2	t_{21}	t_{22}	t_{23}	c_{22}
P_3	t_{31}	t_{32}	t_{33}	c_{32}

III. ONTOLOGY

Ontology [3], [2] represents the relevant concepts (classes) of a domain. Each concept is defined by a set of consensual terms that is not specific to an individual but accepted by a community of users. Specifically, all the defining terms are organized in hierarchy. In semantic web platform, the classes of ontology are used by the experts to annotate the new page created by the users. Uniprot.org web site is an example of semantic web platform where web pages are annotated by keywords (tags) and classes (categories) of gene ontology (GO).

Let Co the set of classes of an external ontology and HC the hierarchy of classes of the ontology. $\forall\, c \in Co$, we denote: $ch(c)$: the set of children classes of c in HC ; $desc(c)$: the set of descendant classes of c in HC ; $sib(c)$: the set of sibling classes of c in HC.

IV. RELATED WORK

The problem of mult-label classification has been studied in the work of [1], [4], [5], [12], [13], [14], [15], [17], [25], [26]. In our context, we apply the ML to predict the categories of a new web page created. In the literature, Multi-label classification approaches [13] can be divided into transformation methods and adaptation methods. An overview on multi-label classification algorithms is given in [13]. We focus on transformation method in this paper. Transformation methods [20] decompose the multilabel problem into a set of binary classification problems. The most popular method is called Binary (BR), which trains a independent binary classifier for each class (against the others). In this paper, we apply a Binary relevance method to categorize web page.

Many similar studies have been realized about web page categorization. The studies differed with the methods used and the use of different algorithms of machine learning [6], [7], [8], [10], [11]. In this paper, we propose a novel method that uses Multi-label Classification and an ontology to categorize a new web page in a web platform used to share knowledge from different communities.

BR [14] is a naturally multi-label classification approach. BR [22] builds one binary data set for each label that contains all examples of the original data set. Examples assigned to label are considered positive examples and the rest are considered to be negative examples. While BR has been used in many practical applications, according to [21], it has been widely criticized for its implicit assumption of labels independence which might be completely incorrect in the data.

BR+ algorithm [16], [23] is an extension of the BR algorithm where the relationship between labels are considered. The differences are its descriptor attributes, which merge all original attributes as well as all labels, except the label to be predicted.

Classifier Chains (CC) [5], [22] generates k binary classifiers. Each classifier incorporates the labels predicted by the previous classifiers as additional attributes. The label correlations are considered randomly.

In this paper, we propose to improve the transformation method of multilabel classification based on BR. So, we propose to use the relationship between labels to select the set of positive examples and negative examples used to build the training dataset of a label. In training dataset of a class cl [24], example assigned to cl are chosen as the positive examples, and other examples are selected as negative examples. An external ontology is used to select the set of positive and negative examples for each label (existing in an ontology) in the learning phase. Similarly, we improve the prediction phase by adding a pruning step if a label is not predicted. Our contribution is described in Section 5.

V. PROPOSED METHODOLOGY

In this section, we describe the methodology used to predict the categories of a new page. The proposed methodology contains two steps. Its main processes are given as follows. The first step is the learning phase. In this step, training data is divided into $|cl|$ subsets, where $|cl|$ means the total number of labels. Then, $|cl|$ binary classifiers are built. The second step is the prediction phase. For a new page created and tagged, this step uses for each label cl, his binary classifier to predict if cl is affected.

A. Step 1: Learning Phase

The first phase is selecting sibling classes, descendant classes for each label by using the hierarchy of ontology and built the training set of cl. For each label cl, we use an ontology to select these siblings ($sib(cl)$) and descendant ($desc(cl)$) classes. For the training set of the category cl, examples assigned to cl or the descendants ($desc(cl)$) $of\ cl$ are chosen as the positive examples, and other assigned to the siblings of cl are selected as negative examples. In the case that the class cl has no correspondent class in an ontology, positive examples of cl are calculated by $g(cl)$ and negative examples are the instances which are not selected by $g(cl)$. The set of positive examples $Tr^+(cl)$ and negative examples $Tr^-(cl)$ are given as follows:

If cl exist in HC then

- $Tr^+(cl) = g(cl) \cup g(desc(cl))$
- $Tr^-(cl) = g(sib(cl))$

Else

- $Tr^+(cl) = g(cl)$
- $Tr^-(cl) = P \setminus \{g(cl)\}$

The last phase of this step is the choice of the base classifier. For each label cl a base classifier [18] (for example: SVM, NaiveBayes, J48,…) is trained by using the training dataset generate for this label.

B. Step 2: prediction phase

This step uses the built classifiers to predict the label of a new example. For improving the prediction phase, if a label is not predicted, then these descendants are pruned in the list of candidates labels.

C. Proposed Algorithm

The proposed algorithm **(**Algorithm 1) takes as input, P, C, T, HC the hierarchy of classes of ontology and the base classifier, the new example. Ontology is used to select the descendant ($desc(cl)$), sibling ($sib(cl)$) labels of cl. The Algorithm generates all the set of positive examples and negative examples for the label cl (line 10).

For each example $p \in Tr(cl)$, it generates the rows (line 14) of the instance $p \in Tr(cl)$ of the training set. The algorithm traverses the set of labels and for each label, the corresponding classifier h_{cl} is invoked (line 26). For improving the prediction phase, if a class is not predicted, then these descendants (line 30) are pruned in the list of candidate labels. Finally, the algorithm returns the set of labels predicted (line 33) for a new example x.

Algorithm 1: ML using an ontology

Input:

$\boldsymbol{P}$: set of examples, $\boldsymbol{C}$:set of label,
$\boldsymbol{T}$: set of attributes,
$\boldsymbol{HC}$:Hierarchy classes of ontology,
classifier :base classifier (example :SVM)
$\boldsymbol{x}$: new example created and tagged

Output:

Y: classes predicted

Begin

1. *For each cl in C do*
2. *// set of positve and negative examples*
3. $Tr(cl) = \emptyset$ *If(cl exist in HC)*
4. $Tr^+(cl) = g(cl) \cup g(desc(cl))$
5. $Tr^-(cl) = g(sib(cl))$
6. Else
7. $Tr^+(cl) = g(cl)$
8. *//all instance without g(cl)*
9. $Tr^-(cl) = P \setminus \{g(cl)\}$
10. End if
11. $Tr(cl) = Tr^+(cl) \cup Tr^-(cl)$
12. For each example $p \in Tr(cl)$ do
13. //set of attributes of a instance p
14. $x_p = \emptyset$
15. For each tag $t \in T$ in BK
16. $x_p = x_p \cup \{ R_T(p,t) \}$
17. End for
18. *//build the training set of cl*
19. $D(p, cl) = x_p \cup \{R_C(p, cl)\}$
20. *InstancesTrain=D*
21. *//build the binary classifier h_{cl} of cl*
22. *h_{cl}=classifier.buildClassifier(instancesTrain)*
23. $h = h \cup \{ h_{cl} \}$*// add h_{cl} to h*
24. End for
24. $Y = \emptyset$
25. for each class $cl \in C$ do
26. *// v=1 if the label cl is predit*
27. $v = h_{cl}(x)$
28. *if($v = 1$) then*
29. $Y = Y \cup \{cl\}$
30. *Else*
31. *//delete the descendants of cl*
32. $C = C \setminus desc(cl)$
33. end if
34. End for
35. *// set of* classes predicted of x
36. return Y

End

VI. Experiments

A. Dataset and Experimental Setup

1) Platform: The experiments are implemented under macOS 10.13.4 (17E199), with Processor: Intel Core i5 @ 2,5 GHz and Memory RAM: 8 Go. The code is implemented in Java and used the weka library.

2) Dataset: As an application area we have chosen bioinformatics[2] in view of the fact that it is an important platform that has many pages annotated by some keywords and classes of GO (Gene Ontology). First we extract the pageID, Keywords and Gene ontology IDs to create the pages of web platform. Fig. 1 illustrates the whole process of collecting training data initial (a) and a fraction of Gene ontology (b) called hierarchy of categories HC.

The characteristics of the experimental dataset are summarized as following:

- pages number used for training data : 5199
- pages number used for Testing data: 3985
- Categories number : 630
- Tag number : 2815

The characteristics of ontology used: the number of classes used in hierarchy of categories HC is 630.

B. Evaluation Metrics

The metrics precision (P), recall (R) and Fmeasure (F1) are proposed to evaluate our method. The precision, recall and F1 for the example i are defined as:

$$P_i = \frac{|Y_i \cap Z_i|}{|Y_i|}, \quad R_i = \frac{|Y_i \cap Z_i|}{|Z_i|}, \quad F1_i = \frac{2 * P_i * R_i}{P_i + R_i}$$

where, for an example i, Y_i is the set containing all of the predicted classes, and Z_i the set including all of its true classes. To combine the performance of all instances to evaluate the results measured on a dataset with n instances labeled, we use the macro-averaging of the precision P, recall R and F1:

$$P = \frac{\sum_{i=1}^{n} P_i}{n}, \quad R = \frac{\sum_{i=1}^{n} R_i}{n}, \quad F1 = \frac{\sum_{i=1}^{n} F1_i}{n}$$

C. Experiments Results

In experimental evaluation, we use some base classifiers (SVM, NaiveBayes, J48) to observe the performance of the method proposed to place the pages in the good categories. We compare the proposed method with BR method.

Table III gives the experimental results of proposed method vs BR with some base classifiers.

Table IV gives the experimental results of the proposed method vs BR method from five categories. The base classifiers SVM is used.

D. Analysis and Discussion

The results (Table III) show: (i) with the classifier SVM, The macro-averaging $F1$ for proposed method is 76.96% against 26.29% for BR; (ii) With the classifier NaiveBayes, the macro-averaging $F1$ for proposed method is 65.08% against 3.88% for BR; (iii) With the classifier J48, the macro-averaging $F1$ for Proposed method is 74.25% against 24.22% for BR. These results show that the proposed method gives the good performance than BR with use these base classifiers. For these three base classifiers, proposed method +SVM gives the better performance. These good performances are linked to the ontology used and by exploiting the dependencies between the categories.

Furthermore, we conducted comparisons with BR using the base classifier SVM on five categories. The results (Table IV) show that our approach has the best performance than BR for the five categories used. The Precision of the category GO0008270 (95.15%) is better with BR than the Precision of proposed method (92.36%). This shows that our selection method presents limits in the choice of positive and negative examples. The macro-averaging $F1$ for each category used is better for proposed method than macro-averaging $F1$ of BR. This best performance is due firstly to the use of the ontology and the relation between category. Also, our method uses a method of selecting positive and negative instances in the building of the training set for each category while the BR method does not use it in the construction of the model. Thus, we can come to a conclusion that our method proposed improves the performance of the method BR of Multi-label classification.

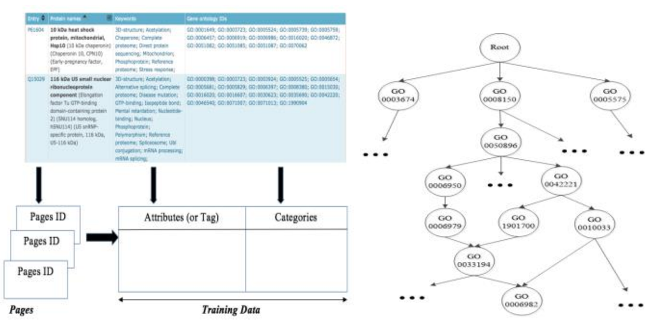

(a) (b)

Fig. 1. (a) The Whole Process of Collecting Training Data (b) a Fraction of the Gene Ontology.

TABLE. III. The Experimental Results of Proposed Method vs BR with Some base Classifiers

Base classifiers	**Proposed method**			**BR**		
	P	***R***	***F1***	***P***	***R***	***F1***
SVM	76.85%	77.67%	76.96%	26.67%	25.92%	26.29%
NaiveBayes	61.25%	69.94%	65.08%	1.99%	74.20%	3.88%
J48	74.81%	73.76%	74.25%	24.83%	23.63%	24.22%

TABLE. IV. BR Method vs Proposed Method for Five Categories

Categories	**BR**			**Proposed method**		
	P	**R**	**F1**	**P**	**R**	**F1**
GO0003700	72.09%	38.59%	**50.27%**	97.54%	98.76%	**98.15%**

[2] https://www.uniprot.org/

GO0016818	81.58%	72.66%	**76.86%**	98.45%	99.22%	**98.83%**
GO0008270	95.15%	63.64%	**76.27%**	92.36%	94.12%	**93.23%**
GO0003735	75.00%	2.80%	**5.398%**	99.03%	95.33%	**97.14%**
GO0003773	66.67%	38.46%	**48.78%**	96.15%	96.15%	**96.15%**

VII. Conclusion

In this paper, we propose a novel method of Multi-label Classification (ML) using an ontology. In the learning phase, the ontology is used to select the set of positive and negative instances for learning and building the training set. In the prediction phase, ontology is used to delete the descendants of the category not predicted. Experiment results on a data downloaded from the biological database Uniprot (www.uniprot.org) show that proposed method improve BR method of ML. The good performance of proposed method demonstrates that our proposal is expected to be a potential approach to solve the automatic web page categorization in a semantic web platform.

In the future work, first we compare our approach with BR+ and CC methods of transformation methods of multi-label classification. Next we will test and compare our approach in more methods of Multi-label classification and more datasets. Also, we will use our approach with the selection methods of features and study their impact in web page categorization.

References

[1] Zhang, M., Zhou, Z.: A review on multi-label learning algorithms. IEEE Transactions on Knowledge and Data Engineering (Volume: 26, Issue:8, Aug. 2014).

[2] Gomez Perez A. Ontological engineering : A state of the art. Expert update 2. Technique et Science Informatiques 28, page 81233–126,1999.

[3] T. R. Gruber. Toward principles for the design of ontologies used for knowledge sharing. in : International Journal of Human-Computer Studies - Special issue : the role of formal ontology in the information technology, V, pages 907 – 928, 1993.

[4] Madjarov G., Kocev D., Gjorgjevikj D., and Dzeroski S. An extensive experimental comparison of methods for multi-label learning. Pattern recognition, 45(9) :3084–3104., 2012.

[5] W. Bi and J. T. Kwok. Multi-label classification on tree-and DAG-structured hierarchies in Proc. 28th Int. Conf. Mach. Learn., Bellevue, WA, USA, 2011, pp. 17–24.

[6] O. W. Kwon and J. H. Lee, Web page classification based on knearest neighbor approach, IRAL, 2003.

[7] O. W. Kwon and J. H. Lee, Web page classification based on knearest neighbor approach, Proceedings of the Fifth International Workshop on Information Retrieval with Asian Languages, 2000, Hong Kong, China, September 30 - October 01, 2000.

[8] Ajay S. Patil, B.V. Pawar. Automated Classification of Web Sites using Naive Bayesian Algorithm, Proceedings of the International Multi Conference of Engineers and Computer Scientists 2012 IMECS 2012, 14-16 March, 2012, Hong Kong.

[9] Noor, A., Chandan, K. R., Farshad, F. Exploiting Label Dependency for Hierarchical Multi-label Classification. In PAKDD (1), 294-305 (2012)

[10] S. Shibu, A. Vishwakarma, and N. Bhargava, A combination approach for web page classification using page rank and feature selection technique, International Journal of Computer Theory and Engineering, 2010.

[11] A. P. Asirvatham and K. K. Ravi, Web Page Categorization Based on Document Structure, 2002.

[12] F. HERRERA, F. CHARTE, A.J. RIVERA, M.J. DEL JESUS, Multi-label Classification Problem Analysis. Metrics and Techniques. Springer International Publishing, ISBN 78-3-319-41111-8, 2016.

[13] Tsoumakas G. and Katakis I. Multi-label classification: An overview. International Journal of Data Warehousing and Mining (IJDWM), 3(3) :1–13, 2007.

[14] Tsoumakas G., Katakis I., and Vlahavas I. Mining multi-label data. In Data mining and knowledge discovery handbook, pages 667–685. Springer, 2010.

[15] Tsoumakas G. and Vlahavas I. Random k-labelsets : An ensemble method for multilabel classification. In Proceedings of the 18th European conference on Machine Learning, 2007.

[16] Cherman EA, Metz J, Monard MC. Métodos multirrótulo independentes de algoritmo: um estudo de caso. In: Anais da XXXVI Conferencia Latinoamericana de Informática (CLEI). Asuncion, Paraguay; 2010. p. 1–14.

[17] Clare A, King RD. Knowledge discovery in multi-label phenotype data. Lect Notes Comp Sci 2001:42–53.

[18] Sun, A.; Lim, E.P.; Liu, Y. On strategies for imbalanced text classification using SVM: A comparative study. Decis. Support Syst. 2009, 48, 191–201.

[19] B. Choi. "Web Page Classification*", Studies in Fuzziness and Soft Computing, 2005.

[20] André Melo, Heiko Paulheim. "Local and global feature selection for multilabel classification with binary relevance", Artificial Intelligence Review, 2017.

[21] Alazaidah, Raed, Fadi Thabtah, and Qasem Al-Radaideh. "A Multi-Label Classification Approach Based on Correlations Among Labels", International Journal of Advanced Computer Science and Applications, 2015.

[22] Gibaja, Eva, and Sebastián Ventura. "Multi-label learning: a review of the state of the art and ongoing research : A review on multi-label learning", Wiley Interdisciplinary Reviews Data Mining and Knowledge Discovery, 2014.

[23] Tanaka, Erica Akemi, Sérgio Ricardo Nozawa, Alessandra Alaniz Macedo, and José Augusto Baranauskas. "A multi-label approach using binary relevance and decision trees applied to functional genomics", Journal of Biomedical Informatics, 2015.

[24] Carlos N. Silla, Alex A. Freitas. "A survey of hierarchical classification across different application domains", Data Mining and Knowledge Discovery, 2010.

[25] Chang Xu, Dacheng Tao, Chao Xu. "Robust Extreme Multi-label Learning", Proceedings of the 22nd ACM SIGKDD International Conference on Knowledge Discovery and Data Mining - KDD '16, 2016.

[26] Amirreza Mahdavi-Shahri, Mahboobeh Houshmand, Mahdi Yaghoobi, Mehrdad Jalali. "Applying an ensemble learning method for improving multi-label classification performance", 2016 2nd International Conference of Signal Processing and Intelligent Systems (ICSPIS), 2016.

Energy Efficient Cluster Head Selection using Hybrid Squirrel Harmony Search Algorithm in WSN

N. Lavanya[1], T. Shankar[2]
Department of Communication Engineering, School of Electronics Engineering
Vellore Institute of Technology, Vellore, Tamil Nadu, India

***Abstract*—The Wireless Sensor Network (WSN) has found an extensive variety of applications, which include battlefield surveillance, monitoring of environment and traffic, modern agriculture due to their effectiveness in communication. Clustering is one of the significant mechanisms for enhancing the lifespan of the network in WSN. This clustering scheme is exploited to improve the sensor network's lifespan by decreasing the network's energy consumption and increasing the stability of the network. The existing cluster head selection algorithm suffers from the inconsistent tradeoffs between exploration – exploitation and global search constraints. Therefore, in this research, the hybridization of two popular optimization algorithms, namely, Harmony Search Algorithm (HSA) and Squirrel Search Algorithm (SSA) is executed for optimal selection of cluster heads in WSN with respect to distance and energy. The proposed Hybrid Squirrel Harmony Search Algorithm (HSHSA) is found to be energy efficient when compared with first node death (FND) and last node death (LND) of existing Cluster Head Selection (CHS) techniques. In addition to this, the proposed HSHSA shows enhancements in overall throughput and residual energy of the wireless sensor network by 31.02% and 85.69%, respectively than the existing algorithms.**

Keywords—Cluster head selection; clustering; harmony search algorithm; squirrel search algorithm; wireless sensor network

I. Introduction

As an improved and innovative data acquisition and processing technology, Wireless Sensor Network (WSN) has an extensive variety of applications in environmental monitoring, military, space exploration, smart furniture, etc. [1]. A WSN can be defined as an autonomous system comprising of a lot of sensor nodes developed for intercommunicating through wireless radio [2]. Energy efficiency is an important aspect of the WSN. Performing routing on a hierarchical basis is a fundamental procedure to decrease the energy consumption in a network [32]. On the other hand, since the cluster heads (CHs) nearer to the base station (BS) are burdened with intense traffic, they drain quicker compared to the rest of the nodes in the cluster. The sensor network algorithms and protocols must be capable of self-organizing. Such a protocol design will improve network lifetime and utilize maximum node energy [10]. In WSN, clustering is a significant routing approach, which can re-configure the network. WSN is divided into clusters, each possessing a coordinator node referred to as the CH, which is accountable for collecting the information from all the members of the cluster and transmitting the gathered information to the base station called the sink node. Sensors are often deployed densely to satisfy the coverage requirement, which enables specific nodes to go to the sleep mode, thus, saving significant energy [11,31]. The cluster heads are chosen either randomly or by checking for one or more criteria. The technique employed for the selection of cluster heads brings a major impact to the lifetime of the WSN. The node which has the highest count of neighbor nodes, the minimum distance from BS, and the maximum residual energy is termed as the ideal cluster head for a cluster [3]. Cluster Heads can aggregate, process and filter the information forwarded by the member nodes of the cluster. This reduces the network bandwidth and conserves energy consumption. Thus, an efficient selection of cluster heads will improve the network's lifespan and maximizes the energy of the sensor nodes. This cluster based reconfiguration of the network is performed based on the desired requirements.

One of the inflexible demands of the nodes in WSN is the effective use of the energy being stored. Numerous techniques have been developed for managing the energy of nodes in WSN efficiently through different clustering techniques [4]. When the search for an optimum solution of the CH becomes exhaustive, meta-heuristic optimizations are preferred. To name a few, Particle Swarm Optimization (PSO), Harmony Search Algorithm (HSA), and Squirrel Search Algorithm (SSA) are such meta-heuristic search optimization algorithms employed for finding an optimal solution. The HSA suffers from the drawback of being bound to only a specific search area. Nevertheless, in PSO, the particle traverses from area to area in search of an optimal solution. However, the PSO suffers from the issue with exploitation and exploration in the problems involving high dimensionality and in the problems which consume a long computational time for achieving local minima or maxima [5].

A. Our Contribution

In contrary to the existing algorithms of cluster head selection, this research work integrates the SSA and HSA optimization techniques. The HSA exhibits high searching efficiency. In SSA, the squirrels move from one locality to another locality in search of a globally optimal solution, hence the exploration is not region specific like HSA. In addition to this, the SSA exhibits high convergence property, unlike PSO. Therefore, the proposed HSHSA scheme utilizes high search efficiency of HSA integrated with the high convergence and dynamic property of SSA for selecting energy efficient cluster heads for the WSN. The important objectives of this research are:

- To deploy nodes in the WSN and form clusters.
- To develop HSHSA optimization for Cluster Head Selection (CHS).
- To improve the overall throughput and residual energy of nodes in the modeled WSN.
- To validate the improved performance of the proposed HSHSA CHS mechanism.

The remaining sections of the research paper are organized in the following manner: Section 2 includes the discussion of the works done by the researchers previously; Section 3 explains the methodology proposed; Section 4 presents all the simulation results and their inferences, and Section 5 provides a conclusion as well as a scope to extend the work in the future.

II. Literature Review

The literature review section of the paper includes the works proposed previously for selecting the cluster heads namely, LEACH protocol, NSGA, PSO, GSA, ABC, HSA, etc. In [7], the authors analyze a scheme that integrates four important clustering techniques such as connectivity based scheme ID based clustering, weighted approach, and probability based clustering. Ant Colony Optimization (ACO) is employed for optimizing the count of clusters and for selecting the optimal cluster heads. However, the time of convergence is very uncertain for ACO algorithms.

The authors in [12] have provided an HSA scheme which is based on the centralized cluster-dependent mechanism. Here, this approach is dependent on music and is a Meta-heuristic optimization technique, which decreases the distance. This method subsists among the cluster heads in addition to the associated nodes, leading to the optimization of energy distribution in the sensor network. However, the HSA method of optimization, the search for an optimal solution is stuck in the local minima. The authors in [13] proposed a modified synchronous FireFly algorithm for the selection of cluster heads in WSN. The Firefly algorithm is a heuristic search optimization technique. This was done to resolve the uneven network degradation and to improve network performance. The results are better compared to the performance of LEACH and conventional firefly technique; however, the lifetime for the nodes can still be improved.

The authors in [14] have examined a PSO clustering method that could enhance the lifetime of the network by disposing of the formation of single nodes. Hence, they suggested an E-OEERP that worked based on both the GSA and PSO. Here, the PSO was employed for eliminating the formation of nodes and the GSA scheme was used for the selection of routes. However, the cluster overhead was the main disadvantage of the clustering approach. The authors in [15] worked on a clustering scheme to improve the network lifetime. Here, a modification to the LEACH algorithm was proposed which worked based on the shortcomings of original LEACH by exploiting the distance measured with the current node was proposed. Hence novel thresholds from node energy as well as the distance factors of the individual node have been developed. But this protocol does not solve the random distribution issue of CHs as well as cluster dimensions [8]. The authors in [16] presented a review on scheduling mechanisms that focused on improving the energy efficiency in WSN having a different architecture of the network compared to the conventional WSN. In order to decrease the whole time taken for transmission and extend the lifespan of the network, the conventional sensor network is substituted by SDN architecture.

The authors in [18] proposed a PSO algorithm for implementing CHS in WSN in an energy efficient manner. This method comprises of efficient fitness function and particle encoding technique. Residual energy, sink distance, and intra-cluster distance are the parameters considered for optimization. The drawback of the PSO technique is the problem of exploration and exploitation. The authors in [19] have presented an ABC meta-heuristic with an enhanced solution search equation to enhance its utilization capability. An enhanced population sampling approach was developed. It needs a single controlling parameter to calculate and save the result. Thus, it increases the efficacy of the suggested methodology. A fine balance between exploitation and exploration was maintained by the use of a proposed approach with minimum memory requirements. However, the ABC algorithm is slow while processing sequential data. The authors in [30] proposed a cluster head selection scheme to improve the network lifetime using hybridization of firefly and grey wolf optimization algorithm. The main motive of this research is to decrease the overhead and stabilize the network. However, the lifetime for the nodes can still be improved.

The authors in [6] suggested the sorting of results of multi-objective problems in a non-dominated manner by the use of a multi-objective evolutionary algorithm (MOEA), referred by Non-dominated Sorting Genetic Algorithm II (NSGA-II) for prolonging the lifespan of the WSN. The optimization of the consumption of energy is carried out for enhancing the lifetime of the network. The drawback of this approach is that the nodes in the network start dying from the initial rounds. The authors in [9] presented an energy efficient scheme of hierarchical clustering for WSN. The nodes form clusters in a hierarchical manner for maximizing coverage and minimizing energy consumption. This method of clustering is decentralized. As an extension, this approach can be formulated as a centralized clustering scheme for improving energy efficiency.

The authors in [17] suggested a spectrum sensing mechanism based on clusters, for minimizing energy consumption. The formation of clusters is implemented by the Fuzzy C-means approach and the CHs are chosen based on locations of sensors which are the members of clusters. However, this method causes nodes to die constantly throughout. The authors in [20] proposed an algorithm for routing which integrates cluster formation, CHS, and multipath routing for data transmission. As a result, energy consumption and routing overheads are decreased. The best path is selected using a Genetic Algorithm, which considers minimal energy dissipation and distance in the objective function. This increases the lifetime of the network by sharing the traffic evenly for all the nodes. From the study of the literature, this research proposes the hybridization of HSA and SSA optimization technique for the energy efficient and optimal selection of cluster heads. The proposed HSHSA technique resolves the problem found in the previously proposed algorithms such as exploration and exploitation and improves the search efficiency and convergence rate.

III. Research Methodology

A. Network Model

The free space network model is taken into consideration for this study. It comprises a receiver section and a transmitter module with d as the separation distance. The transmitter module contains transmission electronics with an amplifier for the transmission and the receiver module contains receiving electronics as a portion for data to be communicated using bits. The network model is assumed to be a group of sensor nodes scattered on a field that is in the shape of a rectangle [21]. The communication energy of the sensor network is calculated using the following equation (1-2). The below mentioned properties are considered for modeling the WSN:

- The sensor nodes in the WSN are assumed to be in the quasi-stationary state.
- Nodes are not aware of their location.
- The sensor nodes in the modeled WSN are in a homogeneous fashion.
- The consumption of energy for the sensor nodes in the network is non-uniform in nature and is dependent on the distance of the sensor node from the cluster head or BS.
- There is no need for monitoring of the nodes after deployment since these nodes are self-organizing. The power levels of all the nodes are fixed.

$$E_{Tx}(l,d) = \begin{cases} lE_{elec} + lE_{fs}d^2, & d < d_0 \\ lE_{elec} + AlE_{mp}d^4, & d \geq d_0 \end{cases} \quad (1)$$

$$E_{Rx}(l) = lE_{elec} \quad (2)$$

where E_{Rx} denotes the energy consumed by the receiver for the message of bit length 1, and E_{Tx} indicaes the energy consumed by the transmitter for that same message. E_{elec} is the electronics energy, which is dependent on the parameters namely, modulation, spreading of the signal, filtering, and digital coding, while the amplifier energy $E_{fs}d^2$ (free space model) or $E_{mp}d^4$ (multi-path model) relies on the distance from the node to the receiver, and the permissible level of bit-error rate. The separation distance is defined using the following equation (3).

$$d = \cos\theta = \frac{A \cdot B}{\|A\|\|B\|} \quad (3)$$

where A and B are the co-ordinates of the cluster head CH and the node i, respectively. In the considered WSN, n number of sensors are randomly arranged in a field of area 'M x N'm^2. For optimizing the approach of selecting CHs and for determining the optimal 'k' CHs, the objective function employed for computing the optimal solution is given in equation (4) [12]:

$$f_{obj} = \epsilon \times f_1 + (1-\epsilon) \times f_2 \quad (4)$$

where f_1 and f_2 are given by

$$f_1 = max_k \left\{ \sum_{\forall, node, i \in C_k} \frac{d(node_i, CH_k)}{||Cluster_k||} \right\} \quad (5)$$

$$f_2 = \frac{\sum_{i=1}^{N} E(node_i)}{\sum_{j=1}^{k} E(CH_j)} \quad (6)$$

where the scaling factor (ϵ) ranges between 0 to 1. In the fitness function given in (4), f_1 is the largest separation distance of the cluster members '$node_i$ $\forall_i \in$ *node cluster* $Cluster_k$' to their corresponding cluster head CH_k and $\|Cluster_k\|$ is the total count of nodes which are the cluster members of $Cluster_k$. Whereas, f_2 denotes the ratio of initial energy of all the sensor nodes that are alive, $E(node_i)$ in the WSN, to the aggregate of the cluster head's current state energy '$E(CH_k)$' of the current iteration of round; ϵ is a constant that denotes the impact of 'f_1' and 'f_2' in the considered fitness function 'f_{obj}'.

B. Proposed Methodology

Harmony Search Algorithm: The Harmony Search Algorithm idealizes the improvisation procedure by a skillful musician. There are three options preferred when a musician improvises: (1) play a similar or known music notes (by altering the pitch to some extent); (2) compose random or new notes; (3) play a popular form of music (a sequence of pitches in the harmony) from the notes of his/her memory. Zong Woo Geem et al. officially announced the above mentioned three choices into a mathematical algorithm of optimization in 2001, and these corresponding elements become pitch adjusting, randomization, and utilization of harmony memory [22]. The utilization of harmony memory is essential, as it is the same as the choice of the best-fit entities in bio-inspired optimizers. This ensures the exploitation of the optimal harmonies in the updated harmony memory. In order to utilize this memory more efficiently, it is generally allotted as a factor $r_{accept} \in [0,1]$, referred to as the harmony memory considering rate (HMCR). When HMCR is very less, only a small number of best harmonies are chosen and that may lead to very slow convergence. When HMCR is exceptionally high (close to 1), almost all the harmonies are employed in the harmony memory, while the rest of the harmonies are not exploited properly, which results in potentially faulty solutions. Hence, r_{accept} is defined between 0.7 and 0.95.

The pitch adjustment is the second element, found using a pitch adjusting rate r_{pa} and a pitch bandwidth b_{range}. Although in music, adjusting the pitch contributes a lot in changing the frequencies, it relates to producing a slightly varied solution in the HSA. The randomization is the third element, which is to improve the solutions of diversity. Though pitch adjustments play a similar part, it is restrained to several local adjustments of pitches and looks for an optimal solution locally. The usage of random assignment can make the system to additionally exploit several diversified solutions, such that the global optimality is found.

1) Squirrel Search Algorithm: The process of search is initialized when the flying squirrels (FSs) begin scavenging. In warm weather conditions (like autumn), these squirrels scavenge for food sources by flying from one tree to another.

This activity changes their locations and begins exploration for food in different regions of the forest. Since the weather conditions are adequately hot, the squirrels can fulfill their day to day requirements of food rapidly on the diet of acorn nuts present abundantly and thus the squirrels eat those acorns right after they're found. When the daily necessity is fulfilled, the squirrels will start to search for the optimal source of food in order to store the requirements during winter (hickory nuts). Storing these nuts aids the squirrels to maintain the requirements of energy during intense weather conditions. This will also decrease the expensive foraging, and thereby raise the survival probability. In winter, the loss of leaves in the forest can result in an elevated risk of predator presence and so the squirrels become less active but do not hibernate in that period of the season. When the winter season comes to an end, these squirrels become active again. These actions of scavenging happen recurrently and continue throughout the lifetime of a flying squirrel. This is also the main reason to form the foundation of SSA [29]. The following are the assumptions taken into consideration for the simplification of the mathematical model:

- In a deciduous forest, n numbers of flying squirrels are considered, out of which only a single squirrel is considered to be on a single tree.
- The entire population of squirrels independently looks for a food source and utilizes the food sources available optimally by demonstrating a dynamic behavior of scavenging.
- In the deciduous forest, three kinds of trees exist; they are normal trees, hickory nut trees, and oak trees (acorn nut trees).
- The area of the forest under the assumption is considered to comprise one hickory tree and three oak trees.

2) Proposed HSHSA for Optimal Cluster Head Selection: The proposed approach of CHS, called the HSHSA, relies on the general attributes of HSA as well as SSA optimization schemes. The optimization technique HSA is capable of producing solutions and metrics of PAR and HMCR, to permit the solution to evade from the optimum solution obtained locally and in order to enhance the optimum solution obtained globally. Because of this reason, HSA is integrated with the SSA to resolve the problem of exploitation and exploration in high dimensionality, thereby achieve optimal solution with good rate of convergence accuracy. The flow diagram of the proposed HSHSA scheme optimal CHS is displayed in the Fig. 1.

In HSHSA optimization, employing SSA permits the squirrels to navigate from one area to other area by changing the locations and seasons at the termination of every iteration of round of data transmission. The dynamic behaviour of SSA agrees to look for optimal solution in n number of regions of the space with higher convergence rate along with high search efficiency of HSA in each area. This functional working of the HSHSA optimization is executed for several rounds of transmission of data. For every round, the CHs conduct transmission of data by collecting information from all the members of the cluster and by transferring to the sink.

The following steps are implemented in the HSHSA:

Step 1: Creation of Network Model: Initial WSN is modelled with nodes. And the energy of all the nodes are initialized.

Step 2: Initialization of Parameters: In a forest, it is considered that there are n number of FS and the position of the i^th^ FS is defined by a matrix. The locations of all the flying squirrels are exemplified in the matrix given below (7):

$$FS = \begin{bmatrix} FS_{1,1} & FS_{1,2} & \dots & \dots & FS_{1,d} \\ FS_{2,1} & FS_{2,2} & \dots & \dots & FS_{2,d} \\ \vdots & \vdots & \vdots & \vdots & \vdots \\ \vdots & \vdots & \vdots & \vdots & \vdots \\ FS_{n,1} & FS_{n,2} & \dots & \dots & FS_{n,d} \end{bmatrix} \tag{7}$$

where $FS_{i,j}$ represents the i^{th} FS in j^{th} dimension. An even distribution is required for allocating the initial position of all the flying squirrels present in the forest as given in the following equation (8) [23].

$$FS_i = FS_{LB} + U(0,1) \times (FS_{UB} - FS_{LB}) \tag{8}$$

where FS_{UB} , FS_{LB} are upper and lower limits respectively of i^{th} FS in the j^{th} dimension; whereas U(0, 1) refers to the uniformly distributed randomly generated number defined in the interval [0, 1]. The initialization of flying squirrels and harmony memory in HSHSA optimization is called as Squirrel Harmonic Memory (SHM). The initial SHM comprises of numerous randomly produced results of the optimization problem considered for the study. The result of the problem being formulated is an index of the 'k' number of CHs. SHM is calculated using the equation (9). The rows of the SHM matrix denote random solutions for the problem of optimization considered. The fitness value for each Hybrid vector is calculated with the help of equation (4).

$$\begin{bmatrix} Fs_1^1 & Fs_2^1 & \dots & Fs_k^1 \\ Fs_1^2 & Fs_2^2 & \dots & Fs_k^2 \\ \vdots & \vdots & \ddots & \vdots \\ Fs_1^{SHM} & Fs_2^{SHM} & \dots & Fs_k^{SHM} \end{bmatrix} \begin{bmatrix} f_{obj\_1} \\ f_{obj\_2} \\ \vdots \\ f_{obj\_n} \end{bmatrix} = \begin{bmatrix} F^1 \\ F^2 \\ \vdots \\ F^{SHM} \end{bmatrix} \tag{9}$$

Step 3: Sorting, Declaration, and Randomized Selection: Upon obtaining the position fitness values of all the FSs, subsequently they are sorted in an ascending manner. The FS having the minimum value of fitness is assumed to stay on the hickory nut trees. The five successive best FSs are assumed to stay on the acorn nut tree. These five squirrels are supposed to fly toward the direction of hickory nut tree. The rest of the FSs are considered to stay on the normal trees. Furthermore, by performing randomized selection, few FSs are supposed to fly toward the direction of hickory nut tree considering that the squirrels have contented with their regular day to day energy demands. The remaining FSs will glide towards the acorn nut tree. The scavenging activity of these squirrels is constantly impacted by the existence of predators. The natural behavior of FSs is developed by formulating the mechanism of updating locations with P_{dp}, known as the predator presence probability. There are three possible scenarios that can take place in the food scavenging activity of flying squirrels. In each scenario, the following conditions are assumed:

- In the absence of a predator, a FS glides and effectively explores for its favorite food throughout the forest.
- In the presence of a predator, the FS is careful. FSs are enforced to perform a small randomized walk to explore a neighboring location for hiding.

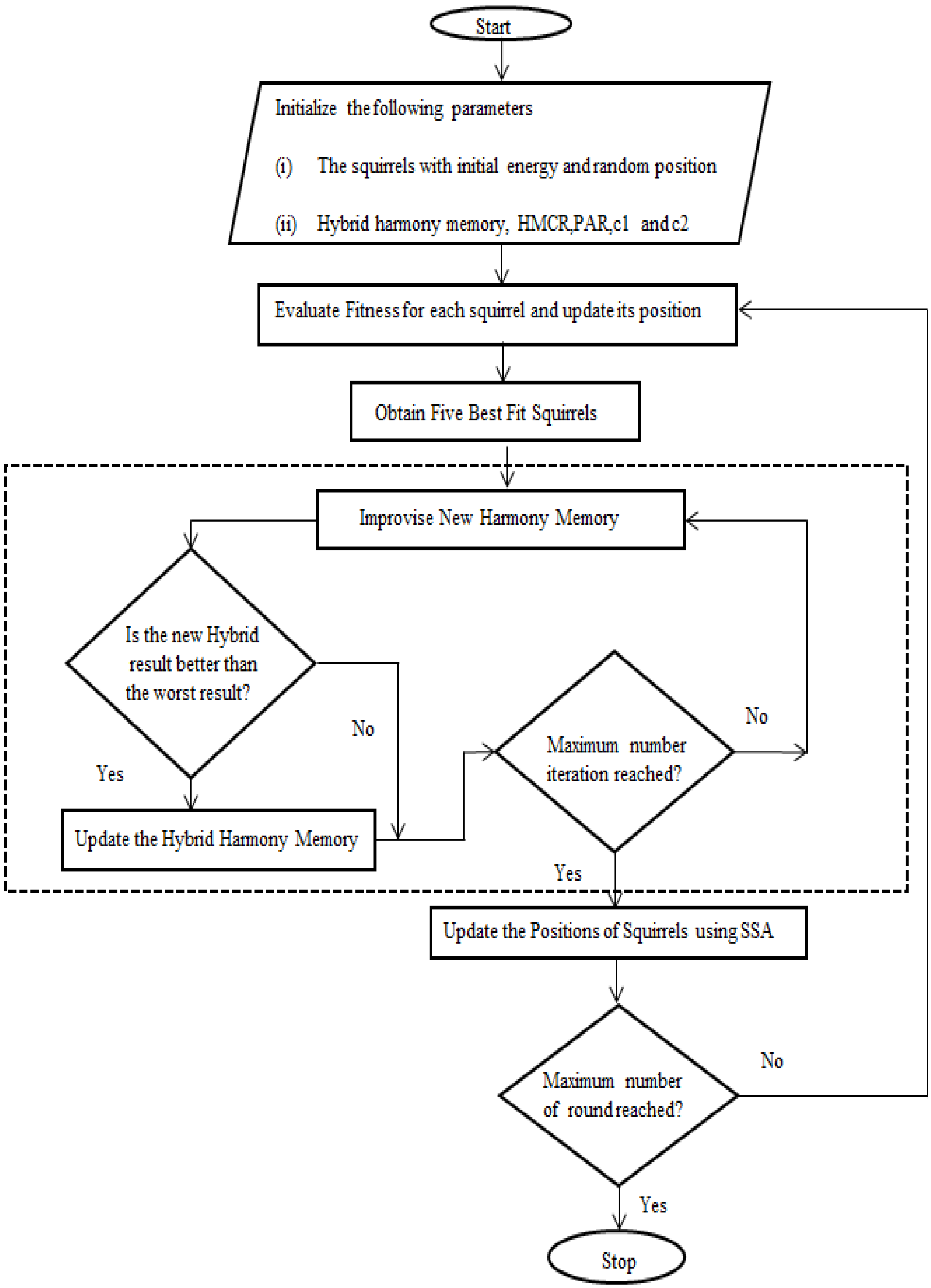

Fig. 1. Flowchart of the Proposed HSHSA.

The dynamic scavenging activity of the FSs can be modeled mathematically for the three situations in the following manner [23]:

Scenario 1: FSs that are on acorn nut tree (FSat) might glide in the direction of hickory nut trees. On considering this situation, the updated positions of the FSs are attained by equation (10):

$$FS_{at}^{t+1} = \begin{cases} FS_{at}^{t} + d_g \times G_c \times (FS_{ht}^{t} - FS_{at}^{t}), & R_1 \geq P_{dp} \\ Randomlocation, & otherwise \end{cases} \quad (10)$$

where d_g is random gliding distance, R_1 denotes the random number in the range of [0, 1], t indicates the current iteration and FS_{ht}^{t} is the position of the flying squirrel which got hold of a hickory nut tree. The balance between exploitation and exploration is attained using the gliding constant G_c mentioned in the mathematical model.

Scenario *2:* FS_{nt}^{t} denotes the FSs that are on the normal trees, and might fly in the direction of acorn nut tree to meet the regular food demands. On considering this situation, the updated position of FS can be achieved in the following equation (11) [23]:

$$FS_{nt}^{t+1} = \begin{cases} FS_{nt}^{t} + d_g \times G_c \times (FS_{at}^{t} - FS_{nt}^{t}), & R_2 \geq P_{dp} \\ Randomlocation, & otherwise \end{cases} \quad (11)$$

where R_2 is a number selected randomly within the interval [0, 1].

Scenario 3: Few FSs from the normal trees that have already consumed acorn nuts might glide in the direction of the hickory nut tree for the purpose of storing the hickory nuts for consuming them when there is scarcity in food. In this situation, the updated positions of FSs can be achieved using the following equation (12) [23]:

$$FS_{nt}^{t+1} = \begin{cases} FS_{nt}^{t} + d_g \times G_c \times (FS_{ht}^{t} - FS_{nt}^{t}), & R_3 \geq P_{dp} \\ Randomlocation, & otherwise \end{cases} \quad (12)$$

where R_3 denotes a number generated randomly from the interval [0, 1]. Predator presence probability P_{dp} is assumed as 0.1.

Step 4: Updating New Harmonic Memory: After declaring the SHM according to the equation (9), the SHM is improved by producing a new vector of harmonies [Fs'_1, Fs'_2,…, Fs'_k]. Every element of the new harmony matrix denoted by 'I_j', is produced with the help of the equation (13) on the basis of the defined HMCR value.

$$Fs'_j \leftarrow \begin{cases} Fs'_j \in SHM \text{ with probablity } HMCR \\ Fs'_j \in Fs_j \text{ with probability } (1 - HMCR) \end{cases} \quad (13)$$

HMCR is referred to the probability of choosing an element from the SHM elements, and (1-HMCR) is, thus, the possibility of randomly producing it. If Fs'_j is produced by the SHM, then Fs_j is furthermore altered or otherwise mutated with respect to the PAR value. This finds the possibility of the SHM candidate to be altered and (1-PAR) gives the possibility of an alternative process. The alteration of the pitch for the chosen Fs'_j can be given as,

$$Fs'_j \leftarrow \begin{cases} Fs_j^n \in SHM \text{ with probablity } PAR \\ Fs'_j \text{ with probability } (1 - PAR) \end{cases} \quad (14)$$

where Fs_j^n refers to a node that is in the closest proximity, having an energy that is higher than the present CHs energy of the respective cluster.

Step 5: Updating the Hybrid Harmony Matrix: This hybrid harmony matrix is generated newly and is assessed with respect to the fitness value obtained for the optimal solution from every row of SSA. If the updated hybrid harmony vector's fitness value is better compared to the fitness value obtained for the SHM's worst harmony, then n updated harmony is comprised in the SHM as well as the prevailing worst harmony is eliminated from the SHM.

Step 6: Update Locations of Flying Squirrels: Gliding behavior of flying squirrels is defined in terms of gliding equilibrium of which the total sum of drag (D) and lift (L) force generates a resultant force (R) having equal magnitude and a direction opposing the weight (Mg) of the FS. Hence, R offers a linear route of gliding for the flying squirrel, which is gliding at a persistent velocity (V) [24]. In this research, an approximated prototype of gliding behavior is employed in developing the technique of optimization. A squirrel flying at constant speed permanently descending with an angle ϕ to the vertical and lift-to-drag or glide ratio is expressed in the following equation (15) [25].

$$\frac{L}{D} = \frac{1}{\tan \phi} \quad (15)$$

The FSs can upsurge their flight-path distance by producing minimal glide angle (ϕ), thereby increasing the glide ratio. In this work, the lift leads to a downward air deflection above the squirrels' wings. This can be expressed in equation (16) [23]:

$$L = \frac{1}{2\rho C_L C^2 A} \quad (16)$$

where ρ (1.204 kgm^{-3}) denotes the density of air, C_L refers to the coefficient of lift, C (5.25 ms^{-1}) indicates the speed, whereas A (154 cm^2) indicates the surface area of squirrel's body. The foraging of FSs is impacted due to the modifications in the weather and including such activity might offer a realistic methodology towards achieving the optimal solution. Thus, a criterion for monitoring the seasons is established in SSA, which stands as a reason to prevent the proposed technique from being bound to the solutions of local optima. The seasonal constant (S_c) is calculated using the following equation (17) [23].

$$S_c^t = \sqrt{\sum_{k=1}^{d} (FS_{at,k}^t - FS_{ht,k})^2} \quad (17)$$

where t = 1, 2, 3. Then the search is processed until the criterion $S_c^t < S_{min}$ is met. where S_{min} is the minimal value of seasonal constant calculated using equation (18):

$$S_{min} = \frac{10E^{-6}}{365^{t/(tm/2.5)}} \quad (18)$$

where t_m and t indicate the maximum and current values of iteration, respectively.

If the criterion for seasonal monitoring is satisfied, then the FSs are randomly relocated which fails to search the forest for an optimum food source for the winter. It is assumed that the squirrels that failed to search the hickory nut tree and still continued to live, will fly to various directions in search of a source of food. The relocation of those FSs is modeled using equation (19) [23]:

$$FS_{nt}^{new} = FS_{LB} + \text{Lévy}(n) \times (FS_{UB} - FS_{LB}) \quad (19)$$

where Lévy distribution ensures the efficient and better exploration of the considered search area.

Step 7: Stopping Criterion: The procedure from step 4 to 6 is repeated until the maximum number of rounds is reached; otherwise, the algorithm continues to search for optimal solutions. The pseudocode of the proposed HSHSA CHS technique is given as follows.

Pseudocode of Hybrid Squirrel Harmony Search Optimization Algorithm:

```
Initialize the WSN model with nodes
Initialize the parameter of squirrel search algorithm
r_max ← Number of iterations for cluster head selection
NI ← Number of iterations for squirrel search
N_Sq ← squirrel search matrix size; SHM = N_Sq
for t ← 1 to r_max do
To construct a random election of normal nodes
for i ← 1 to NI do
for j ← 1 to N_Sq do
FS(j,:) ← Randomly chossen cluster head for Squirrel search.
f_Obj(j) ← Fitness values for FS(j,:) . By using equation (4)
End
Sorting the rows of FS corresponding to f_Obj
Declare FS_ht and FS_at from the fitness values.
Randomly select three sets by Squirrel search algorithm
Using equations (10) − (12) to update the FS
End
Using Harmony search techniques to update the matrix FS
Selecting the best Cluster heads from FS for Data Transmission
End
```

IV. Results and Discussion

The simulation of the suggested HSHSA approach of CHS is implemented in MATLAB R2018a environment. The parameters of the simulation taken into consideration for the proposed method are given in Table I.

The proposed HSHSA is compared with the existing CHS techniques namely, Direct Transmission, LEACH [26], PSO [27], HSA [28], and SSA [29].

The throughput obtained for different algorithms are shown in the Fig. 2. It can be seen that the throughput of DT drops to zero around 315 rounds. This is because the DT allows all the nodes to communicate directly with the BS. The LEACH protocol shows improvement compared to the DT, where the throughput drops to zero at around 715 rounds because of the randomized selection of cluster heads. Then meta-heuristic search algorithms such as PSO, HSA, and SSA algorithms produce throughput that drops to zero at around 1230, 905, and 1637 rounds respectively. And the proposed HSHSA CHS, combining the advantages of both HSA and SSA produces a throughput that lasts up to 1752 rounds. The proposed HSHSA shows 42.86% and 21.43% enhancement in the throughput over the HSA and SSA meta-heuristic algorithms, respectively.

TABLE. I. Simulation Parameters

Parameter	Value
Sensor field region (m^2)	(100*100)
Data packet length (l) (bits)	4096
Initial energy for all the nodes (E_o) (J)	0.5
Number of nodes (n)	100
E_{amp} (pJ/bit/m^2)	120
E_{elec} (nJ/bit)	70
Energy data aggregation (nJ)	5
Number of search iterations	5
Number of rounds (r_{max})	2000
Number of cluster heads selected (k)	5
Predator presence probability (P_{dp})	0.1
Density of air (ρ) (kg/m^3)	1.204
Speed (C) (m/s)	5.25
Surface area of body (A) (cm^2)	154
Lift Coefficient (C_L)	$0.675 \le C_L \le 1.5$
Drag Coefficient (C_D)	0.6
HMCR	0.95

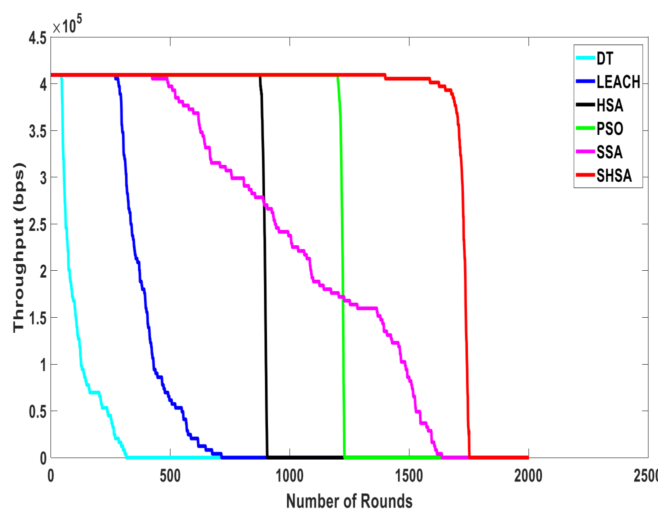

Fig. 2. Comparison of Throughput Obtained for Various Algorithms.

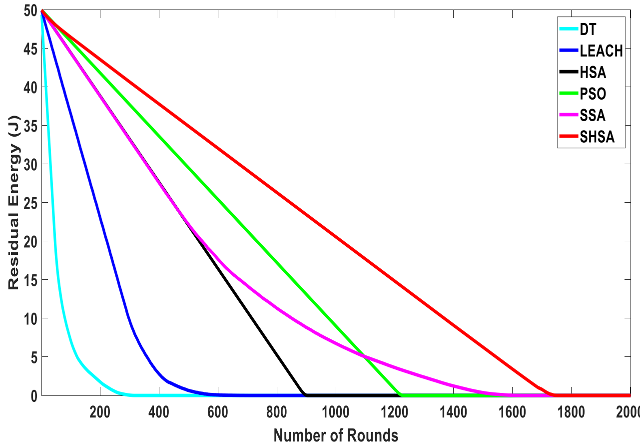

Fig. 3. Comparison of Residual Energy Obtained for Various Algorithms.

The residual energy obtained for different algorithms are shown in the Fig. 3. It can be seen that the residual energy after DT drops to zero at around 315 rounds. This is because the DT allows all the nodes to communicate directly with the BS that causes the nodes to lose energy very quickly. The LEACH protocol shows improvement compared to the DT, where the residual energy drops to zero at around 715 rounds because of the randomized selection of cluster heads. Then meta-heuristic search algorithms such as PSO, HSA, and SSA algorithms show residual energy that drops to zero at around 1230, 905, and 1637 rounds respectively. The proposed HSHSA technique, combining the advantages of both HSA and SSA shows residual energy that lasts up to 1752 rounds. The proposed HSHSA shows 69.84% and 32.43% enhancement in the residual energy over the HSA and SSA algorithms, respectively.

The alive nodes sustained for different algorithms are shown in the Fig. 4. It is evident that the nodes stay alive up to 315 rounds for DT. This is because the DT allows all the nodes to communicate directly with the BS that causes the nodes to lose energy very quickly, thereby, causing the nodes to die. The LEACH protocol shows improvement compared to the DT, where the nodes stay alive till 715 rounds because of the random selection of cluster heads. Then meta-heuristic search algorithms such as PSO, HSA, and SSA algorithms maintain the nodes alive up to 1230, 905, and 1637 rounds respectively. And the proposed HSHSA technique of CHS, combining the advantages of both HSA and SSA maintains the nodes to stay alive up to 1752 rounds. The proposed HSHSA technique of CHS shows 48.29%, 6.57%, and 29.86% enhancement in maintaining the nodes alive compared to the HSA, SSA, and PSO algorithms, respectively.

Fig. 5 provides the dead nodes for different algorithms. It can be seen that the first node dies at the round 44 and eventually all the nodes die in 315 rounds for DT. This is because the DT allows all the nodes to communicate directly with the BS that causes the nodes to lose energy very quickly, thereby causing the nodes to die. The LEACH protocol shows improvement than the DT, in which the first dead node is found at the round 270 and all the nodes become dead in 714 rounds because of the random selection of CHs. Then meta-heuristic search algorithms such as PSO, HSA, and SSA algorithms cause the first node to die at the round 1201, 876, and 424 respectively; and thereby cause all the nodes to die in 1229, 906, and 1637 rounds respectively. The proposed HSHSA CHS, combining the advantages of both HSA and SSA cause all the nodes to die in 1752 rounds. The numerical outcomes are provided in the Table II.

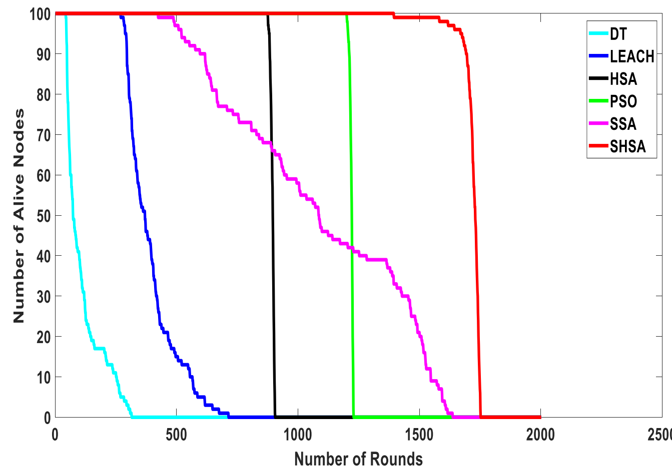

Fig. 4. Comparison of Alive Nodes Obtained for Various Algorithms.

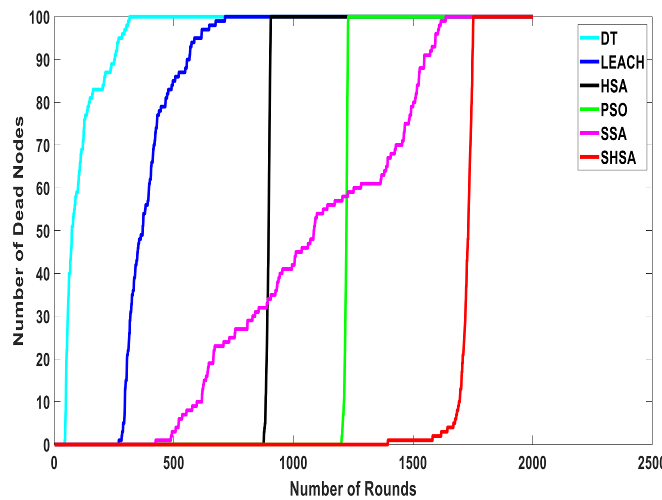

Fig. 5. Comparison of Dead Nodes Obtained for Various Algorithms.

TABLE. II. TABLE OF COMPARISON OF VARIOUS CLUSTER HEAD SELECTION ALGORITHMS

Algorithm	**First node dead**	**Last node dead**	**Residual energy (J) after 300 rounds**	**Throughput (bits/round)**
DT	44	315	0	0
LEACH	270	714	9.5661	305000
PSO	1201	1229	37.6613	409600
HAS	876	906	33.1616	349700
SSA	424	1637	33.1022	405500
Proposed HSHSA	1395	1752	40.6105	415900

Fig. 6 and 10 show the mean residual energy for various sink node positions, and varying count of nodes, respectively. Fig. 7 and 11 show the mean throughput for various sink node positions, and varying count of nodes, respectively. From the bar charts displayed above, the suggested HSHSA outperforms the existing optimization techniques for various positions of the sink node. This is also validated from the standard deviation (SD) of the outcomes obtained. In Fig. 8 and 12, the SD of residual energy is shown for varying sink node positions, and varying count of the nodes respectively. Fig. 9 and 13 show the standard deviation of the throughput for various sink node positions, and varying count of nodes respectively. The standard deviation of residual energy and throughput obtained for the proposed HSHSA are less compared to HSA, SSA, and PSO. This is because, the results of the HSHSA show less deviations, whereas the results of HSA, SSA, and PSO exhibit high deviations. It is inferred from the simulation outcomes that the suggested HSHSA approach of CHS reveals superior performance among other existing cluster head selection techniques.

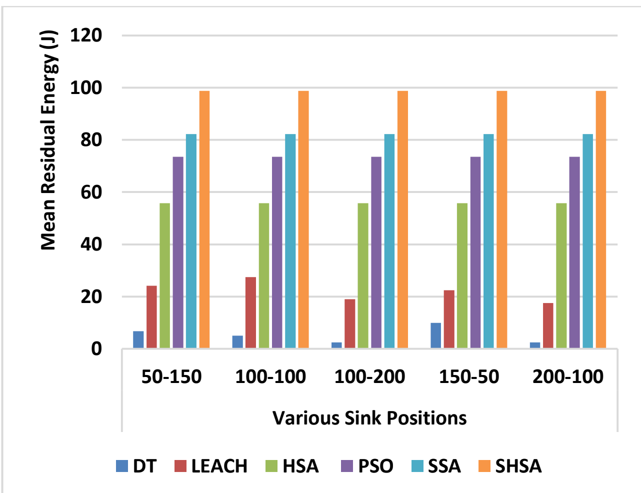

Fig. 6. Mean Residual Energy for Various Positions of the Sink Node.

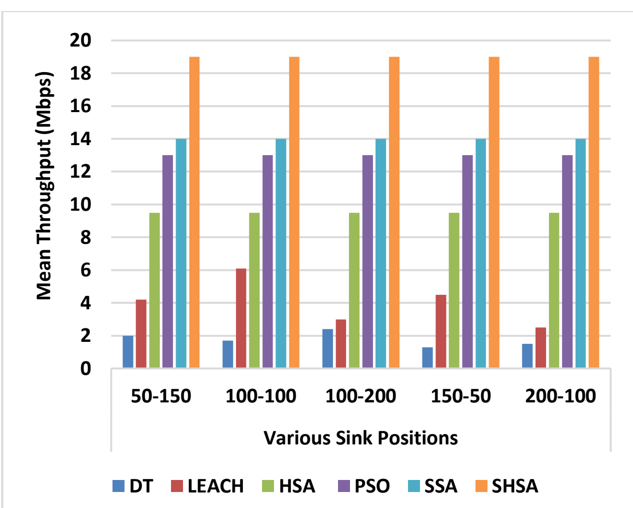

Fig. 7. Mean throughput for Various Positions of the Sink Node.

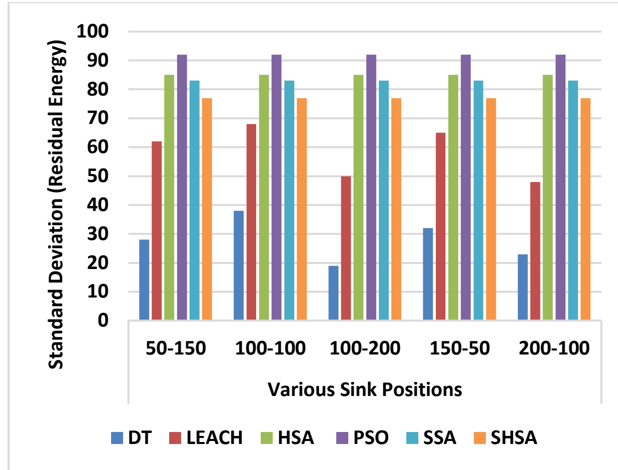

Fig. 8. Standard Deviation of Residual Energy for different Sink Node Positions.

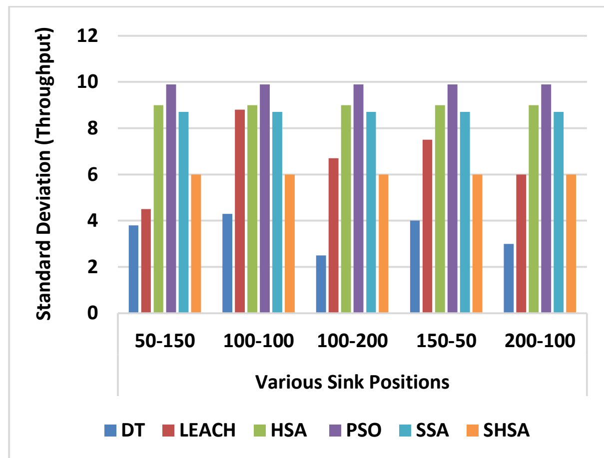

Fig. 9. Standard Deviation of throughput for different Sink Node Positions.

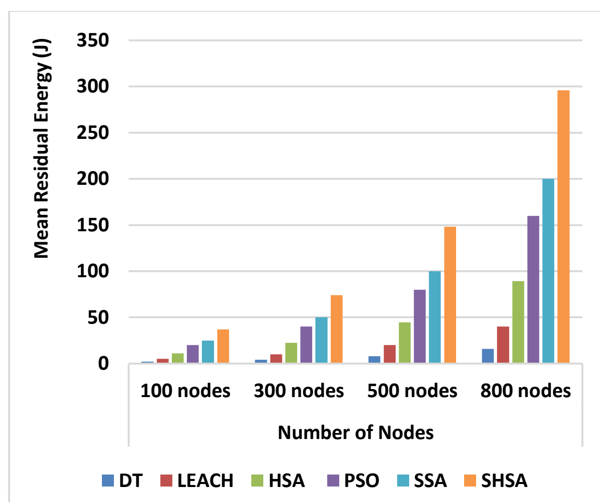

Fig. 10. Mean Residual Energy for Varying Count of Nodes.

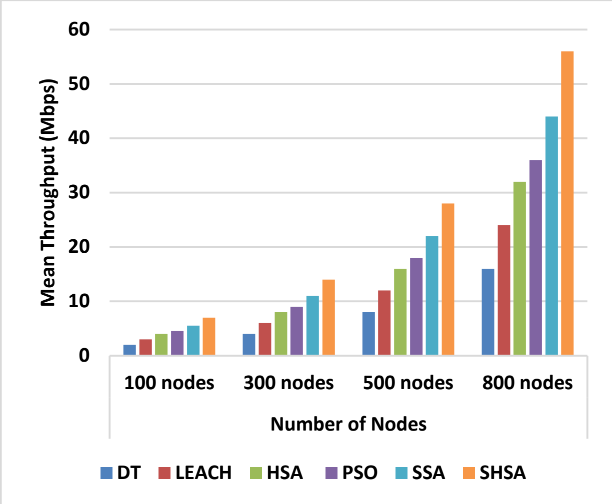

Fig. 11. Mean Throughput for Varying Count of Nodes.

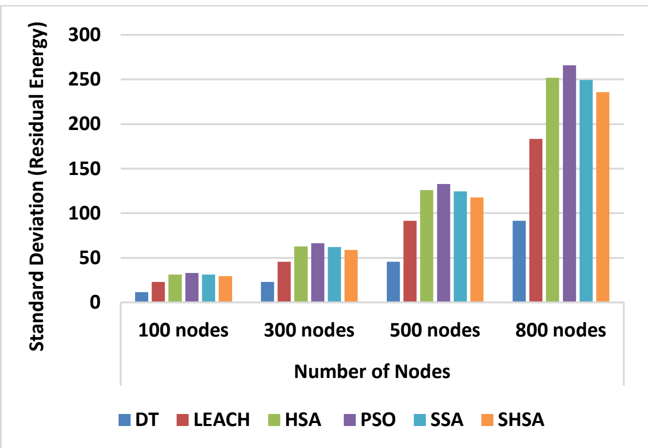

Fig. 12. Standard Deviation of Residual Energy for Varying Count of Nodes.

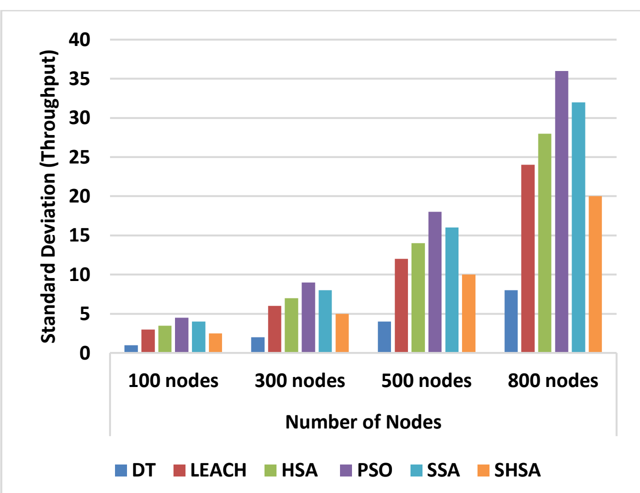

Fig. 13. Standard Deviation of throughput for Varying Count of Nodes

V. CONCLUSIONS

This research proposes HSHSA for optimal selection of cluster heads in WSN based on two parameters namely, energy and distance. The natural behavior of the SSA is developed by employing the mechanism of updating locations of the squirrels with predator presence probability. The balance between the exploitation and the exploration is attained by using the gliding constant. The seasonal monitoring prevents the solution of the proposed technique from being bound to the solutions of local optima. The proposed HSHSA is developed by integrating SSA with a high search efficient optimization algorithm called HSA. These advantages make the proposed optimization algorithm offers better performance than the PSO in terms of residual energy and throughput, with an improvement of 85.69% and 31.02%, respectively. The simulation results prove that the proposed HSHSA is more energy efficient than the existing cluster head selection schemes such as Direct Transmission, LEACH, PSO, HSA, and SSA. The scope for future work lies in the utilization of the different constraints namely, delay and sensing capabilities in different applications.

REFERENCES

[1] I. F. Akyildiz, Y. Sankarasubramaniam, and E. Cayirci, "A survey on sensor networks", IEEE Communications magazine, 2002, 40(8), pp. 102-114.

[2] Z. Jiang, and A. Wei. "An energy balanced algorithm of LEACH protocol in WSN". International Journal of Computer Science Issues (IJCSI), 2013, 10(1), pp. 354.

[3] P. Azad, and V. Sharma, "Cluster head selection in wireless sensor networks under fuzzy environment". ISRN Sensor Networks ,2013.

[4] A. Abbasi, and M. Younis, "A survey on clustering algorithms for wireless sensor networks". Computer communications, 2007, 30(14-15), pp. 2826-2841.

[5] T. Shankar, S. Shanmugavel, and A. Rajesh, "Hybrid HSA and PSO algorithm for energy efficient cluster head selection in wireless sensor networks". Swarm and Evolutionary Computation, 2016, 30, pp. 1-10.

[6] N. Lavanya, and T. Shankar, "Energy Optimization in Wireless Sensor Network using NSGA-II", 2017.

[7] A. Sampath, and S.Thampi, "An ACO algorithm for effective cluster head selection". arXiv preprint arXiv:1111.6218, 2011.

[8] Anindita Ray and Debashis De, "Energy efficient cluster head selection in wireless sensor network", International Conference on Recent Advances in Information Technology (RAIT), 2012.

[9] M. Nasim, S. Qaisar, and S. Lee, "An energy efficient cooperative hierarchical MIMO clustering scheme for wireless sensor networks". Sensors, 12(1), pp.92-114, 2012.

[10] R. N. Enam, M. Imam, and R. I. Qureshi, "Energy consumption in random cluster head selection phase of WSN". International Proceedings of Computer Science & Information Tech, 30, pp.38-44, 2012.

[11] S. Nikolidakis, D. Kandris, D. Vergados, and C. Douligeris, "Energy efficient routing in wireless sensor networks through balanced clustering". Algorithms, 6(1), pp.29-42, 2013.

[12] D. C. Hoang, P. Yadav, R. Kumar, and S. K Panda, "Real-time implementation of a harmony search algorithm-based clustering protocol for energy-efficient wireless sensor networks". IEEE transactions on industrial informatics , 2013, 10(1), pp.774-783.

[13] M. Baskaran, and C. Sadagopan, "Synchronous firefly algorithm for cluster head selection in WSN". The Scientific World Journal,2015.

[14] J. Rejina Parvin, and C. Vasanthanayaki, “Particle swarm optimization-based clustering by preventing residual nodes in wireless sensor networks”. IEEE sensors journal , 2015, 15(8), pp.4264-4274.

[15] R. Sharma, N. Mishra, and S. Srivastava, “A proposed energy efficient distance based cluster head (DBCH) Algorithm: An Improvement over LEACH”. Procedia Computer Science, 2015 , 57, pp.807-814.

[16] N. Lavanya, T. Shankar, “A Review on Energy-Efficient Scheduling Mechanisms in Wireless Sensor Networks”. Indian Journal of Science and Technology , 2016, (9),pp. 32.

[17] D. Bhatti, N. Saeed, and H. Nam, “Fuzzy c-means clustering and energy efficient cluster head selection for cooperative sensor network”. Sensors, 16(9), 2016, pp.1459.

[18] P. S. Rao, P. K. Jana, and H. Banka, “A particle swarm optimization based energy efficient cluster head selection algorithm for wireless sensor networks”. Wireless networks , 2017 , 23(7), pp.2005-2020.

[19] P. S. Mann, and S. Singh, “ Energy efficient clustering protocol based on improved metaheuristic in wireless sensor networks”. Journal of Network and Computer Applications, 2017, 83, pp.40-52.

[20] A. Genta, D. K. Lobiyal, and J.H. Abawajy, “Energy Efficient Multipath Routing Algorithm for Wireless Multimedia Sensor Network”. Sensors, 2019, 19(17), pp.3642.

[21] L. H. Correia, T. Heimfarth, G.M. Pereira, V. F. Silva, and J. L Santana, “Radio channel model of wireless sensor networks operating in 2.4 GHz ISM band”. INFOCOMP, 2010, 9(1), pp.98-106.

[22] Z. W. Geem, J. H Kim, G. V. Loganathan, “A new heuristic optimization algorithm: harmony search”. Simulation ,2001, 76(2), pp.60-68.

[23] M. Jain, V. Singh, and A. Rani, “ A novel nature-inspired algorithm for optimization: Squirrel search algorithm”. Swarm and evolutionary computation , 2019, 44, pp.148-175.

[24] J. W. Bahlman, S. M. Swartz, D. K. Riskin, and K.S. Breuer, “Glide performance and aerodynamics of non-equilibrium glides in northern flying squirrels (Glaucomys sabrinus)”. Journal of The Royal Society Interface, 10(80), 2010, pp.794.

[25] U. M. Norberg, “Evolution of vertebrate flight: an aerodynamic model for the transition from gliding to active flight”. The American Naturalist, 1985, 126(3),pp. 303-327.

[26] W. B. Heinzelman, A. P. Chandrakasan, and H. Balakrishnan, “An application-specific protocol architecture for wireless microsensor networks”. IEEE Transactions on wireless communications, 2002, 1(4), pp. 660-670.

[27] J. Tillett, R. Rao, and F. Sahin, “Cluster-head identification in ad hoc sensor networks using particle swarm optimization”. In IEEE International Conference on Personal Wireless Communications, 2002, pp. 201-205.

[28] Z. W. Geem, J. H. Kim, and G.V Loganathan, “A new heuristic optimization algorithm: harmony search. Simulation”,2001, 76(2), pp.60-68.

[29] M. Jain, V. Singh, and A. Rani, “A novel nature-inspired algorithm for optimization: Squirrel search algorithm”. Swarm and evolutionary computation ,44, 2019, pp.148-175.

[30] T. Senthil Murugan and Amit Sarkar,” Optimal cluster head selection by hybridisation of firefly and grey wolf optimisation”, Int. J. Wireless and Mobile Computing, Vol. 14, No. 3, 2018

[31] Z.Han, J. Wu, J. Zhang, L. Liu, and K Tian, ‘A general self-organized tree-based energy-balance routing protocol for wireless sensor network’, IEEE Transactions on Nuclear Science, Vol. 61, No. 2, pp.732–740, 2014.

[32] A. Puggelli, et al. ‘Routing-aware design of indoor wireless sensor networks using an interactive tool’, IEEE Systems Journal, Vol. 9, No. 3, pp.714–727, 2015.

Knowledge based Soil Classification Towards Relevant Crop Production

Waleej Haider[1, *], Aqeel ur Rehman[3]
Department of Computing
Hamdard University
Karachi, Pakistan

M. Nouman Durrani[2]
Department of Computer Science
FAST-NUCES
Karachi, Pakistan

Sadiq ur Rehman[4]
Department of Computing
Hamdard University
Karachi, Pakistan

***Abstract*—Pakistan's economy is strongly associated with agriculture sector. For a country having 25 % of GDP contributed through agriculture, there is a need to modernize the agriculture by acclimatizing contemporary approaches. Unfortunately, it has become a common trend among farmers to cultivate crops, being used in food items or which can easily be sold out in the market without using knowledge about the suitability or relevancy of crops to the soil environment. Consequently, the farmers face financial losses. Many researchers have proposed soil classification methods for various soils related researches, but they have very little contribution towards guidance of the farmers to select most suitable crops for cultivation at a particular soil type. Without the use of technology and computer-assisted approaches, the process of classifying soil environments could not help the farmers in taking decisions regarding appropriate crop selection in their respective fields. In this paper, an effective knowledge-oriented approach for soil classification in Pakistan has been presented using crowd sourced data obtained from 1557 users regarding 103 agricultural zones. The data were also obtained from AIMS (Govt. of Punjab) and Ministry of National Food Security & Research. In this work, random forest classifier has been used for processing and predicting complex tiered relationship among soil types belonging to agricultural zones and major suitable crops for improving yield production. The proposed model helps in computing the degree of relevancy of crop to agricultural region that help former selecting suitable crops for their cultivated lands.**

Keywords—Knowledge creation; agriculture; soil classification; random forest; knowledge distribution; crop relevancy

I. Introduction

The agriculture has a significant impact on the overall GDP of agricultural countries. As an agricultural country, 25% of Pakistan's GDP is contributed through agricultural revenue. As 2% per year increase in the country's population has given birth to new requirements of: (i) advanced crop production methods and (ii) growing new crop categories over the existing land beside traditional agriculture. Knowing suitable crop or seed type for a particular soil type, may increase the yield. In this work, through crowd sourcing, the knowledge of agricultural experts has been used for the assignment of a crop (or a seed type) to a soil type for helping farmer growing new crops over the existing agricultural lands.

Detailed understanding of soil nature can help in improving overall efficiency of crop productions. Unfortunately, farmers are exploiting customary farming ways which do not tend to meet upcoming agricultural requirements. In this regard, the role of soil environment management is very critical. Further, weather, climate impact, time and type of crop are also very important. Cultivation without having knowledge of appropriateness of context is perilous. In connection to this, current research [1], [2] indicates that researchers, farmers and government officials need to work together for the adequate solutions related to said issues. Moreover, training sessions for the farmers and upholding their preceding experiences related to the crops can help them making efficient decisions for the subsequent crops.

Researchers have proposed methods of classifying soil based on environmental conditions i.e. temperature, moisture, humidity, pH, fertility of soil, mode of formation or structure/texture of soil but these methods could not sufficiently paid attention towards the suitable crop selection criteria [3]–[5].

Modern trends also tend to apply artificial intelligence, machine learning and deep learning mechanisms for the solutions of agricultural problems. One of such solutions expels the use of ML based classifications of soil environment. An effective approach has been proposed for classification of soil environment in Pakistan integrating crowd sourced data, machine learning with local knowledge of experts to take knowledge-based decisions for suitable crop selection.

This paper presents a generic approach for classifying soil types of Pakistan using crowd sourced data. Crop data have been obtained from various regions of Pakistan and worked on crop to soil mapping rules using proposed model, which are further verified by the experts. This model also generates knowledge of soil-crop mapping for those agricultural regions where relevant data is partially available. This knowledge-based classification of soil, mapping to suitable crops, results verification by the experts and crowd sourcing have enhanced the accuracy of the proposed model, provide new directions to the farmers and help in increasing crop production. In this paper, we've also worked on calculating the crop relevancy to different soils that helps in creating knowledge about crop production at various soils and best suitable business-oriented crop selection.

Remaining of the paper has been organized as: literature review of multiple dimensions has presented in the next Section II. Section III contains general categories of soil in Pakistan using different parameters and analytical study about

*Corresponding Author

cultivation of crops on the soil types. Experimental setup is given in Section IV, which is interlinked with Sections V and VI. These sections cover the implementation of the algorithm and discusses the results of different experiments respectively.

II. Existing Systems

The concept of soil classification for different reasons is not new but the use of technology has altogether changed the meaning of classifying soil. It changed the previous ways based on testing soil samples of an agricultural land in the laboratories for examining its fertility, mode of its formation, its textures or existence of different chemicals in soil by which it can be classified. Although, these samples could not represent the whole land, so, the classification could not be performed on the huge landscape using these methods. These approaches based on sample testing are time consuming, have a high frequency of errors and hard to cover maximum agricultural region to collect soil samples to be examined. Evolution of agricultural decision support systems is not ended at computer-assisted solutions, but improved by knowledge-based computerized approached. A comprehensive study covering all the aspects has been presented in this section.

A. Existing Crop Selection Approaches

Researchers have proposed methods for selecting the best crops to be cultivated in the fields. Valipour et al. have presented a model in [6] to evaluate potential evapotranspiration in a specific climate or in a particular agricultural region. Four climate types including arid, mediterranean, semiarid and lastly very humid have been considered. A multidimensional and chronological study of ETo has been done and climatological data of around 50 years (1961 to 2010) of 18 agricultural regions of Iran with several climates on a monthly basis were collected. To estimate ETo, temperature, radiation, mass transfer bases models have selected to check, which model is performing better in a particular climate. It is analyzed that radiation based models were easily adjusted better with climate change [6]. Gornott et al. have tested three regression models for the impact of climate variation on the change of crop yields production. They have focused two major crops, wheat and maize for this analysis [7].

B. Classification of Soil

The soil classification has been done by the researchers using different approaches like i) environmental conditions i.e. temperature, moisture, humidity and pH, were considered, ii) fertility of soil [2], [8], [9] was used as the basic measure for the soil classification, iii) mode of formation of soil iv) structure/texture of soil [5], [10], [11] v) regional or land cover basis [12]–[15], [14], [10], [16], [17] or based on vi) existence of chemicals in the soil [8], [9] were used for the soil classification.

Current computer-assisted methods have been used for classification in the agricultural domain using various types of statistical, AI and ML algorithms like decision trees, random forest and Convolutional Neural Networks (CNN) [18] [19]–[21]. An approach has been presented to modernize large scale, local soil maps using three sourced data. i) used old soil shape classifications, ii) obtained data from visible near infrared classifications spectroscopy, and iii) digital soil class mapping. Using the combined data, Australian Soil Classification maps have been updated. The total error rate was 55.6% after testing the model on independent validation set [3]. Random forest classifier integrated with multivariate regression for classification and to quantify some quality parameters of the soil [11]. Digital soil mapping has been used to update the national map of the soil Drenthe province without extra fieldwork. Multinomial logistic regression has been used on a legacy soil data to measure the association between auxiliary variables and different soil group [13].

Researchers have encouraged towards the design of knowledge oriented methods [22], [23]. This paper deliberates the local knowledge of regular farmers to grow crops, according to soil quality. Interviews of farmers were conducted and most of them have two or more soil types in their agricultural lands. Leigh A et al. have conducted survey and interviewed to realize how farmers living in the remote areas of southeastern Costa Rica are using knowledge of soil for proper allocation and management of crops and to discover how to integrate native and technical knowledge to select sustainable agricultural approach.

III. Context of Soil Type used for Production

Soil can be classified on the basis of their 1) structures and texture 2) regional basis 3) climate 4) vegetation 5) Mode of formation [13], [24] as sown in Fig. 1. In this section, an empirical study about soil types, their existence in different regions, commonly growing crops and the impact on yield obtained has been presented.

1) Variances in structure and texture: There are five main types of soils in Pakistan on the basis of variance in structure and texture as a) clay, b) sand and gravel, c) silt, d) loam and e) organic soil which is less common.

a) Clay soil: Clay soil, composed of smooth and gluey particles and available red, bluish gray, yellow or almost black colors. Since humid nature, it warm and dry up slowly and batter in storing reserves of nutrients it requires regular irrigation and in case of irregular watering, it become very hard during dry and warm weather [11]. In this situation, water absorption ability of the soil become very low and the sprinkling method cannot fulfill the sufficient requirements. Only furrow method can be used in this condition. Cultivators are excavating large amount of organic matters like well- rotted manure compost, peat moss or simply Gypsum in the clay soil to cover the hardness before the sowing stage. This soil is useful for growing wheat, which is one of the major crops being used for food products, gram and paddy crops that is largely cultivated in Pakistan. Clay exists in most of the regions of Punjab, Sindh and KPK provinces where major crops like wheat, rice and sugarcane are cultivated. Unlike other regions, Thatta, Badin zones are not focusing on wheat, which is more suitable for clayey soil. Some regions of Punjab and Sindh are getting good production of cotton and maize. On the other side, according to crowd sources, these zones like Thurparker, NoderoFeroz, Nawabshah, Mirpur Khas, etc. are being used for caster, guar and millat which are not most suitable for Clay soil nor these give sufficient business to the farmers.in the same way some agricultural zones of the KPK province like Peshawar, Noshehra, Mardan and Charsada are growing pears, sugar beet and plum in clayey soil but they can produce tobacco and millet to get more business.

b) Sand and gravel soils: Sand and gravel soils are dominating particles in this type. Cultivation process is very easy on this soil, but it becomes warm and dry up and scattered very quickly [25]. So, its ability to absorb heat may damage vegetables. Pure sandy and gravelly soils have less nutrients and fertility, but mostly these types contain sufficient clay particles which make the soil suitable for cultivation and receptive to fertilizers [3].

Moreover, the quality of this soil can be improved by taking out the larger pebbles and stones and by mixing animal manure or some plant waste with this soil in the fields.

These soils are present in southern and northern irrigated plains and sandy deserts of Sindh and Punjab provinces. Sandy soil is useful in growing vegetables, which thrives in the soil. Wheat, millet, guar are being cultivated in sandy deserts of Sind. Castor is grown in some regions which is less profitable. They can grow melons, maize or oilseeds as in the northern irrigated plains of Punjab province. Same crops are being practiced in sandy deserts of Punjab along with cotton and sugarcane. Sandy and gravel soil do not provide good production of sugarcane but people are traditionally growing this crop.

c) Silt Soils: Silt soils have a transitional size amongst clay and sand with small size gritty particles which make it very hard [25]. Silt present in the soil in a variety of colors like gray, red tan, and yellow. It's usually not very fertile. There is a thick layer of clay at the top, so normally it is less fertile and have low ability of water absorption. This thick layer should be broken by mixing a sufficient amount of peat moss, rotted sawdust, compost, and wood shavings and afterwards, adding organic matter can recover the construction and fertility of this soil type. It is useful for root vegetables and pulses and berseem according to experts from the crowd. This soil exists in southern and northern irrigated plains where mustard, and berseem are being cultivated with sorghum. Regions in the Indus delta like Thatta and Badin are using silty soil for banana fruit and berseem. Pulses and many other crops can give more business to farmers. Wet mountains are used for growing apples with other major crops and people of Barani land near the Punjab province are harvesting fodder crops for animal feed. Mittet, pulses and oilseeds are also being grown there with other major crops. Some farmers are cultivation rice in silty soil which is not relevant to this soil and could not provide more yield. Agronomists from the dry western plateau are growing melons and sorghum as major crops, but some are focusing millet which is less beneficial

d) Loam Soils: Loam contains clay, sand and silt in the different proportions along with organic matters [26]. Various proportions of clay, silt, sand, and organic matter; the magnitudes of these defines the quality, productivity and behavior of the soil towards the cultivation. This soil is best for major crops and vegetables. Pure loamy soil exists in southern irrigated plains i.e. From Hyderabad to Jacobabad where agriculturists are growing sugar cane, sorghum and mustard with other major crops, sandy desert of Sind (Tharparkar to Cholistan) and Punjab (Muzaffar Gharh to Khushab) provinces where wheat, guar and millet are majorly cultivated and some farmers are growing gram and sugar cane in Punjab whereas caster in Sindh. Cotton, mustard, maize and vegetable are also suitable crops for loamy soil. Farmers can earn growing these crops instead of caster and berseem. Regions except Indus delta, northern irrigated plains and dry mountains and Suleiman piedmont, have mixture of loamy and other soils which are fertile and useful for most of the major crops.

e) Organic Soil: Organic Soil is dark in color composed of big amount of peat moss and or leaf mold. It warms up gradually due its moisture retaining capability, but is easy to water, weed and work [11]. It is micronutrient deficient, but the use of special fertilizers cover-up the scarcities.

To analyze the yield production of crops on various soil types and the degree of irrelevancy of crops to the soil environment, knowledge has been created by processing data using statistical models and algorithms have been proposed to calculate the degree of irrelevancy of target crops to the available soil types.

2) Modes of formation: Drought is fundamentally affecting the soil in Pakistan as it is major characteristics of climate which result in shortage of soil moisture. Soil in Pakistan is composed of two parent materials[10] , a) Alluvium, Loess and wind reworked sands, b) Residual material gained from enduring of underlying rocks. The soils of Pakistan have attained different features from the parental material and based on their way of formation. The river-laid residues have established into Muddy Soils. The desert sands have also revolved into a diverse type of soils. The mountains, hills and other highlands have formed Residual Soils with spots of Grainy, loss and other material of the soils. Consequently, the soils of Pakistan have been classified into six types on the basis of its ways of construction or modes of formation as shown in Fig. 1.

3) Soil types according to spatially placed regions: Some fundamental materials may transfer from one place to another through rivers and wind and placed over the surface are called alluvium and Aeolian Soils respectively. This provides a base to another soil categorization according to spatially placed regions.

The Indus plain soil is made-up with the shifting of alluvium by the Indus river and its branches. Rivers are dropping the soil on the earth's surface in the form of layers for the last thousands of years. This soil has sufficient calcium carbonate, lower level of organic matter and further divided into three types. Bangor soils are present over the vast area of the Indus plain like many agricultural portions of the Punjab, Mardan, Kachhi plain, Peshawar and Bannu along with a major part of Sindh province. These soils somehow provide better production. Khaddar soils are present in the nearby regions of the rivers. A layer of salt clay is dropped on the surface and due to this yearly change, this soil has less gratified of salt and organic material. Indus Delta *Soils* present across the river Indus Delta. It maintains its level from Hyderabad and exists in the southern coastal areas. These areas are normally affected by flood so it developed under this floodwater and most of the soil is clay by structure, hence due to its ability to absorb water, this is majorly suitable for cultivation of rice crop. Northern and western zones of Pakistan are highlands, so known as *mountain soil* [25]. The climate of northern mountainous lands is moist and these have large amount of organic matter contents. On the other hand, soils of western mountainous lands are deficient in the organic matter due to dry or semi-arid climate and have a large amount of calcium carbonate. The soils of Pothwar hills have great sea green content. If the sufficient amount of water is provided, this soil become very productive.

Sandy Desert Soils exists in the Cholistan, western side of Balochistan and the desert of Thar. Its structure contains a layer of sands elements and has the medium amount of calcium carbonate. Dry and semi-arid climate [15] effect this type of lands and forcefully disposition the layers of sandy soil. Consequently, this soil type is structured. This is the reason of less economic activities in the deserts.

An effective analysis of three target crops on all available soil types in three target regions has been presented in Table I. An algorithm to compute the degree of crop relevancy has been developed and the results are discussed in detail in Section VII, case-II.

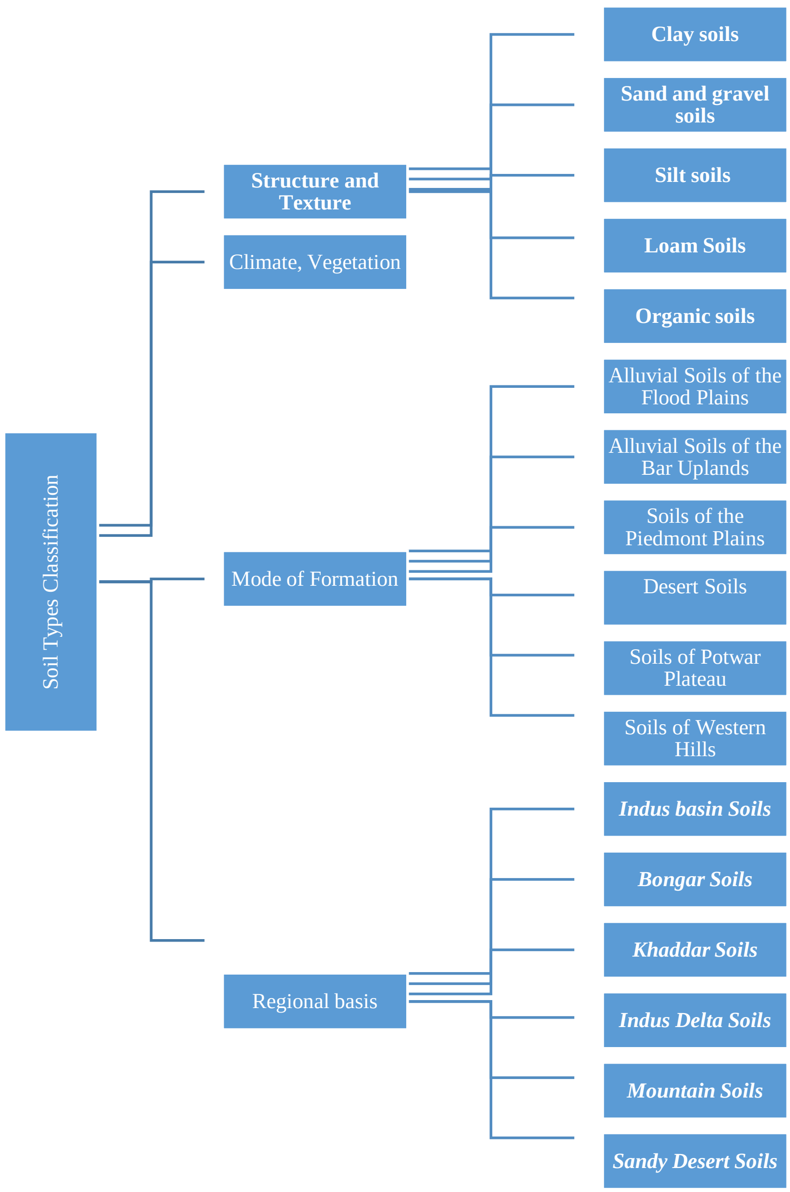

Fig. 1. Hierarchical Structure of Soil Types Classification in Pakistan.

TABLE. I. KNOWLEDGE RESULTANT FROM CROWD SOURCING ABOUT CROP PRODUCTION, INCOME AND RELEVANCY OF CROP

Targeted Regions	**Soil Type**	**Texture & Structure**	**Water Retention Capability**	**Target Crops**	**Business Impact**	**Degree of Irrelevancy (in %)**
Faisalabad	Clay	Smooth , sticky , rock and gluey	High	Rice	Moderate	77.25
				Maize	High	0
				Cotton	Moderate	72.70
	Sandy	Coarse	Low	Rice	low	79.50
				Maize	High	0
				Cotton	Moderate	67.84
	Loam	Mixed	Moderate	Rice	Moderate	72.88
				Maize	High	0
				Cotton	Moderate	67.30
	Silt	Shallow residual and Gritty	Moderate-high	Rice	Moderate	66.73
				Maize	High	20.47
				Cotton	High	0
	Organic	Peat moss or leaf mold	Moderate	Rice	Moderate	85.26
				Maize	High	0
				Cotton	Moderate	74.93
Multan	Clay	Smooth and gluey	High	Rice	Low	93.98
				Maize	Low	93.17
				Cotton	High	0
	Sandy	Gritty	Low	Rice	Low	93.65
				Maize	Low	92.87
				Cotton	High	0
	Loam	Mixed (variable)	Moderate	Rice	Low	90.44
				Maize	Low	92.57
				Cotton	High	0
	Silt	Gritty	Moderate-high	Rice	Low	95.87
				Maize	Low	98.85
				Cotton	High	0
	Organic	Peat moss or leaf mold	Moderate	Rice	Low	95.13
				Maize	Low	97.40
				Cotton	High	0
Bahawalpur	Clay	smooth and gluey	High	Rice	Low	97.84
				Maize	Low	94.58
				Cotton	High	0
	Sandy	Gritty	Low	Rice	Low	98.06
				Maize	Low	94.32
				Cotton	High	0
	Loam	Mixed (variable)	Moderate	Rice	Low	97.50
				Maize	Low	94.29
				Cotton	High	0
	Silt	Shallow residual and Gritty	Moderate-high	Rice	Low	99.69
				Maize	Low	99.46
				Cotton	High	0
	Organic	Peat moss or leaf mold	Moderate	Rice	Low	99.54
				Maize	Low	96.71
				Cotton	High	0

IV. Materials and Methods

Before performing experiments, data from the crowed and online sources has been obtained and the algorithm has been selected for data processing as discussed in the next sections. Workflow of the whole classification process is shown in Fig. 2.

A. Data Acquisition

Data from volunteer users [27] belonging to all over the Pakistan has been obtained and organized. This dataset contains landscape, soil types, agricultural zones or regions and most suitable crops being cultivated in the zones. Around 1600 users has shared the data from 103 different agricultural zones of Pakistan based on four features as shown in the Table II. Another dataset was acquired from the Institute of Soil & Environmental Sciences, University of Agriculture, Faisalabad.

B. Preparation of Data Set

Input data are further processed by testing relativity by correlation, sampling and data cleaning by testing the comprehensiveness and setting missing values in data records. Observations containing missing values have been removed from training dataset. The data has been managed to meet the algorithm requirements as columns of the Table II shows the features of data and rows represents the records. Environmental factors of the soil are characterized by predictors of the environment of any agricultural region R. Finally, the output of the whole process is a function of defined environmental predictors as:

$$\text{Output (R)} = f(st[r], c[r], mc[r], l[r], az[r], ct[r]) \quad (1)$$

For any agricultural region R, representation in the above equation are soil type (st), climate (c), major crops (mc), landscape (l), Agricultural zones (az) and context (ct). Random forest has been used to map four of these factors to output. The data has been divided into two training sets. Two predictor variables from the factors of soil environment initially used in experimentation are, i) soil types and agricultural zones in the first training data and ii) other two predictors, soil types and major crops in the second training datasets which plays a vital role in the classification as presented in Tables III and IV along with statistics of the training data set. Sandy, Clayey exists in 73 agricultural zones which is 16.25 % of the total soil types of the regions. Calcareous, Sandy, Loamy, Silty and Sandy, Loamy are less common in Pakistan. While obtaining the crowd sourced data, there are possibilities of sharing inaccurate, mixed or incomplete data by users. To remove these insufficiencies, this data has been sent to expert community where domain experts are available to rectify the data as depicted in Fig. 2.

This process makes the data cleaner and ultimately improves the accuracy of the results. The sample data of 20 users are shown in the Table II. To produce the clarity in the results, two random forests have been driven using these sets of predictors as discussed in Section VI.

TABLE. II. CROWED SOURCED DATA OF SOIL ENVIRONMENT OF PAKISTAN

User ID	Landscape	Agricultural Zones	Soil Types	Major Crops
1	Western Dry Mountains	Pishin	Calcareous loamy	Apples, Peaches
2	Northern Irrigated Plains (a)	Jhang	Calcareous, Silt-loam	Millet, Maize
3	Southern Irrigated Plains	R.Y. Khan	Calcareous, Loamy	Sorghum, Berseem
4	Wet Mountains	Battagram	Silt loam, Silty clays	Wheat, Apples
5	Sandy Desert (a)	Cholistan	Clayey and Loamy	Guar, Castor
6	Sandy Desert (a)	Nawabshah	Clayey and Loamy	Wheat, Castor
7	Barani Lands	Bhakkar	Silt loam, Silty clay loam	Millet, Fodder crops
8	Western Dry Mountains	Jaffarabad	Calcareous loamy	Peaches, Plums
9	Southern Irrigated Plains	Shikarpur	Silty, Clayey	Berseem, Rice
10	Dry Western Plateau	Chagai	Strongly Calcareous, Silt loams	Wheat, Sorghum
11	Sandy Desert (b)	Layyah	Sandy, Loamy	Cotton, Guar
12	Barani Lands	Lakki Marwat	Silty clay loam, Clay loam	Maize, Oil seeds
13	Northern Irrigated Plains(b)	Charsadda	Clayey, Moderately Calcareous	Maize, Gram
14	Dry Western Plateau	Lasbella	Strongly Calcareous, Silt loams	Wheat, Sorghum
15	Southern Irrigated Plains	Sanghar	Calcareous, Silty	Berseem, Rice
16	Dry Western Plateau	Khuzdar	Strongly Calcareous, Silt loams	Wheat, Sorghum
17	Sandy Desert (b)	Khushab	Calcareous, Loamy	Gram, Millet
18	Sandy Desert (a)	Tharparkar	Sandy, Clayey	Wheat, Castor
19	Barani Lands	Bannu	Silty clay loam, Clay loam	Maize, Oil seeds
20	Western Dry Mountains	Quetta	Calcareous loamy	Apples, Peaches

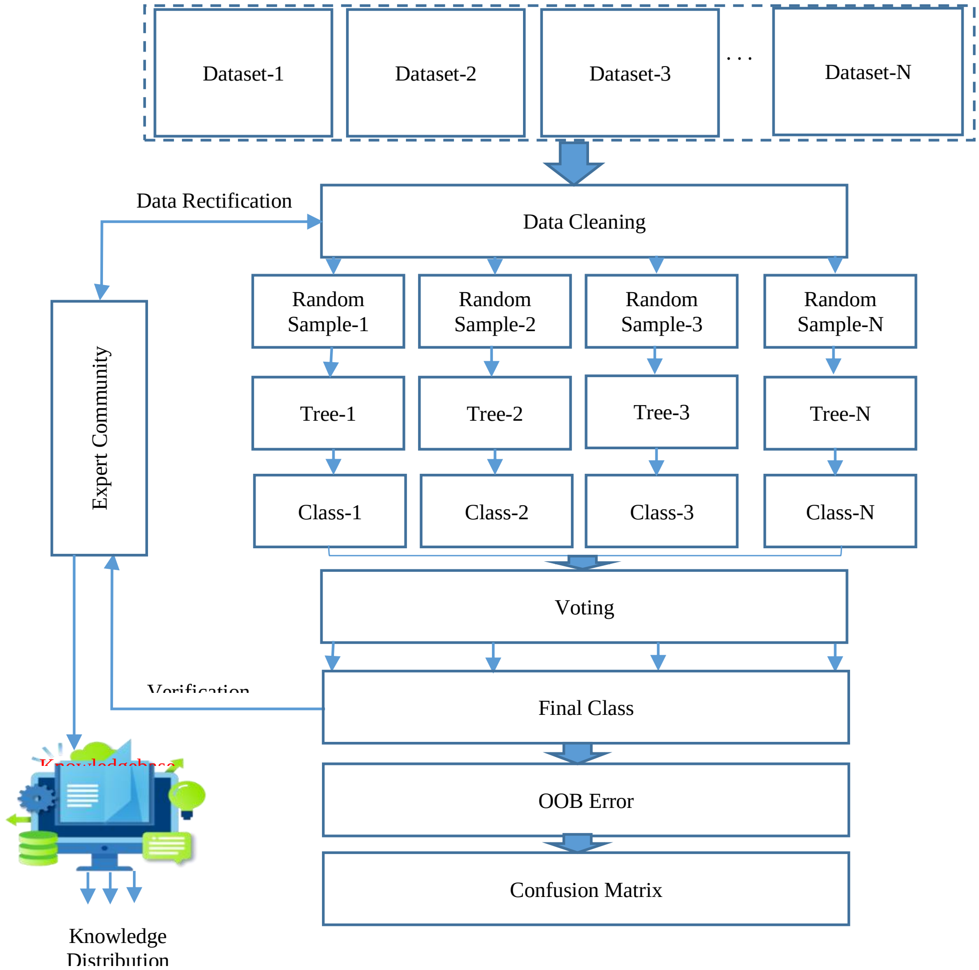

Fig. 2. Workflow of Proposed Approach for Classification of Soil Environment of Pakistan.

TABLE. III. TREE STRUCTURE PREDICTORS, SOIL TYPES AND AGRICULTURAL ZONES

Nodes	**Objects**	**%**	**Test statistic**	**p-value**	**Purity**	**DF**	**Split variable**	**Values**	**Parent node**	**Sons**	**Predicted values**
Node 1	449	100.00%	1677.500	< 0.0001	4.68%	174				2; 3; 4; 5; 6; 7; 8	Badin
Node 2	41	9.13%			51.22%		Soil Types	Clayey and Silty	1		Badin
Node 3	70	15.59%	15.556	0.049	14.29%	8	Soil Types	Calcareous, Loamy; Clayey and Sandy	1	9; 10	Hyderabad
Node 4	85	18.93%	31.481	0.000	17.65%	8	Soil Types	Silty, Clayey; Loamy, Silty; Calcareous, Silty	1	11; 12	Sanghar
Node 5	73	16.26%			6.85%		Soil Types	Sandy, Clayey	1		Tharparkar
Node 6	60	13.36%			16.67%		Soil Types	Clayey and Loamy; Sandy and Loamy	1		Tharparkar
Node 7	40	8.91%			25.00%		Soil Types	Calcareous, Sandy; Sandy, Loamy	1		Muzaffaragarh
Node 8	80	17.82%			12.50%		Soil Types	Clayey, Calcareous; Calcareous, Silt-loam	1		Bahawalnagar
Node 9	45	10.02%			11.11%		Soil Types	Calcareous, Loamy	3		Hyderabad
Node 10	25	5.57%			20.00%		Soil Types	Clayey and Sandy	3		Hyderabad
Node 11	45	10.02%			11.11%		Soil Types	Silty, Clayey	4		Hyderabad
Node 12	40	8.91%			25.00%		Soil Types	Loamy, Silty; Calcareous, Silty	4		Sanghar

TABLE. IV. TREE STRUCTURE PREDICTORS, SOIL TYPES AND MAJOR CROPS

Nodes	Objects	%	Test statistic	p-value	Purity	DF	Split variable	Values	Parent node	Sons	Predicted values
Node 1	199	100.00%	447.503	< 0.0001	22.61%	24				2; 3; 4; 5	Silty, Clayey
Node 2	41	20.60%			100.00%		Major Crops	Rice, Pulses; Berseem, Banana;Pulses , Sugarcane; Pulses, Banana; Rice,Banana; Berseem, Banana;Pulses , Sugarcane; Pulses,Banana; Rice, Banana; Pulses,Banana	1		Clayey and Silty
Node 3	98	49.25%	13.237	0.153	28.57%		Major Crops	Cotton, Wheat; Rice, Wheat; Rice, Sugarcane; Mustard, Sorghum; Sorghum, Berseem	1		Silty, Clayey
Node 4	37	18.59%	21.281	0.007	45.95%	4	Major Crops	Sorghum, Cotton; Sugarcane, Sorghum; Berseem, Rice; Mustard, Wheat; Sugarcane, Berseem	1	6; 7; 8	Silty, Clayey
Node 5	23	11.56%	6.469		43.48%		Major Crops	Guar, Millet; Wheat, Guar; Wheat, Castor; Millet, Wheat; Guar, Castor; Guar, Wheat; Castor, Wheat	1		Sandy, Clayey
Node 6	9	4.52%			100.00%		Major Crops	Sorghum, Cotton; Sugarcane, Sorghum	4		Silty, Clayey
Node 7	24	12.06%			33.33%		Major Crops	Berseem, Rice; Mustard, Wheat	4		Loamy, Silty
Node 8	4	2.01%			100.00%		Major Crops	Sugarcane, Berseem	4		Calcareous, Silty

C. Selection of Algorithm

Various algorithms have been applied to the data e.g., decision trees, K- means, but the random forest from the classification and regression trees seems the most suitable for classification of soil environment of Pakistan. Keeping in view the data set, this algorithm has been selected for classification due to following reasons.

- The random forest algorithm or the random forest classifier can successfully work on both classification and the regression task.
- When the crowd sourcing is used for data acquisition, there may be a chance of missing values in the data [27]. The Random forest classifier can easily handle the missing values in the data.
- As the algorithm builds many decision trees using random samples to be a part of forest, random forest classifier in this situation, won't overfit the applied model.
- Most significantly, in case of classifying agricultural region wise soil environment and mapping these to suitable crops, the data values seem categorical in the sense, the variable have more than one level. The random forest classifier can model for categorical values in this situation.

D. Working of Algorithm

The dataset D containing 1557 observations on 04 useful features was divided into a training set by using the concept of random sampling.

The random forest algorithm can be divided into two stages.

- Creation of random forest.
- To make some predictions from the generated random forest classifier.

First, the process of random forest creation has been discussed.

Random forest is primarily an ensemble of K no. of trees, let say $\{\mathbf{t}_1(j),\ldots,\mathbf{t}_k(j)\}$, where j $=\mathbf{j}_1,\ldots,\mathbf{j}_i$ is an $\mathbf{i}$-dimensional vector of interacting variables (also called predictors) which symbolize the soil environmental factors of Pakistan. The ensemble after processing, provides K outputs as $\{\text{Output}_1 = \mathbf{t}_1(j),\ldots, \text{Output}_K = \mathbf{t}_k(j)\}$, where for OutputK, k = 1,…,K, is the classification of the Soil Environment of Pakistan by the $\mathbf{k}_{th}$ tree. Now to produce a random forest, Outputs of all generated trees are formerly aggregated to perform final classification output, by majority vote from entirely generated trees. Now for prediction from a set of given training data, $T = \{(\mathbf{j}_1, \text{Obs}_1),\ldots, (\mathbf{j}_n, \text{Obs}_n)\}$, where $\mathbf{j}_i$, $\mathbf{i}$ = 1,..…,n, is a vector of interacting variables or predictors and Obs_i is the representing corresponding soil classes as results, hence, training of the current random forest continues according to following steps:

1) Initially, from training rectified data (, K bootstrap samples have been drawn. Each bootstrap provided the foundation for one of the trees which is part of the forest.

2) Afterwards, a classification tree has been grown for every bootstrap sample without any pruning, to originate the classification of soil Environment as Output.

3) Instead of selecting the best split at every node between all predictors to produce a forest, randomly sampled ***m*** no. of predictors and selected the best split among them. While growing the forest, the value of *m* is detained constant.

4) The above steps are repeated so that K trees have been grown. These K no. of trees have created a forest.

5) Now for every tree, the data which is not a part of the bootstrap sample has been predicted (this is also called out-of-bag data) consuming the grown-up of the tree with the bootstrap sample (also called in-the-bag data).

6) After aggregating the predictions which are out-of-bag, and the predicted Output values of processed data are then compared with the ultimate observed values, Obs, of each unit present in the out-of-bag (OOB) sample. Finally, classification error rate (ER) has been calculated as:

$$\sum_{i=1}^{n} I(Output_i^{OOB} \neq Obs_i^{OOB})/n \quad (2)$$

Where equation I represents the indicator function while n is representing the no of data which is out of the bag. On the basis of error rate, confusion matrix for both cases have been generated which shows the performance of algorithms. Each row signifies instances occurred in the predicted class. Whereas each column of the matrix characterizes the instances in a real class. Confusion matrices of both training sets have shown minimal error rate.

V. Verification of Class Assignment

To improve the accuracy of the traditional RF algorithm, experience of domain experts has been used.

Classes obtained after majority voting along with generated rules have been sent to expert community where many domain experts who are already playing their role in data rectification resides are shown in Fig. 2. They have reviewed and verified the classification results and decision rules using their experience. Some rules have been revised as discussed in Section VII and saved in the knowledge-base. This integration of generated results and experience of domain experts has created new knowledge about the soil environment which is used for the improvement of existing decision support systems of the domain. Consequently, the results have been improved after the involvement of expert experience in the system. This created knowledge will be placed on our online system for further distribution among other registered users.

VI. Algorithm Implementation

After data cleaning and management, the crowd sourced data seem categorical in a sense. A random forest algorithm has been implemented by splitting the data set into two portions as by taking soil type as a primary variable. Data have been trained as discussed in the previous section using three predictors, soil type, major crops and agricultural zones. Statistics of the training data are available in Tables V and VI. Soil categories have been counted in the current training data set and the frequency of each type has been calculated. Sandy, Clayey exists in 73 agricultural zones which is in association 16.25 % of the total soil types of the regions besides combination with other soil types. Calcareous, Sandy, Loamy, Silty and Sandy, Loamy are separately 4.45% of the overall soil types hence, less common in Pakistan as shown in Fig. 3. Similarly, Cotton, Wheat, Rice, Sugarcane, Mustard, Sorghum and Berseem are common crop types in Pakistan. During the training and processing of generation decision trees for every random sample, a random with replacement was used in bagging process. The parameter was set as the minimum node size=2, minimum son size=1 and the maximum depth of the tree is 20 while running the random forest algorithm. Further, sample size is set 249 observations for the subset comprising soil types and major crops, maximum trees=100 and stopping condition has been set at 300. After setting these parametric values, the algorithm has run to generate two random forests as: i) to map soil type's classes and agricultural zones, ii) for a subset of predictors, soil types and most suitable major crop for cultivation in that agricultural region. This has provided better representation of results. The tree structure of the data subset i) and ii) is shown in Tables III and IV, respectively. In both trees, no of objects used at each node have been presented along with their frequencies (in %) which shows the existence of predictor variable at each node. Selection of split points on predictor variables which aims to predict membership in various classes of dependent variables. In the both tree structures, initializing the split from the root node, continuing the splits by determining best terminal node in the tree choosing best predictor variable to execute the split. For this, P-values are calculated for each terminal node to examine the significance of association of class membership along with the levels of every predictor variable. After multiple comparisons, if the computed smallest p-value is smaller than the predefined threshold p-value, then the predictor variable which produces smallest p-value has been selected to split the consistent node. Following this practice, node 1, 3 and 4 have been split in the Table III and the node 1 and 4 has performed the split using p-values as presented in Table IV. Then the degree of freedom (DF) has been calculated at each node by computing the (no. of levels of defined categorical variables – 1).

TABLE. V. Summary Statistics of Training Data Set of Soil Types

Variable	Categories	Counts	Frequencies	%
Soil Types	Calcareous, Loamy	45	45	10.022
	Calcareous, Sandy	20	20	4.454
	Calcareous, Silt-loam	40	40	8.909
	Calcareous, Silty	20	20	4.454
	Clayey and Loamy	30	30	6.682
	Clayey and Sandy	25	25	5.568
	Clayey and Silty	41	41	9.131
	Clayey, Calcareous	40	40	8.909
	Loamy, Silty	20	20	4.454
	Sandy and Loamy	30	30	6.682
	Sandy, Clayey	73	73	16.258
	Sandy, Loamy	20	20	4.454
	Silty, Clayey	45	45	10.022

TABLE. VI. SUMMARY STATISTICS OF TRAINING DATA SET OF MAJOR CROPS

Variable	Categories	Counts	Frequencies	%
Major Crops	Berseem, Banana	4	4	2.010
	Pulses, Banana	2	2	1.005
	Pulses,Banana	2	2	1.005
	Pulses, Sugarcane	5	5	2.513
	Berseem, Banana	5	5	2.513
	Berseem, Rice	12	12	6.030
	Castor, Wheat	1	1	0.503
	Cotton, Wheat	20	20	10.050
	Guar, Castor	4	4	2.010
	Guar, Millet	3	3	1.508
	Guar, Wheat	2	2	1.005
	Millet, Wheat	5	5	2.513
	Mustard, Sorghum	23	23	11.558
	Mustard, Wheat	12	12	6.030
	Pulses,Banana	2	2	1.005
	Pulses, Sugarcane	4	4	2.010
	Rice, Banana	3	3	1.508
	Rice, Pulses	10	10	5.025
	Rice, Sugarcane	27	27	13.568
	Rice,Banana	4	4	2.010
	Rice, Wheat	5	5	2.513
	Sorghum, Berseem	23	23	11.558
	Sorghum, Cotton	5	5	2.513
	Sugarcane, Berseem	4	4	2.010
	Sugarcane, Sorghum	4	4	2.010
	Wheat, Castor	5	5	2.513
	Wheat, Guar	3	3	1.508

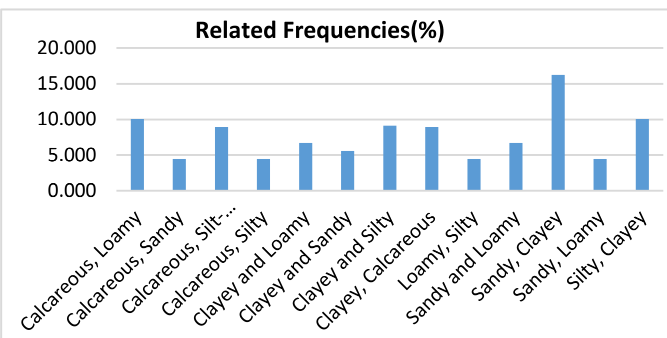

Fig. 3. Existence of Soil Type in no. of Zones as Related Frequencies.

VII. RESULTS AND DISCUSSIONS

This section comprises of two use cases: Case-I contains a) classification of soil environments of Pakistan based on agricultural regions, b) classification crops being cultivated in various soil types and c) mapping of crop(s) to suitable soil types. Case-II encompasses the results of knowledge management using statistical model regarding i) Productions of targeted crops at all available soil types of selected regions, ii) income and business impact of these crops to the farmers and iii) degree of irrelevancy of targeted crops to predict best business-oriented crop(s) for cultivation.

Case-I: Classification of Soil Types and Crop Mapping.

Data set comprising 1557 observations and 4 features has been obtained from various regions of Pakistan.

To achieve final prediction from entire dataset, the training data set has been divided into two parts according to interacting variables (predictors) as i) soil types with major crops taking 199 out of 1557 observations as training sample ii) soil types with agricultural zones having 449 out of 1557 observations as training sample and run the algorithm to generate two random forests using parametric values K=8, m=4, soil type (st=9), climate (c=4), major crops (mc=37), landscape (l=12), Agricultural zones (az=103). To predict output at every new location, the algorithm measured the ration of votes for every class to generate a final class. This is also known as the approximation of probabilities of each class. In the classification, this calculation also gives a measure of confidence. At the end, two random forests have been generated and compared using predictors. For case i), soil type with agricultural zones. Tree structure is available in the Table III. Node 1 has 449 objects with 4.68% purity p-value< 0.0001. Forest is structured with 12 nodes, which split at node 3 and 4. Similarly for case ii) soil type with major crops, tree structure with all statistics is depicted in Table IV which shows that the node 1 have 199 objects, node 2 contains 41 and the last node 8 have only 4 objects. Node 2, 6 and 8 have 100% purity.

As a result, two random forest have been produced along with decision rules for both cases. 11 rules have been made for mapping soil types to agricultural zones as presented in Table VII. These rules are useful to guide the growers to analyze existence of soil types in various agricultural zones. In the same way, 7 decision rules have been generated for mapping suitable major crops to various soil types as shown in Table VIII.

These rules representing different classes have then sent to agricultural community for further verification and knowledge creation of this domain. Four domain experts have participated in the verification process and revised 2 out of eleven rules of case i) and 1 out of seven rules from the case ii), respectively. From Table VII, they have compared rule for the nodes 9 and 10 which are generated for Hyderabad zone and updated the rule no. 10. Also, the rule for node no. 4 and 12 have been compared, reviewed and updated the rule no. 12 where Geographical Coverage is representing agricultural zones. Similarly, after comparing rules of node 4 and 6, the rule 6 has been revised in Table VIII. This integration of expert's experience to the existing decisions obtained using algorithm has generated knowledge of this domain. This knowledge-based decision will improve the DSSs as in this case 16.6% accuracy has been increases using expert's experience. With the use of large training data set and large number of generated rules, more accuracy can be achieved using the proposed approach. These knowledge-based decisions will then place on an online platform for further distribution among many registered users to be utilized in their fields for selection of suitable crops to achieve more production.

TABLE. VII. DECISION RULES OF MAPPING SOIL TYPES TO AGRICULTURAL ZONES

Nodes	Geographical Coverage(Pred)	Rules
Node 1	Badin	
Node 2	Badin	If Soil Types in [Clayey and Silty] then Geographical Coverage = Badin in 9.1% of cases
Node 3	Hyderabad	If Soil Types in [Calcareous, Loamy; Clayey and Sandy] then Geographical Coverage = Hyderabad in 15.6% of cases
Node 4	Sanghar	If Soil Types in [Silty, Clayey; Loamy, Silty; Calcareous, Silty] then Geographical Coverage = Sanghar in 18.9% of cases
Node 5	Tharparkar	If Soil Types in [Sandy, Clayey] then Geographical Coverage = Tharparkar in 16.3% of cases
Node 6	Tharparkar	If Soil Types in [Clayey and Loamy; Sandy and Loamy] then Geographical Coverage = Tharparkar in 13.4% of cases
Node 7	Muzaffaragarh	If Soil Types in [Calcareous, Sandy; Sandy, Loamy] then Geographical Coverage = Muzaffaragarh in 8.9% of cases
Node 8	Bahawalnagar	If Soil Types in [Clayey, Calcareous; Calcareous, Silt-loam] then Geographical Coverage = Bahawalnagar in 17.8% of cases
Node 9	Hyderabad	If Soil Types in [Calcareous, Loamy; Clayey and Sandy] and Soil Types in [Calcareous, Loamy] then Geographical Coverage = Hyderabad in 10.0% of cases
Node 10	Hyderabad	If Soil Types in [Calcareous, Loamy; Clayey and Sandy] and Soil Types in [Clayey and Sandy] then Geographical Coverage = Hyderabad in 5.6% of cases
Node 11	Hyderabad	If Soil Types in [Silty, Clayey; Loamy, Silty; Calcareous, Silty] and Soil Types in [Silty, Clayey] then Geographical Coverage = Hyderabad in 10.0% of cases
Node 12	Sanghar	If Soil Types in [Silty, Clayey; Loamy, Silty; Calcareous, Silty] and Soil Types in [Loamy, Silty; Calcareous, Silty] then Geographical Coverage = Sanghar in 8.9% of cases

TABLE. VIII. DECISION RULES OF MAPPING MAJOR CROPS TO SOIL TYPES

Nodes	Soil Types(Pred)	Rules
Node 1	Silty, Clayey	
Node 2	Clayey and Silty	If Major Crops in [Rice, Pulses; Berseem, Banana; Pulses, Sugarcane; Pulses, Banana; Rice,Banana; Berseem, Banana; Pulses, Sugarcane; Pulses,Banana; Rice, Banana; Pulses,Banana] then Soil Types = Clayey and Silty in 20.6% of cases
Node 3	Silty, Clayey	If Major Crops in [Cotton, Wheat; Rice, Wheat; Rice, Sugarcane; Mustard, Sorghum; Sorghum, Berseem] then Soil Types = Silty, Clayey in 49.2% of cases
Node 4	Silty, Clayey	If Major Crops in [Sorghum, Cotton; Sugarcane, Sorghum; Berseem, Rice; Mustard, Wheat; Sugarcane, Berseem] then Soil Types = Silty, Clayey in 18.6% of cases
Node 5	Sandy, Clayey	If Major Crops in [Guar, Millet; Wheat, Guar; Wheat, Castor; Millet, Wheat; Guar, Castor; Guar, Wheat; Castor, Wheat] then Soil Types = Sandy, Clayey in 11.6% of cases
Node 6	Silty, Clayey	If Major Crops in [Sorghum, Cotton; Sugarcane, Sorghum; Berseem, Rice; Mustard, Wheat; Sugarcane, Berseem] and Major Crops in [Sorghum, Cotton; Sugarcane, Sorghum] then Soil Types = Silty, Clayey in 4.5% of cases
Node 7	Loamy, Silty	If Major Crops in [Sorghum, Cotton; Sugarcane, Sorghum; Berseem, Rice; Mustard, Wheat; Sugarcane, Berseem] and Major Crops in [Berseem, Rice; Mustard, Wheat] then Soil Types = Loamy, Silty in 12.1% of cases
Node 8	Calcareous, Silty	If Major Crops in [Sorghum, Cotton; Sugarcane, Sorghum; Berseem, Rice; Mustard, Wheat; Sugarcane, Berseem] and Major Crops in [Sugarcane, Berseem] then Soil Types = Calcareous, Silty in 2.0% of cases

A maximum tree depth=3 with significance level of 5% and merge threshold is 5% was achieved. The algorithm used the Chi-square Automatic Interaction Detector (CHAID) to control the association among variables. CHAID analysis figures out a predictive model, or possibly a tree, to estimate how independent, interconnecting and dependent variables best merge produce the best output.

Case-II: Region Wise Crop Production in Different Soil Environments.

In order to create knowledge and utilize the advantages of created knowledge, three major cash crops of Pakistan of Khareef season, Cotton, maize and rice have been selected for experimentation. Three agricultural regions, Faisalabad, Multan and Bahawalpur have been used as these have different climate conditions, almost same variety of soil types and have cultivated similar crops. 1000 farmers and experts have participated to provide data about region wise soil types, cultivated crops and verification of soil crop mapping.

The process of knowledge creation has been divided into three phases. In phase-i) The data were obtained about region wise crop cultivation and respective production from online sources e.g. Agriculture Marketing Information Service and ministry of national food security & research. A data related to soil wise crop cultivation has been obtained by crowd sources and data sets have been generated. Knowledge about the existence of soil types in different regions was created using crowd sourcing. Phase ii) covers region wise income of crops at all available soil types to find most business-related crops. Phase iii) encompasses the degree of irrelevancy of crops grown in the targeted regions to avoid growing these crops as presented in Table I.

a) Region-wise Crop Production at different Soil types: First, Knowledge has been created and managed about production of rice crop on available soil types in the Faisalabad region as shown in Fig. 4(a). The covered area was 23.88 (in '000' hectare) and the farmers have achieved the maximum 44000 tons per hectare at loamy soil and lowest yields 7000 tons/ hectare at silt soil. This knowledge has been verified using crowd sourcing to improve the quality of results. Two other crops of 'Khareef' season have been selected and knowledge have been created for cotton and maize crops in this region at same soil environments. More production of all target crops has been observed in loamy soil. Maize produced 162.1 (in '000' tons/hectare) and cotton gives 53 ('000'bales per hectare). Sandy soil has also given good results for maize and cotton, but pure clay has less contributed in rice production. It only produced 32.7 (in '000' tons/hectare). Largely, the yield of maize has achieved the maximum level of production in the Faisalabad region as 162.1 in '000' tons per hectare. Silt soil has given a response in cultivation of cotton as compared to other two crops. It produced 25.4 in '000' bales per hectare. This knowledge created by crowd sources is helpful for farmers in choosing best crop for growing in all available soil types and to predict the combination of soil type and suitable crops for more production.

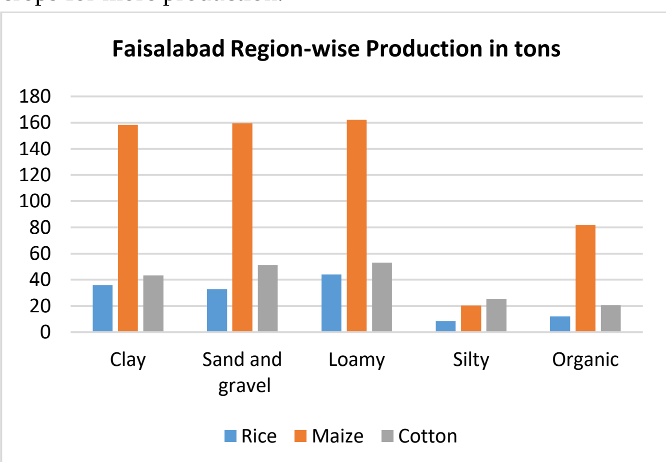

(a)

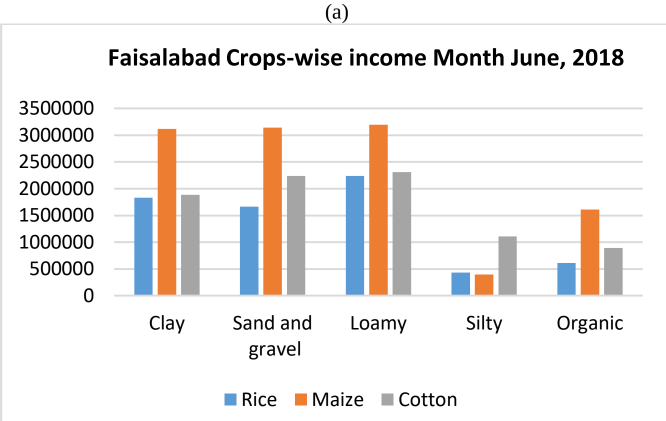

(b)

Fig. 4. (a): Production (in '000'Tons Per Hectare) of Major Crops in Faisalabad, (b): Income of Major Crops in Faisalabad.

Similarly, the dataset about same crops cultivated in two other regions, Multan and Bahawalpur has been obtained. These regions have almost similar soil types and crops, but different climate conditions as compared to Faisalabad region. Results of Multan region show maximum production of 496.8 bales per hectare (in '000' bales/hectare). In the same way, rice yield= 27.76, maize= 63.55 ('000' tons/hectare) and cotton= 1114.65 (bales/hectare) were recorded in loamy soil as shown in Fig. 5(a). Where I bale=170 KG.

b) Region wise income of crops at all available soil types: The has also been obtained from online sources i.e. 'index mundi.com' about prices of the targeted crops in the month of June 2018 and processed the data using statistical models to create the knowledge about most business-oriented yields of Faisalabad regions on various soil types. The knowledge-based results show the maize gives more income to the farmers as compared to cotton and rice in Faisalabad as shown in Fig. 4(b). Maize produced 3.19 million income per hectare (excluding other expenses) to the farmers at loamy soil and a minimum 0.39 million per hectare at silt soil. Loam soil has also given good response to rice and cotton as it has given 2.24 and 2.31 million per hectare to the farmers respectively as depicted in Fig. 5(b).

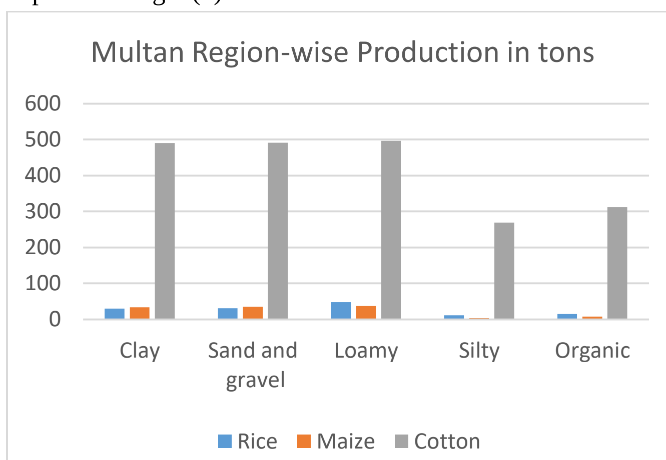

(a)

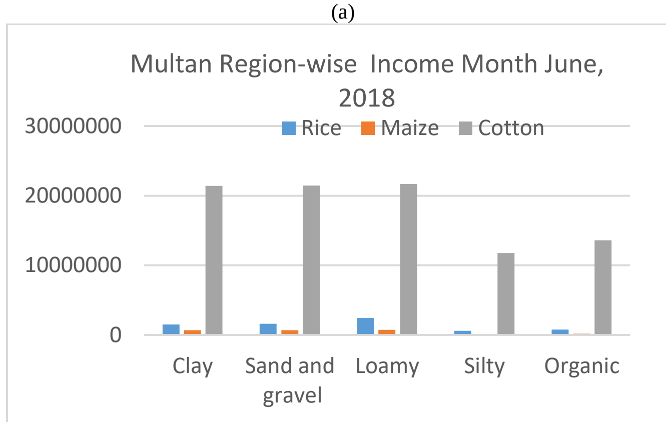

(b)

Fig. 5. (a): Production (in '000'Tons Per Hectare) of Major Crops in Multan Region; (b): Analysis of Income of Major Crops in Multan Region.

c) Towards Knowledge creation about Crop Irrelevancy: In order to predict which crop is not relevant to an agricultural region based on soil types, the data have been obtained from the Agricultural Marketing Information Service of Punjab Government and Pakistan Bureau of Statistics. The data have been processed using statistical models. Also, the data about yield prices has been used. To calculate the degree of crop irrelevancy to an agricultural region based on soil types, a set of steps has been discussed as under:

Consider region as R={ x,y,z…}, soil type as S={l,m,n…} and crop type as C = {a,b,c…}

For a selected region R_i, the degree of crop C_i relevancy DR_i for a soil type S_i can be calculated as:

$$\text{Degree of Relevancy DRi(Si)} = \frac{\text{Production(Ci)}}{\textit{Production in} \ \forall \ \textit{Ci values}} \quad (3)$$

Degree of irrelevancy $DIR_i.(S_i) = (1- DR_i) \times 100$ (4)

Set the threshold value for business impact of Crop $C_i(R_i)$

The degree of relevancy in Table I has been used to calculate the results of crop relevancies in all available soil types of targeted regions. Results have been presented in the Table I. Results show empirical substantiation that at same soil type of two distinct regions, a particular crop gives a completely different response. For example, at clay and loamy soil of Faisalabad and Bahawalpur, Maize and cotton have given different yield production. This shows the importance of knowledge-based results. We could now say that clay or loam soil will always respond to cotton or any particular crop. Similarly, cotton and rice have given different production at the sandy soil in Faisalabad and Multan regions.

The algorithm is generic in nature and can be used for a variety of crops of different agricultural regions where the required data is available. Knowledge verification from crowd sources have not only enhanced the quality of knowledge, but improved the accuracy of results.

VIII. Representation of Results

Decision rules have been generated for both forests to guide the farmers in taking decisions for a) which soil type their agricultural zone have b) Which major crops they may have to cultivate in their respective lands to earn through enhancing yield production. Decision rules for mapping soil types to agricultural zones are presented in Table VII and to select most suitable crop for cultivation on particular soil types is given in Table VIII which have been further elaborated in Section VII case-I. Results of knowledge Creation about crop production at available soil types in the selected regions and regions wise income of target crops at different soil type have been presented in Fig. 4(a) and (b), Fig. 5(a) and (b) and Fig. 6(a) and b. results of presented methodology for crop relevancy to the soil types of any region have been shown in Table I.

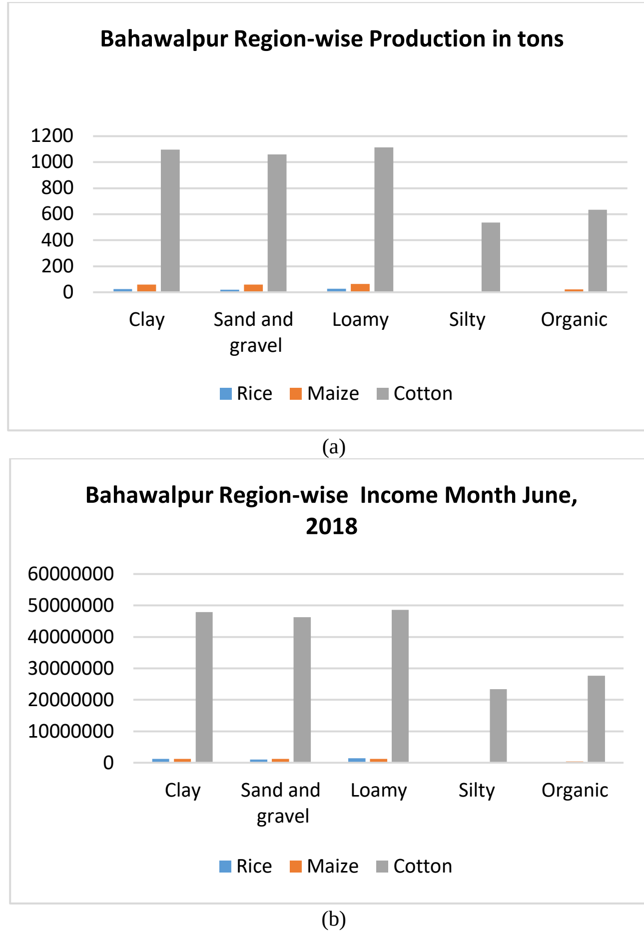

Fig. 6. (a): Production (in '000'Tons Per Hectare) of Major Crops in Bahawalpur Region. (b): Analysis of Income of Major Crops in Bahawalpur Region.

IX. Conclusion

In this paper, a knowledge-based classification approach has been presented to support farmers in taking decisions regarding selection of suitable crops for cultivation in relevant agricultural zones. Moreover, a procedure to calculate the degree of irrelevancy of a crop has also been discussed. The data rectification and verification of classification results from the domain experts have witnessed the improvement towards knowledge-based decisions related to the crops. In this work, a random forest classifier has been used for processing and predicting the multifarious relationship among soil types belonging to agricultural zones and major suitable crops for improving yield production.

Acknowledgment

The authors would like to thank Agriculture Marketing Information Service (AIMS) Government of Punjab, and ministry of national food security & research Pakistan and Institute of Soil & Environmental Sciences, University of Agriculture, Faisalabad for providing data to achieve better results.

References

[1] L. Klerkx and A. Proctor, "Land Use Policy Beyond fragmentation and disconnect : Networks for knowledge exchange in the English land management advisory system," Land use policy, vol. 30, no. 1, pp. 13–24, 2013.

[2] S. Rajeswari and K. Suthendran, "C5. 0 : Advanced Decision Tree (ADT) classi fi cation model for agricultural data analysis on cloud," Comput. Electron. Agric., vol. 156, no. December 2018, pp. 530–539, 2019.

[3] H. Teng, R. A. Viscarra, Z. Shi, and T. Behrens, "Catena Updating a national soil classi fi cation with spectroscopic predictions and digital soil mapping," Catena, vol. 164, no. October 2017, pp. 125–134, 2018.

[4] S. Sinha, A. Norouzi, A. Pradhan, X. Yu, and D. Seo, "A Field Soil Moisture Study Using Time Domain Reflectometry (TDR) and Time Domain Transmissivity (TDT) Sensors," no. Ictim, 2017.

[5] P. Han, D. Dong, X. Zhao, L. Jiao, and Y. Lang, "Original papers A smartphone-based soil color sensor : For soil type classification," Comput. Electron. Agric., vol. 123, pp. 232–241, 2016.

[6] M. Valipour, M. Ali, G. Sefidkouhi, and M. R. Sarjaz, "Selecting the best model to estimate potential evapotranspiration with respect to climate change and magnitudes of extreme events," Agric. Water Manag., vol. 180, pp. 50–60, 2017.

[7] C. Gornott and F. Wechsung, "Agricultural and Forest Meteorology Statistical regression models for assessing climate impacts on crop yields : A validation study for winter wheat and silage maize in Germany," Agric. For. Meteorol., vol. 217, pp. 89–100, 2016.

[8] V. Triantafyllidis, A. Kontogeorgos, C. Kosma, and A. Patakas, "An Assessment of the Soil Quality Index in a Mediterranean Agro Ecosystem," vol. 30, no. 12, pp. 1042–1050, 2018.

[9] K. J. Romanowicz, Z. B. Freedman, R. A. Upchurch, W. A. Argiroff, and D. R. Zak, "Active microorganisms in forest soils differ from the total community yet are shaped by the same environmental factors : the influence of pH and soil moisture," no. July, pp. 1–9, 2016.

[10] B. Heung, C. E. Bulmer, and M. G. Schmidt, "Geoderma Predictive soil parent material mapping at a regional-scale : A Random Forest approach," Geoderma, vol. 214–215, pp. 141–154, 2014.

[11] F. Bachion, D. Santana, A. Marcelo, D. Souza, and R. Jesus, "Spectrochimica Acta Part A : Molecular and Biomolecular Spectroscopy Visible and near infrared spectroscopy coupled to random forest to quantify some soil quality parameters," Spectrochim. Acta Part A Mol. Biomol. Spectrosc., vol. 191, pp. 454–462, 2018.

[12] L. Ma, M. Li, X. Ma, L. Cheng, P. Du, and Y. Liu, "ISPRS Journal of Photogrammetry and Remote Sensing A review of supervised object-based land-cover image classification," ISPRS J. Photogramm. Remote Sens., vol. 130, pp. 277–293, 2017.

[13] B. Kempen, D. J. Brus, G. B. M. Heuvelink, and J. J. Stoorvogel, "Geoderma Updating the 1 : 50 , 000 Dutch soil map using legacy soil data : A multinomial logistic regression approach," Geoderma, vol. 151, no. 3–4, pp. 311–326, 2009.

[14] R. E. Banfield, S. Member, L. O. Hall, K. W. Bowyer, and W. P. Kegelmeyer, "A Comparison of Decision Tree Ensemble Creation Techniques," vol. 29, no. 1, pp. 173–180, 2007.

[15] V. F. Rodriguez-galiano, B. Ghimire, J. Rogan, M. Chica-olmo, and J. P. Rigol-sanchez, "ISPRS Journal of Photogrammetry and Remote Sensing An assessment of the effectiveness of a random forest classifier for land-cover classification," ISPRS J. Photogramm. Remote Sens., vol. 67, pp. 93–104, 2012.

[16] L. Pásztor, A. Laborczi, J. Szabó, and G. Illés, "Geoderma Compilation of a national soil-type map for Hungary by sequential classi fi cation methods," no. April, 2017.

[17] B. Melville, A. Lucieer, and J. Aryal, "Int J Appl Earth Obs Geoinformation Object-based random forest classi fi cation of Landsat ETM + and WorldView- 2 satellite imagery for mapping lowland native grassland communities in," Int J Appl Earth Obs Geoinf., vol. 66, no. November 2017, pp. 46–55, 2018.

[18] D. T. Basics, M. Notation, B. Definitions, R. Trained, D. Trees, and M. Properties, "Decision Forests : A Unified Framework for Classification , Regression , Density Estimation , Manifold Learning and Semi-Supervised Learning By Antonio Criminisi , Jamie Shotton , and Ender Konukoglu," vol. 7, no. 2011, pp. 81–227, 2012.

[19] R. L. Lawrence, S. D. Wood, and R. L. Sheley, "Mapping invasive plants using hyperspectral imagery and Breiman Cutler classifications (RandomForest)," vol. 100, pp. 356–362, 2006.

[20] A. H. Khan, A. Akbar, K. Farooq, N. M. Khan, M. Aziz, and H. Mujtaba, "Soil Classification Through Penetration Tests," vol. 9, no. Figure 1, pp. 76–86, 2011.

[21] H. Ahmed, T. A. Jilani, W. Haider, M. A. Abbasi, and S. Nand, "Establishing Standard Rules for Choosing Best KPIs for an E-Commerce Business Based on Google Analytics and Machine Learning Technique," vol. 8, no. 5, pp. 1–7, 2017.

[22] C. Rica, L. A. Winowiecki, M. P. Whelan, P. A. Mcdaniel, M. Villalobos, and E. Somarriba, "landscape-scale agricultural production and conservation efforts in Local soil knowledge and its use in crop allocation : Implications for landscape-scale agricultural production and conservation efforts in Talamanca , Costa Rica," no. March, 2014.

[23] K. Saito, B. Linquist, and B. Keobualapha, "Farmers ' knowledge of soils in relation to cropping practices : A case study of farmers in upland rice based slash-and-burn systems of northern Laos," vol. 136, pp. 64–74, 2006.

[24] S. Rajeswari and K. Suthendran, "C5.0: Advanced Decision Tree (ADT) classification model for agricultural data analysis on cloud," Comput. Electron. Agric., vol. 156, no. December 2018, pp. 530–539, 2019.

[25] M. Nafees, M. Rasul, J. Hizbullah, and A. Ali, "STATUS OF SOIL Texture and Required Associated Soil Conservation Measure of River Swat Catchments Area , NWFP ," vol. 24, no. 2, 2008.

[26] A. Arooj, "Evaluation of Predictive Data Mining Algorithms in Soil Data Classification for Optimized Crop Recommendation."

[27] Durrani, Muhammad Nouman, and Jawwad A. Shamsi. "Volunteer computing: requirements, challenges, and solutions." Journal of Network and Computer Applications 39 (2014): 369-380.

HCAHF: A New Family of CA-based Hash Functions

Anas Sadak[1], Fatima Ezzahra Ziani[2], Bouchra Echandouri[3], Charifa Hanin[4], Fouzia Omary[5]
Faculty of Science, Mohammed V University
Rabat, Morocco

***Abstract*—Cryptographic hash functions (CHF) represent a core cryptographic primitive. They have application in digital signature and message authentication protocols. Their main building block are Boolean functions. Those functions provide pseudo-randomness and sensitivity to the input. They also help prevent and lower the risk of attacks targeted at CHF. Cellular automata (CA) are a class of Boolean functions that exhibit good cryptographic properties and display a chaotic behavior. In this article, a new hash function based on CA is proposed. A description of the algorithm and the security measures to increase the robustness of the construction are presented. A security analysis against generic and dedicated attacks is included. It shows that the hashing algorithm has good security features and meet the security requirements of a good hashing scheme. The results of the tests and the properties of the CA used demonstrate the good statistical and cryptographic properties of the hash function.**

***Keywords*—Hash function; boolean function; cellular automata; cryptography; information security; avalanche; nist statistical suite; DIEHARDER battery of tests; generic attacks; dedicated attacks**

I. INTRODUCTION

Cryptographic hash functions are of great importance in cryptography and have a major role in modern communication. Most security applications and cryptographic protocols rely on them. They can be used within other schemes (digital signature or message authentication codes (MAC)) or as standalone primitives (password or key generation). They are generally used to ensure data integrity and to provide user authentication. The principle behind a hashing scheme is to compute a digest or hash value of fixed length starting from an arbitrary length message. The digest is considered as a compact identifier of the message [1].

Hashing schemes can be classified according to the nature of the compression function used. Three main categories of hash functions emerge from that classification: hash functions based on block ciphers, hash functions based on modular arithmetic and dedicated hash functions [2]. The hash function proposed in this article falls in this last category. It uses cellular automata in the process of producing the digest. Cellular automata are a class of dynamic systems that are simple in principle but produce chaotic and complex behaviors.

In this article, a new hash function based on cellular automata is presented. It was designed with security in mind. The algorithm described in this paper comprises three phases: a preprocessing phase, a processing phase and a transformation phase. Each of these phases contains elements that provide the algorithm with security measures that help prevent or lower the risk of cryptanalytic attacks against cryptographic hash functions.

The article is organized as follows: in Section 2, a background on cellular automata and hash functions is included. In Section 3, some related works are presented. Section 4 details the hashing scheme proposed. In Section 5, the result of the different statistical tests and the cryptographic properties of cellular automata are provided. Next, in Section 6 a security analysis is performed. Finally, Section 7 summarizes the article.

II. BACKGROUND

A. Cryptographic Hash Functions (CHF)

Cryptographic hash functions with good security properties represent a significant part of cryptography. They are the basis of other cryptographic primitives and protocols. Their major tasks are to ensure data integrity and message authentication. Their major use is hence in digital signature schemes and message authentication protocols [3].

A hash function is a one-way function that maps an arbitrary finite length m-bits input to a fixed length n-bits output, called a hash value or a digest (m>n). The digest is thought of as the unique identifier of the input string.

In general, hash functions are built by iterating a compression function [4]. Depending on the nature of its internal compression function, the hash function can be categorized as either a hash function based on a block cipher, a hash function based on an arithmetic primitive or a dedicated hash function. In this article, the authors are interested in the latter category as the hash function described is based on cellular automata [5].

A hash function must ensure data compression and be easily computable. In addition, to be labeled as "cryptographic" it should guarantee the following basic security criteria [3]:

- Preimage: Given the hash value y = h(x), it is hard to find the message x' such that h(x') = y
- Second preimage: Given x, it is hard to find x' such that h(x') = h(x)
- Collision resistance: It is hard to find x and x' such that h(x) = h(x')

B. Cellular Automata (CA)

Cellular automata are dynamic mathematical models used for modeling physical and real-life phenomena. A cellular automaton is an array of cells arranged as a network that evolves in discrete time and space. Depending on the nature of the network arrangement, the cellular automaton can be one-dimensional or n-dimensional. Each cell assumes a state and evolves in time according to some local rule *f* and the states of its neighbors. The states of all the cells at a given time represent the configuration of the CA. In an *m*-state, *k*-neighborhood cellular automaton, each cell can assume *m* states, the local rule depends on up to *k* neighbors and m^{2^k} rules are possible [6].

They were first studied by von Neumann [7] in the 1960s for self-reproducing systems. They were first used in cryptography by Wolfram [8]. He used elementary cellular automata (ECAs) which are one-dimensional, two-state, three-neighborhood CAs. In this article, the authors are only considering ECAs.

A cellular automaton is said to be uniform if the same rule *f* is applied to all the cells. Otherwise, if two or more rules are used alternately, then the cellular automaton is called non-uniform or hybrid.

The rules can be represented either by a Boolean function or by a truth table. Table I gives the Boolean expression and the truth table of elementary rule 30. In Table I, s_i^{t+1} is the next state of cell *i* and $s_{i-1}^{\ t}$, $s_i^{\ t}$ and $s_{i+1}^{\ t}$ are the states of cells *i-1*, *i* and *i+1* at time *t* respectively.

If the Boolean expression of the local rule(s) involves only the operation, the cellular automaton is called to be linear. Otherwise, it is called non-linear.

How the states of the leftmost and rightmost cells are chosen determines the boundary configuration of the CA. Cellular automata can have a fixed or periodic boundary configuration. In fixed boundary CAs, some fixed states are assigned. An example of fixed boundary is null boundary. In periodic boundary CAs, the boundary cells are neighbors of other boundary cells. For example, in the case of one-dimensional cellular automata, the rightmost and leftmost cells are neighbors [6].

Cellular automata attractiveness lies on their ability to display a complex global behavior from simple local computations and interaction and the possibility of parallel update of the states of the cells.

TABLE. I. RULE 30 BOOLEAN EXPRESSION AND TRUTH TABLE

Algebraic Normal Form							
$s_i^{t+1} = s_{i-1}^{\ t} \oplus (s_i^{\ t} + s_{i+1}^{\ t})$							
Truth Table							
111	110	101	100	011	010	001	000
0	0	0	1	1	1	1	0

III. RELATED WORK

Damgård [9] introduced a method for constructing a hash function that is collision resistant and provided three examples of possible use of his construction, one of which is based on cellular automata. Daemen, Govaerts, and Vandewalle [10] showed the vulnerabilities of the construction proposed by Damgård [9] and presented a framework for constructing practical hash functions. Along with their framework, a newly developed CA-based hash function was introduced: CellHash. The same authors proposed an enhanced version of CellHash called SubHash [11]. Both those constructions were broken by Chang [12]. Mihaljevic, Zheng, & Imai [13] presented a family of fast CA-based hash function over GF(q) without specifying the rules used and the neighborhood configuration used. A hash function based on a cellular automaton using both linear and non-linear rules is proposed by Jeon [14]. Kuila, Saha, Pal, and Chowdhury [15] promoted a hash construction based on cellular automata and inspired by the sponge construction. This construction proved to be as efficient and as secure against known attacks as other well-known hash functions [16] such as SPONGENT [17], GLUON [18], QUARK [19], PHOTON [20] and SHA-3 [21]. In this article, the construction used by the authors is inspired by the wide pipe Merkle-Damgård construction. Therefore, it is an alternative to the work proposed by Kuila et al. [15]. More recently, Hanin, Echandouri, Omary and El Bernoussi [22] proposed a CA-based hash function that uses the MD-construction. The hash algorithm proposed by Hanin et al. [22] lacks however security measures such as a strong padding scheme and the use of hybrid cellular automata and therefore do not have good cryptographic properties and a good pseudorandom behavior. The use of two-dimensional cellular automata for constructing a hash function was explored by Hirose and Yoshida [23]. However, the rule space for two-dimensional cellular automata and the complexity of this kind of cellular automata are beyond the scope of this article.

IV. DESCRIPTION OF HCAHF-256

In this section, the proposed hashing scheme is described. It takes inspiration from the wide pipe hash construction [24], which is a modified Merkle-Damgård construction. The general version with a digest size of *m* bits is named HCAHF while HCAHF-256 designates the 256-bit version.

The algorithm is made of three phases. First, the message is pre-processed. The pre-processed message is then compressed using cellular automata evolutions and the XOR function during the compression phase. Finally, a final transformation is applied before generating the output of HCAHF.

The three phases of HCAHF-256 are detailed in the following subsections. The pseudo-code for the padding scheme and for the digest generation mechanism is also presented.

A. Preprocessing Phase

1) Padding scheme: The first step in the preprocessing of a message M of arbitrary length consists of applying a padding scheme. Padding is always applied even in the case |M| is a multiple of 256.

The padding scheme used in HCAHF-256 is the technique known as Merkle-Damgård strengthening [25]. A single ‘1’ bit is appended to *M*. It is followed by ‘0’ bits and the size of *M* (before padding is applied) encoded in 64 bits. The necessary number of ‘0’ bits must make the padded message size a multiple of 256.

Padding is used as a mean to avoid attacks such as the length-extension attack [3].

2) Message splitting: After the message M is padded, it is split into blocks of size 256 bits.

3) Salt: In the last step of the preprocessing phase, a salt value *salt* is computed using a pseudorandom number generator. It is then prepended to the padded message.

Using a salt value is a security measure that reduces the risk of collisions and prevents pre-computation attacks such as the dictionary attack as hashing the same message with different salt values $salt_1$ and $salt_2$ yields two different hash values [3].

The salt value is generated using the class ThreadedSeedGenerator of the Bouncy Castle Java library.

B. Compression Phase

During the compression phase, a compression function f is repeatedly used to produce a pre-digest value. f takes as inputs a chaining variable h_i from the previous step and message block M_i [16]. The initial chaining variable IV is a 256-bit block also generated using the class ThreadedSeedGenerator of the Bouncy Castle Java library. The final chaining variable $M_{compressed}$ is the pre-digest value.

Starting from (n+1) 256-bit blocks at the beginning of the compression phase, a single 256-bit block is obtained; hence the use of the compression term.

f combines a cellular automaton and the XOR function. The cellular automaton is designated as the function E and the XOR function as $\oplus$.

1) The Function E: The function E is a 3-neighborhood cellular automaton with periodic boundary conditions.

Each block M_i is evolved 128 times using a rule R_i as follows:

$$e_0 = E(salt, R_0)$$

$$e_1 = E(M_1, R_1)$$

$$e_n = E(M_n, R_n)$$

The rule R_i used is obtained from the first 8 bits of each block M_i. For example, if the first 8 bits of a block are 00011110, then the rule to be used is rule 30 ($00011110_2 = 30_{10}$). However, if R_i does not belong to the Wolfram classes 3 and 4 as classified in [26], it is discarded and a rule with good cryptographic properties (non-linearity, algebraic degree, balancedness, resiliency…) is selected at random from the set $R_{process}$. This set has been selected according to the recommendations and cryptographic properties found in [27] and [28]. For a detail of the rules included in this set and their cryptographic properties, the Appendix can be consulted.

2) The XOR Function: At each step, the result of the previous steps is XORed with the evolution of the block M_i.

3) The Function f: The compression function f of this construction can be expressed as:

$$h_0 = IV$$

$$h_1 = f(e_0, h_0)$$

$$h_i = f(e_{i-1}, h_{i-1})$$

$$h_{n+1} = f(e_n, h_n)$$

C. Transformation Phase

During the transformation phase, a function T is applied to $M_{compressed}$, the 256-bit output of the previous phase.

The function T is a 3-neighborhood hybrid cellular automaton with periodic boundary conditions. It evolves $M_{compressed}$ for 128 evolutions using the ruleset R_{digest} = {30, 90, 150, 30, 135, 30, 90, 150}. This ruleset has been chosen using the recommendation found in [27] and a detail of the selection process can be found in the Appendix.

The digest obtained can be expressed as:

$$digest = T(M_{compressed}, R_{digest})$$

Fig. 1 summarizes the different steps of HCAHF.

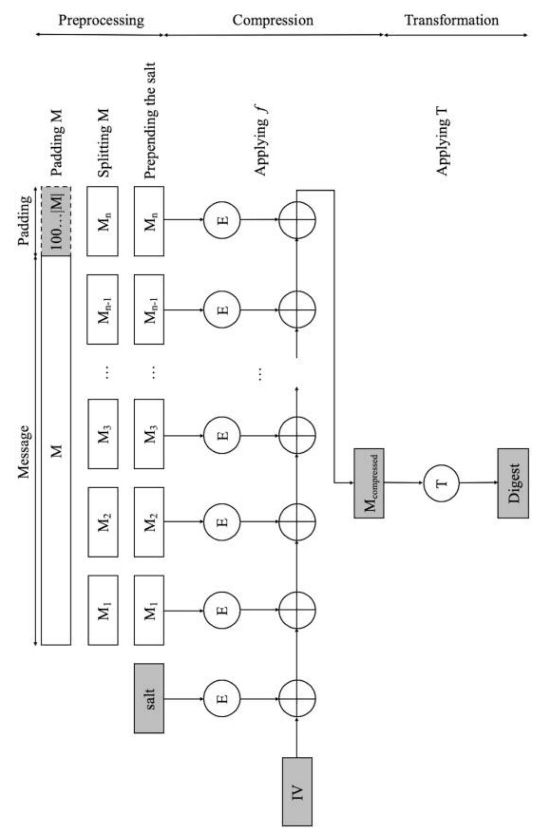

Fig. 1. HCAHF Design.

D. HCAHF-256 Algorithm

1) Pseudo-Code for The Padding Scheme of HCAHF-256

Algorithm 1 details the padding scheme used for HCAHF-256.

Algorithm 1. Pseudo-code of the padding scheme of HCAHF-256

Input: M the message to pad
Output: paddedM

```
begin
    m ← sizeOf(M) mod 256
    x ← 256 - m
    if sizeOf(M) is multiple of 256 then
        NbZero ← 191
    else if sizeOf(M) is not a multiple of 256 then
        if x < 65 then
            y ← x + 256
            NbZero ← y - 65
        else
            NbZero ← x - 65
        end if
    end if
    paddedM ← M || 1 || 0^NbZero||sizeOf(M) in {0,1}^64
    return paddedM
end
```

2) Pseudo-Code for The Generation Mechanism of HCAHF-256

Algorithm 2 shows the different steps by which a 256-bit digest is generated by HCAHF-256.

ALGORITHM 2. PSEUDO-CODE OF HCAHF-256

Input: M the message to hash
Output: digest

```
begin
    Let IV ← randomSequence(256)
    Let salt ← randomSequence(256)
    Let ruleSet← {30, 90, 150, 30, 135, 30, 90, 150}
    paddedM ← padding(M)
    splittedM ← split(paddedM, 256)
    saltedM ← insert (salt, splittedM)
    Xor ← IV
    For each block b in saltedM do
        If IntegerValue(8firstBits(b)) is in S the set of class
        3 and 4 rules then
          rules_i ←IntegerValue(8firstBits(b))
        Else
          rules_i ← randomRule(S)
        End if
        E←evolv(b, rules_i, 128, periodicBoundaries)
        Xor ← Xor ⊕ E
    End for
          s←Xor
    For it from 1 to 128
        For i from 1 to 256
          k ← i - 1 modulo sizeOf(ruleSet)
          If ((k == 0) || (k == 3) || (k == 5)) then
            evolution[i]←s[i-1] ⊕ (s[i]+s[i+1])
          Else if ((k == 1) ||( k == 6)) then
            evolution[i]←s[i-1] ⊕ s[i+1]
          Else if ((k == 2) || (k == 7)) then
            evolution[i] ← s[i-1] ⊕ s[i] ⊕ s[i+1]
          Else
            evolution[i] ←1⊕ s[i-1] ⊕ (s[i].s[i+1])
          End if
        End for
    End for
    digest ← evolution
    return digest
End
```

In this article, the authors chose to use $\frac{n}{2}$ or 128 evolutions in the case of HCAHF-256 for the number of evolutions when cellular automata are used. This is a general rule for guaranteeing a greater period of the cellular automaton [26].

V. RESULTS

In this section, the results of some statistical tests performed on the proposed hash algorithm are presented. Passing those tests does not guarantee the resistance of HCAHF to attacks targeted at hash functions. However, passing those tests is a good indicator of the good security level of a hash function. Pseudorandom behavior and statistical independence between the input and the output are some of the properties desired in cryptographic hash functions. In addition, the complexity of the algorithm is estimated to show the easy computation and implementation of the algorithm proposed.

A. Avalanche Test

The first test performed on HCAHF is the avalanche test. The avalanche effect was first used in cryptography by Feistel [29]. It was introduced as a property of S-boxes and Substitution-Permutation Networks (SPNs). It states that a very small difference in the input, generally a single bit change, produces a substantial difference on the output. More formally, if a function *f* exhibits the avalanche effect, then the Hamming distance between the outputs obtained from M and M', that differ by a single bit, is on average half the digest size. This definition is closely related to the concept of nonlinearity. A function displaying the avalanche effect can be considered as highly non-linear. Mathematically, this concept can be described as follows:

$f:\{0,1\}^m \rightarrow \{0,1\}^n$ has the avalanche effect if:

$$\forall\, M, M' \in \{0,1\}^m : Hamming(M, M') = 1$$

$$\Rightarrow\ average(Hamming(f(M), f(M'))) = \frac{n}{2}$$

In order to conduct the avalanche test on HCAHF, 100 1024-bit messages were generated. For each message M_i, the hash value of the original message and the hash values of its one-bit change replicas ($Hamming(M_i, M'_{i,1\le j\le 1024}) = 1$) are generated by HCAHF. Then, the hamming distances between the hash values are calculated ($Hamming(f(M_i), f(M'_{i,1\le j\le 1024}))$).

The results of the test are presented in Fig. 2. Here the average values for each bit position *j* were taken for the 100 messages and expressed as percentages. The figure shows that the avalanche values are concentrated around 50. This indicates that HCAHF has the avalanche effect and thus its outputs are statistically independent from its inputs.

B. Statistical Tests

In practice, cryptographic hash functions should behave like a random oracle to prevent statistical attacks. Thus, to check this pseudorandom behavior, standard statistical tests are commonly applied. The NIST Statistical Test Suite (STS) and the DIEHARDER battery of tests were used.

1) NIST Statistical Test Suite (STS): The National Institute of Standards and Technology developed a set of tests called the NIST Statistical Test Suite (STS). This test suite is useful to check the randomness property of some cryptographic primitives like hash functions. p-values are computed and evaluated for the generated sequences to verify if the sequences are random. A more detailed description can be found in NIST special publication 800-22 [30].

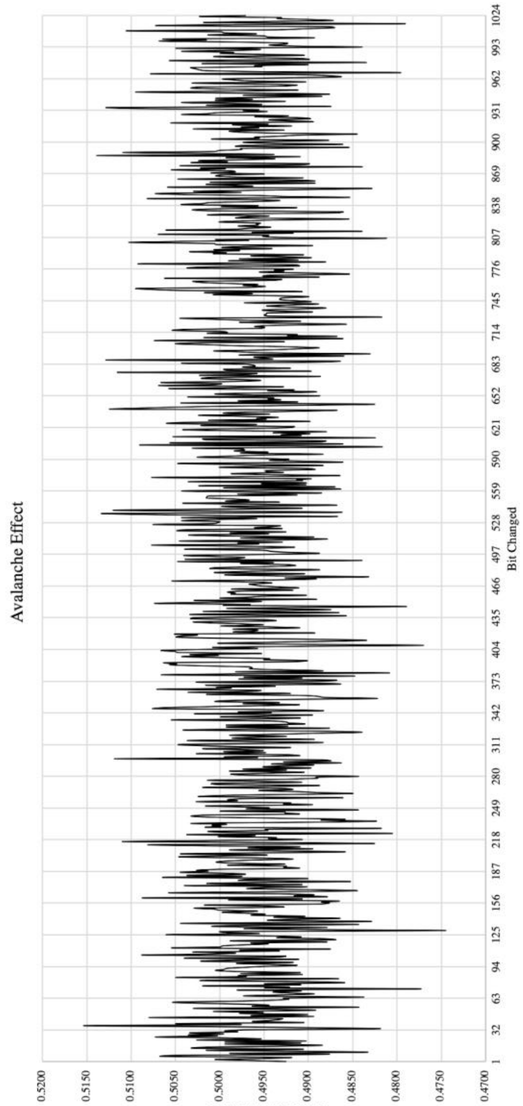

Fig. 2. Avalanche Test Results.

A 10 MB sequence is obtained by concatenating the hash values generated by HCAHF-256. This sequence is used as an input to the test suite. The results of the different tests are presented in Table II. A test is passed if the p-value is between 0.001 and 0.999. Some tests cannot be applied because the size of the output (256 bits) is too short compared to the test requirements (e.g. The Binary Matrix Rank Test requires a sequence of 1000000 bits). HCAHF-256 passes all the applicable tests.

2) Dieharder battery of tests: DIEHARDER is a stronger test battery developed by Brown, Eddelbuettel and Bauer [31] to test all types of random number generators as well as other cryptographic primitives (block ciphers, stream ciphers, hash functions, …). It is a collection of tests that include tests from the DIEHARD battery of tests and from the NIST STS as well as other tests designed by Brown, Bauer, Marsaglia and Tsang. It is an extensible test suite that includes more and more tests with each update. The p-values must be in the range [α ,1- α] to pass a test, α being the significance level. Table III shows the results of the DIEHARDER tests. The significance level used here is α = 0.005. HCAHF-256 passes all the tests.

The results of these two batteries of statistical tests show that HCAHF-256 has a good pseudorandom behavior, which is one of the essential characteristics of a secure hash function. The output generated by HCAHF-256 can then be considered as indistinguishable from the output of a true random number generator.

TABLE. II. NIST STS RESULTS

Test name	p-value	Interpretation
The Frequency (Monobit) Test	0.4963	PASS
Frequency Test within a Block	0.4888	PASS
The Runs Test	0.4927	PASS
Tests for the Longest-Run-of-Ones in a Block	0.4954	PASS
The Binary Matrix Rank Test	-	NOT APPLICABLE
The Discrete Fourier Transform (Spectral) Test	0.4815	PASS
The Non-Overlapping Template Matching Test	0.6973	PASS
The Overlapping Template Matching Test	-	NOT APPLICABLE
Maurer's "Universal Statistical" Test	-	NOT APPLICABLE
The Linear Complexity Test	0.5644	PASS
The Serial p-value1 Test	0.4915	PASS
The Serial p-value2 Test	0.4993	PASS
The Approximate Entropy Test	0.4914	PASS
The Cumulative Sums (Cusums) Forward Test	0.5140	PASS
The Cumulative Sums (Cusums) Reverse Test	0.5132	PASS
The Random Excursions Test	-	NOT APPLICABLE
The Random Excursions Variant Test	-	NOT APPLICABLE

TABLE. III. DIEHARDER TEST SUITE RESULTS

Test name	p-value	Interpretation
Diehard birthdays	0.8559	PASS
Diehard OPERM5	0.9309	PASS
Diehard 32x32 Binary Rank	0.3301	PASS
Diehard 6x8 Binary Rank	0.8151	PASS
Diehard_bitstream	0.7112	PASS
Diehard OPSO	0.9008	PASS
Diehard OQSO	0.1161	PASS
Diehard DNA	0.6635	PASS
Diehard Count the 1s (stream)	0.0808	PASS
Diehard Count the 1s (byte)	0.0082	PASS
Diehard Parking Lot	0.7936	PASS
Diehard Minimum Distance (2d Circle)	0.0254	PASS
Diehard 3d Sphere (Minimum Distance)	0.8868	PASS
Diehard Squeeze	0.9114	PASS
Diehard Sums	0.0138	PASS
Diehard Runs	0.4253	PASS
Diehard Craps	0.5868	PASS
Marsaglia and Tsang GCD	0.3477	PASS
STS Monobit	0.7161	PASS
STS Runs	0.2438	PASS
STS Serial Test (Generalized)	0.5342	PASS
RGB Bit Distribution	0.5511	PASS
RGB Generalized Minimum Distance	0.7152	PASS
RGB Permutations	0.5	PASS
RGB Lagged Sum	0.5330	PASS
RGB Kolmogorov-Smirnov	0.5784	PASS
DAB Byte Distribution	0.5964	PASS
DAB DCT (Frequency Analysis)	0.0541	PASS
DAB Fill Tree	0.7417	PASS
DAB Fill Tree 2	0.4559	PASS
DAB Monobit 2	0.0432	PASS

C. Cryptographic Properties of the Rules used in Function T

In addition to the avalanche effect displayed by HCAHF-256 and the good statistical features of HCAHF-256 proven by the results of the NIST STS and the DIEHARDER statistical tests, the cryptographic properties of the hybrid ruleset used in the transformation phase are presented here. The Appendix provides more clarifications about the selection process of this ruleset and the meaning of each property.

The following tables (Tables IV to VIII) present the cryptographic properties of the hybrid ruleset $R_{digest} = \{30, 90, 150, 30, 135, 30, 90, 150\}$ for eight cells, assumed to be unknown Boolean values x_i, and up to three clock cycles.

From these tables, it can be noted that with the exception of correlation immunity and resiliency, all the other cryptographic properties (algebraic degree, nonlinearity and balancedness) increase with each iteration (algebraic degree, nonlinearity) or remain true (balancedness). The decrease of the values of correlation immunity and resiliency can be explained by the increase in the values of the algebraic degree and the nonlinearity, as some cryptographic properties are self-contradicting [27]. Therefore, a compromise should be found. For a cryptographic hash function, the algebraic degree and the nonlinearity can be judged as more important properties to achieve than the correlation immunity and resiliency properties.

D. Complexity

As stated before, basic requirements for a hash function is the ease of computation and the simplicity of implementation. In this subsection, the complexity of HCAHF is estimated in order to establish those two requirements.

TABLE. IV. ALGEBRAIC DEGREE

Iteration	x_0	x_1	x_2	x_3	x_4	x_5	x_6	x_7
1	2	1	1	2	2	2	1	1
2	3	2	2	3	3	3	2	2
3	4	3	3	4	5	4	3	3

TABLE. V. NONLINEARITY

Iteration	x_0	x_1	x_2	x_3	x_4	x_5	x_6	x_7
1	2	0	0	2	2	2	0	0
2	8	8	8	8	4	8	8	8
3	32	48	48	48	16	36	48	48

TABLE. VI. CORRELATION IMMUNITY

Iteration	x_0	x_1	x_2	x_3	x_4	x_5	x_6	x_7
1	0	1	2	0	0	0	1	2
2	0	2	2	0	0	0	2	2
3	0	0	0	0	0	0	1	1

TABLE. VII. RESILIENCY

Iteration	x_0	x_1	x_2	x_3	x_4	x_5	x_6	x_7
1	0	1	2	0	0	0	1	2
2	0	2	2	0	0	0	2	2
3	0	0	0	0	0	0	1	1

TABLE. VIII. BALANCEDNESS

Iteration	x_0	x_1	x_2	x_3	x_4	x_5	x_6	x_7
1	✓	✓	✓	✓	✓	✓	✓	✓
2	✓	✓	✓	✓	✓	✓	✓	✓
3	✓	✓	✓	✓	✓	✓	✓	✓

The padding requires at most $n+64$ steps, where n is the block size. Splitting the message requires $m=\frac{L}{n}$ steps, where L is the message size after padding. The complexity of generating the salt and the IV is $O(n)$. Applying the function E to blocks involves $(m+1) \times n \times \frac{n}{2}$ steps. The compression phase requires $(m+1) \times n$ mod 2 additions. The last transformation T requires $n \times \frac{n}{2}$ steps. The overall complexity of HCAHF is then $O(m \times n^2)$, n being the digest size and m the number of blocks.

VI. Security Analysis

In this section, a security analysis of the proposed hash algorithm HCAHF is performed. Formally proving the resistance of a given cryptographic primitive to attacks targeted against it is not an easy task. However, since the HCAHF is a wide-pipe MD construction, it can be assumed that its security can be reduced to that of its compression (E and XOR) and transformation (T) functions.

A. Brute Force Attacks against Hash Functions

Brute force attacks targeted at hash functions are attacks that depend only on the length of the hash value and not on the hash algorithm itself. In the case of keyless hash functions, three brute force attacks are possible: the preimage attack, the second preimage attack and the collision attack.

1) Preimage and second preimage attack: The number of trials required for an adversary to find the original message M from a given hash value h (preimage attack) or to find a second message M' given a pair (M,h) (second preimage attack) is 2^n [16], where n is the digest size in bits. In the case of HCAHF-256, the minimum amount of work required for such attacks to be successful is 2^{256} operations. Therefore, HCAHF-256 can be considered as robust against those two attacks.

2) Collision attack: The number of trials required for an adversary to find two messages M and M' that produce the same hash value h (collision attack) is $2^{\frac{n}{2}}$ [16]. In the case of HCAHF-256, the minimum amount of work required for an attacker to find a collision is 2^{128} operations. Thus, HCAHF-256 can be considered as robust against the collision attack.

B. Cryptanalytic Attacks

Cryptanalytic attacks are attacks targeted at the hash algorithm itself. The goal of these attacks is to reduce the complexity of the algorithm and thus reduce the complexity of the brute force attacks. Many different types of cryptanalytic attacks exist. Some examples of cryptanalytic attacks are the length-extension attack [32], the fixed-point attacks by Dean [33] and Kelsey and Schneier [34] and the herding attack [35].

As it is not possible to prevent all kinds of cryptanalytic attacks, the authors chose different techniques to prevent or lower the risk of these attacks. The following paragraphs detail those tools.

The first measure to prevent cryptanalytic attacks is the adoption of MD-strengthening as a padding scheme when preprocessing the message. MD-strengthening was used in HCAHF as a measure to prevent length-extension attacks.

Another measure adopted to avoid cryptanalytic attacks is the use of a salt value. The use of a generated salt value prepended to the message after applying padding helps in preventing attacks [3] such as the length-extension attack [32], the multi-collision attack, the fix point attacks by Dean [33] and by Kelsey and Schneier [34] and the herding attack [35].

The use of cellular automata with linear and non-linear rules (E function), of the bit-by-bit addition modulo 2 (XOR function) and of a non-linear cellular automaton (T function) during the compression and transformation phases of HCAHF also help in preventing cryptanalytic attacks. Differential and linear attacks are avoided by the use of cellular automata. The diffusion property is provided by the XOR operation and the use of cellular automata and was proved by the good avalanche effect of HCAHF. The confusion property is provided by the use of the non-linear cellular automaton (T function) and the non-linear rules cellular automata (E function). It was proved by the good results of the statistical tests performed on HCAHF. Moreover, the cryptographic properties of cellular automata presented in the Appendix point also in that direction.

VII. Conclusion

In this paper, a new family of CA-based hash functions is proposed. The hash algorithm described in the article consists of three phases: a preprocessing phase, a processing phase and a transformation phase. In the preprocessing phase, the input is padded using the MD-strengthening padding scheme, split into blocks of the same size n and prepended with a salt value. Applying a padding scheme and prepending a salt value to the input are measures used to prevent some cryptanalytic attacks targeted at cryptographic hash functions. During the processing phase, each block is first evolved using a cellular automaton then XORed with a chaining variable from a previous step. The first chaining variable is a precomputed n-bit block called IV. The use of cellular automata and the XOR operator during this phase provide the confusion and diffusion properties. The last phase consists of a final transformation by means of a hybrid cellular automaton with a ruleset carefully chosen. The use of the hybrid cellular automaton provides the confusion property and the pseudorandom behavior. In addition to the description of the algorithm and the security measures adopted in design of HCAHF, several statistical tests were performed. The result of these tests proves that HCAHF has good statistical features. These tests show that HCAHF displays the pseudorandom behavior, the statistical independence between the input and the output as well as the sensitivity of the algorithm to changes in the input. Finally, it can be noted that HCAHF has been implemented in software and that it can be presumed to perform better if implemented in hardware due to the simplicity of implementing cellular automata in hardware. Also, two additional properties, the hiding property and the puzzle friendliness property [36], can be verified if HCAHF is to be used in the blockchain technology in a future work. Finally, the number of evolutions used for cellular automata can be the subject of another study in order to maximize the period of the cellular automata used [26].

References

[1] D. R. Stinson and M. B. Paterson, Cryptography: theory and practice. Boca Raton: CRC Press, 2019.

[2] H. C. A. van Tilborg and S. Jajodia, Encyclopedia of cryptography and security. New York: Springer, 2011.

[3] E. Biham and O. Dunkelman, “A framework for iterative hash functions — HAIFA,” IACR Cryptology ePrint Archive 2007: 278, 2007.

[4] B. Preneel, "MACs and hash functions: State of the art," Information Security Technical Report, vol. 2, no. 2, pp. 33-43, 1997.

[5] B. Preneel, “The first 30 years of cryptographic hash functions and the NIST SHA-3 competition,” Topics in Cryptology - CT-RSA 2010 Lecture Notes in Computer Science, pp. 1–14, 2010.

[6] K. Bhattacharjee, N. Naskar, S. Roy, and S. Das, “A survey of cellular automata: types, dynamics, non-uniformity and applications,” Natural Computing, 2018.

[7] J. V. Neumann, Theory of self-reproducing automata. Urbana (U.S.A.): University of Illinois Press, 1966.

[8] S. Wolfram, “Cryptography with cellular automata,” Lecture Notes in Computer Science Advances in Cryptology — CRYPTO ’85 Proceedings, pp. 429–432, 1985.

[9] I. B. Damgård, “A design principle for hash functions,” Advances in Cryptology — CRYPTO’ 89 Proceedings Lecture Notes in Computer Science, pp. 416–427, 1989.

[10] J. Daemen, R. Govaerts, and J. Vandewalle, “A framework for the design of one-way hash functions including cryptanalysis of Damgård’s one-way function based on a cellular automaton,” Advances in Cryptology — ASIACRYPT 91 Lecture Notes in Computer Science, pp. 82–96, 1991.

[11] J. Daemen, R. Govaerts, and J. Vandewalle, “A hardware design model for cryptographic algorithms,” Computer Security — ESORICS 92 Lecture Notes in Computer Science, pp. 419–434, 1992.

[12] D. Chang, “Preimage attacks on CellHash, SubHash and strengthened versions of CellHash and SubHash,” IACR Cryptology ePrint Archive 2006: 412, 2006.

[13] M. Mihaljević, Y. Zheng, and H. Imai, “A cellular automaton based fast one-way hash function suitable for hardware implementation,” Public Key Cryptography Lecture Notes in Computer Science, pp. 217–233, 1998.

[14] J.-C. Jeon, “One-way hash function based on cellular automata,” IT Convergence and Security 2012 Lecture Notes in Electrical Engineering, pp. 21–28, Nov. 2012.

[15] S. Kuila, D. Saha, M. Pal, and D. R. Chowdhury, “CASH: Cellular automata based parameterized hash,” Security, Privacy, and Applied Cryptography Engineering Lecture Notes in Computer Science, pp. 59–75, 2014.

[16] W. Stallings, Cryptography and network security: principles and practice. Hoboken, NJ: Pearson Education, Inc., 2019.

[17] A. Bogdanov, M. Knežević, G. Leander, D. Toz, K. Varıcı, and I. Verbauwhede, “SPONGENT: A lightweight hash function,” Cryptographic Hardware and Embedded Systems – CHES 2011 Lecture Notes in Computer Science, pp. 312–325, 2011.

[18] T. P. Berger, J. D’Hayer, K. Marquet, M. Minier, and G. Thomas, “The GLUON Family: A lightweight hash function family based on FCSRs,” Progress in Cryptology - AFRICACRYPT 2012 Lecture Notes in Computer Science, pp. 306–323, 2012.

[19] J.-P. Aumasson, L. Henzen, W. Meier, and M. Naya-Plasencia, “Quark: A lightweight hash,” Cryptographic Hardware and Embedded Systems, CHES 2010 Lecture Notes in Computer Science, pp. 1–15, 2010.

[20] J. Guo, T. Peyrin, and A. Poschmann, “The PHOTON family of lightweight hash functions,” Advances in Cryptology – CRYPTO 2011 Lecture Notes in Computer Science, pp. 222–239, 2011.

[21] G. Bertoni, J. Daemen, M. Peeters, and G. V. Assche, “The making of KECCAK,” Cryptologia, vol. 38, no. 1, pp. 26–60, Feb. 2014.

[22] C. Hanin, B. Echandouri, F. Omary, and S. E. Bernoussi, “L-CAHASH: A novel lightweight hash function based on cellular automata for RFID,” Ubiquitous Networking Lecture Notes in Computer Science, pp. 287–298, 2017.

[23] S. Hirose and S.Yoshida, “A one-way hash function based on a two-dimensional cellular automaton,” The 20th Symposium on Information Theory and Its Applications (SITA97), pp. 213–216, 1997.

[24] S. Lucks, “A failure-friendly design principle for hash functions,” Lecture Notes in Computer Science Advances in Cryptology - ASIACRYPT 2005, pp. 474–494, 2005.

[25] X. Lai and J. L. Massey, “Hash functions based on block ciphers,” Advances in Cryptology — EUROCRYPT’ 92 Lecture Notes in Computer Science, pp. 55–70, 1992.

[26] S. Wolfram, A new kind of science. USA: Wolfram Media, 2002.

[27] K. Chakraborty and D. R. Chowdhury, “CSHR: Selection of cryptographically suitable hybrid cellular automata rule,” Lecture Notes in Computer Science Cellular Automata, pp. 591–600, 2012.

[28] S. Karmakar, D. Mukhopadhyay, and D. R. Chowdhury, “D-monomial tests of nonlinear cellular automata for cryptographic design,” Lecture Notes in Computer Science Cellular Automata, pp. 261–270, 2010.

[29] H. Feistel, “Cryptography and computer privacy,” Scientific American, vol. 228, no. 5, pp. 15–23, 1973.

[30] A. Rukhin, J. Sota, J. Nechvatal, M. Smid, E. Barker, S. Leigh, M. Levenson, M. Vangel, D. Banks, A. Heckert, J. Dray, and S. Vo, “A statistical test suite for random and pseudorandom number generators for cryptographic applications,” Gaithersburg, MD: U.S. Dept. of Commerce, Technology Administration, National Institute of Standards and Technology, 2000.

[31] R. Brown, D. Eddelbuettel, and D. Bauer, “Dieharder: A random number test suite,” webhome.phy.duke.edu. [Online]. Available: https://webhome.phy.duke.edu/~rgb/General/dieharder/dieharder.abs. [Accessed: Nov-2019].

[32] D. Gligoroski, “Length Extension Attack on Narrow-Pipe SHA-3 Candidates,” Communications in Computer and Information Science ICT Innovations 2010, pp. 5–10, 2011.

[33] R. D. Dean, “Formal aspects of mobile code security,” (Unpublished doctoral dissertation). Princeton University, Princeton, NJ., 1999.

[34] J. Kelsey and B. Schneier, “Second preimages on n-bit hash functions for much less than 2 n work,” Lecture Notes in Computer Science Advances in Cryptology – EUROCRYPT 2005, pp. 474–490, 2005.

[35] J. Kelsey and T. Kohno, “Herding hash functions and the nostradamus attack,” Advances in Cryptology - EUROCRYPT 2006 Lecture Notes in Computer Science, pp. 183–200, 2006.

[36] M. Wang, M. Duan, and J. Zhu, “Research on the security criteria of hash functions in the blockchain,” Proceedings of the 2nd ACM Workshop on Blockchains, Cryptocurrencies, and Contracts - BCC 18, 2018.

[37] C. Carlet, “Boolean functions for cryptography and error-correcting codes,” Boolean Models and Methods in Mathematics, Computer Science, and Engineering, pp. 257–397, 2010.

APPENDIX

Cellular automata were used for the generation mechanism of HCAHF in both the processing phase (function E) and the transformation phase (function T) as they provide some interesting features desired in cryptographic primitives. The randomness property, the maximum period and the high nonlinearity are properties are among the properties provided by cellular automata that ate well suited for cryptographic hash functions.

In this Appendix, some definitions of cryptographic properties are given. In addition, the properties of some of the rules from Wolfram class 3 and 4 used for the function E are presented. Finally, the selection process of the rules of the ruleset R_{digest}, used for the function T of the transformation phase, is detailed.

A. Definitions

Before reporting on the properties of the rules used in the function E and describing the selection process of the ruleset R_{digest}, cryptographic properties are first defined [37].

1) Affine function: An affine function is a Boolean function where only the XOR operator is allowed.

2) Hamming weight: The Hamming weight of a Boolean function corresponds to the number of 1’s in a Boolean function’s truth table.

3) Balancedness (BAL): An n variables Boolean function f is said to be balanced if its Hamming weight is 2^{n-1}.

4) Hamming distance: The Hamming distance between two functions f_1 and f_2 is defined as the Hamming weight of $f_1 \oplus f_2$.

5) Nonlinearity (NL): The nonlinearity of an *n* variables Boolean function *f* is defined as the minimum Hamming distance between *f* and all *n* variables affine functions.

6) Algebraic Degree (AD): The number of variables of the highest order term of a Boolean function determines its algebraic degree.

7) Correlation Immunity (CI): An *n* variables function *f* has correlation immunity of order *k* if its values are statistically independent of any subset of *k* input variables.

8) Resiliency (RES): A Boolean function that is both balanced and has a correlation immunity of order k is said to be a *k*-resilient function.

B. Cryptographic Properties of Class 3 and 4 ECAs

In [25], Wolfram defined four classes of elementary cellular automata. Within these four classes, rules from classes 3 and 4 are assumed to display chaotic and complex behaviors. These behaviors are well suited for cryptographic primitives and thus for cryptographic hash functions. However, some of these rules can be discarded according to their cryptographic properties. Table IX shows all the rules from class 3 and 4 along with their cryptographic properties.

TABLE. IX. CRYPTOGRAPHIC PROPERTIES OF CLASS 3 AND CLASS 4 ECAS

Rule	NL	CI	AD	RES	BAL
18	2	0	2	-1	F
22	1	0	3	-1	F
30	2	0	2	0	T
41	1	0	3	-1	F
45	2	0	2	0	T
60	0	1	1	1	T
75	2	0	2	0	T
86	2	0	2	0	T
89	2	0	2	0	T
90	0	1	1	1	T
101	2	0	2	0	T
102	0	1	1	1	T
105	0	2	1	2	T
106	2	0	2	0	T
110	1	0	3	0	F
120	2	0	2	0	T
121	1	0	3	0	F
122	1	0	3	0	F
124	1	0	3	0	F
126	2	1	2	1	F
128	1	0	3	0	F
135	2	0	2	0	T
137	1	0	3	0	F
146	1	0	3	0	F
147	2	0	2	0	T
149	2	0	2	0	T
150	0	2	1	2	T
151	1	0	3	0	F
161	1	0	3	0	F
165	0	1	1	1	T
169	2	0	2	0	T
182	1	0	3	0	F
183	1	0	2	0	F
193	1	0	3	0	F
195	0	1	1	1	T
225	2	0	2	0	T

From Table IX, the following set has been selected to be used within the processing phase in function *E*:

$R_{process}$ = {18, 22, 30, 41, 45, 60, 75, 86, 89, 90, 101, 102, 105, 106, 110, 120, 121, 122, 124, 126, 128, 135, 146, 147, 149, 150, 151, 161, 165, 169, 182, 183, 193, 195, 225}

C. Selection Process of R_{digest}

A selection procedure for choosing the right ruleset to construct a strong hybrid cellular automaton is presented in [27]. Some linear and nonlinear rules that have good cryptographic properties are shown in Table X. The rules preselected in this table were taken from a preselection process mentioned in [27]. The selection procedure guidelines are summarized in Table XI. This guideline has been proposed in [27].

TABLE. X. CRYPTOGRAPHIC PROPERTIES OF RULES

Rule	AD	NL	BAL	CI
22	7	45	No	1
30	5	40	Yes	1
37	7	49	No	0
41	7	44	No	1
43	5	44	Yes	0
45	4	40	Yes	1
60	1	0	Yes	3
90	1	0	Yes	3
91	7	49	No	0
102	1	0	Yes	3
105	1	0	Yes	4
110	6	38	No	1
120	5	48	Yes	0
135	5	48	Yes	2
150	1	0	Yes	4
165	1	0	Yes	3
180	4	32	Yes	1
195	1	0	Yes	3
210	4	32	Yes	0

TABLE. XI. SELECTION PROCESS FOR THE RULESET

<u>Input:</u> Set L = {60,90,102,105,150,165,195} of linear rules and set NL = {22,30,37,41,43,45,91,110,120,135,180,210} of nonlinear rules

Principle	Choice
For the first cell, pick a nonlinear rule with good cryptographic properties.	Rule 30 selected **[30]**
An equal number of linear and nonlinear rules should be selected for the remaining cells to find a compromise between the algebraic degree and the correlation immunity.	Rules 60, 90 and 135 selected **[30,60, 135,90]**
Two or three nonlinear rules should appear consecutively to increase the algebraic degree.	Rule 30 followed by rule 135 **[30,60,30,135,90]**
One nonlinear rule should be followed by more than one linear rule to increase the order of correlation immunity.	Rule 30 followed by rules 60 and 90 **[30,60,90,30,135,30,60,90]**
Rules with larger period should be chosen to increase the period of the hybrid CA.	Rules 90 and 150 selected **[30,90,150,30,135,30,90,150]**

<u>OUTPUT:</u> A RULESET WITH RULES HAVING GOOD CRYPTOGRAPHIC PROPERTIES [30,90,150,30,135,30,90,150].

Classification Performance of Violence Content by Deep Neural Network with Monarch Butterfly Optimization

Ashikin Ali[1], Norhalina Senan[2]
Faculty of Computer Science and Information Technology, Universiti Tun Hussein Onn Malaysia
Parit Raja, Malaysia

Iwan Tri Riyadi Yanto[3]
Faculty of Mathematics and Natural Sciences, Ahmad Dahlan University
Yogyakarta, Indonesia

Saima Anwar Lashari[4]
College of Computing and Informatics
Saudi Electronic University
Dammam, Kingdom of Saudi Arabia

***Abstract*—Violence is self-sufficient, it is perplexing due to visibility of content dissimilarities among the positive instances that been displayed on media. Besides, the ever-increasing demand on internet, with various types of videos and genres, causes difficulty for a proper search of these videos to ensure the contents is humongous. It involves in aiding users to choose movies or web videos suitable for audience, in terms of classifying violence content. Nevertheless, this is a cumbersome job since the definition of violence is broad and subjective. Detecting such nuances from videos becomes technical without a human's supervision that can lead to conceptual problem. Generally, violence classification is performed based on text, audio, and visual features; to be precise, it is more relevant to use of audio and visual base. However, from this perspective, deep neural network is the current build-up in machine learning approach to solve classification problems. In this research, audio and visual features are learned by the deep neural network for more specific violence content classification. This study has explored the implementation of deep neural network with monarch butterfly optimization (DNNMBO) to effectively perform the classification of the violence content in web videos. Hence, the experiments are conducted using YouTube videos from VSD2014 dataset that are publicly available by Technicolor group. The results are compared with similar modified approaches such as DNNPSO and the original DNN. The outcome has shown 94% of violence classification rate by DNNMBO.**

Keywords*—Deep learning; monarch butterfly; violence video; classification

I. Introduction

Sensible content filtering of media is necessary, as the multimedia content is affecting the internet users significantly. Eventually, every user can provide and be exposed to sensitive media contents over the internet. One sensitive media content type is violence. Through unlimited hours of video being uploaded every day over the internet, the access is by considerable portion of internet users with limited control [1]. Subjective characterization of violence makes impenetrable the violence content displayed based on audio signals, like screams or gunshots. This situation may result in harmful situation to users either mentally or physically. It is evident that numerous web-filtering systems are highly available on internet. Yet, these approaches did not meet user needs to accurately classify violence content that is exposed on internet or social media. To resolve this drawback, artificial neural network will be a feasible solution and has been an efficient method to classify violence content [2],[3],[4]. Currently, Deep neural network (DNN) technique is broadly used for video classification tasks [5],[6],[7],[8],[9],[10]. There are few drawbacks of DNN that it still faces issue regarding complex architecture, specifically on multiple hidden layers, high tendency to get trapped in local minima; moreover, it is also computationally exhaustive. In the long run to ensure DNN perform reliably, big or ample amount of data is required to avoid overfitting [11],[12]. To combat this deficiency, optimization techniques are constantly considered as a solution to this problem. In the relevant literature, these are communal, especially using several optimization algorithms, namely, particle swarm optimization (PSO), chicken swarm optimization (CSO), firefly optimization (FO), whale optimization algorithm (WOA) on deep learning algorithms [13]. Meanwhile, monarch butterfly optimization (MBO) was proposed by Gai-Ge Wang [33], is a new nature-based metaheuristic algorithm, it is carried out by studying the migration behavior of monarch butterflies. Researchers have conducted a comparative study of the performance of MBO with other metaheuristic algorithms, which has shown promising performances [14]. The inspiring simple and robust nature of the algorithm with the ability to deal with the stirring between exploration and exploitation has given strength to the choice. This has motivated this study to embed the MBO with DNN in order to improve the performance accuracy based on the accuracy, precision and recall. From the dataset perspective, researchers focus on audio features [15][16], audio-visual features [17],[18],[19], inter feature and inter-classes [20], multimodal features [21] and exploiting feature and class relationships [22]. Thus, in this study, both the audio-visual features and all the attributes of the features have been used to feed into the proposed classifier.

The paper organized as follows: Section II highlights research methodology adopted to perform this study. Section III proposes the DNN in integration with MBO. The results are reported and discussed in last section of the paper; duly concludes this study, as well as, provides potential research direction.

II. Research Motivation

In line with the literature review, violence could define any circumstances that can cause harm physically or mentally to single or many users. For specific problem on audio signals, the related literature is very limited, and, mostly, it examines audio features and visual features (Krizhevsky, 2012; Dai *et. al.*, 2015) separately. Complex models trained with insufficient data can be prone to overfitting (Caruana, 2001; Shin, 2016; Cortes, 2017). This study intended to examine both the audio and visual features that calculates 68, 830 data instances ensuring it to perform reliably to achieve the violence classification task.

From a computational perspective, as an advantage with Deep Neural Network (DNN) to its supremacy in terms of accuracy is trained with huge amount of data. However, primary drawbacks of using DNN have been identified from its substantial complexity, which require extensively long periods of training time. These are due to nature of its architecture which consist of trillions hidden layers and hidden nodes depends on the loaded input (Bou-Rabee *et. al.*, 2017). Hence, it may cause the algorithm to be stuck at local minima or global minimum. Initially, this research decided to focus to overcome the local minima drawback. Optimization has always been a solution to this problem. However, the implementations are widely used for non-convex (Cortes, 2017), hyper-parameters (Albelwi, 2017), weights (Kietzmann, 2018). Thus, to mitigate the issue this study decided to improve DNN algorithm by optimizing the weights using Monarch Butterfly Optimization (MBO) Algorithm to further reduce the error to an acceptable minimum fitness to improve the classification accuracy. Whereby the initial weighting factor of MBO algorithm proposed by Gai Ge Wang (2015) is $\alpha = S_{max}/t^2$. This study has come to consent that modifying the weighting factor to $\alpha = S_{min}/t^2$ will enable to achieve the goal of minimalize the errors and obtain satisfying accuracy.

III. Research Methodology

A. Research Framework

The five main phases of the proposed methodology are, namely, data acquisition, feature extraction, data pre-processing, classification and classified output, illustrated according to the experimental need. Fig. 1 is the research design of the study.

As a domain in this study, benchmark violence scene dataset (VSD2014) is acquired from Technicolor Group [23][24]. In the whole, the generalization subset of 86 videos have been used but reduced to a meaningful instance to ensure suitability with the available devices. The videos are downloaded from YouTube and are normalized to a frame rate of 25fps (Fig. 2). This dataset contains two classes: 1 represents violence and 0 represents non-violence, respectively.

In pre-processing stage, features were extracted consisting of 29 audio and 405 visual features by total of 434 instances as the input to the network. The data were intertwined with missing values, those missing values were imputed using the ReplaceMissingValues filters from WEKA. By steering this process, it provides eloquent dataset for the learning algorithm, normalized and segregated to provide meaningful dataset for the network.

Classification phase evolves the modified DNNMBO. The optimization process during the training part of deep neural network is performed using MBO algorithm to optimize the weights in DNN to classify the violence content. Performance evaluation is based on the classification metrics like precision, recall and accuracy.

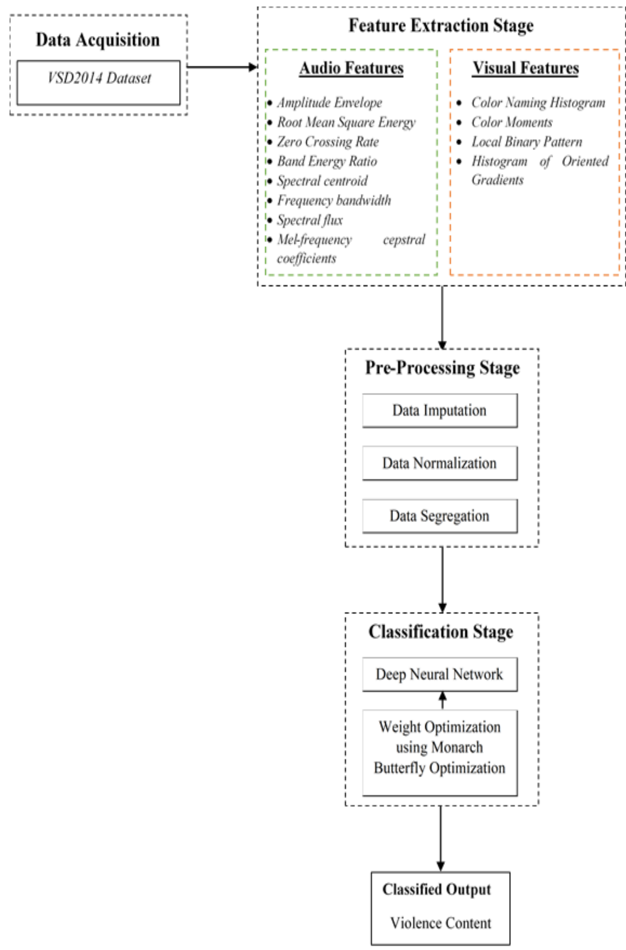

Fig. 1. Methodology of the Study.

Fig. 2. Example Images from the VSD2014 Dataset.

B. Deep Neural Network

The backpropagation is a supervised learning algorithm, acute part of layered feed-forward deep neural network, provided with the inputs and outputs that the network must compute, afterwards calculate the error [25]. Backpropagation algorithm is aware to reduce this error, until the DNN (Fig. 3) learns the training data. The training will begin with random weights till optimized, and the goal is to adjust them so that the error is minimal. The weighted sum of a neuron is written as Equation (1):

$$A_j(x,w) = \sum_{i-0}^{n} X_i\, W_{ji}, \tag{1}$$

where the sum of input X_i is multiplied by their respective weights W_{ji}. If the output function is the identity, then the neuron is called linear. The most used output function is sigmoid function [26], as formulated by Equation (2):

$$O_j(x,w) = \frac{1}{1+e^{-A(x,w)}} \tag{2}$$

The sigmoid function allows a smooth transition between the low and high output of the neuron. The output depends on the activation, which in turn depends on the values of the inputs and their respective weights. The target is to obtain a desired output based on the input given. Since the error is the difference between the actual and desired output, it depends on the weights and preferred to be adjusted to minimize. The error function for the output of each neuron defined as in Equation (3):

$$E_j(x,w,d) = \left(O_j(x,w) - d_j\right)^2 \tag{3}$$

The desired target will be greater when the diffirence is big and lesser, the output considered positive. The error of the network will simply be the sum of the errors of all the neurons in the output layer as in Equation (4):

$$E(x,w,d) = \sum_j \left(O_j(x,w) - d_j\right)^2 \tag{4}$$

where $O_j$is the output and $d_j$is the desired output of the experiment. Afterwards, the weights will be adjusted using the method of gradient descent, Equation (5):

$$\Delta w_{ji} = -\eta \frac{\partial E}{\partial w_{ji}} \tag{5}$$

The Equation (5) infer the adjustments of each weight (Δw_{ji}) will be the negative of a constant eta (η), while η is the learning rate. The size of the adjustment rely on η, and derivative of E in respect to w_{ji} discovered. Initially, the error is dependent on the output, which is the derivative of E in respect to O_j from Equation (3).

$$\frac{\partial E}{\partial O_j} = 2\left(O_j - d_j\right) \tag{6}$$

As of Equation (1) and Equation (2), will alter the output of the activation. That can be seen from Equation (6) and Equation (7):

$$\frac{\partial O_j}{\partial w_{ji}} = \frac{\partial O_j}{\partial A_j}\frac{\partial A_j}{\partial w_{ji}} = O_j\left(1 - O_j\right)x_i \tag{7}$$

$$\frac{\partial E}{\partial w_{ji}} = \frac{\partial E}{\partial O_j}\frac{\partial O_j}{\partial w_{ji}} = 2\ \left(O_j - d_j\right)O_j\left(1 - O_j\right)x_i \tag{8}$$

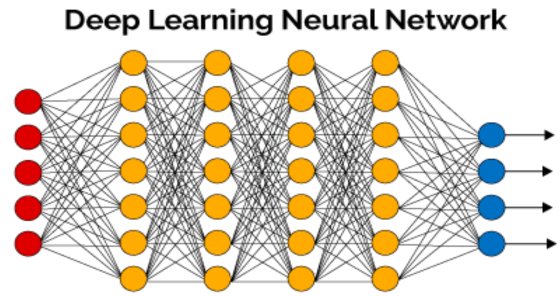

Fig. 3. Architecture of Deep Neural Network.

The adjustment to each weight will begin from Equation (5) and Equation (8):

$$\Delta w_{ji} = -2\eta\left(O_j - d_j\right)O_j\left(1 - O_j\right)x_i \tag{9}$$

Equation (9) can be used as it is for training DNN. These processes clearly visualized in the following architecture of DNN:

The fact that different deep learning networks in general from the common feed-forward multilayer networks that DNN have many hidden layers that are hard to train. More neurons than previous networks and complex way of connecting layers [27],[28]. With backpropagation inside, the errors are sent back through the network again and weights are adjusted to improve the model. This process is constant by adjusting the weights until the error rate cannot be reduced any more. During this process the layers learn the optimal features for the model which derives to learn the optimal weights.

C. Monarch Butterfly Optimization (MBO)

In MBO [29], the spots of the monarch butterflies are updated in two ways. Initially, the offspring are generated to update position by migration operator, which can be adjusted by the migration ratio. Tailed through tuning the positions for other butterflies by means of butterfly adjusting operator. To minimize fitness evaluations and keep the population consistent, the original population and the amount of newly generated butterflies endures equal to the original population which later will be divided into two depending on the fitness. The number of monarch butterflies in land$_1$ and land$_2$ are calculated as subpopulation1 (NP_1) = ceil (p*NP)(NP_1) and subpopulation2 (NP_2) = $NP - NP_1$, respectively, where 'p' is the migration ratio. The positions of monarch butterfly individuals are updated using migration operator (MO) and butterfly adjusting operator (BAO). Next section explains the process of DNNMBO.

IV. Deep Neural Network with Monarch Butterfly Optimization (DNNMBO)

A. Butterfly Adjusting and Migration Operator

Meanwhile, MBO is a latest metaheuristic algorithm, and undoubtedly, it has shown better performance on benchmark evaluation [30],[31],[35]. Hence, this has become a motivation for this study to improve the DNN with MBO. As for migration operator (MO), the offspring are generated to update the position in NP1 by MO and adjust based on ratio of monarch butterflies in land$_1$. The position of each butterfly from NP1 is based on individuals from NP1 and NP2. This initialization aids on finding the optimum weights to provide best error rate and performance accuracy of DNNMBO.

B. Proposed DNNMBO

The initialization of DNNMBO, selected monarch butterflies are considered as $mb_1$and mb_2 from NP1 and NP2 respectively. Meanwhile, $r = rand * peri$, where $rand$ is random number between [0,1] and *peri* is the migration period. Fig. 4 visualizes the implementation process of DNNMBO.

Each one mb_i from the population of *NP* is represented as given as Equation (10):

$$mb_i = \{ w_{i,} b_i \} \tag{10}$$

where $w_{i,}$ denotes the weights of input and hidden layer, b_i denotes bias for hidden layer and output neuron. These weights and biases fulfil the criteria of butterfly positions in the network. The performance is based on the entire training data of size *n*. The MSE is calculated as in Equation (11). Hence the fitness function, *FEs*, of MBO is the average MSE of the entire training set, which is formulated as:

$$Minimise\ FEs = \sum_{j=1}^{n} \frac{E_j}{j} \tag{11}$$

To visualize the proposed DNNMBO, the Algorithm shows the process of DNN training by MBO.

Based on the above clarifications, it is believed that the proposed DNNMBO promises better outcome with best global optimum of 50 generations.

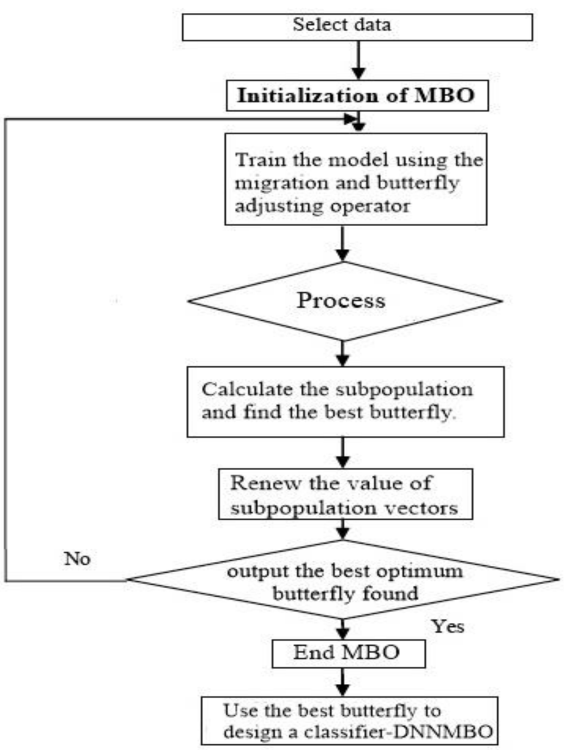

Fig. 4. Flowdiagram of Proposed DNNMBO.

Algorithm: Monarch Butterfly Optimization based training of Deep Neural Network

Step 1: Input *X* denotes n samples, *O* as output the maximum selected attributes.

Step 2: While weights of hidden and input layers updated.

Step 3: Set the population of monarch butterfly individuals NP which is the **weight factors of deep neural networks,** $W_{ji,}$ **where the adjustmen is as in Equation 5 to Equation 8**, randomly in [-1,1], set MaxGen, *NP1* in Land 1 and *NP2* in Land 2, max step is the BAR, *peri* and ratio *p*.

Step 4: for randomly generate numbers by uniform distribution, *mb*<*p* **from** subpopulation 1 monarch butterfly randomly selected **else** select monarch butterfly in subpopulation 2 **end if.** Evolves in Migration Operator.

Step 5: for each monarch butterflies in subpopulation 2 **do** calculate the walk step, calculate the weighting factor $S_{max} = 1.0$ **for** randomly generate by uniform distribution, , **if** *mb*<*p* **then** best monarch butterfly is chosen, **else** randomly select monarch butterfly in subpopulation 2 **end if**.

Step 6: Combine two newly generated subpopulation into one whole population. **Evaluate** monarch butterfly according newly updated positions. The process that evolves weight adjustments in the network.

Step 7: If best solution is not found, butterfly individuals sorted according the fitness. **end If**

Step 8: Finally, gives the best **Output** of weight vector for deep neural network, for best solution.

V. Results and Discussion

A. Experimental Design

The proposed model and similar comparison models are simulated using MATLAB R2016a on MacPro 6, macOS High Sierra operating system, the processor is 8 Core Intel Xeon E5 with the speed of 3 GHz and 32GB RAM.

B. Simulation Results

The experiment is conducted with 5-fold cross validation method [32],[33],[34]. With important parameters of initial momentum of 0.5 and final momentum of 0.9, weight cost of 0.0002. Meanwhile, to obtain optimum weights and biases to present best accuracy, based on [35], the MBO parameters were set as $S_{max} = 1.0$, peri = 1.2, and maximum generation = 50. In the result tables, Tables I to V summarizes the results that have been obtained from different hidden layers. These experiments are simulated using the VSD2014 dataset as the focus domain is on violence classification.

The efficiency of the proposed technique has been thoroughly tested with different hidden layers. This has shown the efficiency of the proposed technique, furthermore able to classify the data correctly at satisfying classification rate of 94% with hidden layer 5 with precision of 0.4471 and recall of 0.8892. It is believed that these parameters and arrangements are appropriate for the classification of violence content in VSD2014 dataset.

TABLE. I. RESULT OF COMPARISONS WITH 3 HIDDEN LAYERS

Approach	Precision	Recall	Acc.	Inc.
DNNMBO	0.5004	0.469	49.98%	50.02%
DNNPSO	0.4947	0.5472	48.60%	51.40%
DNN	0.4638	0.4638	46.29%	53.70%

TABLE. II. RESULT OF COMPARISONS WITH 4 HIDDEN LAYERS

Approach	Precision	Recall	Acc.	Inc.
DNNMBO	0.696	0.702	70.35%	29.65%
DNNPSO	0.5023	0.447	58.67%	41.33%
DNN	0.4856	0.4856	48.57%	51.43%

TABLE. III. RESULT OF COMPARISONS WITH 5 HIDDEN LAYERS

Approach	Precision	Recall	Acc.	Inc.
DNNMBO	0.4471	0.8892	94%	6%
DNNPSO	0.5667	0.6415	75.22%	24.78%
DNN	0.5242	0.5242	52.57%	47.43%

TABLE. IV. RESULT OF COMPARISONS WITH 6 HIDDEN LAYERS

Approach	Precision	Recall	Acc.	Inc.
DNNMBO	0.788	0.631	80.30%	19.70%
DNNPSO	0.5318	0.5222	73.50%	26.50%
DNN	0.5378	0.5374	53.71%	46.29%

TABLE. V. RESULT OF COMPARISONS COMPARISON WITH 7 HIDDEN LAYERS

Approach	Precision	Recall	Acc.	Inc.
DNNMBO	0.5972	0.7963	60.00%	40.00%
DNNPSO	0.5004	0.469	53.58%	46.42%
DNN	0.4571	0.5	45.71%	54.29%

VI. CONCLUSION

As a conclusion, this study implemented MBO optimization algorithm in integration with DNN in favor to enhance the accuracy rate of the conventional DNN. From the conventional DNN, researcher learned that untreated data can be a reason of inefficacy of performance. Thus, in this approach, the data is treated especially on missing values problem and modification of DNN with optimization algorithm has seen the desired outcome. Hence, implementation of monarch butterfly optimization (MBO) algorithm with DNN has contributed in the improvement of the accuracy as it is compatible to each other. As a summary, this employment of DNNMBO considered suitable for violence classification domain.

As a potential research direction, the proposed technique can also be tested with other violence datasets or other focus domain; multiple classifications with more meaningful features, such as using features ranks or feature selection. It is advisable to improve on the weighting factor of monarch butterfly optimization $S_{max} = 1.0$ to MinStep.

ACKNOWLEDGMENT

This research is fully funded by Ministry of Higher Education (MOHE) under the Fundamental Research Grantt Scheme (FRGS) – Vot. No. 1608; in part supported by Research Management Center (RMC), UTHM.

REFERENCES

[1] Cantor, J. (2000). Media violence. Journal of adolescent health, 27(2), 30-34.

[2] Peixoto, B. M., Avila, S., Dias, Z., & Rocha, A. (2018, August). Breaking down violence: A deep-learning strategy to model and classify violence in videos. In Proceedings of the 13th International Conference on Availability, Reliability and Security (p. 50). ACM.

[3] Fenil, E., Manogaran, G., Vivekananda, G. N., Thanjaivadivel, M., Jeeva, S., & Ahilan, A. (2019). Real time Violence Detection Framework for Football Stadium comprising of Big Data Analysis and Deep Learning through Bidirectional LSTM. Computer Networks.

[4] Sudhakaran, S., & Lanz, O. (2017). Convolutional long short-term memory networks for recognizing first person interactions. In Proceedings of the IEEE International Conference on Computer Vision (pp. 2339-2346).

[5] Yue-Hei Ng, J., Hausknecht, M., Vijayanarasimhan, S., Vinyals, O., Monga, R., & Toderici, G. (2015). Beyond short snippets: Deep networks for video classification. In Proceedings of the IEEE conference on computer vision and pattern recognition (pp. 4694-4702).

[6] Simonyan, K., & Zisserman, A. (2014). Two-stream convolutional networks for action recognition in videos. In Advances in neural information processing systems (pp. 568-576).

[7] Wu, Z., Jiang, Y. G., Wang, J., Pu, J., & Xue, X. (2014, November). Exploring inter-feature and inter-class relationships with deep neural networks for video classification. In Proceedings of the 22nd ACM international conference on Multimedia (pp. 167-176). ACM.

[8] Ngiam, J., Khosla, A., Kim, M., Nam, J., Lee, H., & Ng, A. Y. (2011). Multimodal deep learning. In Proceedings of the 28th international conference on machine learning (ICML-11) (pp. 689-696).

[9] Parkhi, O. M., Vedaldi, A., & Zisserman, A. (2015, September). Deep face recognition. In bmvc (Vol. 1, No. 3, p. 6).

[10] Levi, G., & Hassner, T. (2015). Age and gender classification using convolutional neural networks. In Proceedings of the IEEE Conference on Computer Vision and Pattern Recognition Workshops (pp. 34-42).

[11] LeCun, Y., Bengio, Y., & Hinton, G. (2015). Deep learning. nature, 521(7553), 436.

[12] EnterpriceTech, https://www.enterprisetech.com/2017/07/10/deep-neural-networks-not-use/.

[13] Fathollahi-Fard, A. M., Hajiaghaei-Keshteli, M., & Tavakkoli-Moghaddam, R. (2018). The social engineering optimizer (SEO). Engineering Applications of Artificial Intelligence, 72, 267-293.

[14] Wang, GG., Deb, S. & Cui, Z. Neural Comput & Applic (2015). Monarch Butterfly Optimization. Neural Computing & Applications, https://doi.org/10.1007/s00521-015-1923-y.

[15] Giannakopoulos, T., Kosmopoulos, D., Aristidou, A., & Theodoridis, S. (2006, May). Violence content classification using audio features. In Hellenic Conference on Artificial Intelligence (pp. 502-507). Springer Berlin Heidelberg.

[16] Mu, G., Cao, H., & Jin, Q. (2016, November). Violent Scene Detection Using Convolutional Neural Networks and Deep Audio Features. In Chinese Conference on Pattern Recognition (pp. 451-463). Springer Singapore.

[17] Mironică, I., Duţă, I. C., Ionescu, B., & Sebe, N. (2016). A modified vector of locally aggregated descriptors approach for fast video classification. Multimedia Tools and Applications, 75(15), 9045-9072.

[18] Ali, A., & Senan, N. (2016, August). A Review on Violence Video Classification Using Convolutional Neural Networks. In International Conference on Soft Computing and Data Mining (pp. 130-140). Springer, Cham.

[19] Dai, Q., Wu, Z., Jiang, Y. G., Xue, X., & Tang, J. (2014, October). Fudan-NJUST at MediaEval 2014: Violent Scenes Detection Using Deep Neural Networks. In MediaEval.

[20] Wu, Z., Jiang, Y. G., Wang, J., Pu, J., & Xue, X. (2014, November). Exploring inter-feature and inter-class relationships with deep neural networks for video classification. In Proceedings of the 22nd ACM international conference on Multimedia (pp. 167-176). ACM.

[21] Wu, Z., Jiang, Y. G., Wang, J., Pu, J., & Xue, X. (2014, November). Exploring inter-feature and inter-class relationships with deep neural networks for video classification. In Proceedings of the 22nd ACM international conference on Multimedia (pp. 167-176). ACM.

[22] Jiang, Y. G., Wu, Z., Wang, J., Xue, X., & Chang, S. F. (2015). Exploiting feature and class relationships in video categorization with regularized deep neural networks. arXiv preprint arXiv:1502.07209.

[23] Zhang, B., Yi, Y., Wang, H., & Yu, J. (2014, October). MIC-TJU at MediaEval Violent Scenes Detection (VSD) 2014. In MediaEval.

[24] Schedi, M., Sjöberg, M., Mironică, I., Ionescu, B., Quang, V. L., Jiang, Y. G., & Demarty, C. H. (2015, June). Vsd2014: a dataset for violent scenes detection in hollywood movies and web videos. In Content-Based Multimedia Indexing (CBMI), 2015 13th International Workshop on (pp. 1-6). IEEE.

[25] Hecht-Nielsen, R. (1992). Theory of the backpropagation neural network. In Neural networks for perception (pp. 65-93).

[26] Fenil, E., Manogaran, G., Vivekananda, G. N., Thanjaivadivel, M., Jeeva, S., & Ahilan, A. (2019). Real time Violence Detection Framework for Football Stadium comprising of Big Data Analysis and Deep Learning through Bidirectional LSTM. Computer Networks.

[27] Hinton, G., Deng, L., Yu, D., Dahl, G. E., Mohamed, A. R., Jaitly, N., ... & Kingsbury, B. (2012). Deep neural networks for acoustic modeling in speech recognition: The shared views of four research groups. IEEE Signal processing magazine, 29(6), 82-97.

[28] Towards Data Science. (2017). The 10 Deep Learning Methods AI Practitioners Need to Apply. Available: https://towardsdatascience.com/the-10-deep-learning-methods-ai-practitioners-need-to-apply-885259f402c1

[29] Wang, Gai-Ge & Deb, Suash & Cui, Zhihua. (2015). Monarch Butterfly Optimization. Neural Computing and Applications. 10.1007/s00521-015-1923-y.

[30] Wang, Gai-Ge & Deb, Suash & Cui, Zhihua. (2015). Monarch Butterfly Optimization. Neural Computing and Applications. 10.1007/s00521-015-1923-y.

[31] Wang G-G, Zhao X, Deb S (2015c) A novel monarch butterfly optimization with greedy strategy and selfadaptive crossover operator. Paper presented at the 2015 2nd international conference on soft computing & machine intelligence (ISCMI 2015), Hong Kong, Nov 23–24.

[32] Piczak, K. J. (2015, September). Environmental sound classification with convolutional neural networks. In 2015 IEEE 25th International Workshop on Machine Learning for Signal Processing (MLSP) (pp. 1-6). IEEE.

[33] Shin, H. C., Roth, H. R., Gao, M., Lu, L., Xu, Z., Nogues, I., ... & Summers, R. M. (2016). Deep convolutional neural networks for computer-aided detection: CNN architectures, dataset characteristics and transfer learning. IEEE transactions on medical imaging, 35(5), 1285-1298.

[34] Kipf, T. N., & Welling, M. (2016). Semi-supervised classification with graph convolutional networks. arXiv preprint arXiv:1609.02907.

[35] G.G. Wang, S. Deb, Z.H. Cui, Monarch butterfly optimization, Neural Comput. Appl. (2015) http://dx.doi.org/10.1007/s00521-015-1923-y.

Object Detection and Tracking using Deep Learning and Artificial Intelligence for Video Surveillance Applications

Mohana[1]
Department of Electronics and Communication Engineering,
RV College of Engineering® Bengaluru- 560059 and
affiliated to Visvesvaraya Technological University,
Belagavi Karnataka, India

HV Ravish Aradhya[2]
Department of Electronics and Communication Engineering,
RV College of Engineering®, Bengaluru- 560059 and
affiliated to Visvesvaraya Technological University,
Belagavi, Karnataka, India

***Abstract*—Data is the new oil in current technological society. The impact of efficient data has changed benchmarks of performance in terms of speed and accuracy. The enhancement is visualizable because the processing of data is performed by two buzzwords in industry called Computer Vision (CV) and Artificial Intelligence (AI). Two technologies have empowered major tasks such as object detection and tracking for traffic vigilance systems. As the features in image increases demand for efficient algorithm to excavate hidden features increases. Convolution Neural Network (CNN) model is designed for urban vehicle dataset for single object detection and YOLOv3 for multiple object detection on KITTI and COCO dataset. Model performance is analyzed, evaluated and tabulated using performance metrics such as True Positive (TP), True Negative (TN), False Positive (FP), False Negative (FN), Accuracy, Precision, confusion matrix and mean Average Precession (mAP). Objects are tracked across the frames using YOLOv3 and Simple Online Real Time Tracking (SORT) on traffic surveillance video. This paper upholds the uniqueness of the state of the art networks like DarkNet. The efficient detection and tracking on urban vehicle dataset is witnessed. The algorithms give real-time, accurate, precise identifications suitable for real-time traffic applications.**

Keywords*—Artificial Intelligence (AI); Computer Vision (CV); Convolution Neural Network (CNN); You Look Only Once (YOLOv3); Urban Vehicle Dataset; Common objects in Context (COCO); Object detection; object tracking

I. Introduction

Over the past years domains like image analysis and video analysis has gained a wide scope of applications. CV and AI are two main technologies dominating technical society. Technologies try to depict the biology of human. Human vision is the sense through which a perception of outer 3D world is perceived. Human Intelligence is trained over years to distinguish and process scene captured by eyes. These intuitions acts as a crux to budding new technologies. Rich resource is now accelerating researchers to excavate more details form the images. These developments are due to state-of the-art methods like CNN. Applications from Google, Facebook, Microsoft, and Snapchat are all results of tremendous improvement in Computer vision and Deep learning. During time, the vision-based technology has transformed from just a sensing modality to intelligent computing systems which can understand the real world. Computer vision applications like vehicle navigation, surveillance and autonomous robot navigation find Object detection and tracking as important challenges. For tracking vehicles and other real word objects, video surveillance is a dynamic environment. In this paper, efficient algorithm is designed for object detection and tracking for video Surveillance in complex environment.

Object detection and tracking goes hand in hand for computer vision applications. Object detection is identifying object or locating the instance of interest in-group of suspected frames. Object tracking is identifying trajectory or path; object takes in the concurrent frames. Image obtained from dataset is, collection of frames. Basic block diagram of object detection and tracking is shown in Fig. 1. Data set is divided into two parts. 80 % of images in dataset are used for training and 20 % for testing. Image is considered to find objects in it by using algorithms CNN and YOLOv3. A bounding box is formed across object with Intersection over union (IoU) > 0.5. Detected bounding box is sent as references for neural networks aiding them to perform Tracking. Bounded box is tracked in concurrent frames using Multi Object Tracking (MOT). Importance of this research work is used to estimate traffic density in traffic junctions, in autonomous vehicles to detect various kinds of objects with varying illumination, smart city development and intelligent transport systems [18]. Organization of paper is, Section II identifies research gap through extensive literature survey. Section III covers Fundamental Concepts of Object detection and Tracking. Section IV describes design, implementation details and specifications. Section V discusses simulation results and analysis. Section VI describes conclusions and future scope.

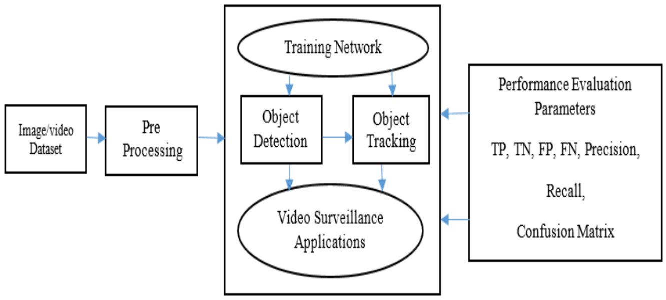

Fig. 1. Block Diagram of Object Detection and Tracking.

II. Literature Survey

Adopting Tile convolution neural network and recursive mode of same network helps in finding objects aiding applications for Driver assistance systems (DAS). Approach includes unsupervised training to help learn and modulate weights based on wide range of training data. Obstacle validation algorithms are included to reduce the count of valid detections [1]. Concepts like Optical flow and Histogram of magnitudes is used to analyze motion of objects, which are not evident to bare eyes. Detection of normal and abnormal events is achieved by classification and localization helping campus environment to differentiate between normal and abnormal events [2]. Features are extracted using pretrained network; classified results are differentiated using SVM. Approach helps in guiding the route for ITS [3]. Many approaches like feature extraction based on color and gradients fail to give spatial positioning in the image. The challenges are overcome by employing Analysis of principal components by PCANet [4] pipeline of image undistortion, image registration, classification and detections based on coordinates and velocities. Approach uses detectors like FAST, FREAK descriptors and followed by classification of Squeeze Net [5]. The workflow of candidate target generation, extracting features from candidate targets, the ground truth boxes around objects assist in tracking. The objects are classified using VGGNet [6]. CNN was designed to classify images, was repurposed to perform the object detection. The approach treats object detection as a relapse for object class to bounding objects detected. Series of gradual improvements has been witnessed from RCNN, Fast RCNN and faster RCNN then finally to YOLO. Instead of assessing image repetitively as in CNN, image is scanned once for all, thereby increasing the processing of frames per second (fps). YOLO is trained based on loss occurred unlike the traditional Classification approach [7]. Paper describes about video analytics part for road traffic. One of main application area apart from vehicle detection and tracking is vehicle counting. One of the novel algorithm called Single Shot Detector (SSD) is employed. Algorithm handles features like Binary large objects. It gives better results in applications like classification of objects. Object tracking employs concepts like background subtraction and virtual coil method. In terms of precision SSD outperforms YOLO versions. Swiftness and precision are always tradeoffs while selecting the right algorithm for object detection with the speed of 58fps performance metric for accuracy exceeds 85% [8], paper explains about upgradation to YOLO was made in the paper. Gradual updating has been witnessed throughout series of YOLO versions namely YOLOv1, YOLOv2, YOLOv3. YOLOv3 is state of the art technology. Upgradation such as thinner bounding boxes without affecting adjacent pixels. YOLOv3's implementation on COCO dataset shows mAP as good as SSD. YOLOv3 gives three times faster results. YOLOv3 promises in detecting smaller objects [9]. With increase in vehicle density in urban region, Single object tracking will no longer cater for the need. Multi object tracking is achieved by employing kernelized correlation filter (KCF). Many KCF are run in parallel. KCF is best suited when images have occlusions. KCF when combined with background subtraction yield reliable results on the urban traffic [10] [12] [14].

Deep Networks require more computer power and time, more data, better performance of Neural Nets. The success of any algorithm lies in parameter tuning. Algorithms are application specific. Fine-tuning of state of the art Neural Nets decreases training time while increasing accuracy. Results are dependent on dataset used, algorithm and network employed.

III. Object Detection and Tracking

There is a wide range of computer vision tasks benefiting society such as object classification, detection, tracking, counting, Semantic Segmentation, Captioning image, etc. Process of identifying objects in an image and finding its position is known as object detection.

Various object detection tasks as shown in Fig. 2. With advancements in field of computer vision assisted by AI, realization of tasks was realizable along t time scale. Semantic segmentation task of clustering pixels based on similarities. Classification + Localization and object detection method of identifying class of object and drawing a bounding box around it to make it distinct. Instance segmentation is semantic segmentation applied to multi objects. The general intuition to perform the task is to apply CNN over the image. CNN works on image patches to carry out the task many such salient regions can be obtained by Region-Proposal Networks like Region Convolution Neural network (RCNN), Fast- Region Convolutional Neural Network (Fast-RCNN), Faster- Region Convolutional Neural Network (Faster-RCNN). To perform selective search for object recognition Hierarchal Grouping Algorithm is used. Few bottlenecks by these approaches are mitigated by state-of the-art algorithms like You Only Look Once (YOLO), Single shot Detector (SSD). The efficient object detection algorithm is one which assures to give bounding box to all objects of vivid size to be recognized, with great computational capabilities, faster processing. YOLO and SSD assure to render promising results, but have a tradeoff between speed and accuracy. Hence, selection of algorithm is application specific [15].

A. Convolutional Neural Networks (CNN)

CNN is widely used neural network architecture for computer vision related tasks. Advantage of CNN is that it automatically performs feature extraction on images i.e. important features are detected by the network itself.

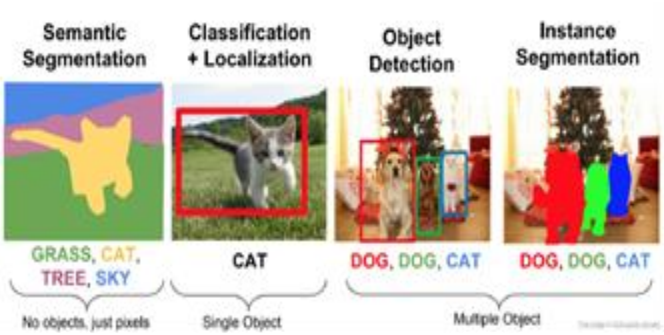

Fig. 2. Object Detection Tasks [7].

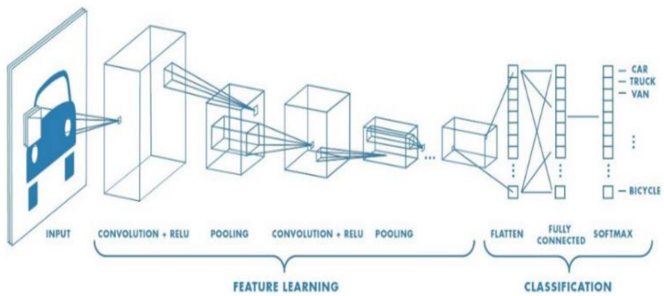

Fig. 3. Overview of CNN Architecture [2].

CNN is made up of three important components called Convolutional Layer, Pooling layer, fully connected Layer as shown in Fig. 3. Considering a gray scale image of size 32*32 would have 1024 nodes in multi-layer approach. This process of flattening pixels loses spatial positions of the image. Spatial relationship between picture elements is retained by learning internal feature representation using small squares of input data.

1) Convolutional layer: Convolutional Layer encompasses filters and feature maps. Filters are processors of a particular layer. These filters are distinct from one another. They take pixel value as input and gives out feature Map. Feature map is output of one filter layer. Filter is traversed all along the image, moving one pixel at a time. Activation of few neurons takes place resulting in a feature map.

2) Pooling layer: Pooling layer is employed to reduce dimensionality. Pooling layers are included after one or two convolutional layer to generalize features learnt from previous feature maps. This helps in reducing chances of over fitting from training process.

3) Fully connected layer: Fully connected layer is used at the end to assign the feature to class probability after extracting and consolidating features from Convolutional Layer and pooling later respectively. These layers use linear activation functions or softmax activation function.

B. You Only Look Once (YOLOv3)

YOLO version 1 and 2 applies softmax functions convert score into probabilities. This approach is feasible when objects are mutually exclusive only. YOLOv3 employs multi label classification. Independent logistic classifier is used to calculate likeliness of input belong to a specific label. Loss is calculated using binary-cross entropy of each label. Since we omit the softmax function complexity is reduced.

1) Optimization of Bounding Boxes: By using Logistic, regression YOLO v3 predicts the score of presence of object. A ground truth box is defined to all objects, if anchor box overlaps the most with ground truth box then objectness score is said to be 1. For the anchor boxes whose overlap is greater than the preselected threshold, the anchor box incurs null cost. Every ground truth box is mapped with only one anchor box. If anchor box is not selected and assigned to bounding box then no classification and localization loss is considered, only confidence loss is calculated.

The anchor box is regressed to the ground truth box by gradual optimization as shown in Fig. 4. Coordinate parameters are now defined as

$$b_x = \sigma(t_x) + c_x \tag{1}$$

$$b_y = \sigma(t_y) + c_y \tag{2}$$

$$b_w = p_w e^{t_w} \tag{3}$$

$$b_h = p_h e^{t_h} \tag{4}$$

Where, t_x, t_y, t_w, t_h are the predictions made by YOLO. c_x, c_y is top left corner of grid cell of the anchor. $p_w p_h$ are the width and height of anchor. b_x, b_y, b_w, b_h are predicted boundary box. $\sigma(t_o)$ is box confidence score.

2) Feature pyramid Network (FPN): YOLOv3 makes three predictions in every point of image. The prediction includes a bounding box, score of objectness followed by 80 class score hence we have S*S*[3*(4+1+80)] predictions. This approach is similar to feature pyramid networks.

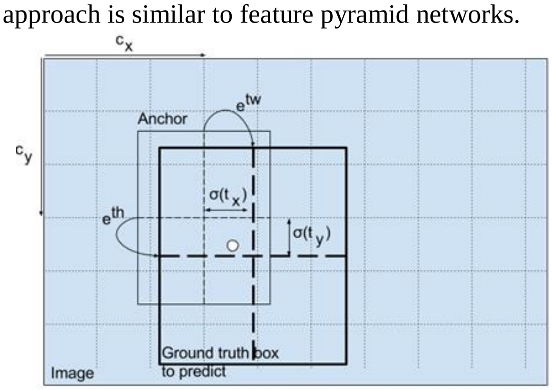

Fig. 4. Anchor Box Regression [9].

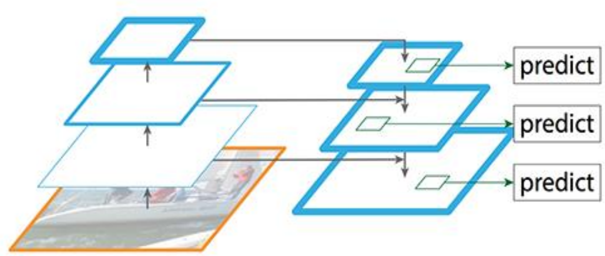

Fig. 5. Feature Pyramid Network [9].

Predictions are made at 3 different scales as in Fig. 5. The initial prediction is made at last feature map layer. Then feature map is up sampled by factor of 2. YOLOv3 merges feature map with up sampled feature using element wise addition. Convolutional layer is applied to obtain second predictions. Repeating second prediction will yield high semantic information.

Two stage algorithms from Region Proposal networks family of algorithms have two different networks for proposing regions and extracting features. FPS of RCNN is 7, which is quite low to handle real-time applications. One stage algorithm overcomes this drawback by employing single shot detectors. Single Shot detectors face trade-off between accuracy and real-time processing. The algorithm faces issues in identifying small objects or objects that are too close. Though SSD networks are equally in boom as much as YOLO, algorithm might outperform YOLO in terms of speed, but spatial resolution has dropped significantly and hence missing out in locating small objects. Solution to challenge is increasing image resolutions. YOLO family upgrades its accuracy, latency. YOLOv3 has DarkNet-53 has its backbone. The network has less BFLOP (Billion floating-point operations) compared to residual Network-512. The inclusion of Feature Pyramid network (FPN) helps in detecting objects that are small. FPN uses both bottom-down and a top-down pathway. Bottom-up approach is used for feature extraction. As we propagate through this approach, spatial resolution minimizes. Semantic value for each layer increases.

C. Object Tracking

Internet is the main network connecting millions of people in world. Main entertainment factor and the source of greater knowledge is video. Video is collection of frames. The negligible time gap between frames makes the stream of photos looks like flow of scenes. When designing algorithm for video processing. Videos are classified into two classes. Video stream is an ongoing process for video analysis. The processor is not aware of future frames. Video sequence is video of fixed length. All the consecutive frames are obtained prior to processing of current frame. Motion is distinct factor that differentiates video form frame. Motion is a powerful visual Que. Object properties and action can be realized by noticing only sparse points in the image.

D. Simple Online Real Time Tracking (SORT)

SORT is a realistic approach to achieve Multi Object Tracking (MOT). Performance of SORT is enhanced by ques such as appearance; this association of appearance to SORT enhances the performance of SORT and increases performance during Scenario like longer periods of occlusion. SORT is a framework that has Kalman filtering has its crux. Image by image data association is achieved by Hungarian method over an association metric like appearance that measures bounding box overlap.

1) Track Handling and state estimation: The assignment problem maps prediction of Kalman filter to that of newly arrived measurements. The task of associating two vectors is performed by Hungarian algorithm. Adding additional information like motion and appearance parameters in conjunction with association helps in better mappings.

$$d^{(1)}(i,j) = (d_j - y_j)^T s_i^{-1} (d_j - y_i) \quad (5)$$

Unlikely association can be removed by thresholding at 95% confidence interval. The decision is given with an indicator.

$$b_{i,j}^{(1)} = 1\left[d^{(1)}(i,j)\right] \leq t^{(1)} \quad (6)$$

When the motion uncertainty is large mahalanobis distance is not suitable, hence another metric to aid in association. Metric computes appearance descriptor for each bounding box detection d_j.

$$d^{(2)}(i,j) = min\left\{1 - {r_i}^T r_k^{(i)} \middle| r_k^{(i)} \in R_I\right\} \quad (7)$$

Combination of both metrics is

$$c_{i,j} = \lambda d^{(1)}(i,j) + (1-\lambda) d^{(2)}(i,j) \quad (8)$$

IV. Design and Implementation

A CNN is designed and is trained on Urban Vehicle dataset, which is an Indigenous dataset for traffic surveillance applications. Specifications of Urban Vehicle Dataset or on road vehicle dataset [11] is tabulated in Table I. And number of images considered for each class is tabulated in Table II.

In total there are 64339 images belonging to 4 classes that are taken under different times of the day and capturing conditions, including NIR images. The images are classified based on utility and size of vehicles. The auto class has images of three wheelers; Heavy class includes buses, trucks, Freight carriers; Light class has cars, SUVs and sedans and two wheelers include motorcycles and bicycles. Most of images have only one object belonging to its respective class.

Some of the sample images of dataset is shown in Fig. 6. Hardware and software requirements are tabulated in Table III and Table IV.

TABLE. I. Dataset Specifications

Source	Traffic Monitoring Cameras
Image Type	RGB, NIR
Image Extension	Jpg
Image Dimension	Variable Size
Image Quality	Medium to Blurred

TABLE. II. Urban Vehicle Dataset

Directory	**Autos**	**Heavy**	**Light**	**Two Wheelers**	**Total**
RGB_Day	2530	2915	12927	13340	31712
RGB_Evening	3122	3709	14654	10027	31512
NIR	124	127	524	340	1115

Fig. 6. Sample Images of urban Vehicle Dataset [11].

TABLE. III. HARDWARE REQUIREMENTS

Processor	Intel i7, 8th Gen quad core
Clock Speed	1.8 GHz
RAM	16 GB
Storage	500 GB SSD
GPU	Nvidia MX

TABLE. IV. SOFTWARE REQUIREMENTS

Distribution	Anaconda Navigator
API	Keras
Library	Tensor Flow, OpenCV
Packages	Matplotlib, numpy, pandas, scikitLearn
Language	Python
IDE	Spyder, Jupyter Notebook
GPU Architecture	CUDA
Applications	LabelImg, TensorBoard

A. Neural Network Training

Flowchart of neural network training is as shown in Fig. 7. First step in training a network using deep learning for an application is to prepare an appropriate dataset and make Train-Test Split depending on the available data. Suitable network is designed or selected (in case of Transfer Learning) for training [13]. Validation Loss is monitored throughout the training process to produce a very less constant value after few epochs, if not then the hyper parameter tuning is performed on model to give lowest possible validation loss values. Model with best validation loss is saved and tested on real world dataset. The model is said to be good if a descent precision and recall values are obtained for new datasets else the model needs to be trained on enhanced dataset for increased performance.

B. Single Object Detection

Fig. 8 shows flow chart of single object detection. Necessary libraries are imported first and training data is given input via the Google drive. Google-Colab, an online simulation tool for python and Tensor-flow algorithms was used. The algorithm then compiles data and learns form it in a supervised manner [16].

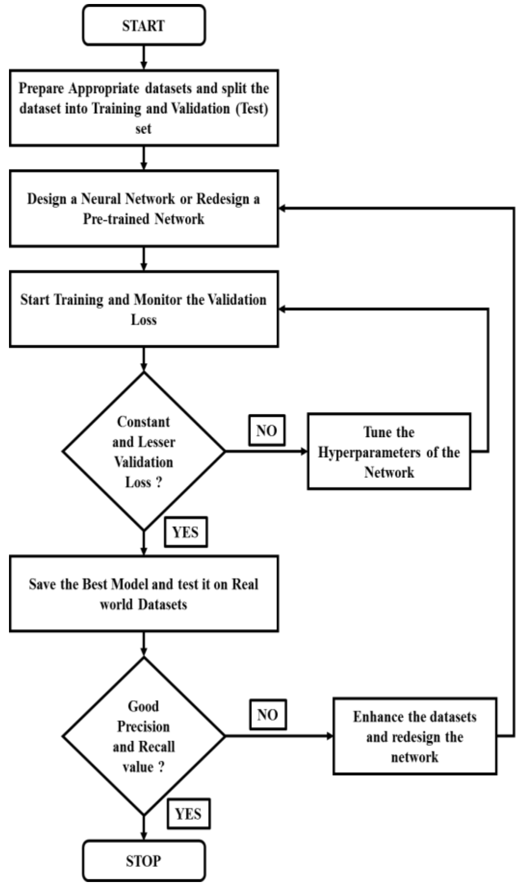

Fig. 7. Flowchart of Neural Network Training.

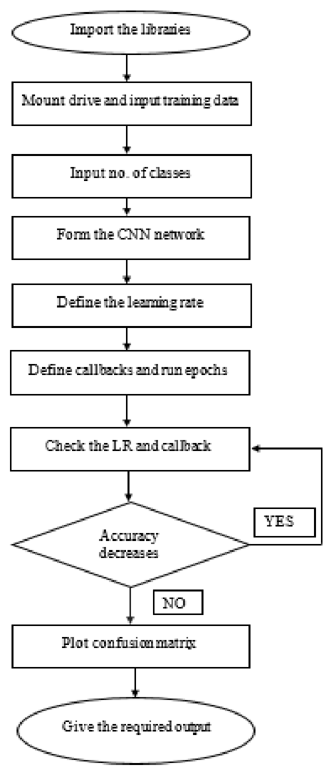

Fig. 8. Flowchart of Single Object Detection.

This algorithm can be described as supervised classification algorithm. Data flows through CNN layers and various operations are performed on data. The learning rate and callbacks are defined. Number of epochs and batch size is also defined. The epochs are then executed through which algorithm learns through training data. Training accuracy and training losses are constantly monitored. If training accuracy starts falling below a threshold, the callback function is invoked and epochs are stopped. Confusion matrix is then plotted using training and testing data. Various performance parameters can be defined and observed using the confusion matrix.

C. *Multiple Object Detection*

Fig. 9 describes working of YOLOv3 multiple object detection algorithm. An image is given as the input to algorithm and transformation is done using CNN. These transformations are done so that, input image is compatible to specifications of algorithm. Following this, flattening operation is performed. Flattening is converting data into a 1-dimensional array for inputting it to next layer. Flattening of output of convolutional layers is to create a single long feature vector and it is connected to final classification model, which is called a fully connected layer. By changing the score threshold, one can adjust how the ML model assigns these labels.

Object detection pipeline has one component for generating proposals for classification. Proposals are nothing but candidate regions for object of interest. Most of approaches employ a sliding window over feature map and assigns foreground/background scores depending on features computed in that window. The neighborhood windows have similar scores to some extent and are considered as candidate regions. This leads to hundreds of proposals. As the proposal generation method should have high recall, we keep loose constraints in this stage. However, processing these many proposals all through the classification network is cumbersome. This leads to a technique, which filters proposals based on some criteria called Non-Maximum Suppression. IOU calculation is actually used to measure the overlap between two proposals.

D. *Multiple Object Tracking*

In multiple object tracking, train the vehicle tracker using YOLOv3 and deep learning methods and optimize the detector's success rate by providing efficient vehicle detection results by testing trained vehicle detector on test data [17]. It consists of six phases such as loading data set, YOLOv3 design, training options configuration, object tracker training, and tracker evaluation, respectively. Flow chart of multiple object detection is shown in Fig. 10.

E. *Performance Metrics*

The trained model using deep learning must be evaluated for its performance on unseen data called as test dataset. The choice of performance metrics will influence the analysis of algorithms. This helps in identifying reasons for mis-classifications so that it can be corrected by taking necessary measures.

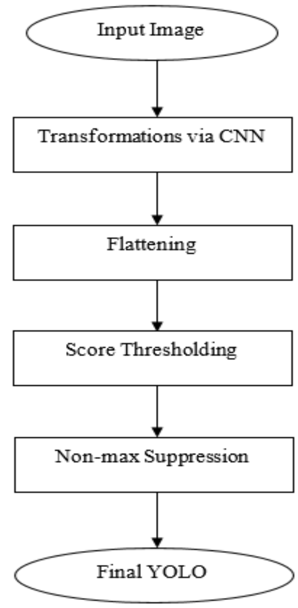

Fig. 9. Flowchart for Multiple Object Detection.

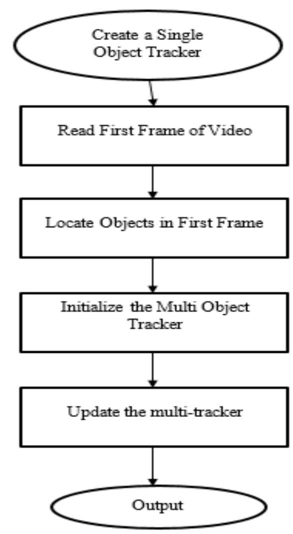

Fig. 10. Flow Chart of Multiple Object Tracking.

1) Confusion Matrix: It gives prediction information of various objects for binary classification as shown in Table V.

2) Accuracy and Loss: Accuracy measure is calculated by using formula $\frac{TP+TN}{TP+TN+FP+FN}$. The accuracy measure, as a stand-alone measure is not reliable since it gives equal costs for both type of errors and works well for a well-balanced dataset. The loss is calculated by loss functions of used for training, and average of the loss is calculated when used batch learning that computes loss after each training each batch.

3) Precision, Recall and F1- score: Precision is the percentage of classification results that are relevant. Recall is the percentage of total relevant results that are classified correctly by algorithm. F-1 score considers both precision and recall values hence must be maximized to make the model better.

TABLE. V. CONFUSION MATRIX FOR BINARY CLASSIFICATION

	Predicted class - 1	**Predicted class - 2**
Actual Class - 1	TP - True Positive Decision is correct	FN - False Negative Error – Type 1
Actual – Class 2	FP - False Positive Error – Type 2	TN - True Negative Decision is correct

The formulas to calculate these metrics are

$$Precision = \frac{TP}{TP+FP} \tag{9}$$

$$Recall = \frac{TP}{TP+FN} \tag{10}$$

$$F-1\,Score = 2 * \frac{Preciison*Recall}{Precision+Recall} \tag{11}$$

$$mAP = \frac{1}{No.of\ divisions} \sum_{r\in(1,0.1,0.001)} p_{interp}(r) \tag{12}$$

The detected objects are bounded with bounding box. Tracking is performed on frames of the videos to identify objects in the successive frames using SORT. The evaluation metrics like True Positive (TP), True Negative (TN), False Positive (FP), False Negative (FN) thereby Precession, Recall and hence mean Average Precession (mAP) is calculated using Intersection over Union (IoU).

F. *Specifications used for Implementation*

Single object detection

Dataset used – On-Road Vehicle Dataset [11]

TABLE. VI. IMAGES USED FOR SINGLE OBJECT DETECTION

Number of classifiers	Three (Autos, Heavy, Light)
Total number of Input Images	12480
Training images	9984
Testing images	2496
Day images	7590
Evening images	4518
Night images	372

Fig. 11. Sample Day Images.

Fig. 12. Sample Evening Images.

Fig. 13. Sample Night Images.

Table VI. Shows total number of images considered for implementation. In this dataset each image contains one object. Further images are captured in different intervals of time, such as day (7590), evening (4518) and night (372); sample images are shown in Fig. 11, 12 and 13 and is tabulated in Table VI.

1) Multiple object detection: Dataset used – KITTI Dataset. All the images are captured in daytime. Dataset contains 80 classes, five classes such as car, bus, truck, motor cycle and Train classes are implemented in this paper. All the images are captured in day time. Total number of images used for implementation 11682, tabulated in Table VII. Sample images of dataset are shown in Fig. 14. Each image contains multiple objects.

TABLE. VII. IMAGES USED FOR MULTIPLE OBJECT DETECTION

Number of classifiers	80
Classifiers used	5 (Car, Bus, Truck, Motor Cycle and Train)
Total number of Input Images	11682
Training images	9736
Testing images	1946

Fig. 14. Sample Images of KITTI Object Detection Dataset.

V. Simulation Results and Analysis

This section describes simulation results and performance parameters observed are accuracy, precision and recall. It also underlines the confusion matrices of different datasets and convolution layers of the algorithms.

A. *Single Object Detection*

CNN is designed for single object detection. The layers and each layer information as shown in Fig. 15.

It encompasses the parameters that were included in each step, layer progression and output image size of every layer. Each layer divides the image matrix into its components and performs an operation on image. The output image size of various layers is different due to manipulations by each layer such as initially the output image size is 28×28 which then reduces to 14×14 due to the max pooling layer which chooses the max valued pixel from the surrounding pixels. It then reduces to 7×7 due to the second max pooling layer. This pixel is then flattened into 7×7×64 which are 3136 sized vector. This vector is then reduced to a less sized vector by proceeding layers and final calculation parameters are displayed.

Designed neural network was trained and tested. Obtained training accuracy and loss as shown in Fig. 16 and 17. Obtained 82% training accuracy through training this model. The loss and accuracy are inversely proportional to each other. As the number of epochs increases, learning rate increases and hence loss decreases. Each time epochs is run, the model trains it itself and weights of the convolution networks gets updated to a more accurate value.

The CNN is successfully able to classify the given object as truck and car with an accuracy of 75.68% and 84.409% respectively as shown in Fig. 18.

Upon simulation, it is able to correctly classify the vehicles by classifying a car with 79.853% accuracy and about 78.122% accuracy for the detection of an auto as shown in Fig. 19.

Upon simulation, it is able to correctly classify the vehicles by classifying it into a car with about 79.036 % accuracy and auto with about 80.064 % accuracy as shown in Fig. 20.

```
Layer (type)                 Output Shape              Param #
=================================================================
conv2d_1 (Conv2D)            (None, 28, 28, 32)        320
_________________________________________________________________
conv2d_2 (Conv2D)            (None, 28, 28, 32)        9248
_________________________________________________________________
max_pooling2d_1 (MaxPooling2 (None, 14, 14, 32)        0
_________________________________________________________________
dropout_1 (Dropout)          (None, 14, 14, 32)        0
_________________________________________________________________
conv2d_3 (Conv2D)            (None, 14, 14, 64)        18496
_________________________________________________________________
conv2d_4 (Conv2D)            (None, 14, 14, 64)        36928
_________________________________________________________________
max_pooling2d_2 (MaxPooling2 (None, 7, 7, 64)          0
_________________________________________________________________
dropout_2 (Dropout)          (None, 7, 7, 64)          0
_________________________________________________________________
flatten_1 (Flatten)          (None, 3136)              0
_________________________________________________________________
dense_1 (Dense)              (None, 256)               803072
_________________________________________________________________
dropout_3 (Dropout)          (None, 256)               0
_________________________________________________________________
dense_2 (Dense)              (None, 3)                 771
=================================================================
Total params: 868,835
Trainable params: 868,835
Non-trainable params: 0
```

Fig. 15. Convolution Layers used in CNN.

```
Use tf.where in 2.0, which has the same broadcast rule as np.where
Epoch 1/10
 - 17s - loss: 7.0876 - acc: 0.4023
Epoch 2/10
 - 11s - loss: 0.7619 - acc: 0.6733
Epoch 3/10
 - 10s - loss: 0.6503 - acc: 0.7470
Epoch 4/10
 - 10s - loss: 0.5791 - acc: 0.7896
Epoch 5/10
 - 11s - loss: 0.5761 - acc: 0.7955
Epoch 6/10
 - 11s - loss: 0.5496 - acc: 0.8031
Epoch 7/10
 - 10s - loss: 0.5387 - acc: 0.8126
Epoch 8/10
 - 10s - loss: 0.5242 - acc: 0.8219
Epoch 9/10
 - 10s - loss: 0.5359 - acc: 0.8173
Epoch 10/10
 - 10s - loss: 0.5501 - acc: 0.8152
```

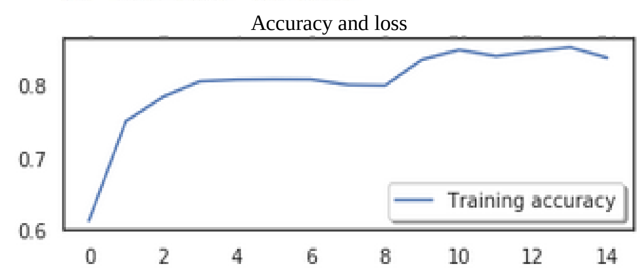

Fig. 16. Training Accuracy.

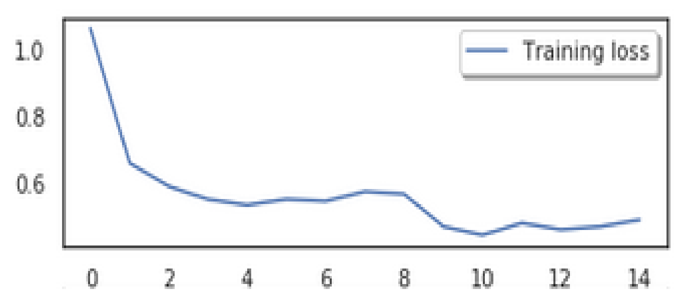

Fig. 17. Training Loss.

Fig. 18. Sample Simulation Results of Day Images.

Fig. 19. Sample Simulation Results of Evening Images.

Fig. 20. Sample Simulation Results of Night Images.

Confusion matrix for day images is tabulated in Table VIII. The performance parameters are extracted from confusion matrix and tabulated in Table IX. Accuracy, precision and recall data is evident for autos, cars and heavy type of vehicles as shown in Fig. 21. The accuracy of autos and cars is almost identical while that of heavy vehicles is slightly better than that of others. Since the number of training images is more for the Day images, the results obtained are better than that of Evening and Night Dataset images. High precision indicates that, the algorithm returned substantially more relevant results than irrelevant ones while high recall means that an algorithm returned most of the relevant results.

TABLE. VIII. CONFUSION MATRIX FOR DAY IMAGES

PREDICTED	Autos	cars	Heavy	All
Autos	2369	117	44	2530
cars	66	2413	70	2530
Heavy	95	89	2346	253

TABLE. IX. PERFORMANCE METRICS OF DAY IMAGES

	TP	TN	FP	FN	Precision	Accuracy	Recall
Auto	2369	4918	161	161	0.936	0.957	0.936
Cars	2413	4853	206	136	0.921	0.955	0.946
Heavy	2346	4965	114	184	0.953	0.960	0.927

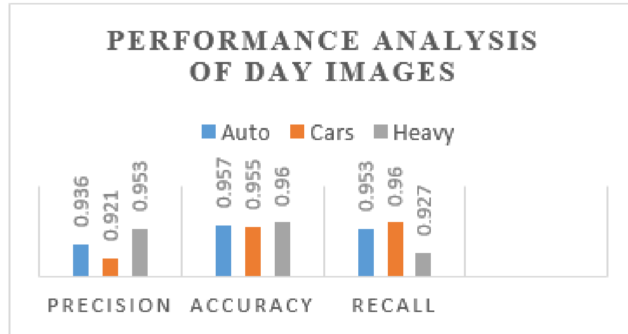

Fig. 21. Performance Analysis of Day Images.

Confusion matrix for evening images is tabulated in Table X. The performance parameters are extracted from confusion matrix and tabulated in Table XI. As shown in Fig. 22, accuracy of evening images has been reduced. This can be accounted due to decrease in number of training images given to the neural network. Because of this, weights may not be as accurate as the day dataset.

TABLE. X. CONFUSION MATRIX FOR EVENING IMAGES

PREDICTED	Autos	cars	Heavy	All
Autos	1456	28	22	1506
cars	16	1480	10	1506
Heavy	42	34	1430	1506

TABLE. XI. PERFORMANCE METRICS OF EVENING IMAGES

	TP	TN	FP	FN	Precision	Accuracy	Recall
Auto	1456	2954	58	50	0.961	0.916	0.966
Cars	1480	2950	62	26	0.959	0.920	0.982
Heavy	1430	2980	32	76	0.978	0.906	0.949

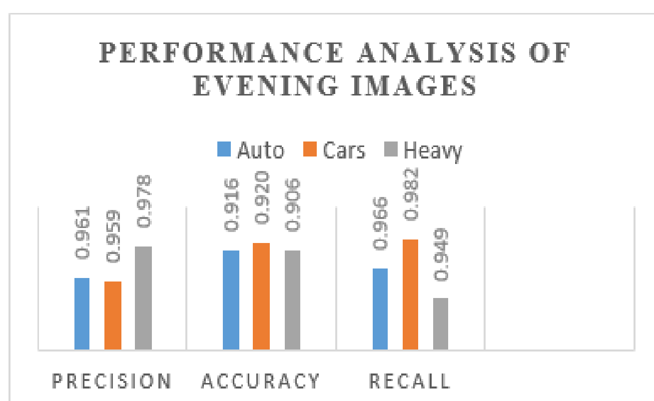

Fig. 22. Performance Analysis of Evening Images.

Confusion matrix for night images is tabulated in Table XII. The performance parameters are extracted from confusion matrix and tabulated in Table XIII. Accuracy of autos, cars and heavy has decreased considerably as shown in Fig. 23. The number of training images is low. Since the Neural Network has received less training images, the weights that are calculated are not very precise. Besides this, illumination of the image plays a major role in Object detection. Since night images have low illumination levels, the accuracy of prediction of class of image is low.

TABLE. XII. CONFUSION MATRIX FOR NIGHT IMAGES

PREDICTED	**Autos**	**cars**	**Heavy**	**All**
Autos	108	4	12	124
cars	14	100	10	124
Heavy	2	16	106	124

TABLE. XIII. PERFORMANCE METRICS OF NIGHT IMAGES

	TP	**TN**	**FP**	**FN**	**Precision**	**Accuracy**	**Recall**
Auto	108	232	16	16	0.87	0.913	0.87
Cars	100	228	20	24	0.833	0.881	0.806
Heavy	106	226	22	18	0.828	0.892	0.854

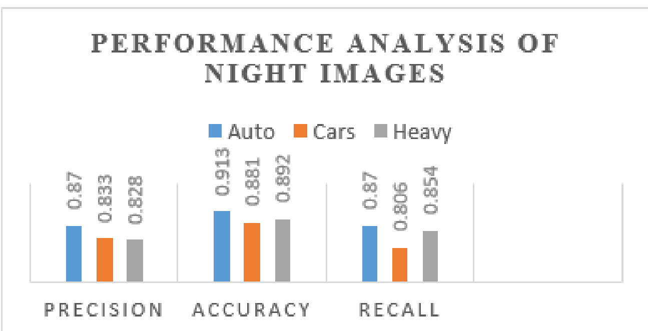

Fig. 23. Performance Analysis of Night Images.

B. Multiple Object Detection

The images collected from [11] have been given as test set. The dataset consisting of three different kinds of images such as day, evening and NIR images (Near Infrared). Object detections by YOLOv3 as shown in Fig. 24, 25 and 26.

The result in Fig. 27 shows algorithm can detect objects of any size and images captured from various camera angle and distance. This attribute is because of FPN used in YOLOv3. Thinner intact bounding boxes as shown in Fig. 28 ensures not to miss out any of the minute details and a greater IoU.

Image considered for performance analysis is as shown in Fig. 29. Performance metrics for car detection is tabulated in Table XIV. Image has various kinds of objects. The precision result is high since objects to be detected are not occluding one another and the recall is 0.8333 since the FN value is 1 as the auto in the image is detected but identified as truck. As result of misclassification, the recall value suffers a loss. Since the precision is high, the mAP value is 100% for given class and considered image.

For on road vehicle dataset [11].

Fig. 24. RGB_Day Image Detections.

Fig. 25. RGB_Evening Images Detections.

Fig. 26. NIR Images Detections.

Fig. 27. YOLOv3 Results for COCO Dataset.

Fig. 28. YOLOv3 Results with Intact Boxes.

Fig. 29. Car Detection.

TABLE. XIV. PERFORMANCE METRICS FOR CAR DETECTION

	TP	TN	FP	FN	Precision	Recall
IoU at.25	5	0	0	1	1	0.8333
IoU at .50	5	0	0	1	1	0.8333
IoU at.75	4	0	0	1	1	0.8333

Image considered has different kinds of objects as shown in Fig. 30 and its performance metrics tabulated in Table XV. Precession result is varied with respect to different IoU's since variations in IoU will results in variations with respect to ground truth boxes. Greater the IoU lesser the detections and hence precession values incur loss. For given class and considered image mAP value is 78.57%. The decrease in mAP value is because of varied precision value.

Fig. 30. Motorbike Detection.

TABLE. XV. PERFORMANCE METRICS FOR MOTORBIKE DETECTION

	TP	TN	FP	FN	Precision	Recall
IoU at.25	6	0	1	0	0.8571	1
IoU at .50	5	0	1	0	0.8333	1
IoU at.75	4	0	2	0	0.6667	1

Object detection in Video: video specifications

Time duration of video = 27 seconds

Type of file = MP4 File (.mp4)

Size = 1.65 MB (17,33,851 bytes)

Size on disk = 1.65 MB (17,36,704 bytes)

Number of Frames = 27*30 = 810

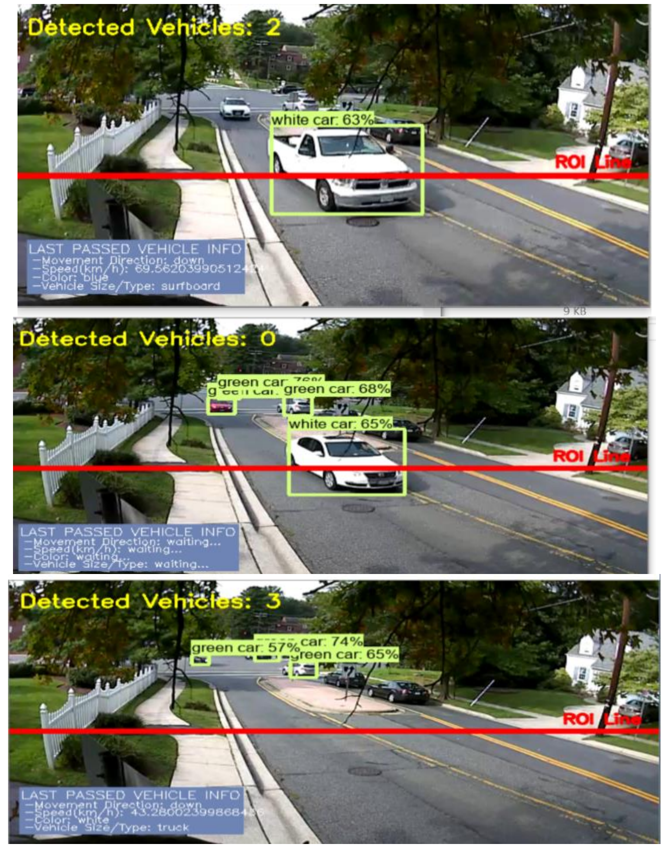

Fig. 31. Results of Object Detection in Video based on Region of Interest (ROI).

Fig. 31 shows detection of objects in video. In addition, the parameters measured are speed and color of vehicle, vehicle type, direction of vehicle movement and number of vehicles in ROI.

1) For KITTI dataset: All images of on road vehicle dataset contains singe object in each image. Hence, for multiple object detection COCO and KITTI vehicle detection dataset is used for simulation. In this dataset, each image contains multiple objects of same class or multiple objects of different class. Objects are detected using YOLOv3 algorithm. Neural network layers information as shown in Fig. 32.

2) Convolution Layers: The convolutional layers of YOLOv3 algorithm when stacked are formed. It contains of 53 convolutional layers, each followed by batch normalization layer and Leaky ReLU activation. No form of pooling is used, and a convolutional layer with stride 2 is used to down-sample the feature maps. This helps in preventing loss of low-level features often attributed to pooling. At the end, all operations performed by the convolutional layers, average pooling and softmax operations are completed.

KITTI dataset contains 80 classes of objects. In this paper, five classes such as cars, truck, bus, train, and motorcycle objects images are considered for simulation. Fig. 33 shows training accuracy and loss values of YOLOv3 for multiple object detection. Fig. 34, 35, 36, 37, 38, 39, 40 and 41 shows multiple object detection using YOLOv3. The YOLOv3 algorithm has successful detected and classified the objects as Car, Truck, Train, Motorcycle. A total of 11,682 images were used from KITTI dataset where 9736 was used for training and 1946 was allocated for testing. An important parameter considered here is IOU which describes the overlap factor of one detected object from the other. It is seen that as the number of vehicles in the image increases the bounding boxes are overlapped.

	Type	Filters	Size	Output
	Convolutional	32	3 × 3	256 × 256
	Convolutional	64	3 × 3 / 2	128 × 128
1×	Convolutional	32	1 × 1	
	Convolutional	64	3 × 3	
	Residual			128 × 128
	Convolutional	128	3 × 3 / 2	64 × 64
2×	Convolutional	64	1 × 1	
	Convolutional	128	3 × 3	
	Residual			64 × 64
	Convolutional	256	3 × 3 / 2	32 × 32
8×	Convolutional	128	1 × 1	
	Convolutional	256	3 × 3	
	Residual			32 × 32
	Convolutional	512	3 × 3 / 2	16 × 16
8×	Convolutional	256	1 × 1	
	Convolutional	512	3 × 3	
	Residual			16 × 16
	Convolutional	1024	3 × 3 / 2	8 × 8
4×	Convolutional	512	1 × 1	
	Convolutional	1024	3 × 3	
	Residual			8 × 8
	Avgpool		Global	
	Connected		1000	
	Softmax			

Fig. 32. Convolutional Layers used in YOLOv3.

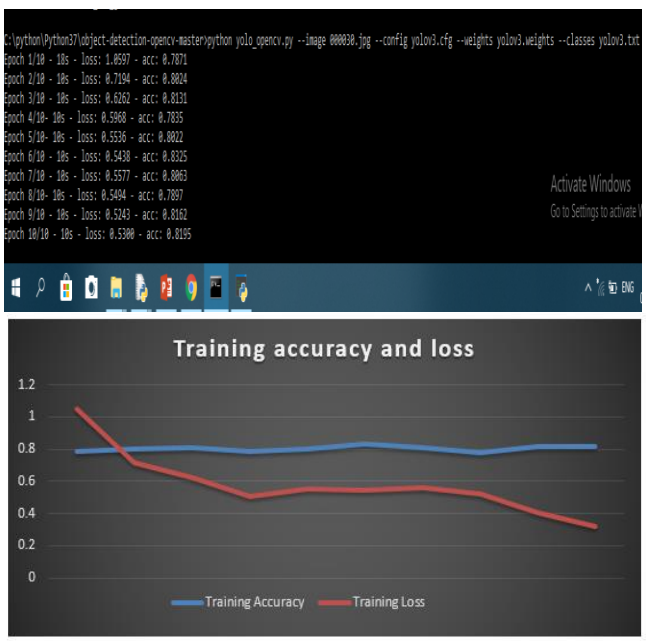

Fig. 33. Training Accuracy and Loss Values of YOLOv3 for Multiple Object Detection.

Fig. 34. Multiple Object Detection – Cars.

Fig. 35. Multiple Object Detection –Cars and Train.

Fig. 36. Multiple Object Detection –Cars and Truck.

Fig. 37. Multiple Object Detection – Cars and Motor Cycle.

Fig. 38. Multiple Object Detection – Four cars are detected and two cars are not detected.

Fig. 39. Multiple Object Detection – All types of cars are detected.

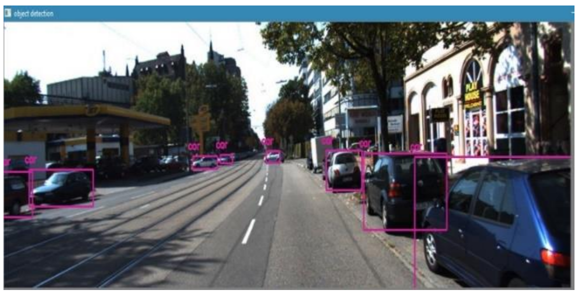

Fig. 40. Multiple Object Detection – Two cars inside petrol bunk not detected.

Fig. 41. Multiple Object Detection – All cars are detected except one car.

C. *Multiple Object Tracking for Trafic Surveillance Video Dataset Specifications*

Name – A3 Road Traffic UK HD – rush hour – British Highway Traffic May, 2017
Format - Mp4
Size - 12.36Mb
Time frame - 245 sec
Video Quality – 720p
Types of objects – Cars and trucks

Fig. 42 shows the images of multiple object tracking for surveillance video, it contains cars and trucks. The vehicle tracker trained on surveillance video using YOLOV3 and deep learning methods. The vehicle tracking process was successfully carried out by testing trained vehicle detector on test data set video. Algorithm divided the video into frames with a rate of 30fps and performed object detection in first frame. In the latter frames, the particular detected image was tracked using its centroid position. Objects are tracked in different frames at different intervals of time as shown in Fig. 43.

Fig. 42. Multiple Object Tracking Snippet.

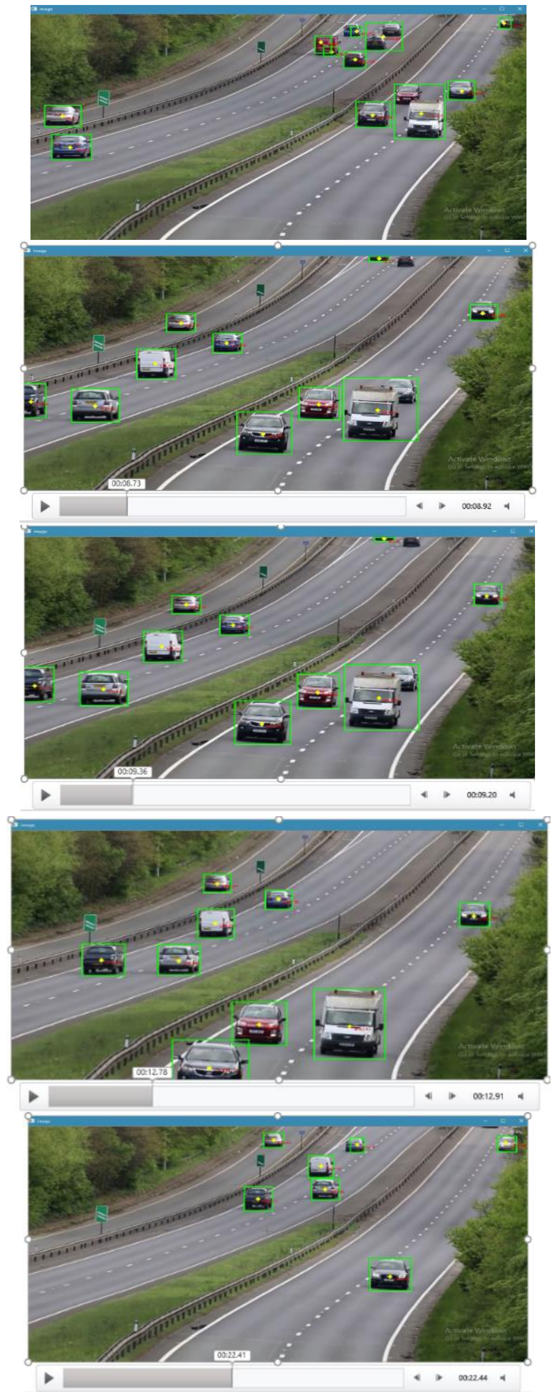

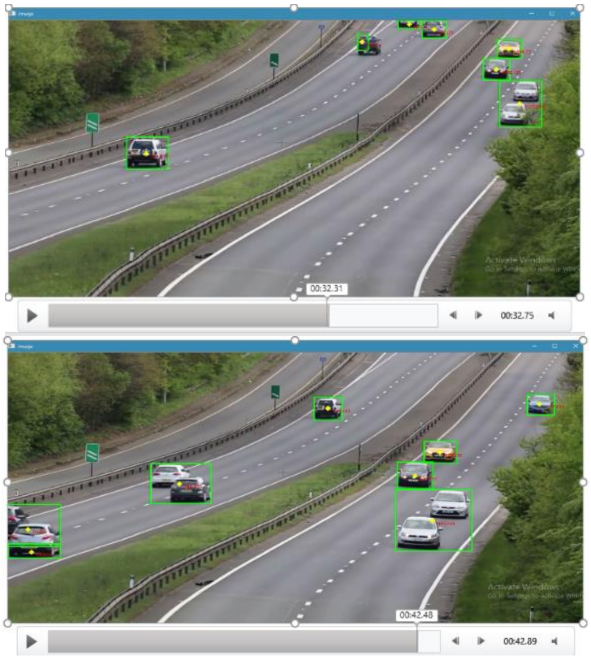

Fig. 43. Images of Multiple Object Tracking at different Frames.

VI. Conclusions

The inclusion of Artificial Intelligence to solve Computer vision tasks has outperformed the image processing approaches of handling the tasks. The CNN model trained to on road vehicle dataset for single object detection, achieved a validation accuracy of 95.7 % for auto, 95.5% for car and 96 % for heavy vehicles for day images. The high validation accuracy is because of huge amount of data on which it is trained from each class. Performance metrics are tabulated for day, evening and NIR images. Multiple object detection is implemented using YOLOv3 for KITTI and COCO dataset. Performance metrics is tabulated for YOLOv3 on considered classes of images. Higher the precession value of class greater will be mAP value. The mAP value depends on image chosen for calculation. IoU of 0.5 is ideal for detection and tracking. mAP values can be enhanced by increasing true positive values. Results of performance metrics is totally dependent on image data set used. Further objects are detected in video based on region of interest. The performance measures measured such as speed and color of vehicle, type of vehicle, direction of vehicle movement and the number of vehicles in ROI. Multiple object tracking is implemented for traffic surveillance video using YOLOv3 and OpenCV. Multiple objects are detected and tracked on different frames of a video. Further training the models on powerful GPUs and by increasing the number of images evaluate the models on other datasets and modify the design if required to make the model more robust and suitable for real-time applications.

References

[1] V. D. Nguyen et all., "Learning Framework for Robust Obstacle Detection, Recognition, and Tracking", IEEE Transactions on Intelligent Transportation Systems, vol. 18, no. 6, pp. 1633-1646, June 2017.

[2] Zahraa Kain et all, "Detecting Abnormal Events in University Areas", 2018 International conference on Computer and Applications(ICCA),pp. 260-264, 2018.

[3] P. Wang et all., "Detection of unwanted traffic congestion based on existing surveillance system using in freeway via a CNN-architecture trafficnet", IEEE Conference on Industrial Electronics and Applications (ICIEA), Wuhan, 2018, pp. 1134-1139.

[4] Q. Mu, Y. Wei, Y. Liu and Z. Li, "The Research of Target Tracking Algorithm Based on an Improved PCANet", 10th International Conference on Intelligent Human-Machine Systems and Cybernetics (IHMSC), Hangzhou, 2018, pp. 195-199.

[5] H. C. Baykara et all., "Real-Time Detection, Tracking and Classification of Multiple Moving Objects in UAV Videos", 29th IEEE International Conference on Tools with Artificial Intelligence (ICTAI), Boston, MA, 2017, pp. 945-950.

[6] W. Wang, M. Shi and W. Li, "Object Tracking with Shallow Convolution Feature", 9th International Conference on Intelligent Human-Machine Systems and Cybernetics (IHMSC), Hangzhou, 2017, pp. 97-100.

[7] K. Muhammad et all., "Convolutional Neural Networks Based Fire Detection in Surveillance Videos", IEEE Access, vol. 6, pp. 18174-18183, 2018.

[8] D. E. Hernandez et all., "Cell Tracking with Deep Learning and the Viterbi Algorithm", International Conference on Manipulation, Automation and Robotics at Small Scales (MARSS), Nagoya, 2018, pp. 1-6.

[9] X. Qian et all., "An object tracking method using deep learning and adaptive particle filter for night fusion image", 2017 International Conference on Progress in Informatics and Computing (PIC), Nanjing, 2017, pp. 138-142.

[10] Y. Yoon et all., "Online Multi-Object Tracking Using Selective Deep Appearance Matching", IEEE International Conference on Consumer Electronics - Asia (ICCE-Asia), Jeju, 2018, pp. 206-212.

[11] H. S. Bharadwaj, S. Biswas and K. R. Ramakrishnan. "A large scale dataset for classification of vehicles in urban traffic scenes", Proceedings of the Tenth Indian Conference on Computer Vision, Graphics and Image Processing,ACM,2016.

[12] Mohana et.al., "Performance Evaluattion of background modeling methods for object Detection and Tracking",International Conference on Inventive systems and Control (ICISC).

[13] G. Chandan et.al., "Real Time Object Detection and Tracking Using Deep Learning and OpenCV", International Conference on Inventive Research in Computing Applications (ICIRCA), 2018.

[14] Mohana et.al., "Elegant and efficient algorithms for real time object detection, counting and classification for video surveillance applications from single fixed camera" International Conference on Circuits, Controls, Communications and Computing (I4C),2016.

[15] Mohana et.al., "Simulation of Object Detection Algorithms for Video Survillance Applications", 2nd International Conference on I-SMAC (IoT in Social, Mobile, Analytics and Cloud),2018.

[16] A. Raghunandan et. al., "Object Detection Algorithms for Video Surveillance Applications," International Conference on Communication and Signal Processing (ICCSP), 2018.

[17] A. Mangawati et al., "Object Tracking Algorithms for Video Surveillance Applications," 2018 International Conference on Communication and Signal Processing (ICCSP), 2018.

[18] Mohana, et al., "Design and Implementation of Object Detection, Tracking, Counting and Classification Algorithms using Artificial Intelligence for Automated Video Surveillance Applications" Advanced Computing and Communication Society (ACCS)- 24th annual International Conference on Advanced Computing and Communications (ADCOM-2018), IIITB, Bangalore.

KNN and SVM Classification for Chainsaw Sound Identification in the Forest Areas

N'tcho Assoukpou Jean GNAMELE[1]
Yelakan Berenger OUATTARA[2]
Laboratoire des Signaux et Systèmes
UFHB, Abidjan, Cote d'Ivoire

Toka Arsene KOBEA[3]
Laboratoire de Physique de l'Atmosphère et Mécanique des Fluides, UFHB, Abidjan, Cote d'Ivoire

Geneviève BAUDOIN[4]
ESIEE-PARIS
UPEM
Marne-la-vallée, France

Jean-Marc LAHEURTE[5]
ESYCOM (FRE 2028)
UPEM, Marne-la-vallée, France

***Abstract*—We present in this paper a comparative study of two classifiers, namely, SVM (support vector machine) and KNN (K-Nearest Neighbors), which we combine to MFCC (Mel-Frequency Cepstral Coefficients) in order to make possible the detection of chainsaw's sounds in a forest environment. Optimization's calculation of the relevant characteristics of the sounds recorded in the forest and the judicious choice of the key parameters of the classifiers allows us to obtain a true positive rate of 95.63% for the SVM-LOG-KERNEL and 94.02% for the KNN. The SVM-LOG-KERNEL classifier offers a better classification result and a processing time 30 times faster than KNN.**

Keywords—KNN Algorithm; SVM Algorithm; MFCC; sound recognition; forest monitoring; machine learning

I. INTRODUCTION

From 16 million hectares at the beginning of the last century, the Ivorian forest decreased to 7 850 864 hectares in 1990 then to 3 401 146 in 2015. Today, the Ivory Coast has around 2 million hectares of natural forest. This situation is largely due to human activities, in particular the overexploitation of the forest with timber and wood energy. To ensure the forest protection, LANDSAT images or military patrols are used. Unfortunately, these solutions are mostly a post observation tool for the evolution of the forest disappearance. A real-time forest monitoring approach is undoubtedly the most appropriate solution to prevent trees cutting. In this work, we propose a monitoring system based on acoustic sensors to classify in-situ forest sounds in real-time.

To date, there is very little work done in sensor networks for real-time monitoring of forest areas. Reference [1] used LANDSAT and RADARSAT images to evaluate the deforestation rate. This work was based on Hidden Markov Models for the multi-source time series analysis. Results showed that the detection of spatial changes in the forest coverage is possible using satellites. However, this method was limited as satellite images have low spatial and temporal resolutions resulting in relatively weak sensitivity. Wang et al. introduced in [2] a Received Signal Strength Indication (RSSI) based method for the detection of deforestation. Sensor nodes were mounted on each guarded tree, and the change in the radio signal strength was used to detect the displacement of the node. It basically means that if a tree falls, the radio signal strength will change between neighboring sensors. While this method is able to detect logging in real-time, it is inefficient for covering large areas since lots of sensors are needed. In [3], it was demonstrated that chainsaw logging can be detected by the analysis of the spectral characteristics of the chainsaw sound signal, the calculations of similarity values and signal-to-noise ratio. However, this approach was not a sound classification method and there was no information about the measurement setup. Authors in [4] presented an approach based on a one-class classifier using a kernel density approach. They show how to find the best combination of parameter σ (Kernel bandwidth) with parameters used in the Mel-Frequency Cepstral Coefficients calculation (MFCCs), and how to choose the optimal decision threshold. With optimized parameters, an accuracy of 98% was achieved.

In [5] Mel-frequency cepstral coefficients are used for audio feature extraction and supervised classification algorithms (support vector machine, k-nearest neighbors, bootstrap aggregation, and random forest) for noise classification. Their data-set is of about 3000 sound samples without animal and chainsaw sound. They explore the parameter of the four algorithms to estimate the optimal parameter values for classification of sound samples in the data-set under study. They achieve a noise classification accuracy in the range 88% – 94%.

For classifying two forest type along with one mixed class of forest of Japanese Cedar Japanese Cypress, based on image classification, authors in [6] **e**valuate four classifiers: Neural Network, Support Vector Machine, Random Forest and NN-GA (Neural Network -Genetic algorithm) . The comparative analysis has revealed that the NN-GA has performed significantly well than all the other classifiers in this study with an accuracy of 95.54 %. The authors in [7] propose a sound recognition method dedicated to environmental sounds, designed with its main focus on embedded applications which is loosely based on the human hearing system, while a robust set of binary features permits a simple k-NN classifier to be used. Sensitivity and specificity were evaluated, and chainsaw sound values, without additional noise, was, respectively, 0.978 and 0.121. With the addition of +6 dB of pink noise, sensitivity and specificity were 0.979 and 0.117, respectively. However, we don't have any information about the recording distances of sounds and the number of samples per category of sounds evaluated, and the database of 29 different environmental sounds, contains only anthropic sounds.

The work in **[**8**]** compared six of the most commonly used machine learning algorithms, including the KNN and SVM algorithms. Twelve (12) sound classes were considered without including chainsaw sounds. The number of samples taken per class being 10, remains insignificant and for the classification based on the twelve classes, neither the value of nearest neighbors nor the kernel function of the SVM is specified. The classification rate is less than 54 % for the six algorithms.

In [9], authors proposed an analysis of the autocorrelation function for the recorded acoustic signals with the help of decision trees, support vector machine (SVM), and K-Nearest Neighbor (KNN). Three sensors were combined to confirm their approach with a best hit rate of 97.7 %.

In this paper, we propose a technique to accurate the detection of the chainsaw sounds in the forest environment by evaluating two method already used in the application of automatic speech recognition, namely the MFCCs analysis. MFCCs are combined with two classifier algorithms: KNN and SVM whose parameters have been optimized. The concerned parameters are: the frame duration of the recorded sounds, the number of cepstral coefficients, the filters band for the MFCCs calculations and for KNN and SVM classifier the parameters are respectively the number K of nearest neighbors and the value of degree of SVM Kernel function. This work could be a real contribution for real time monitoring for protected forest by connecting the chainsaw sound identification system to a wireless network.

The paper is organized as follows: In Section II, MFCC, KNN and SVM algorithms are presented. In Section III, the proposed method is presented, and in Section IV we discuss about the results.

II. Presentation of MFCCs and Classifiers Model

A. *Mel Frequency Cepstral Coefficient (MFCCs)*

MFCCs [10] [11] are coefficients used in automatic speech recognition (ASR) to describe the short-term power spectrum of a speech signal. With MFCCs analysis, the dominant features of different sounds are extracted and are defined as coefficients. These coefficients result from the discrete cosine transform (DCT) of the log power spectrum calculated on a non-linear perceptual Mel-frequency scale of the acoustic signal. The preliminary processing steps for extracting the Cepstral Coefficients from various sounds are presented in Fig. 1.

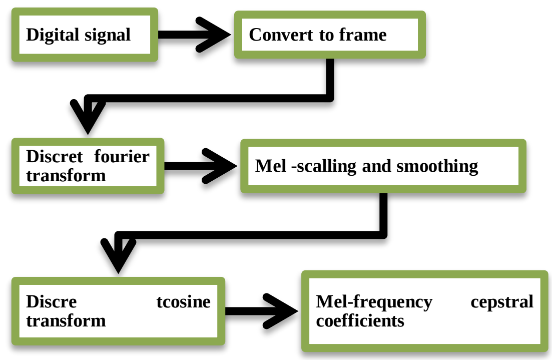

Fig. 1. Diagram Block Showing the MFCC Processing Steps for Extracting Cepstral Coefficients.

The sound signal is converted to frames of 20 ms to 40 ms with overlapping durations between successive frames. Then pre-emphasis and weighting windows are applied on these frames [12]. The discrete Fourier transform (DFT) is calculated for each frame and the log of the amplitude spectrum is taken. The Mel's frequency spectrum is obtained by applying a bank of M band-pass filters using Mel-scaling center frequencies on the previous signal [13], [14], [15]. The Mel's frequency spectrum is given by:

$$P_p = \sum_{v}^{N/2-1}\left(d_{p,v} \times F_v\right),\ p = 0,1,\dots,M \quad (1)$$

where N is the number of sampling points within a speech frame, $d_{p,v}$ is the amplitude of the band-pass filter with the index p at frequency v and F_v the Fourier transform of the signal [16].

Mel's cepstral coefficients are finally obtained by the DCT of the Mel's frequency spectrum:

$$MFCC_k = \sum_{j=1}^{M}\left(L_p \times \cos\left(\frac{k(2j-1)\pi}{2M}\right)\right) \quad (2)$$

With $L_p = \log_{10}\left(P_p\right)$, $= 0,1,\dots,m$, where m is the number of cepstral coefficients chosen for subsequent treatment $(m < M)$.

For Automatic Speech Recognition, $m \epsilon$ [2; 13] and the rest is discarded.

B. *KNN Algorithm (K-Nearest Neighbors) for Sounds Classification*

KNN is a supervised nonparametric instance-based learning algorithm [17]. The classification of a new individual is based on its similarity with the K nearest neighbors. These nearest neighbors are themselves members of predefined classes with given label. The similarity between the new individual X and the constituents $x_{i,j}$ (i being the class and j the individual in this class) of the classes is obtained by calculating the distance between them. This requires that X and $x_{i,j}$ be either scalars or multidimensional vectors [18]. A learning phase on these labeled classes makes it possible to determine the parameter K. In binary classification, it is useful to choose odd K to avoid egalitarian votes. Although several heuristic techniques exist to define the value of K, we keep its value which minimizes classification errors.

C. SVM Algorithm

SVM is an automatic learning algorithm that belongs to the class of linear classifiers. In its approach, a SVM will seek to find an affine hyperplane that separates into two categories processed data. At the end of the training phase, the SVM - consider the sign of Equation (3) to determine the nature of the new individual $x\begin{pmatrix} x_1 \\ \vdots \\ x_n \end{pmatrix}$ to be classified.

$$h(x) = w_1x_1 + \cdots + w_nx_n + b = \sum_{i=1}^{n}(w_i \cdot x_i) + b \quad (3)$$

Where the vector $w\begin{pmatrix} w_1 \\ \vdots \\ w_n \end{pmatrix}$ (the weight vector) and the scalar b (the bias) are the two quantities defining the affine hyperplane and they are determined during the training phase. In practice, there is no separating hyperplane in the study area, to remedy this, the SVM uses "kernel functions". These functions allow the passage of the study space to another space of larger dimension where the determination of the hyperplane will be possible. The most popular kernel functions are shown in [19].

III. Description of the Proposed Model

The proposed method to detect the chainsaw sound among the other sounds consists in the combination of MFCCs to KNN and to SVM leading to MFCCs- KNN and MFCCs-SVM models. Fig. 2 shows the different steps to generate the True Positif Rate with these two classifiers.

Records of chainsaw sounds were carried out in three different forests areas. A first measurement campaign was made in Armainvilliers national forest (Gretz-Armainvilliers, France), the second one in Yapo-Abbé protected forest (Agboville, Côte d'Ivoire) and the third one in the man-made National Floristic Center (Abidjan, Cote d'Ivoire). The sound recordings were made from a distance of 10 meters to 100 meters in WAV format. A sampling rate recording is 44.1 kHz. The training sounds consist in recording sounds : three different STIHL chainsaw machines with simple sounds or cutting trees sounds ; and website sound bank [20], [21] composed by other chainsaw sounds and forest sound (bird; insect, some animal). So that we obtained 3265 sound records of 5 seconds each as presented in Table I.

In the traditional MFCC's calculation for ASR, only the first twelve cepstral coefficients (when using a 8 kHz sampling frequency) are taken into account while rejecting the first coefficient. This is because the first coefficient is regarded as somewhat unreliable and the higher DCT coefficients represent fast changes in the filter-bank energies. In our approach, we take into account this first coefficient considered as the generalized frequency band energy (FBE) [22].

We pay particular attention to the percentage of sounds correctly scored according to the two classes in the presence. This percentage corresponds to the TPR (True Positive Rate) of each classifier. This size is important because it allows both the ability of the classifier to label the sounds and gives us information on the error rate incurred.

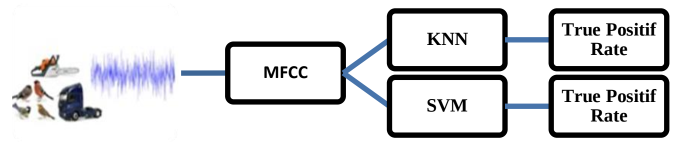

Fig. 2. MFCCs-KNN and MFCCs-SVM Algorithm Blocs for Sound Detection.

TABLE. I. Sounds and Number of Records

Sound	Number of records
Chainsaws	301
Other sounds	2964

The accuracy of these approaches is relative to the optimum parameters of these to be found.

IV. MFCCs-KNN and MFCCs- SVM Parameters Optimization and Results

The optimum parameters yielding a TPR are determined. The parameters to be optimized are:

MFCCs calculation:

- The frequency band for filter arrangement varies from 3170 Hz to 11170 Hz with a frequency sweep of 1000 Hz
- The frame duration (FD) varying from 25 ms to 1000 ms with a sample time of 25 ms
- The cepstral coefficients number (CCN) varying from 9 to 13.Subsequently we examine the need to abandon the cepstral coefficients higher than 13 as is customary in ASR.

The number of filters in the MFCC calculation has been fixed to M= 35 by the fact that it is the best compromise between the calculation time of the algorithm and its accuracy as it is suggested by authors in [20].

KNN (K-Nearest Neighbors)

- The number K of nearest neighbors from 3 to 15 by step of 2.

SVM-LOG-KERNEL

There are a variety of kernel functions as shown [19]. The most used are Linear, Polynomial, Radial Basis, Gaussian Radial, and Sigmoid kernel functions. We are interested, however, by the LOG-KERNEL function [23]. This choice is motivated by the use of the logarithm function in the calculation of MFCCs and also by the fact that the impact of the LOG-KERNEL function in the classification of sounds remains to be demonstrated. Indeed, The LOG-KERNEL seems to be particularly interesting for images. This function is in the following form:

$$k(x, y) = -\log(\|x - y\|^d + 1) \quad (4)$$

In this function, we vary the key parameter d, from 1 to 7 to find its optimum value.

A. Impact of MFCCs Filters Band Arrangement

The curves in the Fig. 3 are comparative TPRs obtained by KNN and SVM algorithms relative to the frequency indexes given in Table II. For each frequency index, we retained only the best TPR after analysis.

TABLE. II. A: FREQUENCY INDEXATION

Frequency Band	3170 Hz-4170 Hz	4170 Hz -5170 Hz	5170 Hz -6170 Hz	6170 Hz -7170 Hz
Index	1	2	3	4

B: FREQUENCY INDEXATION

Frequency Band	7170 Hz -8170 Hz	8170 Hz -9170 Hz	9170 Hz -10170 Hz	10170 Hz-11170 Hz
Index	5	6	7	8

The best TPR is obtained for both classifier at very high-frequency: 94.02 % of TPR at the frequency band [8170 Hz-9170 Hz] for the KNN classifier and 95.63 % at the frequency band [7170 Hz -8170 Hz] for SVM-LOG-KERNEL classifier. That means that the frequency band of Mel's cepstral coefficients impact subsequently the accuracy of TPR. The appropriate frequency of MFCCs must be the audio high frequency band. Therefore, even if the MFCCs are calculated in this frequency, MFCCs-SVM offered a better TPR than MFCCs-KNN.

B. Impact of Frame Duration (FD)

We study the impact of frame duration on the TPR by keeping for each classifier its optimized frequency band obtained in the section IV-A.

In Fig. 4, the classification rate depends on the chosen frame duration. For the KNN, the increase of the frame duration does not improve the classification rate. The best rate obtained is for the smallest frame duration namely 25 ms. On the other hand, the increase of the frame duration improves the classification rate of the SVM-LOG-KERNEL. The maximum value for the SVM is reached for a frame duration of 450 ms.

C. Impact of Cepstral Coefficients Number

In this section, we evaluate the impact of the number of cepstral coefficients on the classification rate. We consider the frame duration for which the classification rate is the most promising following the study of Section IV-B. In Fig. 5, the TPR is better for larger number of cepstral coefficients for both classifiers.

ASR based on the calculation of the cepstral coefficients of MEL, imposes an abandonment of the coefficients number higher than 13. This is because they represent fast changes in the filter bank coefficients and these fine details do not contribute to Automatic Speech Recognition. In our study, we extend their number up to 30 and we evaluate its impact on the TPR value. For the SVM, the increase in the number of MFCCs causes a decrease of about 2% in the classification rate (Fig. 6b) .The values in Fig. 6b are certainly lower than those obtained in Fig. 5b, but they offer TPR at least 93.45%, which is an appreciable rate.

For the KNN (Fig. 6a), where the increase in the number of MFCCs beyond 13 does not offer better results than those in Fig. 5a. The abandonment of the MFCCs above 13 as suggested in framework of the ASR is verified in our study.

D. Impact of the Classifier Parameters

We evaluate the impact of the key parameter of each classifier. For the best frequency band, we take for each frame duration, the best classification rate according to the value of the key parameter of the classifier (Fig. 7).

The number of nearest neighbors that optimizes the classification is 3 (K = 3) while the optimum degree for the SVM-LOG-KERNEL is 1 (d = 1). The increase of the metric dimension in the context of the use of the *LOG-KERNEL* does not favor the exactness of the labeling of sounds. Just as increasing the number of nearest neighbors does not affect positively the ability of the KNN. This increase in the value of the key parameters has the disadvantage of making the calculations more cumbersome.

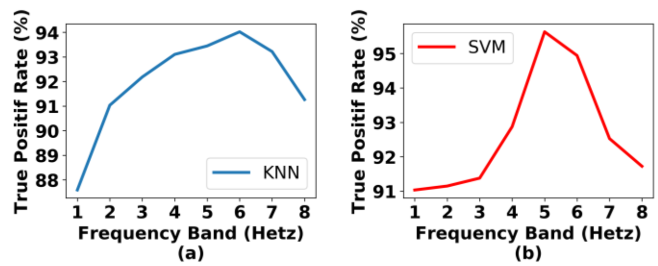

Fig. 3. TPR According to the Frequency Band of Calculated MFCC.

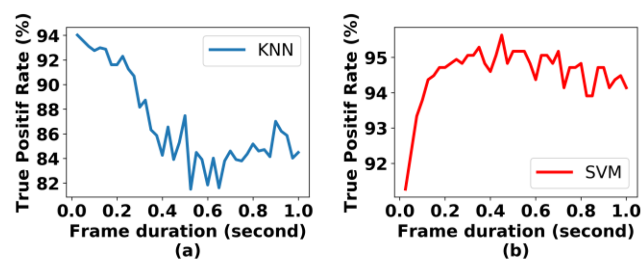

Fig. 4. TPR According to Frames Duration.

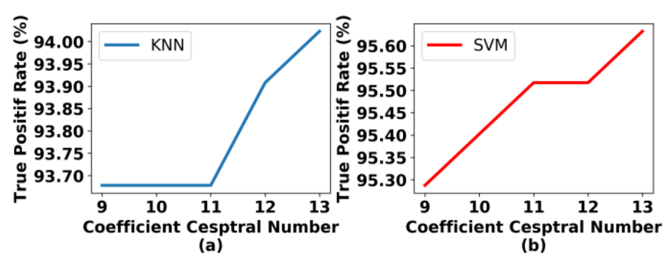

Fig. 5. Impact of the Number of Mel-Frequency Cepstral Coefficients on TPR.

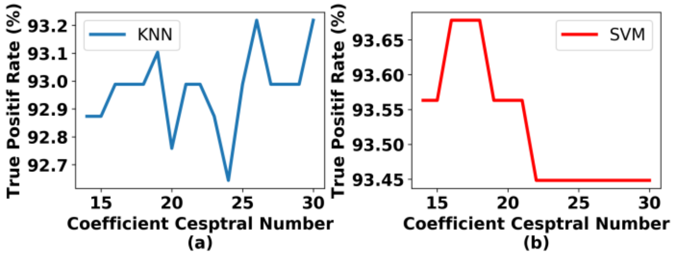

Fig. 6. Impact of the Number of Mel-Frequency Cepstral Coefficients on TPR.

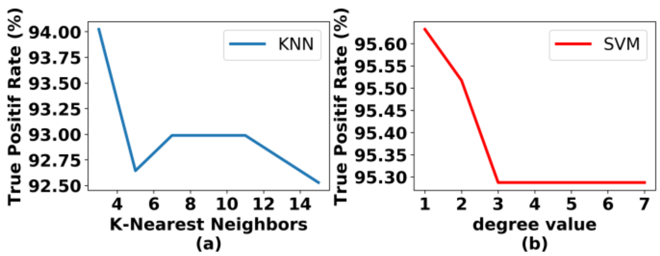

Fig. 7. TPR According to Key Parameter of Classifiers.

E. Comparison of the MFCC-KNN and MFCC-SVM Performances

In Table III, we summarize the TPR for the complete classification of all recorded sounds (general) then individually the TPR for the chainsaw sounds (chainsaw) classification and the TPR for the other sounds (forest) classification are given. The process time for each classification is also display in Table III. An Ubuntu virtual machine installed on a PC running at 2.4 GHz with an 8 GB RAM is used for the tests. The virtual machine has a RAM of 3 GB and 1 processor.

The SVM-LOG-KERNEL classifier offers the best classification rates for a processing time more than 30 times lower than KNN. This process time does not include the MFCCs calculation time because it is similar for both classifiers. As shown, SVM -LOG-KERNEL has a definite advantage in its use for sound labeling.

TABLE. III. RESULT FOR EACH CLASSIFIER

Classifiers	True Positif Rate (%)			Process Time (second)
	general	chainsaw	forest	
KNN	94.02	40.51	99.37	**67**
SVM-LOG-KERNEL	95.63	53.16	99.87	**2**

V. Conclusion and Discussion

The choice of a classifier for the real-time recognition of chainsaw sound in the forest environment has required the comparison of SVM and KNN classifiers with MFCCs calculations. The best TPR we obtained to classify the whole forest sounds are 95.63% and 94.02%, respectively for SVM classifier and KNN classifier. These values are the result of the choice of judicious parameters: number of near Neighbors K=3 for KNN algorithm and the order of the Log-Kernel function in SVM algorithm d=1. The presented results concerned a most extensive database with sounds spectrums near the chainsaw sound i.e. aircraft, motorbike reducing SVM and KNN classification particularly the chainsaw sound. Therefore, we obtained 53.16% and 40.50% respectively for SVM and KNN classifier. For the forest environment, SVM and KNN classifiers give similar results with the more complex algorithm NN-GA but they are simple to implement and fast processing.

The difference between processing time of MFCC-KNN and MFCC-SVM can be understood from the analysis of the classification approach for each of them. The KNN algorithm, focusing on calculating the distance between the new individual and the reference samples, to detect similarities, sees its execution time increases linearly with the size and amount of reference patterns. In contrast, the SVM, whose approach is based only on the provision in a metric space of the new individual in order to identify it, performs less calculation. SVM is most suitable when considering a large number of samples constituting the reference base, which is our case study.

It is important to determine a method able to increase the chainsaw detection rate. This other method will be a complement to MFCC-SVM algorithm. Thus the decision to label a new individual will take into account the results coupled with the two methods.

Acknowledgment

This work was supported by SODEFOR of Cote d'Ivoire Government Company.

References

[1] A.-B. Salberg and Ø. D. Trier. (2012).Temporal analysis of multisensor data for forest change detection using hidden Markov models. Proc. IEEE Int. Geosci. Remote Sens. Symp. (IGARSS), 6749–6752. doi: 10.1109 / IGARSS.2012.6352556.

[2] S. F. Wang, K. Y. Wang, X. J. Wang, Z. Q. Liu. (2012). A Novel Illegal Logging Monitoring System Based on WSN. Advanced Materials Research, 1417-1421. https://doi.org/10.4028/www.scientific.net/AMR.518-523.1417.

[3] Tang Y., Han P., Wang Z., Hu L., Gao Y., Li H. (2012). Based on intelligent voice recognition of forest illegal felling of detecting methods. 2nd International Conference on Cloud Computing and Intelligent Systems, 1153 – 1156. doi: 10.1109/CCIS.2012.6664564.

[4] Colonna, J. G., Gatto, B., Dos Santos, E. M., & Nakamura, E. F. (2016). A framework for chainsaw detection using one-class kernel and wireless acoustic sensor networks into the amazon rainforest. Mobile Data Management (MDM), 17th IEEE International Conference, 2, 34–36. doi: 10.1109/MDM.2016.86.

[5] Y. Alsouda,S. Pllana,A. Kurti (2019). IoT-based Urban Noise Identification Using Machine Learning: Performance of SVM, KNN, Bagging, and Random Forest. In Proceedings of the International Conference on Omni-Layer Intelligent Systems. ACM, 62–67.

[6] Chatterjee S., Ghosh S., Dawn S., Hore S., Dey N.(2016) Forest type classification: a hybrid NN-GA model based approach. In: Satapathy, S.C., Mandal, J.K., Udgata, S.K., Bhateja, V. (eds.) Information Systems Design and Intelligent Applications. AISC, vol. 435, pp. 227–236. Springer, New Delhi. doi: 10.1007/978-81-322-2757-1_23.

[7] Kugler M.; Tossavainen T.; Nakatsu M.; Kuroyanagi S.; Iwata (2016). A. Real-time hardware implementation of a sound recognition system with in-field learning. IEICE Trans. Inf. Syst, 99, 1885–1894.

[8] Bountourakis, V.; Vrysis, L.; Papanikolaou, G. Machine Learning Algorithms for Environmental Sound Recognition: Towards Soundscape Semantics. In Proceedings of the Audio Mostly 2015 on Interaction with Sound, Thessaloniki, Greece, 7–9 October 2015.

[9] L. Czúni, and P. Z. Varga. (2014). Lightweight Acoustic Detection of Logging in Wireless Sensor Networks. The International Conference on Digital Information, Networking, and Wireless Communications (DINWC2014). The Society of Digital Information and Wireless Communication.

[10] J. G. Colonna, A. D. Ribas, E. M. d. Santos, and E. F. N. (2012). Feature subset selection for automatically classifying anuran calls using sensor networks. International Joint Conference on Neural Networks (IJCNN). 1–8doi: 10.1109 / IJCNN.2012.6252794.

[11] D. O'Shaughnesssy. (2008). Invited paper: Automatic speech recognition: History, methods and challenges. Pattern Recognition, 10, 2965–2979. https://doi.org/10.1016/j.patcog.2008.05.008.

[12] Fitch, W. T. (2000a). The evolution of speech: A comparative review. Trends in Cognitive Sciences, 4(7) ,258–267. https://doi.org/10.1016 /S1364-6613(00)01494-7.

[13] Md. Sahidullah ,Goutam Saha. (2012). Design, analysis and experimental evaluation of block based transformation in MFCC computation for speaker recognition. Speech Communication 54,4(2012),543–565. https://doi.org/10. 1016/j.specom.2011.11.004.

[14] H. Fastl and E. Zwicker. (2006).Psychoacoustics - Facts and Models. (3rd ed.). Springer.

[15] B. C. Moore. (2013). An Introduction to the Psychology of Hearing. (6th ed.). BRILL.

[16] K. Kido. (2014). Digital Fourier Analysis: Advanced Techniques. Springer.

[17] K. Lan, D, Wang, S. Fong, L. Liu, K. Wong and N. Dey, "A survey of data mining and deep learning in bioinformatics", Journal of Medical Systems, vol. 42, no. 8, pp. 1-20, 2018.

[18] R.O. Duda, P.E. Hart, D.G. Stork. (2011). Pattern Classification. (2nd ed.). WileyBlackwell.

[19] Souza, César R. "Kernel Functions for Machine Learning Applications." Accessed on 17 October 2019. http://crsouza.blogspot.com/2010/03/ kernel-functionsfor-machine-learning.html.

[20] http://bbcsfx.acropolis.org.uk/ Accessed on 17 october , 2019.

[21] UNIVERSAL-SOUNDBANK Bruitages & sons gratuits (2019) http://www.universal-soundbank.com/forets2.htm / Accessed on 6 May 2019.

[22] Zheng Fang, Zhang Guoliang, Song Zhanjiang.(2001). Comparison of different implementations of MFCC. Journal of Computer Science and Technology,6, 582-589, https://doi.org/10.1007/BF02943243.

[23] S. Boughorbel, J. Tarel, and N. Boujemaa.: Conditionally Positive Definite Kernels for SVM Based Image Recognition.In: IEEE International Conference on Multimedia and Expo (ICME2005), pp.113-116. (2005).

An Efficient Algorithm to Find the Height of a Text Line and Overcome Overlapped and Broken Line Problem during Segmentation

Sanjibani Sudha Pattanayak[1], Sateesh Kumar Pradhan[2]
Department of Computer Science and Application
Utkal University, Bhubaneswar, India

Ramesh Chandra Mallik[3]
P.G. Department of Odia Language and Literature,
Utkal University, Bhubaneswar, India

***Abstract*—Line segmentation is a critical phase of the Optical Character Recognition (OCR) which separates the individual lines from the image documents. The accuracy rate of the OCR tool is directly proportional to the line segmentation accuracy followed by the word/character segmentation. In this context, an algorithm, named height_based_segmentation is proposed for the text line segmentation of printed Odia documents. The proposed algorithm finds the average height of a text line and it helps to minimize the overlapped text line cases. The algorithm also includes post-processing steps to combine the modifier zone with the base zone. The performance of the algorithm is evaluated through the ground truth and also by comparing it with the existing segmentation approaches.**

Keywords—Document image analysis; line segmentation; word segmentation; database creation; printed Odia document

I. Introduction

The Segmentation phase is one of the important phases of the character recognition process which separates the individual lines or words or characters from the image documents. There are several challenges associated with this segmentation process which are intended to discuss taking into consideration of the printed Odia documents.

The Projection profile-based method is a traditional method of segmentation. It has been noticed that a few problems may appear if the projection-profile-bases method will be adopted for segmentation. Therefore, the issues and challenges involved in the process of segmentation are discussed.

Odia language has a rich set of symbols. Approximately, 300 (three hundred) symbols comprising of the consonants, vowels, conjuncts, modifiers, digits, special symbols, etc. The modifiers for a symbol can be placed in different positions; top, bottom, left or right. Odia symbols do not maintain any headlines like other north Indian scripts (Devanagari, Bangla...). Below shown is an example of an Odia line (Fig. 1). The present example shows the different zones, such as base zone, upper modifier zone, and lower modifier zone.

It is not necessary that every text line would contain a lower or upper modifier zone. It may contain only base zone, base zone with any one of the upper/lower modifier zone or base zone with both the modifier zones.

A. Challenges Faced During Text Line Segmentation of Printed Odia Document

During the segmentation, the contents of two text lines might be overlapped or touched in different places making the segmentation process challenging. This is shown here in Fig. 2.

Furthermore, there are cases where during segmentation, the upper and lower modifier zone get separated from the base zone resulting in split or broken lines (Fig. 3).

The skewness of the image document cannot be avoided as manual interpretation for scanning is involved (shown in Fig. 4). There is a problem associated with document base-line detection. Without correcting the skewness, the segmentation becomes difficult.

A document may contain fonts of different sizes e.g. large font for heading or large initial letter (Fig. 5). This is another challenge in front of the text line segmentation.

There might be more than one column in the same document which makes the segmentation process projecting more challenges (Fig. 6).

In the proposed algorithm resolves issues like overlapped text lines, splitted lines and documents with different font sizes. It has been evaluated on different types of documents like good quality, low text density, degraded images, etc.

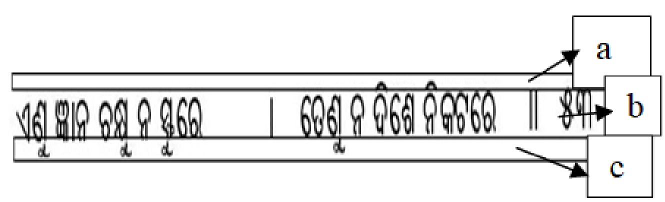

Fig. 1. Different Zones of an Odia Text Line (a) Upper Modifier Zone (b) Base Zone (c) Lower Modifier Zone.

Fig. 2. Example of Overlapped Lines.

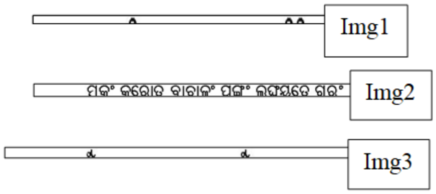

Fig. 3. Demonstration of Text Line Broken into 3 different Images; (Img1:) upper Modifier Zone, (Img2:) base Zone, (Img3:) Lower Modifier Zone of a Single Line.

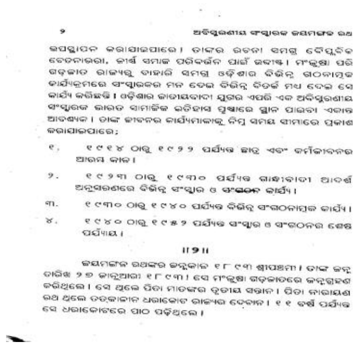

Fig. 4. Example of a Skewed Document.

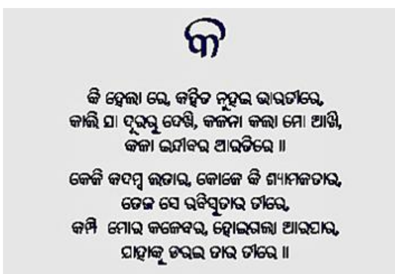

Fig. 5. Document with Large Font for Heading.

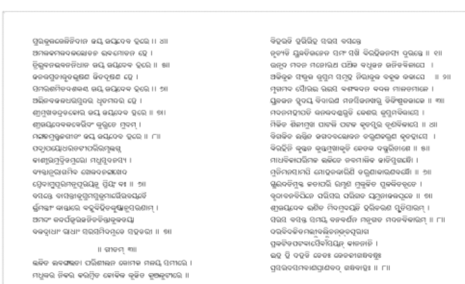

Fig. 6. Document having more than One Columns.

II. Review of Literature

The segmentation algorithms which are successfully applied for the English language, cannot be used for Odia documents due to the inherent nature of Odia scripts. The structure of Roman script and Odia script are different in nature. Different algorithms have been proposed by the researchers for line segmentation earlier. Here few segmentation strategies that have been adopted for Telugu documents are cited as Odia script has lots of similarity with Telugu script [8].

A projection profile is a well-known method for segmentation. In the plotted projection profile, the peaks and valleys of the image are shown. The zero-valued valleys indicate a white line or gap between two lines. When the lines are well separated, the projection profile gives a satisfactory result, whereas in many cases, it results splitting and overlapping. In detail, it has been discussed and demonstrated in the result section.

Kopullu et al. [1] generated connected components from document images for segmentation. The pixels that are connected are labeled with the same blob and then the blob is extracted from the image. They have tested their method on 465 different Telugu documents. It shows good results for high-quality documents but the output degraded with quality. For Odia documents, it will separate the untouched modifiers from the base, thus recognition complexity will increase. Swamy et al. [2] combines the projection profile and connected component for segmenting lines, words as well as characters. It shows good results for high-quality documents but gives segmentation error for touching lines and broken characters. A method using a modified histogram obtained from run-length smearing is proposed by N Priyanka [3]. This method has been verified for different Indic language documents like Telugu, Bengali, Devanagari, Kannada and also for multilingual documents. Kopullu and Negi [4] developed a robust method for text line segmentation using the Fringe map where a fringe map is generated for the input binary image; between text line, peak fringe number is located to construct region between adjacent text lines. Then the segmented path is generated by joining peak fringe number. This method has been tested on 234 images and resulted in 97% accuracy. Tripathy and Pal [5] have proposed a water reservoir based segmentation approach for extracting text lines of unconstrained Odia handwritten documents. Then to extract words, vertical projection profile and structural features of Odia characters are taken into account. Then using structural, topological and water reservoir based features, characters are extracted. Senapati et al. [6] have worked on text line segmentation of printed Odia documents where they have considered the white space between two consecutive lines. For word segmentation, the image is transposed to invert row and column and the same line extraction algorithm is repeated. This method works only in a case where lines are well separated. Segmentation for Odia documents is yet to achieve some milestone.

III. Motivation

There is no substantial work done in the segmentation area in Odia language which is the major motivating factor to work in the same area.

The study of the projection profile output which is shown in the following figure (Fig. 7) motivates height based segmentation. The text line which is not splitted or overlapped is considered as a normal line. The study of the output generated by implementing the traditional projection profile method on the Odia documents, reveals that most of the text lines segmented are normal lines.

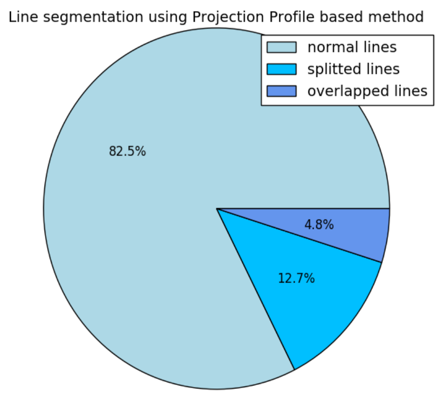

Fig. 7. Overall Line Segmentation Result for all the Documents using the Projection Profile-based Method.

In this case, more than 80% segmented lines are normal lines whereas around 12% segmented lines are broken and around 5% lines are overlapped. Also, document-wise line segmentation results in more normal lines in comparison to splitted or overlapped lines in most of the cases. So, the average height of a normal line can be found easily which will help verify if a line is broken or not. Also, it will help to find the overlapped region between two lines.

IV. Proposed Method

The proposed algorithm named as height_based_ segmentation segments text lines from printed Odia documents having a single column. A variety of documents; good and poor quality, have been collected from different sources. These documents are then converted to image form (jpg, bmp, png, tiff, etc.). The no. of lines present in these documents varies from 5 to 35. The algorithm considers an image document as the input, segments individual text lines and stores these as output. The output images are in jpg format. The segmentation is done based on the approximate height of a text line. So the height of the text line plays a very important role here.

As a part of pre-processing, input image is binarized applying Otsu's method. Here the background of the image document is white whereas the texts are written in black.

Consecutive nonzero rows (The row having at least one black pixel) in the image document form a text line. So counting the consecutive rows gives the height of the text line. These consecutive text lines may include a normal text line, overlapped lines or a broken line that contains the modifier zone. Finding the approximate height of a text line can help us to solve the problem of overlapped lines as well as a broken line.

The text line which is not broken or overlapped is considered as a normal line. To find the approximate height, the frequency of the height of the text lines is considered. If more normal lines are present in a document, the highest frequency is considered as the approximate height of the text line. To confirm the above, the second highest frequency of height is found. If the ratio of the second-highest frequency of height and highest frequency of height is more than 3, then there are more broken lines in the document. (The height of the upper or lower modifier which is separated from the base zone of the text line usually occupies one-third of the height of the base zone.). Here the second highest frequency of height is considered as the approximate height of the normal text line.

When the ratio of the highest frequency of height and second highest frequency of height is more than 2, then there are more overlapped lines in the document. So the second highest frequency of height is considered as the approximate height of the normal text line.

Now for each identified text line, collect the first nonzero row no. Find if the text line is overlapped, broken line or normal line from its height. If it is a normal line, extract the sub-image from the document image within the range (first non-zero row and first non-zero row+ height of the text line).

If the text line is found to be overlapped, the quotient value obtained from the height of the text line and approximate height of the line will give the no. of text lines overlapped. To extract the individual text lines from the overlapped text line, the following code snippet is used.

i) **threshold**=8 *// threshold value 8 gives the best result for this experiment*

ii) **rem**=height of text line% **Approx._height**

q=height of text line/ **Approx._height** *//maximum q no. of text lines is overlapped*

r= **Approx._height** /3 *//r is the approx. height of the upper or lower modifier.*

iii) if (**Approx._height** - rem <= r):

/(all those lines whose height is greater than* ***Approx._height****, doesn't contain an overlapped line. e.g.: calculated approx. height is 18. But, the height of a text line may be slightly more or less than 18.) */*

iv) **starting_point**=first_nonzero_row

v) for all the rows in the range (**starting_point**+**Approx_height**-**r**, **starting_point** + **Approx_height** + **r**):

vi) if a row has less pixel than **threshold**: mark this row **op** as an overlapping row.

vii) Extract the sub-image from the document between **starting_point** and **op**.

viii) **starting_point**=**op**+1. */* The next text line starts from the next row after op/**

viii) repeat step (iv) to (viii) for q no. of times. To extract q text lines.

After extracting images of all the text lines from the document image, post-processing is applied to solve the broken line problem. All the extracted images are saved sequentially in a folder. The height of each text line is computed. If the ratio of the approximate height and the height of the text line is found to be around 3, then it is identified as an upper or lower modifier zone of the text line. It should be merged with the base zone of the text line. Using the algorithm which is mentioned in paper [7], it is identified either as a lower or upper modifier zone image. If the image is found to be an upper modifier zone, then it is merged with the next image in the folder which is supposed to be the image of the base zone. If the image is identified as the lower modifier zone, then it is merged with the previous image in the folder which is supposed to be the image of the base zone.

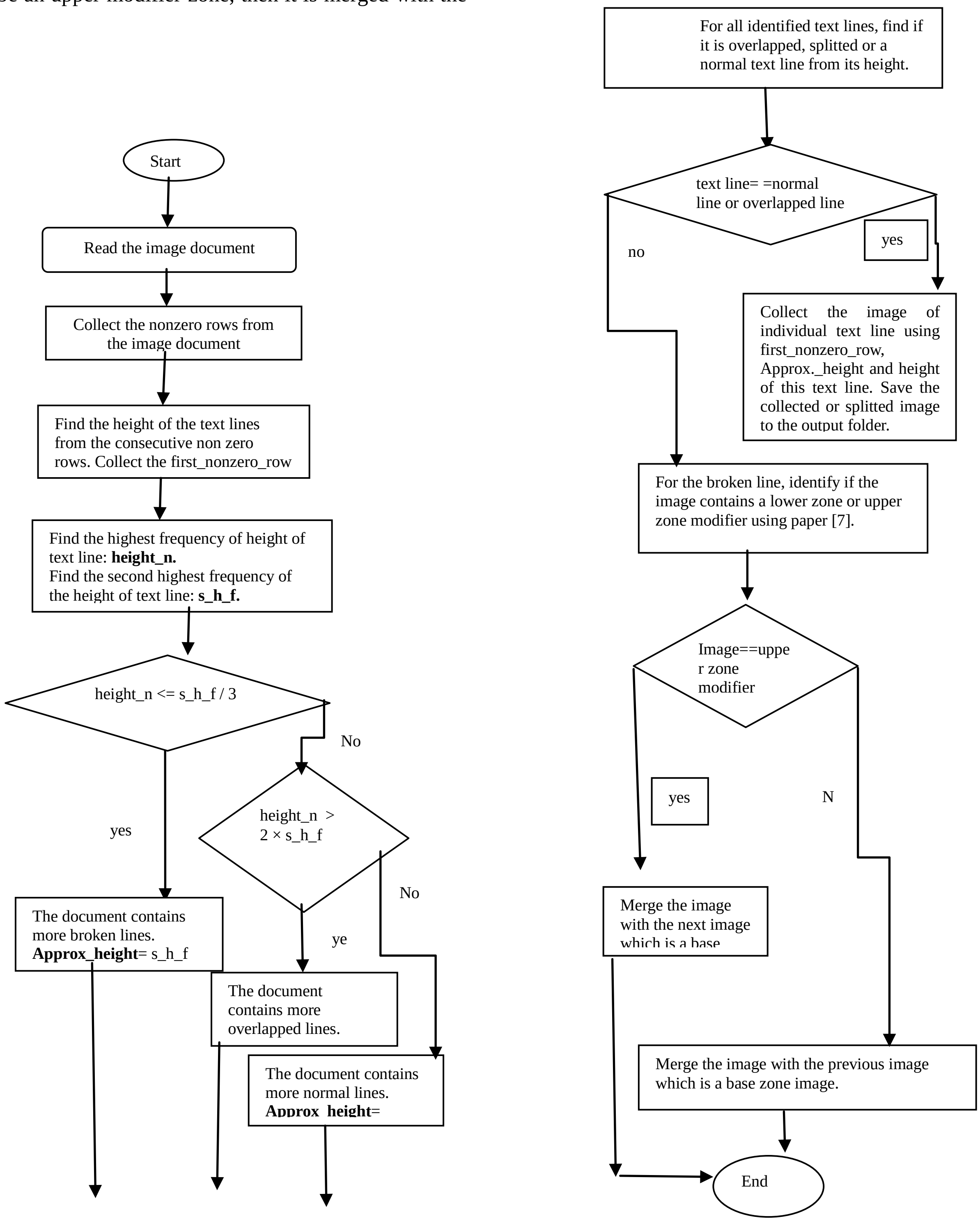

Fig. 8. Flow chart for the height_based_segmentation algorithm:

V. Experimental Result

The Experiment is carried out on a variety of printed Odia books having different font sizes and font types. Few documents are of very high quality and well-spaced whereas many books are of degraded printing quality. There are cases in which the font of the chapter heading is much larger than the body.

The pdf formats of the books are collected from different sources. To maintain heterogeneity, books published in different time period have been chosen. Pages that are considered for the experiment are free from all sorts of graphical contents; contain only textual data. The books contain writing only in a single column.

Then the pdf forms of the books are converted to image documents. These image documents are the input for our segmentation system. Here, a total of 265 documents are considered for the experiment. No. of text lines present in these documents varies from 5 to 40.

The proposed algorithm height_based_segmentation is implemented in Python numpy and scipy package. The performance of the algorithm is evaluated with the ground truth manually as well as with the popular projection profile-based method.

From the result (which is demonstrated in above graph Fig. 8 and Table I), it can be observed that using height_based_segmentation algorithm, broken lines have been reduced by 96% whereas overlapped line cases have been reduced by 71%. Training more varieties of modifiers may reduce more broken lines.

Using a horizontal projection profile-based algorithm, around 26000 nos. of words are segmented from the segmented lines.

With these collected words and lines, two separate databases have been built. The line database contains nearly 6000 normal lines, 300 overlapped lines, and 800 broken lines. Similarly, the word database contains approximately 26000 words. The database contains data of varied font type and size. These databases will be available to the researchers who work in the related field by contacting the authors.

TABLE. I. COMPARISON OF PROJECTION PROFILE-BASED METHOD AND OUR ALGORITHM

Segmentation method	No. of documents	No. of normal lines	No. of broken lines	No. of overlapped lines
Projection profile based method	265	5450	841	319
Our Algorithm	265	5993	26	61

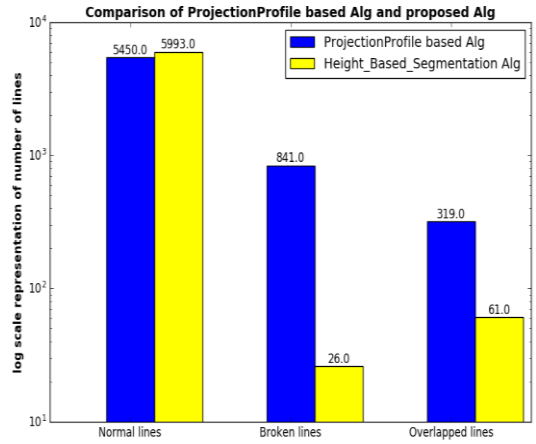

Fig. 9. Comparison of Projection Profile-based Algorithm and Proposed Algorithm.

VI. Conclusion

Line segmentation is a very important phase of the optical character recognition method. The accuracy of the whole system is largely dependent on line-segmentation accuracy. Here, an attempt has been made to experiment line segmentation based on the height of the normal lines as it is observed that comparatively few lines in a document suffer from broken-line or overlapped issues. Here, our new algorithm gives a ray of hope. The accuracy of our algorithm can be increased even more by correcting the skewness of the document. More variations of modifier symbols may be collected and trained to reduce more broken line problem.

References

[1] V. K. Koppula, N. Atul and U. Garain, "Robust Text Line, Word And Character Extraction from Telugu Document Image," Second International Conference on Emerging Trends in Engineering and Technology, Nagpur, 2009, pp. 269-272.

[2] Das, M. Swamy, and Dr. CRK Reddy. "Segmentation of Overlapping Text Lines , Characters in Printed Telugu Text Document Images." 2010.

[3] Nallapareddy Priyanka, Srikanta Pal and Ranju Manda. Article:Line and Word Segmentation Approach for Printed Documents. IJCA,Special Issue on RTIPPR (1):30–36, 2010.

[4] V. K. Koppula and A. Negi, "Fringe Map Based Text Line Segmentation of Printed Telugu Document Images," 2011 International Conference on Document Analysis and Recognition, Beijing, 2011, pp. 1294-1298.

[5] N. Tripathy and U. Pal, "Handwriting segmentation of unconstrained Oriya text," Ninth International Workshop on Frontiers in Handwriting Recognition, Kokubunji, Tokyo, Japan, 2004, pp. 306-311.

[6] D. Senapati, S. Rout and M. Nayak, "A novel approach to text line and word segmentation on Odia printed documents," Third International Conference on Computing, Communication and Networking Technologies (ICCCNT'12), Coimbatore, 2012, pp. 1-6, 2012.

[7] S S Pattanaik, S K Pradhan, R C Malik, Printed Odia Symbols for character Recognition: a Database study, In the proceeding of 3rd Intl. conference on Advanced Computing and Intelligent Engineering,2018, Bhubaneswar, India.

[8] P Mohanty, On script Complexity and the Odia script, Dedicated to Gabriel Altmann on the Occasion of his 75th Birthday,2007.

Adverse Impacts of Social Networking Sites on Academic Result: Investigation, Cause Identification and Solution

Maruf Ahmed Tamal[1], Maharunnasha Antora[2]
Md. Abdul Aziz[4], Pabel Miah[5]
Department of Computer Science & Engineering
Daffodil International University, Dhaka, Bangladesh

Karim Mohammed Rezaul[3]
Faculty of Arts, Science & Technology
Wrexham Glyndŵr University
Wrexham, UK

***Abstract*—Social networking sites (SNS) have become more prevalent over the previous decade. Interactive design and addictive characteristics have made SNS an almost indispensable part of life, particularly among university learners. Previous studies have shown that excessive use of SNS adversely affects learners' academic success as well as mental health. However, still now, there is a lack of clear evidence of the actual rationalization behind these adverse effects. Concurrently, any significant preventive measures are not yet introduced to counter the excessive use of SNS, particularly for students. To bridge this gap, considering a view of 1862 students (male = 1183, female = 659), the current study investigates how and in which way spending time in SNS negatively influences students' academic performance. Correlation and regression analyses showed that there is a powerful negative correlation between students' spending time in social media (STISM) and their educational outcome. Simultaneously, our investigation indicates that classroom standing social media use and late night social media use result in poor educational outcome of the students. Based on the findings of the investigation, an Android based application framework called SMT (Social Media Tracker) is designed and partially implemented to minimize the engagement between students and SNS.**

Keywords*—*Social networking sites; SNS; social media; SM; addiction; mental health; poor academic outcome; sleep disorder; social media tracker introduction

I. Introduction

Social media has now become one of the most important channels of communication. It allows people to connect far and near. Over the previous decade, the popularity of social networking sites like Facebook, WhatsApp, WeChat, Instagram, Twitter, etc. has risen rapidly. This is very likely because it is widely used by college, university and youth pupils to access the world's network. According to Statista [1], in the first quarter of 2019, Facebook had 2.38 billion monthly active users. Twitter had more than 330 million monthly active users worldwide as of the first quarter of 2019 [2]. On the other hand, WhatsApp had more than 500 million monthly active users worldwide as of the first quarter of 2019 [3]. Simultaneously, video games also have become a popular way of virtual communication. This clearly indicates that Social Networking Sites are rapidly getting popular. A large proportion of total users of social media are students and it is exponentially growing day by day. There is no doubt that social media has many beneficial effects. At the same time, today, particularly in students, adverse effects are becoming greater. Social media's dark side involves decreasing academic achievement [4, 5], increasing anxiety [6], cyberbullying [7, 8], addictive behaviour [9], deprivation of sleep [10], sexting [11] and much more, which are major concerns. It is obvious that Social Medias are designed to be addictive as much as possible for financial gain. According to [12], for economic gain, social media businesses intentionally addict consumers to their products. Most of the social media companies hire 'attention engineers' because they want to make sure that their users give as much as time on their sites and they always try to make their product as addictive as possible. As a consequence, individuals in social media are unconsciously wasting a lot of time. The main problem is that students are also using and becoming addicted to social media. Spending enormous time in social media is affecting their academic performance negatively. At the same moment, excessive use of social media creates various health issues such as poorer sleep quality, anxiety, loneliness, and less self-esteem. However, still now, there is a lack of clear evidence of the actual rationalization behind adverse effects of social media. On the other hand, any significant preventive measures are not yet introduced to counter the excessive use of SNS. The purpose of the study is to find out how social media adversely impacts on student's academic result and introduce the effective preventive measures to minimize the negative effects. However, the following specific objectives have been pursued in order to achieve the main goal of this paper:

1) Finding out the correlation between STISM and student's academic outcome (SGPA) and exploring the intensity of this connection.

2) Exploring, how STISM numerically predicts SGPA of students.

3) Investigating on how social media influence male and female students in everyday life.

4) Finding effective solutions against the adverse effects of social media and develop an android based application to minimize the engagement between students and SNS.

II. Literature Review

In order to attain sustainable education, SM (Social Media) currently plays an indispensable role in the learning behavior of university learners [13]. Globally, SM's use is growing. SM's effect on sustainable education is becoming an important and driving factor. It has undoubtedly become a significant means of communication for learners, especially at the stage of higher education. Connecting and communicating through SNS is now one of the most significant characteristics in the life of college learners. Texting, graphical messaging, sharing, and viewing academic and non-academic things may influence the academic lives of learners, particularly their academic performance [14]. Social media has so many beneficial effects on education. As well as multiple dark sides have become a matter of huge concern, particularly for learners at tertiary level. Most of the time students use social media for entertainment, sharing thoughts with friends. In this way they use social media for non–academic purpose rather than academic purpose. According to [4], the use of social media for educational reasons was not an important predictor of academic performance, while the use of social media for non-academic reasons and social media multitasking considerably anticipated to be poor academic performance. Students are concurrently engaged in various tasks and while studying and attending school, they are writing, reading and using social media which contributes to obtaining their lower GPA [15]. In [5], the research reveals that time spent on Facebook was considered to be negative for freshmen. But why does non-academic uses of social media have a negative impact on the student's academic outcome? According to [16], during class session social media uses have a direct and adverse effect on the academic achievement of the student. This distracts learners to focus on the class lessons. The use of social media in classrooms frequently decreases attention towards the quality of lectures which leads to missing lesson information and damaging academic effectiveness. On the other side, the addictive use of social media is associated with reduced self-esteem, anxiety, depression, and bad quality of sleep that adversely affects the academic outcome. According to [17], adolescents who use more social media both in general and at night and those who are more emotionally attached in social media experienced poorer quality of sleep, reduced self-esteem, and greater rates of anxiety and depression. The use of social media over 2 hours per day is linked to bad mental health self-rating and feelings of elevated psychological distress and suicidal ideation [18]. But question is why social media is addictive? Why do individuals spend time there? Probably the answer is dopamine. Dopamine is produced deep in the midbrain and released throughout the brain in many separate fields. These regions are mainly accountable for learning, habit-forming, and addiction-related behaviors [19]. According to [20], dopamine is a neurochemical that is produced in different areas of the brain and is critical in all kinds of brain activities. It improves overall excitement and goal-driven behavior. Ex-Facebook VP of user growth said that Social media (Facebook) promotes short-term dopamine drivers feedback loops which are destroying the society [21]. Another past study [22] revealed that results on social media users from neurological and psychiatric exams indicate that comparable biological and psychological symptoms of alcohol, cigarette and drug addicts are seen in active social media users. In Internet addicts, there are some frequent symptoms shown such as depression, death and suicidal ideas, low self-esteem, loneliness and social isolation (see Table VII). Most of the previous studies have discussed the negative aspects of social media overuse but did not discuss in depth whether and how it has a negative impact on the academic performance of students. At the same time no significant action has been taken to mitigate this issue, particularly for students. A few android-based applications have been identified that can be used to mitigate this issue, but none of them were designed for students in particular (see Table VI).

III. Research Methodology

The primary purpose of the present study is to explore how excessive use of social media negatively impacts on students' academic performance at university level. As well as develop an android based application to minimize the engagement between students and SNS. To present the overall study, the methodological portion has been split into several sections.

A. Primary and Secondary Data

A substantial literature review was performed at the beginning of the study to identify the gap in the existing studies. Simultaneously, significant study issues were found through literature review which assisted to collect relevant data. This study was conducted between July 2018 and June 2019 at Daffodil International University, Dhaka, Bangladesh. Primary data was collected through both field survey and online survey. A web-based questionnaire (Google form) was sent to the students' school e-mail addresses with information about the study and survey paper (offline) were distributed to undergraduate students during class time to participate.

B. Measures and Participants

Five multiple-choice questions along with two general questions where respondents had to input number (SGPA and Spending time in social media), were included in the survey questionnaires. In order to fulfill the research objective and achieve the effective outcome, the following questionnaires were asked to participants "How much time you spend in social media in average?", "What was your SGPA (Semester Grade Point Average) in previous semester", "Do you think social media has positive impact on your academic result?", "Do you ever used social media in classroom?", "When you spend "most of the time" in social media?" and "When you use social media for academic purposes?". A total of 3500 questionnaires were distributed and 1842 valid responses were gathered (field survey: 1267 internet survey: 595), including spontaneous female (35.8%) and male (64.2%) participants. The ethical factors of the respondent have been closely assured to keep their privacy strictly and confidentially secret. The school administration also approved the ethical permission.

C. Data Preprocesing

In order to obtain the precise value, dataset was fully prepossessed until irrelevant, incomplete, inconsistent information were removed. Several python libraries were used to preprocess the raw data. To discover outliers we used box plot and Interquartile Range (IQR) measures as a part of data preprocessing. A boxplot is a graph that provides a good idea of how the information values are distributed. It is a standardized way to display information of distribution. Simultaneously, IQR says how the "center" values are spread out; it can also be used to say when some of the other values are "too far" from the main value. These points "too far" are called "outliers," As outliers negatively influence actual findings, we removed all outliers.

D. Data Analysis

a) Correlation Analysis: 4 correlation statistics (Spearman, Pearson r, Kendalltau and Point Biserial) were followed to assess the strength and direction (either positive or negative) of the relationship between two factors (Spending time in social media (STISM) and Semester Grade Point Average (SGPA)). The value of the correlation coefficient differs between + 1 and -1 in terms of the intensity of the connection. A value of ± 1 refers to an ideal degree of connection between the two variables. The connection will be weaker as the correlation coefficient value goes close to 0. The sign of the coefficient shows the direction of the relationship; + sign shows a positive connection and - sign indicates a negative connection.

b) Regression Analysis: The correlation only determines the relationship between two factors and reflects the linear relationship. But regression depicts the numerical relationship between an independent variable and the dependent variable. As we also required to understand how STISM affects SGPA, we used linear regression determining STISM as an independent variable and SGPA as a dependent variable.

IV. Descriptive Analysis

A. Respondents based on Gender

3,500 survey questionnaires had been distributed to collect the primary data, over the university students. Total 1918 responses were collected and preprocessed. After removing the irrelevant, incomplete, inconsistent records, 1842 records were selected for analysis. Table I shows the frequency distribution and percentage of students according to gender. There was a spontaneous response from both male and female participants. The proportion of participants among male and female were 64.2% and 35.8%, respectively where the participants ' age ranged from 19 to 25.

B. Use of Social Media Affecting Academic Grade

The application of social media has become a prevalent phenomenon among all age groups. This is more common among adolescents and young adults. It is evident that students using social media for a longer period of time adversely affect academic achievement. Table II demonstrates a descriptive summary of academic grades achieved by students and corresponding spending time in social media. At the same time, it shows that the students who are good in terms of academic results spent less time on social media. On the other hand, students spending an enormous amount of time on social media have obtained poor academic results. For male students who achieved A+ (SGPA) and A (SGPA), they used Social Media (SM) for 2.19 hours and 2.02 hours respectively. On the other hand, the majority of them performed poor grades (e.g. C and D) when they spent a longer period of time in SM (e.g. 7.43 and 8.18 hours). Like the male, female also showed the same tendency. Those female students achieved good academic results (e.g. A+, A, A-, B+) spent less amount of time in social media. At the same time, female students with the poor academic result (C+, C, D) spent a longer amount of time on social media.

TABLE I. Frequency Distribution According to Sex

Gender	Frequency	Frequency distribution in percentage
Male	1183	64.2%
Female	659	35.8%

TABLE II. Descriptive Statistics of STISM* According to Grade

Grade	**Spending time in social media**					
	Male			Female		
	N	Mean (Hour)	SD	N	Mean (Hour)	SD
A+	70	2.193	2.022	56	**1.651**	1.147
A	201	**2.019**	1.492	186	2.375	1.914
A-	184	3.587	1.492	101	3.292	1.666
B+	211	4.367	1.576	104	4.361	1.816
B	185	5.051	1.891	100	5.450	1.919
B-	136	7.526	2.037	69	7.623	2.201
C+	59	7.508	2.575	53	8.122	1.715
C	61	7.434	2.169	18	7.361	1.473
D	70	**8.182**	2.793	27	**8.425**	2.567

**N= Number of observations, SD = Standard Deviation, STISM= Spending Time in Social Media

C. Relationship between Spending Time in Social Media (STISM) and Semester Grade Point Average (SGPA)

Addictive use of social media wastes a lot of time that adversely affects the educational outcome of students. To evaluate the correlation between STISM and SGPA, we performed 4 distinct correlation statistics (Spearman, Pearson r, Kendalltau, and Point Biserial). Simultaneously regression analysis was performed to demonstrate how SGPA is numerically related to the STISM. According to the findings of the correlation analysis (see Table III and Table IV), it is shown that STISM and SGPA are highly negatively correlated both for males and females. For male, the correlation coefficients are Spearman = -0.747, Pearson r = -0.720, Kendalltau = -0.595 and Point Biserial = -0.720. Simultaneously, for female the correlation coefficients are Spearman = -0.787, Pearson r = -0.751, Kendalltau = -0.635 and Point Biserial = -0.751.

Regression analysis (see Table III, Table IV, Fig. 1 and Fig. 2) also represents that as an independent factor STISM negatively impacts dependent factor SGPA. For males, the slope of the regression line is b1 = -0.140, R square is 0.519, Adjusted R Square is 0.518 and for females, the slope of the regression line is b1= -0.135, R square is 0.563, Adjusted R Square is 0.5626.

TABLE. III. REGRESSION AND CORRELATION ANALYSIS BETWEEN STISM AND SGPA: MALE

Male										
N	Correlation				Regression					
	Spearman	Pearson r	Kendalltau	Point-Biserial	b_0	b_1	Multiple R	R Square	Adjusted R Square	Std. error
1183	-0.747	-0.720	-0.595	-0.720	3.93	-0.140	0.720	0.519	0.518	0.378

*N= Total observation

TABLE. IV. REGRESSION AND CORRELATION ANALYSIS BETWEEN STISM AND SGPA: FEMALE

Female										
N		Correlation			Regression					
	Point-Biserial	Spearman	Pearson r	Kendalltau	b_0	b_1	Multiple R	R Square	Adjusted R Square	Std. error
659	-0.751	-0.787	-0.751	-0.635	3.93	-0.135	0.750	0.563	0.5626	0.342

**N= Total observation

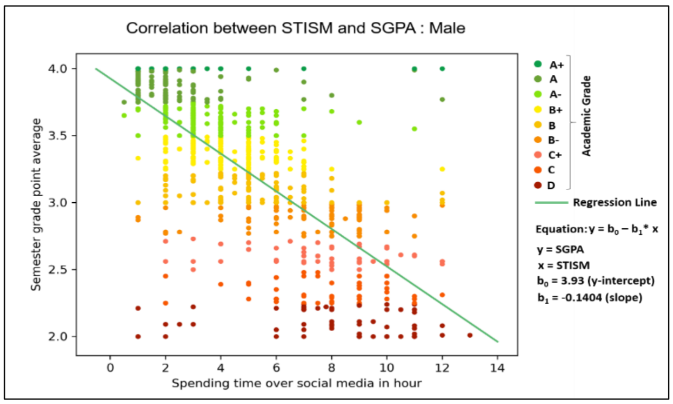

Fig. 1. Correlation between STISM and SGPA (Male)

Fig. 2. Correlation between STISM and SGPA (Female).

D. Using Social Media During Class Time

The use of social media during class time can be distracting, especially when students use their phones to check Facebook, Twitter, Snapchat, YouTube, Instagram or any other social platforms. As a consequence, their concentration diverts to non-academic operations instead of concentrating on the lesson. We questioned students whether they were using social media in the classroom. About 35.05 percent of students said they used social media in classrooms and 64.95 percent said they didn't use social media in classrooms. We further explored the relationship between classroom-standing social media use and the educational outcome of the student. The result from observation shows in Table V that students who used social media in the classroom, their educational outcomes were relatively worse than those who did not use it during school time. More specifically from Table V, it can be concluded that students both male and female who did not use social media during class time achieved higher grades such as A+, A, A-, B+.

E. Social Media for Academic Purpose

Social media provides numerous possibilities for rapid and effective communication with academia. It enables students to interact among themselves both for academic and non-academic purposes. However, we attempted to figure out the length of engagement in social media for academic purposes. Fig. 3 shows that the majority of the students (42%) use social media for academic purposes before the exam. The research also reveals that 26% of students use social media every day and 32% use every week for educational purposes. So, it is clear that the majority of the students use social media as a tool for entertainment rather than academic purposes. We questioned the students whether they believe that social media positively affects their academic outcome. In response to this question, 43.55 % replied that the use of social media did not result in a positive effect. As well as 29.72 % of students thought that social media caused a positive effect on their educational outcome and 26.73 % said that it had both positive and negative effects on their academic outcome.

F. Student's most Preferred time in Getting Engaged at Social Media

The use of social media is associated with significant sleep-related results such as a smaller amount of nighttime sleep hours that leads to poorer quality of sleep. We asked students when they prefer spending most of their time on social media. 40.67% female and 45.48% male students replied that they spend most of their time in social media at late night (see Fig. 4).

TABLE. V. USE OF SOCIAL MEDIA DURING CLASS TIME

Do you frequently use social media during class time?						
Grade	Male			Female		
	N	Yes	No	N	Yes	No
A+	70	**10.0%**	**90.0%**	56	**17.9%**	**82.1%**
A	201	15.4%	84.6%	130	21.5%	78.5%
A-	184	21.2%	78.8%	101	23.8%	76.2%
B+	211	25.6%	74.4%	104	26.0%	74.0%
B	185	43.8%	56.2%	100	42.0%	58.0%
B-	136	64.0%	36.0%	69	44.9%	55.1%
C+	59	62.7%	37.3%	53	60.4%	39.6%
C	61	**78.7%**	**21.3%**	18	**77.8%**	**22.2%**
D	70	58.6%	41.4%	27	63.0%	37.0%

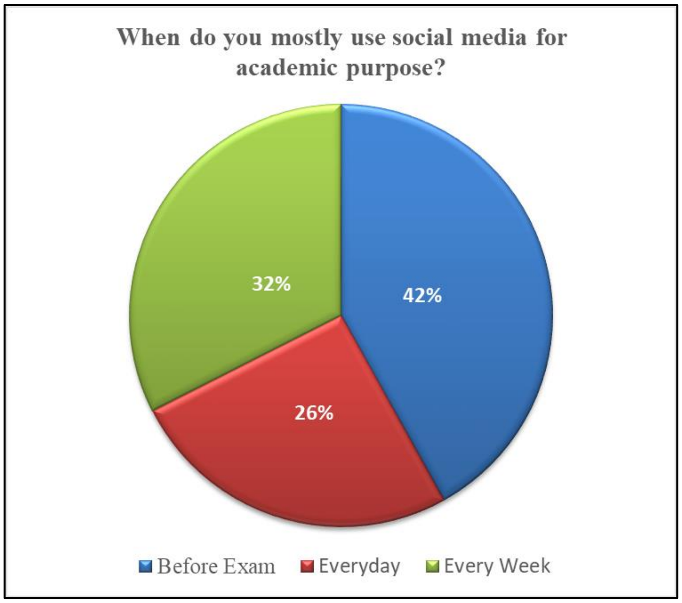

Fig. 3. Social Media use for Academic Purpose.

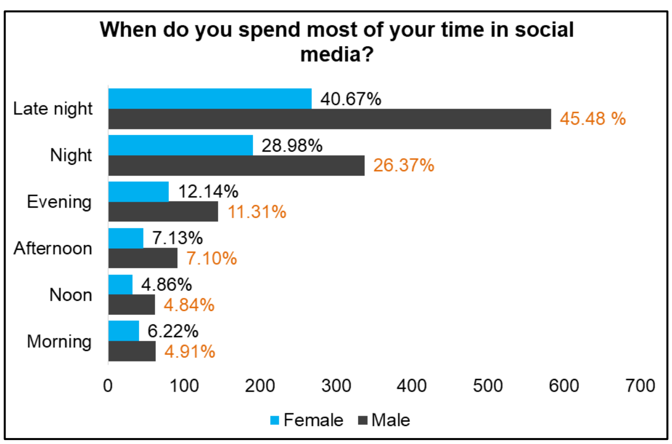

Fig. 4. When Students Spend Time in Social Media Mostly?

28.98% female and 26.37% male students answered that they spend most of their time on social media at night. Also '12.14% female and 11.31% male', '7.13% female and 7.10% male', '4.86% female and 4.84% male' and '6.22% female and 4.91% male' students prefer spending most of their time in social media at evening, afternoon, noon and morning respectively.

V. CAUSE IDENTIFICATION OF ADVERSE EFFECTS OF SOCIAL MEDIA

Some significant factors that negatively impact the academic performance of learners are recognized according to the results of the present research and substantial literature review. All of these factors are directly linked to the excessive use of social media. Fig. 5 represents how SNS impacts on students' academic performance. Excessive SNS use is responsible for aggressive behaviors, lower self-esteem, anxiety, depression, lack of concentration, poor sleep quality, loneliness, fear of missing out, etc. All those factors impact students' academic results badly.

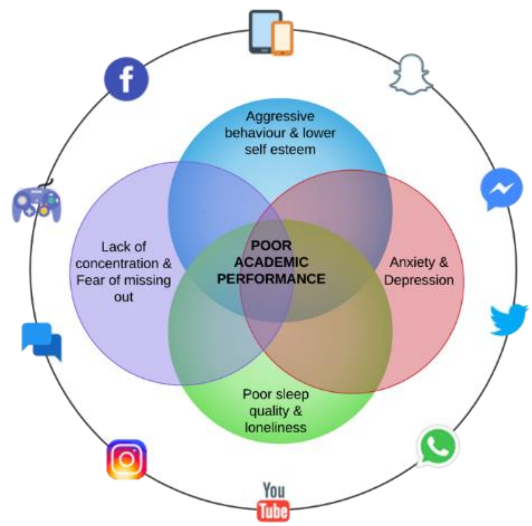

Fig. 5. Factors behind Poor Academic Performance.

VI. SOLUTION

A. Related Android Application Review

Currently, more than 65 social networking sites are available in this world. Among them, 15 to 20 sites are dominating the world. However, there are few apps designed to efficiently regulate social networking sites. Among them, very few are popular and at the same time, they have some common features. The primary objective of these apps is to enable users to monitor their phone time and minimize distraction. These application helps to break users' habits, avoid distracting themselves by their phone, or just offer themselves some time off. As a result, users become able to lead an addiction-free life. This application has some unique features (parental control on SNS) along with the existing features that are different from other applications. At the same time, long research has conducted before designing this application which makes this app to be effective as much as possible. Concurrently this application is specially made for students. From this view, this app is unique to focus on students more than others. Table VI shows that all previous applications are made for all general users. Any of the applications are not specially made for students. However, our proposed are specially made for students to use.

TABLE. VI. EXISTING RELATED APPLICATION'S DETAILS

Serial	App name	Features	Target audience	Ref.
1	AntiSocial: phone addiction	1.Keep tracking on phone unlocking time 2.Track daily phone usage time 3.Reporting daily and weekly view of user's app usage 4. Comparative discussion with others 5. In-depth signature scoring system 6. Try to break user's app addiction habit 7. 3 optional blocking modes which help individual to control phone use, block apps etc.	All general users	[23]
2	AppBlock - Stay Focused (Beat Phone Addiction)	1. Block application 2. Select how long user want to spend in a particular app in a day 3. Highest 15 minutes during working hours 4. Block notifications 5. Use a timer and activate profiles 6. Protect AppBlock application with a PIN code 7. List of blocked notifications 8. Profile lock 9. Strict Mode to lock user's AppBlock settings	All general users	[24]
3	Stay Focused - App Block (Control Phone Addiction)	1.Block apps 2. Block apps at a specified time interval 3. Track daily time spent 4.Quick Play Pause 5. Block notifications off time 6. App usage history 7. App time spent 8. Check phone history 9. Activity history	All general users	[25]
4	OFFTIME - Distraction Free	1. Block calls, texts, and notifications 2. Restrict user's access to apps and internet 3. Limit phone usage 4. Use profiles that fit your needs 5. Track phone and app usage, get analytics	All general users	[26]
5	AppDetox - App Blocker for Digital Detox	1. Calm down users mobile app usage 2. Set user's own rules for apps to detox from heavy usage 3. Stop procrastinating and pubbing. 4. Lock apps with app-locker. 5. Remind to take a break and stop heavy app usage. 6. Keep track of violations in a log	All general users	[27]

B. *Implementation of Android Application*

Finding effective solutions against the adverse effects of social media and develop an android based application to minimize the engagement between students and SNS were the key objects of the current study. An android based framework has been proposed and partially implemented to acquire the desired goal. The proposed framework, named Social Media Tracker (SMT), has been illustrated in Fig. 6. The overall framework was split into three phases (User Authentication, Background Activities, and Foreground Activities). In Back End, both real-time (firebase) and local time (SQLite) database were used to keep the data save. Fig. 7 represents the application diagram which provides a high-level graphical view (Front End) of the overall process of the application.

A starting page (see Fig. 8) will appear at the beginning of the installation of this application and at the same time, users will able to see the usage access of this app as shown in Fig. 9. Users must need to read the terms and conditions (see Fig. 11) before continuing the further steps. They need to explain when establishing a new account if they want parental control on or off (see Fig. 10). If a user permits parental control, he/she has to finish the process of signing up (see Fig. 6); otherwise, the user can just skip this feature. If the registration method is successful, an email will be sent to the parent's email address for verification. In order to monitor children's activities (see Fig. 6), parents need to install this application to parent's android device. After verification, a parent will be able to see (usage time of SNS and other applications) and monitor (Check time limit, set maximum usage limit for SNS) the activities of children from parent's device (see Fig. 14, Fig. 15, Fig. 16 and Fig. 17). If children cross the time limit for any application, a warning message will be appeared to children's devices (see Fig. 13). At the same time, children will not be able to set time limits for SNS while parental control is on (see Fig. 12). But if the user skips parental control during the authentication stage, they will inspect their own activities and set a maximum time limit for any application running on their Android device (see Fig. 6).

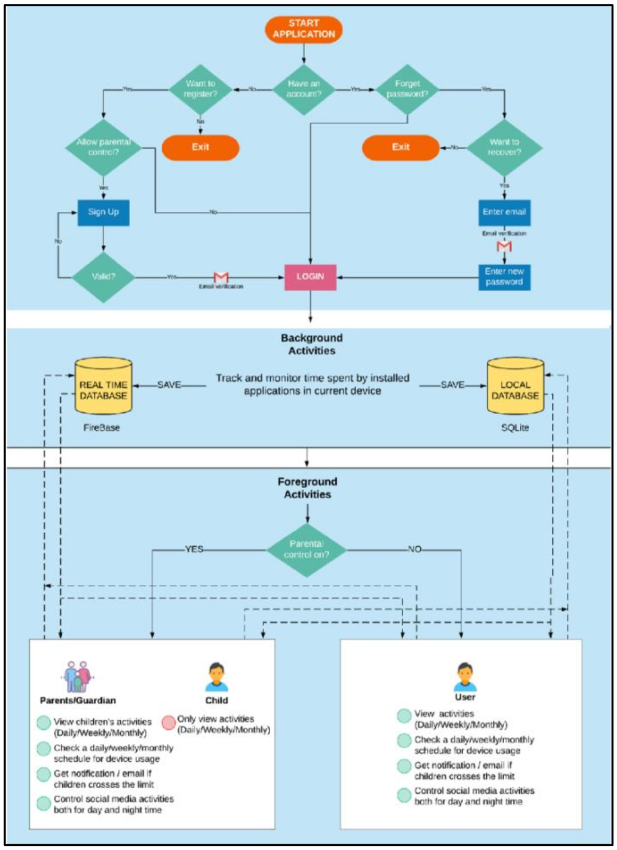

Fig. 6. Proposed Framework (SMT).

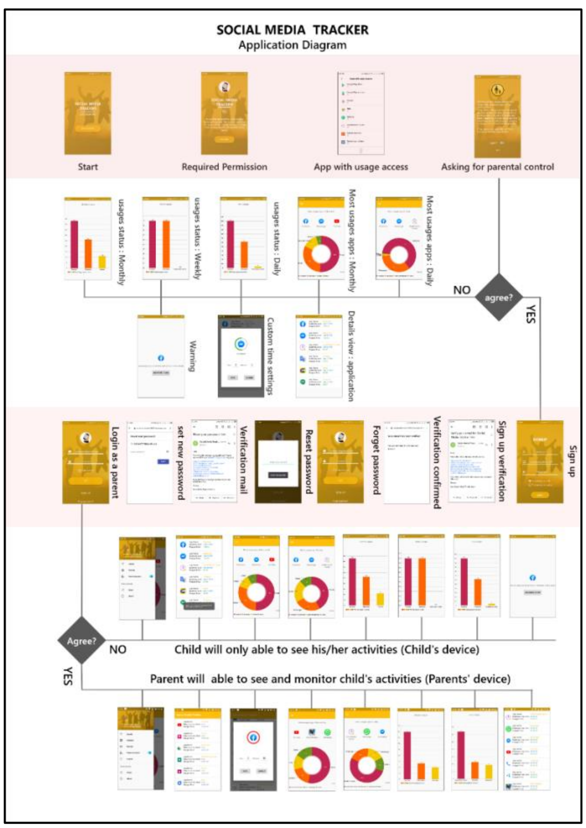

Fig. 7. Application Diagram of SMT.

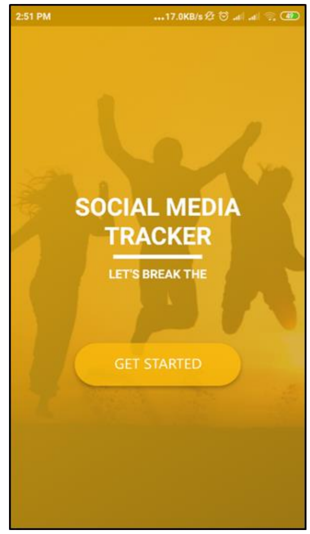

Fig. 8. Start Page.

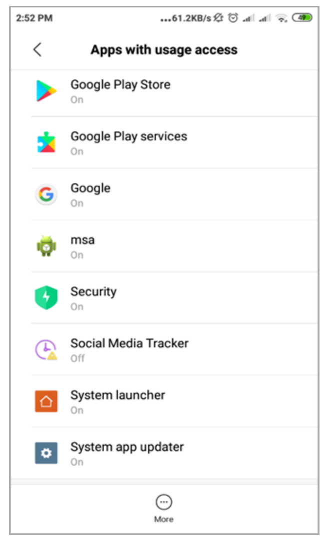

Fig. 9. Apps with usage Access.

Fig. 10. Parental Control Allow.

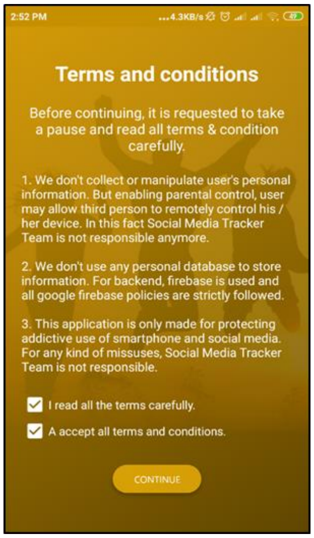

Fig. 11. Terms and Conditions.

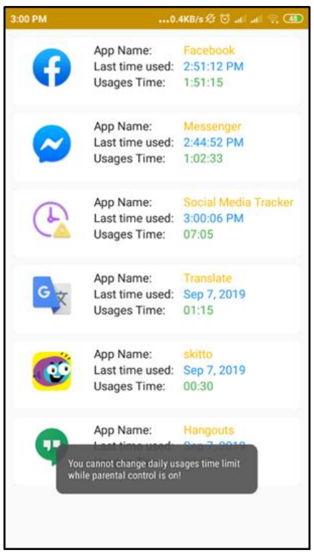

Fig. 12. Children is Notable to Change.

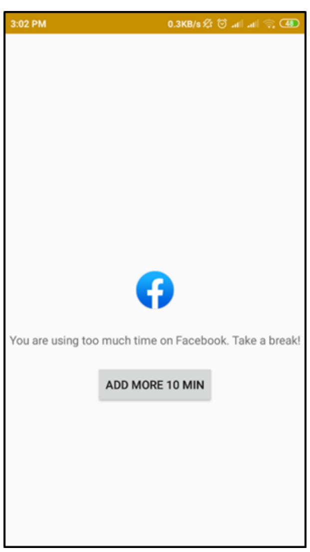

Fig. 13. Warning.

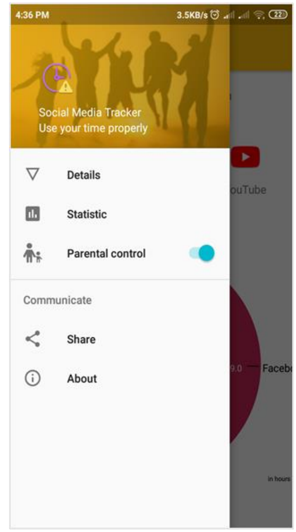

Fig. 14. Child's Activities.

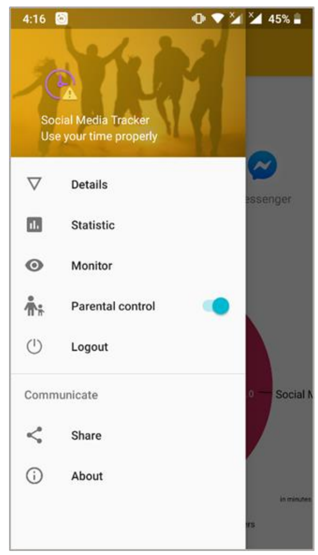

Fig. 15. Parents' Activities

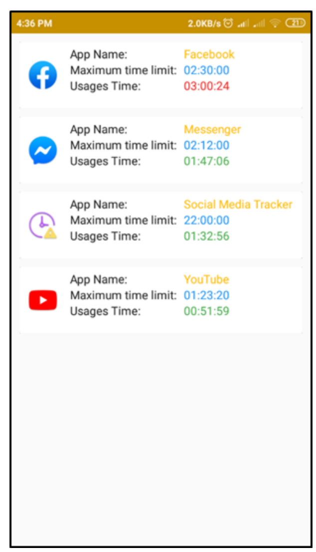

Fig. 16. Childs' Device's usage Time.

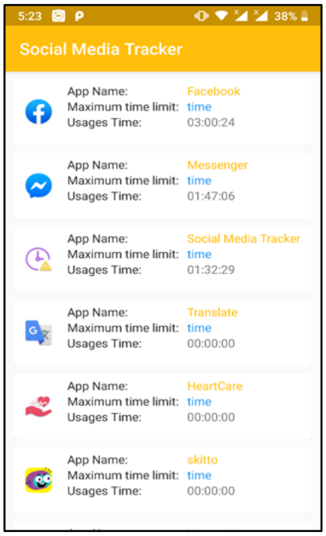

Fig. 17. Monitoring Child by Parents.

VII. Results and Comparative Discussion

SNS is becoming the most significant means of communication. Students use social media both for academic and non-academic purposes. Recently, several studies reported [5, 7, 9, 10, 3] the negative impacts of social media on student's academic outcomes. Engaging in social media for a longer period of time plays an important role to be excessively addictive. The main aim of the research was to find out how adverse effects of social media negatively impacts on the educational outcome of the students and to introduce an effective solution to minimize this problem. We attempted to investigate the correlation between social media spending time and academic performance among students using Regression and correlation analysis. Result shows that spending time on social media and academic outcome of students are strongly negatively correlated both for male (b1=-0.1401, R square = 0.519, Adjusted R Square = 0.518, Spearman = -0.747, Pearson r = -0.720, Kendalltau = -0.595 and Point Biserial = -0.720.) and female (b1=-0.135, R square = 0.563, Adjusted R Square = 0.5626 , Spearman = -0.787, Pearson r = -0.751, Kendalltau = -0.635 and Point Biserial = -0.751). Our findings demonstrate that male students spend an average of 4.74 hours per day on social media and female students spend an average of 4.64 hours per day. The study also reveals that learners who spent less time in social media had excellent SGPA and those who engaged for a longer period in social media have achieved poor SGPA (see Table I). This clearly proves that spending excessive time in social media negatively impacts on the academic result. We also attempted to comprehend the reason for the adverse correlation. Our finding indicates that during class time a big percentage of students (35.05%) use social media. It can be distracting on the way of learning. As a consequence, instead of focusing on the class, their concentration diverts into non-academic activities. It might be a reason behind bad academic outcomes. Our findings indicate that students having good academic results have a lower tendency to using social media in the classroom than students having bad academic results. It has been noticed that most learners use social media at night (male=26.37%, female=28.98%) and late-night (male=45.48%, female=40.67%) which is the key reason behind the poor quality of sleep. It is another reason behind less concentration in the classroom. Since most social media platforms are free, they attempt to get as much attention and time as possible from their users. They pursue the dopamine-driven feedback looping method to capture users' attention to make the platform as addictive as much as possible, which causes poor academic performance, poor sleep quality, anxiety, lack of concentration, waste of time etc. As students unconsciously waste a lot of time in SNS, it negatively impacts their academic performances. Previous studies have shown (see Table VII) that heavy use of SNS has several adverse effects on both the academic and mental health of learners. However, the lack of clear evidence and real rationalization makes the whole thing blurry. At the same time, previous studies did not introduce (see Table VII and Table VI) any significant preventive measures to counter the excessive use of SNS, particularly for students. To cover this gap the current study has proposed and partially implemented an android based application SMT to reduce the engagement students and SNS. Along with adult students, guardians can also use this application to monitor and regulate their children's activities. As a result, this application ensures to protect students from the over-use of SNS and help them not to be addictive to SNS.

TABLE. VII. Summary of the Previous Studies

Year	Context	Sample	Age	Country	Research Objective	Research findings	Developed any preventive measures?	Ref.
2018	SM	2698	12-18	India	To assess the empirical relationships between psychosocial well-being and fatigue in social media.	Compulsive media use significantly triggered social media fatigue, resulting in anxiety and depression	No	[28]
2017	SM	226	14-17	United States	To investigate reports of adolescents and parents regarding the use of social media of adolescents and its relationship to psychosocial adjustment.	Because of using social media, adolescents experienced anxiety, depressive symptoms and high levels of FoMO	No	[29]

2018	SPA	265	21.04±2.63	Turkey	Identify the level of smartphone addiction among learners from different departments at a university foundation	Usages of the smartphone are related to lower GPA. Concurrently, potential risks are found in the case of smartphone addiction.	No	[30]
2017	SM & SMM	348	17-28	Hong Kong	This research examined whether and how academic achievement among university learners is predicted by these two behaviors (heavy use of social media and multitasking social media).	Findings show that using social media for educational reasons was not an important predictor of academic performance as measured by the cumulative grade point average, whereas using social media for non-academic reasons and multitasking social media substantially predicted academic performance.	No	[31]
2016	SPA	490	14 ± 0.89	South Korea	To examine the incidence of young adolescents at risk of SPA and SPA-related psychological variables.	26.61 percent of adolescents experienced considerably higher rates of behavioral and emotional problems, reduced self-esteem and poorer communication with their parents and SPA is related with aggressive behavior.	No	[32]
2017	SM	1787	19-32	United States	This study aimed at evaluating multivariable associations in young adults in the United States between the uses of different SM platforms and self-reporting of depression and anxiety.	The use of various SM platforms is connected with depression and anxiety symptoms separately. These associations are powerful enough for clinicians to ask people with depression and anxiety about the use of various platforms	No	[33]
2015	SNS	753	Mage= 14.1	Canada	This research examined the connection between spending time on SNS and unmet need for mental health assistance, bad self-reported mental health, and reports of psychological distress and suicidal thinking.	Daily more than 2 hours of SNS use is correlated separately with bad mental health self-rating and elevated psychological distress and suicidal ideation experiences. Findings also reveal that excessive SNSs may be the reason for bad mental health.	No	[34]
2019	**SM**	**232**	**Mage= 19.18**	**China**	**This study examined the relationships of SM addiction to mental health and academic performance of college learners by exploring the role of self-esteem as a mediator for relationships, and further evaluated the efficacy of an intervention in decreasing addiction to social media and its potential negative results.**	**The study discovered that SM addiction was negatively correlated with the mental health and academic performance of the learners and that self-esteem mediated the relationship between SM addiction and mental health.**	**No**	**[35]**
2018	SNS	180	16-17	Surabaya	The purpose of this research was to clarify the correlations between family support, academic stress, use of social network site (SNS) and insomnia in adolescents	Major variables connected with adolescent insomnia are the reasons for SNS use, duration of SNS use, and academic stress. In order to decrease insomnia, these elements should be integrated into multi-component instructional interventions aimed at both adolescents and parents.	No	[36]

VIII. Conclusion

Interactive architecture and addictive functionality have made SNS a vital part of life. Excessive use of social media, particularly for students, has nowadays become a global problem. Addictive use of SNS adversely affects the students' academic performance as well as mental health. The current study found a significant negative correlation between the time spent on social media by students and their academic outcomes. Our investigation shows that students who spend an enormous amount of time in SM achieve poor academic performance compared to those who spend less time in SM. The findings of this study also revealed that students usually use social media for academic purposes just prior to the exam and use SM as an entertainment tool for most of their time. Concurrently, students generally prefer using SM at late night which is responsible for their poor quality of sleep. To minimize the engagement between students and SNS (Social Networking Sites), an Android based application framework called SMT (Social Media Tracker) has been proposed and partially implemented.

References

[1] "Facebook users worldwide 2019 | Statista", Statista, 2019. [Online]. Available: https://www.statista.com/statistics/264810/number-of-monthly-active-facebook-users-worldwide/. [Accessed: 17- Jun- 2019].

[2] "Twitter: number of active users 2010-2019 | Statista", Statista, 2019. [Online].

[3] "WhatsApp Status daily active users 2019 | Statistic", Statista, 2019. [Online].Available:https://www.statista.com/statistics/730306/whatsapp-status-dau/. [Accessed: 26- Jun- 2019].

[4] [4] W. Lau, "Effects of social media usage and social media multitasking on the academic performance of university students", Computers in Human Behavior, vol. 68, pp. 286-291, 2017. Available: 10.1016/j.chb.2016.11.043.

[5] R. Junco, "Student class standing, Facebook use, and academic performance", Journal of Applied Developmental Psychology, vol. 36, pp. 18-29, 2015. Available: 10.1016/j.appdev.2014.11.001 [Accessed 17 June 2019].

[6] A. Vannucci, K. Flannery and C. Ohannessian, "Social media use and anxiety in emerging adults", Journal of Affective Disorders, vol. 207, pp. 163-166, 2017. Available: 10.1016/j.jad.2016.08.040.

[7] E. Whittaker and R. Kowalski, "Cyberbullying Via Social Media", Journal of School Violence, vol. 14, no. 1, pp. 11-29, 2014. Available: 10.1080/15388220.2014.949377 [Accessed 17 June 2019].

[8] P. Lowry, J. Zhang, C. Wang and M. Siponen, "Why Do Adults Engage in Cyberbullying on Social Media? An Integration of Online Disinhibition and Deindividuation Effects with the Social Structure and Social Learning Model", Information Systems Research, vol. 27, no. 4, pp. 962-986, 2016. Available: 10.1287/isre.2016.0671 [Accessed 17 June 2019].

[9] C. Andreassen, S. Pallesen and M. Griffiths, "The relationship between addictive use of social media, narcissism, and self-esteem: Findings from a large national survey", Addictive Behaviors, vol. 64, pp. 287-293, 2017. Available: 10.1016/j.addbeh.2016.03.006.

[10] S. Power, C. Taylor and K. Horton, "Sleepless in school? The social dimensions of young people's bedtime rest and routines", Journal of Youth Studies, vol. 20, no. 8, pp. 945-958, 2017. Available: 10.1080/13676261.2016.1273522 [Accessed 17 June 2019].

[11] J. van Oosten and L. Vandenbosch, "Sexy online self-presentation on social network sites and the willingness to engage in sexting: A comparison of gender and age", Journal of Adolescence, vol. 54, pp. 42-50, 2017. Available: 10.1016/j.adolescence.2016.11.006 [Accessed 17 June 2019].

[12] H. Andersson, "Social media is 'deliberately' addictive", BBC News, 2018. [Online]. Available: https://www.bbc.com/news/technology-44640959. [Accessed: 17- Jun- 2019].

[13] Abbas, J., Aman, J., Nurunnabi, M. and Bano, S. (2019). The Impact of Social Media on Learning Behavior for Sustainable Education: Evidence of Students from Selected Universities in Pakistan. Sustainability, 11(6), p.1683.

[14] Rostaminezhad, M., Porshafei, H. and Ahamdi, A. (2018). "Can effective study approaches mediate the negative effect of social networking on academic performance?". Education and Information Technologies, 24(1), pp.205-217.

[15] S. Bellur, K. Nowak and K. Hull, "Make it our time: In class multitaskers have lower academic performance", Computers in Human Behavior, vol. 53, pp. 63-70, 2015. Available: 10.1016/j.chb.2015.06.027 [Accessed 26 June 2019].

[16] A. Flanigan and W. Babchuk, "Social media as academic quicksand: A phenomenological study of student experiences in and out of the classroom", Learning and Individual Differences, vol. 44, pp. 40-45, 2015. Available: 10.1016/j.lindif.2015.11.003.

[17] H. Woods and H. Scott, "#Sleepyteens: Social media use in adolescence is associated with poor sleep quality, anxiety, depression and low self-esteem", Journal of Adolescence, vol. 51, pp. 41-49, 2016. Available: 10.1016/j.adolescence.2016.05.008.

[18] H. Sampasa-Kanyinga and R. Lewis, "Frequent Use of Social Networking Sites Is Associated with Poor Psychological Functioning Among Children and Adolescents", Cyberpsychology, Behavior, and Social Networking, vol. 18, no. 7, pp. 380-385, 2015. Available: 10.1089/cyber.2015.0055 [Accessed 27 June 2019].

[19] T. Haynes, "Dopamine, Smartphones & You: A battle for your time - Science in the News", Science in the News, 2018. [Online]. Available: http://sitn.hms.harvard.edu/flash/2018/dopamine-smartphones-battle-time/. [Accessed: 28- Jun- 2019].

[20] S. Weinschenk, "Why We're All Addicted to Texts, Twitter and Google", Psychology Today, 2012. [Online]. Available: https://www.psychologytoday.com/intl/blog/brain-wise/201209/why-were-all-addicted-texts-twitter-and-google. [Accessed: 27- Jun- 2019].

[21] "Chamath Palihapitiya, Founder and CEO Social Capital, on Money as an Instrument of Change", YouTube, 2017. [Online]. Available: https://www.youtube.com/watch?v=PMotykw0SIk. [Accessed: 27- Jun- 2019].

[22] H. Macit, G. Macit and O. Güngör, "SOSYAL MEDYA BAĞIMLILIĞI VE DOPAMİN ODAKLI GERİBİLDİRİM ÜZERİNE BİR ARAŞTIRMA", Mehmet Akif Ersoy Üniversitesi İktisadi ve İdari Bilimler Fakültesi Dergisi, pp. 882-897, 2018. Available: 10.30798/makuiibf.435845 [Accessed 27 June 2019].

[23] Play.google.com. (2019). [online] Available at: https://play.google.com/store/apps/details?id=com.goozix.antisocial_personal&hl=en [Accessed 1 Aug. 2019].

[24] Play.google.com. (2019). [online] Available at: https://play.google.com/store/apps/details?id=cz.mobilesoft.appblock&hl=en [Accessed 1 Aug. 2019].

[25] Play.google.com. (2019). [online] Available at: https://play.google.com/store/apps/details?id=com.stayfocused&hl=en [Accessed 1 Aug. 2019].

[26] Play.google.com. (2019). [online] Available at: https://play.google.com/store/apps/details?id=co.offtime.kit&hl=en [Accessed 1 Aug. 2019].

[27] Play.google.com. (2019). [online] Available at: https://play.google.com/store/apps/details?id=de.dfki.appdetox&hl=en [Accessed 1 Aug. 2019].

[28] Dhir, A., Yossatorn, Y., Kaur, P. and Chen, S. (2018). Online social media fatigue and psychological wellbeing—A study of compulsive use, fear of missing out, fatigue, anxiety and depression. International Journal of Information Management, 40, pp.141-152.

[29] Barry, C., Sidoti, C., Briggs, S., Reiter, S. and Lindsey, R. (2017). Adolescent social media use and mental health from adolescent and parent perspectives. Journal of Adolescence, 61, pp.1-11.

[30] Dikeç, G. and Kebapçı, A. (2018). Smartphone Addiction Level among a Group of University Students. Journal of Dependence, 19(1), pp.1-9.

[31] Lau, W. (2017). Effects of social media usage and social media multitasking on the academic performance of university students. Computers in Human Behavior, 68, pp.286-291.

[32] Lee, J., Sung, M., Song, S., Lee, Y., Lee, J., Cho, S., Park, M. and Shin, Y. (2016). Psychological Factors Associated With Smartphone

Addiction in South Korean Adolescents. The Journal of Early Adolescence, 38(3), pp.288-302.

[33] Primack, B., Shensa, A., Escobar-Viera, C., Barrett, E., Sidani, J., Colditz, J. and James, A. (2017). Use of multiple social media platforms and symptoms of depression and anxiety: A nationally-representative study among U.S. young adults. Computers in Human Behavior, 69, pp.1-9.

[34] Sampasa-Kanyinga, H. and Lewis, R. (2015). Frequent Use of Social Networking Sites Is Associated with Poor Psychological Functioning Among Children and Adolescents. Cyberpsychology, Behavior, and Social Networking, 18(7), pp.380-385.

[35] Hou, Y., Xiong, D., Jiang, T., Song, L., & Wang, Q. (2019). Social media addiction: Its impact, mediation, and intervention. Cyberpsychology: Journal of Psychosocial Research on Cyberspace, 13(1), article 4.

[36] Nursalam, N., Octavia, M., Tristiana, R. and Efendi, F. (2018). Association between insomnia and social network site use in Indonesian adolescents. Nursing Forum, 54(2), pp.149-156.

A New Method to Find Image Recovery

Nouf Saeed Alotaibi
Computer Science department
College of science, Shaqra University, Shaqra, Saudi Arabia

***Abstract*—Scattering media imagery is degraded during the physical process of image formation, which shifts contrast, color, and turns overall visibility white. With the computer vision system, sight can be amazingly restored. Although the medium transmission in distant artifacts is small, it is vulnerable to amplification of the noise. Here we present / propose the picture recovery of the L0 gradient, which solves the issue discussed previously. In comparison to raw images, the single image is processed and recovered significantly improves while noise amplification discards. The state-of-the-art studies on dehazing have been reviewed in this paper. In addition, L0-gradient minimization of image smoothing was studied in combination with H Kosmedier Image Formation Physical System to solve the dehazing issue as L0 smoothing approximates better results with higher false discovery rate (FDR) .Recovery using L0-Gradient Minimization is formalized in a depth chart that reduces noise adaptively to recover estimated structures marginally in spatially changing media delivery. The minimal gradient is non-zero. Therefore, noise and blur in the nearby objects with low measurement difficulty and impact have been effectively removed, raising the transmitting approximation contributing to the enhancement of the recovered image. We are experimenting with atmospheric, submarine, at night, indoor turbid medium images qualitatively and quantitatively.**

Keywords*—Computer vision; image enhancement; digital image processing

I. INTRODUCTION

A hazy image is distinguished by poor light, dark, low contrast and color dispersion as well as blurriness, vibration and bland appearance under the images. When the atmosphere is turbid, including rain, vogue, smoke, pollen, and wind, the image quality is alarmingly influenced by low visibility. The dispersion of light is influenced by floating misplaced particles in the atmosphere. The radiance emerged from a scenario that decreases steadily from the point of view to the viewer and the dispersing light in the manner that transforms the background contrast, colour and intensity caught down. Visual information is collected with such poor visibility and is highly requested for tracking, navigation, computer vision, oceanography, flight surveillance. It is therefore extremely important either to mechanically restart programs or to evaluate them in real time. In order to solve this problem, several techniques were recommended. Hazy picture recovery differs from standard noise reduction and comparison. Haze influences the dynamic color spectrum in the image Methodiques for remote sensing, airplane boarding, steering, visual aided transportation, driver support device, image captured in the snow, fog, oceanography and many others are of great benefit in various applications. Because of this high demand, physicists invent new and effective inventions day and night. This is the new location in the field of research. The articles published in this region during the time 2000-2018 illustrate this. It's over a thousand men. However, due to the unique characteristic of haze, the research is still unified. In addition, haze image recovery is dependent upon additive as well as multiplier distance of the object and the acquisition device. Those result in the recovery model being completely un-positioned inversely and the optimization problem is constrained (Fig. 1). Few parameters are estimates that are discussed later. There are therefore many scopes for improving the model constantly in order to obtain a finer image.

(a) (b)

Fig. 1. Shows Natural Outdoor, where Haze Sample Hazy (a) and Haze Free Image (b).

The rest of this paper is organized as follows. Section II introduces the dehazing methods according to their classification in Fig. 3 and their principles and characteristics are analyzed in detail. In Section III, different eminent researchers in this field have been studied. Image formation model has been discussed with mathematical details in Section IV. In Section V, L0-Gradient minimization has been examined in detail. In Section VI, Application of L0-Gradient minimization in Image is discussed.

II. CLASSIFICATION OF IMAGE DEHAZING METHODS

Methods of decontamination are divided into three kinds: a) development, b) fusion of the image and c) restoration of the image. Dehazing focused on identity enhancement is not very necessary and is not really welcomed. Contrast and illumination partly strengthens. Dehazing focused on image fusion entails the creation of multiple images on multiple channels without a physical model. This methodology optimizes knowledge from the information provided in multiple channels. Dehazing Photo Restaurant uses optical photo simulation methods based on physics. Inversing the model and calculating certain parameters that induce the distortion is a way to obtain initial image radiance. In principle, three techniques of image restoration are available: a) supplementary information, b) multiple image, and c) prior knowledge. Our approach is based on an optical picture creation model based on previous information physics. Such method includes a single image that makes it the most complicated methodology among the modern technologies, but is the most popular in use because of its lack of information about the current image, i.e. the single image. This technique needs to remove the noise from the target to the installation of cameras, because pixel radiance deteriorates rapidly along with the loss of the so-called blur. Noise amplification is thus a particularly demanding problem during the inversion of the image recovery. Since the haze function is not standardized or constant and the radiance of the scene reduces gradually, the removal of noise will conform to distances. More than nearby objects, distant items are impacted. Tan [5], Fattal [6], He [7], Tarel [8], and Berman [9] are some state-of - the art algorithms for single image dehazing.

III. Related Work

Unconstrained problem is single image dehazing. In this class, dehazing based on prior knowledge has high potential and new algorithms are very promising. Our analysis is based on a single picture unraveling based on prior experience. The following is a significant piece of research under this section.

- 1998 Okley [3]: Daylight signal spread by an aerosol attenuating the gap from the illumination point to the sensor for each pixel. The concept was the reverse H Kosmeider dynamics model [1] and J Marcartney's model was enhanced [2]. Measurement of the signal to noise ratio. Temporary filter configuration that preserves the SNR constant regardless of distance is suggested. Major growth has been achieved. Previous knowledge of scene geometry was required in this procedure. Also restored was the low spatial frequency knowledge. This approach was the first re-search for an inverse pattern of picture creation to preserve visibility.

- Tan in 2008 [5]: one image dehazing based on two knowledge assumptions: i) a foggy image has less contrast than a clear day; ii) an object seen from a point of acquisition exponentially decaes due to air light and, by the presence of atmospheric particles, makes a distant object smooth and invisible because the light absorbs and scatters, modeled on a linear combination of direct attenuation and air light. Automated system and the need for a single image were the main advantage of eliminating all schematic details that rendered the process special. A random field-based cost function was developed that was efficiently optimized with credentials or graphs. A Markov random field based cost function efficiently optimized by belief propagation or graph-cut has been developed. The method is efficient as required single image, but not applicable for real time. The method suffers from "halo" effect due to abrupt depth change which leads to colour over-saturation.

- Fattel Approach [6] in 2008: R Fattal analysis on the basis of single image haze and dispersion light calculation. The knowledge has obtained hazelnut free picture contrast to improve clarity. Transmission and surface filtering have been believed to be uncorrelated locally. Simple statistical inference eliminates certain problems such as albedo level. This method's task is to address the pixels without any communication. Implicit graphical model allowed the solution of these pixels to be extrapolated. R Estimated fattal transmission chart for haze-free image. The dispersion of light to improve illumination is reduced. A latest optical paradigm, where ambiguities in the details are overcome by surface filtering and propagation, is locally irrelevant and effectively eliminates hazel layers and determines the precise color of hazel. Eventually, the system seeks the effective transmitting answer. Due to atmospheric diffusion the algorithm also suffers from blurriness.

- J Kopf [18] in 2008: The primary information included a deep photo system based on existing digital terrain. Hence, huge quantity of Terrain 3D modeling, texture, depth was collected. This information will speed up to rebuild the original color, structure, texture and details of the bright image. But the method is subject to costly system requirements, such as radar, etc.

- He method [7]: DCP (dark channel prior), a statistical prior to haze-free images, was used in certain research projects. This experimental reveals 75% pixels of every dark channel on a standard RGB picture where the lowest intensity channel from three RGB imaging channels is shown by an unknown band. 90% pixels of that channel are below 25. But in cases of degraded weather, the scenario drifts dramatically. This is similar to dark channel high intensity. Due to the atmospheric light, the pixel intensity is shifted to very high value and the image produces almost white. The method is efficient, but due to its high computational complexity, it takes a long time to replicate. Hence, a Dark Channel Prior (DCP) technique has been developed that is essentially beyond two other techniques mentioned above cannot be useful for real-time use. Throughout DCP, strong picture contrast is large and pixel intensities are spread across the whole spectrum evenly, but turbid weathered artifacts do not accurately allocate the intensities, move to the peak of the intensity scale and the image appears as white. This statement describes the central DCP patch and, in effect, determines transmission. Using the scattering model of an environment (see equation 2) the image eventually recovers. As already stated, the image is recuperated by an inversion in this disperse model which is affected by a substantial blocking effect in the map. By sparing laplacian matrix, the transmission diagram can be wisely calculated. The method is not ideal for rapid activity due to its high machine sophistication. This method is still quite satisfactory except for the uncomfortable performance.

- Method Tarel [8]: Fog, haze, smoke and outdoor images fade color and contrast make it difficult to process those images. J P Tarel's algorithm is fast and its difficulty is linear with the amount of picture pixels for color and single gray background. This is done by solving the fog problem and low-color saturation items, which only assume that small objects have low color saturation. Median filter is used to maintain the less complicated and regular image scale borders. Besides this median of the median filter along the axes, edges as well as angles were retained. Only four criteria, a veil approximation, image restoration, smoothing and tone mapping tunes are used to describe the algorithm. The methodology is regulated by the assumption of the environment, the reconstruction of photographs and the softening and tone-maps. There have been extensive qualitative and quantitative studies.

- D Berman [9]: landscape photographs often have haziness that decreases clarity and contrast. Furthermore each pixel is degraded differently depending on the scene point to the camera. The reason for hazing and attenuation is transmission coefficients. It is not a fix previously oriented, unlike previous methods. It is an assumption that is not local D Berman et al. stressed the decay is not clear. The transmission coefficient is different for different pixels of the image and is controlled. The colors of the hazel free picture have been suggested to be grouped and spread uniformly over the RGB file. These pixels are not local color clusters. Based on their varying propagation factors, these pixels are distributed differently. While the hazy photo represents the color line previously grouped, it's called the hazy line. This restores distance chart and haze free image from haze line replication. The algorithm is linear, faster, deterministic and not necessary for training.

- S Roy et al. [10-13]: In [10], three gamma corrections algorithms, contrast controls, sky masking's and directed flowers have been introduced by scientists. Authors of [11-13] stated that DCP methods and picture statistical analysis should be scientifically evaluated. In essence DCP is a patch-based or prior local one. The scale of the patch was 15x15, omega was 0.95. All dimensions have an important role to play. That's proved. DCP is a valuable algorithm for sky masking. But it is difficult to find the worth of the desired value. It is hand-assessed. The Cuckoo Search Algorithm used to restore this difficulty [11]. The resulting image with CSA very well eliminates sky reflection objects. Improving visibility is a classical problem of Inverse. Haze is always linked to blurring. Both were treated and removed here. Computational complexity is an integral part of any computing task. Computational complexity of qualitative and quantitative analytics for fast deployment has been reduced [13].

IV. Image Formation Physics based Model, Inversion and Noise

Restoration based dehazing basically recovers original scene radiance by an inverse transformation. Well known transformation models are: i) Degradation model and ii) Physics based optical scattering model.

Fig. 2 shows degradation model where f(x) is the original scene radiance, g(x) is the degraded image, h(x) is the degradation function, and n(x) is the additive noise. Then, the linear time invariant system is represented by

$$g(x) = f(x) * h(x) + n(x) \tag{1}$$

Koscheder [1] proposed the physical optical dispersion model in 1924, and the McCartney [2] supported it on the basis of the Mie scattering. This model is now a photography research hotpots. In [3] 1998, this pattern was used to improve turbid air visibility. According to this camera-captured model image, two sections are divided: I direct attenuation of light from scene to camera, and ii) air dispersion to the camera. A blurry, low contrast, and poor visibility were the final image created by the camera. Fig. 3 demonstrates this process.

Considering all the above constrains, atmospheric scattering model can be represented by

$$I(x) = J(x) * t(x) + A(1 - t(x)) \tag{2}$$

Where the first term is degraded image, J(x) represents original scene radiance/ image, t(x) is transmission map, and Atmospheric light. In equation 2, three variables are unknown. Out of these three, two variables, J(x) and t(x) are extremely ill-posed. If t(x) and A could be estimated, then J(x) could be recovered. Therefore, it is evident that good or optimum estimations are the key to restore J(x). This t(x) can be estimated from depth estimation, multiple images, or from some prior.

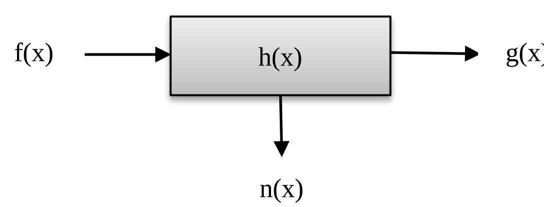

Fig. 2. Image Degradation Model.

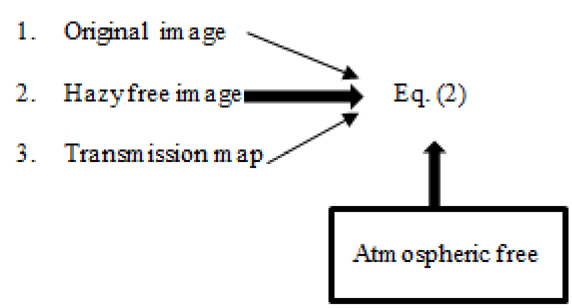

Fig. 3. Image Formation Optical Model.

V. Image Recovery under L0 Norm Regularized (L0Reg) Model

(Positive) scalers to measure length, error, size, distance, etc. depending on the environment is known as Norm. The consistency of the space of a series may be changed by manipulating the option of norm in the infinite dimension. Whereas the convergence of a series is invariant in the case of the final element vector-space. For its efficient use field, however, awareness of different standards is important. For a set of quantities, vectors or matrices in mathematics, the norm reflects the spectrum stands for Common norms: the mean square defect, Euclidean distance, absolute value, Manhattan, p-norm etc.

A. P-Norm (lp Norm)

It is noteworthy here that all Lp norm look alike, but their mathematical as well as application properties shift dramatically. In this work, we are interested in the properties of L0 norm only. L0 norm basically is not a norm, rather cardinality number. This norm has both zeroth root as well as zeroth power. This phenomena makes it problematic to operate. L0 norm recently is in demand due to its sparsity (few number of non-zero elements) , which makes it usable for compress sensing, portability, lastly edge aware smoothing (our main focus). L0 norm optimization is a basically minimization problem and is NP hard problem. Sometimes it is almost unable to solve, and at that point L1 or L2 norm is used as a relaxation. Single image reconstruction is highly challenging, and ill-conditioned in low level vision technique. Main objection of the problem is to estimate robust and accurate kernel for the noisy, blurry image. Here appropriate regularization term or prior estimation is essential to develop sharp images or blur kernel design. Blur kernel design is deeply founded on Bayesian Principal, which encompasses two inference principles: i) Maximum a postrioiri (MAP), ii) Variational Bayes (VB). MAP and VB techniques are sometimes combined sequentially. MAP is exercised more commonly. The reason is: i) intuitive, ii) simple problem formulation, iii) flexible regularisation term, and iv) efficient numerical representation. In practice MAP tracks l0 -norm of various forms to estimate dominant edge where kernel estimation is the main cue, either explicitly or implicitly. It has been experimentally established that l0-norm works far better in blind image de-blurring which will be utilized subsequently in our dehazing algorithm [l0 blind]. L0-norm based image smoothing is a well-known optimization technique which controls globally the number of non-zero gradient to represent prominent structure in a sparsity controlled manner. The special feature of this technique is to sharpen major edges while discarding the unnecessary edges. This trade-off is attainted in an optimization system through L0 gradient minimization [L0-norm Image smoothing]. It is an image editing method, predominantly effective by trade off in optimization framework of L0 gradient minimization sharpening major edges with increasing the steepness of transition while eliminating non prominent, local or noisy information of low-amplitude structures. This is achieved globally control how many non-zero gradients are resulted in to approximate prominent structure in a sparsity-control manner. Unlike other edge-preserving smoothing approaches, our method does not depend on local features, but instead globally locates important edges. It, as a fundamental tool, finds many applications and is particularly beneficial to edge extraction, clip-art JPEG artifact removal, and non-photorealistic effect generation.

B. I-D Smoothing

Main achievement is to get high contrast edges with non-zero gradient without effective geometric structure global smoothing. g is a discrete input function with its smoothed output version f. The concept counts amplitude variations discretely and represented by equation 3.

$$c(f) = \#\{p \mid |f_p - f_{p+1}| \neq 0\} \tag{3}$$

p and p+1 indicated neighboring samples (pixels) index. $|f_p - f_{p+1}|$ indicated forward gradient w.r.t p . #{} indicates count-ing w.r.t p and it is not equal to zero that satisfies L0-norm gradient. Thus $c(f)$ counts only non-zero gradient, not the change in contrast and it is the essence of the algorithm. Now, $c(f)$ is associated with a general constraint of ‘f’ , output , to be structurally similar to that of ‘g’, input. To implement this a cost function or objective function is designed as equation

$$\min_f \sum_p (f_p - g_p)^2 \;\; s.t. \quad c(f) = k \tag{4}$$

Where, c(f)=k indicates non-zero gradients from the result. It has been found by minimizing eq. 4 , k =6, through extensive search. The result is better than BLF, LCIS, WLMS, and TVS. Larger k produces fine approximation. But, in case of 2D images with different resolution, the value of k is in the range of ten to thousands. To get the structural resemblance between input and output image with non-zero gradient equation 4 has to be rewritten as

$$\min_f \sum_p (f_p - g_p)^2 + \lambda.\, c(f) \tag{5}$$

Here, λ is weight or controlling parameter also known as Lagrange Multiplier whose primary work is to balance between c(f) and rest of the equation , so that optimal smoothing can be achieved.

C. 2-D Representation

In 2D Image format, the above mathematical formulation will be represented by I as input and S as output. The gradient for each pixel p is represented as the colour difference between neighboring pixels along x, and y directions.

$$\nabla S_p = (\partial_p S_p, \partial_y S_p)^T \tag{6}$$

The gradient in this context is given by

$$C(S) = \#\{p \mid |\partial_x S_p| + |\partial_y S_p| \neq 0\} \tag{7}$$

The above eq. (7) counts non-zero gradient p whose magnitude is $|\partial_x S_p| + |\partial_y S_p|$. Output image S is computed or estimated by solving the objective function below:

$$\min_f \sum_p (S_p - I_p)^2 + \lambda.\, C(S) \tag{8}$$

For colour image $|S_p|$ is the sum of three channel RGB and the term, $\sum(S - I)^2$, is responsibility for image structure similarity.

D. Solver

Equation 8 involves a separate C(S) test. Due to two opposite criteria, one of them differentiating between two neighboring pixels and the other counting non null pixels (global statistical discontinuity), the above definition is difficult to resolve. There is no suitable classical optimizer such as a decent gradient or discrete optimizer here. Half quadratic fractionation was instead implemented, an alternative approach, in which an auxiliary variable was assumed to expand original conditions and update them on an iterative basis. The stated problem has already been noticed in nature and the regulation problem with L0-Norm is essentially unworkable. Therefore, here an approximation has to be performed to make the problem tractable without losing salient structure of the original image rather strengthening the image. Two auxiliary variables h_p and v_p have been introduced corresponding to $\partial_x S_p and\, \partial_y S_p$ and respectively. Thus, objective function turns out as

$$\min_{s,h,v}\{\sum_p (S_p - I_p)^2 + \lambda\, C(h,v) + \beta((\partial_p S_p - h_v)^2)\} \quad (9)$$

Here, $C(S) = \#\{p||\partial_x S_p| + |\partial_y S_p| \neq 0\}$ and β is an automatic adaptive parameter which tunes the similarity between two variables (h,v) and their corresponding gradients. As β keeps on increasing, eq (9) converges to eq (8). Eq (9) can be solved by minimizing (h,v) and S one by one in a iterative manner.

E. Sub Problem 1: Computing S

From equation (9) it is evident that to estimate S is to minimize the expression without the term that has no S part and is given below

$$\{\sum_p (S_p - I_p)^2 + \beta((\partial_x S_p - h_p)^2) + (\partial_y S_p - v_p)^2)\} \quad (10)$$

The eq. (10) is quadratic, therefore has global minima by gradient decent. Again, by fast Fourier transform for speeding up with diagonal derivative operator this can be written as

$$S = \mathcal{F}^{-1}\left(\frac{\mathcal{F}(I)+\beta(\mathcal{F}(\partial_x)^*\mathcal{F}(h)-\mathcal{F}(\partial_y)^*\mathcal{F}(v))}{\mathcal{F}(1)+\beta(\mathcal{F}(\partial_x)^*\mathcal{F}(\partial_x)-\mathcal{F}(\partial_y)^*\mathcal{F}(\partial_y))}\right) \quad (11)$$

Where F represents FFT operator and F ()*is the complex conjugate. F(1) denotes FFT of delta function. All the normal mathematical operators are component wise operations accordingly. Lastly FFT operation is easier and faster than its spatial domain when large size matrix of image inversion involved.

F. Sub Problem 2: Computing (h,v)

Objective function for minimization (h,v) is derived from equation (9) as

$$\min_{h,v}\{\sum_p (\partial_x S_p - h_p)^2 + (\partial_y S_p - v_p)^2 + \frac{\lambda}{\beta} C(h,v) \quad (12)$$

In the above equation C(h,v) produces non-zero gradient at |h|+|v|. The equation is seemingly sophisticated and complex, but converges quickly due to its spatial processing with individual estimation of h_p , and v_p. Therefore, from equation it is clear that by splitting the equations (9-12) intractable equation becomes tractable even fast. This is the main benefit of this scheme. Thus equation (12) can be equivalently rewritten as

$$\sum_p \min_{h_p, v_p} \{(h_p - \partial_x S_p)^2 + \left(v_p - \partial_y S_p\right)^2 + \frac{\lambda}{\beta} H\left(|h_p| + |v_p|\right)\right\}$$

In the above equation (13), ($|hp|$ + $|vp|$) is a binary function with

$$H(|h_p| + |v_p|) = f(x) = \begin{cases} 1, |h_p| + |v_p| \neq 0 \\ 0, \ otherwise \end{cases} \quad (14)$$

Now, equation (13) is rewritten w.r.t p as

$$E_p = \{(h_p - \partial_x S_p)^2 + \left(v_p - \partial_y S_p\right)^2 + \frac{\lambda}{\beta} H\left(|h_p| + |v_p|\right)\right\} \quad (15)$$

Above equation (15) touches its minima under the condition as

$$(h_p, v_p) = f(x) = \begin{cases} (0.0), \ (\partial_x S_p)^2 + (\partial_y S_p)^2 \\ (\partial_x S_p, \partial_y S_p), otherwise \end{cases} \quad (16)$$

The technique describes above is summed up and presented as algorithm below:

Algorithm I L0 gradient minimization, which can regulate globally how many non-zero gradients contribute to a sparsely regulated approach to the popular framework. In comparison to other smoothing methods to maintaining the edge, our process relies not on local characteristics, but on essential edges worldwide. As an essential tool, it has many uses and is especially useful to strip outlines, erase JPEG artefact clip-art and produce non-photorealistic results. To order to identify distinct but weak edges and rebuild the structure from hazes, a scarce gradient is used with L0-norm. This fundamental is applicable in numerous ways. L0 -norm minimization is a NP-Hard, non-convex problem [14, 15, 17].

VI. Application of L0Reg in Image Formation Model

Image formation model output consists intrinsically and extrinsically of noise. Extrinsic noise is the result of an inherent acquisition system that makes the output image profound and hazy and intricate noise. This paper highlights the need to extract meaning from the distorted file, which makes it easier to relay and eventually creates a hazel-free image. By L0 optimization, the depth map is restored. As already stated, a sparsely regulated method of L0 gradient minimization between non-zero gradient numbers is necessary to approximate prominent structure. Equation (2) is the concept of image loss based on optical mechanics used in this paper [1, 2]. Equation transmission (18) was predicted. The pictures, primary photos, transmittance and ambient light shall be I(x), J(x), t(x), and A. β, d are extinction coefficient and distance, respectively.

$$t = e^{-\beta d} \quad (17)$$

Each pixel is distorted by both additive and multiple noise during transfer from the initial scene point to the acquisition stage. The sound transforms the pixel color, contrast, luminosity and sharpness, rendering the resultant image white and almost invisible. It is difficult to deal with the problem when the tool is a single image. Therefore, the depth map [12,13] is taken into account by a total of three RGB channels, and the optimization of the L0 gradient is performed with this non-noiseless clear communication.

$$I_{cmin} = (\min_{c\in\{r,g,b\}}(I^c(x)) \quad (18)$$

I^c and I_{cmin} indicate individual channel of RGB image and minimum of three channels I^c respectively. A raw depth chart for the retrieval of hazardless artifacts can now be utilized as the noise in I_{cmin} minimal strength channel and quickly noise is made free or smoothed by the L0- Gradient minimizing process of the equation (16).

$$I_{cminL0} = L0(I_{cmin}) \quad (19)$$

Noise-free minimum pressure canal or simplified depth chart is shown in Equation (19). This is the normalization of this screen. Complimenting this method, the L0-Gradient Low Intensity Channel with global non-zero gradient modulation would result in a large image structure and reduced computational complexity. It's a big benefit. In the transmission estimate t(x), this maximum intensity channel is used. This transfer is seriously ill. The minimization of L0-Gradient produces a seamless and high-quality brass-free image without missing a significant image structure. Depth map is more reliable by minimum patch estimates but less common because of its machine cost [7] for easy usage. This theoretical concept is simple and easy to implement computationally. This approximation can be useful for easy implementation without hindering visibility and is defined by equation (20).

$$t_{new}(x) = 1 - kI_{cminL0} \tag{20}$$

t_{new} ,k are refined transmission and a proportionality constant for aerial perspective respectively. The value of k is between 0 to 1. Zero indicates clear visibility like clear day scene, whereas one indicates absolutely no visibility like thick fog. The concept of k, haziness factor have be discussed in detail [7, 12, 13]. Transmission map suggested by equation (20), scene radiance now can be evaluated as

$$J(x) = \frac{I(x)-A}{\max(t(x),t_0)} + A \tag{21}$$

Here, a restriction is imposed by introducing t_0 a lower bound of transmission in such a way that even in dense haze a small amount of transmission will be there. Typical value of t_0 is 0.1. Eq. (21) shows a linear equation of computational complexity O(n).

VII. Importance of Quality Assessment in Image[4]

An essential step in image processing is the image quality assessment (IQA). IQA requires accuracy and picture readability, which is split into (i) subjective evaluation and (ii) quantitative evaluation.

A. Subjective Assessment

The observer's visual vision is significant here. There are few guidelines for determining algorithm performance through visual picture presentation. The scale is separated into five degrees. Table I contains a set of opinions where more opinions from different people support the accuracy of the algorithm. This choice can be rendered by image processing experts or rising consumers.

B. Objective Assessment

Here, image is estimated with respect to objective criteria. Three major aspects are there in image: i) full reference, ii) reduced-reference, and iii) no-reference. Specially dehazing is under no-reference criteria, as it is very difficult to get clear image of the same scene. Therefore, no-reference, also known as single image, dehazing is difficult to design algorithm as well as to evaluate. The evaluation is splitted into two: i) ordinary method, and ii) special method.

1) Ordinary IQA: There are several IQA accessible for visual dehazing purposes, some of which are discussed here. Standard Deviation (SD): This metric shows the amount of dispersion from the mean value of the image and is a measure of the contrast of the subject under consideration. Lower interest is perceived. Mean / Average Gradient (MD): This parameter shows the amount of detail of the file. Information Entropy (IE): is a measure of the energy of the image. High entropy value implies more detail. Low value implies material loss. Mean square error (MSE): Metric is commonly used only to calculate the discrepancy between two images. Low value is desired and shows the proximity between two images. Structural similarity SSIM: is a measure that seeks similarities between two images and has a meaning of [0 1]. Low value means less comparable, while high value implies closeness between the two pictures.

2) Ordinary IQA: There are few IQAs which can only be used to dehaze the graphic. The details was elaborated: i. Visible edge dependent technique: Hautiere et al. proposed a blind contrast improvement argument based on an ambient luminance and illumination degree model initially applied to lighting engineering. This indicates three measures, there are very few IQAs that can be used for face dehazing only. The details was elaborated: (i) Visible edge dependent method: Hautiere et al. proposed a blind contrast enhancement approach based on an ambient luminance and illumination degree model originally applied to lighting engineering. It displays three metrics. Check for contrast improvement details between both the hazy and haze-free images. (ii) Color distortion centered technique: color distortion is an obvious issue in the dahazing method. Li et al. introspected color shift and halo / ring influence and developed color histogram index, histogram similarity and color restoration coefficient. This methodology gives a fair estimation of the degree of color revival. But the method suffers from the complexity and richness of color. It's iii. Contrast-naturalness-colorfulness (CNC) method: Guo et al. proposed a CNC evaluation methodology to determine contrast, color naturalness and colorfulness. The product of this approach is similar to the visual perception of the human eye. Also, the methodology influences the sophistication and the use of parameters. Yeah, iv. Machine learning-based technique Chen et al. stated IQA in terms of classification issues and presented a SVM rank with a performance indicator for foggy, undersea, and low-light images w.r.t recuperated clean images. It has established this scheme as the best NR-IQA technique for image dehazing. However, it is complex and the same classification criteria do not meet all types of images.

TABLE. I. Subjective Assessment Performance Metric

Score	Assessment grade	Quality criteria
1	worst	The worse in the group
2	Worse	Worse than average
3	Average	Average in the group
4	Beter	Better than average
5	Best	the best in the group

VIII. RESULTS

It was already mentioned that subjective and objective evaluations have such a crucial role to play in validating the performance and appropriateness of the algorithm. Many state-of-the-art algorithms have been designed to perform an inspection of quantity and quality together with the suggested one.

A. Subjective Evaluation of Various Methods

Performance of images with qualitative subjective judgment is a really good visual viewpoint attempt. As can be seen, all the accessibility of our work is better, the images are bright, the color fidelity acceptable, the artifact free with extremely low complexity.

B. Objective Analysis of Various Methods

As reported in contrast to visual analysis, objective analysis was carried out using eight different development criteria based on statistical statistics for images PSNR, SSIM, e, r, Entropy, NIQE, BRISQUE [19]. It provides details of the parameters in Table II. This metrics are used on four varying outdoor images with various techniques and are tabulated in Table III. The actual assessment report is useful. It is evident from Table III that each approach has its own perspective. While the estimation of the efficiency of haze removal is a complex problem difficult to address, taking into consideration both the findings of mathematical statistics and the visual effects, the fact that the proposed method is suitable for haze removal can support this.

IX. TIME COMPLEXITY

The most important requirement for any algorithm is performance, how much time and energy is being used to complete a task in terms of seconds and megabytes, respectively. Nonetheless, this is not a subjective evaluation owing to its reliance on the computer system and the data collection used [16]. Computational complexity of the L0-Norm Gradient is O(n) as shown in Algorithm I and that of the proposed method in Suggested Algorithm II is O(n) as well. Overall, however, the suggested methodology retains the computational complexity of O(n) which is significant for rapid activity, such as large-scale real-time image processing. This is not to suggest that the current approach is the highest, but effective with low computational complexity.

X. APPLICATION OF L0-GRADIENT DEHAZING ON DIFFERENT DEGRADED IMAGES [DATASET FRIDA]

Images with different degraded form like underwater, rain, close object, nighttime, etc. have been examined and found remarkable results. Therefore, this can be concluded that the proposed approach is equally applicable for any kind of degraded images as well. (Fig. 4: Application of L0-Norm Dehazing on different degraded images.)

Images with various deteriorated forms such as underwater, fog, near object, nighttime, etc. have been analyzed and impressive findings have been identified.It can therefore be inferred that the proposed solution is equally applicable to any form of degraded image. (Fig. 4: Implementation of L0-Norm Dehazing to distinct deteriorated images.)

Fig. 4. Shows Application of L0-Norm Dehazing on different Degraded Images.

XI. DISCUSSION, SHORTCOMING AND FUTURE SCOPE

The above described approach has been experimented with the natural haze image dataset of K He and FRIDA. Based on the high demand for dehazing, images of day-time, night-time, underwater, rainy, and nearby objects of different types of obscure scene with severe deterioration have been examined as far as possible. So, through studying and evaluating the resulting pictures, it can be concluded that all forms of ambiguous images have also regained their exposure with this algorithm. The state-of-the-art studies on dehazing have been reviewed in this paper. In addition, L0-gradient minimization of image smoothing was studied in combination with H Kosmedier Image Formation Physical System to solve the dehazing issue as L0 smoothing approximates better results with higher false discovery rate (FDR). Depth map has been derived from a total of 3-RGB channels with a L0-gradient pixel smoothing operator to generate a smoothed edge reconstruction in a sparsity-controlled manner. Prediction of a depth chart has been found to be a difficult task. As a consequence, a powerful-principled and well-designed algorithm was introduced along with discreet spatial adjustments that hold prominent and conspicuous edges to form significant structures and discard low amplitude structures as noise. That, in effect, has established an ideal transmission that contributes to the final result of an optimum clear image. This method applies equally to the Dehazing Gray Image. Halo effect during dehazing is a common issue sometimes found in dehazing. The use of this halo effect technique is restricted. In Our method, selecting the parameter lamda is a trade-off between over-sharpening and over-smoothing. Careful use of lama is therefore a fantastic decision-making tool and relies on the specific picture scenario. It has to be kept independent of the particular situation. In the future, this approach can be extended with some alteration to other demonizing and de-blurring issues. Another important field of use is the calculation of depth for textual segmentation, object detection in a perception challenge where the ground reality dataset is inaccessible. Minimizing time variability is a big drawback for any real-time program. Here, this algorithm also faces this challenge. There is significant potential for the improvement of good image performance in the future with the progress in camera technology and computer processing. MATLAB 2017b has been used as tools in Windows 10 settings.

References

[1] K. Koschmieder, Harald, "Theorie der horizontalen Sichtweite," Beitrage zur Physik der freien Atmosphare, vol. 12, pp. 33-53, 1924.

[2] E. McCartney, "Optics of the Atmosphere: Scattering by Molecules and Particles,", New York, NY, USA:Wiley, 1976.

[3] J. P. Oakley and B. L. Satherley, “Improving image quality in poor visibility conditions using a physical model for contrast degradation,” IEEE Trans. Image Process., vol. 7, no. 2, pp. 167-179, Feb. 1998.

[4] W. Wang, X. Yuan, Recent Advances in Image Dehazing, IEEE Journal of Automatica Sinica, Vol. 4, No. 3, July 2017.

[5] R Tan, Visibility in Bad Weather from A Single Image, 2008 CPVR, IEEE Explore, DOI: 10.1109/CVPR.2008.4587643,ISSN: 1063-6919.

[6] R. Fattal, "Single Image Dehazing, ACM Transaction on Graphics (TOG)," vol-27, Issue-3,August 2008.

[7] K.,He, J., Sun, and X., Tang,: Single image haze removal using dark channel prior,” IEEE Conference on Computer Vision and Pattern Recognition, Miami, FL, pp- 1956–1963, 2009.

[8] J. P. Tarel, N. Hautiere, "Fast visibility restoration from a single color or gray level image," IEEE 12th International conference on Computer Vision , pp.2201 – 2208, 2009.

[9] D. Berman, S. Avidan, "Non-local image dehazing," In Proceedings of the IEEE conference on computer vision and pattern recognition, pp. 1674-1682, 2016.

[10] D. Das, S. Roy, S. Chaudhuri, "Dehazing Technique based on Dark Channel Prior model with Sky Masking and its quantitative analysis," CIEC16, IEEE Explore, IEEE Conference ID: 36757.

[11] S .Roy, S. Chaudhuri, "Modelling and control of sky pixels in visibility improvement through CSA" , IC2C2SE2016.

[12] S. Roy, S. Chaudhuri, "Modeling of Ill-Posed Inverse Problem", IJMECS, 2016, 12,pp- 46-55.

[13] S. Roy, S. Chaudhuri, "Low Complexity Single Colour Image Dehazing," Technique,Intelligent Multidimensional Data and Image Processing, June 2018, IGI Global.

[14] Norms, Isometries, and Isometry Groups ,Chi-Kwong Li , "The Americal Mathematical Monthly," Vol. 107, No. 4, pp. 334-340, 2000.

[15] L. Xu, "Image smoothing via L0 gradient minimization," ACM Transactions on Graphics (TOG). Vol. 30. No. 6. ACM, 2011.

[16] C. Huang, C. Lai, K. Cheng, "Fundamentals of Algorithms, Electronic Desigh and Automation," 2009, Elsevier.

[17] H. Deng, W. Shao, "The l0-norm-based Blind Image Deconvolution: Comparison and Inspiration," IJCSI, vol-13, no. 6, 2016.

[18] J. Kopf, B. Neubert, B. Chen, M. F. Cohen, D. Cohen-Or, O. Deussen, M. Uyttendaele, and D. Lischinski, “Deep photo: Model-based pho- tograph enhancement and viewing,” ACM Trans. Graphics (TOG), vol. 27, no. 5, Article ID 116, 2008.

[19] N. Hautiere, J. Tarel, D. Aubert, E. Doumont, "Blind contrast enhancement assessment by gradient rationing at visible edges," Image Analysis & Stereology, vol. 27, no. 2, pp. 87-95, 2011.

APPENDICES

TABLE. II.

Metric	Full Form	Type	Desired Value
PSNR	Peak Signal-to-Noise Ratio	Full Reference Image Quality Metric	High
SSIM	Structural Similarity Index	Full Reference Image Quality Metric	High(0-1)
e	Percent of Newly Visible Edge	Full Reference Image Quality Metric	High
σ	Normalized Newly Found Saturated Pixels	Full Reference Image Quality Metric	High
r	Geometric Mean of the ratio of Visibility Level	Full Reference Image Quality Metric	High
Entropy	Energy (Intensity) of the pixels	No Reference Image Quality Metric	High
NIQE	Naturalness Image Quality Evaluator	No Reference Image Quality Metric	Low
BRISQUE	Blind / No Reference Image Special Quality Evaluator	No Reference Image Quality Metric	Low

TABLE. III.

Metric	Fig. 1	Fig. 2	Fig. 3	Fig. 4
Entropy of original image	7.1535	7.4330	7.4373	7.4436
	7.15335	7.4330	7.4373	7.4436
L0_Dehaze				
PSNR	9.6203	11.9366	12.0643	13.6133
SSIM	0.4118	0.2340	0.5862	0.6431
Antropy of Restored Image	6.4997	7.7436	7.3314	7.8284
NIQE	18.8815	18.8837	18.8773	18.8809
BRISQUE	21.8087	43.6497	24.3925	31.4020
e	-0.0162	-0.0346	0.4580	-0.0484
σ	4.9600	2.56	8.2933	1.1467
r	0.9051	2.5208	1.3836	1.4904
Fattal				
PSNR	16.2893	22.5839	17.1703	19.9720
SSIM	0.8686	0.9146	0.8583	0.9451
Entropy Restored	7.1167	7.7226	7.6079	7.6121
NIQE	18.8814	18.8808	18.8761	18.8812
BRISQUE	15.7537	24.3711	42.7872	46.2568
e	-0.0153	-0.1632	0.0572	0.0264
σ	0.0133	0.4800	0	0.0667
r	1.1740	1.4430	1.1750	1.2636

ALGORITHM I

Algorithm:1	**L0 gradient minimization**	**Complexity**
Input:	Image I, smoothing weight λ, parameter β0 , βmax and rate k	
Initialization:	S←I, β←β0, i←0	O(n)
Repeat:	With $S^{(i)}$, solve for $hp^{(i)}$ and $vp^{(i)}$ in eq(16)	
	With $hp^{(i)\,)}$ and $vp^{(i)}$, solver for $S^{(i+1)}$ with eq(11)	
	β←kβ, i++.	
Until:	β ≥ βmax	
Output:	Result Image S	

ALGORITHM II

Algorithm 2	**Input Hazy Image**	**Computational Com- plexity**
Step I	Average of minimum of three channels as Imin	O(n)
Step II	Average of maximum value of three channels as Imax	O(n)
Step III	Contrast value=Imax –Imin	O(n)
Step IV	Haziness factor, k =Imin / Imax	O(n)
Step V	Airlight Estimation	O(n)
Step VI	Estimation of minimum intensity channel	O(n)
Step VII	Refinement / noise removal of minimum intensity channel by L0-Norm Gradient	O(n) [15]
Step VIII	Transmission Estimation	O(n)
Step IX	Recovery of Dehazed image with image degradation model	O(n)

Distributed SDN Deployment in Backbone Networks for Low-Delay and High-Reliability Applications

Mohammed J.F. Alenazi
College of Computer and Information Sciences
Department of Computer Engineering
King Saud University, Riyadh, Saudi Arabia

***Abstract*—Internet applications, such as video streaming, critical-mission, and health applications, require real-time or near real-time data delivery. In this context, Software Defined Networking (SDN) has been introduced to simplify the network management providing a more dynamic and flexible configuration based on centralizing the network intelligence. One of the main challenges in SDN applications consists of selecting the number of deployed SDN controllers, and their locations, towards improving the network performance in terms of low delay and high reliability. Traditional k-center and k-median methods have been fairly successful in reducing propagation latency, but ignore other important network aspects such as reliability. This paper proposes a new approach for controller placement that addresses both network reliability and reducing network delay. The proposed heuristic algorithm focuses on four different robustness functions, viz, algebraic connectivity (AC), network criticality (NC), load centrality (LC), and communicability, and has been applied in four different real-world physical networks, for performance evaluation based on degree-, closeness-, and betweenness-based centrality-based attacks. Experimental results show that the proposed controller selection algorithms based on AC, NC, LC, and communicability, achieve a high network resilience and low C2C delays, outperforming the latest, widely-used baseline methods, such as k-median and k-center ones, especially when using the NC method.**

Keywords*—*Software Defined Networking (SDN); Controller Placement Problem (CPP); physical network; graph robustness metrics; reliability; resilience

I. Introduction and Motivation

In recent years, the rapid growth in cloud computing coupled with the high demand for massive-scale data centers, have made it crucial to provide efficient network management and resource utilization towards ensuring an optimal system performance [1]. In this dynamic context, network design requirements are subject to change, making it necessary to periodically re-configure network devices, such as switches and routers. Traditionally, this re-configuration used to be performed manually. Nevertheless, as the number of deployed devices increases, re-configuration becomes harder; this situation is particularly noticeable in the case of distributed backbone networks. In recent years, software defined networking (SDN) technologies have been introduced to address such network management and scalability issues [2]. SDN aims at simplifying network management enabling a more dynamic and flexible configuration by centralizing network intelligence. Specifically, SDN decouples the data plane, *i.e.*, the forwarding process of network packets, from the control plane, *i.e.*, the routing process, thereby improving the efficiency and programmability of the former, while centralizing the latter in a single device called an SDN controller that is responsible for defining flow routes at each SDN switch [3]. Fig. 1 shows a typical SDN architecture.

The introduction of SDN technologies signifies a paradigm shift in the field of network infrastructure [4]. In particular, by allowing logical centralization of feedback control, decisions are based on a global view of the network, easing network maintainability and enabling consistency in network policies. In this way, SDN networks provide a favorable environment for the development of innovative applications, and is an important research area for both academia and industry. SDN has been used to improve network performance [5], network resilience [6], [7], [8], and energy consumption [9], [10].

A typical SDN network can operate with one controller [11], which remotely configures SDN switches and routers. However, to avoid single point failure, more than one controller is needed to ensure a higher degree of resilience in the event of network failure that disrupts controller connectivity [12]. In addition, adding more controllers lowers the control message latency between SDN switches, especially for backbone networks where propagation delay can significantly increase the time needed to configure SDN switches remotely. However, adding more controllers can negatively impact the delay in some cases, as the distributed control plane has to consistently exchange to synchronize the global topology among all deployed controllers. Thus, adding more controllers implies additional waiting time for synchronization. The optimal number of deployed controllers can vary from one application to another based on user requirements. Real-time applications, such as video streaming need low-delay to provide the best user experience for content viewers. On the other hand, high-availability applications, such as hosting servers, requires reliable and available connection with a higher emphasis on delivery than instantaneous response. For a successful deployment of SDN network these requirements have to be satisfied while minimizing the deployment cost.

In this paper, a new framework is introduced to help network designers to determine the number of SDN controllers and their locations to satisfy application requirements. This framework includes a greedy algorithm and set of graph metrics to study a given network to improve its overall performance in terms of minimizing latency, improving network resilience while minimizing overall deployment cost. The performance metrics that capture SDN network delays include: switch-to-controller (S2C) and the controller-to-controller (C2C) delays. Our introduced algorithm determines k SDN controller based on four graph-robustness metrics:

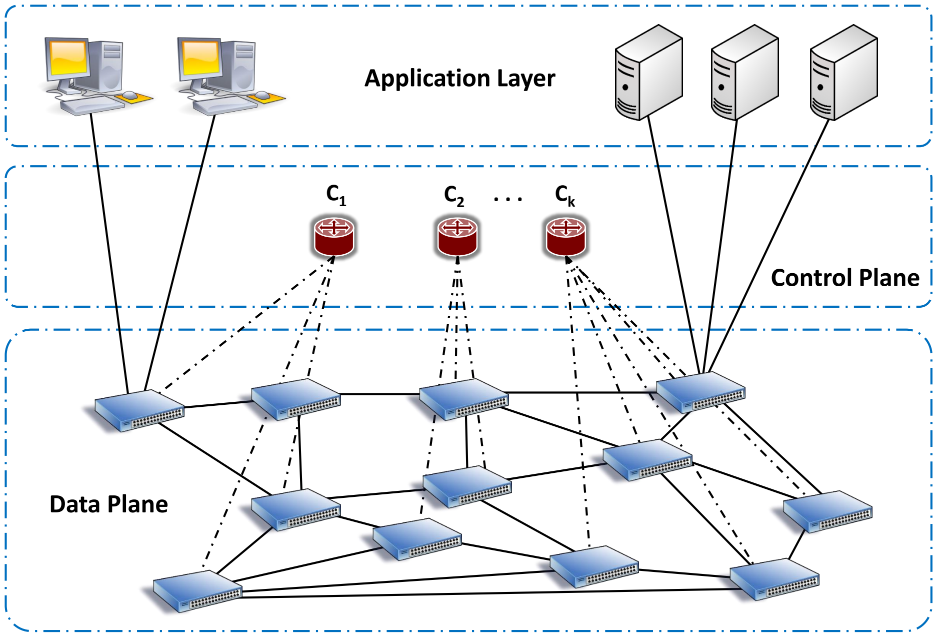

Fig. 1. SDN architecture.

algebraic connectivity (AC) [13], [14], [15], [16], network criticality (NC) [17], load centrality (LC) [18], and communicability [19]. To evaluate the proposed approach within the context of real-world physical networks, the proposed algorithm is applied in four different US-based backbone networks. In addition, the robustness of the proposed approach is evaluated in terms of three different centrality-based attacks, i.e., degree-, closeness-, and betweenness-based ones. Finally, in order to evaluate the network performance of the proposed approach with other state-of-the-art baseline approaches in use at present, the obtained results in terms of S2C and C2C delays and resilience, are compared with the ones obtained with k-median and k-center methods.

The contribution of this paper is threefold. Firstly, it proposes a new framework to aid network designers in determining the number of SDN controller to satisfy network requirements. The greedy-selection algorithm first introduced in a prior work by the author of this paper [20] is generalized towards determining locations of k SDN controllers to meet network requirements in terms of lowering delay, and improving network resilience while reducing deployment cost. In particular, the location algorithm is based on four different objective functions: AC, NC, LC, and communicability. Secondly, the proposed approach is evaluated within the context of four different real-world physical US-based backbone networks. Third, a novel resilience metric, called Attack Resilience, is defined and computed in the presence of three different centrality-based attacks, namely, degree-, closeness-, and betweenness-based ones. Thirdly, a novel resilience metric, called *attack resilience*, is defined and computed in the presence of three different centrality-based attacks, namely, degree-, closeness-, and betweenness-based ones.

The reset of this research article is organized as follows. A brief theoretical background of SDN controller placement and robustness metrics is presented in Section II. In Section III, the relevant related work is discussed. The k-controller selection algorithm proposed in this paper is introduced in Section IV. In Section V, the used evaluation protocol is described. In particular, in Subsection V-A, the used dataset is introduced, while in Subsection V-B, the different graph attack models used to test the proposed controller selection algorithm, are presented. Finally, in Section VI, the obtained results are presented and discussed. In particular, Section VI-A is devoted to the network resilience analysis while Section VI-B is devoted to the network delay analysis. Finally, a summary of our work with some concluding remarks and future directions for research are provided in Section VII.

II. Theoretical Background

In this section, a theoretical background of the controller placement problem (CPP) and graph robustness metrics, is provided in Subsection II-A and Subsection II-B, respectively. In addition, some relevant solutions proposed in the literature to address such issues are also discussed.

A. Controller Placement Problem

In a small-size network one SDN controller can be sufficient to remotely configure a set of SDN switches [11], [21]. However, as the size of the SDN network increases, more than one network controller is needed to maintain scalability requirements. To deploy a set of controllers for a large-size network such as a backbone network, three questions need to be answered during the network design phase [11]:

1) What is the minimum number of controllers to satisfy user-application requirements?
2) Where are the locations of the selected controllers?
3) How many switches should be attached to each selected controller?

In this context, identifying the optimal number of SDN controllers to be deployed and their locations, referred to as the CPP, becomes vital [11]. Several approaches can be found in the literature that addressing the CPP problem from different perspectives, such as reducing network delays [11] or increasing its reliability [22], [23], among others [24]. In [11], controllers are selected based on the k-median method. In this approach, controllers are selected to maintain minimum average delay delay among the SDN switches and controllers. Experimental results in [11], obtained by applying the proposed method on several mid-sized WANs, indicate that the propagation delay decreases as the number of controllers k increases. In [22], a location selection algorithm based on a reliability model computed using link operational probabilities, is proposed. The obtained results on several publicly available network topologies, show that the cost of deployment can be minimized while achieving reliability by carefully determining the placement of controllers. In [23], a control network reliability metric, based on the probability of path failures, is introduced to re-route traffic in case of control path loss. In addition, different placement algorithms are tested such as simulated annealing (SA) [25], which yield improved reliability against network failures. In addition, results in [23] also show that it is possible to find an optimal number of controllers to be deployed in terms of reliability, in the sense that locating more controllers would not further improve the results.

Here it is important to highlight that, although [11], [22] and [23] propose different CPP solutions, not all their results cannot be used for comparison purposes in this paper. In general, in order to be comparable, results should be obtained from a well-designed, clearly explained, and feasible to reproduce evaluation protocol. In particular, many of the parameters used in [23] are randomly selected, making it impossible to reproduce their results. The results in [22], are obtained on a publicly available dataset, making them useful benchmark results. Nevertheless, in [22] the controller locations are determined based on link operational probabilities, which are assumed to be identical, thus providing equally weightage to all the selected nodes. In this context, random results are generated, which cannot be reproduced. Finally, as discussed in Section I, the k-median method used in [11], is used in this paper for comparison. Nevertheless, the results reported in [11] cannot be directly compared with our results as they are not obtained on the same network topologies.

B. Robustness Graph Metrics

Graph metrics are used to evaluate the topological properties of a given network. They are used as indicators to differentiate between network topological designs in terms of performance and resilience. In particular, the topology of a given network can determine, among other essential aspects, its robustness against node removals. For instance, removing the central node in a star network can lead to full dysconnectivity. On the other hand, a full-mesh network can provide optimal resilience against such a challenge. However, a full-mesh network is infeasible in large-area topologies such as backbone, due to its excessive costs [26]. In our earlier studies, we have introduced a graph metric, namely 'nodal path disjoint', which captures the node centrality in terms of the number of disjoint paths to other nodes. This metric has been useful in determining the placement of SDN controllers to achieve network resilience [27].

In this paper, we selected four graph robustness metrics based on a comprehensive evaluation of most graph metrics to capture network resilience against network failures [28], specifically, AC and NC are used. In particular, the AC metric is focused on measuring the graph robustness against node removals [29], [26], while the NC metric measures the network robustness in case of topological failures [17]. In addition, to further evaluate the robustness of the proposed approach, two betweenness-based measures, such as the LC and communicability metrics, are also used. The four selected robustness metrics are described as follows:

- *Algebraic Connectivity:* AC, usually denoted as $a(G) = \lambda_2$, is the second smallest eigenvalue of its Laplacian matrix. AC has been extensively researched, showing several advantages when compared to other well-known robustness metrics, such as, for instance, the average node degree, for evaluating network resilience [30], [31], [32]. In addition, in [14], [15], [16], the AC capability of predicting graphs flow robustness is also highlighted.
- *Network Criticality:* NC, denoted as $\hat{\tau}$, is a spectral graph metric calculated as follows:

$$\hat{\tau} = \frac{2}{n-1}\text{Trace}(\mathcal{L}^{+}) \tag{1}$$

  where n represents the number of nodes while $\text{Trace}(\mathcal{L}^{+})$ is the trace of the Moore–Penrose inverse of the Laplacian matrix of the graph [17]. A lower value of NC, calculated as in Eq. 1, indicates a higher network robustness. A comprehensive study of this metric within the context of different network topologies as well as a comparison with other widely used robustness measures, can be found in [33].
- *Load Centrality*: LC, first introduced in [18], measures the load incurred by other nodes, in terms of node betweenness, by computing the shortest paths passing the given node. A larger value of LC indicates a higher network robustness.
- *Communicability:* The communicability measure, first introduced in [19], evaluates the number of walks that connects every pair of nodes. A larger value of communicability indicates a higher degree of network robustness.

III. Related Work

In recent years, several SDN protocols have been proposed in the literature that implement SDN networks in different scenarios, such as healthcare [34] and traffic [35] applications. One of the most widely used SDN protocols is OpenFlow. Since it was first introduced in 2011, this SDN protocol, originally developed at Stanford University [36], has gained high popularity, calling the attention of both academia and industry. In this section, some of the most relevant works addressing SDN technologies are discussed.

In [34], an SDN protocol is proposed to separate the application from the underlying physical infrastructure towards reducing the total capital and maintenance costs. The proposed protocol allows intelligent health monitoring as well as customized data collecting, transmitting, and processing. The promising results reported in [34] provide a solid for further innovation in the field of healthcare applications. In [4], authors highlight that SDN can favor big data acquisition, transmission, storage, and processing. Further this line, authors in [4] studied the feasibility of applying SDN protocols in the context of big data networking. In particular, the available technologies allowing a joint design of big data and SDN were analyzed towards achieving a synergistic environment capable of exploiting SDN and big data advantages making both of them both benefit from each other. The reported results in [4] are promising highlighting the potential benefits of using SDN technologies in the context of big data applications. In [37], a software-defined IoT infrastructure, consisting of physical, control and application layers, is applied in the context of a new industry concept called Industry 4.0, with the purpose of providing flexible network resource allocation management and improving data exchange. Simulation results in [37], obtained from different Industry 4.0 scenarios, show that SDN technology is essential to the successful development of such new industry concept. In [35], a time-sensitive SDN (TSSDN) is introduced towards providing real-time guarantees in time-sensitive and non-time-sensitive traffic systems. The proposed TSSDN is based on bounding the non-deterministic queuing delays for time-sensitive traffic by exploiting the logical centralization paradigm of SDN to compute a transmission schedule for time-sensitive traffic initiated by the end systems based on a global view. Results in [35], show that the proposed TSSDN achieves deterministic end-to-end delays with low and bounded jitter.

The above discussion shows that SDN technologies can be implemented in diverse scenarios, such as healthcare, big data, industry, and traffic applications, to achieve different objectives, including customizing, reducing costs, minimizing delays, and improving performance. Regardless of the scenario, the successful implementation of SDN networks is highly dependent on network reliability. Although as previously discussed in Subsection II-A, while some network requirements can be fulfilled using only one controller, deploying more controllers, *i.e.*, making the network more redundant, can increase its reliability [24]. Several researchers have focused their works in developing multi-controller approaches towards improving the network reliability and resilience. In [24], a comprehensive survey of multi-controller based on SDN can be found. In Subsection II-A, the proposed approaches in [11], [22], and [23], have been discussed. In addition, some other approaches can be found in [38] and [39]. In [38], the possibility of improving the resilience of smart grids through SDN applications is evaluated using three illustrative use cases, showing that SDN technologies allow the strengthening of smart grid resilience, even under catastrophic circumstances. In [39], a CPP solution based on mobility-aware adaptative flow-rule placement is proposed for a software-defined access network (SDAN) to support IoT applications; good simulation results were obtained in terms of network delay, optimal number of activated access points (APs), control overhead, energy consumption, and costs.

Finally, despite the huge efforts made in the literature towards addressing the CPP problem in SDN applications, researchers agree that there still exist many research gaps and open challenges in the field [24]. In particular, according to the extensive analysis conducted in [24], further research needs to be conducted towards addressing scalability, consistency, reliability, resilience, and load balancing issues. In addition, most of the reported results in the literature have been obtained based on simulation experiments rather than experiments conducted in the real-world scenario. Then, in order to give some insight into the identified research gaps, a novel SDN controller selection approach aimed at improving the network resilience against targeted attacks is proposed in this paper and tested within the context of four different real-world US-based backbone physical networks.

IV. SDN Controller Selection Algorithm

In this section, the proposed approach aimed at selecting the locations of k controllers subject to the four objective functions, namely, AC, NC, LC, and communicability—towards optimizing network performance not only in terms of the S2C and C2C delays, but also of the resilience against centrality-based attacks, is introduced. The proposed greedy algorithm is implemented as follows, being the corresponding pseudocode shown in Algorithm 1. First, the nodes are divided into k

```
Functions:
graphMetric(G) := a generic graph metric of G
k-means(k,G) := k partitions of a graph G
nodeSelection(List) :=select a node based selected
graph metric function
Input:
G_i := input graph
k := number of returned SDN controllers
Output:
kControllers := a list of the selected controllers
begin
    selectedControllers = []
    partitions = k-partitions(k,G_i)
    for partition in partitions do
        graphMetricsVales = []
        for node in partition.nodes() do
            G_i.remove(node)
            nodeImpact = graphMetric(G_i)
            graphMetricsVales.append(node,nodeImpact)
            G_i.add(node)
        end
        bestCandidateNode =
         nodeSelection(graphMetricsVales)
        kControllers.add(bestCandidateNode)
    end
    return kControllers
end
```

Algorithm 1: A greedy algorithm for selecting k-controller.

groups using a k-clustering algorithm. Then, for each cluster, the node satisfying the objective function is selected. The three functions defined in Algorithm 1: graphMetric(G), k-means(G), and nodeSelection($List$), are applied as follows. First, the graphMetric(G) function returns the graph metric value of a given graph G. This function is especially defined to support any graph metric, allowing the use of any of the four metrics proposed in this paper (AC, NC, LC, and

TABLE I. US-BASED BACKBONE NETWORK TOPOLOGIES

Graph	Nodes	Links	Radius	Diameter
Internet2	57	65	8	14
Level 3	99	132	10	19
Sprint	264	313	19	37
AT&T	383	488	20	39

communicability). Then, the k-$\mathsf{means}(G)$ function divides N nodes into k partitions based on their Euclidean locations. Finally, the $\mathsf{nodeSelection}(N)$ function returns the node that maximizes the network robustness.

V. EVALUATION FRAMEWORK

In this section, the evaluation Framework used in this paper is described. In particular, subsection V-A describes the used dataset is introduced, while subsection V-B presents the three different centrality-based attacks used to test the robustness of the proposed approach.

A. Dataset

In this paper, four different backbone fiber-level network topologies available in the KU-TopView Network Topology Tool [40], particularly, Internet2[1], Sprint, Level 3 [41], and AT&T, are used to evaluate the performance of the proposed approach. In order to illustrate their graph properties, some commonly used graph metrics are shown in Table I.

B. Centrality-based Attacks

In this paper, graph-theoretic models are used to attack the network and evaluate its robustness against node removals. In particular, three different centrality-based attacks are considered as follows the degree-, closeness-, and betweenness-based ones [42]. The degree-based attack targets nodes with the highest number of connected links while closeness-based attack targets the nodes closest to central nodes with respect to hop-count. The betweenness-based attack targets the node through which the highest number of shortest paths pass. For each one of them, the list of removed nodes is determined in an adaptive way, allowing a better selection of the highest centrality than in the case of using a single evaluation for selecting the highest number of targeted nodes [43].

VI. RESULTS AND DISCUSSION

In this section, the results obtained from the implementation of the proposed controller selection approach based on the four robustness functions, namely, AC, NC, LC, and communicability, in the four physical-level networks shown in Table I, are presented and discussed. In addition, the k-center and k-median methods are also applied within the context of these four networks for the sake of comparison.

A. Controller Selection Evaluation

In order to select the controller locations with each of the six different tested methods, that is, for the AC, NC, LC, communicability, k-center and k-median methods, the number of controllers is varied from $k = 1$ to $k = 20$. The obtained results are geographically illustrated in Fig. 2, where the optimal controller locations computed by the six methods for the AT&T network are shown. In particular, for the sake of a better visualization, only the locations for $k = 4$, $k = 8$, $k = 12$, and $k = 16$ are shown. The results obtained for the other three physical networks yield similar conclusions and are not included here due to space constraints.

B. Delay Analysis

In this subsection, the obtained end-to-end delay results are analyzed. Typically, while a packet is sent through the Internet it experiences four types of delay: nodal processing, queuing, transmission, and propagation delays. In this paper, the propagation delay is particularly addressed, assuming that routes are selected by means of the shortest lengths or hop-count between the SDN switches and the nearest controllers. In this sense, different delay related metrics, namely, the C2C and the S2C ones, are considered. The former is analyzed in subsection VI-C, while the latter is analyzed in subsection VI-D.

C. Controller-to-Controller Delay

In a distributed SDN network, multiple controllers are deployed to ensure load-balancing and network resilience against attacks. In this context, controllers should be able to deal with real-time data exchange towards sharing a global network view and providing proper flow rules to the switches. In the case of backbone networks, these controllers can be in different cities, increasing the signal propagation time and the number of required hops, causing additional delay. In this paper, the inter-controllers delay is evaluated based on these two factors through the C2C delay and the C2C hop-count, respectively. The former, defined as the average of the propagation delay between the deployed controllers, is computed as the shortest path length divided by the propagation speed[2]. The latter, is defined as the average number of hops corresponding to the shortest paths between the deployed controllers.

In this subsection, the C2C delay is analyzed as a function of the number of deployed controllers k. In particular, the impact of increasing k on the end-to-end delay (C2C delay) and on the number of hops (C2C hop-count) for the four physical networks is shown in Fig. 3 and 4, respectively.

Results in Fig. 3 show that k-median and k-center methods yield high C2C delays, for all the network topologies. For instance, for the Internet2 topology, the maximum value reaches 15 ms. This is due to the fact that these methods select controllers to minimize the S2C delay, rather than the C2C delay. Then, controllers are distributed uniformly, increasing the shortest path distance between them. In addition, Fig. 3 also shows that, for the k-median and k-center methods, the C2C delay decreases as the number of deployed controllers k increases, reaching a maximum for $k = 2$, for all topologies. Note the reader that the C2C delay is not defined for $k = 1$

[1]http://www.internet2.edu

[2]The propagation speed is assumed to be $2 \times 10^8 m/s$.

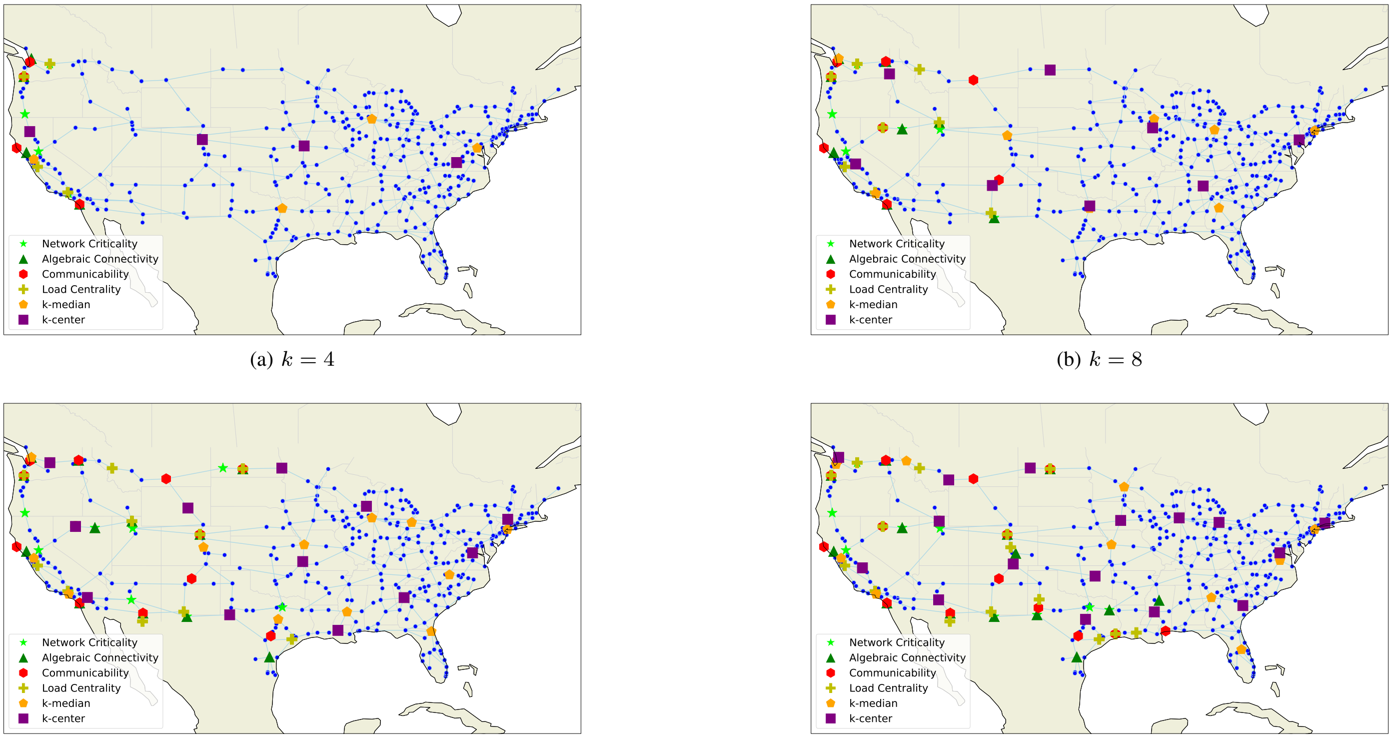

(a) $k = 4$ (b) $k = 8$

(c) $k = 12$ (d) $k = 16$

Fig. 2. Controller Placement for AT&T.

because, in such a case, only one controller is deployed. For the AC, NC, LC and communicability methods, the C2C delay is very low for all the topologies, as they tend to select controller locations that are close to each other, as shown in Fig. 2. In these cases, in contrast to the the k-median and k-center methods, the C2C delay tends to increase as k increases for all the topologies excepting the Internet2 one, where the C2C delay increases for k values between 2 and 4, and for k values greater than 11, but showing no delay penalty as k reaches 11. Nevertheless, even for the largest number of controllers considered here ($k = 20$), the C2C delay obtained with the AC, NC, LC, and communicability methods, are still lower than the ones obtained with the k-median and k-center ones. Finally, similar results can be observed in Fig. 4, making it possible to conclude that the AC, NC, LC, and communicability methods outperform k-median and k-center methods in terms of the C2C delay and hop-count.

D. Switch-to-Controller Delay

In a distributed SDN network, SDN switches are commonly connected to the nearest controller, making it crucial to minimize the delay between them. In this paper, this delay is captured taking into account two delay related metrics, specifically, the S2C delay, defined as the average of the propagation delay between the deployed switches and the nearest controller, and the S2C hop-count, defined as the average number of hops of the shortest paths between the deployed switches and the nearest controller. In this subsection, the S2C delay is analyzed as a function of k. In particular, the impact of increasing k on the end-to-end delay (S2C delay) and on the number of hops (S2C hop-count) for the four physical networks is shown in Fig. 5 and 6, respectively.

The results in Fig. 5 show that the average S2C delay obtained with the k-median and k-center methods are significantly lower than the ones obtained in the case of the C2C delay for all the topologies. This was expected since, as mentioned in Subsection VI-C, k-median and k-center methods select controllers by minimizing the S2C delay. These results are also better than the ones corresponding to the AC, NC, LC and communicability methods for all the topologies. In addition, Fig. 5 also shows that the S2C delay decreases as k increases for all the methods and topologies. This tendency is particularly noticeable in the case of the AC, NC, LC, and communicability methods, because of which the difference between these methods and the k-median and k-center ones to decrease as k increases. Moreover, as k increases, the S2C delay tends to a low value (almost the same one) for all the methods and topologies. Take, for instance, the case of the Internet2 topology, where the S2C delay of k-median and k-center methods for $k = 11$ is around 2.0 ms, while for the other four methods the delay is around 3.6 ms. This difference is not particularly significant. Moreover, depending on the type of application and its requirements, this difference could be taken into consideration or be even neglected.

Finally, the results in Fig. 6, show a similar behavior in terms of the S2C hop-count for all the methods and topologies. As such, the same comments stand.

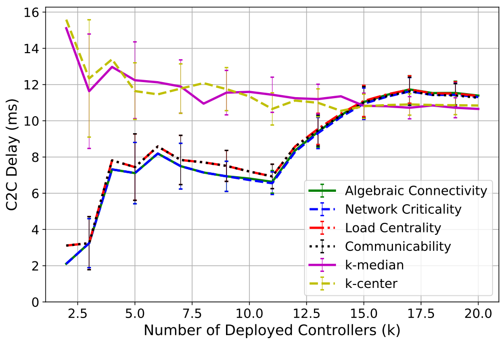

(a) Internet2

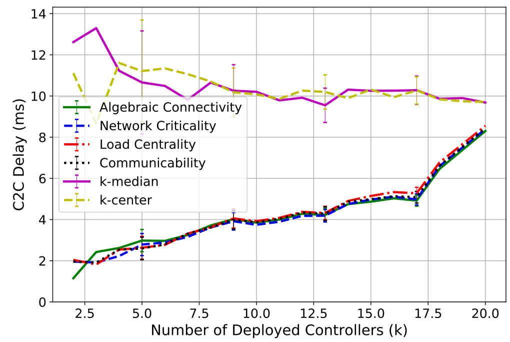

(b) Level 3

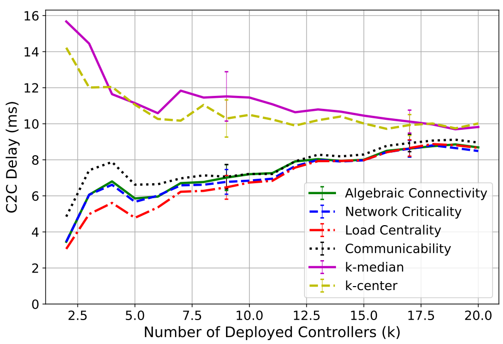

(c) Sprint

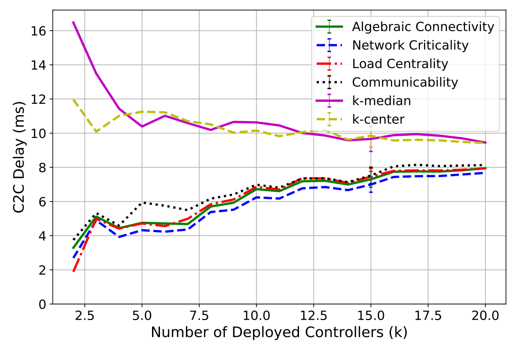

(d) AT&T

Fig. 3. Inter-controller delay.

E. Robustness to Targeted Attacks Analysis

In this section, the network resilience of the proposed approach against targeted attacks is evaluated as a function of the number of deployed controllers k. ITherefore, a new metric, termed as attack resilience (AR), that captures the connectivity to SDN controllers during a given attack, is defined. The AR is computed as the sum of controller reachability, first introduced in [20], during a given attack. The Attack Resilience results of the four physical networks are shown in Fig. 7, 8, 9, and 10, for the six controller selection methods (AC, NC, LC, communicability, k-median and k-center), and the three centrality-based attacks. In particular, Fig. 7a, 7b and 7c show resilience results for the Internet2 topology, Fig. 8a, 8b, and 8c, show the corresponding results for the Level-3 topology, Fig. 9a, 9b, and 9c show the results for the Sprint topology, and Fig. 10a, 10b, and 10c show results for the AT&T topology, for the degree-, closeness- and betweenness-based attacks, respectively. In all cases, the AR is minimum at $k = 1$, confirming that network resilience against targeted attacks is poor when the SDN network has only one controller, as previously suggested in [24]. Similarly, AR increases as k increases for all methods [24]. In all cases, the behavior of all methods remains similar until a particular value of k is reached, becomes different when k further increases, indicating that different methods have different impacts on the network resilience. In this regard, the behavior is similar for all topologies, differing only in the value of k for which the difference among the methods becomes appreciable. These different behaviors are described as follows:

- Internet2:For the Internet2 topology, the resilience values are similar for the six methods for values of k between 1 and 7, after which the NC method outperforms the other ones. For instance, from Fig. 7a it can be seen that for $k = 11$ the attack resilience against the degree-based attack is 75 for the k-median method and 145 for the NC method, showing approximately 95% improvement in resilience. Here, it is important to highlight that, although increasing k does always increase AR, it is not always a good strategy. For instance, the AR against the degree-based attack improves by 3% as k increases from 11 to 17. This will be cost-inefficient since, while there exists a significant extra cost for deploying 6 additional controllers, the corresponding resilience improvement is not significant.
- Level-3: For the Level-3 topology, the AR increases for all methods (and attacks) correspondingly between $k = 1$ and $k = 5$. When k further increases, the AC and NC methods are the ones that most distinguish themselves from the rest. For k values between 5 and 9, the AC method provides the best results, while when k is greater than 9, the NC method outperforms all the

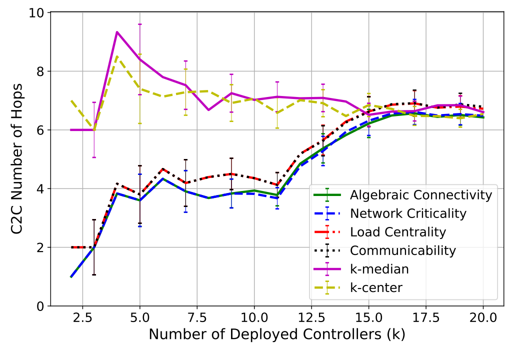

(a) Internet2

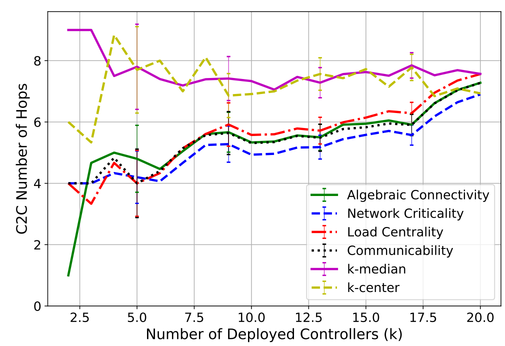

(b) Level 3

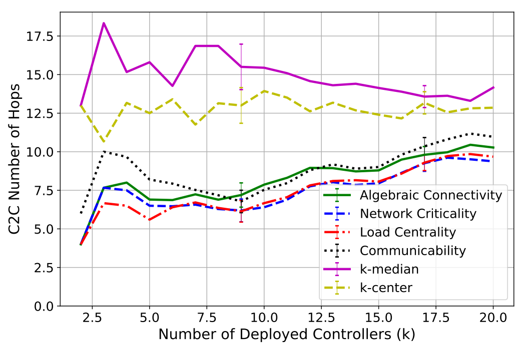

(c) Sprint

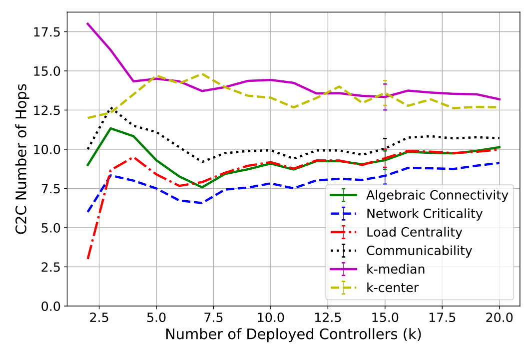

(d) AT&T

Fig. 4. Inter-controller hop-count.

other methods. For instance, when $k = 9$, the AR is 100 for all methods but for the AC one that provides approximately 30% of improvement in the presence of the degree-based attack.

- Spring: For the Spring topology, the AR increases for all the methods in a similar way for k between 1 and 11, for all the attacks, being particularly noticeable in the case of the degree-based one. For k values greater than 11, the NC method outperforms the other methods. For instance, for $k = 14$, the closeness-based Attack Resilience value achieved by the NC method is 350, which is around 75% higher than communicability, which provides the worst results.

- AT&T: For the AT&T topology the AR increases correspondingly for k values between 1 and 3, for all methods and attacks. For this topology, the k-median method provides the best resilience results when k values between 3 and 7 for all the attacks. For greater values of k, the NC method outperforms the other ones for the closeness- and betweenness-based attacks, while for the degree-based attack, the k-median remains as the best one.

Based on the above discussion, it can be concluded that the NC method provides the best results in most of the cases, while AC and k-median methods show better results than the LC, communicability, and k-center. In addition, once the optimal method to place the controllers has been selected, which in this paper is the NC method, the minimum number of deployed controllers should be determined in terms of minimizing both network resilience and deployment costs. The elbow method can be used for finding the minimum k with the maximum resilience gain, in the sense that further increasing k would not result in significant resilience improvement. Based on the elbow method, the optimal k when using the NC method has been computed for each of the four network topologies, being $k = 11$ for the Internet2 topology, $k = 17$ for the Level-3 and AT&T topologies, and $k = 16$ for the Spring topology, showing that this optimal number highly depends on the structure of the physical network.

VII. Conclusions and Future Work

Nowadays, real-time or near real-time data delivery is a crucial aspect in many Internet applications. In this context, SDN technologies can provide efficient solutions, being widely used in diverse scenarios, such as healthcare and traffic applications, for customizing, reducing costs, and minimizing delays. As they are publicly available, the vulnerability of SDN networks is high, making it crucial to evaluate its robustness against different attacks. In this line, increasing the number of deployed controllers can be used to improve reliability through resilience. Nevertheless, deploying multiple controllers is a

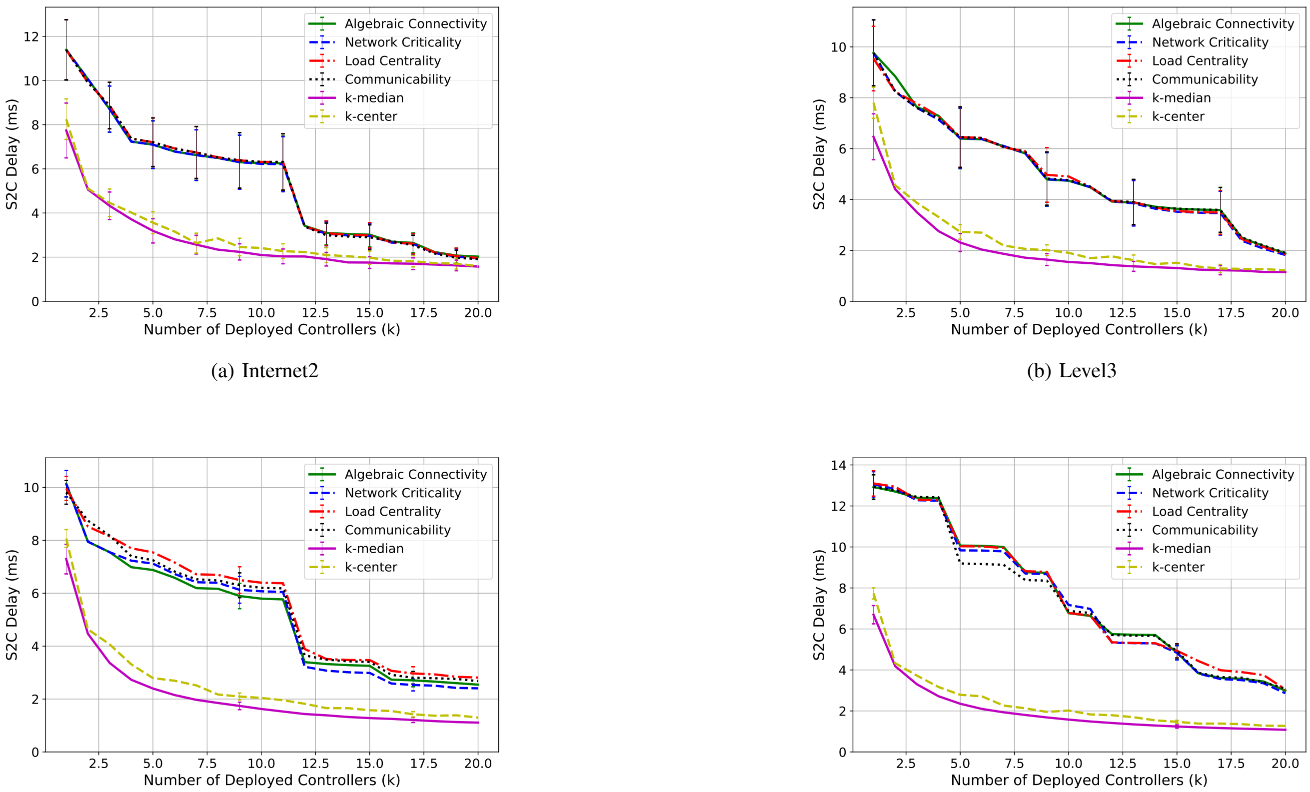

(a) Internet2

(b) Level3

(c) Sprint

(d) AT&T

Fig. 5. Switch delay.

challenging task, especially in terms of determining their number and location. In this paper, a new controller placement approach based on four robustness metrics, namely, AC, NC, LC, and communicability, has been proposed to minimize both S2C and C2C delays, as well as to maximize the network resilience. To bridge the research gap regarding benchmark results obtained in real-world networks, the proposed approach is tested within the context of four different physical graphs, and compared with the present state-of-the-art baseline methods.

The performance of the proposed approach has been evaluated in terms of the C2C and S2C delays as well as the resilience against three different centrality-based attacks, i.e., degree-, closeness-, and betweenness-based methods. In particular, for evaluating the network resilience, a novel robustness metric, the attack resilience, has been defined. The obtained results showed that the NC method serves as a good metric to select the optimal number of deployed controllers for an SDN environment in terms of achieving low C2C delay and high resilience against centrality-based attacks in backbone networks. Moreover, for the S2C delay, although being outperformed by the baseline methods (k-median and k-center), the deployment of the NC method does not have a significant influence.

Finally, for future work, it is the authors' intention to extend the present analysis by applying the proposed controller selection approach to other widely used topologies, such as data centers and smart cities.

Acknowledgments

The authors extend their appreciation to the Deanship of Scientific Research at King Saud University for funding this work through the Research Project No. R5-16-03-03.

References

[1] I. F. Akyildiz, A. Lee, P. Wang, M. Luo, and W. Chou, "Research challenges for traffic engineering in software defined networks," *IEEE Network*, vol. 30, pp. 52–58, May 2016.

[2] H. Kim and N. Feamster, "Improving network management with software defined networking," *IEEE Communications Magazine*, vol. 51, no. 2, pp. 114–119, 2013.

[3] O. N. Fundation, "Software-defined networking: The new norm for networks," *ONF White Paper*, vol. 2, pp. 2–6, 2012.

[4] L. Cui, F. R. Yu, and Q. Yan, "When big data meets software-defined networking: Sdn for big data and big data for sdn," *IEEE Network*, vol. 30, pp. 58–65, January 2016.

[5] M. Wang, N. Karakoc, L. Ferrari, P. Shantharama, A. S. Thyagaturu, M. Reisslein, and A. Scaglione, "A multi-layer multi-timescale network utility maximization framework for the sdn-based layback architecture enabling wireless backhaul resource sharing," *Electronics*, vol. 8, no. 9, 2019.

[6] M. Hussain, N. Shah, and A. Tahir , "Graph-based policy change detection and implementation in sdn," *Electronics*, vol. 8, no. 10, 2019.

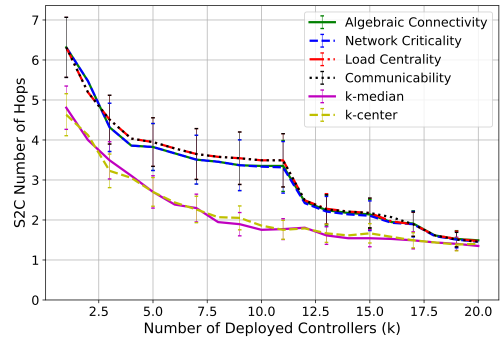

(a) Internet2

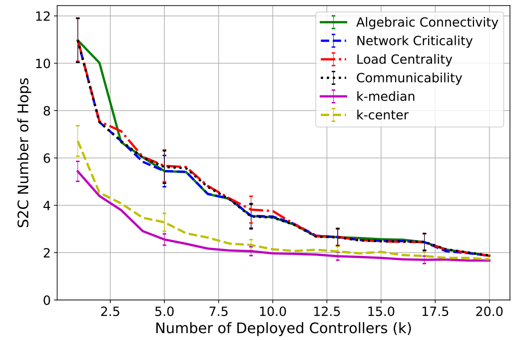

(b) Level3

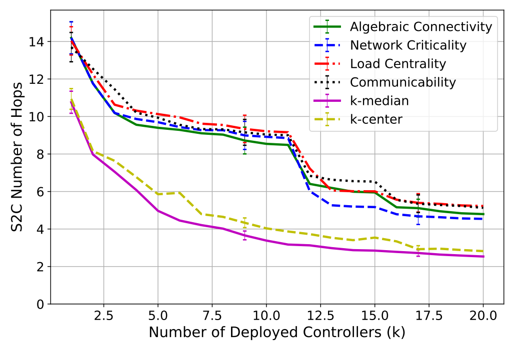

(c) Sprint

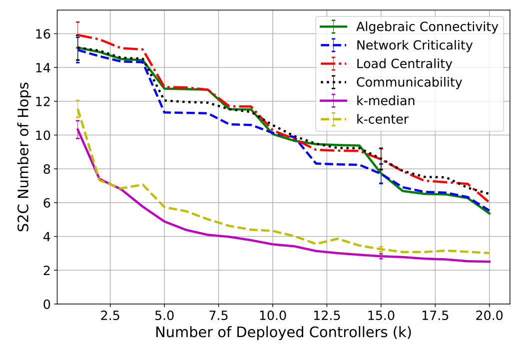

(d) AT&T

Fig. 6. Switch hop-count.

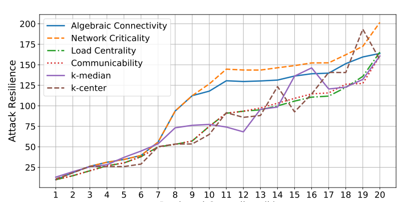

(a) Internet2 degree-based attack

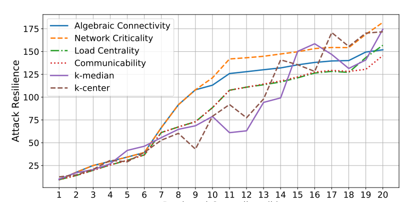

(b) Internet2 closeness-based attack

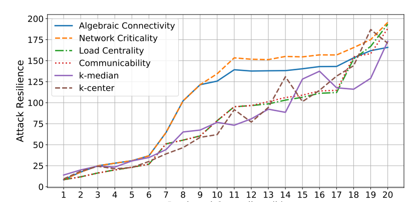

(c) Internet2 betweenness-based attack

Fig. 7. Centrality-based attacks evaluation of internet2 backbone network

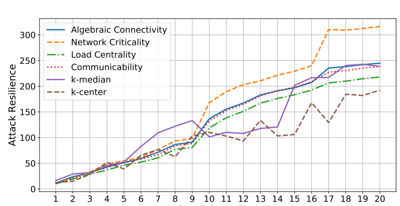

(a) Level 3 degree-based attack

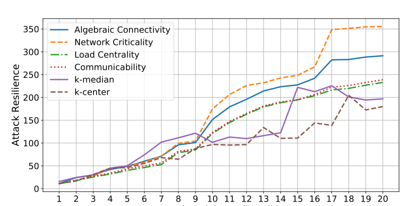

(b) Level 3 closeness-based attack

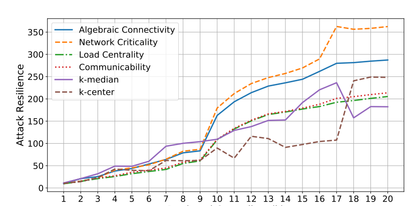

(c) Level 3 betweenness-based attack

Fig. 8. Centrality-based attacks evaluation of Level 3 backbone network

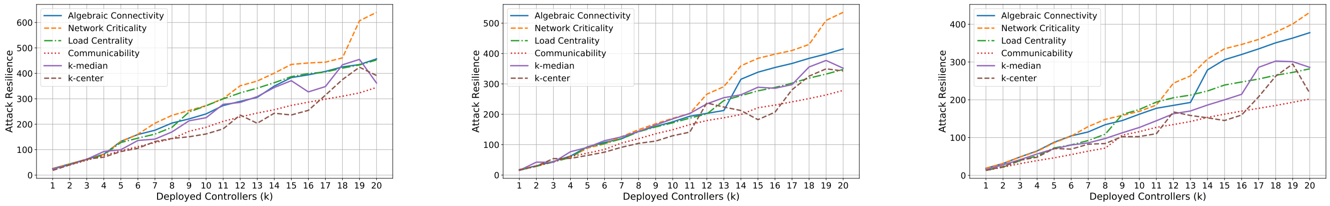

(a) Sprint degree-based attack
(b) Sprint closeness-based attack
(c) Sprint betweenness-based attack

Fig. 9. Centrality-based attacks evaluation of Sprint backbone network

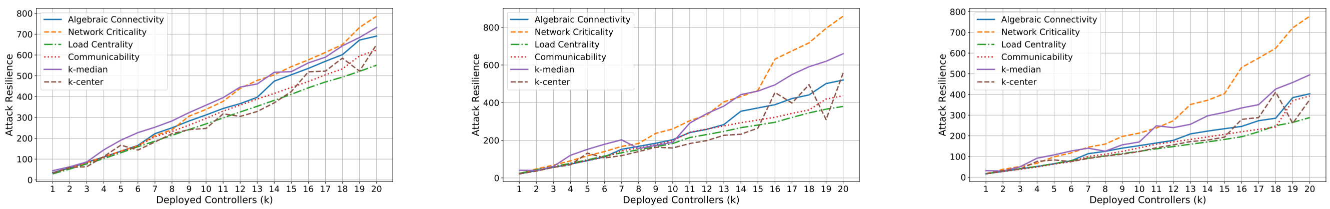

(a) AT&T degree-based attack
(b) AT&T closeness-based attack
(c) AT&T betweenness-based attack

Fig. 10. Centrality-based attacks evaluation of AT&T backbone network

[7] Z. Shah and S. Cosgrove, "Mitigating arp cache poisoning attack in software-defined networking (sdn): A survey," *Electronics*, vol. 8, no. 10, 2019.

[8] M. J.F. Alenazi, "Evaluating multipath tcp resilience against link failures," *The ISC International Journal of Information Security*, vol. 11, no. 3, pp. 113–122, 2019.

[9] P. Charalampou and E. D. Sykas, "An sdn focused approach for energy aware traffic engineering in data centers," *Sensors*, vol. 19, no. 18, 2019.

[10] M. U. Younus, S. u. Islam, and S. W. Kim, "Proposition and real-time implementation of an energy-aware routing protocol for a software defined wireless sensor network," *Sensors*, vol. 19, no. 12, 2019.

[11] B. Heller, R. Sherwood, and N. McKeown, "The Controller Placement Problem," in *Proceedings of the First ACM SIGCOMM Workshop on Hot Topics in Software Defined Networks (HotSDN)*, (Helsinki), pp. 7–12, Proceedings of the 1st ACM SIGCOMM Workshop on Hot Topics in Software Defined Networks (HotSDN), August 2012.

[12] J. P. Sterbenz, D. Hutchison, E. K. Cetinkaya, A. Jabbar, J. P. Rohrer, M. Scholler, and P. Smith, "Redundancy, Diversity, and Connectivity to Achieve Multilevel Network Resilience, Survivability, and Disruption Tolerance," *Telecommunication Systems*, vol. 56, no. 1, 2011.

[13] M. Fiedler, "Algebraic connectivity of graphs," *Czechoslovak Mathematical Journal*, vol. 23, no. 2, pp. 298–305, 1973.

[14] E. K. Çetinkaya, M. J. F. Alenazi, J. P. Rohrer, and J. P. G. Sterbenz, "Topology Connectivity Analysis of Internet Infrastructure Using Graph Spectra," in *Proceedings of the 4th IEEE/IFIP International Workshop on Reliable Networks Design and Modeling (RNDM)*, (St. Petersburg), pp. 752–758, October 2012.

[15] E. K. Çetinkaya, M. J. F. Alenazi, A. M. Peck, J. P. Rohrer, and J. P. G. Sterbenz, "Multilevel Resilience Analysis of Transportation and Communication Networks," *Springer Telecommunication Systems Journal*, 2013. (accepted in July 2013).

[16] M. J. F. Alenazi, E. K. Çetinkaya, and J. P. G. Sterbenz, "Network Design and Optimisation Based on Cost and Algebraic Connectivity," in *Proceedings of the 5th IEEE/IFIP International Workshop on Reliable Networks Design and Modeling (RNDM)*, (Almaty), pp. 193–200, September 2013.

[17] A. Tizghadam and A. Leon-Garcia, "Autonomic traffic engineering for network robustness," *Selected Areas in Communications, IEEE Journal on*, vol. 28, no. 1, pp. 39–50, 2010.

[18] K.-I. Goh, B. Kahng, and D. Kim, "Universal behavior of load distribution in scale-free networks," *Physical Review Letters*, vol. 87, no. 27, p. 278701, 2001.

[19] E. Estrada, D. J. Higham, and N. Hatano, "Communicability betweenness in complex networks," *Physica A Statistical Mechanics and its Applications*, vol. 388, pp. 764–774, March 2009.

[20] M. J. F. Alenazi, "On sdn controller placement to achieve robustness against targeted attacks," in *Complex Networks & Their Applications VI* (C. Cherifi, H. Cherifi, M. Karsai, and M. Musolesi, eds.), (Cham), pp. 633–645, Springer International Publishing, 2018.

[21] A. K. Singh and S. Srivastava, "A survey and classification of controller placement problem in sdn," *International Journal of Network Management*, vol. 28, no. 3, p. e2018, 2018. e2018 nem.2018.

[22] F. J. Ros and P. M. Ruiz, "On reliable controller placements in Software-Defined Networks," *Computer Communications*, vol. 77, pp. 41–51, March 2016.

[23] Y. Hu, W. Wendong, and X. Gong, "Reliability-aware controller placement for Software-Defined Networks," *Integrated Network . . .* , pp. 672–675, 2013.

[24] T. Hu, Z. Guo, P. Yi, T. Baker, and J. Lan, "Multi-controller based software-defined networking: A survey," *IEEE Access*, vol. 6, pp. 15980–15996, 2018.

[25] S. Kirkpatrick, C. D. Gelatt, M. P. Vecchi, *et al.*, "Optimization by simulated annealing," *science*, vol. 220, no. 4598, pp. 671–680, 1983.

[26] M. J. Alenazi, "Graph resilience improvement of backbone networks via node additions," in *2016 8th International Workshop on Resilient Networks Design and Modeling (RNDM)*, pp. 231–237, Sept 2016.

[27] M. J. Alenazi and E. K. Çetinkaya, "Resilient placement of sdn controllers exploiting disjoint paths," *Transactions on Emerging Telecommunications Technologies*, vol. 0, no. 0, p. e3725. e3725 ett.3725.

[28] M. J. Alenazi and J. P. Sterbenz, "Comprehensive comparison and accuracy of graph metrics in predicting network resilience," in *Design of Reliable Communication Networks (DRCN), 2015 11th International Conference on the*, pp. 157–164, IEEE, 2015.

[29] A. Jamakovic and S. Uhlig, "On the relationship between the algebraic connectivity and graph's robustness to node and link failures," in *Proceedings of 3rd EuroNGI Conference on the Next Generation Internet Networks*, pp. 22:1–22:8, 2007.

[30] H. Wang and P. Van Mieghem, "Algebraic connectivity optimization via link addition," in *Proceedings of the 3rd ICST International Conference*

on Bio-Inspired Models of Network, Information and Computing Sytems (BIONETICS), (Hyogo, Japan), pp. 22:1–22:8, November 2008.

[31] W. Liu, H. Sirisena, K. Pawlikowski, and A. McInnes, "Utility of algebraic connectivity metric in topology design of survivable networks," in *Proceedings of the 7th IEEE International Workshop on Design of Reliable Communication Networks (DRCN)*, (Washington, DC), pp. 131–138, October 2009.

[32] A. Sydney, C. Scoglio, and D. Gruenbacher, "Optimizing algebraic connectivity by edge rewiring," *Applied Mathematics and Computation*, vol. 219, no. 10, pp. 5465–5479, 2013.

[33] A. Bigdeli, A. Tizghadam, and A. Leon-Garcia, "Comparison of network criticality, algebraic connectivity, and other graph metrics," in *Proceedings of the 1st Annual Workshop on Simplifying Complex Network for Practitioners*, p. 4, ACM, 2009.

[34] L. Hu, M. Qiu, J. Song, M. S. Hossain, and A. Ghoneim, "Software defined healthcare networks," *IEEE Wireless Communications*, vol. 22, pp. 67–75, December 2015.

[35] N. G. Nayak, F. Dürr, and K. Rothermel, "Time-sensitive software-defined network (tssdn) for real-time applications," in *Proceedings of the 24th International Conference on Real-Time Networks and Systems*, RTNS '16, (New York, NY, USA), pp. 193–202, ACM, 2016.

[36] N. McKeown, T. Anderson, H. Balakrishnan, G. Parulkar, L. Peterson, J. Rexford, S. Shenker, and J. Turner, "OpenFlow: Enabling Innovation in Campus Networks," *SIGCOMM Comput. Commun. Rev.*, vol. 38, pp. 69–74, March 2008.

[37] J. Wan, S. Tang, Z. Shu, D. Li, S. Wang, M. Imran, and A. V. Vasilakos, "Software-defined industrial internet of things in the context of industry 4.0," *IEEE Sensors Journal*, vol. 16, pp. 7373–7380, Oct 2016.

[38] X. Dong, H. Lin, R. Tan, R. K. Iyer, and Z. Kalbarczyk, "Software-defined networking for smart grid resilience: Opportunities and challenges," in *Proceedings of the 1st ACM Workshop on Cyber-Physical System Security*, CPSS '15, (New York, NY, USA), pp. 61–68, ACM, 2015.

[39] S. Bera, S. Misra, and M. S. Obaidat, "Mobi-flow: Mobility-aware adaptive flow-rule placement in software-defined access network," *IEEE Transactions on Mobile Computing*, vol. 18, pp. 1831–1842, Aug 2019.

[40] J. P. Sterbenz, J. P. Rohrer, E. K. Çetinkaya, M. J. F. Alenazi, A. Cosner, and J. Rolfe, "Ku-topview network topology tool." http://www.ittc.ku.edu/resilinets/maps, 2010.

[41] KMI Corporation, "North American Fiberoptic Long-haul Routes Planned and in Place," 1999.

[42] L. C. Freeman, "A Set of Measures of Centrality Based on Betweenness," *Sociometry*, vol. 40, no. 1, pp. 35–41, 1977.

[43] P. Holme, B. J. Kim, C. N. Yoon, and S. K. Han, "Attack Vulnerability of Complex Networks," *Phys. Rev. E*, vol. 65, p. 056109, May 2002.

Vulnerable Road User Detection using YOLO v3

Saranya.K.C[1]
School of Electronics Engineering
Vellore Institute of Technology
Vellore, Tamil Nadu

Arunkumar Thangavelu[2]
School of Computer Science and Engineering
Vellore Institute of Technology
Vellore, Tamil Nadu

***Abstract*—Detection and classification of vulnerable road users (VRUs) is one of the most crucial blocks in vision based navigation systems used in Advanced Driver Assistance Systems. This paper seeks to evaluate the performance of object classification algorithm, You Only Look Once i.e. YOLO v3 algorithm for the purpose of detection of a major subclass of VRUs i.e. cyclists and pedestrians using the Tsinghua – Daimler dataset. The YOLO v3 algorithm used here requires less computational resources and hence promises a real time performance when compared to its predecessors. The model has been trained using the training images in the mentioned benchmark and have been tested for the test images available for the same. The average IoU for all the truth objects is calculated and the precision recall graph for different thresholds was plotted.**

***Keywords*—Yolo v3; Tsinghua-Daimler cyclist benchmark; cyclist detection; pedestrian detection; IoU**

I. Introduction

The past decade has witnessed significant acceleration in the pace of development of automotive technologies which aim at making driving and commutation safe and facile. Deployment of autonomous driving vehicles and building Advanced Driver Assistance Systems (ADAS) to be used in hybrid vehicles are major steps in realizing this. Of the many fields related to these, systems related to improving the driving safety such as pre collision systems, crash imminent braking systems play a very crucial role. However, extensive research has been undertaken over the past few years to protect vulnerable road users (VRUs), including pedestrians, cyclists, motorcyclists. Nearly half of the world traffic deaths occur among vulnerable road users, and road traffic injuries are the eighth leading cause of death for all age groups, according to statistical data provided by WHO [1]. Among the many VRU categories, cyclists and pedestrians are the weakest and fall prey to most accidents because of the lack of protection devices. Hence the development of systems for the detection and identification of VRUs becomes an essential need of the hour, to make their commutes safer and for the ADAS to be practically and widely deployable.

Many approaches based on different sensors are employed in vehicle environment perception systems. The vision based sensors especially monocular cameras, are the most preferred as a standalone or in combination with other sensors when it comes to detection of VRUs, due to the availability of high resolution perception views. Vision based cyclist and pedestrian detection face several challenges due to the diversity in shape, posture, viewpoints, crowded backgrounds, etc. and several algorithms and methodologies have been implemented for the same keeping these considerations in account.

II. Background

Algorithms that are used for the purpose of feature extraction and classification can predominantly be handcrafted or Deep Learning based. The Haar-like feature detector which uses variations in intensities for the detection of the object [2], [3], the Viola and Jones (VJ) detector designed by Viola et al. [4] which uses a detection approach based on cascaded Haar-like features, which also considers the rapid pixel intensity changes ,and the Histogram of Gradients(HOG) detector, suggested by Dalal and Triggs which uses a linear Support Vector Machine for classification [5-8] to find an object's characteristics based on the intensities of the local gradients [2], [6] are some of the common hand-crafted features based methods used in general for pedestrian detection. However, hand-crafted methods which rely on low-level features which are manually designed to find the ROI's [9] are not very efficient as features which complex are arduous to handcraft. Au contraire, Deep Learning (DL) based techniques are highly autonomous by allowing the network to determine features.

Since the advent of DL, several approaches have been designed for pedestrian or cyclist detection. In the method described by Wei Tian [10] cyclists in different views and angles are located using cascade detectors. Together with trajectory planning, this model employs an ROI extraction derived based on geometry but achieves only 11 fps when employed in real time. Ren [11] realized an accuracy of 76.47% for an IoU threshold of 0.7 using a Recurrent Rolling Convolution (RRC) architecture employed on multiscale feature maps. Saleh in [12] use a Faster RCNN based network on synthetic image datasets to perform better than the HOG- SVM classifier by 21% in average precision. Felzenswalb [25] designed the Deformable Part Model (DPM) on the basis of HOG detector to undermine the distortions caused due to non-rigid objects. To ensure swift and accurate detection, Yang in [13] used convolutionary object detector with Scale based pooling and CRCs. The scale-dependent pooling allows the identification of tiny objects to be improved, and the CRCs help to enhance detection speed by rapidly removing false detections.

While all the previously cited works either concentrate on the detection of either the pedestrians or the cyclists, very less literature is available for the simultaneous detection of pedestrians and cyclists [19]. In [5] X. Li propose a unified framework for both cyclist and pedestrian detection using a UB-MPR based detection combined with Fast RCNN and Fu in [26], propose a system based on symmetry of objects to recognize the features of cyclists and pedestrians that appear in an image. However, this method still does not reach the real time speed requirements due to the complex isolated stages that required for the detection and classification.

As emphasized by Huang Ji [16] networks like YOLO which uses a relatively simpler framework for object detection and classification have a slight reduction in accuracy when set against methods like Fast RCNN [14] but expiate for it with real time performance [17] .With optimization, methods like YOLO and its modifications like, YOLO9000, fast YOLO, etc. [18] one can achieve better real time object detection and also makes proper use of the capabilities of the Graphical Processing Unit (GPU) [27].

This paper aims to present and examine the performance of the V3 variant of YOLO for the unified detection of cyclists and pedestrians using the Tsinghua- Daimler Benchmark [15] dataset. The work performed focused on analyzing the performance of the above model on the above dataset in order to establish its efficiency and reliability for the identification of cyclists and pedestrians in real time. A NVidia GTX 1080 Ti GPU was used for training the YOLO V3 network and the detection was run on a Intel Core i7 eighth generation processor CPU system.

The organization of the paper is as follows: Section 2 discusses the methodology elucidating about the dataset, the YOLOv3 network architecture and the procedure followed for training. This is followed by Section 3 and Section 4 which present results and conclusion respectively.

III. Methodology

A. Dataset

The Tsinghua-Daimler Cyclist Benchmark used consists of four subsets namely train, valid, test and non VRU *(Fig. 2)*. Train subset consists of 9741 images and only cyclist objects are annotated. This subset includes cyclists which are fully visible with an occlusion rate of lesser than 10% and greater than 60 pixels. Valid subset contains 1019 images and the objects annotated are pedestrian, cyclist, tri cyclist, moped rider, wheel chair user and motorcyclist. The objects that are labeled have more than 20 pixels. The test set has 2914 images and the same list objects annotated as the valid set. Like the valid set, the objects labeled here also have more than 20 pixels. Non VRU has 1000 images which do not contain any objects of interest such as pedestrian, cyclist, motorcyclist, tricyclist, wheel chair user, moped rider.

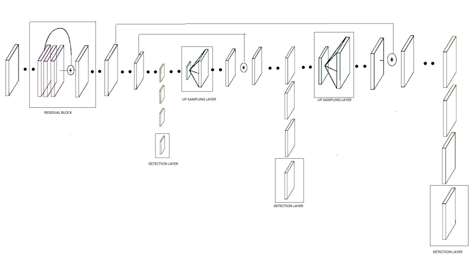

Fig. 1. YOLO V3 architecture

B. Network Architecture

YOLO V3 [20] *(Fig. 1)* uses dimension clusters as anchor boxes for the prediction of bounding boxes [17]. The network

[]
[]
[]
[]

Fig. 2. Sample images from the subsets of Tsinghua-Daimler Cyclist Benchmark: (a)Train (b)Valid (c)Non-VRU (d)Test

predicts 4 coordinates for each bounding box, l_x, l_y, l_w and l_h. If (O_x, O_y) is the offset of the cell from the top left corner of the image and pr_w and pr_h are the the width and height of the previous bounding box respectively, then the predictions correspond to:

$$b_y = \sigma(l_y) + Oy \tag{1}$$

$$b_w = pr_w e^{lw} \tag{2}$$

$$b_h = pr_h e^{lh} \tag{3}$$

Here (b_x, b_y) is the coordinate of the center of the bounding box relative to the location of filter application using a sigmoid function. b_w and b_h are width and height of the bounding box respectively.

The class that the bounding box may contain is predicted using multi label classification. This uses a combination of independent logistic classifier and binary cross entropy loss for class predictions during the training.

Yolov3 uses a feature extractor network called Darknet 53 whose architecture is shown in *(Fig. 3)* which is a hybrid variant of the network used in YOLOv2 , Darknet-19 [17]. This network has 53 convolution layers. The filters consist of

	Type	Filters	Size	Output
	Convolutional	32	3 × 3	256 × 256
	Convolutional	64	3 × 3 / 2	128 × 128
1×	Convolutional	32	1 × 1	
	Convolutional	64	3 × 3	
	Residual			128 × 128
	Convolutional	128	3 × 3 / 2	64 × 64
2×	Convolutional	64	1 × 1	
	Convolutional	128	3 × 3	
	Residual			64 × 64
	Convolutional	256	3 × 3 / 2	32 × 32
8×	Convolutional	128	1 × 1	
	Convolutional	256	3 × 3	
	Residual			32 × 32
	Convolutional	512	3 × 3 / 2	16 × 16
8×	Convolutional	256	1 × 1	
	Convolutional	512	3 × 3	
	Residual			16 × 16
	Convolutional	1024	3 × 3 / 2	8 × 8
4×	Convolutional	512	1 × 1	
	Convolutional	1024	3 × 3	
	Residual			8 × 8
	Avgpool		Global	
	Connected		1000	
	Softmax			

Fig. 3. Darknet 53-network architecture [20]

successive 1x1 and 3x3 filters with shortcut connections. In YOLOv3, features are extracted from the 3 scales congruous to feature pyramid networks [21]. This majorly helps to identify small objects. The last layer predicts the bounding box, probability of box containing object and class predictions. The dimensions of the final prediction vector is

$$L \times L \times [3 \times (4 + 1 + No.of classes)] \quad (4)$$

Where three denotes the number of scales, four the number of bounding box offsets and one is the probability that an object is present is the bounding box. Here, the number of classes is two as this paper concentrates only on the detection of cyclists and pedestrians. $L \times L$ is the splitting of the picture into segments.

C. Training

The training was carried out using the parameters given in *Table I* with keras implementation of YOLOv3, running tensor flow as the backend [22]. For training the first subset labeled as train and a part of the pedestrian subset of the Tsinghua-Daimler benchmark was used. The validation dataset is obtained from a random subset of the above set, which is 10% of the total set. Thus 90% of the above set is used for training and 10% for validation. According to the model's architecture, the training images were divided into batches of 8, enabling the GPU to process 8 images at a time followed by the updation of the corresponding gradients and the related weights.

Initial weights for training were acquired from the weights of a YOLOv3-608 model.

TABLE I. TRAINING PARAMETERS FOR THE NETWORK

Dataset used	Tsinghua-Daimler Cyclist Benchmark
No. of Train samples	8767
No. of Validation samples	974
Initial learning rate	0.001 for 1-60 epochs 0.0001for 61-126 epochs
Beta 1	0.9
Beta 2	0.999
Pre-trained weights	YOLOv3-608
No. of Batches	8
No. of Epochs	126
Train size ($height \times width$)	416 × 416
GPU	Nvidia GTX 1080 Ti

The adam optimizer [23] which has an initial learning rate of 0.001 was used. Learning rate reduction on plateau with a factor of reduction of 0.1 was implemented and validation loss was monitored with early stopping. The beta rates of 0.9 and 0.999 were used.

IV. RESULTS

The results obtained after training 126 epochs *(Table II)* at a rate of 45fps for different scenarios are shown in *(Fig. 5)*. The performance was assessed using Intersection over Union i.e. IoU, Precision recall Graph, and F1 score as metrics *(Table III)*. The prediction was considered for account only when it had at least 0.5 confidence.

TABLE II. TEST PARAMETERS FOR THE NETWORK

Dataset used	Tsinghua-Daimler Cyclist Benchmark
No. of Samples used	2914
Threshold used	Detection :0.5 (50% confidence) IoU :50%
Size specs of test image	1024 × 2048 (height × width in pixels)

A. Intersection over Union (IoU)

Intersection Over Union (IoU), a measure based on Jaccard Index, that evaluates the overlap between the ground truth bounding box BB_g and the predicted bounding box BB_p, was used to identify the accuracy of detection.

$$IoU = \frac{area(BB_p \cap BB_g)}{area(BB_p \cup BB_g)} = \frac{area\,of\,overlap}{area\,of\,union} \quad (5)$$

The predicted objects with an IoU of more than 50% are considered as true objects and the average IoU of all the true objects detected is 73.17%.

B. Precision-Recall Graph

The Precision-Recall graph [24] as shown in the *(Fig. 4)* has been plotted over different threshold values. Here the precision which denotes a model's ability to identify only relevant objects is given by

$$Precision = \frac{T_P}{T_P + F_P} = \frac{T_P}{All\,detections} \quad (6)$$

And recall which is the percentage of true positive detected amongst all relevant ground truths and is given by

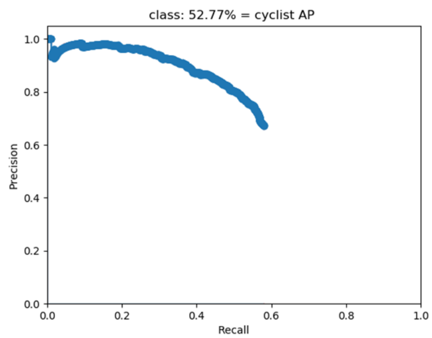

[]

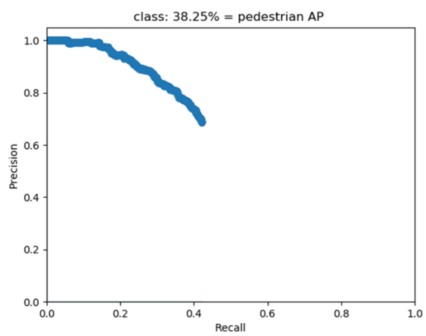

[]

Fig. 4. The precision-recall graph over multiple thresholds.

TABLE III. Consolidated results

Class	Total	TP	FP	FN	Precision	Recall	F1	AP
Cyclist	1541	762	372	779	0.671958	0.494484	0.5697	52.77
Pedestrian	1314	649	297	665	0.686047	0.493912	0.574336	38.25

$$Recall = \frac{T_P}{T_P + F_N} = \frac{T_P}{All\, ground\, truths} \quad (7)$$

Where, True Positives (TP) and False Positives (FP) require predictions to have an IoU and confidence level greater than and less than the threshold value of 0.5, respectively. False Negatives(FN),which is calculated as the difference between the actual number of the object class present and the number of True Positives denotes the failure of the model to identify the ground truth of the particular object class.

By interpolating all precision and the corresponding recall points, the Average Precision (AP) was calculated.

C. F1 score

F_1 score an optimum mix between precision and recall was calculated as the weighted average between precision and recall, thus taking both the false positives and the false negatives into account

$$F_1 score = 2 \times \frac{Recall \times Precision}{Recall + Precision} \quad (8)$$

V. Conclusion

The implemented model shows good performance with regards to accuracy and efficiency with a real time performance at a rate of 45 fps for the scenarios found in the Tsinghua-Daimler benchmark. The deficiencies in the performance can mainly be attributed to situations where the objects of interest are very small or show high degree of occlusion or are limited by the characteristics of the camera used to capture images leading to reduced range of vision causing blind spots and limited field of view. Further studies can be carried out on the above-mentioned difficulties to improve the performance.

References

[1] A. Dominguez-Sanchez, M. Cazorla, and S. Orts-Escolano, “Pedestrian movement direction recognition using convolutional neural networks,” *IEEE transactions on intelligent transportation systems*, vol. 18, no. 12, pp. 3540–3548, 2017.

[2] A. Brunetti, D. Buongiorno, G. F. Trotta, and V. Bevilacqua, “Computer vision and deep learning techniques for pedestrian detection and tracking: A survey,” *Neurocomputing*, vol. 300, pp. 17–33, 2018.

[3] M. Oren, C. Papageorgiou, P. Sinha, E. Osuna, and T. Poggio, “Pedestrian detection using wavelet templates,” in *cvpr*, vol. 97, 1997, pp. 193–199.

[4] P. Viola, M. J. Jones, and D. Snow, “Detecting pedestrians using patterns of motion and appearance,” *International Journal of Computer Vision*, vol. 63, no. 2, pp. 153–161, 2005.

[5] X. Li, L. Li, F. Flohr, J. Wang, H. Xiong, M. Bernhard, S. Pan, D. M. Gavrila, and K. Li, “A unified framework for concurrent pedestrian and cyclist detection,” *IEEE transactions on intelligent transportation systems*, vol. 18, no. 2, pp. 269–281, 2016.

[6] N. Dalal and B. Triggs, “Histograms of oriented gradients for human detection,” in *2005 IEEE Computer Society Conference on Computer Vision and Pattern Recognition (CVPR’05)*, vol. 1, June 2005, pp. 886–893 vol. 1.

[7] R. Benenson, M. Omran, J. Hosang, and B. Schiele, “Ten years of pedestrian detection, what have we learned?” in *European Conference on Computer Vision*. Springer, 2014, pp. 613–627.

[8] D. Tomè, F. Monti, L. Baroffio, L. Bondi, M. Tagliasacchi, and S. Tubaro, “Deep convolutional neural networks for pedestrian detection,” *Signal processing: image communication*, vol. 47, pp. 482–489, 2016.

[9] W. Sun, S. Zhu, X. Ju, and D. Wang, “Deep learning based pedestrian detection,” in *2018 Chinese Control And Decision Conference (CCDC)*, June 2018, pp. 1007–1011.

[10] W. Tian and M. Lauer, “Fast cyclist detection by cascaded detector and geometric constraint,” in *2015 IEEE 18th International Conference on Intelligent Transportation Systems*. IEEE, 2015, pp. 1286–1291.

[11] J. Ren, X. Chen, J. Liu, W. Sun, J. Pang, Q. Yan, Y.-W. Tai, and L. Xu, “Accurate single stage detector using recurrent rolling convolution,” in *2017 IEEE Conference on Computer Vision and Pattern Recognition (CVPR)*. IEEE, 2017, pp. 752–760.

[12] K. Saleh, M. Hossny, A. Hossny, and S. Nahavandi, “Cyclist detection in lidar scans using faster r-cnn and synthetic depth images,” in *2017 IEEE 20th International Conference on Intelligent Transportation Systems (ITSC)*. IEEE, 2017, pp. 1–6.

[13] F. Yang, W. Choi, and Y. Lin, “Exploit all the layers: Fast and accurate cnn object detector with scale dependent pooling and cascaded rejection classifiers,” in *Proceedings of the IEEE conference on computer vision and pattern recognition*, 2016, pp. 2129–2137.

[14] R. Girshick, “Fast r-cnn,” in *2015 IEEE International Conference on Computer Vision (ICCV)*, Dec 2015, pp. 1440–1448.

[15] X. Li, F. Flohr, Y. Yang, H. Xiong, M. Braun, S. Pan, K. Li, and D. M. Gavrila, “A new benchmark for vision-based cyclist detection,” in *2016 IEEE Intelligent Vehicles Symposium (IV)*. IEEE, 2016, pp. 1028–1033.

[16] J. Huang, V. Rathod, C. Sun, M. Zhu, A. Korattikara, A. Fathi, I. Fischer, Z. Wojna, Y. Song, S. Guadarrama *et al.*, "Speed/accuracy trade-offs for modern convolutional object detectors," in *2017 IEEE Conference on Computer Vision and Pattern Recognition (CVPR)*. IEEE, 2017, pp. 3296–3297.

[17] J. Redmon and A. Farhadi, "Yolo9000: Better, faster, stronger," in *2017 IEEE Conference on Computer Vision and Pattern Recognition (CVPR)*. IEEE, 2017, pp. 6517–6525.

[18] M. J. Shaifee, B. Chywl, F. Li, and A. Wong, "Fast yolo: A fast you only look once system for real-time embedded object detection in video," *Journal of Computational Vision and Imaging Systems*, vol. 3, no. 1, 2017.

[19] K. C. Saranya, A. Thangavelu, A. Chidambaram, S. Arumugam, and S. Govindraj, "Cyclist detection using tiny yolo v2," in *Soft Computing for Problem Solving*. Springer, 2020, pp. 969–979.

[20] J. Redmon and A. Farhadi, "Yolov3: An incremental improvement," *arXiv preprint arXiv:1804.02767*, 2018.

[21] T.-Y. Lin, P. Dollár, R. Girshick, K. He, B. Hariharan, and S. Belongie, "Feature pyramid networks for object detection," in *2017 IEEE Conference on Computer Vision and Pattern Recognition (CVPR)*. IEEE, 2017, pp. 936–944.

[22] J. Redmon, "Darknet: Open source neural networks in c," 2013.

[23] D. P. Kingma and J. Ba, "Adam: A method for stochastic optimization," *arXiv preprint arXiv:1412.6980*, 2014.

[24] J. Davis and M. Goadrich, "The relationship between precision-recall and roc curves," in *Proceedings of the 23rd international conference on Machine learning*. ACM, 2006, pp. 233–240.

[25] P. F. Felzenszwalb, R. B. Girshick, D. McAllester, and D. Ramanan, "Object detection with discriminatively trained part-based models," *IEEE transactions on pattern analysis and machine intelligence*, vol. 32, no. 9, pp. 1627–1645, 2009.

[26] L.-C. Fu, P.-Y. Hsiao, C.-E. Wu, Y.-M. Chan, and S.-C. Hu, "Vision based pedestrian and cyclist detection method," Jul. 21 2015, uS Patent 9,087,263.

[27] V. Kharchenko and I. Chyrka, "Detection of airplanes on the ground using yolo neural network," in *2018 IEEE 17th International Conference on Mathematical Methods in Electromagnetic Theory (MMET)*. IEEE, 2018, pp. 294–297.

Fig. 5. (a) Multiple object detection and slightly occluded pedestrian detection (b) Multiple object detection and far object detection (c) Multiple cyclist in different angles (d) Cyclist side view detection (e) Cyclist front view (f) Pedestrian side view detection (note: multiple pedestrian present but others are almost fully occluded)

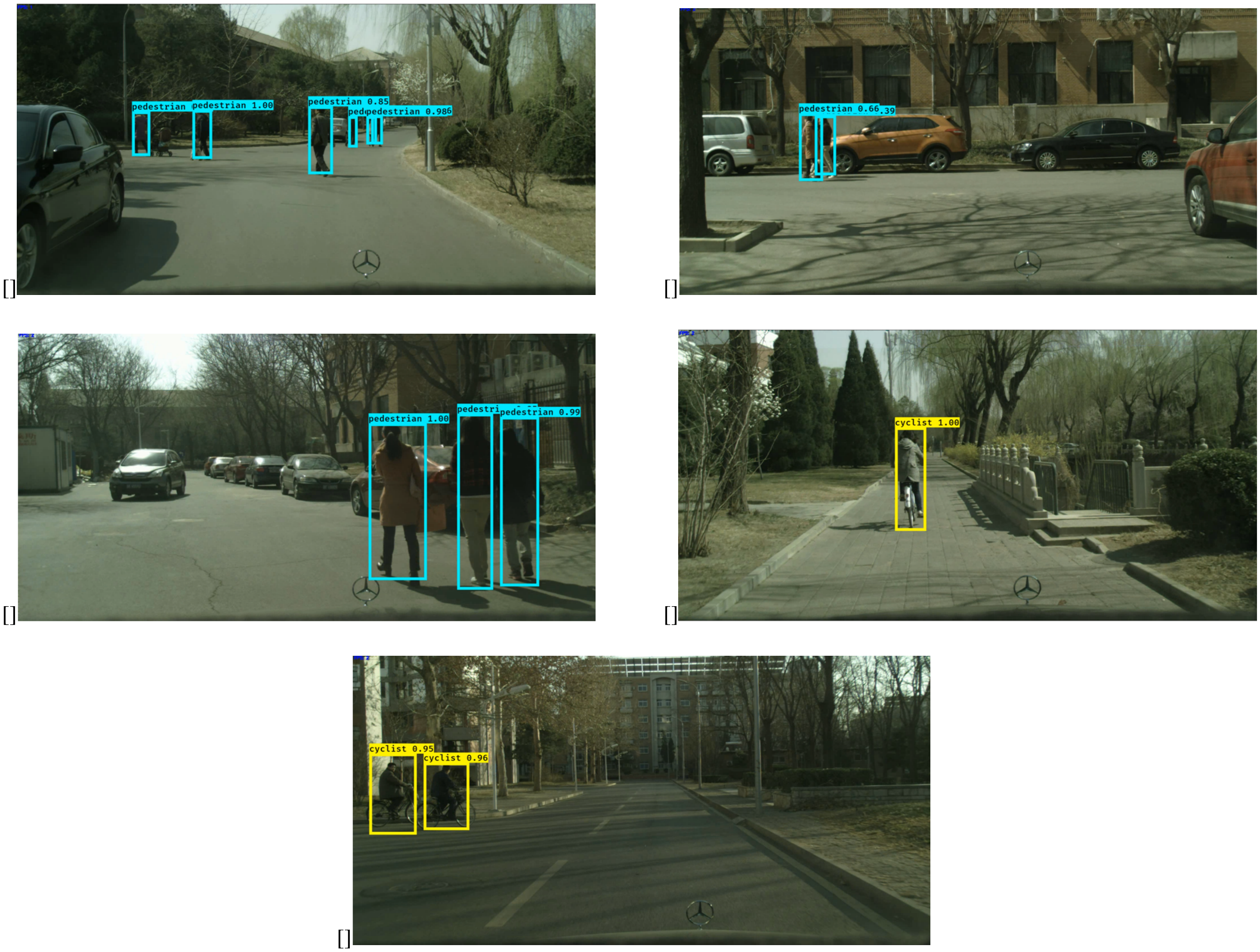

Fig. 5. *(contd.)* (g) Multiple pedestrian detection (h) Multiple pedestrians-side view- occluded (i) Multiple pedestrians-back view (j) Cyclist back view (k) Multiple cyclists side view detection

On Developing an Integrated Family Mobile Application

Subhieh El-Salhi[1], Fairouz Farouq[2], Randa Obeidallah[3], Mo'taz Al-Hami[4]
Department of Computer Information System
Hashemite University, Zarqa, Jordan

***Abstract*—Now-a-days mobile applications have been seen as the most effective, popular and powerful technologies and this is due to the widespread of mobile devices. Moreover, the raising power of mobile devices has a great impact on people of all ages; and more specifically on social relationships including interaction between parents and kids. Therefore, this paper presents a highly integrated Family Mobile Application (FMA) that provides a wide range of services to control, manage, organize and support the different daily tasks of family members effectively. The essential tasks of the FMA are mainly described in terms of facilitating the daily life routine and responsibilities, enhancing the communication between the family members (in different aspects) and supporting the Augmented Reality (AR) which is directed to the children of the family to support educational goals in particular. Moreover, a website has been established to enrich the functionality of the proposed FMA application. The FMA has been analysed, designed, implemented and evaluated on real-world users of the system. The evaluation was con-ducted in terms of the usability testing that considers satisfaction, simplicity and ease of use. More details of the real evaluation are illustrated and presented.**

Keywords*—Mobile technology; social apps; family mobile application; Augmented Reality (AR)

I. Introduction

Generally speaking, parenting can be considered as the most difficult full-time job in the world as the parents need to stay connected with their children all the time to guide, support and take care of them. The difficulties of parenting come from two major factors: (i) to fulfill the parenting responsibilities in providing an adequate supervision constantly and (ii) to overcome the implication of the long hours of work-load. Furthermore, these difficulties become more complicated if both parents are working due to economic, social and cultural reasons. Therefore, the most significant aspect of effective parenting skill requires reaching an ideal work-family balance.

Moreover, Sanders et al. highlights the most important competent parenting aspects [1]. Some of these aspects are summarized as follows (but not limited to): (i) providing positive learning environment, (ii) encouraging good behaviour in kids (assertive discipline), (iii) providing health nutrition, and finally (iv) encouraging cooperative behaviour and caring while handling household chores and family responsibilities. Therefore, there is an essential demand to employ the technology to fulfill the responsibilities of parents effectively.

The mobile apps development process has been increasingly influenced by nowadays-technological revolution and consequently it have been widely employed to facilitate the usage of various services provided by different fields such as health in the work presented in [2], education [3] and marketing [4]. However, most of the intensive work of the existing mobile applications is focused on developing and supporting a single task (service) that serve people in their social life effectively such as the secured mobile chat service application presented in [5].

Regarding mobile apps of social activities, a very limited work has been targeted to serve a group of people that are interested in some common shared tasks. To the best of our knowledge, there is no application directed to a single family. From this prospective, a Family Mobile Application (FMA) is proposed to support family members' lives in easier, simpler and more efficient way. The primary motivation for the work presented was a desire to provide a solution for the growing complexity of managing the daily routines of families and for enhancing the parental role. However, the FMA app is proposed not only to overcome the management challenges of the daily routines but also to provide a wide range of services that would strengthen the relationship between the family members.

Additionally, the family authorization is the key feature of the FMA application since it attempts to simulate the Parent-Child relationships while providing the different services. Therefore, the FMA application can be seen as an integrated application aims to overcome the families social challenges (to some extend) in smooth, effective e and simple technological style.

The FMA app overcomes the major challenges of parenting by providing the following services:

1) Minimize the impact of the long working hours of parents and rigorous working conditions by staying connected with their children using both the chat services and GPS tracker to determine the location of their children accurately.
2) Contribute the entire family members in family decision-making process significantly (i.e. deciding the meal of the day).
3) Increase the collaboration among family members to achieve household duties.
4) Support parents' supervision and control over the assigned household tasks.
5) Increase the level of communication and sharing between the family members by reminding and notifying them with important events.
6) Support real learning environments through presenting some stories using Augmented Reality (AR) technology.

The rest of the paper is organized as follows: Section II presents relevant literature reviews with a brief overview of some related studies. Section III introduces the functional requirement analysis for the proposed FMA app. More details on the interface design and development are demonstrated in Section IV. The evaluation of the application in terms of the usability is presented in Section V. Finally, some conclusions are presented in Section VI.

II. Literature Review

With the rapid growth of internet technology, individuals are eager to obtain the recent new top mobile phones and hand held devices in order to use the latest mobile applications easily. The dynamic revolution of technology redefines the communication process between society members and facilitates the communication between the individuals and their friends and relatives. Recent studies offered by Sanders and Leung indicate the essential role of internet technology on keeping people in touch and enabling them to communicate easily, simply and efficiently more than before [1], [6]. Social researchers have been studying the impact of Information and Communication Technologies (ICT) for individuals, families, and work life in modern societies. Romero-Ruiz et al. in [7] explored and identified perceptions that influence the use of ICT on family life. In modern families, adults and children are using the internet in daily basis. According to Children and Parents: Media Use and Attitudes Report in 2017; 83% of children aged from 12 to 15 have their own smart phones and 55% have their own tablets. Internet, software programs and mobile applications are used for school works, and more for entertainment purposes [6], [7], [8]. Few researchers noticed that family ties are becoming extremely difficult to maintain due to revolution of technology. Tensions between parents and children are increased due to the use of technology [9]. Another common perception showed that ICT do not favour family communication and this perspective found in [10]. However, the effect of ICT on modern family relationships was studied by Kerawalla et al. [8] and Kraut et al. [11] and concluded that family members spend less time in communicating and interacting face to face which may lead to damage family relationships. Romero-Ruiz et al. showed that virtual communication exposes families to feel lacking of affection [7]. On the other hand, Family members benefit of ICT to manage time, money and home activities. ICT helped parents to spend more time with family through taking care of business remotely [12]. Franzen found that internet and e-mail has a positive effect on conserving family social ties [13]. Richer communication methods that include face-to-face communication, phone and video calls showed a positive relationship satisfaction as mentioned by Goodman-Deane et al. [14]. Yet, text messaging and instant messaging were negatively associated. Family life activities are modified and moderated by ICT [15]. The positive or negative impact of ICT is determined by the way ICT is managed by parents. In order to maintain a healthy family relationship, parents need to manage the use of technology inside homes. Technology should be supervised by parents to handle the effect of technology on children's educational, emotional and social development. Parents need to determine what is the appropriate technology to use and the amount of time spent using it at home [16]. Many attempts were made to develop mobile applications to help parents to supervise children's activities, chores and locate child's location. It is familiar that family activities are usually planned and coordinated through a calendar known as family calendar. Digital family calendar is now used as a replacement of paper calendar. Neustaedter et al. proposed a digital family calendar called inkable family calendar (LINC) and examined its positive effect on four families in their study [17]. Another example of family organizer mobile application is Cozi [18]. Cozi has a calendar that can be used by the entire family, "to do list" where you can create a shared to do list, and chore list for the kids, keep family journal and recipes. In modern days, parents need to locate the location of children at all times. An android application was developed by Khan et al. [19] that can be used in emergency cases to send the current address location of a mobile device through an SMS message to a user, in our case the user is the parent. Maghade et al. developed an android application based on GPS and SMS services in Android mobile [20]. SMS service is used when smart phones do not have internet connectivity. Sweidan et al. proposed a system called "kids' tracker" that includes a wearable gadget for the child and an android application installed on parents' smart phone, this system does not need to give a mobile phone to the child [21].

III. The Proposed FMA App Functional Requirement

This section presents a full description for the proposed FMA app through presenting the structure of the FMA app and the functionality of the proposed FMA app in Section III-A and Section III-B, respectively.

A. *The FMA App Structure Overview*

The structure of the proposed FMA is presented in this section using the class diagram. The class diagram presented in Fig. 1 shows the structure of the different types of services that the family members can use and get beneficial from it. Additionally, it shows that the FMA app consists mainly of two types of users: parents and children. Parents start up the app and create the family account. After that the rest of family members including the children start to register and join the family account simply and easily.

Assuming that the FMA app is going to be downloaded on parent's mobile from the website. The complete picture of registration process for different user types and family account creation is fully described in the following steps:

- With respect to parent (considered as admin):
  1) For the first time, one of the parents has to register and create the family account by either (i) filling a sign up form or (ii) using his Facebook account.
  2) Determine the type of user (in this case it would be a parent).
  3) Create the family account so the members can then be added individually.
- With respect to children:
  1) Children apply the above step 1 and determine the type of user as children in step 2.
  2) Then search for the name of their family account. If it is found then they can ask to join

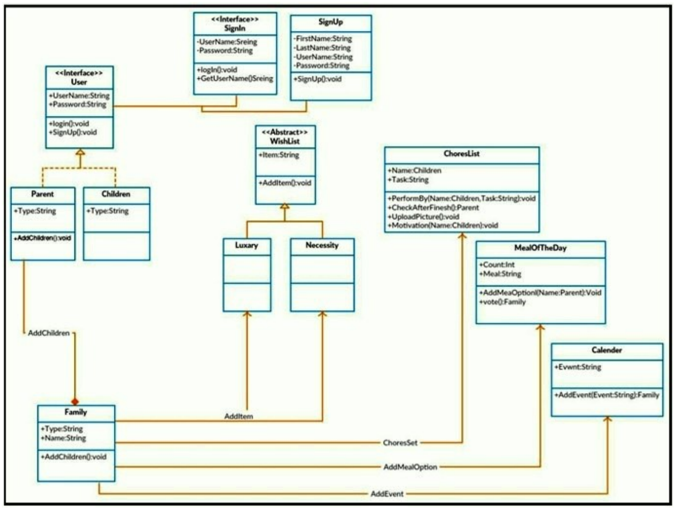

Fig. 1. The class diagram of the FMA app.

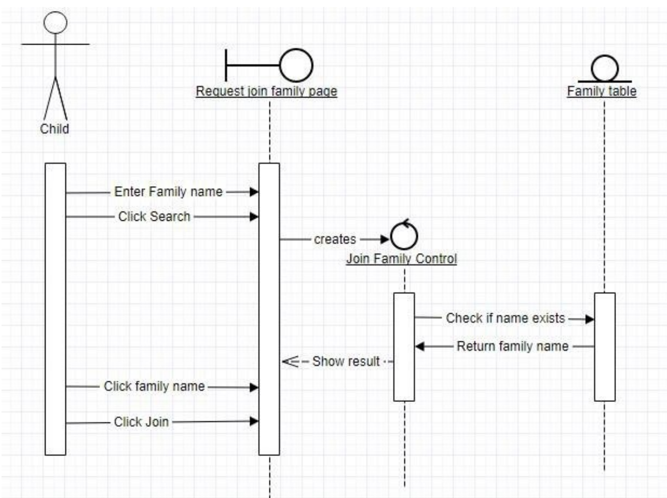

Fig. 2. The Sequence diagram of creating accounts for children.

the family to be a member in (as shown in Fig. 2). Otherwise, they can do nothing but waiting their parents to create the family account.

It is worth to mention that, the concept of parental authority of the parents towards their children appears clearly in the FMA app as the role of creating family account and adding family members are identified as one of the parents' responsibilities and this is a typical example of a real life imitating.

B. System functionality

As previously mentioned, the FMA app provides a wide set of services and functions to the family members once the family account is created. We have two main actors: parents and children. The set of functionality and services are going to be discussed and fully described according to user type.

- For the parents, the main functions are: (i) accepting and rejecting the members request to join the family, (ii) assigning different chores such as vacuuming, sweeping and dusting to children, (iii) monitoring and check the progress of the assigned tasks, (iv) suggesting a meal to the "meal of the day".

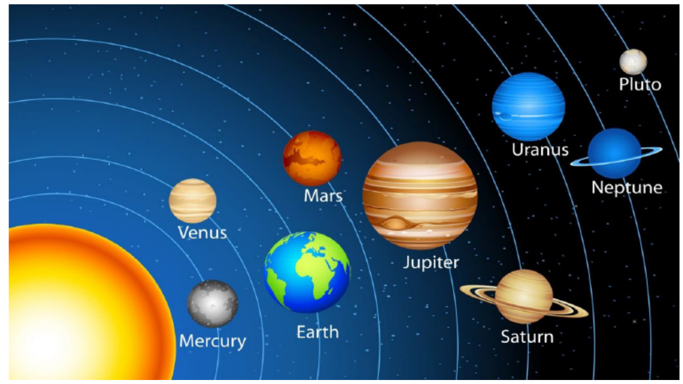

Fig. 3. The Solar system.

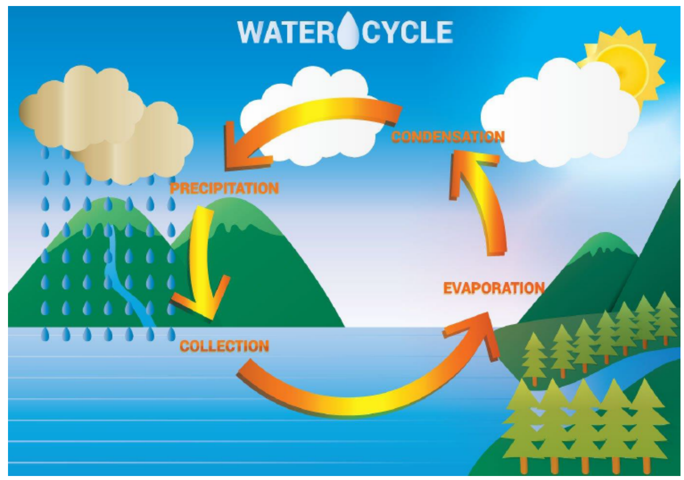

Fig. 4. The Water cycle.

- For the children, the main functions are: (i) reporting the completed as-signed task (chores) and (ii) voting to the preferred meal from the suggested list meals ("meal of the day") where the meal with the majority votes wins.

However, both parents and children have some common set of tasks such as: (i) adding items to the "wishing list", (ii) monitoring and checking the place of family members, (iii) chatting with each other, (iv) adding and viewing significant activities of the dynamic calendar such as parent meetings at schools, exam schedules and doctor appointments, and lastly (v) using AR technology to explore some stories. Two scientific stories have been used with respect to AR stories: the solar system and the Water cycle story shown in Fig. 3 and Fig. 4, respectively.

Furthermore, as good deeds deserve pay off at the end, the concept of rewarding the children appears clearly in the "wishing list" service. The "wishing list" has two different types: (i) luxury list which contains the desired items children wishing to own on different occasions such as branded clothing and accessories (i.e. watches and jewelry) and (ii) ordinary

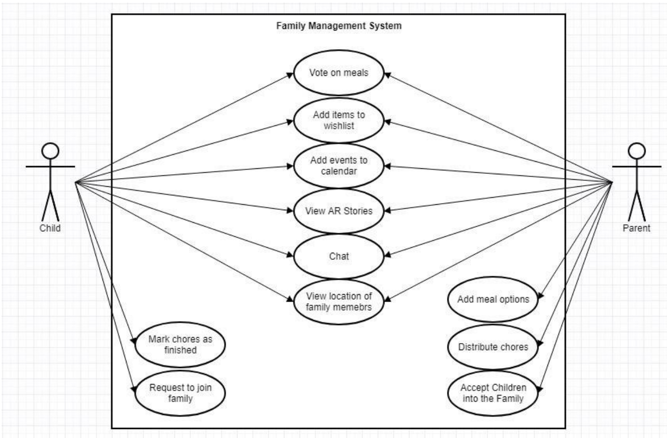

Fig. 5. The Use-case diagram of the provided services of FMA app.

shopping list which contains the basics and daily necessities (i.e. groceries items). It is worth to mention that the children earn points for each successfully completed task that was already as-signed to them by their parents. More accomplished tasks mean more points that are collected. Once the collected points reach certain number of points "level" (determined by the parents), the luxury list is activated and the children are awarded to list their desired valuable items they are willing to obtain. After that, the parents can easily select the items from the luxury list if they decided to reward their children for their high assistance and effective collaboration in household activities especially in special occasions (i.e. birthdays and exams). With reference to Fig. 5, the details of each functional requirement (FR) performed in the FMA app are listed below using Cockburn template [22], [23]:

FR1: Accepting children's request (i.e., registration)
Use case Title: Accepting children's request
Primary Actor: Parent
Stakeholder: Parent, Children
Precondition: Parents create family account successfully and children need to download the FMA app and enter valid data (family name)
Minimal Guarantee: Failed to join the family (reject the request)
Success Guarantee: Children join the family successfully.
Trigger: Download the FMA app from and ask to join the family
Main success scenario:
1. Children download the FMA app from the website successfully
2. Children Search the family name
3. Children send a request to join the family
4. Parent accept the request
Extensions:

1) If the FMA app is not downloaded successfully
   a Children take action to explore the website and download the app again
2) Children cannot find the name of family
   a Children quits the app. Children wait their parent to create family account

FR2: Distribute Chores including the following:
Use case Title: Distribute Chores
Primary Actor: Parent
Stakeholder: Parent, Children
Precondition: Parents and children need to register to the FMA App and join the family account successfully
Minimal Guarantee: Chores are not assigned
Success Guarantee: The application successfully assigns task to one family member.
Trigger: The parents need to check the list of daily chores to distribute among family members.
Main success scenario:
1. Parents check the chores
2. Parents assign the task for a single family member
3. Child checks the assigned task
4. Child finishes the assigned task and marks the task status as completed
5. Parent check the completed tasks and accept it
6. Child collects points for the successfully completed task
Extensions: N/A

FR3: Add meal to the "meal of the day" including the following:
Use case Title: Add meal
Primary Actor: Parent
Stakeholder: Parent, Children
Precondition: Parents and children need to register to the FMA App and join the family account successfully
Minimal Guarantee: N/A
Success Guarantee: The parent can easily update (add or delete) the meal list so the family members can explore the suggested meal list and vote for their favorite one and the meal of the day is successfully determined
Trigger: The parents need to check the meal list in order to update it
Main success scenario:
1. Parents check the meal list
2. Parents add/delete the meal list
3. Parents and children vote for the preferred meal
4. Parent check the completed tasks and accept it
Extensions: N/A

FR4: Add item to list including the following:
Use case Title: Add item to list
Primary Actor: Children
Stakeholder: Parent, Children
Precondition: Parents and children need to register to the FMA App and join the family account successfully. Child needs to collect the minimum number of point to activate the luxury list
Minimal Guarantee: Luxury list is not activated
Success Guarantee: The child can update (add or delete) the most desired items on the luxury list successfully
Trigger: The child needs to activate the luxury list through collecting the required number of points
Main success scenario:
1. The child collects the required points results from the accomplished tasks
2. The collected points activate the luxury list
3. The child can list the desired items on the luxury list
4. Parent can check the luxury list
Extensions: N/A

FR5: Add important event to the calendar including the following:
Use case Title: Add important event to the calendar
Primary Actor: Parent, children
Stakeholder: Parent, Children
Precondition: Parents and children need to register to the FMA App and join the family account successfully.
Minimal Guarantee: N/A
Success Guarantee: The child can update (add or delete) the important events on the calendar
Trigger: The parent and children need to check the calendar
Main success scenario:
1. The parent and children check the calendar
2. The parent or children select the day and time of the important event
3. The parent or children update (add/delete) the calendar
4. The parent or children upload a document or an image for the specified important event
5. All the family member can see and browse the updated events
Extensions: N/A

FR6: View the location of family members including the following:
Use case Title: View (check) the location of family members
Primary Actor: Parent, Children
Stakeholder: Parent, Children
Precondition: Parents and children need to register to the FMA App and join the family account successfully.
Minimal Guarantee: The parents and children cannot determine the location of other family members
Success Guarantee: The child or parent can track and determine the location of other family members accurately
Trigger: The parent and child explore the location
Main success scenario:
1. The child and parents check the location of other family members
Extensions: N/A

IV. Interface Design and Development

Two types of platforms have been developed to support the FMA application; a website and a mobile application. The website is designed to promote the services and the functionality of the mobile application, give a brief description of the App and of course to support the downloading process of the FMA app easily, freely and safely. Different tools have been used in the development process of the mobile application that are: (i) Android Studio IDE that linked via Google API file, Google Firebase and Vuforia [24], [25]. The Firebase is an integrated mobile application development platform that is provided by Google. It is considered as a real time database. Unlike relation database, there are no tables or records. However, Firebase uses JavaScript Object Notation (JSON) tree structure and the stored data is simply represented as a node with reference key. Firebase covers a wide range of services such as authentication, databases, configuration, file storage and messaging. In addition to the aforementioned properties, Firebase has been used due to its

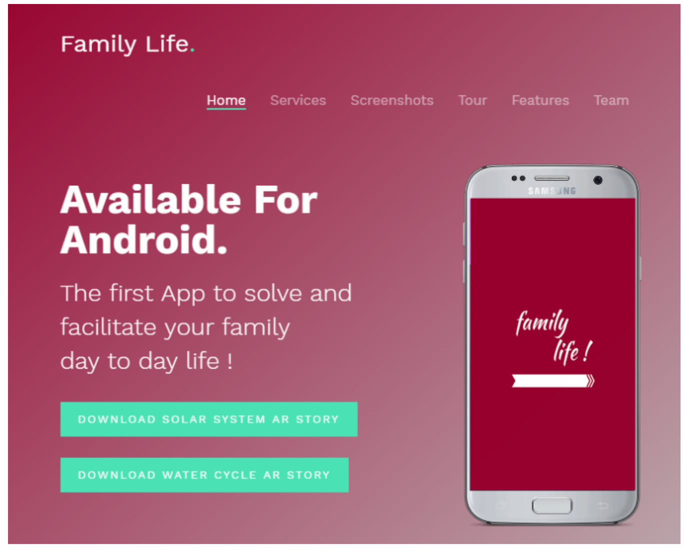

Fig. 6. The website of the FMA mobile application.

reliability, simplicity and popularity. Vuforia has been used to support the Augmented Reality (AR) on mobile applications. Fig. 6 shows the website of the mobile application which consists of six parts (Home, Services, Screenshots, Tours, Features and Team). The screenshots in Fig. 7 illustrates the initial steps of creating accounts for the entire family members. However, the screenshots in Fig. 8 introduces the main services provided by the FMA app.

V. Evaluation

In order to evaluate the FMA mobile app, a simple survey was designed and used. The survey was set to assess the user satisfaction about the provided services of the FMA app taking into consideration each service individually. The obtained results are presented below. In Addition, the evaluation was conducted by selecting 24 families randomly. The total number of members of the selected families was 120 individuals (at a rate of five persons per family approximately). Families were asked to download the application and use it for three months (from February 1^{st}2019 to April 30^{th}2019) then they had been asked to fill the surveys and the results were reported. The survey was designed carefully to consider the families' satisfaction about each service provided by the FMA app. The survey included nine questions reflecting nine essential factors (facts) about the FMA app and the provided services that are listed as follows:

1) The first question concerned about the Simplicity of the FMA app.
2) The second question interested in the Ease of use of the FMA app.
3) The third question interested to show if the app was a Helpful app in terms of deciding the preferred meal of the day and distributing the chores among the family members.
4) The fourth question interested to show if the FMA app improved the communication skills of the family members during the entire day.

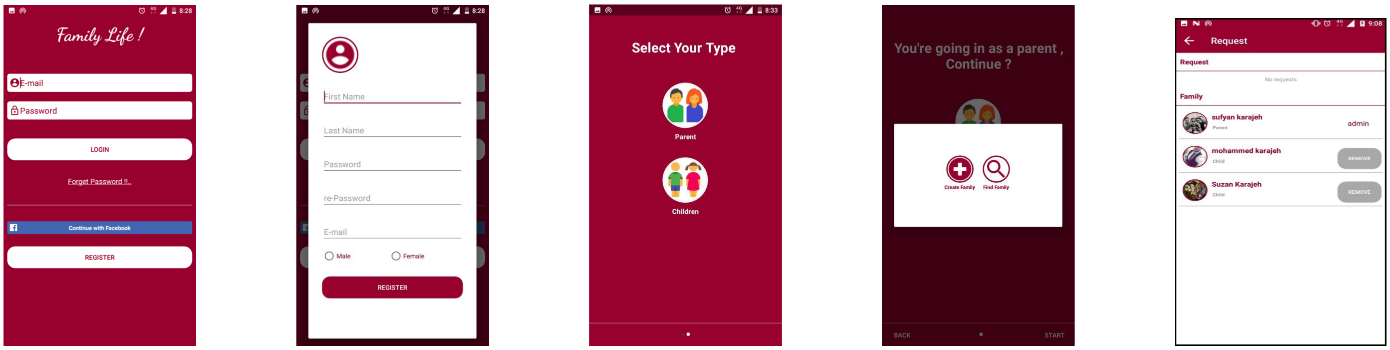

(a) (b) (c) (d) (e)

Fig. 7. A sample of selected screenshots of the FMA app to create family account. (a) Application log-in page, user can choose to log-in or register from this page, registration can be done manually or through using Facebook account. (b) Application sign up page where the user needed to fill the required information. (c) The type of user must be determined to complete the registration process successfully. (d) Users then choose to create a new family count (if user is a parent) or join an existing one. (e) Children request to join the family account.

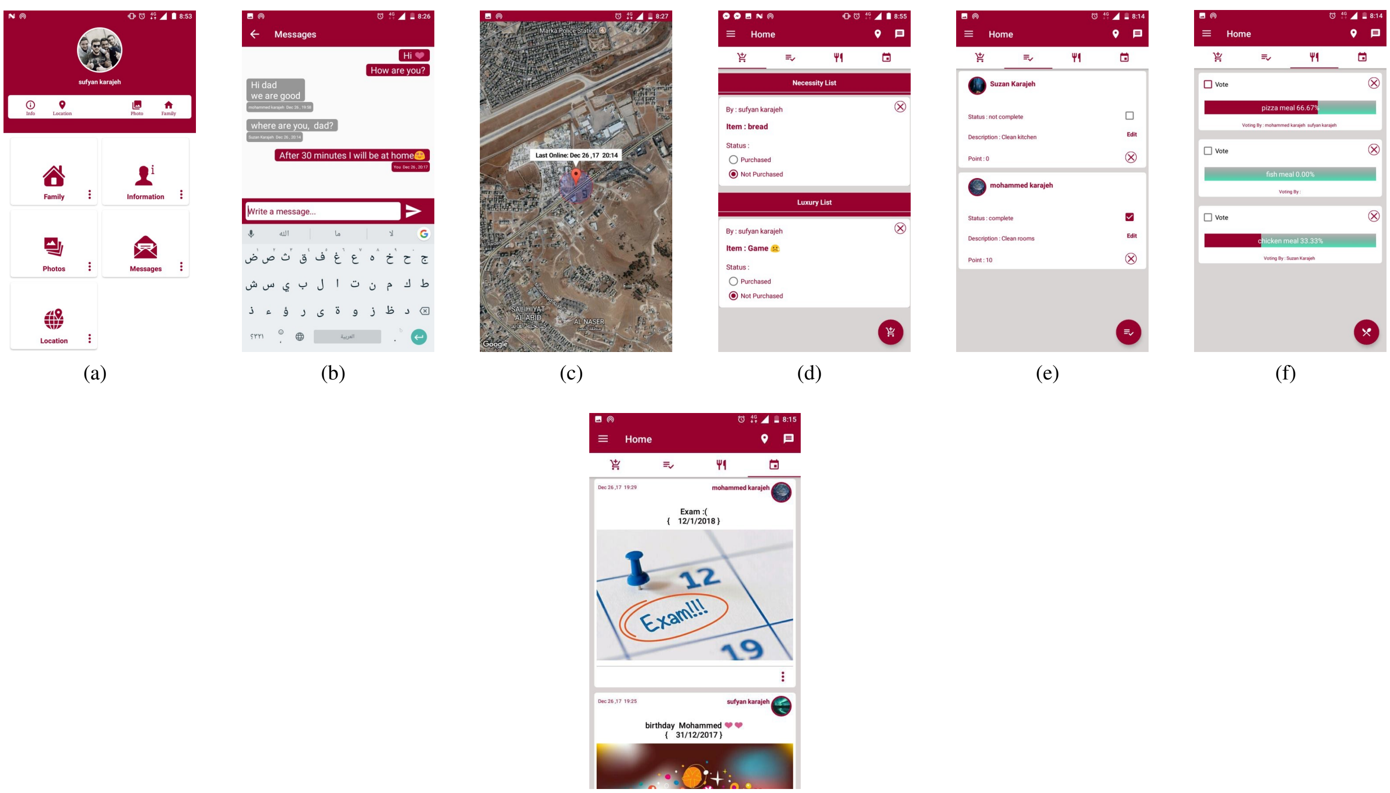

(a) (b) (c) (d) (e) (f)

(g)

Fig. 8. A sample of selected screenshots for the main services of the FMA application. (a) The main page. (b) Chat service. (c) GPS locator presents the last seen place of family members. (d) The wish list: the ordinary shopping list and the luxury list. (e) The chores distributed among the children along with the status (completed or not). (f) The meal of the day service. (g) The dynamic calendar with some of upcoming significant events (i.e. exams and birthday's events) added by family members.

5) The fifth question interested to show an indication about the FMA app time efficiency.
6) The sixth question interested to show if the FMA app was an informative app as it provides information about (but not limited): (i) the daily shopping list, (ii) important events such as exams and school parent meetings and so on and (iii) current position of family members.
7) The seventh question interested to show if the FMA app was capable to follow-up completed tasks that have been distributed to children.
8) The eighth question interested to show if the FMA app improved the educational skills of the children with respect to the provided AR stories.
9) The ninth question asked the users if they would recommend the FMA app to others.

For simplicity, five-scale point of answers was adopted: strongly agree, agree, neutral, disagree and strongly disagree. The results of the questionnaire were reported in Table I. However, the key observations of the obtained results are listed below:

- The average number of participants who agreed on all factors is 86.5% (agree and strongly agree). Therefore, the majority of users are satisfied with the usability of the proposed FSM app.
- The simplicity is the key feature of the FMA application with a percentage of 96% on the satisfaction factor. (as shown in Fig. 9a)
- The results indicated that the FMA application could be seen as an informative application with an average of 97%. (as shown in Fig. 9f)
- A percentage of 98% of participants agreed to recommend this application to other families and friends as shown in Fig. 9i.
- The results also indicated that the FMA is a helpful app with a percentage of 94% followed by the factor of ease of use with a percentage of 93%. (as shown in Fig. 9c and Fig. 9b respectively)
- The task follow-up factor achieved a percentage of 83%. However, an extensive future work is still required to improve this feature where the assigned chore for the children should be reported using a percentage value of the accomplished assigned job (fully or partially completion). (as shown in Fig. 9g)
- The percentage of the satisfaction factor of the provided AR stories achieved only 39% (as shown in Fig. 9h), this is probably due to the limited number of stories (two stories only) and the limited functionality associated with this feature. Therefore, more efforts and elaboration are needed to improve AR service in the future.

However, the reported results show very encouraging results for an early-stage of the FMA app. Further results for each single factor of the survey are presented in Fig. 9 (from Fig. 9a to Fig. 9i).

TABLE I. THE OBTAINED RESULTS OF THE DIFFERENT FACTORS OF THE EVALUATION OF FMA APP

Factors	Strongly Agree	Agree	Neutral	disagree	Strongly disagree
Simplicity	113	2	3	2	0
Ease of use	110	1	6	3	0
Helpful	108	5	2	5	0
Communication skills	102	5	5	3	5
Time efficiency	105	4	10	1	0
Informative app	114	2	3	1	0
Follow-up	94	5	12	7	2
Educational skills	34	13	33	23	17
Recommendation to others	113	4	1	2	0
Average	**99.2**	**4.6**	**8.3**	**5.2**	**2.7**
Percentage	**82.7%**	**3.8%**	**6.9%**	**4.4%**	**2.2%**

VI. CONCLUSION AND FUTURE WORK

This paper presents a comprehensive mobile application that intends to facilitate families' daily life in terms of improving the communication and collaboration between the family members. The Family mobile application can be seen as a very helpful, useful and beneficial app for families to manage their everyday challenges. The proposed FMA application has been developed using two platforms; a website and mobile technology. The proposed FMA app provides a set of services such as suggest the meal of the day, vote on the preferred meal, remind members with important events, track the position of the family members and assign household task to children. The parental responsibilities are carefully adopted and imitated while designing and implementing the different services such as (but not limited): (i) accepting the member request to join the family, (ii) suggesting the meal of the day to be voted by the children (iii) assigning tasks (chores) to children and (iv) checking the completion status of the assigned task. In addition, tracking the position of the family members is one the important services provided by the FMA app. The evaluation of the application was conducted to assess the satisfaction of families. The reported results show very promising results where 86.5% of users were happy, satisfied and very pleased with the provided services of the FMA application. However, for additional future work, a set of suggestions to improve the provided services are listed in the following points: (i) the enhancement of the AR services to cover a wide range of stories, (ii)using machine learning techniques to compare the assigned chore accomplished by the children with a standard previously stored task so that the completed task can be described in terms of percentage value (percentage of completion), and finally (iii)Supporting parents to understand and explore the feelings of children such as sadness, anger, fear, stress and depression (an emotional orientation of the application).

ACKNOWLEDGMENT

The authors would like to thank the Hashemite University for their continuous help and endless support, and acknowledge the implementation inputs of Yazeed Asaad, Ahmed Assaf and Sufyan Karajeh in this research.

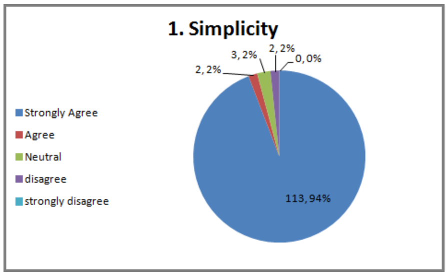

(a) The obtained results of Simplicity factor

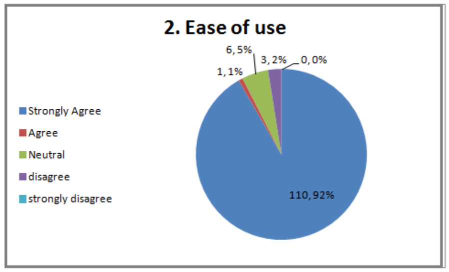

(b) The obtained results of Ease of use factor

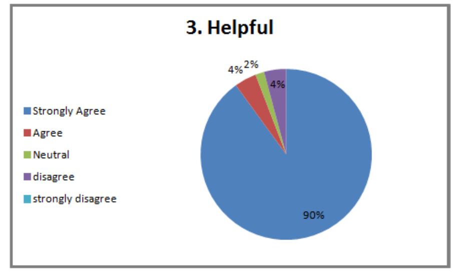

(c) The obtained results of "helpful" factor

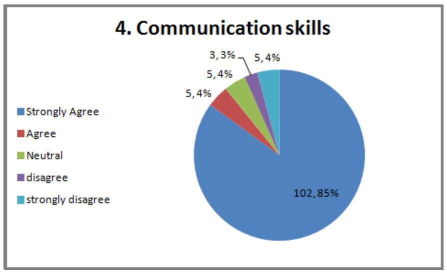

(d) The obtained results of "communication skills" factor

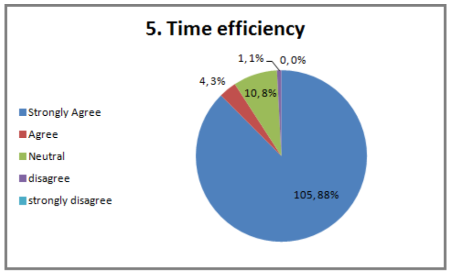

(e) The obtained results of "Time efficiency" factor

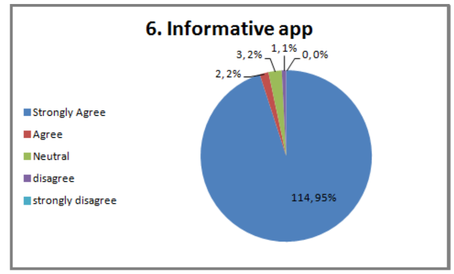

(f) The obtained results of "Informative" factor

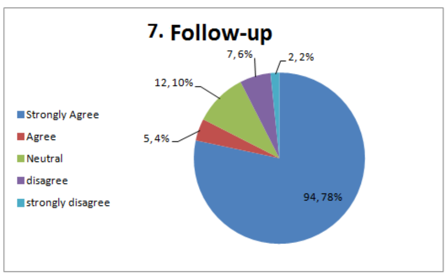

(g) The obtained results of the "Follow-up" factor

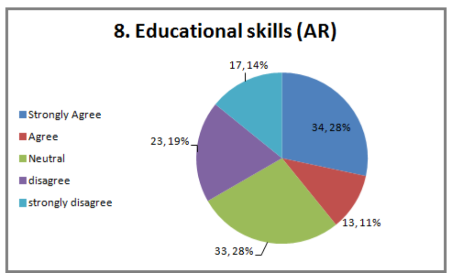

(h) The obtained results of "Educational skills" factor

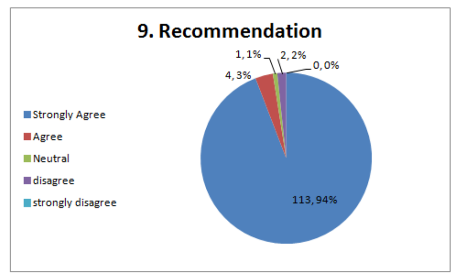

(i) The obtained results of "recommendation" factor

Fig. 9. The obtained results of the distributed survey regarding different factors: (a) Simplicity factor, (b) Ease of use factor, (c) Helpful factor, (d) Communication skills factor, (e) Time efficiency factor, (f) Informative factor, (g) Follow-up factor, (h) Educational skills factor and (i) Recommendation factor.

References

[1] M. R. Sanders, K. Burke, R. J. Prinz, and A. Morawska, "Achieving population-level change through a system-contextual approach to supporting competent parenting," *Clinical child and family psychology review*, vol. 20, no. 1, pp. 36–44, 2017.

[2] C. Doukas, T. Pliakas, and I. Maglogiannis, "Mobile healthcare information management utilizing cloud computing and android os," in *2010 Annual International Conference of the IEEE Engineering in Medicine and Biology*. IEEE, 2010, pp. 1037–1040.

[3] T. Page, "Application-based mobile devices in design education," 2014.

[4] M. Eberl, "An application of pls in multi-group analysis: The need for differentiated corporate-level marketing in the mobile communications industry," in *Handbook of partial least squares*. Springer, 2010, pp. 487–514.

[5] R. N. Akram and R. K. Ko, "End-to-end secure and privacy preserving mobile chat application," in *IFIP International Workshop on Information Security Theory and Practice*. Springer, 2014, pp. 124–139.

[6] L. Leung, "Effects of ict connectedness, permeability, flexibility, and negative spillovers on burnout and job and family satisfaction," *Human Technology: An Interdisciplinary Journal on Humans in ICT Environments*, 2011.

[7] K. Romero-Ruiz, L. Echeverri-Sánchez, J. Peña-Plata, S. Vásquez-Giraldo, M. Aguilera-Cardona, C. Herazo-Avendaño, A. Valencia-Arias, and L. Bran-Piedrahita, "Information and communication technologies impact on family relationship," *Procedia-Social and Behavioral Sciences*, vol. 237, pp. 30–37, 2017.

[8] L. Kerawalla and C. Crook, "Children's computer use at home and at school: context and continuity," *British Educational Research Journal*, vol. 28, no. 6, pp. 751–771, 2002.

[9] L. Blackwell, E. Gardiner, and S. Schoenebeck, "Managing expectations: Technology tensions among parents and teens," in *Proceedings of the 19th ACM Conference on Computer-Supported Cooperative Work & Social Computing*. ACM, 2016, pp. 1390–1401.

[10] M. d. C. Aguilar Ramos and J. J. Leiva Olivencia, "La participación de las familias en las escuelas tic: análisis y reflexiones educativas," *Pixel-Bit. Revista de Medios y Educación, 40, 7-19.*, 2012.

[11] R. Kraut, T. Mukhopadhyay, J. Szczypula, S. Kiesler, and B. Scherlis, "Information and communication: Alternative uses of the internet in households," *Information Systems Research*, vol. 10, no. 4, pp. 287–303, 1999.

[12] A. M. Moore, "A parent's look at technology," *Montessori Life*, vol. 18, no. 2, p. 11, 2006.

[13] A. Franzen, "Does the internet make us lonely?" *European Sociological Review*, vol. 16, no. 4, pp. 427–438, 2000.

[14] J. Goodman-Deane, A. Mieczakowski, D. Johnson, T. Goldhaber, and P. J. Clarkson, "The impact of communication technologies on life and relationship satisfaction," *Computers in Human Behavior*, vol. 57, pp. 219–229, 2016.

[15] M. Lasen, "Education and career pathways in information communication technology: What are schoolgirls saying?" *Computers & Education*, vol. 54, no. 4, pp. 1117–1126, 2010.

[16] S. Huisman, A. Edwards, and S. Catapano, "The impact of technology on families." *International Journal of Education & Psychology in the Community*, vol. 2, no. 1, 2012.

[17] C. Neustaedter, A. Brush, and S. Greenberg, "A digital family calendar in the home: lessons from field trials of linc," in *Proceedings of Graphics interface 2007*. ACM, 2007, pp. 199–20.

[18] S. Razavi Emadi, "Family time management platform," 2018.

[19] S. Khan, W. Ahmad, R. Ali, and S. Saleem, "A research on mobile applications for location tracking through web server and short messages services (sms)," *VFAST Transactions on Software Engineering*, vol. 7, no. 2, pp. 12–17, 2015.

[20] A. Al-Mazloum, E. Omer, and M. Abdullah, "Gps and sms-based child tracking system using smart phone," *Int. J. Electr. Comput. Electron. Commun. Eng*, vol. 7, no. 2, pp. 171–174, 2013.

[21] S. Z. Sweidan, R. Saifan, K. A. Darabkh, S. Abu-Kaff, and S. Al-Ali, "Kids' tracker: An android application for tracking children," *Journal of Software Engineering and Applications*, vol. 10, no. 13, p. 907, 2017.

[22] A. Cockburn, "Structuring use cases with goals," *Journal of Object-Oriented Programming*, vol. 10, no. 5, pp. 56–62, 1997.

[23] ——, *Writing effective use cases*. Addison-Wesley Professional, 2000.

[24] M. Billinghurst, A. Clark, G. Lee *et al.*, "A survey of augmented reality," *Foundations and Trends® in Human–Computer Interaction*, vol. 8, no. 2-3, pp. 73–272, 2015.

[25] C. Xiao and Z. Lifeng, "Implementation of mobile augmented reality based on vuforia and rawajali," in *2014 IEEE 5th International Conference on Software Engineering and Service Science*. IEEE, 2014, pp. 912–915.

Assessing Architectural Sustainability during Software Evolution using Package-Modularization Metrics

Mohsin Shaikh[1*], Dilshod Ibarhimov[2], Baqir Zardari[3]
Westminster International University, Tashkent, Uzbekistan[1,2]
Quaid-e-Awam University of Engineering Science and Technology, Nawabshah, Pakistan[1,3]

***Abstract*—Sustainability of software architectures is largely dependent on cost-effective evolution and modular architecture. Careful modularization, characterizing proper design of complex system is cognitive and challenging task for insuring improved sustainability. Moreover, failure to modularize the software systems during its evolution phases often results in requiring extra effort towards managing design deterioration and solving unforeseen inter-dependencies. In this paper, we present an empirical perspective of package-level modularization metrics proposed by Sarkar, Kak and Rama to characterize modularization quality through packages. In particular, we explore impact of these design based modularization metrics on other well known modularity metrics and software quality metrics. Our experimental examination over open source java software systems illustrates that package-level modularization metrics significantly correlate with architectural sustainability measures and quality metrics of software systems.**

***Keywords*—Software architecture; software modularity; software quality; packages**

I. Introduction

In recent times, conventional conjectures of experimental research and theory have been joined by computational and data-intensive methodologies [1], [2]. These new research mechanisms are driven by software systems that are maintained to avoid complex functional hindrances and operated in distributed e-infrastructure. Integrating the hardware and software components is receiving increasing attention for development of sustainable computational systems. This leads us to understand concept of sustainability which accord with perspective of "capable of being endured or maintained". Secord *et al.* defines software sustainability related to development activities aimed to evolve and modify with changing requirements [3]. However, they also argue that sustainability is influenced by many other factors including the organization, developers, end-users, architecture and design documentation.

Software architecture provides abstract picture of fine-grained development details [4]. Architecture of software systems reflects implementation of major design decisions and their governed methodology. Software architectures postulate division of software into subsystems, components and other functional parts. Software architectures bear an influential importance in evaluating sustainable growth of software (i.e, cost-effectiveness and long lasting) and reliability [5], [6]. Additionally, software architectures metrics help developers to determine maintenance objectives, testing effort and overall design decisions. Typically, during life span of software, it undergoes many corrective and adaptive changes. Evolution of software process takes place through continuous addition, modification and re-organization of source code entities. As these activities are reflected into source code, there can be possible deterioration in software design and its architecture.

In this context, evaluating the sustainability of software architecture for insuring proper maintenance and evolution cost control becomes quite desirable. Architectural sustainability is influenced by many aspects that includes design decisions, evolutionary changes in the software, change-prone requirement and modularization practices. Thus, architecture-level metrics are required to quantify technical sustainability facets of software systems. However, setting a single metric for expressing software sustainability is difficult due to different complications involved in software development life cycle, such as, irrelevant requirement engineering, diverse technology choices, re-factoring of source code and implicit knowledge of software architect [7]. Sustainable architectures are mainly dependent on feasible software deign to insure compatibility with changing requirement.

Software modularization, object-oriented (OO) decomposition in particular, is an approach to ease the development and maintenance. In order to understand the OO software, flexible design with well-connected constituent components is highly demanded for accommodating future changes and requirements. Often, software maintenance costs are higher than its overall development budget [8]. Modularization essentially follows *divide and conquer* strategy for managing the complexity of large source code. Parnas *et al.* introduced concept of information hiding, which became a fundamental paradigm for modularizing the OO systems [9]. There has been significant advancement to reverse engineer the software systems for automatic extraction of its design depicting an aggregate view. Some of notable techniques in this regard are related to partitioning of software systems into subsystems(clusters) and recovering the architecture into module-view [10]. With increasing focus of building tools and methodologies for software maintenance, there has been significant research over mechanism of partitioning the software into subsystems taking into account source code abstractions like classes and packages [11]. In particular, package organization provides higher abstraction and easier way for comprehension, complexity reduction and understanding of software systems. However, due to frequent changes into software, decreasing modularization quality is not an impossible occurrence.

Architectural sustainability can be obtained with implementation of best modularization practices during software development. Some of notable proposed practices include acyclic dependencies, layering organization,testability, encapsulation and concern dispersion [12], [11]. Sarkar *et al.* have proposed a new modularization metrics suite based on packages as its functional components [13]. They have further devised these modularization metrics into three categories, i.e., based on inheritance or association, method invocation and best programming practices. It is worth mentioning that Sarkar *et al.*'s study provided experimental validation of proposed architectural metrics to an extent. Further, they also introduced comparative analysis on modularity achievement between human based development effort and randomized modularization. However, there is still an opportunity to explore application of these metrics in broad spectrum of software quality and software sustainability, particularly during evolutionary phases of software development. As a matter of fundamental perspective of modularization, decay of architectural strength is often expected as the software longevity continues. Therefore, evaluation of architectural metrics during software evolution can provide comprehensive assessment of major sustainability concerns and quality oriented features.

In this paper, we explored Sarkar *et al.*'s package-level modularization metrics for automated optimization of module structure and determine their correlation strength with the metrics related to testing efforts, deficit produced in design of software and overall maintainability. First, we describe the theoretical framework to position our study into big picture of software sustainability. Then, an integrated and empirical approach is presented for evaluating various modularization metrics and software quality attributes during the process of software evolution. There are different determinants of architectural erosion or degradation, but, packages become important architectural subsystems in OO scenario [13]. Precisely, the ability of package components to manage and handle dependencies among classes is quite significant among OO design constituents. While characterizing software system, structural perspective are conventionally analyzed by the class level coupling and cohesion. It was indeed required to explore high level architectural dimension to identify design violations in subsequent releases of software systems. Hence, our motivation to report exploratory study with different architectural metrics becomes obvious with following intended contributions.

- Adding the evidence that package based modularization metrics describing cohesion, coupling and programming practices can be linked to modularization metrics of different engineering domains.
- Evidence that technical aspects of sustainability prescribed by package modularization metrics ultimately help in understanding the composition of software systems.
- Establishing statistical soundness to study as many of studied the modularization metrics show significant correlation from reasonable sample size of data-sets.

Our findings show that Sarkar's modularization metrics bear significant association with already existing modularity metrics. Additionally, significant statistical correlation was also witnessed with metrics quantifying maintainability, design deficit and testing effort. Consequently, these findings help to evaluate software sustainability in terms of architecture. Also, this research study can be utilized to assess the development effort and help taking measures to minimize the design flaws. This paper is organized in nine sections, starting from this introduction. Theoretical Framework is explained in Section 2. Related work is briefly described in Section 3. Section 4 describes the information on architectural level metrics and their summarized definitions. Section 5 illustrates the example for package level metrics. Section 6 presents detailed empirical study with analysis over obtained results. Different aspects of discussion over results obtained and design of study are illustrated in Section 7. Threats to validity are elaborated in Section 8 followed by Conclusion as Section 9.

II. Background

The Software Sustainability Institute relates sustainability[1] with concepts of availability, extensibility and maintainability of software. Despite numerous existing definitions of sustainability, there is an ongoing research to achieve consensus for the setting it's scope within field of software engineering. Taking this direction, we attempt to study system's maintainability and integrity as factors affecting the software sustainability.

In today's technologically motivated business world, evolution and maintenance of software systems are key processes carried out over the decades. Long lasting software systems are inevitable for automating industrial devices, as their longevity insures smoother and uninterrupted business operations. In theoretical terminology, software sustainability covers broad spectrum of measures needed to operate software system for longer time, i.e., stability of its infrastructure, adaptability to functional and environmental changes and inter-interoperability in competitive business strategies.

To define the sustainability in the context of software architecture, an explicit concept is required to confine its notion towards technical concerns of sustainability. Therefore, architectural sustainability of software primarily refers to long living software system that is maintained cost-effectively and evolved over its entire life cycle [14]. Thus, our intended connotation is to incorporate sense of cost-effective longevity and endurance towards sustainability of software systems, covering dimensions of maintainability, modifiablility and evolvability.

III. The Theoretical Framework

This framework aims to position our research into software quality, describing architectural strength during it's evolutionary period as key to software sustainability. Sustainability as quality objective has been targeted by many computer and management based systems [15]. There are various techniques and concepts that have been defined to evaluate architectural quality of software systems. Standard draft of quality models, i.e., ISO/IEC 42030 and ISO/9126[2] for architecture evaluation of software systems describe software, hardware, human and systems components as its major constituents.

[1] http://www.software.ac.uk/about

[2] http:// www.iso.org

However, it is required to incorporate characteristics of sustainability concerns with an existing model. Sustainability analysis framework with empirical evaluation are beginning to appear in research literature of software engineering [14]. Our work discussed here, is an effort to evaluate sustainability at architectural level and emphasize package view of architecture as its determinant.

A. Dimensions of Sustainability

As discussed earlier, sustainability is defined as the "capacity to endure and preserve the function of a system over an extend period of time". Recently, researchers and practitioners analyze the sustainability by its four dimensions, i.e., economic, social, environmental and technical. Social sustainability is concerned with application of software to help communities. Environmental sustainability means protection of natural resources using software based knowledge and application. Technical sustainability seeks to improve longevity and adequate evolution of software systems with changing technological requirements. While evaluating sustainability of software in holistic views a shown in Fig. 1, broader context of inter-dependence among the dimensions should also be considered. Economic sustainability aims at maintaining the business aspects of software systems. Applicability of sustainability analysis is shown through an example of Health Watcher System (WHS) in Fig. 1. Health Watcher System is a basically web-based information system for public health monitoring and complaint registration. This example has been frequently used to depict relevance functional and non-functional requirements of software systems with sustainability [16], [17]. Fig. 1 shows quality requirements of (WHS), sorted by sustainability dimensions and relations among them. This example was particularly selected to show how measurement of a software architectural strength influences sustainability in broader picture.

Sustainability portrays broad view of quality assured software systems that is to be achieved by all dimensions. From developers point of view, understanding the relationships among goals of all these dimensions is important to resolve conflicting aspects. However, setting up all these dimensions into one scope has been shortcoming in current software engineering practice. In particular, sub-characteristics of theses dimensions require quantitative evaluation and evidence of association among each other. The problem, we address here is that how architectural components influence technical sustainability, thereby supporting other dimensions as well.

B. Software Sustainability and Software Architectures

As a basis of discussion about sustainability, architectural evaluation method can provide potential mechanism for sustainability measurement. Architecture is foundation of any software system that expresses fundamental organization of system's components and relationships among them. It is design artifact or blue-print of developing software system [18]. Clements *et al.* argue that successful software development and evolution is highly dependent on design decisions [19]. This position is further endorsed by Koziolek *et al.* who describes quality induced software architecture as determinant of sustainability. They further suggest that methods and metrics should be integrated to evaluate architecture using scenario-based analysis. However, their own analysis highlights the limitations of existing method. A number of methods exist which provide evaluation mechanisms of software architecture using structured approach. The main focus in this regard has been analysis of candidate architecture and identification of potential risks involving non-functional requirements of software design. However, significant difference of approach and methodology is found in all these effort. Bowser *et al.* state that architecture decision represented by design metrics can be instrumental to achieve sustainability [20]. These architectural decisions are characterized by decomposition quality, best practices adherence, change scenario robustness and decision traceability. However, explicit expert knowledge for computing these metrics is challenge as acknowledged by them as well. One of hurdles to this approach is that architecture-level metrics are not yet integrated with evaluation approaches of software architectures. Similarly, appropriate context of applying any metric to evaluate implemented architecture is underpinning concept. Therefore, architectural representation of systems can be effective in understanding broader systems concerns. Deriving suitable measures and metrics towards architectural evaluations is key task.

Comprehension of architectural views of complex software systems entails different perspectives. Clements *et al.* describe three view types as most common and feasible to represent software architecture: *module view*, *Component-and-Connector View* and *Allocation View* [19]. Views mainly represent different units of implementation for an architecture that have composed software system. *Module View* determines construction and decomposition of source code (e.g., clusters, packages, files) at design level. Package view is an intuitive approximation of system's architecture that represent the system's architectural modules. Package structure is reasonably assumed comprehensive approximation of architecture as packages are created by developers of software system [21]. Therefore, package structure of java projects is studied as representative of *module view* architecture in which each module contains several classes and dependencies among them.

IV. Related Work

Different approaches have been proposed in recent research over modularity analysis of software design, which has explored many dimensions for characterizing the object oriented systems on distinct criteria [22], [9], [14]. There exists lot of work in the literature proposing metrics for OO software, the majority of these works centered on characterizing a single class as the criteria of high cohesion, low coupling and structural organization [23], [24], [25]. Evaluation of software architecture has emerged as an important software engineering practice which is evident from the efforts of designing tools and computing mechanisms [26]. Such evaluations are exercised to primarily to determine architectural strengths of software systems. Below we briefly explain the works which are closely related on their application for software sustainability measures.

There is prior empirical evidence in several studies that investigated the relationship between code dependency and software quality [27], [28], [29]. D' Ambrose *et al.* identified the relationships between change coupling and defects and

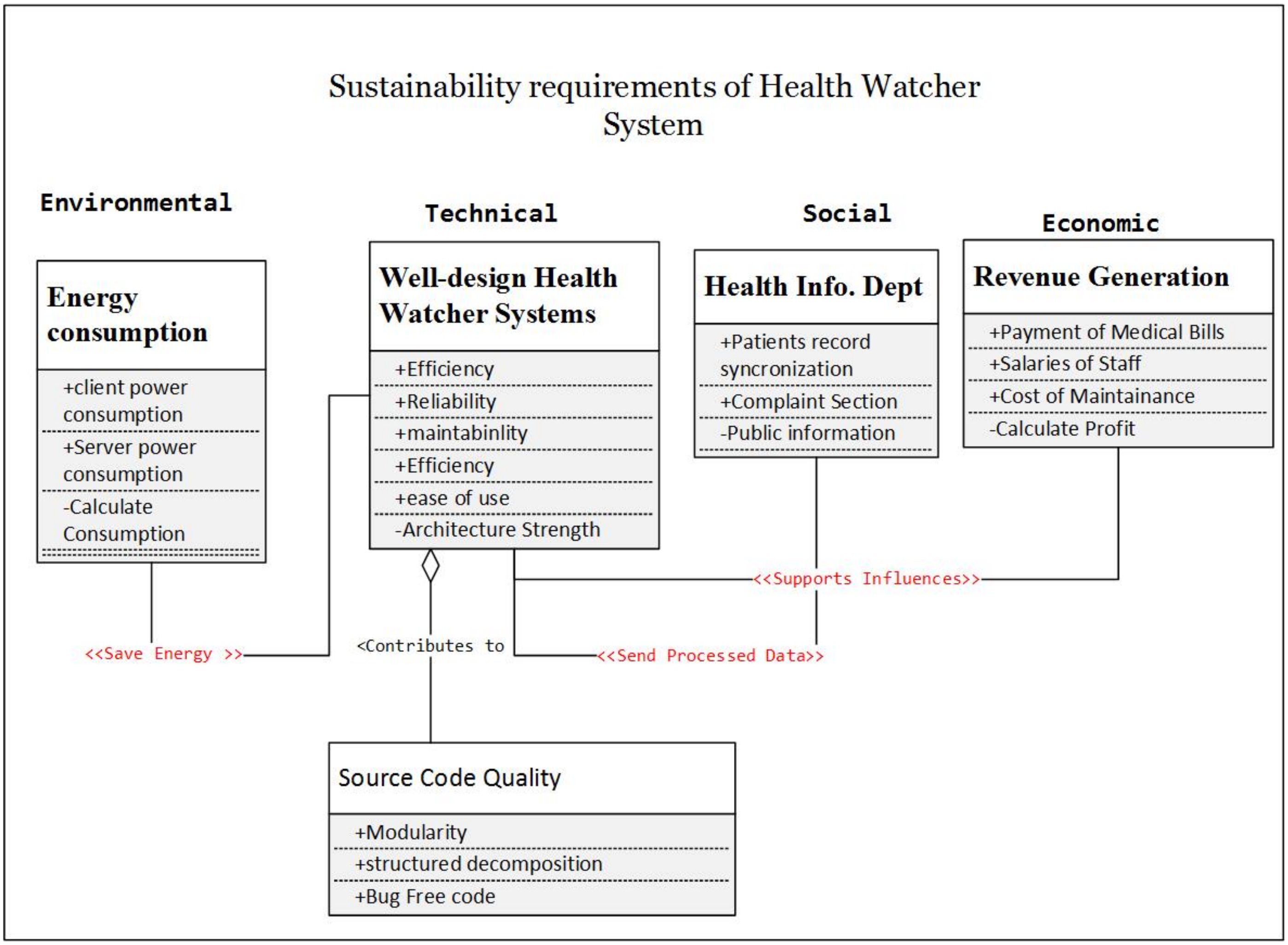

Fig. 1. Four dimensions of Software Sustainablity

class level [27]. Martin introduced Common Closure Principle (CCP) as a design principle about package cohesion, identifying CCP as guideline for decomposition of architecture [27]. Mockus *et al.* found that subsystems modified by a change can be predictor of fault, without defining exact structure(package, cluster, file) of subsystem [28]. Nagappan *et al.* use change-coupling effects to predict faults, however, source-code architecture is not publicly available[29]. In summary, majority of these studies have focused on examining effects of file level coupling on defects, while we approach architectural level evaluation of source code. Moreover, our research is an attempt to show that reverse engineered approximation of system's architecture at package level can be useful for technical sustainability.

According to a systematic review, there are more than 40 architectural-level metrics based on several design principles which assist sustainability evaluation of implemented architectures [14]. It has been reported in the survey that all these metrics are derived from certain design principles, whereas input for computing these metrics varies, e.g., concepts, module size design decisions. Lakos *et al.* proposed metrics known as Cumulative Component Dependency (CCD), which calculates summation of required dependencies in component or module of software systems [30]. CCD metric is numerical value describing strength of module coupling and help in determining maintainability and testability. Martin proposed several metrics, like, efferent and afferent coupling, abstractness, instability, dependency cycles for package entities of software systems [31]. Babar *et al.* carried out the survey to organize architecture-level metrics into framework [32]. These effort targeted the designed architecture and their impact on quality attributes, but, main focus was on differentiation of evaluation methods rather than in-depth quantification or analysis of software modularization and its evolution.

Sethi *et al.* provided an architectural evaluation methodology of software systems on the basis transforming UML component diagram into design structure matrix (DSM) [33]. Evaluation criteria proposed in this work require significant refinement of models and their diagrammatic representation with high precision. This may produce trade-off for large object oriented system and achieving high precision is not always guaranteed. Similarly, there were certain other notable efforts which had its prime focus to analyze architecture during design phases, but, on critical note, all these efforts require complex procedures of collecting and updating relevant data or representing the software systems into graphs [34], [35].

With growing importance of evaluating software architecture, there has been research urge to propose and re-define the architecture-level metrics based on novel object oriented design principles. Sarkar *et al.* put-forward the determination methodology for evaluating well modularized system taking into account size of components and architectural operations [36]. However, proposed architectural measurement framework does not provide any explicit goodness or fitness of metrics, thus it required more rigorous analysis for its practical application. Therefore, Sarkar *et al.* extended architectural level metrics definitions which received notable recognition in research literature, specially for large object-oriented systems [12], [13]. To the best of our knowledge, Zhoa *et al.* studied the capability of Sarkar's package modularization metrics to predict packge level fault-proneness that remains relatively closer to our research direction [37]. Bouwers *et al.* applied research method of metric-based evaluation for software architectures which is also motivation of our study [38]. In simmilar effort, Yu *et al.* has studied the correlation between multiple package dependencies and evolution in correspondence [39]. However, this study does not address the impact of package's co-evolution on software quality. Koziolek *et al.* made remarkable effort for evaluating architectural sustainability, but their study is restricted on architectural tracking in temporary industrial experimental setup [7]. Our study, on the other hand, investigates effects of package's quality from an architectural perspective. Hence, it paves the research direction for application, assessment and evaluation of Sarkar's metrics in determining sustainability concerns and quality attributes of software systems.

V. Modularization and Quality Metrics

This section provides the description and summary of investigated metrics and software quality metrics. Table I summarizes the definitions of three categories of package-level modularization metrics produced with specific methodology of programming design, i.e., inheritance, association and polymorphism, method invocation and programming practices. Table II presents the summary of modularization metrics studied by Lee *et al.*[40]. The main objective of their research was to analyze and compare the various modularity metrics that have been proposed in different domains. Table III describes three quality metrics to evaluate software systems in terms of maintenance, design flaws and testing. These metrics are categorized as follows:

A. Inheritance and Association based Coupling Modularization Metrics

Within object-oriented (OO) design paradigm, inheritance and association are important dependence relationships between classes and packages in a software system. Inheritance is formed when a class extends another class, while association is formed when class uses (through attribute definition into methods) another class. In addition to this, such dependencies among the classes are often seen to be distributed in different modules (Packages in Sarkar's context of study). More specifically, if a class and its subclass exist in two different modules, modification to concrete base class may trigger the change in subclass. Such design phenomenon is known as fragile base-class problem which becomes prominent in particular when maintenance or ownership of packages is taking place across different development teams. In order to insure easier maintainability and re-usability of packages, minimization of inheritance or association based dependencies can be one of the best programming practices.

Sarkar *et al.* describe these metrics to measure the modularization quality of modules with respect to inter-module dependencies. Furthermore, illustration of each metric is given as under:

- **IC(S)**: is a composite metric that measures the extent to which inheritance-based dependencies among and within the packages are minimized. Whereas IC_1 measures extent to which a package extend other packages using inheritance relationship, IC_2 measures the extent to which classes of a package are extended by classes in other package and IC_3 measures the number of classes in a package that are derived in any of the other packages.
- **AC(S)**: is a composite metric that measures the extent to which association-based dependencies among and within the packages are minimized. Whereas AC_1 measures extent to package uses other packages attribute and parameter in method definition, AC_2 measures the extent to which classes of one package are used either as an attribute and parameter in method definition by classes in other packages and AC_3 measures the extent to which number of classes in a package that are used either as an attribute or parameter in method definition into any of the classes of other packages.
- **BCFI(S)**: is a composite metric that measures the extent to which polymorphic design of methods is restricted to the defining packages. Whereas $BCVSet(p)$ is set of classes in the package that contains defined or non-overridden inherited methods from their ancestor classes of other packages and $BCVMax(c)$ for class c measures maximum base-class violation by methods involved in base-class fragility problem.

B. Method Invocation based Coupling Modularization Metrics

Another suite of coupling metrics introduced by Sarkar *et al.* is related to inter-module coupling created by invocation of methods among the modules(packages in their study). In an ideal programming scenario, application programming interfaces (APIs) of a module should be used as service providers to other modules. This sort of design mechanism is established through particular programming pattern of invoking methods or calling methods in inter-module connections of software systems. In a well engineered code, software systems should adhere with principle of maximum segregation and similarity of purpose to avoid any structural decay. However, such modularization practices are violated at times, thus, their quantitative evaluation shall explore more dimension of application.

- **MII(S)**: It measures the extent to which all inter-module interactions are carried out through APIs (designated methods for providing services to other module) of module in entire software system. $MII(P)$ is ratio of $ExtCallRel(i)$ and $ExtCallRel(p)$. Whereas $ExtCallRel(i)$ is set that collects all external calls to API

TABLE I. DESCRIPTION OF SARKAR'S PACKAGE-LEVEL MODULARIZATION METRICS [13]

Metric	Definition
Inheritance based Inter-Module Coupling(IC)	$IC(S) = \frac{1}{\lvert\mathcal{P}\rvert} \sum_{p \in \mathcal{P}} IC(p), \quad IC(p) = \min(IC_1, IC_2, IC_3)$
Association Induced Inter-Module Coupling(AC)	$AC(S) = \frac{1}{\lvert\mathcal{P}\rvert} \sum_{p \in \mathcal{P}} AC(p), \quad AC(p) = \min(AC_1, AC_2, AC_3)$
Base-Class Fragility (BCF)	$BCFI(S) = \frac{1}{\lvert\mathcal{P}\rvert} \sum_{p \in \mathcal{P}} BCFI(p), \quad BCFI(p) = 1 - \frac{1}{BCVSet(p)} \sum_{c \in \mathcal{C}(p)} BCVMax(c)$
Module Interaction Index (MII)	$MII(S) = \frac{1}{\lvert\mathcal{P}\rvert} \sum_{p \in \mathcal{P}} MII(p), \quad MII(p) = \frac{\left\lvert \bigcup_{i \in I(p)} ExtCallRel(i) \right\rvert}{\lvert ExtCallRel(p) \rvert}$
non-API method closedness index (NC)	$NC(S) = \frac{1}{\lvert\mathcal{P}\rvert} \sum_{p \in \mathcal{P}} NC(p), \quad NC(p) = \frac{\lvert M_{na}(p) \rvert}{\left\lvert M_{pub}(p) - \left\{ \bigcup_{i \in I(p)} M(i) \right\} \right\rvert}$
API Usage Index (APIU)	$APIU(S) = \frac{1}{\lvert\mathcal{P}\rvert} \sum_{p \in \mathcal{P}} APIU(p), \quad APIU(p) = \frac{APIUS(p) + APIUC(p)}{2}$
State access violation(SAVI)	$SAVI(S) = \frac{1}{\lvert\mathcal{P}\rvert} \sum_{p \in \mathcal{P}} SAVI(p), \quad SAVI(p) = \frac{1}{\lvert C(p) \rvert} \sum_{c \in \mathcal{C}(p)} SAVI(c)$
Population Pug-in Index (PPI)	$PPI(S) = \frac{1}{\lvert\mathcal{P}\rvert} \sum_{p \in \mathcal{P}} PPI(p), \quad PPI(p) = \frac{\left\lvert \bigcup_{m \in ImplExtn(p)} \{ModuleClosure(m,p)\} \right\rvert}{\lvert M(p) \rvert}$
Size Uniformity Index (CU_m)	$CU_m(S) = \frac{1}{\lvert\mathcal{P}\rvert} \sum_{p \in \mathcal{P}} \frac{\mu_m(p)}{\mu_m(p) + \sigma_m(p)}$
Size Uniformity Index (CU_l)	$CU_l(S) = \frac{1}{\lvert\mathcal{P}\rvert} \sum_{p \in \mathcal{P}} \frac{\mu_l(p)}{\mu_l(p) + \sigma_l(p)}$

Note: S represents entire software system, $\mathcal{P}$ denotes set of packages
$\mathcal{C}$ shows set of classes, M is set of methods, I is set of APIs
$C(p)$ is set of classes in a package p and $I(p)$ is set of API's in package p.
Module and package are used interchangeably in Sarkar's context of study.

methods of packge p, $ExtCallRel(p)$ is set that collects all external calls to public methods in package p.

- **NC(S)**: It measures the extent to which all inter-module interactions are carried out through Non-API methods in entire software system. More precisely, $NC(p)$ determines extent of coupling, a package p establishes through invocation of methods which are explicitly declared as non-abstract.
- **APIU(S)**: It is an average of segregation measure $APIUS(p)$ and cohesiveness measure $APIUC(p)$ of packages in entire software system.

C. Metrics based on Best Modularization Practices

In addition to inter-module coupling, Sarkar *et al.* have proposed third category of modularization metrics which can essentially be applied for best programming practices to insure enhanced software quality. These modularization mechanisms are based on measuring the extent to which inter-module interactions can be minimized. State access violation is phenomenon when communication among software design components is frequently carried out through attribute access. Similarly, third-party plug-ins are integrated within the software systems for their functional and operational extension which also require some design rule evaluation. Additionally, common reuse of software components and their size impact have been shaped into metrics form. These metrics are briefly explained as under:

- **SAVI(S)**: It measures the extent to which the attributes defined in the classes in a package are not directly accessed by other classes for entire software system. $SAVI(c)$ is computed using weighted average of different attribute access cases, i.e., inter/intra-classes and inter/intra-moduels.
- **PPI(S)**: It measures the extent to which the methods that are needed to define extension APIs exist in a plug-in package for entire software system. $ModuleClosure(m, p)$ is set of transitive closure of abstract method implementation in a package p and $M(p)$ is set of methods in package p.
- $\boldsymbol{CU_m}$(S): It measures the extent to which classes in packages of entire software system varies in their sizes taking into account number of methods, whereas $\mu_m(p)$ and $\sigma_m(p)$ are average and standard deviation of package class size in terms of number of methods .
- $\boldsymbol{CU_l}$(S): It measures the extent to which classes in packages of entire software system varies in their sizes taking into account lines of code, whereas $\mu_l(p)$ and $\sigma_l(p)$ are average and standard deviation of package classes size in terms of lines of code.

D. Baseline Modularization Metrics

Below we summarize the definitions, notations used in definitions and interpretation of these metrics in particular context of study by Lee *et al.* [40]. They have conducted an experimental evaluation of these metrics on evolutionary software and reported correlation of different modularity metrics and their sensitivities towards particular modular factors. Moreover, their study is another motivating factor to further examine the modularization metrics proposed with different design paradigms. We set this research work as *baseline* to further investigate the applicability of modularization metrics proposed by Sarkar *et al.* Their definitions with relevant references are mentioned in Table II.

- $\boldsymbol{M_{newm}}$: This metric is well known approach for quantifying modularity of social network represented in graphical structures. Recently, there has been extensive focus on

TABLE II. BASELINE MODULARIZATION METRICS STUDIED IN DIFFERENT DOMAINS

Reference	Definition
Newman *et al.* [41]	$M_{newm} = \frac{1}{2m}\sum_i \sum_j \left(A_{ij} - \frac{k_i k_j}{2m}\right)\delta(g_i, g_j)$
Mancoridis *et al.*[42]	$MQ = \sum_{i=1}^{k} \frac{2\mu_i}{2\mu_i + \sum_{j=1}^{k}(\epsilon_{i,j}+\epsilon_{j,i})}, \quad M_{bunch} = \frac{MQ}{k}$
Guo *et al.*[43]	$M_{g\&g} = \frac{\sum_{k=1}^{M} \frac{\sum_{i=n_k}^{m_k}\sum_{j=n_k}^{m_k} R_{ij}}{(m_k-n_k+1)^2} - \sum_{k=1}^{M} \frac{\sum_{i=n_k}^{m_k}\left(\sum_{j=1}^{n_k-1} R_{ij} + \sum_{j=m_k+1}^{N} R_{ij}\right)}{(m_k-n_k+1)(N-m_k+n_k-1)}}{M}$
MacCormack *et al.* [44]	$M_{rcc} = 1 - \sum_{i=1}^{N}\sum_{j=1}^{N} \frac{DependencyCost(i,j)}{N^{2\lambda}}$

application of this metric into studies pertaining different scientific domains, specially, social network, metabolic network, neural network and the World Wide Web. Computation of metric is based on theoretical heuristic that edges (links between nodes) within a module (community) are greater than expected ones. Further, in the definition, i and j are nodes, A_{ij} represents edges between nodes. m is the number of total edges and k_i indicates expected number of edges in node i. δ is a comparator function that it outputs 1 where its two parameters are same, 0 otherwise. g_i, parameter of δ, represents the module containing node i. This metric ranges between 1 as best value and 0 as worst value.

- $\boldsymbol{M_{bunch}}$: This metric is normalized version of clustering factor (MQ) introduced by Mancoridis *et al.* [42]. MQ is the most frequently used method for evaluation of a software modularity. μ_i is representation of intra-edges of module i, while $\epsilon_{i,j}$ denotes inter-edges between modules i and j in total number of modules k.
- $\boldsymbol{M_{g\&g}}$: This metric was formulated to measure the modularity of complex mechanical products. However, their application in software systems can be interesting towards incorporating mechanical engineering principles and software design theories. Basically, metric quantifies modularity of physical entities using difference of inter and intra edge densities. In the definition, M is number of modules and N is number of mechanical components (total software nodes in our context of study). The numerator of the fraction consists of two part, the sum of intra-edge density of modules and the sum of inter-edge density of the modules. Symbols, i.e., n_k and m_k are the indexes of first node and last node respectively in module k. R_{ij} denotes row and column in dependency between node i and j (software nodes).
- $\boldsymbol{M_{rcc}}$: This metric has its basic application in measuring the modularity of evolving software systems. Computing the Relative Clustered Cost of software systems is key idea of this metric. In perspective of software architectures, software systems having no dependencies shall bear the value 0 and 1 in case of all inter-dependent nodes. *DependencyCost* function returns a weighted dependency between node i and j. N is the number total nodes, n is the size of module, λ is a user defined parameter for the metric. The weight varies along with the dependency types. If a dependency between i and j is an intra-dependency of a single module, the weight is n^{λ}, where n indicates the number of nodes in the module. On the other hand, if it is an inter-dependency between separate modules, the weight becomes N^{λ} to have considerable penalty in terms of poor coupling.

E. Software Quality Metrics

All these quality metrics have been proposed to asses the quality of software systems. Although, there are diverse opinions for setting up any metric as standard for judging the quality of software. Nevertheless, it can be an interesting research direction, if their utility is realized with empirical evidences. Further, they are described below with their definitions in Table III.

- **MI**: HealStead Maintainability Index is composite metric that incorporates number of traditional source code metrics into single value that indicates relative maintainability. The equation presented in Table III for MI is its reformed version that considers *aveV* as Halstead Volume per Module, *aveV(g')* as extended cyclomatic complexity per module and *aveLOC* as average lines of code per module.
- **QDI**: Quality Deficit Index is a positive value aggregating the detected design flaws (i.e., code smells and architectural smells). In terms of computation, each flaw carries a specific weight which accumulates to form a score that determine extent of deficit in particular source code entity(class, package or entire software system).
- **TLOC**: Test Lines of Code metric determines effort required to test the software system. In this regard, TLOC is a size measure that counts physical lines of code within a test class or classes.

VI. AN ILLUSTRATING EXAMPLE

In this section, we use an example of simple architectural design to illustrate the working mechanism of Sarkar's metrics. In order to ease the comprehension, example shows evaluation of metrics for single package interactive modularization scenario. To simplify the presentation, only architectural representation of design for package p is described. Fig. 2 shows system of 6 packages to demonstrate Sarkar's metrics.

As it can be seen, package p is interacting with five other packages $p1, p2, ..., p5$ using *use*, *implement* and *extend* relationships through its classes and interfaces. From Fig. 2, we can see that p has 3 incoming *extend* relationships, i.e., from 2 classes of package $p2$ and 1 class of package $p1$. Further, package p has 1 outgoing *extend* and 1 outgoing *implement* relationship from its 2 classes to package $p5$ and $p2$. It is also visible that package p has 6 incoming *use* relationships from 1 class of package $p1$, 3 classes of package $p3$, 1 class

TABLE III. Description of quality metrics.

Reference	Definition
Welker*et al.* [45]	$MI_1 = 171 - 5.2 \times \log(aveV) - 0.23 \times aveV(g') -16.2 \times \log(aveLOC)$
Marinescu *et al.* [26]	$QDI = \frac{\sum_{all\text{-}flaw\text{-}instances} FIS_{flawinstance}}{KLOC}$
Tahir *et al.*[46]	$TLOC = \frac{\sum_{i=1}^{n} Loc(C_i)}{SLOC},\ C_i$ *is test class*

of package $p4$ and 1 class of package $p5$. Also, package p has 1 outgoing *use* relationship towards package $p2$. Thus, these *extend*, *implement* and *use* relationships form AC and IC coupling for package p respectively. Whereas, only 1 concrete method $m10$ is overridden outside the package p into package $p1$ and $p2$ causing the fragility in base class $C1$ of package p .

Fig. 2 also shows interaction among the packages through invocation of public methods, abstract methods and implementation of abstract methods. For a package p, 3 abstract methods ($m1$,$m2$ and $m7$) are called outside the package which form S-API's[3] of package p. Package p has 2 public methods ($m3$ and $m4$) that are called outside the package p which account non-API external calls for methods.

Fig. 2 further depicts access to attributes in intra-package and inter-package dependency scenarios. Attributes of classes $C6$ and $C7$ of package p are accessed into two packages: $p4$ and $p5$. Classes $C2$ and $C3$ of package p access attributes of $C6$ and $C7$ using intra-package dependency. This information of attribute access is utilized to evaluate the violation of state access to package p. Package p also provides implementation and calls through transitive closure of abstract methods ($m23$ and $m52$) declared outside the package p which serve as extension plug-in to package p using classes $C2$ and $C3$.

VII. Experimental Study

In this section, we describe our experimental evaluation of Sarkar's modularization metrics over open source software system. The measures described for architectural sustainability are pertaining to structural design and source code of software systems. Although, in larger picture there are certain additional indirect measures also discussed in the literature, like, documentation quality, technology choices, employment of human resources, volatile requirement, etc. [14]. However, our scope of our study is towards software design centric metrics.

A. Study Design

Selection of appropriate metric for evaluating the software product is a challenge. Therefore, we tend to adopt most efficient and already utilized methodology in our research with illustrative and insightful aspects [40]. To an examination level, our goal is to better understand the effect and impact of package level modularization metrics over different dimensions of software systems. i.e., modularization metrics, external quality attributes. In this regard following study features are set as research questions for our experiment.

RQ1: Do Sarkar's package modularization metrics correlate with Baseline modularizaton metrics and impact the software quality metrics?

RQ2: Do Sarkar's package modularization metrics provide any significant perspective for improving architectural quality during software evolution?

These research questions are important to understand the critical context of applying Sarkar's metrics. Conventionally, architectural quality of software systems is measured by certain quality metric and their application is not frequently witnessed in practice. Despite their availability comparison or association with existing metrics is rarely performed. Thus it is yet unclear to select particular architectural metrics to quantify the modularization of software system, which leads our motivation behind RQ1. Another objective of RQ1 is to expand the application and usage of Sarkar's metrics (exclusively designed on the basis of OO paradigm) in other dimensions of software quality assurance as restricting them to only modularization metrics may result worthless. The research context of RQ2 is to understand weather architectural facets of evolving software systems can be better explained by package modularization metrics proposed by Sarkar *et al.* This will help both software architects and researchers to understand practical value of applying of Sarkar's metrics to evaluate architectural longevity of evolutionary software systems.

B. Subject Systems

We selected 34 versions of three different open source systems in our experiment. JHotDraw [4]: a Java GUI framework for technical and structured Graphics. Ant[5]: a Java library and command-line tool whose mission is to drive processes described in build files. Google-Web Toolkit(GWT)[6]: an open source set of tools that allows web developers to create and maintain complex JavaScript front-end applications in Java. These systems have reasonable size, manageable degree of complexity, diverse application domain and easily accessible source code. Table IV provides descriptive information of subject systems used in our study, versions involved and their release period.

[3] Sarkar *et al.* described concept of abstract methods and their container entities(abstract classes and interfaces) serving as Application Programming Interfaces for a package. S-API refers to public abstract methods declared, implemented within the package and invoked outside the package.

[4] http://www.jhotdraw.org/

[5] http://ant.apache.org/

[6] http://www.gwtproject.org/overview.html

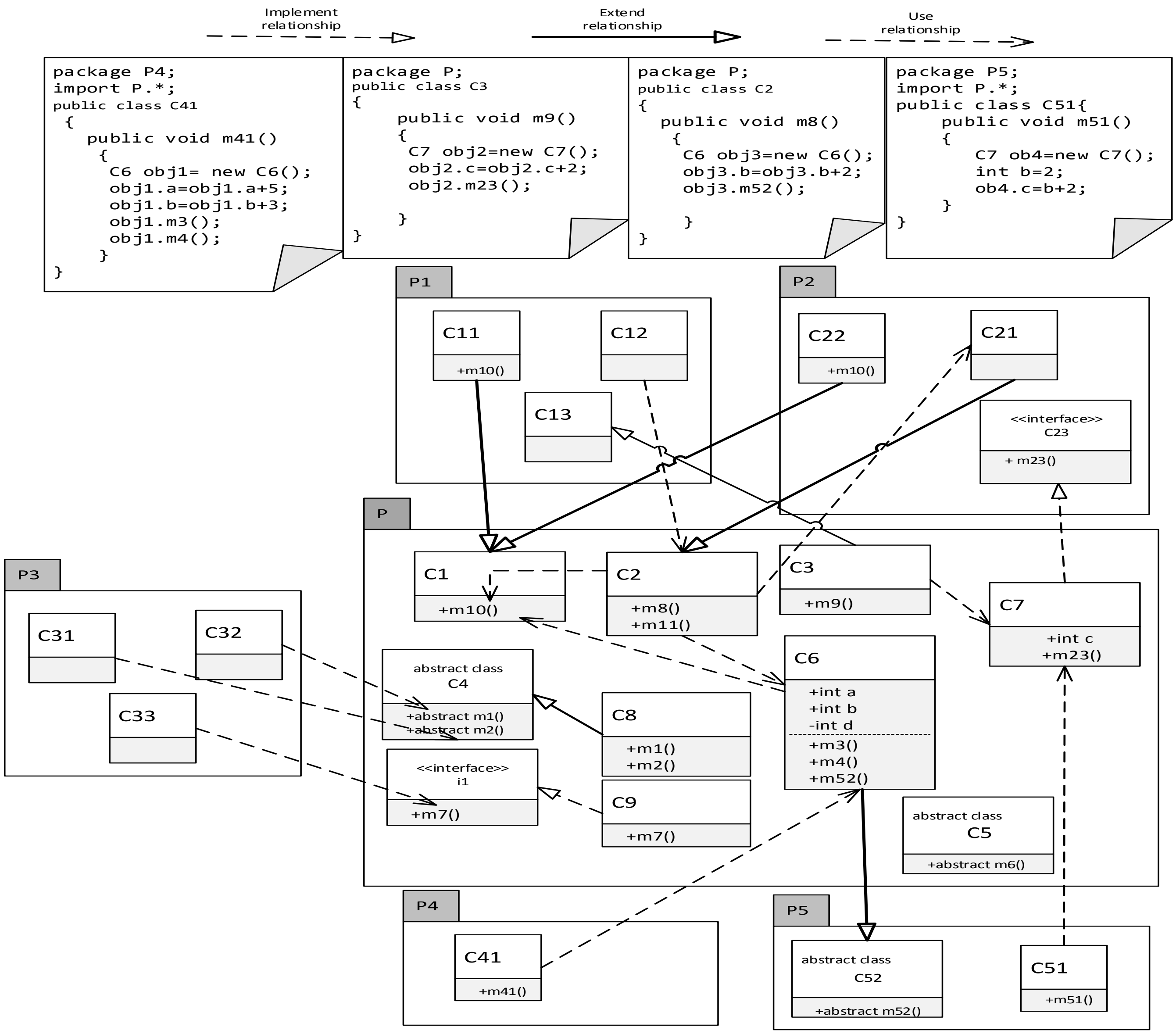

Fig. 2. Simple design for Sarkar's package level metrics

Structural information of subject systems in Table IV provides valuable information. The first to fifth columns report the systems name, versions involved in the study, revised number of entities (Packages, Classes, Interfaces) from initial to final release. The column sixth to nine, revision in number of methods and their invocation on diverse design methodologies are listed. It is evident that release versions experimented in our study have been under development process of over 7 years at-least and considerable changes have taken place in their structural components (Entities and dependencies among them). Since all these open source software systems are frequently utilized in research or industrial areas, it was expected that some of changes their code base would be in correspondence to architectural changes or modularization improvement. Rationale for this expectation was that developers continuously examine and improve structure of evolving software systems.

C. Data Processing

Our purpose of data processing is to compute defined metrics and conduct statistical analysis. To compute Sarkar's metrics, *TLOC* and *MI*, we parsed source code of applications from version archives database using *Understand*[7]: A commercial static analysis tool. We developed our own java code and Understand-Perl API scripts to derive all metric values. To calculate *QDI*, we used evaluation version of open source tool *Infusion*[8]: It parses the source code and provides an in-depth assessment of architecture and design quality. Moreover, the tool mainly detects code smells, architectural flaws and reports quality score for software systems. After collecting metrics information, data-sets for each subject system were

[7]https://scitools.com/
[8]https://www.intooitus.com/products/infusion

TABLE IV. STRUCTURAL INFORMATION OF SUBJECT SYSTEMS

System	Versions	Release Period	Revised packages	Revised classes	Revised interfaces	Revised methods	Revised S-API's	Revised non-API calls	Revised API calls
JHotDraw	(5.2-5.4, 6.0, 7.1-7.5)	2001-02-19 to 2010-08-01	11-62	168-997	23-60	1476-7334	157-291	101-961	127-228
Apache-Ant	(1.5.2,1.5.4, 1.6.0-1.6.5 , 1.7.0,1.71, 1.80-1.8.3)	2003-08-13 to 2012-03-13	62-79	902-1659	48-98	6759-13488	143-222	131-241	128-226
GWT	(1.3-1.7, 2.0-2.5)	2006-5-17 to 2014-11-20	106-498	1655-12390	213-1823	71598-10192	132-272	151-256	230-931

developed. On each data-set, statistical test of correlation is used to obtain correlation coefficient values using R [9] tool. The Spearman's correlation test is particularly applied in our experimental context due to non-parametric nature of data. Additionally, we have made our data sets public on our project site[10] for replication and reproduction. Fig. 3 depicts visual view of our data processing methodology.

Our method for examining the evolving modularity of subject systems builds on source code parsing and extracting the dependency information. Following are keys steps involved in our method.

1) Select the versions to be analyzed and obtain their binary distributions.
2) For each version, extract the dependency information from the parsed code.
3) Compute the required metrics and develop the data-set for each subject system.
4) Report graphical and statistical analysis.

D. Experimental Results

In this section, we report experimental results for modularity correlation between Sarkar's metrics and *baseline* modularization metrics described in Section 2. We have presented correlation between Sarkar's metrics and quality attributes. Further, graphical representation is shown to understand behavior of each category of Sarkar's modularization metrics in different evolving versions of subjects systems.

1) RQ1: Do Sakar's package modularization metrics correlate with Baseline modularizaton metrics and impact the software quality metrics?: To answer RQ1, we employed statistical methodology of correlation test. We briefly describe our results obtained after applying statistical test of Spearman's correlation. Also, we have tried to clarify theoretical and analytical perspectives of values indicated in all the tables. In order to best understand empirical relationship among the each category of Sarkar et al's modularization metrics and baseline metrics, magnitude of statistical association of is shown at significant level of 0.001 (indicated with ***), 0.01 (indicated with **) and 0.05 (indicated with *) in Table V, VI and VII. In particular, all the indicated values employ following rationale.

- Positive and statistically significant correlation with *Baseline* Modularization metrics is desired; meaning package modularization metrics improves architectural quality of software system, while negative and statistically significant correlation values are indication of deterioration in architectural quality.
- Since *QDI* and *TLOC* are measures of quality deficit and testing effort incurred over software system. Therefore, statistically significant and positive correlation values with package modularization metrics indicate that software system is subject to design restructuring or may incur exhaustive testing overhead. In other words, modularization of particular package design has not improved enough to compensate architectural debt or cause reduction in testing effort. This kind of occurrence in software design can be cause of weak modularization that eventually violate the design pattern rules.
- Similarly, *MI* describes strength of maintenance for software, hence, positive and statistically significant correlation of package modularization metrics with *MI* is an evidence of quality enhancement.
- Negative and positive statistically insignificant correlations are considered void of any impact in our scope of study.

Aforementioned implications essentially form experimental scope of our study to determine application of package modularization metrics for diverse objectives. It should be understandable that theoretical construct of each metric is different, thus, correlation analysis with Baseline modularization metrics and quality metrics would be distinctive.

Starting with Table V for Sarkar's coupling modularization metrics based on inheritance and association, some of important observations for different software systems are described: For *JHotDraw*, *BCF* is seen strongly correlated with M_{newm} and M_{rcc}. Whereas, *AC* has shown relatively significant relationship with modularity metrics of M_{bunch}, $M_{g\&g}$ and M_{rcc}. For *Apache-Ant*, strong association of correlation is established only for *IC* with M_{bunch}, $M_{g\&g}$ and M_{rcc}. Interestingly, M_{newm} has shown weak statistical significance with most of coupling metrics in all cases. While in case of *Google-Web ToolKit*, *AC* and *IC* have produced notable statistical relationship with modularity metrics. Such kind of variations in modularity correlation can be result of particular design paradigm of software systems where association based dependencies are minimized as in case of *JHotDraw* or inheritance based dependencies and fragile base classes are abundant as in case of *Apache-Ant*. Results for quality attributes can be elaborated with following specific findings: First, positive significant correlation of *BCF* with *QDI* and *TLOC* employs that fragility of base-class in software may cause design deterioration and testing effort. Thus, less maintenance work will be required as witnessed for correlation coefficients of *JHotDraw* and *Apache-Ant* with *MI*. Second, in most cases,

[9] http://www.r-project.org/
[10] https://github.com/Analyzer2210cau/Package-Sustain

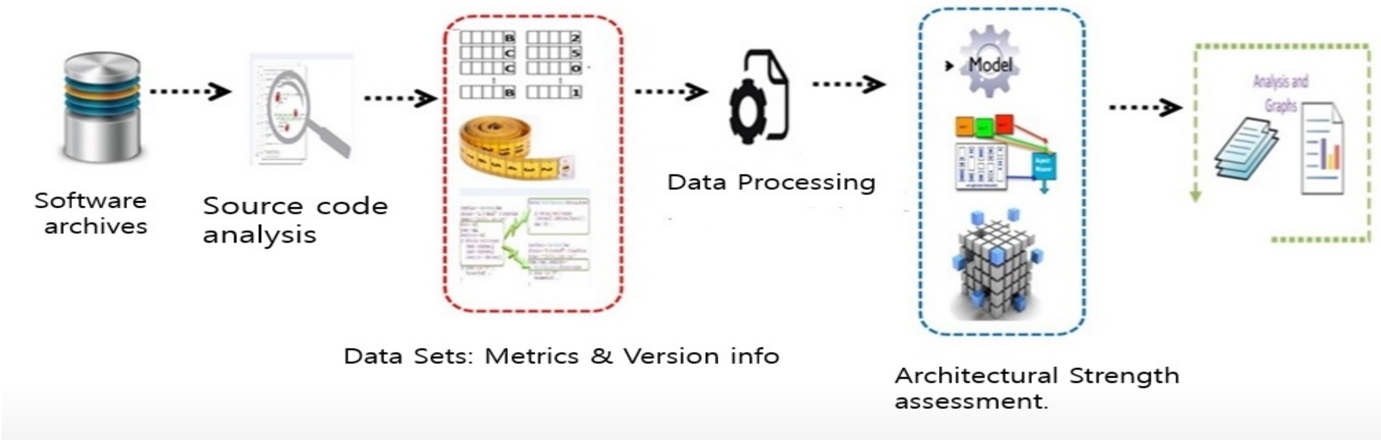

Fig. 3. Data processing Methodology

TABLE V. CORRELATION COEFFICIENT OF COUPLING MODULARIZATION METRICS BASED ON INHERITANCE AND ASSOCIATION

Project	Metric	Baseline Modularization Metrics				Quality Metrics		
		$\mathbf{M}_{newm}$	$\mathbf{M}_{bunch}$	$\mathbf{M}_{g\&g}$	$\mathbf{M}_{rcc}$	**MI**	**QDI**	**TLOC**
JHotDraw(9)	BCF	**0.94*****	**0.77***	0.59	**0.97*****	**-0.86****	**0.92*****	**-0.95***
	IC	**0.94*****	0.66	0.24	**0.84****	**-1.000*****	**0.99*****	**-0.78***
	AC	0.53	**0.72***	**0.78***	**0.70***	-0.18	0.32	-0.65
Apache-ant(14)	BCF	0.41	0.20	0.24	**0.60***	-0.072	**0.75****	**0.64***
	IC	0.27	**0.76****	**-0.79****	**-0.93*****	-0.52	-0.37	**-0.94****
	AC	0.13	**-0.54***	-0.54	0.31	-0.51	0.52	-0.26
GWT(11)	BCF	0.26	0.32	0.12	-0.45	-0.19	-0.49	-0.085
	IC	**0.83****	**0.80****	0.45	**-0.90*****	0.45	0.024	**-0.80****
	AC	**-0.94****	**-0.90***	-0.41	**0.98****	**-0.58***	0.01	**-0.87*****

IC and *AC* are negatively correlated to weak extent with *MI* regardless of their statistical significance that means reducing direct inheritance and association based inter-module coupling shall have influence over maintainability.

Correlation coefficients for Sarkar's coupling modularization metrics based on method invocation are reported in Table VI with following major observations. For *JHotDraw*, only *MII* has developed significant relationship with *Baseline* modularization metrics and quality attributes while *APIU* has shown no as such statistically significance. For *Apache-ant*, *MII*, *NC* and *APIU* are in negative correlation with *Baseline* modularization and quality attributes. Such findings employ that, during the development process, there has been frequent inter-module method call traffic which has in turn decreased the modularization, eventually quality attributes are adversely affected. While in case of *Google-Web ToolKit*, *MII* has depicted significant positive correlation with M_{newman}, M_{rcc} and significant negative correlation with M_{bunch}, however, *NC* and *APIU* do not show similar pattern in the table except for *MI* or *TLOC*. It can be inferred that either the cohesiveness and segregation properties are not followed properly or non-API public methods calls have caused excessive and unnecessary dependencies among the packages. Thus, there are wide variations on this category of modularization metrics which may not account for providing comprehensive view, but its application is yet useful to asses particular software design for inter-module method invocation. A closer examination of these values suggests that inadequate architectural and implementation changes can precipitate decrease in modularity.

Table VII shows correlation values of third category of Sarkar et al.'s metrics. For *JHotDraw*, weak correlation of *SAVI* with M_{bunch} and strong negative and positive correlation with *MI*, *QDI* and *TLOC* should not be surprising due to violation on accessing attributes rules. On the other hand, high trend of correlation in all metrics for CU_m and CU_l is quite visible. For *Apache-Ant*, all the category metrics have developed negative correlation with most of *baseline* modularization metrics and quality metrics, leading to conclude that there has been lack of adopting best modularization practices. For *Google-web-ToolKit*, statistically significant values are quite hard to realize except for *SAVI*, meaning rare violation of state access could be required.

In principle, modularization should reduce complexity of system, allow efficient comprehension of its structural paradigms and enable easier re-factoring process. As a matter of fact, each software system follows certain specific domain of design considering requirements and functional needs. Similarly, as the software evolves, changes in its architecture are quite obvious. All these parameters contribute toward long life of software systems. Although, architectural metrics proposed by Sarkar *et al.* are reported as important to evaluate complementary areas of software sustainability, however, their usage in practice (e.g., software industry) is not too wide. Combining the results of Table V, VI and VII, we can have substantial assessment of software architecture, but, it would not be easy to make general conjecture for single metric. Furthermore, some of metrics have conflicting traits among the each other; as is the case of *IC* and *APIU*, hence

TABLE VI. CORRELATION COEFFICIENT OF COUPLING MODULARIZATION METRICS BASED ON METHOD INVOCATION

Project	Metric	Baseline Modularization Metrics				Quality Metrics		
		$\mathbf{M}_{newm}$	$\mathbf{M}_{bunch}$	$\mathbf{M}_{g\&g}$	$\mathbf{M}_{rcc}$	MI	QDI	TLOC
JHotDraw(9)	MII	**0.89****	**0.75***	0.44	**0.87****	**-0.87****	**0.90*****	**-0.88***
	NC	-0.45	-0.23	0.01	-0.39	**-0.61***	**-0.60***	**0.52**
	$APIU$	0.47	0.31	0.20	0.43	-0.48	0.52	**0.56**
Apache-ant(14)	MII	0.22	**-0.80*****	**-0.82*****	**-0.68****	**-0.69****	**0.06**	**-0.76****
	NC	0.05	**-0.84*****	**-0.85*****	**-0.78*****	**-0.78****	-0.18	**-0.83*****
	$APIU$	-0.20	**-0.72****	**-0.76****	**-0.90*****	**-0.50***	**-0.46***	**-0.97*****
GWT(11)	MII	**0.89****	**-0.75***	0.44	**0.87****	**-0.85****	**0.90*****	**-0.92*****
	NC	-0.45	-0.23	-0.01	-0.39	**0.61***	**-0.60***	**0.90****
	$APIU$	0.47	0.31	0.20	0.43	-0.48	0.52	**-0.79***

TABLE VII. CORRELATION COEFFICIENT OF COUPLING MODULARIZATION METRICS BASED ON INHERITANCE AND ASSOCIATION

Project	Metric	Baseline Modularization Metrics				Quality Metrics		
		$\mathbf{M}_{newm}$	$\mathbf{M}_{bunch}$	$\mathbf{M}_{g\&g}$	$\mathbf{M}_{rcc}$	MI	QDI	TLOC
JHotDraw(9)	$SAVI$	**0.69***	0.38	0.02	**0.63***	**-0.87****	**0.87****	**-0.88****
	PPI	-0.55	**-0.61***	**-0.92****	**-0.80****	0.31	-0.44	0.34
	CU_m	**0.75***	**0.64***	0.50	**0.87****	**-0.67***	**0.77****	**-0.68***
	CU_l	0.365	0.46	**0.80****	0.64	-0.19	0.27	**-0.72***
Apache-ant(14)	$SAVI$	0.17	**-0.93*****	**-0.94*****	**-0.72****	**-0.89*****	0.25	**-0.76****
	PPI	0.09	**0.60***	**0.63***	**0.77****	0.40	**0.52***	**0.87*****
	CU_m	0.019	**-0.84*****	**-0.84*****	**-0.65***	**-0.81*****	0.39	**-0.59***
	CU_l	-0.34	**-0.50***	**-0.53***	**-0.76***	-0.20	-0.37	**-0.74****
GWT(11)	$SAVI$	**0.65***	**0.68***	0.30	**-0.66***	**-0.67***	**0.23*****	**-0.79****
	PPI	0.02	0.045	-016	-0.009	0.014	-0.022	0.009
	CU_m	0.19	-0.032	-0.001	-0.009	**-0.53***	**-0.60***	0.33
	CU_l	-049	-0.51	-0.36	**0.65***	-0.17	0.23	0.44

optimization of certain architectural features may raise unexpected sustainability vulnerabilities[7]. Despite these precise analytical constraints, architectural metrics can help developers to re-asses their design decision to insure modularization in particular during software evolution process. For instance, result of Table VII suggests that excessive state access violation should be avoided during development of *Apache-ant*and results of Table VI indicate that inter-module connections through method invocations can be minimized to improve modularization of *Apache-ant*. Overall, Our results show that package level modularization metrics bear considerably significant relationship with modularization metrics studied in different engineering domains. Such findings can help the software engineer to develop design plan to ensure optimized source code architecture. Additionally, Sarkar's modularization metrics were also analyzed to reveal significant correlation with different software quality metrics.

2) Do Sarkar's package modularization metrics provide any significant perspective for improving architectural quality during software evolution? : Software usually undergoes a continuous process of evolution driven by incremental development processes and design improvement. Modularity of software reflects different design considerations. Modularity of software systems has been linked with growth of software development community, code contribution and reduction of design vulnerabilities. As a theoretical construct, modularity also relates with other domain of research, including organization mechanism, industrial economics and product refinement. However, measuring modularity is crucial for maintenance of complex and large software systems.

To analyze the architecture's sustainability, we assessed the evolution scenario of software systems formed with architectural metrics. Each subject system was separately observed. This kind of analysis towards evolution scenario of software systems is helpful to judge the impact on its structural changes and to identify points where architectural mitigation can be incorporated during software development. To elicit the evolutionary changes, each category of Sarkar *et al.*'s metrics is exclusively represented in Fig. 4, 5, and 6.

Fig. 4 shows patterns of changes taking place in different software systems against modularization values of Inheritance and Association based coupling. In 14 versions of *Apache-ant*, all the coupling based metrics show the constant pattern. In 9 versions of *JHotDraw*, *AC* and *IC* seem to be improving marginally, whereas, *BCF* has gradually improved to significant extent. In 11 versions of *Google-Web Toolkit*, *BCF* and *IC* has shown slight decline as the software evolves, while *AC* has exhibited an improving trend. Our examination from such graphical representation also tells that *BCF* remains as best modularization among two other metrics, however, evolution process is still followed by fluctuating modularization values of *IC*.

Fig. 5 shows patterns of changes taking place in different software systems against modularization values of method invocation based coupling. It can be clearly seen that through out all the evolutionary period of all software systems, only *MII* has achieved an effective modularization while on the other hand *NC* and *APIU* has shown negative and steady trends. Such graphical representation can help us to understand that inter-module method calls through Application programming interfaces declared for each system should be maximized to modularize the software system.

Fig. 6 shows visualization trends for modularization values

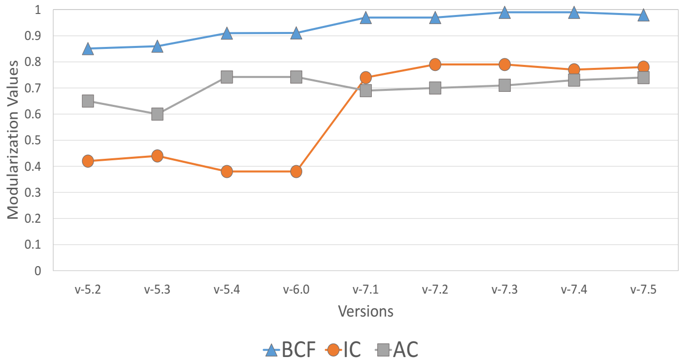

(a) *JHotDraw*

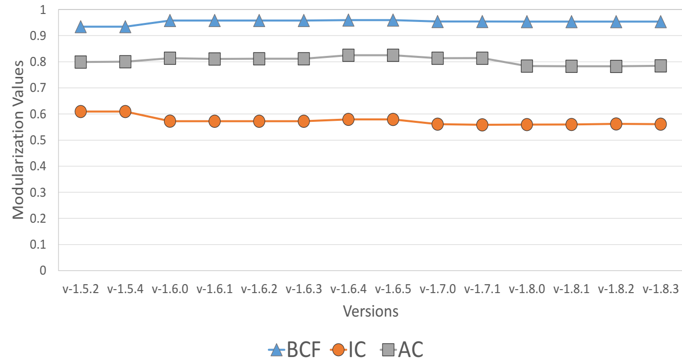

(b) *Apache-ant*

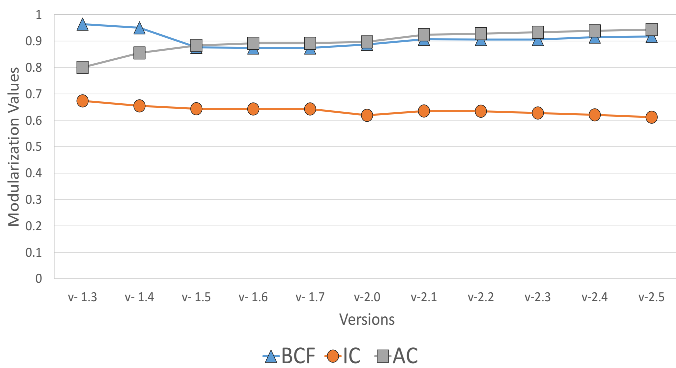

(c) *Google-Web-ToolKit*

Fig. 4. Evolutionary changes against Coupling Based on Inheritance and Association

of best practices defined in category 3 of Sarkar's metrics. An important finding is; managing the size of software components in terms of methods and lines of code improves the modularization during its evolution process as shown by CU_m and Cu_l in all cases. Whereas, *SAVI* and *PPI* show low and unstable values raising the vulnerabilities for sustainability. Hence, development process should avoid extensive violation for integrating third party plug-ins or state access to code base.

In summary, architectural decay or improvement is quite dependent on the particular design phenomenon, the software systems are developed for. Although, flexible architecture allows addition of new functionality during evolution process; however, it may come at the cost of certain sustainability concerns and design deterioration as well. Trend of architectural degradation can be result of design time violations, thereby posing sustainability concerns. If these significant mismatches against original design are identified earlier then maintenance and design improvement strategy can be effectively deployed to insure sustainability of software systems. Additionally, we have noticed that certain architectural metrics bear common modularization trends as well in software systems of diverse nature and domain which can be useful to form opinion for architectural-level metrics towards overall sustainability of software systems.

VIII. Discussion

The subject of software sustainability is emerging as benchmark to realize applications of software in social, economic, operational and technical terms. Hence, relevant empirical studies are required to explore the subject further. We presented an experimental analysis over 34 versions of three different open source java systems that includes research objectives, design, data processing and experimental results. In this regard, we reported statistical relationship of Sarkar's modularization metrics with existing validated modularity metrics studied in different domains of engineering [40] and quality metrics. Indeed, from theoretical standpoint, our study has diverse quality assurance focus but with major emphasis of architectural sustainability. We do not rule out other parameters that may have arguably better explanatory power; however, our effort is to explore significance of package based modularization metrics.

IX. Threats to Validity

In this section, we describe the most important threats to construct, internal and external validity.

Construct Validity

Accuracy of metrics calculation and rationale behind setting up *Baseline* modularization and quality metrics are two major factors which account for threats to construct validity. We

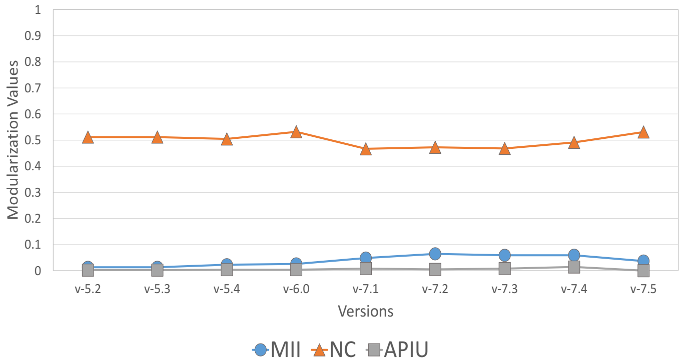

(a) *JHotDraw*

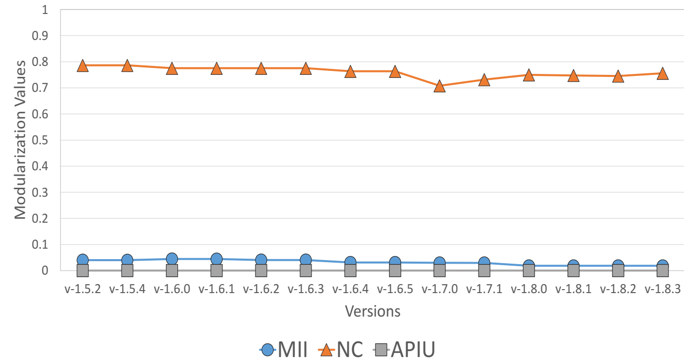

(b) *Apache-ant*

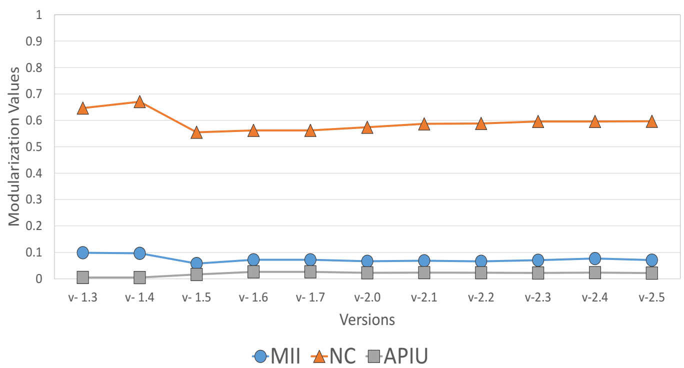

(c) *Google-Web-ToolKit*

Fig. 5. Evolutionary changes against Coupling Based on Method invocation

employed our source code analysis procedure with incremental testing to collect the Sarkar's metrics reliably using *Understand* tool which is already utilized in recent empirical studies [37], [47]. Whereas *Baseline* modularization metrics were computed by co-author using our own java based tool and already recognized in research literature [40]. Therefore, the construct validity of metrics computations can be considered quite satisfactory. Although, independent variables (Sarkar's Package modularization metrics, *Baseline* modularization metrics and software quality metrics) are briefly described with research focus and importance, still, it is required to further insure their validity. For example, *MI* and *MQ* have widely been used as software quality assessment metric [48], [49], [50], but other metrics are novel contribution towards setting up determinants of software sustainability.

Internal Validity

Threats to internal validity can arise from experimental methodology of data analysis applied in our study. Conclusion are drawn on the basis of correlation analysis. We have already mentioned our motivation of using correlation to identify the relationship among the quantities in aforementioned sections. However, these results are not merely based on significance of correlation obtained, but, it expands further through monitoring of evolution scenarios. Moreover, calculating *P-value* for statistical significance in quantitative analysis of software metrics is already utilized methodology [51], [38]. Therefore, sample size and guidelines mentioned by Woh *et al.* [52] and Yin *et al.* [53] counter these threats to internal validity to considerable extent. But, there is need of further study and experimental applications to acquire meaningful conclusion.

External Validity

Our study is based on several versions of open source java systems. This may cause potential threat to external validity due to choice of open source systems developed in particular language. Consequently, it is not possible to generalize the conclusion and results. We experimented our study with open source java system which have been frequently utilized in research literature of empirical software engineering, i.e., *Apache-Ant* and *JhotDraw*. Admitting the fact that this may raise bias over study as software systems of industrial range have not been brought in experimental set up. Indeed, this is an inherent problem in most of empirical software studies. However, we believe that study of 34 versions can substantiate to form at least formidable research opinion.

X. Conclusion

The modularity is an important aspect of software system describing its overall architectural quality and strength. In this paper, we investigated newly proposed modularization metrics based on packages from different perspectives. Our empirical study was mainly based on computation and analysis of modularity metrics through statistical correlation methodology. We presented an assessment for evolution scenarios of

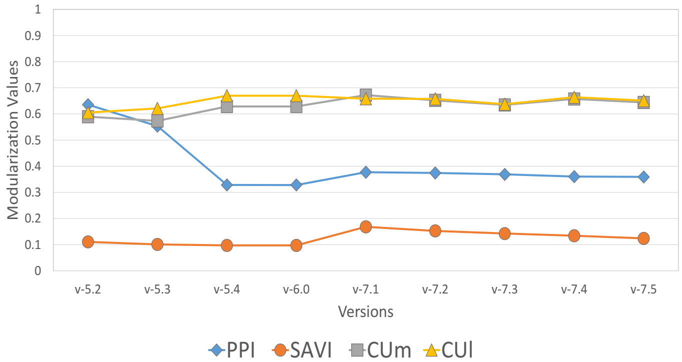

(a) *JHotDraw*

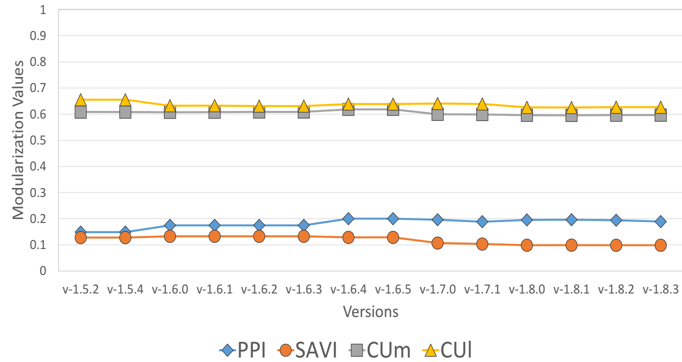

(b) *Apache-ant*

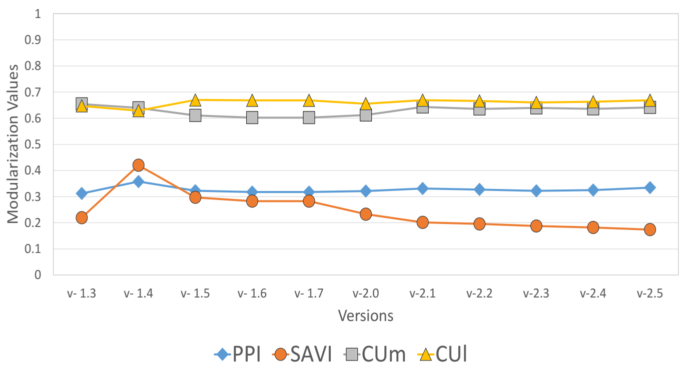

(c) *Google-Web-ToolKit*

Fig. 6. Evolutionary changes against metrics based on Modularization practices

software systems using architectural level metrics. This study can be important to avoid technical risk and develop a formal perspective for managing architectural improvement efforts invested during software development.

Tracking the rules of architectural compliance as the software evolves, there were some unique findings and observation to determine sustainability concerns of software system from different dimensions. Statistical analysis reported on different quality metrics and modularization metrics may help developers to regularly check architectural authenticity and form the code reviews for future quality assurance activities. Due to trade-off among the different architectural metrics, multiple perception are described for software maintenance. In addition to specific empirical view, our study also yielded interesting propositions: First, optimizing of each architectural metrics value is subject to design decisions; however, relative sustainability improvement or decline can be monitored during continuous development process; Second, tracking architectural level metrics and monitoring quality of software design can be possible task when evolution phases of software system are in progress; Third, undesired violations of architectural rules can be controlled with proactive re-factoring or restructuring decisions.

We adopted an integrated approach of evaluating software systems for their sustainable architecture and evolution scenario analysis. Sarkar *et al.* package modularization metrics were statistically tested to check their compliance with existing modularization metrics and their impact over different quality metrics. In addition to this, tracking architectural metrics during software evolution, we could determine ripple effects of different design aspects. Although, there was no as evidence to prioritize these architectural metrics in terms of their application, but, their usage can be helpful to identify critical sensitivities of software sustainability. In broader picture, approach is an effort to explore different dimensions of architectural sustainability.

Acknowledgment

The authors would like to thank Prof. Chan-Gun Lee, Director, RTSE-Lab, Chung-ang University, Seoul, Korea and Dr. Kiseong Lee, Post-doctoral researcher, RTSE-Lab, Chung-ang University, Seoul, Korea for sharing the data of their research work.

References

[1] J. Mitchell, C. Laughton, and S. A. Harris, "Atomistic simulations reveal bubbles, kinks and wrinkles in supercoiled dna," *Nucleic acids research*, p. gkq1312, 2011.

[2] S. R. Mounce, R. B. Mounce, and J. B. Boxall, "Novelty detection for time series data analysis in water distribution systems using support vector machines," *Journal of hydroinformatics*, vol. 13, no. 4, pp. 672–686, 2011.

[3] F. C. Maryland, "Measuring software sustainability," 2003.

[4] P. Oreizy, M. M. Gorlick, R. N. Taylor, D. Heimbigner, G. Johnson, N. Medvidovic, A. Quilici, D. S. Rosenblum, and A. L. Wolf, "An architecture-based approach to self-adaptive software," *IEEE Intelligent systems*, no. 3, pp. 54–62, 1999.

[5] P. C. Clements, "Software architecture in practice," Ph.D. dissertation, Software Engineering Institute, 2002.

[6] R. N. Taylor, N. Medvidovic, and E. M. Dashofy, *Software architecture: foundations, theory, and practice*. Wiley Publishing, 2009.

[7] H. Koziolek, D. Domis, T. Goldschmidt, and P. Vorst, "Measuring architecture sustainability," *Software, IEEE*, vol. 30, no. 6, pp. 54–62, 2013.

[8] W. Albattah and A. Melton, "Package cohesion classification," in *Software Engineering and Service Science (ICSESS), 2014 5th IEEE International Conference on*. IEEE, 2014, pp. 1–8.

[9] D. L. Parnas, "On the criteria to be used in decomposing systems into modules," *Communications of the ACM*, vol. 15, no. 12, pp. 1053–1058, 1972.

[10] B. S. Mitchell and S. Mancoridis, "On the automatic modularization of software systems using the bunch tool," *Software Engineering, IEEE Transactions on*, vol. 32, no. 3, pp. 193–208, 2006.

[11] H. Abdeen, S. Ducasse, and H. Sahraoui, "Modularization metrics: Assessing package organization in legacy large object-oriented software," in *Reverse Engineering (WCRE), 2011 18th Working Conference on*. IEEE, 2011, pp. 394–398.

[12] S. Sarkar, G. M. Rama, and A. C. Kak, "Api-based and information-theoretic metrics for measuring the quality of software modularization," *Software Engineering, IEEE Transactions on*, vol. 33, no. 1, pp. 14–32, 2007.

[13] S. Sarkar, A. C. Kak, and G. M. Rama, "Metrics for measuring the quality of modularization of large-scale object-oriented software," *Software Engineering, IEEE Transactions on*, vol. 34, no. 5, pp. 700–720, 2008.

[14] H. Koziolek, "Sustainability evaluation of software architectures: a systematic review," in *Proceedings of the joint ACM SIGSOFT conference–QoSA and ACM SIGSOFT symposium–ISARCS on Quality of software architectures–QoSA and architecting critical systems–ISARCS*. ACM, 2011, pp. 3–12.

[15] P. Lago, S. A. Koçak, I. Crnkovic, and B. Penzenstadler, "Framing sustainability as a property of software quality," *Communications of the ACM*, vol. 58, no. 10, pp. 70–78, 2015.

[16] C. G. von Wangenheim, A. von Wangenheim, F. McCaffery, J. C. R. Hauck, and L. Buglione, "Tailoring software process capability/maturity models for the health domain," *Health and Technology*, vol. 3, no. 1, pp. 11–28, 2013.

[17] D. Mairiza, D. Zowghi, and N. Nurmuliani, "An investigation into the notion of non-functional requirements," in *Proceedings of the 2010 ACM Symposium on Applied Computing*. ACM, 2010, pp. 311–317.

[18] M. Paulk, "Capability maturity model for software," *Encyclopedia of Software Engineering*, 1993.

[19] P. Clements, R. Kazman, and M. Klein, *Evaluating software architectures*. ACM, 2003.

[20] S. Sehestedt, C.-H. Cheng, and E. Bouwers, "Towards quantitative metrics for architecture models," in *Proceedings of the WICSA 2014 Companion Volume*. ACM, 2014, p. 5.

[21] F. Beck and S. Diehl, "Evaluating the impact of software evolution on software clustering," in *2010 17th Working Conference on Reverse Engineering*. IEEE, 2010, pp. 99–108.

[22] R. Martin, "Oo design quality metrics-an analysis of dependencies," *Proc. Workshop Pragmatic and Theoretical Directions in Object-Oriented Software Metrics*, 1994.

[23] J. Al Dallal and L. C. Briand, "An object-oriented high-level design-based class cohesion metric," *Information and software technology*, vol. 52, no. 12, pp. 1346–1361, 2010.

[24] L. C. Briand, J. W. Daly, and J. Wüst, "A unified framework for cohesion measurement in object-oriented systems," *Empirical Software Engineering*, vol. 3, no. 1, pp. 65–117, 1998.

[25] J. M. Bieman and B.-K. Kang, "Cohesion and reuse in an object-oriented system," in *ACM SIGSOFT Software Engineering Notes*, vol. 20, no. SI. ACM, 1995, pp. 259–262.

[26] R. Marinescu, "Assessing technical debt by identifying design flaws in software systems," *IBM Journal of Research and Development*, vol. 56, no. 5, pp. 9–1, 2012.

[27] M. D'Ambros, M. Lanza, and R. Robbes, "On the relationship between change coupling and software defects," in *Reverse Engineering, 2009. WCRE'09. 16th Working Conference on*. IEEE, 2009, pp. 135–144.

[28] A. Mockus and D. M. Weiss, "Predicting risk of software changes," *Bell Labs Technical Journal*, vol. 5, no. 2, pp. 169–180, 2000.

[29] N. Nagappan and T. Ball, "Use of relative code churn measures to predict system defect density," in *Software Engineering, 2005. ICSE 2005. Proceedings. 27th International Conference on*. IEEE, 2005, pp. 284–292.

[30] J. Lakos, *Large-scale C++ software design*. Addison-Wesley Reading, 1996.

[31] R. C. Martin, *Agile software development: principles, patterns, and practices*. Prentice Hall PTR, 2003.

[32] M. A. Babar, L. Zhu, and R. Jeffery, "A framework for classifying and comparing software architecture evaluation methods," in *Software Engineering Conference, 2004. Proceedings. 2004 Australian*. IEEE, 2004, pp. 309–318.

[33] K. Sethi, Y. Cai, S. Huynh, A. Garcia, and C. Sant'Anna, "Assessing design modularity and stability using analytical decision models," *Drexel University, Philadelphia, PA, Technical Report DU-CS-08-03*, 2008.

[34] A. Tang and J. Han, "Architecture rationalization: a methodology for architecture verifiability, traceability and completeness," in *Engineering of Computer-Based Systems, 2005. ECBS'05. 12th IEEE International Conference and Workshops on the*. IEEE, 2005, pp. 135–144.

[35] E. Bouwers and A. Van Deursen, "A lightweight sanity check for implemented architectures," *Software, IEEE*, vol. 27, no. 4, pp. 44–50, 2010.

[36] C. Sant'Anna, E. Figueiredo, A. Garcia, and C. Lucena, "On the modularity assessment of software architectures: Do my architectural concerns count," in *Proc. International Workshop on Aspects in Architecture Descriptions (AARCH. 07), AOSD*, vol. 7, 2007.

[37] Y. Zhao, Y. Yang, H. Lu, Y. Zhou, Q. Song, and B. Xu, "An empirical analysis of package-modularization metrics: Implications for software fault-proneness," *Information and Software Technology*, vol. 57, pp. 186–203, 2015.

[38] E. M. Bouwers, *Metric-based Evaluation of Implemented Software Architectures*. TU Delft, Delft University of Technology, 2013.

[39] L. Yu, A. Mishra, and S. Ramaswamy, "Component co-evolution and component dependency: speculations and verifications," *IET software*, vol. 4, no. 4, pp. 252–267, 2010.

[40] K.-S. Lee and C.-G. Lee, "Comparative analysis of modularity metrics for evaluating evolutionary software," *IEICE TRANSACTIONS on Information and Systems*, vol. 98, no. 2, pp. 439–443, 2015.

[41] M. E. Newman, "Modularity and community structure in networks," *Proceedings of the National Academy of Sciences*, vol. 103, no. 23, pp. 8577–8582, 2006.

[42] S. Mancoridis, B. S. Mitchell, Y. Chen, and E. R. Gansner, "Bunch: A clustering tool for the recovery and maintenance of software system structures," in *Software Maintenance, 1999.(ICSM'99) Proceedings. IEEE International Conference on*. IEEE, 1999, pp. 50–59.

[43] F. Guo and J. K. Gershenson, "A comparison of modular product design methods based on improvement and iteration," in *ASME 2004 International Design Engineering Technical Conferences and Computers and Information in Engineering Conference*. American Society of Mechanical Engineers, 2004, pp. 261–269.

[44] A. MacCormack, J. Rusnak, and C. Y. Baldwin, "Exploring the structure of complex software designs: An empirical study of open source and proprietary code," *Management Science*, vol. 52, no. 7, pp. 1015–1030, 2006.

[45] K. D. Welker, "The software maintainability index revisited," *CrossTalk*, vol. 14, pp. 18–21, 2001.

[46] A. Tahir, S. G. MacDonell, and J. Buchan, "Understanding class-level testability through dynamic analysis," in *Evaluation of Novel Approaches to Software Engineering (ENASE), 2014 International Conference on*. IEEE, 2014, pp. 1–10.

[47] Y. Zhao, Y. Yang, H. Lu, J. Liu, H. Leung, Y. Wu, Y. Zhou, and B. Xu, "Understanding the value of considering client usage context in package cohesion for fault-proneness prediction," *Automated Software Engineering*, pp. 1–61, 2016.

[48] M. Harman, S. A. Mansouri, and Y. Zhang, "Search-based software engineering: Trends, techniques and applications," *ACM Computing Surveys (CSUR)*, vol. 45, no. 1, p. 11, 2012.

[49] A. Arcuri and L. Briand, "A hitchhiker's guide to statistical tests for assessing randomized algorithms in software engineering," *Software Testing, Verification and Reliability*, vol. 24, no. 3, pp. 219–250, 2014.

[50] G. Bavota, M. Gethers, R. Oliveto, D. Poshyvanyk, and A. d. Lucia, "Improving software modularization via automated analysis of latent topics and dependencies," *ACM Transactions on Software Engineering and Methodology (TOSEM)*, vol. 23, no. 1, p. 4, 2014.

[51] H. Abdeen, H. Sahraoui, O. Shata, N. Anquetil, and S. Ducasse, "Towards automatically improving package structure while respecting original design decisions," in *Reverse Engineering (WCRE), 2013 20th Working Conference on*. IEEE, 2013, pp. 212–221.

[52] C. Wohlin, P. Runeson, M. Höst, M. C. Ohlsson, B. Regnell, and A. Wesslén, *Experimentation in software engineering*. Springer Science & Business Media, 2012.

[53] R. K. Yin, *Case study research: Design and methods*. Sage publications, 2013.

Knowledge Construction by Immersion in Virtual Reality Environments

Luis Alfaro[1], Claudia Rivera[2], Jorge Luna-Urquizo[3], Sofía Alfaro[4], Francisco Fialho[5]
Universidad Nacional de San Agustín de Arequipa, Peru[1,2,3,4]
Federal University of Santa Catarina - Florianópolis - SC, Brazil[5]

Abstract—**The objective of this work is to analyze the potential use of Immersive Virtual Reality technologies as a teaching/learning tool to enrich the organization of the learning environments of educational programs. The study and analysis of human cognition is theoretically based, also considering the Biology of Cognition and various approaches proposed by the theoreticians and researchers of Education Sciences. In the work, the state of the art of immersive technologies is established and their contributions in the construction of the knowledge of cognitive subjects are analyzed as a means for the development of teaching/learning activities, with the support of emerging immersive technologies. The methodology used is that of the bibliographic review of the classic works of printed literature in relation to the Biology of Cognition, and the search in diverse databases of theses and diverse works in universities and digital repositories. The main weakness of the research lies in the fact that the search was limited to documents using English, Spanish, and Portuguese language. To finish, conclusions and recommendations for future work have been established.**

***Keywords*—Computer assisted learning environments; immersive technologies; virtual reality; full immersion in virtual reality environments; knowledge construction by immersion in virtual reality**

I. Introduction

The conception and design of systems to support learning activities, mediated by resources offered by emerging technologies associated with computing, the Web and other sources which incorporate the possibility of adapting activities, learning objects and interaction to the individual profiles and needs of cognoscent subjects [1], [2], [3], is a research topic that has caught the attention of many research groups focusing on the problem, considering different educational philosophies such as: Instructional planning, social-cultural, social learning, the humanist perspective of education, constructivism and constructionism, which notably influenced the architecture and development of these systems during the different stages of development of this important area of research [4], [5].

Likewise, in the contemporary digital world, finding new ways to involve students in educational processes and activities becomes a great challenge, partly because technologies for domestic use, such as mobile phones, tablets and video game consoles, which are increasingly technologically evolved, have also become very popular resources, since the availability for children and adults is practically unrestricted. The fact of establishing a correlation between the possibilities of its use in educational activities associated with those of the classroom can be even more complex, especially if the technology implemented is less attractive than the technology that cognoscent subjects use at home.

In 1993, Winn [6], based on the works of Maturana [7], [8], [9] and Maturana and Varela [10], [11], stated the need for more research on constructivist education currents in order to use the emerging technologies of Virtual Reality (VR), which offered the possibility of constructing knowledge from direct experiences and not from descriptions of these made by third parties, involving symbolic linguistic, textual or computational mediation which inevitably leads to reflection, and which no longer constitutes an experience of its own. In this research, the works of Maturana and Varela and subsequent authors are analyzed in depth, in order to consider the biology of cognition and different concepts such as: Autopoiesis, interpretation and representation (symbolization), learning, behavior, structural coupling and especially cognition, in order to analyze and understand how cognoscent subjects construct their own knowledge in real and/or virtual environments. The answer to this question would enable a better understanding of the processes and elements associated with human cognition, which will undoubtedly influence the quality of the design and conception of environments, objects and interactions that use immersive technologies for educational purposes.

Likewise, the emerging immersive technologies were developed by the end of 2016 to levels at which it is assumed that they would rapidly penetrate large sectors of the consumer market. It is under that perspective that the development of Augmented and Mixed VR begun, which has been called the "Fourth Wave" of technological innovation and change in the world of computing, the first of these being: PCs, Internet and mobile devices, which have made significant changes in the interaction and communication of people, with an impact that managed to change some aspects of life of the general public.

On the other hand, the discipline of Knowledge Management [12], which establishes different types of knowledge, the Tacit [13] and the explicit [14], each of them with its own attributes and characteristics, can also be considered for the conception and design of objects and interactions of educational environments based on immersive technology.

Finally, the main objective of this work is to investigate and review different approaches that deal with human cognition, especially analyzing the approaches related to learning and the construction of the knowledge of cognoscent subjects and the technological resources offered by immersive technology, in order to establish a correlation between the possibilities of their use in educational activities associated with training and education, envisioning contributing towards the theoretical bases for the conception and design of virtual environments, as well as the use of appropriate objects and interactions.

In this work, Section II explores Human Cognition, Section III deals with and explores immersive technologies, and Section IV explores and analyzes the potential of immersive technologies in the construction of knowledge. Finally, conclusions and recommendations for this work are set out in Section V.

II. Human Cognition

In this section, different approaches to knowledge are explored such as: Human Cognition Biological bases, and other Education Sciences methods considering the views and requirements of these areas, whose action impacts organizations and their systems for human talent formation and capacitation.

A. Biological Bases of Human Cognition

In this part of the work, we review the concepts in relation to the organization, plasticity, cognition, learning, and language of living beings, according to the proposal of Maturana and Varela [10], and the reformulations of subsequent authors [15].

In accordance with Maturana [16], living systems are autopoietic entities, with a dynamic structure that allows them to interact with each other on a recurring basis, generating a type of structural ontogeny coupling called consensual domain. Throughout this consensual domain living beings interact with their environment, expanding another type of structural coupling called ontogenic adaptation.

The concept of autopoiesis is not tautological, trivial or unscientific, and neither are its derivations, in contrast to the conclusion of a number of authors [15]. An autopoietic machine is organized as a system of production processes of concatenated components in such a way that they produce components that [11]:

1) Regenerate the production processes (relationships) that produce them, through their continuous interactions and transformations; and
2) Constitute the machine as a unit in physical space.

The understanding of the cited authors about the relationship of an organism with its surrounding environment leads to an epistemological problem. In the Western Culture's theories of knowledge, people "store" representations of concepts "in their minds" based on the information collected through perception. The brain somehow stores the facts, uses them to draw conclusions, and updates them based on experience.

So much so, that Maturana and Varela [10] propose that living organisms, including humans, do not simply take information from outside; they react to the "disturbances" of the environment through adaptations of interior structures. The interaction with the environment does not affect the direct addition of "ingredients" in the physical structure of an organism and in symbols in their mental structure; however, it causes qualitative and quantitative changes in these existing structures. The ability to detect disturbances and the kind of structural change they produce is determined through phylogeny, which is understood as the succession of organic forms that are related to the sequence of reproductive relationships of species and through the history of individual adaptations or ontogeny [11], understood as an integral process of development in the direction of an adult state, through which certain structural forms are achieved, allowing the organism to perform functions in accordance with the innate plane that delimits it in relation to the surrounding environment. The ontogeny of a living system is the history of the conservation of its identity through its continued autopoiesis in the physical space.

The interpretation and representation (symbolization) of the world depend on structural adaptations, depending on the interaction with the disturbances of a symbolic and real environment. Humans usually communicate with someone else symbolically. Communication becomes possible through what Maturana [11] call "structural coupling". Organisms of similar species basically possess similar devices to detect disturbances and adapt to them. On top of that, they inhabit similar environments and are likely to find similar disturbances. As a result, the stories of their structural adaptations can be similar. Their structures are "coupled", so communication with other human beings is possible. According to [17], to make communication possible, an approximation must be made in relation to the meanings of the symbols. Negotiation between members of a group about a meaning is established through a compromise [18], and may result in only temporary concordance. Searle [19], having proposed the problem of meaning, focuses on the structure of language acts. In doing so, he proposes the theory of speech acts, developed by Austin [20] who proposes illocutionary acts, whose purpose is to generate consensus and perlocutionary, whose purpose is to provoke an action [21].

Thus, the organism does not construct a representation of the environment, not does it find a proper behavior for it. For it to operate, there is no means nor memory, only a structural dance in the present, which follows a course consistent with the structural dance of the means. Otherwise it disintegrates. The organism's behavior remains adequate only if it retains its adaptive capacity during its interactions, and what an observer saw as "reminded things" consists precisely in that, in the appearance of behaviors that seem appropriate because the organism retains its adaptation against recurring environment disturbances.

For Maturana [9], learning occurs when the behavior of an organism varies during its ontogeny in a manner consistent with the variations of the environment, which it does following a contingent course in its interactions with it. The fact that the nervous system participates in the phenomena of learning is evident when there is interference caused by damage or alteration in this system. The so-called learning phenomena can be described in different ways: "generation of appropriate behavior towards the environment from previous experience", or "acquisition of a new skill as a result of practice", according to which the observer wants to emphasize. It seems that the characterization proposed above is necessary and sufficient to cover all possible cases.

There are two basic perspectives to explain the learning phenomenon:

- According to one perspective, the observer sees the environment as the world where organisms have to exist and act, and that provides the information, data, and meanings required to represent it, and compute the appropriate behaviors that will allow them to survive in it.

- According to this vision, learning is a process through which an organism obtains information from the environment and builds its representation, storing it in the memory and using it to generate behavior in response to the disturbances of this means. From this point of view, memory consists in finding in memory the representation required to bring adequate answers to the recurrent interactions of the environment.

Under this perspective, the environment is instructive because it specifies in the organism changes of state which, being congruent, constitute a representation of it.

On the other hand, the cited authors see perception as an operation of distinction in which the nervous system, which is an operationally closed system, obtains knowledge [16]. This leads us to a question: How is it that an organism can have knowledge of the world? Learning is not a process of accumulation of environment representations; however, it is a continuous process of behavior transformation going through continuous change in the nervous system's ability to synthesize it. The evocation of representations does not depend on the indefinite retention of a structural invariant which represents an entity (an idea, image or symbol), but on the functional ability of the system to create when there are certain conditions of recurrence, a behavior that meets the recurring demands, classified by the observer as a reactivator [7].

Behavior is not a nervous system invention; it is typical of any unit seen in a medium where a domain of disturbances is specified and maintains its organization as a result of the changes in state that activate it [16]. The usual associations with word conduct are generally actions such as walking, eating, searching, working, etc. Examining all those activities associated with behavior, we see that they relate to movement. The structural coupling is the basis, not only of the changes occurred in the same autopoietic unit or individual throughout their life (learning), but also of those occurring through reproduction (evolution). Indeed, any structural change can be seen as ontogenetic (which occurs during the life of an individual). A genetic mutation is a structural change in a parent that has no direct effect on its state of autopoiesis, until it plays a role in the development of the offspring.

For Maturana [8], "if the observer wishes to discriminate between learned and instinctive behavior, they will discover that in their current realization, both modes are equally determined by the structures of the nervous system and the organism and so, the learned and instinctive behaviors that reside exclusively in the history of the establishment of the structures responsible for them are distinguishable".

The structural coupling [16], generated on the demands of autopoiesis, fulfills the function, naively attributed to having a representation of the world. In the cognitive domain, it is explained how the history of the disturbances of the living being (and its ancestors) leads to the structure that determines them.

- According to another perspective, the observer sees that the behavior of an organism (with its nervous system included) is determined at every moment by its structure, and can only be adapted to the environment if this structure is congruent with that of the environment and its dynamics of change.
- According to this vision, learning is the course of the structural change that the organism follows (including its nervous system) in congruence with the structural changes of the environment, resulting from the reciprocal structural selection that occurs between them during the recurrence of their interactions, retaining their respective identities.
- According to this, there are no instructive interactions, since the medium only selects the structural changes of the organism; it does not specify them.

Maturana [9] is also concerned with understanding the meaning of "cognition" related to the fundamental nature of living beings. This author rejects the metaphor of the treatment of information as the basic element of human cognition, substituting the question of "How does an organism obtain information concerning its environment?" for that of "How does an organism have the structure that allows it to operate adequately in the environment in which it exists?" To answer this question, one must descend to a deeper understanding that cognitive activity is common to all types of life and is determined by the underlying phenomenon of autopoiesis. For the quoted author [7]: "Living systems are cognitive systems and life is a process of cognition. This statement is valid for all organisms with or without a nervous system".

A cognitive system defines a domain of interactions where it can act with relevance to conserving itself, the process of cognition being the actual (inductive) performance or behavior in this domain [7]. A cognitive explanation is related to the relevance of the action for the conservation of autopoiesis and operates in a phenomenological domain, different from the domain of mechanistic behavior determined by the structure.

"... as a result of the structural coupling that takes place throughout history, this takes shape both in the structure of the living nervous system and in the structure of the environment, even though both systems always necessarily operate in the present, by means of processes determined locally as systems determined by the structure ... History is necessary to explain how a given system or phenomenon happens in reality but does not participate in the explanation of the operation of the system or phenomenon in the present" [11].

For observers, it is possible to generate descriptions of the living being's activity in any domain. One of these descriptions, essentially historical, refers to the system's structure and its determination about behavior. No matter how the system becomes what it is, it simply is. At the same time, you can describe (as observers of a history of change within a structure and the environment) the model of interactions through which its structure produces itself and is the relationship of the changes that generate effective actions. This second domain of explanation is called by Maturana [7], "cognitive". This domain refers to the relevance of the mutant structure of the system with an effective behavior for survival.

It is, therefore, in this cognitive domain, that distinctions can be made, based on words such as "intention", "knowledge", and "learning". For Maturana, the cognitive domain is not simply a different (mental) level which provides a mechanistic description of the functioning of an organism, it is the characterization of effective action over time, and essentially temporal and historical. One of Maturana's main objectives [8] is to overcome the tendency (imposed by language), to treat mental terms as descriptions or structure of states. In relation to language, this author considers that two organisms when interacting recurrently generate as a consequence a social coupling in which they are reciprocally involved in the realization of their respective autopoiesis. The behaviors that occur in these domains of social links can be communicative and also innate or acquired.

Language, according to [18], as a consensual domain, is a modeling of "mutually guiding behavior" and not a collection of mechanisms in a "user language" or a "romantic" coupling between linguistic behavior and non-linguistic disturbances experienced by organisms. The basic function of language as a behavior-oriented system is not the transmission of information or the description of an independent universe about which one can speak, but the creation of a consensual domain of behavior between systems which interact linguistically through the development of a cooperative domain of interactions [8].

Language is, then, a consensual (conversational) coordination of consensual (individual) coordination of actions. In this context, the "conversation" is the minimum unit of social interaction oriented to the successful execution of actions [22]. According to Winn [6], the work of biologist Maturana has been particularly influential with some constructivists. The "structural coupling" organisms of the same species have basically the same apparatus for detecting and adapting to perturbations. Also, they inhabit similar environments and are likely to encounter the same perturbations. As a result, the history of their structural adaptations will be similar. Their structures are "coupled", which is why we can communicate with other humans but not with bats.

B. Approaches from the perspective of Education Sciences

In this part of the paper, the authors focus on proposals to explain the development of human autopoietic units, which will be briefly reviewed:

- Behavioral perspectives [23], of learning will contribute to the development of technologies for classroom conduction and instructional realization. Teaching machines, programmed instruction and computerized instruction are among the technologies developed, at least in part, based on these ideas.
- The social learning perspective [24], is driven by behavioral psychologists who considered that operant conditioning offers a limited explanation of learning. They broadened the perspective of learning to include the study of cognitive processes which cannot be observed directly such as expectations, thoughts and beliefs. These psychologists give only a partial explanation of learning and do not adhere to some other important aspects of the subject, such as the social influences of learning.
- Socio-cultural perspective of education: Freire's "Education as a practice of freedom". The ideas of Freire [25] [26] and his followers are located within a socio-cultural approach. You cannot speak rigorously of the Freire method, since it is much more than a theory of knowledge and a philosophy of education than a teaching / learning method. The pedagogical theory of this author proposes an education built on the idea of a dialogue between educator and student, where there are always parts of each other in the other. This education could begin with the educator bringing from his world, from his knowledge, from his teaching method, material for educational activities in classrooms based on culture and values. Within this conception and the one regarding the method, there is the basis that anyone educates anyone and that one educates oneself alone.
- Humanistic perspective of education [27], [28]: Some educators sought student-centered teaching. They did not identify themselves as constructivists, although they developed philosophy and constructivist approaches. Among the basic principles of the humanistic approach, there is a belief that each person creates their own reality. The reality they perceive is important to each individual and one person cannot fully know the reality perceived by another.
  Humanistic interpretations of motivation emphasize intrinsic sources. Humanistic approaches to education emphasize the importance of feelings, free communication and the values of each student. Humanist education is a philosophy, rather than a compilation of strategies. Many actions that teachers can carry out to support self-esteem and make the center or educational resource or place attractive. One approach associated with humanist education is open schools, whose general research shows that these environments promote creativity, cooperation, selfesteem and social adaptation; however, academic performance is not greater than that of traditional classrooms.
- The perspective of teaching in the biology of love: Various forms of body dynamics, which emerged with the evolutionary history that gave rise to humanity, reappear in the ontogenetic drift of the child's physical and mental development. The various forms of free play of children, which emerge without the influence of adults, are organized on the basis of innate forms of actions in a spontaneous way, which include movements and perceptions, which come from human evolutionary history or phylogeny. The forms of free play are not arbitrary; they are forms of body dynamics that are linked to ancestral behavioral territories, as well as to expressions and connections between the living being and its environment, whose current forms are only transformations of archaic Verden-Zöller forms [29]. The future of an organism is never determined by its origin [30]. And it is based on these conceptions that education and the act of "to educate" must be understood and considered. According to these authors, the task of human formation is the foundation of every educational process. Normally, there is no limitation of intelligence as a capacity for consensus; all human beings, except in extreme situations of neurological alterations, are equally intelligent only by communicating through language. Intelligence difficulties arise or result (if there is no neurological damage of any origin) from interference in the biology

of love. Capacitation is an instrument or path in the realization of the task of formation and education.

- Constructivist perspective: The proposals of Gestalt psychologists such as Piaget [31], Vygotsky [17], Dewey [32], and Bruner Bartlett [33], emphasize the active construction of meaning by the cognitive subject. Emphasis is placed on the creation of meaning and construction of knowledge rather than on the memorization of information. Some of these perspectives also consider the social context as one of the fundamental factors of the knowledge that individuals acquire about themselves and the world. Some theories and studies attempt to explain the processing of information carried out by the human autopoietic unit, of how this represents knowledge in memory, concluding with the individual differences of the cognitive subjects.

- The term constructionism [34] [35], was coined by Papert, becoming one of the contemporary approaches of the Cs. According to this proposal, cognitive subjects carry out constructive tasks and activities to foster creativity and motivate learning in order to facilitate the assimilation of knowledge. It is argued that learning is more effective when it is situated in an activity, rather than being received passively.
The approach involves two types of construction [36]: (i) Cognitive subjects actively construct their knowledge and their experiences in the world, according to the approach of Piaget [31]; (ii) Constructionism adds the idea that it is important for cognitive subjects to be involved in the construction of products of personal significance, in order to build new knowledge.

Finally, Winn [6] points out that virtual immersion makes the construction of knowledge possible based on the direct experiences of the cognitive subject which do not become third-person descriptions, since these experiences do not have elements of symbolic mediation such as text, or the spoken language itself, which inevitably lead to reflection, which will be constituted in the experience of another person. The use of a symbolic system, for the communication to another person about the world we have built, will never allow that person to know our world as we know it.

Some reviewed approaches suggest that intelligence or "plasticity" [7], establishes the capacity of organisms to adapt to their environment; Immersive VR can become one of the emerging technologies that allow experiences in real or virtual environments, making it possible to abstract and synthesize some temporal and spatial variables, that will enable first-person experiences without requiring symbolic mediation, enabling learning and training involving tacit and explicit knowledge in an original, direct, unique and unforgettable way.

The immersive technologies will be explored further, envisioning their possibilities and contributions in the construction of knowledge of the cognitive subjects.

III. Immersive Technologies

A. Virtual Reality (VR)

The concept of VR refers to a whole simulated reality which is built with computer systems by using digital formats. Building and visualizing this alternative reality requires hardware and software powerful enough to create a realistic immersive experience (e.g. VR helmets or dedicated glasses and 3D software) [37].

VR [38] is defined as the term used to describe a three-dimensional, computer generated environment which can be explored and interacted with by a person. That person becomes part of this virtual world or is immersed within this environment and whilst there, is able to manipulate objects or perform a series of actions. After many years of research and development, VR hardware and software is now widely available to general users, researchers and entrepreneurs. The following types of applications exist in VR: the "Immersive" applications, which enclose the user's audio and visual perception in the virtual world and remove all external information so that the experience is totally immersive. This type of technology is expensive and has some disadvantages, including less determining images, burden and environmental problems concerning simulators [39]. The user who utilizes the total immersion of VR technology has the ability to feel part of the virtual environment. The "Semi-immersives", which consist of experiences in a VR environment using real world attributes, by incorporating computer-generated graphic objects into the simulated virtual scene. Users enter and control this type of system using a mouse, keyboard, interaction styles, lenses and joystick [40]. They allow the user to interact using hands and sometimes glasses or DataGloves. The information displayed, such as text, graphics and images, is highlighted on the transparent screen to allow the user to interact with the real environment.

The "Non-immersive" [41], non-immersive system also called VR desktop (no input devices) is based on the screens that are displayed to the user; this is a window to the virtual world without additional devices such as HMD, and is sometimes called Window on World (WoW) systems [42].

All these alternatives allow the user to live an entirely immersive experience, in a real world or one created by human imagination. Likewise, it is necessary to emphasize that the fact that the user does not observe his own image within the virtual world, subtracts certain realism from the experience in the system, thus limiting his perception of the surrounding reality. Similarly, a certain feeling of dizziness may occur after a prolonged period of use. Current applications are focused on the world of entertainment, education [43], Marketing [44], Knowledge Management, Rehabilitation [45], etc.

"Stereoscopy" is another important feature of immersive VR, since it allows the user to perceive the depth of the object being observed, thus adapting to the natural way of seeing the world around us, which is generated using binocular vision, to create the illusion of perceiving objects in 3D, using two images taken from different positions, thus recreating human vision in 3D [46]. The sensation of depth is a very important element of VR, which gives the user an idea of the position of the objects shown, for which various configurations of lights, shadows, colors, transparencies, and even shapes are used [44] [47] [48]. That is why stereoscopy is an excellent alternative to improving depth perception [49]. VR has evolved rapidly in recent decades. In the beginning it could only be used by scientific-military laboratories at an excessive level of implementation cost. Due to the development and process of technological innovation, today, it is possible to have VR technology at moderate costs.

B. 2D, 3D and RV viewing modes

The different approaches for using representations related to the visualization of information are 2D, 3D and VR [49]. Short descriptions of each of these approaches will be presented below:

- The type of representation using two dimensions is 2D [40]. The graphs are flat, and are notable for their simplicity, precision and clarity in displaying information. Today, a large part of the interfaces are designed for this type of representation. These environments stand out for their precision and clarity in interpreting information. Generally, interaction is traditional and basic interaction techniques such as Zoom and Select are used.
- The type of 3D representation [39], represents an object allowing to visualize the width, length and height, that are assigned in a 2D surface, like a monitor, obtaining a visual perception of three dimensions. To achieve this effect, visual elements for depth such as lights, shadows and perspectives are used. These environments facilitate navigation and are only the result of an extension of interaction techniques in 2D environments, which use visual effects of light and shadow to generate the illusion of volume, but the final representation remains in 2D. The 3D applications will enhance experiences, even for participants in remote locations, allowing human social interaction [50].
- VR is a technology that allows immersion in a multimodal viewing environment, which also uses stereoscopic images in order to improve depth perception. Thus, it is possible to perceive three dimensions as in the real world. Visualization environments based on VR allow the user to participate in an immersive experience, which allows a different interaction. Some VR interaction techniques include Direct manipulation, in which a virtual hand is available to interact directly with the objects displayed in the system, and the laser beam metaphor, in which a virtual laser pointer is available, with which we can select and manipulate objects and elements.

Fig. 1 shows an example of the three types of environments described above.

C. Immersion

A feature of VR, where users are immersed in a simulated virtual world. Psotka [43], states that the fact that a user is placed in a virtual environment, contributes an important emotional factor, which facilitates cognition and improves information retention, because the user has the feeling that they are part of that virtual world. Additionally, immersion extends the user's range of vision, including travel (which has been very useful in virtual tours) and collaboration (used for manufacturing applications) [41], [51]. For this purpose, immersion was performed through different configurations. For example, a single large screen can be used and an anaglyph lens can be used. Another configuration is that of a CAVE environment consisting of a room with four walls and a projector for each; and another option is the use of a diving helmet or glasses, which have small LCD screens inside, on which images are projected for viewing by the user.

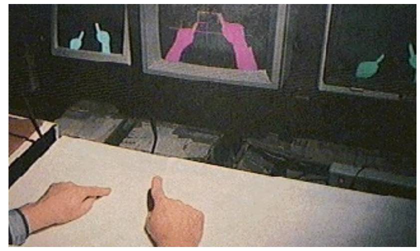

(a) 2D Image. Source: [54]

(b) Scanner captures 3D Image. Source: [54]

(c) Immersive VR Image Composition. Source: [54]

Fig. 1: Visualization Modes: (a) 2D, (b) 3D y (c) RV

D. Immersive RV devices

Recently, different VR devices have emerged which are mostly manufactured for specific purposes and not for traditional use. Some of them are: "Oculus Rift", "Leap Motion" and "Oculus Go". Fig. 2 shows the main VR viewers on the market. Oculus Rift (Fig. 2(a)) is the first to include a series of improvements such as stereoscopy and low latency in the refresh rate. HoloLens (Fig. 2(b)) experiments with mixing VR and augmented reality, as well as creating the first holographic processor. PlayStation (Fig. 2(c)) was created for entertainment purposes that stand out for their sophisticated design. HTC Vive (Fig. 2(d)) on the other hand, stands out for its good performance and development platform. Gear VR (Fig. 2(e)) uses VR with a wireless approach for which it requires a smartphone. Oculus Go (Fig. 2(f)) is a similar alternative, with the difference that its cost is much lower.

In Table I, these viewers are compared considering the main technical characteristics such as: Screen resolution, re-

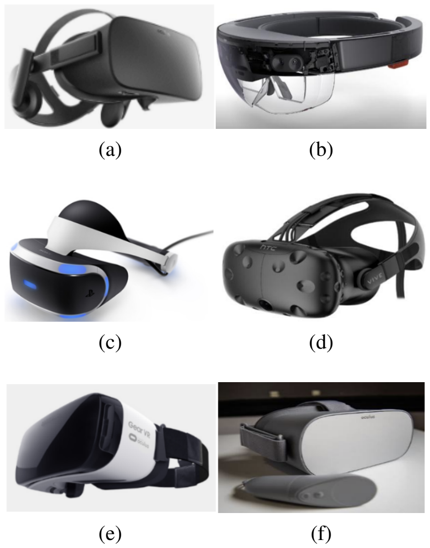

(a) (b) (c) (d) (e) (f)

Fig. 2: Interaction Dispositive Prototypes.

fresh rate, viewing angle and price.

TABLE I. VIEWERS COMPARISON CONSIDERING TECHNICAL ATTRIBUTES AND COST. SOURCE: ADAPTED FROM [47]

Visor	Resolution	Refresh rate	Vision angle	Price $
Oculus Rift	2160x1200	90 Hz.	110°	700.00
Hololens	1920x1080	120 Hz.	110°	3,000.00
PlayStation	1920x1080	120 Hz.	100°	400.00
HTC Vive	2160x1200	90 Hz.	110°	900.00
Gear VR	2560x1440	60 Hz.	96°	100.00
Oculus GO	2560x1440	60 Hz.	110°	169.00

E. Natural User Interfaces (NUI)

Recent developments in input peripherals are changing the way digital displays, the mouse and the keyboard interact with each other, and are already being replaced by tactile interfaces based on body movement [52]. These recent forms of interaction are part of the evolution of interfaces; computing has evolved, changed and diversified. The term NUI, coined by Mann, explores new forms of human-computer interaction, leaving room for research that focuses on new fields of application. NUI and VR are closely related, as the user, as part of the simulation, is expected to act as if he or she were in the real world; for this reason, one of the best options for interacting with the software is to use NUI. The NUI are a revolution in the world of computing, not because they replace the traditional interfaces that are widely used, but because they contribute to the design of new types of applications and new forms of original and innovative interactions that can be applied in Production, Administration, Marketing, etc.

F. Natural Devices Interaction

Fig. 3 shows the main devices necessary for the creation of NUI. Microsoft Kinect 2.0 (Fig. 3(a)) is the first to appear for the consumer market, created for entertainment purposes for games controlled through transduction, but then used for more advanced applications. Nimble VR (Fig. 3(b)) focuses only on the recognition of hands. Similar to Nimble VR (Fig. 3(b)), Leap Motion allows immersion using hands, but differs from the others by using two cameras for hand tracking, providing greater accuracy. Manus VR (Fig. 3(d)), unlike the others, uses motion sensors built into gloves.

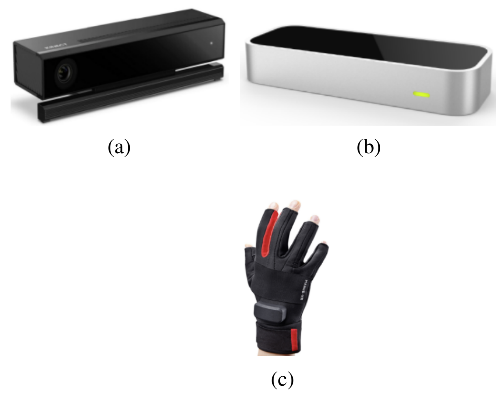

(a) (b) (c)

Fig. 3: Natural Devices Interaction.

Technologies now exist to capture different aspects of a participant's hand, face, and body actions in VR research. However, capturing all aspects of behaviour at the same time remains a challenging problem, and these technical limitations impose critical constraints on what psychology studies can be carried out. Despite the many challenges in the domain of mocap, there are many reasons why we believe that a rich capture of the human behaviour is valuable for social interaction research [53]. The historical review and the establishment of the state of the art allow us to glimpse the enormous potential of the resources and elements of immersive technologies, whose use in marketing strategies will allow innovative and original approaches.

IV. KNOWLEDGE CONSTRUCTION BY INMERSION IN IMMERSIVE TECHNOLOGIES

VR is an emerging technology that allows users to perceive reality through a set of devices that stimulate some sensory organs of a model of a real or fictitious environment. VR provides users with a system of intuitive interaction with the virtual environment and its objects as if they were real, through the possibility of immersion and 3D simulation managed by computer. This system stimulates the understanding of complex systems and allows people to approach diverse and unlimited knowledge and experiences [54]. For Niwhede and Lindgren [55], was not only created to experience games in a 3D environment, but also has great potential for teaching/learning activities in the field of education, as well as in industry, commerce, scientific and technological research and other economic and business activities. Specifically in the field of education, it is possible to create simulated virtual environments, in which students can interact with virtual objects using controllers and interaction devices. In teaching/learning environments, the aim of the use of this technology in principle, is to facilitate and motivate student learning, enabling learning through the creation of experiences in which it is possible to move, interact and understand, through the experiences and actions in the virtual world. The design of a learning experience could, of course, also be done in the real world, but there may be physical, temporal, economic and security limitations, among others that may make the virtual world a better option. VR can also be focused to improve students' motivation, which is also an important aspect of teaching/learning activities.

Contemporary computer-based VR systems have a number of sensors, limiting the user's space. This creates a very high differential value compared to smart phone based systems, because they enable closer to reality sensory experiences within virtual space. In one case, a vertical movement of the user implies a similar movement within the virtual world, which allows to perceive a feeling of immersion when sitting on a chair or a carpet placed on the floor. Additionally, there is the possibility of including trackers, in order to position additional elements within the virtual world [56]. Another similar initiative is the Oculus Rift helmet, with very similar quality and functionality.

The absence of symbolic mediation means that there is no implication of the reflection of conscience, which allows for a first-person experience. For the constructivist approach of the Cs. of education, the construction of knowledge requires first-person experiences, which are those that cannot be completely shared with other individuals Immersive VR allows for first-person experiences through the elimination of interfaces, which occurs in user-computer interaction. In this aspect, VR is unique. This technology allows a synthetic experience, which allows the capture of the essence of meaning for the person, who participates in order to know the virtual world [57]. These experiences, called Plasticity by Maturana [16], are defined as "the greater or lesser capacity of an organism to adapt to its environment", because they are known as intelligence by other approaches. Learning is understood as a process of accumulation of representations of the environment. Maturana [7] refers to the conditions of recurrence as a continuous process of transformation of behavior through a continuous change in the capacity of the nervous system to synthesize it into behavior that satisfies recurrent demands, classified by the observer as reactive. In this case, the virtual world requires the use of appropriate metaphors and some elements of VR such as transduction, reification, simulation of situations, real characters or even avatars, all of which will allow for original and unforgettable experiences.

VR is becoming an important emerging technology, the use of which can achieve enormous benefits. It is considered as a complete visualization environment using appropriate computer technologies. It is in this context that it offers unique experiences in which the student or user experiences an immersion that allows the perception of a reality through the different senses and, as Winn [6], argues, there are possibilities to expand these experiences through transduction, an experience in which the traditional interfaces between the user and the computer are changed and the user literally "sees the computer", which allows experiences using body movements that interact with the system. It is also possible to transform reality through reification, allowing beaches, oceans, swimming pools, etc. to be seen from various angles and even enlarged or minimized.

The reasons why immersive sensory VR is used as a powerful teaching and training tool are as follows [58]:

- It allows direct experiences of a phenomenon,
- It is three-dimensional,
- It allows experiences with multiple reference frames,
- It enables multisensory communication, and
- It is physically immersive.

A learning theory can be developed to cover a wide range of topics, interests and activities for dealing with complex and abstract issues, which can be enhanced by multisensory "immersion" (considering three-dimensional representations; multiple perspectives and frames of reference; multimodal interfaces; simultaneous visualization, auditory and tactile feedback, and various types of interaction that cannot be performed in the real world).

The illustrative themes applicable to virtual worlds are [58]:

- Multisensory stimuli draw learners' attention to important behaviours and relationships, supporting them for better understanding, through different sensory perspectives, also avoiding interaction errors with the use of feedback stimuli and improving usability.
- New representations and perspectives can help students to improve their ability to correct misconceptions, formed through traditional education, and can also help students to develop correct mental models.
- Enabling multimodal representation (voice commands, gestures, menus, virtual controls, and physical controls) will facilitate usability and appear to enhance learning. Multimodal commands are flexible and allow interaction to be tailored to individual preferences, as well as to distribute attention when performing various learning activities.
- Experiences with students and teachers suggest collaborative learning, which can be implemented with two or more students, who "guide the interaction", "remember observations" and "experience activities" in VR. Extending this to collaboration among multiple students sharing synthetic environments can increase attention and improve learning levels.

Likewise, from the pedagogical perspective, which studies the theory, activities and teaching methods, Marton and Booth describe three aspects of learning, the agent of learning, the act of learning and the object of learning [59]. The agent of learning describes what initiates learning. The act of learning describes the intentions of the learning experience, to memorize or understand something. The object of describes the content, the meaning of the phenomenon being learned. The object of learning can be divided into direct and indirect learning object. The direct learning object is the content of what is being learned and the indirect learning object describes the objective of the act of learning, i.e. the competencies that the learner is expected to develop. In other words, the indirect object and act of learning describes the "how" aspect of learning, while the direct object of learning describes the "what" aspect. Marton and Booth also describe three temporary facets or phases of the learning experience. These three facets are: acquisition, knowledge and use of [59]. The learning object can be seen as the link between the three temporary facets.

VR has been used for a long time in educational and training activities, and various simulators have been developed for different types of tasks, such as the operation of airplanes, submarines, power plants, tanks, helicopters, ships, cranes, trains, surgery, automobiles and air traffic control [60]. For Bhat [38], the most common virtual environment used is the 3D environment in various fields, such as: architecture, construction, engineering, etc. 3D visualization allows a better platform for shared and collaborative understanding of each individual in a team. The final users of the application can be people not familiar with technologies, and for them it is necessary to reduce the complexity of the model.

Finally, the different topics covered should be considered for teaching applications, considering the diversity of learner profiles, as well as the learning and thinking styles [4], and the potential of the different hardware and software elements to be used for different types of applications, considering also the costs and technological feasibility for the implementation of these systems, which will undoubtedly contribute in an important way to the teaching/learning activities, and also considering the open problems of immersive technologies.

V. Conclusion and Recommendations

Not only the "autopoiesis theory" and other approaches based on the biology of human cognition, but also most educational theories, suggest that authentic learning takes place in environments that foster first-person experiences since they suppress symbolic mediation and reflection, in addition to capturing the subject's attention, motivating to study and thus reinforcing their learning.

Likewise, in this work, the state of the art of the biological foundations of human cognition of the different approaches of education and of immersive VR has been established, which can allow to take advantage of the enormous potential of this emerging technology, which would make possible the adoption of new approaches, methodologies and techniques for the innovation of human talent education and training practices, since first-person experiences, which are very close to those of the real world, can be a good alternative to consider for the design and development of models of learning teaching systems, which use metaphors that include multisensory actions and perceptions.

The participation of diverse sources of experience is recommended for research in this area, for the conception and development of systems that use immersive technologies and especially the experience of full immersion, requiring the use of working methods for multidisciplinary teams that include specialists in the fields of pedagogy, educational psychology, neurosciences, specialists in the domain of the knowledge they intend to teach, as well as technicians in graphic, artistic, computer, multimedia and project management projects.

It is also advisable to consider the importance of using Artificial Intelligence, which allow teaching and learning systems to be provided with some adaptive characteristics derived from the identification of user profiles, as well as the different environments that may be important and significant.

Acknowledgment

The authors would like to thank the National University of San Agustín of Arequipa (UNSA) – Peru, and the Federal University of Santa Catarina - Florianopolis - Brazil

References

[1] Luis Alfaro, Claudia Rivera, Jorge Luna-Urquizo. *"Using Project-based Learning in a Hybrid e-Learning System Model"*. International Journal of Advanced Computer Science and Applications, Vol. 10, No. 10, 2019.

[2] Luis Alfaro, Erick Apaza, Jorge Luna-Urquizo, Claudia Rivera. *"Identification of Learning Styles and Automatic Assignment of Projects in an Adaptive e-Learning Environment using Project based Learning"*. International Journal of Advanced Computer Science and Applications, Vol. 10, No. 11, 2019.

[3] A. Flores, Luis Alfaro, Jose Herrera, Edward Hinojosa. *"Proposal Models for Personalization of e-Learning based on Flow Theory and Artificial Intelligence"*. International Journal of Advanced Computer Science and Applications, Vol. 10, No. 7, 2019.

[4] Luis Alfaro, Claudia Rivera, Jorge Luna-Urquizo, Sofia Alfaro, Francisco Fialho. *"Virtual Reality Full Immersion Techniques for Enhancing Workers Performance, 20 years Later: A Review and a Reformulation"*. International Journal of Advanced Computer Science and Applications, Vol. 10, No. 10, 2019.

[5] B.M. Quispe, L.A. Casas, O.A. Oviedo, J.H. Quispe, C.V. Chavez, R.V. Pucho, B.D. Joaquin. *"Proceedings of the 10th International Conference on Education Technology and Computers"*. International Journal of Advanced Computer Science and Applications, pp. 341–346, Tokyo, Japan, 2018.

[6] W. Winn.*"A conceptual basis for educational aplications of virtual reality"*. 1993. http://www.hitl.washington.edu/projects/education/winn/winn-R-93-9.txt

[7] H. Maturana. *"Biology of cognition"*. Biological Computer Laboratory Research Report BCL 9.0. Urbana IL: University of Illinois, 1970. http://www.enolagaia.com/M70-80BoC.html

[8] H. Maturana.*"Biology of language: The epistemology of reality. psycology and biology of language and thought"*. New York: academic press, pp. 27-63. 1978. Isbn 0-12-497750-2. http://www.enolagaia.com/umuarchive/m78bol.html

[9] H. Maturana.*"Refexiones: Aprendizaje o deriva ontogénica. In: Desde la biología a psicologia."* Maturana, Humberto R. Santiago de Chile: Editorial Mitech Ltda. Ediciones Synthesis, 1993. p. 82-102. ISBN: 956-7335-01-X

[10] H. Maturana, F. Varela. *"De máquinas y seres vivos - una teoría sobre la organización biológica."* Chile. Editorial Universitaria S.A. 1972.

[11] H. Maturana, F. Varela.*"El árbol del conocimiento."* Octava Edición. Santiago de Chile. Editorial Universitaria. 1992.

[12] Ch. Chauhan, M. Ul Akram. *Knowledge Management, Sustainable Business Performance and Empowering Leadership: A Firm-Level Approach*. International Journal of Knowledge Management, Volume 15, Issue 2, April-June 2019

[13] K. Dampney's, D. Richards, P. Busch. *The Meaning of Tacit Knowledge*. Article in Australasian Journal of Information Systems, January 2007, DOI: 10.3127/ajis.v10i1.438.

[14] Bojan Obrenovic, Slobodan Obrenovic, Akmal Hudaykulov. *The Value of Knowledge Sharing: Impact of Tacit and Explicit Knowledge Sharing on Team Performance of Scientists*. International Journal of Management Science and Business Administration, Vol. 1, No. 2, Pages 33-52, 2015.

[15] P. Razeto-Barry. *"Autopoiesis 40 years Later. A Review and a Reformulation."* in Origins of Life 42(6)· October 2012. DOI: 10.1007/s11084-012-9297.

[16] H. Maturana, G. Guiloff. *"En búsqueda de la inteligencia de la inteligencia."* Santiago de Chile. Editorial Mitech Ltda. Ediciones Synthesis. 1992. pp. 59-81.

[17] M. Mahmoodi-Shahrebabaki. *Vygotsky, Education, and Literacy*. Unpublished manuscript, Department of Literacy Studies, Middle Tennessee State University. February 2019 DOI: 10.13140/RG.2.2.19109.76003

[18] F. Flores, W. Terry. *Hacia la comprensión de la informática y la cognicioń*. Ordenadores y conocimiento para el diseno del siglo XXI. Barcelona. Editorial Hispano Europea. S.A. 1989. pp. 266.

[19] M. Starks. *Review of 'Philosophy in a New Century' by John Searle (2008) (review revised 2019)*. In book: The Logical Structure of Philosophy, Psychology, Mind and Language in Ludwig Wittgenstein and John Searle – Articles and Reviews 2006-2019 2nd Edition Michael Starks, Publisher: Reality Press, pp. 425-444.

[20] Baktir, Hasan. *Speech act theory; Austin and Searle: Derrida's response and Deleuze's Theory of Order-word*. Language, Literature and Cultural Studies. V. 202-211. 10.21533

[21] M. Soler, R. Flecha. *" From Austin's speech acts to communicative acts. Perspectives from Searle, Habermas and CREA."* Revista Signos. 2010 / 43 Número Especial Monográfico Nº 2 363-375. 2010. http://dx.doi.org/10.4067/S0718-09342010000400007

[22] K. Karlgren, R. Ramberg, H. Artman. *Designing interaction: How do interaction design students address interaction?*. Int J Technol Des Educ. 2016. 26: 439. https://doi.org/10.1007/s10798-015-9314-3.

[23] L. Aguilar. *Conductismo radical de B.F. Skinner: coordenadas ontoepistemológicas y visión del ser humano*. CONHISREMI, Revista Universitaria de Investigación y Diálogo Académico, Vol. 14, No. 2, 2015.

[24] S. Lyons, Z. Berge. *Social Learning Theory*. In: Seel N.M. (eds) Encyclopedia of the Sciences of Learning. Boston MA: Springer. 2012

[25] V. Melo. *Emancipatory Education and Youth Engagement in Brazil: A Case Study Bridging the Theory and Practice of Education for Social Transformation*. Educ. Sci. 2019, 9(1), 23; 2019. https://doi.org/10.3390/educsci9010023.

[26] S. Abbasnasab, M. Mohd. *Sociocultural Perspective on Assessment for Learning: The Case of a Malaysian Primary School Procedia*. The 8th International Language for Specific Purposes (LSP) 2012 doi: 10.1016/j.sbspro.2012.11.277.

[27] Lilik Untari. *An epistemological review on humanistic education theory*. Jurnal Bahasa Dan Sastra. Volume 1 Nomor 1 Januari-Juni 2016. P-ISSN: 2527-8088. E-ISSN: 2527-807X.

[28] G. Aikenhead. *Review of Research on Humanistic Perspectives in Science Curricula*. A paper presented at the European Science Education Research Association (ESERA) 2003 Conference, Noordwijkerhout, The Netherlands, August 19-23, 2003.

[29] Verden-Zöller, Gerda. *El juego en la relación materno infantil: Fundamento biológico de la conciencia de si mismo y de la conciencia social*. In: Amor y Juego. Fundamentos olvidados de lo humano. Maturana, Humberto R. e Verden-Zöller, Gerda. Santiago de Chile: Editorial Instituto de Terapia Cognitiva, 1994. p. 71-136. ISBN: 956-7344-01-9.

[30] Maturana, Humberto R. *Emociones y lenguaje en educación y política*. Sexta edición. Santiago de Chile: Editorial Universitaria, 1992. pp. 98.

[31] P. Pérez. *Revisión de las teorías del aprendizaje más sobresalientes del siglo XX*. Tiempo de Educar, vol. 5, núm. 10, julio-diciembre, 2004, pp. 39-76.

[32] W. Arias. *Jerome Bruner 100 años dedicados a la psicología la educación y la cultura*. Rev. peru. hist. psicol. / ISSN 2414-195X / Vol 1 / Enero – Diciembre 2015 / pp. 59-79.

[33] J. Olivo-Franco, Dewey, Freire, Humberto Maturana. *Educación y democracia una década pendiente en Latinoamérica*. DELECTUS. Revista de Capacitación y Educación Continua. 2(1), 9-28. 2019

[34] A. Alanazi. *Critical Review of Constructivist Theory and the Emergence of Constructionism*. American Research Journal of Humanities and Social Sciences (ARJHSS). Volume 2, 8. Pag. 2019.

[35] Chronis Kynigos. *Constructionism: theory of learning or theory of design?*. 12th International Congress on Mathematical Education. 8 July – 15 July, 2012, COEX, Seoul, Korea.

[36] R. Jafari, H. Davatgari. *Review of Constructivism and Social Constructivism*. Journal of Social Sciences, Literature and Languages. Vol. 1(1), pp. 9-16, 30 April, 2015.

[37] Jorge Martín-Gutiérrez, Carlos Efrén Mora, Beatriz Añorbe-Díaz, Antonio González-Marrero. *"Technologies Trends in Education. "* EURASIA Journal of Mathematics Science and Technology Education ISSN 1305-8223 (online) 1305-8215 (print) 2017 13(2):469-486 DOI 10.12973/eurasia.2017.00626a.

[38] Akrati Bhat, Gunjan Bhagwat, Jagannath Chavan. *A Survey on Virtual reality platform and its Applications* International Journal of Advanced Research in Computer Engineering & Technology (IJARCET), vol. 4, number 10, 2015.

[39] Alqahtani, A. S., Daghestani, L. F., Ibrahim, L. F. *"Environments and system types of virtual reality technology in stem: a survey"*. International Journal of Advanced Computer Science and Applications (IJACSA), 8(6), 2017.

[40] Daghestani, L. *The design, implementation and evaluation of a desktop virtual reality for teaching numeracy concepts via virtual manipulatives*. Doctoral dissertation, University of Huddersfield. 2013.

[41] N. Menck, X. Yang, C. Weidig, C. Winkes, C. Lauer, H. Hagen, B. Hamann and J. Aurich, *"Collaborative factory planning in virtual reality,"* Procedia CIRP, vol. 3, p. 317–322, 2012.

[42] N. Sala. *"Multimedia and VR in architecture and in engineering education"*. In Proceedings of the 2nd WSEAS/IASME International Conference on Educational Technologies, Bucharest, Romania, vol. 22, 2006.

[43] J. Psotka, *"Immersive formatiom systems: Virtual reality and education and formatiom,"* Instructional science, vol. 23, no. 5, p. 405–431, 1995.

[44] Luis Alfaro, Claudia Rivera, Juan Zuñiga, Alonso Portocarrero, Jorge Luna-Urquizo, Alberto Barbosa. *"Immersive Technologies in Marketing: State of the Art and a Software Architecture Proposal"*. International Journal of Advanced Computer Science and Applications, Vol. 10, No. 10, pp. 482–490, 2019.

[45] G. Calle, Eveling Castro-Gutierrez, Luis Alfaro. *"Virtual Rehabilitation Using Sequential Learning Algorithms"*. International Journal of Advanced Computer Science and Applications, Vol. 9, No. 11, 2018.

[46] J. Juang, W. Hung, S. Kang, *"Simcrane 3d+: A crane simulator with kinesthetic and stereoscopic vision,"* Advanced Engineering Informatics, vol. 27, no. 4, p. 506–518, 2013.

[47] R. Linares, *"Exploración de artículos científicos con realidad virtual y procesamiento del lenguaje natural,"* Maestría en Ing. Informática. Escuela de Posgrado. Universidad Nacional de San Agustín de Arequipa., 2017.

[48] Luis Alfaro, Ricardo Linares, José Herrera. *"Scientific Articles Exploration System Model based in Immersive Virtual Reality and Natural Language Processing Techniques."* Article Published in International Journal of Advanced Computer Science and Applications(IJACSA), Volume 9 Issue 7, 2018. DOI :10.14569/IJACSA.2018.090736.

[49] B. Zohra, G. Fabrice, R. Paul, B. Julien and P. Fabien, *"An Overview of Interaction Techniques and 3D Representations for Data Mining,"* Applications of Virtual Reality, p. 185, 2012.

[50] L. Rapanotti and J. G. Hall, *"Design concerns in the engineering of virtual worlds for learning"*, Behaviour & Information Technology, vol. 30, no. 1, pp. 27–37, 2011

[51] K. Wanarat and T. Nuanwan, *"Using 3d visualisation to improve public participation in sustainable planning process: Experiences through the creation of koh mudsum plan, thailand,"* Procedia-Social and Behavioral Sciences, vol. 91, p. 679–690, 2013.

[52] A. Cámara, *"Natural user interfaces,"* in In IFIP Conference on HumanComputer Interact, 2011.

[53] X. Pan. A. Hamilton. *"Why and how to use virtual reality to study human social interaction: The challenges of exploring a new research landscape. "* British Journal of Psychology (2018), 109, 395–41, 2018.

[54] L. Alfaro. *"Contribuições para a modelagem de um ambiente inteligente de educação baseado em realidade virtual,"* Doutorado. Programa de Pós-Graduação em Engenharia de Produção. Universidade Federal de Santa Catarina, Brasil, 1999.

[55] J. Niwhede and A. Lindgren. *"VR from a Learning Perspective. "* Masther Thesis: Department of Design Sciences. Faculty of Engineering. Lund University. 2017

[56] H. Skouteris, S. Edwards, H. Morris, R. Cox, L. Baur, L. Wolfenden and T. Huang, *"Early childhood education and health working in partnership: the critical role early childhood educators can play in childhood obesity prevention,"* Early Child Development and Care, vol. 187, no. 8, pp. 1239-1243, 2017.

[57] F. Balan, *"Marketing Experiencial". Tesis de grado. Administración y Dirección de Empresas"*, F. de Cs. Sociales y Jurídicas. Universidad Miguel Hernandez de Elche., Alicante. España, 2015.

[58] C. Dede, M. Salzman, C. Loftin, R. Bowen. *"ScienceSpace: Virtual realities for learning complex and abstract scientific concepts"* 1995. http://www.virtual.qmu.edu/vriaspdf.htm.

[59] F. Marton and S. Booth, *"Learning and Awareness. "* Lawrence Erlbaum Associates, Inc., Publishers, 1997.

[60] W. Jin, *"VR technology in the design of the space environment research, "* in Control, Automation and Systems Engineering (CASE), 2011 International Conference on, 2011, pp. 1–4.

A Technical Guide for the RASP-FIT Tool

Abdul Rafay Khatri
Department of Computer Architecture and System Programming,
University of Kassel, Kassel, Germany.

***Abstract*—Fault injection tools are designed to serve various purposes, such as validate the design under test concerning reliability requirements, find sensitive/critical locations that require error mitigation, determine the expected circuit response in the existence of faults. Fault Simulation/Emulation (S/E) applications are involved in Field Programmable Gate Array (FPGA) based design's verification and simulation at the Hardware Description Languages (HDL) code level. A tool is developed, named RASP-FIT, to perform code modification of FPGA designs, testing of such designs, and finding the sensitive area of designs. This tool works on the FPGA designs written in Verilog HDL at various abstraction levels, gate, data-flow and behavioural levels. This paper presents a technical aspect and the user-guide for the proposed tool in detail, which includes generation of the standalone application (an executable file of the tool for Windows operating system) and installation method.**

***Keywords*—Code-modifier; fault injection; FPGA designs; fault injection tool; Verilog HDL**

I. Introduction

Dependability is the study of error and failure. A robust method that allows assessing the reliability of a target system is the Fault Injection (FI) method. Therefore, fault injection technique can be defined as "the dependability validation technique that is performed in a controlled experiment for the System Under Test (SUT) and observed its response in the presence of faults" [1]. Fault injection technique is used to test the fault-tolerant mechanisms of a system when known faults take place, and evaluate in this way for their effectiveness. The primary goals of fault injection in the design process are validation and design aid.

In the validation process, fault injection is intended to test the mechanisms implemented by the system to achieve dependability (fault tolerance mechanisms) concerning the faults that they are injected during the fault injection campaign. The validation process through fault injection has two primary purposes: fault removal, which is based on the design verification, and fault forecasting, which depends on the assessment of the system. When the objective is fault removal, a qualitative analysis is performed to check if the fault tolerance mechanisms are suitable regarding dependability requirements of the system. On the other hand, in the case of fault forecasting, fault injection is intended to perform quantitative evaluation (with a probabilistic approach), and the coverage of the fault tolerance mechanisms evaluated by the system [2], [3]. In the design aid, fault injection experiments are executed at several steps of the development flow. Results of fault injection are then used to initiate an iterative process that allows improving the test procedures and the fault tolerance mechanisms of the system being exploited.

Fault injection is a useful technique to estimate design characteristics such as reliability, safety, and fault coverage. The method consists of intentionally injecting faults into the device under test and observing the behaviour of faults/errors [1], [4]. Fault injection covers many fundamentals objectives:

1) Validate the design under test concerning reliability.
2) Detect critical areas require mitigation of errors.
3) Determine the expected circuit behaviour in the faulty environment.

The fault injection environment set-up consists of fault location, time of injection, duration of active faults, and the input data for the system.

Hardware Description Language (HDL) has been involved in designing the digital system during the last many years for Field Programmable Gate Array (FPGA) and Application Specified Integrated Circuits (ASIC). Testing and other fault simulation applications can now be applied directly at the HDL code level. Due to this, the gap between the tools and methods used by design and test engineers is reduced [5]. The HDL represents a higher abstraction level in the design flow. Testing should be carried out at lower abstraction levels to obtain the best responses. However, an HDL model at the behavioural level can be simulated to produce useful circuit response vectors for test purposes efficiently. The SUT and its hardware simulation model at the code level can be analysed for testability method.

This paper describes the technical user-guide for a novel fault injection tool and explains the way the user can use this tool for Verilog HDL at any abstraction level. The tool is named RASP-FIT (RechnerArchitektur und SystemProgrammierung-Fault Injection Tool) after the German name of the department in which it is developed. This fault injection tool can be used to modify the design for the Automatic Test Pattern Generation (ATPG) and other fault simulation applications. This tool is programmed in Matlab in a Graphical User Interface Development Environment (GUIDE). This paper presents the method to develop a standalone application, its installation on the computer without having a Matlab tool. Also, it describes the way to use this tool step by step.

The organisation of the paper is as follows: Section II describes the various fault injection techniques and tools for FPGA-based designs. Section III introduces the structure of the RASP-FIT in Matlab along with the method to build and install the standalone application for the user of the tool. The working procedure is also described in the section. Result and discussion for an example design using the RASP-FIT tool are mentioned in Section IV. In the end, Section V concludes the paper.

II. Related Work

Fault injection and fault simulation are typical methods to investigate the impact of a fault on a hardware/software system. Usually, fault injection is performed on abstract models of the system either to retrieve early results when no implementation is available, yet, or to speed up the run-time fast fault simulation of the specified models. Fault injection is mainly used to evaluate fault-tolerant mechanisms [5]. In the last few decades, fault injection has become a popular technique for experimentally determining dependability parameters of a system, such as a fault latency, fault propagation and fault coverage. Types of FI tools for FPGA in the literature are described in the sequel.

A. FI Techniques/Tools based on Simulation

Tools based on simulation involve the simulation model of the design under analysis. The errors or failures for the SUT are distributed with proposed mechanisms [6]. These techniques and tools are divided into two, i.e. Code-Modification (CM) and Simulator Command (SC):

1) Code-Modification technique:- This technique requires the modification of HDL code by adding some fault models such as stuck-at, bit-flip, mutant and saboteur.
2) Simulator Command technique:- In this type of tools and techniques, the particular simulator command is used to change the values of the signal or variable of HDL models available with the simulator (e.g. Modelsim, Xilinx ISIM).

The advantages are summarized below for the Simulation-Based Fault Injection (SBFI) tools [2], [1]:

- As simulation model is used instead of the actual hardware model hence there is no risk of damage.
- Being cost effective.
- Provides higher controllability and observability during FI experiments.
- Different fault models can be modelled with ease.
- Supporting any type of HDL code.

Most the SBFI tools in the literature, are available for the VHDL language, such as VERIFY [7], (MEFISTO-C, HEARTLESS, VFIT (VHDL-based Fault Injection Tool), FTI (Fault Tolerance Injection)) [8], [2], Full System simulator-based Fault Injection (FSFI) [9], etc. These tools are based on simulator command and code-modification techniques. Fault modelling is achieved by a saboteur, and mutant injection. Verilog Programming Language Interface (PLI) application is used in the test generation method during fault simulation applications [5]. The top-level design module can also be modified in some cases to achieve test generation and fault simulation applications with the help of simulator command technique, as presented in [10].

B. FI Techniques/Tools based on Emulation

The emulation-based fault injection tools are most often used with FPGA for speeding up the fault injection experiments to achieve a faster solution. Design from specifications to implementation takes several steps. Emulation-based FI tools are divided by following the stages of the design flow. The two main categories are given in the sequel shortly, i.e. instrumentation and reconfiguration.

1) Instrumentation technique:- This technique requires the modification of HDL code by adding some fault models such as stuck-at, bit-flip, mutant and saboteur in the system, netlist or other formats of the FPGA-based design.
2) Reconfiguration technique:- Reconfiguration or partial reconfiguration is the technique in which the configuration memory of the FPGA is modified or changed with some other logic to inject faults in the SUT.

The fault injection tools develop to work on the net-list obtained by the synthesis process are presented in [11], [12], [13]. Some tools work on the code level and modify the design by instrumentation technique are presented in [14], [15]. However, some hybrid techniques (simulation/emulation) can be achieved by combining two or more fault injection techniques as given in [16], [17], [18], [19]. HDL environment can generate a list of faults, and it is used for fault emulation/simulation of the SUT. The author compared the RASP-FIT tool with the work presented in [20] and found that the RASP-FIT tool uses three fault models (bit-flip and stuck-at (1/0)) provides better performance in testing and hardness analysis.

III. Structure of the RASP-FIT Tool

The RASP-FIT tool, with its Graphical User Interface (GUI) is developed in Matlab. The tool consists of three major functions, namely [21], [22]:

1) Fault Injection Analysis
2) Hardness Analysis
3) Static Compaction

All these functions are developed in Matlab under the function `RASP_FIT()`. It is a tabbed-based GUI as shown in Fig. 4, 5 and 6. Each tab performed certain specific functions and described in this work. To ease of use, a standalone Matlab GUI is developed for the proposed tool using the `deploytool` command [23]. This command generates the executable file for the RASP-FIT tool which can be installed on any computer containing Windows operating systems. The procedure for building a standalone application is given in the sequel.

A. Building a Standalone Tool

The standalone application helps the user of the tool to operate with ease. As described earlier, this tool is programmed in Matlab using the programmatic environment. To run the Matlab code, it is necessary to have a Matlab compiler installed on the computer. The standalone application can be run on any computer without Matlab. To run the RASP-FIT tool, a standalone app is generated. The procedure for creating a standalone application for the RASP-FIT device is described in the sequel.

1) Run the following command on the Matlab prompt.

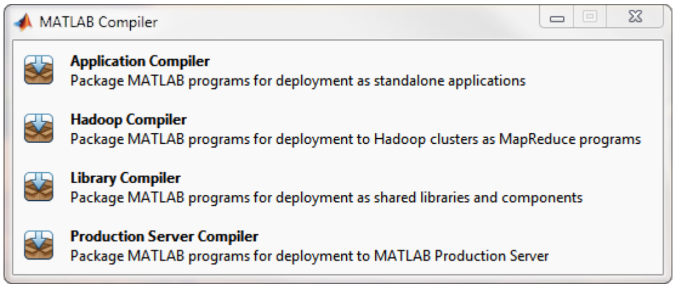

Fig. 1. Matlab compiler

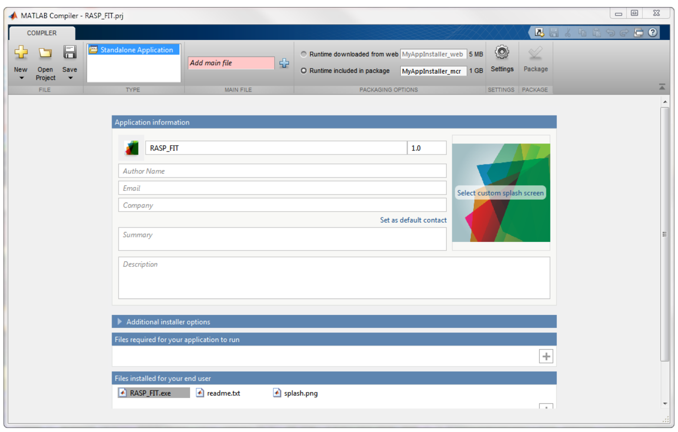

Fig. 2. Matlab compiler window for creating project

```
>> deploytool
```

and press ENTER.

2) A window appears as shown in Fig. 1, select the first option “Application Compiler”.
3) After selecting the above option, another window appears, as shown in Fig. 2. Add the main code file and fill the required pieces of information. Select the option “RASP-FIT_Installer_web” and click on the “Package” option to start the process. After the process, the project is saved under the extension ‘*.prj’ and generates the executable file for the project.
4) When this process stops, the executable file is available in the folder named “for_redistribution”.

B. Installation Procedure

The stepwise procedure is explained to install the standalone application [24].

1) Open the RASP-FIT_Installer executable file located in the *for_redistribution* folder generated by the Matlab compiler.
2) Run the installer file (*.exe) by double click on it. The first window of the Fig. 3 is appeared.
3) Click on the Next option and it leads to the *Installation Options* page.
4) Set the folder location, check the box to generate short-cut to the desktop and click *Next*. See the second window of the Fig. 3.
5) Agree to the license agreement and click yes to it.
6) Click *Next* moves to the confirmation page and press the install button. It checks whether the Matlab runtime is installed in your computer or not. If needed, it also downloads and installs the Matlab runtime. See the third window of the Fig. 3.
7) When the installation is completed, the fourth window of Fig. 3 appears. Click finish and complete the installation.
8) Run the standalone application.

C. Working Procedure

After the successful installation, the user has to double click the RASP-FIT icon available on the desktop. At first, the RASP-FIT tool asks for the user-defined primitive file which is available with the tool by the provider. The user has to locate the file only, and graphical user interface for the tool is opened for use. As described earlier, the RASP-FIT tool performs three functions. The sequel portrays the details of each tab of the device and its related options.

1) Fault Injection Analysis: The second tab of the RASP-FIT tool is the fault injection analysis, as shown in Fig. 4. The user must provide three input for modifying the design for the fault injection analysis.

1) Synthesizable Verilog design file.
2) Select fault model for analysis from a drop-down menu.
3) Enter number of copies the user wants to generate with evenly distributed faults in them.

By clicking on the generate button, faulty modules and top module are produced and stored in a folder where the source file is located. The faulty modules are named (`moduleName_faultycopy1.v`, `moduleName_faultycopy2.v` and so on). The top file consists of fault injection testing logic. This logic contains the comparator logic, dynamic compaction scheme and memory declaration for storing the results of the comparisons, and it is stored under the name (`moduleName_top.v`) in the same folder. These modified designs help design and test engineers to perform fault simulation, digital testing and dependability analysis without much effort. Verilog HDL code modification techniques for each abstraction level are presented in [21], [25], [26]. Along with the faulty copies, the RASP-FIT also provides the number of copies generated, the number of faults per copies which is used to calculate the number of select port pins, the number of total defects injected in the design. In the end, it calculates the select port pins for faults per copy. Eq. 1 describes the method to calculate select port pins [27].

$$FS = \lceil log_2(F_{copy}) \rceil \tag{1}$$

where F_{copy} denotes the number of faults injected per copy of the SUT and Fault Select (FS) is the number of select port pins.

2) Hardness Analysis: Hardness analysis is carried out for the SUT to find the characteristic of those faults which can be detected very often or rarely. The third tab of the RASP-FIT tool is for hardness analysis. It consists of three panels, namely, file merger section, an input data file section of hardness analysis and an input parameters required for

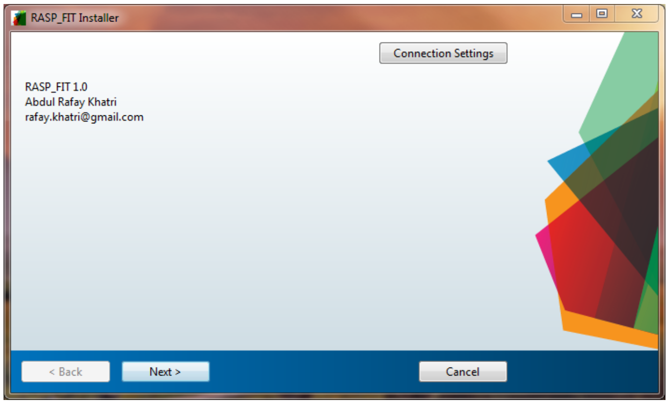

Step 1: First window

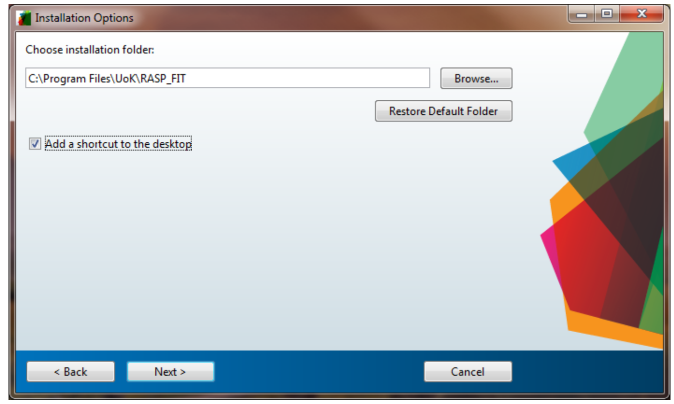

Step 2: Second window (installation folder)

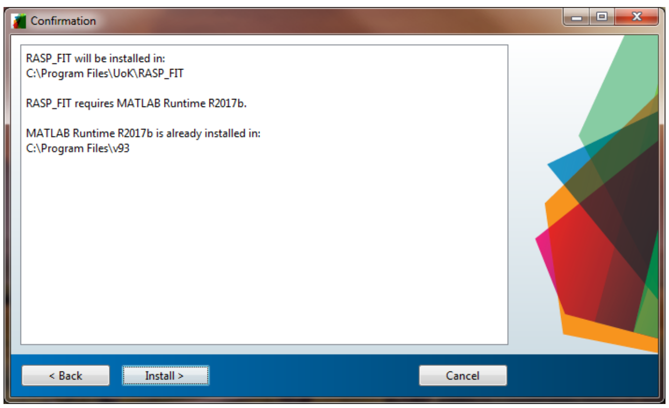

Step 3: Third window (confirmation window)

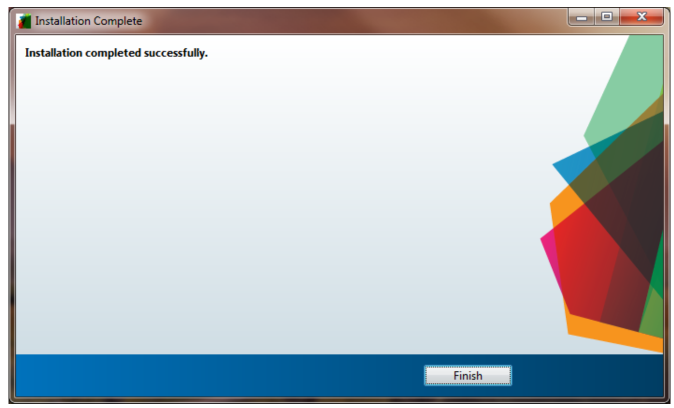

Step 4: Fourth window

Fig. 3. Installation procedure step by step

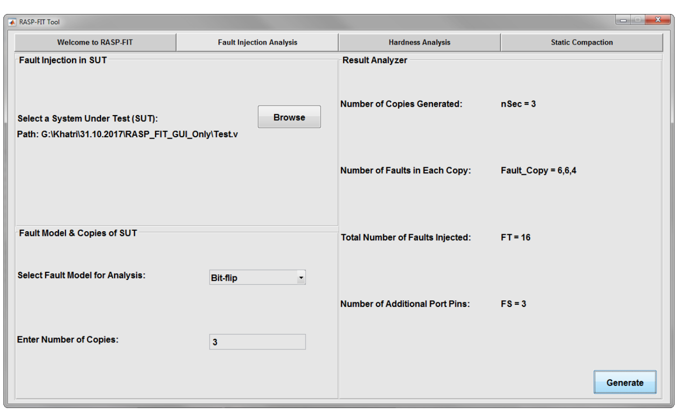

Fig. 4. Fault injection analysis tab.

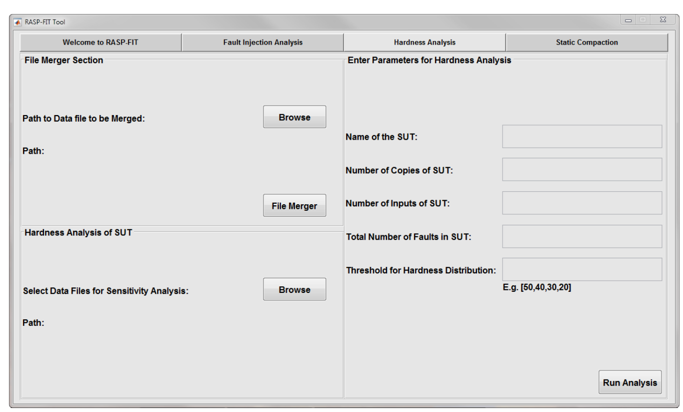

Fig. 5. Hardness analysis tab.

hardness analysis calculations. File merger is a program which takes many data files and merges them to produce one file. It is used if needed. When data files for hardness analysis are imported, and some parameter's information should be provided as inputs to perform hardness analysis. Fig. 5 shows the tab for hardness analysis. These inputs are:

- Name of the SUT: All hardness analysis results are saved under this name.
- Number of copies of SUT: This represents the number

of copies of SUT considered for the project.

- Number of inputs of SUT: Data is stored during experimentation as inputs and outputs. So for the removing of stored input patterns from the data, the user needs to provide this information.
- Total Number of Faults in SUT: This is a crucial parameter to calculate hardness analysis. This information provides the number of fault injection in the SUT during experiments.
- Threshold for Hardness Distribution: To divide the sensitive locations into hard to detect and most often detected, the user assign threshold values.

3) Static Compaction: Static compaction technique reduces the number of test vectors further after their generation. As static compaction techniques are not part of Test Pattern Generation (TPG), hence they do not change the TPG process. Therefore, It can be developed in any programming language or tool. The proposed static compaction algorithm is programmed in the Matlab, which needs few input parameters and data files from experiments. It calculates the fault coverage, compaction and reduces the number of test vectors. Fig. 6 shows the tab for static compaction. All the input parameters required to calculate compact test vectors and fault coverage are the same as that of hardness analysis except the second parameter. This parameter requires the number of fault models used in the test approach. The RASP-FIT uses three fault models at this stage of development. Hence, these parameters get value 3. Also, the user needs to provide three files, one for each fault model. In the next work, other fault models are also developed and added to the RASP-FIT tool easily.

It is seen that this RASP-FIT tool is straightforward, easy to use, and it does not require much computer skills to operate it. It validates our claims about the simplicity, ease of use and user-friendly tool.

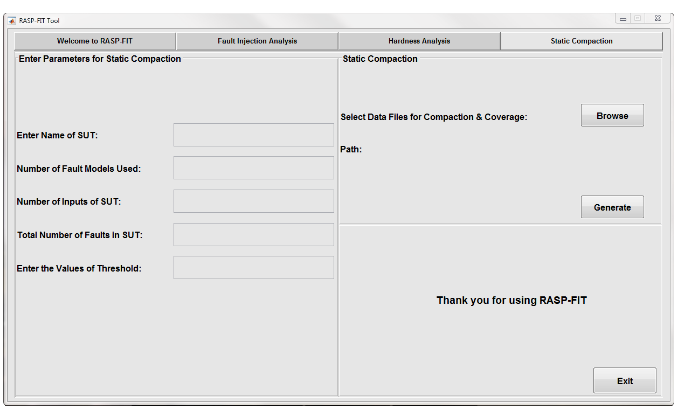

Fig. 6. Static compaction tab.

IV. Result and Discussion

After successful installation of the RASP-FIT tool on the host computer, the user can run it by double click the RASP-FIT icon. Firstly, the tool asks the user to locate the "user-defined-netlist.csv" file, which is provided with the executable file. This file contains the user-defined primitives and functions. There are two columns in the file separated by the semicolon ';'. The first column consists of the name of primitives or task and the second column contains the fault insertion location. When RASP-FIT is run, the contents of the file are read and added to the predefined respective libraries accordingly. For example, the user defines *FD* as a user-defined primitive for a flip-flop with input/output ports in some design, as shown below. Now, the user wants to inject faults in the first three positions.

$$FD \quad fd\_instance(clk, Din, rst, Q, Qn);$$

So, the user needs to define in the "user-defined-netlist.csv" file as follows:

$$FD; [1, 2, 3]$$

The RASP-FIT tool reads the file and adds the *FD* keyword in the file where all primitives are defined, and their positions are concatenated in the library containing positions. When this line of code parsed under RASP-FIT for bit-flip fault model, the output is as follows,

$$FD \quad fd\_inst(f0 \;\hat{}\; clk, f1 \;\hat{}\; Din, f2 \;\hat{}\; rst, Q, Qn);$$

In the above example, f0, f1, f2 represents the bit-flip faults in this line of the code.

The smaller design is considered to illustrate the example for the user-defined primitives or functions. This design is taken from the ISCAS'89 benchmark circuits named 's27.v'. In this design, the user has defined three D-flip-flops as 'dff' as a user-defined-primitive. This user-defined keyword (dff) must be added to the 'user_defined_primitives.csv' file with the desired locations for injection of faults as (dff; [2 3]). The user wants to generate three faulty copies of the design. Therefore, the user needs to provide this file as an input, select fault model (bit-flip in this case) and the number of copies (in this case 3) to the RASP-FIT tool. Fig. 7 shows the original Verilog design with the first faulty copy of the design. It is seen that 'dff' contains only two faults at the positions mentioned above.

After adding the user-defined-netlist file, the RASP-FIT tool can be used for the fault injection modification, fault injection testing, hardness analysis and compaction of test vectors. There are various benchmark designs written in Verilog HDL are considered for these functions. These benchmark designs are ISCAS'85, EPFL designs and some behavioural designs.

V. Conclusion

In this paper, a technical perspective and guidance for the use of this novel tool (RASP-FIT) are presented. It includes the generation of standalone applications in Matlab, installing the RASP-FIT tool on any host computer and usage of the tool for different functions. The RASP-FIT tool can modify the Verilog HDL code for various abstraction levels for fault injection analysis. Also, the tool helps designers and test engineers to perform testing, compaction and hardness analysis. All these functions are used for these fault models (e.g. bit-flip & stuck-at 1/0). The tool is fast, automatic, technology-independent and user-friendly.

```
// s27
// Original design
module s27(GND,VDD,CK,G0,G1,G17,G2,G3);
input GND,VDD,CK,G0,G1,G2,G3;
output G17;

wire G5,G10,G6,G11,G7,G13,G14,G8,G15,G12,
   G16,G9;

dff DFF_0 (CK,G5,G10);
dff DFF_1 (CK,G6,G11);
dff DFF_2 (CK,G7,G13);
not NOT_0 (G14,G0);
not NOT_1 (G17,G11);
and AND2_0 (G8,G14,G6);
or OR2_0 (G15,G12,G8);
or OR2_1 (G16,G3,G8);
nand NAND2_0 (G9,G16,G15);
nor NOR2_0 (G10,G14,G11);
nor NOR2_1 (G11,G5,G9);
nor NOR2_2 (G12,G1,G7);
nor NOR2_3 (G13,G2,G12);
endmodule

// s27
// Faulty Module 1
module s27_1(select,GND,VDD,CK,G0,G1,
   G17_f1,G2,G3);
input GND,VDD,CK,G0,G1,G2,G3;
output G17_f1;
wire G5,G10,G6,G11,G7,G13,G14,G8,G15,G12,
   G16,G9;
input [2:0] select;
wire fis=1;
reg f0,f1,f2,f3,f4,f5,f6,f7;
always @ (select) begin
  if (select == 3'd0) begin
    f0=fis;f1=0;f2=0;f3=0;f4=0;f5=0;f6=0;
       f7=0;end
  else if (select == 3'd1) begin
    f0=0;f1=fis;f2=0;f3=0;f4=0;f5=0;f6=0;
       f7=0;end
  .
  .
  .
  else begin
    f0=0;f1=0;f2=0;f3=0;f4=0;f5=0;f6=0;f7
       =0;end
  end
dff DFF_0 (CK,f0 ^G5,f1 ^G10);
dff DFF_1 (CK,f2 ^G6,f3 ^G11);
dff DFF_2 (CK,f4 ^G7,f5 ^G13);
not NOT_0 (G14,f6 ^G0);
not NOT_1 (G17_f1,f7 ^G11);
and AND2_0 (G8,G14,G6);
or OR2_0 (G15,G12,G8);
or OR2_1 (G16,G3,G8);
nand NAND2_0 (G9,G16,G15);
nor NOR2_0 (G10,G14,G11);
nor NOR2_1 (G11,G5,G9);
nor NOR2_2 (G12,G1,G7);
nor NOR2_3 (G13,G2,G12);
endmodule
```

Fig. 7. Code snippet (original design and modified design).

REFERENCES

[1] M. Kooli and G. Di Natale, "A survey on simulation-based fault injection tools for complex systems," in *2014 9th IEEE International Conference on Design and Technology of Integrated Systems in Nanoscale Era (DTIS)*, (Santorini), pp. 1–6, IEEE, May 2014.

[2] A. Benso and P. Prinetto, *Fault Injection Techniques And Tools For Embedded Systems Reliability Evaluation.* Kluwer Academic Publishers, 2003.

[3] J. Barboza, *Dependability Evaluation of a Critical System by means of Fault Injection Mechanisms.* PhD thesis, 2017.

[4] M. Desogus, L. Sterpone, and D. M. Codinachs, "Validation of a tool for estimating the effects of soft-errors on modern SRAM-based FPGAs," in *2014 IEEE 20th International On-Line Testing Symposium (IOLTS)*, pp. 111–115, IEEE, Jul 2014.

[5] Z. Navabi, *Digital System Test and Testable Design Using HDL Models and Architectures*. Worcester, MA USA: Springer New York Dordrecht Heidelberg London, 2010.

[6] D. Kammler, J. Guan, G. Ascheid, R. Leupers, and H. Meyr, "A Fast and Flexible Platform for Fault Injection and Evaluation in Verilog-Based Simulations," in *2009 Third IEEE International Conference on Secure Software Integration and Reliability Improvement*, pp. 309–314, IEEE, Jul 2009.

[7] V. Sieh, O. Tschache, and F. Balbach, "VERIFY: evaluation of reliability using VHDL-models with embedded fault descriptions," in *Proceedings of IEEE 27th International Symposium on Fault Tolerant Computing*, pp. 32–36, IEEE Comput. Soc, 1997.

[8] H. Ziade, R. Ayoubi, and R. Velazco, "A Survey on Fault Injection Techniques," *The International Arab Journal of Information Technology*, vol. 1, no. 2, pp. 171–186, 2004.

[9] W. Chao, F. Zhongchuan, C. Hongsong, and C. Gang, "FSFI: A Full System Simulator-Based Fault Injection Tool," in *2011 First International Conference on Instrumentation, Measurement, Computer, Communication and Control*, pp. 326–329, IEEE, Oct 2011.

[10] A. Rohani and H. G. Kerkhoff, "Rapid transient fault insertion in large digital systems," *Microprocessors and Microsystems*, vol. 37, pp. 147–154, Mar 2013.

[11] W. Mansour, R. Velazco, R. Ayoubi, H. Ziade, and W. El Falou, "A method and an automated tool to perform SET fault-injection on HDL-based designs," in *2013 25th International Conference on Microelectronics (ICM)*, (Beirut), pp. 1–4, IEEE, Dec 2013.

[12] W. Mansour, M. A. Aguirre, H. Guzman-Miranda, J. Barrientos, and R. Velazco, "Two complementary approaches for studying the effects of SEUs on HDL-based designs," in *2014 IEEE 20th International On-Line Testing Symposium (IOLTS)*, pp. 220–221, IEEE, Jul 2014.

[13] W. Mansour and R. Velazco, "An Automated SEU Fault-Injection Method and Tool for HDL-Based Designs," *IEEE Transactions on Nuclear Science*, vol. 60, pp. 2728–2733, Aug 2013.

[14] M. Shokrolah-Shirazi and S. G. Miremadi, "FPGA-Based Fault Injection into Synthesizable Verilog HDL Models," in *2008 Second International Conference on Secure System Integration and Reliability Improvement*, (Yokohama), pp. 143–149, IEEE, Jul 2008.

[15] W. Mansour and R. Velazco, "SEU Fault-Injection in VHDL-Based Processors: A Case Study," *Journal of Electronic Testing*, vol. 29, pp. 87–94, Feb 2013.

[16] B. Rahbaran, A. Steininger, and T. Handl, "Built-in Fault Injection in Hardware - The FIDYCO Example," in *Second IEEE International Workshop on Electronic Design, Test and Applications*, (Perth, WA, Australia), pp. 327–327, IEEE, 2004.

[17] M. Jeitler, M. Delvai, and S. Reichor, "FuSE - a hardware accelerated HDL fault injection tool," in *2009 5th Southern Conference on Programmable Logic (SPL)*, (Sao Carlos), pp. 89–94, IEEE, Apr 2009.

[18] A. Mohammadi, M. Ebrahimi, A. Ejlali, and S. G. Miremadi, "SCFIT: A FPGA-based fault injection technique for SEU fault model," in *2012 Design, Automation and Test in Europe Conference and Exhibition (DATE)*, (Dresden), pp. 586–589, IEEE, Mar 2012.

[19] L. Naviner, J.-F. Naviner, G. dos Santos, E. Marques, and N. Paiva, "FIFA: A fault-injection–fault-analysis-based tool for reliability assess-

ment at RTL level," *Microelectronics Reliability*, vol. 51, pp. 1459–1463, Sep 2011.

[20] C. Dunbar and K. Nepal, "Using Platform FPGAs for Fault Emulation and Test-set Generation to Detect Stuck-at Faults," *Journal of Computers*, vol. 6, pp. 2335–2344, Nov 2011.

[21] A. R. Khatri, A. Hayek, and J. Börscök, "Validation of the Proposed Fault Injection, Test and Hardness Analysis for Combinational Data-Flow Verilog HDL Designs Under the RASP-FIT Tool," in *2018 IEEE 16th Intl Conf on Dependable, Autonomic and Secure Computing, 16th Intl Conf on Pervasive Intelligence and Computing, 4th Intl Conf on Big Data Intelligence and Computing and Cyber Science and Technology Congress(DASC/PiCom/DataCom/CyberSciTech)*, (Athens, Greece), pp. 544–551, IEEE, Aug 2018.

[22] A. R. Khatri, A. Hayek, and J. Börcsök, "Validation of the Proposed Hardness Analysis Technique for FPGA Designs to Improve Reliability and Fault-Tolerance," *International Journal of Advanced Computer Science and Applications*, vol. 9, no. 12, pp. 1–8, 2018.

[23] A. R. Khatri, A. Hayek, and J. Börcsök, *Applied Reconfigurable Computing*, vol. 9625 of *Lecture Notes in Computer Science*. Cham: Springer International Publishing, 2016.

[24] M. Victoria, O. M. Querin, C. Díaz, and P. Martí, "liteitd a matlab graphical user interface (gui) program for topology design of continuum structures," *Advances in Engineering Software*, vol. 100, pp. 126 – 147, 2016.

[25] A. R. Khatri, A. Hayek, and J. Börcsök, "RASP-FIT: A Fast and Automatic Fault Injection Tool for Code-Modification of FPGA Designs," *International Journal of Advanced Computer Science and Applications*, vol. 9, no. 10, pp. 30–40, 2018.

[26] A. R. Khatri, A. Hayek, and J. Börcsök, "Fault Injection and Test Approach for Behavioural Verilog Designs using the Proposed RASP-FIT Tool," *International Journal of Advanced Computer Science and Applications*, vol. 10, no. 4, pp. 57–63, 2019.

[27] A. R. Khatri, A. Hayek, and J. Börcsök, "ATPG method with a hybrid compaction technique for combinational digital systems," in *2016 SAI Computing Conference (SAI)*, (London, UK), pp. 924–930, IEEE, Jul 2016.

Internet of Things Cyber Attacks Detection using Machine Learning

Jadel Alsamiri[1], Khalid Alsubhi[2]
Faculty of Computing and Information Technology
King Abdulaziz University
Jeddah, KSA

***Abstract*—The Internet of Things (IoT) combines hundreds of millions of devices which are capable of interaction with each other with minimum user interaction. IoT is one of the fastest-growing areas in of computing; however, the reality is that in the extremely hostile environment of the internet, IoT is vulnerable to numerous types of cyberattacks. To resolve this, practical countermeasures need to be established to secure IoT networks, such as network anomaly detection. Regardless that attacks cannot be wholly avoided forever, early detection of an attack is crucial for practical defense. Since IoT devices have low storage capacity and low processing power, traditional high-end security solutions to protect an IoT system are not appropriate. Also, IoT devices are now connected without human intervention for longer periods. This implies that intelligent network-based security solutions like machine learning solutions must be developed. Although many studies in recent years have discussed the use of Machine Learning (ML) solutions in attack detection problems, little attention has been given to the detection of attacks specifically in IoT networks. In this study, we aim to contribute to the literature by evaluating various machine learning algorithms that can be used to quickly and effectively detect IoT network attacks. A new dataset, Bot-IoT, is used to evaluate various detection algorithms. In the implementation phase, seven different machine learning algorithms were used, and most of them achieved high performance. New features were extracted from the Bot-IoT dataset during the implementation and compared with studies from the literature, and the new features gave better results.**

Keywords*—Network anomaly detection; machine learning; Internet of Things (IoT); cyberattacks; bot-IoT dataset

I. Introduction

Concerns over security and privacy regarding computer networks are increasing in the world, and computer security has become a requirement as a result of the spread of information technology in daily life. The raise in the amount of Internet applications and the appearance of modern technologies such as the Internet of Things (IoT) are followed with new and recent efforts to invade computer networks and systems. The Internet of Things (IoT) is a set of interrelated devices where the devices have the ability to connect without the need for human intervention. With IoT, many things that have sensors (such as coffee makers, lights, bicycles, and many others) in areas like healthcare, farming, transportation, etc. can connect to the Internet[1]. By saving time and resources, IoT applications are changing our work and lives. It also has unlimited advantages and opens numerous opportunities for the exchange of knowledge, innovation, and growth.

Every security threat within the Internet exists within the IoT as well because the Internet is the core and center of the IoT. Compared to other traditional networks, IoT nodes have low capacity and limited resources, and do not have manual controls. Also, the rapid growth and broad daily-life adoption of IoT devices makes IoT security issues very troublesome, raising the need to develop security solutions based on networks. While current systems perform well in identifying some attacks, it is still challenging to detect others. As network attacks grow, along with a massive increase in the amount of information present in networks, faster and more effective methods of detection of attacks are required [2] and there is no doubt that there is scope for more progressive methods to improve network security. In this context, in order to provide embedded intelligence in the IoT environment, we can consider Machine Learning (ML) as one of the most effective computational models. Machine learning approaches have been used for different network security tasks such as network traffic analysis [3],[4],[5], intrusion detection[6], and botnet detection [7].

Machine Learning can be described as an intelligent device's ability to modify or automate a knowledge-based state or behavior, which is considered a critical part of an IoT solution. ML has the ability to infer helpful knowledge from data generated by devices or humans, and ML algorithms are used in tasks such as regression, and classification. Likewise, in an IoT network, ML can be used to provide security services. The use of machine learning in attack detection problems is becoming a hotly pursued subject, and ML is being used more and more in different applications in the cybersecurity field. Although many studies in the literature have used ML techniques to discover the best ways to detect attacks, only limited research exists on efficient detection methods suitable for IoT environments.

Machine learning can be applied to the attack detection task via two main types of cyber-analysis: signature-based (sometimes also called misuse- based) or anomaly-based. Signature-based techniques are designed to detect known attacks by using specific traffic characteristics (also known as "signatures") in those attacks. One of the advantages of this class of detection technique is its ability to detect all known attacks effectively without generating an overwhelming number of false alarms. In the literature, some works use signature-based techniques to detect attacks [3], [7]; for instance, in the domain of network traffic analysis, [3] applied four different machine learning techniques as preliminary tools to learn the features of some known attacks. Signature-based techniques were also used in [7] to identify compromised machines by identifying botnet network traffic patterns. The main drawbacks of signature-based approaches are that the efficient use of these approaches requires frequent manual updates of attack traffic signatures and that these approaches cannot detect previously unknown attacks. The second class of detection methods is anomaly-based detection. This class models normal network behavior, and anything abnormal is considered an attack. The ability of this class to detect unknown attacks makes it appealing to use. The essential issue with anomaly-based techniques is the possibility of high false alarm rates (FARs), as previously unknown (even though legal) behaviors can be considered as anomalies. Signature and anomaly detection techniques can be combined as a hybrid technique. One of the hybrid technique examples is presented in [8] where this technique is used to increase the detection rates of known attacks and reduce the false positive (FP) rate for unknown attacks.

In this study, we contribute to the literature as part of a defense against IoT attack behavior by investigating the efficacy of using machine learning approaches to detect IoT network attacks. The detection algorithms are evaluated using a recent dataset, Bot-IoT, that combines legitimate and simulated IoT network traffic along with different types of attacks [9]. Using the Random Forest Regressor algorithm, features were selected from this dataset. In the implementation phase, seven different machine learning algorithms were used, and high performance achieved. The following are the machine learning algorithms that we used: K-nearest neighbours (KNN), ID3 (Iterative Dichotomiser 3),Quadratic discriminant analysis (QDA), Random Forest, AdaBoost, Multilayer perceptron (MLP), and Naıve Bayes (NB).

We can summarize our contributions through this research as:

- Improvement in attack detection in IoT networks by evaluating the performance of machine learning algorithms on a recent IoT dataset.
- Extract new features from the dataset and select the most appropriate features to improve machine learning algorithm performance.
- Contribute to the IoT literature. Since the number of studies done with the Bot-IoT dataset are still few, working with this dataset could be considered to be a possible significant contribution to the literature.

The remainder of the paper is organized as follows: Section II we review related work and discuss the background in this domain; Section IV show our proposed approach, followed by the implementation details in Section V. Experimental results with evaluations are presented in Section VI; and finally, we conclude this paper with a summary in Section VII.

II. Related Work

The domain of using machine learning has been extensively researched in the past [6], and several scholarly papers on intrusion detection by data-mining techniques and machine intelligence have been published [10]. However, most of these prior studies have only used machine learning techniques for intrusion detection in traditional networks. We are therefore extending this area of research in this study by specifically applying machine learning to detect attacks in the context of IoT. The application of machine learning techniques to the IoT field is still in the early stages of research, specifically in IoT security, but it has a huge possibility to discover insights from IoT data [11]. In IoT networks, machine learning principles like pattern recognition, anomaly detection, and behavioral analysis can be used to detect potential attacks and stop abnormal behaviors.

To review recent research on the topic of attack detection using machine learning in IoT networks, we examined various studies and summarized them in Table I. In each study, the machine learning algorithms, datasets, and detection approaches are given. When selecting these studies, we focused on the use of different machine learning algorithms and datasets. The studies provide evidence that machine learning techniques can achieve success for attack detection. From the works discussing the issue of using machine learning for IoT security, the detection methodologies can be categorized as unsupervised methods [10], [12], [13], [14] and supervised methods [15], [16], [17], [9], [18].

Many studies have indicated that machine learning techniques can be applied to support attack detection tasks, including kmeans, artificial neural networks (ANNs), Random Forest (RF), auto-encoder, and others, and several authors have applied unsupervised machine learning algorithms for detection problems. Auto-encoders are some of the most significant unsupervised algorithms that have been used in many works; for example, Mirsky et al. [10] proposed the use of autoencoders to extract features from datasets in order to improve the detection of cyber threats. They introduced Kitsune, which is an unsupervised network intrusion detection system that has ability to learn to detect attacks on networks efficiently. Kitsune's main algorithm (KitNET) uses a set of neural networks, known as autoencoders, to distinguish between normal and anomalous traffic patterns. In [12], Meidan et al. proposed and evaluated a novel detection method that extracts behavioral snapshots from the network and also uses auto-encoders to detect abnormals network traffic from compromised devices. The major drawback of using unsupervised machine learning algorithms for detection problems is that in network traffic, most of the flows are normal and anomalies like attacks and outliers are rare, which negatively affects success rates and the detection of anomalies. For this reason, better results are expected with supervised techniques. On the other hand, many supervised learning algorithms are used to detect attacks and are trained on datasets with labels indicating whether the instances have been pre-classified as attacks or not. In [19], Elike Hodo used ANN and Support Vector Machine algorithms to detect non-Tor traffic attack by using ML techniques on UNBCIC datasets. In order to accurately identifying IoT device types from the whitelist In [15], Random Forest algorithm, was applied to features extracted from network traffic data. A recent work that has a similar approach to our study was presented by Moustafa et al. [9] in the original paper which proposed the Bot-IoT dataset. They used LSTM, SVM, and RNN machine learning models to evaluate the IoT dataset, but in their analysis they did not determine the adversarial robustness of their models. In our work, while we use the same Bot-IoT dataset presented in [9], we focus on extracting new features from the dataset and evaluating different machine learning algorithms on this dataset. [22] is another study that used the BoT-IoT dataset.

TABLE I. SUMMARY OF RELATED STUDIES

Ref.	Year	Detection approach		Machine learning algorithms used							Data For Evaluation
		Signature	Anomaly	Supervised approaches						Unsupervised	
				ANN	RF	SVM	NB	AdaBoost	LSTM		
[9]	2018		✓	✓		✓			✓		Bot-IoT
[10]	2018		✓							✓	Real dataset
[8]	2016	✓									Simulated dataset
[12]	2018		✓							✓	N-BaIoT dataset
[14]	2019		✓							✓	CICIDS2017-Simulated dataset-Bot-IoT
[19]	2016		✓	✓							Simulated dataset
[13]	2017		✓							✓	KDD /DARPA
[20]	2015		✓								Real dataset
[15]	2017	✓			✓						Real dataset
[21]	2018		✓	✓							Real dataset
[18]	2018		✓			✓					Simulated dataset
[16]	2017		✓	✓	✓		✓				USNW-NB15
[22]	2019		✓	✓							Bot-IoT
[23]	2019		✓					✓			Real dataset
[24]	2019		✓				✓				Bot-IoT
[17]	2019	✓		✓							Bot-IoT

They compared the Self-normalizing Neural Network (SNN) performance with the FNN for classifying intrusion attacks in an IoT network. Based on multiple performance metrics in this experiments , the FNN outperformed the SNN in their experimental results for intrusion detection in IoT networks, offering a bright future in the search of secure deep learning in IoT networks. Ferrag, in [14], used the Bot-IoT dataset to evaluate the DeepCoin framework's performance in traffic generated by IoT. DeepCoin is a novel deep learning and blockchain-based energy framework. Through performance evaluations using the Bot-IoT dataset, they demonstrated the efficiency of the proposed DeepCoin framework. In other research, the authors of [17] used the BoT-IoT dataset to generate the rules for IoT-IDS. They used J48, machine learning algorithms for generating effective rules to support lightweight IDS systems appropriate for IoT devices.

III. PROPOSED APPROACH

This section provides a brief description of the dataset used and our proposed approach to detect attacks in IoT networks. In our proposed approach, various pre-processing and actual applications are performed to detect anomalies by machine learning techniques. First, flow-based features from the raw dataset were extracted by CICFlowMeter [25]. Then, the data pre-processing process was performed in the first step before dividing the dataset into two parts: training and test. Data pre-processing is required to transform the data into a format usable by machine learning algorithms. After these operations, the properties to be used by the algorithms are decided in the feature selection step. Finally, our approach ends with the implementation of machine learning algorithms. An overview of the proposed approach is presented in Fig. 1.

We selected the Bot-IoT dataset for the experiments because of its regular updates, wide attack diversity, inclusion of IoT-generated traffic, and ability to generate new features from the raw dataset. The Bot-IoT dataset [10] was created in the Cyber Range Lab at the Australian Centre for Cyber Security (ACCS). This dataset has three main kinds of attacks, which are based on botnet scenarios such as Probing, DoS, and Information Theft. We used CICFlowMeter to extract flow-based features from the raw traffic traces. CICFlowMeter [26] is a network traffic flow generator distributed by CIC to generate 84 network traffic features.

IV. IMPLEMENTATION

As already noted in the previous sections, the major objective of the experiments is to evaluate the performance of machine learning algorithms in detecting IoT network attacks. In this section, we describe the dataset, machine learning algorithms that we used and present our implementation steps.

A. Datasets

Since the applications for various network security tasks use machine learning methods, large datasets are needed to analyze network flows and distinguish between normal and abnormal traffic. Over the years, several experiments have been conducted to generate network datasets. As shown in Table I, most of the studies using machine learning have tested their work against simulated or real network data. Although a good number of those datasets remain private, primarily due to security concerns, some have become publicly available such as DARPA 98, KDD99, UNSW-NB15, ISCX, CICIDS2017, and N-BaIoT. Although several datasets have been produced, however, the development of realistic IoT and network traffic datasets that include new Botnet scenarios are still few. More importantly, some datasets lack the inclusion of IoT-generated traffic, while others neglect to generate any new features. In some cases, the testbed used was not realistic, while in other cases, the attack scenarios were not diverse enough. For instance, in [12], Meidan et al. created a publicly available IoT dataset named N-BaIoT, and many later studies used this dataset for training and to test their classifier models. While this dataset is relatively large and clean, it is unbalanced, and the ratio of normal data is much lower compared to attack data. Moustafa et al. [9] sought to address the shortcomings by designing the Bot-IoT dataset, which we used for our experiments. The Bot-IoT dataset incorporates legitimate and simulated IoT network traffic along with various types of attacks[14]. The BotIoT database attacks are classified into three types: Probing attacks, DoS, and theft information theft.

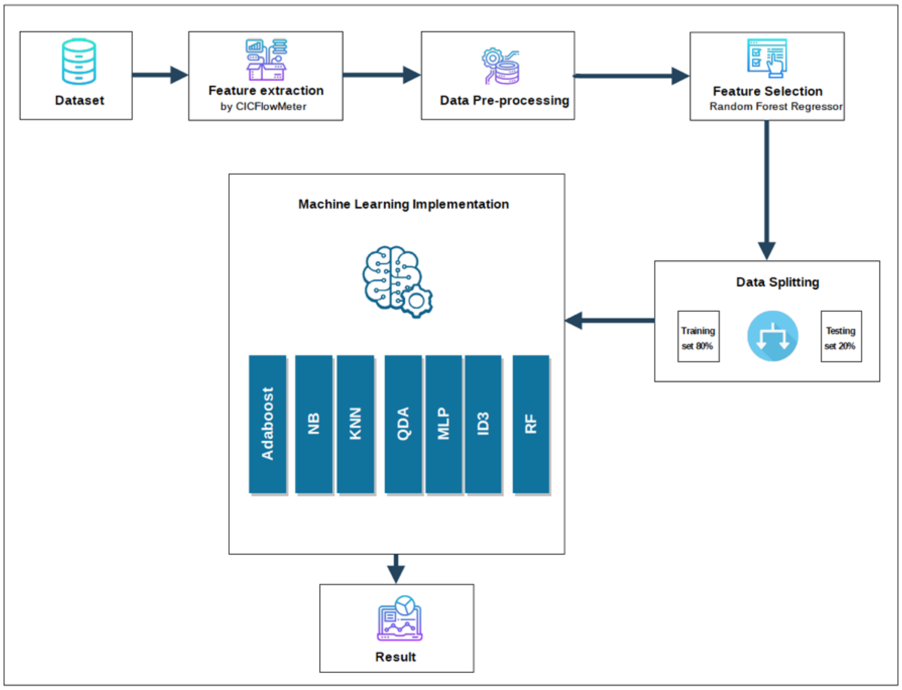

Fig. 1. Proposed Approach Overview.

B. Machine Learning Algorithms

We used the Bot-IoT dataset to evaluate seven well known machine learning classifiers: (K-Nearest Neighbours (KNN), ID3 (Iterative Dichotomiser 3), Random Forest, AdaBoost, Quadratic discriminant analysis (QDA), Multilayer perceptron (MLP), and Naıve Bayes (NB). When choosing these classifiers, the focus is on bringing together popular algorithms with different characteristics. In this context, the algorithms used are briefly examined in the following.

- **K-Nearest Neighbours(KNN):** KNN is one of the simplest and most effective supervised learning algorithm. It is used for searching through the available dataset to associate new data points with similar existing points [24]. KNN, which provides good performance over multidimensional data and is a fast algorithm during the training phase, is relatively slow in the estimation stage.

- **Quadratic discriminant analysis (QDA):** QDA is an ideal algorithm to supervised classification problems. Discriminant analysis is a statistical technique for assigning measured data to one group among many groups. QDA is appropriate to situation where a category is not characterized by much data. In order to be able to apply Quadratic Discriminant Analysis, the number of samples observed must be greater than the number of groups.

- **Iterative Dichotomiser 3(ID3):** ID3 is an algorithm used to create a decision tree from a dataset. It was developed by Ross Quinlan [27]. A decision tree is an algorithm for classification that uses a tree-like decision structure. It is one way to display an algorithm that only contains conditional control statements. The attributes are used as the tree nodes and the criteria are constructed so as to guide from one node to another, with the “leaves” being the class values allocated to the record [16]. ID3 is usually used in the domains of machine learning and natural language processing, and it is the precursor of the C4.5 algorithm.

- **Random Forest(RF):** RF is a machine learning approach that uses decision trees. In this method, a “forest” is created by assembling a large number of different decision tree structures that are formed in different ways[28]. This algorithm has many advantages, such as the ability run on huge datasets efficiently, its light weight compared to other methods, and robustness against noise and outliers when compared to single classifiers.

- **Adaptive Boosting (AdaBoost):** AdaBoost is a machine learning algorithm that focuses on classification issues and tries to convert weak classifiers into efficient ones. It was first proposed by Freund and Schapire in 1996, and can be used in conjunction with many other types of learning algorithm to improve performance. The most important characteristic of the AdaBoost algorithm is its capability to deal with missing values in a dataset.

- **Multilayer Perceptron (MLP):** MLP is a class of feedforward artificial neural network (ANN). Artificial neural networks (ANNs) are a machine learning method that takes inspiration from the way the human brain works, like learning and deriving new information. An MLP include no less than three layers: an input,output and hidden layer. MLP utilizes a

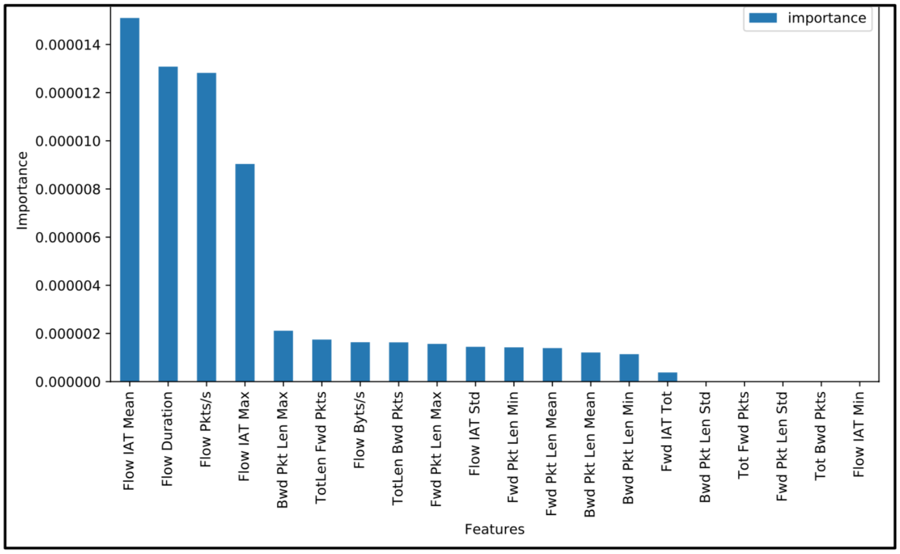

Fig. 2. Graph of Feature Importance of entire dataset

supervised learning technique called back-propagation for training.

- **Naïve Bayes(NB):** The NB is a widely used supervised algorithm, and is famous for its simple principles. The Naïve Bayes method is based on the work of Thomas Bayes [29]. For instance, NB might be utilized to categorize traffic as normal or anomalous for intrusion detection. The traffic classification features used are handled independently by the NB classifier despite the fact that these features may depend on each other. Many attributes make NB user-friendly, like its simplicity, low sample requirement, and ease of implementation[27]. On the other hand, NB deals with features independently and is therefore unable to obtain valuable information from the communication and relationships between features.

C. Implementation Steps

Our method consists of five essential steps:: Feature extraction, data pre-processing, Splitting data, feature selection, and implementation of machine learning algorithms.

- **Feature Extraction:** CICFlowMeter [25] was used to extract flow-based features (in pcap format) from raw network traffic data. CICFlowMeter is a network traffic flow generator distributed by CIC that produces 84 network traffic characteristics. It reads the pcap file and produces a visual document of the features extracted, and also offers a csv file of the dataset. This process was primarily designed to improve classifiers' predictive capabilities by extracting new dataset features.

- **Data pre-processing:** Pre-processing data transformation operations are used to transform the dataset into a structure suitable for machine learning. This step also includes cleaning the dataset by removing irrelevant or corrupted data that can affect the accuracy of the dataset, which makes it more efficient.

- **Splitting Data:** During the machine learning process, data are needed so that learning can take place. In addition to the data required for training, test data are needed to evaluate the performance of the algorithm in order to see how well it works. In our study, we considered 80% of the Bot-IoT dataset to be the training data and the remaining 20% to be the testing data.

- **Feature Selection:** It is significant to decrease the count of features and just use the features needed to train and test the algorithms to find a lightweight security solution appropriate for IoT systems [13]. We used the Random Forest Regressor algorithm as features selection technique. The random forest regressor has been proven to be an effective method of reducing the dimensions of a dataset. Decreasing the input data features from more than 80 network traffic features to 7 makes the model train and respond more quickly. The features' importance weights for the full dataset are shown in Fig. 2.

- **Implementation of Machine Learning Algorithms:** All the experiments were done in Python by relying on Python machine learning libraries (scikit-learn, Matplotlib, Pandas, and NumPy). We organised the evaluation of machine learning algorithms for the dataset in three phases: applying the proposed algorithms on each attack in the dataset separately; applying the algorithms on the entire dataset with a set of features combining the best features for each attack (the list of these features can be seen in Table II); and applying the algorithms on the entire dataset with the seven best features obtained in the feature selection step.

TABLE II. THE FEATURE LIST CREATED FOR ALL ATTACK TYPES

Flow IAT Mean	Flow Duration	Flow Pkts/s
Flow IAT Max	Fwd Pkt_Len_Max	TotLen Fwd Pkts
Fwd Pkt Len Mean	Tot Bwd Pkts	Fwd IAT Tot
Flow IAT Std	Flow Bytss	Tot Fwd Pkts
Flow IAT Min		

V. EVALUATION

A. Evaluation Metrics

When evaluating the performance of machine-learning models, it is crucial to define performance measures that are suitable for the task to be solved. In order to evaluate our results, we used the most important performance indicators for accuracy, precision, f-measure, and recall, as shown in the equations below:

$$Precision = \frac{TP}{TP + FP} \tag{1}$$

$$Recall = \frac{TP}{TP + FN} \tag{2}$$

$$Accuracy = \frac{TP + TN}{TP + FP + TN + FN} \tag{3}$$

$$F - measure = \frac{2}{\frac{1}{Recall} + \frac{1}{Precision}} \tag{4}$$

B. Results

As stated in the previous section, we organised the evaluation of machine learning algorithms for the dataset in three phases, as follows. Phase 1: applying machine learning algorithms on each attack in the dataset separately; Phase 2: applying machine learning algorithms on the entire data set with a set combining the best features for each attack; and Phase 3: applying machine learning algorithms on the entire dataset with the best seven features obtained in the feature selection step. The results of all the experiments are given in the following tables. The performance evaluation procedures were repeated 10 times for each machine learning algorithm, and the numbers given in the tables are the arithmetic means of these 10 processes.

Phase 1: applying machine learning algorithms on each attack in the dataset separately. Seven different machine learning methods are applied to 10 different attack types, and the results are presented in Table III. In the results of the algorithms, if there is an equality in the F-measure, the following values are examined in order to eliminate equality: precision, accuracy, recall, and time.

When observing the results in Table III, it can be noted that all the algorithms, except the Naive Bayes (NB) and Quadratic algorithm(QDA), achieved over 90% success in detecting almost all attack types. The ID3 algorithm was the most successful algorithm, completing 6 out of 10 tasks (DDOS-HTTP, DDOS-UDP, DOS-HTTP, DOS-TCP, Data exfiltration, and Service scan) with the highest score. In fact, for all the tasks, ID3 shares its highest score with at least one other algorithm. However, low processing time puts it ahead of the other algorithms. The last algorithm used in all tasks was Naive Bayes, the lowest F-measure algorithm. Especially with the DOS TCP attack, it had a fairly low score. Even though Naive Bayes performed worse than the other algorithms, it was much better than the alternatives when it came to speed. However, it is also necessary to mention the QDA here, because the QDA had the second-worst performance among the algorithms.

TABLE III. DISTRIBUTION OF RESULTS ACCORDING TO TYPE OF ATTACK

	F-Measures						
Attack Names	**NB**	**QDA**	**RF**	**ID3**	**AB**	**MLP**	**KNN**
DDOS_HTTP	*0.72*	0.85	0.96	**0.96**	0.96	0.95	0.96
DDOS_UDP	*0.73*	0.92	0.98	**0.98**	0.98	0.97	0.98
DDOS_TCP	*0.71*	0.85	0.99	0.99	**1.0**	0.74	0.99
DOS_HTTP	*0.72*	0.82	0.95	**0.96**	0.95	0.95	0.96
DOS_UDP	*0.72*	0.83	0.97	0.97	**0.98**	0.98	0.97
DOS_TCP	*0.64*	0.74	1.0	**1.0**	1.0	0.78	0.99
Data exfiltration	*0.72*	0.76	0.96	**0.97**	0.97	0.94	0.97
Keylogging	*0.72*	0.82	0.95	0.95	0.95	0.91	**0.98**
Service_Scan	*0.73*	0.83	0.95	**0.95**	0.95	0.94	0.94
OS_Scan	*0.72*	0.76	0.94	0.97	0.98	0.97	**0.99**

Phase 2: applying machine learning algorithms on the entire dataset with a set of features the combined the best features for each attack. The whole dataset is used in this phase. Seven different methods of machine learning were implemented on the entire dataset, and we used feature sets that were extracted for each attack separately. Table IV shows the results obtained by using 13 features extracted for the attacks.

TABLE IV. IMPLEMENTATION OF FEATURES OBTAINED FROM PHASE1

ML Algorithm	Accuracy	Precision	Recall	F-Measure	Time
NB	0.78	0.84	0.78	*0.75*	**5.056**
QDA	0.88	0.89	0.88	0.87	6.1964
RF	0.98	0.98	0.98	0.98	27.0328
ID3	0.99	0.99	0.99	0.99	19.3447
Adaboost	1.0	1.0	1.0	**1.0**	308.9403
MLP	0.84	0.88	0.84	0.83	1011.5001
KNN	0.99	0.99	0.99	0.99	*2052.1801*

When observing Table IV, it can be seen that Adaboost was the best performance algorithm, followed by KNN and ID3. ID3 is noticeably faster than KNN, so it takes precedence with this feature. The lowest scoring algorithm was Naive Bayes, with a score of 0.75. From the speed perspective, NB and QDA were the fastest. Although KNN had a high performance score, it was still noticeably slower than the other algorithms.

Phase 3: applying machine learning algorithms on the entire data set with the seven best features obtained in the feature selection step.

From the F-measure perspective, there was no significant change in the algorithms' performance, but from the speed perspective, the running times of all the algorithms were noticeably reduced. The reason for this reduction in execution time is that 13 attributes are used in the method applied in Table V, whereas only 7 attributes are used in Table IV. This reduction in the feature count reduced the running time of the machine learning algorithms.

TABLE V. IMPLEMENTATION OF FEATURES OBTAINED USING RANDOM FOREST REGRESSOR FOR ALL DATASET

ML Algorithm	Accuracy	Precision	Recall	F-Measure	Time
NB	0.79	0.85	0.79	*0.77*	**4.0472**
QDA	0.87	0.89	0.87	0.86	4.4056
RF	0.97	0.97	0.97	0.97	28.9246
ID3	0.97	0.97	0.97	0.97	17.0899
Adaboost	0.97	0.97	0.97	0.97	238.8618
MLP	0.84	0.87	0.84	0.83	949.6977
KNN	0.99	0.99	0.99	**0.99**	*1615.9852*

The final results of the implementation (see Table VI) are compared with a study in the literature. For this comparison, the study conducted by Ferrag et al. [14] in 2019 was chosen. The reason for this is that the mentioned work used the same dataset as well as two machine learning methods similar to the ones we used. These similar machine learning algorithms are Random Forest and Naive Bayse. The key difference between our work and theirs is the feature set used. They used the original feature set while we used a new feature set extracted by CICFLOWMETER. The detection rate (Recall) was determined as the main evaluation criterion. Table VI shows the comparison of the results obtained from the two studies. When the results are examined, it can be seen that the Random Forest algorithm used in our study is higher than that used in [14], and the same thing can be seen for most attack types with the NB algorithm. So, we can see that the new features used in our work increased the performance of both algorithms.

TABLE VI. COMPARISON OF PERFORMANCE OF THE TWO ALGORITHMS

Attack Names	Ferrag et al[14]		Our Work	
	RF	NB	RF	NB
DDOS_HTTP	82.26%	50.78%	96%	71%
DDOS_TCP	88.28%	78.67%	99%	70%
DDOS_UDP	55.26%	78.50%	98%	72%
DOS_HTTP	82.20%	68.68%	95%	71%
DOS_TCP	81.77%	65.56%	100%	63%
DOS_UDP	82.99%	100%	97%	71%
Data exfiltration	86.55%	66.55%	96%	71%
Keylogging	70.12%	65.62%	95%	71%
OS_Scan	82.20%	68.68%	94%	70%
Service_Scan	69.82%	65.21%	95%	72%

VI. CONCLUSION

This paper has aimed to detect IoT network attacks by using machine learning methods. In this context, the Bot IoT [9] was used as a dataset because of its regular updates, wide attack diversity, and various network protocols. We used CICFlowMeter[25] to extract flow-based features from the raw traffic traces. CICFlowMeter generates 84 network traffic features of the dataset which define the network flow. During the implementation, the importance of weight calculations were made with the Random Forest Regressor algorithm to decide which of the features would be used in the machine learning methods. Two approaches were used when making these calculations. In the first approach, the importance weights were calculated separately for each attack type, and in the second approach, all the attacks were collected in a single group and the importance weights for this group were calculated; i.e., the common properties that were important for all attacks were determined. Finally, seven machine learning algorithms which are widely used and have different qualities were applied to the data. These algorithms and the achieved performance ratios according to F-measure are as follows: F-measure had a value between 0 and 1; Naive Bayes was 0.77; QDA was 0.86; Random Forest was 0.97; ID3 was 0.97; AdaBoost was 0.97; MLP was 0.83; and K Nearest Neighbours was 0.99.

In this research we investigated seven supervised algorithms. As a future work ,it would be interesting to evaluate the performance of some unsupervised algorithms. Furthermore, we applied various machine learning algorithms independently from each other. In the future, we sould like to combine different machine learning algorithms as a multi-layered model to improve the detection performance.

ACKNOWLEDGMENT

The computations for the work presented in this paper were supported by the KAU High Performance Computing Center (Aziz Supercomputer) (http://hpc.kau.edu.sa)

REFERENCES

[1] J. Deogirikar and A. Vidhate, "Security attacks in iot: A survey," *International Conference on I-SMAC (I-SMAC)*, pp. 32–37, 2017.

[2] T. Bodström and T. Hämäläinen, "State of the art literature review on network anomaly detection with deep learning," *Internet of Things, Smart Spaces, and Next Generation Networks and Systems*, pp. 64–76, 2018.

[3] I. Arnaldo, A. Cuesta-Infante, A. Arun, M. Lam, C. Bassias, and K. Veeramachaneni, "Learning representations for log data in cybersecurity," *International Conference on Cyber Security Cryptography and Machine Learning*, pp. 250–268, 2017.

[4] M. Du, F. Li, G. Zheng, and V. Srikumar, "Deeplog: Anomaly detection and diagnosis from system logs through deep learning," *Proceedings of the 2017 ACM SIGSAC Conference on Computer and Communications Security*, pp. 1285–1298, 2017.

[5] B. J. Radford, B. D. Richardson, and S. E. Davis, "Sequence aggregation rules for anomaly detection in computer network traffic," *arXiv preprint arXiv:1805.03735*, 2018.

[6] I. Lambert and M. Glenn, "Security analytics: Using deep learning to detect cyber attacks," 2017.

[7] M. Stevanovic and J. M. Pedersen, "Detecting bots using multi-level traffic analysis." *IJCSA*, vol. 1, no. 1, pp. 182–209, 2016.

[8] H. Sedjelmaci, S. M. Senouci, and M. Al-Bahri, "A lightweight anomaly detection technique for low-resource iot devices: A game-theoretic methodology," *IEEE International Conference on Communications (ICC)*, pp. 1–6, 2016.

[9] N. Koroniotis, N. Moustafa, E. Sitnikova, and B. Turnbull, "Towards the development of realistic botnet dataset in the internet of things for network forensic analytics: Bot-iot dataset," *Future Generation Computer Systems*, vol. 100, pp. 779–796, 2019.

[10] Y. Mirsky, T. Doitshman, Y. Elovici, and A. Shabtai, "Kitsune: an ensemble of autoencoders for online network intrusion detection," *arXiv preprint arXiv:1802.09089*, 2018.

[11] X. Yuan, C. Li, and X. Li, "Deepdefense: identifying ddos attack via deep learning," *IEEE International Conference on Smart Computing (SMARTCOMP)*, pp. 1–8, 2017.

[12] Y. Meidan, M. Bohadana, Y. Mathov, Y. Mirsky, A. Shabtai, D. Breitenbacher, and Y. Elovici, "N-baiot—network-based detection of iot botnet attacks using deep autoencoders," *IEEE Pervasive Computing*, vol. 17, no. 3, pp. 12–22, 2018.

[13] M. K. Putchala, "Deep learning approach for intrusion detection system (ids) in the internet of things (iot) network using gated recurrent neural networks (gru)," 2017.

[14] M. A. Ferrag and L. Maglaras, "Deepcoin: A novel deep learning and blockchain-based energy exchange framework for smart grids," *IEEE Transactions on Engineering Management*, 2019.

[15] Y. Meidan, M. Bohadana, A. Shabtai, M. Ochoa, N. O. Tippenhauer, J. D. Guarnizo, and Y. Elovici, "Detection of unauthorized iot devices using machine learning techniques," *arXiv preprint arXiv:1709.04647*, 2017.

[16] N. Koroniotis, N. Moustafa, E. Sitnikova, and J. Slay, "Towards developing network forensic mechanism for botnet activities in the iot based on machine learning techniques," *International Conference on Mobile Networks and Management*, pp. 30–44, 2017.

[17] Y. N. Soe, Y. Feng, P. I. Santosa, R. Hartanto, and K. Sakurai, "Rule generation for signature based detection systems of cyber attacks in iot environments," *Bulletin of Networking, Computing, Systems, and Software*, vol. 8, no. 2, pp. 93–97, 2019.

[18] V. H. Bezerra, V. G. T. da Costa, S. B. Junior, R. S. Miani, and B. B. Zarpelao, "One-class classification to detect botnets in iot devices," *Anais do XVIII Simpósio Brasileiro em Segurança da Informação e de Sistemas Computacionais*, pp. 43–56, 2018.

[19] E. Hodo, X. Bellekens, A. Hamilton, P.-L. Dubouilh, E. Iorkyase, C. Tachtatzis, and R. Atkinson, "Threat analysis of iot networks using artificial neural network intrusion detection system," *International Symposium on Networks, Computers and Communications (ISNCC)*, pp. 1–6, 2016.

[20] D. H. Summerville, K. M. Zach, and Y. Chen, "Ultra-lightweight deep packet anomaly detection for internet of things devices," *IEEE 34th international performance computing and communications conference (IPCCC)*, pp. 1–8, 2015.

[21] F. Y. Yavuz, "Deep learning in cyber security for internet of things," Ph.D. dissertation, 2018.

[22] O. Ibitoye, O. Shafiq, and A. Matrawy, "Analyzing adversarial attacks against deep learning for intrusion detection in iot networks," *arXiv preprint arXiv:1905.05137*, 2019.

[23] I. Cvitić, D. Peraković, M. Periša, and M. Botica, "Novel approach for detection of iot generated ddos traffic," *Wireless Networks*, pp. 1–14, 2019.

[24] Z. A. Baig, S. Sanguanpong, S. N. Firdous, T. G. Nguyen, C. So-In *et al.*, "Averaged dependence estimators for dos attack detection in iot networks," *Future Generation Computer Systems*, vol. 102, pp. 198–209, 2019.

[25] A. H. Lashkari, G. Draper-Gil, M. S. I. Mamun, and A. A. Ghorbani, "Characterization of tor traffic using time based features." *ICISSP*, pp. 253–262, 2017.

[26] S. Yu, "Study on the internet of things from applications to security issues," *International Conference on Cloud Computing and Security*, pp. 80–89, 2018.

[27] S. B. Kotsiantis, I. Zaharakis, and P. Pintelas, "Supervised machine learning: A review of classification techniques," *Emerging artificial intelligence applications in computer engineering*, vol. 160, pp. 3–24, 2007.

[28] K. Kostas, "Anomaly detection in networks using machine learning," Ph.D. dissertation, 08 2018.

[29] M. Panda and M. R. Patra, "Network intrusion detection using naive bayes," *International journal of computer science and network security*, vol. 7, no. 12, pp. 258–263, 2007.

UAV Path Planning for Civil Applications

IDALENE Asmaa[1], BOUKHDIR Khalid[2], and MEDROMI Hicham[3]

[1,2,3]Research and Engineering Laboratory LRI, National School of Electricity and Mechanics Casablanca, Morocco
[1]Pluridisciplinary Laboratory of Research and Innovation (LPRI), EMSI Casablanca, Morocco

***Abstract*—We will present a simple and efficient algorithm for solving the path planning problem for civil UAV operating in a dynamic or incomplete environment. This algorithm searches for a continuous waypoints sequence starting from the initial configuration, visiting all the desired locations and reaching the final position. We will present our proposed algorithm on two steps: The first produces a sorted location set. The second step generates an optimal path for the overall mission. The same algorithm constructs the initial path or re-plans a new one when changes occur to the configuration space. To prove the effectiveness of our proposed algorithm, we will provide computer simulations. A comparison of many results will show that this algorithm yields good experience performance over a wide variety of examples.**

Keywords*—*Unmanned Aerial Vehicle (UAV); path planning; path re-planning; computer simulation

I. Introduction

In recent years, the interest in using Unmanned Aerial Vehicle (UAV) systems for civil purposes has been growing [1], [2], [3], [4]. Civil UAVs are expected to perform autonomously complex tasks. They are used in many applications such as delivery [5], security, surveillance, reconnaissance, tracking [6], inspection [7], monitoring [8]. This increase is thanks mainly to their capacity to fly, their ease of deployment, their low cost, their high mobility, their fast speed, and their ability to collect and send data.

The main challenge to be addressed in the development of civil UAV is path planning [9], [10]. The path planning problem involves computing an appropriate waypoint sequence that enables the UAV to reach the desired targets while avoiding both obstacles and No-Fly Zones [11].

In the case of civil UAV, a good path planning algorithm must fit an optimal path through a set of locations. The generated waypoints sequence should be of a minimal length and also satisfy the aircraft's constraints [12], [13]. The path planning algorithm must solve the planning problem in high-dimensional configuration spaces. It should generate collision-free motions in a 3D workspace [14]. The path planning algorithm must be compatible with the cooperative UAV mission. A complex mission might involve multiple UAVs performing different tasks [15]. The path planning algorithm is expected to be coded in software that runs on the UAV system. It must be computationally efficient. As well as, it should enable the UAV to re-plan its path when a new event occurs [16].

This paper presents a new method for resolving the path planning problem for UAVs operating in the civil domain. Our method produces a path that enables the UAV to visit the desired locations while avoiding obstacles and No-Fly Zone.

This method offers the advantage of finding a fast path of minimal length. It involves two steps: the first step sorts the desired locations according to their distance from the initial position. The second step uses the result of the first one, then computes the free-collision path based on the obstacle's corner.

Furthermore, we present a re-planning algorithm for repairing the initial path if new events occur to the configuration space. Instead of abandoning the invalid solution, our re-planning method determines, removes and repairs the invalid parts, and maintains the rest. This method offers the advantage of searching for a new solution based on recomputing just the path's sections that are no longer valid.

Moreover, we provide computer simulations to confirm the effectiveness of our proposed algorithm. Also, we show a comparison of many results to prove that this algorithm yields good experience performance over a wide variety of examples.

We organize our paper as follows: in the second section, we will present the path planning problem for civil UAVs. We will outline the proposed path planning solution in the third section. In the case of dynamic or incomplete configuration space, the fourth section explains our re-planning algorithm for repairing an invalid path. Section five will show a comparison of many simulations. In section six, we will explain our motivation behind this paper. Finally, we will present a brief conclusion of this work in section seven.

II. Path Planning Problem Formula

The simplest way to represent a mission for civil UAV can be generalized as visiting a set of locations, in which the UAV executes given tasks. Typically, a mission plan defines a set of waypoints and targets [11]. A waypoint represents a simple position to be visited. While a target specifies a location and defines a task command to be executed at this location. For example, a task command can be taking an image, doing a simple take-off, or operating a specific payload.

Fig. 1 illustrates an example of an operating environment of civil UAVs. Starting from the initial point (the red point), the UAV should visit all the targets (the cyan point) and then go to the goal point (the blue point). This environment is enclosed and contains either a set of obstacles or No-Fly zones. Each of which is represented by a simple rectangle (see Fig. 1).

Given the six components presented below:

- w_i : a particular configuration in the UAV's environment.
- w_{init}: the initial configuration of the UAV.
- w_{final}: the final configuration of the UAV.

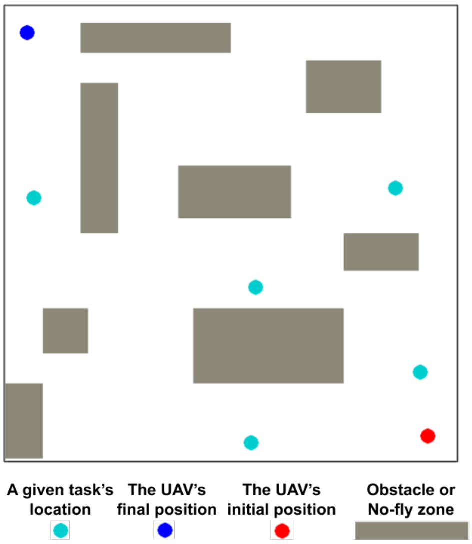

Figure 1. The path planning problem formula

- L_G : a set of target. A target represents a location to be visited by UAV.
- C_{space}: the configuration space.
- $C_{obstacle}$: the obstacle space.
- C_{free}: the free space.

The problem of computing an optimal path planning for civil UAV consists of searching for a continuous waypoint sequence (i.e., an sorted set of w_i) from w_{init} to w_{final} that reaches all the task's locations defined in L_G. Every two successor waypoints must define a free-collision path (i.e., a path in C_{free}).

III. UAV Path Planning Solution

As shown in Fig. 2, the path planning solution described in this paper generates an optimal path. This path starts from the initial point, visits all desired locations and reaches the final configuration. Our proposed solution computes two-step: the first step sorts a set of targets according to their distance from the initial position. The second step generates a free-collision waypoints sequence that visits all the desired targets.

A. First Step

Algorithm 1 describes the process of the first step.

1) Sorting a set of locations according to their cost: The procedure SortTarets sorts a set of targets according to their distance from the initial configuration.

Let T be the final sorted targets set, T is initially empty (line 2). We start the construction by adding the initial point w_{init} to T (line 3). We consider w_{init} as the current node (line 4), and we search for the nearest target to this node (line 6). We add the nearest target to T (line 7) as the next target to visit and we remove it from Lg (line 8). In line 9, we consider the current node as the nearest target, then we repeat the same process until Lg is empty. We add the final point w_{final} as the last node to T (line 11). Finally, we return T (line 12).

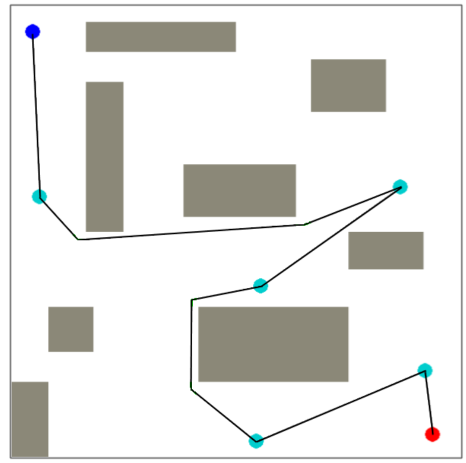

Figure 2. The path planning solution

2) Searching for the nearest target: The NearestTarger procedure finds the nearest target defined in L to the configuration w. To do so, for each target w_i in L, it first calculates the cost between w and w_i, then chooses the target for which the cost is the smallest.

3) Computing the cost between two targets: The Distance procedure calculates the cost between two locations. If the two locations are free-collision, then the Distance procedure calculates the weight of the straight line between the two locations. Otherwise, this procedure sums the Euclidean distance of the line that connects these locations and the result of the FreeDistance function.

4) Computing the distance between two non-connected targets: The FreeDistance procedure calculates the cost of the free-collision path between two non-connected locations (v_i, v_{i+1}). Using the SearchObstacles procedure, this function first searches for the obstacles set $\mathcal{O}$, which collide with the link connecting (v_i, v_{i+1}). Then, the FreeDistance procedure sums the half of each obstacle' perimeter of o_i in $\mathcal{O}$, to Finally returns the computed sum.

5) Searching obstacles between two non-connected targets: Given two non-connected targets (w_i, w_{i+1}), the **SearchObstacles** procedure looks for the current obstacles between (w_i, w_{i+1}). This method first creates a direct link e_i from v_i to v_{i+1}, then identifies all obstacles that intersect with e_i. To do so, this method creates an empty set $\mathcal{O}$ (line 3) for representing the obstacles set that intersect with e_i. For each obstacle o in E (E is the operating environment of the UAV), it checks whether o collides with e_i. If so, o it automatically adds o to $\mathcal{O}$. Finally, this procedure returns $\mathcal{O}$ (line 9).

As shown in Fig. 3, using the first step, the optimal targets set is obtained as: initial point - T1 - T2 - T3 - T4 - T5 - final point.

B. Second Step

Algorithm 2 describes the process of the second step used to establish the optimal free-collision path of the UAV.

Algorithm 1 First step

procedure SORTTARETS(w_{init}, w_{final}, L_G)
  Let $\mathcal{T}$ be an empty way-points sequence
  $\mathcal{T} \leftarrow w_{init}$
  $w_{curr} \leftarrow w_{init}$
  while L_G is not empty **do**
    $w_{near} \leftarrow$ NearestTarget(w_{curr}, L_G)
    add w_{near} to $\mathcal{T}$
    remove w_{near} from L_G
    $w_{curr} \leftarrow w_{near}$
  end while
  add w_{final} to $\mathcal{T}$
  return $\mathcal{T}$
end procedure

procedure NEARESTTARGET(w, L)
  for each w_i target in L **do**
    $d_i \leftarrow$ Distance(w_i, w)
  end for
  return w_i with minimal d_i
end procedure

procedure DISTANCE(w_{init}, w_{goal})
  if freeCollision (w_{init} ,w_{goal}) = True **then**
    return dist (w_{init}, w_{goal})
  else
    $\mathcal{O} \leftarrow$ SearchObstacles(w_{init}, w_{goal})
    return FreeDistance$(\mathcal{O})$ + dist (w_{init}, w_{goal})
  end if
end procedure

procedure SEARCHOBSTACLES(v_i, v_{i+1})
  $e_i \leftarrow (v_i, v_{i+1})$
  Let $\mathcal{O}$ be an empty set
  for each o Obstacle $\in$ E **do**
    if o collides with e_i **then**
      $\mathcal{O} \leftarrow \mathcal{O} \cup o$
    end if
  end for
  return $\mathcal{O}$
end procedure

procedure FREEDISTANCE$(\mathcal{O})$
  sum $\leftarrow 0$
  for each o_i obstacle in $\mathcal{O}$ **do**
    add (width(o_i) + height(o_i)) to sum
  end for
  return sum
end procedure

1) Generating an optimal path planning: The Path planning procedure generates an optimal free-collision path for the overall mission. $\mathcal{V}$ represents the sorted target sequence generated by the first step.

Let $\mathcal{E}$ be the final path. Initially $\mathcal{E}$ is empty (line 2). For each successor targets (v_i, v_{i+1}) in $\mathcal{V}$, the path planning procedure determines whether the link (v_i, v_{i+1}) is collision-free (line 4). If yes (line 5), this process first creates a straight link e_i which connects the two targets (v_i, v_{i+1}), then it adds e_i to the final path (line 6). Otherwise (line 8), this process determines the obstacles that collide with e_i. Then (line 9), it searches for $\mathcal{E}_i$ ($\mathcal{E}_i$ an optimal free-collision sequence of link that reaches v_{i+1} from v_i). It adds $\mathcal{E}_i$ to the final path (line 10).

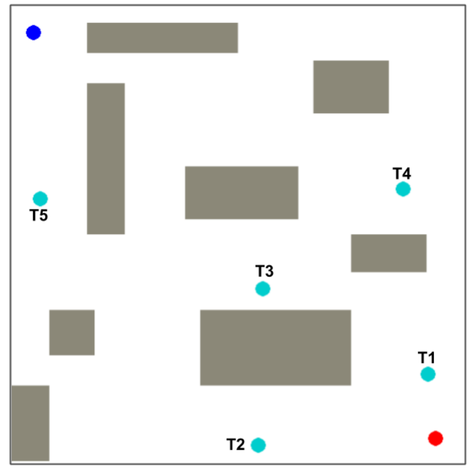

Figure 3. The path planning first step

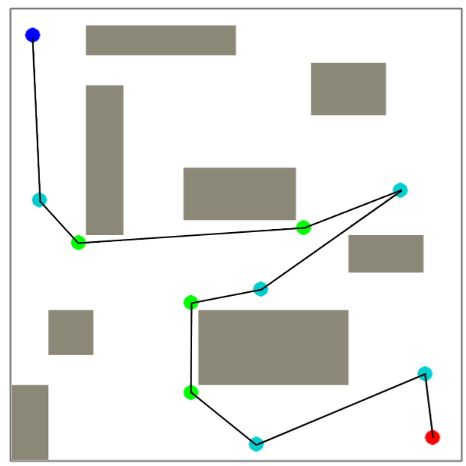

Figure 4. The path planning: second step

The path planning procedure repeats the same process until the $\mathcal{E}$ reaches w_{final}. Finally it returns the final path $\mathcal{E}$ (line 13).

Fig. 4 shows the computer simulation produced by the path planning process.

2) Generating the corners graph: As described in Algorithm 2, CornersGraph procedure constructs a tree based on the obstacle's corners [17].

Initially this procedure creates an oriented graph G_i (line 2) and an empty corners set $\mathcal{C}$ (line 3). The CornersGraph procedure adds the initial point as the root node to G_i (line 4). For each obstacle o_i defined in $\mathcal{O}$, it computes four corners of o_i then, it adds these corners to $\mathcal{C}$ (line 5 to line 7). The CornersGraph procedure connects each corner defined in $\mathcal{C}$ to $\mathcal{G}_i$ according to its distance to the root node (line 8 to line 12). As a result, this procedure creates a tree rooted at v_i and that contains all corners defined in $\mathcal{C}$.

Fig. 5(a) shows the computer simulation got by the execution of **CornersGraph** procedure.

3) Finding the better path between two non-connected target: Fig. 5(b) shows the simulation result generated by the

Algorithm 2 The Second step

1: **procedure** PATH PLANNING($\mathcal{V}$:target set)
2: Let $\mathcal{E}$ be an empty set
3: **for each** $(v_i, v_{i+1}) \in \mathcal{V}$ **do**
4: **if** (v_i, v_{i+1}) is collisionFree **then**
5: $e_i \leftarrow (v_i, v_{i+1})$
6: $\mathcal{E} \leftarrow \mathcal{E} \cup e_i$
7: **else**
8: $\mathcal{O} \leftarrow$ SearchObstacles (v_i, v_{i+1})
9: $\mathcal{E}_i \leftarrow$ FindPath$(v_i, v_{i+1}, \mathcal{O})$
10: $\mathcal{E} \leftarrow \mathcal{E} \cup \mathcal{E}_i$
11: **end if**
12: **end for**
13: **return** $\mathcal{E}$
14: **end procedure**

1: **procedure** CORNERSGRAPH$(v, \mathcal{O})$
2: Let $\mathcal{G}_i = (\mathcal{V}_i, \mathcal{E}_i)$ be an oriented graph
3: Let $\mathcal{C}$ be an empty set
4: $\mathcal{V}_i$.init(v)
5: **for each** $o_i \in \mathcal{O}$ **do**
6: $\mathcal{C} \leftarrow$ Corners(o_i)
7: **end for**
8: **for each** $c \in \mathcal{C}$ **do**
9: $v_{near} \leftarrow$ NearestNode$(\mathcal{V}_i, c)$
10: $\mathcal{V}_i \leftarrow \mathcal{V}_i \cup c$
11: $\mathcal{E}_i \leftarrow \mathcal{E}_i \cup (v_{near}, c)$
12: **end for**
13: **return** $\mathcal{G}_i$
14: **end procedure**

1: **procedure** FINDPATH$(v, \mathcal{G})$
2: Let $\mathcal{P}$ be an empty set
3: $v_{near} \leftarrow$ NearestNode$(\mathcal{G}, v)$
4: $\mathcal{G}$.addVertex(v), $\mathcal{G}$.addEdge(v_{near}, v)
5: $\mathcal{P} \leftarrow$ Path$(v, rootNode)$
6: **return** $\mathcal{P}$
7: **end procedure**

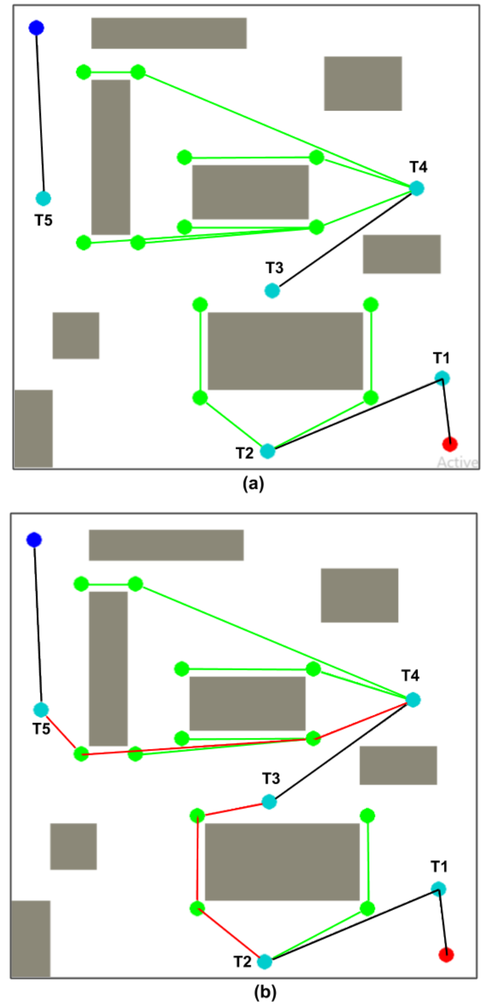

Figure 5. Path planning second step: detailed process

execution of the FindPath procedure. Let the green trees be the oriented graphs computed by the CornerGraph function. For every two non-connected targets, the FindPath procedure looks for an optimal paths that links these targets.

As described in Algorithm 2, the FindPath procedure searches for the optimal free-collision path that connects v to the root node of $\mathcal{G}$. First, this procedure creates an empty set $\mathcal{P}$ (line 2) which represents the optimal path. In line 3, this procedure searches for the nearest corner to v defined in $\mathcal{G}$. Let v_{near} be this corner, the FindPath procedure adds (v_{near}, v) as new link to the oriented graph $\mathcal{G}$ (line 4), then it looks for the path that connects v to the rooted node of $\mathcal{G}$. Finally, it returns $\mathcal{P}$ (line 6).

IV. RE-PLANNING

In real UAV missions, the initial configuration space is often incomplete or dynamic. In these situations, the initial path may become invalid as new information is gathered [18].

Abandoning the invalid path and constructing a new one is a very time-consuming operation. This section presents a re-planning method able to repair the invalid path when changes occur in the configuration space. It does this by finding which parts of the path need to be recomputed and which parts are still valid.

Instead of abandoning the previous solution, our approach efficiently determines, removes, and repairs the invalid parts and maintains the rest. This method presents the advantage of founding a new solution based on re-planing just the sections of the tree that are no longer valid. Our approach, as we will show, resolves the re-planning problem for UAVs navigation. It uses the corners graph, which searches for the collision-free path. Furthers, it found a fast solution, specifically when many changes occur in the configuration space.

Fig. 6 illustrates the re-planning process. Starting with a valid path generated by our previously proposed method. When new obstacles appear in the configuration space, the re-planning process trims just the invalid parts and maintains the rest of the generated path.

The re-planning process recomputes an optimal free-collision path for every two non-connected targets. As a result, the re-planning process produces a valid solution that starts from the initial point, visits all desired targets, and reaches the final point.

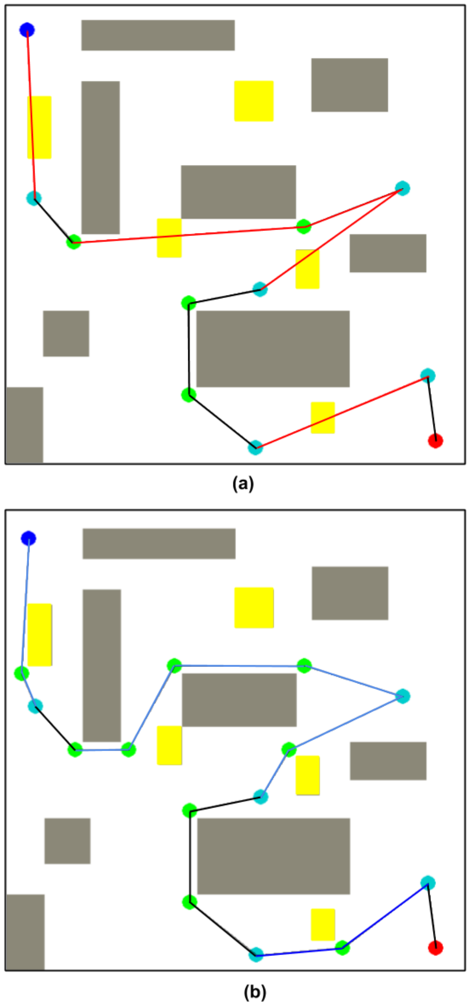

Figure 6. Path Re-planning process

Algorithm 3 describes the process of re-planning a new free-collision path in case of newly added obstacles. Let L be the sorted targets set produced by the first step, and P the optimal waypoints sequence generated by the second step. T is the recomputed path with new changes (line 1). T is initially empty (line 2). For each two successor targets $(t_i, ti+1)$ in L, let P_i be the sub-path that reaches $ti+1$ from t_i (line 5), we first verify if P_i is a free-collision path (line 6). If so, we automatically maintain P_i (line 7). Otherwise, we need to recompute P_i. This involves trimming the sub-path and generating a new valid solution.

Trimming the sub-path involves stepping through P_i in the order in which nodes were added and marking all of them as invalid nodes. As a result, it breaks the branch which collides with new obstacles (line 9). Once the Pi has been trimmed, we recompute it to find a free-collision path. This can be performed by using the same process as described in our path planning algorithm for initial construction (line 10 to line 13).

Depending on how the configuration space has changed, the SearchObstacles method determines which new obstacles collide with Pi (line 10). Based on this result, the CornersGraph method constructs a tree rooted at t_i (line 11) and that contains

Algorithm 3 Re-planning process

1: **procedure** RE-PLANNING ($\mathcal{L}$: targets set, $\mathcal{P}$: initial path)
2: Let $\mathcal{T}$ be the recomputed path
3: $\mathcal{T}$ is initially empty
4: **for each** $(t_i, t_{i+1}) \in \mathcal{L}$ **do**
5: $\mathcal{P}_i \leftarrow$ path reaching t_{i+1} from ti
6: **if** P_i is freeCollision **then**
7: $\mathcal{T} \leftarrow \mathcal{T} \cup \mathcal{P}_i$
8: **else**
9: Trim P_i
10: $\mathcal{O}_i \leftarrow$ SearchObstacles(t_i, t_{i+1})
11: $\mathcal{G}_i \leftarrow$ CornersGraph(t_i, O_i)
12: $\mathcal{T}_i \leftarrow$ FindPath$(t_{i+1}, \mathcal{G}_\rangle)$
13: $\mathcal{T} \leftarrow \mathcal{T} \cup \mathcal{T}_i$
14: **end if**
15: **end for**
16: **return** $\mathcal{T}$
17: **end procedure**

all the obstacle's corners. The FindPath method uses the tree generated by CornersGraph then produces an optimal path that reaches t_{i+1} from t_i (line 12). This solution is then added to the recomputed path T (line 13). We repeat the same process until we reach the final location. The re-planning process returns T as the final result (line 16).

As a summary, when changes occur to the configuration space, the process of re-planning a new path represents a good solution for UAV navigation in a dynamic or incomplete environment.

V. SIMULATION

To prove the effectiveness of the method proposed in this paper, we present computer simulations, as shown in Fig. 7. The configuration space is enclosed and contains a set of static obstacles each of which is in a rectangular shape. We ignore the size of the UAV, we present this aircraft as a "spot robot". The computer simulations presented here show a comparison of many results and yield good experience performance over a wide variety of examples.

Each of Fig. 7-a-1, Fig. 7-b-1, and Fig. 7-c-1 shows a path planning problem to resolve. Starting from the initial point (the red point), the UAV should visit each target (the cyan point) one time, and then reach the final configuration (the blue point).

In each of Fig. 7-a-2, Fig. 7-b-2, and Fig. 7-c-2 an optimal path has been generated using the method described in the third section. The black lines design the computed path. The corners (the green point) represent the intermediate way-points traversed to avoid obstacles.

In each of Fig. 7-a-3, Fig. 7-b-3 and Fig. 7-c-3 new obstacles (the yellow rectangles) have been added. Using the re-planning method presented in section Four, the invalid parts of the tree have been removed and replaced by an optimal free-collision solution (the blue lines).

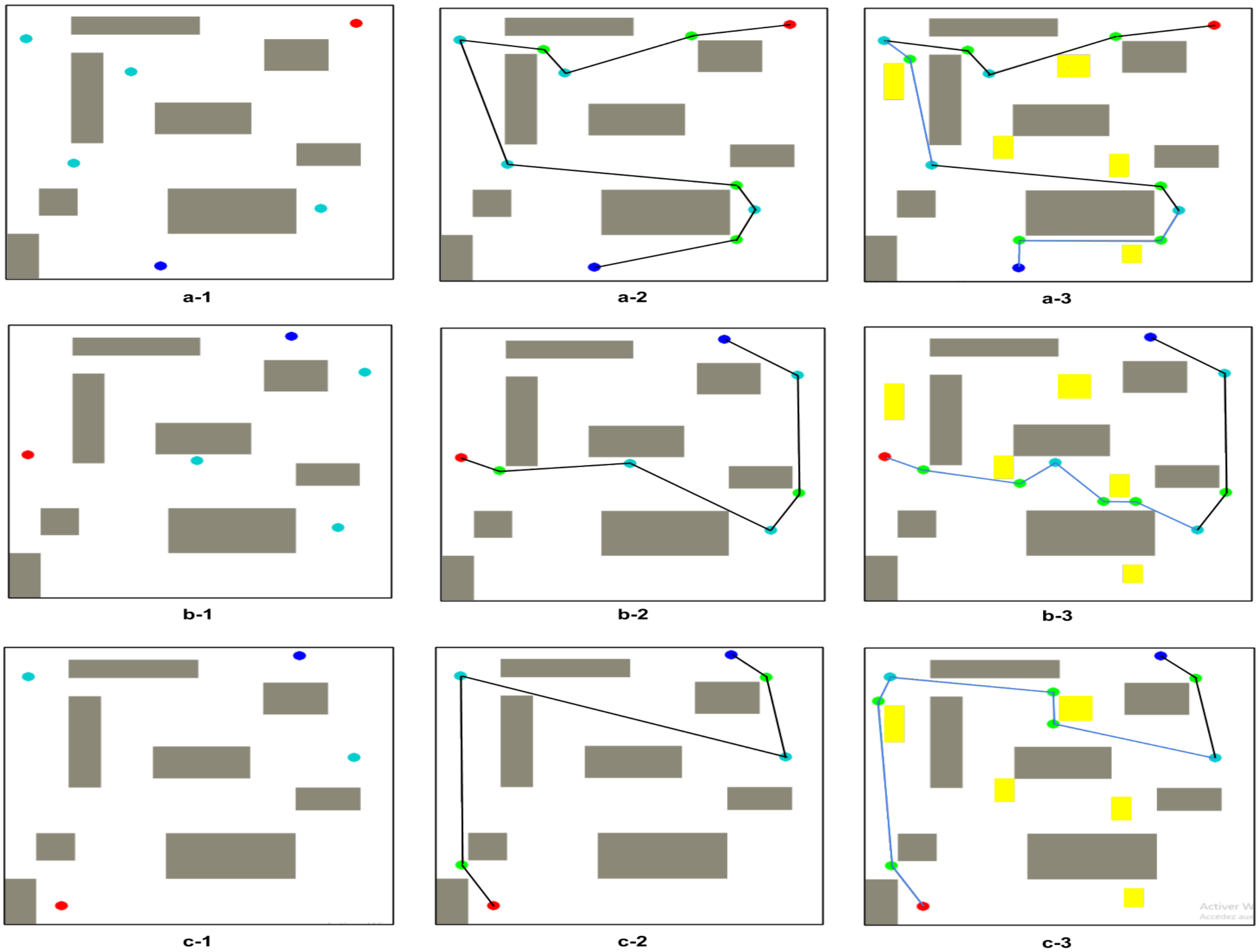

Figure 7. Path planning simulations

VI. Future Work

The motivation behind this work is to develop an efficient UAV path planning for civil application. In particular, we interest in the problem of multi-UAV path planning operating in a dynamic environment, where a team of low-cost UAV is designed to perform complex missions while visiting the desired locations. As the number of UAV increases in the team, path planning algorithms such as A* [19] [20], Dijkstra [21], [22] or RRT [23], [13], may require high-performance capabilities (memory and processing time) to find a valid solution. Our proposed algorithm is a good choice for solving this problem's type since this method is not coupled with its high dimensionality.

Further, this algorithm may be used in high-dimensional configuration spaces, it could be extended to resolve the same path planning problem described in this paper in a 3D work-space. To do so, the obstacles will be represented by cube shape, each of which contains eight corners. Then, based on these corners, the CornerGraph method will generate a tree on minimal length. And finally, the FindMethod will search for an optimal path in a 3D configuration space.

VII. Conclusion

We have presented an efficient algorithm for solving path planning problems for civil UAV operating in a dynamic or incomplete environment. Our algorithm generates an optimal path that starts from the initial configuration, visits all the desired locations, and reaches the final position. We can use the same algorithm to repair the existing path when changes occur on the configuration space. We have proved its effectiveness with the single UAV navigation. The path planning algorithm presented here offers several advantages regarding the problem of fast and optimal UAV path planning. First, our algorithm is simple to implement and involves knowledge of the current obstacles. Second, when new obstacles are added to the configuration space, our algorithm repairs the affected branch rather than compute the path from scratch. This can be very beneficial with UAV navigation in a dynamic environment.

REFERENCES

[1] F. Mancini, M. Dubbini, M. Gattelli, F. Stecchi, S. Fabbri, and G. Gabbianelli, "Using unmanned aerial vehicles (uav) for high-resolution reconstruction of topography: The structure from motion approach on coastal environments," *Remote Sensing*, vol. 5, no. 12, pp. 6880–6898, 2013.

[2] J. Willenborg, "Novel tracking system using unmanned aerial vehicles," May 14 2015. US Patent App. 14/121,686.

[3] W. Immerzeel, P. Kraaijenbrink, J. Shea, A. Shrestha, F. Pellicciotti, M. Bierkens, and S. De Jong, "High-resolution monitoring of himalayan glacier dynamics using unmanned aerial vehicles," *Remote Sensing of Environment*, vol. 150, pp. 93–103, 2014.

[4] J. C. Hodgson, S. M. Baylis, R. Mott, A. Herrod, and R. H. Clarke, "Precision wildlife monitoring using unmanned aerial vehicles," *Scientific reports*, vol. 6, p. 22574, 2016.

[5] G. Kimchi, D. Buchmueller, S. A. Green, B. C. Beckman, S. Isaacs, A. Navot, F. Hensel, A. Bar-Zeev, and S. S. J.-M. Rault, "Unmanned aerial vehicle delivery system," Feb. 21 2017. US Patent 9,573,684.

[6] S. Kamate and N. Yilmazer, "Application of object detection and tracking techniques for unmanned aerial vehicles," *Procedia Computer Science*, vol. 61, pp. 436–441, 2015.

[7] C. Deng, S. Wang, Z. Huang, Z. Tan, and J. Liu, "Unmanned aerial vehicles for power line inspection: A cooperative way in platforms and communications," *J. Commun*, vol. 9, no. 9, pp. 687–692, 2014.

[8] S. d'Oleire Oltmanns, I. Marzolff, K. Peter, and J. Ries, "Unmanned aerial vehicle (uav) for monitoring soil erosion in morocco," *Remote Sensing*, vol. 4, no. 11, pp. 3390–3416, 2012.

[9] F. Kendoul, "Survey of advances in guidance, navigation, and control of unmanned rotorcraft systems," *Journal of Field Robotics*, vol. 29, no. 2, pp. 315–378, 2012.

[10] M. Elbanhawi and M. Simic, "Sampling-based robot motion planning: A review," *Ieee access*, vol. 2, pp. 56–77, 2014.

[11] J. Bellingham, M. Tillerson, A. Richards, and J. P. How, "Multi-task allocation and path planning for cooperating uavs," in *Cooperative control: models, applications and algorithms*, pp. 23–41, Springer, 2003.

[12] M. Noto and H. Sato, "A method for the shortest path search by extended dijkstra algorithm," in *Smc 2000 conference proceedings. 2000 ieee international conference on systems, man and cybernetics.'cybernetics evolving to systems, humans, organizations, and their complex interactions'(cat. no. 0*, vol. 3, pp. 2316–2320, IEEE, 2000.

[13] I. Noreen, A. Khan, and Z. Habib, "Optimal path planning using rrt* based approaches: a survey and future directions," *Int. J. Adv. Comput. Sci. Appl*, vol. 7, no. 11, pp. 97–107, 2016.

[14] L. Yang, J. Qi, J. Xiao, and X. Yong, "A literature review of uav 3d path planning," in *Proceeding of the 11th World Congress on Intelligent Control and Automation*, pp. 2376–2381, IEEE, 2014.

[15] J. S. Bellingham, M. Tillerson, M. Alighanbari, and J. P. How, "Cooperative path planning for multiple uavs in dynamic and uncertain environments," in *Proceedings of the 41st IEEE Conference on Decision and Control, 2002.*, vol. 3, pp. 2816–2822, IEEE, 2002.

[16] L. Meng, S. Qing, and Z. Q. Jun, "Uav path re-planning based on improved bidirectional rrt algorithm in dynamic environment," in *2017 3rd International Conference on Control, Automation and Robotics (ICCAR)*, pp. 658–661, IEEE, 2017.

[17] A. Nash and S. Koenig, "Any-angle path planning," *AI Magazine*, vol. 34, no. 4, pp. 85–107, 2013.

[18] D. Ferguson, N. Kalra, and A. Stentz, "Replanning with rrts," in *Proceedings 2006 IEEE International Conference on Robotics and Automation, 2006. ICRA 2006.*, pp. 1243–1248, IEEE, 2006.

[19] F. Duchoň, A. Babinec, M. Kajan, P. Beňo, M. Florek, T. Fico, and L. Jurišica, "Path planning with modified a star algorithm for a mobile robot," *Procedia Engineering*, vol. 96, pp. 59–69, 2014.

[20] W. Zeng and R. L. Church, "Finding shortest paths on real road networks: the case for a," *International journal of geographical information science*, vol. 23, no. 4, pp. 531–543, 2009.

[21] E. W. Dijkstra, "A note on two problems in connexion with graphs," *Numerische mathematik*, vol. 1, no. 1, pp. 269–271, 1959.

[22] G.-z. Tan, H. He, and S. Aaron, "Global optimal path planning for mobile robot based on improved dijkstra algorithm and ant system algorithm," *Journal of Central South University of Technology*, vol. 13, no. 1, pp. 80–86, 2006.

[23] W. G. Aguilar, S. Morales, H. Ruiz, and V. Abad, "Rrt* gl based optimal path planning for real-time navigation of uavs," in *International Work-Conference on Artificial Neural Networks*, pp. 585–595, Springer, 2017.

Evaluating Programmed Artificial Insemination for Cattle Production

Takuya Yoshihara[1], Yunan He[2], Osamu Fukuda[3]
Hiroshi Okumura[4] and Kohei Arai[5]
Graduate School of Science and Engineering
Saga University, Japan

Iqbal Ahmed[6]
Department of Computer Science
and Engineering
University of Chittagong, Bangladesh

Kenji Endo[7]
Morinaga Dairy Service Co. Ltd.
Tochigi, Japan

Naoki Takenouchi[8]
National Agriculture and Food Research
Organization (NARO), Kumamoto, Japan

Hideo Matsuda[9]
and Tadayuki Yamanouchi[10]
National Livestock Breeding Center, Fukushima, Japan

Junki Egashira[11]
Saga Prefectural Livestock Experiment Station
Saga, Japan

Kenichi Yamashita[12]
The National Institute of Advanced Industrial Science
and Technology (AIST), Saga, Japan

***Abstract*—Cattle productivity in Japan has been declining though livestock farmers and breeders tried to use artificial insemination regularly. The reason behind this declining productivity is the poor evaluation of the applicability of artificial insemination. To address this issue, this research proposes an objective evaluation method to estimate the applicability of programmed Artificial Insemination (pAI). The objective evaluation method tries to estimate the applicability of pAI based on the analysis of various indices from dairy and beef cattle using Bayesian Network Model (BNM). The estimation of the pAI applicability considers 14 and 17 physiological indices for diary and beef cattle respectively. These indices include the basic information (days after childbirth, parity, etc.), diagnosis of appearance, diagnosis of genital organ and the veterinarians' judgments. The overall success rate in estimating the applicability is 89.8% for 1051 records of dairy cattle and 95.6% for 1128 records of beef cattle. The proposed method avoids the subjective error in estimating the applicability of pAI. In addition, the experiment revealed that the applicability of pAI can be evaluated even though the number of measure indices is few.**

***Keywords*—Bayesian network; programmed artificial insemination; cattle production**

I. Introduction

The conception rate of Japanese cattle has been declining for the last 20 years though the livestock companies and veterinaries tried to use artificial insemination regularly [1]. The improvement of conception rate hugely relies on the accurate estimation of estrous cycle. However, the subjective methods of finding estrous cycle sometimes lead to some mistakes and miss the best timing of artificial insemination. The estimation of estrous cycle usually relies on the cattle appearance check or ultrasound image analysis by an experienced inspector. In order to address this issue, many scientists and researchers were trying to use objective indices of a cattle, such as breeding ability, evaluation of dairy cattle conception rate, to estimate the estrous cycle. These studies find many measurement indices that have an relationship with evaluating the productivity of dairy cattle in the industry. In this study, we try to collect these measurement indices of cattle as many as possible and input them to a Bayesian network model (BNM) to estimate the applicability of programmed artificial insemination (pAI). These indices include the basic information (days after childbirth, parity, etc.), the diagnosis of cattle appearance, the diagnosis of genital organ and the uterus condition from the veterinarian's judgment. To collect these data, we got a lot of support from the farmers, the inspectors from dairy company and the veterinarians. With their help, we successfully collected 14 and 16 measurement indices for dairy cattle and beef cattle respectively to build the BNM model. This research discovers that the way of using Bayesian network with many measurement indices achieves more precise estimation of the applicability of pAI in the cattle farming and therefore, assisting the farm management to reduce their overall labor and cost.

The paper layout consists of background checks first, then followed by the selection of cattle indices for the proposed model and the design of BNM model considering selected indices for dairy and beef cattle. Then the validation results of BNM are presented with brief conclusions.

II. Background Checks

Many studies find many measurement indices that are responsible for evaluating the productivity of dairy cattle in the industry. First of all, understanding the ultrasound image analysis of estrous cycle allows the farm management to troubleshoot the productivity problems. Additionally, these are essential for estrous synchronization program and other productive technologies in the livestock industries [2], [3], [4], [5]. The productivity of the cattle is largely identified by whether the cattle shows regular and normal estrous cycles or not. There are many influential factors for the reproductivity of the cattle farming which are already elaborated by various researchers and veterinarian [6], [7], [8], [9], [10], [11], [12], [13]. Understanding the estrous cycle is the first step for the applicability of pAI and many measurement indices are responsible for it

[14], [15], [16]. There were many discovered influential indices for the cattle herd management such as, Body Condition Score (BCS), days after calving and or Postpartum Interval (PPI), parity number, ovarian characteristics, uterine blood flow, progesterone level (P4), climate and nutritional factors, etc. [17], [18], [19], [20]. In addition, different species of beef and dairy cattle also plays vital roles in this case. However, finding out the presence of estrous cycle definitely a distinctive index for the applicability of pAI, which will eventually assists the productive management in the cow herd. Many measurement indices including ultrasound image analysis of the presence or absence of estrous cycles are done by some regular data analytical tools of an experienced veterinarian [21], [22], [23], [24], [25]. The usage of ultrasound image analysis, echo data, BCS, sexual excitement sign for cow and heifers are very much biased, costly and error prone to some extent. Additionally, years of experiences and skills are necessary for understanding ultrasound image, echo data to pinpoint the proper time for the applicability of pAI. Some works have been done on the objective measurement of improving productivity using BNM in the cattle industry [15], [16]. However, the number of measurement indices of cattle is only a few in these researches which leaves us room for further improvement.

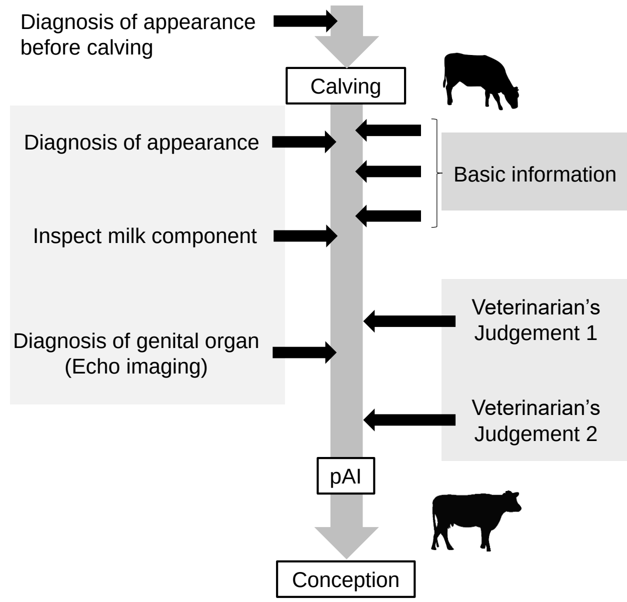

Fig. 1. The steps for collecting various measurement indices in beef and dairy cattle in Japan

III. Measurement Indices and Selection of Important Indices for the Model

Usually, livestock farmers and veterinarians measure various indices of cattle after calving until next pregnancy. The collection of various measurement indices from different sources are shown in Fig. 1. Based on these measured indices, they determine whether pAI is applicable to those cattle or not. For the objective way to analysis, 1051 data (99 dairy cattle) collected from Morinaga Rakunou Co., Ltd. are used for dairy cattle and all this data has 60 measurement indices. On the other hand, 1128 data (71 beef cattle) gathered from Saga Livestock Research Laboratory are used and, in that cases, there are 16 measurement indices. For the data of dairy cattle, a large number of indices are used. But we only select the indexes which are directly related to the applicability of pAI using mosaic plot (Fig. 2) as a primary stage of creating BNM model. In [15], the relationship between the maximum size of corpus luteum and applicability of pAI elaborated shows the importance of pAI for increasing the productivity. Table I lists 14 measurement indices used for the analysis of dairy cattle, and Table II gives 16 measurement indices used for the analysis of beef cattle. Representative and considerable measurement indices will be introduced briefly below.

Among the many factors that have an effect on cattle productivity, the most widely used for herd management is BCS which is defined as “an effective management tool to estimate the energy reserves” of a cow [27], [28], [29]. There are many certified systems for measuring BCS, which varies in different countries [27], [28]. Using BCS to evaluate cattle does not require any special equipment and can be conducted anytime during the year. Poor body condition is associated with reduced income per cow, increased postpartum interval, increased dystocia, and decreased weaning weight. The most common and widely used (USA and Japan) BCS scale ranges from 1 to 5 with 0.25 increments [26]. BCS is related with various factors of cattle, for example postpartum interval (PPI), parity number, RFS, etc. [7], [22], [27] and the reliability of BCS measurement is still questionable to some extent. In the case of beef cattle, BCS is divided into two items: BCS (Body surface) and BCS (Pelvis) in Table II. Although it has somewhat different criteria, it can be considered roughly as BCS for dairy cattle.

Days after calving shown in the first column of Table I and Table II indicates how many days have been passed since the last calving. Since productivity improves as the number of days from the last calving to the next calving is shortened, decreasing days after calving is important.

The objective of this research is to reveal the optimum factors for the pAI applicability using BNM in Japanese cattle. Using BNM for analyzing the applicability of pAI individually in dairy and beef cattle is the most distinctive findings in this field. Moreover, the applicability of pAI using BNM is evaluated even though the number of measurement indices are few.

IV. Designing Bayesian network model (BNM) with identified dairy and beef cattle measurement indices

Bayesian network model (BNM) is a type of graphical model based on Bayesian theory for probability computations. It can reveal the causal relationship by representing conditional dependency using edges in an cyclic directed graph (Fig. 3). Also, by making probabilistic reasoning, it is possible to predict the likelihood and possibility of complicated events. For example, the conditional probability between the random variables X_i, X_j is expressed as $X_i \rightarrow X_j$ in the Bayesian network. Generally, the probability that another event x_2 occurs under the condition that a certain event x_1 has occurred is referred to as a conditional probability and can be expressed as

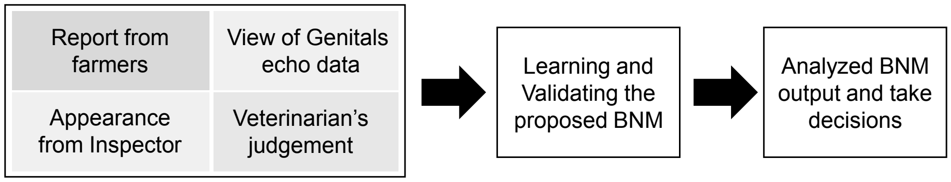

Fig. 2. Analysis of pAI and size of corpus luteum, partial adoption from [15]

TABLE I. MEASUREMENT INDICES OF DAIRY CATTLE

Basic Information	Diagnosis of Appearance	Diagnosis of Genital Organ	Veterinarian's Judgment
Days after Childbirth	BCS	Maximum size of Corpus Luteum	Pregnancy Judgement
Parity	RFS	Blood flow in Luteum	Functional Corpus Luteum
Sexual Excitement Sign	Body Shape	Disorder in genital organ	Uterus Condition
Times of Artificial Insemination	Lochia		

TABLE II. MEASUREMENT INDICES OF BEEF CATTLE

Basic Information	Diagnosis of Appearance	Diagnosis of Genital Organ	Veterinarian's Judgment
Days after Childbirth	BCS (Body surface)	Maximum size of Corpus Luteum	Remaining in Uterus
Parity	BCS (Pelvis)	Blood flow in Luteum	Uterus abnormality
Recurrence of Estrus	RS	Number of Follicle	Uncured puerperalism
Previous Childbirth Condition	Lochia	Ovarian abnormality	
	Uncured Lameness		

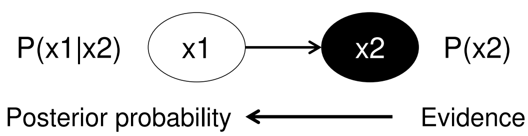

Fig. 3. The basic principle of Bayesian Network

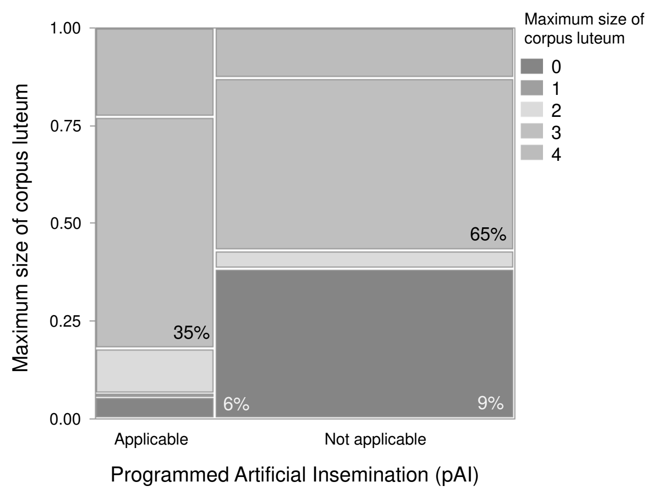

Fig. 4. The proposed BNM of the applicability of pAI in Japanese Cattle

$$P(x_1|x_2) = \frac{P(x_1)P(x_2|x_1)}{P(x_2)}$$

Here, by using Bayes' theorem, it is possible to obtain $P(x_1|x_2)$ which is the probability (posterior probability) that x_1 will occur based on the condition that x_2 has already occurred. Thus, when the result x_2 is obtained, it is found that the cause is x_1.

The proposed method considers four basic information collected from livestock farmers, then four indices from experienced inspectors about the appearance of the cattle. After that, four measurement indices of echo data from the genital organ and veterinarian's judgment are considered. The proposed BNM model is shown in Fig. 4.

The proposed BNM is designed and generated using Bayonet 6 software tool which is developed by AIST, Japan. The data are also visualized using the JMP data analytical tool. The overall proposed work is illustrated in Fig. 5. As shown in the figure, the total posterior probability of the applicability of the pAI is calculated from basic information (days after calving, estrus signs, parity number, times of artificial insemination), appearance indices (BCS, body shape, RFS, lochia), views of genitals or echo data (maximum luteal size, luteal blood flow, genital abnormalities) and veterinarian's judgment (uterus condition, pregnancy judgment).

V. VERIFICATION OF FINDINGS

A. Verification Conditions

For the verification purpose, a cross-validation test of leave-100-out approach is performed. We first randomly select 100 samples from the dataset and use it as validation data, and then create the proposed BNM with the remaining data. This step is repeated to calculate the average accuracy and confirm

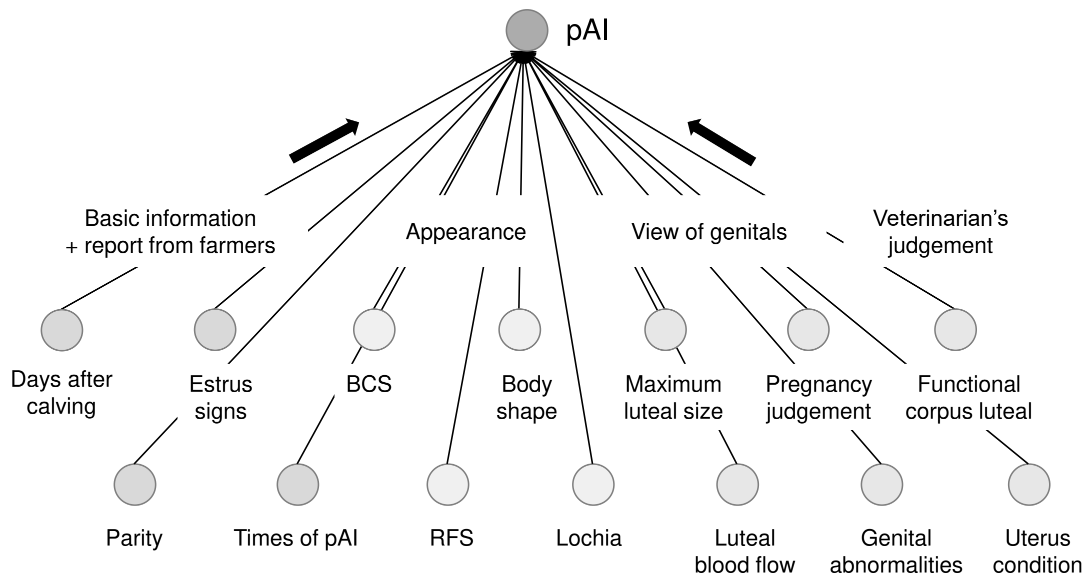

Fig. 5. The overall proposed work

TABLE III. SUMMARY DATA OF DIARY CATTLE

	Ave.	S.D.	Max.	Min.
Days after childbirth	127.7	85.7	467.0	1.0
Parity	2.5	1.8	9.0	1.0
BCS	2.6	0.3	4.5	2.0
RFS	2.4	0.7	4.0	1.0

TABLE IV. SUMMARY DATA OF BEEF CATTLE

	Ave.	S.D.	Max.	Min.
Days after childbirth	56.0	34.4	395.0	5.0
Parity	2.4	1.4	9.0	1.0
BCS (Body surface)	2.8	0.3	3.75	2.0
BCS (Pelvis)	2.9	0.3	3.75	1.5
RS	3.4	0.2	3.5	2.5

TABLE V. VERIFICATION RESULTS OF DAIRY CATTLE WITH ALL INDICES

	Not applicable (NA)		Applicable (A)	
	Records	Rate (%)	Records	Rate (%)
NA	780	92.1	67	7.9
A	41	20.1	163	79.9

TABLE VI. VERIFICATION RESULTS OF DAIRY CATTLE WITHOUT ECHO DATA

	Not applicable (NA)		Applicable (A)	
	Records	Rate (%)	Records	Rate (%)
NA	758	82.3	163	17.7
A	63	48.1	68	51.9

the validity of the analysis. The data used for verification is shown in Table III and IV.

B. Findings / Results

Dairy Cattle: For dairy cattle, Table V represents the verification results of the model for evaluating the applicability of pAI. "Applicable" and "Not applicable" in the first row of the table are the decisions based on the estimated result of proposed model while the first column are Veterinarian's decisions (A = Applicable, NA= Not applicable). Because of missing values, the number of records used to validate the model was 1051. Among the individuals which are judged as "Applicable" by Veterinarian, 79.9% of them are judged as "Applicable" in the proposed model. Also, 92.1% are judged as "Not applicable" in the same model. The overall accuracy rate achieved 89.8% and the average log likelihood was 0.2425.

Table VI shows the results from the similar analysis while not considering echo data from the veterinarian. Without echo data, the proposed model showed slightly lower accuracy (78.6%, average log likelihood 0.4157) for the dairy cattle. The view of genitals and veterinarian's judgments are not considered in this case.

Beef Cattle: For beef cattle, 16 measurement indices (Table II) are used. Fig. 4 shows the proposed model and Table VII represents the verification results for the decision of applicability of pAI or not. "Applicable" and "Not applicable" in the first row of the table are judgments based on the estimated results of this model, and in the first column are Veterinarian's judgments. Because of missing values, the number of records used to validate the model was 1128. Among the individuals which are judged as "Applicable" by Veterinarian, 97.1% of them are judged as "Applicable" in the proposed model. Also, 92.0% are judged as "Not applicable" in the same model. The overall accuracy rate was 95.6% and the average log likelihood was 0.2181. Table VIII illustrates the accuracy rate of beef cattle (90.7%, average log likelihood 0.2509) for evaluating the applicability of pAI with echo data.

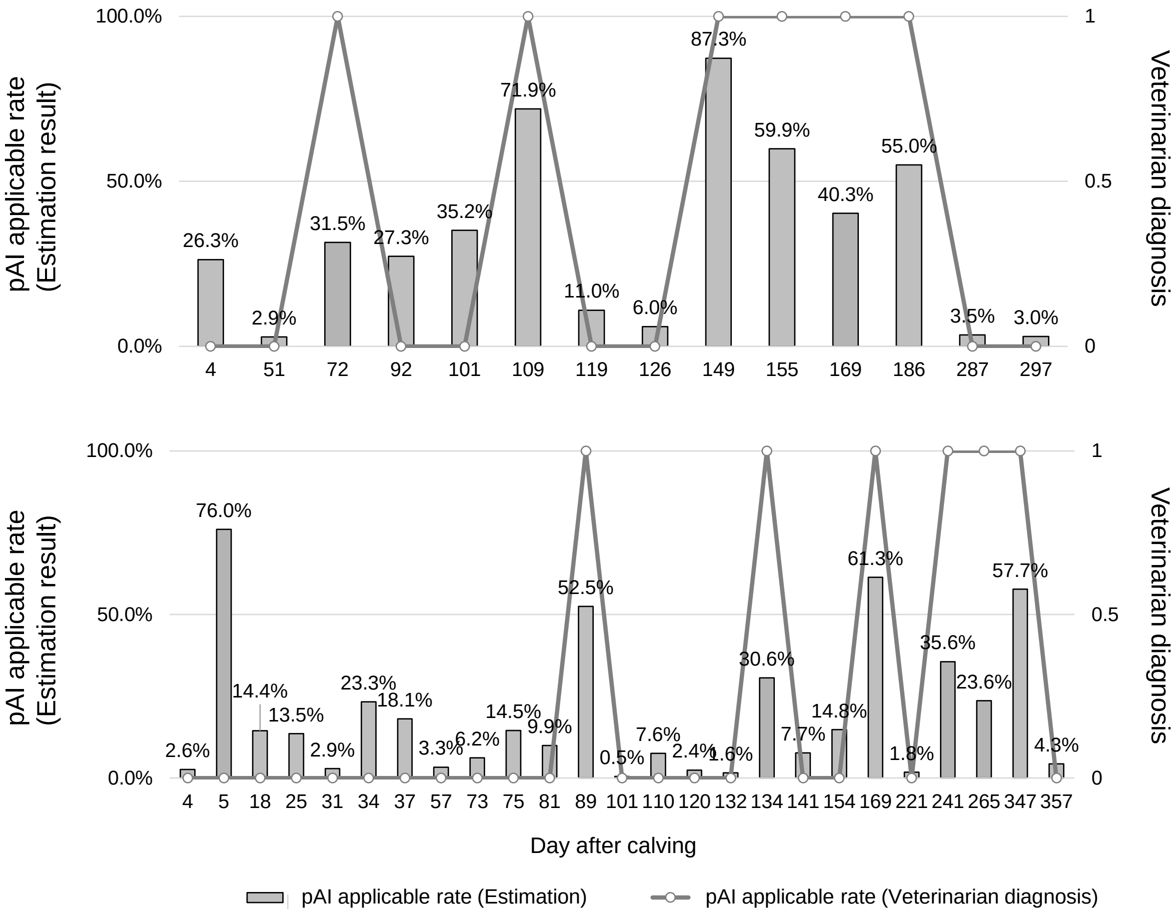

Fig. 6. Comparison between pAI applicability rate estimation by proposed BNM and pAI applicability rate by Veterinarian

TABLE VII. Verification Results of Beef Cattle with all Indices

	Not applicable (NA)		Applicable (A)	
	Records	Rate (%)	Records	Rate (%)
NA	286	92.0	25	8.0
A	24	2.9	793	97.1

TABLE VIII. Verification Results of Beef Cattle without Echo Data

	Not applicable (NA)		Applicable (A)	
	Records	Rate (%)	Records	Rate (%)
NA	263	83.2	53	16.8
A	48	5.9	765	94.1

The summary of the proposed BNM analysis is represented in Table IX. The overall estimation for the applicability of our proposed model is further presented using a time series graph. It shows that the objective estimation for the applicability of pAI is much better than veterinarian's judgments in the cattle feed industry. Fig. 6 depicts the overall comparison of this research findings. In the Fig. 6, the red bar graph represents the pAI applicability rate of the proposed model which is different from veterinarian's diagnosis.

TABLE IX. Summary of the Analysis

Types of Cattle	Index	Accuracy(%)
Dairy Cattle	All indices	89.8
	Without Echo data	78.6
Beef Cattle	All indices	95.6
	Without Echo data	90.7
Overall Average Accuracy		87.7

VI. Conclusion and Future Work

This study finds out an objective method to estimate whether pAI is applicable to the cattle or not. It is achieved by analyzing various of measurement indices of beef and dairy cattle using BNM. The overall accuracy rate of the proposed method exceeds 85%. This objective estimation methods for the applicability of pAI using BNM guide to an eccentric idea to overcome the subjective measurement error of the applicability of artificial insemination in the cattle production in Japan and as well as abroad. In the future, we would like to develop graphical user interfaces for the livestock farmers to help them estimate the applicability of pAI.

ACKNOWLEDGMENT

This research work is funded and supported by Ministry of Agriculture, Forestry and Fisheries(MAFF), Japan under the project name of "Development of technology for enhancement of livestock lifetime productivity by improving fertility through assisted reproduction". Authors would like to gratitude MAFF for their full support and contribution to accomplish the research.

REFERENCES

[1] Report of National Livestock Breeding Center, Japan, 2016. Website: http://www.nlbc.go.jp/en/, Accessed January.

[2] Whittier, J.C., 1993. Reproductive anatomy and physiology of the cow. Extension publications (MU).

[3] Burns, P.D., 2015. The Dairy Cow Heat Cycle. Colorado State University, Accessed December.

[4] Parish, J.A., Larson, J.E. and Vann, R.C. 2010. The Estrous cycle of Cattle. Mississippi State University in cooperation with US Department of Agriculture, Publication, No. 2616.

[5] Perry, G., 2015. The Bovine Estrous Cycle-FS921A. South Dakota State University-Cooperative Extensive Service USDA, Accessed December.

[6] Walker, J. and Perry, G., 2007. Cow Condition and Reproductive Performance. Proceeding of The Range Beef Cow Symposium XX, Colorado, USA

[7] Pfeifer, L.F.M., Leal, S.D.C.B.D., Schneider, A., Schmitt, E. and Corrêa, M.N., 2012. Effect of the ovulatory follicle diameter and progesterone concentration on the pregnancy rate of fixed-time inseminated lactating beef cows. Revista Brasileira de Zootecnia, 41(4), pp.1004-1008.

[8] Matsui, M. and Miyamoto, A., 2009. Evaluation of ovarian blood flow by colour Doppler ultrasound: practical use for reproductive management in the cow. The Veterinary Journal, 181(3), pp.232-240.

[9] Zacarias, T.A., Sena-Netto, S.B., Mendonca, A.S., Franco, M.M. and Figueiredo, R.A., 2015. Ovarian follicular dynamics in 2 to 3 months old Nelore calves (Bos taurus indicus). Embrapa Recursos Genéticos e Biotecnologia-Artigo em periódico indexado (ALICE).

[10] Perry, G.A., Smith, M.F., Roberts, A.J., MacNeil, M.D. and Geary, T.W., 2007. Relationship between size of the ovulatory follicle and pregnancy success in beef heifers. Journal of animal science, 85(3), pp.684-689.

[11] Honnens, A., Voss, C., Herzog, K., Niemann, H., Rath, D. and Bollwein, H., 2008. Uterine blood flow during the first 3 weeks of pregnancy in dairy cows. Theriogenology, 70(7), pp.1048-1056.

[12] Campanile, G., Neglia, G., Di Palo, R., Gasparrini, B., Pacelli, C., Michael, J.D. and Zicarelli, L., 2006. Relationship of body condition score and blood urea and ammonia to pregnancy in Italian Mediterranean buffaloes. Reproduction Nutrition Development, 46(1), pp.57-62.

[13] Perry, G.A., Swanson, O.L., Larimore, E.L., Perry, B.L., Djira, G.D. and Cushman, R.A., 2014. Relationship of follicle size and concentrations of estradiol among cows exhibiting or not exhibiting estrus during a fixed-time AI protocol. Domestic animal endocrinology, 48, pp.15-20.

[14] Arai, K., Suzaki, N., Ahmed, I., Fukuda, O., Okumura, H., Endo, K. and Yamashita, K., 2017. Method for Productive Cattle Finding with Estrus Cycle Estimated with BCS and Parity Number and Hormone Treatments based on a Regressive Analysis. Journal of Advanced Computer Science and Applications (IJACSA), 8(9), pp.191-196.

[15] Yoshihara, T., Ahmed, I., Fukuda, O., Okumura H., Endo, K., and Takenouchi N., 2019. Applicability of Programmed Artificial Insemination (pAI) for evaluting Japnese Cattle Production using Bayesian Network Model (BNM). Proceedings of the 24th International Symposium on Artificial Life and Robotics, pp.1117-1120.

[16] Ahmed, I., Endo, K., Fukuda, O., Arai, K., Okumura, H. and Yamashita, K., 2016. Japanese Dairy Cattle Productivity Analysis using Bayesian Network Model (BNM). International Journal of Advanced Computer Science and Applications, 7(11), pp.31-37.

[17] Kellogg, W., 2016. Body Condition Scoring with dairy cattle- FAS4008. University of Arkansas, Accessed January.

[18] Bewley, J.M. and Schutz, M.M., 2008. An interdisciplinary review of body condition scoring for dairy cattle. The professional animal scientist, 24(6), pp.507-529.

[19] Castro, F.C., Porcayo, J.O., Ake-Lopez, R.J., Monforte, J.G.M. and Montes-Perez, R.C., 2013. Effect of body condition score on estrus and ovarian function characteristics of synchronized beef-master cows. Tropical and Subtropical Agroecosystems, 16(2).

[20] Yamada, K., Nakao, T. and Isobe, N., 2003. Effects of body condition score in cows peripartum on the onset of postpartum ovarian cyclicity and conception rates after ovulation synchronization/fixed-time artificial insemination. Journal of reproduction and development, 49(5), pp.381-388.

[21] Takagi, M., Yamagishi, N., Lee, I.H., Oboshi, K., Tsuno, M. and Wijayagunawardane, M.P.B., 2005. Reproductive management with ultrasound scanner-monitoring system for a high-yielding commercial dairy herd reared under stanchion management style. Asian-australasian journal of animal sciences, 18(7), pp.949-956.

[22] Adams, G.P. and Singh, J., 2011. Bovine bodyworks: Ultrasound imaging of reproductive events in cows. Advances in Dairy Technology, 23, pp.239-54.

[23] Viana, J.H.M., Arashiro, E.K.N., Siqueira, L.G.B., Ghetti, A.M., Areas, V.S., Guimarães, C.R.B., Palhao, M.P., Camargo, L.S.A. and Fernandes, C.A.C., 2013. Doppler ultrasonography as a tool for ovarian management. Animal Reproduction, 10(3), pp.215-222.

[24] Fricke, P.M. and Lamb, G.C., 2002. Practical applications of ultrasound for reproductive management of beef and dairy cattle. Proceedings: Applied Reproductive Strategies in Beef Cattle, Manhattan, KS, pp.228-45.

[25] Lamb, G.C., Dahlen, C.R. and Brown, D.R., 2003. Reproductive ultrasonography for monitoring ovarian structure development, fetal development, embryo survival, and twins in beef cows. The Professional Animal Scientist, 19(2), pp.135-143.

[26] Ferguson, J.D., Galligan, D.T. and Thomsen, N., 1994. Principal descriptors of body condition score in Holstein cows. Journal of dairy science, 77(9), pp.2695-2703. Vancouver

[27] DeJarnette, M., 2004. Estrus synchronization: a reproductive management tool. Select Sires inc. www. selectsires. com. Retrieved on, 31(07), p.2012.

[28] Burkholder, W.J., 2000. Use of body condition scores in clinical assessment of the provision of optimal nutrition. Journal of the American Veterinary Medical Association, 217(5), pp.650-654.

[29] Fukuda, O., Tsuji, T. and Kaneko, M., 2000. A human supporting manipulator based on manual control using EMG signals. Journal of the Robotics society of Japan, 18(3), pp.387-394.

Employing *Takaful* Islamic Banking through State of the Art Blockchain: A Case Study

Mohammad Abdeen[1], Salman Jan[2], Sohail Khan[3], Toqeer Ali[4]
Islamic University of Madinah[1,4]
Malaysian Institute of Information Technology, Universiti Kuala Lumpur & University of Peshawar[2]
Imam Abdulrahman Bin Faisal University[3]

***Abstract*—*Takaful* – an Islamic alternative to conventional insurance – is fast becoming one of the most important constituents of modern Islamic financial market. The fundamental difference between the two forms of risk mitigation is entrenched from the *type of contract* selected. The conventional insurance work on the principle of bilateral contracts between the customer (insured) and insurance provider where the insured pay regular premium in return for payment of compensation, in case of a predefined event occurs. On the other hand, *Takaful* works on the principle of mutual guarantee, cooperation and indemnity where the participants in the scheme mutually insure each other. The *Takaful* providers are mainly responsible for managing, administering and investigating the *Takaful* funds according to *Islamic laws*. This studies provides a decentralized architecture that securely implements *Takaful* risk mitigation system according to its principles. Since all major banking sectors are shifting towards Blockchain technology, as it is currently the only viable solution to offers security, transparency, integrity of resources and ensure trustworthiness among customers. The proposed studies offer state-of-the-art Blockchain technology and focus provide a *Takaful* system that strictly follows the underlying *Islamic laws* for this risk mitigation system. Moreover, the proposed platform provides all *Takaful* transactions over Blockchain that brings confidence and transparency to the community involved in the process.**

Keywords*—*Takaful; hyperledger; blockchain; consensus; decentralized network; muzariba and wakalah

I. Introduction

Digital economy in its current shape is dependent on some form of *trusted entity* that is responsible for building the necessary trust among different participants. Almost all online transactions require a trusted third-party to vouch for authenticity of the participants as well as the transaction itself [1]. For instance, we rely on email service providers to assure that our email has been delivered to the target recipient; similarly, we rely on certification authorities to make sure that a certain digital signature is trustworthy; we rely on banks to assure that our money has been safely delivered to our loved ones remotely. In case of using social media, we rely on social networks like Facebook or Twitter to ensure that our posts or tweets are only shared with our contacts based on our privacy settings and not with the outer world. In fact, in order to keep our digital assets secure and private, we precariously rely on these third party entities, which are much prone to hacking, manipulation and hence can be compromised with ease [1].

Takaful is an elective type of monetary instrument to safeguard resources, liabilities and other individual interests of people and associations. Since its introduction – a few decades ago – the concept of *Takaful* has developed at such a fast rate that its market has extended from Western Asia, South Asia, South East Asia, to Africa, which are prevalently Muslim majority populated nations, to that of some parts of Europe and North America. The great development worldwide and potential venture into new Western markets has a solid ramifications to would-be *Takaful* providers to adapt themselves with creative frameworks for *Takaful* risk mitigation mechanism.

The conception of *Takaful* started back in 1979 in Sudan and currently the business model is implemented in different parts of the world [2]. *Takaful* has achieved significance adoption in the Muslim world as a result of various Islamic finance conferences. It is adopted even by non Muslim countries with Muslims living in majority. *Takaful* business industry has immense potential in the global market. Currently, the market is focused in Gulf Arab nations and some south Asian nations but *Takaful* activities are extending to European Union and as far as Australia. It is projected that this business model will extend to other parts of the world and public will in general receive *Takaful* protection over regular insurance sooner rather than later [3]. Both the conventional insurance and *Takaful* system are tools used for managing and mitigating risk to achieve justice in the society. The primarily and fundamental difference between the two systems is that the former works on the principle of bilateral contracts between the participant and insurance provider where the participant pay regular premium in return for payment of compensation, in case of a predefined event occurs. While later one works on the principle of mutual guarantee, cooperation and indemnity where the participants in the scheme mutually insure each other. The organization providing *Takaful* services are mainly responsible for managing, administering and investigating the *Takaful* funds according to *Islamic laws*. Adherence to these laws are *mandatory* for an insurance scheme to be considered as *shari'h* complaint, which is the essence of *Takaful* scheme and desirable by the wast majority of consumers of such schemes. Therefore, a technological based framework is required for assurance that *Takaful* providers adhere to Islamic laws for providing their services. Furthermore, such a framework should allow consumers to verify these services and ensure trustworthiness of *Takaful* system in its entirety.

In this regard, the Kingdom of Saudi Arabia like other nations is also adopting Blockchain technology in its various sectors for more efficient, reliable and integrated flow of information [4]. Banking sector is shifting towards blockchain as it offer a number of features which are not offered by traditional banking systems [5], [6]. These features among others include transparency, trustworthiness, availability of resources, efficacy, availability and integrity of assets through ledger [7]. To implement transparency in the ledger, Blockchain provides un-tampered public ledger as depicted in Fig. 1.

A number of insurance based systems have been reviewed [8]–[11] and based on the recent trends, the takaful insurance system is proposed to be implemented through Blockchain that will have a bright future. The proposed studies will improve the critical performances and efficiency of the Takaful system and will further ensure transparency in the system. To the best knowledge of the authors after reviewing the literature, such a blockchain based takaful based system is not provided earlier.

Blockchain technology has a number of variants that are used for specific purposes. Based on the nature of the problem in hand, this study propose to use a *permissioned* blockchain as a case study for Saudi Arabia *Takaful* insurance mechanism. The following subsection outlines objectives of the study.

A. Objectives of the Study

The objectives of the proposed study are provided hereunder:

1) To make sure *Sharia* laws are followed in the implementation of *Takaful* insurance mechanism.
2) To implement elements of *Takaful* through state-of-the-art Blockchain technology.
3) To automate Islamic banking laws for implementation on Blockchain multi-node architecture.

To achieve the aforementioned objectives, the study opts for Blockchain technology that offers a number of features explained in the subsequent sections.

The remainder of the paper is organized as follows. Section II presents background of *Takaful* system and also provides details related to Blockchain technology. Section III presents detailed methodology of the proposed solution followed by implementation of the proposed solution, which is detailed in Section IV. At the end, Section V concludes the paper.

II. Background Literature

This section provides details regarding *Takaful* insurance mechanism and elaborates Blockchain core concepts that are essential to comprehend the proposed solution.

A. Evolution of Takaful

Takaful framework is developed with the standard conception of *Ta'awun* meaning, common collaboration and *Tabarru* that is willful and joint contribution. The individuals in *Takaful* plan are capitalists. They pool their contributions with *Takaful* vendor serving as *Mudarib*. This is a single direction exchange which does not guarantee an unmistakable profit for various contribution.*Takaful* insurance mechanism is an unadulterated common build [12]. The idea of *Takaful* depends on common collaboration and deliberate contribution through which the hazard factor is owned among individuals that contribute in *Takaful* and the people that runs the scheme. In the traditional insurance mechanism, risk factor is totally transferred from policy member to the administrators that run the insurance scheme. In *Takaful* scheme, individuals consented to partake in a pool which is further reinvested and the benefits are held in the pool [13], [14]. Later on, if any misfortune happens to any stakeholder; she would be compensated from the pool.

As per Takful schemes, on the off chance that any part or member endures a fiasco or catastrophe, the individual in question would get money related profit by a reserve to help meet that misfortune or harm. The sum is drawn out of a typical pool made with the individual contribution of all members. In this manner, *Takaful*, coming from the Arabic term *kafal*, which means to deal with one's needs. This is rather than traditional protection, which represents various challenges to Muslims.

B. Basic Principles of Takaful

Under Malaysian *Takaful* Act 1984, *Takaful* is defined as, "A scheme based on brotherhood, solidarity and mutual assistance which provides for mutual financial aid and assistance to the participants in case of need whereby the participants mutually agree to contribute for that purpose". While the *Takaful* business model is defined as "business of *Takaful* whose aims and operations do not involve any element which is not approved by the Islamic law". From the perspective of Islamic laws, the essential complaint against insurance offered by conventional system is that it is successfully a bet upon the frequency of the possibility guaranteed against [15], in light of the fact that the interests of the two gatherings are oppositely restricted, and the both parties don't have the foggiest idea about their separate rights and liabilities until the event of the safeguarded occasions.

Dahi et al. [16] provides a mechanism for direct *Takaful* as follows:

1) To partake in *Takaful*, one must have genuine budgetary intrigue.
2) *Takaful* individuals accumulate for their basic great with great confidence and trust, in this way, uncover material data.
3) Every *Takaful*-member adds mutually agreed donation to the pool.
4) If there should be an occurrence of misfortune, the one will be repaid to the degree of the evaluated loss.
5) *Takaful* administrator will be qualified for any addition or recuperation from another party after misfortune remuneration.
6) Hazard will be expelled as for memberships and misfortune remuneration.

The Islamic protection division or *Takaful* has extended in many real markets and in Muslim majority nations around the globe [17]. The insurance business is a feasible solution for risk mitigation, yet does not abide by the Islamic conventions [18]. The insurance systems is being talked about at numerous dimensions by Muslim legal advisers since the eighteenth century. They gave different feelings over the reasonability of protection contracts. Some trusted it is completely prohibited under Islamic laws and some announced admissibility on different grounds. The reasonable decision as per different sentiments proclaimed the current protection contracts illegal.

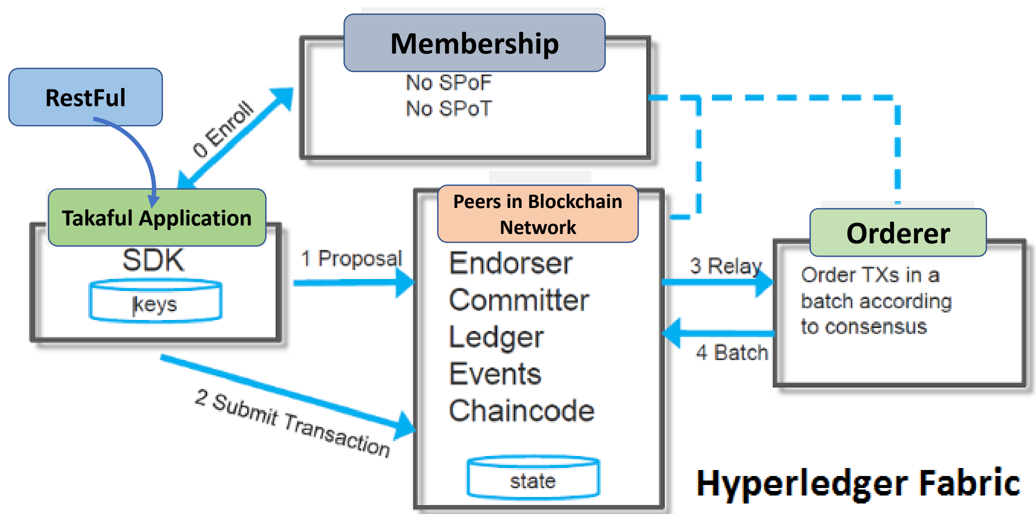

Fig. 1. Generic Blockchain Takaful-HyperLedger Fabric Network

Later on, they contended that common or helpful protection could be substantial. This goals talked about at numerous dimensions and numerous researchers put their endeavors on it [19]. A short time later, Noordin et al. [20] ascertained the goals lead to the foundation of "Islamic protection establishment" in 1979 which accomplished positive reaction from the Muslim world.

C. Blockchain

Digital infrastructure and services are rapidly evolving to embrace the ongoing openness and decentralization approach in technological innovation. One of the most discussed and undeniably ingenious inventions of current era is the blockchain, which allows digital information to be distributed openly but not allowing the same to be copied and/or modified [21]. The blockchain technology facilitate in creating the backbone for a new type of Internet, which was initially perceived to be used only for digital currencies but this perception is briskly changing due to the myriad opportunities offered by this new technology [22]. Although this technology is still in its infancy, the customization, experimental adoption and heavy investment by technological and financial institutes seem to be on the rise since its adaptation by the popular cryptocurrency platform known as Bitcoin [23].

Blockchain is a *distributed, transactional database*, which comprises of a number of *nodes* that are globally distributed, and are linked together by a peer-to-peer *communication network* [21]. These peers use their own layer of protocol messages for peer discovery and node communication. The blockchain nodes use IP addresses to identify each other while users are referenced through their public keys. Each user uses their corresponding private key to perform cryptographic signature over transactions or communications with peers.

The blockchain technology is implemented in the form of public decentralized ledgers and private decentralized ledgers [24]. The former is openly accessible to every user over the Internet. In the public ledgers everyone is free to participate unconditionally in the process of determining the current state of the chain and which blocks are added to it [25]. For validation purposes, these fully decentralized blockchains uses distributed consensus mechanism as proof-of-stake. For instance, Bitcoin considers the "longest chain – the chain with the most proof-of-work – to be the valid ledger" [26]. On the other hand, permissioned or fully private ledger are accessed by assigning write and read permissions. The write permissions are assigned and monitored by a central (private to the organization) decision making entity while the read permissions are either public or restricted [25]. In the permissioned ledger, each organization is responsible to commission the white listing or blacklisting of user identity is based on their organizational procedural structure. The difference between public and private blockchains is the extent to which they are decentralized, or ensure anonymity.

One of the most prevalent examples that is almost inherently tied to blockchain technology is bitcoin [23]. Bitcoin is also the most controversial use case of blockchain technology due to its regularity issues with financial and governments institutes. However, the underlying blockchain technology is not controversial at all and has been adopted flawlessly in both financial and non-financial sectors around the globe [21]. Internet of Things use Blockchain in a number studies [24]. Similarly, blockchain is used health sectors [27] and in collection of Value Added Tax systems [28]. The pundits of global economy and finance consider blockchain invention the same as the invention like steam or combustion engine that most rightly has all potential ingredients to transform the current world of finance and beyond [29]. Similarly, the Silicon Valley's capitalists termed it as one of the most important inventions since the birth of Internet itself [30].

Blockchain-based transactions are not only confined to digital currencies rather blockchain can be adopted in a wider range of use cases both in financial and non-financial sectors [21], [31]. In fact, Blockchain applicability is mostly discussed in the financial sector related to trading and settlement, insurance and private securities insurance [32]–[34]. Other potential application areas include digital marketplace, digital assets, digital notary services [35], [36], health sector [37], energy sector [38] and supply chain information [35]. One of the main reason behind its widespread adoption is that Blockchain-based transactions are verifiable through consensus build from the majority of the participants in the system. This way, Blockchain can be adopted to overcome *trust* issues in the current digital ecosystem. It introduces the concept of *distributed consensus* to revolutionize the digital world. In essence, any transaction that involves digital assets, whether it occurred in past or occurs in present, can easily be verified at any given time in the future [1]. This verification is performed without compromising the privacy of the parties involved and the privacy of the digital assets used. Therefore, *anonymity* and *distributed consensus* are the two paramount features provided by blockchain technology.

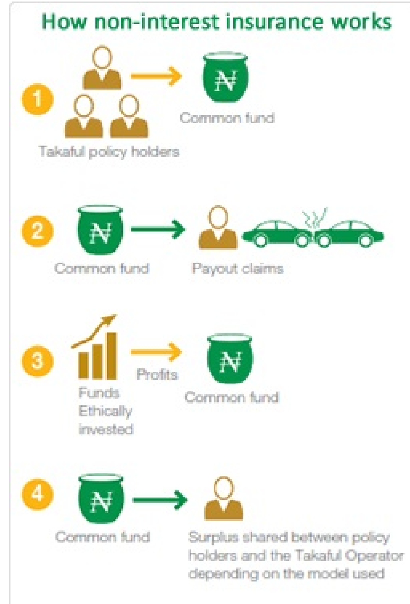

Fig. 2. Takaful Insurance Mechanism

III. Blockchain-based Takaful Insurance Mechanism

Before providing details of how the proposed solution works, we provide brief details regarding the elements of the *Takaful* insurance.

A. Elements of Takaful Insurance Mechanism

The *Takaful* administrator considers five key elements for running the insurance scheme. First, is the cooperative spirit among the stakeholders that is mutual help among participants of the scheme or conformity to the brotherhood. The second element is the ownership of *Takaful* funds that are gathered from various members. The third element is related to investment of the collected funds in an ethical manner. The fourth element accumulates the profits received by investment of the funds. Lastly, the fifth element of the scheme deals with the surplus funds that remains when the use or needs of the individuals are fulfilled. The surplus is shared between policy holders and the *Takaful* operator. A basic flow of this insurance mechanism is provided in Fig. 2.

B. Proposed Solution

Generally, all participants in *Takaful* scheme would like to have a transparent system for the scheme where all transactions such as business investment, profit and loss should be open and trusted upon by the participants. For a risk mitigation scheme like *Takaful* where many participants are interacting with each other and perform various business transactions, Blockchain seems to be a viable solution for trust management, openness and securely managing all transactions. Keeping these requirements in mind, we have proposed a decentralized, transparent and trusted architecture for the *Takaful* system. Since there are various models available for realization of *Takaful* services in the market (see Section II-A), we have incorporated all these models as a smart contract in our proposed architecture. For instance, in *Mudareba* model, the operator and contributors agree on certain percentage of the surplus amount, which is defined through mutual agreement among the participants. The deposited money by the contributors and the surplus received are considered as assets in the Blockchain chain code. Similarly, all participants and their associated assets are added in the system. To perform certain transactions over the assets, participant transactions are defined. Fig. 3 shows various transactions, such as deposit money, define shares, invest money and compensation defaulter in case of any loss to the contributor (in a stipulated event agreed in contract). The basic aim of *Takaful* system is to mutually contribute for the defaulter in case of any loses. Therefore, to provide such services transparency and trust are very important aspects of the system. The transactions mentioned above are endorsed and approved by endorsers. The transactions are further sent to a consensus algorithm called `Orderer node` to agree upon the transaction and commit to the ledger. At the same time, the committed transaction to the ledger is also stored in the world state database. In fact, the correct status of assets are stored along with its current owner. This process is defined in a *Smart Contract* which is called the `Lifecycle of and Asset` in Blockchain. Similarly, our proposed system integrate the *Wakalah* model of the *Takaful* system. The difference between *Wakalah* and *Mudareba* is that in the former model instead of giving percentage to the operator, a predefined fee, based on their expenses are given from the premium. This change of concept is defined as `Second Smart Contract` in the Blockchain network. The complete framework for *Takaful* system over Blockchain is depicted in Fig. 3.

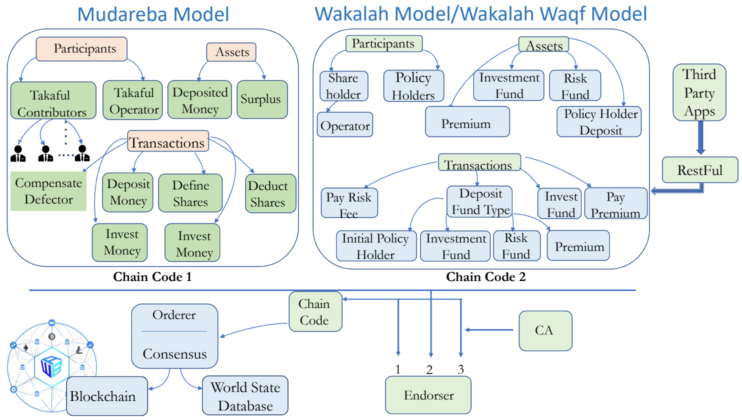

Fig. 3. Proposed Blockchain Based Takaful Insurance Architecture

IV. Selected Implementation Details

In order to provide a more viable solution for *Takful* system over blockchain, a prototype implementation of the proposed system is provided. The architectural framework of *Takaful* is built upon Hyperledger Fabric (HLF) network [39], which connect all members of the system including the operators.

Takaful mechanism is hosted on distributed network of peer nodes that manages and control the entire logical components of Blockchain network including endorsers, orderer node, certification authority, and a peer node of membership service provider (MSP). For a proof of concept, the proposed architecture is deployed using single node implementation where both the `Endorser` and `Orderer` are configured within a single node. The primarily task of the `Endorser` is to validate that the `Chaincode` for the proposed system is deployed and running on different nodes. All payments received as donations in the system from the members are posted to the public ledger through the MSP node, which is also configured to provide opportunity for new members to join the distributed network. For this purpose, a *service subscription* interface is provided that helps new users to subscribe for membership as well as allows existing users to modify their membership information.

The *smart contract* interface incorporates different aspect of *Takaful* business transactions. For instance, we have defined smart contracts for new user subscription, premium selection, contribution and subrogation, indemnity, claims and distribution to name a few. These contracts are combined together to establish *Takaful* business model that govern all of the interactions between participating members. A number of processes and stakeholders are defined regarding how various users shall subscribe to the framework including contributors, operators, takaful providers etc. Using the Hyperledger Fabric network, the rules (defined in the contracts) are automatically enforced when the smart contract is executed during transactions. For instance, one of the transactions ensure collection of the funds from stakeholders and submit to takaful operator. Another example of smart contract ensures that in case of claims, funds are distributed according to prearranged terms. The system authorize and control all members regarding updating the ledger and allow them to connect to the distributor network through peer nodes.

The sequence of events in the proposed *Takaful* system is depicted in Fig. 4. Various transactions can be observed in the same figure. However, one of transactions can be elaborated that a defector make a request for the compensation for his loss. Using the `Takaful Interface`, the defender participant is allowed to invoke claim for compensation when a stipulated event occurs and once all formalities of verification and estimation of cost is conducted and finally the defender is provided with deemed appropriate fund transfer from the Bank. The `Hyperledger` node issue a transaction for the compensation received. The `Chaincode` node requires to validate the participant for the specified claim. The loss claimed by the participant is evaluated and the `Endorser` is asked to execute the particular transaction. The `Endorser` based on the policy mentioned in the endorsement policy performs validation of the claim in terms of its feasibility, i.e. it checks and verifies the blockchain environment wherein a participant is entitled to claim in the framework or not. Any transaction for which approval is granted from the `Endorser`, that transaction is send to the `Orderer` to perform the required consensus before committing it to the public `Ledger`. Order node upon receiving the transactions order these transactions, make a standard block of transactions, as specified in its configuration (e.g. 10, 15, 20 etc), and generate a hash of the block to further communicate it to the network. The nodes that are hosting the Blockchain ledger use consensus mechanism in order to rest assure that the addition to the ledger is updated and synchronized on all the nodes. The ledger becomes updated on the nodes while in response to the execution of transaction, the updated records and data is saved in the couchDB. In this manner, transparency is controlled in the proposed system wherein all the participants can view how various transactions are carried out, and they are informed about the flow of data as well.

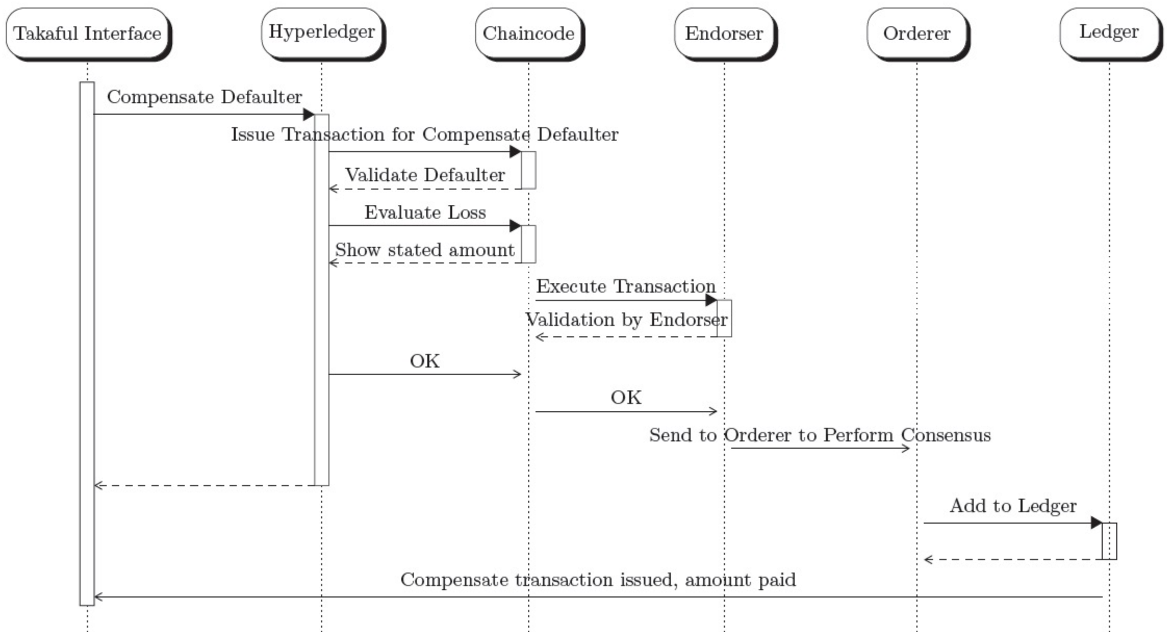

Fig. 4. Sequence Diagram for Takaful Transactions

A. *Deployment of the Hyperledger Fabric*

In the Hyperledger Fabric, a network is built that consist of cluster of servers for hosting *Takaful* participants and operators or administrators that collect donations from participants. A new participant intending to join the permissioned *Takaful* blockchain network is issued certificates by the Certificate Authority (CA) of Saudi Arabia Takaful Operator. These certificates are issued to participants and operators for a particular role. These roles are used to control transactions in the Blockchain.

B. *Deployment of Hyperledger Composer*

The Hyperledger composer business network is deployed over each node for issuance of profile for each member of the *Takaful* insurance scheme. These profiles are used by REST API provided by Hyperledger composer to create URLs for performing different operations such as creation and deletion of records. *Takaful* members are provided with an interface to easily initiate `smart contract` transactions for adding donation to the system and requesting to add transaction to the ledger. In return, the transactions are updated and the donation amount submitted by the members are easily verified.

V. CONCLUSION

Takaful is a widely adopted insurance mechanism spreading across major parts of the world. The banking sector is closely associated with all transactions made under *Takaful* scheme. Monitoring and ensuring security of transactions along with providing transparency, integrity of resources and trustworthiness among all involved stakeholders have become a complex task then ever. This research provides a framework for *Takaful* scheme through implementation of state-of-the-art Blockchain technology, which ensures all rules and regulations required for the *Takaful* system are implemented as per Islamic laws – which is the essence of this scheme and a major difference to that of conventional insurance schemes. We aim to extend our proposed framework to other major Islamic market sectors such Islamic banking market, Islamic money market and Islamic capital market to name a few. For the proof-of-concept, the study opts to select the Kingdom of Saudi Arabia as a use case but it can easily be implemented in any other country that provide Islamic banking system.

ACKNOWLEDGMENTS

This research is supported by Deanship of Research, Islamic University of Madinah.

REFERENCES

[1] M. Crosby, P. Pattanayak, S. Verma, V. Kalyanaraman *et al.*, “Blockchain technology: Beyond bitcoin,” *Applied Innovation*, vol. 2, no. 6-10, p. 71, 2016.

[2] A. R. A. Wahab, M. K. Lewis, and M. K. Hassan, “Islamic takaful: Business models, shariah concerns, and proposed solutions,” *Thunderbird International Business Review*, vol. 49, no. 3, pp. 371–396, 2007.

[3] S. Kassim, “Islamic finance and economic growth: The malaysian experience,” *Global Finance Journal*, vol. 30, pp. 66–76, 2016.

[4] T. Syed, A. Alzahrani, S. Jan, M. S. Siddiqui, A. Nadeem, and T. Alghamdi, “A comparative analysis of blockchain architecture and its applications: Problems and recommendations,” *IEEE Access*, pp. 1–1, 12 2019.

[5] H. Hassani, X. Huang, and E. Silva, “Banking with blockchain-ed big data,” *Journal of Management Analytics*, vol. 5, no. 4, pp. 256–275, 2018.

[6] F. Holotiuk and J. Moormann, “Organizational adoption of digital innovation: the case of blockchain technology.” in *ECIS*, 2018, p. 202.

[7] S. Yoo, "Blockchain based financial case analysis and its implications," *Asia Pacific Journal of Innovation and Entrepreneurship*, vol. 11, no. 3, pp. 312–321, 2017.

[8] D. Singh, N. Stakic, and B. A. Fida, "Comparing the efficiency of national and foreign health insurers in oman."

[9] H. S. Lee, F. F. Cheng, W. M. Har, A. Md Nassir, and N. H. Ab Razak, "Efficiency, firm-specific and corporate governance factors of the takaful insurance," *International Journal of Islamic and Middle Eastern Finance and Management*, 2019.

[10] A. A. Alshammari, S. M. b. S. J. Alhabshi, and B. Saiti, "The impact of competition on cost efficiency of insurance and takaful sectors: Evidence from gcc markets based on the stochastic frontier analysis," *Research in International Business and Finance*, vol. 47, pp. 410–427, 2019.

[11] T. Bhatti and M. Md Husin, "An investigation of the effect of customer beliefs on the intention to participate in family takaful schemes," *Journal of Islamic Marketing*, 2019.

[12] S. Jaffer, F. Ismail, J. Noor, L. Unwin, and D. Ajayi, "Takaful (islamic insurance): Concept, challenges, and opportunities," *Milliman Research Report*, 2010.

[13] Y. Alhumoudi, "Islamic insurance takaful and its arabia," Ph.D. dissertation, 2013.

[14] A. Boztepe, "Green marketing and its impact on consumer buying behavior." *European Journal of Economic & Political Studies*, vol. 5, no. 1, 2012.

[15] K. Mervyn, "Wealth creation through takaful (islamic insurance)," in *International Conference on Islamic Wealth Management. Organized by Durham Summer School of Government and International Affairs, University of Durham and IRTI-Islamic Development Bank, UK*, 2005.

[16] D. E.Q, "Islamic Insurance:," , 2006, [Online; accessed 10-Feb-2019].

[17] I. Finance-Bokhari, "Takaful Takes Off-Islamic-Compliant Insurance-Takaful is Finally Getting off the Mark, with Moody's Predicting a Global Market Work US7 billion by 2015," , 2007, [Online; accessed 02-Feb-2019].

[18] M. Faisal, A. Akhtar, and A. Rehman, "Awareness of islamic banking in india: an empirical study," *J. Manag. Res*, vol. 4, no. 1, pp. 13–27, 2012.

[19] D. a.-B. a.-I. Beirut, "Al-Ta'min al-IslamiyyDirasaFiqhiyyaTa'siliyyaMuqarana bi al-Ta'min al-TijariyyMaa al-Tatbiqat al-Amaliyya." , 2005.

[20] K. Noordin, M. R. Muwazir, A. Madun *et al.*, "The commercialisation of modern islamic insurance providers: A study of takaful business frameworks in malaysia," *International Journal of Nusantara Islam*, vol. 2, no. 1, pp. 1–13, 2014.

[21] F. Glaser, "Pervasive decentralisation of digital infrastructures: a framework for blockchain enabled system and use case analysis," 2017.

[22] H. Hyvärinen, M. Risius, and G. Friis, "A blockchain-based approach towards overcoming financial fraud in public sector services," *Business & Information Systems Engineering*, vol. 59, no. 6, pp. 441–456, 2017.

[23] S. Nakamoto *et al.*, "Bitcoin: A peer-to-peer electronic cash system," 2008.

[24] J. Ali, T. Ali, S. Musa, and A. Zahrani, "Towards secure iot communication with smart contracts in a blockchain infrastructure," *Trans Hash*, vol. 232, p. 9AD, 2018.

[25] V. Buterin, "On public and private blockchains. ethereum blog, 2015," 2018.

[26] T. Swanson, "Consensus-as-a-service: a brief report on the emergence of permissioned, distributed ledger systems," *Report, available online, Apr*, 2015.

[27] M. A. Abdeen, T. Ali, Y. Khan, and M. Yagoub, "Fusing identity management, hl7 and blockchain into a global healthcare record sharing architecture."

[28] A. Alkhodre, S. Jan, S. Khusro, T. Ali, Y. Alsaawy, and M. Yasar, "A blockchain-based value added tax (vat) system: Saudi arabia as a use-case."

[29] J. Borenstein, "A risk- based view of why banks are experimenting with bitcoin and the blockchain." *Spotlight on Risk Technology*, 2016.

[30] J. L. Zhao, S. Fan, and J. Yan, "Overview of business innovations and research opportunities in blockchain and introduction to the special issue," 2016.

[31] M. Pilkington, "Blockchain technology: principles and applications. research handbook on digital transformations, edited by f. xavier olleros and majlinda zhegu," 2016.

[32] R. Beck, J. S. Czepluch, N. Lollike, and S. Malone, "Blockchain-the gateway to trust-free cryptographic transactions." in *ECIS*, 2016, p. ResearchPaper153.

[33] R. Beck and C. Müller-Bloch, "Blockchain as radical innovation: a framework for engaging with distributed ledgers as incumbent organization," 2017.

[34] M. Nofer, P. Gomber, O. Hinz, and D. Schiereck, "Blockchain," *Business & Information Systems Engineering*, vol. 59, no. 3, pp. 183–187, 2017.

[35] K. Korpela, J. Hallikas, and T. Dahlberg, "Digital supply chain transformation toward blockchain integration," in *proceedings of the 50th Hawaii international conference on system sciences*, 2017.

[36] D. Wörner, T. Von Bomhard, Y.-P. Schreier, and D. Bilgeri, "The bitcoin ecosystem: disruption beyond financial services?" 2016.

[37] M. Mettler, "Blockchain technology in healthcare: The revolution starts here," in *2016 IEEE 18th International Conference on e-Health Networking, Applications and Services (Healthcom)*. IEEE, 2016, pp. 1–3.

[38] N. Z. Aitzhan and D. Svetinovic, "Security and privacy in decentralized energy trading through multi-signatures, blockchain and anonymous messaging streams," *IEEE Transactions on Dependable and Secure Computing*, vol. 15, no. 5, pp. 840–852, 2018.

[39] C. Cachin, "Architecture of the hyperledger blockchain fabric," in *Workshop on distributed cryptocurrencies and consensus ledgers*, vol. 310, 2016.

BulkSort: System Design and Parallel Hardware Implementation Considerations

Soukaina Ihirri[1], Ahmed Errami[2], Mohammed Khaldoun[3], Essaid Sabir[4]

NEST Research Group, LRI Lab., ENSEM, Hassan II University of Casablanca, 20000, Morocco[1,2,3,4]
LPRI, EMSI, Casablanca, Morocco[1].

***Abstract*—Algorithms are commonly perceived as difficult subjects. Many applications today require complex algorithms. However, the researchers look for ways to make them as simple as possible. In high time demanding fields, the process of sorting represents one of the foremost issues in the data structure for searching and optimization algorithms. In parallel processing, we divide program instructions among multiple processors by breaking problems into modules that can be executed in parallel, to reduce the execution time. In this paper, we proposed a novel parallel, re-configurable and adaptive sorting network of the BulkSort algorithm. Our architecture is based on simple and elementary operations such as comparison and binary shifting. The main strength of the proposed solution is the ability to sort in parallel without memory usage. Experimental results show that our proposed model is promising according to the required resources and its ability to perform a high-speed sorting process. In this study, we take into account the analysis result of the Simulink design to establish the required hardware resources of the proposed system.**

***Keywords*—Sorting; FPGA; bulk-sort; parallel processing**

I. Introduction

Sorting is taken as one of the most fundamental non-numerical algorithms needed in a multitude of applications. The operation of sorting data became an integral part of many large scale scientific and commercial applications such as data centers, database management or digital signal processing.These applications require parallel processing. Thus, the parallel version of sorting is one of the most required, for which the transition is sophisticate because it demands communication as well as computation. Many sorting algorithms have been developed over the decades. Most important are: Quick sort[1] [2]; Merge sort[3]; Parallel odd-even[4]; bubble sort[5]; Selection sort[6]. The quick sort is a divide-and-conquer algorithm[7] that sorts a sequence by recursively dividing it into smaller sub sequences. The limitation of its parallel version is that it performs the partitioning step serially. Its formulation makes it amenable for parallelization using task parallelism but it impacts the algorithm's scalability. The complexity of the quick sort is $O(n \log n)$ where n is the size of the array. Merge sort is a divide and conquer algorithm where data is divided into two halves and assigned to processors until individual numbers are obtained. After this, each two pair's numbers are merged into sorted list of 2 numbers. This sorted list is again merged to make 4 sorted numbers. This continues till the fully sorted one list is obtained. Merge sort is also easily applied to lists, not only arrays because its worst-case running time is (n log n). Parallel odd-even transposition is an extension of bubble sort, operates in two alternate phases. Even phase in which, values are exchanged between even processors, while the odd processors exchange their values in the odd phase. Its time complexity is$O(n^2)$. Selection sort is an in-place comparison sort. The algorithm finds the minimum value, swaps it with the value in the first position, and repeats these steps for the remainder of the list. It has a hypothetical complexity of $O(n^2)$. Although this algorithm is very slow for sorting larger amount of data, yet is simple.

The difference between these sorting algorithms can be seen in a view of measure of the amount of time and/or space required by an algorithm for an input of a given size (n)[8]. Now-a-days, the amount of information grow rapidly [9] by that a high speed computing to process this huge amount of data[10] is required. So, High performance computing involves parallel processing [11]. A number of research efforts explore how data bases can use the potential of modern hardware architecture. The majority of sorting architectures implemented in hardware use batcher even odd & Bitonic mergers because they are the fasted. Technical literature has called a model frequently used to study sorting algorithms, the sorting networks which have received much interest because of their widespread use in many computations. They represent an abstract machine which accesses the data only through compare-exchange operations by the use of compactors, which are wired together to implement the capability of general sorting. But a various sorting architectures have been presented. Bucket Sorter or FIFO as well as tree based merge sorter which is considered as a target designs for implementation. Bucket sorter follows divide and conquer strategy by distributing the elements of an array into a number of buckets. Each bucket is then sorted individually. FIFO-Based Merge Sorter[12] based on multiple FIFO merge sorters cascaded for sorting on a continuous stream. It shows excellent hardware resource utilization efficiency but requires high buffer memory usage. Merge sorter trees used to merge long sequences from external memory. Elements arranged in trees based structure for sorting sorted sub-sequences to one combined sequences that will be fully sorted. Sorting networks[13] which are models based on algorithms that sort a fixed sequence of numbers by using a fixed sequence of comparators and wires. They require greater number of I/O throughput. Insertion sorter Hardware[14] provides a shift register for storing the search keys.

In view of circuit types, sorting architectures are classified according to 3 categories[13]: combinational sorting circuit, synchronous sorting circuit[15], and piplined circuit[16]. Combinational sorting circuit which is operated without clock signal; signal goes through the sorting stage without following a synchronization signal. The key characteristic of this type is the absence of registers. In view of metrics, the path delay is difficult to estimate, the max delay path depends on number of stages and comparators. Synchronous sorting circuit is a set of stages separated by registers. Signal in this category follows a synchronization signal as a clock. While the pipeline's implementation of sorting network require a new input set every clock cycle. Introducing only registers doesn't make a fully pipelined. Registers are required to buffer the value of wires between stages. The basic element of sorting architecture is the comparison element. It receives 2 numbers on its inputs and presents their Min or Max.

Up to now, there is no easy way to make hardware sorters run in parallel[17]. Research efforts now-a-days are concentrated on network with minimal depth or number of comparators. In parallel processing, program instructions are divided among multiple processors by breaking problems into modules that can be executed in parallel, with the goal of less time execution. Every processor comprehends its piece of general computational issue. But due to the limited number of I/O ports, the existing parallel hardware sorters can sort up to only hundreds of numbers. As sorting large datasets may impose undesired performance degradation too, acceleration units coupled to the embedded processor can be an interesting solution for speeding-up the computations.

Sorting can be implemented in several ways using different technologies. FPGA (Field-Programmable Gate Array)-based systems with re-programmability [18] have become popular for realizing sorting because of the ability to make a trade of between energy and performance. Sorting networks require greater I/O throughput as they consume more sort keys and produce a huge amount of data at the same time. FPGA can be used to almost sorting application. But, sorting a huge amount of data means that it cannot fit into FPGA memory, because of the lack of hardware resources. Despite the limitation in amount of chip space to accommodation functions' parallelism or to sort a huge amount of data, this problem can be managed and estimated. Therefore, FPGA can be added as additional process unit in standard CPU sockets[19] [20]. In some cases, an external memory is required to store intermediate values. This make FPGA good candidates for multicore systems. Latency, throughput and Memory have been used as the metrics for performance evaluation of sorting implementation.

In this context, we presented a novel Bucket sorter architecture designed for the BulkSort algorithm[21]. After the modeling of the BulkSort algorithm, by the use of mathematical equations and the validation by the use of the C++ simulation, we were able to present the system design of the proposed algorithm. We use the Xilinx ISE for FPGA product in order to synthesize our Simulink design to finally present the hardware performance of the pipeline system. Our approach can at best produce $O(nlog_2(n))$-time parallel sorting algorithms. Since a serial simulation that sorts by comparison requires at least $O(n)$ comparisons. The optimal speedup would be achieved when; by using n processors; n elements are sorted in $O(log_2(n))$ parallel comparisons.

This paper is organized as follows. Section II briefly introduces the general idea of the BulkSort. The approach of the BulkSort is presented in Section III, and Section IV provides details about the C++ simulation of the algorithm. System design of our proposed model and its sub-blocks are presented in Sections V and VI. Hardware implementation consideration are presented in Section VII. Finally, Section VIII presents some concluding remarks and perspectives.

II. General idea of the BulkSort

BulkSort, is a novel sorting algorithm that has been presented in [21]. It is an adaptive and parallel algorithm ; based on divide and conquer technique; designed to be implemented in a parallel and re configurable machine for sorting numbers. The concept is easy to understand, we examine the first bit (Must Significant Bit (MSB)) of the concerned unsorted set of elements. After each comparison, each sub set is divided into 2 subsets, winners and losers, each of which undergo the same roles. Fig. 1 illustrate the concept of BulkSort. A set of 6 numbers (5, 2, 10, 4, 6, 8, 10) are firstly converted into binary sequence.Based on a comparison,the whole set is divided into 2 subset representing respectively winners and losers until we have one element elected as the winner of the group.

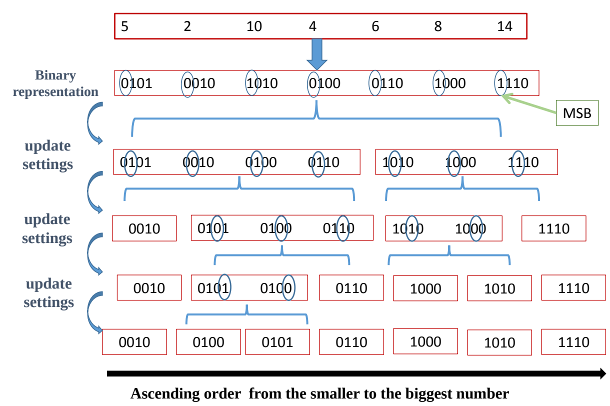

Fig. 1. The Main idea of Bulk Sort [21]

In a binary representation, we have two cases, either 0 or 1.Element with 1 represent a winner, while 0 represent the loser of a subset. The proposed process is based on an iterative pipeline system. Sequence of iterations are executed until a single element is elected as the group winner. Each element in the group is characterized by certain parameters which specify respectively its rank, position, the concerned bit in the current iteration and finally its state (if it is going to be compared or not with the set). We mention that the BulkSort is an iterative algorithm where the iteration is a computation instruction process which loops until stopped condition[21].

III. The Approach of the Bulk Sort

The approach of our algorithm is as follows: all the elements will be compared in a pipe stage system (see Fig. 2).

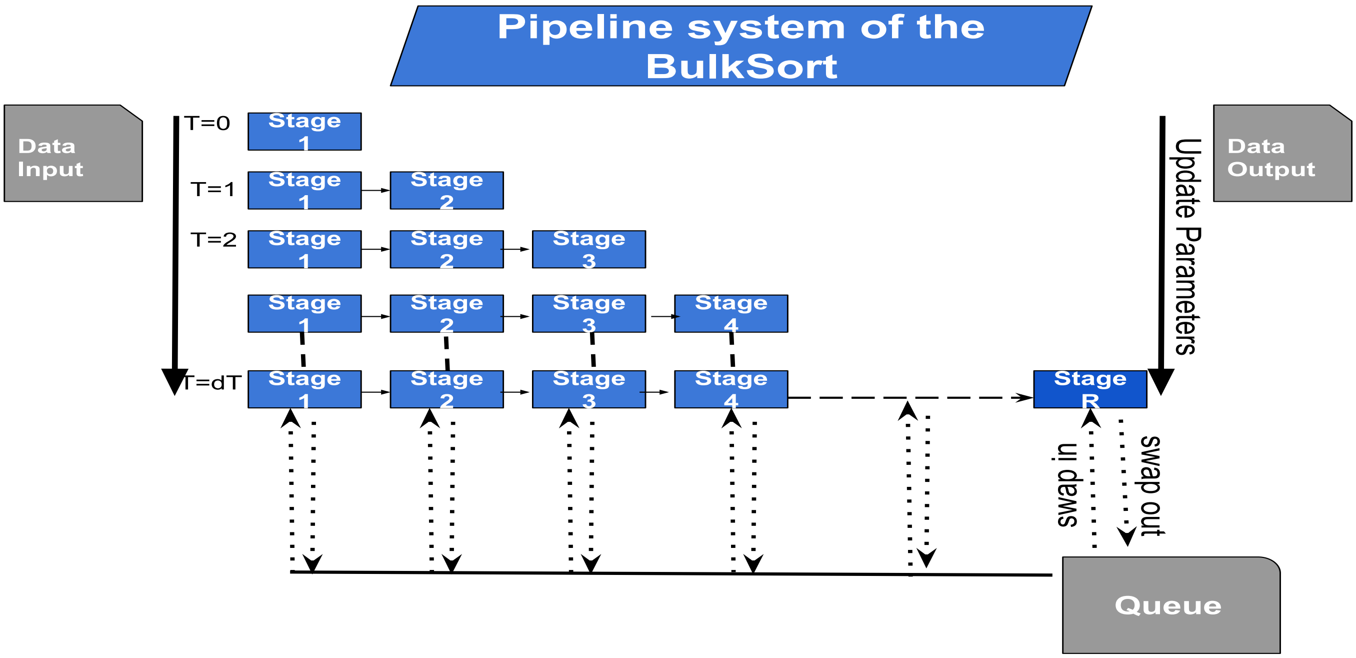

Fig. 2. The approach of the Bulk Sort [21]

We assume that each stage of our system represent a compactor that can compare from 2 to N elements at the same time. At the beginning the set of MSBs of unsorted set will be compared in the first stage. Once we have at least one loser, the whole will be divided into two stages.Then we move to compare the next bit of the 2 sub groups in each stage. And so on until all stages are filled. In this case we are in a scenario where the set of elements are going to be either in a processing or pending state. Elements in the pending state will wait (in the queue) until the concerned stage is emptied. We highlight that elements transit from the pipe to the queue according to the availability of the stages and this process is automatically managed away by a system of mathematical equations.

At each iteration, the parameters of all unsorted elements are updated; according to a specific equations as mentioned below; depending on their state, either processing or pending and if the element is winner or loser. The principal notation used in the following equations are summarized:

- i refers to the current iteration of the sorting process,
- j represents the index of an element in the array, starting in one.
- P_j refers to an element j of the set of the unsorted elements,
- Z_i^j represents the stage index in which the element P_j is going to be processed,
- X_i^j represents the bit index of an element,
- Y_i^j indicates the iteration the element with index j will be processed,
- R_i^j refers to the rank of the element P_j,
- SR_i^k indicates the result of a comparison between elements of the same stage. The value of this parameters is either 0 or 1, depending whether there is a loser or not in the concerned stage k,
- R represents the total number of stages.

A For the processing elements:
Each element in the processing state updates its parameters automatically following the equation presented below:

1 For the rank (R):

- The rank of the winner is computed as follow:

$$R_i^j = R_{i-1}^j - \sum_{k=0}^{Z_{i-1}^j} SR_i^k \tag{1}$$

- The rank of loser is:

$$R_i^j = R_{i-1}^j - \sum_{k=0}^{Z_{i-1}^{j-1}} SR_i^k \tag{2}$$

2 The stage (Z):

- Z_{i+1}^j For winners:

$$Z_{i+1}^j = modulo(Z_i^j + \sum_{k=0}^{Z_i^{j-1}} SR_i^k, R) \tag{3}$$

- Z_{i+1}^{j} For losers:

$$Z_{i+1}^{j} = modulo(Z_i^j + \sum_{k=0}^{Z_i^j} SR_i^k, R) \quad (4)$$

3 The iteration index (Y):
The parameter Y, which refers to the iteration where the element will be processed depend on the the result of the parameter Z as follow:

- If $Z_{i+1}^{j} = 0$

$$Y_{i+1}^{j} = Y_i^j + \frac{\sum_{k=0}^{Z_i^{j-1}} SR_i^k + Z_i^j}{R} + 1 \quad (5)$$

- If $Z_{i+1}^{j} >= 1$

$$Y_{i+1}^{j} = Y_i^j + \frac{\sum_{k=0}^{Z_i^{j-1}} SR_i^k + Z_i^j - 1}{R} + 1 \quad (6)$$

4 Bit Index (X):
This parameter is incremented automatically by one, except the case where element is pending

$$X_{i+1}^{j} = X_i^j + 1 \quad (7)$$

B For the pending elements:
The difference between calculation in the case of pending elements and the processing ones lies in the sum of SR_i^k(indicates the result of a comparison between elements of the same stage. The value of this parameters is either 0 or 1, depending whether there is a loser or not in the concerned stage k) which go from 0 to the total number of stages(R). And also in pending state, we don't talk about loser and winner. Both have the same mathematical equations.

1 The rank(R):

$$R_i^j = R_{i-1}^j - \sum_{k=0}^{R} SR_i^k \quad (8)$$

2 The pipe stage (Z):

$$Z_{i+1}^{j} = modulo(Z_i^j + \sum_{k=0}^{R} SR_i^k, R) \quad (9)$$

3 The iteration index (Y):
For the reason of dependency, we have to check the value of Z each time we compute the iteration index

- If $Z_{i+1}^{j} = 0$

$$Y_{i+1}^{j} = Y_i^j + \frac{\sum_{k=0}^{R} SR_i^k + Z_i^j}{S} + 1 \quad (10)$$

- If $Z_{i+1}^{j} >= 1$

$$Y_{i+1}^{j} = Y_i^j + \frac{\sum_{k=0}^{R} SR_i^k + Z_i^j - 1}{S} + 1 \quad (11)$$

4 Bit Index (X):
This parameter remains in standby until the element goes to the processing state.

$$X_{i+1}^{j} = X_i^j \quad (12)$$

A numerous test has been done (A C++ simulation) to validate the proposed sorting algorithm and examine the proposed idea [21].

We should highlight that the BulkSort is a reconfigured algorithm in view of number of stages. We have proved that by increasing the number of stages, the system become faster. It was also found that we recorded a minimum iteration for very important data numbers.

IV. C++ Simulation

To validate and examine performance of the proposed sorting algorithm; a program was developed in C++, and test results are demonstrated using Intel(R) Core(TM) i5-2430M CPU @ 2.40GHz/2394 MHz. Many experiments with different size of data, different number of pipe stages(communication links) were carried out. We should highlight that the proposed algorithm is iterative and each iteration refers to a clock cycle; in which several operation are executed in parallel.

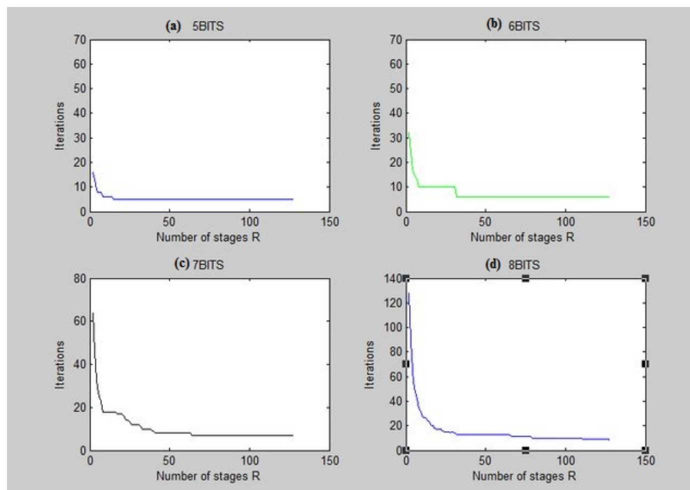

Fig. 3. Illustrate the-number of iteration according to the number of pipe stage.(a),(b),(c) and (d) represent how number of iterations change according to number of stages in case of 5,6,7 and 8 bits [21].

The number of pipe stages is taken as input parameters. By means of this point, our algorithm can be re-configurable. It is found that the number of iterations becomes a constant as the number of pipe stages increases after a while.As shown in Fig. 3, increasing the number of pipe stages until we achieved iteration equal to N (N refers to the total number of bits)with $\frac{2^N}{2}$ pipe stages. It is also found that even with a minimum number of pipe stages (1 pipe stage), the number of iteration is equal to the number of unsorted elements. Our results verify that our algorithm is re-configurable in view of number of pipe stages. More stages we have, the more the system gets faster. A careful analysis reveals also that the number of iterations can be reduced.

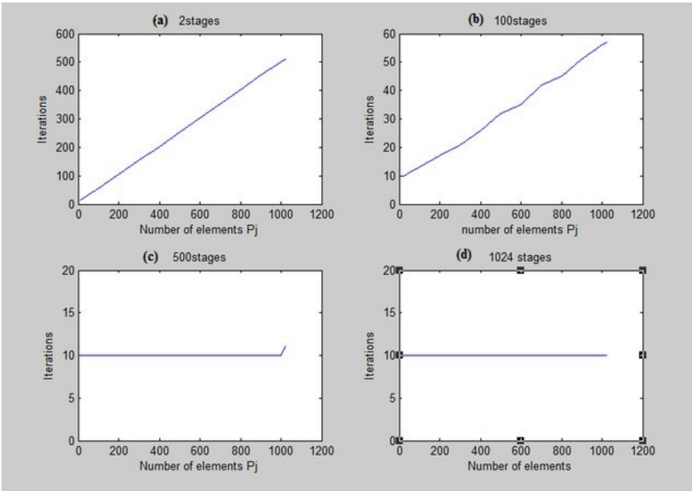

Fig. 4. Illustrate the-number of iteration according to the number of elements.Figures (a),(b),(c) and (d) show the behaviour of number of iterations for different number of stages, according to number of elements. [21].

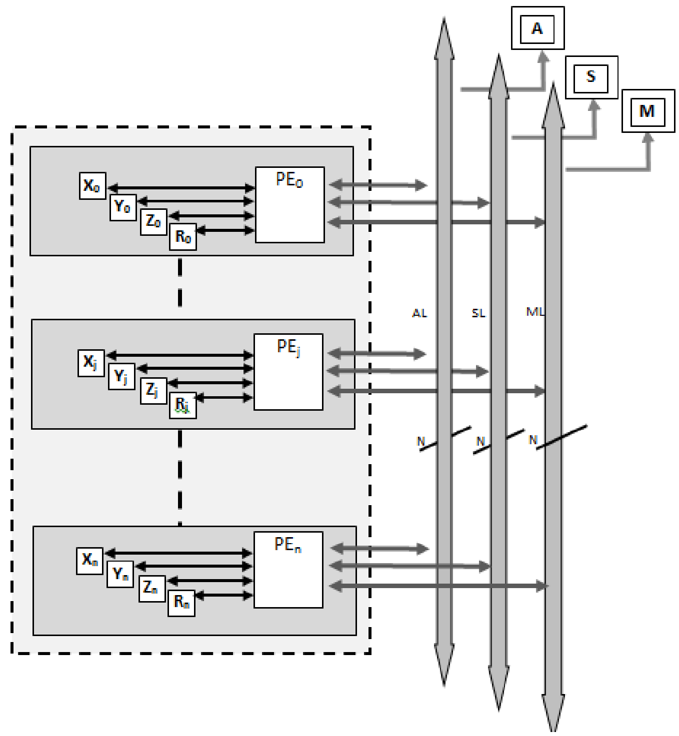

Fig. 5. The external interface of the BulkSort Model.Each Process Element(PE) represent an element to be sorted.It's characterized by the set of parameters.A,S,M represent the communications lines(Buses)

Based on our experiments (see Fig. 4), we reveal that our algorithm recorded minimum sorting iteration for very large data numbers. For example for N=10 bit, the max number of elements is 1024=2^N. With 1 pipe stage, the number of iteration is 2^N , while if we use for example 50 pipe stages, we have just 28 iterations. while with 500 pipe stages, we can reach $10 = log(1024)$ Iterations for 1024 elements. According to more careful analysis, the complexity in view of number of iteration to sort n elements is O(n logn) in the best case and O (n) in its worst case. The main iteration based on a series of computation of the element's rank and parameters used in the next iteration of the sorting process.

V. THE BULKSORT SYSTEM DESIGN

Now it is the time to learn the philosophies of the proposed sorting architecture and the corresponding SIMULINK model. We should mention that certain parameters in this section will be presented otherwise. The clock cycle represents the iteration and the bus is equivalent to the stage of pipeline system.

The BulkSort process relies on synchronous architecture; based on parallel processing distributed among several identical units. Our system performs the process of sorting ; based on a decentralized comparison between these bits; starting from the most significant bits and ending after several clock cycles by the least significant bits. We should emphasize that in hardware, the choice of the data do not affect the sorting network, it affects only the implementation of compactors.

The main strength of our system is the ability to compare a set of elements simultaneously instead of going through them one by one. In order to make the proposed model easy to understand, we use Fig. 5 to illustrate the general model. The BulkSort architecture is composed of n cells PEi with $1 \leq i < n+1$. These cells are interconnected via a communication system distributed between 3 families of lines. Each of these cells is made up of seven units (see Fig. 6).

The process of the bulk Sort system involves several data elements classified into two families: A first family of data which are distributed among all the processing units(PE_i) (X_i, Y_i, Z_i and R_i of Fig. 5). The second family of data, whose elements are shared between all PE_i of our system (S, M, A): Arbitrary(A), Status(S) and Masque lines(M); used in the comparison process, to indicate the status of lines and the computation of the basics parameters of the system

Line (A) of Fig. 5 represent a line where data input/output is transmitted, (S) represent the status line used in the equation (3), (4), (5), (6), (8) and (9) of the system. While (M) refers to a set of lines used as a masque in the process.

Before describing the BulkSort blocks, we should define the use of the data elements in our system.We highlight that data is read from memory and sent to the input of each PE_i at every clock cycle. As a distributed data, we found in each PE_i a binary sequence to be compared. These numbers refers to the ID of the PE_i. The information of Clock cycle (Y_i) is one of the basis distributed data; used in order to indicate when the element PE_i will be transmitted to the comparison process. (Z_i) indicate the concerned shared line AL. At each Clock cycle,PE_i has a specific rank in a view of the other PE_s R_i . During each clock cycle the values of the elements X_i, Y_i,Z_i and R_i are calculated within the processing and calculation unit PE_i by using competing functions which has been described before.

A line is set to the logic state '1' if there is at least one cell PE_i transmitting on this line a binary element = '1', otherwise this line is set to the logic state '0'. Thus, the value of the element and the state of the lines AL ('0' or '1') will make it possible to identify the status of cell (losing cell or winning

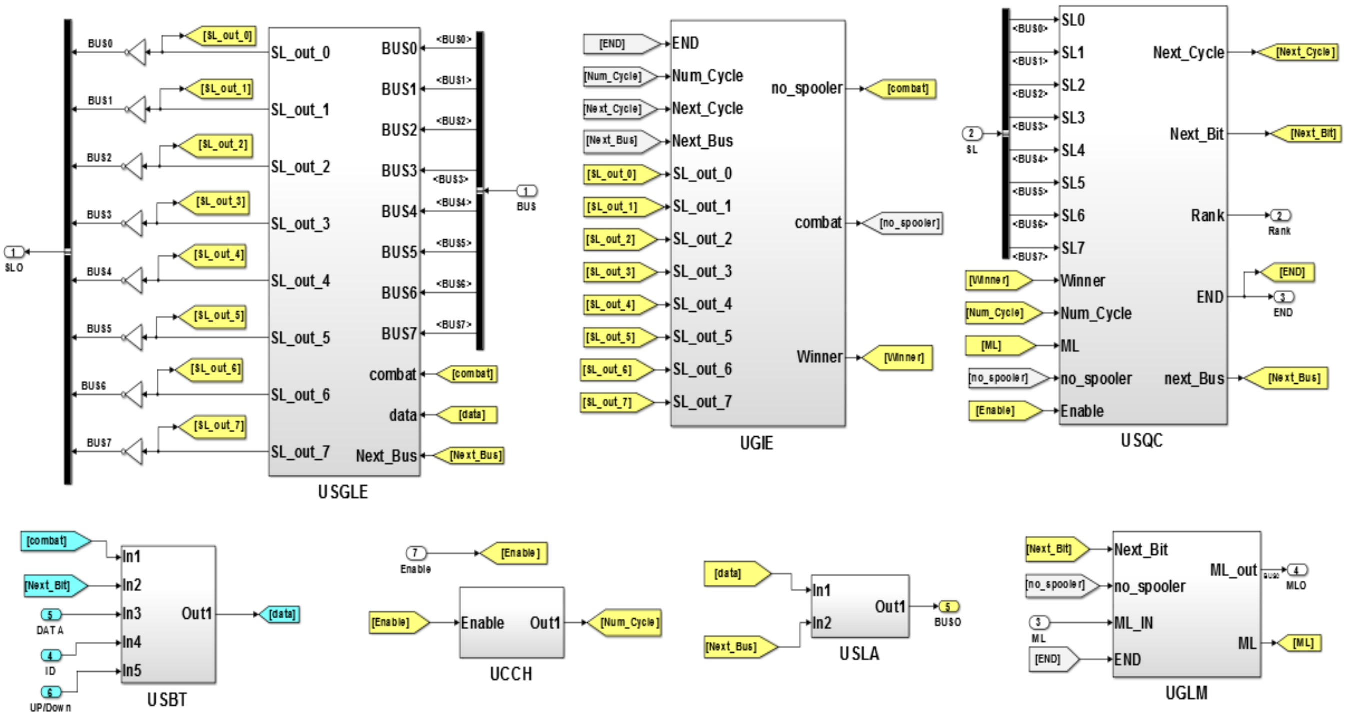

Fig. 6. PE'Sub-Blocks.

cell).

Instead of an iterative treatment, the steps performed by the processors are determined by the clock cycle, which includes reading, interpreting and executing the processes. Indeed, in the hardware implementation, the concept of pending does not exist. The queue refers to shifting in a view of clock cycle.

VI. Description of the BulkSort Sub-Blocks

The BulkSort model is built using Matlab/Simulink in order to be used in the Hardware implementation on FPGA. For the sake of simplicity, the proposed Simulink design will be limited to 7 cells. These cells are interconnected via a communication system. Within each PE_i, there is a system of cooperating units to perform the sorting; each of which has specific tasks (Fig. 6 and 7).

1) USBT (Bit Selection Unit): It generates the respective bit for each PE_i during the concerned clock cycle. The bit generation takes into consideration the result of the combat, either pending or processing state.If the PE_i is in processing state, the USBT unit generates the concerned bit according to the Next Bit set point, otherwise no generation is performed.

2) USQC (Calculation, Selection and counting Unit): Is the pivotal unit of the system, at which the parameters X_i, Y_i, $Z_i$and R_i; are generated. USQC is the unit that communicates with all other units.

Within the USQC unit there are 6 sub units, each of which is dedicated to make a main task in the system (see Fig. 8):

- Sigma SL: The crucial sub-unit for the PE parameters computation. Depends on the state of a PE if it is a loser or a winner. The unit receives the signal (the information) from the BLOCKS Sum_i and next bus, and chooses the sum concerned according to the next bus.
- Bloc Cycle Number:A sub-unit which generates the Next cycleY_i and the current Cycle based on a mathematical equation (Equation 5,6,10 and 11)
- Bloc Process Bus Number:A sub-unit generating the Next Bus and the current Bus according to a mathematical equation (Equation 3,4 and 9)
- Bloc Process Rank Number: Allows to define the rank of each PE at each iteration (Equation 1, 2 and 8)
- Process Bit Number:sub-unit which generates the next bit and current bit as well as the indicator END (Equation 7 and 12)

3) USGLE (Selection & Status Line management Unit): Each PE is connected to the set of state lines. The generation of the result provided by the USGLE unit is based on the following indicators: Next Bit, Data, Bus and Combat, in order to feed the Status Lines (S).

4) UGIE (State Indicator Management Unit): The main reason of this unit is to generate the state indicators of a PE. The different state that a PE can take are: WINNER, Combat and loser. To define the state, each UGIE unit is based on the following indicators to generate the State: num cycle, Next Cycle, End and Masque Lines(ML).

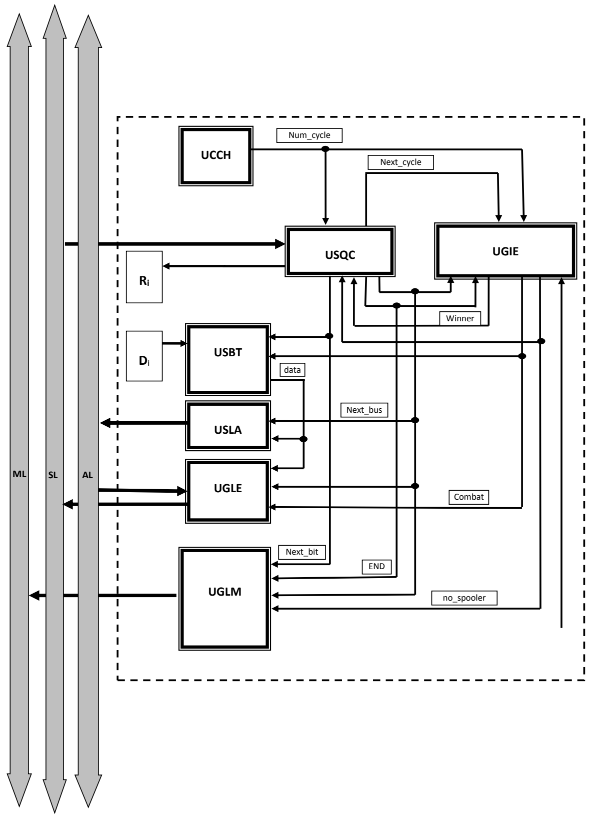

Fig. 7. Interconnection blocks.

5) USLA (Arbitration line selection unit): Responsible for sending the data to the concerned arbitration. It takes into consideration the data: next bit and data to define the concerned arbitration line .

6) UCCH (clock cycle Competing unit): Unit that counts the cycles of sorting processes, and allows us to define the number of iteration at each execution of the system.

7) UGLM (Masque lines Management Unit): It indicates whether there is combat on the bus or not. To carry out this operation, we use Next bit, Next bus and the masks lines.

The interconnection between the different Sub-unit of a PE is shown in Fig. 7. Each sub-unit generate and use as an input several parameters in order to provide at least the corresponding rank of the concerned PE.

To switch from the MATLAB / SIMULINK model to the ISE design model, we proceed as follow: The Simulink model was first checked for compatibility with HDL code generation. We then generated the HDL code in order to synthesize and analyze the timing of our design via the integration with ISE. We finally make an estimation of the resources using ISE.

For the sack of compatibility, before we generate a design report, we specify the characteristics of our FPGA(FPGA Spartan 6 XC6SLX150 (184304 Slice register)) after validating all stages of the HDL advisor. Then an ISE report; providing the required hardware resources; will be generated. The generated report gives as details the device utilization and timing summery of the BulkSort Model.

VII. Results and Discussion

A. Matlab / Simulink Simulation

In this section, we will provide the hardware simulation of our algorithm to demonstrate the effectiveness of the theoretical results in this brief. The C++ Simulation was presented to validate the proposed concept, while the Simulink modeling is in order to have an idea about the required resources.

There has been a question to find an optimal sorting architecture in view of size and depth. The implementation of the majority of sorting algorithm is limited because of the insufficient number of resources.

A number of research efforts are interested on sorting with minimal number of comparators. When we talk about comparators, we ought to think first about the basic devices of an FPGA such as: Slice Registers Look up Tables (LUTs) and others. In this paper, the results will be discussed in view of these parameters.

To simulate, synthesize, and implement HDL code generated from the model, Xilinx ISE Design Suite Version 14.5 is used in this work.The ISE provides an environment to go from design to an implementation of the proposed model by a specification of the design needs.

A various number of models has been synthesized in view of number of Process elements (PE). We should mention that the PEs refer to the set of elements we want to sort. We want to elaborate the variation of slice registers compared to the number of PE for different bus values. The bus refers to the communication link between process elements. Fig. 9 represent the required resources of the BulkSort model in case of 8 and 16 Buses, for 8, 16, 32 and 64 PEs. We found that the percentage do not exceed 21 percent of the available slice LUTs of the used FPGA for the different cases, and remains constant for the slice registers.

It is observed that the variation of LUTs is linear with respect to the number of data to be sorted. We note that using half of Buses we end up with a number of LUTs which is equal to half the number of the beginning. The amount we found is the same when we sort half of the data. The use of LUTs can go up to 1 per cent of the available resources on the platform. These results prove that our model is optimal in view of resources.

For the second parameter which is the Slices registers, we note that a variation of the number of buses for a given data size do not have a very great effect on the slices registers. On the other hand, when acting on the amount of data we are left with the half-slice registers as shown on all tests we performed. The utilization of slice registers did not exceed 1 per cent of the available amount on the platform FPGA Spartan 6.

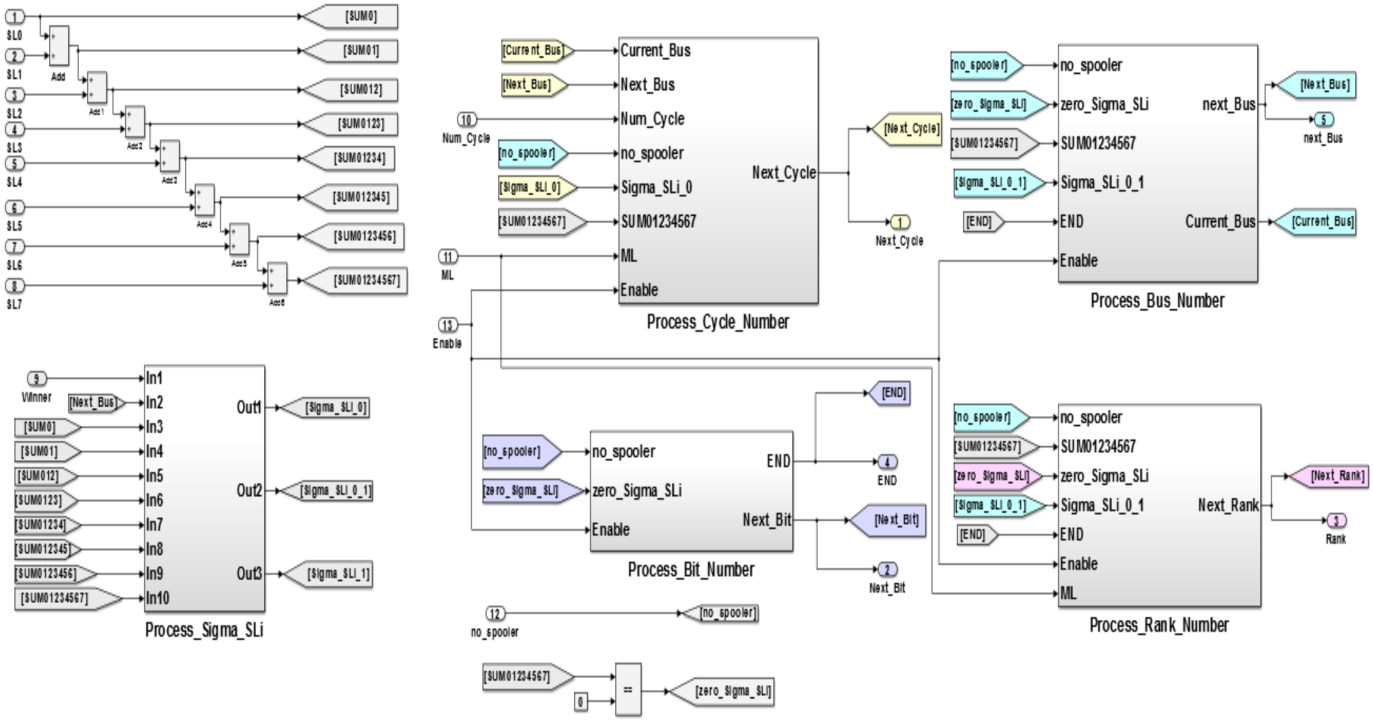

Fig. 8. The USQC $sub_{b}locks$: $Process_{c}ycle_{N}umber$, $Process_{B}us_{N}umber$, $Process_{R}ank_{n}umber$, $Process_{B}it_{N}umber$ and $Process_{S}igma_{S}Li$

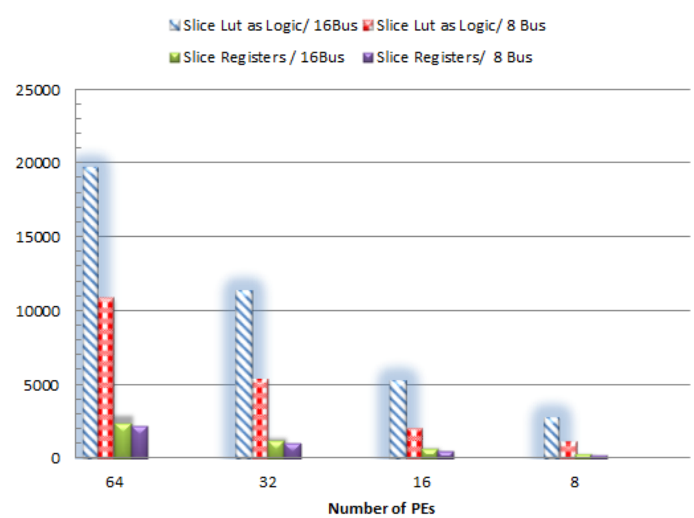

Fig. 9. Required resources of the BulkSort Model in term of slice registers, slice Luck up Tables and clock cycles

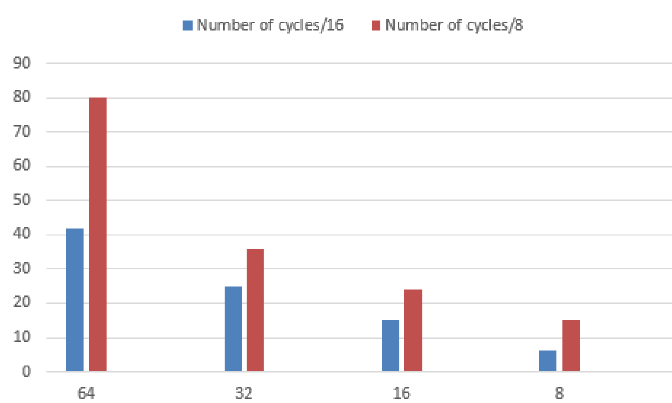

Fig. 10. Number of clock cycles in case of 8 and 16 Buses, for 8, 16, 32 and 64 PEs

In view of clock cycles (see Fig. 10), we found that even if we use half of the Buses to sort the same number of elements, a small increase in clock cycles occurs. So, we can use this point to say that by the use of this model we can sort a big data on a specific clock cycles. We can act also on the number of buses for a model optimization.

The numerical simulation makes it possible to calculate on the computer the solutions of models and to simulate the physical reality in order to have an idea about the hardware implementation. While designing the model of the parallel hardware BulkSort, we focus especially on making an efficient and optimal system. Our central concern is in dividing the required work up into pieces to be processed by several blocks. We proceeded by a partial parallelism (instead of sorting the elements one by one, a single passage allows us to cross the set of elements at each clock stroke).

We should highlight that this model is designed to be implemented in FPGA SPARTAN 6 XC6SLX150 (184304 Slice register). Our system provide both the sorting and ranking list as well as the number of clock cycles of the process.

VIII. Conclusion

In this article, we present a new divide-to-rule-like algorithm, called "BulkSort". We study and exhibit its parallel hardware implementation feasibility. Yet, we implemented it on Matlab-Simulink, and synthesized it using ISE suite design tool. We highlight that our scheme is parallel and reconfigurable according to the number of buses and number of processor elements. We also show that the proposed Simulink design was checked for compatibility with the hardware. Several tests have been conducted to show the applicability and illustrate the performance of our algorithm. Next, we evaluate the BulkSort behaviour in terms of slice registers, slice LUTs and Clock cycles, while varying the number of processor elements. Our proposal exhibits nice performance both in terms of resource utilization as well as sorting time. In view of perspectives, a high-performance, parallel architecture for an FPGA-based accelerator implementing the Bulk-Sort algorithm will be presented. The IP will be modeled using Vivado HLS and an end-to-end system (ZynQ ZC706 board) will be developed in order to assess the performance and resource usage.

References

[1] M. Aumüller and M. Dietzfelbinger, "Optimal partitioning for dual-pivot quicksort," *ACM Transactions on Algorithms (TALG)*, vol. 12, no. 2, p. 18, 2016.

[2] S. Wild, "Quicksort is optimal for many equal keys," in *2018 Proceedings of the Fifteenth Workshop on Analytic Algorithmics and Combinatorics (ANALCO)*. SIAM, 2018, pp. 8–22.

[3] D. P. Singh, I. Joshi, and J. Choudhary, "Survey of gpu based sorting algorithms," *International Journal of Parallel Programming*, vol. 46, no. 6, pp. 1017–1034, 2018.

[4] H. Peng, L. Huang, and J. Chen, "An efficient fpga implementation for odd-even sort based knn algorithm using opencl," in *2016 International SoC Design Conference (ISOCC)*. IEEE, 2016, pp. 207–208.

[5] A. Kazim, "A comparative study of well known sorting algorithms," *International Journal of Advanced Research in Computer Science*, vol. 8, no. 1, 2017.

[6] D. R. Musser, "Introspective sorting and selection algorithms," *Software: Practice and Experience*, vol. 27, no. 8, pp. 983–993, 1997.

[7] S. Mishra, S. Saha, S. Mondal, and C. A. C. Coello, "A divide-and-conquer based efficient non-dominated sorting approach," *Swarm and evolutionary computation*, vol. 44, pp. 748–773, 2019.

[8] R. M. Karp, "A survey of parallel algorithms for shared-memory machines," 1988.

[9] J. M. Liberti and M. A. Petersen, "Information: Hard and soft," *Review of Corporate Finance Studies*, vol. 8, no. 1, pp. 1–41, 2018.

[10] S. G. Akl, *Parallel computation: models and methods*. Prentice Hall Upper Saddle River, 1997, vol. 4.

[11] Y. Zhang, T. Cao, S. Li, X. Tian, L. Yuan, H. Jia, and A. V. Vasilakos, "Parallel processing systems for big data: a survey," *Proceedings of the IEEE*, vol. 104, no. 11, pp. 2114–2136, 2016.

[12] D. Koch and J. Torresen, "Fpgasort: A high performance sorting architecture exploiting run-time reconfiguration on fpgas for large problem sorting," in *Proceedings of the 19th ACM/SIGDA international symposium on Field programmable gate arrays*. ACM, 2011, pp. 45–54.

[13] R. Mueller, J. Teubner, and G. Alonso, "Sorting networks on fpgas," *The VLDB Journal—The International Journal on Very Large Data Bases*, vol. 21, no. 1, pp. 1–23, 2012.

[14] R. Perez-Andrade, R. Cumplido, C. Feregrino-Uribe, and F. M. Del Campo, "A versatile linear insertion sorter based on an fifo scheme," *Microelectronics Journal*, vol. 40, no. 12, pp. 1705–1713, 2009.

[15] H.-T. Hu, J.-R. Chang, and S.-J. Lin, "Synchronous blind audio watermarking via shape configuration of sorted lwt coefficient magnitudes," *Signal Processing*, vol. 147, pp. 190–202, 2018.

[16] M. H. Najafi, D. J. Lilja, M. D. Riedel, and K. Bazargan, "Low-cost sorting network circuits using unary processing," *IEEE Transactions on Very Large Scale Integration (VLSI) Systems*, vol. 26, no. 8, pp. 1471–1480, 2018.

[17] W. Song, D. Koch, M. Luján, and J. Garside, "Parallel hardware merge sorter," in *2016 IEEE 24th Annual International Symposium on Field-Programmable Custom Computing Machines (FCCM)*. IEEE, 2016, pp. 95–102.

[18] S. Hauck, "The roles of fpgas in reprogrammable systems," *Proceedings of the IEEE*, vol. 86, no. 4, pp. 615–638, 1998.

[19] D. Andrews, D. Niehaus, R. Jidin, M. Finley, W. Peck, M. Frisbie, J. Ortiz, E. Komp, and P. Ashenden, "Programming models for hybrid fpga-cpu computational components: a missing link," *IEEE micro*, vol. 24, no. 4, pp. 42–53, 2004.

[20] N. Stekas and D. van den Heuvel, "Face recognition using local binary patterns histograms (lbph) on an fpga-based system on chip (soc)," in *2016 IEEE International Parallel and Distributed Processing Symposium Workshops (IPDPSW)*. IEEE, 2016, pp. 300–304.

[21] S. Ihirri, A. Errami, and M. Khaldoun, "Bulk-sort: A novel adaptive and parallel sorting algorithm," in *Third International Congress on Information and Communication Technology*. Springer, 2019, pp. 725–736.

Semantic Knowledge Transformation for Context-aware Heterogeneous Formalisms

Hafiz Mahfooz Ul Haque[1]
Department of Software Engineering,
The University of Lahore,
Lahore, Pakistan

Sajid Ullah Khan[2]
Department of Computer Science,
The University of Lahore,
Lahore, Pakistan

Ibrar Hussain[3]
Department of Software Engineering,
The University of Lahore,
Lahore, Pakistan

***Abstract*—In recent years, an increasing social dependency has been observed over the cell phones and now evolved into smart devices. Due to the rapid escalation of these smart devices, users are becoming habitual in utilizing these services using smartphones and /or wearable devices in which different applications are running to assist and facilitate users in daily life routine activities. Mobility and context-awareness are the core features of pervasive computing. Context-awareness has the capability to identify the current situation and respond accordingly in the environment whenever and wherever needed. However, it is quite challenging to detect and sense the more appropriate contextual information when various interactive devices communicate among themselves. This paper presents the semantic knowledge transformation techniques for ontology-driven context-aware formalisms to model heterogeneous systems. We propose theoretical as well as practical approaches to transform semantic knowledge into first-order Horn-clause rules format which can be used by context-aware multi-agent systems to achieve their desired goals.**

***Keywords*—Context-aware system; semantic knowledge transformation; ontology; interoperability; smart spaces**

I. Introduction

Smart computing has been considered as one of the most promising research area and rapidly evolving field around the globe. Since the last decade, smart computing has a remarkable upsurge and is continuously progressing towards the development of smarter, faster and tiny devices. Smartphones facilitate the users in daily routine tasks as well as enable interoperability to other active users in the same environment [1]. Smart device dependent technology helps to generate information about user's location, time, and movement to sense and can get a perception about the environment. Usually, knowledge engineers and context-aware computing systems e.g. multiple interacting smart devices and/or multi-agent systems are more user-oriented and formally specified approaches to model context-aware systems. Smart devices need machine-oriented knowledge source intended to make it possible as an intelligent mechanism and smart decisions to perform in a flexible and adjustable way. This trend has been briskly advancing towards pervasive computing environment where smart devices are becoming intelligent enough to analyze the user's current situation and take decision according to the awareness level of the users, which is known as context-awareness. In a pervasive computing environment, semantic knowledge has gained a significant attention for modelling and reasoning heterogeneous systems using context-aware devices. It has been observed that from an individual perspective, a user does not hold the diverse kind of individualized data that can be obtained from heterogeneous sources with their usage pattern, however, it does not disturb their decision on acting [2]. Knowledge representation techniques play vital roles in context-aware computing for understanding contextual information, interpret them, act as a decision support system and then store contextualized information in the knowledge base. Literature has revealed various knowledge representation techniques such as semantic ontologies, frames, rule-based knowledge, knowledge map, decision tables and decision trees [3], [4] etc. Some of them are more useful for human understandability such as semantic knowledge so-called ontologies while some are more suitable for machine requirements for automated inferencing and reasoning process such as rule-based system and object-oriented knowledge representations.

In the literature, several approaches have been proposed using different algorithms [3], [5], transformation functions [6] to improve knowledge representation techniques. It helps knowledge workers to get intrude input knowledge into the system with better machine interoperability. In view of the analysis of the state-of-the-art research approaches, there are few controversial issues and flaws in the conversion of OWL constructs into different desirable knowledge sources [7] as knowledge may exist in different domains in a heterogeneous environment. It may involve inter-agent coordination in distributed nature. Knowledge is conceptualized from the diverse domain, so the flaws or challenging issues might be categorized in different preferences to be adapted. Few of the major challenges are the ambiguity of knowledge, level of automation, the ratio of human intervention & machine intervention to the system, querying efficiency, reasoning & inferring, complex computation and the scope of usability etc. Content-awareness is an appropriate paradigm to process and transmit data in different ways to communicate the content to the end-user. In this paper, we propose semantic knowledge transformation approaches to facilitate the user by introducing a well-defined model and reduce the gap between knowledge engineers and machine users to enhance knowledge interoperability.

The rest of the paper is organized as follows. In Section II, we briefly discuss the background knowledge of context, context-aware systems, contextualizing semantic knowledge and related work. Section III presents a theoretical mapping of ontology axioms to defeasible logic programming rules (DeLP). In Section IV, we show semantic knowledge transformation into a heterogeneous object text file (HOTF). In Section V, we present a contextual defeasible reasoning-based formalism for heterogeneous systems, and finally conclude in

Section VI.

II. Preliminaries and Related Work

A. Context and Context-aware Systems

Literature has revealed several definitions of context so far. The term context can be described as a set of occurring situations essential to the surrounding environment. The situations include in a context setting are persons, objects and the computing resources in the same environment. The ability of smart devices and smart applications to recognize existing working situations or context and adapt their behavior accordingly is known as context awareness [8].

Abowd et al. [9] define context as: *"Context is any information that can be used to characterize the situation of an entity. An entity is a person, place, or object that is considered relevant to the interaction between a user and an application, including the user and applications themselves"*. In a pervasive computing environment, contextual information is of different kinds such as time-context, user-context, physical and computing context. Moreover, the detail about a specific user can be obtained as user profiles, user's location and social situation [10]. More specifically, context provides information related to an entity to know about its current status. It conveys knowledge about a user and application to be interlinked in a specific manner [11]. These devices used for human interactivity e.g. personal digital assistance devices, smart devices or mobile phones, and wireless sensor nodes almost have complex activities to be adapted. Sensors are used to sense the contextual information from the environment which is obtained by the acquisition modules in the context-aware systems. The data generated by the sensors is dynamic and the acquired contextual information can be used to perform reasoning to infer high-level context. The context is interpreted with respect to their scope and describes the context situation at a high-level of interpretation. It is then presented to infer implications and the adaptation process facilitates the users in diverse routine activities manipulating decision-making techniques. The appropriated user's services are discovered and selected in the adaptation process and delivered to the user through the participant devices. The service behavior and the device behavior are adapted with the help of context data accordingly. The application domain is the smart spaces where users interact or communicate smart mobile devices e.g. homes, offices, community areas, healthcare, hotels, campuses and military places [2]. Context-aware approaches should be adaptable as per the changing situation so that user can perfectly complete their desired tasks across the physical locations and smart devices [12].

In the literature, much research efforts have been made to improve interoperability, balancing roles, collaborative work environment among machines and crowd sensing intelligence for human and computing processes design human in the loop architecture [13]. For multiple interacting devices, an agent can be programmed to solve the specific problem. In the multi-agent system, each agent has dedicated a role to capture the knowledge, analyze the situation based on its knowledge base, plan a sequence of actions to achieve the desired goal, enable interoperability in an efficient way, and then finally take decisions dynamically [14]. According to [15] the designing and modeling roles in agent-based systems to facilitate positive interactivity may provide better understandability to the knowledge workers, designer, and development staff. Semantically enriched ontologies are used as a naturally interactive mode among computing devices and active users are shown to be accurate choices [16]. An interoperability refers to the ability to analyze roles in common and to develop schemas in the deployment perspective realizing different methods and tactics. Knowledge interoperability can be further enhanced to cater to complex heterogeneous environments.

B. Contextualizing Heterogeneous Knowledge Sources

Recent years have witnessed the rapid advances in the field of semantic web. The semantic web is a set of standards that can be used for RDF data model, query languages and web ontology language (OWL) to store vocabularies and ontologies. Ontology is an explicit conceptualization of the domain having classes/concepts with their pre-defined relationships [17]. Literature has revealed two different versions of OWL (web ontology language) named as OWL 1 and OWL 2 each having their own sub-languages. A set of fuzzy variables are used for the contextual information and require the rules of fuzzy logic. Local storage stores the collected context data in encrypted form. A history of context is stored to identify preferences. An adequate memory requirement and firm data retrieval mechanisms are required for the context data to achieve efficiency. The missing variables values of the contextual data can be calculated through probabilistic techniques [2].

In literature, researchers have significant contribution in modeling heterogeneous systems by conjoining ontologies with various knowledge representation languages. Description logic with ontology mapping is the most appropriate knowledge representation technique. Distributed description logic (DDL) is a knowledge representation formalism that supports heterogeneity of information. It combines DL knowledge bases to represent distributed information. It also enables inter-ontology mappings using distributed description logics [20]. According to [18], a DDL is mainly a generalization of the description logic frameworks. It aims to conceptualize multiple ontologies that are interconnected by semantic mappings. The core intention of interconnecting ontology axioms is to maintain their unique identity, independence, and preservation of individualized DL knowledge-bases. In DDL, multiple ontologies are interconnected to exchange information using semantic mapping [19] but the axioms of one ontology cannot be shared with other ontology. In DDL, each local ontology contains its local knowledge base with distributed reasoning. The knowledge base of each of the local ontology consists of two kinds of axioms; TBox and ABox. The correspondences of different ontology axioms are called bridge rules (or inter-ontology axioms). By using bridge rules, TBox axioms of one ontology can be interlinked to the corresponding TBox axioms of another ontology in an implicit manner. Example of the inter-ontology axiom is bridge rule which is represented as $C_i \sqsubseteq D_j$; $C_i \sqsupseteq D_j$; Where C_i and D_j belong to concepts of ontologies O_i and O_j correspondingly. A group of different DL knowledge bases is the composition of distributed DL knowledge bases (DKB) that can be expressed as a pair (T, A) that includes distributed TBoxes (DTBox) and distributed

ABoxes (DAbox). For context modeling, ontology-based context modeling approach has been considered to be the most promising one [21].

C. Related Work

In recent years, context-aware applications are rapidly evolving and literature shows the substantial volume of research efforts with the incorporation of heterogeneous systems. Different approaches have been focused on and analyzed in this regard. In [5], semantic knowledge has been transformed into a desirable knowledge format. Authors proposed a transformation mechanism to convert semantic networks into frames. Semantic network ontologies are developed using Protégé ontology editor to get the OWL constructs. The frame is a knowledge representation technique which is more expressive in a sense that it allows the corporate manager or business analyst to predict the current trends in the specified domain. In light of the previous work [6] author has extended his research work and introduced semantic network as ontologies developed in protégé, defined transformation mechanism and provides frames structure as a result. A case study is adapted to show the working flow of the system and to validate the results. Totkov et al. [32] have proposed frame models in e-learning. It introduces the significance of frames and their implications in different real-world application domains such as such as E-learning, which is fanatical to the notion of frames usability as a significant knowledge representation technique. Keeping in view the significance of semantic knowledge transformation into a generalized format for automated reasoning of large-scale ontology management, a mapping of OWL constructs is introduced into relational database schema [33]. It performs the corresponding mapping of classes, properties and individual instances of ontology to the database schema. They use SPARQL and SQL query to query corresponding axioms in ontology and database instances respectively. In [34], an OWL-API based translator, Onto-HCR, was proposed to translate the ontology domain into a set of the plain text of Horn-clause rules format. Later in [35], authors proposed the enhanced version of the tool, D-Onto-HCR. This is also an OWL-API based translator which extracts rules from multiple ontology domains and then transform into horn-clause rules format. It gets input as ontologies and then translates the set of axioms into a set of plain text Horn-clause rules. Apart from this, this tool can be used to generate bridge rules. This work has been further enhanced by the same author in [22]. A translator tool, EDOH was developed which is an extended version of D-Onto-HCR. It is capable to transform mapping rules which help the context-aware defeasible reasoning- based frameworks to deal with inconsistent and incomplete behavior of the system. It takes OWL 2 RL ontology as an input file which is a readable file source using Protégé in the OWL/XML format and provides the resulted output as a text file. In contrast to previous work, the semantic knowledge transformation approaches proposed in this paper provide more flexibility in terms of acquiring contextual information from semantic knowledge sources. We chose the ontology-based context modeling approach and develop the ontologies of smart rescue system and a medical diagnostic system given in the following sections.

III. Transforming Ontology Axioms into DeLP Rules

In this section, we theoretically transform semantic knowledge into horn-clause rules format following the mapping of ontology to DL knowledge-base and then defeasible logic programming (DeLP). To suitably model the system using multiple ontologies and transforming heterogeneous semantic knowledge into defeasible logic programming rules, we adopt the case study of smart rescue system from [22] to illustrate the expressivity and efficacy of the system. We develop two different ontologies of smart rescue system to monitor the fear of flying people and elderly people to provide suitable cure at the right time and in the right place. Fragments of these ontologies can be seen in Fig. 1 and in Fig. 2.

To model the domains, we construct OWL 2 RL ontology (sub-language of OWL 2 [23] to model the case study due to its scalable rule-based reasoning system and expressive power. We show the expressivity and dynamicity of the system by constructing more complex rules using SWRL (Semantic web rule language) [24] in Protégé ontology editor [25]. SWRL provides privileges to users to construct rules using unary predicates (OWL concepts) and binary predicates (roles). In this paper, we explicitly conjoin OWL 2 RL with SWRL rules to solve complex problems using semantic context modeling approach. Contextual knowledge in term of classes and relationships can be defined as concepts and roles respectively in the description logic. Description Logics (DLs) are based on ontology and it has been considered as the best-suited approach to model the domain using ontology with the powerful and expressive DL reasoning. DLs have different sub-languages, among others, we consider DL-SROIQ due to its expressive formalism and its inferencing is decidable [26], [27]. So, ontology axioms can be mapped with the corresponding DL syntax [28] which is shown in Table I. As DL can be used to model the domain, so we transform smart rescue system ontology axiom into corresponding DL axioms. DL Knowledge-base consists of terminology box (TBox) and assertion box (Abox). TBox represents the axioms whereas ABox depicts their substitutions. In Table II, we show the corresponding ontology axioms transformation into DL Knowledge-base.

Description Logic program (DLP) acts as an intermediary knowledge representation mechanism between description logic (DL) and logic programming [28]. DL is a subset of First Order logic (FOL), so DL axioms can be transformed into FOL. Logic programming is closely related to the Horn

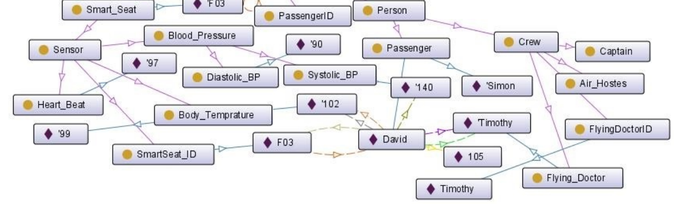

Fig. 1. Smart Seat Ontology Fragment

TABLE I. OWL 2 RL AXIOM TO DL AXIOM

OWL 2 RL Axiom	DL Axiom
SubClassOf	$C \sqsubseteq D$
SubObjectPropertyOf	$R \sqsubseteq S$
EquivalentClassOf	$C \equiv D$
EquivalentObjectPropertyOf	$R \equiv S$
InverseObjectPropertyOf	$R \equiv S^{-}$
ObjectPropertyChain	$R \circ S \sqsubseteq S$
ObjectPropertyRange	$\top \sqsubseteq \forall R.C$
ObjectPropertyDomain	$\top \sqsubseteq \forall R^{-}.C$
SymmetricObjectProperty	$R \equiv R^{-}$
ObjectSomeValuesFrom	$\exists R.C \sqsubseteq D$
ObjectAllValuesFrom	$C \sqsubseteq \forall R.D$

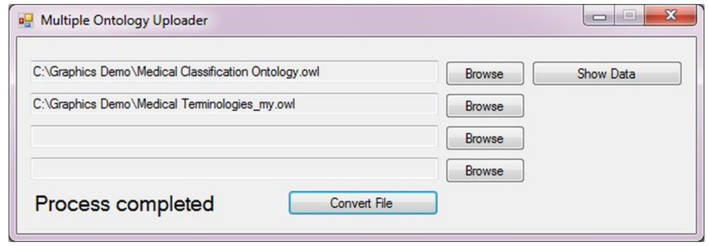

Fig. 3. Multiple Ontology Uploader

fragment of FOL but it is not expressible using FOL [29]. Moreover, DeLP [30] has been considered as one of the most promising approaches to translate DL axioms into non-monotonic horn-clause rules. As this framework is distributed in nature and each domain has to retain its independence, uniqueness, preservation of identity and security. So the acquisition of contextual knowledge from different ontologies and constructing rules could cause inconsistency. To suitably handle this situation, we transform DL knowledge into DeLP rules in the form of strict and defeasible rules as shown in Table III. Strict rules are non-contradictory and interpreted in a classical sense. Defeasible rules perform reasoning to defeat the conflicting contextual information.

IV. Semantic Knowledge To Heterogenous Object Text File (HOTF)

This section presents a systematic tool based approach to transform the semantic knowledge into plain text of OWL constructs. We present a transformation mechanism using HOTF (Heterogeneous Object Text File). Context-aware agents acquire the ontology-driven contextual information from different ontologies using HOTF, perform reasoning and then adapt behavior accordingly. It is more expressive knowledge representation technique and this translation process is automated. The design of HOTF corresponds to the ontology structural specification and hence there is a proximal one-to-one transformation from multiple ontologies constructs to heterogeneous object text file. We illustrate the working flow of HOTF using the case study of medical ontologies. This case study is constructed to assists the patients in diagnostic perspective and for doctors in the treatment plan and health-related services. This ontology is specifically designed to provide complete medical services to patients to take appropriate medical services and this system automatically generates alert messages to doctors whenever needed. We develop ontologies using Protégé [25] ontology editor and it can be saved in

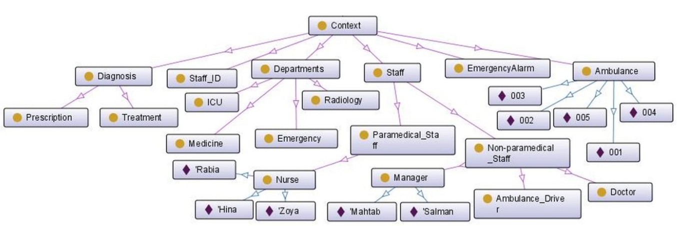

Fig. 2. Smart Rescue System Ontology Fragment

OWL/XML and/or OWL/RDF format. For the translation process, we upload multiple ontologies as input to HOTF as shown in Fig. 3.

Fig. 3 shows a window of multiple ontology uploader which is an input window to get the ontology from different domains of heterogeneous systems. After uploading files, the "Convert File" button executes the transformation function to transform ontological knowledge into Heterogeneous Object Text File. It also classifies OWL constructs based on their object properties and data properties. By clicking "Show Data" button, multiple ontologies OWL constructs can be seen in Fig. 4 in the form of class names with their predefined relationship among classes, methods and relationship types such as aggregation, association etc.

Using this approach, at the moment, four different ontologies can be converted into Object text file simultaneously. However, the number of ontologies can be increased based on user requirement. The results obtained using *HOTF* can be further manipulated to express in the form of horn-clause rules in order to provide better query efficiency. Apart from this, the medical case study discussed above can be interlinked with smart rescue system (mentioned in the previous section) using context-aware multi-agent reasoning based formalism. We draft the ontology-driven context-aware multi-interactive system in Fig. 5 to depict the transformation function from semantic knowledge into rule-based knowledge. The transformation from multiple ontologies to HOTF is implicit in nature; however, from HOTF to rule-based knowledge transformation can be done statically.

V. Contextual Defeasible Reasoning based Formalism for Heterogenous Systems

We present the contextual defeasible reasoning based multi-agent formalism which uses the ontology-driven horn-clause rules to model heterogeneous system. Contextual defeasible reasoning has been emerged from defeasible logic and multi-context system. Contextual Defeasible Logic (CDL) is a rule-based reasoning technique which incorporates defeasible logic in order to defeat and/or derive the contrary evidence. Defeasible logic has been considered as one of the most promising approaches in non-monotonic reasoning. It is a simple and efficient reasoning technique which performs reasoning monotonically as well as non-monotonically [31]. CDL essentially consists of a set of rules (strict, defeasible and defeater), a set of vocabulary and preference ordering. There are two kinds of reasoning in CDL: local reasoning and global reasoning. Local reasoning is performed by either strict rules

TABLE II. MAPPING FROM DL AXIOMS TO STRICT AND DEFESIBLE TERMINOLOGIES

DL Knowledge Base *(KB)*
Strict *TBox* Axioms (Rules)
Rule1:Person $\sqcap$ $\exists$*hasPassengerID.PassengerID* $\sqsubseteq$ *Passenger*
Rule2: Passenger $\sqcap$ *Smart_Seat* $\sqcap$ $\exists$ *isSmartSeatOf* $\sqsubseteq$ *Smart Seat*
Rule3: Passenger $\sqcap$ *Heart Beat* $\sqcap$ *isHeartBeatOf.Heart Beat* $\sqcap$ *greaterThan.100*$\sqsubseteq$ *hasHeartBeat.Abnormal*
Defeasible *TBox* Axioms (Rules)
Rule4: $\exists$*isSmartSeatOf.Smart Seat* $\sqcap$ $\exists$ *hasHeartBeat.Abnormal* $\sqsubseteq$ *NotifyDoctor*
Rule5 : $\exists$*isSmartSeatOf.Smart Seat* $\sqcap$ $\exists$*hasBloodPressure.High* $\sqcap$ $\exists$*hasFever.Yes* $\sqcap$ $\exists$*hasHeartBeat.Abnormal* $\sqsubseteq$ *NotifyDoctor*
Rule6 : $\exists$*isDiagnosedBy.FlyingDoctor* $\sqcap$ $\exists$ *hasHeartBeat.Abnormal*$\sqsubseteq$ $\exists$*hasSituation.Emergency*
Rule7 : $\exists$*isDiagnosedBy.Flying Doctor* $\sqcap$ $\exists$*hasBloodPressure.Stage2hypertension*$\sqcap$ $\exists$*hasHeartBeat.Abnormal*
$\sqsubseteq$ $\exists$hasSituation.Emergency
Rule8 : Passenger $\sqcap$ $\exists$*hasHeartBeat.Abnormal*$\sqsubseteq$ $\exists$ *'Tell 1, 4, hasHeartBeat:Abnormal'*
Rule9 : $\exists$ *'Tell 1, 4, hasHeartBeat.Abnormal'* $\sqsubseteq$ $\exists$ *hasHeartBeat.Abnormal'*
Assertional Box (ABox): *A*
Timothy : Passenger
125 : Heart Beat
David : Flying Doctor
(Timothy, PS00101) : hasPassengerID
(Timothy, F03) : isSmartSeatOf
(Timothy, 125) : isHeartBeatOf
(Timothy, David) : isDiagnosedBy
(Timothy, "Emergency") : hasSituation

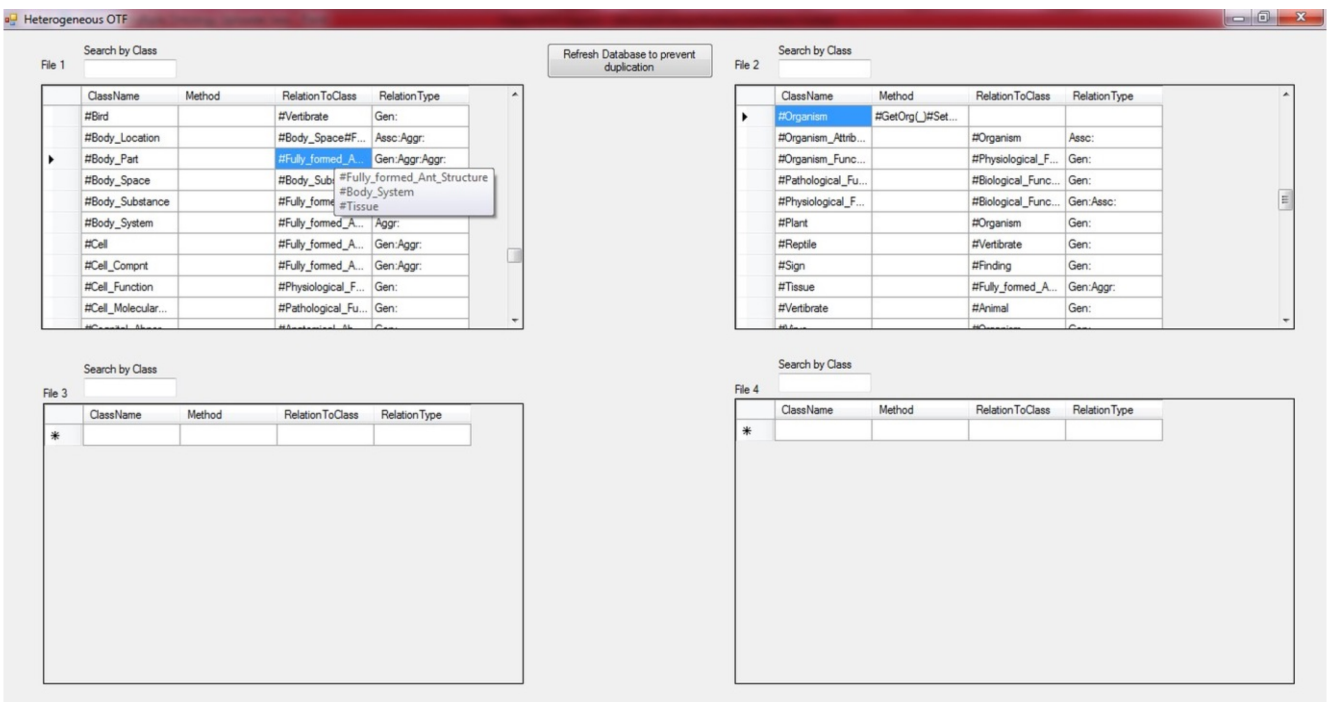

Fig. 4. Heterogenous OTF (HOTF)

or defeasible rules or a combination of both, and these rules are extracted from either a single-domain ontology or multi-domain ontologies. Strict rules are interpreted for local domain ontology in a classical sense whereas defeasible rules are interpreted defeasibly. Global reasoning is performed by firing the rule instances of mapping rules. These rules are formed by combining contextual information extracted from different domains ontologies. More precisely, these rules are formed from local contexts of one domain with the global context of another domain in order to perform successful execution of the system. The set of individualized contextual information and the set of rules taken from corresponding ontology domain is known as local contexts whereas the contextual information extracted from another ontology is known as foreign contexts. These set of local and foreign contexts are formed to make the bridge rules and these rules are interpreted in a classical way using context-aware defeasible reasoning based multi-agent system.

This system includes a set of agents $n_{A_g}(\geq 1)$, i.e., $A_g = \{1, 2, \ldots, n_{A_g}\}$. Each agent is assigned a specific task to solve the problem and it is dedicated for its own specified tasks only. Each agent ($i \in A_g$) in the system having of a set of rules (strict, defeasible, mapping and communication rules) along with the set of contextual information (vocabulary) and

TABLE III. MAPPING FROM STRICT AND DEFEASIBLE TERMINOLOGIES INTO HORN-CLAUSE RULES

DL Axioms to Rules Mapping
Strict TBox Axioms to Strict Rules Mapping
Rule1: Person(?pas), hasPassengerID(?pas, ?pasID), PassengerID(pasID) $\rightarrow$ Passenger(?pas)
Rule2: Passenger(?pas), Smart_Seat(?sid) $\rightarrow$ *isSmartSeatOf (?p, ?sid)*
Rule3: Passenger(?pas), isHeartBeatOf (?hb, ?pas), HeartBeat(?hb), greaterThan(?bh, 100) $\rightarrow$ hasHeartBeat(?pas, "abnormal")
Defeasible TBox Axioms to Defeasible Rules Mapping
Rule4: isSmartSeatOf (?sid, ?pas), hasHeartBeat(?pas, "Abnormal") $\Rightarrow$ NotifyDoctor(?p, ?sid)
Rule5: isSmartSeatOf (?sid, ?pas), hasBloodPressure(?pas, "High"), hasFever(?p, "Yes"), hasHeartBeat(?p, "Abnormal") $\Rightarrow$ NotifyDoctor(?pas, ?sid)
Rule6: isDiagnosedBy(?p, ?doc), hasHeartBeat(?p, "Abnormal") $\Rightarrow$ hasSituation(?p, "Emergency")
Rule7: isDiagnosedBy(?p, ?doc), hasBloodPressure(?p, "Stage2hypertension"), hasHeartBeat(?p, "Abnormal") $\Rightarrow$ hasSituation(?p, "Emergency")
Communication Rules
Rule8: Passenger(?pas), hasHeartBeat(?pas, "Abnormal") $\rightarrow$ 'Tell 1, 4, hasHeartBeat'(?pas, "Abnormal")
Rule9: 'Tell 1, 4, hasHeartBeat'(?pas, "Abnormal') $\rightarrow$ hasHeartBeat(?pas, "Abnormal")

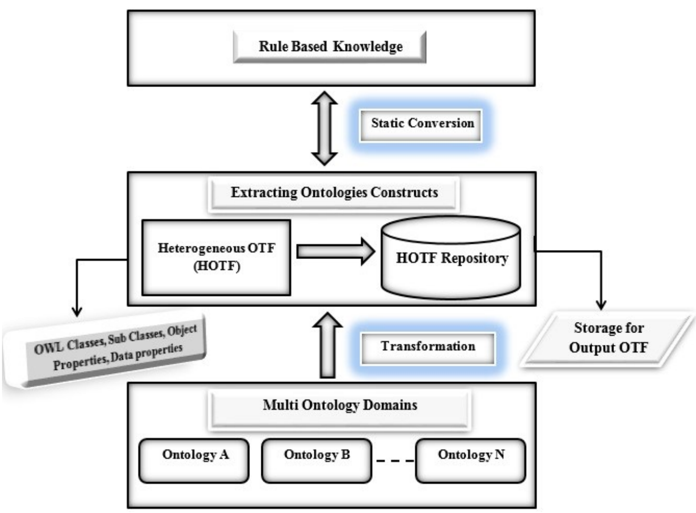

Fig. 5. Ontology-Driven Context-Aware Multi-Interactive System

priority relation, which is represented using a triple $(R, F, >)$, where F is a finite set of individualized contextual information (facts), R represents the set of all rules which are used to infer derivated contextualized information from heterogeneous knowledge sources, and $>$ express superiority relation explicitly on R. As the system is heterogeneous in nature and runs in a highly decentralized and dynamic environment, so agents need to derive and share contextual information autonomously. For contextual modeling and reasoning, the system performs three core actions: *Rule*, *Copy* and *Idle*. *Rule* action is triggered by firing the rule instances of each agent in the system. *Rule* instances are of the type of strict rules, defeasible rules, and mapping rules. *Copy* action is triggered by firing the instance of communication rules whenever agents need to exchange the contextual information. *Idle* action allows agents to remain in idle state but transit to the next state if triggered by the system. The system performs reasoning non-deterministically and non-monotonically, so the rule priorities are static and set at the design time of the system in order to avoid inconsistent behavior of the system.

To illustrate the use of the proposed formalism, we develop the ontologies of smart rescue system and smart seat system to assist the patient's diagnostic perspective and to monitor the vital signs of the fear of flying people during their air travel. We omit the technical details of contextual defeasible reasoning framework in this paper. For this, we refer the interested readers to our earlier work [22]. However, in Section III, we have discussed the implementation of the extended case study in terms of rules transformation.

VI. CONCLUSION AND FUTURE WORK

In this paper, we proposed two approaches of semantic knowledge transformation. The first approach provides a concrete and proximal one-to-one transformation mechanism from ontology axiom to DeLP rules. The second approach provides an automated transformation of ontology axioms into context-aware agent's understandable format in HOTF so that agents automatically acquire contextual information from HOTF to model heterogeneous system and thus achieve their desired goals. In the future, we will develop a systematic application model and implement the case study to check, specify and verify its correctness properties of the system.

REFERENCES

[1] R. Ballagas, J. Borchers, M. Rohs and J. G. Sheridan, *The smart phone: a ubiquitous input device*, in IEEE Pervasive Computing, vol. 5, no. 1, Jan.-March 2006, pp. 70-77.

[2] Grabowski, P., & Samfelt, J. (2016). User awareness of privacy regarding user data in Mobile Health applications and wearables:-Do you know what you are sharing?

[3] Liao, S. H. (2005). Expert system methodologies and applications, a decade review from 1995 to 2004. Expert systems with applications, 28(1), 93-103.

[4] J. D. Wren, Engineering in genomics, in IEEE Engineering in Medicine and Biology Magazine, pp. 87-93, (2004).

[5] Khan, S. U. (2013). Transformation of Semantic Networks into Frames. International Journal of Innovation, Management and Technology, 4(1), 21.

[6] Khan, S. U., Khan, M., & Nauman, M. (2016, August). Semi-automatic knowledge transformation of semantic network ontologies into Frames structures. In Innovative Computing Technology (INTECH), 2016 Sixth International Conference on (pp. 712-717). IEEE.

[7] Afzal, H., Waqas, M., & Naz, T. (2016). OWLMap: Fully Automatic Mapping of Ontology into Relational Database Schema. International journal of advanced computer science and applications, 7(11), 7-15.

[8] Dey, A. K. (2001). Understanding and using context. Personal and ubiquitous computing, 5(1), 4-7.

[9] Abowd, G. D., Dey, A. K., Brown, P. J., Davies, N., Smith, M., & Steggles, P. (1999, September). Towards a better understanding of context and context-awareness. In International Symposium on handheld and ubiquitous computing (pp. 304-307). Springer, Berlin, Heidelberg.

[10] Schilit, B., Adams, N & Want, R. (1994, December). Context-aware computing applications. In Mobile Computing Systems and Applications, 1994. Proceedings., Workshop on (pp. 85-90). IEEE.

[11] Guo, B., Zhang, D., & Imai, M. (2011). Toward a cooperative programming framework for context-aware applications. Personal and ubiquitous computing, 15(3), 221-233.

[12] Li, H., & Wang, J. (2011, August). Application architecture for ambient intelligence systems based on context ontology modeling. In Internet Technology and Applications (iTAP), 2011 International Conference on (pp. 1-4). IEEE.

[13] Nunes, D. S., Zhang, P., & Silva, J. S. (2015). A survey on human-in-the-loop applications towards an internet of all. IEEE Communications Surveys & Tutorials, 17(2), 944-965.

[14] Wooldridge, M. (2009). An introduction to multiagent systems. John Wiley & Sons.

[15] Cabri, G., Ferrari, L., & Leonardi, L. (2004, October). Agent role-based collaboration and coordination: a survey about existing approaches. In Systems, Man and Cybernetics, 2004 IEEE International Conference on (Vol. 6, pp. 5473-5478). IEEE.

[16] Soylu, A., Giese, M., Jimenez-Ruiz, E., Vega-Gorgojo, G., & Horrocks, I. (2016). Experiencing OptiqueVQS: a multi-paradigm and ontology-based visual query system for end users. Universal Access in the Information Society, 15(1), 129-152.

[17] Guarino, N., Oberle, D., & Staab, S. (2009). What is an ontology?. In Handbook on ontologies (pp. 1-17). Springer, Berlin, Heidelberg.

[18] Serafini, L., & Tamilin, A. (2005, May). Drago: Distributed reasoning architecture for the semantic web. In European Semantic Web Conference (pp. 361-376). Springer, Berlin, Heidelberg.

[19] Grau, B. C., Parsia, B., & Sirin, E. (2004, November). Working with multiple ontologies on the semantic web. In International Semantic Web Conference (pp. 620-634). Springer, Berlin, Heidelberg.

[20] Borgida, A., & Serafini, L. (2002, October). Distributed description logics: Directed domain correspondences in federated information sources. In OTM Confederated International Conferences" On the Move to Meaningful Internet Systems" (pp. 36-53). Springer, Berlin, Heidelberg.

[21] Baldauf, M., Dustdar, S., & Rosenberg, F. (2007). A survey on context-aware systems. International Journal of Ad Hoc and Ubiquitous Computing, 2(4), 263-277.

[22] Haque, H. M. U., & Khan, S. U. A context-aware reasoning framework for heterogeneous systems. In International Conference on Advancements in Computational Sciences (ICACS'18), IEEE Xplore Digital Library, pp. 1-9, (2018).

[23] Hitzler, P., Krötzsch, M., Parsia, B., Patel-Schneider, P. F., & Rudolph, S. (2009). OWL 2 web ontology language primer. W3C recommendation, 27(1), 123.

[24] O'connor, M., Knublauch, H., Tu, S., & Musen, M. (2005). Writing rules for the semantic web using SWRL and Jess. Protégé with Rules WS, Madrid.

[25] Protégé: The Protégé ontology editor and knowledge-based framework (Version 4.1). http://protege.stanford.edu/ (July 2011)

[26] Horrocks, I., Kutz, O., & Sattler, U. (2006), The Even More Irresistible SROIQ. Kr, 6, 57-67.

[27] O'Connor, M. J. & Das, A. K. (2012), A Pair of OWL 2 RL Reasoners. In OWLED (Vol. 849).

[28] Grosof, B. N., Horrocks, I., Volz, R., & Decker, S. (2003, May). Description logic programs: combining logic programs with description logic. In Proceedings of the 12th international conference on World Wide Web (pp. 48-57). ACM.

[29] Baral, C. and Gelfond, M. Logic programming and knowledge representation. The Journal of Logic Programming, 19:73148, (1994).

[30] Gómez, S. A., Chesnevar, C. I., & Simari, G. R. (2007). Inconsistent ontology handling by translating description logics into defeasible logic programming. Inteligencia Artificial. Revista Iberoamericana de Inteligencia Artificial, 11(35).

[31] Antoniou, G. (2002). A Nonmonotonic Rule System using Ontologies. In RuleML (Vol. 60).

[32] Totkov G., S. Gaftandzhieva, R. Doneva, Accumulative frame models in e-learning, Scientific works of the Union of Scientists in Bulgaria. Plovdiv, Series C. Technik and Technologies. ISSN 1311-9419, Vol. 15, pp. 17-20, 2017.

[33] Lee, J., Goodwin, R., & Akkiraju, R. (2006). Ontology management for large-scale enterprise systems. In Web Semantics & Ontology (pp. 91-114). IGI Global.

[34] Ul-Haque, H. M. (2017). A formal approach to modelling and verification of context-aware systems (Doctoral dissertation, University of Nottingham).

[35] Haque, H. M. U., Rakib, A., & Uddin, I. (2016, November). Modelling and reasoning about context-aware agents over heterogeneous knowledge sources. In International conference on context-aware systems and applications (pp. 1-11). Springer, Cham.

Performance Analysis of Network Intrusion Detection System using Machine Learning

Abdullah Alsaeedi[1], Mohammad Zubair Khan[2]
Department of Computer Science
College of Computer Science and Engineering
Taibah University, Madinah, KSA

***Abstract*—With the coming of the Internet and the increasing number of Internet users in recent years, the number of attacks has also increased. Protecting computers and networks is a hard task. An intrusion detection system is used to detect attacks and to protect computers and network systems from these attacks. This paper aimed to compare the performance of Random Forests, Decision Tree, Gaussian Naïve Bayes, and Support Vector Machines in detecting network attacks. An up-to-date dataset was chosen to compare the performance of these classifiers. The results of the conducted experiments demonstrate that both Random Forests and Decision Tree performed effectively in detecting attacks.**

***Keywords*—Intrusion Detection System (IDS); classifiers; AI; machine learning; KDD99; CICIDS2017; DoS; U2R; R2L**

I. Introduction

According to January 2019 statistics [1], the number of Internet users has surged compared to the previous year, with more than one million users using the web daily for the first time. There are 5.11 billion mobile users today, increased by 2% compared to the previous year. The number of Internet users worldwide is 4.39 billion, with an expansion of 366 million (9%) compared to January 2018. There are 3.48 billion social media users today, representing a 288 million (9%) increase since this time a year ago. In addition, 3.26 billion users utilized Internet-based social media on cell phones in January 2019. The development of 297 million new users represents a year-on-year increment in excess of 10%. Users are not simply Internet users but hackers too. A computer hacker is a skilled expert who uses technical expertise to hack computers. As per a report generated by AV-TEST [2], there are 350,000 malicious programs (malware) and unwanted applications every day. There are 1,250,000 hackers who make malware [2].

Today, political groups and businesses are progressively engaged in advanced digital warfare to combat harm to and intrusion on PC networks [3], as well as the theft of private content. It is important to ensure reliable measures to guard against the intrusion of powerful attackers over the network. These attacks fall into two categories [4]: passive and active. In passive attacks, the intruders obtain exchanged data through the network without causing any damage or disruption to communication or data. Examples of passive attacks include eavesdropping, non- participation, and monitoring. Active attacks are those that modify communication data or negatively affect operations. Instances of active attacks include jamming, message dropping, debasement, denial of service (DoS), and forging.

In recent years, the number of attacks has increased. Malware, botnets, spam, phishing, and DoS attacks have turned out to be consistent dangers for systems and hosts [5]. Therefore, efficient intrusion detection systems (IDS) have been designed and developed to detect these threats. Intrusion detection [6] is the process of observing and analyzing events in a computer system or network in order to detect possible incidents and to prevent any illegal access. The process commonly begins by automatically gathering information from various network sources and analyzing this information for potential security threats. As the number of threats and attacks are increasing day by day, a powerful IDS is necessary to secure the networks and computer systems. In this paper, detection and identification will be used interchangeably.

Available IDS are commonly categorized as either anomaly-based [7], signature-based [8], or a combination of both. The anomaly-based method focuses on identifying unfamiliar behaviors in a network by examining the network's activities. This method is effective in identifying attacks not encountered before, so it is effective on previously unseen attacks [9], [10]. On the other hand, the signature-based method uses a database that is built to identify attacks. It works by creating a database containing all traffic patterns associated with each detected attack. This strategy is very effective. However, it requires updating the databases continually to handle new data attacks and, regardless of whether the databases are up to date, they are defenseless against previously unseen attacks. Since these attacks are not in the database, they can't be counteracted.

A. Motivation and Objectives

The number of Internet users has increased in parallel with the increasing number of attacks made on the Internet daily. In recent years, dangers have increased in complexity as well, such as application attacks. These kinds of attacks are refreshed continuously. Hence, being able to develop and analyze the performance of the proposed IDS systems on newly released datasets such as the Intrusion Detection Evaluation Dataset (CICIDS 2017) containing up-to-date attacks is another motivation for this study.

As stated in the previous section, there are two fundamental methods to detect and distinguish attacks. These methods aim to guarantee data security and identify attacks based on either signature or anomaly. Developing an effective and reliable anomaly-based IDS to detect attacks properly with few false positives is a challenging task [11], [12]. For this reason, securing the networks and PCs against various kinds of attacks has motivated us to develop a robust anomaly-based IDS by utilizing supervised machine learning classifiers.

The main objectives of this study are:

- to check the performance of machine learning algorithms (classifiers) that can be used to detect network anomalies or attacks.
- to validate the significance of results obtained using an IDS.

The rest of the paper is organized as follows. Section 2 describes the related background of anomaly types and datasets presented in the literature. Section 3 presents the methodology used for developing our IDS. Section 4 presents the experimental results and relevant discussion. Section 5 discusses the related works and Section 6 concludes the paper.

II. Background and Literature Survey

A. Anomaly Types and Network Intrusions

An anomaly is a sample of data that does not behave as well as normal samples [13]. There are three types of anomaly defined in the literature: point, contextual, and collective [14]. An anomaly can be considered as a point anomaly if it differs from the normal pattern of data samples in the entire dataset [14]. If a data sample behaves anomalously in a specific context or under specific conditions, it is referred to as a contextual anomaly. A set of similar instances that behave anomalously compared to other instances in the whole dataset is called a collective anomaly.

System security endeavors to shield the network system from attacks against the following three features: confidentiality, integrity, and availability [14], [15], [16]. The confidentiality feature is introduced to ensure that authorized users can only access data while these data are being transferred through networks. The integrity feature denotes that adding, modifying and deleting data can only be accomplished by the authorized user. The transmission data should maintain availability, which means that the services should always work promptly for the authentic user and that the network should be resilient against any kind of attack.

B. Types of Network Attacks

- Denial of Service (DoS) [14]: This attack is known as one of the most common kinds of intrusion and is intended to prevent legitimate users from accessing system resources or services. The DoS attacker may send a huge number of requests to a web server to prevent legitimate users from accessing services. DoS attacks can perform in two ways [17], [18]. The first way is bandwidth exhaustion, which aims to consume the bandwidth of the victims by flooding it with huge amounts of data. The second way is called resource consumption and its intention is to exhaust the victim's resources such as memory and processor. Many previous works [19], [20] have attempted to detect DoS attacks by utilizing artificial intelligence and machine learning approaches.
- Distributed DoS (DDoS): This attack is very similar to DoS in its intent, which revolves around preventing legitimate users from accessing the services. This kind of attack utilizes various computer systems as attack sources and attempts to flood the victim's devices including PC computers or IoT devices with inessential and useless requests. There are many IDSs [20], [21] proposed in the literature to detect DDoS attacks.
- Probing (information gathering) [14]: This aims to gather information about a machine, network structure, and network-connected devices. It focuses on collecting the security vulnerabilities of machines connected to the network. This kind of attack can be considered as the first step in other attacks.
- R2L/R2U (Remote to Local/Remote to User) [14], [22], [23]: In this attack, an attacker's intention is to gain access to the victim's PC to reveal system vulnerabilities, whereby an attacker attempts to get the privilege of sending packets over the Internet to get access to the system as a local user. The brute force method can be utilized to capture passwords and penetrate the system.
- U2R (User to Root) [14], [24]: In this kind of attack, the attacker focuses on gaining the privilege of administrator in order to access unauthorized files and manipulate important data [14]. The attacker may use system vulnerabilities to gain the privilege of administrator via sniffing passwords or a social engineering approach.
- Port Scan [25]: This aims to discover opened ports by scanning all ports in the victim's system and it can be considered as the initial phase of remote-to-local (R2L) attacks. The attackers use this kind of attack to discover more potential vulnerability that can help them in intruding on the victim's system. A number of IDSs have been proposed using machine learning approaches to detect this kind of attack.
- Botnet: In this kind of attack, the attackers use multiple devices connected to the Internet to get access to the victim's system by sending spams.
- Brute Force [26], [27]: A brute force attack is one of the most common attack types that threaten computer networks and break encryption. In this kind of attack, the attacker attempts to get user credentials by utilizing a repetitive method to guess username and password using automated software to get the valid account information of victims.
- Cross-site Scripting [28]: This is an attack that attempts to inject malicious codes in the client side of a website. It relies on weaknesses in the unencrypted websites and the information entered by users. The attackers may use dynamic content such as JavaScript and Flash to deliver malicious codes.
- SQL injection: This type of attack especially targets webservers, since SQL is a common language used in database servers. To get access to the information contained in the database server, attackers insert customized queries to obtain critical information such as personal information, passwords, or credit card

numbers for further malicious purposes. Also, such as in the case of webservers that contain a content management system (CMS), it is possible to insert the arbitrary code as a database register and execute it, thanks to a vulnerability in the CMS. Usually, most of the SQL injection attacks infect the vulnerable server. It may be possible for an attacker to go to a website's search box and type in a code that would force the site's SQL server to dump all its stored usernames and passwords for the site.

- Heartbleed [29]: This is an attack that can be considered as an impactful vulnerability in the OpenSSL that causes leaking of memory data. It allows attackers to remotely access sensitive data in a memory, including login credentials and private cryptographic keys.

C. Datasets

For evaluating the effectiveness of IDSs that are based on machine learning techniques, a huge amount of risky and riskless network traffic is required to train and test IDSs. Unfortunately, it is very difficult to use live network traffic publicly for security and privacy reasons. To deal with these issues, many datasets are available publicly to be used for testing and training IDSs. In this section, we discuss various datasets that are widely used to compare the performance of IDSs.

1) DARPA 98: DARPA dataset [30] was made by MIT Lincoln research to provide a complete benchmarking IDSs. In this dataset, the training and testing sets is split after simulating PC network of the United States Air Force's local. This dataset includes email and IRC messages, internet browsing, file transmission using FTP, Telnet activities. This dataset contains 38 kind of attacks that fall into the main four categories of attacks: Denial of Service (DoS), User to Remote (U2R), Probe, and Remote to Local (R2L).

2) KDD Cup 99: KDD Cup 99 dataset [31], [32] was made by the University of California for building and evaluating IDSs in the Third International Knowledge Discovery and Data Mining Tools Competition (The KDD Cup '99). It has been used commonly for evaluating anomaly-detection systems. The KDD Cup 99 dataset is split into training and testing sets. The training set comprises 4,898,431 and the test set comprises 311,029 records. The KDD Cup 99 contains 24 attack types in the training set and an additional 14 attack types in the testing set. These attacks fall into four main categories: Dos, R2L, U2R, and Probing. Compared to DARPA, KDD Cup 99 is commonly used for IDSs such as study presented in [33]. However, despite the fact that the KDD 99 dataset is a better option compared to DARPA 98, there are many redundancies in the KDD 99 dataset. These redundancies may affect the result of IDSs. Besides this, the size of the KDD 99 dataset is very large and minimizing the dataset may lead to losing some properties of the datasets.

3) NSL-KDD: In order to mitigate the weaknesses with the KDD dataset, Tavallaee et al. [24] built the NSL-KDD dataset to avoid redundancies by eliminating them. The dataset is not considered as representative of real networks. The NSL-KDD [34] dataset comprises 125,973 training samples and 22,544 testing samples. The size of the dataset is reasonable and experiments can be performed without any minimization [32].

4) ISCX 2012 : Although numerous datasets have been proposed for the identification of intrusions, these datasets are not up-to-date and do not reflect real-world data. To mitigate these problems, the Canadian Institute for Cybersecurity proposed a dataset named Intrusion Detection Evaluation Dataset [12], ISCX-IDS 2012, which was collected by monitoring seven-day network activity. The labeled dataset includes about 1,512,000 packets with 20 features.

The main features of this dataset are described in [35] and can be summarized as follows: real, normal, and malicious streams including FTP, HTTP, IMAP, POP3, SMTP and SSH protocols gathered as made, using real devices. All data are categorized and labelled. The collected datasets include various types of intrusion (Infiltrating, DoS, DDoS and Brute Force SSH).

5) CICIDS2017: The Canadian Institute for Cybersecurity at the University of New Brunswick made a new dataset for Intrusion Detection Evaluation named CICIDS 2017 [36], [37]. The CICIDS 2017 dataset comprises benign and the most up-to-date regular attacks, which takes after the true real-world data (PCAPs). Additionally, it incorporates the results of the network traffic analysis utilizing CICFlowMeter with named streams dependent on the time stamp, source and destination IPs, source and destination ports, conventions and attacks (CSV documents). This dataset contains a 5-day (July 3-7, 2017) data stream on a live network created by computers using up-to-date operating systems such as Windows Vista / 7 / 8.1 / 10, Mac, Ubuntu 12/16 and Kali.

This dataset has a few disadvantages. First, the size of the dataset is very large. Second, unlike KDD 99 and NSL-KDD datasets, there are no separate training and testing datasets. Finally, this is a new dataset so few studies have been used for building IDSs. In this paper, we decided to choose the CICIDS 2017 dataset for our experiment using Python, because it is an up-to-date dataset.

III. Related Work

In this section, different investigations utilizing machine learning to distinguish anomalies on PC networks have been analyzed sequentially. In each examination, the utilized AI algorithms, datasets and execution performance ratios are given. While choosing, these investigations have concentrated on the utilization of various machine learning algorithms and datasets.

Chebrolu et al. [38] applied a feature reduction approach to eliminate less informative attributes and used a Bayesian network (BN), Classification and Regression Trees (CART), and ensemble of both classifiers as intrusion detection systems. The Markov blanket (MB) model and decision tree (DS) were utilized to elect a subset of features. After that, the BN, CART, and the ensemble of both classifiers were examined. A hybrid approach of combining different feature selection approaches and ensemble classifiers utilized this approach on the KDD cup 99 intrusion detection dataset, and achieved different accuracies for each kind of attack: Normal (Benign): 100%, Probe: 100%, DOS: 100%, U2R: 84% and R2L: 84%.

Khan et al. [39] built an anomaly-detection system by combining a dynamically growing self-organizing tree (DGSOT) clustering algorithm with support vector machines (SVM). The intuition behind this combination is to aid SVM to cope with training datasets when they are very large. The random selection was applied to reduce the training data before, in this case, the SVM classifier attained accuracies of 98, 39, 23, 15, and 88% for the following attack kinds: Normal, Dos, U2R, R2L, and Probe, respectively. On the other hand, clear improvements were obtained after combining DGSOT with SVM for DOS, R2L, and prob attacks, achieving accuracies of 97, 43, 91%, respectively.

Yassin et al. [40] proposed an architecture that combines K-Means clustering and Naïve Bayes classifier to increase the detection rate and decrease both false positive and false negatives. They computed the detection rate (precision) and the false alarm (false positive) rate to measure the performance of IDS. The proposed architecture was evaluated using the ISCX 2012 Intrusion Detection Evaluation Dataset. A high accuracy of 0.99 and high detection rate of 98.8 were obtained on the testing data. Besides, a false positive rate of 0.13% was obtained.

Gaikwad et al. [41] proposed a new IDS using a bagging ensemble method with REPTree as the base estimator. Applicable features from the NSL-KDD dataset were selected manually to improve classification accuracy and decrease the false positive rate. The performance of the proposed bagging ensemble method was assessed using classification accuracy, model building time, and false positive rates. The results of the experiments conducted demonstrated that the bagging ensemble method with REPTree as base estimator attained a classification accuracy of 99.67 on 10-fold cross validation and 81.29% on the test dataset.

Divyasree and Sherly [42] proposed an effective IDS utilizing ensemble core vector machine (CVM) approach. CVMs are algorithms which work based on the idea of Minimum Enclosing Ball. The proposed IDS was built to detect attacks such as U2R, R2L, Probe and DoS attacks. The KDD Cup 99 dataset was used to train and test the classifiers. The chi-square test was used to elect the relevant features for each kind of attack to reduce the dimensionality of features. The experimental results demonstrated that CVM models achieved high accuracy for each kind of attack. The CVMs attained accuracies of 0.99, 0.945, 0.76, and 0.937 for Dos, Probe, R2L, and U2R, respectively.

Akram Boukhamla et al. [22] built a new dataset called CICIDS2017 to compare the effectiveness of IDSs. They used principal component analysis (PCA) to reduce the dimensionality of the features. The preprocessing phase included removing missing, redundant or infinite values and removing all nominal feature such as flow ID, source IP, destination IP, timestamp. The minimized CICIDS 2017 dataset was assessed using KNN, C4.5 and naïve Bayes classifiers. The outcomes of their experiment showed that NB attained the highest detection rate (recall) for DDoS, XSS, SqlInjection, and Infiltration attacks, while KNN attained a higher detection rate for PortScan and Botnet attacks. The C4.5 classifier achieved the highest detection rate for Brute Force attacks.

Dong Seong Kim et al. [43] proposed combining Genetic Algorithm (GA) with SVM to improve the performance of the SVM-based IDS. The proposed system in [43] showed the novelty of using GA for selecting optimal features and for choosing optimal parameters for the SVM classifiers. The outcomes of their experiments proved that the system could achieve a detection rate of 0.99 on the KDD 1999 dataset, considering the best performing IDS compared to the traditional SVM.

Ashraf et al. [23] compared the performance of Naive Bayes, J48, and Random Forest (RF) on 20% the NSL-KDD dataset. The valuable attributes were selected using the filter method in WEKA where Info gain was used as attribute evaluator. The collected results proved that RF performed better than NB and J48. Accuracies of 96.27, 99.17, and 99.71 were attained by NB, J48, and RF, respectively. The RF achieved an F-Measure score of 0.997, which is the highest score compared to NB and J48.

Kumar et al. [44] proposed an effective IDS based on a modified NB classifier to overcome the drawback with the traditional NB at detecting intrusions. They compared the performance of modified NB with Naïve Bayes, J48, and REPTree on the NSL-KDD dataset. The modified NB attained the highest accuracy of 92.34. Besides, the performance of the modified NB, traditional NB, J48, and REPTree were measured based on several feature selection methods including Correlation-based, Information Gain, and Gain Ratio. The modified NB attained an accuracy of 98.94 when gain-ratio was used for feature selection.

IV. Methodology

For the experiments, the well-known CICIDS 2017 dataset [36] was chosen. The reason behind selecting this dataset is that it is among the most up-to-date datasets containing the most up-to-date attacks. Table I reports the datasets used in the experiments along with the statistics. Decision Tree (DS), Gaussian Naïve Bayes (GNB), Random Forest (RF), and Linear Support Vector Machines (SVM) were selected as classifiers. The experiments were conducted in a Python environment with the scikit-learn. The classifiers' performances in this study were measured using classification accuracy, precision, recall, and F-score. It is important to highlight that these metrics were computed using the weighted average. The intuition behind selecting the weighted average was to calculate metrics for each class label and take the label imbalance into the account. The performance of classifiers was evaluated based on 5-fold cross-validation to split the datasets into five consecutive folds, one of them for testing and the remaining folds for training.

The following algorithm shows the steps used for the experiments. A list of datasets and a list of classifiers were provided first and then proceeded to iterate over all datasets, as shown in Line 7. The datasets were split into training and testing sets based on 5-fold cross-validation with shuffling of the data before splitting, as shown in Line 8. The loop in Lines 9–20 focused on training the classifiers, obtaining predictions, and computing evaluation metrics for each fold. The average scores were computed since the datasets were split using 5-folds. The process from Lines 7–28 was iterated through all provided datasets.

```
Input : Datasets, Classifiers
Result: AvgAccurecy, AvgRecall, AvgPrecision, and AvgF-score
Datasets ← {DS1, DS2, DS3, DS4, DS5, DS6, DS7};
Classifiers ← {RF, DS, SVM, GNB};
AllAccuracyScores ← {};
AllRecallScores ← {};
AllPrecisionScores ← {};
AllFScores ← {};
for DS ∈ Datasets do
    for Xtrain, Xtest ∈ KFold (nsplits = 5, shuffle = True).split(DS) do
        for clf ∈ Classifiers do
            clf ← TrainClassifier (clf, Xtrain, XtrainLabels);
            predictions ← predict (cls, Xtest);
            Accurecy ← ComputeAccurecy (predictions, XtestLabels);
            Recall ← ComputeRecall (predictions, XtestLabels);
            Precision ← ComputePrecision (predictions, XtestLabels);
            F-score ← ComputeFmeasure (predictions, XtestLabels);
            AllAccuracyScores ← AllAccuracyScores ∪ (clf, Accurecy);
            AllRecallScores ← AllRecallScores ∪ (clf, Recall);
            AllPrecisionScores ← AllPrecisionScores ∪ (clf, Precisionll);
            AllFScores ← AllFscoreScores ∪ (clf, F-score);
        end
    end
    for clf ∈ Classifiers do
        AvgAccuracy ← ComputeAvgAccuracy (AllAccuracyScores.get(clf));
        AvgRecall ← ComputeAvgRecall (AllRecallScores.get(clf));
        AvgPrecision ← ComputeAvgPrecision (AllPrecisionScores.get(clf));
        AvgF-score ← ComputeAvgFmeasure (AllFScores.get(clf));
    end
end
```

Algorithm 1: The experimental procedure for IDS using supervised machine learning algorithms

V. Results

Table I summarizes the average scores achieved by classifiers for the datasets. It is clear that DS and RF attained the highest scores compared to other classifiers. Among these classifiers, the CNB classifier performed badly in all cases.

TABLE I. The average scores obtained for all classifiers

Datasets	Classifier	Accuracy	Precision	Recall	F-score
Dataset1	DS	0.99987	0.999867	0.999867	0.999867
	GNB	0.80790	0.855282	0.807899	0.79449
	RF	0.99996	0.999956	0.999956	0.999956
	SVM	0.96272	0.963079	0.962718	0.962772
Dataset2	DS	0.999895	0.999895	0.999895	0.999895
	GNB	0.690785	0.792843	0.690785	0.64342
	RF	0.99993	0.99993	0.99993	0.99993
	SVM	0.960712	0.960709	0.960712	0.960711
Dataset3	DS	0.999948	0.999948	0.999948	0.999948
	GNB	0.353517	0.989691	0.353517	0.510318
	RF	0.999869	0.999869	0.999869	0.999869
	SVM	0.959693	0.986486	0.959693	0.971018
Dataset4	DS	0.999983	0.999983	0.999983	0.999981
	GNB	0.972659	0.999844	0.972659	0.986003
	RF	0.999965	0.999965	0.999965	0.999957
	SVM	0.997226	0.999741	0.997226	0.998525
Dataset5	DS	0.997709	0.999989	0.997709	0.997741
	GNB	0.773101	0.970593	0.773101	0.865443
	RF	0.997533	0.999978	0.997533	0.997448
	SVM	0.986342	0.982202	0.986342	0.988383
Dataset6	DS	0.999989	0.99778	0.999989	0.999989
	GNB	0.53325	0.988128	0.53325	0.665683
	RF	0.999978	0.997449	0.999978	0.999978
	SVM	0.982744	0.990504	0.982744	0.982443
Dataset7	DS	0.999523	0.999523	0.999523	0.999523
	GNB	0.498051	0.817196	0.498051	0.497581
	RF	0.999429	0.999429	0.999429	0.999429
	SVM	0.833831	0.854528	0.833831	0.834621

Fig. 1 shows the barplots of the mean of accuracy scores attained by the classifiers. It is obvious that DS and RF classifiers attained very similar accuracies. The scores of the classification accuracy showed clear outperforming by DS and RF classifiers. The mean value of accuracy scores attained by DS and RF was 0.999, which is better than any other learners. The worst accuracies were attained by GNB for all datasets.

Table II shows the p-values obtained using the paired t-test after comparing the accuracy scores attained by possible pairs of classifiers. By comparing the DS and RF, the p-values are larger than 0.05, accepting the null hypothesis that the mean difference between accuracies of both classifier is the same. For the comparison of DS and GNB, the p-values are less than 0.05, rejecting the null hypothesis.

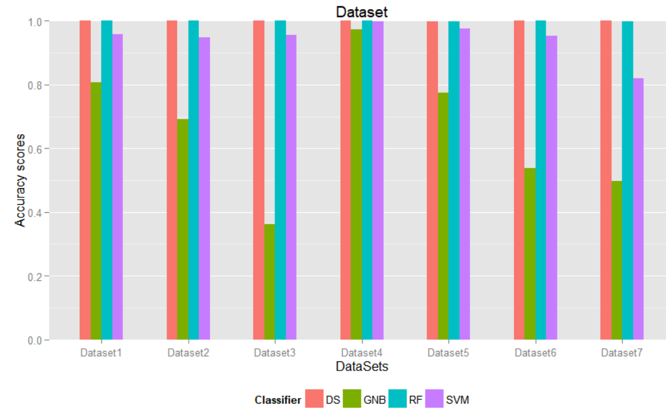

Fig. 1. Accuracy scores obtained by the classifiers

TABLE II. P-values of accuracy scores

	DS vs. RF	DS vs. GNB	DS vs. SVM	RF vs. GNB	RF vs. SVM	GNB vs. SVM
DS1	0.0919	1.321e-11	0.005925	1.691e-11	0.005817	4.66e-05
DS2	0.0919	1.321e-11	0.005925	1.691e-11	0.005817	4.66e-05
DS3	0.01893	8.975e-08	0.004048	8.947e-08	0.004102	1.46e-06
DS4	0.189	5.311e-05	0.05847	5.428e-05	0.05899	0.0001974
DS5	0.829	4.641e-09	0.1661	6.123e-09	0.1655	8.919e-05
DS6	0.7396	1.603e-07	0.1965	1.605e-07	0.1967	0.0001363
DS7	0.02938	6.946e-09	0.005506	7.124e-09	0.005517	0.0005039

Fig. 2 illustrates the barplots of the mean of the precision scores obtained by the four classifiers. It is apparent that both DS and RF classifiers attained the highest precision scores. For all datasets, the mean precision scores attained by DS and RF are about 0.99. For dataset4, it is clear that all classifiers obtained a mean precision value of 0.99 for all classifiers.

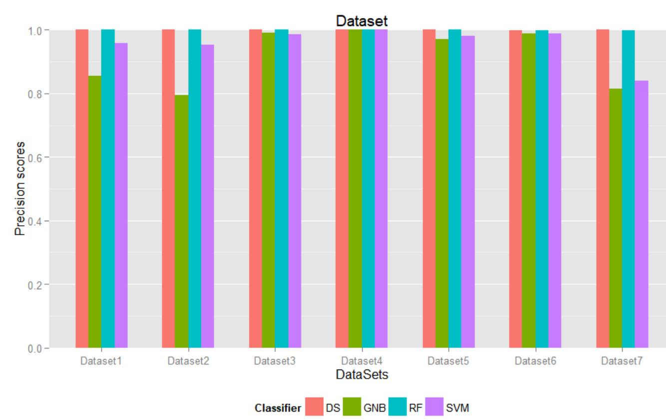

Fig. 2. Precision scores obtained by the classifiers

Table III shows the p-values obtained using the paired t-test after comparing the precision scores achieved by possible pairs of classifiers. By comparing the DS and RF, the p-values are larger than 0.05 in the majority of cases, accepting the null hypothesis that the precision values of both classifiers are the same. The p-values are less than 0.05 after comparing the precision scores attained by DS and GNB, rejecting the null hypothesis that the precision values of DS and GNB are equal.

TABLE III. P-VALUES OF PRECISION SCORES

	DS vs. RF	DS vs. GNB	DS vs. SVM	RF vs. GNB	RF vs. SVM	GNB vs. SVM
DS1	0.0918	2.209e-11	0.006157	2.674e-11	0.006045	0.0002085
DS2	0.07511	2.152e-09	0.02233	2.133e-09	0.02235	0.0002795
DS3	0.0188	4.758e-07	4.674e-05	6.244e-07	4.926e-05	0.006344
DS4	0.1908	0.005962	0.008912	0.002459	0.008954	0.02417
DS5	0.7395	3.091e-08	0.002439	3.144e-08	0.002472	0.03249
DS6	0.3871	2.084e-07	0.01786	3.7e-07	0.01919	0.9129
DS7	0.02711	1.949e-07	0.004181	1.889e-07	0.004191	0.4181

Fig. 3 depicts the barplots of the recall scores obtained by the four classifiers. It is noticeable that the GNB classifier performed badly. It is clear that DS and RF attained the highest recall scores, compared to GNB and SVM. The mean values of recall attained by GNB were 0.807, 0.69, 0.36, 0.97, 0.77, 0.53, and 0.49 for Dataset 1 to Dataset 7, respectively.

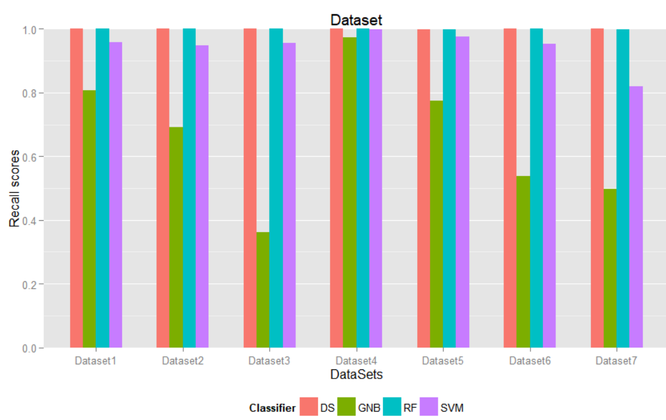

Fig. 3. Recall scores obtained by the classifiers

Table IV shows the p-values obtained using the paired t-test after comparing the accuracy scores attained by possible pairs of classifiers. By comparing the DS and RF, the p-values are larger than 0.05, accepting the null hypothesis that the mean values of both classifiers are the same. For the comparison of DS and GNB, the p-values are less than 0.05, rejecting the null hypothesis.

TABLE IV. P-VALUES OF RECALL SCORES

	DS vs. RF	DS vs. GNB	DS vs. SVM	RF vs. GNB	RF vs. SVM	GNB vs. SVM
DS1	0.0919	1.321e-11	0.005925	1.691e-11	0.005817	4.66e-05
DS2	0.07513	9.111e-09	0.03011	9.145e-09	0.03012	9.354e-05
DS3	0.01893	8.975e-08	0.004048	8.947e-08	0.004102	1.46e-06
DS4	0.189	5.311e-05	0.05847	5.428e-05	0.05899	0.0001974
DS5	0.829	4.641e-09	0.1661	6.123e-09	0.1655	8.919e-05
DS6	0.7396	1.603e-07	0.1965	1.605e-07	0.1967	0.0001363
DS7	0.02938	6.946e-09	0.005506	7.124e-09	0.005517	0.0005039

Fig. 4 illustrates the barplots of the F-scores obtained by the four classifiers. It is clear that the GNB classifier performed badly. The mean values of F-scores attained by GNB were 0.79, 0.646, 0.518, 0.985, 0.866, 0.67, and 0.498 for Dataset 1 to Dataset 7, respectively. Besides, for Dataset 1 to Dataset 7, the mean values of F-scores achieved by SVM were 0.957, 0.948, 0.969, 0.998, 0.98, 0.96, and 0.80, respectively.

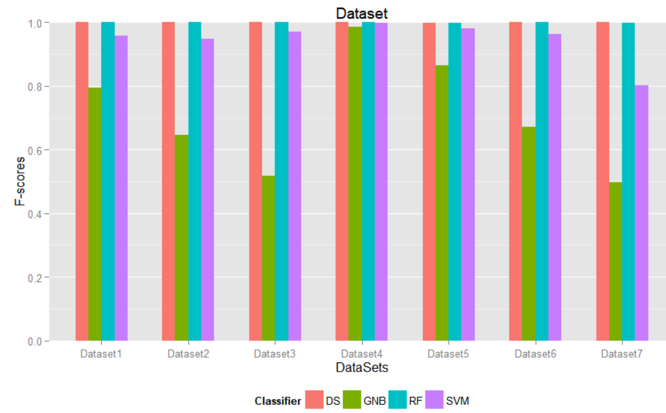

Fig. 4. F-scores obtained by the classifiers

Table V shows the p-values obtained using the paired t-test after comparing the F-scores attained by possible pairs of classifiers. By comparing the DS and RF, the p-values are larger than 0.05, accepting the null hypothesis that the F-scores of both classifiers are the same. For the comparison of DS and GNB, the p-values are less than 0.05, rejecting the null hypothesis, indicating that there is a significant difference between the F-scores of DS and GNB.

TABLE V. P-VALUES OF F-SCORES

	DS vs. RF	DS vs. GNB	DS vs. SVM	RF vs. GNB	RF vs. SVM	GNB vs. SVM
DS1	0.0919	2.437e-11	0.005924	3.133e-11	0.005816	3.453e-05
DS2	0.07513	2.492e-08	0.03122	2.499e-08	0.03123	5.904e-05
DS3	0.01901	4e-07	0.001738	3.99e-07	0.001779	2.05e-06
DS4	0.2133	5.041e-05	0.05023	5.327e-05	0.05101	0.0002019
DS5	0.4132	5.804e-09	0.07611	9.71e-09	0.07645	8.373e-05
DS6	0.7397	2.948e-07	0.1277	2.952e-07	0.128	8.608e-05
DS7	0.02859	6.743e-09	0.009177	6.615e-09	0.009194	0.001743

VI. CONCLUSION AND FUTURE WORKS

In this study, IDSs were proposed to detect network anomalies using machine learning approaches. The CICIDS 2017 [36] was used as the dataset because of its up-to-datedness, wide attack variety, and numerous network protocols (e.g. Mail services, SSH, FTP, HTTP, and HTTPS). This dataset holds more than 80 features that define the network flow. The results showed that DS and RF classifiers achieved near equal accuracies. The best performer in our study was DS and RF. The mean value of accuracy achieved by DS and RF was 0.999, the worst performance given by GNB for all datasets. We performed the paired t-test after comparing the accuracy, recall, precision, and f-score results attained by possible pairs of classifiers. By comparing the DS and RF, the p-values are larger than 0.05, accepting the null hypothesis that the mean values of both classifiers are the same. For the comparison of DS and GNB, the p-values are less than 0.05, rejecting the null hypothesis. In this analysis, a dataset comprising CSV records containing features acquired from the network flow was used as the training and test data. Unfortunately, this strategy isn't basically reasonable in a real system. However, this problem can be solved through live network data using machine learning methods.

An interesting future work might include analyzing and studying the effects of various feature selection approaches to select the optimal set of features for building robust IDSs. One future direction is to develop an IDS based on deep learning and transfer learning approaches to deal with data sparseness issues.

References

[1] S. KEMP, https://thenextweb.com/contributors/2019/01/30/digital-trends-2019-every-single-stat-you-need-to-know-about-the-internet/, 2019. [Online]. Available: https://thenextweb.com/contributors/2019/01/30/digital-trends-2019-every-single-stat-you-need-to-know-about-the-internet/

[2] AV-TEST, https://www.av-test.org/en/statistics/malware/, 2019. [Online]. Available: https://www.av-test.org/en/statistics/malware/

[3] A. Krepinevich, C. f. S. Assessments, and Budgetary, *Cyber Warfare: A "nuclear Option"*. Center for Strategic and Budgetary Assessments, 2012. [Online]. Available: https://books.google.com.sa/books?id=YrxSjwEACAAJ

[4] Y. Xiao, X. Shen, and D. Du, *Wireless Network Security*. Springer US, 2007. [Online]. Available: https://books.google.com.sa/books?id=efCKBrOOqXQC

[5] M. Feily, A. Shahrestani, and S. Ramadass, "A survey of botnet and botnet detection," in *2009 Third International Conference on Emerging Security Information, Systems and Technologies*. IEEE, 2009, Conference Proceedings, pp. 268–273.

[6] K. Scarfone and P. Mell, "Guide to intrusion detection and prevention systems (idps)," National Institute of Standards and Technology, Report, 2012.

[7] V. Jyothsna, V. R. Prasad, and K. M. Prasad, "A review of anomaly based intrusion detection systems," *International Journal of Computer Applications*, vol. 28, no. 7, pp. 26–35, 2011.

[8] H. Holm, "Signature based intrusion detection for zero-day attacks: (not) a closed chapter?" in *2014 47th Hawaii International Conference on System Sciences*, 2014, Conference Proceedings, pp. 4895–4904.

[9] K. Leung and C. Leckie, "Unsupervised anomaly detection in network intrusion detection using clusters," in *Proceedings of the Twenty-eighth Australasian conference on Computer Science-Volume 38*. Australian Computer Society, Inc., 2005, pp. 333–342.

[10] H. H. Volden, "Anomaly detection using machine learning techniques," Thesis, University of Oslo, 2016.

[11] N. Moustafa, E. Adi, B. Turnbull, and J. Hu, "A new threat intelligence scheme for safeguarding industry 4.0 systems," *IEEE Access*, vol. 6, pp. 32 910–32 924, 2018.

[12] N. Moustafa, J. Hu, and J. Slay, "A holistic review of network anomaly detection systems: A comprehensive survey," *Journal of Network and Computer Applications*, vol. 128, pp. 33–55, 2019. [Online]. Available: http://www.sciencedirect.com/science/article/pii/S1084804518303886

[13] S. Agrawal and J. Agrawal, "Survey on anomaly detection using data mining techniques," *Procedia Computer Science*, vol. 60, pp. 708–713, 2015. [Online]. Available: http://www.sciencedirect.com/science/article/pii/S1877050915023479

[14] M. Ahmed, A. Naser Mahmood, and J. Hu, "A survey of network anomaly detection techniques," *Journal of Network and Computer Applications*, vol. 60, pp. 19–31, 2016. [Online]. Available: http://www.sciencedirect.com/science/article/pii/S1084804515002891

[15] W. Stallings, L. Brown, M. D. Bauer, and A. K. Bhattacharjee, *Computer security: principles and practice*. Pearson Education Upper Saddle River (NJ, 2012.

[16] S. F. Yusufovna, "Integrating intrusion detection system and data mining," in *2008 International Symposium on Ubiquitous Multimedia Computing*, 2008, Conference Proceedings, pp. 256–259.

[17] M. Chhabra, B. Gupta, and A. Almomani, "A novel solution to handle ddos attack in manet," *Journal of Information Security*, vol. 4, no. 03, p. 165, 2013.

[18] A. Mishra, B. B. Gupta, and R. C. Joshi, "A comparative study of distributed denial of service attacks, intrusion tolerance and mitigation techniques," in *2011 European Intelligence and Security Informatics Conference*, 2011, Conference Proceedings, pp. 286–289.

[19] I. Ahmad, A. B. Abdullah, and A. S. Alghamdi, "Application of artificial neural network in detection of probing attacks," in *2009 IEEE Symposium on Industrial Electronics and Applications*, vol. 2, 2009, Conference Proceedings, pp. 557–562.

[20] E. Hodo, X. Bellekens, A. Hamilton, P. Dubouilh, E. Iorkyase, C. Tachtatzis, and R. Atkinson, "Threat analysis of iot networks using artificial neural network intrusion detection system," in *2016 International Symposium on Networks, Computers and Communications (ISNCC)*, 2016, Conference Proceedings, pp. 1–6.

[21] Q. Niyaz, W. Sun, and A. Y. Javaid, "A deep learning based ddos detection system in software-defined networking (sdn)," *arXiv preprint arXiv:1611.07400*, 2016.

[22] S. Paliwal and R. Gupta, "Denial-of-service, probing & remote to user (r2l) attack detection using genetic algorithm," *International Journal of Computer Applications*, vol. 60, no. 19, pp. 57–62, 2012.

[23] N. Ashraf, W. Ahmad, and R. Ashraf, "A comparative study of data mining algorithms for high detection rate in intrusion detection system," *Annals of Emerging Technologies in Computing (AETiC)*, vol. 2, no. 1, 2018.

[24] M. Tavallaee, E. Bagheri, W. Lu, and A. A. Ghorbani, "A detailed analysis of the kdd cup 99 data set," in *2009 IEEE Symposium on Computational Intelligence for Security and Defense Applications*, 2009, Conference Proceedings, pp. 1–6.

[25] K. Jaekwang and L. Jee-Hyong, "A slow port scan attack detection mechanism based on fuzzy logic and a stepwise p1olicy," in *2008 IET 4th International Conference on Intelligent Environments*, 2008, Conference Proceedings, pp. 1–5.

[26] M. M. Najafabadi, T. M. Khoshgoftaar, C. Kemp, N. Seliya, and R. Zuech, "Machine learning for detecting brute force attacks at the network level," in *2014 IEEE International Conference on Bioinformatics and Bioengineering*, 2014, Conference Proceedings, pp. 379–385.

[27] M. Garcia, D. Llewellyn-Jones, F. Ortin, and M. Merabti, "Applying dynamic separation of aspects to distributed systems security: A case study," *IET Software*, vol. 6, no. 3, pp. 231–248, June 2012.

[28] K. Gupta, R. R. Singh, and M. Dixit, "Cross site scripting (xss) attack detection using intrustion detection system," in *2017 International Conference on Intelligent Computing and Control Systems (ICICCS)*, 2017, Conference Proceedings, pp. 199–203.

[29] Z. Durumeric, F. Li, J. Kasten, J. Amann, J. Beekman, M. Payer, N. Weaver, D. Adrian, V. Paxson, M. Bailey, and J. A. Halderman, "The matter of heartbleed," in *Proceedings of the 2014 Conference on Internet Measurement Conference*, ser. IMC '14. New York, NY, USA: ACM, 2014, pp. 475–488. [Online]. Available: http://doi.acm.org/10.1145/2663716.2663755

[30] R. Lippmann, https://www.ll.mit.edu/r-d/datasets/1998-darpa-intrusion-detection-evaluation-dataset, 1998. [Online]. Available: https://www.ll.mit.edu/r-d/datasets/1998-darpa-intrusion-detection-evaluation-dataset

[31] S. Hettich and S. D. Bay, "The uci kdd archive," http://kdd.ics.uci.edu/databases/kddcup99/kddcup99.html, 1999. [Online]. Available: http://kdd.ics.uci.edu/databases/kddcup99/kddcup99.html

[32] S. K. Sahu, S. Sarangi, and S. K. Jena, "A detail analysis on intrusion detection datasets," in *2014 IEEE International Advance Computing Conference (IACC)*. IEEE, 2014, Conference Proceedings, pp. 1348–1353.

[33] A. Özgür and H. Erdem, "A review of kdd99 dataset usage in intrusion detection and machine learning between 2010 and 2015," *PeerJ Preprints*, vol. 4, p. e1954v1, 2016.

[34] C. I. for Cybersecurity, https://www.unb.ca/cic/datasets/nsl.html, 2019. [Online]. Available: https://www.unb.ca/cic/datasets/nsl.html

[35] A. Shiravi, H. Shiravi, M. Tavallaee, and A. A. Ghorbani, "Toward developing a systematic approach to generate benchmark datasets for intrusion detection," *Computers and Security*, vol. 31, no. 3, pp. 357–374, 2012. [Online]. Available: http://www.sciencedirect.com/science/article/pii/S0167404811001672

[36] A. H. L. Iman Sharafaldin and A. A. Ghorbaniy, https://www.unb.ca/cic/datasets/ids-2017.html, 2017. [Online]. Available: https://www.unb.ca/cic/datasets/ids-2017.html

[37] A. Gharib, I. Sharafaldin, A. H. Lashkari, and A. A. Ghorbani, "An evaluation framework for intrusion detection dataset," in *2016 International Conference on Information Science and Security (ICISS)*. IEEE, 2016, Conference Proceedings, pp. 1–6.

[38] S. Chebrolu, A. Abraham, and J. P. Thomas, "Feature deduction and ensemble design of intrusion detection systems," *Computers and Security*, vol. 24, no. 4, pp. 295–307, 2005. [Online]. Available: http://www.sciencedirect.com/science/article/pii/S016740480400238X

[39] L. Khan, M. Awad, and B. Thuraisingham, "A new intrusion detection system using support vector machines and hierarchical clustering," *The VLDB Journal*, vol. 16, no. 4, pp. 507–521, 2007. [Online]. Available: https://doi.org/10.1007/s00778-006-0002-5

[40] W. Yassin, N. I. Udzir, Z. Muda, and M. N. Sulaiman, "Anomaly-based intrusion detection through k-means clustering and naives bayes classification," in *Proc. 4th Int. Conf. Comput. Informatics, ICOCI*, vol. 49, 2013, Conference Proceedings, pp. 298–303.

[41] D. P. Gaikwad and R. C. Thool, "Intrusion detection system using bagging ensemble method of machine learning," in *2015 International Conference on Computing Communication Control and Automation*, 2015, Conference Proceedings, pp. 291–295.

[42] T. H. Divyasree and K. K. Sherly, "A network intrusion detection system based on ensemble cvm using efficient feature selection approach," *Procedia Computer Science*, vol. 143, pp. 442–449, 2018. [Online]. Available: http://www.sciencedirect.com/science/article/pii/S1877050918321136

[43] K. Dong Seong, N. Ha-Nam, and P. Jong Sou, "Genetic algorithm to improve svm based network intrusion detection system," in *19th International Conference on Advanced Information Networking and Applications (AINA'05) Volume 1 (AINA papers)*, vol. 2, 2005, Conference Proceedings, pp. 155–158 vol.2.

[44] K. Kumar and J. S. Batth, "Network intrusion detection with feature selection techniques using machine-learning algorithms," *International Journal of Computer Applications*, vol. 150, no. 12, 2016.

Embedded Mission Decision-Making based on Dynamic Decision Networks in SoPC Platform

Hanen Chenini
Microwave Electronics Research Laboratory
Faculty of Sciences of Tunis, University of Tunis El-Manar
Tunis, Tunisia

***Abstract*—This paper tackles a Bayesian Decision Making approach for unmanned aerial vehicle (UAV) mission that allows UAV to quickly react to unexpected events under dynamic environments. From online observations and the mission statement, the proposed approach is designed by means of Dynamic Bayesian Networks (DBN) arising from the safety or performance failures analysis. After proposing a DBN model, a probabilistic approach based on Multiple-Criteria Decision-Making (MCDM) is then applied to find the best configuration reaching a balance between performance and energy consumption, thus decide which tasks will be implemented as SW and which as HW execution units, regarding the mission requirement. The proposal UAV mission decision-making is three-pronged, providing: (1) real time image pre-processing of sensor observations; (2) temporal and probabilistic approach based on Bayesian Networks to continuously update the mission plan during the flight; and (3) low-power hardware and software implementations for online and real time embedded Decision Making using Xilinx System on Programmable Chip (SoPC) platform. The proposed approach is then validated with a practical case UAV mission planning using the proposed dynamic decision-maker implemented on embedded system based on a hybrid device.**

Keywords*—Bayesian Decision Making; Dynamic Bayesian Networks (DBN); Multiple-Criteria Decision-Making (MCDM); SoPC; practical case

I. Introduction

Autonomous system, such as drone known as UAV, is a robot system composed of several components (of hardware or software), fly autonomously according to a pre-programmed mission statement in unknown environment. Now-a-days, UAVs are being more widely used in different applications (military, aerospace reconnaissance, environmental and meteorological monitoring, aerial photography, and geophysical survey, etc.) achieving high performance and reliability combined with reduced size, weight, power consumption and cost. To execute successfully such missions, it was essential that the vehicle able to select appropriate scenario planning under consideration of the current state of the mission and uncertain environmental conditions. In each mission, the UAVs are generally set to perform a particular mission under several requirements and environmental conditions (unexpected obstacles, weather changes and sensor or hardware/software component failures, etc.). For UAVs, sensors are generally embedded on board, and consequently, the embedded systems are constrained to face the hard real-time constraints imposed by moving vehicle applications. In our work, we have focused on combining sensors and algorithms to understand the vehicle environment and to provide some autonomous processing directly into the UAV and achieve the necessary processing power to run the algorithms near the sensors.

These issues increase the demand for providing an online, on-board scenario management system for UAV to produce a response to uncertain environmental events and emergent failures of sensors or software/ hardware components within a specified time. Indeed, it has to provide the system the capability to treat the real time data of uncertain or dynamic elements which might represent a threat for the UAV's mission execution.

Aiming at solving the above problem, the focus of our reasoning is to develop systems that behave differently in different contexts which means they continue to change over time, thus we need an approach capable to model such dynamic systems. For this reason, we are interested in how these systems that evolve over time using Bayesian Network (BN) and particularly its extension DBN [5], [6] to model the temporal evolution/influences of the variables of interest between multiple time series in the same model according to the mission statement. In fact, DBN used especially to relate variables to each other over adjacent time steps in the presence of uncertainty and anomalous observations.

Thanks to the proposed dynamic decision-making approach as depicted in Fig. 1, we may identify successfully the alternative decision that maximize the chance of achieving the mission goal at time $t+1$ using several tasks as well as internal and external constraints of UAV that can affect the mission plan. During the flight, the UAV rely on several applications required to meet mission constraints (path planning, motion detection of aerial or ground targets, tracking, pose estimation to follow a precomputed path, obstacle avoidance, etc.), with computation demands that can vary during a mission. However, the UAV always require accurate measurements and information of the surrounding environment with respect to the current scene. Translating such complex applications for real-time implementation requires making specific choices so that the design meets the constraints. Some of the main processing requirements are speed of processing, accuracy of the results, cost and time involved in the implementation. To tackle with this problem, we are motivated to propose hardware reconfigurable architectures for implementing real time processing applications with stringent resource-consumption and runtime constraints. In this case, it can be beneficial to take advantage of the parallelism, low cost, and low power consumption offered by digital integrated circuits Field-programmable gate arrays (FPGAs) for implementing such reconfigurable systems dedicated to complex image processing algorithms.

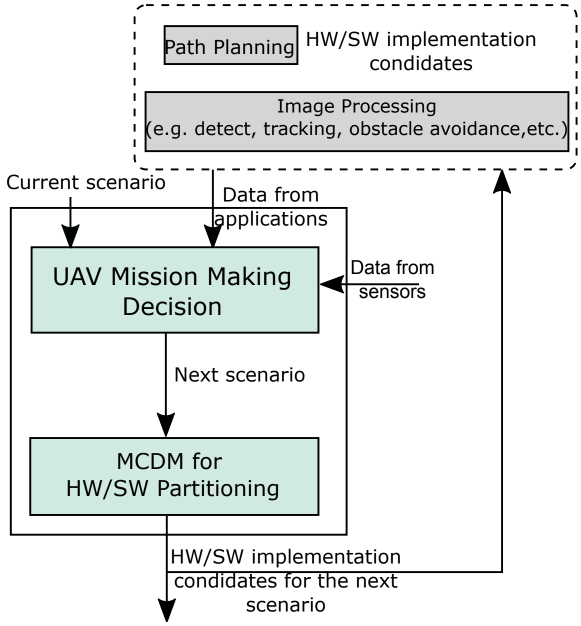

Fig. 1. UAV Mission decision making approach.

The design and implementation of the proposed Mission Decision Making approach can be divided into two main parts software and hardware within a single FPGA device. The software part is implemented on the dual-core ARM Cortex-A9 based Processing System (PS). The hardware partition is called the Programmable Logic (PL), which consists the FPGA programmable logic blocks. With regard to the latter, the different image processing applications is fully performed in FPGA fabric, whereas the control and the reconfiguration of the different functional blocks is managed by processes running on the ARM processor.

In this paper, we specifically propose an embedded Mission Decision Making by means of two contributions as illustrated in Fig. 1. The first one is the introduction based new DBN model is applied to schedule the information and to make on-line decision and provide the new scenario plan in constrained time when immediately required during the flight. Once the mission plan is updated, we then propose a new MCDM model to generate a suitable HW/SW configuration for the mission tasks regarding to performance constraints and resource availability that will allow the development of real time mission decision making module, on System-on-Chip (SoC) using FPGA for deployment on a UAV under extreme and uncertain environmental conditions.

The paper is organized as follows. Section 2 describes the proposed UAV mission decision making approach based on DBN. Section 3 explains how the MCDM deals with the problem of co-design to decide on the most appropriate HW/SW scheduling method and thus keep the embedded system's performance. Section 4 provides the hardware/software (HW/SW) implementations and few performance results concerning FPGA resource costs and execution times of the proposed Dynamic Decision Making module in real case study. Section 5 concludes the paper.

II. Previous Related Work

We confine the related work to Decision-Making approaches based artificial intelligence algorithms in embedded hardware and real-time architecture. Recently, many approaches of embedded Decision-Making are proposed in the literature [1] [2]. We can broadly classify these techniques into three categories: Multicriteria Decision Making [3], Artificial Intelligence and Mathematical Programming techniques [4]. In addition, current research tends to manage the uncertainty of the surrounding environment and the system such as Bayesian Networks introduced as stochastic/probabilistic models [7].

Thus, the development of embedded Decision Making system aims to continuously manage the UAV mission and propose the appropriate recovery action in the case of failure scenarios. This system is able to adapt to the variations in computation requirements during the UAV mission. Digital signal processors (DSP) or FPGAs are used for hardware implementation of such real-time systems. For this reason, a lot of researchers are interested in optimising hardware implementation for Decision-Making mechanism under the constraints of memory or computation.

To implement Decision Making based probabilistic (Bayesian) network onboard, some research has shown encouraging results with FPGA based reconfigurable hardware [19] [18] [15] [16]. In [9], the authors proposed an FPGA implementation based on a BN representation, that allows to continuously monitor the embedded system under time and resource constraints. For this purpose, they proposed off-line framework integrating a high level synthesis tool to generate the hardware version. In [15], the authors have suggested an efficient FPGA hardware design of a BN block written in Hardware Description Languages VHDL and used the development software ALTERA QUARTUS II12 to synthesize the design onto an Altera Cyclone IV EP4CE115 FPGA. Whereas, an embedded processor performed the monitoring of temporal sensor data using Linear Temporal Logic (LTL). In [17], the authors have developed a purely software implementation of their proposed DBN approach through the use of on-board software architecture called Anomaly resolution and prognostic health management for autonomy (ARPHA). This framework is developed to design and implement a specific failure scenario from a set of specifications (diagnosis, prognosis, and recovery) and provide as result an embedded software implementation of a DBN without any hardware alternative.

However, to the best of our knowledge, there is no prior work on hardware implementation of Decision making based on both DBN and MCDM with on-board vision processing on reconfigurable platforms. Our work provides a novel approach of combining DBN with utilizing MCDM techniques to choose between an HW (FPGA) or SW implementation (embedded processor) of the mission tasks.

III. Dynamic Bayesian Networks for UAV Mission Decision Making

A. Dynamic Bayesian Network Model

The goal of this work consists of developing an autonomous on-board management system based on a set of algorithms that will be embedded on-board. In our approach, we started by the model "glues together" proposed by [8] to control the behavior of different hardware/software components for a given task under uncertainty. By adding temporal specification in this model, the proposed mission decision making is a discrete time model of estimating the recovery tasks at the time $t + 1$ based on the evidence obtained at the time t. To avoid critical situations while maintaining safety requirements, the proposed DBN is composed of two types of nodes (**D**ecision **n**odes, **S**ensor **n**odes, **D**ata **s**ources) as depicted in the DBN hierarchy in Fig. 2 over two consecutive time slices.

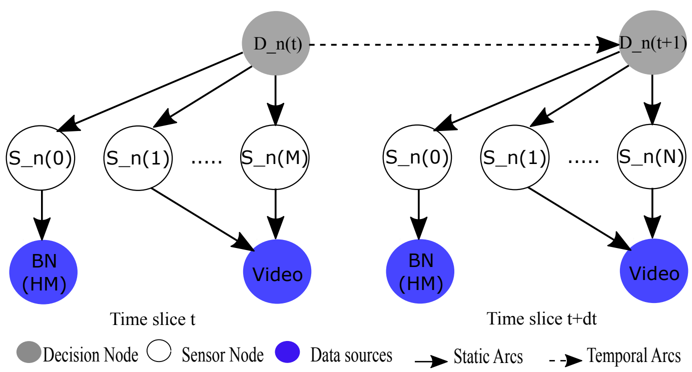

Fig. 2. The proposed dynamic Bayesian network for the mission Decision Making

1) **D**ecision **n**odes (D_n) includes the list of the available decision alternatives, in our case the list of possible scenarios to update the mission plan, modeled explicitly as possible states of the decision node.
2) **S**ensor **n**odes (S_n) representing the data retrieved from the system environment by means of software applications. In practice, the outcome of each sensor node (Observed node) is known certainty with two possible states.
3) **D**ata **s**ources (D_s) indicating process measurements by means of software or hardware sensors (in practice, we used imaging sensors and Health Management HM of the system providing information about the current state of the system environment).

Since the influence of decision nodes with sensor nodes is instantaneous, a regular Bayesian network arc is used as shown in Fig. 2. Considering two successive time slices in the modeling, each node at i^{th} time slice depend not only on its parents node at the same time slice but also on its parents and itself at previous time slices.

B. The Proposed UAV Mission

As previously mentioned, UAVs are considered as critical systems operate in uncertain environments and have to face unexpected obstacles, weather changes and sensor, hardware or software failures. These constraints must be satisfied at all instants during the flight in interaction with the proposed decision maker, to impose the UAV to get to its final destination. At low altitude, we assume that the UAV always keeps the same height level from initial location to the destination location. The decision of re-planning a mission is taken by evaluating the observations to obtain the state of the UAV on every time $t + 1$, from its previous state at time t. To move from a given initial position to a destination position, we attempted to introduce independent solutions for obstacle detection/avoidance, recognition and tracking of the desired object as well as the pose estimation in order to guarantee the accomplishment of detection and tracking mission goals during the flight.

Before we begin our application, the sensor data are aggregated from two cameras mounted in the front of the UAV for simultaneous capturing images in different angles. At any time, the camera can change its field of view θ to detect the presence of ground and/or areal objects. Indeed, the angle θ, which indicates the view angle between the UAV and the observed object, can take two possible values $\theta = \{front, Bottom\}$. Based on the output of these solutions, multiple decision alternatives ($S0$, $S1$, $S2$, $S3$, $S4$, $S5$, $S6$) are proposed to achieve new functionality/applications and to update the mission plan. For simplicity reasons, we suppose that we can receive information from only two processing tasks in each time t in addition to the HM data. After each time slice, we apply the decision maker and the alternatives decisions are sorted according to their priority (starting with urgent decision $P1$ and so on).

1) Scenario $S0$: As shown in Fig. 3, the initial position of the UAV is $(x_0; y_0; z_0)$ and the target position is $(x_d; y_d; z_d)$. To move an UAV from the given initial position to the destination position, two independent image processing algorithms are performed simultaneously:(1) motion detection algorithm is applied in aerial images (captured by the front camera) to detect aerial targets (AT) and (2) pose estimation algorithm is applied in ground images (captured by the bottom camera) to find coordinates of the UAV's location and then verify that it follows a precomputed path.

2) Scenario $S1$: For the second scenario $S1$, if there is any obstacle detected in aerial image i before reaching its final destination, we aim to detect obstacles that are dangerous in the next aerial image $i + 1$ where none, one or more aerial targets can be present. For this purpose, two independent image processing algorithms are performed simultaneously as shown in Fig. 4: (1) Region Labeling algorithm is applied in aerial images to compute region sizes of the detected aerial targets (AT) and then keep only the region with highest size (in our case, it represents obstacles) and (2) motion detection algorithm is applied to detect ground targets (GT).

3) Scenario $S2$: For the next scenario $S2$, whenever there is any obstacle detected between images i and $i+1$, it is highly required to know how far away the UAV is from the largest object observed (i.e. the object of the biggest label). For this purpose, distance measurement algorithm is applied using the two acquired images as shown in Fig. 5.

4) Scenario $S3$: For the scenario $S3$, having found moving objects in ground image i, a method for recognizing a target object in image $i + 1$ is proposed. For this purpose, distance measurement algorithm is applied using the two acquired images as shown in Fig. 6: (1) object recognition algorithm is applied to identify the nature of the detected object (GT) and then check if it can be considered the best match of the target object or not and (2) pose estimation algorithm is applied in

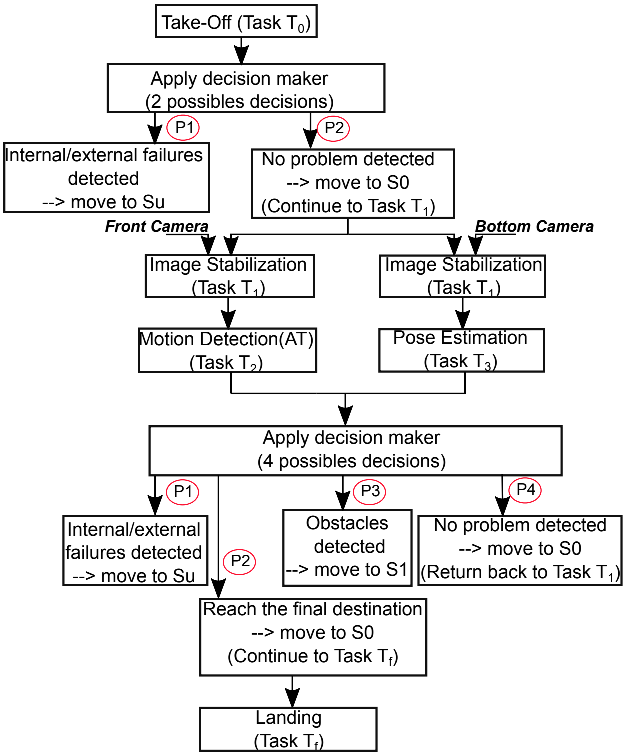

Fig. 3. The different steps of the scenario $S0$

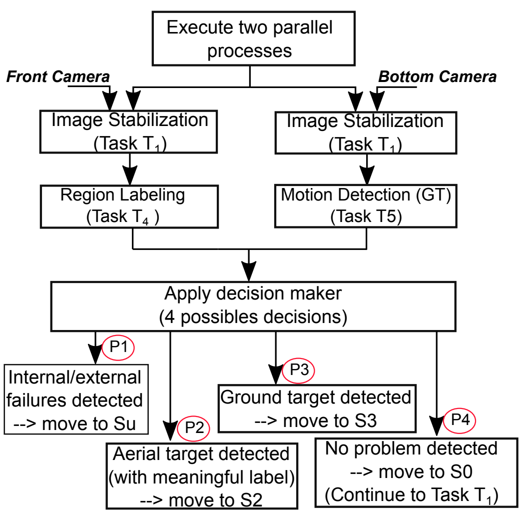

Fig. 4. The different steps of the scenario $S1$

ground images to find coordinates of the UAV's location and then verify that it follow a precomputed path.

5) Scenario $S4$: For the next scenario $S4$, if the distance between the UAV and the observed object (output of distance measurement application) is greater than a threshold distance before reaching its final destination, path planning algorithm is applied in ground image to compute another shortest path to the final destination as shown in Fig. 7

6) Scenario $S5$: For the next scenario $S5$, if the UAV has found the target object in image i before reaching its final destination, two independent image processing algorithms are performed simultaneously as shown in Fig. 8: (1) motion detection algorithm is applied in aerial images to detect aerial targets (AT) and (2) video tracking application is then applied for locating the recognized object over time in ground image $i+1$ to ensure that the target object is not lost from the UAV's view.

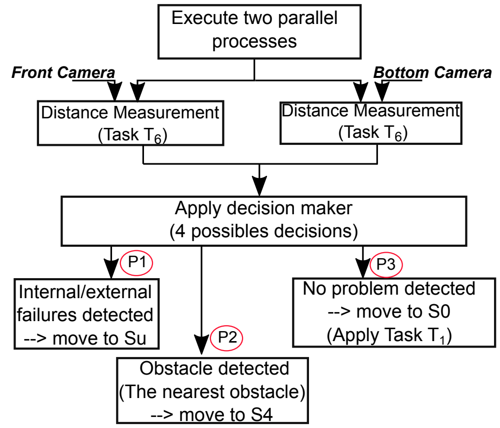

Fig. 5. The different steps of the scenario $S2$

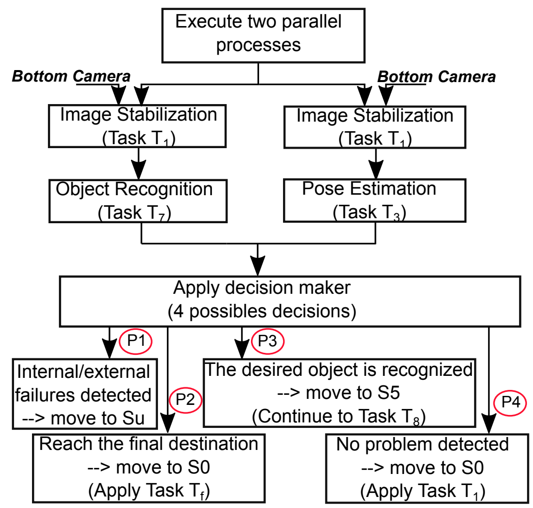

Fig. 6. The different steps of the scenario $S3$

7) Scenario $S6$: For the next scenario $S6$, if the detected object is tracked successfully in moving background before reaching its final destination, the UAV keep track of the target object. For this purpose, two independent image processing algorithms are performed simultaneously as shown in Fig. 9:(1) motion detection algorithm is applied in aerial images to detect aerial targets (AT) and (2) video tracking application is applied for locating the recognized object over time in ground image $i+1$.

8) Scenario Su: For the scenario Su, if any anomalies or failures state are detected during the mission execution, the autonomous UAV need to perform the landing emergency task in the closest safe area.

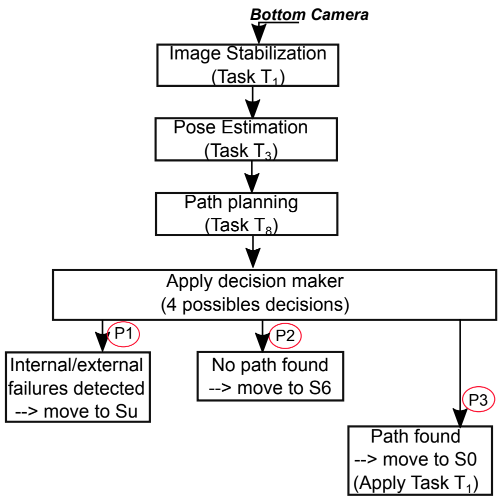

Fig. 7. The different steps of the scenario $S4$

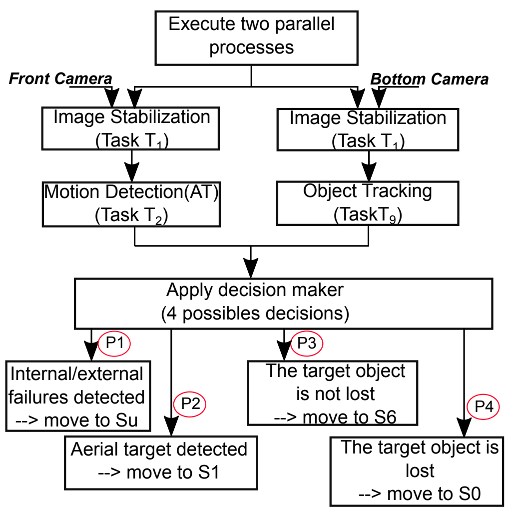

Fig. 8. The different steps of the scenario $S5$

C. DBN Model of the Case Study

For the case study, the proposed dynamic mission decision maker based on DBN, by analyzing influence relations between nodes is illustrated in Fig. 10. This model aims to describe the proposal decision maker that is dynamically evolving over time to update the mission planning and predict what should be the next activity of the UAV following unforeseen circumstances as time proceeds. According to the mission execution, based on online and real time readings given by sensors, the decision is taken whether or not to request intervention in case of anomaly alerts such as internal software and/or hardware failure, changes in the environment (weather, obstacles), or communication problems.

For simplicity reasons, in the example presented, only two sensors nodes can have influence on the same variable or on another variable in the same time slice t with the aim of detecting the anomalous or failed state of the mission plan. In fact, each node in the DBN model can have a different number of states.

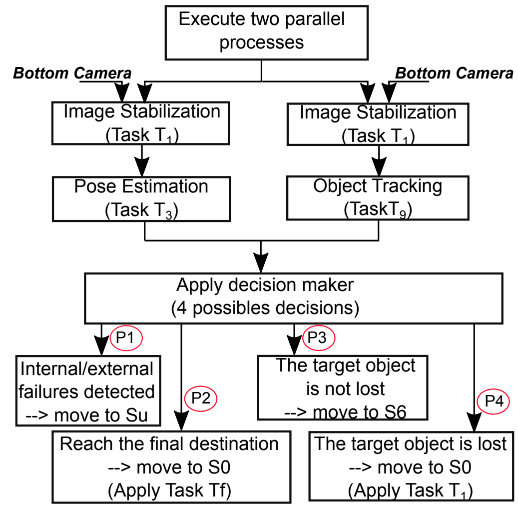

Fig. 9. The different steps of the scenario $S6$

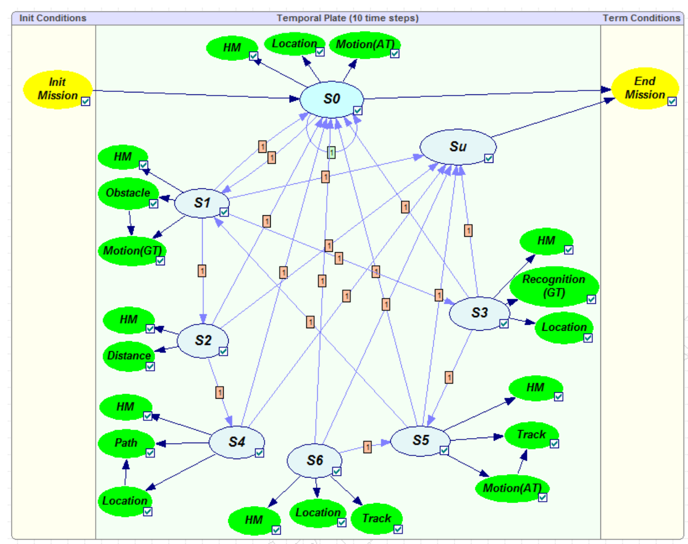

Fig. 10. The implementation of an example of the DBN model in software GeNie.

Since the state of sensor nodes are observable (evidence indicators), this simplify the construction of the DBN model needed to implement the autonomous updating of the mission tasks during the fight. Similarly to inference in a regular Bayesian Network, the inference in a DBN starts by given the evidence indicators for the current state and then calculates the impact of observation of some of its nodes on the posterior probability distribution (pdf) over other nodes as time proceeds.

IV. Multi-Criteria Decision Making (MCDM) for HW/SW Partitioning

To make on-line decision, the autonomous embedded drones, in our case study, have on board management system to allow execution of complex tasks (motion detection, tracking, obstacle avoidance, pose estimation and so on), with computation demands that can vary during a mission. According to some failure scenarios that may arise during the flight, as seen previously, the developed approach includes on-board decision making module to select the future mission tasks. The main objective of this section is to design a partitioning decision module that considers different types requirements to determine which task can be implemented either as a SW or HW components. For this purpose, a comparison between the hardware and software versions is established in the presence of multiple criteria. Indeed, hardware or software task allocation depends essentially on how quickly and how long tasks must be done.

In [10], an extended BN model with influence diagrams is proposed for optimal decision making depending in multiple criteria within the MCDM framework, including decisions alternatives. As illustrated in the BN hierarchy in Fig. 11, the MCDM decision making module of the case study has the following nodes:

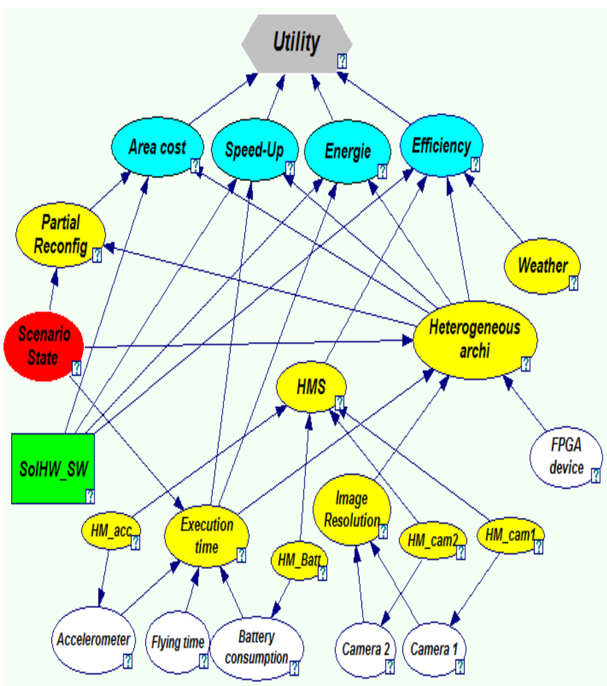

Fig. 11. The implementation of an example of the MCDM Model

1) Input node (red node, evidence node): current scenario state (Output of the decision making module).
2) Objective node (gray nodes, drawn as diamonds): to achieve a balance between different types of criteria cost area/energy consumption/speed-up/efficiency.
3) Decision node (Green node, drawn as rectangles): including the set of possible decision alternatives Di (representing the possible combination of hardware and software : (1) pure HW/HW, (2) pure SW/SW, (3) mixed HW/SW, (4) mixed SW/HW).
4) Criteria nodes (blue nodes, chance nodes): including the set of decision criteria Cj such as cost area, energy consumption, speed up and the efficiency.
5) Sub-criteria nodes (yellow nodes, chance nodes): including a set of variables representing heterogeneous architecture, temporal constraints, internal states of the different sensors, environmental conditions, etc.
6) External factors nodes (white nodes, chance nodes): including a set of variables representing the sensors nodes (IMU, imaging sensors), FPGA platform, flying time (observed nodes).

In our case study, these nodes can have two states (state0,state1). Once the network structure is designed, the probabilities for each node are entered into the network in the form of Conditional Probability Table (CPT). For the criteria nodes, these probabilities are learned from the experimental results. Given observations of some external factors, the CPT entries are fixed on the basis of knowledge of interdependency between nodes and their interactions. The utility function Uf of each decision alternative Uf_{Di} (i from 0 to 3) is equal to the sum of the products of the performance of decision alternative Di, evaluated against the decision criterion Cj with the weights of relative importance of the decision criteria $weight(j)$:

$$Uf_{Di} = \sum_j (\sum_k \sum_t weight(j) * P(Cj_k) * P(Di_t))$$

with k=(state0,state1), t=(state0,state1)

Once the overall utility scores are computed for all the alternatives, the best one is the alternative which has the highest score value and the decision alternative equal to the $Max(Uf_{Di})$.

V. Experimental Results

The experimental section is divided mainly into two parts. First, we present the hardware (FPGA) and software (CPU) implementations of the dynamic decision making module, including the MCDM module for HW/SW Partitioning an on-board heterogeneous architecture. Second, the proposed approach has implemented, and tested using a real case study.

A. The Heterogeneous Architecture

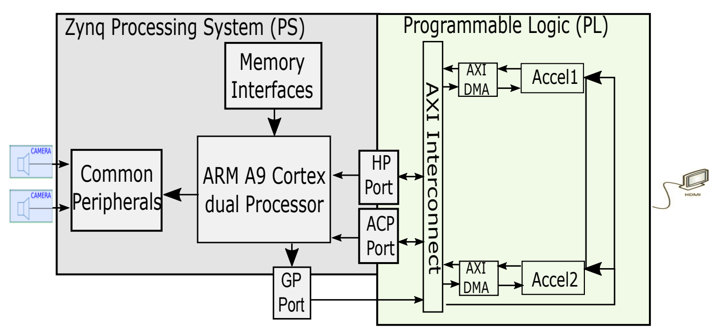

Fig. 12. Overview of the proposed hardware architecture

Our works aim at embedding the decision making module in a mixed hardware and software architecture (CPU and hardware cells) as the best way for low power consumption and high computational performances. In order to do so, the proposed design targets Xilinx Zynq XC7Z020 FPGA as the main processing chip. As shown in Fig. 12, the architecture is built around the ARM CortexA9 processor (Zynq processing system PS). In order to speed up image processing applications, the use of computational HW accelerators components dedicated to some functions make the ARM CortexA9 processor available to adapt its functionality to perform other mission tasks according to mission objectives before the take off or even during the flight. As shown in Fig. 13, the ARM A9 Cortex dual processor can: (1) obtain the sensor data from two USB webcams, (2) communicate with dedicated hardware (HW) accelerators using the programmable logic through an Advanced eXtensible Interface (AXI) bus and (3) display the on a TV screen with the HDMI output.

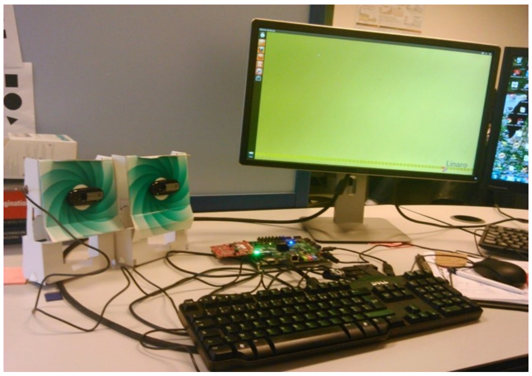

Fig. 13. Setup used to validate the proposed UAV mission decision approach.

B. HW/SW Implementations of The Proposed Mission Decision Making

In this work, we propose an extended framework [9] that can generate an FPGA bitstream from the BN specification. In fact, the hardware implementation of BN inference on synthesizable hardware as FPGAs can be divided into two main phases:

(1) Off-line phase: Once a BN is built, the designer has first to determine, some input BN specifications including evidence indicators (sensor measurement) and network parameters. Based on these specification choices, the developed tool generates the internal representation (Arithmetic circuit (AC) form) and then generates the corresponding C/C++ code (software version).Taken as input, the application written C or C++ languages, Vivado HLS (High Level Synthesis) generates low-level HDL description (Hardware version). The generated HDL code can be instantiated on SoPC Xilinx platform using high level design tools (Vivado) from Xilinx. Afterwards, the HDL code can be verified. Here, if the design does not meet the performance requirements, a first loop enables to re-configure and re-generate the HDL code, regarding resources utilization, speed up and energy consumption.

(2) Execution phase: during the execution of the program, data given by the sensors (evidence indicators) are transferred to the circuit and the developed BN module can be executed and the failure scenario is selected by computing the probability distribution function (pdf) of each node.

In the first experiment, we decide to put the network parameters and the evidence parameters into off-chip memories, with respect to real time processing, and then transmitted to hardware accelerators via the GP AXI bus. After synthesis, the resource requirement for the complete design (using the hardware version) is reported in Table I. Those results demonstrate

TABLE I. ZYNQ XC7Z20-1CLG484 - LOGIC SLICES UTILIZATION

Slice Logic Utilization	Used	Available	Utilization
Slice LUTs	32172	153200	21%
FF	7446	106400	19%
DSP48E	73	220	34%
BRAM (18k)	36	280	13%

that the mapping of of our application is efficient in terms of resource usage.

In the second experiment, we use our design tool to evaluate the performance of the decision making based Bayesian Network module mapped onto the FPGA. In order to test the performance of the FPGA implementation, we measured the experimental times taken by the pure hardware and the pure software implementations to process a single decision making block. In the current implementation, the execution of the decision making module, using its hardware version, took $42ms$. Whereas, the execution of the decision making module (using its software version) running as a program on the CPU took $155ms$. Summarizing the measurements presented above, we obtain a speedup of 3.7 obtained when comparing the software version with the hardware version at clock frequency $100MHz$. However, the processing time obtained during the experiments has shown a considerable shortening of time and we can even improve these results by using high-level transformations.

C. The Proposed Algorithms Applied in our Approach

Before we begin our application, the input for updating the proposed dynamic decision maker comes from the various sensors cameras placed in critical parts of the UAV. The principle is to acquire a sequence of images while the cameras (which will be embedded on UAV) is in motion. In our case, the UAV acquires data from working environment (immediate surroundings), in particular the data given by two cameras putted in the front of the UAV. Thus, the estimate of the decision can be updated based on the dataset collected up to that point in time. To show the validity of the proposed approach, we have conducted a set of experiments on real image sequences with resolution $720x480$ pixels captured with two Logitech webcams. To achieve the mission goals, the algorithms used in the work to verify the viability of our approach include in particular image processing techniques such as: motion detection based on mixture of Gaussian/Background subtraction (Fig. 14), image stabilization [11]), pose estimation [12] (Fig. 15), object recognition [14], object tracking [13]), region labeling and path planning. These applications based image processing are already embedded on-board FPGA in our autonomous UAV. Table II summarizes the different algorithms used in our approach.

Furthermore, we apply a simple method to measure distance between the UAV and the aerial object. For this purpose, we took two cameras slightly separated where the first one must be fixed in the front of the UAV and the second one must be at distance forward as shown in Fig. 16 to capture

TABLE II. THE PROPOSED ALGORITHMS

Application	Description
Region Labeling	Thresholding+Aggregation+Assigning labels
Path Planning	Breadth-First Search
Motion Detection	Application based on mixture of Gaussian Background subtraction
Pose estimation	Harris+Matching+ 3D movement estimation (RANSAC)
Image Stabilization	Application inspired from [11] Harris+Matching+2D Movement Estimation+ Motion Compensation
Object Recognition	Bottom-up visual attention approach
Object tracking	Dynamic Neural Fields (DNFs)

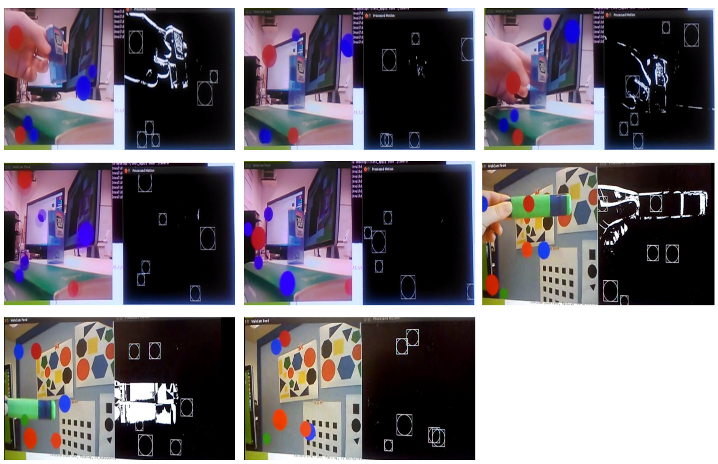

Fig. 14. FPGA motion detection implementation

the same image from two different camera angles at the same time. Thus, the distance between the camera and the aerial object d is given by:

$$d = \frac{m}{1 - \frac{x_1}{x_2}} \tag{1}$$

D. Case Study of the Proposed Approach

In this section, the goal is to validate our proposal on the Zynq platform through a real UAV mission with no anomalous or failed state detected. For example, we consider the following experiment that address only two scenarios ($S0$, $S1$):

1) At time $t0 = 0$, the UAV starts moving in our indoor environment (Fig. 17) and continues moving in the same direction. The two cameras keep the same field of view as the time proceed (front and bottom). During this phase, the task is to detect any motion in the acquired image.
2) At time $t1 = 4s$, the front camera detects movement (aerial target). After motion detection, region labeling application is applied to determine characteristics (shape, size, position, etc.) of each connected group and therefore to determine whether the detected motion is an object or just a noise.

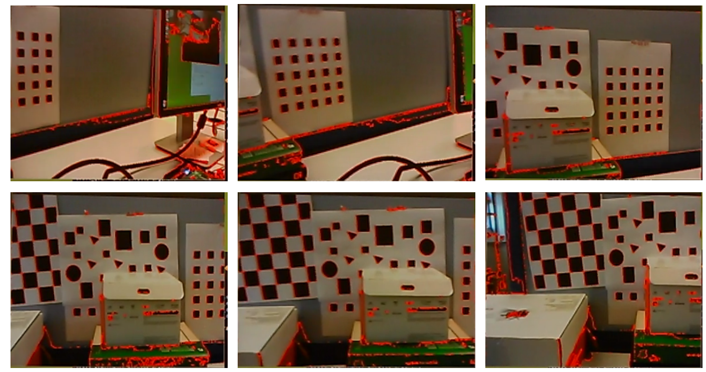

Fig. 15. FPGA pose estimation implementation

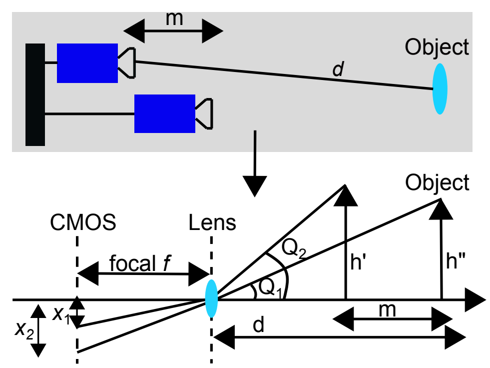

Fig. 16. Distance measurement method

3) At next time $t2 = 5s$, no ground target is detected, and returns no threat detected in the front of the UAV.

After generating the bitstream of the embedded applications, we start to boot Linux on the Zedboard from the SD card divided into two partitions: (1) FAT32 partition including boot.bin (boot image for the Zynq), system.bit (Bitstream file of the custom IPs in the PL), application.elf, zynq_fsbl.elf (First Stage Boot Loader (FSBL)) (2) EXT4 partition including the Linaro file system. For the software implementation on ARM Cortex A9 dual core processor, the pose estimation algorithm takes more than $252ms$ and the execution of the motion detection algorithm based on background subtraction took $78ms$ and finally the region labeling task takes around $42ms$. Table III presents the synthesis results (synthesis under time constraints) in term of FPGA resources utilization and the processing time of each image processing application using hardware accelerators generated by the HLS Vivado tool.

On the basis of the dynamic decision making model, the moving vehicle pursues its goals by means of the developed

TABLE III. FPGA SYNTHESIS RESULTS

Application	Pose estimation	Motion detection
Slice LUTs	9%	13%
FF	2%	7%
BRAM (18k)	31%	28%
Execution times (ms)	127	35

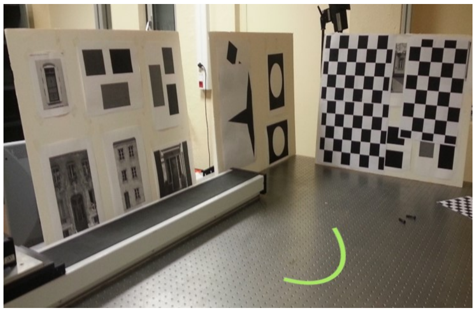

Fig. 17. The indoor environment used to test the different applications

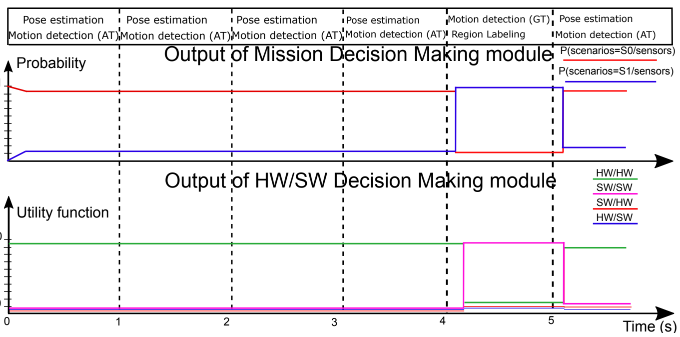

Fig. 18. Example of application of our approach

scenarios according to its available data about the state of the surrounding environment. Our mission decision making will be reactive, that means it will look for new scenarios when something happens according to its current knowledge. As first step, the embedded mission decision making module (the hardware accelerator) takes as evidences the output signals provided by the software and hardware components of the embedded applications. These evidences parameters are stored inside the FPGA using on-chip memories and transmitted by the ARM processor via general purpose (GP) AXI ports. Then, as second step, the choice of a functionality implementation (software version or hardware FPGA version) during the mission is driven by the the developed mission decision making module.

Fig. 18 presents the results obtained for the mission decision making over time with three applications of the case study. From time $t0 = 0s$ to $t1 = 4s$, no problem in the mission is detected. Scenario $S0$ is the best possible scenario in this case since the probability P(S0/evidence on sensors) is equal to 0.9 and the maximum of the utility function is attained for the decision alternative “SW/HW”, i.e., the motion detection is implemented as a hardware accelerator on the FPGA and the pose estimation software implementation on the ARM processor. At time $t1 = 4s$, a moving object is detected. Scenario $S1$ is the best possible scenario in this situation since the probability P(S1/evidence on sensors) increases and the maximum of the utility function is attained for the decision alternative “HW/SW”, i.e., the motion detection is implemented as a hardware accelerator on the FPGA and the region labeling software implementation on the ARM processor. These obtained results showed the ability of the decision making approach to choose the most suitable alternative scenario.

VI. Conclusion

In this paper, we have presented an approach to Decision Making among alternative scenarios for UAV by using mixed DBN for dynamic decision making and MCDM for HW/SW partitioning according to the flying environment conditions as well as the imposed constrains. Thus, the current scenario of UAV can be modified to adapt its functionality to perform different tasks depending on the objectives of the UAV mission. Moreover, real time implementations (hardware and software) of the embedded Decision Making module on FPGA board are given in term of FPGA resource utilization and timing performance. To evaluate the proposed approach, we have demonstrated the implementation of real case study in heterogeneous architecture based on an hybrid device. In the current work, we attempt to validate the complete mission through the use of dynamic and partial reconfiguration at runtime to update the Decision Making and the complete embedded system under certainty. In future work, we may wish to focus on evaluating the performance of our proposal in outdoor environments.

References

[1] K. Noori and K. Jenab, *Fuzzy reliability-based traction control model for intelligent transportation systems*. IEEE Transactions on Systems, Man, and Cybernetics: Systems, 43(1):229–234, 2013.

[2] Hsin-Han Chiang, Yen-Lin Chen, Bing-Fei Wu, and Tsu-Tian Lee, *Embedded driver-assistance system using multiple sensors for safe overtaking maneuver*. IEEE Systems Journal, 8(3):681–698, 2014.

[3] W. Ho, X. Xu, & P. K. Dey, *Multi-criteria decision making approaches for supplier evaluation and selection: A literature review*. European Journal of Operational Research, 202(1), 16–24.

[4] J. Chai, J. N. K. Liu, & E. W. T. Ngai(2013), *Application of decision-making techniques in supplier selection: A systematic review of literature*. Expert Systems with Applications, 40(10), 3872–3885.

[5] P. Dagum, A. Galper, E. Horvitz, A. Seiver, *Uncertain Reasoning and Forecasting*. International Journal of Forecasting. 11 (1): 73–87, 1995.

[6] FV. Jensen, TD. Nielsen, *Bayesian networks and decision graphs*.2nd ed.New York, NY:Springer;2007.

[7] J. Pearl *Probabilistic reasoning in intelligent systems*.San Francisco, CA:Morgan Kaufmann;1988.

[8] J. Schumann, T. Mbaya, O. J. Mengshoel, K. Pipatsrisawat, A. N. Srivastava, A. Choi, and A. Darwiche, *Software health management with Bayesian networks*, ISSE, vol. 9, no. 4, pp. 271–292, 2013.

[9] S. Zermani, C. Dezan, H. Chenini, JP. Diguet, R. Euler, *FPGA implementation of bayesian network inference for an embedded diagnosis-*Prognostics and Health Management (PHM), 2015.

[10] Y. W. Peng Watthayu, *A Bayesian network based framework for multi-criteria decision making*. In Proceedings of the 17th international conference on multiple criteria decision analysis. Whistler, British Columbia CA, 2004.

[11] L. Damez, L. Sieler, A. Landrault, J.P. Derutin: *Embedding of a real time image stabilization algorithm on a parameterizable SoPC architecture a chip multi-processor approach*. J. Real-Time Image Processing 6(1): 47-58 (2011).

[12] H. Chenini, D. Heller, C. Dezan, J.P. Diguet, D. Campbell, *Embedded real-time localization of UAV based on an hybrid device*. ICASSP 2015: 1543-1547.

[13] Chenini. Hanen, *Pipelined architecture for real time detection and tracking of moving objects on an hybrid device*. ATSIP 2017: 1-6.

[14] Chenini. Hanen, *A Bottom-up Approach for Visual Object Recognition on FPGA based Embedded Multiprocessor Architecture*. International Journal of Advanced Computer Science and Applications (IJACSA), 8(5) (2017): 474-482.

[15] Schumann. Johann, Rozier. Kristin Y, Reinbacher. Thomas, Mengshoel. Ole J, Mbaya. Timmy, Ippolito. Corey: *Towards Real-time, Onboard, Hardware-supported Sensor and Software Health Management for*

Unmanned Aerial Systems. Int. J. of Prognostics and Health Management, 6(1) (2015).

[16] I. Sugiarto, C. Axenie,& J. Conradt, *FPGA-Based Hardware Accelerator for an Embedded Factor Graph with Configurable Optimization*. Journal of Circuits, Systems and Computers, 1950031, 2018.

[17] D. Codetta-Raiteri, & L. Portinale, *Dynamic Bayesian Networks for Fault Detection, Identification, and Recovery in Autonomous Spacecraft*. IEEE Transactions on Systems, Man, and Cybernetics: Systems, 45(1), 13–24, 2015.

[18] M. Lin, I. Lebedev, & J. Wawrzynek (2010), *High-throughput bayesian computing machine with reconfigurable hardware*. Proceedings of the 18th Annual ACM/SIGDA International Symposium on Field Programmable Gate Arrays - FPGA '10.

[19] Z. Kulesza, & W. Tylman, *Implementation Of Bayesian Network In FPGA Circuit*. Proceedings of the International Conference Mixed Design of Integrated Circuits and System, 2006. MIXDES 2006.

Adaptive Cluster based Model for Fast Video Background Subtraction

Muralikrishna SN[1], Balachandra Muniyal[2], U Dinesh Acharya[3]
Department of Computer Science & Engineering[1,3]
Department of Information & Communication Technology[2]
Manipal Institute of Technology
Manipal Academy of Higher Education
Manipal, India, 576104

Abstract—**Background subtraction (BGS) is one of the important steps in many automatic video analysis applications. Several researchers have attempted to address the challenges due to illumination variation, shadow, camouflage, dynamic changes in the background and bootstrapping requirement. In this paper, a method to perform BGS using dynamic clustering is proposed. A background model is generated using the K′-means algorithm. The normalized γ corrected distance values and an automatic threshold value is used to perform the background subtraction. The background models are updated online to handle slow illumination changes. The experiment was conducted on CDNet2014 dataset. The experimental results show that the proposed method is fast and performs well for baseline, camera-jitter and dynamic background categories of video.**

***Keywords*—Background subtraction; Gaussian mixture model; K′-means; clustering; object detection; transform**

I. Introduction

Background subtraction refers to the extraction of moving objects, which are of special interest, from a video frame by removing the stationary contents. Background subtraction is one of the key tasks in surveillance video analysis. There are several methods available in the literature to address the issues in background subtraction. Some of the well-known methods for background subtraction can be classified as supervised background subtraction and unsupervised background subtraction.

In a supervised background subtraction, the process of bootstrapping generates a mathematical representation of the background called the background model. Further, the BG subtraction is done using the BG model, by assigning a membership value to the pixels as belonging to the foreground or to the background. In an unsupervised setting, one uses the derivative approach. The difference values from previous frames to current frame and few future frames are considered for background subtraction. Sometimes, the additional spatial information is used to predict the foreground. The frame differencing is one such method where the difference in intensity between two successive frames is used. The double differencing method is an enhancement where the second-order difference is considered for foreground detection. However, these methods fail miserably in situations of dynamic changes in the background [10], and also pose a challenge of ghosts in the foreground detected [5]. In a supervised method, a few frames called the training frames are used to generate a probabilistic model such as in GMM. This method works well in most conditions. However, fixing the number of mixture components k is a challenge and normally it is determined experimentally [32]. Similarly, one can consider $k = 1$ for representing each pixel in the background with a running average value. The soft computing technique like Self-Organizing Background Subtraction (SOBS) maintains a lookup map for each pixel [18]. This self-organizing map is updated subsequently to determine the foreground. SOBS works well in indoor conditions and also does not require bootstrapping.

There are several other background subtraction methods such as Eigen-background, Kernel Density Estimation (KDE), running average etc. All these methods have their own inherent limitations [5]. The major challenges involved in background subtraction are, dynamic changes in the background which may include additional stationary objects in the background, which was not a part of the learning, illumination changes, shadows, camouflage [14]etc. Illumination variation can be a sudden change or a slow change in the lighting condition. In an outdoor setting, this is a common problem. The method such as GMM is simple and can handle a lot of these issues, however, it ignores the lower order distribution in the background model of a pixel. This is due to the fact that in a dynamic background the number of components can vary drastically. In the simplest form, GMM can be implemented using the K-Means algorithm as mentioned in [24]. The major limitation of the K-Means algorithm is that the number of clusters is predetermined and fixed. So, to overcome this difficulty the K′-Means algorithm is implemented for background subtraction in the proposed method. The details of the methodology are given in section III. In section IV, the experimental setup and the results are presented.

II. Review of Existing Techniques

One of the techniques to detect a moving object is using background subtraction. In this, the tasks involved are background modeling and foreground segmentation. Some of the simplest methods for background subtraction are temporal differencing, double differencing, running average and optical flow. The most basic technique is the inter-frame difference with a global threshold. A few others are based on probabilistic methods. These methods often aim at making the detection process more robust to noise, camera jitter and background motion [1]. The motion detection is also achieved using object detection techniques [11]. In this case, the system is trained to detect any objects of interest. A window sliding method is applied to detect the object of different scales. Normally, feature-based or template-based technique is used to represent the object. The classifiers such as Support Vector Machine (SVM), Naive Bayes, and Artificial Neural Network are used to detect the object. Once the object is detected they can be tracked as well. One of the widely used methods for object detection is Histogram of Oriented Gradients (HoG) descriptor-based method. The descriptor based methods are normally invariant to rotation, scaling or illumination changes. The main disadvantage of this method is that it requires training and also window-sliding which is normally time-consuming. These methods are comparatively slower than the background subtraction methods discussed earlier. Several variants of descriptors are available.

The adaptive BGS uses dynamic updates in the background model. In the past decade, a lot of methods have been proposed for background subtraction using parametric and non-parametric background density estimates and spatial correlation. These methods are proven to be effective in background subtraction. Some of the methods from these categories are running Moving average, temporal median filter, KDE, GMM, Sequential KD approximation, Co-occurrence of image variations, Eigen-backgrounds and so on. Evaluations of background subtraction methods with respect to the challenges of video surveillance suffer from various shortcomings. To address this issue, the challenges of background subtraction in the field of video surveillance is studied in [3]. In [4], Conte et al. have conducted a thorough experimental comparison of different foreground detection algorithms on a large dataset of videos. It is concluded that both the techniques, GMM [24] and enhanced background subtraction (EBS), algorithms are adaptable and can be used effectively. Finally, it is given that the statistical background algorithm performs poorly when compared to the others. In some of the works presented in the literature, there have been attempts to capture the spatial dependency of pixels. Instead of using the pixel intensity other features like texture is also considered. In [25] several statistical features such as brightness, inverse contrast ratio, mixed contrast strength, integrated modal variability etc are used. In the training phase, these features are extracted and a bag-of-feature model is used. The background subtraction is done using a distance threshold from the bag-of-feature. This method provides a mechanism to update the background model. Also, this method makes use of majority voting scheme for label fusion. In most of the research presented in the literature, a number of general assumptions are considered as listed in [20].

In [23], a method for BGS is presented based on spatio-temporal binary feature and colour intensity of a pixel. This feature is good to represent the texture and allows to detect camouflaged objects and are not sensitive to illumination changes. The pixel-level feedback loop is maintained to update the model. The adjustments are based on the continuous monitoring, local segmentation noise levels. This approach outperforms most of the previously tested state-of-the-art methods on the Change Detection.net (CDNet) dataset.

The work presented in [22] uses multiple color spaces such as RGB, YCbCr, to create the background model. Unlike the existing techniques in this method multiple background models, called the Background Model Bank (BMB), are used instead of a single background model. Each training image is treated as a background model. Then this set of initial models are clustered into a number of average background model in an iterative way. The absolute difference of the frame and the average background model is used as a clue to perform the final background subtraction. To handle the spatial dependency of pixels super-pixel segmentation and DBSCAN clustering are used. This makes use of color, texture and size information. Here the purpose of DBSCAN is to avoid over-segmentation. The performance of the algorithm is very good in terms of accuracy, however, the algorithm can process approximately 10 frames per second of an image of size 320×240 on a Intel core i5 PC with 8GB of RAM.

Recent developments in the field of convolution neural networks (CNN) and deep neural network (DNN) have contributed largely to background subtraction. Military applications require the detection of moving objects in camouflaged patterns. A detailed review of the existing methods for BGS using DNN is presented in [2]. The DNN based method to detect camouflaged people is presented in [30]. However, most of the existing techniques fail to extract the foreground in the camouflaged videos. BGS still remains a challenge as there are a few unsolved issues [12].

In brief, locating moving objects in a video sequence is the first step of many computer vision applications. Among the various motion detection techniques, background subtraction methods are commonly implemented, especially for applications with a fixed camera. In the second phase, after detecting the object, object classification, tracking is done [11][29][8]. The information from all these stages is crucial in any vision application. So, to implement a robust framework in any surveillance system requires a reliable background subtraction. This would help to speed-up the processing time of the entire system. In this paper, the most widely known algorithms such as SOBS, GMM, Simplified self organizing background subtraction, code-book based method and a few other algorithms are used for comparison. The GMM based method proposed by Zivkovic et al. in [31] addresses the same issue that is discussed in this paper. In the following section, the description of the proposed method is given.

III. Proposed Work

Background modelling is an unsupervised learning task. Clustering techniques have been widely used in unsupervised learning. In the proposed method the key idea is to learn the different variations of pixel intensity values over time for every pixel in the video. This corresponds to the learning of multi-modal distribution of the pixel values. However, the number of components in the distribution is not known and difficult to estimate [22]. In this paper, an extension of the K-Means clustering [9] called the K′-Means clustering [27] is implemented. This method helps to find the optimal number of cluster components $k' < k$ unlike the method given in [24].

In the proposed method, the background subtraction problem is formulated as an unsupervised learning task where the clusters are formed for each pixel location (p, q) varying over time. Given a video with n frames, the set of training frames is denoted by $\mathbf{H} = \{\mathbf{I}^1, \mathbf{I}^2, ...\mathbf{I}^t\}$ where $1 \leq t < n$. The intensity or the colour information of the pixel at location (p, q) at time i is denoted by $\mathbf{I}^i_{p,q} \in \mathbb{R}^d$. For each location (p, q), the clusters with $k'_{p,q}$ components are formed, considering the data $X^t_{p,q} = \{\mathbf{I}^1_{p,q}, \mathbf{I}^2_{p,q}, ...\mathbf{I}^t_{p,q}\}$. The colour information (R, G, B) or the (H, S, I) or any region descriptor can be used to form the background model. Now the data, $X^t_{p,q}$, is clustered to generate the background model. The process of model generation, and background subtraction is explained in the following sections.

A. Background Model Generation

The proposed method uses a two-phase algorithm for background model generation. The first phase is the K-Means algorithm governed by Equation 1.

$$\textbf{Minimize} \quad J_{MSE} = \sum_{i=1}^{k} \sum_{\mathbf{x}_t \in \mathbf{c}_i} ||\mathbf{x}_t - \mathbf{c}_i||^2 \tag{1}$$

Equation 1 is used to assign a point $\mathbf{x}_t$ to a cluster centre $\mathbf{c}_i$ with k clusters, where $\mathbf{x}_t$ and $\mathbf{c}_i \in \mathbb{R}^d$.

The second phase reduces the number of clusters by minimizing information uncertainty in the clusters indicated by J_1 and the mean-square-error J_{MSE}. The modified cost function is given in Equation 2.

$$\textbf{Minimize} \quad J = J_{MSE} + J_1 \tag{2}$$

The distance metric given in Equation 3 is used to assign a point $\mathbf{x}_t$ to a cluster centre $\mathbf{c}_i$. The term $log_2(p(\mathbf{c}_i))$ is the information conveyed by the cluster $\mathbf{c}_i$. The parameter E is a constant defined by the user. In the first phase, the initial k clusters are formed. Further, Equation 3 helps to detect the optimal number of clusters k' starting from a k where $k > k'$.

$$dm(\mathbf{x}_t, \mathbf{c}_i) = ||\mathbf{x}_t - \mathbf{c}_i||^2 - E * log_2(p(\mathbf{c}_i)), \qquad E \in [a, 3a] \tag{3}$$

where $a = average(r) + average(d/2)$, *r*=radius of cluster, *d*=smallest distance between cluster centres. Any input data $\mathbf{x}_t$ is assigned to a cluster i using Equation 4.

$$M(\mathbf{x}_t, i) = \begin{cases} 1 & if \quad i = argmin(dm(\mathbf{x}_t, j)) \quad j = 1...k \\ 0 & otherwise \end{cases} \tag{4}$$

The clusters are formed from the data $X^t_{p,q}$, for each pixel (p, q). The set of cluster centers $C_{p,q} = \{c^i_{p,q}\}$, $i = 1....k'$, for each location p, q in the video frame, and their variances $\sigma^i_{p,q}$ are used as the background model for a given video. It is important to adapt the background model for non-stationary data. The centroids are updated during background subtraction using online K-Means clustering of non-stationary data given in [24] [15]. The algorithm for background model generation is listed in Algorithm 1.

B. Background Subtraction

The background subtraction is done using 2. A distance matrix D_t is constructed for each frame at time instance t. A small distance value in the distance matrix indicates that the pixel belongs to the background and a high value for the foreground pixel. We address two cases in the proposed background subtraction algorithm. The first case is when there are no moving objects in the frame. The second case is when there are one or more moving objects. The first case is handled with a threshold value T which is set to p times the maximum cluster variance $max_i\{\sigma^i_{p,q}\}$. In the second case, we use the Otsu binarization method [21] to automatically detect a threshold for the range normalized distance matrix. In the first case, the centroid of the corresponding model is updated online [24] [15].

Algorithm 1: Background Model Generation

Input: A sequence of spatially smoothed video frames
Parameters: Number of training frames t, the initial value of k, width w, and height h of video frame
Output: A set of cluster centroids $C_{p,q} = \{c^i_{p,q}\}$, $i = 1, 2, ..., k'$
, for each location (p, q) in the video frame.
for $p \leftarrow 1$ **to** w **do**
  for $q \leftarrow 1$ **to** h **do**
    Initialize the cluster centres for the pixel (p, q) ;
    $C_{p,q}$ = `K'-Means`($\mathbf{X}^t_{p,q}$)
  end
end

Algorithm 2: The proposed method for Background Subtraction

Input: A sequence of spatially smoothed video frames
parameter: A threshold value T, Video Frame at time instance t, width w, and height h of video frame
Output: Background subtracted Image
for $p \leftarrow 1$ **to** w **do**
  for $q \leftarrow 1$ **to** h **do**
    dist= **argmin**$_i$ `getDistance`($c^i_{p,q}$, $I^t_{p,q}$)
    if *dist* $< T$ **then**
      $\mathbf{D}_t(p, q) = dist$
      $UpdateCentroid(p, q, i)$
    else
      $\mathbf{D}_t(p, q) = \infty$
    end
  end
end
$\mathbf{D}_t$ = `normalize`($\mathbf{D}_t$);
$\mathbf{D}_t$ = `power`($\mathbf{D}_t, \gamma$);
Foreground$_t$ = `BinarizeDistanceMatrix`($\mathbf{D}_t$);

Another important factor in the proposed method is the introduction of Gamma transformation. The transformation function is given by

$$\mathbf{D}_t = Power(\mathbf{D}_t, \gamma), \quad \gamma \geq 0 \tag{5}$$

The transformation function is shown in Figure 1. This helps to work with a fixed threshold value. The γ parameter is very helpful in the hardware-based implementation of the algorithm. The distance matrix can be transformed so as

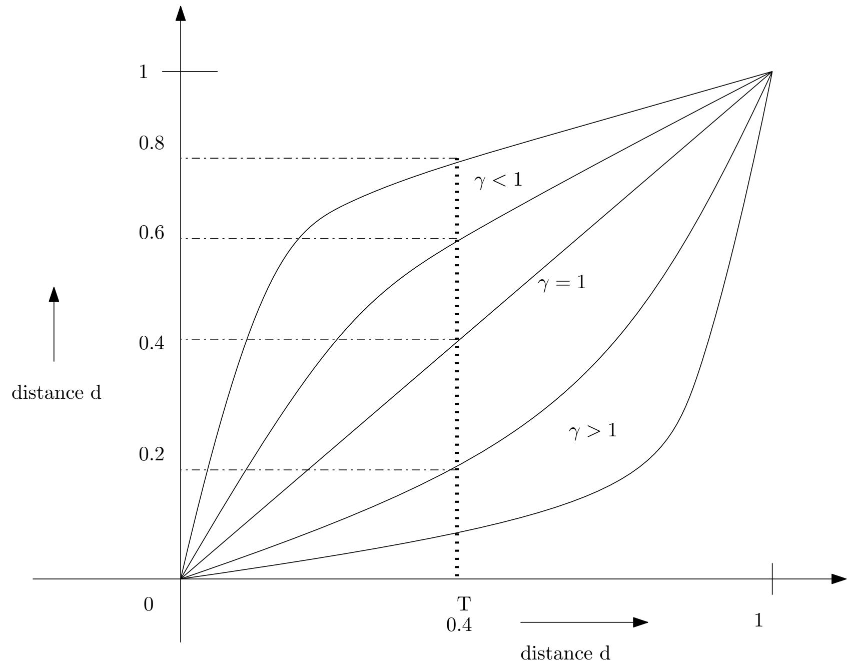

Fig. 1. The transformation using Gamma function on a distance matrix.

to include or exclude pixels which have an almost equal likelihood of belonging to the foreground or background. The value γ helps in adjusting the recall rate. Setting the γ to a lower value increases the recall rate. This can be observed in the example Figure 2. Experimentally it is observed that the γ is significant to fix an optimal threshold.

IV. Experiments and Results

A good background subtraction algorithm must handle challenges such as gradual illumination changes, sudden illumination changes, dynamic background, camouflage, shadows, bootstrapping, and video noise. So the evaluation must be done using the dataset which has all these cases. Some of the most commonly used datasets are Wallflower [26], Performance Evaluation of Tracking and Surveillance (PETS), and Change Detection dataset [7] [6] etc. There are so many other datasets such as CAVIAR, Pedestrian detection dataset, IBM dataset etc.

The proposed method was evaluated quantitatively using the Change Detection (CDNet-2014) dataset [28]. The CDNet-2014 is one of the standard datasets with 11 categories of video. CDNet-2014 dataset contains more challenging cases like camera jitter, low frame rate etc. Each video category has four to six videos in it. The different categories of video are, Baseline, Dynamic Background, Camera-Jitter, Shadow, Intermittent Object Motion, Thermal, Challenging Weather, Low Frame-Rate, Night, PTZ, Air and Turbulence. Totally 53 videos having a resolution of each video frame varying from 160×120 to 720×576. Duration of the videos is from 900 to 7,000 frames. To measure the performance of the algorithm there are several parameters such as precision, recall, specificity, false positive rate (FPR), false negative rate (FNR), the percentage of wrong classification (PWC), and F-measure.

The implementation of the proposed method was done using C++ with OpenCV support. The development and testing were done on Intel(R) Core(TM) i5-6200U CPU @ 2.30GHz processor with 4GB RAM. The size of the video frames was down-sampled to half the original size in all the experiments to speed-up the processing. In the experiments, to perform background subtraction, the first $N = 100$ frames were used as the training data. We have used the parallel implementation of K-Means algorithm for the first phase of the algorithm. The initial k value was set to 10, using the rule of thumb on the best k in K-Means. The value of parameter E is set as 10. To evaluate the performance the threshold T is set as the 3.5 times the maximum standard deviation among the cluster components. The parameter γ is set to 0.85. These parameter values were retained for all the categories of the videos similar to the evaluation method used in the literature. The evaluation was done using the tool given by CDNet-2014 dataset providers.

The baseline category contains the most primitive challenges. The result of the baseline category is presented in Table I. The analysis shows that the proposed method works well on the baseline video category. It is better than some of the state-of-the-art methods like GMM, simplified Self-organized background subtraction, Multi-scale temporal model, DCB, and GraphCutDiff in terms of $F1$-metric for baseline category video. This can be observed in Figure 3.

The dynamic background category is more challenging when compared to the baseline category. In the dynamic background category, the proposed method clearly performs better than all the listed methods in Table II except for SC-SOB [18] method. The PWC is observed to be ≈ 1.15. The result is shown in Figure 4. The result of the experiment on camera-jitter category is presented in Table III. In this category, the performance of the proposed method is better than SC-SOBS and other techniques. The comparison is shown in Figure 5.

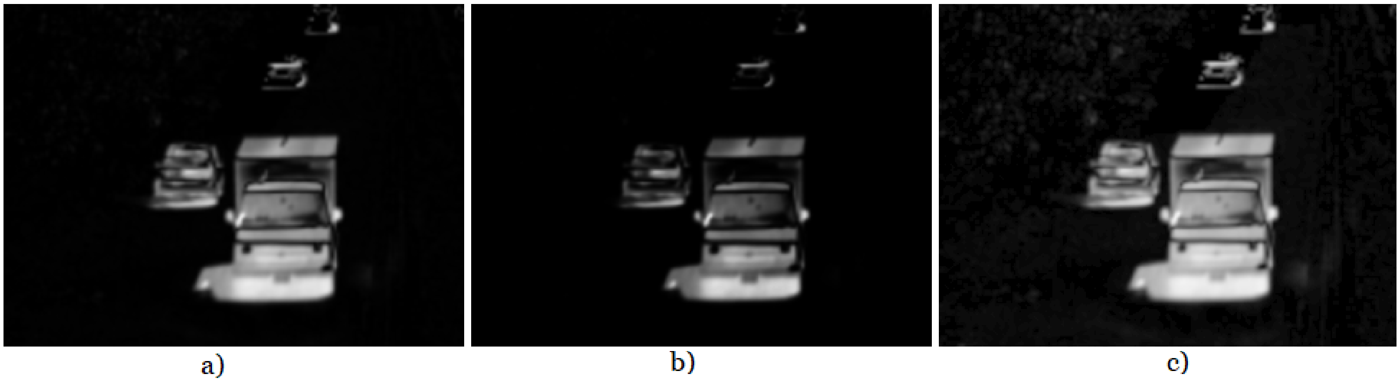

Fig. 2. Distance matrix of the video frame no. 268 from baseline category highway subcategory of changedetection (CDNet2014) dataset. a) Distance matrix with $\gamma = 1$ b)Transformed distance matrix with $\gamma = 0.6$ c) Transformed distance matrix with $\gamma = 1.6$

TABLE I. Comparison of BGS methods on baseline video category.

Method	Average Sp	Average FPR	Average FNR	Average Recall	Average Precision	Average F-Measure
SC-SOBS [18]	0.9980	0.002	0.0673	0.9327	0.9341	0.9333
GMM — Zivkovic[31]	0.9972	0.0028	0.1915	0.8085	0.8993	0.8382
Multiscale Spatio-Temporal BG Model [17]	0.997	0.003	0.1863	0.8137	0.887	0.845
GraphCutDiff [19]	0.9960	0.004	0.2972	0.7028	0.8093	0.7147
Simplified Self-Organized Background Subtraction [13]	0.9965	0.0035	0.5106	0.4894	0.8419	0.6085
DCB [16]	0.9982	0.0018	0.2877	0.7123	0.907	0.7695
Proposed Method	**0.9966**	**0.0034**	**0.1406**	**0.8994**	**0.9165**	**0.9027**

TABLE II. Comparison of BGS methods on dynamic background video category.

Method	Average Sp	Average FPR	Average FNR	Average Recall	Average Precision	Average F-Measure
SC-SOBS [18]	0.9836	0.0164	0.1082	0.8918	0.6283	0.6686
GMM — Zivkovic [31]	0.9903	0.0097	0.1981	0.8019	0.6213	0.6328
GraphCutDiff [19]	0.9063	0.0937	0.2307	0.7693	0.5357	0.5391
DCB [16]	0.9991	0.0009	0.4197	0.5803	0.7632	0.6149
Simplified Self-Organized Background Subtraction [13]	0.9252	0.0748	0.4766	0.5234	0.1013	0.1613
Proposed Method	**0.9721**	**0.0179**	**0.1774**	**0.8126**	**0.6273**	**0.6524**

TABLE III. Comparison of BGS methods on Camera-Jitter video category.

Method	Average Sp	Average FPR	Average FNR	Average Recall	Average Precision	Average F-Measure
DCB [16]	0.9969	0.0031	0.7204	0.2796	0.9107	0.3669
SC-SOBS [18]	0.9768	0.0232	0.1887	0.8113	0.6286	0.7051
GMM — Zivkovic [31]	0.9665	0.0335	0.3100	0.6900	0.4872	0.5670
Multiscale Spatio-Temporal BG Model [17]	0.9477	0.0523	0.2829	0.7171	0.3979	0.5073
GraphCutDiff [19]	0.9222	0.0778	0.3062	0.6938	0.5918	0.5489
Simplified Self-Organized Background Subtraction [13]	0.9373	0.0627	0.4192	0.5808	0.3411	0.4147
Proposed method	**0.9889**	**0.0111**	**0.1650**	**0.8150**	**0.7313**	**0.7326**

There is no single method which performs well in all categories of video. So, the proposed method performs well in primitive challenges. However, the overall performance is degraded because of the certain environmental conditions in the categories such as PTZ, badweather, and turbulence. The proposed method shows a high recall rate in most categories of the video indicating that the method is able to detect moving objects. The result of all the categories of videos is presented in Table IV.

We have compared the performance of the proposed algorithm for its speed. The number of frames the algorithm is able to process per second is considered. The information available in the changedetection.net against each of the existing algorithm is used for comparison. The information is not complete for all resolutions. The proposed algorithm is much faster when compared to the other methods. This is important

TABLE IV. PERFORMANCE OF THE PROPOSED ALGORITHM ON ALL CATEGORIES OF VIDEO.

Method	Recall	Specificity	FPR	FNR	PBC	Precision	FMeasure
Baseline	0.8994	0.9966	0.0034	0.1406	0.4670	0.9165	0.9028
Dynamic background	0.6724	0.9721	0.0179	0.1774	1.1502	0.8126	0.6525
CameraJitter	0.8150	0.9889	0.0111	0.1650	1.7524	0.7313	0.7326
IntermittentObjectMotion	0.8423	0.8606	0.1394	0.1577	13.0122	0.4918	0.5149
LowFramerate	0.7143	0.8896	0.1104	0.2857	11.6353	0.4711	0.4040
NightVideo	0.3877	0.9758	0.0242	0.6123	3.4235	0.2676	0.2622
Shadow	0.6809	0.9479	0.0521	0.3191	6.2910	0.5227	0.4828
Thermal	0.8126	0.9116	0.0884	0.1874	9.3849	0.5287	0.5520
Turbulence	0.7589	0.9193	0.0807	0.2411	8.3041	0.0488	0.0756
PTZ	0.3109	0.7817	0.2183	0.6891	22.1236	0.0178	0.0335
BadWeather	0.7359	0.8474	0.1526	0.2641	15.7556	0.2347	0.2399
Overall:	0.6937	0.9174	0.0817	0.2945	8.4818	0.4585	0.4412

TABLE V. COMPARISON OF EXECUTION SPEED OF THE BACKGROUND SUBTRACTION ALGORITHMS

Method	Resolutions	Hardware	# Frames processed ≈
SOBS	320×240	C code on Core i3-330M for 2.13GHz	23
GraphCutDiff	320×240	video with C++ on a 2.4 Intel Core 2 Duo, single threading	7
Proposed Method	320×240	C++ Intel(R) Core(TM) i5-6200U CPU @ 2.30GHz	**110**
GMM — Zivkovic	720×480	C++ on Core i7 3.4GHz	49
GMM — Stauffer & Grimson	720×480	C++ on Core i7 3.4GHz	21
Proposed Method	720×480	C++ Intel(R) Core(TM) i5-6200U CPU @ 2.30GHz	**49**
SOBS	720×576	C code on Core i3-330M for 2.13GHz	4
Simplified Self-Organized Background Subtraction	720×576	core I7 laptop	0.06
Proposed Method	720×576	C++ Intel(R) Core(TM) i5-6200U CPU @ 2.30GHz	**47**

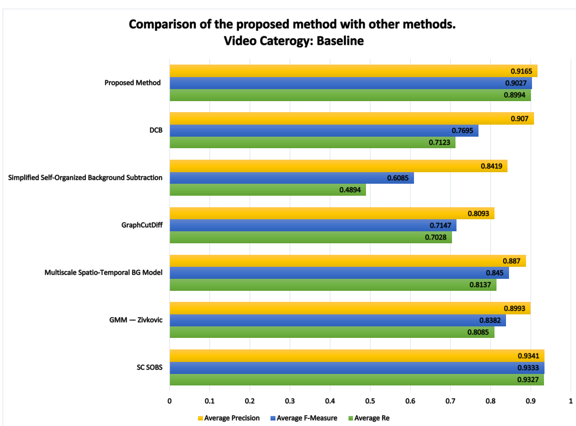

Fig. 3. Average precision, Average recall and Average F1-metric for the baseline video category

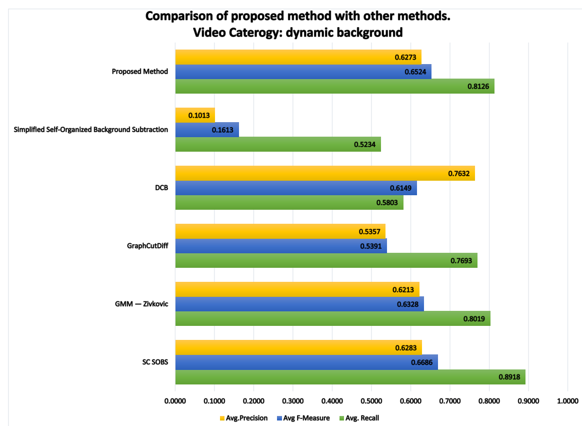

Fig. 4. Average precision, Average recall and Average F1-metric for the dynamic background video category

to develop real-time applications. The result is shown in Table V. The time required for training is not considered in the experiments. The qualitative result of the experiment is shown in Figure 6 and Figure 7.

V. CONCLUSIONS AND FUTURE DIRECTIONS

In this work, a fast background subtraction algorithm based on K′-Means algorithm is presented. The proposed method performs well in videos of baseline category and the camera-jitter, however, requires bootstrapping. Experiments were conducted extensively on the change detection dataset (CDNet2014) to demonstrate that the proposed method works well in challenging conditions. The online centroid-update scheme helps to handle slow and gradual illumination changes. In the proposed work, building the background model is a time-consuming operation, however, the background subtraction can be done in almost real-time on a video of resolution 640×480. The results of the proposed method are compared with various other techniques. It is observed that the proposed method works better than some of the existing techniques in the baseline, dynamic background, and the camera-jitter category. Additional spatial features and texture feature can be used to enhance the results. The parallel implementation of the K′-Means algorithm can be used to speed up the training. The clustering method proposed in this paper is very simple to

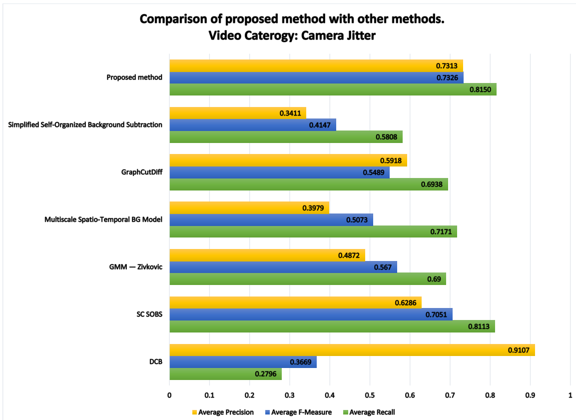

Fig. 5. Average precision, Average recall and Average F1-metric for the camera jitter

a) b) c)

Fig. 6. BGS result of the proposed method Video category: baseline, subcategory: highway, Frame: # 838 a) Input Frame b) Ground truth c) Result

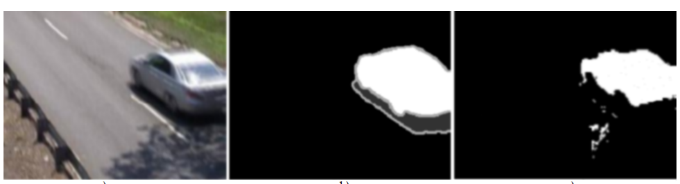

a) b) c)

Fig. 7. BGS result of the proposed method Video category: camera-jitter, subcategory: traffic, Frame: # 1413, a) Input Frame b) Ground truth c) Result

implement and it is suitable for practical applications.

Acknowledgment

Authors would like to thank Manipal Academy of Higher Education for supporting this research work.

References

[1] Y. Benezeth, P.-M. Jodoin, B. Emile, H. Laurent, and C. Rosenberger. Review and evaluation of commonly-implemented background subtraction algorithms. In *Pattern Recognition, 2008. ICPR 2008. 19th International Conference on*, pages 1–4, 2008.

[2] Thierry Bouwmans, Sajid Javed, Maryam Sultana, and Soon Ki Jung. Deep neural network concepts for background subtraction: A systematic review and comparative evaluation, 2019.

[3] S. Brutzer, B. Hoferlin, and G. Heidemann. Evaluation of background subtraction techniques for video surveillance. In *Computer Vision and Pattern Recognition (CVPR), 2011 IEEE Conference on*, pages 1937–1944, 2011.

[4] Donatello Conte, Pasquale Foggia, Gennaro Percannella, Francesco Tufano, and Mario Vento. An experimental evaluation of foreground detection algorithms in real scenes. *EURASIP J. Adv. Signal Process*, 2010:7:1–7:10, February 2010.

[5] R. Cucchiara, C. Grana, M. Piccardi, and A. Prati. Detecting moving objects, ghosts, and shadows in video streams. *IEEE Transactions on Pattern Analysis and Machine Intelligence*, 25(10):1337–1342, Oct 2003.

[6] N. Goyette, P. M. Jodoin, F. Porikli, J. Konrad, and P. Ishwar. Changedetection.net: A new change detection benchmark dataset. In *2012 IEEE Computer Society Conference on Computer Vision and Pattern Recognition Workshops*, pages 1–8, June 2012.

[7] N. Goyette, P. M. Jodoin, F. Porikli, J. Konrad, and P. Ishwar. A novel video dataset for change detection benchmarking. *IEEE Transactions on Image Processing*, 23(11):4663–4679, Nov 2014.

[8] I. Haritaoglu, D. Harwood, and L.S. Davis. W4: real-time surveillance of people and their activities. *Pattern Analysis and Machine Intelligence, IEEE Transactions on*, 22(8):809–830, 2000.

[9] J. A. Hartigan and M. A. Wong. A k-means clustering algorithm. *JSTOR: Applied Statistics*, 28(1):100–108, 1979.

[10] K.K. Hati, P.K. Sa, and B. Majhi. Intensity range based background subtraction for effective object detection. *Signal Processing Letters, IEEE*, 20(8):759–762, 2013.

[11] Weiming Hu, Tieniu Tan, Liang Wang, and S. Maybank. A survey on visual surveillance of object motion and behaviors. *Systems, Man, and Cybernetics, Part C: Applications and Reviews, IEEE Transactions on*, 34(3):334–352, 2004.

[12] Pierre Marc Jodoin, Lucia Maddalena, Alfredo Petrosino, and Yi Wang. Extensive Benchmark and Survey of Modeling Methods for Scene Background Initialization. *IEEE Transactions on Image Processing*, 26(11):5244–5256, 2017.

[13] Jean Meunier Kamal Sehairi, Fatima Chouireb. Comparative study of motion detection methods for video surveillance systems. *Journal of Electronic Imaging*, 26:26 – 26 – 29, 2017.

[14] W. Kim and C. Jung. Illumination-invariant background subtraction: Comparative review, models, and prospects. *IEEE Access*, 5:8369–8384, 2017.

[15] Angie King. Online k-means clustering of nonstationary data. 2012.

[16] R. Krungkaew and W. Kusakunniran. Foreground segmentation in a video by using a novel dynamic codebook. In *2016 13th International Conference on Electrical Engineering/Electronics, Computer, Telecommunications and Information Technology (ECTI-CON)*, pages 1–6, June 2016.

[17] X. Lu. A multiscale spatio-temporal background model for motion detection. In *2014 IEEE International Conference on Image Processing (ICIP)*, pages 3268–3271, Oct 2014.

[18] L. Maddalena and A. Petrosino. The sobs algorithm: What are the limits? In *2012 IEEE Computer Society Conference on Computer Vision and Pattern Recognition Workshops*, pages 21–26, June 2012.

[19] A. Miron and A. Badii. Change detection based on graph cuts. In *2015 International Conference on Systems, Signals and Image Processing (IWSSIP)*, pages 273–276, Sept 2015.

[20] Thomas B. Moeslund and Erik Granum. A survey of computer vision-based human motion capture. *Computer Vision and Image Understanding*, 81:231–268, 2001.

[21] N. Otsu. A threshold selection method from gray-level histograms. *IEEE Transactions on Systems, Man, and Cybernetics*, 9(1):62–66, Jan 1979.

[22] Hasan Sajid and Sen Ching Samson Cheung. Universal multimode background subtraction. *IEEE Transactions on Image Processing*, 26(7):3249–3260, 2017.

[23] P. L. St-Charles, G. A. Bilodeau, and R. Bergevin. Subsense: A universal change detection method with local adaptive sensitivity. *IEEE Transactions on Image Processing*, 24(1):359–373, Jan 2015.

[24] Chris Stauffer and W.E.L. Grimson. Learning patterns of activity using real-time tracking. *Pattern Analysis and Machine Intelligence, IEEE Transactions on*, 22(8):747–757, 2000.

[25] Badri Narayan Subudhi, Susmita Ghosh, Simon C.K. Shiu, and Ashish

Ghosh. Statistical feature bag based background subtraction for local change detection. *Information Sciences*, 366:31–47, 2016.

[26] Kentaro Toyama, John Krumm, Barry Brumitt, and Brian Meyers. Wallflower: Principles and practice of background maintenance. In *ICCV*, 1999.

[27] Krista Rizman Žalik. An efficient k'-means clustering algorithm. *Pattern Recognition Letters*, 29(9):1385 – 1391, 2008.

[28] Y. Wang, P. M. Jodoin, F. Porikli, J. Konrad, Y. Benezeth, and P. Ishwar. Cdnet 2014: An expanded change detection benchmark dataset. In *2014 IEEE Conference on Computer Vision and Pattern Recognition Workshops*, pages 393–400, June 2014.

[29] Xin Xu, J. Tang, Xiaoming Liu, and Xiaolong Zhang. Human behavior understanding for video surveillance: Recent advance. In *Systems Man and Cybernetics (SMC), 2010 IEEE International Conference on*, pages 3867–3873, 2010.

[30] Yunfei Zheng, Xiongwei Zhang, Feng Wang, Tieyong Cao, Meng Sun, and Xiaobing Wang. Detection of people with camouflage pattern via dense deconvolution network. *IEEE Signal Processing Letters*, 26(1):29–33, jan 2019.

[31] Z. Zivkovic. Improved adaptive gaussian mixture model for background subtraction. In *Proceedings of the 17th International Conference on Pattern Recognition, 2004. ICPR 2004.*, volume 2, pages 28–31 Vol.2, Aug 2004.

[32] Zoran Zivkovic and Ferdinand van der Heijden. Efficient adaptive density estimation per image pixel for the task of background subtraction. *Pattern Recogn. Lett.*, 27(7):773–780, May 2006.

High Predictive Performance of Dynamic Neural Network Models for Forecasting Financial Time Series

Haya Alaskar
Department of Computer Science, Collage of Engineering and Computer Sciences
Prince Sattam bin Abdulaziz University, Alkharj, KSA

***Abstract*—The study presents high predictive performance of dynamic neural network models for noisy time series data; explicitly, forecasting the financial time series from the stock market. Several dynamic neural networks with different architecture models are implemented for forecasting stock market prices and oil prices. A comparative analysis of eight architectures of dynamic neural network models was carried out and presented. The study has explained the techniques used in the study involving the processing of data, management of noisy data, and transformations stationary time series. Experimental testing used in this work includes mean square error, and mean absolute percentage error to evaluate forecast accuracy. The results depicted that the different structures of the dynamic neural network models can be successfully used for the prediction of nonstationary financial signals, which is considered very challenging since the signals suffer from noise and volatility. The nonlinear autoregressive neural network with exogenous inputs (NARX) does considerably better than other network models as the accuracy of the comparative evaluation achieves a better performance in terms of profit return. In non-stationary signals, Long short term memory results are considered the best on mean square error, and mean absolute percentage error.**

Keywords*—*Dynamic neural network; financial time series; prediction stock market; financial forecasting; deep learning-based technique

I. INTRODUCTION

Financial time series such as stock markets are considered one of the most common economic activities across the globe. The fluctuations of the stock market are produced by complex activity and their moves are translated into a blend of gains and losses that are represented in time series [1]. The purpose of stock market forecasting is to predict the future values of company stock price or financial instrument dealt on an exchange. This process will provide essential information about the actual stock price movement and its trends that is beneficial for the investors as it enables them to make the right choice about buying/selling strategies [2]. In addition, the successful prediction of a stock's future price might produce a significant profit. Therefore, there is an increase in the importance of analyzing stock markets in the economic world. However, stock market prediction is considered a challenging task and this is related to the structure of data [3]. The stock market price is based on the random walk hypothesis as proposed by Zhang et al. [4]. Few studies have claimed that the stock market is actually unpredictable; however, others are interested in solving this problem [5, 6].

A number of studies have appeared that focus on trying to find the optimum methodology for stock market forecasting. Each technique has shown a good ability to predict future prices. However, the methods can be divided into conventional prediction techniques, described in detail by Box, Jenkins, and Reinsel [7], and unconventional techniques using AI algorithms such as Artificial Neural Network (ANN). The application of conventional methods such as ARIM and ARIXM for financial time series forecasting have been introduced by few studies [8, 9]. However, in the extensive application of these methods, these models suffer from certain limitations in capturing some types of economic behavior, such as non-stationary or economic performance, at specific periods of time [10, 11]. Hence, various artificial neural network architectures (ANNs) have been used recently to predict future values for finical time series data.

ANNs have proven to be extremely successful for predicting this type of time series such as stock market prices [, 12-18]. Furthermore, studies have also attempted to continue to develop more efficient and accurate ANN architectures for solving forecasting problems [18]. In the similar context, the present study aims to compare forecasting performance of eight neural networks. The neural networks are non-linear autoregressive neural network (Nar), NARX neural network with external input, Elman network, layer recurrent neural network (Layer-RNN), Jordan network, echo recurrent neural network (ESN) ,time delay neural network (TDNN) furthermore the deep learning-based network, long short term memory (LSTM) has been used in this study.

These dynamic neural network architectures have been implemented and their performances have been measured by using statistical and financial measurements. The rationale behind selection of the neural network for predicting the prices of the stock market is based on its ability to understand the nonlinear mapping which prevails between input and output. Moreover, various studies supplement that stock market demonstrates chaos, which is a nonlinear deterministic procedure [19]. As the neural network has the ability to learn about the non-linear process, it can help in improving the financial predictions. The study has used dynamic neural network to forecast stock market prices and oil prices time series. It is important for the investors to maximize their returns at an appropriate time through buying or selling of their investments. It is quite challenging to predict the future price of stock because the data of stock market is highly time-variant and presented in a non-linear pattern.

In this study, the chosen time series involves of three different financial indexes. The first two are a global stock markets which are NASDAQ and Oil prices. NAS DAQ and Oil prices are more delicate to changes in the world economy. The last financial index is one of the popular Saudi stock market in which is Al-rajhi bank prices. It was selected because in the literature, there have been insufficient studies on forecasting the Saudi market. These three indexes were selected in order to test the dynamic neural networks (DNNs) on three various time series. The investigation of stock market data to predict the future of stocks is also a great challenge due to the evolution of information technology and the increase in economic globalization. Therefore, the process of predicting valuable information regarding stock market is important concerning the current status of movements in stock prices. This information is likely to help the customers in taking decisions to finalize whether to sell or buy the shares in a given stock. The comparative assessment is likely to depict the accuracy of recent dynamic neural networks as compared to the traditional models. Furthermore, this study will compare between standard dynamic neural network with deep and layered hierarchical neural network long short term memory (LSTM).Moreover, the results would encourage future studies to use the dynamic neural network to forecast volatility in the financial time series.

II. Literature Review

Recently, a series of studies have been presented in the area of financial data analysis using several ANN architectures for financial time series forecasting. ANN has been proved to offer promising results in terms of stock price forecasting. Dase et al. [20] presented a literature review using ANNs to forecast world stock markets. ANNs have been shown to be extremely successful in predicting non-linear and non-stationary time series. Some existing studies have compared the performances of traditional forecasting models with neural networks [12, 13, 15, 21-25]. Empirical results reported in various studies indicated that the neural networks perform better than linear regression techniques using financial evaluation functions or forecasting error measures [26-29]. Kamruzzaman and Sarker [25] investigated the performance of three ANN models that aimed to forecast foreign exchange rates; they were the standard MLP network trained with the back-propagation learning algorithm, the scaled conjugate gradient network, and Bayesian regression. The experiments attempted to predict six foreign currencies against the Australian dollar. The results also showed that ANNs outperformed ARIMA statistical techniques. Bagherifard et al. [30] confirmed that ANNs give a superior performance than the ARIMA model in financial time series prediction in terms of statistical or financial matrices.

Generally, ANN can be characterized into two types on the basis of the architecture. Both the architectures are different and possess different functions for overcoming a specific problem. One type of ANN is the feed-forward neural network where the inputs (signals) go in one direction to layers until they reach the output layer. This type of neural network has been applied for financial time series analyzing [17, 31]. The other type of ANN is the recurrent neural network (RNN), also called the dynamic neural network, in which the direction of the signal is similar to that in feed-forward networks along with recurrent links from some layers. These links provide RNNs with the capability of having a memory that help the RNNs to exhibit a dynamic behavior in the predicted signals, which means that the neural network learning process is based on previous information in addition to current input data. This information will be stored and then it will be used for better prediction of future time series values. Since the data structure in stock markets is dynamic, learning from historical data is essential where future values depend on historic values. Consequently, feedback links in RNNs will leverage the abilities of neural networks (ANNs) for time series forecasting.

Few of the previous studies have shown the application of the dynamic neural network in different areas [1, 18, 32-35]. These applications show the capability that makes them appropriate for time series forecasting with acceptable forecasting results. Elman RNN [36] and echo-state network (ESN) have been used for financial forecasting [37-40]. Lin et al. [39] investigated the ability of the ESN to forecast future stock prices over the short term by using historical S&P 500 data. The result indicated that ESNs achieved a good result. Another type of dynamical model is the non-linear autoregressive model with exogenous inputs (NARX) that is used for financial forecasting by a number of researchers [41-44]. Cocianu and Grigoryan [43] used NARX to forecast the Bucharest Stock Exchange and compare the result with ARIMA models. In addition, the Time Delay Neural Network (TDNN) is another type of dynamic neural network used by Kim et al. [46] for stock market prediction tasks. The network is generating profits (using the annualized return as a financial measure) for the non-stationary data prediction, which has not been achieved by majority of the benchmarked networks.

Other studies have attempted to design novel dynamic neural networks to perform in financial time series forecasting. Ghazali et al. [1] developed a new dynamic neural network including recurrent links in addition to the feed-forward Dynamic Ridge Polynomial Neural Network (DRPNN). The proposed network achieved a better result on the annualized return for the prediction of the exchange rate signals. This network was also applied to predict Standard & Poor's (S&P) 500 stock index future signals [1]. Another developed dynamic neural network is called Dynamic Self Organized Neural Network Inspired by the immune system (DSMIA) [18]. This model was designed to model the dynamics of the stock market by using dynamic links. DSMIA architectures are linked with the recurrent network using self-organized immune algorithm layer. DSMIA was effective in predicting accuracy in forecasting, which was proved by the simulation results. Alaskar et al. [18] used DSMIA for financial market forecasting for stationary and non-stationary data and for one and five forecasting horizons. The network is generating profits (using the annualized return as a financial measure) for the non-stationary data prediction, which most benchmarked networks are unsuccessful at doing.

III. Dynamic Neural Networks (DNNs)

The study has implemented eight Dynamic neural networks models to forecast the financial time series. The model of neural network imitates the working of the human brain. It functions by stimulating various interlinked processing units which are in the form of neuron abstract [47]. Such as, the units responsible for processing are arranged in the form of layers, usually in three layers; namely, input layer (input field), hidden layers and an output layer (target field). All these units are connected together through variable strengths or weights, where the information is passed on from one neuron to other. The networks help in investigating the individual record, where continual predictions are based on every record. This is mostly effective in NN for overcoming time series problem where non-linear dynamics are observed [47]. The eight neural networks have been discussed in this section.

A. Non-Linear Autoregressive Neural Network (NAR)

A non-linear autoregressive neural network is recurrent connection network with multiple layers [44] as presented on Fig. 1. It applies to time series prediction, and modelling non-linear function. NAR model can be written as follows:

$$y(t) = f(y(t-1), y(t-2), .., y(t-d)) + e(t) \tag{1}$$

Where; y(t) is the value of a data series n at time t, d shows the number of past values of the series, y(t−1), y(t−2), ..., y(t−n), are called feedback delays.

B. Non-Linear Autoregressive Neural Network with External Input(NARX)

The non-linear autoregressive neural network with exogenous inputs (NARX) uses past values of the time series to the external input series. NARX was proposed by Lin et al. [48]. The structure of this network is illustrated in Fig. 2 below. The NARX predict future values of the time series by using its last outputs and external data [45]. NARX output is computed by the following equation:

$$y(t) = f(y(t-1), \dots, y(t-d), x(t-1), \dots, x\left(t-d\right) \tag{2}$$

Where; y(t) is the recent prediction value of the dependent output variable y. x is the externally determined variable that influences y. Therefore, it is able to represent dynamic inputs in historical time series sets. This property will help NARX to deal with continuous and discrete inputs.

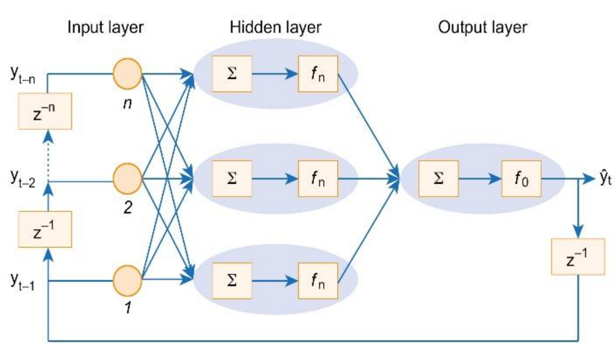

Fig. 1. A Non-Linear Autoregressive Neural Network is Recurrent Connection Network with Multiple Layers.

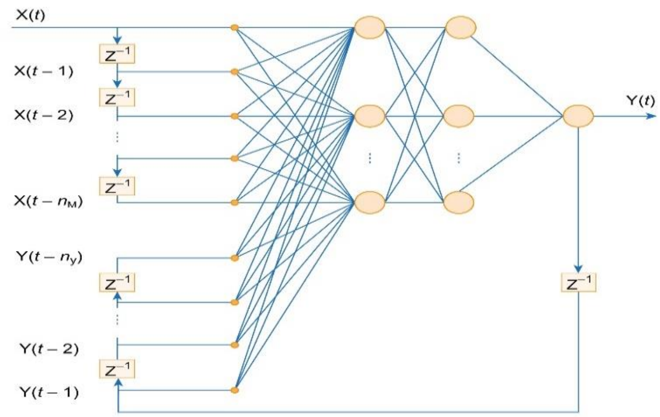

Fig. 2. A Non-Linear Autoregressive Neural Network with External Input.

C. Elman Network

Elman Recurrent Artificial Neural Network (ELMAN) was designed by Jeffrey Elman in 1990. Its first application was to discover patterns in natural languages [49]. The ERNN architecture is similar to the feed-forward neural network, in addition to some context units. The concept of unit context is regarded as the units which store delayed hidden layer of values and represent these in the form of additional network inputs. Such as these context units store the past activation outputs from the hidden layer. Therefore, the feedback links in the ERNN are transformed from the hidden to the input layer through the context-switching nodes, as illustrated in Fig. 3.

The dynamic equations of the ELMAN networks are as follows:

$$u_i(t) = \sum_{j=1}^{n} w_{i,j}^{u}(t) u_j(t-1) + w_i^{x}(k-1) x(t) \tag{3}$$

$$y(t) = \sum_{i=1}^{h} w_i^{y} u_i(t) \tag{4}$$

where n number of output units, w^u refer to the weight connected to context units. Where $u_j(t-1)$ is the context output at time t. h represent number of hidden units. And $u_j(0) = 0$.

D. Layer Recurrent Neural Network (RNNLayers)

This network is similar to the ELMAN network, except that it involves many layers, each of which has a feedback loop from the last layer. Furthermore, it uses arbitrary number of layers and arbitrary transfer functions in each layer.

E. The Jordan Network

The Jordan neural network is similar to the feed-forward network, except that there are feedback links from the output layer to a set of context units. This network was established by Jordan [50], who used the network to learn sequential tasks in language processing. The main aim of designing the Jordan network was to make a neural network that is capable of showing temporal variations and temporal context dependence [50]. In this network, the recurrent links are presented from the output layer to the input layer, in which the input units hold a copy of the values of the external inputs. The context units hold a copy of the values of the feedback link from the previous output units, in addition to self-feedback connections from the context units to themselves Fig. 4.

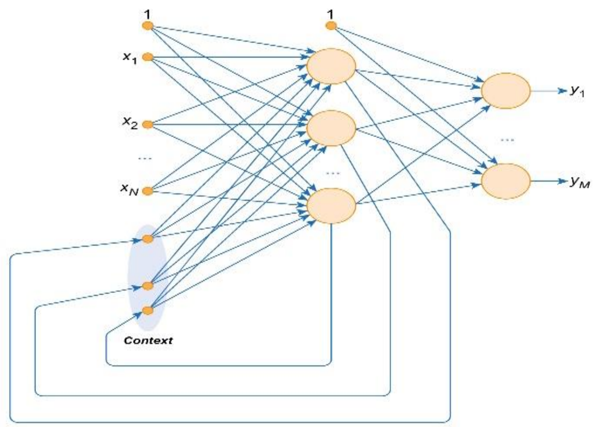

Fig. 3. ELMAN Neural Network.

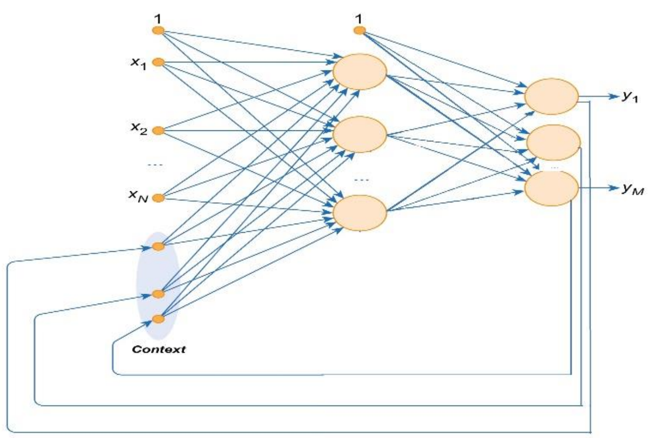

Fig. 4. A Jordan Neural Network.

The dynamic equations of the Jordan neural network can be determined as follows:

$$Z_i(t) = \sum_{j=1}^{n} w_{i,j}^{u}(t) y_j(t-1) + w_i^x(k-1)x(t) \quad (5)$$

$$y(t) = \sum_{i=1}^{h} w_i^y Z_i(t) \quad (6)$$

Where, Z(t) represents the context unit.

F. Echo Recurrent Neural Network (ESN)

The recurrent network of an echo-state network involves an 'echo-state' characteristic [51] that is utilized as a fading memory. Jaeger et al. [52] introduced the echo-state network; however, this network is considered as part of reservoir computing methods based on the recurrent neural network [51]. It involves two parts [52, 53];

- Dynamic reservoir - A recurrent network with a number of units and weights that connect the units with each other.
- Output units - Connected to the neurons of the dynamic reservoir.

The input units are applied to the dynamic reservoir as shown in Fig. 5. The reservoir in the network performs as a fading memory, which is where the echo state name comes from [50].

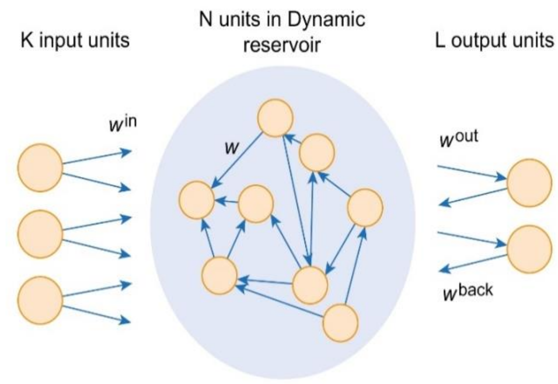

Fig. 5. Echo Recurrent Neural Network.

The activation of the internal units is computed as:

$$u(t) = f(w^{in}x(t) + wu(t-1) + w^{back}y(t-1)) \quad (7)$$

$$y(t) = f(w^{out})(x(t), u(t), y(t-1)) \quad (8)$$

Where; w^{in} is the weight that connects the input units, w^{out} is the weight that connects the output units w^{back}, is the weight connected the output units to internal units ,and fare the transfer function. The output units are y(t). The weights in the dynamic reservoir are trainable by back-propagation algorithm. However, the recurrent weights on the ESN network do not adjust during training.

G. Time Delay Neural Network (TDNN)

The TDNN model design is modular as well as incremental, which forms a larger network using its subcomponents. The TDNN has been illustrated in Fig. 6. The network was designed in 1987, when it was used for speech recognition [54].

It provides an effective way of forming proactive predictions in univariate time series. All input and output variables are scaled between upper and lower boundaries of the network transfer function.

$$\{x(t), x(t-\Delta), x(t-2\Delta), \ldots, x(t-m\Delta)\} \quad (9)$$

This network has been shown to be effective in modelling long-range temporal dependencies [54]. According to Junior et al. [55] the TDNN model will eventually behave as a kind of RNN architecture, since a global loop is needed to feed back the current estimated value into the input regressor.

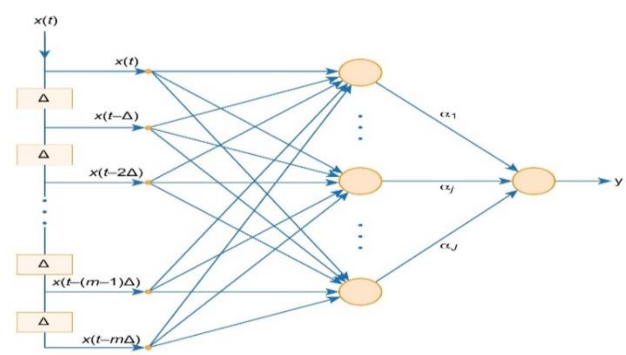

Fig. 6. Time Delay Neural Network (TDNN).

H. Long Short-Term Memory (LSTM) Network

LSTM is a recurrent Neural Network (RNN) with the capability of remembering the values from earlier stages for the purpose of future use. Long Short-Term Memory (LSTM) was first developed by Hochreiter & Schmidhuber (1997) as a variant of Recurrent Neural Network (RNN) [48]. LSTM has been implemented in stock forecasting [46, 48, 58]. LSTM has showed a good performance when compared with traditional-based algorithms such as ARIMA model [58]. LSTM are considered as type of deep learning network. The usual hidden layers are changed with LSTM cells. The LSTM architecture is illustrated below Fig. 7.

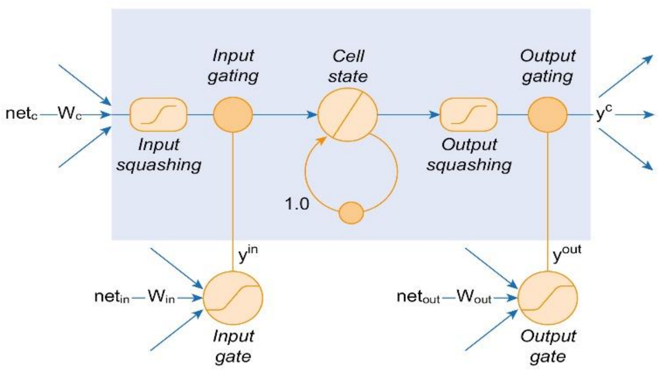

Fig. 7. Long Short-Term Memory (LSTM) Network.

The main aspect of LSTM is having memory block holds memory cells with self-connections storage the temporal state of the network in addition to forget, input gate, and output gate in each LSTM layer [58] has been represented in Fig.7. Gates are able to control the flow of information. The gates and their main functions are as follows:

- Input gate: Input gate contains of the input.
- Cell State: activated through the entire network and its function is to add or eliminate information.
- Forget gate layer: Decides which part of information to be allowed.
- Output gate: It contains of the output produced by the LSTM.
- Sigmoid layer creates numbers between zero and one.
- Tanh layer generates a new vector, which will be added to the state.

IV. Methodology

A. Dataset Description

The experiments conducted in this study are implemented in a MATLAB environment. The performance of the eight neural networks has been evaluated using different time series data. Three noisy financial time series have been studied and used to evaluate the performance of the eight neural network architectures. The data was collected from different resources. The day-by-day stock price of NASDAQ and Al-rajhi has been used as data series. For these companies, the stock movement price for seven years, 2010 to 2017. The historical data consists of daily closing price, opening price, the source of the data can be found at https://finance.yahoo.com. The crude oil price (West Texas Intermediate (WTI) was used in this study. Oil time series was monthly data involving the period between 1st January 1986 and 1st December 2016, with a total of 389 trading months. The source of the data can be found at https://fred.stlouisfed.org/series/DCOILWTICO.

B. Data Processing

The first step before financial forecasting was to select a forecasting horizon. From a trading principle, Cao and Tay [56] declared that a chosen long forecasting horizon might evade over-trading resulting in great transaction rates. However, complexity of the forecasting procedure could increase if the forecasting horizon is very long. In contrast, analysts have claimed that the forecast horizon needs to be small as the persistence of financial time series is for a limited period [1]. This experiment applies one-day ahead predictions from the trading and prediction point of view.

The second step was choosing the pre-processing method, since financial time series are suffering from non-stationary signal [18, 57]. It is also important to transform the data before sending it to the neural network. The transformation technique used is Relative Difference in Percentage of price (RDP) [59], which is used by a number of researchers in this field [1, 18, 57]. It creates a five-day measure of the relative difference in price data. Table I shows the calculations of the data transformation into stationary series.

TABLE. I. The Pre-Processed Data Transformed into Stationary Series

	Indicator	**Calculations**
Input variables	EMA15	$P(i) - EMA_{15}(i)$ $EMA_n(i) = \frac{a^0 p_i + a^1 p_{i-1} + a^2 p_{1-2} + \cdots + a^{n-1} p_{i-n+1}}{a^0 + a^1 + a^3 + \cdots + a^{n-1}}$
	RDP-5	$\frac{p(i) - p(i-5)}{p(i-5) * 100}$
	RDP-10	$\frac{p(i) - p(i-10)}{p(i-10) * 100}$
	RDP-15	$\frac{p(i) - p(i-15)}{p(i-15) * 100}$
	RDP-20	$\frac{p(i) - p(i-20)}{p(i-20) * 100}$
Output variable	RDP + k	$\frac{p(i+k) - p(i)}{p(i) * 100}$ $p(i) = EMA_e(i)$

where α is the weight factor which is experimentally selected in these experiments as 0.85 as recommended on [18], P(i) is the values of signal for the ith day, and k is a horizon of one or five step ahead prediction. Once this process is completed, the signal will be more symmetrical and it will track normal distribution as represented on Fig. 8. RDP helps in reducing the influence of trends on financial time series and smooth the data to reduce noise, which can improve the prediction process [1, 56]. The input variables are calculated from four lagged RDP values based on five-day periods (RDP-

5, RDP-10, RDP-15 and RDP-20) and one transformed signal exponential moving average (EMA15). The main reason for applying (EMA 15) is to keep useful information contained in the original signal, which might be eliminated by the RDP method [18].

Another pre-processing method applied to the data is scaling. This method is implemented to decrease the variances in the data and to reduce the computational time. All input and output variables are scaled between [0.1 0.9]. The procedure steps of this study are represented in Fig. 9.

C. DNNs

The DNNs parameters are 1000 epochs with one unit for input and output layer. The learning algorithm for each DNNs was backpropagation. Table II below represents the different parameters for each DNN.

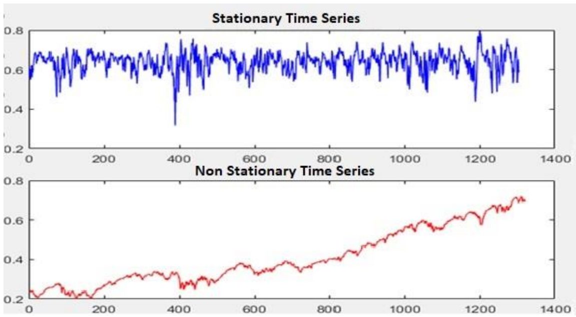

Fig. 8. The Stationary and Non-Stationary Time Series.

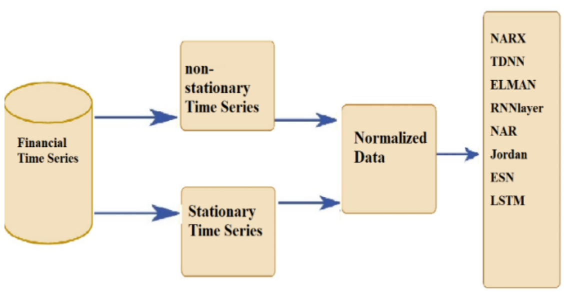

Fig. 9. The Procedure Steps of this Study.

TABLE. II. THE PARAMETERS FOR EACH DNN

	Learning rate	mu	Hidden layer
NARX	0.01	0.001	1
TDNN	0.01	0.001	1
ELMAN	0.01	0.9	1
RNNlayers	0.01	0.001	1
NAR	0.01	0.001	1
Jordan	0.01	0.001	1
ESN	0.01	0	100 hidden units
LSTM	0.01	0.001	1. Sequence input with 1 dimensions 2. LSTM with 200 hidden units 3. 50 fully connected layer 4. Dropout layer 5. 1 fully connected layer 6. Regression Output (MSE)

D. Modelling Performance Criterions

There are different evaluation functions that are applied to estimate the network prediction performance; some of them are related to financial criteria and some of them are statistical criteria. The statistical criteria have been used to evaluate the performance of the neural network prediction model, which includes the functions listed below:

- Mean Square Error (MSE) computes the square of the error between the target and forecasted values:

$$MSE = \frac{1}{N}\sum_{i=1}^{N}(y_i - \hat{y}_i)^2 \quad (10)$$

Where; $\hat{y}_i$ is the predicted value, y_i is the actual value and N is the number of data.

- Mean Absolute Percentage Error (MAPE). The MAPE is defined as follows:

$$MAPE = \frac{100}{N}\sum_{i=1}^{N}\left|\frac{y_i - \hat{y}_i}{y_i}\right|^2 \quad (11)$$

- Correct Directional Change (CDC) CDC defines the ability of a prediction model to forecast accurately the successive actual change of a forecasting variable.

$$CDC = \frac{1}{N}\sum_{i=1}^{N} d_i \quad (12)$$

Where $d_i = \begin{cases} 1 \; if \; (y_i - y_{i-1})(\hat{y}_i - \widehat{y_{i-1}}) \geq 0, \\ \quad 0 \; otherwise \end{cases}$

The financial criterion is likely to be used to determine the quality of the forecasts [13]. These measurements are listed below:

- Annualized Return (AR) computes the ability of forecasting tools to be used as traders. It is a scaled calculation of the observed change in time series value. The better prediction model gains the higher value of AR.

$$AR = \frac{profit}{All\ profit} * 100 \quad (13)$$

$$Profit = \frac{252}{n} * CR, C\ R = \sum_{i=1}^{n} R_i$$

$$R_i = \begin{cases} +|y_i| \; if \; (y_i)(\hat{y}_i) \geq 0, \\ \quad -|y_i| \; otherwise \end{cases} \quad (14)$$

$$All\ profit = \frac{252}{n} * \sum_{i=1}^{n} abs\ (R_i) \quad (15)$$

- The last financial criterion is annualised volatility (AV), which is the function that estimates the investment risk and profit possibilities; thus, a small value of volatility is considered to be a better result.

$$AV = \sqrt{252} * \sqrt{\frac{1}{n-1}\sum_{n-1}^{n}(R_i - \bar{R})^2} \quad (16)$$

V. SIMULATION RESULTS AND DISCUSSION

A. Experimental Results

The simulation results using eight DNNs have been presented in Tables III to VII and Fig. 10 to 13. In this study, the networks are tested in two different sets of signals that are stationary and non-stationary. One-step ahead predictions of financial time series were utilized. In the case of the non-stationary signal, all the data is passed directly to the neural network. On the other hand, for the stationary signal, the original signals have been transformed using RDP.

TABLE. III. THE RESULT OF MSE FOR ONE-STEP AHEAD PREDICTION

	DNNs	Open NASDAQ	Close NASDAQ	Open Al-rajhi	Close Al-rajhi	Oil Prices
Stationary	NARX	0.0001	0.0001	0.000	0.000	0.001
	TDNN	0.0008	0.0010	0.002	0.001	0.003
	ELMAN	0.0310	0.0552	0.022	0.002	0.055
	RNNlayers	0.0139	0.0051	0.092	0.108	0.027
	NAR	0.0002	0.0005	0.001	0.000	0.001
	Jordan	0.0088	0.0067	0.041	0.006	0.014
	ESN	0.0130	0.0096	0.061	0.058	0.115
	LSTM	0.0083	0.0350	0.014	0.022	0.058
Non- Stationary	Narxnet	0.0000	0.00187	0.000	0.000	0.001
	TDNN	0.0006	0.00213	0.001	0.002	0.003
	ELMAN	0.0092	0.01960	0.032	0.015	0.066
	RNNlayers	0.0051	0.0363	0.084	0.717	2.238
	NAR	0.0002	0.00209	0.001	0.001	0.001
	Jordan	0.0028	0.00639	0.001	0.009	0.0261
	ESN	0.0205	0.00024	0.063	0.061	0.086
	LSTM	0.0019	0.00769	0.018	0.818	0.007

TABLE. IV. THE RESULT OF MAPE FOR ONE-STEP AHEAD PREDICTION

	DNNs	Open NASDAQ	Close NASDAQ	Open Al-rajhi	Close Al-rajhi	Oil Prices
Stationary	NARX	4.9638	3.0174	5.8014	8.1437	9.619
	TDNN	6.1601	6.3957	9.8492	10.308	15.52
	ELMAN	12.210	44.518	29.683	26.122	15.68
	RNNlayers	5.3706	14.115	41.355	14.786	33.83
	NAR	4.7291	4.7398	6.8975	8.2749	8.7829
	Jordan	7.3757	21.156	32.222	11.777	19.276
	ESN	8.5551	8.6843	29.6449	14.261	46.569
	LSTM	4.3118	17.281	1.15271	10.218	0.203
Non- Stationary	NARX	1.3911	1.4547	6.14878	5.2597	5.2236
	TDNN	2.5589	3.1934	10.1737	9.2199	9.1529
	ELMAN	13.357	21.752	33.054	10.954	31.655
	RNNlayers	9.2253	17.092	26.929	58.215	159.00
	NAR	1.8488	1.8395	5.14755	6.0778	5.5762
	Jordan	7.6586	9.6192	14.606	14.331	17.823
	ESN	2.3437	2.8355	29.1189	26.861	29.907
	LSTM	2.7303	7.7828	30.6037	1.7817	8.0623

TABLE. V. THE RESULT OF CDC FOR ONE-STEP AHEAD PREDICTION

	DNNs	Open NASDAQ	Close NASDAQ	Open Al-rajhi	Close Al-rajhi	Oil Prices
Stationary	NARX	50.80	50.06	58.24	58.27	48.37
	TDNN	52.62	48.33	63.18	57.66	47.98
	ELMAN	52.89	51.05	59.31	55.77	49.06
	RNNlayers	51.11	48.65	56.65	53.27	48.99
	NAR	54.24	50.84	57.01	58.70	49.26
	Jordan	53.81	50	63.12	61.35	50.22
	ESN	52.43	49.63	57.09	53.67	49.68
	LSTM	45.01	54.03	65.85	63.41	57.60
Non- Stationary	NARX	54.63	59.81	58.53	58.24	55.44
	TDNN	50.18	49.86	63.96	58.21	49.33
	ELMAN	53.35	50.13	57.37	56.29	51.44
	RNNlayers	51.32	53.97	57.20	54.31	51.33
	NAR	57.21	59.26	57.82	58.73	57.44
	Jordan	53.68	50.81	63.19	61.03	53.04
	ESN	50.54	52.52	58.09	54.80	57.93
	LSTM	95.68	88.70	65.04	62.60	72.82

TABLE. VI. THE RESULT OF AR FOR ONE-STEP AHEAD PREDICTION

	DNNs	Open NASDAQ	Close NASDAQ	Open Al-rajhi	Close Al-rajhi	Oil Prices
Stationary	NARX	100	100	100	100	100
	TDNN	100	100	100	100	100
	ELMAN	100	100	94.67	100	100
	RNNlayers	97.70	97.701	98.51	83.56	95.4
	NAR	100	100	100	100	100
	Jordan	100	100	100	100	100
	ESN	99.32	98.614	88.84	90.94	100
	LSTM	100	100	100	100	100
Non- Stationary	NARX	15.62	15.07	4.89	9.15	13.58
	TDNN	12.19	5.20	9.01	3.71	0.31
	ELMAN	5.47	0.49	1.07	2.86	5.15
	RNNlayers	7.55	3.83	0.95	-2.61	1.49
	NAR	13.05	16.86	0.64	6.04	9.82
	Jordan	8.57	8.07	-4.23	-0.06	6.70
	ESN	-1.35	2.17	1.40	-7.85	11.01
	LSTM	0.56	6.2603	-11.48	1.705	8.298

The neural networks achievement of profitability value is the main interest in these experiments; consequently, the network that generates the highest percentage of Annualized Return (AR) is the best model. In contrast, for the Annualized Volatility (AV), a small value of volatility is a better result. The purpose of using the financial criteria to assess the predicting models is that, from a trading point of view, the models must be producing profit. Therefore, it is meaningful for the predicting model to predict the correct direction change of signals. In addition, annualized volatility is the measure of the changeability in asset returns, which exhibit least preferable volatility. The variance in a stock price is demonstrated through annualized volatility and; therefore, it is utilized as a predictor of profit possibilities and investment risk. When predicting investment risk in real trading, the volatility is one of the best measurements for financial analyst to provide information.

The standard deviation is the statistic used for calculating the portfolio price return over a working year. The neural networks results are obtained with the benefits that this network exhibits over the other systems investigated. Tables III to VII have summarized the average result of 10 simulations gained from testing data sets.

From Table III, it can be observed that the NARX model achieved the smallest MSE compared to the other dynamic neural networks on stationary signals and non-stationary signals except Close NASDAQ non stationary signals, ESN has obtained the best result. In term of financial criteria, it can be observed from Table VI that all the neural networks have achieved 100 in AR, except the ESN network ELMAN, and RNNLayers in some signals. Fig. 10 to 13 have summarized the results achieved from all the neural networks on AR and MSE criteria for the stationary and non-stationary data. The annualized return has been used to evaluate the competence of the networks used in this study. It is an actual trading measurement, which it utilized for investigating the potential monetary benefits and for measuring the entire profitability in a year by using the sell and buy signals.

TABLE. VII. THE RESULT OF AV FOR ONE-STEP AHEAD PREDICTION

	DNNs	Open NASDAQ	Close NASDAQ	Open Al-rajhi	Close Al-rajhi	Oil Prices
Stationary	NARX	0.7228	0.6876	1.3226	1.3052	0.700
	TDNN	0.61884	0.6876	1.3226	1.3052	0.700
	ELMAN	0.61886	0.7418	1.7439	1.3052	0.700
	RNNlayers	0.83902	0.6876	1.5354	2.6592	1.087
	NAR	0.61884	0.6876	1.3226	1.3052	0.700
	Jordan	0.61759	0.6862	1.3410	1.3190	0.70
	ESN	0.89579	1.6634	3.0682	2.8541	0.70
	LSTM	0.62310	3.6716	8.5200	8.4516	1.72
Non-Stationary	Narxnet	0.2191	0.20735	6.2688	5.4067	1.28
	TDNN	0.2196	0.20851	9.2093	9.1975	1.302
	ELMAN	0.2204	0.20875	38.537	23.830	1.329
	RNNlayers	0.2201	0.20858	43.135	105.61	1.301
	NAR	0.2194	0.20695	7.3505	6.0990	1.296
	Jordan	0.2205	0.20982	8.6564	16.095	1.290
	ESN	0.2211	0.21084	31.414	31.068	1.322
	LSTM	41.42	0.1376	12.665	1.1388	1.361

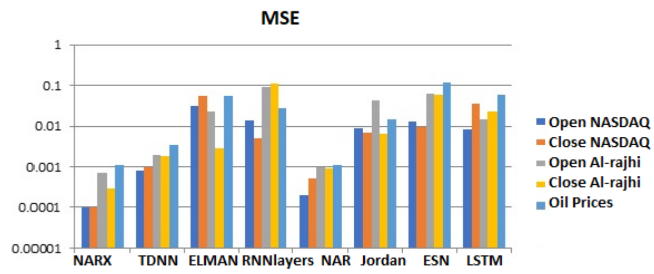

Fig. 10. The Result of MSE using Stationary Signals.

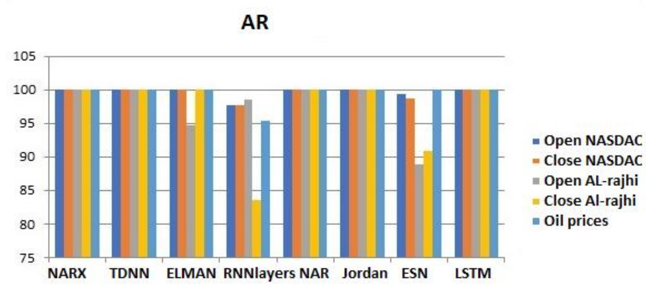

Fig. 11. The Result of AR using Stationary Signals.

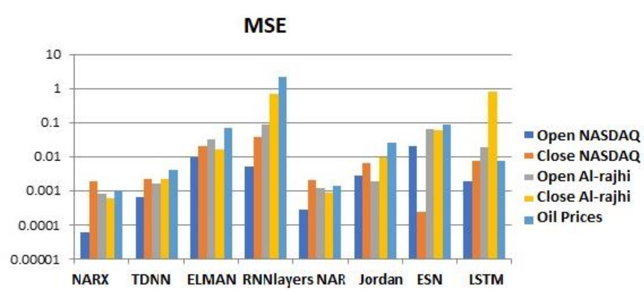

Fig. 12. The Result of MSE using Non-Stationary Signals.

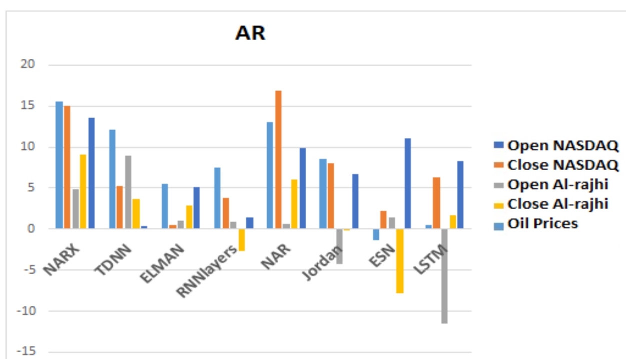

Fig. 13. The Result of AR using Non-Stationary Signals.

It is usually used as the most significant economic parameter for a particular market [18]. This is a scaled calculation of the proposed changes in the time series value where the sign of the change is accurately forecasted. The result of the annualized returns showed that the NARX obtained the best profit return compared to all the other models in the time series data, namely NASDAQ close prices. The NARX has consistently shown the best results with a large margin. Thereby, the NARX has been illustrated as highly favorable performer for this important indicator. From the stationary signals experiment, it can be concluded that the NARX performs better compared to the rest of the dynamic neural networks in most of the financial and statistical measurements. In contrast, the performance of the dynamic neural networks in non-stationary signals varies in five signals. As shown in Fig. 12 to 13, each neural network has achieved a different performance in each signal. In Table VI, the performance of dynamic neural networks is unconsenting, the NARX achieved higher AR in NASDAQ open prices, Al-rajhi close prices, and Oil prices signals. The NAR achieved a higher AR in NASDAQ close prices signals. However, the TDNN showed a good result in Al-rajhi open prices. On the other hand, Mean Absolut percentage Error (MAPE) has exhibited overall standard deviations between measured and predicted values. It is a beneficial parameter for indicating the correct identifying patterns if a system has a low MAPE. In term of stationary signals, LSTM has the best MAPE for the NASDAQ open, Al-rajhi open prices, and Oil prices as can be observed from Table IV. NARX has the best MAPE for the NASDAQ close prices, and Al-rajhi close prices. In term of non-stationary signals, NARX has the best MAPE for NASDAQ open and close prices in addition to Oil prices. However, NAR achieved the lowest values on Al-rajhi open prices whereas LSTM obtained the best result on Al-rajhi close process. The results are clearly represented in Table IV.

B. Discussion

Among the eight networks, as shown from Fig. 10 and 13, the NARX is the best dynamic neural network. The NARX is considered to be a recurrent neural network with inserted memory. Memory allows the NARX to memories the output of the perceptions produced in any layer by unfolding the dependencies of the predicted series far longer than a simplest recurrent neural network. This shows an impact when forecasting nonlinear, aperiodic, and unknown datasets. The NAR is considered to be a good alternative model relating to its simplicity, despite of the NARXs exibility to model exogenous input to help increase performance by modelling external dependencies.

Predicting the stock market future prices has become important because of the successful prediction of stock prices promises attractive benefits. The results for the stock market prediction are validated through evaluation metrics. Specifically, mean square error, and mean absolute percentage error are used to estimate the forecasting accuracy in the stock market. The comparative analysis was carried out on eight dynamic neural network architectures. The first model was non-linear autoregressive neural network (NAR). The second was non-linear autoregressive network with exogenous inputs (NARX), which use external information, caused great improvement in time series forecasting performance.

Also, the deep and layered hierarch neural network LSTM was selected in the comparative analysis in this paper. Despite the success applications of deep layers neural network, deep layered dynamic neural network (LSTM) has filed to achieve the best performance in some signals. In addition, the simplest recurrent neural networks such as Elman, Jordan and ESN network are implemented in this paper. The obtained results show that the performance of each dynamic neural network was different in both stationary and non-stationary predictions. This is related to the non-stationary signals is very difficult since the signals are affected from noise and volatility.

VI. Conclusion

The study has applied dynamic neural network models to forecast high predictive performance of financial time series using stationary and non-stationary data to exploiting the temporal attributes of the neural models in a correct approach. The Elman and Jordan neural networks have been adopted in the neural network models to encode the information for preserving its temporal aspects. From the research experiments, the simulation results showed that the prediction of non-stationary financial signals is very challenging since the signals are suffering from noise and volatility. These unstable behaviours make the signals move and fall sharply at some point during the network training. During the training, the dynamic neural networks are attempting to learn the price values of the non-stationary signals; however, their responses are not sufficient. This is related to the fact that the behaviour of price values was not stable. The extensive experiments of this research confirmed that NARX, NAR and TDNN achieved the best profit values compared to the other networks; although, the prediction for the non-stationary signals usually presents inconsistent results. This study has described the potential of neural networks model for performing more effectively and the applicability of a specific type of neural network models in stationary and non-stationary environments. The improved ways of the neural networks should be explored by the future studies for mapping the data onto the neural networks models and the modification of the grading and classification of candidate solutions for parallel architectures. Thereby, decompositions of the search space of candidate solutions can be used to solve the different parts of the problems.

Acknowledgment

I would like to thank Prince Sattam Bin Abdualziz University for providing me support during these researches.

References

[1] R. Ghazali, "Higher Order Neural Networks for Financial Time Series Prediction". PhD thesis, Liverpool John Moores. 2007.

[2] G. Ristanoski, J. Bailey, "Distribution Based Data Filtering for Financial Time Series Forecasting". In 24 Australasian Joint Conference on Artificial Intelligence. Perth, Australia 122–132. 2011.

[3] M. M. Ali, M. I. Babar, M. Hamza, M. Jehanzeb, S. Habib, M. S. Khan, "Industrial Financial Forecasting using Long Short-Term Memory Recurrent Neural Networks", International Journal of Advanced Computer Science and Applications, 2019.

[4] J. Zhang, "Applying time series analysis builds stock price forecast model". Modern Applied Science 3. 2009.

[5] RA,. Meese, A.K.Rose, "Non-linear, non-parametric, non-essential exchange rate estimation". American Economic Review 80:192-196. Doi: 10.2307/2298014. 1999.

[6] R. Gencay, "Linear, nonlinear and essential foreign exchange rate prediction with simple trading rules". Journal of International Economics 47:91-107.1999.

[7] G.E.P. Box, G.W. Jenkins, G.C. Reinsel, "Time Series Analysis - Forecasting and Control", (3rd ed.), Englewood Cliffs, NJ: Prentice-Hall. 1994.

[8] S. Ho, M. Xie, T.N. Goh., "A comparative study of neural network and BoxJenkins ARIMA modeling in time series prediction". Computers & Industrial Engineering 42:371–375. Doi: 10.1016/s0360-8352(02)00036-0.2002.

[9] S. Porter-hudak, "An Application of the Seasonal Fractionally Differenced Model to the Monetary Aggregates". Journal of the American Statistical Association 85:338–344. 1990.

[10] T. Kamgaing, "Competing Neural Networks as Models for Non Stationary Financial Time Series". Ph.D. Thesis, University of Kaiserslautern. 2005.

[11] M.P. Clements, P.H. Franses, N.R. Swanson, "Forecasting economic and financial time-series with non-linear models". International Journal of Forecasting 20:169-183. Doi: 10.1016/j.ijforecast.2003.10.004, 2004.

[12] J. Kamruzzaman, "ANN-Based Forecasting of Foreign Currency Exchange Rates". Neural Information Processing - Letters and Reviews 3:49–58. 2004.

[13] C.L. Dunis, M. Williams,"Modelling and Trading the EUR / USD Exchange Rate: Do Neural Network Models Perform Better? Trading and Regulation" 8:1–24. 2002.

[14] T.W. Lin, C.C. Yu, "Forecasting Stock Market with Neural Networks". SSRN Electronic Journal. 2009.

[15] W.H. Chen, J.Y. Shih, S. Wu, "Comparison of support-vector machines and back propagation neural networks in forecasting the six major Asian stock markets". International Journal of Electronic Finance 1:49–67.2006.

[16] X. Cai, G. Lai, X. Lin, "Forecasting large scale conditional volatility and covariance using neural network on GPU. The Journal of Supercomputing 63:490–507. 2013.

[17] H. Tawfik, R. Huang, M. Samy, A.K. Nagar. On the Use of Intelligent Systems for the Modelling of Financial Literacy Parameters. Journal of Information Technology Research (JITR) 2:17-35. Doi: 10.4018/jitr.2009062902. 2009.

[18] H. Alaskar. Dynamic self-organised neural network inspired by the immune algorithm for financial time series prediction and medical data classification, PhD Thesis, Liverpool John Moores University. 2014.

[19] M. Sewell, " Chaos in financial markets" 2008.

[20] RK. Dase, DD. Pawar, "Application of Artificial Neural Network for stock market predictions: A review of literature". International Journal of Machine Intelligence 2:1417. Doi: 10.9735/0975-2927.2.2.14-17. 2010.

[21] Z. Vojinovic, V. Kecman, R. Seidel. "A Data Mining Approach to Financial Time Series Modelling and Forecasting". International Journal of Intelligent Systems in Accounting, Finance Management 239:225239. 2001.

[22] CL. Dunis, M. Williams. "Applications of Advanced Regression Analysis for Trading and Investment", it In applied for quantitative method from trading and investment. John Wiley Sons, New York, 1-40. 2003.

[23] D. Pissarenko. "Neural Networks For Financial Time Series Prediction: Overview Over Recent Research", BSc thesis, Computer Studies Thesis, University of Derby in Austria. 2002A.

[24] D.R. Aryal, W. Yao-wu, "Neural Network Forecasting of the Production Level of Chinese Construction Industry". Journal of Comparative International Management 6:45–64. 2003.

[25] J. Kamruzzaman, R.A. Sarker. Forecasting of currency exchange rates using ANN: a case study. In International Conference on Neural Networks and Signal Processing. Nanjing, China: IEEE 1:793797. 2003.

[26] R.G. Ahangar, M. Yahyazadehfar, H. Pournaghshband. "The Comparison of Methods Artificial Neural Network with Linear Regression Using Specific Variables for Prediction Stock Price in Tehran Stock Exchange". (IJCSIS) International Journal of Computer Science and Information Security 7:3846. 2010.

[27] Y. Deniz, SA. Karm. A Comparison of Linear and Nonlinear Models in Forecasting Market Risk: The Evidence from Turkish Derivative Exchange. Journal of Economics and Behavioral Studies 5:164172. 2013.

[28] G. Sermpinis, C. Dunis, J. Laws, C. Stasinakis. Kalman Filters and Neural Networks in Forecasting and Trading. In: Jayne C., Yue S. 2012.

[29] E. Giovanis, Application of Feed-Forward Neural Networks Autoregressive Models in Gross Domestic Product Prediction. World Academy of Science, Engineering and Technology 1:646650. 2010B.

[30] K. Bagherifard, M. Nilashi, O. Ibrahim, N. Janahmadi, L. Ebrahimi. "Comparative Study of Artificial Neural Network and ARIMA Models in Predicting Exchange Rate". Journal of Applied Sciences, Engineering and Technology 4:43974403. 2012.

[31] Y. Kara, M. Acar, B. Boyacioglu. "Predicting direction of stock price index movement using artificial neural networks and support vector machines: The sample of the Istanbul Stock Exchang"e, Expert Systems with Applications 38:53115319. Doi: 10.1016/j.eswa.2010.10.027. 2011.

[32] J.F. Kolen, S.C. Kremer, "A Field Guide to Dynamical Recurrent Networks", WileyIEEE Press. 2001.

[33] V.V. Kondratenko, Y. Kuperin. "Using recurrent neural networks to forecasting of forex". Disordered Systems and Neural Networks.2003.

[34] A.J. Hussain, P. Fergus, H. Al-Askar, D. Al-Jumeily, F. Jager. "Dynamic neural network architecture inspired by the immune algorithm to predict preterm deliveries in pregnant women". Neurocomputing 151:963-974. Doi: 10.1016/j.neucom.2014.03.087. 2015.

[35] S. Siami-Namini , N. Tavakoli , A. Namini . "A Comparison of ARIMA and LSTM in Forecasting Time Series", 17th IEEE International Conference on Machine Learning and Applications (ICMLA). 2018.

[36] I.N. da Silva, D. H. Spatti, R. A. Flauzino, L.H.B. Liboni, S.F. dos Reis Alves. "Forecast of Stock Market Trends Using Recurrent Networks". it In: Artificial Neural Networks. Springer, Cham. 2017.

[37] X. Lin, Z. Yang, Y. Song. "Short-term stock price prediction based on echo state networks". Expert Systems with Applications 36:73137317. Doi: 10.1016/j.eswa.2008.09.049. 2009.

[38] F. Zhai, X. Lin, Z. Yang, Y. Song. "Financial time series prediction based on Echo State Network", in Proceedings of the 6th International Conference on Natural Computation (ICNC 10) 8: 39833987. 2010.

[39] X. Lin, Z. Yang, Y. Song. "Intelligent stock trading system based on improved technical analysis and Echo State Network". Expert Systems with Applications 8:1134711354. 2011Z.

[40] H. Zhang, J. Liang, Z. Chai. "Stock prediction based on phase space reconstruction and echo state networks". Journal of Algorithms Computational Technology 7:87100. Doi: 10.1260/1748-3018.7.1.87. 2013.

[41] J. Dan, W. Guo, W. Shi, B. Fang, T. Zhang. "Deterministic Echo State Networks Based Stock Price Forecasting". Abstract and Applied Analysis 1-7. 2014.

[42] S.J. Abdulkadir, SP. Yong. "Empirical analysis of parallel-NARX recurrent network for long-term chaotic financial forecasting" 2014 International Conference on Computer and Information Sciences, Iccoins 2014 - a Conference of World Engineering, Science and Technology Congress, Estcon 2014 - Proceedings. Doi: 10.1109/ICCOINS.2014.6868354. 2014.

[43] C.L. Cocianu, H. Grigoryan. "An Artificial Neural Network for Data Forecasting Purpose:. Informatica Economic 19:34-45.2015.

[44] C. Wang. "Time series neural network systems in stock index forecasting. Computer Modelling New Technologies:. 2015.

[45] A.D. Chaudhuri, I. Ghosh. "Artificial Neural Network and Time Series Modeling Based Approach to Forecasting the Exchange Rate in a Multivariate Framework." Journal of Insurance and Financial Management, Vol. 1, Issue 5, PP. 92-123, 2016.

[46] H.J.Kim,K.S.Sin. "A hybrid approach based on neural network genetic algorithm for detecting temporal patterns in stock markets". Applied Soft Computing 7:569-576. Doi: 10.1016/j.asoc.2006.03.004. 2007.

[47] T. Kim, H.Y. Kim. Forecasting stock prices with a feature fusion LSTMCNN model using different representations of the same data. PLoS ONE 14(2): e0212320. 2019. ttps://doi.org/10.1371/journal.pone. 0212320}.\bibitem{35}S.Kim, M.Kang.Financialseriespredictionusing AttentionLSTM.{\itCoRRabs}/1902.

[48] T. Lin, B. Horne, P. Tino, C.L. Giles. "Learning long-term dependencies in NARX recurrent neural networks". IEEE transactions on Neural Networks 7:1329. 1996.

[49] LJ. Elman. “Finding Structure in Time”. Cognitive Science 14:179-211. 1990.

[50] MI. Jordan. “Attractor dynamics and parallelism in a connectionist sequential machine”. In Artificial Neural Networks. NJ, USA: IEEE Press Piscataway 112127.1990.

[51] T. Verplancke, S. Looy, K. Steurbaut, D. Benoit, F.D. Turck, G.D. Moor, J. Decruyenaere. “A novel time series analysis approach for prediction of dialysis in critically ill patients using echo-state networks”. BMC medical informatics and decision making 10:4. 2010.

[52] H. Jaeger. “The echo state approach to analyzing and training recurrent neural networks” - with an Erratum note. Available at: ttp://www. faculty.jacobsuniversity. de/jaeger/pubs/EchoStatesTechRep.pdf, 2001.

[53] YI. Al-Mashhadany. “Recurrent Neural Network with Human Simulator Based Virtual Reality”. In M. E. and M. Mysara, ed.Recurrent Neural Networks and Soft Computing Source. InTech. 2012.

[54] Waibel. “Phoneme Recognition Using Time-Delay Neural Networks”, Report of Speech Committee, SP87-100 19-24. Doi: 10.1016/b978-0-08-051584-7.50037-1. 1987.

[55] J.M.P. Junior, G.A. Barreto. “Long-term time series prediction with the NARX network”: An empirical evaluation. Neurocomputing 71:3335-3343. Doi: 10.1016/j.neucom.2008.01.030. 2008C.

[56] L.J. Cao, FEH. Tay. “Financial Time Series Forecasting”. IEEE Transactions on Neural Networks 14:15061518. 2003.M.

[57] A. Mahdi, A.J. Hussain, P. Lisboa. D. Al-Jumeily. “The Application of the Neural Network Model Inspired by the Immune System in Financial Time Series Prediction”. In Developments in eSystems Engineering (DESE) 370376. Doi: 10.1109/dese.2009.39. 2009.X.

[58] X. Pang, Y. Zhou, P. Wang, W. Lin, V. Chang. “Stock Market Prediction based on Deep Long Short Term Memory Neural Network”. In Proceedings of the 3rd International Conference on Complexity, Future Information Systems and Risk (COMPLEXIS 2018), pages 102-108. 2018.

[59] M. Thomason,”The practitioner method and tools. Journal of Computational Intelligence in Finance 7:36–45.1999.

Improving Gated Recurrent Unit Predictions with Univariate Time Series Imputation Techniques

Anibal Flores[1]
Grupo de Investigación en Ciencia de Datos, Universidad Nacional de Moquegua, Moquegua, Perú

Hugo Tito[2]
E.P. Ingeniería de Sistemas e Informática, Universidad Nacional de Moquegua, Moquegua, Perú

Deymor Centty[3]
E.P. Ingeniería Ambiental
Universidad Nacional de Moquegua
Moquegua, Perú

***Abstract*—The work presented in this paper has its main objective to improve the quality of the predictions made with the recurrent neural network known as Gated Recurrent Unit (GRU). For this, instead of making different adjustments to the architecture of the neural network in question, univariate time series imputation techniques such as Local Average of Nearest Neighbors (LANN) and Case Based Reasoning Imputation (CBRi) are used. It is experimented with different gap-sizes, from 1 to 11 consecutive NAs, resulting in the best gap-size of six consecutive NA values for LANN and for CBRi the gap-size of two NA values. The results show that both imputation techniques allow improving prediction quality of Gated Recurrent Unit, being LANN better than CBRi, thus the results of the best configurations of LANN and CBRi allowed to surpass the techniques with which they were compared.**

Keywords*—Gated recurrent unit; local average of nearest neighbors; case based reasoning imputation; GRU+LANN; GRU+CBRi

I. Introduction

In working with time series, forecasting is one of the most exciting and interesting [1]. Today, Deep Learning [2] techniques are used for this type of task, in particular recurrent neural networks such as Long Short-Term Memory (LSTM) [3] and Gated Recurrent Unit (GRU) [4].

Several knowledge areas work with analysis and prediction of time series for different tasks, and greater accuracy are required in the estimated values in order to provide better services or products.

LSTM and GRU has been used successfully in many forecasting works [1], and the changes implemented to improve quality or reduce the error rate in predictions mainly includes tuning of parameters, input adjustments, number of layers, training epochs, batch size, etc.

As it can be seen in [1] the insertion of different NA values in the results produced by LSTM with different gap-sizes and the subsequent recalculation of the NA values produced an improvement in the precision of the LSTM results. Thus, in this work, it is experimented with the results produced by GRU, but instead of just using the Local Average of Nearest Neighbors (LANN) [5] imputation technique, we also experiment with another technique known as Case Based Reasoning Imputation (CBRi) "in press" [6].

Similarly to the analysis performed in [1] for LSTM predictions, Fig. 1 shows a 14-day prediction analysis for Gated Recurrent Unit (GRU). In the first case, the LANN algorithm is applied to a 1 NA gap-size by rebuilding the elements 2, 4, 6, …, 12 of the GRU-predicted series in order to outperform the results. In the second case, LANN is applied for the elements 3, 5, 7, …, 13 in order to improve the results produced by GRU. How it can be appreciated GRU results are improve just in the second case.

The analysis performed in Fig. 1 with the application of the LANN algorithm and the improvement detected on GRU predictions motivate the application of another imputation algorithm known as Case Base Reasoning Imputation (CBRi) "in press" [6].

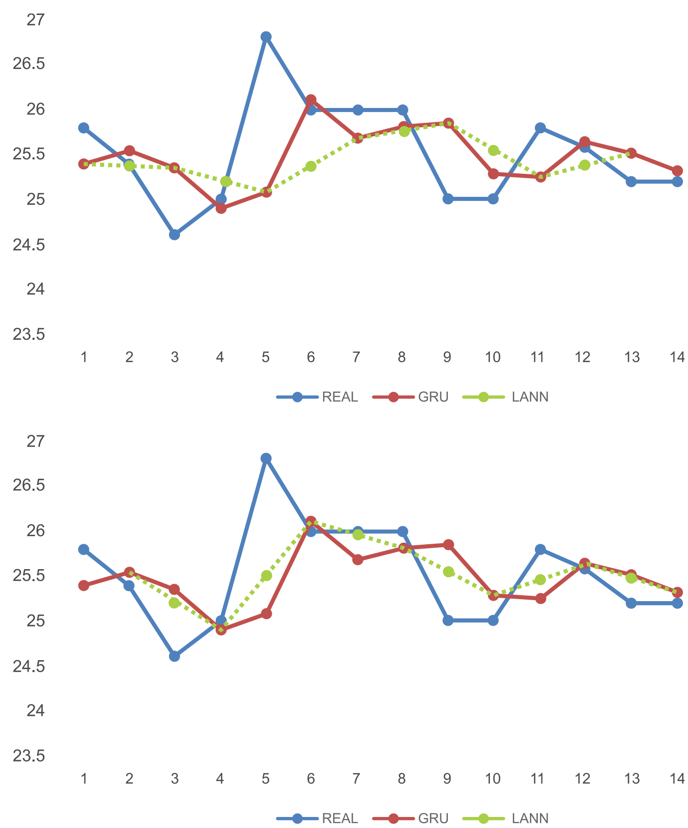

Fig. 1. Improving GRU Predictions with LANN.

The data in [1] is used for analysis and experimentation, it corresponds to maximum temperatures in a meteorological station known as Punta de Coles located in the Moquegua region in south of Peru which is highly seasonal.

The results achieved in this work show that, in the first case, LANN in [1] allowed to considerably improve the results provided by Gated Recurrent Unit (GRU). In the second case, it is experimented with CBRi, taking as a reference the results shown "in press" [6], where CBRi manages to overcome LANN results, however, in this work GRU+CBRi does not surpass GRU+LANN.

This paper has been structured as follows: The second section shows the related work that serves as a point of comparison for the results achieved in this work. In the third section, some concepts that will allow a better understanding of the content of the paper are briefly described. The fourth section shows the process followed for the experiments carried out. In the fifth section, the results achieved after the experiments are shown. In the fifth section, the results are briefly discussed compared to other state-of-the-art techniques. Then, in the sixth section, the conclusions reached at the end of this work are described. And finally, it describes the future work that can be done from the work presented in this paper.

II. Related Work

A. Simple Linear Regression

In the implementation of regression models, one of the most basic and widely used models is known as linear regression. This type of regression consists of a statistical analysis to identify the relationship between two variables, the dependent and the independent one [7]. Equation for Simple Linear Regression can be seen in (1).

$$y(t) = \beta_0 + \beta_1 x_t + \varepsilon_t \tag{1}$$

B. ARIMA

ARIMA [8] stands for Autoregressive Integrated Moving Average. It is a statistical model that works with variations and regressions of time series to find patterns that are used to predict future values. It is a dynamic model, where future estimates are explained by past data and not by independent variables.

Next, some works that implement ARIMA to predict future values in different time series are described.

In [9] the authors worked with wind speed time series and for this work they implemented an ARIMA model and a NNT Back Propagation Neural Network. The results show that the ARIMA model is slightly higher than the Back Propagation Neural Network model.

In [10] to predict the number of epidemic disease, the authors proposed an ARIMA model, which was compared with the results of a model based on Simple Moving Average (SMA). At the end, the ARIMA predictions were better than the SMA ones.

In [11] the authors implement ARIMA and Support Vector Machine (SVM) models to forecast load time series. The results show that ARIMA is better for linear type of load, while SVM is better for non-linear type of load time series.

In [11] the authors implement two models to forecast linear and non-linear load time series, these are ARIMA and Support Vector Machine (SVM). The authors concluded that the ARIMA results are better for the linear load type, while the SVM results are better for the non-linear load type.

C. Prophet

Prophet [12] is a very known forecasting technique developed by the Facebook data science team and it is a forecasting decomposable time series model, it has three main model components: trend, seasonality, and holidays which are combined in equation (2).

$$y(t) = g(t) + s(t) + h(t) + \epsilon_t \tag{2}$$

Where: g(t) is the trend function, s(t) represents periodic changes and h(t) represents the holidays, ϵ_t represents the error.

Some works that used prophet are briefly described below:

In [13] the authors propose the forecasting of bitcoin time series using the ARIMA and Prophet techniques. The results achieved show that Prophet is superior in terms of the accuracy of the results with respect to ARIMA.

In [14] the authors propose the forecasting of groundwater-level time series using the Prophet technique. The results are compared with other techniques such as ARIMA, Linear Regression, and others showing that Prophet offers better accuracy for this type of time series.

In [15] the authors propose the forecasting of time series of microclimate temperatures corresponding to greenhouses using the Prophet technique. Unfortunately, they do not show a comparison of the results with other techniques.

D. Long Short-Term Memory (LSTM)

The LSTM recurrent networks were created in order to address the problem of vanishing gradients, due to the unfold process of a Recurrent Neural Network.

LSTM networks work with special hidden units, whose objective is to remember input data for a long time [2]. Then, it has been proved that LSTM networks are more effective than conventional RNNs [2]. This is because LSTM networks have several layers for each time step. Fig. 2 shows the LSTM architecture.

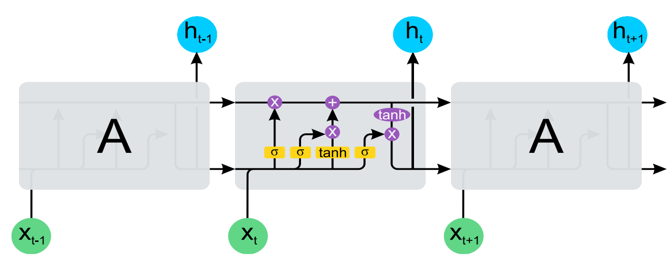

Fig. 2. Architecture of LSTM Network.

Some LSTM works are briefly described below:

In [1], the authors proposed the use of LANN and LANNc to improve the predictions of LSTM in meteorological time series corresponding to maximum temperatures. The results show that on average LANN improves the precision of the LSTM predictions in all the NA values cases: from 1 to 11 NA values.

In [16], the authors proposed the use recurrent neural networks such as LSTM and GRU to forecast electric load time series. The results of the work show that GRU is better than LSTM in terms of the accuracy of the predictions.

In [17] the authors proposed the use of LSTM and GRU networks for forecasting of traffic flow time series, comparing the results achieved with an ARIMA model. The LSTM and GRU results are better than ARIMA for this type of time series.

In [18] the authors propose the forecasting of power load time series for a residential community using Gated Recurrent Unit (GRU). The results obtained from GRU are compared with LSTM results in different settings and show that for this type of time series, the accuracy achieved by GRU is better than that of LSTM.

In [19] the use of a multilayer recurrent neural network called MS-GRU is proposed for forecasting of load electricity time series. The results are compared with LSTM and GRU networks, showing that MS-GRU has better precision than LSTM and GRU.

III. Background

A. *Recurrent Neural Networks (RNN)*

An RNN is a type of neural network that allows modeling time series [3]. The structure of this neural network is similar to that of an MLP (Multilayer Perceptron). This differs from an MLP in the sense that it allows connections between hidden units associated with a time delay. Through these connections, the RNN can retain and remember information from the past [20], allowing it to find temporary correlations between facts that may be far apart in time. Fig. 3 shows the unfolded architecture of an RNN.

The task of training an RNN is difficult to carry out [3] due to the problems of vanishing and exploding gradients. It resulted in the appearance or creation of recurrent neural networks known as LSTM that solve the problems mentioned above.

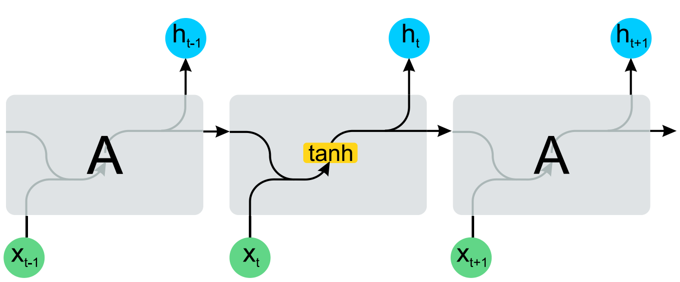

Fig. 3. Architecture of Recurrent Neural Network.

B. *Gated Recurrent Unit (GRU)*

GRUs are a gating mechanism in RNNs introduced by K. Cho et al [4] in 2014. GRU is a variation on the LSTM because both are designed similarly, this can be seen in its architectures. The Gated Recurrent Unit (GRU) has fewer parameters than LSTM, since it lacks an output gate. LSTM is stronger than the GRU, since it can easily perform an unlimited count, while the GRU cannot, that is the reason why GRU fails to learn certain languages that LSTM can [21]. However, in forecasting of univariate time series in many works such as [1], [16], [17], [22], [23], etc. GRU has shown better precision than LSTM, that is why it was chosen as the basis for the present study.

Fig. 4 shows one of the most commonly used GRU architectures.

According to Fig. 3 the following equations:

$$Z_{t=}\sigma_g(W_z x_t + U_z h_{t-1} + b_z) \quad (3)$$

$$r_{t=}\sigma_g(W_r x_t + U_r h_{t-1} + b_r) \quad (4)$$

$$h_{t=}(1 - z_t) \text{ o } h_{t-1} + z_t \text{ o } \sigma_h(W_h x_t + U_h(r_t \text{ o } h_{t-1}) + b_h \quad (5)$$

Where:

x_t : input vector

h_t : output vector

z_t : updated gate vector

r_t : reset gate vector

W,*U* and *b* : matrix parameters and vector

σ_g : sigmoid function

σ_h : hyperbolic tangent

C. *Local Average of Nearest Neighbors (LANN)*

LANN [5] is a fairly simple but very effective algorithm for univariate time series imputation. LANN consists in the calculation of the average of the prior and next values of a block of NA values in a time series according equation (6).

NA=(πριορ + νεξτ)/2 (6)

LANN produces good imputation results since according to the analysis performed in [5]; on average the closest values to a missing value are its closest neighbors, the prior and the next values, therefore the average of these two values produces a very close value to the NA value.

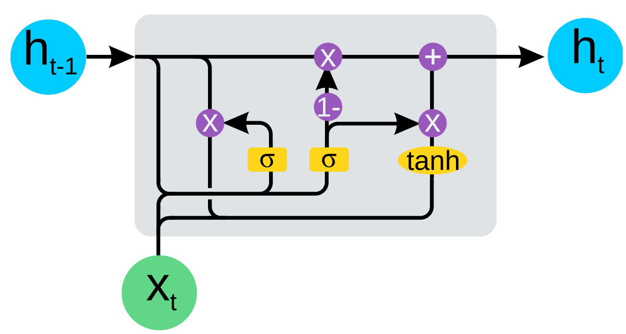

Fig. 4. Architecture of GRU.

D. *Case based Reasoning Imputation (CBRi)*

CBRi "in press" [6] is an imputation technique for univariate time series inspired by Case Based Reasoning that allows to calculate a NA value from a base of cases that stores historical values of a time series.

Fig. 5 graphically shows the architecture of the CBRi system. Hence, initially in the Time Series block, a base of cases is created from a historical time series; the base of cases is a matrix where the rows correspond to the prior values and the columns corresponds to the next values; every matrix cell contains values found for each prior and next value in the historical time series. The CBRi block receives as input a vector with NA values and calculates each NA value from its prior and next values using equation (7). The Testing block allows evaluating the quality of the estimated NA values.

$$NA = \frac{\sum_{i=0}^{n-1}(prior+Vi+next)}{n*3} \quad (7)$$

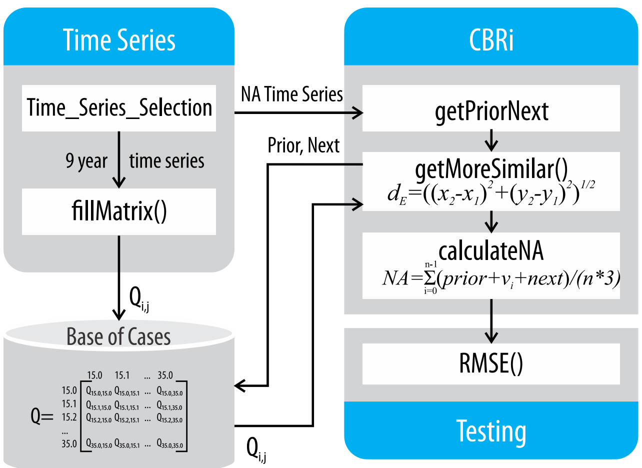

Fig. 5. CBRi System [6].

IV. Process

A. *Time Series Selection*

The time series chosen for experimentation corresponds to maximum daily temperatures that were recorded at the SENAMHI[1] Punta de Coles meteorological station in Ilo city in south of Peru. The data that is used for the training phase correspond to 4 years (from 2012-01-01 to 2015-12-31) and the data that is used for testing correspond to 2016.

B. *GRU Model*

The GRU recurrent neural network architecture used in this work is shown in Fig. 6.

C. *Inserting NAs*

Once the previous phase is completed with 180 days predicted, the NA values are inserted using the same strategy that was used in [1], as shown in Fig. 7.

[1] https://www.senamhi.gob.pe/

```
gru_model = Sequential()

gru_model.add(GRU(units=50, return_sequences=True, input_shape=(gru_ftrs.shape[1], 1)))
gru_model.add(Dropout(0.2))

gru_model.add(GRU(units=50, return_sequences=True))
gru_model.add(Dropout(0.2))

gru_model.add(GRU(units=50, return_sequences=True))
gru_model.add(Dropout(0.2))

gru_model.add(GRU(units=50))
gru_model.add(Dropout(0.2))
gru_model.add(Dense(units = 1))

gru_model.compile(optimizer = 'adam', loss = 'mean_squared_error')
gru_model.fit(gru_ftrs, labels, epochs = 100, batch_size = 32)
```

Fig. 6. Architecture for GRU Model in Python.

20.7	NA	19.5	NA	20.3	NA	21.2	...
20.7	NA	NA	19.2	NA	NA	21.2	...
20.7	NA	NA	NA	20.3	NA	NA	...
20.7	NA	NA	NA	NA	19.1	NA	...
20.7	NA	NA	NA	NA	NA	21.2	...
...							

Fig. 7. NA Values in the GRU Predicted Time Series [1].

D. *Applying LANN/CBRi*

LANN algorithm is used to impute the NA values in the predicted time series according adaptation made in [1] for over 2 NA values.

CBRi algorithm is used to impute NA values according adaptation made in [24] for over 2 NA values. Base of cases corresponds to 9 years (from 2007 to 2015) and it was implemented for CBRi "in press" [6].

E. *Evaluation*

The results of both algorithms are evaluated through Root Mean Squared Error (RMSE) according equation (4)

$$RMSE = \sqrt{\frac{\sum_{i=0}^{n-1}(Pi-Ri)^2}{n}} \quad (8)$$

V. Results

After experimentation, this section shows and describes the results achieved. LANN and CBRi were implemented with different configurations of NA values between 1 to 11 and Table I shows the corresponding RMSE values.

According to Table I, it can be seen that on average both imputation techniques offer their best results between 2 and 6 consecutive NA values, managing to improve GRU results for all cases.

Regarding the first case of insertion of only 1 NA value, on average LANN manages to improve GRU results, however, CBRi fails to improve GRU results.

TABLE. I. GRU, LANN AND CBRI

Technique		**RMSE of Predicted Days**							**Avg**
		15	**30**	**60**	**90**	**120**	**150**	**180**	
GRU		0.5953	0.6917	0.6678	0.6689	0.7076	0.6751	0.6727	0.6684
LANN	1	0.6335	0.6770	0.6340	0.6500	0.6980	0.6558	0.6421	0.6557
	2	**0.5235**	0.6169	0.6064	0.5906	0.6230	0.5880	0.5904	0.5912
	3	0.6071	0.6349	0.6049	0.6010	0.6175	0.5858	0.5961	0.6067
	4	0.5743	0.6598	0.5973	0.5855	**0.6028**	**0.5652**	**0.5891**	0.5962
	5	0.5371	0.6381	0.6174	0.6007	0.6209	0.5853	0.5941	0.5990
	6	0.5287	**0.5759**	**0.5459**	**0.5870**	0.6359	0.6016	0.6197	**0.5849**
	7	0.5553	0.7261	0.6782	0.6435	0.6703	0.6278	0.6302	0.6473
	8	0.5979	0.7271	0.6798	0.6613	0.6844	0.6493	0.6582	0.6654
	9	0.6066	0.6961	0.7451	0.7134	0.7525	0.7080	0.6973	0.7027
	10	0.5480	0.6632	0.6885	0.6903	0.7343	0.7357	0.7636	0.6890
	11	0.5520	0.6616	0.7029	0.6944	0.6968	0.6977	0.7342	0.6770
CBRi	1	0.6278	0.7049	0.6516	0.6599	0.7359	0.6887	0.6738	0.6775
	2	**0.5257**	0.6199	**0.5951**	**0.5900**	0.6386	0.6053	0.6110	**0.5979**
	3	0.6349	0.6457	0.6245	0.6185	**0.6317**	0.5972	0.6115	0.6234
	4	0.5480	0.6757	0.6081	0.6080	0.6231	**0.5870**	**0.6082**	0.6083
	5	0.5831	0.6348	0.6093	0.6107	0.6304	0.5949	0.6113	0.6106
	6	0.5494	**0.5800**	0.6731	0.6779	0.7010	0.6643	0.6746	0.6457
	7	0.8082	0.7443	0.6872	0.6377	0.6690	0.6219	0.6362	0.6863
	8	0.6949	0.7484	0.7688	0.7336	0.7417	0.7006	0.6902	0.7254
	9	0.6654	0.6837	0.7436	0.7077	0.7403	0.6981	0.7471	0.7122
	10	0.5992	0.7597	0.6744	0.6778	0.7321	0.7231	0.7471	0.7019
	11	0.5677	0.7330	0.7873	0.7406	0.7308	0.7308	0.7573	0.7210

Regarding the NA values greater than 6 LANN on average of 5 cases of NAs greater than 6 in two cases it improves the GRU results and in 3 of them it worsens them; with CBRi for the 5 cases of NAs greater than 6 in all of them worsens the GRU results.

According to Fig. 8, it can be seen how the best configuration of NA values for each imputation technique (LANN: 6 consecutive NAs and CBRi: 2 consecutive NAs) allows to improve the accuracy of GRU predictions on different amounts of predicted days.

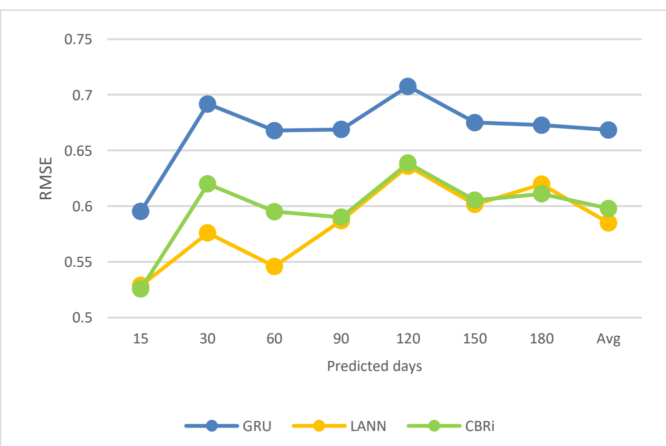

Fig. 8. GRU, GRU+LANN and GRU+CBRi.

VI. DISCUSSION

Next, the results achieved in the previous section are compared with other prediction techniques. It can be seen in Table II.

According to Table II, on average it can be seen how the GRU + LANN combination offers the most accurate results for the predicted time series, it can be seen that from 7 cases in 5 of them, GRU+LANN outperforms other techniques including GRU+CBRi, LSTM, LSTM+LANN, LSTM+LANNc among others. Only in two cases GRU+CBRi manage to surpass GRU+LANN. It demonstrates the importance of the use of univariate time series imputation techniques in the improvement of GRU results for this type of time series.

Fig. 9 clearly shows the difference between the proposals compared to other forecasting techniques.

At this point, it must be highlighted that before applying imputation techniques to GRU prediction results in order to improve them, it is important to take a prior analysis with a simple technique as Local Average of Nearest Neighbors (LANN) as it is showed in Fig. 1 to determine if imputation techniques can really improve GRU results.

TABLE. II. COMPARISON WITH ANOTHER TECHNIQUES

Technique	RMSE of Predicted Days							Avg
	15	30	60	90	120	150	180	
GRU+LANN*	0.5287	**0.5759**	**0.5459**	**0.5870**	0.6359	0.6016	0.6197	**0.5849**
GRU+CBRi**	**0.5257**	0.6199	0.5951	0.5900	0.6386	0.6053	**0.6110**	**0.5979**
GRU	0.5953	0.6917	0.6678	0.6689	0.7076	0.6751	0.6727	0.6684
LSTM	0.6334	0.6637	0.6702	0.7175	0.7649	0.7537	0.7562	0.7085
LSTM+LANN	0.6296	0.6111	0.6097	0.6730	0.7059	0.6910	0.6838	0.6577
LSTM+LANNc	0.5452	0.5918	0.6377	0.6813	0.7302	0.7166	0.7216	0.6606
PROPHET	0.5512	0.7054	1.0516	1.1637	1.1274	1.1274	1.0403	1.0279
ARIMA	0.6134	1.2988	2.2932	2.5240	2.2320	2.2320	2.0440	2.1639

* 6 NAs ** 2 NAs

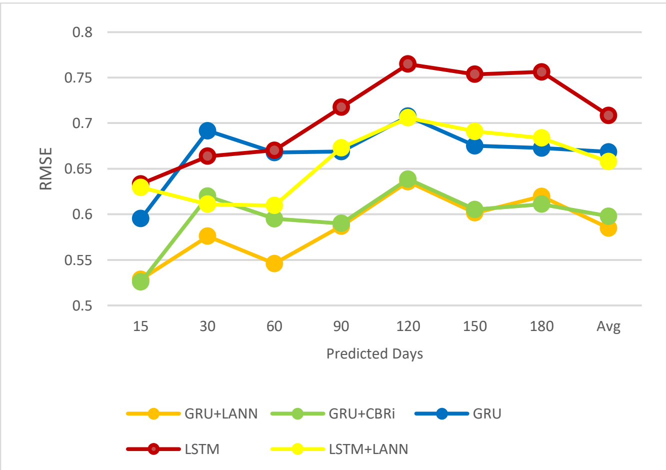

Fig. 9. Comparison with another Techniques.

VII. CONCLUSIONS

The use of univariate time series imputation techniques allows improving the accuracy of the predictions of the Gated Recurrent Unit (GRU).

Of the two imputation techniques experienced in this work, Local Average of Nearest Neighbors (LANN) showed superiority over Case Based Reasoning imputation (CBRi), of seven cases analyzed, LANN was superior to CBRi in five of them, so LANN is highly recommendable for this kind of tasks in this type of time series.

VIII. FUTURE WORK

In this work the results of GRU in time series of maximum temperatures were improved, it would be interesting to analyze if GRU predictions in another kind of time series can be improved in similar or a better way.

In addition, it would be important to determine which is the most appropriate gap-size to obtain the best results for each portion of the time series, since in this work it has been possible to appreciate that the same gap-size does not produce the best results in the entire time series.

REFERENCES

[1] Flores, H. Tito & D. Centty, "Improving Long Short-Term Memory predictions with Local Average of Nearest Neighbors," (IJACSA) International Journal of Advanced Computer Science and Applications, vol. 10, nº 11, pp. 392-397, 2019.

[2] Y. LeCun, Y. Bengio & G. Hinton, "Deep learning," Nature, vol. 521, pp. 436-444, 2015.

[3] R. Pascanu, T. Mikolov, Y. Bengio, "On the dificulty of training recurrent neural networks," de 30th International Conference on Machine Learning, Atlanta, Georgia, USA, 2013.

[4] C. Kyunghyun, V. Bart, G. Caglar, B. Dzmitry, B. Fethi, S. Holger & B. Yoshua, "Learning phrase representations using RNN enconder-decoder for statistical machine traslation," arxiv.org, pp. 1-15, 2014.

[5] A. Flores, H. Tito and C. Silva, "Local average of nearest neighbors: univariate time series imputation," International Journal of Advanced Computer Science and Applications, vol. 10, nº 8, pp. 45-50, 2019.

[6] A. Flores, H. Tito & C. Silva, "CBRi: a case based reasoning-inspired approach for univariate time series imputation. In Press," de 6th IEEE Latin American Conference on Computational Intelligence LA-CCI, Guayaquil, Ecuador, 2019.

[7] S. Kavitha, S. Varuna and R. Ramya, "A comparative analysis on linear regression and support vector regression," de Online International Conference on Green Engineering and Technologies, Coimbatore, India, 2016.

[8] R. Hyndman & G. Athanasopoulos, Forecasting: principles and practice, Melbourne, Australia: OTexts, 2018.

[9] J. Palomares, J. de la Rosa, J. Ramiro, J. Melgar, A. Agüera & A. Moreno, "ARIMA vs neural networks for wind speed forecasting," de International Conference of Computational Intelligence for Measurement Systems and Applications, Hong Kong, China, 2009.

[10] Y. Pan, M. Zhang, Z. Chen, M. Zhou, Z. Zhang, "An ARIMA based model for forecasting the patient number of epidemic disease," de 13th International Conference on Service Systems and Service Management, Kunming, China, 2016.

[11] M. Abdullah, A. Hoque, "Comparison of ARIMA and SVM for short-term load forecasting," de Annual Information Technology, Electromechanical Engineering and Microelectronics Conference, Jaipur, India, 2019.

[12] S. Taylor & B. Letham, "Forecasting at scale," PeerJPreprints, pp. 1-25, 2017.

[13] I. Yenidogan, A. Cayir, O. Kozan, T. Dag & C. Arslan, "Bitcoin forecasting using ARIMA and Prophet," de 3rd International Conference on Computer Science and Engineering (UBMK), Sarajevo, Bosnia-Herzegovina, 2018.

[14] H. Aguilera, C. Guardiola, N. Naranjo & C. Kohfahl, "Towards flexible groundwater-level prediction for adaptive water management: using Facebook's Prophet forecasting approach," Hydrological Sciences Journal, 2019.

[15] Z. Oo, S. Phyu, "Microclimate prediction using cloud centric model based on IoT technology for sustainable agriculture," de IEEE 4th International Conference on Computer and Communication Systems, Singapore, Singapore, 2019.

[16] S. Kumar, L. Hussain, S. Banarjee & M. Reza, "Energy load forecasting using deep learning approach-LSTM and GRU in spark cluster," de Fifth

International Conference on Emerging Applications of Information Technology (EAIT), Kolkata, India, 2018.

[17] R. Fu, Z. Zhang & L. Li, “Using LSTM and GRU neural network methods for traffic flow prediction,” de 31st Youth Academic Annual Conference of Chinese Association of Automation (YAC), Wuhan, China, 2016.

[18] J. Zheng, X. Chen, K. Yu, L. Gan, Y. Wang & K. Wang, “Short-Term power load forecasting of residential community based on GRU neural network,” de International Conference on Power System Technology, Guangzhou, China, 2018.

[19] L. Kuan, Z. Yan, W. Xin, S. Wenxue, J. Zhe, Z. Young, X. Nan, Z. Xing, “Short-term electricity load forecasting method based on multilayered self-organizing GRU network,” de IEEE Conference on Energy Internet and Energy System Integration, Beijing, China, 2017.

[20] M. Paco, C. López Del Alamo & R. Alfonte, “Forecasting of meteorological weather time series through a feature vector based on correlation,” de 18th International Conference Computer Analysis of Images and Patterns CAIP 2019, Salerno, Italy, 2019.

[21] W. Gail, G. Yoav & Y. Eran, “On the practical computational power of finite precision RNNs for language recognition,” arxiv.org, pp. 1-9, 2018.

[22] B. Wang, W. Kong, H. Guan & N. Xiong, “Air quality forecasting based on gated recurrent long short term memory model in internet of things,” IEEE Access, vol. 7, pp. 69524 - 69534, 2019.

[23] A. Tokgoz & G. Unal, “A RNN based time series approach for forecasting turkish electricity load,” de 26th Signal Processing and Communications Applications Conference (SIU), Izmir, Turkey, 2018.

[24] A. Flores, H. Tito & C. Silva, “CBRm: case based reasoning approach for imputation of medium gaps,” (IJACSA) International Journal of Advanced Computer Science and Applications, vol. 10, nº 9, pp. 376-382, 2019.